Acc.
7.43

Cuk-H03518-18-P024404

AJR

(18)

American
Journal of
Roentgenology

July 1987

Precise localization of non-palpable lesions ...from E-Z-EM

PercuGuide™

Regardless of your present method of marking non-palpable lesions, PercuGuide™ can improve upon it.

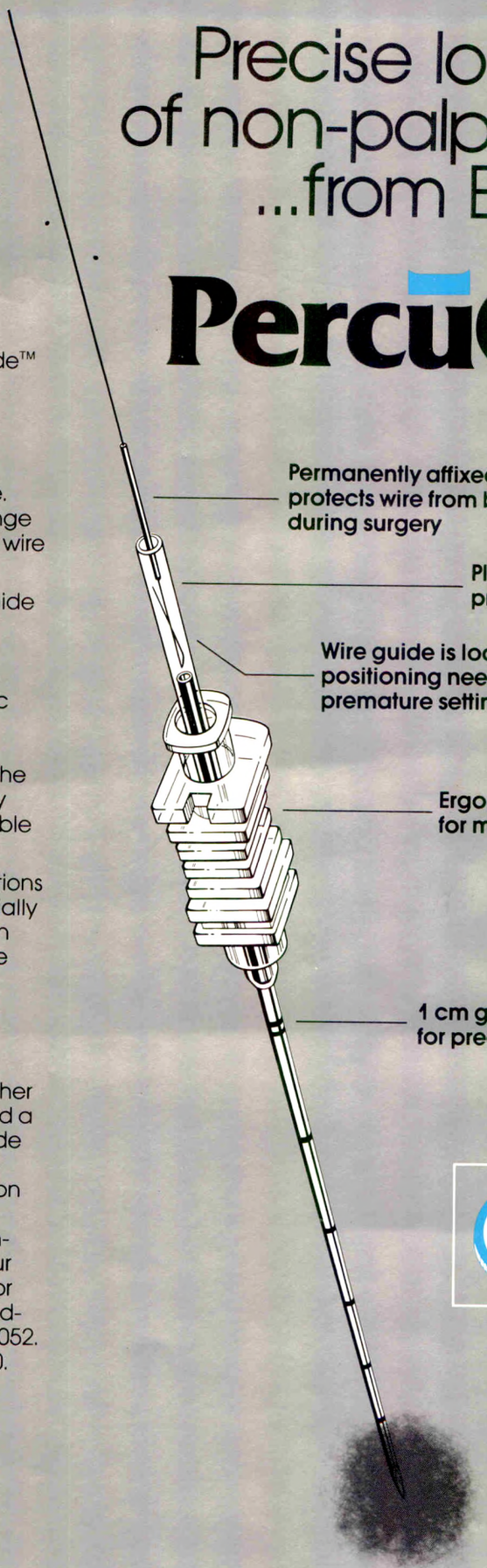
Unlike improvised markers, PercuGuide can't shift with patient movement. It won't disperse over time like a dye. And PercuGuide offers a range of refinements that no other wire guide system can match.

Afterloading of the PercuGuide wire guide eliminates any chance of the barb seating before the needle has been properly positioned. A plastic sheath makes loading easy, and a permanently affixed stiffening cannula protects the wire from being accidentally severed while it acts as a visible guide for the surgeon.

Clearly marked 1 cm gradations on the cannula, and a specially designed gripping hub aid in the precise placement of the needle. And each needle is supplied with an E-Z-MARK® radiopaque marker and a handy ruler.

If you're presently using another system, or if you've never used a wire guide before, PercuGuide can help improve your technique. For more information on PercuGuide, or on any of E-Z-EM's products for interventional medicine, contact your local E-Z-EM representative, or call E-Z-EM Interventional Products Marketing at 1-800-645-3052. In New York call 516-333-8230.

E-Z-EM
More than barium—
much more



E-Z MARK®

E-Z-MARK® radiopaque marker provided with each PercuGuide needle

E-Z-EM®
E-Z-EM, Inc.,
7 Portland Avenue
Westbury, N.Y. 11590

© 1987 E-Z-EM Inc.

Official Journal of the American Roentgen Ray Society

AJR

American Journal of Roentgenology
Diagnostic Imaging and Related Sciences

P24,444

Editor-In-Chief Robert N. Berk, *San Diego, California*

Editor Emeritus Melvin M. Figley, *Seattle, Washington*

Associate Editor Saskia von Waldenburg Hilton, *San Diego, California*

Consulting Editor Juan M. Taveras, *Boston, Massachusetts*

Assistant Editors

John R. Amberg
William L. Ashburn
Lawrence W. Bassett
Charles C. Berry
Gregory P. Borkowski
William G. Bradley
Peter L. Cooperberg
Peter Doubilet
N. Reed Dunnick
David K. Edwards
Ronald G. Evens
David S. Feigen
William R. Hendee
Robert J. Herfkens
John R. Hesselink
Charles B. Higgins
Melvyn T. Korobkin
Thomas L. Lawson
Bruce L. McClennan
Albert A. Moss
Jeffrey H. Newhouse
Donald L. Resnick
Stewart R. Reuter
Stuart S. Sagel
David J. Sartoris
Edward A. Sickles
Barry A. Siegel
Eric vanSonnenberg
David D. Stark
Edward T. Stewart

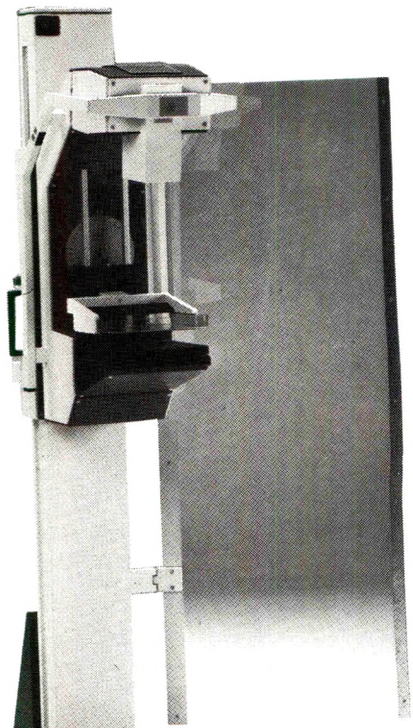
Editorial Staff: Elizabeth A. Whalen, *publications supervisor*; Linda Wood and Barbara Rose, *manuscript editors*; Nancy Rydbeck, *office manager*; Sandra Wood, *administrative assistant*; Valerie Powell, *administrative secretary*.

All business correspondence, including display (not classified) advertising, subscriptions, address changes, reprints, and permission requests should be addressed to Williams & Wilkins, 428 East Preston Street, Baltimore, MD 21202. Correspondence regarding editorial matters and classified advertising should be addressed to the editorial office, AJR, 2223 Avenida de la Playa, Suite 200, La Jolla, CA 92037-3218. For manuscript submission, see Guidelines for Authors, next page. Undelivered or damaged copies replaced within 60 days of publication; 90 days for foreign subscribers. Allow 90 days for address changes.
AJR, AMERICAN JOURNAL OF ROENTGENOLOGY (ISSN 0361 803X) is published monthly by American Roentgen Ray Society, 428 E. Preston Street, Baltimore, MD 21202. Annual dues include $50 for journal subscription. Second class postage paid at Baltimore, MD and at additional mailing offices. Postmaster send address changes (Form 3579) to Williams & Wilkins, 428 East Preston St., Baltimore, MD 21202. Subscription rates $90 ($120 foreign); institutions $100 ($130 foreign); in training $25; single copy $16 ($19). Japanese yen price is available from our sole agent USACO Corporation, 13-12, Shimbashi 1-Chome, Minato-Ku, Tokyo 105, Japan, telephone 03-502-6471. Airmail rates furnished on request. Indexed by *Current Contents* and *Index Medicus*.
Copyright © 1987 by American Roentgen Ray Society.
0361-803X/87$2.00

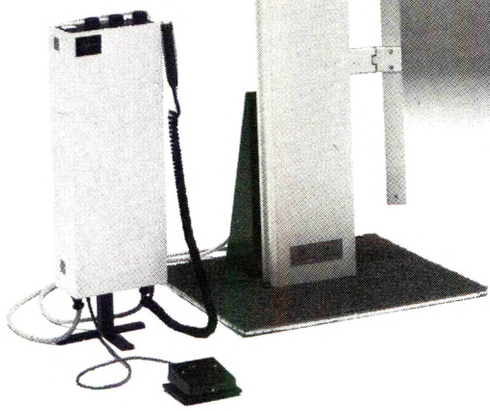
Tecnomed USA

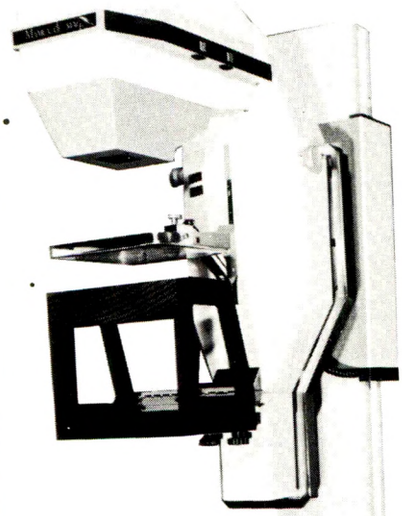
MAMMOGRAPHIC SYSTEMS

The Mamex DC is a complete mammographic system, consisting of a modern, efficient DC generator which virtually eliminates "ripple" and gives a higher resolution image with consistently higher subject contrast; a molybdenum anode x-ray tube; and a motorized compression system with floor remote control. Each feature has been designed, developed, and merged into a single unit to produce an optimal diagnostic system. Compact size, light weight and connection to any standard 220V wall outlet combine to make the Mamex DC easy to install.



Unit of Choice for:
Specialists in Mammography
St. Louis, MO







The best, made better. Mamex DC Mag, with its state-of-the-art, microprocessor-controlled operation DC generator (higher resolution image with consistently higher subject contrast); rotating anode, dual focal spot x-ray tube; and motorized compression system with fine manual adjustment offers you the ability to perform high-quality low-dose films on an efficient, operator-and-patient-friendly machine.

Unit of Choice for:
University of Michigan
Ann Arbor, MI
Melrose-Wakefield Hospital
Melrose, MA

Tecnomed USA 235 South Fehr Way, Bay Shore, New York 11706 • 516/586-1991-Telex II 510-227-9837-Telefax 516/242-4421

AJR Guidelines for Authors

Address new and revised manuscripts, correspondence, and classified ads to the Editor:

AJR Editorial Office
2223 Avenida de la Playa, Suite 200
La Jolla, CA 92037-3218 Telephone: (619) 459-2229

Inquiries regarding subscriptions, display advertising, reprints, or permission to republish *AJR* material should be addressed to the publisher:

The Williams & Wilkins Co.
428 E. Preston St.
Baltimore, MD 21202 Telephone: (301) 528-4133

The *AJR* publishes original contributions to the advancement of medical diagnosis and treatment. Submitted manuscripts should not contain previously published material and should not be under consideration for publication elsewhere. Papers dealing with neuroradiology should be addressed to: American Journal of Neuroradiology, Dept. of Radiology, Massachusetts General Hospital, Boston, MA 02114. At the discretion of the *AJR* Editor, *AJNR* articles that are of interest to the general reader may be republished in the *AJR*. Neuroradiologic papers sent to the *AJR* will be forwarded to the Editorial Office of the *AJNR*.

Manuscript decisions are based on peer review. Reviewers receive manuscripts without title pages to ensure an unbiased review. All accepted manuscripts are subject to editing. Statements made in the article, including changes made by the Editor or manuscript editor, are the responsibility of the author and not of the *AJR* or its publisher. Authors will be sent the edited manuscript, galley proof, and proofs of illustrations. If the corresponding author will be unavailable to review galleys, arrangements should be made for a coauthor or colleague to read and return the proof.

General Guidelines for Major Papers

Abstract. Clearly state (in 200 words or less) the purpose, methods, results, and conclusions of the study. Include actual data.

Introduction. Briefly describe the purpose of the investigation, including relevant background information.

Methods. Describe the research plan, the materials (or subjects), and the methods used, in that order. State in detail the confirmation of disease and control of subjectivity in observations.

Results. Present results in a clear, logical sequence. If tables are used, do not duplicate tabular data in text, but do describe important trends and points.

Discussion. Describe the limitations of the research plan, materials (or subjects), and methods, considering both the purpose and the outcome of the study. When results differ from those of previous investigators, explain the discrepancy.

AUTHOR'S CHECKLIST

For priority handling, please complete the following checklist, sign the copyright form on the reverse side of this page, and mail in both with your manuscript.

_____ Two copies of the manuscript (the original and a photocopy) and two complete sets of figures are submitted. One copy has been retained by the author.

_____ If appropriate, *AJR* Guidelines for case reports, technical notes, pictorial essays, or letters to the Editor have been followed. (See page A5.)

_____ The manuscript, including references, figure legends, and tables, is typed double-spaced throughout on 8½ × 11 in. (21.6 × 27.9 cm) nonerasable paper. Right-hand margins are not justified.

_____ All manuscript pages are numbered consecutively beginning with the abstract. Authors' names do not appear on the manuscript pages.

_____ The manuscript is organized as follows: title page, blind title page (title only), abstract, introduction, methods, results, discussion, acknowledgments, references, tables, figure legends, and figures.

_____ Informed consent has been obtained from patients who participated in clinical investigations. If experiments were performed on animals, authors complied with NIH guidelines for use of laboratory animals.

_____ Use of unfamiliar acronyms and abbrevations is kept to a minimum. When abbreviations are used they are written out at first mention, with the abbreviation following in parentheses.

_____ Metric measurements are used throughout, or the metric equivalent is given in parentheses.

_____ Names and locations (city and state only) of manufacturers are given for equipment and nongeneric drugs.

Title Page

_____ The following information is given: title of article; names and complete addresses (including zip code) of all authors; current addresses of authors who have moved since study; acknowledgment of grant or other assistance. The corresponding author is clearly identified, and a current address and phone number are given.

_____ Two copies of a blind title page are included giving only the title (without the authors' names) for use in the review process.

Abstract

_____ An abstract of approximately 200 words concisely states the purpose, methods, results, and conclusions of the study. Actual data are included.

_____ No abbreviations or reference citations are used in the abstract.

References

_____ References (not to exceed 35) are typed double-spaced starting on a separate page and are **numbered consecutively in the order in which they appear in the text.**

_____ All references are cited in the text and are enclosed in brackets and typed on line with the text (not superscript).

_____ Unpublished data are not cited in the reference list, but are cited parenthetically in the text, for example, (Smith DJ, personal communication), (Smith DJ, unpublished data). This includes papers submitted, but not yet accepted, for publication.

_____ Inclusive page numbers (e.g., 333–335) are given for all references.

_____ Journal names are abbreviated according to *Index Medicus*.

_____ Style and punctuation of references follow the format illustrated in the following examples (all authors are listed when six or less; when seven or more authors, the first three are listed, followed by "et al."):

Journal article

1. Long RS, Roe EW, Wu EU, et al. Membrane oxygenation: radiographic appearance. *AJR* **1986**;146:1257–1260

Book

2. Smith LW, Cohen AR. *Pathology of tumors*, 6th ed. Baltimore: Williams & Wilkins, **1977**:100–109

Chapter in a book

3. Breon AJ. Serum monitors of bone metastasis. In: Clark SA, ed. *Bone metastases*. Baltimore: Williams & Wilkins, **1983**:165–180

Paper presented at a meeting

4. Lau FS, Kirk AN, Beck RA. MR imaging of the spine. Presented at the annual meeting of the American Roentgen Ray Society, Washington, DC, April 1986

Tables

_____ Each table is typed double-spaced on a separate page without vertical or horizontal rules; each has a short, descriptive title. Tables do not exceed two pages in length and contain at least four lines of data.

_____ Tables are numbered in the order in which they are cited in the text.

_____ Abbreviations are defined in an explanatory note below each table.

_____ Tables are self-explanatory and do not duplicate data given in the text or figures.

_____ All arithmetic (percentages, totals, differences) has been double checked for accuracy, and tabular data agree with data given in the text.

Figures and Legends

_____ Two complete sets of original figures are submitted unmounted in labeled envelopes.

_____ Figures are clean, unscratched, 5 × 7 in. (13 × 18 cm) glossy prints with white borders. A separate print is submitted for each figure *part*.

_____ Each figure is labeled on the back with the figure number and an arrow indicating "top." Labeling is done on a gummed label and then affixed to the back of the print. (Never use ink on front or back of figures.)

_____ Author's names are *not* written on the backs of figures.

_____ Only removable (rub-on) arrows and letters are used on the figures. Symbols are uniform in size and style and are not broken or cracked.

_____ Images are uniform in size and magnification.

_____ Line drawings are done in black ink on a white background and are of professional quality. (Only glossy prints, not originals or photocopies, are acceptable.)

_____ Written permission has been obtained for use of all previously published illustrations (and copies of permission letters are included), and an appropriate credit line is given in the legends.

_____ Legends are typed double-spaced, and figure numbers correspond with the order in which the figures are cited in the text.

Transfer of Copyright Agreement and Exclusive Publication Statement

Complete copyright to the article entitled: _____

_____

is hereby transferred to the American Roentgen Ray Society (for United States government employees to the extent transferable), effective if and when the article is accepted for publication in the *American Journal of Roentgenology*. In the case of the authors who are officers or employees of the United States government, the American Roentgen Ray Society recognizes that works prepared by officers or employees of the United States government as part of their official government duties are in the public domain.

Authors reserve all proprietary rights other than copyright, such as patent rights and the right to use all or part of this article in future works of their own. The authors retain the right of replication, subject only to crediting the original source of publication and receiving written permission from the publisher.

Authors guarantee that this manuscript contains no matter that is libelous or otherwise unlawful, invades individual privacy, or infringes any proprietary rights.

Authors understand that they will receive no royalty or other compensation from the American Roentgen Ray Society.

Finally, the authors certify that none of the material in this manuscript has been published previously or is currently under consideration for publication elsewhere.

_____	_____	_____
First author/date	Second author	Third author
_____	_____	_____
_____	_____	_____

This agreement must be signed by all authors in order for the manuscript to be published.

Case Reports

A case report is a brief description of a special case that provides a message that transcends the individual patient.

Format. There is no abstract. The introduction should be a short paragraph giving the general background and the specific interest of the case. No more than one case should be described in detail (similar ones can be mentioned briefly in the discussion). Emphasis should be on the radiologic aspects; clinical information must be limited to that necessary to provide a background for the radiology. The discussion should be succinct and should focus on the specific message and relevance of radiologic methods. A review of the literature is not appropriate.

Length. Maximum of five double-spaced, typewritten pages, including the references but not the title page or figure legends.

References. Maximum of eight.

Figures. Maximum of three or four, unless the text is shortened accordingly. Legends must not repeat the text.

Tables and Acknowledgments. Not appropriate in case reports.

Technical Notes

A technical note is a brief description of a specific technique or procedure, modification of a technique, or equipment of interest to radiologists.

Format. No abstract, headings, or subheadings are required. If headings are used, they should be a combination of "Case Report," "Materials and Methods," "Results," and "Discussion." A brief one-paragraph introduction should be included to give the general background. Discussion should be limited to the specific message, including the uses of the technique or equipment. Literature reviews and lengthy case reports are not appropriate.

Length. Maximum of five double-spaced, typewritten pages, including the references but not the title page or figure legends.

References. Maximum of eight.

Figures. Maximum of two, unless the text is shortened accordingly.

Tables and Acknowledgments. Not appropriate in technical notes.

Pictorial Essays

A pictorial essay is an article that conveys its message through illustrations and their legends. Unlike other *AJR* articles, which are based on original research, pictorial essays serve primarily as teaching tools, like exhibits at a scientific meeting. They are not encyclopedic book chapters. No abstract is necessary.

Length. Maximum of four double-spaced, typewritten pages, including the references but not the title page or figure legends.

References. Maximum of four.

Figures. Maximum of 30 figure *parts*. Number should be as few as necessary to convey the message of the paper.

Tables and Acknowledgments. Not appropriate in pictorial essays.

Letters to the Editor and Replies

Letters to the Editor and Replies should offer objective and constructive criticism of published articles. Letters may also discuss matters of general interest to radiologists.

Format. All letters should be typed double-spaced on nonletterhead paper, with no greeting or salutation. Signature and affiliation should appear at the end of the letter. Titles for letters should be short and pertinent. The title for a reply is simply "Reply."

Length. Maximum of two double-spaced, typewritten pages, including references.

References. Maximum of four.

Figures. Maximum of two.

Tables and Acknowledgments. Not appropriate in Letters to the Editor and Replies.

Opinions, Commentaries, and Perspectives

Opinions, commentaries, and perspectives are special articles dealing with controversial topics or issues of special concern to radiologists.

Format. Include a title page but no abstract. Headings may be used to break up the text.

Length. Maximum of five double-spaced, typewritten pages.

References. Maximum of five.

Tables and Figures. Maximum of four.

Computer Page Articles

Articles published on the computer page deal with practical computer applications to radiology.

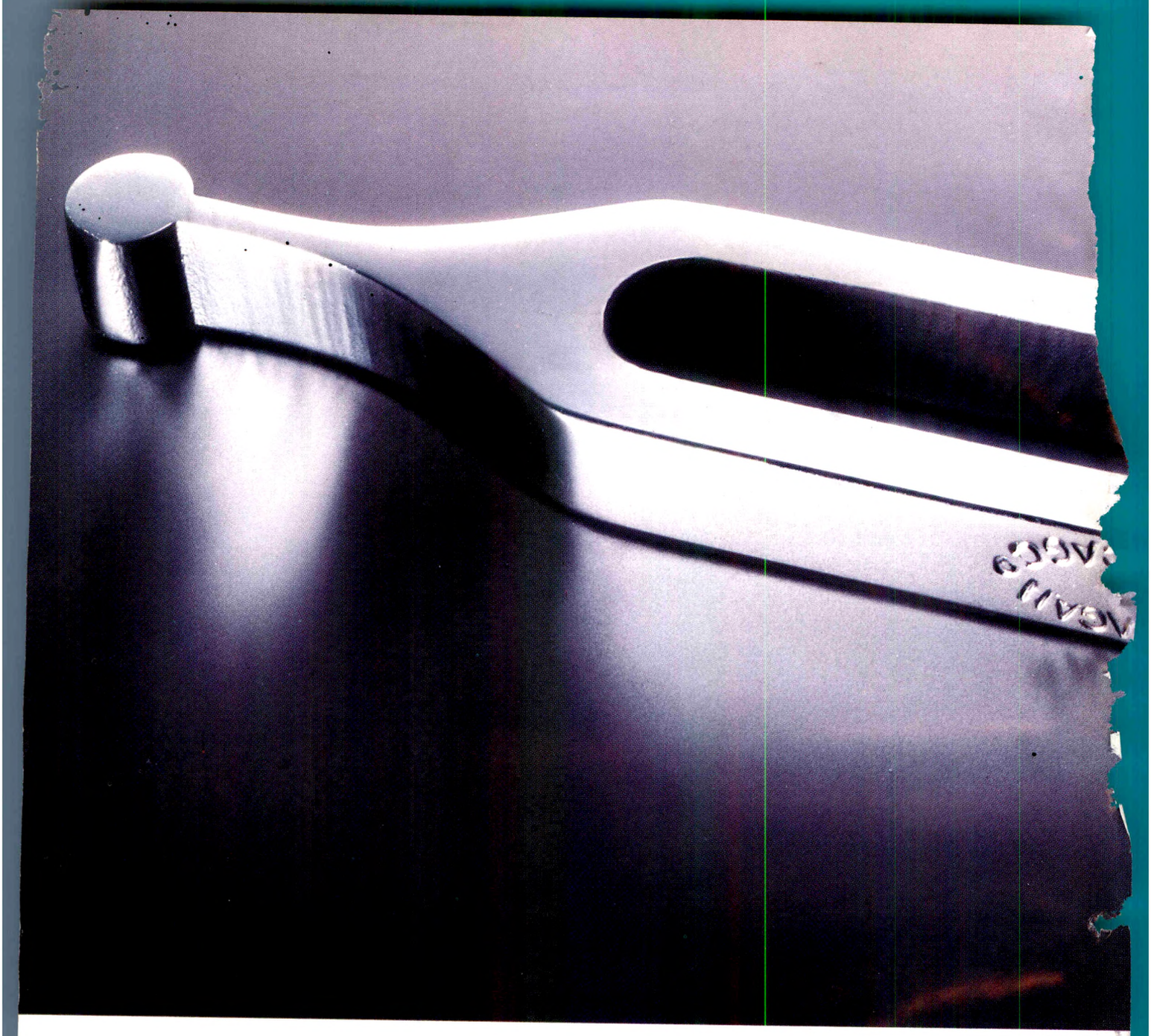
Format. Include a title page but no abstract.

Length. Maximum of eight double-spaced, typewritten pages.

References. Maximum of five.

Figures and Tables. Maximum of five. Computer printouts are not acceptable. Figures must be submitted as 5 × 7 in. glossy prints.

All submissions to the *AJR* must be accompanied by a completed copy of the Author's Checklist and the signed Copyright Agreement.



The art of fine-tuning.
At Kodak, we use it to give you the video image you like.

© Eastman Kodak Company, 1986



Your ideal video image is probably unlike any other. Subtly lighter or darker. A little more contrast. Or a little less. Perhaps your eyes are accustomed to a blue base. Perhaps not. Kodak has the means to *fine-tune* your video images to your personal preferences.

First step: Your Kodak representative adjusts your multiformat cameras to your "look." And measures that look precisely with our exclusive Kodak video display analyzer. And then matches that look to one of Kodak's five video imaging films. More options than anyone else can offer.

Then, to make sure everything works with everything else, there's a complete line of video imaging products from Kodak. Ranging from Kodaflex roomlight film-handling products for speed and efficiency to reliable, proven Kodak X-Omat processors.

For details, ask your Kodak representative, or write Eastman Kodak Company, Dept. 412L-HS, 343 State Street, Rochester, NY 14650.

Can you afford anything less?

Kodak

MAST™ AND STIR™. WHY SETTLE FOR LESS?

Best Image Quality.

Accurate diagnoses depend on it.
Referring physicians demand it.
Your MR service must provide it.
And now you don't have to settle for less.

Motion Artifact Suppression Technique (MAST™).

Only VISTA® offers enhanced spatial resolution with motion artifact suppression so effective that it eliminates artifacts caused by complex motions such as velocity, acceleration and pulsatility. Now with MAST you don't have to settle for anything less than the best image quality.

Short Tau Inversion Recovery (STIR™).

VISTA is the only system to offer Short Tau Inversion Recovery (STIR), which features the best contrast resolution on multi-slice studies of soft tissue. STIR suppresses the signal from fat tissue for a clear delineation between fat and nearby soft tissue. Now, with the high contrast provided with STIR, you don't have to settle for anything less than the best image quality.

Increased Referrals.

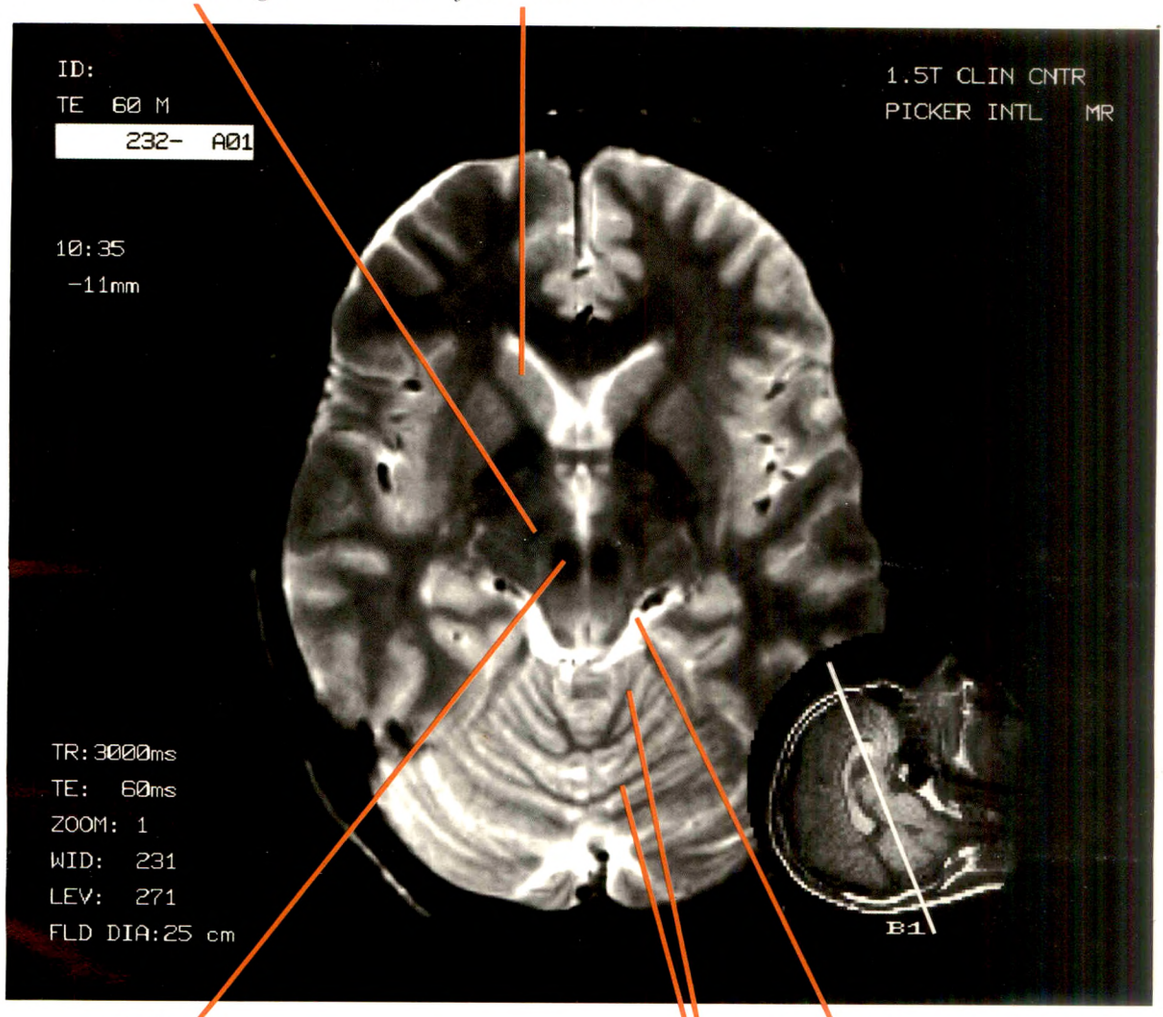
The success of your MR Service depends on its ability to compete. On its ability to build a strong referral base. MAST and STIR are two unique VISTA capabilities which provide uncompromised image quality, a necessity for referral building. But VISTA offers more. 512 x 512 acquisition and display for the highest resolution images available. Three-angle oblique imaging for superior heart and spine studies. Specialized research programs for cardiac, neuro and orthopedic specialties. Reference Pilot Scan for immediate localization of slice position. And much more.

VISTA® . . .Why Settle for Less?

CIRCLE 13 ON READER SERVICE CARD

Some features of Picker's VISTA MR systems are classified as investigational devices and limited by federal law to investigational use. As such, they cannot be made available until necessary government approvals have been granted.

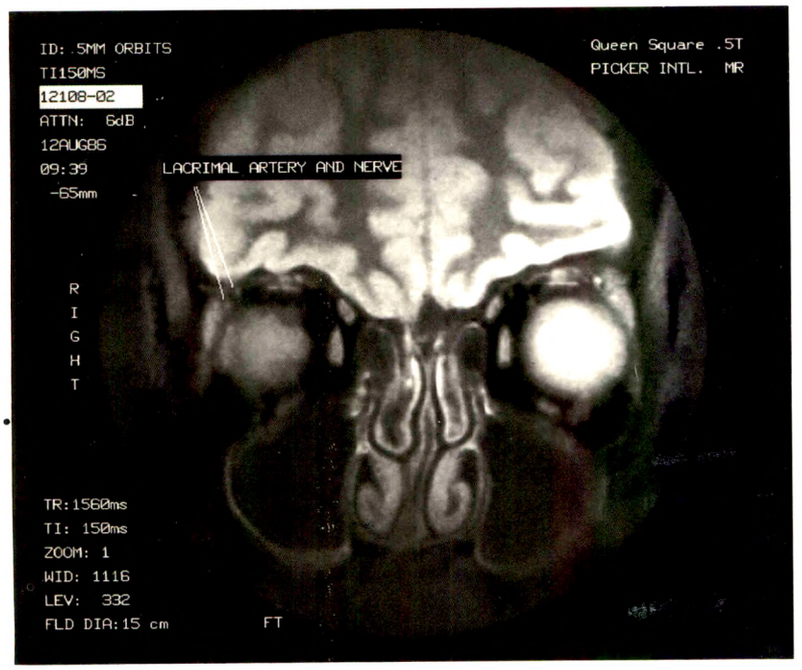
Anatomy of VISTA® MR Image Quality



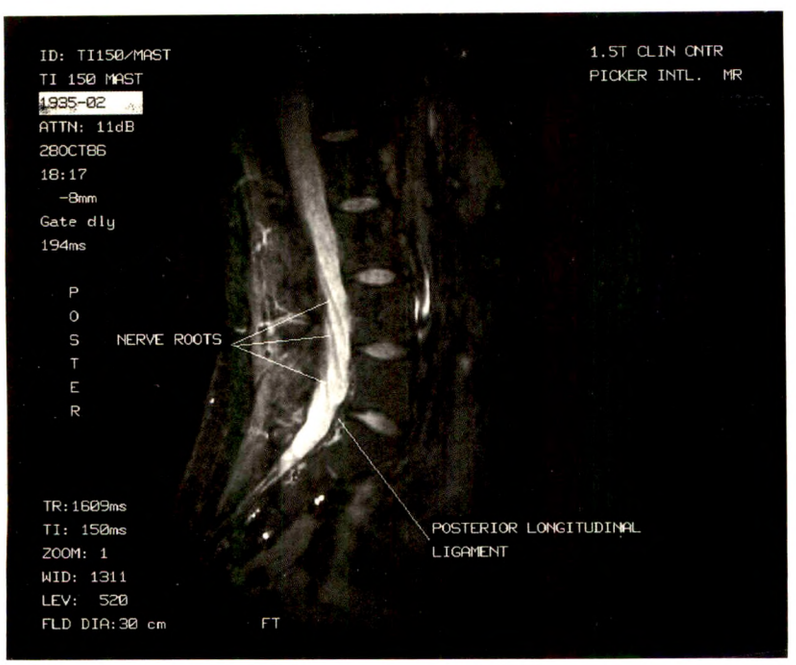
PICKER

THE IMAGE OF EXCELLENCE

VISTA® Referral Building Image Quality



This demyelinating plaque study uses STIR for exquisite delineation of orbital contents. STIR enables fat suppression and highlights structures not easily visualized with other MR protocols, as shown by visualization of the lacrimal artery and nerve.



This unique sequence combination of Short Tau Inversion Recovery (STIR) and Motion Artifact Suppression Technique (MAST) results in excellent fat suppression in vertebral bodies of the normal spine. With MAST, nerve roots are sharply contrasted against the bright signal imparted on the basivertebral drainage system.

PICKER

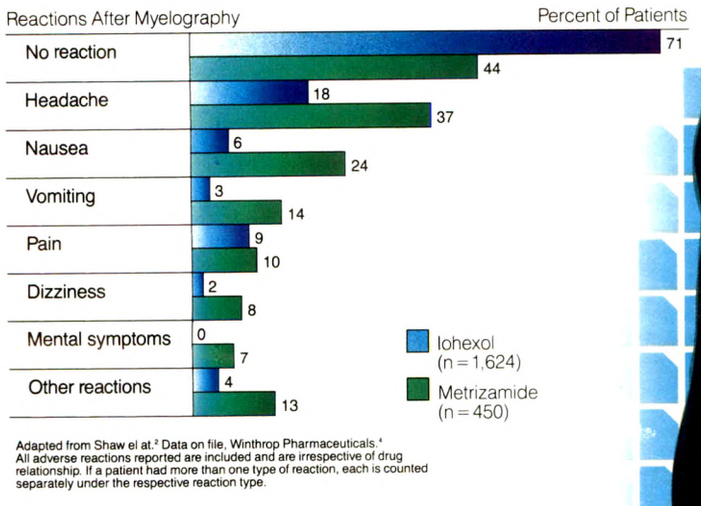
THE IMAGE OF EXCELLENCE

In intrathecal imaging:

Because you can't be sure how every patient will react...

Improve the safety profile.

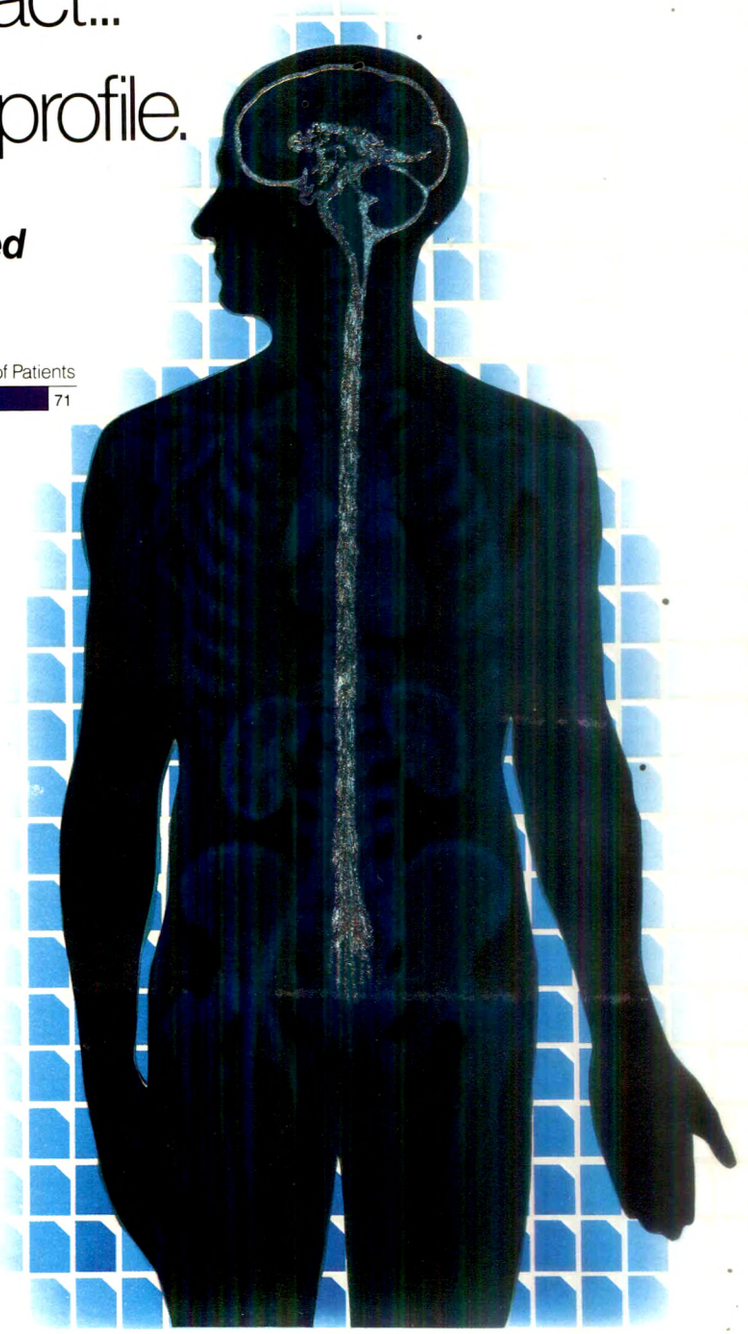
Better patient tolerance, measured subjectively and objectively.[1-5]



Adapted from Shaw et al.[2] Data on file, Winthrop Pharmaceuticals.[4] All adverse reactions reported are included and are irrespective of drug relationship. If a patient had more than one type of reaction, each is counted separately under the respective reaction type.

Lower incidence of EEG changes compared with iopamidol or metrizamide.[2,5]

Excellent diagnostic quality.



NONIONIC

OMNIPAQUE®

(IOHEXOL)

THE NEW STANDARD IN INTRATHECAL IMAGING.

See next page for important product information concerning contraindications, warnings, adverse reactions, patient selection, and precautionary recommendations.



OMNIPAQUE®
INJECTION (IOHEXOL)
INTRATHECAL

180

240

300

PLEASE CONSULT FULL PRODUCT INFORMATION BEFORE USING. A SUMMARY FOLLOWS:

DESCRIPTION: OMNIPAQUE is a nonionic, water-soluble radiographic contrast medium for intrathecal administration in concentrations of 180, 240, and 300 mgI/mL. Each milliliter of iohexol solution contains 1.21 mg tromethamine and 0.1 mg edetate calcium disodium with the pH adjusted between 6.8 and 7.7 with hydrochloric acid or sodium hydroxide. All solutions are sterilized by autoclaving, are nonpyrogenic, and contain no preservatives, so unused portions should be discarded.

CONTRAINDICATIONS–Intrathecal: OMNIPAQUE should not be administered to patients with a known hypersensitivity to iohexol. Myelography should not be performed in the presence of significant local or systemic infection where bacteremia is likely. Intrathecal administration of corticosteroids with OMNIPAQUE is contraindicated. Because of the possibility of overdosage, immediate repeat myelography in the event of technical failure is contraindicated.

WARNINGS–General: If grossly bloody CSF is encountered, the possible benefits of a myelographic procedure should be considered in terms of the risk to the patient.

Caution is advised in patients with a history of epilepsy, severe cardiovascular disease, chronic alcoholism, or multiple sclerosis.

Elderly patients may present a greater risk following myelography. The need for the procedure in these patients should be evaluated carefully. Special attention must be paid to dose and concentration of the medium used, hydration, and technique used.

Patients who are receiving anticonvulsants should be maintained on this therapy. Should a seizure occur, intravenous diazepam or phenobarbital sodium is recommended. In patients with a history of seizure activity who are not on anticonvulsant therapy, premedication with barbiturates should be considered.

Prophylactic anticonvulsant treatment with barbiturates should be considered in patients with evidence of inadvertent intracranial entry of a large or concentrated bolus of the contrast medium, since there may be an increased risk of seizure in such cases.

Drugs that lower the seizure threshold, especially phenothiazine derivatives, including those used for their antihistamine or antinauseant properties, are not recommended for use with OMNIPAQUE. Others include MAO inhibitors, tricyclic antidepressants, CNS stimulants, and psychoactive drugs described as analeptics, major tranquilizers, or antipsychotic drugs. While the contributory role of these medications has not been established, the use of such drugs should be based on physician evaluation of potential benefits and potential risks. Physicians have discontinued these agents at least 48 hours before and for at least 24 hours postprocedure. Care is required in patient management to prevent inadvertent intracranial entry of a large dose or concentrated bolus of the medium. Also, effort should be directed to avoid rapid dispersion of the medium causing inadvertent rise in intracranial levels (eg, by active patient movement). Direct intracisternal or ventricular administration for standard radiography (not CT) is not recommended.

In most reported cases of major motor seizures with nonionic myelographic media, one or more of the following factors were present. Therefore avoid:

- Deviations from recommended procedure or in myelographic management.
- Use in patients with a history of epilepsy.
- Overdosage.
- Intracranial entry of a bolus or premature diffusion of a high concentration of the medium.
- Medication with neuroleptic drugs or phenothiazine antinauseants.
- Failure to maintain elevation of the head during the procedure, on the stretcher, or in bed.
- Excessive and particularly active patient movement or straining.

PRECAUTIONS–General: Diagnostic procedures that involve the use of radiopaque diagnostic agents should be carried out under the direction of personnel with the prerequisite training and with a thorough knowledge of the particular procedure to be performed. Appropriate facilities should be available for coping with any complication of the procedure, as well as for emergency treatment of reactions to the contrast agent itself. After parenteral administration of a radiopaque agent, competent personnel and emergency facilities should be available, since delayed reactions have been reported (see ADVERSE REACTIONS).

Preparatory dehydration may be dangerous and may contribute to acute renal failure in patients with advanced vascular disease, diabetic patients, and in susceptible nondiabetic patients (often elderly with preexisting renal disease). Dehydration in these patients seems to be enhanced by the osmotic diuretic action of contrast agents. *Patients should be well hydrated prior to and following iohexol administration.*

The possibility of a reaction, including serious, life-threatening, fatal, anaphylactoid, or cardiovascular reactions, should always be considered (see ADVERSE REACTIONS). Therefore, it is of utmost importance that a course of action be carefully planned in advance for the immediate treatment of serious reactions, and that adequate and appropriate facilities and personnel be readily available in case of a severe reaction.

The possibility of an idiosyncratic reaction in susceptible patients should always be considered (see ADVERSE REACTIONS). The susceptible population includes patients with a history of a previous reaction to contrast media, patients with a known sensitivity to iodine per se, and patients with a known clinical hypersensitivity: bronchial asthma, hay fever, and food allergies.

A thorough medical history with emphasis on allergy and hypersensitivity, prior to the injection of any contrast medium, may be more accurate than pretesting in predicting potential adverse reactions.

A positive history of allergy or hypersensitivity does not arbitrarily contraindicate the use of a contrast agent where a diagnostic procedure is thought essential, but caution should be exercised (see ADVERSE REACTIONS). Premedication with antihistamines or corticosteroids, to avoid or minimize possible allergic reactions in such patients, should be considered.

In patients with severe renal insufficiency or failure, compensatory biliary excretion of the drug is anticipated to occur, with a slow clearance into the bile. Patients with hepatorenal insufficiency should not be examined unless the possibility of benefit clearly outweighs the additional risk. Sterile technique must be used with any spinal puncture.

When OMNIPAQUE is to be injected using plastic disposable syringes, the contrast medium should be drawn into the syringe and used immediately. If nondisposable equipment is used, scrupulous care should be taken to prevent residual contamination with traces of cleansing agents. **Parenteral drug products should be inspected and discarded if particulate matter or discoloration is present.**

Repeat Procedures. If in the clinical judgment of the physician sequential or repeat examinations are required, a suitable interval of time between administrations should be observed to allow for normal clearance of the drug from the body.

Information for Patients: *When receiving injectable radiopaque diagnostic agents, inform your physician: if you are pregnant; if you are diabetic; if you have multiple myeloma, pheochromocytoma, homozygous sickle cell disease, or known thyroid disorder; if you are allergic to any drugs or food or if you had any reactions to previous injections of dyes used for x-ray procedures; about any other medications you are currently taking, including nonprescription drugs, before you are administered this drug.*

Drug Interactions (See WARNINGS–General): In nonelective procedures in patients on the drugs described, consider prophylactic use of anticonvulsants.

Carcinogenesis, Mutagenesis, Impairment of Fertility: No long-term animal studies have been performed to evaluate carcinogenic potential, mutagenesis, or whether OMNIPAQUE can affect fertility in men or women.

Pregnancy Category B: Reproduction studies have been performed in rats and rabbits with up to 100 times the recommended dose. No evidence of impaired fertility or harm to the fetus has been demonstrated due to OMNIPAQUE; there are, however, no studies in pregnant women. Because animal reproduction studies are not always predictive of human response, this drug should be used during pregnancy only if clearly indicated.

Nursing Mothers: It is not known to what extent iohexol is excreted in human milk. However, many injectable contrast agents are excreted unchanged in human milk. Although it has not been established that serious adverse reactions occur in nursing infants, caution should be exercised when intravascular contrast media are administered to nursing women. Bottle feedings may be substituted for breast feedings for 24 hours following administration of OMNIPAQUE.

Pediatric Use: Safety and effectiveness in children have not been established.

ADVERSE REACTIONS–Intrathecal: The most frequently reported adverse reactions with OMNIPAQUE 180, OMNIPAQUE 240, and OMNIPAQUE 300 are headache, mild to moderate pain including backache, neck ache and stiffness, nausea and vomiting. These reactions usually occur 1 to 10 hours after injection, and almost all occur within 24 hours. They are usually mild to moderate in degree, lasting for a few hours and usually disappearing within 24 hours. Rarely, headaches may be severe or persist for days. Headache is often accompanied by nausea and vomiting and tends to be more frequent and persistent in patients not optimally hydrated. Transient alterations in vital signs may occur and their significance must be assessed on an individual basis. Those reactions reported in clinical studies with OMNIPAQUE are listed below in decreasing order of occurrence, based on clinical studies of 1,624 patients.

Headaches: The most frequently occurring adverse reaction following myelography has been headache, with an incidence of approximately 18%. Headaches may be caused either by a direct effect of the contrast medium or by CSF leakage at the dural puncture site. However, in managing the patient, it is considered more important to minimize intracranial entry of contrast medium by postural management than to attempt to control possible CSF leakage (see PATIENT MANAGEMENT).

Pain: Mild to moderate pain including backache, neck ache and stiffness, and neuralgia occurred following injection, with an incidence of about 8%.

Nausea and Vomiting: Nausea was reported with an incidence of about 6%, and vomiting about 3% (see PATIENT MANAGEMENT). Maintaining normal hydration is very important. The use of phenothiazine antinauseants is not recommended (see WARNINGS–General). Reassurance to the patient that the nausea will clear usually is all that is required.

Dizziness: Transient dizziness was reported in about 2% of the patients.

Other Reactions: Other reactions occurring with an individual incidence of less than 0.1% included: feeling of heaviness, hypotension, hypertonia, sensation of heat, sweating, vertigo, loss of appetite, drowsiness, hypertension, photophobia, tinnitus, neuralgia, paresthesia, difficulty in micturition, and neurological changes. All were transient and mild with no clinical sequelae.

General Adverse Reactions to Contrast Media: Physicians should remain alert for the occurrence of adverse effects in addition to those discussed above, particularly the following reactions which have been reported in the literature for other nonionic, water-soluble myelographic media and rarely with iohexol. These have included, but are not limited to, aseptic and bacterial meningitis and CNS and other neurologic disturbances.

An aseptic meningitis syndrome has been reported rarely (less than 0.01%). It was usually preceded by pronounced headaches, nausea, and vomiting. Onset usually occurred about 12 to 18 hours postprocedure. Prominent features were meningismus and fever, sometimes with oculomotor signs and mental confusion. Lumbar puncture revealed a high white cell count and high protein content, often with a low glucose level and absence of organisms. The condition usually started to clear spontaneously about 10 hours after onset, with complete recovery over 2 to 3 days.

Allergy or Idiosyncrasy: Chills, fever, profuse diaphoresis, pruritus, urticaria, nasal congestion, dyspnea, and Guillain-Barré syndrome.

CNS Irritation: Mild and transitory perceptual aberrations, such as hallucinations, depersonalization, amnesia, hostility, amblyopia, diplopia, photophobia, psychosis, insomnia, anxiety, depression, hyperesthesia, visual or auditory or speech disturbances, confusion and disorientation. In addition, malaise, weakness, EEG changes, meningismus, hyperreflexia or areflexia, hypertonia or flaccidity, hemiplegia, paralysis, quadriplegia, restlessness, tremor, echoacousia, echolalia, asterixis, and dysphasia have occurred.

Profound mental disturbances have also rarely been reported: various forms and degrees of aphasia, mental confusion, or disorientation. Onset is usually at 8 to 10 hours and lasts for about 24 hours. Occasionally, they have been manifest as apprehension, agitation, or progressive withdrawal in several instances to the point of somnolence, stupor, and coma. In a few cases, these have been accompanied by transitory hearing loss or other auditory symptoms and visual disturbances (believed subjective or delusional), including unilateral or bilateral loss of vision, which may last for hours. In one case, persistent cortical loss of vision has been reported in association with convulsions. Ventricular block has been reported; amnesia of varying degrees may be present for the reaction event.

Rarely, persistent though transitory weakness in the leg or ocular muscles has been reported. Peripheral neuropathies have been rare and transitory. They include sensory and/or motor or nerve root disturbance, myelitis, persistent leg muscle pain or weakness, 6th nerve palsy, or cauda equina syndrome. Muscle cramps, fasciculation or myoclonia, spinal convulsion, or spasticity are unusual and have responded promptly to a small intravenous dose of diazepam.

In general, the reactions that are known to occur on parenteral administration of iodinated contrast agents are possible with any nonionic agent. Approximately 95% of adverse reactions accompanying the use of water-soluble contrast agents are mild to moderate in degree. However, severe, life-threatening, anaphylactoid, and fatal reactions, mostly of cardiovascular origin, have occurred. Adverse reactions to injectable contrast media fall into two categories: chemotoxic reactions and idiosyncratic reactions.

Chemotoxic reactions result from the physicochemical properties of the contrast medium, the amount of the dose and the speed of injection. All hemodynamic disturbances and injuries to organs or vessels perfused by the contrast medium are included in this category.

Idiosyncratic reactions occur more frequently in patients 20 to 40 years old and may or may not be dependent on the amount of dose injected, the speed of injection, and the radiographic procedure. They are subdivided into minor, intermediate, and severe. The minor reactions are self-limited and of short duration; the severe reactions are life-threatening, and treatment is urgent and mandatory.

The reported incidence of adverse reactions to the contrast medium in patients with a history of allergy is twice that of the general population. Patients with a history of previous reactions to a contrast medium are three times more susceptible than other patients. However, sensitivity to contrast media does not appear to increase with repeated examination.

Most adverse reactions to injectable contrast media appear within 1 to 3 minutes after the start of injection, but delayed reactions may occur.

OVERDOSAGE: Although clinical consequences of overdosage with OMNIPAQUE have not been reported, physicians should be aware that incorrect management of the patient can permit inadvertent early intracranial entry of normal doses of the medium, thereby increasing CNS reactions.

The intracisternal LD_{50} value of OMNIPAQUE (in grams of iodine per kilogram body weight) is greater than 2.0 in mice.

References: 1. Kieffer SA, Binet EF, Davis DO, et al: Lumbar myelography with iohexol and metrizamide: A comparative multicenter prospective study. *Radiology* 1984; 151:665-670. **2.** Shaw DD, Bach-Gansmo T, Dahlstrom K: Iohexol: summary of North American and European clinical trials in adult lumbar, thoracic, and cervical myelography with a new nonionic contrast medium. *Invest Radiol* 1985; 20(suppl 1):44-50. **3.** Latchaw RE, Hirsch WL Jr, Horton JA, et al: Iohexol vs metrizamide: Study of efficacy and morbidity in cervical myelography. *AJNR* 1985; 6:931-933. **4.** Data on file, Winthrop Pharmaceuticals. **5.** Lamb JT: Iohexol vs. Iopamidol for myelography. *Invest Radiol* 1985; 20(suppl 1):37-43.

© 1987 WINTHROP PHARMACEUTICALS 71171/3777

Winthrop PHARMACEUTICALS

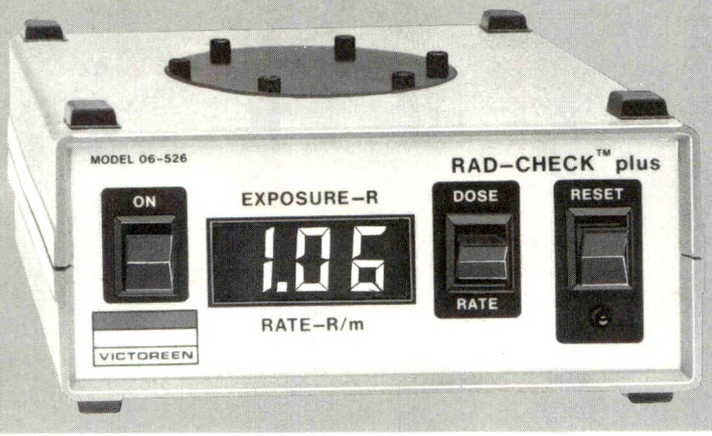
Winthrop Pharmaceuticals
Division of Sterling Drug Inc.
New York, NY 10016

Federal Agency *Recommends...*
PLUS
Joint Commission on Accreditation of Hospitals *Requires...*

HOSPITALS MUST MONITOR DOSES FROM DIAGNOSTIC RADIOLOGY PROCEDURES!

RAD-CHECK® PLUS X-Ray Exposure Meter

Will Perform This Function Plus Many Others!



The Joint Commission on Accreditation of Hospitals requires...

Diagnostic Radiology Services monitor doses from diagnostic radiology procedures. (Accreditation Manual for Hospitals 1987 - DR.2.2.10.2).

Center for Devices and Radiological Health recommends...

1. Diagnostic radiology facilities should be aware of the amount of radiation received by a patient.
2. These exposure levels should fall within acceptable levels. If they don't, appropriate action should be taken. (Publication FDA 85-8247, "Recommendations for Evaluation of Radiation Exposure from Diagnostic Radiology Examinations.") Available from Nuclear Associates.

Over 5 Years of Reliable Service in the Field

APPLICATIONS...

- Entrance skin exposure measurements (ESE).
- Fluoroscopy exposure measurements.
- Exposure checks — radiographic (mR/mAs).
- Beam quality — half-value layer (HVL).
- MAs reciprocity — mA station checks.

ADVANTAGES...

- Fast, easy to use: Battery operation and built-in detector eliminate set-up time. Place RAD-CHECK PLUS on x-ray table, collimate, shoot, and read the result!
- Dual range: Dose up to 2 R; dose rate up to 20 R/min.
- Automatic reset after exposure.
- Optional remote detector.
- Compact: 6″ × 6¼″ × 2¾″ high; weighs 18 oz.

For more information request Bulletin 356-C

CIRCLE 16 ON READER SERVICE CARD

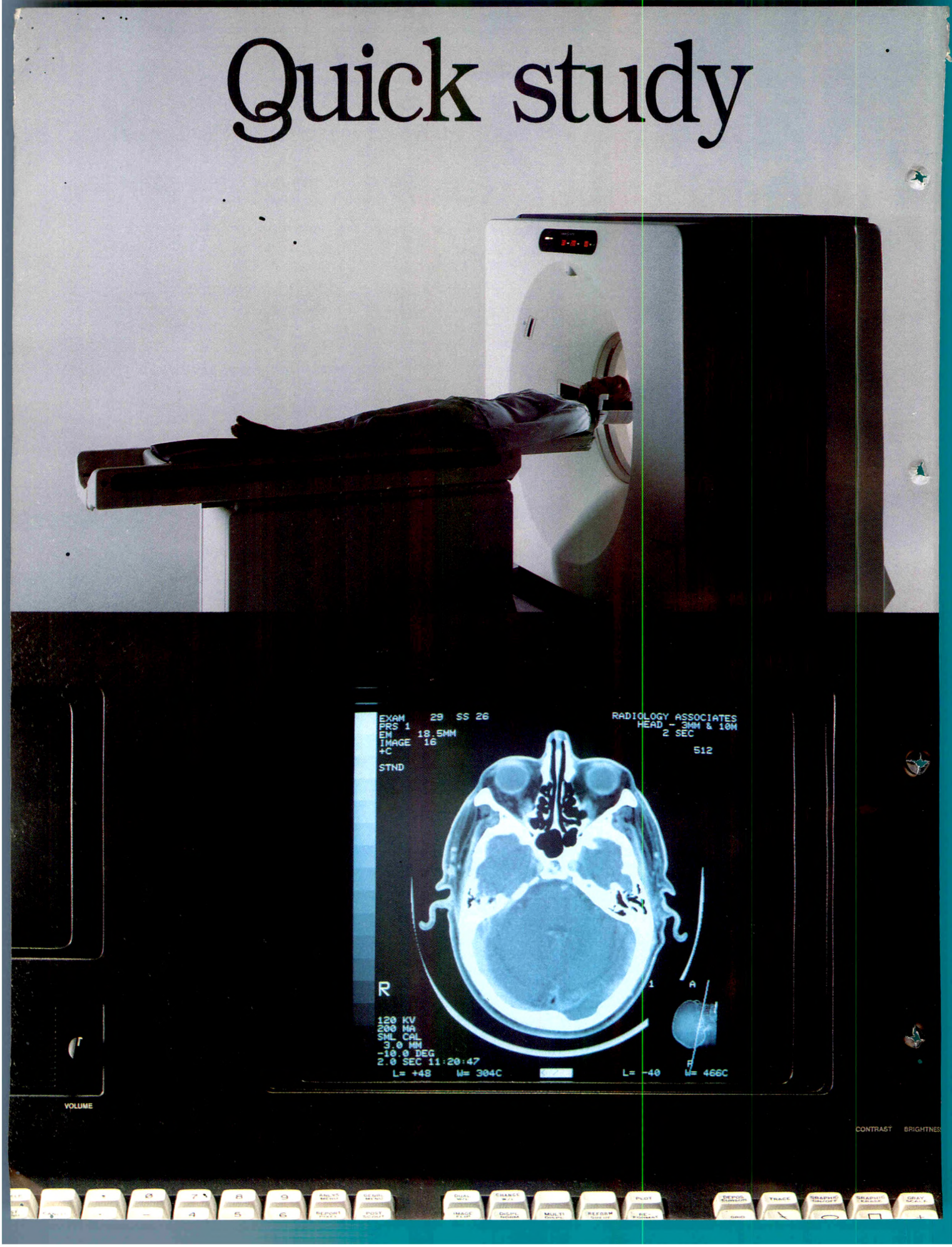
NUCLEAR ASSOCIATES

VICTOREEN

A Division of VICTOREEN, INC.
100 VOICE ROAD
CARLE PLACE, NY 11514-1593
(516) 741-6360
A Subsidiary of Sheller-Globe SG

® Victoreen, Inc.

Quick study


EXAM 29 SS 26
PRS 1
EM 18.5MM
IMAGE 16
+C
STND
RADIOLOGY ASSOCIATES
HEAD - 3MM & 10M
2 SEC
512
R
120 KV
200 MA
SML CAL
3.0 MM
-10.0 DEG
2.0 SEC 11:20:47
L= +48 W= 304C
L= -40 W= 466C
VOLUME
CONTRAST
BRIGHTNESS

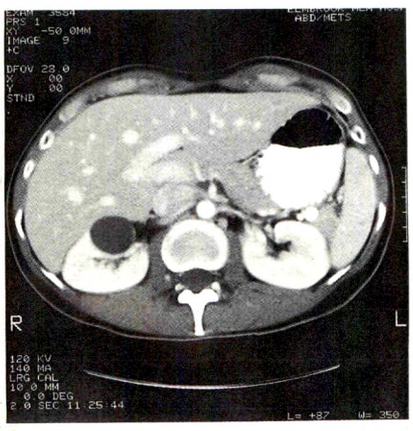
Unequaled image quality. Unprecedented speed. CT 9800 Quick—in a class by itself.

There was only one way to improve the CT 9800 system. Make it even more efficient. The new CT 9800 Quick system from General Electric sets new records for performance—while maintaining the highest image quality.

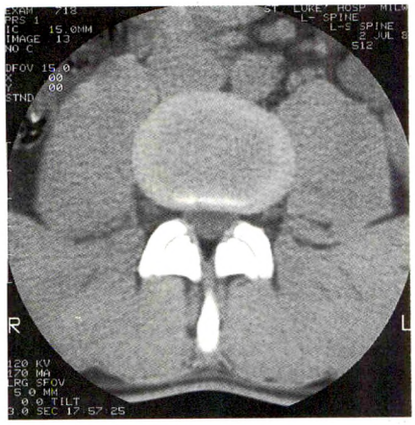
Because time counts

With its Fast Cycle scanning, CT 9800 Quick cuts exam time in half. Images can be acquired, reconstructed, displayed and filmed in less than 16 seconds. For example, a typical 512^2 image begins displaying less than 6 seconds after scan completion; a typical 20-image exam can be completed—scan to film—in less than 6 minutes.

Immediate display of high quality images increases diagnostic accuracy and efficiency. You can respond faster—and with more confidence—especially in trauma cases and interventional procedures. Throughput is accelerated, and referring physicians receive valuable diagnostic information without delay.



Contrast enhanced abdominal scan demonstrating a right kidney cyst and well defined hepatic vasculature.



Five millimeter lumbar spine image demonstrating a clear differentiation of disc material and spinal cord area.

Get a better look

CT 9800 Quick not only produces images quickly, it makes image reading and data manipulation faster than ever before. The pan/zoom feature, for example, lets you pinpoint and magnify areas of interest simply by placing a box cursor over the reference axial or ScoutView™. When the cursor is positioned, the magnified zoom image appears instantaneously.

New software algorithms—edge, smooth and detail— tailor images to your exact specifications. And the special pediatric head scanning mode allows CT 9800 Quick to characterize the bone/soft tissue interface with greater sensitivity.

These are just a few of the CT 9800 Quick features that streamline the diagnostic process and help ensure accuracy across the full range of studies.

The Quick answer

Consistently fine image quality combined with remarkably efficient performance. CT 9800 Quick—it could be the right answer for your computed tomography needs.

To see the CT 9800 Quick system in action, call us today, toll free. 800-433-5566.



CIRCLE 3 ON READER SERVICE CARD

GENERAL ELECTRIC

Tecnomed USA

BAY SHORE MEDICAL EQUIPMENT CORP.

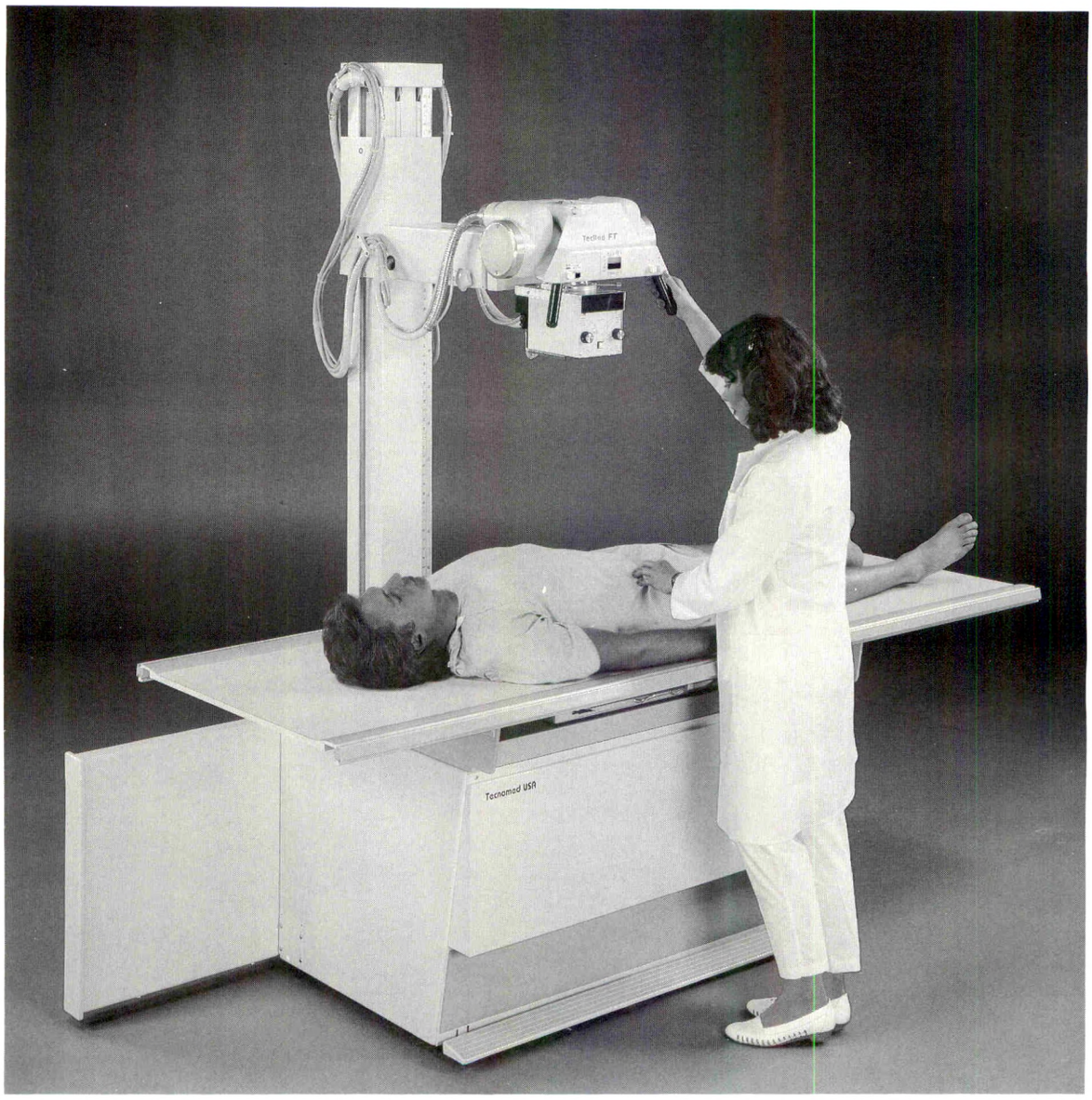
TecRad™ FT Radiographic System

The TecRad FT general radiographic system consists of a 600 mA single phase x-ray generator, a four-way floating top, horizontal bucky table, integrally mounted tubestand with X-ray tube and collimator. The basic system has several optional components that may be added to, or substituted for, basic components to tailor a system to specific needs. System construction makes it suitable for use in hospitals as a back up radiographic room, in outpatient departments, clinics, public health agencies, industrial clinics, or orthopedic clinics.

The TecRad generator consists of a solid state control with a separate high voltage transformer. The transformer is housed within the table body in single room installations. This generator is limited to radiographic capabilities with no provision for fluoroscopic functions.

The TecRad FT table consists of a table base, housing the electronics and high voltage transformer, a bucky assembly, a four-way floating radiographic table top and an integrally mounted tubestand.

The combined tubestand and bucky travel permits a radiographic center to center coverage of 65 inches (1651 mm). This travel permits head to toe radiographic coverage on an average adult patient without having to move the patient. Tubestand motions permit cart radiography behind the table, off table stretcher or wheel chair radiography, cross table laterals and decubitus exposures, angled views of the skull or trunk of the body, and upright studies with wall cassette or erect bucky devices.



™TecRad is a trademark of Bay Shore Medical Equipment Corporation.

235 South Fehr Way, Bay Shore, New York 11706 • 516/586-1991-Telex II 510-227-9837
Telefax 516/242-4421

CIRCLE 28 ON READER SERVICE CARD

IMPROVE YOUR IMAGE



WITH PRECISE OPTICS IMAGE INTENSIFIER SYSTEMS

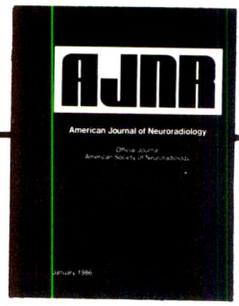
- The world's largest independent manufacturer of Image Intensifier Systems and components
- Over 30 years of experience in design and manufacture
- 6,9,12, and 16-Inch latest series image tubes for optimum performance
- 525/875/1023 line CCTV's, 6fps 100mm/105mm cameras
- Cost effective, versatile, reliable
- Compatible with new or existing x-ray equipment
- Extend the life of existing apparatus
- Worldwide dealer network

Precise® Optics
PHOTO MEDIC EQUIPMENT, INC.

239 South Fehr Way
Bay Shore, New York 11706
Tel.: 516 242-6600
TWX: 510-227-9837

CIRCLE 6 ON READER SERVICE CARD

Increase your expertise in evaluating CNS lesions



AJNR
American Journal of Neuroradiology

Editor: **Juan M. Taveras, MD,** Harvard Medical School; MGH

Outstanding clinical papers on every aspect of CNS imaging, including spinal diagnosis…informed coverage of head and neck radiology…clear, readable CTs, angiographs, MR imaging and ultrasound studies. These are the features you demand of a quality professional journal. You'll find them in every issue of **AJNR: American Journal of Neuroradiology.**

As you are called upon to perform and interpret more and more sophisticated diagnostic tests — from myelography to CT to newborn ultrasound studies — you need a comprehensive, reliable journal that can keep you abreast of all the latest developments. Each bimonthly issue of **AJNR** brings you timely, clinically pertinent information, as well as important clinical research presented with an eye toward immediate practical application.

Here are just a few of the many excellent articles from the November/December 1986 issue:

The MR Appearance of Syringomyelia: New Observations. *Sherman, et al.*

Cranial MR in Spinal Cord MS: Diagnosing Patients with Isolated Spinal Cord Symptoms. *Edwards, et al.*

Time-Dependent Changes in Image Contrast in Brain Tumors After Gadolinium-DTPA. *Schörner, et al.*

Physiology of the CSF Flow-Void Sign: Modification by Cardiac Gating. *Citrin, et al.*

Percutaneous Laser Catheter Recanalization of Carotid Arteries in Seven Cadavers and One Patient. *Choy, et al.*

Focal Necrosis of the White Matter (Periventricular Leukomalacia): Sonographic, Pathologic, and Electroencephalographic Features. *Bejar, et al.*

If you can benefit from articles like these, then you should be a regular reader of **AJNR.** Use the attached coupon to subscribe today.

Bimonthly
Personal $100/yr **Institutions** $120/yr
In-training $65/yr *(add $20.00 outside the US)*

ORDER FREE BY PHONE. Just call 1-800-638-6423 from anywhere in the US except AK. Maryland residents, call 528-4105 *collect.*

Williams & Wilkins
P.O. Box 23291 Baltimore, Maryland 21203
266 Fulham Road London SW10 9EL England

Subscribe to AJNR for 3 years and SAVE

Avoid future rate increases and ensure uninterrupted service by placing a multi-year subscription at current rates.

☐ New subscription ☐ Renewal
☐ 3 yrs ☐ 2 yrs ☐ 1 yr
☐ **Personal** $100 ☐ **Institutions** $120 ☐ **In-training** $65
(add $20.00 outside the US)

☐ Also send me the **1987 Bound Volume** at $45.00 ($50.00 outside the US). $2.00 discount for orders placed before October 1, 1986, and for prepaid orders. I understand that the bound volume is *in addition to* my regular subscription and is available only to subscribers. (To be shipped in early 1988. Sorry, bound volumes for years prior to 1987 are not available.) *All bound volume orders must be received by December 31, 1987.*

☐ Check enclosed ☐ Bill me
☐ VISA ☐ MasterCard ☐ American Express

card # exp.

signature/P.O. #

printed in USA

Name

Address

City/State/Zip

MD residents, please add 5% sales tax. Subscription orders from outside the US must be prepaid in US dollars only.

Residents, Fellows, Interns, and Students: when applying for the in-training rate, available for 3 years, please specify name of institution and training status. Rates valid through October 31, 1987.

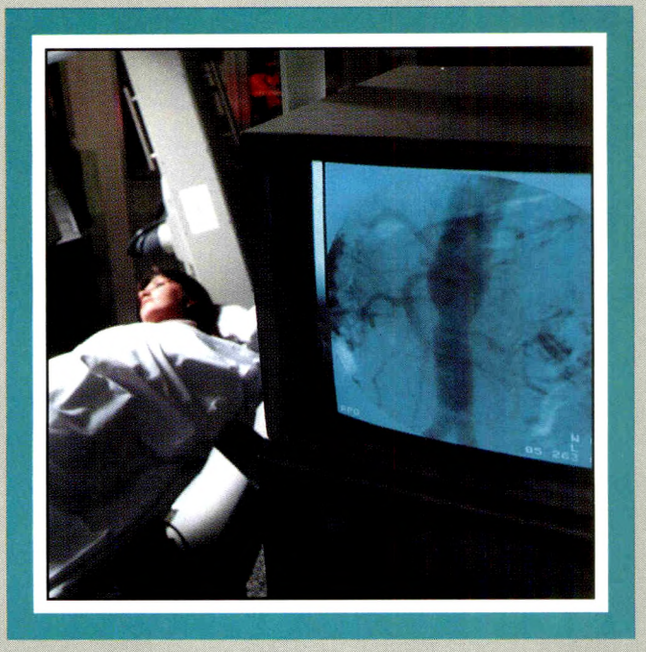
Please allow 8 weeks for order processing and delivery of your first issue. Surface mail delivery to countries outside the US may take up to 16 weeks. Airmail rates available upon request.

Williams & Wilkins
P.O. Box 23291
Baltimore, Maryland 21203

266 Fulham Road
London SW10 9EL
England

AJNRAD 94625 87

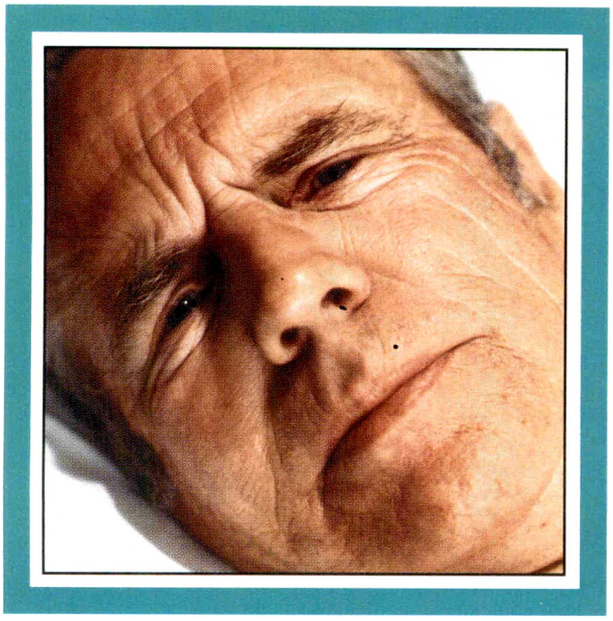
Because you really care....



...about patient comfort
...about diagnostic quality
...about clinical experience

HEXABRIX†

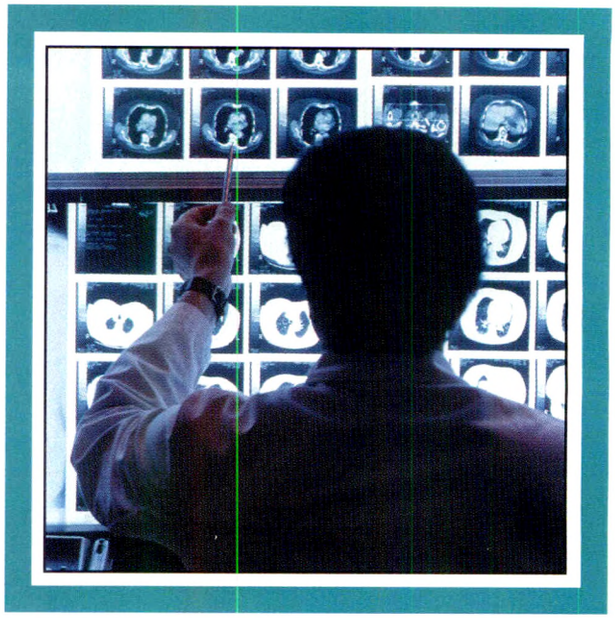
(Ioxaglate Meglumine 39.3% and
Ioxaglate Sodium 19.6% Injection)



Because you care

about patient comfort, tolerance, safety and well-being... you want a contrast agent known for:

- **Reduced pain**
- **Reduced heat**
- **Minimum patient movement**
- **Better patient compliance and cooperation**
- **Completing the procedure with fewer retakes**
- **Visualization comparable to conventional ionic media**
- **Improved nephrotoxic[1-3] and cardiovascular[4-7] profiles versus conventional ionic contrast media**



Because you care

about diagnostic quality...

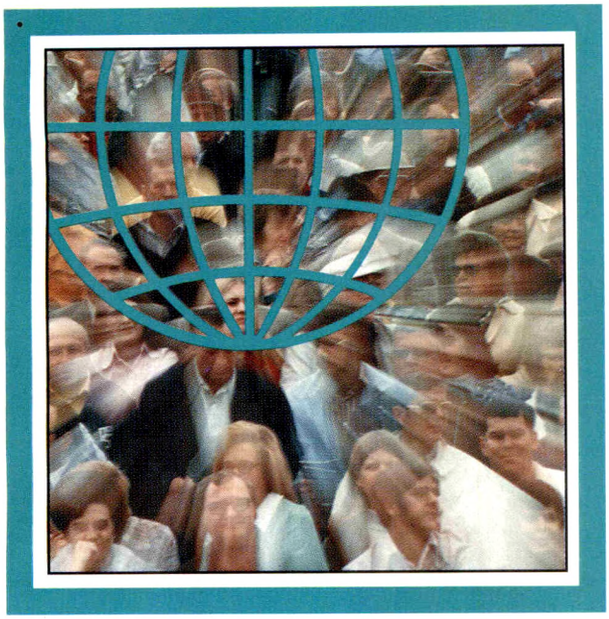
you want the low-osmolality contrast agent that has proved itself time and time again.

- **Hexabrix**—the low-osmolality ionic contrast medium—has been the agent of choice in over 5,000,000 procedures worldwide.
- **Hexabrix** has an osmolality lower than other currently available water-soluble contrast agents with comparable iodine concentrations—*including iopamidol and iohexol.*
- **Hexabrix** helps provide high-quality studies with enhanced patient comfort and fewer procedural problems.
- A recent multi-center U.S. study (893 patients) supports the efficacy and patient tolerance of Hexabrix:
  —95% of patients studied showed good-to-excellent visualization...*and*
  —96% of patients exhibited good-to-excellent toleration in angiographic procedures*

*Data on file at Mallinckrodt

HEXABRIX†

(Ioxaglate Meglumine 39.3% and Ioxaglate Sodium 19.6% Injection)



Because you care

about clinical experience...

you want a proven contrast agent that has passed the test of clinical scrutiny.

Study after study shows that Hexabrix delivers quality diagnostic images with reduced pain, reduced heat and greater patient comfort.[3-6,8-16]

Now...expanded clinical indications to meet procedural requirements for:

- **Peripheral Arteriography,** including percutaneous transluminal angioplasty
- **Selective Visceral Arteriography,** including percutaneous transluminal angioplasty
- **Cerebral Angiography**
- **Selective Coronary Arteriography** (with or without left ventriculography, including percutaneous transluminal coronary angioplasty)
- **Pediatric Angiocardiography**
- **Aortography**
- **Intra-arterial Digital Subtraction Angiography**
- **Intravenous Digital Subtraction Angiography**
- **Peripheral Venography**
- **Excretory Urography**
- **Contrast Enhancement of Computed Tomographic Head Imaging and Body Imaging**
- **Arthrography**
- **Hysterosalpingography**



Because you care

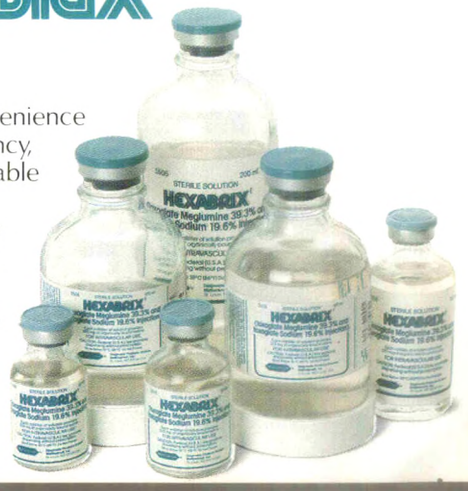
about your patients... and the professionals you work with...

you want the advantages of HEXABRIX†

- **Reduced pain...reduced heat.** ***Patients appreciate that.***
- **Better patient cooperation and compliance throughout the procedure.** ***Nurses and technologists appreciate that.***
- **Hexabrix helps you maintain a smooth-running schedule...cuts costly (and annoying) retakes... helps reinforce patient confidence.** ***Everyone appreciates that.***

HEXABRIX†

For greater convenience and cost-efficiency, Hexabrix is available in a wide range of package sizes to fit procedural needs and minimize waste.



Mallinckrodt®

HEXABRIX† (Ioxaglate Meglumine 39.3% and Ioxaglate Sodium 19.6% Injection)

HEXABRIX®

Each milliliter of HEXABRIX contains 393 mg of ioxaglate meglumine, 196 mg of ioxaglate sodium and 0.10 mg edetate calcium disodium as a stabilizer. The solution contains 3.48 mg (0.15 mEq) sodium in each milliliter and provides 32% (320 mg/mL) organically bound iodine.

CONTRAINDICATIONS

HEXABRIX is contraindicated for use in myelography. Refer to PRECAUTIONS concerning hypersensitivity. Hysterosalpingography should not be performed during the menstrual period; in pregnant patients; in patients with known infection in any portion of the genital tract; or in patients in whom cervical conization or curettage has been performed within 30 days. Arthrography should not be performed if infection is present in or near the joint.

WARNINGS

Serious or fatal reactions have been associated with the administration of iodine containing radiopaque media. It is of utmost importance to be completely prepared to treat any contrast medium reaction.

As with any contrast medium, serious neurologic sequelae, including permanent paralysis, can occur following cerebral arteriography, selective spinal arteriography and arteriography of vessels supplying the spinal cord. The injection of a contrast medium should never be made following the administration of vasopressors, since they strongly potentiate neurologic effects.

In patients with subarachnoid hemorrhage, a rare association between contrast administration and clinical deterioration, including convulsions and death, has been reported. Therefore, administration of intravascular iodinated contrast media in these patients should be undertaken with caution.

A definite risk exists in the use of intravascular contrast agents in patients who are known to have multiple myeloma. In such instances anuria has developed, resulting in progressive uremia, renal failure and eventually death. Although neither the contrast agent nor dehydration has separately proved to be the cause of anuria in myeloma, it has been speculated that the combination of both may be a causative factor. The risk in myelomatous patients is not a contraindication to the procedure; however, partial dehydration in the preparation of these patients for the examination is not recommended since this may predispose to precipitation of myeloma protein in the renal tubules. No form of therapy, including dialysis, has been successful in reversing the effect. Myeloma, which occurs most commonly in persons over 40, should be considered before instituting intravascular administration of contrast agents.

Administration of radiopaque materials to patients known or suspected to have pheochromocytoma should be performed with extreme caution. If, in the opinion of the physician, the possible benefits of such procedures outweigh the considered risks, the procedures may be performed; however, the amount of radiopaque medium injected should be kept to an absolute minimum. The blood pressure should be assessed throughout the procedure, and measures for treatment of a hypertensive crisis should be available.

Since intravascular administration of contrast media may promote sickling in individuals who are homozygous for sickle cell disease, fluid restriction is not advised.

In patients with advanced renal disease, iodinated contrast media should be used with caution and only when the need for the examination dictates, since excretion of the medium may be impaired. Patients with combined renal and hepatic disease, those with severe hypertension or congestive heart failure and recent renal transplant recipients present an additional risk.

Renal failure has been reported in patients with liver dysfunction who were given an oral cholecystographic agent followed by an intravascular iodinated radiopaque agent and also in patients with occult renal disease, notably diabetics and hypertensives. In these classes of patients there should be no fluid restriction and every attempt made to maintain normal hydration prior to contrast medium injection, since dehydration is the single most important factor influencing further renal impairment.

Caution should be exercised in performing contrast medium studies in patients with endotoxemia and/or those with elevated body temperatures.

Reports of thyroid storm occurring following the intravascular use of iodinated radiopaque agents in patients with hyperthyroidism or with an autonomously functioning thyroid nodule, suggest that this additional risk be evaluated before use of this drug. Iodine-containing contrast agents may alter the results of thyroid function tests which depend on iodine estimation, e.g., PBI, and may also affect results of radioactive iodine uptake studies. Such tests, if indicated, should be performed prior to the administration of this preparation.

PRECAUTIONS

Diagnostic procedures which involve the use of iodinated intravascular contrast agents should be carried out under the direction of personnel skilled and experienced in the particular procedure to be performed. All procedures utilizing contrast media carry a definite risk of producing adverse reactions. While most reactions are minor, life-threatening and fatal reactions may occur without warning, and this risk must be weighed against the benefit of the procedure. A fully equipped emergency cart, or equivalent supplies and equipment, and personnel competent in recognizing and treating adverse reactions of all types should always be available. If a serious reaction should occur, immediately discontinue administration. Since severe delayed reactions have been known to occur, emergency facilities and competent personnel should be available for at least 30 to 60 minutes after administration. (See ADVERSE REACTIONS.)

Preparatory dehydration is dangerous and may contribute to acute renal failure in infants, young children, the elderly, patients with pre-existing renal insufficiency, patients with multiple myeloma, patients with advanced vascular disease and diabetic patients.

Acute renal failure has been reported in diabetic patients with diabetic nephropathy and in susceptible non-diabetic patients (often elderly with pre-existing renal disease) following the administration of iodinated contrast agents. Therefore, careful consideration of the potential risks should be given before performing this radiographic procedure in these patients.

Severe reactions to contrast media often resemble allergic responses. This has prompted the use of several provocative pretesting methods, none of which can be relied on to predict severe reactions. No conclusive relationship between severe reactions and antigen-antibody reactions or other manifestations of allergy has been established. The possibility of an idiosyncratic reaction in patients who have previously received a contrast medium without ill effect should always be considered. Prior to the injection of any contrast medium, the patient should be questioned to obtain a medical history with emphasis on allergy and hypersensitivity. A positive history of bronchial asthma or allergy (including food), a family history of allergy, or a previous reaction or hypersensitivity to a contrast agent may imply a greater than usual risk. Such a history may be more accurate than pre-testing in predicting the potential for reaction, although not necessarily the severity or type of reaction in the individual case. A positive history of this type does not arbitrarily contraindicate the use of a contrast agent when a diagnostic procedure is thought essential, but does call for caution. (See ADVERSE REACTIONS.)

Prophylactic therapy including corticosteroids and antihistamines should be considered for patients who present with a strong allergic history, a previous reaction to a contrast medium, or a positive pre-test since in these patients the incidence of reaction is two to three times that of the general population. Adequate doses of corticosteroids should be started early enough prior to contrast medium injection to be effective and should continue through the time of injection and for 24 hours after injection. Antihistamines should be administered within 30 minutes of the contrast medium injection. Recent reports indicate that such pretreatment does not prevent serious life-threatening reactions, but may reduce both their incidence and severity. A separate syringe should be used for these injections.

General anesthesia may be indicated in the performance of some procedures in selected patients; however, a higher incidence of adverse reactions has been reported in these patients, and may be attributable to the inability of the patient to identify untoward symptoms or to the hypotensive effect of anesthesia which can prolong the circulation time and increase the duration of contact of the contrast agent.

Angiography should be avoided whenever possible in patients with homocystinuria because of the risk of inducing thrombosis and embolism.

PRECAUTIONS FOR SPECIFIC PROCEDURES

Pediatric Angiocardiography: It is advisable to monitor for ECG and vital signs changes throughout the procedure.

When large individual doses are administered, sufficient time should be allowed for any observed changes to return to or near baseline prior to making the next injection.

Caution should be used when making right heart injections in patients with pulmonary hypertension or incipient heart failure, since this may lead to increased right side pressures with subsequent bradycardia and systemic hypotension. Patients with pulmonary disease present additional risks.

Caution is advised in cyanotic infants since apnea, bradycardia, other arrhythmias and a tendency to acidosis are more likely to occur.

Since infants are more likely to respond with convulsions than are adults, the amount of total dosage is of particular importance. Repeated injections are hazardous in infants weighing less than 7 kg, particularly when these infants have pre-existing compromised right heart function or obliterated pulmonary vascular beds.

Selective Coronary Arteriography with or without left ventriculography: During the administration of large doses of HEXABRIX, continuous monitoring of vital signs is desirable. Caution is advised in the administration of large volumes to patients with incipient heart failure because of the possibility of aggravating the pre-existing condition. Hypotension should be corrected promptly since it may result in serious arrhythmias.

Special care regarding dosage should be observed in patients with right ventricular failure, pulmonary hypertension, or stenotic pulmonary vascular beds because of hemodynamic changes which may occur after injection into the right heart outflow tract.

Peripheral Arteriography: Moderate decreases in blood pressure occur frequently with intra-arterial (brachial) injections. This change is usually transient and requires no treatment; however, the blood pressure should be monitored for approximately ten minutes following injection.

Extreme caution during injection of the contrast agent is necessary to avoid extravasation and fluoroscopy is recommended. This is especially important in patients with severe arterial disease.

Cerebral Angiography: Cerebral angiography should be performed with special caution in patients with advanced arteriosclerosis, severe hypertension, cardiac decompensation, senility, recent cerebral thrombosis or embolism, and migraine.

Intra-Arterial Digital Subtraction Angiography: The risks associated with IA-DSA are those usually attendant with catheter procedures. Following the procedure, gentle pressure hemostasis is required, followed by observation and immobilization of the limb for several hours to prevent hemorrhage from the site of arterial puncture.

Patient motion, including respiration and swallowing, can result in misregistration leading to image degradation and non-diagnostic studies.

Intravenous Digital Subtraction Angiography: The risks associated with IV-DSA include those usually attendant with catheter procedures and include intramural injections, vessel dissection and tissue extravasation. The potential risk is reduced when small test injections of contrast medium are made under fluoroscopic observation to insure that the catheter tip is properly positioned and, in the case of peripheral placement, that the vein is of adequate size.

Patient motion, including respiration and swallowing, can result in misregistration leading to image degradation and non-diagnostic studies.

Peripheral Venography: Special care is required when venography is performed in patients with suspected thrombosis, phlebitis, severe ischemic disease, local infection or a totally obstructed venous system.

Extreme caution during injection of contrast media is necessary to avoid extravasation and fluoroscopy is recommended. This is especially important in patients with severe arterial or venous disease.

Excretory Urography: Infants and small children should not have any fluid restrictions prior to excretory urography. (See WARNINGS and PRECAUTIONS concerning preparatory dehydration.)

Contrast Enhancement in Body Computed Tomography: Patient cooperation is essential since patient motion, including respiration, can markedly affect image quality. The use of an intravascular contrast medium can obscure tumors in patients undergoing CT evaluation of the liver, resulting in a false negative diagnosis. Dynamic CT scanning is the procedure of choice for malignant tumor enhancement.

Arthrography: Strict aseptic technique is required to prevent the introduction of infection. Fluoroscopic control should be used to insure proper introduction of the needle into the synovial space and prevent extracapsular injection. Aspiration of excessive synovial fluid will reduce the pain on injection and prevent the dilution of the contrast agent. It is important that undue pressure not be exerted during the injection.

Hysterosalpingography: Caution should be exercised in patients suspected of having cervical or tubal carcinoma to avoid possible spread of the lesion by the procedure. Delayed onset of pain and fever (1-2 days) may be indicative of pelvic infection.

Carcinogenesis, Mutagenesis, Impairment of Fertility: No long-term animal studies have been performed to evaluate carcinogenic potential. However, animal studies suggest that this drug is not mutagenic and does not affect fertility in males or females.

Pregnancy Category B: Reproduction studies have been performed in rats and rabbits at doses up to two times the maximum adult human dose and have revealed no evidence of impaired fertility or harm to the fetus due to HEXABRIX. There are, however, no adequate and well-controlled studies in pregnant women. Because animal reproduction studies are not always predictive of human response, this drug should be used during pregnancy only if clearly needed.

Nursing Mothers: Ioxaglate salts are excreted unchanged in human milk. Because of the potential for adverse effects in nursing infants, bottle feedings should be substituted for breast feedings for 24 hours following the administration of this drug.

Pediatric Use: Safety and effectiveness in children has been established in pediatric angiocardiography and intravenous excretory urography. Data have not been submitted to support the safety and effectiveness of HEXABRIX in any other indication.

(Precautions for specific procedures receive comment under that procedure.)

ADVERSE REACTIONS

Adverse reactions to injectable contrast media fall into two categories: chemotoxic reactions and idiosyncratic reactions.

Chemotoxic reactions result from the physiochemical properties of the contrast media, the dose and the speed of injection. All hemodynamic disturbances and injuries to organs or vessels perfused by the contrast medium are included in this category.

Idiosyncratic reactions include all other reactions. They occur more frequently in patients 20 to 40 years old. Idiosyncratic reactions may or may not be dependent on the dose injected, the speed of injection, the mode of injection and the radiographic procedure. Idiosyncratic reactions are subdivided into minor, intermediate and severe. The minor reactions are self-limited and of short duration; the severe reactions are life-threatening and treatment is urgent and mandatory.

NOTE: Not all of the following adverse reactions have been reported with HEXABRIX. Because HEXABRIX is an iodinated intravascular contrast agent, all of the side effects and toxicity associated with agents of this class are theoretically possible, and this should be borne in mind when HEXABRIX is administered.

Severe, life-threatening anaphylactoid reactions, mostly of cardiovascular origin, have occurred following the administration of HEXABRIX as well as other iodine-containing contrast agents. Most deaths occur during injection or 5 to 10 minutes later; the main feature being cardiac arrest with cardiovascular disease as the main aggravating factor. Isolated reports of hypotensive collapse and shock are found in the literature. Based upon clinical literature, reported deaths from the administration of conventional iodinated contrast agents range from 6.6 per 1 million (0.00066 percent) to 1 in 10,000 patients (0.01 percent).

Regardless of the contrast agent employed, the overall estimated incidence of serious adverse reactions is higher with coronary arteriography than with other procedures. Cardiac decompensation, serious arrhythmias, or myocardial ischemia or infarction may occur during coronary arteriography and left ventriculography.

The most frequent adverse reactions are nausea, vomiting, facial flush and a feeling of body warmth. These are usually of brief duration. In double-blind clinical trials, HEXABRIX produced less discomfort upon injection (pain and heat) when compared to various other contrast agents. Other reactions include the following:

Hypersensitivity reactions: Dermal manifestations of urticaria with or without pruritus, erythema and maculopapular rash. Dry mouth. Sweating. Conjunctival symptoms. Facial, peripheral and angioneurotic edema. Symptoms related to the respiratory system include sneezing, nasal stuffiness, coughing, choking, dyspnea, chest tightness and wheezing, which may be initial manifestations of more severe and infrequent reactions including asthmatic attack, laryngospasm and bronchospasm with or without edema, pulmonary edema, apnea and cyanosis. Rarely, these allergic-type reactions can progress into anaphylaxis with loss of consciousness, coma, severe cardiovascular disturbances, and death.

Cardiovascular reactions: Generalized vasodilation, flushing and vasospasm. Occasionally thrombosis or, rarely, thrombophlebitis. Extremely rare cases of disseminated intravascular coagulation resulting in death have been reported. Severe cardiovascular responses include rare cases of hypotensive shock, coronary insufficiency, cardiac arrhythmia, fibrillation and arrest. These severe reactions are usually reversible with prompt and appropriate management; however, fatalities have occurred.

Technique reactions: Extravasation with burning pain, hematomas, ecchymosis and tissue necrosis, vascular constriction due to injection rate, thrombosis and thrombophlebitis.

Neurological reactions: Spasm, convulsions, aphasia, syncope, paresis, paralysis resulting from spinal cord injury and pathology associated with the syndrome of transverse myelitis, visual field losses which are usually transient but may be permanent, coma and death.

Other reactions: Headache, trembling, shaking, chills without fever, hyperthermia and lightheadedness. Temporary renal shutdown or other nephropathy.

Pediatric angiocardiography has been complicated by intramural injection with marked adverse effects on cardiac function.

During selective coronary arteriography with or without left ventriculography, patients may have clinically insignificant ECG changes. The following adverse effects have occurred in conjunction with the administration of iodinated intravascular contrast agents for this procedure: hypotension, shock, anginal pain, myocardial infarction, cardiac arrhythmias (bradycardia, ventricular tachycardia, ventricular fibrillation) and cardiac arrest. Fatalities have been reported. Complications to the procedure include dissection of coronary arteries, dislodgement of atheromatous plaques, perforation, hemorrhage and thrombosis.

Following peripheral arteriography, hemorrhage and thrombosis have occurred at the puncture site of the percutaneous injection. Brachial plexus injury has been reported following axillary artery injection.

The major causes of cerebral arteriographic adverse reactions appear to be repeated injections of the contrast material, administration of doses higher than those recommended, the presence of occlusive atherosclerotic vascular disease and the method and technique of injection. Adverse reactions are normally mild and transient. A feeling of warmth in the face and neck is frequently experienced. Infrequently, a more severe burning discomfort is observed. Transient visual hallucinations have been reported. Serious neurological reactions that have been associated with cerebral angiography and not listed under Adverse Reactions include stroke, amnesia and respiratory difficulties. Visual field defects with anopsia and reversible neurological deficit lasting from 24 hours to 48 hours have been reported. Confusion, disorientation with hallucination, and absence of vision sometimes lasting for one week have also been reported. Cardiovascular reactions that may occur with some frequency are bradycardia and either an increase or decrease in systemic blood pressure. The blood pressure change is transient and usually requires no treatment. Arthrography may induce joint pain or discomfort which is usually mild and transient but occasionally may be severe and persist for 24 to 48 hours following the procedure. Effusion requiring aspiration may occur in patients with rheumatoid arthritis. Fever and pain, cramping and tenderness of the abdomen have been reported following hysterosalpingography.

OVERDOSAGE

Overdosages may occur. The adverse effects of overdosage are life-threatening and affect mainly the pulmonary and cardiovascular systems. The symptoms may include cyanosis, bradycardia, acidosis, pulmonary hemorrhage, convulsions, coma and cardiac arrest. Treatment of an overdose is directed toward the support of all vital functions and prompt institution of symptomatic therapy.

Ioxaglate salts are dialyzable.

The intravenous LD_{50} values of HEXABRIX (in grams of iodine/kilogram body weight) were 11.2 g/kg in mice, >6 g/kg in rats, >6.4 g/kg in rabbits and >10.2 g/kg in dogs.

DOSAGE AND ADMINISTRATION

Details on dosage are provided in the package insert. *CONSULT FULL PACKAGE INSERT BEFORE USE.*

REFERENCES

1. Nilsson PE, Aspelin P, et al: Tolerance and biochemical effects from intravenous injection of ioxaglate in healthy volunteers. *Acta Radiol* (Diagn) 25(6):523-528, 1984.

2. Dawson P: Contrast agent nephrotoxicity. An appraisal. *BR J Radiol* 58:121-124, 1985.

3. Nilsson PE, Holtas SL, Tejler LT: Subjective responses and albuminuria induced by ioxaglate during renal angiography in man. *Radiology* 144:509-512, 1982.

4. Svenson RH: Comparison of the hemodynamic effects of Hexabrix and Renografin 76 following left ventriculography and coronary arteriography. *Invest Radiol* 19(Supp 6):S333-S334, 1984.

5. Hirshfeld Jr JW, Laskey W, Martin JL, Groh WC, Untereker W, Wolf GL: Hemodynamic changes induced by cardiac angiography with ioxaglate: Comparison with diatrizoate. *J AM Coll Cardiol* 2(5):954-957, 1983.

6. Cumberland D: Low-Osmolality Contrast Media in Cardiac Radiology. *Invest Radiol* 19(Supp 6): S270-S274, 1984.

7. Weikl A, Hubmann M: A survey of contrast media used in coronary angiography. *Cardiovasc Intervent Radiol* 5:202-210, 1982.

8. Spataro RF: A comparison of Hexabrix and Renografin-60 in Intravenous Urography. *Invest Radiol* 19(Supp 6):S360, 1984.

9. Ramsey RG, Czervionke L, et al: A double-blind clinical study comparing the safety and efficacy of Hexabrix and Hypaque Meglumine 60% in contrast-enhanced computed cranial tomographic scanning. *Invest Radiol* 19(Supp 6):S317, 1984.

10. Anthony CL, Tonkin ILD, et al: A double-blind randomized clinical study of the safety, tolerability, and efficacy of Hexabrix in pediatric angiocardiography. *Invest Radiol* 19(Supp 6):S335-343, 1984.

11. Tonkin ILD: A double-blind randomized clinical study of the use of Hexabrix in pediatric angiocardiography. *Invest Radiol* 19(Supp 6):S344-349, 1984.

...because you really care

HEXABRIX†
(Ioxaglate Meglumine 39.3% and Ioxaglate Sodium 19.6% Injection)

Mallinckrodt®

CIRCLE 22 ON READER SERVICE CARD

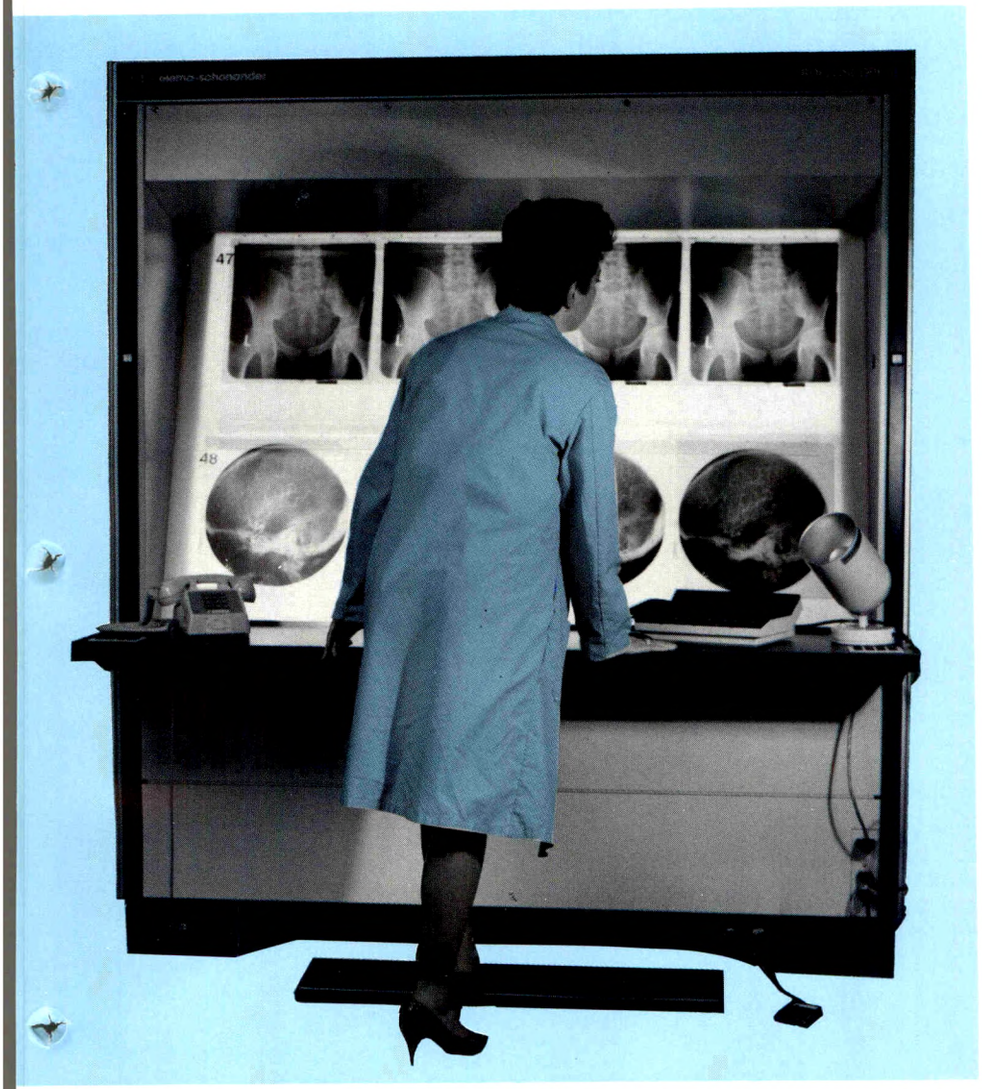
Diagnostic Products Division
Mallinckrodt, Inc.
Post Office Box 5840
St. Louis, MO 63134

For orders, medical and/or professional assistance call (800) 325-3688 TOLL FREE

© Mallinckrodt, Inc. 1987

†Licensed by Guerbet, S.A. Registered U.S. Patent and Trademark Office

What's NEW from Elema-Schonander



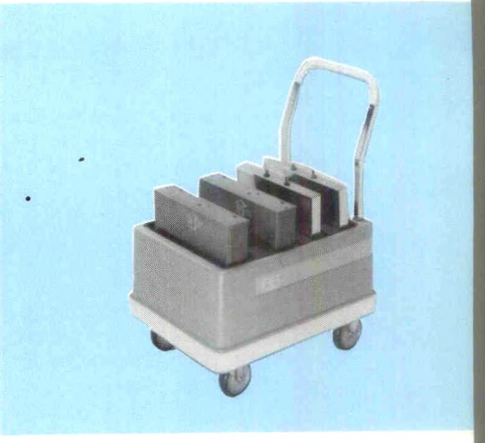
New, improved ROLLOSCOPE II motorized multiple filmviewer allows quick, convenient reading of large and small radiographs



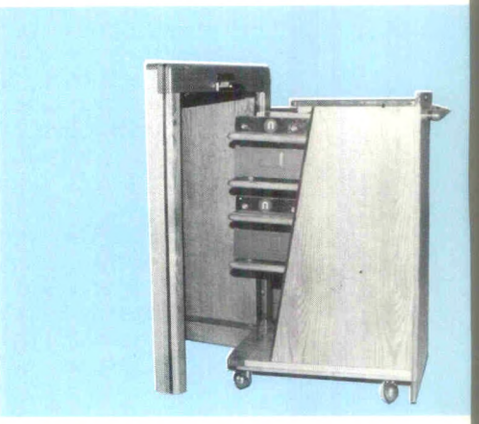
New BINOSCOPE filmviewing binocular enhances radiographic image perception



New PDQ-2 microprocessor-based program control for AOT-S and AOT-R sheet filmchangers



MAG'KART simplifies safe transport and storage of PUCK filmchanger magazines and cassettes



DOC'KART pass-thru cart and dock system links darkroom and special procedures suite

Write for information. Ask for product bulletins on ROLLOSCOPE II, BINOSCOPE, PDQ-2 PROGRAM CONTROL, MAG'KART and DOC'KART.



Elema-Schonander, Inc.
2360 North Palmer Drive, P.O. Box 94517,
Schaumburg, IL 60173-3887

elema-schonander

87215

CIRCLE 4 ON READER SERVICE CARD

You learn from your experience with

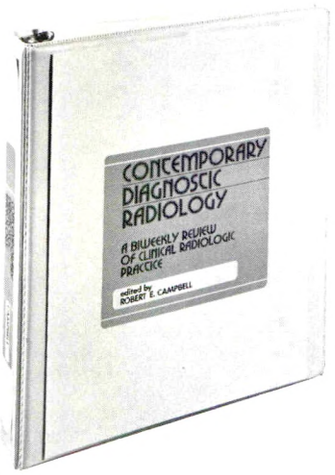
CONTEMPORARY DIAGNOSTIC RADIOLOGY

Editor: **Robert E. Campbell, M.D.**

A Biweekly Review of Clinical Radiologic Practice—26 issues a year!

One of your toughest jobs is keeping up with the many new developments that affect radiology. That's why you want **Contemporary Diagnostic Radiology**... an effective and convenient way to perfect your skills and maintain your professional status.

Contemporary Diagnostic Radiology is designed as a continuing education program that lets you work at your own pace. Every two weeks you'll receive an issue that covers a single topic or procedure in detail. Read the information and study the clearly reproduced radiographs—and then, if you choose, respond to a comprehensive examination in the strictest confidence. You set the pace.
Each biweekly lesson brings you pertinent review of the basics in bone radiology... gastrointestinal radiology... pediatric radiology... genitourinary radiology... MR imaging... and all of the topics you want to know more about.



Contemporary Diagnostic Radiology works *two ways*. You may choose to subscribe to the non-scoring version, receiving every issue as an important element of your professional reading. The scoring version, however, supplements your reading and computer-coded examinations with confidential result responses, making you eligible for Continuing Medical Education credits co-sponsored by the University of Pennsylvania School of Medicine.

"As an organization for continuing medical education, the University of Pennsylvania School of Medicine designates this continuing medical education activity as meeting the criteria for 1 credit hour per bi-weekly issue in Category I for Educational Materials for the Physician's Recognition Award of the American Medical Association provided it has been completed according to instructions."

You can begin this ongoing program **today**. **Contemporary Diagnostic Radiology** is a year-round program, so you can join at any time. To begin your lessons, just fill out the enclosed card and return it to us. Or call **FREE** 1-800-638-6423 (except from Alaska). In Maryland call **COLLECT** 528-4105. You'll find that **Contemporary Diagnostic Radiology** is the most efficient and inexpensive way to keep up with your dynamic field.

Williams & Wilkins

P.O. Box 23291
Baltimore, Maryland 21203

266 Fulham Road
London SW10 9EL England

clip & mail

CONTEMPORARY DIAGNOSTIC RADIOLOGY

☐ **Yes!** I want to keep pace in my field! Begin my 26-issue subscription:
☐ Send me the scoring version ($220)
☐ Send me the non-scoring version ($180)
☐ Send me the resident non-scoring version ($160)
(add $35 for optional air mail delivery outside the U.S.)
☐ new subscription
☐ renewal

name

address

city/state/zip

payment options
☐ payment enclosed ☐ bill me
☐ American Express ☐ MasterCard ☐ VISA

printed in USA

card # expiration date

signature/P.O. #

Maryland residents add 5% sales tax. Subscriptions outside the U.S. must be prepaid in U.S. dollars only. Rates subject to change without notice. Please allow 8 weeks for delivery of your first issue, up to 16 weeks for surface delivery outside the U.S. Optional airmail rates: add $35 per subscription.

Residents are eligible for the special in-training rate for up to three years. When requesting this rate, please include training status and institution.

Don't forget: you can order with a **FREE** phone call at 1-800-638-6423 (except from Alaska). In Maryland, call collect 528-4105.

Williams & Wilkins

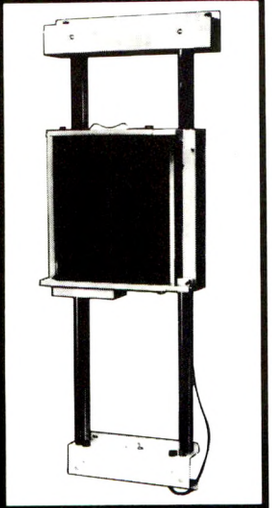
P.O. Box 23291
Baltimore, Maryland 21203

266 Fulham Road
London SW10 9EL England

CDRAD 95191 87

WALL CASSETTE HOLDER

FOR 14x17, 17x14, 10x12 and/or 8x10 CASSETTES.
COMPATIBLE with COLLIMATORS HAVING (PBL) POSITIVE BEAM LIMITING ABILITY.





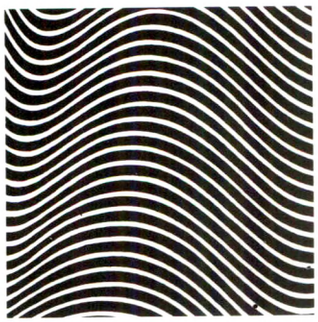
Easy to use: Simply slide the Cassette into the track. Unique S&S flipper design enables change of Cassette size with flip of a finger.

For large and small X-Ray rooms. Built for "Hospital-duty" use—but priced for the small X-Ray user.

FEATURES: Sturdy box girder construction, nylon bearings, dual lock system, constant torque counterbalances and Extra-Heavy plated steel tubes. Requires very minimum of technician's time. Increases productivity Complies with DHEW Regulations.

CIRCLE 9 ON READER SERVICE CARD

S. & S. X-RAY PRODUCTS INC.
The Complete Line of X-Ray Accessories
Accessory Catalog on request.
SOLD BY LOCAL X-RAY DEALERS
87-93 JAY STREET, BROOKLYN, N.Y. 11201
Telephone: 718-852-6900 (800) 221-6634



50th Annual Course

RADIOLOGY/87
Chest-Cardiovascular Imaging and Intervention

September 21–25, 1987
Minneapolis, Minnesota

Presented by
Department of Radiology
University of Minnesota

PROGRAM TOPICS

Radiology/87 will be a comprehensive course emphasizing both conventional diagnostic techniques and advanced imaging modalities, including computed tomography, digital angiography, and magnetic resonance imaging. The pulmonary lectures will focus on many of the practical issues facing radiologists in their daily work. Special imaging and interventional techniques will highlight the two days of cardiac presentations.

GUEST SPEAKERS

Drs. David Godwin, Benjamin Felson, Robert G. Fraser, Paul J. Friedman, Charles B. Higgins, Rogelio Moncada, Charles E. Putman, Carl E. Ravin, Frederick P. Stitik, Leonard E. Swischuk, Elias G. Theros, Ina L. Tonkin, and Jerome F. Wiot.

FEES: $450.
$225. (Resident/Fellow, Military, VA)

ACCREDITATION: 30¼ hours Category 1, AMA

DIRECT INQUIRIES TO: RADIOLOGY/87, Continuing Medical Education, University of Minnesota, Box 202 UMHC, 420 Delaware Street S.E., Minneapolis, MN 55455; telephone (612)626-5525.

"Equal Educational Opportunity"

for prompt subscription service...

attach label here

Please use this coupon and attach a *recent* label in the space provided when writing to us about:

- change of address
- renewal
- questions regarding your subscription

Please use the space below to indicate your *new* address.

Name of Journal_____

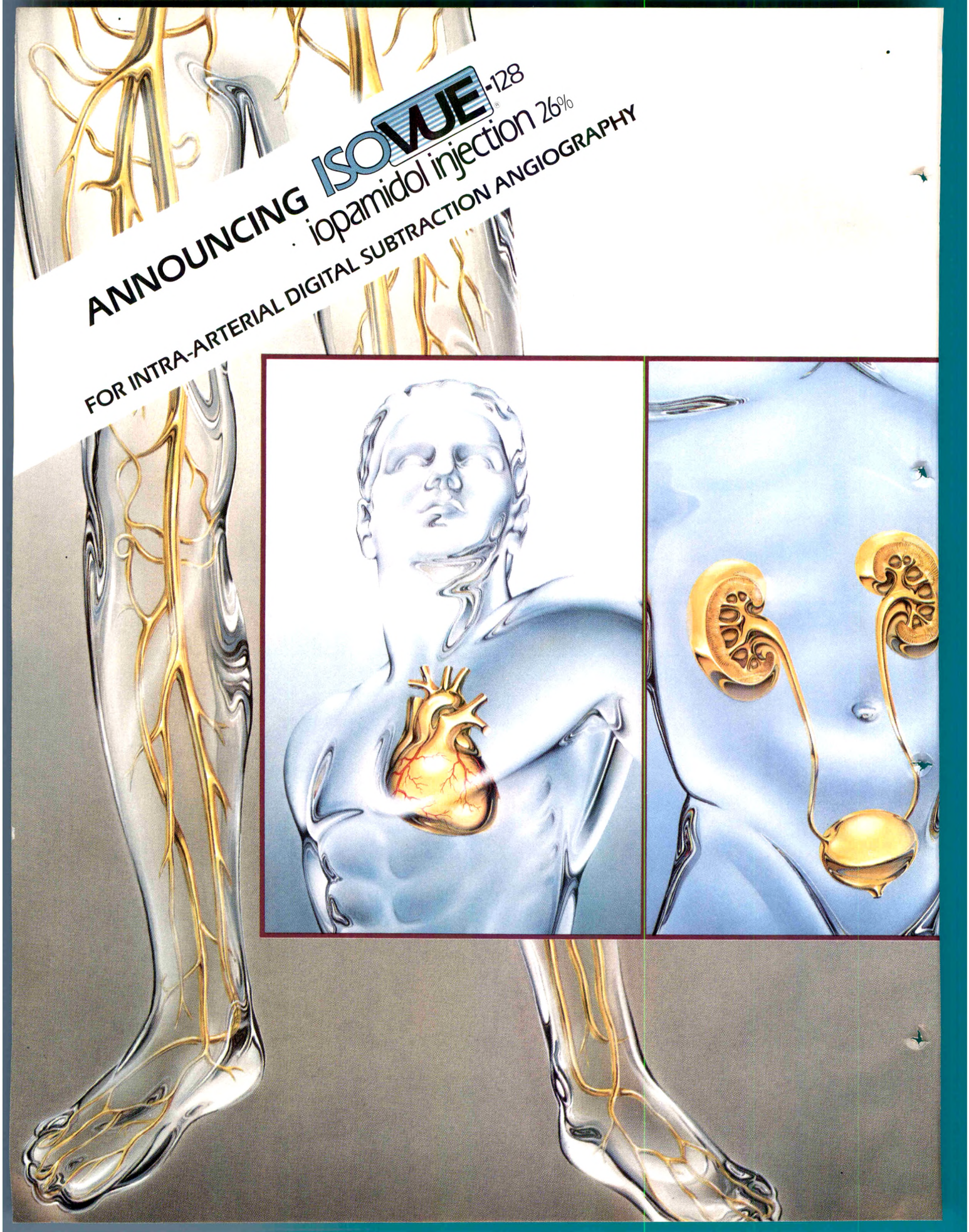
Name_____

Address_____

City/State/Zip_____

THE WILLIAMS & WILKINS COMPANY

428 East Preston Street/Baltimore, Maryland 21202

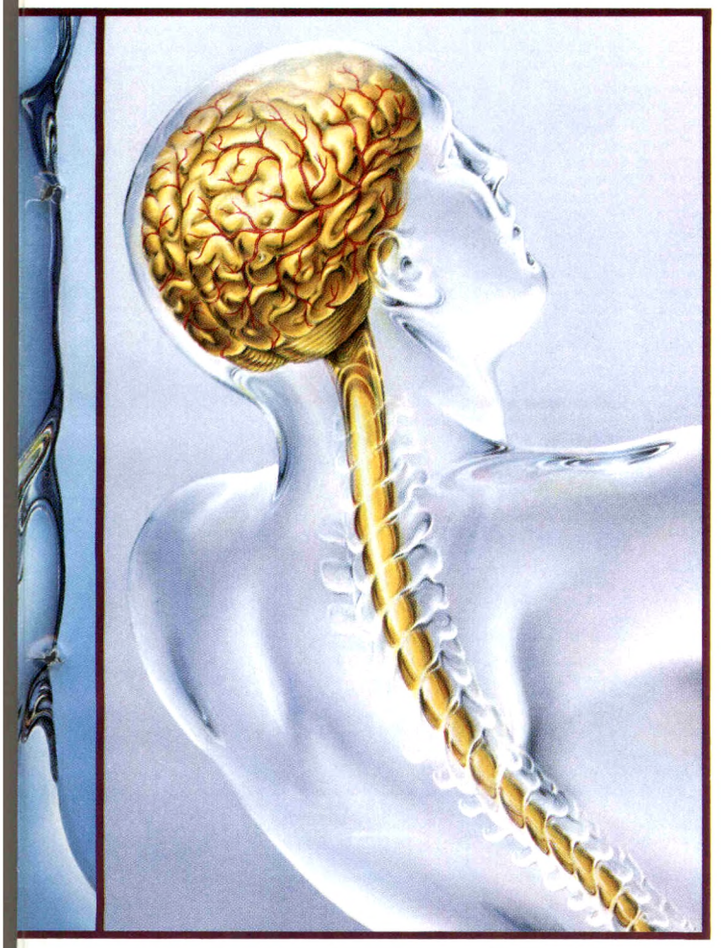

ANNOUNCING ISOVUE®-128
iopamidol injection 26%
FOR INTRA-ARTERIAL DIGITAL SUBTRACTION ANGIOGRAPHY

In radiologic contrast procedures

ISOVUE® iopamidol injection

ISOVUE®-M iopamidol injection

THE CLEAR CHOICE



A broad range of indications

Peripheral arteriography
Coronary arteriography and ventriculography
Excretory urography
Myelography (lumbar, thoracic, cervical, total columnar)
Cerebral arteriography
CT head and body imaging
CT cisternography and ventriculography
Selective visceral arteriography
Aortography
Intra-arterial digital subtraction angiography

The only nonionic contrast agent you need to stock

ISOVUE-M® 200
iopamidol injection 41%

ISOVUE-M® 300/ISOVUE®-300
iopamidol injection 61%

ISOVUE®-370
iopamidol injection 76%

ISOVUE®-128
iopamidol injection 26%

SQUIBB™ Diagnostics

Please see brief summary of prescribing information on following pages.

This product is under license from Bracco Industria Chimica, S.p.A. U.S. Patent #4,001,323

CIRCLE 14 ON READER SERVICE CARD

647-503

ISOVUE®-128 (Iopamidol Injection 26%)
ISOVUE®-300 (Iopamidol Injection 61%)
ISOVUE®-370 (Iopamidol Injection 76%)
ISOVUE-M® 200 (Iopamidol Injection 41%)
ISOVUE-M® 300 (Iopamidol Injection 61%)

INDICATIONS AND USAGE

ISOVUE (Iopamidol Injection) is indicated for intra-arterial digital subtraction angiography (DSA) of the cerebral and abdominal vasculature and for angiography throughout the cardiovascular system, including cerebral and peripheral arteriography, coronary arteriography and ventriculography, selective visceral arteriography and aortography, and intravenous excretory urography and intravenous contrast enhancement of computed tomographic (CECT) head and body imaging.

ISOVUE-M (Iopamidol Injection) is indicated for intrathecal administration in neuroradiology including myelography (lumbar, thoracic, cervical, total columnar), and for contrast enhancement of computed tomographic (CECT) cisternography and ventriculography.

CONTRAINDICATIONS

ISOVUE (Iopamidol Injection)

None.

ISOVUE-M (Iopamidol Injection)

Intrathecal administration of corticosteroids with iopamidol is contraindicated. Because of overdosage considerations, immediate repeat myelography in the event of technical failure is contraindicated (see interval recommendation under DOSAGE AND ADMINISTRATION). Myelography should not be performed in the presence of significant local or systemic infection where bacteremia is likely.

WARNINGS

ISOVUE-M (Iopamidol Injection)

The need for myelographic examination should be carefully evaluated. Iopamidol should be administered with caution in patients with increased intracranial pressure or suspicion of intracranial tumor, abscess or hematoma, those with a history of convulsive disorder, severe cardiovascular disease, chronic alcoholism, or multiple sclerosis, and elderly patients. Particular attention must be given to state of hydration, concentration of medium, dose, and technique used in these patients.

If frankly bloody cerebrospinal fluid is observed, the possible benefits of a myelographic examination should be considered in terms of risk to the patient.

Patients on anticonvulsant medication should be maintained on this therapy.

Direct intracisternal or ventricular administration for standard radiography (without computerized tomographic enhancement) is not recommended. Inadvertent intracranial entry of a large or concentrated bolus of the contrast medium, which increases the risk of neurotoxicity, can be prevented by careful patient management. Also, effort should be directed to avoid rapid dispersion of the medium causing inadvertent rise to intracranial levels (e.g., by active patient movement). If such intracranial entry of the medium occurs, prophylactic anticonvulsant treatment with diazepam or barbiturates orally for 24 to 48 hours should be considered.

Use of medications that may lower the seizure threshold (phenothiazine derivatives, including those used for their antihistaminic properties; tricyclic antidepressants; MAO inhibitors; CNS stimulants; analeptics; antipsychotic agents) should be carefully evaluated. While the contributory role of such medications has not been established, some physicians have discontinued these agents at least 48 hours before and for at least 24 hours following intrathecal use.

Focal and generalized motor seizures have been reported after intrathecal use of water-soluble contrast agents including iopamidol. In several of those cases reported with iopamidol, higher than recommended doses were employed. Therefore *avoid:*

- Deviations from recommended neuroradiologic procedure or patient management.
- Use in patients with a history of epilepsy unless medically justified.
- Overdosage.
- Intracranial entry of a bolus or premature diffusion of a high concentration of the medium.
- Failure to maintain elevation of the head during the procedure, on the stretcher, and in bed.
- Excessive and particularly active patient movement or straining.

ISOVUE (Iopamidol Injection)

Caution must be exercised in patients with severely impaired renal function, those with combined renal and hepatic disease, or anuria particularly when larger doses are administered.

Radiopaque diagnostic contrast agents are potentially hazardous in patients with multiple myeloma or other paraproteinemia, particularly in those with therapeutically resistant anuria. Myeloma occurs most commonly in persons over age 40. Although neither the contrast agent nor dehydration has been proved separately to be the cause of anuria in myelomatous patients, it has been speculated that the combination of both may be causative. The risk in myelomatous patients is not a contraindication; however, special precautions are required.

Contrast media may promote sickling in individuals who are homozygous for sickle cell disease when injected intravenously or intraarterially.

Administration of radiopaque materials to patients known or suspected of having pheochromocytoma should be performed with extreme caution. If, in the opinion of the physician, the possible benefits of such procedures outweigh the considered risks, the procedures may be performed; however, the amount of radiopaque medium injected should be kept to an absolute minimum. The blood pressure should be assessed throughout the procedure and measures for treatment of a hypertensive crisis should be available. These patients should be monitored very closely during contrast-enhanced procedures.

Reports of thyroid storm following the use of iodinated radiopaque diagnostic agents in patients with hyperthyroidism or with an autonomously functioning thyroid nodule suggest that this additional risk be evaluated in such patients before use of any contrast medium.

PRECAUTIONS

General

Diagnostic procedures which involve the use of any radiopaque agent should be carried out under the direction of personnel with the prerequisite training and with a thorough knowledge of the particular procedure to be performed. Appropriate facilities should be available for coping with any complication of the procedure, as well as for emergency treatment of severe reaction to the contrast agent itself. After parenteral administration of a radiopaque agent, competent personnel and emergency facilities should be available for at least 30 to 60 minutes since severe delayed reactions may occur.

Preparatory dehydration is dangerous and may contribute to acute renal failure in patients with advanced vascular disease, diabetic patients, and in susceptible nondiabetic patients (often elderly with preexisting renal disease). *Patients should be well hydrated prior to and following iopamidol administration.*

The possibility of a reaction, including serious, life-threatening, fatal, anaphylactoid or cardiovascular reactions, should always be considered (see ADVERSE REACTIONS). Patients at increased risk include those with a history of a previous reaction to a contrast medium, patients with a known sensitivity to iodine per se, and patients with a known clinical hypersensitivity (bronchial asthma, hay fever, and food allergies). The occurrence of severe idiosyncratic reactions has prompted the use of several pretesting methods. However, pretesting cannot be relied upon to predict severe reactions and may itself be hazardous for the patient. It is suggested that a thorough medical history with emphasis on allergy and hypersensitivity, prior to the injection of any contrast medium, may be more accurate than pretesting in predicting potential adverse reactions. A positive history of allergies or hypersensitivity does not arbitrarily contraindicate the use of a contrast agent where a diagnostic procedure is thought essential, but caution should be exercised. Premedication with antihistamines or corticosteroids to avoid or minimize possible allergic reactions in such patients should be considered (see CONTRAINDICATIONS). Reports indicate that such pretreatment does not prevent serious life-threatening reactions, but may reduce both their incidence and severity.

General anesthesia may be indicated in the performance of some procedures in selected patients; however, a higher incidence of adverse reactions has been reported with radiopaque media in anesthetized patients, which may be attributable to the inability of the patient to identify untoward symptoms, or to the hypotensive effect of anesthesia which can reduce cardiac output and increase the duration of exposure to the contrast agent.

Even though the osmolality of iopamidol is low compared to diatrizoate or iothalamate based ionic agents of comparable iodine concentration, the potential transitory increase in the circulatory osmotic load in patients with congestive heart failure requires caution during injection. These patients should be observed for several hours following the procedure to detect delayed hemodynamic disturbances.

In angiographic procedures, the possibility of dislodging plaques or damaging or perforating the vessel wall should be borne in mind during catheter manipulations and contrast medium injection. Test injections to ensure proper catheter placement are suggested. Following arteriographic procedures, gentle pressure hemostasis is required, followed by observation and immobilization of the limb for several hours to prevent hemorrhage from the site of arterial puncture.

The inhibitory effects of nonionic contrast media on mechanisms of hemostasis have been shown, in vitro, to be less than ionic contrast media at comparable concentrations. For this reason, standard angiographic procedures should always be followed: angiographic catheters should be flushed frequently, and prolonged contact of blood with contrast in syringes and catheters should be avoided.

Selective coronary arteriography should be performed only in selected patients and those in whom the expected benefits outweigh the procedural risk. The inherent risks of angiocardiography in patients with chronic pulmonary emphysema must be weighed against the necessity for performing this procedure. Angiography should be avoided whenever possible in patients with homocystinuria, because of the risk of inducing thrombosis and embolism.

If nondisposable equipment is used, scrupulous care should be taken to prevent residual contamination with traces of cleansing agents.

Information For Patients

Patients receiving injectable radiopaque diagnostic agents should be instructed to:

1. Inform your physician if you are pregnant.
2. Inform your physician if you are diabetic or if you have multiple myeloma, pheochromocytoma, homozygous sickle cell disease, or known thyroid disorder (see WARNINGS).
3. Inform your physician if you are allergic to any drugs, food, or if you had any reactions to previous injections of substances used for x-ray procedures (see PRECAUTIONS, General).
4. Inform your physician about any other medications you are currently taking, including nonprescription drugs, before you have this procedure.

Drug Interactions

Renal toxicity has been reported in a few patients with liver dysfunction who were given oral cholecystographic agents followed by intravascular contrast agents. Administration of intravascular agents should therefore be postponed in any patient with a known or suspected hepatic or biliary disorder who has recently received a cholecystographic contrast agent.

Other drugs should not be admixed with iopamidol.

Drug/Laboratory Test Interactions

The results of PBI and radioactive iodine uptake studies, which depend on iodine estimations, will not accurately reflect thyroid function for up to 16 days following administration of iodinated contrast media. However, thyroid function tests not depending on iodine estimations, e.g., T3 resin uptake and total or free thyroxine (T4) assays are not affected.

Any test which might be affected by contrast media should be performed prior to administration of the contrast medium.

Laboratory Test Findings

In vitro studies with animal blood showed that many radiopaque contrast agents, including iopamidol, produced a slight depression of plasma coagulation factors including prothrombin time, partial thromboplastin time, and fibrinogen, as well as a slight tendency to cause platelet and/or red blood cell aggregation (see PRECAUTIONS, General).

Transitory changes may occur in red cell and leucocyte counts, serum calcium, serum creatinine, serum glutamic oxalacetic transaminase (SGOT), and uric acid in urine; transient albuminuria may occur.

These findings have not been associated with clinical manifestations.

Carcinogenesis, Mutagenesis, Impairment Of Fertility

In animal reproduction studies performed on rats, intravenously administered iopamidol did not induce adverse effects on fertility or general reproductive performance.

In studies to determine mutagenic activity, iopamidol did not cause any increase in mutation rates.

Pregnancy Category B

No teratogenic effects attributable to iopamidol have been observed in teratology studies performed in animals. There are, however, no adequate and well controlled studies in pregnant women. It is not known whether iopamidol crosses the placental barrier or reaches fetal tissues. However, many injectable contrast agents cross the placental barrier in humans and appear to enter fetal tissues passively. Because animal teratology studies are not always predictive of human response, this drug should be used during pregnancy only if clearly needed.

Radiologic procedures involve a certain risk related to the exposure of the fetus to ionizing radiation.

Labor and Delivery

It is not known whether use of contrast agents during labor or delivery has immediate or delayed adverse effects on the fetus, prolongs the duration of labor or increases the likelihood that forceps delivery or other obstetrical intervention or resuscitation of the newborn will be necessary.

Nursing Mothers

It is not known whether iopamidol is excreted in human milk. However, many injectable contrast agents are excreted unchanged in human milk. Although it has not been established that serious adverse reactions occur in nursing infants, caution should be exercised when intravascular contrast media are administered to nursing women because of potential adverse reactions, and consideration should be given to temporarily discontinuing nursing.

Pediatric Use

Safety and effectiveness in children have not been established.

ADVERSE REACTIONS

ISOVUE (Iopamidol Injection)

Adverse reactions following the use of iopamidol are usually mild to moderate, self-limited, and transient.

In a clinical trial with 100 patients undergoing intra-arterial DSA, adverse reactions possibly attributed to ISOVUE-128 administration were nausea (2%), headache (1%) and vomiting (1%). One patient with preexisting renal impairment and severe bilateral renal vascular disease experienced renal failure, possibly secondary to a subsequent acute episode of congestive heart failure and/or drug administration (see Warnings).

In angiocardiography (597 patients), the adverse reactions with an estimated incidence of one percent or higher are: hot flashes 3.4%; angina pectoris 3.0%; flushing 1.8%; bradycardia 1.3%; hypotension 1.0%; hives 1.0%.

Intravascular injection of contrast media is frequently associated with the sensation of warmth and pain, especially in peripheral arteriography; pain and warmth are less frequent and less severe with ISOVUE (Iopamidol Injection) than with diatrizoate meglumine and diatrizoate sodium injection.

The following table of incidence of reactions is based on clinical studies with ISOVUE in about 1835 patients.

Adverse Reactions

System	Estimated Overall Incidence > 1%	≤ 1%
Cardiovascular	none	tachycardia hypotension hypertension myocardial ischemia circulatory collapse S-T segment depression bigeminy extrasystoles ventricular fibrillation angina pectoris bradycardia transient ischemic attack thrombophlebitis
Nervous	pain (1.7%) burning sensation (1.4%)	vasovagal reaction tingling in arms grimace faintness
Digestive	nausea (1.2%)	vomiting anorexia
Respiratory	none	throat constriction dyspnea pulmonary edema
Skin and Appendages	none	rash urticaria pruritus flushing
Body as a Whole	hot flashes (1.5%)	headache fever chills excessive sweating back spasm
Special Senses	warmth (1.1%)	taste alterations nasal congestion visual disturbances
Urogenital	none	urinary retention

Regardless of the contrast agent employed, the overall estimated incidence of serious adverse reactions is higher with *coronary arteriography* than with other procedures. Cardiac decompensation, serious arrhythmias, or myocardial ischemia or infarction may occur during *coronary arteriography and left ventriculography.* Following coronary and ventricular injections, certain electrocardiographic changes (increased QTc, increased R-R, T-wave amplitude) and certain hemodynamic changes (decreased systolic pressure) occurred less frequently with ISOVUE (Iopamidol Injection) than with diatrizoate meglumine and diatrizoate sodium injection; increased LVEDP occurred less frequently after ventricular iopamidol injections.

In *aortography,* the risks of procedures also include injury to the aorta and neighboring organs, pleural puncture, renal damage including infarction and acute tubular necrosis with oliguria and anuria, accidental selective filling of the right renal artery during the translumbar procedure in the presence of preexisting renal disease, retroperitoneal hemorrhage from the translumbar approach, and spinal cord injury and pathology associated with the syndrome of transverse myelitis.

Adverse effects reported in clinical literature for iopamidol include arrhythmia, arterial spasms, hematuria, periorbital edema, involuntary leg movement, malaise, and triggering of deglutition; some of these may occur as a consequence of the procedure. Other reactions may also occur with the use of any contrast agent as a consequence of the procedural hazard; these include hemorrhage or pseudoaneurysms at the puncture site, brachial plexus palsy following axillary artery injections, chest pain, myocardial infarction, and transient changes in hepatorenal chemistry tests. Arterial thrombosis, displacement of arterial plaques, venous thrombosis, dissection of the coronary vessels and transient sinus arrest are rare complications.

ISOVUE-M (Iopamidol Injection)

The most frequently reported adverse reactions following intrathecal administration of iopamidol are headache, nausea, vomiting and musculoskeletal pain. These reactions usually occur 1 to 10 hours after injection, almost all occurring within 24 hours. They are usually mild to moderate in degree lasting for a few hours and usually disappearing within 24 hours. Rarely, headaches may be severe or persist for days. Headache is often accompanied by nausea and vomiting, and tends to be more frequent and persistent in patients not optimally hydrated.

Backache, neck stiffness, numbness and paresthesias, leg or sciatic-type pain occurred less frequently, often in the form of a transient exacerbation of preexisting symptomatology. Transient alterations in vital signs may occur and their significance must be assessed on an individual basis.

The following table of incidence of reactions is based on clinical studies with ISOVUE-M (Iopamidol Injection) in about 615 patients.

Adverse Reactions

System	Estimated Overall Incidence > 1%	≤ 1%
Body as a Whole	headache (18.1%)	pyrexia muscle weakness hot flashes malaise fatigue weakness
Digestive	nausea (7.3%) vomiting (3.7%)	diarrhea heartburn
Musculoskeletal	back pain (2.3%) leg pain (1.4%) neck pain (1.1%)	leg cramps sciatica cervicobrachial irritation meningeal irritation radicular irritation, lumbosacral other musculoskeletal pain involuntary movement burning sensation
Cardiovascular	hypotension (1.1%)	tachycardia hypertension chest pain

Adverse Reactions (con't)

System	Estimated Overall Incidence > 1%	≤ 1%
Nervous	none	emotional stress dizziness paresthesia confusion hallucinations lightheadedness syncope numbness cold extremities
Urogenital	none	urinary retention
Respiratory	none	dyspnea
Skin and Appendages	none	rash
Miscellaneous	none	injection site pain

Other adverse effects reported in clinical literature for iopamidol include facial neuralgia, tinnitus, and sweating.

Major motor seizures have been reported in the clinical literature and since market introduction in the United States. Early onset of seizures (less than two hours) is indicative of early substantial intracranial entry. Transitory EEG changes occur and usually take the form of slow wave activity.

While not observed in controlled clinical studies with ISOVUE-M (Iopamidol Injection), or reported in clinical literature, the following adverse reactions may occur because they have been reported with other nonionic contrast agents: cardiovascular (arrhythmias); aseptic meningitis syndrome; allergy or idiosyncrasy (chills, pruritus, nasal congestion, Guillain-Barre syndrome); CNS irritation (psycho-organic syndrome: mild and transitory perceptual aberrations such as depersonalization, anxiety, depression, hyperesthesia, disturbances in speech, sight, or hearing, and disorientation; in addition, hyperreflexia or areflexia, hypertonia or flaccidity, restlessness, tremor, echoacousia, echolalia, asterixis or dysphasia have occurred). Profound mental disturbances have rarely been reported (various forms and degrees of aphasia, mental confusion or disorientation); the onset is usually at 8 to 10 hours and lasts for about 24 hours without aftereffects.

However, occasionally they have been manifest as apprehension, agitation, or progressive withdrawal to the point of stupor in several instances. In a few cases, these have been accompanied by transitory hearing loss or other auditory symptoms and visual disturbances (believed subjective or delusional). Persistent cortical loss of vision in association with convulsions, and ventricular block have been reported. Rarely, persistent though transitory weakness in the leg or ocular muscles has been reported. *Peripheral neuropathies* have been rare and transitory. They include sensory and/or motor or nerve root disturbances, myelitis, persistent leg muscle pain or weakness, or sixth nerve palsy, or cauda equina syndrome. Muscle cramps, fasciculation or myoclonia, spinal convulsion, or spasticity are unusual.

General Adverse Reactions To Contrast Media

Reactions known to occur with parenteral administration of iodinated ionic contrast agents (see the listing below) are possible with any nonionic agent. Approximately 95 percent of adverse reactions accompanying the use of other water-soluble intravascularly administered contrast agents are mild to moderate in degree. However, life-threatening reactions and fatalities, mostly of cardiovascular origin, have occurred.

Reported incidences of death from the administration of other iodinated contrast media range from 6.6 per 1 million (0.00066 percent) to 1 in 10,000 patients (0.01 percent). Most deaths occur during injection or 5 to 10 minutes later, the main feature being cardiac arrest with cardiovascular disease as the main aggravating factor. Isolated reports of hypotensive collapse and shock are found in the literature. The incidence of shock is estimated to be 1 out of 20,000 (0.005 percent) patients.

Adverse reactions to injectable contrast media fall into two categories: chemotoxic reactions and idiosyncratic reactions. Chemotoxic reactions result from the physico-chemical properties of the contrast medium, the dose, and the speed of injection. All hemodynamic disturbances and injuries to organs or vessels perfused by the contrast medium are included in this category. Experience with iopamidol suggests there is much less discomfort (e.g., pain and/or warmth) with peripheral arteriography. Fewer changes are noted in ventricular function after ventriculography and coronary arteriography.

Idiosyncratic reactions include all other reactions. They occur more frequently in patients 20 to 40 years old. Idiosyncratic reactions may or may not be dependent on the amount of drug injected, the speed of injection, the mode of injection, and the radiographic procedure. Idiosyncratic reactions are subdivided into minor, intermediate, and severe. The minor reactions are self-limited and of short duration; the severe reactions are life-threatening and treatment is urgent and mandatory.

The reported incidence of adverse reactions to contrast media in patients with a history of allergy is twice that for the general population. Patients with a history of previous reactions to a contrast medium are three times more susceptible than other patients. However, sensitivity to contrast media does not appear to increase with repeated examinations. Most adverse reactions to intravascular contrast agents appear within one to three minutes after the start of injection, but delayed reactions may occur (see PRECAUTIONS, General).

Because measurable plasma levels are attained following the intrathecal administration of iopamidol, adverse reactions reported with the use of intravascular contrast agents are theoretically possible. In addition to the adverse drug reactions reported for iopamidol, the following additional adverse reactions have been reported with the use of other intravascular contrast agents and are possible with the use of any water-soluble iodinated contrast agent:

Cardiovascular: vasodilation, cerebral hematomas, petechiae, hemodynamic disturbances, sinus bradycardia, transient electrocardiographic abnormalities, ventricular fibrillation.

Digestive: nausea, vomiting, severe unilateral or bilateral swelling of the parotid and submaxillary glands.

Nervous: paresthesia, dizziness, convulsions, paralysis, coma.

Respiratory: increased cough, asthma, laryngeal edema, pulmonary edema, bronchospasm, rhinitis, dyspnea.

Skin and Appendages: injection site pain usually due to extravasation and/or erythematous swelling, skin necrosis.

Urogenital: osmotic nephrosis of proximal tubular cells, renal failure, pain.

Special Senses: bilateral ocular irritation; lacrimation; conjunctival chemosis, infection, and conjunctivitis; itching.

The following reactions may also occur: neutropenia, thrombophlebitis, flushing, pallor, weakness, severe retching and choking, wheezing, cramps, tremors, and sneezing.

HOW SUPPLIED

ISOVUE-128: 10x50 mL vials; ISOVUE-300: 10x50 mL vials and 10 x 100 mL bottles; ISOVUE-370: 10x50 mL vials and 10 x 100 mL, 10 x 150 mL and 10x200 mL bottles; ISOVUE-M 200: 10x20 mL vials; ISOVUE-M 300: 10 x 15 mL vials.

STORAGE

ISOVUE® and ISOVUE-M® (iopamidol injection) should be stored at room temperature not exceeding 86° F. Protect from light.

For full prescribing information consult package insert.

J3-702A/J3-652D/J3-653E.

© 1987 E.R. Squibb & Sons, Inc., Princeton, NJ 647-503 Issued: June 1987

Evaluation of meniscal tears

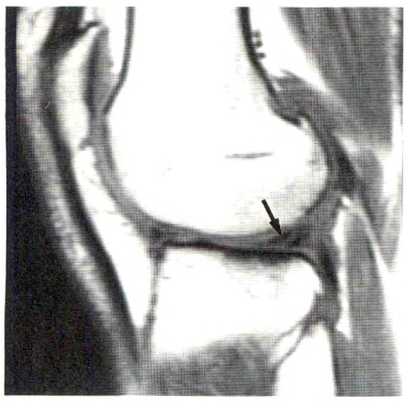
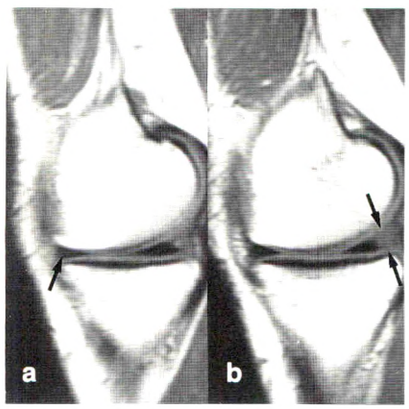


Fig. 1—T1 weighted image defines a linear region of increased signal intensity (arrow) communicating with the inferior articular surface. (TR 800, TE 20)



Figs. 2a,b—Linear signal intensity (Fig. 2a) is present within the anterior horn of the medial meniscus (arrow). A posterior menisco-capsular separation (Fig. 2b) is noted (arrows), as well as increased signal intensity within the posterior horn of the medial meniscus. (Images windowed for maximum visualization of meniscus.) (TR 800, TE 20)

For non-invasive evaluation of the knee, high field magnetic resonance (MR) has become the imaging modality of choice. Its precise imaging of anatomical detail and high sensitivity to pathology permit complete examinations of the knee in less than twenty minutes.

Case study

The patient was a 39-year-old athletic male who had a history of pain and swelling of the lateral aspect of the knee and who had previously undergone an arthrotomy and partial meniscectomy. He presented with non-abated symptoms post-operatively, and was referred to a Signa® user for an MR exam to evaluate the etiology of his knee pain.

MR exam

The MR exam revealed a small residual rim of meniscal tissue in the posterior aspect of the lateral compartment. This retained meniscal region contained a linear area of increased signal intensity communicating with the inferior articular surface (Fig. 1). In the medial compartment, a posterior menisco-capsular separation was noted. The signal intensity within the posterior and anterior horns of the medial meniscus was consistent with a meniscal tear (Fig. 2).

Based on this evaluation, the patient agreed to a second operative procedure. The MR findings were correlated at surgery, and the patient became asymptomatic immediately post-op.

Conclusion

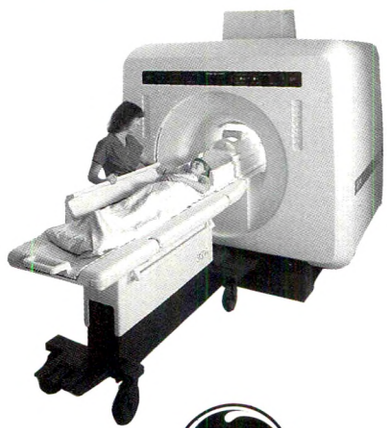
The sensitivity of MR imaging to anatomical detail and pathology demonstrated the locations and details of multiple lesions without employing invasive techniques. This permitted better operative planning and patient management.

Acknowledgement: John V. Crues, III, M.D., Jerrold Mink, M.D., Cedars-Sinai Medical Center, Los Angeles, CA.

Signa . . . the MR reference point

For referring physicians of all specialties, Signa sites are the reference point for optimal image quality across the broadest range of applications in MR.

To receive a detailed discussion of the case presented here, call GE Medical Systems at 1-800-624-5692 and request MR Clinical Symposium No. 7118. We will also be glad to provide a list of the Signa sites in your area.



CIRCLE 15 ON READER SERVICE CARD

©Copyright 1987 GE Medical Systems

7385 Printed in USA

Sonographic Guidance in Diagnostic and Therapeutic Interventions in the Pleural Space

Paul V. O'Moore[1]
Peter R. Mueller
Joseph F. Simeone
Sanjay Saini
Rodney J. Butch
Peter F. Hahn
Edward Steiner
David D. Stark
Joseph T. Ferrucci, Jr.

One hundred eighty-seven diagnostic and therapeutic interventional procedures in the pleural space were performed by using sonographic guidance. These consisted of diagnostic aspiration (118), drainage of malignant and nonmalignant effusions (41), empyema drainage (17), pleural sclerotherapy with tetracycline or bleomycin (7), and pleural biopsy (4). Diagnostic aspiration was performed with 20-gauge needles, and therapeutic and empyema drainages were performed by trocar technique with either a 7-French Sacks catheter or a specially designed empyema drainage catheter. Pneumothoraces were seen in 3% of the patients, and most of these were treated by the radiologist with placement of a Heimlich valve.

We conclude that the use of sonography allows rapid localization of pleural fluid collections and instant monitoring of drainage of noninfected fluid collections and empyemas.

Sonographically guided interventions in the pleural space have been reported infrequently [1, 2]. Both CT and fluoroscopy have been emphasized as the primary techniques for diagnosis and treatment of a variety of pleural abnormalities [2–4]. Yet, because of its ability to visualize superficial fluid collections and its real-time capability, sonography has the potential to be an ideal imaging procedure for monitoring interventional procedures in the pleural space [5–9].

We describe a retrospective review of 187 sonographically guided procedures in the pleural space. The success rate of these procedures approached 95% with a complication rate of 3%.

Materials and Methods

Between January 1983 and February 1986, 187 procedures were performed in the pleural space of 170 patients by using sonographic guidance. Of these, 25% were performed on an outpatient basis and 4% were done on the wards with a portable sonographic unit.

Interventional Procedures

The four types of interventional procedures were diagnostic aspiration, therapeutic drainage, empyema drainage, and miscellaneous interventions.

Diagnostic aspiration.—Diagnostic aspiration was performed in 118 patients. The most common indication was to exclude empyema in febrile patients who had effusions that were not responding to antibiotic therapy (87 cases). Twenty-seven of these were postsurgical patients, 24 had associated preexisting pneumonia, and 36 had multisystem disease. Radiologic guidance was requested because the patient's effusion was not free flowing, because nonguided attempts had already failed, or because the collection was thought to be too small to permit unguided sampling (Fig. 1). Initially (in the first 40 patients), these were the sole reasons for the use of sonographic guidance. However, as it became apparent that diagnostic aspirations could be performed more accurately, more quickly, and with less discomfort to the patient by using sonography, most of the remaining 47 patients were immediately referred

Received January 5, 1987; accepted after revision March 10, 1987.

[1] All authors: Department of Radiology, Massachusetts General Hospital and Harvard Medical School, Boston, MA 02114. Address reprint requests to P. R. Mueller, Dept. of Radiology, Massachusetts General Hospital, Boston, MA 02114.

***AJR* 149:1–5, July 1987**
0361–803X/87/1491–0001
© American Roentgen Ray Society

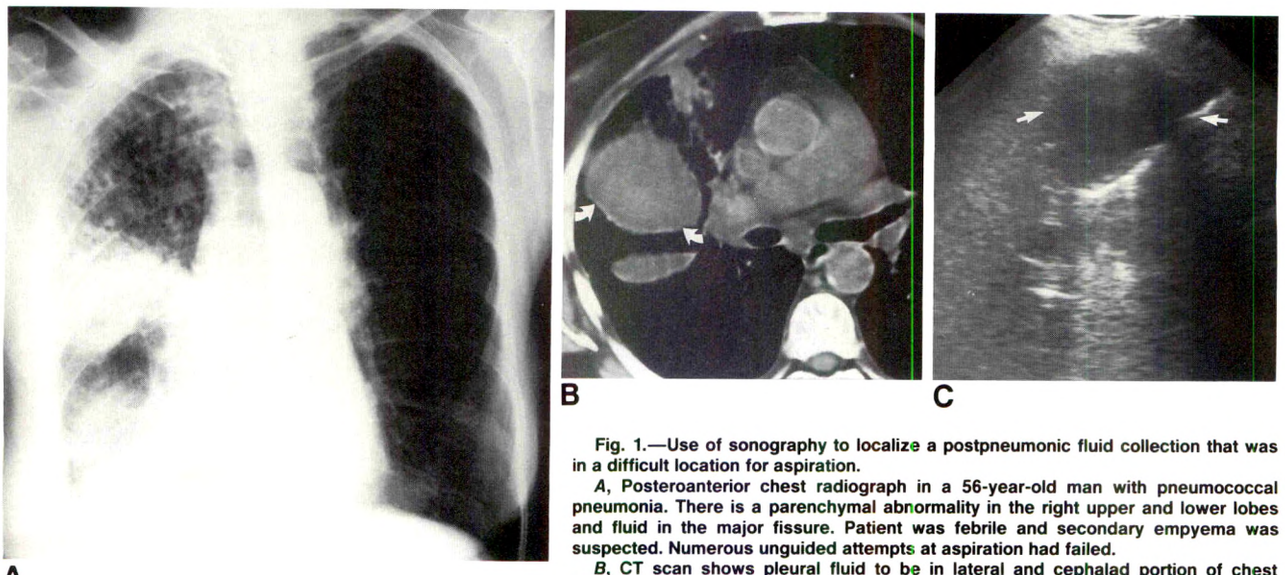


Fig. 1.—Use of sonography to localize a postpneumonic fluid collection that was in a difficult location for aspiration.

***A*, Posteroanterior chest radiograph in a 56-year-old man with pneumococcal pneumonia. There is a parenchymal abnormality in the right upper and lower lobes and fluid in the major fissure. Patient was febrile and secondary empyema was suspected. Numerous unguided attempts at aspiration had failed.**

***B*, CT scan shows pleural fluid to be in lateral and cephalad portion of chest (*arrows*).**

***C*, Sonographic localization was easily performed and showed typical sonolucent and convex appearance of loculated pleural fluid (*arrows*). Actual needle placement was 1 cm inferior and lateral to right nipple.**

for the procedure without attempts on the ward. The second most common indication was in patients with known or suspected malignancy who presented with a new effusion (31 cases). Again, the first 20 patients in this group were referred because of presumed small effusions (i.e., those that were difficult to perceive on lateral decubitus chest radiographs or difficult to detect clinically by percussion of the chest). The other 11 were referred as a direct result of our success with previous chest aspirations.

Therapeutic drainage.—Therapeutic drainage in uninfected collections was performed in 41 cases. These patients had pleural effusions from metastasis, abdominal inflammatory disease (i.e., pancreatitis), and/or severe congestive heart failure, and drainage was performed to relieve dyspnea and associated chest discomfort. The first 25% of patients were referred for sonographically guided drainage because of incomplete drainage done in the ward or office. Ninety percent of the remaining 30 patients were outpatients, and referral was again based on previous success and the perceptions of both clinicians and patients that using sonographic guidance for the procedures caused less patient discomfort.

Empyema drainage.—This procedure was performed in 17 cases with infected postsurgical or postpneumonic collections (Fig. 2). Six (35%) of seventeen drainages were referred because drainage by surgically placed, large-bore chest tube was incomplete. Eleven (65%) of seventeen were referred primarily because the collection visualized by sonography and/or chest radiograph was small (suspected to be less than 100 ml) and would be better localized and drained by sonographic guidance.

Miscellaneous interventions.—These included pleural sclerotherapy (seven patients) and pleural biopsy (four patients). These patients were all referred because previous attempts at sclerotherapy or pleural biopsy without guidance had failed. Seven patients underwent chemical sclerotherapy after the catheter had been placed for removal of malignant effusions. These consisted of injections of 50–100 ml of tetracycline at a dosage of 50–75 mg/ml, or bleomycin at a dosage varying between 60 and 180 mg diluted in saline [10]. In all cases, the agent was injected through the percutaneously placed catheter, which was then immediately removed. The patient was turned 360°, and no attempt was made to withdraw the injected fluid. Pleural biopsies were performed on four patients. These were done with a Cope reversed bevel needle (Becton-Dickinson, Rutherford, NJ). A subpleural mass was biopsied with an 18-gauge spinal needle after sonographic localization.

Data analysis.—For all four types of procedures, data concerning the type of equipment used, the anatomic location of the abnormality, the technique used for guidance, the radiologic findings, and the quantity and character of any specimens obtained were abstracted from the procedure note and radiologic report. Results of laboratory examination of specimens were available in 58% of the patients. These included Gram stain, cell count, bacterial or fungal cultures, cytologic or pathologic examination, and chemistry determinations such as pH, glucose, and protein count. Information concerning the remaining 42% of the patients was obtained either by direct chart review while the patient remained in the hospital or by follow-up through the referring physicians.

For the purpose of defining complication rates, a pneumothorax was defined as air in the pleural space that resulted in symptoms or required insertion of a chest tube. Small amounts of air that were asymptomatic or loculated and that resolved spontaneously were not considered as true complications.

Intervention Technique

Patient positioning.—For most pleural interventions, patients were positioned, when possible, sitting on the side of a stretcher, facing away from the radiologist with arms crossed and resting on a bedside table. Patients who could not tolerate this position were placed in the lateral decubitus position with the diseased side up.

Localization and preparation.—A point of entry in the chest was chosen just above the rib nearest the collection as seen sonographically. A special biopsy transducer was not necessary. Standard aseptic technique and local anesthesia were used. Anesthetizing the periosteum overlying the nearest rib was helpful. The pleura is difficult to anesthetize, but attempts should be made before insertion of the needle.

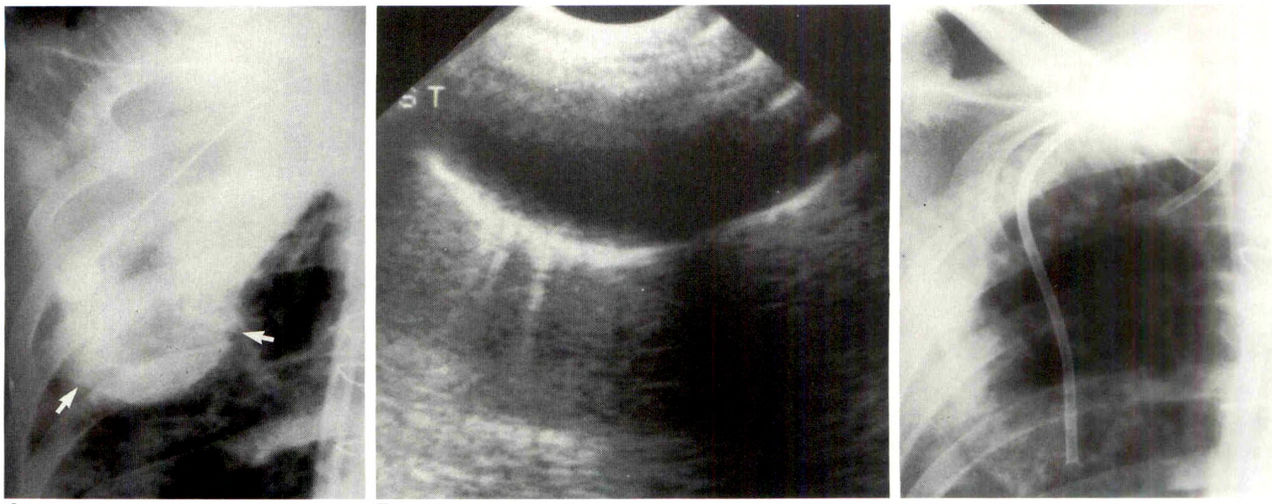


Fig. 2.—Empyema drainage guided by sonography in a 64-year-old man performed 6 days after major mediastinal surgery and tracheal reconstruction. Procedure was performed at patient's bedside in the intensive care unit.

***A*, Portable anteroposterior chest radiograph shows sharply marginated and homogeneous opacity in right upper hemithorax (*arrows*).**

***B*, Sonographic localization 2 cm inferior to right clavicle revealed an ellipsoid sonolucent abnormality in anterior lateral chest corresponding to abnormality on chest radiograph. After initial needle aspiration confirmed presence of purulent material, a 10-French Cook empyema catheter was introduced at bedside and 40 ml of pus were aspirated.**

***C*, Anteroposterior chest radiograph 3 days after procedure showed location of drainage catheter overlying right upper lobe. Pleural collection in right upper chest was gone, and patient was afebrile.**

Diagnostic sampling.—A 20- or 22-gauge spinal needle with or without a 12-ml syringe attached was inserted to the estimated depth of the collection. If a large volume of fluid was to be removed, a three-way stopcock might be inserted between the needle and the syringe. When sufficient material had been collected, the needle was withdrawn. Samples were sent immediately for Gram stain and culture. Cell count of the fluid might be obtained when a traumatic tap is suspected or if the effusion is bloody. In cases of suspected malignancy samples, cytology was routinely performed. Special laboratory studies may be appropriate in suspected diseases such as tuberculosis, rheumatoid arthritis, or systemic lupus erythematosus.

Therapeutic drainage.—Drainage for symptomatic relief in patients with large or loculated benign or malignant fluid collections was performed using a trocar 7-French Sacks catheter with multiple side holes (Electro Cath Group, Rahway, NJ). Once the collection had been localized with sonography, the skin was anesthetized and a small incision was made with a #11 scalpel blade to prevent catheter binding or buckling. The catheter system was introduced into the pleural space to the depth at which fluid was expected. In patients with a thick pleural rind, the catheter might buckle slightly as it meets pleural resistance. For easier catheter placement, an 18-gauge spinal needle can be inserted through the pleura into the fluid collection to create a preliminary tract. The 18-gauge needle was then removed and catheter insertion was attempted. Fluid was withdrawn to confirm proper location. The catheter itself was then advanced over the stiffening cannula into the collection, and a three-way stopcock was attached. Extension tubing was used to connect the stopcock to a sterile vacuum bottle to facilitate rapid drainage of the fluid. When drainage stopped, the catheter could be manipulated to reestablish flow. Once sufficient fluid had been removed to permit the lung to come into contact with the catheter, the patient often had discomfort or coughing. In some cases, a postprocedure sonogram was obtained before removal of the catheter to ensure that residual fluid remained. A postprocedure chest radiograph was obtained in all patients.

Empyema drainage.—If the sample was grossly purulent or if Gram stain indicated the presence of organisms and white cells, a drainage procedure was undertaken with the intent of leaving the catheter in place. Early in our experience, 8.3-French Ring catheters (Cook, Bloomington, IN) were placed using the Seldinger technique. More recently, a specially designed 10- to 12-French empyema catheter (Cook, Bloomington, IN) has been employed, with most of the catheters being placed by trocar technique. This catheter is designed for trocar insertion, has a soft curved tip and distal side holes, and is made of polyethylene that is sufficiently rigid not to be compressed by the ribs. After the catheter was placed in the empyema cavity, irrigation with sterile saline was performed as with standard abscesses.

The catheter was then attached to a standard three-bottle, water-sealed, chest-tube-suction apparatus (Pleur-E-Vac, Deknatel, Division of Pfizer, Hospital Products Group, Queens Village, NY) prepared before insertion. The volume of drainage from the catheter was monitored, and the catheters were inspected daily. A repeat sonogram was obtained 3–5 days after drainage to ensure that no empyema fluid had reaccumulated or remained undrained. Once the drainage stopped, suction was discontinued, and the catheter was placed on water seal for 24 hr and removed if a repeat chest radiograph showed no pneumothorax. The patients were seen on the wards 24–48 hr after chest-tube removal to ensure that no clinical symptoms had recurred.

Treatment for Pneumothorax

If the patient complained of increased dyspnea during the procedure, the catheter was left in place and a chest film was obtained. A symptomatic pneumothorax was treated immediately by connecting a Heimlich valve (Cook, Bloomington, IN) directly to the catheter. The one-way valve chamber outlet may be left open to ambient air or connected to a standard three-bottle, water-sealed, chest-tube-suc-

tion system. Patients were followed with expiration chest radiographs every 30–60 min until complete reexpansion of the lung was determined. The Heimlich valve was left in place but turned off (via a three-way stopcock) for 30 min after the lung was reexpanded. A repeat chest radiograph was performed at 30–60 min, and if the lung remained expanded, the tube was removed and the patient was sent back to the ward or home.

Results

Results can be analyzed in four main categories: diagnostic aspiration, therapeutic drainage, empyema drainage, and miscellaneous (pleural sclerotherapy and biopsy).

Diagnostic Aspiration

Aspiration of fluid was successful in 114 (97%) of 118 patients referred for diagnostic taps. In these patients, the amount of fluid ranged from 1.5 to 350 ml. Significantly, several patients with less than 10 ml of fluid had successful diagnostic aspiration.

Of the patients who underwent diagnostic aspiration to exclude infection, charts were available for review in 58%; the remaining data were recorded by clinical follow-up on the wards or from referring physicians for outpatients. Either (1) a positive Gram stain for WBCs or (2) WBCs with organisms and/or positive culture was considered an indication of infection. Detection of WBCs on a Gram stain was used as a determinant of infection because 41% of the patients were on antibiotics at the time of the aspiration. Any fluid that had WBCs was considered infected and was subsequently drained, or the patient was given a full course of antibiotics. It is difficult to determine the accuracy of these criteria. A prospective study was not carried out to see if the patients would have improved without antibiotic therapy. On the other hand, the absence of both organisms and WBCs on the Gram stain of the fluid was considered evidence of no infection, and no patient who had these findings was found to have an infected pleural space by either reaspiration or clinical follow-up. It is again difficult to follow these patients by size or reappearance of their pleural fluid on repeat examination because over 70% did not have repeat sonograms. Presumably, either the pleural fluid in the patient regressed, or it was the result of other causes such as congestive heart failure and was treated as such when the fluid was determined to be uninfected. The remaining patients either had repeat aspirations that showed no organisms or WBCs on Gram stain, or had less fluid on repeat sonograms or chest radiographs.

It was impossible to determine the false-negative rate of the cytologic results because neither autopsy nor biopsy of the pleura was performed on those with negative thoracentesis. Eighty-seven percent of the patients who had known primary malignant disease and recurrent effusions had positive cytology.

No fluid was obtained in four patients, although sonography and chest radiographs suggested that a small amount of fluid was present. In another patient who had undergone esophageal resection with esophagogastric anastamosis, the initial diagnostic thoracentesis entered an intrathoracic stomach resulting in spurious findings: orange-colored fluid was aspirated, the Gram stain was positive, and culture of the aspirate was positive for yeast. A repeat tap of the actual pleural fluid yielded uninfected fluid.

Therapeutic Drainage

All 41 patients had successful therapeutic drainage of noninfected collections. The amount of fluid removed ranged from 100 to 2500 ml (average, 1000 ml). Eight patients in this group had the procedure two times, four patients three times, and two patients more than three times because of recurring effusions. In four patients, both pleural spaces were drained at one time.

Overall, although postprocedural sonography showed objective evidence of removal of over 90% of the fluid in the pleural space, subjective results were difficult to evaluate. Thirty (73%) of 41 stated that their symptoms had improved, but the other 11 patients noted no change.

Empyema Drainage

Seventeen patients underwent 19 catheter insertions for empyemas. Two patients had two catheters placed because repeat examinations several days after the first catheter placement showed an undrained collection. Of these, 15 had complete resolution of the infected collection and showed clinical improvement over the next 5 days to 3 weeks. Two patients died from unrelated causes, and two underwent surgery for definitive closure of the drained cavity.

Pleural Sclerotherapy and Pleural Biopsy

Only two of the seven patients who had pleural sclerotherapy had an apparent response to chemical pleurodesis. Bleomycin had been injected into both of these patients. The remaining five had subsequent radiographic evidence of recurrent effusion. Three of the four pleural biopsies performed under sonographic guidance yielded pleural tissue and were positive for malignancy (metastases in two cases and mesothelioma in one). In one patient with lymphoma of the pleura (proved at subsequent surgery), a nondiagnostic (false-negative) specimen was obtained.

Complications

Complications were analyzed by the type of procedure performed.

Diagnostic aspiration.—Seven of the patients had asymptomatic, barely detectable air in the pleural space after diagnostic aspiration. None of these patients were symptomatic nor were they treated. Two patients were symptomatic after aspiration and had significant pneumothoraces. One patient was treated with a large-bore chest tube, placed in the usual fashion by a surgeon, and that patient required hospitalization. The other was treated with a radiologically placed Heimlich valve tube, and after several hours of observation was sent home after expansion of the lung.

Therapeutic aspiration.—Eight of 41 cases in this group showed pleural air after aspiration. Of five asymptomatic patients, two had minimal pneumothoraces (<5%) and three had moderate pneumothoraces (>20%). All three had histo-

ries of interstitial lung disease from tumor associated with pleural effusion. Two of the pneumothoraces were treated with Heimlich valve placement, although both were asymptomatic and there was no change in their appearance on radiographs after 48 hr. The catheters were removed, and the fluid reaccumulated. The third patient was sent home with a pneumothorax and with no symptoms, but, in this case too, the pleural fluid reaccumulated.

Three patients has symptomatic pneumothoraces that were treated on an outpatient basis with Heimlich valve placement. All three remained in the Radiology Department until full reexpansion of the lung was documented.

Empyema and Miscellaneous Groups

None of the patients in the empyema or pleural biopsy group had complications. One patient who underwent pleural sclerotherapy had a temperature of 103°F within 3 hr after introduction of tetracycline. This responded to conservative treatment with oral antipyretics.

Discussion

Interventional procedures in the pleural space have evolved as a natural outgrowth of the use of real-time sonography for drainage and biopsy procedures in the abdomen. The combination of its extreme sensitivity in detecting fluid collections, its flexibility, and its use with a portable unit make sonography the ideal technique for diagnosis and treatment of abnormalities in the chest.

In this series, 118 patients underwent diagnostic aspiration because of clinical uncertainty about the cause of a pleural abnormality (infection, tumor, or sympathetic effusions). Many patients had such small amounts of fluid that unguided or fluoroscopically guided aspiration was impossible, and possibly harmful. Several patients had had unsuccessful unguided aspiration in the past with resultant pneumothoraces. Once examined under sonography, the cause of such failures was frequently evident. The site of the attempted aspiration was often not even in the vicinity of the fluid collection.

Therapeutic drainage under sonographic guidance has become a common procedure because of its ease in diagnosing pleural effusions, patient acceptability, and low rate of complications. Sonography has been helpful in the palliative therapy of malignant effusion, in which a frequent cause of failure of drainage without imaging guidance is the presence of a thick pleural peel or multiple loculations. Initially, sonography was only performed when unguided drainage was incomplete, but because of its success and low complication rate, drainage by sonography has become a primary procedure, even for use on outpatients. A small percentage (10%) of patients (4/41) had the procedure performed on both pleural spaces during one visit.

Patients with empyemas had had previous surgical drainage and presented with small loculated collections. Although CT has been described as the ideal technique for monitoring drainage in these patients [2], in our experience sonography is quicker and can be used for real-time monitoring while the drainage procedure is being performed.

The complication rate from any of these procedures is exceedingly low, and, when a complication does occur, it can be treated by the radiologist. In most patients, the major complication is pneumothorax, and treatment is only necessary if the patient complains of dyspnea. If this occurs after therapeutic drainage, a Heimlich valve can be directly attached to the drainage catheter. If a symptomatic pneumothorax occurs after diagnostic aspiration or after removal of the catheter, a small Sacks catheter or Heimlich-type catheter can be placed in the air space, and a Heimlich valve can be attached. In most cases, these patients can be treated as outpatients with periodic follow-up chest radiographs until the lung reexpands.

We noted a subgroup of patients with malignant effusions who also have a combination of severe interstitial lung disease and pleural fluid in whom asymptomatic pneumothoraces developed after fluid removal. Often, after therapeutic drainage of the malignant effusions in these patients, large volumes of air are aspirated at the end of the procedure. The patients experience no pain and no dyspnea, but have a moderate amount of air in their pleural space on a postprocedure chest radiograph. Further catheter drainage with a Heimlich valve placement or even attachment of the drainage catheter to a Pleur-E-Vac usually accomplishes little. In these cases, the relative stiffness of the lung from the diffuse interstitial disease most likely prevents reexpansion, and any attempts at reexpansion are unsuccessful. Furthermore, removal of fluid, while possible, is often not helpful in reducing symptoms. In these patients, placement of a catheter for treatment of pneumothorax is not necessary.

The relative ease of catheter placement under sonographic monitoring and the availability of a Heimlich valve have made pleural aspiration and drainage using sonographic guidance a practical and useful procedure. The procedure has evolved to the point where almost all diagnostic aspirations and drainages can be performed by the radiologist.

ACKNOWLEDGMENT

We would like to thank Lynda Bessette for her help in typing the manuscript.

REFERENCES

1. Izumi S, Tamaki S, Natori H, Kira S. Ultrasonically guided aspiration needle biopsy in disease of the chest. *Am Rev Respir Dis* **1982**;125:460–464
2. vanSonnenberg E, Nakamoto SK, Mueller PR, et al. CT- and ultrasound-guided catheter drainage of empyemas after chest-tube failure. *Radiology* **1984**;151:349–353
3. Gobien RP, Stanley JH, Gobien BS, Vujic I, Pass HI. Percutaneous catheter aspiration and drainage of mediastinal abscesses. *Radiology* **1984**;151:69–71
4. Westcott JL. Percutaneous catheter drainage of pleural effusion and empyema. *AJR* **1985**;144:1189–1193
5. Hirsch JH, Roger JV, Mack LA. Real-time sonography of pleural opacities. *AJR* **1981**;136:297–301
6. Laing FC, Filly RA. Problems in the application of ultrasonography for the evaluation of pleural opacities. *Radiology* **1978**;126:211–214
7. Landay MJ, Conrad MR. Lung abscess mimicking empyema on ultrasonography. *AJR* **1979**;133:731–734
8. Marks WM, Filly RA, Callen PW. Real-time evaluation of pleural lesions: new observations regarding the probability of obtaining free fluid. *Radiology* **1982**;142:163–164
9. Sandweiss DA. Empyema or abscess? Is ultrasound a diagnostic aid? *Chest* **1979**;75:297–298
10. Ostrowski MJ, Halsall GM. Intracavitary bleomycin in the management of malignant effusions: a multicenter study. *Cancer Treat Rep* **1982**;66:1903–1907

Memorial

Robert David Moseley, Jr., 1924–1987



Robert David Moseley, Jr. was born on February 29, 1924, in Minden, LA. He grew up in that state and received most of his formal education there, obtaining his M.D. at L.S.U. in 1947 followed by an internship at the Highland Sanitarium in Shreveport.

In 1949 Dr. Moseley became an Assistant Resident in Radiology at the University of Chicago. In 1950 the University assigned him to a research project at Los Alamos Scientific Laboratory, launching his career as an investigator and, additionally, as Radiologist and Associate Chief of Staff at the Los Alamos Medical Center.

After serving 2 years in the Navy, Bob Moseley returned to the University of Chicago and 1 year later became a Diplomate of the American Board of Radiology. His great intellect, energy, and leadership ability were recognized and Bob rose like a meteor from the position of Instructor in 1954 to that of Professor and Chairman of the Department of Radiology in 1958. His early research included describing a method to destroy the pituitary with the transsphenoidal introduction of radioactive yttrium as well as collaborating on such engineering feats as split-image TV image intensifiers. As Chairman he rebuilt the department and attracted and nourished such luminaries as Kurt Rossmann, Alex Gottshalk, John Fennessy, Paul Hoffer, Roy Strand, Guy Potter, James R. Williams, Galdino E. Valvassori, Klaus Ranniger, Nels Stransjord, and Kunio Doi. During his 20-year tenure, Bob fostered and stimulated research in the radiologic sciences by integrating the Department of Radiology at the University of Chicago with the Argonne Cancer Research Hospital and such scientists as Paul Harper and Bob Beck, a merger that resulted in a golden era of productivity for both institutions. Dr. Moseley also introduced the concept of the radiologic internship and in 1962 went on sabbatical with his family in Lund, Sweden.

In 1971 Dr. Moseley left the high-pressure chairmanship and the big city of Chicago and returned to New Mexico to join B. G. Brogden and become Director of the Division of Diagnostic Radiology at the University of New Mexico. As fate would have it, Dr. Brogdon resigned and Bob took over as Chairman of that Department, a post he held from 1978 through 1985, when he assumed the status of Professor Emeritus.

In 1972 Dr. Moseley became President of the Board of Directors of the James Picker Foundation. At that time the Foundation, which had been established in 1947, was awarding grants and fellowships in radiologic research via a Subcommittee on Radiology of the National Research Council. Under his leadership, the Board of Directors of the Picker Foundation became more directly involved in furthering research and research training in diagnostic radiology. This change ultimately resulted in increasing the Foundation's impact on the academic maturation of our field.

Dr. Moseley contributed his time and effort generously to organizing radiology on a national level. In 1953 he was the youngest of the founding members of the Association of University Radiologists and was president of that organization in 1961–1962. In 1967 he was one of the three drafters of the constitution of the Society of Chairmen of Academic Radiology Departments. Bob was Chairman of the Board of Chancellors of the American College of Radiology in 1972–1973 and President of the American College of Radiology in 1973–1974. He was Chairman of the Advisory Committee on Biology and Medicine to the U.S. Atomic Energy Commission from 1967 to 1973 and a member of the radiation study section from 1971 to 1975.

Bob Moseley was an outstanding international ambassador for American radiology. He was a delegate to five International Congresses. He was the first honorary fellow elected to the Royal College of Radiologists (England) and gave that college's inaugural address. He was the second American radiologist honored with membership in the 200-year-old Royal Physiographic Society of Lund, Sweden. He was also the first corresponding member of the Academic Society of Lund, honorary member of the American Association of Physicists in Medicine, and corresponding member of the Deutsche Rontgengesellschaft. He was, from 1975 to 1986, the official United States representative to the United Nations Scientific Committee on the Effects of Atomic Radiation (UNSCEAR).

During his life, Dr. Moseley was honored by serving as the Annual Orator of The Radiological Society of North America and by receiving Gold Medals from the Association of University Radiologists, The American College of Radiology, and The XIII International Congress of Radiology.

Robert David Moseley was a fighter, a raconteur, a master administrator, a visionary, and an optimist who enjoyed life and his friends. His hobbies included skiing, flying, gardening, gourmet cooking, and linguistics. Bob died on March 5, 1987, leaving his loving wife, Janet; three fine children, David, Richard, and Marianne; a large family of friends; and a huge legacy of achievements in and for radiology.

Joseph Whitley
Baltimore, MD 21201

Book Review

Magnetic Resonance Imaging. A Reference Guide and Atlas. By Allen D. Elster, in collaboration with Stanley F. Handel and Arnold M. Goldman. Philadelphia: Lippincott, 292 pp., 1986. $67.50

This book has three stated goals: to provide a good appreciation of the current state of MR technology, to describe imaging characteristics of most tissues of the body, and to depict complex anatomic relationships of the human body in axial, coronal, sagittal, and oblique planes by using MR images. Unfortunately, the book, through no fault of its own, fails to achieve the first goal simply because the art and science of MR are changing so rapidly; the state of MR technology at the level of 1985 seems relatively dated now.

However, the book succeeds rather nicely in some other ways. The first five chapters ("Physical Foundations") are a good and easily understood introduction to MR physics aimed at the complete neophyte who has no background in the purer sciences. This is good reading for residents or physicians looking for a place to start. Radiologists in practice will eventually need a greater depth of understanding than is provided here, but this is a good first building block.

Chapters 6 through 11 provide MR-technique guides and atlases from various parts of the body, again with end-of-1985-level technology. Chapters on the brain, face, and neck suggest imaging protocols for specific anatomic regions (e.g., brain, brainstem, pituitary, cranial nerves); unfortunately many of these have subsequently changed or are machine (field-strength) dependent. While MR anatomic images are not as good as are currently achievable, major anatomic landmarks are easily identified and well labeled. This is a good reference for normal MR anatomy. Chapters on the chest, abdomen, and pelvis have somewhat better images and equally good labeling of normal anatomy. Chapter 11 discusses surface-coil applications in the spine, breast, and knee—again, this technology has advanced considerably in the past 2 years. The book concludes with a list of the 1985 technical specifications of nine commercial MR scanners, most of which have subsequently changed. The bibliography is quite good up through the end of 1985.

This book should provide a nice introductory text for individuals looking for a place to start in MR. Those who are more advanced in their familiarity with recent developments in MR will find the information and images dated. The MR anatomic depictions are good and serve for general orientation in most of the body.

William P. Shuman
University of Washington Medical School
Seattle, WA 98195

MR Imaging of Congenital Anomalies of the Aortic Arch

Barbara A. Kersting-Sommerhoff[1]
Udo P. Sechtem[1]
Madeleine R. Fisher[1,2]
Charles B. Higgins[1]

Eighteen patients with congenital aortic arch anomalies were evaluated by ECG-gated MR imaging. Transverse images encompassing the heart and thoracic aorta were available in all patients; sagittal or coronal studies were available in 12 patients. Visualization of the aortic arch, its orientation, and the origin and course of the arch vessels was assessed. Associated intracardiac abnormalities were noted, and the effect of aberrant vessels on the trachea or esophagus was determined. Thirteen patients had a right aortic arch. Mirror-image branching was found in 10 cases, and an aberrant left subclavian artery was found in three of these. Three patients had a left aortic arch with aberrant right subclavian artery, and two patients had a double arch. Tracheal compression caused by vascular rings was found in two patients with respiratory symptoms. Corroborating studies (angiography, surgery, CT, and autopsy) in 16 patients confirmed the MR diagnoses in all but one.

We conclude that MR could substitute for other techniques as an effective, noninvasive method for the evaluation of congenital aortic arch anomalies.

Anomalies of the aortic arch and its major branches may be associated with severe congenital heart disease or present as incidental findings in otherwise asymptomatic patients. In other patients aberrant vessels may form vascular rings producing clinical symptoms caused by tracheal or esophageal compression [1, 2]. Several reports have indicated the utility of MR imaging for the demonstration of great vessel anomalies [3–5]. A recent study also showed in a single case the ability of MR to show an aortic arch anomaly as the cause of tracheal compression [6]. Since MR imaging provides definite, noninvasive evaluation of both congenital [7, 8] and acquired [5, 9] abnormalities of the thoracic aorta, the technique should be useful for the diagnosis of aortic arch anomalies. In this study we report our experience with MR for the anatomic demonstration of congenital aortic arch anomalies in 18 patients.

Materials and Methods

MR studies were reviewed of 15 male and three female patients (2 months to 48 years old) with congenital aortic arch anomalies. ECG-gated MR was performed in most of these patients for evaluation of various congenital heart diseases or of other diseases that required imaging of the mediastinum. The aortic arch anomalies were not known before the MR study. Fifteen patients were scanned in a 0.35-T superconducting magnet (Diasonics, Milpitas, CA) and three patients were imaged in a Philips Gyroscan (1.5 T, operating at 0.5 T). All images were acquired with the spin-echo technique with an echo time of 30 msec and a repetition time that depended on the patient's heart rate. Slice thickness was 10 mm except in a 9-month-old infant, in whom 5-mm-thick slices were used. Transverse images encompassing the heart and the thoracic aorta including the aortic arch and the origin of the arch vessels were obtained. One patient did not have images beyond the aortic arch, precluding the evaluation of the branching vessels. Sagittal images were available in three patients, and nine patients had coronal studies. There were corroborating studies in 16 patients: nine had angiography, one CT, five surgery, and one autopsy. In the other two patients the MR finding

Received January 28, 1987; accepted after revision March 24, 1987.

[1] Department of Radiology, University of California Medical Center, San Francisco, CA 94143. Address reprint requests to C. B. Higgins.

[2] Present address: Radiology Department, Northwestern Memorial Hospital, Chicago, IL 60611.

AJR **149:9–13, July 1987**
0361–803X/87/1491–0009
© American Roentgen Ray Society

of an aortic arch anomaly was incidental and without clinical consequences; thus, no further study was warranted.

MR images were evaluated retrospectively by three observers who were unaware of the specific diagnoses or clinical histories of the patients. Each observer assessed separately the visualization of the aortic arch, its orientation, and the origin and course of its branching vessels. Associated intracardiac abnormalities were noted, and the effect of aberrant vessels on the trachea or esophagus was determined.

Results

Right Aortic Arch with Mirror-Image Branching

In nine patients a right aortic arch with a right-sided proximal descending aorta was identified by MR. Mirror-image branching was present with the left innominate artery arising first, followed by the right common carotid and right subclavian arteries. In all but one patient the origin of the branching vessels was identified in the slice cephalad to the top of the arch, and the course of the vessels was followed through the remaining slices (Fig. 1). In the patient who did not have images beyond the aortic arch, this pattern was assumed to be present as no retroesophageal vessel was detected. All nine patients with right aortic arch had associated severe congenital heart disease: three patients had tetralogy of Fallot, four had pulmonary atresia and ventricular septal defect, and two had a single ventricle. MR findings were confirmed by angiography (six cases), surgery (two cases), and autopsy (one case).

In another patient, a 3-year-old girl, MR images suggested a right aortic arch with a retrotracheal left subclavian artery forming a vascular ring. The trachea was narrowed 1 cm proximal to the carina (Fig. 2). At surgery a vascular ring was confirmed, but it consisted of a right aortic arch and a persistent left ductus arteriosus. The aortic arch showed mirror-image branching.

Right Aortic Arch with Aberrant Left Subclavian Artery

Three patients were found to have this anomaly. The right aortic arch was seen with the left common carotid artery arising as the first branch, followed by the right common carotid and the right subclavian arteries. In all subjects, MR showed the aberrant left subclavian artery as a vascular structure behind the esophagus; the vessel originated from the proximal descending aorta. The aberrant subclavian artery

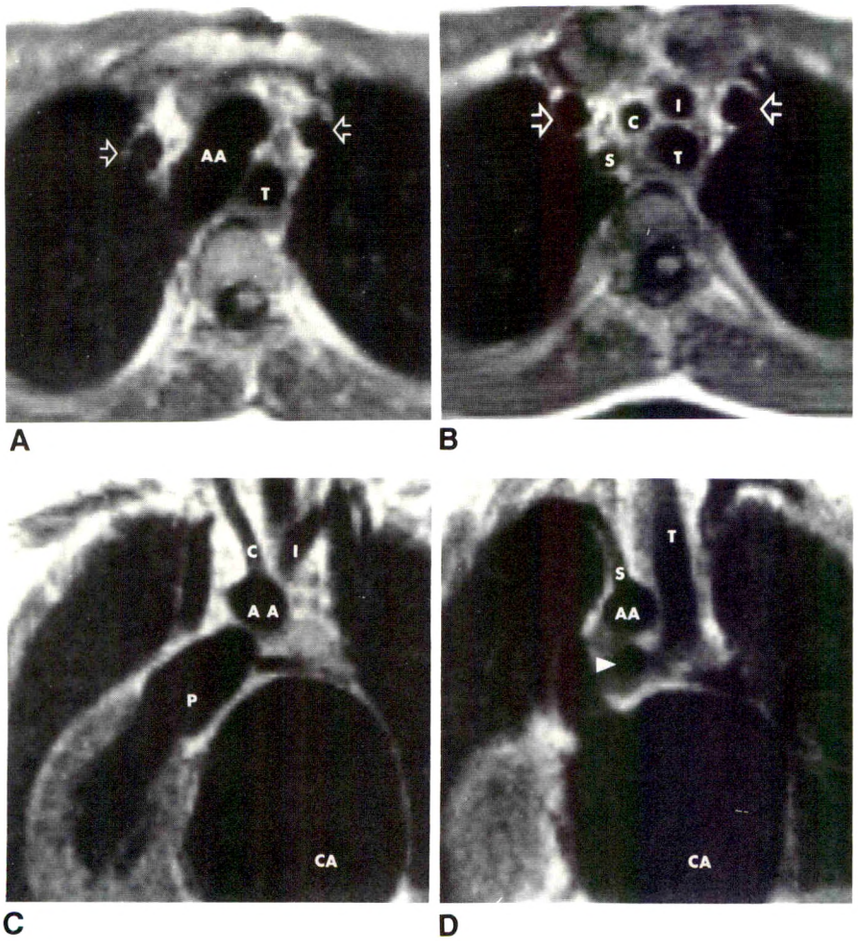


Fig. 1.—Right aortic arch and mirror-image branching in patient with situs inversus, double outlet right ventricle, and common atrium.

***A*, Transverse image of right aortic arch (AA). Bilateral superior venae cavae (*arrows*). T = trachea.**

***B*, Transverse slice 10 mm craniad shows arising left innominate (I), right common carotid (C), and right subclavian (S) arteries. Bilateral superior venae cavae (*arrows*).**

***C*, Coronal image shows right aortic arch (AA) and arising right common carotid (C) and left innominate artery (I). CA = large common atrium; P = main pulmonary artery.**

***D*, Coronal image 10 mm posteriad shows origin of right subclavian artery (S). T = trachea; AA = right aortic arch; CA = large common atrium. Right pulmonary artery (*arrowhead*).**

was usually seen on transverse images in the slice depicting the bottom of the arch and appeared as an outpouching of the aorta extending to the left side posterior to the trachea (Fig. 3).

The origin of the vessel was markedly bulbous in all three cases, representing an aortic diverticulum. In two patients this anomaly of the aortic arch was associated with congenital heart disease: both patients had pulmonary atresia. Angiography confirmed all MR findings in these two patients. In the third patient a large aortic diverticulum was found behind the esophagus on the MR images. A left subclavian vessel could not be identified. This patient had previously undergone surgery for a vascular ring, and the aberrant left subclavian artery had been ligated.

Left Aortic Arch with Aberrant Right Subclavian Artery

Three patients with aberrant right subclavian artery were evaluated. In two cases the finding of an aberrant vessel arising as the last branch from the aortic arch and crossing behind the esophagus was incidental (Fig. 4). The prominent feature on MR transverse images was an outpouching in the region of the proximal part of the descending aorta, the so-called duct of Kommerell. The aberrant subclavian artery was seen arising from this outpouching; one slice higher the vessel could be followed coursing to the right. There was no indentation of the trachea; clinically the patients were asymptomatic. Corroborating studies do not exist, as there was no clinical indication for further evaluation.

In the third patient the aortic arch anomaly was associated with complex congenital heart disease; he had a single ventricle, pulmonary atresia, and atrial septal defect. Angiography confirmed the MR diagnoses.

Double Arch

A double arch was diagnosed by MR in two patients. In one case the descending aorta was seen slightly to the left of the spine, whereas in the other case the aorta descended on the right side. In both patients MR showed a predominant right arch that gave rise to the right common carotid and the right subclavian arteries. The vessels on the left side arose in

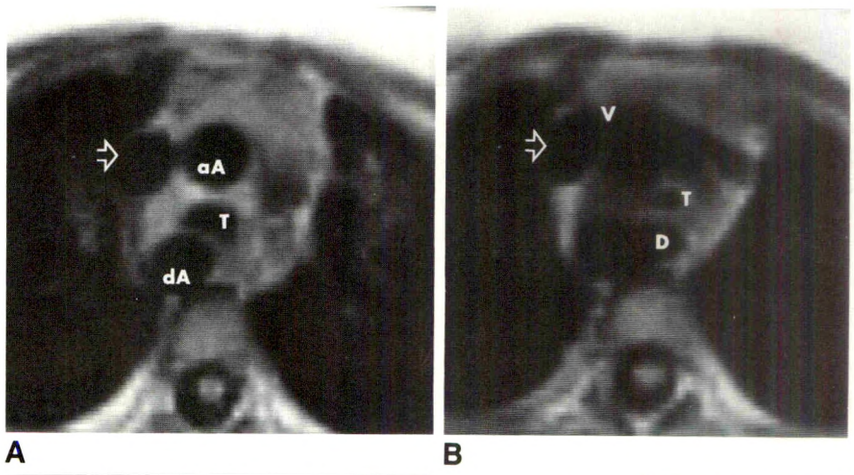


Fig. 2.—Transverse images of patient with vascular ring.

***A*, 15 mm below aortic arch. aA = ascending aorta; dA = descending aorta. *Arrow* indicates right superior vena cava.**

***B*, Slice 10 mm craniad shows origin of patent ductus arteriosus (D) from descending aorta. Note narrowing of trachea (T). Right superior vena cava (*arrow*). V = left brachiocephalic vein.**

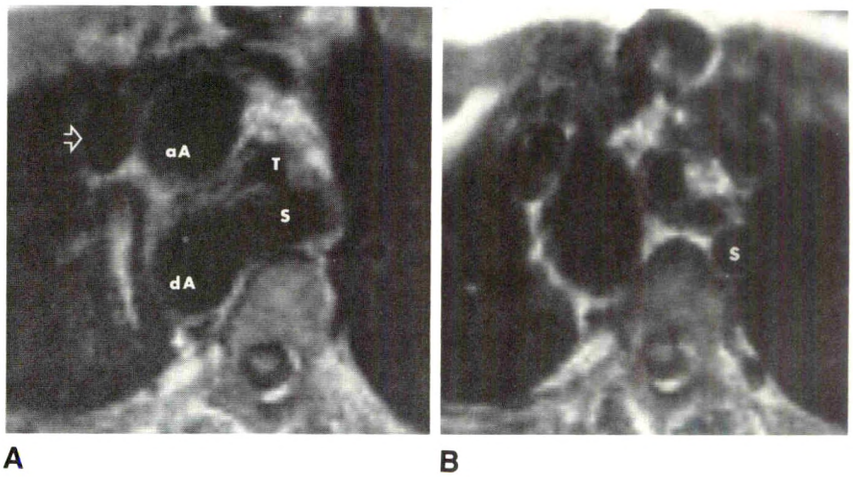


Fig. 3.—Transverse images of patient with tetralogy of Fallot.

***A*, Aberrant left subclavian artery (S) arises from descending part (dA) of right aortic arch. Right superior vena cava (*arrow*). aA = ascending aorta; T = trachea.**

***B*, Scan 2 cm higher shows left subclavian artery (S) in its usual position.**

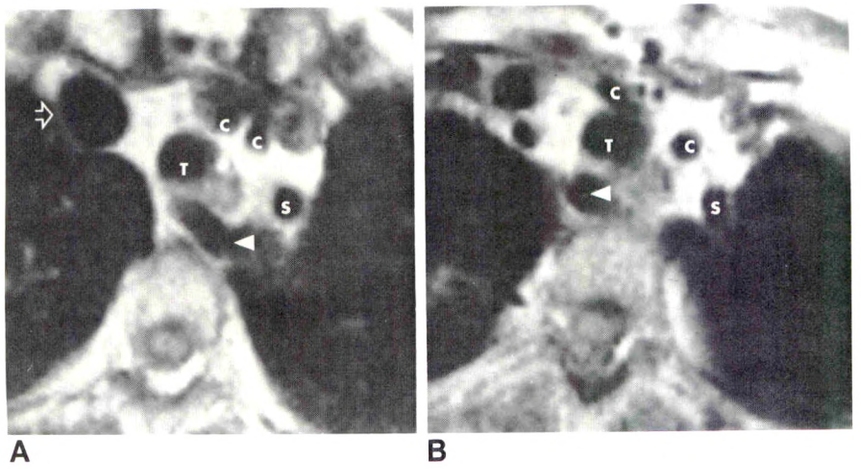


Fig. 4.—Transverse images of patient with left aortic arch and aberrant right subclavian artery.
A, Slice 10 mm above aortic arch shows aberrant right subclavian artery (*arrowhead*) coursing from its left origin to right side. Right superior vena cava (*arrow*).
B, 10 mm craniad. Right subclavian artery (*arrowhead*) has reached its usual position.
C = common carotid artery; S = left subclavian artery; T = trachea.

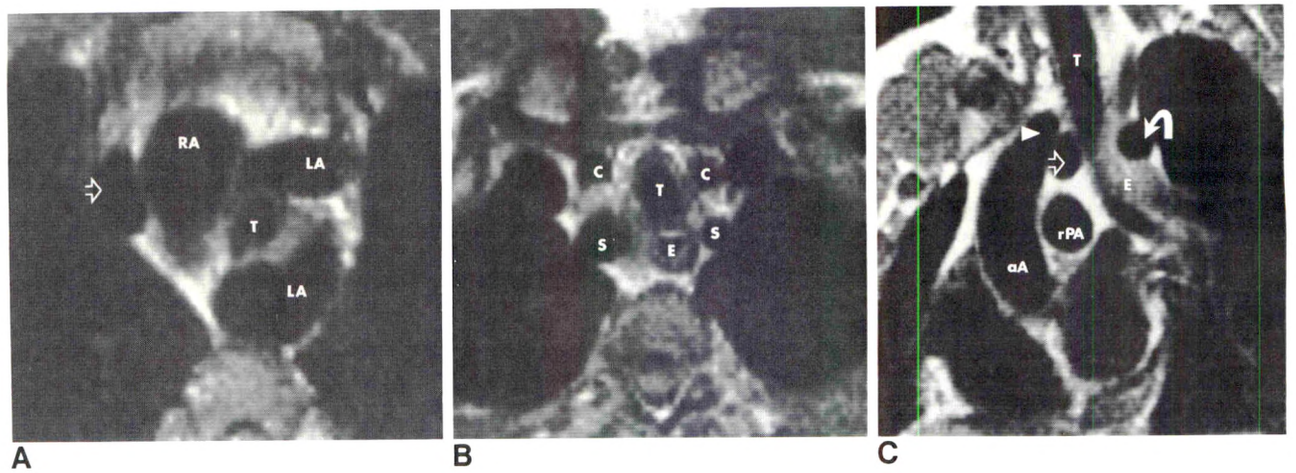


Fig. 5.—Patient with double aortic arch.
A, Transverse image at level of double arch shows right (RA) and left (LA) portions of arch. Right superior vena cava (*arrow*). T = trachea.
B, 20 mm craniad. Right and left common carotid (C) and subclavian (S) arteries arise symmetrically from both portions of arch. T = trachea; E = esophagus.
C, Oblique sagittal image shows anterior (right) portion of aortic arch (*open arrow*) in front of trachea (T) and posterior (left) portion (*curved arrow*) behind trachea and esophagus (E). Origin of right common carotid artery (*arrowhead*). aA = ascending aorta; rPA = right pulmonary artery.

symmetry to the right, consistent with the pattern of double aortic arch. Only a portion of the left arch could be seen on transverse MR images, suggesting either patency of only the anterior portion and atrophy of the posterior portion of the arch or a small left arch component.

In the case of a 9-month-old boy significant narrowing of the trachea (4 mm) was found. The infant presented with respiratory difficulty, and at surgery the double arch proved to be the cause of tracheal compression. In the other patient the double arch was detected incidentally (Fig. 5). He was asymptomatic, and no indentation of the trachea or esophagus was found. This diagnosis was confirmed by a CT scan with IV contrast enhancement.

Effect of Aortic Arch Anomalies on the Trachea

MR showed significant tracheal narrowing as a result of vascular abnormalities in only two patients of our series. One patient had a vascular ring consisting of a right aortic arch and a left ductus; the other patient had a double aortic arch. These were the only two patients with respiratory symptoms in our study population. Thus, the clinical symptoms correlated with the MR findings, and surgery confirmed our diagnoses in both cases. The other seven patients with aberrant subclavian arteries or double aortic arch were asymptomatic and no tracheal indentation was found on the MR images.

Discussion

Anomalies of the aortic arch may present as a double arch or as a single arch with variations in respect to its course and branching pattern [1, 2]. Our current study shows that MR can reliably define the various types of aortic arch anomalies. The main advantage of MR in comparison with angiography and CT is the unique ability of MR to differentiate vessels

from avascular masses without the need for contrast material or radiation exposure. This advantage makes MR a valuable, noninvasive diagnostic method in the evaluation of aortic arch anomalies, despite the higher costs and the longer time that is needed to perform an MR study. In patients with aortic arch anomalies and complex congenital heart disease, MR often provides complete evaluation of the associated intracardiac anomalies within the same study [10, 11].

Our current series contains examples of the various types of congenital aortic arch malformations. A right aortic arch occurs in about 0.1% of adults [12]. Right aortic arch with mirror-image branching is uncommon, but not rare, and almost always is associated with severe congenital heart disease; this type accounted for half of our current cases. Those patients were referred primarily for evaluation of their intracardiac abnormalities, but mediastinal sections were also acquired for the assessment of concomitant vascular anomalies. Right aortic arch with mirror-image branching was associated with tetralogy of Fallot in one-third of our cases and pulmonary atresia/ventricular septal defect or single ventricle in the others. This association would be expected because of the frequency of mirror-image right aortic arch found in various congenital heart diseases in a large autopsy series [12].

Left aortic arch with aberrant right subclavian artery, the most common aortic arch anomaly, is usually found incidentally in asymptomatic patients [13]. In our current study this pattern was found in patients scanned for other diseases that required mediastinal imaging. In these patients MR may help to clarify questionable findings on plain radiographs and obviate further invasive studies.

Aortic arch anomalies that lead to clinical symptoms are vascular rings, which may cause tracheal or esophageal compression. Right aortic arches with a left ductus arteriosus or with an aberrant left subclavian artery may form a vascular ring; the most common cause of a symptomatic vascular ring is a double arch [1]. A double arch is seldom associated with other malformations. In two-thirds of cases, the right arch is larger than the usually obliterated or atretic left arch. To determine the side of the surgical approach, it is necessary to identify the narrower arch, which has to be ligated. MR is able to identify both parts of a double arch and aberrant vessels that form vascular rings. The extent of tracheal narrowing is depicted at the same time.

Barium swallow and angiography are currently used in the evaluation of patients with aortic arch anomalies. Prior reports have also indicated that contrast-enhanced CT can provide the diagnostic information regarding the arch anomaly and the status of the trachea [14–16]. The results of our current study show that MR could substitute for the other techniques as an effective, noninvasive diagnostic method.

REFERENCES

1. Goor DA. *Congenital malformations of the heart. Embryology, anatomy and operative considerations*. New York: Grune & Stratton, **1975**
2. Knight L, Edwards JE. Right aortic arch. Types and associated anomalies. *Circulation* **1974**;50:1047–1051
3. Amparo EG, Higgins CB, Shafton EP. Demonstration of coarctation of the aorta by magnetic resonance imaging. *AJR* **1984**;143:1192–1194
4. Dinsmore RE, Liberthson RR, Wismer GL, et al. Magnetic resonance imaging of thoracic aortic aneurysms: comparison with other imaging methods. *AJR* **1986**;146:309–314
5. Glazer HS, Gutierrez FR, Levitt RG, Lee JK, Murphy WA. The thoracic aorta studied by MR imaging. *Radiology* **1985**;157:149–155
6. Fletcher BD, Dearborn DG, Mulopulos GP. MR imaging in infants with airway obstruction: preliminary observations. *Radiology* **1986**;160:245–249
7. Fletcher BD, Jacobstein MD. MRI of congenital abnormalities of the great arteries. *AJR* **1986**;146:941–948
8. Soulen RL, Donner RM. Advances in noninvasive evaluation of congenital anomalies of the thoracic aorta. *Radiol Clin North Am* **1985**;23(4):727–736
9. Amparo EG, Higgins CB, Hricak H, Sollitto R. Aortic dissection: magnetic resonance imaging. *Radiology* **1985**;155:399–406
10. Fletcher BD, Jacobstein MD, Nelson AD, Riemenschneider TA, Alfidi RJ. Gated magnetic resonance imaging of congenital cardiac malformations. *Radiology* **1984**;150:137–140
11. Higgins CB, Byrd BF, Farmer DW, Osaki L, Silverman NH, Cheitlin MD. Magnetic resonance imaging in patients with congenital heart disease. *Circulation* **1984**;70(5):851–860
12. Hastreiter AR, D'Cruz IA, Cantez T. Right-sided aorta. Part I. Occurrence of right aortic arch in various types of congenital heart disease. *Br Heart J* **1966**;28:722–725
13. Klinkhamer AC. Aberrant right subclavian artery. Clinical and roentgenologic aspects. *AJR* **1966**;97:438–446
14. Webb WR, Gamsu G, Speckman JM, Kaiser JA, Federle MP, Lipton MJ. CT demonstration of mediastinal aortic arch anomalies. *J Comput Assist Tomogr* **1982**;6(3):445–451
15. Baron RL, Gutierrez FR, Sagel SS, Levitt RG, McKnight RC. CT of anomalies of the mediastinal vessels. *AJR* **1981**;137:571–576
16. McLoughlin MJ, Weisbrod G, Wise DJ, Young HPH. Computed tomography in congenital anomalies of the aortic arch and great vessels. *Radiology* **1981**;138:399–403

Book Review

Practical MRI. A Case Study Approach. By Wilson S. Wong, Jay S. Tsuruda, Keith E. Kortman, and William G. Bradley, Jr., Rockville, MD: Aspen, 451 pp., 1987. $74.50

This book uses a teaching-file approach to provide some practical experience for radiologists interested in learning clinical MR imaging. The book draws on the clinical experiences of the authors who have been involved in MR imaging at Huntington Medical Research Institutes since May 1983.

The two introductory chapters summarize the basics of MR imaging physics and technique. These chapters only provide the essentials for understanding basic imaging methods because this book is not intended as a comprehensive text. The appendix provides recommended techniques for a variety of applications. While this explanation may have been satisfactory not too long ago, current instruments provide many more choices in technique than the instrument outlined, including multiple acquisition methods, pulse sequences, timing parameters, and tip angles. Other references may be needed for expanding knowledge in the more current technology. The approach provided gives adequate knowledge for solving the clinical cases provided in the text and will stimulate the reader to maintain familiarity with the fundamentals for future changes in MR imaging technology.

The rest of the book is devoted to the major clinical areas of MR imaging application: CNS, head and neck, spine, musculoskeletal, cardiothoracic, abdominal, and pelvic imaging. A brief introduction is provided to outline the key points in each section with selected references. The introduction is followed by a series of cases presented as a clinical history, questions relating to MR imaging examination technique, images, answers to the technical and clinical questions, and a detailed explanation with references. This approach is similar to that used in the American College of Radiology syllabuses but with the added emphysis on MR imaging technique. The largest and best section deals with the CNS. The head and neck and cardiothoracic sections are reasonably complete. The musculoskeletal section suffers from reduced-resolution images and a smaller spectrum of cases. The image quality in the abdominal section is not state-of-the-art because it lacks fast scans, but it provides a reasonable idea of the potential of abdominal MR imaging applications. The pelvic section is brief but provides information on pelvic anatomy with a good set of cases.

This book is a fresh approach to introductory MR imaging. It makes an often difficult subject fun and entertaining to learn. While not an exhaustive review, the book does cover most of the current applications. The format and references should encourage the reader to expand his knowledge base. The most difficult phase in learning a new area is the early period while struggling with the basics. This book makes that period much less painful. It is highly recommended for all radiologists, residents, and fellows who are beginning their training in MR imaging.

The quality of image reproduction is good. The book has an inexpensive but hard paper binding. If one considers the production quality and length, the book is somewhat expensive at $74.50. The quality and style of the material, however, makes the purchase of this text worthwhile.

Steven Harms
Baylor University Medical Center
Dallas, TX 75246

MR Imaging of Pulmonary Arterial Hypertension and Pulmonary Emboli

Richard D. White[1]
Mark L. Winkler
Charles B. Higgins

Intraluminal signal in the pulmonary arteries on spin-echo, ECG-gated MR images is limited to the diastolic phase of the cardiac cycle in normal subjects. Initial experience has indicated that signal persisting during systole may be characteristic of slow blood flow associated with pulmonary arterial hypertension (PAH) or of thrombotic material secondary to pulmonary embolism. This study analyzes our cumulative experience (31 patients) with multiphasic, double spin-echo MR for assessing PAH and/or suspected pulmonary embolism. In PAH, the abnormal systolic signal showed an intensity increase from first to second echo. This pattern was observed in 92% of PAH patients, including 100% of patients with pulmonary systolic pressures ≥80 mm Hg and 60% of patients with pressures <80 mm Hg. At any focus in the pulmonary arteries, such signal disappeared at some phase of the cardiac cycle. In patients with pulmonary embolism, signal from thrombus was fixed throughout the cardiac cycle and showed little or no increase in relative intensity change from first- to second-echo image. Using this guideline, MR made six confirmed positive and four confirmed negative diagnoses of proximal pulmonary embolism, while it failed to identify thrombus in the one patient with a peripheral pulmonary embolism.

Intraluminal signal in the pulmonary arteries caused by PAH or pulmonary embolism can be differentiated in most instances using multiphasic, double spin-echo, ECG-gated MR. However, at its current stage of development, the procedure does not appear to be useful for the evaluation of peripheral pulmonary embolism.

ECG-gated MR imaging has been useful for noninvasively evaluating the central cardiovascular system in normal [1–3] and various disease states [4–7], because the blood pool is marked by signal void on standard spin-echo images. MR examination of the mediastinal great vessels has concentrated on the various forms of thoracic aortic disease [3, 5, 7–10].

The reported experience with the use of MR to assess acquired pulmonary arterial disease is limited and is largely confined to a few small studies of pulmonary arterial hypertension (PAH) [2, 11–13] or pulmonary embolism (PE) [13–17]. Both PAH and PE can cause abnormal intraluminal signal on spin-echo images. Initial experience has indicated that there are characteristic patterns of intraluminal signal from slow blood flow associated with PAH and from thrombotic material in PE. This study analyzes our cumulative experience (31 patients) with multiphasic, double spin-echo, ECG-gated MR for assessing PAH and/or suspected PE.

Received January 28, 1987; accepted after revision April 8, 1987.

[1] All authors: Department of Radiology, C-309, Box 0628, University of California, San Francisco, CA 94143. Address reprint requests to C. B. Higgins.

AJR 149:15–21, July 1987
0361–803X/87/1491–0015
© American Roentgen Ray Society

Methods

Patient Population

ECG-gated MR was performed in 31 patients (age range, 14–82 years; mean, 46 years; gender, 55% female) for the evaluation of PAH alone (10 patients), suspected PE alone (six patients), or both (15 patients). Nine of the 25 patients with PAH and two of the patients with a PE have been included in earlier reports [11, 13, 15]. In most patients, the specific clinical diagnosis had been established before the MR examination. In fact, most patients were

selected for MR in order to assess the role of this technique in evaluating these particular pulmonary arterial abnormalities.

Confirmatory evidence of the hemodynamic and anatomic abnormalities related to each clinical diagnosis was sought in each patient by review of medical records. Such supportive direct evidence of PAH was obtained in 24 of the 25 patients with PAH alone or in combination with suspected PE from elevated pulmonary pressures (measured during pulmonary angiography or Swan-Ganz catheter placement). Confirmation of PE was derived from results of a pulmonary angiogram (n = 2), a ventilation-perfusion scan (n = 9), or both (n = 3), which were performed in 14 of 21 patients with suspected PE with or without superimposed PAH. The period between the MR imaging studies and such confirmatory examinations ranged from 0 to 16 days (mean, 4 days).

MR Instrument and Imaging Technique

The instrument employed for MR examination has been previously described in detail [2, 3]. Spin-echo images were obtained on a superconducting MR system (Diasonics MT/S) operating at 0.35 T. The corresponding hydrogen resonant frequency was 15 MHz.

Transaxial imaging was performed, with sequential images being acquired from a level just above the bifurcation of the main pulmonary artery down to the level of the right ventricular outflow region. In addition, first spin-echo (echo delay time [TE] = 28 or 30 msec) and second spin-echo (TE = 56 or 60 msec, respectively) images at the five to six adjacent transverse anatomic levels (slice thickness of 7 mm with 3-mm interslice gap in the 11 previously reported patients [11, 15] and thickness of 10 or 11 mm without a gap in the subsequent 20 patients) were obtained in all patients [18]. The delay between each adjacent level was 100 msec [19]; thus, the upper and lower images of the sequence were separated in time by 400 msec (five levels) or 500 msec (six levels).

A multiphasic technique [18] was also employed in 90% (28/31) of the study population to obtain images in various phases of the cardiac cycle at each anatomic level. For multiphasic studies, the normal multilevel imaging sequence was repeated four or five times, with rotation of the temporal order in which the images from each level were obtained. Thus, this technique provided images at five or six phases of the cardiac cycle at each of the five or six anatomic levels. Generally, two or three of these images corresponded to diastole and three to systole. At each phase, two spin-echo images were produced (echo times were 30 and 60 msec, respectively). The imaging time was approximately 35 min for a patient with a heart rate of 75 beats/min. A more detailed description of this multilevel, multiphasic MR imaging technique has previously been published [11, 13, 18, 19].

Image Analysis for Evaluation of Patterns of Intraluminal Signal in the Pulmonary Arterial System

Normally on MR, the blood that is flowing rapidly in the pulmonary arterial system and aorta during systole is manifested as signal void on images that are gated to systolic phases of the cardiac cycle (Fig. 1). On the other hand, images gated to end-diastole normally show intraluminal signal due to slowly flowing blood. This signal typically increases in intensity and distribution on the second-echo image as compared with the first-echo image.

Previous work has shown that with slow pulmonary arterial blood

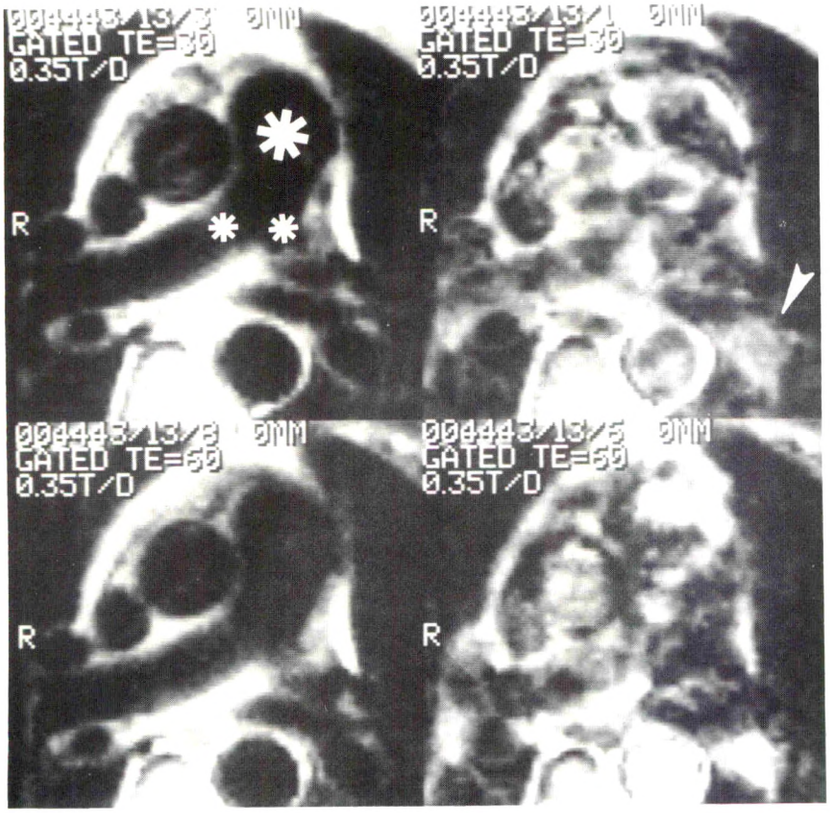


Fig. 1.—Normal intraluminal signal pattern of pulmonary flow on multiphasic MR examination. From same anatomic level, two first-echo (TE = 30 msec) and second-echo (TE = 60 msec) images are presented at top and bottom, respectively. Both images on left represent systole; those on right represent diastole.

On systolic images (*left*), rapidly flowing blood within main pulmonary artery (*large asterisk*) and central right and left pulmonary arteries (*small asterisks*) produces signal void.

Reduced velocity of blood flow in all vascular structures during diastole is manifested as moderately high signal intensity on a first-echo image (*top right*). Note increase in signal intensity on corresponding second-echo image (*bottom right*). This second-echo augmentation of intraluminal signal is particularly evident in descending branch of left pulmonary artery (*arrowhead*).

flow due to PAH, abnormal intraluminal signal may be observed in the pulmonary arterial system during systolic phases, while the normal signal void of rapidly flowing blood is noted in the aorta [11, 12]. Its characteristic absolute increase in intensity [20, 21], visually appreciable from first-echo to second-echo images ("even-echo rephasing"), as well as its fluctuating distribution during the cardiac cycle should differentiate this abnormal pattern of slowly flowing blood within the pulmonary arteries from intraluminal thrombus (i.e., PE). This pattern of abnormal systolic signal within the pulmonary arteries on multiphasic MR was used in this study as the criterion for "evidence of slow flow."

On the other hand, intraluminal thrombotic material of a PE is manifested by a focal area of moderate to moderately high signal intensity with a fixed distribution on both first-echo and second-echo images and throughout the cardiac cycle [12, 13]. In addition, the signal intensity of thrombus, as assessed on region-of-interest or visual analysis, characteristically shows no significant increase from first to second echo [13]. This pattern of fixed, focal, intravascular signal was the criterion for "positive PE." While this pattern could be depicted on standard multislice, double spin-echo, ECG-gated MR examinations, it was more easily discerned when the multiphasic technique was also employed.

During the time frame in which these studies were performed, the multiphasic ECG-gated MR technique was introduced, and it was used to study subsequent patients with PAH or suspected PE to optimize the hemodynamic evaluation and the differentiation between slow flow and thrombus by MR. Consequently, of the 31 patients examined by MR for either condition, only the final 28 were studied with the multiphasic technique.

Results

Pulmonary Arterial Hypertension Alone

The 10 cases of documented PAH alone that were evaluated by multiphasic MR were considered to be either idiopathic (nine patients) or secondary to lung disease (one patient). Evidence of slowly flowing blood on multiphasic examinations, defined as abnormal intraluminal signal during systolic phases of the cardiac cycle with fluctuating distribution and first-echo to second-echo intensity increase (Fig. 2), was found in eight (80%) of 10 patients. Such evidence of slow flow was noted in all eight cases with documented pulmonary systolic pressures ≥80 mm Hg, but in neither of the two cases with systolic pressures <80 mm Hg. In the latter two patients, such abnormal signal was not present in the pulmonary arteries during systole, and thus they could not be differentiated from normal subjects on the basis of this criterion alone.

Suspected Pulmonary Embolism

Twenty-one patients with (n = 15) or without (n = 6) superimposed PAH were evaluated by MR for suspected PE. In those with PAH, documentation of elevated pressure was available in 14 cases. A positive diagnosis of proximal PE was made by MR in nine cases, based on the finding of a focal intraluminal area of moderate to moderately high signal intensity within the main, central, or branch pulmonary arteries that was fixed in distribution during the cardiac cycle and demonstrated little or no increase in relative intensity from first-echo to second-echo (Fig. 3). Because of the absence of these findings, proximal PE was excluded on MR in the remaining 12 cases. However, since MR is not considered adequate at this time for the evaluation beyond the main branches of the central pulmonary arteries, a more distal PE in these 12 cases could not be excluded.

The positive MR diagnoses of PE were substantiated by a confirmatory study in six cases (three patients with definitively

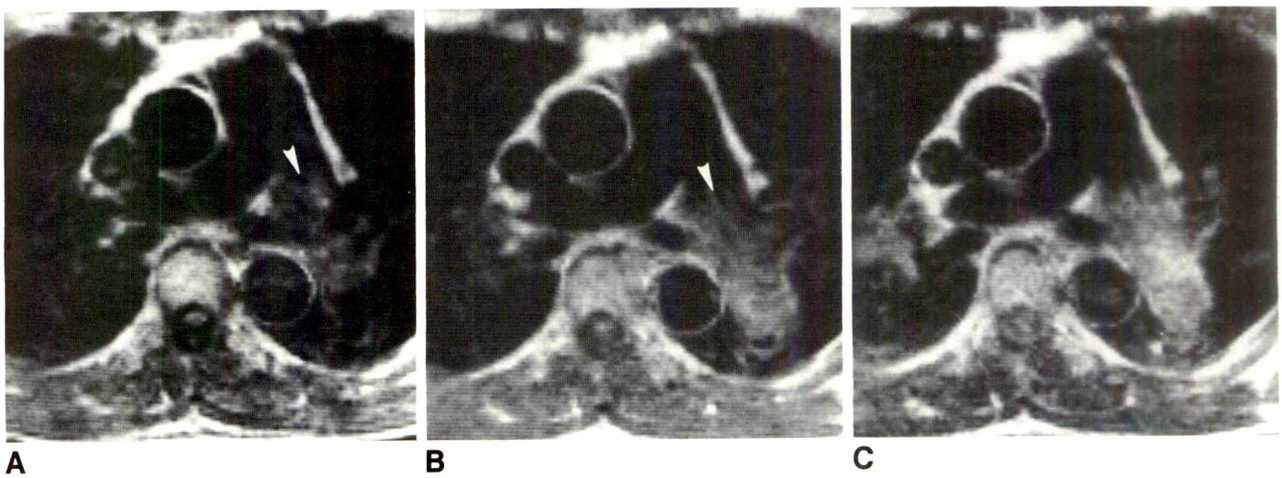


Fig. 2.—Pulmonary arterial hypertension. Two first-echo images (*A* and *B*) from different phases of systole and a corresponding second-echo image (*C*) are shown. Patient had documented pulmonary arterial systolic pressures in excess of 80 mm Hg.

***A* and *B*, Normal signal void of rapidly flowing blood in systole is noted in main and central right pulmonary arteries, but left pulmonary artery shows abnormal signal of moderate intensity that is due to slowly flowing blood (*arrowheads*). Fluctuation of this abnormal signal in distribution during systole is characteristic of slow blood flow.**

***C*, Abnormal slow blood flow signal noted on first-echo image characteristically increases significantly in both distribution and intensity on a second-echo image. Right hilar adenopathy is also noted adjacent to bifurcating central right pulmonary artery.**

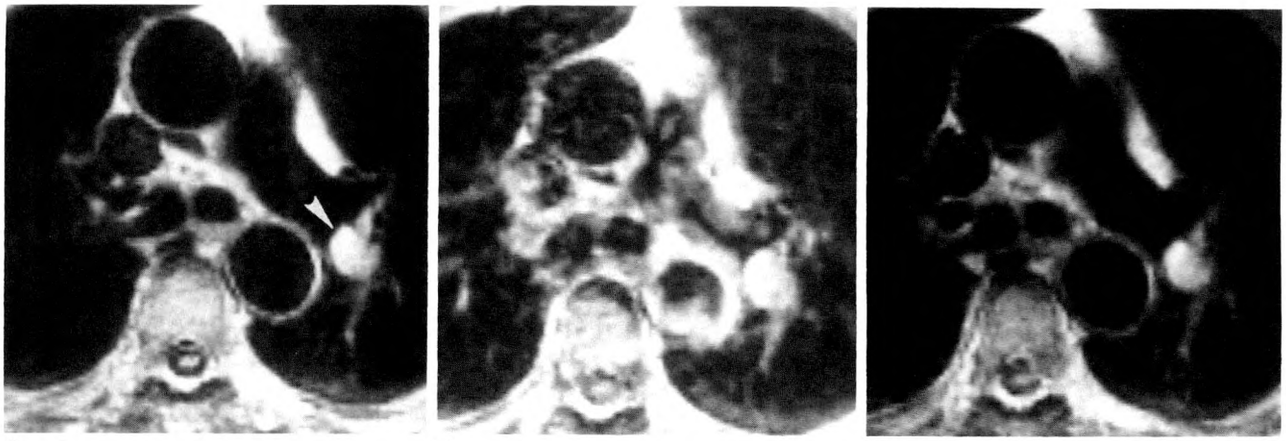


Fig. 3.—Pulmonary embolism. A first-echo image from systole (*A*) and another from diastole (*B*), as well as a corresponding systolic second-echo image (*C*), are shown.

***A* and *B*, A fixed focal area of moderately high signal intensity (*arrowhead*) appears to fill a branch of the bifurcating central left pulmonary artery. Lesion remains well-defined on diastolic image despite adjacent signal from slow blood flow.**

***C*, No significant change in either distribution or relative intensity is noted from first-echo to second-echo image. This pattern characterizes thrombus.**

positive pulmonary angiograms and three patients with high-probability positive ventilation-perfusion scans). The negative MR diagnoses were supported by another study in four cases (one patient with a definitively negative angiogram and three patients with definitively negative or low-probability positive scans), but contradicted in one case. In this last case, MR initially suggested only a pulmonary infiltrate on prospective evaluation. On the other hand, a pulmonary angiogram confirmed the presence of a peripheral PE in a segmental artery in the same region as the infiltrate, which probably represented an area of infarct. An intraluminal thrombus, not identified prospectively, was recognized during retrospective review of all MR cases.

Of the remaining 10 patients with suspected PE, three had inconclusive results from their confirmatory studies (one patient with a positive and two with a negative MR diagnosis of PE who had indeterminant ventilation-perfusion scans). Seven patients had no other study performed to confirm the MR diagnoses (two positive-PE and five negative-PE diagnoses by MR), but at least no follow-up clinical complications were noted in the patients with negative-PE diagnoses to call into question the accuracy of the MR evaluation.

Thus, six of seven proved cases of PE, including all six cases of proximal PE, had intraluminal thrombus detected on MR. However, no thrombus was noted on MR in the four cases in which PE was ruled out by other means.

In all 15 cases of suspected PE superimposed on PAH, evidence of slow blood flow was present. In the setting of PAH, the detection or exclusion of PE by MR was more difficult (Fig. 4). Intraluminal signal within the pulmonary arterial system had to be totally attributed to slow flow to rule out PE. A focus of fixed signal (i.e., present in all phases of the cardiac cycle) in the pulmonary arteries was detected and differentiated from adjacent slow flow signal in five cases.

Implications of Slowly Flowing Blood in Pulmonary Arterial Hypertension Detected by Multiphasic, Double Spin-Echo, ECG-gated MR

For all 25 patients in this study with PAH alone ($n = 10$) or with PAH superimposed on suspected PE ($n = 15$) who underwent multiphasic MR (systolic and mean pulmonary artery pressures ranging from 65 to 175 mm Hg and from 38 to 128 mm Hg, respectively), the prevalence of the intraluminal signal during systolic phases was highest at higher pulmonary arterial pressures. Nineteen of 19 patients (100%) with systolic pressures ≥80 mm Hg and three (60%) of five with pressures between 65 and 80 mm Hg showed evidence of slow flow (i.e., systolic intraluminal signal). When mean pulmonary arterial pressure was considered, all 17 patients (100%) with pressures >50 mm Hg, as compared with five (71%) of seven patients with mean pressures from 38 to 50 mm Hg, showed the slow flow pattern.

Discussion

MR imaging of the great vessels provides excellent contrast between the mediastinal tissues and the vasculature, which normally shows little or no intraluminal signal [1, 2]. In the evaluation of suspected pulmonary arterial abnormalities, this attribute is valuable in the differentiation between primary disease of the pulmonary arterial system and disease involving adjacent structures. This study examines the common causes of intraluminal MR signal within the pulmonary arterial system. On ECG-gated studies, intraluminal signal is normally

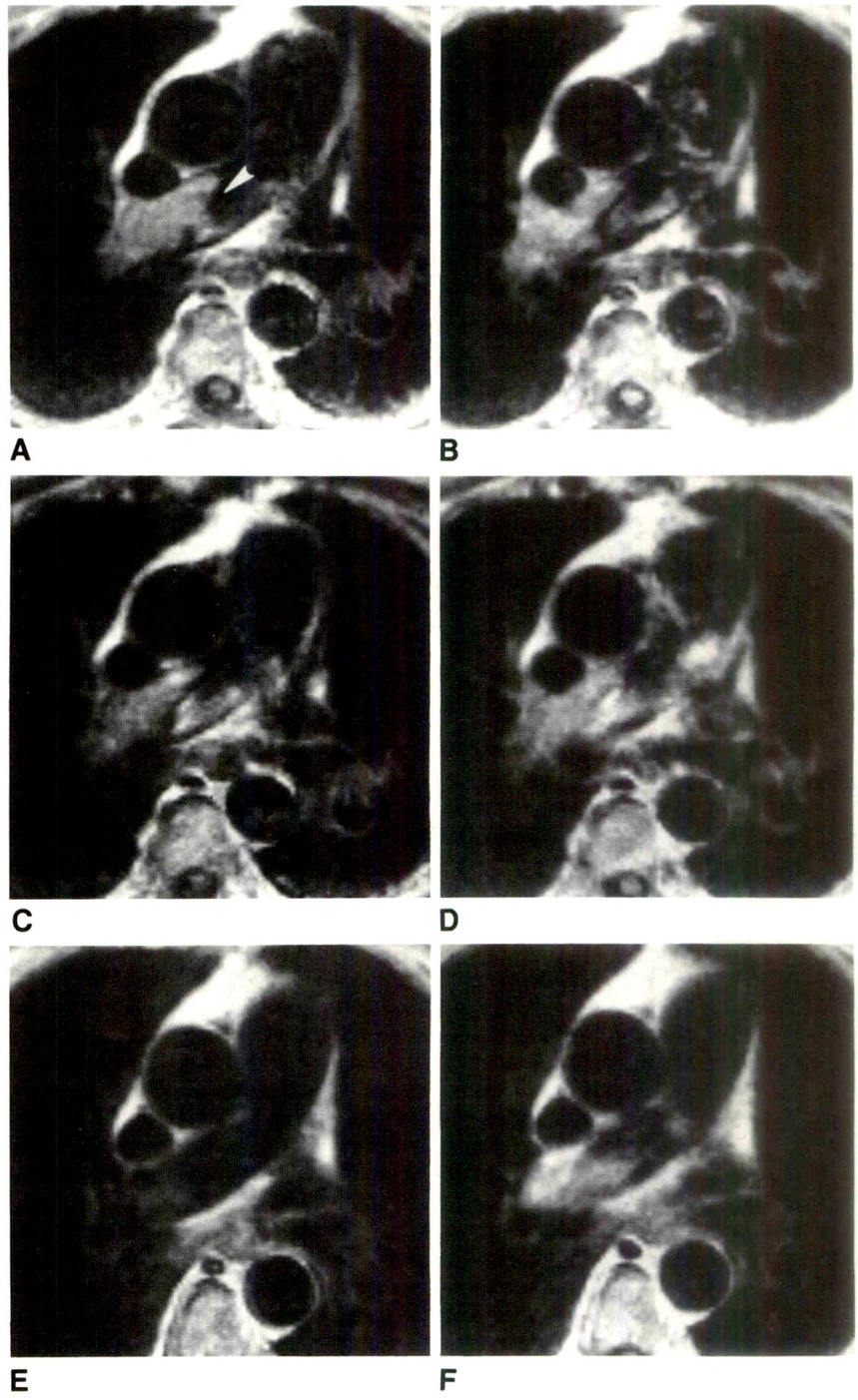


Fig. 4.—Pulmonary embolism superimposed on pulmonary arterial hypertension. Two systolic first-echo images (*A* and *B*) and their corresponding second-echo images (*C* and *D*) are presented. Also shown are a first-echo (*E*) and corresponding second-echo (*F*) systolic image from a 6-month follow-up examination.

***A* and *B*, Within dilated pulmonary arteries, a mass of moderately high signal intensity (*arrowhead*) appears to almost totally occlude lumen of central right pulmonary artery, starting at level where it passes posterior to ascending aorta. Fluctuating abnormal systolic signal, which is adjacent to this thrombotic material, is due to slow blood flow.**

***C* and *D*, Second echo accentuates distribution and intensity of slow flow signal, while no significant distribution or intensity change is noted in the appearance of the pulmonary embolus.**

***E* and *F*, Although evidence of abnormal systolic signal of slow pulmonary arterial blood flow persists, no residual thrombus is noted.**

present on images acquired near end-diastole, but normally is not present on systolic images. When present on systolic as well as diastolic images, it is usually due to abnormally slow blood flow as occurs in PAH, thrombus from PE, or both. While the current study indicates guidelines for distinguishing between these possibilities, it must be recognized that the appearance of blood flow and thrombotic material may vary among MR systems since both have shown variations in signal intensity using different field strengths and imaging techniques. The observations in this report regarding

the nature of intraluminal signal are pertinent at a medium field strength using the spin-echo technique. The appearances of both flowing blood and thrombus are markedly different using the recently introduced fast MR techniques, which employ narrow flip angles and gradient-refocused echoes [22].

Noninvasive evaluation of PAH is desirable because procedures such as angiography, which require contrast injection, may be hazardous [23]. In the setting of PAH, MR provides information about associated pathologic changes in the pulmonary arterial system and heart [12]. Use of the multiphasic, double spin-echo technique also depicts the functional abnormality of slow blood flow in the pulmonary arteries in PAH. This intraluminal systolic signal, with fluctuating distribution and appreciable increase in intensity from the first- to second-image [20, 21], is indicative of slow blood flow found in the more severe cases of PAH. As suggested in previous studies [11, 12], the slow blood flow pattern was found to be an indicator of higher pulmonary arterial pressures, usually ≥80 mm Hg systolic. The actual intensity of the blood signal has been shown to correlate best with pulmonary arterial vascular resistance [11].

Several factors govern the appearance of flowing blood on spin-echo images, and the role of each factor is variable [24]. These factors can be grouped into those actually related to blood flow and those related to the nature of MR imaging. Flow factors include the direction of flow; the motion characteristics (velocity, acceleration, and so forth), which depend strongly on the phase of the cardiac cycle; and the flow profile (i.e., spatial distribution of velocities and accelerations across the vessel lumen). MR imaging-related factors include the pulse sequence (i.e., spin-echo vs inversion-recovery, characterized by TR, TE, and inversion time); the position of a section in two-dimensional multilevel imaging; the spin-echo type (i.e., odd vs even); the spatial direction; and the type of imaging gradients (e.g., linear gradients). Finally, it is important whether a MR examination is acquired in an untriggered or ECG-gated mode. However, in the present study, the unifying feature of the hemodynamic alteration in patients with PAH seems to be that the blood flow velocity in the pulmonary arteries is often below the threshold for high-velocity signal loss in systolic phases of the cardiac cycle [11, 20].

For the differentiation between PAH and PE, the signal generated by slow flow must be distinguished from that of intraluminal thrombus. Such thrombotic material shows a focal area of signal that persists in all of the phases of the cardiac cycle represented on multiphasic MR [13], whereas the signal emanating from slowly flowing blood fluctuates during the cardiac cycle, depending on its velocity and acceleration. The differentiation between slow flow and thrombus is additionally accomplished by noting on a double spin-echo study that slow flow, but not thrombus, produces signal that markedly increases in intensity relative to other tissues from the first-echo to the second-echo image [11, 20, 21, 25]. In the current study, fixed signal during the cardiac cycle was observed in all patients with proved proximal PE who had multiphasic MR studies.

The actual intensity of intraluminal thrombus seems to be variable and possibly related to its age [26]. However, it has been reported that thrombotic material observed clinically over 4 weeks maintains a constant appearance of high intensity on T2-weighted spin-echo images [27]. Consequently, recognition of thrombus on spin-echo images based on intensity alone seems to be problematic.

To date, several experimental studies [14, 17, 28] and case reports [13, 15, 16] have suggested a potential clinical use for MR in the evaluation of suspected PE. This study offers initial results in a group of patients evaluated for possible PE by MR. The results indicate that MR may provide an accurate means of noninvasively confirming or excluding the presence of proximal PE. Unfortunately, MR may be limited in its sensitivity for the detection of peripheral PE of segmental or more distal branches of pulmonary arteries. This deficiency might represent either limitations in spatial resolution or effects of volume averaging. With the latter, it is conceivable that the signal emanating from a peripheral PE could be diluted or "averaged out" by the signal void of the adjacent lung or patent vascular structures. This situation would presumably be accentuated by excessive respiratory motion or inadequate ECG gating.

In addition, the detection and delineation of PE in any location is more difficult when there is superimposed PAH with slow flow signal. However, the results of the current study suggest that detection is usually possible when the multiphasic, double spin-echo technique is employed. Potential sources of false-positive diagnoses of PE by MR might include incorrect identification of nodes or vessel wall and, of course, misinterpretation of intraluminal signal from slow blood as that of thrombus.

In conclusion, multiphasic, double spin-echo, ECG-gated MR can be used for the noninvasive evaluation of both PAH and proximal PE. It serves as an alternative to angiography for the high-risk patient with suspected proximal PE.

REFERENCES

1. Herfkens RJ, Higgins CB, Hricak H, et al. Nuclear magnetic resonance imaging of the cardiovascular system: normal and pathologic findings. *Radiology* **1983**;147:749–759
2. Higgins CB, Byrd BF III, McNamara MT, et al. Magnetic resonance imaging of the heart: a review of the experience in 172 subjects. *Radiology* **1985**;155:671–679.
3. Higgins CB, Stark D, McNamara MT, Lanzer P, Crooks LE, Kaufman L. Multiplane magnetic resonance imaging of the heart and major vessels: studies in normal volunteers. *AJR* **1984**;142:661–667
4. Didier D, Higgins CB, Fisher MR, Osaki L, Silverman NH, Cheitlin MD. Congenital heart disease: gated MR imaging in 72 patients. *Radiology* **1986**;158:227–235
5. Glazer HS, Gutierrez FR, Levitt RG, Lee JKT, Murphy WA. The thoracic aorta studied by MR imaging. *Radiology* **1985**;157:149–155
6. McNamara MT, Higgins CB, Schechtmann N, et al. Detection and characterization of acute myocardial infarction in man with the use of gated magnetic resonance. *Circulation* **1985**;71:717–724
7. McNamara MT, Higgins CB. Magnetic resonance imaging of chronic myocardial infarcts in man. *AJR* **1986**;146:315–320
8. Geisinger MA, Risius B, O'Donnell JA, et al. Thoracic aortic dissections: magnetic resonance imaging. *Radiology* **1985**;155:407–412
9. Dinsmore RE, Liberthson RR, Wismer GL, et al. Magnetic resonance imaging of thoracic aortic aneurysms: comparison with other imaging

methods. *AJR* **1986**;146:309–314
10. Webb WR, Jensen BG, Gamsu G, Sollitto R, Moore EH. Coronal magnetic resonance imaging of the chest: normal and abnormal. *Radiology* **1984**;153:729–735
11. von Schulthess GD, Fisher MR, Higgins CB. Pathologic blood flow in pulmonary vascular disease as shown by gated magnetic resonance imaging. *Ann Intern Med* **1985**;103:317–323
12. Bouchard A, Higgins CB, Byrd BF III, Amparo EG, Osaki L. Axelrod R. Magnetic resonance imaging in pulmonary arterial hypertension. *Am J Cardiol* **1985**;56:938–942
13. Fisher MR, Higgins CB. Central thrombi in pulmonary arterial hypertension detected by MR imaging. *Radiology* **1986**;158:223–226
14. Gamsu G, Hirji M, Moore EH, Webb WR, Brito A. Experimental pulmonary emboli detected using magnetic resonance. *Radiology* **1984**;153:467–470
15. Moore EH, Gamsu G, Webb WR, Stulbarg MS. Pulmonary embolus: detection and follow-up using magnetic resonance. *Radiology* **1984**; 153:471–472
16. Thickman D, Kressel HY, Axel L. Demonstration of pulmonary embolism by magnetic resonance imaging. *AJR* **1984**;142:921–922
17. Stein MG, Crues JV III, Bradley WG Jr, et al. MR imaging of pulmonary emboli: an experimental study in dogs. *AJR* **1986**;147:1133–1137
18. Crooks LE, Barker B, Chang H, et al. Magnetic resonance imaging strategies for heart studies. *Radiology* **1984**;153:459–465
19. Lanzer P, Barta C, Botvinick EH, Wiesendanger HUD, Modin G, Higgins CB. ECG-synchronized cardiac MR imaging: method and evaluation. *Radiology* **1985**;155:681–686
20. Bradley WG, Waluch V. NMR even echo rephasing in slow laminar flow. *J Comput Assist Tomogr* **1984**;8:594–598
21. Kucharczyk W, Brant-Zawadzki M, Lemme-Phlaghos L, et al. MR technology: effect of even-echo rephasing on calculated T1 values and T2 images. *Radiology* **1985**;157:95–101
22. Sechtem U, Pflugfelder PW, White RD, et al. Cine MR imaging: potential for the evaluation of cardiovascular function. *AJR* **1987**;148:239–246
23. Sostman HD, Rapoport S, Gottschalk A, Greenspan RH. Imaging of pulmonary embolism. *Invest Radiol* **1986**;21:443–454
24. von Schulthess GK, Higgins CB. Blood flow imaging with MR: spin-phase phenomena. *Radiology* **1985**;157:687–695
25. Amparo EG, Hoddick WK, Hricak H, et al. Comparison of magnetic resonance imaging and ultrasonography in evaluation of abdominal aortic aneurysm. *Radiology* **1985**;154:451–456
26. Rapoport S, Sostman HD, Pope C, Camputaro C, Holcomb W, Gore JC. Venous clots: evaluation with MR imaging. *Radiology* **1987**;162:527–530
27. Erdman WA, Weinreb JC, Cohen JM, Buja LM, Chaney C, Peshock RM. Venous thrombosis: clinical and experimental MR imaging. *Radiology* **1986**;161:233–238
28. Crues JV III, Stein MG, Bradley W, et al. The origin of abnormal MR imaging signal intensity in acute pulmonary emboli (abstr). *Radiology* **1985**;157(P):183

P24,444

Book Review

Progress in Radiopharmacy. Edited by P. H. Cox, S. J. Mather, C. B. Sampson, and C. R. Lazarus. The Hague: Nijhoff, 615 pp., 1986. $155

This textbook is a compilation of papers presented to the Second European Symposium on Radiopharmacy and Radiopharmaceuticals, held at St. Catharine's College Cambridge in March 1985.

The text is divided into seven sections. The first section, on generator systems for ultra-short-lived radionuclides, discusses parent-daughter selection criteria, separation systems, limitations, and potential for clinical use. Specific topics include the current status of the Os^{191}-Ir^{-191m} generator and a new approach to the preparation of the Yt^{87}-Sr^{87m} generator. The second section describes the production of positron-emitting radionuclides using generators and/or cyclotrons to produce radiopharmaceuticals for medical applications. The third section, on radiochemistry, presents reviews on the advances made in the radiochemistry of Tc^{99m}, the use of indium chemistry in radiopharmaceutical development, and methods of radiohalogenation. Specific methods explained are new aspects of technetium complexation with DTPA ligand and the development of iodine-labeled 5-iodo-2-thiouracil for the diagnosis and treatment of melanoma. The fourth section deals with recent developments in radiopharmacy practice. Task-related activities from record keeping and adverse-reaction reporting to automated dispensing are suggested with the use of computers and automated equipment. The training and education of pharmacists in radiopharmacy are surveyed, with specific goals recommended in the United Kingdom. Recent developments in analytical techniques for quality control of radiopharmaceuticals are described.

An overview of existing methods of diagnostic imaging is presented with emphasis on encouraging research and development of radionuclide and paramagnetic tracers. The fifth section, on the biologic fate of radiopharmaceuticals, presents topics on the biologic fate of renal agents, the in vivo and in vitro behavior of technetium bone-seeking phosphate compounds, the biologic behavior and quality control of colloids for functional studies of the reticuloendothelial system, myocardial agents (including $T1^{201}$, Tc^{99m} cationic complexes, and fatty acids), and adrenal cortex imaging with I^{131} metaiodobenzylguanidine MIBG. The sixth section lists radionuclides in drug-formulation studies that describe methods of following the fate of formulation and quality tests for antibodies labeled with iodine, indium, and technetium. The seventh section, on radiopharmaceutical aerosols, describes methods of production, the deposition and clearance of inhaled aerosols, and the use of a Tc^{99m} aerosol system for ventilation studies.

As expected in a book of this type, most of the illustrations are diagrams rather than scintigraphic images. Several software programs presented, written in Basic, may be useful for radiopharmaceutical quality control. The editors believe that this book complements earlier publications of the series *Developments in Nuclear Medicine* to give current and on-going state-of-the-art practices of radiopharmacy in Europe. Although many typographic errors have crept into the text, it is adequately referenced and contains both technical and practical information. The text is addressed to individuals who are involved in radiopharmacy and the production of radiopharmaceuticals.

Physicians active in the use of radiopharmaceuticals will be familiar with most of the information on biologic fate and clinical use of radiopharmaceuticals, but overall the book is not particularly directed at that audience.

Tom Kawada
Michael E. Siegel
Los Angeles County-USC Medical Center
Los Angeles, CA 90033

Pulmonary Complications of Cytosine-Arabinoside Therapy: Radiographic Findings

Richenel T. O. Tjon A Tham[1]
Wim G. Peters[2]
Francisca T. de Bruïne[1]
Roel Willemze[2]

Sixty-four patients underwent 66 remission induction courses with intermediate-dose cytosine-arabinoside (Ara-C) for treatment of acute myelogenous leukemia, acute lymphoblastic leukemia, or high-grade malignant non-Hodgkin's lymphoma. The Ara-C was administered in combination with amsacrine with or without VP16-213 and prednisone. After complete remission was achieved, 27 patients received 38 consolidation courses consisting of high-dose Ara-C either alone or in combination with amsacrine with or without VP16-213 and prednisone. Seven (11%) of 66 induction courses and eight (21%) of 38 consolidation courses were complicated by respiratory failure that was considered a pulmonary reaction to Ara-C therapy. The initial findings on chest radiographs in the 15 cases included a diffuse interstitial pattern (two), a mixed interstitial-alveolar pattern (eight), an alveolar pattern (three), and a normal pattern (two). In 11 cases, the abnormalities were diffuse throughout both lungs with a preference for the lower lobes in five. The changes were localized in two cases. A small pleural effusion was observed in two patients. In the majority of cases, the initial radiographic changes progressed to a predominantly alveolar pattern. Thirteen patients recovered clinically within 2–9 days, and two patients died of pulmonary complications. Radiologic recovery took 7–21 days. Rapid regression of alveolar consolidations within 3–7 days was the first sign of radiologic improvement. The interstitial pattern gradually regressed.

We conclude that the spectrum of radiologic abnormalities in cases of pulmonary reaction to Ara-C therapy includes diffuse interstitial, mixed interstitial-alveolar, or alveolar pulmonary changes.

Iatrogenic pulmonary disease with respiratory failure is a well-known complication of cytotoxic drug therapy. The clinical and radiographic findings of these pulmonary conditions are nonspecific [1]. Three recent reports [2–4] described diffuse lung disease induced by the antineoplastic agent cytosine-arabinoside (Ara-C). Ara-C is a pyrimidine nucleoside analog that produces rapid and potent inhibition of DNA synthesis in mammalian cells, primarily through inhibition of DNA polymerase by Ara-CTP (cytosine-arabinoside triphosphate). The drug is important in the treatment of acute leukemia and non-Hodgkin's lymphoma [5]. Because the radiographic features of the pulmonary complications associated with Ara-C therapy have not been well described in the literature, we analyzed the radiographic findings in 15 patients with this complication.

Materials and Methods

Between 1982 and 1986, 64 patients underwent a total of 66 remission induction therapy courses that included intermediate-dose Ara-C (1 g/m^2 twice daily for 6 days) for either (1) previously untreated, primary refractory, or relapsed acute myelogenous leukemia, (2) acute lymphoblastic leukemia, or (3) high-grade malignant non-Hodgkin's lymphoma. For 42 patients, induction therapy also included amsacrine at a dose of 115 mg/m^2 daily for 1 or 3 days; the remaining 22 patients additionally received amsacrine for 2 days in combination with VP16-213 at a dose of 120 mg/m^2 daily for 2 days and prednisone (60 mg/m^2) daily for 7 days.

Received February 9, 1987; accepted after revision March 25, 1987.

[1]Department of Diagnostic Radiology, Leiden University Medical Center, Leiden, the Netherlands. Address reprint requests to R. T. O. Tjon A Tham, Dept. of Diagnostic Radiology, Building 1: C2-S, University Hospital Leiden, Rijnsburgerweg 10, 2333 AA Leiden, the Netherlands.

[2]Department of Hematology, Leiden University Medical Center, Leiden, the Netherlands.

AJR 149:23–27, July 1987
0361–803X/87/1491–0023
© American Roentgen Ray Society

After achievement of complete remission 22 patients received a total of 33 consolidation therapy courses that included high-dose Ara-C (3 g/m^2 twice daily for 4 days). In 14 cases consolidation therapy also included amsacrine (115 mg/m^2) for 1 day; the remaining eight patients additionally received amsacrine for 2 days, VP16-213 (120 mg/m^2) for 2 days, and prednisone (60 mg/m^2) for 5 days. Five additional patients underwent consolidation therapy with Ara-C alone at a dose of 2 g/m^2 twice daily for 6 days, after remission induction therapy with vincristine, daunorubicin, 1-asparaginase, and prednisone.

Fifteen of all therapy courses that included Ara-C were complicated by respiratory failure that was attributed to Ara-C therapy. The group of patients with this complication consisted of 11 men and four women ranging in age from 15 to 57 years (median, 29 years). Five patients had acute myelogenous leukemia, one had acute lymphoblastic leukemia, five had lymphoblastic non-Hodgkin's lymphoma, and four had Burkitt's lymphoma. The diagnosis of an adverse reaction of the lungs to Ara-C therapy was based on the fact that other causes of diffuse lung disease, such as cardiac failure, hypoalbuminemia, renal failure with fluid overload, CNS disease, and lung infiltration by leukemia or lymphoma, were excluded. Exclusion of opportunistic infections was based on the clinical course, sputum cultures, and repeated serologic investigations. Fourteen patients could not undergo invasive diagnostic procedures because of their critical condition. One patient underwent a thoracoscopic lung biopsy. The lung specimen did not show specific histologic or microbiological abnormalities, possibly because of sampling error. Remarkable was the fact that 12 patients developed *Streptococcus* viridans septicemia a median of 2 days (range, 1–3 days) before respiratory failure. All patients received appropriate antibiotic therapy; blood cultures taken at the onset of respiratory failure were negative.

The clinical records and chest radiographs of all 15 cases were reviewed, and the radiographic findings were correlated with the clinical data.

Results

All 15 patients developed acute or subacute respiratory failure a median of 16 days (range, 8–20 days) after the start of Ara-C therapy. Seven (11%) of 66 induction courses resulted in pulmonary complications after induction therapy with intermediate-dose Ara-C (cumulative dose, 12 g/m^2), and eight (21%) of 38 courses resulted in complications after consolidation therapy with high-dose Ara-C (cumulative dose, 24 g/m^2).

Clinical findings included fever in all cases, dry cough (10/15), dyspnea (12/15), tachypnea (14/15), rales (10/15), and hypoxemia (13/15).

At the start of chemotherapy all patients had normal chest radiographs. In 13 cases these became abnormal on the day respiratory failure developed. The chest radiographs of two patients who received high-dose methylprednisolone immediately after the onset of respiratory symptoms remained normal. The initial chest radiographs showed a predominantly interstitial or mixed interstitial-alveolar pattern (Figs. 1 and 2) in two and eight cases, respectively; an alveolar pattern (Fig. 3) was observed in three cases. All patients had bilateral abnormalities with a preponderance in the left or right lung in one and four cases, respectively. The abnormalities were scattered diffusely throughout both lungs in 11 patients, although there was a preference for the lower lobes in five of

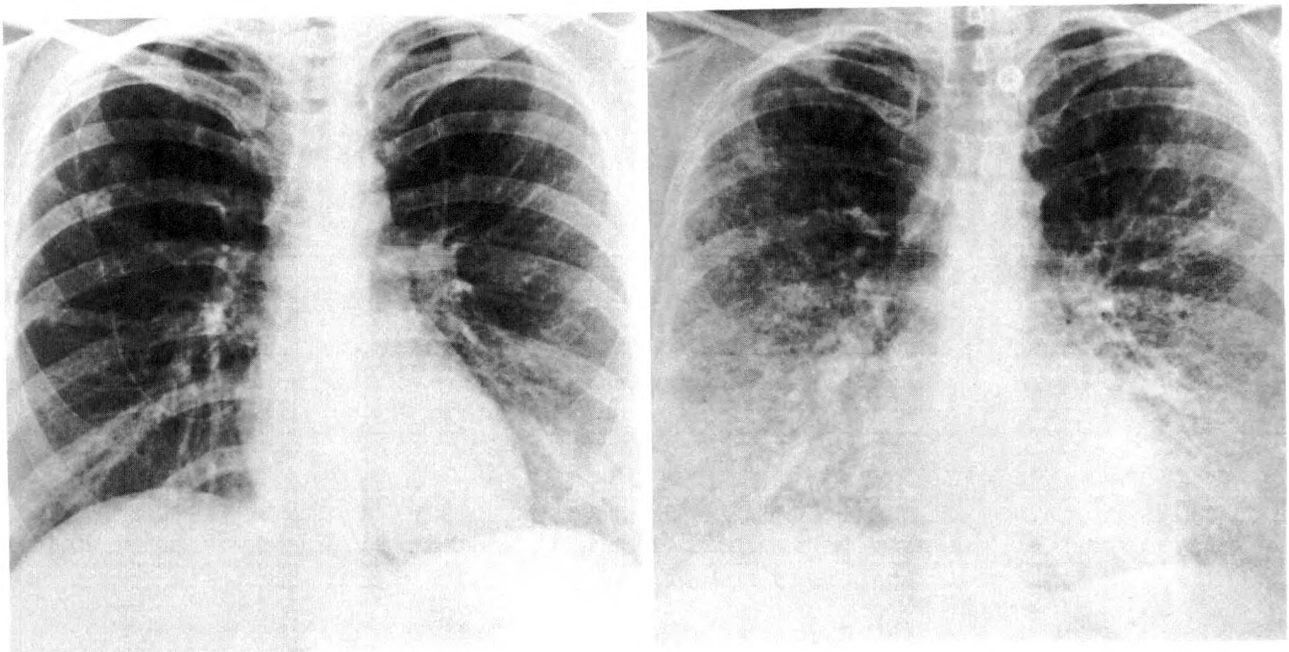
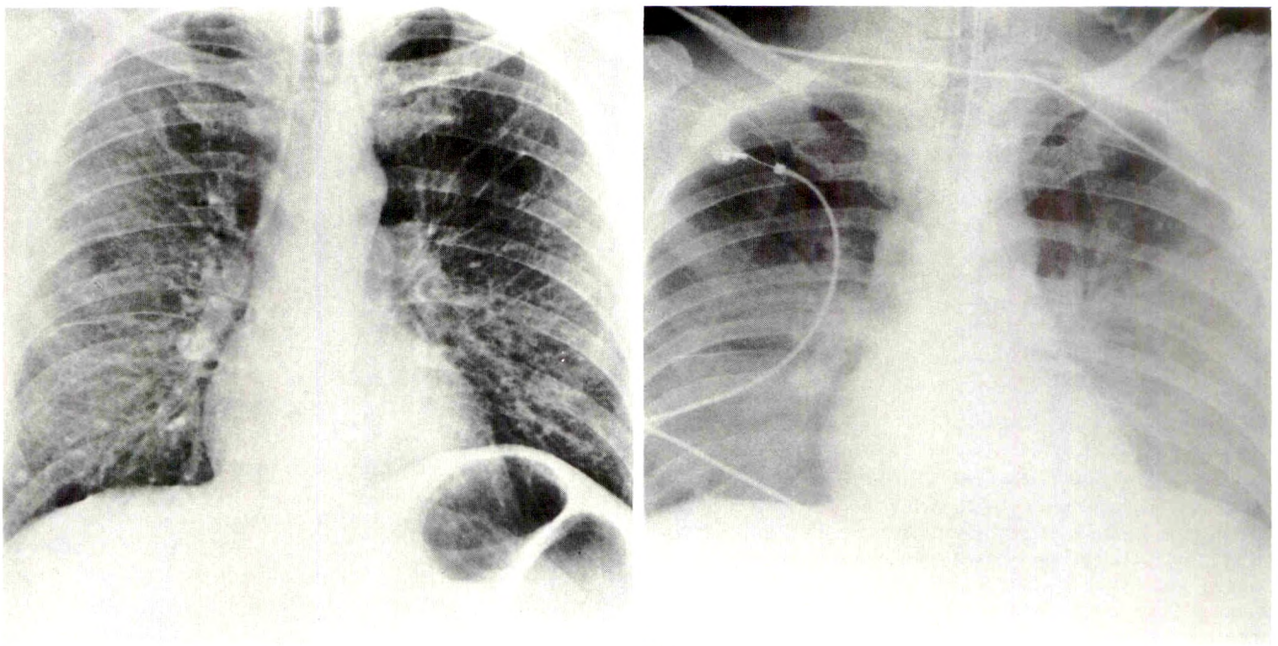


Fig. 1.—A 23-year-old woman with acute lymphoblastic leukemia who developed acute respiratory failure 13 days after start of consolidation therapy with high-dose Ara-C. Chest radiograph showed a diffuse interstitial infiltrate (*A*) that progressed rapidly to a diffuse interstitial-alveolar pattern, localized mainly in basal lung fields (*B*). Patient recovered completely.



A B

Fig. 2.—A 55-year-old man with acute myelogenous leukemia exhibited diffuse interstitial pulmonary changes 9 days after start of induction therapy with intermediate-dose Ara-C. Chest radiograph showed slight predominance in right lung (*A*). Abnormality progressed to a diffuse alveolar pattern (*B*). Patient died of combined pulmonary and gastrointestinal toxicity complicated by acute tubular necrosis. Autopsy showed massive pulmonary edema with a highly proteinaceous interstitial and intraalveolar exudate, occasionally accompanied by extravasation of erythrocytes, diffusely scattered throughout both lungs.



Fig. 3.—A 29-year-old woman with lymphoblastic non-Hodgkin's lymphoma. Consolidation therapy with high-dose Ara-C was complicated by respiratory failure 13 days after start of therapy. Chest radiograph showed a diffuse alveolar pattern. Patient recovered completely. Radiographic recovery took 9 days; diffuse alveolar pattern changed into a diffuse interstitial pattern, which was followed by a complete return to normal.

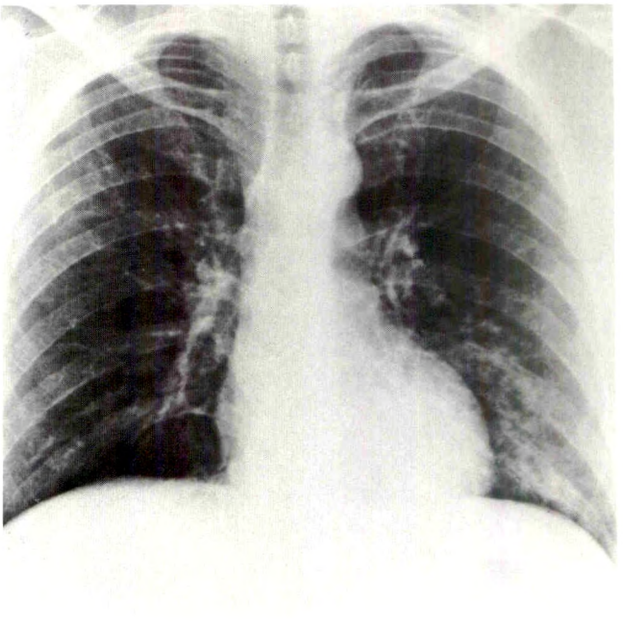


Fig. 4.—A 49-year-old man with acute myelogenous leukemia who developed respiratory failure 15 days after start of high-dose Ara-C. Chest radiograph showed localized patchy alveolar pattern in left lower lobe. Patient recovered completely with a normal follow-up chest radiograph.

these cases (Fig. 1). In two other cases the radiographic changes were local (Figs. 4 and 5); in one patient both lower lobes were affected and in the other patient the changes were observed in the left lower and right upper lobes. A small pleural effusion was observed in two patients (Fig. 5); one had a bilateral pleural effusion and the other had an effusion in the right costophrenic sulcus. None of the chest radiographs revealed cardiomegaly or other signs of cardiac failure. During the course of the respiratory failure the initial predominantly interstitial pattern changed into a predominantly alveolar pattern in the majority of cases (Figs. 1 and 2).

The clinical course was characterized by the complete recovery of 13 patients within 2–9 days of the start of respiratory failure. They did not receive specific therapy or artificial ventilation. Four patients were given high-dose methylprednisolone (10 mg/kg IV); two showed partial clinical improvement and radiographic stabilization; the remaining two improved clinically and did not even develop radiographic changes, probably because the corticosteroids were administered at the beginning of respiratory failure. In 11 patients definite clinical improvement was accompanied by granulocyte recovery. In two cases the course was fatal: one died of respiratory failure and the other of combined pulmonary and gastrointestinal toxicity complicated by acute tubular necrosis. The postmortem examination of the lungs of both patients showed massive pulmonary edema without cardiac abnormalities. Postmortem bacterial, protozoal, fungal, and viral examinations were negative. In one patient a highly proteinaceous interstitial and intraalveolar exudate, occasionally accompanied by extravasation of erythrocytes, was scattered diffusely throughout both lungs (Fig. 2).

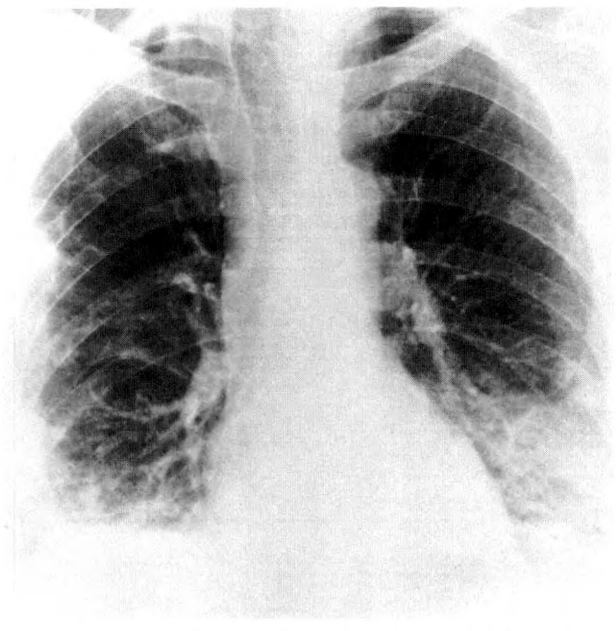


Fig. 5.—A 56-year-old man with lymphoblastic non-Hodgkin's lymphoma who had respiratory failure 18 days after start of consolidation therapy with high-dose Ara-C. Chest radiography showed patchy alveolar changes in basal lung fields with pleural effusion. Patient recovered clinically; follow-up chest radiographs were not available.

For the patients who survived and who were available for follow-up, the radiographic course was characterized by complete resolution of all abnormalities. Return to normal condition took 7–21 days. Rapid regression of alveolar consolidations within 3–7 days was the first sign of radiologic recovery, whereas the interstitial pattern persisted longer, with a more gradual regression to normal.

Discussion

Cytosine-arabinoside, a pyrimidine nucleoside analog that produces a rapid and potent inhibition of DNA-synthesis in mammalian cells, is important in the therapy for acute leukemia and, to a lesser extent, non-Hodgkin's lymphoma [5]. The success rate appears to be dose-dependent since Ara-C administered as the single agent in doses of 10–30 mg/m^2 leads to remission in 10–15% of previously untreated cases, whereas doses of 100–200 mg/m^2 are effective in approximately 30% of these cases [6]. In combination with an anthracycline antibiotic, complete remission can be achieved in 60–80% of untreated patients. Higher dosages of Ara-C (500–3000 mg/m^2) have been shown to be effective therapy for patients with refractory or relapsed acute leukemia or non-Hodgkin's lymphoma when used either as a single agent or in combination with an anthracycline antibiotic, amsacrine, or 1-asparaginase [7]. Remission induction therapy with these agents leads to complete remission in 50–70% of the patients. In addition, the use of high-dose Ara-C for consolidation therapy possibly results in the prolongation of remissions [7].

Side effects commonly seen with Ara-C therapy are fever, rashes, nausea and vomiting, diarrhea with or without paralytic ileus, keratoconjunctivitis, myalgia and arthralgia, liver function abnormalities, and pancytopenia [8]. With the introduction of higher Ara-C dosages, the incidence and severity of some of these side effects increased, and some new side effects, like CNS abnormalities, appeared [8]. Pulmonary toxicity caused by Ara-C is considered to be rare and was first reported by Haupt et al. [2] and later by Willemze et al. [3] and Andersson et al. [4]. Haupt et al. [2] performed a postmortem study on leukemic patients receiving Ara-C–containing chemotherapy. They found a high incidence of unexplained noncardiogenic pulmonary edema in patients who received courses of Ara-C within 30 days before death and suggested a relationship between pulmonary edema and Ara-C administration. The pathologic findings consisted of highly proteinaceous interstitial and intraalveolar edema, occasionally accompanied by extravasation of RBCs.

Andersson et al. [4] reported respiratory failure in 16 (22%) of 72 patients who had received high-dose Ara-C therapy. They observed a significant increase in pulmonary toxicity with increasing numbers of Ara-C doses. From this report it is not clear whether other causes of pulmonary edema were fully excluded, since some of the patients experienced peripheral edema and/or showed radiographic signs of definite cardiac enlargement. In the present study diffuse lung disease occurred after 11% of remission induction courses and 21%

of consolidation courses. In the majority of patients, clinical signs of respiratory failure and the radiologic abnormalities developed simultaneously. The clinical signs consisted of the acute (or subacute) onset of fever, cough, dyspnea, tachypnea, rales, and hypoxemia. The pattern noted on radiographs in the majority of cases was either diffuse interstitial or mixed interstitial-alveolar.

The diagnosis of Ara-C toxicity was made by excluding other causes of diffuse pulmonary disease. Conditions such as cardiac failure, hypoalbuminemia, renal failure with fluid overload, CNS disease, and tumor infiltration of the lungs could be ruled out completely. Since clinical signs of cardiac failure were lacking, the contribution of previous anthracycline or recent amsacrine therapy, both of which might cause cardiomyopathy [9, 10], could be excluded. Diffuse lung disease caused by VP16-213 has not been reported [11]. Opportunistic infections such as those caused by *Pneumocystis carinii*, cytomegalic virus, herpes viruses, and fungi were unlikely in view of the sputum cultures, repeated serologic investigations, and the rapid and spontaneous improvement of the majority of patients. The abatement of symptoms and signs in four patients after corticosteroid therapy supports the diagnosis Ara-C toxicity and is in agreement with the findings of Andersson et al. [4].

A normal chest radiograph and the existence of a pleural effusion do not exclude the presence of cytotoxic lung injury, although these findings are uncommon [12]. The postmortem pathologic findings in one of the two patients who died were in agreement with the pathologic results of Haupt et al. [2], although they were not specific for Ara-C toxicity [13].

The pathogenesis of the Ara-C toxicity remains unclear. Haupt et al. [2] suggested that the permeability of the alveolo-capillary membrane increases because of the relative aging of the constituents of the membrane, which is induced by inhibition of DNA synthesis by Ara-C. The resulting disease resembles the adult respiratory distress syndrome. On the basis of the sequence of events, it seems that in the present study the *Streptococcus* viridans septicemia might have played an additional role in the majority of patients. Bacterial products might lead to further disruption of the preexisting damaged alveolo-capillary membranes, resulting in capillary leakage. However, statistically the role of *Streptococci* remains unclear since the incidence of septicemia due to these bacteria among these patients did not differ significantly from that found in patients without diffuse lung disease [14].

ACKNOWLEDGMENTS

We are grateful to M. Popkes for his excellent photographic art work and to Clary Labee and Ineke Lek for their secretarial assistance.

REFERENCES

1. Cooper JAD, White DA, Matthay RA. Drug-induced pulmonary disease. Part I. Cytotoxic drugs. *Am Rev Respir Dis* **1986**;133:321–340
2. Haupt HM, Hutchins GM, Moore GW. Ara-C lung: non-cardiogenic pulmonary edema complicating cytosine arabinoside therapy of leukaemia. *Am J Med* **1981**;70:256–261
3. Willemze R, Zwaan FE, Keuning JJ, Colpin G. Treatment of refractory acute leukaemia with high-dose cytosine arabinoside. *Br J Haematol* **1982**;51:497–498
4. Andersson BS, Cogan BM, Keating MJ, Estey EH, McCredie KB, Freireich EJ. Subacute pulmonary failure complicating therapy with high-dose Ara-C in acute leukaemia. *Cancer* **1985**;56:2181–2184
5. Kremer WB. Cytarabine. *Ann Intern Med* **1975**;82:684–688.
6. Gale RP. Advances in the treatment of acute myelogenous leukemia. *N Engl J Med* **1979**;300:1189–1199
7. Gale RP, Foon KA. Acute myeloid leukaemia: recent advances in therapy. *Clin Haematol* **1986**;15(3):781–810
8. Herzig RH, Wolff SN, Lazarus HM, Phillips GL, Karanes C, Herzig GP. High-dose cytosine arabinoside therapy for refractory leukemia. *Blood* **1983**;62:361–369
9. Tokaz LK, Von Hoff DD. The cardiotoxicity of anticancer agents. In: *Toxicity of chemotherapy*. Perry MC, Yarbro JW, eds. Orlando, FL: Grune & Stratton, **1984**:199–226
10. Weiss RB, Grillo-López AJ, Marsoni S, et al. Amsacrine-associated cardiotoxicity: an analysis of 82 cases. *J Clin Oncol* **1986**;4:918–928
11. O'Dwyer PJ, Leyland-Jones B, Alonso MT, Marsoni S, Wittes RE. Etoposide (VP16-213): current status of an active anticancer drug. *N Engl J Med* **1985**;312:692–700
12. Sostman HD, Putman CE, Gamsu G. Diagnosis of chemotherapy lung. *AJR* **1981**;136:33–40
13. Bedrossian CWM. Pathology of drug-induced lung diseases. *Semin Respir Med* **1982**;4:98–106
14. Peters WG, Willemze R, Colly LP, Guiot HFL. Side effects of intermediate and high-dose cytosine arabinoside during treatment of refractory or relapsed acute leukaemia and non-Hodgkin's lymphoma. *Neth J Med* **1987**;30:64–74

Books Received

Receipt of books is acknowledged as a courtesy to the sender. Books that appear of sufficient interest will be reviewed as space permits. If the book has been reviewed in the *AJR* during the current year, the date of its review is given in parentheses.

Nuclear Cardiac Imaging. Principles and Applications. By A. S. Iskandrian. Philadelphia: Davis, 552 pp., 1987. $75 (3/87)

Ultrasound-Guided Biopsy and Drainage. By Rainer Ch. Otto and Josef Wellaue, Berlin: Springer-Verlag, 160 pp., 1986. (3/87)

Cranial Computed Tomography in Infants and Children. By Eric N. Faerber. Philadelphia: Lippincott, 237 pp., 1986. $39.59 (3/87)

Atlas of Fetal Sectional Anatomy with Ultrasound and Magnetic Resonance Imaging. By G. Isaacson, M. C. Mintz, and E. S. Crelin. New York: Springer-Verlag, 184 pp., 1986. $89 (3/87)

Guide to the Ultrasound Examination of the Abdomen. By M. Leon Skolnick. New York: Springer-Verlag, 240 pp., 1986. $51 (3/87)

Bone Tumors. General Aspects and Data on 8,542 Cases, 4th ed. By David C. Dahlin and Krishnan K. Unni. Springfield, IL: Thomas, 522 pp., 1986. $82 (3/87)

Ultrasound Diagnosis in Obstetrics and Gynecology. By M. Hansmann, B. J. Hackeloer, and A. Staudach. New York: Springer-Verlag, 495 pp., 1986. $100 (4/87)

Subarachnoid Haemorrhage. By R. P. Sengupa and V. L. McAllister. Berlin: Springer-Verlag, 378 pp., 1986. $135 (4/87)

Nuclear Techniques in Diagnostic Medicine. Edited by P. P. van Rijk. The Hague, The Netherlands: Nijhoff, 527 pp., 1986, $156.50 (4/87)

The Radiologic Clinics of North America. Vascular Imaging: Angiography and the New Modalities: Edited by Harvey A. Koolpe. Philadelphia: Saunders, 525 pp., 1986, $60 (4/87)

Diagnostic Imaging in Surgery. By Ronald L. Eisenberg. New York: McGraw-Hill, 834 pp., 1987. $135 (4/87)

Asbestos-Related Malignancy. Edited by Karen Antman and Joseph Aisner. Orlando, FL: Grune & Stratton, 412 pp., 1987. $64.50 (4/87)

Urologic Pathology. By Robert O. Petersen. Philadelphia: Lippincott, 762 pp., 1986. $87.50 (4/87)

New Developments in Imaging. Edited by Rainer Ch. Otto and Charles B. Higgins. New York: Thieme, 172 pp., 1986, $47 (4/87)

Basic Imaging in Congenital Heart Disease. By Leonard Swischuk and David W. Sapire. Baltimore: Williams & Wilkins, 312 pp., 1986. $58.95 (5/87)

Radiology of Bone Diseases. By George B. Greenfield. Philadelphia: Lippincott, 926 pp., 1986, $87.50 (5/87)

Quantitative Obstetrical Ultrasonography. By Russell L. Deter, Ronald B. Harrist, Jason C. Birnholz, and Frank P. Hadlock, New York: Wiley, 377 pp., 1986. $45 (5/87)

Guide to the Ultrasound Examination of the Abdomen. By M. Leon Skolnick. New York: Springer-Verlag, 240 pp., 1986. $51 (5/87)

Pediatric Imaging Doppler Ultrasound of the Chest: Extracardiac Diagnosis. By James C. Huhta, Philadelphia: Lea & Febiger, 225 pp., 1986. $42.50 (5/87)

Ultrasound Annual 1986. Edited by Roger C. Sanders and Michael C. Hill. New York: Raven, 261 pp., 1986. $79 (5/87)

Recent Advances in Radiology and Medical Imaging—8. Edited by R. E. Steiner and Thomas Sherwood. New York: Churchill Livingstone, 213 pp., 1986. $76.50 (5/87)

Radiology of the Acute Abdomen. By Jovitas Skucas and Robert F. Spataro. New York: Churchill Livingstone, 727 pp., 1986. $125 (5/87)

Cancer in Atomic Bomb Survivors. Edited by Itsuzo Shigematsu and Abraham Kagan. New York: Plenum, 196 pp., 1986. $55 (5/87)

State of the Art in Quantitative Coronary Arteriography. Edited by J. H. C. Reiber and P. W. Serruys. Dordrecht, The Netherlands: Nijhoff, 274 pp., 1986. $96.50 (5/87)

Skeletal Development of the Wrist and Hand in *Macaca Mulatta* and Man. By Maria Michejda. Basel, Switzerland: Karger, 124 pp., 1987. $192.25 (5/87)

Angiocardiography. Current Status and Future Developments. Edited by H. Just and P. H. Heintzen. Berlin: Springer-Verlag, 403 pp., 1986. $103 (5/87)

Magnetic Resonance of the Musculoskeletal System. Edited by Thomas H. Berquist, R. L. Ehman, and M. L. Richardson. New York: Raven, 220 pp., 1986. $28 (5/87)

Neuroradiology, 2nd ed. By Ruth G. Ramsey. Philadelphia: Saunders, 852 pp., 1987. $85 (5/87)

Concepts in Pediatric Neurosurgery 7. Edited by Arthur E. Marlin. Basel: Karger, 240 pp., 1987. $95.50

Treatment Planning in the Radiation Therapy of Cancer. Edited by J. M. Vaet and J. Meyer. Switzerland: Karger, 342 pp., 1987. $180.75

Magnetic Resonance Annual 1987. Edited by Herbert Y. Kressel. New York: Raven, 347 pp., 1986. $69

A Colour Atlas of Gastrointestinal Endoscopy. By K. F. R. Schiller, Roy Cockel, and Richard H. Hunt. Philadelphia: Saunders, 240 pp., 1987. $110

Traumatic Hip Dislocation in Childhood. By Antonio Barquet. New York: Springer-Verlag, 146 pp., 1987. $71

Interpretation of the Chest Roentgenogram. By Michael J. Landay. Boston: Little, Brown, 189 pp., 1987. $19.50 (6/87)

Radiology of Congenital Heart Disease, vol. 1. By Kurt Amplatz, James H. Moller, and Wilfrido R. Castaneda-Zuniga. New York: Thieme, 542 pp., 1986. $125 (6/87)

Radiologic Management of Musculoskeletal Tumors. By Holger Pettersson, Dempsey S. Springfield, and William F. Enneking. New York: Springer-Verlag, 153 pp., 1987. $89 (6/87)

Pediatric Ultrasonography. Edited by C. Keith Hayden, Jr., and Leonard E. Swischuk. Baltimore: Williams & Wilkins, 403 pp., 1987. $59.95 (6/87)

Clinical Imaging of the Colon and Rectum. By Frederick M. Kelvin and Richard Gardiner. New York: Raven, 507 pp., 1987. $79 (6/87)

Cranial Computed Tomography and MRI, 2nd ed. By Seungho Howard Lee and Krishna C. V. G. Rao. New York: McGraw-Hill, 858 pp., 1987. $125 (6/87)

Pocket Atlas of MRI Body Anatomy. By Thomas H. Berquist, Richard L. Ehman, and Gerald R. May. New York: Raven, 95 pp., 1987. $12.50 (6/87)

Imaging in Internal Medicine. Edited by Robert L. Siegle. Boston: Little, Brown, 262 pp., 1987. $35 (6/87)

Computed Tomographic Angiography of the Mediastinum. By Lee Chiu, William Stanford, and Vicky S. Yiu-Chiu. St. Louis: Green, 214 pp., 1986. $55 (6/87)

Essentials of Cardiac Roentgenology. By James T. T. Chen. Boston: Little, Brown, 334 pp., 1986. $75 (6/87)

Paracardiac Adenopathy: CT Evaluation

Steven K. Sussman[1,2]
Robert A. Halvorsen, Jr.[3,4]
Paul M. Silverman[1,5]
Mohsin Saeed[1]

To establish the normal CT appearance of lymph nodes in the paracardiac area, we reviewed the CT scans of 50 patients without known malignancy or benign causes of lymphadenopathy. Five patients (10%) showed soft-tissue densities in the paracardiac region. The largest of these measured 3.5 mm. No more than two rounded soft-tissue densities were seen in any of the normal CT studies. Forty-five patients with paracardiac adenopathy were subsequently evaluated. In 27 (60%) of these the masses were due to either carcinoma, sarcoma, or benign disease. In 40%, the cause of paracardiac adenopathy was lymphoma. Features that favor a diagnosis of lymphoma are bilateral disease, multiple nodes, nodes greater than 2 cm in diameter, a lobulated or "matted" appearance, and associated pericardial thickening/effusion. Chest radiographs obtained within 2 weeks of the CT scans in 38 patients revealed only nine cases in which a paracardiac mass could be seen.

This study suggests that 1 cm is the upper limit for the diameter of lymph nodes in the paracardiac region, and that paracardiac adenopathy may be caused by a wide variety of nonlymphomatous malignant and benign diseases in addition to lymphoma. Compared with CT, chest radiographs are insensitive for detecting paracardiac lymph-node enlargement.

Although the normal size of lymph nodes in the mediastinum has been documented [1], no size criteria are available for lymph nodes in the paracardiac region. To establish the normal CT appearance of the paracardiac area, we reviewed the CT scans of 50 patients who had no known cause for malignant or benign lymphadenopathy. A second purpose of this investigation was to study the appearance of paracardiac adenopathy with particular reference to etiologies other than Hodgkin's and non-Hodgkin's lymphoma [2–5]. This part of the study was based on CT examinations of 45 patients with solid masses in the paracardiac region. Finally, we compared the relative abilities of chest radiography and CT to detect paracardiac lymphadenopathy.

Materials and Methods

The CT scans of 50 patients (26 women and 24 men, 24–68 years old) with no known malignant or benign causes of lymphadenopathy were examined to assess the detectability and size of presumed normal lymph nodes in the paracardiac region. The CT scans evaluated were either chest or abdominal scans obtained with 1-cm contiguous slices in which the paracardiac region was well seen. Any soft-tissue density was noted in the cardiophrenic angles, along the cardiac silhouette, or in the most inferior portion of the internal mammary lymph-node chain. The size and number of these nodes, as well as their sites, were recorded. Nodes were classified as either anterior prepericardiac or lateropericardiac (or posterior), on the basis of the anatomic classification of Rouviere [6]. The anterior group of nodes is subdivided into right, middle, and left components, whereas the posterior group has a left and a right component (Fig. 1).

In addition, all CT scans obtained over a 4-year period in 45 patients (17 women and 28 men, 16–77 years old) with solid masses in the paracardiac region were reviewed by two

Received June 25, 1986; accepted after revision February 25, 1987.

[1] Department of Radiology, Box 3808, Duke University Medical Center, Durham, NC 27710. Address reprint requests to S. K. Sussman at Duke University.

[2] Present address: Department of Radiology, Hartford Hospital, Hartford, CT 06115.

[3] Department of Radiology, Durham Veterans Administration Hospital, Durham, NC 27705.

[4] Present address: Department of Radiology, University of Minnesota Hospital and Clinic, Minneapolis, MN 55455.

[5] Present address: Department of Radiology, Georgetown University Hospital, Washington, DC 20007.

AJR 149:29–34, July 1987
0361–803X/87/1491–0029
© American Roentgen Ray Society

radiologists. Any single soft-tissue density in the paracardiac region 1 cm or larger was considered abnormal. Three or more solid-appearing masses in the paracardiac area, even if less than 1 cm in diameter, were considered abnormal. Specific note was made of mass size, location, and multiplicity. Associated findings such as pleural effusions, other associated adenopathy, and pericardial effusion/thickening were noted. Patients with purely cystic and fatty paracardiac masses were excluded. The masses were seen at the time of abdominal CT in 27 patients, chest CT in 12 patients, and combined chest and abdominal CT in six patients. Chest CT scans were obtained with 1-cm collimation at 1-cm intervals, and abdominal CT scans were obtained with 1-cm collimation at either 1-cm (22 patients) or 2-cm (11 patients) intervals. Most patients received IV contrast material as a bolus followed by a rapid drip infusion. All scanning was performed on either a GE 8800 or GE 9800 CT scanner.

All patients underwent posteroanterior and lateral chest radiographs. The mean interval between chest radiograph and CT scan was 8.8 days (range, 0–52 days). In the majority (30 patients) the time interval was less than 1 week. In all patients who had chest radiographs within 2 weeks of the CT scan (38 patients), the chest radiograph reports were reviewed to determine if a paracardiac mass had been described. Two authors reviewed the chest radiographs together and rated the films on a 1–3 scale: 1 = no paracardiac mass seen, 2 = equivocal, and 3 = paracardiac mass seen. The scores were arrived at by consensus.

Direct pathologic proof of the CT finding of paracardiac adenopathy (that is, biopsy or surgical removal of the mass itself) was available in 11 patients (three lymphomas, two colon carcinomas, one neurofibrosarcoma, one osteosarcoma, one breast carcinoma, one neuroblastoma, one endometrial carcinoma, and one histoplasmosis). Biopsy material confirming the patient's underlying diagnosis from a site other than the paracardiac mass (the primary tumor in nonlymphoma patients and other involved nodal regions in lymphoma patients) was available in the other 34 patients.

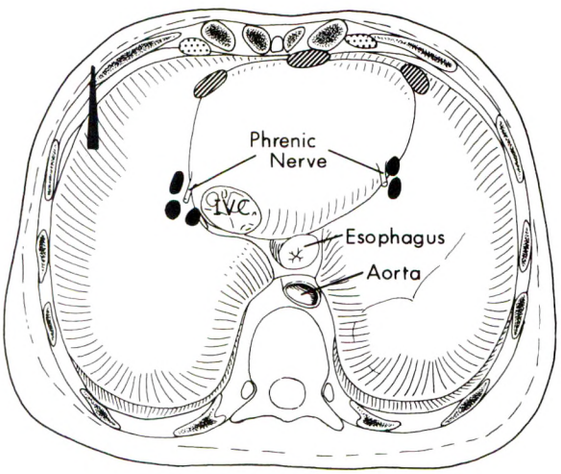


Fig. 1.—Diagram of the diaphragm as viewed from above showing the location of the paracardiac lymph nodes. Anterior prepericardiac nodes (*hatched*), lateropericardiac group (*black*); internal mammary nodes (retrosternal) and parietal pericardial nodes are not shown because they are located more cranially.

Results

Review of the CT scans in 50 patients with neither a known malignancy nor a known benign etiology for lymphadenopathy revealed rounded soft-tissue densities in the paracardiac region in only five patients (10%). In all five patients the soft-tissue densities were seen on only one CT slice. Two patients had single 2.0-mm-diameter rounded soft-tissue densities in the right anterior prepericardiac region. One patient had a single 3.5-mm-diameter rounded soft-tissue density in the mid anterior prepericardiac region (Fig. 2). Two patients had two rounded paracardiac soft-tissue densities each measuring 1.5

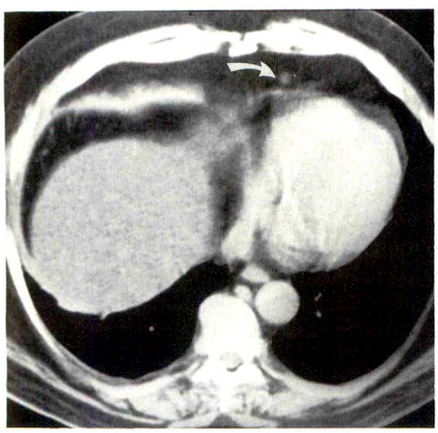


Fig. 2.—Normal-sized lymph node in patient without malignancy. Small 3.5-mm rounded soft-tissue density anterior to pericardium (*arrow*) presumably represents normal-sized anterior prepericardiac *lymph node in* patient with no underlying malignancy.

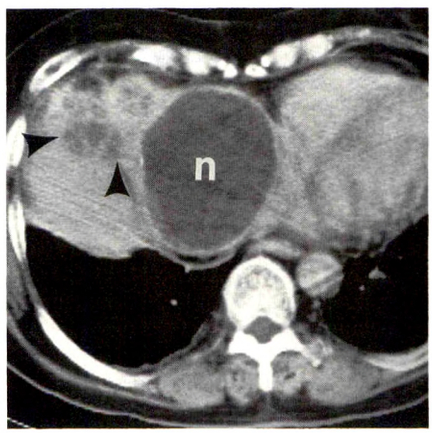


Fig. 3.—Right-sided large necrotic node (n) in patient with metastatic colon carcinoma (biopsy-proved). Liver is also involved by metastatic disease (*arrowheads*). Additional CT sections, as well as sonography, showed node to be separate from liver.

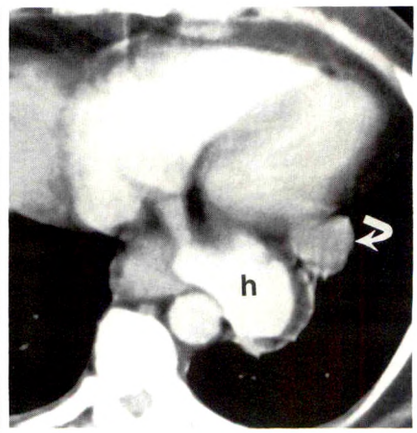


Fig. 4.—Left-sided lateropericardiac node in patient with colon carcinoma (*arrow*). Small hiatal hernia (h) is noted incidentally.

mm in diameter. These were in the right and left anterior prepericardiac region in one patient and in the right and mid anterior prepericardiac region in the other. The other 45 patients showed no measurable soft-tissue densities in the paracardiac region.

In 27 (60%) of the 45 patients with paracardiac adenopathy, the masses were nonlymphomatous in origin. Twenty-five (93%) of the 27 nonlymphoma patients with masses in the paracardiac region had known malignancies from a variety of carcinomas and sarcomas. Primary tumors included colon carcinoma (five patients) (Figs. 3 and 4), lung carcinoma (four patients) (Fig. 5), carcinoid (three patients), breast carcinoma (two patients), and a variety of other tumors encountered in one patient each (melanoma [Fig. 6], hepatoma, neurofibrosarcoma [Fig. 7], neuroblastoma, somatostatinoma, renal cell carcinoma, osteosarcoma, endometrial carcinoma, ovarian carcinoma, transitional cell carcinoma, and adenocarcinoma of unknown primary). One patient with *Aspergillus* of the chest wall had multiple anterior bilateral nodes measuring about 1.5 cm in diameter. An isolated paracardiac lymph node that measured 1 cm in diameter was seen in the patient with histoplasmosis. In 18 (40%) of 45 patients paracardiac adenopathy was secondary to malignant lymphoma (Figs. 8 and 9). Seven patients had Hodgkin's lymphoma while the remainder were non-Hodgkin's.

Isolated right-sided anterior prepericardiac adenopathy was the most common site, occurring in 47% of patients. Isolated left anterior prepericardiac nodes and isolated midline anterior prepericardiac nodes were less common, occurring in 17% and 9% of patients, respectively. In 23% of patients, combinations of several sites were involved in the anterior prepericardiac group. Posterior nodes (lateropericardiac) were uncommon, present in only two patients (4%). Nodal size, multiplicity, and associated CT findings in the 45 patients with paracardiac adenopathy are listed in Table 1. Paracardiac nodes varied in size from as small as 3 mm (in a patient with more than four masses, one of which was larger than 1 cm) to masses with a single dimension as large as 9 cm. In only two patients were the lymph nodes multiple and less than 1.0 cm in diameter: a patient with colon carcinoma had four detectable lymph nodes and a patient with lymphoma had five detectable lymph nodes, all less than 1.0 cm in size. In

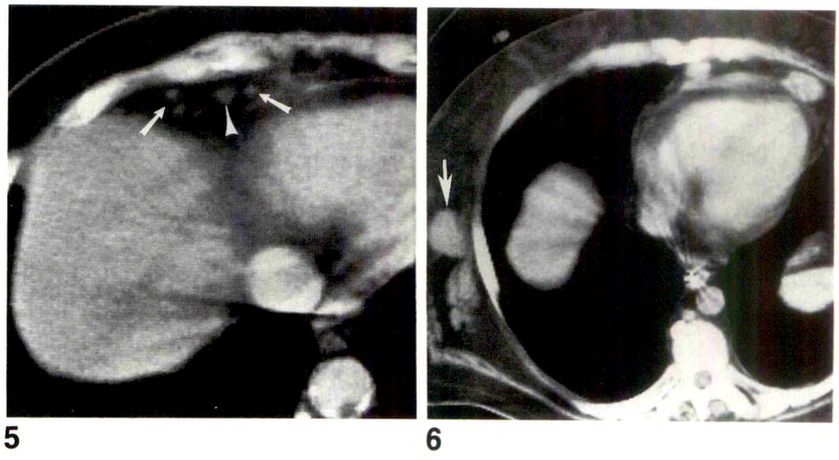


Fig. 5.—Multiple small lymph nodes in patient with metastatic lung carcinoma. A single node (*arrowhead*) measures 1 cm. There are at least three other discrete rounded soft-tissue densities (*arrows*) in right anterior prepericardiac region, all measuring less than 1 cm.

Fig. 6.—Bilateral anterior prepericardiac nodes in patient with melanoma. There is associated pericardial thickening as well as subcutaneous tumor nodule (*arrow*) in right chest wall.

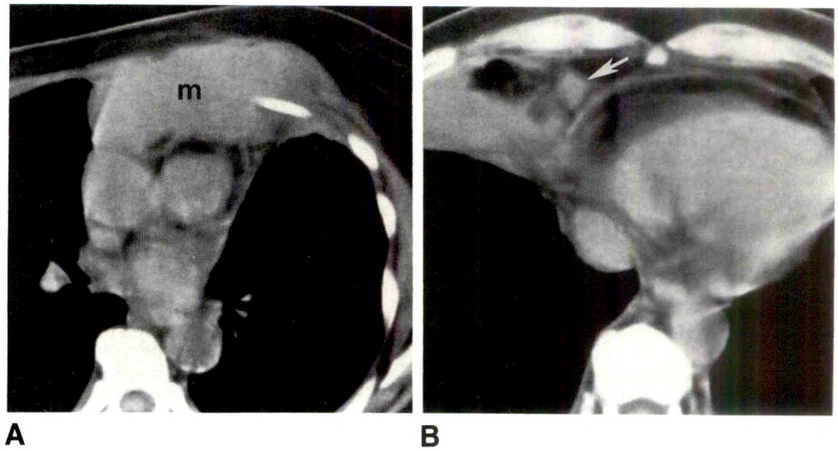


Fig. 7.—Isolated right anterior prepericardiac node in patient with neurofibrosarcoma of chest wall.

***A*, Large soft-tissue mass (m) involves right anterior chest wall.**

***B*, CT slice 6 cm lower shows right anterior prepericardiac node (*arrow*). Mild pericardial thickening is present.**

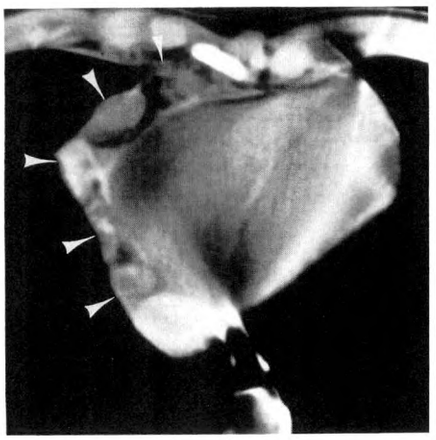
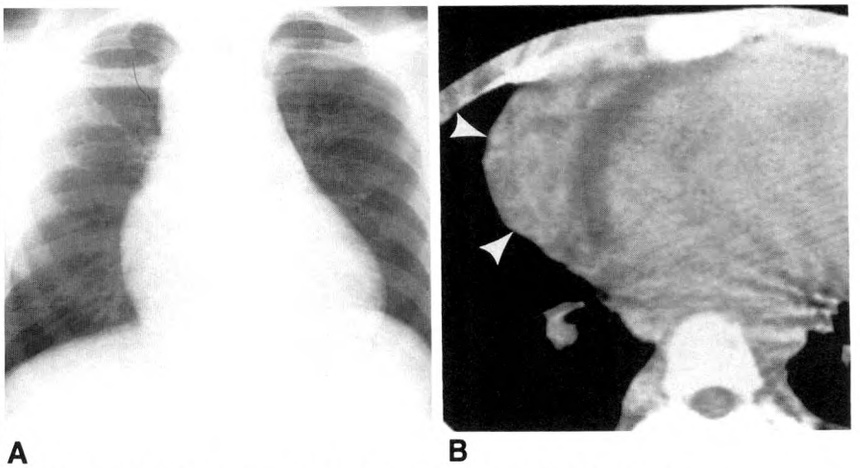


Fig. 8.—Multiple discrete nodes (*arrowheads*) encircle right heart border in patient with Hodgkin's disease.



A B

Fig. 9.—Adenopathy mimics cardiomegaly in patient with Hodgkin's disease.
A, Chest radiograph shows enlarged cardiac silhouette as well as prominent azygous and right paratracheal regions.
B, CT scan shows multiple "matted" nodes with lobulated appearance (*arrowheads*). 6 months later, after therapy, cardiac silhouette returned to normal, coinciding with resolution of paracardiac adenopathy detected on CT.

TABLE 1: Ancillary CT Findings in 45 Patients with Paracardiac Nodes

CT Findings	No. of Patients	
	Lymphoma (n = 18)	Nonlymphoma (n = 27)
Multiple nodes	10	6
Bilateral nodes	6	3
Node size:		
≤2 cm	6	22
>2 cm	12	5
Lobulated nodes	6	3
Other associated adenopathy	10	9
Pericardial thickening or effusion	5	2

neither of these two cases was biopsy proof obtained directly from these nodes. The mean lymph-node size for Hodgkin's lymphoma was 5.3 cm, and the mean size for non-Hodgkin's lymphoma was 2.5 cm.

A retrospective review of all chest radiographs obtained within 2 weeks of the CT scan is presented in Table 2. In only nine cases could a paracardiac mass be seen. In four of these cases, this finding was not mentioned in the original interpretation. The mean size of the largest node detected by CT in these nine cases was 5.4 cm, compared with a mean size of 2.6 cm in the patients with no mass detected on chest radiographs.

Discussion

Paracardiac lymph nodes is a general term for lymph nodes surrounding the heart. These lymph nodes consist of (1) nodes in the cardiophrenic angles, (2) nodes in the most caudal portion of the internal mammary chain, and (3) nodes along the pericardium [3]. *Paracardiac adenopathy* is somewhat misleading, as these nodes do not drain the myocardium. The lymphatics of the heart preferentially drain into anterior mediastinal nodes at the level of the transverse aortic arch [7].

The cardiophrenic-angle nodes were originally classified by Rouviere [6] and were described further by Castellino and Blank [8]. More recently, Glazer et al. [9] have added *superior diaphragmatic nodes* to the American Thoracic Society classification of regional nodes. These are nodes seen within 2 cm of the diaphragm, and they can be considered the equivalent to cardiophrenic-angle nodes. The cardiophrenic-angle nodes consist of two major groups, an anterior prepericardiac group and a lateropericardiac group (Fig. 1). The anterior prepericardiac group has a medial retroxiphoid component as well as paired lateral components. The anterior prepericardiac-node groups drain the diaphragm, liver, pleura, and anterior abdominal wall and empty into the internal mammary chain. The paired lateral component of the anterior prepericardiac group are the nodes that, when enlarged, produce a characteristic cardiophrenic-angle mass seen on frontal chest radiographs. The lateropericardiac group is located in the cardiophrenic angle more posteriorly at the position of the phrenic nerves. These nodal groups drain the diaphragm, liver, pleura, and pericardium and empty into the anterior mediastinal chain [3].

The internal mammary-lymph-node chain parallels the internal mammary vessels, extending up from the level of the diaphragm. Although the internal mammary lymph nodes are sparse near the diaphragm [10], the most inferior aspect of this chain should be considered paracardiac nodes. CT cannot consistently distinguish adenopathy in the most inferior aspect of the internal mammary chain from adenopathy in the

TABLE 2: Retrospective Review of Chest Radiographs in 38 Patients with Paracardiac Adenopathy and Chest Radiographs Obtained within 2 Weeks of CT Scan

Radiographic Rating	No. of Patients	CT Findings					
		No. with Multiple Nodes	No. with Single Nodes	Mean Size of Largest Node (cm)	No. with Small Nodes (≤2 cm)	No. with Intermediate (>2 cm, <4 cm)	No. with Large Nodes (≥4 cm)
1	23	5	18	2.6	15	2	6
2	6	1	5	4.6	1	3	2
3	9	5	4	5.4	2	2	5

Note.—1 = no paracardiac mass seen; 2 = equivocal, that is, a paracardiac mass could not be excluded because of overlying structures (such as effusion, collapse, and consolidation); 3 = paracardiac mass detected.

medial retroxiphoid component of the anterior prepericardiac group. Therefore, we group these nodes together as anterior prepericardiac nodes. In addition, lymph nodes sometimes may be present on the surface of the parietal pericardium and drain the central portion of the diaphragm [7].

We suggest 1 cm as an upper limit of normal for lymph-node size in the paracardiac region. Of the 50 patients studied who had neither an underlying malignancy nor a benign cause of lymphadenopathy, no patient showed a soft-tissue density greater than 3.5 mm in diameter. This conservative upper limit was chosen to decrease the number of false-positive examinations. Smaller nodes may be considered suspicious if multiple. A patient with colon carcinoma had a single 1-cm node as well as multiple other smaller adjacent nodes that presumably were abnormal (Fig. 5). Also, nodes larger than 1 cm are not necessarily caused by malignant processes. The two patients in our series with benign causes of paracardiac adenopathy (a patient with *Aspergillus* and a patient with histoplasmosis) had 1.5- and 1.0-cm nodes, respectively.

Paracardiac adenopathy is an uncommon finding, reported predominantly in patients with malignant lymphoma, both Hodgkin's and non-Hodgkin's [2–5]. Even within the subgroup of lymphoma patients, involvement in this area is said to occur in only 3%, although the incidence of paracardiac adenopathy during relapse may be somewhat higher [4, 8].

Reports of involvement of paracardiac lymph nodes by a process other than lymphoma are rare in the radiologic literature. Recently Vock and Houler [11] reported nine cases of nonlymphomatous cardiophrenic-angle adenopathy. Before this, there had been only a single report of two cases of nonlymphomatous cardiophrenic-angle adenopathy [12]. Our series clearly emphasizes that paracardiac adenopathy is not limited to only lymphoma patients, as in 60% of our cases the cause was nonlymphomatous, encompassing a wide range of causes.

On chest radiographs, the paracardiac area is difficult to evaluate, as detection of masses usually is possible only when a mass is large enough to project beyond the cardiac silhouette. In only five of the 38 patients in whom chest radiographs were obtained within 2 weeks of the CT scan was a paracardiac mass described on the original chest radiographic report. Retrospective review of the chest radiographs with specific attention to the paracardiac regions revealed another four patients in whom masses could be seen. This insensitivity of the chest radiograph was reiterated recently by Castellino et al. [13]; of 16 patients with Hodgkin's disease and cardiophrenic-angle adenopathy detected by CT, these nodes were detected on chest radiographs in only two patients. In our study there was a significant correlation between mass size and visibility on chest radiographs (Table 2). While larger masses are detected more frequently on chest radiographs, a small mass may be visible if positioned so that its edge is border-forming. Of the nine patients in whom paracardiac masses were seen in retrospect, three patients had masses measuring only 2 cm in diameter. On the other hand, the presence of a large mass does not ensure detection on chest radiographs—six of the 23 patients with normal paracardiac regions on chest radiographs had masses of 4 cm or greater in diameter on CT. In two of these patients large nodal masses blended with the cardiac silhouette mimicking cardiomegaly (Fig. 9) [14, 15]. All masses visible on chest radiographs were in the lateral components of the anterior prepericardiac group. No patients with only midline anterior prepericardiac or posterior nodes had masses visible on chest radiographs.

Patients with lymphoma and paracardiac adenopathy had a number of features that were helpful in differentiating them from patients with paracardiac adenopathy from nonlymphomatous causes (Table 1). Features favoring the diagnosis of lymphoma consisted of bilateral disease, multiple nodes greater than 2 cm in diameter, a lobulated appearance, and associated pericardial thickening/effusion.

Recognizing the presence of paracardiac adenopathy can be significant in terms of patient care. Paracardiac adenopathy was the only sign of active disease in some patients. In seven of the 18 patients with lymphoma, the paracardiac site was the only site of nodal involvement detected on the CT scans (chest CT in three patients, abdominal CT in three patients, and both chest and abdominal CT in one patient). In two of the three patients with recurrent carcinoid tumors, paracardiac adenopathy was the only evidence of disease detected by abdominal CT. In three of four patients with lung carcinoma, the paracardiac area was the only site of associated nodal disease. All six patients with colon carcinoma and paracardiac adenopathy underwent contrast-enhanced CT of the liver with 1-cm contiguous slices. Although liver metas-

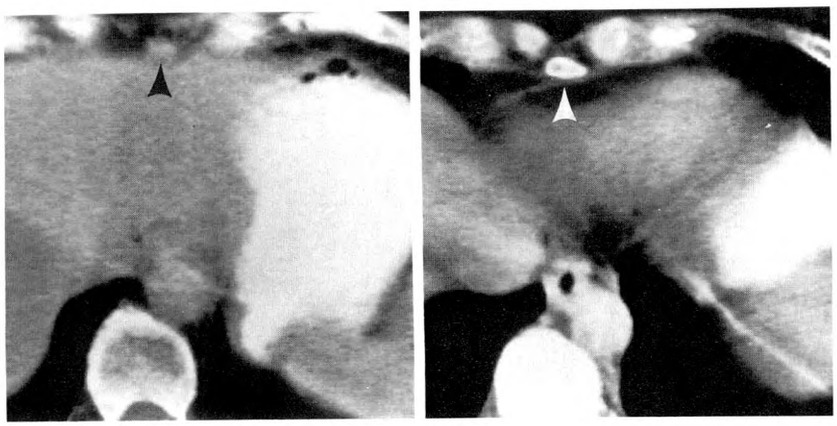


Fig. 10.—Partial volume of xiphoid tip mimicking paracardiac adenopathy.
***A*, Rounded soft-tissue density (*arrowhead*) is seen in midline at base of heart.**
***B*, Next slice cephalad shows that soft-tissue density is immediately contiguous with bony xiphoid tip (*arrowhead*) above.**

tases were seen in three patients, three showed adenopathy despite the lack of liver metastases detected by CT. Detecting the presence of paracardiac adenopathy may alter clinical treatment plans. A decision not to place an intrahepatic chemotherapy pump in the patient with a hepatoma was made on the basis of the presence of extrahepatic disease as evidenced by the paracardiac adenopathy. Castellino et al. [13] recently reported that the CT finding of cardiophrenic-angle nodes in patients with Hodgkin's disease had modified treatment in 18%. Such changes might include an increase in the radiotherapy dosage to the cardiophrenic angle or enlargement of treatment ports to encompass this previously unrecognized disease site [13].

In this study, only 11 of the 45 patients had biopsy proof directly from the paracardiac node. Of the other 34 patients, biopsy was not obtained from the paracardiac region, but from the primary tumor or infected site. Therefore, we cannot be sure that in these 34 patients the adenopathy was from underlying disease rather than from another unknown disease process, although the latter is unlikely. Another concern in those patients with enlarged paracardiac lymph nodes with biopsy proof only from other sites is that the lymph-node enlargement was from benign reactive hyperplasia rather than from neoplastic disease. Therefore, if an important therapeutic decision hinges on the cause of the nodal enlargement, one may need biopsy proof from the node itself.

Pitfalls in the diagnosis of paracardiac masses seen by us include lung parenchymal masses abutting the pericardium, loculated pericardial effusions, atelectatic lung abutting the pericardium, focal postoperative blood collections, partial volume of the xiphoid tip (Fig. 10), and a liver mass protruding up through the diaphragm, presumably through a foramen of Morgagni hernia.

A 1-cm upper limit of normal for lymph-node size in the paracardiac region may be used, although smaller nodes, if numerous, must be viewed with suspicion. In conclusion, paracardiac adenopathy may be caused by a wide variety of nonlymphomatous malignant and occasionally benign diseases.

ACKNOWLEDGMENT

We thank Janice Waters for secretarial assistance in preparing this manuscript.

REFERENCES

1. Cho CS, Blank N, Castellino RA. CT evaluation of cardiophrenic angle lymph nodes in patients with malignant lymphoma. *AJR* **1984**;143:719–721
2. Jochelson MS, Balikian JP, Mauch P, Liebman H. Peri- and paracardial involvement in lymphoma: a radiographic study in 11 cases. *AJR* **1983**;140:483–488
3. McLoud TC, Meyer JE. Mediastinal metastases. *Radiol Clin North Am* **1982**;20:453–467
4. Glazer GM, Gross BH, Quint LE, Francis IR, Bookstein FL, Orringer MB. Normal mediastinal lymph nodes: number and size according to American Thoracic Society mapping. *AJR* **1985**;144:261–265
5. Meyer JE, McLoud TC, Lindfors KK. CT demonstration of cardiophrenic angle lymphadenopathy in Hodgkin disease. *J Comput Assist Tomogr* **1985**;9:485–488
6. Rouviere H. *Anatomy of the human lymphatic system* (a compendium translated from the original by Tobias MJ). Ann Arbor, MI: Edward Grothers, **1938**:86–88
7. Weinberg JA. The intrathoracic lymphatics. In: Haggensen CD, Feind CR, Herter FP, Slanetz CA, Weinberg JA, eds. *The lymphatics in cancer*. Philadelphia: Saunders, **1972**:231–245
8. Castellino RA, Blank N. Adenopathy of the cardiophrenic angle (diaphragmatic) lymph nodes. *AJR* **1972**;114:509–515
9. Glazer HS, Aronberg DJ, Sagel SS, Friedman PJ. CT demonstration of calcified mediastinal lymph nodes: a guide to the new ATS classification. *AJR* **1986**;147:17–25
10. Lein HH, Lund G. Computed tomography of mediastinal lymph nodes. *Acta Radiol [Diagn] (Stockh)* **1985**;26:641–647
11. Vock P, Houler J. Cardiophrenic angle adenopathy: update of causes and significance. *Radiology* **1986**;159:395–399
12. Bledin A, Bernardino ME, Libshitz HI. Cardiophrenic angle nodes: an unusual CT finding of advanced metastatic disease. *J Comput Tomogr* **1980**;4:193–198
13. Castellino RA, Blank N, Hoppe RT, Cho C. Hodgkin disease: contributions of chest CT in the initial staging evaluation. *Radiology* **1986**;160:603–605
14. Anglelini GD, Butchart EG. Lymphoma mimicking cardiomegaly. *Thorax* **1984**;39:72–73
15. Crowe JE. Cardiophrenic adenopathy in Hodgkin's disease. *Am J Dis Child* **1975**;129:116–117

Mammographic Changes After Reduction Mammoplasty

Cynthia L. Miller[1]
Stephen A. Feig[1]
James W. Fox IV[2]

Mammograms obtained in 24 patients after reduction mammoplasty were reviewed retrospectively to define the mammographic findings seen after this procedure. Nine characteristics were found. The most frequent findings were skin thickening and retraction of the lower portion of the breast, transposition of breast parenchyma from a high to a low position, and a high nipple. The image characteristics were then correlated with the surgical type of mammoplasty performed, that is, dermal transposition of the nipple vs full-thickness nipple-areolar graft. All patients who had dermal transposition had complete or partial preservation of continuity between the subareolar ducts and the nipple. Patients who had nipple-areolar grafts showed either disruption of the subareolar ducts or very fatty breasts without visible ductal tissue.

Reduction mammoplasty produces characteristic and predictable mammographic changes.

The role of mammography in association with plastic surgery of the breasts has been confined predominantly to augmentation mammoplasty and to screening before breast surgery in patients over 35 years old [1]. Mammographic findings after reduction mammoplasty have been described only briefly in the surgical literature [2].

Reduction mammoplasty is becoming more popular. Since the establishment and increasing acceptance of the American College of Radiology's guidelines for screening the general population, radiologists are more likely to encounter mammograms of reduced breasts. Reduction mammoplasty is usually performed to improve cosmetically bilateral macromastia or to achieve a symmetric result after mastectomy and reconstruction of a cancerous breast. The patients included in our study had one of two procedures: pedicle flaps with dermal nipple transposition or pedicle flaps with full-thickness nipple-areolar grafts. The mammographic changes were evaluated and correlated with the surgical type of mammoplasty performed.

Surgical Technique

Although there are many techniques for reduction mammoplasty, all include nipple elevation, glandular resection, and contouring of skin removal. In the transposition procedure, the nipple areolar complex remains connected to its subareolar ducts. In the transplantation procedure, a full-thickness nipple-areolar graft is severed from its underlying ducts.

In both procedures a keyhole pattern is drawn on the patient's breasts preoperatively (Fig. 1A). The top of the "keyhole" outlines the new position for the nipple. The design creates medial and lateral skin flaps that provide support for the new breast. The area within the keyhole is deepithelialized, sparing the areola. This creates a vertically oriented dermal pedicle flap. The medial and lateral triangles, formed by the inferior dermal pedicle medially, the medial and lateral skin flaps superiorly, and the inframammary fold inferiorly, are resected (skin, breast, and fat). This constitutes most of the glandular resection of the mammoplasty. The superior pedicle is then folded on itself, thereby elevating the nipple to its new position

Received December 15, 1986; accepted after revision March 10, 1987.

[1] Department of Radiology, Thomas Jefferson University Hospital, 111 S. 11th St., Philadelphia, PA 19107. Address reprint requests to C. L. Miller.

[2] Department of Surgery, Thomas Jefferson University Hospital, Philadelphia, PA 19107.

AJR **149:35–38, July 1987**
0361–803X/87/1491–0035
© American Roentgen Ray Society

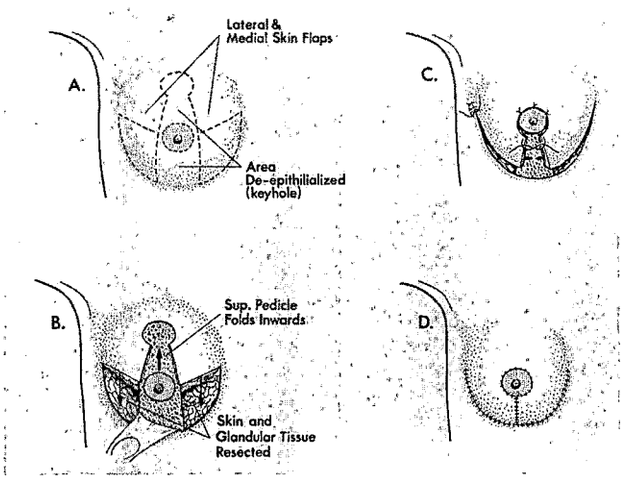


Fig. 1.—Surgical technique of reduction mammoplasty. Sup. = superior. (See text for description of *A–D*.)

in the upper keyhole (Fig. 1B). The medial and lateral skin flaps are then brought together below the nipple, followed by closure of the inframammary wound (Figs. 1C and 1D). The transposition mammoplasty performed at our institution follows the modifications described by McKissock [3] and Strombeck [4].

In larger breasts and in women beyond childbearing years, the transplantation procedure is preferred because it carries less risk of avascular necrosis of the nipple [5].

Materials and Methods

The mammograms of 24 women who had undergone reduction mammoplasty at Thomas Jefferson University Hospital were reviewed to determine the mammographic changes and to correlate these with the surgical procedures. The interval between the surgery and the mammogram was longer than 6 months in all cases. The patients were 32–68 years old. In six cases unilateral mammograms were obtained in patients with cancer of the opposite breast; 18 patients had had bilateral reduction mammoplasties. Ten patients (19 breasts) had had nipple transplantation, and 14 patients (23 breasts) had had dermal transposition. Two radiologists viewed the mammograms together and were in agreement when a positive rating was given in a category. Nine characteristic changes were identified.

Results

The results are summarized in Table 1. Some patients exhibited many characteristics whereas others showed only one characteristic.

The most striking finding was a downward shift of the ductal and fibroglandular tissue, as seen on the mediolateral view (Figs. 2 and 3). Ten of our cases showed most fibroglandular tissue below the level of the nipple, an appearance distinctly altered from the normal breast, where most of the ductal and fibroglandular tissue generally is concentrated in the upper outer quadrants.

An elevation of the nipple with respect to the skin circumference of the breast was seen on the mediolateral view in nine cases. Compared with the normal breast, less skin was above the nipple and more skin was below it (Fig. 2). In addition, the nipple was seen to be directed upward in two cases bilaterally and in three cases unilaterally (Fig. 2).

TABLE 1: Mammographic Changes According to Mammoplasty Type

Mammographic Change	No. of Patients	
	Transposition (n = 14)	Transplantation (n = 10)
Parenchymal redistribution	6	4
High nipple	5	4
Nipple tilt	5	0
Retroareolar band	7	1
Areolar thickening	9	6
Areolar calcification	1	2
Skin thickening, lower breast	3	7
Retraction, lower breast	3	6
Continuity of subareolar ducts:		
Continuous	13	0
Discontinuous	0	4
90–100% fatty breast	1	6

Skin thickening of the lower breast was seen in 10 cases. Skin thickening is caused by the vertical scar that runs between the nipple and inframammary fold (Fig. 1D). Skin retraction was present in nine cases (Fig. 3). Except for one case of mild retraction, all of these cases were associated with skin thickening.

Thickening of the skin of the areola was present in 15 patients. A skin thickness of greater than 3 mm was considered abnormal (Fig. 2). Three patients had 1- to 2-mm skin calcifications scattered in a random distribution in the areola (Fig. 4). Two patients had bilateral calcifications; the third patient had only one remaining breast. These postsurgical calcifications all had a benign appearance.

Another characteristic finding was the presence of a retroareolar fibrotic band about 0.5-cm thick and parallel to the skin contour. The retroareolar band usually was seen best on the craniocaudal view (Fig. 5) and was observed in eight patients; seven of these had had transposition procedures.

Disruption of the subareolar ducts was seen in four of the 10 patients who had undergone nipple transplantation. The ducts were seen to terminate abruptly within fatty tissue deep to the nipple (Fig. 6). In the other six cases, insufficient ductal tissue was present for evaluation. In contrast, all but one of the patients with nipple transposition surgery had mammographic continuity between the subareolar ducts and the nipple (Fig. 7). The one exception was in a fatty breast that had little remaining ductal tissue. Two cases showed a typical convergence of all of the ducts leading into the nipple and 11 showed continuity of only some ducts with the nipple.

Discussion

The mammographic findings after reduction mammoplasty are predictable. Transposition of parenchyma to an unusually

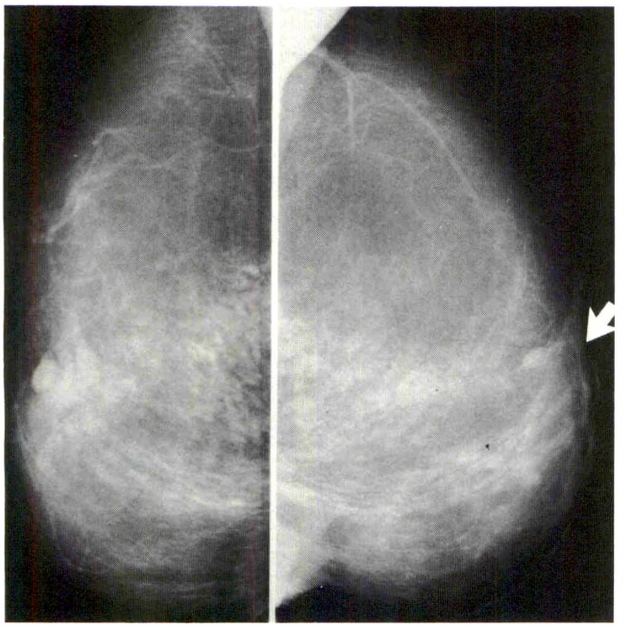


Fig. 2.—Transposition. Mediolateral views, right and left breasts of same patient. Note preponderance of fibroglandular tissue in lower half of breast. Thickening of right areola (*arrow*). Nipples, which are tilted up, occupy a high position. Ducts in inferior breasts connect with nipple, typical of transposition-type surgery.

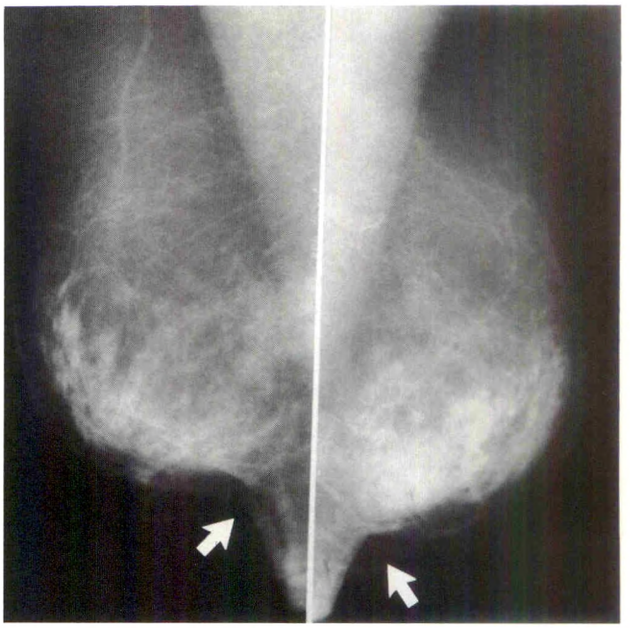


Fig. 3.—Transplantation. Mediolateral views, right and left breasts of same patient. Abrupt discontinuity between glandular tissue and nipple. Skin retraction of lower breast is severe (*arrows*). Remaining parenchyma is shifted to lower part of breast.

low position is explained by a relative shift with respect to the nipple. The new nipple site in a ptotic breast has little parenchyma behind it inasmuch as most of the parenchyma is shifted to the dependent portion of the breast.

All patients are left with a linear vertical scar between the nipple and inframammary fold (Fig. 1D). This accounts for the frequent finding of skin thickening of the lower breast.

In all types of mammoplasty, the areola is sutured circum-

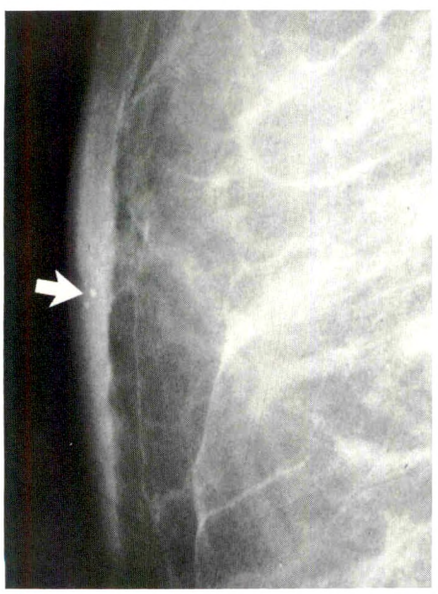


Fig. 4.—Transplantation. Craniocaudal view, magnification. Note punctate, benign-appearing areolar calcifications (*arrow*).

4

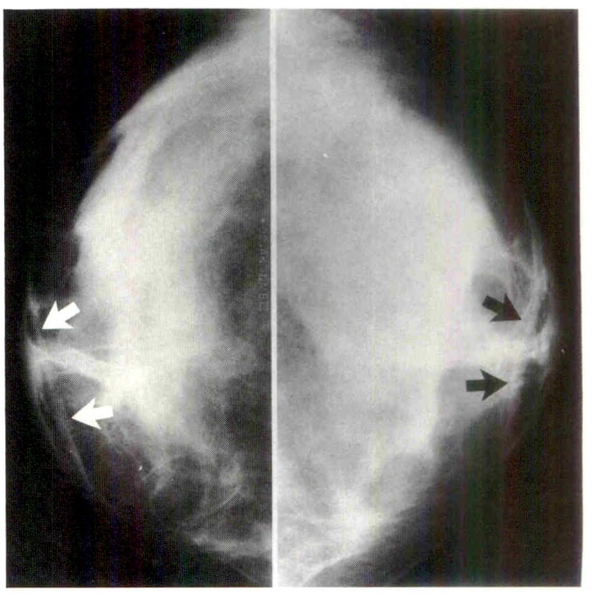


Fig. 5.—Transposition. Craniocaudal view. Subareolar ducts connect to nipple. Note thick, retroareolar bands (*arrows*).

5

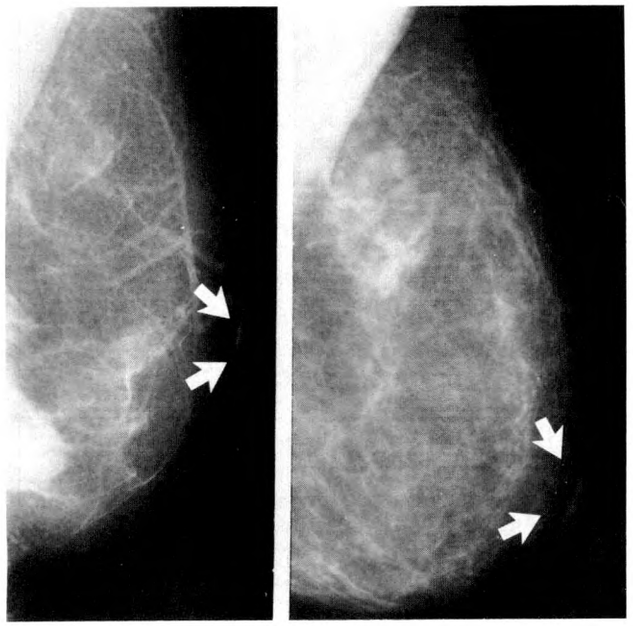


Fig. 6.—Transplantation. Mediolateral views, different patients. Subareolar area is occupied by fat (*arrows*) after transplantation.

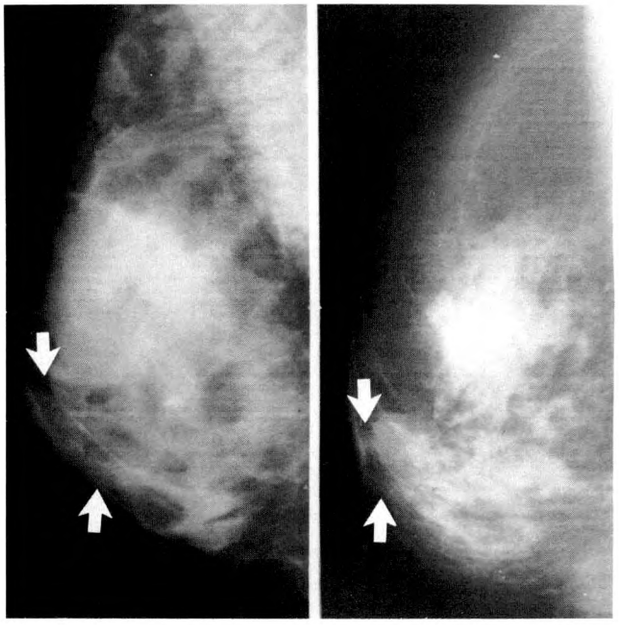


Fig. 7.—Transposition. Mediolateral views, different patients. Transposition-type surgery has maintained subareolar duct continuity (*arrows*).

ferentially into its new site. The thickened areola is related to the suture line surrounding the areola. Fat necrosis after reduction mammoplasty, presenting as irregular partially calcified masses, has been reported [6] but was not encountered in our series.

The status of the subareolar ducts correlated well with the type of mammoplasty (Figs. 6 and 7). In a dermal transposition procedure, the subareolar ducts are left intact and connect with the nipple. In the transplantation procedure, the subareolar ducts are transected. Mammography of these patients showed ducts that were either disrupted or not visible at all. The transplantation technique is the procedure of choice for reducing large breasts by more than two or three brassiere sizes. In the transplantation group, we found fatty breasts in which the ducts were often atretic or absent.

With increased use of this surgical procedure and the widespread implementation of mammographic screening, it is likely that mammographers will see an increasing number of patients who have undergone reduction mammoplasty. A postreduction mammogram would aid in the interpretation of subsequent annual screening mammograms in this patient population.

REFERENCES

1. Perras C, Papillon J. The value of mammography in cosmetic surgery of the breasts. *Plast Reconstr Surg* **1973**;52:132–137
2. Isaacs G, Rozner L, Tudball C. Breast lumps after reduction mammaplasty. *Ann Plast Surg* **1985**;15:394–399
3. McKissock PK. Correction of macromastia by the bipedicle vertical dermal flap. In: Goldwyn RM, ed. *Plastic and reconstructive surgery of the breast*. Boston: Little, Brown **1976**;215–229
4. Strombeck JO. Mammaplasty: report of a new technique based on the two-pedicle procedure. *Br J Plast Surg* **1961**;13:79–90
5. Wise RJ, Gannon JP, Hill JR. Further experience with reduction mammaplasty. *Plast Reconstr Surg* **1963**;32:12–20
6. Baber CE, Libshitz HI. Bilateral fat necrosis of the breast following reduction mammoplasties. *AJR* **1977**;128:508–509

Localization of Breast Lesions Identified on Only One Mammographic View

Daniel B. Kopans[1]
Ellen D. Waitzkin[1]
Lidia Linetsky[1]
Cynthia A. Swann[1, 2]
Kathleen A. McCarthy[1]
Deborah A. Hall[1]
George White[1]

Occasionally, a breast lesion is visible in only one mammographic projection. A simplified method of using parallax in a dedicated mammographic system has been devised to locate accurately lesions that are not visible in two orthogonal projections. In eight patients, a parallax approach from essentially a single mammographic position was used to place a hookwire preoperatively at nonpalpable suspicious abnormalities detected by mammography. Needles were inserted parallel to the chest wall while the breast was compressed in the mammographic unit. In each case, the tissue containing the lesion was pierced by a needle chosen to be longer than the distance from the skin to the abnormality. Simple geometric ratios were used to determine the position of the lesion along the needle shaft after slightly changing the mammographic projection and viewing the needle obliquely.

In all cases, this parallax approach permitted accurate localization of the lesion.

The use of dedicated mammographic equipment has led to a marked improvement in mammography. The need to compress the breast for optimal film/screen imaging has required modifications in localization techniques that have led ultimately to safer, more accurate placement of needles and guidewires [1]. Occasionally, a lesion is encountered that cannot be imaged on 90° projections. Such a lesion poses a challenge. We previously have described methods to triangulate and preoperatively locate such difficult lesions by using sonography or CT of the breast [2, 3]. On rare occasions, however, a lesion visible in only one mammographic view is not amenable to localization by these methods. Some clustered microcalcifications, for example, will not be visible on CT because of volume averaging, and sonography cannot detect microcalcifications. We have devised a simple but quite accurate method for the localization of such lesions.

Subjects and Methods

In eight patients with nonpalpable mammographically detected lesions, we undertook preoperative radiographically guided localization from essentially a single mammographic position. Seven of the eight lesions were visible in orthogonal projections, but because the new technique required the same number of exposures as our standard procedure, the lesions were located by using the parallax technique. The eighth lesion, a small cluster of calcifications, was visible only in the mediolateral oblique and straight lateral view. It could not be seen in the craniocaudal projection and could be located only by using this new technique.

All localizations were performed by using a dedicated mammography unit (Model 500T, Thomson-CGR Medical Corp., Columbia, MD) and the DKBL-A 20-gauge springhook wire localization guide (Cook, Inc., Bloomington, IN). The localizations were begun by using our standard approaches parallel to the chest wall with the breast compressed between a fenestrated compression plate and cassette holder [1]. The breast was positioned so that the lesion would project within the opening in the compression plate (Fig. 1). Needles were selected to be longer than the distance to the lesion from the skin surface should the breast be compressed in the orthogonal projection. This was to ensure that the lesion could be

Received October 10, 1986; accepted after revision March 25, 1987.

[1] Department of Radiology and the Cancer Center, Massachusetts General Hospital, 32 Fruit St., Boston, MA 02114 and Harvard Medical School, Boston, MA 02115. Address reprint requests to D. B. Kopans, Department of Radiology and the Cancer Center, Massachusetts General Hospital, 32 Fruit St., Boston, MA 02114.

[2] Present address: Department of Radiology, Holy Cross Hospital of Silver Spring, 1500 Forest Glen Rd., Silver Spring, MD 20910.

***AJR* 149:39–41, July 1987**
0361–803X/87/1491-0039
© American Roentgen Ray Society

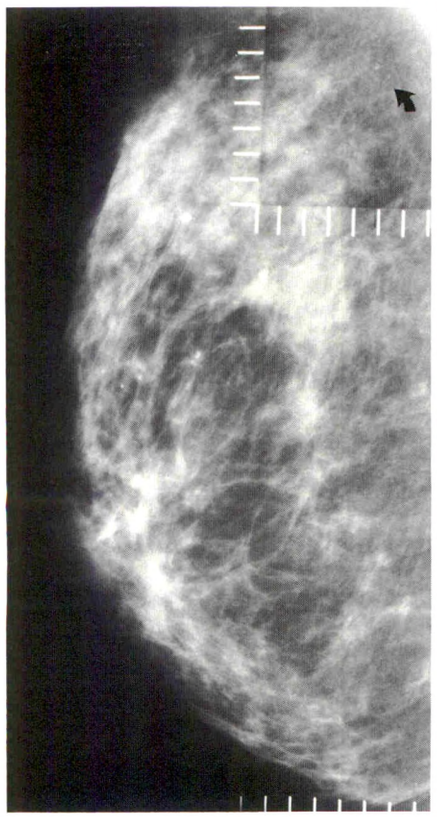


Fig. 1.—Mammogram shows microcalcifications (*arrow*) in upper left breast in window of compression plate.

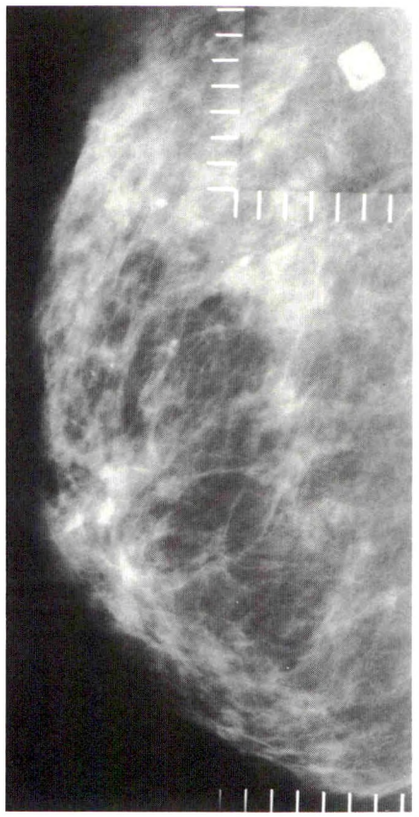


Fig. 2.—Mammogram shows view looking down needle, which is superimposed on calcifications.

1 2

transfixed along the shaft of the needle. All needles were introduced parallel to the chest wall in the direction of the X-ray beam.

In all eight patients, the hub of the needle was superimposed on the shaft of the needle, and this in turn was superimposed on the lesion. This guaranteed that the lesion would be within 5 mm of the shaft of the needle.

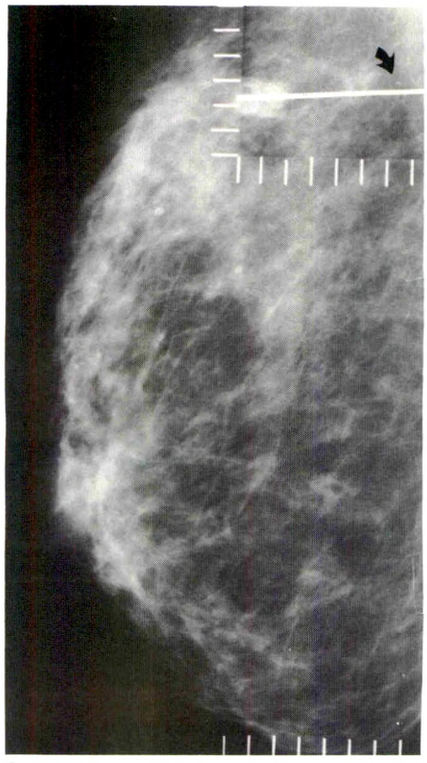
With the patient remaining in compression, the superimpositions were confirmed by a mammogram (Fig. 2), and then, without removing the patient from the mammographic unit, the compression was relaxed. The needle was kept within the window of the compression plate, and the breast was repositioned slightly and then recompressed so that the needle was oblique to the X-ray beam. The degree of obliquity was not important. A mammogram obtained in this orientation produced a foreshortened projection of the entire needle and the lesion along its shaft (Fig. 3). By noting that the true distance of the lesion from the tip of the needle bears the same relationship to its projected distance from the tip as the true length of the needle does to its projected length (Fig. 4), we were able to determine the actual distance beyond the lesion that we had passed the needle. We then pulled the needle back this distance and afterloaded the hookwire and engaged it at the proper depth (Fig. 5).

Results

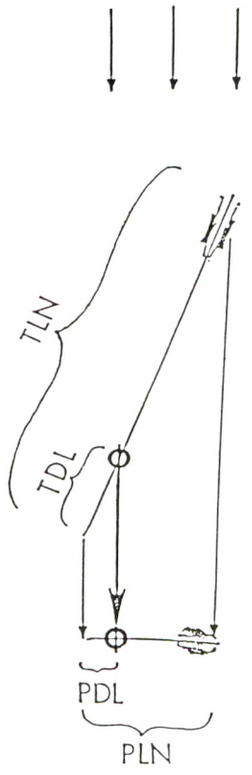
All eight lesions were located successfully by using this technique. In seven of the eight cases, the position of the lesion along the wire was confirmed by obtaining a final image in the orthogonal projection perpendicular to the wire. In these cases, the lesion was no more than 5 mm from the wire and was positioned optimally along the thickened segment of the wire 1 cm proximal to the hook. The eighth lesion was very close to the pectoralis fascia and was too deep to be seen in the orthogonal projection. However, the location of the calcifications was confirmed by using this parallax technique (Fig. 5), and at surgery the calcifications were found along the thickened segment of wire.

Discussion

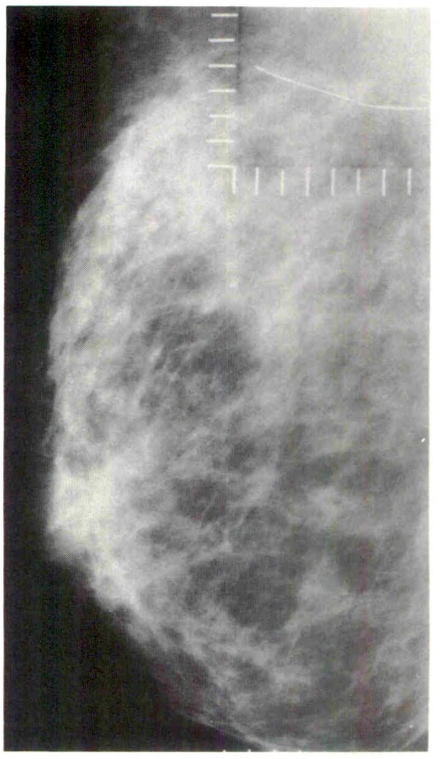
Localization of a lesion requires knowledge of the lesion's general position. This is accomplished most easily by seeing a lesion in two mammographic projections that are orthogonal to each other. However, when this is not possible, the three-dimensional location of the lesion can be narrowed down to the medial, mid, or lateral third of the breast by noting the lesion's projected shift between two mammographic positions that are at slightly different angles. For example, by obtaining a straight lateral mammogram and a mediolateral oblique view, the apparent shift of the lesion between these two projections can be observed [4]. A lesion in the lateral aspect of the breast will appear to move up within the breast between the straight lateral and mediolateral oblique views, whereas a lesion located medially in the breast will appear to move down when these two views are compared. By knowing which third



3



4



5

Fig. 3.—Mammogram shows how recompression projects needle obliquely. Calcifications are visible along shaft (*arrow*).

Fig. 4.—Schematic drawing shows simple geometric relationship between true needle and lesion relative to projected lesion and projection of needle. TDL = True distance of lesion from needle tip; this is distance needle must be pulled back to position its tip in the lesion. TLN = True length of needle. PLN = Projected length of needle. PDL = Projected distance of lesion from needle tip. Because TLN, PLN, and PDL are known lengths, TDL can be calculated by the following equation: TDL = (TLN/PLN) × PDL.

Fig. 5.—Mammogram shows hookwire projected at an oblique angle at calcifications.

of the breast the lesion is in, one can choose an appropriate needle that is longer than the expected distance to the lesion. Once the lesion is along the shaft of the needle, this parallax technique and simple geometry can be used to determine the true distance.

This technique is slightly more complicated than our usual procedure, but it provides a method for positioning guides at lesions that are not visible in 90° projections. Because of beam divergence, the ratios are not exact, but with long source-to-image distances this lack does not, in practice, affect accuracy.

Measurements of the true length of the needle must take into account that the projected needle includes the entire shaft. If, for example, springhook wires are used, the 9-cm needle actually measures 11.4 cm from the point to the proximal end. This number is used in the calculations.

When using this parallax technique, one also must be aware that the breast is compressed when the hook is engaged. The breast will reexpand when uncompressed, and the hook will move with the tissue volume in which it is engaged. Because of this basic elasticity, distances are amplified with reexpansion. To account for this, the needle tip should be pulled back to the lesion to engage the hook of the wire at the lesion. Then, when the breast reexpands, the lesion will be at or proximal to the hook along the thick segment.

REFERENCES

1. Kopans DB, Meyer JE, Lindfors KK, McCarthy KA. Spring-hookwire breast lesion localizer: use with rigid compression mammographic systems. *Radiology* **1985**;157:505–507
2. Kopans DB, Meyer JE, Lindfors KK, Bucchianeri SS. Breast sonography to guide cyst aspiration and wire localization of occult solid lesions. *AJR* **1984**;143:489–492
3. Kopans DB, Meyer JE. Computed tomography guided localization of clinically occult breast carcinoma: the "N" skin guide. *Radiology* **1982**;145:211–212
4. Swann CA, Kopans DB, McCarthy KA, White G, Hall DA. Localization of occult breast lesions: practical solutions to problems of triangulation. *Radiology* **1987**;163:577–578

FORTHCOMING ARTICLES

BILIARY LITHOTRIPSY

Perspective. Biliary lithotripsy—what will the issues be? *Ferrucci JT*

Perspective. The promise of extracorporeal shock-wave lithotripsy for the treatment of gallstones. *Burhenne HJ*

CARDIOPULMONARY RADIOLOGY

Measurement of myocardial infarct size using MR imaging: an experimental study in dogs. *Caputo GR, Sechtem U, Tscholakoff D, Higgins CB*

Instant images of the human heart using a new, whole-body MR imaging system. *Rzedzian RR, Pykett IL*

Vascular rings: MR imaging. *Bisset GS III, Strife JL, Kirks DR, Bailey WW*

Reliability of selective pulmonary arteriography in the diagnosis of pulmonary embolism. *Quinn MF, Lundell CJ, Klotz TA, et al.*

Penetrating injuries of the thoracic aorta and brachiocephalic arteries: angiographic findings in eighteen cases. *Fisher RG, Ben-Menachem Y*

Giant right atrium after mitral valve replacement: plain film findings in 15 patients. *Rubin SA, Hightower CW, Flicker S*

Case report. Compression of left main bronchus and left pulmonary artery by thoracic aortic aneurysm. *Duke RA, Barrett MR II, Payne SD, Salazar JE, Winer-Muram HT, Tonkin ILD*

Nonspecific interstitial pneumonitis in patients with AIDS: radiologic features. *Simmons JT, Suffredini AF, Lack EE, et al.*

Thymic atrophy and regrowth in response to chemotherapy: CT evaluation. *Choyke PL, Zeman RK, Gootenberg JE, Greenberg JN, Hoffer F, Frank JA*

Case report. Congenital absence of the azygos vein: a cause for "aortic nipple" enlargement. *Hatfield MK, Vyborny CJ, MacMahon H, Chessare JW*

Evaluation of optical unsharp masking and contrast enhancement of low-scatter chest radiographs. *Sorenson JA, Mitchell CR*

BREAST RADIOLOGY

Two-view specimen radiography in surgical biopsy of nonpalpable breast masses. *Rebner M, Pennes DR, Baker DE, Adler DD, Boyd P*

GASTROINTESTINAL RADIOLOGY

Pictorial essay. Imaging of surgically relevant hepatic vascular and segmental anatomy. Part I. Normal anatomy. *Mukai JK, Stack CM, Turner DA, et al.*

Pictorial essay. Imaging of surgically relevant hepatic vascular and segmental anatomy. Part II. Extent and resectability of hepatic neoplasms. *Mukai JK, Stack CM, Turner DA, et al.*

Abdominal sonography after hepatic transplantation: results in 36 patients. *Letourneau JG, Day DL, Ascher NL, et al.*

Case report. Gallium-67 detection of occult gastric lymphoma in AIDS. *Gianfelice D, Rosenthall L, Falutz J*

Esophageal radiography and manometry: correlation in 172 patients with dysphagia. *Ott DJ, Richter JE, Chen YM, Wu WC, Gelfand DW, Castell DO*

GENITOURINARY RADIOLOGY

Case report. Urethroplasty with balloon catheter in prostatic hypertrophy. *Castaneda F, Johnson S, Hulbert J, et al.*

The accuracy of CT in the staging of carcinoma of the prostate. *Platt JF, Bree RL, Schwab RE*

Case report. Control of postoperative vaginal hemorrhage by embolization of the medial circumflex femoral artery. *Odurny A, Colapinto RF*

Case report. Duplex Doppler evaluation of puerperal ovarian vein thrombosis. *Baran GW, Frisch KM*

MUSCULOSKELETAL RADIOLOGY

Vertebral erosions in patients undergoing maintenance hemodialysis for chronic renal failure. *Sundaram M, Seelig R, Pohl D*

Stress fractures of the distal tibia and calcaneus subsequent to acute fractures of the tibia and fibula. *Zlatkin MB, Bjorkengren A, Sartoris DJ, Resnick D*

MR imaging of marrow changes adjacent to end plates in degenerative lumbar disk disease. *de Roos A, Kressel H, Spritzer C, Dalinka M*

MR imaging of the shoulder: diagnosis of rotator cuff tears. *Kneeland JB, Middleton WD, Carrera GF, et al.*

Skeletal measurements using a flying spot digital imaging device. *Wilson AJ, Ramsby GR*

Percutaneous biopsy of the cervical spine using CT guidance. *Kattapuram SV, Rosenthal DI*

Technical note. A device for maintaining cervical spine stabilization and traction during CT scanning. *Stimac GK, Burch D, Livingston RR, Anderson P, Dacey RG*

PALEORADIOLOGY

Arctic paleoradiology: portable radiographic examination of two frozen sailors from the Franklin Expedition (1845–1848). *Notman DNH, Anderson L, Beattie OB, Amy R*

NEURORADIOLOGY

MR signal abnormalities at 1.5 T in Alzheimer's dementia and normal aging. *Fazekas F, Chawluk JB, Alavi A, Hurtig HI, Zimmerman RA*

Reduced signal intensity on MR images of thalamus and putamen in multiple sclerosis: increased iron content. *Drayer B, Burger P, Hurwitz B, Dawson D, Cain J*

Study of movement disorders and brain iron by MR. *Rutledge JN, Hilal SK, Silver AJ, Defendini R, Fahn S*

MR of craniopharyngiomas: tumor delineation and characterization. *Pusey E, Kortman KE, Flannigan BD, Tsuruda J, Bradley WG*

Adverse reactions after iohexol lumbar myelography: influence of postprocedural positioning. *Kuuliala IK, Göransson HJ*

Technical note. New needle for MR-guided aspiration cytology of the head and neck. *Lufkin R, Teresi L, Hanafee W*

PEDIATRIC RADIOLOGY

Hepatic regenerating nodules in hereditary tyrosinemia. *Day DL, Letourneau JG, Allan BT, et al.*

Anorectal atresia: prenatal sonographic diagnosis. *Harris RD, Nyberg DA, Mack LA, Weinberger E*

Sonographic measurements of the normal bladder wall in children. *Jequier S, Rousseau O*

Case report. Gallbladder contraction in biliary atresia. *Weinberger E, Blumhagen JD, Odell JM*

The coexistence of obstruction at the ureteropelvic and ureterovesical junctions. *McGrath MA, Estroff J, Lebowitz RL*

Multicystic dysplasia and crossed renal ectopia. *Nussbaum AR, Hartman DS, Whitley N, McCauley RGK, Sanders RC*

TECHNICAL DEVELOPMENTS

Technical note. Use of light localizer in fluoroscopically guided percutaneous procedures. *Hayt DB*

COMPUTER PAGE

Computerized reference management—filing the literature. *Gurney JW, Wigton RS*

RESIDENT EDUCATION

Instruction in image processing for residents in diagnostic radiology. *Huang HK, Bassett LW, Mankovich N, Cho P, Kangarloo H, Seeger L*

PERSPECTIVE

Women in academic radiology. *Whitley NO*

Preoperative Needle Localization of Lesions in the Lower Half of the Breast:

Needle Entry from Below

Marc J. Homer[1]

For preoperative localization of lesions in the lower part of the breast, an inferior approach provides the shortest skin-to-lesion distance. This paper describes the successful inferior approach in 48 of 49 consecutive localizations. No special grid localization device is needed. This technique permits accurate localization of small foci of microcalcifications and other nonpalpable breast lesions.

Since most of the new mammography units are equipped with some type of grid localization device, preoperative needle localization for nonpalpable breast lesions has become technically feasible. However, for lesions in the lower portion of the breast, where the shortest approach might be from below, these devices are awkward to use. Since 1977, I have been localizing all lesions in the lower third of the breast via an inferior approach with the needle entering essentially parallel to the chest wall with slight angulation. The purpose of this communication is to review this 10-year experience.

Materials and Methods

Between the period of July 1977 and September 1986, a total of 287 percutaneous needle localizations were performed for nonpalpable mammographic abnormalities. Of these, 234 employed a superior approach, three used a lateral approach, and one needle was placed obliquely under sonographic guidance. The remaining 49 localizations were performed using an inferior approach, and they form the basis of this report. One of two needle-wire systems were used: either the curve-end retractable wire [1] or a needle hook-wire system [2]. All specimens were radiographed to document complete excision of the lesion.

The position of the lesion relative to the nipple is measured from the craniocaudad view. Posterior and medial or lateral coordinates can be taken from the original mammogram if the nipple is in profile. A small metallic marker is taped to the undersurface of the breast at the site of the lesion. A mammogram is then obtained in the craniocaudad projection with enough compression to eliminate patient motion and visualize the lesion (Fig. 1). If the metallic marker is not within 1 cm of the lesion, it is repositioned and the craniocaudad view is repeated. Then, without removal of the marker, a lateral view is obtained, again with an appropriate degree of compression (Fig. 2). The marker is then removed after its position is marked with indelible ink. This marks the entry site of the needle. Its relationship to the lesion determines the precise depth of the lesion from the skin as well as the degree of needle angulation required. The patient is now placed supine on a stretcher, and the area is prepped and draped in the usual fashion. While holding the breast and manually compressing it with one hand, the needle is angled appropriately either ventrally or dorsally and poised parallel to the sagittal plane (Fig. 3). When these two directions appear to be visually correct, the needle is inserted. The patient is helped off the stretcher, and postlocalization craniocaudad (Fig. 4) and lateral (Fig. 5) mammograms are obtained. If repositioning is necessary, it is done with the patient again lying supine on the stretcher with the breast compressed manually as described above. All specimens are radiographed to verify complete excision of the lesion (Fig. 6).

Received September 10, 1986; accepted after revision March 17, 1987.

[1] Department of Radiology, New England Medical Center and The Tufts University School of Medicine, Boston, MA 02111. Address reprint requests to M. J. Homer, Mammography Section, Box 388, Dept. of Radiology, New England Medical Center, 750 Washington St., Boston, MA 02111.

AJR 149:43–45, July 1987
0361–803X/87/1491–0043
© American Roentgen Ray Society

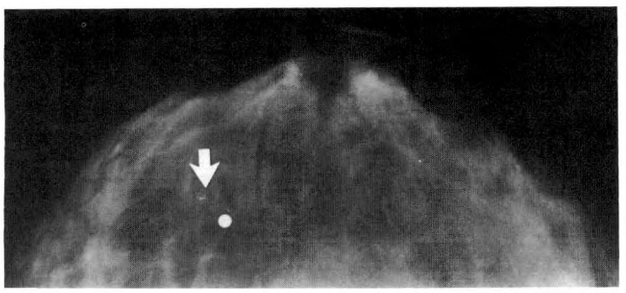


Fig. 1.—Needle localization was performed on a geographic cluster of microcalcifications located in lower outer quadrant. Metallic marker taped on undersurface of breast projects over geographic cluster of microcalcifications (*arrow*) on craniocaudad view.



Fig. 2.—A lateral view was then obtained. In lateral compression geometry, distance of lesion (*arrow*) from skin is A and angle θ represents angle of needle relative to horizontal plane.

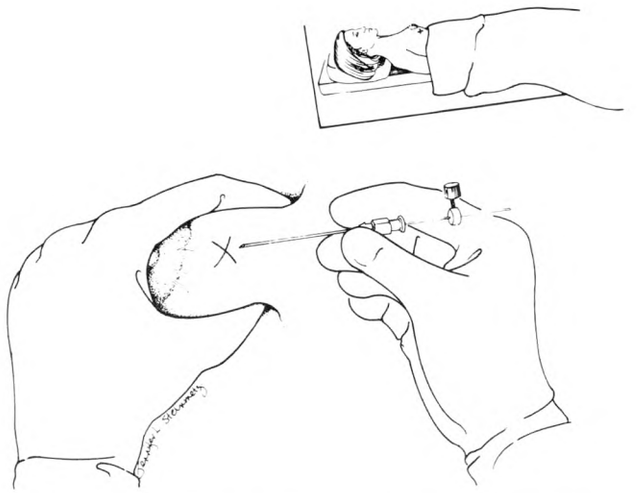


Fig. 3.—Positions of patient and physician during needle insertion are shown. With patient lying supine on a stretcher, physician holds localization needle with one hand and the breast with the other to simulate lateral compression geometry as needle is inserted.

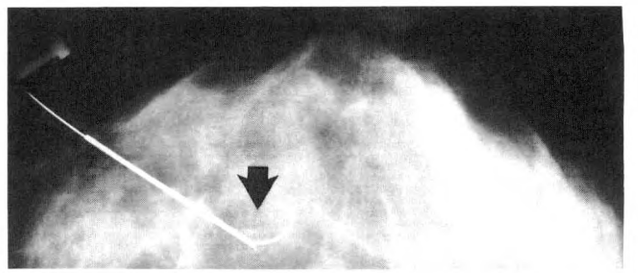


Fig. 4.—Craniocaudad postlocalization film confirms close proximity of microcalcifications (*arrow*) to wire. Needle-wire system, although inserted parallel to sagittal plane, appears to be at a slight angle because of moderate compression applied during filming.

Results

Of the 49 inferior localizations performed, 48 (98%) were successful, 13 (27%) lesions proved to be cancer, and 36 (73%) were benign. In one case the lesion, a cluster of microcalcifications, was not contained in the specimen, and a second localization and biopsy were required for successful excision. In six cases (12%), the localization wire had to be repositioned closer to the lesion. The average time for performance of the localization was 20 min.

Discussion

This inferior approach is easy to use and requires no special equipment. The failure to excise one lesion on the initial biopsy in this series remains unexplained as postlocalization films showed the needle position to be accurate. We consider a localization acceptable when the needle is within 5 mm of the lesion. The failure rate of 2% in this series is even lower than the failure rate of other series using more conventional approaches [3].

If the postlocalization films are obtained with the needle in place, as I prefer with a needle-wire system that I now use [4], the technologist has no difficulty in obtaining the craniocaudad mammograms as the needle is inserted up to its hub. Even though the film holder is pressing on the needle hub in the craniocaudad projection, this causes no difficulty because a curved-end wire protects the sharp needle tip. Similarly, there is no difficulty with other systems that do not require an unprotected straight needle in place during postlocalization filming [2]. However, I have never used this approach with a spring-hookwire system [5] in which postlocalization films are obtained with an unprotected rigid needle in the breast before springing the wire.

The needle is always inserted up to its hub, even if its tip

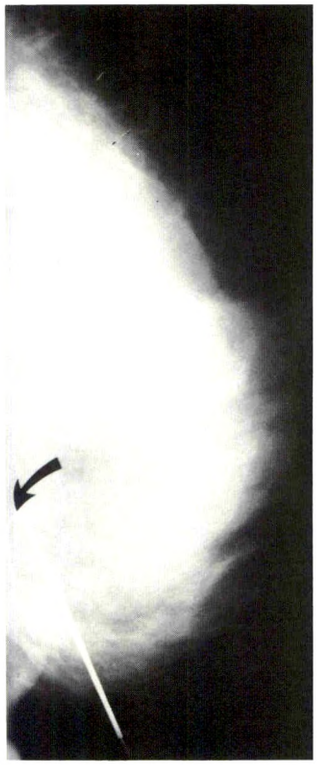


Fig. 5.—Lateral postlocalization film shows lesion (*arrow*) at tip of curved wire.

goes beyond the lesion. Since the localization needle and wire are left in place, providing the surgeon with an anchored palpable guide, there is no reason to have the lesion precisely at the needle tip. The surgeon easily palpates the needle during the dissection and can determine the location of the lesion by its relationship to the needle shaft, as defined by lateral compression mammograms. This eliminates the need for many needles of different lengths.

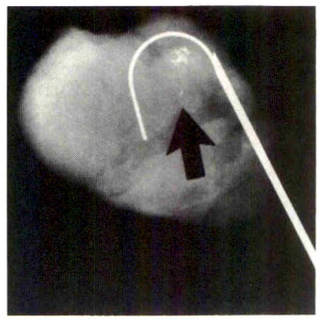


Fig. 6.—Specimen radiography confirms total excision of microcalcifications. Note small size of specimen made possible by accurate needle placement. Histologic studies showed intraductal carcinoma with foci of microinvasion.

The key to the accuracy of this approach is the simulation of the geometry of the lateral compression mammogram while inserting the needle, since measurements of depth and angle are obtained from this geometry. This goal is easily achieved by having the patient lie supine and inserting the needle while compressing the breast with one hand. This technique can serve as an alternative for the radiologist in selected cases in which the optimal approach to the lesion is from below. However, this technique is so easy to use and accurate that I employ it in every case in which the lesion is in the lower third of the breast.

REFERENCES

1. Homer MJ. Nonpalpable breast lesion localization using a curved-end retractable wire. *Radiology* **1985**;157:259–260
2. Frank HA, Hall FM, Steer ML. Preoperative localization of nonpalpable breast lesions demonstrated by mammography. *N Engl J Med* **1976**;295:259–260
3. Homer MJ. Localization of nonpalpable breast lesions: technical aspects and analysis of 80 cases. *AJR* **1985**;140:807–811
4. Homer MJ., Pile-Spellman ER. Needle localization of occult breast lesions with a curved-end retractable wire: technique and pitfalls. *Radiology* **1986**;161:543–548
5. Kopans DB, Meyer JE. Versatile spring hookwire breast lesion localizer. *AJR* **1982**;138:586–587

Book Review

Radiology of the Liver, Biliary Tract, Pancreas and Spleen. Edited by Arnold C. Friedman. Baltimore: Williams & Wilkins, 1110 pp., 1987. $118

This comprehensive text is the newest addition to the *Golden's Diagnostic Radiology Series*. The goal of the series as stated in the foreword is to "present a contemporary, authoritative text that will serve as reference sources for radiologists and others with particular interest in the title subject." Friedman and his contributors have accomplished this well.

The text is divided into five separate sections—four are based on anatomic sections (liver, gallbladder and biliary tract, pancreas, and spleen), and a short fifth section discusses biopsy and drainage procedures in the upper abdomen. The four anatomically oriented sections form the bulk of the text and are each composed of five to 10 chapters. Each section is logically organized with an initial chapter on embryology and anatomy with good correlation to diagnostic images and discussion of normal techniques and normal anatomy encountered in the multitude of imaging methods currently available. The following chapters in each section then discuss the variety of disease processes involving each organ. The chapters are organized around disease processes, rather than imaging techniques, which makes for concise, yet thorough descriptions of the disease processes. Each disease process is thoroughly discussed with subsections on clinical findings, pathology, and radiologic findings. The radiology sections are usually separated into separate discussions of appropriate imaging studies. MR imaging, however, is not included in these sections, but presented as a separate chapter at the end of each organ system. The information is presented in an encyclopedic fashion as a reference source organized by disease processes. The book would not be helpful as a source for differential diagnosis evaluation and is not set up as are some more limited texts on the basis of imaging techniques and imaging findings. The organization throughout the text is excellent with no significant duplications or gaps. This is a tribute to the editor and probably due to the fact that he is also an author listed on most all of the chapters except those on the spleen and interventional radiology.

The spleen, well covered in section IV, is an unusual addition to the other organs in this text. It is not one of the accessory digestive organs and does not relate intimately with the other organs. While I am uncertain why this section was included in this text, it is well done and will be a helpful reference source. Section V represents two short chapters on biopsy and drainage procedures. Although these short chapters are well written, I question whether such procedurally oriented chapters belong in a reference text such as this and I doubt that they will be used because most physicians will use other textbooks on interventional techniques.

The references provided are thorough and complete, although predominantly noted through 1984 with a few 1985 references. This time interval between reference material and publication date is to be expected in an undertaking of this size. This does, however, limit the discussions and references for MR imaging. Appropriate references are easily located, since they are listed after each short subsection within chapters rather than in a long listing at the end of each chapter. The index appeared complete, although realistically one would probably rarely use it because the table of contents is lengthy and the organization of the material in the text so good that it is quicker to use the table of contents to locate information.

A complete review should mention some faults, but I found this difficult to do. Occasionally, separate small sections were written that might have been more optimally included within larger topics. For example, the section on CT evaluation of hepatocellular carcinoma should include the discussion of Lipiodol-CT studies rather than have separate short discussion on these studies elsewhere. Another minor criticism is that some of the CT images are not optimally reproduced, although overall the reproduced images are of good quality. In summary, this text fills the need for a complete reference text in this area and will be helpful to radiologists and others in the evaluation of patients with disorders of the upper abdomen.

Richard L. Baron
University of Washington School of Medicine
Seattle, WA 98195

Radiographic Appearance of Mucosal Dysplasia Associated with Ulcerative Colitis

Joseph R. Hooyman[1]
Robert L. MacCarty[1]
Herschel A. Carpenter[2]
Kenneth W. Schroeder[3]
Harley C. Carlson[1]

The radiographic appearance of dysplasia, a precancerous histologic change that is frequently present in colitic colons at high risk for cancer, was analyzed. Over a 5-year period, 170 patients with long-standing ulcerative colitis participated in a cancer surveillance program at our institution. On entry, all patients underwent radiography with a double-contrast barium enema and colonoscopy with multiple random biopsies. All radiographs were reviewed retrospectively and were correlated with the colonoscopic and histologic findings. Dysplasia, ranging from mild to severe, was found in the biopsy specimens from 26 (15%) of these patients (in 59 different regions). Thirteen of the 26 patients with dysplasia had colectomies, and the specimens were available for review. Most dysplasia is not radiographically visible, as was the case in 40 (68%) of the 59 regions found histologically to have dysplasia. In the 19 regions in which dysplasia was visible radiographically, it appeared as a solitary nodule or as several separate nodules in 11 (19%) of the 59 regions or as a close grouping of multiple adjacent nodules with apposed, flattened edges in 8 (14%) of the 59 regions. The radiographic finding of a nodule or of several separate nodules was not specific because these nodules were indistinguishable from the inflammatory nodules often present in colitic colons. On the other hand, the radiographic finding of a close grouping of adjacent nodules with apposed, flattened edges was associated with dysplasia 50% of the time. This radiographic appearance was seen in five of our 26 patients who had dysplasia.

Our study shows that barium examinations are useful in some patients with chronic ulcerative colitis by suggesting the presence of dysplasia and directing the endoscopist to specific locations for biopsy.

Patients with chronic ulcerative colitis are at an increased risk for colon cancer [1]. The subset of these patients most likely to develop colon cancer are believed to have dysplasia scattered in their colonic epithelium. Dysplasia is thought to be a risk indicator for subsequent or concurrent cancer, in part because of the frequent finding of dysplasia in resected colons containing cancer (Fig. 1) [2–4]. Thus, there is great interest in detecting dysplasia, and the presence of dysplasia in a colitic colon is a factor favoring prophylactic colectomy.

There have been few detailed studies on the radiographic appearance of dysplasia. Dysplasia may not be visible radiographically because random endoscopic biopsies can find histologic dysplasia in mucosa containing no visible lesion. However, radiographically visible dysplasia may be more significant [5, 6]. One radiographically visible form of dysplasia has been described as a grouping of irregular nodular areas with sharply angulated edges [7–9]. The frequency and specificity of this finding have yet to be established.

We set out to evaluate the radiographic appearance of dysplasia in a large group of patients with long-standing ulcerative colitis by correlating radiographic findings with findings obtained from (1) surveillance colonoscopy with biopsies and (2) pathologic evaluation of colectomy specimens.

Received December 16, 1986; accepted after revision February 27, 1987.

Presented at the annual meeting of the American Roentgen Ray Society, Washington, DC, April 1986.

This work was supported by research funds from the Research Committee of the Mayo Clinic Department of Diagnostic Radiology.

[1] Department of Diagnostic Radiology, Mayo Clinic and Mayo Foundation, Rochester, MN 55905. Address reprint requests to R. L. MacCarty.

[2] Section of Surgical Pathology, Mayo Clinic and Mayo Foundation, Rochester, MN 55905.

[3] Division of Gastroenterology and Internal Medicine, Mayo Clinic and Mayo Foundation, Rochester, MN 55905.

***AJR* 149:47–51, July 1987**
0361–803X/87/1491–0047
© American Roentgen Ray Society

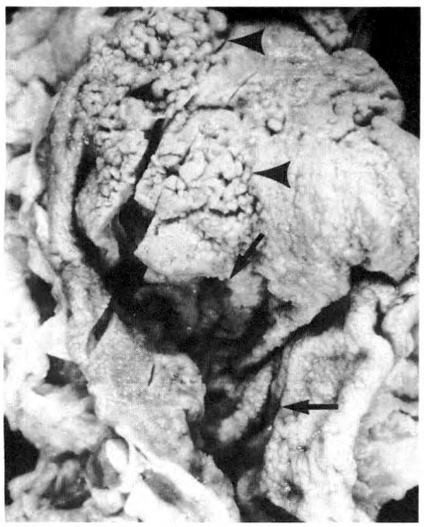


Fig. 1.—Dysplasia associated with carcinoma. Ascending colon, from colectomy specimen, is distorted by annular infiltrating carcinoma (*arrows*). Proximal to carcinoma are areas of nodular dysplasia (*arrowheads*).

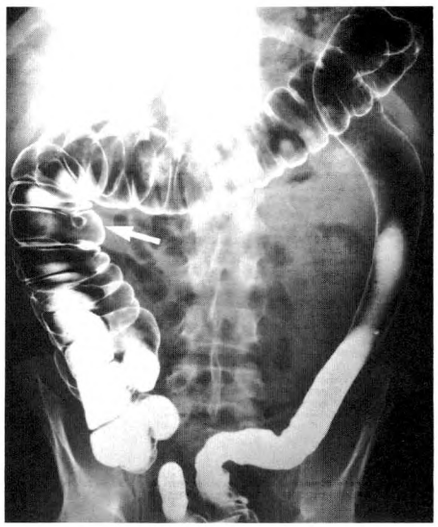


Fig. 2.—Air contrast enema shows diffuse symmetric narrowing of much of left colon, consistent with ulcerative colitis. A nodule is present in ascending colon (*arrow*). Random colonoscopic biopsies of flat mucosa in left colon showed widespread mild and moderate dysplasia. Nodule in ascending colon contained moderate dysplasia.

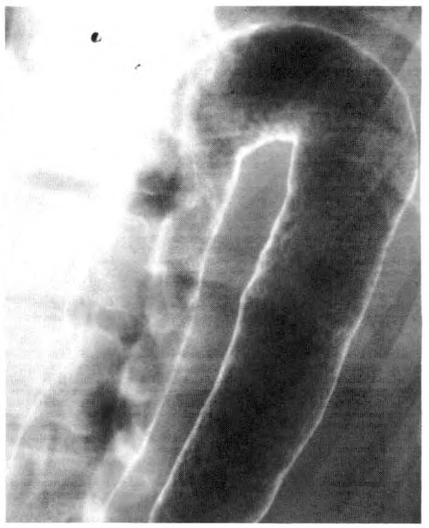


Fig. 3.—Air contrast radiograph of splenic flexure shows coarse granularity of mucosa, consistent with inflammatory disease. No visible lesions are present to suggest dysplasia. Random colonoscopic biopsies showed widespread dysplasia in this region of colon.

Subjects and Methods

The 170 patients who entered a cancer surveillance program in the period 1980 through 1984 generally had had pancolitis for 7 years or more and were referred to the program by their internists because of their increased cancer risk. All patients had undergone radiographic study with a double-contrast barium enema and colonoscopy with multiple biopsies during the initial year of surveillance. Results of follow-up examinations were available for all patients who had been in the study for more than a year, and these were referred to for confirmation or classification of findings seen on the initial radiographic and colonoscopic examinations. Generally in the second year of the study, patients underwent repeat colonoscopy with biopsies; in the third year, repeat radiography (double-contrast barium enema) and flexible proctosigmoidoscopy with biopsy were performed. For patients in the study for 4 or more years, colonoscopy with biopsies during one year alternated with double-contrast barium-enema radiography and flexible proctosigmoidoscopy with biopsy during the next year. The sequence and time frame between examinations frequently were altered if a significant disease condition was seen—that is, dysplasia or cancer. This generally resulted in more frequent follow-up with biopsy or colectomy.

Double-contrast barium examinations were performed by both staff and residents in radiology. In examinations performed by residents, the examinations were reviewed with a staff radiologist before the final reading. The examinations were performed by a standard technique with 10 films (14 × 17 in., 35.6 × 42.2 cm), including posteroanterior, anteroposterior, angled left posterior oblique, and angled right anterior oblique views; both upright oblique views; both lateral decubitus views; and both horizontal-beam views of the rectum. Polibar Plus barium suspension (E-Z-EM, Westbury, NY) was used as the contrast medium.

The initial 170 double-contrast barium-enema radiographs were reviewed retrospectively by two staff radiologists and one resident without prior knowledge of the colonoscopist's observations or of the histologic findings from the colonoscopic biopsies. Any radiographic findings suspected to represent carcinoma or dysplasia were recorded. The colonoscopic and histologic findings were then correlated with the radiographic findings. All radiographs of colons known to contain histologic dysplasia were again studied. The radiographic appearance of regions of dysplasia were recorded and correlated with prior observations.

All colonoscopies were performed by experienced endoscopists. Written reports of the colonoscopic findings were available for all patients. At colonoscopy, the endoscopist divided the colon into eight equal regions for biopsy and descriptive purposes, and four biopsy specimens were taken at random from each region to detect dysplasia. In addition, regions suspected to harbor dysplasia or carcinoma at colonoscopy were described and biopsied. Each colonoscopic examination produced at least 32 biopsy specimens.

The pathologic criteria and terminology used to grade dysplasia were standardized [10] near the end of the study period. As a result, the grades of dysplasia were from mild to severe, even though these terms are not used in this recent classification scheme. (Mild, moderate, and severe grades of dysplasia have been reclassified as positive dysplasia of low or high grade.) Because of this standardization, all biopsy specimens initially interpreted to contain dysplasia were reexamined by an additional pathologist who applied this recent classification scheme to our cases to ensure that the criteria needed for dysplasia were met. The biopsy specimens had to be at least "positive" for dysplasia of low grade by this new classification for a patient to be included in our study. Areas "indefinite" for dysplasia were not considered. A colonic region was considered to contain dysplasia if at least one of the four biopsy specimens from the region was "positive" for dysplasia.

All patients who had regions of dysplasia found by colonoscopic biopsy had follow-up colonoscopic biopsies or a colectomy with histologic sampling to help confirm the grade and location of the

dysplasia. Occasionally, dysplasia was not confirmed on follow-up; this has been reported in previous studies [11]. In these circumstances, the original biopsies that had been interpreted as showing dysplasia were reviewed to ensure that "positive" dysplasia had indeed been present.

Thirteen patients with dysplasia eventually had colectomies, eight within 1 year after their original radiographs. All colectomy specimens were available for review.

TABLE 1: Radiographic Forms and Frequencies of Dysplasia in 26 Patients

Form	No. of Regions (%) (n = 59)
Close grouping of adjacent nodules with apposed, flattened edges	8 (14)
Discrete nodule or several separate nodules	11 (19)
No visible lesion	40 (68)

Results

Twenty-six of the 170 patients with long-standing ulcerative colitis were found to have 59 regions of dysplasia histologically out of a possible 208 (26 colons with eight possible regions per colon). The radiographic forms of this dysplasia and their relative frequencies are outlined in Table 1.

No visible evidence of dysplasia was apparent radiographically or endoscopically for 40 regions (68% of the total number of regions) of histologic dysplasia from 21 patients. In these cases the histologic evidence of dysplasia had been obtained by random biopsy of colonic mucosa. This mucosa was involved by the inflammatory bowel disease (Fig. 2), sometimes with coarse granularity (Fig. 3), but there was no visible evidence to suggest anything more than inflammatory disease. Therefore, most dysplasia was not detectable radiographically.

Radiographically visible dysplasia occurred in two forms. The first consisted of a grouping of multiple adjacent nodules with apposed, flattened borders (Figs. 4–7). This nodular

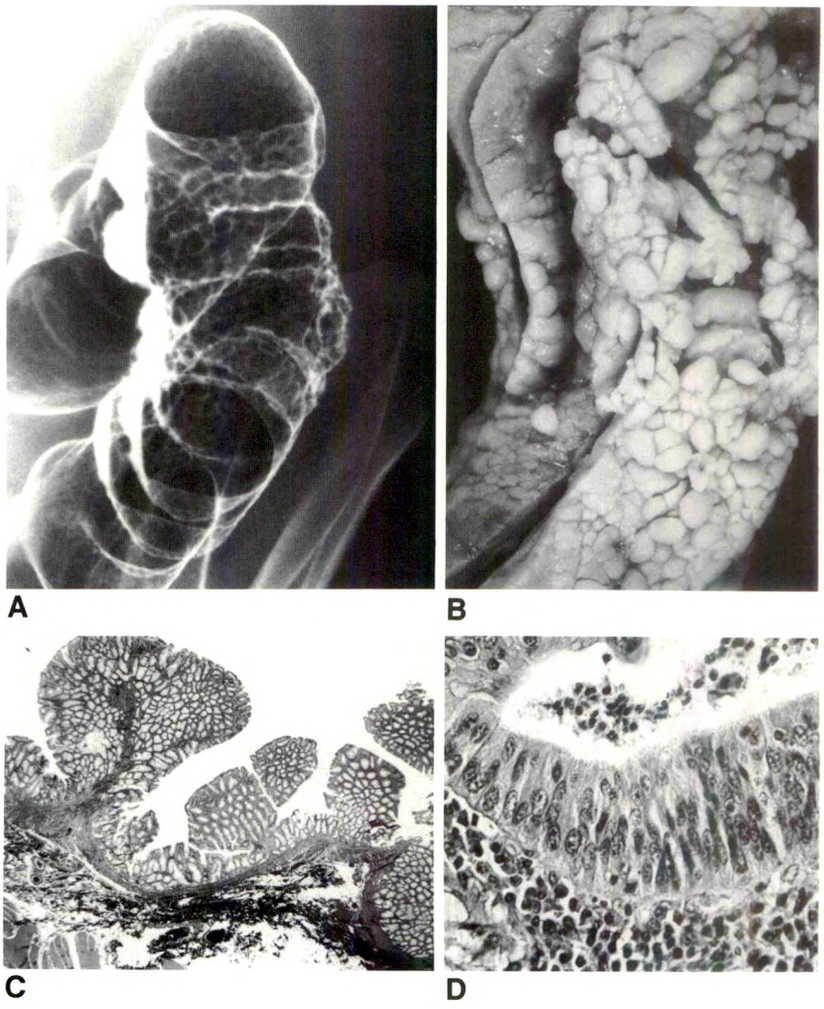


Fig. 4.—Dysplasia appearing as multiple adjacent nodules with apposed, flattened borders.

***A*, Air contrast radiograph of descending colon.**

***B*, Corresponding region on colectomy specimen (specimen had been sampled previously).**

***C*, Histologic section of nodules. Nodules are primarily formed by cytologically atypical colonic glands crowded together in lamina propria. This architectural pattern is frequently seen in dysplastic nodules and is the pattern seen in tubular adenomas. (×40)**

***D*, Histologic section of one gland within nodule shows pathognomonic cytologic features of dysplasia. Cells are crowded with stratification of nuclei. Nuclei are enlarged, are hyperchromatic with stippled chromatin pattern, and vary in size and shape. There are increased numbers of mitotic figures. (×400)**

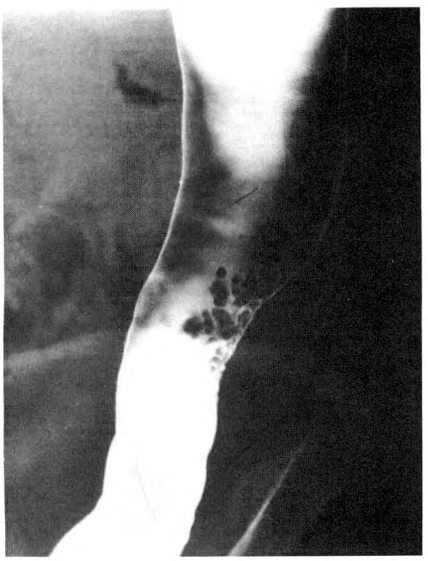
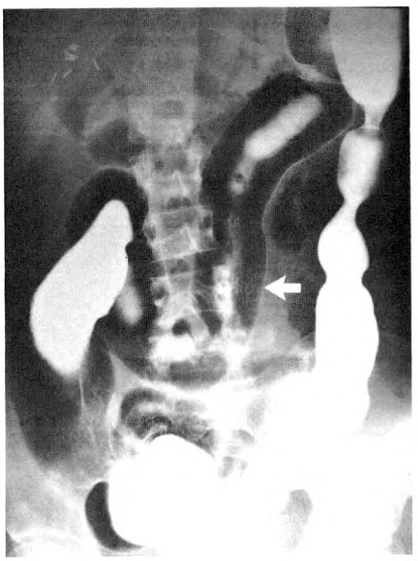


Fig. 5.—Barium enema examination shows close grouping of nodules in descending colon, which contained dysplasia.



A

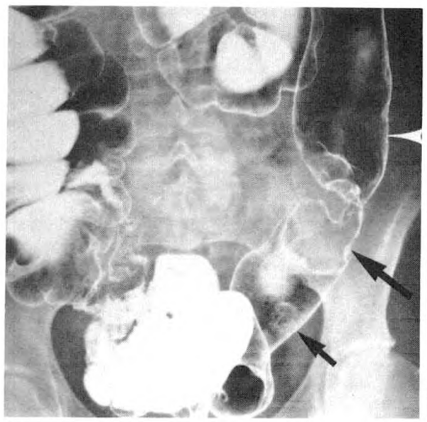


B

Fig. 6.—Barium enema shows close grouping of fine dysplastic nodules in mid transverse colon (*arrow*) with apposed, flattened borders.

A, Air contrast radiograph.

B, Localized view of nodules. Nodular abnormality in mid transverse colon was described endoscopically as having an "unusual cobblestoned appearance." Multiple biopsies showed dysplasia.



A

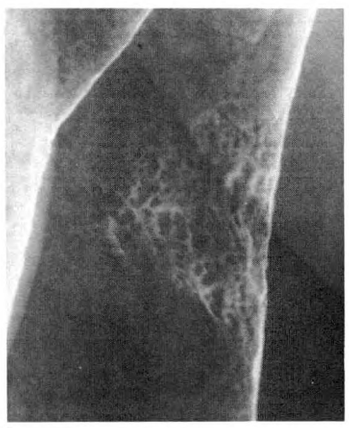


B

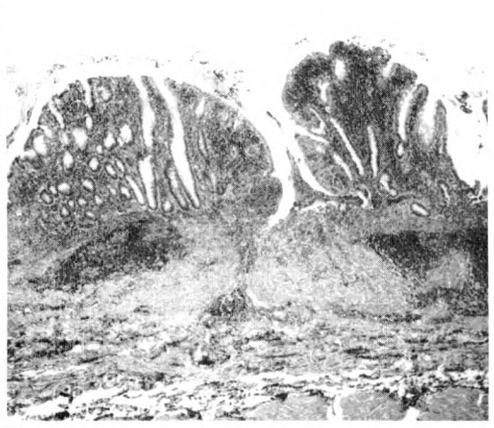
Fig. 7.—Barium enema examination shows dysplasia associated with carcinoma.

A, Air contrast radiograph shows carcinoma in proximal sigmoid colon (*large arrow*). Solitary nodule distal to carcinoma contained severe dysplasia (*small arrow*). Although not well seen on this view, fine dysplastic nodules were proximal to carcinoma (*arrowhead*).

B, Histologic section of solitary dysplastic nodule in *A* shows that surface of nodule is composed of delicate papillary folds, an architectural pattern seen in villous adenomas. (×40)



A



B

Fig. 8.—Barium enema shows group of nodules with apposed, flattened borders. Nodules were formed by inflammatory infiltrates and there was no dysplasia.

A, Localized air contrast view of nodular region near splenic flexure.

B, Histologic section of nodules, obtained from colectomy specimen, shows nodules to be composed of chronic inflammatory infiltrates that expand lamina propria and separate colonic glands. There is no dysplasia. Contrast this histologic appearance of inflammatory nodules with that of dysplastic nodules (Fig. 4C), which are formed from proliferation of cytologically atypical glands.

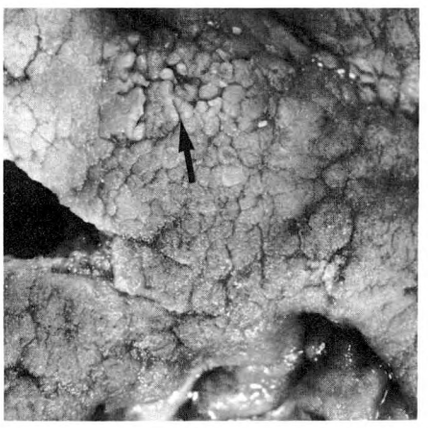


Fig. 9.—Magnified view (×4) of mucosa in ascending colon, from colectomy specimen. Subtle, slightly elevated, dysplastic lesion has papillary surface (*arrow*). This lesion was not seen on prior radiographic or endoscopic studies.

pattern of dysplasia may be coarse (Figs. 4 and 5) or fine (Figs. 6 and 7) and was seen radiographically in eight (14%) of the 59 regions of histologic dysplasia. In five of the 26 patients with dysplasia, this form of dysplasia was evident on barium examination. Histologically, these grouped nodules were formed by dysplasia with varying amounts of inflammatory infiltrate. This radiographic appearance of grouped nodules was not specific for dysplasia. In five other patients, among the 170 surveillance patients, radiographs showed nodular areas with apposed, flattened borders, and no dysplasia was found in these nodular areas on follow-up colonoscopic biopsies or colectomies. The grouped nodules in these cases were formed by inflammatory change (Fig. 8). Thus, only half of the patients who had this radiographic pattern actually had dysplasia.

The second form of radiographically visible dysplasia, present in 11 regions (19% of the total number of regions) of dysplasia from seven patients, appeared as a solitary nodule or as several separate nodules (Figs. 2 and 7) up to 1 cm in diameter (mean diameter, 5 mm). These nodules were adenomatous polyps. The surface of some of these nodules had delicate papillary folds that gave them a villous configuration. However, this fine architecture generally was too subtle to be evident on the radiographs and was best appreciated by low-power examination of histologic sections of the nodule (Fig. 7B).

These separate dysplastic nodules were indistinguishable radiographically from the much more numerous inflammatory nodules seen in the colons of many of these patients. Therefore, this radiographic appearance is nonspecific.

No correlation was found between the degree or severity of dysplasia and its radiographic form. In our study, radiographically visible dysplasia was as likely to be mild as it was to be severe: Three patients had multiple regions of dysplasia with regions of severe dysplasia, six had multiple regions of dysplasia with regions of moderate dysplasia, 12 had multiple regions of mild dysplasia, and five had one region of mild dysplasia.

Three patients with dysplasia had coexisting carcinoma in another region of the colon. One of the carcinomas was not evident radiographically. Visible forms of dysplasia were present in these three colons, appearing as solitary nodules in all and, in addition, as closely grouped nodules in one (Fig. 7).

Discussion

Although no large study on the radiographic appearance of visible dysplasia has been reported, an article by Butt et al. [12] in the pathologic literature describes the appearance of visible dysplasia on the basis of close visual inspection of colectomy specimens in a large study. Of 105 areas of visible dysplasia, Butt et al. found, as we did in our study, elevated nodular areas and nodules to be characteristic forms of visible dysplasia.

Studies based on the close visual inspection of colectomy specimens also reveal that some visible dysplastic lesions can be subtle. The subtle forms of visible dysplasia typically are slightly elevated lesions that may have a finely villous or papillary surface configuration. This subtle form of visible dysplasia can easily elude radiographic and endoscopic detection (Fig. 9).

Radiography would be expected to detect only larger forms of visible dysplasia. One of these larger forms has been described in radiographic case reports [7–9] and was seen radiographically in our study as a group of adjacent nodules with apposed, flattened edges.

Most dysplasia does not form a visible lesion, a fact confirmed by other investigators [11]. Exactly how frequently dysplasia occurs in flat mucosa or in mucosa involved by inflammatory bowel disease without any detectable lesion is difficult to determine. The frequency of this form of dysplasia is certainly higher than the 68% found in our study, and it may be much higher because it is not feasible to biopsy the entire colonic surface.

The role of radiography in detection of dysplasia therefore is limited. Our study found that, when dysplasia was visible radiographically, it appeared as a separate nodule or as a close grouping of nodules with apposed, flattened edges. Neither radiographic appearance was pathognomonic for dysplasia, although the grouped nodular appearance was suggestive, being associated with dysplasia in 50% of instances. This radiographic finding, seen in five of the 26 patients who had dysplasia, should alert the radiologist to the possible presence of dysplasia, and it is an indication for endoscopic examination and biopsy.

REFERENCES

1. Devroede GJ, Taylor WF, Sauer WG, Jackman RJ, Stickler GB. Cancer risk and life expectancy of children with ulcerative colitis. *N Engl J Med* **1971**;285:17–21
2. Cook MG, Goligher JC. Carcinoma and epithelial dysplasia complicating ulcerative colitis. *Gastroenterology* **1975**;68:1127–1136
3. Fuson JA, Farmer RG, Hawk WA, Sullivan BH. Endoscopic surveillance for cancer in chronic ulcerative colitis. *Am J Gastroenterol* **1980**;73:120–126
4. Ransohoff DF, Riddell RH, Levin B. Ulcerative colitis and colonic cancer. Problems in assessing the diagnostic usefulness of mucosal dysplasia. *Dis Colon Rectum* **1985**;28:383–388
5. Blackstone MO, Riddell RH, Rogers BHG, Levin B. Dysplasia-associated lesion or mass (DALM) detected by colonoscopy in long-standing ulcerative colitis: an indication for colectomy. *Gastroenterology* **1981**;80:366–374
6. Butt JH, Morson B. Dysplasia and cancer in inflammatory bowel disease (editorial). *Gastroenterology* **1981**;80:865–868
7. Frank PH, Riddell RH, Feczko PJ, Levin B. Radiological detection of colonic dysplasia (precarcinoma) in chronic ulcerative colitis. *Gastrointest Radiol* **1978**;3:209–219
8. Kelvin FM, Woodward BH, McLeod ME, Fetter BF, Jones RS. Prospective diagnosis of dysplasia (precancer) in chronic ulcerative colitis. *AJR* **1982**;138:347–349
9. Stevenson GW, Goodacre R, Jackson R, Ragbeer M, Rowland R. Dysplasia to carcinoma transformation in ulcerative colitis. *AJR* **1984**;143:108–110
10. Riddell RH, Goldman H, Ransohoff DF, et al. Dysplasia in inflammatory bowel disease: standardized classification with provisional clinical applications. *Hum Pathol* **1983**;14:931–968
11. Granqvist S, Gabrielsson N, Sundelin P, Thorgeirsson T. Precancerous lesions in the mucosa in ulcerative colitis: a radiographic, endoscopic, and histopathologic study. *Scand J Gastroenterol* **1980**;15:289–296
12. Butt JH, Konishi F, Morson BC, Lennard-Jones JE, Ritchie JK. Macroscopic lesions in dysplasia and carcinoma complicating ulcerative colitis. *Dig Dis Sci* **1983**;28:18–26

Book Review

Radiology in Emergency Medicine. By Richard C. Levy, Hugh Hawkins, and William D. Barsan. St. Louis: Mosby, 468 pp. 1986. $72.75

This book is intended primarily for novice emergency room physicians. It is organized into seven major anatomic divisions: head, neck, chest, abdomen, pelvis, back, and upper and lower extremities. Each anatomic area is subdivided into trauma and nontrauma sections, resulting in 14 chapters. Each chapter consists of three sections: a narrative description of selected entities with a short list of references; a tabulation of imaging techniques and principal indications; and an atlas of illustrations showing some of the more common radiographic findings and, in certain cases, sonographic, scintigraphic, and CT findings.

The descriptions are short and most are devoted to clinical information with only a brief description of findings on imaging examinations. Terms, such as "thumbprinting" and "central echo complex," are used without further explanation. There is no reference in the description section to illustrations in the atlas.

Errors were encountered in the narrative. In a description of Kerley Lines, the authors state that "Kerley B lines are short, touch the pleural surface, and are perpendicular to that pleural surface. Kerley A and C lines are located more centrally and are longer." Describing pulmonary embolism, the authors state "Westermark's sign is a dilated pulmonary artery with decreased segmental perfusion"; in the description of abdominal trauma, the text reads "The accumulation of blood in the paracolonic gutters creates the so-called rabbit-ear or dog-ear appearance in the pelvis." Regarding the evaluation of trauma to the urinary tract the reader is admonished, "In males the urethra should be cleared by retrograde urethrography before an IVP is undertaken." The radiograph of a classic example of sigmoid volvulus is described as "the classic coffee bean sign of sigmoid volvulus."

The tabulation of indications is brief and not all inclusive. The description of the procedures is equally brief, presented in tabular form, obviously incomplete, and questionably informative.

Twenty or more illustrative cases are presented at the end of each chapter in an atlas format with a short comment and usually no more than two images to a case. Arrows and letters designate the principal findings. There is no narrative description of the images. Most of the illustrations are too small, and the page is never filled by the comment, legends, and images. Many of the illustrations are too dark and occasionally marred by significant artifacts.

There are two excellent texts in radiology devoted to emergency medicine, *Radiology of Emergency Medicine* by Harris and Harris and *Emergency Radiology by Keats*. Both are more informative than the book under review.

I cannot recommend *Radiology in Emergency Medicine* to radiologists or departments of radiology. Perhaps the book might be of value to emergency room physicians. Certainly its level of sophistication is far below that required of radiology trainees, and it would seem that an emergency room physician's time would be better spent in reading and referring to the alternative texts named above.

Lee F. Rogers
Northwestern University
Chicago, IL 60611

High-Resolution Sonography of Acute Appendicitis

Monzer M. Abu-Yousef[1]
Jon J. Bleicher[1]
James W. Maher[2]
Luis F. Urdaneta[2]
Edmund A. Franken, Jr.[1]
Amanda M. Metcalf[2]

During a 7-month period high-resolution sonography was used in the evaluation of 68 patients with an equivocal clinical diagnosis of acute appendicitis. The sonographic findings were correlated with surgical-pathologic outcome in 32 cases and with clinical follow-up in the remainder. This technique was found to be accurate in the diagnosis of acute appendicitis with a specificity of 95%, a sensitivity of 80%, and an accuracy of 90%. The predictive value of a positive test was 91%; that of a negative test was 89%.

The results show that high-resolution sonography is indicated to establish the diagnosis of acute appendicitis in patients with equivocal clinical findings.

Although the clinical presentation of acute appendicitis is typical in more than 70% of the cases, about 30% of the patients have an uncertain preoperative diagnosis [1, 2]. Consequently, the rate of unnecessary laparotomy for acute appendicitis is as high as 20–25% [3]. The rate is even higher (35–45%) in women of childbearing age because of the prevalence of diseases of the female pelvic organs and complications of pregnancy in this group [2, 4–7].

Several imaging techniques have been used to improve the diagnostic accuracy of this disease. Of these, the plain film of the abdomen is of limited value, since abnormalities are present in less than 50% of the examinations [8]. Moreover, most of these findings are nonspecific. The accuracy of the barium enema examination in the diagnosis of acute appendicitis ranges from 50% [9] to as high as 84% [10].

Although the normal and inflamed appendix can occasionally be seen by CT [11], more often the CT diagnosis of acute appendicitis is presumptive as it depends on the demonstration of a right lower quadrant abscess or fluid collection rather than on visualizing the inflamed appendix [11–13]. Similarly, sonography has also been used mainly in the diagnosis of the complications of this disease and to exclude other diagnoses [14, 15]. Recent reports have suggested that high-resolution sonography is fairly accurate in showing the inflamed appendix in patients with uncomplicated acute appendicitis [3, 16], while others have shown that it is only accurate in the diagnosis of phlegmonous and gangrenous appendicitis [17]. We present our experience with high-resolution sonography in the diagnosis of 68 cases with equivocal clinical diagnosis of acute appendicitis.

Subjects and Methods

During a 7-month period we obtained sonograms on 68 patients with atypical clinical and laboratory findings suggestive but not diagnostic of acute appendicitis. Most of these patients had either atypical pain, normal body temperature, normal WBC count, absence of nausea and vomiting, and/or symptoms lasting more than 24 hr.

Only 26 patients experienced nausea and vomiting. Forty-nine patients had pain and tenderness localized to the right lower quadrant of the abdomen, and the other 19 had pain

Received December 17, 1986; accepted after revision March 17, 1987.

[1] Department of Radiology, The University of Iowa Hospitals and Clinics, Iowa City, IA 52242. Address reprint requests to M. M. Abu-Yousef.

[2] Department of Surgery, The University of Iowa Hospitals and Clinics, Iowa City, IA 52242.

AJR 149:53–58, July 1987
0361–803X/87/1491–0053
© American Roentgen Ray Society

in the flanks or one of the other quadrants or diffuse abdominal pain. Forty had a body temperature of more than 37°C, while 28 had normal temperature. Twenty-two had a normal WBC count. Thirty-two patients had symptoms for more than 24 hr. Plain abdominal radiographs were obtained in 38 patients, and five patients had a barium enema examination.

There were 32 men and 36 women ranging in age from 2 to 64 years with an average age of 26 years. Eighty-five percent of the patients were between 18 and 35 years old. Seven were pregnant women. Three other patients were excluded from the study as the appendiceal area was not well seen because of lack of cooperation, severe obesity, and/or significant gas blocking.

The sonographic examinations were done using the 5-MHz, phased linear-array transducer (Acuson 128 Computed Sonography, Mountain View, CA 94043). Examinations were performed according to the method described by Puylaert [3]. Graded pressure was applied with the transducer to compress the bowel loops and displace the air, thus allowing visualization of retroperitoneal structures such as the iliopsoas muscle and iliac vessels. Scanning was usually started in the transverse plane from the upper ascending colon down to below the level of the cecum, and then in the longitudinal plane starting lateral to the cecum and progressing to the midline. The inflamed appendix, when identified, was seen medial and inferior to the cecum. Transverse and longitudinal views of the appendix were obtained with magnification. If the inflamed appendix was not seen, a quick survey of the abdomen with this transducer and occasionally a pelvic examination with a 3-MHz sector transducer were performed. The images were then recorded on a hard copy. Most patients tolerated the pain caused by the transducer pressure fairly well. The sonographic findings were correlated with the surgical results in 31 cases, with the findings at laparoscopy in one case, and with the results of clinical follow-up in 36 cases.

Results

Twenty-five of the 68 cases with equivocal clinical diagnoses had surgically and pathologically proved acute appendicitis, while 43 had no evidence of appendicitis either at laparoscopy in one case, at laparotomy in six cases, or at clinical follow-up in 36 cases. The average temperature for those with appendicitis was 37.7°C and for those without was 37.4°C. The average WBC count was 16,100/ml in the positive cases and 11,900/ml in the negative cases; 12% of the former group did not have leukocytosis while 56% of the latter group did. There was, however, such a high rate of variation in the presence and duration of nausea, vomiting, fever, location of pain, and the presence of leukocytosis that the clinical findings were not helpful in identifying patients with appendicitis in individual cases (Table 1).

Plain films of the abdomen were obtained in 19 cases with acute appendicitis, and were suggestive of acute appendicitis in four cases and unremarkable in the other 15. On the other hand, of the 19 negative cases that had plain films, three showed ileus.

Barium enema examination was performed on five patients without appendicitis. The appendix showed normal filling in four and partial filling in one, a finding that was consistent with appendicitis.

In our series, a negative sonographic diagnosis of acute appendicitis was based on nonvisualization of the appendix in 95% of the cases or visualization of a normal appendix in 5% (Figs. 1A and 1B). The former criterion was based on Puylaert's study [3]. The normal small bowel loops were seen as tubular or round structures with mucosal folds and thin hypoechoic walls (≤2 mm), and almost always showed active peristalsis (Figs. 1C and 1D). The colon was seen as a large tubular structure with occasional peristalsis, haustra, and a wall thickness of 2–5 mm (Fig. 1E). The iliac artery and vein, which could be mistaken for an inflamed appendix, were seen as parallel tubular structures medial to the psoas muscle (Figs. 1C and 1D). The anterior abdominal wall muscles were usually compressed against the iliopsoas muscle (Figs. 1A and 1C).

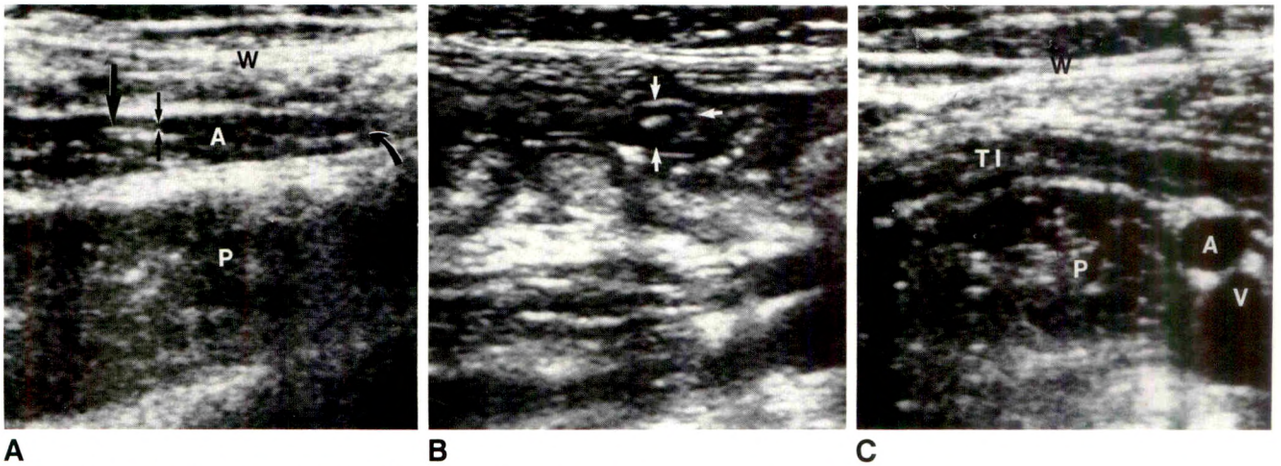
Depending on the plane of scanning, the inflamed appendix was visualized as a sausage-shaped, blind-ending structure on longitudinal imaging (Fig. 2A) or as a target lesion on transverse sections (Fig. 2B). The wall, which is the hypoechoic peripheral zone of the appendix, is thickened to more than 2 mm. Depending on the presence and degree of obstruction of the appendix, the lumen may be seen as an echogenic area or as an anechoic area because of fluid distension (Fig. 3). The mucosa, which had no folds, was seen as a thin echogenic line surrounding the lumen. The muscular wall was surrounded on the outside by an echogenic area representing the periappendiceal fat or serosa. The size, shape, location, and lack of demonstrable peristalsis or of change in configuration helped to differentiate the inflamed appendix from the small and large bowel loops.

The criteria used in the diagnosis of appendiceal perforation were asymmetric appendiceal wall thickening (Fig. 4), periappendiceal mass or abscess (Fig. 5), and lack of significant tenderness during the examination in the presence of positive findings, probably due to relief of intraappendiceal pressure after its rupture. Fluid distension of the appendix (Fig. 3) with or without an appendicolith was used as a sign of suppurative or gangrenous appendicitis. Appendicoliths were seen as intraluminal hyperechoic structures with or without shadowing (Fig. 6).

Sonography correctly diagnosed 20 of 25 pathologically

TABLE 1: Correlation of Clinical Findings with Final Outcome

Clinical Finding	Appendicitis (%) (n = 25)	No Appendicitis (%) (n = 43)
Fever	14 (56)	26 (60)
Nausea and vomiting	10 (40)	16 (37)
Right lower quadrant pain	18 (72)	31 (72)
Symptoms present 24 hr or less	13 (52)	23 (53)
Leukocytosis	22 (88)	24 (56)



A B C

Fig. 1.—Normal anatomy (normal appendix is not usually imaged).

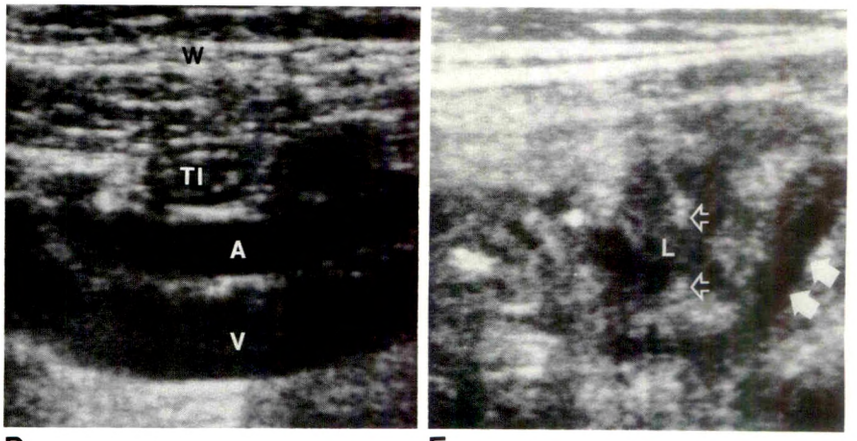
A, Longitudinal view of right lower quadrant with compression shows normal appendix (A) between anterior abdominal wall (W) and psoas muscle (P). Note tapering end of appendix (*curved arrow*), thin muscular wall (*small arrows*), and thin echogenic mucosal outline (*large arrow*) surrounding collapsed lumen.

B, Transverse view of normal appendix (*arrows*).

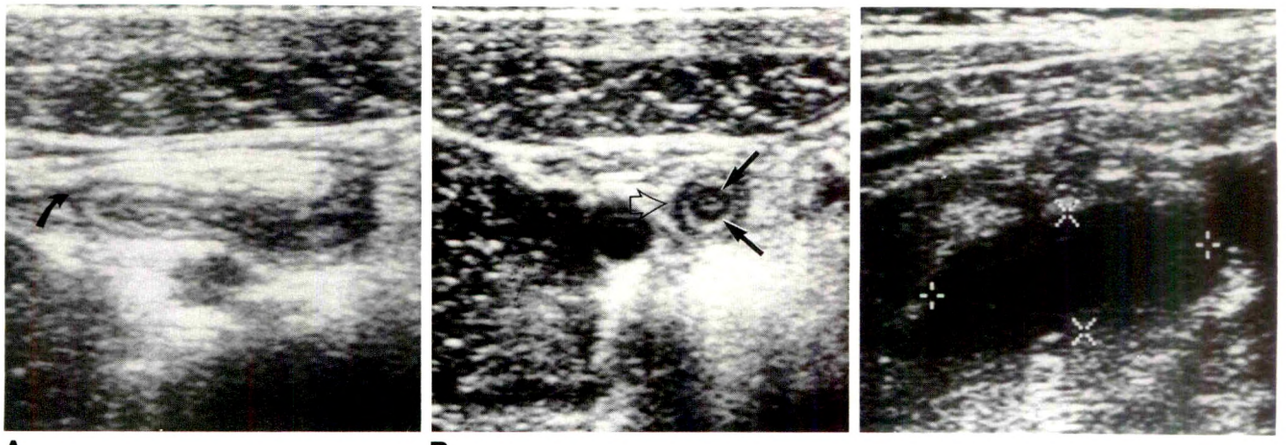
C, Transverse scan of right lower quadrant shows a cross section of iliac artery (A) and vein (V), medial to psoas muscle (P). Terminal ileum (TI) is shown between anterior abdominal wall (W) and psoas muscle showing characteristic features of small bowel loops on high-resolution sonography.

D, Oblique view of right lower quadrant shows iliac artery (A) and vein (V) in their length. TI = terminal ileum; W = anterior abdominal wall muscles.

E, Transverse scan of right lower quadrant shows colon with its large size, typical haustra (*open arrows*), hypoechoic wall (*solid arrows*), and wide lumen (L).



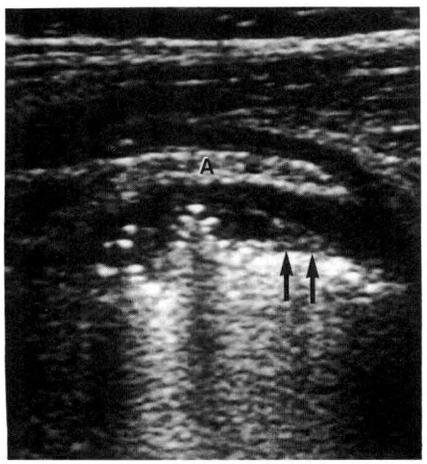
D E



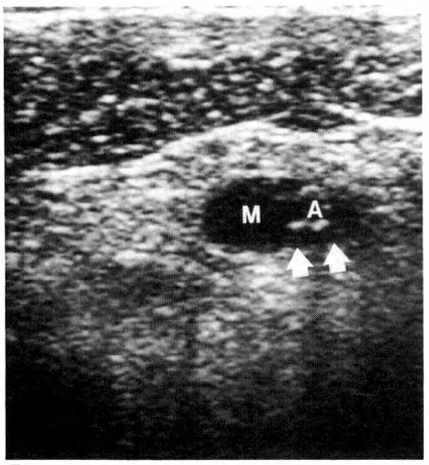
A B

Fig. 2.—Sagittal (*A*) and transverse (*B*) sonograms of uncomplicated, acutely inflamed appendix with slightly thickened muscular wall (*open arrow* on *B*) and submucosa (*closed arrows* on *B*). Note its sausage shape and blind end (*curved arrow* on *A*) on longitudinal view and its target appearance on transverse view. Note also that lumen, which is surrounded by echogenic mucosa, is collapsed.

Fig. 3.—Longitudinal sonogram of inflamed appendix (*between cursors*) shows marked fluid distension in addition to wall thickening. Proved gangrenous appendicitis.



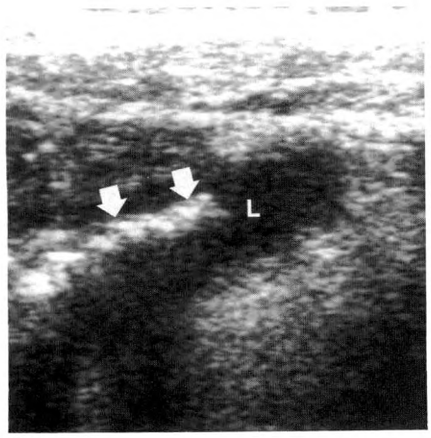
4



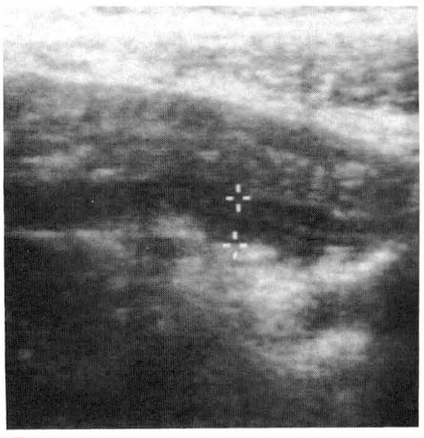
5

Fig. 4.—Longitudinal sonogram of appendix (A) shows asymmetric wall thickening with posterior wall (*arrows*) more thickened than anterior wall. Note also intramural shadowing echogenic structures in posterior wall, which were due to gas. Proved acute appendicitis with perforation.

Fig. 5.—Cross section of appendix (A) shows an almost anechoic periappendiceal mass (M) with some enhancement. Dilated appendiceal lumen seems to communicate with this mass. Note also thickened wall (*arrows*). Proved perforation with periappendiceal abscess.



6



7

Fig. 6.—Longitudinal sonogram of inflamed appendix shows a shadowing hyperechoic linear structure (*arrows*) within appendiceal lumen (L), which is severely distended by fluid. Proved gangrenous appendicitis with appendicolith.

Fig. 7.—Longitudinal sonogram of inflamed appendix shows moderate thickening of muscular wall (*between cursors*) with no significant lumen distension or periappendiceal fluid collection. Proved Crohn's disease of the appendix.

proved cases of acute appendicitis. Of these 25 cases, six had uncomplicated acute appendicitis, eight had nonperforated gangrenous appendicitis, 10 had perforation, and one had granulomatous appendicitis. Sonography missed the diagnosis in no cases from the first or last group, four from the second group, and one from the third group. Suppurative or gangrenous appendicitis without perforation was predicted in all four cases seen by sonography. An appendicolith was present in three cases and sonography predicted two of these. Intramural echogenic foci were seen in two other cases with appendiceal perforation and were attributed to intramural air (Fig. 4). Perforation was predicted in five of the nine cases seen by sonography, while three others showed sonographic evidence of gangrenous appendicitis without perforation. One false-positive diagnosis of perforation was made on the basis of bowel wall thickening. This was the case of Crohn's disease of the appendix. The sonographic findings were similar to some of the cases of acute appendicitis, except that the wall was slightly thicker, the lumen was not distended, and there was associated colonic wall thickening (Fig. 7).

Forty-three patients did not have appendicitis, as proved by surgery in seven cases and clinical follow-up in 36. The latter group was followed from 1 to 3 days until the signs and symptoms completely resolved and the laboratory findings returned to normal. Of the seven patients with normal appendices who were operated on, one had pyelonephritis, one had cholelithiasis, one had *Legionella* pneumonia, one had mesentric adenitis, one had tubovarian abscess, one had endometriosis, and in one pregnant woman the pain was attributed to the stretching of the round ligament. Of the 43 negative cases, sonography was correct in 41 cases; two patients, one of whom was a pregnant woman, were erroneously diagnosed as having acute appendicitis. Of the seven pregnant women, one had acute appendicitis, which was accurately diagnosed by sonography; sonographic diagnosis correctly excluded appendicitis in all but one of the other six pregnant women.

Discussion

The clinical diagnosis of acute appendicitis can sometimes be difficult [1, 2]. In our study, there was no significant

difference between the groups of negative and positive cases in WBC count, temperature elevation, or the presence of right lower quadrant abdominal pain and tenderness. Nausea and vomiting and the duration of symptoms were also not helpful in separating positive from negative cases.

In a study of 100 patients with suspected acute appendicitis, Kniskern et al. [14] found sonography to be accurate in detecting both cases of complicated appendicitis, unhelpful in detecting either of the two cases of early acute appendicitis, and helpful in depicting other pelvic pathology in 11 of 19 patients without appendicitis.

Until recently, demonstration of the acutely inflamed appendix by sonography was thought to be impossible for three reasons: interference from gas-filled bowel loops in the right lower quadrant; concern about pain and tenderness that could be caused by compressing the abdomen with the transducer in this region; and lack of high-resolution transducers necessary to image small structures such as the inflamed appendix. Not only are new high-resolution transducers now available, but it is now possible to apply graded compression without intolerable pain, thus facilitating the displacement of intestinal gas and the visualization of the inflamed appendix. In our experience and that of Puylaert [3], nonvisualization of the inflamed appendix is strongly suggestive but not diagnostic of a normal appendix.

Our findings concur with those of Puylaert [3], who evaluated 60 consecutive patients with suspected acute appendicitis. While 47% of his patients had acute appendicitis, only 37% of our group did. This may be attributed to the method of patient selection, since he scanned all patients with suspected appendicitis whereas we scanned only patients with equivocal clinical diagnosis of acute appendicitis. Patients with a clear clinical diagnosis of acute appendicitis at our institution were not included in the study, because they were operated on without sonography. Our 90% accuracy (95% confidence interval: 82%, 97%); 80% sensitivity (64%, 96%); 95% specificity (89%, 100%); 91% positive predictive value (79%, 100%); and 89% negative predictive value (80%, 98%) were comparable to the 95% accuracy, 89% sensitivity, 100% specificity, 89% positive predictive value, and 91% negative predictive value in Puylaert's study [3]. One of our two false-positive diagnoses was in a pregnant woman; a dilated uterine vein was probably mistaken for a dilated inflamed appendix despite the absence of Doppler signal in that structure. The patient's signs and symptoms resolved in 2 days. In the other false-positive case, the patient left the hospital against medical advice and follow-up was not possible. On retrospective analysis of the sonographic examination of the five false-negative cases, the inflamed appendix could be seen in two, raising the accuracy of sonography to 93% (86%, 99%); the sensitivity to 88% (75%, 100%); the positive predictive value to 92% (81%, 100%); and the negative predictive value to 93% (86%, 100%). In these two cases the sonographic appearance of the inflamed appendix could be seen retrospectively in one or two scans, and lack of adequate documentation of several different views was due to failure to recognize the diagnosis during real-time examination.

Takada et al. [17] found that the rate of detection of acute appendicitis by sonography depends on the severity of the inflammation. While they were able to detect 100% of the cases of phlegmonous or suppurative appendicitis, they detected only 32% of catarrhal appendicitis cases. Our results, on the other hand, showed no significant difference in the detection accuracy of the two groups, since none of the seven cases of acute uncomplicated and Crohn's appendicitis was missed while four of the eight cases of gangrenous and one of the 10 cases of perforated appendicitis were. This is probably because patients with gangrenous nonperforated appendicitis have more pain and tenderness than the other two groups due to fluid distension of the appendix, and this severe tenderness prevents the compression needed to visualize the inflamed appendix. The one perforated appendix that was missed was retrocecal.

Using the criteria suggested by Takada et al. [17], gangrenous or suppurative changes were predicted in all cases seen by sonography. Sonography was less accurate in cases of perforated appendicitis. Using the criteria suggested by Puylaert [3], it was possible to diagnose perforation in 56% of the cases. In three other cases (33%), it was not possible to differentiate perforation from gangrenous appendicitis. These findings were not consistent with those of Puylaert [3], who was able to predict perforation in all cases proved as such. Overall, sonography was correct in detecting complications of acute appendicitis in 92% of the cases seen by this technique.

Appendiceal calculi are present in about 10–14% of the cases of acute appendicitis and are associated with perforation in 50% [8, 18]; however, plain abdominal films can detect one-third of these [18]. Although we were able to detect appendicoliths by sonography in two of three cases, their sonographic appearance could be mimicked by intraluminal air, mucus, or fecal material [3].

Crohn's disease of the appendix occurs as part of Crohn's ileocolitis in 25% of the cases [19, 20]. Rarely, Crohn's disease can be localized to the appendix. Preoperative and even intraoperative clinical diagnosis is always difficult. Fortunately, however, the rate of recurrence of Crohn's disease in the colon or small bowels after appendectomy is low (14%), and fistula formation has never been reported [20]. Although it was not possible in our series to differentiate the case of Crohn's appendicitis from acute appendicitis, recent reports suggest that the presence of excessive thickening of the appendiceal muscular wall without significant lumen distension is suggestive of Crohn's appendicitis [15]. The wall thickening in our case was similar to several other cases of acute appendicitis. The presence of adjacent bowel wall thickening does not help in the differentiation, since this can occur in acute appendicitis from extension of the inflammatory process to the adjacent bowel loops.

In conclusion, our study confirms the findings of Puylaert's study that high-resolution sonography is fairly accurate and specific, although slightly less sensitive, in the diagnosis of acute appendicitis. This technique is also fairly accurate in detecting complications of acute appendicitis. Sonography should be performed in all patients in whom the clinical diagnosis of acute appendicitis is equivocal, especially women of childbearing age, because it is sometimes difficult to differentiate clinically between acute appendicitis and pelvic inflam-

matory disease and the complications of pregnancy that are prevalent in this population.

ACKNOWLEDGMENTS

The authors thank Patricia Donovan for secretarial assistance, Phyllis Bergman for editorial assistance, Steve Moon for photographic help, and the sonographers in the Department of Radiology for their dedication.

REFERENCES

1. Deal DR. Acute appendicitis. In: Sleisenger MH, Fordtran JS, eds. *Gastrointestinal disease. Pathophysiology, diagnosis, management*. Philadelphia: Saunders, **1973**:1494–1500
2. Lewis FR, Holcroft JW, Boey J, Dunphy JE. Appendicitis: a critical review of diagnosis and treatment in 1,000 cases. *Arch Surg* **1975**;110:677–684
3. Puylaert JBCM. Acute appendicitis: US evaluation using graded compression. *Radiology* **1986**;158:355–360
4. Dunn EL, Moore EE, Elerding SC, Murphy JR. The unnecessary laparotomy for appendicitis—can it be decreased? *Am Surg* **1982**;48:320–323
5. Bongard F, Landers DV, Lewis F. Differential diagnosis of appendicitis and pelvic inflammatory disease. A prospective analysis. *Am J Surg* **1985**;150:90–96
6. Horowitz MD, Gomez GA, Santiesteban R, Burkett G. Acute appendicitis during pregnancy: diagnosis and management. *Arch Surg* **1985**;120:1362–1367
7. Bailey LE, Finley RK Jr, Miller SF, Jones LM. Acute appendicitis during pregnancy. *Am Surg* **1986**;52:218–221
8. Mindelzun RE, McCort JJ. Acute abdomen. In: Margulis AR, Burhenne HJ, eds. *Alimentary tract radiology*, Vol. 1, 3rd ed. St. Louis: Mosby, **1983**:391–455
9. Fedyshin P, Kelvin FM, Rice RP. Nonspecificity of barium enema findings in acute appendicitis. *AJR* **1984**;143:99–102
10. Schey WL. Use of barium in the diagnosis of appendicitis in children. *AJR* **1973**;118:95–103
11. Balthaza EJ, Megibow AJ, Hulnick D, Gordon RB, Naidich DP, Beranbaum ER. CT of appendicitis. *AJR* **1986**;147:705–710
12. Gale ME, Birnbaum S, Gerzof SG, Sloan G, Johnson WC, Robbins AH. CT appearance of appendicitis and its local complications. *J Comput Assist Tomogr* **1985**;9:34–37
13. Feldberg MAM, Hendriks MJ, van Waes PFGM. Computed tomography in complicated acute appendicitis. *Gastrointest Radiol* **1985**;10:289–295
14. Kniskern JH, Eskin EM, Fletcher HS. Increasing accuracy in the diagnosis of acute appendicitis with modern diagnostic techniques. *Am Surg* **1986**;52:222–225
15. Parulekar SG. Ultrasonic findings in diseases of the appendix. *J Ultrasound Med* **1983**;2:59–64
16. Deutsch A, Leopold GR. Ultrasonic demonstration of the inflamed appendix: case report. *Radiology* **1981**;140:163–164
17. Takada T, Yasuda H, Uchiyama K, Hasegawa H, Shikata J. Ultrasonographic diagnosis of acute appendicitis in surgical indication. *Int Surg* **1986**;71:9–13
18. Tegtmeyer CJ, Thistlethwaite JR, Sneed TF. Roentgen findings in acute appendicitis. *Med Ann* **1969**;38:127–130
19. Early CK, Kouri S. Granulomatous disease of the appendix manifesting as a cecal mass: report of a case. *Dis Colon Rectum* **1980**;23:421–422
20. Yang SS, Gibson P, McCaughey RS, Arcari FA, Bernstein J. Primary Crohn's disease of the appendix: report of 14 cases and review of the literature. *Ann Surg* **1979**;189:334–339

Percutaneous Drainage of Periappendiceal Abscesses: Review of 20 Patients

R. Brooke Jeffrey, Jr.[1]
Corito S. Tolentino
Michael P. Federle
Faye C. Laing

Twenty patients with periappendiceal abscesses diagnosed by CT underwent percutaneous catheter drainage. Eighteen (90%) of the 20 patients were successfully treated by percutaneous drainage and antibiotic therapy alone. In two of these patients, however, small recurrent abscesses were diagnosed by CT 4 and 6 weeks after drainage, but these abscesses resolved with additional antibiotic therapy. Surgery was performed in two patients in whom percutaneous drainage failed. One was a diabetic patient who had a gas-forming abscess that extended into the posterior pararenal space. Surgery was necessary in a second patient because of a technical failure of catheter insertion, which resulted in perforation of the abscess cavity and peritonitis. Abscess sinograms in eight (44%) of 18 patients showed fistulas between the abscess cavity and the base of the cecum or appendix. However, the fistulas did not pose a problem in clinical management, and all closed within 14 days.

Percutaneous drainage is an effective alternative to surgery in selected patients with periappendiceal abscesses.

Recent reports have documented the accuracy and clinical utility of CT in distinguishing periappendiceal abscesses from phlegmons [1–5]. In addition, percutaneous drainage has been shown to be a useful alternative to surgical drainage [6]. This report summarizes our clinical experience with 20 patients undergoing percutaneous catheter drainage for periappendiceal abscesses and analyzes the role of percutaneous drainage in the management of periappendiceal abscesses.

Materials and Methods

From January 1983 to December 1986, 20 patients with fever, leukocytosis, and CT evidence of pericecal fluid collections were diagnosed as having periappendiceal abscesses. There were 13 men and seven women 6–74 years old (mean age, 26 years). The CT criteria for diagnosis of a periappendiceal abscess included a low-density mass (less than 20 H) adjacent to the inferior aspect of the cecum. The presence of a calcified appendicolith was considered diagnostic of periappendiceal abscess. Nineteen (95%) of the 20 patients had had right lower quadrant pain for more than 72 hr. A palpable mass was present in 17 (85%) of the 20 patients.

Each patient who had well-defined and well-localized periappendiceal abscess with a safe access route for catheter insertion was considered a candidate for percutaneous drainage. Patients with more extensive and poorly defined abscesses (eight patients during the same interval) underwent early surgical drainage.

Percutaneous drainage was performed under CT guidance (18 patients) or sonographic guidance (two patients). A standard guidewire-exchange method was used in all patients. Smaller periappendiceal abscesses (3.5–5 cm) were generally drained with 8.3- to 10-French nephrostomy pigtail catheters. Larger abscesses were drained with 12-French sump catheters. Periappendiceal abscesses were drained via either an anterior or right lateral approach (Figs. 1 and 2). Routine abscess sinograms were obtained 3 days after initial catheter drainage to document the abscess cavity size and the presence of any fistulas (Fig. 3).

After resolution of clinical symptoms, drainage catheters were gradually withdrawn when abscess sinograms showed closure of any existing fistulas and when catheter drainage was

Received February 2, 1987; accepted after revision March 11, 1987.

[1] All authors: Departments of Radiology, University of California, San Francisco, San Francisco, CA 94143, and San Francisco General Hospital, San Francisco, CA 94110. Address reprint requests to R. B. Jeffrey, Department of Radiology 1X55, San Francisco General Hospital, 1001 Potrero Ave., San Francisco, CA 94110.

AJR 149:59–62, July 1987
0361–803X/87/1491–0059
© American Roentgen Ray Society

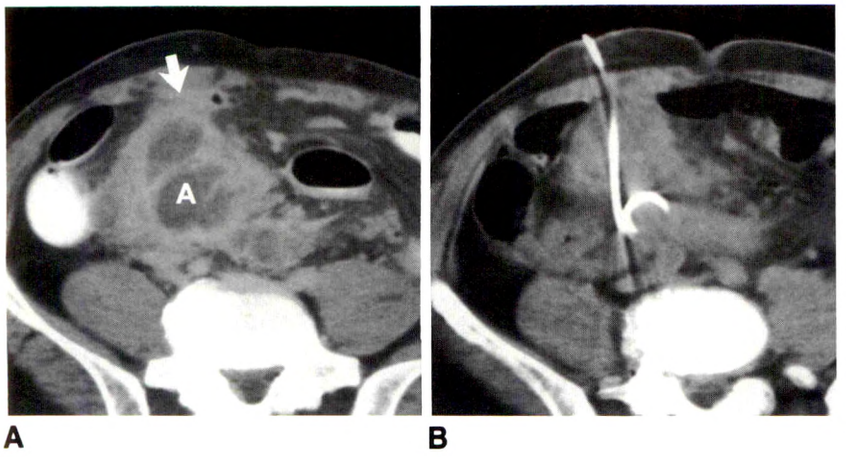


Fig. 1.—Medially located periappendiceal abscess.
***A*, CT shows precise access route between bowel loops for catheter insertion (*arrow*). A = periappendiceal abscess.**
***B*, After drainage. Complete evacuation of abscess.**

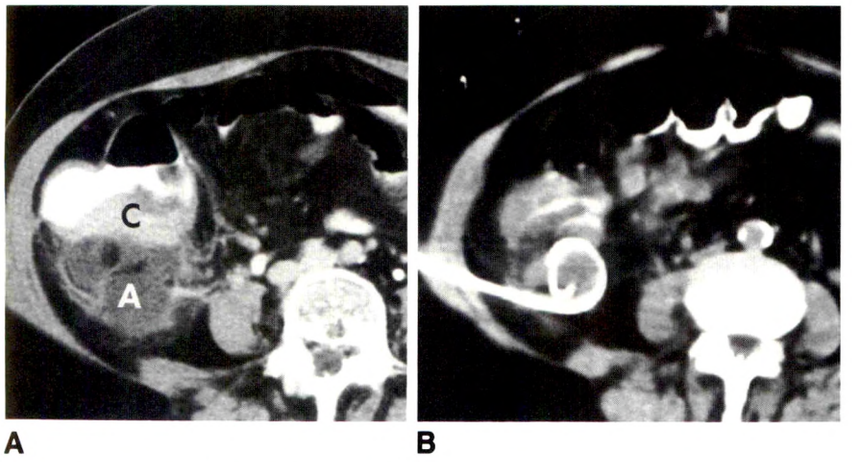


Fig. 2.—CT demonstration of retrocecal periappendiceal abscess.
***A*, Note mural thickening of adjacent cecum (C). A = periappendiceal abscess.**
***B*, Abscess completely evacuated via right lateral approach.**

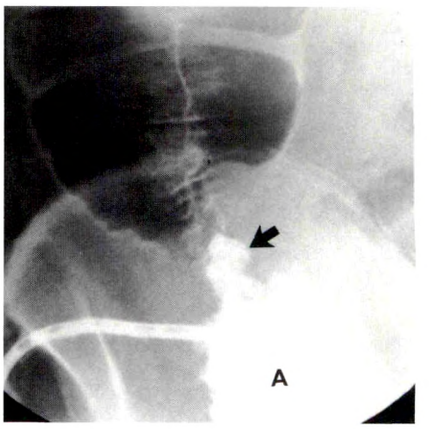


Fig. 3.—Cecal fistula after percutaneous drainage. Abscess sinogram 3 days after initial catheter placement shows communication (*arrow*) between abscess cavity (A) and base of cecum. Patient was discharged on day 7 and fistula closed on day 10.

minimal (<20 ml/day). Patients with persistent evidence of a fistula often were discharged from the hospital with the catheter in place for outpatient sinograms at 3- to 5-day intervals.

Results

In 18 (90%) of the 20 patients treated with percutaneous drainage and antibiotics, the periappendiceal abscess resolved without surgical intervention. However, two patients developed small recurrent abscesses documented by CT at 4 and 6 weeks after initial drainage (Fig. 4). In both patients the abscesses were smaller than 2.5 cm and promptly resolved with additional IV antibiotics. The abscess sinograms before catheter removal in both these patients did not disclose a cecal or appendiceal fistula.

In two patients percutaneous therapy failed, and surgery was required. One patient was a 56-year-old diabetic woman with a gas-forming pericecal abscess extending into the posterior pararenal space (Fig. 5). On the basis of the CT appearance of the abscess, the patient was not believed to be a good candidate for percutaneous drainage. However, percutaneous drainage was performed as a temporizing measure to improve the patient's medical condition before definitive surgical drainage. Two 12-French sump catheters were placed both in the pericecal area and in the posterior pararenal space. The patient failed to respond to percutaneous drainage and underwent surgical debridement 72 hr later, which confirmed the presence of a perforated appendix. Because of persistent sepsis, two further surgical reexplorations were required for drainage and debridement of the posterior pararenal space. The patient died from pulmonary and renal failure after 82 days of hospitalization.

In a second patient, percutaneous drainage was not successful because the abscess cavity was inadvertently perfo-

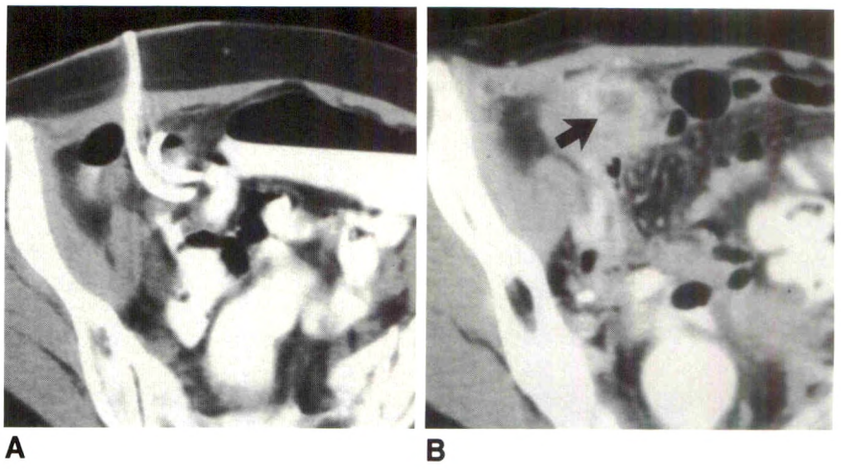


Fig. 4.—CT diagnosis of small (2-cm) recurrent abscess 6 weeks after percutaneous drainage.
***A*, Initial scan after abscess drainage reveals complete evacuation of abscess.**
***B*, 6 weeks later. Small abscess recurred (*arrow*), but it resolved completely on antibiotic therapy.**

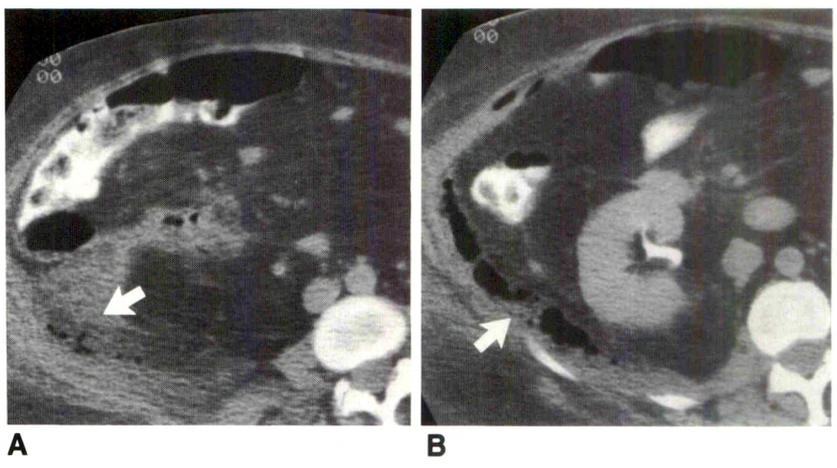


Fig. 5.—Diabetic patient with extraperitoneal extension of periappendiceal abscess.
***A*, Gas-forming pericecal abscess (*arrow*) is seen with inflammatory changes in adjacent abdominal wall.**
***B*, Extension to posterior pararenal (*arrow*). Surgery revealed gangrenous perforated appendix. Percutaneous drainage with two catheters was performed as temporizing measure but failed to provide definitive drainage.**

rated during guidewire insertion. Six hours later peritonitis had developed, and emergent surgical drainage was required.

After percutaneous drainage, cecal or appendiceal fistulas were demonstrated on routine abscess sinograms in eight (44%) of 18 patients. Although the duration of catheter drainage in this group of patients (average, 9 days) was longer than in patients without a fistula (average, 6.5 days), all fistulas were of low output (less than 50 ml/24 hr) and ultimately closed within 14 days. The average length of hospitalization for the 18 patients undergoing successful percutaneous drainage was 6.7 days. Seven patients were discharged from the hospital with a drainage catheter in place and were managed as outpatients.

Interval Appendectomy

In nine patients interval appendectomies were performed 4–6 weeks after catheter drainage. In two other patients appendectomies were performed at the time of initial surgical exploration and drainage. Interval appendectomies were not performed in the other nine patients in this series. No known episodes of recurrent appendicitis have occurred to date; clinical follow-ups have ranged from 4 months to 3½ years (average, 8 months).

Discussion

Recent surgical reports have documented an overall decline in the prevalence of periappendiceal abscesses. Bradley and Isaacs [7] reported appendiceal abscess formation in only 2% of 2621 patients with acute appendicitis. Surgical opinion, however, is divided with regard to the initial therapy (surgical drainage vs conservative therapy) for appendiceal inflammatory masses [7–16]. Often these patients present with a palpable right lower quadrant mass, often referred to as the "appendix mass" [7–16]. This mass may represent a liquified abscess, a phlegmon consisting of inflamed omentum and adherent bowel loops, or a combination of these two entities. Prior surgical reports evaluating operative vs nonoperative therapy for an appendix mass have emphasized the clinical difficulty in distinguishing an abscess from a phlegmon or in predicting the size of the abscess preoperatively [15].

Our results concur with those of Nunez et al. [6] in that patients with well-localized periappendiceal abscesses shown

by CT generally can be managed successfully with percutaneous drainage. Eighteen (90%) of our 20 patients undergoing percutaneous drainage required no surgical intervention. Of the two patients in whom percutaneous drainage failed, technical failure during guidewire insertion caused perforation of the abscess cavity in one patient. In a second, diabetic patient with a gas-forming appendiceal abscess involving the right posterior pararenal space, surgical debridement was required (Fig. 5). Because of the retroperitoneal extension and gas-forming nature of the abscess, it was anticipated that percutaneous drainage alone would not prove definitive. Percutaneous drainage was attempted, primarily as a temporizing measure to improve the patient's general condition before surgery.

Two patients who underwent percutaneous drainage of periappendiceal abscesses had late recurrences of small abscesses 4 and 6 weeks after percutaneous drainage. In both patients the recurrent abscess (smaller than 2.5 cm) resolved on antibiotic therapy alone. It is unclear why these abscesses developed, as neither patient had evidence of a cecal or appendiceal fistula documented on the initial abscess sinogram 72 hr after drainage. An occult fistula may have been present but not recognized. Premature catheter withdrawal may then have led to subsequent recurrence of a small abscess.

Although eight patients in our series (44% of patients with successful percutaneous drainage) had cecal or appendiceal low-output fistulas documented by abscess sinograms, the fistulas ultimately closed with percutaneous catheter drainage alone. This is in agreement with prior reports of successful percutaneous management of low-output fistulas [17–18]. Patients with fistulas often were discharged from the hospital with the catheter in place, and follow-up sinograms were obtained on an outpatient basis. The catheter was withdrawn when the fistula had closed and catheter output was minimal.

The main advantage of percutaneous drainage of periappendiceal abscess is that it avoids the morbidity and expense associated with surgical drainage and attempted appendectomy. The surgical morbidity is 24–36% [10, 11, 15]. The most common postoperative complications include wound infections, fecal fistulas, ileus, and recurrent abscess [15]. Paull and Bloom [10] reported a 24% prevalence of postoperative complications (four of 17 patients) after surgical drainage of a periappendiceal abscess with attempted appendectomy. These included one patient with a fecal fistula (18 days), one patient with a hematoma requiring surgical drainage, one patient with a pulmonary embolism and a drug rash, and one patient readmitted for antibiotic therapy. In this same report complications occurred in five (16%) of 32 patients undergoing drainage alone without attempted appendectomy [10]. Complications included subhepatic, subphrenic, and scrotal abscesses and a fecal fistula draining for 58 days. Jordan et al. [15] noted a 34% prevalence of complications in 15 patients after drainage of a periappendiceal abscess and appendectomy. These included six patients with wound infections, five patients with intraabdominal infections (three of whom required a second operation for drainage of a residual abscess), three patients with a prolonged ileus, and one patient with a fecal fistula. In our series, complications occurred in four (20%) of the 20 patients undergoing percutaneous drainage. These included two patients in whom catheter drainage failed and surgery was required and two patients with small recurrent abscesses that resolved with additional antibiotic therapy. When compared with percutaneous drainage, the increased surgical morbidity may result in part from patient selection, as the surgical series include patients with more extensive abscesses in whom a higher complication rate is anticipated. Nevertheless, this comparison underscores the relative lack of morbidity in patients treated with percutaneous drainage.

Interval appendectomy was performed in nine patients in this series 4–6 weeks after percutaneous drainage. Appendectomies were performed in two patients in whom catheter drainage failed and surgery was required. Nine additional patients did not undergo interval appendectomy, and no known cases of recurrent appendicitis have been noted to date (average follow-up, 8 months). Whether interval appendectomy is necessary at all remains controversial, and the issue will only be settled when the results are reported of large series of patients treated conservatively [11, 12].

In the absence of calcified appendicolith or direct communication between the abscess and the appendix on sinography, the CT diagnosis of an appendiceal abscess is nonspecific. We previously reported a small percentage of patients in whom an incorrect diagnosis of a periappendiceal abscess was made with CT [4]. If there is any doubt about the diagnosis, a barium-enema examination should be performed in adult patients after percutaneous drainage to exclude coexisting colonic disease.

REFERENCES

1. Gale ME, Birnbaum S, Gerzof SG, Sloan G, Johnson WC, Robbins AH. CT appearance of appendicitis and its local complications. *J Comput Assist Tomogr* **1985**;9(1):34–37
2. Jones B, Fishman EK, Siegelman SS. Computed tomography and appendiceal abscess: special applicability in the elderly. *J Comput Assist Tomogr* **1983**;7(3):434–438
3. Fish B, Smulewicz JJ, Barek L. Role of computed tomography in diagnosis of appendiceal disorders. *NY State J Med* **1981**;81:900–904
4. Barakos JA, Jeffrey RB, Federle MP, Wong VW, Laing FC, Hightower DR. CT in the management of periappendiceal abscesses. *AJR* **1986**; 146:1161–1164
5. Balthazar EJ, Megibow AJ, Hulnuk D, Gordon RB, Nadich DP, Beranbaum ER. CT of appendicitis. *AJR* **1986**;147:705–710
6. Nunez D Jr, Huber JS, Yuzarry JM, Mendez G, Russell E. Nonsurgical drainage of appendiceal abscesses. *AJR* **1986**;146:587–589
7. Bradley EL, Isaacs J. Appendiceal abscess revisited. *Arch Surg* **1978**;113:130–132
8. Vakele C. Operative treatment of appendix mass. *Am J Surg* **1976**; 131:312–314
9. McPherson AG, Kinmoth JB. Acute appendicitis and the appendix mass. *Br J Surg* **1945**;32:365–370
10. Paull DL, Bloom GP. Appendiceal abscess. *Arch Surg* **1982**;117:1017–1019
11. Hoffman J, Lindhard A, Jensen H. Appendix mass: conservative management without interval appendectomy. *Am J Surg* **1984**;148:379–382
12. Foran B, Berne TV, Rosoft L. Management of the appendiceal mass. *Arch Surg* **1978**;113:1144–1145
13. Skoubo-Kristensen E, Hvid I. The appendiceal mass: results of conservative management. *Ann Surg* **1982**;196(5):584–587
14. Ainbjournsson E. Management of appendiceal abscess. *Curr Surg* **1984**; 41:4–9
15. Jordan JS, Kovalcik PJ, Schwab CW. Appendicitis with a palpable mass. *Ann Surg* **1981**;193(2):227–229
16. Thomas DR. Conservative management of the appendix mass. *Surgery* **1973**;73(5):677–680
17. Papanicolaou N, Mueller PR, Ferucci JT Jr, et al. Abscess-fistula associations: radiologic recognition and percutaneous management. *AJR* **1984**;143:811–815
18. Kerlan RK Jr, Jeffrey RB Jr, Pogany AC, Ring EJ. Abdominal abscess with low-output fistula: successful percutaneous drainage. *Radiology* **1985**; 155:73–75

Performance of Barium Examinations After Acute Myocardial Infarction: Report of a Survey

Herbert J. Smith[1]

A survey of members of the Society of Gastrointestinal Radiologists was conducted to ascertain the standards of practice and timing for elective barium studies of the gastrointestinal tract in patients recovering from acute myocardial infarction. Sixty-two percent of respondents do not have cardiac monitoring apparatus readily available in the fluoroscopy suite. When readily available, such equipment is rarely (42%) or never (58%) used during *routine* barium examinations. Twenty-four percent of respondents take special precautions when performing examinations on these patients by reducing patient movement, the length of the examination, and the number of radiographs exposed, and by employing cardiac monitoring. Seventy-two (89%) of 81 respondents noted at least one adverse cardiovascular reaction. This was most often chest pain, but there were 10 deaths from cardiac causes. Two-thirds of respondents delay *elective* barium examinations of any kind for at least 4 weeks after acute myocardial infarction. The remaining one-third perform these studies earlier than 4 weeks. The latter typically limit their studies to the upper gastrointestinal tract (82%), 42% of which are single-contrast; the rest are equally divided between double-contrast and biphasic studies. This minority of radiologists is twice as likely to perform a single-contrast barium enema than a double-contrast barium enema during this period. No such preference for single-contrast (47%) over double-contrast (53%) barium enema is revealed by the majority who delay their elective barium enemas 4 or more weeks.

The data indicate a strong preference to defer elective barium examinations a minimum of 4 weeks after acute myocardial infarction. A sizable minority (one-third) of radiologists, however, feel comfortable performing a single-contrast upper gastrointestinal examination at an earlier time.

Although data exist concerning the expected frequency of recurrent myocardial infarction and its relation to stress and to noncardiac surgery [1–4], few reports directly describe the cardiac stress involved with upper gastrointestinal tract examinations and barium enema, or the proper timing for these elective diagnostic barium examinations during the postinfarction period. This report gives the results of a survey of experienced radiologists concerning their practices in this regard.

Materials and Methods

Questionnaires were mailed to 165 members of the Society of Gastrointestinal Radiologists inquiring about their experiences and customs in performing barium studies on patients after acute myocardial infarction. Eighty-six (52%) of the surveys were returned. The responses of three radiologists who limit their practices to pediatrics were excluded from this tabulation. The 83 remaining respondents represent 76 different institutions. Responses from more than one radiologist from the same institution were individually tabulated (in the absence of a departmental policy, individual responses were assumed to reflect individual experiences and practices). This group comprised 15 persons from seven institutions. Sixty-eight (89%) of all institutions responding were university hospitals or their affiliates. Radiologists were queried about the availability and use of cardiac monitoring apparatus in the fluoroscopy suite, the timing of nonemergency (elective) barium studies in patients recovering from acute myocardial

Received December 29, 1986; accepted after revision March 2, 1987.

[1] Radiology Service, Veterans Administration Medical Center and The University of Texas Health Science Center, Dallas. Address reprint requests to H. J. Smith, VA Medical Center, Radiology Service (114), 4500 S. Lancaster Rd., Dallas, TX 75216.

AJR 149:63–65, July 1987
0361–803X/87/1491–0063
© American Roentgen Ray Society

infarction, the types of gastrointestinal studies performed in this circumstance, special precautions taken during these examinations, and their experiences with specific cardiovascular reactions related to these barium studies.

Results

Cardiac Monitoring

Equipment for cardiovascular monitoring (e.g., ECG, telemetry) was readily available in 31 (38%) of 81 cases. This figure reflects the location of equipment both in and near the fluoroscopy suites. When available, cardiac monitoring was used rarely (42%) or never (58%) during routine barium examinations.

Timing and Types of Contrast Studies

Radiologists were questioned about the earliest time (1–3 weeks, 1–3 months, 4–6 months) that they would perform specific types of elective barium examinations on patients recovering from myocardial infarction. Five individuals either provided no answer or indicated that the wishes of the clinical services were determinative. Forty-eight (67%) of 72 radiologists who responded delayed the performance of nonemergency barium studies at least 4 weeks after the acute infarction, seven of the 48 preferring an even longer delay of up to 4 months. Twenty-four (33%) of 72 examiners, however, performed such studies 1–3 weeks after myocardial infarction. Most (82%) of these examinations were upper gastrointestinal tract examinations. The barium enemas (18%) done at an earlier time were weighted 2:1 in favor of single-contrast studies (15 vs 7). Several practitioners (10) provided more specific information about timing: one would perform all types of studies after 1 week; four after 2 weeks, but two of these would restrict the studies to the single-contrast upper gastrointestinal tract study; another would delay all studies of the upper gastrointestinal tract for 3 months and all barium enemas for 4 months; three other radiologists chose to examine at 3 weeks. All three would limit their examinations to studies of the upper gastrointestinal tract, and two of the three would perform only single-contrast studies. One radiologist requires written cardiology consultation before performing any type of barium study during the period before 4 weeks. There was no overall difference in the timing of the earliest study between the 63 (76%) who indicated no special precautions and the 20 (24%) who did; 34% of all studies were done before 4 weeks by the former, 35% by the latter. However, for those indicating special precautions, barium enemas formed a larger proportion (25% vs 16%) of their studies.

Special Precautions

Twenty-four percent of respondents indicated that they took special precautions when examining a patient recovering from myocardial infarction. These special precautions included suggestions to limit the examination to the recumbent position; to reduce the number of films taken; and to work fast, make the patient comfortable, talk to the patient, leave the lights on in the fluoroscopy room, and use cardiac monitoring, if available.

Cardiovascular Reactions

Seventy-two of 81 (89%) noted at least one cardiovascular reaction associated with the performance of barium examinations in these patients. At least one instance of chest pain, hypotension, or syncope was reported by 32%, 22%, and 21%, respectively, of the 72 radiologists. The development of acute heart failure was seen in one patient. Ten deaths were reported, six related to barium enema, one to upper gastrointestinal tract examination, and three to unspecified barium studies. At least three of the barium-enema–related deaths involved single-contrast barium enema; the type of barium enema was unspecified in the remainder.

Discussion

Barium studies of the gastrointestinal tract may be requested for patients recovering from acute myocardial infarction. Although barium examinations have a remarkable record of safety, these studies carry potential and actual risks [5–9]. Unforeseen hazards continue to be reported [10–11]. This report provides some information on several aspects of the conduct of barium studies on patients recovering from myocardial infarction. It provides no means, however, of ascertaining prevalence data on adverse cardiovascular reactions, for example. There are other obvious limitations to surveys of this type: they are retrospective and subjective, and they rely on recall of incidents that may have occurred years ago. The tendency to remember "unusual cases" helps in this regard.

The present data reveal a wide variety of opinion and practice among individual radiologists. However, a sizable majority of examiners (67%) delay elective barium studies of any kind for at least 4 weeks after acute myocardial infarction. For the one-third who perform these studies earlier, examinations are typically limited to single-contrast studies. If a barium enema were performed during this earlier period, 15 (68%) of 22 radiologists would use a single-contrast technique. These preferences seem to reflect a shared belief that single-contrast examinations of both the upper and lower tracts are less stressful than those that use air. Furthermore, they suggest that barium enemas of any sort are more stressful than upper gastrointestinal tract studies. The definitions of the various types of studies are those of the respondents.

The 67% of examiners who delay all elective barium study at least 4 weeks seem to be in agreement with the current timing (21–42 days) of a patient's initial return to physical activity (via symptom-limited exercise testing) after uncomplicated myocardial infarction [12]. This seems to represent a conservative yet workable policy on barium examinations in the postinfarction period, on the basis of application of available evidence. The approaches to high-risk patients (those with complicated myocardial infarction) must be individual-

ized, with especially careful weighing of known risks and presumed benefits of nonemergency barium examinations.

REFERENCES

1. Goldman L, Caldera DL, Southwick FS, et al. Cardiac risk factors and complications in non-cardiac surgery. *Medicine (Baltimore)* **1978**;57:357–370
2. Goldman L. Cardiac risks and complications of noncardiac surgery. *Ann Intern Med* **1983**;98:504–513
3. Gibson RS, Watson DD, Craddock GB, et al. Prediction of cardiac events after uncomplicated myocardial infarction: a prospective study comparing predischarge thallium-201 scintigraphy and coronary angiography. *Circulation* **1983**;68:321–336
4. Mukharji J, Rude RE, Poole WK, et al. Risk factors for sudden death after myocardial infarction: two-year follow-up. *Am J Cardiol* **1984**;54:31–36
5. Gelfand DW. Complications of gastrointestinal radiologic procedures. I. Complications of routine fluoroscopic studies. *Gastrointest Radiol* **1980**;5:293–315
6. Berman CZ, Jacobs MG, Bernstein A. Hazards of the barium enema examination as studied by electrocardiographic telemetry: preliminary report. *J Am Geriat Soc* **1965**;13:672–686
7. Roeske WR, Higgins C, Karliner JS, Berk RN, O'Rourke RA. Incidence of arrhythmias and ST-segment changes in elderly patients during barium enema studies. *Am Heart J* **1975**;90:688–694
8. Higgins CB, Roeske WR, Karliner JS, O'Rourke R, Berk RN. Predictive factors and mechanisms of arrhythmias and myocardial ischaemic changes in elderly patients during barium enema. *Br J Radiol* **1976**;49:1023–1027
9. Amberg JR. Complications of colon radiography. *Gastrointest Endosc* **1980**;26[Suppl]:15S–17S
10. Schwartz EE, Glick SN, Foggs MB, Silverstein GS. Hypersensitivity reactions after barium enema examination. *AJR* **1984**;143:103–104
11. Janower ML. Hypersensitivity reactions after barium studies of the upper and lower gastrointestinal tract. *Radiology* **1986**;161:139–140
12. DeBusk RF, Blomqvist CG, Kouchoukos NT, et al. Identification and treatment of low-risk patients after myocardial infarction and coronary-artery bypass graft surgery. *N Engl J Med* **1986**;314:161–166

1988 AMERICAN ROENTGEN RAY SOCIETY MEETING

MAY 8–13, 1988
SAN FRANCISCO HILTON HOTEL
SAN FRANCISCO, CA

See p. 208 and forthcoming issues for further information.

Book Review

Color Doppler Flow Imaging and Other Advances in Doppler Echocardiography. Edited by J. Roelandt. The Hague: Nijhoff, 221 pp., 1986. $86

This short book is a series of independently authored and submitted chapters written by qualified and experienced authors and edited by a major contributor to the field of two-dimensional Doppler echocardiography, Jos Roelandt of Erasmus University in Rotterdam. The book addresses a variety of new clinical applications of Doppler but is somewhat misleadingly stressed as a color-flow-imaging treatise because only about 90 of its 200 pages deal with Doppler color-flow imaging. As in many multiauthored books, the best contributions are by the editor himself and some of his associates, and the other contributions vary in quality. Unfortunately, in a rapidly changing field, and for a book prepared a year ago, some of the statements about the application and impact of color-flow imaging represent a contrast between Japanese investigators in the field with vast clinical experience and other investigators who are giving their first impressions of first-generation instruments of what was a new technology to them. The result is a book that is quite informative and relatively state-of-the-art, but of mixed quality.

The book is organized quite rationally with chapters in technical aspects of instruments, Bernoulli (pressure velocity), hydrodynamics, and computer processing. The first section is, in general, quite useful and represents a nice collection of basic science papers and an extremely good review of principles. Next comes the color-flow imaging section with a variety of clinical papers from Japan, Europe, and the United States. This is followed by a clinical impact and advances section that discusses a variety of Doppler applications, mainly related to noncolor applications.

The first chapter on bidimensional pulse Doppler instruments (a technical chapter) by Peronneau and his associates is a little difficult to read. It is probably a too sophisticated approach for the average reader. However, the general description of the technology of color-flow-mapping systems at the end of the chapter is quite good.

The chapter by Rijsterborgh and Roelandt on the Bernoulii relationship and its applications is an excellent review of a variety of simplifications and transmutations of the Doppler velocity pressure relationship. It is, while sophisticated, extremely well written and clinically important since much of what is being done around the world in clinical Doppler represents significant oversimplification of hydrodynamic principles dealing with concepts of flow relaminarization, pressure recovery, proximal energy loss, and other important concepts.

Section 2 of the book relates to color-coded Doppler. Pioneering investigators, such as Omoto and his associate, present vast clinical experience in well-illustrated and important chapters. These are mixed with early experiences by Yock and coworkers showing early generation and relatively poor quality images. Similarly, Stevenson's experience, while extensive in non–color-flow Doppler, was, when he prepared this chapter, a mixed one. A nice chapter by Kyo and coworkers from Japan on congenital heart disease discusses opportunities for bypassing the catheter laboratory when referring patients for surgery and represents significant experience.

A review chapter ending the color Doppler section by Roelandt, Vletter, Rijsterborgh, and Gussenhoven contains illustrations of outstanding and exciting quality and is generally an important and well-referenced review of the subject. This chapter by the editor himself is the most impressive part of the color-flow section.

The last section of the book, the clinical advances section, is not as impressive as Roelandt's chapter. The chapter by Skjaerpe on continuous-wave Doppler and gradients is a well-written and comprehensive review. The chapter by Dennig represents a scholarly experience with a large number of patients with prosthetic valves. The last two chapters are a review of the impact of Doppler in pediatric cardiology.

The illustrations in this book are of mixed quality. Those by Roelandt and coworkers have been prepared with diligence and extremely high quality photographic technique, whereas others appear to have mixed exposures and some are quite difficult to see.

In summary, this treatise has a somewhat misleading title. It contains informative and important basic science material, some extensive reviews of color-flow-mapping experience from Japan, applications in prosthetic and native-heart valve disease in adults mainly related to continuous-wave Doppler in Europe, and an extremely well written and elegantly illustrated chapter by the editor and his coworkers from Rotterdam. There are a few truly comprehensive works in this field that are state-of-the-art and, certainly, in view of a paucity of good writing on the subject, this short treatise still serves an important place for education in Doppler technologies. Like many multiauthored textbooks, it varies in the quality of the contributions. Despite this drawback, the book will be useful as a review of the recent state-of-the-art of Doppler sonographic technologies and as a well-written series of chapters on basic principles of Doppler and the hydrodynamics of flow in the heart.

David J. Sahn
Erkki Pesonen
UCSD Medical Center
San Diego, CA 92103

Case Report

Sonographic Findings in Pancreatic Lipomatosis

C. Benny So,[1] Peter L. Cooperberg,[1] Robert G. Gibney,[1] and Abraham Bogoch[2]

In pancreatic lipomatosis there may be complete replacement of the pancreas by fat associated with pancreatic insufficency [1]. On CT, this has the expected appearance of the pancreatic lobules completely replaced by fatty tissue [2]. To our knowledge, the sonographic appearance in this condition has not been previously reported. We present a case in which the pancreas appeared normal on sonography, despite the fact that CT showed complete replacement of the pancreas with fat.

Case Report

A 57-year-old woman had a 22-year history of chronic diarrhea. She had bloating, eructation, and flatulence, and she described her stools as "frothy with mucus." There was an elevated fecal fat content. An initial sonogram in 1976 and a subsequent sonogram at the time of admission both showed a "normal" appearance of the pancreas (Fig. 1A). CT showed that the pancreas had been completely replaced by fat (Fig. 1B).

Discussion

Fatty infiltration or replacement of the pancreas is a condition that frequently occurs with aging and increased body fat [3]. Although lesser degrees of fatty replacement are not associated with any clinical abnormality, malabsorption syndrome can occur with severe fatty replacement also known as pancreatic lipomatosis [1]. The etiology of this condition is unknown, but it has been associated with a variety of diseases including cystic fibrosis, obesity, diabetes mellitus, hereditary pancreatitis, and chronic pancreatitis [2, 4]. There was no apparent predisposing disease in our patient.

In pancreatic lipomatosis, the primary disorder is replacement of the pancreatic parenchyma by adipose tissue [4]. The pancreas may appear normal in size, as in our patient, or may be massively enlarged, resulting in a condition known as lipomatous pseudohypertrophy [5]. On the other hand, an atrophic gland with a variable degree of fatty replacement may be seen in cystic fibrosis, pancreatic duct obstruction by tumor, or calculus [2, 6].

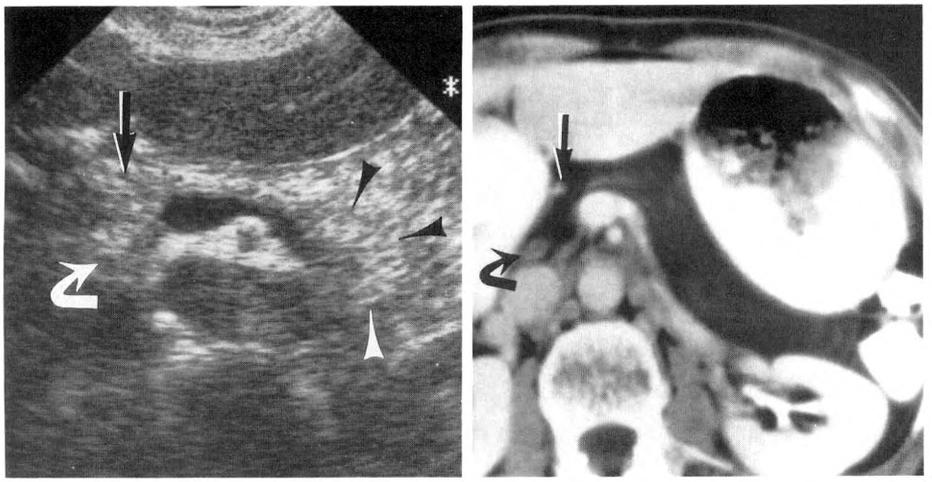
The normal sonographic appearance of the pancreas has been well described [7]. The echo texture of the pancreas is greatly dependent on the degree of fatty infiltration but can also be affected by transducer frequency, focal depth of the transducer, and gain settings [8]. The pancreas should be slightly more echogenic than the liver but less echogenic than the surrounding retroperitoneal fat [3]. In a small percentage of patients (9.3% in one study [3] and 14% in another [7]), the echogenicity of the normal pancreas was found to be undifferentiable from that of the surrounding fat. Thus, in a significant minority of subjects, the pancreas can only be identified by inference from its characteristic relationship to the adjacent vessels (that is, the splenic vein, portal confluence, gastroduodenal artery, and inferior vena cava) and the common bile duct. If these structures are well seen and the tissue in the expected position of the pancreas has an expected echogenicity, the pancreas is considered normal, and total replacement by fat may not be appreciated.

Received December 29, 1986; accepted after revision February 13, 1987.

[1] Department of Radiology, University of British Columbia, and Vancouver General Hospital, 855 W. 12th Ave., Vancouver, British Columbia V5Z 1M9, Canada. Address reprint requests to P. L. Cooperberg.

[2] Department of Medicine, University of British Columbia, and Vancouver General Hospital, Vancouver, British Columbia V5Z 1M9, Canada.

AJR 149:67–68, July 1987 0361–803X/87/1491–0067 © American Roentgen Ray Society



A B

Fig. 1.—*A*, Transverse sonogram through pancreas. Pancreas appears normal (*arrowheads* outline distal pancreatic body and proximal tail). Note normal vascular landmarks of splenic vein and portal confluence posterior to body of pancreas, gastroduodenal artery (*straight arrow*) in anterolateral aspect of head, and common bile duct (*curved arrow*) in posterolateral aspect of head. Liver is clearly seen anteriorly and shows echogenicity less than that of "pancreas."

***B*, CT scan at level of pancreas. Pancreas has been completely replaced by tissue of fat density. Note same landmarks of splenic vein and confluence posteriorly, gastroduodenal artery (*straight arrow*) anterolaterally, and common bile duct (*curved arrow*) posterolaterally. Pancreatic duct can also be seen anterior to portal confluence.**

REFERENCES

1. Bogoch A, ed. *Gastroenterology*, New York: McGraw-Hill, **1973**:978–979
2. Patel S, Bellon EM, Haaga J, Park CH. Fat replacement of the exocrine pancreas. *AJR* **1980**;135:843–845
3. Worthen NJ, Beabeau D. Normal pancreatic echogenicity: relation to age and body fat. *AJR* **1982**;139:1095–1098
4. Freeny PC, Lawson TL, eds. *Radiology of the pancreas*. New York: Springer-Verlag, **1982**
5. Nakamara M, Katanda N, Sakalibara A, et al. Huge lipomatous pseudohypertrophy of the pancreas. *Am J Gastroenterol* **1979**;72:171–174
6. Daneman A, Gaskin K, Martin DJ, Cutz E. Pancreatic changes in cystic fibrosis: CT and sonographic appearances. *AJR* **1983**;141:653–655
7. Mark WM, Filly RA, Callen PW. Ultrasound evaluation of normal pancreatic echogenicity and its relationship to fat deposition. *Radiology* **1980**;137:475–479
8. Filly RA, London SS. The normal pancreas: acoustic characteristics and frequency of imaging. *JCU* **1979**;7:121–124

Case Report

Uptake of ^{99m}Tc–Methylene Diphosphonate by Pancreatic Insulinoma

Jeremy Price,[1] Clive S. Cockram,[2] Lloyd J. McGuire,[3] Trevor J. Crofts,[4] Iain E. T. Stewart,[1] and Constantine Metreweli[1]

Despite the use of dynamic CT and the improved resolution of sonography, pancreatic insulinomas remain difficult to detect. Some 40% of tumors are smaller than 1 cm, and multiple tumors occur in 10% of cases [1]. It is in these situations, when imaging is particularly difficult, that preoperative localization is most useful to the surgeon. A scintigraphic method would have an inherent advantage in locating tumors, regardless of site, size, and number. We report a case in which ^{99m}Tc–methylene diphosphonate (^{99m}Tc-MDP) concentrated in an insulinoma.

Case Report

A 23-year-old Chinese man presented in spontaneous hypoglycemic coma. During admission, a plasma immunoreactive insulin of 21 mU/l was recorded at a plasma glucose level of 25 mg/dl (1.4 mmol/l), confirming the presence of an insulinoma on biochemical grounds.

Dynamic CT was performed using a GE 8800 scanner with 5-mm sections obtained at selected levels during injection of a total of 60 ml of 76% Urografin (Schering, Berlin, West Germany). This revealed a 2.5-cm-diameter lesion in the pancreatic tail showing dense uniform enhancement typical of an islet-cell tumor (Fig. 1A). Sonography was performed with a Philips SDU 7000 real-time unit with a 3.5-MHz probe, and a 2.5-cm-diameter hypoechoic lesion was found, also within the pancreatic tail.

Routine biochemical tests showed an elevation of plasma alkaline phosphatase (bone isoenzyme) to 186 IU/l (normal range, 40–136 IU/l). A bone scan was obtained with 15 mCi (555 MBq) of ^{99m}Tc-MDP (Mallinckrodt Diagnostica, Petten, Holland) with 2-hr delayed imaging on a Philips Diagnost C gamma camera (Philips, Eindhoven, Holland). This showed a single area of marked uptake of isotope in the left upper quadrant (Fig. 1B). An oblique view showed the activity centered between two ribs indicating its extraosseous origin (Fig. 1C). There were no areas of increased activity in bone.

The soft-tissue uptake on the bone scan corresponded exactly to the lesion shown by the other imaging techniques. It seemed likely that this represented uptake of ^{99m}Tc-MDP by the insulinoma. Before surgical exploration, injection of ^{99m}Tc-MDP was repeated to allow imaging of the resected specimen.

At laparotomy a firm 2.5-cm tumor was palpable in the pancreatic tail. A 1.5-cm splenunculus was also noted in close proximity. A distal pancreatectomy with splenectomy was performed. The intact specimen was then imaged on the gamma camera by using a cobalt-57 source to check the relative positions of the tumor and the splenunculus (Fig. 1D). This confirmed the pancreatic tumor as the source of intense activity, with a low level of activity from the adjacent spleen and splenunculus.

Histology showed a benign islet-cell tumor, with numerous granules of calcification seen throughout the tumor stroma on light microscopy and confirmed by von Kossa's stain.

Discussion

Several tumors in the neuroendocrine series, to which islet-cell tumors belong, have been reported to concentrate ^{99m}Tc bone-scanning agents. This has a clinical application in the management of neuroblastoma, where a high proportion of primary tumors [2, 3] and some extraosseous secondary deposits [4] accumulate activity. However, we found only one previous report of uptake of a ^{99m}Tc bone scanning agent in

Received January 5, 1987; accepted after revision February 20, 1987.

[1] Department of Diagnostic Radiology and Organ Imaging, The Prince of Wales Hospital, The Chinese University of Hong Kong, Shatin, New Territories, Hong Kong. Address reprint requests to J. Price.

[2] Department of Medicine, The Prince of Wales Hospital, The Chinese University of Hong Kong, Shatin, New Territories, Hong Kong.

[3] Department of Morbid Anatomy, The Prince of Wales Hospital, The Chinese University of Hong Kong, Shatin, New Territories, Hong Kong.

[4] Department of Surgery, The Prince of Wales Hospital, The Chinese University of Hong Kong, Shatin, New Territories, Hong Kong.

AJR 149:69–70, July 1987 0361–803X/87/1491–0069 © American Roentgen Ray Society

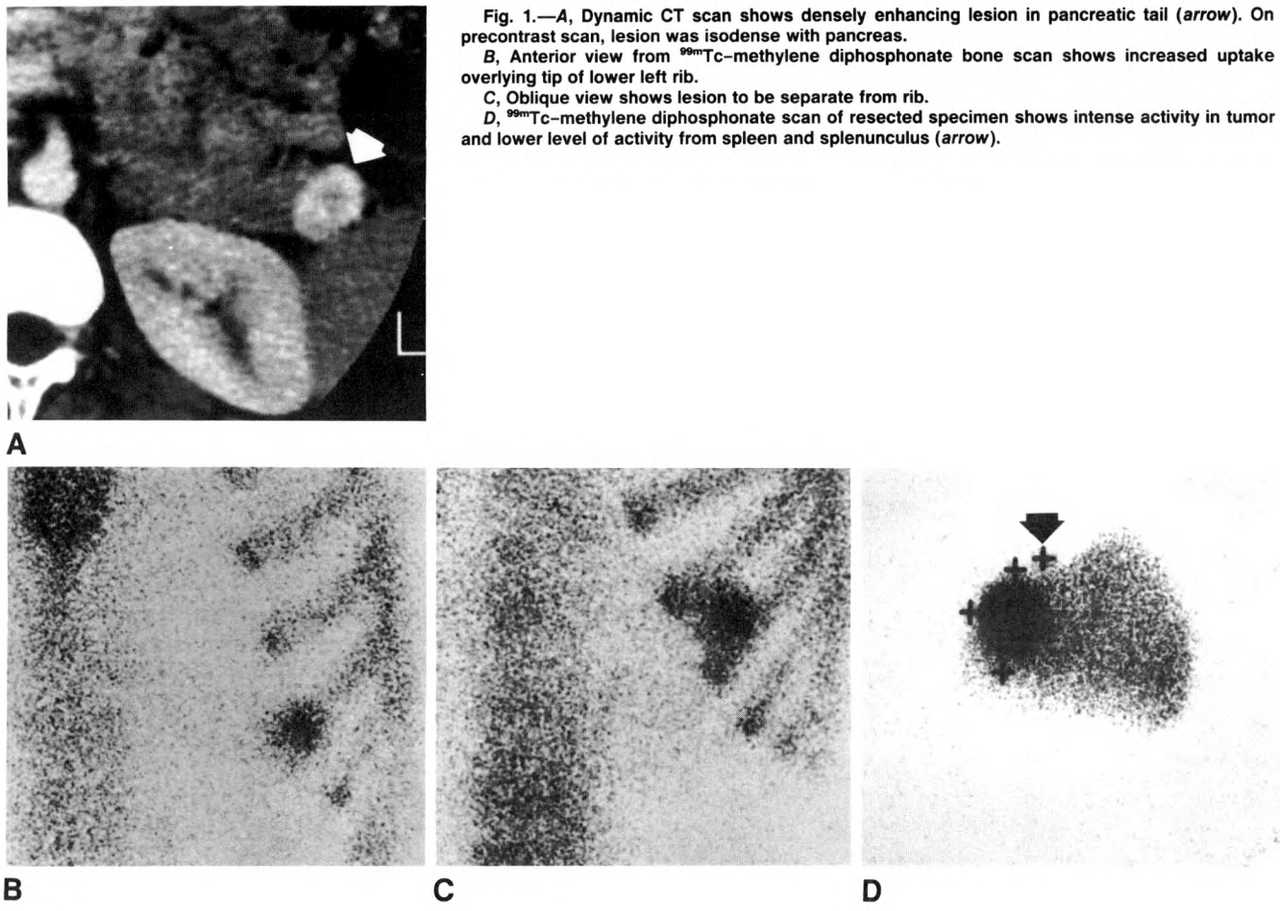


Fig. 1.—*A*, Dynamic CT scan shows densely enhancing lesion in pancreatic tail (*arrow*). On precontrast scan, lesion was isodense with pancreas.

***B*, Anterior view from ^{99m}Tc-methylene diphosphonate bone scan shows increased uptake overlying tip of lower left rib.**

***C*, Oblique view shows lesion to be separate from rib.**

***D*, ^{99m}Tc-methylene diphosphonate scan of resected specimen shows intense activity in tumor and lower level of activity from spleen and splenunculus (*arrow*).**

a pancreatic islet-cell tumor, which occurred in a nonfunctioning malignant lesion [5]. To our knowledge this is the first time this phenomenon has been reported in a benign insulin-secreting tumor.

The mechanism by which bone-scanning agents are taken up by soft-tissue tumors is poorly understood. Hypervascularity alone cannot explain the prolonged and intense uptake seen in some cases. Excessive capillary leakage from the abnormal vessels of the tumor circulation may be the additional factor.

Many cases may also be explained by the presence of tumor calcification. Bone uptake of ^{99m}Tc bone scanning agents is thought to be caused by a process of adsorption onto the hydroxyapatite crystals of bone. These crystals are also present in calcified soft-tissue tumors, and their uptake may result from the same process. This could account for uptake by this insulinoma, which showed microscopic calcification.

Another hypothesis invokes the presence of a specific enzyme receptor. Schmitt et al. [6] found high levels of acid and alkaline phosphatase activity in both normal and diseased noncalcified breast tissue that had shown uptake of bone-scanning agents. These enzymes, also present in normal bone, act on phosphate substrates. Uptake in bone and in these soft tissues could then be explained by binding of the polyphosphate and diphosphonate bone agents as false substrates. Zimmer et al. [7] provided evidence that such binding of methylene diphosphonate does occur, at least in vitro. This could offer an alternative explanation for uptake in this insulinoma, where a high level of plasma alkaline phosphatase activity was found.

Further experience is needed to assess the possible value of ^{99m}Tc-MDP scanning as a diagnostic investigation for insulinoma. We suggest that when conventional methods have failed to locate a documented insulinoma, a ^{99m}Tc-MDP scan should be considered.

REFERENCES

1. Stefanini P, Carboni M, Patrassi N, Basoli A. Beta-islet cell tumors of the pancreas: results of a study on 1,067 cases. *Surgery* **1974**;75:597–609
2. Martin-Simmerman P, Cohen MD, Siddiqui A, Mirkin D, Provisor A. Calcification and uptake of Tc-99m diphosphonates in neuroblastomas: concise communication. *J Nucl Med* **1984**;25:656–660
3. Garty I, Koren A, Goshen Y, Siplovich L. The complementary role of sequential 99mTc-MDP and 67Ga-citrate scanning in the diagnosis and follow-up of neuroblastoma. *Eur J Nucl Med* **1985**;11:224–229
4. Mandell GA, Heyman S. Extraosseous uptake of technetium-99m MDP in secondary deposits of neuroblastoma. *Clin Nucl Med* **1986**;11:337–340
5. LeBovic J, Waxman AD, Siemsen JK. Localization of 99mTc-pyrophosphate in an islet cell tumour of the pancreas. *Clin Nucl Med* **1978**;3:289–291
6. Schmitt GH, Holmes RA, Isitman AT, Hensley GT, Lewis JD. A proposed mechanism for 99mTc-labeled polyphosphate and diphosphonate uptake by human breast tissue. *Radiology* **1974**;112:733–735
7. Zimmer AM, Isitman AT, Holmes RA. Enzymatic inhibition of diphosphonate: a proposed mechanism of tissue uptake. *J Nucl Med* **1975**;16:352–356

Duplex Doppler Examination in Portal Hypertension:
Technique and Anatomy

Heidi Patriquin[1]
Michel Lafortune[2]
Peter N. Burns[3]
Michel Dauzat[4]

Three hundred fifty duplex Doppler examinations were performed in 195 patients (150 adults and 45 children) with radiologically and/or clinically proved portal hypertension. In this paper we describe this duplex Doppler technique for the qualitative assessment of splanchnic venous hemodynamics in these patients. The caliber of and the presence and direction of flow in the following veins are assessed: splenic, superior mesenteric, portal and intrahepatic portal, and portasystemic collateral. This examination can be performed on patients of any age without sedation and can establish the diagnosis of clinically significant portal hypertension. Technical success rate was 95%, although 10% of examinations were incomplete because of intestinal meteorism.

We conclude that the combined use of Doppler and routine sonography permits precise evaluation of the vascular anatomy in portal venous hypertension.

Real-time sonography has become increasingly useful in the examination of patients with long-standing liver disease and/or possible portal hypertension (PHT) [1–3]. Doppler has been a reliable tool in the investigation of vessel patency and flow direction [4–6]. Combined, these examinations yield anatomic and functional information and are synergistic in the evaluation of chronic liver disease and PHT.

Investigations of PHT using the duplex Doppler technique have concentrated largely on the quantitative estimation of flow velocity and volumetric rate in the portal vein [6–13]. These measurements usually require specialized, dedicated equipment; they are time consuming and not always accurate [11, 14, 15]. A broad, although less quantitative, understanding of the portal circulation may be obtained by using a conventional duplex scanner. We present a protocol for a qualitative examination of the portal system, suitable for clinical use by radiologists experienced in abdominal sonography. The method is a systematic Doppler examination of the portal circulation and its potential portasystemic collaterals.

Materials and Methods

Between June 1985 and October 1986, we examined 195 patients with chronic liver disease (150 adults and 45 children, aged 2 weeks to 18 years) and 20 normal controls, with real-time B-mode sonography and pulsed Doppler, using commercially available equipment (Advanced Technology Laboratories, Seattle, WA; MK 600, UM8 and UM4, Aloka SSD 800). Imaging was performed at 3, 5, and 7.5 MHz, Doppler at 3 and 5 MHz.

Adults were examined both after a 12-hr fast and 0.5–2 hr after a meal. Children were examined after a meal, and infants were fed during the examination to decrease motion. Maximal portal venous velocity in the normal subjects was calculated using standard methods [14].

B-mode Examination

The B-mode examination included a general abdominal survey with evaluation of the size and architecture of both liver and spleen. Collateral veins were sought in the lesser omentum; near the spleen, kidneys, umbilicus, pancreas, liver hilum, or colon; or in the pelvis.

Received December 18, 1986; accepted after revision March 17, 1987.

[1] Department of Radiology, Université de Montréal and Hôpital Sainte-Justine, 3175 Chemin Cote Ste. Catherine, Montreal, Quebec H3T 1C5, Canada. Address reprint requests to H. Patriquin.

[2] Department of Radiology, Hôpital Saint-Luc 1058 Rue St. Denis, Montreal H2X 3J4, and Université de Montréal, Montreal, Quebec, Canada.

[3] Radiology Department, Yale University School of Medicine, New Haven, CT 06510.

[4] Unité d'Exploration Vasculaire, Centre Hospitalier Regional BP26, Nimes, France.

***AJR* 149:71–76, July 1987**
0361–803X/87/1491–0071
© American Roentgen Ray Society

Doppler Examination

The abdominal vessels were insonated using established techniques [12, 13]. The Doppler sample volume was adjusted to encompass but not exceed the diameter of the vessel studied. The spatial peak temporal average (SPTA) acoustic-output power was kept under 170 mW/cm^2, in keeping with the current guidelines of the Food and Drug Administration [16]. The pulse-repetition frequency (PRF) was adjusted automatically but corrected manually when aliasing occurred. Since the velocity of flow in the veins examined is often low, low PRF and the lowest available filter of the Doppler receiver (50–100 Hz) were used. A low-frequency transducer (3 MHz) was chosen for the examination of deep vessels and/or for the detection of high velocities, and a higher frequency (5–7.5 MHz) was used for the examination of superficial vessels, the studies of children, and/or the detection of low blood-flow velocities (e.g., veins with decreased blood flow). Where imaging and Doppler frequencies were fixed, the latter took priority over B-mode requirements in the duplex exploration, even if image quality suffered slightly. The B-mode images and Doppler signals were recorded on film.

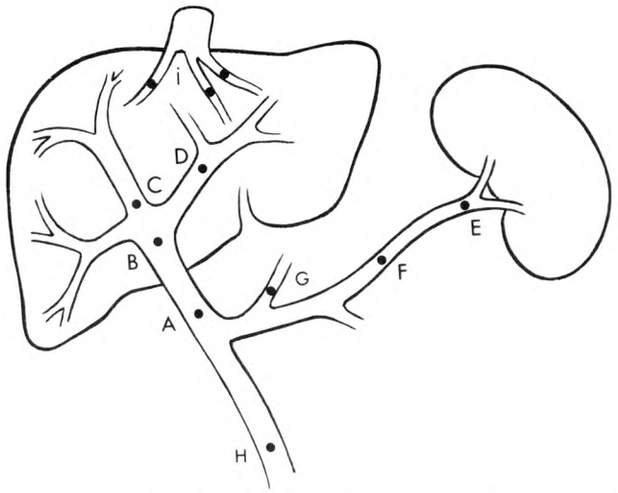


Fig. 1.—Sites of duplex insonation of splanchnic venous system in patients examined for possible portal hypertension. Letters A–I correspond to parts of Fig. 2 (2A–2I).

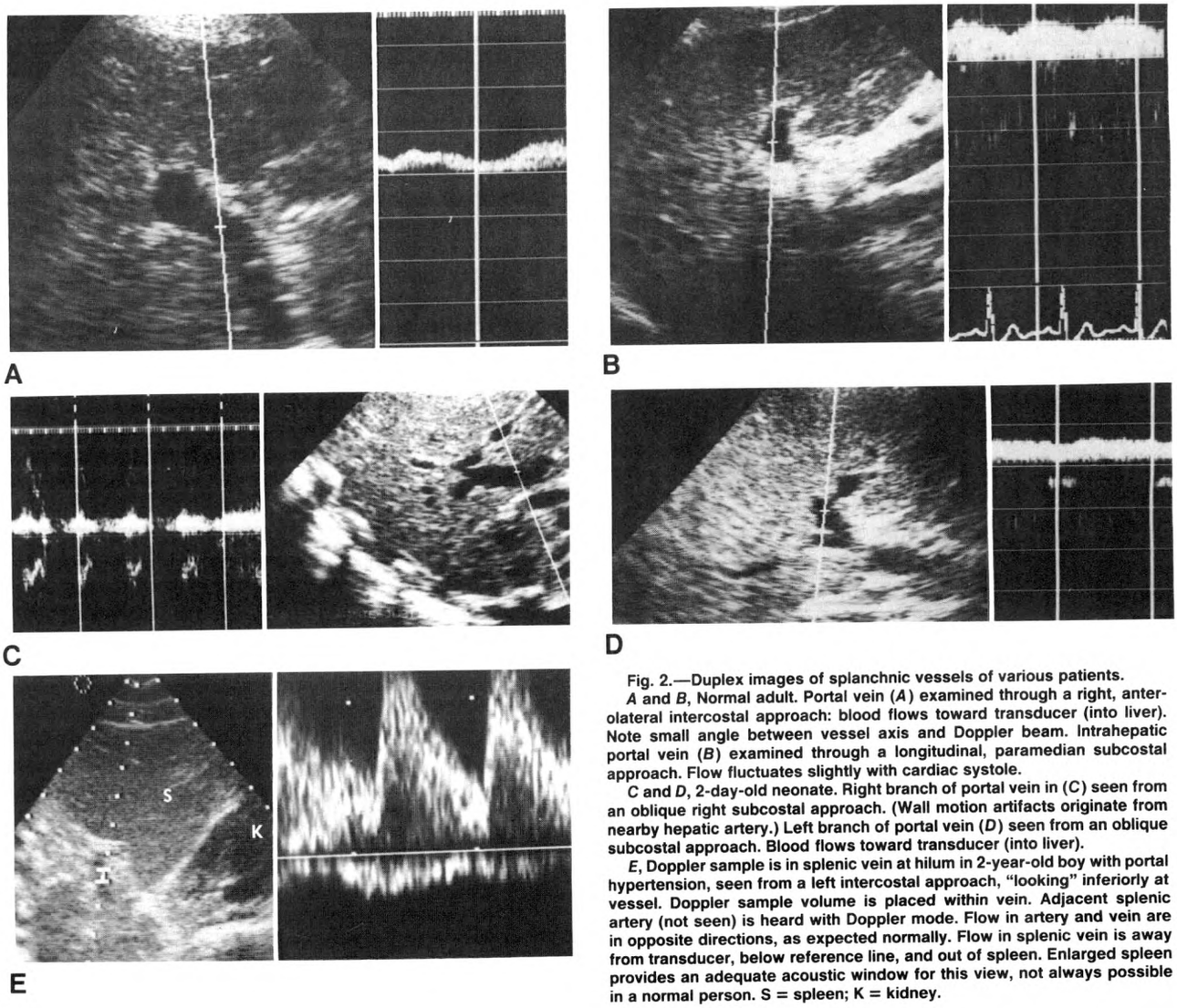


Fig. 2.—Duplex images of splanchnic vessels of various patients.

***A* and *B*, Normal adult. Portal vein (*A*) examined through a right, anterolateral intercostal approach: blood flows toward transducer (into liver). Note small angle between vessel axis and Doppler beam. Intrahepatic portal vein (*B*) examined through a longitudinal, paramedian subcostal approach. Flow fluctuates slightly with cardiac systole.**

***C* and *D*, 2-day-old neonate. Right branch of portal vein in (*C*) seen from an oblique right subcostal approach. (Wall motion artifacts originate from nearby hepatic artery.) Left branch of portal vein (*D*) seen from an oblique subcostal approach. Blood flows toward transducer (into liver).**

***E*, Doppler sample is in splenic vein at hilum in 2-year-old boy with portal hypertension, seen from a left intercostal approach, "looking" inferiorly at vessel. Doppler sample volume is placed within vein. Adjacent splenic artery (not seen) is heard with Doppler mode. Flow in artery and vein are in opposite directions, as expected normally. Flow in splenic vein is away from transducer, below reference line, and out of spleen. Enlarged spleen provides an adequate acoustic window for this view, not always possible in a normal person. S = spleen; K = kidney.**

Duplex Doppler Examination Method

The vessels examined and the sites of diameter measurement and Doppler insonation are outlined in Figures 1 and 2. The portal vein is the most readily accessible vessel in the portal system. The entire length of the portal vein was examined from an anterior abdominal, subcostal approach, using a right paramedian, slightly oblique plane (Fig. 2A). A left paramedian approach was sometimes necessary to find a convenient angle of incidence. From the hilum to the intrahepatic bifurcation, the portal vein was imaged though a right lateral intercostal window (Fig. 2A). In this position, the transducer is close to the portal vein even in obese patients and those with ascites. This vertical view of the portal vein results in a small angle between the vessel axis and the ultrasonic beam. Whenever possible, the portal vein was examined as it crosses the hepatic artery. At this point, the portal venous signal was easily obtained and the direction of flow could be compared with that of the hepatic artery. Flow direction in all portal vein branches was recorded using an intercostal or subcostal, transverse or oblique approach (Figs. 2C and 2D). The falciform or round ligament was then examined to exclude a patent paraumbilical vein [17, 18] coursing from the left portal vein to the umbilicus. A right paramedian or axillary longitudinal approach was used to examine the superior mesenteric vein. Collateral veins were sought and traced to the pelvis. The inferior mesenteric vein was rarely seen, only when enlarged, through the left kidney on axillary view.

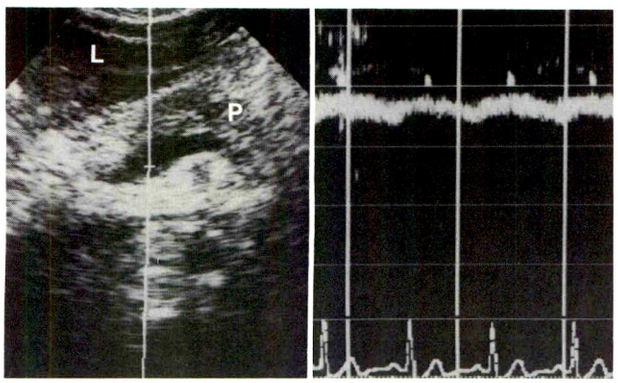
The splenic vein was examined at the splenic hilum, by angling the transducer to follow the long axis of the vessel (Fig. 2E). Whenever possible, the nearby splenic artery was used as reference for splenic-vein flow direction (Fig. 2E). The remainder of the splenic vein to its confluence with the superior mesenteric vein was examined in transverse cuts (Fig. 2F), made increasingly difficult as the left lobe of the liver atrophies with advancing cirrhosis. The medial edge of the spleen was screened for short gastric vein branches, with possible hepatofugal collateral flow. Similarly, the relation between the left renal vein and the splenic vein was outlined for possible splenorenal shunting.

Near the splenoportal confluence, the left gastric vein was examined in transverse and oblique-longitudinal cuts, as it courses from the gastric cardia to the splenic or portal vein in the lesser omentum [11–13, 17] (Fig. 2G).

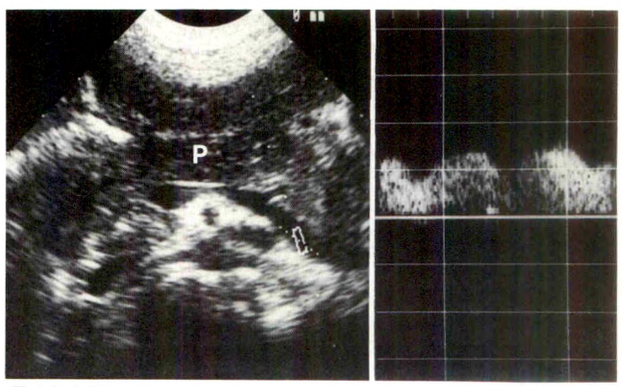
The superior mesenteric vein was examined through a longitudinal, right paramedian, upper abdominal approach (Fig. 2H).

The inferior vena cava was insonated along its visible length, noting any localized increase in caliber and/or flow velocity. The hepatic veins usually were explored easily through an oblique, subcostal or intercostal approach, yielding excellent Doppler signals (Fig. 2I).

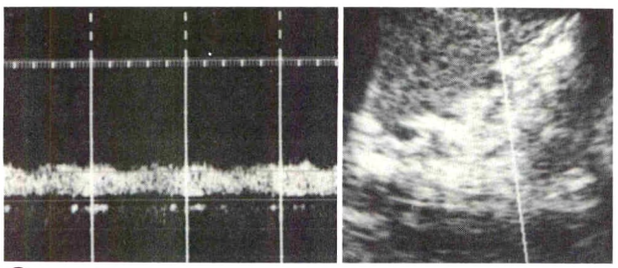
The pelvis was screened for collateral veins, especially the right ovarian vein (receiving the blood from the superior mesenteric vein) and pararectal veins posterior to the bladder (inferior mesenterico-iliocaval collaterals).



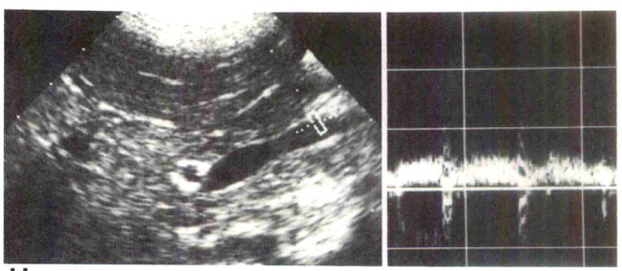
F (left)



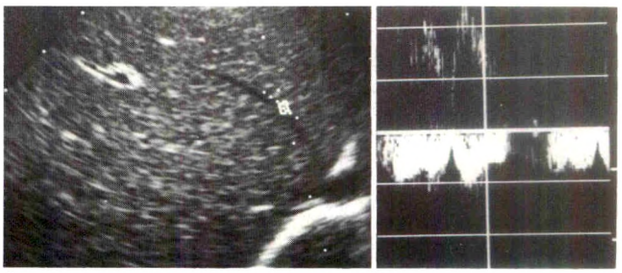
F (right)



G



H



I

Fig. 2.—Continued.

***F*, Splenic vein. Doppler sample volume is in vein near splenomesenteric confluence in an adult (left) and in its midthird in a 5-year-old boy (right). Note cardiac-related modulation of flow. P = pancreas; L = left liver lobe.**

G, Enlarged left gastric vein in 17-year-old boy with cirrhosis. Left paramedian longitudinal view shows a thickened lesser omentum and a tortuous vein. Flow is directed anteriorly and superiorly toward esophagus.

***H*, Superior mesenteric vein in 1-month-old boy, right paramedian longitudinal view. Flow modulation is synchronous with wall pulsations from adjacent superior mesenteric artery. Flow is directed toward Doppler sampler, superiorly toward liver.**

***I*, Hepatic vein in 1-week-old girl, transverse subcostal view, with flow away from transducer and modulated by pulsations of nearby right atrium.**

The hepatic artery was insonated at its origin at the celiac axis and where it crosses the portal vein. Intrahepatic branches were examined adjacent to portal venous branches. These intrahepatic arterial branches were usually heard with Doppler without being seen in real-time, especially in infants and young children. The splenic artery was examined concomitantly with the vein, at the splenic hilum, and within the spleen.

Duplex Data Analysis and Interpretation

For each examined vessel, the following were determined: (1) presence or absence of the vessel image on real-time imaging; (2) vessel diameter recorded at standard sites (Fig. 1); (3) presence or absence of intraluminal echogenic material; (4) presence or absence of a Doppler signal; and (5) normal (orthograde) or reversed (retrograde) flow.

A written report was made and the results were summarized on a comprehensive diagram, showing vessel diameter and flow direction and rate, with blind spots inaccessible to sonography noted as such (see Fig. 4D).

Duration of the Duplex Examination

Our average time for a duplex examination of the liver and portal system in patients with chronic liver disease was 40 min. With increased complexity of collateral circulation and progressing liver cirrhosis (increased sound attenuation and/or atrophy), the examination time lengthened, and some patients required more than one study for complete examination of their splanchnic and portal circulatory abnormalities.

As our experience increased, the examination time shortened. Not all vessels were seen in every patient. However, the portal vein and its intrahepatic branches as well as the splenic vein were seen and insonated in all patients.

Results

Real-Time Imaging

Suggestive signs for portal hypertension included splenomegaly, ascites, hepatomegaly, a thickened lesser omentum in children [19–22], and large, tortuous, abnormal venous channels (possibly portosystemic collaterals). In addition, liver size and architecture are gross indicators of steatosis and cirrhosis [23, 24]. Masses in the liver parenchyma, at the hilum, or near the head of the pancreas offer clues to the cause of PHT.

Duplex Doppler Examination

The normal Doppler examination of the portal venous system consisted of the examination of orthograde, hepatopetal flow in the splenic vein and superior mesenteric vein, as well as in the portal vein and its intrahepatic branches. The flow in the portal and splenic veins is slightly modulated by cardiac systole in some patients (Figs. 2B and 2F). Thus, portal vein blood flow was easily distinguished from the inferior vena caval flow, which was deeply modulated by right atrial contractions. Maximal portal venous flow velocities in normal, nonfasting children ranged from 10 to 30 cm/sec and in fasting adults from 8 to 18 cm/sec. Portal vein velocities increased from 50% to 100% in adults after eating. The velocity range was similar to those in previously published reports [8, 11].

Inversion of flow in the superior mesenteric vein generally implied the presence of mesenterico-caval shunting via renal [25] or gonadal veins, thus necessitating identification of collateral veins in the pelvis. Reversed blood flow in the splenic vein, together with an enlarged renal vein and locally enlarged inferior vena cava, indicated spontaneous splenorenal shunting [26]. The shunt was directly examined with Doppler and usually showed a high-velocity circulatory pattern.

The common collateral routes in PHT were examined directly with Doppler and showed hepatofugal blood flow in the left gastric vein, paraduodenal or periportal collaterals, and the paraumbilical vein (Figs. 3 and 4).

Since esophageal varices constitute the most important clinical complication of portal hypertension, duplex Doppler exploration of the left gastric vein is essential, and the examiner must be familiar with its anatomy and variants [21, 22]. Its course from the lower esophagus to the splenomesenteric junction through the lesser omentum usually is easily accessible if the upper abdominal aorta and the pancreas are visible [20] (Fig. 2H). The diameter of the left gastric vein should not exceed 5 mm in adults [27], and the vein was not visible in normal children. Direction of flow in the left gastric vein was at times difficult to detect because of a wide angle between vessel axis and Doppler beam. Scanning caudally from a subxiphoid position sometimes decreased this angle, and simultaneous insonation of the left gastric artery at times defined flow direction. Direction of flow was also difficult to discern when the vein was tortuous.

The inferior vena cava normally showed a well-modulated blood flow, with a typical triphasic right atrial modulation and a superimposed respiratory modulation [4]. A focal increase of caliber and/or flow velocity suggested the recipient site for shunted portal blood. The hepatic veins normally showed an inferior vena cava–like modulated blood flow, most marked near their junction with the inferior vena cava (Fig. 2H).

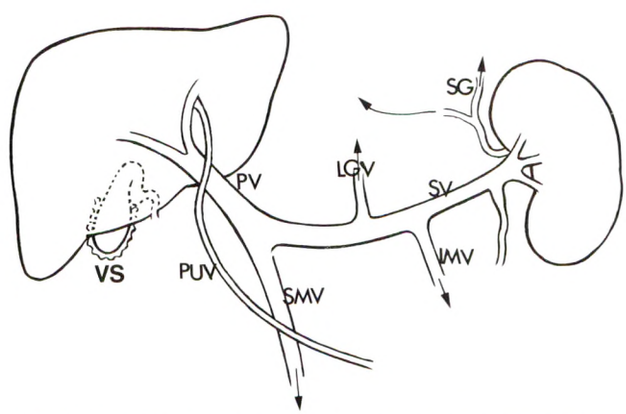


Fig. 3.—Common spontaneous portasystemic collateral venous routes in portal hypertension. PV = portal vein; SMV = superior mesenteric vein; IMV = inferior mesenteric vein; SV = splenic vein; LGV = left gastric vein; SGV = short gastric vein; PUV = paraumbilical vein; VS = veins of Sappey.

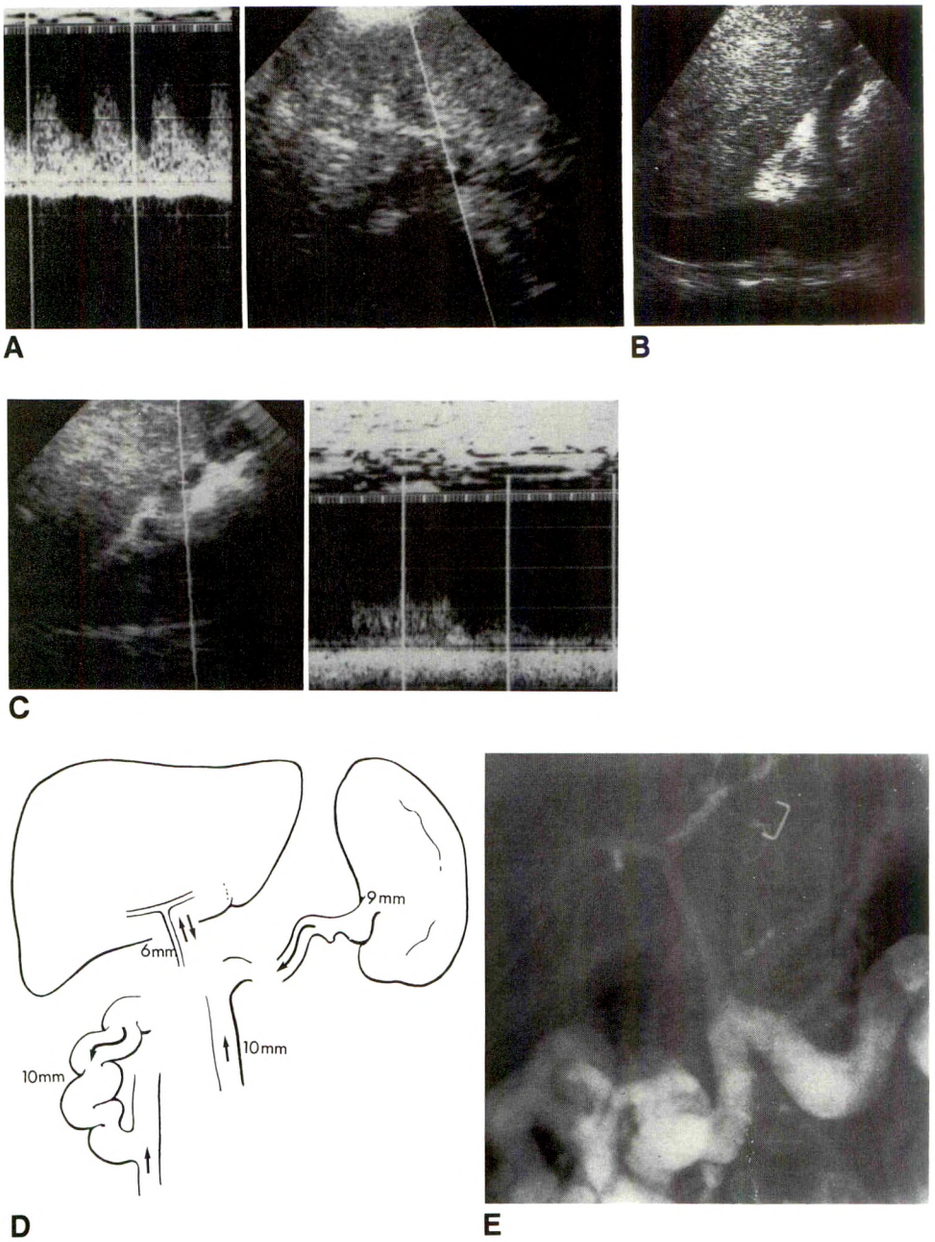


Fig. 4.—Duplex Doppler mapping of splanchnic venous circulation in 11-year-old girl with biliary cirrhosis; main portal vein (not illustrated) was tiny. Flow was hepatofugal.

***A*, Transverse subcostal view of liver. The Doppler sampler is within the barely visible left branch of the portal vein. Flow is opposite (below reference line) to that of hepatic artery (above line) and, therefore, hepatofugal. Liver architecture is heterogeneous.**

***B*, A large collateral vein enters inferior vena cava (IVC) near right edge of liver, augmenting the IVC diameter (longitudinal right paramedian view).**

***C*, Same collateral vein as in *B*, seen more anteriorly, is tortuous and sends its blood toward IVC (flow is directed below reference line, away from transducer, or posteriorly).**

***D*, Schematic drawn at the end of the duplex examination showing concept of splanchnic vein circulation, vessel diameter, and flow direction. Blind areas are blank (e.g., splenomesenteric confluence and origin of collateral vein).**

***E*, Splenoportogram shows small portal vein and huge paraduodenal collateral vein. (Left gastric vein shown here was not seen by duplex examination.)**

Discussion

Most previous investigations of the portal venous system by Doppler techniques have concentrated on quantitative flow measurements in the portal or splenic veins [21–23]. As flow rate is itself determined by the ratio of pressure and resistance, a determination of the presence and degree of PHT from these measurements is imprecise. Normal portal venous flow rates vary in the same individual: they increase after a meal [28] and decrease after exercise or when the patient is upright [9]. In PHT, portal venous inflow also depends on the degree of portasystemic collateral outflow [29].

Measurements of portal inflow require repeated and even insonation of the portal vein, as well as accurate measurements of vessel cross-sectional area and of the angle formed between the Doppler beam and the long axis of the vessel [11, 14]. These meticulous measurements may not be possible in ill or agitated patients. Although attempts to measure exact flow rates in our normal population proved promising in

adults and in calm children and infants, we found that in sick, distressed infants, children, and adults, these measurements became impossible because of rapid respiratory rates, uncontrolled movement or crying, and difficulty in obtaining several measurements in the same segment of a vein.

In a patient with PHT, the key clinical question is not the portal venous pressure but rather the likelihood of gastroesophageal variceal hemorrhage.

We chose to study our patients with a "qualitative" duplex Doppler technique, concentrating on presence and direction of flow in the splanchnic veins and attempting to see and insonate collateral vessels. Results thus gleaned from these veins coupled with a knowledge of the altered abdominal anatomy in PHT usually led us to discover portasystemic collateral veins in patients with PHT (Fig. 4). The discovery of these collateral routes establishes the diagnosis of portal hypertension and allows follow-up. There is a significant relationship between the risk of gastrointestinal bleeding and the size of the left gastric vein [30]. In addition, reversal of flow in the left gastric vein signals the opening of a network of esophageal varices. Because the diameter of the left gastric vein usually can be assessed when this vessel is large, patients with potential hemorrhage from gastroesophageal varices can thus be identified. These patients can be simultaneously investigated with esophagoscopy and treated with sclerotherapy.

Selected flow-velocity measurements, however, may prove valuable in the assessment of the progression of liver disease [7–12], as recent studies show that portal vein velocity is decreased in patients with cirrhosis [7, 31], severe PHT, or chronic hepatitis [9].

This "qualitative" or "anatomic" duplex Doppler analysis of patients with possible PHT is valuable in a clinical setting. The technical Doppler adjustments are learned quickly, and the skills required for the examination are finding appropriate acoustic windows and defining parenchymal and vessel anatomy. The information allows a physiologic overview of presence and direction of flow in the splanchnic/portal venous system without the need for potentially nonphysiologic injections of intravascular contrast medium.

ACKNOWLEDGMENTS

We thank Sylvie Tassé for preparing the manuscript and Richard Veillette, Denise Collins, and Richard Leblanc for illustrations.

REFERENCES

1. Subramanyam BR, Balshazar EJ, Modamba MR, Raghvendra BN, Horii SC, Lefleur RS. Sonography of portosystemic venous collaterals in portal hypertension. *Radiology* **1983**;146:161–166
2. Dach JL, Hill MC, Pelaez JC, LePage JR, Russel E. Sonography of hypertensive portal venous system: correlation with arterial portography. *AJR* **1981**;137:511–517
3. Dökmeci AK, Kimura K, Matsutani S, et al. Collateral veins in portal hypertension: demonstration by sonography. *AJR* **1981**;137:1173–1177
4. Taylor KJW, Burns PN. Duplex Doppler scanning in the pelvis and abdomen. *Ultrasound Med Biol* **1985**;11:643–658
5. Milles VE, Berland LL. Pulsed Doppler duplex sonography and CT of portal vein thrombosis. *AJR* **1985**;145:73–76
6. Ohnishi K, Saito M, Koen H, Nakayama T, Nomura F, Okuda K. Pulsed Doppler flow as a criterion of portal venous velocity: comparison with cineangiographic measurements. *Radiology* **1985**;154:495–498
7. Zoli M, Marchessini G, Cordiani MR, et al. Echo-Doppler measurement of splanchnic blood flow in control and cirrhotic patients. *JCU* **1986**;14:429–435
8. Moriyasu F, Nishida O, Ban N, et al. Measurement of portal vascular resistance in patients with portal hypertension. *Gastroenterology* **1986**;90:710–717
9. Ohnishi K, Saito M, Nakayama T, et al. Portal venous hemodynamics in chronic liver disease: effects of posture change and exercise. *Radiology* **1985**;155:757–761
10. Moriyasu F, Nishida O, Ban N, et al. Congestion index of the portal vein. *AJR* **1986**;146:735–739
11. Gill RW. Pulsed Doppler with B-mode imaging for quantitative blood flow measurements. *Ultrasound Med Biol* **1979**;5:223–235
12. Gill RW. Splanchnic blood flow measurement. In: Altobelli SA, Voyles WF, Greene ER, eds. *Cardiovascular ultrasonic flowmetry*. New York: Elsevier, **1985**:369–388
13. Taylor KJW, Burns PN, Woodsock JP, Wells PNT. Blood flow in deep abdominal and pelvic vessels: ultrasonic pulsed Doppler analysis. *Radiology* **1985**;154:487–493
14. Burns PN, Jaffe CC. Quantitative flow measurements with Doppler ultrasound: techniques, accuracy and limitations. *Radiol Clin North Am* **1985**;23:641–657
15. Gill RW. Measurement of blood flow by ultrasound: accuracy and sources of error. *Ultrasound Med Biol* **1985**;5:223–235
16. AIUM/NEMA safety standard for diagnostic ultrasound equipment. AIUM/NEMA Standard Publication ULI-1981. *J Ultrasound Med* **1983**;2 [suppl]:S1–S50
17. Lafortune M, Constantin A, Breton G, Legaré AG, Lavoie P. The recanalized umbilical vein in portal hypertension: a myth. *AJR* **1985**;144:549–553
18. Smith-Laing S, Camile ME, Dick R, Sherlock S. Percutaneous transhepatis portography in the assessment of portal hypertension. *Gastroenterology* **1980**;78:197–205
19. Patriquin H, Tessier G, Grignon A, Boisvert J. Lesser omental thickness in normal children: baseline for detection of portal hypertension. *AJR* **1985**;145:693–696
20. Doehner GA, Ruzicka FF, Hoffman G, Rousselot LM. The portal venous system: its roentgen anatomy. *Radiology* **1955**;64:675–688
21. Takashi M, Igarashi M, Hino S, et al. Esophageal varices: correlation of left gastric venography and endoscopy in patients with portal hypertension. *Radiology* **1985**;155:327–331
22. Brunelle F, Alagille D, Pariente D, Chaumont P. Etude échographique de l'hypertension portale chez l'enfant. *Ann Radiol (Paris)* **1981**;24:121–130
23. Taylor KJW, Riely CA, Hammers L, et al. Quantitative US attenuation in normal liver and in patients with diffuse liver disease: importance of fat. *Radiology* **1986**;160:65–72
24. Dewbury KC, Clark BE. The accuracy of ultrasound in detection of cirrhosis of the liver. *Br J Roentgenol* **1979**;52:945–948
25. Doehner GA, Ruzicka FF, Rousselot LM, Hoffman G. The portal venous system: on its pathological roentgen anatomy. *Radiology* **1956**;66:206–217
26. Kobayashi C, Musha H, Okuda K. Sonographic detection of large spontaneous spleno-renal shunts and its clinical significance. *Br J Radiol* **1984**;57:565–570
27. Lafortune M, Marleau D, Breton G, Viallet A, Lavoie P, Huet PM. Portal venous system measurements in portal hypertension. *Radiology* **1984**; 151:27–30
28. Madjar H, Gill RW, Griffiths KA, Kossoff G. Liver function tested by pulsed Doppler measurements of portal venous flow fasting and following a standard meal. In: Gill RW, Dadd MJ, eds. *Proc 4th meeting World Fed Ultrasound Med Biol.* Sydney: Pergammon Press, **1985**:70
29. Burns PN, Taylor KJW, Blei AT. Doppler flowmetry and portal hypertension. *Gastroenterology* (in press)
30. Lebrec D, De Fleury P, Rueff B, Nahum H, Benhamou JP. Portal hypertension, size of esophageal varices, and risk of gastrointestinal bleeding in alcoholic cirrhosis. *Gastroenterology* **1980**;79:1139–1144
31. Reichle FA, Sovak M, Soulen RC, Rosemond GP. Portal vein flow determination in the unanesthetized human by umbilicoportal cannulation. *J Surg Res* **1972**;12:146–150

Comparison of Pulsed Doppler Sonography and Angiography in Patients with Portal Hypertension

Rendon C. Nelson[1]
Karen E. Lovett
Judith L. Chezmar
Joseph H. Moyers
William E. Torres
Frederick B. Murphy
Michael E. Bernardino

Pulsed Doppler sonography and liver panangiography were performed in 43 patients with cirrhosis. Fourteen patients were evaluated preoperatively, and 28 patients were evaluated after a variceal decompressive shunt. One patient was studied before and after undergoing a shunt. The direction of portal blood flow by Doppler sonography was compared with both the grading pattern and direction of flow by angiography. When portal blood flow was determined to be antegrade by Doppler sonography, angiography showed antegrade flow in 84% (grade I, II, or III portal venous pattern). Six percent had retrograde flow (grade IV), and 10% had portal vein thrombosis. When the portal blood flow was determined to be retrograde by Doppler sonography, angiography showed retrograde flow (grade IV portal venous pattern) in 80% and antegrade flow (grade I, II, or III) in 20%. When an inadequate Doppler tracing was obtained from the portal vein, angiography showed either grade I, II, or III in 38%; grade IV in 50%, and portal vein thrombosis in 13%. There was poor correlation between the calculated mean flow rates, as determined by Doppler sonography, and the angiographic grade.

We conclude that pulsed Doppler sonography is accurate in determining the direction of portal flow when an adequate tracing is obtained (36 of 44 studies). When an inadequate tracing is obtained, retrograde portal flow or portal vein thrombosis is likely.

Duplex sonography, the combination of real-time and pulsed Doppler sonography, has been advocated as having the ability to provide meaningful information about the portal venous system in patients with cirrhosis [1–7]. Because frequent follow-up of patients with portal hypertension is important, especially in those who have undergone a portosystemic shunt or sclerotherapy, a noninvasive screening technique would be advantageous. Angiography, even though invasive, continues to be the gold standard for evaluating the status of the portal and hepatic venous systems. At present, both techniques have certain intrinsic limitations. Angiography can determine vascular pressures but cannot assess blood flow rates. Doppler sonography, on the other hand, can determine relative flow rates but cannot assess vascular pressures. The purpose of this study was to evaluate the information provided by angiography and Doppler sonography in terms of three comparisons: (1) the direction of portal blood flow as determined by Doppler sonography and the angiographic grading of the portal venous branching pattern and penetration into the hepatic parenchyma, (2) the direction of portal flow by Doppler sonography and the direction of flow by angiography, and (3) the calculated mean portal venous flow rates determined by Doppler sonography and the angiographic grade of the portal venous branching pattern and penetration into the hepatic parenchyma.

Subjects and Methods

Forty-four pulsed Doppler sonographic and liver panangiographic procedures were performed over a 5-month period in 43 patients with hepatic cirrhosis. The population included 29 men and 14 women 16–71 years old (mean, 49 years). The average interval between Doppler sonography and angiography was 1.8 days (range, 0–5 days). Fourteen patients

Received January 28, 1987; accepted after revision March 23, 1987.

Presented at the annual meeting of the American Roentgen Ray Society, Miami Beach, April 1987.

[1] All authors: Department of Radiology, Emory University School of Medicine, 1364 Clifton Rd., N.E., Atlanta, GA 30322. Address reprint requests to R. C. Nelson.

AJR 149:77–81, July 1987
0361–803X/87/1491–0077
© American Roentgen Ray Society

were evaluated preoperatively; nine of these had undergone sclerotherapy for esophageal varices. Twenty-eight patients were evaluated after a variceal decompressive shunt. These included 23 patients with distal splenorenal shunts [8], three with portacaval shunts, one with a mesoatrial shunt, and one with a splenocaval shunt. In addition, one patient was evaluated both before and after a distal splenorenal shunt.

All duplex sonographic examinations were performed on an Acuson 128 Computed Sonography unit (Mountain View, CA), which combines real-time sonography with pulsed Doppler sonography. A 3.5-MHz sector transducer was used in all cases. The patients were then scanned in either the supine or left lateral decubitus position during quiet respiration. The patients were not in the fasting state. The transducer was oriented along the longitudinal axis of the main portal vein. The Doppler gate width was varied so that it was consistent with the vessel lumen. The angle between the Doppler pulse wave and the vessel was maintained at less than 70°. The mean velocity and direction of blood flow were obtained from the main portal vein for a total of 10 tracings, and these measurements were averaged. The diameter of the vessels was measured at the site of the velocity tracing. The mean portal venous flow rate was subsequently calculated from the product of the mean velocity (cm/sec) and the cross-sectional area (cm^2) assuming that the vessel was circular in cross section. The Doppler sonography was interpreted without knowledge of the angiographic findings and vice versa.

The panangiographic procedure [9] for the patient consists of wedge hepatic vein, free hepatic vein, inferior vena cava, right atrium, and left renal vein pressure measurements. Wedge hepatic and left renal venography was also performed. Superior mesenteric and splenic arteriograms were obtained to evaluate portal perfusion and patency of the splenic and portal veins. After surgery the study included shunt catheterization, pressure measurements, and a superior mesenteric arteriogram for evaluation of portal flow.

The portal venous grading system was as follows [10]: grade I, normal hepatopetal flow with visualization of the branches of the portal vein to the periphery of the liver and staining of the hepatic parenchyma; grade II, hepatopetal flow with visualization of tertiary portal venous branches not extending to the liver periphery but with staining of the liver parenchyma; grade III, poor hepatopetal flow with visualization of only first- and second-order portal branches and no liver stain; and grade IV, hepatofugal flow with nonvisualization of the portal vein on superior mesenteric arterial injection and reversal of flow on hepatic wedge venography.

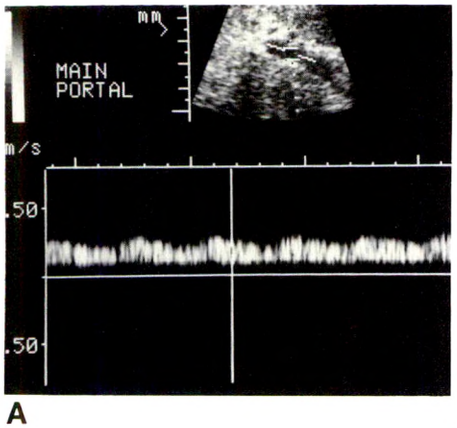
TABLE 1: Comparison of Direction of Portal Flow by Doppler Sonography with Angiographic Grade

Angiographic Grade	Doppler Sonography: No. of Studies (%)		
	Antegrade Flow	Retrograde Flow	No Flow Tracing
I	12 (39)	1 (20)	1 (13)
II	10 (32)	0	2 (25)
III	4 (13)	0	0
IV	2 (6)	4 (80)	4 (50)
Portal vein thrombosis	3 (10)	0	1 (13)
Total	31	5	8

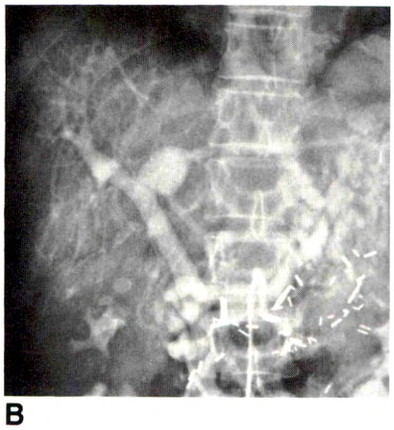
Results

Table 1 shows the comparison of Doppler findings for direction of portal flow with angiographic grade. Doppler sonography agreed with angiographic findings of antegrade flow in 84% of cases (Fig. 1). Two cases of retrograde flow were mistakenly identified by Doppler sonography as antegrade (Fig. 2). In three patients with portal vein thrombosis, Doppler sonography showed antegrade flow, and angiography showed not only a clot in the portal vein but also antegrade flow within collateral vessels in the porta hepatis (Fig. 3). In one patient with a grade I angiographic pattern (antegrade flow), Doppler sonography mistakenly showed retrograde portal flow. In four other patients who did have retrograde flow, Doppler sonography and angiographic findings agreed (Fig. 4).

In eight studies inadequate Doppler tracings were obtained from the main portal vein. In four patients this vein was not seen (two were grade II, and two were grade IV). In the other four patients the main portal vein was imaged by sonography, but an inadequate Doppler tracing was obtained. In one patient Doppler sonography noted a 13-mm portal vein without flow, and angiography showed a thrombus in the portal vein due to a large hepatocellular carcinoma. In one patient an inadequate Doppler tracing was obtained from a small,



A



B

Fig. 1.—58-year-old woman examined 2 years after distal splenorenal shunt.

***A*, Doppler sonogram shows antegrade flow in main portal vein measuring 8 mm in diameter. Flow is antegrade since Doppler frequency shift is directed toward transducer (above baseline).**

***B*, Venous phase of superior mesenteric arteriogram shows grade I angiographic pattern with visualization of portal vein branches to hepatic periphery.**

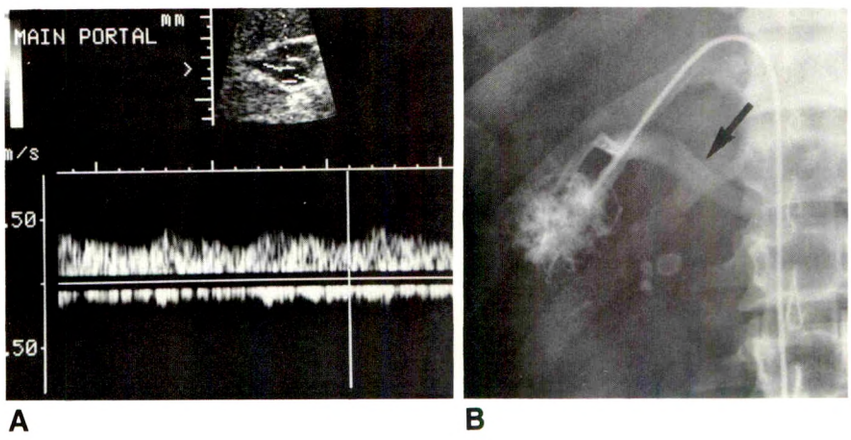


Fig. 2.—32-year-old man evaluated before decompressive surgery.

***A*, Doppler sonogram shows predominantly antegrade flow in main portal vein measuring 12 mm in diameter. Most blood flow is toward transducer, but some is retrograde; therefore Doppler frequency shift is represented both above and slightly below baseline.**

***B*, Wedge hepatic venogram shows retrograde flow into main portal vein (*arrow*). Incidentally noted are gallstones.**

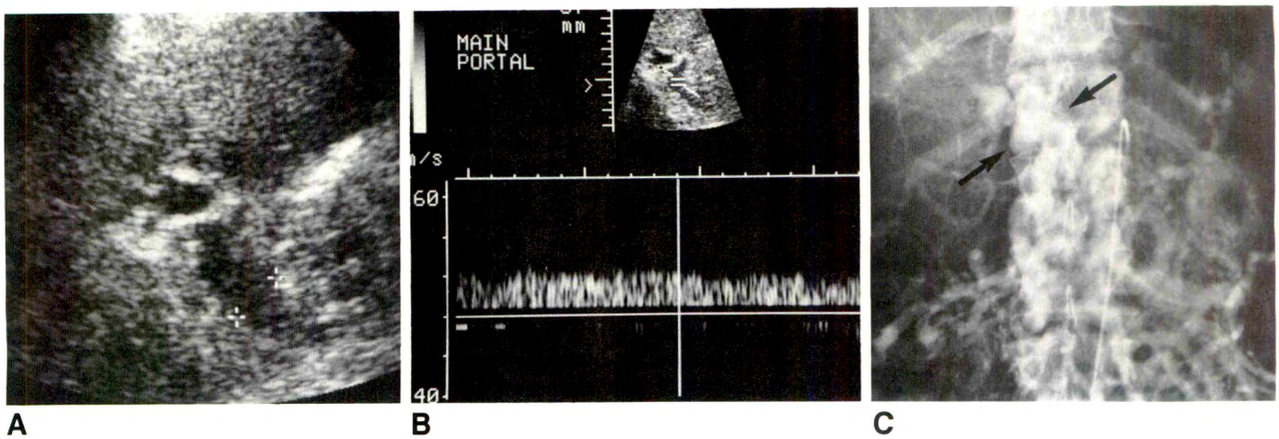


Fig. 3.—24-year-old man after mesoatrial shunt for Budd-Chiari syndrome.

***A*, Oblique sonogram through porta hepatis shows fine internal echoes within lumen of 13-mm vessel.**

***B*, Doppler sonogram reveals antegrade flow within this vessel.**

***C*, Venous phase of superior mesenteric arteriogram shows nest of serpiginous vessels in region of porta hepatis (*arrows*) consistent with portal vein thrombosis and cavernous transformation.**

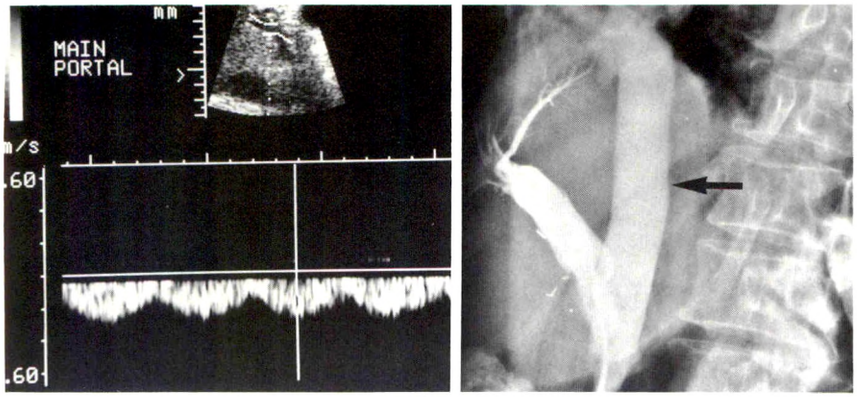
5-mm portal vein, and angiography showed retrograde flow (grade IV). In another patient, with grade I flow by angiography, the Doppler tracing was inadequate because of a suboptimal Doppler angle (>70°). In the fourth patient, retrograde flow (grade IV) was shown by angiography, and, while the Doppler tracing was somewhat faint, the flow in retrospect was also retrograde.

Table 2 shows the results for direction of portal venous flow as determined by angiography. In the one patient with antegrade flow that was shown mistakenly as retrograde on sonography, a study in this patient before decompressive shunt placement had revealed antegrade flow. For the four thrombosis patients, three patients had adequate Doppler tracing, and antegrade portal blood flow was noted in all three. Angiography in this same group of patients not only revealed a thrombus in the main portal vein but also showed antegrade flow within collateral vessels located in the porta hepatis, consistent with cavernous transformation (Fig. 3).

Table 3 shows the comparisons for the calculated mean blood flow rate in the main portal vein and the angiographic grade for the 36 studies in which an adequate Doppler tracing was obtained. The flow rates for grades I, II, and III were seen to decrease as the severity of hepatic parenchymal disease increased. When there was retrograde flow (grade IV) or portal vein thrombosis, the flow rates were relatively high, although the number of patients in these groups was not high enough to determine clinical significance.

Discussion

Duplex Doppler sonography has recently been advocated as an important method for studying the effect of physiologic stimuli and pathologic processes, such as cirrhosis, on the portal venous system. Several authors [1–3] have noted an increase in the caliber of the main portal vein as well as a decrease in the velocity of portal flow, resulting in overall



A B

Fig. 4.—49-year-old man after portocaval shunt.

***A*, Doppler sonogram shows retrograde flow in main portal vein, which measures 8 mm in diameter.**

***B*, Angiogram of portocaval shunt reveals retrograde flow from main portal vein into inferior vena cava (*arrow*).**

TABLE 2: Comparison of Direction of Portal Flow by Angiography with Direction of Flow by Doppler Sonography

Doppler Sonography	Angiography: No. of Studies (%)		
	Antegrade Flow	Retrograde Flow	Portal Vein Thrombosis
Antegrade flow	26 (87)	2 (20)	3 (75)
Retrograde flow	1 (3)	4 (40)	0
No flow tracing	3 (10)	4 (40)	1 (25)
Total	30	10	4

TABLE 3: Comparison of Angiographic Grade and Calculated Mean of Portal Venous Flow Rates by Doppler Sonography in 36 Studies

Angiographic Grade	Flow Rate (ml/min)
I	641 ± 330
II	394 ± 337
III	353 ± 209
IV	545 ± 292
Portal vein thrombosis	552 ± 417

maintenance of a normal volume of portal flow. Moriyasu et al. [4] determined that the normal portal venous blood flow rate in the fasting state was 889 ± 284 ml/min. No correlation, however, was found between portal venous pressures and the flow rates. Ohnishi et al. [5] determined portal venous velocity both by cineangiography and Doppler sonography, and, although the absolute flow rates differed by a factor, there was good correlation over a wide range of values. The question that arises on evaluation of these data is whether or not the information obtained from noninvasive Doppler sonography can supplant angiography, which, although invasive, is currently the gold standard. With this in mind we attempted to look at how the direction of flow and parenchymal extent of portal venous branching by angiography compare with the direction and volume flow rates by Doppler sonography.

In our study, there was an 83% agreement between Doppler sonography and angiography on the direction of portal flow when an adequate Doppler tracing was obtained (36 of 44 studies). Furthermore, diagnostic Doppler flow data were obtained from the main portal vein in 82% of cases. This portal Doppler information rate is similar to that noted in a previous study performed at our institution in a different group of patients (Nelson RC, unpublished data).

In this study, when no diagnostic data were obtained from the main portal vein by Doppler sonography (eight of 44 studies) even though the portal vein may have been imaged, retrograde flow (grade IV) and portal vein thrombosis were documented by angiography in 63% of patients. Nonvisualization or a poor Doppler tracing, therefore, cannot simply be attributed to intervening bowel gas; large body habitus; increased sound attenuation by fatty or cirrhotic liver; or the existence of a small, shrunken liver in a high subcostal location. Van Gansbeke et al. [11] similarly suggested a relationship between sonographic nonvisualization and portal vein thrombosis. They were also able to demonstrate an intraluminal thrombus in 67% of patients, increase in diameter of the thrombosed segment in 57%, and periportal collaterals in 48%. In our four cases of main portal vein thrombosis, Doppler sonography was nondiagnostic in one patient (25%), an intraluminal thrombus was not seen in any patient, the mean diameter of the portal vein was normal (9.3 ± 3.4 mm) in all four patients, and antegrade flow was noted in periportal collaterals (cavernous transformation) in three patients (75%).

There are several possible reasons for false results in terms of direction of portal flow. These include patient-related problems such as body habitus and difficulty with breath-holding, as well as technical problems such as cursor placement. As previously mentioned, false results may also arise when sampling is obtained from collateral vessels or varices in and about the porta hepatis in patients with either retrograde flow (grade IV) or portal vein thrombosis. While careful examination of the porta hepatis for multiple, perhaps serpiginous, vessels with venous flow may be helpful in detecting cavernous transformation, it will continue to be a diagnostic problem when a single large collateral vessel coexists with a small main portal vein.

In our study there was poor correlation between the mean flow rates calculated by Doppler sonography and the angiographic grade for the portal venous pattern. The mean flow rates in all patient groups were less than the normal value of 889 ± 284 reported by Moriyasu et al. [4]. There are several possible sources for error in flow-rate determination by Doppler sonography. Not only has it been assumed that the main portal vein is circular in cross section (πr^2), but a 1-mm difference in measuring the diameter of the vessel can result in an error in the calculated flow rate of 12–36% for this group of patients. Other technical sources of error include variations in cursor placement, nonparallel alignment of the velocity cursor, suboptimal Doppler angulation, as well as the size of the sample gate relative to the diameter of the vessel. There may also be variations in the flow rates related to changes in the patient's position, phase of respiration, and dietary status, whether fasting or not.

We conclude that, while Doppler sonography cannot supplant angiography in evaluating patients with portal hypertension, it can be used as a complementary method for determining the direction of portal blood flow. When an inadequate Doppler tracing is obtained from the main portal vein, it cannot simply be attributed to large body habitus, intervening bowel gas, or a shrunken liver, as retrograde portal flow and portal vein thrombosis may be present. Thus, angiography is more valuable in patients with portal hypertension.

REFERENCES

1. Zoli M, Marchesini G, Cordiani MR, et al. Echo-Doppler measurement of splanchnic blood flow in control and cirrhotic subjects. *JCU* **1986**;14:429–435
2. Moriyasu F, Nishida O, Ban N, et al. "Congestion index" of the portal vein. *AJR* **1986**;146:735–739
3. Ohnishi K, Saito M, Nakayama T, et al. Portal venous hemodynamics in chronic liver disease: effect of posture change and exercise. *Radiology* **1985**;155:757–761
4. Moriyasu R, Ban N, Nishida O, et al. Clinical application of an ultrasonic duplex system in the quantitative measurement of portal blood flow. *JCU* **1986**;14:579–588
5. Ohnishi K, Saito M, Koen H, et al. Pulsed Doppler flow as a criterion of portal venous velocity: comparison with cineangiographic measurements. *Radiology* **1985**;154:495–498
6. Smith DF, Lawson TL, Berland LL, et al. Pulsed Doppler evaluation of portosystemic collaterals in portal hypertension. *J Ultrasound Med* **1982**;1[suppl]:59
7. Foley WD, Gleysteen JJ, Lawson TL, et al. Dynamic computed tomography with pulsed Doppler ultrasonography in the evaluation of splenorenal shunt patency. *J Comput Assist Tomogr* **1983**;7:106–112
8. Warren WD, Salam AA, Hutson D, Zepa R. Selective distal splenorenal shunt: technique and results of operation. *Arch Surg* **1974**;108:306–314
9. Oliver TW, Sones PJ. Hepatic angiography: portal hypertension. In: Bernardino ME, Sones PJ, eds. *Hepatic radiology*. New York: Macmillan, **1984**:243–275
10. Henderson JM, Gong-Liang J, Galloway J, et al. Portaprival collaterals following distal splenorenal shunt: incidence, magnitude and associated portal perfusion changes. *J Hepatol* **1985**;1:649–661
11. Van Gansbeke D, Avni EF, Delcour C, et al. Sonographic features of portal vein thrombosis. *AJR* **1985**;144:749–752

Book Review

The Radiologic Clinics of North America. Radiology of Inflammatory Bowel Disease. Guest editors: Peter J. Feczko and Robert D. Halpert. Philadelphia: Saunders, January 1987;25(1). By subscription, 4 issues annually, $60

This symposium of 232 pages packs a maximum of useful information into its limited length. The editors have drawn upon the talents of some of the best in gastrointestinal radiology and medicine. The 16 chapters are divided into three major sections: I. Imaging the Gastrointestinal Tract in Inflammatory Bowel Disease, II. Complications of Inflammatory Bowel Disease, and III. Clinical Aspects of Inflammatory Bowel Disease. The contributions are generally well written and tightly edited to limit redundancy and duplication of information. Although much of the information relates to traditional radiologic methods, the writing is up-to-date, the images are numerous and of very high quality, and the reference lists are complete without being intimidating.

The initial chapter, Radiologic—Pathologic Correlation of Inflammatory Bowel Disease, sets the tone of the volume with a crisp, relevant, and well-illustrated correlative exposition of the pathologic basis for the barium radiography images of the intestinal tract afflicted by inflammatory bowel disease. Subsequent chapters review the radiologic findings in patients with Crohn's disease of the upper gastrointestinal tract, small intestine, and colon, and ulcerative colitis. Chapters describing inflammatory bowel disease in children, the use of CT and MR imaging in inflammatory bowel disease, and the value of nuclear medicine in these diseases follow. The section on complications includes chapters on intestinal and extraintestinal complications, toxic dilatation of the colon, malignancy, hepatobiliary, enteropathic arthropathies, and genitourinary complications. The final section describes, in two chapters, the modern clinical aspects and current management of inflammatory bowel disease.

This is a well-chosen topic for general radiologists as well as those interested in gastrointestinal disease. It updates the clinical and radiographic information relating to these disorders and will, therefore, be a welcome and useful reference after its initial reading.

Charles A. Rohrmann, Jr.
University of Washington
Seattle, WA 98195

CT of Giant Cavernous Hemangioma

John C. Scatarige[1, 2]
Janis M. Kenny[1]
Elliot K. Fishman[1]
Franklin H. Herlong[3]
Stanley S. Siegelman[1]

Giant hepatic cavernous hemangiomas are clinically distinct from smaller asymptomatic ones and may be confused with primary or metastatic malignancy. Hemangiomas exceeding 8 cm in diameter (mean, 13.7 cm) were studied in eight women 28–71 years old, six of whom presented with right upper quadrant discomfort and/or hepatomegaly. On unenhanced CT, seven of the masses were less dense than surrounding normal liver and one was slightly more dense than adjacent fatty liver. All masses contained additional stellate or cleftlike low-density zones, and two contained calcification. After bolus IV contrast administration, all exhibited early peripheral enhancement and partial centripetal isodense fill-in. None became completely isodense on delayed scans.

Familiarity with these CT characteristics and a high index of suspicion should facilitate correct diagnosis and avert needle biopsy.

The expanding application of sonography and CT in evaluating the oncologic patient for possible space-occupying liver disease has produced the need for a reliable, noninvasive means of differentiating the incidental hemangioma from primary or metastatic neoplasm [1, 2]. In this regard, the CT enhancement pattern after bolus IV injection of contrast material has received particular attention [1–9].

In contrast to small incidentally discovered hemangiomas, the uncommon giant cavernous hemangioma is more likely to produce symptoms [10]. We examined the CT behavior of eight large hemangiomas on nonenhanced and bolus dynamic scans.

Subjects and Methods

Between January 1978 and July 1986, 39 patients with 49 cavernous hemangiomas underwent standardized CT examinations. A giant hemangioma, defined as one in which at least one dimension exceeded 8 cm, was present in eight patients, all women, 28–71 years old (mean, 55). Final proof was based on angiography, laparotomy or laparoscopy, ^{99m}Tc-labeled RBC scintigraphy, or a lack of change over a 1- to 2-year interval of observation. None of the hemangiomas was surgically resected and available for pathologic study. Six of the women complained of right upper quadrant pain or fullness or had an upper abdominal mass palpable on physical examination. In the other two, the mass was discovered serendipitously on cross-sectional imaging performed for other reasons. In one elderly patient with known breast cancer, the hemangioma was discovered on thoracic CT performed after a slow drip infusion of contrast material. A diagnosis of metastasis was suggested and two percutaneous biopsies were performed without incident, both revealing hepatocytes and no evidence of malignancy. Liver function studies were normal except for minimal elevation of the serum alkaline phosphatase in two patients.

The CT studies were performed either on a Siemens Somatom DR3 scanner with an 8-mm slice thickness, 125 kVp, and 230 mAs or on the Pfizer/AS & E Model 0500 body scanner with a 10-mm slice thickness, 5- or 10-sec scan time, 20 or 50 mA, and 125 kVp. Unenhanced scans of the entire liver were obtained, and one or two representative scan levels through the suspect mass were selected. A 100-ml bolus of 60% iodinated contrast material was then delivered via a peripheral vein. Injection time did not exceed 60 sec. Scans at the

Received February 23, 1987; accepted after revision March 31, 1987.

[1] Russell H. Morgan Department of Radiology and Radiological Sciences, The Johns Hopkins Medical Institutions, 600 N. Wolfe St., Baltimore, MD 21205.

[2] Present address: Department of Radiology, DePaul Hospital, Eastern Virginia Medical School, 150 Kingsley Lane, Norfolk, VA 23505. Address reprint requests to J. C. Scatarige.

[3] Department of Medicine, The Johns Hopkins Medical Institutions, Baltimore, MD 21205.

AJR 149:83–85, July 1987
0361–803X/87/1491-0083
© American Roentgen Ray Society

preselected level(s) were then acquired at 15 sec, 30 sec, 1 min, 2 min, 3 min, and 5 min from end-injection. Scanning at progressively longer intervals continued until no further increase in lesion density or degree of fill-in was discernible on serial delayed sections. At this point, the examination was terminated, and no additional delayed scans were acquired.

The CT examinations were reviewed to determine the size, location, and precontrast appearance of the hemangiomas, as well as changes after bolus contrast enhancement.

Results

Unenhanced CT

The giant hemangiomas were 8–22 cm (mean, 13.7 cm) in maximum diameter. Five arose in the right lobe and three in the left lobe. Seven hemangiomas were less dense than surrounding normal liver, and all contained additional stellate or cleftlike zones of decreased density (Figs. 1A and 2A). One large hemangioma that arose in a fatty liver was slightly more dense than surrounding liver. No hemorrhage or fluid-debris levels were visible. Punctate and globular calcifications were present in two of the eight masses. Multiple smaller hemangiomas (less than 5 cm) were present in one patient.

Bolus-Enhanced CT

Contrast enhancement at the periphery of the mass was visible on the first postinjection scan in every patient (Figs. 1B and 2B). The early enhancement was often dense and assumed a nodular configuration. Delayed imaging at the preselected reference levels revealed further centripetal enhancement in each of the lesions. However, complete fill-in was never observed. More precisely, the cleftlike zones of decreased density did not enhance completely on delayed scans (Figs. 1C and 2C). The delayed enhancement was hyperdense (higher density than surrounding liver) in the one patient with fatty liver and isodense in the other seven. The time interval from end-injection to maximal observed fill-in was 8–35 min (mean, 18.5 min); this time interval was shortest for a 12-cm hemangioma and longest for an 8-cm lesion.

Discussion

During the past 8 years, several authors have suggested that hepatic hemangiomas exhibit features on CT sufficiently distinctive to permit a specific diagnosis without resorting to angiography [2–4]. Controversy still exists, however, concerning which CT criteria must be met to diagnose a hemangioma reliably. In recent reports, Freeny and Marks [7, 8] define three CT requirements for the diagnosis of hepatic hemangioma: (1) a mass with density less than liver on precontrast scan, (2) peripheral enhancement after bolus IV contrast injection, and (3) complete isodense fill-in on delayed scans. Only 32 (55%) of 58 of proved hemangiomas in their series fulfilled all criteria. In contrast, Ashida et al. [9] used a different scheme. They proposed five criteria: (1) low-density lesion on unenhanced scan, (2) early peripheral contrast enhancement, (3) progressive centripetal opacification, (4) a delay of at least 3 min before total opacification, and (5) eventual isodense fill-in with or without unopacified clefts. CT diagnosis of a hemangioma required fulfillment of the last two and at least two more of the five criteria. Forty-three (90%) of 48 proved hemangiomas met the CT requirements in this series and 38 (79%) satisfied all five.

The eight giant cavernous hemangiomas we report behaved similarly on CT. Seven were less dense than surrounding liver on precontrast scans, and each contained one or more additional cleftlike or stellate zones of low density. All masses displayed early peripheral enhancement and some degree of centripetal fill-in. However, none became completely isodense on delayed images. Because of the latter feature, none of our patients fulfilled the criteria for a typical hemangioma used by Freeny and Marks [7, 8]. However, all would have been acceptable under the conditions proposed by Ashida et al. [9].

The few large hemangiomas reported previously exhibited CT findings similar to those presented here. One giant hemangioma occupying the left hepatic lobe was illustrated by Johnson et al. [4]. This mass contained two discrete low-density zones on a precontrast scan and exhibited peripheral enhancement and partial isodense fill-in. In addition, Freeny

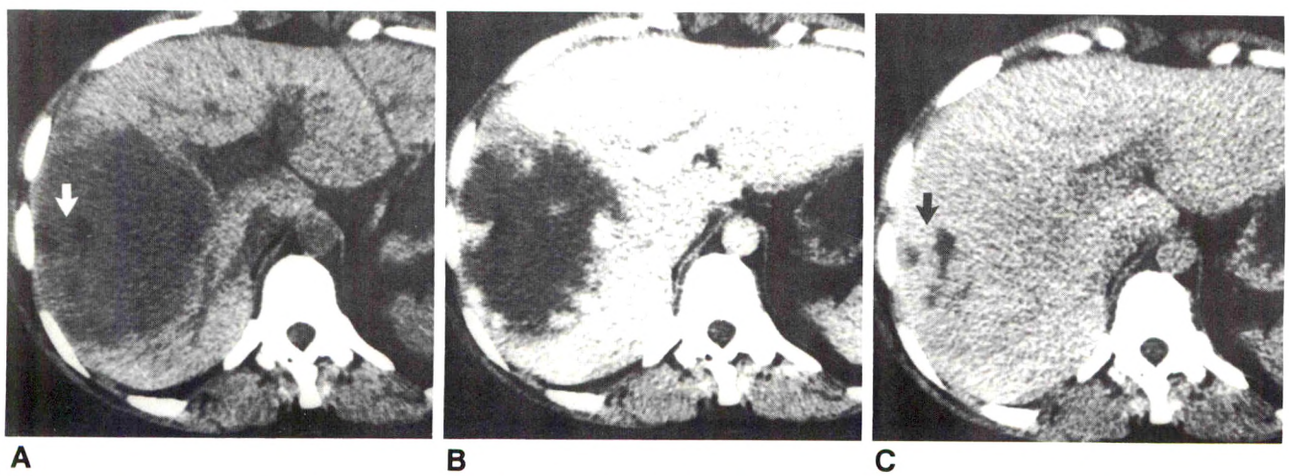


Fig. 1.—Giant cavernous hemangioma in 28-year-old woman with right upper quadrant pain.
***A*, Unenhanced CT scan shows a 10-cm hypodense mass in right lobe. Cleftlike zones of lower density are present laterally (*arrow*).**
***B*, 1 min postinjection image reveals peripheral contrast enhancement.**
***C*, Delayed scan 17 min after injection shows nearly complete isodense fill-in that spares eccentric low-density clefts (*arrow*).**

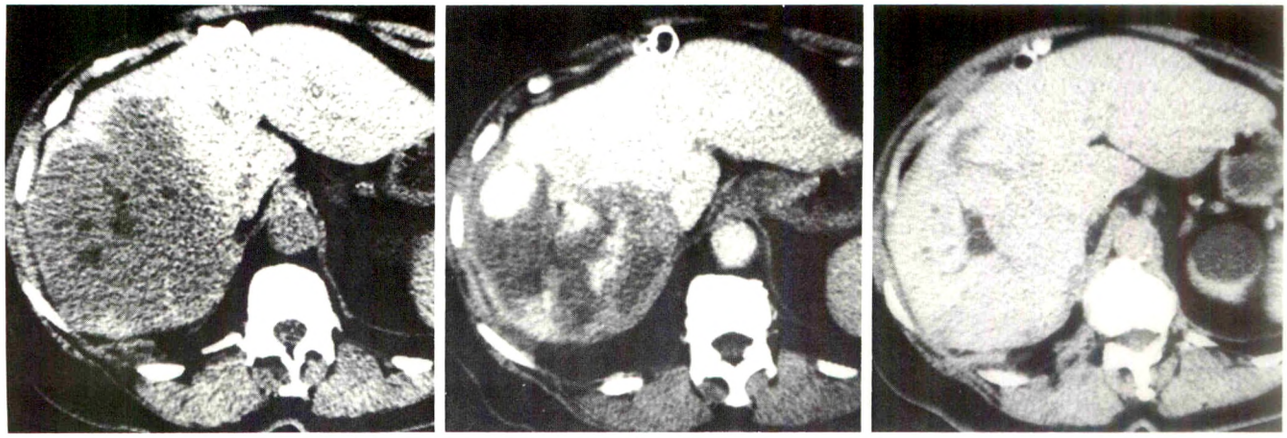


Fig. 2.—CT scans of 71-year-old woman with history of breast carcinoma. Large right hepatic mass was discovered on chest CT after drip infusion of contrast material. Two percutaneous biopsies yielded blood and hepatocytes.

***A*, Unenhanced CT shows lobulated hypodense mass with numerous low-density clefts.**

***B*, 1 min after bolus injection of contrast material, scan through cephalad border of mass reveals dense puddles of enhancement. Subsequent images showed centripetal fill-in.**

***C*, Delayed scan 8 min after injection, at maximal fill-in, shows that most of mass is now isodense. Small left renal cyst is present also.**

and Marks [8] illustrated a large, calcified hemangioma in the right lobe with similar pre- and postcontrast appearances. The same authors also reported complete isodense fill-in of a 12-cm hemangioma, documented on 90-min delayed scanning.

The cleft-like and stellate zones of low density visible on precontrast scans that did not become isodense after contrast administration probably represent areas of fibrosis, thrombosis, or hemorrhage [2, 4], although none of the eight lesions we report was available for pathologic examination. Indeed, incomplete central opacification of large hemangiomas has been observed at angiography [4]. Low-attenuation, nonenhancing clefts were reported in five of six hemangiomas studied by Barnett et al. [2]. In the 48 hemangiomas in the series of Ashida et al. [9], 22 (46%) had unopacified clefts.

Lesion size appears to affect at least two CT features of cavernous hemangiomas. First, the frequency of nonenhancing central clefts, present in each of our eight cases, is probably size-dependent. In reviewing the data of Ashida et al. [9], clefts were absent in hemangiomas smaller than 2 cm, present in 17% of hemangiomas 2–4 cm in diameter, and present in 78% of hemangiomas larger than 4 cm. Second, the time to maximal isodense enhancement appears to be at least loosely related to lesion size. In the series of Ashida et al., the mean diameter of hemangiomas requiring 2–4 min for maximum fill-in was 3.0 cm, while those needing 10–20 min for maximum enhancement averaged 7.5 cm in diameter. The data from Freeny and Marks [8] and our present report suggest that this relationship is not direct or linear, however. For example, the longest interval to maximum fill-in in our series (35 min) occurred in the smallest hemangioma.

Large hemangiomas examined by CT after slow drip infusion of IV contrast material may be mistaken for metastases or hepatocellular carcinoma. The confusion occurs because the early peripheral enhancement and serial centripetal fill-in are not ideally revealed by this scanning technique. One of our patients, initially studied in such a manner, underwent large-needle percutaneous biopsy after a tentative CT diagnosis of hepatic metastasis. A similar experience was reported by Itai et al. [3]. Freeny and Marks [8] suggested that, in addition to a single-level bolus study, use of the incremental-bolus dynamic technique for examining the liver may also be effective in displaying the enhancement properties of hemangiomas.

In summary, a diagnosis of giant cavernous hemangioma should be considered when CT shows a large hepatic mass that contains irregular areas of decreased density, peripherally enhances on bolus dynamic study, and exhibits centripetal but incomplete isodense fill-in on delayed images.

REFERENCES

1. Freeny PC, Vimont TR, Barnett DC. Cavernous hemangioma of the liver: ultrasonography, arteriography and computed tomography. *Radiology* **1979**;132:143–148
2. Barnett PH, Zerhouni EA, White RI, Siegelman SS. Computed tomography in the diagnosis of cavernous hemangioma of the liver. *AJR* **1980**;134: 439–447
3. Itai Y, Furui S, Araki T, Yashiro N, Tasaka A. Computed tomography of cavernous hemangioma of the liver. *Radiology* **1980**;137:149–155
4. Johnson CM, Sheedy PF, Stanson AW, Stephens DH, Hattery RR, Adson MA. Computed tomography and angiography of cavernous hemangiomas of the liver. *Radiology* **1981**;138:115–121
5. Itai Y, Ohtomo K, Araki T, Furui S, Iio M, Atomi Y. Computed tomography and sonography of cavernous hemangioma of the liver. *AJR* **1983**;141:315–320
6. Itai Y, Ohtomo K, Furui S, Minami M, Yashiro N. Noninvasive diagnosis of small cavernous hemangioma of the liver: advantage of MRI. *AJR* **1985**; 145:1195–1199
7. Freeny PC, Marks WM. Patterns of contrast enhancement of benign and malignant hepatic neoplasms during bolus dynamic and delayed CT. *Radiology* **1986**;160:613–618
8. Freeny PC, Marks WM. Hepatic hemangioma: dynamic bolus CT. *AJR* **1986**;147:711–719
9. Ashida C, Fishman EK, Zerhouni EA, Herlong FH, Siegelman SS. Computed tomography of hepatic cavernous hemangioma. *J Comput Assist Tomogr* (in press)
10. Ishak KG, Rabin L. Benign tumors of the liver. *Med Clin North Am* **1975**;59:995–1013

Book Review

Physics in Nuclear Medicine, *2nd ed.* By James A. Sorenson and Michael E. Phelps. New York: Grune & Stratton, 590 pp., 1987. $47.50

This book is intended to be an introductory textbook for the teaching of the physics of nuclear medicine and nuclear medicine instruments. In the preface, the authors state "there is a need for an introductory text covering the physics and instrumentation of nuclear medicine in sufficient depth to be of permanent value to the trainee or student, but not at such depth to be of interest only to the physics or instrumentation specialist." It is the opinion of this reviewer that the authors have achieved their stated goal. This revised edition not only covers the traditional topics in books of this type, but it also includes much more up-to-date information about emission tomography and kinetic modeling that is currently being used in research and clinical nuclear medicine laboratories. I believe that the book is appropriate for essentially any training program in nuclear medicine and, in fact, is quite useful for the physics instrumentation specialist in addition to the physicians training in the field.

The book is organized into 23 chapters and seven appendices. At the end of each chapter is a list of references and suggested material for further reading. This is particularly important since several of the chapters are terse and many readers may need to refer to a more complete text to understand all the information that is contained within this book.

The first chapter deals with basic atomic and nuclear physics. The second chapter goes into general modes of radioactive decay. Chapter 3 gives a more complete discussion of the decay process. The fourth chapter gets into radiation detectors. Chapter 5 presents a basic discussion of electronic instrumentation used in radiation detectors. In chapter 6, nuclear counting statistics are presented. Chapter 7 goes into the methods of production of radionuclides. Chapter 8 deals with the passage of charged particles through matter and the basic concept of ionization. Chapter 9 focuses on the passage of photons through matter and the traditional interactions of interest to nuclear medicine. Chapter 10 addresses internal radiation dosimetry and practical problems of dosimetry in nuclear medicine. Chapter 11 deals with pulse height spectrometry. Chapter 12 is titled "Problems in Radiation Detection and Measurement" and covers a potpourri of topics including detector efficiency, absorption, scatter, and calibration techniques. Chapter 13 presents the first of two chapters in counting systems. The first chapter deals primarily with problems in in vitro counting. Chapter 14 deals with details on solid state and liquid scintillation counting systems. Chapter 15 begins the imaging chapters with a basic discussion of the Anger camera. Chapter 16 continues the theme with a discussion of performance characteristics. Chapter 18 addresses image quality in nuclear medicine. Chapter 19 begins a series of chapters that has long been overdue in a general textbook on nuclear medicine and physics; these chapters cover the general area of emission tomography. It includes a discussion of filtered back projection with good examples. The chapter also includes several major topics of quantitative aspects of tomography. Chapter 20 extends the discussion of chapter 19 into specific instrumentation including focal plane systems, single-photon tomography systems, and positron systems. Chapter 21 deals with digital image processing. Chapter 22 begins an introduction of tracer-kinetic modeling in considerably more detail than I'm used to seeing in a textbook of this type. The final chapter, Chapter 23, deals with radiation safety and health physics. The appendixes include a summary of the properties of the elements, characteristics of some of the most commonly used radionuclides, table of exponential functions, mass attenuation coefficients for selected materials, some tables of dose estimates, numograms converting conventional units to SI units, and finally a discussion of convolution.

The book covers a broad range of material and is extraordinarily useful with good references and illustrations. As is true with any textbook, there are some areas that any given reviewer may take fault with. In my case, I was somewhat disappointed that the positron tomography section dealt extensively with bismuth-germanate-oxide (BGO) detector systems with little detail for some of the other alternatives. In the introduction the authors mentioned that they wanted to rely primarily on describing systems that are commercially available, and yet they did not include as much information on time-of-flight systems (which are offered by two commercial firms) as they did on non–time-of-flight systems. The material that they give in the text would be adequate, except that they do not give any references for the source for the time-of-flight gain equation presented in the text, nor do they include any further reading appropriate for either time-of-flight machines or the two-dimensional NaI (T1) detectors. In the tracer-kinetic modeling section, I would like to have seen references for some of the newer distributed modeling systems being developed in positron tomography, since so much detail was presented on compartmental models.

Overall, the text is extremely useful and is the most up-to-date textbook that I am aware of for the teaching of physics instrumentation in nuclear medicine. I found some of the chapters to be terse with just enough information to get a reader interested, but in general the references sections provided an appropriate avenue to the reader to find additional material. I have no hesitation in recommending this book and I congratulate the authors in achieving their goal.

Thomas K. Lewellen
University Hospital
Seattle, WA 98195

Hepatic Infarcts: New Observations by CT and Sonography

Anna S. Lev-Toaff[1]
Arnold C. Friedman
Lawrence M. Cohen
Paul D. Radecki
Dina F. Caroline

Until recently hepatic infarcts were rarely diagnosed before autopsy and were nearly always fatal. Four cases of hepatic infarcts, three of them nonfatal, were diagnosed and followed by CT (three cases), sonography (two cases), arteriography (two cases), and sulfur colloid liver-spleen scan (one case). In three patients with multiple subsegmental hepatic infarcts, most of the lesions were round or oval and centrally located. Only a minority of the lesions were wedge-shaped and peripheral. The early lesion appears hypoechoic on sonography, and CT shows a poorly demarcated low-density region. Later, lesions become confluent with more distinct margins. Bile lakes are a late sequela of large infarcts. Gas formation within sterile infarcts is newly described in two cases.

Hepatic infarcts have a variable appearance on CT and sonography and are not reliably distinguished from other lesions such as abscess or necrotic neoplasm.

In the era before sonography and CT, the diagnosis of hepatic infarction was rarely made before autopsy. Cases were nearly always fatal [1]. Now hepatic infarcts can be detected before death, even when the infarcts are small, and their evolution can be followed. Hepatic infarcts are most commonly due to hepatic arterial occlusion, and their extent (total, segmental, subsegmental) depends on the site of the occlusion and the development of collateral blood supply [2, 3]. We described the radiologic features in four cases, two of which had gas formation in proved sterile infarcts.

Materials and Methods

The imaging studies and clinical records of four patients with hepatic infarcts were reviewed. The patients included a 57-year-old white woman with polycythemia vera who had right intrahepatic arterial thrombosis. The second patient was a 68-year-old white man who presented with mesenteric infarction. At laparotomy an embolus to the superior mesenteric artery with a replaced right hepatic artery was found. The third patient was a 64-year-old black man who had had accidental ligation of a left hepatic artery during gastrectomy for gastric carcinoma. The fourth patient was a 37-year-old black woman who had had an accidental ligation of the common hepatic artery during total pancreatectomy for chronic pancreatitis. Three of the four patients presented with postoperative complications. All four patients had abdominal pain, either epigastric or right upper quadrant, and fever. They had moderate to marked leukocytosis and markedly elevated liver function tests.

Imaging studies included CT scans in three patients 3–12 days after surgery (embolism or ligation of an artery). In addition, follow-up CT scans were obtained 13 days to 9 months later. The CT scanners were third or fourth generation (General Electric 9800, Milwaukee, or Siemens Somatom DR3, Iselin, NJ). IV contrast material (150 ml of 60% meglumine diatrizoate) was administered with the rapid infusion technique. Sonography was performed in two patients. In one patient sonograms were obtained 3 and 13 days after surgery; in another patient a single study was performed 11 days after surgery. The sonography was real time with 3.5- or 5.0-MHz mechanical sector transducers (Diasonics DRF-400, Milpitas, CA). Arteriography was performed in two cases. In one case, a celiac angiogram followed a sulfur-

Received February 4, 1987; accepted after revision March 27, 1987.

[1] All authors: Department of Diagnostic Imaging, Temple University Hospital, Broad and Ontario Sts., Philadelphia, PA 19140. Address reprint requests to A. S. Lev-Toaff.

AJR 149:87–90, July 1987
0361–803X/87/1491–0087
© American Roentgen Ray Society

colloid liver-spleen scan in the acute phase of hepatic infarction. In another patient, an arteriogram was obtained 25 days after surgery (after CT and sonography) and revealed the unrecognized common hepatic artery ligation.

The diagnosis of hepatic infarction was confirmed in two patients by arteriography. In one case arteriography delineated abrupt occlusion of several right hepatic arterial branches with three round, unperfused defects in the parenchymal phase. In the second case, arteriography showed occlusion of the common hepatic artery, and multiple CT-guided aspirations of the lesions yielded sterile fluid. These two patients recovered clinically in 8–10 weeks. A third patient with mesenteric infarction died of multisystem failure 3 weeks after surgery, and a postmortem examination confirmed the presence of hepatic infarction. In this patient, CT-guided aspirates and autopsy specimens also revealed no evidence of infection. In the fourth case, the surgical report documented the accidental ligation of the left hepatic artery during a complicated gastrectomy. This patient recovered clinically in 3 weeks, and the liver function tests returned to normal in 2 months.

Results

Review of the imaging studies in four cases of hepatic infarction, including three cases with follow-up examinations, reveals several new observations regarding the location, appearance, and evolution of these lesions. Figures 1–3 show the CT scans and sonograms of three patients. Hepatic infarcts are commonly round and centrally located. A liver-spleen scan and celiac angiogram in one case revealed three small, round, central lesions in the right lobe of the liver and no wedge-shaped or peripheral infarcts. In two other patients who were followed by CT and sonography (Figs. 1A, 1E, and

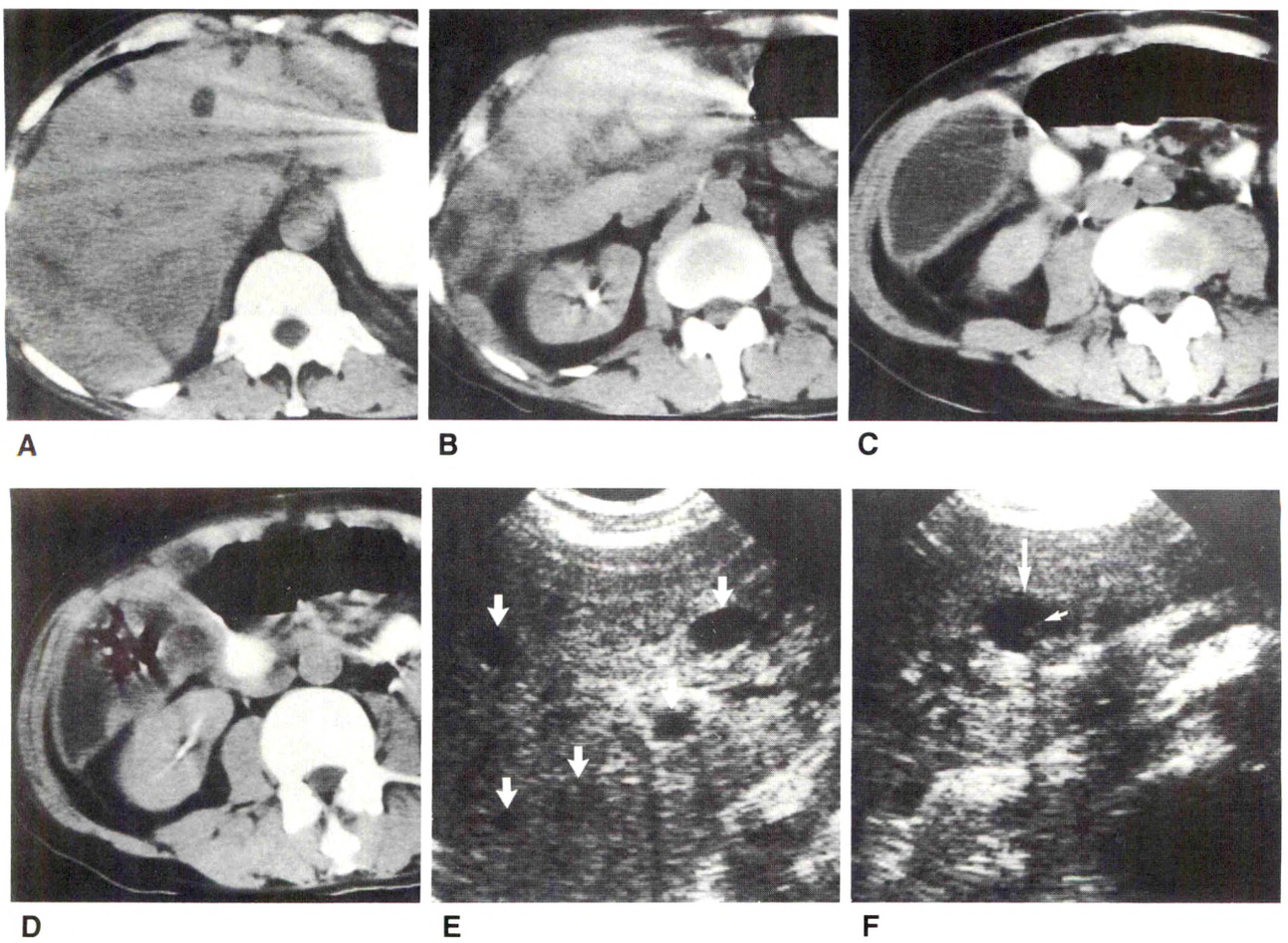


Fig. 1.—Images from a 68-year-old man with multiple right hepatic infarcts caused by superior mesenteric artery embolus with replaced right hepatic artery.

***A–C*, Postcontrast CT scans of liver 3 days after surgery show various manifestations of hepatic infarction: multiple small round foci of decreased attenuation in right lobe of liver (*A*), poorly defined low-density zone located more inferiorly in right lobe (*B*), and large cystic region occupying inferior tip of right lobe (*C*). Various appearances of infarction may represent infarcts of different ages caused by recurrent arterial emboli.**

***D*, CT scan 10 days later at same level as *C* shows well-defined fluid-density region (bile lake) containing gas.**

***E*, Transverse sonogram of liver corresponding to region in *A* 3 days after surgery. Multiple hypoechoic areas in right lobe, some with poorly defined margins (*arrows*).**

***F*, 10 days later. Larger anechoic region (*large arrow*) is seen containing necrotic debris (*small arrow*) with enhanced through-transmission.**

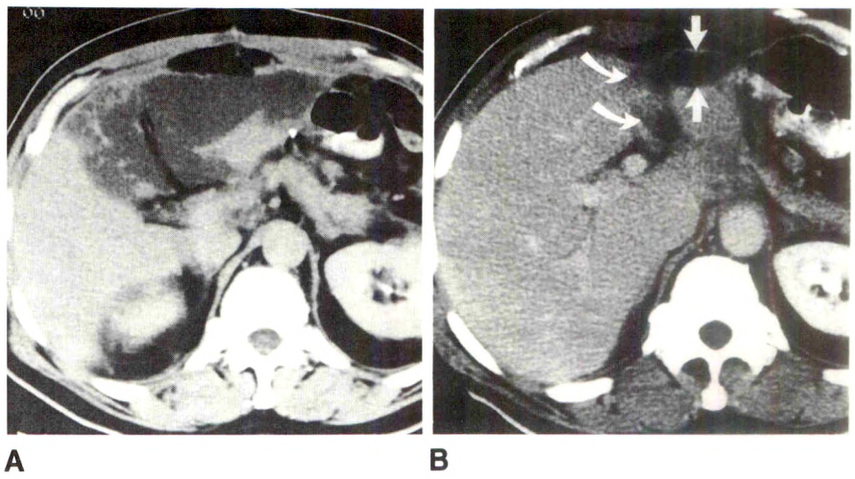


Fig. 2.—CT scans in a 64-year-old man with left lobar hepatic infarction from accidental ligation of left hepatic artery during gastrectomy for gastric carcinoma.

***A*, Postcontrast CT scan 12 days after surgery shows hypodense region involving most of left lobe without contrast enhancement.**

***B*, 9 months later. Left lobe has decreased in size with residual small hypodense areas (*curved arrows*) and small cystic area (bile lake) (*straight arrows*).**

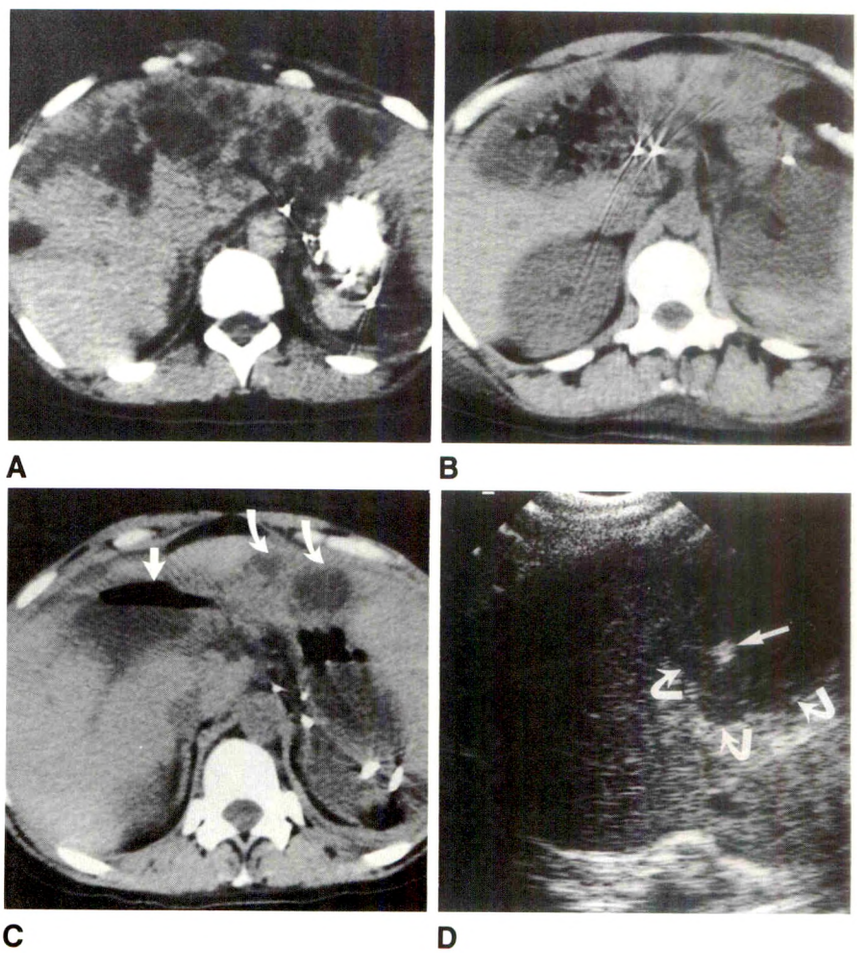


Fig. 3.—Images from a 37-year-old woman with multiple hepatic infarcts after accidental ligation of common hepatic artery during total pancreatectomy for chronic pancreatitis.

***A*, Postcontrast CT scan 9 days after surgery shows unenhancing multiple amorphous hypodense regions in both lobes of liver.**

***B*, 3 weeks after surgery. Large, rounded central low-density region in right lobe contains gas. (There is a left perirenal hematoma after thoracentesis.)**

***C*, 2 months after surgery. Large bile lake containing gas-bile level (*straight arrow*) in right lobe. Round areas of infarction in left lobe (*curved arrows*).**

***D*, Transverse subcostal sonogram of liver 11 days after surgery shows irregular zone of decreased echogenicity (*curved arrows*) with bright echo suspicious for gas (*straight arrow*).**

3A), nine round or oval central lesions were identified. In addition, there were several poorly defined central and peripheral infarcts and only three wedge-shaped, peripheral lesions. In one case, the lesion involved almost the entire left lobe (Fig. 2A). The appearance of hepatic infarcts changed with time. Initially they appeared as poorly marginated regions of decreased attenuation on CT, without evidence of contrast enhancement (Figs. 1B and 3A). They were round, oval,

wedge-shaped, or of poorly defined configuration. With time, these lesions became more discrete. Some poorly defined adjacent lesions became confluent with a fluid density (Figs. 1C, 2B, and 3C) corresponding to bile-lake formation. Over time, the necrotic areas shrunk significantly (Figs. 2, 3A, and 3B).

On sonography, foci of hepatic infarction were initially depicted as poorly defined hypoechoic zones (Fig. 1E). On follow-up study, these regions became more discrete and anechoic with enhanced through-transmission indicating cystic change (Fig. 1F).

Gas formation was demonstrated in two cases of hepatic infarction (Figs. 1D, 3B, and 3D). In both cases, the gas formed in relatively large subsegmental infarcts that evolved into bile lakes. On sonography, gas was demonstrated as a bright echogenic focus without shadowing within the hypoechoic infarct (Fig. 3D). In both cases, the lesions demonstrating gas formation were sterile, as evidenced by CT-guided aspiration and culture.

Discussion

There have been few reports on cross-sectional imaging of hepatic infarction [4–6]. Our cases of hepatic infarction were due to interference with the arterial blood supply to the liver. The classic description of hepatic infarction is a well-circumscribed, peripheral, and wedge-shaped lesion [2, 6, 7]. In three of our cases, most of the infarcts demonstrated a round or oval configuration located centrally within the liver parenchyma. The other case involved almost the entire left lobe. We found that the appearance of the infarct, particularly the distinctness of its borders, depends on the stage in which the imaging is performed. In general, the areas of infarction developed progressively more distinct margins with time. The absence of contrast enhancement on CT was a uniform finding.

The development of bile-duct cysts secondary to hepatic infarction has been described [4, 8]. Doppman et al. [4] postulated that these cysts result from ischemic necrosis of bile-duct epithelium. The extravasated bile is eventually surrounded by fibrous tissue forming a localized dilatation of the intrahepatic bile ducts. In three of our cases in which follow-up CT scans were available, we observed the formation of bile cysts or lakes. These findings suggest that bile-lake formation may be a common sequela of large hepatic infarctions.

Spontaneous formation of gas in hepatic infarcts has not been described previously. Gas within hepatic tumors after therapeutic arterial embolization has been reported [9]. The sonographic appearance of gas within the liver was reviewed by Gosink [10]. The finding of intraparenchymal hepatic gas is usually considered a sign of abscess formation. In two of our cases gas collections developed in the infarcted regions, which showed bile-lake formation. There was no evidence of infection on aspiration of these regions. Thus, gas formation does not serve to distinguish between infection and sterile infarction.

In our experience it is difficult to differentiate hepatic infarcts from abscesses or necrotic tumors by CT, sonography, or any other imaging technique, and percutaneous aspiration is frequently required to rule out an infectious process or neoplasm. This is crucial since the clinical and laboratory data in hepatic infarction may be entirely compatible with hepatic abscess, which is excluded only by negative smears and cultures of aspirated material.

ACKNOWLEDGMENT

We thank Frederick E. Cosco, Department of Radiology, George Washington University Hospital, for assistance with one of the cases.

REFERENCES

1. Sherlock S. *Diseases of the liver and biliary system*. Oxford, England: Blackwell Scientific, **1981**:178
2. Woolling KR, Baggenstoss AH, Weir JF. Infarcts of the liver. *Gastroenterology* **1951**;17:479–493
3. Carroll R. Infarction of the human liver. *J Clin Pathol* **1963**;16:133–136
4. Doppman JL, Dunnick NR, Girton M, Fauci AS, Popovsky MA. Bile duct cysts secondary to liver infarction. *Radiology* **1979**;130:1–5
5. Dammann HG, Hagemann J, Runge M, Kloppel G. In vivo diagnosis of massive hepatic infarction by computed tomography. *Dig Dis Sci* **1982**;27:73–79
6. Adler DD, Glazer GM, Silver TM. Computed tomography of liver infarction. *AJR* **1984**;142:315–318
7. Seeley TT, Blumenfeld CM, Ikeda R, Knapp W, Ruebner BH. Hepatic infarction. *Hum Pathol* **1972**;3:265–276
8. Peterson IM, Neumann CH. Focal hepatic infarction with bile lake formation. *AJR* **1984**;142:1155–1156
9. Bernardino ME, Chuang VP, Wallace S, Thomas JL, Soo CS. Therapeutically infarcted tumors: CT findings. *AJR* **1981**;136:527–530
10. Gosink BB. Intrahepatic gas: differential diagnosis. *AJR* **1981**;137:763–767

Addendum

Since the preparation of this manuscript we have encountered a patient with a clinical history and sonographic and CT findings indistinguishable from our other cases of hepatic infarction who proved to have an abscess that was probably an infected infarct. Accidental surgical ligation of the replaced right hepatic artery during a pancreatectomy was proved by arteriography, and the infection was proved by percutaneous aspiration and catheter drainage.

Technical Note

External-Internal Cross-Connection for Bilateral Percutaneous Biliary Drainage

Christoph D. Becker,[1] J. Stephen Fache, Robert G. Gibney, and H. Joachim Burhenne

Percutaneous biliary drainage by catheter often is difficult in patients with multisegmental obstruction of the bile ducts. In many cases, only one catheter can be advanced through a strictured area for internal drainage. If necessary, a second catheter is then left to drain externally. We report our experience with a new drainage technique that we used in two such situations to avoid the disadvantages of external biliary drainage.

Subjects, Methods, and Results

Two patients, a 48-year-old woman and a 65-year-old man, both with unresectable cholangiocarcinoma of the hepatic bifurcation, underwent percutaneous transhepatic biliary drainage for palliative treatment. Both patients had drainage catheters inserted through the right hepatic duct and the biliary stricture into the duodenum for internal drainage (Cope biliary catheter, 12-French, Cook, Bloomington, IN). Although satisfactory biliary decompression was achieved at first, separate drainage of the isolated left hepatic lobe became necessary later in each patient because of cholangitis and recurrent jaundice. In both cases, the additional catheter on the left (Mueller biliary catheters, 8.3-French and 12-French, respectively; Cook, Bloomington, IN) drained externally into a bile bag because internal drainage was not feasible. Before the patients were discharged from the hospital, cholangiograms of the tubes on the right side were obtained to confirm patency. In each case, the catheter on the left side was then disconnected from the bile bag, the hub was cut off, and the end of the tube was introduced into the hub of the catheter on the right. Both catheter ends were secured together with waterproof tape. This cross-connection allowed the bile draining from the left lobe to drain first externally and then internally through the catheter on the right side (Fig. 1).

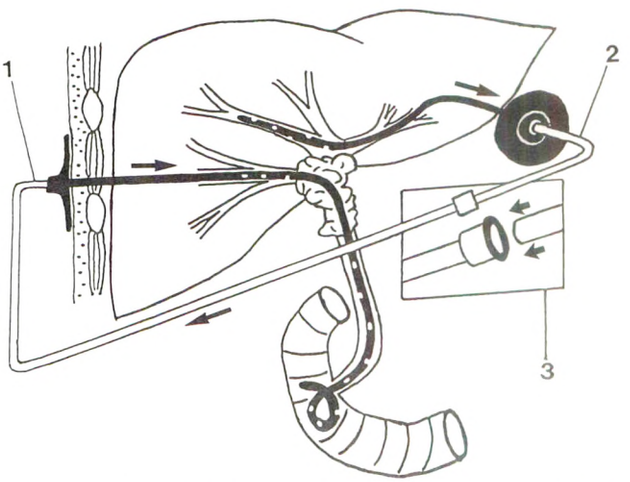


Fig. 1.—Schematic drawing of external-internal cross-drainage. Right internally draining catheter (1) and left externally draining catheter (2) are secured to the skin by Molnar disks (*black*) and connected externally. Bile flows from left catheter to right catheter (*long arrows*). The two catheter ends can be connected by cutting off hub of one catheter and advancing its tube into hub of other catheter (*short arrows*) (3).

Received January 26, 1987; accepted after revision February 19, 1987.

[1] All authors: Department of Radiology, University of British Columbia and Vancouver General Hospital, 855 W. 12th Ave., Vancouver, British Columbia V5Z 1M9, Canada. Address reprint requests to C. D. Becker.

AJR 149:91–92, July 1987 0361–803X/87/1491–0091 © American Roentgen Ray Society

After the patients were discharged, catheters were replaced periodically to maintain patency, but no other catheter-related problems occurred. The two catheters were secured by Molnar disks (Cook, Bloomington, IN), the cross-connection tube system was taped to the skin, and each patient wore an elastic Fastanet bandage (Roussel, Paris, France). Both patients experienced only minimal discomfort and impairment of activities due to their catheters. One of the two patients died after 6 months; the other was able to resume manual labor during a follow-up period of 9 months.

Discussion

Patients with unresectable cholangiocarcinoma may survive for a considerable period of time if effective biliary drainage is established and maintained. Tumors of the hepatic bifurcation may progress to cause isolated obstruction of several biliary segments, often necessitating the use of more than one drainage catheter [1–4]. A single catheter usually can be advanced through a strictured area for unilateral internal drainage. Decompression of one hepatic lobe offers sufficient relief. As the tumor progressively obstructs more proximal radicles, however, pruritus and jaundice may recur. Furthermore, cholangitis developing in undrained intrahepatic radicles may require additional drainage. If a second catheter cannot be advanced through the stricture, it must be left to drain externally. Cholangitis usually responds rapidly to biliary decompression and antibiotic treatment. Once the patient has been afebrile for several days with clear bile draining externally from the previously obstructed duct, cross-connection can be performed. We think that the risk of septic complications due to bacterial contamination from one lobe to another is low as long as the flow of bile through the drainage system into the duodenum is unimpeded. External-internal cross-drainage avoids the discomfort of a bile bag and depletion of bile salts. This technique thus permits improved palliation in patients with malignant obstruction of multiple biliary ducts.

REFERENCES

1. Mueller PR, vanSonnenberg E, Ferrucci JT Jr. Percutaneous biliary drainage: technical and catheter-related problems in 200 procedures. *AJR* **1982**;138:17–23
2. McLean GK, Ring EJ, Freiman DB. Therapeutic alternatives in the treatment of intrahepatic biliary obstruction. *Radiology* **1982**;145:289–295
3. Kerlan RK, Pogany AC, Goldberg HI, Ring EJ. Percutaneous biliary drainage in the management of cholangiocarcinoma. *AJR* **1983**;141:1295–1298
4. Ferrucci JT Jr, Wittenberg J, Mueller PR. Percutaneous biliary drainage: special considerations. In: Ferrucci JT Jr, Wittenberg J, Mueller PR, Simeone JF, eds. *Interventional radiology of the abdomen*, 2nd ed. Baltimore: Williams & Wilkins, **1985**:219–249

Transcystic Biopsy: A New Approach to Posterior Pelvic Lesions

Edward Steiner[1]
Peter R. Mueller
Joseph F. Simeone
Sanjay Saini
Peter F. Hahn
Joseph T. Ferrucci, Jr.

Six patients with masses located posterior to the bladder were biopsied using an anterior transcystic approach. Conventional biopsy needles were introduced through the bladder with both sonographic (five) and CT guidance (one). Clinically important diagnoses of recurrent carcinoma (four) or cytology-negative fluid (two) were made in all patients. One patient had a transient episode of minimal hematuria immediately after the biopsy. Otherwise, there were no complications.

Transcystic biopsy appears to be a safe and effective technique for biopsy or aspiration of posterior pelvic masses.

The safety of percutaneous needle biopsy of tumors of intraabdominal organs and retroperitoneal structures is well documented. Many studies have shown that transgression of bowel or vascular structures while biopsying solid lesions does not significantly increase the complication rate [1–6]. Lesions situated posteriorly in the pelvis, however, particularly those posterior to the bladder, have often required more complex biopsy approaches. These include transvaginal and/or transrectal routes, which can be cumbersome and can be uncomfortable for the patient [7]. Similarly, a transgluteal approach (via the greater sciatic foramen) requires CT guidance and is technically more difficult because of the proximity of neural structures [8]. The anterior transcystic approach in most patients is the most direct pathway for biopsy of these types of masses and usually can be done easily with sonography, avoiding the need to use extensive CT time or patient manipulation.

We report our experience with six patients using the transcystic approach. Although there has been some use of this approach in aspirating human ovarian follicles [9, 10] no series of patients with percutaneous transcystic pelvic biopsies has been published.

Materials and Methods

Six women ranging in age from 30 to 77 years were included in this study (Table 1). All had masses posterior to the bladder seen by CT or sonography. Three patients had gynecologically related tumors (two cervical carcinomas, one ovarian carcinoma) that had been operated on within the previous 24 months. One patient had a previously resected colonic carcinoma, one developed complex masses after a total abdominal hysterectomy and bilateral salpingo-oophorectomy, and one had a large ovarian cyst palpated on routine physical examination. Five of the six patients had had a surgical hysterectomy. The biopsied masses ranged in size from $3 \times 2 \times 2$ cm to $5 \times 6 \times 8$ cm.

All six were outpatients. The biopsy procedure was performed with sonographic guidance on five patients and with CT guidance on one. Patients who underwent the procedure by sonographic guidance were prepared by having a bladder full enough that the mass could be seen, but the patient was still comfortable (Fig. 1). Local anesthesia was used in all cases. Although three of the patients had perineal discomfort during the biopsy, none required further medication.

Received December 22, 1986; accepted after revision February 6, 1987.

[1] All authors: Department of Radiology, Massachusetts General Hospital and Harvard Medical School, Boston, MA 02114. Address reprint requests to P. R. Mueller.

AJR 149:93–95, July 1987
0361–803X/87/1491–0093
© American Roentgen Ray Society

TABLE 1: Lesions Biopsied by Transcystic Route

Case	Age (yr)	Clinical Diagnosis	Reason for Biopsy	Technique	Needle size (gauge)	Result
1	30	Extensive pelvic adenomyosis	Paraovarian fluid collection	Sonography	22	Brownish fluid aspirated consistent with ovarian cyst
2	73	Carcinoma of sigmoid colon	Pelvic mass suspicious for tumor recurrence	CT	22	Positive for recurrent sigmoid carcinoma
3	34	Cervical carcinoma (Stage III)	Recurrent pelvic mass	Sonography	18–20	Positive for poorly differentiated carcinoma
4	75	Cervical carcinoma	Recurrent pelvic mass	Sonography	22	Positive for metastatic squamous cell carcinoma
5	77	Ovarian carcinoma	Recurrent pelvic mass	Sonography	18–20	Positive cytology for ovarian carcinoma
6	77	Endometrial carcinoma	Complex cystic parauterine mass	Sonography	20	150 ml of brown fluid aspirated; cytology: epithelial cells consistent with benign cyst

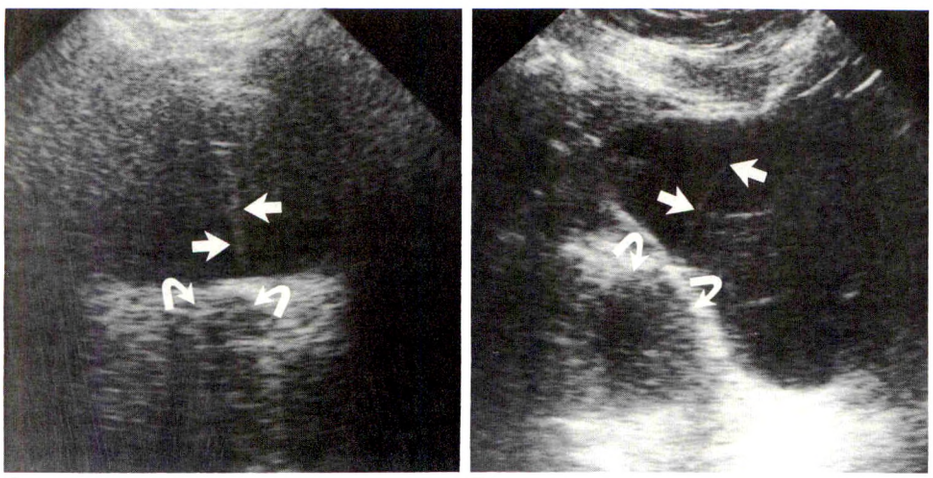


Fig. 1.—Case 3: 34-year-old woman with stage III cervical carcinoma (previously treated with hysterectomy) presented with 5-cm mass posterior to bladder that was easily seen by sonography.

***A*, Transverse scan shows 22-gauge needle (*straight arrows*) within bladder. Tip of needle is at anterior portion of the mass (*curved arrows*).**

***B*, Sagittal scan shows needle (*straight arrows*) positioned at anterior portion of mass (*curved arrows*).**

Biopsy was positive for poorly differentiated carcinoma.

Four patients were biopsied using standard 20- or 22-gauge cutting needles (Bernardino-Sones from Medi-tech, Watertown, MA; Turner from Cook Co., Bloomington, IN) and two were biopsied using a combination of 20- and 18-gauge needles. In these cases a 20-gauge needle (Turner) was positioned first and an 18-gauge needle (Turner) was then placed in a tandem fashion into the lesion. Three passes were made into each mass. In cases 1 and 6, where fluid was encountered, only one pass was made.

In all five patients who had the biopsy performed with sonography, direct visualization of the needle was maintained as it was placed through the bladder and into the mass. In four patients with solid lesions, cytologic material was aspirated and sent to the pathology department. A brownish fluid was aspirated from two of the patients (30 ml and 150 ml). This was sent for culture and cytology.

Results

All six biopsies yielded diagnostic material (Table 1). Four specimens were positive for recurrent carcinoma. In two patients with cystic mass, cytology was negative for carcinoma and epithelial cells were detected suggesting diagnoses most consistent with benign hemorrhagic ovarian cysts.

No significant complications were encountered either during or after the procedure. One patient had an immediate episode for minimal gross hematuria. The patient was observed for several hours, remained completely asymptomatic, and was discharged after a clear urine sample. No patient had hematuria on clinical followup.

Discussion

An anterior transcystic approach for biopsying solid masses in the posterior pelvis appears to be safe and expeditious.

The urine-filled bladder makes an ideal acoustic window for biopsies guided by sonography (Fig. 1). No significant complications were encountered with this approach.

The use of a percutaneous approach to the bladder to confirm or rule out urinary tract infections in children has been documented as a safe and common practice in pediatric and adult surgery [11]. Biopsy of a mass by transgressing both walls of the bladder is merely an extension of this technique. Because the bladder contains sterile fluid, the transcystic approach to aspirate fluid-containing structures in the posterior pelvis is not a contraindication; however, the transgression of bowel during these aspiration procedures should be avoided so as not to contaminate a previously sterile bladder. Performing the biopsy with the bladder full helps to ensure that small and large bowel will be displaced away from the anterior abdominal wall and to minimize the danger of transgression. Similarly, if the collection might be infected, the transcystic route would be contraindicated.

Biopsy and aspiration of posterior, pelvic, solid and cystic collections using an anterior transcystic approach is tolerated well by most patients. The ease of needle visualization, especially by sonography, makes this procedure practical and simple to perform.

REFERENCES

1. Holm HH, Als O, Gammelgaard J. Percutaneous aspiration and biopsy under ultrasound visualization. In: Taylor KJW, ed. *Clinics in diagnostic ultrasound: diagnostic ultrasound in gastrointestinal disease*. New York: Churchill Livingstone, **1978**:137–149
2. Lundquist A. Fine-needle aspiration biopsy of the liver. *Acta Med Scand [Suppl]* **1971**;520:1–28
3. Ferrrucci JT Jr, Wittenberg J, Mueller PR, et al. Diagnosis of abdominal malignancy by radiologic fine-needle aspiration biopsy. *AJR* **1980**;134:323–330
4. Kuligowska E, Olsen WL. Pancreatic pseudocysts drained through a percutaneous transgastric approach. *Radiology* **1985**;154:79–81
5. Bernardino ME, Amerson JR. Percutaneous gastrocystostomy: a new approach to pancreatic pseudocyst drainage. *AJR* **1984**;143:1096–1097
6. Ho CS, Taylor B. Percutaneous transgastric drainage for pancreatic pseudocyst. *AJR* **1984**;143:623–625
7. Graham D, Sanders RC. Ultrasound directed transvaginal aspiration biopsy of pelvic masses (Abstr). *Radiology* **1984**;150:1299
8. Butch RJ, Mueller PR, Ferrucci JT Jr. Drainage of pelvic abscesses through the greater sciatic foramen. *Radiology* **1986**;158:487–491
9. Lenz S, Lauritsen JG. Ultrasonically guided percutaneous aspiration of human follicles under local anesthesia: a new method of collecting oocysts for in vitro fertilization. *Fertil Steril* **1982**;38:673–677
10. Wikland M, Nilsson L, Hansson L, Hamberger L, Janson PO. Collection of human oocytes by the use of sonography. *Fertil Steril* **1983**;39:603–608
11. Belman AB. GU infections. In: Kelalis PP, King LR, Belman AB, eds. *Clinical pediatric urology*. Philadelphia: Saunders, **1985**:237

Book Review

Bone Scanning in Clinical Practice. Edited by Ignac Fogelman. Berlin: Springer-Verlag, 260 pp., 1987. $165

Although bone scintigraphy is covered in all general textbooks of nuclear medicine, the subject is, unfortunately, never covered in sufficient depth to satisfy the needs of the advanced student. On the other hand, in-depth reviews are usually found as separate chapters regarding bone scanning in monographs devoted to other subjects, such as metastatic disease, osteomyelitis, sports medicine. This text, which offers a complete and well-organized review of the entire subject, is a welcome addition to the nuclear medicine literature.

The editor is an expert in the field of bone scintigraphy and has written (or co-written) the obligatory introductory chapters concerning radiopharmaceuticals of the past and present and their mechanism of uptake by bone. These chapters cover more material than is required (or desired) by most practitioners of nuclear medicine, but the clear labeling of the sections within the chapters makes it easy to skip over the more esoteric information.

The remaining chapters of the text, which were predominantly written by other authors, discuss the role of scintigraphy in the evaluation of specific clinical problems. These topics include the evaluation of metastatic disease, primary bone and marrow tumors, metabolic bone disease, Paget's disease, infection, trauma, arthritis, and avascular necrosis. Separate chapters regarding the use of scintigraphy for pediatric disorders and the gamut of soft-tissue uptake of tracers are also included.

The reviews of these subjects are quite complete. In fact, I suspect that some would say "exhaustive," since a synopsis of all important research in the field is included in the text. However, the inclusion of such detail is the aim of the book. Much to their credit, the authors have included views both for and against the use of bone scanning in these various situations, and the reader is allowed to form his or her own opinion of the usefulness of the test. At the end of each section, the consensus of opinion is summarized and the personal approach of the author is presented.

As expected, the book concentrates on the role of ^{99m}Tc diphosphonate imaging, but the use of ^{67}Ga citrate, ^{111}In WBC, and ^{99m}Tc colloid imaging is also covered when appropriate. Good quality illustrations of scintigraphs and, when necessary, correlative radiographs are incorporated into the text and a long list of references are included at the end of each chapter. The reading of this excellent text should be required of all residents in radiology and nuclear medicine. It is also highly recommended to all who frequently use bone scintigraphy in their practice. Those who perform these studies less often will still find it to be a valuable reference.

My only reservation about this text is that the cost seems quite high. Read it yourself, but find someone to buy it for you.

James L. Buck
Armed Forces Institute of Pathology
Washington, DC 20306-6000

Potential Contrast Agents for MR Arthrography: In Vitro Evaluation and Practical Observations

Paul C. Hajek[1]
David J. Sartoris[1]
Christian H. Neumann[2]
Donald Resnick[1]

In an attempt to identify an ideal contrast agent for MR arthrography, signal behavior as well as T1 and T2 values for articular cartilage, menisci, and ligaments were determined in knees from cadavers and normal volunteers. Comparison was made with similar data derived for intraarticular blood, varying concentrations of an albumin-saline solution (simulating synovial fluid) and Gd-DTPA, 0.9% saline, Renografin 60%, and air. Cadaveric specimens were imaged after intraarticular administration of each substance. A 500-μM volume of Gd-DTPA proved to be an ideal contrast agent for MR arthrography, exhibiting excellent contrast differences with articular structures on T1-weighted images. An albumin concentration of 12%, potentially occurring in severe inflammatory arthritis, also manifested adequate contrast to articular cartilage on T1-weighted images. Renografin and saline provided inadequate contrast on T1-weighted images, and saline necessitated the use of T2-weighted sequences. Air was not found to be an optimal contrast agent. Intraarticular blood exhibited insufficient contrast differences with articular cartilage during the acute hemorrhagic phase. Synovial fluid associated with severe arthritis as compared with fresh intraarticular hemorrhage may thus prove to be a better biological contrast agent for MR arthrography.

Saline is currently recommended for use in arthrography, but Gd-DTPA offers significant advantages and should be safety-tested for potential clinical use.

Recent reports have indicated the diagnostic potential of MR imaging in the evaluation of normal and abnormal articulations [1–5]. In contrast to conventional arthrography, MR allows direct visualization of the major anatomic structures including ligaments, menisci, and periarticular soft tissues; however, the articular cartilage, joint capsule, and smaller (but nevertheless structurally important) ligaments cannot be imaged reliably with MR. Identification or exclusion of abnormalities of some intraarticular structures, therefore, can be accomplished only with some degree of uncertainty [1–3]. Recent studies have shown that the delineation of many intraarticular structures is enhanced by the presence of a joint effusion [4–8]. Furthermore, visualization of normal articular anatomy and depiction of subtle abnormalities are facilitated by iatrogenically introduced effusion, so-called MR arthrography [7]. Many articular disorders are accompanied by a joint effusion, the composition of which depends on the underlying disease [9]. In general, these effusions contain variable quantities of protein or blood, or both. Since synovial fluid contains chiefly albumin [10], the MR characteristics and signal behavior of various concentrations of this protein were investigated. A comparable study of intraarticular blood was also performed, as well as a quantitative evaluation of various potential contrast agents that might be suitable for MR arthrography.

Materials and Methods

A 1.5-T imaging system (Signa, General Electric, Milwaukee) equipped with the 2.0 software package [11] and a standard-head imaging coil was used in this investigation. Specimens were imaged by using a 13.5-cm circular surface coil.

Received January 8, 1987; accepted after revision March 6, 1987.

This work was supported in part by Veterans Administration grant SA 360, the Erwin Schrodinger Fellowship Stipendium J0062, Republic of Austria, and a grant from the Panhandle Diagnostic Imaging Center, Amarillo, TX.

[1] Department of Radiology, University of California Medical Center, and Veterans Administration Medical Center, 3350 La Jolla Village Dr., San Diego, CA 92161. Address reprint requests to D. Resnick.

[2] Department of Radiology, French Hospital and Medical Center, San Francisco, CA 94118.

AJR **149:97–104, July 1987**
0361–803X/87/1491–0097
© American Roentgen Ray Society

In Vitro Analysis

Six different dilutions of 24% (weight/volume [w/v]) human serum albumin in saline were prepared and placed into 15-ml glass tubes. The final albumin-saline concentrations ranged from 0.1% (w/v) to 24% (w/v). Three additional tubes containing 0.9% (w/v) saline, Renografin 60% (Squibb, Princeton, NJ), or air were also prepared. This nine-tube phantom was then placed in a plastic cylinder filled with 2 l of saline. A second phantom was constructed consisting of seven glass tubes filled with gadolinium-DTPA–dimeglumine (Magnevist Schering AG, Berlin) diluted by variable proportions of saline. The final concentrations of this contrast agent were 50 μM to 1 mM.

Phantoms were imaged by using spin-echo (SE) pulse techniques with repetition times (TRs) of 600 and 2000 msec and echo times (TEs) of 25 and 25/70 msec, respectively. Slice thickness was 10 mm with a 5-mm increment and a 256 × 128 data-acquisition matrix displayed on a 512 × 512 matrix. Signal intensities of the various compounds were evaluated with system software [10]. Longitudinal (T1) and transverse (T2) relaxation times were determined using TRs of 200, 400, 800, 1500, and 2500 msec and a TE of 25 msec, as well as a TR of 4000 msec with TEs of 25, 50, 75 and 100 msec, respectively. One signal average was used for all scans. Each pulse sequence was repeated three times for each phantom in order to define a mean value and standard deviation as an indication of reproducibility.

In Vivo and Cadaveric Analysis

The left knees of three normal volunteers (25, 33, and 42 years old) without prior knee trauma were imaged in the sagittal plane with a standard 13.5-cm circular surface coil. SE technique was used, with TRs of 600 and 2000 msec and TEs of 25 and 25/70 msec, respectively, in conjunction with 5-mm slice thickness, 2.5-mm interslice gap, 16-mm field of view, 128 × 256 data-acquisition matrix, and one signal average. Signal intensities (mean value of five measurements per knee) of the articular cartilage (in the posterior circumference of the lateral femoral condyle), the meniscus, and the posterior cruciate ligament were determined using the region-of-interest system software. A single sagittal slice through the lateral femoral condyle was selected to define T1 and T2 values for the articular cartilage and the meniscus by applying TRs of 200, 400, 800, 1500, and 2000 msec with a TE of 25 msec for T1 and a TR of 4000 msec with TEs of 25, 50, 75, and 100 msec for T2. An identical experimental approach was applied to three fresh (3–6 days postmortem) cadaveric knees, with measurement of signal intensities and determination of T1 and T2 values.

Cadaveric Analysis

Fourteen additional fresh cadaveric knees were evaluated by MR arthrography [6]. Intraarticular injections of 500 μM Gd-DTPA in five cadavers, air in two, saline in five, and Renografin 60% in two were performed with standard arthrographic technique, and an injection volume of 30 ml. MR imaging was performed by using SE techniques (TR = 600 msec, TE = 25 msec, and TR = 2000 msec, TE = 25/70 msec) with 5-mm slice thickness.

Thirty milliliters of fresh blood or 12% (w/v) albumin solution was injected into a fresh cadaveric knee. Imaging was performed by using the methods already outlined. The joint with the artificially introduced hemarthrosis was imaged with TR = 600 msec, TE = 25 msec, and TR = 2000 msec, TE = 20/70 msec, at 6-hr intervals over a period of 48 hr. Signal intensities of albumin, blood, articular cartilage, meniscus, and posterior cruciate ligament were measured with system software.

Results

In Vitro Analysis

A clear effect of albumin on relaxation times of saline was apparent (Table 1) with observed linear relationships (Fig. 1).

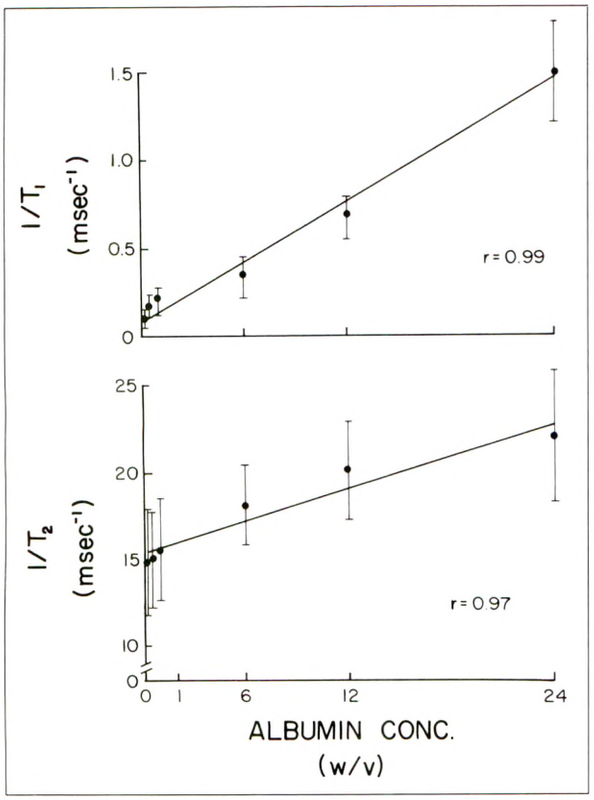
The influence of albumin on signal behavior is shown in Figure 2. For the TR = 600-msec, TE = 25-msec sequence, a steady increase in signal intensity was observed for albumin concentrations between 0.1% and 12%, whereas the slope of this relationship decreased at higher concentrations. For the TR = 2000 msec, TE = 25 msec sequence, peak signal intensity was observed for concentrations of 12–24%. For the TR = 2000 msec, TE = 70 msec sequence, the brightest signal intensities were achieved for a 12% solution, whereas intensity for a 24% solution decreased to the value of saline owing to increased shortening of T2 relaxation times.

Gd-DTPA–dimeglumine is the dimeglumine salt of the chelated form of gadolinium (Gd^{3+}), which is highly paramagnetic and therefore produces strong relaxation effects on adjacent hydrogen nuclei [12–16]. With an increase in the concentration of Gd-DTPA, a decrease in both T1 and T2 relaxation times occurred (Table 1). In this investigation, a linear relationship was noted between the concentration and the reciprocal values of relaxation times over the range from 50 μM to 1 mM (Fig. 3). The signal behavior of the Gd-DTPA solutions is depicted in Figure 4. For the TR = 600 msec, TE = 25 msec sequence, a progressive increase in signal intensity was noted up to 500 μM, whereas the curve flattened for higher concentrations. Since the influence of Gd-DTPA on proton-relaxation parameters is concentration dependent [12–15], this phenomenon can be explained by the increasing importance of T2 reduction at higher concentrations. For the TR = 2000 msec, TE = 25-msec sequence, signal intensities exhibited a dramatic increase for concentrations as great as 500 μM, whereas overall signal intensity decreased slowly for concentrations exceeding 600 μM, owing to an increasing T2 influence. The relatively T2-weighted sequence of TR = 2000 msec, TE = 70 msec showed a peak signal intensity at even lower concentrations of Gd-DTPA and a steady decrease in

TABLE 1: T1 and T2 Relaxation Times of Articular Cartilage, Meniscus, and Various MR Contrast Agents

Fluid	Mean Relaxation Time ± 1 SD (msec)	
	T1	T2
Vital cartilage	1017 ± 217	36 ± 6
Vital meniscus	1124 ± 146	30 ± 5
Cadaveric cartilage	455 ± 108	46 ± 8
Cadaveric meniscus	476 ± 93	51 ± 21
0.9% (w/v) saline	3660 ± 864	289 ± 69
Renografin 60%	3510 ± 720	310 ± 72
Gd-DTPA (1 mM)	237 ± 42	86 ± 16
Gd-DTPA (500 μM)	357 ± 75	112 ± 16
Gd-DTPA (100 μM)	2313 ± 462	152 ± 26
Albumin 24% w/v	661 ± 125	45 ± 8
Albumin 12% w/v	1476 ± 170	50 ± 7
Albumin 0.1% w/v	3730 ± 852	101 ± 23

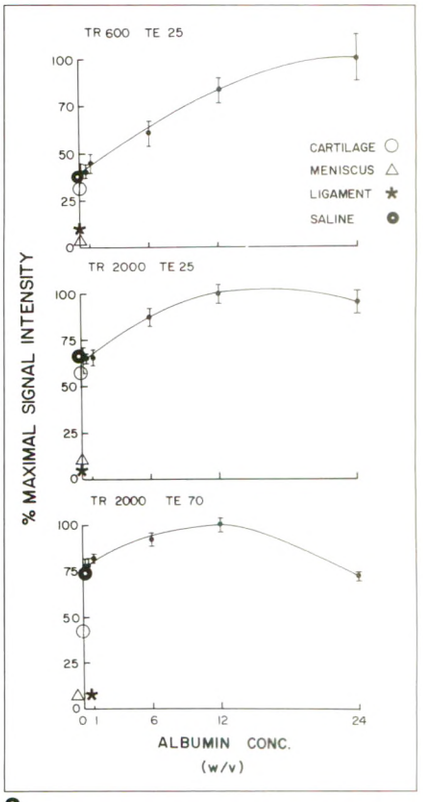
Note.—w/v = weight (of solute) per volume (of solvent).



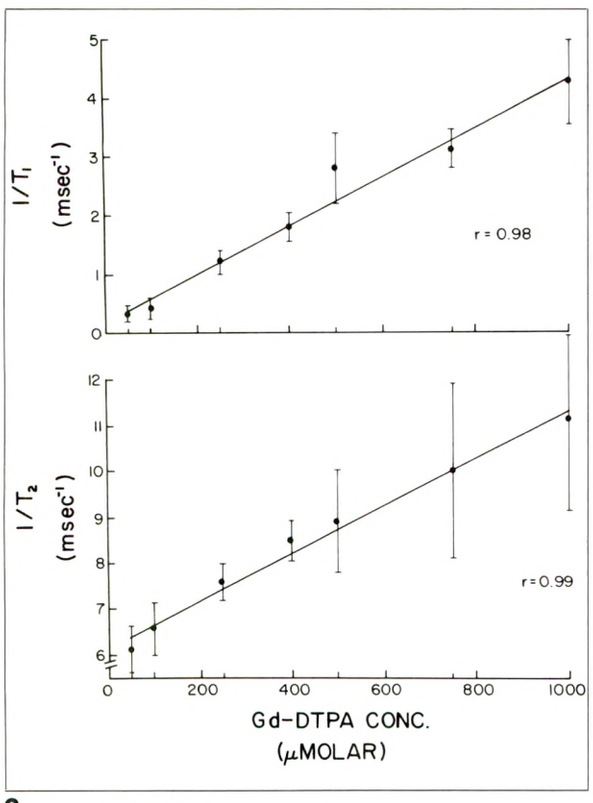
1

Fig. 1.—Relationship between T1 and T2 relaxation rates and various concentrations of human serum albumin in 0.9% (w/v) saline. Data represent mean ± 1 SD of three experiments. *Solid line* shows linear best fit to the data.

Fig. 2.—Relationship between percentage of maximum signal intensity and various concentrations of human serum albumin in 0.9% (w/v) saline for three different imaging sequences. 100% is defined as highest signal intensity for each specific imaging sequence. For comparison, relative signal intensities of cartilage, meniscus, ligaments, and 0.9% (w/v) saline are plotted on abscissa. Each point represents arithmetic mean of five measurements ± 1 SD. Flattening of curves and decrease in signal intensity for concentrations above 12% (w/v) result from increasing T2 effect.



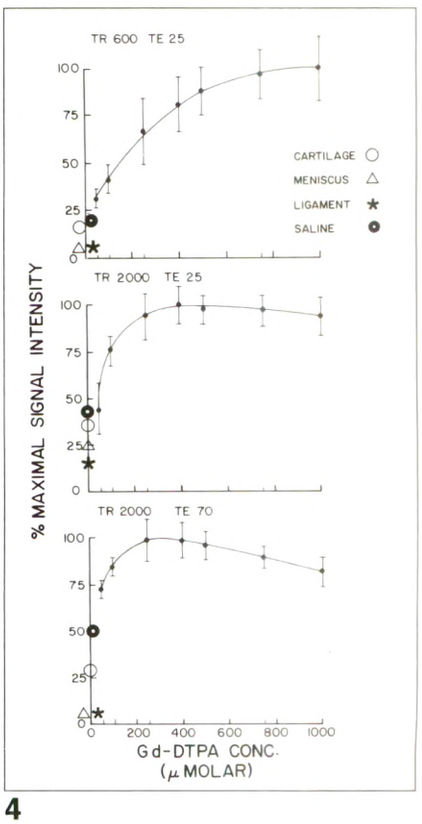
2



3

Fig. 3.—Relationship between T1 and T2 relaxation rates and various concentrations of Gd-DTPA–dimeglumine in 0.9% (w/v) saline. Data represent mean ± 1 SD of three experiments. *Solid line* shows linear best fit to the data.

Fig. 4.—Percentage of maximum signal intensity of various solutions of Gd-DTPA–dimeglumine in 0.9% (w/v) saline for different imaging sequences. 100% is defined as highest signal intensity for each specific imaging sequence. Relative signal intensities for cartilage, meniscus, ligaments, and 0.9% (w/v) saline are plotted on abscissa. Each point represents arithmetic mean of five measurements ± 1 SD. Flattening of curves and decrease in signal intensity at high concentrations result from accentuated influence of decreasing T2 values.



4

intensity for concentrations greater than 400 μM.

Saline and Renografin 60% revealed comparable T1 and T2 values (Table 1) and similar relative signal intensities for all imaging sequences (Figs. 2 and 4). As system software, SE pulse techniques, and a limited number of three experiments were used for each substance tested, a standard deviation of up to 25% was derived.

In Vivo and Cadaveric Analysis

The absolute values of relaxation times for menisci and articular cartilage of living subjects are listed in Table 1. Cadaveric values for T1 were considerably lower and for T2 only slightly higher than those of living individuals. The observed difference can be explained by postmortem alterations, which chiefly shorten T1 values without greatly influencing T2 values [17, 18].

The quantitative signal behavior of the meniscus and articular cartilage varied in a predictable manner. Cartilage manifested higher signal intensities on all sequences included in this study, as compared with meniscus and ligaments (Figs. 2 and 4). The latter structures exhibited comparable signal intensities on all sequences. Signal intensity was generally higher for cadaveric cartilage and meniscus as compared with those in the living subjects (particularly on the TR = 600 msec, TE = 25 msec sequence), explainable by the shorter T1 values of cadaveric tissue [17, 18]. With increasing TR values, both meniscus and articular cartilage exhibited slightly increasing signal intensity (Fig. 5).

When compared with the signal intensities derived for substances tested in vitro, signal intensities of menisci and ligaments were sufficiently different on all imaging sequences to ensure their clear recognition. Signal-intensity differences ranged from 21% for meniscus vs saline (TR = 600 msec, TE = 25 msec) to 100% for ligaments vs 1 mM Gd-DTPA (TR = 600 msec, TE = 25 msec) (Figs. 2 and 4). Signal-intensity differences for the various contrast agents vs articular cartilage were (1) TR = 600 msec, TE = 25 msec: 7.2% for saline and Renografin, 24% for air, 62% for 500 μM Gd-DTPA, and 41% for 12% albumin; (2) TR = 2000 msec, TE = 20 msec: 5% for saline and Renografin, 36% for air, 60% for 500 μM Gd-DTPA, and 41% for 12% albumin; and (3) TR = 2000 msec, TE = 70 msec: 20% for saline and Renografin, 32% for air, 65% for 500 μM Gd-DTPA, and 57% for 12% albumin solution. In general, signal-intensity differences were highest for Gd-DTPA and lowest for saline and Renografin. Insufficient contrast (values below about 20%, the lowest observed signal intensity difference for saline vs meniscus) was achieved for

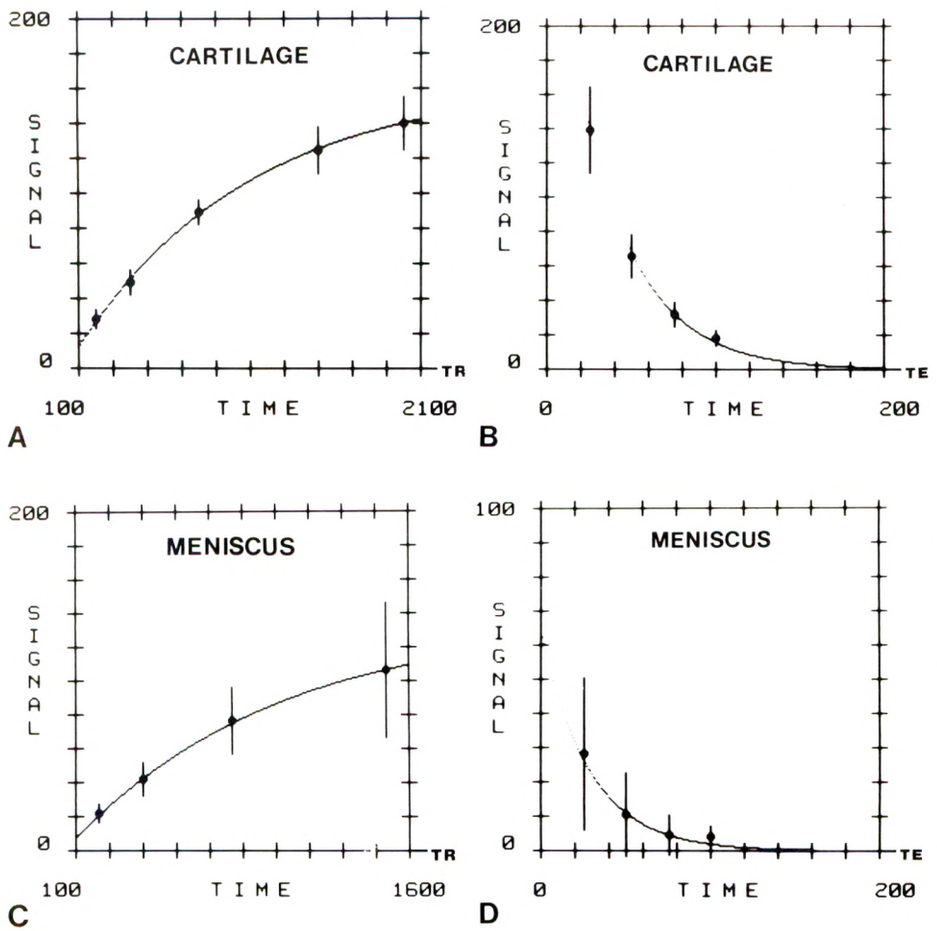


Fig. 5.—Change in relative signal intensity of living human cartilage and meniscus for increasing TR and TE values (msec). Signal values are related to lowest possible signal intensity for cartilage. Each point represents the mean of three measurements ± 1 SD.

***A*, Cartilage exhibits progressive increase in signal intensity with increasing TR.**

***B*, Exponential decrease in signal intensity for cartilage is noted with increasing TE values.**

***C*, Meniscus exhibits relatively smaller increase in intensity for longer TRs, as compared with cartilage.**

***D*, Decrease in signal intensity with increasing TE values is of lesser magnitude as compared with that for cartilage.**

Consequent to these differences in signal behavior, contrast between articular cartilage and meniscus is greater for T1-weighted sequences as compared with T2-weighted sequences.

saline and Renografin 60% on T1-weighted sequences (Figs. 2 and 4).

Cadaveric Analysis

To evaluate the practical significance of these data, 500 μM Gd-DTPA (Fig. 6), 12% (w/v) human albumin (Fig. 7), 0.9% (w/v) saline (Fig. 8), Renografin 60% (Fig. 9), air, and 30 ml human blood (Fig. 10) were injected into fresh cadaveric knees. The difference in signal intensities between cartilage and intraarticular blood as measured over a period of 48 hr did not change significantly (Fig. 10). With increasing age, blood exhibited an inhomogeneous appearance (Fig. 10B). Signal-intensity differences between blood and articular cartilage were 12–23% for TR = 600 msec, TE = 25 msec; 4–6% for TR = 2000 msec, TE = 20 msec; and 19–29% for TR = 2000 msec, TE = 70 msec. In general, poor contrast was noted between blood and cartilage. All other solutions exhibited expected signal behavior after intraarticular injection. Gd-DTPA demonstrated excellent contrast to all articular structures (Fig. 6) on T1-weighted sequences. Adequate contrast was exhibited with 12% albumin, even on T1-weighted images (Fig. 7), whereas saline and Renografin necessitated the use of T2-weighted sequences (Figs. 8 and 9). Air exhibited sufficient contrast to cartilage on all pulse sequences, but delineation of low-signal-intensity structures such as ligaments and meniscus was poor. In addition, bubble formation significantly hindered detail recognition.

Discussion

MR imaging has been shown to be an effective diagnostic tool in the evaluation of articular disorders [1–8]. Advantages

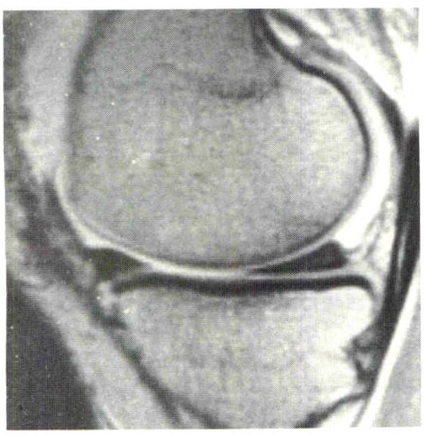
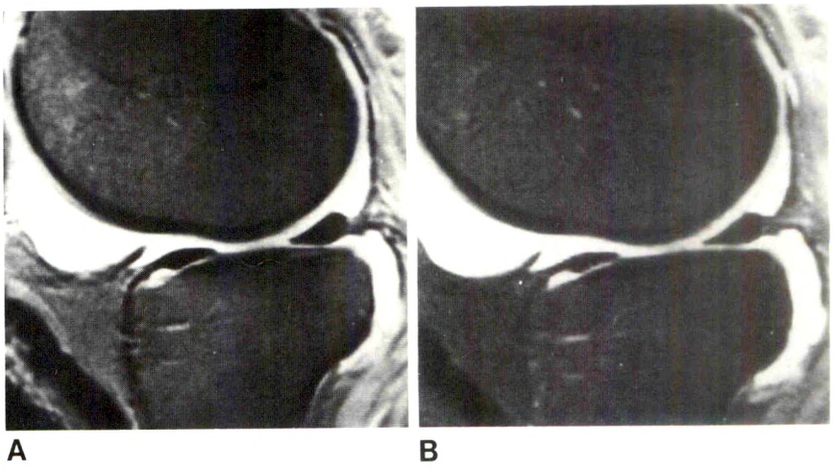


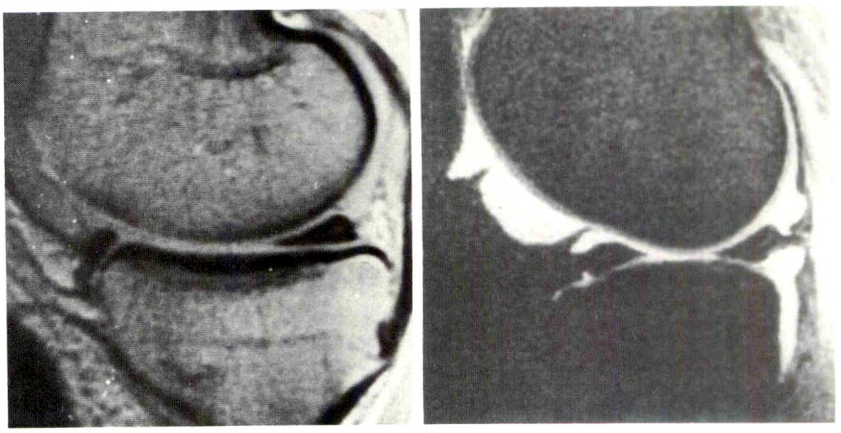
Fig. 6.—Cadaveric knee after intraarticular injection of 500 μM Gd-DTPA–dimeglumine. TR = 600 msec, TE = 25 msec. Excellent contrast enhancement of all intraarticular structures.



A B

Fig. 7.—Cadaveric knee after intraarticular injection of 12% (w/v) albumin solution.
A, T1-weighted image, TR = 600 msec, TE = 25 msec.
B, T2-weighted image, TR = 2000 msec, TE = 70 msec. Intraarticular albumin solution simulates conditions possible in severe inflammatory arthritis. Sufficient contrast is achieved between joint fluid and articular cartilage.

Fig. 8.—Cadaveric knee with intraarticular saline. On T1-weighted sequence (TR = 600 msec, TE = 25 msec), intraarticular saline failed to delineate articular cartilage. Comparable signal characteristics were observed for Renografin 60%.



8 9

Fig. 9.—Cadaveric knee after intraarticular injection of Renografin 60%. T2-weighted image with TR = 2000 msec, TE = 70 msec. Renografin exhibited adequate signal-intensity difference as compared with intraarticular structures. Comparable signal behavior was observed for saline.

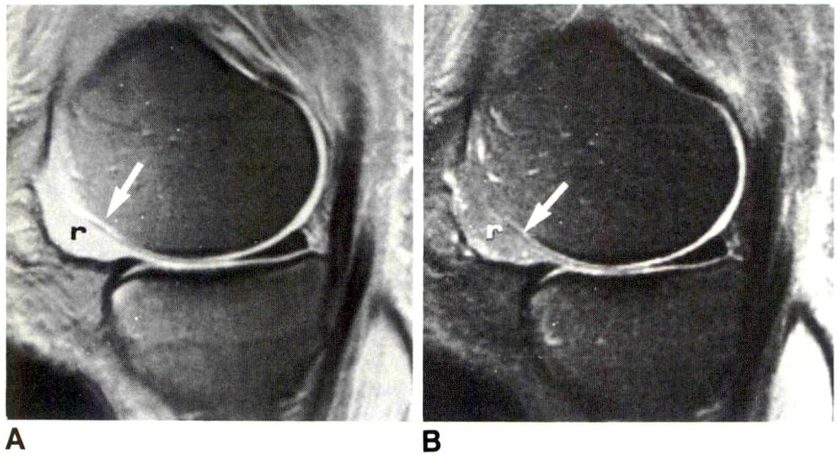


Fig. 10.—Cadaveric knee after intraarticular injection of 30 ml of fresh human blood.
***A*, T1-weighted sequence, TR = 600 msec, TE = 25 msec, 60 min postinjection.**
***B*, T2-weighted sequence, TR = 2000 msec, TE = 70 msec, 48 hr postinjection.**
Poor signal-intensity difference between blood (r) and articular cartilage (*arrow*). Signal characteristics did not change over a 48-hr interval.

over existing imaging techniques [19] include noninvasiveness, excellent inherent contrast resolution, and direct visualization of various articular components. Such visualization is principally confined to major anatomic structures [5–7] and to gross pathologic alterations. The articular cartilage, the joint capsule, and the intraarticular surface of various ligaments cannot be demonstrated effectively [5]. Furthermore, subtle abnormalities of even large anatomic structures such as the cruciate ligaments and menisci in the knee and the glenoid labrum in the shoulder are imaged inconsistently [7], leading in many instances to a diagnostic dilemma. A previous investigation has shown that intraarticular injection of various fluids prior to MR (MR arthrography) can significantly enhance the diagnostic capabilities of MR and permit demonstration of small anatomic structures and subtle alterations [7]. More importantly, MR arthrography has the potential to definitively exclude disease owing to its ability to display the normal intraarticular surfaces of these structures.

Prior reports of MR imaging have emphasized its noninvasive nature [1–4]. The clinical applicability of MR, however, is strongly influenced by its accuracy and potential ability to replace other diagnostic methods [5–8]. Indeed, the relatively expensive cost of MR demands high diagnostic yield. Therefore, it is our belief that the diagnostic advantages of MR arthrography justify its moderately invasive nature.

The ultimate success of MR arthrography depends on identification of a suitable contrast medium. In general, such a medium should have a strong influence on T1 relaxation times (shortening or lengthening) as compared with that of synovial fluid, resulting in either a very high or a very low signal intensity on imaging sequences that use a short TR (below 1000 msec). As T1-weighted sequences offer high contrast and spatial resolution owing to a high signal-to-noise ratio and, of greatest practical importance, short imaging times, they are preferable to T2-weighted sequences [20–22]. As shown in previous investigations, sufficient differences in inherent contrast exist between fibrocartilage or major ligaments and synovial fluid in all major joints [1, 3–7]. The joint capsule, small ligaments, and articular cartilage, however, may exhibit insufficient differences in signal intensity when compared with each other, with normal synovial fluid, and with other articular soft tissues, rendering them diagnostically inaccessible to MR, particularly when T1-weighted sequences are used [7]. An ideal contrast agent for MR arthrography must provide high contrast compared with that of articular cartilage. In addition, an intense signal is preferred because normal ligaments and fibrocartilage inherently manifest very low signal intensity.

Many articular disorders are associated with the presence of a joint effusion that, conceivably, could provide the characteristics necessary for MR arthrography. The major constituent of synovial fluid other than water is albumin, which constitutes 80% of all proteins [9, 10]. The albumin content normally is 1–4% (w/v) and can increase to as much as 12% (w/v) in the setting of inflammatory disease [10]. The effect of protein macromolecules such as albumin on relaxation times is extremely complex and controversial on the basis of results in the literature [17, 18, 23–25]. Most investigators concur, however, that relaxation rates chiefly depend on particular structure and size, water binding capability, and viscosity, as well as magnetic field strength, pH, and temperature. Protein concentration is, however, the most important factor. In general, albumin shortens T1 and T2 relaxation rates of saline, and this effect is greater for lower field strengths (0.1–0.5 T). As shown in this investigation with 1.5 T, an albumin concentration of 1–4% offers an insufficient amount of contrast to allow analysis of articular cartilage on T1-weighted sequences, thus necessitating T2-weighted sequences for diagnostic purposes (Fig. 2). An albumin concentration of 12%, which may accompany a severe inflammatory disorder [10], provides sufficient positive contrast to allow evaluation of cartilage, thereby serving as a biological MR contrast agent on T1-weighted images (Fig. 2). The relatively high viscosity of such an effusion [9, 10], however, may preclude filling of small defects in articular structures, thus limiting its usefulness. Lower albumin concentrations in synovial fluid would necessitate T2-weighted sequences; contrast would be excellent because signal intensity would be higher than that of cartilage (Fig. 2). Iatrogenic removal of the joint effusion with subsequent injection of a contrast agent

for MR arthrography might thus be avoided if a longer imaging time could be accepted.

As acute trauma constitutes an important indication for diagnostic MR imaging of joints [19], the MR appearance of hemarthrosis was investigated as a potential MR arthrographic agent by injecting fresh human blood into a cadaveric knee. The characteristic signal behavior of an evolving hematoma has been extensively studied by other investigators [26–28]. However, we studied differences in signal intensity between blood and articular cartilage to determine whether a hematoma could obviate other contrast agents. A fresh hematoma (0–2 days old) typically consists of intact red corpuscles containing Fe^{2+} desoxyhemoglobin, which has four unpaired electrons and is paramagnetic [29, 30]. Since Fe^{2+} desoxyhemoglobin exhibits minimal proton-electron dipolar-dipolar proton relaxation enhancement [26–28], its influence on T1 relaxation times is negligible, even for the high magnetic strength used in this study [28]. Therefore, the T1 of fresh hematoma is chiefly determined by its protein content [23, 24], with contrast characteristics similar to those of articular cartilage (Fig. 10A). As Fe^{2+} desoxyhemoglobin within a clotted hematoma induces significant local heterogeneity of magnetic susceptibility [26–28], it causes considerable shortening of T2 relaxation times. The magnitude of the effect is dependent on the hematocrit, and shortening is most extensive in clotted hematomas [26–28]. Consequently, an acute hemarthrosis exhibits low signal intensity relative to that of normal synovial fluid on T2-weighted sequences, and only minor differences in contrast relative to articular cartilage (Fig. 10B).

An increase in signal inhomogeneity (Fig. 10B) has been observed with increased duration of hematomas [26–28]; this phenomenon was also apparent during the observation time of 48 hr in our investigation. These alterations in signal behavior on T2-weighted images occur exclusively with magnetic field strengths greater than 0.5 T [28]. As the hematoma "ages," Fe^{3+} methemoglobin appears within intact RBCs [26, 27]. Since Fe^{3+} methemoglobin is paramagnetic and accessible to proton-electron dipolar-dipolar proton relaxation enhancement, it causes shortening of T1 and a bright signal on T1-weighted sequences [26–28]. The low signal intensity of fresh hematoma on T2-weighted sequences disappears subsequent to lysis of red blood cells [26]. These fundamental concepts indicate that in the setting of acute hemarthrosis (0–2 days after injury), MR imaging may not be diagnostic because of limited contrast differences between the blood and the articular cartilage and because of signal inhomogeneity (Fig. 10). Imaging in the subacute stage (1–3 weeks after injury) should improve the delineation of articular cartilage (and other structures) on T1-weighted sequences owing to the formation of methemoglobin. Signal inhomogeneity may again limit diagnostic utility.

The dimeglumine salt of gadolinium-DTPA (Gd^{3+}-DTPA) has been used as an IV and intrathecal contrast agent both in experimental animals and in humans [12–16, 31]. In this investigation, the same complex was used as a potential intraarticular contrast agent for MR arthrography. It was our belief that its very short T1 values (Table 1), which yield high signal intensity on T1-weighted images (Figs. 3 and 6), would enhance contrast differences between intraarticular fluid and the various joint structures, particularly articular cartilage. As shown in Figure 6, Gd-DTPA afforded the most disparate signal intensity when compared with other structures. A maximal signal intensity on T1-weighted images combined with the lowest possible concentration is achieved by a solution of 400–600 μM (Fig. 3). Higher concentrations of gadolinium result in a smaller increase in signal intensity on T1-weighted sequences as well as a decreased signal intensity on T2-weighted images. The homogeneity of signal and waterlike viscosity of Gd-DTPA are additional desirable characteristics that render it capable of delineating even small contour irregularities of intraarticular structures. Owing to these combined qualities, we believe Gd-DTPA is an ideal contrast agent for MR arthrography.

Saline and Renografin 60% exhibited equivalent signal behavior. On T1-weighted sequences, both substances showed inadequate contrast differences with articular cartilage (Fig. 8); on T2-weighted images, however, signal-intensity differences were sufficient relative to all intraarticular structures (Fig. 9), indicating the necessity for T2-weighted sequences in clinical imaging with these agents. Renografin may, therefore, be an acceptable contrast material when MR imaging follows standard single-contrast arthrography. MR evaluation after double-contrast arthrography, however, is not practical owing to the formation of many bubbles. Air provided considerable contrast differences with articular cartilage on all of the imaging sequences used. It exhibits very low signal intensity on both T1- and T2-weighted images, however, and delineation of low-signal-intensity structures such as fibrocartilage and ligaments is poor when compared with Gd-DTPA. In addition, bubbles related to admixture with existing synovial fluid hinder image resolution.

Conclusions

With SE imaging techniques, Gd-DTPA is an ideal agent for MR arthrography, providing excellent contrast to all important joint structures by exhibiting bright signal intensity on T1-weighted sequences [20]. Intraarticular Gd-DTPA may greatly enhance the diagnostic capabilities of MR imaging in the setting of articular disease. In addition, it permits the use of T1-weighted imaging sequences, which result in shorter imaging times and offer the greatest possible contrast and spatial resolution [20–22]. No toxic side effects have been reported after IV injection of Gd-DTPA in concentrations below 0.5 mM/kg [12, 13, 31]. the absence of documented anaphylactoid reactions [13, 15, 31] to Gd-DTPA and its short half-life in blood and urine suggest a high in vivo tolerance [15, 16, 31]. Therefore, animal experiments are warranted to study the synovial effects of Gd-DTPA and its absorption and excretion characteristics.

Since Gd-DTPA is not yet approved for human use by the Food and Drug Administration, we currently recommend 0.9% (w/v) saline as a safe contrast agent for MR arthrography. Saline has no known biological side effects. T2-weighted sequences with long imaging times and reduced contrast and spatial resolution [7, 20] are necessary for diagnostic pur-

poses. Ultimately, the fortuitous presence of a joint effusion can obviate any iatrogenic contrast medium, although T2-weighted imaging sequences are required. In the presence of severe inflammatory arthritis, the preferred T1-weighted sequences may be applicable, owing to the potentially high albumin content of the synovial joint. Hemarthroses should be imaged only in the subacute phase (1–3 weeks old), although inhomogeneity may interfere with interpretation of MR images.

ACKNOWLEDGMENT

We thank Carol Latham, without whose dedication this work would not have been possible.

REFERENCES

1. Reicher MA, Bassett LW, Gold RH. High resolution magnetic resonance imaging of the knee joint: pathologic correlations. *AJR* **1985**;145:903–909
2. Steinbrich W, Beyer D, Friedmann A, Ermers JWLM, Bunke J. MRI of the knee joint using surface coils. Presented at the annual meeting of the Society of Magnetic Resonance in Medicine. London, August **1985**
3. Turner DA, Prodromos CC, Petasnick JP, Clark JW. Acute injury of the ligaments of the knee: magnetic resonance evaluation. *Radiology* **1985**;154:717–722
4. Huber DJ, Sauter R, Mueller E, Requardt H, Weber H. MR imaging of the normal shoulder. *Radiology* **1986**;158:405–408
5. Hajek PC, Baker LL, Bjorkengren A, Sartoris DJ, Neumann CH, Resnick D. High-resolution magnetic resonance imaging of the ankle: normal anatomy. *Skeletal Radiol* **1986**;15:536–540
6. Baker LL, Hajek PC, Bjorkengren A, et al. High-resolution magnetic resonance imaging of the wrist: normal anatomy. *Skeletal Radiol* **1987**;16:128–132
7. Hajek PC, Baker LL, Sartoris DJ, Neumann CH, Resnick D. MR arthrography: an anatomic-pathologic investigation. *Radiology* **1987**;163:141–147
8. Beltran J, Noto AM, Herman LJ, Mosure JC, Burk JM, Christoforidis AJ. Joint effusions: MR imaging. *Radiology* **1986**;158:133–137
9. Castor CW. The study of the connective tissue. In: Hollander JL, McCarty DJ, eds. *Arthritis and allied conditions*, 8th ed. Philadelphia: Lea & Febiger, **1976**:51–66
10. Jessar RA. The study of synovial fluid. In: Hollander JL, McCarty DJ, eds. *Arthritis and allied conditions*, 8th ed. Philadephia: Lea & Febiger, **1976**:67–81
11. General Electric Medical Systems: *Operating the Signa system (0.5, 1.0, and 1.5 Tesla) OMSI*, rev 7. Milwaukee: General Electric, **1986**
12. Weinmann HJ, Brasch RC, Press WR, Wesbey GE. Characteristics of gadolinium DTPA complex: a potential NMR contrast agent. *AJR* **1984**;142:619–624
13. Carr DH, Brown J, Bydder GM, et al. Gadolinium-DTPA as a contrast agent in MRI: initial clinical experience in 20 patients. *AJR* **1984**;143:215–224
14. Barnhart JL, Berk RN. Influence of paramagnetic ions and pH on proton NMR relaxation of biologic fluids. *Invest Radiol* **1986**;21:132–136
15. Gadian DG, Payne JA, Bryant DJ, Young IR, Carr DH, Bydder GM. Gadolinium-DTPA as a contrast agent in MR imaging—theoretical projections and practical observations. *J Comput Assist Tomogr* **1985**;9:242–251
16. Di Chiro G, Knop RH, Girton ME, et al. MR cisternography and myelography with Gd-DTPA in monkeys. *Radiology* **1985**;157:373–377
17. Daszkiewicz OK, Hennel JW, Lubas B, Szczepkowski TW. Proton magnetic relaxation and protein hydration. *Nature* **1963**;200:1006–1007
18. Bottomley PA, Foster TH, Argersinger RE, Pfeifer LM. A review of normal tissue hydrogen NMR relaxation times and relaxation mechanisms from 1–100 MHZ: dependence on tissue type, NMR frequency, temperature, species, excision, and age. *Med Phys* **1984**;11:425–448
19. Resnick D, Niwayama G. *Diagnosis of bone and joint disorders*. Philadelphia: Saunders, **1981**:510–560
20. Slichter CP. *Principles of magnetic resonance*. Berlin: Springer Verlag, **1980**
21. Bloembergen N, Purcell EM, Pound VR. Relaxation effects in nuclear magnetic resonance absorption. *Phys Rev* **1948**;73:679–712
22. Koenig SH, Brown RD, Adams D, Emerson D, Harrison CG. Magnetic field dependence of 1/T1 of protons in tissue. *Invest Radiol* **1984**;10:76–81
23. Koenig SH, Schillinger WE. Nuclear magnetic relaxation dispersion in protein solutions. *J Biol Chem* **1969**;244:3283–3289
24. Fullerton DG, Cameron IL, Ord VA. Frequency dependence of magnetic resonance spine-lattice relaxation of protons in biological materials. *Radiology* **1984**;151:135–138
25. Fullerton DG, Potter JL, Dornbluth NC. NMR relaxation of protons in tissues and other macromolecular water solutions. *Magnetic Resonance Imag* **1982**;1:209–228
26. Sipponen JT, Sepponen RE, Sivula A. Nuclear magnetic resonance (NMR) imaging of intracerebral hemorrhage in the acute and resolving phases. *J Comput Assist Tomogr* **1983**;7:954–959
27. Dela Paz RL, New PFJ, Buonanno FS, et al. NMR imaging of intracranial hemorrhage. *J Comput Assist Tomogr* **1984**;8:599–607
28. Gomori JM, Grossman RI, Goldberg HI, Zimmerman RA, Bilaniuk LT. Intracranial hematomas: imaging by high-field MR. *Radiology* **1985**;157:87–93
29. Fabry TL, Reich HA. The role of water in deoxygenated hemoglobin solutions. *Biochem Biophys Res Commun* **1966**;22:700–703
30. Eisenstadt M. NMR relaxation of protein and water protons in methemoglobin solutions. *Biophys J* **1981**;33:469–474
31. Brasch RC, Weinmann HJ, Wesbey GE. Contrast enhanced NMR imaging: animal studies using gadolinium-DTPA complex. *AJR* **1984**;142:625–630

Symptomatic Intraspinal Synovial Cysts: Opacification and Treatment by Percutaneous Injection

Ann G. Bjorkengren[1]
Lawrence T. Kurz[2]
Donald Resnick[1]
David J. Sartoris[1]
Steven R. Garfin[2]

Intraspinal synovial cysts are usually located in the lower lumbar spine in association with osteoarthritis of the facet joints, and they are most accurately diagnosed by using CT. Surgical removal of intraspinal synovial cysts implicated in the development of radiculopathy has resulted in symptomatic relief. A nonoperative method of treatment consists of CT-guided needle placement into the facet joint adjacent to the cyst, followed by (1) injection of contrast material to show communication between the joint and the cyst and (2) injection of corticosteroids. Three outpatients were treated in this fashion without complications. Complete relief of symptoms was achieved in two cases and partial relief was achieved in one. Follow-up CT scans performed 2 months after the procedure showed no change in the size of the cysts in two of the patients. A 6-month follow-up CT scan in the third patient, however, showed significant improvement in cyst size.

These preliminary results suggest that this procedure is an alternative to surgical management of intraspinal synovial cysts.

Synovial cysts, or ganglia, can occur adjacent to any synovium-lined articulation. Several cases of intraspinal synovial cysts associated with osteoarthritis of contiguous facet joints have been described [1–8], most frequently involving the L4–L5 level. The diagnosis is best established radiographically by using CT [6]. In patients with radiculopathy attributed to this space-occupying lesion, surgical removal of the synovial cyst has resulted in symptomatic relief [1, 2, 4, 7]. Potential communication between the cyst and the adjacent facet joint has been mentioned by previous investigators [6, 7] but has not been documented. This investigation was undertaken to evaluate whether such a communication could be shown by arthrography and whether intraarticular injection of corticosteroids could provide symptomatic relief and perhaps delay or eliminate the need for surgery.

Materials and Methods

Three patients (two women and one man, ages 44, 56, and 77 years, respectively) with the CT diagnosis of intraspinal synovial cyst in the lumbar spine were evaluated and treated by percutaneous injection of the adjacent facet joint. The initial CT examination was obtained to investigate low back pain and radiculopathy in each case. In each patient, the synovial cyst occurred at the L4–L5 level, adjacent to the right facet joint in two cases and the left articulation in one case. Osteoarthritis involving the facet joint adjacent to the cyst was present in each instance, and in two cases mild degenerative spondylolisthesis was also observed. All three patients had radicular pain. One patient had a normal neurologic examination, whereas the remaining two manifested mild motor and sensory abnormalities.

The CT-guided percutaneous injections were performed on an outpatient basis and did not require premedication. Local anesthesia was used. The patient was positioned prone on the CT table, and a pillow was placed beneath the abdomen in order to reduce the lumbar lordosis and distract the facet joints. A digital localization image was obtained and the position of the involved facet joint was determined and thereafter marked on the skin. Under sterile conditions and with CT guidance, a 20-gauge spinal needle was introduced into the facet

Received January 14, 1987; accepted after revision March 26, 1987.

This work was supported in part by Veterans Administration Grant #SA306.

[1] Department of Radiology, Veterans Administration Medical Center and the University of California, San Diego, Medical Center, San Diego, CA 92103. Address reprint requests to D. Resnick, Dept. of Radiology, Veterans Administration Medical Center, 3350 La Jolla Village Dr., San Diego, CA 92161.

[2] Department of Orthopedic Surgery, Veterans Administration Medical Center and the University of California, San Diego, Medical Center, San Diego, CA 92103.

AJR **149:105–107, July 1987**
0361–803X/87/1491–0105
© American Roentgen Ray Society

joint. In one case, approximately 0.3 ml of viscous fluid was aspirated. A small amount of contrast material (Angiovist 370, Berlex Laboratories, Wayne, NJ) was then injected to verify the intraarticular position of the needle tip, followed by introduction of approximately 1.5 ml of Angiovist. In each of the three cases, CT images showed sequential contrast opacification of the facet joint, a slightly tortuous channel, and the intraspinal synovial cyst. Subsequently, 100 mg (1.6 ml) of methylprednisolone in two cases and triamcinolone in the third case were injected into the facet joint. The needle was then removed, and CT images were again obtained. Extravasation of contrast material was not observed in any of the patients.

Results

The entire procedure required approximately 45 min and was well tolerated by the patients. No change was noted in symptoms immediately after the injection. All of the patients reported that their radiculopathy had completely resolved on the day after the injection. One patient (Fig. 1) with radiating leg pain noted complete absence of symptoms for several months. A repeat CT examination 6 weeks after the procedure revealed no change in the size or appearance of the cyst (Fig. 1C). One year later only 20% of her pain had returned.

The second patient reported complete absence of radiculopathy for 3 days following the procedure, after which mild pain recurred following vigorous garden work. Six weeks after the injection, a repeat CT examination again revealed the cyst, which had not changed in appearance. The patient underwent myelography and repeat CT examination 8 months later owing to progressive bilateral symptoms. The left-sided intraspinal synovial cyst, compressing the L5 nerve root, was again evident as was a herniated nucleus pulposus located in the midline at the L5–S1 spinal level. The patient opted not to have surgery and requested a repeat injection procedure for the left-sided synovial cyst, which was performed without complications. At 6-month follow-up, he reported intermittent discomfort but improvement compared with his condition before the last injection.

The third patient had L5 root symptoms, including leg weakness, that prevented her from engaging in physical exercise. On the initial CT scan, a synovial cyst with a calcific rim was seen (Fig. 2A). Opacification and corticosteroid injection were performed (Fig. 2B). At 6-month follow-up, she remained asymptomatic and actively participated in tennis and aerobics. A follow-up CT scan obtained 6 months after the procedure showed that the calcific rim of the synovial cyst was absent, and a vacuum phenomenon (gas) was seen in a small residual cyst (Fig. 2C).

Discussion

Although predominantly found in the extremities, synovial cysts can arise from any synovium-lined joint or tendon sheath. A small number of intraspinal synovial cysts have been reported in patients under investigation for low back pain and radiculopathy [1–8]. The L4–L5 spinal level is typically involved, and the adjacent facet joint reveals characteristic alterations of osteoarthritis. The diagnosis of an intraspinal synovial cyst cannot be made on the basis of conventional radiography, and although myelography shows an extradural defect, it does not generally yield a specific diagnosis. However, CT can be diagnostic [6–8] by documenting a cystic structure, occasionally containing gas within its lumen [9] or calcification within its wall, that may compress the adjacent dural sac or nerve roots. Such compression is believed to result in low back pain, radiculopathy, or both. In 13 of 15 previously reported cases [1–8], surgical removal of the cyst yielded immediate relief of pain and, on follow-up examination, the patients had normal neurologic examinations. In one case

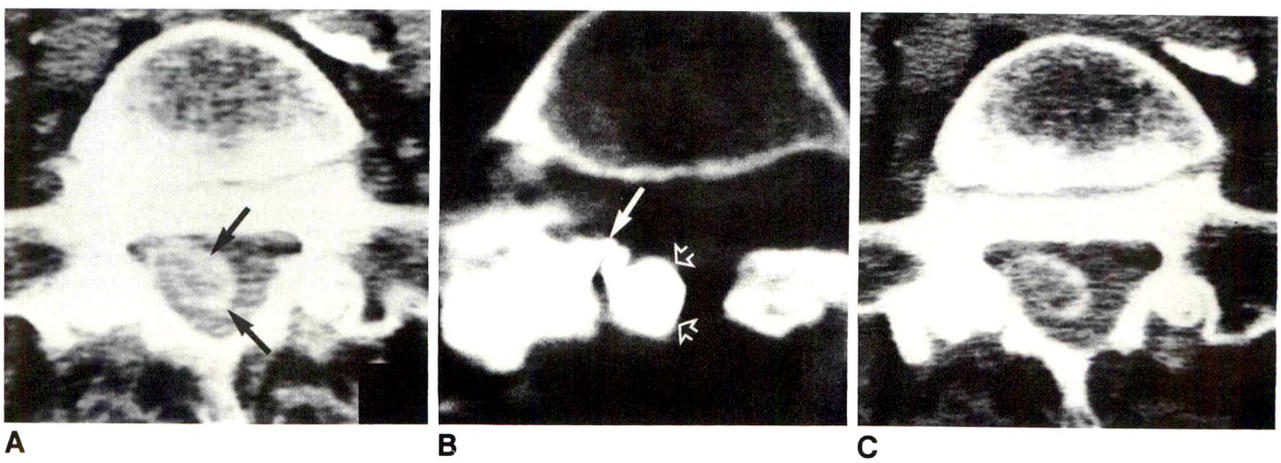


Fig. 1.—*A*, CT scan of lumbar spine in a 77-year-old woman with back pain radiating to right leg shows an intraspinal cystic structure with a calcified rim (*arrows*). Cystic structure is located adjacent to right L4–L5 facet joint, which exhibits articular space obliteration and osteophyte formation. There is also evidence of L4–L5 spondylolisthesis. CT findings are diagnostic of a synovial cyst.

***B*, After injection of contrast material into facet joint, cyst (*open arrows*) and its tortuous neck (*white arrow*) have opacified, indicating its communication with the articulation; corticosteroids were then injected.**

***C*, A follow-up scan 6 weeks later shows no change in size or appearance of cyst.**

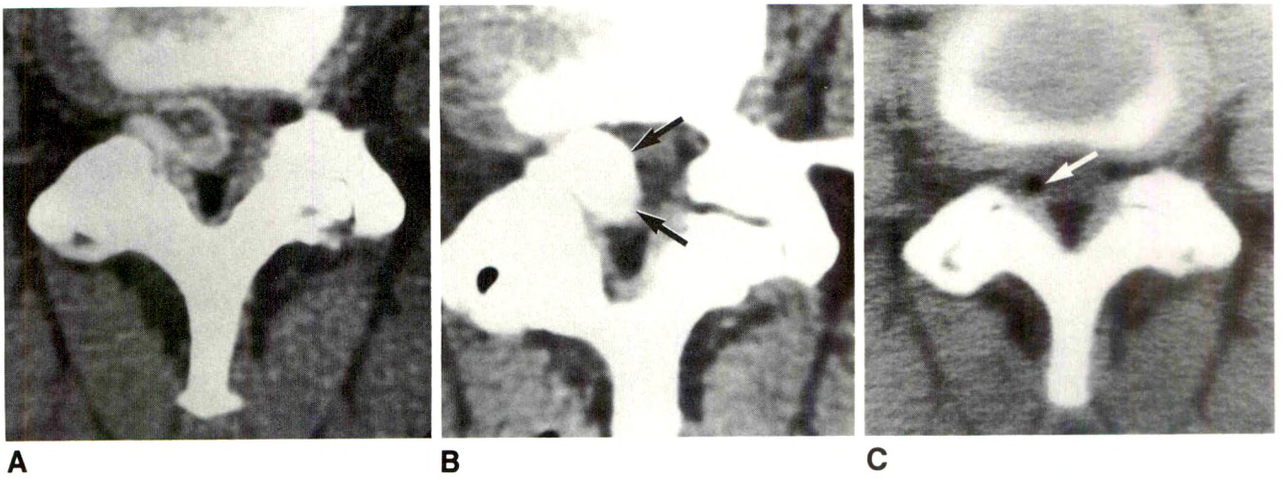


Fig. 2.—*A*, CT scan of lumbar spine in a 44-year-old woman with back pain radiating to right leg shows an intraspinal synovial cyst. Note a cystic structure with a calcified rim adjacent to an osteoarthritic right L4–L5 facet joint. A diffuse disk bulge is also present.

***B*, After percutaneous injection of contrast material into this joint, cyst (*arrows*) has opacified; then corticosteroids were injected. Small collections of air are seen in facet joint and in soft tissues along needle path.**

***C*, On a follow-up CT scan 6 months after procedure, calcific rim is no longer present and synovial cyst, which has markedly decreased in size, now contains gas (*arrow*).**

the recovery from cauda equina syndrome was partial [3], and in another case no follow-up clinical examination was mentioned [6]. Histologic examination of these intraspinal cysts has shown either a distinct synovial lining [3, 4, 6, 7] or fibrous tissue [1, 2, 5, 8].

Recently, a case of symptomatic intraspinal cyst adjacent to a facet joint was described in a patient with rheumatoid arthritis [10]. The diagnosis was made on CT and was followed by surgical removal of the cyst. Histologically, synovial tissue with alterations typical of rheumatoid arthritis was found. Two months later the symptoms recurred, and the cyst was again identified on CT and was punctured under CT guidance, followed by contrast instillation confirming the cystic nature of the lesion. Corticosteroids were then injected, resulting in complete relief of symptoms. In three reports [11–13] synovial cysts of the ligamentum flavum, which were not communicating with the facet joints, have been described. The patients exhibited signs of lumbar nerve root compression, and myelography revealed posterolateral extradural defects. CT examinations were not performed. Surgical exploration found cysts within the ligamentum flavum, which histologically contained a mesothelial lining of a synovial cyst and degenerated mucinous material.

Previous reports have suggested that injection of contrast material into the adjacent facet joint might opacify an intraspinal synovial cyst [6], although the procedure to our knowledge has not been previously performed. In each of our three patients, the technique resulted in successful opacification of the synovial cyst as well as the connection between it and the neighboring apophyseal joint.

Our results suggest that the percutaneous therapeutic approach may constitute a useful alternative to surgical management in patients with symptomatic intraspinal synovial cysts. Our clinical follow-up period is short, however, and the number of patients is small. Therefore, further studies with longer periods of observation are necessary before this treatment can be recommended in all cases of symptomatic intraspinal synovial cysts. This mode of treatment, however, depends on the existence of communication between the facet joint and the synovial cyst.

REFERENCES

1. Kao C, Uihlein A, Bickel W, Soule E. Lumbar intraspinal extradural ganglion cyst. *J Neurosurg* **1968**;29:168–172
2. Brish A, Payan H. Lumbar intraspinal extradural ganglion cyst. *J Neurol Neurosurg Neuropsych* **1972**;35:771–775
3. Sypert G, Leech R, Harris B. Posttraumatic lumbar epidural true synovial cyst. Case report. *J Neurosurg* **1973**;39:246–248
4. Bhushan C, Hodges FJ III, Wityk JJ. Synovial cyst (ganglion) of the lumbar spine simulating extradural mass. *Neuroradiology* **1979**;18:263–268
5. Maresca L, Meland B, Maresca C, Field M. Ganglion cyst of the spinal canal. Case report. *J Neurosurg* **1982**;57:140–142
6. Hemminghytt S, Daniels D, Williams A, Haughton V. Intraspinal synovial cysts: natural history and diagnosis by CT. *Radiology* **1982**;145:375–376
7. Kurz L, Garfin S, Unger A, Thorne R, Rothman R. Intraspinal synovial cyst causing sciatica. *J Bone Joint Surg [Am]* **1985**;67A:865–871
8. Baum J, Hanley E Jr. Intraspinal synovial cysts simulating spinal stenosis: a case report. *Spine* **1986**;11:487–489
9. Schulz EE, West WL, Hinshaw DB, Johnson DR. Gas in a lumbar extradural juxtaarticular cyst: sign of synovial origin. *AJR* **1984**;143:875–876
10. Jacobs J, Weisman M, Mink J, et al. Reversible cause of back pain and sciatica in rheumatoid arthritis: an apophyseal joint cyst. *Arthritis Rheum* **1986**;29:431–435
11. Abdullah A, Chambers R, Daut D. Lumbar nerve root compression by synovial cysts of the ligamentum flavum. *J Neurosurg* **1984**;60:617–620
12. Moiel R, Ehni G, Anderson M. Nodule of the ligamentum flavum as a cause of nerve root compression. Case report. *J Neurosurg* **1967**;27:456–458
13. Haase J. Extradural cyst of ligamentum flavum L4—a case. *Acta Orthop Scand* **1972**;43:32–38

Book Review

Diagnosis of Metabolic Bone Disease. By Paul Grech, T. J. Martin, N. A. Harrington, and P. J. Ell. Philadelphia: Saunders, 374 pp., 1985. $65

The normal and aberrant systemic control of skeletal metabolic dynamics has always intrigued radiologists. Acknowledging that metabolic bone disease is still a somewhat loosely circumscribed concept rather than a strictly defined discipline, the authors have brought together a large amount of information regarding physiologic, hormonal, and other processes that affect the radiologic appearance of bone. With the aim of integrating current knowledge in radiology, nuclear medicine, and biochemistry, this book is specifically directed to radiologists. A multidisciplinary approach is taken, reflecting the interests of the authors (two radiologists and two internists).

A metabolic bone disturbance, as defined by the authors, is one that alters the entire skeleton and that is mediated by biochemical, endocrine, nutritional, or pharmacologic mechanisms. The 10 chapters are introduced by a clear and succinct summary of bone anatomy, physiology, and hormonal control. Basic radiologic principles are also described. This is followed by a discussion of the general manifestations of bone loss or gain, with emphasis on osteoporosis and osteomalacia. The remaining chapters are more specifically oriented and deal with endocrine disturbance, malnutrition, renal bone disease, major states of increased bone turnover (e.g., Paget's), extraskeletal mineralization, drug- and chemical-induced abnormalities (environmental and therapeutic), and metabolic disorders associated with tumors. A final chapter discusses in more detail radionuclide diagnosis in these disorders.

In each chapter the basic physiology, biochemistry, and anatomy are given as background for the radiologic discussion. The 277 figures are appropriately chosen and are generally good. All are essentially adequate to make the points described, but some are not quite of the quality seen in specialty radiologic journals.

The references are mainly those published during the 1970's and early 1980's, with the latest in 1984. They are inserted into the text at appropriate places and are easy to use for reference. The binding is sturdy, the typography is clear, and the resultant layout is pleasing to read. Typographic errors are infrequent. The style is usually clear but some of the sentence constructions are not as elegant or easy to follow as they should be.

As with any text, there are areas where one might believe that emphasis is misplaced or lacking, but there is no serious deficiency in objective or practice. In general, this is an excellent summary of the physiologic control of bone metabolism, which is valuable for any radiologist. The latest information and theories are either discussed sufficiently or alluded to and referenced, which is a valuable aspect of the book. The radiologic discussions, however, are disappointingly meager in many sections and often do not go into great detail or discuss variations of the classic findings. Personal experience is rarely reflected or mentioned. The supporting figures also tend to show the most obvious changes and omit subtleties. Part of this is a result of the organization of the book; for example, the changes of hyperparathyroidism would have to be discussed many times in each chapter in which this is an important influence. In many cases, however, the radiologic discussions are almost too basic for those with any radiologic experience. In addition, the brevity of many of the topics precludes use of this book as a reference text. For example, the authors describe the general principles of morphometric analysis but do not give normal values, and the discussion of Turner's syndrome specifically mentions three "signs" but does not indicate what they are.

This book is useful as a compendium of the latest ideas on many aspects of metabolic bone disease. The radiologic aspects are much less detailed than can be found in Resnick and Niwayama (*Diagnosis of Bone and Joint Disorders*, Saunders, 1981) or Greenfield (*Radiology of Bone Diseases*, Lippincott, 1986), both detailed texts on bone disease, or even in the general radiology text by Taveras (*Radiology. Diagnosis—Imaging—Intervention*, Lippincott, 1986), but it is valuable to have the material gathered into one source. The advantages of this book also are that it is more current than most books devoted to bone disease in general and a few minutes spent with the discussion of bone physiology will be rewarding in the reader's approach to bone disease in general. It is recommended as a text that should be available in any facility that treats patients with bone disease.

M.B. Ozonoff
Newington Children's Hospital
Newington, CT 06111

CT for Determining the Results of Treatment of Fractures of the Wrist

Stephen F. Quinn[1,2]
William Murray[1]
Troy Watkins[3]
John Kloss[3]

Eighteen CT examinations of the wrist were performed in 13 patients to evaluate the results of treatment for carpal fractures. In four cases with metal objects and in seven with cast materials, there was no difficulty achieving adequate CT studies. In 13 cases CT was found to be helpful in determining bony union in the presence of advanced osteoporosis. In six cases CT was excellent in evaluating bone-graft incorporation. CT affords improved detection of fractures perpendicular to the plane of the scan and also shows small areas of bone disruption, even with osteoporosis. Axial CT images can evaluate Lister's tubercle, a bony prominence on the dorsum of the distal radius, for hypertrophy, which can occur secondary to traumatic and degenerative changes. A hypertrophied tubercle can impinge on the extensor pollicis longus tendon and cause atrophy and disruption. The high cost of CT is offset by the possibility of reducing the patient's period of immobilization and, thereby, the length of time the patient is unable to participate in normal activities. In addition, since CT is often definitive, the number of supplemental or follow-up radiologic procedures or clinical appointments should be reduced.

We conclude that CT is useful in evaluating the results of treatment of wrist injuries.

Evaluation of complex wrist problems that continue after treatment of carpal fractures is difficult. Problem diagnostic cases include continued pain after proper immobilization, internal fixation with a metallic pin, bone graft, or arthrodesis. Plain radiography and tomography are often inadequate or equivocal because of osteoporosis, metallic devices, cast material, or difficulty in obtaining proper wrist positioning. Several authors have reported their experience using CT to image the carpal region [1–4]. We used CT specifically to depict the alignment of complex fractures, to evaluate Lister's tubercle, to image subtle areas of bony fusion, to evaluate bone-graft incorporation, and to exclude occult fractures.

Subjects and Methods

In a 48-month period, 13 patients underwent 18 high-resolution carpal CT examinations for evaluation of alignment and union after treatment of fracture or attempted arthrodesis. All patients were imaged with a GE 9800 CT scanner.

Axial, sagittal, and occasionally coronal images were obtained with contiguous 1.5- or 3-mm sections at 2-mm intervals. To provide high detail, the GE review target reconstruction program was used with both bone and soft-tissue algorithms. A 512 × 512 matrix was used with a large-calibration file. For axial images of both wrists a field of view of 17.4 cm was used with a pixel size of 0.34 mm. If only one wrist was imaged, field size was reduced to 15.87 cm with a pixel size of 0.31 mm. Hard copies of the targeted bone images were made at a window setting of 4000 H and a center of 400 H. Hard copies were also obtained with soft tissue (window, 500 H; center, 50 H) and bone (window, 2000 H; center, 250 H) settings.

To evaluate surgical fusion, scans were obtained at right angles to the fusion plane. Sagittal images were obtained by positioning the wrist above the patient's head with the forearm flat on the table, oriented parallel to the plane of the gantry (Fig. 1A). Even with an above-the-elbow cast, this position was easily assumed and tolerated by the patient. When the wrist

Received December 8, 1986; accepted after revision March 2, 1987.

[1] Department of Diagnostic Imaging, St. Alphonsus Regional Medical Center, 1055 N. Curtis Rd., Boise, ID 83706.

[2] Present address: Department of Diagnostic Imaging, H. Lee Moffitt Cancer Center and Research Institute, University of South Florida, College of Medicine, P.O. Box 280179, Tampa, FL 33682–0179. Address reprint requests to S. F. Quinn.

[3] Department of Orthopedics, St. Alphonsus Regional Medical Center, Boise, ID 83706.

AJR **149:109–111, July 1987**
0361–803X/87/1491–0109
© American Roentgen Ray Society

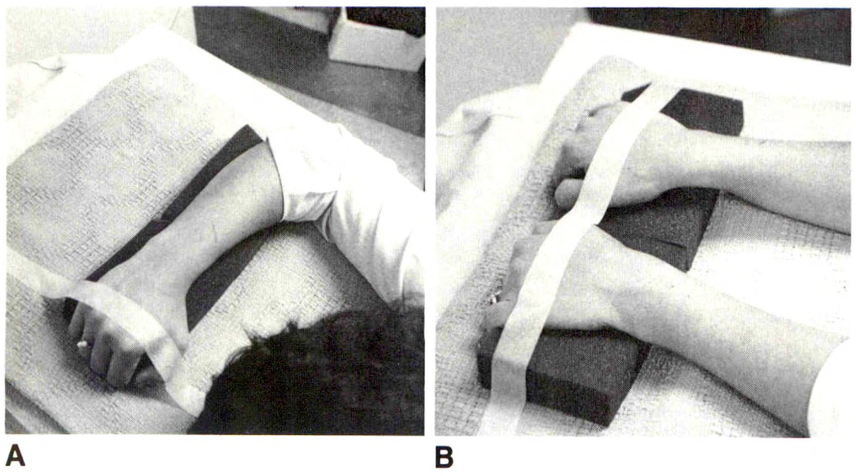


Fig. 1.—Position of wrist for CT images.
***A*, Sagittal plane. Patient is prone with arm above head. Forearm is placed on sponge and secured with tape.**
***B*, Axial plane. Patient is prone with forearms and wrists flat on table supported by sponge and secured with tape.**

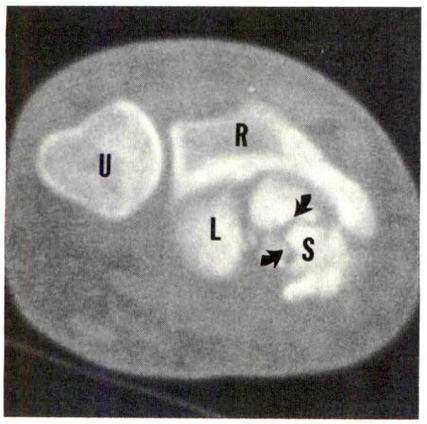


Fig. 2.—Nonunited fracture of scaphoid. Axial image (palm down) 8 weeks after injury shows nonunion of scaphoid fracture. Bony margins of fracture fragments are easily identified (*arrows*). U = ulna; R = radius; L = lunate; S = scaphoid.

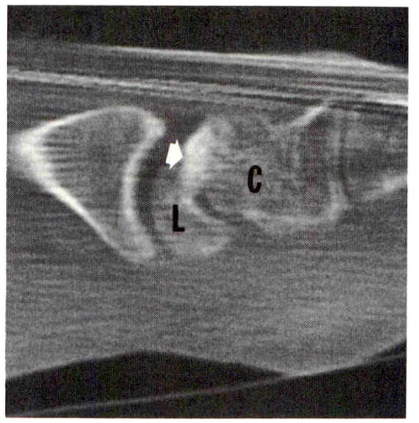


Fig. 3.—Partial bony union after arthrodesis. Sagittal image (palm down) 10 weeks after surgery to determine degree of fusion between lunate and capitate shows partial bony union between dorsal aspects of lunate and capitate (*arrow*). L = lunate; C = capitate.

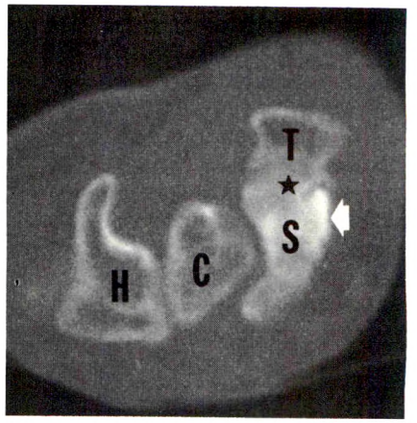


Fig. 4.—Complete bony union after arthrodesis. Axial image (palm up) shows complete bony union between triquetrum and scaphoid (*star*). Bone graft is visible (*arrow*). T = trapezium; S = scaphoid; C = capitate; H = hamate.

was imaged in the axial plane, the patient was placed prone with both arms above the head and with the wrists resting flat on the table (Fig. 1B). Placing a sponge under the chest increased patient comfort, thereby decreasing patient motion.

Results

CT scans allowed accurate assessment of alignment and union of carpal fractures in all 18 patients with a high degree of confidence in evaluating the degree of bony fusion. In four instances of nonunion, the bony margins at the fracture site were easily seen (Fig. 2). In 15 cases of partial union (Fig. 3) and in two of complete fusion (Fig. 4), the percentage of bony fusion could be measured easily and the progression of fusion could be monitored (Fig. 5). Significant osteoporosis was seen on 13 of 17 scans obtained for assessment of bony union, but did not prevent evaluation of the degree of fusion.

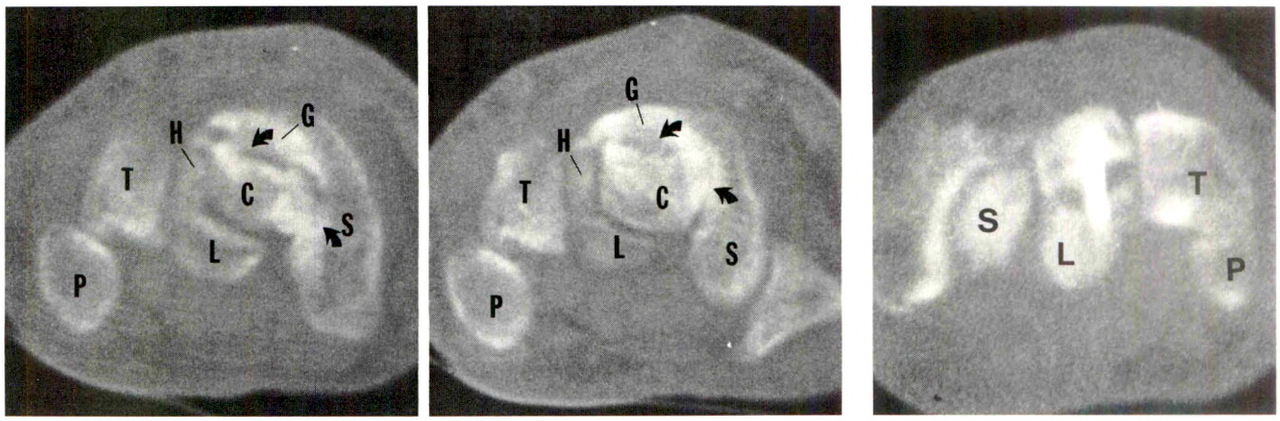
In four wrists with metal devices near the region of interest and in seven with cast material, the image quality was not significantly compromised (Fig. 6). In six cases of previous bone graft, the degree of bony incorporation could be determined (Fig. 7). In one patient, overgrowth of Lister's tubercle was seen (Fig. 8).

Discussion

Our results suggest that CT is often superior to standard tomography or fluoroscopy in evaluating the wrist after treatment of carpal fractures. This is in keeping with the experience of others [2–4]. CT is useful in evaluating the results of carpal fusions. It is helpful in patients whose osteoporosis resulted from prolonged immobilization, because assessment of the percentage and character of fusion with or without bone-graft incorporation can be crucial in clinical management.

Prior review of plain films and consultation with the clinician are important in selecting the best CT scanning planes. The ability to image in the axial plane often allows improved visualization of areas of interest, such as fractures, compared with standard radiographs or tomograms.

CT in the axial plane also allows the best visualization of Lister's tubercle. Lister's tubercle is a bony protuberance on the dorsal aspect of the distal radius. After a fracture of the distal radius, there may be bony overgrowth of this tubercle as part of the remodeling process. Secondary degenerative changes may continue to aggravate this growth process. Hypertrophy and spurring of this tubercle may cause atrophy and/or rupture of the extensor pollicis longus tendon (Fig. 8).



A B

Fig. 5.—Progression of bony healing, left hand.

***A*, Axial image (palm down) 8 weeks after arthrodesis with bone graft for pain and instability resulting from fracture-dislocation injury shows areas of partial bony fusion between capitate and scaphoid (*arrows*).**

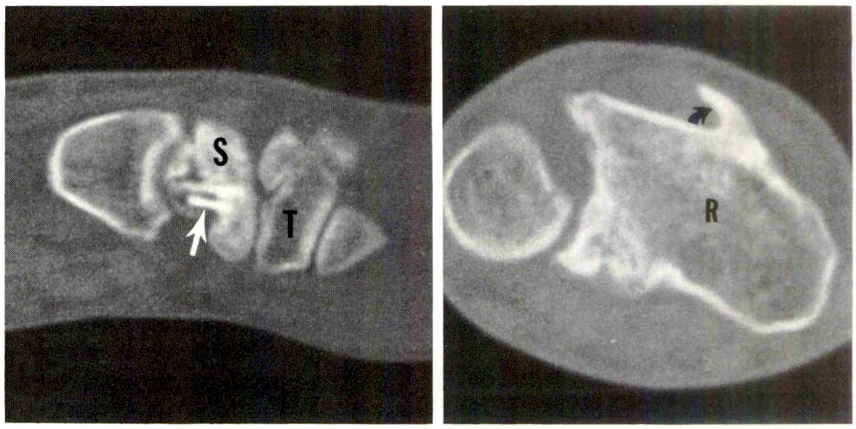
***B*, Follow-up study 6 weeks later shows progressive bony healing (*arrows*). Because of positioning, sections through exact area as *A* are unavailable.**

S = scaphoid; C = capitate; L = lunate; T = triquetrum; P = pisiform; H = hamate; G = bone graft.

Fig. 6.—Metallic fixation pin through nonunited fracture of lunate, which had failed to fuse with conservative treatment. Axial image (palm down, right hand) 6 weeks after placement shows metallic fixation pin spanning unfused lunate fracture. There is virtually no artifact. P = pisiform; T = triquetrum; L = lunate; S = scaphoid.

Fig. 7.—Assimilation of bone graft after arthrodesis. Bone-graft material was implanted after failure of conservative treatment of scaphoid fracture. Sagittal image (palm down) 6 weeks after implantation shows incomplete assimilation of iliac bone-graft struts into healing fracture site (*arrow*). S = scaphoid; T = trapezium.

Fig. 8.—Overgrowth of Lister's tubercle on dorsum of distal radius in patient without appreciable weakening of extensor pollicis longus tendon. Axial image (palm down) 2 months after fracture of distal radius shows overgrowth of Lister's tubercle (*arrow*), which could cause atrophy and/or rupture of extensor pollicis longus tendon. R = radius.



7 8

Axial, sagittal, and coronal images may be used to assess complex fracture dislocations of the carpus. In addition to the unique display of axial anatomy, CT has advantages over standard methods in assessing surrounding soft tissues and is better able to detect small, displaced fracture fragments or foreign bodies.

Because of its greater cost, CT should be used only for selected cases in which standard techniques carry a high probability of suboptimal examination. This is most likely to be the situation with patients who are undergoing prolonged immobilization with internal metallic fixation wires or screws, overlying metallic electric stimulators, or casts, in whom definite information about the degree and character of healing is required. Appropriate timing of mobilization will minimize time lost from normal activities and obviate repeated clinical and radiologic evaluations.

ACKNOWLEDGMENTS

We thank Sally Hammer and Julie Fox for manuscript preparation and Karen Noyes, Linda Snider, Sherry Pierce, and Julli Hopkins for technical assistance.

REFERENCES

1. Zucker-Pinchoff B, Hermann G, Srinivasan R. Computed tomography of the carpal tunnel: a radioanatomical study. *J Comput Assist Tomogr* **1981**;5(4):525–528
2. Mino DE, Palmer AK, Levinsohn EM. Radiography and computerized tomography in the diagnosis of the incongruity of the distal radioulnar joint. *J Bone Joint Surg [Am]* **1985**;67(2):247–252
3. Sciafani SA. Dislocation of the distal radioulnar joint. *J Comput Assist Tomogr* **1981**;5(3):450
4. Hermann G, Rose JS. Computed tomography in bone and soft tissue pathology of the extremities. *J Comput Assist Tomogr* **1979**;3(1):58–66

Book Review

Atlas of Pediatric Orthopedic Radiology. By Alan E. Oestreich and Alvin B. Crawford. Stuttgart: Thieme-Stratton, 334 pp., 1985. $96

This book is an extremely well-illustrated atlas that covers all major areas of musculoskeletal disease in infants and children. The text discusses general principles, including bone growth and development, as well as specific categories of abnormality. Dysplasia, trauma, infection, metabolic bone disease, and positional derangements are considered, with subdivision according to the upper extremity, lower extremity, and trunk. The text material is sparse but appropriate for the visual atlas-type format of the book.

Positive features of the book include the exceptional quality of the illustrations, an attractive page-layout style, and a print size that is benevolent to the eye. Many of the figures are clarified by arrows or other labels, and the diagnosis for each case is highlighted by boldface type in the legend. Boldface referencing of each figure in numeric order is helpful. The illustrations encompass both conventional radiography and advanced imaging techniques, including arthrography, sonography, CT, and skeletal scintigraphy. A substantial number of supplementary diagrams and clinical photographs greatly enhance the reader's understanding of the material presented.

Negative aspects of the book are few and readily justified by its atlas-type format. The concise text makes abrupt transitions from one topic to the next and is written in a manner akin to the well-known textbook of normal variants by A. Kohler and E. A. Zimmer (*Borderlands of the Normal and Early Pathologic in Skeletal Roentgenology*). The index is brief, and the reference list is current but is extremely short and lacks several important citations, including the outstanding sections in J. Caffey's *Pediatric X-Ray Diagnosis* on musculoskeletal disease. A notable drawback, unavoidable because of publication schedules, is the omission of MR imaging, an increasingly important technique in the evaluation of pediatric orthopedic disorders.

This atlas constitutes a valuable complement to the book by M. B. Ozonoff entitled *Pediatric Orthopedic Radiology*. Whereas the text of the latter book is far superior, it lacks the exquisite quality and broad scope of imaging techniques encompassed by the illustrations in this book. The book would be a useful addition to the radiology library of any department that evaluates a significant number of pediatric patients. In addition, it has the potential to serve as an important study guide for residents-in-training. Not only can the book be read completely in a short period of time, but it also can be used as a self-test by viewing the high-quality illustrations with their legends obscured. The book is well worth its cost and is highly recommended with the few reservations outlined above.

David J. Sartoris
University of California, San Diego, Medical Center
San Diego, CA 92103

The Apical Oblique View of the Shoulder: Its Usefulness in Acute Trauma

Phyllis J. Kornguth[1]
Ana M. Salazar

A retrospective analysis of the radiographs of the shoulder in 511 patients examined for acute trauma was performed to evaluate the usefulness of the apical oblique view (45° posterior oblique with 45° caudal angulation of the central ray). Each study included anteroposterior, transthoracic lateral, and scapular "Y" (60° anterior oblique) views as well as the apical oblique projection. Radiographic evidence of injury detected on each view was recorded. The apical oblique view detected 153 (81%) of the 190 injuries. Twenty abnormalities were seen only in this view. These included 11 glenoid rim fractures, seven Hill-Sachs lesions, one posterior subluxation, and one case of soft-tissue calcification. Additional clinically useful information, such as fracture extension into the joint space and displacement of clavicular fracture fragments, was also uniquely provided in this view. The anteroposterior view was more effective than the apical oblique view in detecting acute shoulder injuries, showing 168 (88%) injuries. However, the two views were often complementary, and in this series, if only the anteroposterior and apical oblique views had been obtained, 188 of 190 injuries would have been seen.

The results show that the apical oblique view is useful for the detection of shoulder injuries.

Most routine radiographic studies of the shoulder in trauma patients include a frontal view (anteroposterior) and at least one additional projection [1–4]. These additional views may include a transthoracic lateral, a 45° posterior oblique (Grashey's tangential view of the glenohumeral joint), or a 60° anterior oblique (scapular "Y" view) [5, 6]. In each of these projections, the shoulder is imaged from a different point in the same horizontal plane. The axillary projection [7] images the shoulder along the orthogonal (cephalocaudal) plane, but that projection requires abduction of the arm, which is often painful in patients with shoulder injuries.

Garth et al. [8] in 1984 described a new view of the shoulder, the apical oblique projection, which images the shoulder in a different plane (Fig. 1). The central ray is directed 45° caudad and provides a unique coronal view of the glenohumeral joint (Fig. 2). This projection can be obtained rapidly; it is simple for the technologist to obtain and painless for the patient. In this report we review the effectiveness of this projection for detecting abnormalities in 511 trauma patients in whom the view was added to the routine radiographic examination of the shoulder.

Materials and Methods

Between August 1, 1985, and July 31, 1986, 790 patients had radiographic examinations of the shoulder in the Yale–New Haven Hospital Emergency Room for a chief complaint of shoulder pain. Eight patients had bilateral examinations and ten had pre- and postreduction films, making a total of 808 studies. Five hundred sixty-seven of these cases had a history of acute shoulder trauma and had the following series of radiographs performed: anteroposterior, transthoracic lateral, scapular "Y," and apical oblique views. The last film was obtained by placing the injured shoulder in a 45° posterior oblique position and angling the X-ray beam 45° caudad. Fifty-six studies were not available for review. Thus, 511 studies constitute the

Received February 2, 1987; accepted after revision March 26, 1987.

[1] Both authors: Department of Diagnostic Radiology, Yale University School of Medicine, 333 Cedar St., New Haven, CT 06510. Address reprint requests to P. J. Kornguth.

AJR 149:113–116, July 1987
0361–803X/87/1491–0113
© American Roentgen Ray Society

basis of this report. All examinations were reviewed simultaneously by both authors. The four views were reviewed together, and the presence or absence of any evidence of injury was recorded for each of the projections.

Results

There were 350 normal and 161 abnormal studies. Three hundred twenty-two patients were men (222 normal and 100 abnormal cases), and 189 were women (128 normal and 61 abnormal studies).

The radiographic findings and the frequency with which they were seen on each of the four views are shown in Table 1. The most common injury was fracture of the humerus. The fracture was shown on the anteroposterior view in all 56 cases. This projection also showed all 14 acromioclavicular separations and all seven rib fractures. None of the other views showed these injuries as well.

There were 34 glenohumeral dislocations; 33 anterior and one posterior. Fifty percent of the dislocations had associated fractures. Dislocations were shown on all four projections. The posterior dislocation, although present on all four views, was best seen on the apical oblique view (Fig. 3). Of the five glenohumeral subluxations, one was seen only on the apical oblique.

All 22 clavicle fractures were visible on the anteroposterior view. However, the apical oblique view was particularly helpful for evaluation of this injury, since in two cases it was the only view that showed displacement of the fracture fragments in the anteroposterior direction and the extent of fragment overriding (Fig. 4).

The anteroposterior view showed nine of the 10 scapular fractures. Although the apical oblique view was less sensitive in detecting this injury, it clearly showed extension of the fracture line into the glenohumeral joint in one case (Fig. 5). One case of comminuted scapular fracture was seen only on the lateral and "Y" views.

Fracture of the glenoid rim was present in 18 cases. The anteroposterior view showed less than half of them and the lateral and "Y" views were even less effective. The apical oblique view showed 17 of the 18 fractures. In 11 cases, the fracture was visible only in this view (Fig. 6).

The apical oblique view showed all 12 of the Hill-Sachs deformities that were present (Fig. 7); seven were seen only in this projection.

Soft-tissue calcifications were seen on the anteroposterior and apical oblique views; one case was seen only on the apical oblique projection.

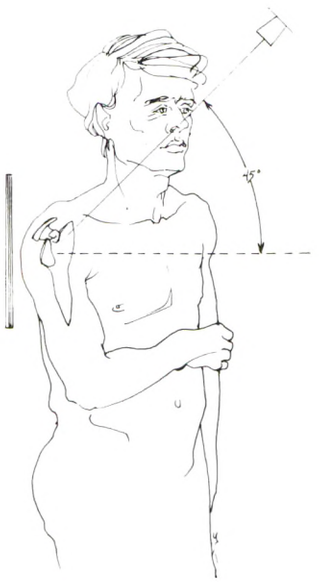
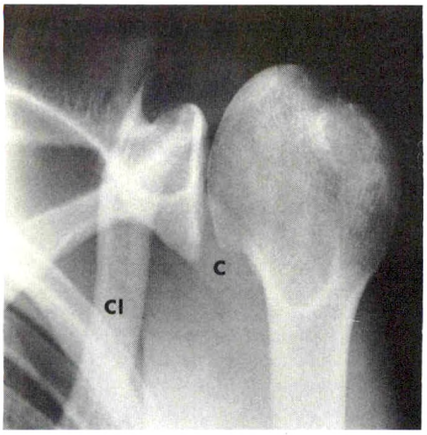


Fig. 1.—Diagram showing positioning for apical oblique view of shoulder. Injured shoulder is placed in 45° posterior oblique position, and central ray is angled 45° caudad.

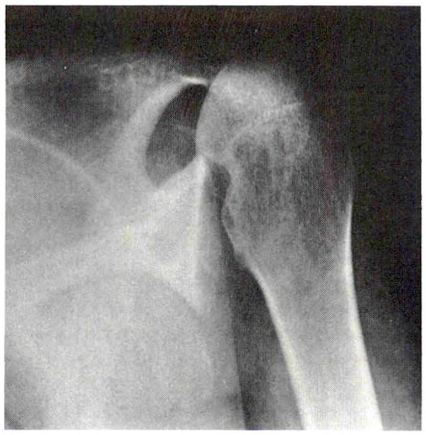
Discussion

The frontal anteroposterior view of the shoulder was the most effective view for showing fractures and dislocations; 168 of the 190 injuries (88%) were present on this projection. It was the best view for detecting fractures of the humerus, ribs, scapula, and clavicle, as well as separations of the acromioclavicular joint. It showed all of the shoulder dislocations and most of the soft-tissue calcifications as well as the foreign body.

Although overall the apical oblique view was less sensitive than the anteroposterior view, showing 153 (81%) of the 190



2



3

Fig. 2.—Normal apical oblique view of shoulder. Cl = clavicle, C = coracoid process of the scapula.

Fig. 3.—Posterior dislocation of shoulder clearly shown on apical oblique view.

TABLE 1: Frequency of Radiographic Abnormalities

Abnormality	*n*	AP (%)	Lateral (%)	Y-View (%)	AO (%)
Humerus fracture	56	56 (100)	39 (70)	38 (68)	52 (93)
Glenohumeral dislocation	34	34 (100)	32 (94)	31 (91)	34 (100)
Clavicle fracture	22	22 (100)	2 (9)	15 (68)	16 (73)
Glenoid rim fracture	18	7 (39)	0 (0)	2 (11)	17 (94)
Acromioclavicular separation	14	14 (100)	2 (14)	3 (21)	2 (14)
Hill-Sachs deformity	12	5 (42)	1 (8)	1 (8)	12 (100)
Scapular (body/spine) fracture	10	9 (90)	3 (30)	5 (50)	5 (50)
Soft-tissue calcification	10	9 (90)	1 (10)	1 (10)	10 (100)
Rib fracture	7	7 (100)	0 (0)	4 (57)	1 (14)
Superior subluxation	2	2	2	1	1
Posterior subluxation	2	0	1	1	1
Inferior subluxation	1	1	0	0	0
Acromion fracture	1	1	0	1	1
Foreign body (bullet)	1	1	1	1	1

Note.—*n* = number of patients; AP = anteroposterior view; Y-View = 60° anterior oblique view; AO = apical oblique view.

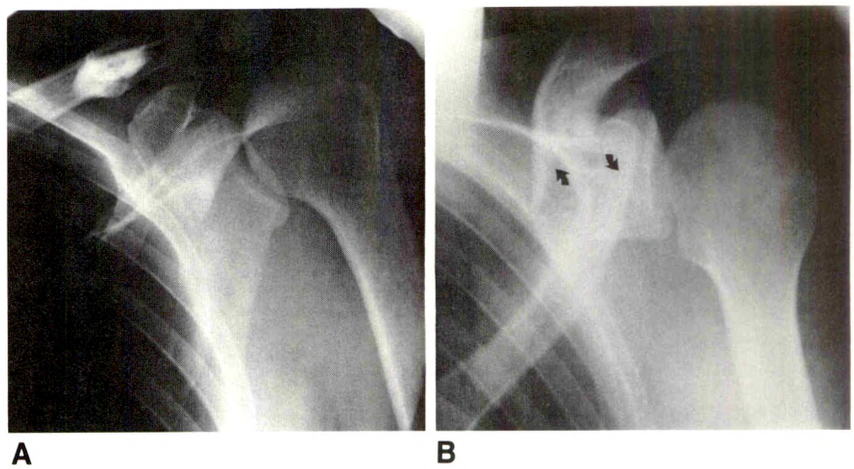


Fig. 4.—Clavicle fracture.
***A*, Anteroposterior view.**
***B*, Apical oblique projection shows displacement and overriding of fracture fragments (*arrows*).**

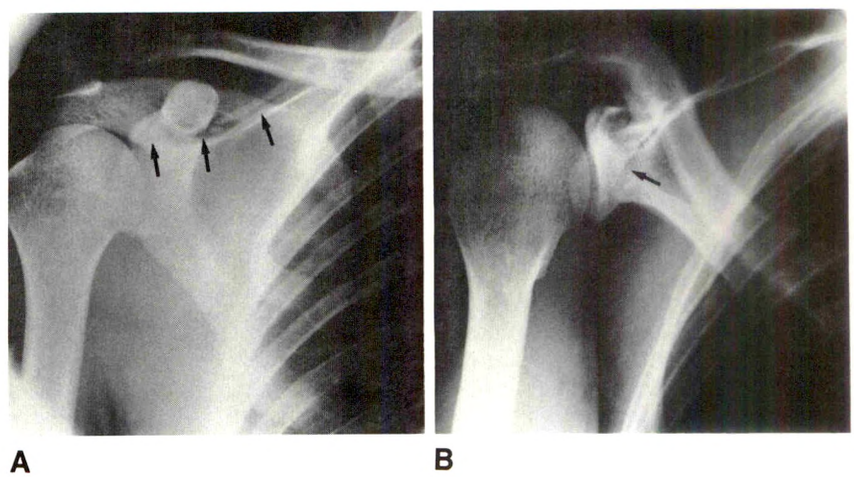


Fig. 5.—Scapular fracture.
***A*, Anteroposterior view shows fracture of superior surface through spine and base of coracoid process (*arrows*).**
***B*, Apical oblique view shows extension into joint space (*arrow*).**

injuries, it was more sensitive for some specific injuries. It was the only view that showed all of the Hill-Sachs fractures of the humeral head and 94% of the glenoid rim fractures. Twenty abnormalities (11 glenoid rim fractures, seven Hill-Sachs lesions, one posterior subluxation, and one case of soft-tissue calcification) were detected only on the apical oblique projection. It was the view that most clearly showed the posterior dislocation. In several instances it provided unique information that was not available on the frontal film. It was the only projection that showed the intraarticular extension of a scapular fracture and the anteroposterior displacement and overriding of clavicular fracture fragments.

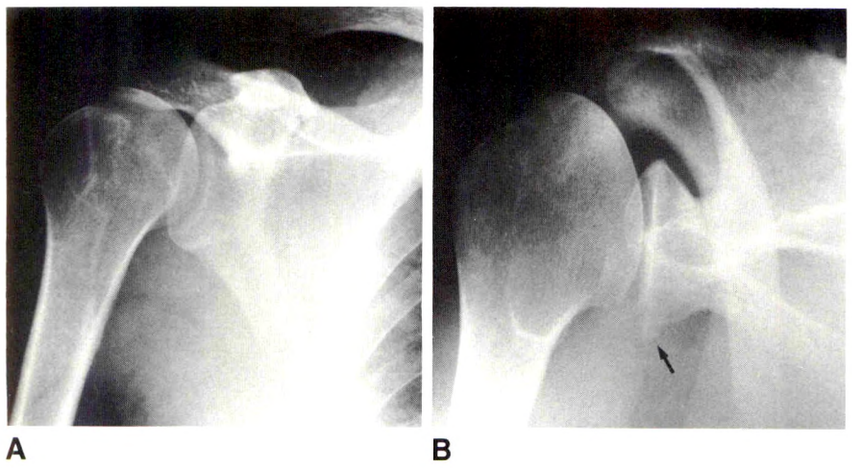


Fig. 6.—Anterior glenoid rim fracture.
***A*, Postreduction anteroposterior view is normal.**
***B*, Small fragment (*arrow*) fractured from anterior surface of glenoid rim shown on postreduction apical oblique view.**

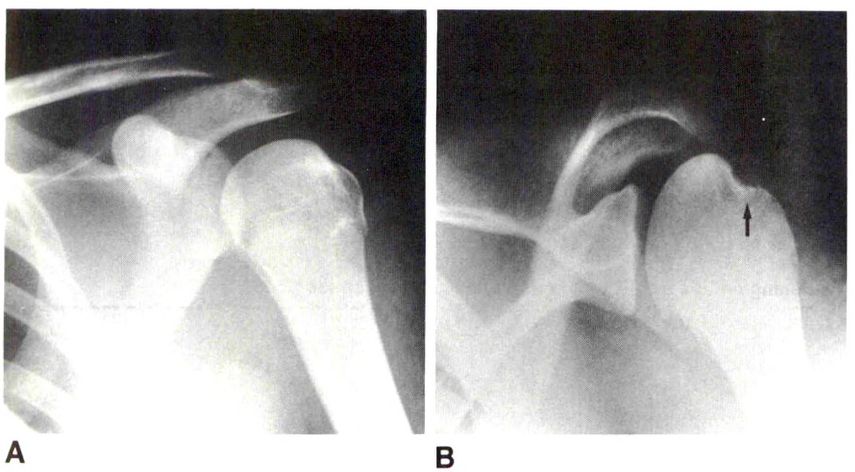


Fig. 7.—Acute Hill-Sachs fracture of humerus.
***A*, Postreduction anteroposterior view is normal.**
***B*, Postreduction apical oblique view shows cortical compression and interruption (*arrow*).**

This information is clinically important for making therapeutic decisions.

The "Y" view and the transthoracic lateral were less sensitive than the apical oblique projection. The "Y" view showed 55% of the abnormalities (104/190); the transthoracic lateral view showed 44% (84/190). The "Y" view gave no information that was not available on another projection. The transthoracic lateral view was useful, however, in showing anteroposterior displacement of fragments in proximal humeral fractures.

The apical oblique view was originally suggested for showing shoulder instability, that is, glenohumeral subluxations or dislocations as well as intraarticular fractures [8]. This study supports this indication. In addition, this view provided important diagnostic information for other types of acute shoulder injury. In many instances, this information was unique and not available on any other projection. It was the single most useful projection in addition to the anteroposterior view for detection of acute shoulder injuries. In the present series, if only anteroposterior and apical oblique projections had been obtained, 188 of 190 injuries would have been detected. A comminuted fracture of the scapula and a posterior glenohumeral subluxation would have been missed. Without the apical oblique view, 20 injuries would have gone undetected. Therefore, it is recommended that the apical oblique projection be included in routine radiographic series for acute shoulder trauma.

ACKNOWLEDGMENT

The authors wish to thank Morton Glickman for his help in preparing this manuscript.

REFERENCES

1. Harris JH, Harris WH. *The radiology of emergency medicine*, 2nd ed. Baltimore: Williams & Wilkins, **1981**:166–171
2. Rogers LF. *Radiology of skeletal trauma*. New York: Churchill Livingstone, **1982**:377–381
3. Simpson EM, Dalinka MK, Stewart VL. Trauma to the shoulder and elbow. In: Dalinka MK, Kaye JJ, eds. *Radiology in emergency medicine*. New York: Churchill Livingstone, **1984**:25–42
4. Weissman BN, Sledge CB. *Orthopedic radiology*. Philadelphia: Saunders, **1986**:215–222
5. DeSmet AA. Anterior oblique projection in radiography of the traumatized shoulder. *AJR* **1980**;134:515–518
6. Rubin SA, Gray RL, Green WR. The scapular "Y": a diagnostic aid in shoulder trauma. *Radiology* **1974**;110:725–726
7. DeSmet AA. Axillary projection in radiography of the nontraumatized shoulder. *AJR* **1980**;134:511–514
8. Garth WP Jr, Slappey CE, Ochs CW. Roentgenographic demonstration of instability of the shoulder: the apical oblique projection. *J Bone Joint Surg [Am]* **1984**;66:1450–1453

The Widened Teardrop Distance: A Plain Film Indicator of Hip Joint Effusion in Adults

John P. Sweeney[1]
Clyde A. Helms[2]
Hideyo Minagi[2]
Kevin W. Louie[3]

The teardrop distance is defined as the distance from the lateral margin of the pelvic teardrop to the most medial aspect of the femoral head as seen on anteroposterior pelvic radiographs. The structure responsible for the teardrop is the anteroinferior portion of the acetabular fossa with contributions from the ischium and from the superior pubic ramus. Anteroposterior pelvic radiographs of 10 patients with documented cases of unilateral hip effusion were retrospectively evaluated for teardrop distance widening on the affected side. Proof of the presence of hip effusion was based on the results of percutaneous hip joint aspirations as described in the patient's medical records. A teardrop distance widening of 1 mm or more was always consistent with hip joint fluid. In addition, radiographs from 20 patients with no known hip abnormalities were reviewed as a control population. These showed side-to-side symmetry in 16 cases (80%) and widening of less than 1 mm in the remaining four cases (20%).

Thus, hip joint effusion in adults can be accurately diagnosed from plain radiographs in the presence of a teardrop asymmetry of 1 mm or more and in the absence of degenerative joint disease.

The presence of excess hip joint fluid is indicative of inflammatory processes and other joint abnormalities. Detection of hip joint effusion in association with clinical symptoms characteristic of joint inflammation warrants aspiration for culture to evaluate the possibility of infection. Prompt diagnosis of such infections is paramount, if the destructive consequences that often accompany these infections are to be avoided.

The value of MR imaging in the diagnosis of hip joint effusions has recently been documented [1]. However, plain film signs that are helpful in evaluating hip joint effusions have only been described for children [2–4]. To the best of our knowledge, no such plain film signs have been documented in adults. This study reports a widened teardrop distance as a subtle sign of hip joint effusion in adults.

Materials and Methods

Anteroposterior radiographs of the pelvis in 10 patients (age range, 14–74 years) with documented hip joint fluid were obtained from the Department of Orthopedics at San Francisco General Hospital and from the teaching files of the Radiology Department at the University of California, San Francisco. Radiographs of children, patients with hip prostheses, and those with degenerative joint disease were excluded from the study. The radiographs of a 14-year-old girl were included because the epiphyses were fully closed. In addition, radiographs of the pelvis in 20 patients with no clinical findings or obvious radiologic signs of hip disease were reviewed. Patients in the control group ranged in age from 27 to 65 years.

The teardrop distance is defined as the distance from the lateral margin of the pelvic teardrop [5, 6] to the most medial aspect of the femoral head as seen on anteroposterior pelvic radiographs [4, 6] (Fig. 1). The distances were measured to the closest 0.5 mm using a millimeter ruler. Each measurement was made twice to ensure reproducibility. Teardrop distances from each hip were then compared. The effects of minimal rotation of the pelvis on the teardrop distance were not evaluated. The presence of hip fluid was confirmed by

Received December 29, 1986; accepted after revision March 10, 1987.

[1] University of California, San Diego, School of Medicine, San Diego, CA 92093.

[2] Department of Radiology, University of California, San Francisco, San Francisco, CA 94143. Address reprint requests to C. A. Helms.

[3] Department of Orthopedic Surgery, University of California, San Francisco, San Francisco, CA 94143.

AJR 149:117–119, July 1987
0361–803X/87/1491–0117
© American Roentgen Ray Society

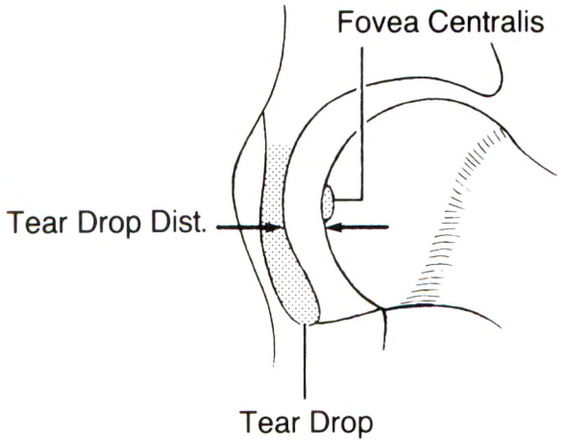


Fig. 1.—Diagram of hip joint as seen on frontal radiograph of pelvis. Note teardrop configuration of anteroinferior portion of acetabulum, fovea centralis, and teardrop distance (*arrows*). Lateral demarcation is most medial aspect of femoral head. Medial demarcation is lateral margin of teardrop.

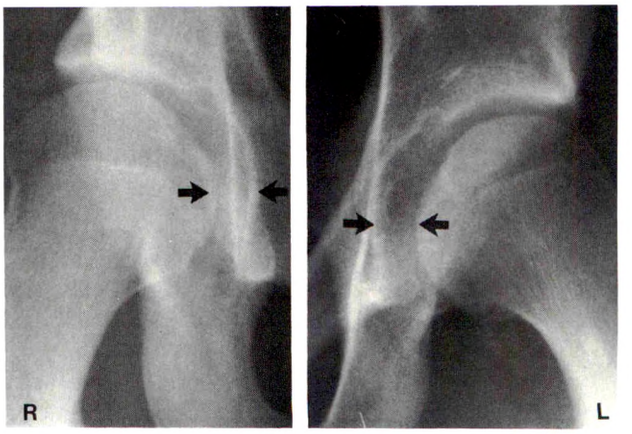


Fig. 2.—Case 1: Widened teardrop distance due to fluid in left hip joint caused by pneumococal arthritis. Right and left teardrop distances (*arrows*) measure 8.0 mm and 9.0 mm, respectively. Fluid aspirated from left hip joint cultured *Pneumococcus*. Ilioischial line, seen superimposed on teardrop distance on the right, should not be confused with medial demarcation of teardrop distance.

percutaneous aspiration of the joint, and the presence of hip infection was ascertained from culture data on the aspirate.

Results

The teardrop distance measurements and hip aspiration results are given in Table 1. All patients with symptoms in whom the teardrop distance was widened by 1 mm or more on one side had joint fluid aspirated from that hip. In 16 (80%) of the 20 control subjects, side-to-side symmetry was noted. In the other four, the differences were less than 1 mm. Thus, a widened teardrop distance in the presence of clinical symptoms was always indicative of joint fluid. Widening of the teardrop distance by as little as 1 mm proved to be an adequate indication of joint effusion (sensitivity 90%, specificity 100%).

Although a widened teardrop distance was indicative of joint effusion, an adequate measurement could not be obtained for both hips in every case. For example, a satisfactory teardrop distance measurement could not be made on the left side in a patient who had an enlarged fovea that obscured the most medial aspect of the femoral head. Although the patient's left joint space seemed wider upon inspection of the radiographs, no point at which a satisfactory absolute measurement could be made was apparent. This was the only case in this series in which a definite measurement could not be made.

One patient with Legg-Calvé-Perthes disease showed progressive widening of the right hip teardrop distance and subsequent right hip destruction. Because of remodeling changes in the right hip from previous Legg-Calvé-Perthes, no valid comparison of the left and right teardrop distances could be made on the initial films. On subsequent films with the left hip teardrop distance unchanged, widening of the teardrop distance on the right was noted. An aspiration was performed after the last film in the series was taken and culture of the purulent fluid disclosed *Staphylococcus*. This course of events suggests an ongoing hip infection that ultimately ended in irreversible hip destruction.

TABLE 1: Teardrop Distance Measurements (mm) and Results of Hip Joint Aspirations

Case	Age (yr)	Right	Left	Results of Aspiration
1	14	8.0	9.0	Left effusion (*Gonococcus*)
2	23	7.0	6.0	Right effusion (sterile)
3	60	8.0	9.0	Left effusion (*Pneumococcus*)
4	41	10.0	8.0	Right effusion (sterile)
5[a]	28	15.0	8.0	Right effusion (*Staphylococcus*)
		18.0	8.0	
6	50	—	—	Left effusion (*Staphylococcus*)
7	20	6.5	8.0	Left effusion (*Staphylococcus*)
8	20	8.0	10.0	Left effusion (sterile)
9	18	8.0	6.0	Right effusion (culture results unavailable)
10	74	4.0	6.0	Left effusion (culture results unavailable)

Note.—yr = year; dash (—) = not definable.

[a] This patient had remodeling changes in the right hip from previous Legg-Calvé-Perthes disease; therefore, no comparison of the left and right teardrop distances could be made on the initial films (first line, 2/11/83). On subsequent films (second line, 8/21/85), with the left teardrop distance identical to the measurement made 6 months earlier, the right teardrop distance had increased by 3 mm. Results of aspiration were obtained 6/19/84.

Discussion

Since the detection of fat pad displacement on plain films has been shown to have no value in the detection of hip joint

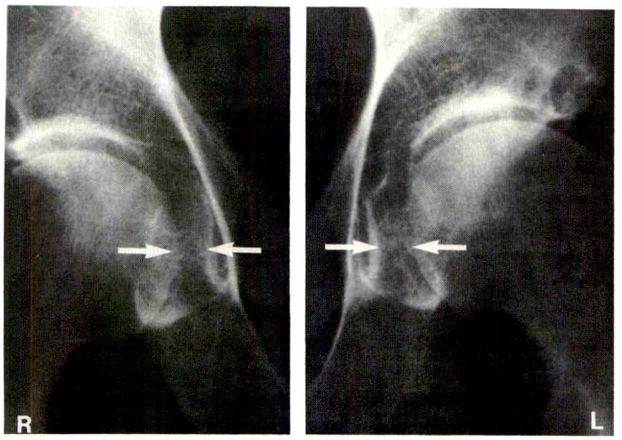


Fig. 3.—Case 2: Widened teardrop distance due to fluid in left hip joint caused by pneumococcal arthritis. Right and left teardrop distances (*arrows*) measure 8.0 mm and 9.0 mm, respectively. Fluid was aspirated from left hip, and culture revealed *Pneumococcus*. (Case courtesy of Richard Gross.)

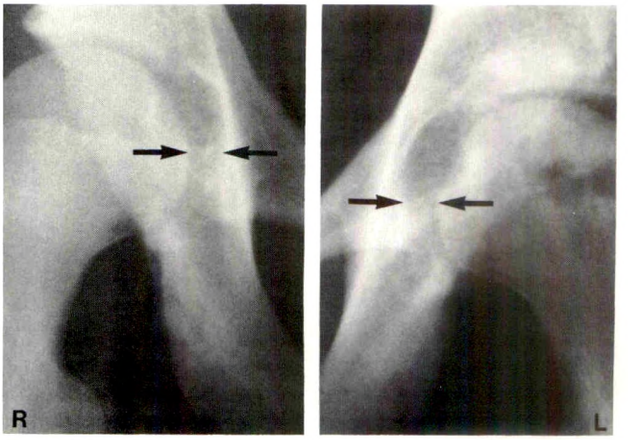


Fig. 4.—Case 8: Widened teardrop distance caused by fluid in left hip joint due to septic arthritis of unknown cause. Right and left teardrop distances (*arrows*) measure 8.0 mm and 10.0 mm, respectively. Purulent fluid was aspirated from left hip; however, no organisms were reported.

fluid [7], no valid plain film criteria for hip joint effusion in adults have been reported. This investigation was undertaken to evaluate the value of another plain film finding for this purpose. In particular, we were interested in diagnosing the presence of joint fluid associated with hip infections. A widened teardrop distance proved to be accurate.

The teardrop distance is defined as the distance between the lateral aspect of the teardrop [5, 6] and the most medial aspect of the femoral head [4, 6] (Fig. 1). The structure responsible for the teardrop is the anteroinferior portion of the acetabular fossa, which consists primarily of the ischium with some contribution from the superior pubic ramus of the pubis [8].

Swischuk described the use of a widened teardrop distance in diagnosing pyogenic arthritis and transient synovitis in children [2, 3]. In addition, Eyring et al. [4] reported teardrop distance widening of 2 mm or more as an early indicator of Legg-Calvé-Perthes disease. To our knowledge, this is the first report to document a correlation between widening of the teardrop distance and the presence of joint effusion in adults.

Although the teardrop distance was easily measured on most of the radiographs in the study, this was difficult in cases in which the ilioischial line obscured the lateral border of the teardrop shadow. In such cases, additional radiographs in which the ilioischial line did not obscure the teardrop shadow could be used, and this was done in two of our cases. In three cases, careful examination of the ilioischial line itself yielded an approximate lateral border of the teardrop shadow. Another difficulty involved the presence of a unilaterally enlarged fovea centralis of the femoral head, which made the decision regarding the lateral measurement of the teardrop distance difficult. In one patient an enlarged fovea obscured the lateral demarcation to such an extent that no accurate measurement could be made. In another patient with bilaterally enlarged foveas, a satisfactory teardrop distance measurement was obtained using the inferior border of the fovea.

A pressing problem in the management of patients with hip pain is the exclusion of pyogenic arthritis and/or osteomyelitis [2]. A widened teardrop distance along with clinical findings suggestive of inflammation is a compelling reason to aspirate the hip to ascertain the presence of infection and identify the offending organism (Figs. 2–4). While treatment for other hip diseases can be delayed with relative impunity, hip infection requires immediate attention and represents an acute condition requiring immediate, vigorous antibiotic treatment [2]. Prompt diagnosis is essential for successful treatment or the joint cartilage will be destroyed. A widened teardrop distance in the appropriate clinical setting indicates the presence of hip effusion. Aspiration and culture of the fluid will facilitate such an early diagnosis.

REFERENCES

1. Beltran J, Noto AM, Herman LJ, Mosure JC, Burk JM, Christoforidis AJ. Joint effusions: MR imaging. *Radiology* **1986**;158:133–137
2. Margulis AR, Gooding CA. *Diagnostic radiology 1975.* San Francisco: University of California, San Francisco Extended Programs in Medical Education, **1975**:61
3. Swischuk LE. *Radiology of the newborn and young infant.* Baltimore: Williams & Wilkins, **1980**:647
4. Eyring EJ, Bjornson DR, Peterson CA. Early diagnostic and prognostic signs in Legg-Calvé-Perthes disease. *AJR* **1965**;93:382–387
5. Halkier E. "Tear-shaped phenomenon" in Calvé-Perthes disease. *Acta Orthop Scand* **1956**;25:287–295
6. Meschan I. An atlas of anatomy basic to radiology. Philadelphia: Saunders, **1975**:146
7. Resnick D, Niwayama G. *Diagnosis of bone and joint disorders.* Philadelphia: Saunders, **1981**:123–125
8. Bowerman JW, Sena JM, Chang R. The teardrop shadow of the pelvis: anatomy and clinical significance. *Radiology* **1982**;143:659–662

Opinion

Bone-Mineral Screening for Osteoporosis

Ferris M. Hall[1]

Osteoporosis in postmenopausal women is an important public health problem accounting for 1 to 2 million fractures per year in the United States. The morbidity, mortality, and monetary ramifications associated with this disease are most evident in hip fractures, which occur in approximately one-third of women who live to the age of 90 [1, 2].

Recent events have focused attention on both the diagnosis and treatment of osteoporosis. The Health Care Financing Administration is currently under mounting pressure to change its previous decision not to permit reimbursement for bone-mineral screening in patients receiving Medicare [3]. Similar pressures have recently led a number of third-party payers, including some State Blue Cross and Blue Shield programs, to agree to reimburse for osteoporosis screening. Last year the Food and Drug Administration for the first time permitted the labeling of estrogens for use in osteoporosis [4]. Finally, in the past 4 years, awareness of osteoporosis among physicians and the public has increased in parallel with a variously estimated 10- to 30-fold increase in the number of offices, clinics, and hospitals offering screening examinations for bone mineral.

Bone-mineral screening for osteoporosis is similar in principle to mammographic screening for breast cancer, since almost all perimenopausal and postmenopausal women are eligible for these evaluations. For both examinations, opinions differ as to methodology, interpretation, reimbursement, when screening should begin, how often it should be repeated, and how long it should continue. Techniques for measuring bone mineralization have recently been reviewed [5, 6]. The traditional examinations of radiogrammetry, photodensitometry, and single-photon absorptiometry (SPA) measure predominantly cortical bone in the appendicular skeleton and are not sensitive to changes in more metabolically active trabecular bone. However, interest has been renewed in SPA of the extreme distal radius and os calcis as an accurate and less costly measure of general bone mineralization, and one large company has recently made a major commitment to this method [7].

Dual-photon absorptiometry (DPA) and single- or dual-energy quantitative CT (QCT) are considered to be the examinations of choice for assessing osteoporosis and have the advantage of permitting measurements of the proximal femur [8, 9] as well as the spine. Dual-energy digital radiography is another promising method for assessing bone mineral. However, although protoype units have been available for some time and have been accurate in assessing calcification in pulmonary nodules [10], the methodology for bone-mineral assessment is just emerging and not yet available on the commercial market. The advantage of dual-energy techniques is that by comparing the transmission of two different energy photon levels (in the case of a radioisotope) or two radiographs with different energy levels (in the case of CT), one can distinguish the attenuation attributable to calcium from that due to the adjacent soft tissues.

The methodology chosen for bone-mineral screening has many economic and political ramifications. CT equipment is costly and QCT, when compared with DPA, is more expensive per test ($150–300 vs $75–200) and exposes the patient to

Received March 2, 1987; accepted April 8, 1987.

This paper is based on a recent article by the author in the *New England Journal of Medicine* (Hall FM, Davis MA, Baran DT. Bone mineral screening for osteoporosis. *N Engl J Med* **1987**;316:212–214). Because of its relevance to radiology and with the encouragement of the *AJR* Editor, it has been revised for publication here.

[1] Department of Radiology, Beth Israel Hospital, 330 Brookline Ave., Boston, MA 02215.

more radiation. CT machines are rarely dedicated to bone-mineral measurements and are usually supervised by a third-party radiologist in a hospital or large clinic setting. DPA equipment, traditionally found in hospital departments of nuclear medicine or endocrinology, is one-tenth as expensive ($40,000–80,000), is easy to operate, and is increasingly being purchased by venture capital for use by such diverse groups as primary care physicians, general internists, rheumatologists, endocrinologists, radiologists, gynecologists, and orthopedists. Monetary factors also make DPA a popular examination in free-standing health centers.

Dual-energy QCT is probably the most accurate measure of bone mineralization. It avoids the major disadvantage of DPA, which is that vertebral trabecular bone measurements are summed with those of adjacent calcium deposits in cortical bone, compression fractures, osteophytes, and the aorta. It also avoids a major disadvantage of single-energy QCT, the confounding effect of variable bone-marrow fat. Dual-energy QCT is, however, less reproducible than single-energy QCT and precision may be more important than accuracy in serial comparison screening. Precision of QCT and DPA varies from 2% to 5% [2, 9, 11, 12], with the variability of DPA relating to both the age of the gadolinium-153 source and the speed with which the scan is performed. Depending on the precision of the method in relation to the rate of bone loss (average, 1–2% per year after menopause), serial examinations at approximately 6- to 12-month intervals over 2 to 3 years may be required to assess a significant change. This is because therapy is predicated not on treatment at some arbitrary bone-mineral threshold for fracture but on prevention through early detection of accelerated bone loss. Subsequent periodic monitoring of both treated and untreated patients may also be necessary.

Obviously, a marked increase in bone-mineral examinations can be expected if third-party reimbursement becomes more liberal. The inevitability of self-referral in many instances and the lack of accepted screening standards create the potential for excessive use. Finally, as pointed out by one investigator: "Measuring bone mineral is not a simple procedure and is subject to many errors. Screening in inexperienced hands is probably more harmful than helpful" (Rosenthal D, personal communication).

The rationale for bone-mineral screening is the assumption that it is possible to identify persons at risk for fracture. Many studies have shown a good correlation between vertebral fractures and the mineral content of the spine. Recent investigations, however, which have used a variety of methods and areas of measurement (including the proximal femur), show a weak correlation between hip fractures and bone mineralization [8, 13, 14]. This is important because hip fractures are clinically and economically far more important than spine or wrist fractures. A recent review summarizes this problem: "In general, measurements of bone mass in elderly women with hip fractures overlap the measurements of other elderly women to such a degree that the groups are indistinguishable" [15]. Although bone mineralization undoubtedly has an etiologic role in hip fractures, other factors, such as a predisposition to falls, are also important determinants [8, 14, 16, 17].

A crucial question concerning bone-mineral screening is how test results influence therapy. Most researchers agree that the postmenopausal use of estrogen deters bone loss and reduces associated fractures [1, 2, 18–20], but it also increases the risk of endometrial carcinoma. In this regard, an important statement came from the 1984 National Institutes of Health Consensus Development Conference on Osteoporosis [1]: "estrogen replacement therapy is highly effective for preventing osteoporosis in women" and results in "a substantial reduction in hip and wrist fractures in women whose estrogen replacement was begun within a few years of menopause. Studies also suggest that estrogen reduces the rate of vertebral fractures . . .Estrogen therapy should be given to women whose ovaries are removed before the age of 50 in whom there are no specific contraindications. Women who have had a natural menopause also should be considered for cyclic estrogen replacement . . .Estrogen-associated endometrial cancer is usually manifested at an early stage and is rarely fatal when managed appropriately." The conference statement did not mention bone-mineral screening.

Recent discussions of postmenopausal estrogen replacement have considered the addition of sequential progestins to reduce the risk of endometrial carcinoma [21, 22], the effect of estrogen dose on bone mineral [23], and the possible effect of estrogen on ischemic heart disease [24, 25]. The potential importance of estrogen in heart disease was discussed in a recent article [25]: "estrogen therapy provides a significant gain in quality-adjusted life expectancy" and "if the beneficial effect of estrogen on cardiovascular mortality is confirmed, it will overshadow all other effects".

The routine use of estrogen in postmenopausal women remains controversial, although I believe that many—perhaps most—authorities would agree with a recent review that concluded: "estrogen treatment is appropriate for many—perhaps most—postmenopausal women" [22]. In so far as this statement is true, there is less rationale for widespread bone-mineral screening. Such screening would in most cases only document what is known, that women lose bone mineral rapidly after menopause, primarily in response to estrogen loss [26]; that thin women are at greater risk probably because they have less bone mineral initially and lower circulating estrogen levels; and that all postmenopausal women become relatively osteoporotic, losing an average of 35% of their cortical and 50% of their trabecular bone during their lifetimes [2]. Indeed, as pointed out by Riggs and Melton [2], knowledge of age alone permits the bone density of the lumbar spine or femoral neck to be predicted with a standard deviation of only about 10%. Widespread uncontrolled screening for osteoporosis would contribute little to our understanding of this disease or its treatment. It would not tell us the specific levels or interval changes of measured bone mineral at which treatment should be started, nor would it provide further information about the optimal estrogen dose [23] or the value of other therapy such as estrogen-progestin combinations [21, 22], fluoride [27], calcium, calcitonin, low-dose parathyroid hormone, vitamin D, or exercise. On the other hand, bone-mineral screening to investigate these questions is now being performed in many centers, and this research should be encouraged and supported.

I believe that large-scale bone-mineral screening of perimenopausal and postmenopausal women is not justified at this time, and that third-party reimbursement for this examination should be discouraged. I question the usefulness of a screening examination that is based on controversial data and unanswered questions and that identifies a disease with an extremely high eventual prevalence. This is particularly true when there is a known effective treatment that an increasing number of authorities think may be indicated, regardless of bone-mineral measurements. Screening for osteoporosis is an extremely useful research tool and obviously can be helpful in specific patients or clinical situations. I certainly would not preclude its widespread use in the future. At the present time, however, bone-mineral screening would appear to have a low priority for our restricted health resources. A substantially better case can be made for mammographic screening, an examination that is applicable to a similar population and that also is not reimbursed by most third-party payers.

REFERENCES

1. National Institutes of Health. Consensus conference: osteoporosis. *JAMA* **1984**;252:799–802
2. Riggs BL, Melton LJ III. Involutional osteoporosis. *N Engl J Med* **1986**;324:1676–1686
3. Society of Nuclear Medicine. Bone mineral densitometry: society responds to HCFA and Blue Cross/Blue Shield subcommittee. *J Nucl Med* **1985**;26:115–117
4. Food and Drug Administration. Oral estrogen for postmenopausal osteoporosis; drug efficacy study implementation: reevaluation. *Fed Regist* **1986**;51:12,568–12,570
5. Wahner HW, Dunn WL, Riggs BL. Assessment of bone mineral. *J Nucl Med* **1984**;25:1134–1141, 1241–1253
6. Health and Public Policy Committee, American College of Physicians. Radiologic methods to evaluate bone mineral content. *Ann Intern Med* **1984**;100:908–911
7. Hess TP. Commerical infighting may be blurring value of bone mineral analysis systems. *Diagn Imaging* **1986**;June:53–56
8. Riggs BL, Wahner HW, Seeman E, et al. Changes in bone mineral density of the proximal femur and spine with aging. *J Clin Invest* **1982**;70:716–723
9. Sartoris DJ, André M, Resnick C, Resnick D. Trabecular bone density in the proximal femur: quantitative CT assessment. *Radiology* **1986**; 160:707–712
10. Frazer RG, Hickey NM, Niklason LT. Calcification in pulmonary nodules: detection with dual-energy digital radiography. *Radiology* **1986**;160:595–601
11. Rosenthal DI, Ganott MA, Wyshak G, Slovik DM, Doppelt SH, Neer RM. Quantitative computed tomography for spinal density measurement: factors affecting precision. *Invest Radiol* **1985**;20:306–310
12. Genant HK, Ettinger B, Cann CE, Reiser U, Gordan GS, Kolb FO. Osteoporosis: assessment by quantitative CT density. *Orthop Clin North Am* **1985**;16:557–568
13. Firooznia H, Rafii M, Golimbu C, Schwartz MS, Ort P. Trabecular mineral content of the spine in women with hip fracture: CT measurement. *Radiology* **1986**;159:737–740
14. Cummings SR. Are patients with hip fractures more osteoporotic? *Am J Med* **1985**;78:487–494
15. Cummings SR, Black D. Should perimenopausal women be screened for osteoporosis? *Ann Intern Med* **1986**;104:817–823
16. Ray WA, Griffin MR, Schaffner W, Baugh DK, Melton J III. Psychotropic drug use and the risk of hip fracture. *N Engl J Med* **1987**;316:363–369
17. Kelsey JL, Hoffman S. Risk factors for hip fracture. *N Engl J Med* **1987**;316:404–406
18. Hutchinson TA, Polansky SM, Feinstein AR. Post-menopausal oestrogens protect against fractures of hip and distal radius: a case-control study. *Lancet* **1979**;2:705–709
19. Weiss NS, Ure CL, Ballard JH, Williams AR, Daling JR. Decreased risk of fractures of the hip and lower forearm with postmenopausal use of estrogen. *N Engl J Med* **1980**;303:1195–1198
20. Ettinger B, Genant HK, Cann CE. Long-term estrogen replacement therapy prevents bone loss and fractures. *Ann Intern Med* **1985**;102:319–324
21. Padwick ML, Pryse-Davies J, Whitehead MI. A simple method for determining the optimal dosage of progestin in postmenopausal women receiving estrogens. *N Engl J Med* **1986**;315:930–934
22. MacDonald PC. Estrogen plus progestin in postmenopausal women—act II. *New Engl J Med* **1986**;315:959–961
23. Horsman A, Jones M, Francis R, Nordin C. The effect of estrogen dose on postmenopausal bone loss. *New Engl J Med* **1983**;309:1405–1407
24. Petitti DB, Perlman JA, Sidney S, et al. Postmenopausal estrogen use and heart disease (letter to the editor). *New Engl J Med* **1986**;315:131–136
25. Hilner BE, Hollenberg JP, Pauker SG. Postmenopausal estrogens in the prevention of osteoporosis: benefit virtually without risk if cardiovascular effects are considered. *Am J Med* **1986**;80:1115–1127
26. Richelson LS, Wahner HW, Melton LJ III, Riggs BL. Relative contributions of aging and estrogen deficiency to postmenopausal bone loss. *New Engl J Med* **1984**;311:1273–1275
27. Riggs BL, Seeman E, Hodgson SF, Taves DR, O'Fallon WM. Effect of the fluoride/calcium regimen on vertebral fracture occurrence in postmenopausal osteoporosis. *New Engl J Med* **1982**;306:446–450

Case Report

Antibiotic-Containing Acrylic Beads: Radiographic Appearances

Richard H. Daffner[1] and David E. Foss[2]

Radiographic changes that occur as a result of a surgical procedure often are misinterpreted by radiologists who are unfamiliar with the procedure. The use of antibiotic-containing polymethylmethacrylate (PMMA) to anchor prosthetic components began in 1970 [1] in an attempt to reduce infections in total joint implants. More recently, antibiotic-impregnated beads of PMMA have been used in the periarticular areas to treat osteomyelitis as well as infected total joint prostheses [2, 3]. To our knowledge, this procedure has not been mentioned in the radiologic literature. Although the radiographic appearance of the PMMA beads is characteristic, they could be misinterpreted as dense synovial osteochondromas. The following case illustrates the characteristic radiographic appearance of these beads.

Case Report

A 56-year-old man underwent implantation of a Miller-Galante total condylar prosthesis (Zimmer Manufacturing Co., Warsaw, IN). Despite antibiotic irrigation and postoperative administration of IV antibiotics, infection of the joint developed. Six months after implantation, the prosthesis was removed, and 32 pellets of PMMA impregnated with cephapirin sodium were implanted (Fig. 1). The patient was placed in a long leg cast, and the joint was irrigated with antibiotics. Six weeks later, a joint fusion was performed, and 24 of the PMMA pellets were left in place. The joint remained sterile, and the fusion healed. Future removal of the pellets was contemplated because of irritation of the quadriceps tendon.

Discussion

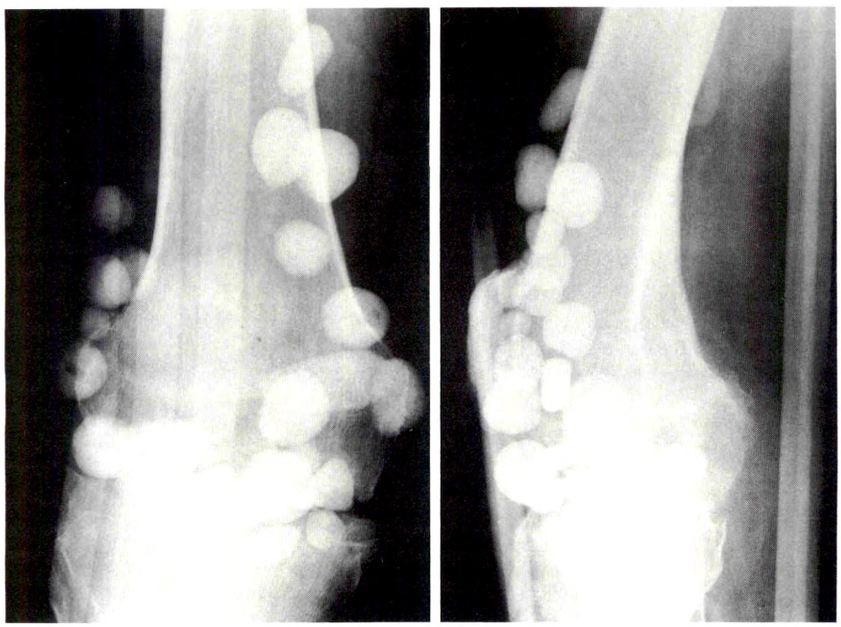
The use of antibiotic-impregnated acrylic bone cement began in 1970 [1, 4]. Although this procedure is popular in Europe, it has been approved for use in the United States only recently. Experimental findings show that the antibiotics incorporated into acrylic cement diffuse out of the cement both in vivo and in vitro [2, 4, 5–7].

Antibiotic-containing PMMA is used in two forms. In the first form, the original way the compound was used, the cement is used to anchor prosthetic components. No radiographic method can distinguish between plain and antibiotic-containing PMMA when the cement is used in this way. In the second form, beads of antibiotic-impregnated PMMA are placed either in osteomyelitic cavities or in the periarticular space after removal of infected prostheses [5–7]. The beads often are placed on a string, which allows easier removal at a later date.

The radiographic appearance of antibiotic-containing PMMA beads is characteristic. The materials for making PMMA cement are supplied in kits containing packets of powder and vials of liquid that are added to complete the polymerization process [8]. Because the beads are prepared at the time of surgery, they are round to ovoid, of various sizes, and extremely dense. Small radiolucencies representing air trapped within the beads at the time of preparation may be present (Fig. 1). Because of their size and location, these beads may be confused with synovial osteochondro-

Received December 18, 1986; accepted after revision February 4, 1987.
[1] Department of Diagnostic Radiology, Allegheny General Hospital, 320 E. North Ave., Pittsburgh, PA 15212. Address reprint requests to R. H. Daffner.
[2] Department of Orthopedic Surgery, Allegheny General Hospital, Pittsburgh, PA 15212.

AJR **149:123–124, July 1987** 0361–803X/87/1491–0123 © American Roentgen Ray Society



A B

Fig. 1.—Radiographs of antibiotic-impregnated polymethylmethacrylate pellets implanted after removal of a condylar knee prosthesis. Pellets are uniformly dense and contain occasional radiolucencies that represent trapped air bubbles. *A*, Frontal view. *B*, Lateral view.



Fig. 2.—Lateral radiograph of knee of a patient with synovial osteochondromatosis. Osteochondromas have punctate curvilinear calcification typical of chondroid tissue and are much less dense than polymethylmethacrylate beads.

mas (Fig. 2). The latter osteocartilaginous loose bodies usually are smaller than the PMMA beads. In addition, the density of the osteochondromas is less than that of the beads, is less homogeneous, and shows the characteristic punctate or curvilinear "*C*'s and *O*'s" appearance of chondroid calcification.

REFERENCES

1. Buchholz HW, Engelbrecht A, Uber die Depotwirkung einiger Antibiotica bei Vermischung mit dem Kunstharz Palacos. *Chirurg* **1970**;41:511–515
2. Picknell B, Mizen L, Sutherland R. Antibacterial activity of antibiotics in acrylic bone cement. *J Bone Joint Surg [Br]* **1977**;59:302–307
3. Murray WR. Use of antibiotic-containing bone cement. *Clin Orthop* **1984**;190:89–95
4. Buchholz HW, Elson RA, Heinert K. Antibiotic-loaded acrylic cement: current concepts. *Clin Orthop* **1984**;190:96–108
5. Majid SA, Lindberg LT, Gunterberg B, Siddiki MF. Gentamicin-PMMA beads in the treatment of chronic osteomyelitis. *Acta Orthop Scand* **1985**;56:265–268
6. Marcinko DE. Gentamicin-impregnated PMMA beads: an introduction and review. *J Foot Surg* **1985**;24:116–121
7. Walenkamp GHIM, Vree TB, van Rens TJG. Gentamicin-PMMA beads: pharmacokinetic and nephrotoxicological study. *Clin Orthop* **1986**; 205:171–183
8. Calandruccio RA. Arthroplasty of the hip. In: Crenshaw AH, ed. *Campbell's operative orthopaedics*, 7th ed. St. Louis: Mosby, **1987**:1240–1242

Peroneal Tendon Injury Associated with Calcaneal Fractures: CT Findings

Zehava Sadka Rosenberg[1,2]
Frieda Feldman[1]
Rolando D. Singson[1]
Grant J. Price[1]

Injury to the peroneal tendons is one of the major long-term complications of intraarticular calcaneal fractures and heretofore has been difficult to diagnose by noninvasive radiography. Retrospective review of CT scans of 24 intraarticular calcaneal fractures, obtained shortly after injury, identified 22 cases (92%) of acute peroneal tendon abnormalities. In most of these cases, multiple findings were present. These included lateral displacement in 14 (58%) of 24, impingement by bony fragments in eight (33%), subluxation or dislocation in six (25%), soft-tissue masses around the tendons representing hematomas or early scar tissue in five (21%), and entrapment of the tendons in three (13%). In 10 cases with long-term follow-up, impingement on the tendons by bony fragments correlated well with the subsequent development of peroneal tenosynovitis, while hematoma around the tendons or lateral displacement of the tendons was clinically insignificant.

Thus, CT in the immediate postfracture period, can be used to detect and categorize acute peroneal tendon injuries as well as possibly to predict the likelihood and nature of subsequent development of peroneal tenosynovitis.

One of the major long-term complications of intraarticular calcaneal fractures is injury to the peroneal tendons [1–7]. The fracture is produced by an axial force applied to the foot, so that the talus is driven downward into the calcaneus. This splits the calcaneus into two major fragments with outward bulging of the lateral one. As a result, displacement of the peroneal tendons, as they course along the calcaneal wall, occurs [8, 9]. In addition to being laterally displaced, the peroneal tendons may be impinged on by bony fragments, entrapped between the fibula and calcaneal fragments, or dislocated anteriorly about the fibula. Chronic or stenosing tenosynovitis may then develop as a sequela of scarring or impingement by bony fragments on the tendon sheath [1–7, 10–11].

Although peroneal tendon injury is potentially correctable with surgery [1, 5, 12–16], it cannot be studied adequately by routine imaging techniques. It may be inferred, but not definitively diagnosed, by lateral broadening of the calcaneus or outward displacement of bony fragments on plain films. Peroneal tenography can identify displaced tendons and tendon-sheath abnormalities [1, 2], yet it is an invasive technique that requires special skills and has not gained widespread use. Also, it does not allow direct visualization of adjacent scar or bony spurs impinging on the tendons. MR imaging may be valuable in assessing tendon injuries around the ankle [17], but to our knowledge, no reports are available dealing specifically with peroneal tendon injuries.

The normal CT anatomy of the peroneal tendons has been described in recent literature [18]. Also, CT of intraarticular calcaneal fractures is beginning to gain popularity [19–21]; however, associated peroneal tendon injury diagnosed by CT have been discussed only briefly [18–21]. We retrospectively analyzed 30 CT studies in 21 patients with 24 intraarticular calcaneal fractures with two goals in mind: (1) delineate and categorize peroneal tendon injuries in the immediate postfracture period and (2) determine the ability of CT, performed shortly after

Received December 29, 1986; accepted after revision March 10, 1987.

[1] Department of Radiology, Presbyterian Hospital, College of Physicians and Surgeons, Columbia University, New York, NY 10032.

[2] Present address: Department of Radiology, Hospital for Joint Diseases/Orthopedic Institute, 301 E. 17th St., New York, NY 10003. Address reprint requests to Z. S. Rosenberg.

AJR 149:125–129, July 1987
0361–803X/87/1491–0125
© American Roentgen Ray Society

trauma, to predict the likelihood and nature of subsequent peroneal tendon dysfunction.

Materials and Methods

CT was performed shortly after trauma in 21 patients with 24 intraarticular calcaneal fractures for assessing the position and joint involvement of fracture fragments. Retrospective analysis was performed on peroneal tendon abnormalities such as lateral displacement, entrapment, impingement by bone fragments, hematoma, and scar tissue. The initial CT scans were obtained between 5 days and 3 months (mean, 20 days) after injury. Repeat scans were obtained in six cases 5 days to 11 months after injury (mean, 6½ months). The total number of scans reviewed was 30.

In 10 cases, clinical follow-up was performed 9–12 months (mean, 10 months) after fracture. Symptoms and signs consistent with peroneal tenosynovitis were recorded. These included pain, tenderness, and swelling posterolaterally along the course of the tendons, as well as complaints of involuntary inversion of the foot during walking and weakness of the tendons on resisted eversion.

All patients were studied on a Siemens DR 3 CT scanner with a 512 × 512 matrix, a 5-sec scanning time, a 4-mm slice thickness, and a 3-mm overlapping interval. Axial slices were obtained with the feet in the neutral anatomic position and the patient supine. Coronal scans, obtained by angling the gantry 20°, were occasionally used to facilitate delineation of the relationship between the tendons and bony structures, but were unnecessary in most cases. Routine sagittal and coronal reconstructions served to supplement axial scans and improve delineation of the peroneal tendons throughout their course in all patients studied.

Results

The normal CT anatomy of the peroneal tendons is outlined in Figure 1. The peroneal tendons were positioned normally in only two (8%) of the 24 fractures studied shortly after injury. These fractures had resulted in minimal outward displacement of the lateral bony fragments (Fig. 2). In the other cases specific abnormalities were seen alone or in various combinations. Fourteen (58%) of 24 fractures were associated with laterally displaced tendons (Fig. 3). Impingement by bony fragments arising from either the calcaneus (Figs. 3 and 4) or lateral malleolus (Fig. 5) was present in eight cases (33%). In six cases (25%) the tendons were dislocated or subluxed (Figs. 6 and 7). Soft-tissue prominence about the tendons was present in five cases (21%) (Figs. 3B and 8). This was presumed to represent either hematoma or early scar tissue, depending on the age of injury. In three cases (13%) the tendons were entrapped between the lateral malleolus and calcaneal fragments (Fig. 7). Two patients (8%) scanned 3 weeks after injury had bony densities posterior to the tendons (Fig. 9) that were thought to represent either small fracture fragments or early ectopic bone formation.

Definitive clinical and radiologic correlation was obtained in 10 cases 9–12 months after fracture. In five of these, the clinical findings were consistent with peroneal tenosynovitis, and initial CT studies showed displacement of tendons with impingement by bony fragments. One of these patients had significant relief of pain after surgical resection of bone spike

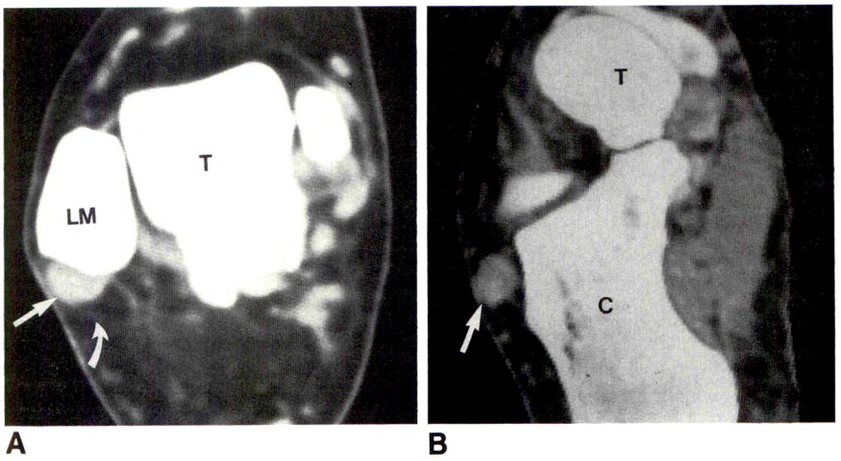


Fig. 1.—Normal axial CT anatomy of right peroneal tendons.

***A*, Slightly below ankle joint, both peroneus longus and brevis tendons (*straight arrow*) are situated posterior to lateral malleolus. Superior peroneal retinaculum (*curved arrow*) is faintly seen posterolateral to tendons.**

***B*, More distally, at level of subtalar joints, tendons (*arrow*) are noted lateral to calcaneal wall.**

C = calcaneus; LM = lateral malleolus; T = talus.

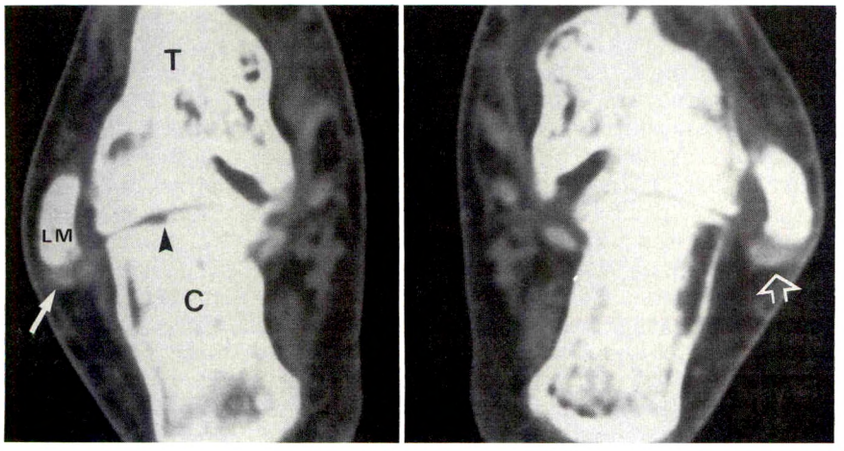


Fig. 2.—Axial CT scan shows right nondisplaced intraarticular calcaneal fracture with incongruent posterior calcaneal facet (*arrowhead*). Right peroneal tendons (*solid arrow*) are in normal position posterior to lateral malleolus. Note normal left peroneal tendons (*open arrow*). Except for mild right ankle stiffness, the patient was asymptomatic 1 year later. C = calcaneus; LM = lateral malleolus; T = talus.

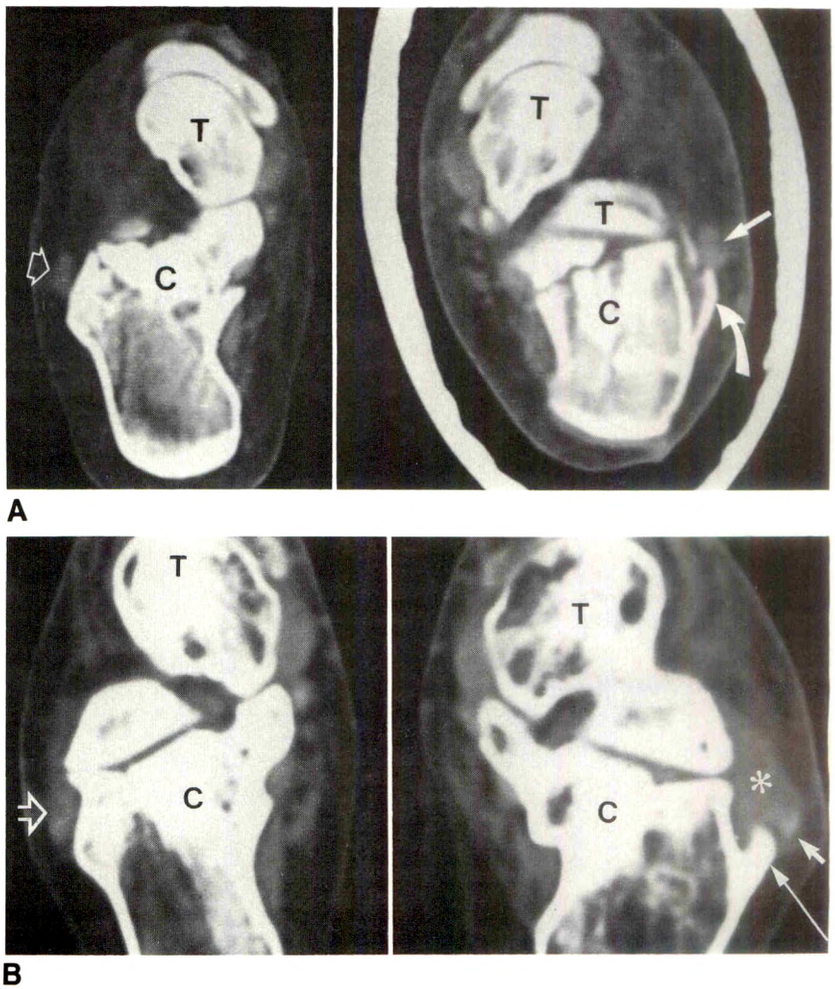


Fig. 3.—*A*, Axial CT scan shows bilateral acute intraarticular calcaneal fractures. Left peroneal tendons (*straight solid arrow*) are laterally displaced and impinged on by fragment arising from comminuted calcaneal wall (*curved arrow*). Right peroneal tendons are mildly displaced laterally because of buckling of right calcaneal wall (*open arrow*).

***B*, 1 year after injury the patient complained of pain and swelling along the course of the left peroneal tendons and weakness of the left foot on eversion, consistent with left peroneal tenosynovitis. Right foot was relatively asymptomatic. On repeat CT left peroneal tendons (*short solid arrow*) were displaced outwardly by lateral calcaneal wall spur (*long solid arrow*). Scar tissue was present around tendons (*asterisk*). No significant abnormalities were seen in right peroneal tendons (*open arrow*). Resection of left-sided bony spike and scar with release of tendons resulted in significant pain relief.**

C = calcaneus; T = talus.

and lysis of scar around the tendons (Fig. 3). In a sixth patient, CT 2 months after injury illustrated a peritendonous soft-tissue mass representing either hematoma or early scar. Nine months after fracture, the patient complained of "snapping" of the tendons but had only mild posterolateral pain along the course of the tendons (Fig. 8). The last four cases were relatively asymptomatic. One had no CT evidence of tendon injury (Fig. 2), one had hematoma around the tendons, and the last two had only mild lateral displacement of the tendons (Fig. 3, right side).

Discussion

The peroneus longus and brevis tendons descend together posterior to the fibular malleolus and proceed obliquely along the lateral calcaneal wall toward their respective insertion sites. They are held tightly in position by both the superior and inferior peroneal retinacula [18, 22]. The peroneal muscles and their tendons serve as pronators and evertors of the foot, contribute to ankle stability, and are involved in the second stage of walking and push-off [22]. Peroneal tenosynovitis results in pain, swelling, and tenderness along the course of the tendons, as well as involuntary inversion of the foot, particularly when walking on rough surfaces. This frequently leads to lateral ankle instability, twisting, or repeated ankle sprains [1]. Weakness of the tendons on passive or resistive eversion may also be present. Peroneal tenosynovitis commonly occurs after intraarticular calcaneal fractures [1, 2, 4, 23, 24]. In a long-term follow-up of 50 cases with intraarticular calcaneal fractures, Deyerle [1] found that the most common complaint was inability to resist inversion during ambulation due to peroneal tenosynovitis. Slatis et al. [23] reviewed 86 cases of calcaneal fractures and found that pain along the peroneal tendons was a common sequela of calcaneal fractures. Lateral ankle pain and peroneal motor dysfunction have also been found in other studies of long-term results of intraarticular calcaneal fractures [4, 24].

Our series shows a high frequency of acute peroneal tendon abnormalities present immediately after intraarticular calcaneal fractures. Because of the retrospective nature of our study and the transient nature of the patient population, we were able to correlate our radiographic findings with long-term follow-up in only 10 cases. In the five with clinical diagnosis of peroneal tenosynovitis, CT obtained shortly after fracture showed impingement on the tendons by small bony fragments arising from either fibular malleolus or comminution of the calcaneus (Fig. 3, left side). In four patients who had no complaints relating to peroneal tendon dysfunction, CT

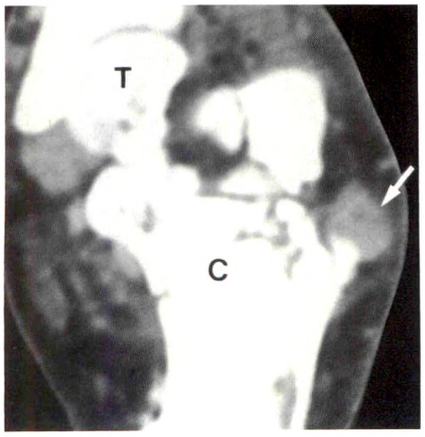


Fig. 4.—Calcaneal bony fragment impinges on left peroneal tendons (*arrow*). C = calcaneus; T = talus.

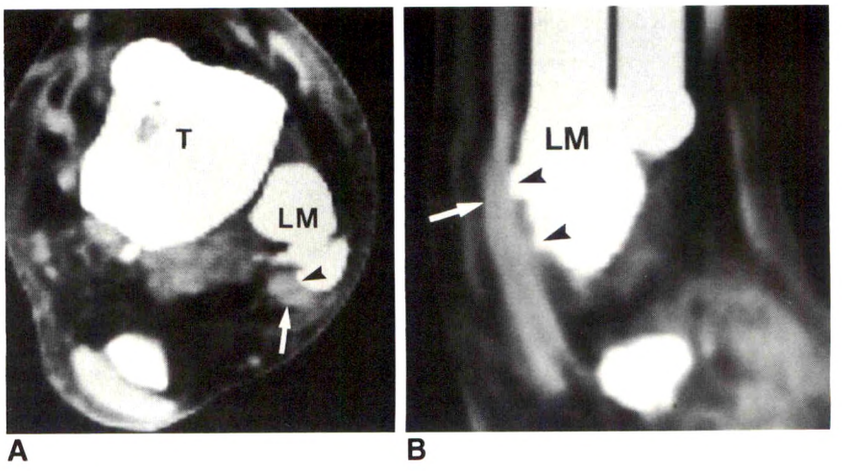
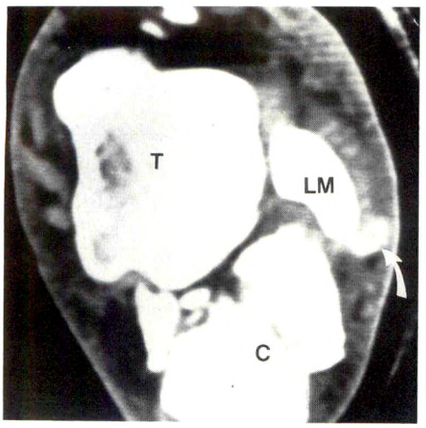


Fig. 5.—*A*, Axial scan shows left lateral malleolar fragment (*arrowhead*) abutting peroneal tendons (*arrow*).

B, Sagittal reconstruction shows displacement of tendons (*arrow*) by lateral malleolar fragments (*arrowheads*).

LM = lateral malleolus; T = talus.



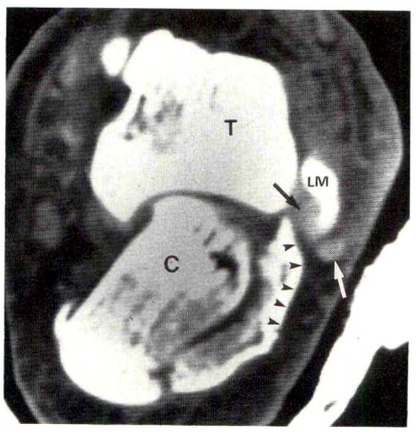


Fig. 6.—CT scan after calcaneal fracture shows dislocation of left peroneal tendons lateral to fibular malleolus (*arrow*). C = calcaneus; LM = lateral malleolus; T = talus.

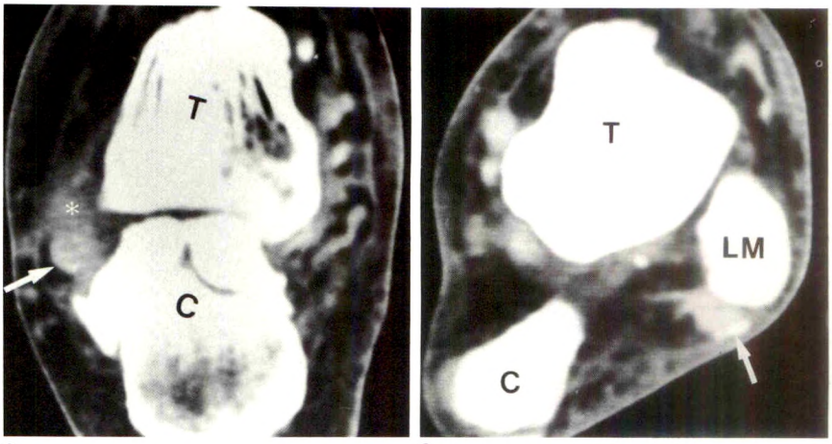
Fig. 7.—Axial CT scan of left foot shows laterally displaced calcaneal fragment (*arrowheads*) trapping left peroneus brevis (*black arrow*) between itself and tip of fibular malleolus. Peroneus longus tendon is subluxed laterally (*white arrow*). C = calcaneus; LM = lateral malleolus; T = talus.

showed either normal position of the tendons (Fig. 2), mild lateral displacement (Fig. 3, right side), or hematoma around the tendons. In the last case, snapping of the tendons with only minimal pain along their course was associated with a soft-tissue density around the tendons, representing either hematoma or early scar tissue (Fig. 8). Too few cases were studied to draw definite conclusions, but the data suggest that initial CT evidence of impingement by bony fragments correlates well with the subsequent development of peroneal tenosynovitis. Mild lateral displacement of the tendons or hematoma around them, on the other hand, may be clinically insignificant later. Therefore, the nature and likelihood of long-term peroneal tendon dysfunction may be predicted on the basis of the initial CT findings. This information can be valuable when immediate open reduction of intraarticular calcaneal fractures is planned. Presurgical knowledge and recognition of the possible predictive value of a peroneal tendon abnormality may lead to repair, and thus reduce subsequent tendon dysfunction.

Since peroneal tenosynovitis is a source of severe disability and is surgically correctable, it is important to differentiate it from other complications of calcaneal fractures including posttraumatic subtalar arthritis, loss of plantar soft tissue, and excessive new bone formation on the heel surface [25]. In the past, these entities have been differentiated solely on a clinical basis, with peroneal tenography serving only as an occasional aid [1, 2, 26]. While tenography is a valuable study, it is invasive and often is difficult to perform, particularly when swelling obscures ankle landmarks or when the tendon sheath is scarred down. Unlike tenography, CT is noninvasive and simple to perform. It also affords direct visualization of the tendons as well as bony fragments and hematoma or scar around them, while tenography can only indicate displacement or scarring of the tendons' sheath. Theoretically, ten-

Fig. 8.—2 months after calcaneal fracture a soft-tissue density representing hematoma or early scar tissue (*asterisk*) partially engulfs peroneal tendons (*arrow*). 10 months after injury the patient had only mild posterolateral discomfort but complained of lateral "snapping sensation" on dorsiflexion of foot. C = calcaneus; T = talus.

Fig. 9.—CT scan 3 weeks after left intraarticular calcaneal fracture shows calcification posterior to peroneal tendons (*arrow*) representing either small bone fragment or early ectopic bone formation. C = calcaneus; LM = lateral malleolus; T = talus.



8 9

ography would be more sensitive than CT in the diagnosis of complete rupture of the tendons. However, this is an unusual complication of intraarticular calcaneal fractures, and sagittal and coronal reconstruction should increase the sensitivity of CT in this respect.

In summary CT is a sensitive, noninvasive, easily performed technique for delineating and categorizing peroneal tendon injuries in the immediate postfracture period. The findings may also serve to predict the future development of peroneal tenosynovitis. Thus, in situations where immediate surgical repair of intraarticular calcaneal fracture is attempted, prior knowledge of the status of the peroneal tendons with attempt at surgically removing abutting bony fragments and repositioning of the tendons may reduce the subsequent incidence of tendon dysfunction.

ACKNOWLEDGMENTS

We thank Joan Boykin, Ruth Harvey, Patricia Kunzler, and Bridget Torres for manuscript preparation.

REFERENCES

1. Deyerle WH. Long term follow up of fractures of the os calcis. Diagnostic peroneal synoviagram. *Orthop Clin North Am* **1973**;4:213–227
2. Resnick D, Goergen TG. Peroneal tenography in previous calcaneal fractures. *Radiology* **1975**;115:211–213
3. Stover CN, Bryan DR. Traumatic dislocation of the peroneal tendons. *Am J Surg* **1962**;103:180–186
4. Pozo JL, Kirwan EOG, Jackson AM. The long-term results of conservative management of severely displaced fractures of the calcaneus. *J Bone Joint Surg [Br]* **1984**;66(3):386–390
5. McReynolds IS. Trauma to the os calcis and heel cord. In: Jahss MH, ed. *Disorders of the foot*. Philadelphia: Saunders, **1982**:1497–1542
6. Watson-Jones R. Injuries of the foot. In: Wilson JN, ed. *Fractures and joint injuries*, 6th ed. Edinburgh: Churchill Livingstone, **1982**:1156–1175
7. Fitzgerald RH, Coventry MB. Post-traumatic peroneal tendinitis. In: Bateman JE, Trott AW, eds. *The foot and ankle*. New York: Thieme-Stratton, **1980**:103–109
8. Palmer I. The mechanism and treatment of fractures of the calcaneus. *J Bone Joint Surg [Am]* **1948**;30(1):2–8
9. Essex-Lopresti P. Fractures of the os calcis. The mechanism, reduction technique and results in fractures of the os calcis. *Br J Surg* **1952**;39:395–419
10. Burman M. Stenosing tendovaginitis of the foot and ankle. *Arch Surg* **1953**;67:686–698
11. Trevino S, Gould N, Korson R. Surgical treatment of stenosing tenosynovitis at the ankle. *Foot Ankle* **1981**;2(1):37–45
12. Jones E. Operative treatment of chronic dislocation of the peroneal tendons. *J Bone Joint Surg* **1932**;14:574–576
13. Mortiz JR. Ski injuries. *Am J Surg* **1959**;98:493–505
14. Murr S. Dislocation of the peroneal tendons with marginal fracture of the lateral malleolus. *J Bone Joint Surg [Br]* **1961**;43:563–565
15. Marti R. Dislocation of the peroneal tendons. *Am J Sports Med* **1977**;5(1):19–22
16. McLaughlin HL. Treatment of late complications after os calcis fractures. *Clin Orthop* **1983**;30:111–115
17. Beltran J, Noto AM, Mosure JC, Shamam OM, Weiss KL, Zueller WA. Ankle: surface coil MR imaging at 1.5 T. *Radiology* **1986**;161:203–209
18. Rosenberg ZS, Feldman F, Singson RD. Peroneal tendon injuries: CT analysis. *Radiology* **1986**;161:743–748
19. Guyer BH, Levinsohn EM, Frederickson BE, Bailey GL, Formikell M. Computed tomography of calcaneal fractures: anatomy, pathology, dosimetry, and clinical relevance. *AJR* **1985**;145:911–919
20. Heger L, Wulff K, Seddiqi MSA. Computed tomography of calcaneal fractures. *AJR* **1985**;145:131–137
21. Seltzer SE, Weissman BN, Braunstein EM, Adams DF, Thomas WH. Computed tomography of the hind foot. *J Comput Assist Tomogr* **1984**;8(3):488–497
22. Warwick R, Williams PL. *Gray's anatomy*, 35th ed. Philadelphia: Saunders, **1973**:573–579
23. Slatis P, Kiviluoto O, Santavirta S, Laasonen EM. Fractures of the calcaneum. *J Trauma* **1979**;19:939–943
24. Lindsay WRN, Dewar FP. Fractures of the os calcis. *Am J Surg* **1958**;95:555–576
25. Heckman JD. Fractures and dislocations of the foot. In: Rockwood CA, Green DR, eds. *Fractures in adults*, 2d ed. Philadelphia: Lippincott, **1975**:1760–1789
26. Gilula LA, Oloff L, Caputi R, Destouet JM, Jacobs A, Solomon M. Ankle tenography: a key to unexplained symptomatology. *Radiology* **1984**;151:581–587

Book Reviews

Renal Sonography, 2nd ed. By Francis S. Weill, Edmond Bihr, Paul Rohmer, and Francois Zeltner. Berlin: Springer-Verlag, 208 pp., 1986. $95

This second edition follows *Atlas ot Ultrasonic Radiography* by these authors, published in 1973, and represents the cumulative experience of 18 years. Most of the text concerns the kidney, but sections also deal with the retroperitoneum and the lower urinary tract. Chapters cover echoanatomy: tissue echo patterns, examination techniques, hydronephrosis, renal cysts, renal tumors, evaluation of tumoral spread, the retroperitoneal space, infections and inflammatory processes, renal trauma and juxtarenal collections, adrenals, and lower urinary tract. A short chapter addresses sonographic differential diagnosis and diagnostic policies in synoptic form based on the sonographic appearances. The technique of renal sonography is extensively described, as are the pitfalls and artifacts that may be observed. Throughout this book renal sonography is placed in the context of addressing a clinical finding or problem, with the sonographic examination usually being the primary radiologic imaging procedure. Although the IV urogram may often be the initial procedure ordered, many (like these authors) would argue that sonography should be the primary imaging procedure and that the sonographic findings should dictate what other examinations (if any) are necessary. The general layout of the text is excellent, and it is easy to read. The authors' unique humor enlivens the text to emphasize certain fundamentals. Useful diagrams of excellent quality are included. Numerous well-labeled sonograms are included, generally of high quality, although some of the illustrations are too small. In very few cases are any urographic or CT images included with these sonograms. No reference is made to the use of nuclide studies in the evaluation of any of the disorders discussed. The section on renal transplantation could well have been expanded to encompass the increasing role of sonography in this field. These, however, are minor criticisms. Overall, this is a most useful textbook for the radiologist and full of practical information. Beginning sonographers will benefit from the inclusion of considerable basic and technical details while the experienced radiologist can improve his diagnostic skills with this practical approach. Urologists, nephrologists, and internists will also find much of interest herein.

Noel K. Allan
Northwest Diagnostic Imaging
Bremerton, WA 98310

The Radiologic Clinics of North America. Interventional Uroradiology. Guest editor: Erich K. Lang. Philadelphia: Saunders, December 1986;24(4). By subscription, 4 issues annually, $60; single issue: $22.95

A good book is informative, interesting, easy to read, well produced and illustrated, and available at a reasonable price. This issue of *Radiologic Clinics of North America* fulfills these criteria nicely. The editor has produced a multiauthored book with 24 contributors representing 10 major institutions. This issue, which is devoted to interventional techniques in uroradiology, has 14 chapters that include discussions on renal cyst management, drainage of abscesses and urinomas, antegrade pyelography, antegrade maneuvers in the ureter including stent applications and dilatation, renal calculus management by percutaneous techniques and extracorporeal shock-wave lithotripsy, and procedures involving the lower urinary tract. In addition, there are selected chapters on transluminal renal angioplasty, embolization techniques, and renal neoplasm evaluation.

The value of the book to radiologists, urologists, and residents in training from both fields is that each chapter is concise yet contains a wealth of facts and helpful hints for success. Indications, radiographic features, patient selection, techniques, results, and complications are presented in a manner to benefit both a novice and an experienced radiologist. The chapter material overlaps anatomic areas appropriately and the various approaches to similar problems in different regions enhance the quality of the book. Images and drawings illustrate appropriately the principles and clinical problems.

The excellent quality of the contents of this book and its readable size and low price make it a recommended purchase for all radiologists doing interventional procedures in the genitourinary tract. It will also be a valuable book for urologists and urology residents, since it concisely presents newer and innovative treatment options now available to their patients.

William H. Bush
Virginia Mason Clinic
Seattle, WA 98111-0900

Sonographic Evaluation of Renal Stones Treated by Extracorporeal Shock-Wave Lithotripsy

Bruce R. Baumgartner[1]
Harvey V. Steinberg[1]
Samuel S. Ambrose[2]
Kenneth N. Walton[2]
Michael E. Bernardino[1]

Real-time sonography was performed on 94 patients the day before and at 24 and 48 hr after extracorporeal shock-wave lithotripsy (ESWL) therapy. The ability of sonography to detect renal stones before ESWL, changes in the calculi after ESWL, and the occurrence of pre- and post-ESWL hydronephrosis was evaluated. Abdominal radiographs and linear renal tomography were used as the standard of comparison. Six other patients had sonography only either before or after ESWL. One hundred patients had a total 105 kidneys treated; 18 kidneys with more than three stones were not included. The other 87 kidneys had 102 stones evaluated by sonography before having ESWL; 66 stones (65%) were identified and 36 were not. Of those calculi not seen, 10 were ≤5 mm in diameter. Nineteen of the other 26 stones were in the ureter or at the ureteropelvic junction. Comparison of sonograms of 80 kidneys obtained before and after ESWL revealed no change in 37 (46%), more stones or fragments detected in 23 (29%), fewer stones or a change in location in 12 (15%), and an apparent decrease in the size of the original stone in eight (10%). Hydronephrosis was detected by pre-ESWL sonography in 16 kidneys (20%) and was noted to develop after ESWL in 20 (31%) of the 64 other kidneys.

These results indicate that the ability of sonography to detect renal calculi is related not only to stone size but also to location. The clinical significance of pre- and post-ESWL hydronephrosis found by sonography must be considered in conjunction with the patient's symptoms, laboratory data, and other radiographic studies. Therefore, the routine use of sonography in the post-ESWL patient does not seem warranted.

Sonography has been considered an excellent diagnostic imaging technique for the detection of both opaque and nonopaque renal calculi [1–5]. The sonographic diagnosis of a calculus is usually based on the demonstration of a highly echogenic focus with an associated acoustic shadow. Banner [6] has stated that stones as small as 5 mm can be reliably detected in this manner. The recent development of extracorporeal shock-wave lithotripsy (ESWL) has resulted in an increased number of patients being treated for stone disease; the techniques of this new therapy have been discussed elsewhere [7–10]. The purpose of this report is to demonstrate the accuracy of sonography in detecting renal stones before ESWL as well as changes occurring after ESWL. The occurrence of pre- and postlithotripsy hydronephrosis as well as complications after ESWL are also reported.

Materials and Methods

Sonography was performed using a Philips SDU 3000 real-time scanner with either a 3.5- or 5.0-MHz transducer. Of 100 consecutive patients undergoing ESWL, 94 were studied the day before treatment and at 24 and 48 hr after the treatment. Four additional patients had only post-ESWL sonography, and two other patients had only pre-ESWL sonography. The images were evaluated with the knowledge that each patient was being examined before or after ESWL, but without other radiographic studies for comparison. The diagnosis of a calculus was made when a highly echogenic focus was detected within the collecting system associated with distal acoustic shadowing. In a few cases, the calculus was identified as an

Received January 30, 1987; accepted after revision March 17, 1987.

[1] Department of Radiology, Emory University School of Medicine, Atlanta, GA 30322. Address reprint requests to B. R. Baumgartner.

[2] Department of Surgery, Division of Urology, Emory University School of Medicine, Atlanta, GA 30322.

AJR 149:131–135, July 1987
0361–803X/87/1491–0131
© American Roentgen Ray Society

echogenic focus without shadowing (Fig. 1).

The findings were compared with abdominal radiographs and renal linear tomography obtained before and after ESWL. These 100 patients (65 men, 35 women) had 105 kidneys treated; 18 kidneys with more than three stones were not included in the study. The other 87 kidneys had 111 stones distributed as follows: one stone in 65, two stones in 20, and three stones in two patients. Three pairs of adjacent stones were considered as one calculus for size determination and sonographic evaluation, thereby resulting in a total of 108 calculi studied. All stones were radiopaque except seven. Pre-ESWL sonograms were not available for six stones in five kidneys. Three stones in two kidneys had no post-ESWL sonograms.

The size of each calculus was determined on the abdominal radiograph when possible. The measurement was made on the linear tomogram only when the stone was not localized on the abdominal radiograph. A contrast medium was administered by IV or retrograde route for nonopaque stones. The 102 calculi with comparative pre-ESWL sonograms were grouped by size according to longest diameter as follows: ≤5 mm (10), 6–10 mm (45), 11–15 mm (22), 16–20 mm (15), and >20 mm, including staghorn calculi (10).

Results

Of the 102 calculi seen on conventional radiography done with or without contrast medium and studied by sonography before ESWL, 66 (65%) were seen and 36 were not (Table 1). Of those not seen, 10 were less than or equal to 5 mm in diameter, representing all calculi in that size group. Twenty-four stones in the 6–15 mm range were undetected by sonography; of these, 19 were in the ureter or at the ureteropelvic junction (UPJ) and only five were in a calyx. Of the 25 stones 16–20 mm and larger, only two were undetected by sonography. One was a partial staghorn calculus in the lower pole, and the other was a large, ovoid, nonopaque calculus in the renal pelvis (Fig. 2). Of the seven nonopaque calculi, five were detected by sonography. These included two calculi that were unsuspected on previous radiographic evaluation but that were subsequently confirmed by contrast studies.

Comparison of the sonograms of calculi in 80 kidneys before and after ESWL revealed no change in the apparent size, location, or number of calculi in 37 kidneys (46%). An increase in the number of stones or fragments was seen in 23 kidneys (29%), while a decrease in the number of stones was identified in eight (10%); a decrease in size of the original echogenic focus was noted in eight kidneys (10%), and a change in location was apparent in four kidneys (5%).

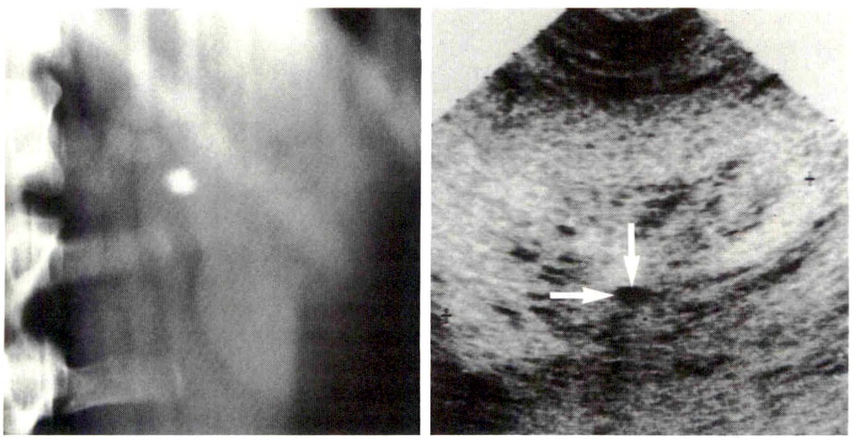
Hydronephrosis was detected by sonography before ESWL in 16 kidneys (Fig. 3A). Fourteen of these kidneys had calculi in the renal pelvis (two), UPJ (five), or ureter (seven), and only two were located in the calyx. After ESWL, the hydronephrosis did not change in seven; it decreased in three, resolved in five, and increased in only one. Hydronephrosis was noted on sonography to develop after ESWL in 20 (31%) of the other 64 kidneys studied before and after ESWL. The distribution of the calculi by size in these 20 kidneys is as follows: ≤10 mm (five), 11–15 mm (seven), 16–20 mm (five), and >20 mm (three). Thus, 19% (5/27) of kidneys with calculi ≤10 mm in size developed hydronephrosis, while 41% (7/17), 42% (5/12), and 38% (3/8) of kidneys in each group of larger stones developed hydronephrosis after ESWL.

Other complications of ESWL treatment were detected by sonography in only two (3%) of the 80 kidneys studied before and after ESWL. Sonography detected an intrarenal fluid collection with debris compatible with hematoma in one patient, while the other was found to have a new perinephric fluid collection after lithotripsy (Fig. 3B).

TABLE 1: Sonography of Renal Calculi Before ESWL

Size (mm)	Stones Detected (66)	Stones Not Detected (36)			
		Calyx or Pelvis	UPJ	Ureter	Total
≤5	0	9	0	1	10
6–10	26	4	8	7	19
11–15	17	1	2	2	5
16–20	15	0	0	0	0
>20	8	2	0	0	2

Note.—ESWL = extracorporeal shock-wave lithotripsy; UPJ = ureteropelvic junction.



A B

Fig. 1.—Stone calculi may be detected without acoustic shadowing.

***A*, Pre-ESWL tomogram. A densely opaque calculus is noted in left renal pelvis near ureteropelvic junction.**

***B*, Pre-ESWL sonogram. Sagittal image of same left kidney reveals calculus delineated as an echogenic focus (*arrows*), although no shadowing is apparent.**

Discussion

Sonography is extremely useful in the detection of both opaque and nonopaque renal calculi [1–5] and was initially investigated as the imaging technique for ESWL therapy [9]. The detection of calculi is enhanced by the presence of acoustic shadowing. Stone size has been reported to be the most important variable in the production of this acoustic shadowing. The location of the calculus (amount of intervening tissue and the focal zone placement) also affect shadow-

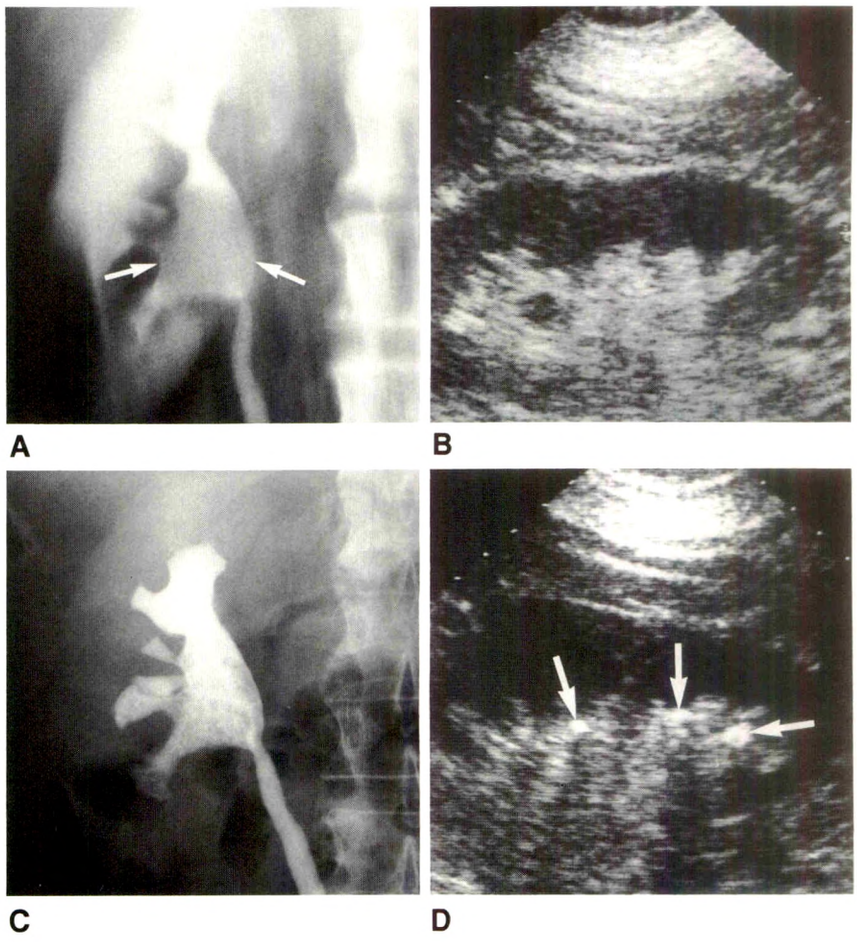


Fig. 2.—Even large calculi may not be delineated by sonography.

***A*, Pre-ESWL IV pyelogram. A 40 × 30 mm nonopaque calculus (*arrows*) is seen in right renal pelvis.**

***B*, Pre-ESWL sonogram. Sagittal image of same kidney shows no hyperechoic focus and no acoustic shadowing. Stone, pelvis, and peripelvic fat are of equal echogenicity.**

***C*, Post-ESWL retrograde pyelogram. Marked fragmentation of calculus has occurred with distribution of particles in calyces and renal pelvis.**

***D*, Post-ESWL sonogram. Sagittal image of right kidney now reveals several echogenic foci (*arrows*) with acoustic shadowing from stone fragments.**

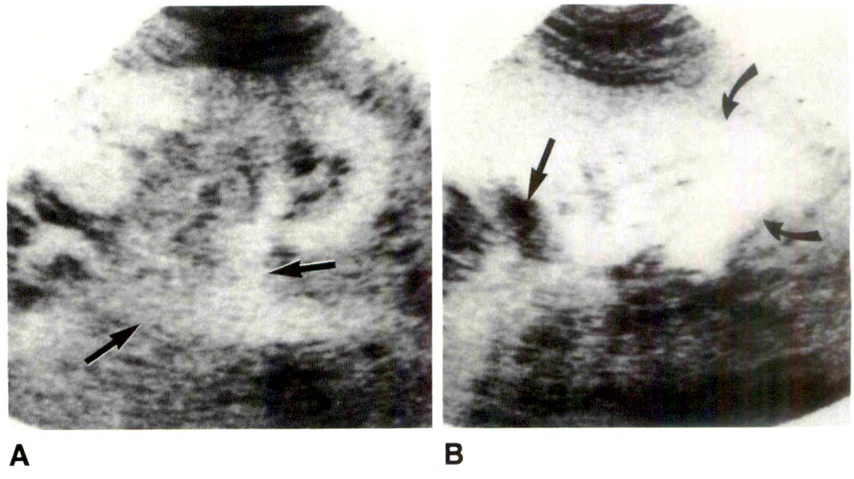


Fig. 3.—Complications were rarely identified with sonography after ESWL.

***A*, Pre-ESWL sonogram. Sagittal image of left kidney shows mild pelvic dilatation (*arrows*). No calculus is identified.**

***B*, Post-ESWL sonogram. Sagittal image of same left kidney reveals resolution of hydronephrosis with development of a small fluid collection (*curved arrows*) adjacent to lower pole. A fragment of calculus (*arrow*) is now noted in renal pelvis with acoustic shadowing.**

ing. The chemical composition of the calculi does not seem to be a contributing factor [11].

In our series of 102 calculi, 36 (35%) were not detected by sonography. It would seem that a large number of stones were missed by sonography, until we examine their size and location. Calculi ≤5 mm in diameter account for 28% of the undetected stones. Of the 26 stones >5 mm that were not detected, only seven were within a calyx or the renal pelvis. Ninety percent of stones >5 mm within a calyx or renal pelvis were delineated by sonography. This is similar to a recent report that found that sonography detected 90% of stones 4–40 mm in diameter in 100 random patients with opaque renal or upper ureteral calculi shown by abdominal radiography [12]. The other 19 calculi not detected by sonography were in the UPJ or were located more distally in the ureter. In the nondistended urinary tract, diagnosis of a calculus is usually dependent on the identification of an acoustic shadow [11]. Urinary calculi outside the kidney are more difficult to localize. Ureteral calculi may be shown more easily when hydronephrosis and ureteral dilatation are present to the level of the stone [13], assuming that proper techniques are used and that there is no intervening intestinal gas.

Seven nonopaque calculi, all >10 mm, were included in the study. Five (71%) of these seven were detected by sonography. The other two were in the renal pelvis or a calyx. In two patients, a nonopaque stone that was not suspected prior to sonography was demonstrated and subsequently was treated by ESWL. Of note is the 40 × 30 mm nonopaque calculus filling the renal pelvis that was not shown by sonography (Figs. 2A and 2B). The explanation for this may be related to the position of the calculus relative to the focal zone of the transducer, and the fact that the echogenicity of the stone was similar to that of the surrounding collecting system and renal sinus fat. Additional careful scanning with the same or different sonographic equipment probably could have revealed some acoustic shadowing.

Pre- and post-ESWL comparison of calculi by sonography did not result in a significant alteration of the subsequent therapeutic regimen. The findings by tomography after lithotripsy were more useful in evaluating the degree of stone fragmentation that had occurred whether or not there was a sonographic change in the size, location, or number of echogenic foci in the kidney (Fig. 4). No change was seen in these parameters in 46% of the sonographic studies, despite comparative radiographic evaluation revealing various degrees of fragmentation of the calculi. Although stone size is an important factor for the delineation of acoustic shadowing [11] and stone detection, the amount of shadowing is not necessarily related to the size of the stone fragments after ESWL. The multiple small fragments often layer together and present multiple impedance interfaces that may cause stronger acoustic shadows than the original calculus [12]. Only when the size, number, and amount of shadowing of the treated stones decrease by sonography does that technique become useful for following the patient's post-ESWL course as compared with abdominal radiography.

Hydronephrosis was detected by sonography before ESWL in only 16 patients. It is not surprising that 14 of these kidneys had calculi in the renal pelvis, UPJ, or ureter; the hydronephrosis either did not change, decreased, or resolved in virtually all of these patients after ESWL. In many of these patients, fragmentation of a partially obstructing calculus likely resulted in the improvement of the degree of hydronephrosis. Hydronephrosis developed after lithotripsy in 31% of the other kidneys; the likelihood of this occurring was greater when a larger volume of stones was present before therapy, since

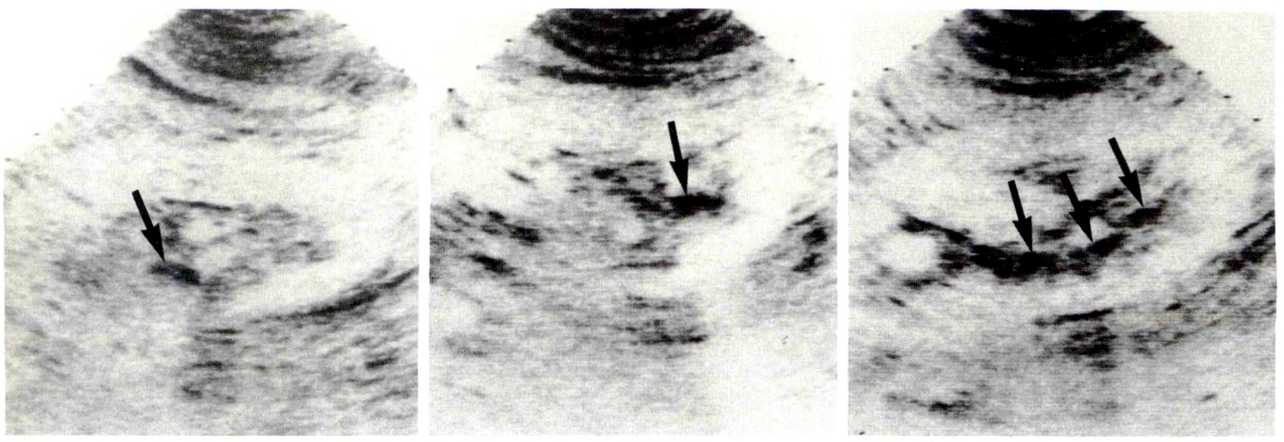


Fig. 4.—Although excellent fragmentation was shown by tomography in this patient, sonography alone does not define the size of residual particles that are clustered together.

***A*, Pre-ESWL sonogram. Sagittal image of left kidney shows a solitary calculus in renal pelvis (*arrow*) with shadowing.**

***B*, Post-ESWL sonogram. Sagittal image of left kidney now reveals an echogenic focus (*arrow*) in lower pole that is the same size as the original stone but with more prominent shadowing.**

***C*, Post-ESWL sonogram. Additional stone fragments (*arrows*) are also seen elsewhere in kidney.**

hydronephrosis developed twice as often in kidneys with larger stones. Many kidneys, even those with large calculi, did not develop hydronephrosis detected by sonography within 48 hr after ESWL. Postlithotripsy interventional therapy is usually based on clinical signs and symptoms, laboratory data, and the apparent fragmentation of the calculi and distribution of the particles as determined by conventional radiography. Rarely are sonographic findings of hydronephrosis the primary reason for additional treatment or intervention.

The incidence of hematoma or perirenal fluid collection detected by sonography after lithotripsy was only 3%. Our recent report noted the presence of small perinephric fluid collections in 25% of patients studied after ESWL by MR imaging, which may be a more sensitive technique than sonography for these findings [14].

In conclusion, the detection of urinary calculi by sonography in this study is related not only to the size of the stone but also to its location. The use of sonography before ESWL in patients with nonopaque calculi may be helpful in detecting additional, unsuspected stones. Furthermore, the variable sonographic findings after ESWL as compared with findings of renal tomography indicate that the latter is more useful in evaluating the effectiveness of shock-wave therapy. The significance of pre- and post-ESWL hydronephrosis must be considered in conjunction with the clinical picture and other radiographic studies. Also, the sonographic delineation of significant complications after ESWL is too infrequent to justify the routine use of sonography for their detection.

REFERENCES

1. Edell S, Zegal H. Ultrasonic evaluation of renal calculi. *AJR* **1978**;130:261–263
2. Amis ES, Hartman DS. Renal ultrasonography 1984: a practical overview. *Radiol Clin North Am* **1984**;22:315–332
3. Brennan RE, Curtis JA, Kurtz AB, Dalton JR. Use of tomography and ultrasound in the diagnosis of non-opaque renal calculi. *JAMA* **1980**;244:594–596
4. Jeffrey RB, Federle MP. CT and ultrasonography of acute renal abnormalities. *Radiol Clin North Am* **1983**;21:515–525
5. Pollack HM, Arger PH, Goldberg BB, Mulholland SG. Ultrasonic detection of non-opaque renal calculi. *Radiology* **1978**;127:233–237
6. Banner MP. Nephrocalcinosis and stone disease. In: Taveras JM, ed. *Radiology: diagnosis-imaging-intervention*. Philadelphia: Lippincott, **1986**
7. Chaussy CH, Schmiedt E, Jocham D, et al. First clinical experience with extracorporeally induced destruction of kidney stones by shock waves. *J Urol* **1982**;127:417–420
8. Chaussy CH, Schmiedt E. Shock wave treatment for stones in the upper urinary tract. *Urol Clin North Am* **1983**;10:743–750
9. Chaussy CH, Schmiedt E, Jocham D. Extracorporeal shock wave lithotripsy for treatment of urolithiasis. *Urology* **1984**;23:59–66
10. Chaussy C, Schmiedt E. Extracorpeal shock wave lithotripsy (ESWL) for kidney stones. An alternative to surgery? *Urol Radiol* **1984**;6:80–87.
11. King W, Kimme-Smith C, Winter J. Renal stone shadowing: an investigation of contributing factors. *Radiology* **1985**;154:191–196
12. Yoder IC, Chafey JH, Pfister RC, Papanicolaou N. Evaluation of renal stones by abdominal radiography and ultrasonography in extracorporeal shock wave lithotripsy. Presented at the annual meeting of the Society of Uroradiology, St. Thomas, U.S. Virgin Islands, March **1985**
13. Erwin BC, Carroll BA, Sommer FG. Renal colic: the role of ultrasound in initial evaluation. *Radiology* **1984**;152:147–150
14. Baumgartner BR, Dickey KW, Ambrose SS, Walton KN, Nelson RC, Bernardino ME. Kidney changes after extracorporeal shock wave lithotripsy: appearance on MR imaging. *Radiology* **1987**;163:531–534

Book Review

Magnetic Resonance of the Reproductive System. By Shirley McCarthy and Florence Haseltine. Thorofare, NJ: Slack, 230 pp., 1987. $49.50

This book originated from a workshop on "The Evaluation of Reproductive Processes by Magnetic Resonance Imaging and Spectroscopy" held at the Center for Population Research at the National Institutes of Health in May 1976. The 17 contributors consist primarily of scientists involved in basic research dealing with the reproductive system. A number of fields are represented, including biochemistry, biophysics, physiology, spectroscopy, obstetrics and gynecology, zoology, pathology, physics, and radiology. A sampling of the hopes for clinical MR is provided by individuals considered to be experts from a wide range of fields. Because of the wide divergence of interests, the book is not a well-coordinated text on the clinical use of pelvic MR.

The physics of MR is reviewed in the introductory two chapters. The description of the physics is reasonably well written but is brief and not well coordinated with the rest of the book. Some of the other chapters repeat similar information. Spectroscopy is reviewed briefly in chapters 3 and 4. Biohazards are reviewed in the last chapter. The remainder of the book is devoted to selected topics related to each author's particular area of expertise. Many of the chapters suffer from the lack of sufficient scientific data. A few of the chapters, however, provide excellent data and information not currently available in the MR literature. These chapters may provide additional insights for other workers in the field. As was the purpose of the conference, exposure of preliminary data aids in stimulating further research in the field. The chapters on ^{31}P spectroscopy of the breast, spectroscopy of reproductive organs and associated malignancies, uterine bioenergetics by ^{31}P spectroscopy, and MR in egg metabolism and lipid metabolism in semen are among the most useful, especially to those interested in spectroscopy. One article describes MR microscopy and demonstrates its use in developing live chick embryo. Three chapters deal with imaging of the uterus, uterus and ovaries, and scrotum. These chapters are short reviews of the MR imaging applications. The imaging chapters suffer from brevity and poor image reproductions. In the short time since the conference in the spring of 1986, MR imaging of the reproductive system has progressed dramatically in terms of image quality and clinical experience. Because of the fast progression of pelvic imaging, the imaging chapters are somewhat dated.

The book is recommended for researchers in MR spectroscopy and reproductive biochemistry. It may be of interest to others who are intensely involved in MR imaging and who wish to increase their knowledge of related applications. The book is not a textbook on imaging applications and is not recommended as a basic reference for students, residents, or radiologists.

The editorial quality is flawed by a number of misprinted words and equations. The quality of the image reproduction is poor. The book does have a hard cover but the binding is not cloth. Although not a radiology text, there is a role in radiology for a book that collects a set of fast-breaking research topics and publishes these as a forum for enhancing the research effort. Unfortunately, at $49.50 a copy, this book is not likely to sit on many radiologists' shelves.

Steven Harms
Baylor University Medical Center
Dallax, TX 75246

Case Report

Seminal Vesicle Abscess After Vasectomy: Evaluation by Transrectal Sonography and CT

Ronald J. Zagoria,[1,2] Nicholas Papanicolaou,[1] Richard C. Pfister,[1] Susan A. Stafford,[1] and Hugh H. Young II[3]

Seminal vesicle disease is often difficult to diagnose. While isolated bacterial infection of these structures appears to be rare, unrecognized infection involving the seminal vesicles may occur in association with prostatitis in 25% of patients [1]. Seminal vesiculography can show most structural abnormalities, but there is the potential risk of resultant stenosis of the vas deferens at the puncture site [2, 3]. We encountered a case in which a seminal vesicle abscess developed after vasectomy, and the abscess was diagnosed by transrectal sonography and CT and confirmed by endoscopic surgery.

Case Report

A 43-year-old man was transferred to our institution for further evaluation of a pelvic infection refractory to antibiotic (gentamicin, carbenicillin) therapy. Three weeks after a vasectomy the patient developed hematuria, dysuria, fever, and purulent drainage from the scrotal incision site. A CT scan at the referring hospital showed a mass, presumed to be an abscess, arising from the prostatic region (Fig. 1A).

On admission to this institution a transrectal sonogram was performed, using a General Electric RT 3600 scanner with a 5-MHz linear-array transrectal transducer. This study revealed a thick-walled 5-cm lesion with complex echotexture in a greatly enlarged left seminal vesicle consistent with an abscess (Fig. 1B). Endoscopy was performed and approximately 40 ml of purulent material were evacuated from the left seminal vesicle by a transurethral approach. *Staphylococcus aureus* was cultured from this exudate. The patient improved rapidly. A follow-up transrectal sonogram performed 2 months later was normal (Fig. 1C).

Discussion

Over 500,000 vasectomies are performed each year for sterilization. Complications have included superficial wound infection, postoperative epididymitis, vasocutaneous fistula, spermatic granuloma, arteriovenous fistula, and hematoma [3, 4].

CT and transrectal sonography can be useful in the evaluation and localization of lower genitourinary tract disease. CT of the pelvis remains helpful in the recognition of many seminal vesicle abnormalities; however, determining the origin of the disease using only the axial plane of imaging is often difficult. In addition, CT beam-hardening artifacts caused by the bony pelvis and a contrast-filled bladder may obscure detail of abnormalities in this region.

Transrectal sonography allows imaging in numerous longitudinal and/or transverse planes with good resolution of the seminal vesicles [5], prostate [6], and bladder neck [7]. Since transrectal sonography has the added advantage of not using ionizing radiation, it is an excellent technique for suspected disorders of the seminal vesicles. In our case, although the CT scan clearly showed a deep pelvic mass, the exact origin of the abscess was ascertained by transrectal sonography as has been previously reported [5].

Received February 13, 1987; accepted after revision March 17, 1987.
[1] Department of Radiology, Massachusetts General Hospital and Harvard Medical School, Boston, MA 02114. Address reprint requests to R. C. Pfister.
[2] Department of Radiology, Bowman Gray School of Medicine, Winston-Salem, NC 27103.
[3] Department of Urology, Massachusetts General Hospital and Harvard Medical School, Boston, MA 02114.

AJR **149:137–138, July 1987** 0361–803X/87/1491–0137 © American Roentgen Ray Society

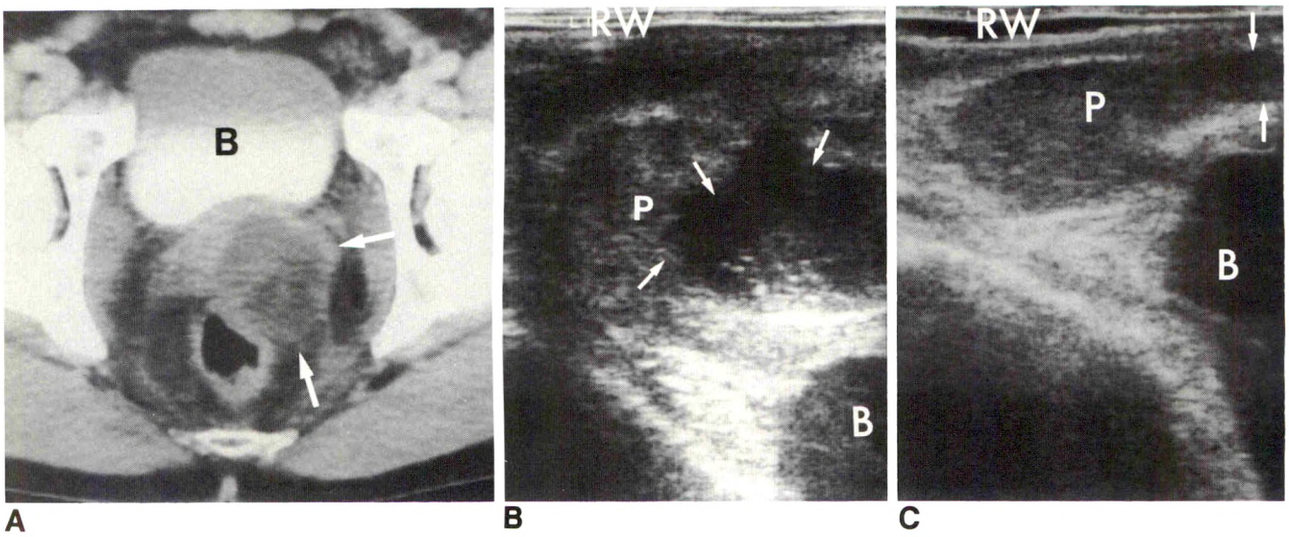


Fig. 1.—Left seminal vesicle abscess after vasectomy.

***A*, CT scan shows a large mass with thick wall and low density center (*arrows*) to left of midline behind bladder (B).**

***B*, Transrectal sagittal sonogram shows an enlarged left seminal vesicle (*arrows*) with a thick wall and a hypoechoic center containing echogenic debris. Inferiorly located prostate (P) is not clearly separable from inflamed seminal vesicle. Bladder (B) lies anteriorly and rectal wall (RW) posteriorly.**

***C*, Transrectal sagittal sonogram after transurethral drainage of abscess shows a normal prostate (P) and left seminal vesicle (*arrows*). Bladder (B) and rectal wall (RW) are identified.**

REFERENCES

1. Meares EM Jr. Urinary tract infections in men. In: Harrison JH, Gittes RF, Perlmutter AD, Stamey TA, Walsh PC, eds. *Campbell's urology*. Philadelphia: Saunders, **1978**:509–537
2. Meyer JJ, Hartig PR, Koos GW, McKinley CR. Transrectal seminal vesiculography. *J Urol* **1979**;121(1):129–130
3. Squires JW, Pinch LW. The morbidity of vasectomy. *Surg Gynecol Obstet* **1976**;143:237–240
4. Auman JR. Spermatic cord arteriovenous fistula: an unusual complication of vasectomy. *J Urol* **1985**;134:768
5. Lee SB, Lee F, Solomon MH, Kumasaka GH, Straub WH, McCleary RD. Seminal vesical abscess: diagnosis by transrectal ultrasound. *JCU* **1986**;14:546–549
6. Lee F, Gray JM, McLeary RD, et al. Prostatic evaluation by transrectal sonography. *Radiology* **1986**;158:91–95
7. Perkash I, Friedland GW. Posterior ledge at the bladder neck; crucial diagnostic role of ultrasonography. *Urol Radiol* **1986**;8:175–183

Case Report

Giant Cyst of the Seminal Vesicle with Renal Agenesis

John A. Heaney,[1,2] Richard C. Pfister,[3] and Edwin M. Meares, Jr.[1]

Cysts of the seminal vesicle associated with ipsilateral renal agenesis are rare [1–5]. Usually, the cysts are 5 cm or less in diameter and are either asymptomatic or present during early adulthood with symptoms related to voiding or epididymitis. Infrequently, cysts larger than 12 cm occur; such giant cysts can result in bladder or colon obstruction as we observed in two recent patients. These cases were evaluated by cross-sectional imaging (sonography and CT) and needle puncture, and one is described here in detail.

Case Report

A 30-year-old man presented with a 3-week history of cramping left suprapubic and flank pain that occurred upon defecation. A 15-cm smooth, rubbery-firm, spherical, nontender suprapubic mass was palpable bimanually. Rectally, the prostate could not be distinguished from the mass.

An abdominal radiograph revealed peripherally located, curvilinear calcification in the mass (Fig. 1A). Urography showed a hypertrophied left kidney (17.5 cm) with mild hydronephrosis and hydroureter to the ureterovesical junction; no right kidney was seen. Retrograde urethrocystography showed extrinsic compression of the bladder and a normal urethra (Fig. 1B). A 20-gauge needle was passed percutaneously into the mass, and viscous brown liquid was aspirated. A contrast medium was introduced revealing a cyst adjacent to the bladder base. CT confirmed the presence of a thick-walled cystic structure (17 H) displacing the bladder (Fig. 1C). Neither seminal vesicle was identified.

At resection, the right vas deferens was found to enter the mass, but neither the right ureter nor the right kidney was identified. Histopathologic examination confirmed the diagnosis of seminal vesicle cyst by its epithelial membrane and the presence of degenerating spermatids.

Discussion

Although congenital anomalies of the urinary tract are more common in men than women (1.5–2.0:1), anomalies of the reproductive tract are less frequently encountered in men. Genital anomalies with unilateral renal agenesis are found in 12% of men and in 40% of women [1].

An association is made between ipsilateral renal agenesis and cysts of the seminal vesicle because of the common origin of the ureteral bud and seminal vesicle from the mesonephric (Wolffian) duct. With isolated failure of development of the ureteral bud, renal agenesis ensues, but the genital tract is unaffected. However, maldevelopment of the mesonephric duct in the 12th gestational week affects the ipsilateral seminal vesicle and vas deferens, as well as the ureter and kidney [3, 4].

Cysts of the seminal vesicle are uncommon, with fewer than 100 cases reported. Approximately two-thirds (68%) of them are associated with ipsilateral renal agenesis [1]. The majority of seminal vesicle cysts are small (<5 cm). Most are either asymptomatic or present clinically during the years of maximal sexual activity. The clinical presentation is either dysuria or actual (or simulated) infection of the epididymis, prostate, or the cyst itself. In most instances, partial or complete ejaculatory duct obstruction with retention of seminal fluid containing spermatozoa is present.

Both congenital factors and postinfection fibrosis have been suggested as causes. However, the larger cysts (>12 cm), those associated with ipsilateral renal agenesis and often with atresia of the ureter, are congenital. Of the five patients with seminal vesicle cysts encountered by the authors in the last

Received March 3, 1986; accepted after revision February 13, 1987.

[1] Department of Urology, New England Medical Center, Tufts University, 171 Harrison Ave., Boston, MA 02114.
[2] Present address: Section of Urology, Department of Surgery, Dartmouth-Hitchcock Medical Center, Hanover, NH 03756.
[3] Department of Radiology, Massachusetts General Hospital and Harvard Medical School, Boston, MA 02114. Address reprint requests to R. C. Pfister, Dept. of Radiology, Massachusetts General Hospital, Boston, MA 02114.

AJR **149:139–140, July 1987** 0361–803X/87/1491–0139 © American Roentgen Ray Society

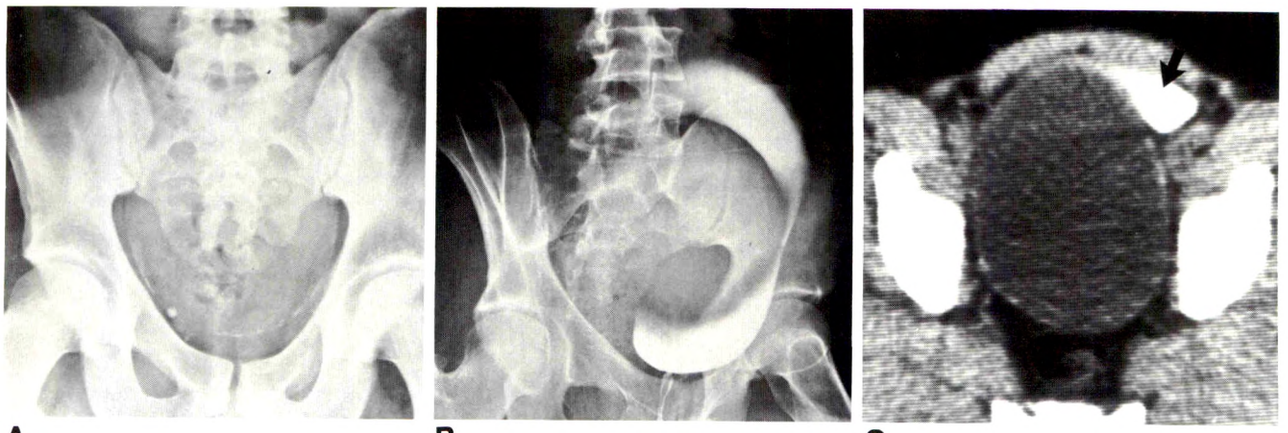


Fig. 1.—*A*, Abdominal radiograph shows peripheral curvilinear calcification in large pelvic mass. *B*, Retrograde urethrography shows mass displacing bladder to left. *C*, CT shows cyst with thick calcified wall occupying pelvis and displacing bladder (*arrow*) anteriorly and to the left.

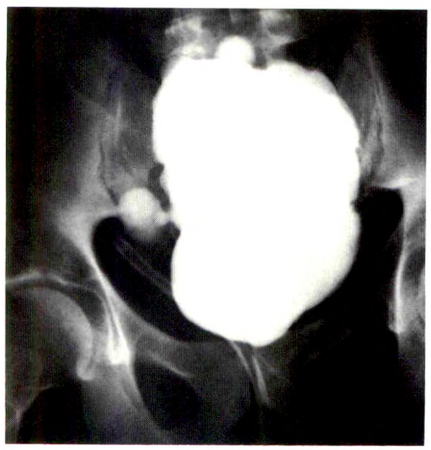


Fig. 2.—Cystogram after percutaneous aspiration and introduction of contrast medium into left seminal vesicle cyst in another patient. Note urethral-bladder catheter displaced to right.

5 years, two had such giant cysts that they resulted in symptomatic obstruction of bladder outlet and rectum.

Seminal vesicle cysts require differentiation not only from other deep pelvic cysts arising from the genital tract (e.g., prostatic, utricular, and Müllerian) but also from hydronephrotic pelvic kidneys, abscesses, and benign or malignant tumors arising from bladder, rectum, sacrum, spinal cord meninges, and lymph nodes [1, 6]. Urethrography, seminal vesiculography, sonography [6, 7], and CT [2, 5, 6, 8] are useful in this differentiation.

Unilateral renal agenesis may be suspected by urography or scintigraphy. Sonography and particularly CT are useful in excluding a rudimentary or ectopic kidney, as well as ureteroceles within the bladder. Angiography has a lesser role.

Evaluation of pelvic masses in men by sonography may be performed with standard abdominal, transrectal, or intravesical transducers [4, 6]. In general, they permit separation of solid and cystic lesions, unless low-level internal echoes suggest a mixed or complex component [3, 4]. The presence of hemorrhage in the cyst may lead to such confusion.

CT has a definitive role in evaluating a pelvic mass. The identification of one normal and one absent seminal vesicle with an associated thick-walled ipsilateral cystic structure is definitive [2, 5, 6, 8]. In smaller cysts of the seminal vesicle this is expected; however, in giant cysts the anatomy of the prostatic urethra and bladder floor may be so distorted that they cannot be located with certainty by CT. Coronal and sagittal MR imaging may be helpful in such cases [8].

Invasive studies include vasography and percutaneous fine-needle puncture [1]. Both are capable of preoperative confirmation of seminal vesicle cysts. The choice can be directed by the size of the cyst. Needle placement through the anterior abdominal wall or perineum allows aspiration of fluid for chemical analysis, culture, and microscopy for cytology and spermatozoa; only a seminal vesicle cyst will contain spermatozoa. Contrast medium may be introduced to delineate internal architecture and anatomic relationships to adjacent organs, as in both our cases (Fig. 2).

REFERENCES

1. Case records of the Massachusetts General Hospital. Weekly clinicopathological exercises. *N Engl J Med* **1980**;302:1246–1251
2. Lantz E, Berquit TH, Hattery R, Mattson M, Lieber M. Seminal vesical cyst associated with ipsilateral renal agenesis: a case report. *Urol Radiol* **1981**;2:265–266
3. Ejeckam GC, Govatsos S, Lewis AS. Cyst of seminal vesicle associated with ipsilateral renal agenesis. *Urology* **1984**;24:372–374
4. Roehrborn CG, Schneider HJ, Rugendorff EW, Hamann W. Embryological and diagnostic aspects of seminal vesicle cysts associated with upper urinary tract malformation. *J Urol* **1986**;135:1029–1032
5. Kenney PJ, Leeson MD. Congenital anomalies of the seminal vesicles: spectrum of computed tomographic findings. *Radiology* **1983**;149:247–251
6. Raskin MM, Cunningham, JB, Cohen GH. Complimentary role of computed tomography and ultrasound of pelvic masses. *J Comput Tomogr* **1978**;2:221–224
7. Meyer JJ, Hartig PR, Koos GW, McKinley Cr. Transrectal seminal vesiculography. *J Urol* **1979**;121:129–130
8. Kneeland JB, Auh YH, McCarron JP, et al. Computed tomography, sonography, vesiculography and MR imaging of a seminal vesicle cyst. *J Comput Assist Tomogr* **1985**;9:964–966

Midtrimester Screening for Open Neural Tube Defects: Correlation of Sonography with Amniocentesis Results

Karen K. Lindfors[1]
John P. McGahan[1]
Frances P. Tennant[2]
Frederick W. Hanson[2]
John P. Walter[1]

Eight pregnancies with open neural tube defects were detected in 70 midtrimester patients referred for sonography and amniocentesis because of elevated maternal serum alpha-fetoprotein levels. Two cases of anencephaly were detected by sonography, aborted without aminocentesis, and confirmed by pathologic examination. Six cases of open spina bifida were detected through amniocentesis by elevation of alpha-fetoprotein and acetylcholinesterase levels. In only three of these six was the abnormality seen on sonography. All six pregnancies were terminated, and open spina bifida defects were confirmed on pathologic examination. Amniocentesis was 100% sensitive for diagnosis of open spina bifida, while sonography was only 50% sensitive.

Our results indicate that, in patients with elevated serum alpha-fetoprotein and a normal fetal sonogram, amniocentesis should be performed to rule out open spina bifida.

As screening for open neural tube defects through determination of maternal serum alpha-fetoprotein (AFP) becomes more prevalent in this country, an increasing number of patients will be referred for early second trimester fetal sonography. Such sonograms can often determine the cause of the elevated maternal serum AFP, frequently obviating amniocentesis, and can identify conditions such as gastroschisis and omphalocele, which may be surgically correctable. Sonography has also been recommended as a procedure that can identify morphologically normal fetuses in cases of elevated or equivocal amniotic fluid AFP [1, 2].

A statewide maternal serum AFP screening for open neural tube defects began recently in California, and through this program at our institution, we have to date successfully identified with sonography two cases of anencephaly and three cases of open spina bifida. However, three cases of open spina bifida were not diagnosed by sonography but were subsequently detected by amniotic fluid AFP and acetylcholinesterase (AChE) determination. These cases form the basis of this report.

Materials and Methods

From April 1986 through November 1986, 70 pregnant women were referred for early-second-trimester sonography and amniocentesis because of elevated levels of maternal serum AFP. An elevated maternal serum AFP is defined as one that is greater than 2.5 multiples of the mean for menstrual age. The mean maternal serum AFP level is determined by certified laboratories of the state of California. Accurate fetal age was determined by biparietal diameter and femur length in each case. If correlation of the maternal serum AFP level with the correct menstrual age revealed a consistently elevated maternal serum AFP level, a full fetal sonographic examination was performed by a radiologist with expertise in obstetric sonography. Particular attention was given to the cranial bones and intracranial anatomy. The fetal head was examined in the axial plane and in the coronal and/or sagittal plane when possible. The ratio of the lateral ventricular width to the hemispheric width was calculated. The fetal spine was fully examined both in transverse and longitudinal planes. Standard documentation of the remainder of the fetal anatomy was obtained. Examinations were performed with a variety of state-of-the-art real-time scanners including a General

Received February 5, 1987; accepted after revision March 23, 1987.

[1] Department of Diagnostic Radiology, University of California, Davis, Medical Center, Room 109R UCD Professional Bldg., 4301 X St., Sacramento, CA 95817. Address reprint requests to K. K. Lindfors.

[2] Department of Obstetrics and Gynecology, University of California, Davis, Medical Center, Sacramento, CA 95817.

AJR **149:141–145, July 1987**
0361–803X/87/1491–0141
© American Roentgen Ray Society

Electric RT 3000 and an ACUSON-128 (Mountain View, CA) with transducer frequencies of 3.0–5.0 MHz in all cases.

Patients in whom an explanation of the maternal serum AFP levels could not be determined by sonography underwent amniocentesis. The amniotic fluid AFP level was determined by our laboratory. If the amniotic fluid AFP level was elevated, fluid was sent to an independent laboratory (University of California, Los Angeles, Medical Center) for confirmation. In all cases of confirmed elevated amniotic fluid AFP, samples of amniotic fluid were analyzed for the presence of AChE.

Amniotic fluid AFP and AChE levels were correlated with sonographic findings, and patients were then counseled as to the significance of these results and offerred therapeutic options. All patients with fetal open neural tube defects diagnosed by sonography and/or amniocentesis elected to terminate their pregnancies. Fetal pathology was correlated with the results of sonography and amniocentesis.

Results

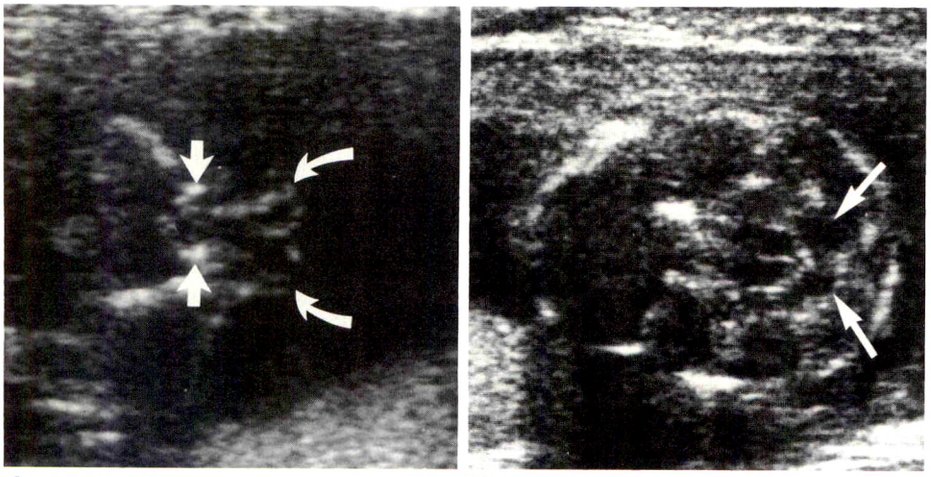
Among the women referred for elevated maternal serum AFP levels, eight cases of neural tube defects were diagnosed. There were two cases of anencephaly. Both were imaged by sonography. One case was accompanied by polyhydramnios. Amniocentesis was not performed in either case. Termination of these two pregnancies and subsequent pathologic examination confirmed the sonographic findings.

Six cases of open spina bifida were found in the examined population. Five cases had amniotic fluid AFP levels that were over 5 multiples of the mean; the sixth case had an amniotic fluid AFP level of 3.86 multiples of the mean. All were positive for AChE.

Three cases of open spina bifida were correctly diagnosed by sonography. The menstrual ages of the fetuses at diagnosis were 16–20 weeks. All were manifested by a divergence of the posterior spinal ossification centers on transverse sonograms of the lumbosacral spine. The sizes of these defects ranged from 0.4 to 1 cm in width and 1 to 2 cm in length. Dorsal sacs representing herniated meninges were seen in two of the three cases as well (Fig. 1). These sacs were 1.5–2.0 cm long and 1.5 cm wide. Associated ventriculomegaly as well as scalloping of the frontal bones ("lemon sign") and obliteration of the cisterna magna with cerebellar compression ("banana sign") indicative of an Arnold-Chiari II malformation [3] were noted in all sonographically identified cases (Fig. 1).

In two of three cases of open spina bifida seen by sonography the diagnosis was made after amniotic fluid AFP and AChE levels were known. In one of these cases the initial sonogram at 17 weeks menstrual age suggested only possible ventriculomegaly (ratio of lateral ventricular width to hemispheric width = 0.56) by biparietal diameter and fetal length [4]. There was slight separation of the medial wall of the ventricle from the choroid plexus (Fig. 2). Compression of the cerebellum was also noted. No spinal abnormality was seen. When the patient returned at 18.5 weeks menstrual age, after the amniocentesis results showed an elevated AFP and a positive AChE, there was definite ventriculomegaly (ratio of lateral ventricular width to hemispheric width = 0.65) by biparietal diameter and femur length. Scalloping of the frontal bones and obliteration of the cisterna magna with cerebellar compression indicating an Arnold-Chiari II malformation also were clearly evident on the second scan. Careful scanning of the spine revealed minimal flaring of the posterior ossification centers at the lower lumbar level (Fig. 2). The pregnancy was terminated, and open spina bifida that was 0.4 cm wide and 1 cm long and did not have an associated dorsal sac was evident on gross inspection at the lower lumbar level. Gross inspection of the brain demonstrated hydrocephalus, but a full examination of the neural structures was not performed.

In the other case of open spina bifida diagnosed by sonography after amniocentesis results were obtained, reexamination was first done on a GE RT 3000 sonographic unit. Ventriculomegaly was noted with obliteration of the cisterna magna and scalloping of the frontal bones. A slight flaring of the posterior ossification centers was detected, but a dorsal sac was not seen. A subsequent sonogram the same day on a computerized unit (ACUSON, Mountain View, CA) clearly showed a flaring of the posterior ossification centers with a



A B

Fig. 1.—Open spina bifida with dorsal sac in 18-week (menstrual age) fetus.

***A*, Transverse sonogram shows flaring of posterior spinal ossification centers (*straight arrows*) of sacrum with associated dorsal sac (*curved arrows*).**

***B*, Axial sonogram of fetal head shows obliteration of cisterna magna with compression of cerebellum (*arrows*).**

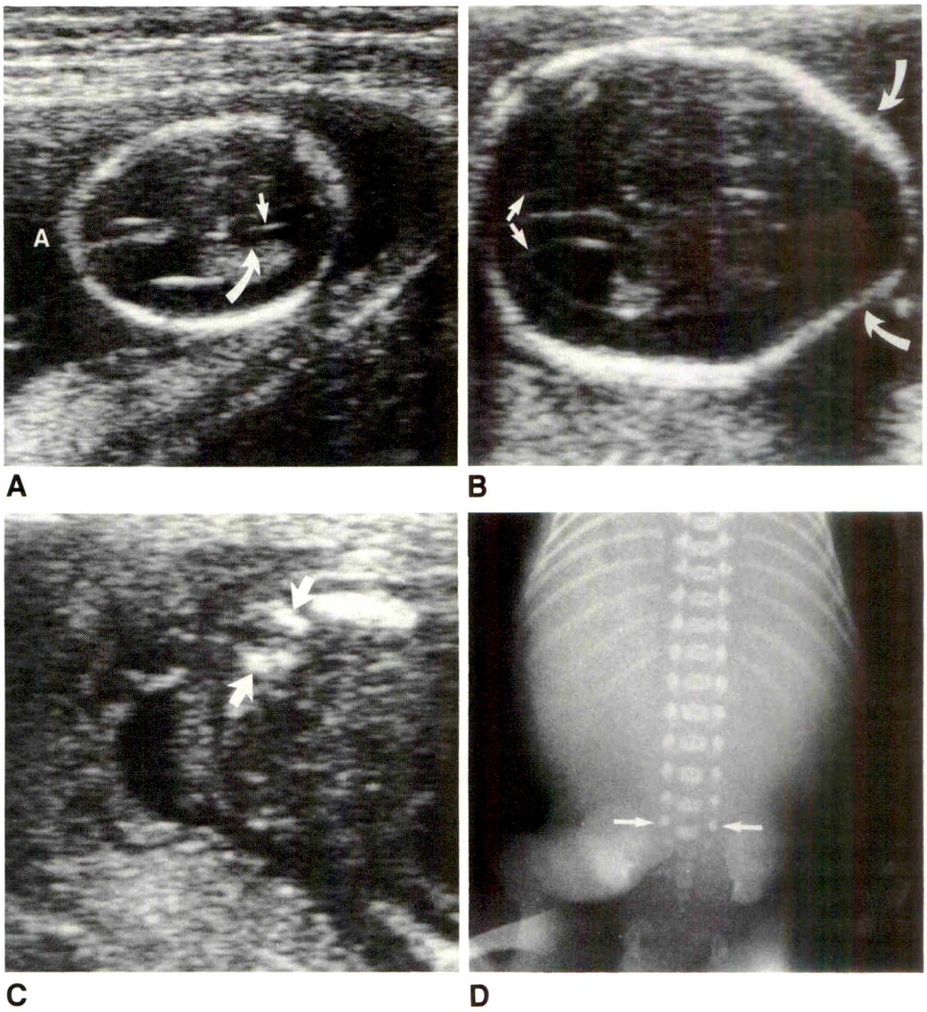


Fig. 2.—Open spina bifida without dorsal sac.

***A*, Axial sonogram through head of 17-week (menstrual age) fetus shows separation of choroid plexus (*curved arrow*) from medial wall of lateral ventricle (*straight arrow*), suggesting ventriculomegaly. A = anterior. No spinal abnormality was seen.**

***B*, 2 weeks later. Ventriculomegaly with separation of occipital horns (*straight arrows*) and scalloping of frontal bones (*curved arrows*).**

***C*, Transverse sonogram of spine shows slight widening of posterior ossification centers (*arrows*) at lower lumbar level, suggestive of open spina bifida.**

***D*, Frontal radiograph of aborted fetus shows slight widening of interpediculate distance at L5 level (*arrows*), corresponding to caudal edge of open spina bifida.**

dorsal sac in the lumbosacral area (Fig. 3). After termination of the pregnancy these findings were confirmed by pathologic examination. The dorsal sac was 2.0 cm long and 1.5 cm wide, and the open spina bifida was 2.0 cm long and 0.8 cm wide.

Three cases of open spina bifida referred for screening because of elevated maternal serum AFP levels were not detected by sonography. The fetal ages ranged from 16 to 18 weeks. The amniotic fluid AFP levels were all greater than five multiples of the mean, and all cases were positive for AChE. These three women elected to terminate their pregnancies on the basis of these results, even though the preamniocentesis sonograms had been reported as normal. In retrospect, one fetus had a scalloping of the frontal bones, but ventriculomegaly was not noted in any of these cases. Sonography was not repeated after amniotic fluid AFP and AChE levels were obtained in these patients. On pathologic examination, all three fetuses had open lumbar spina bifida defects 0.8–1.5 cm long and 0.4–0.6 cm wide. Only one had an associated dorsal sac with herniation of dura and leptomeninges containing spinal cord elements; all had skin and soft-tissue defects visible on gross inspection. Radiographs of two of these fetuses after termination of the pregnancies revealed minimal flaring of the posterior elements in the areas of the open spina bifida. Pathologic examination of the brain was completed in one case and no abnormality was noted. In the case in which signs indicative of an Arnold-Chiari II malformation were seen, a full examination of the neural structures was not performed.

Discussion

The frequency of neural tube defects in this country is between one and two per 1000 births [1]. It is now mandatory in California that pregnant women be offerred a maternal serum AFP screening test for these devastating, potentially lethal abnormalities. Previous reports have estimated that one in 10 women with elevated maternal serum AFP levels will have a fetus with an open neural tube defect [5]. Our results from this series substantiate these findings.

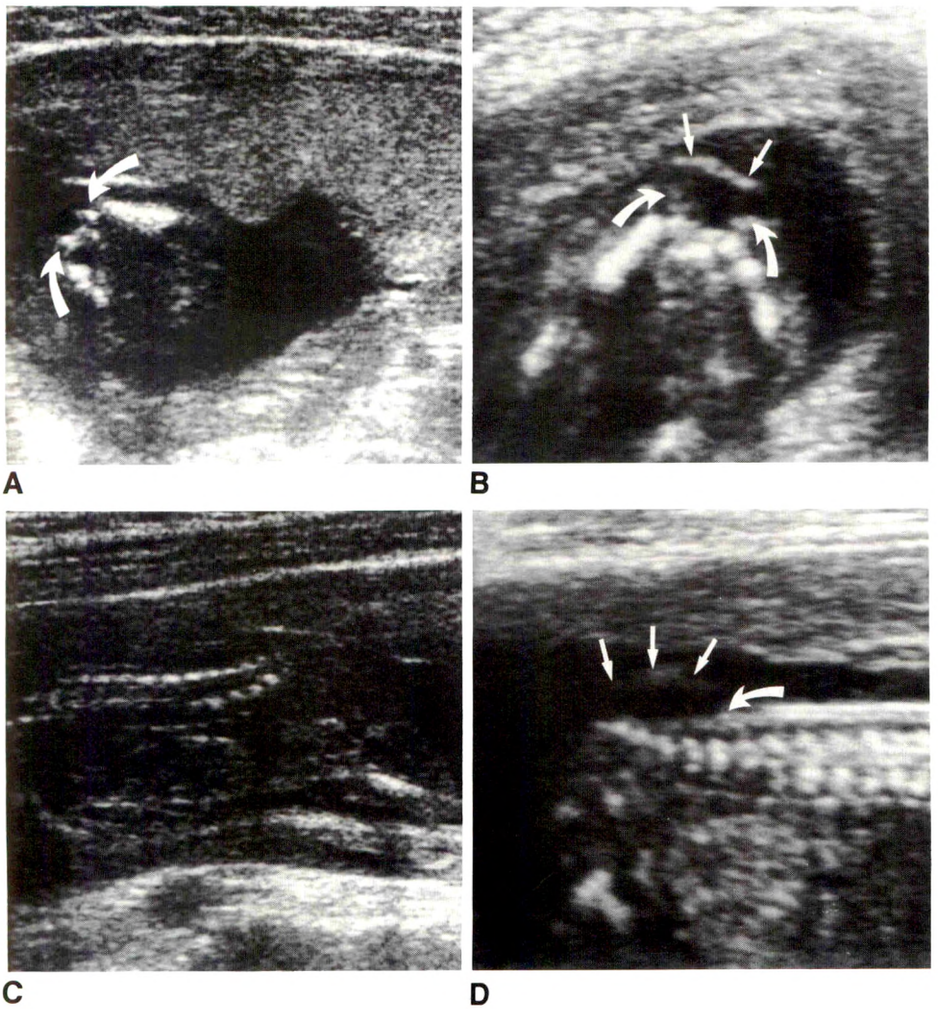


Fig. 3.—Open spina bifida with dorsal sac.

***A*, Transverse sonogram on GE RT 3000 unit through lower lumbar spine of an 18-week (menstrual age) fetus shows slight flaring of posterior ossification centers (*arrows*) without evidence of dorsal sac.**

***B*, Transverse sonogram on computerized sonographic unit clearly shows dorsal sac (*straight arrows*) posterior to open spina bifida in lower lumbar area. Skin and subcutaneous tissues are interrupted by sac (*curved arrows*). Similar findings were noted in longitudinal plane.**

***C*, Longitudinal sonogram on GE RT 3000 unit shows no definite evidence of open spina bifida or dorsal sac.**

***D*, Longitudinal sonogram the same day on computerized unit clearly shows dorsal sac (*straight arrows*) and interruption of skin and subcutaneous tissues (*curved arrow*).**

Sonography has been useful in determining the cause of the elevated maternal serum AFP. Incorrect fetal age, fetal demise, and multiple gestations, which are all causes of elevated maternal serum AFP, can be readily diagnosed by sonography. Potentially correctable defects that cause elevated maternal serum AFP levels (such as omphalocele, gastroschisis, urinary tract obstruction, and cystic hygroma) can also be imaged sonographically. Often amniocentesis can be avoided if a satisfactory explanation for the maternal serum AFP elevation can be determined by sonography. If, however, the anomaly is associated with genetic abnormalities (e.g., omphalocele, cystic hygroma), amniocentesis should be performed for chromosomal analysis.

Neural tube defects that can be detected by maternal serum AFP screening include anencephaly, encephalocele, and open spina bifida. Sonographic findings in anencephaly include absence of the cranial vault above the level of the orbits and absence of cerebral tissue. Polyhydramnios may accompany this anomaly. Sonography has been shown to be 100% sensitive in identifying cases of anencephaly [2, 6, 7], and both cases in our series were easily diagnosed. When the sonogram is diagnostic for this anomaly, amniocentesis need not be performed. Termination of the pregnancy is usually elected for this lethal anomaly.

Encephaloceles are also easily imaged with sonography. This anomaly appears as a midline fluid-filled sac most commonly extending from the bony calvarium. The sac may contain brain tissue, and the bony defect in the skull may be seen on sonography. If the sac is not intact, an encephalocele may be missed sonographically [8]. We have not encountered any cases of encephalocele through our maternal serum AFP screening program.

Open spina bifida is the most difficult of the open neural tube defects to diagnose by sonography. Such anomalies are sonographically manifested by splaying of the posterior ossification centers of the spine. The transverse plane has been reported as the most useful plane for scanning these defects [9]. Meticulous scanning is necessary, as a slight widening of the interpediculate distance is a normal finding in the cervical and lumbar areas [8]. All three of the open spina bifida defects missed in our series were in the lumbosacral region and were small (0.4–0.6 cm wide).

In addition to the splaying of the posterior ossification centers in open spina bifida, a sac containing meninges, CSF, and possibly neural tissue may be seen posterior to the bony defect on sonography. Of the six cases of open spina bifida reported here, one of the three that were detected by sonography and two of the three that were missed by sonography had no associated dorsal masses. In the case with a dorsal sac that was missed by sonography, the fetal spine was closely apposed to an anterior placenta, apparently obliterating visualization of the dorsal sac. If such a sac exists, the identification of an open spina bifida may be facilitated if fetal position is appropriate.

Other positional factors may also influence the ease with which open spina bifida can be detected sonographically early in the second trimester. Excessive fetal movement and kyphosis may make precise transverse examination of the spine difficult.

On the basis of these cases, we believe that the type of sonographic equipment is important is assuring accurate diagnosis of open spina bifida. In one of our cases the dorsal sac accompanying the open spina bifida was not detected with standard real-time equipment, but was clearly visible on our computerized unit because of the increased detail and contrast resolution offered by this unit [10]. In our department all patients with elevated maternal serum AFP are now examined by computed sonography.

Associated sonographic findings may also facilitate discovery of open spina bifida. Ventriculomegaly usually is associated with open spina bifida, although it may not be manifest early in the second trimester. One case reported here had mild ventriculomegaly on the initial sonogram, but 2 weeks later had definite dilatation of the ventricles (Fig. 2). Equivocal cases should be reexamined.

Recently, a new cranial and a new cerebellar sign were seen retrospectively in an entire series of 70 fetuses with open spina bifida [3]. The cranial sign of open spina bifida consists of a scalloping of the frontal bones (lemon sign) and the cerebellar sign reflects compression of the cerebellum in a crescent shape with obliteration of the cisterna magna (banana sign). These appear to reflect an Arnold-Chiari II malformation. These associated findings were noted in all of our sonographically identified cases of open spina bifida and were seen retrospectively in one missed case. They may be helpful in identifying future cases.

In one report, sonography was found to be 100% sensitive in the diagnosis of open spina bifida [2]. The cases reported were all meningomyeloceles, so it must be presumed that dorsal sacs were present in all cases on sonography. Fetal ages were not reported. Other authors have reported sensitivities of 33–80% in sonographic diagnosis of all types of open spina bifida [6]. These results more closely reflect our experience.

Because of the difficulties encountered in the diagnosis of small open spina bifida deformities in the second trimester by sonography, we believe that patients presenting with elevated maternal serum AFP levels and apparently normal fetal sonograms should always undergo amniocentesis. Amniotic fluid AFP and AChE levels can then be determined. A recent series reported no false-negative results for open spina bifida with elevated amniotic fluid AFP levels and a positive AChE [10].

False-positive results have been reported in the presence of fetal blood, but these are usually distinguishable from the true-positive results by examination of the fluid for blood and by the distinctiveness of the AChE band on electrophoresis. One case that was false positive for open spina bifida was also reported with elevated amniotic fluid AFP and positive AChE [11]; this fetus had a cystic hygroma, an abnormality easily diagnosed by sonography. Other series have produced similar results when second-trimester amniotic fluid was analyzed [12]. In the three cases of false-negative sonographic examinations for open spina bifida in this series, decisions to terminate the pregnancies were made solely on the basis of the amniocentesis results. Rescanning after the amniocentesis results were available might have yielded a positive sonographic diagnosis, as it did in two of the cases identified correctly by sonography.

In summary, second-trimester fetal sonography can be extremely useful in determining the cause of an elevated maternal serum AFP and does, in selected circumstances, obviate amniocentesis. However, when a satisfactory explanation for the maternal serum AFP level cannot be determined by sonography, amniocentesis for amniotic fluid AFP and AChE determination should always be carried out. Contrary to previous reports [2], fetal sonography is not 100% sensitive in identifying open spina bifida and cannot be used early in the second trimester to positively identify morphologically normal fetuses.

REFERENCES

1. Hobbins JC, Venus I, Tortora M, Mayden K, Mahoney MJ. Stage II ultrasound examination for the diagnosis of fetal abnormalities with an elevated amniotic fluid alpha-fetoprotein concentration. *Am J Obstet Gynecol* **1982**;142:1026–1029
2. Hashimoto BE, Mahoney BS, Filly RA, Golbus MT, Anderson RL, Callen PW. Sonography, a complementary examination to alpha-fetoprotein testing for fetal neural tube defects. *J Ultrasound Med* **1985**;4:307–310
3. Nicholaides KH, Campbell S, Gabbe SG, Guidetti R. Ultrasound screening for spina bifida: cranial and cerebellar signs. *Lancet* **1986**;2:72–74
4. Rumack CM, Johnson ML. *Perinatal and infant brain imaging: role of ultrasound and computed tomography*. Chicago: Year Book Medical, **1985**:65
5. U.K. collaborative study on alpha-fetoprotein in relation to neural tube defects. Maternal serum alpha-fetoprotein measurement in antenatal screening for anencephaly and spina bifida in early pregnancy. *Lancet* **1977**;1:1323–1332
6. Campbell S. Early prenatal diagnosis of neural tube defects by ultrasound. *Clin Obstet Gynecol* **1977**;20:351–359
7. Roberts CJ, Evans KT, Hibbard BM, Laurence KM, Roberts EE, Robertson IB. Diagnostic effectiveness of ultrasound in detection of neural tube defect. *Lancet* **1983**;2:1068–1069
8. Fiske CE, Filly RA. Ultrasound evaluation of the normal and abnormal fetal neural axis. *Radiol Clin North Am* **1982**;20:285–296
9. Filly RA, Golbus MS. Ultrasonography of the normal pathologic fetal skeleton. *Radiol Clin North Am* **1982**;20:311–323
10. Maslak S. Computed sonography. In: Sanders RC, Hill MC, eds. *Ultrasound annual 1985*. New York: Raven, **1985**:1–16
11. Crandall BF, Matsumoto M. Routine amniotic fluid alphafetoprotein assay: experience with 40,000 pregnancies. *Am J Med Genet* **1986**;24:143–149
12. Regemorter N, Defleur V, Delbeke D, Vamos E, Rodesch F. Alphafetoprotein (AFP), concanavalin A non-reactive AFP and specific acetylcholinesterase in amniotic fluid from pathological pregnancies. Predictive values for open spina bifida. *Eur J Obstet Gynecol Reprod Biol* **1983**;16:9–18

Book Review

A Practical Guide to Ultrasound in Obstetrics and Gynecology. By Eric E. Sauerbrei, Khanh T. Nguyen, and Robert L. Nolan. New York: Raven, 185 pp., 1987. $24.50

This little book seems to have begun as a good idea. In the authors' words it is meant to be a "short guide [the purpose of which is] to portray the ultrasound appearance of the normal structures in obstetrics and gynecology and the abnormalities most commonly found in our clinical practice." In 168 pages, the text offers a review of ultrasound in obstetrics and gynecology, well illustrated and reasonably readable. The scans published are well executed and have been clearly reproduced and annotated. Although the text is brief, it includes helpful quick summaries of such subjects as hormonal control and cycles, early gestational bleeding, and polyhydramnios. Now, why isn't this book the answer to every ultrasonologist's dream?

First, it is incomplete. Brevity is a virtue, but it can be carried too far. The omission of a description of the technique of performing a satisfactory ultrasound examination of either the pelvis or the pregnant uterus in a textbook on obstetrics and gynecology is a serious deficiency and compromises the usefulness of the book for most purposes. Other similar omissions are in the sections on the diabetic mother and on twins, both areas in which ultrasound is of paramount importance. They are inadequate because they do not include information necessary to perform satisfactory ultrasound examinations and would leave the uninitiated ill-equipped to handle many of the problems in these areas.

Second, the organization is confusing and often ineffective. This is most obvious in the section on the fetus. The parts are mostly there, however, they are not assembled well. Again, there is no indication of how one should organize the examination of the fetus systematically to avoid overlooking important features. Also, the catalog of anomalies is uneven. The catalog is based on the authors' experience, and since no one can have seen every abnormality, the list is spotty. This reviewer was especially distressed by the handling of urinary tract problems. Most of the important entities are described, but nowhere is an overview given. In microcosm this reveals the weakness of the book's organization, a flaw that makes learning from it difficult. Finally, the authors' approach to fetal measurement is somewhat unorthodox. They recommend using several combinations of parameters, which have not proved useful in most hands and could be seriously misleading to the neophyte.

This book is up against formidable competition in the field of obstetric and gynecologic ultrasound, because there are several excellent texts already available. Although they are more expensive, the extra investment will buy a great deal more; for this reason I cannot recommend the present book except perhaps as a convenient, pocket-sized vehicle for review for Board examinations.

Harte C. Crow
Mary Hitchcock Memorial Hospital
Hanover, NH 03756

Case Report

Diprosopus: Diagnosis In Utero

Joel R. Okazaki,[1] James L. Wilson, Stephen M. Holmes, and Linda L. Vandermark

Conjoined twins have been reported in the medical literature since 1864; however, their existence has been known for centuries [1]. The frequency has been reported as 10.25 per 1 million births [2] in the United States. Diprosopus (two faces) is a rare form of symmetric conjoined twins consisting of a single neck and body and a spectrum of duplication of craniofacial structures. In the mildest form, isolated duplication of the nose occurs; in the most severe form, the fetus has two complete faces. The term *tetrophthalmos* is applied to a fetus with four eyes. The two median eyes may be fused partially, may be separate but share a central orbit, or may occupy completely separate orbits.

Fewer than 30 cases of diprosopus have been reported in the obstetric, pathologic, embryologic, and related literature [1, 3–5]. To our knowledge, no case has been published of definitive diagnosis of diprosopus in utero. Because the resolution of real-time sonographic equipment now allows detailed evaluation of fetal facial and intracranial structures, radiologists should be aware of the sonographic appearance of this condition. Antenatal diagnosis will permit optimal obstetric management.

Case Report

A 27-year-old pregnant Filipino woman was referred to us. Gestational age was 28 weeks by menstrual weeks. A sonographic examination at another institution had shown polyhydramnios, a biparietal diameter of 90+ mm, and cystic intracranial structures that were thought to represent hydrocephalus.

Our first sonographic examination showed polyhydramnios and a single live fetus. Measurements of abdominal circumference and femur length indicated a gestational age of 28 weeks. An adequate biparietal diameter could not be obtained, and evaluation of fetal facial and intracranial structures was poor because of continuous fetal movement compounded by the presence of polyhydramnios. Because of the patient's discomfort, a therapeutic amniocentesis was performed, without complication, and 1000 ml of clear yellow fluid were aspirated from the amniotic cavity. The level of alpha-fetoprotein in the amniotic fluid was 1.85 μg/ml, which is normal at our institution.

A second sonographic examination was performed the day after the amniocentesis and showed a biparietal diameter of 120 mm. Craniofacial structures were seen much better than in the first study because fetal movement was limited after the withdrawal of amniotic fluid. Assessment of fetal facial structures showed two mouths, two noses, two ears, and four eyes. The two median globes shared a single orbit and were directly adjacent to each other (Fig. 1). The intracranial structures were duplicated partially. There were two pairs of lateral ventricles, one set of which was dilated, and a single large cystic structure involving the posterior fossa (Fig. 2). Dextrocardia was noted, but no other abnormalities of the thoracic or abdominal organs were detected.

Three weeks later the fetus died in utero, and a stillborn female diprosopus infant was delivered by cesarean section (Fig. 3). A CT scan of the fetal head, which had partially duplicated facial and intracranial structures, was obtained for educational purposes.

Discussion

Conjoined twins are always of the same sex and share a single chorion and placenta [6]. This finding suggests that they arise from a single ovum that has undergone abnormal fission. Animal experiments in which conjoined twins were

Received January 20, 1987; accepted after revision March 11, 1987.

The opinions and assertions contained herein are the private views of the authors and are not to be construed as official or as reflecting the views of the Department of the Army or the Department of Defense.

[1] All authors: Department of Radiology, Tripler Army Medical Center, Honolulu, HI 96859-5000. Address reprint requests to J. L. Wilson.

AJR **149:147–148, July 1987** 0361–803X/87/1491–0147 © American Roentgen Ray Society

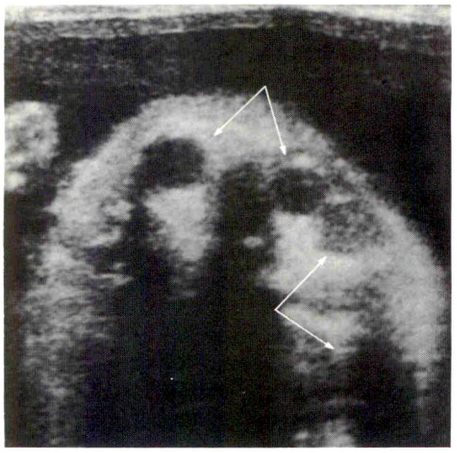


Fig. 1.—In utero real-time sonogram of fetal face shows four globes (*arrows*). Two median globes are adjacent to each other and share a single orbit. Fourth globe is slightly out of scan plane.

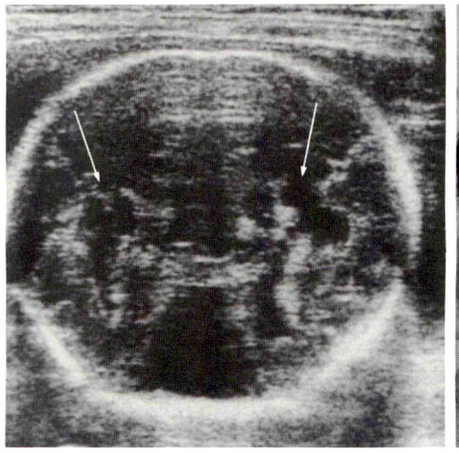


Fig. 2.—Sonogram from angled axial scan through fetal head shows duplication of lateral ventricles (*arrows*). Large posterior midline cystic structure is confluence of ventricular systems in posterior fossa.



Fig. 3.—Stillborn diprosopus fetus delivered by cesarean section at 31 weeks' gestation. Note duplication of facial structures and single large midline orbit.

formed have indicated that stress from the fetal environment in the time just before gastrulation is the dominant factor in pathogenesis; however, one study suggested that genetic transmission also may play a significant role [7]. Lowering temperature or reducing oxygen concentration in the growth medium has produced anterior duplication in fish that is similar to diprosopus. Various teratogens also have been shown to cause conjoined twins in other animal models [8].

Reports have indicated an increased incidence of neural tube defects in monozygotic twinning [2], and case reports of diprosopus have shown a common association with both neural tube defects and anterior duplication [1, 3–5]. These findings support the possibility that similar pathogenetic processes are involved, such as a disorder of embryonic migration or fusion [2]. Our case had mild spinal dysraphism of the thoracic spine, but a significant neural tube defect was absent.

As with many neuraxial anomalies, the first indication of diprosopus may be polyhydramnios, which is manifested clinically as increasing fundal height or a weight gain out of proportion to gestational age. As seen in this case, significant polyhydramnios and fetal motion can make evaluation of the craniofacial structures difficult. Reduction in amniotic fluid by means of therapeutic amniocentesis can facilitate the examination. Sonographic demonstration of four globes can distinguish this entity from other causes of hydrocephalus, macrocephaly, and cranial deformity. If only two orbits are present, the finding of partial duplication of the lateral ventricles or other intracranial structures can aid in the diagnosis. Early diagnosis is desirable because termination of pregnancy is a therapeutic option before 24 weeks of gestation. If diprosopus is diagnosed later, the patient can be advised of the prognosis and of the possibility that cesarean delivery may be necessary because of cephalopelvic disproportion. If significant hydrocephalus is the major cause of macrocephaly, cephalocentesis under sonographic guidance may be offered to avoid cesarean delivery [5].

REFERENCES

1. Turpin IM, Furnas DW, Amlie RN. Craniofacial duplication (diprosopus). *Plast Reconstr Surg* **1981**;67:139–142
2. Edmonds LD, Layde PM. Conjoined twins in the United States, 1970–1977. *Teratology* **1982**;25:301–308
3. Changaris DG, McGavran MH. Craniofacial duplication (diprosopus) in a twin. Arch Pathol Lab Med **1976**;100:392–394
4. Riccardi VM, Bergmann CA. Anencephaly with incomplete twinning (diprosopus). *Teratology* **1977**;16:137–140
5. Chervenak FA, Pinto MM, Heller CI, Norooz H. Obstetric significance of fetal craniofacial duplication: a case report. *J Reprod Med* **1985**;30:74–76
6. Nishimura H, Okamoto N, Tanimura T, Ikeda T. Classified malformations, multiple pregnancy. In: Nishimura H, ed. *Sequential atlas of human congenital malformations*. Baltimore: Univ. Park Press, **1976**:18–27
7. Chai CK, Crary DD. Conjoined twinning in rabbits. *Teratology* **1971**;4:433–444
8. Ferm VH. Conjoined twinning in mammalian teratology. *Arch Environ Health* **1969**;19:353–357

CSF Pulsations Within Nonneoplastic Spinal Cord Cysts

Dieter R. Enzmann[1]
James O'Donohue[2]
Jeremy B. Rubin[1]
Larry Shuer[3]
Phil Cogen[3]
Gerald Silverberg[3]

Because of its sensitivity to fluid motion, MR imaging was used to investigate fluid dynamics in syringomyelia. Three major findings characterized syringomyelia: pulsatile fluid in cysts, nonpulsatile fluid in cysts, and damaged cord tissue. The fluid in preoperative syrinx cavities pulsated in a fashion similar to subarachnoid CSF. Pulsation was more prominent in large cysts but was also seen in small cysts. Nonpulsatile cysts were generally of smaller diameter, were shorter in length, and often were single; they could, however, coexist with pulsatile cysts. Nonpulsatile cysts had etiologies similar to those of pulsatile cysts: Chiari malformation, trauma, and unknown. Damaged cord, characterized by abnormal high signal on T2-weighted sequences, was seen in 15 of 16 patients and could be either focal or diffuse but was always adjacent to syrinx cavities. Postsurgical MR scans had a lower incidence of pulsatile cysts. In five patients with both pre- and postoperative MR scans, shunting of the cyst reduced the size of the pulsating cyst (two patients) or reduced the size of the cyst and eliminated pulsation altogether (three patients). Axial, T2-weighted images are recommended in the investigation of spinal cord cysts to determine the presence or absence of pulsatile fluid. The presence of pulsation indicates a nonneoplastic cyst. The absence or reduction of CSF pulsation may prove to be a valuable indicator of the success of a shunting procedure.

Nonneoplastic spinal cord cysts are associated with a variety of clinical entities, the Chiari I and II malformations and traumatic spinal cord injury being the most common [1–6]. In each entity, however, the etiology and pathogenesis of cyst development is poorly understood. Although there is still disagreement as to proper terminology we will use the term *syrinx* to refer to nonneoplastic cysts of the spinal cord.

MR imaging in comparison with CT has greatly simplified the diagnosis of syrinx and promises to expand our understanding of its pathogenesis and natural history [5–12]. Numerous MR pulse sequences are known to be sensitive to the oscillatory motion of CSF [13–16]. These sequences can be used to study the dynamics of fluid motion in the spinal canal and within the syrinx. A specific, prospective protocol with pulse sequences designed to take advantage of this sensitivity to flow was used to study pre- and postoperative syrinx patients.

Subjects and Methods

Sixteen syrinx patients were studied (Table 1). The etiology of syringomyelia was related to trauma in six patients, Chiari I (seven) or II (one) malformation in eight patients, and unrelated to a specific etiology in two. The syrinx was in the cervical cord in 10 pateints, in the thoracic cord in two, in the cervical and thoracic cords in three, and in the thoracolumbar region in one. Preoperative MR scans were available in 15 patients, five of whom were also scanned postoperatively. In one patient only a postoperative scan was available. Of the six patients with a shunting procedure, two were syringoperitoneal and four were syringosubarachnoid. Diagnoses were confirmed by surgery in all but six patients, three of whom had posttraumatic syringes and three of whom had Chiari malformations. For comparison, six

This article appears in the May/June 1987 issue of *AJNR* and the July 1987 issue of *AJR*.

Received July 22, 1986; accepted after revision December 16, 1986.

[1] Department of Diagnostic Radiology, Stanford University School of Medicine, Stanford, CA 94305. Address reprint requests to D. R. Enzmann.

[2] Department of Radiology, Good Samaritan Hospital, San Jose, CA 95124.

[3] Department of Neurosurgery, Stanford University School of Medicine, Stanford, CA 94305.

***AJR* 149:149–157, July 1987**
0361–803X/87/1491–0149
© American Roentgen Ray Society

TABLE 1: MR of Nonneoplastic Spinal Cord Cysts: Pre- and Postoperative MR Findings

Cause: Case No.	Age	Gender	Site	Preoperative MR		Postoperative MR	
				Pulsation: Width (mm)/Length (cm)	Myelomalacia	Pulsation: Width (mm)/Length (cm)	Myelomalacia
Chiari I							
1	27	M	C, T	Pulsatile: 4/14	Focal	Nonpulsatile: 2/10	Focal
2	40	F	C	Pulsatile: 7/>40[a]	Diffuse	Pulsatile: 2/>25[a] Nonpulsatile: portion	Diffuse
3	25	F	C	Pulsatile: 8/>16[a]	Focal	. . .	. . .
4	56	M	C, T	Pulsatile: 8/>30[a] Pulsatile: 8	Diffuse	. . .	. . .
5	11	M	C	Pulsatile: 10/17	Diffuse	. . .	. . .
6	33	M	C, T	Nonpulsatile: 3/4	Focal	. . .	. . .
7	9	F	T, L	Nonpulsatile: 20/15	Diffuse	. . .	. . .
Chiari II							
8	1½	M	T	Nonpulsatile: 4/3	Diffuse	. . .	. . .
Trauma							
9	44	M	C	Pulsatile: 8/9 Nonpulsatile: 5/2	Diffuse	Nonpulsatile: 5/7 Nonpulsatile: 5	Diffuse
10	33	M	C	Pulsatile: 9/>22[a]	Diffuse	Nonpulsatile: 2/5	Diffuse
11	29	M	T	Pulsatile: 8/>20[a] Nonpulsatile: 4/5	Focal	. . .	. . .
12	62	M	C	Nonpulsatile: 12/1.5	None	. . .	. . .
13	52	M	C	Nonpulsatile: 1/4.5	Focal	. . .	. . .
14	51	M	C	. . .	. . .	Nonpulsatile: 6/4	Focal
Unknown							
15	60	M	C	Pulsatile: 2/4 Nonpulsatile: 3/3	Focal	Pulsatile: 1/2	Focal
16	41	M	C	Nonpulsatile: 5/15	Diffuse	. . .	. . .

Note.—C = cervical; T = thoracic; L = lumbar.

[a] The exact length could not be measured because separate coils were used and the syrinx extended beyond the field of view.

patients with large cysts associated with intrinsic spinal cord tumors were studied with a similar protocol.

All scans were obtained on a 1.5-T MR scanner (GE Signa) with 5-in. (13-cm) circular and 7- by 12-in. (18- by 30-cm) rectangular surface coils by using the following protocol. Each patient had a sagittal T1-weighted scan with a repetition time (TR) of 600–800 msec and echo time (TE) of 20–25 msec; the number of excitations (NEX) was two, and a 256 × 256 matrix, 24-cm field of view (FOV), and 3-mm slice thickness were used to delineate cord morphology and the low-signal cystic component. In all but one patient, an axial T1-weighted scan (TR = 800–1000 msec, TE = 20 or 25 msec, NEX = 4 or 6, 256 × 128 matrix, 24-cm FOV, 3- or 5-mm slice thickness) was obtained to delineate cord size and the size of the low-signal areas presumed to represent cystic space(s). Each patient had an ungated scan (TR = 2000 msec, TE = 20 or 25 msec and 80 msec, NEX = 2, 256 × 256 matrix, 26-cm FOV, 3-mm slice thickness) in either the axial or sagittal view; in two patients, both views were obtained. Pulsatile flow could be identified by areas of signal loss on the TR = 2000-msec scan (sagittal or axial view). In addition, pulsations in subarachnoid CSF and cyst fluid were detected by two additional flow-sensitive sequences: (1) selective saturation recovery, gradient refocusing (SSRGR) [16], and (2) gradient recalled acquisition in the steady state (GRASS) with low flip angles [17]. Both of these sequences were single-slice scans that relied on the "time-of-flight" phenomenon of unsaturated protons entering the slice of interest so that flow was seen as an area of high signal, that is, flow-related enhancement. The parameters for SSRGR were TR = 500 msec, inversion time (TI) = 400 msec, TE = 12 msec, NEX = 2, 256 × 256 matrix, 24-cm FOV, and 3-mm slice thickness. For GRASS the parameters were TR = 22 msec, TE = 12 msec, NEX = 8, 256 × 256 matrix, 24-cm FOV, and 5-mm slice thickness. SSRGR and GRASS were performed in the axial projection, since in this view CSF pulsation caused inflow of unsaturated protons perpendicular to the slice and thus generated flow-related enhancement. The term ultralow is used to describe the flip angle because it was only 6°. These latter two pulse sequences were compared with the cord morphology depicted on axial T1-weighted sequences and with areas of signal loss on axial ungated long TR sequences (TR = 2000, TE = 80). CSF gating, performed in one patient, was accomplished by triggering the finger capillary blush with a photoplethysmograph. The trigger was set to about 400–500 sec after the pulse onset to achieve diastolic gating.

Results

The most important and most consistent finding on preoperative scans was pulsating fluid within the syrinx cavity. This was seen in five of eight Chiari malformation–associated syringes, in three of five posttraumatic syringes, and in one of two syringes of unknown etiology. Therefore, nine of 15 preoperative patients had this finding. Fluid pulsation was seen as an area of signal loss or signal void within the cord on long-TR, long-TE pulse sequences in either the axial or the sagittal projection (Figs. 1–3). When performed, the SSRGR (three patients) and GRASS (four patients) sequences confirmed the presence of motion in the cyst fluid, correlating closely with the area of low signal on T1-weighted images and with areas of signal loss or signal void on the axial

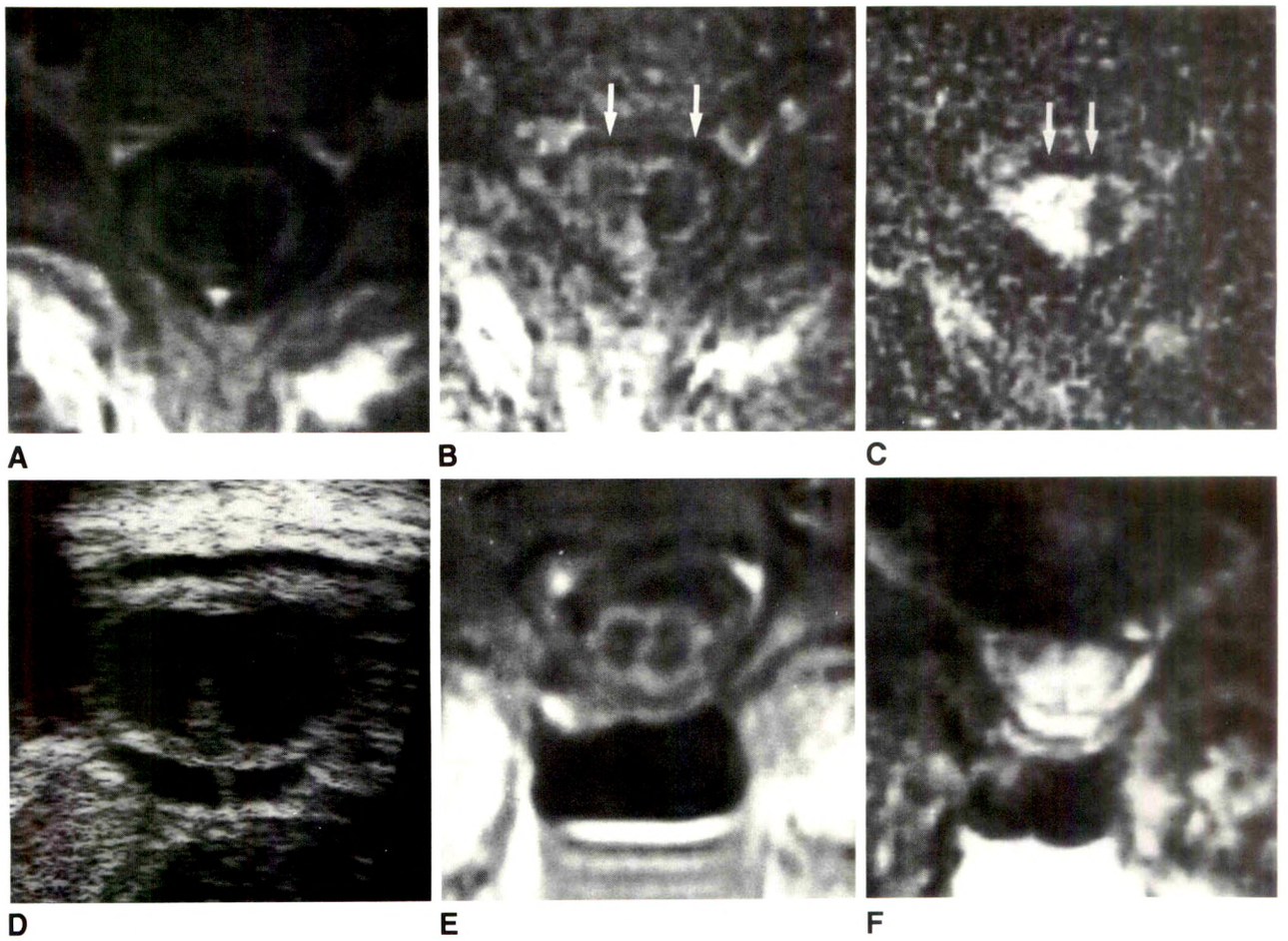


Fig. 1.—Case 9: Traumatic syrinx. Axial MR scans show three main components of syringomyelia: (1) cyst with pulsating fluid, (2) cyst with nonpulsating fluid, (3) myelomalacia.

***A*, Enlarged cord with two cysts was well seen with TR = 1000, TE = 20, slice thickness = 10 mm.**

***B* and *C*, 3-mm axial scans, TR = 2000, TE = 20 (*B*) and TE = 80 (*C*), show pulsatile and nonpulsatile nature of cysts. Cyst on left showed prominent signal loss on both echoes, whereas cyst on right showed the high signal intensity expected from static water (*C*). CSF anterior to cord also showed signal loss indicative of normal pulsation (*arrows*). The cord should have had a lower signal intensity than static CSF on this pulse sequence, but this cord had diffusely high signal indicative of some type of damage, which we termed myelomalacia.**

***D*, Intraoperative sonogram oriented to match MR images confirms two cysts.**

***E*, Postoperative proton density scan (TR = 1000, TE = 20) shows both cysts in cord to be decreased in size.**

***F*, T2-weighted scan (TR = 2000, TE = 80) at same level shows high signal intensity within both cysts. Left cyst no longer shows evidence of pulsation.**

ungated long-TR scans (Fig. 3). When compared with axial T1-weighted scans, the area of flow sometimes did not encompass the entire area of low signal intensity. The remainder of the low-signal-intensity area was assumed to be either static cyst fluid or possibly cord tissue damage. Intraoperative sonography in the two patients in whom it was performed confirmed that the cysts corresponded to the low-signal areas on T1-weighted images (Fig. 1).

In 11 preoperative patients, the axial view showed the syrinx to be a single cavity occupying varying proportions of the cord, whereas in four patients, two cystic spaces were observed (Table 1). Of interest were the differences in pulsation between these various cystic spaces. Of the 11 patients with a single cystic cavity (2- to 20-mm diameter), five had pulsatile fluid (four Chiari malformations, one posttrauma) and six had static fluid (three Chiari, two posttrauma, one unknown etiology). The axial TR-2000, TE-80 scans and the flow-sensitive sequences (SSRGR and GRASS) were consistent in discriminating between pulsating and nonpulsating cysts. Four patients had two distinct cysts: In one patient (Chiari I) both cysts were pulsatile, and in the other three (two posttrauma, one unknown etiology) one cyst had pulsatile fluid while the other had static fluid. Static cyst fluid could be identified as a separate cyst by identifying a septation on the T1-weighted scan. In only one patient with multiple complex but incomplete septations was there apparently static fluid in the same cavity as moving fluid.

The nonpulsatile cysts in general were of smaller diameter

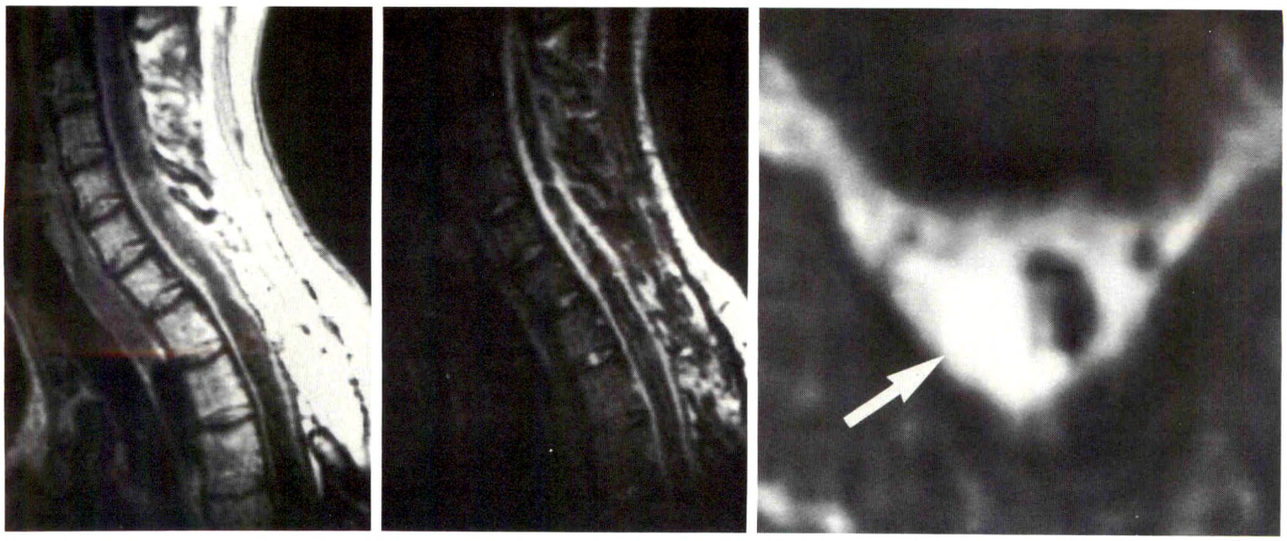


Fig. 2.—Case 10: Traumatic syrinx involving cervical and thoracic cords. *A*, T1-weighted scan. Areas of signal loss, indicative of pulsation, are evident on sagittal (*B*) and axial (*C*) T2-weighted scans. This is seen in this large traumatic syrinx on the sagittal scan (TR 2000, TE = 80) (*B*), in which signal loss correlates with low-signal area on T1-weighted scan (TR = 800, TE = 20) (*A*). *C*, Axial scan (TR = 2000, TE = 80) shows large signal void caused by pulsating fluid. Entire cord is of abnormal high signal, best appreciated on axial view (*arrow*), but also seen on sagittal view as high-signal parallel lines (*B*). Findings were consistent with myelomalacia.

and shorter length than pulsatile cysts. In two posttrauma patients, one such cyst was in a very atrophic cord (4 mm) and the other was a small, focal cyst (1.5 cm long). In the former patient, there was no surgical proof, and this thin (1-mm), low-signal area could have represented myelomalacia without true cyst formation, although it extended for 4.5 cm. Clinically this patient has been stable and has shown no evidence of progression. In Chiari patients (Fig. 4), two static cysts were only 3–4 cm long and 3–4 mm wide, but one was large, 20 mm in maximum diameter and 15 cm long. Two nonpulsatile cysts reached 15 cm in length.

On presurgical scans, if the cystic cord was large, CSF pulsations in the markedly narrowed subarachnoid space were not seen. In general when cord enlargement was present, the signal intensity of subarachnoid-space CSF was higher than expected because of reduced CSF pulsation. The subarachnoid flow voids were either absent or less prominent than normal. If the cord was not large enough to obliterate the subarachnoid space, CSF pulsations within it were normal. Gating to the peripheral pulse in one patient showed that the fluid motion within the cyst had the same periodicity as the normal oscillatory motion of CSF in the subarachnoid space (Fig. 5).

On the T2-weighted sequence (TR = 2000, TE = 80) the normal cord was usually of lower signal intensity than surrounding nonpulsating CSF. In 15 of the 16 syrinx patients it could be determined on either the pre- or postsurgical scan that the cord exhibited abnormal high signal (Figs. 1–3 and 5). High-signal areas could represent either abnormal cord tissue (myelomalacia and/or gliosis) or static cyst fluid. Comparison with the axial short-TR sequence, which yielded excellent cord morphology, helped differentiate static fluid (low signal intensity and discrete septations) from damaged cord tissue, which did not have as low a signal and showed no septations. These areas of noncystic abnormal signal intensity could involve the cord diffusely around the cystic cavity (eight patients) or they could be more localized, occupying only a portion of the cord (seven patients). In patients with both pre- and postoperative scans this abnormal cord signal intensity remained essentially unchanged after surgery, except in one patient in whom it decreased.

Postshunt scans differed from presurgical scans (Table 1). Of the six postsurgical scans, only two patients had pulsatile cyst fluid, and it was small, in the range of 1–2 mm. In the five patients in whom both pre- and postsurgical scans were available for comparison, the postsurgical scans showed a marked reduction in both the cord and cystic cavity (Figs. 1 and 6). Of these five patients, three cysts with prominent pulsations before surgery showed no pulsation after shunting (Fig. 1). Two cysts had residual pulsation, but it had diminished (Fig. 6). Overall, the average presurgical anteroposterior diameter of the cord was 12 mm; after shunting this decreased to an average of 5 mm. In all patients, the reduction of the cystic cavity accounted for this difference. Concomitant with a decrease in cord size was a return of normal flow voids in the subarachnoid space.

In the six spinal cord tumor patients with large associated cysts, each cyst showed high signal intensity on T2-weighted sequences (TR = 2000–2500, TE = 80). There was *no* evidence of cyst pulsation in any of the tumor patients, even when the subarachnoid space was completely obliterated by the large cyst (Fig. 7). No areas of signal loss were seen on

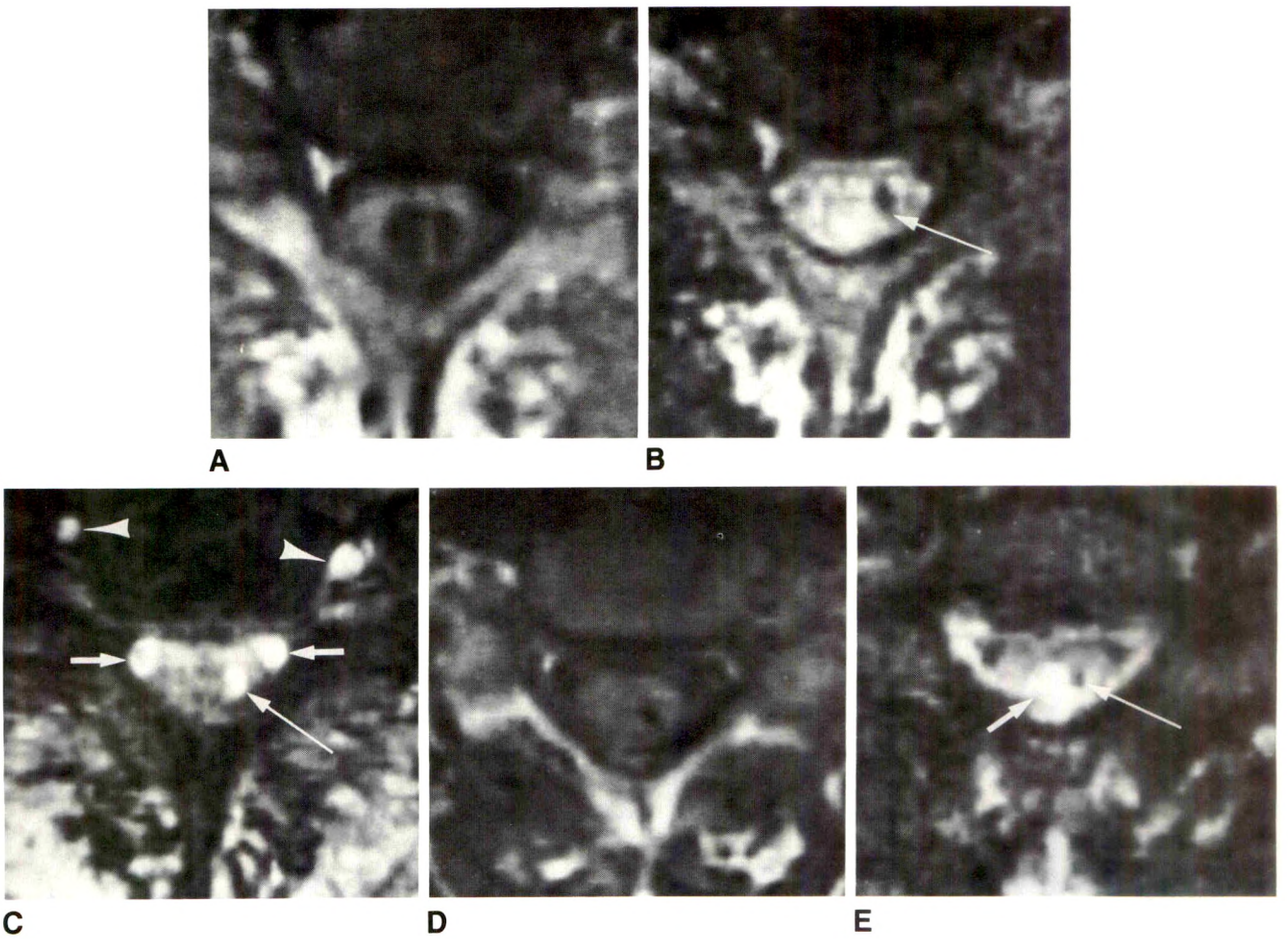


Fig. 3.—Case 15: Syrinx of unknown etiology.

***A*, T1-weighted axial scan (TR = 1000, TE = 20) shows two areas of low signal suggesting adjacent cysts.**

***B*, Axial scan (TR = 2000, TE = 80) within 2 mm of *A* shows area of signal void in left cyst indicating that fluid in cyst was pulsating (*arrow*). Fluid in right cyst is of high signal and, therefore, nonpulsatile.**

***C*, Selective saturation recovery, gradient refocusing pulse sequence, which is sensitive to flow and displays it as high signal, shows increased signal in same region as signal loss, confirming pulsatile fluid in cyst (*long arrow*). Right cyst does not show high signal (that is, no moving fluid). Areas of increased signal in vertebral arteries (*arrowheads*), in anterolateral recesses of subarachnoid space (*short arrows*), and to a lesser degree anterior to cord all indicate fluid moving perpendicular to slice. At a higher cervical level only pulsatile cyst was seen as well as abnormal cord.**

***D*, Axial T1-weighted scan (TR = 1000, TE = 20) shows homogeneous cord with a small cyst of low signal intensity.**

***E*, T2-weighted scan (TR = 2000, TE = 80) shows signal void in cyst indicating pulsation (*long arrow*) and segmental area of abnormal high signal within cord, myelomalacia (*short arrow*).**

ungated long-TR sequences, and no areas of high signal were observed on flow-sensitive sequences.

Discussion

Numerous theories have been proposed regarding the etiology of syringomyelia. None has been definitively proven or gained widespread acceptance. It is doubtful that hemorrhagic cysts play a significant role in posttrauma patients since none of the MR scans had evidence for old hemorrhage (that is, hemosiderin-laden macrophages) in the form of the magnetic susceptibility effect on T2-weighted images [18]. It is accepted that the pathogenesis of syrinx includes a role for altered CSF dynamics, but the nature of the alteration is not clear. Many of the disease states associated with syrinx, Chiari malformation, ankylosing spondylitis, and trauma have associated with them some changes in CSF motion. It is not surprising, therefore, that this investigation has found unusual CSF dynamics in syrinx cavities. Preoperative patients had a high incidence of fluid pulsation within the syrinx. Lack of pulsation was generally seen in the smaller cysts. The presence or absence of pulsation was not related to etiology of the syrinx but was more related to cyst size. Subarachnoid space and peritoneal shunting reduced the size of pulsating cysts in five of five patients; in three of the five, shunting not only reduced the cyst size but eliminated pulsations entirely.

The sensitivity of many MR pulse sequences to fluid motion can be used to advantage in the diagnosis and characteriza-

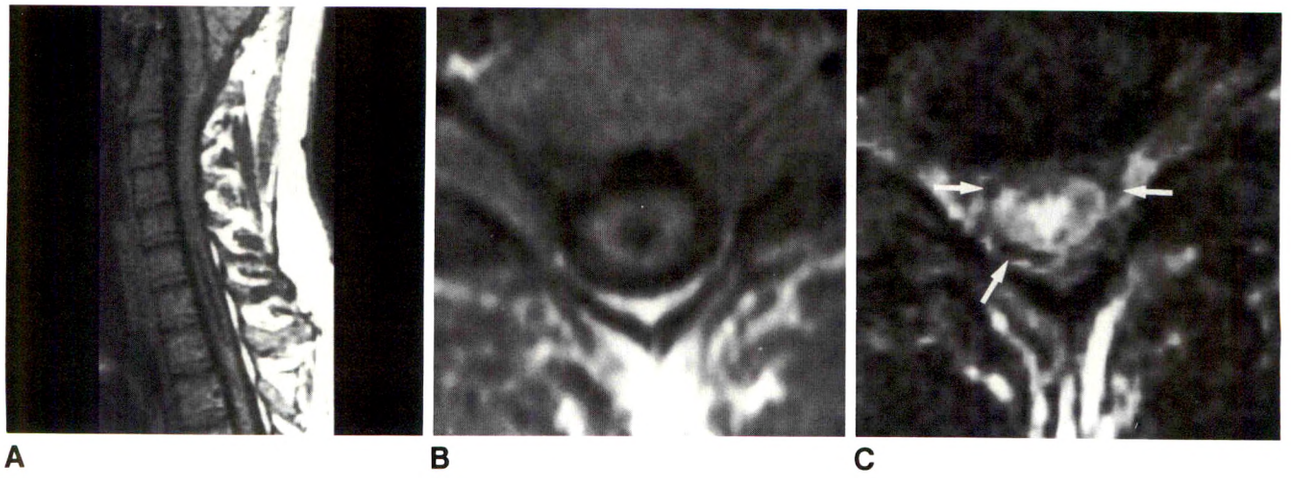


Fig. 4.—Case 6: Syrinx with Chiari I malformation.
A and *B*, Sagittal (TR = 600, TE = 20) (*A*) and axial (TR = 1000, TE = 20) (*B*) T1-weighted scans. Low cerebellar tonsils in *A*.
C, T2-weighted scan (TR = 2000, TE = 80). Cyst does not have pulsatile fluid, as shown by high signal from cyst fluid in central cord. Cord is of normal signal intensity, and areas of signal loss (*arrows*) are present in subarachnoid space, indicative of pulsatile CSF.

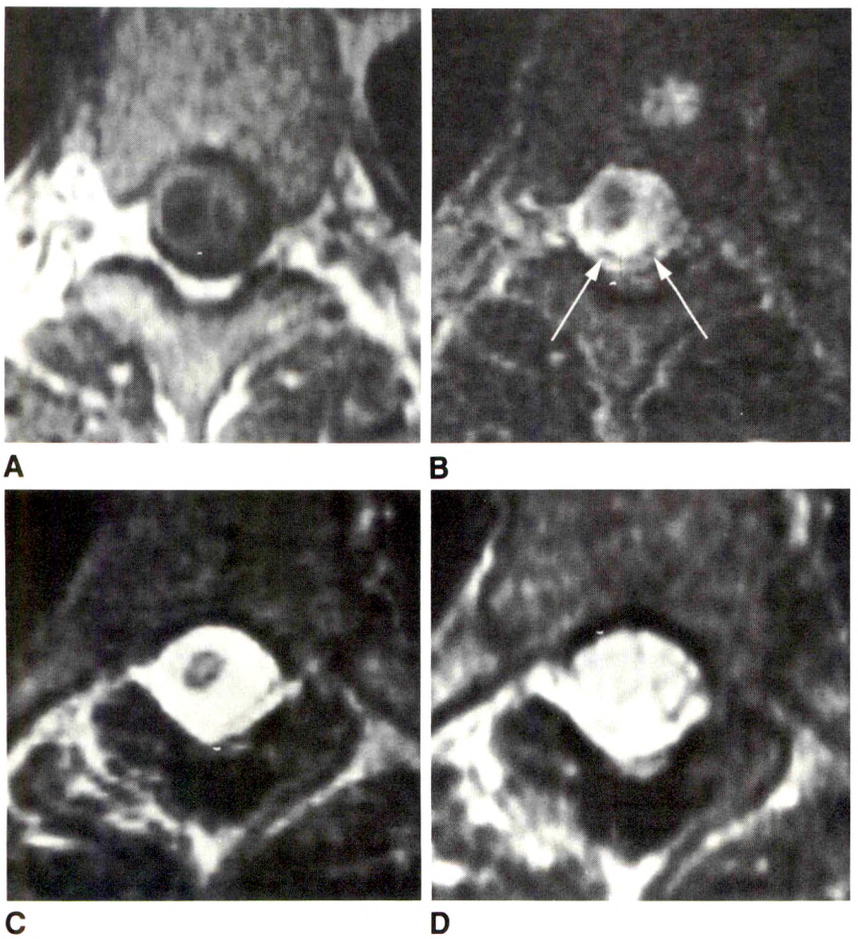


Fig. 5.—Case 11: Traumatic syrinx. Series of axial MR scans show pulsatile cyst, nonpulsatile cyst, myelomalacia, and synchronicity of pulsation with peripheral pulse.
A, T1-weighted sequence (TR = 1000, TE = 20) shows enlarged cord in thoracic region with two cysts of unequal size.
B, Thin-section (3-mm) axial scan (TR = 2000, TE = 80) shows large cyst to be pulsatile because of significant area of signal loss. Small cyst is nonpulsatile at this level. Posterior central region of cord just behind both cysts shows high signal indicative of myelomalacia. Thin black line posterior to cord represents pulsating CSF manifest as signal loss (*arrows*) and helps outline cord.
C and *D*, Thin-section (3-mm) axial scans compare ungated (TR = 2000, TE = 80) (*C*) and gated (*D*) scan at exact same level, but gated scan has an effective TR of about 1800 msec and a TE of 80 msec. Area of signal loss in *C* is not seen on gated image, where it is replaced by high signal intensity expected from static CSF. This showed that fluid within pulsatile cysts behaved in fashion similar to CSF in subarachnoid space in that pulsations were synchronous with peripheral pulse.

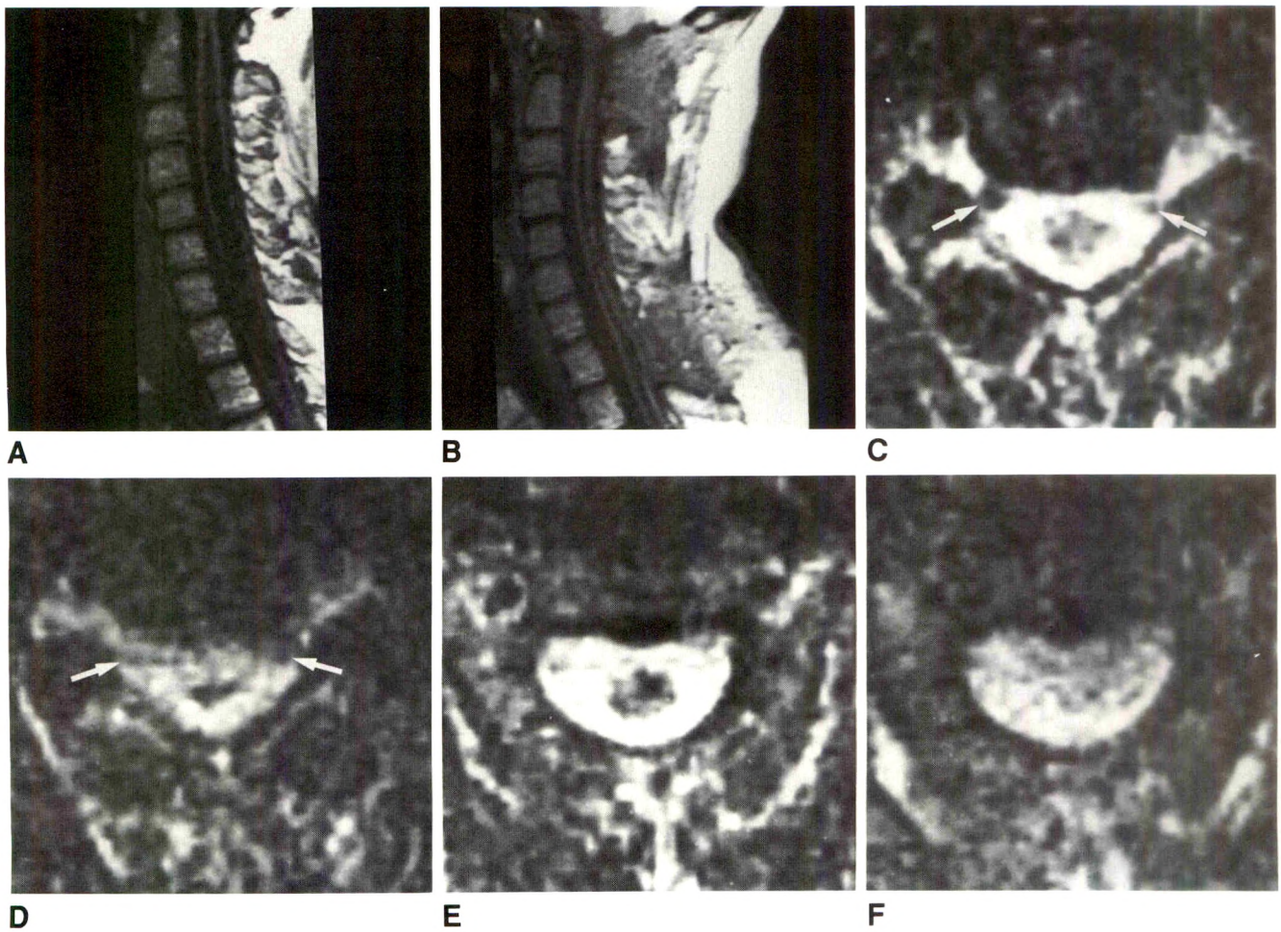


Fig. 6.—Case 2: Chiari I–related syrinx. Pre- and postshunt axial MR scans.

***A*, T1-weighted sagittal scan (TR = 400, TE = 25) before shunting shows large single cyst.**

***B*, After shunting, cyst has decreased as diameter (TR = 600, TE = 25).**

***C* and *E*, Before surgery. Single, large, pulsating cyst within cervical cord is seen well on scans with TR = 2000, TE = 80. Cord was of diffuse high signal making it difficult to discern from relatively static CSF in subarachnoid space. Anterolateral signal voids were seen but were less prominent than normal (*arrows*).**

***D* and *F*, After shunting, pulsating cyst has diminished on scans obtained at presurgery levels with the same scanning parameters. On *D*, cyst fluid still pulsates, but in a smaller cyst. Pulsations in anterolateral areas have become more prominent (*arrows*). At another level (*F*), pulsations within syrinx cavity have virtually disappeared with cord, becoming indistinguishable from surrounding CSF (*D*). The inability to differentiate cord tissue from surrounding CSF on both studies indicated diffuse abnormal signal within cord.**

tion of syringomyelia. Oscillating fluid such as CSF in the spinal canal causes a well-known phenomenon, that of signal loss or signal void on thin-slice long-TR, long-TE scans [13, 14]. This is caused by the combination of harmonic modulation of proton precessional phase induced by CSF pulsation and the two-dimensional Fourier transform method of image reconstruction [14]. The effect is greatest on axial thin slices because of the higher gradient strength used [14]. The increased gradient strength increases the phase shift caused by moving protons and thereby accentuating the signal loss [14]. Other flow-sensitive sequences confirmed fluid pulsation within the syrinx by exhibiting flow-related enhancement. The response to peripheral pulse gating showed the pulsation period to be determined by the heart rate in a fashion similar to normally pulsating CSF in the subarachnoid space.

This cardiac-related pulsation has implications for the pathogenesis of syringomyelia. Pulsation was most prominent in large cysts but was also observed in small cysts. The presence of pulsation in small cysts suggests this may be one mechanism of cyst enlargement. However, cysts do enlarge without the presence of pulsation. There may be two mechanisms for cyst enlargement: (1) cyst fluid production in nonpulsatile cysts and (2) a "water hammer" effect caused by pulsatile cyst fluid. How and where pulsations are transmitted to the cyst fluid is unknown, but presumably this is related to some type of communication with the subarachnoid space or

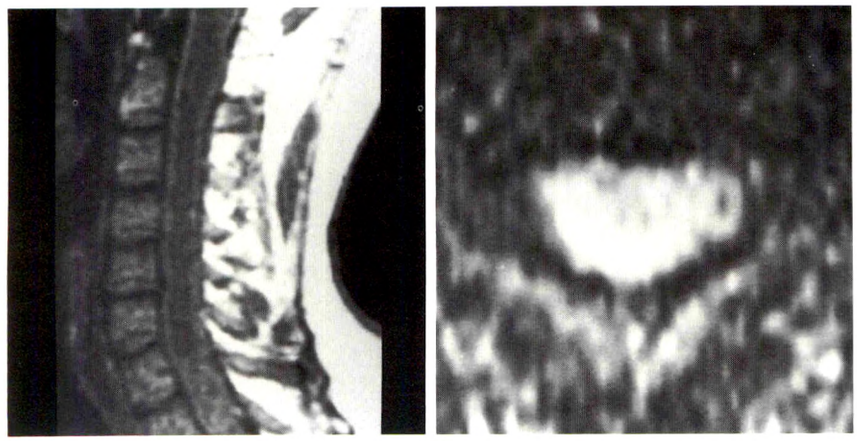


Fig. 7.—Large spinal cord cyst in cervical cord associated with ependymoma.

***A*, T1-weighted sequence shows large area of low signal in enlarged cord.**

***B*, Axial T2-weighted scan (TR = 2000, TE = 80, 3-mm slice thickness) shows high signal from cyst fluid with no evidence of pulsation.**

fourth ventricle. Clefts in the spinal cord have been reported between the cyst and subarachnoid space in the posttrauma type of syrinx but not in other types [19]. The possibility for such communications requires further elaboration. Simple transmission from the subarachnoid space through the cord is unlikely since tumor cysts that are much larger than syringes and that also compress the subarachnoid space showed no similar pulsation. Our investigation detected pulsation within the syrinx but did not characterize the direction or magnitude of the velocity components relative to systole and diastole or to location within the syrinx. Quantitative assessment of several segments of a syrinx is necessary to fully understand its fluid dynamics and the source and direction of pulsations.

Normally the cervical and thoracic subarachnoid spaces act as a conduit for CSF pulsations with the lumbar area, which serves as the area of compliance. In syringomyelia the cystic cavity seems to serve as a conduit for pulsations, especially when the cord is large enough to obliterate the subarachnoid space. If the cystic cavity has a distal blind pouch then the pulsations must be transmitted through the cord to the lumbar sac, which can still serve as the major area of compliance. This may be one mechanism of cord damage. After spine trauma, which causes high-grade or complete canal stenosis, the ability of the lumbar sac to provide compliance in the system may be compromised. In such instances the cord may be subjected to greater pulsatile stress. If the syrinx cavity has a distal opening then it would serve primarily as a conduit and the cord would be subjected to less stress compared with a syrinx cavity with a blind pouch. One benefit afforded by current surgical treatments, which create such openings to the subarachnoid space or the peritoneal cavity, may be relief of such pulsatile stress on the cord [20]. If shunting collapses the cyst, it may remain collapsed and show no pulsation.

Cord damage in syringomyelia is complex. Three structural changes seem relevant: cysts with pulsating fluid, cysts with static fluid, and intrinsic cord-tissue damage. When pulsating and nonpulsating cysts coexist, the nonpulsating cystic fluid collections are smaller and appear not to communicate with the main, usually larger pulsating cyst in the presurgical state. Significant cord damage was observed and was manifested as areas of high signal intensity on T2-weighted images. We have no histologic data to further define the cause of the abnormal high signal. Given the mechanical stress on the cord, gliosis is the most likely explanation. Local reabsorption of CSF could have a small role, but the lack of significant change after shunting suggests it was not a major factor. This abnormal signal could involve a thinned cord diffusely or could be more segmental in a more normal-sized cord. The degree of involvement was greater with pulsating cysts than with nonpulsating cysts. This cord abnormality could exhibit normal signal intensity on T1-weighted images but was easily identified as abnormal high signal of the spinal cord on T2-weighted scans. Cord damage, when more severe, could exhibit low signal intensity on T1-weighted images. When this occurs it cannot always be differentiated definitively from small static fluid cysts except by intraoperative sonography [3, 4, 21]. Metrizamide CT also cannot make this differentiation reliably [3, 4, 21, 22]. In our limited series, the cord damage was not reversed by surgery except for partial resolution in one patient.

Decompressing and shunting a syrinx seems to have a beneficial clinical effect in that it can reduce pain and sometimes improve, but usually only halt, the progression of motor and sensory deficits [4, 20, 21]. At present the best criterion for shunting seems to be the size of the cyst, the larger cysts seemingly responding better than the smaller ones [4]. If symptoms are related primarily to cord-tissue damage, surgical intervention does not seem indicated [4]. Given our findings, it would seem worthwhile for investigations to correlate the progression of symptoms and the response to treatment with two factors: (1) changes in cyst size and (2) changes in the presence and nature of fluid pulsation. This could be taken one more step, quantitation of pulsation throughout the syrinx. Since the large cysts are usually the pulsatile ones, their favorable response to surgery is not surprising [4]. Many posttrauma patients remain stable. This

may be because they have only small, localized, nonpulsatile cysts. The MR scan has opened up numerous avenues for investigating the natural history of all types of syrinx and the opportunity to better select patients for surgical intervention. We consider the presence of pulsation in the syrinx to be an important new variable in assessing its correlation with clinical findings, its progression, and its response to surgery.

Nonneoplastic cystic disease of the spinal cord appears to be somewhat more common than initially suspected. In many patients, especially those with the Chiari I malformation, syringomyelia is relatively easy to diagnose with MR. But as the spectrum of nonneoplastic cystic disease of the spinal cord broadens, differentiation from cyst associated with cord tumor may become more difficult [8, 23]. A syrinx with prominent, thick septations can mimic neoplasm, especially when the cord is enlarged. The diagnosis of neoplasm can be made confidently if cord enlargement can be identified at another level of the cord where no cyst has formed. Such a region may not be readily apparent. Axial long-TR, long-TE scans through a cystic region can be used to help make the neoplastic/nonneoplastic differentiation. In our experience, cysts associated with intrinsic spinal cord tumors, even when they are quite large, exhibit high signal and show no areas of signal loss that would indicate fluid pulsation. This differs from our syrinx patients with large cysts, all of whom had evidence for fluid pulsation. Techniques for detecting pulsation, therefore, can be helpful in differentiating neoplastic from nonneoplastic spinal cord cysts.

ACKNOWLEDGMENT

We thank Andrew Yeates for contributions to the case material.

REFERENCES

1. Scher AT. Syringomyelia secondary to paraplegia due to fractures of the thoracic spine. *S Afr Med J* **1976**;50:1406–1408
2. Shannon N, Symon L, Gogue V, Cull D, Kang J, Kendall B. Clinical features, investigation and treatment of post-traumatic syringomyelia. *J Neurol Neurosurg Psychiatry* **1981**;44:35–42
3. Quencer RM, Green BA, Eismont FJ. Posttraumatic spinal cord cysts: clinical features and characterization with metrizamide computed tomography. *Radiology* **1983**;146:415–423
4. Gebarski SS, Maynard FW, Gabrielsen TO, Knake JE, Latack JT, Hoff JT. Posttraumatic progressive myelopathy. *Radiology* **1985**;157:379–385
5. Aubin ML, Vignaud J, Jardin C, Bar D. Computed tomography in 75 clinical cases of syringomyelia. *AJNR* **1981**;2:199–204
6. Foster NL, Wing SD, Bray PF. Metrizamide ventriculography in syringomyelia. *Neurology* **1980**;30:1323–1326
7. Bonafe A, Manelfe C, Espagno J, Guiraud B, Rascol A. Evaluation of syringomyelia with metrizamide computed tomography myelography. *J Comput Assist Tomogr* **1980**;4:797–802
8. Resjo IM, Harwood-Nash DC, Fitz CR, Chuang S. Computed tomographic metrizamide myelography in syringohydromyelia. *Radiology* **1979**; 131:405–407
9. Kokmen E, Marsh WR, Baker HL. Magnetic resonance imaging in syringomyelia. *Neurosurgery* **1985**;17:267–270
10. Lee BCP, Zimmerman RD, Manning JJ, Deck MDF. MR imaging of syringomyelia and hydromyelia. *AJNR* **1985**;6:221–228
11. Pojunas K, Williams AL, Daniels DL, Haughton VM. Syringomyelia and hydromyelia: magnetic resonance evaluation. *Radiology* **1984**;153:679–683
12. Yeates A, Brant-Zawadzki M, Norman D, Kaufman L, Crooks LE, Newton TH. Nuclear magnetic resonance imaging of syringomyelia. *AJNR* **1983**;4:234–237
13. Rubin JB, Enzmann DR. Harmonic modulation of proton MR precessional phase by pulsatile motion: origin of spinal CSF flow phenomenon. *AJNR* **1987**;8:307–318
14. Rubin JB, Enzmann DR. CSF gated spine MRI: theory and clinical implementation. *Radiology* (in press)
15. Enzmann DR, Rubin JB, DeLaPaz R, Wright A. Benefits and pitfalls in MRI scanning resulting from CSF pulsation. *Radiology* **1986**;161:773–778
16. Wehrli FW, Shimakawa A, Gullberg GT, MacFall JR. Time-of-flight MR flow imaging revisited: selective-saturation recovery with gradient refocusing. *Radiology* **1986**;160:781–785
17. Perkins TG, Wehrli FW. CSF signal enhancement in short TR gradient echo images. *Magnetic Resonance Imag* (in press)
18. Gomori JM, Grossman RI, Goldberg HI, Zimmerman RA, Bilaniuk LT. Intracranial hematomas: imaging by high-field MR. *Radiology* **1985**;157:87–93
19. Post MJD, Quencer RM, Green BA, Montalvo BM, Eismont FJ. Radiologic evaluation of spinal cord fissures. *AJNR* **1986**;7:329–335
20. Barbaro NM, Wilson CB, Gutin PH, Edwards MSB. Surgical treatment of syringomyelia. *J Neurosurg* **1984**;61:531–538
21. Quencer RM, Sheldon JJ, Post MJD, et al. Magnetic resonance imaging of the chronically injured cervical spinal cord. *AJNR* **1986**;7:457–464
22. Quencer RM, Morse BM, Green BA, Eismont FS, Brost P. Intraoperative spinal sonography: adjunct to metrizamide CT in the assessment and surgical decompression of post-traumatic and surgical decompression of posttraumatic spinal cord cysts. *AJNR* **1984**;5:71–79
23. Rubin JM, Aisen AM, DiPietro MA. Ambiguities in MR imaging of tumoral cysts in the spinal cord. *J Comput Assist Tomogr* **1986**;10:395–398

Book Review

Magnetic Resonance Imaging of the Central Nervous System. Edited by Michael Brant-Zawadzki and David Norman. New York: Raven, 404 pp., 1987. $89.50

As stated in the preface, this text attempts to collate the accumulated knowledge of MR imaging of the CNS and transmit it to the "individual for whom the clinical applications of MRI are fairly new." Material is presented in four distinct sections, including basic physical principles (seven chapters), clinical aspects of brain MR imaging (nine chapters), spine imaging (two chapters), and head and neck MR imaging (two chapters). Each chapter is written by a different author or authors, all of whom are experts in their particular subjects of discussion. Overall, there are 23 contributors, and the book varies in style and is sometimes repetitious.

A thorough treatment of the physical principles of MR imaging begins the work. It is in this portion of the book that the greatest differences in style and emphasis are encountered. The initial chapter simplifies the discussion of the generation of the MR signal and T1 and T2 relaxation but includes few line drawings to aid understanding. Succeeding chapters more completely address how the generated MR signal is modified by flowing blood and cerebrospinal fluid, and by such important pathologic processes as edema and hemorrhage. The liberal use of line drawings, graphs, and other figures help the reader to grasp these fundamentals. The chapter on image artifacts and technical limitations in MR imaging is a most complete and readable treatment of pitfalls and annoyances encountered in clinical imaging, and it deserves special attention.

Clearly, the greatest strength of the work is in the presentation of the clinical aspects of brain and spine imaging. In these 11 chapters are included a museumlike display of common and uncommon MR appearances of intra- and extraaxial CNS lesions with succinct and uniformly helpful explanatory text. The separate chapters on brain tumors, ischemia, congenital anomalies, intracranial infection, pituitary lesions, white-matter diseases, and spine MR are particularly authoritative. Both the novice and the veteran MR physician can benefit from thorough study of this material.

Imaging of the neck and nasopharynx are described in separate chapters. After discussion of the normal anatomy of these complex regions (aided by profuse MR illustrations) common pathologic entities are demonstrated. Although this treatment of head and neck disease is most useful, there is no mention of orbital or ocular disease, a curious omission.

The format of the book and completeness of the index lends itself to easy reference and encourages use on an as-needed basis. The small number of typographic errors and mislabeled figures is certainly acceptable and does not place a great burden on the reader.

I can strongly recommend this book to clinically oriented MR physicians at all levels of experience as well as to radiology residents and fellows. In addition, referring clinicians in neurosurgery, neurology, and ENT may find this book helpful in interpreting the results generated by this important new imaging method.

Gary A. Press
University of California, San Diego, Medical Center
San Diego, CA 92103-9981

Differentiation of Intramedullary Neoplasms and Cysts by MR

Alan L. Williams[1]
Victor M. Haughton
Kathleen W. Pojunas
David L. Daniels
David P. Kilgore

To determine the MR criteria that are effective for differentiating intramedullary neoplasms from syringo- or hydromyelia, we reviewed MR scans made on prototype and commercial imagers of 33 patients with surgically confirmed cord abnormalities, including nine intramedullary neoplasms and 20 cysts (syringo- or hydromyelia). Two radiologists who did not know the clinical and radiologic diagnoses were asked to evaluate the scans with respect to (1) cord expansion, (2) distinctness of the disease margin, (3) homogeneity, and (4) signal intensity. These observations were correlated with the proved diagnoses. The combination of distinct margins and uniform signal intensity equal to that of CSF correlated consistently (88%) with spinal cord cysts. Other combinations were less reliable for diagnosing a cyst or tumor.

MR imaging has been shown to demonstrate, effectively and noninvasively, a variety of spinal diseases [1–14]. However, previously described MR criteria for differentiating intramedullary neoplasms and cysts have not been evaluated objectively. Therefore, for the purpose of selecting the most accurate MR criteria, we reviewed a series of patients with surgically confirmed intramedullary abnormalities.

Materials and Methods

MR scans were reviewed in 33 patients (14 males and 19 females ranging in age from 6 to 71 years) with intramedullary lesions studied between May 1983 and November 1985. Scans were acquired on various prototype (0.5–1.5 T) MR imagers at the General Electric facility in New Berlin, WI, or on a 1.5-T commercial MR scanner (GE Signa) at the Milwaukee County Medical Complex. All patients were studied with short TR spin-echo pulse sequences (TR = 500–800 msec,TE = 20–25 msec) and 16 were also studied with long TR spin-echo pulse sequences (TR = 2000–2500 msec,TE = 20–25 msec and 80–100 msec). Scans were obtained with a standard body coil in 16 patients and with 7.5- or 10-cm "butterfly" surface coils (Medical Advances, Inc., Milwaukee, WI) in 17 patients [15]. Other imaging parameters included 3–10 mm slice thickness, 0–2 mm slice interspacing, 2–4 excitations, 4–10 min acquisition time, 128 × 256 or 256 × 256 matrixes, and 16–25 cm field of view. Imaging was routinely performed in the sagittal plane; additional images in the axial plane were obtained in seven patients.

MR scans in the 33 patients were evaluated by two senior radiology residents who did not know the clinical and radiologic diagnoses. The readers were asked to report four different MR observations: (1) expanded cord (larger anteroposterior diameter than the remainder of the cord), (2) distinct or indistinct margins in the disease, (3) uniform or nonuniform signal intensity in the disease, and (4) signal intensity of the disease isointense with CSF or not.

Results

The intramedullary abnormalities included nine neoplasms (five astrocytomas, three ependymomas, and one lipoma), 20 cysts (syrinx or hydromyelia), two cases of myelomalacia, one case of viral myelitis, and one case of hematoma. Diagnoses

This article appears in the May/June 1987 issue of *AJNR* and the July 1987 issue of *AJR*.

Received June 6, 1986; accepted after revision November 21, 1986.

Presented at the annual meeting of the American Society of Neuroradiology, San Diego, January 1986.

[1] All authors: Department of Radiology, Medical College of Wisconsin, Froedtert Memorial Lutheran Hospital, 9200 West Wisconsin Ave., Milwaukee, WI 53226. Address reprint requests to A. L. Williams.

***AJR* 149:159–164, July 1987**
0361–803X/87/1491–0159
© American Roentgen Ray Society

were verified at surgery by biopsy, cyst puncture, or, in cases of myelomalacia, intraoperative sonography.

The data are tabulated in two ways: the percentage of cysts or tumors with the MR observation is recorded in Table 1, and the percentage of MR observations in which a cyst was found is recorded in Table 2. In the cases of intramedullary cyst, an expanded cord was reported in 78% of patients, distinct margins in 73%, uniform signal intensity in

TABLE 1: Frequency* (%) of MR Observations in 33 Spinal Cord Lesions

Nosologic Diagnosis	Observation			
	Expanded Cord	Distinct Margins	Uniform Signal Intensity	Isointensity
Neoplasm	78	44	44	17
Syringohydromyelia	78	73	75	78
Other**	38	50	25	38

* Frequency = percentage of the nosologic category with the MR finding.
** Includes myelomalacia, viral myelitis, and hematoma.

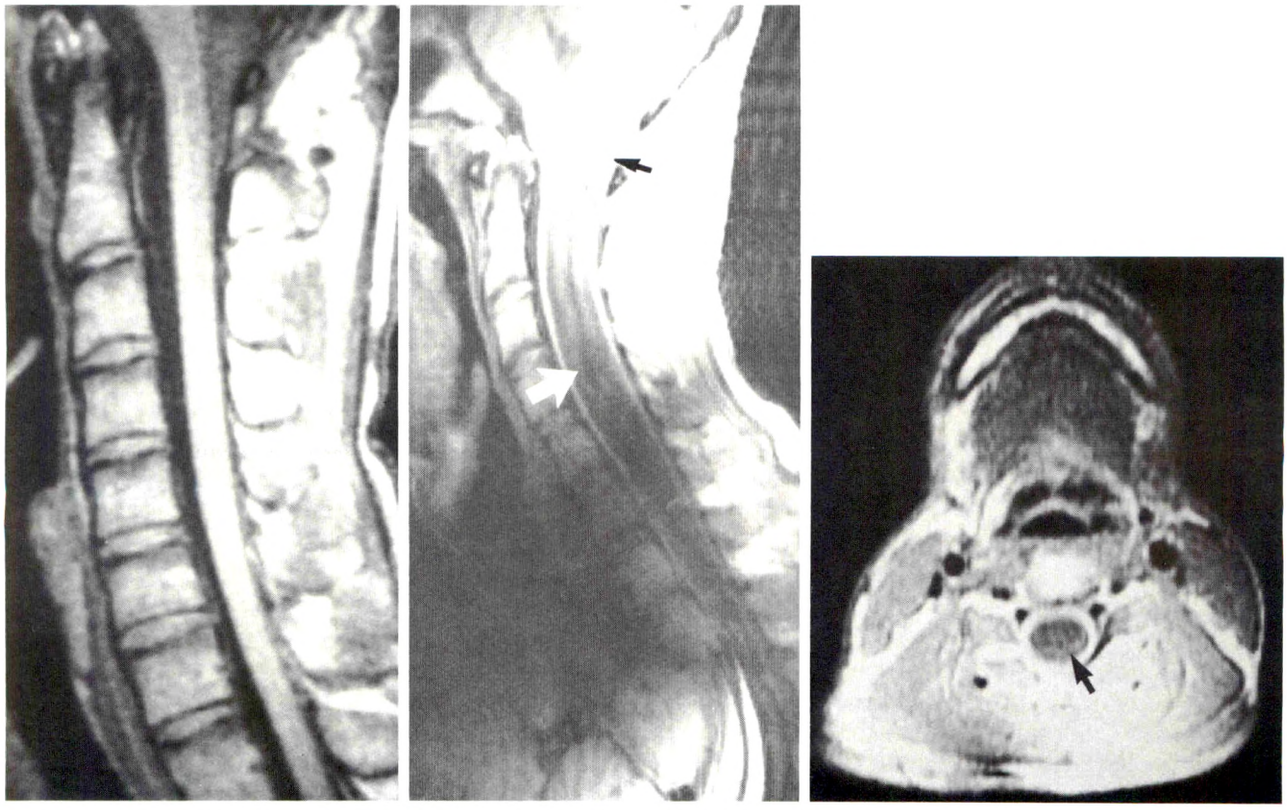
TABLE 2: Accuracy* of MR Findings in Predicting a Diagnosis

MR Observation	Nosologic Diagnosis	Diagnostic Accuracy (%)
Distinct margins	Syringohydromyelia	78
Uniform signal intensity	Syringohydromyelia	76
Isointensity (CSF)	Syringohydromyelia	85

* Accuracy = percentage of cases with the MR finding that had the specific nosologic diagnosis.

TABLE 3: Accuracy of MR Findings in Predicting a Diagnosis

MR Observation	Nosologic Diagnosis	Diagnostic Accuracy (%)
Distinct margins, uniform signal intensity, and isointensity (CSF)	Syringohydromyelia	88
Indistinct margins, nonuniform signal intensity, and nonisointensity (CSF)	Neoplasm	60



A B

Fig. 1.—Normal cervical cord. In sagittal T1-weighted spin-echo image (TR = 800 msec, TE = 25 msec), cervical spinal cord has virtually uniform anteroposterior dimension and homogeneous signal intensity.

Fig. 2.—Typical MR appearance of hydromyelia in 19-year-old man. Sagittal (*A*) and axial (*B*) short TR spin-echo images (TR = 400 msec, TE = 25 msec) demonstrate marked expansion of cervical central canal (*large arrow*). Cyst margins are well defined and cyst fluid is homogeneous and isointense with CSF. Note low-lying cerebellar tonsils (*small arrow*) in this patient with Chiari I malformation.

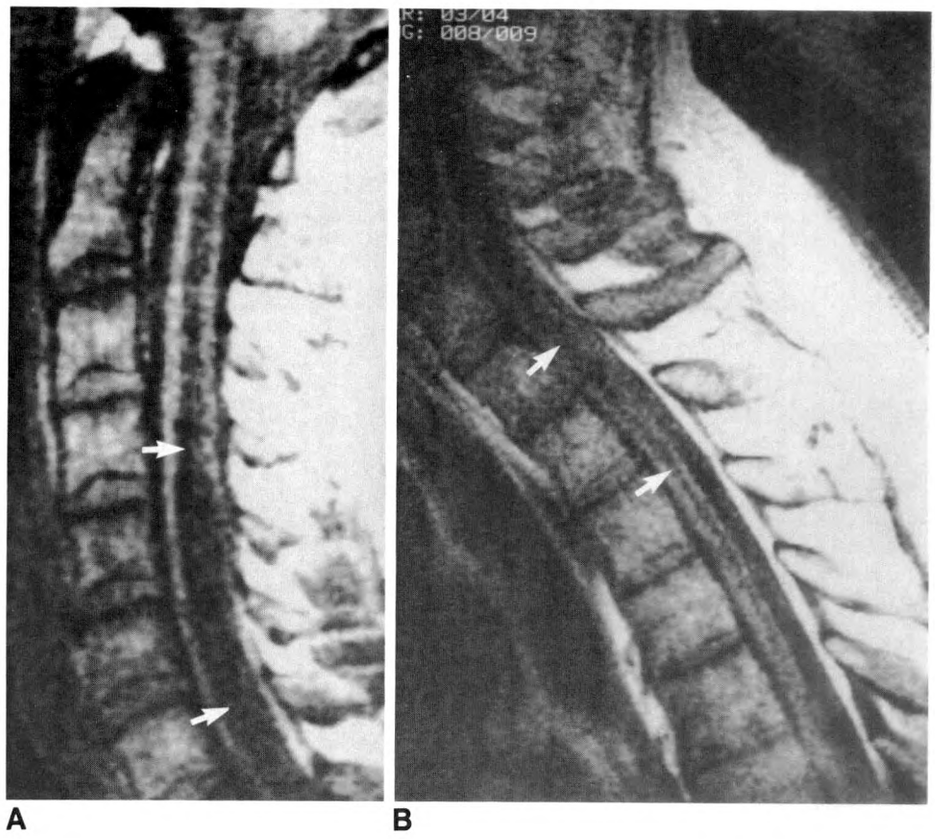


Fig. 3.—Characteristic MR findings in syringomyelia. Sagittal short TR spin-echo images (TR = 600 msec, TE = 25 msec) through cervical (*A*) and cervicothoracic (*B*) regions in 38-year-old man show expansion of mid and lower cervical cord secondary to extensive syrinx (*arrows*). Syrinx margins are well defined and cyst fluid is isointense with CSF.

75%, and isointensity with CSF in 78%. In patients with neoplasm, cord expansion was also reported in 78% of patients, distinct margins in 44%, uniform signal intensity in 44%, and isointensity in 17%. A cyst was confirmed surgically in 78% of reported distinct margins, in 76% of reported uniform signal intensities, and in 85% of reported signal isointensity. When the three criteria—distinct margins, uniform signal intensity, and isointensity—were observed in the same patient, the likelihood of syringo- or hydromyelia was 88% (Table 3). With a combination of indistinct margins, nonuniform signal intensity, and nonisointensity the likelihood of neoplasms was only 60%.

Discussion

Syringomyelia refers to a glial-lined cavity within the spinal cord. Hydromyelia represents cystic dilatation of the cord's central canal. Syringohydromyelia, a nonspecific term describing a nonneoplastic intramedullary cyst, encompasses both syringomyelic and hydromyelic abnormalities.

Conventional CT or myelographic imaging is imperfect in distinguishing intramedullary neoplasm and syringo- or hydromyelia. Myelography does not reliably differentiate intramedullary tumor from cyst because both abnormalities typically show a fusiformly expanded cord as a filling defect within the subarachnoid contrast column [16]. Unenhanced CT may show the cord [17]; however, artifacts from adjacent osseous structures or body parts outside the reconstruction circle tend to obscure the cord margins and small intramedullary cysts. Intrathecally enhanced CT effectively shows cord margins and may demonstrate opacification of intramedullary cysts on immediate or delayed CT scans [18–20]. However, not all cases of syringo- or hydromyelia show intramedullary contrast enhancement, and cystic neoplasms and myelomalacia may also show enhancement within cord substance [21, 22].

The sensitivity of MR for detecting spinal disease is high. Because of its excellent contrast resolution, MR effectively demonstrates the spinal cord (Fig. 1) and detects various intramedullary abnormalities, including syringo- or hydromyelia (Figs. 2 and 3), neoplasm (Figs. 4–7), myelomalacia (Fig. 8), hematoma (Fig. 9), and arteriovenous malformation.

The typical intramedullary cyst is characterized by a glial cell (syringomyelia) or ependymal (hydromyelia) lining, which provides a sharp interface with the cyst fluid. Thus, most cysts appear in MR images as an abnormality with sharply defined margins, uniform signal intensity, and isointensity with CSF (Figs. 2 and 3). Occasionally, collagenous bands or synechiae crossing the cyst cavity from one wall to the other or a high protein concentration in the cyst fluid may produce nonuniform signal intensity, hyperintensity, or ill-defined mar-

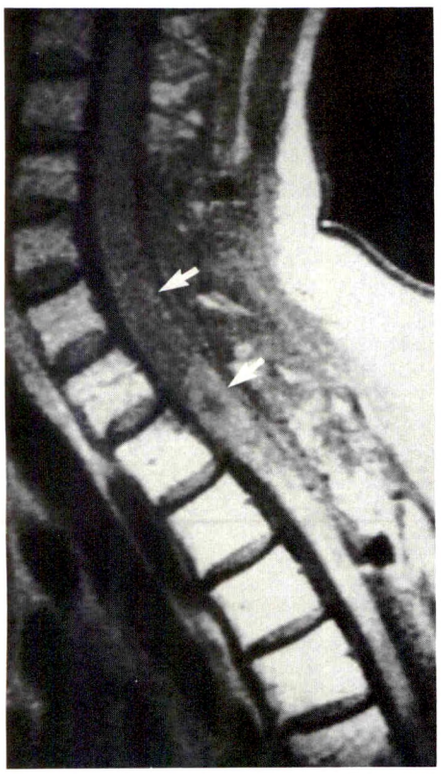


Fig. 4.—Characteristic MR findings in astrocytoma. Short TR spin-echo image (TR = 800 msec, TE = 25 msec) in 53-year-old-woman shows lower cervical cord expanded by inhomogeneous, poorly marginated, intramedullary neoplasm (*arrows*). Signal intensity of tumor is greater than that of CSF.

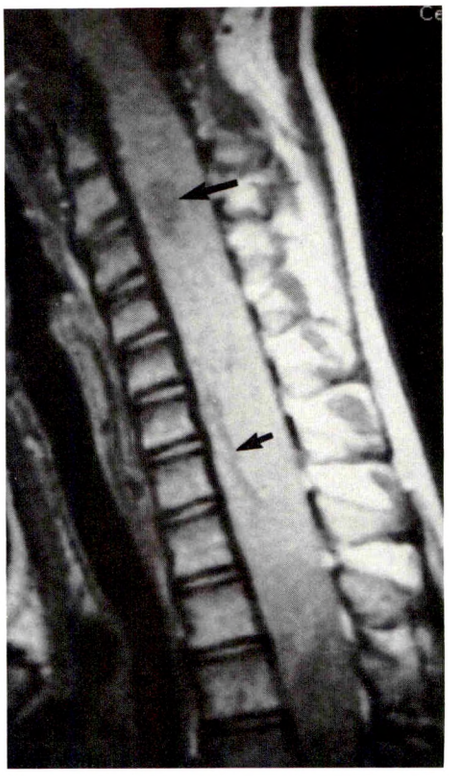


Fig. 5.—Indistinct margins in an ependymoma in 6-year-old boy with neurofibromatosis. Sagittal T1-weighted spin-echo image (TR = 600 msec, TE = 25 msec) shows diffuse expansion of cervical and upper thoracic cord. Tumor margins cannot be distinguished. Note area of cystic degeneration (*large arrow*) and dilated vessel (*small arrow*).

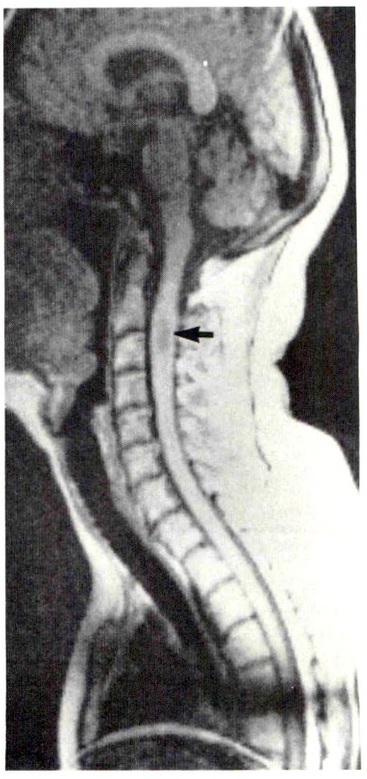
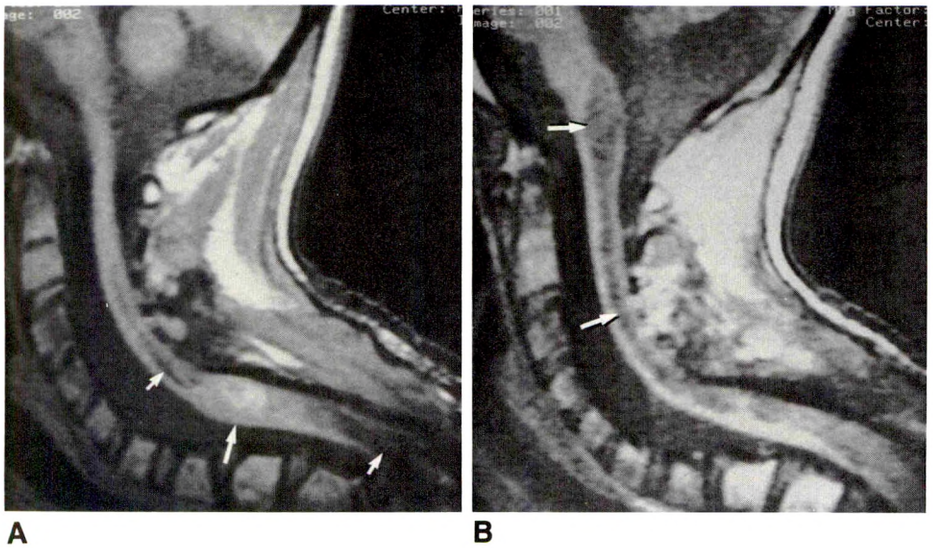
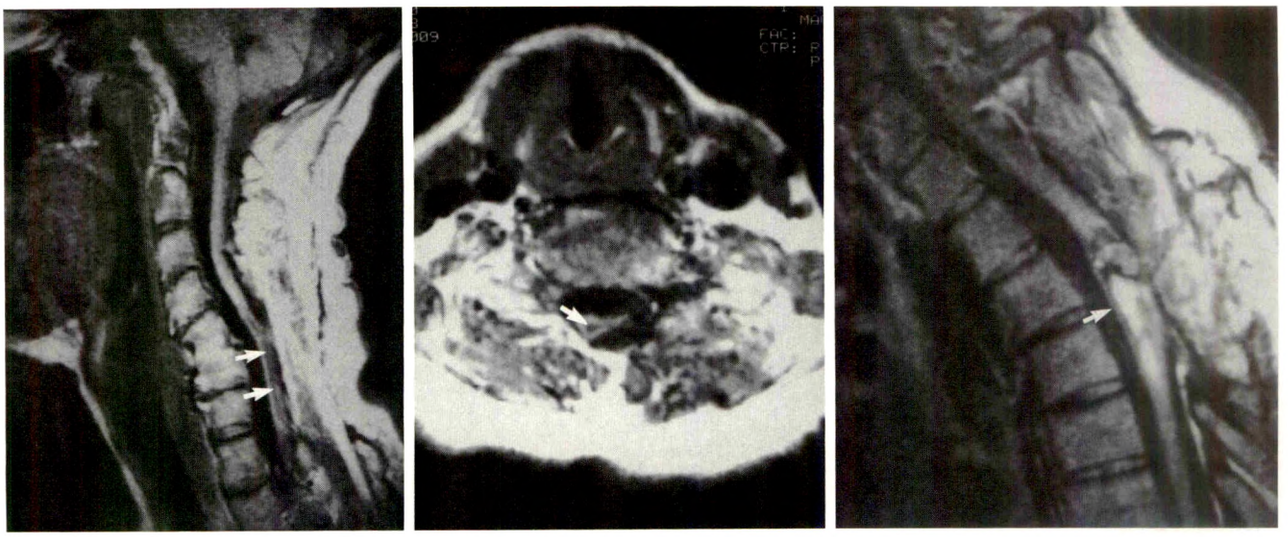


Fig. 6.—Cervical ependymoma. Focal expansion of cord in 43-year-old woman secondary to indistinctly marginated tumor (*arrow*) is identified in T1-weighted spin-echo image (TR = 350 msec, TE = 20 msec). Signal intensity of tumor is intermediate between normal cord and CSF.



A B

Fig. 7.—*A* and *B*, Astrocytoma with syrinx in 13-year-old boy. Short TR sagittal spin-echo images (TR = 600 msec, TE = 25 msec) show inhomogeneous, hyperintense expansile process (*large arrow* in *A*) at cervicothoracic junction associated with extensive, sharply marginated cervicomedullary and upper thoracic cyst (*small arrows* in *A* and *B*). Patient has had previous surgery and radiation therapy.



A B

Fig. 8.—Myelomalacia in 53-year-old woman with a history of chronic posttraumatic myelopathy. Sagittal (*A*) and axial (*B*) T1-weighted spin-echo images (TR = 600 msec, TE = 25 msec) show an atrophic, misshapen, lower cervical cord associated with intramedullary zone of decreased signal intensity (*arrows*). Myelomalacia was confirmed by intraoperative sonography. Note solid C5–C6 anterior vertebral fusion and abnormal spinal curvature.

Fig. 9.—Intramedullary hematoma in 30-year-old woman with a history of previous spontaneous intramedullary hemorrhage. Recurrent symptoms prompted MR examination. Sagittal short TR spin-echo image (TR = 800 msec, TE = 25 msec) shows focal expansion of cervicothoracic cord secondary to inhomogeneous process (*arrow*) containing both high and low signal intensity tissue that represents subacute hematoma.

gins [23]. In addition, pulsatile CSF movement may occasionally cause inhomogeneous signal intensity within an intramedullary cyst in T2-weighted images [24]. However, our study suggests that when a combination of three criteria—distinct margins, uniform signal intensity, and isointensity (with CSF)—are observed in MR scans in a patient with an expanded cord, the diagnosis of syringo- or hydromyelia can be made with a high degree of accuracy. In these cases additional imaging studies may not be needed. As surface coil advances and other technical improvements increase MR resolution, even greater accuracy should be noted.

MR is less accurate in characterizing intramedullary tumors. Primary tumors such as astrocytomas and ependymomas tend to infiltrate adjacent cord tissue and evoke reactive edema [25]. This combination of infiltrating tumor and edema results in ill-defined margins in MR images (Figs. 4–6). Necrosis, cystic degeneration, or hemorrhage may cause tumors to have an inhomogeneous MR appearance (Figs. 4, 5, 7). Highly proteinaceous fluid within zones of cystic degeneration may produce hyperintensity or nonuniform signal intensity on MR. Thus, poorly defined margins, inhomogeneity, and lack of isointensity suggest neoplasm. The combination of indistinct margins, nonuniform signal intensity, and nonisointensity was present in a small majority of our tumors but cannot be considered diagnostic of neoplasm. In cases where an intramedullary neoplasm is associated with a syrinx, MR may show features of both abnormalities (Fig. 7).

REFERENCES

1. Norman D, Mills CM, Brant-Zawadzki M, Yeates A, Crooks LE, Kaufman L. Magnetic resonance imaging of the spinal cord and canal: potentials and limitations. *AJR* **1983**;141:1147–1152, *AJNR* **1984**;5:9–14
2. Moon KL, Genant HK, Helms CA, Chafetz NI, Crooks LE, Kaufman L. Musculoskeletal applications of nuclear magnetic resonance. *Radiology* **1983**;147:161–171
3. Han JS, Kaufman B, El Yousef SJ, et al. NMR imaging of the spine. *AJNR* **1983**;4:1151–1159
4. Modic MT, Weinstein MA, Pavlicek W, et al. Nuclear magnetic resonance imaging of the spine. *Radiology* **1983**;148:757–762
5. Modic MT, Weinstein MA, Pavlicek W, Boumphrey F, Starnes D, Duchesneau PM. Magnetic resonance imaging of the cervical spine: technical and clinical observations. *AJNR* **1984**;5:15–22
6. Bradley WG, Waluch V, Yadley RA, Wycoff RR. Comparison of CT and MR in 400 patients with suspected disease of the brain and cervical spinal cord. *Radiology* **1984**;152:695–702
7. Pojunas K. Williams AL, Daniels DL, Haughton VM. Syringomyelia and hydromyelia: magnetic resonance evaluation. *Radiology* **1984**;153:679–683
8. Gebarski SS, Maynard FW, Gabrielsen TO, Knake JE, Latack JT, Hoff JT. Posttraumatic progressive myelopathy. Clinical and radiologic correlation employing MR imaging, delayed CT metrizamide myelography and intraoperative sonography. *Radiology* **1985**;157:379–385
9. Spinos E, Laster DW, Moody DM, Ball MR, Witcofski RL, Kelly DL. MR evaluation of Chiari I malformations at 0.15 T. *AJNR* **1985**;6:203–208
10. Hyman RA, Edwards JH, Vacirca SJ, Stein HL. 0.6 T MR imaging of the cervical spine: multislice and multi-echo techniques. *AJNR* **1985**;6:229–236
11. Lee BCP, Zimmerman RD, Manning JJ, Deck MDF. MR imaging of syringomyelia and hydromyelia. *AJNR* **1985**;6:221–228

12. Baker HL, Berquist TH, Kispert DB, et al. Magnetic resonance imaging in a routine clinical setting. *Mayo Clin Proc* **1985**;60:75–90
13. Kucharczyk W, Brant-Zawadzki M, Sobel D, et al. Central nervous system tumors in children: detection by magnetic resonance imaging. *Radiology* **1985**;155:131–136
14. DiChiro G, Doppman JL, Dwyer AJ, et al. Tumors and arteriovenous malformations of the spinal cord: assessment using MR. *Radiology* **1985**;156:689–697
15. Kneeland JB, Jesmanowicz A, Froncisz W, Grist TM, Hyde JS. High-resolution MR imaging using loop-gap resonators. *Radiology* **1986**; 158:247–250
16. Shapiro R: *Myelography*, 4th ed. Chicago: Year Book Medical, **1984**:218–222, 346–358
17. Haughton VM, Williams AL. *Computed tomography of the spine*. St. Louis: Mosby, **1982**:31–41
18. Aubin ML, Vignaud J, Jardin C, Bar D. Computed tomography in 75 clinical cases of syringomyelia. *AJNR* **1981**;2:199–204
19. Dorwart RH, LaMasters DL, Watanabe TJ. Tumors. In Newton TH, Potts DG, eds. *Computed tomography of the spine and spinal cord: modern neuroradiology*, vol. 1. San Anselmo, CA: Clavadel Press, **1983**:115–147
20. Seibert CE, Dreisbach JN, Swanson WB, Edgar RE, Williams P, Hahn H. Progressive post-traumatic cystic myelopathy: neuroradiologic evaluation. *AJNR* **1981**;2:115–119
21. Kan S, Fox AJ, Vinuela F, Barnett HJM, Peerless SJ. Delayed CT metrizamide enhancement of syringomyelia secondary to tumor. *AJNR* **1983**;4:73–78
22. Quencer RM, Green BA, Eismont FJ. Posttraumatic spinal cord cysts: clinical features and characterization with metrizamide computed tomography. *Radiology* **1983**;146:415–423
23. Adams JH, Corsellis JAN, Duchen LW, eds. *Greenfield's neuropathology*, 4th ed. New York: Wiley Medical, **1984**:396–402
24. Sherman JL, Citrin CM, Gangarosa RE, Bowen BJ. The MR appearance of CSF pulsations in the spinal canal. *AJNR* **1986**;7:879–884
25. Rubenstein LJ. Tumors of the central nervous system. In *Atlas of tumor pathology*, 2nd series, fascicle 6. Washington, DC: Armed Forces Institute of Pathology, **1972**:10–12

Radiation Effects on Cerebral White Matter:
MR Evaluation

Jay S. Tsuruda[1, 2]
Keith E. Kortman[1, 3]
William G. Bradley[1, 3]
Donald C. Wheeler[1]
William Van Dalsem[1]
Thomas P. Bradley[1]

The purpose of this study was to evaluate the white-matter changes associated with cranial radiation by MR imaging. The MR scans of 95 patients receiving conventional external beam radiation for a wide variety of central nervous system tumors were reviewed. Moderately T2-weighted spin-echo images with a 2000-msec repetition time and 56-msec-echo time were analyzed for white-matter abnormalities without knowledge of the patient's history. These were correlated with radiation dose, port, and time interval since completion of therapy, and then compared with an age-matched control group of 180 patients with nonirradiated, space-occupying, intracranial lesions. Radiation-related lesions were characterized as symmetric, high-signal foci in the periventricular white matter. Relative sparing of the posterior fossa, basal ganglia, and internal capsules was noted. In patients older than 20 years, these changes paralleled those seen in ischemia but were more prevalent ($p < .005$). In 25 patients with sequential MR scans, these findings remained stable. In those patients with limited treatment fields, for example, pituitary adenomas, no statistical differences were seen between radiation-treated and nontreated groups. Cerebral white-matter changes that mimic deep white-matter infarction are frequently seen in response to therapeutic radiation. There is a variable incidence of radiation effects, becoming more marked in older patients. MR interpretation must consider the neuropathologic consequences of therapeutic radiation, which include demyelination, microvascular occlusion, and blood-brain barrier breakdown.

The goal of therapeutic radiology is to provide a sufficient dose to treat central nervous system (CNS) tumors without affecting adjacent healthy tissue. As more therapeutic regimens have been implemented, long-term effects of neurotoxicity in the surviving patients have been recognized [1–3]. A spectrum of CNS changes has been noted on CT including atrophy, decreased attenuation of the deep cerebral white matter, and rarely focal, enhancing radionecrosis [4–7]. The findings of neurotoxicity have been correlated with clinical findings in both patients and clinical experiments [1]. More recently, similar findings of radiotherapy-related lesions of the brain have been described with MR [8–10]. Of interest, is the formation of deep white-matter periventricular foci characterized by prolonged T1 and T2 relaxation times compared with normal white matter [10] in a pattern suggestive of either demyelination or ischemia. Both can be identified readily by MR [11]. Since the natural prevalence and severity of focal periventricular abnormalities (e.g., deep white-matter infarction) increase with age [11, 12], these abnormalities must be considered before ascribing changes to radiotherapy. For this reason, a retrospective review of a large patient population was undertaken; MR was used to further characterize the effects of radiation on cerebral white matter with respect to age, prevalence, time of onset, and both the temporal and spatial stability of these lesions.

Materials and Methods

MR imaging was performed using a Diasonics MT/S system operating at 0.35 T. Multiple-

This article appears in the May/June 1987 issue of *AJNR* and the July 1987 issue of *AJR*.

Received August 20, 1986; accepted after revision December 16, 1986.

Presented at the annual meeting of the American Roentgen Ray Society, Washington, DC, April 1986.

[1] NMR Imaging Laboratory, Huntington Medical Research Institutes, 10 Pico St., Pasadena, CA 91105. Address reprint requests to W. G. Bradley.

[2] Present address: Department of Radiology, University of California, San Francisco, CA 94143.

[3] Department of Radiology, Huntington Memorial Hospital, Pasadena, CA 91105.

***AJR* 149:165–171, July 1987**
0361–803X/87/1491–0165
© American Roentgen Ray Society

slice spin-echo scans were performed with a repetition time (TR) of 2000 msec and an echo time (TE) of 28 and 56 msec. Four excitations were used. Axial images were obtained in the majority of patients (90%) in both the therapeutic and control groups. The remainder had coronal studies only. In selected patients, additional images were obtained with a TR of 500 and/or 1000 msec in either the axial, sagittal, or coronal plane; however, these images were not included in this study. The acquisition matrix was 128 × 128, corresponding to a spatial resolution of 1.7 mm. Slice thickness was 7 mm with a 3-mm gap between sections. In two patients, an axial study was performed with a 256 × 256 matrix (0.95-mm spatial resolution) and 10-mm contiguous sections having a TR of 2000 msec and a TE of 30 and 60 msec. The images were graded for white-matter abnormalities as described below.

Radiation Therapy Group

We reviewed retrospectively 95 patients imaged between May 1983 and April 1986 who had received external beam-radiation therapy. All patients received conventional therapy except for five patients who were treated with charged-particle radiation or iridium brachytherapy. Patients who received only interstitial implant therapy were not included in this study. In each case, the estimated radiation dose, fractionation schedule, and prior systemic chemotherapy were noted. A wide variety of CNS tumors was represented, including gliomas of all grades, meningiomas, pituitary adenomas, lymphoproliferative disorders, and metastases (Fig. 1).

The therapeutic group was subdivided into six different age subgroups (Fig. 2). The average time interval between the MR scan and the completion of radiation therapy in the age subgroups between 20 and 59 years was 38 months. This time interval was less in the <20-year subgroup (18 months) and greater in the >60-year subgroup (71 months).

The estimated radiation dose and percentage of patients in each age subgroup with a history of previous chemotherapy are shown in Figures 3 and 4, respectively. In six of the 95 patients, the history of prior systemic chemotherapy was not known; however, they were included in this study. This radiation therapy group (n = 95) excluded patients with other suspected causes of deep white-matter abnormalities such as intrathecal chemotherapy, obstructive hydrocephalus, periventricular extension of tumor, or evidence of prior or present shunt-tube placement.

Control Group

One hundred-eighty age-matched patients (30 in each age subgroup) with no history of radiation therapy were randomly selected as the control group. All patients had either benign or malignant intracranial lesions, which included gliomas of all grades (37%), neurinomas (10%), pituitary adenomas (9%), metastases (9%), arachnoid cysts (8%), arteriovenous malformations (6%), meningiomas (5%), empty sellae (3%), abscess (1%), miscellaneous tumors (9%) (including tuberous sclerosis, pineal region tumor, osteoma, craniopharyngioma, glomus jugulare, hemangioblastoma, epidermoid, lipoma), and unknown (3%). As with the radiation therapy group, patients with other possible causes of deep white-matter changes were excluded from the study.

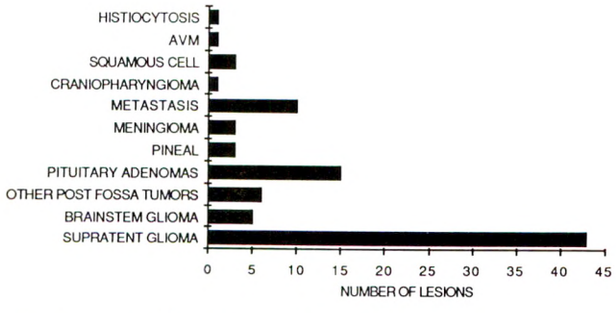


Fig. 1.—Lesion type and number treated in therapeutic group. AVM = arteriovenous malformation; post = posterior; supratent = supratentorial.

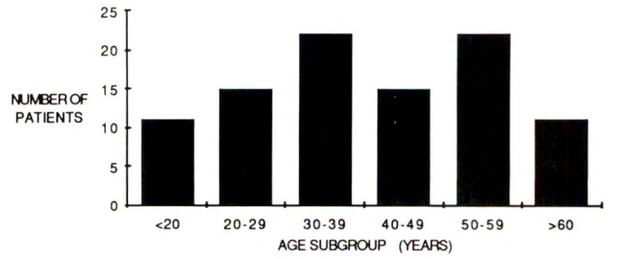


Fig. 2.—Distribution of therapeutic group into age subgroups.

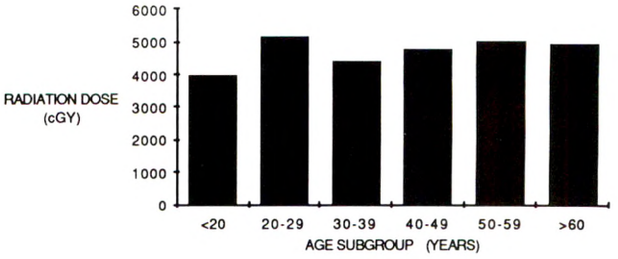


Fig. 3.—Estimated radiation dose in each age subgroup.

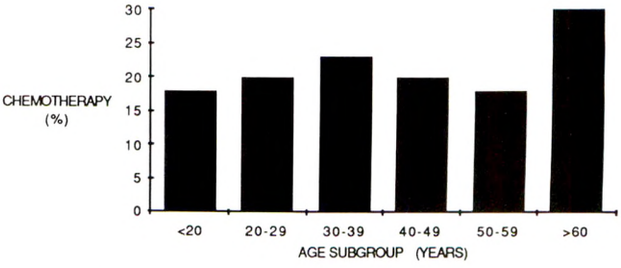


Fig. 4.—Percentage of patients who received systemic chemotherapy in each age subgroup. Patients treated with intrathecal chemotherapy were not included in this study.

MR Review

The MR studies from both groups were reviewed retrospectively by two observers without knowledge of age, gender, or prior radiation therapy. The images were then graded on a 0–4 scale for high-intensity changes involving the white matter in nine separate areas: frontal horn tip, occipital horn tip, lateral aspect of ventricular body, lateral aspect of occipital/temporal horns, centrum semiovale, basal

ganglia, internal capsules, brainstem, and cerebellum. Zero indicated the absence of intensity change compared with normal white matter, and 4 indicated extensive, confluent white-matter abnormalities. Both hemispheres were graded. The actual site of tumor involvement, the immediately surrounding edema, and postoperative gliosis were not included.

The patient's scores including mean, standard deviation, and standard error for each area were then tabulated into either the control or radiotherapy group and respective age subgroups. Statistical significance between similar age subgroups of the control vs radiotherapy groups was determined by an unpaired, two-sample Student's t test. The relationship between each age subgroup within either the control or radiotherapy group was determined from second-order polynomial regression analysis and resulting correlation coefficients.

Results

Radiation-related lesions were characterized as high-signal foci in the periventricular, supratentorial white matter. The areas most often involved were adjacent to the frontal horn tip, occipital horn tip, lateral aspect of the ventricular body, lateral aspect of the occipital and temporal horns, and centrum semiovale. Relative sparing of the brainstem, cerebellum, internal capsules, and basal ganglia was noted (Fig. 5). This involvement tended to be symmetric and equally severe in the contralateral hemisphere and was remote from either the tumor or the operative site. There was no mass effect associated with even the highest grade (4) lesions (Fig. 6).

From a qualitative standpoint, any patient in the radiation therapy group with a score of one or greater in two separately graded areas of the periventricular white matter was suspected of having radiation-related changes. No patients under 20 years old were considered to have radiation-related changes. However, in the remainder of the age subgroups the number of suspected patients was as follows: 20–29 years, three patients (20%); 30–39 years, nine patients (41%); 40–49 years, five patients (33%); 50–59 years, 10 patients (45%); and older than 60 years, nine patients (82%). When these supratentorial periventricular white-matter changes were compared in each age subgroup, statistically significant ($p < .005$) differences were noted between the radiotherapy and control groups except in patients younger than 20 years old (Table 1). Areas of the brainstem, cerebellum, internal capsule, and basal ganglia showed no significant difference between the radiotherapy and control-age subgroups.

The severity of deep white-matter changes in both the

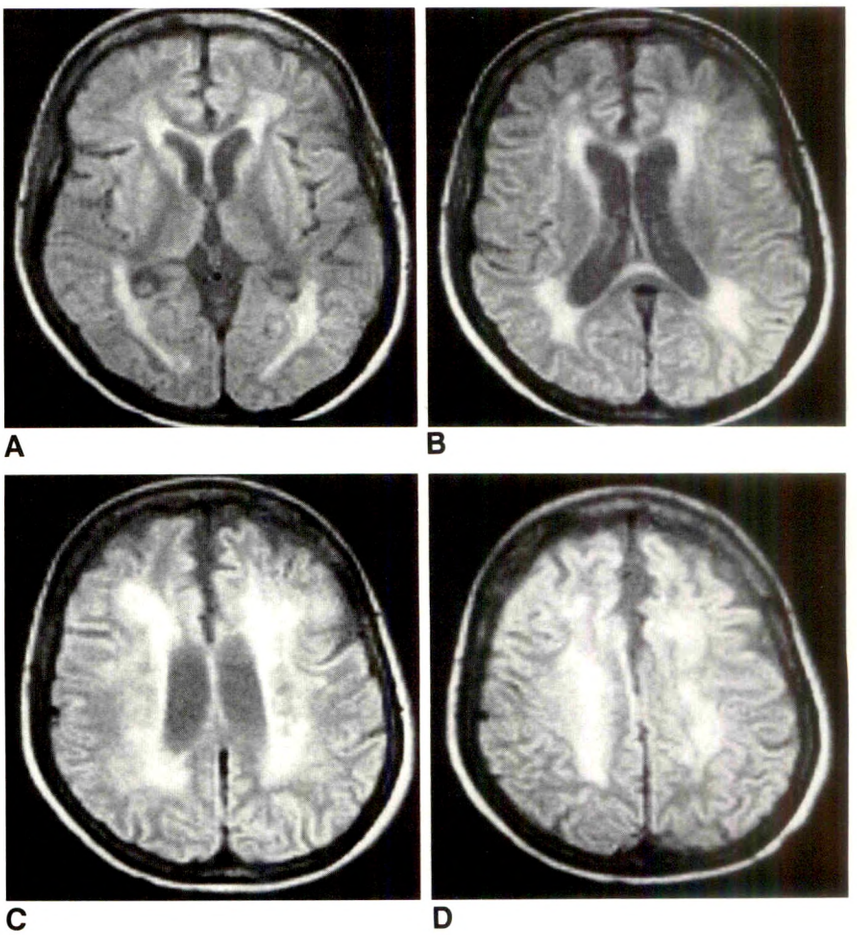
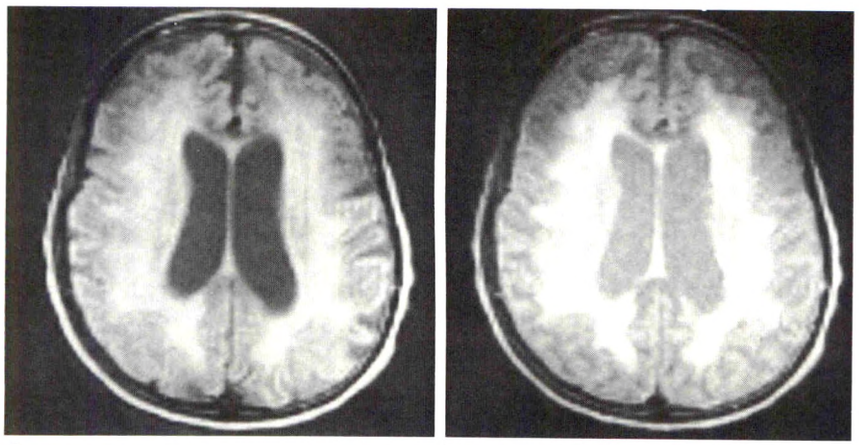


Fig. 5.—Series of T2-weighted (SE 2000/28) axial images in 61-year-old woman who, 11 months before this study, was treated with 5000 cGy by using 14- by 17-cm bilateral ports fractionated over 38 days. Bilateral and symmetric distribution of periventricular white-matter foci without mass effect. Sparing of basal ganglia, internal capsules, and posterior fossa (not shown) was noted.



A B

Fig. 6.—SE 2000/28 (*A*) and SE 2000/56 (*B*) images in 70-year-old woman treated for metastatic lung carcinoma with whole-brain radiation, 3000 cGy, 2 years 8 months before this study. There are extensive (grade 4) periventricular white-matter changes and associated atrophy.

TABLE 1: Supratentorial Periventricular White-Matter Changes: Radiation vs Control Groups

Age Subgroup	Mean Score ± SEM		Significance
	Radiotherapy Group	Control Group	
<20	0.09 ± 0.02	0.03 ± 0.01	NS
20–29	0.20 ± 0.05	0.02 ± 0.007	$p < .005$
30–39	0.41 ± 0.05	0.06 ± 0.01	$p < .005$
40–49	0.60 ± 0.09	0.06 ± 0.01	$p < .005$
50–59	0.87 ± 0.10	0.12 ± 0.02	$p < .005$
>60	1.64 ± 0.16	0.23 ± 0.03	$p < .005$

Note.—Scores are based on a 0–4 scale: 0 = no intensity change relative to normal white matter; 4 = extensive, confluent white-matter abnormalities. NS = not significant.

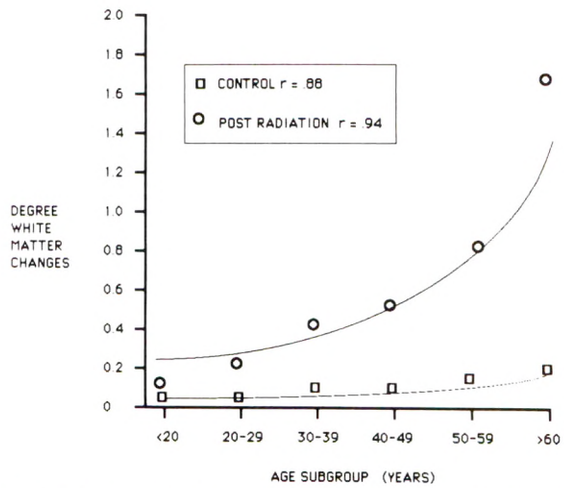


Fig. 7.—Comparison between average degree of supratentorial white-matter changes with advancing age for both therapeutic and control groups obtained from data in Table 1. Connecting curves and correlation values were computed from second-order polynomial regression analysis (see text).

radiotherapy and control groups was found to increase with advancing age (Table 1). Nonlinear regression analysis of the data (Fig. 7) resulted in the second-order polynomial equations: $y = 0.23 - 0.158x + 0.063x^2$ ($r = .94$) for the radiotherapy group and $y = 0.07 - 0.049x + 0.012x^2$ ($r = .88$) for the controls, where x represents age and y is the degree of white-matter changes.

Within the radiotherapy group, 29 of 95 had two or more sequential scans. Nine patients (31%) had sequential studies that were interpreted to have positive findings attributed to radiation therapy. In all but two patients, the findings were noted to remain stable over an average interval of 10.5 months. In 15 patients, (52%) the first MR study was performed before or during the course of radiotherapy with an average follow-up MR study 6 months after completion of therapy. In two of these patients, definite new lesions within the deep white matter were noted 7 and 9 months after the completion of therapy (Figs. 8 and 9).

Sixteen patients had limited treatment fields for pituitary tumors. The mean age was 40.5 years and the average interval between completion of radiotherapy and the MR study was 4.6 years. The estimated average radiation dose to the sella was 4234 cGy (4234 rad). From the 180 control patients, 22 (mean age, 48.6 years) had sellar region abnormalities including newly diagnosed adenomas (60%), empty sellae (27%), and adenomas treated by surgery or bromocriptine therapy (13%). When all graded areas were compared between the radiotherapy and control groups for patients with pituitary lesions, no statistical differences were seen.

Discussion

The delayed pathophysiologic changes encountered in brain tissue as a response to radiotherapy have been investigated thoroughly, and several target sites have been implicated. First, delayed capillary endothelial cell damage may occur leading to breakdown of the blood-brain barrier with resulting vasogenic edema [13]. This edema has been de-

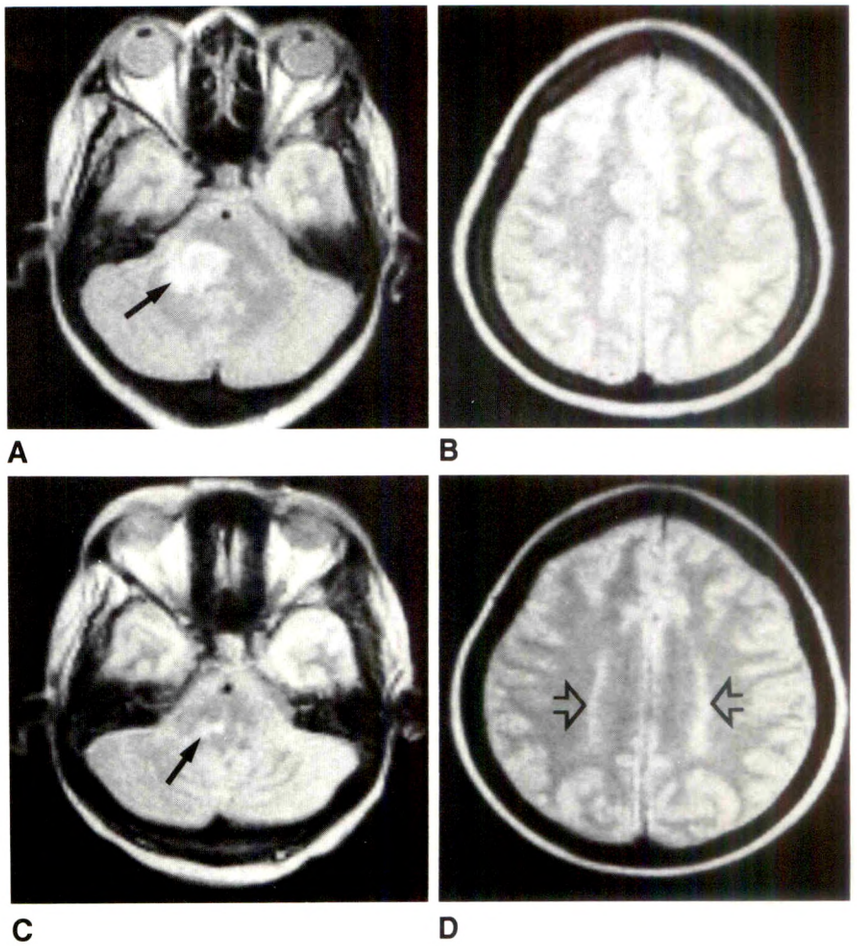


Fig. 8.—SE 2000/56 images. Evolving radiation-related white-matter changes in 55-year-old woman.

***A* and *B*, Before radiotherapy. Posterior fossa glioma (*arrow*) and normal white matter in centrum semiovale.**

***C* and *D*, 7 months after completion of radiotherapy. Interval tumor response (*solid arrow*) and formation of additional supratentorial white-matter changes (*open arrows*) remote from tumor site.**

scribed after necropsy as occurring remote from the site of primary radiation exposure and results in impaired CSF circulation due to elevated CSF pressures. Cerebral blood flow may also be reduced [13]. Heterogeneous endothelial hyperplasia [14], fibrinoid necrosis of penetrating arterioles within the white matter [4, 9], and morphologic changes suggestive of atherosclerosis involving large-sized arteries have been noted [13]. Animal studies have shown that focal demyelination occurs, with associated proliferation of glial elements and mononuclear cells weeks or months after completion of radiotherapy [13]. In addition, white matter may develop small necrotic foci [13], vacuolation [3, 9], and petechial hemorrhage [15] months to several years after radiotherapy. Ventriculomegaly and widening of the sulci due to atrophy is commonly noted on both CT and gross pathology [7, 9, 13]. Depending on the severity of these changes, patient age, and total radiation dose, these lesions may partially resolve, stabilize, or progress over a protracted course of several months to several years, leading to widespread, potentially fatal brain destruction characterized by coagulation necrosis [7, 16]. When this stage is reached, clinical symptoms may suggest a recurrent intracranial mass, and CT may show an enhancing mass [5–7], which is difficult to distinguish from recurrent or residual cancer. This latter form of extensive coagulation necrosis has been called "radiation necrosis" or "late delayed reaction" [15]. To our knowledge, none of the patients in the radiotherapy group had biopsy-proven or clinically suspected radiation necrosis; however, this distinction cannot be made on the basis of MR findings alone [10].

Our MR findings agree with previous studies [8–10]. The pattern of involvement is symmetric, with involvement of the deep white matter. These abnormalities are often remote from the tumor site (which presumably received the highest radiation dose). Since the majority of the patients were alive, histologic correlation was not performed; however, our MR findings concur with the expected pathophysiologic changes previously described. Prolongation of T1 and T2 relaxation values were noted, with resulting MR intensity and distribution similar to either multiple sclerosis plaques or deep white-matter infarcts. This is understandable since the known histologic findings of white-matter radiation changes are demyelination, microvascular occlusion, and vasogenic edema. These white-matter changes have a variable delay of onset [13] measured in weeks to months. In two of 15 patients with sequential scans obtained during and after radiotherapy, radiation-related lesions appeared 7 and 9 months after com-

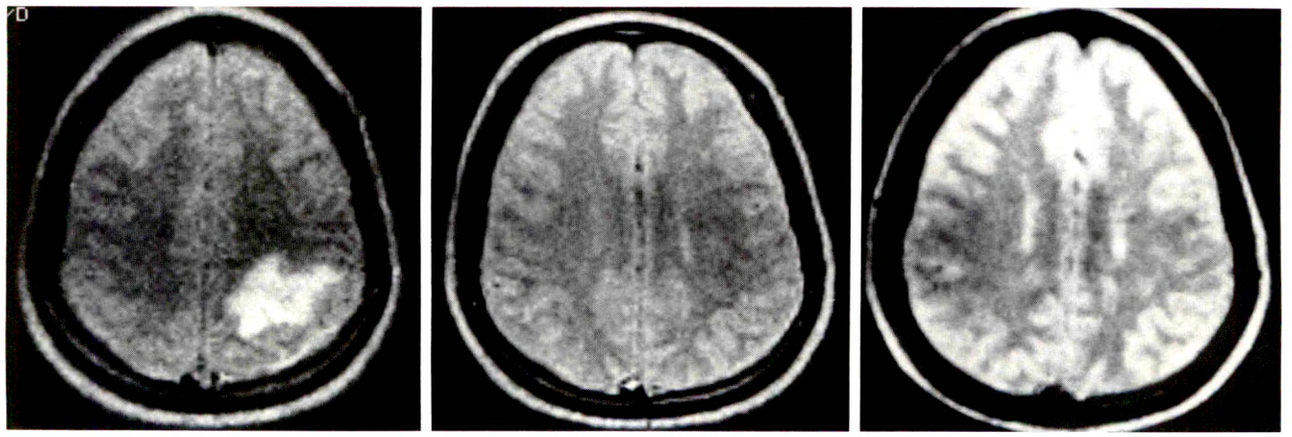


Fig. 9.—Sequential SE 2000/56-images in 28-year-old man with left parietal testicular carcinoma metastasis.
***A*, Before combined systemic chemotherapy and radiotherapy. Radiotherapy consisted of opposed 18- by 12-cm whole-brain ports for 4000 cGy and opposed lateral coned-down ports for an additional 1000 cGy.**
***B*, 4 weeks later, MR study is essentially normal.**
***C*, Follow-up study 8 months later shows new, faint periventricular high-intensity lesions that can be regarded as definite new findings when compared with previous examination.**

pletion of therapy. The remainder of these 15 patients showed no new white-matter abnormalities; however, the follow-up interval may not have been sufficiently long (6 months). In the future, additional prospective studies are needed to document these changes accurately.

In our experience, the pattern of involvement mimics the changes seen in older patients and in patients with risk factors for cerebral vascular disease. There is a greater tendency for these periventricular lesions to be more confluent, as seen with deep white-matter infarction, than more focal, as seen with multiple sclerosis (Kortman KE, Bradley WG, Rauch RA, et al., unpublished data). Morphologically, the deep white-matter changes in both the radiation and control groups had similar MR patterns. Both groups showed an increase in changes with advancing age, but these occurred at a greater rate in the radiotherapy group. This raises the possibility that treating "at-risk" middle-aged and elderly patients with radiotherapy tends to accelerate the normal, involutional white-matter changes expected with advancing age, which are presumably caused by small, often clinically silent infarcts. In Table 1, it should be noted that the mean changes of the entire age group, based on a 0- to 4-point scale, is quite low even with advancing age. This directly reflects the variable incidence of radiation-related changes in patients who are close in age. Even in the advanced age groups, there are patients who will have minimal or no-white matter changes after therapy. This variable incidence of radiation changes has also been experimentally demonstrated on monkeys of similar ages [13].

Although no attempt was made to correlate the degree of white-matter changes with the presence of adverse clinical effects, we did note anecdotally that the majority of patients, without evidence of tumor recurrence of extension, showed variable clinical expression. Patients ranged from being asymptomatic to having signs of neurotoxicity "characterized by varied degrees of irreversible dementia, confusion, ataxia, and psychomotor retardation" [1]. This lack of correlation has also been described in elderly individuals with leukoencephalopathy as a response to normal and pathologic aging [17–19]. In addition, extensive radiation changes of the deep white matter may potentiate the effects of an underlying disorder such as Alzheimer's disease or multiinfarct dementia [17, 19].

We are unable to explain the lack of statistical increase in deep white-matter changes in the youngest age group. It has been reported previously that the age of the recipient at the time of radiotherapy may determine the severity of parenchymal damage, with the most significant changes seen in younger patients [13]. A follow-up interval of less than 2 years and a higher percentage (45%) of posterior fossa tumors may have biased the results in the under-20 subgroup.

The stability of the MR findings confirms the histologic results in experimental models [13]. Although it has been postulated that remyelination and reversal of microvascular changes may occur [4], we were unable to document this by MR over the time interval covered by this study.

Since cerebral edema has been reported to lower brain resistance to radiation injury [4, 13, 20], it could be predicted that peritumoral edema would be the most sensitive site. Unfortunately, this could not be verified with MR since MR signal alterations cannot discriminate between tumor edema and white-matter radiation changes. As a result, these regions were excluded from the grading process.

We are uncertain of the influence of systemic chemotherapy, either alone or in combination with radiotherapy, on the MR appearance of the deep white matter compared with radiotherapy alone. A significant percentage of these patients in all age subgroups received combined therapy, and this may

have influenced our conclusions. This is especially true in the subgroup older than 60 and may partially account for the greater degree of white-matter changes shown in Figure 7. In a recent study, the MR findings of leukoencephalopathy were noted in five patients with clinical signs of neurotoxicity treated with combined therapy [1]; however, no comparison was made with patients who were treated by radiation alone. In another study of brain radiation lesions evaluated by MR in 55 patients [10], there was no mention of chemotherapy being administered to patients with positive findings.

In the pituitary tumor subgroup, we were able to select a large population with limited treatment fields for statistical analysis. Although, radiation necrosis has been described in the temporal and frontal lobes, hypothalamus, thalamus, basal ganglia, cerebral white matter, and brainstem in patients with pituitary adenomas [5, 15], these findings were not present in any of our cases and no statistical differences were seen compared with the age-matched controls.

In conclusion, cerebral white-matter changes are often seen as a delayed response to therapeutic radiation. The pattern of involvement is symmetric and mimics deep white-matter infarction. There is a variable incidence of radiation effects that become more marked in older patients. MR interpretation must consider the neuropathologic consequences of therapeutic radiation including demyelination, microvascular occlusion, and blood-brain barrier breakdown and may serve as a useful adjunct in assessing neurotoxicity in these long-term survivors.

ACKNOWLEDGMENTS

We thank Gail Thompson for help in manuscript preparation; Terry Andrues, Jay Mericle, and Leslee Watson for technical help; and Richard A. Yadley, Irwin Grossman, and Michael R. Kadin for comments.

REFERENCES

1. Frytak S, Earnest F, O'Neill BP, Lee RE, Creagan ET, Trautman JC. Magnetic resonance imaging for neurotoxicity in long-term survivors of carcinoma. *May Clin Proc* **1985**;60:803–812
2. Rottenberg DA, Horten B, Kim J, Posner JB. Progressive white matter destruction following irradiation of an extracranial neoplasm. *Ann Neurol* **1980**;8:76–78
3. Wang A, Skias DD, Rumbaugh CL, Schoene WC, Zamani A. Central nervous system changes after radiation therapy and/or chemotherapy: correlation of CT and autopsy findings. *AJNR* **1983**;4:466–471
4. Groothuis DR, Vick N. Radionecrosis of the central nervous system: the perspective of the clinical neurologist and neuropathologist. In: Gilbert HA, Kagan AR, eds. *Radiation damage to the nervous system*. New York: Raven, **1980**:93–106.
5. Fukamachi A, Wakao T, Akai J. Brain stem necrosis after irradiation of pituitary adenoma. *Surg Neurol* **1982**;8:343–350
6. Safadari GH, Fuentes J-M, Dubois J-B, Alirezai M, Castan P, Vlahovitch B. Radiation necrosis of the brain: time of onset and incidence related to total dose and fractionation of radiation. *Neuroradiology* **1985**;27:44–47
7. Safadari GH, Boluix B, Gros C. Multifocal brain radionecrosis masquerading as tumor dissemination. *Surg Neurol* **1984**;21:35–41
8. Bydder GM, Pennock JM, Steiner RE, Orr JS, Bailes DR, Young IR. The NMR diagnosis of cerebral tumors. *Magnetic Resonance Med* **1984**;1:5–29
9. Curnes JT, Laster DW, Ball MR, Moody DM, Witcofski RL. Magnetic resonance imaging of radiation injury to the brain. *AJNR* **1986**;7:389–394
10. Dooms GC, Hecht S, Brant-Zawadzki M, Berthiaume Y, Norman D, Newton TH. Brain radiation lesions: MR imaging. *Radiology* **1986**;158:149–155
11. Bradley WG, Waluch V, Brant-Zawadzki M, Yadley RA, Wycoff RR. Patchy, periventricular white matter lesions in the elderly: a common observation during NMR imaging. *Noninvas Med Imag* **1984**;1:35–41
12. Brant-Zawadzki M, Fein F, Van Dyke C, Kiernan R, Davenportt L, de Groot J. Magnetic resonance imaging of the aging brain: patchy white matter lesions and dementia. *AJNR* **1985**;6:675–682
13. Cavenes WF. Experimental observations: delayed necrosis in normal monkey brain. In: Gilbert HA, Kagan AR, eds. *Radiation damage to the nervous system*. New York: Raven, **1980**:1–38
14. Denekamp J, Folwer JF. Cell proliferation kinetics and radiation therapy. In: Becker FE, ed. *Cancer—a comprehensive treatise*. New York: Plenum, **1977**:101–137
15. Sheline GE. Irradiation injury of the human brain: a review of clinical experience. In: Gilbert HA, Kagan AR, eds. *Radiation damage to the nervous system*. New York: Raven, **1980**:39–58
16. Rizzoli HU, Paggnanelli DM. Treatment of delayed radiation necrosis of the brain. *J Neurosurg* **1984**;60:5589–5594
17. George AE, de Leon MJ, Gentes CI, et al. Leukoencephalopathy in normal and pathologic aging: 1. CT of brain lucencies. *AJNR* **1986**;7:561–566
18. George AE, de Leon MJ, Kalnin A, Rosner L, Goodgold A, Chase N. Leukoencephalopathy in normal and pathologic aging: 1. MRI of brain lucencies. *AJNR* **1986**;7:567–570
19. Lotz PR, Ballinger WE, Quisling RG. Subcortical arteriosclerotic encephalopathy: CT spectrum and pathologic correlation. *AJNR* **1986**;7:817–822
20. Burger PC, Mahaley MS, Dudka L, Vogel FS. The morphologic effects of radiation administered therapeutically for intracranial gliomas. A postmortem study of 25 cases. *Cancer* **1979**;44:1256–1272

Book Reviews

Clinical Neurosonography. Ultrasound of the Central Nervous System. Edited by Thomas P. Naidich and Robert M. Quencer. New York: Springer-Verlag, 276 pp., 1987, $110

This monograph is a reissue of volume 28, issues 5–6, 1986, of *Neuroradiology*. A chapter by Yousefzadeh and Naidich, "US anatomy of the posterior fossa in children: correlation with brain sections," has been added to section II, "The neonatal head." A subject index also has been added to the monograph.

This book is divided into seven topics: fetal neurosonography, the neonatal head, the neonatal spine, intraoperative neurosonography, postoperative neurosonography, duplex carotid sonography, and orbital echography. Thirty-two contributors present 19 papers, which include discussions on normal anatomy of the head and spine in the fetus and neonate as well as in utero and neonatal diseases subdivided into congenital, infections, hydrocephalus, tumors and cysts, premature brain, and septo-optic dysplasia. The text contains 300 figures, which include 740 images, 86 brain sections, 36 drawings, and 15 tables.

The editors' purpose for this monograph was to have "authorities discuss basic diagnosis, present recent advances ... and provide new information ... so we may utilize the full potential of ... recent advances in ultrasound technology." These several papers succeed in this purpose by providing informative text and high-quality figures. The keys for the images and brain slices are clear, detailed, and accurate in most cases. Errors in correlation of text to the image occur in six figures. Typographic errors are few and present no difficulty in correctly understanding the text or images.

The paper on in utero brain neuropathology presents a detailed discussion with differential diagnoses of developmental abnormalities, infections, intracranial hemorrhage, and mass lesions. The text, although informative, is inadequately supported by appropriate images. The paper on premature brain, although informative, is not supported by images and text as well as are some recent papers on the subject in the literature.

The papers on normal anatomy are superb. The figures are detailed, and the images are of extremely high quality. This is also true of the intraoperative and postoperative papers. The methods of performing the scans, the best projections, common technical problems, and artifacts are presented frequently. These hints should be useful to those less familiar with this form of imaging.

Overall I found this monograph to be excellent. The text is well organized and well written. The images are generally of superb quality as are their legends. The subject of neurosonography is concisely organized in one monograph. I know of no other monograph that accomplishes that task so well. This text is recommended to anyone interested in learning more about this area of sonography. It should be beneficial to radiologists, neonatologists, pediatric neurologists, and neurosurgeons, as well as those caring for the fetus and neonate. Residents in these fields will find it useful. Sections of the book also are valuable for orthopedic surgeons, vascular surgeons, and ophthalmologic surgeons. However, this book would not be of benefit to those who subscribe to *Neuroradiology*.

Richard A. Flom
St. Joseph's Hospital
Phoenix, AZ 85001

High-Resolution Computed Tomography of the Paranasal Sinuses, Pharynx and Related Regions. Impact of CT Identification on Diagnosis and Patient Management. By Gertrude Maatman. The Hague: Nijhoff, 171 pp., 1986. $60.50

The opening chapter deals with the author's technique in performing CT of the sinuses and pharynx. A short discussion of the anatomy of these regions and appropriate line drawings follow. The next two sections deal with normal axial and coronal CT anatomy. The photographs are excellent and clearly labeled. Frequently, a nonlabeled duplicate image at a different window setting accompanies them. The text here is brief and confined mainly to adding points not obvious on the films. In the final chapter the author documents the usefulness of CT in determining the extent of disease and its help in therapy. Although specific cases are illustrated here, the author does not attempt to cover completely the pathologic gamut.

This is an excellent reference book of normal axial and coronal CT anatomy of the paranasal sinuses and pharynx and should be part of the library of any radiologist or ear, nose, and throat specialist who deals with these regions.

Norman N. Keep
1676 W. Bullard
Fresno, CA 93711

Radiographic Characteristics of Skull Fractures Resulting from Child Abuse

Clifford J. Meservy[1, 2]
Richard Towbin[1, 4]
Robert L. McLaurin[3, 4]
Patricia A. Myers[5]
William Ball[1, 4]

Radiographic characteristics of skull fractures in 39 cases of documented child abuse were compared with skull fractures in 95 cases of accidental injury to determine if differential features could be identified. All children were less than 2 years old. Emergency room and hospital records for these patients were also reviewed. The results of this study show that clinical features did not provide any clues as to whether the children had been injured by abuse or by accident. However, it was found that multiple fractures, bilateral fractures, and fractures crossing sutures occurred significantly more often in abuse cases than in accidental injury. When such fractures are present, abuse should be suspected.

The ability to identify child abuse constitutes an important concern to those involved in the medical care of children. Estimates of the number of cases of physical abuse occurring yearly in the United States range from 585,000 [1] to 1.7 million [2]. Studies show that at least 10% of children under 5 years old who are brought to the emergency room with alleged accidents have actually suffered nonaccidental trauma [3]. Since as many as 65% of all abuse cases are initially seen in the emergency room [4], the first step in correctly identifying abuse is to train hospital staff members to recognize abuse indicators. Radiographic findings of suspected child abuse have been described in the literature [5–7]. The importance of these findings is enhanced when features are identified that enable one to differentiate injuries occurring in abuse from those occurring in accidental injury. This differentiation gives the radiographic studies great import from the clinical, social, and medicolegal standpoints. Previous reports have not described the differential features between the radiographic appearance of skull fractures that result from abuse and those that result from accidental injury [8–11]. Skull fractures in abused children have been described as simple linear fractures most commonly occurring in a parietooccipital location. Depressed, comminuted, and diastatic fractures are uncommon. However, Hobbs [12] has recently reported that skull fractures resulting from child abuse often have features that make the skull radiograph an important asset in differentiating suspected child abuse from accidental trauma. We reviewed 134 pediatric cases of skull fracture to determine if Hobbs' observations are reproducible in a nonselected population.

Subjects and Methods

Radiographs of skull fractures in 134 children under 2 years of age were reviewed. The injuries all occurred between January 1981 and December 1985. Of this group, 39 had skull fractures resulting from abuse and 95 suffered accidental injury. Suspected abuse cases were referred to the multidisciplinary child abuse team for assessment. The major criteria for referral included (1) inadequate, unlikely, or no explanation of the child's injury, (2) history of injury inconsistent with the child's development, (3) discrepancy in history given by caretakers or other family members, (4) multiple injuries or injuries of various ages, (5) past history of suspicious injuries or previous abuse reports, (6) delay in seeking medical treatment, (7) the

This article appears in the May/June 1987 issue of *AJNR* and the July 1987 issue of *AJR*.

Received July 22, 1986; accepted after revision October 7, 1986.

[1] Department of Radiology, University of Cincinnati College of Medicine, Cincinnati, OH 45229.

[2] Present address: Department of Radiology, LeBonheur Children's Medical Center, 848 Adams Ave., Memphis, TN 38103. Address reprint requests to R. Towbin.

[3] Department of Neurosurgery, University of Cincinnati College of Medicine, Cincinnati, OH 45229.

[4] Department of Pediatrics, University of Cincinnati College of Medicine, Cincinnati, OH 45229.

[5] Department of Social Service, Children's Hospital Medical Center, Cincinnati, OH 45229.

***AJR* 149:173–175, July 1987**
0361–803X/87/1491–0173
© American Roentgen Ray Society

child's response to medical examination, since an abused or neglected child frequently accepts procedures in a passive manner, and (8) parent-child interactions suggesting lack of parental concern.

Motor vehicle accidents were not included, as these events are quite easily identified and would not be confused with abuse. Therefore, all patients included in this study were initially suspected to be possible victims of abuse. Children who did not meet the criteria established for identification of abuse were presumed to have sustained accidental injury. However, we have no absolute criteria for identification of accidental injury. It is possible, therefore, that cases of undetected abuse may have been included in the group of accidental injury cases.

With rare exceptions, accidental injury occurred by falling down stairs; by being dropped while carried; or by falling from a raised surface, such as a changing table, couch, or bed.

Skull fractures were evaluated for site, size, number, depression, configuration, and patient age at time of fracture. The classification of configuration was described by Hobbs [12]. He described both a single linear and complex type of fracture. A single linear fracture is a single unbranched line in straight, zigzagged, or angled configuration. A complex fracture consists of two or more distinct fractures of any type or a single fracture with multiple components. Branched linear fractures are included in this category.

The incidence of each parameter was examined in the two groups of patients. The results were subjected to statistical analysis, and *p* values were determined.

The emergency room and hospital records were reviewed for the entire group of 39 abused infants and a random series of 42 accidentally injured infants. The purpose of this review was to determine if there were any distinguishing features on clinical presentation that might serve as clues to the method of trauma. The specific features noted included the neurologic state on arrival (especially the level of consciousness), external evidence of trauma about the head and neck, and the presence or absence of retinal hemorrhages.

Results

Thirty-nine cases of abuse and 95 cases of accidental injury were included in the study. Eighty-five percent of each group was under 12 months old. Owing to the presence of multiple fractures, there were 56 total fractures in the abused population and 104 in the accidentally injured children. Fractures ranged in length from 1 to 12 cm in both groups. The parietal bone was the most common site of fracture in both groups, occurring in 49 of 56 (87.5%) abused children and 95 of 104 (91.3%) of those accidentally injured.

No significant differences between the effects of abuse and accidental injury were identified with regard to (1) nonparietal fracture, (2) depressed fracture, (3) diastatic fracture ≥ 3 mm, and (4) complex fracture (Table 1).

Despite these similarities of skull fracture, we found three characteristics that were more frequent after trauma of abuse than after accidental injury. These characteristics were (1) multiple fractures, (2) bilateral fractures (Fig. 1), and (3) fractures that cross sutures (Fig. 2 and Table 2).

TABLE 1: Fracture Characteristics of No Statistical Significance

	Abuse (n = 39)	Accidental Injury (n = 95)	*p* Value
Nonparietal fracture	1 (2.6%)	6 (6.3%)	0.6461
Depressed fracture	6 (15.4%)	12 (12.6%)	0.8842
Diastatic fracture ≥ 3 mm	6 (15.4%)	14 (14.8%)	0.8640
Complex fracture	9 (23.1%)	12 (12.6%)	0.2116

Clinical features reviewed did not provide any clues as to whether the individual had been injured by abuse or by accident. All but three of the abused infants were conscious on admission although a few were reported to have mild lethargy or irritability. Of the accidentally injured patients, one was comatose on arrival. In both groups the most common external signs of trauma were scalp swelling and discoloration in the parietal region. Scalp lacerations were rarely seen in either group. Depression of the skull was usually not detected until radiologic study because of overlying hematoma. Retinal hemorrhages were seen initially in one abused infant and in one case of accidental injury. It was not surprising that retinal hemorrhages were not more common in the abused infants since this characteristically occurs in the "shaken baby" syndrome, which is usually not associated with skull fracture.

Review of the presenting and follow-up social histories from the caretakers of abused children indicated that in 33% of cases no history of trauma could be determined (i.e., "I just found him that way"). In a surprising percentage of cases (15%) some history of specific abuse or neglect was elicited (i.e., "I think my boyfriend might have hurt him"). Other histories included falling from a bed, couch, or other low surface. Fairly frequently, the history was conflicting; less commonly, it was inconsistent or changed (Table 3).

Discussion

The skull radiograph has been of use in clinical and legal matters for identification of the presence of skull fractures but until recently has been considered of little value in differentiating abuse from accidental injury. Hobbs has reported specific characteristics that he found to occur more frequently in abuse than in accidental injury. These include: (1) depressed fractures, (2) diastatic fractures ≥ 3 mm in width, (3) nonparietal fractures, (4) fractures having the complex configuration, (5) multiple calvarial fractures, (6) bilateral fractures, and (7) fractures that cross sutures. Abuse is suggested by the presence of one or more of these features. He stated that most of his cases of abuse had more than two of these features, while most of his cases of accidental injury had none. However, no statistical information was given to support his conclusions. He also reported that a depressed occipital fracture is virtually pathognomonic of abuse.

Hobbs' study appears to be biased toward severe abuse. The study included 29 cases of abuse of which 13 were obtained through the Department of Forensic Medicine. Six of the remaining 16 cases also were fatal. Our group of patients represents a more typical cross section of less severely injured children seen at a community hospital.

In contrast to Hobbs' observations, our results indicate that there are no significant differences between the appearance of skull fractures in abuse and accidental injury with regard to (1) depressed fractures, (2) diastatic fractures ≥ 3 mm, (3) nonparietal fractures, and (4) fractures having the complex

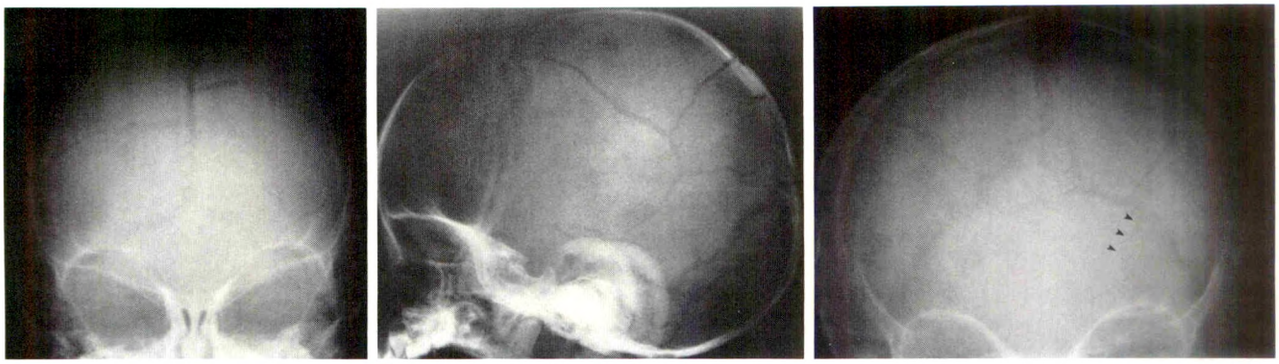


Fig. 1.—8-month-old abused boy. Anteroposterior (*A*) and lateral (*B*) skull radiographs reveal multiple, bilateral parietal fractures.

Fig. 2.—6-month-old abused girl. Multiple, bilateral skull fractures. Left parietal fracture crosses lambdoid suture (*arrowheads*).

TABLE 2: Fracture Characteristics of Statistical Significance

	Abuse (n = 39)	Accidental Injury (n = 95)	*p* Value
Multiple fractures	12 (30.8%)	9 (9.5%)	0.0036
Bilateral fractures	7 (18%)	5 (3.2%)	0.0395
Fractures crossing sutures	10 (25.6%)	9 (9.5%)	0.0264

TABLE 3: History Given in 39 Cases of Suspected Child Abuse

Description	*n*
No history of trauma	13 (33.3%)
History of fall from bed, couch, or other low surface	10 (25.6%)
Conflicting history that later appeared to be abusive	7 (17.9%)
History indicating abuse or neglect	6 (15.3%)
Inconsistent or changed history	3 (7.6%)

configuration. Our one patient with a depressed occipital fracture sustained this in accidental injury.

Several of the characteristics described by Hobbs were reproduced in our study. In spite of his apparent bias toward severe abuse, we concur with Hobbs in his opinion regarding the differential significance of certain radiologic features. These features are (1) multiple fractures, (2) bilateral fractures, and (3) fractures that cross suture lines. These occurred much more frequently in abuse and were found to be statistically significant with p values $< .05$.

The clinical presentation was of no help in distinguishing whether the infant had been injured by abuse or by accident. Frequently, there was either no stated history of trauma or only a minor fall. We therefore conclude that one must suspect abuse when skull fractures are identified that are multiple, bilateral, or cross suture lines. This suspicion is greatly enhanced when there is no history of trauma or when only a minor fall is reported. Awareness of the characteristics of abuse and a well-defined hospital protocol for suspicious cases is essential for identification.

REFERENCES

1. The American Humane Association, Child Protective Division. *National analysis of official child neglect and abuse reporting 1982*. Denver: American Humane Association, **1982**
2. Straus MA. Family patterns and child abuse in a nationally representative sample. *Child Abuse Negl* **1979**;3:213–225
3. Schmitt B. *The child protection team handbook*. New York: Garland STPM Press, **1978**:23–24
4. Deitz S, Shutty M, Cary T. Child abuse: a physician's guide. *Generics* **1985**;1(3):15–22
5. Caffey J. Multiple fractures in the long bones of infants suffering from chronic subdural hematoma. *AJR* **1946**;56:163–173
6. Silverman FN. The roentgen manifestations of unrecognized skeletal trauma in infants. *AJR* **1953**;69:413–427
7. Kempe CH, Silverman FN, Steele BF, et al. The battered child syndrome. *JAMA* **1962**;181:105–112
8. Merten DF, Osborne DRS, Radkowski MA, Leonidas JC. Craniocerebral trauma in the child abuse syndrome: radiological observations. *Pediatr Radiol* **1984**;14:272–277
9. Merten DF, Radkowski MA, Leonidas JC. The abused child: a radiological reappraisal. *Radiology* **1983**;146:377–381
10. Helfer RE, Slovis TL, Black M. Injuries resulting when small children fall out of bed. *Pediatrics* **1977**;60:533–535
11. Silverman FN. Unrecognized trauma in infants, the battered child syndrome and the syndrome of Ambroise Tardieu. *Radiology* **1973**;104:337–350
12. Hobbs CJ. Skull fracture and the diagnosis of abuse. *Arch Dis Child* **1984**;59:246–252

Book Review

A Manual of Radiographic Equipment. By Sybil M. Stockley. New York: Churchill Livingston, 304 pp., 1986. $22.50

Books by British authors tend to be written in concise lucid prose. The volume under consideration is an exception to this rule only because of terms that will be unfamiliar to the novice radiologist or technologist because the terms are uniquely British or because of expressions that assume a technical background that most of her North American readership are unlikely to have.

The author intends to aid "student radiographers" in their understanding of the design and function of diagnostic radiographic equipment and accessories. The aim is to supply basic and general information, and to illuminate in simple terms the principles that underlie their function. In this, the book succeeds admirably with the exceptions noted above.

The text is divided into two major sections: X-ray generation, and handling and use of the X-ray beam. Each of these is treated in detail, with diagrams and drawings used extensively and effectively to reinforce points made in the text. Elements of equipment are discussed, beginning with the electrical supply and proceeding with consideration circuits, the generator, the tube filament, and the high voltage system. Discussion of X-ray tubes and their connections occupy nearly 40 pages. The discussion of the principles of fluoroscopy and image intensification is particularly clear, concise, and detailed. Chapters also deal with radiographic tables, grids, tube supports, and cassette/film holders, as well as specialized units including portable and mobile units.

Unfortunately, the author has touched on sonography only briefly and confines her presentation of CT to a few paragraphs and a single figure. One is advised to seek technical information concerning these techniques from other sources. Nevertheless, Stockley appears to have succeeded in reaching the goals set out in her preface. This book should be particularly useful to teachers of radiographic technology and should be a welcome addition to any radiology department's library. A glossary of technical and engineering terms would make it even more useful to many students.

John W. Loop
University of Washington
Seattle, WA 98104

Thrombosed Dialysis Grafts: Efficacy of Intrathrombic Deposition of Concentrated Urokinase, Clot Maceration, and Angioplasty

Gary B. Davis[1]
Christopher F. Dowd[1]
Joseph J. Bookstein[1]
Timothy P. Maroney[1,2]
Elvira V. Lang[1]
Nicholas Halasz[3]

Forty-one thrombosed polytetrafluoroethylene hemodialysis grafts in 26 patients were treated by a modified method of fibrinolytic therapy and transluminal angioplasty. The modifications included the use of highly concentrated urokinase, intrathrombic injection of urokinase into mechanically macerated thrombi, use of a crossed two-catheter technique, observation of the patient in the angiography suite during the entire procedure, and transluminal angioplasty to correct underlying stenosis immediately after partial or complete thrombolysis. Lysis was initially successful in 37 (90%) of 41 procedures. Successful treatment, defined as a functional graft for longer than 6 months without intervening surgery, was achieved in 16 (62%) of 26 patients.

In comparison with previous transluminal or surgical regimens, this modified method permits marked acceleration of thrombolysis, immediate transluminal angioplasty, and sparing of potential future graft sites.

In our initial experience with fibrinolysis of thrombosed hemodialysis grafts [1], we used selective infusion of streptokinase. Although lysis was successful in eight of nine cases, surgery was eventually necessary in five because of hemorrhage or residual anastomotic stenosis. Young et al. [2] reported similar results and recommended against fibrinolysis for graft thrombosis because of the high prevalence of hemorrhage and the ultimate need for surgical revision of underlying graft stenoses.

To overcome some of the difficulties associated with thrombolysis, we undertook a laboratory investigation of factors that determined the consistency and rate of thrombolysis [3]. Results indicated advantages of intrathrombic vs parathrombic infusion, advantages of high concentration of urokinase vs streptokinase, and the value of increasing the area of interface between clot and fibrinolytic agent by means of clot maceration.

As a result of these considerations, we have continued to use fibrinolytic therapy in the clinical management of thrombosed hemodialysis grafts, but we have modified our approach in five respects: (1) streptokinase has been replaced by highly concentrated urokinase; (2) two catheters with bent tips are used in a crisscross manner, allowing maceration of the clot and deposition of fibrinolytic agent throughout the entire thrombus; (3) the entire fibrinolytic procedure is carried out within a few hours while the patient remains in the angiography suite; (4) after the pulse returns to the graft, fluoroscopy or filming is performed to show any underlying abnormality; and (5) after full heparinization, any stenosis is treated with transluminal dilatation.

The purpose of this study was to evaluate the efficacy of these modifications in comparison with previously reported techniques and to assess their usefulness in the long-term management of dialysis patients.

Subjects and Methods

Between December 1984 and August 1986, 26 patients were referred for treatment of 41 episodes of acute thrombosis of polytetrafluoroethylene hemodialysis grafts (Gortex, W. L.

Received January 16, 1987; accepted after revision March 23, 1987.

[1] Department of Radiology, Veterans Administration Medical Center, 3550 La Jolla Village Dr., La Jolla, CA 92161, and the University of California, San Diego, Medical Center, San Diego, CA 92103. Address reprint requests to G. B. Davis, Department of Radiology, Veterans Administration Medical Center, 3550 La Jolla Village Dr., La Jolla, CA 92161.

[2] Present address: Department of Radiology, University of California Hospitals, San Francisco, CA 94143.

[3] Department of Surgery, University of California, San Diego, Medical Center, San Diego, CA 92103.

AJR 149:177–181, July 1987
0361–803X/87/1491–0177
© American Roentgen Ray Society

Gore Assoc. Inc., Flagstaff, AZ; or Impra, Impra Co., Tempe, AZ). Sixteen patients had one procedure, six had two procedures, three had three, and one had four. Grafts were located in the forearm in 31 instances, in the upper arm in eight, and in the thigh in two. Often a history of recent difficulty during dialysis suggested increased venous pressures. Duration of occlusion was less than 3 days in all cases and usually was 1 day.

Two catheters were used to allow simultaneous access to both the arterial and the venous ends, and the catheters were crossed to allow deposition of urokinase throughout the entire graft. A 30° hockey-stick bend was placed 1 cm from the distal tip of each catheter to facilitate disruption of the clot and relatively homogeneous deposition of urokinase during catheter rotation.

The graft was punctured at the junction of the middle and distal (i.e., arterial) thirds. Successful needle entry into the graft was shown by return of a small amount of serosanguinous fluid and/or by easy passage of a Bentson guidewire (Cook, Inc., Bloomington, IN). The guidewire was advanced until it was well within native venous circulation. A 5-French dilator was passed over the wire until the tip was shortly beyond the probable level of the venous anastomosis. Similarly, from the junction of the middle and proximal thirds of the graft, a guidewire and then a dilator were passed beyond the arterial anastomosis (Fig. 1A). By slowly withdrawing the catheters until blood could no longer be aspirated freely, or by injecting minute amounts of contrast medium, we were able to place the catheter tips exactly at the proximal and distal ends of the thrombus.

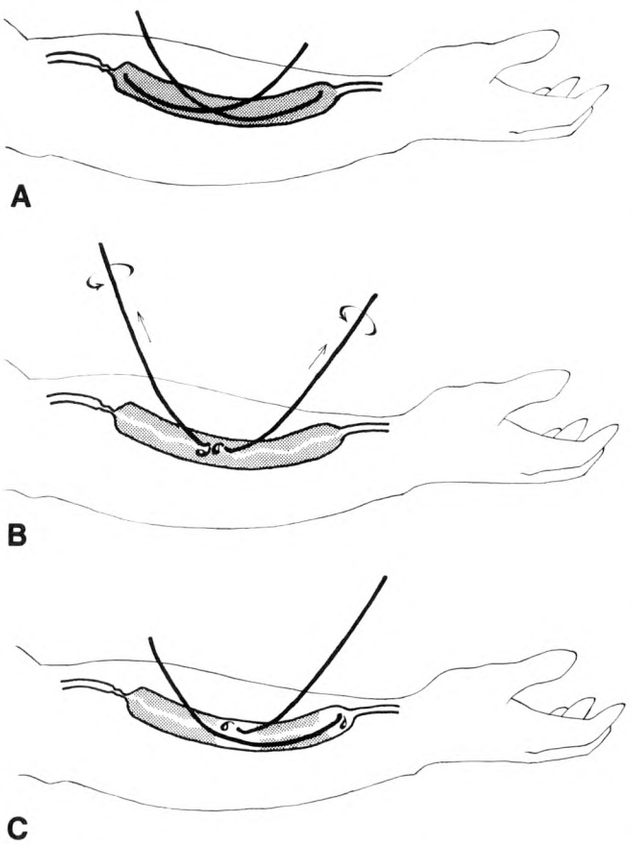


Fig. 1.—Schematic diagram of crossed two-catheter technique for fibrinolysis of thrombosed hemodialysis grafts.

***A*, Two 5-French dilators placed in opposite directions cross each other at proximal and distal ends of middle third of graft. The 30° bend at each dilator tip aids in clot maceration.**

***B*, Both catheters are partially withdrawn while they are rotated to macerate and lace entire thrombus with urokinase.**

***C*, Catheters are then positioned for optimal continuous infusion of urokinase. One catheter tip lies at proximal extent of clot; second catheter tip lies at middle of graft.**

The hook-shaped catheters were then partially withdrawn and slowly rotated to macerate the clot while concentrated urokinase (25,000 units/ml) was deposited via each catheter for a total of 100,000–150,000 units (Fig. 1B). This procedure, termed *lacing*, markedly increased the clot-agent interface. Care was taken to lace all portions of the clot. Failure to lace small parts near the anastomotic ends usually meant failure of lysis of those parts.

After lacing, the catheter tips were repositioned at the arterial end and at the middle of the graft. Urokinase (4000 units/ml) was infused via each catheter at a rate of 2000 units/min (Fig. 1C). Patients were given heparin IV during lacing and infusion; an initial bolus of 2000–3000 units was followed by an infusion of 1000 units/hr.

Return of graft flow was indicated by return of graft pulse or by onset of bleeding from previous dialysis puncture sites. Fluoroscopy and/or venography were then performed to confirm graft patency and to show possible underlying causes of thrombosis. Usually a venous stenosis was identified, either at the graft-venous anastomosis or more proximally in a draining vein. After additional administration of 5000 units of heparin (smaller amounts were used in some cases), any identified stenoses were dilated by means of high-pressure angioplasty balloon. Venous stenoses usually were overdilated via an 8-mm balloon; smaller balloons were used for arterial stenoses. The residual clot also was compressed by means of the balloon catheter at this time.

After lysis and dilatation, the catheters were removed, and hemostasis was achieved by careful application of digital pressure to the puncture sites. Very small amounts of residual thrombus were ignored. If moderate amounts of thrombus persisted after restoration of flow, administration of heparin was continued for 24 hr.

Lysis was considered successful if flow was restored and if the underlying cause of graft failure was shown. Treatment was considered successful if one or more thrombolytic procedures maintained satisfactory graft function for 6 months or longer without the need for surgery.

Results

Therapeutic Response

Of the 41 thrombolytic procedures, with or without associated transluminal angioplasty, 37 (90%) resulted in successful lysis (Table 1). The four thrombolytic failures (in three patients) were due to spasm and endovenectomy during withdrawal of the guidewire, extraluminal passage of the catheter, inadequate lysis in an infected graft, or rethrombosis during transluminal angioplasty because of inadequate heparinization.

The average time for restoration of flow was 86 ± 57 min (range, 15 min–4 hr). Clots were laced with 127,000 ± 48,000 units of urokinase; the total dose per procedure was 389,000 ± 191,000 units. In the last 10 cases, the average time for lysis was reduced to 70 min, and the average dose of urokinase was reduced to 260,000 units. This was possible because of earlier use of balloon catheters for dilatation of stenoses and maceration of clots.

TABLE 1: Summary of Results of Fibrinolysis of Thrombosed Hemodialysis Grafts

Results	No. (%)
Initially successful procedures	37/41 (90)
Patients classified as clinical successes	16/26 (62)
Patients classified as clinical failures	10/26 (38)
Underlying graft abnormality not amenable to angioplasty	4/26 (15)
Initial failure of recanalization	3/26 (12)
Inadequate dilatation or prompt rethrombosis	3/26 (12)

Note.—41 procedures were performed in 26 patients. A useful graft 6 months after the procedure was classified as a clinical success.

Fibrinogen levels were determined in 17 patients. Unfortunately, the analytic method did not consistently allow for the presence of heparin in the sample, and these results must be disregarded.

Sixteen (62%) of 26 patients were considered therapeutic successes. Their grafts were patent for 6–18 months after initial transluminal therapy. At the time of data analysis, none of these patients had required surgery yet. Continued patency required one and two transluminal procedures in 11 and four patients, respectively; one patient required three transluminal procedures.

The remaining patients required surgical revision. For reasons indicated in the first paragraph of the Results section, the first attempt at thrombolysis failed in three patients (four procedures). Four other patients had underlying graft abnormalities that were not amenable to angioplasty (two graft pseudoaneurysms, one distal venous outflow obstruction, and one arterial steal); two had stenoses that could not be dilated; and one had reocclusion of the graft after 5 days for unknown cause.

Thrombolysis allowed determination of the major underlying graft abnormality as follows: 26 venous stenoses (Fig. 2), three arterial stenoses, two instances (one patient) of inadequate arterial inflow due to arteriovenous fitula causing a steal syndrome, two instances (one patient) of subclavian vein stenoses, and two instances (one patient) of embolus from clot in a graft aneurysm. Systemic hypotension and infection were considered the primary factors causing graft thrombosis in one case each, and in four cases no underlying cause of thrombosis was determined.

In five of the 10 clinical failures (19% of 26 patients), significant information aided the surgical approach. Two cases of occlusion due to graft pseudoaneurysm were diagnosed. In a case of outflow obstruction in a subclavian vein, a new graft was placed in the opposite arm. An arterial steal from an arteriovenous fistula to graft anastomosis was shown. This was treated with ligation of the venous end of the arteriovenous fistula. One arterial stenosis was not amenable to angioplasty and was revised surgically.

A subgroup of four patients required repeated thrombolysis (three or more) at approximately bimonthly intervals, despite initially successful results. All four patients also had recurrence of thrombosis one or more times within 2 months of surgical revision. This sequence suggests that the recurrences may be attributable to an unexplained propensity of the patient rather than to the particular method (transcatheter or surgical) used to achieve recanalization.



Fig. 2.—Venograms show thrombolysis and transluminal angioplasty of a venous stenosis.

***A*, After 1 hr of infusion with urokinase, venous stenosis and significant residual clot are present.**

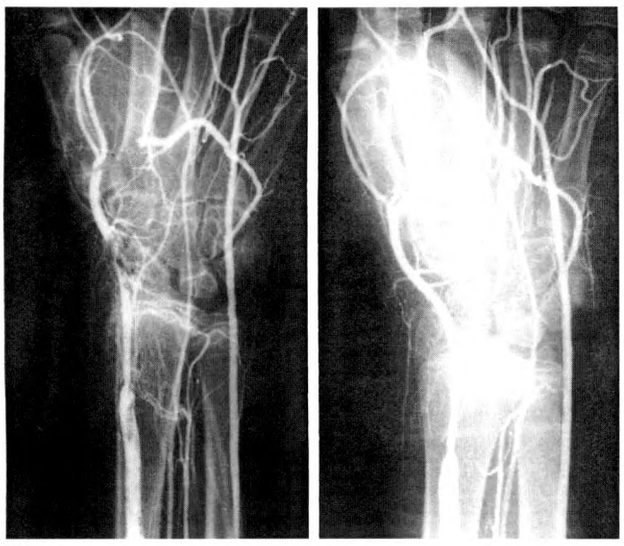
***B*, After balloon dilatation of both stenoses and graft, only minimal clot is present, and venous end is open.**

Complications

Significant hemorrhage occurred in no patients, and hemostasis usually was achieved easily. The longest duration over which direct digital pressure was required for hemostasis was 80 min. One patient had surgery at 1 month for a suspected pseudoaneurysm that proved to be hematoma at the puncture site used for both thrombolysis and dialysis.

An extreme degree of venospasm, shown by fluoroscopy, complicated four procedures. In one case, a guidewire was held so forcefully by venous spasm that its withdrawal resulted in endovenectomy and procedural failure.

No clinically recognizable episodes of pulmonary embolism occurred. Clot was embolized into the arteries of the hand in one case (Fig. 3) but was lysed after additional intraarterial infusion of urokinase. No clinical sequelae occurred. General sepsis and failure of lysis occurred in one infected graft, indicating that infected grafts should be considered a contraindication for lysis.



A B

Fig. 3.—Venograms show embolization to the hand after fibrinolysis of thrombosed hemodialysis graft.

***A*, Palmar arcade shows an embolus that originated from dialysis graft.**

***B*, Continued intraarterial infusion of urokinase has lysed embolus.**

Discussion

Two nonsurgical methods are available for restoring patency to thrombosed dialysis grafts: thrombolysis and/or transluminal angioplasty. Transluminal angioplasty without administration of a fibrinolytic agent has been used with mixed results [4–11]. Grafts have been infused with a variety of fibrinolytic agents in various doses and concentrations [12–19], including tissue plasminogen activator, streptokinase, and urokinase. Although one recent paper [20] reported encouraging results with the use of intraarterial high-dose urokinase, other studies [2, 15] have found unfavorable risk-benefit ratios. Reported difficulties encountered with fibrinolytic agents include local and remote hemorrhage, inordinately prolonged infusion, insufficient thrombolysis, and necessity for surgery despite lysis. For these reasons, Young et al. [2] firmly recommended against the use of fibrinolysis in the treatment of thrombosed dialysis grafts.

Our experience with fibrinolysis has been more favorable. The response rate has been high, and complications have been infrequent. Even when graft function could not be restored, demonstration of the underlying cause of graft failure (e.g., high venous stenosis, aneurysm) was helpful in planning surgical therapy. We think the several major advantages of our technique make transluminal therapy of graft thrombosis a preferred first alternative to surgical revision.

The selection of urokinase over streptokinase was based on previous in vitro laboratory studies that showed a marked increase in the rate of thrombolysis with increasing concentrations of urokinase up to 100,000 units/ml [3]. Use of streptokinase caused a decreased rate of thrombolysis when used at concentrations greater than 2500–5000 units/ml. Use of high concentrations of urokinase also permitted intrathrombotic deposition (lacing) of large doses in small volumes, thereby reducing the chance of arterial embolization.

Because of the frequent need for repeated treatments within a period of months, the lack of antigenicity of urokinase is another important advantage over streptokinase [21]. We observed no evidence of diminished efficacy of subsequent treatments with urokinase, as opposed to reputed failure of second treatments with streptokinase, despite initial success [22]. Inefficacy of subsequent treatments with streptokinase probably is due to the marked elevation of antibodies to streptokinase that may persist for months after streptokinase treatment [23]. Urokinase, however, exists normally in human serum [24] and urine, and antibodies against urokinase do not develop after its administration [21].

Our laboratory studies showed that intrathrombic administration of a fibrinolytic agent combined with maceration of the thrombus accelerated thrombolysis by as much as 50% over parathrombic infusion without maceration [3]. Rotation of our L-shaped catheters during lacing is a simple clinical method for achieving a modicum of maceration.

Crossed placement of two catheters has several advantages. The entire thrombus can be laced fully with urokinase, whereas transgraft placement of a single catheter would result in lack of urokinase deposition in at least part of the thrombus. It seems likely that infusion of urokinase through two catheters allows more rapid lysis than infusion through one catheter. Finally, two directions of puncture allow access to any part of the graft for transluminal angioplasty.

Once a palpable pulse returns, therapy can be directed precisely toward residual thrombus or stenosis. The majority of our occluded grafts had a stenosis at or beyond the venous anastomosis. After additional injection of about 5000 units of heparin, transluminal angioplasty of any significant stenosis was performed. Successful dilatation with long-term benefit often required use of a relatively large high-pressure balloon. Residual clot usually was macerated by means of the same balloon catheter. We observed no episodes of pulmonary embolus, probably because the clots had softened and lysed partially; the clots had, so to speak, been laced with "the seeds of their own destruction."

A major advantage of our technique is the decrease in the time required to restore graft patency. Our mean lysis time of 86 min compares favorably with the 3.6 hr or more cited in other studies [13, 20]. In our earlier experiences with streptokinase [1], mean lysis times were longer than 12 hr. The current short lysis times allow performance of the entire procedure within the angiography suite, where bleeding from previous puncture sites can be controlled immediately, lysis can be stopped as soon as patency is reestablished, and transluminal angioplasty can be performed via the same puncture sites before rethrombosis or contamination can occur.

Another advantage of our technique is its high success rate. Although flow was reconstituted in 37 of 41 cases, lysis actually occurred in two others that either rethrombosed promptly because of inadequate heparinization or became obstructed because of venospasm. Thus, lysis actually occurred in 39 (95%) of 41 cases; other studies [12, 13, 16, 17,

20, 25] have reported lysis rates of 47–92%. Although 10 patients did require subsequent surgery, 62% had functioning grafts for 6 months or longer, and an additional 19% derived significant diagnostic benefit from the procedure.

Other investigators [2, 25] found that hemorrhage was the major complication. Indeed, Young et al. [2] contended that the risk of hemorrhage outweighed the benefits of transcatheter thrombolysis. Once fibrinolysis has been achieved and graft patency reestablished, bleeding is liable to occur from recent dialysis puncture sites. This is particularly true in the presence of a venous stenosis, which functions to maintain high pressures within the graft. However, with the constant observation of the patient that is possible with our technique, bleeding from these sites can be controlled promptly and easily with digital pressure while transluminal angioplasty of venous stenosis is begun. Once a venous stenosis is dilated, the graft becomes a low-pressure system, and leakage is managed easily. The biologic half-life of urokinase is only about 10 min [26]. Thus, immediately after dilatation, the catheters can be removed, and prompt hemostasis can be expected.

Transcatheter therapeutic methods are a useful adjunct to surgery. If thrombolysis and angioplasty are successful, the graft is immediately available for dialysis, as opposed to several days that may be required after placement of a new graft. In any one patient, the number of potential graft sites is limited. Nonsurgical methods tend to prolong the life of each graft, thus extending the total time over which hemodialysis is feasible. Transluminal angioplasty causes less scarring in the operative site than does surgical revision, thus simplifying future revisions should they become necessary. Even if thrombolysis and angioplasty fail to restore graft function fully, useful information may be provided. When thrombolysis shows the underlying cause of the thrombus, such as arterial or venous anastomotic stenosis, aneurysm, kinks, or more proximal venous obstructions, surgical revision can be tailored to the specific abnormality.

Although some of our patients developed recurrent venous stenosis and thrombosis within 2 months of transcatheter therapy, these patients often also developed prompt recurrence after surgical revision. We have observed four patients with this apparent predisposition to occlusion after both transcatheter therapy and surgery.

The goal of therapy in thrombosed access grafts is to preserve functioning graft sites for as long as possible. Our results indicate that transcatheter restoration of graft patency via fibrinolytic therapy and transluminal angioplasty is a preferred first alternative to immediate surgical revision of the graft. Exploitation of current methodology requires examination of the patient within the angiography suite, use of highly concentrated urokinase, initial lacing and maceration of the clot, use of the crossed two-catheter technique, continuous infusion of urokinase, and immediate balloon dilatation. In those cases in which graft function cannot be restored fully by transcatheter methods, thrombolysis nevertheless reveals the underlying abnormalities and facilitates proper planning and conduct of surgery.

REFERENCES

1. Rodkin RS, Bookstein JJ, Heeney DJ, Davis GB. Streptokinase and transluminal angioplasty in the treatment of acutely thrombosed hemodialysis access fistulas. *Radiology* **1983**;149:425–428
2. Young AT, Hunter DW, Castaneda-Zuniga WR, et al. Thrombosed synthetic hemodialysis access fistulas: failure of fibrinolytic therapy. *Radiology* **1985**;154:639–642
3. Bookstein JJ, Saldinger E. Accelerated thrombolysis: in vitro evaluation of agents and methods of administration. *Invest Radiol* **1985**;20(5):731–735
4. Hunter DW, So SKS, Castaneda-Zuniga WR, Coleman CR, Sutherland DER, Amplatz K. Failing or thrombosed Brescia-Cimino arteriovenous dialysis fistulas. *Radiology* **1983**;149:105–109
5. Glanz S, Gordon D, Butt KMH, Hong J, Adamson R, Sclafani SJA. Dialysis access fistulas: treatment of stenoses by transluminal angioplasty. *Radiology* **1984**;152:637–642
6. Tortolani EC, Tan AHS, Butchart S. Percutaneous transluminal angioplasty: an ineffective approach to the failing vascular access. *Arch Surg* **1984**;119:221–223
7. Probst P, Mahler F, Krneta A, Descoeudres C. Percutaneous transluminal dilatation for restoration of angio access in chronic hemodialysis patients. *Cardiovasc Intervent Radiol* **1982**;5:257–259
8. Zajko AB, Mclean GK, Freiman DB, Oleaga JA, Ring EJ. Percutaneous puncture of venous bypass grafts for transluminal angioplasty. *AJR* **1981**;137:799–802
9. Glanz S, Gordon DH, Butt KMH, Hong J, Adamsons R, Sclafani SJA. Stenotic lesions in dialysis-access fistulas: treatment of transluminal angioplasty using high pressure balloons. *Radiology* **1985**;156:236
10. Motarjeme A, Kleifer JW, Zuska AJ, Nabawi P. Percutaneous transluminal angioplasty for treatment of subclavian steal. *Radiology* **1985**;155:611–613
11. Smith TP, Hunter DW, Darcy MD, Castaneda-Zuniga WR, Amplatz K. Thrombosed synthetic hemodialysis access fistulas: the success of combined thrombectomy and angioplasty (technical note). *AJR* **1986**;147:161–163
12. Zeit RM. Arterial and venous embolization: declotting of dialysis shunts by direct injection of streptokinase. *Radiology* **1986**;159:639–641
13. Pernes JM, Vitoux JF, Brenoit P, et al. Acute peripheral arterial and graft occlusion: treatment with selective infusion of urokinase and lysyl plasminogen. *Radiology* **1986**;158:481–485
14. Mori KW, Bookstein JJ, Heeney DJ, et al. Selective streptokinase infusion: clinical and laboratory correlates. *Radiology* **1983**;148:677–682
15. Becker GJ, Holder RW, Rabe FW. Contrast extravasation from a Gortex graft: a complication of thrombolytic therapy. *AJR* **1984**;142:573–574
16. Mangiorotti G, Canavese C, Thea A, et al. Urokinase treatment for arteriovenous fistulae declotting in dialysed patients. *Nephron* **1984**;36:60–64
17. Horvath L. Percutaneous transluminal angioplasty: importance of anticoagulant and fibrinolytic drugs. *AJR* **1980**;135:951–954
18. Risius B, Graor RA, Geisinger MA, et al. Recombinant human tissue-type plasminogen activator for thrombolysis in peripheral arteries and bypass grafts. *Radiology* **1986**;160:183–188
19. Becker GJ, Rabe FE, Richmond BD, et al. Low dose fibrinolytic therapy: results and new concepts. *Radiology* **1983**;148:663–670
20. McNamara TO, Fischer JR. Thrombolysis of peripheral arterial and graft occlusion: improved results using high-dose urokinase. *AJR* **1985**;144:769–775
21. Genton E, Claman HN. Urokinase: antigenic studies in patients following thrombolytic therapy. *J Lab Clin Med* **1970**;75:619–621
22. van Breda A, Katzen BT, Scales FE. Streptokinase vs urokinase in local thrombolytic infusion. *Radiology* (in press)
23. Kostering H, Barth U, Naidu R. Changes of antistreptokinase-titer following long term streptokinase therapy. In: Martin M, Schoop W, Hirsch J, eds. *New concepts in streptokinase dosimetry*. Bern: Huber, **1978**:110–115
24. Wun T-C, Schleuning W-D, Reich E. Isolation and characterization of urokinase from human plasma. *J Biol Chem* **1982**;257:3276–3283
25. Hallett JW, Greenwood LH, Yrizarry JM, Pierson WP, Robison JG, Brown SB. Statistical determinant of success and complications of thrombolytic therapy for arterial occlusion of lower extremity. *Surg Gynecol Obstet* **1985**;161:431–437
26. Collen D. On the regulation and control of fibrinolysis. *Thromb Haemost* **1980**;43:77–89

Book Review

Surgical Neuroangiography. Vol. 1. Functional Anatomy of the Craniofacial Arteries. By P. Lasjaunias and A. Berenstein. New York: Springer-Verlag, 426 pp., 1987. $165.50

This is the first of four volumes devoted to endovascular therapy of the head, neck, brain, and spine. As the title indicates, this volume describes the functional anatomy of the craniofacial arteries. There are 21 chapters with 316 figures and 684 separate illustrations.

The first chapter discusses the embryology of the carotid and vertebral arterial systems with a description of the usual anatomy and common anatomic variants. Chapters 2 through 6 discuss the internal maxillary system, the pharyngooccipital system, the ascending and deep cervical arteries, the arteries of the scalp, face, and floor of the mouth, and the thyrolaryngeal arteries. Chapter 7 is a discussion of the transosseous arterial supply of the cranial nerves and cervical roots. Chapter 8 is a discussion of dangerous vessels that must be recognized before embolization because they can give origin to the ophthalmic artery, supply cranial nerves, or supply the brainstem and cerebellum. Chapters 9 through 13 discuss collateral circulation in general terms, specific collateral patterns involving the pharyngooccipital, internal maxillary, and linguofacial systems, and the expected collateral patterns that might develop in response to embolization. The last eight chapters of the book discuss angiographic protocols in general and specific protocols for the parasellar, posterior base of skull, carotid, nasomaxillary, maxillomandibular, temporofacial and scalp, and the thyrolaryngeal regions.

The book is written in great detail and profusely illustrated with drawings, subtraction angiograms, and injected anatomic specimens, which are all excellent. Most of the book deals with normal arterial anatomy and does not discuss specific embolic materials or techniques. My only minor criticism is that the language is at times unclear and not concise. Some of the information in this volume has been published in two earlier works.

The authors are recognized leaders in neuroradiologic endovascular therapy. This volume is recommended to all who have an interest in this field. The adjective "surgical" in the title was chosen by the authors to indicate the additional demands on the physician and additional risks to the patient involved in these procedures.

Paul M. Chikos
Valley Medical Center
Renton, WA 98055

Case Report

Leiomyosarcoma of the Portal Vein

Stephanie R. Wilson[1] and Andrew L. Hine

Leiomyosarcomas originating from a vein wall are rare tumors. Their most common site of origin is the inferior vena cava, although tumors arising in other major and minor veins have been described [1–4]. In the abdomen this tumor is frequently advanced at the time of clinical presentation, making the site of origin difficult to determine [5]. We describe a patient in whom a leiomyosarcoma of the portal vein was discovered incidentally. A literature search failed to reveal a report of a leiomyosarcoma in this site.

Case Report

A 28-year-old asymptomatic woman was referred for sonographic evalulation of a palpable pelvic mass. Sonograms showed bilateral, 10-cm-diameter, complex, septated pelvic masses of nonspecific morphology. As part of our routine procedure in such a case, the upper abdomen was also evaluated, and extensive incidental abnormalities were revealed. A large mass filled and expanded the lumen of the portal vein from the venous confluence to the intrahepatic portion of both the right and left portal venous branches (Figs. 1A and 1B). The liver was normal. A 3-cm-diameter node was present in the porta hepatis. The splenic vein and superior mesenteric vein proximal to the venous confluence were dilatated and the enlarged spleen measured 15 cm in length. Huge tortuous venous collaterals were present in the porta hepatis, peripancreatic, and pericholecystic regions (Fig. 1C). These findings suggested a slow-growing tumor in the portal vein. Sonography-guided percutaneous aspiration biopsy revealed a pleomorphic spindle-cell tumor diagnostic of leiomyosarcoma. CT confirmed the sonographic findings (Fig. 1D). Angiography showed abnormal tumor vessels corresponding to the documented portal vein tumor and portal venous obstruction at the level of the venous confluence with collateral formation.

Laparotomy was performed, and benign pelvic masses related to endometriosis were resected. The portal vein leiomyosarcoma was unresectable and liver transplantation could not be performed.

Discussion

This incidentally noted portal vein leiomyosarcoma presented confusing sonographic findings when viewed in conjunction with the large, nonspecific pelvic masses. Percutaneous aspiration biopsy of the portal vein mass was most useful in making the diagnosis of a primary leiomyosarcoma arising in an unusual site. This suggested that the pelvic and portal diseases were unrelated, which was subsequently confirmed at laparotomy.

Previous authors have described the sonographic features of portal vein thrombosis. Van Gansbeke et al. [6] reported enlargement of the thrombosed segment of the portal vein in 38% of 21 cases. Of these, five of eight were malignant. They did not give the specific size of the vein in their three benign cases of portal vein thrombosis with vein enlargement. The tremendous enlargement of the caliber of the vein in our case suggested the presence of a tumor rather than benign thrombosis. The enlarged lymph node in the porta hepatis was also suggestive of a neoplastic etiology. However, the presence of extensive collateral circulation is usually associated with benign disease, as the development of the collateral pathways occurs slowly [7].

Hepatoma is the most common tumor associated with portal vein tumoral thrombosis, although it has been described in isolated cases of hepatic metastases [8]. In both of these, involvement of the hepatic parenchyma is seen in association with the portal vein thrombosis. Extensive collateral circulation is uncommonly associated with these malignant throm-

Received December 29, 1986; accepted after revision February 3, 1987.

[1] Both authors: Department of Radiology, Toronto General Hospital, 200 Elizabeth St., Toronto, Ontario M5G 2C4, Canada. Address reprint requests to S. R. Wilson.

AJR 149:183–184, July 1987 0361–803X/87/1491–0183 © American Roentgen Ray Society

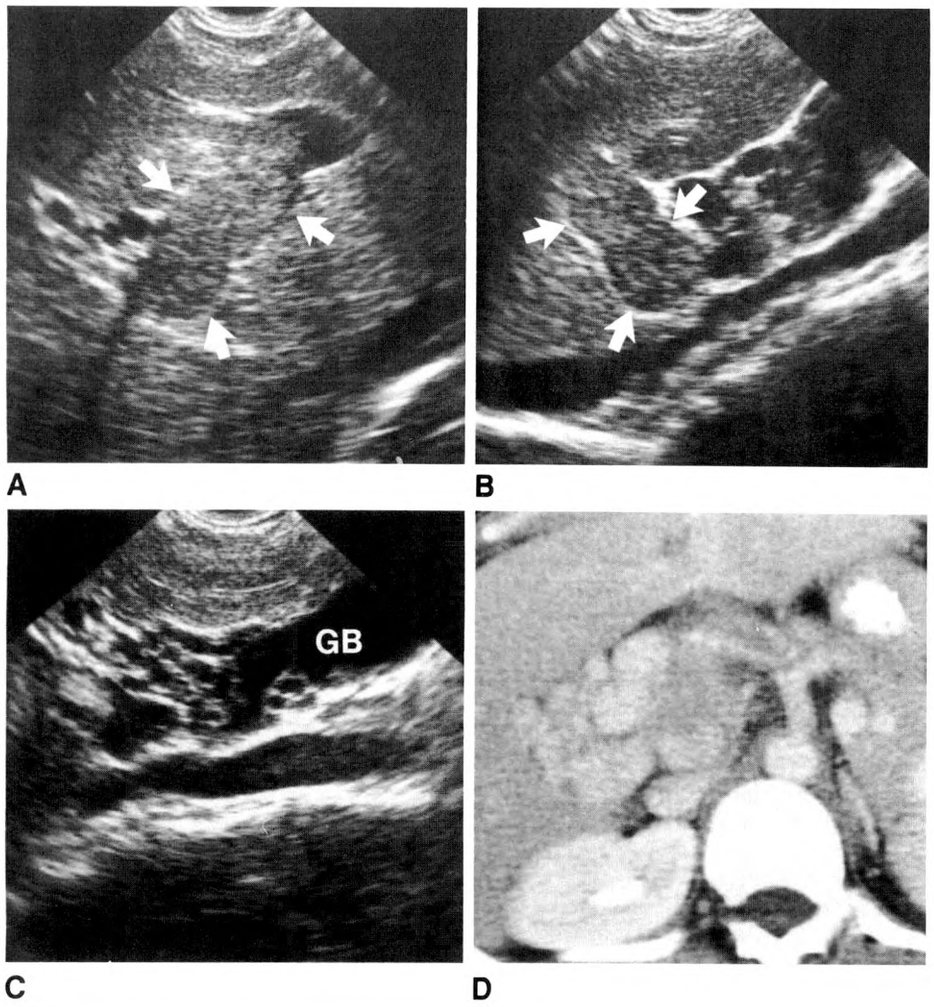


Fig. 1.—*A*, Subcostal oblique sonogram. Large solid mass (*arrows*) fills and distends main portal vein at bifurcation.

***B*, Sagittal sonogram through porta hepatis. Portal vein mass (*arrows*) extends from venous confluence to portal vein bifurcation in liver.**

***C*, Sagittal sonogram shows extensive pericholecystic and porta hepatis venous collaterals. GB = gallbladder.**

***D*, CT scan with contrast enhancement shows extensive portal venous collaterals.**

boses because of the poor prognosis and consequent lack of time for the development of collateral vessels.

The imaging findings in our case are explained by the presence of a slow-growing primary malignant tumor in the portal vein, causing both marked expansion of the vein and cavernous transformation.

Despite the incidental diagnosis of this portal vein leiomyosarcoma when it was still localized to the region of the porta hepatis, the tumor was unresectable.

REFERENCES

1. Kevorkian J, Certo DP. Leiomyosarcoma of large arteries and veins. *Surgery* **1973**;73:390–400
2. Bailey RV, Stribling J, Weitzner S, Hardy JD. Leiomyosarcoma of the inferior vena cava: report of a case and review of the literature. *Ann Surg* **1976**;184:169–173
3. Bruyninckx CMA, Derkson OS. Leiomyosarcoma of the inferior vena cava. Case report and review of the literature. *J Vasc Surg* **1986**;3:652–656
4. Leu HJ, Makek M. Intramural venous leiomyosarcoma. *Cancer* **1986**;57:1395–1400
5. McLeod AJ, Zornoza J, Shirkhoda A. Leiomyosarcoma: computed tomographic findings. *Radiology* **1984**;152:133–136
6. Van Gansbeke D, Avni EF, Delcour C, Engelholm L, Struyven J. Sonographic features of portal vein thrombosis. *AJR* **1985**;144:749–752
7. Kane RA, Katz SG. The spectrum of sonographic findings in portal hypertension: a subject review and new observations. *Radiology* **1982**;142:453–458
8. Mathieu D, Grenier P, Larde, Vasile N. Portal vein involvement in hepatocellular carcinoma: dynamic CT features. *Radiology* **1984**;152:127–132

Case Report

Transcatheter Occlusion of a Profunda Femoral Artery Pseudoaneurysm Using Thrombin

T. Gregory Walker,[1] Stuart C. Geller,[1] and David C. Brewster[2]

The treatment of pseudoaneurysms usually involves surgery because of the danger of eventual rupture. In some situations, however, the size and location of the pseudoaneurysm, as well as the patient's clinical status, may complicate or increase the difficulty of an operative approach [1]. In these situations, interventional radiologic procedures may be of use as an adjunct to surgery to stop bleeding before the operation [2–4].

A wide variety of embolic agents have been used, depending on the clinical situation and the technical feasibility. Thrombin, a vascular occlusive agent, has been reported to be of use in inducing aneurysm thrombosis, either intraoperatively or via direct needle puncture [2, 3]. We report a case in which thrombin was injected by a transcatheter technique to thrombose a pseudoaneurysm of the profunda femoris artery.

Case Report

A 33-year-old man presented with an 8-month history of a right thigh mass, which had developed 1 week after open reduction and internal fixation of a right femoral neck fracture. The mass had increased significantly in size over 24 hr. Physical examination revealed a pulsatile mass in the anterior aspect of the proximal portion of the right thigh, measuring approximately 18 × 20 cm by palpation. Arteriography showed a 5 × 7 cm pseudoaneurysm of a proximal branch of the right profunda femoris artery (Fig. 1A). A decision was made to occlude the feeding artery, using percutaneous techniques, to facilitate subsequent surgical repair.

From a left femoral artery approach, a catheter was advanced over the aortic bifurcation, and the tip was positioned in the branch of the right profunda femoris artery supplying the pseudoaneurysm. Initial attempts to occlude the feeding artery with 5 mm × 5 cm Gianturco coils were unsuccessful, as the coils repeatedly fell into the pseudoaneurysm owing to the large size of the mouth of the pseudoaneurysm. Subsequently, the catheter tip was introduced into the pseudoaneurysm, and several small Gelfoam pledgets were deposited without inducing thrombosis (Fig. 1B). After this, 1000 units of thrombin dissolved in 1 ml of saline were slowly injected. Within 20 sec, an angiogram showed complete thrombosis of the pseudoaneurysm (Fig. 1C). A 5 mm × 5 cm Gianturco coil was then placed into the feeding artery at the mouth of the thrombosed pseudoaneurysm. Repeat arteriography showed occlusion of the pseudoaneurysm and preservation of the remaining branches of the profunda femoris artery (Fig. 1D).

The next day the patient underwent surgical evacuation of the contents of the pseudoaneurysm. At exploration, a combination of fresh clot and older organized thrombotic material was found. No point of origin of the pseudoaneurysm could be identified, and ligation of the feeding artery was not required. The patient is still doing well 2 months after the procedure and there has been no recurrence of pseudoaneurysm.

Discussion

Pseudoaneurysm formation involving the femoral artery or its branches is generally the result of penetrating soft-tissue injury, bone trauma, or iatrogenic causes such as transfemoral catheterization or surgery in and around the hip. Before surgical repair, arteriography usually is done to define the point of origin of the pseudoaneurysm. A large, actively bleeding aneurysm, or a pseudoaneurysm of the profunda femoris artery located deep in the thigh musculature, requires a complicated surgical procedure since adequate surgical exposure may be more difficult to obtain under such circumstances. In these situations, transcatheter occlusion of the pseudoaneurysm before surgical repair may greatly facilitate the surgery by allowing better control of the feeding vessel, minimizing blood loss, and preventing the sacrifice of adjacent

Received December 16, 1986; accepted after revision February 3, 1987.

[1] Department of Radiology, Massachusetts General Hospital and Harvard Medical School, Boston, MA 02114. Address reprint requests to G. Walker, Dept. of Radiology, Massachusetts General Hospital, Boston, MA 02114.

[2] Surgical Services, Massachusetts General Hospital and Harvard Medical School, Boston, MA 02114.

AJR 149:185–186, July 1987 0361–803X/87/1491–0185 © American Roentgen Ray Society

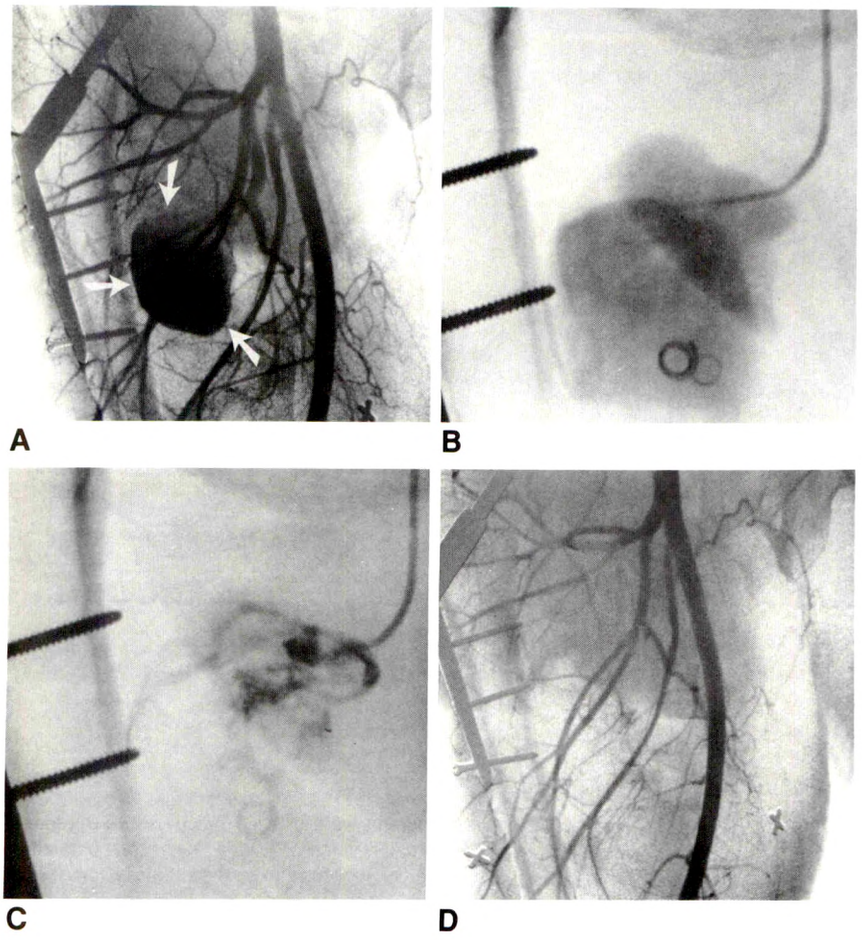


Fig. 1.—*A*, Arteriogram of right femoral artery shows pseudoaneurysm (*arrows*) of profunda femoris artery.

***B*, After embolization with Gelfoam and coils, pseudoaneurysm is not thrombosed.**

***C*, Immediately after thrombin injection into pseudoaneurysm, there is thrombus formation.**

***D*, Follow-up arteriogram shows obliteration of pseudoaneurysm and preservation of surrounding vessels.**

vessels. Occlusion may be achieved by either obstructing the mouth of the pseudoaneurysm or by inducing thrombosis within it.

In the case reported here, the size and location as well as the acute expansion of the mass prompted initial angiographic intervention. Because surgical evacuation of the contents of the pseudoaneurysm was planned, the use of temporary occlusive agents was acceptable. The initial attempt to occlude the mouth of the pseudoaneurysm was unsuccessful, because Gelfoam pledgets and coils passed freely through the arterial defect. Larger coils or detachable balloons might have been adequate to occlude the mouth, but this would have required exchange for a larger delivery catheter. Disadvantages to large delivery systems are difficult both in negotiation of tortuous vessels and in attaining a subselective position.

To induce thrombosis, the large size of the pseudoaneurysm required an agent that would occlude a large vascular space. Gelfoam and coils alone did not induce thrombosis when placed within the pseudoaneurysm. Therefore, an alternative thrombogenic agent was sought.

Thrombin has been used to induce thrombosis of aneurysms either by direct percutaneous administration or by soaking and coating Gelfoam particles or coils [2–5]. It is available as a sterile powder that can be reconstituted in varying concentrations using sterile saline as a diluent. When administered into an area of blood stasis, as in the case of a saccular aneurysm, thrombosis is induced by the formation of fibrin from fibrinogen with subsequent development of a fibrin mesh. Intravascular use of thrombin must be accompanied by measures to prevent extensive intravascular clotting and/or disseminated intravascular coagulopathy. In this case, 1000 units of thrombin in a small volume (1 ml) were injected into a circumscribed space. Contrast injection showed there was no reflux into the efferent vessel.

The advantages of using thrombin as an occlusive agent include its ready availability as an inexpensive formulary item, its high thrombogenicity, and its ability to induce thrombosis using only a small volume. It is a liquid and can be administered through catheter delivery systems of all sizes. A further advantage of a liquid occlusive agent is its ability to occlude a large vascular space.

REFERENCES

1. Berguer R, Schneider J, Wilner HI. Induced thrombosis of inoperable abdominal aortic aneurysm. *Surgery* **1978**;84:425–429
2. Rogoff PA, Stock JR. Percutaneous transabdominal embolization of an iliac artery aneurysm. *AJR* **1985**;145:1258–1260
3. Cope C, Zeit R. Coagulation of aneurysms by direct percutaneous thrombin injection. *AJR* **1986**;147:383–387
4. Reuter SR, Carson SN. Thrombosis of a common iliac artery aneurysm by selective embolization and extraanatomic bypass. *AJR* **1980**;*134*:1248–1250
5. McLean GK, Stein EJ, Burke DR, Meranze SG. Steel occlusion coils: pretreatment with thrombin. *Radiology* **1986**;158:549–550

Computer Page

Microcomputer Applications for the Academic Radiologist

Edward S. Amis, Jr.[1]

The academic radiologist does research, writes for publication, teaches medical students, residents, and fellows, and lectures in-house and by invitation at courses, meetings, and other institutions. To facilitate these efforts, most departments of radiology in academic centers provide support services such as medical illustration and photography. Yet, for enhancing productivity, the individual radiologist must organize and maintain his or her own support systems. The personal computer is ideal for this purpose, and can become a very powerful instrument with many functions if properly set up and used [1].

The computer system described in this article has proven useful to the author and may serve as an example for those considering the purchase of a system for their own practice. A decision on the cost-effectiveness of the system described must be based on the services duplicated by the department or hospital vs the convenience of having them available in one's own office.

Materials and Methods

Table 1 lists the computer hardware and software that make up the author's system and gives the manufacturers' list prices. Though mention of items by brand name is not meant as an endorsement, the equipment and programs described have been found compatible, user friendly, and powerful.

To obtain easy and rapid access to each software function, appropriate directories were created on the hard disk using the IBM Disk Operating System software (DOS). The various software programs were then installed in the directories. For the neophyte computer user (as was the author), a book such as *Hard Disk Management* [2] is mandatory, as it takes the user step by step through the organization and configuration of the disk.

Once the desired programs were installed, batch files were created, again using DOS. Batch files consist of a series of commands activated by a single entry. Sequential execution of these commands then occurs, changing directories and starting the desired program. A special batch file, the automatically executed batch file (Autoexec.bat) starts up (boots) the computer when it is switched on, displaying the Radiology Functions Menu (Fig. 1). From that point, a separate batch file for each menu function is activated by the selection of the letter assigned to that function on the menu. For example, selection of "C" (word processor) from the menu activates a batch file named "C.bat" that, through a series of permanently installed commands, takes the user to the word processor. Exiting the word processing program reactivates the remainder of C.bat and returns the user to the Radiology Functions Menu. Menus containing as many or as few functions as desired can be created using DOS. *Hard Disk Management* [2] also contains complete directions for creating menus and batch files, as well as other interesting options, with DOS.

The menu-driven system, as described above, allows one-keystroke access to those functions useful to the academic radiologist: database management, word processing, accessing Medline, 35-mm slide production, and numeric data manipulation (spreadsheet).

Discussion

Database management is probably the most important and frequently used function in the system, as reference to one's files regarding a specific case or in preparing a paper is necessary almost daily. Computerization of personal literature

Received January 26, 1987; accepted after revision March 12, 1987.

The opinions and assertions expressed are the private ones of the author and are not to be construed as official or reflecting the views of the Navy Department, the Naval Service at large, or the Department of Defense.

[1]Department of Radiology, Naval Hospital and Uniformed Services University of the Health Sciences, Bethesda, MD 20814. Address reprint requests to E. S. Amis at the Naval Hospital.

AJR **149:187–190, July 1987** 0361–803X/87/1491–0187

TABLE 1: Recommended Computer Hardware and Software, Including List Prices

Component	Supplier	Price
Hardware		
IBM-XT Microcomputer 640k memory 360k floppy disk drive 20 megabyte hard disk Color graphics adapter card Printer adapter card	International Business Machines Corp. (IBM), Boca Raton, FL	$2979
IBM color monitor		680
IBM ProPrinter and cable		594
Polaroid Palette Computer Image Recording System	Polaroid Corporation, Cambridge, MA	1999
Hayes 1200B Internal Modem	Hayes Microcomputer Products, Inc., Norcross, GA	549
Software		
IBM Disk Operating System (DOS 3.2)	IBM	95
Cardbox (electronic card-indexing database)	Caxton Software Publishing Company, London	91
Word Processor	Choice deferred to user	50–500
Grateful Med (software for searching Medline)	National Technical Information Service, Springfield, VA	30
35 mm Express, Version 4.0 (graphics program)	Business and Professional Software, Cambridge, MA	695
Lotus 1-2-3 (spreadsheet)	Lotus Development Corporation, Cambridge, MA	495

Note.—Although the total list price of approximately $8500 seems staggering at first, it should be noted that judicious shopping can result in acquisition of the complete system at a 30% or greater discount.

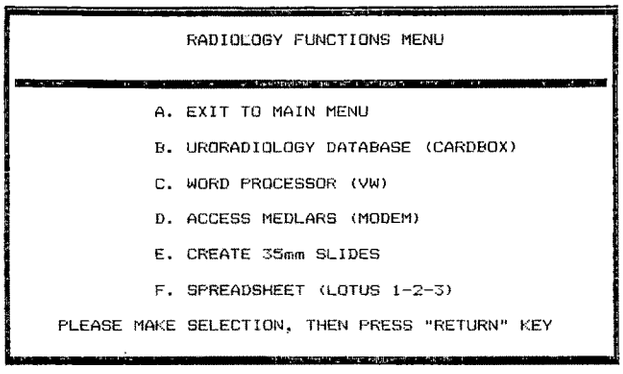


Fig. 1.—Radiology Functions Menu. Each function can be brought into use by selecting appropriate letter and pressing return key.

files is time consuming only while initially entering existing large files into the database. For the average typist, about 1 min is required for each file entry. If a secretary is to make the entries, it is necessary to jot the key words on the article as it is reviewed to ensure that it can be easily searched.

Any current database software can be used as long as it is text oriented and allows indexing of unlimited numbers of key words. Cardbox (Caxton Software Publishing Company, London) meets these criteria, allows the user to draw a file card on the screen, and has a maximum capacity of 65,000 files. Haynes et al. [3] have addressed in detail the storage and retrieval of medical literature. The simplest computerized method is sequential numeric filing, in which articles, regardless of topic, are numbered sequentially beginning with 1, entered into the computer, and then placed in file folders labeled with the numbers of the articles contained in each. In the system described here, 25 articles are placed in each file folder.

Figure 2 is a reproduction of the card seen on the screen when entering a publication. Authors, title, and journal are entered in standard fashion. The file number in the upper right corner is the location of the article in the file. All words listed under modality, organ, and pathology are automatically indexed as they are entered and may therefore be searched. Most database software will allow the indexing of any word in the entry (e.g., the primary author). To illustrate search and cross-reference possibilities, the article in Figure 2 would be found if one searched for "CT of angiomyolipoma" or "ultrasound of renal masses." Cardbox can also be configured to

Fig. 2.—Typical file entry for personal literature database. Any word on card can be indexed, allowing it to be searched. In this file, all words in modality, organ, and pathology sections are indexed, facilitating cross referencing.

```
CARDBOX(U)     File = C:GUFILE.FIL     READY
Level  0 - 1888 RECORDS SELECTED
```

Author: Raghavendra BN, Bosniak MA, Megibow AJ	File # 784
Title: Small angiomyolipoma of the kidney: sonographic-CT evaluation	
Journal: AJR 141:575-578, September 1983	
Modality: US, CT	
Organ: KIDNEY	
Pathology: ANGIOMYOLIPOMA, HAMARTOMA, MASS, TUMOR, BENIGN	

allow computer filing of radiograph teaching files and slide files, though it is much simpler to store the latter in a slide library where the entire collection can be easily seen while preparing presentations.

A word processing program on the menu is essential, even if full secretarial support is available. It is useful in developing outlines and for preparing rough drafts. There are many inexpensive, user-friendly programs currently available, as well as more sophisticated packages designed for the production of quality scientific manuscripts. Several programs now incorporate a spelling checker and thesaurus.

A modem is necessary for rapid and easy access to all medical literature available via telephone lines. The main database, Medline, is located at the National Library of Medicine (NLM). Application for an access code is free (Medlars Management Section, National Library of Medicine, 8600 Rockville Pike, Bethesda, MD 20894), and formal training in searching the database, although desirable, is not mandatory. The NLM publishes a monograph entitled "The Basics of Searching Medline: A Guide for the Health Professional," and has also produced an inexpensive software program, Grateful Med, for use in directly accessing Medline. Grateful Med features automatic log-on, a simplified search process, and downloading of citations to the user's computer. Gurney and Wigton [4] provide more useful information on searching the literature via computer.

Quick, simple production of 35-mm slides is one of the more exciting functions now available with the personal computer. Although there are several computer image recording systems available, the Polaroid Palette is relatively inexpensive and produces multicolored, high-quality slides (Fig. 3). The Palette includes a device for instant processing of all the various 35-mm films that Polaroid produces. Thus, not only can color text and graphic slides be produced from computer-derived images using Polachrome film, radiographs can also be photographed using Polapan film (ASA 125) in a hand-held 35-mm camera with macro lens, and the film can be processed in the office immediately. The quality of such slides is quite good. Both types of slides produced this way cost approximately 40 cents each. If more time is available, it is recommended that Ektachrome 100 film (Eastman Kodak Company, Rochester, NY) be used for color work with the Palette and developed in standard fashion. The colors are brighter, and the cost of each slide is reduced to about 30 cents.

Documentation accompanying the Palette lists several graphics software programs that will drive the Palette directly. An extremely powerful software package is 35-mm Express, which produces high-quality text and graphics slides and can program the Palette to automatically expose batches of up to 32 slides at a time. The program also allows computer drawing using the cursor control keys or a hand-directed mouse. Text and graphs can be produced without the Palette by using a graphics printer and slides made from the printout (Fig. 4), though they will be black and white only and not of the same quality. Whereas 35-mm Express produces only black-and-white graphics on the screen, other graphics programs yield full-color results, allowing direct photography of the image on the monitor screen. Again, resolution is significantly less than that attainable with the Palette.

The final function that is essential to the academic radiologist is the spreadsheet, which allows manipulation of numeric data derived from clinical or laboratory research. A widely accepted program is Lotus 1-2-3. This software interfaces with 35-mm Express and other graphics programs, allowing formulation of various types of graphs from the data recorded in the Lotus program.

While tape systems are available for backing up—or saving—the entire contents of the hard disk, they are quite expensive. Therefore, backup of the contents of the entire hard disk with floppy disks, even though 15 to 20 disks may be required, is highly recommended after the initial installation of programs and creation of menus and batch files. This will save a tremendous amount of effort in reconfiguring the hard disk in the unusual event of failure. Once the initial backup is done, it is simple to create another batch file that allows backup of important permanent files on the hard disk, such as a personal literature database. For example, the author backs up his literature file after every 100 or so entries. It now contains over 2000 entries, and yet requires only two floppy disks for backup.

The microcomputer system and software described in this article can significantly enhance the productivity of the academic radiologist by placing all desired functions within a couple of keystrokes. Certainly several of these functions, such as maintaining a literature file and the ability to access the national medical databases, can also be useful to the radiologist in private practice. Those functions readily available in one's department or hospital need not be included, or can be added to a basic system as the need arises.

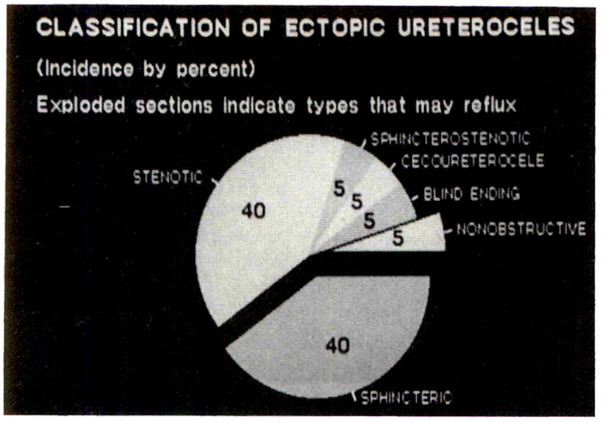


Fig. 3.—Computer-derived graphic produced by 35-mm Express software with Polaroid Palette. Software permits multiple styles, colors, and other manipulations such as "exploding," or separating, pie sections requiring emphasis.

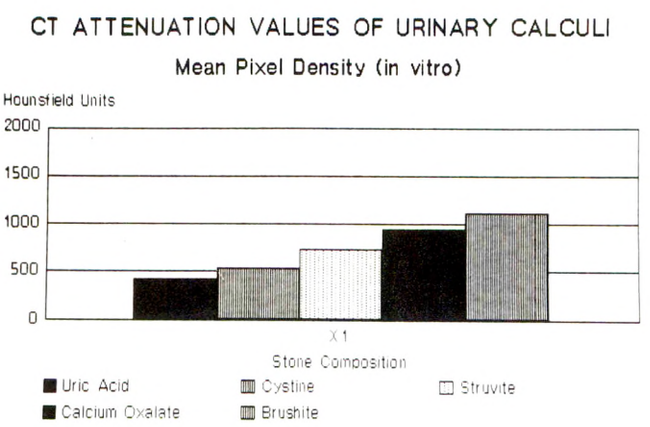


Fig. 4.—Printout of computer-derived bar graph. Data is entered in a simple grid; user can then choose various types of graphs that are automatically formatted. 35-mm slides are produced by photographing printout, if Polaroid Palette is not included in system.

REFERENCES

1. Newell JD, Hunter TB. Personal computer needs for the radiologist. *Invest Radiol* **1986**;21:167–169
2. Cain T, Cain NW. *Hard disk management for the IBM PC XT, AT and compatible systems.* New York: Brady, **1986**
3. Haynes RB, McKibbon KA, Fitzgerald D, Guyatt GH, Walker CJ, Sackett DL. How to keep up with the medical literature: VI. how to store and retrieve articles worth keeping. *Ann Intern Med* **1986**;105:978–984
4. Gurney JW, Wigton RS. Computerized reference management: searching the literature. *AJR* **1986**;147:641–645

Computer Page

A Computerized Filing System for Radiology Teaching Cases

Christopher L. Sistrom[1] and William C. Black[1]

A teaching file can be a valuable asset to academic radiology departments and private practice groups, providing that the retrieval of cases for specific needs can be performed easily and quickly. Traditionally, cases from a teaching file are selected either randomly or sequentially according to their indexing system, usually the anatomic region or organ system. However, to take full advantage of a large teaching file, which potentially could be used to illustrate presentations, books, and articles, specific cases must be retrievable on the basis of any one of several elements, for example, disease, body part, chief complaint, technique used, or any combination of the above. The practical application of such a complex filing system requires the use of a data base tailored for the radiology department. We developed a data-base management program called DBRAD that runs on a personal computer and performs case-searching and other tasks. The program is completely menu-driven and provides its users easy and quick access to a large radiologic data base as well as a complete set of maintenance functions.

Materials and Methods

We used a personal computer that is compatible with an IBM PC XT (International Business Machines, Boca Raton, FL); it has a 10-megabyte hard-disk drive and 0.5 megabyte of random-access memory in combination with a popular data-base management system for personal computers, dBase III (Ashton Tate, Inc., Culver City, CA). Each case in the radiology data base is represented by a record consisting of 12 fields. The various functions of our program enable the user to search the entire data base for all the records that satisfy specified field conditions and then list those records, as well as to modify or add to the existing data base. Commands are also available to print a "catalogue" of the teaching file and to generate labels for the film jackets. The American College of Radiology has promulgated a numeric system for coding the radiologic manifestations of diseases (ACR code). This widely accepted coding system is defined by a two-part number that is kept as two separate fields (anatomic and pathologic), which serve as the primary filing keys for records in the data base. Other fields, which include the imaging technique used, patient identification information, descriptive diagnosis, chief complaint, and comment field for additional information, are depicted in Figure 1, a typical case record. The size of each record is about 170 bytes. Our teaching file of about 5000 cases will occupy about 1.5 megabytes of storage, which is easily within the 10-megabyte capacity of our fixed disk (a standard 5¼-in. [13.3-cm] 350-kilobyte flexible disk can hold just under a thousand cases).

On start-up a menu screen (Fig. 2) is presented to the user. Striking a single letter command quickly selects the function desired. The centerpiece of the data-base system is a search routine that allows the user to specify ACR code, modality, diagnosis, chief complaint, and comment information, in any combination. If one of these parameters is not specified, that field is not included in the search. Initially, only the number of matching cases is presented on the screen to the user. These cases can then be listed on the screen or printed. Alternatively, a new set of parameters can be specified if the initial search produces too many or too few matches. Figure 3 shows the screen used to specify searches. We designed the search algorithm to minimize the time required to produce the number of matching cases. If an ACR code is specified, the counting phase of the search takes about 4 sec. When diagnosis, chief complaint, or comment (for example, radiographic findings) are specified without an ACR code, a period of about 10 sec is required for counting. This applies to a file of 400 cases residing on a fast fixed-disk drive.

Received December 24, 1986; accepted after revision February 9, 1987.
[1] Department of Radiology, Box 170, University of Virginia Medical Center, Charlottesville, VA 22908. Address reprint requests to C. L. Sistrom.

AJR **149:191–193, July 1987** 0361–803X/87/1491–0191 © American Roentgen Ray Society

FIELD NAME	SAMPLE CONTENTS	LENGTH AND DATA TYPE
PATIENT NAME	PSEUDONYM, IMA	15 ALPHANUMERICS
HISTORY NUMBER	123456	6 DIGITS
PATIENT AGE	53	2 DIGITS
SEX MALE = T, FEMALE = F	T	1 LOGICAL*
ACR CODE	811.243	4&5 DIGITS**
MODALITY	U (ULTRASOUND)	1 ALPHANUMERIC
DIAGNOSIS	LYMPHOMA	30 ALPHANUMERICS
CHIEF COMPLAINT	HEMATURIA	30 ALPHANUMERICS
COMMENT	HYPOECHOIC MASS	75 ALPHANUMERICS
SIGNATURE	CSIS	4 ALPHANUMERICS
DATE OF ENTRY	10/10/86	DATE FORMAT***

*ALLOWS ONLY "T" (TRUE) AND "F" (FALSE)
**STORED AS TWO SEPARATE FIELDS
***SPECIAL FORMAT KEPT BY SYSTEM

Fig. 1.—Structure of individual records in teaching-file data base. Field name, sample contents, and data type are shown. ACR = American College of Radiology.

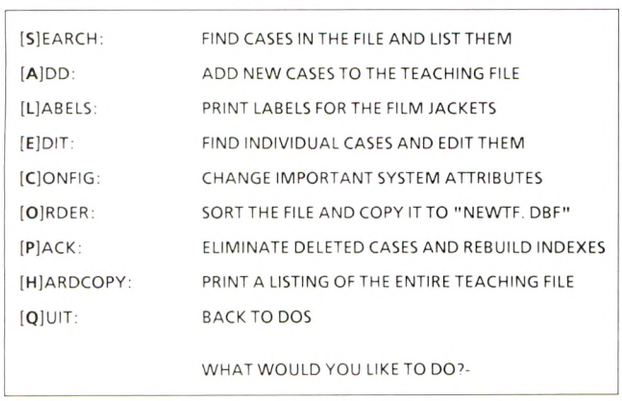


Fig. 2.—Main menu screen. Typing highlighted command letters allows execution of each command. DOS = disk operating system.

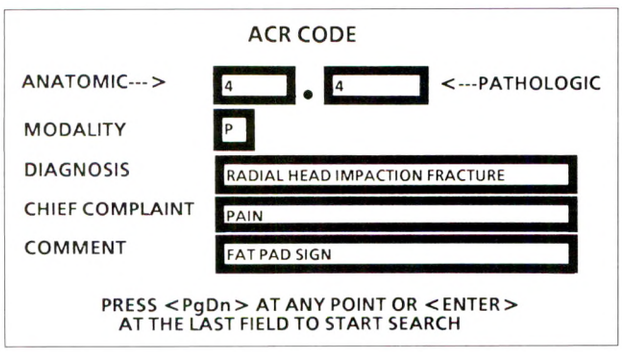


Fig. 3.—Screen used to specify enter search parameters. Rectangular border denotes reverse video display. P in modality stands for plain film.

The "ADD" command allows entry of new case material to the file. A blank case-record form is presented allowing rapid entry of the patient information and radiographic findings. Extensive data checking and error correction are used to ensure future retrievability of the record. For example, if the patient name is left blank during case entry, that field is automatically filled to allow the record to be uniquely identified. A blank hospital number field is replaced by the term "OUTSID." Only digits are allowed in the ACR code field, and blanks are automatically trimmed from all fields. Before filing, the corrected record is redisplayed and further modifications are allowed. To aid in adding cases where two or more ACR codes apply, a "carry-over" feature is supplied that files the current record and creates a duplicate record to which minor modifications (for example, ACR code) can be made.

The "EDIT" command finds individual cases by name, hospital number, or ACR code. The first matching case is displayed. The user can then step through the file forward or backward from that point. The order in which the cases are presented is determined by the parameter that was used to gain entry into the file. Thus the file can be searched according to almost any order, including name, hospital number, anatomic code, and pathologic code. The contents of any case can be changed, or the case may be deleted. This feature replaces a bulky manual filing system that would require four large, separate card files.

The "LABELS" command prints labels for the corners of the film jackets, which facilitates locating and refiling cases. Since the date of entry is kept for each record, labels for the most recently added cases can be produced on a periodic basis. A set of four labels is printed for each film jacket. The two front corners are marked with the ACR code, patient identifying information, age, and chief complaint. The back of the jacket displays the same information as the front, but the chief complaint is replaced by the diagnosis. Another command, "HARDCOPY," prints a listing of the entire teaching file. The order of this "catalogue" is determined by the user.

Selection of the above functions is by single key strokes from the main menu screen (Fig. 2). Simple instructions are shown at each point input is required. Data entry, case editing, and search specification are facilitated by a full-screen editing mode, which allows all fields to be viewed at once and changed independently (Fig. 4).

After this data-base system was written with dBase III and tested, we used another software product, a dBase compiler called Clipper (Nantucket Corp., Culver City, CA) to produce a single program file called DBRAD that can run (by itself) on any IBM-compatible computer.

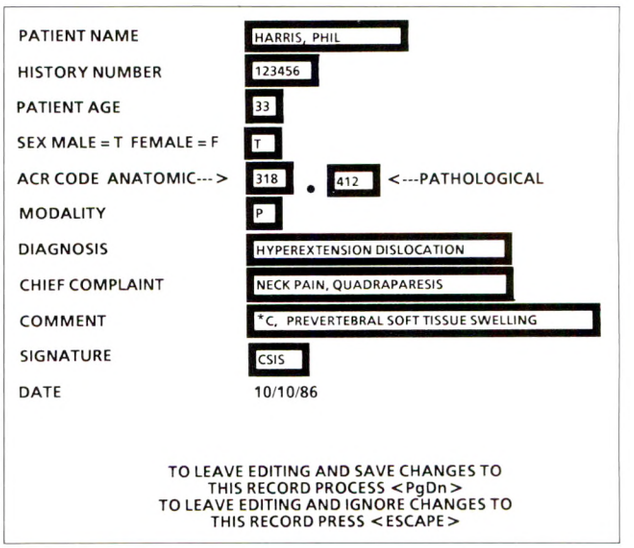


Fig. 4.—Replica of edit-mode screen for editing individual cases. Fields can be individually changed until desired content is displayed. Rectangular border represents reverse video display. Opposite modality, P = plain film; opposite comment, *C means CT scans are also included.

Discussion

There are two organizational features of the ACR coding system that greatly facilitate the searching of a large radiology data base. First, in its tree-structure form higher precision numbers specify more detailed anatomic locations or pathologic entities. Second, the pathologic codes are similar, often identical, across the anatomic fields (at least in the first two or three digits). Our search algorithm was designed specifically to take advantage of these coding features. Thus, in searching the teaching file, anatomic location can be specified very tightly by entering a full precision number while the pathologic code may be broadly defined, or vice versa. For example, all cases of neoplasms in and around the knee can be found by specifying 45.3 in the ACR code. Alternatively, findings related to tuberculosis throughout the skeletal system are easy to extract (ACR code = 4.23). By not specifying the anatomic code, all cases of a particular disease will be listed regardless of the anatomic location. Diseases such as lymphoma, rheumatoid arthritis, or sarcoidosis, which affect many different anatomic regions, can be accessed completely. If the modality field and ACR code are specified, more refined searches are possible. Thus, CT findings in renal tumors can be found by using an ACR code of 8.3 and "C" in the modality.

To make the most efficient use of the diagnosis, chief complaint, and comment fields, consistent terms and abbreviations should be used. In specifying chief complaint, diagnosis, and radiographic findings, considerable brevity can be used by realizing that some anatomic and pathologic information is already contained in the ACR code. The search algorithm will find cases that contain a user-specified text string within these fields. Because the matching string can occupy any position within the field, a powerful method of case retrieval is available if chief complaints and radiographic findings have been entered carefully. For example, all cases associated with the chief complaint of seizure or gastrointestinal bleeding or the radiologic finding of periosteal reaction are easy to extract. These free text fields allow considerable flexibility in tailoring the system to the specific needs of the department or an individual. For example, our residents add the string "*BR" to expedite retrieval of cases most suitable for board review, and one faculty member has modified the input of data on his own copy of the program according to his special interests in chest radiology and body CT. He uses "*FU" in the diagnosis field for current cases needing follow-up pathology. A subset of data fields and program functions can be used to make a personal data base that is easy to use and well suited to individual needs.

By using the Clipper compiler we were able to generate a program, DBRAD, that will work alone on any IBM-compatible personal computer. The dBase III product is not required to run the program. A diskette containing DBRAD and a short users' guide are available to anyone interested; a nominal amount ($25–$35) is charged to cover the cost of diskettes, duplication, and postage. For more information, contact the first author.

American Roentgen Ray Society:
Officers, Committees, and Meeting Information

Officers

President: Raymond A. Gagliardi
President-elect: Lee F. Rogers
1st Vice-president: Gerald D. Dodd
2nd Vice-president: Rosalind H. Troupin
Secretary: Glen W. Hartman
Treasurer: Ronald G. Evens

Executive Council: E. Gedgaudas, J. F. Wiot, L. F. Rogers, R. A. Gagliardi, R. G. Evens, R. N. Berk, F. L. Angell, J. E. Madewell, M. P. Capp, G. W. Hartman, B. G. Brogdon, R. H. Troupin, G. R. Leopold, G. D. Dodd, A. K. Poznanski, A. E. James, Jr., J. T. Ferrucci, Jr., T. C. Beneventano, E. J. Ferris, J. A. Kirkpatrick, Jr., chairman

Committees 1987–1988

Editorial Policy: S. S. Sagel, W. J. Casarella, J. T. Ferrucci, Jr., N. C. Whitley, S. Hilton, J. M. Taveras, R. N. Berk, M. P. Capp, chairman

Education and Research: C. E. Putman, A. R. Margulis, B. J. Hillman, R. A. McLeod, J. T. Ferrucci, Jr., ex officio, B. G. Brogdon, chairman

Finance and Budget: B. P. Wood, L. R. James, J. A. Kirkpatrick, Jr., A. E. James, F. L. Angell, chairman

Nominating: W. J. Casarella, H. C. Carlson, A. E. James, chairman

Publications: W. J. Casarella, S. S. Sagel, N. C. Whitley, C. A. Rohrmann, Jr., M. P. Capp, chairman

Membership: A. E. James, chairman

Representatives to Other Organizations

American Board of Radiology: E. C. Klatte, T. C. Beneventano, L. F. Rogers

American College of Radiology: L. F. Rogers, G. A. Kling, R. A. Gagliardi, J. M. Dennis, E. J. Ferris, J. E. Madewell

American Medical Association House of Delegates: S. F. Ochsner, K. L. Krabbenhoft, alternate

American National Standards Institute: M. Haskin

National Council on Radiation Protection and Measurements: E. L. Saenger, H. L. Friedell

Meeting Arrangements

Annual Meetings: May 8–13, 1988, Hilton, San Francisco; May 7–13, 1989, Hilton, New Orleans; May 13–18, 1990, Sheraton Washington, Washington, D.C.

Annual Meeting Committee: H. C. Carlson, G. P. Janetos, G. D. Dodd, T. C. Beneventano, chairman (Montefiore Hospital, Bronx, NY 10467; (212) 920-4200).

Instruction Courses: R. A. McLeod, associate chairman, J. T. Ferrucci, Jr., chairman

Program: R. A. Gagliardi, G. W. Hartman, J. A. Kirkpatrick, Jr., A. E. James, M. P. Capp, J. E. Madewell, B. G. Brogdon, J. T. Ferrucci, Jr., G. A. Kling, S. A. Feig, G. P. Janetos, L. F. Rogers, chairman

Scientific Exhibits: K. H. Vydareny, A. V. Proto, S. M. Goldman, J. E. Madewell, chairman

ARRS Membership

Send applications to: Paul Fullagar, administrative director, American Roentgen Ray Society, 1891 Preston White Dr., Reston, VA 22091; (703) 648-8900. The ARRS has two membership categories: active and in-training. For active membership, applicants must practice radiology in the U.S. or Canada. Each must have graduated in good standing from an approved medical school or hold an advanced degree in a physical, chemical, or biological science and be certified by the American Board of Radiology, the Royal College of Physicians and Surgeons of Canada, or otherwise adequately document training and credentials. A member-in-training must be in a radiology residency or a postresidency fellowship program, or be a postgraduate student in an allied science. Status must be verified by the program director. For consideration during the 1988 ARRS meeting, completed applications must be received by Paul Fullagar no later than Feb. 1, 1988.

Business Information

Business Office: Paul Fullagar, administrative director, American Roentgen Ray Society, 1891 Preston White Dr., Reston, VA 22091; (703) 648-8900.

Computer Page

Computer-Aided Design and Realization of Scientific Exhibits in Radiology

Felix S. Chew[1] and Martha L. Hefner[2]

Scientific exhibits are an integral and popular component of national radiology meetings. Sessions of scientific exhibits are well attended, and prizes awarded for the best exhibits are highly coveted. Their purpose is educational: to communicate a body of knowledge, a group of concepts, or a set of images. Typically placed in close proximity to one another in a large room, the design of these exhibits has two functions: to attract and hold the attention of the viewer and to communicate effectively. This poses an interesting blend of science and tastefully restrained advertising, with the bright colors and lights of a scientific exhibit not far removed from the neon signs and billboards of commercial enterprises. This article describes the use of a personal computer in the design and realization of scientific exhibits in radiology. Computers offer speed, accuracy, adaptability, and low operating cost. An effective and versatile tool for graphic design [1], the computer can replace tedious work with big sheets of graph paper, ruler, scissors, and paste. The ease of editing and the ability to make several different versions encourage innovation and experimentation.

Materials and Methods

Two microcomputer systems were used: (1) an Apple Macintosh Plus computer with an internal 800-kilobyte 3.5-in. (8.9-cm) floppy-disk drive, a second similar external-disk drive, and an Imagewriter II dot-matrix impact printer and (2) an Apple Macintosh Plus computer with an internal 800-kilobyte 3.5-in (8.9-cm) floppy-disk drive, an Apple Hard Disk 20 (20-megabyte hard-disk drive), and an Apple Laserwriter Plus laser-xerographic printer (Apple Computer, Cupertino, CA). The ease of use of these computer systems, their speed, and their generous memory capacity (1 megabyte of random access memory) are important to frustration-free exhibit design. The usable portion of the Macintosh monitor screen is relatively small—17.3 × 11.7 cm—but its 512 × 342 matrix and normal aspect ratio provide relatively high resolution for a personal computer. The Laserwriter is a powerful, dedicated microcomputer that interprets commands from the Macintosh to control a laser-xerographic printing mechanism. Full descriptions of these off-the-shelf systems are available from the manufacturer [2–4]. The software programs used were Apple MacDraw (Apple Computer, Cupertino, CA); Cricket Graph (Cricket Software, Philadelphia, PA); and Microsoft Word (Microsoft, Redmond, WA). Other microcomputers and other software programs may also be suitable for exhibit design and realization.

One backboard exhibit [5] was completely designed and produced. This exhibit occupied a 1.22 × 1.22 m area and consisted of two title signs (96.5 × 14.0 cm and 31.8 × 13.3 cm) and seven smaller signs (26.0 × 33.0 cm) with exposition in text and graphics. The signs were constructed by mounting paper on colored matboard. The exhibit was viewed with reflected light.

One panel (74.7 × 47.0 cm) of a view-box exhibit [6] was designed. The panel produced from this design consisted of radiographs, photographs, and blocks of text sandwiched between two sheets of Plexiglas (Fig. 1). The entire exhibit had 12 such panels and was viewed with transmitted light.

Exhibit Design

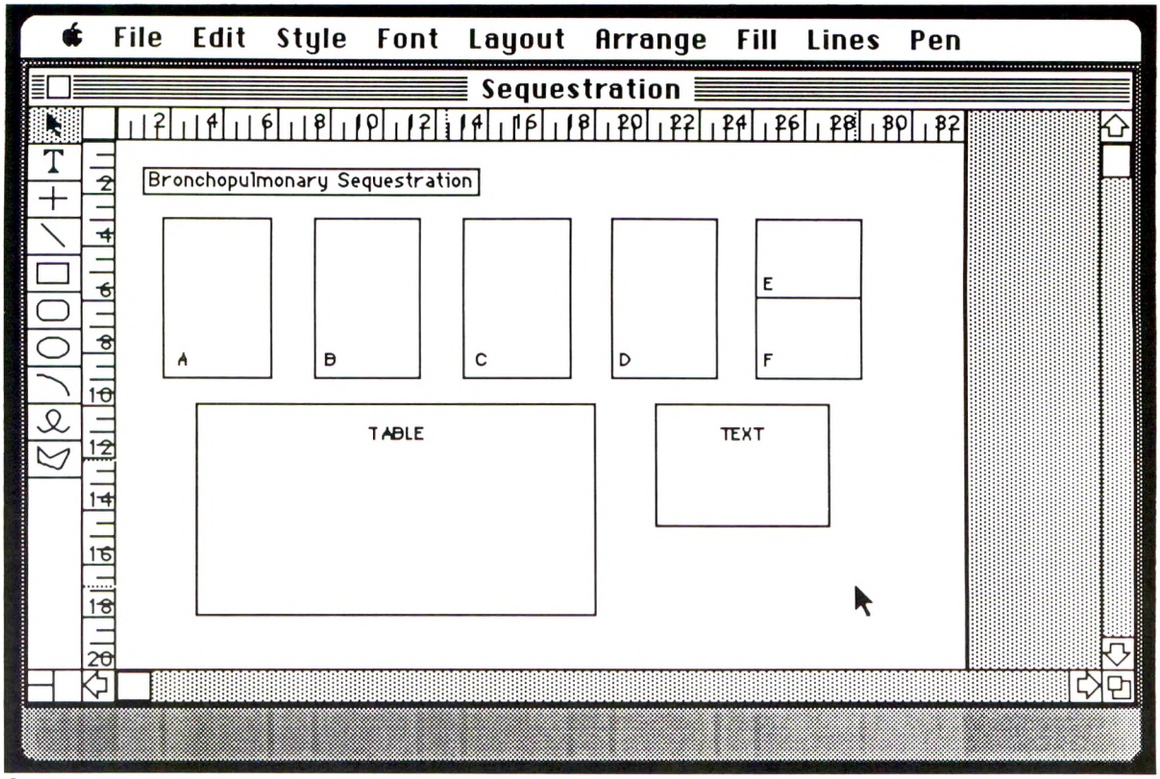
MacDraw is a structured graphic design program capable of creating standard objects (squares, rectangles, circles, ovals, curves, and straight lines) in any proportion and dimension. Once created, these objects can be duplicated, moved, overlayed, rotated, arranged, aligned with each other, grouped together, edited, or deleted. Illustrations, graphic material, and blocks of text can be represented by rectangles; then these are arranged and grouped on the computer (Fig.

Received December 29, 1986; accepted after revision February 18, 1987.

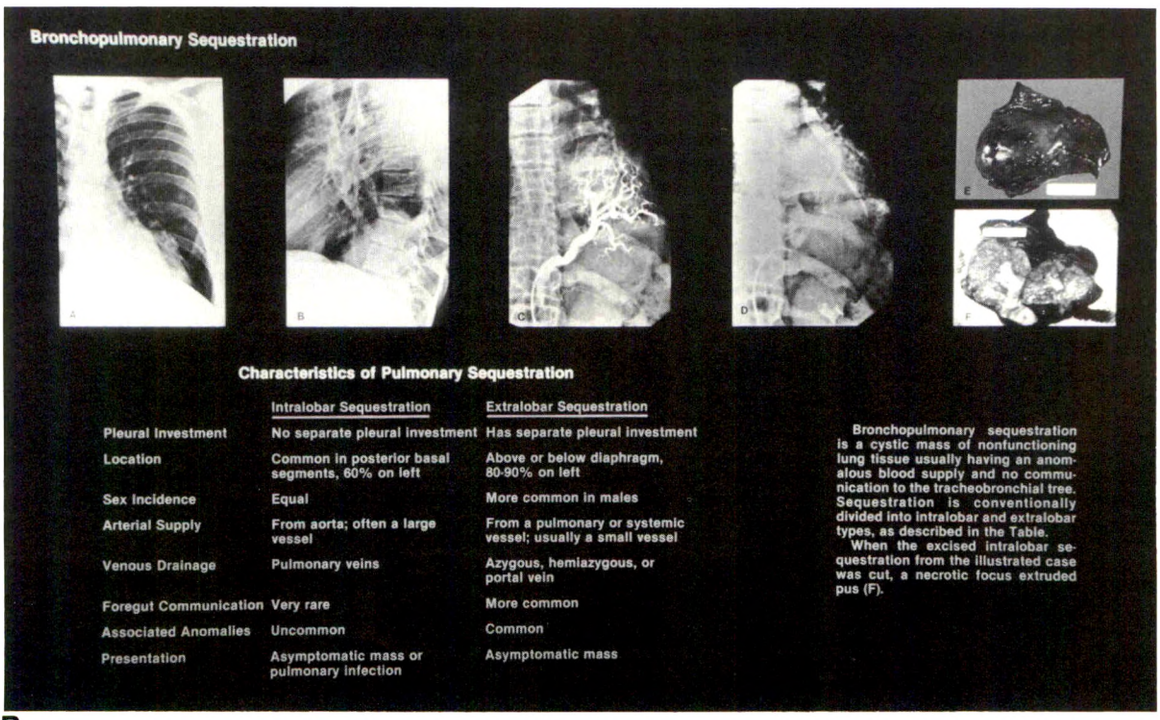
[1] Department of Radiology, State University of New York, Health Science Center at Syracuse, 750 E. Adams St., Syracuse, NY 13210. Address reprint requests to F. S. Chew.

[2] Division of Medical Illustration, State University of New York, Health Science Center at Syracuse, Syracuse, NY 13210.

AJR 149:195–198, July 1987 0361–803X/87/1491–0195 © American Roentgen Ray Society



A



B

Fig. 1.—*A*, Layout on Macintosh monitor screen for one panel of view-box exhibit with program MacDraw. Radiographs, photographs, and blocks of text are represented by rectangles. Note rulers along edges. Graphic design tools for creating text, lines, curves, and shapes are selected on left by mouse-controlled cursor. Menu bar along top of screen has commands for saving, printing, enlarging, and so forth. Scroll bars along right side and bottom allow display of any portion of document on screen.

B, Photograph of actual exhibit panel.

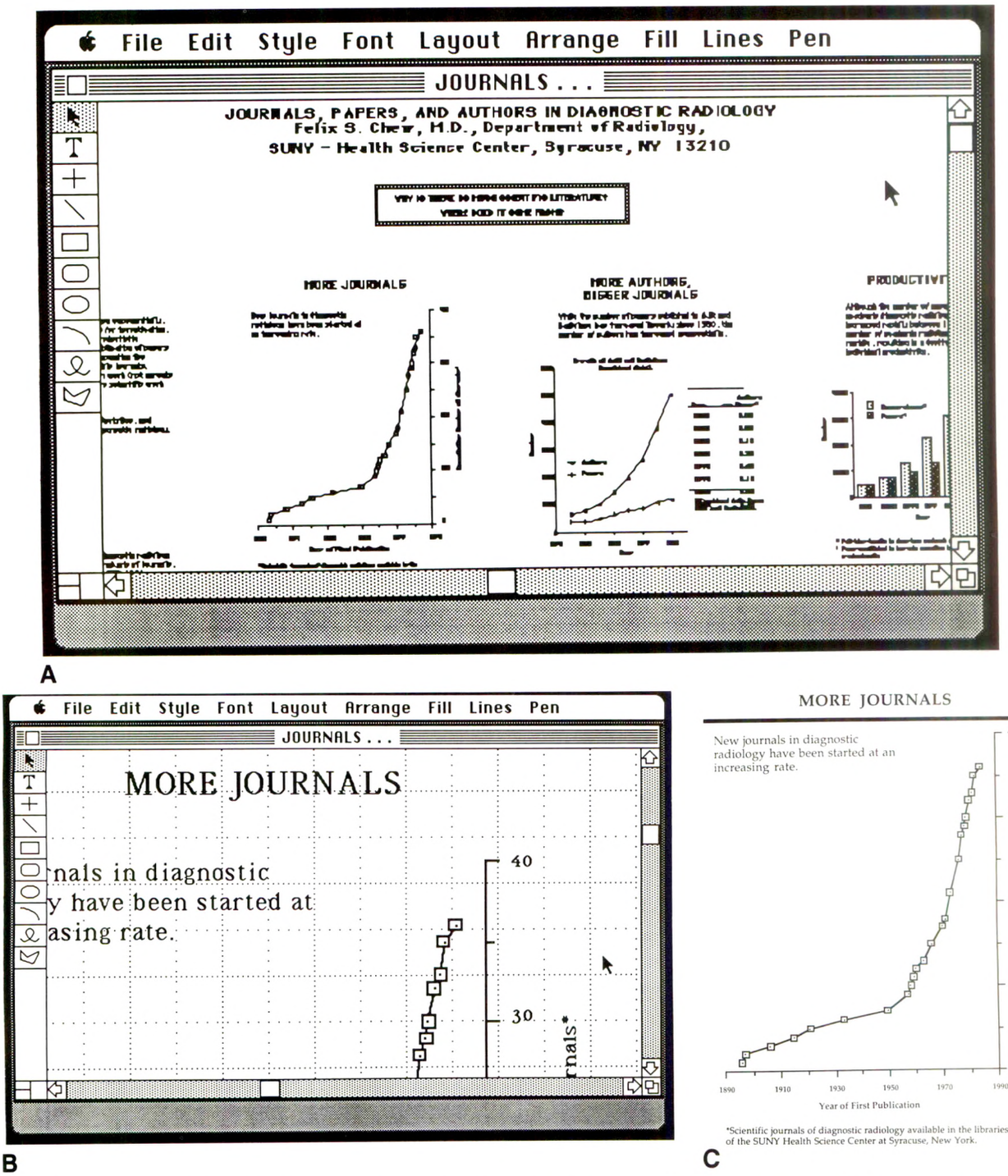


Fig. 2.—*A*, Part of a backboard exhibit design is shown on computer monitor in reduced size. All graphs were created from numeric data with program Cricket Graph.

***B*, Full-size display on monitor. Grid lines help with layout and accurate positioning of objects.**

***C*, Portion of actual exhibit. Resolution of laser-xerographic printer exceeds that of monitor screen.**

1A). One can also work with the actual text and graphics (Fig. 2A). Layout is simplified by grids and ruler lines on the design surface (Fig. 2B) and the ability to show the dimensions of objects. Drawing sizes up to 2.44 × 1.22 m can be accommodated. Graphics from other programs such as Cricket Graph can be inserted into MacDraw and altered. MacDraw also has text-editing capability and can accept text from word-processing programs such as Microsoft Word. The amount

and size of the text can be scaled to the size of the illustrations and fitted to the available space; alternatively, the space can be arranged to accommodate the text. The computer allows this process to occur in an interactive and dynamic fashion.

Adherence to a few general principles of typography [7] may help the exhibitor maintain the attention of the viewer amidst the many distractions of the exhibit floor. Astute choice of typefaces can enhance readability. A combination of upper- and lower-case letters is better than the use of upper-case letters alone. Typefaces with serifs—ending cross strokes on the ends of the principal strokes of letters—may be more comfortable to read than typefaces without serifs (sans serifs) when a body of text is used. For titles, sans serif typefaces are more easily recognizable; the larger the size of the letter, the simpler its design can be. Unusual typefaces should be avoided. The use of heavy-weight letters such as boldface is appropriate for emphasis or subheadings, but a body of text with too much contrast is uninviting and difficult to read. Opaque letters on a light background are far more comfortable to read than light letters on a dark background. Line spacing should be adequate for legibility, but not so generous as to require too much space. Line length should be short enough that neither turning of the head nor use of the hands is required for reading. Optimal line length is related to the size of the letters used. Justification of both margins often introduces odd and distracting spacing of words, resulting in awkward vertical patches of space; a ragged right margin is usually better.

During any part of the design phase, the exhibit can be printed out for inspection in full or reduced scale. The Imagewriter can produce a reduction to 50% of original size; the Laserwriter can produce continuously variable reduction down to 25% of original size.

Exhibit Realization

MacDraw is capable of printing the entire exhibit full-scale on multiple sheets of paper. These can be taped together and used as templates for cutting matboard or for masking Plexiglas.

The Laserwriter can produce copy suitable for photography with a resolution of 118 dots/cm [3]; the resolution of the Imagewriter II, 28 dots/cm in the vertical direction [4], is inadequate for this purpose. Professional typesetters have a resolution of 394 dots/cm or better [8]. Copy from the Laserwriter can be used directly on the exhibit (Fig. 2). Because the horizontal and vertical resolutions of the Laserwriter are identical, text and graphics are equally sharp in either orientation. The maximum print areas possible with the Laserwriter are 20.3 × 27.7 cm centered on letter-size paper and 17.1 × 33.0 cm centered on legal-size paper. The Laserwriter can produce continuously variable enlargement of MacDraw documents up to 400% of original size, so that large signs for titles can be made (in sections). For very large signs, output from the Laserwriter can be enlarged on a stat camera (direct positive photographic process for enlarging material to poster size), as was the large title sign for the background exhibit described above. For reflected light text, printing onto paper can be followed by mounting onto matboard or other backing. When wax is used as an adhesive, coated paper similar to that used in magazine production may provide a more attractive surface and may eliminate the problem of adhesive bleeding through and marring the viewing surface. Opaque signs for viewing with reflected light in combination with transilluminated radiographs may be difficult to read if the ambient lighting is inadequate. For transilluminated exhibits, opaque letters on a transparent background are created by printing with the Laserwriter onto standard medium-weight overhead transparency material. Such transparencies can be mounted directly onto the viewing panel. Sheets of colored cellophane interposed between the copy and the light source will reduce or eliminate glare. Additional photographic steps are necessary to obtain clear letters on an opaque background.

Discussion

The microcomputer systems described above could have been purchased at the time of writing for about $2200 for the system with the impact printer and $6700 for the system for the laser-xerographic printer; the software programs would have cost about $130–150. The prices for computer hardware and software have continually declined. Purchase of these systems for the sole purpose of occasional exhibit design and production may be difficult to justify, but there are many other useful applications. Computer output services are available in many cities; one can use, on an hourly or per-page basis, a Laserwriter or even an Allied Linotronic 100 (Allied Linotype, Hauppauge, NY) professional typesetter, which can be driven by the Macintosh [7]. In producing final copy for exhibits, the computer can enhance the productivity of a graphic artist and save the time and cost of photography. The use of the Laserwriter in playing out text has eliminated the need for expensive and time-consuming typesetting. When heavy-weight coated stock is used, stat photography is no longer necessary unless the maximum paper size or the print area of the Laserwriter is too small. When time is of the essence, the speed of these computers and their powerful, easy-to-use software programs allow the scientific exhibitor and medical illustrator to design and produce an economical but high-quality professional exhibit or poster presentation in a relatively short time.

ACKNOWLEDGMENT

The transilluminated exhibit was produced by Allen Ayres & Assoc., Syracuse, NY.

REFERENCES

1. Taylor GA. Microcomputer-based graphics for radiology. *AJR* **1986**; 147:1319–1321
2. Apple Computer. *Macintosh Plus* (manual). Cupertino, CA: Apple Computer, **1986**
3. Apple Computer. *LaserWriter Plus* (manual). Cupertino, CA: Apple Computer, **1986**
4. Apple Computer. *ImageWriter II owner's manual*. Cupertino, CA: Apple Computer, **1985**
5. Chew FS. Journals, papers, and authors in diagnostic radiology (abstr). *Radiology* **1986**;161(P):372
6. Panicek DM, Heitzman ER, Randall PA, Chew FS, Lane EJ, Markarian B. The continuum of developmental pulmonary anomalies (abstr). *Radiology* **1986**;161(P):391
7. Ernst SB. *The ABC's of typography*. New York: Art Direction, **1977**
8. Bove T, Rhodes C, Thomas W. *The art of desktop publishing: using personal computers to publish it yourself*. New York: Bantam, **1986**

Opinion

Diagnostic Imaging Interpretation: Comprehensiveness Means Quality

David J. Sartoris[1]

Accuracy is without a doubt the most important goal in the clinical practice of diagnostic imaging. The well-being of a patient can be jeopardized more by an incorrect diagnosis than by the absence of a diagnosis, since the former may result in inappropriate management with secondary adverse complications. While no radiologist would intentionally misinterpret an examination, it has recently come to my attention that a significant number of practitioners may make such errors because of failure to employ a comprehensive approach.

Ideally, comprehensiveness in the interpretation of any diagnostic imaging study involves three major actions: (1) consultation with referring physicians regarding clinical presentation and laboratory findings, (2) review of all previously performed diagnostic imaging examinations, and (3) communication with and examination of the patient. Unfortunately, a variety of factors frequently prevent one or more of these interactions from taking place. Clinicians are often unavailable for consultation or fail to provide adequate information on written request forms. Previous imaging studies may have been performed at other institutions or, if in-hospital, may be misplaced, checked out to clinicians, or sequestered in other file rooms. Often patients are no longer in the department at the time that their examinations are interpreted, or the radiologist who is in a busy practice may have insufficient time to talk with patients about their symptoms.

Although the foregoing situations must be accepted as realities to varying degrees, steps can be taken to minimize their detrimental impact on the quality of patient care. The need for enhanced comprehensiveness in diagnostic imaging interpretation is undeniable. The current situation fosters unnecessary therapeutic and additional diagnostic maneuvers, which only add to the rising costs of health care in general. Of greater importance, potentially avoidable patient morbidity and mortality can result, which may prompt legal action in the form of medical malpractice suits.

Despite the fact that at least one study has shown awareness of clinical information to be detrimental to diagnostic accuracy [1], most radiologists would agree that such knowledge is desirable. In order to encourage the availability of this data, a department can make it a policy not to perform examinations unless acceptable histories are included on request forms. Daily or weekly imaging conferences can facilitate communication with otherwise aloof clinicians. However, it ultimately becomes the individual radiologist's responsibility to seek out clinical information whenever it is unavailable or inadequate, either by calling the referring physician or by requesting and reviewing the patient's medical records.

Consolidation of diagnostic imaging film libraries can greatly enhance the availability of previous studies during interpretation of a current examination. Maintenance of separate files for radiographic, scintigraphic, and MR imaging studies in different areas of the hospital, for example, either discourages correlative review or requires additional staff time and effort to bring the examinations together. This situation also increases the likelihood that a given study is either checked out or lost from its respective library. File-room staffing should be a major departmental priority, as the level of conscientiousness exhibited by these individuals can mean the difference between organizational success and chaos with regard to

[1] Department of Radiology, Musculoskeletal Section, University of California, San Diego, Medical Center, San Diego, CA 92103. Address reprint requests to D. J. Sartoris.

AJR **149:199–200, July 1987** 0361–803X/87/1491–0199 © American Roentgen Ray Society

locating specific studies. Availability of outside films can be improved by a requirement that they be maintained in the main file room rather than in the offices of referring physicians, and by a hospital policy that encourages patients to obtain such records from previous health care providers. Again, however, the conscientiousness and personal effort of the individual radiologist are critical if we are to avoid interpretations based on limited clinical data. Since the findings on a current examination may be nonspecific, the previously performed studies are frequently essential for an accurate diagnosis and can minimize or eliminate the need for equivocation. In my experience, unnecessary percutaneous bone biopsy requested on the basis of vague or missed interpretation of films reviewed in isolation can be avoided by taking the time to analyze all aspects of a case. For example, an MR examination had suggested discitis in a child, until absence of septic clinical signs, negative bone-scan findings, and stable sequential radiographs compatible with Scheuermann's disease were uncovered. Similarly, a CT study in a middle-aged woman with colon carcinoma revealed probable metastatic disease in the sacrum; a history of previous radiation therapy, decreasing pain, and evolving radiographic findings compatible with stress fracture through an area of radiation necrosis laid this erroneous diagnosis to rest.

As a resident in diagnostic radiology, I learned that the optimal means of explaining a confusing finding is to interview and examine the patient. As practicing radiologists, we should avoid the temptation to rely exclusively on our clinical colleagues to perform these tasks. The additional time and personal effort involved frequently yield valuable insight into the problem, allowing for a more accurate and specific diagnosis. Through this correlative aspect of imaging interpretation, the noninterventional radiologist is also appropriately reminded that patients are thinking and feeling individuals as opposed to simply images on a viewbox.

In conclusion, the provision of high-quality diagnostic imaging services demands a comprehensive, patient-oriented approach to the interpretation of examinations. Although departmental policy, clinician cooperation, and ancillary personnel are key determinants of success in this regard, the individual radiologist is ultimately responsible for the consequences from the standpoint of patient care. The practicing members of our specialty can and should routinely engage in the strategies outlined above.

REFERENCE

1. Eldevik OP, Dugstad G, Orrison WW, Haughton VM. The effect of clinical bias on the interpretation of myelography and spinal computed tomography. *Radiology* **1982**;145:85–89

Review of Current Literature

Beginning with this issue, a more comprehensive and predictable review of the current medical literature will replace the Journal's previous abstract section. The editors hope that this new system will make it easier for *AJR* readers to stay abreast of important new advances in general medicine as well as radiology.

Each month the *AJR* will publish the original abstract of the single best article of interest to radiologists from a select number of clinical and radiology-subspecialty journals. The delay between the original publication and publication of the abstract in the *AJR* will be 2 months.

Selection of the abstracts will be made by radiologists who are authorities in each imaging subspecialty. The same journals will be featured on a regular basis. Subspecialty imaging journals are also included for those *AJR* readers whose busy schedules preclude a careful review of the expanding number of these publications.

Abstracts will be selected from the following journals: *The New England Journal of Medicine, Cancer, Chest, Circulation, Gastroenterology, Digestive Diseases and Sciences, Gastrointestinal Endoscopy, Gastrointestinal Radiology, The Journal of Bone and Joint Surgery, Clinical Orthopaedics and Related Research, The Journal of Urology, British Journal of Urology, Urology, Pediatrics, The Journal of Pediatrics, Pediatric Radiology, The Journal of Nuclear Medicine, Journal of Ultrasound in Medicine, Journal of Computer Assisted Tomography, CT: Journal of Computed Tomography*, and *Magnetic Resonance Imaging*.

We hope that this new system will offer a comprehensive and efficient survey of important medical journals.

Saskia von Waldenburg Hilton
Associate Editor

Initials and addresses of corresponding authors are provided in parentheses for each article so that the reader can obtain reprints directly. Abstracts are printed verbatim from each journal.

CLINICAL LITERATURE

The New England Journal of Medicine

Prevalence and importance of pigmented ocular fundus lesions in Gardner's syndrome. Traboulsi EI, Krush AJ, Gardner EJ, et al. (Irene H. Maumenee, Wilmer Ophthalmological Institute, Johns Hopkins Hospital, Maumenee Bldg., Rm. 321, 600 N. Wolfe St., Baltimore, MD 21205). *N Engl J Med* 316:661–667, 1987

We examined 134 members of 16 families with Gardner's syndrome for pigmented ocular fundus lesions. Of 41 patients with documented Gardner's syndrome, 37 (90.2 percent) had such lesions. The lesions were bilateral in 32 of the patients (78.1 percent) and in 2 of 42 controls (4.8 percent). Twenty (46.5 percent) of 43 first-degree relatives at 50 percent risk for Gardner's syndrome had bilateral pigmented fundus lesions, indicating that they had probably inherited the abnormal gene. The presence of bilateral lesions, multiple lesions (more than four), or both appeared to be a specific (specificity, 0.952) and sensitive (sensitivity, 0.780) clinical marker for Gardner's syndrome. The lesions are probably congenital; they were observed in a three-month-old baby at risk. The multiplicity of the pigmented fundus lesions and their association with diffuse disturbances of the retinal pigment epithelium in the same eye suggest a widespread expression of the abnormal gene in the retinal pigment epithelial cells.

Cancer

Bone sarcomas associated with Ollier's disease. Liu J, Hudkins PG, Swee RG, Unni KK (KKU, MBBS, Mayo Clinic, 200 First St. SW, Rochester, MN 55905). *Cancer* 59:1376–1385, 1987

Of 55 patients with Ollier's disease seen at the Mayo Clinic between 1907 and 1985, 16 had malignant bone neoplasms: 12 chondrosarcomas, two dedifferentiated chondrosarcomas, one chordoma, and one osteosarcoma. One patient had a chondrosarcoma in two different bones. These findings suggest that approximately 30% of patients with Ollier's disease will develop a malignant bone neoplasm, most probably chondrosarcoma. The prognosis for most patients is good. Five of the 16 patients survived more than 13 years after treatment.

Reprinted with permission by the American Cancer Society.

Chest

Colonization of the respiratory tract with *Pseudomonas cepacia* in cystic fibrosis: risk factors and outcomes. Tablan OC, Martone WJ, Doershuk CF, et al. (OCT, Centers for Disease Control, Bldg. I-5044, Atlanta, GA 30329). *Chest* 91(4):527, April 1987

Between 1981 and 1983, some 85 patients with cystic fibrosis at Rainbow Babies and Childrens Hospital, Cleveland, developed colonization or infection of the respiratory tract with *Pseudomonas cepacia*. Twenty-nine (34 percent) of the colonized patients died; four were female patients with fulminant bacteremia with *P cepacia* prior to death. Case-control studies showed that increasing severity of underlying cystic fibrosis, increasing age, having a sibling with cystic fibrosis who was colonized with *P cepacia*, and previous hospitalizations were associated with increased risk of colonization. In patients with mild cystic fibrosis, no differences in clinical outcome were seen during the period of study; however, patients colonized with *P cepacia* who had moderate or advanced cystic fibrosis were hospitalized longer and died sooner after colonization, compared with control subjects with similar severity of cystic fibrosis. The excess mortality associated with such colonization varied in magnitude and trend according to the patient's sex and severity of underlying cystic fibrosis, reflecting the combined influence of colonization with *P cepacia*, sex, and severity of cystic fibrosis on the mortality of the patients. The source and mode of transmission of *P cepacia* were not determined, but the data suggest a possible nosocomial source. The results of this investigation showed that colonization with *P cepacia* most often affected patients with moderate or advanced cystic fibrosis and was associated with an adverse clinical outcome in these patients.

Circulation

Cystic medial necrosis in coarctation of the aorta: a potential factor contributing to adverse consequences observed after percutaneous balloon angioplasty of coarctation sites. Isner JM, Donaldson RF, Fulton D, Bhan I, Payne DD, Cleveland RJ (JMI, Box 70, Tufts–New England Medical Center, 171 Harrison Ave., Boston, MA 02111). *Circulation* 75(4):689–695, 1987

Percutaneous transluminal angioplasty has been shown to be both feasible and efficacious for the treatment of aortic coarctation. Recent reports, however, have indicated that the development of aortic aneurysms at or near the coarctation segment may complicate attempts to treat this lesion by catheter-based intervention. Accordingly, we examined the light microscopic features of coarctation segments excised at surgery (n = 31) or obtained at autopsy (n = 2) in 33 patients with coarctation of the aorta. Cystic medial necrosis, defined as depletion and disarray of elastic tissue, was observed in each of the 33 specimens. In the majority of coarctation specimens (22 of 33 or 67%) the extent of cystic medial necrosis, graded semiquantitatively on a scale of 0 (normal aorta) to 3 +, was severe (3 +). The finding that cystic medial necrosis represents a consistent histologic feature of coarctation of the aorta provides a pathologic basis for the formation of aneurysms observed after balloon angioplasty of coarctation sites.

Gastroenterology

Screening for colorectal cancer in a high-risk population. Eddy DM, Nugent FW, Eddy JF, et al. (DME, Director, Center for Health Policy Research and Education, Duke University, Box GM, Duke Station, Durham, NC 27706). *Gastroenterology* 92:682–692, 1987

A mathematical model was used to estimate the cost-effectiveness of colorectal cancer screening strategies for people who are at high risk because of a first-degree relative with colorectal cancer. The model uses indirect evidence about such factors as cancer incidence, sensitivity and specificity of different tests, and treatment effectiveness. The analysis indicates that for screening people over 40 yr old (a) an annual fecal occult blood test may reduce colorectal cancer mortality by about one-third, (b) either colonoscopy or barium enema may reduce mortality by ~85%, (c) a 3–5-yr frequency for endoscopies or barium enemas preserves 70%–90% of the effectiveness of an annual frequency, and (d) beginning screening at age 50 reduces effectiveness by 5%–10%. Although both barium enemas and colonoscopies appear to be effective in reducing mortality, the lower cost of the barium enema makes it a more cost-effective strategy. All of these estimates depend on the baseline estimates of each of the factors incorporated in the model; the conclusions are most sensitive to assumptions about the natural history of adenomatous polyps, the bleeding of adenomas and presymptomatic cancers, and the sensitivity of the fecal occult blood test. Recommendations about colorectal cancer screening must also consider factors such as discomfort, inconvenience, and the availability of various technologies.

Reprinted with permission by the American Gastroenterological Association.

Digestive Diseases and Sciences

Aggressive angiographic diagnosis in acute lower gastrointestinal hemorrhage. Koval G, Benner KG, Rösch J, Kozak BE (KGB, Division of Gastroenterology, Oregon Health Sciences University, 3181 SW Sam Jackson Park Rd., Portland, OR 97201). *Dig Dis Sci* 32(3):248–253, March 1987

To assess the value of recently developed aggressive pharmacologic angiographic techniques for the diagnosis of acute lower gastrointestinal hemorrhage, we reviewed our experience with 63 consecutive patients referred for angiography. Hemorrhage was severe as indicated by a mean blood transfusion requirement of 9.4 units. Extravasation of contrast (46%), or an obvious vascular abnormality suggestive of a bleeding site (32%), was identified in 78% of patients. Extravasation was seen more frequently in patients with ≥3 units of transfusion (66%) than in those with <3 units of transfusion (17%, $P < 0.001$). After the introduction of pharmacologic techniques using heparin, tolazoline, streptokinase, and indwelling arterial catheters, the percentage of studies with extravasation of contrast increased from 32 to 65% ($P < 0.01$). Application of aggressive angiographic techniques increases the diagnostic yield of angiography in acute severe lower gastrointestinal hemorrhage while exposing the patient to modest increased procedure-related risks which can be accepted in selected patients.

Gastrointestinal Endoscopy

Primary panendoscopy. Overholt BF, Hargrove RL, Farris RK, Porter FR (BFO, Weisgarber Medical Center, 1112 Weisgarber Rd., Ste. 201, Knoxville, TN 37909). *Gastrointest Endosc* 33:1–3, 1987

Primary panendoscopy is defined as a limited-consultative, diagnostic, UGI endoscopic examination that provides, in non-critically ill patients with dyspeptic symptoms, an accurate and cost-effective alternative to the standard UGI x-ray examination. The procedure was instituted at St. Mary's Medical Center's hospital in February 1985. During the first 12 months, a total of 321 patients were

examined: 212 inpatients and 109 outpatients. In those patients with complete information, primary panendoscopy changed the diagnosis in 67% and the treatment in 52%. As expected, the number of esophagogastroduodenoscopies decreased during this time, but the combined numbers of primary panendoscopies and esophagogastroduodenoscopies exceeded the projected increase of esophagogastroduodenoscopies. Similarly, the number of UGI x-ray examinations fell sharply. With a physician fee of $150.00 and a facility fee of $50.00, theoretical savings of some $117,000.00 to the patients were estimated. The authors conclude that primary panendoscopy provides a cost-effective and beneficial patient service that warrants broad consideration by gastroenterologists as they face the cost constraints being imposed within the health care system of the 1980s.

The Journal of Bone and Joint Surgery

The use of computerized tomography in evaluating non-visualized vertebral levels caudad to a complete block on a lumbar myelogram. Herkowitz HN, Garfin SR, Bell GR, Bumphrey F, Rothman RH (HNH, 16800 W. Twelve Mile Rd., Ste. 100, Southfield, MI 48076-2176). *J Bone Joint Surg [Am]* 69A(2):218–224, February 1987

In thirty-two patients who demonstrated a complete or almost complete block on a lumbar myelogram, computerized tomography of the non-visualized vertebral levels caudad to the block was performed prior to surgical intervention. The purpose of this study was to evaluate the clinical value of computerized tomography in detecting a lesion that is caudad to the level of a myelographic block. For twenty-three patients the cause of the myelographic block was stenosis of the spine; for five patients, a combination of stenosis of the spine and herniation of a disc; for one patient, herniation of a disc between the fourth and fifth lumbar vertebrae alone; for two patients, arachnoiditis; and for one patient, kyphosis secondary to fracture. A total of fifty vertebral levels that could not be visualized because of the block were evaluated. Thirty (60 per cent) of the non-visualized vertebral levels, in nineteen (59 per cent) of the thirty-two patients, demonstrated stenosis of the spine or a herniated disc that was confirmed at the time of surgical treatment.

The value of computerized tomography for the evaluation of the vertebral levels caudad to the level of a complete or almost complete block on a lumbar myelogram was threefold. First, it provided visualization of the vertebral levels that could not be evaluated by the myelography. Second, the findings on computerized tomography provided information that was essential for preoperative planning and it removed the so-called exploratory element from the operative procedure. Third, in two patients, computerized tomography demonstrated a lesion that was amenable to surgical treatment below the level of a block that had been caused by arachnoiditis, an entity that does not require surgical treatment.

Based on the results of this study, it is recommended that all patients who have a complete or almost complete block on a lumbar myelogram undergo computerized tomography to evaluate the non-visualized vertebral levels below the block.

The Journal of Urology

Incidence, extent and location of unsuspected pelvic lymph node metastasis in patients undergoing radical cystectomy for bladder cancer. Wishnow KI, Johnson DE, Ro JY, Swanson DA, Babaian RJ, von Eschenbach AC. (KIW, Dept. of Urology, Box 110, University of Texas M. D. Anderson Hospital and Tumor Institute, 6723 Bertner Ave., Houston, TX 77030). *J Urol* 137:408, March 1987

Between March 1, 1983 and December 31, 1985, 18 of 130 patients (14 per cent) undergoing radical cystectomy had unsuspected metastasis. In 17 patients (94 per cent) only 1 or 2 nodes were involved. The mean size of the involved nodes was 0.81 cm. and the mean size of metastasis was 0.39 cm. In patients with 1 or 2 positive nodes metastasis was not observed above the bifurcation of the common iliac arteries or lateral to the external iliac arteries. In patients in whom the primary bladder tumor was localized clearly to 1 side of the bladder unsuspected metastasis was observed only in ipsilateral lymph nodes. In accordance with these findings, we advocate a restricted pelvic lymphadenectomy in patients in whom gross examination reveals no evidence of nodal metastasis at radical cystectomy.

British Journal of Urology

Haematuria following a marathon run: source and significance. Reid RI, Hosking DH, Ramsey EW (EWR, Dept. of Surgery, University of Manitoba, Winnipeg, Canada). *Br J Urol* 59:133–136, 1987

Urine specimens were obtained from 98 runners before and immediately after running a half (21 km) or full (42 km) marathon. Specimens were examined for the presence of proteinuria, haematuria and whether the erythrocytes were normomorphic or dysmorphic as determined by phase contrast microscopy. Proteinuria occurred in 35% of those running the half and 69% running the full marathon. Haematuria with or without proteinuria occurred in 21% running the half and 22% running the full marathon.

In runners with haematuria, dysmorphic erythrocytes were found in 30% of the half and 81% of the full marathon group. No urinary abnormalities were found on repeat examination 4 to 12 weeks after the run. These results suggest that non-glomerular bleeding, possibly from bladder contusions, predominates at shorter distances. With greater distances glomerular bleeding occurs. These abnormalities disappear with rest and do not appear to signify underlying urinary tract disease.

Urology

Spontaneous rupture of ureter. Kaplan LM, Farrer JH, Lupu AN (ANL, Dept. of Surgery, Division of Urology, UCLA School of Medicine, Los Angeles, CA, 90024). *Urology* 29(3):313–316, March 1987

A patient with spontaneous ureteral rupture in the absence of obstruction or calculus disease is presented. In addition to ureteral rupture this patient also had a penile squamous cell carcinoma and infected inguinal lymph nodes. A review of the literature discloses that all reported cases with spontaneous rupture of the ureter had an underlying process leading to that rupture. It is considered therefore, that rupture of the ureter should be designated as "traumatic" or "nontraumatic." The term "spontaneous," implying a primary event, is a misnomer. No such case has been reported occurring in an otherwise healthy individual.

Pediatrics

Declining frequency of circumcision: implications for changes in the absolute incidence and male to female sex ratio of urinary tract infections in early infancy. Wiswell TE, Enzenauer RW, Holton ME, Cornish JD, Hankins CT. (TEW, Brooke Army Medical Center, Box 64, Ft. Sam Houston, TX 78234-6200). *Pediatrics* 79(3):338–342, 1987

The results of an investigation examining the circumcision frequency rate and its effect on the incidence of urinary tract infections in a large, widely dispersed population base during the 10-year period since the 1975 report of the American Academy of Pediatrics Ad Hoc Task Force on Circumcision are reported. Our study population included the 427,698 infants born in all United States Army hospitals, worldwide, from Jan 1, 1975, through Dec 31, 1984. There was an initial plateau in the circumcision frequency rate at approximately 85% during the first 4 years of the study period. In the subsequent 6 years

there was a steady, significant decrease ($P < .001$) of 1.4% to 4.0% per year through 1984, when the circumcision frequency rate reached its nadir of 70.5%. There was a concomitant increase in the total number of urinary tract infections among male infants ($P < .02$) as the circumcision rate declined. This increase was due to the increase in the overall number of uncircumcised boys (who had a greater than 11-fold increased infection rate compared with circumcised boys). During the first half of the study period, there was a female predominance for urinary tract infections from birth onward. As the number of circumcised boys decreased (with a resultant increase in the total number of boys with infection), the male to female ratio of urinary tract infections during the first 3 months of life reversed, reflecting a movement toward a male predominance for infection in early infancy. This is the first, well-documented report of a decreasing rate of circumcisions performed on the American male population. We conclude that the number of urinary tract infections in male infants, as well as the male to female sex ratio, is affected by the circumcision practices of the population examined.

Reproduced with permission by *Pediatrics* © 1987.

The Journal of Pediatrics

Atlantoaxial instability in Down syndrome: roentgenographic, neurologic, and somatosensory evoked potential studies. Pueschel SM, Findley TW, Furia J, Gallagher PL, Scola FH, Pezzullo JC (SMP, Director, Child Development Center, Rhode Island Hospital, 593 Eddy St., Providence, RI 02902). *J Pediatr* 110(4):515–521, April 1987

To identify patients with Down syndrome and asymptomatic atlantoaxial instability who are at increased risk for developing neurologic symptoms, we studied 27 patients with this skeletal disorder and compared them with an age- and sex-matched group of 27 patients with Down syndrome without atlantoaxial instability. A third group of six patients had symptomatic atlantoaxial instability. The mean atlanto-dens intervals and the mean spinal canal widths among the three groups were significantly different. There were no significant differences in mean composite neurologic scores and somatosensory evoked responses between patients in the asymptomatic group and those in the control group. However, when a subsample of patients with high and low latencies (>1 SD below and above the mean) was formed and comparisons were made with roentgenographic findings, there was a high correspondence between somatosensory evoked potential latencies and atlanto-dens interval measurements. We conclude that no single assessment technique, but a combined approach using roentgenographic, CT scan, neurologic, and neurophysiologic investigations, will provide information of the risk status of patients with Down syndrome and atlantoaxial instability.

RADIOLOGY SUBSPECIALTY JOURNALS

Pediatric Radiology

Dyskinetic cilia syndrome: clinical, radiographic and scintigraphic findings. de la Rocha SR, Pysher TJ, Leonard JC (SR de la R, Dept. of Pediatrics, Pulmonary Division, Primary Children's Medical Center, University of Utah, School of Medicine, Salt Lake City, UT 84112). *Pediatr Radiol* 17:97–103, 1987

The clinical, electron microscopic and radiographic data of 9 patients with dyskinetic cilia syndrome (DCS) are presented. Scintigraphic evaluation of mucociliary dynamics in six patients showed evidence of dyskinesia. Ventilation and perfusion studies were performed to evaluate obstructive lung disease. Retrospectively, bronchiectasis could be detected in 77% of the patients by analysis of the chest radiograph and lung scintigraphy, and bronchography potentially avoided in the seven patients who underwent this procedure.

Gastrointestinal Radiology

Limiting overhead views in double-contrast colon examinations does not affect diagnostic accuracy. Feczko PJ, Halpert RD (PJF, Dept. of Diagnostic Radiology, Henry Ford Hospital, 2799 W. Grand Blvd., Detroit, MI 48202). *Gastrointest Radiol* 12:175–177, 1987

A prospective study was undertaken to evaluate whether reducing overhead (technician-performed) films in double-contrast colon examinations had any effect on diagnostic accuracy. Only 4 overhead films were obtained routinely: supine, both decubitus, and prone cross-table rectal views. A high detect rate was maintained, comparable to our accuracy when 7 or 8 overhead films were obtained. Our study confirms that with double-contrast colon examinations, the need for overhead films is diminished. A significant decrease in cost, radiation exposure, and examination time can be obtained. We continued to use this method without any noticeable decrease in diagnostic accuracy.

The Journal of Nuclear Medicine

Radionuclide diagnosis and therapy of neural crest tumors using iodine-131 metaiodobenzylguanidine. Hoefnagel CA, Voûte PA, de Kraker J, Marcuse HR (CAH, Dept. of Nuclear Medicine, Antoni van Leeuwenhoekhuis, The Netherlands Cancer Institute, Plesmanlaan 121, 1066 CX Amsterdam, The Netherlands). *J Nucl Med* 28:308–314, 1987

The successful application of [^{131}I]metaiodobenzylguanidine (MIBG) in diagnosis and therapy of pheochromocytoma has led to its use in other tumors which derive from the neural crest and potentially concentrate this radiopharmaceutical as well. In the present series, [^{131}I]MIBG total-body scintigraphy was used for detection of neuroblastoma in 47 patients and 47 cases of other neural crest tumors. The method was found to be as reliable in neuroblastoma (sensitivity 95%, specificity 100%), as it is in pheochromocytoma. Although other neural crest tumors may concentrate [^{131}I]MIBG, this is not a consistent finding; however, it is useful to investigate which tumors do, as this may provide an alternative treatment modality for some patients. Although followup is still very short, preliminary results of therapeutic use of [^{131}I]MIBG in 21 patients indicate that this treatment modality may be effective in neuroblastoma and malignant pheochromocytoma.

Journal of Ultrasound in Medicine

Ectopic pregnancy: diagnosis by sonography correlated with quantitative HCG levels. Nyberg DA, Filly RA, Laing FC, Mack LA, Zarutskie PW (DAN, Dept. of Radiology SB-05, University of Washington Hospital, Seattle, WA 98195). *J Ultrasound Med* 6:145–150, 1987

Pelvic sonograms were correlated with simultaneous human chorionic gonadotropin (HCG) determinations in 150 women with early intrauterine pregnancy ($N = 76$) and ectopic pregnancy ($N = 74$). Of the 76 patients with intrauterine pregnancy (IUP), 55 had HCG levels exceeding 1,800 mIU/ml (Second International Standard), and in each case a gestational sac was identified. In comparison, 35 of 74 (47%) patients with ectopic pregnancy had HCG levels of 1,800 mIU/ml or more, and no case demonstrated a gestational sac. Although six patients (8%) with ectopic pregnancy demonstrated a "pseudogestational sac," no case was confused with a true gestational sac. We conclude that, when the HCG level exceeds 1,800 mIU/ml, an intrauterine gestational sac is normally detected and its absence is evidence for an ectopic pregnancy.

Reprinted with permission by the American Institute of Ultrasound in Medicine.

Journal of Computer Assisted Tomography

Limitations of CT in evaluation of neoplasms involving chest wall. Pearlberg JL, Sandler MA, Beute GH, Lewis JW Jr, Madrazo BL (JLP, Dept. of Diagnostic Radiology, Henry Ford Hospital, Detroit, MI 48202). *J Comput Assist Tomogr* 11(2):290–293, March/April 1987

We reviewed the CT of 20 patients with peripheral lung malignancies in which CT appearance suggested chest wall invasion on the basis of extension of mass around ribs into fat or muscle of the chest wall, or definite bone destruction. We correlated these findings with other radiographic studies and surgical and autopsy results. All 11 cases in which CT indicated chest wall involvement on the basis of definite bone destruction were confirmed. Tumor extension into the chest wall was disproven in six of the remaining nine cases in which invasion was suggested on the basis of tumor infiltration between ribs or extension of tumor into fat or soft tissue planes. Our findings confirm the lack of reliability of CT findings in determining the extension of malignancy into the chest wall, except when definite bone destruction is present.

CT: The Journal of Computed Tomography

Role of computed tomography in diverticulitis. Raval B, Lamki N, St. Ville E (BR, Dept. of Radiology, University of Texas Medical School, 6431 Fannin, Rm. 2. 134, Houston, TX 77030). *J Comput Tomogr* 11:144–150, 1987

Fourteen patients with diverticulitis who were clinically believed to require radiologic investigation form the basis of this report. An inflammatory mass (n = 10) or abscess (n = 2) were reliable findings on computed tomography. Other signs encountered were abnormal density of pericolic fat, thickening of colonic wall, and narrowing of the lumen of the colonic wall. Colovesical fistulas, all of which were suspected clinically, occurred in three patients. Computed tomography should be performed with administration of rectal contrast medium to demonstrate the origin of inflammation from the colon, assess pericolic extent, and confirm colovesical fistula.

Magnetic Resonance Imaging

Gated acquisition of MR images of the thorax: advantages for the study of the hila and mediastinum. Mark AS, Winkler ML, Peltzer M, Kaufmann L, Higgins CB (CBH, Dept. of Radiology, Box 0628, University of California Medical School, San Francisco, CA 94143). *Mag Reson Imag* 5:57–63, 1987

Gated and nongated magnetic resonance (MR) scans of the chest were compared in five normal volunteers and 20 patients with chest disease to determine possible advantages of gated MR for delineation of noncardiac mediastinal anatomy. In order to compare gated and nongated images of the chest using similar imaging parameters, five spin-echo sequences were obtained in each of five normal volunteers: (a) TR: 1000 msec, TE: 30 msec; (b) gated to every heart beat (TR approximately 1000 msec, TE: 30 msec); (c) TR: 2000 msec, TE: 30 msec; (d) gated to every other heart beat (TR approximately 2000 msec), TE: 30 msec; (e) TR: 500 msec, TE: 30 msec. In the 20 patients, the gated images were gated to every heart beat and the nongated images were obtained using a TR of 2000 msec, both with a TE of 30 msec. The noise in the periphery and in the center of the gated and nongated images at the level of the carina was compared in the five normal volunteers, using the signal intensity of the posterior chest wall as a control. There was 92% ± 44% greater noise in the central region and 63% ± 60% greater noise in the peripheral region on the nongated studies (TR: 1000 msec), than on the studies gated to every heart beat. In three of the five volunteers, the measured noise was greater on the nongated long TR (2000 msec) images than on the images gated to every other heart beat. However, the mediastinal structures below the level of the aortic arch were much better defined on the gated images in all five subjects. In 17 of the 20 patients, the gated images provided superior definition of hilar and/or mediastinal structures. The gated images were equal to the nongated ones in two patients and inferior in one patient, in whom the gating was unsuccessful. The anatomic regions where gating proved most beneficial were the hila, aortopulmonary window, ascending aorta and aortic arch. Gating was less helpful in the superior mediastinum and descending aorta. Because of the marked improvement in image quality, we recommend, whenever possible, the use of ECG gated sequences for the evaluation of hilar and mediastinal pathology at and below the level of the aortic arch.

Letters

Imaging in Acute Renal Infection in Children

Sty et al. [1] prefer glucoheptonate to dimercaptosuccinic acid in children because of the lower radiation dose to the kidneys. While it is true that for each millicurie administered, ^{99m}Tc–dimercaptosuccinic acid (Tc-DMSA) results in a higher radiation dose to the kidney than ^{99m}Tc-glucoheptonate (Tc-Glu), this is not an adequate reason for selecting the latter for imaging children with renal infections. A larger portion (greater than 80%) of the administered Tc-Glu is excreted by the kidneys and is "wasted" in the bladder, which receives a significant radiation dose. Tc-DMSA is bound more to the renal tubules (<60% excreted at 1 hr). Hence, for a given concentration of technetium in the kidneys, a lower dose of Tc-DMSA is needed and results in a lower absorbed dose to the bladder [2]. Additionally, the images obtained with Tc-DMSA are indisputably superior to Tc-Glu [3, 4]. Since a flow study was not required, a relatively low dose of Tc-DMSA can be used (approximately half the μCi/kg of Tc-Glu used). Only if a flow study is performed does Tc-DMSA have a disadvantageous radiation burden because the same minimal dose of technetium must be administered whether bound to DMSA or gluheptonate [5].

Michael J. Daly
Meridian Park Hospital
Tualatin, OR 97062

REFERENCES

1. Sty JR, Wells RG, Starshak RJ, Schroeder BA. Imaging in acute renal infection in children. *AJR* **1987**;148:471–477
2. Merrick MV, Uttley WS, Wild SR. The detection of pyelonephritic scarring in children by radioisotope imaging. *Br J Radiol* **1980**;53:544–556
3. Handmaker H, Young BW, Lowenstein JM. Clinical experience with ^{99m}Tc-DMSA (dimercaptosuccinic acid), a new renal-imaging agent. *J Nucl Med* **1975**;16:28–32
4. Englander D, Weber PM, dos Remedios LV. Renal cortical imaging in 35 patients: superior quality with ^{99m}Tc-DMSA. *J Nucl Med* **1974**;15:743–749
5. Daly MJ, Henry RE. Defining renal anatomy and function with ^{99m}technetium dimercaptosuccinic acid: clinical and renographic correlation. *J Urol* **1981**;126:5–9

Reply

Dr. Daly's statements regarding the use of ^{99m}Tc–dimercaptosuccinic acid (Tc-DMSA) as a renal cortical imaging agent are correct. Nonetheless, it is our preference to use ^{99m}Tc-glucoheptonate (Tc-GH) because our renal imaging technique involves sequential imaging (1, 3, 6, 9, 12 min) in addition to 2- to 4-hr delayed images. We consider this sequential evaluation of renal function and anatomy of the pelvocalyceal system and ureters to be essential for the appropriate evaluation of the pediatric urinary tract. This imaging strategy can detect hydronephrosis and duplication abnormalities that may be associated with upper urinary tract infection. Also, decreased function with delayed appearance of the pelvocalyceal system may indicate renal edema, a complication of parenchymal infection. In addition, Tc-GH provides adequate demonstration of renal cortical morphology at an acceptable radiation dose.

Concerning the dose to the urinary bladder with Tc-GH, this can be significantly lowered by hydrating the patient and by encouraging frequent voiding. Therefore, the excreted Tc-GH that is not retained in the kidney does not represent "wasted" radiation exposure but rather constitutes a significant portion of the examination that provides both functional and anatomic information.

John R. Sty
Children's Hospital of Wisconsin
Milwaukee, WI 53201

Ruptured Appendix in Rabbit Model

I wish to express my confusion about the article by Dachman et al. in the February 1987 issue of the *AJR* [1]. As I understand the article, the authors surgically obstructed the rabbit appendix, emptied it of its contents, flushed the appendix with a 10% iodine solution, and placed gentamicin directly into the appendix. The animals were also given systemic gentamicin for 1 week after surgery. The authors subsequently extrapolate their results to the development of a mucocele in humans.

The authors are not dealing with a naturally obstructed appendix but with an experimental model. The emptying of the appendix and the flushing with iodine and antibiotics are obviously quite different from what happens in the intact human. I think that it is unjustified to extrapolate their experimental results from their model to the intact human. Certainly, their description of what happens in their experimental model is of great interest, but why should one think that these unnatural conditions would be applicable to a human?

M. L. Janower
Saint Vincent Hospital, Inc.
Worcester, MA 01605

REFERENCE

1. Dachman AH, Nichols JB, Patrick DH, Lichtenstein JE. Natural history of the obstructed rabbit appendix: observations with radiography, sonography, and CT. *AJR* **1987**;148:281–284

Reply

We appreciate Dr. Janower's comments and acknowledge the limitations of extrapolating from any animal model to the human

condition. The "unnatural" method used to produce appendiceal obstruction was not intended to mimic the pathophysiology of human appendiceal obstruction. Rather, the method creates a hypothetical phase postulated to occur sometime after the appendix is obstructed (regardless of its cause) and host defenses have rendered the contents of the appendix relatively sterile. This is based on our current understanding of appendicitis and mucoceles in humans, both of which are thought to be caused by appendiceal obstruction, and on our knowledge that the contents of human mucoceles are sterile. Thus, we hypothesize that in some cases of appendiceal obstruction, host defenses must render the obstructed appendix relatively sterile.

Our use of the phrase "natural history," therefore, refers to the histologic changes that are seen after this hypothetical phase is reached, not to the events leading up to it. Given the established histopathologic similarity between mucoceles in animals and humans, we believed that certain conclusions were reasonable. We did not conclude that our model proves the existence of chronic appendicitis in humans. Rather, given existing data from human surgical material that chronic appendicitis occurs, we believe that this animal experiment supports that data. This is the limited extrapolation from the experimental model to the human condition that we think is justified.

We appreciate the opportunity to clarify this point.

Abraham H. Dachman
Uniformed Services University School of Medicine
Bethesda, MD 20814-4799

An Improved Method for Viewing Small-Format Images on Standard Viewboxes

The standard 35 × 43 cm illuminated viewbox is ill-suited for viewing small-format images commonly used in nuclear medicine and sonography. In our department, almost all studies are imaged with 12.7 × 17.8 cm, 10.2 × 12.7 cm, or 20.3 × 25.4 cm films. Most viewboxes have one row of film hangers at the top, which are adequate for use of about half the illuminated viewing surface. Often, a length of clear monofilament fishing line is employed to hold a second row of films along the bottom of the viewbox; however, this is clumsy as the lower edge of most viewboxes is not designed to support a film adequately. Additionally, with use of the monofilament line, a large portion of the viewbox remains unused in the center when 12.7 × 17.8 cm or smaller films are viewed.

We have tried several approaches to improve this inconvenient situation, including the placement of a clear Plexiglas strip along the center of the viewbox to support a central row of films. Several disadvantages made this unworkable, however. Small films often slid down behind the Plexiglas. The viewbox was also rendered unusable for review of large films. Application of this strip also damaged the viewbox surface.

For the past year, we have applied horizontal rows of double-sided transparent tape (Scotch brand 665 Double-Coated Tape, 3M Company, Minneapolis, MN) to the viewbox surface; films adhere securely to the tape strips during review and are easily removed after use.

All films in our department are the single-sided emulsion type and thus the emulsion does not contact the adhesive surface of the tape. However, our limited experience with double emulsion films has been satisfactory and no film damage has been noted.

The tape allows flexible use of the entire viewbox surface with smaller images, yet because it is clear, the entire viewbox surface can be employed for review of large films, such as chest radiographs.

The tape remains usable for about 4 weeks; it is not difficult to remove from the viewbox, although at times we have simply applied a second or third piece of tape over the original one. If dirt or foreign material become stuck to the tape, it may be cleaned gently with an alcohol swab.

In our department, we have found this method quite satisfactory, allowing flexible use of the viewing surface. It is a simple, nondestructive viewbox modification.

Edward B. Cronin
Gerald M. Kolodny
Dace Jansons
Beth Israel Hospital
Boston, MA 02215

The Radiology of Aging: A New Subspeciality?

With progressive advances in modern medicine and increasing availability of health-care services, the elderly have become a large proportion of the total patient population in the United States. In response to this demographic trend, a new subspeciality of general practice and internal medicine, geriatric medicine, has recently been created. The impact on radiology has been an increase in the demand for radiologic services rendered to older individuals. This raises the question of whether specialized training is warranted within diagnostic radiology to deal adequately with the unique health-care problems of the elderly.

The subspecialty of pediatric radiology is founded on the basic premise that children are not merely small adults. Many disease processes are unique to the younger age group and, from a diagnostic imaging perspective, demand expertise that may exceed that of the general radiologist. An equivalent argument can be legitimately advanced for the geriatric patient population; osteoporosis with its associated fractures, degenerative joint disease, atherosclerosis and vascular insufficiency, atrophic disorders of the CNS, colonic diverticular disease, many types of cancer, and benign prostatic enlargement are but a few of the numerous disorders encountered almost exclusively in the elderly.

The need for subspecialists in geriatric radiology is potentially greatest in hospitals and clinics located in retirement areas, such as Florida, Arizona, and southern California. However, senior-citizen medical clinics, nursing homes, and other health-care institutions catering specifically to the needs of the aged in any part of the country would also benefit from such an individual. Ideally, the geriatric radiologist should possess advanced technical and interpretive skills in areas such as noninvasive bone densitometry, mammography, angiography, CT, MR imaging of the brain, and imaging of joints. Most importantly, such a subspecialist would possess personality characteristics conducive to positive interaction with the older patient, including a gentle approach to the performance of procedures, a compassionate understanding of attitudes and expectations among the aged, and a sincere willingness to face often difficult or unpleasant situations.

While the creation of fellowship positions in geriatric radiology for graduating residents may not be practical because of the broad range of organ systems and imaging technologies involved, such subspecialty training is feasible. Greater emphasis can be placed on teaching technical and interpretive knowledge relevant to diseases of aging in residency programs. Postgraduate courses and categorical seminars on the subject at national radiology meetings constitute a viable means of enhancing knowledge in geriatric imaging among generalists. The formation of a subspecialty society, akin to the Society of Pediatric Radiologists, with its own annual meeting is also a possible approach. Such an organization would attract leading academicians with expertise and/or interest relevant to the elderly from specific existing subspecialty areas of radiology, and might also attract members from clinical fields such as rheumatology, pathology, and gerontology.

Demographic changes in American society in the 1980s and beyond suggest the need for a diagnostic imaging subspecialist devoted to the unique health-care problems of the elderly. Diagnostic imaging is currently at the forefront in most areas of the patient-oriented approach to medical practice, and we should not ignore the one disorder that ultimately affects all human beings, if they live long enough.

David J. Sartoris
University of California, San Diego, Medical Center
San Diego, CA 92103

American Roentgen Ray Society 88th Annual Meeting May 8–13, 1988, San Francisco, CA San Francisco Hilton Hotel

Registration and Hotel Reservations

Forms for advance registration and hotel reservations will be in the February and March 1988 issues of the *AJR*.

Scientific Program

Abstracts of papers to be considered for the program must reach the president-elect by Oct. 1, 1987. Forms on which to submit abstracts are in this issue of the *AJR*. Please photocopy if additional copies are needed. The ARRS Program Committee will select papers in October and notify the authors by November 1. The *AJR* has first rights to all papers accepted for presentation at the ARRS meeting. Send abstract to:

Lee F. Rogers, M.D.
Dept. of Radiology
Olson Pavillion, Room 3426
Northwestern University Medical School
710 N. Fairbanks
Telephone (312) 908-5103 Chicago, IL 60611

Refresher Course Program

A summary of the refresher courses will appear in the *AJR* in February along with advance registration forms. Early registration is an advantage in assuring preferred courses in this popular program. Dr. J. T. Ferrucci, Jr., is program director.

Scientific Exhibits

Proposals for scientific exhibits must reach the Chairman of Exhibits by Oct. 1. Forms, which may be photocopied, are in this issue of the *AJR*. Send completed form to:

John E. Madewell, M.D.
Dept. of Radiology
Baylor College of Medicine
One Baylor Plaza
Telephone (713) 799-6362 Houston, TX 77030

Local Program

A program of sightseeing, shopping, and entertainment will be developed by Dr. George Janetos, the Local Arrangements Chairman. Information and advance registration forms will be in the February issue of the *AJR*.

Residents' Award Papers

The society offers several cash awards for the best scientific papers prepared by residents in radiology. The President's Award has a $1000 prize. There are two Executive Council awards of $500 each. All are presented at the annual meeting. Papers should be submitted by Jan. 31, 1988, for consideration in this competition. Send entries to:

B. G. Brogdon, M.D.
Dept. of Radiology
University of South Alabama Medical Center
2451 Fillingim Street
Mobile, AL 36617

Associated Society Meetings

Society for Pediatric Radiology

The Society for Pediatric Radiology will hold its 31st annual meeting April 27–May 1, 1988, at the Hotel Del Coronado, Coronado, CA (San Diego, CA). The SPR 1989 annual meeting will be April 5–9, 1989, at La Mansion Del Rio Hotel, San Antonio, TX. For details contact: Donald R. Kirks, M.D., Secretary, Society for Pediatric Radiology, c/o Dept. of Radiology, Childrens Hospital Medical Center, Elland and Bethesda Aves., Cincinnati, OH 45229-2899, (513) 559-8058.

Deadlines

Abstracts of papers: October 1, 1987
Scientific exhibit proposals: October 1, 1987
Residents' Award papers: January 31, 1988

Call for Scientific Exhibits

American Roentgen Ray Society 1988 Annual Meeting: May 8–13, 1988, San Francisco, CA

FOR COMMITTEE USE ONLY

Date Received _____ Application No. _____
Subject _____ Score _____
Rejected _____ Accepted _____
Assigned _____ Space No. _____

Principal Exhibitor's Professional Mailing Address:

Name: _____ Institution: _____

Department: _____ Street Address: _____ City: _____

State: _____ Zip Code: _____ Telephone: work ( ) _____ home ( ) _____

Are you a member of ARRS? (Please circle one.) yes or no

Names of Exhibitors:
(List principal exhibitor first and telephone number of each person.)

Last	First	Middle	Telephone	Degree (one only)	Member ARRS? Yes	No

Title of Exhibit:

Type Abstract in This Space Single Spaced:
(Instructions are on reverse.)

Instructions for Abstract

A brief resume of the exhibit is requested. State purpose, principal information, and conclusions. Promissory statements are not acceptable. Type single-spaced in the space provided on the reverse side. Brevity is desirable but not at the expense of factual information. The abstract **will appear in the program book as submitted.** Exhibitors will receive detailed instructions for exhibit preparation. Please use typewriter and complete the application form on both sides. Type must be fully legible. List space requirements.

What Sort of Exhibit Is Proposed? (Check one and complete all appropriate places.)

_____**Free Standing.** This is a self-contained display created in total by the exhibitor and may be a fold-open unit, a unit shipped in cases and assembled on site, or a table top unit. Linear feet required: _____

_____**Poster Board (Backboard Panels).** Backboard panels are 4 × 6 or 4 × 8 feet. Number of panels required: _____ 4 × 6 or _____ 4 × 8. If two panels are needed, there will be a ¼-in frame separating the panels, thus requiring a separation in the presentation.

_____**Viewbox.** Mounted materials (radiographs and other transparencies) for display on the society's illuminators. Each illuminator is 39.5 × 59.5 inches. Number of illuminators required: _____ . Slides should be nonglass mounted.

_____**Audiovisual.**

Please Indicate Most Appropriate Category for Your Exhibit.

Diagnostic Radiology:
_____Bone _____ Cardiovascular System _____ Chest _____ Pediatric Radiology
_____Gastrointestinal Tract _____ Genitourinary Tract _____ Neuroradiology

Other:
_____Medical Physics _____ Nuclear Medicine _____ Radiation Oncology _____ Radiobiology
_____Ultrasound
Has the exhibit been shown in whole or part at any previous meeting? _____ (Previous display does not preclude acceptance.)

Where? _____ When? _____

Nature of meeting or name of society _____

_____
Signature of Principal Exhibitor

Applications must be received no later than October 1, 1987.
Mail original (*and five copies*) to: John E. Madewell, M.D.
Department of Radiology
Baylor College of Medicine
One Baylor Plaza
Houston, TX 77030

Telephone (703) 799-6362

Call for Papers

American Roentgen Ray Society 1988 Annual Meeting: May 8–13, 1988, San Francisco, CA

FOR COMMITTEE USE

Received _____ No. _____
Subject _____ Score _____
Rejected _____ Accepted _____
Assigned: Day _____ Session _____
Time _____ No. _____

Title of Paper:

Names of Authors (Last, First, Middle):
(Use asterisk to indicate who will present paper.)

Degree (one only) | Member ARRS? Yes | No

. . . . . .

. . . . . .

. . . . . .

Professional Address of Corresponding Author: _____

_____

City State Zip Code Telephone

Type Abstract in This Space Single Spaced:
(Instructions are on reverse.)

Has this been presented elsewhere? yes no. If yes, please describe on reverse.

Projection Requirements: _____ 35 mm (2 × 2), single or double (circle which); _____ 16 mm silent movie. (Note: video tapes must be converted to 16-mm films.)

(This Form May Be Photocopied)

Instructions for Scientific Abstracts

Proposals are judged by topic and content. New information is preferred, but careful reviews of subjects important to the practice of radiology are also acceptable. The content is treated as confidential information. If the material has been presented elsewhere, notice to that effect is required.

The abstract should contain the four essentials of a scientific communication. It should describe the purposes of the study, the material and methods used, the principal observations, and their significance to radiologic practice. Brevity is desired but not at the expense of information. Factual data are essential. The abstract should be a succinct summary of work done rather than a promissory note. Acceptance for publication is encouraged by well-organized, factual abstracts. The abstract will remain confidential until the program is distributed at the meeting.

PLEASE USE TYPEWRITER. Supplemental information may be attached. Photocopies of the abstract will be distributed to the Program Committee for evaluation. Keep a copy for yourself.

Manuscripts presented on the scientific program become the property of the Society and will be considered for publication in the *American Journal of Roentgenology*. If publication is not offered by the Journal, publication rights return to the author.

Deadline for submission of abstract is October 1, 1987

Telephone (312) 908-5103

Mail abstract to: Lee F. Rogers, M.D.
Dept. of Radiology
Olson Pavillion, Room 3426
Northwestern University Medical School
710 N. Fairbanks
Chicago, IL 60611

Meeting News

International Congress of Radiology, 1989–Paris, France

France is proud to host the 17th International Congress of Radiology (ICR) in Paris during the first of week of July 1989. We undertake this enormous responsibility and exciting task with a great awareness of the importance of such an international congress for radiologists.

The science of radiology has spanned almost 100 years and many countries. Roentgen's discovery of the X-ray in 1895 was made known to the whole civilized world within 1 week. Since then, this science has steadily grown—despite two world wars, many economic and political crises, the skepticism of many physicians, the discovery of the deleterious effects of the ionizing radiation, and the increasing cost of equipment.

Most inventions in radiology have come from countries whose language is either English (CT, MR, sonography, gamma cameras); French (curietherapy, artificial isotopes); or German (X-ray, contrast media). However, Portuguese and Danish radiologists introduced angiography. Mammography was developed in Uruguay, and subtraction radiography and axial transverse tomography were first used in the Netherlands and Italy, respectively. The first nonionic contrast medium came from Norway. National organizations and journals have helped disseminate these advances within countries. The purpose of the ICR is to provide an *international* forum for radiologists to share knowledge and freely discuss important issues.

The International Society of Radiology sponsors the quadrennial ICR and has chosen France, with its great scientific and industrial heritage and 4000 radiologists, to host the 1989 meeting. The French radiologic community promises that ICR '89 will be a high-standard international scientific event. Multilingual scientific sessions, symposia, workshops, scientific exhibits, and refresher courses will be provided. The meeting will include an exceptional technical exhibit. With the cooperation of international manufacturers of radiologic equipment, the technical exhibits will include new equipment available from these companies for export around the world. Finally, ICR '89 will be an international political meeting, because international relationships in radiology must be regulated on new bases. In the setting of the bicentennial celebrations of the French Revolution, Bastille Day, and the first Human Rights Act, the bylaws of the International Society of Radiology will be reformed and the International Committee and the four commissions of the International Society of Radiology will hold their sessions.

This ICR will not copy former ICRs—we are even now preparing a complex and expansive system to suit a heterogeneous audience. We wish to invite all radiologists to attend this important international event—a conference, technical exhibit, and forum for exchange of ideas across national lines.

Jean-Francois Moreau, M.D.
Department of Radiology
Hôpital Boucicaut
78 rue de la Convention
75015 Paris
France

News

Two-day Seminar on Breast Imaging

The Continuing Education Committee of the Los Angeles Radiological Society will sponsor a 2-day seminar on breast imaging, July 11–12, at the Century Plaza Hotel, Los Angeles, CA. A workshops-and-lectures format will be used to give an overview of film-screen and xeromammography, sonography, biopsy, and localization techniques, and medicolegal problems. Category 1 credit: 10 hr. Fee: $200: regular registrant; $175: LARS member; $25: residents and technologists. Information: Los Angeles Radiological Society, Attn. Diane L. Johnson, 5200 Century Blvd., Ste. 920, Los Angeles, CA 90045; (213) 642-0921.

Diagnostic Imaging Postgraduate Course

The Dept. of Radiology, Duke University Medical Center, will present a 5-day postgraduate course in diagnostic imaging, July 27–31, in Pine Knoll Shores, NC. This course is designed to update participants in a number of newer imaging techniques in diagnostic radiology including MR imaging, nuclear medicine, sonography, angiography, and general radiology for pediatric and adult patients. Category 1 credit: 20 hr. Fee: $350: advance registration; $425: on-site registration. Information: Carl E. Ravin, M.D., Professor and Chairman, Dept. of Radiology, Duke University Medical Center, P. O. Box 3808, Durham, NC 27710; (919) 681-5268.

MRI for Technologists

The Dept. of Radiology, Hospital of the University of Pennsylvania, will sponsor MRI for Technologists: A Practical Introduction, Aug. 1–2, at the Penn Tower Hotel, Philadelphia, PA. This course will provide an overview of the equipment and technical aspects of MR imaging and will also highlight areas of important clinical applications. Cross-sectional anatomy as depicted on MR images will be reviewed, and the program will include workshops and demonstrations of techniques and technical problems commonly encountered. Credit: 12 hr (pending). Fee: $175. Information: Janice Ford, CME Coordinator, Dept. of Radiology, Hospital of the University of Pennsylvania, 3400 Spruce St., Philadelphia, PA 19104; (215) 662-6904/6982.

Workshop of Magnetic Resonance Imaging, 1987

The Section on Radiology of the National Medical Association will present a workshop on MR imaging, Aug. 2, at the Hyatt Regency Hotel in New Orleans, LA. Topics will include MR imaging in back pain, female genital tract, soft tissues, metabolic brain disorders, and imaging strategies. Faculty: L. M. Hinds, L. Saint-Louis, H. Butler, J. D. Collins, S. E. Byrd. Category 1 credit: 3 hr (pending). Fee: nonmembers: $30; residents: $5. Information: A. Oestreich, M.D., Radiology, Children's Hospital Medical Center, Cincinnati, OH 45229-2899; (513) 559-4255.

Annual Scientific Meeting, Section on Radiology

The annual scientific meeting of the Section on Radiology of the National Medical Association will take place Aug. 2–6 at the Hyatt Regency, New Orleans, LA. Topics will include diagnostic radiology (including MR, CT, and sonography), nuclear medicine, radiation therapy, pediatric radiology, and socioeconomic problems. Faculty: R. H. Timpton, A. L. Goldson, C. M. Mansfield, R. A. Holmes, L. W. Young, E. M. Mapp, E. A. Patterson, G. C. Evans. Category 1 credit: 21 ¾ (pending). Fee: members: approximately $100; nonmembers: $395. Information: A. Oestreich, M.D., Radiology, Children's Hospital Medical Center, Cincinnati, OH 45229-2899; (513) 559-4255.

Modern Radiology Practice

The Dept. of Radiology, University of California, San Diego, School of Medicine, will present a postgraduate course, Modern Radiology Practice, Aug. 3–7, at the Red Lion Ocean Resort, Santa Barbara, CA. The course is an update emphasizing new imaging techniques and practice management. Category 1 credit: 30 hr. Fee: $425: physicians; $250: residents, fellows, and technologists. Information: Dawne Ryals, Ryals & Assoc., P. O. Box 920113, Norcross, GA 30092-0113; (404) 641-9773.

Magnetic Resonance Imaging Update and New Techniques

The Hoag Memorial Presbyterian Hospital, Newport Beach, CA, will sponsor a course, Magnetic Resonance Imaging Update and New Techniques: A Mini-Symposium, Aug. 8–9, at the Ritz-Carlton Hotel, Laguna Niguel, CA. Guest faculty: W. Bradley, M. Brant-Zawadski, D. M. Cassel, J. V. Crues III, A. Hasso, and M. Modic. Program director: Michael Brant-Zawadzki. Category 1 credit: 12 hr. Fee: $175. Information: Dawne Ryals, Ryals & Assoc., P. O. Box 920113, Norcross, GA 30092-0113; (404) 641-9773.

Napa Valley Imaging Update

The Sacramento Radiology Research and Education Foundation and the Northern California Radiology Society will sponsor the annual Napa Valley Imaging Update, Aug. 15–19, at the Silverado Country Club in Napa, CA. This course is designed for practicing diagnostic radiologists with a particular interest in clinical radiology. Guest faculty: W. P. Dillon, C. R. Bird, P. W. Ralls, and W. R. Webb. Category 1 credit: 20 hr. Fee: $385: physicians; $285: residents and fellows. Information: John P McGahan, M.D., Sacramento Radiology Research and Education Foundation, P. O. Box 19184, Sacramento, CA 95819.

Hepatobiliary Radiology Review Course

The Dept. of Radiologic Pathology of the Armed Forces Institute of Pathology will hold its 1st annual hepatobiliary radiology review course, Aug. 24–25, at the Holiday Inn of Bethesda, Bethesda, MD. Category 1 credit: 16 hr. Military and other full-time federal salaried physicians should contact the Associate Director for Education, (EDZ), Armed Forces Institute of Pathology, Washington, DC 20306; (202) 576-2934/9. Information: Mrs. Cunningham, Dept. of Radiologic Pathology, Rm. G051, Armed Forces Institute of Pathology, Washington, DC 20306; (202) 576-2534/5.

Radiology Seminar: Postgraduate Course

The University of Southern California School of Medicine—Postgraduate Division—and the Dept. of Radiology will hold the annual radiology seminar, Aug. 24–28, at the Marriott Hotel, Maui, HI. Category 1 credit: 28 hr. Fee: $525. Information: Beverly J. Johnson, University of Southern California School of Medicine—Postgraduate Division, 1975 Zonal Ave. KAM 314, Los Angeles, CA 90033; (213) 224-7051.

Third Annual Physics and Biology of Radiology

The Dept. of Radiology, University of California, San Diego, School of Medicine, will hold its annual Physics and Biology of Radiology course, Aug. 27–30, at the Town & Country Hotel, San Diego, CA. Program director: Michael André. Category 1 credit: 26 ½ hr. Fee: $395. Information: Dawne Ryals, Ryals & Assoc., P. O. Box 920113, Norcross, GA 30092-0113; (404) 641-9773.

Third Annual Sonographers' Update and Review

The Dept. of Radiology, University of California, San Diego, School of Medicine, will present its postgraduate course, Third Annual Sonographers' Update and Review, Aug. 28–30, at the Bahia Resort Hotel, San Diego, CA. Program directors: Deborah Wolf Ehlers and John R. Forsythe. Category 1 credit: 16 hr. Fee: $275. Information: Dawne Ryals, Ryals & Assoc., P. O. Box 920113, Norcross, GA 30092-0113; (404) 641-9773.

Advances in Sectional Imaging

The Dept. of Radiology, University of California, San Diego, School of Medicine, will present a postgraduate course, Advances in Sectional Imaging, Sept. 10–12, at the U. S. Grant Hotel, San Diego, CA. Guest faculty: M. D. Rifkin and E. A. Zerhouni. Program director: Robert F. Mattery. Category 1 credit: 14 hr. Fee: $375: physicians; $275: residents, fellows, and technologists. Information: Dawne Ryals, Ryals & Assoc., P. O. Box 920113, Norcross, GA 30092-0113; (404) 641-9773.

Organ Imaging Review—Toronto 1987

The Dept. of Radiological Sciences, University of Toronto, will present a conference, Organ Imaging Review—1987, Sept. 14–18, at the Four Seasons Hotel, Toronto, Ontario. The conference will cover practical aspects of modern imaging, emphasizing the interaction of conventional and newer techniques in assessment of specific organ systems. Topics will include chest, cardiac, genitourinary, gastrointestinal, and musculoskeletal organ systems. Discussions concerning pediatric and interventional radiology will be presented in conjunction with the appropriate organ system. Guest faculty: J. Burhenne, A. Davidson, R. Heitzman, E. Kazam, E. Lyona. Category 1 credit: 30 hr. Fee: $550 Canadian ($425 U.S.): physicians; $350 Canadian ($270 U.S.): residents and fellows. Information: E. E. Kassel, M.D., Program Director, Department of Radiology, University of Toronto, Room 127 FitzGerald Bldg., Faculty of Medicine, Toronto, Ontario, M5S 1A8 Canada; (416) 987-6801.

Refresher Course of the International Skeletal Society: Musculoskeletal Disorders

The International Skeletal Society will sponsor its 14th annual refresher course, Musculoskeletal Disorders, Sept. 16–19, in Cannes, France. The course is designed to present a review of current knowledge and future trends in musculoskeletal disorders. An interdisciplinary faculty of over 70 radiologists, orthopedic surgeons, and pathologists will consider various aspects of bone and joint disease. Newer concepts and recent developments in the area of skeletal radiology, including MR imaging, CT, arthrography, and bone scanning will be provided. Fee: $50: member; $400: nonmember physicians; $175: residents and fellows; 2000 French francs: physicians native to France. Information: Janice Ford, Convention Manager, International Skeletal Society, 39 Dunlin Way, Erial, NJ 08081; (215) 662-6904.

Diagnostic Ultrasound in Obstetrics and Gynecology

The Dept. of Radiology and Radiological Science of the Johns Hopkins Medical Institutions will sponsor a course in diagnostic ultrasound in obstetrics and gynecology, Sept. 18–20, at the Baltimore Marriott–Inner Harbor Hotel, Baltimore, MD. Guest faculty: J. Bowie, G. DeVore, R. Filly, B. J. Hackeloer, S. Kunari, G. Phillip, B. Topol. Category 1 credit: 19 hr. ACOG cognates will be available; ASRT credit. Fee (3 days): $325: physicians; $250: sonographers and RNs. Information: Carlita M. Kearney, Program Coordinator, Office of Continuing Education, 22 Turner, 720 Rutland Ave., Baltimore, MD 21205; (301) 955-3168.

Ultrasound Update

The Sacramento Radiology Research and Education Foundation and the Northern California Radiology Society will hold their annual Ultrasound Update conference, Sept. 19–20, at the Red Lion Inn, Sacramento, CA. This course is designed as a refresher course for the diagnostic radiologist, obstetrician, and ultrasound technologist with an interest in obstetrical and gynecologic ultrasound. A review

of controversial areas relating to imaging in clinical obstetrics and gynecology and an update of newer applications of ultrasound will be presented with a focus on Doppler. Guest faculty: P. N. Burns, D. E. Strandness, Jr., G. R. De Vore. Category 1 credit: 10.5 hr. Fee: $145: physicians; $90: residents and technologists. Information: John P. McGahan, M.D., Sacramento Radiology Research and Education Foundation, P.O. Box 19184, Sacramento, CA 95819; (916) 453-3766.

Nuclear Cardiology Symposium

The Cardiovascular Disease Center, University of Wisconsin School of Medicine, Milwaukee Clinical Campus, Mount Sinai Medical Center, Milwaukee, and Continuing Medical Education, University of Wisconsin, will sponsor the 12th Annual Nuclear Cardiology Symposium, Sept. 21–22, at the Red Carpet Hotel, Milwaukee, WI. The symposium will provide a comprehensive review of current techniques in nuclear cardiology for physicians and technologists who either provide cardiovascular imaging services or make use of the information derived from nuclear cardiology procedures in patient management. Category 1 credit, University of Wisconsin CEUs, and VOICE credits for technologists available. Information: Sarah Z. Aslakson, Continuing Medical Education, 465B WARF Bldg., 610 Walnut St., Madison, WI 53705; (608) 263-2856.

Computed Tomography/MRI Update: 1987

The Dept. of Radiology, Brigham and Women's Hospital, and the Dept. of Continuing Education, Harvard Medical School, will sponsor the annual postgraduate CT/MRI course Sept. 28–Oct. 2, at the Hyatt Regency Hotel, Cambridge, MA. The seminar format, supplemented with film reading panels and plenary lectures will be used. Key topics include clinical applications of CT and MR imaging in the head, neck, chest, abdomen, pelvis, and spine. Interventional procedures, bone densitometry, arthrography, contrast agent use, and MR physics and instrumentation will also be covered. Program directors: Steven E. Seltzer, Douglass F. Adams, and Calvin L. Rumbaugh. Category 1 credit: 32 hr. Fee: $550: physicians; $325: residents, fellows, and technologists. Information: Dept. of Continuing Education, Harvard Medical School, 25 Shattuck St., Boston, MA 02115.

MRI and Neuroimaging

The Ministry of Health, the Ministry of Research, the Medical University of Bordeaux II, and the French Society of Radiology and Neuroradiology will sponsor a symposium on MR imaging and neuroimaging, organized by Pr. J. M. Caillé and Ph. Castan, Oct. 1–3, in Bordeaux, France. The symposium will cover research, development, and future uses of NMR; MRI; positron emission tomography; MRI contrast media; NMR and MRI of spine and spinal cord CSF; and NMR and MRI of cerebral diseases, arteriovenous malformations, stroke, epileptic seizures, gliomas, movement disorders, and hypophysis tumors. Fee: 1500 French francs. Information: Secrétariat Service Neuroradiologie, Groupe Hospitalier Pellegrin, 33076 Bordeaux Cédex, France; Telephone: 56.96.83—poste 14604.

Angiography and Interventional Radiology: 1987

The Dept. of Radiology, Brigham and Women's Hospital, and the Dept. of Continuing Education, Harvard Medical School, will hold their 17th annual postgraduate course, Angiography and Interventional Radiology: 1987, Oct. 5–8, at the Hyatt Regency Hotel, Cambridge, MA. Sessions will focus on recent advances in angioplasty and thrombolysis, abdominal diagnostic and interventional techniques, equipment (digital imaging, catheters, lasers), and issues in billing, interventional practice, and risk management. Program director: Michael A. Bettmann. Category 1 credit: 27 hr. Fee: $495: physicians; $324: residents, fellows, and technologists. Information: Dept. of Continuing Education, Harvard Medical School, 25 Shattuck St., Boston, MA 02115.

Practical Radiology

The University of Virginia will offer its 10th annual postgraduate course, Practical Radiology, Oct. 12–14, at the Boar's Head Inn, Charlottesville, VA. Guest faculty: William G. Bradley, David G. Bragg, and Manuel Viamonte, Jr. Category 1 credit: 20 hr. Fee: $350. Information: Theodore E. Keats, M.D., Professor and Chairman, Dept. of Radiology, University of Virginia School of Medicine, Charlottesville, VA 22908.

Chest Disease: 1987

The Dept. of Radiology, Brigham and Women's Hospital, and the Dept. of Continuing Education, Harvard Medical School, will hold their 13th annual postgraduate course, Chest Disease: 1987, Oct. 13–16, at the Ritz-Carlton Hotel, Boston, MA. This comprehensive 4-day course emphasizes current controversies and state-of-the-art reviews of thoracic surgery and oncology. Key topics include a comprehensive review of CT in evaluating the mediastinum, lung cancer, pulmonary parenchyma, and pleural disease, oncoradiology, intensive-care-unit radiology, MR imaging, and digital chest radiography. Program director: Robert D. Pugatch. Category 1 credit: 22 hr. Fee: $475: physicians; $315: residents, fellows, and technologists. Information: Dept. of Continuing Education, Harvard Medical School, 25 Shattuck St., Boston, MA 02115.

Twelfth Annual San Diego Postgraduate Course

The Dept. of Radiology, University of California, San Diego, School of Medicine will present its 12th Annual Postgraduate Course, Oct. 19–23, at the Hotel del Coronado, Coronado (San Diego), CA. Guest faculty: L. L. Berland, M. Reicher, M. J. Siegel, R. A. Zimmerman. Program director: Barbara Gosink. Category 1 credit: 28 hr. Fee: $425. Information: Dawne Ryals, Ryals & Assoc., P. O. Box 920113, Norcross, GA 30092-0113; (404) 641-9773.

International Symposium on Diagnostic Imaging

The Centro Radiologico Computarizado de Barcelona of the Universidad de Barcelona and Mount Sinai Medical Center, Miami Beach, FL, will present the 4th International Symposium on Diagnostic Imaging, Oct. 19–23, in Barcelona, Spain. Subjects covered will include sonography, nuclear medicine, CT, digital subtraction angiography, MR imaging, positron emission tomography. Official languages: Catalan, Spanish, and English. Director: C. Sanpons, Barcelona, Spain; Co-director: Manuel Viamont, Jr., Miami Beach, FL. Fee: $400 ($500 after Oct. 1): physicians; $200 ($250 after Oct. 1): residents. Registration limited to 400. Information: Nuria de Arana, c/o Centro Radiologico Computarizado de Barcelona, Tavern, 82, 08006 Barcelona, Spain.

ASTRO Meeting Dates Changed

The 29th annual scientific meeting of the American Society for Therapeutic Radiology and Oncology will be held Oct. 19–23, at the Sheraton-Boston Hotel, Boston, MA. The dates have been changed to 1 week earlier than previously announced. Categorical courses on hyperthermia, radiation biology, brachytherapy techniques, monoclonal antibody treatment for cancer, and intraoperative radiation therapy will be offered for the first time. Information: John Ciccone, American Society for Therapeutic Radiology and Oncology, 1891 Preston White Dr., Reston, VA 22091; (703) 648-8900.

Recent Advances in the Systemic Therapy of Genitourinary Malignancies

The University of Texas M. D. Anderson Hospital and Tumor Institute will sponsor the 31st annual clinical conference, Recent Advances in the Systemic Therapy of Genitourinary Malignancies, Nov. 11–14, at the Westin Galleria Hotel, Houston, TX. The conference will include comprehensive presentations on bladder cancer, renal-cell carcinoma, germ-cell tumors, and prostatic carcinoma. Innovative aspects to be discussed include new hormonal therapies, integration of chemotherapy and locoregional therapy in genitourinary cancer, cytotoxic chemotherapy in advanced cancer of the prostate and bladder, and immunologic therapy in renal-cell carcinoma. Information: Office of Conference Services, Box 131, M. D. Anderson Hospital and Tumor Institute, 1515 Holcombe Blvd., Houston, TX 77030; (713) 792-2222.

Temporomandibular Joint Conference

The University of Rochester School of Medicine and Dentistry will hold its 5th annual Temporomandibular Joint—Pain and Dysfunction Course, Nov. 12–14, at the Four Seasons Hotel, Philadelphia, PA. Special emphasis will be given to mechanics of joint function, sonographic diagnosis, MR imaging with surface coils, arthroscopy, and laser surgery. Other topics will include pros and cons of splint therapy—surgical vs nonsurgical philosophies; surgical techniques—plication, implants, and meniscectomy. Category 1 credit: 24 hr. Fee: $420: physicians and dentists; $195: students and residents. Information: Judy Olevnik, University of Rochester, Dept. of Radiology, P. O. Box 648, Rochester, NY; (716) 275-2622.

The Society of Gastrointestinal Radiologists Meeting and Postgraduate Course

The Society of Gastrointestinal Radiologists announces its 17th annual meeting and postgraduate course, Jan. 16–20, 1988, at the Cable Beach Hotel, Nassau, Bahamas. Information: Lynne K. Tiras, International Meeting Managers, P. O. Box 271411, Houston, TX 77277-1411; (713) 729-6418.

The Society of Thoracic Radiology—Annual Postgraduate Course

The Society of Thoracic Radiology will present its annual postgraduate course, March 27–31, 1988, at the Willard-Intercontinental Hotel, Washington, DC. Program director: Eric Milne. Category 1 credit: 30 hr. Fee: $425. Information: Dawne Ryals, Ryals & Assoc., P. O. Box 920113, Norcross, GA 30092-0113; (404) 641-9773.

1986 Winners of the Radiology News Awards

The American Roentgen Ray Society, The American College of Radiology, and The Radiological Society of North America announce the following winners of the 1986 Radiology News Awards. Medical science category: 1st place, Barry Vincour, *Diagnostic Imaging*; 2nd place, Mitchel L. Zoler, *Medical World News*. General publications category: 1st place, Jon Van, *Chicago Tribune*; 2nd place, Jane Collins and Walter Froehlich, *The World and I Magazine*. Broadcast media category: 1st place, Daniel C. Rutz, Cable News Network, Inc.; 2nd place, Margie Manning, KMOX Radio, St. Louis, MO.

Robert D. Moseley, Jr., Memorial Fund

The National Council on Radiation Protection and Measurements (NCRP) announces the establishment of the Robert D. Moseley, Jr., Fund for young physicians and others in radiation protection. The aim of the Fund is to foster in young physicians and others an interest in radiation protection and the work of the NCRP. Donations may be sent to the Robert D. Moseley, Jr., Fund, National Council on Radiation Protection and Measurements, Suite 1016, 7910 Woodmont Ave., Bethesda, MD 20814.

Correction: Congress on Ultrasonic Examination of the Breast

Two corrections need to be made to the description in Feb. 1987 *AJR* concerning the fifth International Congress on the Ultrasonic Examination of the Breast. The congress will be held Oct. *4–5*, and the phone number for Dr. Elizabeth Kelly-Fry is (317) *630*-6131. The complete correct information for this congress is in the following paragraph.

The fifth International Congress on the Ultrasonic Examination of the Breast will be held Oct. 4–5 in New Orleans, LA. The meeting is open to all clinicians and technologists interested in breast disease diagnosis. Proffered presentations are encouraged and will be reviewed after an abstract is submitted to Elizabeth Kelly-Fry, Dept. of Radiology, Wishard Memorial Hospital, 1001 W. 10th St., Indianapolis IN 46202; (317) 630-6131; telefax (317) 636-3198. Guest faculty: D. Amy, J. C. Bamer, J. Croll, B. J. Hackeloer, J. Jellins, T. Kobayashi, M. McSweeney, T. S. Reeve, J. Teubner, and T. Wagai. Category credit: available. Information: Catherine Cole-Beuglet, Dept. of Radiological Sciences, University of California Medical Center, Irvine, University Hospital, 101 City Dr. S., Orange, CA 92668.

Meeting and Course Review

For reader convenience, a summary of upcoming meetings and courses is provided. Detailed listings are given in the *AJR* issue noted in parentheses.

UC San Diego Courses; Physicians Imaging Courses 1987, times arranged, San Diego, CA (Nov)
UC San Diego Visiting Fellowships in MR Imaging, times arranged, San Diego, CA (Feb)
International Conference on Computer Assisted Radiology. July 1–4, West Berlin (Feb 1986)
Diagnostic Imaging Seminar: an Imaging Spectrum Analysis, July 6–10, Martha's Vineyard, MA (April)
Radiology Conference at the Greenbrier, July 8–13, White Sulphur Springs, WV (June)
Planning Functional Endoscopic Surgery by CT, July 9, Baltimore, MD (May)

Diagnostic Course on Imaging Techniques, July 10–12, Rochester, NY (May)
Body Imaging: Ultrasound and Computed Tomography Course, July 17–19, Stowe, VT (April)
Breast Imaging Seminar, July 24–26, Pittsburgh, PA (June)
International Continuing Medical Education Series: Topic to be announced, July 24–30, Pebble Beach, CA; Topic to be announced, Aug., Gstaad, Switzerland (Oct)
Symposium on Breast Disease: Diagnostic Imaging and Current Management, Aug. 9–14, Grand Traverse Village, MI (June)
Symposium on Diagnostic Imaging, August 10–13, Providence, RI (April)
Summer Imaging and Interventional Techniques V, August 10–14, Hilton Head, SC (May)
Masters International Diagnostic Radiology Conference, August 23–28, Paris, France (March)
Sarcoidosis and Granulomatous Disorders, Sept. 6–11, Milan, Italy (June 1986)
Magnetic Resonance Imaging: a Technologist's New World, Sept. 10–12, Orlando, FL (June)
Physics of Diagnostic Radiology, Nuclear Medicine, and Radiation Biology, Sept. 10–13, Davis, CA (June)
Magnetic Resonance Imaging for Technologists, Sept. 11–12 and Dec. 4–5, Houston, TX (June)
Radiology in Yorkshire, Sept. 13–20, Yorkshire, England (March)
Physics of Radiology, Nuclear Medicine, and Radiobiology, Sept. 14–16, New York, NY (June)
Registry Review Courses for Sonographers, Sept. 14–19, Arlington, VA (May)
Diagnostic Ultrasound Course, Sept. 17–19, Ann Arbor, MI (April)
The Asian-Oceanian Congress of Radiology, Sept. 21–25, Seoul, South Korea (Nov 1986)
International Workshop on Bone and Soft Tissue Densitometry, Sept. 22–25, Buxton, Derbyshire, UK (March)
Congress on Ultrasonic Examination of the Breast, Oct. 3–5, New Orleans, LA (Feb)
Mammography Courses, Oct. 5–8, Nov. 2–5, Boston, MA (Jan)
The American Board of Radiology Examinations. Written examinations: Oct. 8–9, 1987; Oct. 6–7, 1988; Oct. 5–6, 1989.
Oral examinations: May 23–27, 1988; June 5–9, 1989, all oral examinations at Louisville, KY (Dec 1986)
Neuroradiology and Head and Neck Radiology Course, Oct. 12–16, Boston, MA (April)
Current Trends in Diagnostic Radiology, Intervention, and Cross-Sectional Imaging—1987, Oct. 19–22, Boston, MA (April)
The Johns Hopkins Medical Institutions Courses in Abdominal and Obstetric Ultrasound: Basic Practicum, Nov. 16–20; **Advanced Practicum in Ultrasound,** Dec. 7–11, Baltimore, MD (Feb)
Congress of the Indian Radiological and Imaging Association, Jan. 14–16, 1988, Coimbatore, India (June)

AJR carries announcements of courses, symposia, and meetings of interest to its readers if received a minimum of 5 months before the event. There is no charge; receipt of items by the *AJR* Editorial Office is not acknowledged. Submit items for publication typed double spaced. Provide title, date, location, brief description, sponsor, course directors, fees, category I credit, and address and telephone number for additional information. Faculty from the host institution will not be listed. Guest faculty names will appear **only** if initials are provided. Mail news items to *AJR* Editorial Office, 2223 Avenida de la Playa, Suite 200, La Jolla, CA 92037-3218.

Classified Advertising

Positions Available

ISRAEL, DIAGNOSTIC RADIOLOGY. Opportunities for 3–4 week or longer working vacations in a number of Israeli medical centers, on a volunteer basis. Positions varied, arrangements flexible. For information contact: Jonathan H. Fish, M.D., 1844 San Miguel Dr., #302, Walnut Creek, CA 94596; (415) 947-0560. 8xa

ASSOCIATE DIAGNOSTIC RADIOLOGIST needed for new community hospital in scenic Michigan upper-peninsula town. Practice includes ultrasound (Doppler), nuclear medicine, CT, mammography, and some special procedures. Generous salary and liberal benefits leading to early partnership. Send CV to Mario Nunez, M.D., 750 Lake Shore Dr., Escanaba, MI 49829; (906) 786-7350. 7–9ap

BOARD-CERTIFIED RADIOLOGISTS—Exciting opportunities with expanding group. Dept. chairman and staff positions available in both urban and rural settings. Send CV to Box U90, *AJR* (see address this section). 7–8a

NEURORADIOLOGIST—A 7-member multispecialty radiology group is recruiting a board-certified radiologist with a minimum of 1 yr (preferable 2 yr) fellowship training in neuroradiology. MRI training would be expected. An interest and expertise in interventional neuroradiology is desired. The position is in a private hospital, licensed for 540 beds, situated in S. California. A private office is located in a building adjacent to the center. Submit CV to Patrick J. Cahill, M.D., St. Mary's Radiology Medical Group, 1050 Linden Ave., Long Beach, CA 90801. 7ap

PROFESSOR AND CHAIRMAN, DEPT. OF DIAGNOSTIC RADIOLOGY—Stanford University School of Medicine invites nominations and applications of candidates for appointment to the full-time faculty as Professor and Chairman of the Dept. of Diagnostic Radiology and Nuclear Medicine. Interested candidates should send a CV and supporting documentation to H. Barrie Fairley, M.B., B.S., Chairman, Search Committee for Diagnostic Radiology, Dept. of Anesthesia, Stanford University School of Medicine, Rm. S286A, Stanford, CA 94305. Stanford University is committed to increasing representation of women and members of minority groups on its faculty and particularly encourages applications from such candidates. 7a

CARDIOVASCULAR-INTERVENTIONAL RADIOLOGIST position available July 1, 1987, at University of Rochester Medical Center, Strong Memorial Hospital, a 750-bed tertiary care facility. State-of-the-art angiography equipment recently installed. An appointment as assistant professor or higher is available at a level appropriate to experience. One-year fellowship training or equivalent experience is required. Research and teaching opportunities are available in a strong academic dept. Send letters of inquiry to Robert E. O'Mara, M.D., Acting Chairman, Diagnostic Radiology, Box 648, University of Rochester Medical Center, Rochester, NY 14642. EO/AA/M-F employer. 7a

ABDOMINAL IMAGING—A staff position is available at The Cleveland Clinic Foundation in the Section of Abdominal Imaging. The Cleveland Clinic is a 1000-bed tertiary care facility with a large outpatient population and international referral base. The Section of Abdominal Imaging encompasses body CT, ultrasound, body MR, gastrointestinal radiology, and mammography. Sectional applicants should be fellowship trained or possess equivalent experience. Send CV to David M. Paushter, M.D., Head, Section of Abdominal Radiology, Hospital Radiology, Cleveland Clinic Foundation, 9500 Euclid Ave., Cleveland, OH 44106. 7a

ACADEMIC FACULTY POSITIONS AVAILABLE—The Dept. of Radiology at the University of Colorado Health Sciences Center is planning to undergo rapid and dynamic expansion within the next academic year. We would like to begin recruitment for full-time faculty in the following areas: body imaging, chest radiology, general radiology, GI radiology, and GU radiology. The level of faculty appointment will depend on the applicant's experience and previous appointment. Principle criteria for review of applicants are devotion to patient care, dedication to teaching, interest in independent or collaborative research, and experience. For more information, write to Michael L. Manco-Johnson, M.D., Professor and Acting Chairman, Dept. of Radiology, University of Colorado School of Medicine, 4200 E. Ninth Ave., C277, Denver, CO 80262; (303) 394-7817. UCHSC is an AA/EOE and invites applications from all qualified individuals. 7a

BOARD-CERTIFIED RADIOLOGIST to join 12-member dept. and 625-bed hospital and associated private office. All modalities of radiology performed. Have a 1.5-T GE MRI operation and 2 CT scanners, one of which is a GE 9800 quick scan. Large ultrasound and nuclear medicine section. New angiographic suite being completed. Active residency program. Please send resume to H. E. Yeagley, M.D., Dept. of Radiology, Reading Hospital and Medicine Center, Reading, PA 19603. 7–10a

INTERVENTIONAL RADIOLOGIST—University hospital is seeking a board-certified radiologist experienced in nonvascular and vascular interventional procedures to participate in an active clinical/teaching program affiliated with local VA hospital. Salary and rank commensurate with experience. Please contact William W. Olmsted, M.D., Professor and Director, Diagnostic Radiology Division, The George Washington University Hospital, 901 23rd St., NW, Washington, D.C. 20037. Affirmative action/equal opportunity employer. 7a

NEURORADIOLOGIST—Applications are being sought for a neuroradiologist for a 560-bed teaching hospital/private office. New 1.5-T MRI unit soon to be operational. Candidate should be board certified preferably with 2 yr of neuroradiology fellowship. Training in MR, CT, angiography, and myelography necessary. Send current CV to R. William McConnell, M.D., Chairman, Dept. of Radiology, Number 9, Doctor's Park, Greenville, NC 27834. 7–12a

EXCELLENT OPPORTUNITY—Seeking board-certified radiologist with additional training in interventional radiology or board certification in nuclear medicine to join 12-man private-practice group covering 2 hospitals in suburban St. Louis. Applicant should have experience in CT, nuclear medicine, ultrasound, and mammography. Very competitive salary with excellent benefits. Send CV to A. C. Hooper, M.D., Ernst Radiology Clinic, Inc., Ste. 110, 14377 Woodlake Dr., Chesterfield, MO 63017; (314) 878-4680. 7–9ap

POSITION WITH 5-MAN RADIOLOGY GROUP in a busy, multispecialty clinic for an experienced neuroradiologist. Primarily an outpatient practice at the present time, soon to expand to include a new fully-equipped hospital. Contact J. Moyle, M.D., Austin Diagnostic Clinic, 801 W. 34th St., Austin, TX 78705; (512) 459-1111. 7a

DIAGNOSTIC RADIOLOGIST—Very busy group urgently needs 2 BC/BE radiologists. Recent training preferred, with skills in routine work, sonography, mammography, CT, nuclear medicine, interventional, and MRI. Two-yr work up to full equal partner, generous benefits, and great Texas weather year-round. Population of area served is approximately 150,000. Submit current CV and other information to *AJR*, Box T80 (see address this section). 6xa

BOARD-CERTIFIED RADIOLOGIST wanted for community of 10,000 (45,000 service area) in the lush Yakima Valley of central Washington. Superior diagnostic radiologic skills required with experience in ultrasound, angiography, and CT. Generous practice assistance package. Excellent school system and outdoor recreation. Contact PROSEARCH, 305 NE 102nd Ave., Portland, OR 97220; (503) 256-2070. 7–9ap

DIRECTOR, SECTION OF INTERVENTIONAL RADIOLOGY—The Dept. of Radiology at Harper Hospital is seeking a board-certified radiologist with competence in all aspects of interventional radiology. Harper Hospital is the major institution in the Detroit Medical Center and is affiliated with Wayne State University. Please send CV or inquiries to George A. Kling, M.D., Chairman, Dept. of Radiology, Harper Hospital, 3990 John R, Detroit, MI 48201; (313) 745-8405. 7–9a

CT/ULTRASOUND—The University of Texas Health Science Center, San Antonio is seeking a board-certified radiologist with experience in CT/ultrasound to join our faculty. Contact Robert L. Siegle, M.D., Chief, Diagnostic Radiology, Dept. of Radiology, University of Texas Health Science Center at San Antonio, 7703 Floyd Curl Dr., San Antonio, TX 78284. Equal Opportunity/Affirmative Action Employer. 7–9a

NORTHWEST OPPORTUNITY—Board-certified diagnostic radiologist to join group of 4 at busy 160-bed hospital and private-office practice. Minimum requirements include competence in angiography, CT, and ultrasound. Some limited interventional skills are desirable. Prefer university-trained applicant with imaging fellowship. Excellent benefits and early partnership. Community of 60,000 located on the Columbia River in the beautiful Pacific Northwest 1 hr from Portland, OR. Send CV and inquiries to Michael L. Hanslits, M.D., Longview Radiologists, 1020 11th Ave., Longview, WA 98632. 7–8a

RADIOLOGICAL SCIENCES RESEARCH DIRECTOR—Applications are invited for a tenure-track full-time faculty position as Radiological Sciences Research Director in the Dept. of Radiology at the University of Nebraska Medical Center. Candidates must be a Ph.D. and/or M.D. with postdoctoral research experience including thorough knowledge of biostatistical analysis and knowledge in physiology and anatomy. The Director will be expected to prepare grants and obtain external funding from local, state, and federal agencies, to coordinate developmental research projects, and to be responsible for basic science and clinical experimental design. The Director will be encouraged to pursue independent research projects in areas complimenting those of the current faculty. Applications should be received no later than Oct. 1, 1987, by Thomas J. Imray, M.D., Professor and Chairman, Dept. of Radiology, University of Nebraska Medical Center, Omaha, NE 68105. Telephone (402) 559-6396 for further details. An equal opportunity/affirmative action employer M/F/H/V/. 6–7a

ULTRASOUND AND MAMMOGRAPHY—This is an outstanding opportunity for a radiologist to join a well-respected, growing, office-based private practice in a highly desirable metropolitan area. Fellowship training or equivalent experience is required. Send CV to Box T78, *AJR* (see address this section). 6–8a

BOARD-CERTIFIED GENERAL DIAGNOSTIC RADIOLOGIST—Immediate opening with 17 radiologists in rapidly growing south central Florida communities. Join two radiologists to cover two 100-bed hospitals, private office, and two mammography centers. Expertise in all modalities, with emphasis on CT (MRI not urgent). Send CV to L. S. Ross, M.D., Radiology Consultants, 114 Medical Center, Sebring, FL 33870. 6–7a

DIAGNOSTIC RADIOLOGIST with special interest in CT and ultrasound to join growing hospital-based practice. 125-bed hospital with adjoining office building located near downtown Seattle. Send CV to K. Wade Brunette, M.D., 16775 16th Ave. NW, Seattle, WA 98177; (206) 583-2675. 7–9a

BODY MAGNETIC RESONANCE IMAGING, DEPARTMENT OF RADIOLOGY—The University of Texas Health Science Center at Dallas has an available Assistant Professor position. The successful candidate will be experienced in body MRI and have demonstrated ability in research and teaching. Contact William Erdman, M.D., Director of Nuclear Medicine at Dallas, 5323 Harry Hines Blvd., Dallas, TX 75235; (214) 590-6364. An equal employment/affirmative action employer. 7a

DIAGNOSTIC RADIOLOGIST to join established group of 10 in greater Philadelphia area. Two hospitals and imaging center. Growing practice. State-of-the-art in all modalities. Fellowship a plus but not essential. Position available ASAP. Reply to Box T82, *AJR* (see address this section). 6–8a

PART-TIME POSITION AVAILABLE for general diagnostic radiologist to serve as permanent locum tenens for busy three-person group. Outpatient work only; MRI, angiography not required. Guaranteed 20 weeks/yr. Beautiful southern California location. Contact Wm. Duge, M.D., P.O. Box 2985, Laguna Hills, CA 92654. 6–7a

NEW ENGLAND MEDICAL CENTER, TUFTS UNIVERSITY SCHOOL OF MEDICINE is seeking a radiologist in the general radiology section. The candidate should have expertise in bone radiology and a desire to participate in all modalities of bone and joint imaging including contrast arthrography. The candidate should also have an interest in orthopedic radiology. The hospital is a 469-bed (112 pediatric) hospital and the principal teaching affiliate of Tufts University School of Medicine. The candidate should be eligible for a faculty position at the medical school. Please direct inquiries and CV to Robert C. Sarno, M.D., Dept. of Radiology, New England Medical Center Hospitals, 750 Washington St., Boston, MA 02111. 6–7ap

BC/BE DIAGNOSTIC RADIOLOGIST to join 5-man group covering two major hospitals. Position available July 1987. All modalities except MR which is in planning stages. Background in sonography, CT, and angiography required. Administrative skills preferred. Beautiful mountain setting in a university town of 50,000. "Unlimited" recreational opportunities including skiing, fishing, hunting, hiking. Send CV to Missoula Radiology, Inc., P.O. Box 2039, Missoula, MT 59806. 6–7a

BOARD-CERTIFIED RADIOLOGIST, university trained, wanted for a salaried position in a free-standing imaging center and part-time hospital practice. The center facilities include an Acuson 128, GE 9800, low-rad dedicated mammography, dedicated digital angiography, and routine fluoroscopic and radiographic imaging. Regular hours with minimal on-call responsibilities. Beautiful town in Indiana-Illinois-Kentucky tri-state. Part-time or locum tenes considered. Send CV to Box T88, *AJR* (see address this section). 6–9a

RADIATION ONCOLOGIST. 180-member multispecialty group seeks a board-certified/board-eligible radiation oncologist to expand the service offerings of the Oncology Dept. In addition to provision of care, radiation oncologist will have considerable latitude in design of services including planning of the proposed radiation therapy plant. Duties will include design of facilities, selection of equipment, and selection and training of personnel. Community of 143,000 offers three universities, fine cultural opportunities, and four-season recreational activities. Please send CV and references to John Weir, Associate Administrator, Dakota Clinic, Ltd., P. O. Box 6001, Fargo, ND 58108. 5–7a

BC/BE RADIOLOGIST for general radiology practice including ultrasound, nuclear medicine, CT, and angiography to join group of 15 physicians in northwestern Minnesota community of 9,000 serving 40,000 patient area. Clinic is part of a 185-physician group with facilities in 21 locations throughout Minnesota and North Dakota. Applicant should have experience in angiography (including carotid catheterization) and interventional radiology including percutaneous transluminal angioplasty. Competitive salary, excellent benefits. Summertime fun in lake country, excellent fall hunting and wintertime sports. Send inquiry and CV to Arnold Carriere, Administrator, Falls Clinic, 120 LaBree Ave. South, Thief River Falls, MN 56701. 5–7a

A 400-BED COMMUNITY HOSPITAL staffed by private practice group seeks a second neuroradiologist, preferably with MR experience. Ongoing neuroradiologic service includes state-of-the-art CT, angiography with digital, and myelography. MR unit on order. Must be capable and willing to do general radiology also. Contact Ben R. Mayes, Jr., M.D., Radiology Dept., St. Luke's Hospital, 232 So. Woods Mill Rd., St. Louis, MO 63017, (314) 434-1500, ext. 4250. 4xa.

RADIOLOGIST—A board certified/board eligible radiologist with experience is needed to join the staff of the Alaska Native Medical Center, 170-bed referral facility for a state-wide system of Indian Health Service hospitals and clinics. Practice stimulating and challenging radiology in a relaxed and casual atmosphere. State-of-the-art in-house CT, sonography, and mammography. Send C.V. to C.J. Heitz, Jr., M.D., P.O. Box 7-741, Anchorage, AK 99510. EOE 2–7a

DIAGNOSTIC RADIOLOGIST. Need aggressive associate to perform all aspects of diagnostic radiology in well-equipped hospital with large outpatient component in South Texas. MR training a plus but not essential. Excellent salary and early partnership available. For confidential consideration please submit CV to Box H70, *AJR* (see address this section). 11xa

TWO YOUNG RADIOLOGISTS seek a third radiologist in expanding hospital-based practice near Canadian border in northern New York. All modalities available. Write P. Berman, HC 61 Box 454, Massena, NY 13662. 8–7a

Positions Desired

BOARD-CERTIFIED AIR FORCE RADIOLOGIST desires general outpatient (private/HMO/multispecialty) position beginning August 1988. Has 12-yr experience that includes chairmanships of three major USAF Medical Center dept. Reply A. Daley, M.D., 6306 Wilmington Dr., Burke, VA 22015; office (301) 981-4222. 7b

BOARD-CERTIFIED RADIOLOGIST—52, all modalities, permanent or locum. Administrative and academic experience as Chief Radiologist. Ivy-league training, licensed in many states. Write Box P28, *AJR* (see address this section). 7bp

Fellowship and Residencies

ADVANCED IMAGING FELLOWSHIP—A position is now available for a board-certified or board-eligible radiologist in a University of Rochester teaching-hospital complex. The fellowship emphasizes in-depth exposure to CT, ultrasound, and MRI integrated with invasive procedure exposure. Additional positions will be available in January 1988. Please respond to Steven G. Herbert, M.D., Director, Fellowship Program, Diagnostic Radiology Dept., The Genesee Hospital, 224 Alexander St., Rochester, NY 14607. 7–8c

FELLOWSHIP SOUGHT—Radiologist, 53, DABR, DABNM, DABMR. Retired 4 yr. Imaging preferred but flexible. Available Jan. 1988. Reply Box U92, *AJR* (see address this section). 7–8cp

IMAGING FELLOWSHIP IN DIAGNOSTIC IMAGING with emphasis on diseases of children and women. Diasonics MRI, Imatron CT, and Acuson Ultrasound. Opportunity for clinical or basic research. Must be eligible for oral board exam. Reply Jerald Kuhn, M.D., Director, Radiology Dept., Children's Hospital, 219 Bryant St., Buffalo, NY 14222; (716) 878-7525. 7–10c

MAMMOGRAPHY—GENERAL RADIOLOGY FELLOWSHIP—The New England Medical Center Hospital announces a new 1-yr fellowship starting July 1, 1987, combining training in general radiology with emphasis in mammography and GI radiology (double-contrast technique). Breast imaging equipment includes 2 new CGR Senographe units and an automated whole-breast scanner. Clinical responsibilities will include an active role in the multidisciplinary Breast Health Center that serves as both a primary-care and regional-referral center. This position carries an appointment at Tufts University School of Medicine. For further information contact Marc J. Homer, M.D., Box 388, Dept. of Radiology, New England Medical Center, 750 Washington St., Boston, MA 02111. 7–8cp

ANGIOGRAPHY/NEURORADIOLOGY FELLOWSHIP, BOSTON—Unexpected new position available immediately. Fellows participate in cerebral, peripheral, and abdominal angiography; interventional procedures and myelography; CT and MRI. Send inquiries to Laura Feldman, M.D., Head, Angiography Section, VAMC, 150 S. Huntington Ave., Boston, MA 02130; (617) 739-3435. 7–9c

IMAGING FELLOWSHIP, BOSTON—Unexpected new position available immediately. Fellows participate in CT, ultrasound, nuclear medicine, MRI, and related procedures. Send inquiries to Stephen Gerzof, M.D., Chief, Ultrasound and Body CT, VAMC, 150 S. Huntington Ave., Boston, MA 02130; (617) 739-3435. 7–9c

VISCERAL IMAGING AND INTERVENTIONAL RADIOLOGY FELLOWSHIP to begin July 1988. 612-bed teaching hospital. Fellows will be actively involved in diagnostic CT and sonography. Fellows will also participate in all vascular and nonvascular/interventional procedures including angioplasties, biliary, GU, biopsies, abscess drainages, and angiography. Send inquiries to Harvey L. Neiman, M.D., Chairman, Dept. of Radiology, West Penn Hospital, 4800 Friendship Ave., Pittsburgh, PA 15224. 6–8c

INTERVENTIONAL RADIOLOGY—Rhode Island Hospital, Dept. of Radiology, seeks one fellow in the Special Procedures section to begin July 1988. We are the major affiliate of Brown University Medical School and serve a 715-bed general hospital. During the calendar year 1986 we performed approximately 2400 procedures. The fellow will perform vascular and nonvascular interventional procedures of all types; including angiography, angioplasty, infusions, embolizations, biopsies, aspirations, abscess drainages, transhepatic cholangiograms, biliary drainages, nephrostomies, stone extractions, and percutaneous endoscopies. All imaging modalities are integrated in this busy and diverse service with emphasis on fluoroscopy, sonography, and CT. Requirements include a minimum of 3-yr training in an accredited radiology residency and expectations of board certification before start date. Send inquiries to Daniel J. Hanson, M.D., Radiologist-in-Chief, Dept. of Diagnostic Radiology, Rhode Island Hospital, 593 Eddy St., Providence, RI 02902. 6–7c

VISITING ULTRASOUND FELLOWSHIPS, VANCOUVER, B.C. Year-round basis. Fellowships are 1–12 wk at the University of British Columbia, under Peter L. Cooperberg, M.D. Heavy ultrasound caseload, with Doppler and real-time techniques emphasized. Contact Ultrasound Dept., Vancouver General Hospital, 855 West 12th Ave., Vancouver, B.C., V5Z 1M9, Canada. 7c

FELLOWSHIP IN DIAGNOSTIC IMAGING at Rhode Island Hospital to begin July 1988. Rhode Island Hospital is the major affiliate of Brown University Medical School. The radiology staff serves this 715-bed general hospital and a 200-bed lying-in hospital. Over 165,000 examinations are performed yearly in the Radiographic Dept. All imaging modalities are integrated into this busy and diverse service. The fellowship will emphasize sonography and CT, along with associated interventional procedures, a busy mammography area, and MRI. Requirements include completion of an accredited radiology training program. Send inquiries to Daniel J. Hanson, M.D., Radiologist-in-Chief, Dept. of Diagnostic Radiology, Rhode Island Hospital, 593 Eddy St., Providence, RI 02902. 6–7c

ABDOMINAL IMAGING FELLOWSHIP to begin July 1988. 612-bed teaching hospital. Over 120,000 examinations are performed yearly in the radiology dept. All imaging modalities are integrated into the Fellowship Program which will emphasize body CT, diagnostic sonography including obstetric, and MRI. Send inquiries to Harvey L. Neiman, M.D., Chairman, Dept. of Radiology, West Penn Hospital, 4800 Friendship Ave., Pittsburgh, PA 15224. 6–8c

Tutorials/Courses

MAUI, HAWAII—12TH ANNUAL BODY IMAGING CONFERENCE—October 10–18, 1987. Diagnostic Imaging, Category I Accreditation, University Faculty. Registration and information: Body Imaging Conference, 21915 Roscoe Blvd., Ste. 222, Canoga Park, CA 91390; (818) 719-7380. 7–9d

INTERNATIONAL TRENDS IN BREAST ULTRASOUND—International Congress on the Ultrasonic Examination of the Breast: New Orleans, LA, Oct. 4–5, 1987 (AIUM Annual Convention, Oct. 6–9, same host Hotel Sheraton, New Orleans). International faculty CME-1. Topics include the multimodality approach to breast examination. Congress registration fee: $200 Physicians, Scientists, Engineers; $125 Technologists, Research Assistants. Checks (US funds) payable to The International Congress on the Ultrasonic Examination of the Breast. Send to Elizabeth Kelly-Fry, M.D., Indiana University Medical Center, Indianapolis Center for Advanced Research, 611 N. Capitol Ave., Indianapolis, IN 46204, USA; (317) 630-6131, (317) 262-5008. 7–8d

MRI TUTORIAL PROGRAM—Diagnostic Radiological Imaging Medical Group offers 1-wk training programs in clinical MRI for physicians with limited or no experience in MRI. The program is individualized to the applicant, and the physician may subscribe to 1 or more weeks. Only 2 physicians per week are accepted. The 1.5-T MRI scanner is used in an outpatient imaging facility and 12–16 examinations per day are performed. Individual tutorials in MRI physics, equipment evaluation, clinical indications for MRI examination, performance of MRI studies, discussion of case material, and review of an extensive teaching file are offered. The faculty are A. B. Dublin and M. H. Reid. The fee is $600 and 40 hr Category I credit are available/week. For further information contact Michael H. Reid, Ph.D., M.D., Diagnostic Radiological Imaging, 79 Scripps Dr., Ste. 100, Sacramento, CA 95825. (916) 921-1300. 6–9d

THE UNIVERSITY OF MINNESOTA, DEPT. OF RADIOLOGY will present its 50th Annual Continuation Course, September 21–25, 1987 in Minneapolis. Thirteen guest faculty will participate in this 5-day, comprehensive review. This year's subject, Chest-Cardiovascular Imaging and Intervention, will be a comprehensive course emphasizing both conventional diagnostic techniques and advanced imaging modalities, including computed tomography, digital angiography, and magnetic resonance imaging. The pulmonary lectures will focus on many of the practical issues facing radiologists in their daily work. Special imaging and interventional techniques will highlight the 2 days of cardiac presentations. Registration fee: $450 (inquire about the reduced fee for medical fellows, military personnel and VA physicians). 30¼ hr Category 1 credit. For information contact Office of Continuing Medical Education, University of Minnesota, Box 202 UMHC, 420 Delaware St. S.E., Minneapolis, MN 55455. (612) 626-5525. 5–7d

LONDON—PARIS FALL ULTRASOUND. Attend one or both, September 19–27, 1987, CME I accreditation. For registration and information contact Medical Seminars International, 21915 Roscoe Blvd., Ste. 222, Canoga Park, CA 91304, (818) 340-0580 ext. 280. 3–8d

Other

RADIOLOGY PRACTICE FOR SALE. Established Breast Center, So. California. Excellent location. Good referral base. Potential for broader base radiology. All negotiating options considered. P.O. Box 4893, Lancaster, CA 93539-4893. 6e

AJR Classified Advertising Information

Box Responses and Address for Ad Placement

Write Box _____, AJR, Suite 200, 2223 Avenida de la Playa, La Jolla, CA 92037; (619) 459-2229.

How to Place an Ad

AJR accepts classified advertising for Positions Available, Positions Desired, Fellowships and Residencies, and Tutorials/Courses. Ads are accepted by mail or telephone. Institutions should supply purchase orders.

Rates: $6.00/line with a $30 minimum charge. Box service is $10 additional for each month the ad appears. There are discounts for multiple insertions: 10% for 2–3 insertions; 20% for 4 or more. To estimate lines, count all words and divide by 5.5.

Billing: Ads may be prepaid or invoices will be sent after the ad appears.

Deadlines. About 3 weeks before the issue mails. *AJR* issues mail in the middle of the month preceding the cover date (e.g., July mails June 17). For specific deadlines, write or telephone the AJR editorial office.

Estimating Ad Charges

Line charge: divide total words by 5.5 and multiply by $6.00 .... $ _____

Multiple insertions? If so, multiply by number ..... × _____

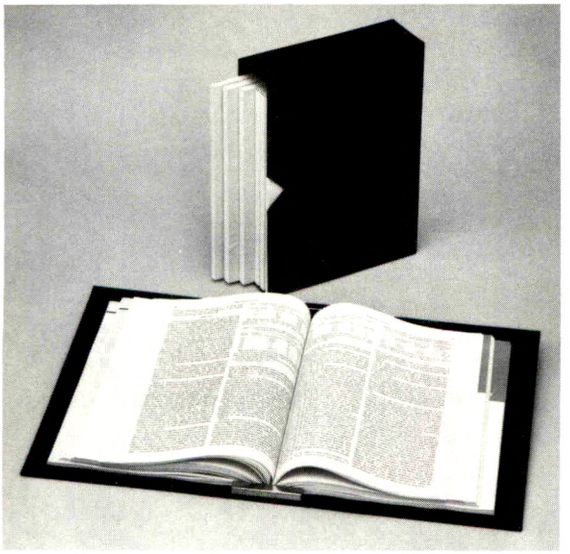
Subtotal ..... $

Box response requested? If so, multiply number of months by $10.00 ..... + _____

Subtotal ..... $

Discount applies to two or more insertions. Subtract 10% if ad appears 2–3 months, 20% if 4 months or more ..... – _____

Approximate advertising charge ..... $



Protect your copies of

AJR: AMERICAN JOURNAL OF ROENTGENOLOGY

with Jesse Jones Binders or Files

Keep your journals clean, orderly, and readily accessible with Jesse Jones Binders or Files. Two Binders or two box style Files are all you need to accommodate a full year's worth of issues. Both Binders and Files are handsomely made with rich black leatherette covers and gold leaf embossed lettering.

Jesse Jones Binders open flat for easy reading and reference and are economically priced at only $9.95 each; 3 for $27.95, or 6 for $52.95 postpaid. The rugged, compact box Files are only $7.95 each; 3 for $21.95, or 6 for $39.95. Add $1.00/unit postage and handling. (Outside the U.S. add $2.50/unit.)

For charge orders call toll free 1-800-972-5858. ($15.00 minimum).

Free gold transfer slips included for indexing volume and year.

Please allow four to five weeks for delivery.

TO: Jesse Jones Industries
499 E. Erie Avenue, DEPT. AJR
Philadelphia, PA 19134

I enclose my check or money order for $_____
(PA residents add 6% sales tax)

Send me ____ ☐ Files ☐ Binders for my journals

Name

Address (will not ship to P.O. Box)

City/State/Zip

Satisfaction guaranteed.

INDEX TO ADVERTISERS

Eastman Kodak A6, A7

Elema Schonander, Inc. A23

E-Z-EM Company ..... Cover 2

FUJI ..... Cover 3

General Electric A14, A15, A30

Mallinckrodt, Inc. A19, A20, A21, A22

Nuclear Associates A13

Picker International A8, A9, A10

Precise Optics/PME, Inc. A17

E. R. Squibb & Sons, Inc .. A26, A27, A28, A29

S & S X-Ray A25

Tecnomed USA A2, A16

University of Minnesota A25

Winthrop Laboratories A11, A12, A33, A34

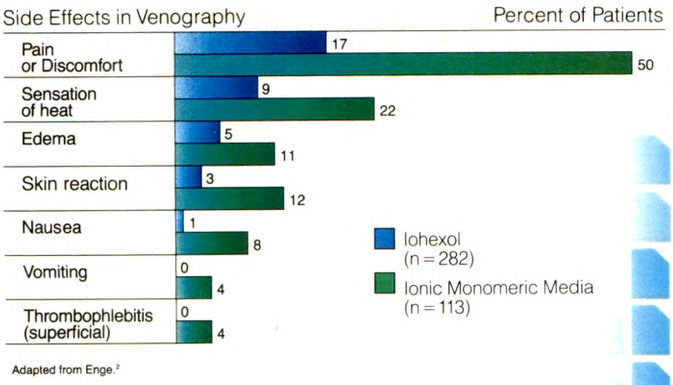
We try to present an accurate index. Occasionally this may not be possible because of a last-minute change or an omission.

In peripheral arteriography/venography:

Because you can't be sure how every patient will react...

Improve the safety profile.

Significant improvement in patient comfort.
Lower incidence of adverse reactions than with conventional ionic media.[1-4]

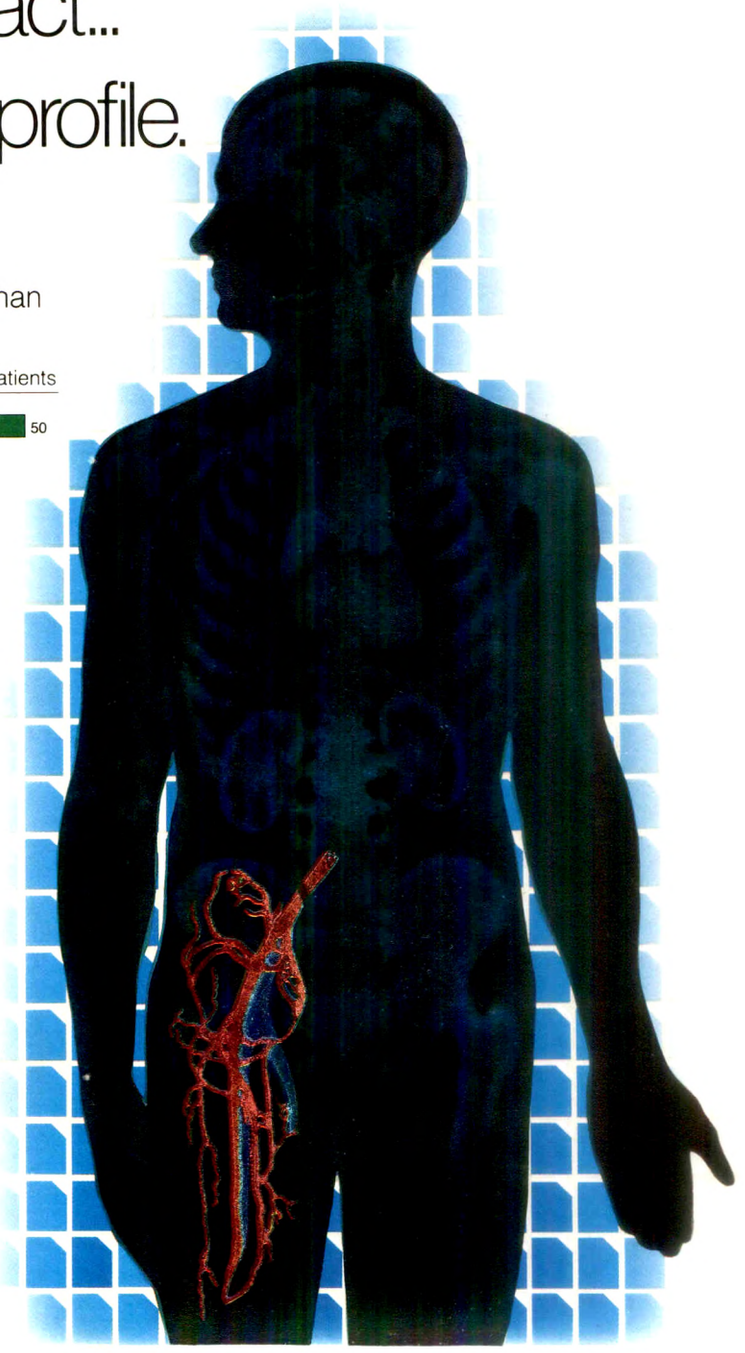


Adapted from Enge.[2]

Excellent vascular tolerance.
Lower incidence of thrombophlebitis.[2]

Excellent cardiovascular profile.
Reduced effect on blood pressure and heart rate.[4,5]

Pulsation should be present in the artery to be injected.



NONIONIC

OMNIPAQUE®

(IOHEXOL)

THE NEW STANDARD IN

See next page for important product information concerning contraindications, warnings, adverse reactions, patient selection, and precautionary recommendations.



OMNIPAQUE®
INJECTION (IOHEXOL)
INTRAVASCULAR

240

300

350

PLEASE CONSULT FULL PRODUCT INFORMATION BEFORE USING.
A SUMMARY FOLLOWS:

DESCRIPTION: OMNIPAQUE is a nonionic, water-soluble radiographic contrast medium for intravascular administration and is provided in iodine concentrations of 240, 300, and 350 mgI/mL. Each milliliter of iohexol solution contains 1.21 mg tromethamine and 0.1 mg edetate calcium disodium with the pH adjusted between 6.8 and 7.7 with hydrochloric acid or sodium hydroxide, but it contains no preservatives.

CONTRAINDICATIONS: OMNIPAQUE should not be administered to patients with a known hypersensitivity to iohexol.

WARNINGS: OMNIPAQUE should be used with extreme care in patients with: severely impaired renal and/or hepatic function; severe thyrotoxicosis, hyperthyroidism, or an autonomously functioning thyroid nodule, diabetes with a serum creatinine level above 3 mg/dL. Not recommended for use in patients with anuria.

Patients with known or suspected pheochromocytoma should receive a minimum of contrast medium if benefit of the exam is judged to outweigh risk; blood pressure should be monitored throughout the procedure, and measures for the treatment of hypertensive crisis should be readily available.

Contrast agents are potentially hazardous in patients with multiple myeloma or other paraproteinemia, particularly those with therapeutically resistant anuria. The combination of contrast agent and dehydration may precipitate myeloma protein in the renal tubules. No form of therapy, including dialysis, has been successful in reversing the effect. Myeloma, which occurs most commonly in persons over age 40, should be considered before instituting intravascular administration of contrast agents.

PRECAUTIONS: Diagnostic procedures that involve the use of radiopaque diagnostic agents should be carried out under the direction of personnel with the prerequisite training and with a thorough knowledge of the particular procedure to be performed. Appropriate facilities should be available for coping with any complication of the procedure, as well as for emergency treatment of severe reactions to the contrast agent itself. Competent personnel and emergency facilities should be available for at least 30 to 60 minutes postprocedure. The possibility of serious, life-threatening, fatal, anaphylactoid, or cardiovascular reactions should always be considered (see ADVERSE REACTIONS). It is of utmost importance that a course of action be carefully planned in advance for immediate treatment of serious reactions. Preparatory dehydration is dangerous and may contribute to acute renal failure in patients with advanced vascular disease, diabetic patients, and in susceptible nondiabetic patients (often elderly with preexisting renal disease). *Patients should be well hydrated prior to and following iohexol administration.* Careful consideration to the potential risk of acute renal failure should be given before performing excretory urography in diabetic patients with diabetic nephropathy and in susceptible nondiabetic patients (often elderly with preexisting renal disease). Immediately following surgery, excretory urography should be used with caution in renal transplant recipients. The possibility of an idiosyncratic reaction in susceptible patients should always be considered (see ADVERSE REACTIONS). The susceptible population includes patients with a history of a previous reaction to contrast media, patients with a known sensitivity to iodine per se, and patients with a known clinical hypersensitivity: bronchial asthma, hay fever, and food allergies. A thorough medical history with emphasis on allergy and hypersensitivity, prior to the injection of any contrast media, may be more accurate than pretesting in predicting potential adverse reactions.

A positive history of allergies or hypersensitivity does not arbitrarily contraindicate the use of a contrast agent where a diagnostic procedure is thought essential, but caution should be exercised (see ADVERSE REACTIONS). Premedication with antihistamines or corticosteroids to avoid or minimize possible allergic reactions in such patients should be considered. Recent reports indicate that such pretreatment does not prevent serious, life-threatening reactions but may reduce both their incidence and severity.

Even though the osmolality of OMNIPAQUE is low compared to diatrizoate- or iothalamate-based ionic agents of comparable iodine concentration, the potential transitory increase in circulatory osmotic load in patients with congestive heart failure requires caution during injection. These patients should be observed for several hours following the procedure to detect delayed hemodynamic disturbances.

Angiography should be avoided whenever possible in patients with homocystinuria, because of the risk of inducing thrombosis and embolism.

In angiographic procedures, the possibility of dislodging plaques or damaging or perforating the vessel wall should be borne in mind during the catheter manipulations and contrast medium injection. Test injections to ensure proper catheter placement are recommended.

Selective coronary arteriography should be performed only in those patients in whom the expected benefits outweigh the potential risk. The inherent risks of angiocardiography in patients with chronic pulmonary emphysema must be weighed against the necessity for performing this procedure.

When OMNIPAQUE is to be injected using plastic disposable syringes, the contrast medium should be drawn into the syringe and used immediately.

The inhibitory effects of nonionic contrast media on mechanisms of hemostasis have been shown, in vitro, to be less than those of ionic contrast media at comparable concentrations. For this reason, standard angiographic procedures should always be followed: angiographic catheters should be flushed frequently, and prolonged contact of blood with contrast media in syringes and catheters should be avoided.

If nondisposable equipment is used, scrupulous care should be taken to prevent residual contamination with traces of cleansing agents.

Drug/Laboratory Test Interaction: If iodine-containing isotopes are to be administered for the diagnosis of thyroid disease, the iodine-binding capacity of thyroid tissue may be reduced for up to 2 weeks after contrast medium administration. Thyroid function tests which do not depend on iodine estimation, eg, T_3 resin uptake or direct thyroxine assays, are not affected.

Carcinogenesis, Mutagenesis, Impairment of Fertility: No long-term animal studies have been performed to evaluate carcinogenic potential, mutagenesis, or whether OMNIPAQUE can affect fertility in men or women.

Pregnancy Category B: Reproduction studies have been performed in rats and rabbits with up to 100 times the recommended human dose. No evidence of impaired fertility or harm to the fetus has been demonstrated due to OMNIPAQUE. There are, however, no studies in pregnant women. Because animal reproduction studies are not always predictive of human response, this drug should be used during pregnancy only if clearly needed.

Nursing Mothers: It is not known to what extent iohexol is excreted in human milk. However, many injectable contrast agents are excreted unchanged in human milk. Although it has not been established that serious adverse reactions occur in nursing infants, caution should be exercised when intravascular contrast media are administered to nursing women. Bottle feedings may be substituted for breast feedings for 24 hours following administration of OMNIPAQUE.

Pediatric Use: Safety and effectiveness in children have not been established.

ADVERSE REACTIONS: Usually mild to moderate in severity. However, serious, life-threatening, and fatal reactions, mostly of cardiovascular origin, have been associated with the administration of iodine-containing contrast media including OMNIPAQUE. The injection of contrast media is frequently associated with the sensation of warmth and pain, especially in peripheral angiography; pain and warmth are less frequent and less severe with OMNIPAQUE than with many contrast media.

Cardiovascular System: Arrhythmias including PVCs and PACs (3%), angina/chest pain (2%), and hypotension (1%). Others including cardiac failure, asystole, bradycardia, tachycardia, and vasovagal reaction were reported with an individual incidence of less than 0.8%. In controlled clinical trials involving 900 patients, one fatality occurred. A cause-and-effect relationship between this death and iohexol has not been established.

Nervous System: Pain (6%), photomas (3%), headache (2%), and metallic taste (0.8%). Others including anxiety, blurred vision, dizziness, fever, motor and speech dysfunction, convulsion, lightheadedness, paresthesia, somnolence, vertigo, stiff neck, hemiparesis, and nystagmus were reported, with an individual incidence of less than 0.3%.

Respiratory System: Dyspnea and laryngitis, with an individual incidence of 0.1%.

Gastrointestinal System: Nausea (2%) and vomiting (0.5%). Others including diarrhea, dyspepsia, and dry mouth were reported, with an individual incidence of 0.1%.

Skin and Appendages: Urticaria (0.3%) and purpura (0.1%).

General Adverse Reactions to Contrast Media: The following reactions have been reported after administration of other intravascular iodinated contrast media. *Reactions due to technique:* hematomas and ecchymoses. *Hemodynamic reactions:* vein cramp and thrombophlebitis following intravenous injection. *Cardiovascular reactions:* rare cases of cardiac arrhythmias, reflex tachycardia, chest pain, cyanosis, hypertension, hypotension, peripheral vasodilatation, shock, and cardiac arrest. *Renal reactions:* occasionally, transient proteinuria; rarely, oliguria or anuria. *Allergic reactions:* asthmatic attacks, nasal and conjunctival symptoms, dermal reactions such as urticaria with or without pruritus, as well as pleomorphic rashes, sneezing, and lacrimation; rarely, anaphylactic reactions. Rare fatalities have occurred due to these or unknown causes. *Signs and symptoms related to the respiratory system:* pulmonary or laryngeal edema, bronchospasm, dyspnea; or *to the nervous system:* restlessness, tremors, convulsions. *Other reactions:* flushing, pain, warmth, metallic taste, nausea, vomiting, anxiety, headache, confusion, pallor, weakness, sweating, localized areas of edema (especially facial cramps), neutropenia, and dizziness. Rarely, immediate or delayed rigors can occur, sometimes accompanied by hyperpyrexia. Infrequently, "iodism" (salivary gland swelling) from organic iodinated compounds appears 2 days after exposure and subsides by the sixth day.

In general, the reactions that are known to occur upon parenteral administration of iodinated contrast agents are possible with any nonionic agent. Approximately 95% of adverse reactions accompanying the use of water-soluble intravascularly administered contrast agents are mild to moderate in degree. However, severe, life-threatening anaphylactoid reactions, mostly of cardiovascular origin, have occurred.

Reported incidences of death range from 6.6 per 1 million (0.00066%) to 1 in 10,000 (0.01%). Most deaths occur during injection or 5 to 10 minutes later, the main feature being cardiac arrest, with cardiovascular disease as the main aggravating factor. Isolated reports of hypotensive collapse and shock are found in the literature. The incidence of shock is estimated to be 1 out of 10,000 (0.005%) patients.

Adverse reactions to injectable contrast media fall into two categories: chemotoxic reactions and idiosyncratic reactions.

Chemotoxic reactions result from the physicochemical properties of the contrast media, the amount of dose injected, and the speed of injection. All hemodynamic disturbances and injuries to organs or vessels perfused by the contrast medium are included in this category.

Idiosyncratic reactions include all other reactions. They occur more frequently in patients 20 to 40 years old. Idiosyncratic reactions may or may not be dependent on the amount of dose injected, the speed of injection and the radiographic procedure. Idiosyncratic reactions are subdivided into minor, intermediate, and severe. The minor reactions are self-limited and of short duration; the severe reactions are life-threatening and treatment is urgent and mandatory.

The reported incidence of adverse reactions to contrast media in patients with a history of allergy is twice that in the general population. Patients with a history of previous reactions to a contrast medium are three times more susceptible than other patients. However, sensitivity to contrast media does not appear to increase with repeated examinations.

Most adverse reactions to injectable contrast media appear within 1 to 3 minutes after the start of injection, but delayed reactions may occur.

Regardless of the contrast agent employed, the overall estimated incidence of serious adverse reactions is higher with angiocardiography than with other procedures. Cardiac decompensation, serious arrhythmias, angina pectoris, or myocardial ischemia or infarction may occur during angiocardiography and left ventriculography. Electrocardiographic and hemodynamic abnormalities occur less frequently with OMNIPAQUE than with diatrizoate meglumine and diatrizoate sodium injection.

References: 1. Gordon IJ, Skoblar RS, Chicatelli PD, et al: A comparison of iohexol and Conray-60 in peripheral arteriography. *AJR* 1984; 142:563-565. **2.** Enge I: Phlebography: Survey and present state. *Acta Radiol* 1983; suppl 366, pp 50-53. **3.** Wolf GL: Adult peripheral angiography: Results from four North American randomized clinical trials of ionic media versus iohexol. *Acta Radiol* 1983; suppl 366, pp 166-170. **4.** Egsgaard H, Hørup A, Praestholm J: Iohexol and diatrizoate in aortofemoral angiography: a controlled clinical trial. *Acta Radiol* 1983; suppl 366, p 173. **5.** Higgins CB, Mancini GBJ, Bloomquist JN, et al: Cardioangiography in man using iohexol and meglumine-Na diatrizoate: A comparison of hemodynamic and electrocardiographic effects. *Acta Radiol* 1983; suppl 366, pp 111-114.

Winthrop PHARMACEUTICALS

Winthrop Pharmaceuticals
Division of Sterling Drug Inc.
New York, NY 10016

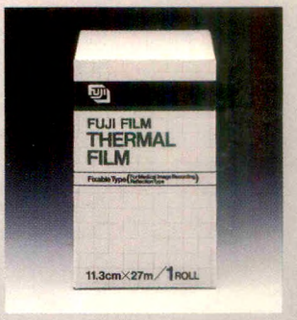
© 1987 WINTHROP PHARMACEUTICALS 7+73-3779



FUJI...Quality and Convenience!

FUJI FILM THERMAL IMAGING SYSTEM ■ World's only self-fixing, polyester base, thermal film ■ Sharper, clearer images ■ Superior archival quality ■ Fast – records up to 4 images per minute ■ Hard copy in only 22 seconds ■ No trips to the darkroom ■ 100% room light loading (300 exposures per roll) **■ No film processor required ■ Tough film base eliminates wrinkling**

With the push of a button or foot switch you can make a hard copy from a standard video signal – in room light – in just 22 seconds and make duplicate or enhanced originals using the built-in image memory. FUJI Thermal Film produces images that are sharper, clearer and last longer when compared to conventional thermal paper. FUJI's MI (Micro-Isolating) technology protects the images from the effects of heat and chemicals. Contact your FUJI MEDICAL SYSTEMS representative for a demonstration.



The world's only self-fixing polyester base, thermal film.

FUJI QUALITY UNCOMMONLY CONSISTENT.

I&I *Imaging & Information*

FUJI MEDICAL SYSTEMS U.S.A., INC.
90 Viaduct Road, Stamford, CT 06907
1-(800) 431-1850 (In CT-(203) 353-0300)

CIRCLE 7 ON READER SERVICE CARD

Volume 149 **American Journal of Roentgenology** July 1987

CHEST RADIOLOGY

1 **Sonographic guidance in diagnostic and therapeutic interventions in the pleural space.** *O'Moore PV, Mueller PR, Simeone JF, et al.*

9 **MR imaging of congenital anomalies of the aortic arch.** *Kersting-Sommerhoff BA, Sechtem UP, Fisher MR, Higgins CB*

15 **MR imaging of pulmonary arterial hypertension and pulmonary emboli.** *White RD, Winkler ML, Higgins CB*

23 **Pulmonary complications of cytosine-arabinoside therapy: radiographic findings.** *Tjon A Tham RTO, Peters WG, de Bruine FT, Willemze R*

29 **Paracardiac adenopathy: CT evaluation.** *Sussman SK, Halvorsen RA Jr, Silverman PM, Saeed M*

BREAST RADIOLOGY

35 **Mammographic changes after reduction mammoplasty.** *Miller CL, Feig SA, Fox JW IV*

39 **Localization of breast lesions identified on only one mammographic view.** *Kopans DB, Waitzkin ED, Linetsky L, et al.*

43 **Preoperative needle localization of lesions in the lower half of the breast: needle entry from below.** *Homer MJ*

GASTROINTESTINAL RADIOLOGY

47 **Radiographic appearance of mucosal dysplasia associated with ulcerative colitis.** *Hooyman JR, MacCarty RL, Carpenter HA, Schroeder KW, Carlson HC*

53 **High-resolution sonography of acute appendicitis.** *Abu-Yousef MM, Bleicher JJ, Maher JW, Urdaneta LF, Franken EA Jr, Metcalf AM*

59 **Percutaneous drainage of periappendiceal abscesses: review of 20 patients.** *Jeffrey RB Jr, Tolentino CS, Federle MP, Laing FC*

63 **Performance of barium examinations after acute myocardial infarction: report of a survey.** *Smith HJ*

67 **Case report. Sonographic findings in pancreatic lipomatosis.** *So CB, Cooperberg PL, Gibney RG, Bogoch A*

69 **Case report. Uptake of ^{99m}Tc-methylene diphosphonate by pancreatic insulinoma.** *Price J, Cockram CS, McGuire LJ, Crofts TJ, Stewart IET, Metreweli C*

71 **Duplex Doppler examination in portal hypertension: technique and anatomy.** *Patriquin H, Lafortune M, Burns PN, Dauzat M*

77 **Comparison of pulsed Doppler sonography and angiography in patients with portal hypertension.** *Nelson RC, Lovett KE, Chezmar JL, et al.*

83 **CT of giant cavernous hemangioma.** *Scatarige JC, Kenny JM, Fishman EK, Herlong FH, Siegelman SS*

87 **Hepatic infarcts: new observations by CT and sonography.** *Lev-Toaff AS, Friedman AC, Cohen LM, Radecki PD, Caroline DF*

91 **Technical note. External-internal cross-connection for bilateral percutaneous biliary drainage.** *Becker CD, Fache JS, Gibney RG, Burhenne HJ*

93 **Transcystic biopsy: a new approach to posterior pelvic lesions.** *Steiner E, Mueller PR, Simeone JF, Saini S, Hahn PF, Ferrucci JT Jr*

MUSCULOSKELETAL RADIOLOGY

97 **Potential contrast agents for MR arthrography: in vitro evaluation and practical observations.** *Hajek PC, Sartoris DJ, Neumann CH, Resnick D*

105 **Symptomatic intraspinal synovial cysts: opacification and treatment by percutaneous injection.** *Bjorkengren AG, Kurz LT, Resnick D, Sartoris DJ, Garfin SR*

109 **CT for determining the results of treatment of fractures of the wrist.** *Quinn SF, Murray W, Watkins T, Kloss J*

113 **The apical oblique view of the shoulder: its usefulness in acute trauma.** *Kornguth PJ, Salazar AM*

117 **The widened teardrop distance: a plain film indicator of hip joint effusion in adults.** *Sweeney JP, Helms CA, Minagi H, Louie KW*

120 **Opinion. Bone-mineral screening for osteoporosis.** *Hall FM*

123 **Case report. Antibiotic-containing acrylic beads: radiographic appearances.** *Daffner RH, Foss DE*

125 **Peroneal tendon injury associated with calcaneal fractures: CT findings.** *Rosenberg ZS, Feldman F, Singson RD, Price GJ*

GENITOURINARY RADIOLOGY

131 **Sonographic evaluation of renal stones treated by extracorporeal shock-wave lithotripsy.** *Baumgartner BR, Steinberg HV, Ambrose SS, Walton KN, Bernardino ME*

137 **Case report. Seminal vesicle abscess after vasectomy: evaluation by transrectal sonography and CT.** *Zagoria RJ, Papanicolaou N, Pfister RC, Stafford SA, Young HH II*

139 **Case report. Giant cyst of the seminal vesicle with renal agenesis.** *Heaney JA, Pfister RC, Meares EM Jr*

FETAL RADIOLOGY

141 **Midtrimester screening for open neural tube defects: correlation of sonography with amniocentesis results.** *Lindfors KK, McGahan JP, Tennant FP, Hanson FW, Walter JP*

147 **Case report. Diprosopus: diagnosis in utero.** *Okazaki JR, Wilson JL, Holmes SM, Vandermark LL*

NEURORADIOLOGY

149 **CSF pulsations within nonneoplastic spinal cord cysts.** *Enzmann DR, O'Donohue J, Rubin JB, Shuer L, Cogen P, Silverberg G*

159 **Differentiation of intramedullary neoplasms and cysts by MR.** *Williams AL, Haughton VM, Pojunas KW, Daniels DL, Kilgore DP*

165 **Radiation effects on cerebral white matter: MR evaluation.** *Tsuruda JS, Kortman KE, Bradley WG, Wheeler DC, Van Dalsem W, Bradley TP*

173 **Radiographic characteristics of skull fractures resulting from child abuse.** *Meservy CJ, Towbin R, McLaurin RL, Myers PA, Ball W*

VASCULAR RADIOLOGY

177 **Thrombosed dialysis grafts: efficacy of intrathrombic deposition of concentrated urokinase, clot maceration, and angioplasty.** *Davis GB, Dowd CF, Bookstein JJ, Maroney TP, Lang EV, Halasz N*

183 **Case report. Leiomyosarcoma of the portal vein.** *Wilson SR, Hine AL*

185 **Case report. Transcatheter occlusion of a profunda femoral artery pseudoaneurysm using thrombin.** *Walker TG, Geller SC, Brewster DC*

COMPUTERS IN RADIOLOGY

187 **Microcomputer applications for the academic radiologist.** *Amis ES Jr*

191 **A computerized filing system for radiology teaching cases.** *Sistrom CL, Black WC*

195 **Computer-aided design and realization of scientific exhibits in radiology.** *Chew FS, Hefner ML*

OPINION

199 **Diagnostic imaging interpretation: comprehensiveness means quality.** *Sartoris DJ*

OTHER CONTENT

6 **Memorial, Robert David Moseley, Jr.**

42 **Forthcoming articles**

28 **Books received**

194 **American Roentgen Ray Society officers and information**

201 **Review of current literature**

206 **Letters**

208 **ARRS 1988 meeting summary, calls for papers and exhibits**

213 **Meeting news. ICR, 1989**

214 **News**

219 **Classified ads**

Book reviews 8, 14, 22, 46, 52, 66, 82, 86, 96, 108, 112, 130, 136, 146, 158, 172, 176, 182

A3 **Guidelines for authors**

Hea.
7.4.88

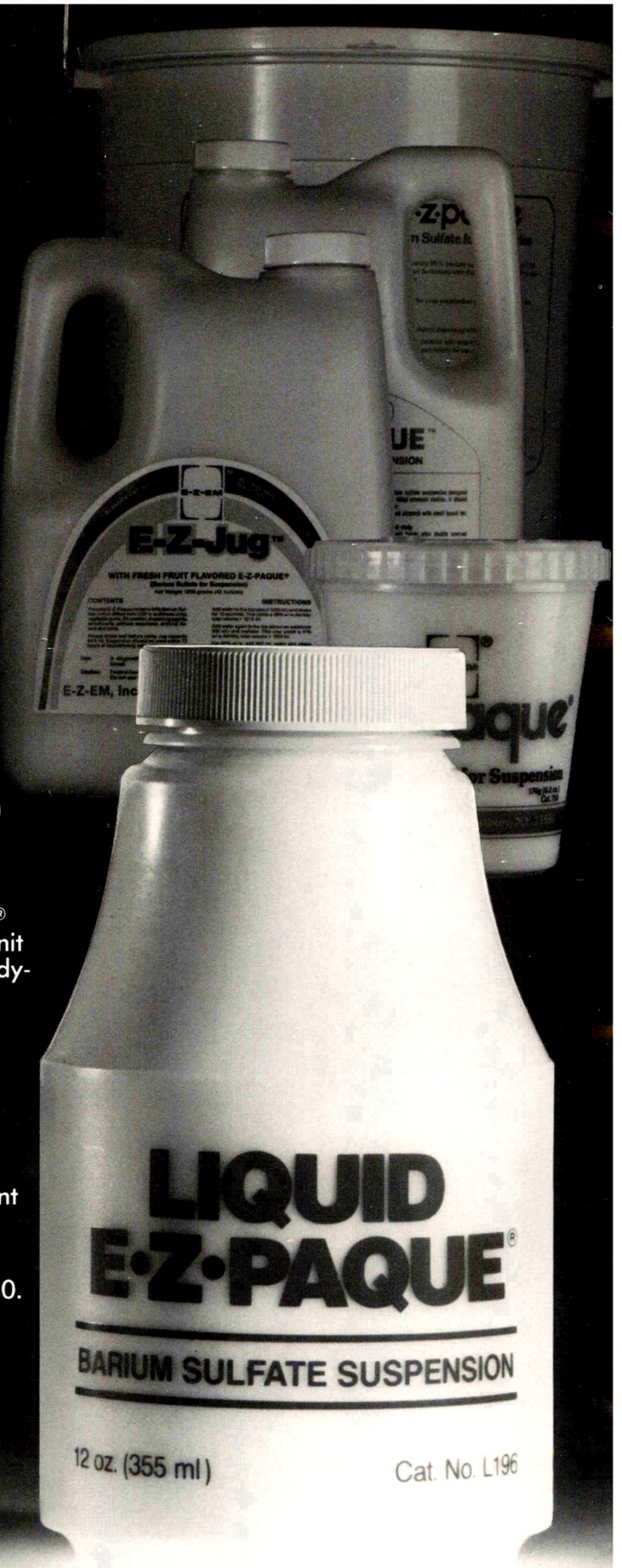
AJR

American
Journal of
Roentgenology

SUBSCRIBER

August 1987

A NEW ADDITION TO THE BEST-SELLING FAMILY OF BARIUM PRODUCTS



E-Z-EM introduces a new product to the E-Z-Paque® line of barium suspensions—Liquid E-Z-Paque® in unit dose bottles. This new packaging combines the ready-to-use convenience and consistency of a prepared suspension with the time-saving advantages of disposable, single-use bottles.

Improved Liquid E-Z-Paque in unit dose bottles is a multi-purpose, 60% w/v barium sulfate suspension which provides excellent results when used in small bowel and filled stomach studies. And, of course, it has a pleasant fruit flavor that gives excellent patient acceptance.

Ask your E-Z-EM dealer for a free sample, or call us at 1-800-645-3052. In New York, call 516-333-8230.

Cat. No. L196
24 bottles per case

E-Z-EM®
E-Z-EM, Inc.
7 Portland Ave.
Westbury, NY 11590
CIRCLE 30 ON READER SERVICE CARD

© E-Z-EM, Inc., 1987

Official Journal of the American Roentgen Ray Society

AJR

American Journal of Roentgenology
Diagnostic Imaging and Related Sciences

Editor-In-Chief Robert N. Berk, *San Diego, California*

Editor Emeritus Melvin M. Figley, *Seattle, Washington*

Associate Editor Saskia von Waldenburg Hilton, *San Diego, California*

Consulting Editor Juan M. Taveras, *Boston, Massachusetts*

Assistant Editors

John R. Amberg
William L. Ashburn
Lawrence W. Bassett
Charles C. Berry
Gregory P. Borkowski
William G. Bradley
Peter L. Cooperberg
Peter M. Doubilet
N. Reed Dunnick
David K. Edwards
Ronald G. Evens
David S. Feigin
William R. Hendee
Robert J. Herfkens
John R. Hesselink
Charles B. Higgins
Melvyn T. Korobkin
Thomas L. Lawson
Bruce L. McClennan
Albert A. Moss
Jeffrey H. Newhouse
Donald L. Resnick
Stewart R. Reuter
Stuart S. Sagel
David J. Sartoris
Edward A. Sickles
Barry A. Siegel
Eric vanSonnenberg
David D. Stark
Edward T. Stewart

Editorial Staff: Elizabeth A. Whalen, *publications supervisor*; Linda Wood, Barbara Rose, and Barbara L. Halliburton, *manuscript editors*; Nancy Rydbeck, *office manager*; Sandra Wood, *administrative assistant*.

All business correspondence, including display (not classified) advertising, subscriptions, address changes, reprints, and permission requests should be addressed to Williams & Wilkins, 428 East Preston Street, Baltimore, MD 21202. Correspondence regarding editorial matters and classified advertising should be addressed to the editorial office, AJR, 2223 Avenida de la Playa, Suite 200, La Jolla, CA 92037-3218. For manuscript submission, see Guidelines for Authors, next page. Undelivered or damaged copies replaced within 60 days of publication; 90 days for foreign subscribers. Allow 90 days for address changes.
AJR, AMERICAN JOURNAL OF ROENTGENOLOGY (ISSN 0361 803X) is published monthly by American Roentgen Ray Society, 428 E. Preston Street, Baltimore, MD 21202. Annual dues include $50 for journal subscription. Second class postage paid at Baltimore, MD and at additional mailing offices. Postmaster send address changes (Form 3579) to Williams & Wilkins, 428 East Preston St., Baltimore, MD 21202. Subscription rates $90 ($120 foreign); institutions $100 ($130 foreign); in training $25; single copy $16 ($19). Japanese yen price is available from our sole agent USACO Corporation, 13-12, Shimbashi 1-Chome, Minato-Ku, Tokyo 105, Japan, telephone 03-502-6471. Airmail rates furnished on request. Indexed by *Current Contents* and *Index Medicus*.
Copyright © 1987 by American Roentgen Ray Society.
0361-803X/87$2.00

Tecnomed USA

BAY SHORE MEDICAL EQUIPMENT CORP.

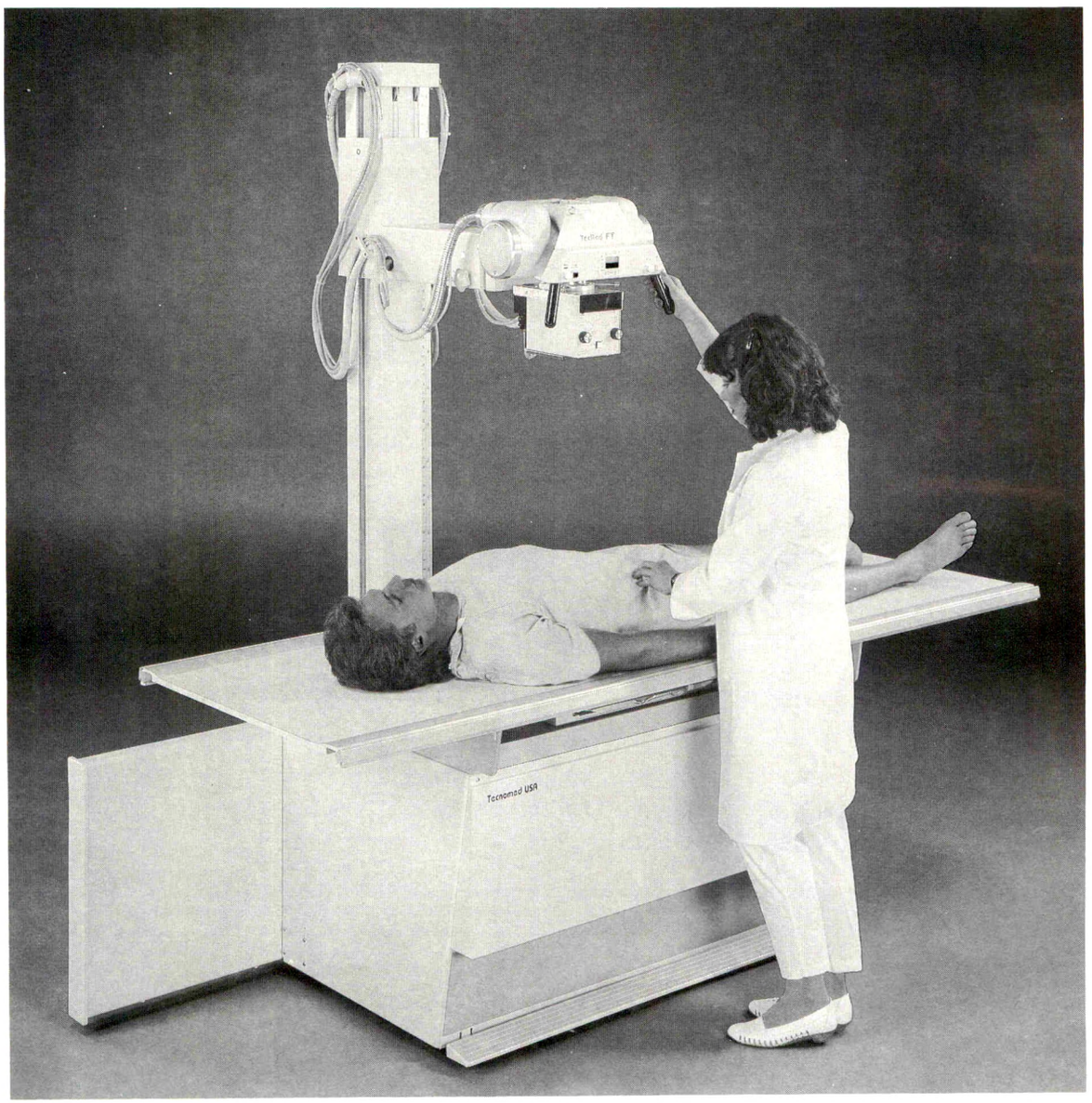
TecRad™ FT Radiographic System

The TecRad FT general radiographic system consists of a 600 mA single phase x-ray generator, a four-way floating top, horizontal bucky table, integrally mounted tubestand with X-ray tube and collimator. The basic system has several optional components that may be added to, or substituted for, basic components to tailor a system to specific needs. System construction makes it suitable for use in hospitals as a back up radiographic room, in outpatient departments, clinics, public health agencies, industrial clinics, or orthopedic clinics.

The TecRad generator consists of a solid state control with a separate high voltage transformer. The transformer is housed within the table body in single room installations. This generator is limited to radiographic capabilities with no provision for fluoroscopic functions.

The TecRad FT table consists of a table base, housing the electronics and high voltage transformer, a bucky assembly, a four-way floating radiographic table top and an integrally mounted tubestand.

The combined tubestand and bucky travel permits a radiographic center to center coverage of 65 inches (1651 mm). This travel permits head to toe radiographic coverage on an average adult patient without having to move the patient. Tubestand motions permit cart radiography behind the table, off table stretcher or wheel chair radiography, cross table laterals and decubitus exposures, angled views of the skull or trunk of the body, and upright studies with wall cassette or erect bucky devices.



™ TecRad is a trademark of Bay Shore Medical Equipment Corporation.

235 South Fehr Way, Bay Shore, New York 11706 • 516/586-1991-Telex II 510-227-9837
Telefax 516/242-4421

CIRCLE 28 ON READER SERVICE CARD

AJR Guidelines for Authors

Address new and revised manuscripts, correspondence, and classified ads to the Editor:

AJR Editorial Office
2223 Avenida de la Playa, Suite 200
La Jolla, CA 92037-3218 Telephone: (619) 459-2229

Inquiries regarding subscriptions, display advertising, reprints, or permission to republish *AJR* material should be addressed to the publisher:

The Williams & Wilkins Co.
428 E. Preston St.
Baltimore, MD 21202 Telephone: (301) 528-4133

The *AJR* publishes original contributions to the advancement of medical diagnosis and treatment. Submitted manuscripts should not contain previously published material and should not be under consideration for publication elsewhere. Papers dealing with neuroradiology should be addressed to: American Journal of Neuroradiology, Dept. of Radiology, Massachusetts General Hospital, Boston, MA 02114. At the discretion of the *AJR* Editor, *AJNR* articles that are of interest to the general reader may be republished in the *AJR*. Neuroradiologic papers sent to the *AJR* will be forwarded to the Editorial Office of the *AJNR*.

Manuscript decisions are based on peer review. Reviewers receive manuscripts without title pages to ensure an unbiased review. All accepted manuscripts are subject to editing. Statements made in the article, including changes made by the Editor or manuscript editor, are the responsibility of the author and not of the *AJR* or its publisher. Authors will be sent the edited manuscript, galley proof, and proofs of illustrations. If the corresponding author will be unavailable to review galleys, arrangements should be made for a coauthor or colleague to read and return the proof.

General Guidelines for Major Papers

Abstract. Clearly state (in 200 words or less) the purpose, methods, results, and conclusions of the study. Include actual data.

Introduction. Briefly describe the purpose of the investigation, including relevant background information.

Methods. Describe the research plan, the materials (or subjects), and the methods used, in that order. Explain in detail how disease was confirmed and how subjectivity in observations was controlled.

Results. Present results in a clear, logical sequence. If tables are used, do not duplicate tabular data in text, but do describe important trends and points.

Discussion. Describe the limitations of the research plan, materials (or subjects), and methods, considering both the purpose and the outcome of the study. When results differ from those of previous investigators, explain the discrepancy.

AUTHOR'S CHECKLIST

For priority handling, complete the following checklist, sign the copyright form on the reverse side of this page, and include both with the manuscript.

_____ Two copies of the manuscript (the original and a photocopy) and two complete sets of figures are submitted. One copy has been retained by the author.

_____ If appropriate, *AJR* Guidelines for case reports, technical notes, pictorial essays, or letters to the Editor have been followed. (See page A5.)

_____ The manuscript, including references, figure legends, and tables, is typed double-spaced on 8½ × 11 in. (21.6 × 27.9 cm) nonerasable paper. Right-hand margins are not justified.

_____ All manuscript pages are numbered consecutively beginning with the abstract. Authors' names do not appear on the manuscript pages.

_____ The manuscript is organized as follows: title page, blind title page (title only), abstract, introduction, methods, results, discussion, acknowledgments, references, tables, figure legends, and figures.

_____ Informed consent has been obtained from patients who participated in clinical investigations. If experiments were performed on animals, authors complied with NIH guidelines for use of laboratory animals.

_____ Use of unfamiliar acronyms and abbrevations is kept to a minimum. When abbreviations are used they are defined at first mention, followed by the abbreviation in parentheses.

_____ Metric measurements are used throughout, or the metric equivalent is given in parentheses.

_____ Names and locations (city and state only) of manufacturers are given for equipment and nongeneric drugs.

Title Page

_____ The following information is given: title of article; names and complete addresses (including zip code) of all authors; current addresses of authors who have moved since study; acknowledgment of grant or other assistance. The corresponding author is clearly identified, and a current address and phone number are given.

_____ Two copies of a blind title page are included giving only the title (without the authors' names) for use in the review process.

Abstract

_____ An abstract of approximately 200 words concisely states the purpose, methods, and results of the study in one paragraph. Actual data are included.

_____ No abbreviations or reference citations are used.

_____ Conclusions are stated in a second, summary paragraph.

References

_____ References (not to exceed 35) are typed double-spaced starting on a separate page and are **numbered consecutively in the order in which they appear in the text.**

_____ All references are cited in the text and are enclosed in brackets and typed on line with the text (not superscript).

_____ Unpublished data are not cited in the reference list, but are cited parenthetically in the text, for example, (Smith DJ, personal communication), (Smith DJ, unpublished data). This includes papers submitted, but not yet accepted, for publication.

_____ Inclusive page numbers (e.g., 333–335) are given for all references.

_____ Journal names are abbreviated according to *Index Medicus*.

_____ Style and punctuation of references follow the format illustrated in the following examples (all authors are listed when six or less; when seven or more authors, the first three are listed, followed by "et al."):

Journal article

1. Long RS, Roe EW, Wu EU, et al. Membrane oxygenation: radiographic appearance. *AJR* **1986**;146:1257–1260

Book

2. Smith LW, Cohen AR. *Pathology of tumors*, 6th ed. Baltimore: Williams & Wilkins, **1977**:100–109

Chapter in a book

3. Breon AJ. Serum monitors of bone metastasis. In: Clark SA, ed. *Bone metastases*. Baltimore: Williams & Wilkins, **1983**:165–180

Paper presented at a meeting

4. Lau FS, Kirk AN, Beck RA. MR imaging of the spine. Presented at the annual meeting of the American Roentgen Ray Society, Washington, DC, April 1986

Tables

_____ Each table is typed double-spaced on a separate page without vertical or horizontal rules; each has a short, descriptive title. Tables do not exceed two pages in length and contain at least four lines of data.

_____ Tables are numbered in the order in which they are cited in the text.

_____ Abbreviations are defined in an explanatory note below each table.

_____ Tables are self-explanatory and do not duplicate data given in the text or figures.

_____ All arithmetic (percentages, totals, differences) has been double checked for accuracy, and tabular data agree with data given in the text.

Figures and Legends

_____ Two complete sets of original figures are submitted unmounted in labeled envelopes.

_____ Figures are clean, unscratched, 5 × 7 in. (13 × 18 cm) glossy prints with white borders. A separate print is submitted for each figure *part*.

_____ All figure parts relating to one patient are in one figure.

_____ Each figure is labeled on the back with the figure number and an arrow indicating "top." Labeling is done on a gummed label, which is then affixed to the back of the print. (Never use ink on front or back of figures.)

_____ Author's names are *not* written on the backs of figures.

_____ Only removable (rub-on) arrows and letters are used on the figures. Symbols are uniform in size and style and are not broken or cracked.

_____ Images are uniform in size and magnification.

_____ Line drawings are done in black ink on a white background and are of professional quality. (Only glossy prints, not originals or photocopies, are acceptable.)

_____ Written permission has been obtained for use of all previously published illustrations (and copies of permission letters are included), and an appropriate credit line is given in the legends.

_____ Legends are typed double-spaced, and figure numbers correspond with the order in which the figures are cited in the text.

Transfer of Copyright Agreement and Exclusive Publication Statement

Complete copyright to the article entitled: _____

_____

is hereby transferred to the American Roentgen Ray Society (for United States government employees to the extent transferable), effective if and when the article is accepted for publication in the *American Journal of Roentgenology*. In the case of the authors who are officers or employees of the United States government, the American Roentgen Ray Society recognizes that works prepared by officers or employees of the United States government as part of their official government duties are in the public domain.

Authors reserve all proprietary rights other than copyright, such as patent rights and the right to use all or part of this article in future works of their own. The authors retain the right of replication, subject only to crediting the original source of publication and receiving written permission from the publisher.

Authors guarantee that this manuscript contains no matter that is libelous or otherwise unlawful, invades individual privacy, or infringes any proprietary rights.

Authors understand that they will receive no royalty or other compensation from the American Roentgen Ray Society or the publisher.

Finally, the authors certify that none of the material in this manuscript has been published previously or is currently under consideration for publication elsewhere.

_____	_____	_____
First author/date	Second author	Third author
_____	_____	_____
_____	_____	_____

This agreement must be signed by all authors in order for the manuscript to be published.

Case Reports

A case report is a brief description of a special case that provides a message that transcends the individual patient.

Format. There is no abstract. The introduction should be a short paragraph giving the general background and the specific interest of the case. No more than one case should be described in detail (similar ones can be mentioned briefly in the discussion). Emphasis should be on the radiologic aspects; clinical information must be limited to that necessary to provide a background for the radiology. The discussion should be succinct and should focus on the specific message and relevance of radiologic methods. A review of the literature is not appropriate.

Length. Maximum of five double-spaced, typewritten pages, including the references but not the title page or figure legends.

References. Maximum of eight.

Figures. Maximum of three or four, unless the text is shortened accordingly. Legends must not repeat the text.

Tables and Acknowledgments. Not appropriate in case reports.

Technical Notes

A technical note is a brief description of a specific technique or procedure, modification of a technique, or equipment of interest to radiologists.

Format. No abstract, headings, or subheadings are required. If headings are used, they should be a combination of "Case Report," "Materials and Methods," "Results," and "Discussion." A brief one-paragraph introduction should be included to give the general background. Discussion should be limited to the specific message, including the uses of the technique or equipment. Literature reviews and lengthy case reports are not appropriate.

Length. Maximum of five double-spaced, typewritten pages, including the references but not the title page or figure legends.

References. Maximum of eight.

Figures. Maximum of two, unless the text is shortened accordingly.

Tables and Acknowledgments. Not appropriate in technical notes.

Pictorial Essays

A pictorial essay is an article that conveys its message through illustrations and their legends. Unlike other *AJR* articles, which are based on original research, pictorial essays serve primarily as teaching tools, like exhibits at a scientific meeting. They are not encyclopedic book chapters. No abstract is necessary.

Length. Maximum of four double-spaced, typewritten pages, including the references but not the title page or figure legends.

References. Maximum of four.

Figures. Maximum of 30 figure *parts*. Number should be as few as necessary to convey the message of the paper.

Tables and Acknowledgments. Not appropriate in pictorial essays.

Letters to the Editor and Replies

Letters to the Editor and Replies should offer objective and constructive criticism of published articles. Letters may also discuss matters of general interest to radiologists.

Format. All letters should be typed double-spaced on nonletterhead paper, with no greeting or salutation. Signature and affiliation should appear at the end of the letter. Titles for letters should be short and pertinent. The title for a reply is simply "Reply."

Length. Maximum of two double-spaced, typewritten pages, including references.

References. Maximum of four.

Figures. Maximum of two.

Tables and Acknowledgments. Not appropriate in Letters to the Editor and Replies.

Opinions, Commentaries, and Perspectives

Opinions, commentaries, and perspectives are special articles dealing with controversial topics or issues of special concern to radiologists.

Format. Include a title page but no abstract. Headings may be used to break up the text.

Length. Maximum of five double-spaced, typewritten pages.

References. Maximum of five.

Tables and Figures. Maximum of four.

Computer Page Articles

Articles published on the computer page deal with practical computer applications to radiology.

Format. Include a title page but no abstract.

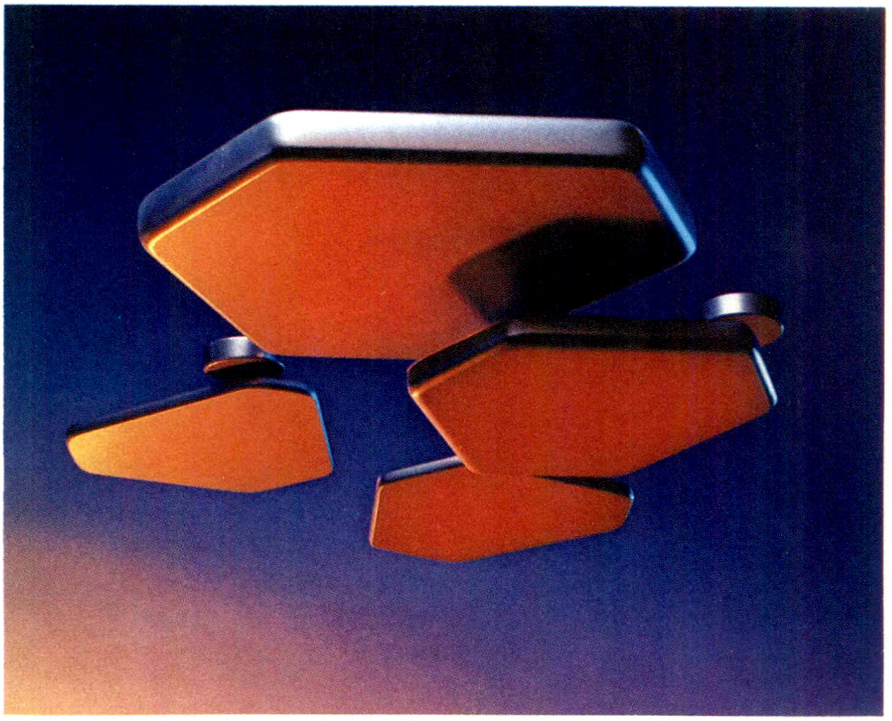
Length. Maximum of eight double-spaced, typewritten pages.

References. Maximum of five.

Figures and Tables. Maximum of five. Computer printouts are not acceptable. Figures must be submitted as 5 × 7 in. glossy prints.

All submissions to the *AJR* must be accompanied by a completed copy of the Author's Checklist and the signed Copyright Agreement.

A SHARPER PORTRAIT FROM KODAK



Exclusive Kodak T-Grain emulsions give Kodak T-Mat films extra sharpness that can only mean more detailed "portraits" for better diagnoses. See the difference on your viewbox.

Kodak T-Mat films. The only x-ray films in the world with the sharpness of T-Grain emulsions. A sharpness your Kodak representative can show you, on your own viewbox, in a side-by-side comparison with your present film. It's sharpness you can see, plus all the benefits of rare-earth imaging, including the exposure-reducing speed. At no increase in cost, with even more processing latitude.

And now there is Kodak CFT film, an extremely fine-grain film for cinefluorography with T-Grain emulsion. For a demonstration of the sharpness difference T-Mat films can make, talk to your Kodak representative.

The new vision of Kodak

Kodak

©Eastman Kodak Company, 1987

MAST™ AND STIR™. WHY SETTLE FOR LESS?

Best Image Quality.

Accurate diagnoses depend on it.
Referring physicians demand it.
Your MR service must provide it.
And now you don't have to settle for less.

Motion Artifact Suppression Technique (MAST™).

Only VISTA® offers enhanced spatial resolution with motion artifact suppression so effective that it eliminates artifacts caused by complex motions such as velocity, acceleration and pulsatility. Now with MAST you don't have to settle for anything less than the best image quality.

Short Tau Inversion Recovery (STIR™).

VISTA is the only system to offer Short Tau Inversion Recovery (STIR), which features the best contrast resolution on multi-slice studies of soft tissue. STIR suppresses the signal from fat tissue for a clear delineation between fat and nearby soft tissue. Now, with the high contrast provided with STIR, you don't have to settle for anything less than the best image quality.

Increased Referrals.

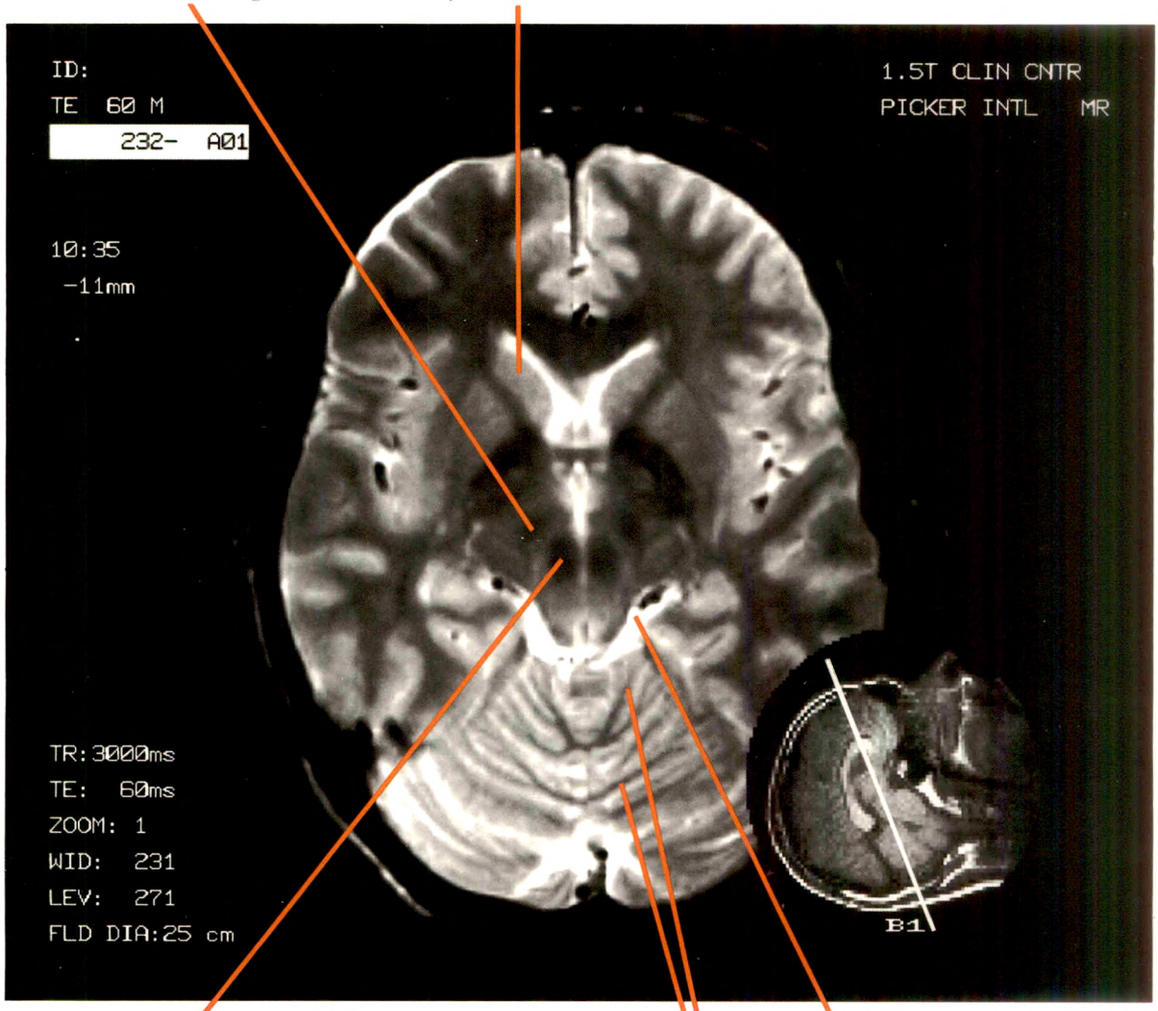
The success of your MR Service depends on its ability to compete. On its ability to build a strong referral base. MAST and STIR are two unique VISTA capabilities which provide uncompromised image quality, a necessity for referral building. But VISTA offers more. 512 x 512 acquisition and display for the highest resolution images available. Three-angle oblique imaging for superior heart and spine studies. Specialized research programs for cardiac, neuro and orthopedic specialties. Reference Pilot Scan for immediate localization of slice position. And much more.

VISTA® . . .Why Settle for Less?

CIRCLE 13 ON READER SERVICE CARD

Some features of Picker's VISTA MR systems are classified as investigational devices and limited by federal law to investigational use. As such, they cannot be made available until necessary government approvals have been granted.

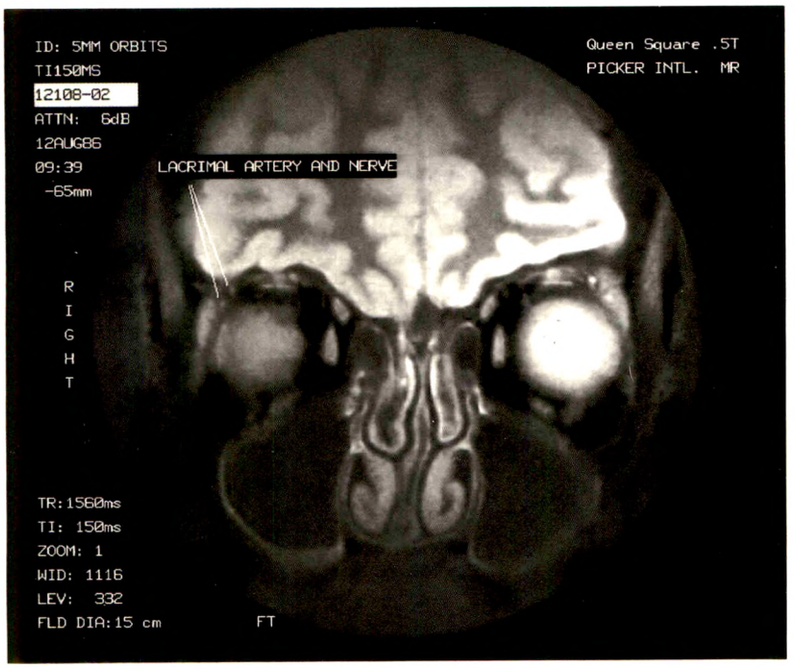
Anatomy of VISTA® MR Image Quality



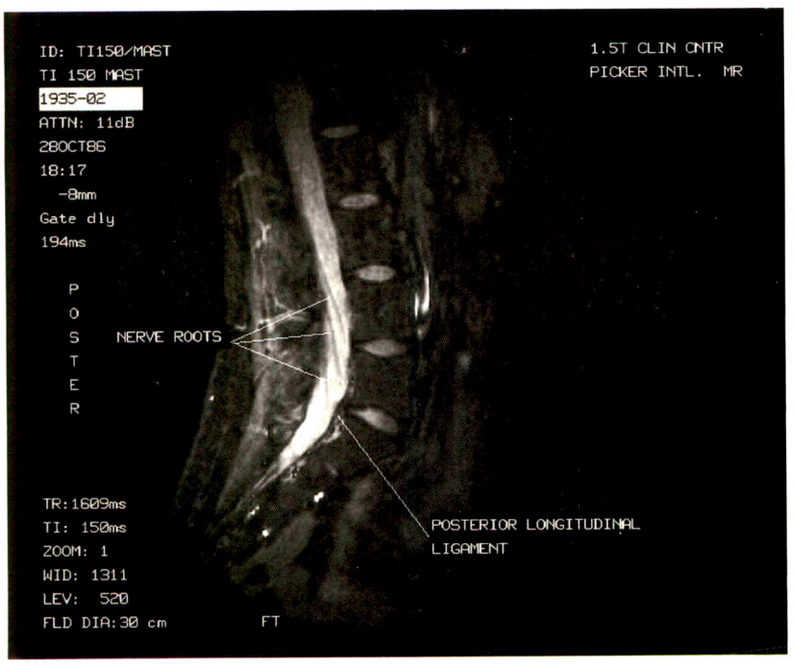
PICKER

THE IMAGE OF EXCELLENCE

VISTA® Referral Building Image Quality



This demyelinating plaque study uses STIR for exquisite delineation of orbital contents. STIR enables fat suppression and highlights structures not easily visualized with other MR protocols, as shown by visualization of the lacrimal artery and nerve.



This unique sequence combination of Short Tau Inversion Recovery (STIR) and Motion Artifact Suppression Technique (MAST) results in excellent fat suppression in vertebral bodies of the normal spine. With MAST, nerve roots are sharply contrasted against the bright signal imparted on the basivertebral drainage system.

PICKER

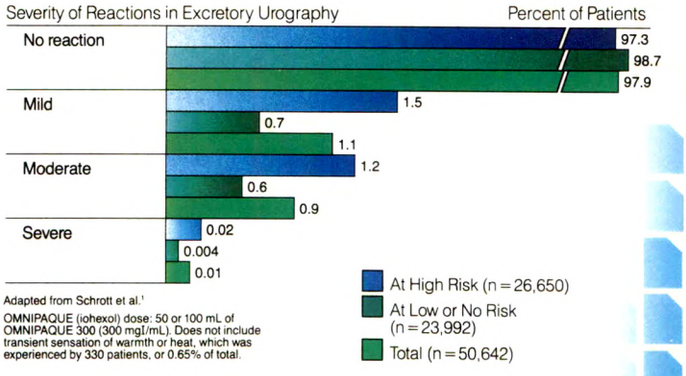
THE IMAGE OF EXCELLENCE

In excretory urography:

Because you can't be sure how every patient will react...

Improve the safety profile.

In a 50,642-patient clinical study, 97.9% had no reported adverse reactions.



Adapted from Schrott et al.[1]

OMNIPAQUE (iohexol) dose: 50 or 100 mL of OMNIPAQUE 300 (300 mgI/mL). Does not include transient sensation of warmth or heat, which was experienced by 330 patients, or 0.65% of total.

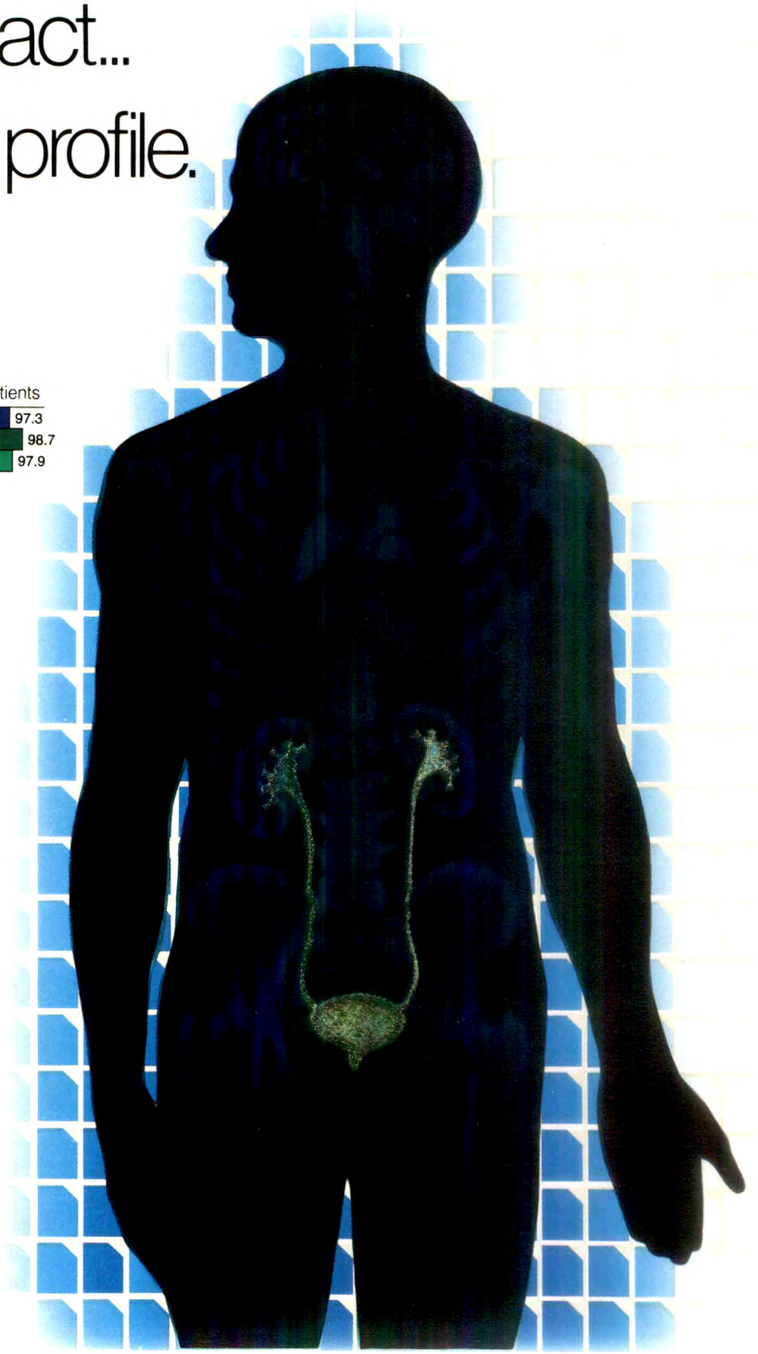
Of 26,650 patients considered high risk, 97.3% had no reported adverse effects.[1]

Of 7,629 patients hypersensitive to iodinated contrast media, 95.9% had no reported adverse effects.[1]

Excellent patient comfort.[2]

Excellent diagnostic quality.[2]

Physicians should consider the potential benefit-to-risk ratio prior to radiographic procedures.



NONIONIC

OMNIPAQUE®

(IOHEXOL)

THE NEW STANDARD IN

See next page for important product information concerning contraindications, warnings, adverse reactions, patient selection, and precautionary recommendations.



OMNIPAQUE
INJECTION (IOHEXOL) INTRAVASCULAR

240

300

350

PLEASE CONSULT FULL PRODUCT INFORMATION BEFORE USING.
A SUMMARY FOLLOWS:

DESCRIPTION: OMNIPAQUE is a nonionic, water-soluble radiographic contrast medium for intravascular administration and is provided in iodine concentrations of 240, 300, and 350 mgI/mL. Each milliliter of iohexol solution contains 1.21 mg tromethamine and 0.1 mg edetate calcium disodium with the pH adjusted between 6.8 and 7.7 with hydrochloric acid or sodium hydroxide, but it contains no preservatives.

CONTRAINDICATIONS: OMNIPAQUE should not be administered to patients with a known hypersensitivity to iohexol.

WARNINGS: OMNIPAQUE should be used with extreme care in patients with: severely impaired renal and/or hepatic function; severe thyrotoxicosis, hyperthyroidism, or an autonomously functioning thyroid nodule; diabetes with a serum creatinine level above 3 mg/dL. Not recommended for use in patients with anuria.

Patients with known or suspected pheochromocytoma should receive a minimum of contrast medium if benefit of the exam is judged to outweigh risk; blood pressure should be monitored throughout the procedure, and measures for the treatment of hypertensive crisis should be readily available.

Contrast agents are potentially hazardous in patients with multiple myeloma or other paraproteinemia, particularly those with therapeutically resistant anuria. The combination of contrast agent and dehydration may precipitate myeloma protein in the renal tubules. No form of therapy, including dialysis, has been successful in reversing the effect. Myeloma, which occurs most commonly in persons over age 40, should be considered before instituting intravascular administration of contrast agents.

PRECAUTIONS: Diagnostic procedures that involve the use of radiopaque diagnostic agents should be carried out under the direction of personnel with the prerequisite training and with a thorough knowledge of the particular procedure to be performed. Appropriate facilities should be available for coping with any complication of the procedure, as well as for emergency treatment of severe reactions to the contrast agent itself. Competent personnel and emergency facilities should be available for at least 30 to 60 minutes postprocedure. The possibility of serious, life-threatening, fatal, anaphylactoid, or cardiovascular reactions should always be considered (see ADVERSE REACTIONS). It is of utmost importance that a course of action be carefully planned in advance for immediate treatment of serious reactions. Preparatory dehydration is dangerous and may contribute to acute renal failure in patients with advanced vascular disease, diabetic patients, and in susceptible nondiabetic patients (often elderly with preexisting renal disease). *Patients should be well hydrated prior to and following iohexol administration.* Careful consideration to the potential risk of acute renal failure should be given before performing excretory urography in diabetic patients with diabetic nephropathy and in susceptible nondiabetic patients (often elderly with preexisting renal disease). Immediately following surgery, excretory urography should be used with caution in renal transplant recipients. The possibility of an idiosyncratic reaction in susceptible patients should always be considered (see ADVERSE REACTIONS). The susceptible population includes patients with a history of a previous reaction to contrast media, patients with a known sensitivity to iodine per se, and patients with a known clinical hypersensitivity: bronchial asthma, hay fever, and food allergies. A thorough medical history with emphasis on allergy and hypersensitivity, prior to the injection of any contrast media, may be more accurate than pretesting in predicting potential adverse reactions.

A positive history of allergies or hypersensitivity does not arbitrarily contraindicate the use of a contrast agent where a diagnostic procedure is thought essential, but caution should be exercised (see ADVERSE REACTIONS). Premedication with antihistamines or corticosteroids to avoid or minimize possible allergic reactions in such patients should be considered. Recent reports indicate that such pretreatment does not prevent serious, life-threatening reactions but may reduce both their incidence and severity.

Even though the osmolality of OMNIPAQUE is low compared to diatrizoate- or iothalamate-based ionic agents of comparable iodine concentration, the potential transitory increase in circulatory osmotic load in patients with congestive heart failure requires caution during injection. These patients should be observed for several hours following the procedure to detect delayed hemodynamic disturbances.

Angiography should be avoided whenever possible in patients with homocystinuria, because of the risk of inducing thrombosis and embolism.

In angiographic procedures, the possibility of dislodging plaques or damaging or perforating the vessel wall should be borne in mind during the catheter manipulations and contrast medium injection. Test injections to ensure proper catheter placement are recommended.

Selective coronary arteriography should be performed only in those patients in whom the expected benefits outweigh the potential risk. The inherent risks of angiocardiography in patients with chronic pulmonary emphysema must be weighed against the necessity for performing this procedure.

When OMNIPAQUE is to be injected using plastic disposable syringes, the contrast medium should be drawn into the syringe and used immediately.

The inhibitory effects of nonionic contrast media on mechanisms of hemostasis have been shown, in vitro, to be less than those of ionic contrast media at comparable concentrations. For this reason, standard angiographic procedures should always be followed: angiographic catheters should be flushed frequently, and prolonged contact of blood with contrast media in syringes and catheters should be avoided.

If nondisposable equipment is used, scrupulous care should be taken to prevent residual contamination with traces of cleansing agents.

Drug/Laboratory Test Interaction: If iodine-containing isotopes are to be administered for the diagnosis of thyroid disease, the iodine-binding capacity of thyroid tissue may be reduced for up to 2 weeks after contrast medium administration. Thyroid function tests which do not depend on iodine estimation, eg, T$_3$ resin uptake or direct thyroxine assays, are not affected.

Carcinogenesis, Mutagenesis, Impairment of Fertility: No long-term animal studies have been performed to evaluate carcinogenic potential, mutagenesis, or whether OMNIPAQUE can affect fertility in men or women.

Pregnancy Category B: Reproduction studies have been performed in rats and rabbits with up to 100 times the recommended human dose. No evidence of impaired fertility or harm to the fetus has been demonstrated due to OMNIPAQUE. There are, however, no studies in pregnant women. Because animal reproduction studies are not always predictive of human response, this drug should be used during pregnancy only if clearly needed.

Nursing Mothers: It is not known to what extent iohexol is excreted in human milk. However, many injectable contrast agents are excreted unchanged in human milk. Although it has not been established that serious adverse reactions occur in nursing infants, caution should be exercised when intravascular contrast media are administered to nursing women. Bottle feedings may be substituted for breast feedings for 24 hours following administration of OMNIPAQUE.

Pediatric Use: Safety and effectiveness in children have not been established.

ADVERSE REACTIONS: Usually mild to moderate in severity. However, serious, life-threatening, and fatal reactions, mostly of cardiovascular origin, have been associated with the administration of iodine-containing contrast media including OMNIPAQUE. The injection of contrast media is frequently associated with the sensation of warmth and pain, especially in peripheral angiography; pain and warmth are less frequent and less severe with OMNIPAQUE than with many contrast media.

Cardiovascular System: Arrhythmias including PVCs and PACs (3%), angina/chest pain (2%), and hypotension (1%). Others including cardiac failure, asystole, bradycardia, tachycardia, and vasovagal reaction were reported with an individual incidence of less than 0.8%. In controlled clinical trials involving 900 patients, one fatality occurred. A cause-and-effect relationship between this death and iohexol has not been established.

Nervous System: Pain (6%), photomas (3%), headache (2%), and metallic taste (0.8%). Others including anxiety, blurred vision, dizziness, fever, motor and speech dysfunction, convulsion, lightheadedness, paresthesia, somnolence, vertigo, stiff neck, hemiparesis, and nystagmus were reported, with an individual incidence of less than 0.3%.

Respiratory System: Dyspnea and laryngitis, with an individual incidence of 0.1%.

Gastrointestinal System: Nausea (2%) and vomiting (0.5%). Others including diarrhea, dyspepsia, and dry mouth were reported, with an individual incidence of 0.1%.

Skin and Appendages: Urticaria (0.3%) and purpura (0.1%).

General Adverse Reactions to Contrast Media: The following reactions have been reported after administration of other intravascular iodinated contrast media. *Reactions due to technique:* hematomas and ecchymoses. *Hemodynamic reactions:* vein cramp and thrombophlebitis following intravenous injection. *Cardiovascular reactions:* rare cases of cardiac arrhythmias, reflex tachycardia, chest pain, cyanosis, hypertension, hypotension, peripheral vasodilatation, shock, and cardiac arrest. *Renal reactions:* occasionally, transient proteinuria; rarely, oliguria or anuria. *Allergic reactions:* asthmatic attacks, nasal and conjunctival symptoms, dermal reactions such as urticaria with or without pruritus, as well as pleomorphic rashes, sneezing, and lacrimation; rarely, anaphylactic reactions. Rare fatalities have occurred due to these or unknown causes. *Signs and symptoms related to the respiratory system:* pulmonary or laryngeal edema, bronchospasm, dyspnea; or *to the nervous system:* restlessness, tremors, convulsions. *Other reactions:* flushing, pain, warmth, metallic taste, nausea, vomiting, anxiety, headache, confusion, pallor, weakness, sweating, localized areas of edema (especially facial cramps), neutropenia, and dizziness. Rarely, immediate or delayed rigors can occur, sometimes accompanied by hyperpyrexia. Infrequently, "iodism" (salivary gland swelling) from organic iodinated compounds appears 2 days after exposure and subsides by the sixth day.

In general, the reactions that are known to occur upon parenteral administration of iodinated contrast agents are possible with any nonionic agent. Approximately 95% of adverse reactions accompanying the use of water-soluble intravascularly administered contrast agents are mild to moderate in degree. However, severe, life-threatening anaphylactoid reactions, mostly of cardiovascular origin, have occurred.

Reported incidences of death range from 6.6 per 1 million (0.00066%) to 1 in 10,000 (0.01%). Most deaths occur during injection or 5 to 10 minutes later, the main feature being cardiac arrest, with cardiovascular disease as the main aggravating factor. Isolated reports of hypotensive collapse and shock are found in the literature. The incidence of shock is estimated to be 1 out of 10,000 (0.005%) patients.

Adverse reactions to injectable contrast media fall into two categories: chemotoxic reactions and idiosyncratic reactions.

Chemotoxic reactions result from the physicochemical properties of the contrast media, the amount of dose injected, and the speed of injection. All hemodynamic disturbances and injuries to organs or vessels perfused by the contrast medium are included in this category.

Idiosyncratic reactions include all other reactions. They occur more frequently in patients 20 to 40 years old. Idiosyncratic reactions may or may not be dependent on the amount of dose injected, the speed of injection and the radiographic procedure. Idiosyncratic reactions are subdivided into minor, intermediate, and severe. The minor reactions are self-limited and of short duration; the severe reactions are life-threatening and treatment is urgent and mandatory.

The reported incidence of adverse reactions to contrast media in patients with a history of allergy is twice that in the general population. Patients with a history of previous reactions to a contrast medium are three times more susceptible than other patients. However, sensitivity to contrast media does not appear to increase with repeated examinations.

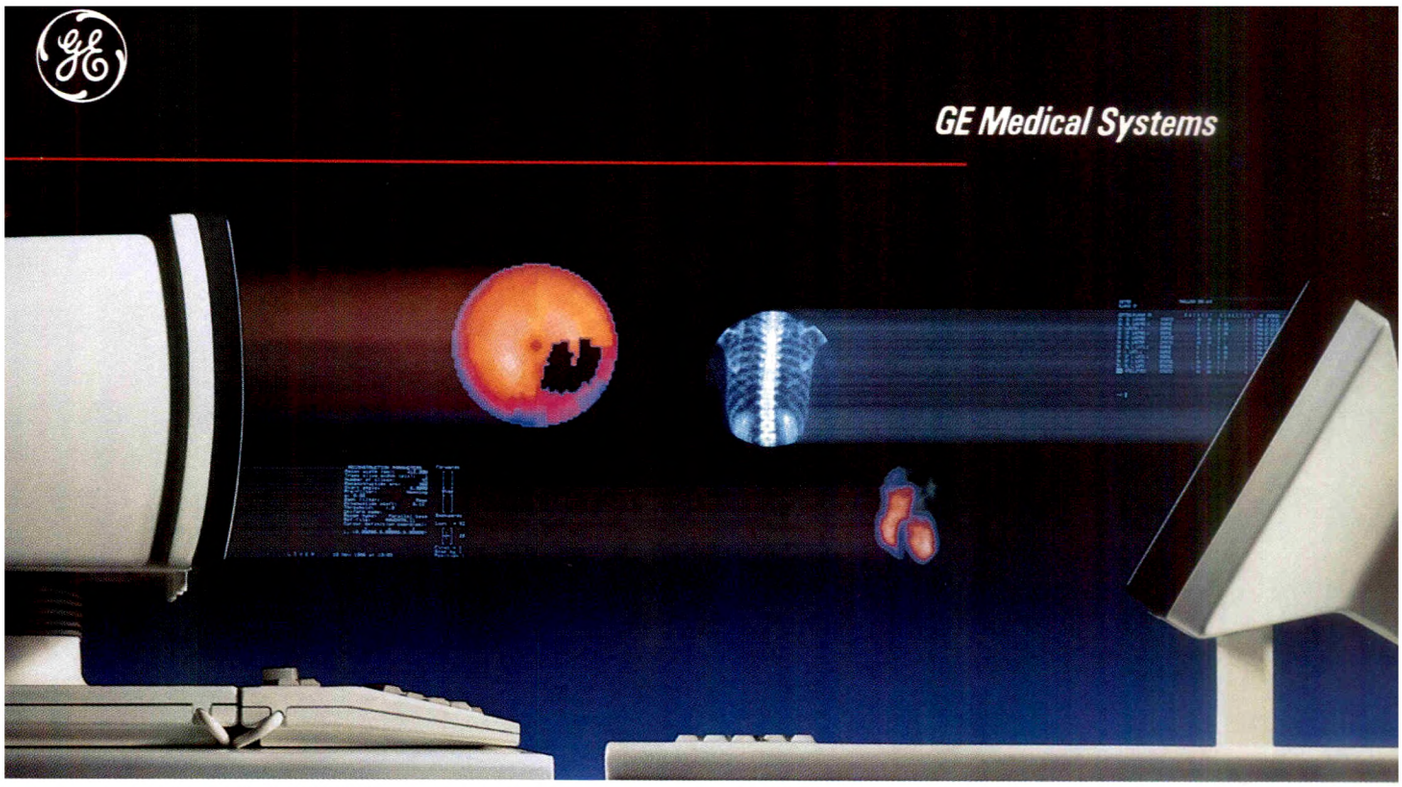
Most adverse reactions to injectable contrast media appear within 1 to 3 minutes after the start of injection, but delayed reactions may occur.

Regardless of the contrast agent employed, the overall estimated incidence of serious adverse reactions is higher with angiocardiography than with other procedures. Cardiac decompensation, serious arrhythmias, angina pectoris, or myocardial ischemia or infarction may occur during angiocardiography and left ventriculography. Electrocardiographic and hemodynamic abnormalities occur less frequently with OMNIPAQUE than with diatrizoate meglumine and diatrizoate sodium injection.

References: 1. Schrott KM, Behrends B, Clauss W, et al: Iohexol in excretory urography: Results of a drug monitoring study. *Fortschr Med* 1986; 7:153-156. **2.** Data on file, Winthrop Pharmaceuticals.

© 1987 WINTHROP PHARMACEUTICALS 71172/3778

Winthrop PHARMACEUTICALS
Winthrop Pharmaceuticals
Division of Sterling Drug Inc.
New York, NY 10016



Starlink

Introducing the intelligent network from GE. A Local Area Network to integrate your nuclear imaging department.

Busy nuclear medicine departments need quick access to images and information, often in several places at once. Starlink—a sophisticated local area network from GE—delivers speed, power and economy.

With Starlink, for example, a physician can access an image stored in a Starcam integrated system, send it to a Star II computer for processing, and retrieve it for viewing on a Starview viewing station. The whole process takes only a few seconds, and won't disrupt activities at the access point. And because data is available in electronic form, you eliminate the expense of redundant hardware such as array processors and hard copy formatters.

Invisible access

Starlink gives you access to all the systems in your network—invisibly—without interrupting work on those systems. Images stored in archives, computers or digital camera systems can be accessed without so much as a flicker. Operators won't even know you have made contact—their efficiency is maintained, yours is enhanced.

Processing power allows rapid transmission of medical images. Starlink was created to efficiently handle the large amounts of information contained in images, unlike many network systems designed for simple data transfer.

This quiet activity is possible because of Starlink's "intelligence." The system hardware doesn't need to lend its processing "brains" to access information—powerful Starlink hardware and software do all the work.

Your link to the future

Starlink's Ethernet™ bus topology allows multiple systems to be connected on a single coaxial cable. This permits fast, simultaneous image transfer, high reliability and easy expansion. Starlink—the right choice for today and tomorrow.

Ethernet is a trademark of Xerox Corp.

Inside intelligence

Find out how Starlink can help increase efficiency in your nuclear medicine department. Call your GE Representative today, toll free:

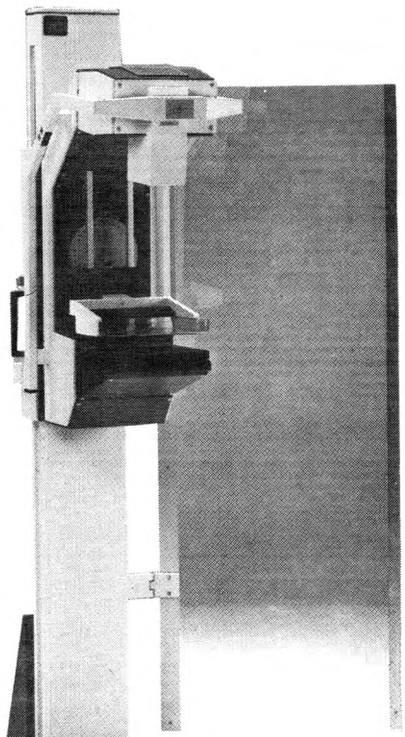
1-800-624-5692.

CIRCLE 15 ON READER SERVICE CARD

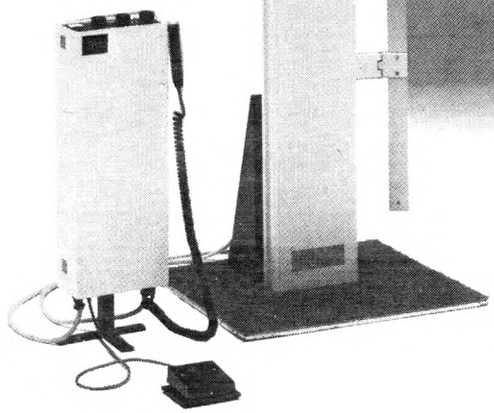
Tecnomed USA

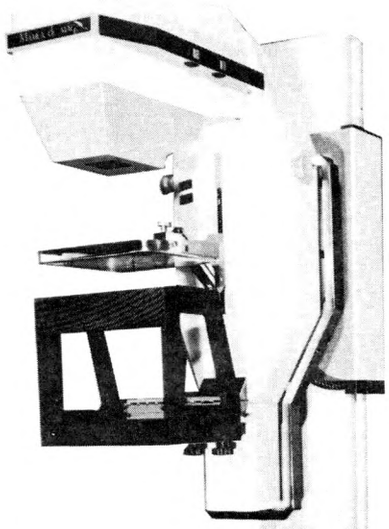
MAMMOGRAPHIC SYSTEMS

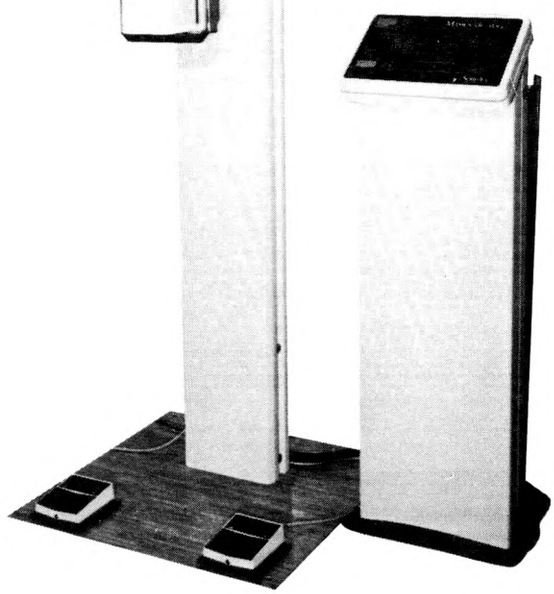
The Mamex DC is a complete mammographic system, consisting of a modern, efficient DC generator which virtually eliminates "ripple" and gives a higher resolution image with consistently higher subject contrast; a molybdenum anode x-ray tube; and a motorized compression system with floor remote control. Each feature has been designed, developed, and merged into a single unit to produce an optimal diagnostic system. Compact size, light weight and connection to any standard 220V wall outlet combine to make the Mamex DC easy to install.



Unit of Choice for:
Specialists in Mammography
St. Louis, MO







The best, made better. Mamex DC Mag, with its state-of-the-art, microprocessor-controlled operation DC generator (higher resolution image with consistently higher subject contrast); rotating anode, dual focal spot x-ray tube; and motorized compression system with fine manual adjustment offers you the ability to perform high-quality low-dose films on an efficient, operator-and-patient-friendly machine.

Unit of Choice for:
University of Michigan
Ann Arbor, MI
Melrose-Wakefield Hospital
Melrose, MA

Tecnomed USA 235 South Fehr Way, Bay Shore, New York 11706 • 516/586-1991-Telex II 510-227-9837-Telefax 516/242-4421

Evac-Q-Kwik® advantages are as clear as the X-ray you get.

Use this checklist to compare other bowel preps:

	EVAC-Q-KWIK	Other Preps
Taste	Pleasant, cherry flavor	
Fluid intake	40 fl oz	
Reconstitution	No	
Enema	No	
Cost	Low	
Adminstration time	6 hours	
Sugar	No	
Alcohol	No	
Sodium content	Low	



Evac-Q-Kwik thoroughly cleans the colon. Patients arrive ready for X-ray. No staff time or extra prepping needed. One take is all—virtually every time. This means better work flow, cost containment and patient comfort.

Everything is in the kit, including easy-to-follow instructions. No mixing, no enemas, no alcohol, no sugar, low sodium… and low cost. Easy to use for better compliance.

Seeing is believing. Give Evac-Q-Kwik a trial.

There's more.

Take advantage of our service materials:
☐ Inservice film for nurses ☐ Multi-language instruction sheets ☐ Radiology work sheets ☐ "What to expect" booklet for patients. Ask your Adria Representative, or drop us a line. Adria Laboratories, Columbus, Ohio 43215.

Evac-Q-Kwik®

Clean colon, clear advantages.

Adria®

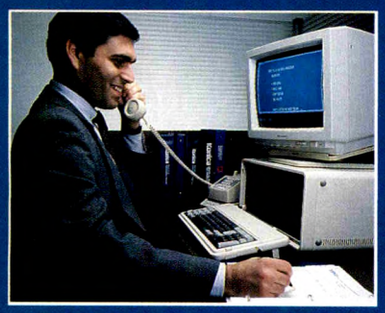
Adria Laboratories
Columbus, OH 43215



When it comes to Medical Imaging... We work harder for you.

©1986 Konica Medical Corp.

Konica®



People Serving People.

Part of an International Fortune 500 Company with over $1 billion in sales, Konica has an important resource no other company can claim. Our people! Konica people! And serving you is what we do best. Because having the best value in medical imaging products alone isn't enough. You also need the best value in service and support. Konica people. We work harder for you.



Nationwide Service And Support By Dedicated Professionals

Our imaging specialists and technical representatives are dedicated professionals. They stand behind every box of film. Through Radiology Support programs and National Accounts Programs for Materials Management, they give you the right support for your specific medical imaging needs. Helping you get the most out of your radiology departments is what we're all about. We're Konica. And we work harder for you.



Technology & Products For State-Of-The-Art Imaging.

Konica continues creating and exploring today's technologies to meet your future medical needs. And we're meeting your present needs with sophisticated technologies in electronic imaging, automatic film processing, digital radiography systems and the latest breakthrough in imaging film, new High Ortho Mono-Dispersed Grain Technology. At Konica, we never stop working on new ideas for better imaging products. And we never will. We're Konica. We work harder for you.

Konica...The Image Of Perfection, Since 1873.

Konica Medical Corporation, 411 Newark Pompton Turnpike, Wayne, New Jersey 07470 (201) 633-1500

CIRCLE 18 ON READER SERVICE CARD

BREAK THE LEAD-GLASS HABIT!

CLEAR-Pb is a lead-impregnated, transparent plastic sheet that combines superb light transmission and complete radiation protection. It gives you many unique benefits:

- *Panoramic viewing areas.*
- *Simple, quick, on-site modular barrier installation. Modules can be moved or changed without expensive labor or renovations.*
- *Attractive, space-saving, decorator look. Walls are only about 1½" thick.*
- *Shatter resistance.*
- *Choice of lead equivalency—0.5 to 1.5 mm.*

There is a Complete Line of CLEAR-Pb® X-Ray Shielding Products to Meet All Your Shielding Requirements:

- ***Modular Barriers • Single-Panel Windows • Mobile Barriers***
- ***Adjustable-Height Mobile Barriers . . . and more!***

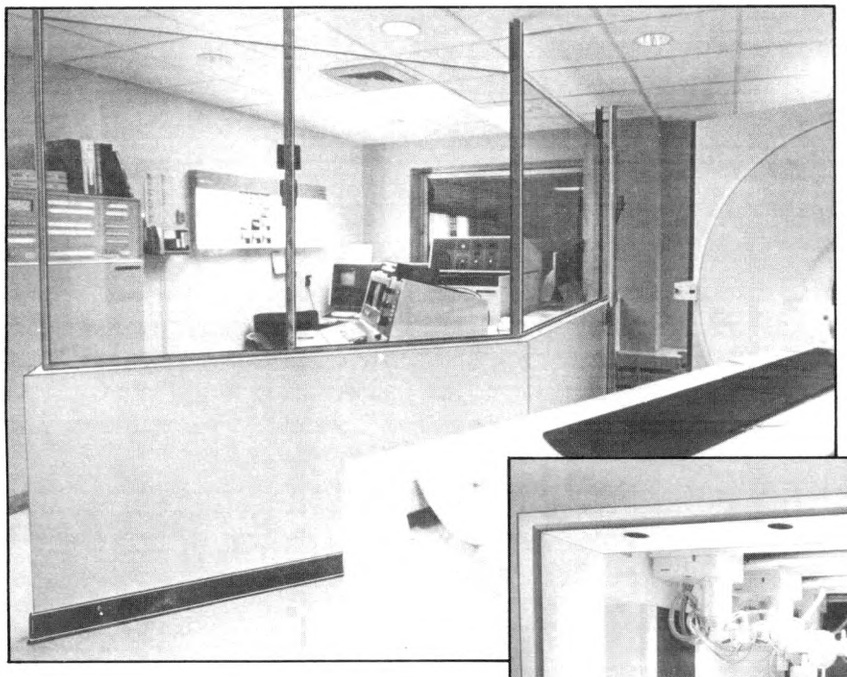
CLEAR-Pb® Lead-Plastic Modular X-Ray Barriers and Windows

FOR MORE INFORMATION, send for Bulletin 3188-B or phone our CLEAR-Pb Product Specialist.

FREE

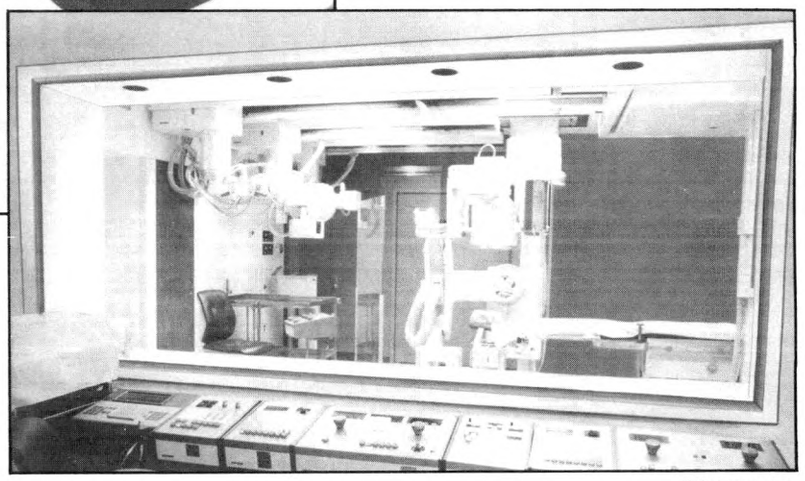
- **CLEAR-Pb LEAD-PLASTIC SAMPLES.**
- **CLEAR-Pb "PLANNING GUIDE."** Beautifully illustrates dozens of user-designed x-ray room shielding installations to assist you in your planning efforts.

*Call or write today for your **FREE** materials.*



Left:
In this CT scanner room, the *CLEAR-Pb* Modular Barrier provides an unparalleled view of the exam area. Large windows (two 48" x 72" and one 18" x 48") allow the technologist and patient to see each other, giving both a greater feeling of security. *Southern Baptist Hospital, New Orleans, LA.*

Below:
Note the distortion-free clarity of the equipment behind the large *CLEAR-Pb* window (96" x 48") of this special-procedures room. *Designed by Arthur E. Rosenbaum, M.D., Neuroradiology Section, The Johns Hopkins Hospital, Baltimore, MD, and Robert Pfeifer, Architect.*



CIRCLE 16 ON READER SERVICE CARD

NUCLEAR ASSOCIATES

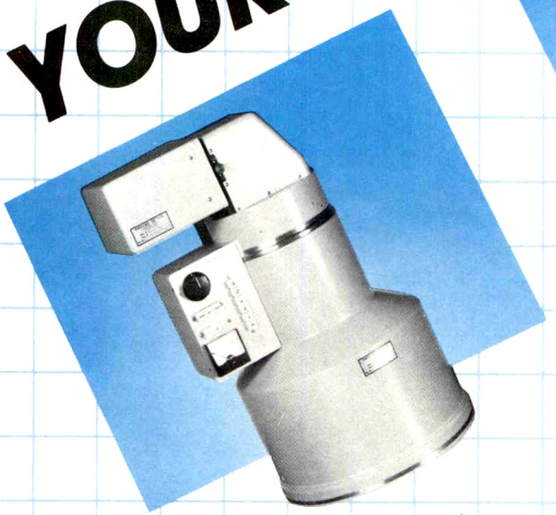
VICTOREEN

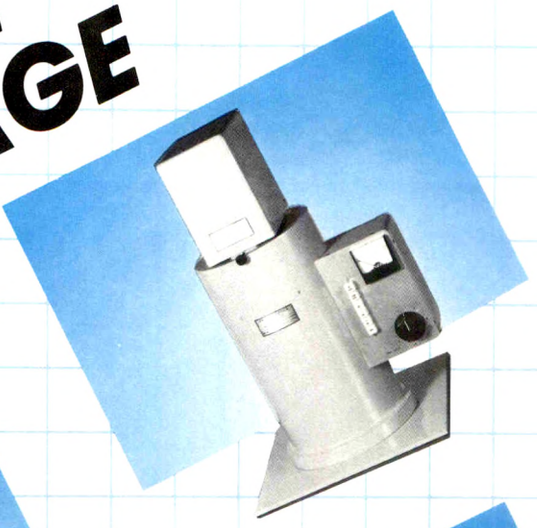
A Division of VICTOREEN, INC.
100 VOICE ROAD
CARLE PLACE, NY 11514-1593
(516) 741-6360
A Subsidiary of Sheller-Globe SG

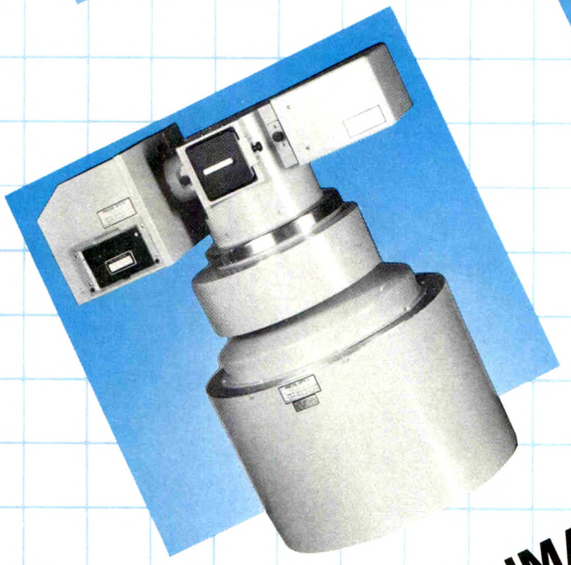
® Victoreen, Inc.

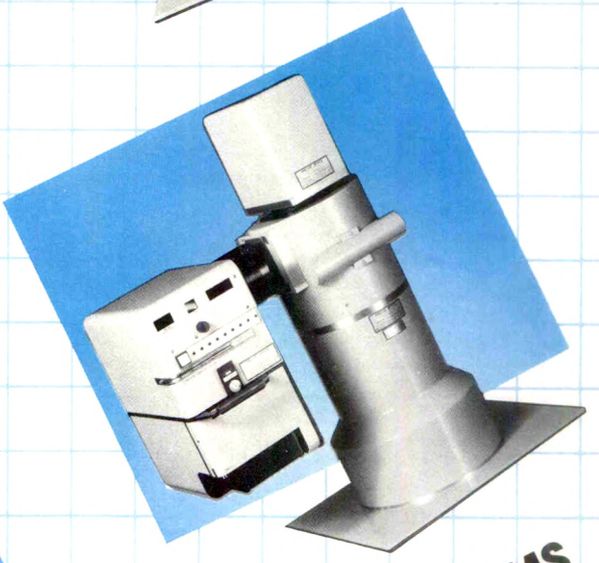
CLEAR-Pb® MODULAR BARRIERS AND WINDOWS . . . THE STATE OF THE ART IN X-RAY ROOM SHIELDING

IMPROVE YOUR IMAGE









WITH PRECISE OPTICS IMAGE INTENSIFIER SYSTEMS

- The world's largest independent manufacturer of Image Intensifier Systems and components
- Over 30 years of experience in design and manufacture
- 6,9,12, and 16-inch latest series image tubes for optimum performance
- 525/875/1023 line CCTV's, 6fps 100mm/105mm cameras
- Cost effective, versatile, reliable
- Compatible with new or existing x-ray equipment
- Extend the life of existing apparatus
- Worldwide dealer network

Precise® Optics
PHOTO MEDIC EQUIPMENT, INC.

239 South Fehr Way
Bay Shore, New York 11706
Tel.: 516 242-6600
TWX: 510-227-9837

CIRCLE 6 ON READER SERVICE CARD

WALL CASSETTE HOLDER

FOR 14x17, 17x14, 10x12 and/or 8x10 CASSETTES.
COMPATIBLE with COLLIMATORS HAVING (PBL) POSITIVE BEAM LIMITING ABILITY.

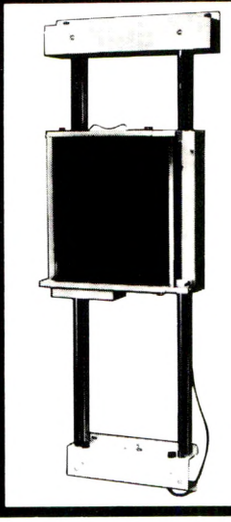


Easy to use: Simply slide the Cassette into the track. Unique S&S flipper design enables change of Cassette size with flip of a finger.

For large and small X-Ray rooms. Built for "Hospital-duty" use—but priced for the small X-Ray user.

FEATURES: Sturdy box girder construction, nylon bearings, dual lock system, constant torque counterbalances and Extra-Heavy plated steel tubes. Requires very minimum of technician's time. Increases productivity Complies with DHEW Regulations.

CIRCLE 9 ON READER SERVICE CARD



S. & S. X-RAY PRODUCTS INC.
The Complete Line of X-Ray Accessories

Accessory Catalog on request.
SOLD BY LOCAL X-RAY DEALERS

87-93 JAY STREET, BROOKLYN, N.Y. 11201
Telephone: 718-852-6900 (800) 221-6634

CIRCLE 17 ON READER SERVICE CARD

The NEW Ackrad H/S Catheter Set for Hysterosalpingography

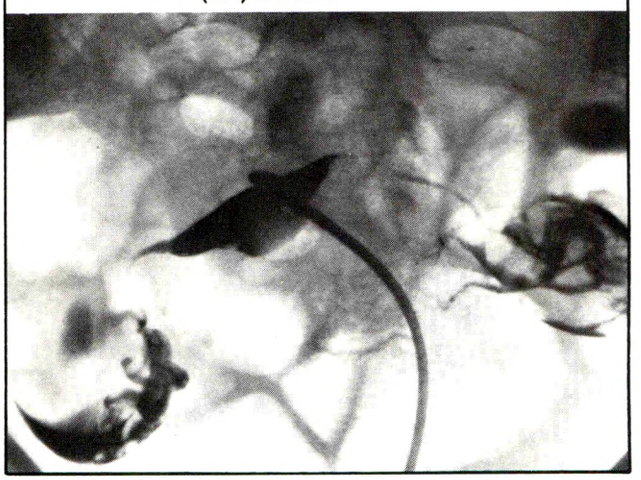


Now: Easier on the Patient . . . Better for the Physician

The unique small sizes (5 and 7F) of the flexible balloon-bearing catheter provide previously unavailable freedom from trauma for the patient. A placement sheath and inflation syringe are included in the set for a rapid and efficient procedure.

Sample furnished on request.

ACKRAD LABORATORIES, Inc.
70 Jackson Drive, P.O. Box 1085, Cranford, NJ 07016
(201) 276-6390



DIAGNOSTIC RADIOLOGIST

Guthrie Clinic recruits a diagnostic radiologist to join 9 other radiologists with general and subspecialty interests. This tertiary level, multispecialty group staffs 160 physicians representing all disciplines in medicine and surgery.

The Guthrie Clinic affords physicians a dynamic and progressive practice opportunity, excellent salaries and benefits as well as a rural, Northeast Pennsylvania setting.

Candidates should submit their CV and three references to:

Donald R. Weaver, M.D.
Medical Director
Guthrie Clinic Ltd.
Sayre, PA 18840
(717) 888-5858

THE OHIO STATE UNIVERSITY HEALTH CENTER SECOND ANNUAL CONFERENCE ON ADVANCES IN MAGNETIC RESONANCE IMAGING

September 24–26th, 1987

THE HYATT REGENCY, AT THE OHIO CENTER COLUMBUS, OHIO

This conference will provide participants with the most recent advances in Clinical MRI and also focus on financial considerations, surface coil utilization and new research applications.

OSU FACULTY	GUEST FACULTY
A. John Christoforidis, M.D., Ph.D.	Anton Hasso, M.D.
Javier Beltran, M.D.	William A. Kennedy, M.B.A.
Donald W. Chakeres, M.D.	Shirley McCarthy, M.D.
William W. Hunter, M.D., D.V.M.	Robert Parkey, M.D.
Alan Marshall, Ph.D.	David Sparks, M.D.
Petra Schmalbrock, Ph.D.	Felix Wehrli, Ph.D.

For more information contact:

Renate Young
OSU-MRI Facility
1630 Upham Drive
Columbus, Ohio 43210 (614) 293-8181

THE INNOVATION CONTINUES

We're building a case for being #1 in Ultrasound.



EXAMINE THE EVIDENCE

Exhibit A: Symme

The best sector images in the industry.

Who really provides the best image quality and technology? We believe the evidence is there for everyone to see. Take a close look at Diasonics' superior images. Then you be the judge.

With our SPA 1000, you'll find the superior spatial and contrast resolution that leads to greater diagnostic confidence. And the ease of use that increases patient throughput.

Quite simply put, the SPA 1000 produces the best sector imaging available anywhere. Superior image quality is established by our wide aperture, symmetrical phased array technology, with all of its inherent advantages over standard phased linear and annular array technologies.

Symmetrical focusing produces the thinnest tomographic sector slice over the entire depth. Our wider apertures — up to 30 mm — allow you to see the subtle gray scale tissue differences that you miss with other technologies.

Our 10 MHz probe technology and digital RF signal processing set the industry standard for vascular and small parts imaging. The higher frequencies achievable with symmetrical phased array technology enable you to visualize subtle pathologies.

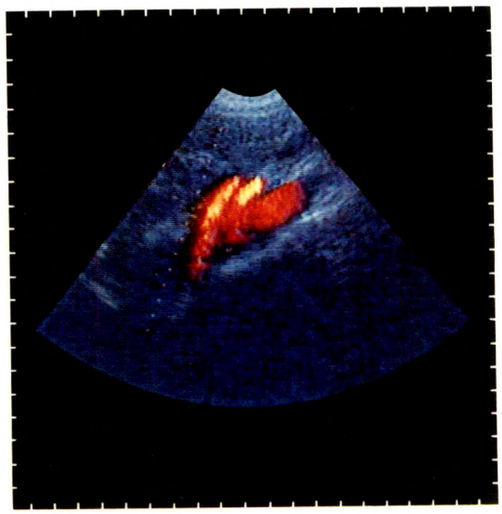
Symmetrical phased arrays provide superior sensitivity, which permits you to scan obese patients at higher frequencies. There's no need to revert to the lower resolution produced by lower transducer frequencies.

Along with such extensive imaging advantages, the SPA 1000 provides deep abdominal Doppler to analyze the hemodynamics of blood flow and expand your clinical capabilities.

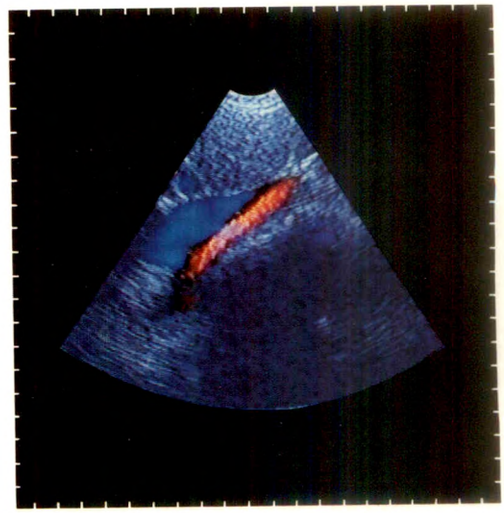
That's only some of the evidence that proves the superiority of the Diasonics SPA 1000. But don't take our word for it. Examine the images and the technology, and judge for yourself.



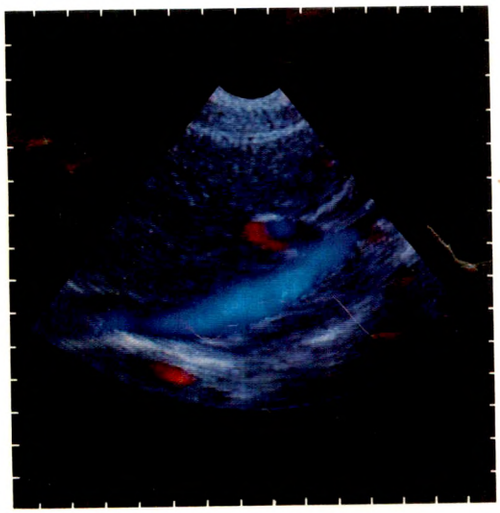
Exhibit C: Color



A sagittal image depicting the origin of the celiac trunk and SMA branching from the abdominal aorta.



Coronal scan through the liver demonstrating the IVC and right renal artery.



High-resolution abdominal array image showing blood flow within the IVC and portal venous system.



Carotid bifurcation showing the CCA, ECA, ICA and the superior thyroid artery posterior to the bifurcation.

Specialty Probes

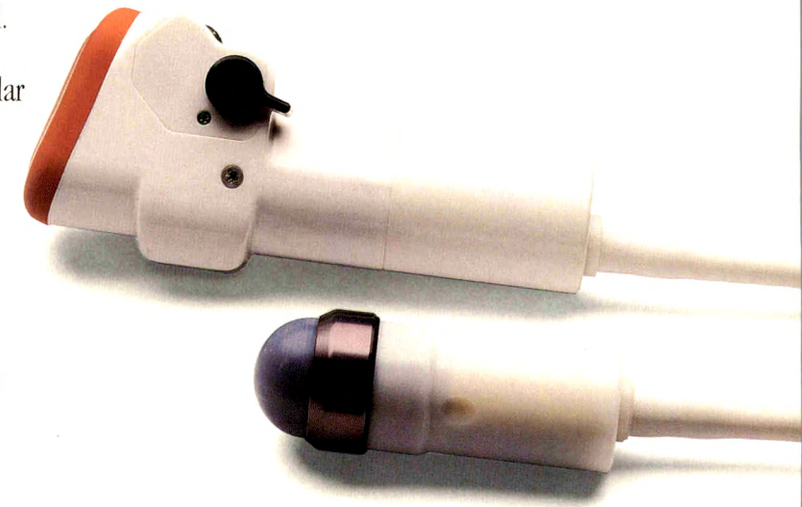
see the detail and structures that other probes fail to reveal.

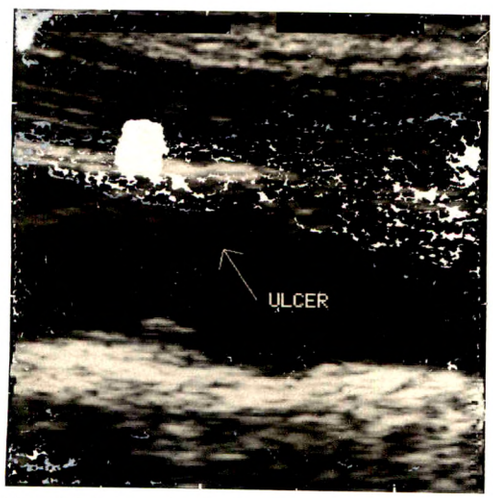
For simultaneous imaging and Doppler for vascular exams, you need the higher resolution of our 10 MHz vascular and small parts probe. To eliminate the compromises of single-transducer probes, our unique design incorporates two separate transducers: one clinically optimized for Doppler, the other for imaging.

The 10 MHz probe also provides the high resolution you need for confident diagnoses in thyroid, breast and testicular exams.

Our Micro-Sector probe provides high-quality images and sensitive pulsed Doppler for precise deep abdominal studies. The probe's small size facilitates ease of use and improves anatomical accessibility.

There's only one way to find out if an ultrasound company is using the right technology for the right application. Ask some probing questions. We have the answers.





True 10 MHz axial and lateral resolution provides the ability to detect a 4 mm ulceration in a soft plaque.



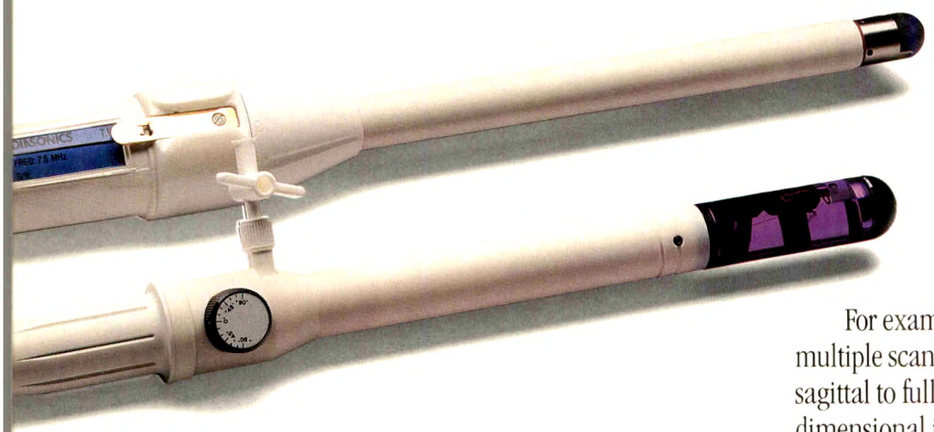
High-resolution 10 MHz sagittal image of an abnormal neonatal spine.

DIASONICS

A Habit of Innovation

EXAMINE THE EVIDENCE

Exhibit B: The



The right technology for the right clinical application.

Some ultrasound companies claim that a single probe can work for many different applications. But they don't tell you about the compromises they made to generalize their probe technology.

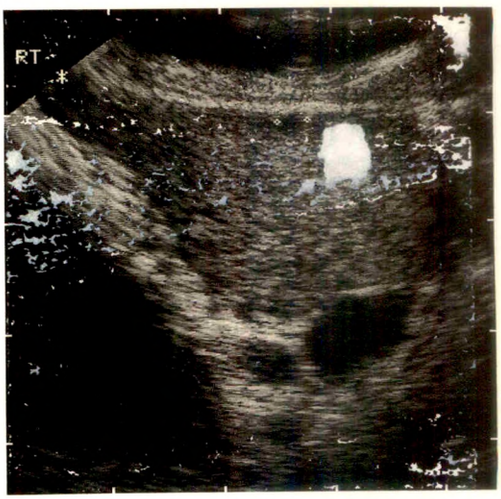
We're more specific about our probe technology. We've developed a wide variety of probes, each one optimized for a specific clinical application. That way, you never have to compromise on performance or your diagnosis.

For example, our unique transrectal probe gives you multiple scan planes for continuous imaging from full sagittal to full transverse. As a result, you achieve full, three-dimensional interrogation of the prostate, something you can't do with either linear or phased arrays.

Our transvaginal probe, which operates at 7.5 MHz, was specifically designed for early fetal viability studies, IVF and other obstetric and pelvic applications. This probe produces a wider sector image with higher resolution, so you

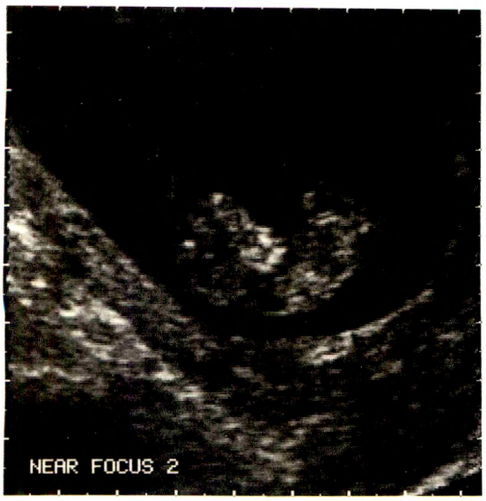


7.5 MHz transvaginal scan depicting multiple follicles in the right ovary.

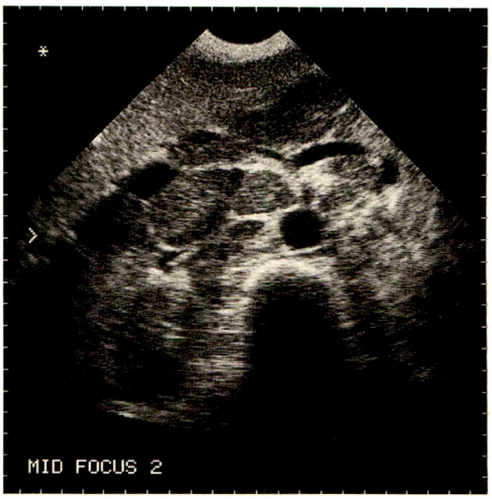


7.5 MHz transrectal sagittal scan demonstrating a 2.7 mm lesion in the peripheral zone of the prostate.

trical Phased Array



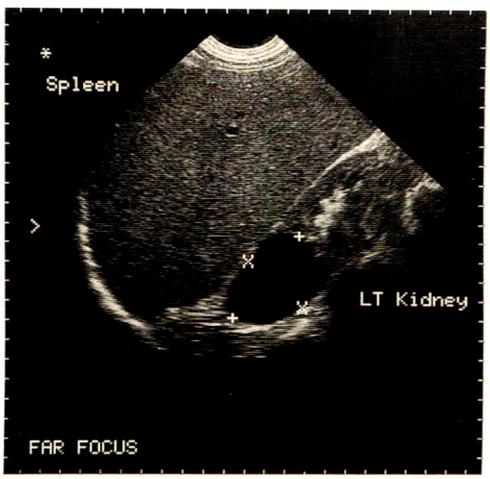
Excellent spatial resolution shows facial detail on a 9-week fetus.



Transverse view of the upper abdomen showing enlargement of the lymph nodes due to chronic lymphocytic leukemia.



Both renal arteries are visualized with excellent detail as they branch from the abdominal aorta.



Intercostal sagittal scan demonstrating a large cyst on the upper pole of the left kidney and an enlarged spleen.

DIASONICS

A Habit of Innovation

Flow Mapping

Whole-body CFM without clinical compromise.

For abdominal Doppler and high-resolution peripheral vascular exams, Color Flow Mapping adds new dimensions to your diagnoses. CFM allows you to quickly see blood flow and complements your gray scale image to increase the speed and accuracy of your exams.

These advantages are being established in cardiology, where Diasonics is a CFM leader. Now we're bringing all of our CFM experience and expertise to abdominal and vascular ultrasound.

In keeping with our philosophy of the right technology for the right application, we're developing a series of clinically optimized CFM probes for a variety of specific applications.

Other companies may try to get by with one CFM probe for many different clinical applications. But we won't settle for clinical compromises.

Only a company with expertise in CFM technology and proven abilities in high-resolution imaging can provide the ultrasound medical community with the best Color Flow Mapping system. Diasonics has clearly demonstrated abilities in probe technology, image processing, Doppler and mainframe system architecture — the essential components of the best CFM system.

That's the kind of sound experience we bring to Doppler Color Flow Mapping. Soon you'll be able to see for yourself exactly what we mean.

DIASONICS

A Habit of Innovation

YOU BE THE JUDGE

A commitment that extends beyond product excellence.

Diasonics has designed a customer support program that's as advanced and complete as our products.

To begin with, we've built out obsolescence — bringing our product advances back to our installed base as upgrades. No one is left behind because we still offer upgrades on our very first products.

All Diasonics products are built for reliable performance and maximum uptime. For example, we feel so confident about the dependability of our SPA 1000 symmetrical phased array system that we offer the industry's first 36-month warranty.

We also support our products with direct national service, clinical educational support, and a research and development program devoted exclusively to medical imaging.

So before you judge which ultrasound company is best for your needs, examine all the evidence.

800-538-7021. In California, 800-662-6293.

DIASONICS

A Habit of Innovation

U.S.
Ultrasound
1656 McCarthy Boulevard
Milpitas, CA 95035
408-432-9000
800-662-6293 (in CA)
800-538-7021

Europe
Sonotron Holding AG
Steinhauserstrasse 74
P.O. Box 4737
CH-6304 Zug
Switzerland
(41) 42 41 64 64

Australia
Diasonics Pty Ltd
576 St. Kilda Road
Melbourne 3004
Australia
(03) 529-6111

Acoustic neuromas

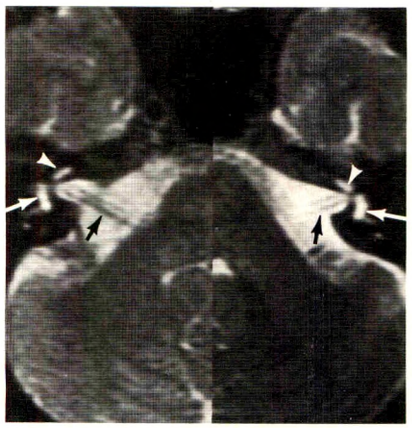
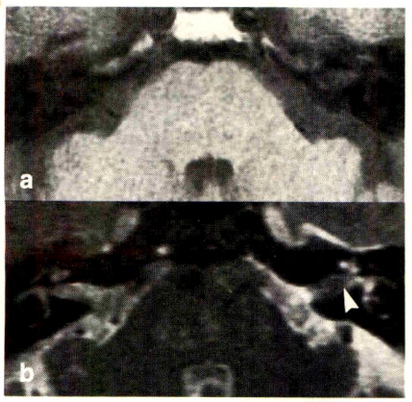


Fig. 1—T2 weighted images show normal VII and VIII cranial nerves (short arrows), vestibular apparatus (long arrows), and cochlea (arrowheads) bilaterally. (TR 4000, TE 120)



Figs. 2a,b—T1 weighted image (Fig. 2a) demonstrates both IACs. T2 weighted 3 mm slice at same location (Fig. 2b) shows obvious asymmetry between IACs. Normal CSF intensity pattern is seen within normal right IAC. Signal intensity from left IAC is markedly diminished due to displacement of CSF by tumor (arrow). (Fig. 2a: TR 600, TE 25; Fig. 2b: TR 4000, TE 90)

For non-invasive evaluation of acoustic neuromas, high field magnetic resonance imaging is the modality of choice. Alone, it can provide definitive diagnosis in a majority of cases.

The thin slices and small fields of view possible with the Signa® system permit the very small voxel volumes essential for visualization of minute anatomic structures in the head, such as the VII and VIII cranial nerves, vestibular apparatus and cochlea. (Fig. 1).

This enables the accurate evaluation of tiny or early lesions which do not exhibit IAC widening.

The following case study demonstrates Signa's capability for excellent soft tissue contrast without artifacts, a distinct advantage in this potentially difficult diagnostic situation.

Case study

A 76-year-old female with a history of bilateral sensorineural hearing loss presented with dysequilibrium and left-sided tinnitus.

Evaluation confirmed left-sided hearing loss with mild right-sided loss.

A CT scan suggested a mass in the left IAC, with minimal widening of bony margins.

The patient was referred to a Signa user for MR evaluation.

MR exam

A Signa T1 weighted image demonstrated the appearance of the IACs (Fig. 2a).

A T2 weighted image (Fig. 2b) at the same slice location showed cerebrospinal fluid (CSF) and cranial nerves filling the normal right IAC. The expected signal intensity from within the left IAC is markedly diminished. The mass in the left IAC has a weaker signal than the CSF it displaces. This confidently confirms the presence of a purely intracanalicular tumor.

Conclusion

Early or small acoustic neuromas may not demonstrate characteristic IAC widening despite significant symptomatology. These tumors are not as readily imaged by CT due to beam hardening artifacts and poor soft tissue contrast.

Signa MR imaging, however, provides the clinical advantages of high signal-to-noise and high contrast-to-noise imaging. This permits the non-invasive acquisition of diagnostically successful 3 mm slices in clinically realistic scan times.

Acknowledgement: Emanuel Kanal, M.D., Pittsburgh NMR Institute, Hugh Curtin, M.D., Eye and Ear Hospital, Pittsburgh.

Signa . . . the MR reference point

For referring physicians of all specialties, Signa sites are the reference point for optimal image quality across the broadest range of applications.

To receive a detailed discussion of the case presented here, call GE at 1-800-624-5692 and request MR Clinical Symposium No. 7135. We will also be glad to provide a list of the Signa sites in your area.

CIRCLE 3 ON READER SERVICE CARD



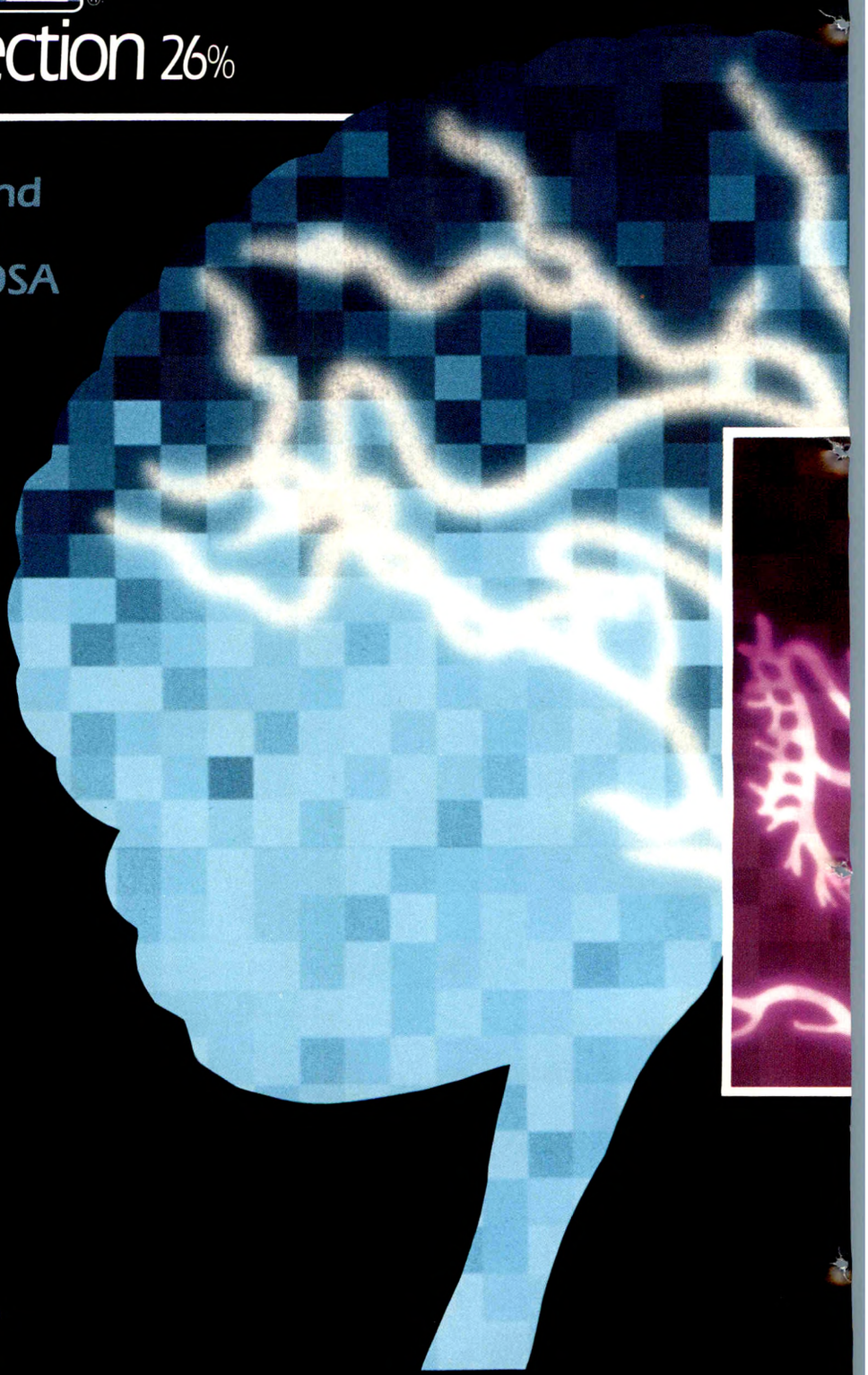
GE

ANNOUNCING

ISOVUE®-128

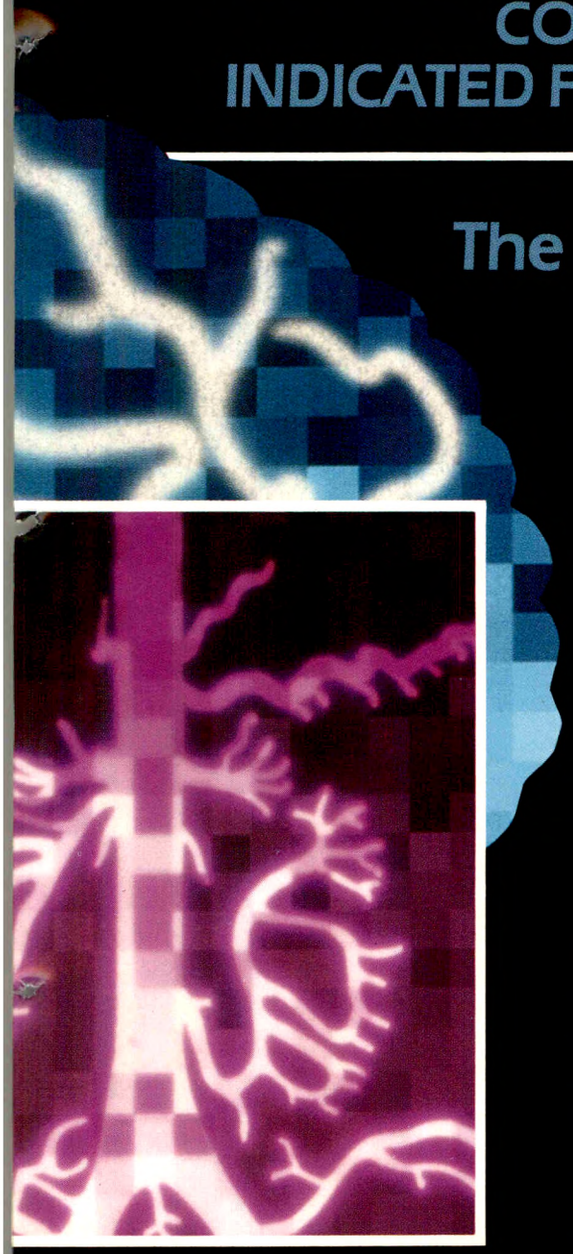
iopamidol injection 26%

For cerebral and abdominal intra-arterial DSA



From SQUIBB™ Diagnostics

THE ONLY NONIONIC, LOW-OSMOLALITY CONTRAST AGENT INDICATED FOR INTRA-ARTERIAL DSA



The ISOVUE Advantages:

Approximately isotonic to plasma.

The osmolality of ISOVUE-128 is 290 mOsm/kg H_2O, compared with 285 mOsm/kg H_2O for plasma. As with all injectable contrast agents, patients with CHF may experience a transient increase in circulatory osmotic load.

Low incidence of patient motion.

Well-tolerated ISOVUE-128 has been associated with a low incidence of patient motion, which may mean fewer retakes. In a clinical trial, 2% (9 of 520) sets of images were technically inadequate due to patient motion.*

High-quality images.

For both cerebral and abdominal studies, ISOVUE-128 has been shown to produce images of diagnostic quality in 98% (502 of 511) of cases.*

As with all injectable contrast agents, the possibility of severe adverse reactions should be borne in mind. (See brief summary on adjacent page for WARNINGS, PRECAUTIONS, and ADVERSE REACTIONS.)

*Data on file, Squibb Institute for Medical Research.

This product is under license from Bracco Industria Chimica, S.p.A.
U.S. Patent #4,001,323

ISOVUE®-128
iopamidol injection 26%

CIRCLE 14 ON READER SERVICE CARD

© 1987 E.R. Squibb & Sons, Inc., Princeton, NJ

647-505

Issued: August 1987

ISOVUE®-128
Iopamidol Injection 26%

INDICATIONS AND USAGE
ISOVUE-128 (Iopamidol Injection 26%) is indicated for intra-arterial digital subtraction angiography (DSA) of the cerebral and abdominal vasculature.

CONTRAINDICATIONS
None.

WARNINGS
Caution must be exercised in patients with severely impaired renal function, those with combined renal and hepatic disease, or anuria, particularly when larger doses are administered.

Radiopaque diagnostic contrast agents are potentially hazardous in patients with multiple myeloma or other paraproteinemia, particularly in those with therapeutically resistant anuria. Myeloma occurs most commonly in persons over age 40. Although neither the contrast agent nor dehydration has been proved separately to be the cause of anuria in myelomatous patients, it has been speculated that the combination of both may be causative. The risk in myelomatous patients is not a contraindication; however, special precautions are required.

Contrast media may promote sickling in individuals who are homozygous for sickle cell disease when injected intravenously or intraarterially.

Administration of radiopaque materials to patients known or suspected of having pheochromocytoma should be performed with extreme caution. If, in the opinion of the physician, the possible benefits of such procedures outweigh the considered risks, the procedures may be performed; however, the amount of radiopaque medium injected should be kept to an absolute minimum. The blood pressure should be assessed throughout the procedure and measures for treatment of a hypertensive crisis should be available. These patients should be monitored very closely during contrast enhanced procedures.

Reports of thyroid storm following the use of iodinated radiopaque diagnostic agents in patients with hyperthyroidism or with an autonomously functioning thyroid nodule suggest that this additional risk be evaluated in such patients before use of any contrast medium.

PRECAUTIONS
General
Diagnostic procedures which involve the use of any radiopaque agent should be carried out under the direction of personnel with the prerequisite training and with a thorough knowledge of the particular procedure to be performed. Appropriate facilities should be available for coping with any complication of the procedure, as well as for emergency treatment of severe reaction to the contrast agent itself. After parenteral administration of a radiopaque agent, competent personnel and emergency facilities should be available for at least 30 to 60 minutes since severe delayed reactions may occur.

Preparatory dehydration is dangerous and may contribute to acute renal failure in patients with advanced vascular disease, diabetic patients, and in susceptible nondiabetic patients (often elderly with preexisting renal disease). *Patients should be well hydrated prior to and following iopamidol administration.*

The possibility of a reaction, including serious, life-threatening, fatal, anaphylactoid or cardiovascular reactions, should always be considered (see ADVERSE REACTIONS). Patients at increased risk include those with a history of a previous reaction to a contrast medium, patients with a known sensitivity to iodine per se, and patients with a known clinical hypersensitivity (bronchial asthma, hay fever, and food allergies). The occurrence of severe idiosyncratic reactions has prompted the use of several pretesting methods. However, pretesting cannot be relied upon to predict severe reactions and may itself be hazardous for the patient. It is suggested that a thorough medical history with emphasis on allergy and hypersensitivity, prior to the injection of any contrast medium, may be more accurate than pretesting in predicting potential adverse reactions. A positive history of allergies or hypersensitivity does not arbitrarily contraindicate the use of a contrast agent where a diagnostic procedure is thought essential, but caution should be exercised. Premedication with antihistamines or corticosteroids to avoid or minimize possible allergic reactions in such patients should be considered. Recent reports indicate that such pretreatment does not prevent serious life-threatening reactions, but may reduce both their incidence and severity.

General anesthesia may be indicated in the performance of some procedures in selected patients; however, a higher incidence of adverse reactions has been reported with radiopaque media in anesthetized patients, which may be attributable to the inability of the patient to identify untoward symptoms, or to the hypotensive effect of anesthesia which can reduce cardiac output and increase the duration of exposure to the contrast agent.

Although the osmolality of iopamidol 128 mgI/mL is comparable to that of plasma, the potential transitory increase in circulatory volume load in patients with congestive heart failure requires caution during injection. These patients should be observed for several hours following the procedure to detect delayed hemodynamic disturbances.

In angiographic procedures, the possibility of dislodging plaques or damaging or perforating the vessel wall should be borne in mind during catheter manipulations and contrast medium injection. Test injections to ensure proper catheter placement are suggested. Following arteriographic procedures, gentle pressure hemostasis is required, followed by observation and immobilization of the limb for several hours to prevent hemorrhage from the site of arterial puncture. Angiography should be avoided whenever possible in patients with homocystinuria, because of the risk of inducing thrombosis and embolism.

Drug Interactions
Renal toxicity has been reported in a few patients with liver dysfunction who were given oral cholecystographic agents followed by intravascular contrast agents. Administration of intravascular agents should therefore be postponed in any patient with a known or suspected hepatic or biliary disorder who has recently received a cholecystographic contrast agent.

Other drugs should not be admixed with iopamidol.

Drug/Laboratory Test Interactions
The results of PBI and radioactive iodine uptake studies, which depend on iodine estimations, will not accurately reflect thyroid function for up to 16 days following administration of iodinated contrast media. However, thyroid function tests not depending on iodine estimations, e.g., T3 resin uptake and total or free thyroxine (T4) assays are not affected.

Any test which might be affected by contrast media should be performed prior to administration of the contrast medium.

Laboratory Test Findings
In vitro studies with animal blood showed that many radiopaque contrast agents, including iopamidol, produced a slight depression of plasma coagulation factors including prothrombin time, partial thromboplastin time, and fibrinogen, as well as a slight tendency to cause platelet and/or red blood cell aggregation.

Transitory changes may occur in red cell and leucocyte counts, serum calcium, serum creatinine, serum glutamic oxalacetic transaminase (SGOT), and uric acid in urine; transient albuminuria may occur.

These findings have not been associated with clinical manifestations.

Carcinogenesis, Mutagenesis, Impairment of Fertility
In animal reproduction studies performed on rats, intravenously administered iopamidol did not induce adverse effects on fertility or general reproductive performance.

In studies to determine mutagenic activity, iopamidol did not cause any increase in mutation rates.

Pregnancy Category B
No teratogenic effects attributable to iopamidol have been observed in teratology studies performed in animals. There are, however, no adequate and well controlled studies in pregnant women. It is not known whether iopamidol crosses the placental barrier or reaches fetal tissues. However, many injectable contrast agents cross the placental barrier in humans and appear to enter fetal tissues passively. Because animal teratology studies are not always predictive of human response, this drug should be used during pregnancy only if clearly needed.

Radiologic procedures involve a certain risk related to the exposure of the fetus to ionizing radiation.

Labor and Delivery
It is not known whether use of contrast agents during labor or delivery has immediate or delayed adverse effects on the fetus, prolongs the duration of labor or increases the likelihood that forceps delivery or other obstetrical intervention or resuscitation of the newborn will be necessary.

Nursing Mothers
It is not known whether iopamidol is excreted in human milk. However, many injectable contrast agents are excreted unchanged in human milk. Although it has not been established that serious adverse reactions occur in nursing infants, caution should be exercised when intravascular contrast media are administered to nursing women because of potential adverse reactions, and consideration should be given to temporarily discontinuing nursing.

Pediatric Use
Safety and effectiveness in children have not been established.

ADVERSE REACTIONS
Adverse reactions following the use of iopamidol are usually mild to moderate, self-limited, and transient.

In a clinical trial with 100 patients, adverse reactions possibly attributed to ISOVUE-128 administration were nausea (2%), headache (1%) and vomiting (1%). One patient with preexisting renal impairment and severe bilateral renal vascular disease experienced renal failure, possibly secondary to a subsequent acute episode of congestive heart failure and/or drug administration (see Warnings).

The following table of incidence of reactions is based on clinical studies with ISOVUE in about 1835 patients. While the following reactions may or may not occur with ISOVUE-128 with the same frequency, the data are presented to provide a more complete profile of ISOVUE (Iopamidol Injection).

Adverse Reactions

System	Estimated Overall Incidence >1%	≤1%
Cardiovascular	none	tachycardia hypotension hypertension myocardial ischemia circulatory collapse S-T segment depression bigeminy extrasystoles ventricular fibrillation angina pectoris bradycardia transient ischemic attack thrombophlebitis
Nervous	pain (1.7%) burning sensation (1.4%)	vasovagal reaction tingling in arms grimace faintness
Digestive	nausea (1.2%)	vomiting anorexia
Respiratory	none	throat constriction dyspnea pulmonary edema
Skin and Appendages	none	rash urticaria pruritus flushing
Body as a Whole	hot flashes (1.5%)	headache fever chills excessive sweating back spasm
Special Senses	warmth (1.1%)	taste alterations nasal congestion visual disturbances
Urogenital	none	urinary retention

In *aortography,* the risks of procedures also include injury to the aorta and neighboring organs, pleural puncture, renal damage including infarction and acute tubular necrosis with oliguria and anuria, accidental selective filling of the right renal artery during the translumbar procedure in the presence of preexisting renal disease, retroperitoneal hemorrhage from the translumbar approach, and spinal cord injury and pathology associated with the syndrome of transverse myelitis.

Adverse effects reported in clinical literature for iopamidol include arrhythmia, arterial spasms, hematuria, periorbital edema, involuntary leg movement, malaise, and triggering of deglutition; some of these may occur as a consequence of the procedure. Other reactions may also occur with the use of any contrast agent as a consequence of the procedural hazard; these include hemorrhage or pseudoaneurysms at the puncture site, brachial plexus palsy following axillary artery injections, chest pain, myocardial infarction, and transient changes in hepatorenal chemistry tests. Arterial thrombosis, displacement of arterial plaques, venous thrombosis, dissection of the coronary vessels and transient sinus arrest are rare complications.

General Adverse Reactions To Contrast Media
Reactions known to occur with parenteral administration of iodinated ionic contrast agents (see the listing below) are possible with any nonionic agent. Approximately 95 percent of adverse reactions accompanying the use of other water-soluble intravascularly administered contrast agents are mild to moderate in degree. However, life-threatening reactions and fatalities, mostly of cardiovascular origin, have occurred. Reported incidences of death from the administration of other iodinated contrast media range from 6.6 per 1 million (0.00066 percent) to 1 in 10,000 patients (0.01 percent). Most deaths occur during injection or 5 to 10 minutes later, the main feature being cardiac arrest with cardiovascular disease as the main aggravating factor. Isolated reports of hypotensive collapse and shock are found in the literature. The incidence of shock is estimated to be 1 out of 20,000 (0.005 percent) patients.

Adverse reactions to injectable contrast media fall into two categories: chemotoxic reactions and idiosyncratic reactions. Chemotoxic reactions result from the physicochemical properties of the contrast medium, the dose, and the speed of injection. All hemodynamic disturbances and injuries to organs or vessels perfused by the contrast medium are included in this category. Experience with iopamidol suggests there is much less discomfort (e.g., pain and/or warmth) with peripheral arteriography. Fewer changes are noted in ventricular function after ventriculography and coronary arteriography.

Idiosyncratic reactions include all other reactions. They occur more frequently in patients 20 to 40 years old. Idiosyncratic reactions may or may not be dependent on the amount of drug injected, the speed of injection, the mode of injection, and the radiographic procedure. Idiosyncratic reactions are subdivided into minor, intermediate, and severe. The minor reactions are self-limited and of short duration; the severe reactions are life-threatening and treatment is urgent and mandatory.

The reported incidence of adverse reactions to contrast media in patients with a history of allergy is twice that for the general population. Patients with a history of previous reactions to a contrast medium are three times more susceptible than other patients. However, sensitivity to contrast media does not appear to increase with repeated examinations. Most adverse reactions to intravascular contrast agents appear within one to three minutes after the start of injection, but delayed reactions may occur (see PRECAUTIONS, General).

In addition to the adverse drug reactions reported for iopamidol, the following additional adverse reactions have been reported with the use of other intravascular contrast agents and are possible with the use of any water-soluble iodinated contrast agent:
Cardiovascular: vasodilation, cerebral hematomas, petechiae.
Nervous: paresthesia, dizziness, convulsions, paralysis, coma.
Respiratory: increased cough, asthma, laryngeal edema, pulmonary edema, bronchospasm, rhinitis.
Skin and Appendages: injection site pain usually due to extravasation and/or erythematous swelling, skin necrosis.
Urogenital: osmotic nephrosis of proximal tubular cells, renal failure, pain.
Special Senses: bilateral ocular irritation; lacrimation; conjunctival chemosis, infection, and conjunctivitis.

The following reactions may also occur: neutropenia, thrombophlebitis, flushing, pallor, weakness, severe retching and choking, wheezing, cramps, tremors, and sneezing.

OVERDOSAGE
Treatment of an overdose of an injectable radiopaque contrast medium is directed toward the support of all vital functions, and prompt institution of symptomatic therapy. Intravenous LD_{50} values (gI/kg) for iopamidol in animals: 21.8 (mice), 13.8 (rats), 9.6 (rabbits), 17.0 (dogs).

HOW SUPPLIED
ISOVUE-128 (Iopamidol Injection 26%)
Ten 50 mL single dose vials (NDC 0003-2153-10)

J3-702 A

© 1987 E.R. Squibb & Sons, Inc., Princeton, NJ 647-505 Issued: August 1987

Special Report

High-Temperature Superconductors: Will New Materials Take the Chill off Our Magnets?

Lawrence E. Crooks[1] and Douglas Kelley

Recent press coverage [1–3] has focused attention on the discovery of materials that have the property of superconductivity at relatively high temperatures. The prospect that such materials will reduce or eliminate the need for cryogenic cooling of superconducting magnets poses a number of questions for the medical MR community: Should I postpone purchase of my MR system until a new magnet design is available? Will the money I save on cryogens pay for a replacement magnet? Will a new design give me more or less field strength? Should I sell my niobium mining stock and reinvest in a company producing the new materials?

The work reported is at an early stage. The researchers have concentrated on investigation of the superconducting properties of the materials. We must know a number of other properties and processing aspects to determine their suitability for use in magnets. It is also a challenge to theoreticians to explain why the materials work.

Present Superconducting Magnets: What Can Be Eliminated?

To appreciate the potential of the new materials, one needs to understand the present design and materials used in magnets. The wire in superconducting magnets used for MR is made of niobium-titanium supported by copper. The niobium-titanium is superconducting below 18°K at the field strengths and electrical currents used in typical magnets. For human-sized magnets, the wire is wound on a horizontal cylinder that is immersed partly in a tank of liquid helium. This tank is surrounded by the vacuum of the cryostat and another tank of liquid nitrogen. The liquid nitrogen (temperature, 77°K) is a shield that intercepts ambient heat from the surrounding room (temperature, 300°K). Some heat is radiated or conducted by the magnet supports from the nitrogen to the liquid helium tank. This heat boils the helium at 4°K, so periodic refilling of the helium is required. Liquid helium covers the bottom of the magnet; the top is surrounded by cold helium gas. This combination keeps the wire below 18°K, the critical temperature for superconductivity in the wire. If some part of the wire heats up above this temperature, it becomes resistive. The magnet then quenches. Magnet designs thus include safety margins so that no part of the magnet gets too warm.

Cryogen consumption of superconducting magnets is typically 0.7 l/hr for helium and 1.0 l/hr for nitrogen. At prices in the United States of $4.50 and $0.60 per liter, respectively, the total annual consumption costs are $27,600 and $5300, respectively. Contracts for cryogen supplies include these costs, labor, insurance, and a reserve to refill the magnet if it quenches. Medium-field magnet contracts cost about $39,000, and high-field ones about $65,000. Part of the difference is due to the quench reserve. At medium field only about 10% of the magnet's helium content boils away, dissipating the magnet's energy, whereas at high field, energy equivalent to more than 100% of the helium content is dissipated. Thus, the magnet partially warms up and must be recooled, consuming, additional liquid helium. Liquid helium thus accounts for $28,000–38,000 annual cryogen cost, depending on field strength.

[1] Both authors: Dept. of Radiology, University of California, San Francisco, San Francisco, CA 94080. Address reprint requests to L. E. Crooks, UCSF Radiologic Imaging Laboratory, 400 Grandview Dr., South San Francisco, CA 94080.

AJR **149:223–225, August 1987** 0361–803X/87/1492–0223 © American Roentgen Ray Society

If new materials raise the critical temperature required for superconductivity, simplified magnet design will result, first by reducing safety margins and eventually by eliminating cryogens. Materials with a critical temperature below 77°K will reduce margins and may require only cooling by a helium refrigerator. Even if refrigeration is possible, liquid helium may still be used as insurance during electric utility failures. Once the critical temperature is above 77°K, all the complexities of the helium cryostat are eliminated. A single liquid nitrogen tank can house the magnet, eliminating one cryogen tank and a heat shield. This reduces magnet size and weight. Vacuum seals would need only to be airtight, rather than helium-tight. Optimistically, these factors could drop cryostat construction costs by 50%. Because the cryostat and magnet winding each account for half of the total cost, the magnet cost would drop by 25%. As the critical temperature moves above 200°K, conventional refrigeration becomes possible, with additional cost reductions. When the critical temperature rises above room temperature (300°K), the magnet structure is freed from all cooling constraints. The magnet would need only to have enough structure to support the forces on it. These forces can be significant at high fields because the current in each turn interacts with the field from all the other turns.

For MR machines used for human imaging, new materials will have little impact on the value of the maximum available field strength. This is because the ability of niobium-titanium to provide fields up to about 10 T is not the limiting factor in the construction of high-field magnets. Extrapolating to 0°K, the new materials have better high-field performance, accommodating fields of 60 T or more.

Properties of the New Superconducting Materials

The October 1986 report of a barium-lanthanum-copper-oxygen compound with a critical temperature of 30°K broke the 1973 record of 23°K [4]. Since this discovery, rapid increases have been made, pushing the temperature up to 40°K [5] and then 94°K [6], with the suggestion that 240°K may be possible.

In addition to critical temperature, two other parameters are important to maintain superconductivity in a magnet wire. One is critical field, the field above which superconductivity is lost. All materials tested have indications of high values at low temperatures, which is good for magnet designers. At higher temperatures, the performance drops but is adequate for imaging systems. The other parameter is maximum current density. A given cross section of wire can carry only up to a certain current. Maximum current density has been disappointing so far in the new materials. One material drops from a capacity of 1000 A/cm^2 at 4°K to only 15 A/cm^2 at 77°K. Present low-current magnets use 20 A to produce 0.35-T magnetic fields. Thus, they would require a solid conductor with a cross section of 1 cm^2, 100 times larger than their present wire. Such a size would be impractical. The same type of limitation has been overcome in niobium-titanium by distributing the current over many fine wire filaments that are bundled together to carry the total current.

The new materials are ceramics, so that once they are baked into their final form, they are brittle. Thus, their suitability as wire is dominated by properties such as ductility, the ability to be drawn out or thinned. For usual superconductors, niobium-titanium rods are inserted in a copper billet that is drawn through dyes to form wire. The copper supports the multiple filaments of superconductor and provides ductility, heat capacity, and a path for current if the wire quenches. Such a support material may be possible for the new materials. Alternatives are (1) to form the material into the final desired shape and then bake it or (2) to deposit it as a thin film. Such approaches are different from present magnet construction, but they may have advantages in making the current paths a pattern that is easily repeated from one unit to the next.

The ceramic compounds consist of two material phases. It is thought that one is superconducting and the other is not. Production of only the superconducting phase is the goal of improvements in processing. The critical field and temperature may be higher when only one phase is present.

Several years of work will be needed to understand the limitations and opportunities provided by the new materials. Adapting magnet factories to new techniques will also take time.

Availability of the New Materials

Because the new materials are ceramics, their constituents (including the rare earths) are readily available. So far no bulk samples have been produced. Once these are made, and the basic processing steps are understood, the ceramics industry will be able to produce quantities of material. The United States government and corporate research sponsors are pushing development in the hope that American industry can establish a leading position in the world market. The military also will support development for its own uses.

As production accelerates, will MR be able to obtain the materials for use in MR magnets? Competition among customers (such as the military) will have a strong influence. Probably the largest financial benefit will be in the electric utility industry. Large energy savings will be available by replacing inefficient power lines with superconducting ones. Off-peak energy storage in large superconducting magnets also is being considered. Although such uses are capital intensive and slow to start, they would require a tremendous amount of material, assuming that materials that would function at room temperature were used (ones cooled by liquid nitrogen will be less attractive). Magnet levitation of trains also is expected. Fortunately for MR, most customers of superconductivity are interested in magnets. The magnet suppliers thus will have early access to the materials and should have useful products designed before the large projects are started. The public's perception that MR diagnostics are desirable also will help.

Conclusions

If room-temperature superconductors with satisfactory performance become available, the structure and operation of

MR magnets will be simplified greatly. Because the magnet accounts for less than one-third of the system's cost, some cost reduction would occur. Maximum available field will not increase, as other factors are more important. At low fields, the stability of superconductivity makes it an attractive replacement for resistive and permanent magnet elements. Relative economics will determine the approach chosen. Iron cores might remain in use, when fringe field or mechanical strength are overriding concerns.

Answers to many of the practical questions about material properties will be available in the next 1 or 2 years. Material production will begin at the same time. Incorporation of the materials into magnet design and production will be somewhat slower. If present problems are solved, at least operation at the temperature of liquid nitrogen will be possible. At the present rate of progress, if room-temperature operation is not achieved in the next year, we may again be at a performance plateau that will last for years.

An MR unit purchased now will remain competitive for at least 5 years. When a magnet cooled only by liquid nitrogen becomes available, purchase price will be reduced by about 8% (25% reduction in the cost of the magnet times one-third of system cost). New systems would operate at a lower cost, but not low enough to justify replacing an existing magnet. The reduction of cryogen cost is $28,000–38,000 per year, small compared with the maintenance cost of a mid-field unit ($150,000) and other operating costs [7]. System performance in terms of signal-to-noise, contrast, and resolution will continue to improve much as they have in the past. These performance parameters are only slightly affected by the kind of superconductor that produces the basic magnetic field.

The intangible benefits of eliminating cooling with liquid helium are that magnet operation is more convenient and that the supply of helium need not be a concern.

Niobium mining stock will not be as good an investment as it once was. Products based on mass-marketable room-temperature superconductivity would have a profound effect on technological capabilities. Routine levitation of vehicles and frictionless motors are two examples. More energy would be available as electric transmission losses are reduced. Fusion energy also will become more accessible, although other major problems remain to be solved. As with all technology, the benefits are derived at the cost of dependence on the technology. Failure modes of the new materials will have to be assessed and perhaps learned in hard ways [8].

REFERENCES

1. Gleick J. New superconductors offer chance to do the impossible. *The New York Times* **1987**; April 9:1
2. Robinson AL. Record high-temperature superconductors claimed. *Science* **1987**;235:531–533
3. Robinson AL. Superconductor claim raised to 94K. *Science* **1987**;235:1137–1138
4. Bednorz JG, Muller KA. Possible high T_c superconductivity in the Ba-La-Cu-O system. *Z Phys B* **1986**;64:189–193
5. Chu CW, Hor PH, Meng RL, Gao L, Huang ZJ, Wang YQ. Evidence for superconductivity above 40 K in the La-Ba-Cu-O compound system. *Phys Rev Lett* **1987**;58:405–407
6. Wu MK, Ashburn JR, Torng, et al. Superconductivity at 93 K in a new mixed-phase Y-Ba-Cu-O compound system at ambient pressure. *Phys Rev Lett* **1987**;58:908–910
7. Di Monda R. Economic impact and cost justification (of MRI). Presented at the annual meeting of the Radiological Society of North America, Chicago, November **1985**
8. Niven L. *The ringworld engineers*. New York: Ballantine Books, **1980**

Book Review

La Radiologia Interventiva delle Vie Biliari. By Paolo Mannela, Giorgio Benea, Massimo Borrelli, and Roberto Galeotti. Milano: Co. GRAF., 127 pp., 1986. Lire 50,000

This book is a well-planned and comprehensive review of the present state of interventional radiology of the biliary tract. It opens with a short history of the progress of radiology in the investigation of pathologic processes involving the biliary system, including a description of the radiological-surgical table of Caroli-Champeau-Porcher or "le sarcophage," as it was called by those who had the good fortune of being associated with the Hôpital St. Antoine in Paris. Correctly the authors state that the radiologist has moved from under the table ("le sarcophage") to the side of the surgeon to participate actively in the investigation and management of the patient with biliary tract disease.

The book is divided into six main chapters and each one is accompanied by up-to-date references. The first chapter deals with the most recent and accepted techniques of intrahepatic cholangiography and discusses their roles in the demonstration and diagnosis of the various pathologic processes. The second chapter reviews in detail the "collateral investigations" that are performed either at the time of the percutaneous cholangiography or at a later date. Among the immediate investigations are the analysis of the cytology of the bile; evaluation of the carcinoembryonic antigen in the aspirated bile; cholangiomanometry and flow-rate tests; and bile cultures. Brush biopsy, transcatheter biopsy, transhepatic biopsy, percutaneous choledoscopy, radiomanometry, and flow-rate studies are all procedures that can also be performed at a later stage. Chapter three discusses the advantages and disadvantages of external biliary drainage, transhepatic duodenal drainage, internal biliary drainage, and internal biliary drainage using endoprostheses. The various techniques and types of catheters and prostheses are also reviewed in detail. The fourth chapter deals with the techniques of percutaneous transhepatic removal of retained biliary calculi, which are illustrated by several examples. In chapter five the nonsurgical management of the benign biliary stenoses is reviewed, and in the last chapter the role of the percutaneous drainage of hepatobiliary abscesses is discussed.

The text is not in English, and this is the main limitation of this informative book. However, the numerous and clear illustrations that accompany each chapter are quite demonstrative and self explanatory.

Antonio F. Govoni
The New York Hospital–Cornell Medical Center
New York, NY 10021

Perspective

Biliary Lithotripsy: What Will the Issues Be?

Joseph T. Ferrucci[1]

Inasmuch as gallstones occur with 10 times the frequency of kidney stones, the recent report by Sauerbruch et al. [1] of successful extracorporeal shock-wave lithotripsy (ESWL) of gallstones using a modified Dornier kidney lithotripter rivals the clinical implications of the first reports of successful renal lithotripsy by Chaussy et al. 3 years ago [2]. However, instead of the universal awe that attended the early descriptions of the ESWL phenomenon, biliary lithotripsy emerges in the context of a broader set of technologic, metabolic, and clinical issues that will be the focus of this review.

At this stage, data on clinical results are scanty and derived entirely from preliminary trials in Europe. Moreover, confidentiality and disclosure concerns of manufacturers have tended to suppress release of information into the competitive marketplace.

Nevertheless, some 200–250 patients have now been treated in Europe on at least three different systems, all three of which will be installed in the United States by late 1987. Evidence that the stakes in biliary lithotripsy are high is seen from the intense interest of many diverse groups: different medical specialties (radiologists, surgeons, gastroenterologists); manufacturers of radiographic, sonographic, and lithotriptic systems; pharmaceutical and interventional product firms; hospital administrators; the Food and Drug Administration (FDA); and, predictably, venture capitalists. It is this atmosphere that suggests that the diffusion of equipment and knowledge will be less tightly controlled than in the case of urologic ESWL. Thus, there is reason to believe that with biliary lithotripsy, radiology as a specialty will have another chance to participate in the application of this important imaging-based technology.

Gallbladder vs Kidney Lithotripsy

Distinctions immediately arise between lithotripsy of biliary and urinary tract calculi. In 90% of cases of renal calculi, mechanical fragmentation is followed by spontaneous passage of fragments through the ureter. Endourologic or radiologic interventions may be required in the remainder, but adjuvant chemolytic drug therapy is not a routine part of acute management. However, successful therapy of gallbladder calculi will likely require a combination of mechanical fragmentation plus chemical solvent dissolution. This derives from both anatomic and biochemical considerations. The spiral valves of Heister in the cystic duct constitute a tortuous barrier to expulsion of fragments from the gallbladder lumen, while gallbladder contractility will probably be impaired by the combination of chronic calculus disease and the local trauma of shock-wave therapy. Distally in the common bile duct the choledochoduodenal sphincter presents a second potential site of relative obstruction with the risk of calculus obstruction of the pancreatic duct as well. Further, unlike the ureter, the common bile duct has no inherent peristaltic capability. Thus, in addition to biliary colic, cholecystitis, cholangitis, and pancreatitis are all possible serious complications. The biliary passages will not be as forgiving of a "steinstrasse" (stone street) as the ureter.

On the other hand, about 85% of gallstones are composed of cholesterol (the remaining 15% are bilirubin pigment) and have proved susceptible to complete dissolution by chemical compounds with cholesterol solvent activity, such as monooctanoin, methyl tertiary butyl ether (MBTE), and cheno or ursodeoxycholic acid (CHENO/URSO) [3, 4]. Widely pub-

Received April 13, 1987; accepted after revision May 8, 1987.
Presented at the annual meeting of the American Roentgen Ray Society, Miami Beach, FL, April 1987.
[1] Department of Radiology, Massachusetts General Hospital and Harvard Medical School, Boston, MA 02114. Address reprint requests to J. T. Ferrucci.

AJR 149:227–231, August 1987 0361–803X/87/1492–0227 © American Roentgen Ray Society

licized clinical trials in the United States and Europe have shown that oral bile salt chemolitholytic therapy with CHENO and/or URSO can achieve a 30–40% dissolution rate of cholesterol gallstones when given continuously over a 1- to 2-year period [5–7]. In general, the effect of oral bile salt therapy is greatest for small gallstones that have larger surface areas. Thus, there should be a complementary effect of initial shock-wave fragmentation followed by a short course of oral drug therapy to dissolve the inevitable residual fragments. The other cholesterol solvents such as monooctanoin and MTBE are highly potent and can produce dissolution within hours or days but require an invasive needle or catheter procedure for direct instillation into the biliary tract [7–10].

A second difference between renal and gallstone lithotripsy is the use of sonography rather than fluoroscopy for gallstone targeting since 85% of gallstones are noncalcified, as well as the primacy of real-time sonography as the diagnostic standard for gallstone detection. It can also be anticipated that the expertise of diagnostic radiologists in the technical and clinical aspects of sonography will be recognized as essential to successful development of the technique. This would represent another vital difference from the renal ESWL experience.

The Dornier Advantage

Visitors to West Germany have observed continued clinical success with gallstone ESWL since the original report appeared in the *New England Journal of Medicine*, further extending the competitive advantage of the Dornier approach in the field of lithotripsy [1]. Preferred candidates are patients with one or two gallstones less than 2.5 cm in diameter that are noncalcified on plain radiographs. Even though stone consistency in the biliary tract is much softer than that of the average calcified urinary calculus, shock-wave fragmentation either in the gallbladder or common bile duct appears highly effective. A functioning oral cholecystogram is required to assure cystic duct patency so that residual fragments can be evacuated. There must also be free passage into the gallbladder of orally administered CHENO/URSO after hepatic excretion. Fewer patients are said to require general anesthesia with the majority receiving only IV analgesia. Presently, a large immersion water tank is still employed, but a smaller second-generation production model has been designed without the water tank using only a compressible, membrane-covered water bag housing an electrode-ellipsoid assembly. Two real-time diagnostic sonographic transducers provide multidimensional spatial localization of the stone. Ten sites have already been identified in the United States for clinical trials of this system commencing in late 1987. Radiologists have been invited to participate in the planning of these trials, and the presence of a Dornier technical exhibit at the recent meeting of the Radiological Society of North America confirms a new willingness on the part of the company to deal with radiologists.

Other Second-Generation Systems

Some six to eight other manufacturers in the United States and Europe are developing second-generation systems with varying combinations of approaches for shock-wave generation and target imaging apparatus. All but one have replaced the water immersion tank with a compressible, movable water bath container that transmits the focused shock wave across the body wall. Most are being marketed primarily as renal devices and include an operating type table with stirrups for cystoscopy. However, many have the potential capability for treating biliary calculi with appropriate operational and patient position modifications. Nearly all are more compact in design, require less floor space and less site preparation, and are presumably less expensive to own and operate than the original Dornier kidney device. Currently active manufacturers and their system features are shown in Table 1. The FDA has issued investigational device exemptions for a number of manufacturers, and clinical trials for kidney stones are already underway in the United States for Technomed International, Medstone, Siemens, and EDAP International. In France, both Technomed International and EDAP International have already treated several dozen patients with gallstones.

Techniques for shock-wave generation include electrostatic spark discharge (Dornier, Technomed, Medstone), electromagnetic shock waves (Siemens), and pulsed piezoelectric shock generation (EDAP, Wolf). One company (Labsonics) uses a specially constructed high-intensity, low-frequency sonographic source to agitate the calculi after an appropriate amount of cholesterol solvent has been introduced into the gallbladder. This innovative technique relies primarily on the chemical dissolution effect rather than on the mechanical fragmentation and is an approach that may be nearly specific for gallstones. Systems using sonographic imaging for stone target localization include Dornier Medical Systems, EDAP International, Technomed International, and Labsonics.

Gallbladder vs Common Bile Duct Stones

Despite the deserved excitement over the potential for gallbladder lithotripsy, the broader term, biliary lithotripsy, is probably more appropriate since common bile duct stones are readily fragmented as well. In their initial report, Sauerbruch et al. [1] reported four of five patients who showed disintegration of common duct stones when treated on a conventional kidney device. Their experience has subsequently been further extended, while we and other groups [11] have accumulated similar positive results in individual cases (Fig. 1). Thus, in contradistinction to gallstone lithotripsy, which has not yet been performed in the United States, common duct stone lithotripsy is a currently available method using existing installed equipment. However, FDA approval for ESWL of common duct stones on a kidney system will be required and Dornier is implementing such a protocol.

The management of common duct stones by lithotripter techniques will differ from gallstone treatment in several other respects. For example, there will be a requirement for direct contrast opacification most likely via a nasobiliary catheter after endoscopic papillotomy. As in the case of kidney stone localization, biplane image-intensified fluoroscopy is used. Care will be required to avoid undue shock trauma to the head of the pancreas, and if possible stones should be positioned cephalad into the mid-duct. The volume of potential

TABLE 1: Second Generation Lithotripter Systems with Potential Suitability for the Biliary Tract

Manufacturer	Model	Nature of Shock/Energy Source	Stone Target Imaging Technique	Water Path Design	Installed US Sites[a]	Approximate Cost ($)	Comments
Dornier Medical Systems (Munich, W. Germany)	GM-2	Spark-gap electrode	Sonography	Compressible bag	No	1,000,000	Proved technology; specifically designed for gallstones
EDAP (Marne la Vallee, France)	LT 01	Piezoelectric pulse	Sonography	Compressible bag	Yes	750,000	Fixed relation of therapeutic sonographic probe to imaging probe
Medstone International (Costa Mesa, CA)	1000	Spark-gap electrode	Fluoroscopy and radiography	Compressible bag	Yes	850,000	Current device will need sonographic imager for gallbladder applications
Siemens (Erlangen, W. Germany)	Lithostar	Electromagnetic shock wave	Fluoroscopy	Compressible bag	Yes	1,300,000	Will need sonographic imager for gallbladder applications
Technomed International (Paris, France)	Sonolith 2000	Spark-gap electrode	Sonography	Immersion tank	Yes	850,000	Water tank design poor for gallbladder
Labsonics (Indianapolis, IN)	—	Low-frequency, high-intensity sonography	Sonography	Compressible bag	No	500,000	Probably specific for gallstone applications but technology unproved

[a] As of May 1, 1987.

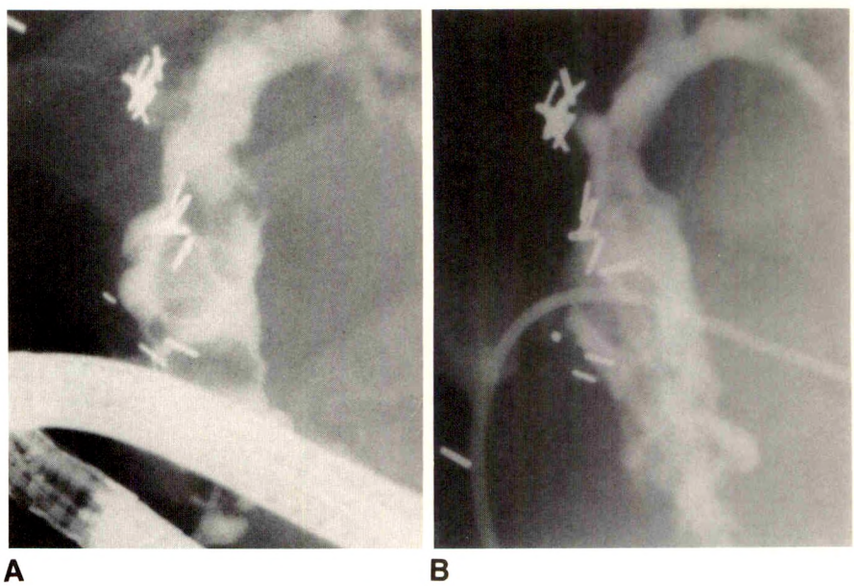


Fig. 1.—Extracorporeal shock-wave lithotripsy of multiple large common bile duct stones. Procedure was performed on a Dornier renal device after contrast opacification via an indwelling endoscopically placed nasobiliary catheter. Papillotomy with basket extraction was unsuccessful.

***A*, Multiple large calculi before lithotripsy.**

***B*, Numerous smaller fragments after lithotripsy with 1000 shocks. A second lithotripsy session was ultimately carried out with complete spontaneous passage of all fragments.**

cases will be relatively small as there are other effective surgical and nonsurgical techniques for management of common duct stones, for example, endoscopic papillotomy with basket extraction or monooctanoin infusion. Further, many patients with common duct stones present with acute life-threatening complications including cholangitis, pancreatitis, and jaundice, and they often require more urgent therapy. Finally, because of the likely requirement for an endoscopic papillotomy to facilitate fragment passage, only patients who fail a preliminary effort with that form of therapy will be logical candidates for subsequent shock-wave fragmentation. Thus, gallabladder lithotripsy probably will be more widely used as a primary treatment technique than will ESWL of common duct stones.

CHENO/URSO and the Food and Drug Administration

Extensive clinical experience in the United States and Europe has established that oral administration of the naturally occurring bile salts, chenodeoxycholic acid (CHENO) and its 7-beta epimer ursodeoxycholic acid (URSO) or a combination of both, decreases cholesterol saturation of human gallbladder bile [5–7]. When bile becomes sufficiently unsaturated with cholesterol, an appreciable proportion of cholesterol stones will slowly dissolve.

An exhaustive literature has accumulated detailing the physical, biochemical, and clinical factors affecting biliary lipid metabolism and the rate of gallstone dissolution [3–7]. Critical elements include a functioning gallbladder on oral cholecystography, the presence of predominant cholesterol stone composition, and lack of stone calcification. Perhaps most important is the relatively small stone size, which increases the surface area for exposure to the desaturated gallbladder bile bathing the stones. It is in this context that acute direct mechanical disruption to small fragments supplemented by several months of oral bile salt therapy seems to be emerging as the optimal combination for effective therapy of gallbladder calculi. It should be noted that CHENO/URSO is not appropriate as an oral regimen for dissolution of common bile duct stones as they are less often due to cholesterol and the concentration of the agent in hepatic bile is too low.

There are significant differences among the mechanism of action, side effects, cost, and availability of these two drugs which presently affect their clinical use as chemolitholytic agents for cholesterol gallstones in the United States. While the dissolution efficacy and optimal dose range (10–15 mg/kg/day at bedtime) of the two agents are comparable, CHENO is associated with a moderate frequency of liver function abnormalities (10–20%) and diarrhea (30–40%) as well as increases in serum low-density lipoprotein cholesterol [3–7]. Thus, although CHENO was the first drug evaluated, its use as a single agent has not gained much popularity. In contrast to CHENO, URSO is not yet FDA approved but has been found to be safe with no adverse effects or signs of toxicity in large clinical trials in Europe [5–7]. Because URSO is 25–50% more expensive than CHENO, the two drugs have been widely used in a half-strength combination (8 mg/kg/day of each at bedtime). More recently, URSO alone at a full 10–12 mg/kg/day dose has given a high 30–40% dissolution rate of smaller (<15 mm) cholesterol gallstones essentially without side effects [7]. At present, therefore single drug therapy with URSO appears to be the preferred regimen.

Related Alternative Techniques

Numerous ingenious approaches have been described for mechanical disruption or solvent dissolution of gallbladder and common bile duct stones over the years. Direct contact fragmentation using lithotripters with laser, ultrasonic, or electrohydraulic energy has been used for retained biliary duct stones [12–15]. Direct instillation of various high potency cholesterol solvents has also been carefully investigated [3, 4, 8–10, 16–19]. Monooctanoin dissolution of cholesterol-containing common bile duct stones has had the widest success [8, 16, 17]. However, occasional complications such as cholangitis and duodenitis have been described [18–20]. More recently, the development of safe sonography-guided percutaneous catheter access to the gallbladder has allowed successful rapid (6–8 hr) dissolution of cholesterol gallstones by instillation of MTBE [9–10]. This technique is highly effective in skilled hands but is invasive and personnel intensive, and it requires familiarity with the drawbacks of MTBE including its volatility, foul odor, tendency for CNS depression, and solvent damage of catheter materials. A combination of initial lithotripsy fragmentation followed by intracholecystic instillation of MTBE (monooctanoin in the gallbladder is less well tolerated) has also been proposed. Whether the costs and risks of such combination therapy will be worth the extra benefit remains unclear.

Other Clinical Issues

If the early efficacy and safety of gallstone lithotripsy is confirmed, other clinical issues will arise. For example, gallstones recur in up to 40% of patients after initially successful oral bile salt therapy [21]. Because cholesterol gallstones are the end product of a chronic metabolic disorder, a finite rate of recurrence after extracorporeal lithotripsy is highly likely. Thus, small fragments remaining after lithotripsy or a nondissolved core matrix of calcium and/or a protein mucin plug could serve as a nidus for reformation of a cholesterol stone. In this regard, the merits, nature, and cost of a prophylactic postlithotripsy drug program will require study. Will a calcium binding agent such as EDTA be required? Will it be important to predict gallstone composition as is now recommended prior to entry into long-term oral drug therapy protocols [22, 23]? Will the sheer mechanical effectiveness of the lithotripsy approach render these considerations academic?

Further, the cost-benefit trade-offs of gallstone lithotripsy vs conventional cholecystectomy, which provides a permanent cure at a small but definite operative risk, remain a much larger issue. This is particularly relevant in the new era of cost-aware medical practice where surgical groups are now reporting hospital discharge 24 hr after cholecystectomy [24]. The final issues of turf (who will control the procedure) and the potential for overutilization (in patients with asymptomatic gallstones) are obviously interrelated and could become most important if the technique reaches wide clinical acceptability.

REFERENCES

1. Sauerbruch T, Delius M, Paumgartner G, et al. Fragmentation of gallstones by extracorporeal shock waves. *New Engl J Med* **1986**;314:818–822
2. Chaussy C, Schmiedt E, Joacham D, et al. Extracorporeal shock-wave lithotripsy (ESWL) for treatment of urolithiasis. *Urology* **1984**;23:59–66
3. Neoptolemos JP, Hofmann AF, Moossa AR. Chemical treatment of stones in the biliary tree. *Br J Surg* **1986**;73(7):515–524
4. Fromm H. Gallstone dissolution therapy: current status and future prospects. *Gastroenterology* **1986**;91:1560–1567
5. Schoenfield LJ, Lachin JM, et al. Chenodiol (chenodeoxycholic acid) for dissolution of gallstones. The National Cooperative Gallstones Study: a controlled trial of efficacy and safety. *Ann Intern Med* **1981**;95:257–282.
6. Roda E, Bazzoli F, Morselli M, et al. Ursodeoxycholic acid vs chenodeoxycholic acid as cholesterol gallstone-dissolving agents: a comparative randomized study. *Hepatology* **1982**;2:804–810

7. Ward A, Brogden RN, Heel RC, et al. Ursodeoxycholic acid: a review of its pharmacological properties and therapeutic efficacy. *Drugs* **1984**;27: 95–131
8. Thistle JL, Carlson GL, Hofmann AF, et al. Monooctanoin, a dissolution agent for retained cholesterol bile duct stones: physical properties and clinical application. *Gastroenterology* **1980**;78:1016–1022
9. Allen MJ, Borody TJ, Bugliosi TF, et al. Rapid dissolution of gallstones by methyl tert-butyl ether: preliminary observations. *New Engl J Med* **1985**;312:217–220
10. vanSonnenberg E, Hofmann AF, Neoptolemus J, et al. Gallstone dissolution with methyl tert-butyl ether via percutaneous cholecystostomy: success and caveats. *AJR* **1986**;146:865–867
11. Gelfand E, McCullough DL, Myers RT, D'Sousa VJ, Leinbach LB, Faust KB. Choledocholithias: successful treatment with extracorporeal lithotripsy. *AJR* **1987**;148:1114–1116
12. Burhenne HJ. Electrohydrolytic fragmentation of retained common duct stones. *Radiology* **1975**;117:721–722
13. Gadacz TR. Ultrasonic fragmentation of gallstones in vitro. *Surgery* **1985**;97(5):511–513
14. Lear JL, Ring EA, Macoviak JA, Baum S. Percutaneous transhepatic electrohydraulic lithotripsy. *Radiology* **1984**;150:589–590
15. Bean WJ, Daughtry JD, Rodan BA, Mullin D. Ultrasonic lithotripsy of retained common bile duct stone. *AJR* **1985**;144:1275–1276
16. vanSonnenberg E, Wittich GR, Casola G, et al. Diagnostic and therapeutic percutaneous gallbladder procedures. *Radiology* **1986**;160:23–26
17. Teplick SK, Pavlides CA, Goodman LR, et al. In vitro dissolution of gallstones: comparison of mono-octanoin, sodium dehydrocholate, heparin, and saline. *AJR* **1982**;138:271–273
18. Train J, Dan SJ, Cohen LB, et al. Duodenal ulceration associated with mono-octanoin infusion. *AJR* **1983**;141:557–558
19. Crabtree TS, Dykstra R, Kelly J, Preshaw RM. Necrotizing choledochomalacia after use of mono-octanoin to dissolve bile duct stones. *Can J Surg* **1982**;25:644–646
20. Minuk GY, Hoofnagle JH, Jones EA. Systemic side effects from the intrabiliary infusion of mono-octanoin for the dissolution of gallstones. *J Clin Gastroenterol* **1982**;4:133–135
21. Ruppin DC, Dowling RH. Is recurrence inevitable after gallstone dissolution by bile-acid treatment? *Lancet* **1982**;January 23:181–185
22. Dolgin SM, Schwartz JS, Kressel HY, et al. Identification of patients with cholesterol or pigment gallstones by discriminant analysis of radiographic features. *New Engl J Med* **1981**;304(14):808–811
23. Hickman MS, Schwesinger WH, Bova JD, et al. Computed tomographic analysis of gallstones: an in vitro study. *Arch Surg* **1986**;121:289–291
24. Moss G. Discharge within 24 hours of elective cholecystectomy. *Arch Surg* **1986**;121:1159–1161

Book Review

Pioneers and Early Years: A History of British Radiology. By Edward H. Burrows. Alderney, England: Colophon, 264 pp., 1986. £32.50

The field of radiology, now approaching its centennial, makes a tidy historical package that only a few investigators have chosen to open. Unlike any other major specialty, radiology can point to a clear beginning in 1896—a specific point from which all professional and technical achievements arose. And what an educating, entertaining, and cautionary spectacle the earliest years offer both the profession and the public! From popular ditties to bicycle-powered diagnostic units to personal triumphs and tragedies, the story of the X-ray is unique in the history of medicine.

In an admirably thorough fashion, Edward Burrows, senior consultant neuroradiologist at Southampton and a diligent historian of the field, looks at the first 35 years of radiology in England, with substantial reference to other venues. Including military, professional, technical, and institutional aspects of the field, Burrows has compiled a readable book that also serves as a valuable reference work. With useful histories of individual hospital X-ray departments, an essay on the development of journals (of special note to scholars), and a mine of vintage illustrations, the book becomes a guided tour of British organized radiology. Frequent biographies of figures great and small constitute something of an intrusion in the text, but are of substantial research interest.

This volume is a must for the radiologic history buff and certainly accessible to the historian who is not a practicing radiologist. Perhaps more important is its potential on the shelves of medical school libraries and departmental collections. Having recently talked to a group of young radiology residents who found the term "X-ray martyr" both unfamiliar and risible, I am concerned that our relatively short and fascinating history not be lost. Although the cost of Dr. Burrows's book (£32.5) is a bit steep for a nontechnical work, its value as a rare and readable resource on our past makes it a notable contribution to the field.

Nancy Knight
American College of Radiology
Reston, VA 22091

Perspective

The Promise of Extracorporeal Shock-Wave Lithotripsy for the Treatment of Gallstones

H. Joachim Burhenne[1]

A promise is in the air for a leap forward in the treatment of cholelithiasis, which in recent years has become a worldwide public health concern. In the United States alone 25 million patients are estimated to have cholelithiasis, over 10% of the population [1]. Gallstone disease is the most common indication for abdominal surgery, accounting for more than 500,000 operations annually in the United States [2].

In 1882, Langenbuch performed the first successful cholecystectomy and yet today, a century later, surgery is still the safest, most effective, and most widely recommended treatment for calculus biliary disease. The overall surgical mortality for cholecystectomy is less than 1% in most centers [3], but this rate will increase as the population advances in age. Although it is difficult to improve on this classical therapy, investigators continue to search for a treatment that is less expensive and that involves less morbidity. During the past decade several new approaches to the treatment of cholelithiasis have been proposed. Experience in treating gallstones with techniques designed to dissolve the stones has increased considerably. Two compounds—chenodeoxycholic acid and ursodeoxycholic acid, two bile acids naturally occurring in humans—have proved particularly effective in dissolving gallstones. These systemically administered compounds are naturally secreted in bile, but the 1- to 2-year treatment is expensive. A cholelitholytic effect is only achieved in stones that are composed mainly of cholesterol and that do not have a significant admixture of calcium salts, pigments, or mucus. A 10% recurrence rate has been reported within 1 year after discontinuation of bile acid medication [4].

Another cholelitholytic treatment involves the local application of dissolving agents via transhepatic or endoscopic catheter infusion. The use of the monoglyceride monooctanoin for the treatment of common duct stones requires instillation for several days [5]. Monooctanoin caused no response in 12 of 17 patients with intrahepatic calculi [6]. More recent reports on monooctanoin showed moderate-to-severe inflammation and ulceration of the gallbladder in animal experiments [7].

More rapid dissolution of cholesterol stones with the transhepatic instillation of methyl tert-butyl ether for the treatment of stones in the gallbladder and common duct is more promising [8]. Partial or total stone dissolution was achieved in 29 of 30 patients by means of percutaneous cholecystostomy [9]. The concept of using chemicals to dissolve gallstones is exciting, but the future of this form of therapy is uncertain.

The principle of electrohydraulic disintegration of stones was first tested in the 19th century [10]. Successful fragmentation by this mechanical method was reported in the transurethral treatment of bladder stones in 1970 [11]. In 1982 shock-wave application was successfully extended to extracorporeal treatment in the destruction of kidney stones by using a lithotripter with a Dornier water bath [12] (Munich-Germering, West Germany). The shock waves are generated by a high-voltage condenser spark discharged from an electrode. The electrode is placed under water in a geometric focus of an ellipsoid reflector. The high-voltage discharge of the condenser causes a sudden evaporation of water, and the associated expansion of the water results in the genera-

Received March 25, 1987; accepted after revision April 15, 1987.
[1] Department of Radiology, University of British Columbia, 855 W. 12th Ave., Vancouver, B.C., Canada V5Z 1M9. Address reprint requests to H. J. Burhenne.

AJR **149:233–235, August 1987** 0361–803X/87/1492–0233 © American Roentgen Ray Society

tion of a shock wave. Shock waves are reflected from the ellipsoid surrounding wall and are bundled into a second focus. Shock waves can be distributed evenly throughout the body since the acoustic impedance of most body tissue is similar to that of water. The kidney stone is located by means of a two-axis fluoroscopic X-ray system whose axes intersect in the second focus of the shock-wave reflector.

The use of hydraulic shock-wave for the successful fragmentation of biliary tract stones in vitro and in vivo was first reported in 1975 [13]. Further successful cholelithotripsy was also reported subsequently in the radiologic literature [14, 15]. These reports involved intracorporeal lithotripsy, which was successfully extended to extracorporeal treatment in 1986 by Sauerbruch et al. [16]. This group, working at the Munich Medical School in Grosshadern, West Germany, used a modified Dornier extracorporeal renal lithotriper to disintegrate gallbladder stones in nine patients. Patients were treated in a prone position in the water bath, but sonography instead of radiologic monitoring was used for targeting. The five common bile duct stones described in this report were treated with the unmodified Dornier renal extracorporeal lithotripsy equipment. Both animal and human studies indicate that extracorporeal lithotripsy is well tolerated without serious side effects. Lung tissue, however, must be avoided in the shock-wave path as wave exposure on the thoracic region of the rat resulted in extensive lung damage [17]. The great difference in the acoustic properties of air, as opposed to tissue in the alveoli of the lung, creates a great number of acoustic interfaces so that a tensile stress is created on the membranes.

Extracorporeal cholelithotripsy carries some risk in that gallstone fragments could obstruct the cystic or common bile ducts. In the initial report from the group in Germany [16], three of their nine patients did not experience complete stone disappearance after cholelithotripsy. Sludge or fragments persisted in these three patients during a follow-up period of 22–34 weeks, but did not cause biliary pain. These changes were noted, even though all patients received systemic application of both ursodeoxycholic acid and chenodeoxycholic acid. This treatment was started 1 week before shock-wave therapy and was continued for up to 6 months. No randomized trial was obtained to ascertain the additional benefit from adjuvant chemotherapy to cholelithotripsy. Furthermore, the recurrence of gallstones is likely.

The promise of extracorporeal biliary lithotripsy is enormous, especially when the prevalence of the disease and the prospects for noninvasive treatment are considered. All initial reports are encouraging, and success rates are higher than those reported for chemical stone dissolution.

We have started to treat bile duct stones at Vancouver General Hospital with an unmodified Dornier renal lithotripsy unit and have had complete success in our first three cases. No adjuvant cholelitholytic therapy was used. Two patients passed their fragments spontaneously. In the third patient, who had two large retained cystic duct stones, the remaining fragments were removed with the basket technique through a T-tube tract. Targeting of the bile duct stones in these three cases was accomplished under fluoroscopic control after contrast application through a transhepatic or trans–T-tube tract catheter.

The use of a modified Dornier renal lithotripter to fragment gallbladder stones has been reported only by the group in Germany [16]. In contrast to the renal lithotripsy equipment, this Dornier modification uses sonography for targeting the stones. More work is now required to determine what type of gallbladder stones (other than cholesterol stones) can be successfully fragmented. During my recent visits to the University of Munich, I have observed successful fragmentation of calcified gallbladder stones.

The small number of patients reported so far undergoing biliary lithotripsy were all symptomatic. Is lithotripsy treatment of silent gallstones indicated in the future? A survey of several reports showed that only 5–28% of persons with cholelithiasis at autopsy had biliary symptoms during their lifetime [18]. Available data favor a policy of expectant management, but there is evidence in the literature both in favor of and against surgery for silent gallstones. Biliary lithotripsy could certainly be substituted in patients with silent gallstones who are scheduled for elective surgery.

The ideal extracorporeal lithotripsy apparatus will treat both renal and biliary stones. It should provide both sonographic and X-ray facilities for targeting. A single X-ray C-arm with fluoroscopy in two different positions should suffice for triangulation. Improvement in spatial and contrast resolution is required for better visualization of fragments. Detail can be further improved with added digital manipulation of the image. The recent installation and successful use of the Siemens Lithostar (Siemens, Erlangen, West Germany) for renal stone treatment has enhanced competition and should stimulate further research and development. New lithotripsy apparatus with contact skin positioning of the shock-wave applicator permits omission of the water bath. This technical advance can be expected to lead to smaller and, possibly, portable units.

Extracorporeal renal lithotripsy was first applied successfully by urologists and now is used almost universally by urologists. The radiologist is a member of the lithotripsy team in less than six institutions. This is unfortunate if we realize that the imaging aspect of renal lithotripsy is the most difficult part of the treatment. Targeting small fragments with the renal lithotripsy equipment that is currently available is difficult [19]. The radiologist, however, has been important in the development of biliary lithotripsy [13–15, 20, 21], and we believe that a team approach to the treatment of gallstone disease should result in the highest possible success rates. At the University of British Columbia in Vancouver, we have formed a team of radiologists, surgeons, and gastroenterologists to implement cholelithotripsy. The clinician can best evaluate the patient and decide whether biliary lithotripsy is appropriate, while the radiologist is best qualified to target the stones using fluoroscopy and sonography. Cholelithotripsy can be facilitated by the interventional radiologist, but managing patients with complex medical problems is best accomplished by the clinician [22]. This is certainly not the time for the radiologist to act as the primary physician [23].

Biliary lithotripsy is still in its infancy, but its use is growing

rapidly. A large amount of investigation is required before this therapeutic technique will find its proper place in medicine. Radiologists are well advised to initiate research on biliary lithotripsy, preferably by using an interdisciplinary approach. The Dornier Company in Munich manufactures a small laboratory lithotripter that is well suited for animal research. It is likely that interventional radiologic procedures complementary to biliary lithotripsy will have to be developed and employed in the future.

REFERENCES

1. Tyor MP. Gallstone disease. Washington, DC: National Digestive Disease Education and Information Clearing House, Health and Human Services, **1982**
2. Simeone JT, Ferrucci JT Jr. New trends in gallbladder imaging. *JAMA* **1981**;246:380–383
3. Dempsey DT, Rosato EF. Surgical management of cholelithiasis. In: Cohen S, Soloway RD, eds. *Gallstones*. New York: Churchill Livingstone, **1985**
4. Fromm H. Gallstone dissolution therapy. Current status and future prospects. *Gastroenterology* **1986**;91:1560–1567
5. Thistle JL, Carlson GL, Hofman AF, et al. Monooctanoin, a dissolution agent for retained cholesterol bile duct stones: physical properties and clinical application. *Gastroenterology* **1981**;78:1016
6. Butch RJ, MacCarty RL, Mueller PR, et al. Monooctanoin perfusion treatment of intrahepatic calculi. *Radiology* **1984**;153:375–377
7. McGahan JP, Lee LL, Tesluk H, Nyland TG, Ruebner B, Schmidt B. Dissolution of gallstones using cholecystostomy tube in the pig. *Invest Radiol* **1987**;22:201–205
8. Allen MJ, Borody TJ, Bugliosi TF, May GR, LaRusso NF, Thistle JL. Rapid dissolution of gallstones by methyl tert-butyl ether, preliminary observations. *N Engl J Med* **1985**;312:217–220
9. May GR, Thistle JL. Percutaneous cholecystostomy for gallstone dissolution by methyl tert-butyl ether. Presented at the annual meeting of the Radiological Society of North America, Chicago, December **1986**
10. Riches E. The history of lithotomy and lithotrity. *Ann R Coll Surg Engl* **1968**;43:185–199
11. Reuter HJ. Electronic lithotripsy: transurethral treatment of bladder stones in 50 cases. *J Urol* **1970**;104:834–838
12. Chaussy C, Schmiedt E, Jocham D, Brendel W, Forssmann B, Walther V. First clinical experience with extracorporeally induced destruction of kidney stones by shock waves. *J Urol* **1982**;127:417–420
13. Burhenne HJ. Electrohydrolytic fragmentation of retained common duct stones. *Radiology* **1975**;117:721–722
14. Martin EC, Wolff M, Neff RA, Casarella WJ. Use of the electrohydraulic lithotripter in the biliary tree in dogs. *Radiology* **1981**;139:215–217
15. Lear JL, Ring EA, Macoviak JA, Baum N. Percutaneous transhepatic electrohydraulic lithotripsy. *Radiology* **1984**;150:589–590
16. Sauerbruch T, Delius M, Paumgartner G, Holl J, et al. Fragmentation of gallstones by extracorporeal shock waves. *N Engl J Med* **1986**;314:818–822
17. Chaussy CH, ed. *Extracorporeal shockwave lithotripsy: new aspects in the treatment of kidney stone disease*. Basel, Switzerland: Karger, **1982**
18. Gracie WA, Ransohoff DR. Natural history and expectant management of gallstone disease. In: Cohen S, Soloway RD, eds. *Gallstones*. New York: Churchill Livingstone, **1985**
19. Barth KH, Pahira JJ, Elliott LP. Extracorporeal shockwave lithotripsy: role of the radiologist. *Radiology* **1985**;155:835–836
20. Gacetta DJ, Cohen MJ, Crummy AB, Joseph DB, Kuglitsch M, Mack E. Ultrasonic lithotripsy of gallstones after cholecystostomy. *AJR* **1984**;143:1088–1089
21. Davies H, Bean WJ, Barnes FS. Breaking up residual gallstones with an ultrasonic drill. *Lancet* **1977**;2(1):278–279
22. Burhenne HJ. Open forum. Interventional cholelithotomy as an alternative to cholecystectomy: with or without the surgeon? *Invest Radiol* **1986**;21:594–595
23. Evens RG. The radiologist as an attending physician: routine or special procedure? *Radiology* **1985**;154:545–546

Book Review

Functional Studies Using NMR. Edited by V. Ralph McCready, Martin Leach, and Peter J. Ell. New York: Springer-Verlag, 206 pp., 1987. $69.50

Based on a series of lectures regarding the functional and metabolic aspects of MR, this text has 11 chapters and several contributors. As stated by the authors, the main objective is to provide the reader with background information and a summary of the advances and current work in metabolic and functional MR studies.

In the first four chapters, the authors concisely and clearly explain the physical basis of MR and functional parameters of MR as well as flow, cardiac, sodium, and fast imaging methods. Good illustrations accompany the text. The applications of MR spectroscopy to metabolic research and clinical studies of the brain, heart, and liver are also well discussed.

While both chapters five and six discuss functional MR imaging of the heart and cardiovascular systems, chapter five deals mainly with echo-planar imaging of the heart and great vessels. In chapter seven the authors extensively cover the different pharmaceuticals available for functional studies. Particularly well illustrated, chapter eight discusses most aspects of the clinical use of gadolinium-DTPA in MR of the CNS. Chapter nine clearly presents tissue characterization, its measurement methods, and MR parameters in normal and abnormal tissues. The influence of MR parameters on imaging are presented in chapter 10. The book ends with a discussion of a correlative approach to nuclear medicine and MR imaging.

The text is well written and beautifully illustrated, printing is adequate, and legends are clear. Unfortunately the quality of the illustrations in chapter five is lower than in the rest of the text. Also, the authors use a right and left standard different from the standard used in the other chapters. In chapter six, again, a schematic view of the chest does not correspond to the other illustrations. Also, many radiologists will not favor the use of the abbreviation NMR for MR imaging in the title and throughout the text.

Despite the few shortcomings described above, this text provides a good basis for the applications of MR to the study of different organ functions, particularly for those readers with a background in nuclear medicine. Despite the fact that the book has several contributors, it is well organized and meets the objectives stated by the authors.

Juan F. Lois
UCLA School of Medicine
Los Angeles, CA 90024

Measurement of Myocardial Infarct Size at Early and Late Time Intervals Using MR Imaging: An Experimental Study in Dogs

Gary R. Caputo[1,2]
Udo Sechtem[1]
Dimiter Tscholakoff[1,3]
Charles B. Higgins[1]

The current study assessed the capability of ECG-gated MR imaging to quantitate both the percentage of the left ventricle involved by acute myocardial infarction and the mass of acute myocardial infarction at 3 and 21 days after coronary occlusion in dogs. Infarct mass was measured from gated transverse MR images using computer-generated calculated-T2 images. T2 images provided accentuation of the boundary between infarcted and normal myocardium as well as objective, reproducible calculation of image voxels representing infarcted myocardium. Postmortem and in vivo MR infarct mass and percentage correlated closely at 3 days (r = .98, SEE = 0.73 g; r = .97, SEE = 1.2%), and 21 days (r = .94, SEE = 1.54 g; r = .95, SEE = 1.61%). Left ventricular mass, infarct mass, and percentage of infarct were measured on end-diastolic MR images. Infarct mass at 3 and 21 days was not significantly different, with a mean deviation of 0.63 g. There was close intra- and interobserver reproducibility (r = .99 and r = .90, respectively) for measurement of infarct mass.

The quantitative technique employed for determining the mass of acute myocardial infarctions, based on the different T2 relaxation times of infarcted and normal myocardium, provides for objective analysis and reproducibility. With this technique, MR provides an accurate method for assessing the mass of acute infarcts and the percentage of the left ventricle involved by the infarct both early and late after coronary occlusion.

Considerable effort has been devoted to the development and evaluation of noninvasive techniques for quantitation of acute myocardial infarction. These techniques have included precordial ST segment and R wave mapping [1], serum creatinine-phosphokinase analysis [2–4], echocardiography [5], radionuclide imaging [6–10], and transmission CT [11–12]. An accurate, reproducible, and noninvasive method for the quantitation of infarct size provides an insight into prognosis [3]. It might be useful to guide therapy and to evaluate interventions used to limit the amount of ischemically damaged myocardium. In this regard, such a technique could be useful for assessing the result of thrombolytic therapy in acute myocardial infarction.

MR imaging is a new noninvasive technique for imaging the cardiovascular system [13]. It does not require the use of ionizing radiation or contrast media. MR imaging of the heart offers the advantages of having natural contrast between the blood pool and cardiac structures, because flowing blood produces minimal MR signal [14] and high soft-tissue contrast, enabling direct visualization of the myocardium and sharp delineation of the myocardium from blood pool and pericardium [13]. Several studies in animals [15, 16] and humans [17] have shown that the acutely infarcted myocardium can be recognized on gated MR images because of an increase in signal intensity compared with normal myocardium.

The present study was designed to develop a technique to measure infarcted myocardial mass with MR imaging and to evaluate the accuracy and reproducibility of this technique in dogs. The accuracy of infarct quantitation at early and late time intervals after coronary occlusion was also evaluated.

Received December 11, 1986; accepted after revision May 5, 1987.

G. R. Caputo and D. Tscholakoff were research fellows in MR Imaging. G. R. Caputo was supported by NRSA grant 5T32 HL 07278–08. D. Tscholakoff was supported by NIH Fogarty International Center grant FOST WO 34 37.

[1] Department of Radiology, University of California School of Medicine, San Francisco, CA 94143. Address reprint requests to C. B. Higgins.

[2] Present address: Department of Cardiology, Advanced Cardiac Imaging, LDS Hospital, 8th Ave. and C St., Salt Lake City, UT 84143.

[3] Present address: Zentrales Institute Sur Radiodiagnostik der Universitat, 4 Alser Str., Vienna, Austria.

AJR 149:237–243, August 1987
0361–803X/87/1492–0237
© American Roentgen Ray Society

METHODS

Experimental Model

Eleven adult mongrel dogs weighing 15–29 kg were premedicated intramuscularly with droperidol and fentanyl citrate (Innovar 0.1 ml/kg), intubated and anesthetized with IV sodium pentobarbital (20–25 mg/kg), and ventilated with a Harvard respirator. The heart was exposed via left thoracotomy, and the left anterior descending coronary artery was dissected free. A ligature was placed around the vessel, the artery was occluded, and the chest wound was closed.

At 3 and 21 days after surgery, MR imaging was performed by anesthetizing the dogs with Innovar intramuscularly (0.1 ml/kg) and with IV sodium pentobarbital (20–25 mg/kg). The imaging at 3 days for one dog was technically inadequate because of excessive noise produced by the imager, and this imaging sequence was excluded from the study. However, the 21-day images were adequate for analysis in this animal and were included in the analysis.

Postmortem Examination

The dogs were sacrificed after the last MR examination at 21 days after occlusion. At autopsy, the right ventricle, both atria, the semilunar valve, and the atrioventricular valve were removed from each heart. The left ventricle was weighed with a Mettler balance and then sliced transversely into 10-mm-thick sections from apex to base. The slices were incubated in a 2% solution of 2,3,5-triphenyltetrazolium chloride for 10 min at 37°C. Although at 3 and 21 days the infarcted region could be discerned without staining, this process provided vivid delineation of the infarcted myocardium. The endocardial and epicardial borders of the left ventricular wall and the area of grossly visible myocardial infarction were traced onto clear film overlays. For each section, the total area and the area of infarcted myocardium were measured by planimetry using a digitizer interfaced to a PDP 11-70 computer (Digital Equipment Corp., Maynard, MA). The thickness of each myocardial slice was measured with a micrometer, five times for each section. The average thickness for each section was multiplied by its respective area to determine volume. These myocardial volumes were summed from each section to determine total, normal, and infarcted myocardial volumes. These volumes were multiplied by the specific gravity of myocardium (1.05 g/ml) to obtain the corresponding masses. The percentage of the entire myocardium involved by infarction was also calculated as: % infarct = (infarct mass/total mass) × 100.

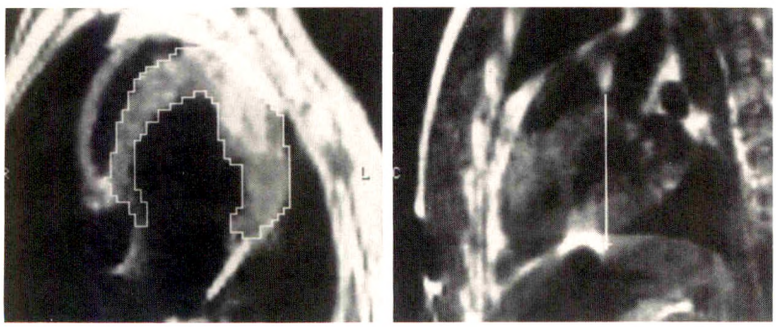
MR Imaging

Imaging was performed with a superconducting magnet operating at 0.35 T (Diasonics MT/S, Milpitas, CA) with a corresponding resonance frequency of 15 MHz, as previously described [18]. ECG-gated, dual spin-echo sequences (first echo, TE = 30 msec; second echo; TE = 60 msec) with multislice acquisition were used to image the left ventricle from apex to base with contiguous slices that were positioned at 10-mm intervals. This required two separate sets of multislice images. Each set consisted of five images. The two sets were positioned so that the caudal slice of set 1 coincided with the cranial slice of set 2. In this manner, a total of nine contiguous slices covering the entire heart were obtained. Transaxial, multisection imaging was implemented to allow the imaging of each section at multiple times in the cardiac cycle. This cycle-gated sequence obtained first-echo (TE = 30 msec) and second-echo (TE = 60 msec) images at each of the five contiguous anatomic sections at five phases of the cardiac cycle [14]. Each of the five sections were obtained at end-diastole and, additionally, at four 100-msec intervals extending into the cardiac cycle. Time for the total imaging of the entire heart was approximately 40–70 min. After completion of the transaxial cycled sequences, a standard 10-slice, single-echo, sagittal-imaging sequence lasting between 7 and 10 min was used to measure the height of the left ventricle.

Image Analysis

Although the signal-to-noise ratio varied from animal to animal because of such factors as respiratory motion, artifacts, and coil-filling factor, a standard approach for setting display windows was used. Using the first-echo image, each observer set the maximum gray-scale value to the intensity of the epicardial fat in each animal. The upper window was set to 100% of the maximum gray-scale value, and the lower window was set to 6% background subtraction. This was done for every image in each dog.

The measurements of infarct size and left ventricular mass were done on end-diastolic images of each anatomic level. Regions of interest were constructed, encompassing the endocardial and epicardial borders of the left ventricle for each transaxial level acquired at end-diastole. The end-diastolic images were all acquired at 10 msec after the R wave, and a midventricular sagittal slice was used to measure the height of the left ventricle to correct for partial-volume effects (Fig. 1). This was used to define the height of the left ventricle, and this measurement was employed for partial-volume corrections



A B

Fig. 1.—*A*, Transaxial midventricular MR image acquired at end-diastole with left ventricular myocardial region of interest.
***B*, Sagittal MR image through left ventricle showing height measurement used to correct the most caudal slices for partial-volume effects.**

of the slice at the caudal end of the ventricle. Each of these regions was drawn by two independent observers for the 3- and 21-day images.

Determination of Left Ventricular Mass

An oil-filled, lucite phantom was used to determine the milliliter per voxel in the x (1.79 mm), y (1.79 mm), and z (9.45 mm) planes using a 48-cm field of view, yielding a calculated value of 0.0334 ml/voxel. This calibration was found to vary less than 1% throughout the course of the study. For end-diastole, the total number of left ventricular myocardial voxels was determined, using regions of interest encompassing the left ventricle (Fig. 1). The total number of left ventricular myocardial voxels was multiplied by 0.0334 ml/voxel to determine myocardial volume. The specific gravity of myocardium (1.05 g/ml) was then multiplied by the myocardial volume to yield myocardial mass [18]. Since the most inferior transaxial slice was most affected by partial-volume problems, its number of voxels was adjusted using the length of the left ventricle (Fig. 1). If the length of the ventricle was measured as a number of centimeters and a fraction of a centimeter, then the caudal boundary section was multiplied by this fraction to minimize partial-volume errors (i.e., in a left ventricle that would measure 9.5 cm in height, only 50% of the volume of the caudal slice would contribute to total myocardial volume). Partial-volume correction was not complete since it was done for only the caudal end of the heart. However, assignment of partial volume to both ends would have had to be done in an arbitrary way and was not considered necessarily more accurate.

Previous work from our laboratory has shown that the mean T2 relaxation time of infarcted canine myocardium in vivo was 59 ± 13 msec [16]. Normal in vivo myocardium had a mean T2 of 37 ± 4 [16]. High-intensity flow signal caused by stasis of blood adjacent to akinetic and dyskinetic regions of myocardium results in negative values for T2 relaxation times or a T2 value greater than 100 msec [17]. When T2 is calculated for an entire tomographic image on a pixel-by-pixel basis, a new image can be generated that has the T2 relaxation times for each pixel encoded into the gray scale (range, 0–300 msec). T2 values of 300 msec are set to the maximum value of the range and are displayed as white, while T2 values of 0 are displayed as black.

Pixels showing an absolute increase in signal intensity from the first- to second-echo image have a negative value using the double spin-echo formula. This only occurs to pixels containing tissue in motion and is due to second-echo rephasing [17, 19]. With our software, such pixels are also given the brightest intensity on calculated-T2 images. Based on the T2 value of infarct found from previous work in our laboratory [16–17], criteria for pixels on the calculated-T2 images containing infarcted myocardium were set as values between 50 and 100 msec, inclusive. To facilitate the delineation of such pixels, the maximum value of the gray scale was reduced from 300 to 100 msec.

This resulted in all pixels of values 100–300 msec being displayed as white. The display window settings were 100% maximum gray-scale value with 50% background subtraction. This resulted in all pixels with T2 values between 0 and 50 msec (normal myocardium) being displayed as black, those with values between 50 and 100 msec (infarcted myocardium) being displayed as gray, and those with values greater than 100 msec (nonmyocardial structures and intracavitary flow signal) being displayed as white (Fig. 2).

For each calculated-T2 image, contiguous infarct pixels were defined using region-of-interest analysis and summed to yield total pixels containing myocardial infarct. The boundary of the region of interest was determined by interrogating each contiguous gray myocardial pixel with a cursor to verify that the contained T2 value of the pixel was between 50 and 100 msec, inclusive. The number of pixels was

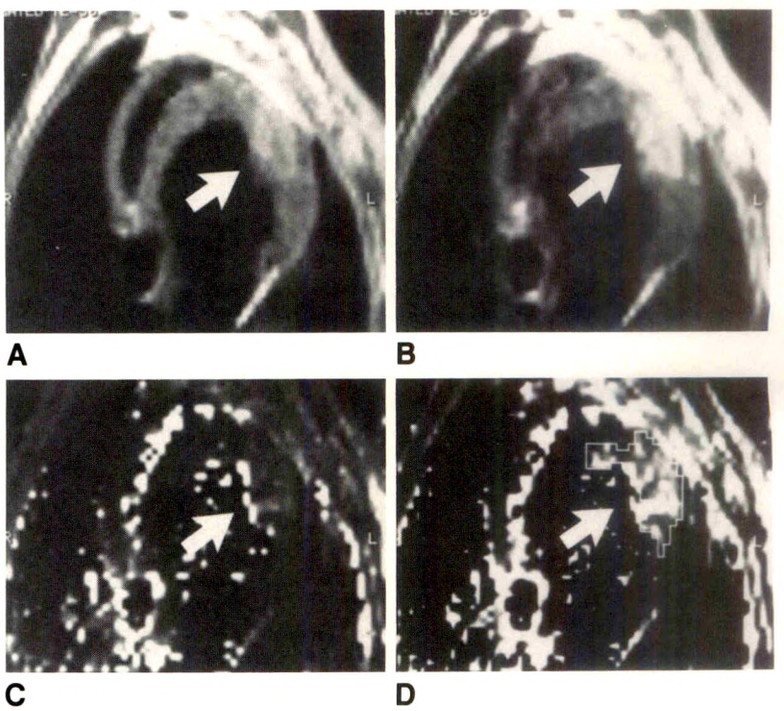


Fig. 2.—*A*, First-echo (TE = 30 msec), transaxial midventricular MR image acquired at end-diastole showing region of infarcted myocardium as a region of high signal intensity (*arrow*).

***B*, Second-echo (TE = 60 msec), transaxial midventricular MR image acquired at end-diastole showing region of infarcted myocardium as a region of increased signal intensity (*arrow*) compared with normal myocardium.**

***C*, Transaxial, calculated-T2 MR image acquired at end-diastole through same level of left ventricle as in *A* and *B*, showing region of infarcted myocardium as an area of increased T2 (*arrow*). Maximum intensity is set to 300 msec, with window settings of 100% maximum scale, 0% background subtraction.**

***D*, Transaxial, calculated-T2 MR image acquired at end-diastole at same level as *C*, showing region of infarcted myocardium as gray pixels with region of interest drawn (*arrow*) and flow signal as white pixels. Maximum intensity is set to 100 msec, with window settings of 100% maximum scale, 50% background subtraction.**

multiplied by 0.0334 ml/pixel and then by 1.05 g/ml to yield total mass of infarcted myocardium.

The percentage of infarcted myocardial mass was calculated for both the 3- and 21-day images using the formula: % infarcted myocardium = [total infarcted mass)/total myocardial mass)] × 100.

Statistical Analysis

Total left ventricular mass and infarcted mass determined by weighing tissue, by planimetry of traced overlays of autopsy specimens, and by MR imaging were compared using linear regression with calculation of correlation coefficients and standard errors of the estimate. Intra- and interobserver reproducibility were evaluated in a similar fashion using linear regression.

Results

Measurement of Left Ventricular Mass

Figures 3–10 show the comparisons of infarct measurement by MR imaging and the two postmortem techniques. The infarct produced high signal intensity on MR images compared with surrounding normal myocardium. This region could be followed on tomograms extended from base to apex to the left ventricle (Fig. 3). Left ventricular mass determined by weighing tissue correlated closely with digital planimetry of traced overlays of the postmortem tissue slices ($r = .94$, SEE = 8.0 g) (Fig. 4). Mass determined by left ventricular weight correlated well with the left ventricular mass determined from MR images ($r = .96$; SEE = 5.1 g) (Fig. 5). Mass determined by postmortem planimetry and MR also showed good correlation ($r = .93$, SEE = 6.42 g). Thus, MR provided an accurate estimation of left ventricular mass when compared with the two postmortem measurements.

Measurement of Infarct Size

At 3 days, myocardial infarct mass and percentage of the left ventricle involved by infarcted myocardium as determined by MR correlated well with autopsy planimetry measurements ($r = .98$ and .97, respectively) (Figs. 6 and 7). The similar comparison made at 21 days yielded a correlation coefficient of .94 and infarct mass and .95 for percentage of infarcted myocardium (Figs. 8 and 9). There was also close correlation between the 3- and 21-day MR measurements of both infarct mass ($r = .94$) and percentage of infarcted myocardium ($r = .94$) (Fig. 10). The mean difference in infarct mass at the two time intervals was ±0.63 g. There was no significant difference in infarct mass determined by MR at 3 days and 21 days.

Calculations of intraobserver reproducibility for both myocardial infarct mass and percentage of infarcted myocardium yielded a correlation coefficient of .99, while the calculations of interobserver reproducibility yielded correlation coefficients of .90 and .89, respectively.

Discussion

The clinical course of patients after acute and chronic myocardial infarction is directly related to the total amount of left ventricular muscle mass that has been irreversibly damaged [3, 20, 21]. Consequently, the determination of infarct

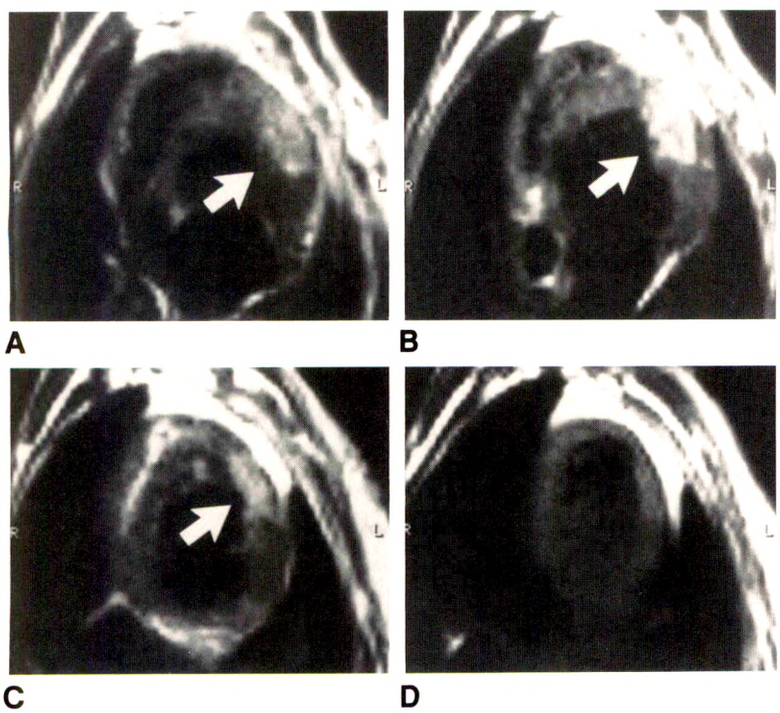


Fig. 3.—*A–D*, Transaxial MR images (TE = 60 msec) extending from cranial to caudal aspects of the left ventricle showing region of infarcted myocardium as having increased contrast (*arrows*) compared with normal myocardium.

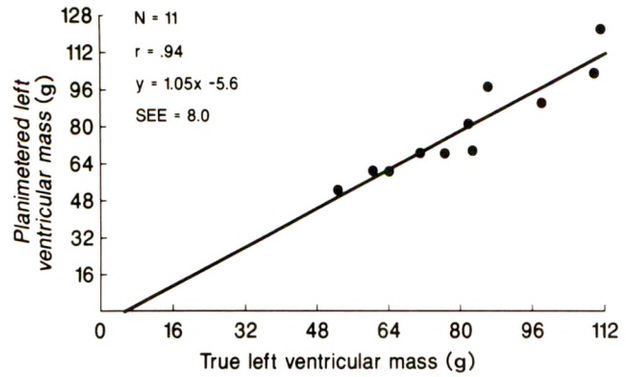


Fig. 4.—Left ventricular mass determined by planimetry at autopsy compared with that determined by weighing at autopsy. r = correlation coefficient, SEE = standard error of estimate.

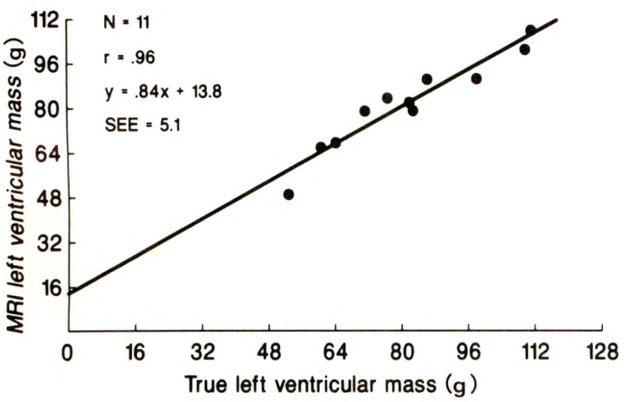


Fig. 5.—Left ventricular mass determined by MR imaging (MRI) at 21 days compared with that determined by weighing at autopsy. r = correlation coefficient, SEE = standard error of estimate.

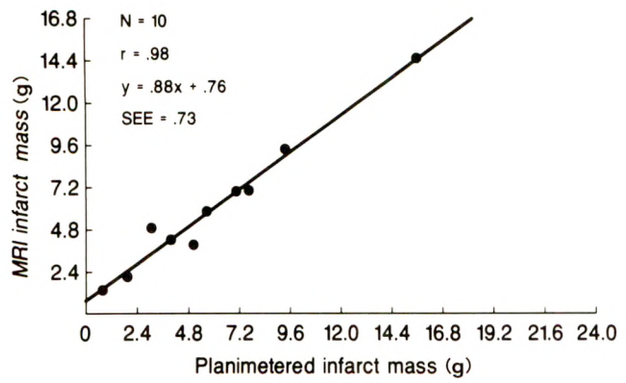


Fig. 6.—Left ventricular infarct mass determined by MR imaging (MRI) at 3 days compared with that determined by planimetry at autopsy. r = correlation coefficient, SEE = standard error of estimate.

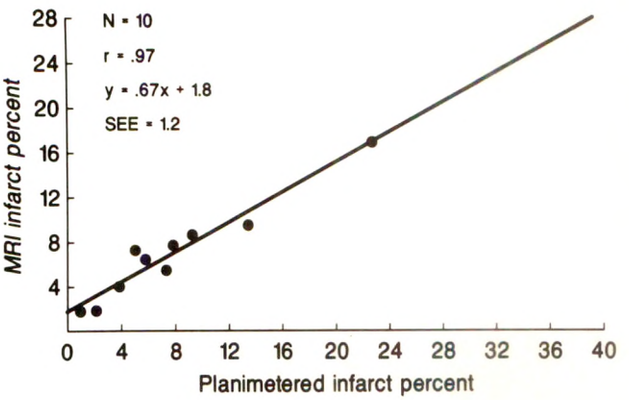


Fig. 7.—Left ventricular percentage of infarcted myocardium determined by MR imaging (MRI) at 3 days compared with that determined by planimetry at autopsy. r = correlation coefficient, SEE = standard error of estimate.

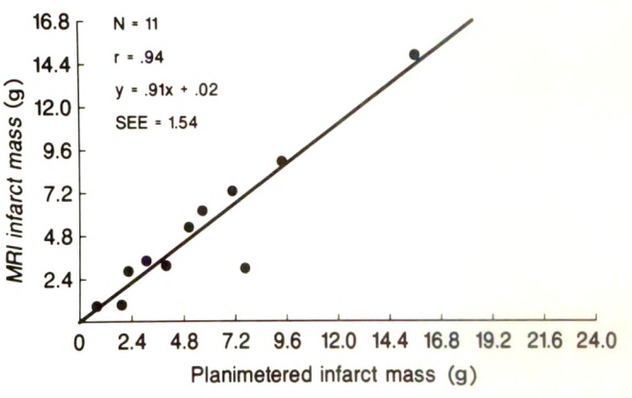


Fig. 8.—Left ventricular infarct mass determined by MR imaging (MRI) at 21 days compared with that determined by planimetry at autopsy. r = correlation coefficient, SEE = standard error of estimate.

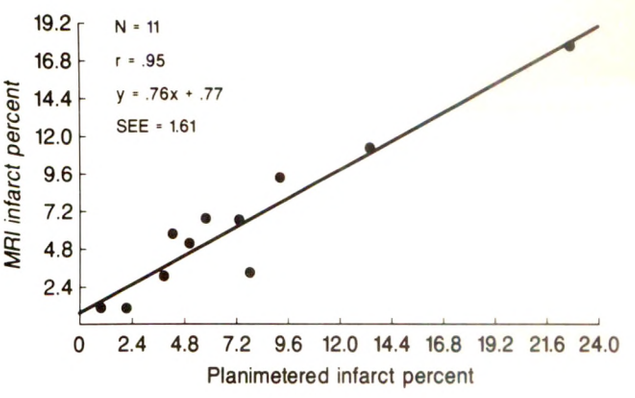


Fig. 9.—Left ventricular percentage of infarcted myocardium determined by MR imaging (MRI) at 21 days compared with that determined by planimetry at autopsy. r = correlation coefficient, SEE = standard error of the estimate.

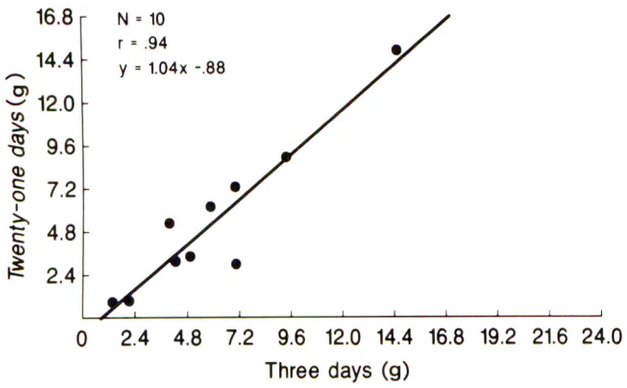


Fig. 10.—Left ventricular infarct mass determined by MR imaging at 3 days compared with that determined at 21 days. r = correlation coefficient, SEE = standard error of estimate.

size is an important prognostic indicator. Patients who develop pump failure after myocardial infarction usually have more than 40% of their left ventricular muscle mass irreversibly damaged [20]. Refractory ventricular arrhythmias developing after an acute myocardial infarction may also be related to infarct size [22]. The extent of myocardial injury may be modified by therapeutic interventions [23]. However, the accuracy of noninvasive techniques for sizing infarcts remains unknown.

The present study shows the capability of gated MR imaging to quantitate the mass of acutely infarcted myocardium in dogs. In addition to MR imaging, several other methods of infarct sizing have been developed, including precordial S-T segment and R wave maps [2]. However, precordial mapping is relatively insensitive in the identification of small anterior infarcts. Methods employing serum creatine-phosphokinase release measurements [2, 4] when obtained for 24 hr after infarction tend to underestimate the size of large anterior infarcts.

Techniques employing technetium-99m pyrophosphate [7, 9, 10] for infarct sizing are limited because although technetium-99m is a marker of myocardial necrosis, its accumulation in regions of ischemically damaged myocardium depends on a threshold level of residual myocardial perfusion [24]. Technetium-99m myocardial scintigrams may fail to recognize anterior infarcts weighing less than 3 g and may overestimate the size of small, predominantly subendocardial infarcts.

While technetium-99m pyrophosphate and iodinated contrast material are taken up by damaged cells, thallium-201, like other potassium analogs, is also taken up by normal myocardial cells. Thallium-201 myocardial concentration is related to the level of myocardial perfusion [25] and the integrity of active membrane transport by myocardial cells [26]. Previous studies [24] have shown reduced thallium-201 activity at the margin of the infarct, where technetium-99m pyrophosphate activity is most intense. This is apparently a zone of considerable residual blood flow that is insufficient to maintain viability of many myocardial cells. Infarct sizing methods using thallium-201 [6, 8] have this limitation; this technique has considerably overestimated infarct volumes after the first few days beyond the acute event [6].

Attempts to quantitate infarct size from echocardiograms [5] show that identification of regions with reduced wall thickening achieved some degree of separation of normal from infarcted myocardium; although zones adjacent to but not part of the infarction frequently showed abnormal endocardial motion as well. Overlap of functional measurements of distant normal, adjacent normal, and infarcted zones persisted, even using wall-thickening analysis. Thus, regional contraction abnormalities on two-dimensional echocardiography do not necessarily define the extent of an ischemic or infarcted zone.

Contrast-enhanced CT has yielded accurate, reproducible estimates of infarct volume in dogs [12]. However, the need for ECG-gated acquisition of cardiac CT scans in patients has not been realistic for clinical evaluation using conventional CT scanners. The recent introduction of millisecond CT scanners may make such capability useful for patient studies.

The present study shows that ECG-gated, spin-echo MR imaging detects acutely infarcted myocardium as a region having significantly prolonged T2 relaxation times. Previous work in our laboratory in ex vivo [15] and in vivo [16] canine hearts has shown a significant increase in percentage of water content of infarcted compared with normal canine myocardium, and a close linear relationship between T2 relaxation time and water content in acutely infarcted myocardium. This is probably related to local changes in tissue water resulting from myocardial edema, but is apparently not the only factor responsible for increased signal intensity and relaxation time of the infarct [27].

A recent ex vivo canine study [28] using a similar technique to quantitate acutely infarcted myocardial mass found a close correlation ($r = .98$) between infarct size determined by MR imaging and histochemical staining. Since this study did not have the problems inherent in imaging the beating heart, the results must be considered the best attainable with MR imaging.

The relatively small change in myocardial infarct size between 3 and 21 days as determined by MR imaging suggests that MR imaging detects irreversibly damaged myocardium and is insensitive to areas of jeopardized and reversibly injured myocardium in the early phases of evolution of the infarct. On the other hand, infarct size within the first 24 hr was not evaluated by the current study, and no conclusion can be drawn about the accuracy of infarct estimation at this earlier time. However, a recent canine study from our laboratory [29] suggests that reversible myocardial injury does not alter magnetic relaxation time or signal intensity on MR images, while irreversible injury causes alterations in relaxation time and increased signal intensity of the damaged myocardium. Imaging with contrast-enhanced CT scans has estimated larger infarcts within the first week, compared with 3 weeks after infarction [12].

Although it is not realistic to expect constancy of the positioning of the heart in the scanner on both the 3- and 21-day images, MR is a three-dimensional technique allowing accurate and comparative volumes of myocardial tissue to be

attained. This is not true for comparing the area of similar slices at different times, but holds true for the measurement of total volume.

A potential pitfall exists in quantitating subendocardial regions of myocardial infarct by MR imaging. A prior report from our laboratory [30] has shown that high signal intensity can be caused by stasis of blood adjacent to akinetic and dyskinetic regions of myocardium on the second spin-echo images. However, this phenomenon can be discriminated from acutely infarcted myocardium on the calculated-T2 image, since measurement of T2 relaxation time in a high-intensity region caused by stasis of blood results in a negative value of T2. Only even-echo rephasing of slowly moving blood results in a negative T2 value [19] that is encoded in the T2 image as a prolonged positive value; measurements of solid tissue will not produce negative T2 values.

The present study only addresses the accuracy of this technique in quantitating anterior-wall myocardial infarcts using the transaxial cardiac imaging plane. If the same imaging plane was employed in an attempt to quantitate infarcts involving the inferior wall, partial-volume effects would probably result in decreased accuracy. However, this problem should be eliminated by the use of short-axis cardiac-imaging planes obtainable by oblique-angle MR imaging techniques.

In summary, the current study shows that MR can accurately and reproducibly measure acutely infarcted myocardial mass and percentage of infarcted myocardium. ECG-gated MR imaging is an accurate, reproducible, and noninvasive approach for determining the mass of acutely infarcted myocardium. A quantitative technique based on different T2 relaxation times of infarcted and normal myocardium provides for objective analysis and reproducibility.

REFERENCES

1. Henning H, Hardarson T, Francis G, O'Rourke RA, Ryan W, Ross J. Approach to the estimation of myocardial infarct size by analysis of precordial S-T segment and R wave maps. *Am J Cardiol* **1978**;41:1–8
2. Grande P, Hansen BF, Christiansen C, Naestoft J. Estimation of acute myocardial infarct size in man by serum CK-MB measurements. *Circulation* **1982**;65:756–764
3. Sobel BE, Bresnahan GF, Shell WE, Yoder RD. Estimation of infarct size in man and its relation to prognosis. *Circulation* **1972**;46:640–648
4. Rogers WJ, McDaniel HG, Smith LR, Mantle JA, Russell RO, Rackley CE. Correlation of angiographic estimates of myocardial infarct size and accumulated release of creatine kinase MB isoenzyme in man. *Circulation* **1977**;56:199–205
5. Lieberman AN, Weiss JL, Jugdutt BI, et al. Two-dimensional echocardiography and infarct size: relationship of regional wall motion and thickening to the extent of myocardial infarction in the dog. *Circulation* **1981**;63:739–746
6. Wackers FJ, Becker AE, Samson G, et al. Location and size of acute transmural myocardial infarction estimated from thallium-201 scintiscans: a clinicopathological study. *Circulation* **1977**;56:72–78
7. Stokely M, Topton DM, Buya LM, et al. Quantitation of experimental canine infarct size using multipinhole single-photon tomography. *J Nucl Med* **1981**;22:55–61
8. Keyes JW, Brady TJ, Leonard PF, et al. Calculation of viable and infarcted myocardial mass from thallium-201 tomograms. *J Nucl Med* **1981**;22:339–343
9. Keyes JW, Leonard PF, Brody SL, Svetkoff DJ, Rogers WL, Lucchesi BR. Myocardial infarct quantification in dog by single photon emission computed tomography. *Circulation* **1978**;58:227–232
10. Holman BL, Goldhaber SZ, Kirsch CM, et al. Measurement of infarct size using single photon emission computed tomography and technetium-99m pyrophosphate: a description of the method and comparison with patient prognosis. *Am J Cardiol* **1982**;50:503–511
11. Doherty PW, Lipton MJ, Berninger WH, Skioldebrand CT, Carlsson E, Redington RW. Detection and quantification of myocardial infarction in vivo using transmission computed tomography. *Circulation* **1981**;63:597–606
12. Peck WW, Mancini J, Slutsky RA, Mattrey RF, Higgins CB. In vivo assessment by computed tomography of the natural progression of infarct size, left ventricular muscle mass and function after acute myocardial infarct in the dog. *Am J Cardiol* **1984**;53:929–935
13. Herfkens RJ, Higgins CB, Hricak H, et al. Nuclear magnetic resonance imaging of the cardiovascular system: normal and pathologic findings. *Radiology* **1983**;147:749–759
14. Crooks LE, Banker B, Chang H, et al. Magnetic resonance imaging strategies of heart studies. *Radiology* **1984**;153:459–465
15. Higgins CB, Herfkens R, Lipton MJ, et al. Nuclear magnetic resonance imaging of acute myocardial infarction in dogs: alterations in magnetic relaxation times. *Am J Cardiol* **1983**;52:184–188
16. Tscholakoff D, Higgins CB, McNamara MT, Derugin N. Early phase myocardial infarction: evaluation by MR imaging. *Radiology* **1986**;159:667–672
17. McNamara MT, Higgins CB, Schectmann N, et al. Detection and characterization of acute myocardial infarction in man with the use of gated magnetic resonance imaging. *Circulation* **1985**;71:717–724
18. Caputo GR, Tscholakoff D, Sechtem U, Higgins CB. Measurement of canine left ventricular mass by using MR imaging. *AJR* **1987**;148:33–38
19. Walach V, Ka-Siu L, Fernandez EJ, Spalter C. The appearance of rapidly flowing blood on magnetic resonance imaging. *AJR* **1984**;143:1167–1174
20. Alonso DR, Scheidt S, Post M, Killip T. Pathophysiology of cardiogenic shock. Quantification of myocardial necrosis, clinical pathologic and electrocardiographic correlations. *Circulation* **1973**;48:588–596
21. Willerson JT, Curry GC, Watson JT, et al. Intra-aortic balloon counterpulsation in patients in cardiogenic shock. Quantification of myocardial necrosis, clinical, pathologic and electrocardiographic correlations. *Circulation* **1973**;48:588–596
22. Sehapayak GK, Watson JT, Curry GC, et al. The late development of intractable ventricular tachycardia after acute myocardial infarction. *J Thorac Cardiovasc Surg* **1974**;67:818–825
23. Shell WE, Sobel BE. Protection of jeopardized ischemic myocardium by reduction of ventricular afterload. *N Engl J Med* **1974**;291:481–486
24. Buja M, Parkey RW, Stokely EM, Bonte FJ, Wilkerson JT. Pathophysiology of technetium-99m stannous pyrophosphate and thallium-201 scintigraphy of acute anterior myocardial infarcts in dogs. *J Clin Invest* **1976**;57:1508–1522
25. Strauss HW, Harrison K, Langan JK, Lebowitz E, Pitt B. Thallium-201 for myocardial imaging. Relationship of thallium-201 to regional myocardial perfusion. *Circulation* **1975**;51:641–645
26. Gehring PJ, Hammond PB. The inter-relationship between thallium and potassium in animals. *J Pharmacol Exp Ther* **1966**;155:187–201
27. Evanochko WT, Reeves RC, Pohost EM. Investigation of the mechanism of T1 and T2 elevation in 24-hour canine myocardial infarctions (abstr). In: *Proc Society Mag Resonance Med*. London, August **1985**
28. Rokey R, Verani MS, Bolli R, et al. Myocardial infarct quantification by MR imaging early after coronary artery occlusion in dogs. *Radiology* **1986**;158:771–774
29. McNamara MT, Tscholakoff D, Revel D, et al. Differentiation of reversible and irreversible myocardial injury by MR imaging with and without gadolinium-DTPA. *Radiology* **1986**;158:766–769
30. Higgins CB, Lanzer P, Stark D, et al. Imaging by nuclear magnetic resonance in patients with chronic ischemic heart disease. *Circulation* **1984**;69:523–531

Book Review

Clinics in Chest Medicine. Diagnostic Techniques. Guest Editor: Deborah Shure. Philadelphia: Saunders, March 1987; 8(1):1–175, iii–xii

This, the latest issue of *Clinics in Chest Medicine*, consists of a discussion of diagnostic techniques in pulmonary medicine. Although the focus is on pulmonary physiology, the multiplicity of techniques used in pulmonary diagnosis is explored. Newer techniques and experimental techniques are included. The first chapter summarizes the present capabilities of fiberoptic bronchoscopy, focusing on its utility in diagnosis of lung cancer. The clinical applications of bronchoalveolar lavage are next assessed as an aid in management of individual patients. Interventional procedures are next described, beginning with percutaneous fine-needle aspiration biopsy of the mediastinum and continuing with mediastinoscopy and other surgical procedures. In addition to brief discussions of diagnostic imaging techniques, more detailed analyses include terse discussions of exercise testing and a detailed description of forms of diaphragmatic dysfunction. Individual chapters are devoted to the diagnosis of sleep-related breathing disorders, bacterial infections of the lung, serodiagnostic tests and skin tests of fungal disease, cytology in the diagnosis of benign lung diseases, and DNA molecular biology including hybridization, isolation, separation, and gene cloning.

These subjects are discussed primarily by pulmonologists with strong clinical orientation. The entire volume is a valuable reference for radiologists and is worth reading to better understand the needs and orientation of clinicians in pulmonary medicine.

David S. Feigin
University of California, San Diego
La Jolla, CA 92093

Instant Images of the Human Heart Using a New, Whole-Body MR Imaging System

Richard R. Rzedzian[1]
Ian L. Pykett

An extremely rapid MR imaging technique is described, and its use on a new 2.0-T high-speed MR system is demonstrated. This implementation permits complete filling of the two-dimensional spatial-frequency domain (k-space) within an acquisition window of 26 msec. With this acquisition window placed under the spin-echo signal envelope generated by a 90–180° pulse pair, the image contrast is the same as that of a conventional spin-echo pulse sequence. Resultant proton images have a motion-independent voxel resolution of 0.08 cm^3 and a signal-to-noise ratio for cardiac muscle of approximately 30:1 (for TE = 30 msec) with no signal averaging. The pulse sequence yields images that are chemical shift–resolved. The total proton density distribution is optionally presented with lipid and water signals displayed in two different colors. Cardiac function is observed by displaying multiple images, acquired at different times in successive cardiac periods, in a cyclic movie format. Such motion pictures are obtained within a single period of suspended respiration, thereby assuring freedom from respiratory related motion artifacts. As preliminary examples, we present MR images of the normal adult human heart that have total acquisition times of only 40 msec/image and that show the major cardiac anatomy. Frames from movie loops show contraction of cardiac chambers and left ventricular wall thickening.

The extremely rapid acquisition time of this technique suggests that it may hold promise for the routine and cost-effective evaluation of cardiac anatomy and function.

Since the early 1980s, MR imaging has become established as the technique of choice for the diagnosis of many CNS disorders [1, 2]. This is in part a result of MR's intrinsically high soft-tissue contrast (and, hence, its high diagnostic sensitivity), its ability to obtain images directly at arbitrary slice orientations, and its lack of known side effects. However, another reason MR is the method of choice is that the organs of the CNS are not subject to involuntary motions and thus can tolerate the long acquisition times (several minutes) typical of commercially available MR systems.

The potential of MR for imaging the cardiovascular system is also tremendous [3]. Under certain conditions, MR is able to show most cardiac morphology noninvasively and with high resolution; it can also provide significant inherent tissue contrast. However, the long acquisition times currently required with MR have limited the extent of its clinical practicality for cardiac investigations [4].

The concept of high-speed MR imaging, in which a complete tomographic image is acquired within a fraction of a second, was introduced almost a decade ago [5, 6]. The particular technique proposed was coined "echo planar imaging," and by 1983 this method had produced clinically useful images of infants and young children [7]. However, the poor spatial resolution (32 × 32 pixels) of these images raised doubts about the usefulness of echo planar imaging for clinical work. More recently, images of the human head have been obtained with acquisition times of about 100 msec using a reduced-size system [8].

We describe herein a new technique of MR imaging that is capable of acquiring whole-body images of the adult human in only 40 msec, and we demonstrate its

Received January 26, 1987; accepted after revision April 17, 1987.

[1] Both authors: Advanced NMR Systems, Inc., 30 Sonar Dr., Woburn, MA 01801. Address reprint requests to R. R. Rzedzian.

AJR **149:245–250, August 1987**
0361–803X/87/1492–0245
© American Roentgen Ray Society

implementation on a new 2.0-T MR imaging system. The potential application of this technology in cardiac imaging is discussed.

Materials and Methods

All data were obtained on a high-field, high-speed MR imaging system developed by Advanced NMR Systems (Woburn, MA). The static magnetic field strength is 2.0 T, corresponding to a proton resonance frequency of 85.1 MHz. The general characteristics of the pulse sequence used are shown in Figure 1A, and the corresponding k-space trajectory [9] is shown in Figure 1B. Data sufficient to generate a 128-point x 64-line image are all acquired within a 26-msec acquisition window, centered under the envelope of a traditional spin echo. The spin-echo envelope is generated by application of a 90° and a 180° RF pulse pair, as in conventional spin-echo imaging. During the data acquisition interval, the readout gradient G_y is rapidly oscillated in order to generate a large number of closely spaced gradient echoes, each one of which is rapidly sampled to provide sufficient data to fill in one line, k_y, in k-space. Between successive k_y lines, incremental amounts of phase encoding are applied via the gradient G_x to scan over all of k_x during the short acquisition window. The k-space scan is thus a single rasterlike trajectory, completed in just 26 msec.

For the present images the 180° pulse was rendered frequency-selective, so that only the water or the lipid proton signals contributed to the spin echo. The initial 90° pulse was slice-selective to yield, together with the slice-selection gradient G_z, a plane thickness of 4.7 mm, and a consequent voxel dimension of 80 mm^3. Also, for all images presented herein, TE was set to 30 msec. Thus, the total acquisition time per image, including preparatory RF excitation, was 40 msec. No signal averaging was performed; all images are the result of a single application of a pulse sequence of the type shown in Figure 1. Prior to display, the data are interpolated in real time as desired to produce a fine-grid display matrix.

ECG electrodes were connected to the patient in positions that remained outside the physical confines of the RF coil during the entire imaging study. The high-speed image acquisition can be initiated either after receipt of an ECG gating pulse, derived from the R wave of the QRS complex, or independently of it. In the former case (ECG-gated study), either the image acquisition can be initiated following a fixed and predetermined delay after receipt of the gating pulse ("fixed delay mode"), or a series of successive high speed acquisitions can be initiated at successively increasing precalculated delays after receipt of the gating pulse ("progressive time delay mode"). This latter mode enables successive high-speed images to be acquired and then played back in a repetitive "movie" sequence in order to observe cardiac dynamics. It is important to note that in an ECG-gated study, a complete image is produced for every ECG gating pulse; it is not required that acquisitions be performed over many cardiac cycles in order to generate an image, as is traditionally the case. In the progressive time delay mode, either eight or 16 images were obtained with TR (image repetition period) values of about 1, 2, or 3 sec corresponding to one, two, or three cardiac periods. Choice of TR depended on the extent of T1 contrast desired and the capacity of the subject for suspending respiration. Thus, the complete cardiac cycle is typically covered in one breath-hold of approximately 20 sec, with time delay increments progressively increased by either 60 or 120 msec.

The procedures were fully explained to the study participants, who gave their informed consent for the study. Studies were approved by the Human Research Review Board of the Philadelphia Association for Clinical Trials.

Results

The lipid-suppressed transaxial images shown in Figure 2 were obtained from a normal 33-year-old man at three adjacent levels, 6 mm apart and several centimeters cephalad to the diaphragm. The data were obtained in the progressive

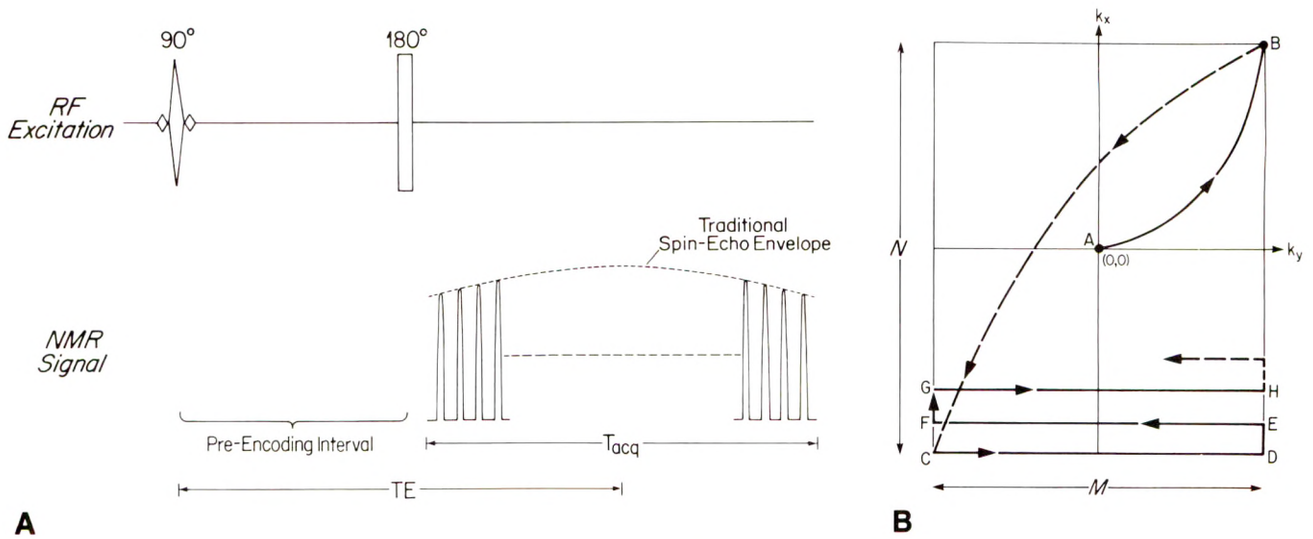


Fig. 1.—Typical instant imaging pulse sequence (*A*) and corresponding k-space trajectory (*B*). After initial slice-selective 90° pulse, preencoding gradient pulses are applied to effect a trajectory in k-space from point A to point B. Application of 180° pulse commences refocusing of magnetization dephased as a result of T_2* decay, and a trajectory from point B to the conjugate position at C is mapped out. Subsequent rapid reversals of readout gradient during data acquisition period T_{acq} generate multiple gradient echoes. Each echo is digitally sampled and trajectories are swept out in k_y (C–D; E–F; G–H; and so on). Between each echo an increment of phase-encoding gradient is applied, causing trajectory to scan in k_x (D–E; F–G; and so on). For simplicity and clarity, magnitudes of gradient echo signals in schematic (*A*) do not reflect dephasing effect of phase-encoding gradient. For images presented herein, N and M on (*B*) were set to 64 and 128, respectively.



Fig. 2.—Lipid-suppressed transaxial images of a normal adult volunteer. Three adjacent levels shown in (*A*), (*B*), and (*C*) are 4.7 mm in thickness and are spaced 6 mm apart. Each separate image was acquired in 40 msec, and for each level, all images were acquired in one breath-hold. For *A*, *B*, and *C*, the temporal order of acquisition is from top left (R wave) to bottom right (end-diastole).

time-delay mode with the times between successive images kept sufficiently long (about 3 sec) to minimize T1 relaxation-time contrast. For each level, all images were acquired during a single breath-hold. The temporal order of the images is from

top left (immediately after the R wave) to bottom right (end-diastole). The data are shown with the anterior body wall uppermost and the subject's left side on the right of each image.

For the TE value of 30 msec employed in these examples, the signal-to-noise ratio (SNR) from cardiac muscle (defined as signal from cardiac muscle divided by the standard deviation of the background noise level) is approximately 30:1. All major cardiac anatomy sectioned by these planes is well seen, including the left ventricle, papillary muscle, right ventricle and right atrium, septum, and descending aorta. When the images are played in a cyclic movie sequence, contraction of the right atrium and left ventricle is well demonstrated, with left ventricular myocardial wall thickening observed during the systolic phase. Also, motion of the anterior leaflet of the tricuspid valve frequently can be tracked. As with conventional spin-echo MR imaging methods, blood yields a strong signal only when relatively static. Thus the intensity of the blood in the aorta varies in synchrony with the cardiac cycle. Similarly, pulmonary vessels in the lung are typically noticeable in particular cardiac phases. A further advantage of the movie display format is that the brain tracks the highly correlated images in the movie against a constantly changing uncorrelated noise background, thereby enhancing real features and improving the perceived SNR.

Immediately after obtaining each of the three MR movies of water distribution shown in Figure 2, a corresponding lipid movie was generated at each level. The lipid and water images have been combined and are shown in Figure 3 for the level corresponding to that in Figure 2A. In order to clearly distinguish between the lipid and the water components, each is displayed in a separate color; red for the lipid and blue for the water distributions. For each color scale the brightness is proportional to signal intensity, as for conventional monochrome displays. Pixels that contain both lipid and water (e.g., the signals from bone marrow in the vertebral body) are displayed in colors that are a linear combination of the two component colors, in proportion to the respective intensities of the lipid and water signals.

Discussion

Signal-to-Noise-Ratio and Acquisition Time

An acquisition window of 26 msec was used for this pulse sequence in order to minimize the effects of T2 decay during the acquisition period (T2 of mobile protons is typically 50 msec for cardiac muscle) and to effectively "freeze" the motion of even rapidly moving organs, such as the heart. The acquisition of 64 lines in 26 msec mandates that the incremental phase encoding, the gradient-echo generation, and the data collection all occur within a time interval of approximately 400 μsec for each k_y line. This extremely rapid scan time has been achieved using a new design for the magnetic field gradient subsystem and a high-speed control computer.

Because instant techniques require high-signal bandwidths in order to achieve such short acquisition times, the images generated contain more noise. The nuclear signal, when all factors are taken into account, increases approximately linearly with field strength [10], and it is therefore desirable to operate at high field. Additionally, a high field is indicated in order to maintain the high RF-coil Q's necessary for high SNR and to accommodate the wide-signal bandwidth. The magnet used in this study was a 2.0-T superconducting magnet. The SNR of approximately 30:1 in these images is 50% higher than the (somewhat subjective) value of 20:1 considered adequate for "good image quality" [10].

Spatial Resolution and Motion Degradation

The methods presently used to obtain MR cardiac images include the gated traditional spin-echo methods and the gated variable RF pulse angle, gradient-echo ("variable flip angle") methods. In the traditional spin-echo case, it has been reported that spatial resolution is degraded when long TE values (greater than about 50 msec) are used; when images are obtained near the cardiac apex; and when images are acquired at temporal positions far from the R wave (e.g., late diastole) [11]. In addition, inconsistent triggering or arrhyth-

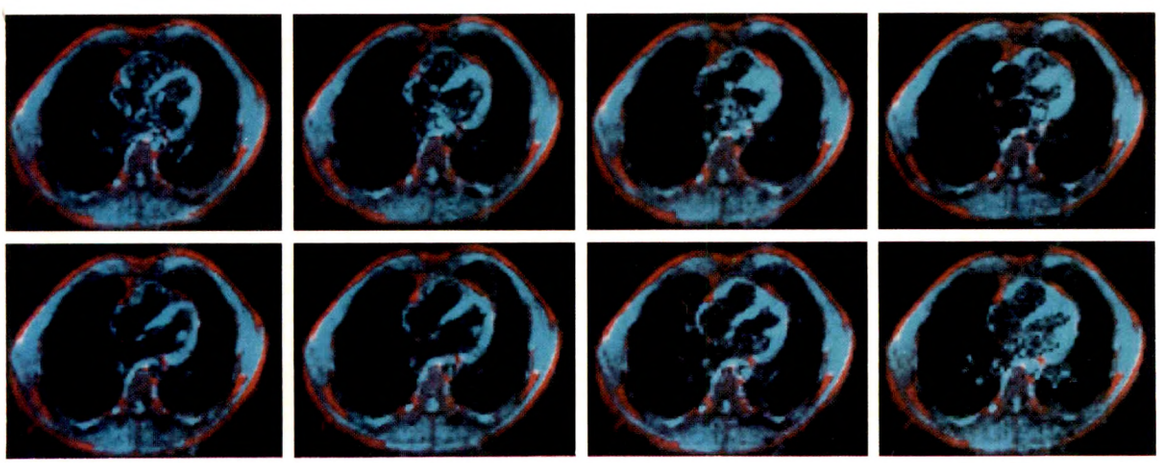


Fig. 3.—Composite "total proton density" MR-movie image set. Lipid and water distributions are shown in red and blue, respectively.

mias will adversely affect image quality. In preliminary variable flip angle studies, image quality has also been determined to be adversely affected when the heart rate is irregular, and when imaging is performed close to the diaphragm [12]. These and other data confirm the expectation that, in many circumstances, the spatial resolution will be less than the resolution matrix would imply. If these contraindicated circumstances are avoided as much as possible, the diagnostic yield of cardiac MR studies can be high [13], but such restrictions clearly limit the extent to which the full potential of MR techniques can actually be achieved.

In the present method, the spatial resolution of an individual image is quite independent of variations in heart rate or inconsistent gating. Indeed, ECG triggering is not required for acquisition of single cardiac images. Also, both single images and multiple-image movies, the latter of which can be obtained during a period of suspended respiration, are free of respiratory motion artifacts even when imaging at the cardiac apex. Deleterious effects of using a long TE value, such as a lower SNR, are, however, the same for this method as for the traditional gated spin-echo methods.

The size of the resolution voxel used in various cardiac MR imaging protocols varies from about 20 mm^3 [13] to 97 mm^3 [14] depending on methodologic, technical, and clinical considerations. Our present voxel dimension of 80 mm^3 falls within this range, but in our case this spatial resolution is not subject to any motion-related degradation. A variety of tradeoffs between spatial resolution, SNR, and acquisition time potentially can be made, and these are currently under investigation in our laboratory.

Image Contrast

The image contrast is defined primarily by the pulse sequence used. An important feature of the present method is that the images retain the same relaxation-time intensity dependence as do those obtained with conventional spin-echo pulse sequences. The option of generating a high degree of relaxation-time contrast is important inasmuch as most lesions are visualized by virtue of their abnormal relaxation time behavior [15]. At the same time, it is desirable that an image with relatively little relaxation-time weighting also can be obtained, since this yields good visibility of anatomic features independent of their relaxation times and optimizes the SNR. The present pulse sequence maintains the flexibility to alter soft-tissue T2 contrast via the TE parameter, and T1 contrast may be obtained by acquiring several images at the desired TR interval. (Acquisition of a single image results in a TR = infinity scan in which there is no T1 contrast). In the special case of single breath-hold cardiac MR movies, choices among long TR values are restricted by the minimum acceptable number of frames and the capacity of the patient for suspending respiration. The pulse sequence is amenable to modifications such as introduction of a preparatory 180° inversion pulse to obtain an "inversion-recovery" type image.

The image contrast function in variable flip-angle methods depends on the RF pulse angle as well as on TR and TE [16]. However, in their preliminary applications to dynamic cardiac imaging, variable flip-angle methods have found their greatest diagnostic potential in their sensitivity to flow. In such applications, the TR is typically set short (about 20–50 msec) so that a large number of images per cardiac period can be reconstructed; this requires that the TE also be short. The blood-pool signal then emanates largely from previously unexcited nuclei that flow into the imaging plane, intraventricular blood signal being greatest for low-RF pulse angles [12]. In this regime (short TR and TE; short RF pulse angle) soft-tissue contrast is not optimized and visualization of cardiac muscle is therefore somewhat compromised. In this sense, the cardiac applications of variable flip-angle methods may be complementary to the present pulse sequence. In nondynamic variable flip-angle applications, there are fewer restrictions on the choice of pulse sequence parameters, and higher soft-tissue contrast is then available. Low-RF pulse angle variants of a modified echo planar imaging technique have been demonstrated [17], although only with low SNR and spatial resolution and at low field. Real-time visualization of intraventricular blood-pool phenomena is similarly possible using our system, in which case image contrast would be analogous to that of the variable flip-angle methods.

Chemical Shift Resolution

In high-field imaging systems, the chemical shift difference between (primarily) lipid and water protons can lead to undesirable artifacts [18]. In chemical shift imaging schemes, this same effect is used to advantage to provide an extra dimension of potentially useful diagnostic information [19]. In cardiac work, chemical shift imaging of fatty acids at the border zone surrounding myocardial infarction may provide diagnostic information to help manage this disease [20]. Further, the concentration of mobile lipids in myocardium has been found to be significantly elevated in regions of moderately reduced blood flow [21]. These data indicate that the property of chemical shift resolution of this instant-scan pulse sequence may be of clinical value.

In conclusion, the present images—among the first 40 msec MR images of adults we have obtained—demonstrate the feasibility of very high speed imaging at high-field strength. Cardiac gating is not required to obtain single images, and the image quality is independent of heart rate irregularities, including arrythmias. In these images, major cardiac anatomy is visualized, with the same relaxation-time contrast characteristic of traditional spin-echo MR methods. Cardiac MR movies may be obtained in a single period of suspended respiration, thereby permitting observation of cardiac function with no respiration-related image degradation. The capability of interactive manipulation of scan parameters (e.g., plane position; pulse sequence parameters) should enable more rapid tailoring and optimization of the imaging protocol for a given patient. Finally, the advanced technology required for high-speed imaging does not preclude the use on the same machine of any of the other more traditional imaging approaches.

ACKNOWLEDGMENTS

We acknowledge with thanks Thomas J. Brady, Robert E. Dinsmore, and Mark R. Goldman for their critical reviews of our initial

high-speed data and for their professional assistance and advice. We also thank the team at Advanced NMR Systems, who helped make it all possible, and Priscilla Stark for her most efficient preparation of the manuscript.

REFERENCES

1. Brant-Zawadzki M, Norman D, Newton TH, et al. Magnetic resonance of the brain: the optimal screening technique. *Radiology* **1984**;152:71–77
2. Richardson M, Genant H, Helms C. MRI of the musculoskeletal system. In: James TL, Margulis AR, eds. *Biomedical magnetic resonance*. San Francisco: Radiology Research and Education Foundation, **1984**:397–414
3. Lieberman JM, Alfidi RJ, Nelson AD. Gated MRI of the normal and diseased heart. *Radiology* 1984;152:465–470
4. Peshock RM. Clinical applications: cardiac. In: Thomas SR, Dixon RL, eds. *NMR in medicine: the instrumentation and clinical applications*. Medical physics monograph no. 14. New York: American Institute of Physics, **1986**:339–349
5. Mansfield P. Multi-planar image formation using NMR spin echoes. *J Phys* **1977**;C10:L55–L58
6. Mansfield P, Pykett IL. Biological and medical imaging by NMR. *J Mag Reson* **1978**;29:355–373
7. Rzedzian R, Mansfield P, Doyle M, et al. Real-time NMR clinical imaging in paediatrics. *Lancet* **1983**;December 3:1281–1282
8. Crooks LE, Arakawa M, Hale JD, et al. Echo planar imaging at 0.35T with one half of a data set. *Proc annual meeting Society Mag Reson Med,* Montreal, August **1986**:946–947
9. Twieg DB. The k-trajectory formulation of the NMR imaging process with applications in analysis and synthesis of imaging methods. *Med Phys* **1983**;10:610–621
10. Edelstein WA, Glover GH, Hardy CJ, Reddington RW. The intrinsic signal-to-noise ratio in NMR imaging. *Mag Reson Med* **1986**;3:604–618
11. Lanzer P, Barta P, Botvinick EH, Wiesendanger HUD, Modin G, Higgins CB. ECG-synchronized cardiac MR imaging: method and evaluation. *Radiology* **1985**;155:681–686
12. Utz J, Herfkens R, Glover G, Shimakawa A, Fram E, Heinsimer J. Rapid Dynamic NMR imaging of the heart. *Proc annual meeting Society Mag Reson Med,* Montreal, August **1986**:930–931
13. Higgins CB, Byrd BF II, McNamara MT et al. Magnetic resonance imaging of the heart: a review of the experience in 172 subjects. *Radiology* **1985**;155:671–679
14. Edelman RR, Thompson R, Kantor H, Brady TJ, Leavitt M, Dinsmore R. Cardiac function: evaluation with fast-echo MR imaging. *Radiology* **1987**;162:611–615
15. Modic MT. Magnetic resonance imaging of the brain and spine: clinical considerations. In: Thomas SR, Dixon RL, eds. *NMR in medicine: the instrumental and clinical applications*. Medical physics monograph no. 14. New York: American Institute of Physics, **1986**:229–248
16. Buxton RB, Edelman RR, Rosen BR, Wismer GL, Brady TJ. Contrast in rapid MR imaging: T1- and T2-weighted imaging. *J Comput Assist Tomogr* **1987**;11:7–16
17. Worthington BS, Doyle M, Chapman B et al. Real-time cardiac imaging of adults using variations of echo planar imaging (abstr). *Radiology* **1986**;161(P):338
18. Babcock EE, Brateman L, Weinreb JC, Horner SD, Nunnally RL. Edge artefacts in MR images: chemical shift effect. *J Comput Assist Tomogr* **1985**;9:252–257
19. Pykett IL. Chemical shift imaging. In: Thomas SR, Dixon RL, eds. *NMR in medicine: the instrumental and clinical applications*. Medical Physics Monograph No. 14. New York: American Institute of Physics, **1986**:281–288
20. Herfkens RJ, Hedlund LW, Foley D, Brazzamano S, Reimer KA, Coleman RE. Visualization of fat by proton chemical shift imaging in experimental myocardial infarction. *Proc annual meeting Society Mag Reson Med,* London, August **1985**:159–160
21. Evanochko WT, Reeves RC, Sakai TT, Canby RC, Pohost GM. Proton NMR spectroscopy in myocardial ischemic insult. *Mag Reson Med* (in press)

Vascular Rings: MR Imaging

George S. Bisset III[1, 2]
Janet L. Strife[1, 2]
Donald R. Kirks[1, 2]
Warren W. Bailey[3]

The purpose of this study was to assess the utility of MR imaging in identifying anatomic features of vascular rings. MR imaging of the thorax was performed in five consecutive children with symptoms and findings of vascular rings on barium esophagography. The diagnoses were subsequently proved at surgery and/or angiography. Preoperative definition of the anatomy was adequate and accurate in each case.

Our preliminary experience with MR imaging in five patients with vascular rings suggests that this technique is an excellent alternative to angiography when further anatomic delineation of the abnormality is required.

The term *vascular ring* has been used to define a developmental anomaly in which there is encirclement and compression of the trachea and esophagus by the aortic arch and its associated vascular structures [1, 2]. Vascular rings result from failure of the embryonic vascular arches to fuse and regress in the usual manner during formation of the aortic arch, pulmonary arteries, and ductus arteriosus. The diagnosis and differentiation of vascular rings is dependent on the findings on plain chest radiographs and barium esophagograms [3].

The necessity for preoperative angiography in these patients has been controversial [4–6]. Several surgical problems can be avoided if extensive preoperative evaluation is performed [2, 7]. Tonkin et al. [4] and Keith [5] have stated that all patients suspected of having vascular rings should undergo angiography (either digital subtraction or cineangiography).

MR imaging has proved to be excellent for evaluating the thoracic aorta [8–11]. This technique is particularly useful in children, since it is noninvasive, provides excellent spatial resolution, and uses no ionizing radiation. We report our experience in five consecutive patients with various symptomatic vascular rings.

Subjects and Methods

From September to November 1986, five consecutive patients with a diagnosis of vascular ring were studied. At the time of diagnosis the patients were 8 months to 12 years old (mean, 6 years). The three youngest patients presented with the chief complaint of intermittent stridor. The two older patients had difficulty swallowing. Each patient had chest radiography and barium esophagography before MR.

All patients underwent MR imaging with a General Electric 1.5-T Signa System scanner. Each study was ECG-gated, and a spin-echo imaging technique was used. The echo-delay time (TE) was 20 msec and the repetition time (TR) was equivalent to the R-R interval of the ECG. The TR ranged from 536 to 800 msec. Two signal averages and a 256 × 128 matrix size were used to acquire images with plane thicknesses of 5 mm (1-mm gaps between sections).

Initial localizing scans were obtained in the sagittal plane, followed by axial and coronal images through the region of interest of the aortic arch. Total imaging time ranged from 45 min to 1 hr.

All diagnoses made prospectively with MR were confirmed by surgery (four patients) or angiography (one patient).

Received January 30, 1987; accepted after revision April 28, 1987.

[1] Department of Radiology, Children's Hospital Medical Center, Elland and Bethesda Aves., Cincinnati, OH 45229–2899. Address reprint requests to G. S. Bisset III.

[2] Departments of Radiology and Pediatrics, University of Cincinnati College of Medicine, Cincinnati, OH 45267.

[3] Department of Pediatric Cardiovascular Surgery, Children's Hospital Medical Center, Cincinnati, OH 45229–2899, and Department of Surgery, University of Cincinnati College of Medicine, Cincinnati, OH 45267.

***AJR* 149:251–256, August 1987**
0361–803X/87/1492–0251
© American Roentgen Ray Society

Results

Four of the five patients are described in Figures 1–4. The fifth patient, an 8-month-old white girl who presented with recurrent episodes of "croup," is not illustrated. A high-kilovoltage film of the airway revealed a right aortic arch. The chest radiograph and barium swallow were consistent with a double aortic arch. MR scanning confirmed the diagnosis, which was proved at surgery. None of the children had congenital heart disease.

Discussion

MR has been used successfully to image aortic disease in adults [8, 11]. In childhood, isolated cases of vascular ring evaluation with MR have been described [12–14]. In our group of children with vascular rings, MR provided excellent preoperative definition of each abnormality. No discrepancies were identified between MR and surgical findings. The only detail that could not be detected with MR was the exact site of the ligamentum arteriosum. The aortic branches were accurately defined, and axial, coronal, and sagittal images enabled detailed anatomic relationships to be evaluated.

This technique is especially useful in children because it is noninvasive. No ionizing radiation is used, spatial resolution is excellent, and inherent natural contrast between intraluminal blood and vessel walls obviates IV or intraarterial contrast material administration.

The controversy concerning imaging evaluation of patients with vascular rings is difficult to resolve. Many authors believe that chest radiographs and barium esophagography provide adequate evaluation [2, 3]. These individuals believe that preoperative distinction between double aortic arch (the most common type of vascular ring in infancy) and the right aortic

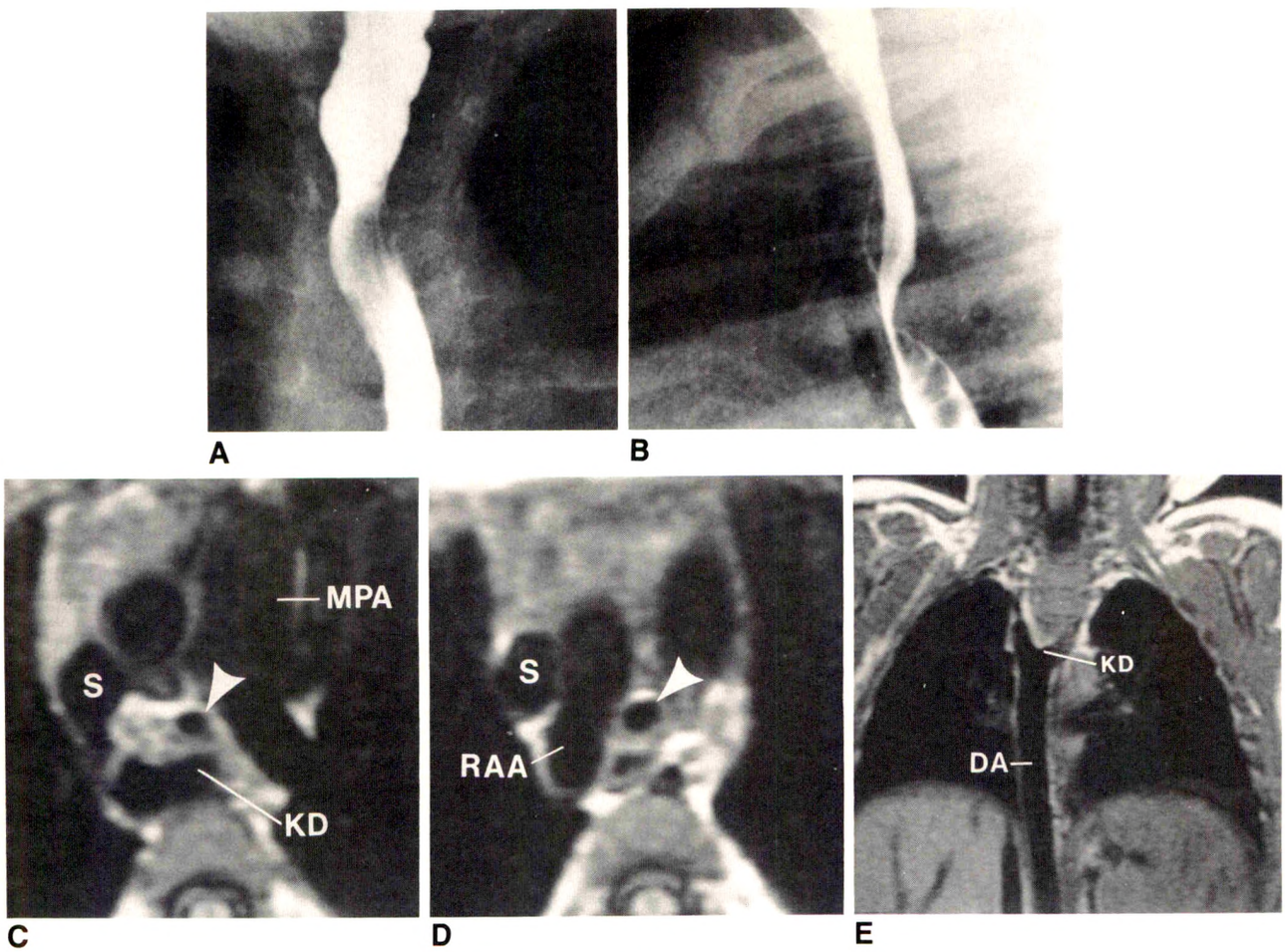


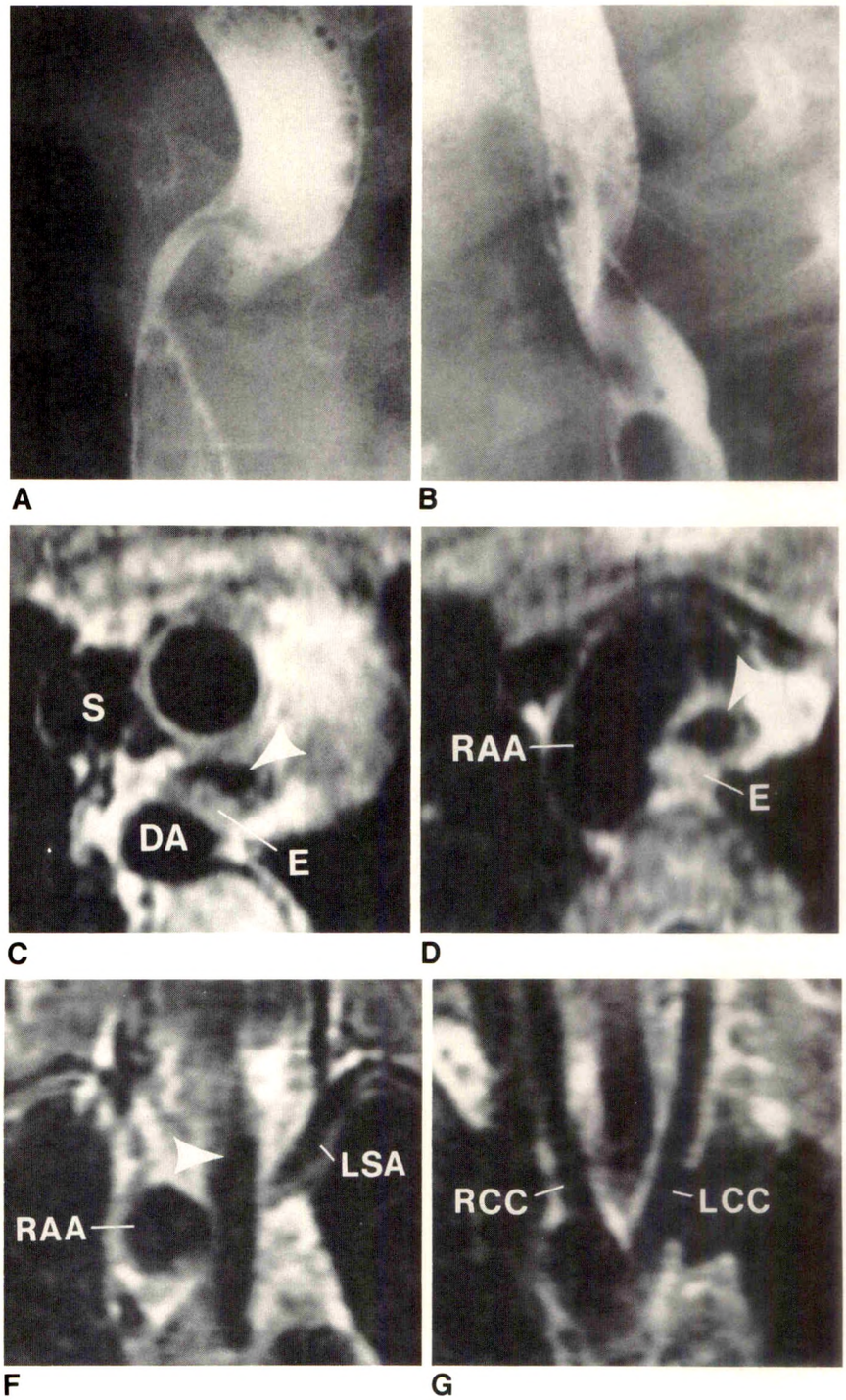
Fig. 1.—1-year-old boy referred for evaluation of recurrent inspiratory stridor.
***A* and *B*, Anteroposterior (*A*) and lateral (*B*) views of barium esophagogram show superior right esophageal indentation and posterior esophageal compression that extends from right inferiorly to left superiorly.**
***C* and *D*, Contiguous axial MR images through right aortic arch (RAA). Trachea (*arrowheads*).**
E, Coronal image through descending aorta (DA). Diagnosis was subsequently proved surgically.
KD = Kommerell diverticulum (left dorsal arch aortic diverticulum); MPA = main pulmonary artery, S = superior vena cava.

Fig. 2.—9-year-old girl with recurrent episodes of stridorous upper respiratory infections since infancy. She also had history of occasional dysphagia and mild exercise intolerance. Exercise testing indicated restrictive large airway disease.

***A* and *B*, Anteroposterior (*A*) and lateral (*B*) views of barium esophagogram show posterior esophageal indentation.**

***C* and *D*, Contiguous axial MR sections through right aortic arch (RAA). Trachea (*arrowheads*). S = superior vena cava; E = esophagus; DA = descending aorta.**

***E–G*, Contiguous coronal MR images through right aortic arch and descending aorta (DA). Aberrant left subclavian artery (LSA) and retroesophageal passage of descending aorta are seen clearly. Diagnosis was confirmed at surgery. RSA = right subclavian artery; KD = Kommerell diverticulum; LSA = left subclavian artery; RCC = right common carotid artery; LCC = left common carotid artery. Trachea (*arrowhead*).**



arch–left ductus complex is not required, since a left posterolateral thoractomy is the standard surgical approach to either lesion [15]. Proponents of angiography have stated that anatomic variations make angiography necessary in preoperative planning [4, 16]. McFaul et al. [17] noted a 10–20% prevalence of vascular rings, which were best approached through a right thoracotomy. Berdon and Baker [2] documented a patient (similar to our patient in Fig. 4) who required a right thoracotomy despite having features on plain films of a "typical" vascular ring [2]. Tonkin et al. [4] emphasized the need for all vascular rings to undergo angiography with complex views. We have seen two patients with coarctation

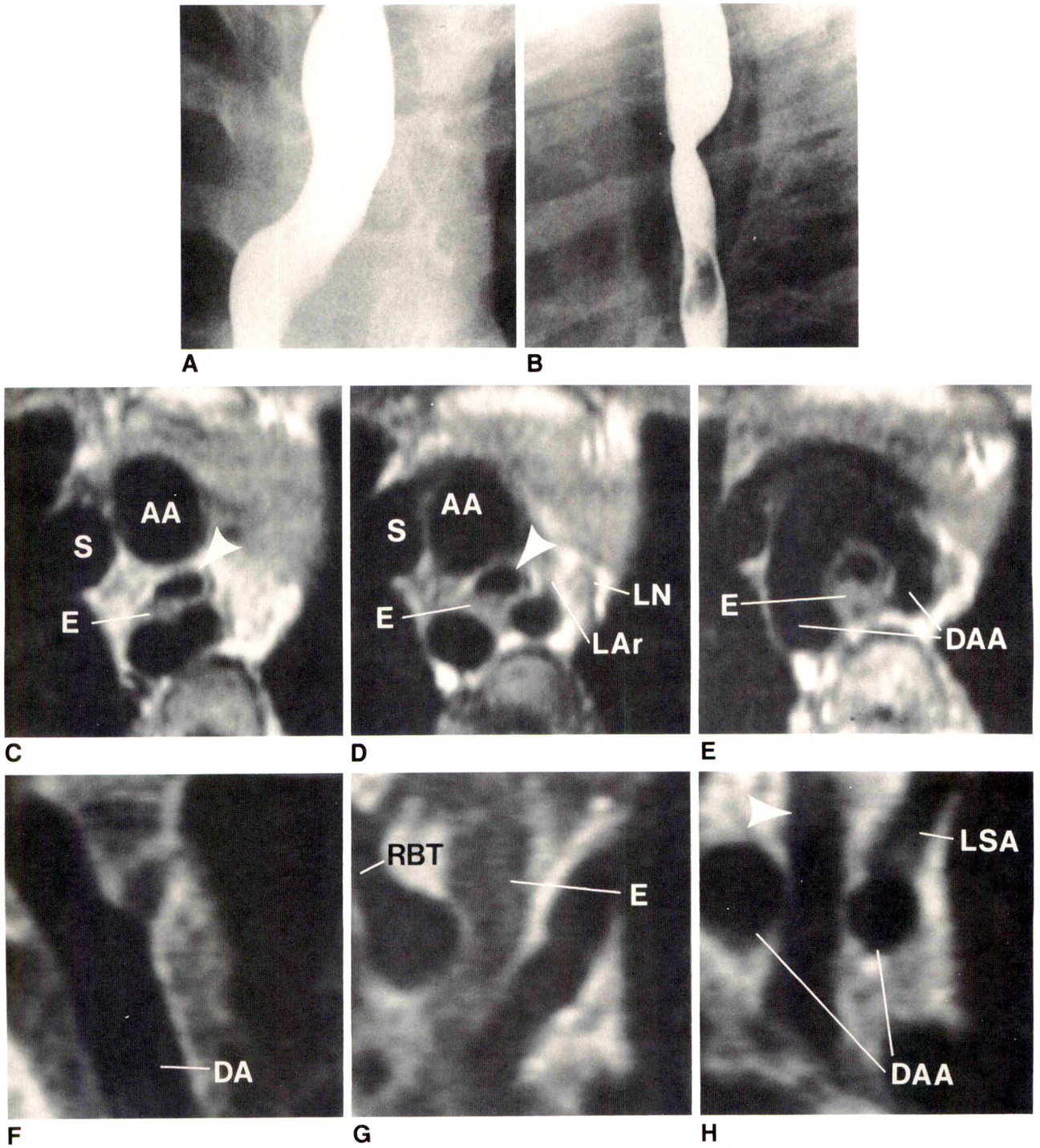


Fig. 3.—9-year-old boy with mild dysphagia and history of recurrent episodes of pneumonia.

A and *B*, Anteroposterior (*A*) and lateral (*B*) views of barium esophagogram show what was initially believed to represent right aortic arch with aberrant left subclavian artery.

C–E, Contiguous 5-mm axial MR sections through double aortic arch (DAA). Trachea (*arrowheads*). Small left ligamentum arteriosum (LAr) was identified at surgery, immediately adjacent to 1-cm lymph node (LN). Both are seen on *D*. E = esophagus; S = superior vena cava; AA = ascending aorta.

F–H, Contiguous coronal MR images through double aortic arch (DAA). DA = descending aorta; RBT = right brachiocephalic trunk; LSA = left subclavian artery; E = esophagus. Trachea (*arrowhead*).

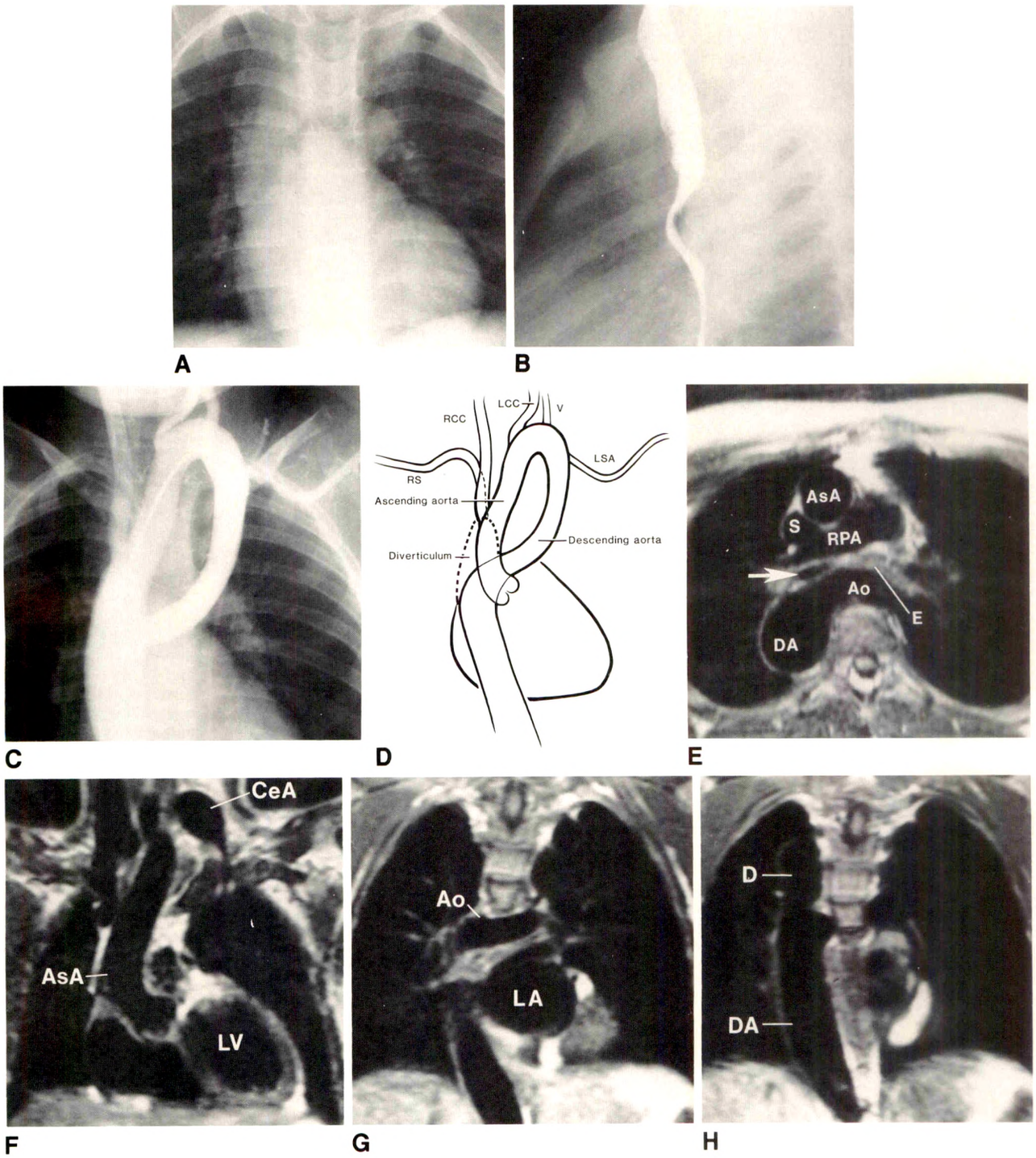


Fig. 4.—12-year-old boy, initially seen 3½ years of age, with history of dysphagia and recurrent upper respiratory infections.

***A* and *B*, Initial posteroanterior chest radiograph (*A*) and lateral chest radiograph with barium in esophagus (*B*) show wide superior mediastinum and rounded posterior impression on mid portion of esophagus.**

***C*, Anteroposterior aortogram shows left cervical aortic arch and right descending aorta.**

***D*, Diagram of anatomy. RS = right subclavian artery; RCC = right common carotid artery; LCC = left common carotid artery; V = left vertebral artery; LSA = left subclavian artery. Right ligamentum arteriosum was suspected because of the symptoms indicating a vascular ring.**

***E*, Axial MR scan through retroesophageal component of aorta (Ao). Right main bronchus (*arrow*). S = superior vena cava; AsA = ascending aorta; RPA = right pulmonary artery; DA = descending aorta; Ao = retroesophageal aortic component; E = esophagus.**

***F–H*, Coronal MR images extending from anterior to posterior through various components of cervical aortic arch. Kommerell diverticulum was noted arising from descending aorta (DA). AsA = ascending aorta; LV = left ventricle; CeA = cervical arch; LA = left atrium; Ao = retroesophageal aortic component; D = diverticulum.**

associated with a double aortic arch. If coarctation is unsuspected in the posterior arch, and the anterior (left) arch is divided, the patient's anatomy may be converted to discrete aortic coarctation.

Therefore, imaging studies in addition to barium esophagography may permit more accurate preoperative surgical planning. Specifically, MR may prevent "wrong-sided" thoracotomy and may permit detection of unsuspected coarctation.

Our early experience with MR of vascular rings shows the utility of this technique. If preoperative evaluation of these anomalies is required, MR provides an excellent noninvasive alternative to conventional or digital angiography.

REFERENCES

1. Kirks DR. *Practical pediatric imaging*, 1st ed. Boston: Little, Brown, **1984**:387–390
2. Berdon WE, Baker DH. Vascular anomalies and the infant lung: rings, slings and other things. *Semin Roentgenol* **1972**:39–64
3. Swischuk LE. *Plain film interpretation in congenital heart disease*, 2d ed. Baltimore: Williams & Wilkins, **1979**:205–225
4. Tonkin IL, Elliott LP, Bargeron LM. Concomitant axial cineangiography and barium esophagography in the evaluation of vascular rings. *AJR* **1980**;135:69–75
5. Keith HH. Vascular rings and tracheobronchial compression in infants. *Pediatr Ann* **1977**;6:91–103
6. Billig DM. Congenital anomalies of the thoracic aorta and its branches: pathophysiology, clinical course, and management. *Prog Cardiovasc Dis* **1973**;16:43–67
7. Nikaidoh H, Riker WL, Idriss FS. Surgical management of "vascular rings." *Arch Surg* **1972**;105:327–333
8. Amparo EG, Higgins CB, Hoddick W, et al. Magnetic resonance imaging of aortic disease. Preliminary results. *AJR* **1984**;143:1203–1209
9. Higgins CB, Stark D, McNamara M, Lanzer P, Crooks LE, Kaufman L. Multiplane magnetic resonance imaging of the heart and major vessels. Studies in normal volunteers. *AJR* **1984**;142:661–667
10. Dooms GC, Higgins CB. The potential of magnetic resonance imaging for the evaluation of thoracic arterial diseases. *J Thorac Cardiovasc Surg* **1986**;92:1088–1095
11. Boxer RA, Fishman MC, LaCorte MA, Singh S, Purnell VA Jr. Diagnosis and postoperative evaluation of supravalvar aortic stenosis by magnetic resonance imaging. *Am J Cardiol* **1986**;58:367–368
12. Julsrud PR, Ehman RL. Magnetic resonance imaging of vascular rings. *Mayo Clin Proc* **1986**;61:181–185
13. Fishman MC, Naidich JB, Stein HL. Vascular magnetic resonance imaging. *Radiol Clin North Am* **1986**;24:485–501
14. Soulen RL, Donner RM. Advances in noninvasive evaluation of congenital anomalies of the thoracic aorta. *Radiol Clin North Am* **1985**;23:727–736
15. Binet JP, Langlois J. Aortic arch anomalies in children and infants. *J Thorac Cardiovasc Surg* **1977**;73:248–252
16. Tonkin ILD, Gold RE, Moser D, Laster RE Jr. Evaluation of vascular rings with digital subtraction angiography. *AJR* **1984**;142:1287–1291
17. McFaul R, Millard P, Nowicki E. Vascular rings necessitating right thoracotomy. *J Thorac Cardiovasc Surg* **1981**;82:306–309

Giant Right Atrium After Mitral Valve Replacement:
Plain Film Findings in 15 Patients

Sanford A. Rubin[1]
Cheryl White Hightower[2]
Stephanie Flicker[3]

We reviewed the radiographs of 166 patients who had undergone mitral valve replacement and found 15 (9%) with giant right atrium. It was confirmed in 13 cases by angiography and/or echocardiography. It was proved at autopsy in one case and confirmed by a Swan-Ganz catheter delineating the lateral right atrial wall in another case. Tricuspid insufficiency of varying severity was present in all patients. Progressive bulging of the right heart border on frontal radiographs and an anterior masslike density on lateral radiographs were the important findings. The bulging right heart border was seen in all 15 patients. The anterior masslike density was noted in seven of nine patients with lateral radiographs; its upper border was sharp in four and indistinct in three.

Giant right atrium may be misdiagnosed as pleural effusion, pericardial effusion, and mediastinal neoplasm. Correct diagnosis is important so that unnecessary procedures are not performed.

Extreme enlargement of the right atrium is uncommon. It may be idiopathic or associated with a number of conditions including left-to-right shunts, Uhl's anomaly (chamber dilatation with a parchment thin wall), Ebstein's anomaly, and rheumatic heart disease. Although there have been many reports of left atrial abnormalities associated with rheumatic heart disease, there have been few reported cases of right atrial abnormalities. Because extreme enlargement of the right atrium is uncommon, it may be misdiagnosed on plain radiographs, being confused with such abnormalities as pleural effusion, pericardial effusion, and mediastinal neoplasm. Such errors have led to unnecessary diagnostic radiologic procedures as well as invasive procedures such as thoracentesis, pericardiocentesis, mediastinoscopy, and thoracotomy [1–6]. This study was undertaken to assess the plain film findings of giant right atrium in order to facilitate correct diagnosis of this condition. Medical records were also studied to further elucidate the cause and effect of giant right atrium.

Materials and Methods

We reviewed the radiographs of 166 patients who had undergone mitral valve replacement, most of whom had a long history of rheumatic heart disease and had been hospitalized many times for congestive heart failure. All 15 patients identified as having giant right atrium had frontal radiographs, nine of the 15 had lateral radiographs, and serial radiographs were available in 11. Oblique radiographs were not evaluated because they were obtained infrequently. The diagnosis of giant right atrium was based on bulging of the right heart border on frontal radiographs and an anterior masslike density on lateral radiographs.

The medical records of those patients identified as having giant right atrium were studied to determine its cause as well as its effect on the patient's clinical status.

Thirteen patients with giant right atrium had confirmation by contrast angiocardiography, echocardiography, or both. It was proved at autopsy in one patient and confirmed by the course of a Swan-Ganz catheter as it outlined the lateral wall of the giant right atrium in another case.

Received January 7, 1987; accepted after revision April 29, 1987.

Presented at the annual meeting of the Society of Thoracic Radiology, Scientific Session, Bal Harbour, FL, March 1985.

[1] Department of Radiology, The University of Texas Medical Branch, Galveston, TX 77550. Address reprint requests to S. A. Rubin.

[2] Department of Radiology, Midland Memorial Hospital, 2200 W. Illinois, Midland, TX 79701.

[3] Department of Radiology, Deborah Heart and Lung Center, Browns Mills, NJ 08015.

AJR 149:257–260, August 1987
0361–803X/87/1492–0257
© American Roentgen Ray Society

Results

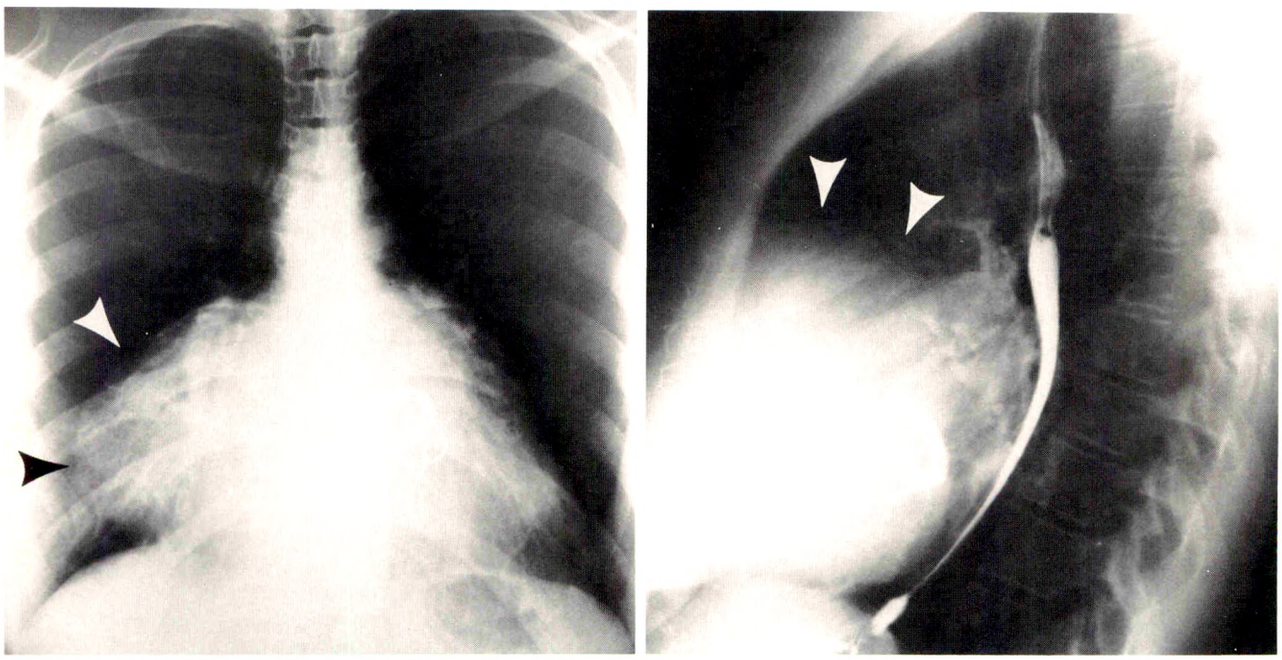
We found giant right atrium in 15 (9%) of 166 patients who had undergone mitral valve replacement. Twelve (80%) of the 15 patients had extreme bilateral atrial enlargement, and the remaining three (20%) had giant right atrium and a much smaller left atrium. All patients had some degree of tricuspid insufficiency diagnosed by physical examination or angiocardiography, but whether it was organic or functional could not be determined. Review of the medical records of each patient suggested that giant right atrium was caused by the tricuspid insufficiency but did not worsen the clinical status. The clinicians concurred and considered it unimportant in 10 of the 15 cases, but because of the bulging right heart border they were concerned that the other five patients might have either a mediastinal mass or a pericardial effusion.

Giant right atrium could be diagnosed on both frontal and lateral views (Figs. 1–3). Bulging of the right heart border was the most important finding and was seen on frontal radiographs of all 15 patients. Serial films available in 11 of the 15 patients showed a progressive increase in the bulging right heart border as the right atrium enlarged. Lateral radiographs available in nine of the 15 patients showed an anterior masslike density in seven. It was more easily recognized when its upper margin was sharply defined as was seen in four of the seven. The upper margin was indistinct in the remaining three.

Discussion

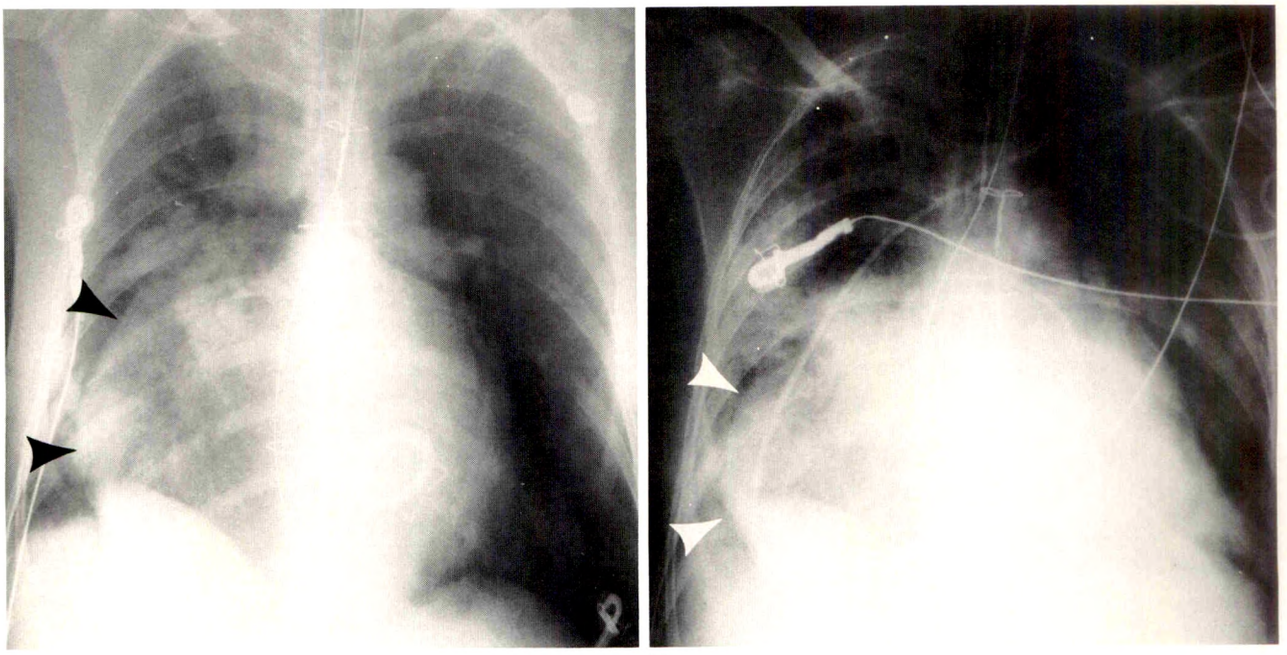
Cardiomegaly is infrequently attributed to enlargement of the right atrium, as this chamber is difficult to evaluate on conventional frontal and lateral chest radiographs. Minimal right atrial enlargement is probably not detectable on plain radiographs. We believe that the bulging right heart border on frontal views and the masslike density on lateral views are sufficient to suggest the diagnosis of giant right atrium, especially in patients who have undergone mitral valve replacement. If the diagnosis is in doubt, it can be confirmed by echocardiography.

Enlargement of the right atrium has been associated with organic changes in the right atrial wall and/or tricuspid valve or chordae tendineae, both of which may lead to tricuspid insufficiency. Pham and Fenoglio [7] studied the pathology of the right atrial wall in two groups of patients with comparable right atrial pressures. The group with rheumatic heart disease showed a number of abnormalities including severe interstitial myocardial fibrosis, extensive cellular degeneration, and marked cellular hypertrophy. The nonrheumatic group showed a lesser degree of cellular hypertrophy, but fibrosis and cellular degeneration were absent. The right atrial wall of our patients undergoing an autopsy was not examined pathologically. Dilatation of the tricuspid annulus caused by chronic right heart failure [8], right ventricular hypertension



A B

Fig. 1.—29-year-old woman with rheumatic heart disease since age of 14. Mitral valve replaced by Starr-Edwards valve 6 years earlier. Chest radiographs show (*A*) marked bulging of right heart border (*arrowheads*) and (*B*) anterior masslike density with sharp upper margin (*arrowheads*). These findings of giant right atrium were misinterpreted as a mediastinal mass, and additional diagnostic procedures were contemplated. Giant right atrium (1000 ml) was found at autopsy.



A B

Fig. 2.—47-year-old woman with rheumatic heart disease since age of 15. Mitral valve replaced by Beall valve 7 years earlier. Patient was admitted for congestive heart failure.

***A*, Initial radiograph shows marked bulging of right heart border (*arrowheads*) misinterpreted by clinicians as a mediastinal mass. We suggested correct diagnosis based on findings of previous case.**

***B*, Subsequently placed Swan-Ganz catheter follows contour of lateral wall of giant right atrium (*arrowheads*) thus confirming diagnosis.**

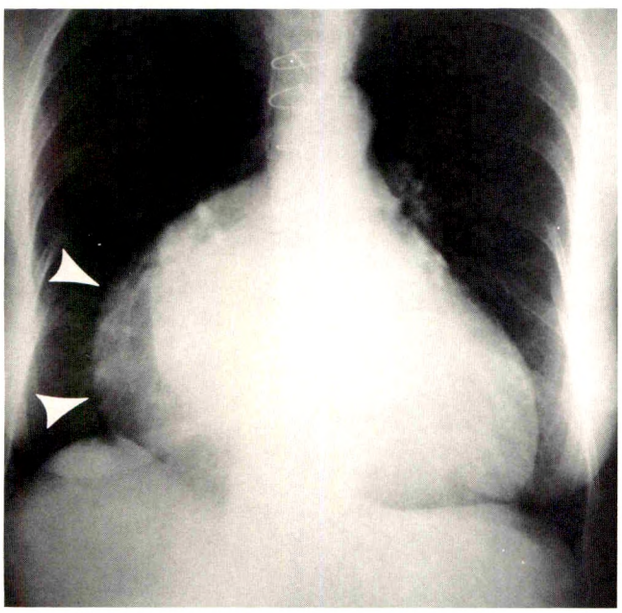


Fig. 3.—59-year-old woman with long history of rheumatic heart disease seen as a clinically well outpatient 4 years after mitral valve replaced by Beall valve. Note giant right atrium (*arrowheads*) and extreme enlargement of left atrium (double density and markedly increased subcarinal angle).

[9], and stretching of the atrial septum by an enlarged left atrium [10] have also been implicated as causes of right atrial enlargement.

Eight of our 15 patients with giant right atrium are still alive. Four are doing well clinically, but the other four have been hospitalized for recurrent episodes of heart failure.

Twelve of our 15 patients had extreme enlargement of both atria, the left atrium being as large as or larger than the right. This has been attributed to less severe and shorter duration of involvement of the tricuspid valve than the mitral valve [11].

Three of our patients had giant right atrium with a much smaller left atrium. To our knowledge, this has been reported only twice previously. Roberts et al. [10] reported three patients with enormous dilatation of the right atrium and only slight enlargement of the left atrium. All three had diffuse calcification of the left atrial wall and atrial septum but no calcification of the right atrial wall. The tricuspid valve leaflets and chordae tendineae demonstrated fibrous thickening in all three, and extensive changes were seen in both the pulmonary vasculature and lung parenchyma. The authors believed calcification of the left atrial wall and septum prevented enlargement of the left atrium by decreasing its compliance thus causing retrograde reflection of the elevated left atrial pressure to the pulmonary vessels and right ventricle leading to tricuspid insufficiency and dilatation of the more compliant right atrium. Taussig [12] described a patient with mitral and

tricuspid valve disease, probably of rheumatic etiology, with an enormously dilated right atrium (2150 ml) and a normal left atrium. The left atrial wall was not calcified and the cause of the giant right atrium was not known. Our three patients with giant right atrium and only minimal enlargement of the left atrium did not show radiographic evidence of calcification of the left atrial wall or atrial septum.

Severe mitral valve disease, which may persist or recur after mitral valve replacement, often masks the clinical and radiographic diagnosis of concomitant tricuspid valve disease [13, 14]. Giant right atrium heralds the presence of tricuspid insufficiency whether its cause is organic or functional. Surgical correction of tricuspid insufficiency has been shown to be beneficial to these patients [9, 13, 14].

REFERENCES

1. Tajik AJ, Broadbent JC, Shattenberg TT. Idiopathic right atrial enlargement with pericardial effusion. *Chest* **1973**;63:450–453
2. Tenckhoff L, Stamm SJ, Beckwith JB. Sudden death in idiopathic (congenital) right atrial enlargement. *Circulation* **1969**;40:227–235
3. Asayama J, Matsuura T, Endo N, Matsukubo H, Furukawa K. Idiopathic enlargement of the right atrium. *Am J Cardiol* **1977**;40:620–623
4. Mahapatra S, Goldberg MJ, Ryan JM, Rubenfire M, Cascade PN. Progressive extreme biatrial enlargement following mitral valve replacement. *Chest* **1983**;84:306–308
5. Saigusa M, Morimoto K, Koike T, Hori T, Sato T. Idiopathic enlargement of the right atrium. *Jpn Heart J* **1962**;3:373–379
6. Pastor BH, Forte AL. Idiopathic enlargement of the right atrium. *Am J Cardiol* **1961**;8:513–518
7. Pham TD, Fenoglio JJ. Right atrial ultrastructure in chronic rheumatic heart disease. *Int J Cardiol* **1982**;1:289–304
8. Chopra P, Tandon HD. Pathology of chronic rheumatic heart disease with particular reference to tricuspid valve involvement. *Acta Cardiol (Brux)* **1977**;32:423–434
9. Asano K, Washio M, Eguchi S. Results of mitral valve replacement, with special reference to the functional insufficiency. *Jpn Heart J* **1971**;12:507–516
10. Roberts WC, Humphries JO, Morrow AG. Giant right atrium in rheumatic mitral stenosis: atrial enlargement restricted by mural calcification. *Am Heart J* **1970**;79:28–35
11. Rogers WR, Wittels B. Extreme bilateral atriomegaly: review of the literature and report of a case. *Circulation* **1957**;15:434–441
12. Taussig BL. A case of tricuspid stenosis with enormous dilatation of the right auricle. *Am Heart J* **1937**;14:744–752
13. Boyd AD, Engelman RM, Isom OW, Reed GE, Spencer FC. Tricuspid annuloplasty: five and one-half years' experience with 78 patients. *J Thorac Cardiovasc Surg* **1974**;68:344–351
14. Lillehei CW, Gannon PG, Levy MJ, Varco RL, Wang Y. Valve replacement for tricuspid stenosis or insufficiency associated with mitral valvular disease. *Circulation* **1966**;33:34–42

Case Report

Compression of Left Main Bronchus and Left Pulmonary Artery by Thoracic Aortic Aneurysm

Robert A. Duke,[1,2] Milton R. Barrett II,[1,2] Steven D. Payne,[1,3] Jorge E. Salazar,[1,2] Helen T. Winer-Muram,[1,2] and Ina L. D. Tonkin[1,4]

We describe a patient in whom an aneurysm of the transverse thoracic aorta extended inferiorly into the aortopulmonary window with compression of the left mainstem bronchus and left pulmonary artery. Plain film findings revealed aneurysmal dilatation of the thoracic aorta, progressive atelectasis of the left lung, and a mass in the aortopulmonary window. CT and MR imaging showed that the obstructing lesion was a saccular aortic aneurysm with mural thrombus.

Case Report

A 71-year-old man with longstanding systemic hypertension had a gradual onset of persistent cough and hoarseness over several months. He had no previous history of syphilis or thoracic trauma. On physical examination a grade III/IV systolic ejection murmur was noted at the left sternal border. Blood pressure was 180/90 mm Hg. A chest radiograph taken in 1981 revealed aneurysmal dilatation of the ascending and transverse aortic arch with intimal calcifications. Chest radiographs obtained in November 1985 showed progressive enlargement of the thoracic aorta with compression and inferior displacement of the left main bronchus and a mass in the aortopulmonary window (Figs. 1A and 1B). A repeat examination 2 months later showed some volume loss of the left hemithorax. CT of the chest, done to evaluate the thoracic aorta and exclude a mediastinal neoplasm, showed a 5-cm mass adjacent to the inferior aspect of the transverse thoracic aorta. The mass had peripheral calcification and its superior portion enhanced to the same degree as the aorta (Fig. 1C). Inferiorly, the mass was less dense than aorta (Fig. 1D). Oblique reconstruction images supported the impression that the mass was an aneurysm of the transverse thoracic aorta. The mass caused nearly complete obstruction of the left main bronchus and the left main pulmonary artery, resulting in diminished left-lung volume and subtle hyperlucency relative to the contralateral lung. Flexible bronchoscopy revealed no endobronchial lesion, but pulsatile extrinsic compression of the left main bronchus was noted just past the carina. A follow-up chest radiograph obtained 1 month later on an outpatient basis (Fig. 1E) showed complete atelectasis of the left lung. The patient was readmitted.

Chest MR imaging, performed with ECG-gated acquisition of T1-weighted sagittal slices, showed marked dilatation of the proximal left pulmonary artery and elongation of the aortic arch (Fig. 1F). The 5-cm aneurysm with a 4-cm mouth was well visualized, containing multiple, well-delineated layers of thrombus inferiorly. Marked compression of left hilar structures and compression of the superior aspect of the left atrium were also present.

At surgery, a large saccular aneurysm of the transverse thoracic aorta was found compressing the left mainstem bronchus and left pulmonary artery; the left recurrent laryngeal nerve was stretched by the aneurysm.

Discussion

In nonradiological literature, compressions of the trachea, bronchi, and pulmonary arteries are well-known, although uncommon, complications of thoracic aortic aneurysm [1–3]. In the radiology literature, compressions of the left main

Received February 2, 1987; accepted after revision March 19, 1987.
[1]Department of Radiology, University of Tennessee, Memphis, 800 Madison Ave., Memphis, TN 38163. Address reprint requests to R. A. Duke.
[2]Department of Radiology, Veterans Administration Medical Center, 1030 Jefferson Ave., Memphis, TN 38104.
[3] Baptist Memorial Hospital/University of Tennessee, Memphis, 10 North Pauline, Memphis, TN 38146.
[4]Department of Radiology, LeBonheur Children's Medical Center, 848 Adams Ave., Memphis, TN 38103.

AJR 149:261–263, August 1987 0361–803X/87/1492–0261 © American Roentgen Ray Society

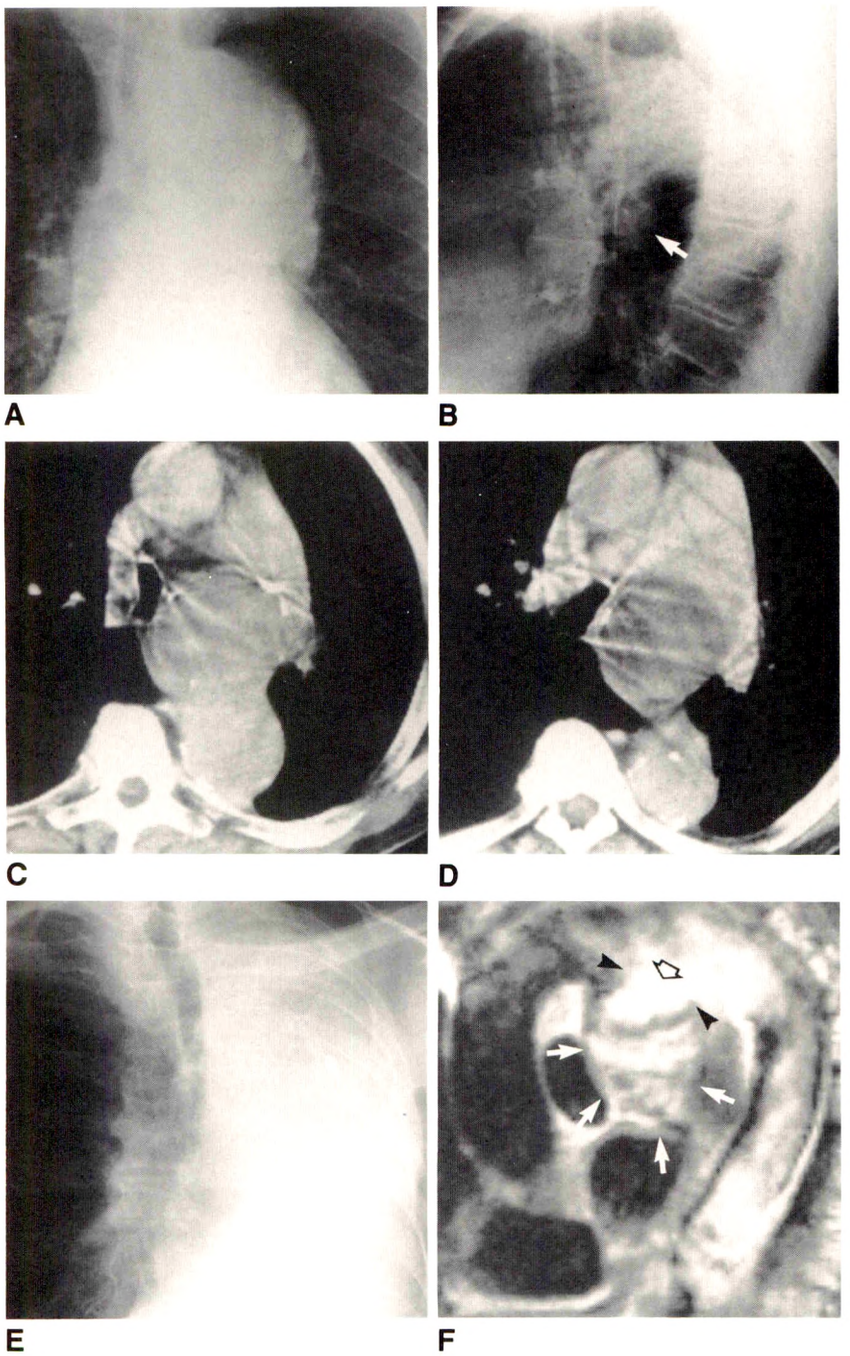


Fig. 1.—*A* and *B*, Chest radiograph (November 1985) shows dilated thoracic aorta with intimal calcifications. There is compression and inferior displacement of left main bronchus. Soft-tissue mass in aortopulmonary window is visible in *B* (*arrow*).

***C* and *D*, Chest CT with bolus IV contrast material (January 1986) *C*, Superior. *D*, Inferior. There is mass in aortopulmonary window that enhances to same degree as aorta superiorly (*C*), but less than aorta on more inferior images (*D*).**

***E*, Chest radiograph obtained 1 month after CT shows complete atelectasis on left.**

***F*, Sagittal T1-weighted MR image (SE 500/60). Layers of thrombus show in inferior aspect of aneurysm (*white arrows*). Wide mouth of aneurysm also shows well (*arrowheads*). High-signal intensity in superior aspect of aneurysm (*open arrow*) that was shown to be patent by contrast-enhanced CT. This, as well as similar high-intensity signal in distal arch and descending aorta, is considered to be due to slow and/or turbulent flow.**

bronchus and left pulmonary artery by aortic aneurysm have not been widely recognized.

Differential diagnosis of obstruction of the left pulmonary artery includes congenital absence or hypoplasia of the pulmonary artery, granulomatous disease such as histoplasmosis, pulmonary artery sarcoma, pulmonary embolism, postirradiation fibrosis, and pulmonary Takayasu's arteritis. Bronchial obstruction may be due to an endobronchial lesion such as tumor, foreign body, or mucous plugging or to extrinsic compression such as tumor or infection.

In recent years, CT has become widely used in evaluating the thoracic aorta and has made easier the differentiation between aortic aneurysm and mediastinal neoplasm [4–6]. Even more recently, MR has proved valuable in imaging abnormalities of the thoracic aorta [7].

In the case presented here, a thoracic aortic aneurysm

enlarged to such a degree that it obstructed the left main bronchus and produced complete atelectasis of the left lung. Differential diagnosis included a central neoplasm with post-obstructive atelectasis and pneumonia. The aneurysm also enlarged enough to stretch the recurrent laryngeal nerve and produce hoarseness. This may mimic a neoplasm or metastasis in the aortopulmonary window involving the recurrent laryngeal nerve.

Although, as in this case, a part of the aneurysm may contain thrombus, it may communicate with the aortic lumen and enhance on CT with bolus IV contrast material administration. MR may show blood flow within a portion of the aneurysm as well as multilaminar mural thrombus. Slow and/or turbulent flow may produce high signal intensity, however, and make differentiation from thrombus difficult. Both studies show anatomic relationships to mediastinal structures including bronchi and pulmonary arteries in great detail, an obvious benefit in planning surgical resection. In cases of noncalcified aneurysm completely filled with thrombus, differentiation from tumor may not be possible and percutaneous thin-needle biopsy may be necessary [4].

REFERENCES

1. Verdant A. Chronic traumatic aneurysm of the descending thoracic aorta with compression of the tracheobronchial tree. *Can J Surg* **1984**;27:278–279
2. Charrett EJP, Winton TL, Salerno TA. Acute respiratory insufficiency from an aneurysm of the descending thoracic aorta. *J Thorac Cardiovasc Surg* **1983**;85:467–470
3. Varkey B, Tristani FE. Compression of pulmonary artery and bronchus by descending thoracic aortic aneurysm. *Am J Cardiol* **1974**;34:610–614
4. Miller GA, Heaston DK. Moore AV, Korobkin M, Braun SD, Dunnick NR. CT differentiation of thoracic aortic aneurysms from pulmonary masses adjacent to the mediastinum. *J Comput Assist Tomogr* **1984**;8:437–442
5. Smith TR, Khoury PT. Aneurysm of the proximal thoracic aorta simulating neoplasm: the role of CT and angiography. *AJR* **1985**;144:909–910
6. Cramer M, Foley WD, Palmer TE, et al. Compression of the right pulmonary artery by aortic aneurysms: CT demonstration. *J Comput Assist Tomogr* **1985**;9:310–314
7. Glazer HS, Gutierrez FR, Lee JKT, Murphy WA. The thoracic aorta studied by MR imaging. *Radiology* **1985**;157:149–155

American Roentgen Ray Society
Resident Award Papers, 1988

The ARRS announces competition for the 1988 President's Award and two Executive Council's Awards for the best papers concerning the clinical application of the radiologic sciences.

Awards

The winner of the President's Award will receive a certificate and a $1000 prize. The winners of the two Executive Council Awards will each be given a certificate and a prize of $500. The winners will be announced on March 15, 1988. Winning papers will be presented at the ARRS annual meeting at the San Francisco Hilton Hotel, San Francisco, CA, May 7–12, 1988. Winning papers will be submitted for early publication in the *American Journal of Roentgenology*. All other papers will be returned to the authors.

Regulations

Eligibility is limited to residents or fellows in radiology who have not yet completed 4 years of approved training in a radiologic discipline. A letter from the resident's department chairman attesting to this status must accompany the manuscript. The resident must be the sole or senior author and be responsible for all or most of the project.

Submitted manuscripts must not exceed 5000 words and have no more than 10 illustrations. Four copies of the manuscript and illustrations are required.

Deadline for submissions is January 29, 1988. Send papers to:

B. G. Brogdon, M.D.
Chairman, Committee on Education & Research
American Roentgen Ray Society
Department of Radiology
University of South Alabama Medical Center
2451 Fillingim Street
Mobile, AL 36617

Nonspecific Interstitial Pneumonitis in Patients with AIDS: Radiologic Features

J. Thayer Simmons[1, 2]
Anthony F. Suffredini[3]
Ernest E. Lack[4]
Matthew Brenner[3]
Frederick P. Ognibene[3]
James H. Shelhamer[3]
H. Clifford Lane[5]
Anthony S. Fauci[6]
Henry Masur[3]

Chest radiographic abnormalities in patients with AIDS usually are associated with opportunistic infection or neoplasm. One hundred five patients with AIDS and clinical evidence of pneumonitis had chest radiographs and underwent bronchoscopy with bronchoalveolar lavage, transbronchial biopsy, or open-lung biopsy. Chest radiographs were abnormal in 73 (70%). *Pneumocystis carinii* pneumonia was identified at bronchoscopy or open-lung biopsy in 52 (50%). Nonspecific interstitial pneumonitis occurring in the absence of an identifiable infection was documented histologically in 36 (34%). Twenty (56%) of these 36 patients had abnormal chest radiographs. No currently recognized infectious agents were recovered from lavage fluid or were seen histopathologically in patients with nonspecific interstitial pneumonitis.

The results show that nonspecific interstitial pneumonitis is clinically and radiologically indistinguishable from *Pneumocystis carinii* pneumonitis and should be considered in the differential diagnosis of AIDS patients with interstitial infiltrates.

Pneumocystis carinii pneumonia is the most common opportunistic lung infection in patients with AIDS and in 27% of cases is accompanied by a coexisting infection [1]. Neoplastic involvement, although less common than infections, usually is caused by Kaposi's sarcoma [1]. Typical findings on chest radiographs vary from a normal radiograph to gross bilateral interstitial and alveolar infiltrates [2–5].

Little attention has been given to the fact that a substantial fraction of transbronchial lung biopsies, open-lung biopsies, or autopsies in patients with AIDS reveal diffuse alveolar damage and interstitial inflammation of variable severity, with no identifiable pathogen [6–9]. Clinically, these patients often have symptoms and signs that are indistinguishable from *Pneumocystis* pneumonia. The cause of this nonspecific pneumonitis has not been established.

We retrospectively reviewed the radiographs and bronchoscopic findings in 105 consecutive patients with AIDS who had clinical evidence of pneumonitis to define the frequency of nonspecific interstitial pneumonitis and to compare its radiographic presentation with that of *Pneumocystis carinii* pneumonia.

Materials and Methods

One hundred ten patients with AIDS were referred to the Clinical Center, National Institutes of Health, for evaluation of clinical pneumonitis. Patients were referred for experimental drug protocols and thus were almost never on antibiotic therapy at the time of referral. Each patient was evaluated by means of a chest radiograph and underwent bronchoscopy with bronchoalveolar lavage and transbronchial biopsy or bronchoalveolar lavage followed by open-lung biopsy. All patients in this study were evaluated at the Clinical Center between November 1982 and May 1986.

The radiographs could not be located in four cases. In one patient, the results of bronchoscopy were inconclusive.

Eighty-five of the remaining 105 patients had bronchoalveolar lavage and transbronchial biopsy, 14 had bronchoalveolar lavage only, four had open-lung biopsy only, and two had bronchoalveolar lavage followed by open-lung biopsy.

Received March 2, 1987; accepted after revision May 4, 1987.

[1] Diagnostic Radiology Department, The Clinical Center, Bldg. 10, Rm. IC660, National Institutes of Health, Bethesda, MD 20892. Address reprint requests to J. T. Simmons.

[2] Department of Radiology, Georgetown University Medical Center, Washington, DC 20007.

[3] Critical Care Medicine Department, The Clinical Center, National Institutes of Health, Bethesda, MD 20892.

[4] Laboratory of Pathology, National Cancer Institute, Bethesda, MD 20892.

[5] Laboratory of Immunoregulation, National Institute of Allergy and Infectious Diseases, Bethesda, MD 20892.

[6] Office of the Director, National Institute of Allergy and Infectious Diseases, Bethesda, MD 20892.

***AJR* 149:265–268, August 1987**
0361–803X/87/1492–0265
© American Roentgen Ray Society

All chest radiographs were obtained within 24 to 72 hr before the diagnostic procedure was performed. All patients had at least one pulmonary symptom: cough, fever, dyspnea, or sputum production. Further clinical information on these patients has been provided by Suffredini et al. [9]. Bronchoscopy with transbronchial biopsy and bronchoalveolar lavage was performed as previously described [10]. Lavage fluid was centrifuged, and the cell pellet was examined by using toluidine blue stain for *Pneumocystis carinii*, Gram stain, wet mount for fungus, fluorochrome for acid-fast bacilli, and direct fluorescent antibody for *Legionella*. Histologic stains of biopsy specimens included hematoxylin-eosin, Giemsa, PAS, Fite stain, and Gomori's methenamine silver stain. Cultures performed included routine ones for bacteria, cultures for mycobacteria and fungi, and charcoal yeast extract cultures for *Legionella*.

Histologically, nonspecific interstitial pneumonitis was defined by evidence of diffuse alveolar damage associated with increased numbers of alveolar macrophages, alveolar hemorrhage, or, rarely, lymphoid aggregates in the absence of identifiable infections or tumor [9]. All radiographs and histopathologic data were interpreted by a radiologist and a pathologist, respectively, who had no knowledge of the clinical data but were aware that the patients had AIDS.

Interstitial infiltrates were classified on a scale of I to IV. Grade I represented subtle increased perihilar markings and early infiltrate, and grade II represented more prominent interstitial infiltrates extending laterally beyond the hila. Grade III changes represented gross interstitial infiltrates with early alveolar infiltrates, and grade IV changes corresponded to gross interstitial and alveolar disease.

Seventy-three patients (70%) had abnormal radiographs immediately before the diagnostic procedure was performed. Ninety-five patients (90%) had abnormal findings on bronchoscopy or open-lung biopsy; *Pneumocystis carinii* was identified in 52 patients (50%). Other pathogens identified included *Mycobacterium avium intracellularae* (three patients), cytomegalovirus (one patient), and *Legionella* (one patient). Kaposi's sarcoma was identified in two cases.

Results

Thirty-six patients (34%) had a nonspecific interstitial pulmonary inflammation documented histologically by transbronchial or open-lung biopsy. No organisms could be shown histologically, and no causative agent was cultured from lavage specimens. Eighteen of these patients had a history of previous pulmonary infection and/or drug therapy or IV drug abuse. Five patients had nonspecific interstitial pneumonitis and Kaposi's sarcoma shown on follow-up bronchoscopic or open-lung biopsy performed within 2 weeks of initial evaluation. The remaining 13 patients had no history of previous pulmonary disease.

Twenty (56%) of the 36 patients with nonspecific interstitial pneumonitis had abnormal chest radiographs. The most common radiographic finding was a diffuse interstitial infiltrate varying from subtle increased perihilar markings (grade I) to coarser infiltrates with pleural effusions (grade IV) (Figs. 1 and 2). Eight patients had pleural effusions; in four patients, these were the only abnormalities. Forty-two (81%) of the 52 cases of *Pneumocystis carinii* pneumonia had abnormal chest radiographs. As in nonspecific interstitial pneumonitis, the most common finding was a diffuse interstitial infiltrate. These findings are summarized in Table 1.

Figure 3 shows the number of cases with normal and abnormal radiographic patterns. The relative likelihood of a given radiographic pattern being associated with either *Pneumocystis* pneumonia or nonspecific interstitial pneumonitis is shown as a ratio of the respective heights of the bars. Figure 3 shows that *Pneumocystis* pneumonia was more likely to be manifested as a higher grade of infiltrate than nonspecific

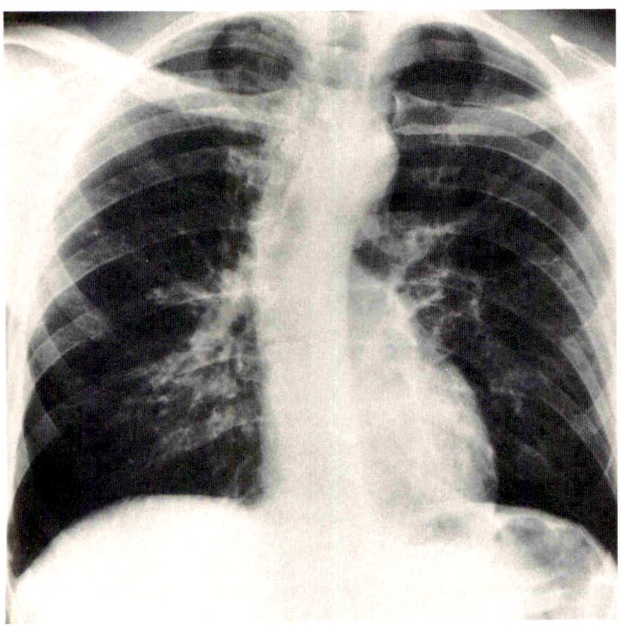


Fig. 1.—Posteroanterior radiograph shows grade I increased perihilar interstitial markings due to nonspecific interstitial pneumonitis.

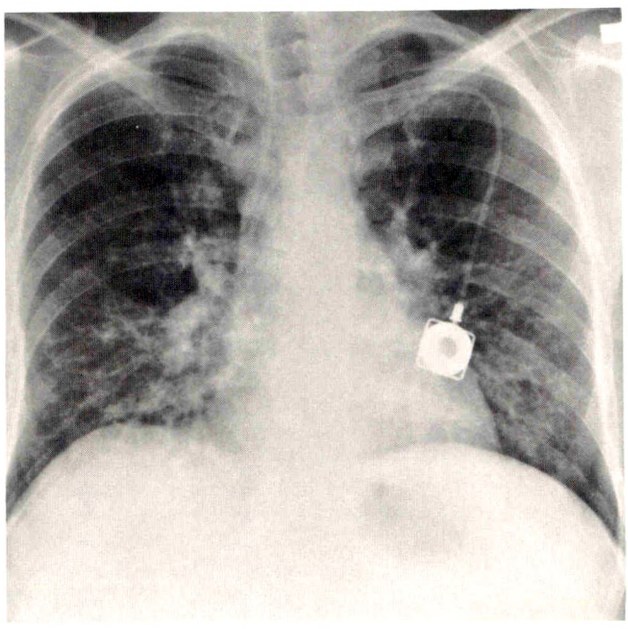


Fig. 2.—Posteroanterior radiograph shows grade III interstitial infiltrate due to nonspecific interstitial pneumonitis.

TABLE 1: Comparison of Radiographic Findings in AIDS Patients with *Pneumocystis* Pneumonia and Nonspecific Interstitial Pneumonitis

Radiographic Abnormality	Nonspecific Interstitial Pneumonitis (%, $N = 36$)	*Pneumocystis* Pneumonia (%, $N = 52$)
Interstitial infiltrates	39	75
Alveolar infiltrates	3	2
Pleural effusion only	11	2
Nodular masses	3	2
None	44	19

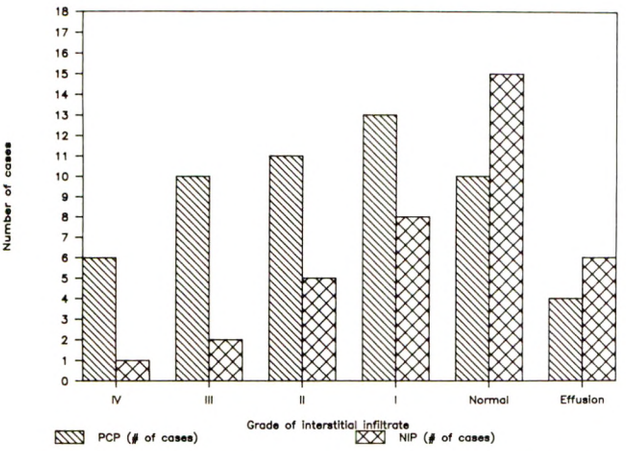


Fig. 3.—Bar graph shows the relative likelihood of a given radiographic pattern (abscissa) representing *Pneumocystis carinii* pneumonia (PCP) vs nonspecific interstitial pneumonitis (NIP).

interstitial pneumonitis was. Patients with nonspecific interstitial pneumonitis were more likely to have normal radiographs or grade I or II interstitial infiltrates; however, the small sample size precluded statistical significance.

Discussion

Pulmonary involvement in AIDS is common, and more than 65% of patients with AIDS present with *Pneumocystis* pneumonia [11]. Mortality due to the respiratory failure was 41% in one study [6]. *Pneumocystis carinii* pneumonia is the most commonly recognized source of pulmonary morbidity and the most commonly recognized opportunistic infection in patients with AIDS [12].

The radiographic patterns of opportunistic lung infections in patients with AIDS have been well documented [2–5]. Findings vary from a normal chest radiograph to diffuse bilateral interstitial and alveolar infiltrates. Other patterns include adenopathy [2, 3], a reticulonodular pattern [2, 5], lobar consolidation [3, 5], cavities, and pleural effusions [5]. The usual causative agent identified in a multicenter collaborative study [1] was *Pneumocystis carinii* (84%). Others included cytomegalovirus (4%), *M. avium intracellularae* (8%), *Mycobacterium tuberculosis* (1%), *Legionella* (2%), and fungi (4%). *Pneumocystis* pneumonia often is accompanied by a coexisting infection (27%). Neoplastic pulmonary disease (8%), although less common than infections, is usually due to Kaposi's sarcoma [1].

In our series, *Pneumocystis carinii* was identified in 50% of patients; 34% had nonspecific interstitial pneumonitis. The reasons for the relatively high percentage of patients with nonspecific interstitial pneumonitis remains unclear. Unlike the study of Suster et al. [13], most of our patients were male homosexuals; very few immigrants were part of the study group. All patients had symptoms of pneumonitis; however, few were critically ill. The symptomatic state of our study group may be a factor in the prevalence of nonspecific interstitial pneumonitis we observed; however, this probably is not significant. It is unlikely that we misinterpreted an early opportunistic infection as nonspecific interstitial pneumonitis; pneumonitis due to identifiable pathogens did not develop in any of the patients in the several months after the diagnosis of nonspecific interstitial pneumonitis.

Other investigators have reported nonspecific interstitial pneumonitis as part of their findings. Stover et al. [6] and Ramaswamy et al. [7] reported seven and 12 cases, respectively, of nonspecific interstitial pneumonitis; their pathologic findings were similar to ours. A more recent study by Barrio et al. [8] found a 29% prevalence of nonspecific interstitial pneumonitis in a series of 286 bronchoscopies of patients with AIDS.

The cause of nonspecific interstitial pneumonitis in patients with AIDS remains obscure. Although 23 of the patients in our series had possible reasons for their pathologic findings, 13 had no history of previous infection, drug abuse, or drug therapy. Those with Kaposi's sarcoma had disease confined to the skin, with no evidence of visceral involvement. The recent detection of human immunodeficiency virus ribonucleic acid in pulmonary parenchyma may lead to further clues in establishing an infectious cause in these cases of nonspecific pneumonitis [14].

The clinical appearance of nonspecific interstitial pneumonitis is indistinguishable from that of *Pneumocystis carinii* pneumonia. In both diseases, patients can have cough, fever, dyspnea, or sputum production. Laboratory findings include a decreased alveolar-arterial oxygen gradient. The radiographic features of nonspecific interstitial pneumonitis likewise are similar to those of *Pneumocystis* pneumonia. When the findings are abnormal, both diseases usually are manifested as bilateral interstitial infiltrates, with *Pneumocystis carinii* pneumonia tending to have more severe involvement of lung parenchyma (Fig. 3). Pleural effusions, although uncommon, were seen in both diseases. Patients with nonspecific interstitial pneumonitis were more likely to have normal radiographs.

Seventy-three patients in our series had abnormal radiographs, and 58% of these had *Pneumocystis* pneumonia at diagnosis vs 27% who had nonspecific interstitial pneumonitis. Thus, patients in our series who had abnormal radiographs were more than twice as likely to have *Pneumocystis carinii* pneumonia found at diagnostic procedure than to have nonspecific interstitial pneumonitis.

The relatively common occurrence of nonspecific interstitial pneumonitis in patients with AIDS should be considered when chest radiographs are interpreted in these patients. Therefore, when a patient with AIDS has an abnormal chest radiograph, a diagnostic procedure should not be delayed. If the findings of the biopsy are nondiagnostic, or if the patient does not respond to drug therapy, nonspecific interstitial pneumonitis should be a strong consideration.

REFERENCES

1. Murray JP, Felton CP, Garay S, et al. Pulmonary complications of AIDS: report of National Heart, Lung, and Blood Institute. *N Engl J Med* **1984**;310(25):1683–1688
2. McCauley DI, Naidich DP, Leitman BS, Reede DL, Laubenstein L. Radiographic patterns of opportunistic lung infection and Kaposi sarcoma in homosexual men. *AJR* **1982**;139:653–658
3. Gamsu G, Hecht ST, Birnberg FA, Coleman DL, Golden JA. *Pneumocystis carinii* pneumonia in homosexual men. *AJR* **1982**;139:647–651
4. Vanley GT, Huberman R, Lufkin RB. Atypical *Pneumocystis carinii* pneumonia in homosexual men with unusual immunodeficiency. *AJR* **1982**;138:1037–1041
5. Cohen BA, Pomeranz S, Rabinowitz JG, et al. Pulmonary complication of AIDS: radiologic features. *AJR* **1984**;143:115–122
6. Stover DE, White DA, Romano PA, Gellene RA, Robeson WA. Spectrum of pulmonary diseases associated with the acquired immune deficiency syndrome. *Am J Med* **1985**;78:429–437
7. Ramaswamy G, Jagadha V, Tchertkoff V. Diffuse aveolar damage and interstitial fibrosis in acquired immunodeficiency syndrome patients without current pulmonary infection. *Arch Pathol Lab Med* **1985**;109:408–412
8. Barrio JL, Harcup C, Baier JH, Pitchenik AE. Value of repeat fiberoptic bronchoscopies and significance of nondiagnostic bronchoscopic results in patients with the acquired immunodeficiency syndrome. *Am Rev Respir Dis* **1987**;135:422–425
9. Suffredini AF, Ognibene FP, Lack EE, et al. Nonspecific interstitial pneumonitis: a common cause of pulmonary disease in the acquired immunodeficiency syndrome. *Ann Intern Med* **1987**;107:7–13
10. Ognibene FP, Shelhamer J, Gill V. The diagnosis of *Pneumocystis carinii* pneumonia in patients with the acquired immune deficiency syndrome using subsegmental bronchoalveolar lavage. *Am Rev Respir Dis* **1984**;129:929–932
11. Centers for Disease Control. Update: acquired immunodeficiency syndrome (AIDS). *MMWR* **1986**;35:17–21
12. Macher AM. Infection in the acquired immune deficiency syndrome. *Ann Intern Med* **1984**;100:94–96
13. Suster B, Akerman M, Orenstein M, Wax MR. Pulmonary manifestations of AIDS: review of 106 episodes. *Radiology* **1986**;161:87–93
14. Chayt KJ, Harper ME, Marselle LM, et al. Detection of HTLV-III RNA in lungs of patients with AIDS and pulmonary involvement. *JAMA* **1986**;256(17):2356–2359

Thymic Atrophy and Regrowth in Response to Chemotherapy: CT Evaluation

Peter L. Choyke[1]
Robert K. Zeman[1]
Joseph E. Gootenberg[2]
Jay N. Greenberg[2]
Frederic Hoffer[3]
Joseph A. Frank[4]

Twenty-nine consecutive patients 2–35 years old underwent serial thoracic CT evaluations for metastatic disease. Thymic volumes were determined for each patient during cycles of chemotherapy and were compared with the patient's clinical status. This group included patients with Hodgkin's disease (13 patients), osteogenic sarcoma (five), testicular neoplasm (four), Wilms' tumor (three), rhabdomyosarcoma (two), malignant fibrous histiocytoma (one), and Ewing's sarcoma (one). Seven patients with mediastinal lymphoma had tumor involvement of the thymus and therefore were excluded. The 22 remaining patients showed cyclic thymic volume changes in response to chemotherapy or its discontinuance. During the first course of chemotherapy the thymic volume decreased by an average of 43% in 20 of 22 patients. Between the first and second course, regrowth was observed in all 20 of these patients. Among the six patients who received a second course of therapy, an average volume decrease of 36% was observed during the second course with regrowth again occurring during recovery from chemotherapy. Thymic rebound (regrowth 50% greater than baseline volume) occurred in five patients, three of whom were in clinical remission.

The thymus appears to atrophy during the administration of chemotherapy and regrow during the recovery phase of chemotherapy in 90% of the patients studied. Thymic hyperplasia or rebound is a relatively common phenomenon occurring in 25% of patients. The size of the thymus appears to be extremely sensitive to chemotherapy.

The thymus undergoes considerable change in size in response to systemic stress. During prolonged periods of illness the thymus involutes, a process most likely mediated by endogenous steroids [1]. During recovery, the thymus regrows and occasionally overgrows or "rebounds." Young patients receiving chemotherapy for malignancies undergo similar alterations in thymic volume. These changes in thymic volume can mimic metastatic disease in the anterior mediastinum. In this study, we measured the thymic volumes of young patients receiving courses of chemotherapy in order to establish the frequency and degree of thymic volume changes that occur during chemotherapy in this age group.

Subjects and Methods

Between 1984 and 1986, 29 patients 35 years old or younger (mean age, 17 years; median, 19 years; range, 2–35 years) underwent serial thoracic CT studies to detect metastatic disease. Primary tumors included Hodgkin's lymphoma (13 patients), osteogenic sarcoma (five), testicular neoplasm (four), Wilms' tumor (three), rhabdomyosarcoma (two), malignant fibrous histiocytoma (one), and Ewing's sarcoma (one). An average of 4.3 scans were obtained per patient during this period.

Of the 29 patients initially reviewed, seven were found by surgical biopsy to have tumor involvement of the thymus (lymphoma in all seven) and therefore were excluded from further analysis. The remaining 22 patients had no evidence of thymic tumor involvement, and no tumor involvement has been discovered on subsequent clinical follow-up (mean period of follow-up, 18 months). Absence of thymic involvement was determined by (1) normal size of thymus, (2) absence of adjacent tumor, (3) discordant changes in the thymus with respect to

Received February 6, 1987; accepted after revision April 29, 1987.

Presented in part at the annual meeting of the American Roentgen Ray Society, Washington, DC, April 1986.

[1] Department of Radiology, Georgetown University Hospital, 3800 Reservoir Rd., N.W., Washington, DC 20007. Address reprint requests to P. L. Choyke.

[2] Department of Pediatrics and the Vincent T. Lombardi Cancer Research Center, Georgetown University School of Medicine, Washington, DC 20007.

[3] Department of Radiology, Children's Hospital Medical Center, 300 Longwood Ave., Boston, MA 02115.

[4] Department of Radiology, The National Institutes of Health, Bldg. 10—Clinical Center, Bethesda, MD 20814.

AJR 149:269–272, August 1987
0361–803X/87/1492–0269
© American Roentgen Ray Society

the patient's tumor and metastases, and (4) no enlargement of thymic tissue on CT scans 18 months after chemotherapy.

Various chemotherapeutic agents were used in these patients: adriamycin, BCNU (bischloroethylnitrisourea), bleomycin, cyclophosphamide, dactinomycin, dacarbazine, 5-fluorouracil, methotrexate, mustard, cis-platinum, prednisone, vincristine, and vinblastine. Only the patients with lymphoma received steroids (prednisone) as part of their regimen. One additional patient with osteogenic sarcoma received a single dose of 20 mg of Decadron (Merck Sharp & Dohme, West Point, PA) for treatment of side effects from his chemotherapy.

CT scans were timed to correspond to the time of minimum WBC counts during the course of chemotherapy and to the plateau of normal white counts before beginning the next course of chemotherapy. CT scans were obtained on a Philips 350 or GE 9800 scanner using 9- to 10-mm thick sections at 9- to 10-mm intervals. Thymic volumes were computed in the following manner: The area occupied by thymus on each slice was multiplied by the slice thickness and the appropriate magnification factor to obtain measurements in cubic centimeters. These "slice volumes" were added together; the first and last slice volumes were halved to account for partial-volume averaging. This technique has been validated by Breiman et al. [2] and Friedman et al. [3] and was adopted for smaller thymic volumes. It has an error rate of about 3–5% but is extremely reproducible.

Thymic volumes were graphed over time and related to courses of chemotherapy, absolute neutrophil count, absolute lymphocyte count, and total WBC count. The absolute neutrophil, lymphocyte, and WBC counts were used because they represent sensitive indicators of chemotherapy toxicity [4]. *Thymic atrophy* is defined as any decrease in volume relative to baseline, *thymic regrowth* as any increase in volume relative to the previous scan, and *thymic rebound* as a greater than 50% increase in volume over baseline.

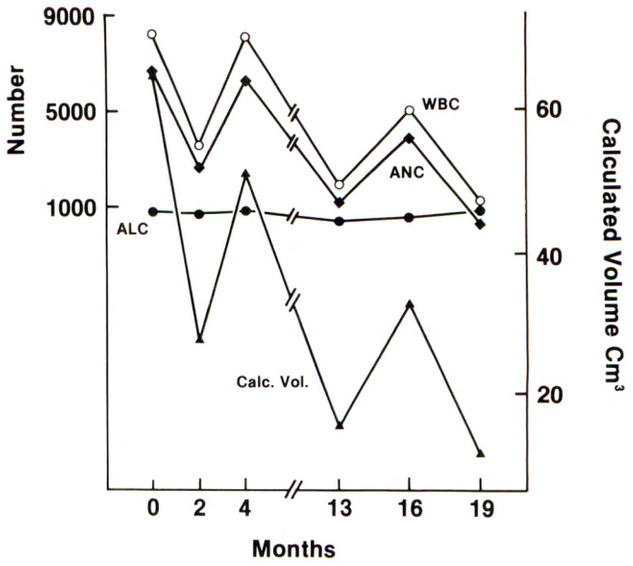


Fig. 2.—Graphic depiction of calculated thymic volume changes and WBC counts, absolute neutrophil counts (ANC), and absolute lymphocyte counts (ALC). Note good correlation between WBC, ANC, and thymic volumes. There is no correlation with ALC. (Left vertical axis is number of cells/mm³.)

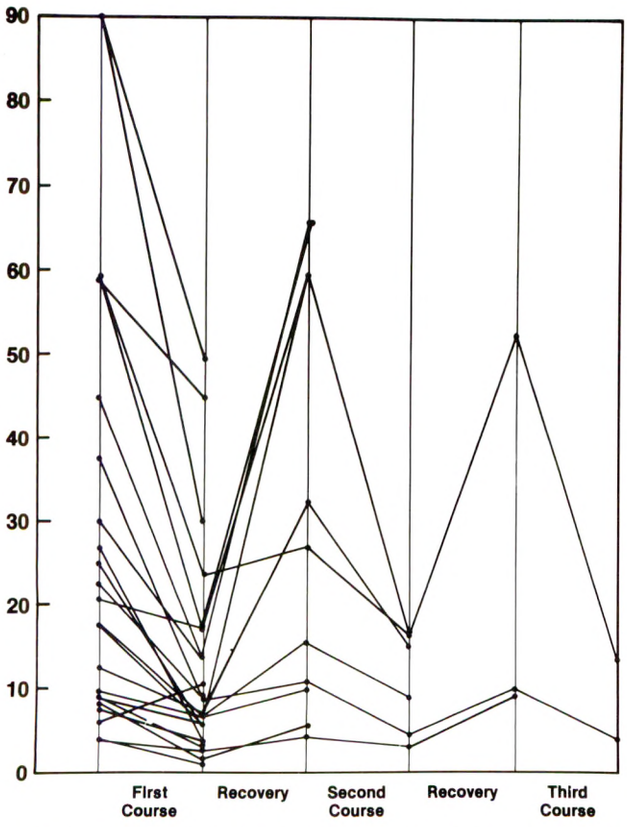


Fig. 1.—Graph depicting thymic volume changes during first, second, and third courses of chemotherapy. Vertical axis is thymic volume (in cm³).

Results

Twenty of 22 patients showed a decrease in thymic volume after their first course of chemotherapy (Fig. 1). Twenty of 22 patients also showed regrowth occurring 3–5 months after cessation of chemotherapy (Figs. 2–4). The first course of chemotherapy produced the largest average volume decrease 10.4 ± 0.5 cm^3 (mean initial volume, 24.0 ± 1.2 cm^3; mean posttreatment volume, 13.6 ± 0.7 cm^3). A range of volume changes (Fig. 1) was observed, from 2.0 ± 0.1 cm^3 to 60 ± 3.0 cm^3. Regrowth occurred over a period of 4–6 weeks after chemotherapy was terminated in 20 patients (Fig. 1). A mean increase of 19.4 ± 1.0 cm^3 was observed with a range from 1.0 ± 0.1 cm^3 to 47.0 ± 2.4 cm^3. In six patients CT scans were obtained during a second course of chemotherapy. An average decrease in volume of 17.1 ± 0.9 cm^3 with a range from 1.7 ± 0.1 cm^3 to 41.1 ± 2.05 cm^3 occurred during the second course followed by regrowth when the course was complete. Too few patients (two) were followed beyond three courses to allow further evaluation. Thymic rebound occurred in five of the 22 patients. Rebound (greater than 50% increase in volume) occurred several months (range, 3–8 months; mean, 4.2 months) after cessation of chemotherapy. Three of five patients with thymic rebound required additional treatment for their primary lesion. Thymic rebound prompted thymic biopsy in three cases and close clinical follow-up in

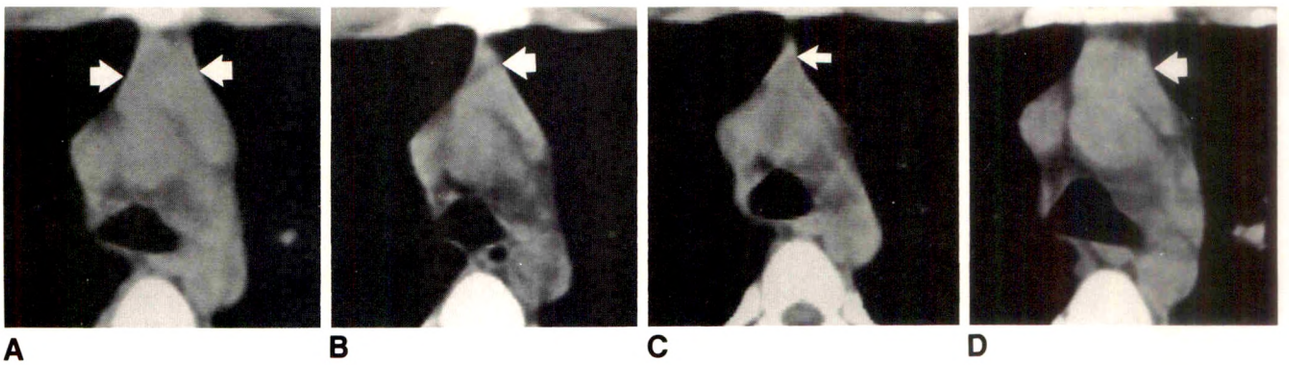
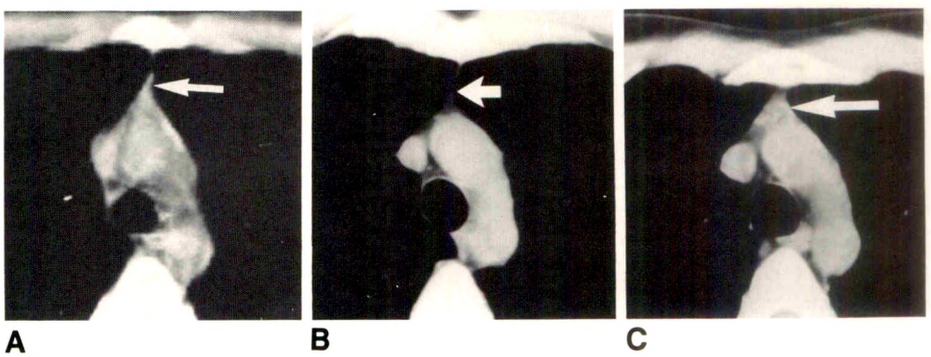


Fig. 3.—18-year-old man with osteogenic sarcoma of right humerus.
***A*, Baseline CT scan at level of aortic arch shows normal-sized thymus before treatment (*arrows*) (volume = 17 cm^3).**
***B*, 3 months after first course of chemotherapy. Thymus gland (*arrow*) is reduced in size (volume = 14 cm^3).**
***C*, After 5 months of treatment. Thymus (*arrow*) is further reduced in volume (volume = 7 cm^3).**
***D*, 24 months since diagnosis (8 months after last treatment). Thymus (*arrow*) has returned to normal size (volume = 18 cm^3).**

Fig. 4.—19-year-old woman with Hodgkin's lymphoma who had thymic enlargement after treatment.
***A*, Baseline CT scan shows normal thymus (*arrow*) before therapy (7 cm^3).**
***B*, Decrease in thymic volume (*arrow*) (3 cm^3) is noted during chemotherapy.**
***C*, Overgrowth of thymus (*arrow*) 5 months after cessation of chemotherapy (22 cm^3).**



the remaining two. Thymic hyperplasia was the cause of enlargement in all three biopsied cases.

The cyclic volume changes occurred in near synchrony with the WBC and absolute neutrophil counts in 20 of 22 patients (Fig. 2). The absolute lymphocyte count showed a poor correlation with thymic volumes. In 20 of 22 patients the thymic volumes were lowest within 1–5 months after the beginning of chemotherapy at the time the WBC and absolute neutrophil counts were at a minimum. Initial WBC counts were 4000–11,500/mm^3 (mean, 6600/mm^3); absolute neutrophil counts were 2000–8000/mm^3 (mean, 5600/mm^3). Post-treatment WBC counts were 100–4500/mm^3 (mean, 1100/mm^3), and absolute neutrophil counts were 5–2000/mm^3 (mean, 900/mm^3). Minimal thymic volumes were observed at maximal myelosuppression. Thymic regrowth coincided with the return to baseline cell counts. Subsequent cycles produced similar changes in six patients.

Thymic volumes actually increased during administration of chemotherapy in the remaining two of 22 patients (one with osteogenic sarcoma and one with malignant fibrous histiocytoma). Of interest, neither patient experienced significant alteration in the WBC count or absolute neutrophil count during treatment. One of these patients received a lowered dose of chemotherapy because of intolerance of side effects.

Discussion

CT of the thorax has become a common means of evaluating patients for metastatic disease. This is especially true for young patients with tumors that have a predilection for spread to the lungs and mediastinum such as lymphoma, testicular carcinoma, osteogenic sarcoma, and Wilms' tumor. It can be disconcerting to observe that an anterior mediastinal mass, which was originally thought to be a thymus, has increased or decreased significantly in size on serial CT scans while the patient is receiving chemotherapy. These changes can be mistaken for metastatic disease. This study shows that volume changes in the absence of tumor involvement are not only common, but occur predictably in response to the administration of or recovery from chemotherapy. Such changes are not necessarily a result of steroids in the regimen, since only six of 22 patients in our series received steroids as part of their therapy. Minimum thymic volumes are seen at the time of maximum leukopenia in over 90% of patients, and maximum thymic volumes are seen several months after the cessation of chemotherapy or just before starting the next course.

Cushing's disease, exogenous steroids, burns, starvation, and fever are all known causes of thymic atrophy [1, 5–7].

On CT the anterior mediastinum becomes replaced with fat. To our knowledge, atrophy of thymus during chemotherapy has not been documented previously, yet the finding is not surprising in view of the cytotoxic effects of chemotherapy.

Steroids are well documented to cause thymic atrophy [1, 5–7]. In our study, only patients with lymphoma received steroids as part of their chemotherapy, and thymic changes in these patients may have been caused by this component of their regimen. The other 16 patients, however, did not receive steroids as part of their therapy, and thymic changes in these patients appear to have been a result of nonsteroidal chemotherapeutic agents.

Much attention has been focused on the phenomenon of thymic hyperplasia or rebound. Pathologically, thymic hyperplasia is divided into two types [8]. The first represents an increase in the number of germinal centers and medullary lymphocytes [8]. This "follicular" type is not associated with marked enlargement, although minimal growth does occur. This type can be seen in myasthenia gravis, systemic lupus erythematosus, and autoimmune hemolytic anemia [8]. The second type is caused by overgrowth of normal thymic elements in normal proportions and with normal histology. This latter type, which is truly a hyperplasia, occurs not only in the cortex and medulla of thymus but also in the "extraparenchymal" zone of the thymus, which lies in the anterior mediastinal fat [8]. The changes we observed were documented surgically to represent the latter type in three patients. The remainder of the patients were presumed to have hyperplasia to varying degrees. No tumor has developed in any of the 22 patients after 18 months of follow-up.

No clear distinction has been made between hyperplasia, regrowth, and "rebound" of the thymus [9, 10]. Regrowth of the thymus is common after chemotherapy. Rebound occurs when the thymus enlarges over its baseline, although a significant change must occur for it to become visually obvious. Numerous reports document the phenomenon of rebound after cessation of either chemotherapy or endogenous or exogenous steroids [10–15]. Thymic rebound has been described after treatment of lymphoma, Ewing's sarcoma, Wilms' tumor, leukemia, osteosarcoma, ovarian tumors, and testicular tumors. Hyperplasia after cessation of chemotherapy does not appear to be unique to specific types of tumor, but appears to be a common response to the withdrawal of chemotherapy, nor does it appear limited to children, since it occurred in patients as old as 35. Cohen et al. [10] described seven patients with thymic hyperplasia showing mediastinal widening on chest radiographs after chemotherapy. They suggested that rebound was more common than previously thought and concluded that "thymic rebound [may] represent a positive prognostic sign." Our experience tends to support the concept that rebound is common after cessation of chemotherapy (since it occurred in 25% of our patients); however, in two of five patients with thymic rebound it occurred while the patient's neoplasm was still clinically active. Thymic volume changes appear to reflect a response of the body to the cessation of chemotherapy rather than a response of the tumor itself.

In conclusion, over 90% of young patients in our series who were receiving chemotherapy for malignancies showed thymic atrophy during their first course of therapy. The minimum thymic volume coincided with maximal myelosuppression caused by the direct effects of chemotherapy. Withdrawal of chemotherapy, either because of planned cyclic administration or side effects, resulted in variable enlargement of the thymus gland. In about 25% of patients, thymic rebound was observed. Subsequent courses of chemotherapy appear to result in similar although less marked changes. Thymic atrophy during chemotherapy is very common and usually is reversible. Thymic regrowth after chemotherapy does not necessarily reflect thymic metastasis. In nonlymphomatous tumors, such regrowth should be correlated with the general status of the patient's disease and timing of chemotherapy. In the appropriate setting thymic enlargement can be followed. Nevertheless, because patients with lymphoma are at high risk for anterior mediastinal metastasis, a progressively enlarging thymus in such patients may signal recurring tumor, and biopsy or close clinical follow-up is indicated.

ACKNOWLEDGMENTS

We thank Lynda Terry and Adam Choyke for data analysis and Krystine M. Williams for manuscript preparation.

REFERENCES

1. Levine GD, Rosai J. Thymic hyperplasia and neoplasia: a review of current concepts. *Hum Pathol* **1978**;9:495–515
2. Breiman RS, Beck JW, Korobkin M, et al. Volume determinations using computed tomography. *AJR* **1982**;138:329–333
3. Friedman MA, Resser KJ, Marcus FS, Moss AA, Cann CE. How accurate are computed tomographic scans in assessment of changes in tumor size? *Am J Med* **1983**;75:193–198
4. DeVita VT Jr. Principles of chemotherapy. In: DeVita VT Jr, Hellman S, Rosenberg SA, eds. *Cancer: principles and practice of oncology*. Philadelphia: Lippincott, **1982**:132–155
5. Caffey J. *Pediatric x-ray diagnosis*, 7th ed. Chicago: Year Book Medical, **1978**:510–527
6. Caffey J, Silbey R. Regrowth and overgrowth of the thymus after atrophy induced by the oral administration of adrenocorticosteroids to human infants. *Pediatrics* **1960**;26:762–770
7. Doppman JL, Oldfield EH, Chrousos GP, et al. Rebound thymic hyperplasia after treatment of Cushing's syndrome. *AJR* **1986**;147:1145–1147
8. Katz SM, Chatten J, Bishop HC, Roseblum H. Massive thymic enlargement: report of a case of gross thymic hyperplasia in a child. *Am J Clin Pathol* **1977**;68:786–790
9. Baron RL, Lee JKT, Sagel SS, Peterson RR. Computed tomography of the normal thymus. *Radiology* **1982**;142:121–125
10. Cohen M, Hill CA, Cangir A, Sullivan MP. Thymic rebound after treatment of childhood tumors. *AJR* **1980**;135:151–156
11. Carmosino L, DiBenedetto A, Feffer S. Thymic hyperplasia following successful chemotherapy. A report of two cases and review of the literature. *Cancer* **1985**;56:1526–1528
12. Tartas NE, Korin J, Dengra CS, Barazzutti LM, Blassetti A, Avalos JCS. Diffuse thymic enlargement in Hodgkin's disease. *JAMA* **1985**;254:406
13. Woodhead PJ. Thymic enlargement following chemotherapy. *Br J Radiol* **1984**;57:932–934
14. Shin MS, Ho KJ. Diffuse thymic hyperplasia following chemotherapy for nodular sclerosing Hodgkin's disease. An immunologic rebound phenomenon? *Cancer* **1983**;51:30–33
15. Kissin CM, Husband JE, Nicholas D, Eversman W. Benign thymic enlargement in adults after chemotherapy: CT demonstration. *Radiology* **1987**;163:67–70

Case Report

Congenital Absence of the Azygos Vein: A Cause for "Aortic Nipple" Enlargement

Malcolm K. Hatfield,[1] Carl J. Vyborny,[2] Heber MacMahon,[1] and Joseph W. Chessare[2]

The left superior intercostal vein, often referred to as an "aortic nipple," frequently is visualized along the margin of the aortic knob on posteroanterior chest radiographs. When the hemiazygos system is distended, the aortic nipple may become enlarged and simulate lymphadenopathy or focal aneurysmal dilatation of the aorta. We report a case in which congenital absence of the azygos vein resulted in enlargement of the left superior intercostal vein. Absence of the azygos vein is a rare finding in man. To our knowledge, only one case has been reported previously in the medical literature.

Case Report

A 35-year-old man without chest complaints had routine posteroanterior and lateral radiographs of the chest before an outpatient surgical procedure was performed. The frontal view showed a prominent bulge along the inferolateral portion of the aortic knob (Fig. 1). Enlargement of the left superior intercostal vein was considered the most likely explanation, although aortopulmonary window lymphadenopathy or focal aneurysmal dilatation of the aorta could not be excluded. On the frontal view, the azygos vein was not visible in its usual location. The patient had no history of malignancy or previous major trauma.

The patient subsequently underwent contrast-enhanced CT of the chest and upper abdomen. The findings confirmed complete absence of the azygos vein. Marked distension of the hemiazygos vein was evident; a distended accessory hemiazygos was also visualized (Fig. 2). An enlarged left superior intercostal vein adjacent to the aortic arch was observed.

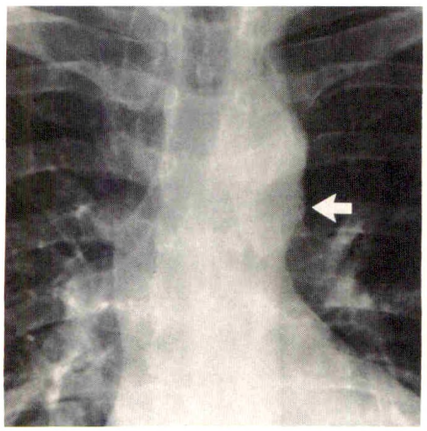
Discussion

The left superior intercostal vein gives the appearance of an aortic nipple on frontal chest radiographs in up to 10% of normal subjects [1]. The left superior intercostal vein may be enlarged in conditions that produce distension in the hemiazygos–accessory hemiazygos system. These include congenital absence of the inferior vena cava and left innominate vein, congestive heart failure, portal hypertension, Budd-Chiari syndrome, and obstruction of the superior or inferior vena cava [2–5]. When the left superior intercostal vein appears enlarged on radiographs, it may not be possible to exclude mediastinal tumor, lymphadenopathy, or small aneurysm of the aortic arch on the basis of the findings on plain films [2]. This is particularly true if the enlarged vein projects over the inferolateral portion of the aortic knob [1], as was the case in our patient.

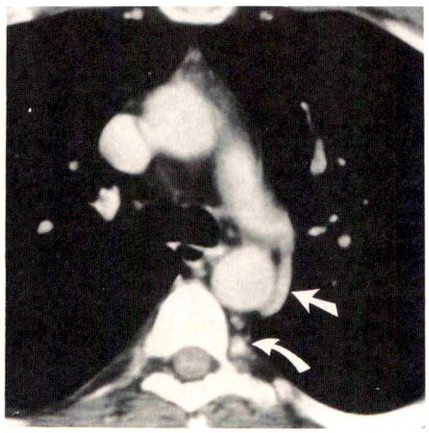
The marked enlargement of the aortic nipple in this patient was attributed to the absence of the azygos vein and resulting distension of the hemiazygos system. Congenital absence of the azygos is uncommon. Although the actual prevalence is not known, only one case has been reported previously [6, 7]. The azygos vein develops embryologically from the subcardinal veins; the right subcardinal vein corresponds to the azygos vein, and the left subcardinal vein corresponds to the hemiazygos vein [8]. An anastomosis develops between the left and right subcardinal veins, usually at the level of the sixth

Received February 9, 1987; accepted after revision March 31, 1987.
[1] Department of Radiology, Box 429, The University of Chicago, 5841 S. Maryland Ave., Chicago, IL 60637. Address reprint requests to H. MacMahon.
[2] Department of Radiology, LaGrange Memorial Hospital, 5101 S. Willow Springs Rd., LaGrange, IL 60525.

AJR 149:273–274, August 1987 0361–803X/87/1492–0273 © American Roentgen Ray Society



1



2

Fig. 1.—Chest radiograph shows well-defined convex density (*arrow*) caused by enlarged superior intercostal vein. Note absence of azygos vein. (The linear density above the right hilum was shown by CT to represent a scar rather than an azygos pseudolobe.)

Fig. 2.—CT scan with contrast infusion confirms absence of azygos vein and marked enlargement of superior intercostal vein (*arrow*) and accessory hemiazygos vein (*curved arrow*).

or seventh thoracic vertebra. The left subcardinal vein undergoes complete or partial atrophy cranial to the anastomosis, or it may persist as the accessory hemiazygos vein. The accessory hemiazygos vein meets the left superior intercostal vein medial to the distal aortic arch [5]; the left superior intercostal vein is derived from the embryonic posterior cardinal veins [5]. The left superior intercostal vein then turns anteriorly adjacent to the aortic arch to empty into the left innominate vein posteriorly [2, 3, 9]. Enlargement of the aortic nipple in our patient is presumably the result of increased blood flow through the superior intercostal vein from the distended hemiazygos system.

Although congenital absence of the azygos vein is an unusual cause for an enlarged aortic nipple, the diagnosis may be suggested by the findings on plain chest radiographs, especially when the shadow caused by the azygos vein is absent.

REFERENCES

1. Ball JB, Proto AV. The variable appearance of the left superior intercostal vein. *Radiology* **1982**;144:445–452
2. Friedman AC, Chambers E, Sprayregen S. The normal and abnormal left superior intercostal vein. *AJR* **1978**;131:599–602
3. Pagniez B, Denies JD, Dupus C, Remy J. The left superior intercostal vein. *J Radiol* **1975**;56:285–298
4. Berk RN. Dilatation of the left superior intercostal vein in the plain film diagnosis of chronic superior vena caval obstruction. *AJR* **1964**;83:419–423
5. Lane EJ, Heitzman ER, Dinn WM. The radiology of the superior intercostal veins. *Radiology* **1976**;120:263–267
6. Karpowicz S. Une variation de la veine mediane de dos en coincidence avec le défaut de la veine azygos. *C R Seances Acad Sci [III]* **1934**;27(4)
7. Adachi, Buntaro. *Das Venensystem der Japaner*, vol. II. Kyoto: Druckanstalt Kenkyusha Tokyo, **1940**:92
8. Kjellberg SR, Mannheimer E, Rudhe U, Jonsson B. *Diagnosis of congenital heart disease*, 2nd ed. Chicago: Year Book Medical, **1959**:11–12
9. McDonald CJ, Castellino RA, Blank N. The aortic "nipple": the left superior intercostal vein. *Radiology* **1970**;96:533–536

Evaluation of Optical Unsharp Masking and Contrast Enhancement of Low-Scatter Chest Radiographs

James A. Sorenson[1]
Christopher R. Mitchell

Conventional chest radiography poses a challenging technical problem because of its requirement for simultaneous high-contrast display and wide-latitude recording across the entire image. We developed and evaluated a method of producing chest radiographs by using a tantalum air-interspace grid for highly efficient scatter rejection, wide-latitude X-ray film for recording the low-scatter image, and a LogEtronics printer for optical unsharp masking and contrast enhancement of the recorded image (TWL technique). TWL images can be readily obtained and have excellent contrast and detail across the entire image. In comparison with a conventional technique, the TWL technique provides about a 15% improvement in image contrast in well-penetrated areas and a threefold to tenfold improvement in poorly penetrated areas. A detection study using simulated lung nodules and a chest phantom showed about 10% overall improvement in nodule detection with the TWL technique (51% vs 42%), most of which was due to improvement in detection rates in poorly penetrated areas of the chest (62% vs 26%). In well-penetrated areas, there was a decrease in detection rates (52% vs 44%) using TWL images despite measured improvements in image contrast in these areas. Possibly this was due to the observers' unfamiliarity with the reversed-contrast TWL images.

Our results show the TWL technique to be valuable for improving image quality and diagnostic accuracy in chest radiography.

Although it is the most frequently performed study in a typical radiology department, chest radiography remains a challenging technical problem. Many of the structures and features of interest—for example, pulmonary vasculature and lung nodules—have inherently low contrast. The display of such features is optimized by the use of high-contrast film, low-kilovoltage exposures, and highly efficient scatter rejection. On the other hand, recording the wide range of exposure levels across the chest, which can have a 10:1 range between lungs and mediastinum [1, 2], favors the use of wide-latitude film, higher kilovoltage, and less efficient scatter rejection [3]. Therefore, when choosing technique factors for chest radiography, one is faced with unsatisfactory compromises between the need for wide-latitude recording to encompass a wide exposure range and the need for high-contrast display for visibility of low-contrast details.

Several research groups currently are working on techniques to overcome these display problems [1, 4–7]. Research efforts also are underway to develop methods for decreasing scattered radiation in chest radiography [8–10], which in some areas of the chest can exceed the levels encountered in the abdomen and other thick body parts [11]. We describe here a technique for chest radiography that combines the use of (1) a tantalum air-interspace crossed grid for highly efficient scatter rejection, (2) a wide-latitude film (Du Pont WDR, wide dynamic range) for faithful recording of the entire chest image, and (3) a LogEtronics printer for unsharp masking and contrast enhancement to improve the display of the recorded image. For simplicity, we will refer to the tantalum grid/WDR film/LogEtronics technique as the TWL technique.

Received December 29, 1986; accepted after revision April 3, 1987.

This work was supported by NIH research grant 5-ROI-CA32548 and by University of Utah Institutional Research Funds.

[1] Both authors: Department of Radiology, University of Utah Medical Center, Salt Lake City, UT 84132. Address reprint requests to J. A. Sorenson, Lunar Radiation, 313 W. Beltline Hwy., Madison, WI 53713.

AJR 149:275–281, August 1987
0361–803X/87/1492–0275
© American Roentgen Ray Society

Materials and Methods

The tantalum air-interspace grid has been described previously [10]. Briefly, it consists of two 10:1 linear grids crossed at right angles to achieve a crossed-grid effect. The grid strips are made of 0.1-mm-thick tantalum and are separated by 1 mm, and their centers are separated by 1 mm. For comparison, conventional antiscatter grids typically have lead strips 0.05-mm thick with centers separated by about 0.25 mm. The greater thickness, higher density, and more favorably located K-absorption edge of tantalum within the X-ray energy spectrum results in significantly better scatter rejection than is achieved with conventional grids. The interspace material is air, so that primary transmission is comparable with that of a conventional low-ratio linear grid. The tantalum grid has scatter-rejection characteristics that are comparable with those of some scanning-slit devices [12], but it makes more efficient use of X-ray tube output; thus it can be used with the same tube loading and X-ray exposure times as those normally used for chest radiography.

The low-scatter chest radiographs were recorded by using medium-speed intensifying screens (Du Pont Fast Quanta Detail) and Du Pont WDR film [13]. This film has less contrast than the conventional "latitude" film types commonly used for chest radiography, but it records with a constant and useful level of contrast over a wide range of exposure levels (Fig. 1A). For film densities greater than about 0.6 optical density (OD) units, WDR film has a relatively constant contrast (gamma) of about 1.3. By comparison, a conventional "latitude" film type has a gamma between 0 and 2.5, depending on the density to which it is exposed (Fig. 1B). Conventional chest radiographs typically are exposed to achieve a film density of about 1.7 OD units in well-penetrated areas of the lungs. This provides maximum film contrast in these areas; however, other areas then are displayed with less contrast.

We accomplished simultaneous unsharp masking and contrast enhancement by printing the low-scatter WDR chest radiograph onto a high-contrast print film (Du Pont MRF-31, Fig. 1C) using a LogEtronics model 4050 printer (LogEtronics, Springfield, VA) [14]. The LogEtronics printer uses a scanning light beam generated by a cathode ray tube to make a contact print (Fig. 2). A lens system blurs the light beam to a diameter of approximately 2 cm and projects it onto the original image and the print film. As the exposing beam scans over the image, the amount of light transmitted through the original image and print film is monitored by a photomultiplier tube. The photomultiplier tube generates a feedback signal that modulates the brightness and scanning speed of the exposing light beam, so that lighter areas of the image are exposed with less light and, conversely, darker areas with more light. This results in an unsharp masking effect by which large-area contrast (e.g., lungs vs medias-

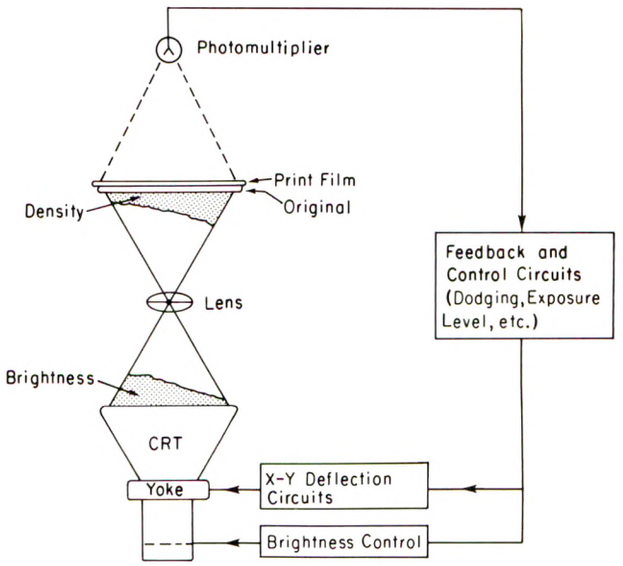


Fig. 2.—Principles of LogEtronics printer. (Adapted with permission from Street et al. [14].)

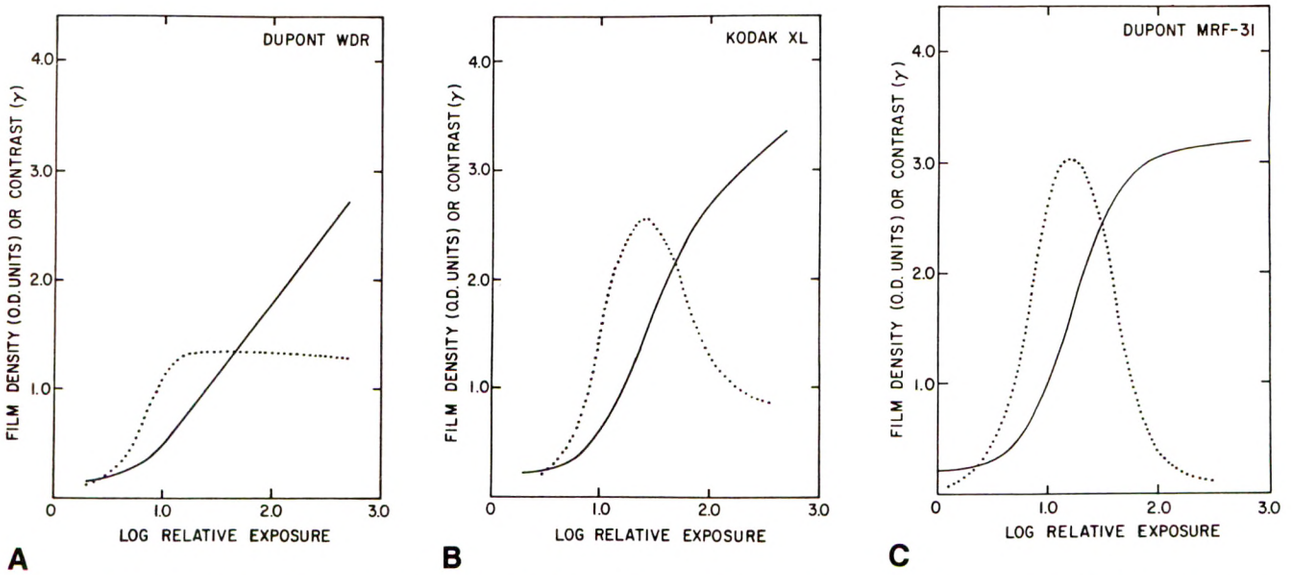


Fig. 1.—*A–C*, Sensitometric curves for film types used in this study. Unbroken line = film density; dotted line = contrast (γ). WDR = wide dynamic range; O.D. = optical density.

tinum) is suppressed; however, the contrast of details smaller in size than the scanning light beam is not suppressed and indeed may be enhanced by printing onto a high-contrast print film. Du Pont MRF-31 film provides a contrast-enhancement factor (film gamma) of about 3 when exposed to optical densities of 1–2 OD units (Fig. 1C).

The LogEtronics printer was modified by replacing the original 100-mm (diameter) projection lens with a 25-mm (diameter) lens that has variable aperture settings. This was done to decrease lens flare and provide a more accurate unsharp masking effect. Although this also decreased the speed of the system, the required exposure times with MRF-31 film still were acceptable, typically about 10 sec.

We also found it helpful to calibrate the printer with an additional 0.3-OD neutral-density filter placed over the lens system. The filter was removed for subsequent printing exposures. The effect of adding an optical attenuator was to "offset" the operating range of the printer and thus better match the density range usually encountered on WDR chest radiographs.

To evaluate the effect of the TWL technique on nodule contrast, we obtained images of a polystyrene chest phantom [1]; Teflon beads (diameter, 1.25 cm; density, 2.1 g/cm^3) were attached to the surface of the phantom to simulate lung nodules. This phantom contained no anatomic details and was designed specifically for measurements of image contrast. Although more dense than soft tissue, the composition of Teflon (primarily fluorocarbons) is reasonably close to that of soft tissue; thus it is suitable for measurements of relative soft-tissue contrast. Beads were positioned over areas representing mid-lung, retrocardiac, and mediastinal regions. Radiographs were obtained with a three-phase generator (General Electric MSI-850II, GE Medical Systems, Milwaukee, WI) using 140-kV exposures and 0.6-mm (nominal) focal-spot size. Total X-ray beam filtration was 3-mm Al equivalent. Technical factors for conventional and low-scatter WDR films are summarized in Table 1.

The WDR images were copied onto Du Pont MRF-31 film using the LogEtronics printer, with the printer set for "maximum dodging" and the lens aperture set to *f*/16. We used MacBeth Model TD502 densitometer (Kollmorgen, Newburgh, NY) to measure regional film densities and nodule contrasts (density difference between center of nodule shadow and surround) on the conventional film image and on the original and LogEtronics copies of the WDR film images.

Conventional and TWL chest radiographs were obtained on patients with known cancer who were referred to our laboratory from the Oncology/Hematology Division of the University of Utah Hospital. Approximately 100 patients have been studied to date in this ongoing clinical evaluation. Technical factors were as described in Table 1. Informed consent was obtained from all patients.

To evaluate the effects of the TWL technique on nodule detection, we performed an observer study employing images of an anthropomorphic chest phantom (Humanoid Systems, Irvine, CA) and 0.8-cm diameter plastic beads, as previously described [1, 15]. This phantom contained fixed lungs to create anatomic background structures. We compared nodule detection on conventional films, WDR films, and TWL films. A total of 18 films containing 0–6 nodules each (42 nodules total) was obtained by the conventional and WDR/Ta grid technique. The latter were used to prepare the TWL films. The 42 individual nodule locations were carefully matched, but the distribution of nodules on individual films was varied between the conventional and WDR film series. The nodules also were categorized by location: L = well-penetrated lung regions (26 nodules) and R = poorly penetrated "retro" regions, that is, retrohilar, retrocardiac, and subdiaphragmatic (16 nodules). Films of different types were randomly sorted into packets of 18 films each. Five radiologists and a physicist experienced with nodule detection studies served as observers. The observers marked the nodules they detected and indicated their confidence level by using a four-level confidence rating scale. Films on which no nodules were detected were marked "0" or "no nodules."

Results

Table 2 summarizes measured contrasts of images of the Teflon beads and surround film densities in different regions of the polystyrene chest phantom. In comparison with conventional film images, the images recorded on WDR film had greater contrast in the retrocardiac and mediastinal areas but significantly less contrast in the mid-lung areas. The TWL images had greater contrast than the conventional or WDR film images in all areas.

Figures 3–5 show the results obtained in patients. The images shown include the conventional chest radiograph (Fig. 3A), the original Ta grid/WDR radiograph (Fig. 3B), a copy of the Ta grid/WDR radiograph printed on MRF-31 film using the LogEtronics printer (TWL image, Fig. 3C), and a copy of the conventional chest radiograph printed by the same technique (Fig. 3D). Note that image contrast is reversed on the LogEtronics images owing to the sensitometric characteristics of MRF-31 film.

The images in Figure 3 demonstrate the contrast comparisons shown in Table 2 and typify the general appearance and quality of results achieved to date. In comparison with the conventional chest radiograph (Fig. 3A), the WDR radiograph

TABLE 1: Technical Factors Used in Chest Radiography

	Conventional Film-Screen and Scatter Rejection	Very Wide Latitude Film, Low-scatter
Film	Kodak XL	Du Pont WDR
Screen	Du Pont Hi-Plus	Du Pont Fast Quanta Detail
FFD (cm)	183	200
Antiscatter grid	Conventional: 12:1, 33.5 l/cm	Tantalum, crossed; 10:1, 10 l/cm
mAs	1	4
Entrance exposure (mR[a])	12	40

Note.—WDR = Wide dynamic range; FFD = focus-film distance.
[a] 1 mR = 2.58 × 10^{-7} C/kg.

TABLE 2: Nodule Contrast and Surround Film Density in Different Regions of Chest Radiographs

Film Type	Contrast[a]/Surround Film Density[b]		
	L	R	M
Conventional	0.5/1.6	0.2/0.6	0.03/0.3
WDR[c]	0.3/2.2	0.3/1.5	0.2/0.9
TWL[d]	0.6/1.2	0.7/1.3	0.4/2.0

[a] Difference in optical density between Teflon beads and surround film density on polystyrene chest phantom. L = mid-lung; R = retrocardiac; M = mediastinum.
[b] Measured adjacent to shadow of simulated nodule.
[c] Wide dynamic range.
[d] Tantalum grid, WDR film, LogEtronics printer.

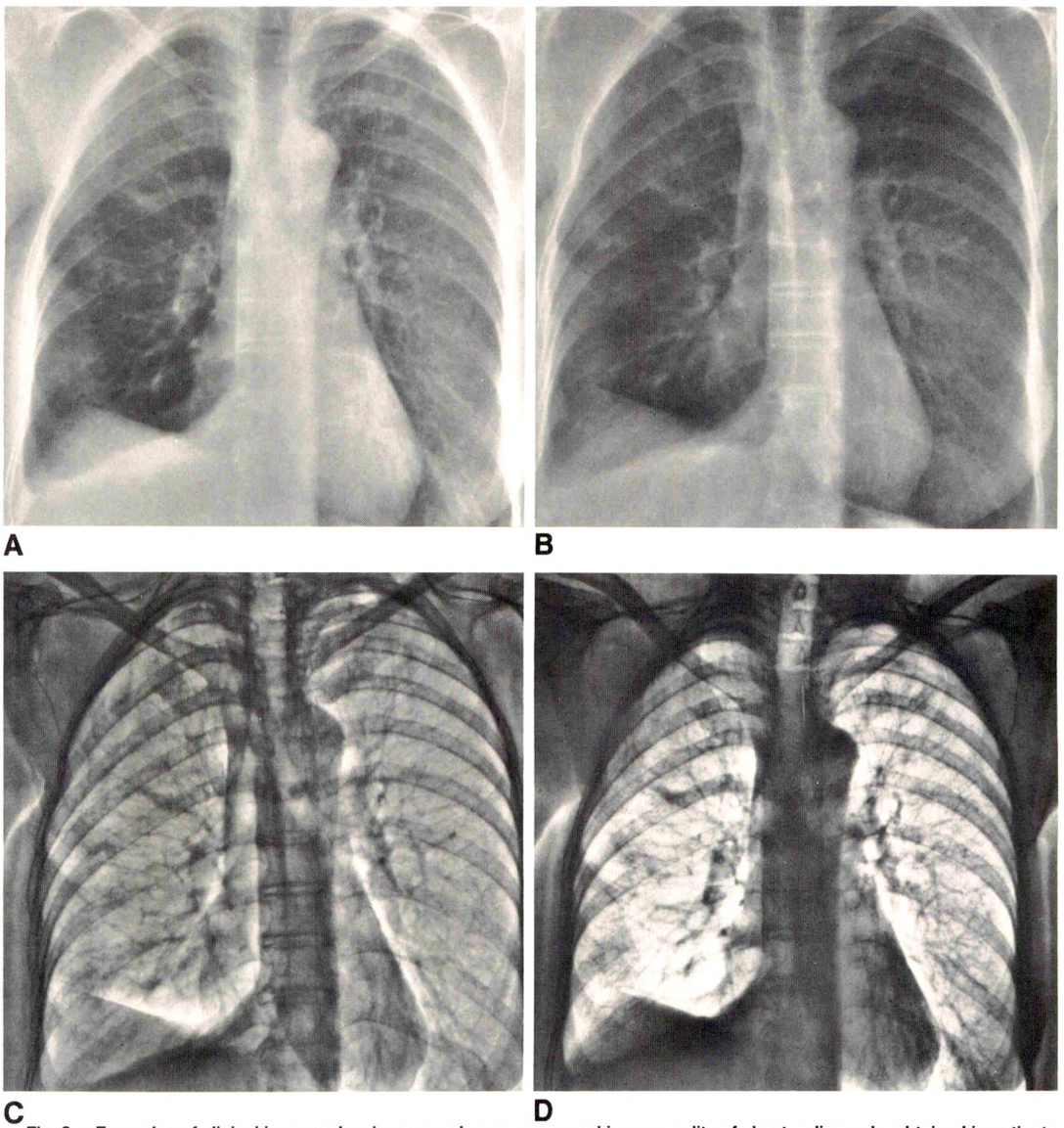


Fig. 3.—Examples of clinical images showing general appearance and image quality of chest radiographs obtained in patients in this study.

***A*, Conventional chest radiograph recorded on Kodak XL film.**

***B*, Low-scatter (Ta grid) chest radiograph recorded on Du Pont WDR film.**

***C*, LogEtronics print of *B* on Du Pont MRF-31 film (TWL image).**

***D*, LogEtronics print of *A* on Du Pont MRF-31 film.**

Note also that each of these images was copied onto standard copy film using the LogEtronics printer in order to preserve the contrast of the original images for this figure.

(Fig. 3B) has greater contrast in poorly penetrated areas, but less contrast in well-penetrated areas. The TWL image (Fig. 3C) has greater contrast than either the conventional or WDR image in all areas. The LogEtronics copy of the conventional film (Fig. 3D) is noticeably inferior to the TWL image in several respects. It has uneven contrast across the image, greater in well-penetrated areas than in poorly penetrated areas. This reflects the difference in contrast between these areas on the original image. It also has both very dark and very light areas in which anatomic structures are not well visualized.

Figure 4 shows segments of conventional and TWL images of another patient in a region containing lung nodules. In this example, nodules that were virtually invisible on the conventional film were obvious on the TWL film. Although the nodules were projected differently on the two films, improved contrast appears to be the major difference affecting nodule visibility in this demonstration. These nodules were proved on follow-up films. We have encountered several similar examples in our clinical studies, which number about 100 patients to date. Objective receiver-operating-characteristics (ROC) nodule de-

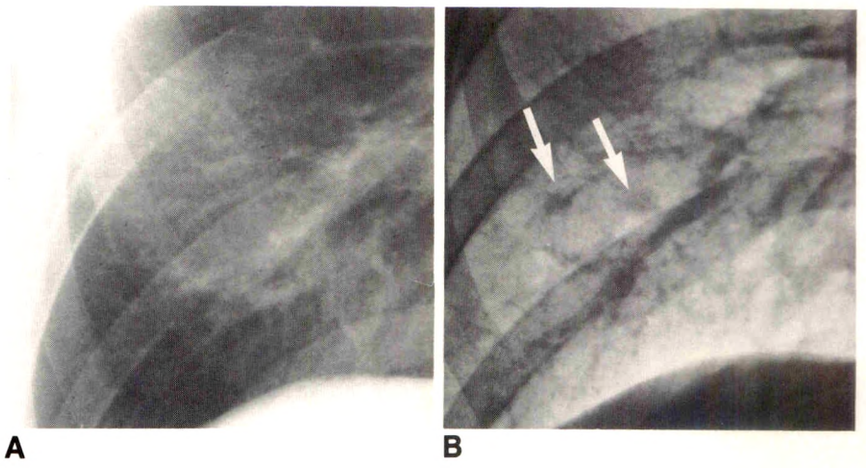


Fig. 4.—Closeup of region containing nodules (*arrows*) on conventional chest radiograph (*A*) and TWL radiograph (*B*). Nodule visibility is noticeably superior on TWL image.

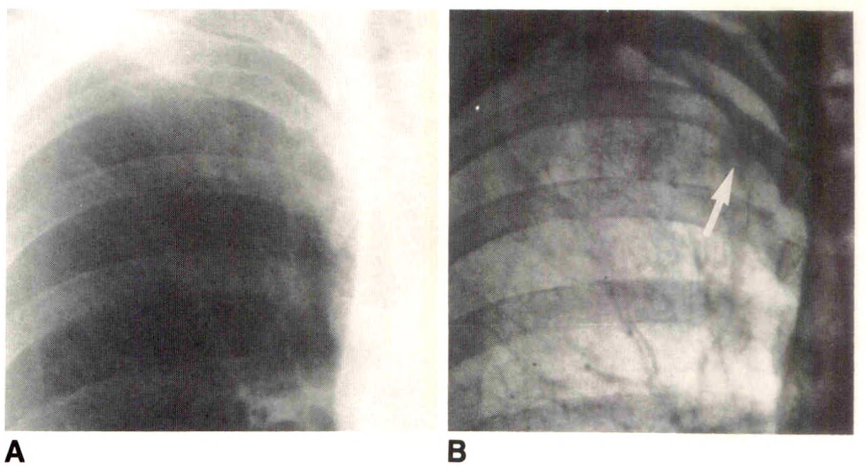


Fig. 5.—*A*, Conventional chest radiograph. *B*, Closeup on TWL radiograph shows potential false-positive finding (*arrow*). Density is probably caused by focal calcification in costal cartilage at sternal end of right first rib. It was initially suspected to be a nodule, illustrating potential for false-positive finding resulting from increased contrast on TWL image.

tection studies [16] will be required to determine the statistical and clinical significance of these findings.

Figure 5 shows comparative images of another patient in a region containing a potential false-positive nodule. In this example, the faint structure on the TWL film, initially identified as a nodule, was not seen on CT scans and probably was due to focal irregular calcification of costal cartilage at the sternal end of the right first rib. This is the only example of a confirmed false-positive finding in our clinical studies to date. The statistical and clinical significance of false positives also will be evaluated by objective ROC studies using clinical films.

The results of the phantom nodule-detection study were not analyzed by ROC methods because of the relatively small number of false-positive findings detected—in some cases, none or only one of a series of films for an individual reader. This probably was the result of a lack of variable background structure in the phantom. For this reason, only the true-positive rates, combining all confidence levels, were compared.

Table 3 summarizes the mean true-positive detection rates and the standard deviations of the means for the six readers in different regions of conventional, WDR, and TWL films. In poorly penetrated retro (R) regions, the results were as expected from the measured differences in contrast (Table 2), with the highest detection rates being recorded on the TWL film, followed by the original WDR film and then the conventional film. By a paired t-test [17], the differences in the retro (R) regions between conventional vs WDR films and between conventional vs TWL films were significant at the $p < .01$ level and between WDR vs TWL films at the $p < .05$ level.

TABLE 3: Lung Nodule Detection Rates in Different Regions of Chest Phantom (± SD of Mean for Six Observers)

Film Type	Region		
	Lung (L)	Retro[a] (R)	All (L + R)
Conventional	0.520 (± 0.044)	0.262 (± 0.041)	0.422 (± 0.038)
WDR[b]	0.405 (± 0.029)	0.458 (± 0.044)	0.425 (± 0.031)
TWL[c]	0.442 (± 0.032)	0.615 (± 0.044)	0.508 (± 0.032)

[a] Retrohilar, retrocardiac, or subdiaphragmatic.
[b] Wide dynamic range.
[c] Tantalum grid, WDR film, LogEtronics printer.

In well-penetrated lung (L) regions, TWL films were superior to the WDR films, as expected from the relative contrast measurements in these areas; however, the conventional films were unexpectedly superior to TWL films. By a paired t-test, none of the differences in the lung (L) regions were significant at the .05 level, although the differences between conventional vs both WDR and TWL films were of marginal significance ($p < .1$).

Combining all regions (L + R), nodule detection was virtually identical on conventional and WDR films owing to offsetting advantages in lung and retro regions between these two film types. TWL films were superior to both, although by a paired t-test, only the advantage over the conventional films was significant ($p < .05$).

Discussion

TWL images have been well received by our clinical colleagues, including both radiologists and referring oncologists. The reversed-contrast ("black bone") image also has been well received, as has been noted previously by other investigators [9]. Our clinical experience to date suggests that the TWL technique may improve nodule detectability (Fig. 4). This was supported by the results of the phantom nodule-detection study for nodules in poorly penetrated areas (Table 3). The improvement may have been due in part to the higher doses used for the TWL films; however, the advantage of improved image contrast for nodule detection in poorly penetrated areas has been well documented in several previous studies [1, 9, 15, 16].

The unexpected superiority of conventional films over TWL films in well-penetrated areas in the phantom nodule-detection study, although only of marginal statistical significance, will require further study. MacMahon et al. [18] recently reported similar findings in a clinical study comparing different display formats for digital chest radiography. They also found that, whereas their observers subjectively preferred the reversed-contrast display, diagnostic accuracy, measured by ROC techniques, was superior on images displayed with conventional "white bone" contrast.

We explored the use of positive-contrast print films with the TWL technique to avoid the potential complications of contrast reversal. Unfortunately, the selection of available film types is quite limited, particularly for 90-sec processors. Positive contrast film types that we have identified tend to have either too little contrast enhancement (gamma about 1, e.g., conventional copy film) or too much contrast (gamma about 4 or greater, e.g., graphic arts films such as Kodak Kodalite or Du Pont CRR). In addition, all positive-contrast print films are slow and require long exposure times (up to 1 hr) with the small lens aperture that we use for the TWL technique. For these reasons, our efforts have focused on the use of contrast-reversing film types.

The TWL technique requires about three times as much patient dose as a conventional chest radiograph; however, the recorded image has excellent contrast and density over the entire chest. The usual approach for acquiring an image with adequate contrast in poorly penetrated regions is to obtain an "overpenetrated" film in addition to a conventional film. In comparison to this approach, the TWL technique actually requires a lower dose by providing all of the desired information with a single X-ray exposure. An additional factor affecting dose for the TWL technique is the highly efficient cleanup of scattered radiation by the tantalum grid. Additional primary radiation is needed to replace the scattered radiation to achieve adequate film blackening. This is an unavoidable consequence of efficient scatter rejection [3].

Image processing with the LogEtronics printer is a simple and rapid procedure. Exposure times for MRF-31 film typically are about 10 sec. After an initial daily warm-up and calibration procedure that requires a few minutes to complete, the instrument is stable and needs only occasional recalibration. In only a few cases have we found it necessary to repeat an exposure to obtain an acceptable result. Optical image-processing techniques also have been described by Kattan [19] and McSweeney et al. [20]. They prepared a blurred negative of the original film and used this as an unsharp mask to compress the overall density range for high-contrast printing. We experimented with this technique for chest radiography but found it to be impractical because of the need for careful adjustment of film densities and exposure times in the printing process. The ability to achieve a good result on the first try is a major advantage of the LogEtronics approach.

In comparison with digital unsharp masking and contrast enhancement, the TWL technique lacks flexibility in selection of "algorithm parameters"; however, the TWL method can be implemented with equipment that is much less costly. Also, it does not introduce loss of detail and aliasing artifacts, which result from the finite sampling aperture size and sampling interval used for digital images [21]. Although sampling requirements for digital chest radiography have not been firmly established yet, it appears that at least 1024 × 1024 and possibly 2048 × 2048 elements will be needed to avoid loss of diagnostically important information [22, 23]. As illustrated by the close-up views in Figure 4 and 5, the spatial resolution of TWL images is comparable with that of conventional chest radiographs. Also, the dose requirements for the TWL technique are comparable with those of the Picker digital chest unit [9].

ACKNOWLEDGMENTS

We thank Du Pont and Kodak for providing film samples for evaluation of the TWL technique. We also thank G. Nicholas Baldwin, Marcia Bilbao, Patrick Leurs, Howard Mann, and William Zweibel for serving as observers in the phantom nodule-detection study and Philip Bossart for assistance in preparing phantom images. Finally, we thank John D. Armstrong II, David G. Bragg, Howard Mann, and James A. Nelson for their helpful comments on clinical images and John Street of LogEtronics for his helpful comments on the manuscript.

REFERENCES

1. Sorenson JA, Niklason LT, Nelson JA. Photographic unsharp masking in chest radiography. *Invest Radiol* **1981**;16(4):281–288
2. Tesic MM, Sones RA, Morgan DR. Single-slit digital radiography: some practical considerations. *AJR* **1984**;142:697–702

3. Sorenson JA, Nelson JA. Slit radiography: problems and potential. *Proc SPIE* **1980**;233:240–247
4. Wieder S, Adams PL. Improved routine chest radiography with a trough filter. *AJR* **1979**;137:695–698
5. Hasegawa BH, Naimuddin S, Dobbins JT III, et al. Digital beam attenuator technique for compensated chest radiography. *Radiology* **1986**;159: 537–543
6. Plewes DB, Vogelstein E. A scanning system for chest radiography with regional exposure control: practical implementation. *Med Phys* **1983**;10:655–663
7. Mitchell CR, Sorenson JA. Digital image processing in chest radiography. *Proc SPIE* **1986**;626:259–267
8. Sorenson JA, Nelson JA, Niklason LT, Jacobsen SC. Rotating disk device for slit radiography of the chest. *Radiology* **1980**;134(1):227–231
9. Fraser RG, Breatnach E, Barnes GT. Digital radiography of the chest: clinical experience with a prototype unit. *Radiology* **1983**;148:1–5
10. Sorenson JA, Niklason LT, Jacobsen SC, Knutti DF, Johnson TC. Tantalum air-interspace crossed grid: design and performance characteristics. *Radiology* **1982**;145:485–492
11. Niklason LT, Sorenson JA, Nelson JA. Scattered radiation in chest radiography. *Med Phys* **1981**;8:677–681
12. Sorenson JA, Floch J. Scatter rejection by air gaps. An empirical model. *Med Phys* **1985**;12(3):308–316
13. Schwenker RP. Film-screen digital radiography. *Proc SPIE* **1984**;486: 146–149
14. Street JN, McIntosh WL, Manack AW, Gibson RC. Optimizing photographic information transfer by CRT—a technology and application review. *Proc SPIE* **1984**;496:162–171
15. Armstrong JD, Sorenson JA, Nelson JA, et al. Clinical evaluation of unsharp masking and slit scanning techniques in chest radiography. *Radiology* **1983**;147:351–356
16. Sorenson JA, Mitchell CR, Armstrong JD, et al. Effects of improved contrast on nodule detection: a clinical ROC study. *Invest Radiol* (in press)
17. Sorenson JA, Phelps ME. *Physics in nuclear medicine*, 2nd ed. Orlando, FL: Grune & Stratton, **1987**:137.
18. MacMahon H, Metz CE, Doi K, Kim T, Giger ML, Chan H-P. Effect of display format on diagnostic accuracy in digital chest radiography (abstr). *Radiology* **1986**;161(P):203
19. Kattan KR. A modified blurred undersubtraction method (BUS) and its applications. *Radiology* **1980**;134:782–783
20. McSweeney MB, Sprawls P, Egan RL. Enhanced-image mammography. *Recent Results Cancer Res* **1984**;90:79–89
21. Giger ML, Doi K. Investigation of basic imaging properties in digital radiography. *Med Phys* **1984**;11:287–295
22. Foley WD, Wilson CR, Keyes GS, et al. The effect of varying spatial resolution on the detectability of diffuse pulmonary nodules. *Radiology* **1981**;141(1):25–31
23. MacMahon H, Vyborny C, Powell G, Doi K, Metz CE. The effect of pixel size on the detection rate of early pulmonary sarcoidosis in digital chest radiography systems. *Proc SPIE* **1984**;486:14–20

Book Review

Textbook of Radiographic Science. Edited by H. Brian Bentley. New York: Churchill Livingstone, 216 pp., 1986. $24

This is an eclectic collection of chapters written by a number of senior radiographers (technologists) primarily from Great Britain. The stated purpose is to cover some of the "more specialized areas of radiology" and to give the radiographic technologists studying for examinations some scientific background for these special procedures. The editor states that he is not attempting to make this an inclusive textbook but since technology is changing so rapidly he will try in the book to point out some of the specialized areas with a somewhat in-depth coverage. The individual chapters are written at a technologist's level, and a lot of the information in these individual chapters would be interesting to technologists and technology students. The book itself is written on high-quality paper so that the illustrations reproduce well. Included among the 10 chapters are "Radiography of Trauma in the Cervical Spine in Patients with Associated Spinal Cord Injuries," "Pediatric Radiography," "Urodynamic Studies in the Patient with Severe Cord Injury," "Radiography of the Heart and Great Vessels," and a concluding chapter on research techniques for those interested in pursuing research projects.

I found the book to be poorly organized, and the subject material is esoteric for technologists. This book might be useful for technologists who wish to learn more about certain "special procedures" or as a reference book in the library of a school of radiographic technology. This book is not appropriate for radiologists.

Ronald D. Harris
Geisinger Medical Center
Danville, PA 17822

Two-View Specimen Radiography in Surgical Biopsy of Nonpalpable Breast Masses

Murray Rebner[1]
David R. Pennes
David E. Baker
Dorit D. Adler
Pamela Boyd

Nonpalpable, low-density, noncalcified lesions sometimes can be difficult to see on an initial specimen radiograph. In 57 consecutive wire localizations, 37 patients had obvious microcalcifications and did not require a second specimen radiograph. Twenty-six patients had nonpalpable, noncalcified lesions, and a second specimen radiograph was obtained in 24 of these. In four of these cases the initial specimen radiograph failed to show the suspected lesion, and a second specimen radiograph orthogonal to the original plane of orientation of the specimen showed the lesion to be contained within the biopsied material. Although it is seldom necessary to use this technique, it may obviate a second biopsy specimen as well as reduce operative time.

We found that a second orthogonal specimen radiograph provided important information in 7% of cases.

The increased use of mammography as a screening tool for the detection of breast cancer has resulted in an increase in the number of nonpalpable breast lesions detected in asymptomatic women. Excisional biopsy of these nonpalpable lesions has allowed for the diagnosis and treatment of breast cancer at an earlier stage. Specimen radiography is an essential step in confirming excision of the suspicious lesion [1]. For nonpalpable, low-density lesions that do not contain calcifications, it sometimes can be difficult to determine whether the lesion has been removed. We present our experience with 57 patients who underwent wire localization and specimen radiography.

Subjects and Methods

A prospective study was undertaken from July 1, 1986, through March 10, 1987, to determine the utility of a second orthogonal specimen radiograph. The series comprised 57 women. All had routine mammograms. Of the 57 patients requiring a surgical biopsy, 26 had nonpalpable, noncalcified lesions and 37 had suspicious microcalcifications. Six women had both microcalcifications and a mass. Axillary, mediolateral, and craniocaudal views of each breast were obtained with a dedicated mammography unit (Thomson CGR 500-T, Paris) with Kodak Ortho-M film and Min-R screens (Rochester, NY). The examinations were performed at 28 or 30 kVp, and reciprocating grids were used in all cases.

Specimen radiographs were obtained for all 57 patients within 1 hr of the surgical biopsy. A second orthogonal image was obtained for 24 of the 26 noncalcified masses. With use of the grid, radiographs were obtained with compression at 28 kVp and about 10 mAs, with a target-to-film distance of 65 cm. After the initial specimen radiograph, a second specimen radiograph was obtained in an orthogonal projection with the same exposure factors.

Results

In 20 of the 24 two-view specimen radiographs the lesion was clearly visible on the first and second views. In four cases the second view provided critical information. In two of these cases (Figs. 1A and 2A) the initial specimen radiographs

Received January 30, 1987; accepted after revision April 6, 1987

[1] All authors: Department of Radiology, University of Michigan Medical Center, Taubman Center 2910/0326, 1500 E. Medical Center Dr., Ann Arbor, MI 48109–0326. Address reprint requests to M. Rebner.

AJR 149:283–285, August 1987
0361–803X/87/1492–0283
© American Roentgen Ray Society

failed to show the lesions unequivocally (Figs. 1B and 2B), and they were identified only on the orthogonal image (Figs. 1C and 2C). In one patient (Fig. 3A) the initial specimen radiograph showed the lesion at the edge of the specimen (Fig. 3B). The orthogonal view (Fig. 3C) revealed that the specimen had been transected, with separation of the two parts. The fourth patient (Fig. 4A) had two adjacent lesions. The initial specimen radiograph (Fig. 4B) showed only one of the lesions, whereas the orthogonal radiograph (Fig. 4C) showed both lesions, which had been superimposed on the initial radiograph.

Discussion

Viewing a lesion in more than one projection is a standard practice in radiology. This aids in geographic localization and may allow features of the lesion to be appreciated in one plane that cannot be seen in another plane. Detection of microcalcifications in a specimen radiograph usually is not a problem because of their high density relative to adjacent breast parenchyma. However, low- to moderate-density lesions, which do not differ greatly from surrounding breast tissue, may be difficult to identify in the biopsy specimen. Various maneuvers have been used in specimen radiography to enhance lesion identification, including placing the biopsy specimen in a water-filled container [2–4] and using magnification [5].

Although a lesion is usually identified on two or three standard mammographic views before excision, the orientation of the lesion in the final specimen may not correspond to any of the three preoperative projections. The advantage provided by orthogonal specimen radiography is the probability of reproducing the geometry of one of the standard

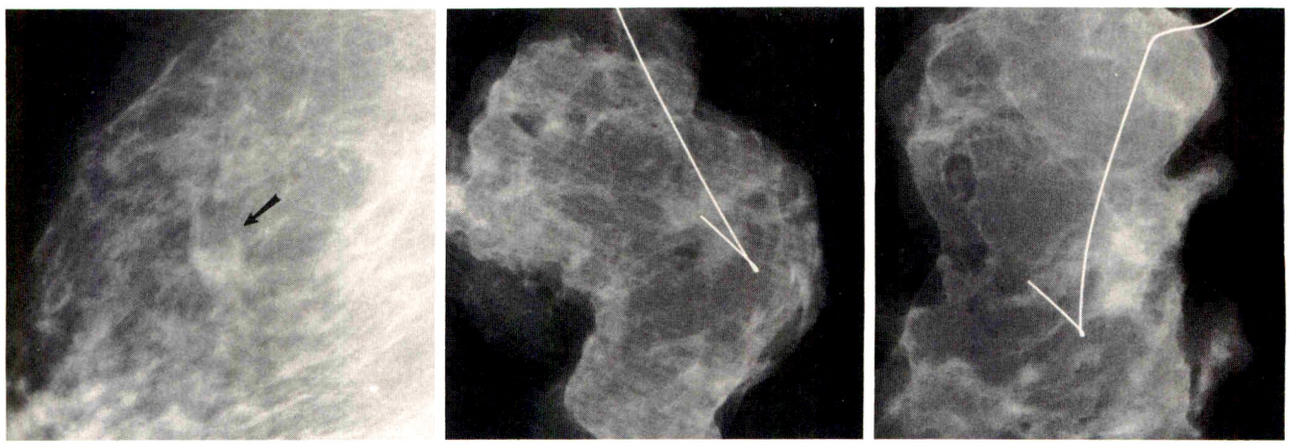


Fig. 1.—71-year-old woman.
***A*, Oblique view from screening mammogram shows a small stellate density (*arrow*).**
***B*, Initial specimen radiograph shows low-density area adjacent to hook-wire tip. This finding was not clearly the same density as that seen in *A*.**
***C*, Second specimen radiograph after rotating specimen 90° shows density more closely resembling that on original mammogram. (*A*). Finding represented fibrosis with epithelial hyperplasia.**

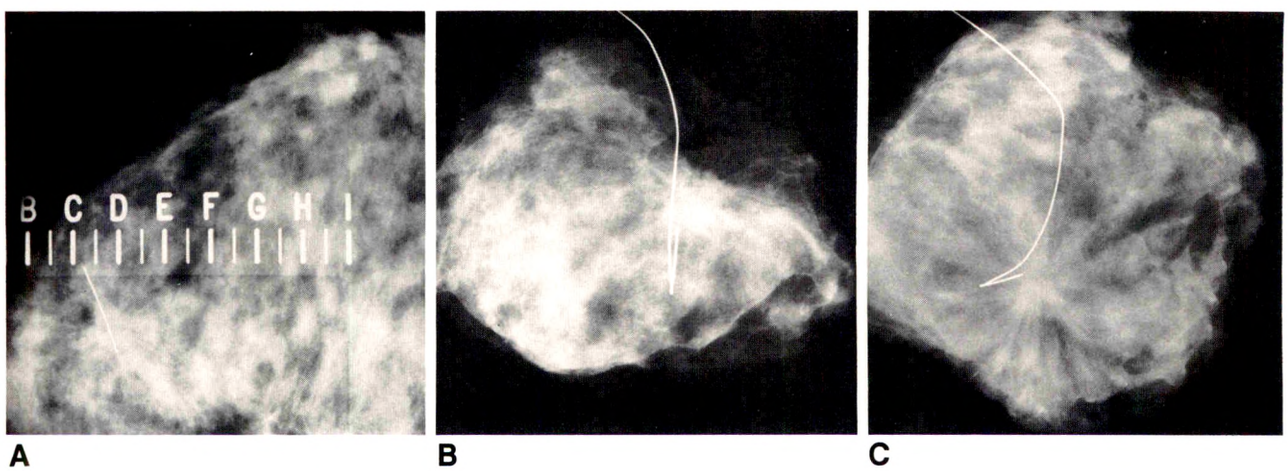


Fig. 2.—48-year-old woman.
***A*, Craniocaudal view from wire localization shows hook-wire tip projected over center of small spiculated mass.**
***B*, Initial specimen radiograph shows density adjacent to hook-wire tip, which probably represents lesion.**
***C*, Second specimen radiograph in orthogonal projection better defines spiculated nature of lesion. Findings represented intraductal carcinoma.**

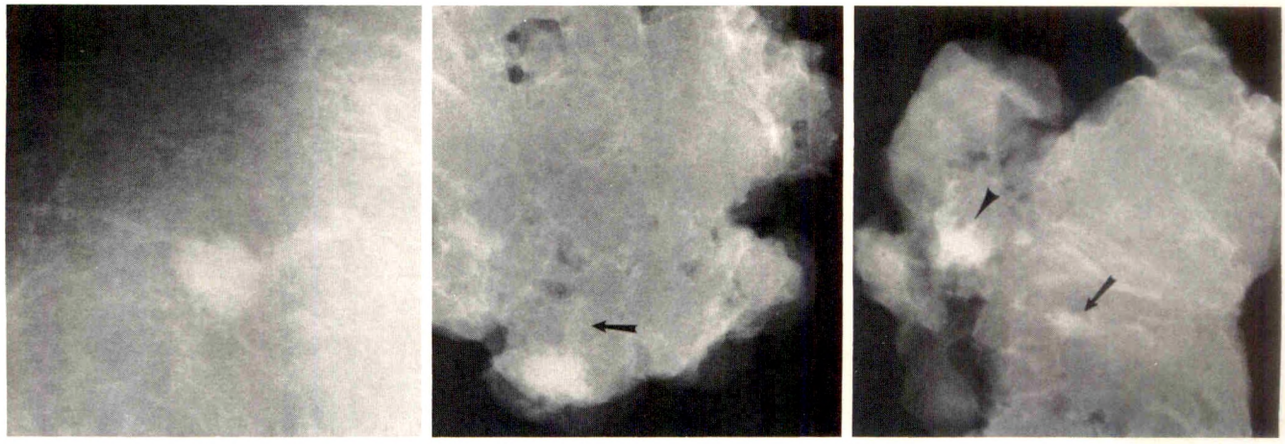


Fig. 3.—48-year-old woman.
***A*, Detail from lateral view shows low-density comma-shaped lesion that had enlarged since mammogram 1 year earlier.**
***B*, Initial specimen radiograph shows lesion at edge of specimen; linear structure (*arrow*) was believed to represent "tail" of lesion.**
***C*, Second specimen radiograph in orthogonal projection shows transection of specimen, with separation of tail (*arrow*) from main portion of lesion (*arrowhead*). Main portion of mass was a radial sclerosing lesion, and tail contained intraductal papilloma.**

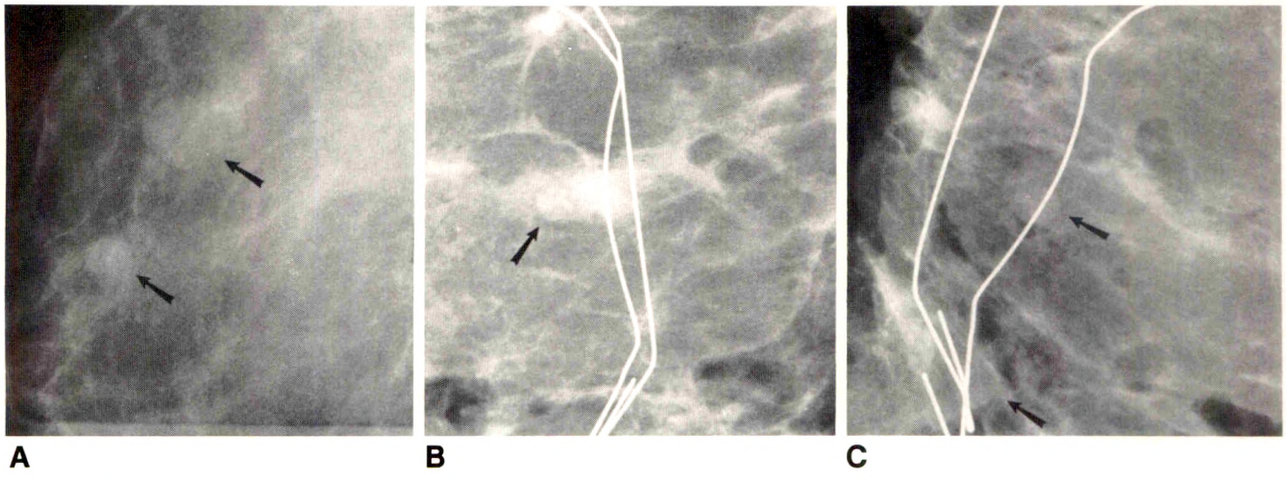


Fig. 4.—45-year-old woman.
***A*, Detail from craniocaudal view obtained at time of wire localization shows two small, low-density nodules (*arrows*). Despite benign appearance, patient desired surgical excision.**
***B*, Initial specimen radiograph shows one of the lesions (*arrow*).**
***C*, Orthogonal view shows two separate lesions, with inferior lesion partly obscured by hook wire (*arrows*). Findings represented two small fibroadenomas.**

preoperative mammogram films. If incomplete excision of the lesion is suspected by the surgeon, orthogonal specimen radiography can define whether the lesion is located at the edge of the specimen. Routine use of orthogonal specimen radiography to evaluate incomplete excision has yet to be evaluated.

The vast majority of nonpalpable lesions requiring specimen radiography can be detected on the initial view. However, in our experience, a second orthogonal view was beneficial in 7% of the cases. It should be emphasized that equal compression of the specimen for each view and proper exposure factors are vital in providing diagnostic images.

REFERENCES

1. Bavermeister DE, McClure HH. Specimen radiography: a mandatory adjunct to mammography. *Am J Clin Pathol* **1973**;59:782
2. Pitzen RH, Urdaneta LF, Al-Jurf AS, et al. Specimen xeroradiography after needle localization and biopsy of non-calcified non-palpable breast lesions. *Am Surg* **1985**;51(1):50–57
3. Phillip J, Harris WG, Rustage JH. Radiology of breast biopsy specimens. *Br J Surg* **1982**;69:126–127
4. Eastgate RJ, Gilchrist KW, Matallana RH. Enhancement of tissue structure visualization in breast specimen radiography. *Radiology* **1979**;132:744–746
5. Holland R. The role of specimen x-ray in the diagnosis of breast cancer. *Diagn Imag Clin Med* **1985**;54:178–185

1988 AMERICAN ROENTGEN RAY SOCIETY MEETING

MAY 8–13, 1988
SAN FRANCISCO HILTON HOTEL
SAN FRANCISCO, CA

See page 430 and forthcoming issues for further information.

Pictorial Essay

Imaging of Surgically Relevant Hepatic Vascular and Segmental Anatomy. Part 1. Normal Anatomy

John K. Mukai,[1] Caryn M. Stack,[1] David A. Turner,[1] Robert J. Gould,[1] Jerry P. Petasnick,[1] Terence A. S. Matalon,[1] Alexander M. Doolas,[2] and Marcia Murakami[1]

A major role of the radiologist in evaluating hepatic neoplasms is to assist the surgeon in determining the feasibility of hepatic resection. Disease confined to the liver must be accurately localized relative to important intrahepatic structures, particularly those that determine hepatic segmental anatomy [1, 2]; moreover, extrahepatic spread must be defined if present.

The first part of this essay reviews normal hepatic vascular anatomy and its relationship to segmental anatomy, as seen on CT, MR imaging, and sonography. Emphasis is placed on the formation of a three-dimensional concept of hepatic vascular and segmental anatomy. Such a concept is essential in real-time sonography, since the liver is imaged in nonorthogonal planes. Moreover, it enables the radiologist to take full advantage of sagittal and coronal images when evaluating the liver with MR imaging.

Materials and Methods

We selected CT, MR, and sonographic images that demonstrate normal anatomy to highlight vascular and segmental anatomy. The CT images are from a patient with fatty liver, who also had air in the biliary tree and reflux of oral contrast medium into the gallbladder because of surgical alteration of the biliary tract. The sonograms are from a patient who had right-sided congestive heart failure and dilated hepatic veins. The MR images are from two patients who had abdominal aortic aneurysms.

The CT scans were obtained with a whole-body scanner (Somatom DR3, Siemens, Islen, NJ). Contrast medium (meglumine diatrizoate) was administered intravenously as a 50-ml bolus (0.28 g I/ml) followed by a 150-ml drip infusion. Contiguous 8-mm-thick sections were obtained through the entire liver. The sonograms were obtained with a sector scanning, phased-array system operated at 3.5 MHz (Accuson, Mountain View, CA). The MR images were acquired with a system based on a superconducting magnet operating at approximately 0.5 T (Teslacon, Technicare, Solon, OH). Relatively T1-weighted (echo time = 30 msec, repetition time = 530 msec) spin-echo transaxial, coronal, and sagittal images were obtained through the liver with software provided by the manufacturer of the imaging device. Relatively T2-weighted (echo time = 45 or 90 msec, repetition time = 2090 msec), and inversion spin-echo (echo time = 30 msec, inversion time = 300 msec, repetition time = 1800 msec) images were acquired in a transaxial orientation only. The nominal slice thickness was 7.5 mm (full width at half maximum) with 2.5-mm gaps.

Figure 1A is provided as a guide to the location of image planes illustrated in subsequent figures. Four representative transaxial (levels a–d, Figs. 2–5) and four sagittal (levels e–h, Figs. 6–9) planes have been chosen for illustration, as marked on Figure 1A. A labeled diagram is included in each figure to aid in identifying anatomic structures.

Figure 1B shows the liver with three planes (A, B, and C) drawn along the boundaries between the hepatic segments, which are defined by the hepatic veins. These planes indicate the boundaries between the right posterior segment and the right anterior segment (plane A), the right anterior segment and the left medial segment (plane B), and the left medial segment and the left lateral segment

Received January 5, 1987; accepted after revision May 4, 1987.
Presented at the annual meeting of the American Roentgen Ray Society, Washington, DC, April 1986.
This work was supported in part by a grant from the Robert R. McCormick Charitable Trust.
[1] Department of Diagnostic Radiology and Nuclear Medicine, Rush–Presbyterian-St. Luke's Medical Center, 1753 W. Congress Parkway, Chicago, IL 60612. Address reprint requests to D. A. Turner.
[2] Department of General Surgery, Rush–Presbyterian-St. Luke's Medical Center, Chicago, IL 60612.

AJR 149:287–292, August 1987 0361–803X/87/1492–0287 © American Roentgen Ray Society

(plane C). The locations of these boundaries also are marked on each transaxial diagram (Figs. 2A, 3A, 4A, and 5A). Plane C, which divides the medial and lateral segments of the left lobe, passes through the falciform ligament and the ligamentum teres in addition to the left hepatic vein. Thus, on transaxial images in which the left hepatic vein cannot be identified, these ligaments can be used to find the boundary between the two segments of the left lobe.

Observations

Hepatic vascular anatomy is well delineated by CT and sonography [1, 2]. MR imaging, a relatively new technique, also defines vascular structures well without IV contrast material [3]. Unlike CT, MR can obtain images directly in coronal and sagittal (as well as transaxial) orientations.

As noted above, the hepatic veins define the boundaries between the segments of the liver. The branches of portal structures (vein, artery, and bile duct) generally lie within the hepatic segments (Fig. 1) [1]. The intrahepatic biliary and arterial branches approximate the portal venous anatomy.

Key to Abbreviations Used in Figures 1–9

CBD	common bile duct
CL	caudate lobe
FL	falciform ligament
FLV	fissure for ligamentum venosum
GB	gallbladder
HA	hepatic artery
IVC	inferior vena cava
LHV	left hepatic vein
LLS	left lateral segment
LMS	left medial segment
LPV	left portal vein
LT	ligamentum teres
MF	major fissure
MHV	middle hepatic vein
MPV	main portal vein
PROX	proximal
R	right
RAS	right anterior segment
RHV	right hepatic vein
RPV	right portal vein
RPS	right posterior segment
RRA	right renal artery
SMV	superior mesenteric vein
SV	splenic vein

Transaxial Planes

Four transaxial planes are illustrated (Figs. 2–5). The most cephalad plane (level a, Fig. 1A) is at the level of the confluence of the right, middle, and left hepatic veins with the inferior vena cava (Fig. 2). The next plane caudad (level b) contains the left portal vein (Fig. 3). The plane below (level c) passes through the right portal vein (Fig. 4). The main portal vein and the gallbladder lie in the most caudal plane (level d) (Fig. 5).

As noted above and shown in Figure 1B, the hepatic segments are defined by the hepatic veins. The boundaries between segments can be estimated on transaxial images by lines drawn from the inferior vena cava through each vein (Fig. 2A). However, it is only on images through upper levels of the liver that all three hepatic veins can be identified readily. Thus, other structures (falciform ligament, ligamentum teres, and the gallbladder) must be identified at lower levels to estimate segmental boundaries (Figs. 3A, 4A, and 5A).

Sagittal Planes

Orientation to segmental anatomy in sagittal planes is most easily attained by identifying the hepatic veins and inspecting the images sequentially from right to left. The two planes farthest to the right (levels e and f, Fig. 1A) demonstrate the middle and right hepatic veins (Figs. 6 and 7), which converge as one moves to the left toward their confluence with the inferior vena cava (Figs. 6B and 7B). A lesion posterior to the right hepatic vein is in the right posterior segment. A lesion anterior to the right hepatic vein and posterior to the middle hepatic vein is in the right anterior segment. A lesion anterior to the middle hepatic vein and to the right of the left hepatic vein is in the left medial segment. The inferior vena cava and the proximal portion of the middle hepatic vein lie in the next

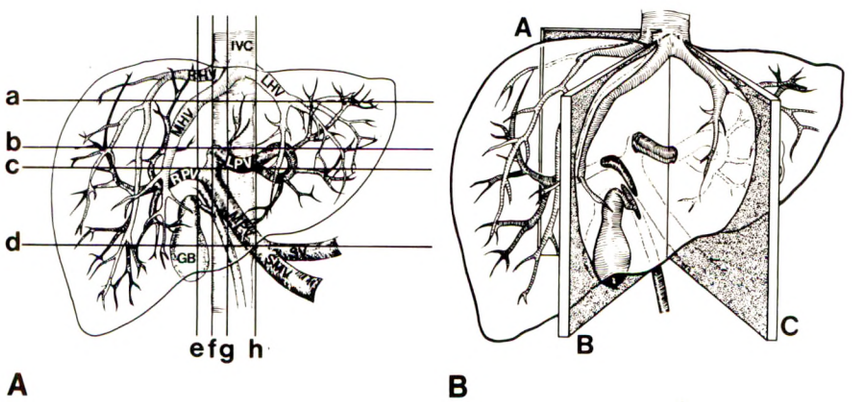


Fig. 1.—*A*, Major vascular structures are shown in relation to outlines of the liver. Lines indicate the levels of images shown in subsequent figures.
***B*, Intersegmental boundaries (planes A, B, and C) are defined by hepatic veins.**

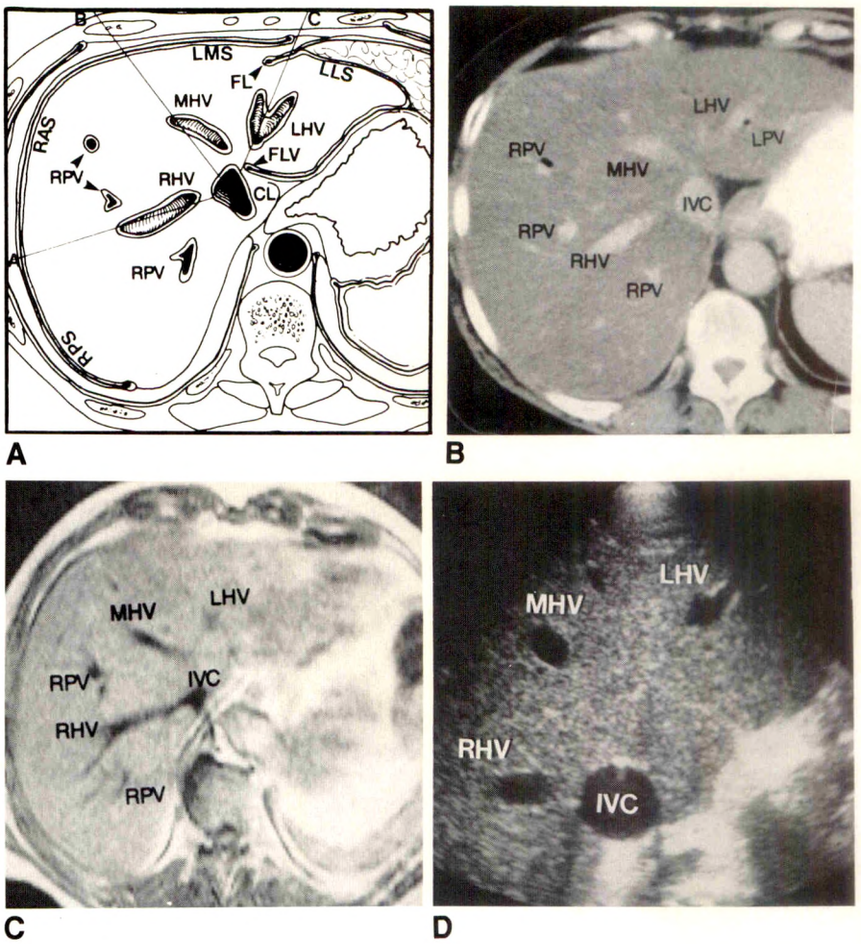


Fig. 2.—Transaxial diagram and images at level a.

A, Lines A, B, and C indicate intersection of intersegmental planes A, B, and C (Fig. 1B) with transaxial plane at this level. Note that lines, which are boundaries of hepatic segments, radiate from the inferior vena cava and pass through hepatic veins.

B, CT image. Vessels are seen particularly well because of fatty infiltration of liver. Air in distal biliary radicles, within left lateral and right anterior segments, is from previous surgery.

C, MR image of another patient shows similar vascular anatomy.

D, Transaxial sonogram at same level.

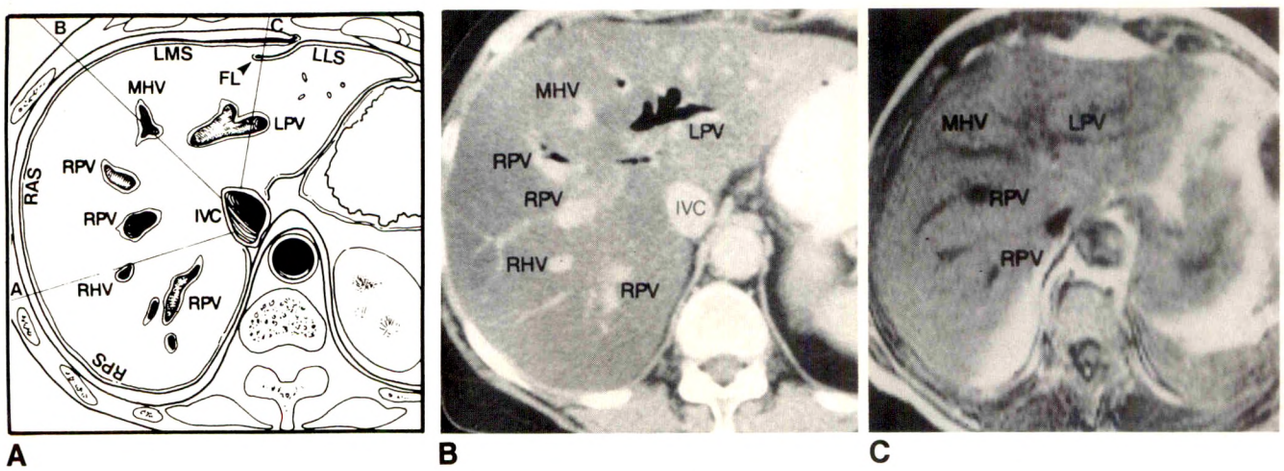


Fig. 3.—Transaxial images at level b. Transverse portion of left portal vein is seen at this level.

A, Left hepatic vein is not seen at this level. Therefore, line from inferior vena cava through falciform ligament (line C) is a guide to boundary between left lateral and left medial segments.

B, CT scan, same patient as in Figure 2B. Air in left hepatic duct obscures transverse portion of left portal vein.

C, MR image, same patient as in *A*, shows anatomy similar to that in *B*. Biliary system was normal and therefore is not seen.

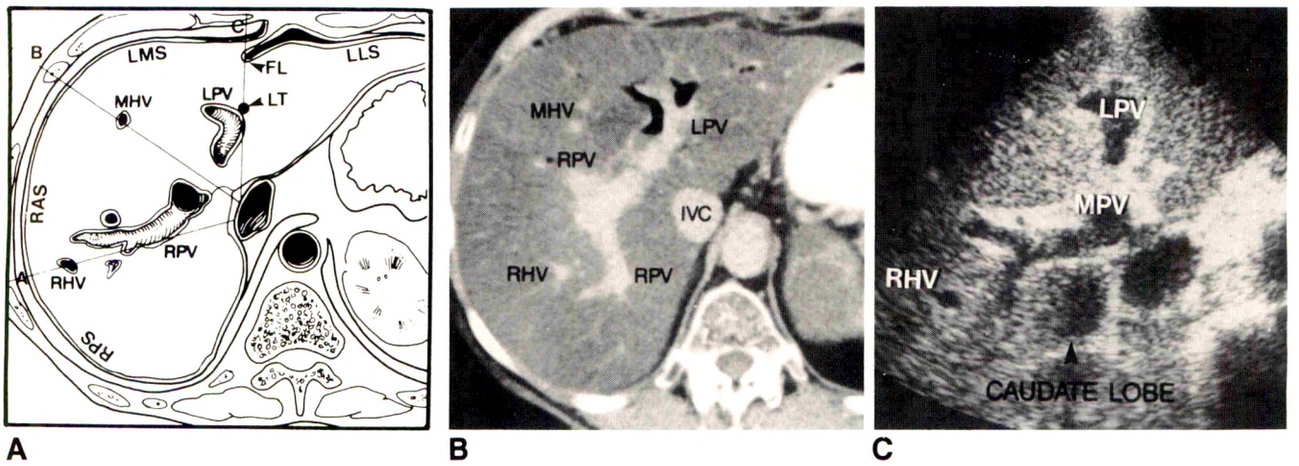


Fig. 4.—Transaxial images at level c.

***A*, Boundary between left medial and left lateral segments is denoted by line C, which runs from inferior vena cava through falciform ligament and ligamentum teres. At this level left portal vein lies in boundary between medial and lateral segments, rather than within single segment.**

***B*, CT scan, same patient as in Figure 3B, shows division of main portal vein to form right and left portal veins, as well as division of right portal vein into anterior and posterior branches. At this level posterior branch of right portal vein crosses boundary between anterior and posterior segments of right lobe (line A, *A*). As in Figure 3B, air is seen in biliary system, adjacent to branches of left portal vein.**

***C*, Sonogram, including a small portion of liver at same level as *B* and *C*, shows anatomy similar to that seen in the other two studies.**

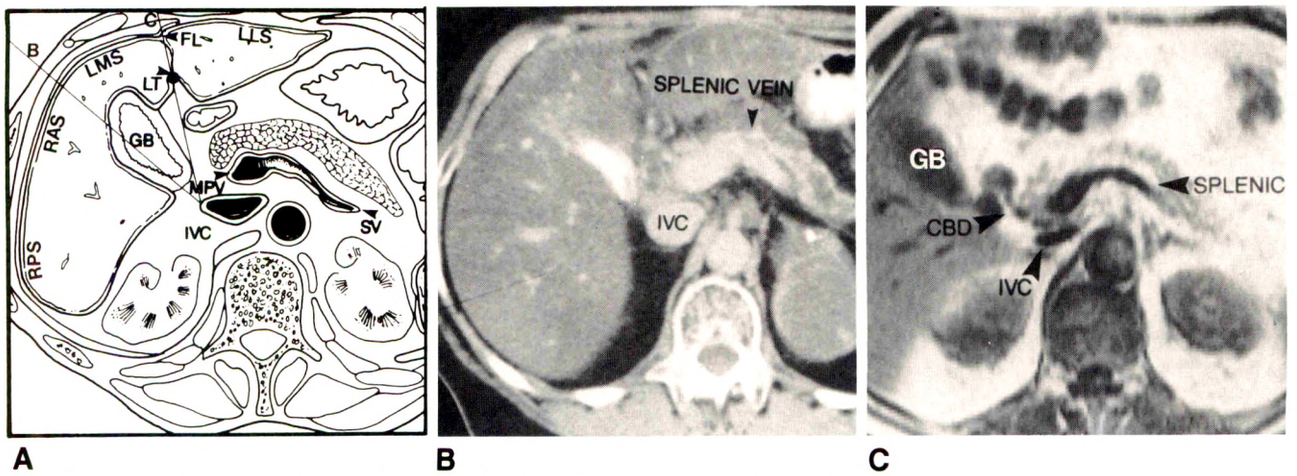


Fig. 5.—Transaxial images at level d, level at which splenic and superior mesenteric veins join to form main portal vein.

***A*, Hepatic veins are not readily identified at this level. Line drawn through gallbladder and inferior vena cava approximates boundary between left and right lobes (plane B, Fig. 1B). Line through ligamentum teres and inferior vena cava denotes boundary between left medial and left lateral hepatic segments (plane C).**

***B*, CT scan, same patient as in Figure 4B, shows radiopaque contrast medium in gallbladder due to previous choledochojejunostomy. Left adrenal mass is present.**

***C*, MR image, same patient as in Figure 4C, shows anatomy similar to that in *A* and *B*.**

plane to the patient's left (level g) (Fig. 8). The most leftward plane (level h) is through the confluence of the left hepatic vein and inferior vena cava (Fig. 9). A lesion just to the right of this plane is in the left medial segment. A lesion just to the left is in the left lateral segment.

Once the hepatic veins are identified, elements of the portal venous system can be found. In the most rightward plane represented (level e), the right portal vein is seen on end, in line with the gallbladder (Fig. 6). The major hepatic fissure "points" caudad to the gallbladder, a feature that is helpful for localization of the gallbladder during real-time sonography. Proceeding leftward to the next level (level f), the left portal vein is seen along its long axis as it originates from the main portal vein (Fig. 7). In the two images farthest to the left (levels g and h) the distal left portal vein is seen on end (Figs. 8 and 9, respectively).

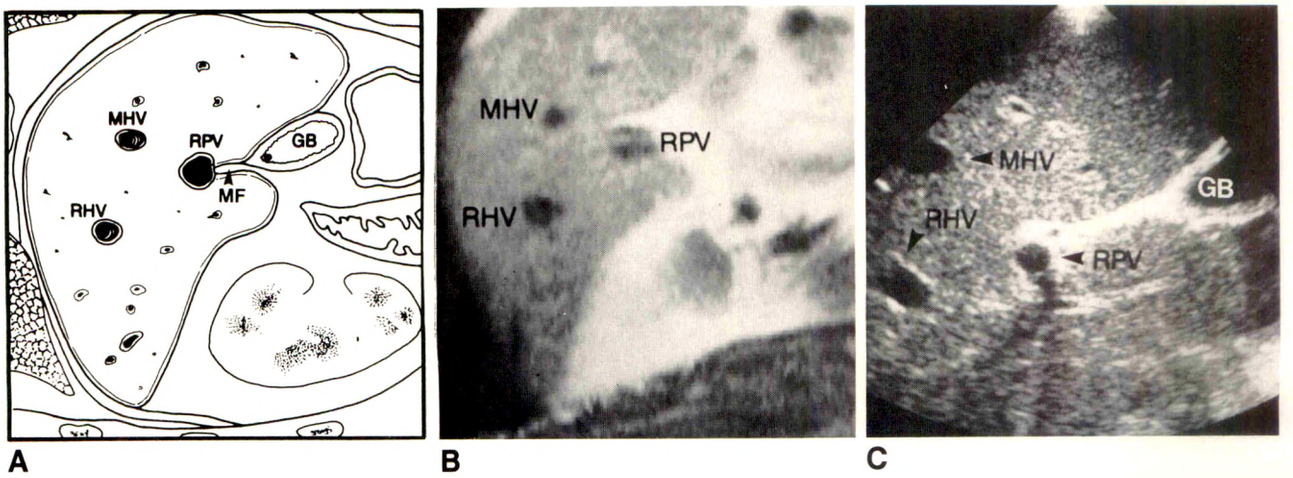


Fig. 6.—Sagittal images at level e. Diagram, sonogram, and MR image are in standard sonographic orientation (head to left of image, anterior toward top of image).

***A*, Images at this level pass through middle and right hepatic veins, right portal vein, and gallbladder. Hepatic tissue posterior to right hepatic vein is right posterior segment; tissue anterior to right hepatic vein and posterior to middle hepatic vein is right anterior segment; and tissue anterior to middle hepatic vein (and to right of left hepatic vein, not seen at this level) is left medial segment.**

***B*, Sagittal MR image, same level. Gallbladder is not well seen. Intensity of gallbladder on spin-echo MR image can vary from low signal (black) to high (white), depending on concentration of bile, echo time, and repetition time.**

***C*, Sagittal sonogram, same level.**

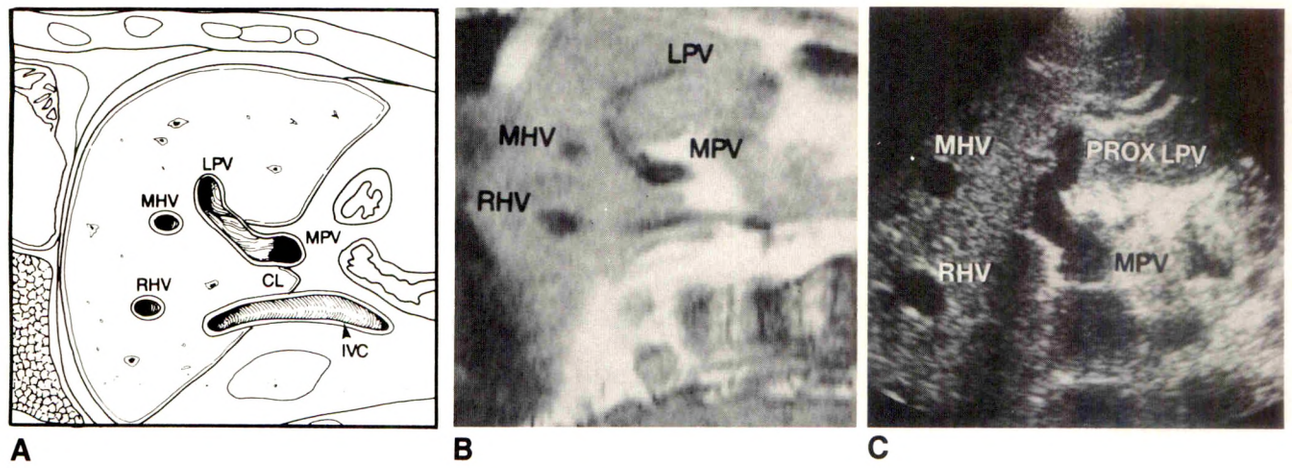


Fig. 7.—Sagittal images at level f. Image orientation is same as in Figure 6.

***A*, Plane passes through portion of inferior vena cava and confluence of left portal and main portal veins.**

***B*, MR image shows anatomy similar to that in *A*. Right and middle hepatic veins have converged slightly as compared with MR image at level e (Fig. 6B).**

***C*, Sonogram shows anatomy similar to that shown in *A* and *B*.**

Coronal Planes

Coronal images (not shown because of space limitations) can be obtained readily by both MR imaging and sonography. Although these images can be very helpful in special tasks, such as evaluating patency of the main portal vein, the segmental anatomy of the liver can be recognized only approximately in coronal images. Moreover, coronal MR images of the liver are usually inferior to MR images acquired in a transaxial orientation, possibly because respiratory movement occurs primarily perpendicular to transaxial images, but along an axis of good spatial resolution on coronal images. In any case, coronal images are of limited usefulness in demonstrating segmental hepatic anatomy and in determining the resectability of hepatic masses.

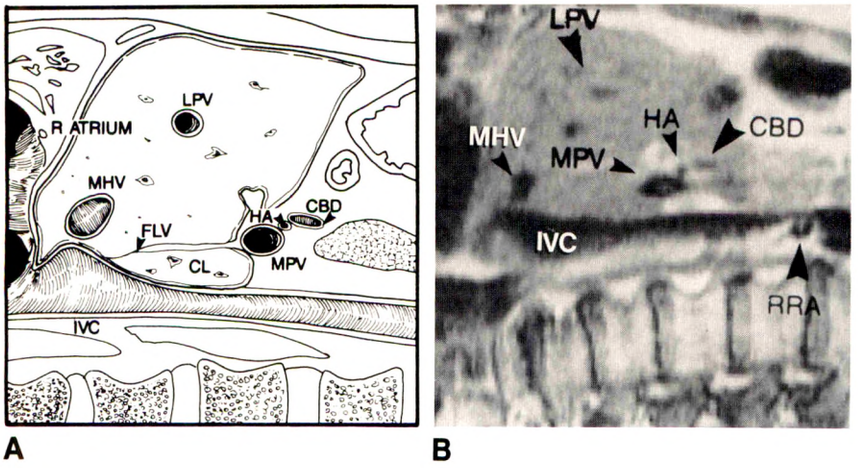


Fig. 8.—Sagittal images at level g. Image orientation same as that in Figures 6 and 7. Image plane passes through inferior vena cava, proximal middle hepatic vein, main portal vein, common bile duct, and hepatic artery.

***A*, Right hepatic vein, seen in more rightward sagittal images (Figs. 6 and 7) has merged with inferior vena cava and disappeared. Middle hepatic vein is seen on end as it courses to left. Anterior to main portal vein is hepatic artery, seen on end between main portal vein and common bile duct.**

***B*, MR clearly shows common bile duct, hepatic artery, and other indicated structures. Demonstration of anatomy is similar to that usually seen on sonography.**

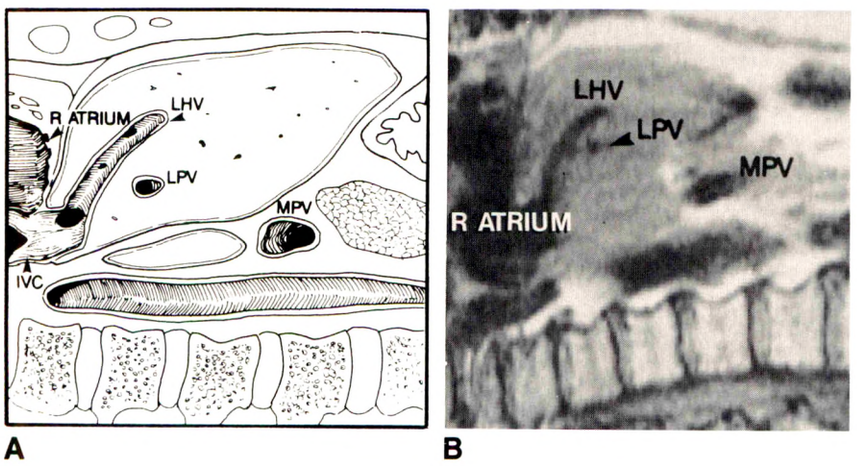


Fig. 9.—Sagittal images at level h through confluence of left hepatic vein with inferior vena cava. Same image orientation as in Figures 6–8.

***A*, Venous confluence (left hepatic vein and inferior vena cava) marks posterior end of intersegmental boundary between left medial and left lateral segments (plane C, Fig. 1B). Left portal vein is seen on end as it courses into left lobe. Tubular structure just anterior to spine is aorta.**

***B*, MR shows anatomy similar to that in *A*.**

Conclusions

The hepatic venous and portal anatomy has been illustrated, with emphasis on major landmarks as a guide to recognizing hepatic segmental anatomy. A three-dimensional visual concept of vascular segmental hepatic anatomy is necessary to correlate two-dimensional images obtained in standard orthogonal (transaxial, sagittal, coronal) and nonorthogonal planes. Integration of the spatial relationships of hepatic and portal veins as they course through the liver aids in segmental localization of lesions seen on orthogonal and nonorthogonal images obtained with MR, CT, and sonography. Part 2 of this essay [4] discusses the application of these concepts in determining the extent and resectability of hepatic neoplasms.

ACKNOWLEDGMENTS

We thank Patricia Piescinski and Heidi Hoffer for illustrating this work and Barbara Marciano and Yvonne Allen for typing the manuscript.

REFERENCES

1. Pagani JJ. Intrahepatic vascular territories shown by computed tomography (CT). *Radiology* **1983**;147:173–178
2. Sexton CC, Zeman RK. Correlation of computed tomography, sonography, and gross anatomy of the liver. *AJR* **1983**;141:711–718
3. Fisher MR, Wall SD, Hricak H, McCarthy S, Kerlan RK. Hepatic vascular anatomy on magnetic resonance imaging. *AJR* **1985**;144:739–746
4. Mukai JK, Stack CM, Turner DA, et al. Pictorial essay. Imaging of surgically relevant hepatic vascular and segmental anatomy: 2. Extent and resectability of hepatic neoplasms. *AJR* **1987**;149:293–297

Pictorial Essay

Imaging of Surgically Relevant Hepatic Vascular and Segmental Anatomy. Part 2. Extent and Resectability of Hepatic Neoplasms

John K. Mukai,[1] Caryn M. Stack,[1] David A. Turner,[1] Terence A. S. Matalon,[1] Robert J. Gould,[1] Jerry P. Petasnick,[1] Alexander M. Doolas,[2] and Marcia Murakami[1]

The resectability of hepatic neoplasms depends largely (but not exclusively) on the distribution of lesions in the liver and their relationships to vascular structures [1]. CT and sonography currently play an important role in the preoperative determination of the resectability of these lesions because of their ability to demonstrate, in a noninvasive manner, hepatic vascular (and thus segmental) anatomy, as well as hepatic neoplasms [2, 3]. Early studies have indicated that MR imaging also provides excellent demonstration of hepatic tumors and normal vascular anatomy [4, 5], suggesting that MR may be particularly well suited to determining the resectability of hepatic lesions. Part 1 of this pictorial essay illustrated the demonstration of normal hepatic anatomy by CT, sonography, and MR [6]. Part 2 illustrates the use of noninvasive imaging methods to determine the extent and resectability of hepatic neoplasms.

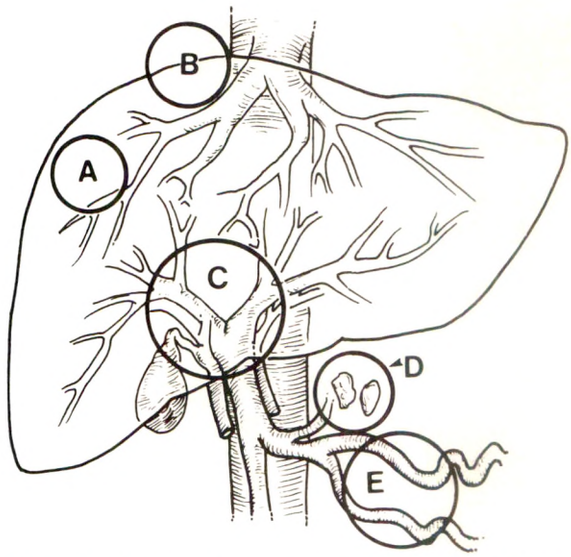


Fig. 1.—Categories of extent of disease: *category A*, Intrahepatic disease sparing porta hepatis and not contiguous with inferior vena cava; *B*, Lesions with local, contiguous, extraluminal extension to porta hepatis and/or margin of inferior vena cava, also lesions extending contiguously to structures adjacent to liver; *C*, Lesions encasing, invading, and/or obstructing the main portal vein or one or both of its major branches or the main hepatic artery or duct or one or both of its major branches; *D*, Lesions with metastatic spread to regional lymph nodes or distant sites; and *E*, Secondary signs of diffuse, benign, or malignant hepatic disease, such as ascites or splenoportal varices.

Extent of Disease

For the purposes of this discussion we have defined the anatomic extent of disease in terms of five categories, representing a logical progression of disease extent (Fig. 1). *Category A* is defined as intrahepatic disease that spares the porta hepatis and is not contiguous with the inferior vena cava. *Category B* includes lesions with local, contiguous, extraluminal extension to the porta hepatis and/or the margin

Received January 5, 1987; accepted after revision May 4, 1987.
Presented at the annual meeting of the American Roentgen Ray Society, Washington, DC, April 1986.
This work was supported in part by a grant from the Robert R. McCormick Charitable Trust.
[1] Department of Diagnostic Radiology and Nuclear Medicine, Rush–Presbyterian-St. Luke's Medical Center, 1753 W. Congress Parkway, Chicago, IL 60612. Address reprint requests to D. A. Turner.
[2] Department of General Surgery, Rush–Presbyterian-St. Luke's Medical Center, Chicago, IL 60612.

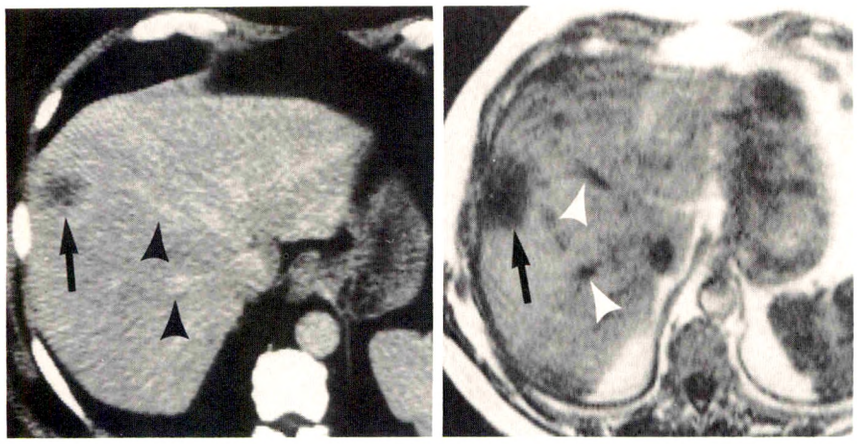


Fig. 2.—Adenocarcinoma of colon, metastatic to liver, correctly classified as resectable.

A, Contrast-enhanced CT scan reveals lesion in right lobe of liver (*arrow*). Lesion is in anterior segment, that is, between right and middle hepatic veins (*arrowheads*).

B, Inversion spin-echo MR image (inversion/echo/repetition times = 300/30/1400 msec, respectively) shows same lesion as low-intensity (dark) area (*arrow*). Right and middle hepatic veins are easily seen as low-intensity linear structures (*arrowheads*).

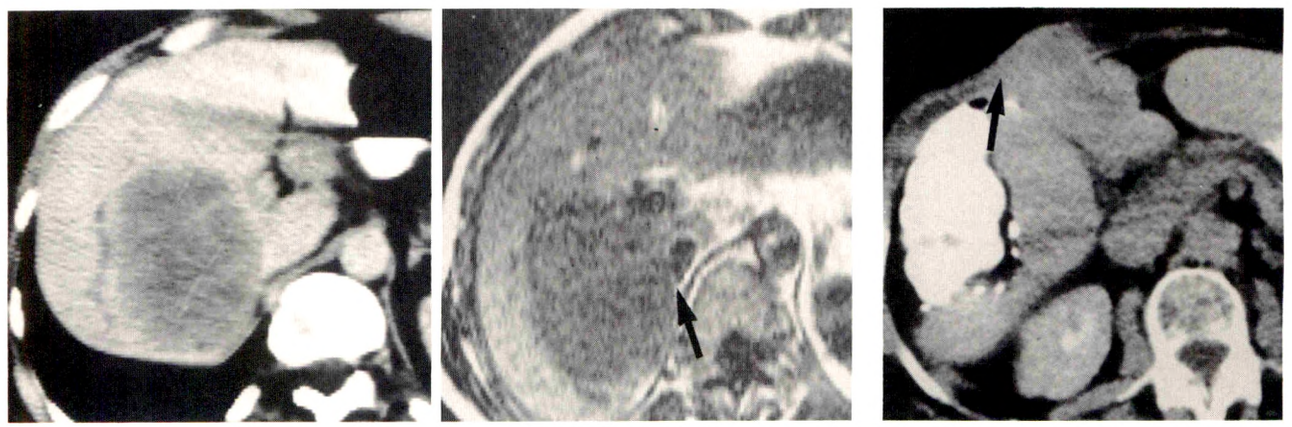


Fig. 3.—Metastatic adenocarcinoma of colon with extension to extraluminal margin of inferior vena cava. Classified as technically difficult.

A, CT scan of liver immediately after bolus infusion of contrast material. Large lesion is well seen, but inferior vena cava is not.

B, Inversion spin-echo MR image (inversion/echo/repetition times = 300/31/1800 msec, respectively) shows low-intensity lesion in right lobe, contiguous with inferior vena cava. Note partial loss of pericaval fat plane (*arrow*) and effacement of inferior vena cava. This suggests that lesion may invade vessel, but final judgment of resectability can be made only at laparotomy. Lesion proved to be resectable.

Fig. 4.—Local, extrahepatic extension of adenocarcinoma of colon in patient who had previously undergone right hepatic lobectomy. Classified as technically difficult. Postinfusion CT study shows lesion extending into anterior abdominal wall (*arrow*). Lesion was successfully resected (tumor-free margins), but abdominal wall reconstruction was required.

of the inferior vena cava, as well as lesions that extend contiguously to structures adjacent to the liver, such as the abdominal wall or diaphragm. *Category C* includes lesions that involve the portal region *and* encase, invade, and/or obstruct the main portal vein or one or both of its major branches or the main hepatic artery or duct or one or both of its major branches. *Category D* includes lesions with metastatic spread to regional lymph nodes or distant sites. Cases are placed in *category E* if there are secondary signs of diffuse, benign, or malignant hepatic disease, such as ascites or splenoportal varices.

Hepatic Resections

Two cardinal rules guide a surgeon in hepatic resections. The first is that the volume of liver left behind must be sufficient to support life. The second is that the vascular supply and venous and biliary drainage of the remaining hepatic tissue must be left intact [7]. Beyond these restrictions, technical problems may be associated with resection of specific regions of the liver. For example, resection of the posterior segment of the right lobe alone is technically quite difficult, and thus rarely is done.

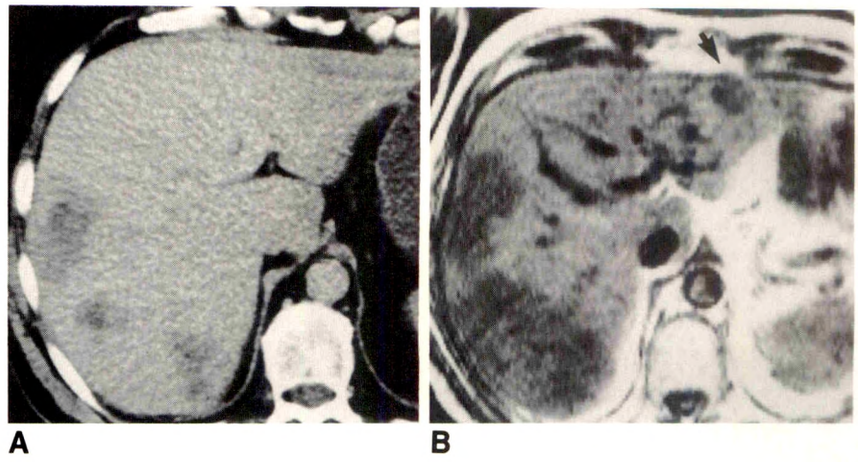


Fig. 5.—Metastatic adenocarcinoma of colon, confined to liver but classified as unresectable because of extent of lesions.

***A*, CT scan reveals multiple, low-density lesions in right lobe. Left lobe was interpreted as normal.**

***B*, Inversion spin-echo MR image (inversion/echo/repetition times = 300/30/1400 msec, respectively) shows lesion in lateral segment of left lobe, undetected by CT (*arrow*). Disease in right lobe is more extensive than shown on CT.**

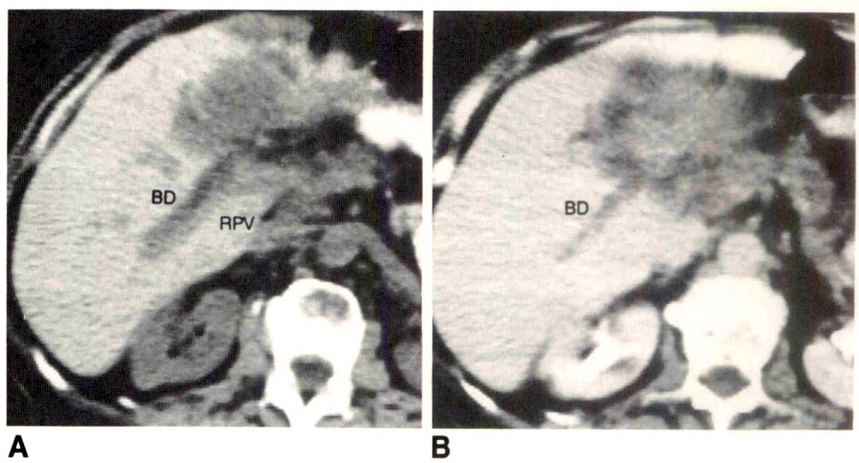


Fig. 6.—Metastatic adenocarcinoma, primary unknown, unresectable because of involvement of both segments of left lobe, right portal vein, and right hepatic duct.

***A*, Preinfusion CT study shows tumor in both segments of left lobe. Dilated right intrahepatic bile duct (BD) is seen anterior to right portal vein (RPV).**

***B*, Postinfusion study shows enhancing tumor; opacification of portal vein; and dilated, low-density right intrahepatic bile duct (BD). Right portal vein obscured by IV contrast medium**

The need to preserve the hepatic venous drainage of liver remaining after resection dictates that resection margins generally must be along planes parallel to the main hepatic veins, approximating the intersegmental boundaries depicted in part 1 of this essay [6]. However, the intersegmental boundaries are shown as being perfectly flat, whereas resection margins cannot be so. Deviation of resection margins from planar segmental boundaries is necessary, particularly in the region of the porta, in order to preserve the portal venous supply. Moreover, the variability of the hepatic and portal venous systems is such that any a priori description of hepatic resections can be only an approximation. The surgeon will modify procedures considerably from case to case, depending on the anatomy encountered. Nonetheless, major hepatic resections are defined relative to the same landmarks that determine the intersegmental boundaries of the liver.

As a result of the above considerations, only four types of major resections are commonly performed. Two of these are right-sided, namely, the right lobectomy and "trisegmentectomy," and two are left-sided, namely, the left lobectomy and left lateral segmentectomy. Recently, selective resection of the medial segment of the left lobe ("median lobectomy") has been employed at some centers.

In a right lobectomy, the entire right lobe of the liver is removed, up to but not including the middle hepatic vein. The surgeon is guided during the procedure by surface landmarks. The liver is divided approximately along a line running from the inferior vena cava to the gallbladder fossa; blunt dissection is used to avoid severing major intrahepatic vessels. In a trisegmentectomy the entire right lobe and the medial segment of the left lobe are removed, up to the right side of the falciform ligament. The middle hepatic vein is removed in this procedure, along with the territory it drains. In a left lateral segmentectomy the lateral segment of the left lobe is removed, up to the left side of the falciform ligament. If it is necessary to extend the resection to the right of the falciform ligament, the medial segment must be removed also, that is, a left lobectomy must be performed. This is because a plane of resection just to the right of the falciform ligament disrupts the portal venous supply of the medial segment: As illustrated

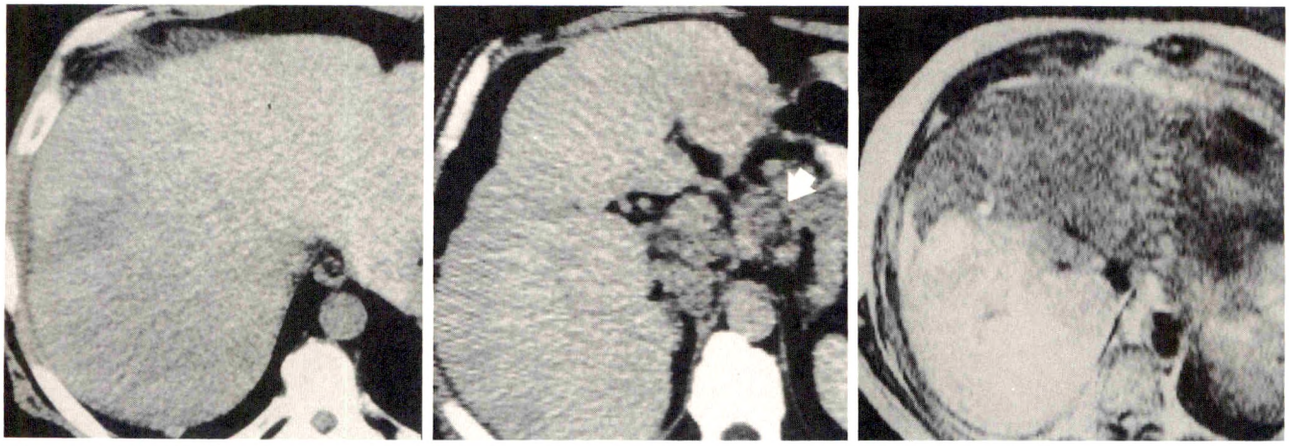


Fig. 7.—Hepatoma, unresectable because of spread to regional lymph nodes.
A, Postinfusion CT study shows subtle, large, heterogeneous lesion occupying much of right lobe.
B, Multiple enlarged lymph nodes (*arrow*) surround celiac axis.
C, T2-weighted spin-echo MR image (echo/repetition times = 60/2120 msec) shows high-intensity right-lobe lesion with better contrast than with CT.

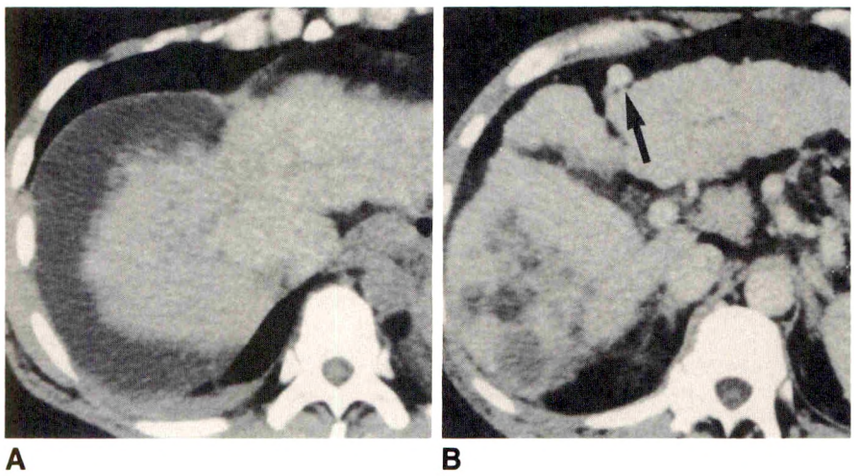


Fig. 8.—Hepatoma, inoperable because of ascites.
A, Preinfusion CT study shows ascites.
B, Postinfusion study shows nodular liver with multiple right-lobe lesions, "recanalized" umbilical vein (*arrow*), and varices. Enlarged spleen also present (not shown).

in part 1 of this essay, the proximal portion of the left portal vein lies in the boundary between the left medial and lateral hepatic segments.

Resectability of Lesions

We classify hepatic lesions as resectable if it is technically feasible to remove all gross tumor with tumor-free margins, without violating the two cardinal rules discussed above (Fig. 2). If there is local, contiguous spread to the extraluminal margins of the inferior vena cava or the main portal vein or local extension into adjacent, extrahepatic structures, resection may still be possible, but the procedure will be technically difficult (Figs. 3 and 4). Moreover, the attainability of a tumor-free margin frequently cannot be predicted by imaging studies (Fig. 3). If tumor is present in all hepatic segments, it generally cannot be resected completely (that is to say, it cannot be completely removed with tumor-free margins, leaving hepatic tissue sufficient to sustain life, an intact vascular supply, and venous and biliary drainage). Such lesions, therefore, usually are classified as unresectable (Fig. 5). Lesions are also classified as unresectable if they encase or invade the main portal vein, the proper hepatic artery, the common hepatic duct, or the major contralateral branch of these structures (Fig. 6). Similarly, lesions are unresectable if spread of tumor to regional lymph nodes or distant metastases are present (Fig. 7). Finally, we classify patients as inoperable if we detect signs of cirrhosis, portal hypertension, and/or ascites (Fig. 8).

Although criteria for resectability may vary among surgeons, the guidelines presented in this essay are consistent with those suggested in the current literature [1, 2, 7]. By

using this approach to radiologic classification of resectability we have been able to accurately predict surgical outcome in 24 of 25 cases by MR imaging and in 21 of 25 cases by CT. Moreover, the classification system has been well received by the surgeons at our institution. However, the system can be modified to suit the needs of individual surgeons. The radiologist's goal should be to tell the surgeon "what [he/she] wants to know . . . about a tumor in the liver before he/she decides or tries to take it out or not. Success or failure may depend in part on the radiologist" [8].

Conclusions

The purpose of part 2 of this essay has been to describe and illustrate surgically relevant radiologic classifications of the extent and resectability of hepatic neoplasms. The goal of the radiologist should be to provide the surgeon with information needed for management decisions. Visualization of the hepatic veins and other landmarks of hepatic segmental anatomy is the cornerstone of this process. Seven illustrative, surgically confirmed cases have been presented that depict a spectrum of anatomic extent and resectability.

ACKNOWLEDGMENTS

We thank Patricia Piescinski and Heidi Hoffer for illustrating this work and Barbara Marciano and Yvonne Allen for typing the manuscript.

REFERENCES

1. LaBerge, JM, Laing FC, Federle MP, Jeffrey RB Jr, Lim RC Jr. Hepatocellular carcinoma: assessment of resectability by computed tomography and ultrasound. *Radiology* **1984**;152:485–490
2. Pagani JJ. Intrahepatic vascular territories shown by computed tomography (CT). *Radiology* **1983**;147:173–178
3. Sexton CC, Zeman RK. Correlation of computed tomography, sonography, and gross anatomy of the liver. *AJR* **1983**;141:711–718
4. Stark DD, Wittenberg J, Middleton MS, Ferrucci JT Jr. Liver metastases: detection by phase-contrast MR imaging. *Radiology* **1986**;158:327–332
5. Fisher MR, Wall SD, Hricak H, McCarthy S, Kerlan RK. Hepatic vascular anatomy on magnetic resonance imaging. *AJR* **1985**;144:739–746
6. Mukai JK, Stack CM, Turner DA, et al. Pictorial essay. Imaging of surgically relevant hepatic vascular and segmental anatomy: 1. Normal anatomy. *AJR* **1987**;149:287–292
7. Joishy SK, Balasegaram MB. Hepatic resection for malignant tumors of the liver: essentials for a unified surgical approach. *Am J Surg* **1980**;139:360–369
8. Adson MA. Hepatic metastases in perspective. *AJR* **1983**;140:695–700

Book Review

Computed Tomography in Trauma. Edited by Barry D. Toombs and Carl M. Sandler. Philadelphia: Saunders, 224 pp., 1987. $49.95

After a few brief chapters on trauma patients and their evaluation, the authors present chapters on acute chest and abdominal trauma and complications of chest and abdominal trauma. R. M. Steinberg supplies a chapter on pelvic trauma and K. F. Lee a chapter on craniofacial trauma. The longest chapter, written with eight other authors, is on spinal trauma. The book reads well and the illustrations are generally good. Unfortunately, the authors include a few illustrations from earlier publications that are not done with state-of-the-art equipment. Both editors are advocates of suspending respiration with Pavulon (pancuronium-bromide), and they are perhaps a bit too persistent in making this point. The section on craniofacial trauma is supplemented with three-dimensional reconstruction images. The spinal chapter demonstrates only a single MR study, but MR is apparently beyond the scope of this book. The pelvic section includes a very nice discussion of pelvic fractures. The text is virtually error free.

This book would be a welcome addition to the library of any general radiologist and is of great utility for the radiology resident in an emergency room setting. Much of the material it covers is of value for the general surgical or orthopedic surgical resident as well.

David H. Carlson
Newton-Wellesley Hospital
Newton Lower Falls, MA 02162

Abdominal Sonography After Hepatic Transplantation:
Results in 36 Patients

Janis G. Letourneau[1]
Deborah L. Day[1]
Nancy L. Ascher[2]
Dale C. Snover[3]
John W. Steely[1]
Jeffrey R. Crass[1,4]
John S. Najarian[2]
Samuel B. Feinberg[1]

Hepatic transplantation was performed in 46 patients over a 2-year period at the University of Minnesota. Thirty-six of these patients subsequently underwent 166 sonographic examinations of the upper abdomen. Forty-three examinations were performed within 2 weeks of transplantation, 47 between 2 and 8 weeks after transplantation, and 76 more than 8 weeks after transplantation. The sonograms were reviewed retrospectively and correlated with the available clinical and histopathologic data. Diffuse, nonspecific parenchymal abnormalities were seen in 27 patients. Focal regions of parenchymal abnormality seen in four patients were associated with abscess and infarction. Moderate to severe biliary dilatation was seen in seven patients with biliary obstruction diagnosed by percutaneous or T-tube cholangiography. Obstruction was seen most commonly in children who had undergone cholecystojejunostomy biliary reconstruction, and it required radiologic or surgical intervention. Routine sonographic assessment of the upper abdominal vasculature showed thrombosis of the portal vein in two cases, thrombosis of the inferior vena cava in one case, thrombosis of the donor aorta in three cases. Focal intraabdominal fluid collections were identified in 14 patients and represented hematomas in all but one. Free peritoneal fluid was detected in 19 patients. Sonography was used to guide percutaneous aspiration of abdominal fluid and to guide fine-needle puncture for percutaneous transhepatic cholangiography.

Upper abdominal sonography provides a noninvasive means of evaluating and confirming a wide spectrum of complications that can follow hepatic transplantation. Because clinical and laboratory findings often are nonspecific in these patients, sonographic detection of focal parenchymal abnormalities, biliary dilatation, and vascular compromise is especially valuable.

Hepatic transplantation is an accepted treatment for end-stage liver disease and is performed with increasing frequency and success at a number of institutions both in the United States and elsewhere [1–3]. At the University of Minnesota, triple-drug immunosuppression (azothioprine, prednisone, and cyclosporine-A) of hepatic transplant recipients was begun in April 1984. This procedure has been associated with an improvement in the 6-month survival rate from 50% in 1984 to 86% in 1985 [4].

Diagnosis of posttransplantation complications often is difficult in recipients of hepatic transplants because clinical data and laboratory findings are nonspecific [5]. In particular, biliary obstruction can mimic rejection clinically. Specific and accurate diagnosis, however, best determines treatment of both medical and surgical complications. Abdominal imaging frequently provides valuable information in the assessment of transplant recipients who have graft dysfunction [6–12].

We retrospectively reviewed the sonographic findings in 36 recipients of hepatic transplants who were treated with a consistent triple-drug immunosuppressive regimen. We focused our assessment on the ability of sonography to characterize posttransplantation complications that clinically can mimic rejection.

Materials and Methods

In the 2-year interval from April 1, 1984, to March 31, 1986, 46 patients underwent hepatic transplantation. Causes of hepatic failure included extrahepatic biliary atresia (19), primary

Received March 2, 1987; accepted after revision April 7, 1987.

[1] Department of Radiology, University of Minnesota, Box 292 UMHC, Harvard Street at East River Rd., Minneapolis, MN 55455. Address reprint requests to J. G. Letourneau.

[2] Department of Surgery, University of Minnesota, Minneapolis, MN 55455.

[3] Department of Surgical Pathology, University of Minnesota, Minneapolis, MN 55455.

[4] Present address: Dept. of Radiology, State University of New York, Stony Brook, NY 11794.

AJR 149:299–303, August 1987
0361–803X/87/1492–0299
© American Roentgen Ray Society

biliary cirrhosis (6), alpha-1 antitrypsin deficiency (5), fulminant hepatitis, (4), sclerosing cholangitis (2), Wilson's disease (2), glycogen storage disease (1), hepatoblastoma (1), tyrosinemia (1), and congenital hepatic fibrosis (1). In four patients, the cause of hepatic failure was not determined precisely. Details of the surgical techniques for hepatic transplantation at the University of Minnesota have been described elsewhere [5]. Because of technical limitations, arterial reconstructions in small children originally were accomplished by means of an end-to-side aorto–aortic anastomosis; later in the series, end-to-side hepatic artery–celiac axis anastomoses were used. In the beginning, cholecystojejunostomies were used for biliary reconstructions in children; later in the series, choledochojejunostomies were used. In older children and adults, end-to-end hepatic arterial and end-to-end choledochocholedochostomy anastomoses were performed routinely. End-to-end portal venous and inferior vena caval anastomoses were performed in all patients. All of these patients received azothioprine, prednisone, and cyclosporine-A for immunosuppression.

Between April 1, 1984, and June 30, 1986, 36 patients (25 children and 11 adults) underwent 166 sonographic examinations of the upper abdomen. Nine patients had one study, 15 had two to five, and 12 had six or more. Forty-three studies were done within 2 weeks of transplantation, 47 between 2 and 8 weeks, and 76 after more than 8 weeks. Indications for abdominal sonography after transplantation included fever, jaundice, abdominal pain or distension, and laboratory evidence of hepatic dysfunction or blood loss. The sonographic findings were correlated with clinical, laboratory, and histopathologic data, including the results of 182 percutaneous and open liver biopsies in 33 patients. Sonography was used to guide percutaneous aspiration of intraabdominal fluid in six patients and to guide percutaneous transhepatic cholangiography in two.

A complete sonographic examination of the upper abdomen, including the hepatic parenchyma, biliary system and hepatic vasculature, was performed in transverse and sagittal planes, if at all feasible. A 5.0-MHz transducer was used for both static and real-time scanning of children. For adults, a 3.5-MHz transducer was used for static scanning and a 5.0-MHz transducer for real-time scanning. During most of the study period, a phased-array unit was used for real-time scanning. When deep Doppler capabilities became available in our hospital, studies were expanded to include duplex Doppler examinations of the portal vein, inferior vena cava (IVC), and hepatic artery.

Results

Sonographic Assessment of Liver Parenchyma

Sonographic findings in the hepatic parenchyma included diffuse abnormalities, diminished graft volume, and focal defects. Widespread parenchymal abnormalities were seen in 27 patients. These included increased overall echogenicity (21), diffuse inhomogeneity (12), and increased periportal echogenicity (11); some patients had more than one abnormality. Increased diffuse and periportal echogenicity were first detected as early as 1 day and as late as 7 months after transplantation (mean, 2.1 months). Once present, these two abnormalities never resolved. Parenchymal inhomogeneity was detected within 1 month of transplantation in all but two of the 11 patients who had this finding (mean, 1.5 months) and resolved with time if the patient survived. No consistent association between these widespread sonographic abnormalities could be made with the histopathologic conditions identified by biopsy, including ischemia, rejection, nonspecific inflammation, infection, toxic reactions to drugs, and fibrosis.

Serial sonographic examinations in 11 patients showed a decrease in the size or contraction of the inferior margins of the graft (Fig. 1). Histopathologic correlation was available for all of these patients; the findings showed chronic inflammation (5), chronic rejection (3), and hepatic fibrosis (1). In one patient, the results of a biopsy and angiographic evidence indicated portal vein thrombosis, and in one patient, no cause of the decrease in graft volume could be identified.

Focal regions of mixed, but primarily decreased, echogenicity (Fig. 2) were seen in four of the 36 patients. Two of these patients had surgically proved hepatic abscesses. One patient had massive hepatic infarction at autopsy, and histopathologic data for the fourth patient showed hepatocellular necrosis in conjunction with severe rejection.

Sonographic Assessment of the Biliary System

Thirteen of the 36 patients had sonographic evidence of biliary dilatation. In five patients, it was minimal and resolved spontaneously. In another patient, minimal biliary dilatation became moderately severe, and percutaneous transhepatic cholangiography confirmed the dilatation, but not obstruction. Seven patients had moderate to severe dilatation (Fig. 3) and all had obstruction. Five of these had undergone cholecystojejunostomy biliary reconstruction (Fig. 3); in three of the five, the cystic duct was obstructed, in one the anastomosis was obstructed, and in one the level of obstruction was indeterminant. One patient with a choledochojejunostomy had an incomplete obstruction at the anastomosis, and another who had undergone choledochocholedochostomy had an obstruction that was due to kinking of the T-tube.

Sonographic Assessment of Upper Abdominal Vasculature

In three patients, sonographic findings suggested abnormalities in the portal vein that were corroborated by angiography or MR imaging. Suspected thrombosis of the portal vein was documented angiographically in two patients (Fig. 4), and a portal vein aneurysm containing nonobstructing thrombosis was seen in one by MR. In a fourth patient, sonograms showed a small, presumably patent portal vein, but angiographic studies indicated thrombosis and collateralization. Irregularity of the portal vein wall and luminal echogenicity at the anastomosis suggestive of nonobstructive thrombus were seen in five patients; these findings were not evaluated further by angiography or MR imaging.

Sonographic findings of thrombosis of the IVC in one patient (Fig. 5) and of IVC patency in two patients were confirmed angiographically. A large azygous vein was misidentified sonographically as the IVC in one patient with congenital absence of the IVC. The presence of possible obstructing thrombus in two patients and nonobstructing thrombus in 17 patients was not evaluated further by angiography.

Suspected thrombosis of the donor aorta was confirmed angiographically or surgically in three patients (Fig. 6) and was not found at autopsy or surgery in another three patients. Two large pseudoaneurysms of the hepatic artery seen angiographically in one patient were not seen sonographically.

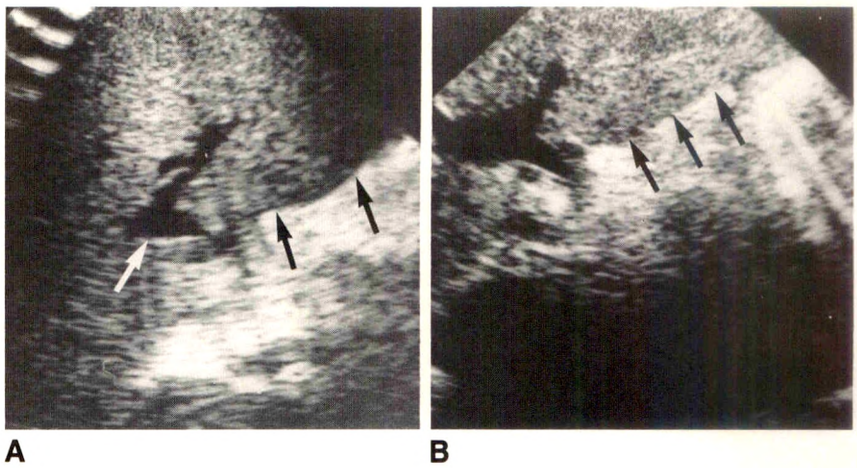


Fig. 1.—15-year-old girl with multiple episodes of acute rejection after hepatic transplantation.

***A*, Transverse sonogram of hepatic allograft 1 week after transplantation shows a convex liver contour. *Black arrows* show liver margin; *white arrow* shows portal vein.**

***B*, Transverse sonogram 4 months later shows development of marginal concavity of left hepatic lobe (*arrows*), indicating a loss of volume of graft. Results of a contemporaneous biopsy indicated severe chronic rejection.**

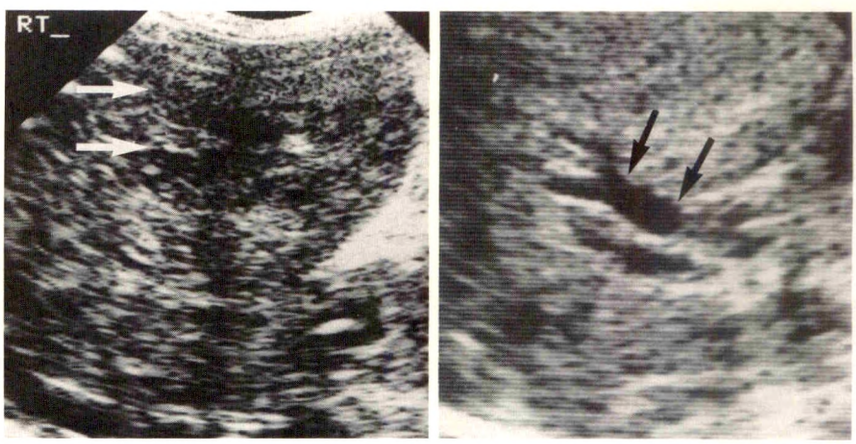


Fig. 2.—4-year-old girl with choledocholithiasis, cholangitis, and hepatic abscess after hepatic transplantation. Transverse sonogram shows decreased echogenicity (*arrows*) near hilum of liver. CT shows low attenuation in same area. Cultures obtained by sonography-guided percutaneous aspiration yielded streptococci, and transhepatic cholangiography showed communication with the biliary system. Open surgical drainage of abscess ultimately was required.

Fig. 3.—18-month-old girl with jaundice 1 week after hepatic transplantation. Biliary reconstruction was accomplished via a cholecystojejunostomy. Transverse sonogram shows moderate dilatation of central biliary system (*arrows*). Transhepatic cholangiography confirmed biliary dilatation and showed obstruction of cystic duct. Biliary drainage was revised via a choledochojejunostomy.

Evaluation of Intraabdominal Fluid

Sixteen focal fluid collections were identified by sonography in 14 patients. Eleven of the collections were seen in the early postoperative period. Surgical and autopsy evidence indicated that these collections, which were located in the upper abdomen and in the subphrenic spaces, represented hematomas. Four focal fluid collections were identified immediately after percutaneous liver biopsy and were thought to be hematomas. An additional uncharacterized collection was seen in the subhepatic space by sonography after percutaneous transhepatic cholangiography. Scant to massive amounts of free peritoneal fluid were identified sonographically in 19 patients.

Sonographically Guided Percutaneous Procedures

Sonography was used successfully to guide percutaneous aspiration of noninfected focal fluid collections in three patients, sterile-free peritoneal fluid in two patients, and a hepatic abscess in another patient. Fine-needle puncture for percutaneous transhepatic cholangiography was directed by sonography in two patients; it was successful in the one with biliary dilatation and unsuccessful in the one without biliary dilatation.

Discussion

Hepatic transplantation is being offered as treatment for end-stage liver disease, and improved survival rates are attributed to wider availability of suitable donor organs, technical advances, and more effective immunosuppression [1–4]. Nevertheless, medical and surgical complications continue to threaten survival of grafts and patients [4, 5]. Of particular importance is clinical differentiation of rejection from other causes of graft dysfunction, more commonly biliary obstruction or less commonly vascular insufficiency.

Sonographic examination of the parenchyma of the transplanted liver does not provide specific information about the cause of graft dysfunction. Diffuse parenchymal abnormalities are seen in the majority of patients and are associated with a variety of histopathologic conditions, including rejection, ischemia, nonspecific inflammation, systemic infection, and

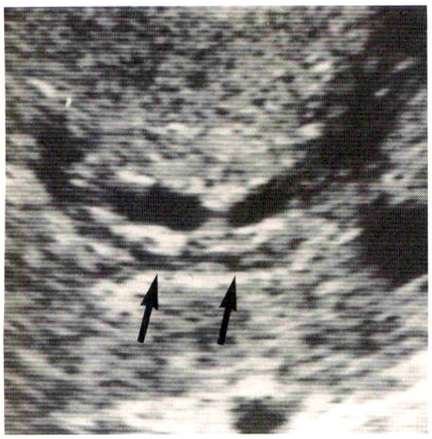


Fig. 4.—12-year-old boy with graft dysfunction 5 weeks after hepatic transplantation due to portal vein thrombosis. Transverse sonogram shows echogenicity within lumen of portal vein, suggesting thrombus (*arrows*). Wedged-hepatic venogram showed filling of intrahepatic portal venous system without opacification of main portal vein or washout of smaller portal vein branches. These findings indicated occlusion of extrahepatic portal vein.

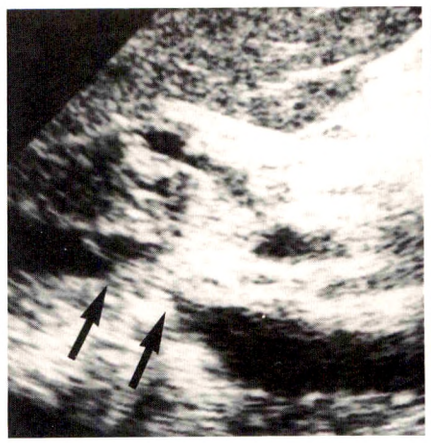


Fig. 5.—37-year-old woman with obstruction of inferior vena cava detected 2 days after hepatic transplantation. Parasagittal sonogram shows narrowing of inferior vena cava and obliteration of vessel lumen by echogenic material at level of infrahepatic anastomosis (*arrows*). Venacavography showed obstruction of flow of contrast within inferior vena cava and opacification of paravertebral collateral vessels.

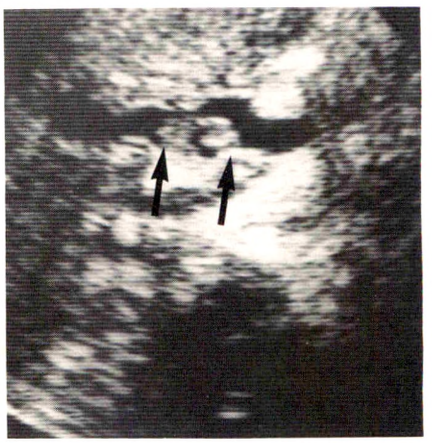


Fig. 6.—7-year-old boy with incomplete aortic thrombosis detected 2 weeks after hepatic transplantation. Parasagittal sonogram obtained at that time shows a rounded echogenic defect within donor aorta (*arrows*), suggesting presence of nonobstructing thrombus. Aortography confirmed this finding.

toxic reactions to drugs. We did not find, as had been reported earlier [9], that parenchymal mixed hyperechogenicity was more suggestive of hepatic infarction than other possible diagnoses. Unfortunately, to date no noninvasive imaging examination, including sonography, can be used to diagnose rejection accurately [8]. Consequently, pathologic evaluation of biopsy material has been an integral part of the assessment of graft dysfunction at our institution [13, 14]. Focal sonographic abnormalities of the hepatic parenchyma are seen in the more limited settings of abscess, infarction, and necrosis.

Overall volume of the allograft is difficult to assess after transplantation, as disproportion of the graft to the patient is common. However, a decrease in the size or contraction of the margins of the allograft is associated with chronic inflammation, chronic rejection, and portal venous insufficiency.

Detection of biliary dilatation in hepatic transplant recipients is an important capability of sonography because exclusion of biliary obstruction is one step in the evaluation of the patient with suspected rejection. Mild biliary dilatation tends to resolve spontaneously. In one patient with hepatic artery thrombosis, it did not resolve but progressed; arterial insufficiency was thought to contribute to impaired biliary contractility in this patient. Moderate to severe dilatation indicates obstruction; it was seen most commonly in the children who underwent cholecystojejunostomy, and it required radiologic intervention or surgical revision. A choledochojejunostomy is preferred now for pediatric biliary reconstruction.

Real-time sonography alone can be valuable in the vascular assessment of hepatic transplant recipients [15]. Expanded use of deep Doppler capabilities undoubtedly will improve sonographic assessment of the hepatic vasculature [15, 16]. Doppler capabilities will be especially important in determining the hemodynamic significance of luminal irregularity in the portal vein and IVC when these irregularities are seen in conjunction with apparently nonobstructing thrombi. It is hoped that these techniques will decrease the need for angiographic procedures [4, 9, 11, 17].

Intraabdominal fluid, both localized and free, frequently is seen after hepatic transplantation because of the massive blood loss and replacement that occur during surgery. Most fluid collections and free peritoneal fluid can be aspirated by using sonographic or CT guidance. The frequent sterility of these collections reflects the preponderance of systemic, rather than focal, infections in recipients of hepatic transplants [5]. Sonographic guidance also can be of value in other percutaneous procedures in these patients, such as percutaneous transhepatic cholangiography.

In summary, we have used sonography extensively in the evaluation of hepatic transplant recipients. Although its usefulness in the characterization of diffuse parenchymal processes is limited, it has value in the identification of focal parenchymal, biliary, and vascular complications. In particular, the detection of biliary obstruction in the setting of suspected allograft rejection is critical, as it determines an entirely different therapeutic course. Detection of fluid within the abdomen is accomplished easily with sonography,and characterization of the fluid obtained by sonographically guided percutaneous aspiration can have an effect on patient management.

REFERENCES

1. Starzl TE, Iwatsuki S, Byers BS, et al. Analysis of liver transplantation. *Hepatology* **1984**;4:475–495
2. Scharschmidt BF. Human liver transplant: analysis of data on 540 patients

from four centers. *Hepatology* **1984**;4:955–1015
3. Najarian JS, Ascher NL. Liver transplantation. *N Engl J Med* **1984**;311:1179–1181
4. Stock PG, Estrin JA, Fryd D, Payne W. Factors influencing early survival following liver transplantation. Presented at the meeting of the American Society of Transplant Surgeons, Chicago, May **1986**
5. Ascher NL. Simmons RL, Najarian JS. Host hepatectomy and liver transplantation. In: Simmons RL, Finch ME, Ascher NL, Najarian JS, eds. *Manual of vascular access, organ donation and transplantation*. New York: Springer-Verlag, **1985**:255–286
6. Cardella JF. Evaluation and treatment of nonvascular complications of liver transplantation. *Semin Intervent Radiol* **1986**;3:139–147
7. Cardella JF, Castaneda-Zuniga WR, Hunter DW, Young A, Amplatz K. Angiographic and interventional radiologic considerations in liver transplantation. *AJR* **1986**;146:143–153
8. Dominguez R, Cuervas-Mons V, Van Thiel DH, Lecky JW, Starzl TE. Radiographic features of liver allograft rejection. *Gastrointest Radiol* **1986**;11:326–329
9. Dominguez R, Young LW, Ledesma-Medina J, et al. Pediatric liver transplantation. Part II: Diagnostic imaging in postoperative management. *Radiology* **1985**;157:339–344
10. Letourneau JG, Day DL, Maile CW, Crass JR, Ascher NL, Frick MP. Liver allograft transplantation: postoperative CT findings. *AJR* **1987**;149:1099–1103
11. Zajko AB, Bron KM, Starzl TE, et al. Angiography of liver transplantation patients. *Radiology* **1985**;157:305–311
12. Zajko AB, Campbell WL, Bron KM, et al. Cholangiography and interventional biliary radiology in adult liver transplantation. *AJR* **1985**;144:127–133
13. Snover DC. The pathology of acute rejection. *Transplant Proc* **1986**;18:123–127
14. Snover DC, Freese Dk, Sharp HL, Bloomer JR, Najarian JS, Ascher NL. Liver allograft rejection: an analysis of the use of biopsy in determining outcome of rejection. *Am J Surg Path* (in press)
15. Taylor KJW, Morse SS, Weltin GG, Riely CA, Flye MW. Liver transplant recipients: portable duplex US with correlative angiography. *Radiology* **1986**;159:357–363
16. Berland LL, Lawson TL, Foley WD. Porta hepatis: sonographic discrimination of bile ducts from arteries with pulsed Doppler with new anatomic criteria. *AJR* **1982**;138:833–840
17. Wozney P, Zajko AB, Bron KM, Point S, Starzl T. Vascular complications after liver transplantation: a 5-year experience. *AJR* **1986**;147:657–663

Book Review

Transcranial Doppler Sonography. Edited by R. Aaslid. New York: Springer-Verlag, 177 pp., 1986. $35

This small, soft-covered book is well written and illustrated and summarizes the current state of transcranial Doppler sonography. The technique was pioneered in 1981 by the editor, Dr. Aaslid, yet this technique now rivals the more conventional methods (such as angiography and xenon assessment of cerebral blood flow) for investigating intracranial hemodynamics.

The first chapter is a biography of Christian Doppler that has been carefully researched. It is essential reading for anyone involved with Doppler applications since the author points out that many of our current beliefs about this man are fallacious. The well-researched problems of ultrasonic transmission through bone are summarized in the second chapter, while the third chapter deals with the basic principles of Doppler. The fourth chapter details the examination technique for obtaining recordings from all of the major intracranial arteries. Chapter five is a helpful review of cerebral hemodynamics and is followed by a chapter on cerebral arteriovenous malformations. A comparison of transcutaneous Doppler recordings and intraoperative vascular patterns confirm that it is possible to record from each of the major intracranial vessels through the intact skull.

Chapter eight is devoted to the evaluation of cerebral vasospasm using transcranial Doppler, an important use for a noninvasive technique in patients with subarachnoid hemorrhage. This technique can therefore be used continuously for monitoring hemodynamic changes after surgery. Prototype probes are described that can be attached to the temporal region to allow continuous monitoring after surgery.

In summary this is an excellent book and provides state-of-the-art information on transcranial Doppler. It will be particularly valuable for neurologists and neurosurgeons. For all radiologists who wish to be aware of the scope and the development of these new applications, this book is an excellent educational resource.

Kenneth Taylor
Yale University
New Haven, CT 06510

Case Report

Gallium-67 Detection of Occult Gastric Lymphoma in AIDS

D. Gianfelice,[1] L Rosenthall,[2] and J. Falutz[1]

AIDS has been reported almost exclusively in certain high-risk population groups: namely, homosexual men, drug abusers, hemophiliacs, and Haitians [1]. These patients are at increased risk for opportunistic infections [2], a variety of malignancies including Kaposi's sarcoma, both Hodgkin's and non-Hodgkin's lymphoma, squamous cell carcinoma of the oral cavity, and anal carcinoma [3]. We present one case of a homosexual man with AIDS who had a primary gastric lymphoma that was first detected by gallium-67 citrate scanning at a time when it was asymptomatic.

Case Report

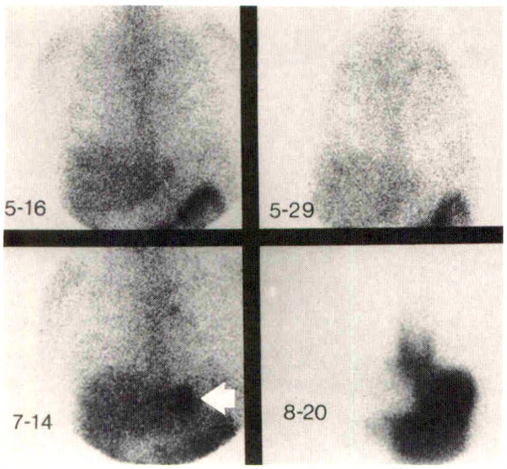
A 46-year-old homosexual man was admitted to Montreal General Hospital with a diagnosis of AIDS. He was positive for HTLV-III antibody, had *Pneumocystis carinii* of the lung (proved by biopsy), and perianal herpes simplex infection. Gallium-67 citrate scans were obtained 48 hr after IV injection of 148 MBq using a large field-of-view, medium-energy, parallel-hole collimator. The pulse-height analyzer was set to include the 93, 185, and 300 keV photopeaks individually. The first gallium-67 citrate scan showed low-grade uptake in the upper lungs consistent with opportunistic infection (Fig. 1). Five weeks after appropriate therapy with antibiotic and antiherpetic agents began, a repeat gallium-67 citrate scan was normal except for an area of intense activity in the esophagogastric region (Fig. 1). Radiocolloid and sonographic studies of the liver were normal, and because the patient was asymptomatic, no further investigation was undertaken. Three weeks later he complained of vomiting and a blocking sensation in the retrosternal area. Endoscopy was normal. One week later, he complained of an intolerable progressive dysphagia. He had lost 13 kg since he was discharged from the hospital 2 months earlier. A repeat gallium-67 citrate scan showed a lesion involving the distal esophagus and most of the stomach (Fig. 1). The differential diagnosis of this gallium-67 citrate uptake in the stomach included both primary and secondary Ga-67 avid tumors, inflammatory conditions, infections (predominantly opportunistic), and possibly normal uptake of gallium-67 citrate in the stomach [4]. CT showed a diffusely thickened gastric wall (Fig. 2). Percutaneous biopsy with CT guidance and endoscopic biopsy of the stomach were nondiagnostic. A left tonsillar biopsy 1 week later revealed a high-grade non-Hodgkin's lymphoma. The patient received one full course of chemotherapy consisting of cyclophosphamide, hydroxydoxorubicin, Oncovin, and prednisone (CHOP), but deteriorated rapidly and died 2 weeks later. Autopsy showed a large-cell immunoblastic lymphoma involving the entire stomach and esophagus with extension up to the tonsil and into the mediastinum without evidence of lymphoma elsewhere. The time between detection of the occult focus in the stomach and death was approximately 7 weeks.

Discussion

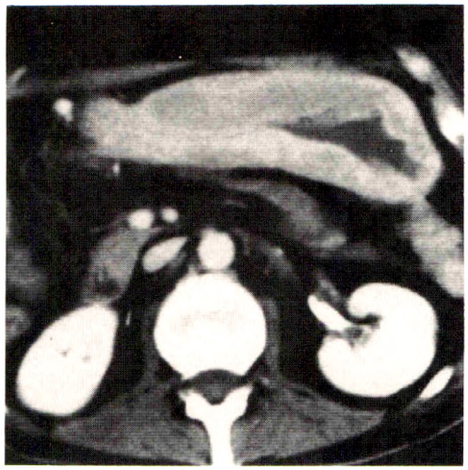
Several recent studies have reported an increased incidence of both Hodgkin's and non-Hodgkin's lymphoma in patients with AIDS. Lymphomas associated with AIDS tend to be high-grade, undifferentiated tumors and there is a high frequency of extranodal involvement and a poor prognosis [5, 6]. The response to appropriate chemotherapy is generally poor.

The use of gallium-67 citrate as a screening method for detection of certain malignancies has been well documented in the literature. Gallium-67 citrate tumor detection is particularly helpful in Hodgkin's disease, Burkitt's lymphoma, and hepatoma, and is also moderately sensitive for non-Hodgkin's lymphomas [7]. Ichiya et al. [8] showed a good correlation

Received January 8, 1987; accepted after revision March 19, 1987.
[1]Department of Radiology, Montreal General Hospital, 1650 Cedar Ave., Montreal, Quebec, H3G 1A4, Canada.
[2]Department of Nuclear Medicine, Montreal General Hospital, 1650 Cedar Ave., Montreal, Quebec, H3G 1A4, Canada. Address reprint requests to L. Rosenthall.
AJR **149:305–306, August 1987** 0361–803X/87/1492–0305 © American Roentgen Ray Society



1



2

Fig. 1.—Serial anterior gallium-67 citrate studies in a patient with AIDS, *Pneumocystis carinii* of the lung, and lymphoma. Initial study on May 16 shows low-grade uptake in the upper portion of the lungs consistent with *Pneumocystis carinii* infection, persisting on image obtained on May 29. Six weeks later (July 14) the lungs were improved, but there was a lesion in the cardia of the stomach (*arrow*). Follow up 5 weeks later (August 20) shows an intense concentration of gallium-67 citrate in the stomach and distal end of the esophagus.

Fig. 2.—CT shows diffuse thickening of gastric wall.

between upper gastrointestinal series and gallium-67 citrate uptake in 13 patients with documented gastric lymphoma.

Our patient's clinical course is significant for several reasons. First, he was shown to have an increased focus of gallium-67 citrate uptake in the left upper quadrant on a routine follow up for opportunistic lung infection at a time when he was relatively asymptomatic. A repeat scan 5 weeks later revealed marked uptake in the region of the stomach and distal esophagus accompanying a deteriorated clinical status. Autopsy confirmed a B-cell, immunoblastic, high-grade lymphoma, the extent of which correlated well with the gallium-67 citrate scan.

This sequence of events illustrates several points concerning AIDS and its complications. First, it reconfirms both the association and aggressive nature of lymphomas reported in this disease. Second, it illustrates the usefulness of whole-body gallium-67 citrate scanning in AIDS patients for detection of clinically occult processes, whether they are infectious or neoplastic. Third, it suggests that an incidental abnormality on a gallium-67 citrate scan may indicate the need for aggressive investigation in AIDS patients to assure the earliest possible diagnosis.

REFERENCES

1. Levine A, Meyer P, Begandy MK, et al. Development of B-cell lymphoma in homosexual men. *Ann Intern Med* **1984**;100:7–13
2. Soulen MC, Fishman EK, Scatarige JC, Hutchins D, Zerhouni EA. Cryptosporidiosis of the gastric antrum: detection using CT. *Radiology* **1986**;159:705–706
3. Ioachim H, Cooper M, Hellman E. Lymphomas in men at high risk for acquired immune deficiency syndrome (AIDS). *Cancer* **1985**;56:2831–2842
4. MacMahon H, Vyborny C, Sephordari S, Kirschner P, Ryon J. Gallium accumulation in the stomach: a frequent incidental occurrence. *Clin Nucl Med* **1985**;10:719–723
5. Kalter S, Riggs S, Cabanillas F, et al. Aggresive non-Hodgkin's lymphomas in immunocompromised homosexual males. *Blood* **1985**;66(3):655–659
6. Jeffrey BR, Nyberg DA, Bottles K, et al. Abdominal CT in acquired immunodeficiency syndrome. *AJR* **1986**;146:7–12
7. Hoffer P. Status of gallium-67 in tumor detection. *J Nucl Med* **1980**;21:394–398
8. Ichiya Y, Oshiumi Y, Kamoi I, et al. Ga scanning and upper gastrointestinal series for gastric lymphomas. *Radiology* **1982**;142:187–192

Esophageal Radiography and Manometry: Correlation in 172 Patients with Dysphagia

David J. Ott[1]
Joel E. Richter[2]
Yu Men Chen[1]
Wallace C. Wu[2]
David W. Gelfand[1]
Donald O. Castell[2]

Radiographic and manometric examinations of the esophagus were correlated in 172 patients with dysphagia. Esophageal manometry was abnormal in 66 (38%), with diagnoses of nonspecific esophageal motor disorder (26), achalasia (19), nutcracker esophagus (12), diffuse esophageal spasm (seven), and scleroderma (two). Compared with manometry, radiographic sensitivities were 95% (18 of 19) for achalasia, 71% (five of seven) for diffuse esophageal spasm, and 46% (12 of 26) for nonspecific esophageal motor disorder. Nutcracker esophagus was not diagnosed specifically on the radiographic examination. Overall radiographic sensitivity was 56% (37 of 66) but increased to 89% by excluding nutcracker esophagus and nonspecific esophageal motor disorders. In 106 manometrically normal patients, radiographic specificity was 91% with 10 false-positive diagnoses of nonspecific motor disorder.

We conclude that radiographic examination of the esophagus is useful in patients with dysphagia for evaluating functional esophageal abnormalities, although detection rates vary widely with the type of motor disorder.

Dysphagia is a common reason for radiographic examination of the esophagus to assess structural or functional abnormalities [1–5]. If a structural abnormality is not implicated radiographically, endoscopy is usually recommended, primarily to exclude carcinoma. However, in three recent radiologic reports [3–5] evaluating a total of 408 patients with dysphagia who had endoscopy, all carcinomas of the esophagus were detected radiographically. Consequently, endoscopy may not be the most appropriate recommendation if the barium esophagram has excluded structural lesions. Esophageal dysmotility, another important cause of dysphagia, can also be evaluated radiographically. We reviewed the radiologic and manometric records in 172 patients with dysphagia to define better the role of radiology in evaluating esophageal motility and its disturbances.

Materials and Methods

We reviewed the esophageal manometric and radiologic records for a 2-year period. The patients were selected consecutively on the basis of having had both examinations performed within 2 weeks of each other and of having a clinical history of dysphagia. A total of 172 patients entered the study, which consisted of 84 women and 88 men with a mean age of 55 years (range, 15–89 years). In addition to all patients having dysphagia, 130 also had heartburn, 111 chest pain, and 31 odynophagia.

Esophageal manometry was performed with a round, eight-lumen polyvinyl catheter with each lumen infused continuously by using a low-compliance infusion system (Arndorfer Specialities, Inc., Greensdale, WI). Lower esophageal sphincter pressure was measured and relaxation assessed at mid-expiration by the station pull-through technique [6]. The catheter was then positioned in the esophageal body with openings at 3, 8, 13, and 18 cm above the lower esophageal sphincter. The esophageal contractions were recorded in response to 10 wet swallows (5 ml H_2O) at 30-sec intervals. The normal mean distal amplitude in our laboratory is 100 ± 80 mm Hg (mean ± 2 SD) [6].

Received February 9, 1987; accepted after revision May 4, 1987

Presented at the annual meeting of the Society of Gastrointestinal Radiologists, Scottsdale, AZ, February 1987.

[1] Department of Radiology, Bowman Gray School of Medicine, Wake Forest University, Winston-Salem, NC 27103. Address reprint requests to D. J. Ott.

[2] Department of Medicine, Bowman Gray School of Medicine, Wake Forest University, Winston-Salem, NC 27103.

AJR 149:307–311, August 1987
0361–803X/87/1492–0307
© American Roentgen Ray Society

Manometric diagnoses included (1) normal, (2) nonspecific esophageal motor disorder (NEMD), (3) achalasia, (4) nutcracker esophagus, (5) diffuse esophageal spasm, and (6) scleroderma [7–9]. The manometric criteria for achalasia were esophageal aperistalsis and lower esophageal sphincter dysfunction, primarily incomplete relaxation. Nutcracker esophagus was defined in patients with chest pain or dysphagia who had normal esophageal peristalsis but distal peristaltic contractions with mean amplitudes above 180 mm Hg. Diffuse esophageal spasm was diagnosed in patients with chest pain showing intermittently normal peristalsis and simultaneous contractions after >10% of wet swallows [10]. NEMD, a catchall term, was used for symptomatic patients whose manometric abnormalities defied specific classification, and included intermittent absence of peristalsis, low-amplitude peristalsis, prolonged duration of contractions, occasional repetitive contractions, or incomplete relaxation of the lower esophageal sphincter.

A multiphasic radiographic examination of the esophagus was performed with remote control machinery [11]. Esophageal motility was assessed fluoroscopically with the patient in the prone oblique position by observing single swallows or barium traversing the length of the esophagus. All examinations were performed by gastrointestinal radiologists or residents, the latter being supervised during film interpretation but not always during fluoroscopy. Videotaping and solid bolus examination, with barium tablets or marshmallows, were used in a minority of patients. The status of primary esophageal peristalsis and the level of esophageal involvement if motility was poor were noted. Tertiary activity and its severity were also recorded along with structural and other functional abnormalities, if present.

Radiographic criteria for achalasia included aperistalsis of the esophagus and failure of relaxation of the lower esophageal sphincter segment, showing the characteristic "tapered beaking" at the level of the esophageal hiatus [12–14]. The esophagus was usually dilated and occasionally contained excess secretions and food. Radiographic findings suggesting diffuse esophageal spasm included intermittently discoordinated peristalsis and segmental nonperistaltic contractions [12–14]. The esophagus was typically not dilated and the lower esophageal sphincter segment usually functioned normally. Other less specific abnormalities of esophageal motility, as observed radiographically, were diagnosed as NEMD, unless the clinical history suggested a secondary motor disorder, such as scleroderma or diabetes mellitus. No specific radiographic criteria have been determined for nutcracker esophagus [15, 16].

Results

Esophageal manometry was abnormal in 66 (38%) of the 172 patients. The overall radiographic sensitivity was 56% (37 of 66), with a wide range of detection rates (Table 1). The radiographic examination most accurately identified achalasia and scleroderma, with a combined sensitivity of 95%. One patient with achalasia was diagnosed radiographically as having NEMD. Diffuse esophageal spasm was suggested radiographically in 71% of cases (Figs. 1 and 2). Nearly half of the patients with NEMD manometrically were similarly diagnosed radiographically (Fig. 3). As expected, nutcracker esophagus

TABLE 1: Radiographic Diagnoses in Esophageal Motor Disorders Detected by Manometry

Manometric Diagnosis	No. of Patients	
	Total	Diagnosed Radiographically (%)
Nonspecific esophageal motor disorder	26	12 (46)
Achalasia	19	18 (95)
Nutcracker esophagus	12	0 (0)
Diffuse esophageal spasm	7	5 (71)
Scleroderma	2	2 (100)
Total	66	37 (56)

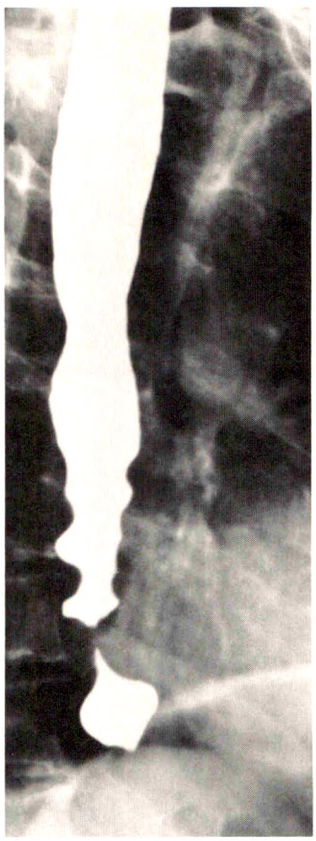
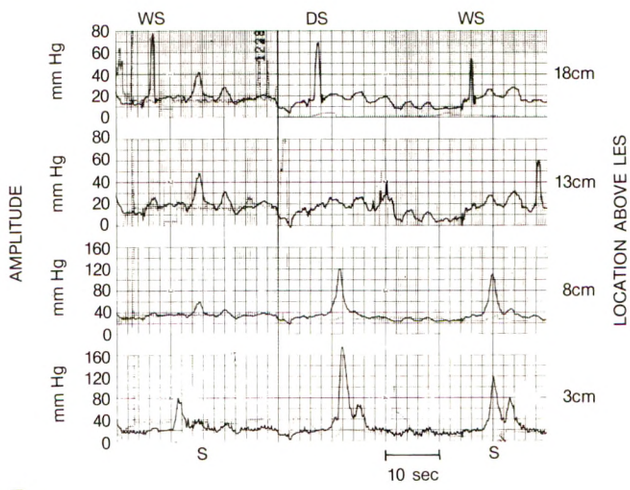


Fig. 1.—*A*, Barium esophagram shows diffuse esophageal spasm. At fluoroscopy, there was intermittent disruption of primary peristalsis associated with simultaneous tertiary contractions.

***B*, Manometry shows multiple simultaneous (S) and repetitive contractions occurring with wet swallowing (WS). DS = dry swallow; LES = lower esophageal sphincter.**

A



B

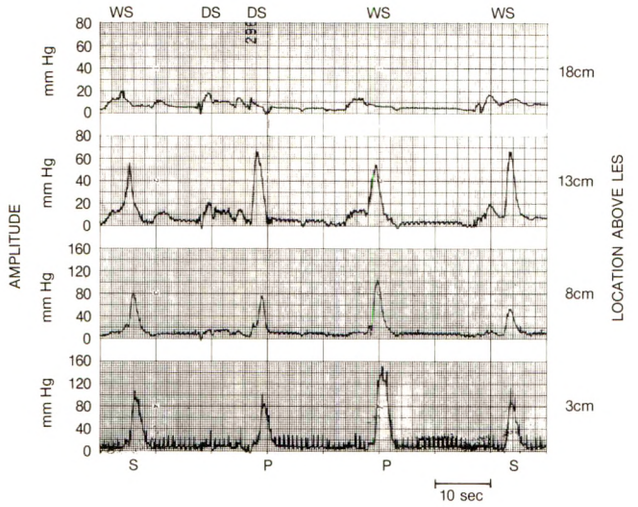


Fig. 2.—Manometry shows diffuse esophageal spasm in patient with normal radiographic examination. Tracings show intermittent normal peristalsis (P) with more than 10% simultaneous (S) contractions with swallowing. WS = wet swallow; DS = dry swallow; LES = lower esophageal sphincter.

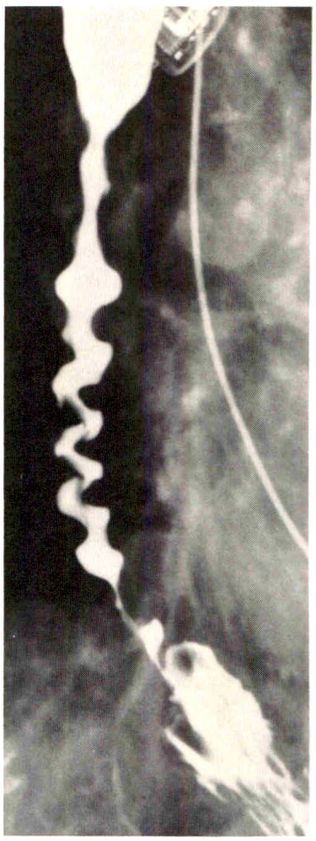
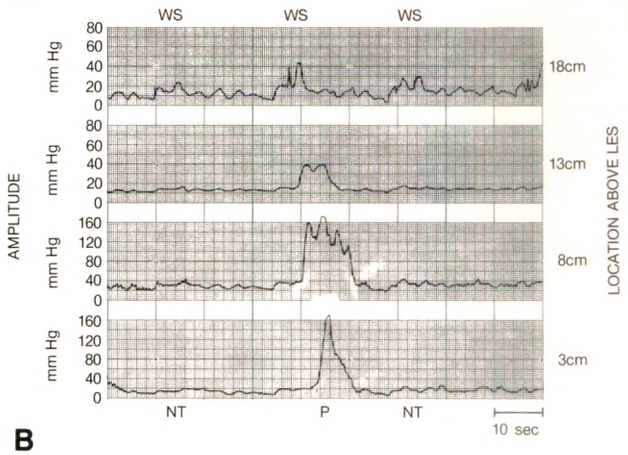


Fig. 3.—*A*, Barium esophagram shows nonspecific esophageal motor disorder with severe tertiary activity causing so-called "curling" or "corkscrew" appearance.

A



B

***B*, Manometry in another patient with nonspecific esophageal motor disorder shows nontransmitted (NT) peristalsis in lower leads and repetitive contractions during transmitted peristalsis (P). WS = wet swallow; LES = lower esophageal sphincter.**

was primarily a manometric and clinical diagnosis (Fig. 4). If the patients with NEMD and nutcracker esophagus are excluded, the radiographic sensitivity was 89% (25 of 28).

The most common manometric disorder was NEMD, accounting for 39% of all observed abnormalities. Table 2 compares the true-positive and false-negative radiographic groups in NEMD. The patients diagnosed radiographically as having NEMD were older, had a lower mean esophageal body pressure manometrically, and showed more tertiary activity in the esophagus radiographically than did the group with false-negative diagnoses. Perhaps, lower amplitude esophageal peristalsis, which more commonly occurs in older patients [17], and the presence of tertiary activity facilitated the radiographic diagnosis of NEMD.

Esophageal manometry was normal in 106 patients, and 96 also had normal motility radiographically, for a specificity of 91%. Ten false-positive diagnoses of NEMD were made radiographically. Comparing this latter group with the true-negative radiographic group showed that the patients with false-positive diagnoses were older (62 vs 52 years) and had a lower mean esophageal body pressure manometrically (68 vs 91 mm Hg). The positive predictive value for a radiographic diagnosis of the esophageal motor abnormality was 79% (37 of 47). The negative predictive value was 77% (96 of 125), which improved to 85% by eliminating the patients with nutcracker esophagus.

Structural abnormalities of the esophagus were also present radiographically in 108 (63%) of the 172 patients (Table 3). Sixty-one of these patients had a single abnormality while 47 had multiple findings. Hiatal hernia was seen most often and was occasionally associated with reflux esophagitis and peptic stricture. This abnormality occurred predominantly (87%) in patients with normal motility or NEMD. The reflux-related abnormalities and mucosal rings in patients with normal esophageal motility most likely explain their dysphagia. The reflux-related changes that occurred in a few of the patients with NEMD may be an alternative reason for their dysphasia.

Discussion

Radiographic evaluation of patients with esophageal dysphagia is useful for assessing both structural and functional

abnormalities of the esophagus. Excluding mild cases of esophagitis, the radiographic examination is capable of showing about 90–95% of structural abnormalities that may cause dysphagia, including esophageal carcinoma, peptic stricture, mucosal ring, and more severe forms of reflux esophagitis [11, 18–21]. In addition to evaluating structural disease, the radiographic examination also evaluates esophageal function and its abnormalities. In our investigation, however, radiographic detection depended on the type of esophageal motor disorder; the overall sensitivity of 56% improved to 89% by excluding NEMD and nutcracker esophagus.

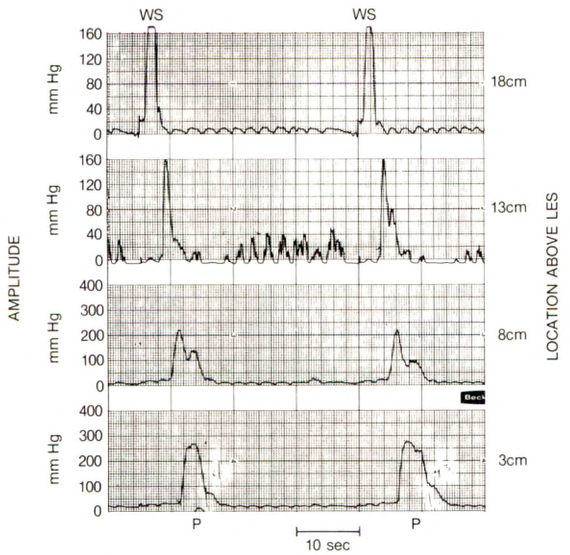


Fig. 4.—Manometry shows nutcracker esophagus in patient with normal radiographic examination. Normal primary peristalsis (P) manometrically with high-amplitude contractions (over 200 mm Hg, lower two leads). Accentuated baseline activity in 13-cm lead represents cardiac artifact. WS = wet swallow; LES = lower esophageal sphincter.

TABLE 2: Comparison of True-Positive and False-Negative Radiographic Diagnoses in Manometrically Detected Nonspecific Esophageal Motor Disorder

Parameter	Radiographic Diagnosis	
	True Positive	False Negative
No. of patients	12	14
Mean age ± 1 SD	69 ± 14	53 ± 13
Mean esophageal peristaltic pressure (mm Hg) ± 1 SD	72 ± 41	102 ± 63
No. with tertiary activity radiographically	8	4

Achalasia requires accurate diagnosis because it can be treated effectively by pneumatic dilatation or surgical myotomy. In our series, radiographic sensitivity in 19 patients with achalasia was 95%, which confirms the value of radiology in detecting this disorder. The single patient with achalasia not diagnosed specifically was believed to have had NEMD radiographically, which prompted manometric evaluation. The radiologic diagnosis of achalasia is made easily in most patients. However, in patients with early disease, esophageal dilatation and tapering of the distal esophagus may not be as apparent, making detection of aperistalsis critical for proper diagnosis [22].

Compared with achalasia, diffuse esophageal spasm is less well defined. Many manometric criteria have been used to describe diffuse esophageal spasm, but the most important are the presence of frequent simultaneous contractions and intermittent normal peristalsis [7–9]. Because these criteria have been applied variably, the prevalence of diffuse esophageal spasm is difficult to estimate. In our manometric laboratory diffuse esophageal spasm represented only 11% of esophageal motor disorders diagnosed among patients with dysphagia and was less common than achalasia (29%). Although the diagnosis of diffuse esophageal spasm requires manometric confirmation, our radiographic sensitivity of 71% suggests that many patients with this disorder have radiographic abnormalities that suggest the appropriate diagnosis [12–14].

Nutcracker esophagus is a recently described esophageal motor disorder seen in some patients with chest pain and/or dysphagia [8, 9, 15, 16]. It is characterized manometrically by normal primary peristalsis with distal contractions of higher amplitude and of increased duration. Nutcracker esophagus is a common esophageal motor disorder that is being recognized increasingly with the advent of higher fidelity infusion systems and microtransducers [8, 9]. As expected, normal primary peristalsis was observed radiographically in most of our patients with nutcracker esophagus, although mild to severe tertiary activity was present occasionally.

TABLE 3: Other Radiographic Abnormalities in Manometrically Normal and Abnormal Patients

Manometry	Hiatal Hernia	Mucosal Ring	Reflux Esophagitis	Peptic Stricture
Normal	77	12	25	13
Abnormal:				
Nonspecific esophageal motor disorder	13	2	1	6
Achalasia	1	0	0	0
Nutcracker esophagus	7	0	1	0
Diffuse esophageal spasm	4	1	1	0
Scleroderma	2	0	1	2
Subtotal	27	3	4	8
Total	104	15	29	21

Note.—Forty-seven of 108 patients had multiple findings.

The most common esophageal motility disorder manometrically affecting 39% of our patients was NEMD. Unfortunately, NEMD is less clearly defined and is a catchall term for patients whose symptoms defy more definite classification. The natural history and clinical significance of NEMD remain controversial. Some of these patients may progress to more specific esophageal motor disorders or show evidence of systemic disease, such as diabetes mellitus. The manometric diagnosis of NEMD is based primarily on peristaltic abnormalities, such as intermittently absent or low-amplitude peristalsis, prolonged duration contractions, lower esophageal sphincter dysfunction, or frequent spontaneous or repetitive contractions [8, 9]. These abnormalities may be minimal or intermittent, and difficult to detect radiographically.

About half of our patients with NEMD were detected radiographically. Generally NEMD was diagnosed in older patients with lower esophageal body pressures, often accompanied by tertiary activity. The limited time used to examine patients fluoroscopically and the use of only several swallows of barium to assess primary peristalsis made radiographic assessment of these milder forms of esophageal dysmotility less sensitive. Furthermore, residents were not always supervised directly while performing fluoroscopy, and their more limited experience probably contributed to our poor detection in this category. An experienced radiologist would likely have had a better sensitivity in evaluating patients with NEMD.

Radiographic specificity in this series was 91%, indicating that the barium examination effectively evaluated normal esophageal motility. This compares favorably with other reports, suggesting a 95% correlation between radiology and manometry in patients with normal esophageal peristalsis [21]. Our 9% false-positive fraction resulted from 10 radiographic diagnoses of NEMD in patients with normal manometry. Although these patients may have had intermittent functional abnormalities of the esophagus that were not present during the manometric examination, it is more probable that the radiographic assessment was incorrect. Similarly, the more limited experience of radiology residents may have contributed to this false-positive radiographic error. Patients who are repetitive swallowers or demonstrate proximal escape of barium during normal peristalsis may be misinterpreted radiographically as having disruption of primary peristalsis.

In addition to the variability of experience among radiologic examiners in our investigation, several other methodologic problems warrant discussion. We did not routinely use motion-recording techniques to supplement our fluoroscopic impressions nor were bolus size and number of swallows standardized. Ideally, at least five single swallows of barium should be used to determine the frequency of peristalsis [12–14]. Videotaping or cinerecording would also have allowed precise review of the fluoroscopic examinations. But even without these limitations, our results probably would have been similar except for some improvement in detection of NEMD. Prospective and simultaneous radiologic-manometric studies of esophageal motor disorders, particularly NEMD and the nutcracker esophagus, are needed to better assess the efficacy of radiographic detection.

In summary, radiographic examination is useful in patients with dysphagia for evaluating structural and functional esophageal abnormalities. The presence of primary esophageal peristalsis can be determined confidently with proper fluoroscopic evaluation. Achalasia is accurately diagnosed. Diffuse esophageal spasm can be suggested in most patients with appropriate symptoms. NEMD is evaluated less well radiographically. Nutcracker esophagus is primarily a manometric diagnosis.

REFERENCES

1. Edwards DAW. Discriminative information in the diagnosis of dysphagia. *J R Coll Physicians Lond* **1975**;9:257–263
2. Castell DO, Knuff TE, Brown FC, Gerhardt DC, Burns TW, Gaskins RD. Dysphagia. *Gastroenterology* **1979**;76:1015–1024
3. DiPalma JA, Prechter GC, Brady CE III. X-ray–negative dysphagia: is endoscopy necessary? *J Clin Gastroenterol* **1984**;6:409–411
4. Ott DJ, Wu WC, Gelfand DW. Efficacy of radiology of the esophagus for evaluation of dysphagia. *Gastrointest Radiol* **1981**;6:109–110
5. Halpert RD, Feczko PJ, Spickler EM, Ackerman LV. Radiological assessment of dysphagia with endoscopic correlation. *Radiology* **1985**;157:599–602
6. Richter JE, Wu WC, Johns DN, et al. Esophageal manometry in 95 healthy adult volunteers: variability of pressures with age and frequency of "abnormal contractions." *Dig Dis Sci* (in press)
7. Cohen S. Motor disorders of the esophagus. *N Engl J Med* **1979**;301:184–192
8. Blackwell JN, Castell DO. Motility disorders of the lower esophagus. *Surv Dig Dis* **1983**;1:157–168
9. Katz PO, Castell DO. Review. Esophageal motility disorders. *Am J Med Sci* **1985**;290:61–69
10. Richter JE, Castell DO. Diffuse esophageal spasm: a reappraisal. *Ann Intern Med* **1984**;100:242–245
11. Ott DJ. Radiologic evaluation of the esophagus. In: Castell DO, Johnson LF, eds. *Esophageal function in health and disease*. New York: Elsevier Science, **1983**:211–235
12. Margulis AR, Koehler RE. Radiologic diagnosis of disordered esophageal motility. *Radiol Clin North Am* **1976**;14:429–439
13. Stewart ET. Radiographic evaluation of the esophagus and its motor disorders. *Med Clin North Am* **1981**;65:1173–1194
14. Dodds WJ. Motility disorders. In: Margulis AR, Burhenne HJ, eds. *Alimentary tract radiology*, vol. 1, 3d ed. St. Louis: Mosby, **1983**:538–553
15. Chobanian SJ, Curtis DJ, Benjamin SB, Cattau EL Jr. Radiology of the nutcracker esophagus. *J Clin Gastroenterol* **1986**;8:230–232
16. Ott DJ, Richter JE, Wu WC, Chen YM, Gelfand DW, Castell DO. Radiologic and manometric correlation in "nutcracker" esophagus. *AJR* **1986**;147:692–695
17. Khan TA, Shragge BW, Crispin JS, Lind JF. Esophageal motility in the elderly. *Dig Dis Sci* **1977**;22:1049–1054
18. Ott DJ, Gelfand DW, Lane TG, Wu WC. Radiologic detection and spectrum of appearances of peptic esophageal strictures. *J Clin Gastroenterol* **1982**;4:11–15
19. Ott DJ, Chen YM, Gelfand DW, Munitz HA, Wu WC. Analysis of a multiphasic radiographic examination for detecting reflux esophagitis. *Gastrointest Radiol* **1986**;11:1–6
20. Ott DJ, Chen YM, Wu WC, Gelfand DW, Munitz HA. Radiographic and endoscopic sensitivity in detecting lower esophageal mucosal ring. *AJR* **1986**;147:261–265
21. Dodds WJ. Current concepts of esophageal motor function: clinical implications for radiology. *AJR* **1977**;128:549–561
22. Katz PO, Richter JE, Cowan R, Castell DO. Apparent complete lower esophageal sphincter relaxation in achalasia. *Gastroenterology* **1986**;90:978–983

Editorial

AJR Achieves Goal to Speed Publication

The members of the American Roentgen Ray Society's Publications Committee and the *AJR* editors are dedicated to the notion that manuscripts submitted to the Journal must be published in a timely fashion if the Journal is to be of maximal value to its readers. Medical journals, in general, have a reputation for having an egregious delay between submission of papers and their appearance in print. This time varies, but it is often 8 months or even 1 year, long enough that the information is already outdated by the time it is published. The *AJR* considers this unacceptable.

Consequently when the San Diego editorial office was organized 20 months ago, the new editors determined to create a system whereby the expeditious handling of submitted manuscripts was ensured and the peer-review and revision processes were facilitated. Dedicated and talented editorial and administrative assistants, a new computer system, and a generous budget, allocated for this purpose, guaranteed the increased efficiency of the new office.

The goal to speed publications into print has been achieved. The mean time between submission of manuscripts and notification of authors of the initial editorial decision has been reduced from 8.3 weeks in 1984 and 1985 to 4.8 weeks in 1986, a reduction of 42%. In the first quarter of 1987, the time was reduced even further to 3.8 weeks.

The mean time between first submission of manuscripts and final publication was unchanged in 1986 compared with 1984 and 1985 (7 months). However, in the first quarter of 1987, after a backlog of manuscripts was published, the time fell to 5.2 months, a reduction of 26%. On average, this period now includes approximately 1 month for the editors to make an initial decision, 1 month for authors to prepare a revision, and 3 months for editing and printing.

This goal could not have been achieved without the commitment of more than 700 manuscript reviewers. These authorities take time from their busy practices, without remuneration or recognition, to give first priority to the detailed evaluation of manuscripts. Initial editorial decisions are reached quickly only because reviewers agree to judge manuscripts within 2 weeks, an enormous commitment considering the extent of their other responsibilities.

The ARRS Publications Committee and the editors are proud of this accomplishment. We rest assured knowing that the information brought to *AJR* readers is as current as the publication process allows.

Robert N. Berk
Editor-in-Chief

Case Report

Urethroplasty with Balloon Catheter in Prostatic Hypertrophy

Flavio Castaneda,[1] Steven Johnson, John Hulbert, Gunnar Lund, Janis G. Letourneau, Augusto Brazzini, David W. Hunter, Wilfrido R. Castaneda-Zuniga, and Kurt Amplatz

Benign prostatic hypertrophy is seen in more than 80% of men over the age of 50 years [1]. Consequently, it represents a significant medical problem. Despite the widespread use of interventional techniques for diseases of the genitourinary tract and technical advances in balloon catheters, percutaneous methods have not been used in the treatment of this common ailment. Burhenne et al. [2] recently described a patient who was treated by retrograde transurethral dilatation using a balloon catheter 8 mm in diameter. After an in vivo study in dogs at our institution indicated that large balloons (20-mm diameter or greater) were necessary to achieve long-lasting dilatation [3], we used the technique on one patient.

Case Report

Benign prostatic hypertrophy was diagnosed in a 62-year-old man with a progressive history of hesitancy, nocturia, dribbling, urgency, and frequency of urination. A voiding cystourethrogram confirmed moderate prostatic urethral narrowing (Fig. 1).

Mild sedatives and prophylactic antibiotics were administered before the procedure. After sterile preparation and draping, 2% viscous lidocaine was instilled into the urethra for topical anesthesia. The urethra was catheterized with a 5-French curved angiographic catheter over a 0.035 in. (0.09 cm) floppy-tip guidewire.

Once the guidewire was coiled within the bladder, the angiographic catheter was removed and then reinserted into the urethra alongside the guidewire. Contrast medium was injected through this catheter to localize the position of the external sphincter. A clamp was placed externally in the surgical drapes to mark the position of the external sphincter fluoroscopically. The 5-French catheter was removed, and a balloon catheter 10 mm in diameter (Medi-tech, Inc., Watertown, MA) was positioned just in the urethra proximal to the external sphincter. The balloon was inflated to 5 atm (5.06×10^5 Pa) for 3 min. No discomfort was reported by the patient. Immediate voiding cystourethrography showed an inadequate increase in the diameter of the prostatic urethra. Consequently, the 10-mm balloon was replaced with a 20-mm urethroplasty balloon (Medi-tech, Watertown, MA), which was inflated twice to 5 atm for 3 min each time. The patient had a sensation of urgency during maximal inflation, but no pain. After removal of the balloon catheter, a 14-French Foley catheter was advanced into the bladder over the guidewire, and the guidewire was removed. The Foley catheter was left in place for 24 hr. Prophylactic antibiotics were continued for 48 hr.

Minimal, postprocedural hematuria cleared after 12 hr. Mild dysuria persisted for 48 hr. After removal of the Foley catheter, the patient had immediate improvement in terms of urgency, frequency, hesitancy, and nocturia. By 2 weeks, when the postprocedure edema had resolved and healing had taken place, all these symptoms had disappeared completely. Minimal dribbling continued but was significantly reduced.

In an effort to avoid any further trauma to the urethra, retrograde or voiding cystourethrograms were not obtained immediately, especially because this was the first human urethra to be dilated to these large diameters.

Voiding cystourethrograms obtained 1 and 6 months after dilatation showed persistent, undiminished improvement in the caliber of the prostatic urethra (Figs. 2 and 3). Surface-coil MR imaging at 1 and 6 months showed an enlarged prostate with homogeneous signal on both T1- and T2-weighted sequences in the sagittal and coronal planes. No masses or parenchymal or periprostatic abnormalities were identified.

Received January 15, 1987; accepted after revision March 11, 1987.

[1] All authors: Department of Radiology, University of Minnesota Hospital and Clinic, Minneapolis, MN 55455. Address reprint requests to K. Amplatz, Department of Radiology, Box 292 UMHC, University of Minnesota Hospital and Clinic, Harvard Street at East River Road, Minneapolis, MN 55455.

AJR 149:313–314, August 1987 0361–803X/87/1492–0313 © American Roentgen Ray Society

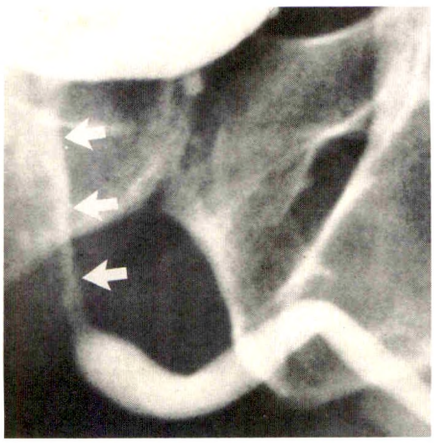


Fig. 1.—Voiding cystourethrogram shows marked narrowing and scalloping of prostatic urethra (*arrows*).

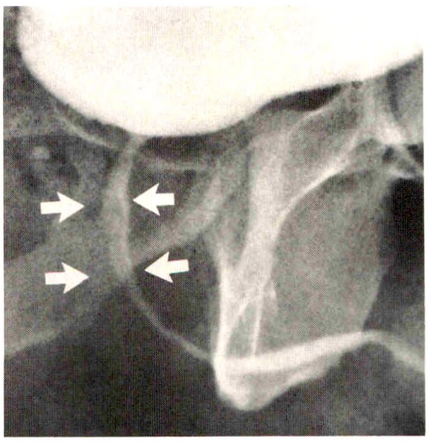


Fig. 2.—Voiding cystourethrogram obtained 3 months after dilatation shows widening of prostatic urethra (*arrows*) in comparison with predilatation width (Fig. 1).

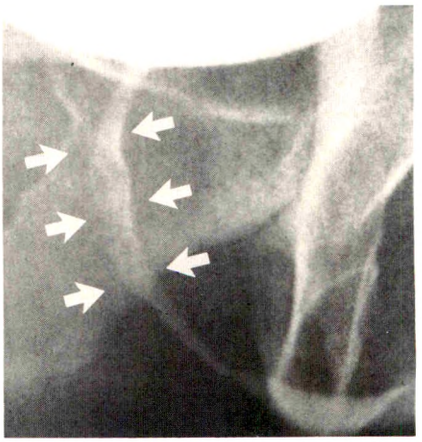


Fig. 3.—Voiding cystourethrogram obtained 6 months after balloon dilatation shows persistent widening of prostatic urethra at site of dilatation (*arrows*).

The patient has remained completely asymptomatic 11 months after the procedure, and voiding cystourethrography and MR imaging will be repeated at 1 year.

Discussion

The clinical and radiographic results obtained in this patient are encouraging. They suggest that the procedure is not traumatic and, if performed carefully, should be associated with few complications. This case suggests that even if the clinical improvement lasts only for a relatively short period, balloon-catheter dilatation can be repeated as needed.

This is the first case in which a human urethra was dilated to 20 mm; in the case reported by Burhenne et al. [2] dilatation was to 8 mm only. Our case highlights several important technical considerations. A careful retrograde urethrogram, obtained with the patient in the oblique position in which the dilatation will be performed, is important because it allows precise localization of the position of the external sphincter. Inadvertent dilatation of this structure could cause incontinence. Firm traction on the penis facilitates catheter manipulations in the urethra, but care must be taken to remember the position of the external sphincter. Dilatation of the bladder neck and internal sphincter, structures usually affected by benign prostatic hypertrophy, appears to be critical to the success of the procedure.

The 10- and 20-mm balloon catheters used for this procedure probably are unnecessarily small. Even though the animal studies [3] had suggested that 20 mm would be the smallest size that would produce a long-lasting effect, we decided to be cautious with the first patient. We used the balloons sequentially to determine the effects of dilatation on the patient. We now routinely use a 25-mm balloon catheter (Medi-tech, Watertown, MA) that is inflated for 10 min as a first step.

Hematuria, as seen in this case, also was seen in all the animal cases [3] and should clear within 24 hr. Dysuria also seems to be a minimal, transient postprocedural symptom.

Although the current surgical therapy for benign prostatic hypertrophy is associated with a relatively low morbidity and mortality, balloon-catheter dilatation promises to be safer. If its effects are long-lasting, percutaneous dilatation of the prostatic urethra could have a tremendous impact on the personal and social costs of treating this common problem. It can be performed on patients who are poor candidates for surgery, and it would be associated with minimal morbidity and no mortality. Balloon dilatation can be performed on an outpatient basis and by using only topical anesthesia. Therefore, it would be an appealing alternative to surgical treatment of benign prostatic hypertrophy.

REFERENCES

1. National Institute of Health, Education, and Welfare. Lower urinary tract diseases: obstruction. In: *Research needs in nephrology*, vol. 1. Washington, DC: US Government Printing Office, **1978**:19 (DHEW publication no. (NIH) 78-1481)
2. Burhenne HS, Chisholm RJ, Quenville NF. Prostatic hyperplasia radiological intervention. *Radiology* **1984**;152:655–657
3. Castaneda F, Lund G, Larson BW, et al. Experimental retrograde transurethral balloon dilatation of the prostate. Presented at the annual meeting of the Radiological Society of North America, Chicago, December **1986**

The Accuracy of CT in the Staging of Carcinoma of the Prostate

Joel F. Platt[1,2]
Robert L. Bree[1]
Richard E. Schwab[1,3]

Previous studies have reported the accuracy of CT in distinguishing stages of prostatic carcinoma, but they lack uniform surgical proof of histopathologic stage. We evaluated CT scans in 32 patients who underwent radical prostatectomy to assess its role in the preoperative staging of prostatic carcinoma. Two experienced radiologists blindly interpreted CT scans of the pelvis; they looked for evidence of tumor beyond the prostatic capsule and involvement of the seminal vesicles (stage C) or involvement of pelvic lymph nodes (stage D). Sixty-four interpretations in 32 patients yielded a specificity of 75% for predicting stages A or B disease (local disease), a sensitivity of 50% for the prediction of stages C or D, and an overall accuracy of staging of 67%. Interpretation errors were due to an inability to detect lymph node metastases, errors in evaluating the seminal vesicles, and errors in interpreting densities surrounding the prostate gland.

Our data suggest that CT should not be used to influence decisions concerning surgical vs nonsurgical treatment in patients with clinically staged local disease and is only useful when unsuspected metastatic nodal disease is detected.

Carcinoma of the prostate accounts for 20% of cancers in men and ranks as the third leading cause of cancer mortality. There are 90,000 new cases and 26,000 deaths each year due to prostatic carcinoma [1]. Accurate staging of newly diagnosed prostatic carcinoma is essential when deciding on appropriate therapy. Although no uniform treatment regimen exists, the proper decision requires distinguishing local from more extensive disease. Patients with localized tumor are often considered candidates for radical surgery, while those with more extensive involvement generally are treated with radiation or chemotherapy [2]. Digital rectal examination, serum levels of acid phosphatase, bone scans, and cystoscopy are often performed to assess the clinical stage, but are known to underestimate the true stage of disease [3–5]. CT can be used to assess the extent of tumor in patients considered to be surgical candidates. Previous CT studies have reported an overall accuracy of staging ranging from 47% to 75%, but in general these studies were limited by small numbers of patients and their reliance on clinical staging rather than staging based on histopathologic proof [6–10]. The purpose of the study was to assess the accuracy of preoperative staging of prostatic carcinoma by CT in patients in whom the actual stage of the tumor was subsequently verified by surgery.

Materials and Methods

Thirty-two consecutive patients with prostatic carcinoma diagnosed by biopsy who were scheduled for radical prostatectomy were evaluated by CT. Each patient was clinically staged as having local disease and was considered as a candidate for radical surgery. Clinical staging included physical examination and laboratory and bone scan results. CT results did not influence clinical stage. Most CT scans were performed on a Siemens DRIII scanner. Scan time was 3–4 sec with scans performed at 8-mm intervals from the iliac crest to the symphysis pubis. When possible, patients received 180 ml of IV contrast material either by bolus or by

Received January 30, 1987; accepted after revision April 14, 1987.

Presented at the annual meeting of the American Roentgen Ray Society, Washington, DC, April 1986.

[1] Department of Diagnostic Radiology, William Beaumont Hospital, 3601 W. 13 Mile Rd., Royal Oak, MI 48072. Address reprint requests to R. L. Bree.

[2] Present address: Department of Radiology, University of Michigan, Ann Arbor, MI 48109.

[3] Present address: Department of Radiology, Bay Pines Veterans Administration Hospital, Tampa, FL 33612.

AJR **149:315–318, August 1987**
0361–803X/87/1492–0315
© American Roentgen Ray Society

constant infusion using an automatic injector. All patients were given oral contrast material and contrast enemas before the CT examination. In each patient, proof of the stage of the disease was based on histologic study of the radical prostatectomy and pelvic lymphadenectomy specimens. Ten patients were found to have stage C or D disease, and 22 patients had histologic stage A or B.

Two experienced radiologists, unaware of the number of patients with each stage, blindly interpreted the CT scans retrospectively in an effort to stage the carcinoma. The following staging system was used: occult or nonpalpable cancer (stage A); cancer confined within the prostatic capsule (stage B); cancer extending locally beyond the capsule involving surrounding structures such as seminal vesicles, periprostatic fat, and urinary bladder (stage C); and distant metastases including nodal involvement (stage D).

Since both observers interpreted each examination in 32 patients, a total of 64 interpretations were available for analysis. Ten patients had invasive or metastatic prostatic carcinoma and 22 had local disease. Thus there were 20 positive and 44 negative interpretations that were considered correct.

An overall stage was then given to each examination. Criteria for local invasion included marked asymmetry of the periprostatic fat or seminal vesicles, distinct focal masses, obliteration of the seminal vesicle angle, or involvement of an adjacent structure such as the urinary bladder [6–8]. A lymph node was considered abnormal if it was 1.5 cm or more in diameter. The interpretations were then analyzed separately for the two observers and the disagreements were tabulated.

Results

The results of the CT evaluation of specific tumor invasion and overall accuracy of staging of prostatic carcinoma with CT are outlined in Table 1. In all instances, CT findings were compared with the histopathologic findings to determine the accuracy of CT. CT was least accurate in estimating the absence or presence of seminal vesicle invasion (58%). Three patients had proved seminal vesicle invasion; however, only one had abnormal findings suggested on CT by both observers (Figs. 1 and 2). In 23 observations, seminal vesicle involvement was suggested on the basis of the CT scans with no evidence of invasion on the surgical specimen (Fig. 3). Local invasion into periprostatic fat had somewhat better accuracy but still suffered from low specificity (60%) (Fig. 4). Of the individual parameters analyzed, CT was most accurate in the evaluation of lymph nodes largely because of a high specificity (96%). In the sole patient with a lymph node larger than 1.5 cm detected on CT, no tumor was found histopathologically (Fig. 5). Of the five patients with nodal metastases proved

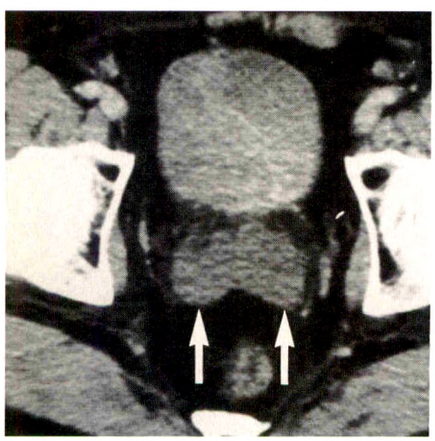
TABLE 1: Accuracy of CT in Detection of Invasive Prostate Cancer (32 Patients, 64 Observations)

	No. of Patients	Sensitivity[a] (%)	Specificity[b] (%)	Accuracy[c] (%)
Seminal vesicle invasion	3	33 (2/6)	60 (35/58)	58 (37/64)
Periprostatic fat invasion	8	75 (12/16)	60 (29/48)	64 (41/64)
Pelvic nodal metastases	5	0 (0/10)	96 (52/54)	81 (52/64)
Overall accuracy for invasive or metastatic cancer	10	50 (10/20)	75 (33/44)	67 (43/64)

[a] $\frac{\text{Number of positive observations}}{\text{Number of proved positive} \times 2} \times 100$

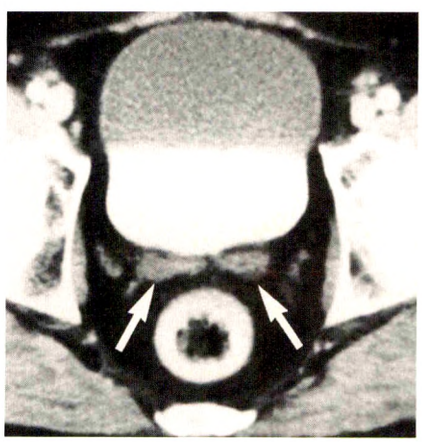
[b] $\frac{\text{Number of negative observations}}{\text{Number of proved negative} \times 2} \times 100$

[c] $\frac{\text{Number of correct observations}}{\text{Number of patients} \times 2} \times 100$



1

Fig. 1.—CT scan showing invasion of seminal vesicles by carcinoma of the prostate. Bilateral enlarged asymmetric seminal vesicles (*arrows*) in patient with pathologically proved seminal vesicle invasion.



2

Fig. 2.—CT scan that is false negative for seminal vesicle invasion by prostatic carcinoma. Seminal vesicles (*arrows*) appear normal. At surgery, tumor was found to be invading seminal vesicles.

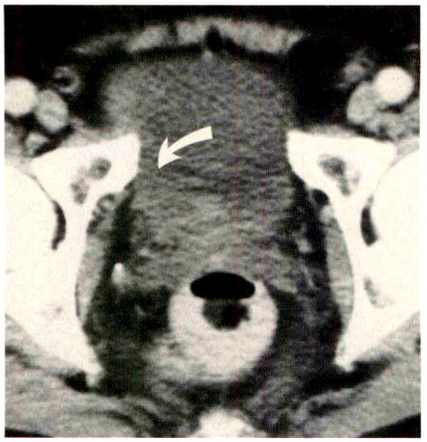


Fig. 3.—CT scan that is false positive for seminal vesicle invasion by prostatic carcinoma. Scan suggests extension of carcinoma to seminal vesicles with apparent obliteration of acute angle between bladder and right seminal vesicle (*arrow*) and asymmetric enlargement of right seminal vesicle. Surgical specimen revealed carcinoma confined to the prostate.

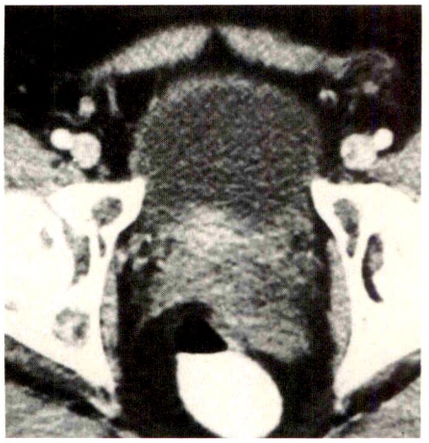


Fig. 4.—CT scan that is false positive for periprostatic invasion by carcinoma of the prostate. Scan reveals apparent extensive prostatic carcinoma in patient with pathologically proved local cancer and extensive changes of benign prostatic hypertrophy. Presence of benign disease mimicked local invasion.

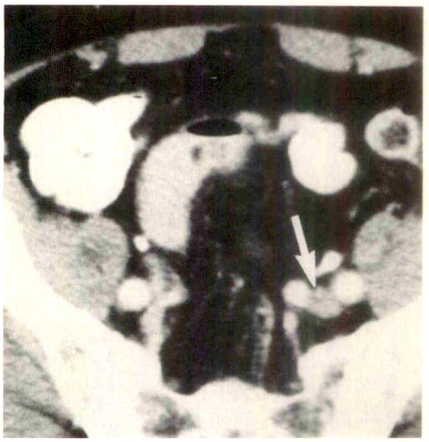


Fig. 5.—CT scan that is false positive for lymph node metastasis. Scan appears to show an enlarged pelvic lymph node (*arrow*). No evidence of nodal metastases was found during careful lymph node dissection before radical prostatectomy.

histologically, none had abnormalities detected by CT. CT, in general, exhibited a greater specificity for stages A–B lesions than sensitivity for the detection of C or D stage tumor. As seen in Table 1, some patients had more than one parameter determining the presence of metastases.

Between the two observers, there was total agreement in 23 (72%) of 32 patients. Of these 23, there were three false-negative and three false-positive interpretations by both observers. Three other patients were interpreted differently and incorrectly (stages B or C) by both observers, all of whom had positive lymph nodes not detected by CT, indicating stage D. Six patients (19%) had discordant interpretations, five of the six were stage B but were interpreted as stage C by at least one of the two observers.

Discussion

Accurate staging of biopsy-proved prostatic carcinoma is essential in deciding on an appropriate treatment plan and in determining prognosis. Patients with local disease are estimated to have a 5-year survival of 85%, while patients with more extensive carcinoma have a 5-year survival of 46% [1]. At least one-third of patients with newly diagnosed carcinoma of the prostate have stage C or D disease at the time of diagnosis [1]. Previous reports have discussed the ability of CT to evaluate the spread of prostatic carcinoma [7, 9–12]. This report analyzes the role of CT in preoperative staging of patients with clinically presumed local disease. Since clinical staging suffers from inaccuracy, a number of patients in this series were understaged preoperatively both clinically and with CT. This allowed us to compare our results with histopathologic proof rather than with presumed clinical stage. The presumed ability of CT to separate patients with stage A or B from those with stage C and D was tested in this study, since in most centers only patients with stages A or B undergo radical surgery. Radiation therapy is an alternative to surgical treatment of prostatic carcinoma and is useful in all stages, particularly in patients with high surgical risk factors. In these patients, CT can be used for therapy planning without absolute staging accuracy. CT detection of pelvic lymph node metastases from prostate carcinoma has been previously studied with a reported sensitivity range of 17–100% [2, 9–11, 13, 14]. Our low sensitivity for the detection of nodal metastases (0%) is similar to that reported in previous studies [7, 9, 11]. In our five patients with undetected nodal metastases, the pathologic studies generally revealed only small or microscopic foci of tumor within the involved pelvic lymph nodes, demonstrating once again that CT cannot identify nodal metastases unless there is gross nodal enlargement [13]. Our data suggest that patients with clinical stage A or B are more likely to have microscopic foci in the lymph nodes than to have bulky nodal disease, which is occasionally seen in patients with more extensive prostatic and periprostatic tumors.

The evaluation of the local extension of prostatic carcinoma to seminal vesicles and periprostatic fat has been less extensively studied than lymph node metastases. Previous reports have described an accuracy of 47–73% for detection of locally invasive prostatic carcinoma [7, 9]. Our overall accuracy was 61% for the detection of local extension. CT was less accurate in the detection of local extension than in the evaluation of pelvic nodal metastases because of the fewer false-positive interpretations.

Determination of seminal vesicle invasion is crucial because in addition to indicating stage C disease, it often coexists with microscopic nodal metastases suggesting an even worse

prognosis [5]. The results of seminal vesicle analysis in our study group were disappointing. Three patients had seminal vesicle invasion documented by surgery, despite being clinically staged as having local disease. CT revealed abnormalities consistent with invasion in only one of these patients, with the abnormal findings being detected by both observers. Of more concern were the 23 observations of CT seminal vesicle abnormalities in which no invasion was evidenced in the surgical specimen. These false-positive observations could lead to the exclusion of surgery as a treatment plan in the patient with localized prostatic carcinoma.

CT evaluation of periprostatic fat invasion was somewhat better than seminal vesicle analysis, with a sensitivity of 75%. As with seminal vesicle analysis, the specificity was only 60%, with numerous instances of suspected fat invasion on CT but with no abnormalities on the surgical specimen. In two patients, both observers detected findings consistent with invasion of the surrounding fat and seminal vesicles on CT indicative of stage C disease. Histopathologic correlation revealed the carcinoma to be entirely confined within the prostatic capsule. In both these patients the local carcinoma was associated with extensive changes of benign prostatic hypertrophy, and these marked benign changes may account for the false appearance of extensive cancer on CT (Fig. 4).

In our study, 31% of the patients had histopathologic proof of extensive prostatic carcinoma despite their being considered as surgical candidates with clinically localized disease. With CT, 33% of the patients could not be accurately staged, suggesting that there was no benefit to the patients from the CT. In 10 instances, CT correctly suggested stage C or D disease in patients clinically thought to have local carcinoma. In 11 other instances, CT incorrectly suggested extensive cancer in patients with clinically suspected and pathologically proved local carcinoma. As seen by the analysis of the individual observers, only 19% of the patients were staged differently by the two reviewers. This suggests that the individual parameters assessed do represent real interpretation dilemmas and that the high rate of false-positive findings in our series is a function of the CT examination itself and not of the individual observer.

Our results suggest that CT is not useful for determining the presence of local spread of prostatic carcinoma. We believe that CT should not be used to influence decisions concerning surgical vs nonsurgical treatment in patients with clinically staged local disease. CT is only useful when unsuspected metastatic nodal disease is detected, but often these patients have clinical evidence of advanced local disease and bony metastases.

REFERENCES

1. Silverberg E, Lubera J. Cancer statistics 1986. *CA* **1986**;36:9–25
2. Vick CW, Walsh JW. CT staging of pelvic neoplasms. *Appl Radiol* **1984**;13(5):74–84
3. Byar DP, Mostofi FK. Carcinoma of the prostate: prognostic evaluation of certain pathologic features in 208 radical prostatectomies examined by step section technique. *Cancer* **1972**;30:5–13
4. Yam LT. Clinical significance of the human acid phosphatase: a review. *Am J Med* **1974**;56:604–616
5. Lange PH, Narayan P. Understaging and undergrading of prostate cancer. *Urology* **1983**;21:113–118
6. Bonney WW, Chiu LC, Culp DA. Computed tomography of the pelvis. *J Urol* **1978**;120:457–464
7. Emory TH, Reinke DB, Hill AL, Lange PH. Use of CT to reduce understaging in prostatic cancer: comparison with conventional staging techniques. *AJR* **1983**;141:351–354
8. Seidelman FE, Reich NE, Cohen WN, Haagad R, Bryant PJ, Havrilla TR. Computed tomography of the seminal vesicles and seminal vesicle angle. *Comput Axial Tomogr* **1977**;1:281–284
9. Golimbu M, Morales P, Al-Askari S, Shulman Y. CAT scanning in staging of prostatic cancer. *Urology* **1981**;18:305–308
10. Lee JKT, Stanley RJ, Sagel SS, McClennan BL. Accuracy of CT in detecting intraabdominal and pelvic lymph node metastases from pelvic cancers. *AJR* **1978**;131:675–679
11. Morgan CL, Calkins RF, Cavalcanti EJ. Computed tomography in the evaluation, staging and therapy of carcinoma of the bladder and prostate. *Radiology* **1981**;140:751–761
12. Sawczuk IS, White RV, Gold RP, Olsson CA. Sensitivity of computed tomography in evaluation of pelvic lymph node metastases from carcinoma of bladder and prostate. *Urology* **1983**;21:81–84
13. Levine MS, Arger PH, Coleman BG, Mulhern CB, Pollack HM, Wein AJ. Detecting lymphatic metastases from prostatic carcinoma: superiority of CT. *AJR* **1981**;137:207–211
14. Weinerman PM, Arger PH, Coleman BG, Pollack HM, Banner MP, Wein AJ. Pelvic adenopathy from bladder and prostate carcinoma: detection by rapid-sequence computed tomography. *AJR* **1983**;140:95–99

Case Report

Control of Postoperative Vaginal Hemorrhage by Embolization of the Medial Circumflex Femoral Artery

Allan Odurny[1] and Ronald F. Colapinto

Hemorrhage from branches of the internal iliac artery after pelvic surgery is a potentially life-threatening complication. Ligation of the internal iliac artery is frequently unsuccessful because of the extensive collateral circulation to the pelvic organs. Angiography is being used increasingly to identify the source of hemorrhage and enable therapeutic embolization to be performed.

We report a case in which vaginal bleeding from collateral channels from the deep femoral artery persisted despite surgical ligation of one internal iliac artery and embolization of the other. Embolization of the medial circumflex branch of the deep femoral artery successfully controlled hemorrhage.

Case Report

A 41-year-old woman presented with vaginal bleeding 19 days after an uneventful abdominal hysterectomy for fibroids. Vaginal packing failed to control the hemorrhage. At reoperation, attempted suturing of bleeding points from the right uterine pedicle was unsuccessful and proximal ligation of the right internal iliac artery controlled the bleeding only temporarily. The patient was referred for angiography after receiving 10 units of packed RBCs and 2 units of fresh frozen plasma.

A pelvic arteriogram was obtained via a right common femoral artery puncture, confirming the ligation of the right internal iliac artery with retrograde filling of the vessel to the site of ligation (Figs. 1A and 1B). There was contrast extravasation from vaginal branches of the anterior division of the right internal iliac artery.

Selective catheterization of the left internal iliac artery did not show contrast extravasation. Embolization of the anterior division was performed because of the potential for collateral supply.

Another pelvic arteriogram confirmed occlusion of the left internal iliac artery but showed continued contrast extravasation, with the right internal iliac artery filling via deep femoral collaterals.

Selective catheterization of the medial circumflex branch confirmed this as the major vessel supplying the bleeding point (Fig. 1C). Angiography after embolization with ethanol and a steel coil confirmed that the bleeding had stopped (Fig. 1D). The patient tolerated the procedure satisfactorily.

No significant vaginal bleeding occurred after embolization. No ischemic symptoms attributable to embolization were apparent. The patient was discharged 19 days after embolization.

Discussion

Although surgical intervention is commonly performed to control intractable pelvic bleeding, it is often unsuccessful, and ligation of the internal iliac artery is then the only procedure possible [1]. Furthermore, surgery may release the tamponading effect of a pelvic hematoma and result in further deterioration in an unstable patient [2].

After internal iliac artery ligation an extensive collateral circulation develops from the aorta and ipsilateral external iliac and femoral arteries. After unilateral or bilateral proximal ligation of the internal iliac arteries, blood flow in the distal portion decreases only by about 50% [3]. These findings may explain the low success rate of surgical ligation.

Percutaneous embolization for the control of pelvic bleeding has been used as an alternative treatment. Its use in controlling hemorrhage during the postpartum period, after trauma, and from pelvic malignancy is well documented [2, 4, 5]. Its use in postoperative vaginal bleeding has been reported [6].

Distal embolization occludes vessels proximal to the terminal arterioles, resulting in more effective control of bleeding than proximal embolization or ligation, which preserves potential collateral pathways [4]. Surgical ligation will also pre-

Received February 2, 1987; accepted after revision March 27, 1987.

[1] Both authors: Department of Radiological Sciences, Toronto General Hospital, 200 Elizabeth St., Toronto, Ontario M5G 2C4, Canada. Address reprint requests to R. F. Colapinto.

AJR **149:319–320, August 1987** 0361–803X/87/1492–0319 © American Roentgen Ray Society

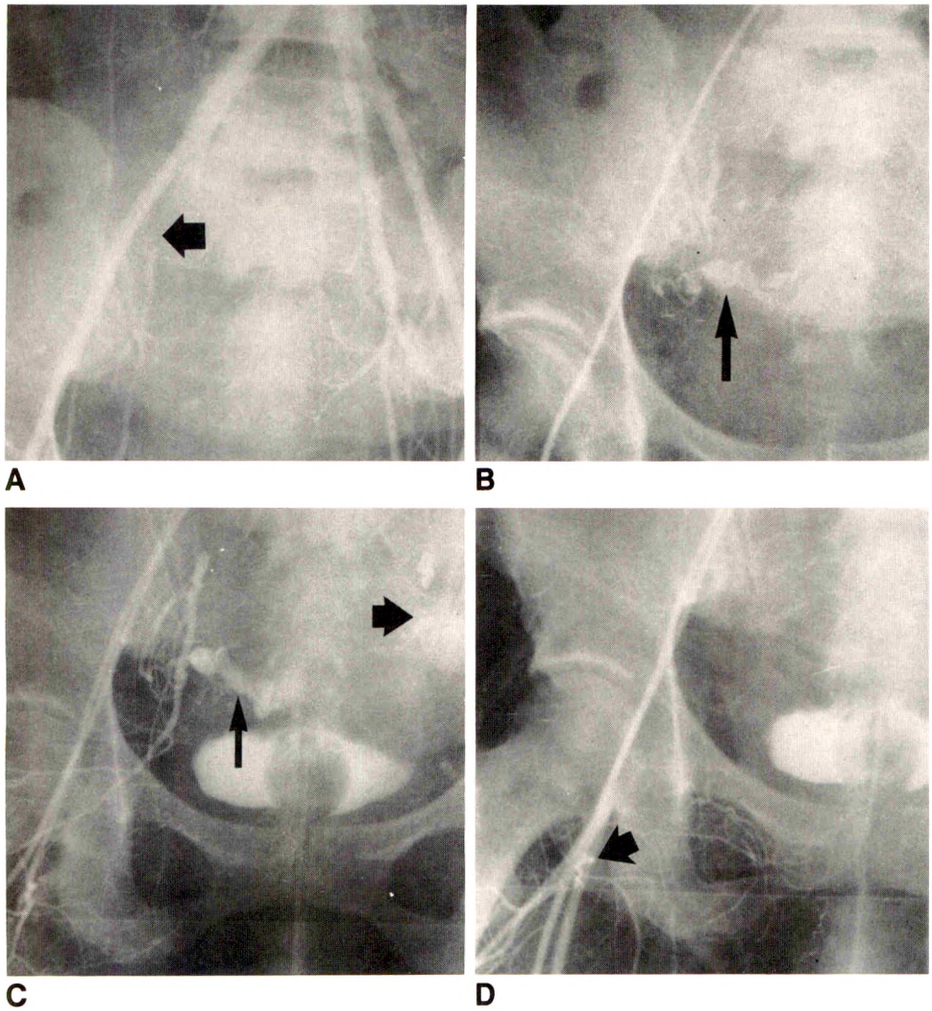


Fig. 1.—*A*, Pelvic arteriogram shows retrograde filling of right internal iliac artery to site of surgical ligation (*arrow*).

***B*, Late film shows contrast extravasation from vaginal branches of internal iliac artery (*arrow*).**

***C*, Selective injection of right medial circumflex femoral artery shows persistent extravasation of contrast material (*long arrow*). Note coils in occluded anterior division of left internal iliac artery (*short arrow*).**

***D*, Angiogram after embolization shows cessation of bleeding with medial circumflex femoral artery occluded by coil (*arrow*).**

vent subsequent embolization of the internal iliac artery, necessitating more difficult embolization of collaterals. This is well illustrated by the case presented.

Collaterals tend to develop along pathways from the aorta, and external iliac and femoral vessels to branches of the internal iliac artery. There is little collateral flow across the midline [2]. This is illustrated in our case, in which ipsilateral deep femoral collaterals supplied the bleeding point after embolization of the contralateral internal iliac artery failed to control hemorrhage.

To our knowledge, this is the first report of a case in which embolization of the medial circumflex femoral artery was used to control postoperative bleeding. Heaston et al. [7] reported a case of postpartum vaginal bleeding controlled by embolization of the same vessel. In their case, bilateral internal iliac artery ligation had also been performed, with the bleeding point being supplied by deep femoral collaterals from the ipsilateral side.

We suggest that, after internal iliac ligation, the contralateral femoral artery should be punctured, since the collaterals that develop are likely to arise from the same side as the bleeding point and are more easily embolized from a contralateral puncture.

Complications related to internal iliac artery embolization are rare [8]. However, embolization of collateral branches after bilateral internal iliac occlusion increases the risk of ischemic sequelae. The risk is particularly high in those with impaired inferior mesenteric arterial circulation. Embolization of internal iliac collaterals may produce rectal ischemia. Although not usually a problem in the younger patient, in the elderly it is important to confirm patency of the inferior mesenteric artery before embolization.

REFERENCES

1. Fahmy K. Internal iliac artery ligation and its efficiency in controlling pelvic hemorrhage. *Int Surg* **1969**;51:244–250
2. Ring EJ, Athanasoulis C, Waltman AC, Margolies MN, Baum S. Arteriographic management of hemorrhage following pelvic fracture. *Radiology* **1973**;109:65–70
3. Burchell RC. Physiology of internal iliac artery ligation. *Br J Obstet Gynaecol* **1968**;75:642–651
4. Lang EK. Transcatheter embolization of pelvic vessels for control of intractable hemorrhage. *Radiology* **1981**;140:331–339
5. Pais SO, Glickman M, Schwartz P, Pingoud E, Berkowitz R. Embolization of pelvic arteries for control of postpartum hemorrhage. *Obstet Gynecol* **1979**;55:754–758
6. Rosenthal DM, Colapinto RF. Angiographic arterial embolization in the management of postoperative vaginal hemorrhage. *Am J Obstet Gynecol* **1985**;151:227–231
7. Heaston DK, Mineau DE, Brown BJ, Miller FJ. Transcatheter arterial embolization for control of persistent massive puerperal hemorrhage after bilateral surgical hypogastric artery ligation. *AJR* **1979**;133:152–154
8. Hare WS, Holland DJ. Paresis following internal iliac artery embolization. *Radiology* **1983**;146:47–51

Case Report

Duplex Doppler Evaluation of Puerperal Ovarian Vein Thrombosis

Gregory W. Baran[1] and Kay M. Frisch

Puerperal ovarian vein thrombosis is a potentially life-threatening condition that requires prompt medical treatment. Despite the estimated frequency of 1 (0.17%) in 600 cases [1], only 71 cases have been reported in the literature [1–8]. The diagnosis of ovarian vein thrombosis by surgery, CT scanning, sonography, and MR imaging has been described previously [3–7]. We wish to present the use of pulsed duplex Doppler examinations in the evaluation of this syndrome.

Case Report

A 27-year-old gravida 2 para 1 woman with a viable 32-week twin gestation was admitted because of premature labor and vaginal spotting. She was treated unsuccessfully with tocolytics, and on the fourth hospital day a partial placenta abruptio developed. A low transverse cesarean delivery was performed; the estimated blood loss was 1000 ml. Postoperatively, the patient's hemoglobin was 9.1 g/dl, and she received a transfusion of packed RBCs. Leukocytosis was documented on the day of admission and continued throughout the patient's hospital stay. Two days postpartum, the patient experienced chills, spiking fever, and vague abdominal pain. Cultures of blood, endocervical, and urine specimens were negative. The patient was given IV heparin and antibiotic therapy. A pelvic sonogram performed 5 days postpartum showed an enlarged uterus with air in the endometrial canal and a right adnexal mass (Fig. 1). A CT scan of the abdomen confirmed the sonographic findings and showed a retroperitoneal inflammatory mass with the suggestion of thrombus formation in the inferior vena cava. Pulsed duplex Doppler studies (3-MHz ATL Ultramark 8, Bothell, WA) and real-time sonography (Toshiba SAL 77A, Tustin, CA) of the inferior vena cava and right ovarian vein, with the patient in the left posterior oblique position, showed a dilated, thrombus-filled right ovarian vein extending from the adnexal mass to the inferior vena cava (Fig. 2). Thrombus formation also was noted within the inferior vena cava at the origin of the right ovarian vein. Doppler examination of the right ovarian vein showed no demonstrable flow (Fig. 3, top image). Normal flow with characteristic respiratory variation was documented within the inferior vena cava above and below the thrombus formation. The findings of duplex Doppler examination of the right renal and femoral veins were normal. A sonogram obtained 4 weeks after treatment was begun showed complete resolution of the thrombus formation within the right ovarian vein and inferior vena cava. Normal flow spectra were seen in both structures (Fig. 3, bottom image).

Discussion

Puerperal ovarian vein thrombosis is heralded by abdominal pain and fever, which usually commence 1 to 4 days postpartum. The abdominal pain is usually right-sided and may radiate to the flank or groin. Direct abdominal tenderness usually is found on abdominal palpation. The most reliable physical finding is a ropelike mass felt in the right lower abdominal quadrant. The right-sided nature of this disorder occurs as a result of antegrade flow in a distended venous system that propagates the infectious process upward into the right ovarian vein [1, 8]. Leukocytosis is common in this syndrome.

The underlying causes of puerperal ovarian vein thrombosis are venostasis, a hypercoagulable state in pregnancy, and an underlying infection that either precipitates or accentuates the phlebitic process. The ovarian veins distend from a diameter

Received February 9, 1987; accepted after revision March 17, 1987.
[1] Both authors: Department of Radiology, Hackley Hospital, 1700 Clinton St., Muskegon, MI 49442-5592. Address reprint requests to G. W. Baran.

AJR 149:321–322, August 1987 0361–803X/87/1492–0321 © American Roentgen Ray Society

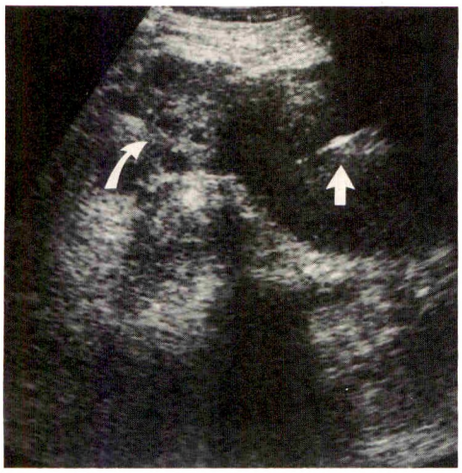


Fig. 1.—Transverse pelvic sonogram shows air within the endometrial canal (*straight arrow*) consistent with endometritis and a right adnexal mass (*curved arrow*).

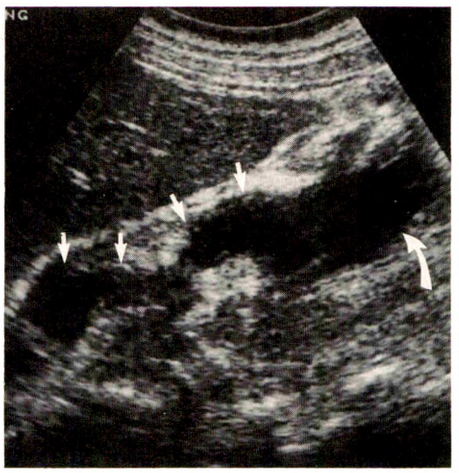


Fig. 2.—Sagittal sonogram shows a completely thrombosed right ovarian vein (*small arrows*) extending superiorly from right adnexa (*curved arrow*).

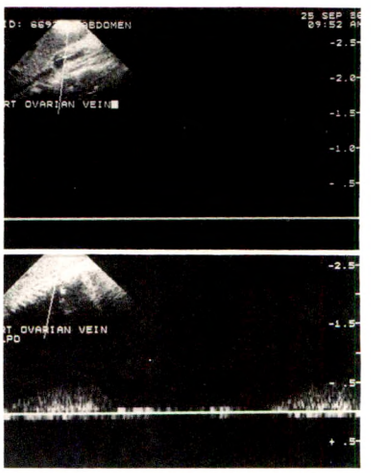


Fig. 3.—Pulsed duplex Doppler images show no demonstrable flow in the right ovarian vein (*top image*) and reestablished flow 4 weeks after clinical treatment (*bottom image*).

of 9 mm to a mean diameter of 26 mm during pregnancy. The veins collapse during parturition, and venostasis develops [2]. Failure to identify a causative organism, as in our case, is not uncommon [1, 8]. Endometritis occurs in approximately 23–45% of patients with ovarian vein thrombosis and usually precedes the clinical symptoms by 1 day [1].

A prompt noninvasive diagnosis is essential because pulmonary thromboembolism is the second leading cause of death in the postpartum period, and surgical mortality is approximately 16% [8]. Sonography, CT, and, recently, MR imaging [6] have proved useful in the noninvasive diagnosis of this syndrome. Pulsed duplex Doppler examination offers some distinct advantages when compared with MR imaging and CT. The equipment for a duplex Doppler study is portable, allowing bedside examination; is less expensive; and requires no contrast material. Moreover, venous structures such as the renal and femoral veins can be examined for thrombus formation. Overlying bowel gas is the major hindrance in visualizing the inferior vena cava and right ovarian vein, but by placing the patient in the left posterior oblique position, an acoustic window for evaluation of this area can be created.

REFERENCES

1. Brown TK, Munsick RA. Puerperal ovarian vein thrombophlebitis: a syndrome. *Am J Obstet Gynecol* **1971**;109:263–273
2. Maull KI, van Nagell JR, Greenfield LJ. Surgical implications of ovarian vein thrombosis. *Am Surg* **1978**;44:727–733
3. Shaffer PB, Johnson JC, Bryan D. Diagnosis of ovarian vein thrombophlebitis by computed tomography. *J Comput Assist Tomogr* **1981**;5:436–439
4. Angel JL, Knuppel RA. Computed tomography in diagnosis of puerperal ovarian vein thrombosis. *Obstet Gynecol* **1984**;63:61–64
5. Wilson PC, Lerner RM. Diagnosis of ovarian vein thrombophlebitis by ultrasonography. *J Ultrasound* **1983**;2:187–190
6. Martin B, Mulopulos GP, Bryan PJ. MRI of puerperal ovarian-vein thrombosis. *AJR* **1986**;147:291–292
7. Rubio PA, Farrell EM, Del Castillo H. Postpartum thrombophlebitis of the ovarian vein. *South Med J* **1979**;72:356–358
8. Munsick RA, Gillanders LA. A review of the syndrome of puerperal ovarian vein thrombophlebitis. *Obstet Gynecol Surv* **1981**;36:57–66

Vertebral Erosions in Patients Undergoing Maintenance Hemodialysis for Chronic Renal Failure

Murali Sundaram[1]
Robert Seelig
David Pohl

Unlike articular erosions in the appendicular skeleton, the frequency, appearance, and clinical relevance of vertebral erosions in azotemic osteodystrophy are not known. Lateral vertebral radiographs of 118 patients on maintenance hemodialysis were reviewed to assess the frequency, distribution, and rate of progression of vertebral erosions. Thirty (25%) of 118 patients showed a superficial corner erosion resembling the so-called Romanus lesion of ankylosing spondylitis. Their presence, whether at a single level or at multiple levels, did not correlate with erosive changes in the phalanges or sacroiliac joints that are known to occur in renal osteodystrophy. Vertebral erosions may progress slowly with time, but seem to have limited bearing on clinical symptoms. In two patients, however, the radiographic changes progressed dramatically, simulating an infection. Biopsy and surgical intervention were considered but not carried out because one patient declined and in the other an infected graft was identified as the source of infection. Both patients had negative scintiscans, and their subsequent clinical courses excluded infectious spondylitis.

Vertebral erosions in patients on maintenance hemodialysis are frequent, and there appears to be a spectrum of changes from superficial erosions to large resorptive defects. Further diagnostic evaluation of these erosive changes appears to be warranted only rarely.

Articular erosions are noted frequently on radiographs in patients with azotemic osteodystrophy, in both small and large bones of the appendicular skeleton [1, 2]. Ten years ago, a study of a cadaver with azotemic osteodystrophy demonstrated extensive subchondral bony resorption in the axial skeleton including the vertebrae, sternoclavicular joints, sacroiliac joints, and symphysis pubis [3]. More recently, there have been reports describing a destructive-appearing spondyloarthropathy in patients on maintenance hemodialysis [4, 5]. The primary objectives of this study were to assess the frequency and clinical relevance of vertebral erosions in patients on maintenance hemodialysis, to determine whether their presence correlated with the widely known phalangeal and sacroiliac erosive changes, and to describe the spectrum of vertebral changes from early erosions to the more aggressive resorptive changes.

Subjects and Methods

A total of 118 radiographs of the dorsolumbar vertebral column of patients in chronic renal failure and on maintenance hemodialysis were retrospectively reviewed. These radiographs were from skeletal surveys, when such surveys were routinely obtained on uremic patients on dialysis. Sequential radiographs were available in about 60% of these patients, and the time interval between skeletal surveys ranged from 3 months to 18 years. Only two patients were prospectively evaluated by scintigraphy and CT because of symptoms and radiographic abnormalities. The patients' ages ranged from 32 to 78 years, with the duration of dialysis ranging from 1 to 15 years. This patient population was drawn from two institutions, and the review was carried out by two radiologists independently, each one limiting his review to

Received January 20, 1987; accepted after revision April 8, 1987.

[1] All authors: Department of Radiology, St. Louis University Medical Center, 1325 S. Grand Blvd., St. Louis, MO 63104. Address reprint requests to M. Sundaram.

AJR 149:323–327, August 1987
0361–803X/87/1492–0323
© American Roentgen Ray Society

patients from his respective institution. There were five patients in this group with lateral radiographs of the cervical vertebrae.

The radiographs were examined for the presence of erosions. Patients with spondylotic changes were excluded. Radiographs with positive findings were then matched for age and gender with controls and subsequently reviewed by a third radiologist who was unaware of the findings of the other two. Independent agreement on the presence of erosion by both observers constituted a positive finding. Disagreement, equivocation, and suboptimal radiographs for the purpose of this study were considered negative for erosions. Medical records and radiographs of patients with erosions were reviewed to exclude a seronegative spondyloarthropathy.

Pelvic and hand radiographs of patients with positive erosive vertebral changes were then examined for sacroiliac and phalangeal and wrist erosions. During the course of this study, one of the patients in the positive group presented as a problem of clinical management because of the extent of vertebral destruction, while another patient (not in the previously reviewed group) rapidly developed progressive vertebral resorption.

Results

Erosions at the anterosuperior or anteroinferior margins of the vertebral bodies were the most frequently encountered abnormality. Thirty patients showed such erosions. In 29 of these patients the abnormality occurred in the dorsal or lumbar vertebral column (Fig. 1), and in one patient it was in the cervical vertebral column. Erosions at a single level, all limited to the lumbar vertebrae, were found in three patients. The other 27 showed erosions at multiple levels.

Multiple erosions in the lower thoracic vertebral column were seen in nine patients. Twelve patients showed multiple erosions in the thoracic and lumbar vertebral column, and one of these 12 patients had an erosion in the cervical vertebral column. Six patients showed more than one erosion limited to the lumbar vertebrae. All patients with erosions had been on maintenance hemodialysis for at least 3 years. On review of radiographs and medical records, there was no evidence that any of these patients had a seronegative spondyloarthropathy. There was poor correlation between the presence of vertebral erosions and sacroiliac and phalangeal erosions of uremic osteodystrophy; three patients had sacroiliac changes and three had phalangeal changes. Neither of the two patients with the large destructive or resorptive vertebral lesions had any predisposing disease to explain these changes on the basis of a neuroarthropathy.

Only two of the 118 patients showed large, destructive, aggressive-appearing resorptive changes of the vertebrae (Figs. 2 and 3). These two patients had CT scans and scintigraphy that excluded an abscess and infection, respectively. Although biopsy and surgery were considered, neither of these options was performed on either patient. One patient declined any form of interventional procedure and is mobile with the help of a walker. In the other patient (Fig. 3), an infected vascular graft was identified and replaced. Clinical follow-up has not revealed an infectious spondylitis in either of these patients. The precise cause and mechanism that results in these large resorptive vertebral lesions remains uncertain.

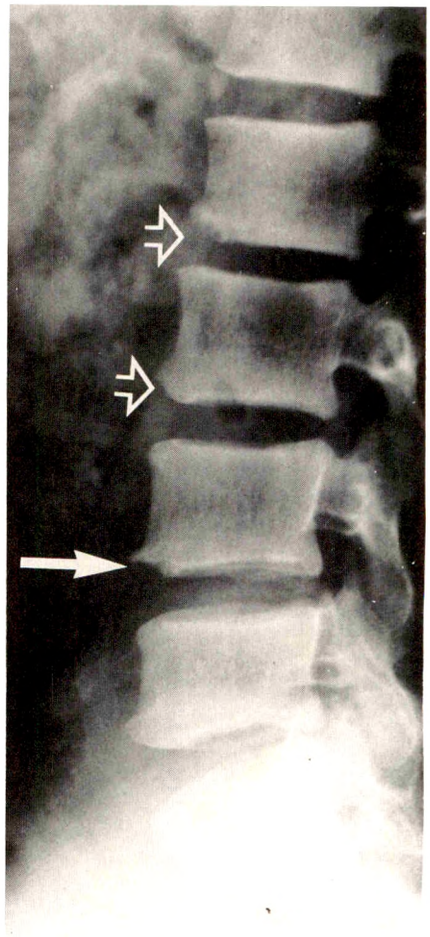


Fig. 1.—Erosions of L2, L3, and L4 resembling enthesopathy of early ankylosing spondylitis. L2 and L3 show minimal cortical resorption (*open arrows*), while at L4 there is an accompanying bony excrescence resembling an early syndesmophyte (*solid arrow*). All vertebrae show varying degrees of the "rugger-jersey" appearance of renal osteodystrophy.

Discussion

This study was undertaken because we were impressed with the resemblance between the erosions at the anterior corners of the vertebral bodies and the erosive precursor of the bony syndesmophyte in ankylosing spondylitis (Fig. 1). This latter lesion has been referred to as the Romanus lesion [6]. The small corner erosions (Figs. 1 and 2) are not significant clinically, except that they could be mistaken for early erosions of ankylosing spondylitis. None of our patients had any evidence of a coexisting seronegative spondyloarthropathy. The erosions in our patients mostly occurred in multiple vertebral bodies but were also found, less commonly, as solitary abnormalities. These lesions were either slowly progressive or not progressive at all, and an increase in the size

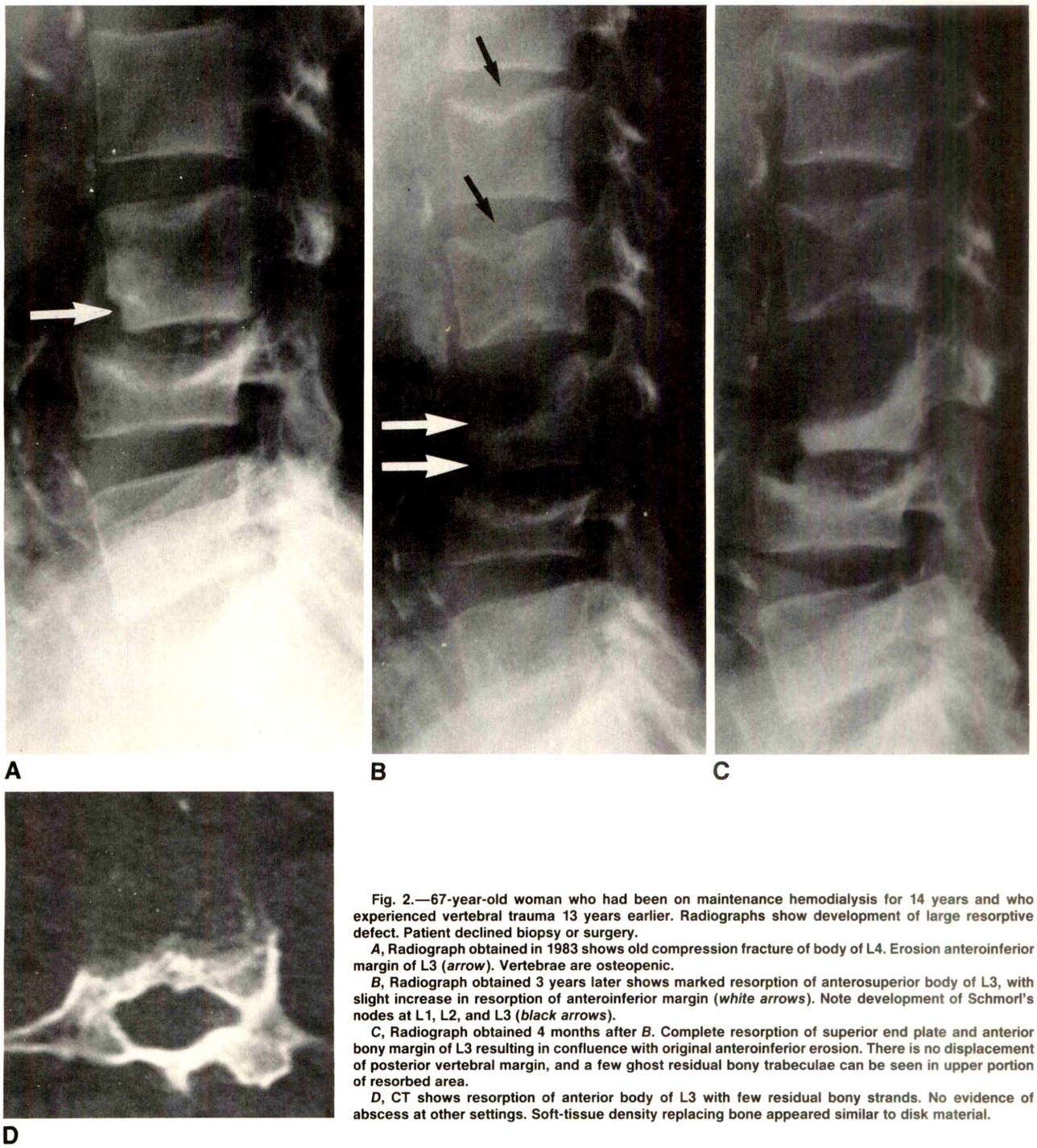


Fig. 2.—67-year-old woman who had been on maintenance hemodialysis for 14 years and who experienced vertebral trauma 13 years earlier. Radiographs show development of large resorptive defect. Patient declined biopsy or surgery.

***A*, Radiograph obtained in 1983 shows old compression fracture of body of L4. Erosion anteroinferior margin of L3 (*arrow*). Vertebrae are osteopenic.**

***B*, Radiograph obtained 3 years later shows marked resorption of anterosuperior body of L3, with slight increase in resorption of anteroinferior margin (*white arrows*). Note development of Schmorl's nodes at L1, L2, and L3 (*black arrows*).**

***C*, Radiograph obtained 4 months after *B*. Complete resorption of superior end plate and anterior bony margin of L3 resulting in confluence with original anteroinferior erosion. There is no displacement of posterior vertebral margin, and a few ghost residual bony trabeculae can be seen in upper portion of resorbed area.**

***D*, CT shows resorption of anterior body of L3 with few residual bony strands. No evidence of abscess at other settings. Soft-tissue density replacing bone appeared similar to disk material.**

of the erosions usually was observed over a period of years (Figs. 2A and 2B). Our estimate of the frequency of these erosions is conservative because we excluded cases in which two observers did not independently agree on their presence and also because of a lack of follow-up skeletal surveys on several patients. Cervical vertebral column involvement may represent an underestimation because of the few cervical X-rays available in this study. There was no correlation between

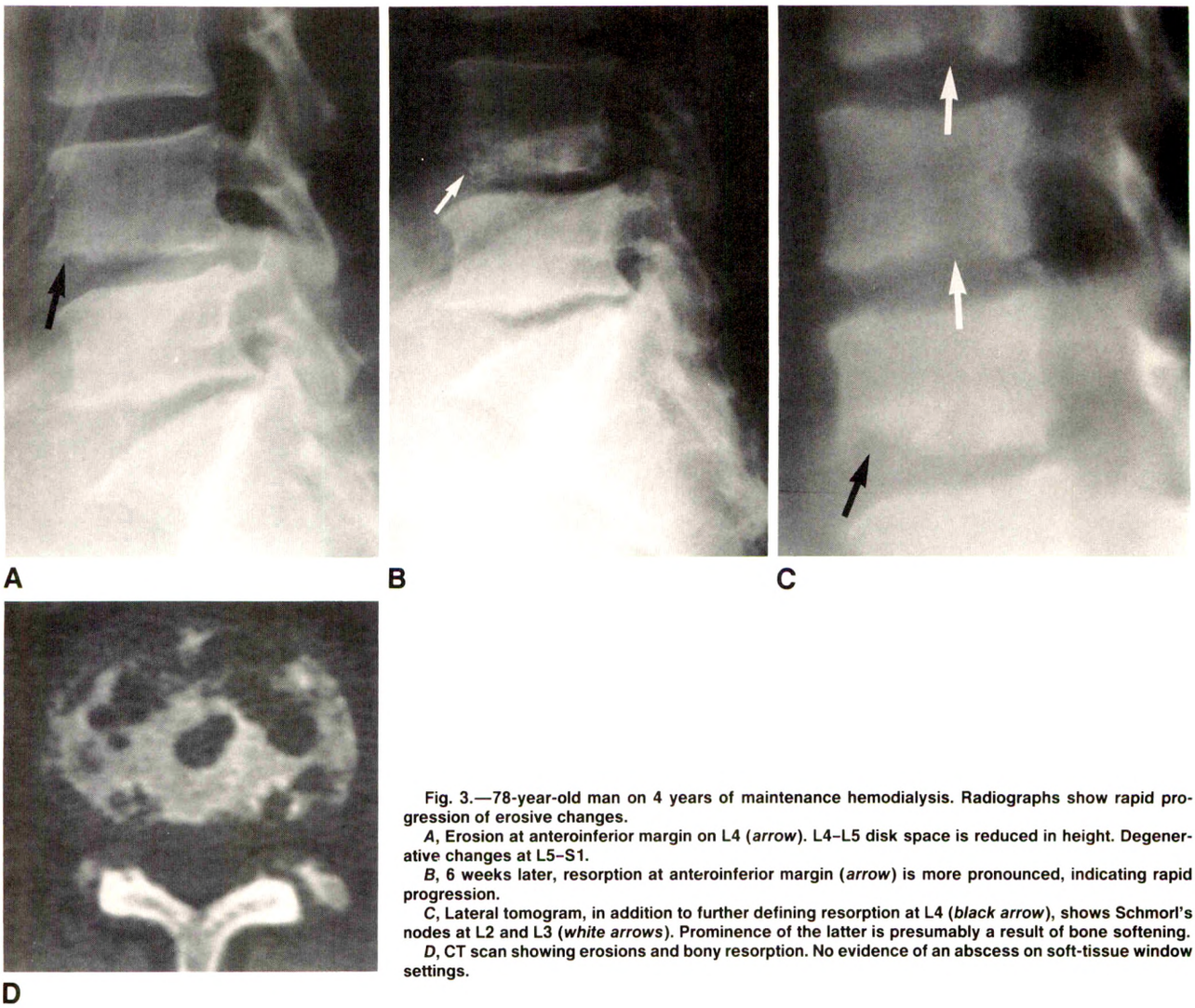


Fig. 3.—78-year-old man on 4 years of maintenance hemodialysis. Radiographs show rapid progression of erosive changes.

A, Erosion at anteroinferior margin on L4 (*arrow*). L4–L5 disk space is reduced in height. Degenerative changes at L5–S1.

B, 6 weeks later, resorption at anteroinferior margin (*arrow*) is more pronounced, indicating rapid progression.

C, Lateral tomogram, in addition to further defining resorption at L4 (*black arrow*), shows Schmorl's nodes at L2 and L3 (*white arrows*). Prominence of the latter is presumably a result of bone softening.

D, CT scan showing erosions and bony resorption. No evidence of an abscess on soft-tissue window settings.

the presence of vertebral erosions and phalangeal signs of azotemic osteodystrophy. Vertebral erosions were not seen in any patient who had been on maintenance hemodialysis for less than 3 years. It would appear that these erosions are a result of the sustained uremic state and represent a further skeletal manifestation of azotemic osteodystrophy and maintenance hemodialysis.

Most patients with chronic renal failure on maintenance hemodialysis have histologic evidence of varying degrees of hyperparathyroidism, osteomalacia, and osteoporosis [7]. It is virtually impossible to determine which of these components is most responsible for this appearance, and thus the cause would have to be considered multifactorial. Other workers have shown histologically that these erosions in the axial and appendicular skeleton are a result of subchondral bony resorption and have postulated that they may represent a collapse of softened subchondral bone [3, 8].

Of particular interest were the two patients who showed advanced resorptive vertebral changes (Figs. 2 and 3). Figure 2 shows resorptive changes in the lumbar vertebral body occurring over several years. The CT scan of this patient showed no evidence of a mass. The patient declined any form of interventional procedure and remains mobile with a walker. The patient illustrated in Figure 3 was the only case in which the resorptive changes were rapid, developing over a period of a few weeks. The rapidity of the radiographic changes in the presence of a low-grade fever suggested an underlying infectious spondylitis. Further examination revealed infection in a pseudoaneurysm of a bovine graft that was successfully treated. No specific treatment was directed toward the vertebral abnormality in view of the negative scintiscan and CT appearances. This patient remains free of symptoms. The radiographs of these two patients resemble reports of destructive spondyloarthropathy in hemodialyzed patients [4,

5]. Since crystal deposits have been identified in two of the previously reported 14 cases, the possibility that this destructive change was crystal induced has been suggested [4, 5]. On the basis of one case, hydroxyapatite rather than calcium pyrophosphate dihydrate was suggested as the cause [4]. The other study showed, in a single case, the presence of calcium pyrophosphate dihydrate crystals [5] in the destructive lesion. The underlying causes for the remaining 12 cases and the two reported in this paper remain speculative. We do not know if these changes represent the extreme end of the spectrum of vertebral uremic osteodystrophy and bone softening, or if they are due to amyloid or iron deposition (as has been reported in other joints) [9, 10], or if they are indeed a crystal-induced process. The most immediate remediable concern is that an infectious process is present. However, in none of the cases reported so far has an infectious etiology been identified. Thus, despite the radiographic appearances, there is a place for clinical observation, especially when scintiscans and CT do not suggest the presence of infection (Figs. 2 and 3). In neither of our patients did scintiscans suggest infection. The greater concern may be the eventual need for surgery to provide mechanical support for the disintegrating vertebrae. We are unaware that cord compression has been reported as a complication of azotemic osteodystrophy, although this has been reported in primary hyperparathyroidism [11].

In summary, there is a spectrum of erosive vertebral changes in patients on maintenance hemodialysis. Most frequently encountered are erosions at the anterosuperior and anteroinferior margin of the vertebral bodies. These erosions, reminiscent of the Romanus lesion of ankylosing spondylitis, are common, may progress slowly, and do not warrant further investigation. Extensive resorptive vertebral changes that may develop either slowly or rapidly may be seen. These patients must be observed for the presence of an underlying infectious process, although such a process has not yet been confirmed. This extreme form of vertebral resorption may be due simply to uremic osteodystrophy and prolonged maintenance hemodialysis rather than to any single complicating factor.

ACKNOWLEDGMENT

We most gratefully acknowledge the considerable secretarial assistance provided by Ann Smith.

REFERENCES

1. Sundaram M, Wolverson MK, Heiberg E, Grider RD. Erosive azotemic osteodystrophy. *AJR* **1981**;136:363–367
2. Bonavita JA, Dalinka MK. Shoulder erosions in renal osteodystrophy. *Skeletal Radiol* **1980**;5:105–108
3. Resnick D, Niwayama G. Subchondral resorption of bone in renal osteodystrophy. *Radiology* **1976**;118:315–321
4. Kuntz D, Nareau B, Bardin T, Doueke T, Treves R, Dryll A. Destructive spondyloarthropathy in hemodialyzed patients. *Arthritis Rheum* **1984**;27:369–375
5. Kaplan P, Resnick D, Murphey M, et al. Destructive noninfectious spondyloarthropathy in hemodialysis patients: a report of four cases. *Radiology* **1987**;162:241–244
6. Romanus R, Yden S. Destructive and ossifying spondylitic changes in rheumatoid ankylosing spondylitis. *Acta Orthop Scand* **1952**;22:88–99
7. Parfitt AM. Clinical and radiographic manifestations of renal osteodystrophy. In: David DS, ed. *Calcium metabolism in renal failure and nephrolithiasis*. New York: Wiley, **1977**:145–195
8. Bywaters EGL, Dixon ASG, Scott JT. Joint lesions of hyperparathyroidism. *Ann Rheum Dis* **1963**;22:171–187
9. Huaux JB, Noel H, Malghem J, Maldague B, Devogelar JP, Deuxchaisnes CN. Erosive azotemic osteoarthropathy: possible role of amyloidosis. *Arthritis Rheum* **1985**;28:1075–1076
10. Cary NRB, Sethi D, Brown EA, Erhardt CC, Woodrow DF, Gower PE. Dialysis arthropathy: amyloid or iron? *Br Med J* **1986**;293:1392–1394
11. Sundaram M, Scholz C. Primary hyperparathyroidism presenting with acute paraplegia. *AJR* **1977**;128:674–676

Book Review

The Radiology of Joint Disease, Vol. 2., 3rd ed. By D. M. Forrester and J. C. Brown. Philadelphia: Saunders, 576 pp., 1987. $60

This is the third edition of a monograph on the radiologic aspects of joint diseases. John W. Nesson, a coauthor on the previous two editions, is no longer associated with the book. This reviewer has had the opportunity to use the first edition of the book as a resident and the second edition in subsequent years in the daily practice of skeletal radiology. The third edition incorporates changes in terminology and technology, especially advanced imaging techniques and their use in the diagnosis of arthritis. Although the third edition is 58 pages shorter than its predecessor, it has 18 additional illustrations. The basic size of the text remains the same, as does the content (using the newer accepted terminology). This economy of size is the result of a different size print which makes the text, tables, and illustrations much easier to read. The book has basically kept the same format as its two predecessors. There are 11 chapters contained in three separate sections. Section I, "The ABC's of Arthritis: The Hand," has individual chapters on abnormalities of alignment, bony mineralization, cartilage space, and soft tissues. Section II, "Arthritis from Head to Foot," reviews the radiologic features of arthritis in each of the joints exclusive of the hand. Section III, "Clinical Approach to Arthritis," contains a single chapter on the differential diagnosis of arthritis. Each section has several pages devoted to introductory material followed by the individual chapters. The chapters are easy to read and each is well referenced with appropriate and relatively up-to-date references.

The general format of each chapter is to initially discuss the ABC's for that particular joint and then go into the various alterations produced by specific diseases. This approach, successful in the previous two editions, has been maintained. Thus the overall approach is to deal with an analysis of radiographs in relation to the alteration each disease produces. This may offend some individuals who want to read about a specific disease such as rheumatoid arthritis. However, since patients rarely come labeled with their disease, the authors' approach is a sound one and is geared toward the practicing radiologist who, upon being confronted with a patient with an erosive arthropathy of the hand, may use the book as a ready reference to allow him to reach a correct diagnosis. Those purists among us who wish to read about a specific disease and all of its manifestations would do well to consult a general textbook of skeletal radiology, such as Resnick's *Diagnosis of Bone and Joint Diseases* or Edeiken's *Roentgen Diagnosis of Disease of Bone*, or a textbook on rheumatology.

The quality of the illustrations is excellent. The publisher is to be congratulated for maintaining the same quality of illustrations as those carried over from previous editions. Many of the illustrations go to the edge of the page giving more room for the picture.

This reviewer would have preferred that the authors had adhered to the sequence given in the title. For example, Section I on the ABC's of arthritis begins with an analysis of the soft tissues, followed by alignment, bony mineralization, and cartilage space abnormalities. In addition, Section II on arthritis from head to foot actually begins at the foot and works cephalad, finishing with the spine.

In summary, the third edition of this monograph has fulfilled its goal as a ready reference on rheumatologic disease for the practicing radiologist who needs help in establishing a diagnosis when confronted by a patient with joint symptoms. Residents will also find the book extremely useful, but they are advised to consult it only after having learned about individual forms of arthritis from a textbook on skeletal radiology.

Richard H. Daffner
Allegheny General Hospital
Pittsburgh, PA 15212

Stress Fractures of the Distal Tibia and Calcaneus Subsequent to Acute Fractures of the Tibia and Fibula

Michael B. Zlatkin[1]
Ann Bjorkengren
David J. Sartoris
Donald Resnick

Stress fractures (two in the calcaneus and four in the distal tibia) occurring distal to the site of a healing fracture of the tibia or fibula were discovered in five patients. Three of these fractures were identified radiographically at the time of their occurrence, and three were identified only after retrospective review of the radiographs of 74 patients with previous tibial or fibular fractures. Three of the patients were less than 10 years old. All five patients had disuse osteopenia and recently had begun weight-bearing. Four patients had healing of their acute fractures with angulation or displacement. Stress fractures can easily be overlooked on radiographic studies in this setting and may be a source of pain that mistakenly can be attributed to malunion or nonunion.

Stress fractures should be considered in patients with fractures of the lower extremity, particularly those who experience new or persistent pain or discomfort.

Complications of fractures of the tibia and fibula include delayed union, nonunion, malnunion, infection, limb shortening, vascular and neurologic injury, compartment syndrome, joint stiffness and ankylosis, posttraumatic dystrophy, and refracture [1]. To our knowledge, however, complicating stress fractures of the distal tibia and calcaneus that occur during the course of treatment for traumatic fractures of the tibia and fibula have not been described.

We report the occurrence of four stress fractures of the distal tibia and two stress fractures of the calcaneus in five patients with traumatic fractures of the tibia or fibula or both. Three of these injuries were recognized radiographically at the time of their occurrence, and three were identified only on retrospective review of radiographs from similar patients.

Materials and Methods

The discovery of three stress fractures (two in the calcaneus and one in the tibia) occurring distal to the site of healing fractures of the tibia or fibula or both prompted a retrospective analysis to define the frequency and significance of these lesions. The conventional radiographs of 74 patients with fractures of the tibia and/or fibula treated at the University of California Medical Center in San Diego during the 1-year period from June 1985 to June 1986 were reviewed. Thirty of these patients had comprehensive sequential radiographic follow-up examinations during a period of 6 months or longer.

Results

Among the 74 patients evaluated, three additional examples of stress fracture were identified; all were located in the distal tibia. One fracture was identified in a patient with a known stress fracture of the calcaneus. These lesions had been overlooked during the initial radiographic assessment of these patients.

The age range of the patients was 5–38 years. Three of the patients were less than 10 years old. A total of six lesions were identified: four in the distal tibia and two in the calcaneus. All patients had a significant degree of disuse osteopenia at

Received February 25, 1987; accepted after revision April 20, 1987.

This work was supported in part by Veterans Administration grant #SA306.

[1] All authors: Department of Radiology, Veterans Administration Medical Center, San Diego, CA 92161, and the University of California Medical Center, San Diego, CA 92103. Address reprint requests to D. Resnick, Dept. of Radiology, Veterans Administration Medical Center, 3350 La Jolla Village Dr., San Diego, CA 92161.

AJR 149:329–332, August 1987
0361–803X/87/1492–0329
© American Roentgen Ray Society

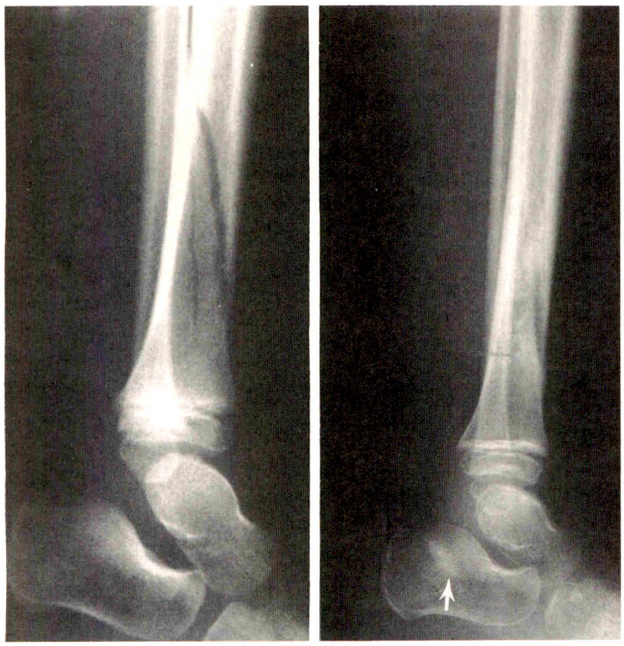


Fig. 1.—A stress fracture of the calcaneus developed 1 month after resumption of full weight-bearing in a 5-year-old boy who had sustained an acute fracture of the distal tibia.

***A*, Lateral radiograph of lower leg at time of injury shows an oblique fracture of distal third of tibia without displacement or angulation.**

***B*, Lateral radiograph obtained 3 months after initial injury shows interval healing and disuse osteopenia. Obliquely oriented band of sclerosis characteristic of a stress fracture is seen in calcaneus (*arrow*).**

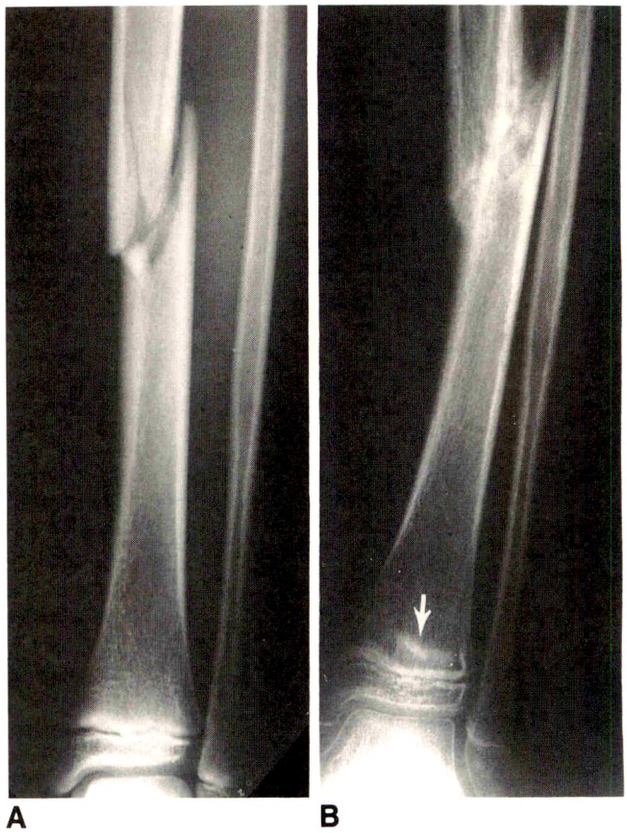


Fig. 2.—A stress fracture of the distal tibia developed 1 month after resumption of weight-bearing in a 9-year-old girl who had sustained an acute fracture of the tibia.

***A*, Frontal radiograph of lower leg at time of injury shows a fracture of midshaft of tibia.**

***B*, Frontal radiograph obtained approximately 4 months later shows interval healing with varus angulation of distal fragment and disuse osteopenia. A horizontal band of sclerosis consistent with a stress fracture (*arrow*) is seen in distal tibia.**

the time of appearance of the stress fracture (Figs. 1–4). All had begun partial or full weight-bearing shortly before the lesions were identified. Two of the patients (both adults) had symptoms and signs in the foot and ankle that could be attributed to these stress injuries. Four of the patients had acute tibial and/or fibular fractures that had healed with some displacement or angulation. The stress fractures were noted 2 to 3 months after the acute fractures in the children and 6 months after in the adults. Radiographically, the stress fractures appeared as linearly oriented, dense bands of sclerosis. All of these fractures subsequently healed without further complications.

Discussion

Stress fractures can be categorized by their cause into two broad types [2]: fatigue fractures, which result from abnormal muscular stress or torque applied to a bone with normal elastic resistance, and insufficiency fractures, which occur when a bone that is deficient in mineral or elastic resistance is subjected to normal or physiologic stresses.

The lower extremities are the most common site of stress fractures. The radiographic appearance of these lesions is related to the site of occurrence and the time at which they are imaged [2]. In general, the appearance of a stress fracture in the cancellous bone in the metaphysis of a long bone (such as the tibia) or calcaneus initially involves a focal zone of sclerosis. As healing occurs, solid or thick laminar periosteal reaction may be seen [2]. These typical alterations may require 2 to 3 weeks for development; hence, conventional radiography is insensitive for early diagnosis [3]. Techniques such as skeletal scintigraphy are more reliable for detection at this stage.

Fatigue fractures of the tibia may be caused by such activities as running, marching, and ballet dancing [4–7]. Fatigue and insufficiency fractures also are common after certain surgical procedures that result in altered stress or imbalance of muscular force on normal or abnormal bones. Examples include stress fractures of the tibia after knee arthodesis or arthroplasty [8, 9]. Insufficiency fractures of the tibia are common in patients with rheumatoid arthritis [9]. Osteoporosis caused by corticosteroid therapy and the underlying disease, joint stiffness, contracture and angular de-

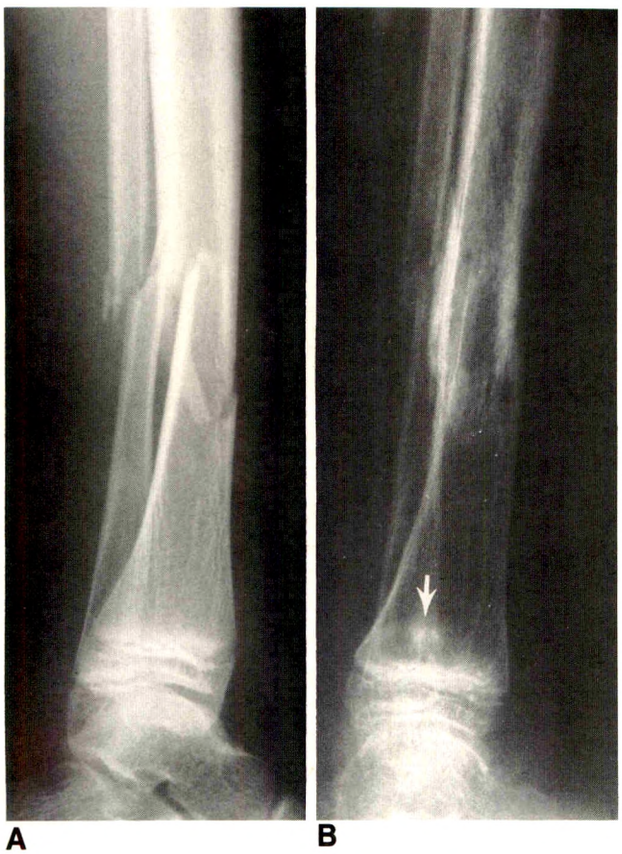


Fig. 3.—A 17-year-old boy was on steroid treatment for a chronic respiratory illness and had long-standing osteopenia. A stress fracture of the distal tibia developed 1 month after resumption of full weight-bearing after an acute fracture of the tibia and fibula.

***A*, Lateral radiograph of lower leg at time of injury shows acute fractures of distal tibia and fibula with mild displacement and angulation.**

***B*, Lateral radiograph obtained 3 months later shows interval healing with mild angulation, persistent disuse osteopenia, and a stress fracture in distal tibia (*arrow*).**

formity of the extremity, and unaccustomed exercise after reconstructive joint surgery combine to predispose such patients to the development of stress fractures. Thus, although stress fractures of the tibia are common, localization in the distal tibia is infrequent. Such lesions generally have been reported in inactive middle-aged and older individuals [7]. Among the series of Schneider and Kaye [9] of rheumatoid patients with stress fractures, however, two of the 12 lesions occurred in the distal tibia.

Stress fractures of the calcaneus also are not rare. Fatigue fractures at this site may occur among military recruits [10], and insufficiency fractures can accompany rheumatoid arthritis, neurologic disorders [11], and recent immobilization [2].

Complications of fractures involving the tibia and fibula have been well documented and are discussed extensively in most standard orthopedic textbooks. We have been unable to find a description of stress fractures in the distal tibia or calcaneus among such patients. These lesions, which the present study



Fig. 4.—Pain developed in the ankle and heel of a 38-year-old woman 6 months after she had sustained oblique fractures of the distal tibia and fibula. She recently had started partial weight-bearing with crutches.

***A*, Lateral radiograph shows a linear band of sclerosis in distal tibia suggestive of a stress fracture (*arrow*). It was clinically and radiographically unrecognized at that time. Calcaneus is normal.**

***B*, Patient continued weight-bearing, and her symptoms worsened. Lateral radiograph obtained 1 month later shows abnormality in distal tibia had resolved. A vertically oriented stress fracture of calcaneus is seen now (*arrow*), along with persistent disuse osteopenia.**

indicates are common, most likely are overlooked because of a lack of awareness of their occurrence. Failure to obtain radiographs of the entire lower leg including the calcaneus (as in the group of patients we reviewed) is an additional factor. In addition, symptoms that might occur secondary to these lesions, such as pain, tenderness, and swelling in the foot and ankle, may be ascribed wrongly to problems related to fracture union, joint stiffness from immobilization, or the reflex sympathetic dystrophy syndrome.

The stress fractures observed among our patients most likely occurred as a result of resumption of partial or full weight-bearing in the setting of disuse osteopenia. It is well recognized that osteopenia of any cause predisposes patients to the development of insufficiency fractures [2]. The resumption of weight-bearing ultimately leads to an increase in strength of both muscle and bone. However, reacquisition of normal muscle tone occurs at a faster rate than remineralization of osteopenic bone, resulting in an imbalance of forces and the potential development of a stress fracture. Presumably, altered biomechanical stress resulting from healing of the acute tibial and fibular fractures with abnormal angulation or displacement (seen in four of our patients) is important as well.

The absence of documented symptoms or signs among three of the five patients in this series (including all of the children) is difficult to explain. Most likely, pain and swelling are not sufficiently disabling or distinctive for patients to ascribe them to new lesions unrelated to healing of the acute injuries. Alternatively, incomplete documentation of subjective complaints must be considered.

In conclusion, physicians involved in the management of such patients should be aware that secondary stress fractures can occur. These lesions represent a potential source

of pain or discomfort that may be mistaken clinically for malunion, nonunion, or other complications of the original fracture. Furthermore, they may be overlooked easily on radiographic examinations. Our results indicate that stress fractures of the distal tibia or calcaneus are not infrequent after acute tibial and fibular fractures and must be considered whenever new or persistent pain or discomfort develops, particularly if weight-bearing has recently been resumed. Appropriate diagnostic studies in this setting include radiographs of the entire lower leg and calcaneus, possibly with skeletal scintigraphy if these radiographs are normal. Follow-up radiographs are reliable if a diagnostic delay is acceptable and for documentation of healing. Recognition of these lesions is important so that proper therapy can be used and the potential complication of complete fracture at the affected site can be avoided.

ACKNOWLEDGMENTS

Special thanks to Cynde Roche for secretarial assistance and to Debra Turdell for technical assistance.

REFERENCES

1. Pillsbury SL, Gossling HR. Complications of tibial fracture management. In: Gossling HR, Pillsbury SL, eds. *Complications of fracture management*. Philadelphia: Lippincott, **1984**:487–531
2. Daffner RH. Stress fractures: current concepts. In: *ACR syllabus for the categorical course on musculoskeletal trauma*. Reston, VA: American College of Radiology **1983**:103–131
3. Prather JL, Nusynowitz ML, Snowdy HA, et al. Scintigraphic findings in stress fractures. *J Bone Joint Surg* [*Am*] **1977**;59:869–874
4. Hallel T, Amit S, Segal D. Fatigue fractures of the tibial and femoral shaft in soldiers. *Clin Orthop* **1976**;118:35–43
5. Schneider JH, King AY, Bronson JL, Miller EH. Stress injuries and developmental change of lower extremities in ballet dancers. *Radiology* **1974**;113:627–632
6. Orava S, Puranen J, Ala-Ketola L. Stress fractures caused by physical exercise. *Acta Orthop Scand* **1978**;49:19–27
7. Singer M, Maudsley RH. Fatigue fractures of the lower tibia: a report of five cases. *J Bone Joint Surg* [*Br*] **1954**;36:647–650
8. Rand JA, Coventry MB. Stress fractures after total knee arthroplasty. *J Bone Joint Surg* [*Am*] **1980**;62:226–233
9. Schneider R, Kaye JJ. Insufficiency and stress fractures of the long bones occurring in patients with rheumatoid arthritis. *Radiology* **1975**;116:595–599
10. Winfield AC, Dennis JM. Stress fractures of the calcaneus. *Radiology* **1959**;72:415–418
11. Stein RE, Stellin FH. Stress fracture of the calcaneus in a child with cerebral palsy. *J Bone Joint Surg* [*Am*] **1977**;59:131

MR Imaging of the Shoulder:
Diagnosis of Rotator Cuff Tears

J. Bruce Kneeland[1]
William D. Middleton[1]
Guillermo F. Carrera[1]
Robert C. Zeuge[2]
Andrzej Jesmanowicz[1]
Wojciech Froncisz[1]
James S. Hyde[1]

Twenty-five patients with known or suspected tears of the rotator cuff in 26 shoulders underwent MR imaging. All patients also underwent arthrography or surgery. MR visualized abnormalities consistent with a tear in 20 of the 22 tears diagnosed by arthrography or surgery. In most cases, tears were seen as regions of increased signal intensity within the cuff on long-TR pulse sequences, although two cases simply showed an almost complete absence of normal cuff. The MR appearance of the two cases with partial tears was similar to that of full-thickness tears. Of the four cases with normal arthrograms, one case had MR findings consistent with a tear.

We conclude that MR has good potential for the noninvasive diagnosis of rotator cuff tears. Its ultimate role in this diagnosis must await prospective studies comparing its accuracy with that of sonography, CT, and arthrography.

The rotator cuff consists of the supraspinatus, infraspinatus, teres minor, and subscapularis muscles together with their tendons. Rotator cuff tears are both common and important [1].

The radiologic diagnosis of rotator cuff tears has traditionally been performed with arthrography and more recently with sonography [2–4] with CT [5]. Arthrography is quite accurate in detecting complete tears, but it is an invasive procedure with some associated risk and discomfort [6]. In addition, arthrography is insensitive to partial tears involving the superficial surface or the substance of the cuff. It will only detect tears involving the deep surface [7]. Sonography is noninvasive and has an accuracy similar to that of arthrography for the diagnosis of tears [2]. However, it is highly operator-dependent, requires a dedicated small-parts transducer, and is incapable of visualizing portions of the cuff beneath the acromion [2]. Postarthrography CT, although more sensitive to the presence of partial tears than arthrography, entails the same risk and discomfort [5].

MR imaging with surface coils has proved of great value in the assessment of disorders of the peripheral joints [8–11]. In previous papers, we presented a detailed correlation between MR and cryomicrotome sections of the rotator cuff [12] and the preliminary results of imaging a small number of patients with known rotator cuff tears using a novel coil design [13]. In this paper, we present the results of MR imaging of 25 patients with suspected rotator cuff tears on whom arthrography or surgery was performed.

Materials and Methods

Twenty-five patients (15 men, 10 women; ages, 24–67) with the clinical signs and symptoms of rotator cuff tears underwent MR imaging of either one (24) or both (one) shoulders. Thus, in total, 26 shoulders were imaged. Arthrography was performed on 24 of 26 shoulders within 30 days of the MR examination. In the other two cases no arthrograms were obtained but surgery was performed within 30 days.

MR imaging was performed on a Signa MR system (General Electric) operating at 1.5 T. An angled pair of 7.5-cm diameter, counter-rotating current-loop-gap resonators were used

Received January 28, 1987; accepted after revision April 3, 1987.

This work was supported in part by NIH grants RR01088 and CA41464 and a grant from General Electric Medical Systems.

[1] Department of Radiology, Medical College of Wisconsin, Milwaukee WI. Address reprint requests to J. B. Kneeland, Dept. of Radiology, Milwaukee County Medical Complex, 8700 W. Wisconsin Ave., Milwaukee, WI 53226.

[2] Department of Orthopedic Surgery, Columbia Hospital, 3321 N. Maryland Ave., Milwaukee, WI 53211.

AJR 149:333–337, August 1987
0361–803X/87/1492–0333
© American Roentgen Ray Society

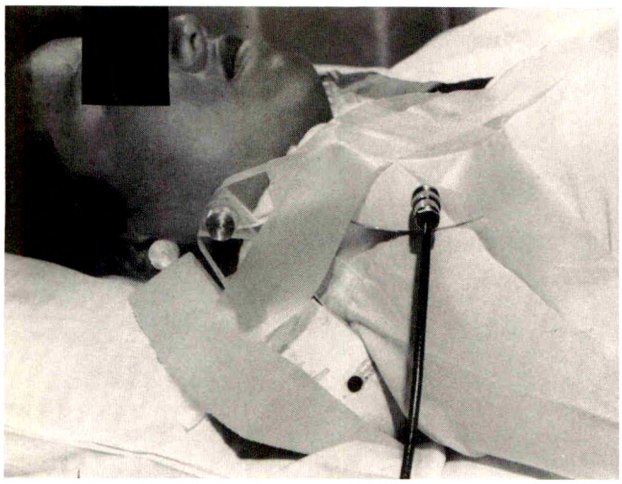


Fig. 1.—Local coil for shoulder imaging shown in place on a normal volunteer.

as the receiver coils [13, 14] with the body coil as the transmitter. The coil was placed over the shoulder as shown in Figure 1 with the arm held in neutral position. Spin-echo pulse sequences with TR/TE = 2500 msec/20 msec (proton-density weighted) and TR/TE = 2500/60–80 (T2 weighted) were obtained in both coronal and sagittal planes for all patients. (TR = repetition time; TE = echo delay time.) Images in the coronal plane were obtained by using the off-center field-of-view method described previously [13].

The MR images and arthrograms were reviewed in conference by three of the authors. A tear was diagnosed on the MR study if a discontinuity of the cuff could be identified. All diagnoses were established by consensus of the three reviewers.

Results

Of the 24 shoulder joints on which arthrography was performed, 20 were interpreted as having tears and four as normal. In the remaining two cases in which arthrography was not performed, tears were found at surgery in both cases. Of the 22 cases diagnosed as complete tears by arthrography

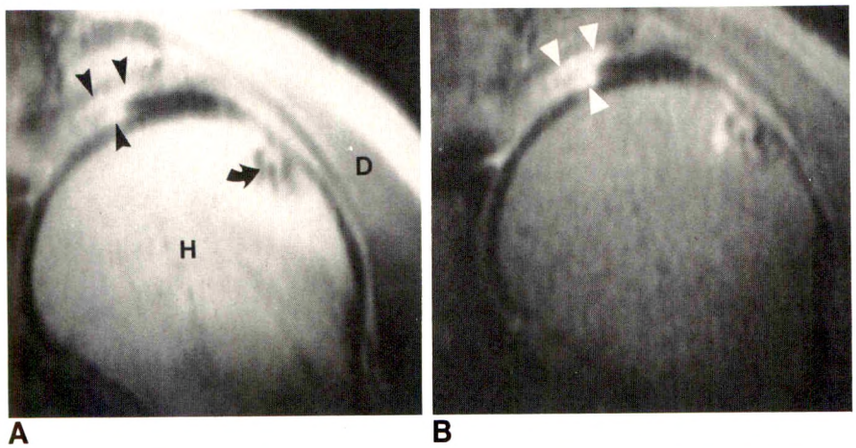
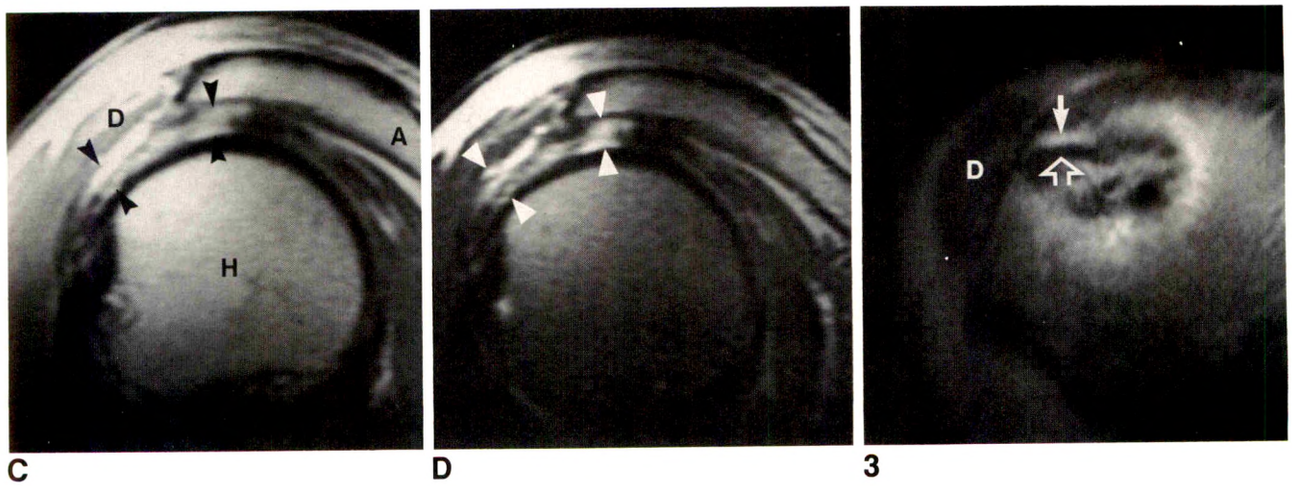


Fig. 2.—Coronal (*A* and *B*) and sagittal (*C* and *D*) sections through a tear in supraspinatus tendon of left shoulder obtained with TR/TE = 2500/20 (*A* and *C*) and TR/TE = 2500/70 (*B* and *D*). Tear (*arrowheads*) is seen as a high-intensity discontinuity in rotator cuff. Area indicated by *curved black arrow* probably represents early subchondral cyst formation. H = humeral head; A = acromion; D = deltoid muscle.

Fig. 3.—Coronal section through extreme anterior aspect of right shoulder obtained with TR/TE = 2500/20. *White arrow* points to high-intensity region, probably fluid, adjacent to site of normal insertion of supraspinatus tendon onto cortex of greater tuberosity (*open white arrow*). D = deltoid muscle.



or surgery, MR imaging detected abnormalities consistent with tears in 20. Analysis of the MR appearance of the tears revealed that all but two of the tears were seen as areas of increased signal intensity on T2-weighted images. The exact appearance and the ease of detectability varied among the patients. Figure 2 shows the typical appearance of a moderate-sized tear in the supraspinatus tendon. Figure 3 shows a small tear at the distal insertion of the supraspinatus tendon.

Of the 20 tears seen with MR images, 10 were seen only in the coronal plane, eight were seen in both coronal and sagittal planes, and two were seen only in the sagittal plane. Of the eight tears seen in both planes, the sagittal sections gave information in regard to location of extent that was not present on the coronal sections in at least two cases. Figure 4 shows an unusual longitudinal tear at the junction of the supraspinatus and infraspinatus muscles.

In two of the tears, MR showed the almost complete absence of cuff over the humeral head in several sections without any regions of increased signal intensity (Fig. 5). Both of these tears were large at arthrography and presumed to be long-standing from the clinical history.

Two partial tears were seen with MR (Fig. 6). The MR

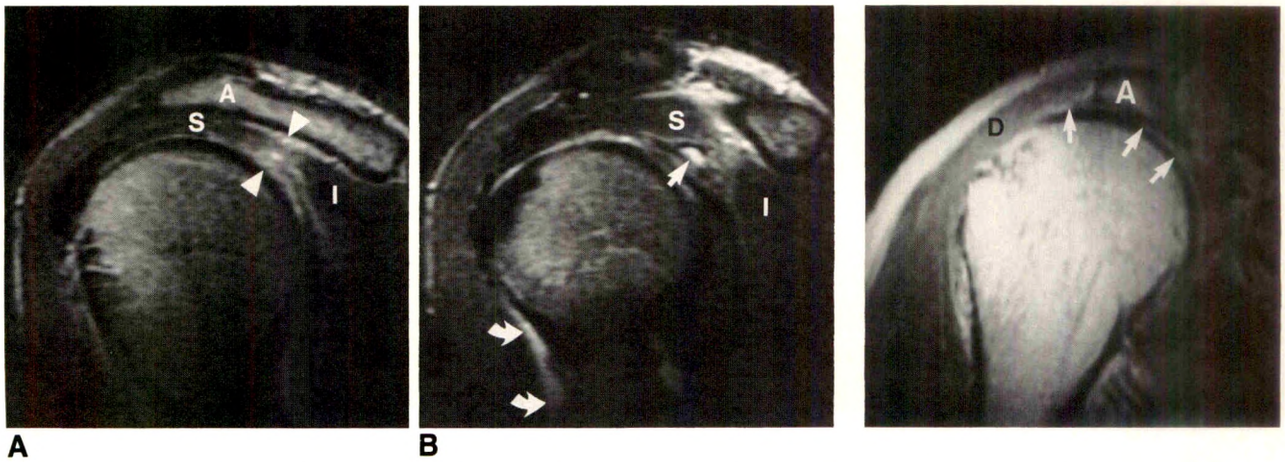


Fig. 4.—Sagittal sections through right shoulder obtained with TR/TE = 2500/70. *A* is lateral to *B*. A tear (*white arrowheads*) is present between supraspinatus (S) and infraspinatus (I) muscles and extends deep to supraspinatus muscle (*straight white arrow*) on *B*. *Curved white arrows* = effusion of the sheath of the biceps tendon.

Fig. 5.—Coronal section through right shoulder in a patient with almost complete destruction of rotator cuff obtained with TR/TE = 2500/20. *White arrows* point to a medium-intensity layer just superficial to black cortex, which represents hyaline cartilage and possibly a small amount of fat. No normal cuff tissue is seen. A = acromion, D = deltoid muscle.

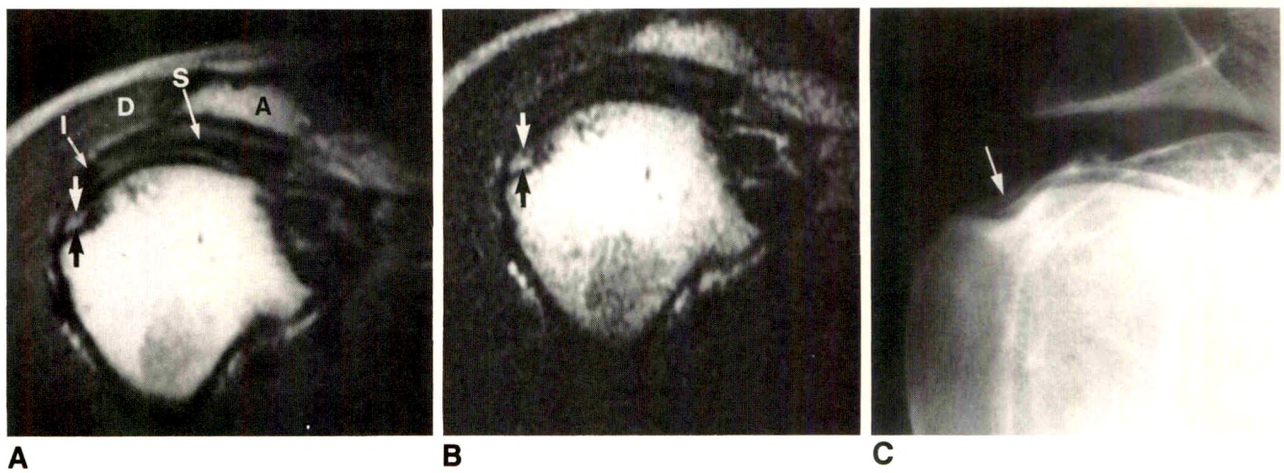


Fig. 6.—Coronal sections (*A* and *B*) and film from a post-exercise arthrogram (*C*) of right shoulder in a patient with a partial tear of infraspinatus tendon. *A* was obtained with TR/TE = 2500/20, *B* with TR/TE = 2500/70. *Black* and *white arrows* in *A* and *B* denote tear; *arrow* in *C* points to area of partial extravasation of contrast material that corresponds to tear in *A* and *B*. I = infraspinatus tendon; S = supraspinatus tendon; A = acromion; D = deltoid muscle.

appearance of these cases was similar to that seen with full-thickness tears.

No tear was seen by MR in two cases with confirmed tears. In one of these two cases image quality was degraded considerably by motion artifacts. Of the four cases with normal arthrograms, MR detected no abnormalities in three and an apparent tear in one (Fig. 7).

Discussion

In these 25 patients MR was accurate for the detection of rotator cuff tears. This investigation does, however, have the limitation of being retrospective in nature. A prospective study of a large number of patients will be necessary to determine the sensitivity and specificity of MR imaging.

Our choice of proton-density–weighted and T2-weighted pulse sequences was based on our preliminary work involving four patients studied with MR imaging using only T1-weighted images (not included in this series) and two others who were studied with both T1- and T2-weighted images. With T1-weighted images identification of rotator cuff tears was difficult for several reasons. The normal rotator cuff is a complex structure with the central tendons of the rotator cuff muscles having low intensity and the intervening cuff having medium intensity on all pulse sequences. Defects in the rotator cuff are filled with either fluid, granulation tissue, or hypertrophied synovium. These will all tend to have a low or medium intensity on relatively T1-weighted images and will thus be difficult to distinguish from the normal parts of the cuff. Proton-density–weighted and, to an even greater extent, T2-weighted images increase the signal intensity of fluid or abnormal tissue at the site of the tear relative to normal cuff, making the tears more visible. Figure 8 illustrates the difficulty of using a T1-weighted sequence to detect even large tears, which are seen quite easily with proton-density–weighted and T2-weighted sequences.

Partial tears are difficult to diagnose with arthrography, which relies on the passage of contrast material out of the

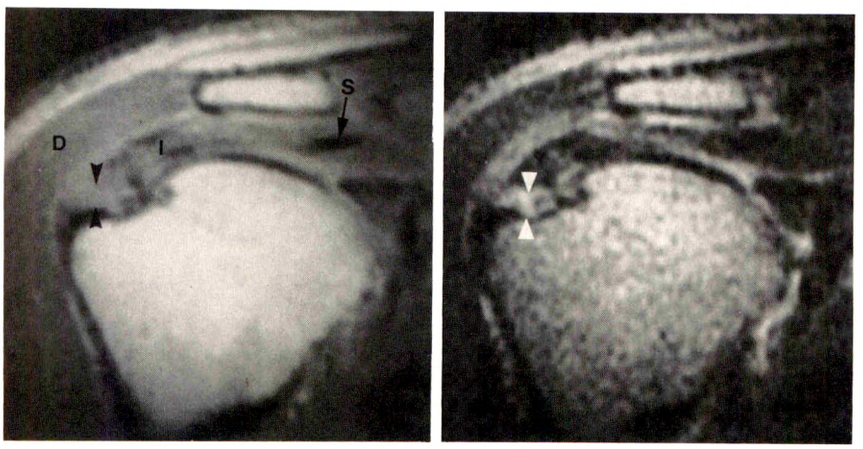


Fig. 7.—Coronal section through right shoulder obtained with TR/TE = 2500/ 20 (*A*) and TR/TE = 2500/70 (*B*). MR images show apparent tear of infraspinatus tendon (*arrowheads*), although arthrogram was negative. I = infraspinatus tendon; S = supraspinatus tendon; A = acromion; D = deltoid muscle.

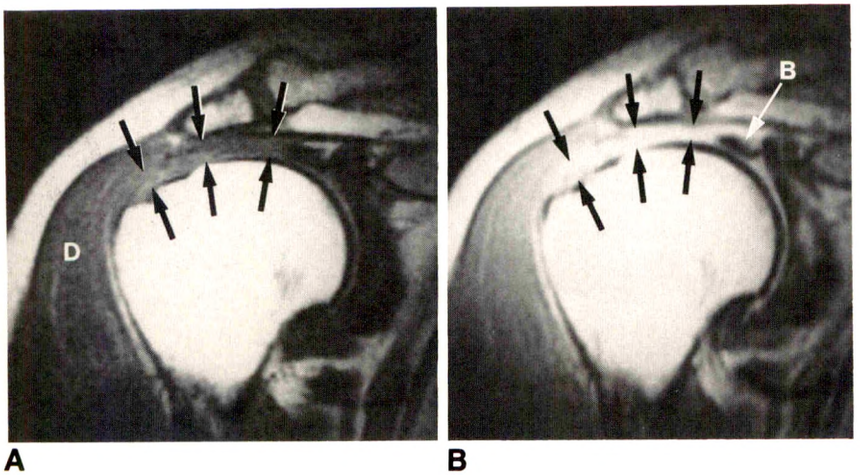


Fig. 8.—Coronal section through left shoulder of a subject in whom fluid (*arrows*) occupies the site of a large tear in rotator cuff. *A* was obtained with TR/TE = 500/25; *B* with TR/TE = 2500/25. On short-TR sequence fluid has same intensity as medium-intensity component of normal cuff, but on longer-TR sequence fluid is clearly visible. D = deltoid muscle; B = biceps tendon.

joint space into the subacromial/subdeltoid bursa. The diagnosis of partial tears, however, is particularly important because many orthopedic surgeons will operate to relieve impingement of the supraspinatus tendon before it progresses to a full-thickness tear. Although both of the partial tears in this series were seen at arthrography, the relative ease with which they were seen on the MR images suggests that MR may have a role in their diagnosis.

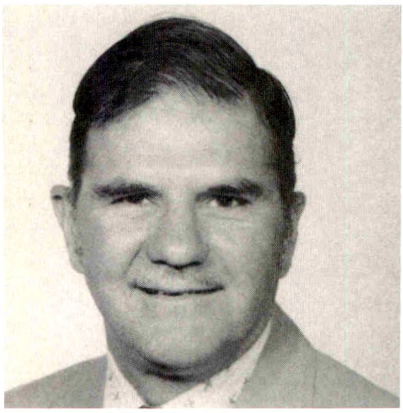
The ultimate role of MR imaging in the diagnosis of rotator cuff tears must await the results of larger prospective series involving direct comparison with the competing techniques. Although noninvasive, MR is considerably more expensive than sonography and will probably not replace it as a screening procedure for those trained in its use. For those cases in which the sonogram yields indeterminate results or in those institutions in which no one is trained to do sonography of the shoulder, MR may be a useful screening test. In addition, it may also be able to determine the size and location of the tear more precisely than either sonography or arthrography.

REFERENCES

1. Colfield RH. Rotator cuff disease of the shoulder. *J Bone Joint Surg* [*Am*] **1985**;67A:974–979
2. Middleton WD, Edelstein G, Reinus WR, Melson GL, Totty WG, Murphy WA. Sonographic detection of rotator cuff tears. *AJR* **1985**;144:349–353
3. Mack LA, Matsen FA III, Kilcoyne RF, Davies PK, Sickler ME. US evaluation of the rotator cuff. *Radiology* **1985**;157:205–209
4. Cross JR, Craig EV, Thompson RC, Fienberg SB. Ultrasonography of the rotator cuff: surgical correlation. *JCU* **1984**;12:487–492
5. Beltran J, Gray LA, Bools JC, Zuelzer W, Weis L, Unverferth LJ. Rotator cuff lesions of the shoulder: evaluation by direct sagittal CT arthrography. *Radiology* **1986**;160:161–165
6. Hall FM, Rosenthal DI, Goldberg RP, Wyshak G. Morbidity from shoulder arthrography: etiology, incidence, and prevention. *AJR* **1981**;136:59–62
7. Goldman AB, Ghelman B. The double-contrast shoulder arthrogram. *Radiology* **1978**;127:655–663
8. Reicher MA, Hartzman S, Duckwiler GR, et al. Meniscal injuries: detection using MR imaging. *Radiology* **1986**;159:753–757
9. Weiss KL, Beltran J, Lubbers LM. High-field MR surface coil imaging of the hand and wrist. Part II. Pathologic correlations and clinical relevance. *Radiology* **1986**;160:147–152
10. Middleton WD, Kneeland JB, Kellman GM, et al. MRI of the carpal tunnel: normal anatomy and preliminary findings in the carpal tunnel syndrome. *AJR* **1987**;148:307–316
11. Beltran J, Noto Angela M, Mosure JC, et al. Ankle: surface coil imaging at 1.5 T. *Radiology* **1986**;161:203–209
12. Middleton WD, Kneeland JB, Carrera GF, et al. High-resolution magnetic resonance imaging of the normal rotator cuff. *AJR* **1987**;148:559–564
13. Kneeland JB, Carrera GF, Middleton WD, et al. Rotator cuff tears: preliminary application of high-resolution MR imaging with counter rotating current loop-gap resonators. *Radiology* **1986**;160:695–699
14. Froncisz W, Jesmanowicz A, Kneeland JB, Hyde JS. Counter rotating current local coils for high resolution magnetic resonance imaging. *Magn Resonance Med* **1986**;3:590–603

Memorial

Alan Ward Shriver, 1920–1987



On Monday, April 13, 1987, Dr. Alan W. Shriver, 66, died as a result of an automobile accident near Savannah, GA.

Born June 23, 1920, to Karl W. and Beth Shriver, he was raised near Pittsburgh, PA. He attended Mt. Lebanon High School and Alleghany College. He attended the University of Pittsburgh Medical School while serving in the Army Reserves during World War II. After internship at the University of Pittsburgh Hospitals, he was commissioned a captain in the Army Air Corps. After his discharge, he relocated to Greensburg, PA, where he established a general practice. He returned to the University of Pittsburgh in 1954 for a residency in Diagnostic and Therapeutic Radiology and Nuclear Medicine. He was a staff radiologist at Westmoreland Hospital in Greensburg, McGinnis Hospital in Ligonier, and Western Pennsylvania Hospital in Pittsburgh, PA. After retirement in 1981, he moved to North Carolina and later Virginia, where he practiced part time on a locum tenens basis throughout the eastern United States until his death.

Society memberships included The American Medical Association, The American College of Radiology, The Radiologic Society of North America, The Pennsylvania Medical Society, Westmoreland County Medical Society (PA), and The New Hanover County Medical Society (NC).

Honors included Fellowship in the American College of Radiology; President, Pittsburgh Roentgen Ray Society (1975–1976); President, Westmoreland Hospital medical staff (1970–1971); President, Wainwright Tumor Clinic Assoc. (1976); Vice President, American Cancer Society, Westmoreland County (1975); and Secretary, Westmoreland County Medical Society (1956–1957).

He is survived by his wife Sara, sons David and Peter, daughters Polly and Maggie, and their families. He was a man of immeasurable patience, resilience, and kindness and will forever be a source of the fondest of memories to all who were fortunate enough to know him. He will be deeply missed.

Jeffrey P. Kochan, M.D.
Polly Shriver Kochan, M.D.
Peter A. Shriver, D.O.
Lansdowne, PA 19050

Skeletal Measurements Using a Flying Spot Digital Imaging Device

Anthony J. Wilson[1]
Gale R. Ramsby

A flying spot digital imaging unit was devised to measure skeletal length and angles. This device uses a spinning chopper wheel and fixed slit collimator in front of a conventional X-ray tube to produce a scanning pencil beam that passes through the patient and onto an electronic detector. The beam scans the patient transversely and the device moves longitudinally, creating a digital image with a skin dose of less than 2 mrad (0.02 mGy). Patients can be imaged both when upright and when recumbent. A large field of view makes it possible for the entire length of the spine or lower extremities to be included in a single image. Built-in computer algorithms are used to make measurements of skeletal lengths and angles. The accuracy of the digital device was tested by making measurements of known angles and lengths using protractors and rulers. Skeletal measurements were then made on a number of patients. Interobserver error was tested using both patient and nonpatient images. The following patient measurements were made: (1) Cobb angle in 166 patients with scoliosis; (2) knee joint angles in 120 patients undergoing knee surgery; (3) lower extremity lengths in 78 patients with length inequalities; (4) bony fragment angulation and displacement in 30 patients with healing fractures. These studies have shown the device to be accurate with low interobserver error, while delivering much lower patient dose than more conventional methods. The ability to manipulate window levels and widths enables visualization of thick and thin body parts on the same image.

Our experience both in the laboratory and with patients has been encouraging, and the method appears to have several advantages over more conventional techniques.

Since the 1920s numerous radiographic techniques have been proposed for measuring a variety of skeletal lengths and angles [1–11]. Most of these methods are aimed at eliminating, minimizing, or correcting for radiographic distortion while attempting to provide a large field of view. Orthogonal projections [2, 3] and 36-in. (92-cm) cassettes [4] are used most frequently, although other procedures, such as slit radiography [5], also have merit.

Recently, digital radiographs obtained with CT scanners used in the scout-film mode have been advocated because they substantially reduce patient dose and allow accurate length measurements [10, 11].

All of the available methods have certain deficiencies. For this reason, a Microdose scanner (American Science and Engineering, Cambridge, MA) was evaluated as an alternative method of obtaining skeletal measurements.

Materials and Methods

The Microdose scanner, described previously [12–14], is designed for general digital radiography, including chest imaging. The scanner uses a conventional X-ray tube and generator. Positioned in front of the tube is a spinning metal disk containing radial slits (chopper wheel) in front of which is a fixed transverse slit. The chopper wheel and slit together collimate the X-ray beam into a thin pencil shape that scans from one side of the table to the other (Fig. 1). The beam passes through the patient and impinges on an electronic detector, the output from which is digitized and fed to a computer. The source and detector move

Received February 9, 1987; accepted after revision April 3, 1987.

[1] Both authors: Department of Radiology, University of Connecticut Health Center, 263 Farmington Ave., Farmington, CT 06032. Address reprint requests to A. J. Wilson.

AJR 149:339–343, August 1987
0361–803X/87/1492–0339
© American Roentgen Ray Society

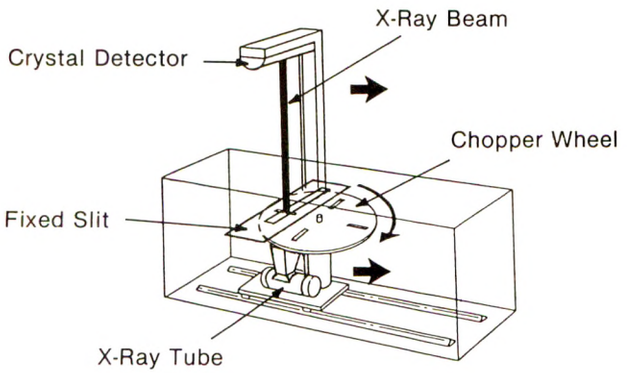


Fig. 1.—Diagram of Microdose unit. Spinning chopper wheel and stationary slit combine to form a pencil beam that scans from side to side. Source and detector move together to scan area of interest in a longitudinal direction.

together, scanning the area of interest in a longitudinal plane. The computer then generates a digital image, which is displayed on a video monitor. Because the scanning beam is always perpendicular to the longitudinal axis, distortion is eliminated in the longitudinal direction, as with slit radiography, orthogonal scanograms, and CT scout films. The unit has separate horizontal and vertical gantries, making it possible to obtain examinations in both the upright (weight-bearing) and recumbent positions. Similar to CT and other digital imaging devices, window levels and widths can be manipulated to compensate for various patient thicknesses.

Length measurements are obtained by placing cursors on the cathode-ray tube image at the points of interest using one of several computer algorithms available at the console. These algorithms allow lines to be drawn along any plane or between any two points, thus allowing measurement of any lengths or angles that the operator chooses. For example, lines may be drawn across the end plates of the vertebrae to measure the Cobb angle (the angle between the end plates of the vertebrae at the extremes of a scoliotic curvature) (Fig. 2) and across joints for both length and angle measurements (Fig. 3).

Angles calculated by the computer are affected by distortion in the transverse plane only. The computer, however, can mathematically correct for this transverse distortion if the level of the measurement plane, above the table top, is known and provided to the computer.

Images were made of rulers and protractors placed against and above the table top in varying increments to 30 cm to measure the amount of longitudinal and transverse distortion and to estimate the resultant errors that might be introduced by this distortion in clinical practice. The rulers and protractors were positioned at the edge of the beam where the transverse distortion is greatest. Various lengths were measured from 1 to 30 cm (31 cm is the greatest transverse length measurable at the table top), and angles were measured from 0° to 90°.

Interobserver errors were studied by using two individuals who were familiar with the operation of the machine. Each was asked to place cursors at certain points on several different images, to draw lines between the cursors, and to calculate angles between the lines. Five lower extremity cases were used, with eight cursors placed on each image, defining four lines and two angles. Two ruler images were used, with cursors placed at ten points defining five lines for the computer to calculate. No attempt was made to study interobserver error in placing lines or measuring angles on conventional radiographs.

Five goniometers were selected at random from among practicing radiologists and orthopedists. These devices (three manufactured by

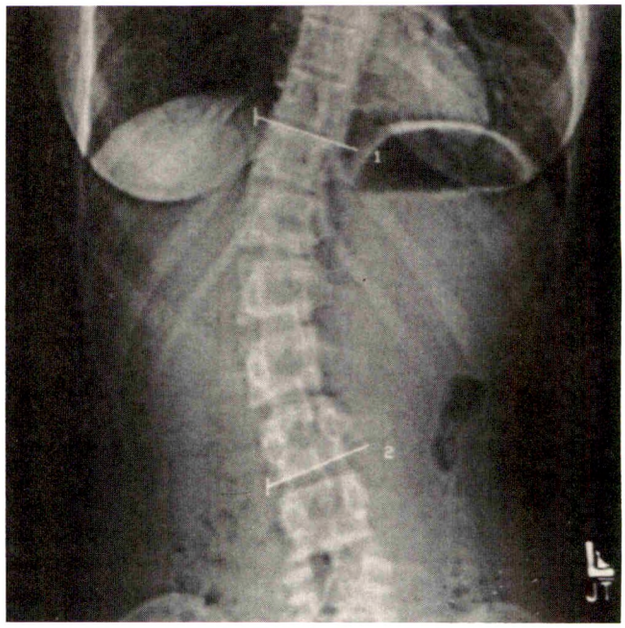


Fig. 2.—Patient with idiopathic scoliosis of the spine was examined using digital scanner. Lines were placed as shown for Cobb angle measurement, and angle of curvature was calculated by computer. Patient dose was less than 2 mrad (0.02 mGy).

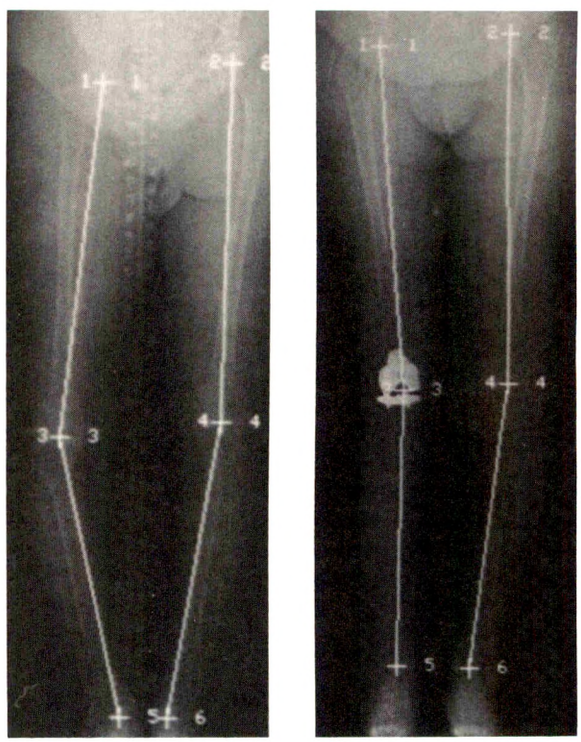


Fig. 3.—Patient with severe osteoarthritis of the knee had a total joint prosthesis inserted. Comparison of preoperative (*A*) and postoperative (*B*) digital scans shows correction of a severe varus deformity. Angle measurements give a quantitative evaluation of surgical result.

X-ACT Design, Boston, MA; one distributed by Upjohn Pharmaceuticals, Kalamazoo, MI; and one distributed by Winthrop Laboratories, New York, NY) were carefully examined for construction errors that could affect their accuracy. The goniometers were all in active clinical use at the time.

In order to test the effect of decentering errors on conventional scanograms, we reproduced an experiment previously reported by Aitken et al. [11]. Conventional X-ray exposures of a cadaveric femur were made by using an 8 × 10 in. (18 × 24 cm) X-ray cassette. Three exposures were made on a single film without moving the femur, but with the central ray in three different positions along the longitudinal axis of the bone. A standard scanogram ruler was included on the film for measurement purposes.

After completing initial measurements, patient studies were undertaken. The technique was used for measurement of extremity lengths in patients with growth inequalities, follow-up of trauma patients, measurement of Cobb angles in scoliosis patients, and planning and follow-up of knee joint surgery for arthritis. Before knee joint replacement and high tibial osteotomy, a number of angles were measured including the mechanical and anatomic axes of the joint [15]. These measurements were repeated postoperatively to give a quantitative assessment of surgical correction. One hundred sixty-six scoliosis, 78 extremity length, 120 knee joint, and 30 trauma studies were performed.

Results

The machine is calibrated to an accuracy of ±1 mm for linear measurements and ±0.1° for angular measurements. Ruler measurements in the longitudinal plane were accurate to within 1 mm when care was exercised in placing the cursors. Transverse plane measurements were found to be within 4 mm (1%) (Table 1) and angle measurements within 0.3° when the distance from the table top to the plane of measurement was correctly given to the computer.

When the distance from the table top to the measurement plane was incorrectly stated, errors were seen in both transverse linear measurements and angle measurements, while longitudinal linear measurements remained accurate. These errors increased as the discrepancy between the true and measured planes became greater. Transverse linear measurement errors increased as line lengths became longer. Angle errors were greatest around 45° and always within 0.1° at 0° and 90°. The relationship between transverse linear measurement errors and distance from the plane of measurement is shown in Table 1. A typical distribution of angle errors, with an incorrect plane of measurement, is shown in Table 2.

Interobserver error in placement of lines and cursors rarely exceeded 1 pixel, with a maximum of 2 pixels. The angle and length errors generated by 1 pixel differences are a function of both line length and pixel size. Pixel size varies with the length of the scan from a minimum of 0.24 × 0.32 mm to a maximum of 0.62 × 0.78 mm. With the field size used for spine and lower extremity examinations, the angle errors created by a single pixel misplacement of the cursor are less than 2° when the line length is 2 cm or more (Table 3). The computer algorithm that is used for scoliosis patients has a fairly short fixed line length (approximately 5 cm) and gives a 1-pixel misplacement error of 0.7° with the frame size normally used for these scans. The line lengths used for mechanical axis measurement in preoperative knees are the full

TABLE 1: Horizontal Measurements and Errors[a]

Distance Above Table (cm)	True Length (cm)	Uncorrected Measurement (cm)	Corrected Measurement (cm)	Uncorrected Error (cm)	Corrected Error (cm)
0.0	30.0	30.4	30.4	0.4	0.4
3.5	30.0	27.6	29.9	2.4	0.1
8.0	30.0	25.3	30.1	4.7	0.1
11.5	30.0	23.4	30.0	6.5	0.0
17.0	30.0	21.4	30.1	8.6	0.1
25.5	30.0	18.5	29.8	11.5	0.2
30.5	30.0	17.5	30.2	12.5	0.2

[a] Errors produced when measuring a 30-cm ruler at different levels above the table top with and without using the corrective algorithm.

TABLE 2: Angle Measurement and Errors[a]

True Angle (degrees)	Measured Angle (degrees)	Error (degrees)
0.0	0.0	0.0
2.9	2.9	0.0
4.3	4.4	0.1
7.1	7.3	0.2
9.9	10.4	0.5
14.0	14.6	0.6
20.5	21.5	1.0
26.5	27.7	1.2
36.9	38.3	1.4
45.0	46.6	1.6
53.1	54.7	1.6
54.8	56.3	1.5
63.5	64.9	1.4
69.5	70.6	1.1
70.5	71.6	1.1
76.0	76.9	0.9
80.1	80.7	0.6
82.9	83.4	0.5
85.7	86.0	0.3
87.1	87.5	0.4
90.0	90.0	0.0

[a] A typical distribution of errors in angle measurement when distance above the table is incorrectly stated (in this case, the corrected plane was 2.5 cm from the true plane).

TABLE 3: Single Pixel Angles[a]

Line Length (cm)	Direction of Line	Angle (degrees)
1.0	Transverse	4.5
2.0	Transverse	1.9
5.0	Transverse	0.9
10.0	Transverse	0.4
20.0	Transverse	0.2
30.0	Transverse	0.1
1.0	Longitudinal	4.7
2.0	Longitudinal	1.7
5.0	Longitudinal	0.7
10.0	Longitudinal	0.4
20.0	Longitudinal	0.2
30.0	Longitudinal	0.1

[a] Angle produced by displacing the cursor, at one end of a line, 1 pixel from its correct position.

length of the femur and tibia. A 1-pixel misplacement error with lines this long is 0.1° or less.

The study of pocket goniometers revealed construction errors of up to 2°, with all of the devices having alignment errors that were visible to the naked eye. These devices were all calibrated in 1° increments, giving a calibration error of ± 0.5°. This yields measurement errors up to 2.5° without taking into account any interobserver error. If we assume an interobserver error of only 1°, we then have a total error of up to 3.5° for angle measurements on conventional radiographs. In practice, the errors may be greater.

The ruler used for our conventional scanograms is calibrated in 5-mm increments, giving a calibration error of ±2.5 mm, in addition to interobserver error. This is much greater than the 1 mm observed accuracy for the Microdose unit. While more accurate rulers are available, all those we have seen have calibration errors > ±1mm.

The conventional scanogram experiment yielded results similar to those found by Aitken et al. [11]. Measurement errors were caused when the point of measurement was not in the plane of the central ray. Errors as high as 1 cm were produced by deliberate decentering of only 10 cm.

Spatial resolution with the Microdose scanner was measured at the time of installation and, while this varies with scan length and exposure factors, the highest resolution currently available is 1.6 line pairs/mm. Patient entry dose was also measured on installation and was found to be always less than 2 mrad (0.02 mGy) with the exposure factors used in this study. The maximum skin dose that can be delivered by the machine is less than 6 mrad (0.06 mGy).

In most patients studied, there were no problems in providing the referring physician with the measurement data required for management. The main problems encountered were (1) in those patients who were unable to stand upright when erect images were requested, (2) in patients taller than 6½ ft. (195 cm) whose lower extremities and pelvis could not be entirely covered with a single scan, and (3) in one obese patient in whom the images were so photon deficient that the spine could not be seen.

Discussion

A major drawback of conventional radiography is the high dose of radiation involved. This is particularly significant in children with thoracolumbar scoliosis, in whom almost the whole spine must be included on the film. Although numerous methods have been suggested to reduce the gonad dose in these children, large, accumulated doses are difficult to avoid because many of these patients require repeated follow-up examinations. The use of 36-in. cassettes poses the difficulty of balancing exposures over a wide range of patient thicknesses. Wedge filters and variable speed screens can be used to diminish this problem, but do not always help in patients who have unusual body shapes.

CT scanograms address both of the above problems; however, the area that can be covered with a single scan is limited, and it is not possible to scan the patient in an upright, weight-bearing position.

The Microdose scanner addresses all of these problems. The radiation dose of 2 mrad (0.02 mGy) is considerably lower than the 15–20 mrad (0.15–0.2 mGy) used for CT scanograms and the 200–250 mrad (2–2.5 mGy) used for conventional scanograms [11]. Patients can be scanned in either the upright or recumbent position, window manipulation allows for thick and thin areas of the body to be visualized on the same image, and the amount of coverage is greater than that of any other method currently in use. The maximum patient length we can cover with the Microdose unit is 104 cm, which is significantly greater than that possible with either a CT scanner (50 cm or less) or conventional 36-in. cassettes (85 cm or less). A single view of the spine from the base of the skull to the tip of the coccyx or a single view of the lower extremities from the iliac crest to the feet can be obtained in patients as tall as 6 ft. 6 in.

Small errors in angle measurements are generated by the machine whenever the exact plane of measurement is not known. This is usually the case in clinical practice; however, these errors are constant and reproducible from one examination date to another, giving useful comparative information. Interobserver errors are usually less than 1°, unless very short lines are used. When the distance from the table top to the plane of measurement is known, the angle measurements are accurate. Even when this distance is incorrectly estimated, the error rarely exceeds 1.5°, which is significantly less than that which occurs with more conventional methods.

At 1.6 line pairs/mm (1p/mm), the resolution is less than many currently available film/screen systems (2–10 lp/mm), but it is more than adequate for the measurements described. A hardware update is expected in the future, which should lead to a major improvement in resolution. Scan time varies with the length of the scan, to a maximum time of 16 sec; therefore, patient movement can be a problem, but it produces distortion rather than blurring. The distortion is usually obvious and does not necessarily affect the areas of interest. If the distortion does interfere with the measurements, a repeat scan does not constitute a significant increase in patient risk and, in practice, we have had few patients requiring repeat scans.

Because the in vitro measurements appeared to be accurate, we decided that the extra radiation dose associated with a double-blind comparison between the Microdose scanner and conventional methods was not warranted. Patient studies were therefore undertaken using digital examination alone.

Despite the accuracy of computer measurements, a standard radiographic ruler is included in the beam in all scanograms to make direct measurements possible from hard copy, to guard against calibration errors, and to make the images more familiar in appearance for the referring physician.

One major drawback of this machine is its initial cost. Cost effectiveness has not been addressed in our study, but it remains an important issue that must be resolved. Another drawback is that the amount of time spent on these examinations by the technologist is often much greater than that spent for more conventional studies. While patient examination does not take long, edge enhancement, drawing lines, measuring angles, and other poststudy processing of the

image can be very time consuming; however, this time is saved for the physician.

Although our present experience with this device is limited, it appears to offer several advantages over previously described methods. The reduction in radiation dose to the patient is considerable, the area of coverage is greater, and the accuracy is equal to or greater than that of other methods. The ability to manipulate window level and width makes examination of different patient thicknesses possible on the same image and has eliminated the need for repeat examinations due to wrong exposure.

ACKNOWLEDGMENT

We would like to thank Jill Tolasi. Her help was invaluable both in collecting the material and in performing many of the examinations.

REFERENCES

1. Hickey PM. Teleroentgenography as an aid in orthopedic measurements. *AJR* **1924**;11:232–233
2. Merrill OE. A method for the roentgen measurement of long bones. *AJR* **1942**;48:405–406
3. Green WT, Wyatt GM, Anderson M. Orthoroentgenography as a method of measuring bones of the lower extremities. *J Bone Joint Surg* **1946**;28:60–65
4. Young, LW, Oestreich AE, Goldstein LA. Roentgenology in scoliosis: contribution to evaluation and management. *AJR* **1970**;108:778–795
5. Millwee RH. Slit scanography. *Radiology* **1937**;28:483–486
6. Cobb JR. Outline for the study of scoliosis. In: *Instructional course lectures. The American Academy of Orthopaedic Surgeons*, vol 5. Ann Arbor, MI: J.W. Edwards, **1948**:261–267
7. Ferguson AB. *Roentgen diagnosis of the extremities and spine.* New York: Paul B. Hoeber, **1945**
8. George K, Ripstein J. A comparative study of the two popular methods of measuring scoliotic deformity of the spine. *J Bone Joint Surg* [Am] **1961**;43:809–818
9. Kittleson AC, Lim LW. Measurement of scoliosis. *AJR* **1970**;108:775–777
10. Helms CA, McCarthy S. CT scanograms for measuring leg length discrepancy. *Radiology* **1984**;151:802
11. Aitken GF, Flodmark O, Newman DE, Kilcoyne RF, Shuman WP, Mack LA. Leg length determination by CT digital radiography. *AJR* **1985**;144:613–615
12. Bjorkholm PJ, Annis M, Frederick EE. Digital radiography. Applications of optical instrumentation in medicine. *Proc SPIE*, **1980**;233:137
13. Stein J, Swift RD. Flying spot x-ray imaging systems. *Materials Eval* **1972**;30:137–141
14. Stein J. X-ray imaging with a scanning beam. *Radiology* **1976**;117:713–716
15. Laskin RS, Denham RA, Apley AG. *Replacement of the knee.* New York: Springer-Verlag, **1984**;59

1988 AMERICAN ROENTGEN RAY SOCIETY MEETING

MAY 8–13, 1988
SAN FRANCISCO HILTON HOTEL
SAN FRANCISCO, CA

See page 430 and forthcoming issues for further information.

Technical Note

A Device for Maintaining Cervical Spine Stabilization and Traction During CT Scanning

Gary K. Stimac,[1,2] Deborah Burch,[2] Robert R. Livingston,[2] Paul Anderson,[3] and Ralph G. Dacey[4]

Although plain films are often the first images obtained in the evaluation of spinal injuries, CT reveals the most useful diagnostic information [1, 2]. CT can show a greater number of fractures and indicate their precise positions relative to the spinal canal. When water-soluble contrast material is administered intrathecally, these scans can show compression of the spinal cord and compression of nerve roots.

In most patients suspected of cervical fracture, a CT scan is obtained immediately after resuscitation in the emergency room. When a patient has a significant cervical spinal fracture, stabilization is achieved with traction in the axial direction via a metallic device fixed to the head, the force applied by weights and pulleys. Such traction works well for the patient on a stretcher or in a hospital bed. However, maintaining traction using weight and pulley systems during CT examinations is awkward and is potentially catastrophic if the proper traction cannot be maintained at all times. The greatest problems are (1) possible dislodgment of the pulley system as the CT table moves through the scanning ring and (2) the table being unlatched because of the excess force of the weights, causing misregistration of scan slices.

Although various techniques for scanning the cervical spine have been described [1–4], we are unaware of any method devised to ensure safe maintenance of traction during scanning. Thus, to achieve this goal, we devised a spring-loaded traction device that mounts directly on the GE 9800 scanner. This system is easy to use, reliably maintains traction, and can be adapted for use with all commercially available CT systems.

Materials and Methods

The dedicated CT traction device was designed by one of us and has been used at Harborview Medical Center, a level I trauma center, since July 1984. The device was constructed by the Scientific Instrument Division of the University of Washington, Seattle.

The main components of the system are a pair of braces to be placed against the shoulders and a spring scale that attaches to the halo, tongs, or other traction hardware (Fig. 1). The braces, attached to the CT table, apply force to depress the shoulders. These braces are made of radiolucent plastics that do not degrade the CT images. They offer the additional benefit of keeping the shoulders down during scans of the cervical areas, thus reducing the image degradation due to shoulder artifact. The spring scale, attached to the CT table and the halo or tongs, pulls the head superiorly and registers the applied force. Thus, the device provides axial traction on the cervical spine by pulling the cranium against the shoulders. Adjustments allow the device to accommodate all body types and various circumstances encountered in traumatized patients. In addition, after initial positioning, any anatomic part may be scanned without attention to maintaining traction.

The device is easily used (Fig. 2). The patient is placed on the CT table while manual traction is applied. Next the hook on the spring-scale is inserted into the skull stabilization hardware and the braces are engaged at the shoulders. A screw is turned to achieve the desired traction force as determined by the clinical circumstances.

Received January 29, 1987; accepted after revision March 24, 1987.

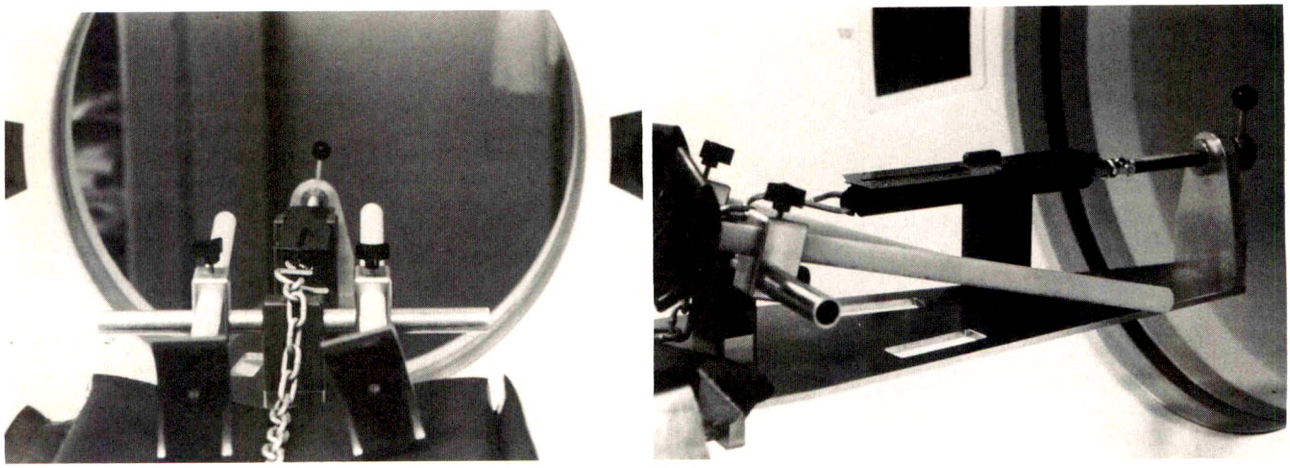
[1] Department of Radiology, SB-05, University of Washington Hospitals, 1959 N.E. Pacific St., Seattle, WA 98195, and First Hill Diagnostic Imaging Center, 1001 Boylston, Seattle, WA 98104. Address reprint requests to G. K. Stimac at the First Hill Diagnostic Imaging Center.

[2] Department of Radiology, Harborview Medical Center, 325 Ninth Ave., Seattle, WA 98104.

[3] Department of Orthopedic Surgery, University of Washington, and Harborview Medical Center, Seattle, WA 98104.

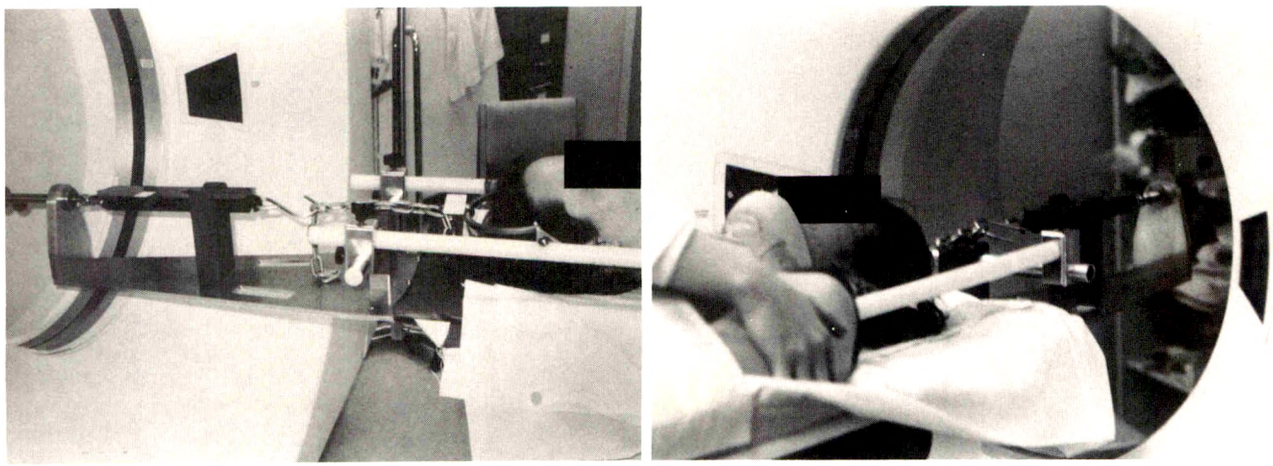
[4] Department of Neurosurgery, University of Washington, and Harborview Medical Center, Seattle, WA 98104.

AJR **149:345–346, August 1987** 0361–803X/87/1492–0345 © American Roentgen Ray Society



A B

Fig. 1.—Traction device. Front (*A*) and side (*B*) views. C-shaped braces engage shoulders from above and maintain them in a neutral or depressed position. Long, plastic rods allow for adjustment for all types of body habitus. Spring scale attaches to halo or tongs at one end and to an adjustable screw at the other end. Screw allows application of desired traction force in axial direction.



A B

Fig. 2.—Use of traction device.
A, Scale, by means of chain, applies axial traction on halo.
B, Shoulders are maintained in lowered position by cupped pads attached to adjustable (white) plastic rods.

Results

Since July 1984, 325 patients with unstable cervical injuries have had CT scans with our device. The system functioned well in all patients, and there have been no known complications in its use. We now use the system routinely in all patients who require spinal traction, including those who are unstable, and even when time is limited. The technologists have had no difficulty using the device.

Specific advantages are (1) constant, stable traction; (2) elimination of weights and pulleys that can become tangled in the scanner and cause injury; (3) elimination of excessive tension that may cause the scanner table to unlatch; (4) rapid attachment to the CT table; (5) ease of use by technologists; (6) maintenance of shoulders in a lowered position, reducing image degradation due to shoulder artifacts; and (7) ease of scanning additional body parts without attention to maintaining traction.

REFERENCES

1. Orrison WW, Johansen JG, Eldevik OP, Haughton VM. Optimal computed tomographic techniques for cervical spine imaging. *Radiology* **1982**;144:180–182
2. Acheson MB, Livingston RR, Richardson ML, Stimac GK. High-resolution CT scanning in the evaluation of cervical spine fractures: comparison with plain film examinations. *AJR* **1987**;148:1179–1185
3. Boger D, Ralls PW. New traction device for radiography of the lower cervical spine. *AJR* **1981**;137:1202–1204
4. Boger DC. Traction device to improve CT imaging of lower cervical spine. *AJNR* **1986**;7:719–721

Commentary

Arctic Paleoradiology: Portable Radiographic Examination of Two Frozen Sailors from the Franklin Expedition (1845–1848)

Derek N. H. Notman,[1] Lawrence Anderson,[1] Owen B. Beattie,[2] and Roger Amy[3]

The bodies of three British sailors who died in 1846 lie buried in the permafrost of Beechey Island in the Canadian Arctic, only 900 nautical miles from the North Pole. They were members of the ill-fated Franklin expedition, which perished in an attempt to complete a Northwest Passage. In 1984 the Franklin Expedition Forensic Anthropology Project was established by coauthor Owen Beattie and his colleagues at the University of Alberta. The principal objectives of this multidisciplinary field and laboratory study were to determine the cause of death and the presence of disease in these individuals. The body of John Torrington was subjected to a limited autopsy in 1984 [1]. In 1986, we performed a more detailed study of John Hartnell and William Braine, which included a complete portable radiographic examination and formal autopsy at the grave sites.

This investigation likely represents the first use of portable radiographic equipment under Arctic field conditions. Pathologic findings are discussed, but of parallel interest are the technical aspects of obtaining radiographs of diagnostic quality under adverse climatic and topographic conditions.

Materials and Methods

A Quonset-shaped, white canvas long-house tent was erected next to the graves to serve as a clinic (Fig. 1). The graves themselves were also sheltered by long-house tents until the bodies were reinterred. A specially designed darkroom was assembled inside the laboratory tent. This remarkable two-person structure, made of a double layer of 4-ml black landscaping plastic and supported by an 18-kg steel conduit frame, proved to be entirely light-tight, even in brightly sunlit conditions. The Port-a-Ray (Deer Park, NY) 9100A unit was mounted on a sturdy quadrapod and positioned directly over the body, which lay on a plastic sheet next to the darkroom tent (Fig. 2A). Snow was melted and filtered to provide about 250 l of water for mixing chemicals and washing the films. The film-screen combination was Kodak's (Rochester, NY) X-Omatic Regular screen with XRP film, which provided a 200-speed system. There was concern initially that this system would be too slow for a low-power radiographic unit, but specialists at Kodak believed that a faster 400-speed system would be too sensitive to the cold conditions. By using the time-temperature method, with Kodak's GBX Chemistry, films could be developed in 3–5 min, fixed for an equal time, and then washed for 15 min. The films were then dried on a clothesline for

Received March 9, 1987; accepted after revision May 4, 1987.

Canadian funding for this work was provided in part by the Social Sciences and Humanities Research Council. Additional substantial support was provided by the Polar Continental Shelf Project of Energy, Mines and Resources, Canada. United States financial support was provided by the Park Nicollet Medical Foundation, Minneapolis, MN. Additional support was provided by Northern X-Ray Co., Minneapolis; Kodak, Rochester, NY; Hoigaard's, Inc., St. Louis Park, MN; National Camera Exchange, Golden Valley, MN; Nikon Cameras; and Browning Boots, Morgan, UT.

[1] Department of Radiology, Park Nicollet Medical Center, 5000 W. 39th St., Minneapolis, MN 55416. Address reprint requests to D. N. H. Notman.

[2] Department of Anthropology, University of Alberta, Edmonton, Alta., Canada T6F 2E1.

[3] Department of Pathology, University of Alberta Medical Center, Edmonton, Alta., Canada T6G 2E1.

AJR **149:347–350, August 1987** 0361–803X/87/1492–0347 © American Roentgen Ray Society

about 2 hr, a process that was aided by Kodak's Photo-Flo solution. Essential equipment inside the darkroom included a mechanical timer, a photographic dial thermometer, and a battery-operated safelight with a GBX-2 filter.

Constant wind and occasional snow flurries buffeted the tents, but the darkroom tent inside remained adequately protected. Several Coleman stoves, used primarily for melting snow, provided heat inside the laboratory tent, maintaining an average temperature of 6°C. The temperature of the water bath itself was kept at 24°C by a 200-W fish-tank heater that was plugged into the main generator. The Honda 4.5-kW generator had to be placed at a distance of 50 m from the laboratory tent to reduce noise and to permit documentary filming of activities inside the tents. The generator worked remarkably well, especially at such a distance from the radiographic unit. Only during the multiple 3-sec exposures required to penetrate the lateral thoracic and lumbar spines did the generator "dip" momentarily, indicating that we were nearing its power limit.

The film cassettes and 8-1 wafer-type grid (when used) were wrapped in plastic bags and positioned under the region of interest. As the emaciated and dehydrated bodies continued to thaw, their limbs became almost lifelike in flexibility and could be handled much like those of living patients; foam sponges and masking tape were used for proper positioning.

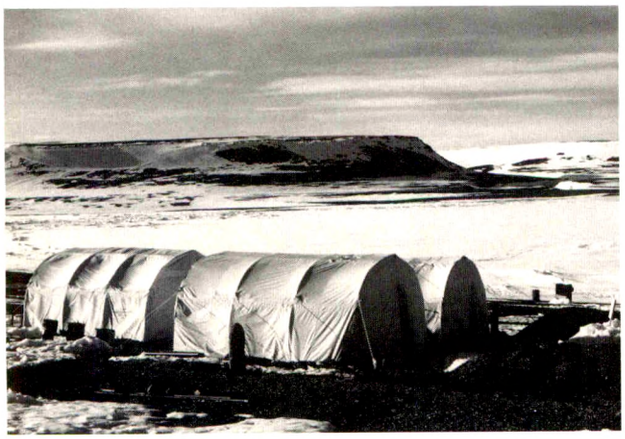
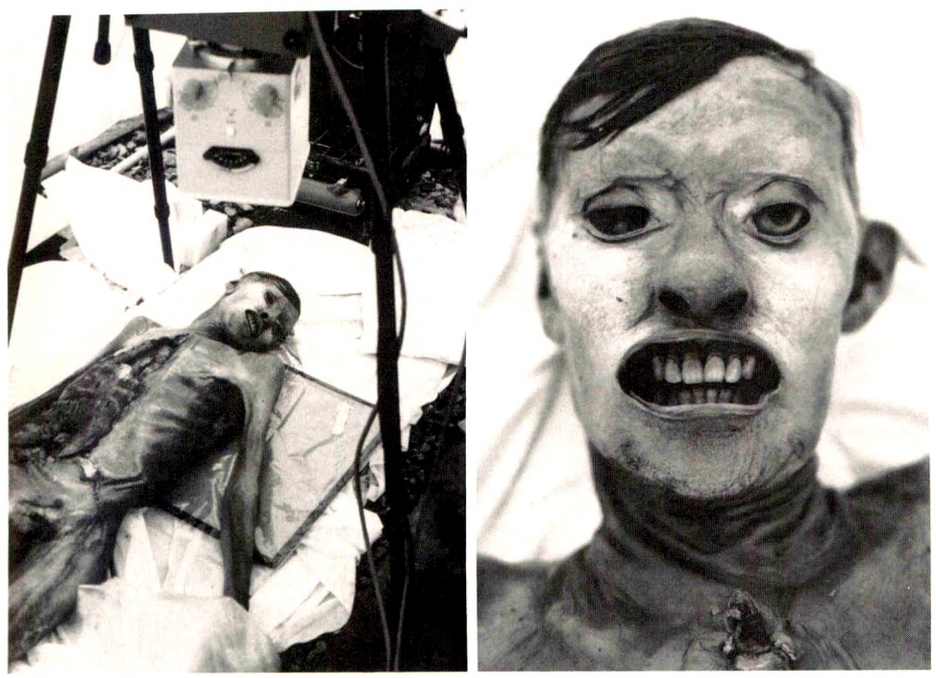


Fig. 1.—Three long-house tents at grave site on Beechey Island, N.W.T. Two tents on right stand over excavated graves of William Braine and John Hartnell. They are flanked by laboratory tent. (Photograph taken at midnight.)

Results

At the beginning of the radiographic examination, the bodies were frozen solid. Ice artifacts created such opacity within John Hartnell's skull on initial films that a considerable adjustment in technique was necessary to penetrate it. The ice opacity eventually diminished with thawing. We have radiographed phantoms through water and ice and have confirmed by simple optical densitometry that a significant increase in density occurs during the transition from liquid to solid. Once the brain had thawed, outlines of the dura and convolutions of the brain were readily visible, probably because of dehydration and autolysis (Fig. 2B). No intracranial abnormalities were detected in either John Hartnell or William Braine. There is some evidence that the crews had been exposed to elevated lead levels [2]. However, calcifications in the basal ganglia, which can be seen in chronic lead poisoning, were not evident on the radiographs.

The initial anteroposterior chest radiograph of John Hartnell, obtained before his clothing had been removed, showed a



A B

Fig. 2.—John Hartnell, 25 years old, died January 4, 1846.

***A*, In position under portable radiographic unit (Portaray 9100-A). Note original autopsy incision.**

***B*, Dehydration has caused thinning and retraction of eyelids and lips.**

bizarre mediastinal pattern of bony structures and soft tissues (Fig. 3). Once the body was exposed, however, it was discovered that the patient had been subjected to a previous postmortem examination in 1846, via an inverted Y incision. This autopsy probably had been performed by the ship's surgeon. The sternum and attached ribs had been replaced upside-down in the chest cavity, and the thoracic anatomy consequently had been disturbed by dissection of the roots of the lungs and mediastinal tissues. The frozen contents were otherwise unremarkable, although ice artifacts obscured radiographic details. Calcified granulomas (probably tuberculous) were identified on pathologic examination of lung specimens and mediastinal lymph nodes, although these were not imaged radiographically. No bony abnormalities were seen in Hartnell's body. His right shirt-sleeve had been torn during a brief and superficial examination of his grave by members of an expedition in 1852, but no fractures were seen where an errant pick had struck.

William Braine's body required more thawing than Hartnell's with buckets of warm water before it could be freed from the ice inside the coffin. This additional time also promoted internal thawing and considerably reduced the dense ice artifacts on the skull and chest films. Braine had not been autopsied in 1846. His skull and upper extremities were normal, but a slight angular kyphosis of the lower thoracic spine was discovered, with anterior collapse and wedging of the body of T11 (Fig. 4). There was considerable joint-space narrowing at T10–T11 and some narrowing at T11–T12, with reactive sclerosis and irregularity of articular margins. There were no paraspinal soft-tissue masses. These findings, taken in historical context, suggest Pott's disease rather than syphilis, which should have caused greater bony destruction and loss of contiguous joint spaces. Old trauma, a less plausible explanation, probably would not be associated with such irregularity of the end-plates. Although the frontal radiograph shows a symmetric, cleftlike appearance of the body of T11, a congenital butterfly vertebra would not exhibit anterior wedging with kyphosis on the lateral projection.

The radiographic examinations were followed immediately by detailed autopsies. Pathologic studies showed caseating, largely noncalcified granulomas in the lungs. The granulomas contained acid-fast mycobacteria, almost certainly *Mycobacterium tuberculosis*.

John Hartnell was carefully and formally reburied at midnight on June 21, 1986, and within 24 hr a similar ceremony was conducted for William Braine.

Discussion

A full account of the third Sir John Franklin expedition will probably never be written. It is known that by the end of 1848, all 129 men on the H.M.S. *Erebus* and H.M.S. *Terror* had died in what has become the worst tragedy in the history of Arctic exploration. John Torrington, John Hartnell, and William Braine were the first to die, early in 1846. Shipmates buried them on Beechey Island, where Franklin had decided to spend the winter of 1845–1846.

Since the beginning of the searches for Franklin, questions have centered on reasons for the loss of the expedition. Most explanations suggest that scurvy and eventual starvation accounted for many if not all of the deaths of the men. However, these theories were based on the discoveries of Franklin campsites and the distribution of artifacts and bones. The preserved human remains on Beechey Island had not been used as a source of information by the many search expeditions. To investigate this perspective, we hoped to obtain radiographs of diagnostic quality that might shed some light on the medical condition of John Hartnell and William Braine. The decision to attempt a radiographic survey of the bodies posed a number of unique problems.

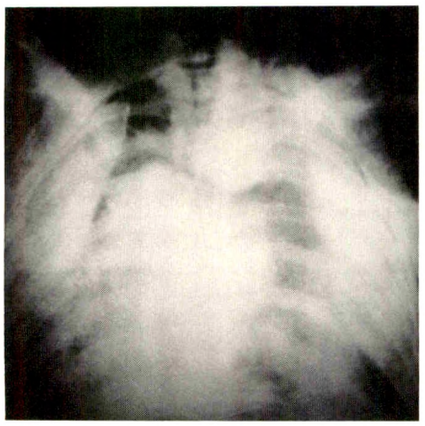
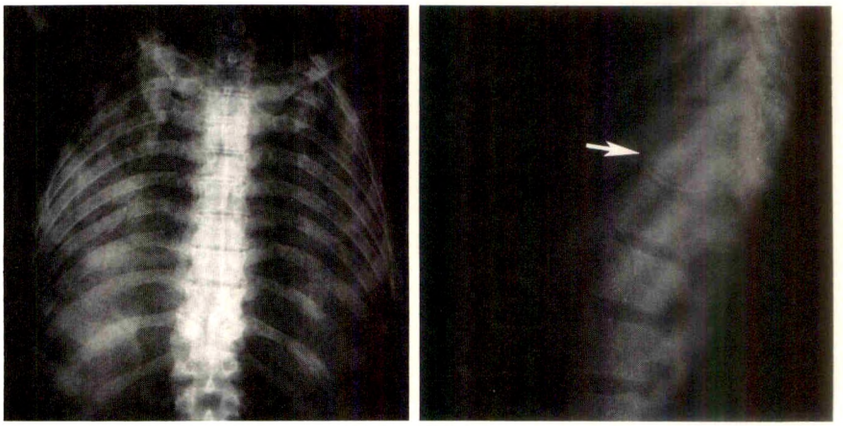


Fig. 3.—Anteroposterior chest radiograph of John Hartnell before clothing was removed. Ice artifacts obscure disturbed thoracic contents. (Imaging parameters: 80 kVp, 15 mA, 1.0 sec, with grid.)



A **B**

Fig. 4.—William Braine, 34 years old, died April 4, 1846.

***A*, Anteroposterior chest and thoracic spine with cleft appearance of T11. (Imaging parameters: 80 kVp, 15 mA, 1.0 sec, with grid.)**

***B*, Lateral thoracolumbar spine with anterior wedging of T11 (*arrow*). Loss of T10–T11 interspace with irregular articular margins. (Imaging parameters: 100 kVp, 13 mA, 9.0 sec [3 × 3.0 sec with 45-sec intervals], with grid.)**

Once the radiographic equipment had been flown to Beechey Island (via Edmonton, Alta., and Resolute, N.W.T.), we were faced with the immediate task of constructing a clinic on the wind-swept, uninhabited beach. Twenty-four-hr daylight and freezing conditions had been our main concerns from the beginning and directed the careful planning of a darkroom tent that could be erected inside a heated long-house tent. Melting snow was time-consuming but relatively simple and provided plentiful water for developing the radiographs. Initially, it was believed that the generator had been placed at too great a distance from the radiographic unit and that the extra length of heavy 14-gauge extension cord would draw too much power, but the 4.5-kW output proved to be adequate for all exposures.

One problem that was not anticipated was the constant threat of polar bears. There were numerous sightings of bears on the ice, forcing the personnel to be armed and on guard at all times while the bodies were exposed.

The radiographic findings did not prove to be significant. Pulmonary tuberculosis was common among early nineteenth century sailors, and one might expect to find lung and even spinal involvement in members of a British crew from that era. However, there was no radiographic evidence to suggest a cause of death in these men. In particular, there were no signs of trauma or dietary deficiency such as scurvy.

Emphasis should be placed on the accomplishment of producing diagnostic radiographs in such a restricted environment and with limited equipment. This goal was achieved in a spirit of true international cooperation.

Modern imaging has become increasingly important in the study of ancient remains. This project on Beechey Island shows that portable radiography can be undertaken successfully in harsh polar conditions, and that paleoradiologists undoubtedly will continue to explore the remote, uninhabited regions of the Arctic.

We feel privileged to have participated in the unique scientific investigation of John Hartnell and William Braine and to have been in attendance when those two young men who died 141 years ago were returned to their graves. The grave sites were carefully reconstructed, stone for stone, from Polaroid photographs and scaled drawings made at the start of the excavation, and if someone were to visit the site now, no trace of our camp would be found.

ACKNOWLEDGMENTS

We thank Arne Carlson, Eric Damkjar, Walt Kowal, Joelee Nungaq, James Savelle, Barbara Schweger, and Brian Spenceley.

REFERENCES

1. Amy R, Bahatnagar R, Damkjar E, Beattie O. Report of a post-mortem exam on a member of the last Franklin expedition. *Can Med Assoc J* **1986**;135:115–117
2. Beattie OB. Elevated bone lead levels in a crewman found from the last arctic expedition of Sir John Franklin. In: *The Franklin Era in Canadian Arctic history: 1845–1859*, Mercury Series Archaeological Survey of Canada paper no. 131. Ottawa, Ont.: National Museum of Man, **1985**: 141–148

MR Signal Abnormalities at 1.5 T in Alzheimer's Dementia and Normal Aging

Franz Fazekas[1]
John B. Chawluk[2]
Abass Alavi[1]
Howard I. Hurtig[2]
Robert A. Zimmerman[1]

The type, frequency, and extent of MR signal abnormalities in Alzheimer's disease and normal aging are a subject of controversy. With a 1.5-MR unit we studied 12 Alzheimer patients, four subjects suffering from multiinfarct dementia and nine age-matched controls. Punctate or early confluent high-signal abnormalities in the deep white matter, noted in 60% of both Alzheimer patients and controls, were unrelated to the presence of hypertension or other vascular risk factors. A significant number of Alzheimer patients exhibited a more extensive smooth "halo" of periventricular hyperintensity when compared with controls (p = .024). Widespread deep white-matter hyperintensity (two patients) and extensive, irregular periventricular hyperintensity (three patients) were seen in multiinfarct dementia. Areas of high signal intensity affecting hippocampal and sylvian cortex were also present in five Alzheimer and two multiinfarct dementia patients, but absent in controls. Discrete, small foci of deep white-matter hyperintensity are not characteristic of Alzheimer's disease nor do they appear to imply a vascular cause for the dementing illness. The frequently observed "halo" of periventricular hyperintensity in Alzheimer's disease may be of diagnostic importance. High-signal abnormalities in specific cortical regions are likely to reflect disease processes localized to those structures.

Alzheimer's disease is estimated as the underlying cause in 50–60% of dementia cases [1]. Therefore, it represents a serious health problem for the elderly, with about 15% of those over 65 demonstrating some degree of dementia [2]. Although the ability to diagnose Alzheimer's disease clinically has improved [3], there is still a need to increase the accuracy of in vivo diagnosis. MR imaging has shown unprecedented sensitivity in detecting pathologic changes of the brain and has the potential to contribute to this goal.

The occurrence of white-matter signal abnormalities on MR has been noted with increasing age [4–6], and extensive white-matter damage has been demonstrated in patients suffering from presumed vascular dementia [5, 7, 8]. However, reports dealing with the MR appearance of Alzheimer's disease have been anecdotal and controversial. Whereas some investigators have found no signal abnormalities in Alzheimer's disease [9], others have reported almost as many abnormalities as are seen in multiinfarct dementia (MID) [10]. More information is needed to evaluate fully the potential of MR in the diagnosis of dementia.

This report attempts to describe the type and frequency of signal abnormalities that may be observed in patients with a clinical diagnosis of Alzheimer's disease and contrasts these with findings in healthy elderly controls and patients with MID. To our knowledge this is the first time a high-field MR system has been used to address this question.

Subjects and Methods

The 25 subjects in this study were selected from a group of elderly individuals currently under investigation at our institution for cerebral abnormalities associated with normal aging

This article appears in the May/June 1987 issue of *AJNR* and the August 1987 issue of *AJR*.

Received September 19, 1986; accepted after revision December 9, 1986.

This work was supported by NIA Teaching Nursing Home grant P01AG03934 and NIH Clinical Research Center grant 5-M01RR00040.

[1] Department of Radiology, Divisions of Nuclear Medicine and Neuroradiology, Hospital of the University of Pennsylvania, 3400 Spruce St./G1, Philadelphia, PA 19104. Address reprint requests to A. Alavi (Nuclear Medicine).

[2] Department of Neurology, Cerebrovascular Research Center, Hospital of the University of Pennsylvania, Philadelphia, PA 19104.

***AJR* 149:351–356, August 1987**
0361–803X/87/1492-0351
© American Roentgen Ray Society

and dementia. These subjects were carefully screened by a neurologist and underwent a comprehensive laboratory evaluation consisting of an automated blood chemistry battery, tests for vitamin B12 deficiency and thyroid dysfunction, as well as ECG, electroencephalogram, and chest radiograph. All subjects underwent CT, MR, and positron emmission tomography scanning. The mini-mental state examination [11] and the Blessed dementia scale [12] were included as part of the neuropsychological test battery.

In 12 subjects a diagnosis of Alzheimer's disease was established according to clinical diagnostic criteria set forth in the DSM III (*Diagnostic and Statistical Manual of Mental Disorders*) [13] and expanded on by an NINCDS–ADRDA consensus committee [14]. All Alzheimer patients scored 2 or less on a modification of Hachinski's vascular dementia scale [15] and demonstrated no other clinical cause for their dementing illness. In four other demented subjects a Rosen-Hachinski score [15] of greater than 4 suggested a multiinfarct state as the cause of dementia. Impairment was defined by mini-mental state examination scores as mild (>20), moderate (11–20), and severe (10 or less). Nine healthy elderly control subjects were also studied and were found to be free of any neurologic, psychiatric, or major systemic illnesses, although one subject had diabetes and two had a history of hypertension. The mean ages in these groups were 69 (Alzheimer), 70 (MID), and 68 (healthy controls) years old, respectively.

MR was performed on a General Electric imaging unit with a superconducting magnet to generate a field strength of 1.5 T. Image acquisition was performed with a spin-echo technique, the pulse sequences being repetition time (TR) 600–800 msec/echo time (TE) 20–25 msec for T1-weighted and TR 1500–2500 msec/TE 25–120 msec for T2-weighted images. Sagittal, axial, and coronal scans were available in every subject and interpreted by a neuroradiologist blinded to the clinical diagnosis.

A modification of suggested rating scales [5, 6] was used to describe the different types of hyperintense signal abnormalities surrounding the ventricles and in the deep white matter. Periventricular hyperintensity (PVH) was graded as 0 = absence, 1 = "caps" or pencil-thin lining, 2 = smooth "halo," 3 = irregular PVH extending into the deep white matter. Separate deep white matter hyperintense signals (DWMH) were rated as 0 = absence, 1 = punctate foci, 2 = beginning confluence of foci, 3 = large confluent areas.

The occurrence of these types of abnormality as well as the presence of other signal intensity changes were recorded for dementia patients (Alzheimer and MID) and controls, and compared among the groups. The effects of age, vascular risk factors, and dementia severity on the degree and nature of the signal abnormalities were assessed.

Results

MR revealed a variety of signal abnormalities in controls, as well as in patients with Alzheimer's disease and MID. These findings together with the subjects' clinical data are listed in Table 1 and are discussed below.

TABLE 1: Clinical Features and MR Findings in Alzheimer's Disease, Multiinfarct Dementia, and Normal Aging

Group: Case No.	Age	Duration (years)	Severity	Risk Factors	Grade		Other
					PVH	DMWH	
Probable Alzheimer's disease:							
1	70	3	Mild	H, CAD	2	0	CH
2	66	3	Mild	H	0	0	...
3	66	3	Moderate	H	2	0	...
4	77	6	Moderate	...	2	0	CH
5	80	4	Moderate	...	1	2	CH
6	61	3	Severe	...	1	1	...
7	68	10	Severe	H	1	2	...
Possible Alzheimer's disease:							
8	52	1	Mild	...	0	0	...
9	62	6	Moderate	...	2	2	CH
10	71	2	Moderate	...	2	2	CH
11	77	3	Moderate	H, D	1	1	...
12	73	5	Severe	...	2	1	...
Multiinfarct dementia:							
13	64	6	Mild	H	3	3	BGL, I
14	74	3	Moderate	H, CAD	3	3	BGL, CH
15	63	3	Moderate	H	3	2	I
16	80	1	Severe	H	1	1	BGL, CH
Control:							
17	52	...	...	D	0	1	...
18	70	...	...	...	1	1	...
19	64	...	...	...	0	0	...
20	61	...	...	H	0	0	...
21	68	...	...	...	0	2	...
22	76	...	...	...	1	0	...
23	76	...	...	...	1	2	BGL
24	83	...	...	H	3	2	...
25	65	...	...	...	0	0	...

Note.—PVH = periventricular hyperintensity; DWMH = deep white-matter hyperintensity; H = hypertension; CAD = coronary artery disease; CH = cortical hyperintensity; D = diabetes mellitus; BGL = basal ganglionic lesions; I = "classical" infarcts (infarcts confined to typical vascular territories).

Periventricular Hyperintensity

In controls, areas of abnormal high signal intensity around the ventricles were either absent or seen as caps or a pencil-thin lining of periventricular hyperintensity (PVH) (Fig. 1). The sole exception was a grade-3 PVH pattern in a healthy 83-year-old individual with a history of hypertension. PVH was noted in 10 of 12 Alzheimer subjects, with six showing a halo (Fig. 2C) of high signal intensity around the ventricles. The proportion of Alzheimer patients with a PVH score of 2 was significantly different from that in controls (Table 2). In contrast to Alzheimer patients and controls, three MID subjects (75%) showed an irregular PVH extending into the deep white matter (Fig. 3B).

Deep White-Matter Hyperintensity

The incidence and extent of deep white-matter hyperintensity (DWMH) seen in Alzheimer patients was comparable to that observed in controls. About 60% of all subjects had some foci of DWMH. However, confluent areas of DWMH (Fig. 3) were present only in MID (two patients) (Table 2).

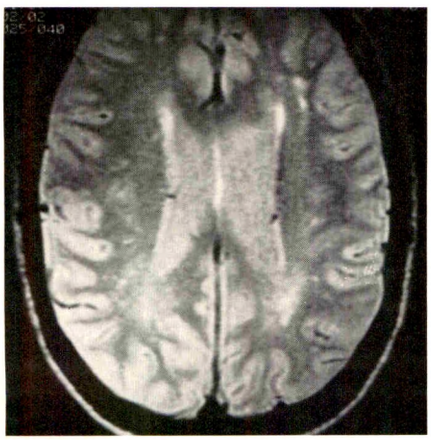
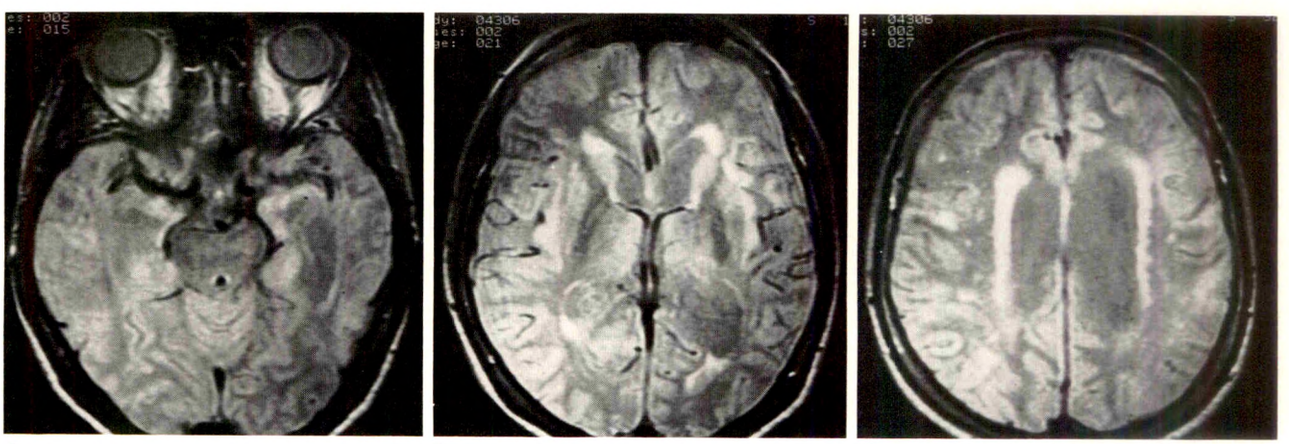


Fig. 1.—Case 18: 70-year-old male control subject with no vascular risk factors. Pencil-thin line of hyperintensity (grade 1) surrounds ventricles. Punctate foci of high signal intensity (grade 1) in deep white matter.

TABLE 2: Incident and Extent of MR Abnormalities in Alzheimer's Disease, Multiinfarct Dementia, and Normal Controls

Abnormality	No. of Patients		
	Controls	Alzheimer's disease	Multiinfarct Dementia
Periventricular hyperintensity (grade):			
0–1	8	6	1
2	0	6*	0
3	1	0	3
Deep white-matter hyperintensity (grade):			
0	4	5	0
1	2	3	1
2	3	4	1
3	0	0	2
Type of lesion:			
Cortical hyperintensity	0	5	2
Basal ganglionic foci	1	0	3
Infarct	0	0	2

* The proportion of Alzheimer patients with grade 2 periventricular hyperintensity differs significantly from that in controls ($p = .024$).



A **B** **C**

Fig. 2.—Case 9: 62-year-old woman with Alzheimer's disease and no vascular risk factors.
***A*, Signal intensity of hippocampal cortex is increased bilaterally.**
***B*, Sylvian cortex on left and right are of high signal intensity; hyperintense areas are present at tips of ventricles.**
***C*, Smooth halo of hyperintensity (grade 2) surrounds ventricles; punctate foci of high signal intensity are noted in subcortical white matter. Beginning confluence of these foci (not shown) was present on more inferior sections.**

Miscellaneous Findings

Areas of high signal intensity in cortical regions were also noted on some MR studies. In five Alzheimer patients the cortex of the sylvian and/or hippocampal-uncal regions appeared bright on T2-weighted images (Figs. 2A and 2B). Similar changes were seen in two MID subjects but were not seen in any of the controls. MR of Alzheimer subjects revealed no basal ganglionic lesions or "classical" infarcts. However, such abnormalities were common in MID (Table 2).

Correlation of MR Findings with Clinical Data

The presence of a halo of PVH in Alzheimer subjects was not correlated with the severity of dementia, nor was there a correlation of dementia severity with any other signal abnormality detected in these individuals. There was no relationship between a type 1 or 2 PVH or DWMH and vascular risk factors (see Table 1). There was a history of hypertension, however, in all subjects with an irregular PVH extending into the deep white matter or with confluent areas of DWMH (grade 3 lesions). PVH and DWMH were observed more often in the older subjects in this series, but the presence or type of white-matter signal abnormality could not be predicted on the basis of a subject's age. All subjects without any PVH abnormalities, however, were younger than 70 years.

Discussion

In recent years the routine neuroimaging study of the brain in Alzheimer's disease has been CT, the aim being to exclude possible treatable causes of the dementia. Otherwise, the capabilities of CT in supporting the diagnosis of Alzheimer's disease have been restricted to imaging diffuse cerebral atrophy considered inappropriate for the patient's age. Reports on changes in brain density with Alzheimer's disease have been controversial [16, 17].

Early experience with MR has already demonstrated its greater sensitivity in detecting cerebral abnormalities in comparison with CT [18, 19]. This is particularly true for white-matter lesions, which can be detected readily by highlighting T2 relaxation with a long spin-echo pulse-sequence method [20]. The possibility of a distinct white-matter disorder in Alzheimer's disease reported recently in a pathoanatomic study by Brun and Englund [21] supports the rationale of applying MR in the evaluation of this disease. Nevertheless, the number of white-matter signal abnormalities observed in Alzheimer's disease in this study is somewhat surprising.

Our results support the observation that foci of high signal intensity in the deep white matter are commonly seen in clinically normal elderly individuals [5, 22]. In contrast to a report by Erkinjuntti et al. [9], a similar frequency and extent of such deep white-matter lesions were seen in Alzheimer patients. The more extensive signal changes in the deep white matter seen in two of our MID patients were recently described with vascular dementia [7, 8]. In our series such widespread lesions were not present either in Alzheimer patients or in controls. Therefore, such a finding should rule against a diagnosis of pure Alzheimer's disease. The extensive deep white-matter changes observed in an 85-year-old Alzheimer patient with a gait disturbance in the series of George et al. [22] presumably reflects marked vascular damage in addition to Alzheimer's disease. Therefore, this case would be classified as a mixed type of dementia [23], a speculation supported by the neuropathologic observations

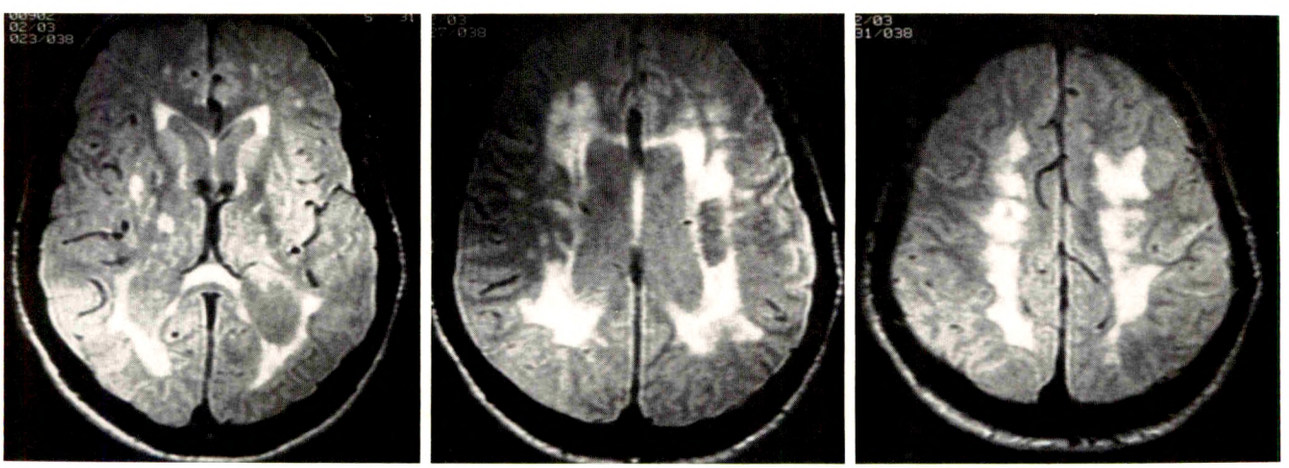


Fig. 3.—Case 13: 64-year-old man with multiinfarct dementia and history of hypertension.
***A*, Two hyperintense lesions in right putamen and thalamus; punctate foci of hyperintensity in left basal ganglia. Areas of hyperintensity surround tips of ventricles.**
***B*, Diffuse irregular hyperintensity surrounds ventricles and extends into deep white matter (grade 3).**
***C*, Confluent lesions of high signal intensity (grade 3) involve almost entire supraventricular deep white matter.**

of similar patients by the same authors [24]. In our experience the smaller white-matter lesions (punctate foci of hyperintensity or even beginning confluence of DWMH) are of no value in distinguishing Alzheimer patients from controls.

The white-matter signal abnormalities we have seen in our Alzheimer patients do not appear to be identical to the white-matter pathology described by Brun and Englund [21]. They observed large, diffuse, predominantly symmetric areas in the deep white matter with partial loss of axons, myelin sheaths, and oligodendroglial cells, accompanied by a mild reactive astrocytosis; in our series MR revealed only punctate or slightly confluent areas of high signal abnormality. Either these lesions do not produce enough change in tissue proton arrays to be fully detected by MR—their pathologic appearance being different from pronounced ischemic damage—or they have not been present in our patients. Pathologically confirmed severe ischemic changes in the deep white matter have been shown to cause extensive signal hyperintensity [7].

The similar extent, frequency, and distribution of the deep white-matter signal abnormalities seen in both healthy elderly individuals and Alzheimer patients suggest a common etiology. Possibilities include local ischemia or focal parenchymal degeneration due to aging. Whereas the presence of vascular risk factors was not correlated with the occurrence of such minor signal abnormalities, all patients (cases 13, 14, 15, and 24) with extensive deep white-matter disease or irregular PVH extending into the deep white matter (grade 3) had a history of hypertension.

The most distinctive finding in Alzheimer's disease in this study was a halo of high signal intensity surrounding the ventricles. This abnormality was detected in 50% of Alzheimer patients and was not present in controls or MID. In a review of 365 cerebral cases studied by MR, a similar pattern of PVH was invariably associated with a specific disease process, for example, hydrocephalus, supratentorial neoplasms, trauma, and rarely white-matter disease [6]. Given the smooth margin of this halolike abnormality, it seems unlikely that ischemia or demyelination would be the cause. It may rather represent an exaggeration of a similar process that has been hypothesized to cause the pencil-thin lining of PVH, more often observed in older subjects with otherwise normal MR studies [6]. This latter hypothesis is supported by our data, since all patients without PVH were younger than 70 years. It has been suggested that the periventricular subependymal lining of hyperintensity reflects an increase in interstitial water reabsorption from the white matter into the ventricles [6]. This explanation is consistent with the observation that caps of PVH seem to be present first, since the area that has to be drained of interstitial water will be greatest for the tips of the ventricles. In patients with Alzheimer's disease this bulk flow to the ventricles would therefore seem to be further enhanced. Unfortunately, no studies directly address the question of interstitial water content in Alzheimer's disease, although there is some indirect support from previous radiologic studies. Besson et al. [25], calculating the proton density of white matter on MR scans, reported a water content of white matter in Alzheimer's disease that was significantly increased over that of both controls and MID patients. Similarly, the finding of decreased white-matter density on CT [16] is consistent with increased interstitial water. White-matter changes such as those described by Brun and Englund [21] might be the underlying pathologic substrate, and MR might detect their distant effects as increased periventricular water rather than as the actual lesion.

Although its pathologic basis may not be clear, the appearance of the halo of hyperintensity in Alzheimer's disease is an important empirical observation. To date this pattern of PVH has been mostly ascribed to hydrocephalus [6] and has been claimed to be a very reliable diagnostic sign in normal-pressure hydrocephalus [26]. Since normal-pressure hydrocephalus might be considered in the differential diagnosis of Alzheimer's disease, yet requires substantially different management, the notion of a similar PVH pattern in Alzheimer's disease may be critical. Our subjects suffering from Alzheimer's disease had no clinical or radiologic signs suggestive of normal-pressure hydrocephalus.

On the basis of the above discussion, one may speculate that the rim of PVH in normal subjects widens with advancing age, making it similar to that of Alzheimer patients. Our experience with MR in normal patients over 80 years old is too limited to evaluate this possibility.

In accordance with pathologic [23] and CT data, MR detected no typical infarcts or basal ganglionic lesions in Alzheimer patients. Such abnormalities were also absent in controls, except for a tiny lenticular nucleus signal abnormality seen in one normal individual. Basal ganglionic lesions seem to be an important feature in MID, however, confirming previous CT reports [27].

Areas of cortical hyperintensity were present in five Alzheimer and two MID patients. It is likely that such abnormalities affecting the hippocampus reflect changes that have occurred in the cortical structure. A disturbed quantitative relationship of neurons to glia and associated degenerative changes (that is, a high number of senile plaques and fibrillary tangles) may be the basis for these signal-intensity changes. The topography of these histopathologic alterations seen in Alzheimer's disease corresponds well with the hippocampal hyperintensity detected on MR [28]. Congophilic angiopathy affecting cortical vessels with secondary parenchymal changes may represent another possible explanation for the observed hyperintense cortical signals. Pathologically those changes have been reported to occur less often in the hippocampus, however, than in other regions of the brain [29].

In summary, MR has demonstrated its ability to detect parenchymal changes in the brains of Alzheimer patients who have not been seen before with high-resolution CT. The implication of a signal abnormality differs with its type. Small discrete foci of DWMH are neither characteristic of Alzheimer's disease nor do they implicate a vascular cause of dementia, since they are seen to a similar extent in healthy elderly individuals. Furthermore, these punctate lesions appear to be unrelated to the presence of vascular risk factors. A smooth halo of PVH, however, is a distinctive finding in Alzheimer's disease. Areas of cortical signal hyperintensity observed in Alzheimer patients may reflect the disease process itself.

REFERENCES

1. Terry RD, Katzman R. Senile dementia of the Alzheimer type. *Ann Neurol* **1983**;14:497–506
2. Katzman R. The prevalence and malignancy of Alzheimer disease. *Arch Neurol* **1976**;33:217–218
3. Ron MA, Toone BK, Garralda ME, Lishman WA. Diagnostic accuracy in presenile dementia. *Br J Psychiatry* **1979**;134:161–168
4. Bradley WG Jr, Waluch V, Brant-Zawadzki M, Yadley RA, Wycoff RR. Patchy, periventricular white matter lesions in the elderly: a common observation during NMR imaging. *Noninvasive Med Imaging* **1984**;1:35–41
5. Brant-Zawadzki M, Fein G, Van Dyke C, Kiernan R, Davenport L, de Groot J. MR imaging of the aging brain: patchy white-matter lesions and dementia. *AJNR* **1985**;6:675–682
6. Zimmerman RD, Fleming CA, Lee BCP, Saint-Louis LA, Deck MDF. Periventricular hyperintensity as seen by magnetic resonance: prevalence and significance. *AJNR* **1986**;7:13–20, *AJR* **1986**;146:443–450
7. Kinkel WR, Jacobs L, Polachini I, Bates V, Heffner RR Jr. Subcortical arteriosclerotic encephalopathy (Binswanger's disease). Computed tomographic, nuclear magnetic resonance, and clinical correlations. *Arch Neurol* **1985**;42:951–959
8. Alavi A, Fazekas F, Chawluk J, Zimmerman R. Magnetic resonance imaging of the brain in normal aging and dementia. Presented at the Conference on Cerebrovascular Disease, Salzburg, Austria, September **1986**
9. Erkinjuntti T, Sipponen JT, Iivanainen M, Ketonen L, Sulkava R, Sepponen RE. Cerebral NMR and CT imaging in dementia. *J Comput Assist Tomogr* **1984**;8:614–618
10. Cherryman GR, Gemmell HG, Sharp PF, Besson JAO, Crawford J, Smith FW. NMR demonstration of white matter changes in the watershed area of patients with dementia. Correlation with psychiatric evaluation and J-123-isopropylamphetamine cerebral blood flow imaging. Presented at the international meeting of the Society of Magnetic Resonance in Medicine, London, August **1985**
11. Folstein MF, Folstein SE, McHugh PR. "Mini-mental state": a practical method for grading the cognitive state of patients for the clinician. *J Psychiatr Res* **1975**;12:189–198
12. Blessed G, Tomlinson BE, Roth M. The association between quantitative measures of dementia and of senile change in the cerebral gray matter of elderly subjects. *Br J Psychiatry* **1968**;114:797–811
13. American Psychiatric Association. *Diagnostic and statistical manual of mental disorders*, 3d ed. Washington, DC: American Psychiatric Association, **1980**
14. McKhann G, Drachman D, Folstein M, Katzman R, Price D, Stadlan EM. Clinical diagnosis of Alzheimer's disease. *Neurology* **1984**;34:939–944
15. Rosen WG, Terry RD, Fuld PA, Katzman R, Peck A. Pathological verification of ischemic score in differentiation of dementias. *Ann Neurol* **1980**;7:486–488
16. Naeser MA, Gebhardt C, Levine HL. Decreased computerized tomography numbers in patients with presenile dementia. *Arch Neurol* **1980**;37:401–409
17. George AE, de Leon MJ, Ferris SH, Kricheff II. Parenchymal CT correlates of senile dementia (Alzheimer disease): loss of gray-white matter discriminability. *AJNR* **1981**;2:205–213
18. Bradley WG, Waluch V, Yadley RA, Wycoff RR. Comparison of CT and MR in 400 patients with suspected disease of the brain and cervical spinal cord. *Radiology* **1984**;152:695–702
19. Baker HL, Berquist TH, Kispert DB, et al. Magnetic resonance imaging in a routine clinical setting. *Mayo Clin Proc* **1985**;60:75–90
20. Brant-Zawadzki M, Norman D, Newton TH, et al. Magnetic resonance of the brain: the optimal screening technique. *Radiology* **1984**;152:71–77
21. Brun A, Englund E. A white matter disorder in dementia of the Alzheimer type: a pathoanatomical study. *Ann Neurol* **1986**;19:253–262
22. George AE, de Leon MJ, Kalnin A, Rosner L, Goodgold A, Chase N. Leukoencephalopathy in normal and pathologic aging: 2. MRI of brain lucencies. *AJNR* **1986**;7:567–570
23. Tomlinson BE, Blessed G, Roth M. Observations on the brains of demented old people. *J Neurol Sci* **1970**;11:205–242
24. George AE, de Leon MJ, Gentes CI, et al. Leukoencephalopathy in normal and pathologic aging: 1. CT of brain lucencies. *AJNR* **1986**;7:561–566
25. Besson JAO, Corrigan FM, Foreman I, Eastwood LM, Smith FW, Ashcroft GW, Nuclear magnetic resonance (NMR): 2. Imaging in dementia. *Br J Psychiatry* **1985**;146:31–35
26. Kortman KE, Bradley WG. Magnetic resonance imaging of normal pressure hydrocephalus. Presented at the annual meeting of the American Society of Neuroradiology, New Orleans, February **1985**
27. Ladurner G, Iliff LD, Sager WD, Lechner H. A clinical approach to vascular (multiinfarct) dementia. In: Meyer JS, Lechner H, Reivich M, Ott EO, eds. *Cerebral vascular disease 4*. Amsterdam: Excerpta Medica, **1983**:236–243
28. Englund E, Brun A. Senile dementia—a structural basis for etiological and therapeutic considerations. In: Perris C, Struwe G, Jansson B, eds. *Biological psychiatry*. Amsterdam: Elsevier, **1981**:951–956
29. Vinters HV, Gilbert JJ. Cerebral amyloid angiopathy: incidence and complications in the aging brain. 2. The distribution of amyloid vascular changes. *Stroke* **1983**;14:924–928

Reduced Signal Intensity on MR Images of Thalamus and Putamen in Multiple Sclerosis: Increased Iron Content?

Burton Drayer[1-3]
Peter Burger[4]
Barrie Hurwitz[2]
Deborah Dawson[5]
John Cain[1]

High-field-strength (1.5-T) MR imaging was used to evaluate 47 patients with definite multiple sclerosis and 42 neurologically normal control patients. Abnormal, multiple foci of increased signal intensity on T2-weighted images, most prominent in the periventricular white matter, were apparent in 43 of 47 MS patients and in two of 42 control patients. A previously undescribed finding of relatively decreased signal intensity most evident in the putamen and thalamus on T2-weighted images was seen in 25 of 42 MS patients and correlated with the degree of white-matter abnormality. In the normal control patients a prominently decreased signal intensity was noted in the globus pallidus, as compared with the putamen or thalamus, correlating closely with the distribution of ferric iron as determined in normal Perls'-stained autopsy brains. The decreased signal intensity (decreased T2) is due to ferritin, which causes local magnetic field inhomogeneities and is proportional to the square of the field strength. The decreased T2 in the thalamus and striatum in MS may be related to abnormally increased iron accumulation in these locales with the underlying mechanism remaining speculative.

MR imaging has become the primary imaging technique for the diagnosis of multiple sclerosis (MS) [1, 2]. The basic MR abnormality, an increase in signal intensity on a T2-weighted image, results from an increase in mobile protons from either edema, gliosis, or neutral sudanophilic lipid (cholesterol esters and triglycerides) accumulation [3]. Our studies with high-field-strength (1.5-T) MR suggest that additional functional information concerning MS may be derived by delineating an abnormally decreased signal intensity on T2-weighted images in the thalamus and putamen. This investigation analyzes the origin of this decreased T2 relaxation time and its detectability in relationship to disease severity.

Subjects and Methods

We studied 47 patients aged 23–57 years old (mean, 40) with a clinical diagnosis of definite MS as established with standard diagnostic criteria [4]. MR studies were compared with those of 42 neurologically normal control individuals aged 21–58 (mean, 38) studied for headache, vertigo, depression, or orbital or middle-ear disorders.

MR imaging was performed with a high-field-strength (1.5-T) superconducting GE Signa or prototype system. After obtaining a multislice T1-weighted partial-saturation (PS) pulse sequence in the sagittal plane with a 500-msec repetition time (TR) and a 25-msec echo time (TE) (PS 500/25), a multislice T2-weighted spin-echo (SE) sequence was obtained with TR 2000 or 2500 and TE 100 or 80 msec (SE 2500/80) in both axial and coronal projections. Intermediate-weighted SE sequences with TR 2000 or 2500 and TE 30 or 40 msec (SE 2500/40) were also routinely obtained simultaneously with the T2-weighted images (a multislice, multiecho pulse sequence). An image acquisition matrix of 128 × 256 was used with a slice thickness of 5 or 10 mm and a single signal average. The total imaging time for the entire brain with all pulse sequences was only 19 min 12 sec.

The images were analyzed for areas of abnormal signal intensity. MS lesions were defined as localized regions of abnormally increased signal intensity (increased T2 relaxation time) on T2-weighted images. A visual rating of lesion number and severity was made and the MS

This article appears in the May/June 1987 issue of *AJNR* and the August 1987 issue of *AJR*.

Received July 23, 1986; accepted after revision November 5, 1986.

Presented at the annual meeting of the American Society of Neuroradiology, San Diego, January 1986.

[1] Department of Radiology, Duke University Medical Center, Durham, NC 27710.

[2] Department of Medicine (Neurology), Duke University Medical Center, Durham, NC 27710.

[3] Present address: Department of Radiology, St. Joseph's Hospital and Medical Center, and Division of Neuroradiology, Barrow Neurological Institute, 350 W. Thomas Rd., Phoenix, AZ 85013. Address reprint requests to B. P. Drayer.

[4] Department of Pathology, Duke University Medical Center, Durham, NC 27710.

[5] Department of Community and Family Medicine (Biometry), Duke University Medical Center, Durham, NC 27710.

***AJR* 149:357–363, August 1987**
0361–803X/87/1492-0357
© American Roentgen Ray Society

patients and normal controls were separated into four groups on the basis of degree of MR abnormality (normal, mild, moderate, severe). The T2-weighted images were also evaluated to compare the relatively decreased signal intensity (decreased T2) in the thalamus and putamen with that in the globus pallidus. A simple three-point visual rating scale was used to analyze the T2-weighted images at the basal ganglia–thalamic level, in which *normal* = decreased signal intensity in the globus pallidus more prominent than in the putamen and far more prominent than in the thalamus, *equivocal* = decreased signal intensity in the globus pallidus slightly more prominent than in the putamen and more prominent than in the thalamus, and *abnormal* = decreased signal intensity in the globus pallidus equal to or less prominent than that in the putamen and caudate and only minimally more prominent or equally prominent to that in the thalamus.

Perls' stain [5–7] was used in four normal autopsy brains (18, 21, 43, and 44 years old) to determine the normal topographic distribution of ferric iron in the brain. In addition, an autopsy brain from one individual with MS was analyzed. Each brain was fixed in 20% formalin for at least 1 week, and horizontal 1-cm-thick sections were cut with at least two sections through the basal ganglia and thalamus. The brain sections were washed in tap water for 15 min and rinsed with three changes of distilled water. The specimens were immersed in Perls' stain for ferric iron with intermittent agitation over 30 min. The Perls' staining solution was decanted and the specimens washed for 5 min in tap water before color and black-and-white photography.

An estimate of the T2 relaxation time was made with the multislice SE 2500/40–80 msec pulse sequence in 13 normal control patients 23–54 years old (mean, 39) and in 13 of the MS patients 23–54 years old (mean, 39). Computed T2 and pseudodensity values were derived as described by MacFall [8] by performing a weighted linear regression on the logarithms of the source signal values for each pixel. The negative reciprocal of the slope of the fitted line represented T2, while the exponential of the intercept at TE equal to zero represented the pseudodensity. Operator-selected, region-of-interest cursors containing 12 (3 × 4) pixels were placed in the globus pallidus, putamen, and thalamus bilaterally to determine mean T2 and SD.

Relationships between number and severity (normal, mild, moderate, severe) of white-matter lesions and signal intensity ratings (normal, equivocal, or abnormal) on SE 2500/80 images were evaluated using Kendall's tau-b statistic, which is a measure of the association between two ordinal measurements [9]. It takes on values between −1 and +1 and is interpreted in the same way as a correlation coefficient: tau-b > 0 implies a direct relationship between the two measures under study and tau-b < 0 implies an inverse relationship. The closer tau-b is to +1 or −1, the stronger the association. In testing the hypothesis that there is no increasing or decreasing relationship between lesion severity and T2 rating (tau-b = 0), significance probabilities (p values) were obtained according to the approximation of Brown and Benedetti [10]. The nonparametric Wilcoxon rank sum test was used to compare MS and control groups with respect to the distributions of estimated T2 relaxation times in the globus pallidus, putamen, and thalamus, as well as in terms of the globus pallidus/putamen and globus pallidus/thalamus T2 ratios.

Results

There was no significant abnormality in the 42 neurologically normal patients except for a few scattered discrete areas of increased signal intensity in the cerebral white matter in two individuals. High-signal-intensity abnormalities on the SE 2500/80 and SE 2500/40 images were apparent in the cerebral white matter with a periventricular predominance in 43 of 47 patients with definite MS. The degree of MR abnormality was rated as normal in four, mild in 21, moderate in 17, and severe in five. No lesions were seen on the PS 500/25 images that were not delineated on the T2-weighted images. The number and extent of white-matter lesions were characterized equally well on axial and coronal SE images. The majority of white-matter lesions were periventricular in location with additional abnormalities in the more peripheral centrum semiovale, internal and external capsules, brainstem, and cerebellum. There was no association between patient age and the number and extent of MS lesions.

The visual analyses of the decreased-signal-intensity ratings for the globus pallidus, putamen, and thalamus and their relationship to the number and severity of high-signal-intensity lesions in the white matter are summarized in Table 1. A dominant decrease in signal intensity in the globus pallidus as compared with the putamen was noted in 40 of 42 control patients and as compared with the thalamus in all 42 control patients (Fig. 1). A relative prominence of decreased signal intensity in the thalamus as compared with the globus pallidus was differentiated on the SE 2500/80 images on visual inspection in moderate (10 of 17) and severe (five of five) MS as compared with patients with fewer (one of 21) or no (zero of four) white-matter lesions (Figs. 2 and 3). Abnormally decreased signal intensity in the putamen was also prominent in moderate (12 of 17) and severe (five of five) MS (Figs. 3 and 4) and was noted also with less extensive white-matter involvement (seven of 21).

The correlational measures of association (Kendall's tau-b) between lesion severity (number and extent of white-matter lesions) and T2 ratings were 0.609 + 0.067 using T2 ratings for the putamen vs globus pallidus comparison and 0.687 + 0.048 for the thalamus vs globus pallidus contrast. Since $p <$

TABLE 1: Putamen/Thalamic vs Globus Pallidus Signal-Intensity (T2) (SE 2500/80) Ratings in Multiple Sclerosis

Region: Signal Intensity	No. of Lesions				
	Normal Control	Normal MS	Mild MS	Moderate MS	Severe MS
Putamen:					
Normal	39	3	13	3	0
Equivocal	1	0	1	2	0
Abnormal	2	1	7	12	5
Total	42	4	21	17	5
Thalamus:					
Normal	42	4	18	4	0
Equivocal	0	0	2	3	0
Abnormal	0	0	1	10	5
Total	42	4	21	17	5

Note.—MS = multiple sclerosis. Signal-intensity rating scale: *normal*—decreased signal intensity (T2) in the globus pallidus was strikingly more apparent than in the putamen or thalamus; *equivocal*—decreased signal intensity in the globus pallidus was only slightly more apparent than in the putamen or thalamus; *abnormal*—decreased signal intensity in the globus pallidus was similar to that in the putamen and thalamus; that is, increased thalamic and putamen iron. The statistical measures of association between severity and T2 ratings with a Kendall tau-b statistical analysis were tau-b 0.609 (0.687), asymptomatic error 0.067 (0.048), and significance probability $p < .0001$ ($p <$ .0001) for the putamen (thalamus).

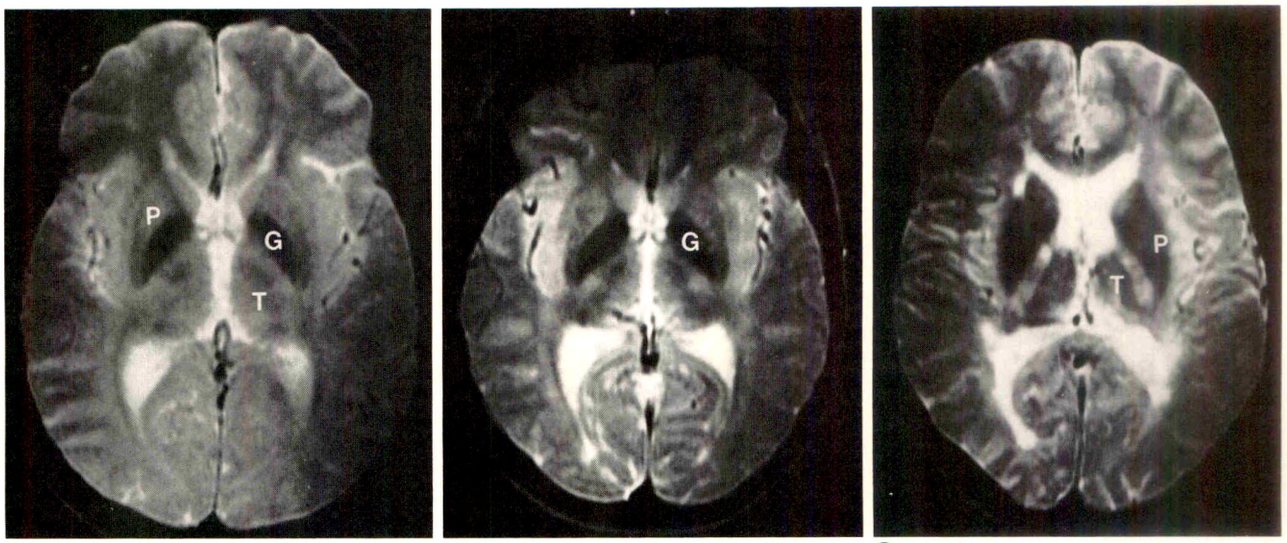


Fig. 1.—Normal, mild, and severe multiple sclerosis. SE 2000/100 msec (T2-weighted) axial MR images with 1.5-T MR unit.
***A*, Normal iron distribution—decreased signal intensity in globus pallidus (G) vs putamen (P) or thalamus (T)—in control patient (age 34).**
***B*, Normal iron distribution in mild multiple sclerosis patient (age 32).**
***C*, Abnormal decreased signal intensity (increased iron) as compared with normal in putamen and thalamus in 32-year-old patient with moderate multiple sclerosis.**

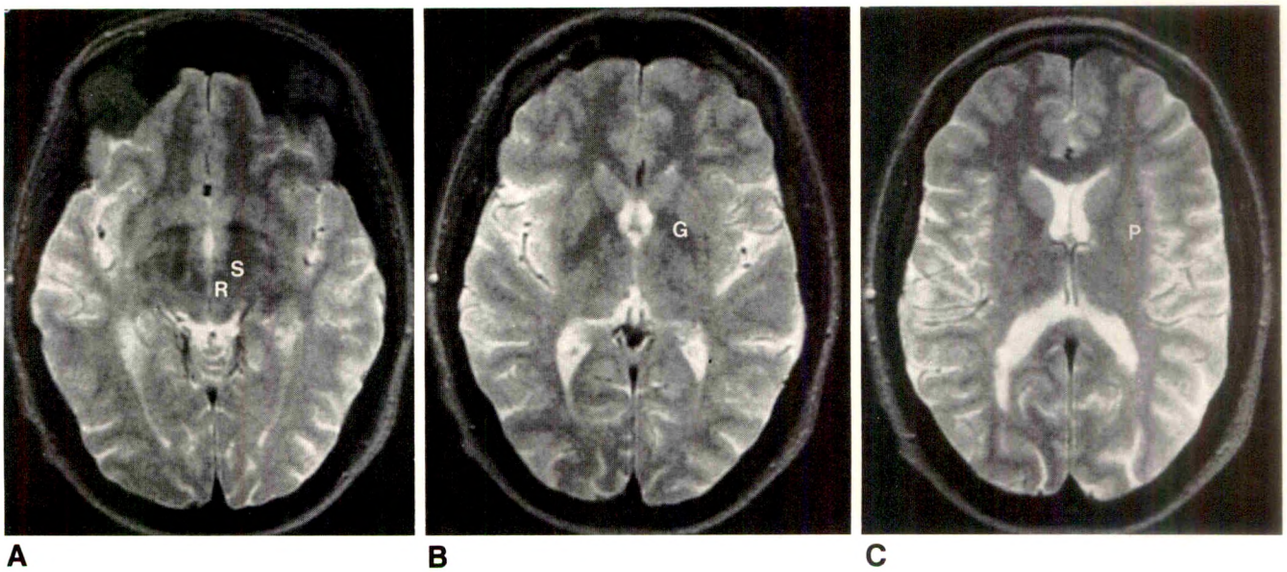


Fig. 2.—Mild multiple sclerosis (normal iron). SE 2500/80 msec (T2-weighted) axial MR images define normal distribution of decreased signal intensity in the red nucleus (R), substantia nigra (S), and globus pallidus (G) (age 35). P = putamen.

.0001 in both cases, these data provide very strong evidence of a positive association between lesion severity and T2 rating in both instances. There was no significant correlation with patient age or duration of disease.

Although the mean estimated T2 relaxation time in the thalamus was somewhat decreased in the MS group as compared with normal controls (Table 2), no statistically significant differences between MS and control patients were found in the globus pallidus, the putamen, or the thalamus using the Wilcoxon test ($p > .10$). However, a significant elevation in the globus pallidus vs thalamus T2 ratio was found in the MS group relative to controls ($p < .05$). There

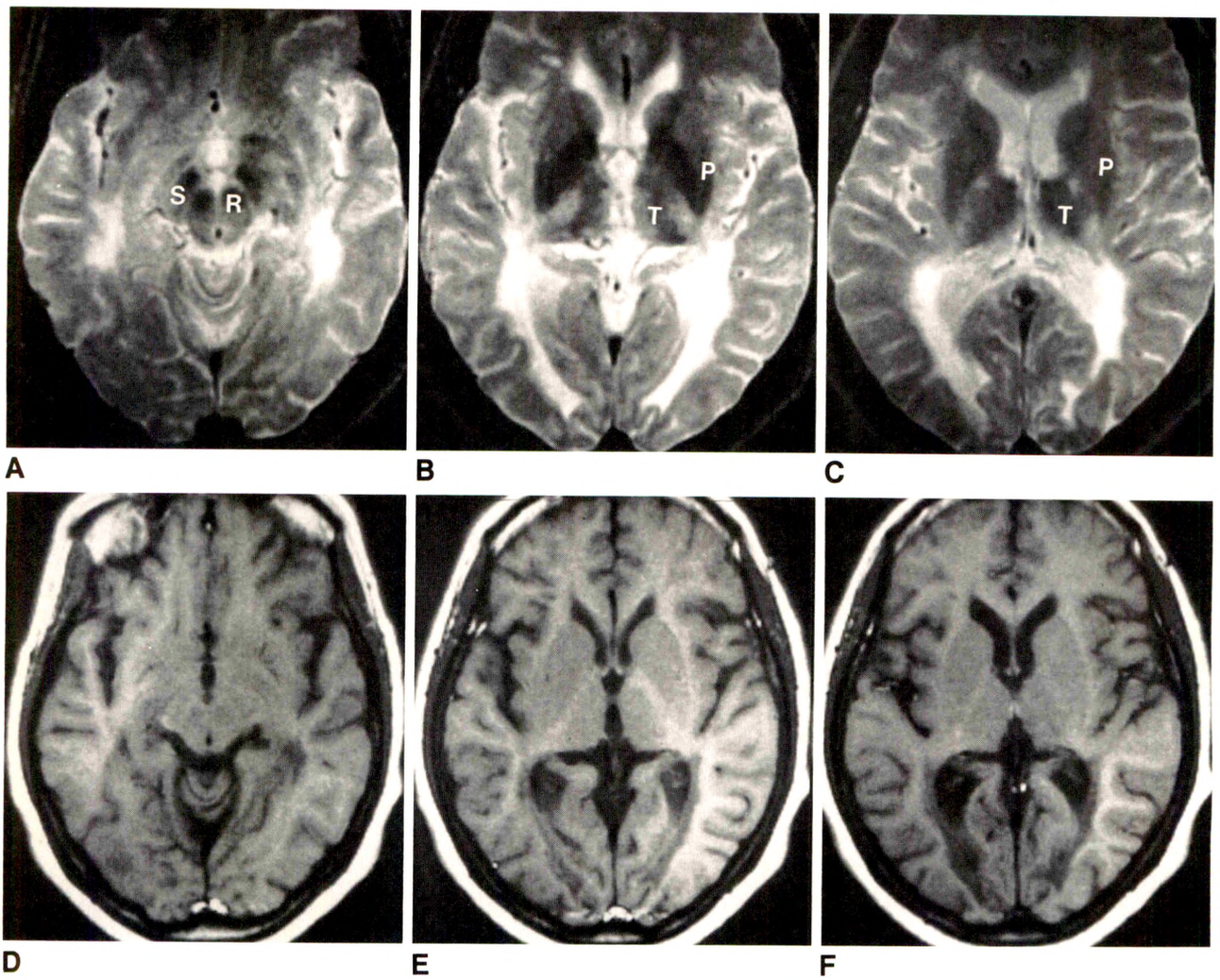


Fig. 3.—Moderate multiple sclerosis (abnormal iron).

***A–C*, SE 2500/80 msec (T2-weighted) images display abnormally decreased signal intensity in putamen (P) and thalamus (T) as compared with normal in 30-year-old patient. Decreased signal intensity in globus pallidus, red nucleus (R), and reticular substantia nigra (S) is prominent but within normal limits.**

***D–F*, SE 500/25 msec (partial-saturation, T1-weighted) images at same levels show no evidence of abnormal signal intensity in basal ganglia structures.**

was also some suggestion ($.05 < p < .10$) of an increase in the globus pallidus vs putamen T2 ratio for MS patients (Table 2). The T2 ratios were neither age nor gender dependent.

The intensity of blue staining in all four normal autopsy brains after Perls' staining for ferric iron correlated closely with the degree of decreased signal intensity seen in the 42 normal control brains using the SE 2500/80 (T2-weighted) pulse sequence. The most blueness (iron) was always noted in the globus pallidus with less blueness in the putamen and caudate and the least blue staining in the thalamus, cerebral cortex, and cerebral white matter (Fig. 5). The ferric iron distribution was increased in the putamen and thalamus as compared with the globus pallidus in the MS brain (Fig. 4).

Discussion

High-field-strength (1.5-T) MR imaging was abnormal (areas of increased signal intensity on T2-weighted images) in 43 (91%) of 47 patients with definite MS. This finding confirms other studies that have reported the sensitivity of T2-weighted MR imaging for the diagnosis of MS [1–3]. This series describes a previously unreported finding in MS, decreased signal intensity on T2-weighted images in the thalamus and putamen. The prominence of the decreased signal intensity directly correlated with the extent and number of white-matter lesions. This selective decrease in signal intensity is consistent with an abnormally increased accumulation of a transition

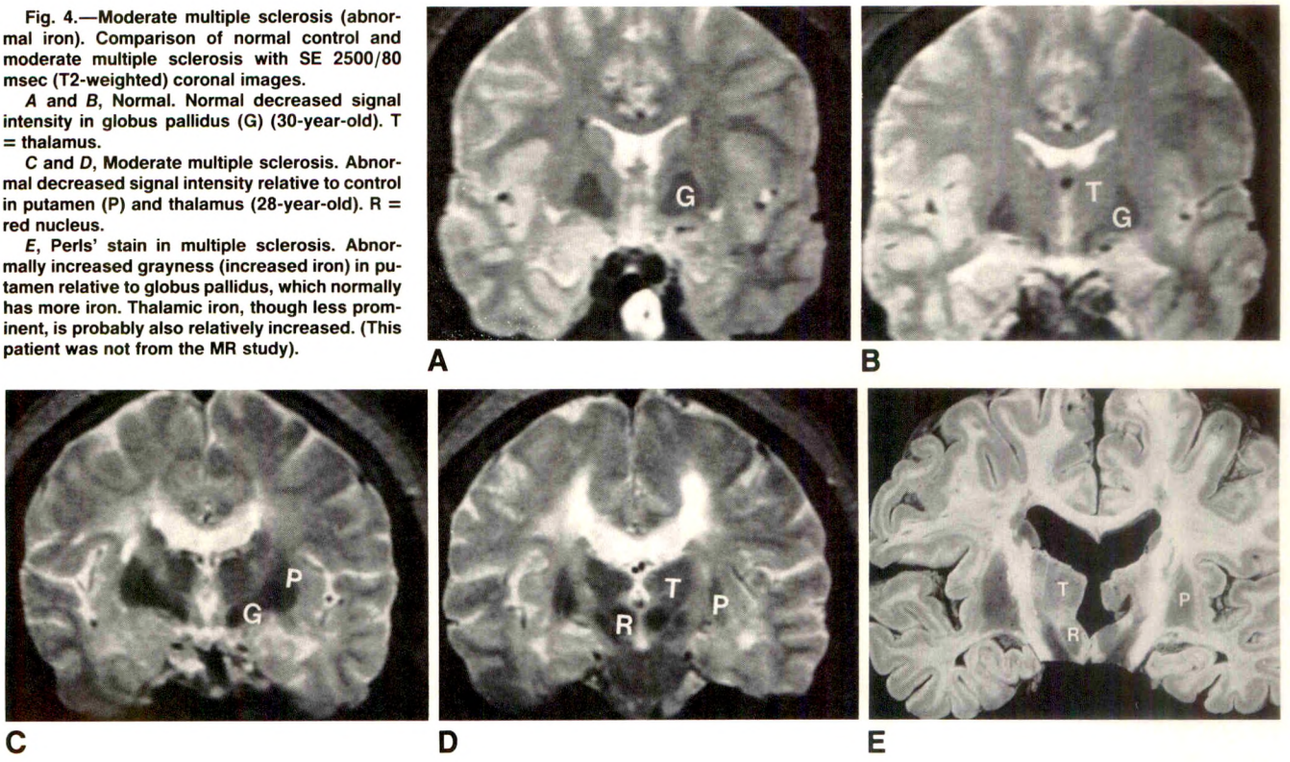


Fig. 4.—Moderate multiple sclerosis (abnormal iron). Comparison of normal control and moderate multiple sclerosis with SE 2500/80 msec (T2-weighted) coronal images.

***A* and *B*, Normal. Normal decreased signal intensity in globus pallidus (G) (30-year-old). T = thalamus.**

***C* and *D*, Moderate multiple sclerosis. Abnormal decreased signal intensity relative to control in putamen (P) and thalamus (28-year-old). R = red nucleus.**

***E*, Perls' stain in multiple sclerosis. Abnormally increased grayness (increased iron) in putamen relative to globus pallidus, which normally has more iron. Thalamic iron, though less prominent, is probably also relatively increased. (This patient was not from the MR study).**

TABLE 2: T2 Relaxation Times in Multiple Sclerosis Estimated from SE 2500/40–80 Multislice Images

Region	Relaxation Times	
	MS (n = 13)	Controls (n = 13)
Globus pallidus	46.1 ± 3.2	45.1 ± 4.7
Putamen	52.4 ± 3.0	53.6 ± 6.1
Thalamus	56.5 ± 2.5	59.3 ± 6.8
T2 ratio of globus pallidus/		
Putamen	0.88 ± 0.05[a]	0.84 ± 0.05
Thalamus	0.82 ± 0.06[b]	0.76 ± 0.06

Note.—The ages for both multiple sclerosis (MS) and control groups were 23–54 years old (mean 39 years).

[a] Wilcoxon text ($.05 < p < .10$).

[b] Wilcoxon text ($p < .05$).

element, most likely iron, in the thalamus and striatum associated with MS.

When imaging with a 1.5-T-field-strength magnet, normal adults always exhibited a decrease in signal intensity on T2-weighted images (decreased T2 relaxation time) in a specific topographic distribution (globus pallidus, red nucleus, substantia nigra, and dentate nucleus of cerebellum) correlating with Perls' stain and other autopsy studies [5, 11–13]. The normal iron concentration in the brain is four times greater in the globus pallidus and 2.5 times greater in the putamen than in the thalamus [13]. No stainable iron is present at birth [14], but there is a progressive accumulation of nonheme brain iron until stable adult levels are attained at about 20–25 years of age [13–15].

Brain iron concentration is most likely independent of hemoglobin metabolism and the iron reserves of other body organs. The passage of iron across the blood-brain barrier is poorly understood but may occur at sites of transferrin receptors on brain capillary endothelial cells [16]. Iron is present in other animal systems in a distribution similar to that found in humans [17, 18]. Finely granular brain iron is mainly in the form of ferritin [13, 15] and found predominantly in the mitochondria and microsomes of oligodendrocytes and glial cells, with much smaller deposits in the neuropil, inner and outer loops of myelin sheaths, and scattered neurons [13, 15, 18].

Iron and copper are the key trace metals used in brain metabolism. Iron enzymes play an important role in oxidative reactions [15]: (1) DPNH-cytochrome-C-reductase has a high iron content, (2) iron and lactoflavin contents of the brain are parallel except for low lactoflavin in the globus pallidus, and (3) iron-containing flavoproteins (DPNH dehydrogenase, succinic acid dehydrogenase) play a role in cellular respiration. Iron is an important cofactor in dopamine synthesis and degradation [19, 20] as well as in glutamate synthesis [21]. An important reaction in normal aging is the dismutation of superoxides to produce hydrogen peroxide, which in turn reacts with ferrous (II) iron to produce highly reactive and likely toxic hydroxyl free radicals and ferric iron [22].

Iron is the most likely candidate for producing the topographically specific, decreased signal intensity in basal ganglia

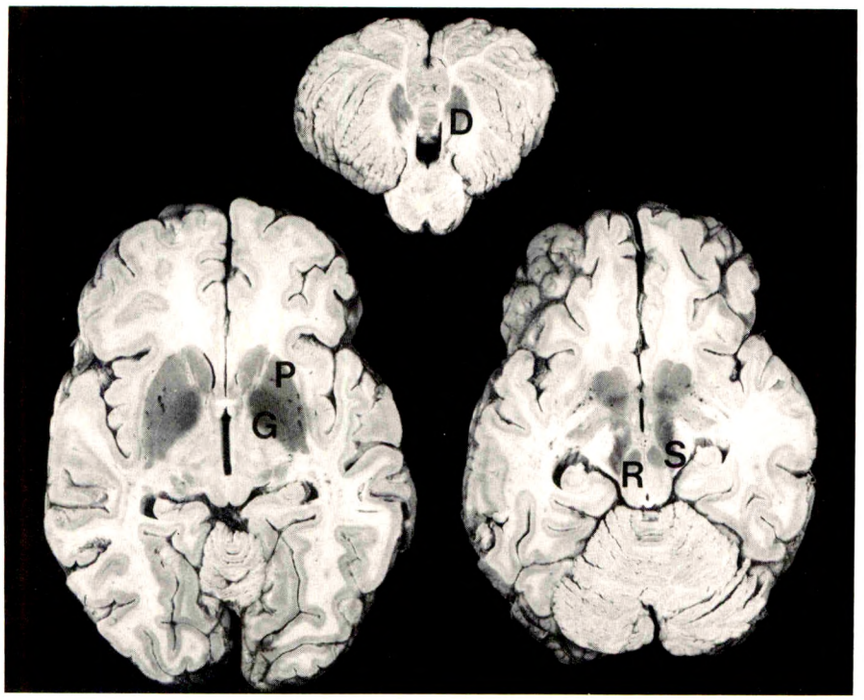


Fig. 5.—Perls' stain for ferric iron (normal brain). Greater intensity of blue staining (gray on black-and-white photographs) represents greatest concentration of ferric iron. Maximal blue (gray) staining in globus pallidus (G), red nucleus (R), reticular substantia nigra (S), and dentate nucleus (D) coincide with lowest signal intensity (decreased T2) on T2-weighted MR images. Gray staining in putamen (P) is less intense and in thalamus far less intense than in globus pallidus, consistent with normally lower iron concentrations in putamen and thalamus.

structures with high-field-strength MR imaging [3, 12]. Ferritin (molecular weight 480,000) is composed of a crystalline fericoxyhydroxide core with up to 4000 ferric ions per molecule. The ferritin is encased by a 25-Å protein shell, and therefore theories of paramagnetic relaxation effects would suggest no significant alteration in T1 or T2 relaxation time [23]. Intracellular iron, however, does create slow, statistical fluctuations in the magnetization of each ferritin core, resulting in local magnetic field gradients and inhomogeneities and a resultant decline in the transverse (T2) relaxation time and signal intensity on the T2-weighted image [5, 11, 23–26]. The effect of brain iron is better discerned at high field because this heterogeneity in magnetic susceptibility is proportional to the square of the magnetic field strength [25].

An abnormally increased concentration of brain iron has been reported in Hallervorden-Spatz disease [27], Huntington's disease [28], Parkinson's disease, and Parkinson's plus (multisystem atrophy) syndromes [12, 29, 30]. Individuals over 80 years old may normally have increased iron deposition in the striatum [12, 13]. There are, however, no disorders in which elevated iron concentration has been reported in the thalamus, although we have seen this finding after intracranial radiation therapy [12]. Rojas et al. [31] reported discrete foci of increased iron in only the ventrolateral thalamic nucleus with Parkinson's disease.

The question arises as to the reason for decreased signal intensity on T2-weighted images in the thalamus and putamen in a disease that predominantly affects the white matter. No trace metal or chemical compound in the brain other than iron normally preferentially accumulates as described [5, 13, 32] and preferentially affects T2 relaxivity. The decreased T2 in the thalamus and striatum is not related to calcium or vascularity, which would similarly affect T1 relaxivity. The relative appearance of an abnormally decreased signal intensity in the putamen and thalamus does not seem highlighted by internal capsule plaques (increased signal intensity) as one would expect the globus pallidus decreased T2 to be equally accentuated.

Iron might accumulate as a result of a decline in iron-requiring oxidative reactions (hypometabolism) in deep gray-matter structures. MS is a disease of the oligodendroglia-myelin system. Since iron is predominantly found in the oligodendroglia, dysfunction may result in an excessive accumulation of iron in structures that normally have relatively high iron stores [18]. The increased iron accumulation might also result from an accelerated rate of hydroxyl free radical formation causing increased membrane peroxidation and ferric iron production [22]. Another possibility is that iron may pass into the brain more freely in MS because of an underlying blood-brain barrier abnormality [5].

Increased iron accumulation has been reported in ovoid bodies at a distance of about 150 μm from the MS plaque margin [33]. Walton and Kaufman [34] were unable to confirm this observation, although they occasionally found hemosiderin-laden macrophages within an acute plaque. Craelius et al. [33] reported iron along fiber tracts with occasional iron-containing microglia in close proximity to axons. The globus pallidus contains far fewer white-matter tracts than does the thalamus or putamen. Although these researchers did not see ovoid bodies in the gray matter, they noted that intravascular Prussian blue (iron) staining was extensive in the gray matter adjacent to the plaques. Enlarged, densely staining lysosomes, possibly containing iron, may be found in a perivascular location within glial cells near MS plaques. Craelius et

al. [33] proposed various potential mechanisms for iron accumulation in MS, including abnormal blood-brain barrier permeability, increased lysosomes and microglia that store iron, and increased iron in blood-vessel walls in the gray matter. They also mention that both hemochromatosis (disorder of iron metabolism) and MS are associated with similar histocompatibility loci, HLA–A3 and HLA-B7.

Whatever the mechanism, the results of high-field-strength MR studies strongly suggest that abnormally dominant decreased signal intensity on T2-weighted images in the thalamus and striatum is directly proportional to the severity of associated white-matter lesions. The possibility that iron accumulation is causally related to demyelination or disease progression in MS is unproved, although it provides an interesting new avenue for investigation. Even if iron accumulation proves epiphenomenal, the MR finding of decreased thalamic and striatal signal intensity may provide an important new diagnostic clue and marker of disease activity. Further studies are needed to determine the specificity of this finding for MS as compared with other white-matter disorders.

REFERENCES

1. Sheldon JJ, Siddharthan R, Tobias J, et al. MR imaging of multiple sclerosis: comparison with clinical and CT examinations in 74 patients. *AJNR* **1985**;6:683–690
2. Young IR, Hall AS, Pallis CA, et al. Nuclear magnetic resonance imaging of the brain in multiple sclerosis. *Lancet* **1981**;2:1063–1066
3. Drayer BP, Barrett L. Magnetic resonance imaging and CT scanning in multiple sclerosis. *Ann NY Acad Sci* **1984**;436:294–314
4. Poser CM, Paty DW, Scheinberg L, et al. New diagnostic criteria for multiple sclerosis. Guidelines for research protocols. *Ann Neurol* **1983**;13:227–231
5. Drayer BP, Burger P, Darwin R, et al. Magnetic resonance imaging of brain iron. *AJNR* **1986**;7:373–380
6. Nguyen-Legros J, Bizot J, Bolesse M, et al. Noir de diaminobenzidine: une nouvelle methode histochimique de revelation du fer exogene. *Histochemistry* **1980**;66:239–244
7. Perls M. Nachweis von Eisenoxyed in giwissen Pigmenten. *Virchows Arch [A]* **1867**;39:42–48
8. MacFall JR. Pulse sequence considerations for computed T1, T2, and spin density images. In: Essen PD, Johnston RE, eds. *Technology of nuclear magnetic resonance*. New York: Society of Nuclear Medicine, **1984**:79–86
9. Agresti A. *Analysis of ordinal categorical data*. New York: Wiley, **1984**
10. Brown MB, Benedetti JK. Sampling behavior of tests for correlation in two-way contingency tables. *J Am Stat Assoc* **1977**;72:309–315
11. Darwin R, Drayer B, Wang HZ, et al. Comparison of T2 estimates using various magnetic resonance pulse sequences in man. *Radiology* **1986**;160:375–381
12. Drayer BP. *Neurometabolic applications of magnetic resonance*. Categorical course on magnetic resonance (syllabus). Reston, VA: American College of Radiology, **1985**
13. Hallgren B, Sourander P. The effect of age on the non-haemin iron in the human brain. *J Neurochem* **1958**;3:41–51
14. Diezel PB. Iron in the brain: a chemical and histochemical examination. In: Waelsch H, ed. *Biochemistry of the developing nervous system*. London: Academic Press, **1955**:145–152
15. Seitelberger F. Pigmentary disorders. In: Minckler J, Blakistan Division, eds. *Pathology of the nervous system*. New York: McGraw Hill, **1972**: 1324–1338
16. Hill JM, Ruff MR, Weber RJ, et al. Transferrin receptors in rat brain: neuropeptide-like pattern and relationship to iron distribution. *Proc Natl Acad Sci* **1985**;82:4553–4557
17. Francois C, Nguyen-Legros J, Percheron G. Topographical and cytological localization of iron in rat and monkey brain. *Brain Res* **1981**;215:317–322
18. Hill JM, Switzer RC III. The regional distribution and cellular localization of iron in the rat brain. *Neuroscience* **1984**;11:595–603
19. Youdim MBH, Yehuda S, Ben-Shachar D, et al. Behavioral and brain biochemical changes in iron deficient rats: the involvement of iron and dopamine receptor function. In: Pollitt E, Leibel RL, eds. *Iron deficiency: brain biochemistry and behavior*. New York: Raven, **1982**:39–56
20. Fahn S. Regional distribution studies of GABA and other putative neurotransmitters and their enzymes. In: Roberts E, Chase TN, Tower DB, eds. *GABA and nervous system function*. New York: Raven, **1976**:169–186
21. Michaelis EK, Belieu RM, Grubbs RD, et al. Differential effects of metal ligands on synaptic membrane glutamate binding uptake systems. *Neurochem Res* **1982**;7:423–436
22. Floyd RA, Zaleska MM, Harmon HJ. Possible involvement of iron and oxygen free radicals in aspects of aging in brain. In: Armstrong D et al., eds. *Free radicals in molecular biology, aging, and disease*. New York: Raven, **1984**:143–161
23. Koenig SH. A theory of solvent relaxation by solute clusters of noninteracting paramagnetic ions, as exemplified by ferritin. *Magnetic Resonance Med* **1985**;2:873–874
24. Brittenham GM, Farrell DE, Harris JW. Magnetic susceptibility measurements of human iron stores. *N Engl J Med* **1982**;307:1671–1675
25. Gomori JM, Grossman RI, Goldberg HI, et al. Intracranial hematomas: imaging by high-field MR. *Radiology* **1985**;157:87–93
26. Packet KJ. The effects of diffusion through locally inhomogeneous magnetic fields on transverse nuclear spin relaxation in heterogeneous systems: proton transverse relaxation in striated muscle tissue. *J Magnetic Resonance* **1973**;9:438–443
27. Vakili S, Drew AL, Von Schucking S, et al. Hallervorden-Spatz syndrome. *Arch Neurol* **1977**;34:729–738
28. Klintworth GK. Huntington's chorea—morphologic contributions of a century. In: Barbeau A, Chase TN, Paulson GW, eds. *Advances in neurology*. New York: Raven, **1973**:353–368
29. Drayer BP, Olanow W, Burger P. High field magnetic resonance imaging of brain iron. The diagnosis of Parkinson's plus (multisystem atrophy) syndromes. *Radiology* **1986**;159:493–498
30. Earle KM. Studies on Parkinson's disease including x-ray, fluorescent spectroscopy of formalin-fixed brain tissue. *J Neuropathol Exp Neurol* **1968**;27:1–14
31. Rojas G, Asenjo A, Chiorino R, et al. Cellular and subcellular structure of the ventrolateral nucleus of the thalamus in Parkinson disease. Deposits of iron. *Appl Neurophysiol* **1965**;26:362–376
32. Hock A, Demmel U, Schicha H, et al. Trace element concentration in human brain. *Brain* **1975**;98:49–64
33. Craelius W, Migdal MW, Luessenhop CP, et al. Iron deposits surrounding multiple sclerosis plaques. *Arch Pathol Lab Med* **1982**;106:397–399
34. Walton JC, Kaufman JCE. Iron deposits and multiple sclerosis. *Arch Pathol Lab Med* **1984**;108:755–756

Book Review

Neurosurgical Applications of Transcranial Doppler Sonography. By Albrecht Harders. New York: Springer-Verlag 134 pp., 1986. $35

This slim cloth-covered volume succinctly summarizes the state-of-the-art in this new noninvasive technique. It has the advantage of single authorship and is copiously illustrated. Dr. Harders established a technique for measuring blood velocity in all the major branches of the circle of Willis. The ability to detect vasospasm before and after surgery has been invaluable in patient management. This book summarizes this exciting work. The first two chapters review elementary hemodynamics and the physical principles of Doppler, a consistent feature of all Doppler books. Another chapter is devoted to the positions from which the various arteries are detected, followed by the normal velocity ranges for the obtained Doppler signals. The detection of vasospasm after subarachnoid hemorrhage is succinctly summarized. The next chapter deals with the flow patterns within cerebral aneurysms, and there are further sections on arteriovenous malformations and extracranial/intracranial bypass. The final chapters deal with the hemodynamic response to meningitis and the diagnosis of brain death by transcranial Doppler.

In summary, this book is well written and concise and will be particularly valuable for neurologists and neurosurgeons. However, blind Doppler has never been the radiologist's forte and with the other techniques available to the radiologist for direct visualization of cerebral arterial flow, I think few radiologists will attempt to use this interesting technique. However, for those who want to learn about these new applications, this book can provide valuable information.

Kenneth Taylor
Yale University
New Haven, CT 06510

Study of Movement Disorders and Brain Iron by MR

J. Neal Rutledge[1, 2]
Sadek K. Hilal[1]
A. John Silver[1]
Richard Defendini[3]
Stanley Fahn[4]

Heavily T2-weighted high-field MR images provide a unique opportunity for the evaluation of the extrapyramidal motor system. The images are affected by the presence of small amounts of naturally occurring paramagnetic substances—principally iron—that delineate the neostriatum (caudate and putamen), globus pallidus, red nucleus, substantia nigra, and dentate nucleus, primarily by a decrease in signal secondary to the T2* effect. Movement disorders are associated with either increased or decreased signal or both in these structures, depending on the pathologic process. In the initial evaluation of 113 patients with a variety of movement disorders, good correlation of imaging abnormalities can be made with a simplified schema of the extrapyramidal pathways and a system of classification of abnormal movements, parkinsonism/tremor, dystonia, chorea, myoclonus, and hemiballismus. Parkinsonisms are characterized by abnormalities of the cortico-ponto-cerebello-dentato-rubro-thalamo-cortico-spinal tract or the nigrostriatal tract. Dystonias are characterized by abnormalities of the neostriatum predominantly affecting the putamen. Choreas are also characterized by abnormalities of the neostriatum but predominantly affecting the caudate nucleus. Hemiballismus is characterized by lesions affecting the subthalamic nucleus or associated pathway.

Iron

Interest in movement disorders is heightened by the recent ability to map the distribution of macromolecular complexes of Fe(III) in the brain with heavily T2-weighted images. This is accomplished through contrast created by the T2* effect, a local inhomogeneity in the magnetic field that dephases spin and results in loss of signal [1]. This effect is different from the paramagnetic effect of smaller soluble contrast agents, such as gadolinium, and corresponds roughly with the ferric iron distribution demonstrated by Perls' Prussian blue reaction (Fig. 1) [2].

The signal loss observed varies according to the concentration of the macromolecular complexes and the square of the field strength. Normally a statistically characteristic distribution of iron exists that varies with age: none is present at birth; then a rapid accumulation of iron occurs with the majority being present between the ages of 8 and 25 years. After this, a gradual accumulation occurs with prominence seen in the globus pallidus, putamen, and substantia nigra in old age [3–5].

It is a unique characteristic of the extrapyramidal system that its nuclei contain high concentrations of iron. Especially rich are the substantia nigra and globus pallidus. Lesser amounts of iron are found in the red nucleus, dentate nucleus, nigrostriatal tract, putamen, caudate nucleus, and the fifth layer of cortical gray matter [6]. The reasons for increased concentration of iron in nuclei related to movement are unknown; these reasons are reviewed in our discussion.

Other trace metals found in the brain in significant amounts include copper, magnesium, and zinc [3, 4]. In the normal state they appear to contribute little to MR imaging. But in pathologic states, for example, Wilson's disease with increased copper concentrations, their effect becomes apparent and applicable to the study of the extrapyramidal system.

This article appears in the May/June 1987 issue of *AJNR* and the August 1987 issue of *AJR*.

Received July 10, 1986; accepted after revision November 20, 1986.

Presented at the annual meeting of the American Society of Neuroradiology, San Diego, January 1986.

This work was supported in part by National Institutes of Health grant CA 28881 and by Philips Medical Systems, Inc.

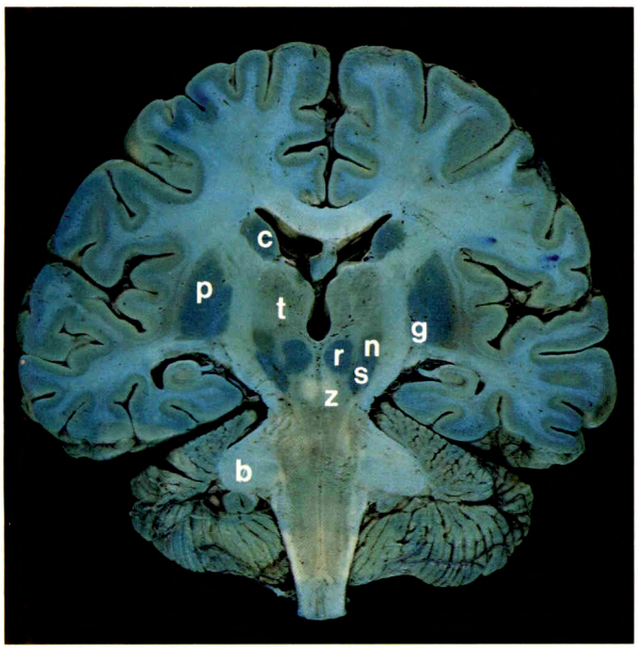
[1] Department of Radiology, Division of Neuroradiology, Columbia-Presbyterian Medical Center, New York, NY 10032.

[2] Present address: 10 Medical Arts Square, Austin, TX 78705. Address reprint requests to J. N. Rutledge.

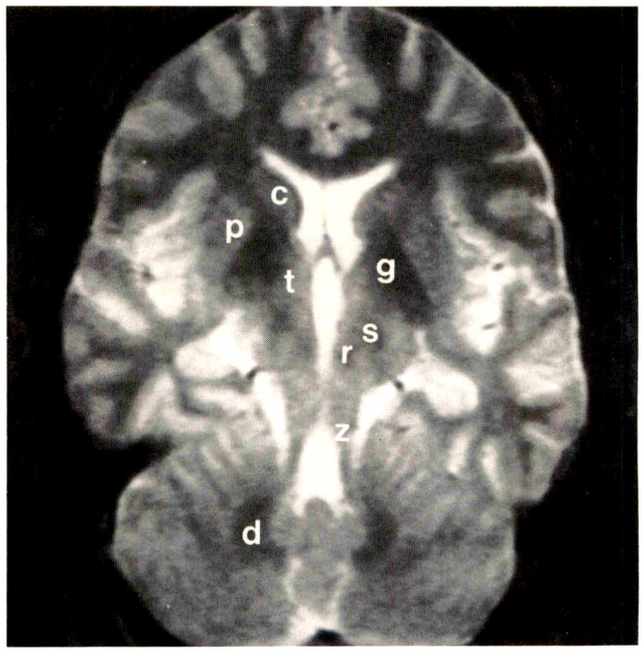
[3] Department of Pathology, Division of Neuropathology, Columbia-Presbyterian Medical Center, New York, NY 10032.

[4] Department of Neurology, Division of Movement Disorders, Columbia-Presbyterian Medical Center, New York, NY 10032.

***AJR* 149:365–379, August 1987**
0361–803X/87/1492-0365
© American Roentgen Ray Society



A



B

Fig. 1.—Semicoronal sections of normal brain.
***A*, Perls' stain in 47-year-old shows most extrapyramidal nuclei and tracts.**

***B*, Heavily T2-weighted MR image in 30-year-old shows decreased signal in corresponding extrapyramidal nuclei. c = caudate nucleus; p = putamen; t = thalamus; g = globus pallidus; n = subthalamic nucleus; r = red nucleus; z = brachium conjunctivum; b = brachium pontis; s = substantia nigra; d = dentate nucleus.**

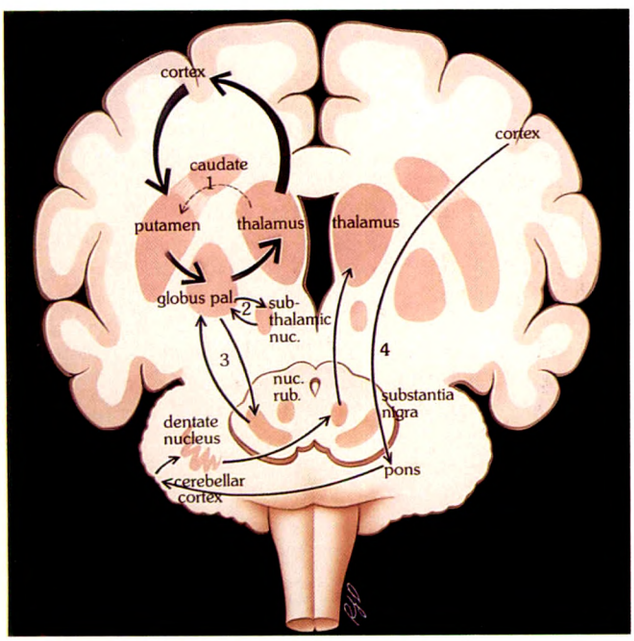


Fig. 2.—Simplified extrapyramidal pathway shows circuits frequently involved in movement disorders: dystonias and choreas (*loop 1*), hemiballismus (*loop 2*), and parkinsonisms (*loops 3 and 4*).

Movement Disorders

Classically, movement has been found to be mediated by multiple neural pathways that can be divided into pyramidal, extrapyramidal, and cerebellar systems. This classification, however, belies the fact that multiple coordinated interaction between these artificial divisions is required for purposeful movement. In the radiologic conceptualization of movement disorders, a simplified model of the involved anatomic pathways can be useful. The extrapyramidal system can then be thought of as a major circuit and several minor circuits that modify the control of movement. Damage to these circuits causes involuntary movement and other nonparalytic disorders by release of inhibition, dyscoordination, or loss of modulation on the pyramidal tract.

The major extrapyramidal motor circuit is a loop consisting of projections from the cortex to the neostriatum (caudate and putamen nuclei), globus pallidus, thalamic nuclei, and finally returning to the cortex (see loop 1 in Fig. 2). Damage to this circuit is manifest by signal changes on MR and results in a clinically manifest spectrum of abnormal movements ranging from dystonia to chorea. Accessory or minor extrapyramidal motor circuits are formed between the subthalamic nucleus and globus pallidus (see loop 2 in Fig. 2); the lenticular nuclei (caudate, putamen, and globus pallidus) and substantia nigra (loop 3); and a complex loop originating in the cortex, passing through the pons, brachium pontis, and cerebellum

TABLE 1: Definitions of Terms Descriptive of Movement Disorders

Term	Definition
Tremor	Involuntary, rhythmic, oscillatory movements of opposing muscles
Myoclonus	Abrupt, shocklike contraction of a single or group of muscles
Hemiballismus	Sudden, violent, swinging movements of arm and/or leg
Dystonia	Usually slow, sustained, continual, repetitive, and twisting contractions that can result in postural abnormality
Athetosis	Slow, sinuous, writhing, purposeless movements flowing into one another
Chorea	Rapid, arrhythmic, nonrepetitive, nontwisting, flowing movements affecting proximal and distal muscles

and returning to the thalamus via the brachium conjunctivum and red nucleus (cortico-ponto-cerebello-dentato-rubro-thalamo-cortico-spinal tract, loop 4). Hemiballismus is caused by damage to loop 2. Parkinsonisms result from damage to loops 3 and/or 4 [7, 8].

Understanding the extrapyramidal system is made more difficult by the classification and description of the resulting abnormal movements. The definitions set out in Table 1 were used in this study [9]. Patients were then grouped according to these definitions, and their images correlated for specific changes. Athetosis was not assessed separately because of the lack of characteristic pathologic changes and difficulty distinguishing it clinically from a chorea or a dystonia.

Subjects and Methods

To analyze the phenomenon of decreased signal delineating the extrapyramidal system, eight pathologic specimens 8–72 years old were stained for iron and compared with normal heavily T2-weighted images. One hundred thirteen patients with a variety of movement disorders were then imaged and assessed for differences in signal patterns.

The pathologic specimens were prepared for iron staining by preserving them in formalin for 5 days, instead of the conventional 4 weeks, to minimize any leaching of the iron. They were then sectioned and stained in a two-step process: 15 min in 2.5% potassium ferrocyanide only and 15 min in 1% hydrochloric acid [10]. This results in Perls' Prussian blue reaction, with maximum color-contrasting areas containing ferric iron (Fig. 3). Prolonging the staining process tends to reduce the intensity differences.

The MR images were obtained using a 1.5-T prototype system (Columbia-Philips). A spin-echo pulse sequence was used with an echo time (TE) of 70–120 msec and a repetition time (TR) of 4300 msec along with an acquisition matrix of 512 × 768 or 256 × 768 to produce contiguous 5-mm slices, primarily in the axial plane.

Between October 1984 and September 1985 113 consecutive patients with a variety of movement disorders were studied. The patients were 3 months to 78 years old. IV sedation was required in most cases. The images were grouped according to the type of abnormal movement and assessed for any signal changes. In the subgroup of parkinsonisms 30 age-matched controls were used to help assess subtle changes and their significance. The images were then grouped according to clinical diagnosis to assess any further characteristics.

Results

Iron Staining

Excellent demonstration of the nuclei containing ferric iron is obtained by the methods outlined by Gans [10]. Extrapyramidal nuclei stain a deep blue color in a dynamic process corresponding to their concentrations of iron, as documented by Harrison et al. [3] (Table 2).

Other staining occurs near the gray-white-matter border in the deep cortical gray layers and is easily mistaken for white-matter U fibers (Fig. 3F). Also the frontal white matter is usually noted to stain more deeply than the occipital white matter.

Areas with lack of staining are also present. The internal capsule, corpus callosum, and anterior and posterior commissures show little staining grossly. Closer inspection of the internal capsule demonstrates fine, intensely staining tracts traversing it (Fig. 4).

The optic system is also dramatically devoid of staining. The optic tracts, lateral geniculate body, and optic radiations can all be seen to stain less than adjacent white matter.

An important observation is the intensity with which caudate and putamen stain. Even considering the naturally darker color of the neostriatum, the amount of ferric iron staining present is intense. This is significant when comparison is made with the MR images.

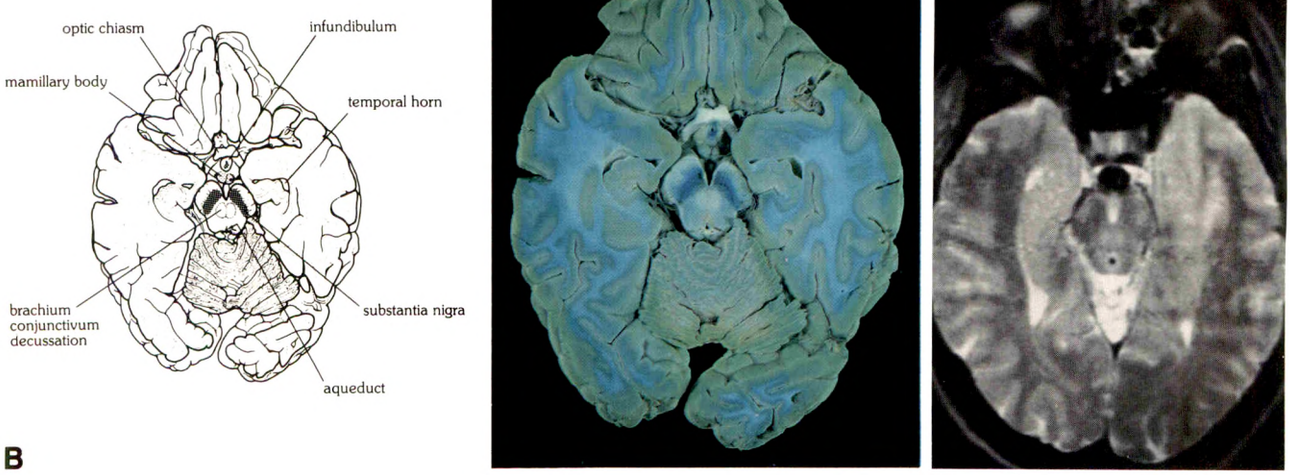
MR Images

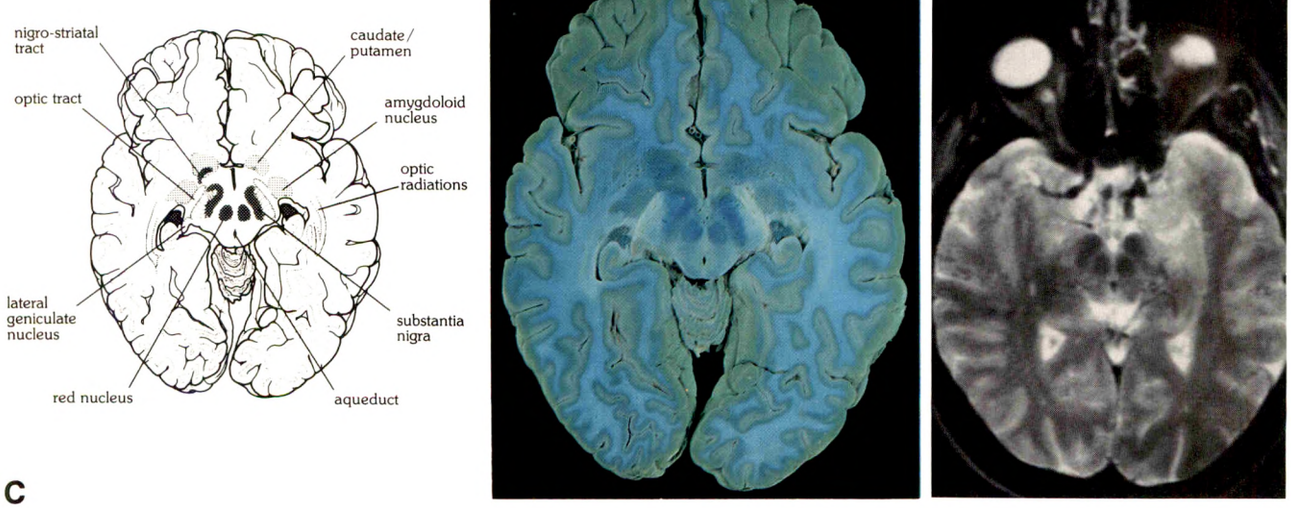
Comparison of the heavily T2-weighted images and Perls' stain shows a close but imperfect relationship between the signal void on MR and the intensity of the stain. The low signal intensity seen in the substantia nigra, red nucleus, dentate nucleus, globus pallidus, deep cortical layers, and some white-matter areas correlates perfectly with the stained specimens (Figs. 3 and 4). Areas like the optic system (optic tract, radiations, and lateral geniculated body) also correlate closely. This includes an area of high signal commonly seen at the posterior end of the putamen, the pars retrolenticularis of the optic tract. This has been attributed to the internal capsule [11] (Fig. 3C).

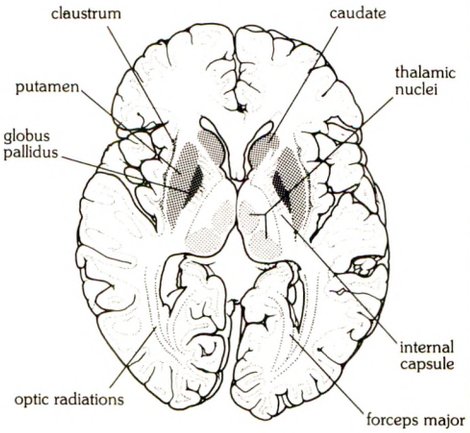
In contrast to previous observers, we did not find that MR signal correlation between Perls' stain and the signal void exists everywhere. The putamen and caudate show relatively little loss in signal when compared with the loss expected by the iron concentration or Perls' stain. Also the internal capsule, commissures, and corpus callosum show a much larger decrease in signal than Perls' stain predicts (Fig. 4A). This lack of correlation will be discussed.

Fig. 3.—Axial diagrams (*left*) corresponding to Perls' stain (*middle*) and heavily T2-weighted MR images (*right*) in normal 25-year-old document correlation between regions of ferric staining and signal loss.

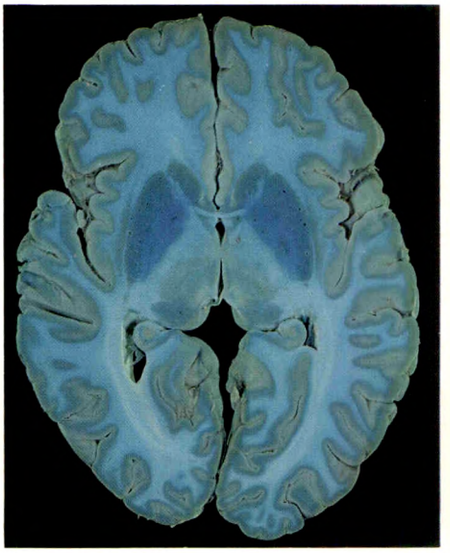




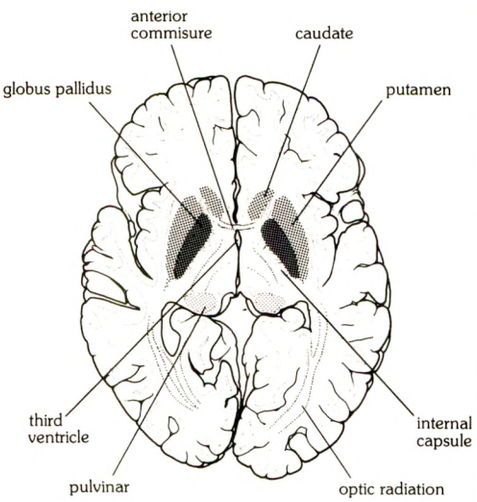



claustrum
caudate
putamen
thalamic nuclei
globus pallidus
internal capsule
optic radiations
forceps major

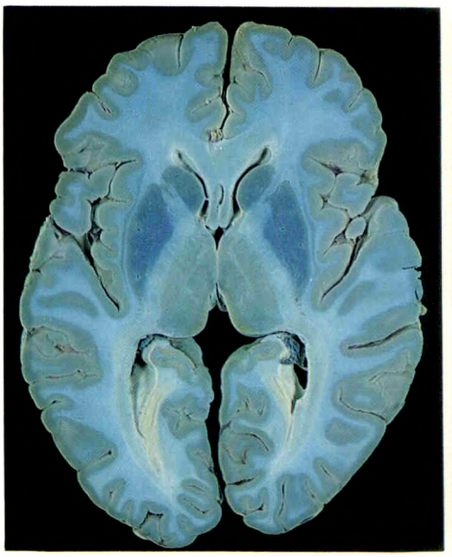
D



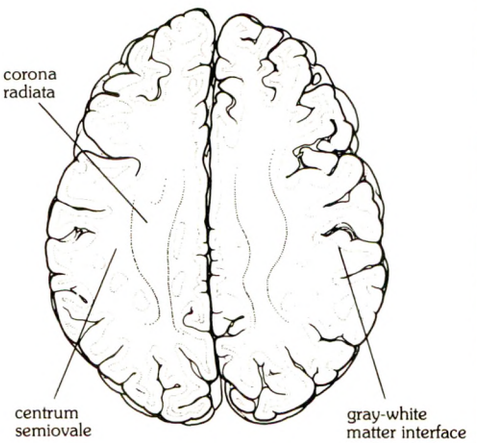



anterior commisure
caudate
globus pallidus
putamen
third ventricle
internal capsule
pulvinar
optic radiation

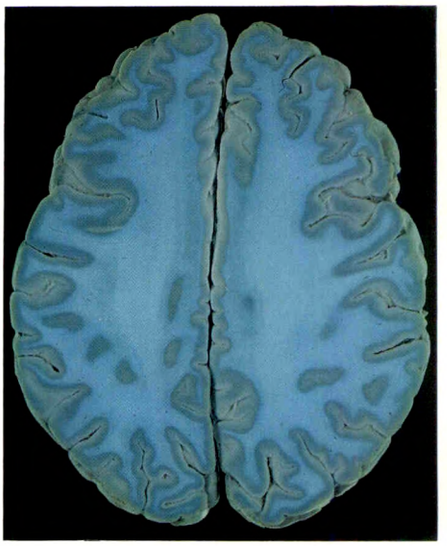
E

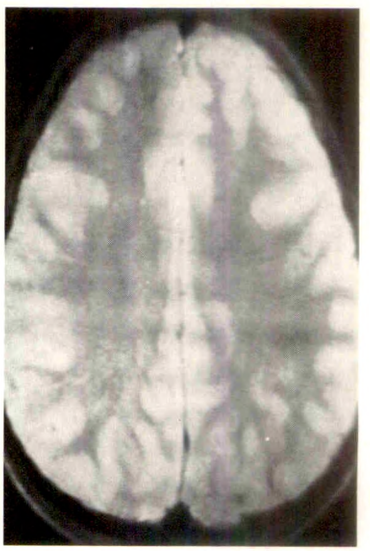





corona radiata
centrum semiovale
gray-white matter interface

F





Parkinsonisms and Myoclonus

Thirty-five patients with parkinsonism/tremors were studied (Table 3). All patients had been treated pharmacologically at least 3 years before being imaged. These were compared with 30 age-matched controls who had no symptoms of parkinsonism or other abnormalities.

The most common abnormality identified was a restoration of signal in the area of void normally observed in the dorsal lateral aspect of the substantia nigra seen at the superior collicular level of the midbrain. By restoration we mean that the decreased signal seen in normal patients was changed to a signal level similar to that of brain parenchyma without iron. In patients with parkinsonism, 75% showed restoration of signal, while only 53% of age-matched patients (without symptoms) showed this change (Figs. 3C and 5). The odds ratio for this finding is 2.63 with a 90% confidence interval (0.76–9.10). The sample size is too small for a significant chi square.

Comparison of degrees of general atrophy demonstrated increased atrophy in 86% of patients with parkinsonism vs 56% in age-matched controls. Focal atrophy was found to be an excellent marker of secondary parkinsonism and the heterogeneous system degenerations, being present at least to some degree in 73%. This focal atrophy was not present in the control group. A loss of signal seen by other examiners [12, 13] in the dorsal lateral aspect of the putamen was seen in 20 (67%) of our 30 normal controls and was associated with increasing age (Fig. 6). We found a similar amount of decreased signal in 25 (71%) of the 35 patients with parkinsonism.

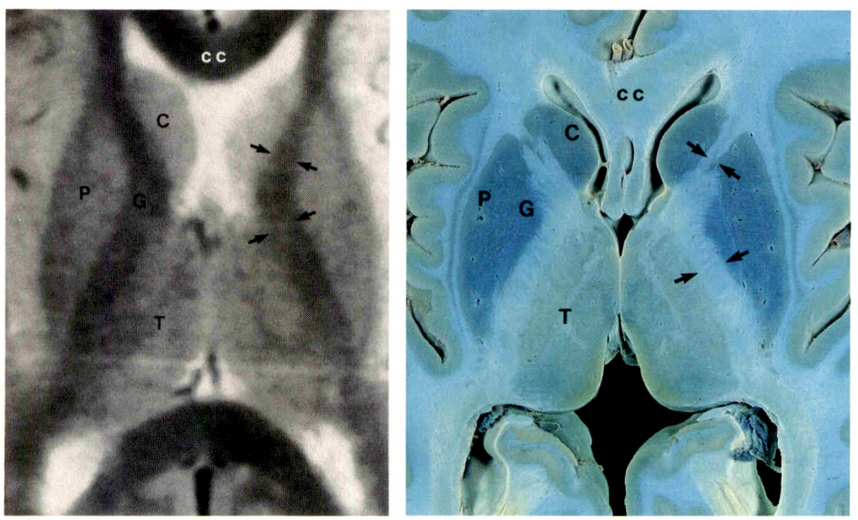
Greater correlation occurred after separating these patients into subgroups corresponding to their clinical diagnosis. Of the 12 patients with primary parkinsonism (Parkinson's disease), no additional changes were noted, but among second-

TABLE 2: Elemental Concentrations of Iron in Brain Tissue

Region	mg Fe/100 g Tissue
Globus pallidus	21.3
Red nucleus	19.5
Substantia nigra	18.5
Putamen	13.2
Dentate nucleus	10.4
Caudate nucleus	9.3
Thalamus	4.8
Cerebellar cortex	3.4
Motor cortex	5.0
Prefrontal cortex	3.0
Frontal white matter	4.2
Liver	13.4

TABLE 3: MR Findings in Parkinsonian Syndromes

Group: Finding	No.
Parkinsonism (n = 35):	
Striatonigral tract abnormality (restoration of signal in substantia nigra)	25
Cortico-ponto-cerebello-dentate tract abnormality (focal atrophy or increased signal)	23
Generalized atrophy	30
Decreased signal in dorsolateral putamen	25
Normal age-matched controls (n = 30):	
Decreased signal in dorsolateral putamen	20
Restoration of signal in substantia nigra	16
Parkinson's disease (n = 12):	
Restoration of signal in substantia nigra	9
Secondary parkinsonism—infarct (n = 4):	
Striatonigral tract abnormality	3
Cortico-ponto-cerebello-dentate tract abnormality	4
Heterogeneous system degenerations (n = 19):	
Striatonigral tract abnormality	13
Cortico-ponto-cerebello-dentate tract abnormality	19



A B

Fig. 4.—Magnified axial MR image (*A*) and Perls' stain (*B*) show areas of greatest disparity between ferric staining and signal loss. Caudate nucleus (C) and putamen (P) are stained without signal loss. Internal capsule (*arrows*) and corpus callosum (cc) show little staining and moderate signal loss. G = globus pallidus; T = thalamus; or = optic radiations.

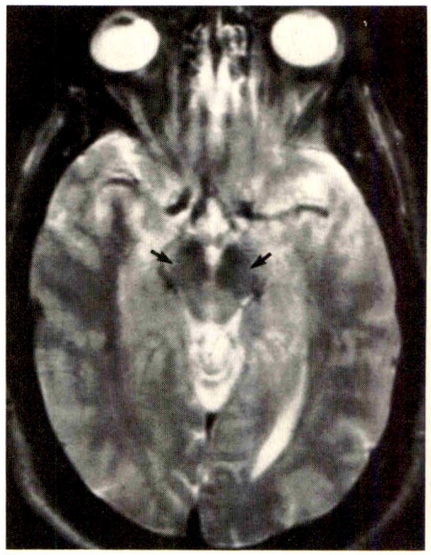


Fig. 5.—Axial, 1.5-T SE 4300/80 image of Parkinson's disease shows restoration of signal in dorsal lateral substantia nigra (*arrows*).



Fig. 6.—Axial 1.5-T SE 4300/80 image of normal 56-year-old shows decreased signal in lateral putamen (*arrows*).

5 6

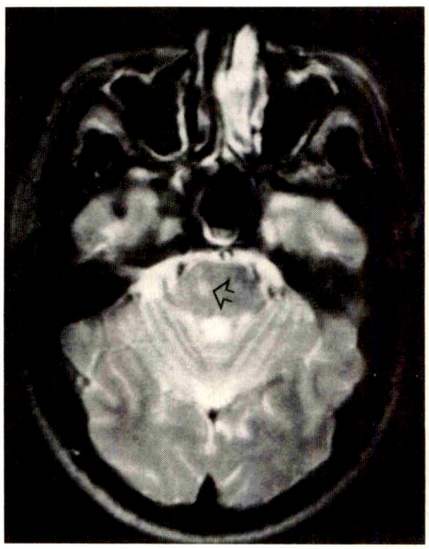


Fig. 7.—Axial 1.5-T SE 4300/80 image of secondary parkinsonism–midbrain infarct (*arrow*).



Fig. 8.—Axial 1.5-T SE 4300/80 image of early progressive supranuclear palsy with increased signal in tectum (*arrows*).

7 8

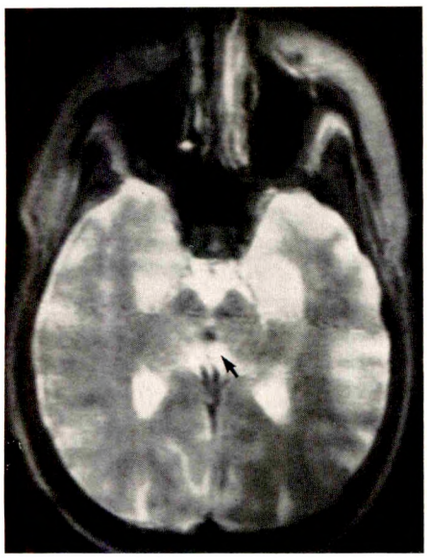
ary parkinsonisms and heterogeneous system degenerations numerous changes were found.

Secondary parkinsonisms can occur after infection, be drug- or toxin-induced, or result from trauma or vascular causes. No drug-induced or postinfection cases were available for study. Excellent correlation occurred in acute parkinsonism suspected to be secondary to stroke. All four cases studied showed focal areas of increased signal in the midbrain at the level of the decussation of the brachium conjunctivum or upper pons compatible with infarcts (Fig. 7).

A third category of parkinsonism consists of heterogeneous system degenerations; that is, parkinsonism plus other clinical signs. Among this subgroup are several diseases: progressive supranuclear palsy, olivo-ponto-cerebellar atrophy, Shy-Drager syndrome, and striatonigral degeneration.

Of this subgroup we studied six patients with progressive supranuclear palsy, all of whom had focal atrophy of the midbrain, particularly the tectum, with concurrent dilatation of the aqueduct, quadrigeminal plate cistern, and posterior portion of the third ventricle. In three of the cases increased signal was seen in the periaqueductal region and in one case the tectum. These cases were encountered early in their clinical course and showed less atrophy than the chronic cases (Figs. 8 and 9).

In four cases of olivo-ponto-cerebellar atrophy focal atrophy of the olives, pons, brachium pontis, medulla, and cerebellum



9



10

Fig. 9.—Axial 1.5-T SE 4300/80 image of chronic progressive supranuclear palsy with focal atrophy of tectum and enlargement of quadrigeminal plate cistern (*arrow*).

Fig. 10.—Axial 1.5-T SE 4300/80 image of olivo-ponto-cerebellar atrophy shows marked focal atrophy of pons (*large arrow*) and brachium pontis (*small arrows*).



11



12

Fig. 11.—Axial 1.5-T SE 4300/80 image in Shy-Drager syndrome shows increased signal in globus pallidus (*arrows*).

Fig. 12.—Axial 1.5-T SE 4300/80 image of unclassified parkinsonism with homogeneous decreased signal throughout neostriatum (*arrows*).

was observed. No change in parenchymal signal was noted (Fig. 10).

In seven cases of Shy-Drager syndrome, atrophy similar to that of olivo-ponto-cerebellar atrophy was seen; and in four cases, increased signal was seen in the globus pallidus, which we attributed to advanced degeneration of the globus pallidus with gliosis (Fig. 11).

One case of striatonigral degeneration was observed and demonstrated atrophy of the caudate without other abnormality; motion limited fine detail in this case.

In addition, two cases of an unclassified disease with dramatic changes were observed. The cases demonstrated markedly decreased signal in the entire neostriatum, unlike the normal controls, where signal void was spotty. Signal void in the putamen was pronounced and homogeneous with sharp margins (Fig. 12). Clinically, these cases manifested prominent rigidity, ataxia, and a poor response to treatment.

Six patients with myoclonus, two with focal and four with diffuse forms, were examined and showed no imaging abnormality.

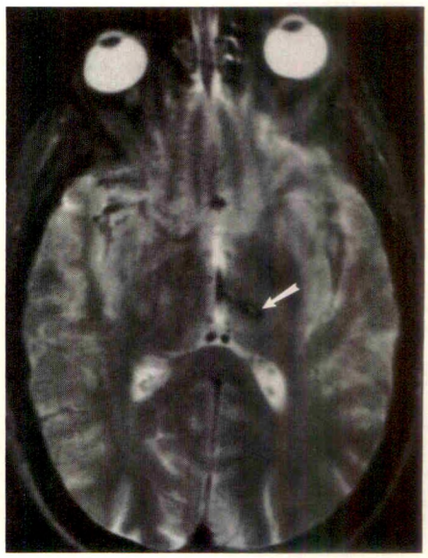
Choreic Disorders and Hemiballismus

Eight patients with choreic disorders were imaged, four with Huntington's disease, three with chorea-acanthocytosis



13

Fig. 13.—Axial 1.5-T SE 4300/80 image in Huntington's chorea shows decreased signal and atrophy of neostriatum, predominantly caudate nucleus (*arrows*).



14

Fig. 14.—Axial 1.5-T SE 4300/80 image in hemiballismus secondary to hemorrhagic infarct in left subthalamic nucleus (*arrow*).

TABLE 4: MR Findings in Secondary Dystonias

Pathology: Signal Abnormality	No. of Patients (n = 41)
Leigh's disease and subacute necrotizing encephalopathy:	
Increased signal, putamen, midbrain, and cortex	5
Postinfarct dystonia:	
Increased signal, putamen	3
Decreased signal, putamen (hemorrhagic)	3
Postinfection dystonia:	
Increased signal and atrophy, putamen	2
Metabolic aciduria (glutaric):	
Increased signal, neostriatum (primarily putamen)	1
Glioma:	
Increased signal, basal ganglia	1
Wilson's disease:	
Decreased signal, neostriatum, at high field	1
Previous perinatal ischemic insult:	
Mild decreased signal, neostriatum	3
Hallervorden-Spatz disease:	
Increased and *decreased* signal, globus pallidus	4
Unknown metabolic disorder:	
Multiple areas decreased signal basal ganglia	1
Unclassified (for example, ?Leigh's disease, ?neuroaxonal dystrophy):	
Increased signal, neostriatum	9
Total	33

(CAC), and one with Sydenham's chorea. In this series, all patients with Huntington's disease and CAC showed decreased signal in the neostriatum, caudate, and putamen (Fig. 13). Generalized atrophy as well as focal atrophy of the neostriatum, predominantly of the caudate, with resulting enlargement of the frontal horns was seen in six of the seven cases. The patient without significant atrophy was in an early stage of Huntington's disease with only mild choreic movements. No significant difference was noted between images of Huntington's disease and CAC. One CAC patient was imaged twice over a 6-month period. A modest decrease in the signal of the neostriatum accompanied a progressive worsening of his clinical symptoms. The single case of Sydenham's chorea imaged showed no abnormalities. The patient was improving at the time of examination and went on to full recovery.

Four patients with hemiballismus were studied. All cases were of acute onset and demonstrated signal changes in the contralateral subthalamic nucleus region. Three of the patients demonstrated increased signal compatible with infarct, and one patient demonstrated increased signal surrounded by decreased signal compatible with subacute hemorrhage (Fig. 14).

Dystonias

Sixty patients with various dystonic conditions were examined. Nineteen were classified as primary dystonias and 41 were classified as secondary dystonias. No specific anatomic changes were noted in the dystonia group as a whole. The primary dystonia group comprised eight generalized (dystonia musculorum deformans) and 11 focal (for example, spasmodic torticollis and Meige syndrome) dystonias. No signal abnormalities were seen in any patient with a primary dystonia.

Thirty-three (80%) of the 41 patients with secondary dystonia, sudden- or delayed-onset dystonia, demonstrated signal changes in the neostriatum or paleostriatum. Twenty-one of these showed increased signal in the caudate and putamen, eight showed decreased signal in the caudate and putamen, and four showed mixed increased and decreased signal in the globus pallidus. Focal atrophy was seen in three patients in the putamen associated with increased signal.

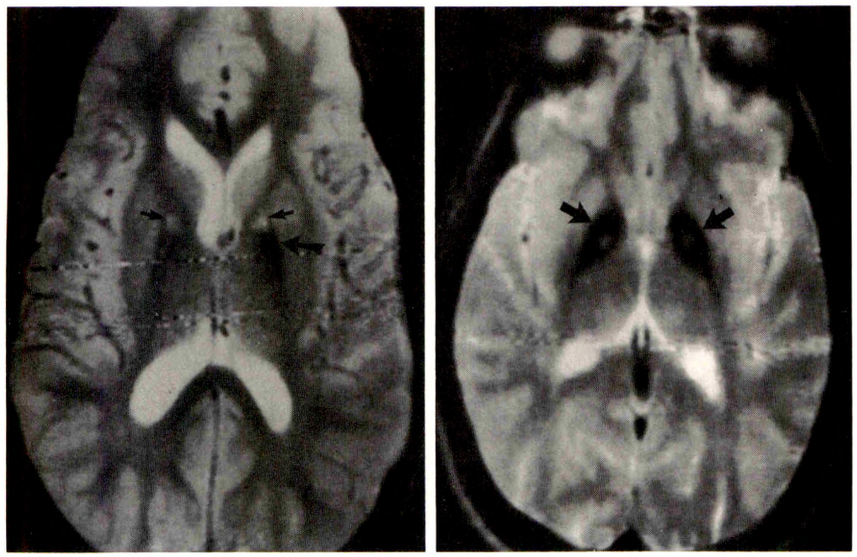


Fig. 15.—Axial 1.5-T SE 4300/80 images in Hallervorden-Spatz disease.
***A*, Increased (*small arrows*) and decreased (*large arrow*) signal in globus pallidus.**
***B*, Another patient. More uniformly decreased signal in globus pallidus bilaterally with slight central increased signal in long-standing disease (*arrows*).**

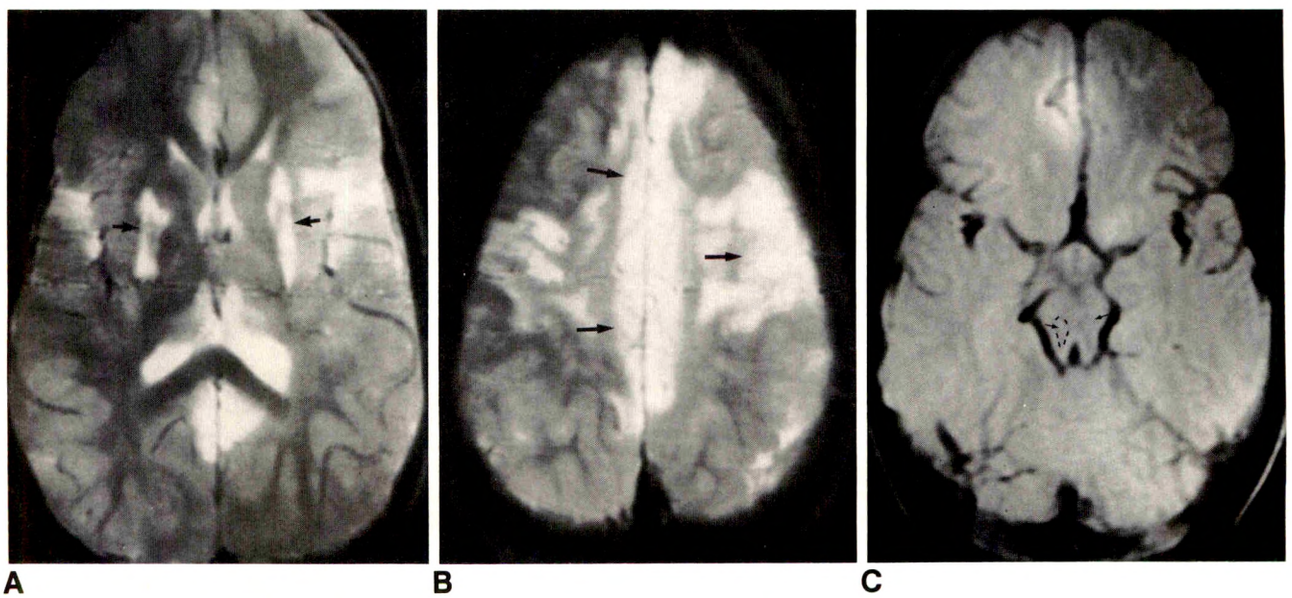


Fig. 16.—Axial 1.5-T MR images in Leigh's disease.
***A*, SE 4300/80. Increased signal in both putamen (*arrows*).**
***B*, Additionally increased signal in cortical areas (*arrows*) in subacute necrotizing form.**
***C*, SE 2000/80 image. "Butterfly" pattern of periaqueductal increased signal (*arrows*) is characteristic of Leigh's disease.**

When assessed by clinical diagnosis, even more discernible patterns were found in secondary dystonia (Table 4). Four patients with strong clinical/familial evidence of Hallervorden-Spatz disease (HSD) demonstrated markedly decreased signal in the globus pallidus when compared with the normal signal loss in the red nucleus (Fig. 15). Small areas of increased signal were also seen within the areas of decreased signal. No focal atrophy was seen in these patients. Their CT scans demonstrated little or no calcification in the globus pallidus. Several cases of clinically suspected neuroaxonal dystrophy, believed by some to be related to HSD (symptomatically similar but with an earlier age of onset), were grouped with cases of progressive unclassified dystonias; all showed increased signal in the putamen.

Four cases of confirmed Leigh's disease showed changes similar to those of the unclassified group of progressive dystonias with increased signal in the neostriatum, predominantly the putamen. In addition, in one patient with subacute

necrotizing encephalopathy, a cortical form of Leigh's disease, increased signal was observed in the cortex and midbrain and was equivalent to the described diagnostic pathologic changes (Fig. 16).

One patient with glutaric aciduria was studied at 6 and 8 months of age. The first images were normal for age; the second showed increased signal in the neostriatum similar to that of the above cases (Fig. 17). Other cases demonstrating increased signal in the neostriatum included two cases of postinfection dystonia and three cases of infarct-induced dystonia (Figs. 18 and 19). These cases also demonstrated atrophy in associated structures. In one case of basal ganglionic glioma with dystonia increased signal was seen also.

Three patients with a history of perinatal ischemic insults with resulting dystonia showed mildly decreased signal in the neostriatum. Two cases with this tenuous diagnosis were normal. One case of Wilson's disease showed bilateral decreased signal in neostriatum (Fig. 20). Three cases of infarct-induced dystonia showed decreased signal unilaterally in the putamen compatible with posthemorrhagic deposition of hemosiderin. One presumed metabolically caused dystonia showed multiple areas of decreased signal throughout the basal ganglia in a heterogeneous pattern.

Nine patients fell into an unclassified group because of a lack of definitive pathologic or clinical/laboratory proof. These cases all had similar findings with increased signal observed in the neostriatum predominantly the putamen. No changes in the globus pallidus were seen in the suspected neuroaxonal dystrophy. Several cases that may be Leigh's disease were also left unclassified pending pathologic proof.

Of the eight cases of secondary dystonias with no signal abnormality, two were believed to have been caused by perinatal ischemic insults, one was a 69-year-old with marked generalized atrophy, one was associated with Behr's syndrome, one was later determined to be a hysterical dystonia, two were believed to have resulted from drugs or toxins, and one occurred after head trauma.

Discussion

General

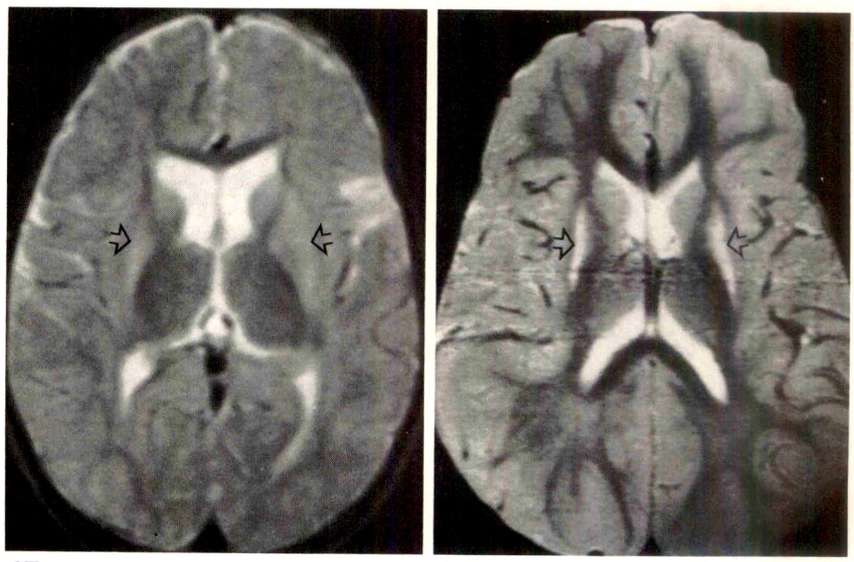
The clinical features of movement disorders often bear little resemblance to the gross pathologic changes. Biochemical abnormalities are the cause of many manifestations and are reflected only secondarily by structural changes such as atrophy or cell loss. The nature of movement disorders is also, like most neurodegenerative disorders, associated with a long clinical course that does not allow simple clinicopathologic correlation. The final autopsy findings also may not reflect the dynamic changes that can be captured by in vivo imaging methods. Because of these limitations, our analysis tried to group patient images first by the overt clinical dyskinesia and second by the clinical diagnosis. Limitations in the ability to verbally describe movement has always been a handicap and of necessity required a simplified group of definitions (Table 1). The rarity of many of the disorders also limits observation. Some of the diseases, therefore, are poorly defined. The simplified extrapyramidal system schema was then introduced to correlate anatomic regions of abnormality in relation to abnormal movement and to avoid memorizing the findings in a large number of rare diseases.

Iron/MR Correlation

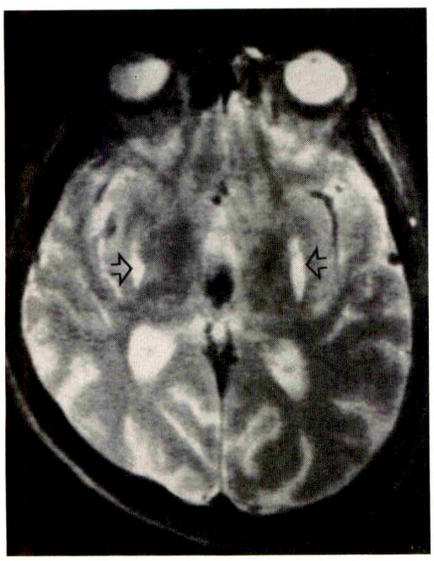
To fully exploit the ability of MR imaging to map iron, more precise knowledge about its functions in the brain, its distribution at the cellular level, and the physical state in its many roles is required. Also, an explanation for the close but imperfect correlation with iron staining is necessary (Fig. 4).

Fig. 17.—Axial 1.5-T SE 4300/80 image in 8-month-old patient with glutaric aciduria. Increased signal in neostriatum, predominantly putamen (*arrows*).

Fig. 18.—Axial 1.5-T SE 4300/80 image in subacute postinfection dystonia shows atrophy and increased signal in putamen (*arrows*).

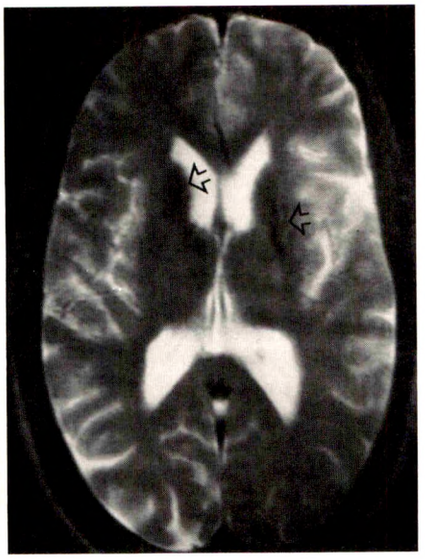


17 18



19

Fig. 19.—Axial 1.5-T SE 4300/80 image after anoxic infarct-induced dystonia shows increased signal in putamen bilaterally (*arrows*).



20

Fig. 20.—1.5-T SE 4300/80 image in Wilson's disease shows decreased signal and atrophy secondary to copper deposition in neostriatum (*arrows*).

Functionally, iron is required in oxidative metabolism at every step of the electron transport chain. This alone cannot, however, account for the very large variation of iron concentration in different parts of the brain, since there are no significant differences in metabolic rates of the cerebral cortex and basal ganglia as evaluated by positron emission tomography (PET) and other methods. Iron also participates in enzymatic synthesis of biogenic amines (dopamine, norepinephrine, and serotonin), and this may be relevant to regional metabolism. It should be noted, however, that high levels of iron are not always found in catecholaminergic (for example, nigra compacta, locus ceruleus) or serotonergic (for example, median raphe) systems [14–16]. The coincidence of iron and gamma-aminobutyric acid (GABA)-rich structures [17] is also imperfect (for example, the hypothalamus and superior colliculus) [18], while possible roles for iron in peptidergic systems are speculative [19].

If these known enzymatic requirements for iron are added to the amount stored as ferritin (estimated at one-third to one-half of the total), the sum still does not account for the high content of iron in specific regions of the brain. Therefore, it is possible that the regional concentrations of iron reflect neural system-specific functions that remain unknown.

Perls' Prussian blue reaction, long considered a highly sensitive method for the histochemical detection of ferric iron, colors specific regions consistently, but what proportion of the iron in the tissue is reactive (hemoglobin iron is not) and how much of it is solubilized in the process and subject to diffusion has not been determined. Also, cellular localization and changes with age and maturity are not always in accord [20–27]. With advancing age, encrustations of blood vessels in the globus pallidus, cerebellum, and hippocampus are seen and doubtless represent a special aspect of regional iron metabolism in tissue assay and imaging.

The biochemical versatility of iron is understandable in terms of this metal's extraordinary range of oxidation states, from Fe(-II) to Fe(VI), which explains its active presence along the entire chain of electron transfer reactions [28]. Only Fe(II) and Fe(III) are stable in aqueous solution, but with ligands, marked displacements of valence electrons from the d orbit take place. Such spatial rearrangements have profound effects on stereochemical binding properties, and in this regard, it is interesting to speculate that the disparity between the neostriatal and pallidonigral imaging and iron staining is caused by iron in the two structures in predominantly different forms (and subserves different functions).

In a study of the relaxation of water in the presence of ferritin, Koenig et al. [1] showed that the relaxation behavior of ferritin changes with the amount of iron within its core. A core substantially loaded with iron has no effect on T1, but has a substantial shortening effect on T2. Ferritin molecules with partially loaded cores do not demonstrate these changes. Koenig et al. postulated that the pronounced T2* effect is the result of small ferrimagnetic domains of ferric or mixed valence oxides produced within the core. This suggests that at least some of the failure of correlation between Perls' Prussian blue reaction and the heavily T2-weighted images can be attributed to states in which ferric iron is isolated within ferritin.

Parkinsonism

Describing changes in the images of patients with parkinsonism finds clinical utility in the ability to differentiate primary parkinsonism (Parkinson's disease) from secondary parkinsonisms and hereditary system degenerations. Clinically, Parkinson's disease consists of a tetrad of findings: rigidity, bradykinesia, postural instability, and resting tremor. Secondary parkinsonisms and hereditary system degeneration may also manifest these symptoms initially. That these groups of diseases can be differentiated by imaging has been suggested

by CT studies [29], and imaging is improved with MR because of its increased sensitivity to pathology and ability to differentiate the iron-containing extrapyramidal nuclei.

This sensitivity is seen in Parkinson's disease as restoration of signal in the dorsal lateral substantia nigra, hypothesized to be caused by either depletion of iron by increased cellular metabolic activity or by local cell death resulting in expansion of the extracellular space, which overwhelms the T2* effect by increasing signal locally [30]. Supporting this, PET has documented increased metabolism in the basal ganglia, and drug therapy has been shown to increase metabolic activity in the region [31, 32]. The inconstant occurrence (75%) requires further assessment regarding the age of the patient, therapeutic regimen, angle of the imaging plane, and specific clinical manifestations. That 53% of normal patients over 50 also have this change may suggest a threshold effect is present.

In secondary parkinsonism the increased sensitivity to cell loss; demyelination; and edema from infarcts, trauma, infections, toxins, and multiple sclerosis allows differentiation. In the group of heterogeneous system degenerations increased sensitivity is reflected primarily by detection and assessment of atrophy patterns. Occasionally, signal changes also are helpful. In supranuclear palsy these signal changes preceded the clinical changes. In these early cases, we hypothesize that increased signal seen in the periaqueductal and tectal regions represents gliosis and that atrophy occurs as the condition progresses [33]. In Shy-Drager syndrome, differentiation from olivo-ponto-cerebellar atrophy can be made by increased signal changes in the globus pallidus. This was only present in half of our cases and underscores the pathologic similarity between these diseases [34, 35]. Unlike other descriptions, we found no excess in iron. This is not surprising, as a review of this disorder by Schwarz [36] found no pathologic increase in iron. We suspect that, because of their similarity, olivo-ponto-cerebellar atrophy and Shy-Drager syndrome are linked in the multifocal atrophies. Another similar condition, striatonigral degeneration, is noteworthy in that it also does not demonstrate increased iron pathologically [37].

The two cases with homogeneous signal loss in the neostriatum underscore the utility of MR imaging. While clinically these patients were characterized by changes similar to olivo-ponto-cerebellar atrophy (ataxia, bradykinesia, mild tremor, and rigidity), they were clinically differentiated by poor responses to treatment. Other investigators have attributed this pattern to Shy-Drager syndrome, but our patients had no autonomic findings, considered a prerequisite of the syndrome [12]. Taking this into account, we believe that this change is either nonspecific, that it represents a separate disease, or that Shy-Drager syndrome may not always manifest with autonomic dysfunction.

Although the myoclonus cases imaged demonstrated no changes, it is believed that this group is worth imaging. An acquired form (hypoxic, infectious, and degenerative), as well as a familial form, exists. Pathologic changes described in the familial form may be too subtle for imaging, but changes in the acquired form may be recognizable [38].

Choreic Disorders and Hemiballismus

The prototypic choreic disorder is Huntington's disease, which is caused by a genetic abnormality in the short arm of the fourth chromosome resulting in loss of a specific set of cholinergic and GABA-nergic neurons and metabolic activity in the neostriatum [8, 30]. The recent ability to detect the chromosomal abnormality precludes much of the potential utility of the MR changes, even the suggestive loss of signal before atrophic changes. In the similar pathologic entity of chorea-acanthocytosis, distinguished by acanthocytes in the blood, MR changes are identical to those in Huntington's disease and suggest a residual utility and commonality of findings and location for choreic disorders. The decreased neostriatal signal corresponds to the increased iron described by Hallervorden [39] and Terplan [40]. In our one case of Sydenham's chorea with no MR abnormalities, progressive improvement, and full recovery, it is interesting to speculate if imaging findings are predictive.

Hemiballismus is a rare disorder caused by stroke, hemorrhage, or tumors damaging the contralateral subthalamic nucleus or, less often, the striatum or thalamic nuclei. Since the pathology is so well described and specific, imaging changes should be present and diagnostic in all cases. Imaging may be of value in subacute and borderline choreic cases and for differentiating the rare neoplastic etiologies.

Dystonia

Like the other groups, this group showed greatest correlation when subdivided by clinical diagnoses. That this assessment can then differentiate primary and secondary dystonia is not surprising. Primary dystonias (for example, dystonia musculorum deformans) have no known pathology, and secondary dystonias, which are associated with metabolic diseases, have several known pathologic changes. In this context, primary dystonias are defined as action dystonias, insidious in onset and slowly progressive with late posturing. Secondary dystonias are defined as sudden- or delayed-onset dystonias at rest with sustained postures and a more rapidly progressive course [41].

In trying to classify the secondary dystonias, it was found that an association with individual disease was stronger than any classification, such as hereditary and acquired forms. Wilson's disease is a good example, demonstrating a decreased signal in the putamen from the T2* effect of the copper, deposited due to a derangement in metabolism. Leigh's disease, a defect in pyruvate metabolism with a resulting elevation in lactate levels, demonstrates the opposite, increased signal in the putamen. At low field strengths, increased signal has been reported in Wilson's disease [42, 43] and probably reflects the inability to detect T2* effects at low field or variation in the amount of copper deposition.

When considering separately the diagnosis of HSD, a high field strength is advantageous in detecting the T2* of the increased iron in the globus pallidus. Pathologically, the globus pallidus also shows demyelination, neuronal loss, gliosis, and focal axonal swelling [44], which on T2-weighted images are reflected by increased signal. It is suspected that these

changes account for the heterogeneous signal pattern on our images. That our suspected cases of neuroaxonal dystrophy have no decreased signal on T2-weighted images in the globus pallidus suggests that HSD and neuroaxonal dystrophy should be considered as separate diseases despite the arguments of a shared metabolic defect [45–47].

In considering Leigh's disease, in addition to the increased signal in the putamen denoting its dystonic nature, signal changes in the midbrain and cortex suggest a feature differentiating it from the other dystonias. Pathologically, the periaqueductal signal changes correlate with gliosis and vacuolation [48]. In the cortical form a spongiform degeneration has been described. All the pathologic changes share the common MR finding of increased signal.

The one case of glutaric aciduria is important because it represents a large group of amino acid metabolic defects that are potentially treatable. The pathologic lesions manifest by these disorders are probably secondary to local acidosis, hypoglycemia, or hyperammonemia. The resulting cell loss and gliosis is detected by increased signal on T2 images. Also described histologically is a failure of myelination that we have seen in another case of aminoaciduria without dystonia or lesions in the putamen.

In the two cases of postinfection secondary dystonia increased signal and mild atrophy were seen in the putamen. No additional distinguishing features were found to separate this diagnosis from the others. An immunologic etiology is suspected, and little pathologic data are available.

In the five patients with the clinical diagnosis of perinatal ischemia a strong clinical interest exists because, unlike most of the other dystonias, these disorders are relatively static. The lack of a well-defined subset of asphyxia neonatorum producing pathologic changes consistent with our findings and the sparse historical data available make any conclusions highly speculative. However, experimental work by Windle [49] on rhesus monkeys suggests that perinatal ischemic insults as well as other factors may result in hemorrhage or other abnormalities such as mineral deposition that could result in decreased signal.

In the eight cases of infarct-induced dystonia a consistent pattern of putamenal lesions was found. Unique to MR was the ability to differentiate whether these were hemorrhagic or not, even when the ictus was in the distant past. The posthemorrhagic deposition of hemosiderin demonstrates a decrease in signal on the T2 image secondary to the T2* effect. The vascular distribution in the neostriatum is such that it is rarely affected by embolic events in isolation, and so generalized ischemia (such as carbon monoxide poisoning) and localized ischemia, hemorrhage, or thrombosis (by atherosclerosis or dystrophic changes of the lenticulostriate arteries associated with hypertension or occlusive arterial diseases) can be considered as causes of these secondary dystonias.

The unclassified group of dystonias may represent several diagnoses, including Leigh's disease, neuroaxonal dystrophy, or other metabolic abnormalities, but gives support to the idea that increased signal in the putamen is closely associated with dystonic movements. Further histologic investigation will determine if separate disease entities are present.

In the eight cases of secondary dystonias in which no signal abnormality was seen, it can only be assumed, without pathologic data, that these represent metabolic abnormalities not identified or structural abnormalities beyond the resolution of MR. In the case of hysterical dystonia, the normal examination strongly weighted the approach to treatment.

Conclusions

The ability to image the nuclei of the extrapyramidal motor system allows us to correlate, in life, many structural defects with functional deficits. Two of the largest gaps in this correlation at the present time are (1) the lack of correlation between chemically demonstrated iron distribution and metabolism and (2) imperfect correlation between the signal void on T2-weighted images and sections of the brain treated with Perls' stain.

In general, the MR brain findings in patients with movement disorders consist of complex patterns of focal atrophy, regions of pronounced signal void on T2-weighted images, and regions of increased signal in the various extrapyramidal nuclei. More specifically, in parkinsonisms we see a restoration of signal in the substantia nigra as well as less specific forms of atrophy. In choreas we see decreased signal in and atrophy of the caudate nucleus and to a lesser extent the putamen. In hemiballismus we see an increased signal in the subthalamic nucleus. In dystonias, we see no specific abnormalities in primary dystonia but often see abnormal signal in the neostriatum, especially the putamen in secondary dystonias (Tables 3–5).

While strict anatomic localization of pathology in these conditions is still in its early stages, we believe that this classification, while simplified [50, 51], has significant utility in clinical diagnosis.

ACKNOWLEDGMENTS

We thank Susan Bressman, Mitchel Brin, Lucien Cote, and Darryl DeVivo for sharing their patients and clinical diagnoses; Howard Radzyner for photography; and Charles Deschamps for imaging.

REFERENCES

1. Koenig SH, Brown RD, Peters TJ, Ward RJ. Relaxometry of ferritin solutions and the influence of the Fe(III) core ions. *Magnetic Resonance Med* **1986**;3:755–767
2. Rutledge JN, Hilal SK. MRI imaging of movement disorders (abstr). *Radiology* **1985**;157:290
3. Harrison WW, Netsky MG, Brown MD. Trace elements in human brain: copper, zinc, iron, and magnesium. *Clin Chim Acta* **1968**;21:55–60
4. Hock A, Demmel U, Schicha K. Trace element concentration in human brain. *Brain* **1975**;98:49–64
5. Ule G, Volkl A, Berlet H. Trace elements in human brain. *Neurology* **1974**;206(2):117–128
6. Hallgren B, Sourander P. The effect of age on the non-haemin iron in the human brain. *J Neurochem* **1958**;3:41–51
7. Seab JA. Anatomy and pathology of extrapyramidal diseases. *Brain Res Bull* **1983**;11:135–141
8. Cote L, Crutcher M. Motor functions of the basal ganglia and diseases of transmitter metabolism. In: Kandel ER, Schwartz JH, eds. *Principles of neural science*, 2d ed. New York: Elsevier, **1985**:523–534

9. Yung CY. Clinical features of movement disorders. *Brain Res Bull* **1983**;11:167–171
10. Gans A. Iron in the brain. *Brain* **1923**;46:128–136
11. Drayer B, Burger P, Darwin R, Riederer S, Herfkens R, Johnson GA. Magnetic resonance imaging of brain iron. *AJNR* **1986**;7:373–380
12. Drayer BP, Olanow W, Burger P, Johnson GA, Herfkens R, Riederer S. Parkinson plus syndrome: diagnosis using high field MR imaging of brain iron. *Radiology* **1986**;159:493–498
13. Pastakia B, Polinsky R, DiChiro G, Simmons JT, Brown R, Wener L. Multiple system atrophy (Shy-Drager syndrome): MR imaging. *Radiology* **1986**;159:499–502
14. Mackler B, Person R, Miller LR, Indamar AP, Finch CA. Iron deficiency in the rat: biochemical studies of brain metabolism. *Pediatr Res* **1978**;12:217–220
15. Sourkes TL. Transition elements and the nervous system. In: Pollitt E, Leibel RL, eds. *Iron deficiency: brain biochemistry and behavior*. New York: Raven, **1982**:1–29
16. Youdim MBH, Green AR, Bloomfield MR, Mitchell BD, Heal DJ, Grahame-Smith DG. The effects of iron deficiency on brain biogenic monamine biochemistry and function in rats. *Neuropharmacology* **1980**;19:259–267
17. Francois C, Nguyen-Legros J, Percheron G. Topographical and cytological localization of iron in rat and monkey brains. *Brain Res* **1981**;215:317–322
18. Roberts E, Chase TN, Tower DB, eds. *GABA and central nervous system function*. New York: Raven, **1976**:169–186
19. Sullivan S, Akil J, Blacker D, Barchas JD. Enkephalinase: selective inhibitors and partial characterization. *Peptides* (Fayettesville) **1950**;1:31–35
20. Hill JM. Brain iron: sex difference and changes during the estrous cycle and pregnancy. In: Saltman P, Hegenauer J, eds. *The biochemistry and physiology of iron*. New York: Elsevier Biomedical, **1982**:599–601
21. Dallman PR, Siimes MA, Manies EC. Brain iron: persistent deficiency following short-term iron deprivation in the young rat. *Br J Haematol* **1975**;31:209–215
22. Dallman PR, Spirito RA. Brain iron in the rat: a possible basis for irreversible depletion of brain non-heme iron following a brief period of iron deficiency. In: Brown EB, Aissen P, Fielding J, Crichton RR, eds. *Proteins of iron metabolism*. New York: Grune & Stratton, **1977**:381–386
23. Hill JM, Switzer RC. The regional distribution and cellular localization of iron in the rat brain. *Neuroscience* **1984**;11:596–603
24. Barden H. The histochemical distribution and localization of copper, iron, neuromelanin and lysosomal enzyme activity in the brain of aging rhesus monkey and the dog. *J Neuropathol Exp Neurol* **1971**;30:650–667
25. Kishi R, Ikeda T, Miyake H, et al. Regional distribution of lead, zinc, iron, and copper in suckling and adult rat brains. *Brain Res* **1982**;215:180–182
26. Spatz H. Eisennachweis im Gehirn, besonders in Zentren de extrapyramidalen Systems. *Eur Arch Psychiatry Neurol Sci* **1922**;77:261
27. Martin TL, Switzer RC, Joshi J, et al. Ferritin localization in rat brain by immunocytochemistry. *Soc Neurosci Abstr* **1985**;11:502
28. Spiro TG. Chemistry and biochemistry of iron. In: Brown EB, ed. *Proteins of iron metabolism*. New York: Grune and Stratton **1977**:xxiii–xxxii
29. Ambrosetto P, Michelucci R, Forti A, et al. CT findings in PSP. *J Comput Assist Tomogr* **1984**;8(3):406–409
30. Schoene WC. Degenerative diseases of the central nervous system. In: Davis RL, Robertson DM ed. *Textbook of neuropathology*. Baltimore: Williams & Wilkins, **1985**:788–823
31. Martin WR. Positron emission tomography in movement disorders. *Can J Neurol Sci* **1985**;12:6–10
32. Weiner W, Nausieda P, Klawans H. Effect of chlorpromazine on CNS concentration of manganese, iron and copper. *Life Sci* **1977**;20:1181–1186
33. Behrman S, Carrol J, Janata I, et al. Progressive supranuclear palsy: clinico-pathological study of 4 cases. *Brain* **1969**;92:663–678
34. Shy GM, Drager GA. A neurological syndrome associated with orthostatic hypotension. *Arch Neurol* **1959**;42:511–527
35. Petito CK, Black IB. Ultrastructure and biochemistry of sympathetic ganglia in idiopathic orthostatic hypotension. *Ann Neurol* **1978**;4:417–433
36. Schwarz GA. Dysautonomic syndromes in adults. In: Vinken PY, Bruyn GW, eds. *Handbook of clinical neurology*, vol 22. Part 2. *System disorders and atrophies*. New York: Elsevier, **1975**:243–280
37. Adams RD, Bogaert LV, Ecken HV. Striato-nigral degeneration. *J Neuropathol Exp Neurol* **1964**;23:584–608
38. Hoehn MM, Cherington M. Spinal myoclonus. *Neurology* **1977**;27:942–946
39. Hallervorden J. *Handbuch der speziellen pathologischen Anatomie und Histologie*. Berlin: Springer-Verlag, **1957**:793
40. Terplan K. Zur pathologischen anatomie der chronischen progressiven chorea. *Virchows Arch [Cell Pathol]* **1924**;252:146–176
41. Fahn S. The varied clinical expressions of dystonia. *Neurol Clin* **1984**;2(3):541–553
42. Lukes SA, Aminoff MJ, Crooks L, et al. Nuclear magnetic resonance imaging in movement disorders. *Ann Neurol* **1983**;13(6):690–691
43. Aisen AM, Martel W, Gabrielsen TO, et al. Wilson's disease of the brain: MR imaging. *Radiology* **1985**;157:137–141
44. Dooling E, Schoene W, Richardson E. Hallervorden-Spatz syndrome. *Arch Neurol* **1974**;30:70–83
45. Cowen D. Infantile neuroaxonal dystrophy. *J Neuropathol Exp Neurol* **1963**;22(2):175–236
46. Vakili S, Drew AL, Von Schuching S, et al. Hallervorden-Spatz syndrome. *Arch Neurol* **1977**;34:729–738
47. Littrup PJ, Gebarski SS. MR imaging of Hallervorden-Spatz disease. *J Comput Assist Tomogr* **1985**;9(3):491–493
48. Egger J, Pincott JR, Wilson J, et al. Cortical subacute necrotizing encephalomyelopathy. *Neuropediatrics* **1984**;15:150–158
49. Windle WF. Brain damage at birth. Functional and structural modification with time. *JAMA* **1968**;209(9):1967–1972
50. Young AB, Penney JB. Neurochemical anatomy of movement disorders. *Neurol Clin* **1984**;2(3):417–433
51. Marsden CD. The patholphysiology of movement disorders. *Neurol Clin* **1984**;2(3):435–459

Technical Note

New Needle for MR-Guided Aspiration Cytology of the Head and Neck

R. Lufkin,[1] L. Teresi, and W. Hanafee

CT-guided aspiration cytology is valuable in the work-up of many deep head and neck lesions [1]. Since MR imaging is rapidly replacing CT as the imaging study of choice for evaluating many areas of head and neck pathology, the ability to perform MR-guided aspiration cytology is becoming increasingly important. Attempts at MR-guided biopsy with conventional stainless steel CT needles result in images with unacceptably large image artifacts that obscure underlying anatomy.

A needle for MR-guided biopsies of the liver first developed by Mueller et al. [2] has decreased the number of artifacts and is ideal for relatively thick MR sections of the liver. The decreased artifact of the liver needle necessary for thick-section liver studies is still too large to locate small lesions in areas of complex head and neck anatomy where higher resolution and thinner MR sections are necessary. Other investigators are studying nonferrous plastic sheaths with larger diameters for MR-guided percutaneous drainage procedures [3].

Finally, new field-echo imaging techniques with narrow flip angles, which probably will be the most practical pulse sequences for MR-guided biopsy because of their speed, tend to accentuate magnetic susceptibility artifacts of all needle types because of the increased T2 sensitivity of gradient refocusing techniques [4].

We describe a new MR needle with fewer artifacts on both spin-echo and gradient-echo sequences that is ideal for MR-guided aspiration cytology of head and neck lesions using high-resolution, thin-section MR imaging.

Materials and Methods

A variety of stainless steel needle alloys were tested. For each needle, the effects of length, composition, annealing, degree of beveling, internal and external diameter, and pulse sequence on the image artifact were studied.

Standard spinal CT needles made of 304 stainless steel as well as the Mueller needle made of 316 stainless steel were also examined [5]. In an attempt to decrease the number of artifacts on MR, a new needle was developed from c-276 stainless steel that has four times the nickel content of the Mueller needle and five times the nickel present in the standard CT needle. The needle compositions are summarized in Table I. The needles were suspended in a phantom made of 2.5 mM NiCl solution (T1 = 460 msec at 0.3 T) for imaging.

MR scans were performed on a 0.3-T permanent magnet (Fonar Beta 3000, Melville, NY) MR whole-body imager. With one signal excitation on a 256 × 256 matrix, 2DFT images were obtained. A 25.6-cm field of view yielded 1.0 × 1.0 mm pixels; 3.5-mm-thick image slices were obtained. Field-echo sequences using a reduced flip angle of 30° and standard spin-echo sequences were employed with an echo time (TE) of 14 msec and a repetition time (TR) of 400 msec.

Imaging during an MR-guided clinical aspiration cytology was performed with the new needle. In a patient with a parapharyngeal space squamous carcinoma, the needle was placed using a subzygomatic approach.

Results

Images of needles of comparable size that were made of the three stainless steel alloys described above are shown in

Received January 26, 1987; accepted after revision March 19, 1987.
This work was supported by the E-Z-EM Corporation, Westbury, NY, and PHS grant number 1KO8 CA 00979-01, awarded by the National Cancer Institute, Department of Health and Human Services.
[1] All authors: Department of Radiological Sciences, UCLA School of Medicine, Los Angeles, CA 90024. Address reprint requests to R. B. Lufkin.

TABLE 1: Needle Composition (%)

	Carbon	Chrome	Nickel
Standard CT needle (alloy 304)	0.8	19	9
MR liver needle (alloy 316)	0.8	17	12
New MR needle (alloy c-276)	0.01	16	49

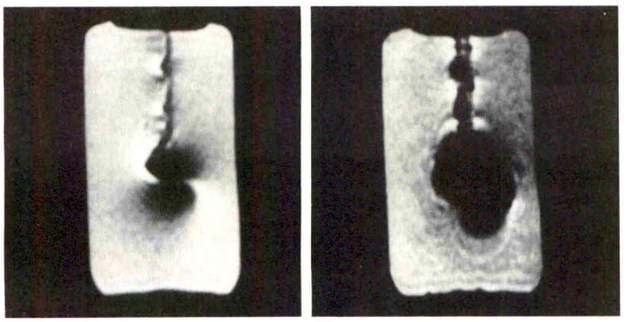


Fig. 1.—Standard CT needle in phantom.
***A*, Image obtained with spin-echo sequence (SE/400/14) shows significant number of susceptibility artifacts.**
***B*, Increased artifacts with a field-echo sequence (FE/400/14).**

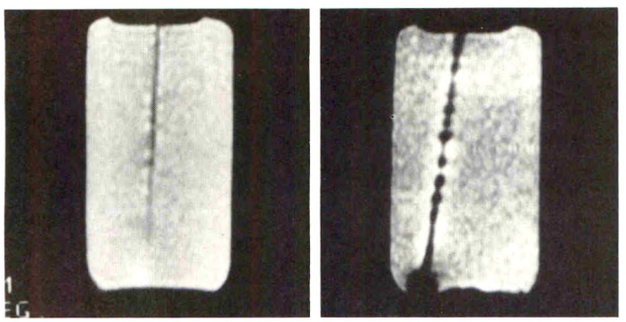


Fig. 2.—Mueller MR liver needle in phantom.
***A*, Spin-echo sequence (SE/400/14) shows fewer artifacts.**
***B*, Field-echo image (FE/400/14) shows minimal increase in number of artifacts allowing for positioning that obscures needle tip.**

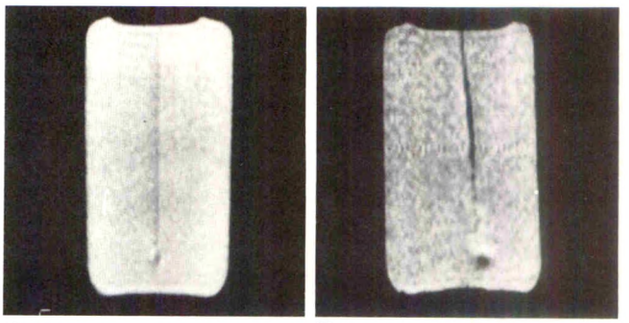


Fig. 3.—New head and neck needle in phantom.
***A*, Spin-echo sequence (SE/400/14) shows still fewer artifacts.**
***B*, Field-echo sequence (FE/400/14) results in slightly more but still acceptable number of artifacts.**

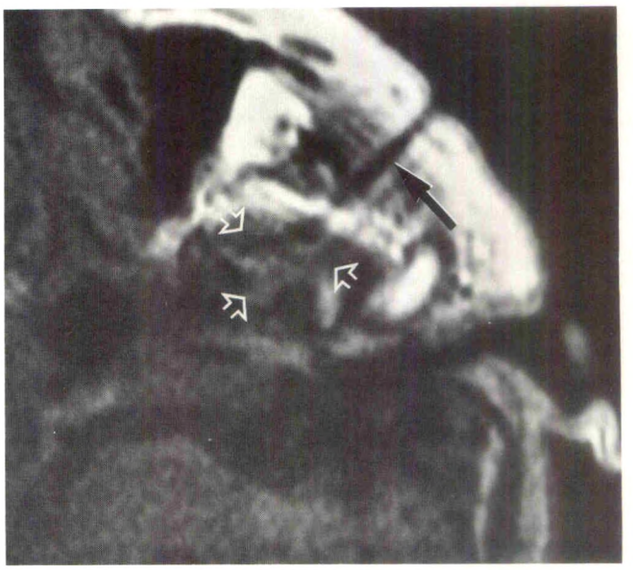


Fig. 4.—Spin-echo sequence (SE/500/28) obtained with 10-cm planar surface coil during MR-guided biopsy in patient with parapharyngeal mass (*white open arrows*) using new needle. A subzygomatic approach was used. Needle appears as a linear, low-signal region (*black arrow*). Number of artifacts is somewhat increased compared with those in Figure 3 owing to different relation of needle to the readout axis [6].

Figures 1–3. Artifacts produced by the standard stainless steel CT needle tended to obscure accurate needle tip localization. The Mueller liver needle produced fewer artifacts than the standard CT needle but still tended to obscure the needle tip on the thin-section images used. For each needle tested, the artifacts were increased on the field-echo sequences relative to spin-echo sequences. Figure 3 shows the new head and neck needle which, of the needles studied, produced the fewest artifacts with both spin-echo and field-echo sequences.

As noted by others, the degree of needle tip bevel, annealing, or length had no significant effect on image artifacts [2]. A minimal increase in artifacts occurred when the needle diameter was increased for each alloy.

During the clinical study of the patient with squamous carcinoma, the position of the needle was confirmed with an MR image obtained using a 10-cm planar surface coil (Fig. 4).

Discussion

The main difference between the new needle and the other needles tested is the increased nickel content of the stainless steel alloy. Nickel reduces the ferromagnetic properties of the iron in the alloy and generally decreases magnetic susceptibility differences between the alloy and surrounding tissues [7]. The nickel works by changing the highly susceptible form of alpha iron into less susceptible gamma iron.

Abrupt local changes in induced magnetic field (susceptibility) result in magnetic field inhomogeneities that interfere with gradient fields used in imaging. The result is local geometric image distortions oriented along the read gradient [6]. Alterations in image intensity also occur with a similar orientation. A combination of these geometric and brightness distortions can completely obscure underlying anatomy and pathology.

The lack of the 180° refocusing pulse allowing an extremely short TE and TR with gradient refocusing techniques also means that the imaging sequences are generally much more sensitive to magnetic inhomogeneities and susceptibility differences [4]. Therefore, the magnetic susceptibility artifacts produced by all the needles are accentuated by using gradient refocusing techniques. Because of the high speed of field-echo imaging, this technique will be useful for MR-guided biopsies. Thus, MR needles with minimal differences in susceptibility are especially valuable. The overall trend toward higher resolution, thinner section imaging will also make needles with smaller artifacts increasingly important for MR-guided biopsies throughout the body.

We describe a new needle for MR-guided biopsies of the head and neck. Standard CT needles and other MR needles designed for thick-section liver imaging are unsatisfactory in the head and neck because the artifacts produced are unacceptable for high-resolution, thin-section MR imaging.

REFERENCES

1. Abemayor E, Lung B, Larsson S, Ward P, Hanafee W. CT-directed aspiration biopsies of masses in the head and neck. *Laryngoscope* **1985**;95:1382–1386
2. Mueller PR, Stark DD, Simeone JF, et al. MR-guided aspiration biopsy: needle design and clinical trials. *Radiology* **1986**;161:605–609
3. vanSonnenberg E, Hajek P, Baker L, et al. Materials for MR-guided interventional radiology procedures: laboratory and clinical experience (abstr). *Radiology* **1986**;161(P):121
4. Edelman RR, Johnson K, Buxton R, et al. MR of hemorrhage: a new approach. *AJNR* **1986**;7:751–756
5. American Society for Metals. *Metals handbook*, vol. 3, 9th ed. Metals Park, OH: American Society for Metals, **1980**
6. Ludeke KM, Roschmann P, Tischler R. Susceptibility artefacts in NMR imaging. *Mag Resonance Imag* **1985**;3:329–343
7. New PFJ, Rosen BR, Brady TJ, et al. Potential hazards and artifacts of ferromagnetic and nonferromagnetic surgical and dental materials and devices in nuclear magnetic resonance imaging. *Radiology* **1983**;147:139–148

MR of Craniopharyngiomas: Tumor Delineation and Characterization

Elizabeth Pusey[1]
Keith E. Kortman[2]
Bonnie D. Flannigan[1,3]
Jay Tsuruda[2]
William G. Bradley[2]

MR imaging and CT (with and without contrast enhancement) were performed in 20 patients with an established or clinically suspected diagnosis of craniopharyngioma. Fifteen had biopsy-proven craniopharyngioma and five had presumed craniopharyngioma based on clinical and CT findings. In two cases MR was superior to contrast-enhanced CT in demonstrating the tumor. A variable appearance on T1-weighted MR images reflected the pathologic appearance of craniopharyngiomas. High intensity on T1-weighted images corresponded to high cholesterol content or presence of methemoglobin. MR was the preferred method in the evaluation of tumor extent, especially in the cavernous sinus and posterior clival region. CT was superior to MR in detecting the presence of calcification, which with the clinical history correctly suggested the diagnosis of craniopharyngioma. Both MR and CT studies are desired initially to establish the diagnosis and to evaluate tumor extent. MR was the preferred method in detecting the presence of recurrent tumor.

Clinical experience with MR has demonstrated its superiority over CT in the evaluation of many brain tumors, and it has been cited by some authors as the examination of choice in screening and delineating tumor extent [1–3] due to its increased sensitivity and direct multiplanar capabilities. The variable histologic appearances of craniopharyngiomas and the difficulty in identifying calcifications with MR has cast doubt on its applicability in suspected craniopharyngioma. Previous reports have included isolated cases in larger studies of brain tumors [4–8]. Because the spectrum of MR appearances of this tumor has not previously been described fully, we correlated the results of MR, CT, and histopathology in 20 patients to characterize the MR appearance and to determine its role in diagnosis.

Subjects and Methods

Twenty-seven MR studies were performed in 20 patients 7–66 years old. Fifteen patients with surgical proof and five with clinical and CT diagnosis of craniopharyngioma are included in the study. MR was performed as part of the preoperative workup in 13 patients. In seven patients it was performed after biopsy or partial surgical resection.

MR and CT studies were performed in all cases. MR studies were performed on one of three imagers. Relative T1-weighted and T2-weighted spin-echo (SE) sequences were obtained in all patients. Sixteen patients were scanned with a 0.35-T scanner (Diasonics). Multislice multiecho images were obtained with a repetition time (TR) of 1000 or 2000 msec and an echo time (TE) of 28 or 56 msec. Three patients were scanned with a 0.3-T imager (Fonar) Multislice single-echo images were obtained with TR = 500/2000 msec, TE = 28/56 msec. Two patients were scanned on a 0.5-T instrument (Picker) Multislice, dual-echo images were obtained with TR = 1000/2000 msec, TE = 40/80 or 60/120 msec. Images were obtained in at least two planes. Surgical pathology reports were reviewed in all cases. Surgical pathologic specimens were reviewed by the authors in six cases. In one case analysis of the hemosiderin content of the specimen was performed by ultraviolet light spectroscopy.

This article appears in the May/June 1987 issue of *AJNR* and the August 1987 issue of *AJR*.

Received June 27, 1986; accepted after revision October 5, 1986.

Presented at the annual meeting of the American Roentgen Ray Society, Washington, DC, April 1986.

[1] Department of Radiologic Sciences, University of California, Los Angeles, Center for Health Sciences, Los Angeles, CA 90024. Address reprint requests to E. Pusey.

[2] Department of Radiology, Huntington Memorial Hospital, and NMR Imaging Laboratory, Huntington Medical Research Institutes, Pasadena, CA 91105.

[3] Present address: Department of Radiology, Valley Presbyterian Hospital, Van Nuys, CA 91405.

***AJR* 149:383–388, August 1987**
0361–803X/87/1492-0383
© American Roentgen Ray Society

Results

MR studies demonstrated a wide range of appearances of craniopharyngiomas, especially on T1-weighted images. In nine patients the tumor showed an increase in intensity on T1-weighted images consistent with T1 shortening (Fig. 1). Ten studies demonstrated a tumor of intermediate intensity on T1-weighted images (Fig. 2) with signal intensity greater than CSF and variable homogeneity (Fig. 3). In one case a cystic tumor showed decreased intensity on T1-weighted images (Fig. 4). The craniopharyngiomas were of high signal intensity on T2-weighted images in all but one case, suggesting a long T2 relaxation time (Figs. 1B and 2B).

Pathologic specimens were reviewed in an attempt to correlate the varying MR appearances with the wide histologic appearances of craniopharyngiomas. High-intensity signal on T1-weighted images was found to correspond to a high liquid cholesterol content in the tumor, as demonstrated pathologically (Fig. 1), or to the presence of methemoglobin, as demonstrated by ultraviolet visible spectroscopy (Fig. 5). Moderate-intensity signal on T1-weighted images was found in tumors without high cholesterol content (Fig. 2). In each case the tumor demonstrated a high signal intensity on T2-weighted images. In a single case (Fig. 4), the tumor demonstrated low-intensity signal on both T1- and T2-weighted images. This corresponded to a cystic tumor with a high keratin content and delicate bone trabecular network. The presence of extensive ossification throughout the aspirated specimen was a surprising finding. Apparently, the delicate bone trabecular network collapsed with suction and could be aspirated with cyst fluid at surgery. In each case the typical adamantinomatous pattern was present in some of the pathologic sections, confirming the diagnosis. Overall, CT was superior to MR in demonstrating calcifications within the tumors. MR failed to demonstrate areas of calcification in three of 14 cases in which calcification was demonstrated by CT (Figs. 1 and 6). In one case, calcification would have been incorrectly suspected on the basis of MR. The areas of low signal on MR corresponded to low-density regions on CT believed to represent areas of cystic necrosis (Fig. 3).

MR imaging was very sensitive in detecting the presence of pathology. In two cases MR was superior to contrast-infused CT in demonstrating tumor. In one case in which tumor was confined to the suprasellar region the tumor was not appreciated on contrast-infused CT. CT with metrizamide cisternography performed the same day and MR studies

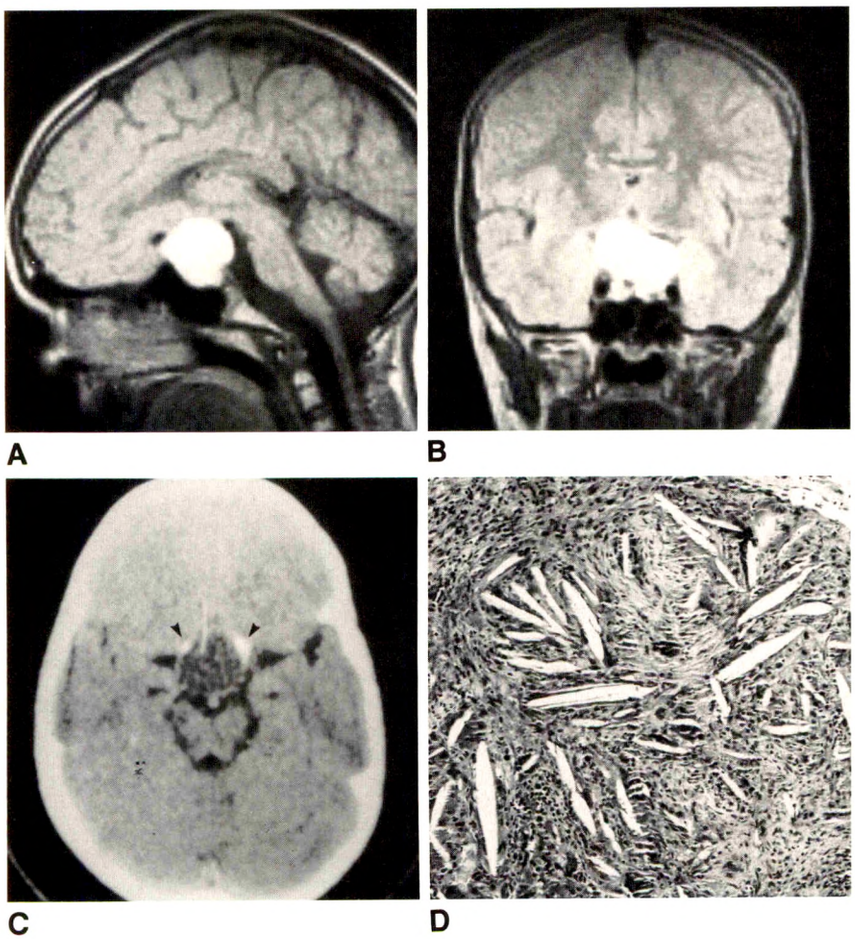


Fig. 1.—8-year-old boy who had multiple surgical resections for recurrent craniopharyngioma. MR was performed as part of periodic monitoring of tumor.

***A*, Sagittal SE image (TE = 28, TR = 1000 msec) with relative T1-weighting. Suprasellar tumor of high signal intensity.**

***B*, Coronal SE image with T2-weighting (TE = 56, TR = 2000 msec). Long T2 of tumor and cavernous sinus extension was important in planning radiation therapy.**

***C*, Axial noninfused CT scan shows peripheral calcification (*arrowheads*) not apparent on MR scans.**

***D*, Pathologic specimen shows large number of cholesterol clefts. High cholesterol tumor content was found to be one cause of high-intensity signal on T1-weighted images.**

Fig. 2.—41-year-old man with headache and visual field deficits.

A, Sagittal image with relative T1-weighting shows moderate signal intensity of suprasellar tumor (TE = 28, TR = 500 msec).

B, Sagittal image with relative T2-weighting shows high signal intensity of tumor (TE = 56, TR = 2000 msec).

C, Coronal MR image shows tumor impinging on right optic nerve (*arrow*), which correlated with symptoms.

D, Metrizamide axial CT scan shows suprasellar tumor. Contrast-enhanced CT before metrizamide study failed to show pathology.

E, Pathologic specimen shows striking lack of cholesterol clefts. Representative section is shown with moderate amounts of keratin (*black arrow*) and typical adamantinomatous cells of craniopharyngioma (*white arrow*). Lack of cholesterol or hemorrhage and presence of keratin may account for longer T1 of this tumor compared with Figure 1.

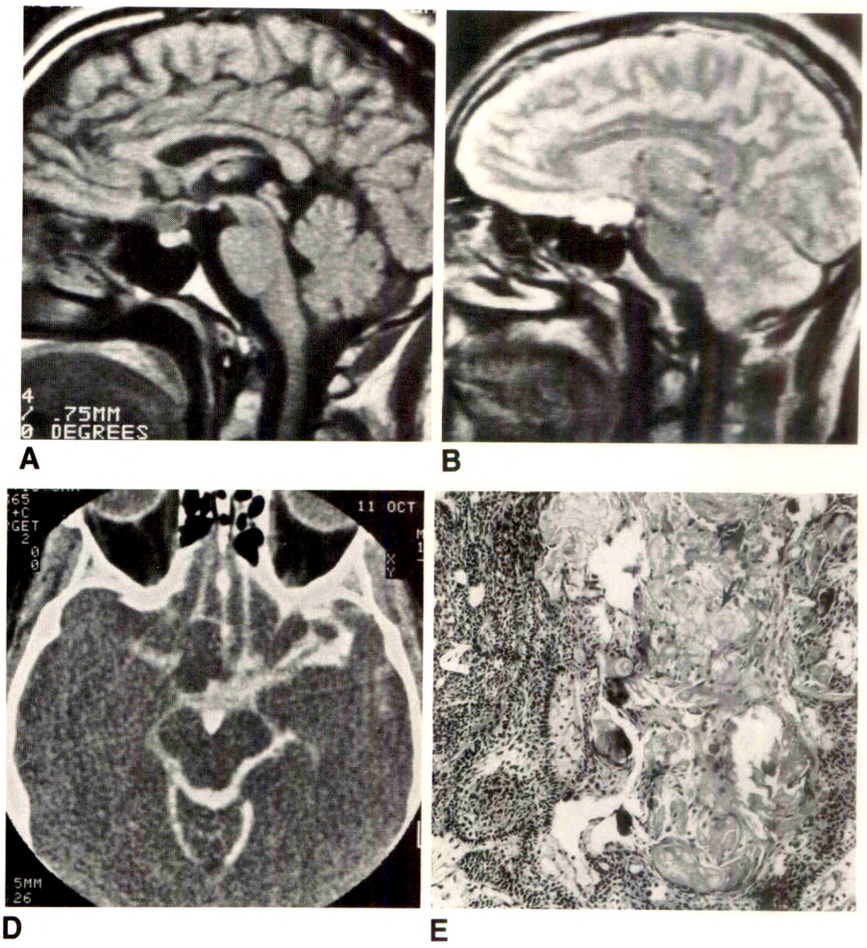
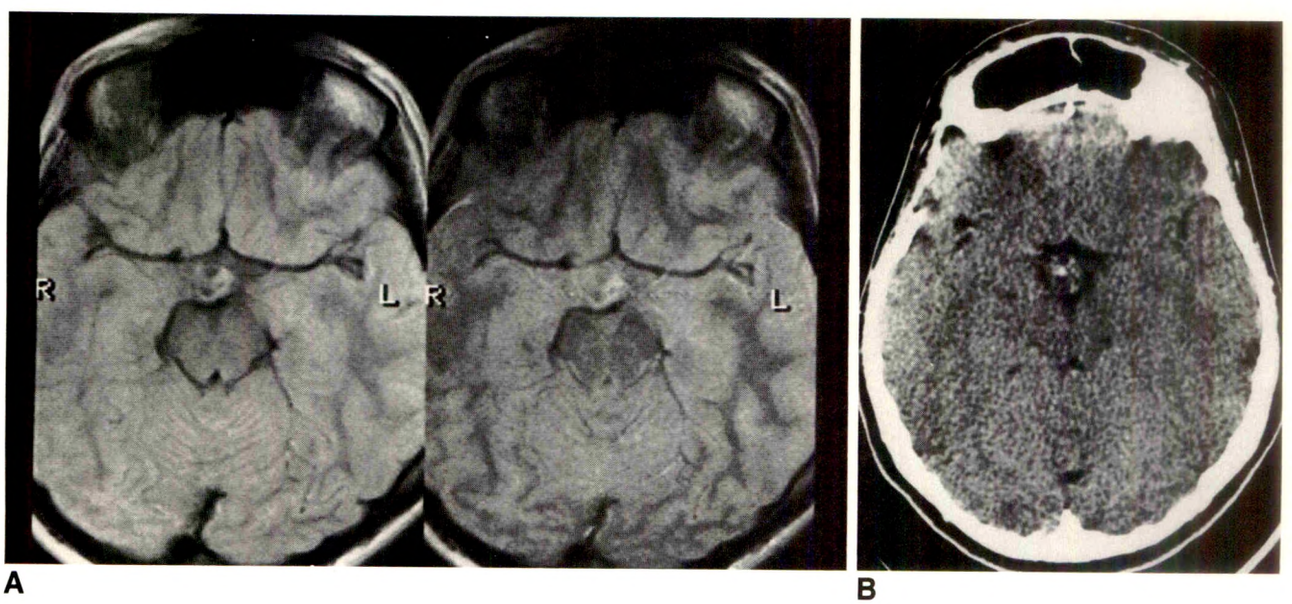
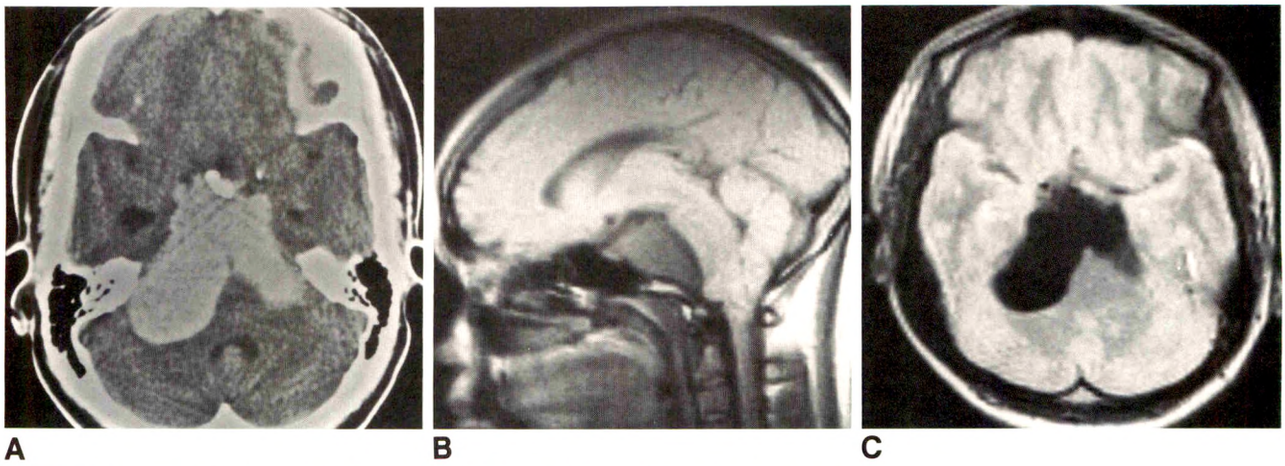


Fig. 3.—19-year-old woman with subsequent surgical resection demonstrating craniopharyngioma.

A, T2-weighted axial MR study shows areas of focal decreased signal intensity also present on T1-weighted images (TE = 30, TR = 2000 msec). Calcification could be suspected on basis of MR study alone.

B, CT scan shows focal areas of decreased density corresponding to areas of decreased signal on MR, believed to represent areas of cystic necrosis.





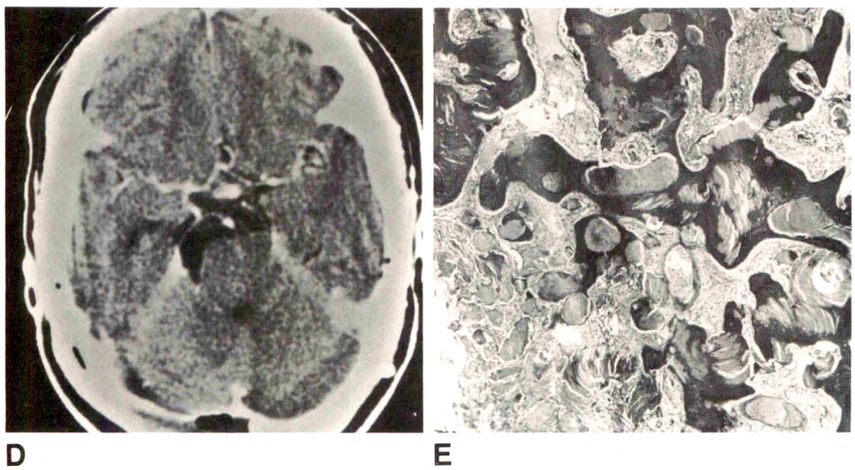


Fig. 4.—17-year-old girl with headaches.
A, Unenhanced CT scan shows hyperdense mass with suprasellar and posterior extension.
B and *C*, Sagittal (TE = 28, TR = 1000 msec) and axial (TE = 56, TR = 2000 msec) SE images, respectively, show low signal-intensity mass.
D, Axial contrast-enhanced CT scan after tumor drainage shows collapse of cyst walls.
E, Pathologic specimen of cyst aspirate shows delicate bone trabecular network and keratin.

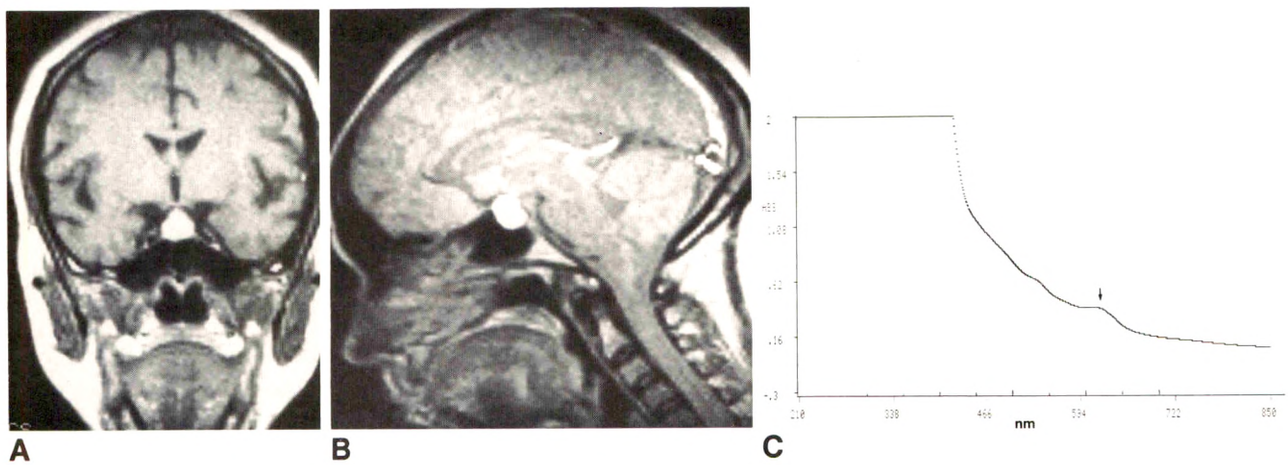


Fig. 5.—38-year-old woman with bitemporal visual field loss.
A, Coronal relative T1-weighted SE image (TE = 28, TR = 500 msec) shows high-intensity-signal suprasellar tumor.
B, Sagittal T2-weighted image shows high-intensity signal of tumor (TE = 56, TR = 1500 msec). Pathologic specimen showed numerous RBCs with few cholesterol clefts.
C, Ultraviolet light spectroscopy of cyst contents shows photopeak at 630 nm indicating presence of methemoglobin (*arrow*). Presence of methemoglobin was found to be one cause of T1 shortening.

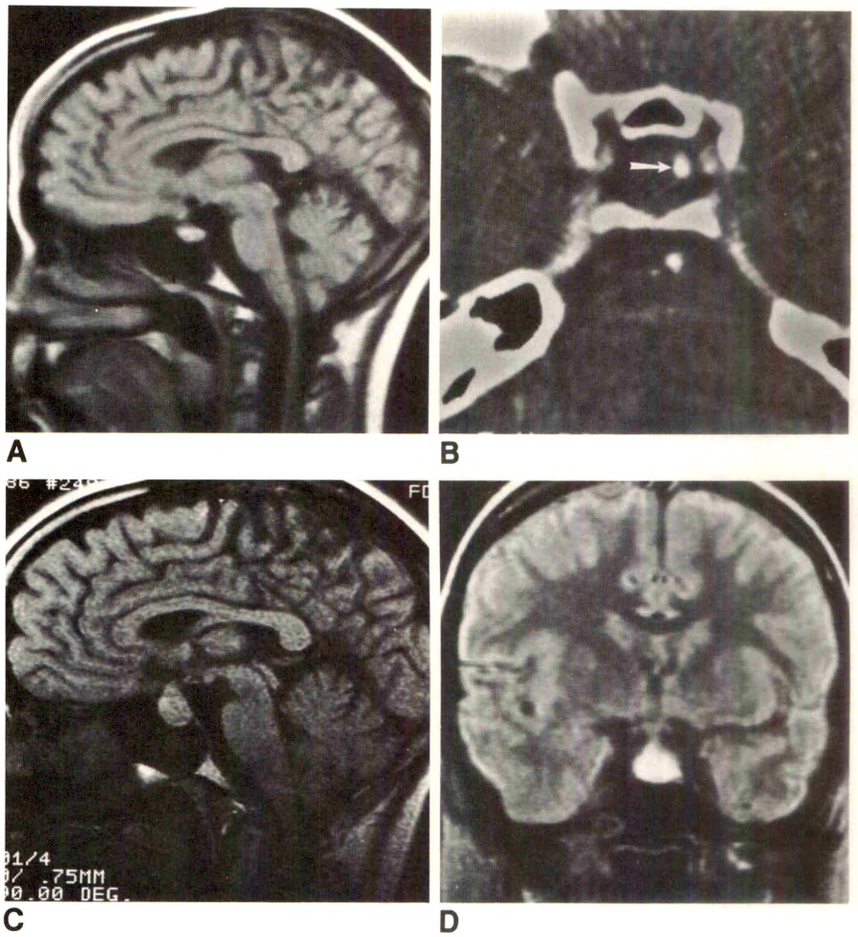


Fig. 6.—19-year-old woman seen for routine follow-up studies after surgical removal of intrasellar craniopharyngioma.

***A*, Recurrence of tumor shows moderate signal intensity on T1-weighted images (TE = 28, TR = 500 msec).**

***B*, Punctate calcification (*arrow*) identified by CT was not seen on MR study.**

***C*, 6 months later. Patient returned with increasing visual field deficits. Enlargement of tumor mass with suprasellar extension is seen on T1-weighted image (TE = 28, TR = 500 msec).**

***D*, Coronal T2-weighted image shows extension of tumor to level of optic chiasm (TE = 56, TR = 2000 msec).**

performed 4 days later clearly demonstrated the abnormality (Fig. 2). In a second patient, pathology was suspected on CT due to the presence of an enlarged sella without demonstration of tumor. MR 2 weeks later showed a 2.5-cm tumor with suprasellar extension. In 10 patients the tumor was located above and within the sella. In nine the tumor was entirely suprasellar. In one the tumor was located only within the sella (Fig. 6). Posterior extension in five cases was well demonstrated on sagittal MR images, which was significant in planning the surgical approach in these cases. In one of these patients the posterior location of the tumor was not appreciated on CT, and the tumor was missed during transnasal biopsy. Subsequent MR revealed the posterior location of the tumor (Fig. 7). Coronal images were especially useful in demonstrating cavernous sinus extension, which was present in one case (Fig. 1) and was important in planning postsurgical radiation therapy.

Discussion

Craniopharyngiomas originate from squamous epithelial rests of Rathke's pouch. They are benign, slow-growing tumors. Although primarily tumors of children and young

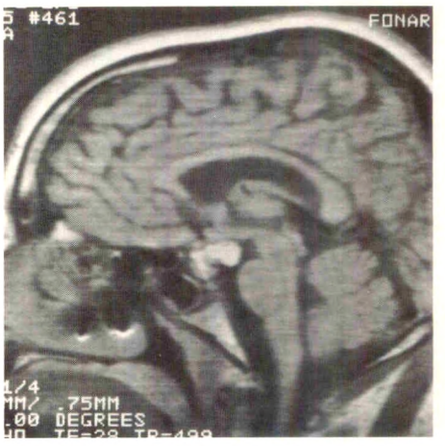


Fig. 7.—27-year-old man with double vision and headaches. Sagittal SE image (TE = 28, TR = 499 msec) shows high-intensity suprasellar tumor extending posteriorly. Biopsy was performed through transnasal approach and normal tissue was obtained. Posterior extension of tumor is important in preoperative surgical planning. Subtemporal exposure may be preferred in cases with significant posterior extension.

adults, some may have delayed presentation in middle age or older. They present with headache, visual symptoms, and symptoms caused by dysfunction of the hypothalamus and pituitary gland. Growth failure is often the mode of presentation in a child.

The histologic pattern of craniopharyngiomas [9, 10] is variable and includes a variety of cell types. Diagnosis is made histologically by the identification of nests or cords of stratified squamous or columnar epithelium in loose fibrous stroma reminiscent of the enamel organ of the tooth, and they are considered to have an adamantinomatous pattern. Craniopharyngiomas may be cystic, often with high cholesterol content, or solid, and they contain calcium in 75% of cases.

The wide range of histologic appearances of craniopharyngiomas was reflected in their MR appearances. Although definitive statements concerning calcium and cholesterol content cannot be made without complete sectioning of the entire specimen, qualitative examination of the sections correlated well with the several MR patterns. High intensity on T1-weighted images was noted in cystic lesions with high cholesterol content or containing methemoglobin. Kjos et al. [4] described high-intensity signal on T1-weighted images of hemorrhagic cysts. Bradley and Schmidt [11] showed that methemoglobin formation with T1 shortening at least partially accounts for the increasing MR signal intensity of subarachnoid hemorrhage with time. Moderate intensity on T1-weighted images was noted in tumors lacking significant cholesterol or blood. Both these groups demonstrated high signal intensity on T2-weighted images. In a single case (Fig. 4), low signal intensity was demonstrated on both T1- and T2-weighted images in a cystic lesion high in keratin and having extensive bone trabeculae. In this case CT demonstrated a hyperdense lesion. Braun et al. [12] described hyperdense cystic craniopharyngiomas in four of 63 cases in their series. Their analysis of cyst contents demonstrated a high protein content in these cases. However, the MR appearance of low T1 and T2 signal intensity in our series was explained by the delicate bone trabecular network found at pathologic examination of the cyst aspirate. Despite the presence of ossification, the tumor behaved as a cyst at surgery, and collapse of the cyst walls was seen on postaspiration CT studies.

In the evaluation of craniopharyngioma the presence of calcification is often of diagnostic significance. Holland et al. [8] have shown CT to be superior to MR in the detection of calcification, which was also demonstrated in our study. The failure of MR to demonstrate tumoral calcification is of less importance in the evaluation of tumor recurrence when the tissue diagnosis is known.

MR has proved to be valuable in preoperative and radiation therapy planning due to its multiplanar capabilities. Accurate preoperative knowledge of the tumor extent may lead to a change in the surgical approach [13]. A transnasal approach may be sufficient for an entirely intrasellar tumor. Suprasellar tumor may require a subfrontal approach to allow optimal exposure of the optic chiasm. Cryoprobes may need to be available in this case to peel tumor away from the optic chiasm. Supra- and intrasellar tumor extension may additionally require unroofing of the sphenoid sinus. If the tumor extends posteriorly along the clivus a subtemporal approach may be preferred. A cystic craniopharyngioma may allow a more conservative surgical approach with drainage without removing the walls and with implantation of radioisotopes. MR offers superior information in identifying tumor in the cavernous sinus (Fig. 1B), which would not usually be explored at surgery and would be treated with radiation therapy. Tumor extension into the sphenoid sinus is not as easily identified by MR due to its resemblance to benign conditions such as sinus disease and changes resulting from transnasal biopsy. In cases with supra- and intrasellar tumor, a subfrontal approach with unroofing of the sphenoid sinus would be used, and extension into the sinus would be discovered at surgery.

In summary, MR is more sensitive than CT in identifying the presence and extent of tumor. The wide range of appearances on T1-weighted images reflects the range of histologic appearances of craniopharyngiomas. T1 shortening may reflect the presence of high cholesterol content or methemoglobin. CT is superior to MR in detecting calcifications. Currently, CT is more specific in establishing the diagnosis of craniopharyngioma. MR is preferred in the evaluation of tumor extent for presurgical and radiation planning. MR is valuable in detecting recurrent tumor, particularly in children, to limit radiation exposure.

ACKNOWLEDGMENTS

We thank Harry Vinters, UCLA neuropathology department, for photography of pathologic specimens and discussions on pathology of craniopharyngiomas and Ed Helmer for Figures 4A and 4D.

REFERENCES

1. Brant-Zawadzki M, Badami JP, Mills CM, Norman D, Newton H. Primary intracranial tumor imaging: a comparison of magnetic resonance and CT. *Radiology* **1984**;150:435–440
2. Bradley WG, Waluch V, Yadley RA, Wycoff RR. Comparison of CT and MR in 400 patients with suspected disease of the brain and cervical spinal cord. *Radiology* **1984**;152:695–702
3. Hawkes RC, Holland GN, Moore WS, et al. The application of NMR imaging to the evaluation of pituitary and juxtasellar tumors. *AJNR* **1983**;4:221–222
4. Kjos BO, Brant-Zawadzki M, Kucharczyk W, Kelly W, Norman D, Newton T. Cystic intracranial lesions: magnetic resonance imaging. *Radiology* **1985**;155:363–369
5. Kucharczyk W, Brant-Zawadzki M, Sobel D, et al. Central nervous system tumors in children: detection by magnetic resonance imaging. *Radiology* **1985**;155:131–136
6. Peterman SB, Steiner RE, Bydder GM. Magnetic resonance imaging of intracranial tumors in children and adolescents. *AJNR* **1984**;5:703–709
7. Rinck P, Meindl S, Higer HP, Bieler EU, Pfannenstiel P. Brain tumors: detection and typing by use of CPMG sequences and in vivo T2 measurements. *Radiology* **1985**;157:103–106
8. Holland BA, Kucharczyk W, Brant-Zawadzki M, Norman D, Haas DK, Harper PS. MR imaging of calcified intracranial lesions. *Radiology* **1985**;157:353–356
9. Petito CK, DeGirolami U, Earle KM. Craniopharyngiomas: a clinical and pathological review. *Cancer* **1976**;37:1944–1952
10. Burger PC, Vogel FS. *Surgical pathology of the nervous system and its coverings*. New York: Wiley, **1982**:511–528
11. Bradley WG, Schmidt PG. Effect of methemoglobin formation on the MR appearance of subarachnoid hemorrhages. *Radiology* **1985**; 156:99–103
12. Braun IF, Pinto RS, Epstein F. Dense cystic craniopharyngiomas. *AJNR* **1982**;3:139–141
13. Rand RW, Konovalov AN. Craniopharyngiomas. In: Rand RW. *Microneurosurgery*. St. Louis: Mosby, **1985**:187–195

Adverse Reactions After Iohexol Lumbar Myelography: Influence of Postprocedural Positioning

Ilkka K. Kuuliala[1]
Hans J. Göransson

A prospective study of 110 patients having iohexol lumbar myelograms indicates that patient positioning does not significantly influence the frequency of adverse postprocedural reactions. Thus, after the procedure, patients may be allowed to choose either ambulation or bed rest with their heads raised.

Adverse postmyelographic reactions may be due to either CSF leakage caused by lumbar puncture or CNS irritation caused by contrast material [1]. Management of those symptoms should be the opposite of each other (bed rest or erect position, respectively) depending on which of the possible causes is primarily responsible. Bed rest for 24 hr after lumbar puncture is a common practice. In myelograms performed with metrizamide (currently the most widely used contrast agent), CNS irritation has been reported to be the major cause of postprocedural symptoms, with the incidence of side effects about equal in ambulatory patients and those confined to bed [1–3]. Iohexol (Omnipaque) has been noted to cause less postmyelographic morbidity than metrizamide [4–7]. With the advent of a safer contrast agent it is possible that CSF leakage surpasses the irritative effect of contrast material as the major cause of postprocedural symptoms. On this basis we undertook a prospective study to determine whether postprocedural positioning after iohexol myelography has any influence on postmyelographic symptoms.

Materials and Methods

One hundred and ten consecutive iohexol lumbar myelograms form the basis of this study. The myelograms were divided into two groups, each consisting of 55 consecutive patients. Group 1 patients were kept in bed with their heads raised about 30° after the procedure until the following morning (however, lavatory use was allowed). Patients in group 2 were encouraged to be ambulatory after the procedure, depending on their condition. Patients in both groups were encouraged to drink sufficiently after the myelographic procedure.

Before the procedure, patients were informed of the purpose of the study, otherwise myelography was performed according to strict routine practice. Patients were usually referred because of a suspected lumbar disk herniation or spinal stenosis.

Preprocedural symptoms were registered and patients were premedicated with rectal diazepam (10 mg). Myelography was performed via L2–L3 or L3–L4 puncture using a 22-gauge needle. A few milliliters of CSF were removed. Iohexol concentration was 240 mgI/ml, with the typical dose being 12 ml of contrast. Radiographs in the prone, lateral decubitus, and oblique positions were obtained so that the lumbar spinal canal and conus region were thoroughly visualized.

The following morning every patient was interviewed and asked to describe his or her postprocedural symptoms. Patients were specifically asked about headache, nausea, vomiting, worsening of radicular pain, and accentuation of preprocedural symptoms. They graded their symptoms as none, slight, moderate, or severe, and the duration of the symptoms was also registered via inquiries later on as needed. The frequency and severity of adverse reactions in the two patient groups were then compared.

This article appears in the May/June 1987 issue of *AJNR* and the August 1987 issue of *AJR*.

Received October 2, 1986; accepted after revision December 14, 1986.

[1] Both authors: Department of Radiology, Central Hospital of Kanta-Häme, 13530 Hämeenlinna, Finland. Address reprint requests to I. K. Kuuliala, Kankaantaustantie 43 D, 13100 Hämeenlinna, Finland.

***AJR* 149:389–390, August 1987**
0361–803X/87/1492-0390
© American Roentgen Ray Society

Results

Table 1 summarizes the patient groups with respect to several variables; no significant differences are seen. Postmyelographic adverse reactions are noted in Table 2. Seventy-one percent of patients in the nonambulatory groups and 66% in the ambulatory group were totally symptom-free. Adverse reactions typically lasted less than 24 hr. The most common symptom was slight or moderate headache either alone or in conjunction with nausea, vomiting, or accentuation of radicular pain. No one with these symptoms of short duration graded his or her symptoms as severe. One patient reported having diarrhea and another patient had tingling sensations all over her body. Five patients experienced accentuated radicular pain as the only symptom. Altogether, 15 patients in the nonambulatory group and 16 in the ambulatory group had these mild or moderate symptoms on the day of the examination but not longer.

One patient in group 1 and three patients in group 2 had symptoms lasting for several days. These are summarized in Table 3. These patients graded their symptoms as moderate or severe, and they typically were accentuated in erect position, causing the patients to be confined to bed for up to 1 week.

TABLE 1: Comparison of Nonambulatory and Ambulatory Patient Groups

	GROUP 1 (Bed Rest)	GROUP 2 (Ambulation)
Gender		
Female	23	25
Male	32	30
Age (years)	16–73 (mean, 44.5)	18–72 (mean, 43.7)
Volume of contrast	12–15 ml (mean, 12.7 ml)	10–15 ml (mean, 12.8 ml)
Cranial extension of contrast		
Th 9–12	5	10
Th 6–8	41	41
Th 1–5	9	4

Note.—Group 1 and group 2 each consisted of 55 consecutive patients.

TABLE 2: Incidence of Adverse Reactions

	GROUP 1 (Bed Rest)	GROUP 2 (Ambulation)
No adverse reactions	39 (71%)	36 (66%)
Mild or moderate symptoms during the examination day	15 (27%)	16 (29%)
Headache and/or nausea	10	14
Mild	7	9
Moderate	3	5
Severe	0	0
Accentuation of radicular pain only	3	2
Diarrhea	1	None
Tingling sensations	1	None
Prolonged symptoms (see Table 3)	1	3

Note.—Group 1 and group 2 each consisted of 55 consecutive patients.

TABLE 3: Prolonged Symptoms

GROUP 1 (Bed Rest)
Patient 1. Moderate headache, nausea, and vomiting, lasting 3 days; worse in erect position.

GROUP 2 (Ambulation)
Patient 1. Severe headache and mild nausea, lasting 6 days; worse in erect position.
Patient 2. Severe headache, mild nausea, and vomiting, lasting 7 days; worse in erect position.
Patient 3. Moderate headache and nausea, starting 2 days after the procedure and lasting 3 days; worse in erect position.

Discussion

Our study results indicate that positioning after iohexol lumbar myelography does not seem to have a significant influence on the incidence of adverse postprocedural reactions. About two-thirds of patients in both groups were completely free of symptoms. Among the ambulatory and nonambulatory patients who did experience symptoms, they were usually mild or moderate, lasting no longer than the examination day. A slight tendency toward more frequent nausea and/or headache was seen in the ambulatory group, but the number of patients with different mild symptoms was not dependent on postmyelographic positioning.

One patient in the nonambulatory group and three in the ambulatory group had symptoms lasting for several days, which worsened in the upright position (see Table 3). Postmyelographic adverse reactions may be due to either the lumbar puncture or the irritative effect of contrast, or both [1–2]. The rather rapid elimination of intrathecally injected iohexol [8] with respect to the duration of symptoms and the influence of position on the severity of headache speaks in favor of the role of lumbar puncture as the major causative alternative in these patients. Prolonged symptoms are now and then seen after a lumbar puncture [9] and it may be possible that some patients are especially sensitive, experiencing nausea and/or headache after a spinal puncture whatever the postprocedural position might be. However, we cannot with certainty explain the reason or determine the possible influence of positioning on this kind of symptom prolongation seen in some of the patients in our study.

Results of this prospective study thus indicate that after iohexol lumbar myelography patients may be allowed to choose either ambulation or bed rest with their heads raised. According to our experience, positioning does not significantly correspond to adverse postprocedural reactions.

REFERENCES

1. Sykes RHD, Wasenaar W, Clark P. Incidence of adverse effects following metrizamide myelography in nonambulatory and ambulatory patients. *Radiology* **1981**;138:625–627
2. Robertson WD, Lapointe JS, Nugent RA, Robinson RG, Daly LF. Positioning of patients after metrizamide lumbar myelography. *AJNR* **1980**;1:197–198
3. MacPherson P, Teasdale E, MacPherson PY. Radiculography: is routine bed rest really necessary? *Clin Radiol* **1983**;34:325–326
4. Gabrielsen TO, Gebarski SS, Knake JE, Latack JT, Yang PJ, Hoff JT. Iohexol versus metrizamide for lumbar myelography: double-blind trial. *AJNR* **1984**;5:181–183, *AJR* **1984**;142:1047–1049
5. Kieffer SA, Binet EF, Davis DO, et al. Lumbar myelography with iohexol and metrizamide: a comparative multicenter prospective study. *Radiology* **1984**;151:665–670
6. Sortland O, Nestvold K, Kloster R, Aandahl MH. Comparison of iohexol with metrizamide in myelography. *Radiology* **1984**;151:121–122
7. Laasonen EM. Iohexol and metrizamide in lumbar myelography. Comparison of side effects. *Acta Radiol Diagn* **1985**;26(6):761–765
8. Holz E, Michelet AA, Jacobsen T. Absorption after subarachnoid and subdural administration of iohexol, ^{51}Cr-EDTA, and ^{125}I-albumin to rabbits. *AJNR* **1983**;4:338–341
9. Fishman RA. Cerebrospinal fluid. In: Baker AB, ed. *Clinical neurology*. New York: Harper & Row, **1962**:350–384

Hepatic Regenerating Nodules in Hereditary Tyrosinemia

Deborah L. Day[1]
Janis G. Letourneau[1]
Bradford T. Allan[1]
Harvey L. Sharp[2]
Nancy Ascher[3]
Louis P. Dehner[4]
William M. Thompson[1]

Hereditary tyrosinemia is an autosomal recessive, enzymatic disorder that results in micro- and macronodular cirrhosis in early childhood. Hepatocellular carcinoma occurs in approximately one-third of affected children. We evaluated the imaging studies performed in five children with this disorder. Pathologic examination of all five of the livers revealed cirrhosis and multiple regenerating nodules; hepatocellular carcinoma was present in two of the five livers. All five patients had high-attenuation or high- and low-attenuation foci within the liver. These high-attenuation foci were not apparent as focal lesions in three of four hepatic sonograms or in one of two hepatic nuclear scans. Angiography showed tumor vascularity in one patient with a focal hepatocellular carcinoma, but was indeterminate in a second patient with severe cirrhosis and multifocal hepatocellular carcinoma.

Children with cirrhosis due to tyrosinemia may develop regenerating nodules that appear as high-attenuation hepatic foci on CT scans. It is difficult to differentiate regenerating nodules from multifocal hepatocellular carcinoma in these patients.

Hereditary tyrosinemia (tyrosinosis) is an autosomal recessive, inherited, enzymatic defect that causes progressive liver disease in early childhood. Affected individuals develop liver failure, cirrhosis, and portal hypertension [1]. Thirty-seven percent of patients with hereditary tyrosinemia surviving beyond 2 years of age develop hepatocellular carcinoma (HCC) [2]. Hepatic imaging techniques (including CT, sonography, nuclear scintigraphy, and angiography) were evaluated in five children with hereditary tyrosinemia. Regenerating nodules in these patients may be seen as high-attenuation foci on hepatic CT scans. It is difficult to detect the development of HCC in cirrhotic livers secondary to tyrosinemia with any of these imaging techniques.

Patients and Methods

Hepatic imaging studies were obtained in five children prior to liver transplantation. The four girls and one boy ranged in age from 11 months to 9 years (mean, 3.5 years). Imaging studies included IV contrast-enhanced liver CT scans in all five patients, unenhanced liver CT scans in four, liver sonography in four, hepatobiliary scintigraphy in one, sulfur-colloid liver-spleen scintigraphy in one, and hepatic angiography in two. The results of all imaging studies were correlated with available pathologic data.

Results

All five patients in our series had multifocal high-attenuation hepatic lesions shown on either unenhanced (three patients) or contrast-enhanced (two patients) CT scans (Figs. 1A, 2, and 3A). Multifocal low-attenuation foci were also evident in two patients on unenhanced or contrast-enhanced CT scans (Figs. 3A and 3B). Sonographically, one liver was normal and two other livers showed slightly increased hyperechogenicity but no focal abnormalities (Fig. 1B). Sonography in the

Received January 26, 1987; accepted after revision April 30, 1987.

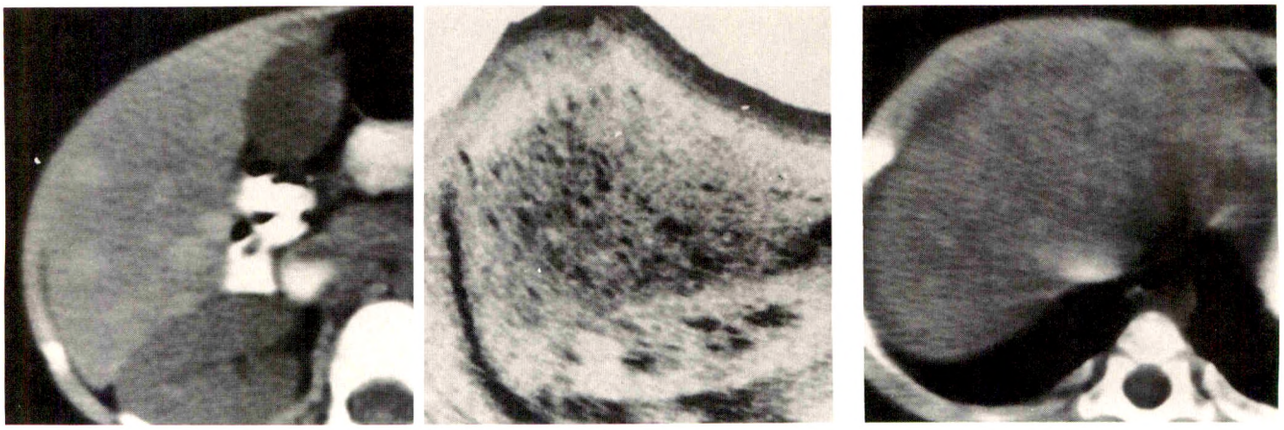
[1] Department of Diagnostic Radiology, UMHC Box 292, University of Minnesota Hospital, Harvard St. and E. River Rd., Minneapolis, MN 55455. Address reprint requests to D. L. Day.

[2] Department of Pediatrics, University of Minnesota Hospital, Minneapolis, MN 55455.

[3] Department of Surgery, University of Minnesota Hospital, Minneapolis, MN 55455.

[4] Department of Laboratory Medicine and Pathology, Division of Surgical Pathology, University of Minnesota Hospital, Minneapolis, MN 55455.

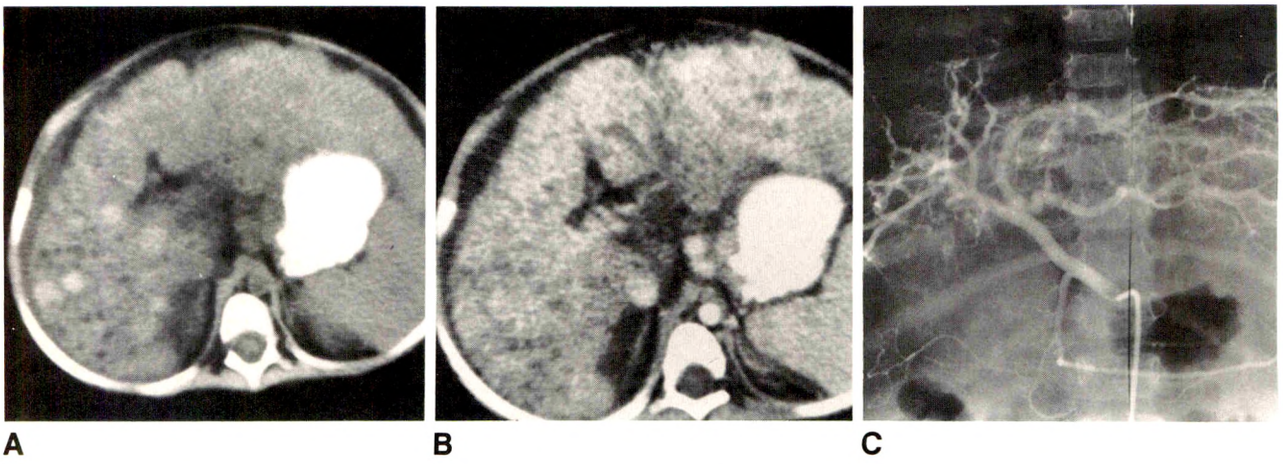
AJR 149:391–393, August 1987
0361–803X/87/1492–0391
© American Roentgen Ray Society



A B

Fig. 1.—Case 1: 2½-year-old boy with cirrhosis and multiple regenerating nodules.
A, Unenhanced upper abdominal CT scan shows multiple high-attenuation foci (approximately 80 H) scattered throughout diffusely low dense liver (approximately 60 H). Lesions became almost isodense with adjacent hepatic parenchyma after IV contrast administration.
B, Right parasagittal liver sonogram reveals diffuse increased echogenicity consistent with diffuse fatty infiltration or fibrosis. No focal lesions are evident.

Fig. 2.—Case 2: 11-month-old girl with multiple regenerating nodules and fatty changes secondary to cirrhosis. Unenhanced upper abdominal CT scan shows multiple high-attenuation foci scattered throughout the liver.



A B C

Fig. 3.—Case 3: 4-year-old girl with severe cirrhosis, portal hypertension, and multifocal hepatocellular carcinoma.
A, Unenhanced upper abdominal CT scan shows splenomegaly, ascites, and hepatomegaly with irregular hepatic contour. Multiple low- and high-attenuation foci are scattered throughout the hepatic parenchyma.
B, Contrast-enhanced CT scan at the same level shows that high-attenuation foci have become isodense.
C, Arterial phase of hepatic angiogram reveals enlargement of left hepatic lobe. Marked tortuosity and beading of hepatic vessels are consistent with advanced cirrhosis with or without diffuse malignancy.

fourth patient, who had multiple high- and low-attenuation foci on CT, showed marked inhomogeneity with areas of hypo- and hyperechogenicity. A normal disophenin nuclear scintigram was obtained in a patient with multifocal lesions on CT scan. A sulfur-colloid liver-spleen scan showed diffuse inhomogeneity and a photopenic defect in the region of a focal HCC. Hepatic angiography in this patient revealed a hypervascular mass. A hepatic angiogram in a second patient revealed multiple distorted irregular vessels but was indeterminate in differentiating changes of malignancy from severe cirrhosis (Fig. 3C).

Pathologic examination of all five native livers, which were resected for transplantation, showed mixed micro- and macronodular cirrhosis with fatty changes in the parenchyma and regenerating nodules. The pathologic abnormalities varied in severity, with relative worsening with advancing age. HCC had developed in the two older children (4 and 9 years old).

Discussion

Tyrosinemia is an autosomal recessive, enzymatic defect that causes progressive liver disease in early childhood. Af-

fected individuals present with hepatosplenomegaly, abnormal liver function, anemia, increased plasma alpha fetoprotein, increased levels of serum tyrosine and methionine, and elevated levels of urinary succinyl acetone [1]. Acute and chronic forms occur. The acute form is associated with fulminant liver failure and death, often by 1 year of age. In the chronic form, cirrhosis, Fanconi's syndrome with renal tubular dysfunction, vitamin-D–resistant rickets, and acute intermittent porphyria-like symptoms may be present [1]. One-third of individuals surviving beyond 2 years of age develop HCC [2].

The hepatic pathology of hereditary tyrosinemia is distinctive but not pathognomonic [3]. The liver may be smooth and normal in size, particularly in infants, or it may be nodular. There is progressive hepatocyte atrophy with fatty change, fibrosis, and nodular regeneration of the hepatic parenchyma. Nodules of regenerating hepatocytes are abundant in those patients surviving beyond infancy.

It has been reported that regenerating nodules are low or isodense compared with the surrounding liver on CT scans [4]. However, in our cases, regenerating nodules were hyperdense relative to the surrounding low-attenuation liver parenchyma. In one patient, these lesions were histologically proved regenerating nodules (Fig. 1A). High-attenuation lesions in two other cases probably also represented regenerating nodules as no other focal abnormalities were found on pathologic examination (Fig. 2). In a fourth patient, the centrally located high-attenuation lesions also most likely represented regenerating nodules since the focal HCC found in this patient was a single peripheral mass in the right hepatic lobe. The fifth patient had multifocal high- and low-attenuation lesions and histologically had severe cirrhosis with multiple regenerating nodules and multifocal HCC (Figs. 3A and 3B). However, since no histologic and imaging correlation was done, it cannot be determined which nodules represented regenerating nodules and which represented HCC. The other patient who had multifocal high- and low-attenuation lesions was found to have cirrhosis, regenerating nodules, and no malignancy. Therefore, all multifocal low-attenuation lesions do not represent HCC. It is likely that these regenerating nodules generally appear hyperdense because of their relatively normal hepatic architecture superimposed on a background of diffuse fatty change and secondary cirrhosis. Conversely, HCC can have attenuation characteristics similar to that of the surrounding background hepatic parenchyma as seen on enhanced CT scanning in one patient in this series.

Four of the five patients underwent hepatic sonography. The sonograms of three patients with cirrhosis and multiple regenerating nodules showed normal architecture, diffuse hyperechogenicity (Fig. 1B), or slight inhomogeneous hyperechogenicity despite the finding of multifocal high- or mixed-attenuation lesions on CT scans. This corresponds to previously described sonographic findings of regenerating nodules in cirrhotic livers [5]. Cirrhosis with multifocal HCC in a fourth patient was seen sonographically as markedly inhomogeneous hepatic parenchyma with focal areas of hypo- and hyperechogenicity.

Scintigraphic liver scanning was performed in two patients. Disophenin liver scintigraphy was normal in one of the patients who had multiple regenerating nodules and multifocal high-attenuation lesions on CT scans. A focal photopenic area seen on sulfur-colloid liver-spleen scintigraphy corresponded to focal HCC in the right hepatic lobe of another patient.

Hepatic angiography was helpful in one case in defining malignant neovascularity, but it was indeterminate in another in whom the tumor was diffuse and cirrhosis advanced (Fig. 3C).

We have drawn two conclusions from evaluation of the hepatic imaging in five children with hereditary tyrosinemia. First, high-attenuation focal lesions seen on unenhanced or contrast-enhanced hepatic CT scans that are not detectable as discrete abnormalities on hepatic sonography or scintigraphy likely represent regenerating nodules within a cirrhotic liver. Second, as in adults with cirrhosis, the radiographic determination of the presence of HCC in a cirrhotic liver in a child with tyrosinemia is not straightforward. The radiographic features of cirrhosis are variable, and there is considerable overlap seen between the imaging findings of cirrhosis alone [4] and the findings of HCC in a cirrhotic liver [6].

REFERENCES

1. Goldsmith LA. Tyrosinemia and related disorders. In: Stanbury JB, Wyngaarden JB, Fredrickson DS, Goldstein JL, Brown MS, eds. *The metabolic basis of inherited disease*, 5th ed. New York: McGraw-Hill, **1983**:287–299
2. Weinberg AG, Mize CE, Worthen HG. The occurrence of hepatoma in the chronic form of hereditary tyrosinemia. *J Pediatr* **1976**;88:434–438
3. Hardwick DF, Dimmick JE. Metabolic cirrhosis of infancy and childhood. *Perspect Pediatr Pathol* **1976**;3:103–144
4. Stanley RJ. Liver and biliary tract. In: Lee JKT, Sagel SS, Stanley RJ, eds. *Computed body tomography*. New York: Raven, **1983**:172–173, 186–189
5. Freeman MP, Vick CW, Taylor KJW, Carithers RL, Brewer WH. Regenerating nodules in cirrhosis: sonographic appearance with anatomic correlation. *AJR* **1986**;146:533–536
6. Edmondson HA, Peters RL. Tumors of the liver: pathologic features. *Semin Roentgenol* **1983**;18:75–83

Software Review

Basic Baby II (BBII). By Terry J. DuBose, 1987. Purchase directly from the author at 3606 Grooms St., Austin, TX, 78706. $50 use fee per workstation

Basic Baby II (BBII) is a dedicated spread-sheet/data-base program for evaluation of sonographic fetal measurements. It is designed for the IBM PC/XT and compatibles, requires the DOS 2.1 operating system, and uses 200K of RAM memory. It comes on a non–copy-protected disk with a 27-page users' manual. BBII is offered under the "share ware" concept and the users' fee should be paid if one decides to use BBII for fetal calculations.

Basic Baby II provides an extensive fetal analysis. The fetal age may be computed for gestational sac measurements, crown-rump length, biparietal diameter (BPD), transverse and coronal head circumferences, cardiac volume, abdominal circumference, cardiac volume, femur and humerus lengths, and biocular distance. BBII will also give both the average menstrual age and the age range from 10 parameters and will estimate fetal weight from BPD and abdominal-circumference measurements. A report is generated and a disk file is maintained for each fetus whose data are entered into the program. Of course, the interpretation of the measurements is solely the responsibility of the sonographer.

The users' manual is reasonably clear and well written. It does, however, have somewhat small print and may be difficult to read easily without a magnifying glass. The manual walks the user through the program, and the program can be learned with ½–1 hr of practice. It offers a remarkably large amount of patient data, fetal-measurement entry, and calculation possibilities. There is also a surprisingly good, albeit brief, discussion of various fetal-measurement parameters in the manual and a superb reference list. The program produces rapid, consistent calculations that match the standard reference charts found in most sonography laboratories. Because of its relative simplicity and ease of use, BBII is ideal for a busy referral clinic that has limited computer resources but desires to keep a detailed, accurate archive of multiple high-risk patients and their respective fetal parameters. It is probably less useful for a clinic whose patients are more routine and are seen only once or twice during their pregnancy and whose measurements are easily archived in the official report.

The BBII disk contains an ASCII text translator for BBII files and will translate the data files into comma delimited files that can be read by larger, more advanced data bases such as dBASE III or Frame Work II. This is a useful feature. Nevertheless there are aspects of BBII that need improvement. It is designed for two floppy disk drives (A and B) and will not allow direct assignment of data files to a hard-disk drive (C). BBII's author suggests using the DOS ASSIGN.COM command to assign B = C drives and to load BBII each time it is used. This is awkward and ought to be automatically implemented by the program software. Data entry can sometimes be clumsy. Column numbers must be entered for each new measurement entry. Most users would probably prefer to move around the spread sheet with cursor arrows or at least have this option available. Unfortunately, the patient's file number must be less than seven digits. This is a serious program flaw as many institutions, such as our own, use a seven-digit file number or the patient's social security number. We found the screen color combinations to be unpleasant to the eye and decided to use the black-and-white screen version. All data entries must be in millimeters with no allowance in the program for conversion to centimeters or vice versa.

BBII is a helpful, convenient software package. It does have its flaws, but it performs its stated function well and is moderately priced.

Tim B. Hunter
K. Rebecca Hunt
The University of Arizona
Tucson, AZ 85724

Anorectal Atresia: Prenatal Sonographic Diagnosis

Robert D. Harris[1]
David A. Nyberg
Laurence A. Mack
Edward Weinberger

To determine the prenatal sonographic findings of anorectal atresia (ARA), we retrospectively reviewed 12 proven cases. Sonography showed abnormally dilated bowel segments in five cases (42%), four of which were identified prospectively; at autopsy, two other cases showed mild colon dilatation not evident on sonograms. Bowel dilatation was not associated with the location of atresia or the presence of a fistula, but was possibly related to menstrual age. Eleven fetuses (92%) had significant other anomalies primarily related to the VACTERL syndrome (vertebral defects, anal atresia, tracheoesophageal fistula with esophageal atresia, radial and renal dysplasia, and limb malformations) and/or the caudal regression syndrome; of these, sonography identified one or more concurrent anomalies in seven cases. In two cases, bowel dilatation was the primary sonographic finding. Death in nine cases resulted from termination of pregnancy (four cases) or perinatal demise (five cases); three patients are still alive.

We conclude that some cases of ARA can be suspected on prenatal sonograms by demonstration of dilated colon, and that the sensitivity of this finding may be related to menstrual age at the time of the examination. Distinguishing ARA from other causes of fetal-bowel dilatation is important because of the frequency of concurrent anomalies associated with ARA.

Anorectal atresia (ARA) is a major congenital malformation that occurs in about one of 5000 live births [1]. Recognition of ARA is important not only because surgical correction is required after delivery but also because it is frequently associated with other anomalies [2–7]. An association between vertebral, anal, cardiovascular, tracheoesophageal, renal, and limb malformations has been recognized and termed the VACTERL syndrome [2–7]. Anorectal anomalies are also found frequently in association with sacral agenesis and lower limb hypoplasia as part of the caudal regression syndrome [8].

Prenatal detection of ARA has been reported infrequently. Two previously published case reports suggest that dilated fetal bowel seen on prenatal sonography may result from ARA as well as from other causes of bowel obstruction [9, 10]. Recently, we also encountered several cases of ARA that presented with abnormally dilated fetal bowel segments. However, the frequency and significance of this observation and its association with other sonographic findings remain unknown. Furthermore, quantitative comparison with normal bowel measurements has not been studied previously. To determine the usual sonographic findings in fetuses with ARA, we undertook the present study of 12 proved cases.

Materials and Methods

Our review of clinical and pathologic records covering a 5-year period (1981–1986) yielded 12 fetuses with ARA for whom a prenatal sonogram was available for evaluation. Anorectal malformations that were considered a part of ARA included imperforate anus, anal agenesis, anorectal agenesis, and rectal atresia. Indications for sonography included size less than dates (four cases), determination of menstrual age (three cases), premature labor (three

Received February 4, 1987; accepted after revision April 7, 1987.

[1] All authors: Department of Radiology, SB–05, University of Washington Medical Center, Seattle, WA 98195. Address reprint requests to D. A. Nyberg.

AJR 149:395–400, August 1987
0361–803X/87/1492–0395
© American Roentgen Ray Society

cases), maternal diabetes (one case), and suspected absent fetal heart tones by Doppler (one case).

All sonograms were obtained with commercially available real-time sonographic equipment. The prospective sonographic findings were noted, and each sonogram was also reviewed retrospectively by two sonographers for the presence, size, and location of fetal bowel segments. When discrete colon segments were identified, the diameter was measured from the inner bowel wall. These results were compared with colon diameter measurements made from 120 randomly selected normal fetuses seen between 20 to 40 menstrual weeks who had normal clinical evaluations after birth.

Fetal outcome for the 12 fetuses with ARA included termination of pregnancy (four cases), perinatal demise (five cases), or survival beyond the neonatal period (three cases). All patients were proved to have ARA by surgery (three cases) or autopsy (nine cases). The location of atresia was categorized as either high (above the levator sling) or low (below the levator sling). The presence of an associated distal colonic fistula was also noted, when known. The presence of

TABLE 1: Sonographic, Clinical, and Pathologic Findings in Anorectal Atresia (ARA)

Case No.	Age (weeks)	Sonographic Findings		Pathologic and Surgical Findings			
		Colon Diameter (mm)	Other	Fetal Outcome	Location of ARA	Fistula	Other Anomalies
1	18	Not seen	Omphalocele, meningomyelocele	VTOP	NA	Yes	Omphalocele, small-bowel atresia, sacral agenesis, meningomyelocele
2	22	Not seen	Anhydramnios hydrocephalus	VTOP	High	No	Sirenomelia, renal agenesis, radial dysplasia, hydrocephalus
3	24	Not seen	Anhydramnios, renal agenesis	VTOP	High	Yes	Sirenomelia, absent genitalia, renal agenesis, mildly dilated distal colon
4	23 27 33	Not seen 9 27	Multicystic dysplastic kidney	Alive	High	No	Small-bowel astresia, annular pancreas, renal dysplasia, sacral agenesis
5	30	13 (retrospective)	Hydrocephalus, anhydramnios, renal agenesis, sacral agenesis	Death	High	No	Sirenomelia, renal agenesis, radial dysplasia, atrial septal defect, hydrocephalus, dilated distal colon
6	29	20	Polyhydramnios, fetal ascites	Death	High	Yes	Esophageal atresia with tracheoesophageal fistula, vertebral malformations, renal dysplasia, dilated distal colon
7	35	22	Anhydramnios	Died 1 week after birth	High	No	Esophageal atresia with tracheoesophageal fistula; absent genitalia; right cystic dysplastic kidney, left renal agenesis; tetralogy of Fallot; short extremities, rocker-bottom feet; dilated colon filled with meconium
8	26	20	Anhydramnios	Death	High	Yes	Urethral atresia, meningocele, ambiguous genitalia, mildly dilated colon
9	26	Not seen	. . .	Death	Low	Yes	Ambiguous genitalia, dilated colon/ileum, club foot
10	19	Not seen	Hydrocephalus, meningomyelocele, scoliosis	VTOP	High	No	Hydrocephalus, meningomyelocele, scoliosis
11	27	Not seen	Oligohydramnios (premature rupture of membranes)	Alive	High	No	Tetralogy of Fallot, cryptorchidism
12	21	Not seen	. . .	Alive	Low	NA	None

Note.—VTOP = voluntary termination of pregnancy; NA = information not available from pathology report.

concurrent anomalies was determined by clinical, surgical, and autopsy examination.

Results

Sonographic findings are compared with pathologic and clinical results in Table 1. Of the 12 fetuses studied, five showed at least one segment of abnormally dilated fetal bowel (Figs. 1 and 2). In four of these cases, the abnormality was prospectively recognized at the time of the initial sonogram; in one other case, it was seen on retrospective review. In each case, the location and appearance of the bowel segment suggested that it represented colon. Colon diameters for these five cases were greater than 2 SD above normal colon diameters, as determined from 120 normal cases (Fig. 3). In the other seven cases, discrete bowel segments were not identified either prospectively or retrospectively.

Of the five cases with sonographically detectable bowel dilatation, four showed an anechoic segment of bowel located in the pelvis or lower abdomen, and three demonstrated a V or U configuration (Figs. 1 and 2). In one case, a long segment of dilated colon, filled with echogenic meconium, was imaged around the periphery of the abdomen (Fig. 4). This case also demonstrated active colon peristalsis, noted prospectively on real-time sonography.

The presence of colon dilatation seen by sonograph and/or at autopsy appeared to be related to menstrual age. Colon dilatation was not seen sonographically in any of the four cases examined at or before 22 weeks, whereas all three cases seen after 27 weeks demonstrated dilated colon. Between 23 and 27 weeks, one of five cases had sonographically detectable colon dilatation, and two other cases had dilated colons on pathologic examinations. The earliest that colon dilatation was detected by sonography was 26 weeks, although mild colon dilatation was found pathologically as early as 24 weeks. One case with minimal colon dilatation (9 mm) at 27 weeks enlarged significantly to 27 mm by 33 weeks (Fig. 4).

No correlation was observed between colon dilatation and the site of atresia or the presence of a fistula. The location of ARA was reported by surgical or autopsy findings as high (supralevator) in nine cases, low (infralevator) in two cases, and not reported in one case. A fistula was identified in five cases; two of these showed bowel dilatation.

Eleven cases (92%) had concurrent malformations in addition to ARA (Table 1); of these, seven had three or more cardinal features of the VACTERL syndrome (cases 1–7) and four had two features (cases 8–11). Five fetuses (cases 1–5) also had characteristic features of the caudal regression syndrome, including sacral agenesis (two cases) or sireno-

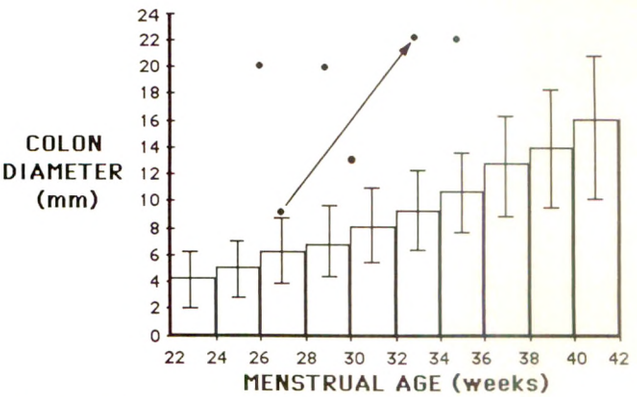


Fig. 3.—Colon diameters from four fetuses with anorectal atresia (*dots*) compared with values obtained from 120 normal fetuses (mean ± 2 SD). One case (case 4) showed progressive (*arrow*) colon dilatation from 27 to 33 weeks.

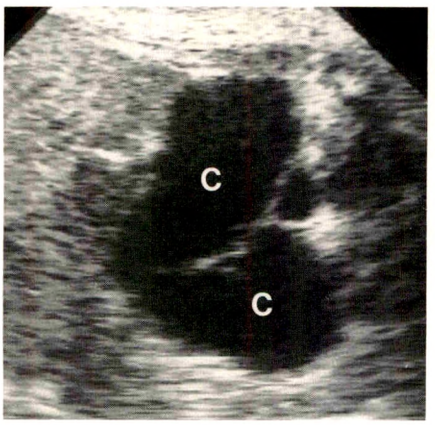


Fig. 1.—Case 7. Coronal sonogram at 35 weeks shows segment of dilated colon (C) in fetal pelvis measuring 22 mm in diameter. Note V configuration of dilated bowel segment.

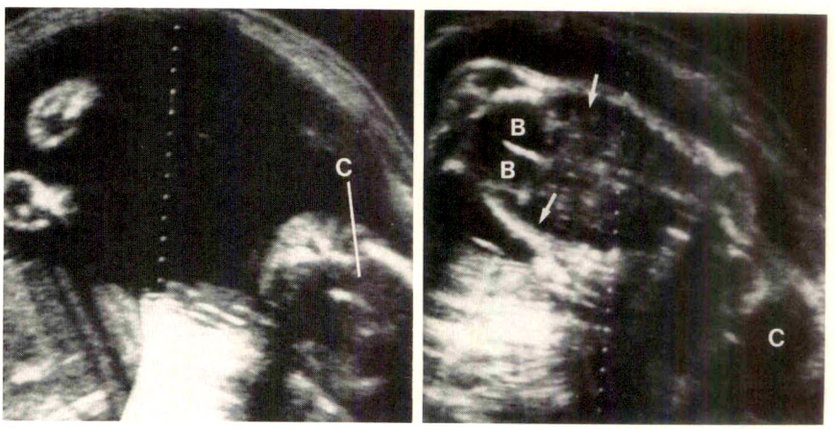


Fig. 2.—Case 6.
***A*, Sagittal sonogram at 29 weeks shows polyhydramnios. C = fetal cranium.**
***B*, Adjacent sonogram shows dilated segment of bowel (B) in fetal pelvis and ascites (*arrows*). At birth, infant was found to have multiple anomalies including both anorectal atresia and esophageal atresia with tracheoesophageal fistula. The infant died 1 week after delivery.**

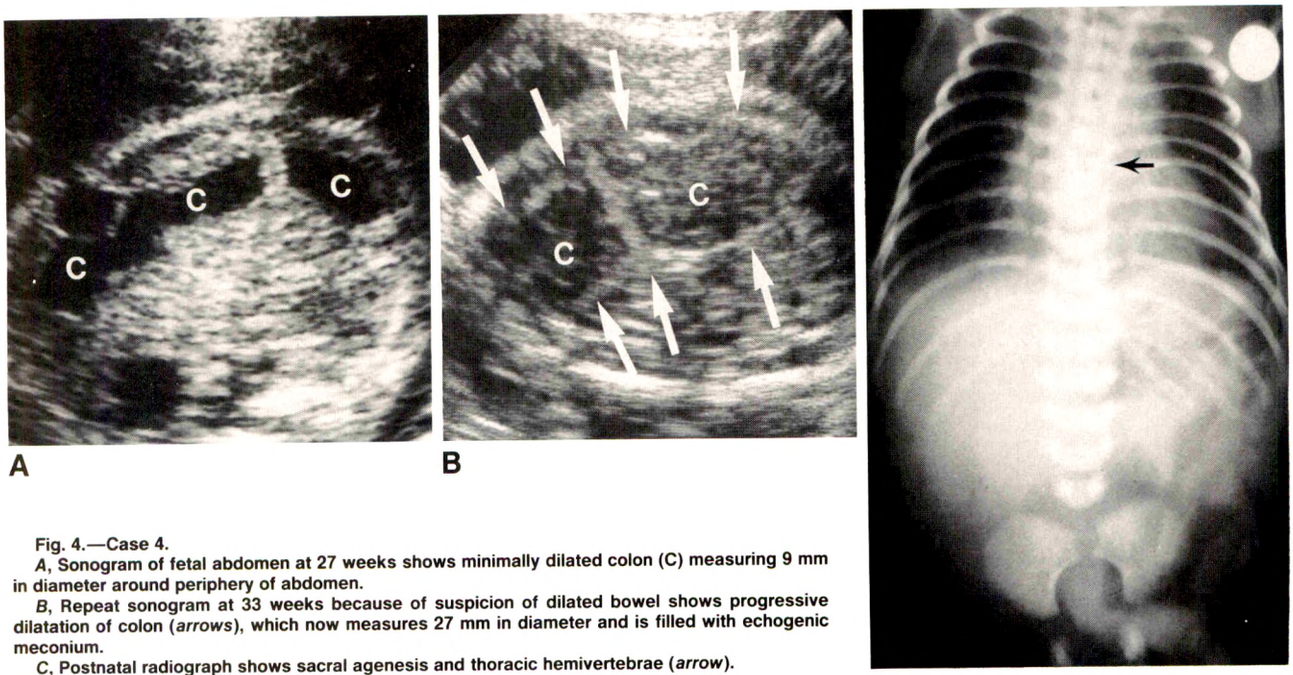


Fig. 4.—Case 4.
A, Sonogram of fetal abdomen at 27 weeks shows minimally dilated colon (C) measuring 9 mm in diameter around periphery of abdomen.
B, Repeat sonogram at 33 weeks because of suspicion of dilated bowel shows progressive dilatation of colon (*arrows*), which now measures 27 mm in diameter and is filled with echogenic meconium.
C, Postnatal radiograph shows sacral agenesis and thoracic hemivertebrae (*arrow*).

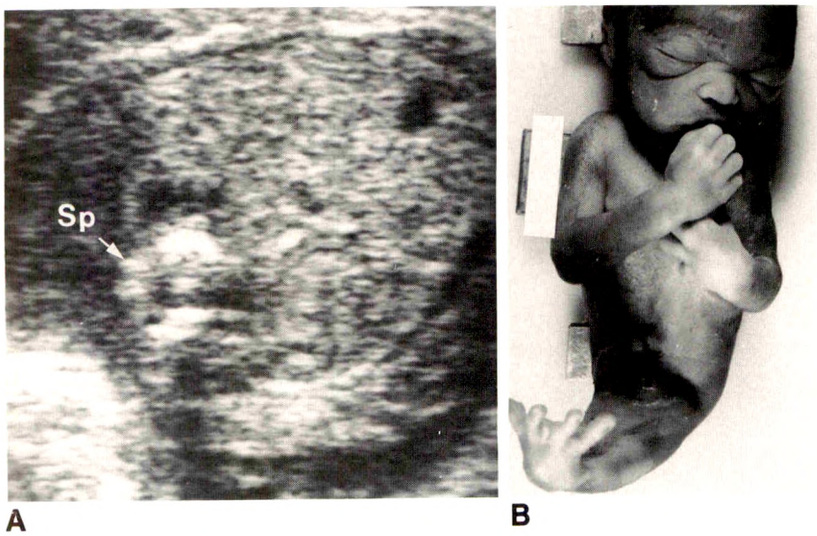


Fig. 5.—Case 3.
A, Sonogram at 24 weeks shows anhydramnios and renal agenesis, consistent with Potter's disease. Sp = spine.
B, Photograph of fetus after termination of pregnancy shows sirenomelia with fused lower extremities. Anorectal atresia was also present.

melia (three cases) (Figs. 5 and 6). At autopsy, the most common concurrent anomalies included sacral agenesis (two cases), sirenomelia (three cases) (Figs. 5 and 6), renal agenesis (three cases bilateral, one case unilateral) (Fig. 5), cystic dysplastic kidney (three cases), esophageal atresia with tracheoesophageal fistula (two cases) (Fig. 2), hydrocephalus (three cases), and meningomyelocele (three cases).

Sonography identified one abnormality or more in seven fetuses, including four with hydrocephalus (Fig. 6) and/or a meningomyelocele. Of the five remaining cases, three had severe oligohydramnios that limited sonographic evaluation. Of the six cases with oligohydramnios, five were associated with renal anomalies and one had premature rupture of membranes. The only case with polyhydramnios had esophageal atresia with tracheoesophageal fistula (Fig. 2).

Discussion

The classification of anorectal malformation is variable, reflecting the complexity of malformations involving the cloaca and hindgut [7]. We have included under ARA a spectrum of malformations including imperforate anus, anal agenesis, an-

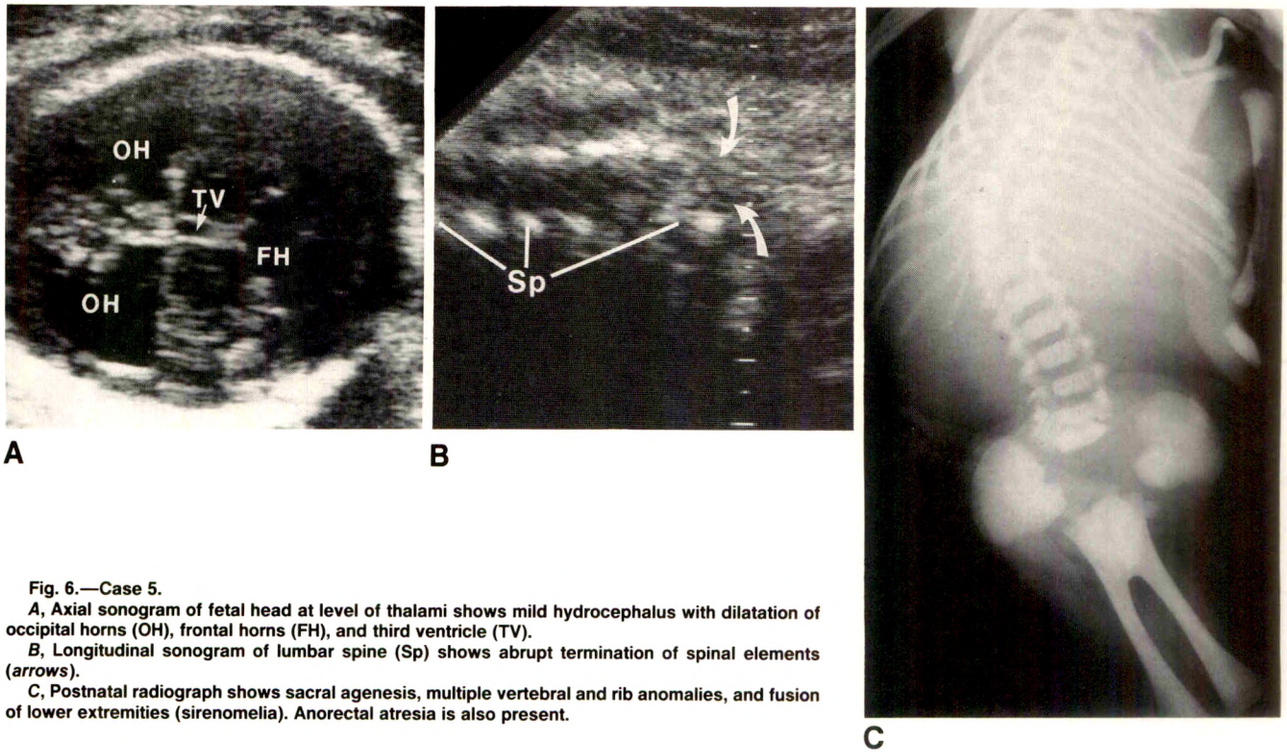


Fig. 6.—Case 5.

***A*, Axial sonogram of fetal head at level of thalami shows mild hydrocephalus with dilatation of occipital horns (OH), frontal horns (FH), and third ventricle (TV).**

***B*, Longitudinal sonogram of lumbar spine (Sp) shows abrupt termination of spinal elements (*arrows*).**

***C*, Postnatal radiograph shows sacral agenesis, multiple vertebral and rib anomalies, and fusion of lower extremities (sirenomelia). Anorectal atresia is also present.**

orectal agenesis, and rectal atresia [7]. Any of these lesions may also have an associated fistula. For simplification, ARA can be divided into two groups: high (supralevator) lesions that terminate above the levator sling and low (infralevator) lesions that terminate below the levator sling. High lesions are the most common type of ARA and are associated more often with fistulas and genitourinary malformations [7].

Our present study confirms previous observations [9, 10], suggesting that dilated fetal bowel may result from ARA (Figs. 1 and 2) in addition to more commonly recognized causes of fetal bowel obstruction (Figs. 1 and 2). A U- or V-shaped segment of dilated bowel in the lower abdomen or pelvis is particularly suggestive of ARA and was seen in three of our cases. Bean et al. [9] showed nearly identical sonographic features in a fetus with ARA scanned at 34 weeks. Similarly, Barss et al. [10] suspected dilated bowel at 28.5 weeks in another fetus with imperforate anus. Sonographic and pathologic findings suggest that such bowel segments represent distal colon.

Four of five fetuses with visibly dilated bowel were recognized prospectively in our present series, indicating that experienced sonographers can identify pathologic bowel segments in the fetus. However, distinguishing abnormally dilated colon from normal colon occasionally may be difficult since normal fetal colon progressively enlarges during pregnancy and can approach 2 cm in diameter toward term [11–13]. In questionable or borderline cases of colon dilatation, comparison with age-adjusted normal measurements may be helpful (Fig. 3).

While the number of patients studied was relatively small, our results suggest that colon dilatation is probably related to menstrual age. The earliest case detected in the present series was at 26 menstrual weeks and the earliest previously reported case of ARA was at 28.5 weeks [10]. One case in our series showed minimally dilated bowel at 27 weeks that progressed significantly by 33 weeks (Fig. 4). Also, the case described by Bean et al. [9] showed normal findings at 24 weeks but dilated bowel at 34 weeks. Pathologically, mild colon dilatation was found as early as 24 weeks but was not seen in any of four cases examined before 22 weeks. These results are consistent with known formation of meconium, since meconium normally does not accumulate in the colon before 20 weeks [11, 12].

The reason that some fetuses with ARA demonstrate colon dilatation is unclear and is a question that has not been addressed previously. As meconium normally does not pass through the anus in uncomplicated pregnancies [11], in order for colon dilatation to occur from a distal obstruction, one must postulate an increased amount of ingested amniotic fluid, a decreased absorption of fluid, or an increased production of meconium. ARA could also be associated with segmental aganglionosis, permitting colon distension to occur, although this has not been studied specifically. In cases of ARA in which colon dilatation is absent, a possible explanation is that a distal colorectal fistula decompresses the obstructed bowel. However, while the number of cases in our study was small, no direct correlation was observed between the presence or absence of a fistula and colon dilatation.

In addition to colon dilatation, other bowel abnormalities occasionally may be demonstrated in ARA. Colon peristalsis

was observed on real-time sonography in one ARA case in our study but was not observed in any of 120 normal fetuses. Intraluminal meconium calcification has been noted in some cases of ARA [14], including one case detected in utero [15], although it was not observed in any case in our present series. The etiology of calcification in these cases is uncertain, but some authors propose that alkaline urine from an associated bladder fistula may be contributory [14].

Concurrent anomalies often are associated with ARA. Additional anomalies were present in 92% of cases in our present study and have been reported in up to 72% of cases in neonatal series [16, 17]. The association between ARA and other types of anomalies led to description of the VATER (vertebral defects, anal atresia, tracheoesophageal fistula with esophageal atresia, radial and renal dysplasia) acronym [2], which was subsequently modified to the VACTERL (vertebral, anal, cardiovascular, tracheoesophageal, renal, and limb) syndrome [3]. Other authors have emphasized a broad overlap between the VACTERL syndrome and the caudal regression syndrome [8, 18], which may include ARA, sacral agenesis, lower limb hypoplasia, renal agenesis or dysplasia, and its most severe form, sirenomelia [19, 20].

On the basis of our experience, we suggest that when fetal bowel dilatation is identified and ARA is suspected, a specific search should be conducted for concurrent anomalies. Associated abnormalities, excluding oligohydramnios, were prospectively identified by sonography in seven (64%) of the 11 fetuses with concurrent anomalies. In one case, polyhydramnios was the only clue to the presence of esophageal atresia with tracheoesophageal fistula (Fig. 2). Central nervous system anomalies including hydrocephalus and/or meningomyelocele were correctly identified in four of five cases and have also been associated with ARA [16, 17]. In two cases, however, dilated fetal bowel was the primary sonographic evidence for ARA and the VACTERL syndrome (cases 7 and 8).

In contrast to ARA, other causes of fetal bowel obstruction are usually an isolated abnormality not associated with concurrent anomalies. Other causes of fetal colon dilatation include the meconium-plug syndrome [21] and Hirschsprung's disease [22], while small-bowel dilatation may be from small-bowel atresia, volvulus, Ladd's bands, meconium ileus [23], or Hirschsprung's disease [24]. Identification of additional malformations may influence the obstetric management of fetuses found to have bowel dilatation because of the high mortality and morbidity associated with ARA.

In summary, the diagnosis of ARA should be considered when dilated fetal bowel is detected by prenatal sonography, particularly when it involves the distal colon. This finding should alert the sonographer to possible concurrent malformations associated with the VACTERL or caudal regression syndrome.

REFERENCES

1. Murken JD, Albert A. Genetic counseling in cases of anal and rectal atresia. *Prog Pediatr Surg* **1976**;9:115–118
2. Quan L, Smith DW. The VATER association: vertebral defects, anal atresia, tracheoesophageal fistula with esophageal atresia, radial dysplasia. *Birth Defects* **1972**;8(2):75–78
3. Nora RH, Nora JJ. A syndrome of multiple congenital anomalies associated with teratogenic exposure. *Arch Environ Health* **1975**;85:17–21
4. Temtamy SA, Miller JD. Extending the scope of the VATER association: definition of the VATER syndrome. *J Pediatr* **1974**;85:345–349
5. Barnes JC, Smith WL. The VATER association. *Radiology* **1978**;126: 445–449
6. Ludd WE, Gross RF. Congenital malformations of the anus and rectum: report of 162 cases. *Am J Surg* **1937**;23:167–183
7. Stephens FD, Smith ED. *Ano-rectal malformations in children*. Chicago: Year Book, **1971**:212–256
8. Duhamel B. From the mermaid to anal imperforation. The syndrome of caudal regression. *Arch Dis Child* **1961**;36:152–155
9. Bean WJ, Calonge MA, Aprill CN, Geshner J. Anal atresia: a prenatal ultrasound diagnosis. *JCU* **1978**;6:111–112
10. Barss VA, Benacerraf BR, Frigolotto FD. Antenatal sonographic diagnosis of fetal gastrointestinal malformation. *Pediatrics* **1985**;76:445–449
11. Windle WF. *Physiology of the fetus*. Springfield, IL: Thomas, **1971**:94–100
12. Grelin ES. *Functional anatomy of the newborn*. New Haven: Yale University, **1973**:54–60
13. Nyberg DA, Mack LA, Patton BM, Cyr DR. Fetal bowel: normal sonographic findings. *J Ultrasound Med* **1987**;6:3–6
14. Berdon WE, Baker DH, Wigges HJ, et al. Calcified intraluminal meconium in newborn males with imperforate anus. *AJR* **1975**;125:449–455
15. Shalev E, Weiner E, Zuckerman H. Prenatal US diagnosis of intestinal calcifications with imperforate anus. *Acta Obstet Gynecol Scand* **1983**;62:95–96
16. Moore TC, Lawrence EA. Congenital malformations of the rectum and anus: associated anomalies encountered in a series of 120 cases. *Surg Gynecol Obstet* **1952**;95:281–288
17. Haase W. Associated malformation with anal and rectal atresia. *Prog Pediatr Surg* **1976**;9:99–102
18. Khoury MJ, Cordero JF, Greenberg F, James IM, Erickson JD. A population study of the VACTERL association: evidence for its etiologic heterogeneity. *Pediatrics* **1983**;71:815–820
19. Kallen B, Winberg J. Caudal mesodermal pattern of anomalies: from renal agenesis to sirenomelia. *Teratology* **1973**;9:99–112
20. Bearn JG. The association of sirenomelia with Potter's syndrome. *Arch Dis Child* **1960**;35:254–258
21. Nyberg DA, Hastrup W, Watts H, Mack LA. Dilated fetal bowel: a sonographic sign of cystic fibrosis. *J Ultrasound Med* **1987**;6:257–260
22. Vermesh M, Mayden KL, Confino E, Giglia RV, Gleicher N. Prenatal sonographic diagnosis of Hirschsprung's disease. *J Ultrasound Med* **1986**;5:37–39
23. Boricelli L, Rizzo N, Orsini LF, Gianluigi P. Prenatal diagnosis and management of fetal gastrointestinal abnormalities. *Semin Perinatol* **1983**;7: 109–117
24. Wrodleski D, Wesselhoeft C. Ultrasonic diagnosis of prenatal intestinal obstruction. *J Pediatr Surg* **1979**;5:598–600

Case Report

Gallbladder Contraction in Biliary Atresia

Edward Weinberger,[1] Joel D. Blumhagen,[1] and J. Michael Odell[2]

When persistent neonatal jaundice is present and metabolic, hemolytic, and infectious causes have been excluded, two major diagnoses must be considered: idiopathic intrahepatic cholestasis (usually caused by neonatal hepatitis) and biliary atresia. Both these entities are probably different manifestations of a single inflammatory process; their clinical features are often indistinguishable, especially in infants from 1–4 months old. Differentiation is critical, however, because neonatal hepatitis is treated medically, whereas biliary atresia requires early surgical intervention (usually hepatoportoenterostomy by 8 weeks of age) to achieve adequate, sustained bile drainage and to avoid biliary cirrhosis [1–3].

In many of the articles written about using hepatobiliary scintigraphy and sonography to assess this problem, the sonographic appearance of the gallbladder is a focus of attention [1, 2, 4]. The gallbladder is usually small or absent in biliary atresia, but rarely it can appear normal in length (≥1.5 cm) [2, 4]. It has been suggested recently that if the gallbladder contracts after an oral feeding, the diagnosis of biliary atresia is unlikely [5, 6]. Our case of gallbladder contraction in biliary atresia may not represent an unusual finding.

Case Report

After an uncomplicated pregnancy and delivery at term, a 3-day-old girl was readmitted to the hospital for jaundice (total bilirubin, 17.8 mg/dl [304 μmol/l]; direct fraction, 3.2 mg/dl [54 μmol/l]). The patient's 3-year-old sibling had had biliary atresia. Sonography at 4 days old reportedly showed a normal gallbladder. Appropriate laboratory studies were initiated to evaluate the possibility of infection or metabolism error as a cause for the hyperbilirubinemia. The next day the patient began receiving 5 mg/kg per day of phenobarbital. Sonography 3 days later showed a gallbladder of normal size (Fig. 1A), which contracted 20 min after the start of a feeding (Fig. 1B). Direct serum bilirubin remained elevated (7.3 mg/dl [124 μmol/l] on the tenth day), and hepatobiliary scintigraphy showed poor hepatic extraction and marked retention of the radiotracer with no activity in the gallbladder or extrahepatic ducts after 24 hr. Although these results were consistent with biliary atresia, severe neonatal hepatitis with intrahepatic cholestasis and the inspissated bile syndrome were considered. Phenobarbital therapy was continued, but direct bilirubin remained elevated. At 5 weeks old the patient underwent open-liver biopsy that showed marked cholestasis and periportal inflammation as well as bile duct proliferation, a hallmark of biliary atresia [3]. The gallbladder, however, appeared normal and contained clear fluid. Intraoperative cholangiogram showed contrast material exiting the cystic duct into a narrow, but patent, common bile duct leading to the duodenum (Fig. 2). No retrograde flow into hepatic ducts occurred. A cholecystostomy tube was left in place for continuous heparin irrigation to evaluate the possibility of a plugged, but partially patent, proximal ductal system. Postoperative drainage remained clear and repeat cholangiograms showed findings similar to those found in the intraoperative study. At 6 weeks old the patient underwent hepatoportocholecystostomy. Biopsy of the liver at this time showed progressive changes of biliary atresia with periportal fibrosis and ductal obliteration.

Discussion

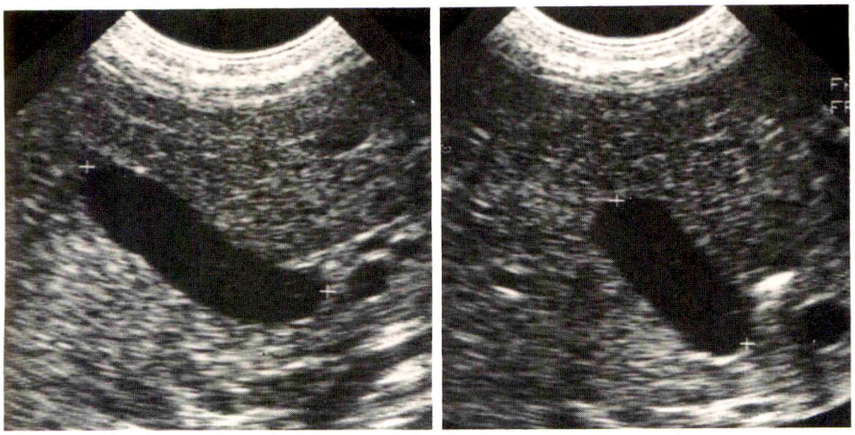
The bile ducts are patent in neonatal hepatitis, whereas in biliary atresia, any or all parts of the biliary tract (usually

Received January 16, 1987; accepted after revision March 17, 1987.

[1] Department of Radiology, Children's Hospital and Medical Center, 4800 Sand Point Way N.E., P.O. Box C5371, Seattle, WA 98105. Address reprint requests to E. Weinberger.

[2] Department of Pathology, Children's Hospital and Medical Center, 4800 Sand Point Way N.E., Seattle, WA 98105.

AJR 149:401–402, August 1987 0361–803X/87/1492-0401 © American Roentgen Ray Society



A B

Fig. 1.—Transverse sonograms in newborn with biliary atresia showing normal contraction after feeding.
***A*, Fasting, gallbladder is 28 mm long and 8 mm wide.**
***B*, 20 min after feeding was begun, gallbladder is smaller (21 mm long and 8 mm wide).**

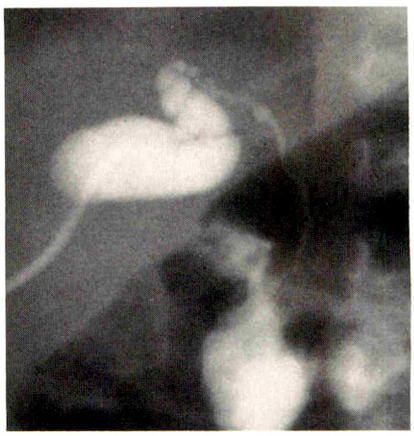


Fig. 2.—Transcholecystostomy cholangiogram shows narrowed but patent common bile duct. No retrograde filling of hepatic ducts occurs.

extrahepatic ducts or intrahepatic ducts near the porta hepatis) are obliterated [2, 3]. In this case, the hepatic duct was obliterated, but cystic and common bile ducts were patent, thus establishing communication between gallbladder and duodenum. It is therefore not surprising that the gallbladder, in response to feeding, would contract and empty part of its contents into the duodenum. In fact, this type of biliary atresia is common. In a series by Kasai [7], of 116 surgically proved cases of biliary atresia, 23 (20%) had a patent communication between gallbladder and duodenum. In his textbook on pediatric gastrointestinal imaging, Franken [3] published an illustration of a similar case as an example of biliary atresia.

We believe that sonography and radionuclide scintigraphy play complementary roles in the attempt to differentiate biliary atresia from neonatal hepatitis [8]. Sonography alone is not sufficient to establish the diagnosis. Rather, its principal role is to exclude other possible causes of obstructive jaundice such as choledochal cyst (which may or may not coexist with biliary atresia), biloma due to perforation of a bile duct, or a mass at the porta hepatis [8]. In addition, sonography may show other important coexistent conditions such as polysplenia and preduodenal portal vein, both of which are associated with biliary atresia. Sonographic demonstration of gallbladder contraction is indirect evidence for patency of the biliary tract from the cystic duct to the duodenum, but this finding does not imply patency of the more proximal bile ducts.

Hepatobiliary scintigraphy complements the primarily structural sonographic information by evaluating function, which usually helps establish the correct diagnosis [1, 2]. Excretion of radiotracer into the intestine indicates that the entire length of at least a portion of the biliary tract is patent from the hepatocytes to the duodenum. In cases where scintigraphy after phenobarbital stimulation is equivocal (usually because of poor hepatic uptake and/or marked retention of the radiotracer, which may occur with either severe neonatal hepatitis or biliary atresia), surgery for hepatic biopsy and intraoperative cholangiography is indicated [2, 3].

REFERENCES

1. Gerhold JP, Klingensmith WC III, Kuni CC, et al. Diagnosis of biliary atresia with radionuclide hepatobiliary imaging. *Radiology* **1983**;146:499–504
2. Kirks DR, Coleman RE, Filston HC, Rosenberg ER, Merten DF. An imaging approach to persistent neonatal jaundice. *AJR* **1984**;142:461–465
3. Smith WL. The liver. In: Franken EA Jr, ed. *Gastrointestinal imaging in pediatrics*. New York: Harper & Row, **1982**:427–429
4. Abramson SJ, Treves S, Teele RL. The infant with possible biliary atresia: evaluation by ultrasound and nuclear medicine. *Pediatr Radiol* **1982**;12:1–5
5. Green D, Carroll BA. Ultrasonography in the jaundiced infant: a new approach. *J Ultrasound Med* **1986**;5:323–329
6. Hayden CK Jr, Swischuk LE. *Pediatric ultrasonography*. Baltimore: Williams & Wilkins, **1987**:176
7. Kasai M. Treatment of biliary atresia with special reference to hepatic porto-enterostomy and its modifications. *Prog Pediatr Surg* **1974**;6:5–52
8. Blumhagen JD, Weinberger E. Pediatric gastrointestinal ultrasonography. In: Sanders RC, Hill MC, eds. *Ultrasound annual*. New York: Raven, **1986**:99–140

The Coexistence of Obstruction at the Ureteropelvic and Ureterovesical Junctions

Mary Anne McGrath[1]
Judy Estroff
Robert L. Lebowitz

Obstructions at the ureteropelvic junction and ureterovesical junction were found to coexist in 14 children seen over an 11-year period. The coexistence of these two conditions made the diagnosis of each difficult. In only three children were both diagnoses made preoperatively; in the others, the second diagnosis was either suspected at surgery or was made on postoperative uroradiologic studies. Of five children in whom the initial diagnosis was obstruction at the ureteropelvic junction, only two have needed surgery for obstruction at the ureterovesical junction. Seven children had an initial diagnosis of obstruction at the ureterovesical junction, and all required subsequent pyeloplasty to relieve coexisting obstruction at the ureteropelvic junction.

Therefore, our experience suggests that when both obstructions are known to exist or are suspected preoperatively, it is advisable to repair the stenosis at the ureteropelvic junction first, as distal ureteral surgery may not be necessary.

Obstruction at the ureteropelvic junction (UPJ) is the most common cause of hydronephrosis in children [1]. It is commonly discovered in the fetus during obstetric sonography, but patients with this condition can present at any age with a flank mass, hematuria, pain, or urinary tract infection [2]. Obstruction occurs with all degrees of severity; it may worsen as the child grows and the production of urine per unit of time increases while the size of the stenotic lumen remains fixed [1–3]. The obstruction is bilateral in one-fourth to one-third of cases, but the degrees of severity usually are different on each side [2, 4]. With appropriate uroradiologic evaluation, UPJ obstruction usually is easy to diagnose and is corrected readily by surgery (pyeloplasty). However, diagnosis may be more difficult when other conditions coexist [4].

Obstruction at the distal end of the ureter, the ureterovesical junction (UVJ), is another common cause of hydronephrosis in children [5]. In the most common type, primary megaureter, the ureter and collecting system are dilated because of a functional obstruction in the juxtavesical segment of the ureter. This occurs with all degrees of severity and is bilateral in 15–40% of cases [1, 3, 5]. The condition usually is easy to diagnose after other causes of hydroureteronephrosis, such as vesicoureteral reflux, ectopic ureterocele, or stricture, have been excluded [5]. This diagnosis also is more difficult when other conditions coexist [6, 7].

Obstructions at the UPJ and UVJ can coexist, and when they do, the presence of one may make detection of the other problematic. In this report we describe 14 such cases and discuss the pitfalls encountered in their diagnosis and treatment.

Materials and Methods

A review of medical records and imaging studies performed over an 11-year period (1975–1986) identified 14 children with coexisting obstructions at the UPJ and UVJ.

Received January 20, 1987; accepted after revision April 28, 1987.

[1] All authors: Department of Radiology, The Children's Hospital and Harvard Medical School, 300 Longwood Ave., Boston, MA 02115. Address reprint requests to R. L. Lebowitz.

AJR 149:403–406, August 1987
0361–803X/87/1492–0403
© American Roentgen Ray Society

Results

During the 11-year period, 14 children were found to have coexisting obstructions at the UPJ and UVJ. Seven patients were male. The ages at presentation ranged from birth (prenatal diagnosis) to 11 years. In 11 cases the left ureter was affected; in two of these it was draining the child's only kidney. The diagnosis was made preoperatively in only three patients (Figs. 1 and 2). In three the second obstruction was initially suspected at surgery (Fig. 3); in the other eight the second obstruction was diagnosed during follow-up uroradiologic studies performed 2 weeks to 2½ years after surgery.

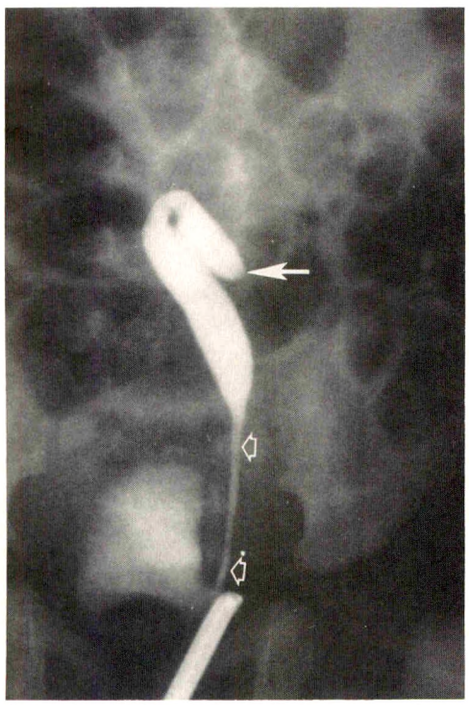
In five children the diagnosis of obstruction at the UPJ was made first. Three children presented with a mass in the flank; in the other two hydronephrosis was detected during prenatal sonography. The obstruction was severe in all five, and all underwent pyeloplasty. Only two of the five children with UPJ obstruction needed surgery for obstruction at the UVJ, one at 7 months and one at 20 months after pyeloplasty; in the other three the obstruction was mild or moderate, and these children are being followed.

In six children the diagnosis of obstruction at the UVJ was made first. Two presented with a mass in the flank. Hydronephrosis was detected during prenatal sonography in one patient and in another during evaluation for a cloacal anomaly. In one patient the condition was noted incidentally on cineurography after cardiac catheterization for a ventricular septal defect; in the sixth patient hydronephrosis was detected during evaluation for hematuria after minor trauma. The obstruction was severe in five and moderate in one. All had excision of the aperistaltic segment and reimplantation of the ureter to relieve what was thought to be an isolated distal ureteral obstruction. In this group, all needed a subsequent pyeloplasty to relieve the unrecognized obstruction at the UPJ.

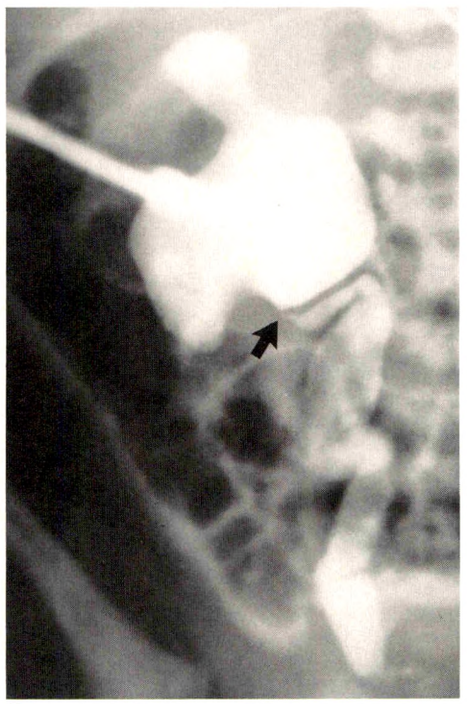
In only three children were coexisting obstructions at the UPJ and UVJ diagnosed simultaneously. In one, in whom hydronephrosis was detected during obstetric sonography, both obstructions were severe and were repaired at the same operation (Fig. 1). In another both were seen on percutaneous antegrade pyelography (Fig. 2). The third child presented with urinary tract infection, both obstructions were mild, and she is being followed.

Discussion

The coexistence of obstructions at the proximal and the distal ends of the ureter is rare. We found 14 cases after reviewing about 225 cases of UPJ obstruction and 115 cases of UVJ obstruction that had been diagnosed over an 11-year period. Only one prior case report was found that dealt specifically with these coexisting conditions [8], and two articles on primary megaureter mention the coexistence of these lesions [5, 9]. Pfister and Hendren [5] reported 150 primary megaureters (predominantly in children) and described five patients (3%) who had coexisting UPJ obstruction [5]. Pitts and Muecke [5] reviewed 80 patients (about one-half were children) with primary megaureter and noted that 20 (25%) had simultaneous UPJ obstruction. In the one illustration of this coexistence, however, there is clearly a



1



2

Fig. 1.—Male neonate found to have hydronephrosis on maternal sonography. Retrograde ureterogram shows long distal aperistaltic segment (*open arrows*) and obstruction at ureteropelvic junction (*solid arrow*). Voiding cystourethrogram was normal. Excretory urogram and sonogram showed left hydroureteronephrosis to the level of aperistaltic segment. Pyeloplasty and excision of distal ureter with reimplantation were performed.

Fig. 2.—Male neonate with flank mass. Percutaneous antegrade pyelogram shows stenosis at ureteropelvic junction (*arrow*) and distal ureteral obstruction. Voiding cystourethrogram was normal. Sonography showed a dilated pelvicalyceal system and ureter.

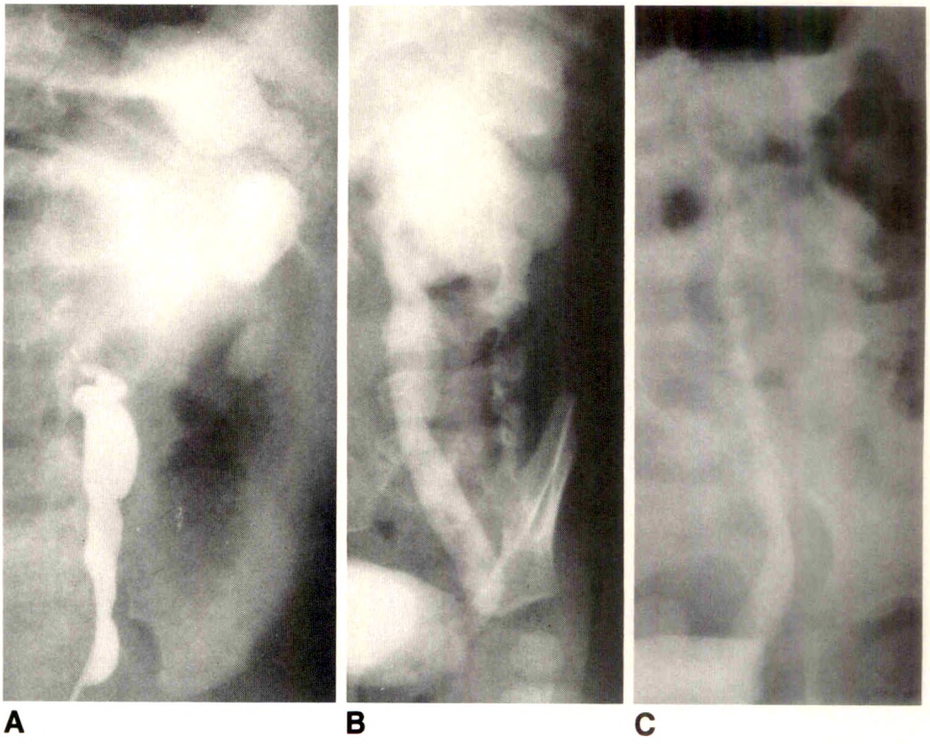


Fig. 3.—2-month-old girl with abdominal mass.

***A*, Retrograde ureterogram shows not only obstruction at ureteropelvic junction but also irregularly dilated ureter. Excretory urography and sonography were typical for severe left ureteropelvic junction obstruction. Voiding cystourethrogram was normal.**

***B*, Excretory urogram after excision of ureteropelvic junction stenosis and pyeloplasty shows moderate dilatation of ureter and pelvicalyceal system.**

***C*, Excretory urogram soon after excision of distal ureter and reimplantation shows decrease in pelvicalyceal and ureteral dilatation.**

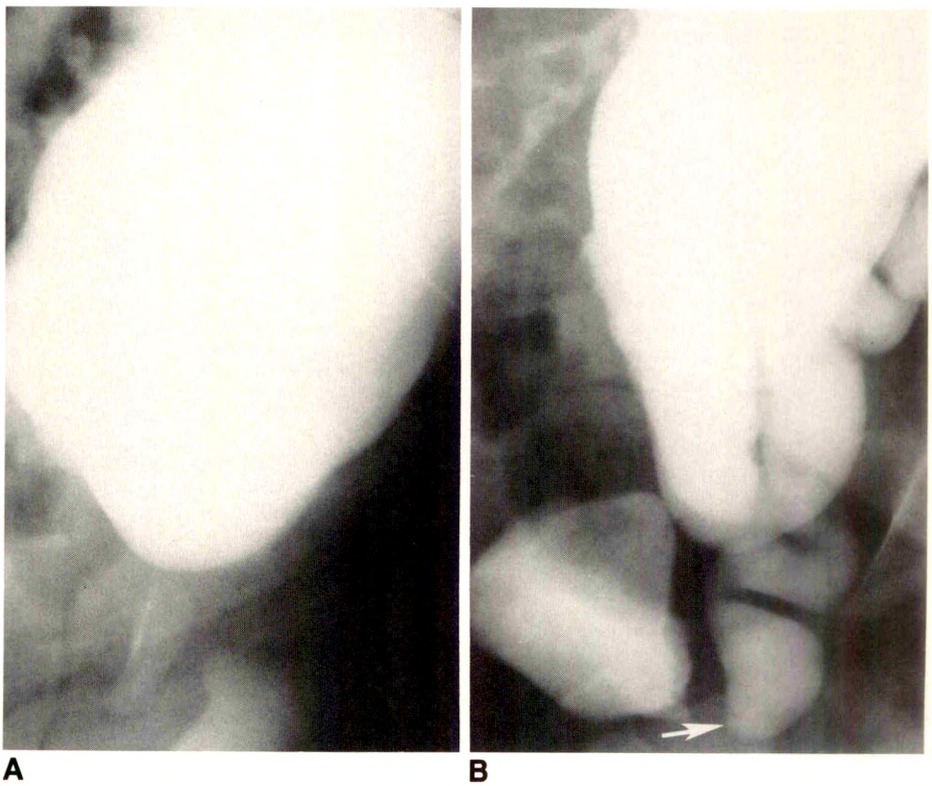


Fig. 4.—Male neonate with flank mass.

***A*, Percutaneous antegrade pyelogram shows complete obstruction at ureteropelvic junction. Excretory urography was not diagnostic and voiding cystourethrography was normal. Sonography was not performed.**

***B*, Nephrostogram after excision of ureteropelvic junction stenosis and pyeloplasty shows megaureter with juxtavesical obstruction (*arrow*). Distal aperistaltic segment of ureter was excised and ureter reimplanted.**

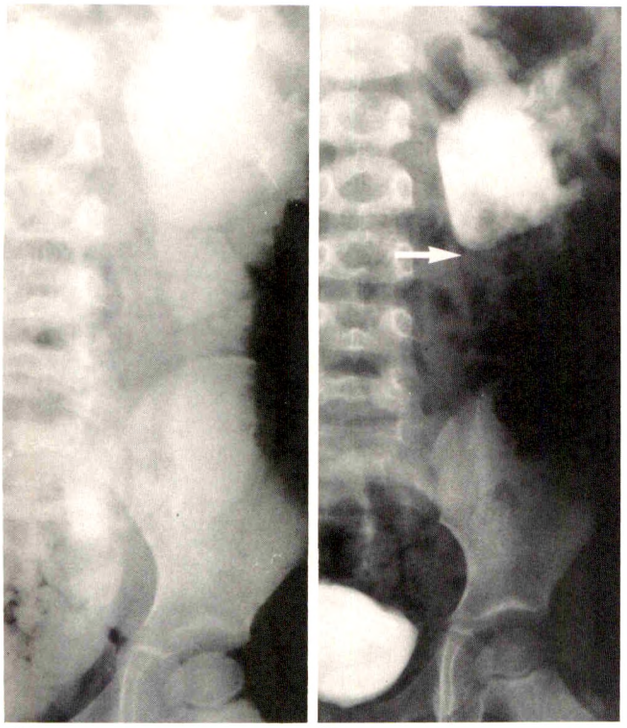


Fig. 5.—3-year-old boy with solitary left kidney.
***A*, Excretory urogram shows severe hydroureteronephrosis consistent with primary megaureter. Voiding cystourethrogram was normal.**
***B*, Excretory urogram (45-min film) after excision of distal aperistaltic segment of ureter and reimplantation. Ureter drained well. Obstruction at ureteropelvic junction is now evident (*arrow*). Instrinsic stenosis was found at time of subsequent pyeloplasty.**

widely patent UPJ, so that the frequent association of the two lesions in their report is suspect [9].

In the rare instances when these conditions do coexist they do so independently. Any degree of one can occur with any degree of the other, and therefore, the urographic picture is variable. The diagnosis of their coexistence is usually not made preoperatively for several reasons. First, in some instances it may be difficult or even impossible to diagnose both before one has been corrected. Severe obstruction at one end of the ureter may completely mask the second obstruction (Figs. 4 and 5). For example, severe obstruction at the UPJ may keep an obstructed ureter from dilating because so little of the contrast material reaches it per unit time (Fig. 4). Similarly, a high-grade obstruction at the UVJ may cause such severe hydroureteronephrosis that the UPJ stenosis is overlooked (Fig. 5). When the ureter is not well seen on an excretory urogram showing UPJ obstruction, sonography (or retrograde ureterography) should always be performed preoperatively to evaluate the ureter. If it is dilated, a distal obstruction should be suspected. Obstruction at the UVJ, however, can be present even in the absence of ureteral dilatation. Second, the coexisting lesion may be missed, simply because the diagnosis is not considered.

Because both diagnoses frequently cannot be made preoperatively, routine uroradiologic studies are mandatory after correction of either. Excretory urography, sonography, nuclear scintigraphy, nephrostography, or antegrade pyelography with pressure/flow studies are all acceptable imaging methods, and each has the potential for demonstrating the unsuspected second obstruction (Figs. 3–5).

In this review, the obstructed UPJ required surgery in all cases, whether or not it was diagnosed first. This was not the case for obstruction at the UVJ; only two of five had surgery when the diagnosis was made after pyeloplasty. This suggests that when both conditions are suspected, repair of the UPJ should be the first procedure. A nephrostomy tube placed during surgery is then an ideal route for a postoperative study of the UVJ, at which time the presence and severity of UVJ obstruction can be assessed either by the flow of contrast agent (Fig. 4) or by a formal pressure/flow study. If the obstruction is mild it may be followed.

Either condition is a common cause of urinary tract obstruction in children. Their coexistence is unusual and makes the diagnosis challenging. Although making simultaneous diagnoses often is not possible, the second obstruction can be recognized on a routine postoperative uroradiologic examination.

REFERENCES

1. Young DW, Lebowitz RL. Congenital abnormalities of the ureter. *Semin Roentgenol* **1986**;21(3):172–187
2. Snyder HM III, Lebowitz RL, Colodny AH, Bauer SB, Retik AB. Ureteropelvic junction obstruction in children. *Urol Clin North Am* **1980**;7(2):273–290
3. Perlmutter A, Retik AB, Bauer SB. Anomalies of the ureteropelvic junction. In: Walsh PC, Gittes RF, Perlmutter AD, Stamey TA, eds. *Campbell's urology*, 5th ed. Philadelphia: Saunders, **1986**:1709–1713
4. Lebowitz RL, Blickman JG. The coexistence of ureteropelvic junction obstruction and reflux. *AJR* **1983**;140:231–238
5. Pfister PC, Hendren WH. Primary megaureter in children and adults: clinical and pathophysiologic features of 150 ureters. *Urology* **1980**;12:160–176
6. Vargas B, Lebowitz RL. The coexistence of congenital megacalyces and primary megaureter. *AJR* **1986**;147:313–316
7. Blickman JG, Lebowitz RL. The coexistence of primary megaureter and reflux. *AJR* **1984**;143:1053–1057
8. Pak K, Konishi T. Horseshoe kidney in an infant associated with ureteropelvic junction and ureterovesical junction obstructions. *Hinyokika Kiyo* **1985**;31(3):457–461
9. Pitts WR, Muecke EL. Congenital megaloureter: a review of 80 patients. *J Urol* **1974**;111:468–473

Multicystic Dysplasia and Crossed Renal Ectopia

A. R. Nussbaum[1]
D. S. Hartman[2]
N. Whitley[3]
R. G. K. McCauley[4]
R. C. Sanders[1]

Multicystic renal dysplasia in a crossed fused or nonfused ectopic kidney is a rare occurrence that produces unusual imaging findings. In four such cases in neonates, three presented with a palpable abdominal mass and one was discovered in utero with maternal sonography. In three cases, sonography showed a multicystic mass, contiguous with the lower pole of the orthotopic kidney. In the fourth infant, a crossed, tiny dysplastic kidney was not visualized, but its markedly dilated ectopic ureter was seen traversing the spine on CT. Ureteropelvic junction obstruction was present in the three fused orthotopic kidneys.

The characteristic imaging findings of multicystic dysplasia and crossed renal ectopia include (1) a multicystic mass of variable size that is contiguous with the lower pole of a hydronephrotic, malrotated kidney; (2) ureteral displacement and/or dilatation; and (3) contralateral absence of the kidney and its renal artery.

Multicystic renal dysplasia is one of the most common causes of a palpable abdominal mass in the neonate [1]. Although the entire kidney is usually involved with cysts, the disease may be segmental, involving only one moiety of a duplex kidney, one-half of a horseshoe kidney, or a crossed fused ectopic kidney [1–13]. Multicystic dysplasia in a crossed fused or nonfused ectopic kidney is a rare phenomenon that can produce a palpable abdominal mass; the imaging findings may be confusing. In the four cases we report here, three were associated with ureteropelvic junction (UPJ) obstruction in the orthotopic kidney.

Materials and Methods

Three cases of crossed fused ectopia with multicystic dysplasia were retrieved from the files of the Armed Forces Institute of Pathology and The Johns Hopkins Hospital. One case of crossed nonfused ectopia was obtained from the New England Medical Center. The clinical histories, imaging studies, and histologic findings were reviewed.

Results

Crossed ectopia with multicystic dysplastic kidney (MCDK) was discovered in four neonates, three because of a palpable abdominal mass and one because of maternal sonography that showed fetal hydronephrosis and nonvisualization of the contralateral kidney. Histologic analysis of the four ectopic kidneys revealed Potter type 2 multicystic dysplasia.

Case 1

Sonography in a 4-day-old girl with a palpable right abdominal mass showed an echogenic right kidney that was mildly hydronephrotic and malrotated; both the calyces and kidney were horizontally oriented (Fig. 1A). The inferior border of the

Received February 2, 1987; accepted after revision April 28, 1987.

The opinions or assertions contained herein are the private views of the authors and are not to be construed as official or as reflecting the views of the Department of Navy or the Department of Defense.

[1] Russell H. Morgan Department of Radiology and Radiological Science, The Johns Hopkins Medical Institutions, Baltimore, MD 21205. Address reprint requests to A. R. Nussbaum, Dept. of Radiology and Radiological Science, Nelson/Tower B-173, The Johns Hopkins Medical Institutions, 600 N. Wolfe St., Baltimore, MD 21205.

[2] Department of Radiology, Naval Hospital, National Naval Medical Center, Bethesda, MD 20814.

[3] Department of Radiology, University of Maryland Medical Systems Hospital, Baltimore, MD 21201.

[4] Department of Radiology, New England Medical Center, Boston, MA 02111.

***AJR* 149:407–410, August 1987**
0361–803X/87/1492–0407
© American Roentgen Ray Society

kidney was flattened and contiguous with a 10 × 7 cm multicystic septated mass that extended into the pelvis and crossed the midline (Fig. 1B). The cysts varied in size, and no solid tissue was identified around or between the cysts. No renal tissue was present in the left renal fossa. A voiding cystourethrogram showed vesicoureteral reflux into the distal two-thirds of the right ureter and extrinsic compression of the posterior bladder. Reflux occurred into a distal left ureter, which was tiny but located in a normal posterolateral position. A technetium-99m dimercaptosuccinic acid scan showed functioning parenchyma only in the right upper flank (Fig. 1D). An aortogram performed after a cardiac catheterization for congenital heart disease (ventricular septal defect and patent ductus arteriosus) showed (1) a high bifurcation of the aorta and (2) absent left renal artery and internal iliac vessels (Fig. 1C). Vascular supply to the orthotopic right kidney was from both the aorta and right common iliac artery. Cystoscopy showed a normal ureteral orifice on each side of the trigone. Retrograde pyelography showed that the right ureter narrowed at the UPJ and deviated laterally and that the left ureter crossed from left to right. At surgery, the right ureter was seen to cross over an ectopic left multicystic kidney. The multicystic kidney was removed and the right UPJ obstruction was repaired. Multiple small cysts were also present in the isthmus joining the right and left kidneys. Histology showed Potter type 2 multicystic dysplasia.

Case 2

A newborn boy was evaluated for right-sided fetal hydronephrosis and "absent" left kidney. Sonography revealed a moderately dilated right renal pelvis and a markedly dilated and tortuous ureter that was medial to the lower pole of the kidney and could not be traced into the right renal pelvis (Fig. 2A). The right kidney was minimally elongated (5.5 cm), but the appearance of the renal parenchyma was otherwise normal. No left kidney was present. Voiding cystourethrography excluded vesicoureteral reflux, but the bladder appeared compressed by a left pelvic mass. IV urography showed a mild right UPJ obstruction and absence of left-sided function, which was confirmed by a technetium-99m diethylenetriaminepentaacidic acid renogram (Fig. 2B). A CT scan showed a dilated, nonopacified left ureter anterior to the right renal pelvis, which crossed from right to left anterior to the spine (Fig. 2C). It widened considerably in the left pelvis, and compressed and entered the left posterior bladder. Surgery confirmed the presence of left crossed fused renal ectopia, with the 2-cm ectopic left kidney composed of multiple small cysts and attached to the lower pole of the right kidney. The proximal left ureter was atretic and then dilated markedly in caliber distal to the atresia. A second area of atresia was present in the distal ureter. The proximal right ureter was located just behind the left multicystic kidney. Histologic analysis of the left kidney showed Potter type 2 multicystic dysplasia.

Case 3

A 1-month-old boy had an IV urogram to evaluate a left flank mass. The left kidney was slightly displaced superiorly and laterally and had moderate left-sided hydronephrosis compatible with a UPJ obstruction. The right kidney was not visualized. A cystogram was normal. Sonography revealed a 6 × 6 cm multicystic mass attached to the lower pole of the hydronephrotic left kidney. At surgery, the left ureter was noted to cross over the multicystic dysplastic right kidney, creating the obstruction at the UPJ.

Case 4

An IV urogram in this 1-week-old boy with a palpable right lower abdominal mass showed a normal right kidney with a mildly dilated ureter. The lower third of the ureter was deviated to the right. No function was seen on the left side. A renal scan with ^{99m}Tc glucoheptonate confirmed the absence of left-sided function and the normal function of the right kidney. Sonography revealed a right pelvic mass composed of multiple variable-size cysts that compressed the bladder and extended upward to the lower pole of the right kidney. At surgery, a crossed ectopic nonfused multicystic kidney was removed. The kidney had a small artery and vein, and its ureter was small and tortuous and entered the left side of the bladder. Histologic examination confirmed multicystic dysplasia.

Discussion

Crossed renal ectopia is a congenital malformation in which both kidneys lie on the same side of the spine, usually side by side longitudinally [4]. The ectopic kidney is smaller than normal and malrotated, and it lies caudal to the orthotopic kidney [4]. Most often, the anomaly is right-sided [4]. Fusion of the two renal units is eight times more common than nonfusion [4]. There is great variability in the aberrant vascular supply, which can arise from either side of the lower aorta, or from the common or external iliac arteries [4].

Multicystic dysplasia of the crossed unit has been previously described [1–10]. Some were composed of large cysts, while others were small cystic remnants associated with a dilated, ectopic ureter [1–10]. In a review of 443 crossed ectopic kidneys, seven were multicystic [4, 5]. We found eight other cases in the literature [2, 3, 6–10], and case 3 was previously reported by Evans et al. [1].

This unusual entity merits consideration in an infant with a flank mass and/or hydronephrosis, an unexplained course or dilatation of a ureter, and apparent contralateral renal agenesis. Since most cases of MCDK do not have functional parenchyma, both IV urography and isotope renography show function of the orthotopic kidney but lack of function in the ipsilateral lower mass and contralateral flank. These two imaging techniques cannot readily disprove renal agenesis or explain the flank mass in neonates with this type of anomaly.

The diagnosis can be established preoperatively with sonography because it allows direct visualization of the orthotopic kidney and ipsilateral caudal mass [1, 3]. In three of our four cases, the mass had the typical sonographic features of MCDK: multiple noncommunicating cysts that varied in size and were randomly distributed, a lobular renal contour with lack of peripheral parenchyma, and absent sinus echo complex [14]. In the other case, the ectopic kidney was not identified because it manifested a diminutive form of dysplasia [13].

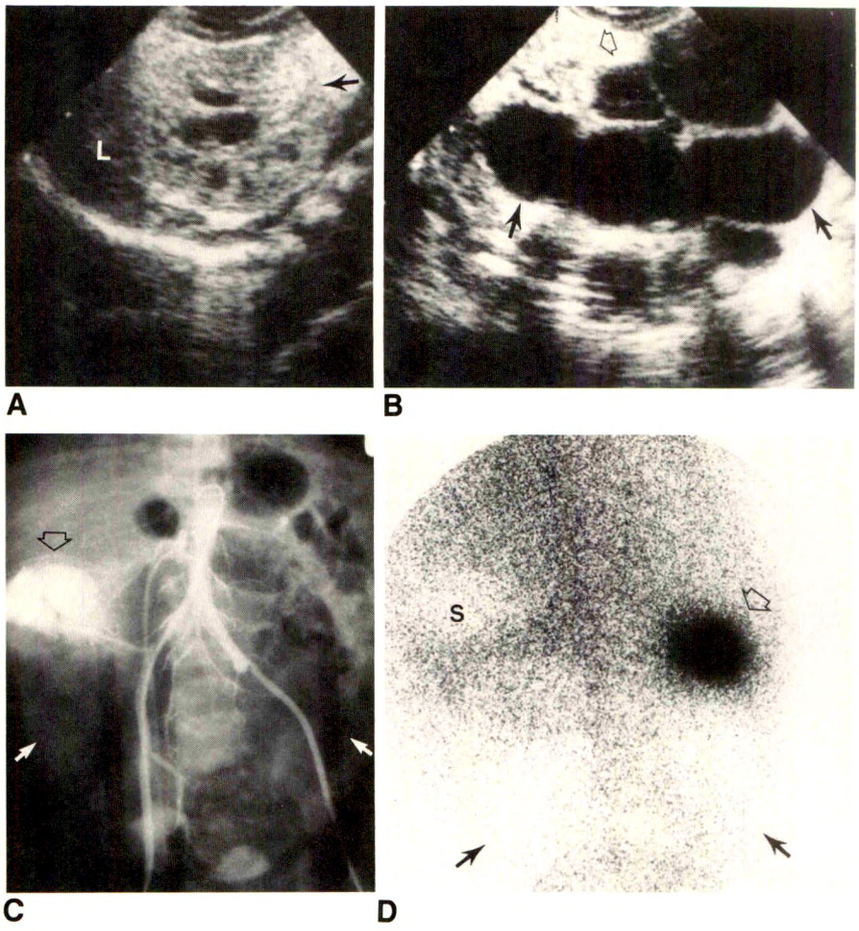


Fig. 1.—Case 1: 4-day-old girl with right abdominal mass.

A, Longitudinal sonogram in right upper abdomen shows hydronephrotic, malrotated right kidney (*arrow*). Parenchyma is echogenic. L = liver.

B, Longitudinal sonogram in right lower abdomen shows lower pole of right kidney (*open arrow*) and multiple cysts (*black arrows*) in dysplastic crossed left kidney. Septations between a few of the cysts are not shown because sonic beam is not perpendicular to their interface.

C, Aortogram shows hydronephrotic right kidney (*open arrow*), which has anomalous vascular supply. Left renal artery is absent. Note large lower abdominal mass (*white arrows*) that distorts iliac vessels.

D, Posterior DMSA scan shows functioning renal tissue in right upper flank (*open arrow*). Photopenic areas on both sides of midline are nonfunctioning cysts (*arrows*). S = stomach.

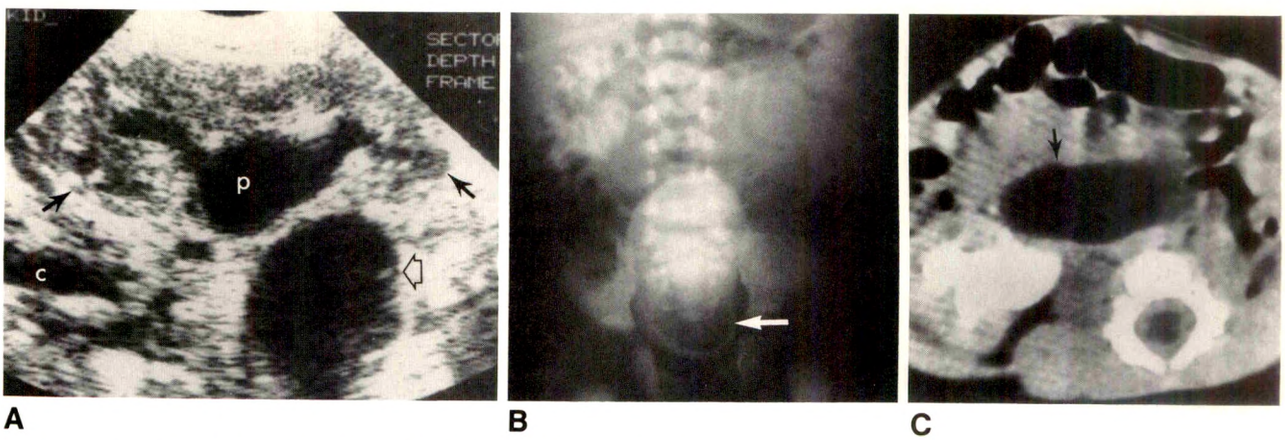


Fig. 2.—Case 2: Newborn boy. Diminutive dysplasia in crossed fused ectopic kidney.

A, Right coronal scan. Right kidney (*black arrows*) is hydronephrotic. Crossed left ureter (*open arrow*) is markedly dilated and traverses spine. P = renal pelvis; c = inferior vena cava.

B, IV urogram confirms a right ureteropelvic junction obstruction. No functioning left renal tissue is evident. A large lucency in bladder (*arrow*) is caused by extrinsic compression by dilated, distal, crossed left ureter.

C, CT scan clearly shows dilated nonopacified left ureter crossing spine (*arrow*).

Sonography is the imaging technique of choice in a neonate with an abdominal mass or abnormal prenatal renal sonogram. In many cases of crossed fused ectopia with MCDK, the diagnosis can be strongly suspected from the sonogram, and no other studies may be necessary. However, a renogram is useful to assess the function of the crossed kidney and the degree of obstruction in the orthotopic kidney. A voiding cystourethrogram may help to determine ureteral presence and course.

Moderate hydronephrosis was present in the orthotopic kidney in the three cases with renal fusion. All had ureteral narrowing at the UPJ, most likely related to in utero obstruction or ischemia created by compression from the adjacent multicystic kidney. Support for this theory is evidenced by the position of the ureter, which crossed over the MCDK in two of the neonates and crossed behind it in the third. Alternatively (case 4), lateral deviation and dilatation of the ureter and/or renal pelvis, without an intrinsic ureteral stenosis, can occur [4, 6].

The simultaneous occurrence of two relatively uncommon congenital genitourinary anomalies is interesting. The two kidneys fuse early in utero, and variation in the axial deviation of the fused renal elements is common [4]. Current belief is that MCDK results from early in utero ureteral obstruction [15]. Possibly, in crossed fused ectopia, MCDK results from obstruction created by the renal fusion. Also, the renal pelvis or ureter may be constricted by the anomalous blood supply [5]. In cases with marked dilatation of the crossed ureter, cystic dysplasia is usually caused by the obstruction that occurs with ureteral ectopia and the associated ureterocele [8–10].

Recognition of the following imaging features may permit a preoperative diagnosis of MCDK in crossed ectopia: (1) a multicystic mass of variable size that is contiguous with the lower pole of a hydronephrotic, malrotated kidney; (2) ureteral displacement and/or dilatation; and (3) contralateral absence of the kidney and its renal artery.

REFERENCES

1. Evans WP, Sumner TE, Lorentz WB Jr, Resnick MI. Association of crossed fused renal ectopia and multicystic kidney. *J Urol* **1979**;122:821–822
2. Herczeg T, Rutkai P, Deak J. Metanephrogenic cystic remnant of crossed dystopic kidney. *J Urol* **1956**;76:488–498
3. Rosenberg HK, Snyder HM III, Duckett J. Abdominal mass in a newborn: multicystic dysplasia of crossed fused renal ectopia—ultrasonic demonstration. *J Urol* **1984**;131:1160–1161
4. Abeshouse BS, Bhisitkul I. Crossed renal ectopia with and without fusion. *Urol Int* **1959**;9:63–91
5. Abeshouse BS. Crossed ectopia with fusion: review of literature and a report of four cases. *Am J Surg* **1947**;73:658–683
6. Daniel WW, Datnow B. Crossed fused ectopia with renal dysplasia. *AJR* **1977**;128:845–846
7. Tanenbaum B, Sanford S, Pochaczevsky R, Weinberg SR, Rosenkranz W. Crossed fused renal ectopia with calcific cystic dysplasia mimicking a malignant renal neoplasm. *J Can Assoc Radiol* **1972**;23:142–144
8. Hendren WH, Donahoe PK, Pfister RC. Crossed renal ectopia in children. *Urology* **1976**;7:135–144
9. Fishman M, Borden S. Crossed fused renal ectopia with single crossed ectopic ureterocele. *J Urol* **1982**;127:117–118
10. Farkas A, Earon J, Firstater M. Crossed renal ectopia with crossed single ectopic ureterocele. *J Urol* **1978**;119:836–838
11. Walker D, Fennell R, Garin E, Richard G. Spectrum of multicystic renal dysplasia: diagnosis and management. *Urology* **1978**;11:433–436
12. Diard F, Le Dosseur P, Cadier L, Calabet A, Bondonny JM. Multicystic dysplasia in the upper component of the complete duplex kidney. *Pediatr Radiol* **1984**;14:310–313
13. Nussbaum AR, Dorst JP, Jeffs RD, Gearhart JP, Sanders RC. Ectopic ureter and ureterocele: their varied sonographic manifestations. *Radiology* **1986**;159:227–235
14. Sanders RC, Hartman DS. The sonographic distinction between neonatal multicystic kidney and hydronephrosis. *Radiology* **1984**;151:621–625
15. Beck AD. The effect of intrauterine urinary obstruction upon the development of the fetal kidney. *J Urol* **1971**;105:784–789

Computer Page

Computerized Reference Management—Filing the Literature

Jud W. Gurney[1] and Robert S. Wigton[2]

The next best thing to knowing something is knowing where to find it.
—Samuel Johnson (1709–1784)

According to Jeghers [1], the amount of medical knowledge doubles every 10 years. Therefore, the radiologist faces a deluge of information. It is difficult to keep up with the weekly flow of journals or even to remember the location of a recent article. Many solve this problem by saving important citations in a personal file. A well-organized filing system gives the physician a tool for improved patient care, continuing education, research proposals, and lecture preparation. The organization and maintenance of files are, however, a tedious task, consuming a considerable amount of time. Those in the medical profession are forever plagued by the question: "Where did I see that paper?" [2]. The personal computer, which is useful for searching the medical literature, can also relieve much of the work associated with bibliographic organization and filing [3]. The purpose of this article is to describe some computerized techniques for the management of bibliographic citations.

Data-Base Management

The process of structuring information in a standard format is known as data-base management. An example of this familiar form of organization is filing radiologic cases in a teaching file according to the American College of Radiology coding system. Ordinarily, once references have been selected for filing, the standard method is to group related papers into manila folders. The clinician confronted with a stuffed filing cabinet faces a real challenge in deciding which folder gets the new article, especially when any one of several folders could qualify.

The storage problem is compounded by the need for cross-references. The information from a journal article such as author, volume number, key words, abstract, and page number can be indexed on cards and cross-referenced for later use. For most radiologists, this sort of project would be too time consuming to be practical. On the other hand, software programs for data-base management quickly accomplish the tasks of arranging, sorting, and filing citations, facilitating the retrieval of desired information.

Computerized Literature Storage

The general format for reference storage is similar in all data-base management computer programs (Fig. 1). The bibliographic data from a journal article make up a single record. Each record or citation has an identical template divided into several fields. Each field contains a specific element of the citation, such as the author, title of the article, key words, and other pertinent information. A collection of similar records constitutes a file or data base. Once the desired citations have been entered into the computer, the information is stored on magnetic media. Depending on the storage media, roughly 1000 records can be stored on a single floppy disk, or over 100,000 records on a hard-disk system. Journal citations stored in this manner can be recalled later by any clue—author's name, key words, or journal name

Received March 2, 1987; accepted after revision April 20, 1987.
[1] Department of Radiology, Creighton University, Omaha, NB 68131. Address reprint requests to J. W. Gurney, Dept. of Radiology, St. Joseph Hospital, 601 N. 30th St., Omaha, NB 68131.
[2] Section of General Internal Medicine, University of Nebraska Medical Center, 42nd & Dewey, Omaha, NB 68105.

AJR **149:411–413, August 1987** 0361–803X/87/1492–0411 © American Roentgen Ray Society

REFERENCE #	
FILE	FILE Chest
AUTHOR(S)	AUTHOR(S)
TITLE	TITLE
JOURNAL	JOURNAL
VOLUME	VOLUME
PAGE(S)	PAGE(S)
YEAR	YEAR 1970-1980
KEYWORD(S)	KEYWORD(S) Carcinoma or Adenoma
ABSTRACT	ABSTRACT
JOURNAL BOOK	JOURNAL BOOK
PUBLISHER	PUBLISHER
1	2

Fig. 1.—Typical template for reference management. Information is typed (or downloaded directly from MEDLINE search) into respective fields. Bibliographic data from an article constitute a single record. Multiple records constitute a data base.

Fig. 2.—Data base with a file name "Chest" containing 3000 articles on pulmonary disease. Desired years and keywords entered. Search will be for those citations published between 1970 and 1980 with keywords carcinoma *or* adenoma. Boolean operators (and, or, not) are advantageous in narrowing or enlarging scope of search. Selected references may be ordered in any journal style.

(Fig. 2). Articles vaguely remembered can be retrieved if only a fraction of the citation is known. Bibliographies for articles, teaching, and research can be compiled quickly and easily.

Several noncommercial computer programs developed for reference management by individuals have been described in the literature [4–6]. The programs were simple, straightforward, and filled an in-house need for citation storage. Designed on early microcomputers, compatibility between different computers may be a problem. A program that was developed on one system may have to be modified to work on another. An advantage is that these programs can usually be obtained from the authors free of charge or at nominal cost. To those with computer expertise, these programs may be tailored to specific needs. Overall, they tend to be more error prone, less sophisticated, and more difficult to maintain than the commercial programs that have now been marketed for bibliographic management.

Commercial Programs

Two categories of commercial programs for bibliographic management exist (Table 1). All-purpose data-base management programs such as Personal Filing System (PFS) and dBaseIII may be adapted for reference storage, but the user must create the template desired for citations. Programs range from simple to complex. On one end, a program such as PFS electronically simulates an index card. This system is easy to learn, takes little time, and the commands are in simple English. The simplicity, however, limits the overall capabilities of the system. The abilities to search, sort, and combine fields are limited. Care must be taken in designing the template. Once formatted, it may be impossible to change at a later date without having to enter thousands of already stored citations again. More complex, sophisticated programs such as dBaseIII have their own programming language, allowing the user to query the data base in a variety of ways. Complex searching requests can be performed and sorting routines can be invoked to place references into many formats. Such complexity requires a considerable apprenticeship in computer programming and is suitable only for the more serious user [7]. The general-purpose data-base management programs are flexible and may be used for other filing purposes, such as maintaining a radiologic teaching file [8].

Data-base management programs specifically designed for citation management offer several advantages (Table 1). The programs have defined templates for journal articles, books, and theses, requiring the user to simply key in the required information. Several programs combine MEDLINE searching with personal data-base management. The retrieved citations are then automatically entered into the data-base manager for later searching and editing. This saves the steps of either formatting downloaded references for the data-base management software on the word processor, or for some programs, entering the journal articles by hand on the keyboard.

All of these programs handle the basic tasks of sort, search, and retrieval. Unique features of each may be desirable for the individual user. For example, PAPERBASE has the capability of reading through a manuscript and listing all citations to produce a flawless reference list. MINI MEDFILE contains a utility program to print self-adhesive labels for file folders. For record entry, ARTFILE users can set up a two-letter code for the 10 most commonly cited publications. Use of these abbreviated keystrokes reduces the time needed to fill in the journal name on the form. ARTFILE also has a spelling checker that quickly detects errors as they are entered into the computer. When names or keywords are entered, the words are saved in a separate file. The program produces an audible "beep" when a new word is entered. This is a useful feature notifying the typist if an author's name has been misspelled.

One of the most unusual programs is PAPERBASE. It consists of a booklet that contains a list of programs written in BASIC and provides a full explanation of how they work. Programmers may then modify the programs for use on their computers or add personal enhancements. The programs are also available on disk for most computers. An enhanced version, PAPERBASE DeLuxe, is available separately.

One of the most useful features contained in several programs is the ability to print references in any journal style. Any author who has devoted the time and effort to rearranging the style of references for journal resubmission will appreciate the ease with which these computer programs can accomplish this task [9].

The dissemination of medical literature remains the key to unifying education, research, and patient management. Computerized reference storage provides the means for the individual physician to rapidly gather and store information.

ACKNOWLEDGMENT

We thank Dawn Temple for her help in preparing the manuscript.

TABLE 1: Reference Data-Base Management Software

Programs*	System Requirements	Comments
GENERAL		
Personal Filing System (PFS) Software Publishing Corp. 2021 Landings Dr. Mountain View, CA 94043 Tel: (415) 962-8910	Apple II line or IBM PC & compatible	
dBaseIII Ashton-Tate 20101 Hamilton Ave. Torrance, CA 90502 Tel: (800) 437-4329	IBM PC or compatible	
SPECIFIC		
Sci-Mate Manager, Sci-Mate, Editor Version 2.0 ISI Institute for Scientific Information 3501 Market St. Philadelphia, PA 19104 Tel: (800) 523-4092	IBM PC or compatible, 128K RAM min or CP/M 80	1, 2
PRO-CITE* Professional Bibliographic System* Personal Bibliographic System** Personal Bibliographic Software, Inc. P.O. Box 4250 Ann Arbor, MI 48106 Tel: (313) 996-1580	* IBM PC, 128K RAM min, PC DOS 2.0 ** Apple II line 64K, 2-disk drive, 80 column display	1, 2
Bookends, MED TRANS Sensible Software, Inc. 210 South Woodward, Suite 229 Birmingham, MI 48011 Tel: (313) 258-5566	Apple II line IBM & compatibles with 256K	1, 2
Quick-Search Librarian Interactive Microware, Inc. P.O. Box 139 State College, PA 16804 Tel: (814) 238-8294	Apple II line	
REF-ED Skandigen Reference Systems AB Radmansgatan 50 S-11357 Stockholm, Sweden Tel: +46(8)165455	IBM PC, MS DOS 3.10	1, 2
PAPERBASE PAPERBASE DeLuxe Wight Scientific 44 Roan Street London SE10 9JT England Tel: 01-858-2699	IBM, 64K min, DOS 2.0 MacKintosh	1, 2
MINI MEDFILE Medical Software Consortium P.O. Box 429342 Cincinnati, Ohio 45242 Tel: (513) 871-0145	Apple II line	1
ARTFILE Frambach Software Systems P.O. Box 8815 Boston, MA 02114 Tel: (617) 497-4384	IBM & compatible, 128K RAM min	1, 2

Note.—Comments. 1 = Customized journal style; 2 = Can accept download from MEDLINE search.

* Price varies considerably between programs from a few dollars (PAPERBASE-book) to several hundred dollars (Sci-Mate). In general, higher-priced programs have greater flexibility and ease of use. A listing of current prices is useless, since prices are constantly subject to change. Contact the manufacturer or a local computer store for an up-to-date listing.

PC = personal computer; RAM = random access memory; min = minimum; CP/M, DOS = computer operating systems.

REFERENCES

1. Jeghers H. Medical care, education and research. *N Engl J Med* **1964**;271:1297–1301
2. Elkinton JR. Where did I see that paper? *Ann Intern Med* **1967**;67:459–460
3. Gurney JW, Wigton RS. Computerized reference management: searching the literature. *AJR* **1986**;147:641–645
4. Bertrand D, Bader CR. Storage and retrieval of bibliographic references using a microprocessor system. *Int J Biomed Comput* **1980**;11:285–293
5. Hunter TB. Simple interactive computer program to store literature references. *AJR* **1983**;140:169
6. McCabe JR, McCabe BH. Microcomputer-based filing system for emergency medicine literature. *Ann Emerg Med* **1981**;10:87–90
7. Kunin CM. Managing bibliographic citations using microcomputers. *Am J Med* **1985**;78:627–634
8. Smith DF, Rowberg AA. Data-base management system on a CT scanner computer: application to teaching file and procedure records. *AJR* **1984**;142:1219–1223
9. O'Connor M. Standardization of bibliographical reference systems. *Br Med J [Clin Res]* **1978**;1:31–32

FORTHCOMING ARTICLES

1987 ARRS EXECUTIVE COUNCIL AWARD

Results of intraarterial fibrinolytic therapy for popliteal and tibial artery obstruction: comparison of streptokinase and urokinase. *Traughber PD, Cook PS, Micklos TJ, Miller FJ*

RADIOLOGIC PROGRESS

MR imaging of the musculoskeletal system: current and future status. *Sartoris DJ, Resnick D*

CARDIOPULMONARY RADIOLOGY

Reliability of selective pulmonary arteriography in the diagnosis of pulmonary embolism. *Quinn MF, Lundell CJ, Klotz TA, et al.*

Intrathoracic manifestations of metastatic testicular seminoma: a comparison of chest radiographic and CT findings. *Williams MP, Husband JE, Heron CW*

Case report. Aberrant right subclavian artery with a large diverticulum of Kommerell: a potential for misdiagnosis. *Walker TG, Geller SC*

ENDOCRINE RADIOLOGY

Selective intraarterial DSA of the parathyroid glands in patients with persistent or recurrent hyperparathyroidism after parathyroidectomy. *Lacombe P, Foster D, Dubost C, et al.*

GASTROINTESTINAL RADIOLOGY

Cholangiographic findings in hepatic artery occlusion following liver transplantation. *Zajko AB, Campbell WL, Logsdon GA, et al.*

Focal fatty change of the liver adjacent to the falciform ligament: CT and sonographic findings in five surgically confirmed cases. *Yoshikawa J, Matsui O, Takashima T, et al.*

The inferior accessory hepatic fissure: sonographic appearance. *Lim JH, Ko YT, Han MC, Kim CW, Choi BI, Im JG*

Sonographic features of amebic and pyogenic liver abscesses: a blinded comparison. *Ralls PW, Barnes PF, Radin DR, Colletti P, Halls J*

Case report. Focal acute acalculous cholecystitis. *Warshauer D, Scott G, Gottschalk A*

Pancreas transplantation with pancreatico-duodeno-cystostomy for exocrine drainage: cystographic findings. *Woolsey EJ, Tauscher JR, Dafoe DC*

Case report. Ascaris-induced pancreatitis. *Leung JW, Mok SD, Metreweli C*

Technical note. Esophageal deviation: pushed or pulled? *Levine MS, Gilchrist AM*

Appendicitis as the initial manifestation of Crohn's disease: radiologic features and prognosis. *Agha FP, Ghahremani GG, Panella JS, Kaufman MW*

Technical note. Double-contrast examination of the colon with carbon dioxide: the use of effervescent powder. *Pochaczevsky R*

Opinion. Primary panendoscopy—a radiologist's response. *Gelfand DW, Ott DJ, Chen YM*

GENITOURINARY RADIOLOGY

The distinction between acute renal transplant rejection and cyclosporine nephrotoxicity: value of duplex sonography. *Buckley AR, Cooperberg PL, Reeve CE, Magil AB*

The evaluation of gross hematuria in anticoagulated patients: efficacy of IV urography and cystoscopy. *Cuttino JT Jr, Clark RL, Feaster SH, Zwicke DL*

Case report. Spermatic granuloma complicating abdominoperineal resection of the rectum: diagnosis by CT, MR imaging, and percutaneous biopsy. *Feaster SH, Kinard RE, Yancey JM, Marsh RL*

MUSCULOSKELETAL RADIOLOGY

MR imaging of marrow changes adjacent to end-plates in degenerative lumbar disk disease. *de Roos A, Kressel H, Spritzer C, Dalinka M*

The effect of restricting the indications for lumbosacral spine radiography in patients with acute back symptoms. *Baker SR, Rabin A, Lantos G, Gallagher EJ*

Percutaneous biopsy of the cervical spine using CT guidance. *Kattapuram SV, Rosenthal DI*

Pictorial essay. MR imaging of the normal elbow: anatomic correlation. *Middleton WD, Macrander S, Kneeland JB, Froncisz W, Jesmanowicz A, Hyde JS*

Technical note. A CT table attachment for parasagittal scanning of the axilla. *Roger DJ, Richli WR*

MR imaging of solitary osteochondromas: report of eight cases. *Lee JK, Yao L, Wirth CR*

Perspective. Arthrography: past, present, and future. *Hall FM*

PEDIATRIC RADIOLOGY

Sonographic measurements of the normal bladder wall in children. *Jequier S, Rousseau O*

Case report. Cor triatriatum: diagnosis by MR imaging. *Bisset GS III, Kirks DR, Strife JL, Schwartz DC*

Case report. Atrial ventricular diverticulum: sonographic diagnosis. *Karnaze MG, Shackelford GD, Abramson CL*

NEURORADIOLOGY

ASNR: the Silver Anniversary. Neuroradiology: the next 25 years. *Taveras JM*

Lymphomas of the head and neck: CT findings at initial presentation. *Lee Y-Y, Van Tassel P, Nauert C, North LB, Jing B-S*

An early CT sign of ischemic infarction: increased density in a cerebral artery. *Pressman BD, Tourje EJ, Thompson JR*

Carotid cavernous fistulae: indications for urgent treatment. *Halbach VV, Hieshima GB, Higashida RT, Reicher M*

Pitfalls in the CT diagnosis of atlantoaxial rotary subluxation. *Kowalski HM, Cohen WA, Cooper P, Wisoff JH*

VASCULAR RADIOLOGY

Role of CT in excluding major arterial injury following blunt thoracic trauma. *Mirvis SE, Kostrubiak I, Whitley NO, Goldstein LD, Rodriguez A*

Penetrating injuries of the thoracic aorta and brachiocephalic arteries: angiographic findings in 18 cases. *Fisher RG, Ben-Menachem Y*

Angiography in patients with arterial trauma: correlation between angiographic abnormalities, operative findings, and clinical outcome. *Rose SC, Moore EE*

INTERVENTIONAL RADIOLOGY

Technical note. Use of light localizer in fluoroscopically guided percutaneous procedures. *Hayt DB*

Technical note. Percutaneous atheroma removal using a wire basket. *Kim D, Turkel DH, Orron DE, Steer ML*

Technical note. Improved guidewire immobilization technique for interventional procedures. *Gavant ML*

RADIOLOGIC PHYSICS

An improved method for estimating the entrance exposure in diagnostic X-ray examinations. *Zamenhof RG, Shehabi S, Morgan HT*

OPINIONS

Wall Street entrepreneurs and imaging centers: an insidious threat to radiology. *Berlin L*

Risk management for the radiologist: some advice in prospect. *Smith JP*

ARRS Presidential Address

1987 ARRS Meeting–Presidential Address

Raymond A. Gagliardi[1]



At this time I would like to welcome you to Miami Beach for the 87th annual meeting of the American Roentgen Ray Society—a stopping place on the long journey that started in Wurzburg in 1895 and continues this day. The tremendous technological triumphs of the past 15 years may lead us to believe that this journey has been one of uninterrupted triumph. However, I remind you that the one constant has been the presence of serious recurring obstacles to the development and even the survival of the specialty. It is not news that the medical profession and radiology face a new series of attacks growing in intensity from legal and legislative quarters that threaten the educational, scientific, and economic stability of the profession and the specialty. We truly are facing a major crisis. This morning I would like to review with you the crises radiology has faced in the past and try to deepen your sense of our history. Together we can evaluate the responses of organized radiology to previous confrontations, and perhaps we can see what is possible in devising new solutions for new problems.

On December 28, 1895, Professor Wilhelm Roentgen submitted his famous communication to the President of the Physical Medical Society of Wurzburg, and within 10 days the news spread throughout the civilized world. The announcement was met with incredible enthusiasm and with an equally incredible lack of understanding of its real application and true potential. Everyone who owned or had access to a static machine was advertising and providing X-ray services, both medical and otherwise. Its use in reputable medical installations was far overshadowed by its use in quasi-medical sideshows. It is not surprising that the medical uses of Roentgen's spectacular discovery almost fell into disrepute.

On March 26, 1900, less than 5 years after the announcement of the new kind of ray, a small group of physicians met in the office of Dr. Heber Robarts in St. Louis and formed the Roentgen Society of the United States. Hoping to establish responsible standards for the use of the roentgen ray, the group held its first annual meeting in December 1900 and changed its name to the American Roentgen Ray Society. With the exception of two meetings modified by wartime restrictions, the Society has continued ever since to hold its annual meeting as a major scientific occasion. Our gathering this week is a direct benefit of their planning. The Society fought to exclude electricians, engineers, radiographers, and indeed, many out-and-out charlatans from the field. Slowly and surely the American Roentgen Ray Society won the first and most significant turf battle of all, identifying radiology as a medical discipline and identifying the radiologist as a medical specialist providing an essential medical service. No action by organized radiology since then has surpassed this landmark achievement. Reviewing our early rosters, we find the names of all the great American pioneers in and martyrs to radiology.

However, this was not achievement enough for these men. There was recognized a need to disseminate the new knowledge, and in 1900 was born the *American X-Ray Journal*,

Presented at the annual meeting of the American Roentgen Ray Society, Miami Beach, FL, April 1987.
[1] Department of Radiology, St. Joseph Mercy Hospital, Pontiac, MI 48053.

AJR **149:415–417, August 1987** 0361–803X/87/1492–0415 © American Roentgen Ray Society

which became the *American Quarterly of Radiology* and then the *American Journal of Roentgenology*, still serving as a premier scientific journal at almost 90 years of age.

A monumental crisis had been surmounted by the oldest radiologic society in North America. In a brief period, a start was made in the definition of radiology, the organization of radiologic knowledge, and a system for its dissemination. The identification of radiology as an integral part of medical practice has never been challenged since that day. Little wonder we are proud of the heritage and the contribution of the American Roentgen Ray Society and the *American Journal of Roentgenology*.

As the ARRS was quickly developing into an organization of fully trained specialists, it limited its membership to those who had been in the field for 3 years and who practiced only radiology. Distances and travel conditions precluded attendance by members in the Plains States and on the Pacific Coast, so the society provided regional meetings, bringing the information to the membership. The regional meetings ended in 1925, but the ARRS continued the rule that new members must devote the major share of their practice time to radiology. In a word, the Society had become elitist and was excluding a whole segment of younger men who were doing radiology but were unable, for local or economic reasons, to abandon their other areas of practice. Happily, under the leadership of Colin Holman, rule changes presently allow membership for all certified radiologists. Even at that time, however, radiology was facing its next major crisis in the form of fragmentation of the specialty.

In 1915, a group of midwestern radiologists met in St. Louis in the old offices of Dr. Russell Carman, and later that year, in Chicago, the Western Roentgen Society was organized. Membership was available to those physicians who devoted a major portion of their practice time to radiology for only 1 year rather than the 3 years demanded by the senior organization. Its original bylaws fixed Chicago as the annual meeting site, making attendance less expensive and more convenient for the growing group of radiologists in the central United States. Its membership burgeoned, and in 1918 the Western Roentgen Society became officially the Radiological Society of North America. After some fits and starts, its journal—the *Journal of Roentgenology*—became in 1923 *Radiology*. The RSNA is now the largest radiologic society in the world, and its journal has the largest circulation.

The Radiological Society of North America almost 70 years ago recognized the problem of fragmentation as a major threat to the specialty and attacked that problem by broadening its organizational base and, at the same time, providing new strength. Today we pay tribute to their foresight.

Radiology still did not enjoy the prestige freely given other major medical specialties. In truth, it was not considered a major medical specialty. In my own personal experience, military radiology toward the close of World War II was a subdivision of the Department of Medicine, and the radiologists were required to rotate as medical officer of the day. Earlier, in medical school at Yale, the Chief Radiologist was designated as Associate Professor of Surgery (Radiology), and this was 50 years after Roentgen's discovery. In 1923, in San Francisco, a group of radiologists met to discuss and implement the formation of an American College of Radiology (ACR), with a program of invited honored fellows to rival their peers in the American College of Surgery. The College made little significant impact until 1936, in the dark days of the Great Depression, when the College expanded its activities not only of advancing radiology as a science and improving service to the sick and the poor but also of studying the economics of radiologic practice. Once on this path, the College became increasingly active in the area of radiologic socioeconomics and worked zealously as government intervention and third-party payers became significant forces in medical practice. There were problems that could not be dealt with even by the most effective individuals but required trained and knowledgeable professionals. Their work with early Blue Cross–Blue Shield plans usually succeeded in establishing radiology as a medical rather than a hospital service. More recently, the College worked with Congress through its Washington representatives to reaffirm the place of radiology as a medical discipline and establish professional component billing as the preferred system for all providers. In the new Congress, that battle is renewed and joined again. The attempt to include radiologic services under the DRG system is a resurrection of previous attempts to separate the radiologist from other medical colleagues as a separate species under the hospital genus. In these instances, we see again how a major radiologic organization has taken on new crises and continues to serve us all as economics and legislative activities have become so crucial to our very survival.

In 1932, at the ACR meeting, Dr. Arthur Christie raised the issue of an examination process for the certification of radiologists and asked for steps toward implementation of that process. In 1933, an attempt at multisociety unification had led to the American Congress of Radiology, held under the presidency of Henry Pancoast. The Congress lasted only 1 year, but it provided an opportunity for representatives of the major societies to consider joint sponsorship of an examining board. In 1933, the American Roentgen Ray Society, the Radiological Society of North America, the American College of Radiology, the Section on Radiology of the American Medical Association, and the American Radium Society joined to form the American Board of Radiology. The new Board sought protection for the public against irresponsible and unqualified practitioners, the elevation of the standards of practice, and the advancements of the interests of radiology by ensuring that only the truly qualified should offer this service. Modifications have been made over the years as well as timely adjustments to the new technology, such as nuclear radiology and sonographic imaging. We have been well served and continue to be well served by our Board.

In recent years, following the lead of Seymour Ochsner, an annual summit meeting has been held for intersocietal discussions. This meeting has become an increasingly productive one. Old problems, once thought solved, have a way of recurring, and narrow subspecialization and the proliferation of journals have again raised concerns about excessive fragmentation of radiologic influence. This is a justifiable concern only if subspecialists abandon their roles as complete radiol-

ogists and their commitments to the interests of radiology in general. Diagnostic radiologists who deny their abilities to interpret a chest radiograph or find a fracture are, in my judgment, not worthy of the name.

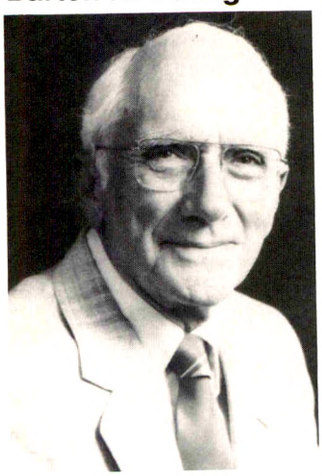
Where are we now? Are the crises of DRGs, medical malpractice, traveling doctors, or turf struggles any worse than those faced by our predecessors? I think not. The early members of this society were forced to define radiology, identify its training requirements, extend its scope, and enhance its prestige, making possible the development of the noble specialty we now practice. They achieved this by doing the job better, with a total commitment to excellence of performance and to a unity of purpose. I warn you that the difficult journey that started in Wurzburg is a never-ending one, but I remind you that several generations of radiologists before us have faced steeper mountains in their path and never have failed to reach the summit. I repeat that they did this by a total commitment to excellence and a unity of purpose.

It is in the certain knowledge that we, too, shall prevail that I urge you to be one of us in the science and education of this meeting and this society, and I ask you to assume your obligation to serve as a coparticipant in the battles we now face as radiologists, as physicians, and as Americans.

1987 ARRS Awards for Distinguished Service to Radiology

Raymond A. Gagliardi

Barton R. Young



In 1934, Barton Young published his first scientific paper, entitled "Hodgkin's Disease," in coauthorship with W. Edward Chamberlain. In the intervening 53 years, Dr. Young has been and continues to be a giant in the speciality. Still in active practice, he finds time to attend meetings and postgraduate seminars to keep abreast of new developments in radiology.

During his career, he has published more than 60 papers, several book chapters, and a classic monograph, *The Skull, Sinuses, and Mastoids.* He was appointed professor of radiology at Temple University in 1943, and he has served as an examiner and inspector for the American Board of Radiology and as a member of the Residency Review Committee. He cofounded the Committee on Radiology of the National Research Council and served as a consultant to the United States Navy. He served as a chancellor of the American College of Radiology, Vice President of the Radiological Society of North America, as a founder and President of the Eastern Radiological Society, and as President of the Philadelphia Roentgen Ray Society. He has delivered almost every one of the significant named radiology lectures in this country.

He is honored by the American Roentgen Ray Society for all of these contributions to radiologic practice, education, and organization, but more particularly for his long service to this Society. Dr. Young served 8 years as Secretary, from 1949 to 1957, and as President-elect and President in 1958. These were difficult years of new priorities and new challenges for the expanding specialty. For his dedication and wise guidance, the American Roentgen Ray Society is pleased to present Dr. Barton R. Young its Distinguished Service Award.

Colin B. Holman

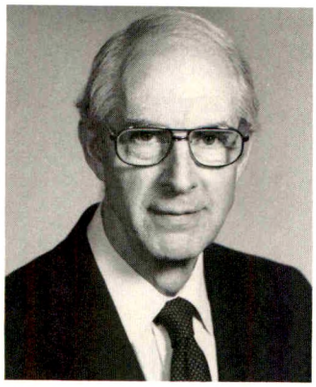


Pray's © 1986

If one were to characterize Dr. Colin Holman, he would best be described as a gentle man of surpassing modesty. Despite his reticence, we in radiology, and the American Roentgen Ray Society in particular, are well aware of his major contributions.

After college at Dartmouth and medical school at the University of Pennsylvania, Dr. Holman went to the Mayo Clinic in Rochester and spent his entire career during the rebirth of that great institution. His professional career includes countless scientific papers, book chapters, and named lectures, mostly in the area of neuroradiology. The many Mayo residents remember with warmth his gentle patience with them as they struggled with the veins of the posterior fossa. This fine teacher's skills were recognized when he was appointed Professor of Radiology at Mayo Graduate School and the Mayo Medical School, posts he held until his retirement in 1980. In 1961 he was awarded the Billings Gold Medal of the American Medical Association. Dr. Holman was one of the founders of the American Society of Neuroradiology and served as its president in 1968–1969. However, it was in the American Roentgen Ray Society that Colin Holman's sensitivity to the needs of the specialty and his organizational skills were used best. Having served as Treasurer, he was chosen President for 1974–1975. It was during that time that he started the process of reorganizing the membership structure of the American Roentgen Ray Society to convert it from a rather elitist group to a truly international organization serving the scientific and educational needs of young and mature radiologists alike. For his many contributions to neuroradiologic education and science, but especially for his major efforts to restore the vitality of a great radiologic organization, the American Roentgen Ray Society is pleased to award its Distinguished Service Award to Dr. Colin B. Holman.

William R. Eyler



The contributions to radiology by Dr. William R. Eyler are well known to everyone who practices that specialty. After attending Harvard University and its medical school, Dr. Eyler served his residency at the Massachusetts General Hospital. He served briefly on the Harvard faculty and, after a brief flirtation with private practice, became Chairman at Henry Ford Hospital in Detroit, gracing that position with great distinction from 1955 until his retirement from the chairmanship, but not radiology, in 1983. Dr. Eyler is best known for his service as Editor of *Radiology,* but his scientific contributions are truly more impressive. While managing a large department always on the leading edge of new technology, he built one of the finest residency programs in the country and published more than 100 scientific papers and editorials and contributed chapters to no fewer than six books. No new development was too much of a challenge for him. From personal knowledge of his work and a review of his bibiliography, it is easy to see that this was a general radiologist who became the peer of the most narrow subspecialist. As editor of *Radiology* from 1966 to 1985, he converted that great journal from a comfortable senior to a vibrant, aggressive youngster at a time when radiology was expanding by quantum leaps and when new approaches to dissemination of medical knowledge were needed. Dr. Eyler supplied those approaches and in so doing served his journal, his society, and all of radiology.

In gratitude for a lifetime of service to radiology, the American Roentgen Ray Society is pleased to award its Distinguished Service Award to one of our own long-serving and loyal members, Dr. William R. Eyler.

Stephen W. Brown



Elson-Alexandre, Los Angeles, CA

On entering the private practice of radiology in 1947, Dr. Stephen Brown made a commitment to excellence in that practice, and he has never failed that commitment. Georgia-born and Georgia-bred, Dr. Brown has devoted his entire career to service in Augusta, GA, except when attending Louisiana State University in New Orleans and for military service during World War II. As Chairman of the Department of Radiology at the University Hospital in Augusta from 1955 until 1986, he built an impressive organization whose technology and staff are more like an academic institution than most academic institutions. Dr. Brown founded the Georgia Radiation Therapy Center, a magnificent modern facility now serving all Augusta area hospitals and clinics. He is perhaps prouder of the technology training program, named on his retirement the Stephen W. Brown School of Radiography, or of the Stephen W. Brown Endowment Fund that provides scholarship aid and educational support. These last two honors were established to demonstrate the esteem of his peers, already shown by previous elections to president of the medical staff at two Augusta hospitals, president of the Georgia Radiological Society, and president of the Radiological Section of the Southern Medical Association, and as a founding member of the Eastern Radiological Society. The American Roentgen Ray Society was well served by Dr. Brown as Treasurer from 1961–1967 during an uncertain period in the financial fortunes of the Society. He was honored by the Presidency in 1968–1969, and the American Roentgen Ray Society reaffirms its debt to a man who has demonstrated the unlimited horizons of quality practice and quality service by presenting its Distinguished Service Award to Dr. Stephen W. Brown.

87th Annual Meeting of the American Roentgen Ray Society: Secretary's Report

Glen W. Hartman[1]

The 87th annual meeting of the American Roentgen Ray Society (ARRS) was held April 26–May 1, 1987, at the Fontainebleau Hilton in Miami Beach, FL. True to its reputation as the Sunshine State, the weather in Florida remained perfect throughout the week. The meeting facilities at the Fontainebleau were well suited for the outstanding scientific and educational program.

The meeting officially began on Monday morning with the installation of Raymond Gagliardi of Pontiac, MI, as the 87th President of the ARRS. He was installed in his new office by retiring President Jerome Wiot and Executive Council Chairman Rosalind Troupin. In a first for the Society, the President was given a congratulatory kiss by the Chairman of the Executive Council. Dr. Gagliardi's address to the Society is presented elsewhere in this issue. In an upbeat message, he traced the history of the ARRS and other radiologic organizations, emphasizing how our predecessors had resolved prior crises that faced our specialty, and urged us to confront current challenges in a similar manner.

Dr. Gagliardi had selected 189 papers covering all phases of radiology for the scientific program that began on Monday. A record number of papers were submitted this year, far in excess of the number that could be presented. Three parallel sessions were held for a total of 18 scientific sessions.

Under the direction of Joseph Ferrucci and Richard McLeod, 48 instructional courses were offered. Again, none of these conflicted with the scientific sessions or the categorical course. These 90-min sessions continue to be one of the most popular segments of the program.

The categorical course for 1987 was arranged by Gary Ghahremani and Richard Gore. The subject, gastrointestinal radiology, attracted over 500 attendees. A thorough update on gastrointestinal imaging is provided in the outstanding syllabus prepared by the faculty and edited by Dr. Ghahremani. The categorical course will continue to provide an important element of the educational program next year when Dr. Stephen A. Feig will arrange a breast imaging course.

The scientific exhibit space at the Fontainebleau Hilton made it possible to exhibit a record 217 scientific exhibits under the leadership of Dr. John Madewell. They were well arranged and allowed ample room for quiet viewing and study. The Case of the Day was centrally located and attracted wide participation. The cases were prepared by Dr. Marvin E. Goldberg, who incorporated a computer into the program for the first time.

Elsewhere in this issue the abstracts of the award-winning scientific exhibits appear along with the titles and exhibitors of the exhibits especially honored. Major awards were Gold Medal for "High Resolution CT of the Lung Parenchyma with Pathologic Correlation" by Moulay A. Meziane, Elias A. Zerhouni, Ralph H. Hruban, Paul S. Wheeler, Nagi F. Khouri, Elliot K. Fishman, Grover M. Hutchins, and Stanley S. Siegelman of Baltimore, MD; the Silver Medal for "Ultrasound-Guided Biopsy of Small ($\leq$ 3 cm) Masses: A Review of 126 Cases" by Carl C. Reading, J. William Charboneau, E. Meredith James, and Mark R. Hurt of Rochester, MN; and the Bronze Medal for "Magnetic Resonance of the Pelvis and Perineum in Children" by Rosalind B. Dietrich, Hooshang Kangarloo, M. Ines Boechat, Franklin N. Tessler, and Theodore R. Hall of Los Angeles, CA.

On Wednesday, the Special Awards Program was held. In addition to the Roscoe E. Miller Paper of the Society of Gastrointestinal Radiologists, the special papers by residents in radiology were presented. The President's Award paper, with an honorarium of $1000, was "High Resolution, Real-Time Ultrasonography of Artificially Produced Meniscal Lesions in Human Cadaveric Knee Specimens" by Bayne Selby, Michael L. Richardson, Brent D. Nelson, Daniel O. Graney, and Laurence A. Mack of Seattle, WA. The Executive Council Award papers, with honoraria of $500, were "Initial and Long Term Results of Intra-Arterial Fibrinolytic Therapy for the Popliteal and Trifurcation Arteries: Comparison of Streptokinase and Urokinase" by Paul D. Traughber, Timothy J. Micklos, and Franklin J. Miller of Salt Lake City, UT, and Philip S. Cook of Denver, CO; and "Retrograde Prostatic Urethroplasty with Balloon Catheter" by Flavio Castaneda and Kurt Amplatz of Minneapolis, MN.

Special awards from the American Roentgen Ray Society for Distinguished Service to Radiology were given by President Gagliardi to Stephen W. Brown of Augusta, GA; William R. Eyler of Detroit, MI; Barton R. Young of Santa Barbara, CA; and Colin B. Holman of Port Ludlow, WA. The four

[1] Secretary, American Roentgen Ray Society, Dept. of Radiology, Mayo Clinic, 200 Front St. S.W., Rochester, MN 55901.

AJR 149:420–421, August 1987 0361–803X/87/1492–0420 © American Roentgen Ray Society

recipients were recognized not only for their contributions to the ARRS but also for their outstanding service to the entire specialty.

The 67th Caldwell Lecture was presented by M. Paul Capp, Professor of Radiology, Arizona Health Sciences Center. Dr. Capp chose as his topic "The Future Practice of Radiology: Art vs Science." It was a scholarly dissertation on the progress of science in medicine and the important role of radiology in this transition.

The program for accompanying persons was arranged by Manuel Viamonte, Jr., and Lucy Kelley. A boat trip on the inland waterways and to the Vizcaya Museum and Gardens was especially popular. The Society is deeply indebted to them for their outstanding efforts.

The annual golf and tennis tournaments were well organized by Neil Messinger and Reuven Porges; both were held at the Turnberry Country Club under ideal conditions. The Manges Trophy was won by Jules O. Sumkin, while the Exhibitor Trophy was presented to Ralph Alfidi for their performance on the links. The winners of the tennis tournament were Arlene Berens and William J. Casarella.

Once again, the ARRS/ACR luncheon speakers presented timely and informative topics. These included "The 100th Congress: What It Will Do To Radiology" by Otha Linton; "Resource-Based Relative Value Scales: The Harvard/AMA Study" by Franklin L. Angell; "Alternative Health Delivery Systems: Problems for Radiology" by Thomas G. Dehn; and "Malpractice/Risk Management Issues for Radiologists" by Harold N. Schwinger.

The Friday Symposium titled "Genitourinary Imaging Update" featured an outstanding faculty and was presented under the direction of Harry Z. Mellins and David S. Hartman. This popular program is tentatively scheduled to feature chest imaging in 1988.

During the ARRS business meetings, the following officers were elected for 1987–1988: President-Elect, Lee F. Rogers; First Vice President, Gerald D. Dodd; Second Vice President, Rosalind H. Troupin; Secretary, Glen W. Hartman, Rochester, MN; Treasurer, Ronald G. Evens, St. Louis, MO; Chairman of the Executive Council, John A. Kirkpatrick, Jr.; and Executive Council (5-year term), Ernest J. Ferris.

New committee members elected were Publications and Editorial Policy Committee (5-year term), Charles A. Rohrmann, Jr.; Scientific Exhibits Committee (3-year term), Kay H. Vydareny; Finance and Budget Committee (3-year term), Beverly P. Wood; and Advisory Committee on Education and Research (5-year term), Bruce J. Hillman.

The Constitution and Bylaws were amended to form an Annual Meeting Committee chaired by Thomas C. Beneventano, a Scientific Program Committee chaired by the President-Elect, and a Membership Committee chaired by the Vice-Chairman of the Council.

The Society was pleased to welcome 402 new active members in addition to a large number of members-in-training and corresponding members.

Plans are under way for the 1988 meeting at the San Francisco Hilton, May 8–13. This hotel is undergoing extensive renovation and will provide excellent facilities for a springtime meeting. President-Elect Lee Rogers will be the director of what promises to be an outstanding educational experience. Watch for future announcements of the program in this Journal.

ARRS Award-Winning Scientific Exhibits, 1987

Over 215 scientific exhibits were selected for display at the ARRS 1987 meeting in Miami Beach. The Committee on Awards selected three medal winners and named 19 exhibits for certificates of merit.

Elsewhere in this issue are an application form and instructions for submitting scientific exhibits for the 1988 ARRS meeting in San Francisco, CA, May 8–13.

The 1987 meritorious exhibits are:

Gold Medal Exhibit

High resolution CT of the lung parenchyma with pathologic correlation. Meziane MA, Zerhouni EA, Hruban RH, Wheeler PS, Khouri NF, Fishman EK, Hutchins GM, Siegelman SS (The Johns Hopkins Medical Institution, Baltimore, MD)

The use of high-resolution CT of the lung parenchyma has been advocated in the investigation of the diffuse pulmonary process. The lack of detailed pathologic correlation has hampered the interpretation of the various CT patterns seen. This exhibit presents the results of a systematic study performed on a series of lungs obtained from autopsies over a 1-year period. The lungs were prepared by using the method developed at the Upstate Medical Center, Syracuse, NY. The specimens were scanned with 2-mm slides with 0.3 × 0.3 mm pixels. Pathologic sections of the same levels were then correlated. The appearance of normal lung is characterized. The basic CT signs of diffuse parenchymal disease with their pathologic correlates are presented and compared with the plain radiographic appearance and the premortem studies.

Silver Medal Exhibit

Ultrasound-guided biopsy of small (≤ 3 cm) masses: a review of 126 cases. Reading CC, Charboneau JW, James EM, Hurt MR (Mayo Clinic, Rochester, MN)

It has often been reported that percutaneous needle biopsy under sonographic guidance is primarily useful for large or superficially located masses and that CT-guided biopsy is reserved for masses less than 3- to 5-cm in size. This exhibit demonstrates that today, successful sonography-guided biopsy of smaller masses is possible because of several factors, including: (a) continuous real-time monitoring of needle position primarily using phased-array transducers, (2) use of larger-bore (18–19 gauge) needles to improve cytologic/histologic yield and, (3) frequent use of an echogenic screw-biopsy stylet that markedly improves needle visibility. Real-time sonography-guided biopsy of 126 consecutive masses less than or equal to 3 cm in size (25 ≤ 1 cm, 47 were 1–2 cm, 69 were 2–3 cm) were carried out to diagnose primary or secondary neoplasm. The correct cytologic/histologic diagnosis was established in 91% of these small lesions. The accuracy was 79% for masses ≤ 1 cm, 88% for masses 1–2 cm, and 98% for masses 2–3 cm in size. The accuracy for hepatic masses, which represented the greatest number of patients in this series, was 96%. Ninety-two masses were located in the abdomen (76 liver, nine pancreas, five kidney, two retroperitoneum); 31 in the neck (16 thyroid, 12 lymph nodes, three parathyroid); two in the breast; and one in the lower extremity. Ninety-five biopsies were positive for malignancy, and 20 were negative for malignancy yielding benign tissue. Only 11 of 126 biopsies of these small masses were considered nondiagnostic by the pathologist. No complications other than mild local discomfort were encountered. Sonography-guided biopsy is a highly accurate and safe technique to document or exclude malignancy in small (≤ 3 cm) masses.

Bronze Medal Exhibit

Magnetic resonance of the pelvis and perineum in children. Dietrich RB, Kangarloo H, Boechat MI, Tessler FN, Hall TR (University of California at Los Angeles, Los Angeles, CA)

The pelvises of 112 children (aged 6 days to 19 years) were evaluated by using 0.3-T echo MR imaging. The MR scans of 54 of these patients, who had normal pelvic studies, were compared to cadaver cryosections and reviewed to assess the optimal imaging plane(s) and sequence(s) for showing specific pelvic structures. The remaining 58 patients imaged showed a spectrum of pelvic and peritoneal disease. Results were correlated with sonography (45) and CT (13). Twenty-eight patients had surgical or biopsy correlation. Lesions imaged were divided into three categories: congenital (31), cystic and fluid collections (11), and neoplastic (20). The ability of MR to differentiate pelvic abnormalities with optimal imaging sequences and planes is shown. MR imaging gave a better global view of the pelvis than did sonography and was especially useful in evaluating pelvic neoplasms and lesions not directly adjacent to the bladder. It was superior to CT in evaluating the extent of lesions because of its ability to image in any plane and its better tissue differentiation.

Certificate of Merit Exhibits

US guided fine-needle aspiration biopsy of breast masses. Fornage BD, Djelassi L, Pluot M, Faroux MJ. (Institut Jean Godinot, Reims, France)

The continuum of developmental pulmonary anomalies. Panicek DM, Heitzman ER, Randall PA, Groskin SA, Chew FS, Lane EJ, Markarian B. (SUNY Health Science Center, Syracuse, NY)

Central nervous system injury in fatally abused infants: a computed tomographic-neuropathologic analysis. ter Meulen DC, Kleinman PK, Deveikis JP, Smith TW, Blackbourne BD, Adams V, Greenwald M (University of Massachusetts Medical Center, Worcester, MA)

MRI of the knee: assessment of clinical utility. Bellon EM, Keith MW, Sacco DC, Shah ZR, Benson JE (Cuyahoga County Hospital, Cleveland, OH)

Silicone-induced erosive arthritis. Schneider HJ, Weiss MA, Stern PJ (University of Cincinnati Medical Center, Cincinnati, OH)

3-D CT in acute cervical spine trauma. Harris JH Jr, Wojcik G (University of Texas, Houston, TX)

Aluminum toxicity in dialysis patients: radiographic findings and establishment of biopsy-sparing criteria. Kriegshauser JS, Swee RG, McCarthy JT, Hauser MG (Mayo Clinic, Rochester, MN)

The solitary colonic polyp: radiologic-histologic differentiation and significance. Olmsted WW, Ros PR, Sobin LH, Dachman AH (The George Washington University Hospital and Armed Forces Institute of Pathology, Washington, DC)

Interventional radiology in the gallbladder. vanSonnenberg E, Casola G, Wittich GR, Hofmann AF, Zakko S, Christenson R, Keightley AM (University of California, San Diego, Medical Center, San Diego, CA)

Duplex Doppler ultrasound examination of pre- and post-liver transplantation patients. Longley DG, Skolnick ML, Zajko A, Bron K (University of Pittsburgh School of Medicine, Pittsburgh, PA)

Transvaginal ultrasound scanning of the pelvis: normal anatomy and pathologic findings. Joseph N, Mendelson EB, Neiman HL, Bohm-Velez M, Kellman G, Russo J (The Western Pennsylvania Hospital, Pittsburgh, PA)

The lips of the renal sinus: the sensitive signposts. Morettin LB, Pope KL, Jennings AJ (University of Texas Medical Branch, Galveston, TX)

Retrograde transurethral prostatic dilatation. Castaneda F, Amplatz K (University of Minnesota Hospital, Minneapolis, MN)

The CT and MRI features of acute toxic encephalopathies. Batnitzky S, Nelson DL, McMillan JH, Rosenthal SJ (The University of Kansas Medical Center, Kansas City, KS)

Intraoperative DSA for control of aneurysmal clipping and endarterectomy procedures. Litvin GK, Baran SA, Cacayorin ED, Petro GR, Hodge CJ, Bredenberg CE, Winfield JA, Moro JJ (SUNY Health Science Center at Syracuse, Syracuse, NY)

Cerebral infarction in the young adult. Grosman H, Gray RR, St. Louis EL (The Wellesley Hospital, Toronto, Ont., Canada)

Percutaneous Greenfield IVC filter: caveats in patient selection and placement technique. Dorfman GS, Cronan JJ, Haas RA, Lambiase RE, Paolella LP (Rhode Island Hospital, Providence, RI)

Standardized imaging and Doppler criteria for cerebrovascular diagnosis using duplex sonography. Bluth EI, Marich KW, Stavros AT, Wetzner SM, Aufrichtig D, Baker JD (Ochsner Medical Foundation, New Orleans, LA)

Diagnosis and management of complications of central venous catheters: a radiologic approach. Charnsangavej C, Chasen MH, Carrasco CH, Richli WR, Wallace S (M. D. Anderson Hospital and Tumor Institute, Houston, TX)

American Roentgen Ray Society New Members

At the 1987 annual meeting of the American Roentgen Ray Society (ARRS) in Miami Beach, FL, 402 applicants were elected to active membership and five to corresponding membership. Two hundred and fifty-seven applicants were added to in-training membership during the year preceding the 1987 annual meeting. John F. Roach and William B. Seaman were elected to life membership in recognition of their contributions to the Society and the specialty of radiology.

Active members of the society must be graduates in good standing of an approved medical school or hold an advanced degree in one of the physical, chemical, or biologic sciences. They must be board certified, active in radiology or one of its branches in the U.S. or Canada, and sponsored by two ARRS members.

Members-in-training are physicians in a radiology residency or in a postresidency fellowship program.

Corresponding members are physicians residing in foreign countries who are active in the science of radiology or allied sciences.

An application form is printed elsewhere in this issue or may be obtained by writing: Paul Fullagar, Administrative Director, American Roentgen Ray Society, 1891 Preston White Dr., Reston, VA 22091.

Active Members

Dorit D. Adler, Ann Arbor, MI
Yolanda T. Adler, Chicago, IL
Naomi P. Alazraki, Atlanta, GA
Daniel D. Alterman, Bronx, NY
Robert S. Altin, Browns Mills, NJ
Judith M. Aronchick, Philadelphia, PA
Harold L. Atkins, Stony Brook, NY
David E. Baker, Ann Arbor, MI
Mark E. Baker, Durham, NC
Stephen R. Baker, Scotch Plains, NJ
John L. Bardsley, St. Louis, MO
Merle H. Barth, Houston, TX
Georgine B. Bartiromo-DeMarino, Iowa City, IA
Hanae L. Belfar, Pittsburgh, PA
Paul Berger, Long Beach, CA
Vidor Bernstien, Wayne, NJ
Diran R. Bezirdjian, Richmond, VA
Drupadi G. Bhagwanani, Pittsburgh, PA
Ronda Bixon, New York, NY
Jeffrey D. Blonstein, Millburn, NJ
James R. Bos, Royal Oak, MI
Pierre M. Bourgouin, Boston, MA
Richard A. Bowerman, Ann Arbor, MI
James D. Bowie, Durham, NC
Lawrence M. Boxt, Pomona, CA
Michael N. Brant-Zawadzki, Newport Beach, CA
William H. Brewer, Richmond, VA
Marvin Brodie, Oakhurst, NJ
Klaus M. Bron, Pittsburgh, PA
Barbara G. Bronitsky, Camp Hill, PA
Abraham J. Bronner, Oak Brook, IL
Betty S. Brooks, Augusta, GA
Kathleen Brown, Los Angeles, CA
Patrick J. Bryan, Cleveland, OH
Shalom S. Buchbinder, Riverdale, NY
James L. Buck, Washington, DC
Dana R. Burke, Narberth, PA
Henry Burko, Milwaukee, WI
Richard N. Cadotte, Montreal, Que., Canada
A. Frank Campbell, FPO New York
Michael Capek, Des Plaines, IL
David H. Carlson, Newton Lower Falls, MA
Raymond F. Carmody, Tucson, AZ
C. Humberto Carrasco, Houston, TX
Barbara A. Carroll, Durham, NC
Philip N. Cascade, Detroit, MI
Giovana Casola, La Jolla, CA
Edward S. Casselman, Everett, WA
Robert P. Cavallino, Winnetka, IL
Less T. Chafen, San Francisco, CA
Caroline Chiles, Durham, NC
Robert H. Choplin, Winston-Salem, NC
W. Peter Cockshott, Hamilton, Ont., Canada
Alan M. Cohen, Shaker Heights, OH
Bradley M. Cohen, Boca Raton, FL
Douglas M. Coldwell, Washington, DC
John C. Collingwood, Granger, IN
Harry A. Cooperman, Voorhees, NJ
Herbert B. Copeland, Baltimore, MD
Jack A. Copeland, Baltimore, MD
Ronald R. Cordell, Charleston, WV
Gerald W. Coueslan, Brandon, Man., Canada
Robert D. Crane, Seattle, WA
Donald A. Cubberley, Salt Lake City, UT
John T. Curnes, Chapel Hill, NC
Hugh D. Curtin, Pittsburgh, PA
Richard J. D'Amico, Orange, NJ
Robert B. Danley, Urbana, IL
Paul K. Danner, Littleton, CO
Michael A. David, Westwood, MA
David J. Delany, Chapel Hill, NC
Terrence C. Demos, Maywood, IL
Praful C. Desai, Midland, MI
Sheila M. Deshmukh, Pelham, NY
Peter A. Dietrich, Shelburne, VT
Francoise M. Dion, Vezdun, Que., Canada
Wylie J. Dodds, Milwaukee, WI
Peter Doubilet, Boston, MA
Gerard Duprat, Jr., Montreal, Que., Canada
Shigeru Ehara, Iowa City, IA
Robert A. Ellwood, Royal Oak, MI
Linda M. Fahr, Loma Linda, CA
Joseph Fakhry, Valhalla, NY
Jalil Farah, Royal Oak, MI
Abdol V. Fatemi, San Marino, CA
Michael P. Federle, Foster City, CA
Augene F. Foley, Jr., Jamestown, NY
W. Dennis Foley, Milwaukee, WI
Julian B. Foreman, New Orleans, LA
Stephen M. Fry, Atlanta, GA
Manohar P. Gandhi, Granada Hills, CA
David W. Gelfand, Winston-Salem, NC
Stuart C. Geller, Boston, MA
Kenneth H. Gerber, Solana Beach, CA
Bijan Ghorashi, Atlanta, GA
James S. Gilley, Salt Lake City, UT
Seth N. Glick, Philadelphia, PA
Morton Glickman, New Haven, CT
Thomas G. Goergen, Rancho Santa Fe, CA
Leonard Goldberg, Toronto, Ont., Canada
Lawrence E. Goldberger, Del Mar, CA
Nancy J. Goldenberg, Gladwyne, PA
Harold S. Goldman, New York, NY
Antoinette S. Gomes, Los Angeles, CA
Allen Goodman, New York, NY
Neal Goodman, Englewood, CO
Edward V. Grayson, Hollywood, FL
James L. Greve, Miami Shores, FL
Diana F. Guthaner, Stanford, CA
Agnes Marie Guthrie, Houston, TX
Peter F. Hahn, Boston, MA
Theodore Hall, Marina Del Rey, CA
Jack O. Haller, Teaneck, NJ
Gregory L. Hanson, Omaha, NE
Steven D. Harlan, Hickory, NC
Paul S. Harper, Mountain Brook, AL
Irvin F. Hawkins, Jr., Gainesville, FL
William T. Hawkins, Gainesville, FL
Richard G. Hayes, Birmingham, MI
Clyde A. Helms, San Francisco, CA
William R. Hendee, Chicago, IL
Daniel A. Henry, Midlothian, VA
Milton J. Herba, Westmount, Que., Canada
Robert Herfkens, Durham, NC
Hans Herlinger, Philadelphia, PA
Michael M. Herskowitz, Teaneck, NJ
C. Thomas Hill, Jr., Clovis, NM
Paul B. Hoffer, New Haven, CT
Brian A. Holtan, Rock Springs, WY
Daniel F. Housholder, Wichita, KS
Kuei-Tang G. Hsiang, Miami, FL
Karl F. Hubner, Knoxville, TN
Steven T. Hunt, Salt Lake City, UT
Robert D. Hunter, Englewood, CO
William T. Huskison, Fort Smith, AR
Frank L. Hussey, Jr., Park Ridge, IL
Gerald A. L. Irwin, East Meadow, NY
Robert J. Isler, Falmouth, ME
Richard B. Jaffe, Salt Lake City, UT
Syed Z. H. Jafri, Birmingham, MI
Paul F. Jaques, Chapel Hill, NC
Bruce R. Javors, New York, NY
Bruce F. Jeffery, Hanover, NH
Brooke Jeffrey, San Francisco, CA
Maxine Jochelson, Boston, MA
Gordon C. Johnson, Silver Spring, MD
Mary Ann Johnson, Edmonton, Alta., Canada
Daniel M. Jones, Exeter, CA
Gary J. Jones, Salem, OR
R. Gilbert Jost, St. Louis, MO
George W. Kabalka, Knoxville, TN
Saadoon Kadir, Baltimore, MD
A. Robert Kagan, Los Angeles, CA

Joseph D. Kalowsky, Conyngham, PA
Krishna Kandarpa, Boston, MA
Gregory B. Kapala, Bloomington, IL
David Karasick, Philadelphia, PA
Sheldon R. Karasick, Penn Valley, PA
Nolan Karstaedt, Winston-Salem, NC
Chandra S. Katrgadda, Corpus Christi, TX
Michael E. Katz, Detroit, MI
Richard W. Katzberg, Rochester, NY
Stephen L. Kaufman, Baltimore, MD
Chester Kay, Pittsburgh, PA
Kenneth M. Kays, Moberly, MO
Marc S. Keller, New Haven, CT
Richard H. Keller, Salt Lake City, UT
Charles R. Kersh, Charlottesville, VA
Reiley Kidd, Seattle, WA
Henri L. G. Kieffer, Asheville, NC
Gregery D. Kienzle, Des Moines, IA
Charles W. Kieser, Bloomington, IL
Peter T. Kirchner, Iowa City, IA
Alan D. Kirsh, Macon, GA
David L. Klein, San Francisco, CA
Richard M. Klein, Kettering, OH
John B. Kneeland, Milwaukee, WI
David R. Knopf, Savannah, GA
E. Ute Knowlton, Kaysville, UT
Eduard V. Kotlyarov, Kensington, MD
Dan Kramer, Fairfax, VA
Frederick L. Kramer, Media, PA
Henry J. Krebs III, Palm Beach, FL
Herbert Y. Kressel, Philadelphia, PA
Adrian G. Krudy, Mayfield Heights, OH
Madan V. Kulkarni, Houston, TX
Gerald J. Kurlander, Indianapolis, IN
David C. Kushner, Boston, MA
Ian M. Lande, Washington, DC
David D. Lawrence, Jr., Houston, TX
Edward A. Lebowitz, Saratoga, CA
Robert L. Lebowitz, Boston, MA
Chung Min Lee, Woodbury, MN
S. Christopher Lee, Columbus, OH
Johnsey L. Leef, Jr., Charleston, WV
Roger N. Leekam, Toronto, Ont., Canada
James L. Lehr, Chicago, IL
A. Jill Leibman, Atlanta, GA
Andrew J. LeRoy, Rochester, MN
David B. Lewall, Edmonton, Alta., Canada
David K. Li, Vancouver, B.C., Canada
Timothy A. Lind, Tulsa, OK
Martin J. Lipton, San Francisco, CA
Joseph P. LiPuma, Cleveland Heights, OH
William W. M. Lo, Los Angeles, CA
Wende Logan, Rochester, NY
Juan F. Lois, Los Angeles, CA
Patricia A. Lowry, Houston, TX
Herman W. Lubetsky, New York, NY
Patrick R. Luers, Sandy, UT
Caroline J. Lundell, Los Angeles, CA
Byron C. Machen, Mobile, AL
Kenneth W. Mackie, Kingston, Ont., Canada
John T. Mail, Indianapolis, IN
M. Nabil F. Maklad, Houston, TX
Daniel Maklansky, New York, NY
Michael L. Manco-Johnson, Denver, CO
Thomas L. March, Winter Park, FL
William R. Martin, McAllen, TX
Salutario Martinez, Durham, NC
Thomas J. Masaryk, Cleveland, OH
Alan H. Maurer, Philadelphia, PA
Gerald R. May, Seattle, WA
Kathleen A. McCarroll, Bloomfield Hills, MI
Gordon K. McLean, Philadelphia, PA
Kerrianne K. McMurdo, Honolulu, HI
H. Erik Meema, Toronto, Ont., Canada
Theodore L. Megremis, Bloomington, IN
Raymond A. Mencini, Aurora, CO
Ellen B. Mendelson, Pittsburgh, PA
Leslie Menuck, Escondido, CA
Clifford J. Meservy, Memphis, TN
Reuben S. Mezrich, New Brunswick, NJ
Duane Mezwa, Rochester Hills, MI
Cynthia L. Miller, Philadelphia, PA
Franklin J. Miller, Salt Lake City, UT
Rudolph M. Miller III, Dallas, TX
Rogelio Moncada, Maywood, IL
Barbara Monsees, St. Louis, MO
Paul Montgomery, Snyder, NY
Patrick T. Moore, Denver, CO
William E. Moore, Rochester, NY
James M. Moorefield, Sacramento, CA
Richard P. Moser, Washington, DC
Frank M. Mroz, Bangor, ME
James M. Mylrea, Dubuque, IA
Thomas P. Naidich, Chicago, IL
Laurence Needleman, Philadelphia, PA
E. Harold Nelson, Augusta, GA
James A. Nelson, Salt Lake City, UT
Fredrick L. Netherton, Windsor, Ont., Canada
John D. Newell II, Albuquerque, NM
Alex Norman, New York, NY
Elizabeth W. O'Connell, Brooklyn, NY
Michael O'Donovan, Montreal, Que., Canada
Linda K. Olson, San Diego, CA
Michael R. Paling, Charlottesville, VA
Julio C. Palmaz, San Antonio, TX
Timothy W. Parker, Albuquerque, NM
Steven R. Parmett, Brookline, MA
William Pavlicek, Cleveland, OH
Wallace Peck, San Francisco, CA
Patrick J. Perkins, Orinda, CA
James C. Peters, Albany, NY
Robert G. Peyster, Philadelphia, PA
Stephen W. Phillips, Columbia, MO
Daniel D. Picus, St. Louis, MO
Rita J. Pink, Birmingham, MI
Ronald M. Pomerantz, Potomac, MD
David H. Porter, Newton, MA
Rodney V. Pozderac, Ann Arbor, MI
Myron A. Pozniak, Madison, WI
Dolores H. Pretorius, Del Mar, CA
Leland A. Prewitt, Jr., Minneapolis, MN
Richard P. Puckett, Bloomington, IL
E. Thomas Pulaski, Silver Spring, MD
Neil H. Puller, Highland Park, IL
David A. Raetz, Denver, CO
Mahvash Rafii, New York, NY
Jack B. Rampton, Salt Lake City, UT
Michael I. Rauchway, St. Petersburg, FL
Helen C. Redman, Dallas, TX
Kenneth B. Reynard, Englewood, CO
Carlos J. Reynes, Maywood, IL
Melissa J. Riedy, Charlottesville, VA
Usha S. Rishi, Pittsburgh, PA
Barry Robbins, San Jose, CA
John L. Roberts, Birmingham, MI
Ralph G. Robinson, Kansas City, KS
Spencer L. Robnik, Willmar, MN
John O. F. Roehm, Jr., Houston, TX
Bonna Rogers-Neufeld, Fresno, CA
F. David Rollo, Louisville, KY
Steven C. Rose, Durham, NC
Robert J. Rosen, New York, NY
Daniel Rosenthal, Boston, MA
Lawrence S. Ross, Avon Park, FL
Myer Roszler, Oak Park, MI
Susan G. P. Roux, Mendota Heights, MN
Alan Rowberg, Seattle, WA
Victor A. Rowley, Vancouver, B.C., Canada
Val M. Runge, Boston, MA
Edward Russell, Miami, FL
Margaret J. Sabine, Burlington, Ont., Canada
Richard Sacknoff, Lexington, MA
Vijay K. Sadhu, Columbia, MO
Mohsin Saeed, Durham, NC
Sanjay Saini, Boston, MA
Seppo J. Saksanen, Tulsa, OK
Shia Salem, Burlington, Ont., Canada
Steven K. Sargent, Hanover, NH
Yutaka Sato, Iowa City, IA
Eric Sauerbrei, Kingston, Ont., Canada
Kathleen A. Scanlan, Madison, WI
Dennis A. Schmidt, St. Louis, MO
Stephanie G. Schoenberger, New Orleans, LA
Salvatore J. A. Sclafani, Port Washington, NY
Arthur J. Segal, Rochester, NY
Mark C. Segel, Southfield, MI
Ratan Shah, Jeannette, PA
A. Hamid Shadinfar, Utica, NY
Sheng C. Shaw, Pittsburgh, PA
Douglas R. Shearer, Providence, RI
Brixey R. Shelton, Memphis, TN
P. C. Shetty, Troy, MI
Hano A. Siegel, San Diego, CA
Michael E. Siegel, Los Angeles, CA
Burton Silbert, Nashville, TN
Gary S. Silverstein, Cherry Hill, NJ
Allan L. Simon, San Diego, CA
Jack Slivka, San Diego, CA
James G. Smirniotopoulos, Washington, DC
Kenneth W. Sniderman, Toronto, Ont., Canada
Douglas M. Solonick, San Antonio, TX
Livia G. Solti-Bohman, Los Angeles, CA
Sat Somers, Burlington, Ont., Canada
Robert A. Songe, Dearborn, MI
Benigno Soto, Birmingham, AL
Renate L. Soulen, Baltimore, MD
David B. Spring, San Francisco, CA
Robert C. Stadalnik, Sacramento, CA
Thomas L. Stahly, Summersville, WV
Robert J. Stanley, Birmingham, AL
Terry L. Stake, Wheeling, WV
Lynne Steinbach, San Francisco, CA
Neil D. Steinmetz, Atlantis, FL
Richard K. Stevens, Hermiston, OR
Giles Stevenson, Ancaster, Ont., Canada
David A. Stringer, Toronto, Ont., Canada
Karen J. Stuck, Northville, MI
John A. Sullivan, Springfield, MO
M. Jill Sullivan, Springfield, IL
Jules H. Sumkin, Pittsburgh, PA
Steven Sussman, Burham, NC
Bennett S. Sweren, Owings Mills, MD
Lee Talner, San Diego, CA
Kenneth Taylor, New Haven, CT
Rita Teele, Boston, MA
Bruce R. Thomas, Roanoke, VA
F. Deaver Thomas, Syracuse, NY
Richard Towbin, Cincinnati, OH
Paul S. Tower, Andover, MA
David A. Turner, Chicago, IL
James A. Usselman, La Jolla, CA
Carolyn W. Van Dyke, Cleveland Heights, OH
Ronald L. Van Heertum, New York, NY
C. Whitley Vick III, Rome, GA
James B. Vogler III, Durham, NC
John P. Walter, Sacramento, CA
Joseph F. Walter, Palo Alto, CA
Victor Waluch, Pasadena, CA
Felix W. Wehrli, Milwaukee, WI
Edward Weinberger, Seattle, WA
Michael A. Weiss, Rockville, MD
Barbara N. Weissman, Boston, MA
Dennis M. Welch, Sandy, UT
Richard L. Wesenberg, Calgary, Alta., Canada
Jack L. Westcott, New Haven, CT
Louis H. Wetzel, Westwood, KS
Lewis Wexler, Stanford, CA
Dana H. Whaley, Latrobe, PA
Edward R. Wheatley, Charleston, WV
Scott D. Wiedenmann, Port Royal, SC
Marion A. Wier, Augusta, GA
Brian R. J. Williamson, Charlottesville, VA
Michael R. Williamson, Little Rock, AR
Gary A. Wilson, Phoenix, AZ
Stephanie Wilson, Toronto, Ont., Canada
Peter F. Winter, Burlington, MA
Jack Wittenberg, Boston, MA
Fred S. Wittenstein, Winchester, MA
Gerald L. Wolf, Pittsburgh, PA
Nancy J. Worthen, Torrance, CA
John B. Wyly, Atlanta, GA
Chune-Woo Yeh, Naperville, IL
David L. Yerzley, Shadow Hills, CA
Isabel C. Yoder, Brookline, MA
Patricia Youngblood, Mundelein, IL
William T. C. Yuh, Iowa City, IA
Charles E. Zacherias, Des Moines, IA
Michael A. Zerbini, Pontiac, MI
Carl J. Zylak, Waterdown, Ont., Canada

ARRS Corresponding Members

Jean-Michel Bigot, Paris, France
Yuji Itai, Tokyo, Japan
Denis F. Matter, Strasbourg, France
Rik L. Prevo, Enschede, The Netherlands
Frans van der Voorde, Utrecht, The Netherlands

Invitation to Membership in the American Roentgen Ray Society

During the American Roentgen Ray Society's (ARRS) 1985 meeting in Boston, society members approved several fundamental changes in the membership application process and created a new category of membership: members-in-training. Also, active members are no longer required to document contributions to radiology by way of teaching or scientific publications.

Active Membership

Candidates for active membership must be graduates of an approved medical school or hold an advanced degree in one of the physical, chemical, or biological sciences. Each must be board certified and active in the practice of radiology or one of its branches in the United States or Canada. Applicants must be endorsed by two members of the ARRS, not necessarily residents of the same community.

Members-in-Training

The new members-in-training membership category is reserved for physicians in a radiology residency or a postresidency program approved by the Radiology Residency Review Committee of the American Council of Graduate Education and for postgraduate students in allied sciences. The status is limited to 5 years, starting with the entrance date into the radiology residency. In the fifth year, members-in-training are eligible for transfer to active membership.

Corresponding Members

Corresponding members shall be physicians and/or scientists residing in foreign countries who are active in the science of radiology or allied sciences and who are in good ethical standing in the respective countries. They shall pay dues, but shall not have the privilege of voting nor of holding elective office. They may be members of special committees.

Dues and Initiation Fees

A new schedule of fees and dues has been established. Initiation fee for active members is $50. There is no initiation fee for members-in-training. Annual dues for active and corresponding members are $125, payable on July 1 of each year. The dues payment includes a 1-year subscription to the *American Journal of Roentgenology* (*AJR*) and waiver of the annual meeting registration fee. Dues for members-in-training are $25 and include a year's subscription to the *AJR* and waiver of meeting fees. *AJR* subscription rates for domestic nonmembers will be $90 for 1987. The resident subscription rate will remain $25 for residents who do not elect to become members-in-training. Nonmember residents will have a $25 meeting registration fee.

A membership application form is in this issue of the journal. Applications for active membership should be received by February 1 for action during the annual meeting in May. Members-in-training will be eligible for membership upon receipt and processing of the completed application form.

Initiation fees and dues should not accompany the application but are payable after election upon notice by the treasurer.

The American Roentgen Ray Society continues to be a vital force in providing an educational forum for the radiologic community. As it embarks on a program of a broader base of membership, we cordially welcome all those who are eligible. Thus, I urge you to complete the application and forward it to Paul Fullagar, Administrative Director, ARRS, 1891 Preston White Dr., Reston, VA 22091

Glen W. Hartman
Secretary

American Roentgen Ray Society Membership Application

Date _____ Category (check one) ☐ Active ☐ Corresponding ☐ In-Training

Name (in full) _____ Age _____

Address & zip code _____ Date of Birth _____

_____ Birthplace _____

Education — Institution — Years — Degree/Type

Undergraduate: _____

_____

Graduate (medical school, graduate school, etc.):

_____

_____

Postgraduate (internship, residency, fellowship, etc.):

_____

_____

_____

Licensed to practice _____ (type) in _____ (state, province, etc.)

Active and corresponding membership applicants, complete this section. In-training applicants, turn to reverse side.

Practice limited to radiology or one of its branches for _____ years, since (date) _____

Present appointments: Academic _____

_____

Hospitals _____

_____

Membership in scientific societies _____

_____

Offices or committee memberships in scientific societies _____

_____

Government service (military, civilian) _____

Credentials

I hereby certify that I was issued a certificate of qualification in _____

by the _____ (an American Medical Specialty Board or the Royal College of Canada)

continued overleaf

Other credentials _____

Signature _____

We, active members in good standing of the American Roentgen Ray Society and personally acquainted with the applicant, do recommend him/her for Active Membership in the society. **Two references are required.**

Name (print/type) _____ _____

Address _____ _____

_____ _____

Signature _____ _____

In-training applicants must complete this section

Credentials

I certify that I am serving as a resident/fellow in _____

at _____ Date program begins (began) is _____
(institution)

_____. It ends _____. I understand the in-training membership is limited to 5 years and in my 5th year I may transfer to active membership.

Signed _____

Program director or department chairman (name and address) _____

_____

Training director's certification.

I certify the applicant is a trainee at the institution named and qualifies for enrollment as a member-in-training of the American Roentgen Ray Society. Name (print) _____ Signature _____

Address _____

General Information

Candidates for Active Membership

1. An active member must be a graduate of an approved medical school or hold an advanced degree in one of the physical, chemical, or biological sciences and be certified by the American Board of Radiology, the Royal College of Physicians of Canada, or document training and credentials that are adequate to qualify for membership. Active members shall actively practice radiology or one of its branches in the United States or Canada. Such members are eligible to participate in all activities of the society, including membership on committees, and have full voting privileges.
2. Application must be on an official form, signed by the applicant and at least two active members of the American Roentgen Ray Society, in good standing, who endorse the applicant.
3. Initiation fee is $50.
4. Annual dues are $125, payable on July 1 of each year. Of this amount, $50 is for a 1-year subscription to the *American Journal of Roentgenology*, beginning with the July issue for the year following election to membership.
5. Application must be received by February 1 for action during the 1988 meeting.

Candidates for In-Training Membership

1. In-training members must be serving in a radiology residency or a postresidency fellowship program approved by the Radiology Residency Review Committee of the American Council of Graduate Medical Education or be a postgraduate student in an allied science. Training status must be verified by the program director. In-training members have special consideration in fees and subscription rates to the society journal. Such members cannot hold society offices or vote.
2. Application must be on an official form and signed by the applicant and by the applicant's training or residency program director.
3. In-training status is limited to 5 years starting with the entrance date into the radiology residency. In the fifth year, each in-training member will receive an application for transfer to active membership from the society secretary. Those who do not apply for transfer to active membership shall be dropped from membership at the end of the fifth year.
4. There is no initiation fee. Annual dues are $25. Membership includes a subscription to the *American Journal of Roentgenology* and admission to the annual meeting without registration fees.
5. Membership applications will be acted on when received.

All Applicants

1. Do not remit initiation fee or dues until requested by the treasurer.
2. Send completed forms to: Paul Fullagar
   Administrative Director
   American Roentgen Ray Society
   1891 Preston White Dr.
   Reston, VA 22091

American Roentgen Ray Society:
Officers, Committees, and Meeting Information

Officers

President: Raymond A. Gagliardi
President-elect: Lee F. Rogers
1st Vice-president: Gerald D. Dodd
2nd Vice-president: Rosalind H. Troupin
Secretary: Glen W. Hartman
Treasurer: Ronald G. Evens

Executive Council: E. Gedgaudas, J. F. Wiot, L. F. Rogers, R. A. Gagliardi, R. G. Evens, R. N. Berk, F. L. Angell, J. E. Madewell, M. P. Capp, G. W. Hartman, B. G. Brogdon, R. H. Troupin, G. R. Leopold, G. D. Dodd, A. K. Poznanski, A. E. James, Jr., J. T. Ferrucci, Jr., T. C. Beneventano, E. J. Ferris, J. A. Kirkpatrick, Jr., chairman

Committees 1987–1988

Editorial Policy: S. S. Sagel, W. J. Casarella, J. T. Ferrucci, Jr., N. C. Whitley, S. Hilton, J. M. Taveras, R. N. Berk, M. P. Capp, chairman

Education and Research: C. E. Putman, A. R. Margulis, B. J. Hillman, R. A. McLeod, J. T. Ferrucci, Jr., ex officio, B. G. Brogdon, chairman

Finance and Budget: B. P. Wood, L. R. James, J. A. Kirkpatrick, Jr., A. E. James, Jr., F. L. Angell, chairman

Nominating: W. J. Casarella, H. C. Carlson, A. E. James, Jr., chairman

Publications: W. J. Casarella, S. S. Sagel, N. C. Whitley, C. A. Rohrmann, Jr., M. P. Capp, chairman

Membership: E. J. Ferris, G. R. Leopold, A. K. Poznanski, A. E. James, Jr., chairman

Representatives to Other Organizations

American Board of Radiology: E. C. Klatte, L. F. Rogers, T. C. Beneventano

American College of Radiology: L. F. Rogers, G. A. Kling, R. A. Gagliardi, J. M. Dennis, E. J. Ferris, J. E. Madewell

American Medical Association House of Delegates: S. F. Ochsner, K. L. Krabbenhoft, alternate

American National Standards Institute: M. Haskin

National Council on Radiation Protection and Measurements: E. L. Saenger, H. L. Friedell

Meeting Arrangements

Annual Meetings: May 8–13, 1988, Hilton, San Francisco; May 7–13, 1989, Hilton, New Orleans; May 13–18, 1990, Sheraton Washington, Washington, DC

Annual Meeting Committee: H. C. Carlson, G. P. Janetos, G. D. Dodd, T. C. Beneventano, chairman (Montefiore Hospital, Bronx, NY 10467; (212) 920-4200)

Instruction Courses: R. A. McLeod, associate chairman, J. T. Ferrucci, Jr., chairman

Program: R. A. Gagliardi, G. W. Hartman, J. A. Kirkpatrick, Jr., A. E. James, Jr., M. P. Capp, J. E. Madewell, B. G. Brogdon, J. T. Ferrucci, Jr., G. A. Kling, S. A. Feig, G. P. Janetos, L. F. Rogers, chairman

Scientific Exhibits: K. H. Vydareny, A. V. Proto, S. M. Goldman, J. E. Madewell, chairman

ARRS Membership

Applications: An application form is printed in this issue of the Journal. For consideration at the 1988 ARRS meeting, send completed forms before February 1, 1988, to Paul Fullagar, administrative director, American Roentgen Ray Society, 1891 Preston White Dr., Reston, VA 22091. Active members are graduates of an approved medical school or hold an advanced degree in an allied science. They must practice radiology or work in an associated science in the United States or Canada and be certified by the American Board of Radiology or the Royal College of Physicians of Canada or otherwise adequately document training and credentials. Corresponding members are foreign radiologists or scientists who are active in radiology or an allied science. Members-in-training are residents or fellows in radiology or postgraduate students in an allied science.

Business Information

Business Office: Paul Fullagar, administrative director, American Roentgen Ray Society, 1891 Preston White Dr., Reston, VA 22091; (703) 648-8900

American Roentgen Ray Society 88th Annual Meeting May 8–13, 1988, San Francisco, CA San Francisco Hilton Hotel

Registration and Hotel Reservations

Forms for advance registration and hotel reservations will be in the February and March 1988 issues of the *AJR*.

Scientific Program

Abstracts of papers to be considered for the program must reach the president-elect, Lee F. Rogers, by October 1, 1987. Forms on which to submit abstracts are in this issue of the *AJR*. Please photocopy if additional copies are needed. The ARRS Program Committee will select papers in October and notify the authors by November 1. The *AJR* has first rights to all papers accepted for presentation at the ARRS meeting. Send abstract to:

Lee F. Rogers, M.D.
Dept. of Radiology
Olson Pavillion, Rm. 3426
Northwestern University Medical School
710 N. Fairbanks
Telephone (312) 908-5103 Chicago, IL 60611

Refresher Course Program

A summary of the refresher courses will appear in the *AJR* in February along with advance registration forms. Early registration is an advantage in assuring preferred courses in this popular program. J. T. Ferrucci, Jr., is program director.

Scientific Exhibits

Proposals for scientific exhibits must reach the Chairman of Exhibits by October 1. Forms, which may be photocopied, are in this issue of the *AJR*. Send completed form to:

John E. Madewell, M.D.
Dept. of Radiology
Baylor College of Medicine
One Baylor Plaza
Telephone (713) 799-6362 Houston, TX 77030

Local Program

A program of sightseeing, shopping, and entertainment will be developed by George Janetos, the Local Arrangements Chairman. Information and advance registration forms will be in the February issue of the *AJR*.

Residents' Award Papers

The society offers several cash awards for the best scientific papers prepared by residents in radiology. The President's Award has a $1000 prize. There are two Executive Council awards of $500 each. All are presented at the annual meeting. Papers should be submitted by January 31, 1988, for consideration in this competition. Send entries to:

B. G. Brogdon, M.D.
Dept. of Radiology
University of South Alabama Medical Center
2451 Fillingim St.
Mobile, AL 36617

Associated Society Meetings

Society for Pediatric Radiology

The Society for Pediatric Radiology will hold its 31st annual meeting April 27–May 1, 1988, at the Hotel Del Coronado, Coronado, CA (San Diego, CA). The SPR 1989 annual meeting will be April 5–9, 1989, at The Four Seasons Hotel, San Antonio, TX. For details, contact Donald R. Kirks, M.D., Secretary, Society for Pediatric Radiology, c/o Dept. of Radiology, Childrens Hospital Medical Center, Elland and Bethesda Aves., Cincinnati, OH 45229-2899, (513) 559-8058.

Deadlines

Abstracts of papers: October 1, 1987
Scientific exhibit proposals: October 1, 1987
Residents' Award papers: January 31, 1988

Call for Papers

American Roentgen Ray Society 1988 Annual Meeting: May 8–13, 1988, San Francisco, CA

FOR COMMITTEE USE

Received _____ No. _____
Subject _____ Score _____
Rejected _____ Accepted _____
Assigned: Day _____ Session _____
Time _____ No. _____

Title of Paper:

Names of Authors (Last, First, Middle):
(Use asterisk to indicate who will present paper.)

Degree (one only) | Member ARRS? Yes | No

_____

_____

_____

Professional Address of Corresponding Author: _____

_____

City | State | Zip Code | Telephone

Type Abstract in This Space Single Spaced:
(Instructions are on reverse.)

Has this been presented elsewhere? _____ yes _____ no. If yes, please describe on reverse.

Projection Requirements: _____ 35 mm (2 × 2), single or double (circle which); _____ 16 mm silent movie. (Note: video tapes must be converted to 16-mm films.)

(This Form May Be Photocopied)

Instructions for Scientific Abstracts

Proposals are judged by topic and content. New information is preferred, but careful reviews of subjects important to the practice of radiology are also acceptable. The content is treated as confidential information. If the material has been presented elsewhere, notice to that effect is required.

The abstract should contain the four essentials of a scientific communication. It should describe the purposes of the study, the material and methods used, the principal observations, and their significance to radiologic practice. Brevity is desired but not at the expense of information. Factual data are essential. The abstract should be a succinct summary of work done rather than a promissory note. Acceptance for publication is encouraged by well-organized, factual abstracts. The abstract will remain confidential until the program is distributed at the meeting.

PLEASE USE TYPEWRITER. Supplemental information may be attached. Photocopies of the abstract will be distributed to the Program Committee for evaluation. Keep a copy for yourself.

Manuscripts presented on the scientific program become the property of the Society and will be considered for publication in the *American Journal of Roentgenology*. If publication is not offered by the Journal, publication rights return to the author.

Deadline for submission of abstract is October 1, 1987

Telephone (312) 908-5103

Mail abstract to: Lee F. Rogers, M.D.
Dept. of Radiology
Olson Pavillion, Room 3426
Northwestern University Medical School
710 N. Fairbanks
Chicago, IL 60611

Call for Scientific Exhibits

American Roentgen Ray Society
1988 Annual Meeting:
May 8–13, 1988, San Francisco, CA

FOR COMMITTEE USE ONLY

Date Received _____ Application No. _____
Subject _____ Score _____
Rejected _____ Accepted _____
Assigned _____ Space No. _____

Principal Exhibitor's Professional Mailing Address:

Name: _____ Institution: _____

Department: _____ Street Address: _____ City: _____

State: _____ Zip Code: _____ Telephone: office ( ) _____ home ( ) _____

Are you a member of ARRS? (Please circle one.) yes or no

Names of Exhibitors:
(List principal exhibitor first and telephone number of each person.)

Last	First	Middle	Telephone	Degree (one only)	Member ARRS? Yes	No

Title of Exhibit:

Type Abstract in This Space Single Spaced:
(Instructions are on reverse.)

Instructions for Abstract

A brief resume of the exhibit is requested. State purpose, principal information, and conclusions. Promissory statements are not acceptable. Type single-spaced in the space provided on the reverse side. Brevity is desirable but not at the expense of factual information. The abstract **will appear in the program book as submitted.** Exhibitors will receive detailed instructions for exhibit preparation. Please use typewriter and complete the application form on both sides. Type must be fully legible. List space requirements.

What Sort of Exhibit Is Proposed? (Check one and complete all appropriate places.)

_____**Free Standing.** This is a self-contained display created in total by the exhibitor and may be a fold-open unit, a unit shipped in cases and assembled on site, or a table top unit. Linear feet required: _____

_____**Poster Board (Backboard Panels).** Backboard panels are 4 × 6 or 4 × 8 feet. Number of panels required: _____ 4 × 6 or _____ 4 × 8. If two panels are needed, there will be a ¼-in frame separating the panels, thus requiring a separation in the presentation.

_____**Viewbox.** Mounted materials (radiographs and other transparencies) for display on the society's illuminators. Each illuminator is 39.5 × 59.5 inches. Number of illuminators required: _____ . Slides should be nonglass mounted.

_____**Audiovisual.**

Please Indicate Most Appropriate Category for Your Exhibit.

Diagnostic Radiology:
_____Bone _____ Cardiovascular System _____ Chest _____ Pediatric Radiology
_____Gastrointestinal Tract _____ Genitourinary Tract _____ Neuroradiology

Other:
_____Medical Physics _____ Nuclear Medicine _____ Radiation Oncology _____ Radiobiology
_____Ultrasound

Has the exhibit been shown in whole or part at any previous meeting? _____ (Previous display does not preclude acceptance.)

Where? _____ When? _____

Nature of meeting or name of society _____

_____
Signature of Principal Exhibitor

Applications must be received no later than October 1, 1987.
Mail original and (*five copies*) to: John E. Madewell, M.D.
Department of Radiology
Baylor College of Medicine
One Baylor Plaza
Houston, TX 77030

Telephone (713) 799-6362

Resident Education

Instruction in Image Processing for Residents in Diagnostic Radiology

H. K. Huang,[1] Lawrence W. Bassett, Nicholas J. Mankovich, Paul Cho, Hooshang Kangarloo, and Leanne Seeger

Computers are increasingly important in the practice of radiology, and image processing has been an integral part of every new imaging technique introduced in the past 10 years. Yet, in traditional training in diagnostic radiology, residents do not receive instruction in this changing technology. Therefore, in 1983 the Curriculum Committee of the Department of Radiological Sciences at UCLA School of Medicine asked us to develop a 2-week rotation in image processing for residents in diagnostic radiology. The factors to be considered included the clinical and training responsibilities of the resident, scheduling of the rotation, and availability of imaging equipment and instructors. After 1 year of preparation, the 2-week rotation was approved formally and implemented by the department. Since then, 15 residents have participated in this 2-week course.

Background

In anticipation of the transition to a digital radiology department, a dedicated image processing laboratory was established at UCLA in 1982 [1]. The laboratory has a threefold purpose: (1) to suggest research agenda relating to diagnostic imaging and its associated technology, (2) to accumulate and interpret imaging-related information, and (3) to participate in the training of radiology residents, graduate students, and postdoctoral scholars.

The original funding and space allocation of the image processing laboratory consisted of a $200,000 endowment and 1000 square feet of space. With support from federal agencies and private industry, the value of the laboratory equipment has increased to about $1.2 million. Satellite laboratories for image processing also have been established in diagnostic sections (e.g., pediatric radiology). In 1985, the Medical Imaging Division was recognized formally. This division offers Ph.D. training in medical imaging under the Radiological Sciences Graduate Program and also accepts medical students for elective studies and postdoctoral fellows for 1–2 years of training in medical imaging.

Course Description

Training Facilities and Personnel

Image processing facilities and equipment used for this training include two VAX-11/750 computers; two Gould IP8500 image processors; two laser film scanners; one laser film printer [2]; a digital optical disk library with two disk drives [3]; a PIXAR image computer [4]; a picture archiving and communication system (PACS) with 512-, 1024-, and 2048-line display stations; and a computed radiography (CR) system [5]. The division designates approximately 10 staff members to supervise radiology residents during these 2 weeks of training. These include three faculty members, three postdoctoral scholars, visiting research scientists and engineers, and senior graduate students who are Ph. D. candidates in medical imaging.

Received February 24, 1987; accepted after revision March 31, 1987.
[1]All authors: Department of Radiological Sciences, University of California, Los Angeles, Los Angeles, CA 90024. Address reprint requests to H. K. Huang.

AJR **149:435–437, August 1987** 0361–803X/87/1492–0435 © American Roentgen Ray Society

Prerequisites and Schedule

The prerequisites for this course are 3 months experience in basic radiologic physics and knowledge of the terminology of computers and image processing. The residents fulfill these basic requirements during classroom lectures in their first 3 months of residency. The majority of the residents start this rotation in their second year. One or two residents rotate through at any one time, so the Medical Imaging Division devotes about 10 weeks each year to this rotation.

Course Contents

The training includes tutorial lectures, hands-on experience with the hardware and software of image processing, and projects in image processing. A training manual [6] (available upon request from the authors) is provided for each participant.

Each day of the course begins with a 30-min lecture. Topics include architecture of an image processor; representations of a radiologic image in the spatial and frequency domains; measurement of the quality of digital images; applications of Fourier transformation; methods of picture reconstruction; terminology used in CT, MR imaging, and CR; and image filtering. These lectures, which emphasize an intuitive approach and try to avoid mathematical derivations whenever possible, provide the resident with an understanding of the foundations of image processing in radiology.

An overview of laboratory procedures is given in the first half of the first week; both show-and-tell and hands-on experiences are included. The following topics are covered in this overview: the VAX-11/750 computer and peripherals, concepts of computer and image memory, magnetic disk drive and tape drive, Gould IP8500 image processor, video digitizer, laser film digitizer, laser film printer, image display station, optical disk storage, and image communication systems. In the overview of software, the resident learns some basic commands in the VMS operating system for the VAX-11/750, the structure of computer files, and the operating system (software) for the IP8500 image processor. The completion of this introduction provides the resident with the basic terminology used in image processing and a knowledge of the basic components in a digital chain of a diagnostic imaging technique.

A set of laboratory exercises, given in the second half of the first week, is designed for in-depth, hands-on experience. The resident actually uses the image processor and image processing commands on radiologic images. Exercises include use of the image memories, digital video processor, video output controller, image processing and measurement functions, and systems for managing image files. Mastery of these exercises provides the resident with a basic knowledge of the image processing skills commonly used in digital subtraction angiography (DSA), CT, MR imaging, and CR.

During the second week, the resident is expected to carry out 15 projects in image processing under staff supervision. In the category of image input and output, the resident learns to do the following: use the magnetic tape, magnetic disk, and optical disk drives; acquire images from the CR system; transfer CT, MR, CR, and DSA images from the acquisition system to optical disk storage via magnetic tapes; digitize an X-ray film from a laser film scanner and a video scanner and display the digitized image on a high-resolution monitor; produce a hard copy of a digital image by using a matrix camera and a laser film printer; and photograph digital images for presentation. For clinical applications, the resident performs real-time image subtraction from radiographs by using either hip arthrograms [7] or neuroangiograms; calculates organ or tumor volumes from multislice CT or MR imaging contour data; reconstructs three-dimensional surfaces from CT or MR images by means of the MOVIE.BYU 3-D surface display package [8]; computes mineral content in bone by using sectional CT scans [9]; and estimates motion of the cardiac wall by means of sonographic or ventriculographic images. To understand image quality, the resident learns to average images to compute the signal to noise ratio of an imaging acquisition system, perform image filtering in the spatial domain (median, averaging, Laplacian) and in the frequency domain (Fourier transformation), and use the programs for analysis of receiver operating characteristics [10]. Finally, the resident learns PACS [11], including concept and method of image acquisition, archiving, communication, and viewing. The resident acquires one clinical case that has images derived by more than one imaging technique, inputs the information into the PACS, and reviews the images at a multiple-image display station.

Discussion

We have outlined the contents and schedule of a 2-week rotation in image processing for radiology residents. At the end of the 2 weeks, each resident is expected to comprehend the material covered in the course. During the last day, the course director and the residents discuss the 2-week experience, and the director evaluates each resident's performance using a standard departmental evaluation form.

To date, 15 residents have taken this rotation. Following are some general remarks from them: (1) The 2-week training is extremely useful and is definitely worthwhile for a basic understanding of image processing and its applications to radiology. The terminology learned through this training provides a better understanding of the clinical imaging equipment. (2) Ninety to 95% of the material that was included in the training is helpful in later clinical experience. (3) The rotation is a bridge between the clinical sciences and the basic sciences. This experience exposes residents to research resources and, in turn, may help them use these resources to generate teaching material, research reports, abstracts, papers, and exhibits.

The only negative comment from residents has been that the image processors and the computer systems employed in the course are not user friendly. This is true; the image processing laboratory is a research facility, and the image processing consoles often differ from those designed for clinical use. We hope this will evoke in the resident a better appreciation of the design of clinical imaging equipment.

We also see the program as positive because it brings

residents and departmental scientists together. During the 2 weeks, the resident often brings up interesting clinical problems, leading to a useful dialogue and, we hope, a long-term understanding of the value of collaboration with basic scientists.

We plan to continue offering this course in our residency training program, and we are considering extending the course to residents from other programs.

ACKNOWLEDGMENT

The authors thank the staff of the Medical Imaging Division who have participated in developing and running this training program and the residents who provided us feedback to improve the course contents.

REFERENCES

1. Huang HK, Mankovich NJ, Wilson GH, Barbaric Z. Development of a dedicated image processing laboratory for the radiology department. *Noninvasive Med Imaging* **1984**;1:227–232
2. Lo S-C, Taira RK, Mankovich NJ, Huang HK, Takeuchi H. Performance characteristics of a laser scanner and laser printer system for radiological imaging. *Comput Radiol* **1986**;10:227–237
3. Mankovich NJ, Cho PS, Taira RK, Wong A, Stewart BK, Huang HK. A general purpose optical disk system with radiological applications. *Proc SPIE. PACS IV for Medical Applications*, **1986**;626:676–684
4. Fishman EK, Magid D, Drebin R, St Ville JA, Brooker, AF Jr, Zerhouni EA. Volumetric image processing for three-dimensional display of hip disorders (abstr). *Radiology* **1986**;161(P):381
5. Sonoda M, Takano M, Miyahara J, Kato H. Computed radiography utilizing scanning laser stimulated luminescence. *Radiology* **1983**;148:833–838
6. *Manual for resident rotation in image processing*. Los Angeles: Medical Imaging Division, Department of Radiological Sciences, UCLA, March **1986**
7. Bassett LW, Loftus A, Mankovich NJ. Computer-processed subtraction arthrograms (abstr). *Radiology* **1985**;157:821
8. Mankovich NJ, Curtis DA, Kugawa T, Beumer J. Comparison of computer-based fabrication of alloplastic cranial implants with conventional techniques. *J Prosthet Dent* **1986;** 55:606–609
9. Cann CE, Genant HK, Kalb FO, Ettinger B. Quantitative computed tomography for prediction of vertebral fracture risk. *Bone* **1985**;6:1–7
10. Swets JA, Pickett RM. *Evaluation of diagnostic systems: methods from signal detection theory*. New York: Academic Press, **1982**
11. Huang HK, Mankovich NJ, Cho PS, et al. PACS at UCLA: a status report. *J Med Imaging Tech* **1986**;4:69–93

Perspective

Women in Academic Radiology

Nancy O. Whitley[1]

In May of 1984, Charles Putman, incoming president of the Association of University Radiologists (AUR), formed an ad hoc committee to determine the status of women in academic departments of radiology. This was done because of the increasing number of women entering radiology and the concomitant interest in the status of women in academic radiology. I was asked to be chairman of a committee composed of Ronald Evens, Joseph Sackett, and Kay Vydareny. The committee prepared a questionnaire that was sent to the chairmen of academic radiology departments. The survey was sent out in 1985, and the paper published in the May issue of *Investigative Radiology* [1] is the culmination of 2 years of gathering and analyzing the data.

We had 1199 responses from 89 of 129 departments of diagnostic radiology in the United States and Canada. This represented 59% of the male faculty members of the responding institutions and 66% of the female faculty members. Analysis of the results showed that women were overrepresented at the levels of instructor and assistant professor (71% vs 40% for their male counterparts) and underrepresented at the levels of associate and full professor (29% vs 60% for their male counterparts). A trend existed toward women staying in rank longer than men. Men had significantly more grant support than women (19% and 12%, respectively). The overall number of publications in *AJR*, *Investigative Radiology*, and *Radiology* was significantly different; the women published an average of 4.5 articles, and the men, 10.8 articles. When the publications were analyzed in terms of specialty journals, foreign medical journals, or prestigious clinical journals, such as *The New England Journal of Medicine* or *JAMA*, the findings were similar. Men had a mean number of 13 articles as first author, whereas women had only 5.8 articles; this also was a statistically significant difference. The number of total publications also was significantly different; the women averaged 14.4 articles, and the men, 35.9 articles. No significant differences were found between the age of completion of residency, board certification, or hours spent in formal teaching. Female professors of radiology had fewer articles than their male counterparts (an average of 39 vs 69.5, respectively).

It has been suggested that the poorer representation in the higher ranks was related to the female faculty members being younger [2]. To evalute the possibility of age-related factors, each woman was matched randomly and compared with a man of the same age. The findings of the study basically were unaffected. More men than women were in the higher ranks, and more men than women had extramural grant support and publications in *AJR*, *Investigative Radiology*, and *Radiology*. With age matching, the difference in the total number of articles published was still statistically significant. The women published an average of 14.4 articles, and the men, 28.3 articles. As research productivity and publications are generally the most significant factors considered in promotion at most medical schools, the findings of fewer publications and fewer grants appear to refute the argument that sex discrimination is the reason for the lack of advancement of women in academic medicine.

The survey did not consider the question of why women lag behind in these respects. It is not logical to assume that women who have competed as successfully in medical school and residency as their male peers suddenly would cease to achieve [3, 4]. One compelling explanation is the fact that

Received March 10, 1987; accepted after revision April 10, 1987.

[1] Department of Diagnostic Radiology, University of Maryland Medical System/Hospital, 22 S. Greene St., Baltimore MD 21201. Address reprint requests to N. O. Whitley.

AJR **149:438–439, August 1987** 0361–803X/87/1492–0438 © American Roentgen Ray Society

only women bear children. In many instances, female radiologists chose to have a child and to assume responsibility for family care. A woman's potential childbearing years are limited and usually coincide with the time when professional advancement for academicians is most rapid. One strategy is for women to delay childbearing until they are in their late 30's, but this delay can involve only a few years. It seems a shame to waste this potential gene pool in the population, but the other choice is to forego having children. This choice is an unacceptable option for most women, although Paula Diamond [5] found that only 6.4% of all married women age 40 to 44 were childless, whereas 15% of all married women physicians age 40 to 44 were childless.

If a female radiologist has children, the question of primary responsibility for family care and management of the household becomes a factor in her career. The classic American view of a well-rounded "successful female professional" is a woman who has a full-time career, runs a perfect household, and raises a model family. This has been termed the *superwoman syndrome*. It presents a goal that is difficult to attempt and even more difficult to achieve. If the phrase "a successful female professional" is dissected, the qualifier "female" distinguishes her from her male counterpart (who is simply known as a successful professional). The qualifier implies that she is different. This implied difference may be in the comparative standard of excellence and/or in the number of handicaps, such as being a mother and running a household while having a career. Most male professionals attempt only a career. Superwomen aside, delegation of most of the household duties is a necessity for women in the full-time practice of radiology, particularly for those in academic radiology. Preparing lectures and professional manuscripts and keeping current with literature are tasks usually performed in the evenings and weekends and not during a routine workday.

Although delegation of major household tasks is possible, a number of female physicians with children want to work only part-time when their children are young and return to full-time work when their children are older. Part-time practice is a compromise made to have time with the young children and yet maintain a career. Academic advancement via the part-time route is routinely slow, but this pace does not indicate less intelligence, less drive, or a lack of commitment to the profession [3, 4]. These women should not feel like, or be treated as, second-class citizens. Incorporation of women who work part-time into an academic department, even in a limited way, makes their eventual return to full-time radiology more likely and easier. Most women still will have 20 years or more left to practice radiology after their children are grown [6]. Statistically, they are likely to practice longer than their male peers [7].

Lack of a mentor for the "professional socialization process" is another reason for the slower pace of professional achievement of some female radiologists. This process is common to all professions and entails learning the values deemed appropriate and techniques (such as research) necessary in that profession. This process ensures that those novices selected usually will be promoted and, with promotion, obtain more rewards and thus more prestigious positions. Those beginners who may (1) be undervalued already and (2) lack a mentor are relegated to slower progress, lower rank, and, most likely, eventual elimination for academia. Even though a man or a woman may be a mentor, this so-called professional "gatekeeping" in the male-dominated profession tends to exclude women automatically.

Because men are the traditional gold standard against which women are measured, I wish that other questions had been incorporated into the survey conducted by the AUR: Are you a parent? If so, how many children do you have, and what are their ages? Who bears primary responsibility for the nurturing and care of the children? Who has the primary responsibility for housekeeping? Do you or did you have a mentor? Detail the amount of service to the institution (number of committee appointments, etc.) that is required or to which you have commitments. Answers to these questions might aid in providing a better definition of the time commitment of male and female academic radiologists.

What can academic radiology do to address these problems? The solution begins with understanding the reasons for the discrepancy in the rate of advancement in academic radiology between men and women. Female radiologists do not want favoritism; they want only to be a part of the team and to fulfill their potential. It has been estimated that in the 1990's, one-third of radiologists will be women [3] and that the number of women entering academic radiology will increase proportionally. All academic departments should make an effort to furnish each junior faculty member, man or woman, with a mentor. If during certain periods of a woman's life, her productivity is less than that of her male counterparts, both her peers and those responsible for promotions in an academic setting should understand and adapt.

REFERENCES

1. Whitley NO, Evens RG, Moody MM, Putman CE, Sackett JF, Vydareny KH. Advancement of women in academic radiology. *Invest Radiol* **1987** (in press)
2. Jolly P. Research activities of women in internal medicine. Presented at Women in Medicine Research Symposium. Chicago, October **1984**
3. Braslow JB, Heins M. Women in medical education. *N Engl J Med* **1983**;304(19):1129–1135
4. Heins M. Women in medicine: two points of view. II. Medicine and motherhood. *JAMA* **1982**;249(2):209–210
5. Diamond P. The private lives of women doctors: second annual survey. *Medica* **1984**; December:40–45
6. Angell M. Women in medicine: beyond prejudice. *N Engl J Med* **1981**;304(19):1161–1162
7. Dimond EG. Women in medicine: two points of view. I. The future of women physicians. *JAMA* **1983**;249(2):207–208

Letters

Xeroradiography in the Evaluation of Below-Knee Prosthetic Devices

In their article in the January 1987 issue of *AJR*, Irwin et al. [1] failed to cite a recent article on this subject by Varnau et al. [2]. I believe that an article on xeroradiography is remiss if it does not address itself to the increased levels of radiation delivered with this technique over the more conventional radiographic techniques, even though the actual dosage might not be of major consequence.

I also take exception to the authors' comment that "the [patellar tendon] bar should lie midway between the tibia tubercle and the inferior aspect of the patella." Often there are anatomic anomalies present, such as patella alta or patella infera, or evidence of previous trauma to the knee that would contradict this interpretation. In modern prosthetic fittings, there is no longer a markedly identified patella bar, but rather a molding of the prosthesis over the inferior patella ligament area creating a total-contact, total-tissue, weight-bearing surface.

The authors also state that the fibula should be transected at least 1 cm proximal to the tibia. This has been the more conventional approach. But this surgical treatment can result in a conical, mature residual limb. Prosthetically, it would be best to have the fibula transected just a few millimeters proximal to the tibia. This provides for a better-shaped residual limb, which ultimately will offer increased medial lateral stability in the prosthesis, resulting in decreased energy expenditure during gait.

All of the illustrations in the article show poor prosthetic fittings. If adequate prosthetic fitting techniques were employed, it would not be necessary to use xeroradiography for these levels of problem solving—for example, the problem of pistoning. Xeroradiography is a costly method of observing piston action of the residual limb when it can be objectively evaluated clinically. The indiscriminate use of this procedure for poor and antiquated prosthetic techniques is not warranted.

Keith E. Vinnecour
Beverly Hills Prosthetics Orthotics, Inc.
Beverly Hills, CA 90211

REFERENCES

1. Irwin GAL, Friedman L, Shapiro D. Prosthetic fit in below-knee amputation: evaluation with xeroradiography. *AJR* **1987;** 148:99–101
2. Varnau D, Vinnecour K, Luth M, Cooney D. The enhancement of prosthetics through xeroradiography. *Orthot Prosthet* **1985;** 39:14–28.

Reply

It is refreshing to know that people other than radiologists took interest in our article. Vinnecour raised several points in his letter that should be addressed. First, it is true that we did not reference his article, and for this we apologize.

Vinnecour also mentions that we failed to discuss the increased levels of radiation delivered with xeroradiography. Frankly, we did not think it was necessary to address this issue in a technical note directed at radiologists. We did, however, make it clear that we were aware of this problem, as evidenced by our use of "the negative xerographic mode to decrease radiation dosage."

Comments regarding the patellar tendon bar are noted. It should be pointed out that our article was written for radiologists who do not see xeroradiographs of prostheses on a regular basis; it was also intended to provide some general guidelines for interpretation and reporting to the amputee team. While the patellar tendon bar may be less prominent in some prosthetic fittings, the prominent patellar tendon bar is still the most common shape. If a patellar tendon bar is seen on the radiograph, then the location should be specified.

Vinnecour's comment on the length of the fibula is also interesting. While a longer fibula gives a better shape early on, patients with a longer fibula experience more pain when the stump matures, both at the distal end of the fibula and at the tibial-fibular joint. Medial-lateral stability is not enhanced, as claimed in the letter, since the fibula will not tolerate distal-lateral pressure. There is also no evidence in the literature that energy expenditure is lower with a longer fibula. We believe that Vinnecour's comments on the energy expenditure issue are purely speculative. Finally, he comments that all of our illustrations demonstrate poor prosthetic fittings. Apparently, the article was not carefully read. We clearly state in the first paragraph of the Method's section: "Those patients who because of faulty prosthetic fit have pain or skin irritations over bony prominences that cannot be resolved by routine modification of the prosthesis are referred for radiographic study." We do not advocate routine xeroradiography for everyone with a prosthetic device. Our recommendations are that only in poorly fitting sockets, where a reason for the problem is not clinically identifiable, are the cost and X-ray exposure justified.

Gerald A. L. Irwin
Lawrence Friedman
Daniel Shapiro
Nassau County Medical Center, SUNY at Stony Brook
East Meadow, NY 11554

Localization Devices for Occult Breast Lesions

In the April issue of *AJR* Parekh and Wolfe [1] described a breast-lesion localization device with "a fenestrated plate with multiple small holes located 3-mm apart and a cassette tunnel . . ." As noted by these authors, we described a very similar device in 1983 [2]. The market for our instrument was negligible and will soon be nonexistent because virtually every dedicated mammographic unit made since that time has a localization apparatus incorporated into the machine. These built-in devices have numerous advantages over free-standing units. The latter require various adaptations to the specific mammographic machine with which they are used and they must provide their own less optimal breast compression (Velcro straps in the unit described by Parekh and Wolfe). Suboptimal compression assumes particular importance with film-screen mammography when locating faint calcifications in large breasts or close to the chest wall.

Current-generation dedicated mammographic units have many advantages over older machines. In addition to built-in localization devices, these advantages include smaller focal spots and improved resolution, grid and magnification capabilities, phototiming, pneumatic compression, and, in many cases, decreased radiation. Any reader who is contemplating replacing their old mammographic unit or acquiring an additional one, should probably not be in the market for a free-standing localization device.

Ferris M. Hall
Ronald P. Goldberg
Beth Israel Hospital and Harvard Medical School
Boston, MA 02215

REFERENCES

1. Parekh NJ, Wolfe JN. Localization device for occult breast lesions: use in 75 patients. *AJR* **1987;**148:699–701
2. Goldberg RP, Hall FM, Simon M. Preoperative localization of nonpalpable breast lesions using a wire marker and perforated mammographic grid. *Radiology* **1983;**146:833–835

Reply

We agree with Hall and Goldberg that the localization grid is included with most of the newer dedicated mammographic units and that many larger institutions such as theirs have devised their own localizer apparatus. There are, however, a large number of institutions that use xeroradiography, which do not necessarily have dedicated units. Although the localizer apparatus we described can be adapted, with some modification, to most mammography units, we believe that it will be particularly useful to the group of radiologists who do not have dedicated units.

In our experience, we have found this device to be simple to use. The degree of compression has been found sufficient for xeroradiography to delineate even faint calcifications located deep near the chest wall. One of the 75 cases in our report included a small carcinoma that presented with fine calcifications near the chest wall where localization attempts using a standard grid with a dedicated unit at another institution had failed because the calcifications could not be identified. Also, we think that the closely placed small holes in the compression plate and our use of a wire hook needle with a detachable hub has been helpful in accurate localization.

Navin J. Parekh
John N. Wolfe
Hutzel Hospital
Detroit, MI 48201

Letters are published at the discretion of the Editor and are subject to editing.

Letters to the Editor must not be more than two *doubled-spaced* typewritten pages. One or two figures may be included. See Author Guidelines for letters, page A5.

Letters concerning a paper published in the *AJR* will be sent to the authors of the paper for a reply to be published in the same issue. Opinions expressed in the Letters to the Editor do not necessarily reflect the opinions of the Editor.

Review of Current Literature

Initials and addresses of corresponding authors are provided in parentheses for each article so that the reader can obtain reprints directly. Abstracts are printed verbatim from each journal.

CLINICAL LITERATURE

The New England Journal of Medicine

Alcohol consumption and breast cancer in the Epidemiologic Follow-up Study of the First National Health and Nutrition Examination Survey. Schatzkin A, Jones DY, Hoover RN, et al. (AS, National Institutes of Health, National Cancer Institute, Blair Bldg., Rm. 6A-01, Bethesda, MD 20892). *N Engl J Med* 316:1169–1173, 1987

We investigated the relation between alcohol consumption and breast cancer in the Epidemiologic Follow-up Study of the first National Health and Nutrition Examination Survey, a cohort study based on a sample of the U.S. population. A total of 7188 women 25 to 74 years of age who were examined during the period 1971 through 1975 were included in the analysis. Information about alcohol consumption was obtained during the base-line interview. The median follow-up period for this cohort was 10 years. One hundred twenty-one cases of breast cancer that developed after the baseline examination were identified through hospital records or death certificates.

The relative-risk estimate for any amount of drinking relative to no drinking was 1.5 (95 percent confidence interval, 1.1 to 2.2). The estimates for three levels of consumption, from the lowest to the highest, were 1.4 (confidence interval, 0.9 to 2.3), 1.5 (0.9 to 2.6), and 1.6 (1.0 to 2.7), in comparison to no drinking at all. These relative-risk estimates were not materially affected by adjustment for known risk factors for breast cancer or for several dietary factors.

The results of this study, consistent with those of two other cohort studies and a number of case-control studies, suggest that moderate alcohol consumption is associated with an elevation in the risk of breast cancer of 50 to 100 percent.

Long-term follow-up after percutaneous transluminal coronary angioplasty: the early Zurich experience. Gruentzig AR, King SB III, Schlumpf M, Siegenthaler W (SBK, Interventional Cardiology, Emory University Hospital, 1364 Clifton Rd. N.E., Atlanta, GA 30322). *N Engl J Med* 316:1127–1132, 1987.

The first 169 patients in whom percutaneous transluminal coronary angioplasty was performed have now been followed for five to eight years. The procedure was technically successful in 133 patients (79 percent). In the follow-up period, nine of the 133 patients died (five of cardiac disease), and actuarial cardiac survival was 96 percent at six years. All patients were symptomatic before angioplasty, but 67 percent of the 133 who had technically successful procedures were asymptomatic at the last follow-up evaluation. Exercise stress testing, positive in 97 percent before angioplasty, was positive at the last follow-up study in only 10 percent of the patients who had technically successful procedures.

Stenosis recurred during the first six months in 30 percent of the patients, and six more recurrences were observed among the 41 patients who had follow-up angiograms at two to seven years. A second angioplasty was required in 27 patients, and coronary bypass surgery was subsequently needed in 19. Actuarial event-free survival (freedom from death, myocardial infarction, and coronary bypass surgery) was 79 percent at six years. Follow-up of patients with multivessel disease showed a higher mortality from cardiac causes and a lower rate of long-term success than occurred among patients with single-vessel disease.

These long-term results indicate that most episodes of restenosis occurred within six months of angioplasty, but some late recurrences were seen. Patients with single vessel disease had a better long-term outcome after angioplasty than those with multivessel disease.

Cancer

Anticancer effects of arterial administration of the anticancer agent SMANCS with lipiodol on metastatic lymph nodes. Ohtsuka N, Konno T, Miyauchi Y, Maeda H (NO, First Dept. of Surgery, Kumamoto University Medical School, Kumamoto 860, Japan). *Cancer* 59:1560–1565, 1987

A new method of arterially administering an oily anticancer agent was successfully established for the selective targeting of metastatic lymph nodes. A high molecular weight anticancer agent, a conjugate of copolymer (styrene maleic acid) to neocarzinostatin (SMANCS) was prepared in our laboratory and dissolved in a lymphographic oily contrast medium, Lipiodol (SMANCS/Lipiodol). SMANCS/Lipiodol was administered intraoperatively to eight patients with colorectal cancer and preoperatively to one patient with gastric cancer with lymph node metastases. In six of the patients with colorectal cancer, the drug was administered via an artery and in the other two patients, the drug was injected into the wall of the colon near the primary cancer. In the patient with gastric cancer, the drug was administered via the left gastric artery. Delivery of the drug to the lymph nodes was examined roentgenologically and the anticancer effect was examined histologically. The results showed that SMANCS/Lipiodol could be delivered to the metastatic lymph node via the artery, but it could not be delivered to the metastatic lesion of the lymph node via the lymphatic route. In the patient with gastric cancer, SMANCS/Lipiodol preoperatively administered via an artery was found to remain selectively in a metastatic lymph node and an anticancer effect was histologically proved in all three of the metastatic lymph nodes.

Reprinted with permission by the American Cancer Society.

Chest

The role of open lung biopsy in patients with the acquired immunodeficiency syndrome. Fitzgerald W, Bevelaqua FA, Garay SM, Aranda CP (FAB, 650 First Ave., New York, NY 10016). *Chest* 91(5):659, May 1987

To assess the role of open lung biopsy in patients with the acquired immunodeficiency syndrome (AIDS), we retrospectively reviewed the cases of 42 patients with AIDS who underwent this procedure for the diagnosis of pulmonary infiltrates. Four patients had no preceding bronchoscopy because the severity of the respiratory failure or abnormalities of coagulation precluded the safe performance of this procedure. Twenty-nine cases had a preceding nondiagnostic bronchoscopic procedure, and nine others underwent open lung biopsy because of progressive deterioration despite treatment for diseases diagnosed bronchoscopically. We found that open lung biopsy was likely to be useful diagnostically when bronchoscopy could not be safely performed or when a preceding bronchoscopic procedure was not diagnostic. Open lung biopsies done on patients whose condition continued to deteriorate despite treatment for disorders established bronchoscopically were not likely to yield information therapeutically useful. In only one of nine such cases was a new treatable diagnosis obtained (Legionella). The others showed either severe pulmonary fibrosis or persistence of the initial disease process diagnosed at the time of bronchoscopy.

Journal of Thoracic Imaging

Retrieval of intravascular foreign bodies. Gerlock AJ Jr, Mirfakhraee M (MM, Dept. of Radiology, LSUMC-Shreveport, PO Box 33932, Shreveport, LA 71130). *J Thorac Imag* 2(2):52–60, 1987

The use of intravascular catheters for diagnostic and therapeutic purposes has resulted in an increased number of foreign body embolizations. The retained foreign body is a potential source of morbidity and mortality. In this communication we describe the different techniques that are used to remove foreign bodies from various locations within the heart or vascular tree. A brief review of the literature concerning the reported complications from retained foreign bodies is made to underline the importance of early percutaneous removal of these fragments.

Circulation

Increased embolic risk in patients with left ventricular thrombi. Stratton JR, Resnick AD (ADR, Cardiovascular Disease Section (111-C), Seattle VA Medical Center, 1660 S. Columbian Way, Seattle WA 98108). *Circulation* 75(5):1004–1011, 1987

Although left ventricular thrombi are associated with an increased embolic risk in the first few weeks after acute myocardial infarction, the long-term risk remains undefined. To ascertain the incidence of strictly defined systemic emboli, we followed 85 patients with echocardiographically documented left ventricular thrombi. At the time of the entry echocardiogram, most patients ($n = 57$) had remote myocardial infarction, while 19 had recent (<1 month) infarction, and nine had idiopathic cardiomyopathy. Because of the difficulty in classifying events as embolic in patients with advanced atherosclerosis, a matched control group of 91 patients without thrombi was also studied. The thrombus and control groups were similar with regard to recent myocardial infarction, remote infarction, anterior infarction, ejection fraction, atrial fibrillation, echocardiographic referral for source of emboli, and warfarin therapy. During a mean follow-up of 22 months after echocardiography, embolic events occurred in 13% (11 of 85) of patients with thrombi compared with 2% (two of 91) of control patients ($p < .01$). The actuarial probability of being embolus free at 2 years after echocardiography was 86% in patients with thrombi compared with 97% in control patients ($p < .01$). All embolic events occurred greater than 1 month after myocardial infarction (range 1 to 96 months). The only clinical or echocardiographic features predictive of embolization were protrusion and mobility of thrombus (both $p < .02$). We conclude that the incidence of embolic events is definitely increased in patients with left ventricular thrombi compared with control subjects during long-term follow-up. The increased embolic risk is not restricted to the immediate postinfarction period, documenting that chronic thrombi continue to embolize. Whether long-term anticoagulation can reduce the embolic rate with an acceptable risk of bleeding remains to be determined.

Gastroenterology

Early invasive cancer in adenomatous colonic polyps ("malignant polyps"). Evaluation of the therapeutic options by decision analysis. Wilcox GM, Beck JR (GMW, Dept. of Gastroenterology, Maine Medical Center, Portland, ME 04102). *Gastroenterology* 92:1159–1168, 1987.

The management alternatives of segmental colonic resection versus follow-up alone for colonic adenomas containing early invasive carcinoma (i.e., polypectomy resection margin free of tumor) were evaluated by decision tree analysis. Using data from the literature, the major variables influencing the decision were as follows: (a) probability of residual disease after polypectomy, (b) operative efficacy (defined as the chance of curing a tumor that would otherwise recur without surgery), and (c) operative mortality. For a hypothetical patient with low operative risk (operative mortality of 0.2%), resection would yield the best outcome in terms of life expectancy as long as the probability of residual disease was >0.5%. Extensive analysis of the impact of changes in assumptions about the parameters characterizing the problem showed this conclusion to be unchanging over wide ranges of operative efficacy and probability of residual disease. However, the decision to do a secondary resection in this situation was still close because surgery was only marginally justifiable on economic grounds. Observation would be preferred in patients with higher operative risk (operative mortality >2%).

Reprinted with permission by the American Gastroenterological Association.

Digestive Diseases and Sciences

Indium-111–labeled autologous leukocyte imaging and fecal excretion. Comparison with conventional methods of assessment of inflammatory bowel disease. Leddin DJ, Paterson WG, DaCosta LR, et al. (LRD, Division of Gastroenterology, Hotel Dieu Hospital, Kingston, Ontario K7L 5G2, Canada). *Dig. Dis Sci* 32(4):377–387, 1987.

This study was designed to evaluate the role of ^{111}In-labeled leukocyte imaging and fecal excretion in the assessment of inflammatory bowel disease. We compared these tests to various indices of disease activity in Crohn's disease, to Truelove's grading in ulcerative colitis, and to endoscopy, x-ray, and pathology in both diseases. Eleven controls, 16 patients with Crohn's disease, 13 with ulcerative colitis, and 3 with other types of acute bowel inflammation were studied (positive controls). Indium scanning was performed at 1, 4, and 24 hr. Fourteen of 16 patients with active Crohn's disease had positive scans but in only five was localization accurate. One patient had inactive ulcerative colitis, and the scan was negative. Of 12 patients with active ulcerative colitis, 10 had positive scans but disease localization was accurate in only four. Disease extent was correctly defined in 1 of the 3 Positive Controls. There was no significant difference in the accuracy of scanning at 1, 4, or 24 hr. ^{111}In fecal excretion was significantly higher in patients with inflammatory bowel disease than in controls, and there was correlation between ^{111}In fecal excretion and most of the indices of disease activity in Crohn's disease. In ulcerative colitis, ^{111}In fecal excretion did not correlate with Truelove's grading but reflected colonoscopic assessment of severity. In conclusion, ^{111}In-labeled leukocyte scan-

ning lacks sensitivity with respect to disease extent, but fecal excretion of ^{111}In correlates well with disease severity as determined by other methods.

Gastrointestinal Endoscopy

Primary panendoscopy. Overholt BF, Hargrove RL, Farris RK, Porter FR (BFO, Weisgarber Medical Center, 1112 Weisgarber Rd., Ste. 201, Knoxville, TN 37909). *Gastrointest Endosc* 33:1–3, 1987

Primary panendoscopy is defined as a limited-consultative, diagnostic, UGI endoscopic examination that provides, in non-critically ill patients with dyspeptic symptoms, an accurate and cost-effective alternative to the standard UGI x-ray examination. The procedure was instituted at St. Mary's Medical Center's hospital in February 1985. During the first 12 months, a total of 321 patients were examined: 212 inpatients and 109 outpatients. In those patients with complete information, primary panendoscopy changed the diagnosis in 67% and the treatment in 52%. As expected, the number of esophagogastroduodenoscopies decreased during this time, but the combined numbers of primary panendoscopies and esophagogastroduodenoscopies exceeded the projected increase of esophagogastroduodenoscopies. Similarly, the number of UGI x-ray examinations fell sharply. With a physician fee of $150.00 and a facility fee of $50.00, theoretical savings of some $117,000.00 to the patients were estimated. The authors conclude that primary panendoscopy provides a cost-effective and beneficial patient service that warrants broad consideration by gastroenterologists as they face the cost constraints being imposed within the health care system of the 1980s.

The Journal of Bone and Joint Surgery

Proximal tibial osteotomy for osteoarthritis with varus deformity. A ten to thirteen-year follow-up study. Hernigou PH, Medevielle D, Debeyre J, Goutallier D (PHH, Dept. of Orthopaedic Surgery, Centre Hospitalo-Universitaire Henri Mondor, 51 Avenue du Maréchal de Lattre de Tassigny, 94010 Creteil, France). *J Bone Joint Surg [AM]* 69(A):332, 1987

The results in ninety-three knees that had been treated by proximal tibial opening-wedge osteotomy for varus deformity and osteoarthritis of the medial compartment were evaluated after a mean length of follow-up of 11.5 years (range, ten to thirteen years). After ten years, only forty-two (45 per cent) of the ninety-three knees had an excellent or good result, and in fifty-one knees there was recurrent pain for which seventeen had another operation. At five years, on the other hand, 90 per cent of the knees had a good result. Deterioration occurred at an average of seven years after the osteotomy and was always associated with recurrence of pain.

Although the results deteriorated with time, time was not the only determinant of the result. Alignment, measured as the hip-knee-ankle angle on radiographs of the whole limb that were made with the patient bearing weight, was also a determinant of long-term results. The best results were obtained in the twenty knees that had a hip-knee-ankle angle of 183 to 186 degrees. In these knees, there was no pain and no progression of the arthrosis in either the medial or the lateral tibiofemoral compartment. Of the five knees that had an angle of more than 186 degrees, all five had progressive degenerative changes in the lateral compartment. In the sixty-eight undercorrected knees (an angle of less than 183 degrees), the results were less satisfactory, and there was a tendency toward recurrence of the varus deformity and progression of the arthritis of the medial compartment. However, when the correction was insufficient the deterioration was slow (average, seven years), and it was not associated with lateral laxity and deterioration of the lateral compartment, which are the changes that characterize the natural course of gonarthrosis as described by Hernborg and Nilsson[19]. Therefore, proximal tibial osteotomy is a very suitable operation for patients who have gonarthrosis of the medial compartment, but a rigidly standardized and precise operative technique is required as well as accurate radiographic measurements of the mechanical axis of the limb, because exact postoperative alignment is the prerequisite for the longest possible period of relief of symptoms after osteotomy.

The Journal of Urology

Reduction of cyst volume for symptomatic management of autosomal dominant polycystic kidney disease. Bennett WM, Elzinga L, Golper TA, Barry JM (WMB, Oregon Health Sciences University, Portland, OR 97201). *J Urol* 137:620, April 1987

A total of 11 patients with refractory pain secondary to autosomal dominant polycystic kidney disease underwent ultrasound guided percutaneous aspiration of cyst fluid on the affected side. Surgical reduction of cyst volume was performed if pain recurred. Dramatic relief of pain was observed after both procedures. The probability of a patient being free of renal pain at 18 months was 33 ± 17 per cent for aspiration and 81 ± 12 per cent for an operation. Individual patients had relief of pain for more than 4 years. There was no deleterious effect on renal function after either aspiration or an operation. Blood pressure improved in the 5 patients with hypertension. There were no complications of percutaneous cyst aspiration. One patient required neurolysis of the drain site after cyst reduction.

Urology

Neoplastic potential in patients with disorders of sexual differentiation. Beheshti M, Hardy BE, Mancer K, McLorie G, Churchill BM (MB, Division of Urology, Dept. of Surgery, The Hospital for Sick Children, Toronto, Ontario, Canada). *Urology* 29(4):404, 1987

The occurrence of tumors was determined in 157 patients with disorders of sexual differentiation at a major pediatric hospital from 1960 to 1980. Gonadoblastoma developed in 2 of the 4 patients with mixed gonadal dysgenesis (MGD) who had not had bilateral gonadectomy; this indicates the need for early gonadectomy in such cases. Gonadal embryonal carcinoma developed in 1 child with Turner's syndrome (1 of 71). Four cases of nephroblastoma occurred, 1 in a child with MGD (1 of 18) and 3 in male pseudohermaphrodites (3 of 35). The nature of the defect linking male pseudohermaphroditism with Wilms tumor remains to be established.

Pediatrics

Pediatric brain injuries: the nature, clinical course, and early outcomes in a defined United States' population. Kraus JF, Fife D, Conroy C (JFK, Division of Epidemiology, School of Public Health, University of California, Los Angeles, CA 90024). *Pediatrics* 79(4):501–507, April 1987

Acute brain injury is the cause of approximately 100,000 pediatric hospital admissions per year in the United States. This report examines the nature of the brain injury, clinical diagnosis, hospital course, and discharge outcome of all pediatric cases in the population of San Diego County, California, for 1981 (N = 709). Brain-injured children were identified from hospital records, death certificates, and coroners' records. Severity of injury was determined using the Abbreviated Injury Scale and the Glasgow Coma Scale. Three percent of brain-injured children died at the accident site; an additional 3% died in the hospital. All in-hospital deaths occurred among the 5% of children with Glasgow Coma Scale scores of 8 or less, and in this group the case fatality rate was 59%. Fractures of the skull, present in 23% of cases, seemed to be associated with excess mortality even after type of lesion was considered. Type of lesion, but not presence or absence of a skull fracture, had some predictive power for disability

among survivors. Concussion was the most frequent diagnosis. Mildly brain-injured children accounted for 93% of all cases and about 90% of all hospital days.

Reproduced with permission by *PEDIATRICS* © 1987.

Journal of Pediatrics

Brain death in children: characteristic common carotid arterial velocity patterns measured with pulsed Doppler ultrasound. Ahmann PA, Carrigan TA, Carlton D, Wyly B, Schwartz JF (TAC, Dept. of Pediatrics, 2040 Ridgewood Dr. N.E., Atlanta, GA 30322). *J Pediatr* 110:723–728, May 1987

The clinical criteria for brain death in children remain controversial. An accepted confirmatory test for brain death is the documented absence of intracranial blood flow, the most common methods being arteriography and radionuclide cerebral angiography. We correlated the common carotid arterial blood velocity patterns measured by pulsed Doppler ultrasound in 32 brain-dead infants and children with results of their clinical examinations and, whenever possible, with radionuclide cerebral angiography. A distinct, characteristic carotid arterial blood velocity waveform indicating absent cerebral blood flow appeared in 19 of the 23 brain-dead patients 4 months of age or older. The velocity patterns of the other four older children were similar, but not identical, to the characteristic waveform. The remaining nine brain-dead patients were infants 4 months of age or younger. These infants had velocity waveforms different from those of healthy infants, but also were totally different from the characteristic brain death pattern of older children. No patient had the characteristic brain death waveform without being clinically brain dead. Measurement of carotid arterial blood velocity with pulsed Doppler ultrasound is a repeatable, noninvasive, portable test useful for confirmation of brain death in children.

RADIOLOGY SUBSPECIALTY JOURNALS

The Journal of Nuclear Medicine

Interpretation and classification of bone scintigraphic findings in stress fractures. Zwas ST, Elkanovitch R, Frank G (STZ, Dept. of Nuclear Medicine, The Chaim Sheba Medical Center, Tel-Hashomer 52621 Israel). *J Nucl Med* 28:452–457, 1987

A new system for classification of stress fractures identified by bone scintigraphy was developed and divided into four grades according to lesion dimension, bone extension, and tracer accumulation. The scintigraphic findings were evaluated for severity of lesions by extent of the visualized bone response, ranging from ill-defined cortical lesions with slightly increased activity (I) to well-defined intramedullary transcortical lesions with intensely increased activity (IV). Bone scintigraphies using [^{99m}Tc]MDP were obtained in 310 military recruits suspected of having stress fractures. In 235 patients, 391 stress fractures were diagnosed. Forty percent of the lesions were asymptomatic. Most of the lesions were in the tibiae (72%), and 87% of the patients had one or two lesions, while 13% had three to five lesions. Eighty-five percent of the lesions were classified as mild and showed early and more complete resolution on follow-up studies after treatment as compared to the severe grades. Furthermore, specific scintigraphic patterns have been introduced for distinguishing inflammatory shin-splints from stress fractures, allowing for their appropriate early treatment. Thus, early recognition of mild stress fracture scintigraphic patterns representing the beginning of pathologic bone response to stress enabled a prompt and effective treatment to prevent progression of lesions, protracted disability, and complications.

The Journal of Ultrasound in Medicine

Total parenteral nutrition (TPN) and gallbladder diseases in neonates. Sonographic assessment. Matos C, Avni EF, Van Gansbeke D, Pardou A, Struyven J (CM, Dept. of Radiology, Hôpital Erasme, route de Lennick 808, B 1070 Brussels, Belgium). *J Ultrasound Med* 6:243–248, 1987

During a 1-year period, a prospective ultrasound (US) study of the biliary tract was performed in 41 neonates receiving total parenteral nutrition (TPN). Gallbladder sludge appeared in 18 neonates (44%) after a mean period of 10 days of TPN. The occurrence of this abnormality seems related to three main factors: prematurity with immaturity of the enterohepatic circulation of bile acids, duration of TPN, and lack of enteral nutrition. In five neonates (12%), an evolution of sludge to "sludge balls" was observed. Two neonates (5%) went on to develop uncomplicated gallstones and a spontaneous resolution occurred in one of them 6 months after the examination. This finding suggests conservative management in such cases. However, since cholecystitis or biliary tract obstruction are classical complications in older children, a US survey of neonates receiving TPN is useful to follow the abnormal gallbladder content, and rapid introduction of enteral feeding is advisable. KEY WORDS: ultrasonography; parenteral nutrition; gallbladder stasis; gallstones.

Reprinted with permission by the American Institute of Ultrasound in Medicine.

Magnetic Resonance Imaging

MRI in staging of endometrial and cervical carcinoma. Fishman Javitt MC, Stein HL, Lovecchio JL (MCFJ, North Shore University Hospital, Manhasset, NY 11030). *Mag Reson Imag* 5:83–92, 1987

MRI of 54 patients with endometrial and cervical carcinoma was performed on a 0.6-T superconducting magnet. In 18 of 24 cases of surgically proved endometrial carcinoma, MRI accurately showed the depth of myometrial invasion. MRI was superior to CT scan for defining the primary site and extent of the tumor in 14 of 24 cases. Of 25 patients with cervical carcinoma studied, MRI was superior to CT scan in 15 of 19 cases with CT correlation for localizing the primary site. MRI showed parametrial extension and invasion of surrounding structures but is probably less reliable than CT scan for detection of adenopathy because of false positive findings from volume averaging with bowel.

News

Annual Wendell G. Scott Lecture

The Mallinckrodt Instute of Radiology, Washington University Medical Center, announces that Dr. Lee F. Rogers, Chairman, Dept. of Radiology, Northwestern University Medical School, Chicago, IL, will deliver the 16th Annual Wendell G. Scott Lecture on Sept. 9, 1987, at the Mallinckrodt Institute of Radiology, Washington University School of Medicine. Dr. Rogers' topic will be "Osteoporosis: The Marketing of Medicine." Information: Ronald G. Evens, M.D., Director, Mallinckrodt Institute of Radiology, 510 S. Kingshighway, St. Louis, MO 63110.

Visiting Fellowship in MR Imaging

The Dept. of Radiology of the University of California, San Diego, Medical Center/AMI Magnetic Resonance Institute is offering a 1- to 4-week visiting fellowship in Magnetic Resonance Imaging. The program includes 2 hr of lectures each day as well as daily interpretation sessions with the faculty. Program director: J. R. Hesselink. Category 1 credit: up to 34 hr. Fee: (1 week) $1000; (additional weeks) $750/week. Information: Vicki Broughton, Dept. of Radiology, University Hospital, 225 Dickinson St., San Diego, CA 92103.

Fellowships in Imaging and Interventional Radiology for Physicians, 1987–1988

The Dept. of Radiology, University of California, San Diego, Medical Center offers a 1- to 8-week program for physicians interested in updating their knowledge in diagnostic sonography—including carotid Doppler, or a combination of sonography-abdominal CT, and/or interventional radiology. Sonography and sonography-abdominal CT are offered weekly; abdominal CT alone is offered as an independent rotation. Interventional radiology is available any week throughout the year as arranged with Dr. Eric vanSonnenberg. Trainees may choose to concentrate on one specialty at a time or two or three together in the same session. Category 1 credit: 40 hr/week attendance. Information: Elizabeth Novak, Ultrasound Division, UCSD Medical Center, 225 Dickinson St., San Diego, CA 92103; (619) 543-6657; or to arrange participation in interventional radiology, call Dr. Eric vanSonnenberg (619) 543-6657

Doppler Echocardiography Seminar

The Center for Medical Ultrasound, Bowman Gray School of Medicine will sponsor the Advanced Echocardiography Seminar, Sept. 10–12, at the Innisbrook Resort Conference Center, Tarpon Springs, FL. This course will focus on Doppler echocardiography with emphasis on recent developments and applications. Correlations with measurements will be presented. Sessions demonstrating cardiac pathology offer the participant physicians and sonographers instruction in obtaining and evaluating Doppler and echocardiography studies. Category 1 credit: 17 hr. Fee: $375. Information: Registrar, Ultrasound Center, Bowman Gray School of Medicine, 300 S. Hawthorne Rd. Winston-Salem, NC 27103; (919) 748-4505.

The Asian-Oceanian Congress of Radiology

The 5th Asian-Oceanian Congress of Radiology will be held Sept. 21–25, at the Seoul Hilton International Hotel, Seoul, Korea. The official language will be English. The congress will sponsor scientific papers, scientific exhibits, and technical exhibits. Fee: $300: physicians; $150: residents, trainees, and accompanying persons. Information: Man Chung Han, M.D., Secretary General, The 5th Asian-Oceanian Congress of Radiology, Dept. of Diagnostic Radiology, Seoul National University Hospital, 28, Yunkun-dong, Chongro-ku, Seoul 110, Korea (K.P.O. Box 1880, Seoul 110, Korea). Telex:SNUHK25501; telephone: 745-6826, 7601-2514.

Breast Imaging Conference

The Department of Radiology and Continuing Medical Education of the Medical College of Wisconsin and the Ausonics Corporation will sponsor the 7th annual breast imaging conference, Sept. 27–29, at the Americana Canyon Hotel, Palm Springs, CA. Faculty: L. W. Bassett, P. J. Dempsey, G. Frankl, S. Fox, R. H. Gold, V. Jackson, D. Kopans, J. R. Milbrath, M. Moskowitz, D. L. Murray, C. W. Sewell, E. A. Sickles, C. Swan, and L. Tabar. Category 1 credit: 16.5 to 22.5 hr. Fee: $450: physicians; $275: technologists and nurses; $500: commercial; $225: partial registration (per day); $50: exhibits only (1-day pass). Information: Conference Coordinator, Jill M. Blazek, Breast Imaging Conference, Continuing Medical Education, Medical College of Wisconsin, 8701 Watertown Plank Rd., Milwaukee, WI 53226; (414) 747-1030 or (800) 558-6120.

American Institute of Ultrasound in Medicine Convention

AIUM will hold its 32nd annual convention Oct. 6–9, in the Rivergate Convention Center, New Orleans, LA. The convention, which is directed toward physicians, sonographers, scientists, engineers, and members of the ultrasound industry, will include a schedule of more

than 35 categorical courses and scientific sessions in the areas of abdomen, basic science, cardiovascular Doppler, obstetrics, gynecology, neurosonology, pediatrics, tissue characterization, and instrumentation. Program chairman: Gretchen A. W. Gooding; vice-chairman: Thomas L. Slovis. Information: AIUM, 4405 East-West Highway, Ste. 504, Bethesda, MD 20814; (301) 656-6117.

Society for Medical Decision Making Meeting

The 9th annual meeting of the Society for Medical Decision Making will be held Oct. 12–14, at the Sheraton Society Hill Hotel, Philadelphia, PA. Information about scientific program: J. Sanford (Sandy) Schwartz, M.D., Section of General Medicine-Silverstein 3, Hospital of the University of Pennsylvania, 3400 Spruce St., Philadelphia, PA 19104, (215) 662-3798; or Alan B. Cohen, Sc.D., The Robert Wood Johnson Foundation, P.O. Box 2316, Princeton, NJ 08540, (609) 452-8701. Abstract forms and information about the Society: John C. Tomeny, Administrator, Society for Medical Decision Making, P.O. Box 447, West Lebanon, NH 033784; (603) 298-9929. The Society announces the 6th annual Lee B. Lusted Student Prizes to be given for original research in medical decision making. The prizes consist of cash awards of up to $750 and certificates of recognition, as well as the opportunity to present research at the Society's annual meeting. Information concerning competition: Robert S. Wigton, M.D., Dept. of Internal Medicine, University of Nebraska Medical Center, 42nd & Dewey St., Omaha, NE 68105; (402) 559-7426.

Advanced Applied Ultrasound in Obstetrics

The Center for Medical Ultrasound, Bowman Gray School of Medicine, will sponsor a seminar in advanced applied ultrasound in obstetrics Nov. 5–7, at the Registry Resort Hotel, Naples, FL. The course will focus on advanced problems in application of diagnostic ultrasound as well as correlation with surgical and clinical management. Guest faculty: F. P. Hadlock, D. J. Sahn, J. P. Crane, and L. D. Platt. Program director: Lewis H. Nelson. Category 1 credit: 12 hr. This course is approved for 12 cognates, Formal Learning, by the American College of Obstetrics and Gynecologists. Fee: $375. Information: Registrar, Ultrasound Center, Bowman Gray School of Medicine, 300 S. Hawthorne Rd., Winston-Salem, NC 27103; (919) 748-4505.

Progress in Impotence: Workshops/Seminars

The Urology Research and Education Foundation and the Office of Continuing Medical Education, The University of California, San Diego, School of Medicine will hold the 2nd Annual Progress in Impotence: Workshops/Seminars Nov. 12–14, at the Hyatt Islandia Hotel, San Diego, CA. Category 1 credit: 13 hr. Fee: $295. Information: Edith Bookstein/UREF, P.O. Box 2586, La Jolla, CA 92038; (619) 454-3212.

Computed Tomography Head to Toe

The New York University Medical Center will sponsor a course, Computed Tomography Head to Toe, Dec. 14–19, at the Grand Hyatt Hotel, New York, NY. This intensive course is dedicated to the practical updating of the entire field of CT with correlative presentations in MR imaging. Small-group, in-depth seminars, addressing most of the subspecialties, will augment the lectures. Each registrant will be able to attend eight different workshops and will be able to select subjects of particular interest. The course is divided into two sections that can be taken independently or consecutively. Category 1 credit: 37.5 hr. Fee: $575. Information: NYU Medical Center, Post-Graduate Medical School, 550 First Ave., New York, NY 10016; (212) 340-5295.

Meeting and Course Review

For reader convenience, a summary of upcoming meetings and courses is provided. Detailed listings are given in the *AJR* issue noted in parentheses.

MRI for Technologists, Aug. 1–2, Philadelphia, PA (July)
International Continuing Medical Education Series: Aug., Gstaad, Switzerland; Sept. 5–12, Banff, Canada (Oct)
Workshop of Magnetic Resonance Imaging, 1987, Aug. 2, New Orleans, LA (July)
Annual Scientific Meeting, Section on Radiology, Aug. 2–6, New Orleans, LA (July)
Modern Radiology Practice, Aug. 3–7, Santa Barbara, CA (July)
Magnetic Resonance Imaging Update and New Techniques, Aug. 8–9, Newport Beach, CA (July)
Symposium on Breast Disease: Diagnostic Imaging and Current Management, Aug. 9–14, Grand Traverse Village, MI (June)
Symposium on Diagnostic Imaging, Aug. 10–13, Providence, RI (April)
Summer Imaging and Interventional Techniques V, Aug. 10–14, Hilton Head, SC (May)
Napa Valley Imaging Update, Aug. 15–19, Napa, CA (July)
Masters International Diagnostic Radiology Conference, Aug. 23–28, Paris, France (March)
Hepatobiliary Radiology Review Course, Aug. 24–25, Bethesda, MD (July)
Radiology Seminar: Postgraduate Course, Aug. 24–28, Maui, HI (July)
Third Annual Physics and Biology of Radiology, Aug. 27–30, San Diego, CA (July)
Third Annual Sonographers' Update and Review, Aug. 28–30, San Diego, CA (July)
Sarcoidosis and Granulomatous Disorders, Sept. 6–11, Milan, Italy (June 1986)
Magnetic Resonance Imaging: A Technologist's New World, Sept. 10–12, Orlando, FL (June)
Advances in Sectional Imaging, Sept. 10–12, San Diego, CA (July)
Physics of Diagnostic Radiology, Nuclear Medicine and Radiation Biology, Sept. 10–13, Davis, CA (June)
Magnetic Resonance Imaging for Technologists, Sept. 11–12 and Dec. 4–5, Houston, TX (June)
Radiology in Yorkshire, Sept. 13–20, Yorkshire, England (March)
Physics of Radiology, Nuclear Medicine, and Radiobiology, Sept. 14–16, New York, NY (June)
Organ Imaging Review—Toronto 1987, Sept. 14–18, Toronto, Ontario, Canada (July)
Registry Review Courses for Sonographers, Sept. 14–19, Arlington, VA (May)
Refresher Course of the International Skeletal Society: Musculoskeletal Disorders, Sept. 16–19, Cannes, France (July)
Diagnostic Ultrasound Course, Sept. 17–19, Ann Arbor, MI (April)
Diagnostic Ultrasound in Obstetrics and Gynecology, Sept. 18–20, Baltimore, MD (July)
Ultrasound Update, Sept. 19–20, Sacramento, CA (July)
Nuclear Cardiology Symposium, Sept. 21–22, Milwaukee, WI (July)
International Workshop on Bone and Soft Tissue Densitometry, Sept. 22–25, Buxton, Derbyshire, UK (March)
Computed Tomography/MRI Update: 1987, Sept. 28–Oct. 2 (July)

MRI and Neuroimaging, Oct. 1–3, Bordeaux, France (July)
Congress on Ultrasonic Examination of the Breast, Oct. 4–5, New Orleans, LA (July)
Angiography and Interventional Radiology: 1987, Oct. 5–8, Cambridge, MA (July)
Mammography Courses, Oct. 5–8, Nov. 2–5, Boston, MA (Jan)
The American Board of Radiology Examinations. Written examinations: Oct. 8–9, 1987; Oct. 6–7, 1988; Oct. 5–6, 1989. **Oral examinations:** May 23–27, 1988; June 5–9, 1989, all oral examinations at Louisville, KY (Dec 1986)
Practical Radiology, Oct. 12–14, Charlottesville, VA (July)
Neuroradiology and Head and Neck Radiology Course, Oct. 12–16, Boston, MA (April)
Chest Disease: 1987, Oct. 13–16, Boston, MA (July)
Current Trends in Diagnostic Radiology, Intervention, and Cross-Sectional Imaging—1987, Oct. 19–22, Boston, MA (April)
Twelfth Annual San Diego Postgraduate Course, Oct. 19–23, Coronado, CA, San Diego (July)
International Symposium on Diagnostic Imaging, Oct. 19–23, Barcelona, Spain (July)
ASTRO Meeting Dates Changed, Oct. 19–23, Boston, MA (July)
Recent Advances in the Systemic Therapy of Genitourinary Malignancies, Nov. 11–14, Houston, TX (July)
Temporomandibular Joint Conference, Nov. 12–14, Philadelphia, PA (July)
The Johns Hopkins Medical Institutions Courses in Abdominal and Obstetric Ultrasound: Basic Practicum, Nov. 16–20; **Advanced Practicum in Ultrasound,** Dec. 7–11, Baltimore, MD (Feb)
Congress of the Indian Radiological and Imaging Association, Jan. 14–16, 1988, Coimbatore, India (June)
The Society of Gastrointestinal Radiologists Meeting and Postgraduate Course, Jan. 16–20, 1988, Nassau, Bahamas (July)
The Society of Thoracic Radiology—Annual Postgraduate Course, March 27–31, 1988, Washington, DC (July)

AJR carries announcements of courses, symposia, and meetings of interest to its readers if received a minimum of 5 months before the event. There is no charge; receipt of items by the *AJR* Editorial Office is not acknowledged. Submit items for publication typed double spaced. Provide title, date, location, brief description, sponsor, course directors, fees, category I credit, and address and telephone number for additional information. Faculty from the host institution will not be listed. Guest faculty names will appear **only** if initials are provided. Mail news items to *AJR* Editorial Office, 2223 Avenida de la Playa, Suite 200, La Jolla, CA 92037-3218.

Classified Advertisements

Positions Available

BC/BE RADIOLOGIST—Immediate opportunity available to join 6-member group. All modalities present. Group services 2 hospitals and has 2 offices in south Florida, East Coast. Interventional fellowship would be beneficial. David Harr, M.D., 1845 Tarpon Ln., G-101, Vero Beach, FL 32960. 8–9ap

BOARD-CERTIFIED GENERAL-DIAGNOSTIC RADIOLOGIST with academic credentials to become Director of Residency Training Program in a 700-bed university-affiliated teaching hospital with a fully approved residency program. Experience in clinical research mandatory. Send CV to David Bryk, M.D., Director of Radiology, Maimonides Medical Center, 4802 Tenth Ave., Brooklyn, NY 11219. 8ap

UNIVERSITY OF CALIFORNIA, SAN FRANCISCO CLINICAL INSTRUCTORSHIP—1-yr position available beginning July 1988 in the Body Computed Tomography/Gastrointestinal Radiology Section. Active, combined section includes body CT imaging with state-of-the-art equipment, including an Ultrafast scanner. Some body MRI exposure is also available. The University of California is an equal opportunity/affirmative action employer. Women, handicapped, and minorities are encouraged to apply. For further information, contact Henry Goldberg, M.D., Dept. of Radiology, University of California, San Francisco, CA 94143-0628. (415) 476-1781. 8a

SOUTH ORANGE COUNTY DIAGNOSTIC RADIOLOGIST—Excellent position available, ASAP, in multispecialty hospital and office practice located in Orange County (Southern California). Position is for interventional radiologist with training in cardiovascular radiology. Excellent salary and benefits. Hospital is in a beautiful, growing area. Reply with CV to Box W54, *AJR* (see address this section). 8–9ap

ULTRASOUND/CT/MRI—Seeking board-certified radiologist specializing in sectional body imaging to pursue academic practice at the University of Alabama at Birmingham. Expanding 1400-bed medical complex performs over 10,000 imaging examinations per yr with state-of-the-art equipment, including 2 Acuson units, 2 G.E. 9800 CT scanners, and high- and low-field MRI units. Special interest in abdominal Doppler ultrasound. Position includes clinical, teaching, and research responsibilities. Send CV to Lincoln L. Berland, M.D., Dept. of Radiology, University of Alabama at Birmingham, 619 S. 19th St., Birmingham, AL 35233. 8–11a

ASSOCIATE DIAGNOSTIC RADIOLOGIST needed for new community hospital in scenic Michigan upper-peninsula town. Practice includes ultrasound (Doppler), nuclear medicine, CT, mammography, and some special procedures. Generous salary and liberal benefits leading to early partnership. Send CV to Mario Nunez, M.D., 750 Lake Shore Dr., Escanaba, MI 49829; (906) 786-7350. 7–9ap

DIRECTOR OF MUSCULOSKELETAL RADIOLOGY—The University of Michigan Medical School is seeking to recruit a board-certified radiologist to serve as Director of Musculoskeletal Radiology in the Dept. of Radiology. In-depth experience in musculoskeletal radiology in an academic dept. is essential. This individual will direct the clinical service, medical student and house-officer education, and research programs of the Skeletal Division. The Dept. provides excellent facilities and academic opportunities. Rank and salary commensurate with experience. Contact William Martel, M.D., Chairman, Dept. of Radiology, University Hospital B1G503/0030, 1500 E. Medical Center Dr., Ann Arbor, MI 48109-0030. A nondiscriminatory, affirmative action employer. 8a

RADIOLOGIST, BOARD-CERTIFIED/ELIGIBLE—4 Mayo Clinic-trained radiologists have a position available in a hospital-based practice that includes angiography and other invasive procedures, diagnostic radiology, CT, ultrasound, nuclear medicine, and MRI. 4-yr university training required. Liberal vacation and seminar time. Low buy-in and early full partnership. Locum tenens assistance desired until a permanent associate is obtained. Send CV and 3 references with initial letter of inquiry to Box 2818, Waterloo, IA 50704. 8–10a

OPPORTUNITY FOR YOUNG, WELL-TRAINED, AGGRESSIVE GENERAL RADIOLOGIST to join 3-man group in a small midwestern city 20 min from St. Louis metropolitan area. All modalities, including mobile MRI. Excellent equipment. Competitive salary leading to early partnership. Reply Box W56, *AJR* (see address this section). 8ap

BC/DIAGNOSTIC RADIOLOGIST WITH NEURORADIOLOGY OR MR FELLOWSHIP TRAINING to join progressive 5-man group in central Maine. 1.0-T MR unit to go on-line 1/88. 280-bed hospital. 52,000 exams/yr. 5000 CT. Brand new dept. to be completed by 1990 with state-of-the-art equipment. Position available 1/88–7/88. Excellent salary and benefits to partnership in 2 yr. Unique opportunity to join a progressive private group doing university-level practice in a regional referral center. Send CV to X-Ray P.A., 583 Main St., Lewiston, ME 04240; (207) 795-2400. 8–9a

BOARD-CERTIFIED, DIAGNOSTIC RADIOLOGIST to join established group at active, acute-care, 500-bed voluntary-teaching hospital in New York City. Well-equipped, modern dept. with all imaging modalities, plus nearby private outpatient office. Good location and attractive financial opportunity. Broad-based interest and competence in quality clinical radiology required; fellowship and/or postresidency experience at university institution preferred. Also available, in late 1988, a second opening for individual with expertise in MRI and neuroradiology. 8xa

DIAGNOSTIC RADIOLOGIST—7-man group seeking BC/BE radiologist to join busy practice in 530-bed community hospital. State-of-the-art in all modalities. Position available 10/87. Nuclear medicine training a plus. Contact Arthur F. Bishop, M.D., Methodist Medical Center, 221 N.E. Glen Oak, Peoria, IL 61636; (309) 672-5586. 8–10a

NEURORADIOLOGIST—Applications are being sought for a neuroradiologist for a 560-bed teaching hospital/private office. New 1.5-T MRI unit soon to be operational. Candidate should be board certified preferably with 2 yr of neuroradiology fellowship. Training in MR, CT, angiography, and myelography necessary. Send current CV to R. William McConnell, M.D., Chairman, Dept. of Radiology, Number 9, Doctor's Park, Greenville, NC 27834. 7–12a

EXCELLENT OPPORTUNITY—Seeking board-certified radiologist with additional training in interventional radiology or board certification in nuclear medicine to join 12-man private-practice group covering 2 hospitals in suburban St. Louis. Applicant should have experience in CT, nuclear medicine, ultrasound, and mammography. Very competitive salary with excellent benefits. Send CV to A. C. Hooper, M.D., Ernst Radiology Clinic, Inc., Ste. 110, 14377 Woodlake Dr., Chesterfield, MO 63017; (314) 878-4680. 7–9ap

BOARD-CERTIFIED RADIOLOGIST wanted for community of 10,000 (45,000 service area) in the lush Yakima Valley of central Washington. Superior diagnostic radiologic skills required with experience in ultrasound, angiography, and CT. Generous practice assistance package. Excellent school system and outdoor recreation. Contact PROSEARCH, 305 NE 102nd Ave., Portland, OR 97220; (503) 256-2070. 7–9ap

TEXAS, DIAGNOSTIC RADIOLOGIST—Immediate opportunity for board-certified physician as associate with existing group of 3 radiologists in northeast Texas community of 27,000 (service area population, 150,000). All modalities, including MRI and interventional radiology, required for regional medical center. This position offers a quality lifestyle in a family-oriented community with a strong economy and easy access to major metropolitan area. Competitive incentive package and option for early ownership. Please send CV in confidence or call Physician Resource Network, P.O. Box 37102, Fort Worth, TX 76117; (817) 595-1128. 8ap

FULL-TIME, PART-TIME, OR LOCUM TENENS (LEADING TO PERMANENT) office/hospital-based position in south Texas urban community. Board certification, friendly attitude, good training, motivation, and Texas license required. General radiology practice with fluoroscopy, mammography, nuclear medicine, sonography, CT, and limited MRI. Comfortable hours and remuneration with potential to expand. Reply Box W60, *AJR* (see address this section). 8a

GENERAL RADIOLOGIST with training in all phases of diagnostic and invasive radiology is being recruited by a 6-man group of radiologists in northeastern Connecticut. The practice includes 3 offices and a small, progressive hospital. The hospital currently offers a full range of services including nuclear medicine, ultrasound, and CT. There is a new 1-day surgical center (recently completed), a regional dialysis center, and a busy outpatient dept. Send CV to Jonathan Berger, M.D., 142 Echo Dr., Vernon, CT 06066. 8a

ISRAEL, DIAGNOSTIC RADIOLOGY. Opportunities for 3–4 week or longer working vacations in a number of Israeli medical centers, on a volunteer basis. Positions varied, arrangements flexible. For information contact: Jonathan H. Fish, M.D., 1844 San Miguel Dr., #302, Walnut Creek, CA 94596; (415) 947-0560. 8xa

BOARD-CERTIFIED RADIOLOGISTS—Exciting opportunities with expanding group. Dept. chairman and staff positions available in both urban and rural settings. Send CV to Box U90, *AJR* (see address this section). 7–8a

BOARD-CERTIFIED RADIOLOGIST to join 12-member dept. and 625-bed hospital and associated private office. All modalities of radiology performed. Have a 1.5-T GE MRI operation and 2 CT scanners, one of which is a GE 9800 quick scan. Large ultrasound and nuclear medicine section. New angiographic suite being completed. Active residency program. Please send resume to H. E. Yeagley, M.D., Dept. of Radiology, Reading Hospital and Medicine Center, Reading, PA 19603. 7–10a

ULTRASOUND AND MAMMOGRAPHY—This is an outstanding opportunity for a radiologist to join a well-respected, growing, office-based private practice in a highly desirable metropolitan area. Fellowship training or equivalent experience is required. Send CV to Box T78, *AJR* (see address this section). 6–8a

CT/ULTRASOUND—The University of Texas Health Science Center, San Antonio is seeking a board-certified radiologist with experience in CT/ultrasound to join our faculty. Contact Robert L. Siegle, M.D., Chief, Diagnostic Radiology, Dept. of Radiology, University of Texas Health Science Center at San Antonio, 7703 Floyd Curl Dr., San Antonio, TX 78284. Equal Opportunity/Affirmative Action Employer. 7–9a

DIAGNOSTIC RADIOLOGIST to join established group of 10 in greater Philadelphia area. Two hospitals and imaging center. Growing practice. State-of-the-art in all modalities. Fellowship a plus but not essential. Position available ASAP. Reply to Box T82, *AJR* (see address this section). 6–8a

DIAGNOSTIC RADIOLOGIST—Very busy group urgently needs 2 BC/BE radiologists. Recent training preferred, with skills in routine work, sonography, mammography, CT, nuclear medicine, interventional, and MRI. Two-yr work up to full equal partner, generous benefits, and great Texas weather year-round. Population of area served is approximately 150,000. Submit current CV and other information to *AJR*, Box T80 (see address this section). 6xa

NORTHWEST OPPORTUNITY—Board-certified diagnostic radiologist to join group of 4 at busy 160-bed hospital and private-office practice. Minimum requirements include competence in angiography, CT, and ultrasound. Some limited interventional skills are desirable. Prefer university-trained applicant with imaging fellowship. Excellent benefits and early partnership. Community of 60,000 located on the Columbia River in the beautiful Pacific Northwest 1 hr from Portland, OR. Send CV and inquiries to Michael L. Hanslits, M.D., Longview Radiologists, 1020 11th Ave., Longview, WA 98632. 7–8a

DIAGNOSTIC RADIOLOGIST with special interest in CT and ultrasound to join growing hospital-based practice. 125-bed hospital with adjoining office building located near downtown Seattle. Send CV to K. Wade Brunette, M.D., 16775 16th Ave. NW, Seattle, WA 98177; (206) 583-2675. 7–9a

DIRECTOR, SECTION OF INTERVENTIONAL RADIOLOGY—The Dept. of Radiology at Harper Hospital is seeking a board-certified radiologist with competence in all aspects of interventional radiology. Harper Hospital is the major institution in the Detroit Medical Center and is affiliated with Wayne State University. Please send CV or inquiries to George A. Kling, M.D., Chairman, Dept. of Radiology, Harper Hospital, 3990 John R, Detroit, MI 48201; (313) 745-8405. 7–9a

BOARD-CERTIFIED RADIOLOGIST, university trained, wanted for a salaried position in a free-standing imaging center and part-time hospital practice. The center facilities include an Acuson 128, GE 9800, Low-Rad dedicated mammography, dedicated digital angiography, and routine fluoroscopic and radiographic imaging. Regular hours with minimal on-call responsibilities. Beautiful town in Indiana-Illinois-Kentucky tri-state. Part-time or locum tenens considered. Send CV to Box T88, *AJR* (see address this section). 6–9a

DIAGNOSTIC RADIOLOGIST. Need aggressive associate to perform all aspects of diagnostic radiology in well-equipped hospital with large outpatient component in South Texas. MR training a plus but not essential. Excellent salary and early partnership available. For confidential consideration please submit CV to Box H70, *AJR* (see address this section). 11xa

Positions Desired

BOARD-CERTIFIED AIR FORCE RADIOLOGIST desires general outpatient (private/HMO/multispecialty) position beginning August 1988. Has 12-yr experience that includes chairmanships of three major USAF Medical Center dept. Reply A. Daley, M.D., 6306 Wilmington Dr., Burke, VA 22015; office (301) 981-4222. 7–10b

Fellowship and Residencies

ANGIOGRAPHY/NEURORADIOLOGY FELLOWSHIP, BOSTON—Unexpected new position available immediately. Fellows participate in cerebral, peripheral, and abdominal angiography; interventional procedures and myelography; CT and MRI. Send inquiries to Laura Feldman, M.D., Head, Angiography Section, VAMC, 150 S. Huntington Ave., Boston, MA 02130; (617) 739-3435. 7–9c

PULMONARY RADIOLOGY FELLOWSHIP—July 1, 1988, to June 30, 1989. The program provides intensive training in all phases of thoracic and pulmonary radiology, including cross-sectional imaging, plain film analysis, invasive thoracic procedures, pulmonary function testing, fiberoptic bronchoscopy, cytopathologic specimen examination, and clinical patient evaluation. Research projects are encouraged. Applicants should be ABR eligible. For information, contact S. David Rockoff, M.D., Professor and Head of Thoracic Radiology, The George Washington University Medical Center, 901 23rd St. NW, Washington, D.C. 20037; (202) 994-4646. The George Washington University is an EEO/affirmative action employer. 8c

INTERVENTIONAL RADIOLOGY FELLOWSHIP. The Dept. of Radiology of the University of South Florida offers a 1- and 2-year fellowship in interventional radiology. Procedures include all noncardiac diagnostic angiography, angioplasty, chemoembolization, lymphangiography, arthrography, biopsies, GI and GU drainages, ganglion and facet blocks, and gastrostomies. The 2-year program will include a year as junior faculty. There is extensive exposure to MRI, CT, and ultrasound. Send CV to Stephen F. Quinn, M.D., U.S.F., H. Lee Moffitt Cancer Center and Research Institute, Dept. of Diagnostic Imaging, P.O. Box 280179, Tampa, FL 33682-0179. 8c

DIAGNOSTIC RADIOLOGY RESIDENCY—Unexpected vacancy at second- or third-yr diagnostic radiology resident level. Fully accredited 705-bed Northeastern teaching hospital, 104,000 exams yearly, major university affiliation. Modern equipment with MRI this fall. For further information contact Lester Kalisher, M.D., Saint Barnabus Medical Center, 94 Old Short Hills Rd., Livingston, NJ 07039; (201) 533-5822. We are an equal opportunity employer, M/F/H/V/. 8cp

PEDIATRIC NEURORADIOLOGY FELLOWSHIP—Childrens Hospital of Los Angeles has an opening for a pediatric neuroradiology fellow starting July 1, 1988, for 1 yr. Childrens Hospital of Los Angeles is the largest children's hospital on the West Coast. The neuroradiology facilities include a new Siemens angiographic suite and a GE 9800 scanner; a GE magnetic resonance imager has been ordered. Applications should be sent to John L. Gwinn, M.D., Radiology, Childrens Hospital of Los Angeles, 4650 Sunset Blvd., Los Angeles, CA 90027. Childrens Hospital of Los Angeles is an equal opportunity employer. 8–9c

FELLOWSHIPS IN DIAGNOSTIC IMAGING (MRI, ULTRASOUND, AND CT)—3 fellowships available July 1988 at Rhode Island Hospital, a major affiliate of Brown University Medical School. The radiology staff serves this 715-bed general hospital and a 200-bed lying-in hospital. Over 190,000 exams are performed yearly. The fellowships will emphasize MRI, ultrasonography, and CT, along with associated interventional procedures. A busy mammography area is included. Send inquiries to Daniel J. Hanson, M.D., Radiologist-in-Chief, Dept. of Diagnostic Radiology, Rhode Island Hospital, 593 Eddy St., Providence, RI 02902. 8c

IMAGING FELLOWSHIP, BOSTON—Unexpected new position available immediately. Fellows participate in CT, ultrasound, nuclear medicine, MRI, and related procedures. Send inquiries to Stephen Gerzof, M.D., Chief, Ultrasound and Body CT, VAMC, 150 S. Huntington Ave., Boston, MA 02130; (617) 739-3435. 7–9c

IMAGING FELLOWSHIP IN DIAGNOSTIC IMAGING with emphasis on diseases of children and women. Diasonics MRI, Imatron CT, and Acuson Ultrasound. Opportunity for clinical or basic research. Must be eligible for oral board exam. Reply Jerald Kuhn, M.D., Director, Radiology Dept., Children's Hospital, 219 Bryant St., Buffalo, NY 14222; (716) 878-7525. 7–10c

MAMMOGRAPHY—GENERAL RADIOLOGY FELLOWSHIP—The New England Medical Center Hospital announces a new 1-yr fellowship starting July 1, 1987, combining training in general radiology with emphasis in mammography and GI radiology (double-contrast technique). Breast imaging equipment includes 2 new CGR Senographe units and an automated whole-breast scanner. Clinical responsibilities will include an active role in the multidisciplinary Breast Health Center that serves as both a primary-care and regional-referral center. This position carries an appointment at Tufts University School of Medicine. For further information contact Marc J. Homer, M.D., Box 388, Dept. of Radiology, New England Medical Center, 750 Washington St., Boston, MA 02111. 7–8cp

FELLOWSHIP SOUGHT—Radiologist, 53, DABR, DABNM, DABMR. Retired 4 yr. Imaging preferred but flexible. Available Jan. 1988. Reply Box U92, *AJR* (see address this section). 7–8cp

ADVANCED IMAGING FELLOWSHIP—A position is now available for a board-certified or board-eligible radiologist in a University of Rochester teaching-hospital complex. The fellowship emphasizes in-depth exposure to CT, ultrasound, and MRI integrated with invasive procedure exposure. Additional positions will be available in January 1988. Please respond to Steven G. Herbert, M.D., Director, Fellowship Program, Diagnostic Radiology Dept., The Genesee Hospital, 224 Alexander St., Rochester, NY 14607. 7–8c

ABDOMINAL IMAGING FELLOWSHIP to begin July 1988. 612-bed teaching hospital. Over 120,000 examinations are performed yearly in the radiology dept. All imaging modalities are integrated into the Fellowship Program which will emphasize body CT, diagnostic sonography including obstetric, and MRI. Send inquiries to Harvey L. Neiman, M.D., Chairman, Dept. of Radiology, West Penn Hospital, 4800 Friendship Ave., Pittsburgh, PA 15224. 6–8c

VISCERAL IMAGING AND INTERVENTIONAL RADIOLOGY FELLOWSHIP to begin July 1988. 612-bed teaching hospital. Fellows will be actively involved in diagnostic CT and sonography. Fellows will also participate in all vascular and nonvascular/interventional procedures including angioplasties, biliary, GU, biopsies, abscess drainages, and angiography. Send inquiries to Harvey L. Neiman, M.D., Chairman, Dept. of Radiology, West Penn Hospital, 4800 Friendship Ave., Pittsburgh, PA 15224. 6–8c

Tutorials/Courses

MAUI, HAWAII—12TH ANNUAL BODY IMAGING CONFERENCE—October 10–18, 1987. Diagnostic Imaging, Category I Accreditation, University Faculty. Registration and information: Body Imaging Conference, 21915 Roscoe Blvd., Ste. 222, Canoga Park, CA 91390; (818) 719-7380. 7–9d

INTERNATIONAL TRENDS IN BREAST ULTRASOUND—International Congress on the Ultrasonic Examination of the Breast: New Orleans, LA, Oct. 4–5, 1987 (AIUM Annual Convention, Oct. 6–9, same host Hotel Sheraton, New Orleans). International faculty CME-1. Topics include the multimodality approach to breast examination. Congress registration fee: $200 Physicians, Scientists, Engineers; $125 Technologists, Research Assistants. Checks (US funds) payable to The International Congress on the Ultrasonic Examination of the Breast. Send to Elizabeth Kelly-Fry, M.D., Indiana University Medical Center, Indianapolis Center for Advanced Research, 611 N. Capitol Ave., Indianapolis, IN 46204, USA; (317) 630-6131, (317) 262-5008. 7–8d

MRI TUTORIAL PROGRAM—Diagnostic Radiological Imaging Medical Group offers 1-wk training programs in clinical MRI for physicians with limited or no experience in MRI. The program is individualized to the applicant, and the physician may subscribe to 1 or more weeks. Only 2 physicians per week are accepted. The 1.5-T MRI scanner is used in an outpatient imaging facility and 12–16 examinations per day are performed. Individual tutorials in MRI physics, equipment evaluation, clinical indications for MRI examination, performance of MRI studies, discussion of case material, and review of an extensive teaching file are offered. The faculty are A. B. Dublin and M. H. Reid. The fee is $600 and 40 hr Category I credit are available/week. For further information contact Michael H. Reid, Ph.D., M.D., Diagnostic Radiological Imaging, 79 Scripps Dr., Ste. 100, Sacramento, CA 95825. (916) 921-1300. 6–9d

LONDON—PARIS FALL ULTRASOUND. Attend one or both, September 19–27, 1987, CME I accreditation. For registration and information contact Medical Seminars International, 21915 Roscoe Blvd., Ste. 222, Canoga Park, CA 91304, (818) 340-0580 ext. 280. 3–8d

Other

USED EQUIPMENT—Mobile mammography unit. 27-ft Itasca motor home with Kramex 43-S Mammographic System and onboard processor. $97,000. Reply to P.O. Box 2440, Sanford, FL 32772-2440 or call (305) 321-7000 (ask for Camellia). 8d

WANTED, RADIOLOGY PRACTICE—Desire private-office practice or outpatient clinic. Prefer sunbelt/mountain location. Reply Box W58, *AJR* (see address this section). 8–9d

AJR Classified Advertisements Information

Box Responses and Address for Ad Placement

Write Box _____, AJR, Suite 200, 2223 Avenida de la Playa, La Jolla, CA 92037; (619) 459-2229.

How to Place an Ad

AJR accepts classified advertising for Positions Available, Positions Desired, Fellowships and Residencies, and Tutorials/Courses. Ads are accepted by mail or telephone. Institutions should supply purchase orders.

Rates: $6.00/line with a $30 minimum charge. Box service is $10 additional for each month the ad appears. There are discounts for multiple insertions: 10% for 2–3 insertions; 20% for 4 or more. To estimate lines, count all words and divide by 5.5.

Billing: Ads may be prepaid or invoices will be sent after the ad appears.

Deadlines. 6 weeks prior to issue date. For specific deadlines telephone the AJR editorial office.

Estimating Ad Charges

Line charge: divide total words by 5.5 and multiply by $6.00	$
Multiple insertions? If so, multiply by number	×
Subtotal	$
Box response requested? If so, multiply number of months by $10.00	+
Subtotal	$
Discount applies to two or more insertions. Subtract 10% if ad appears 2–3 months, 20% if 4 months or more	−
Approximate advertising charge	$

You learn from your experience with

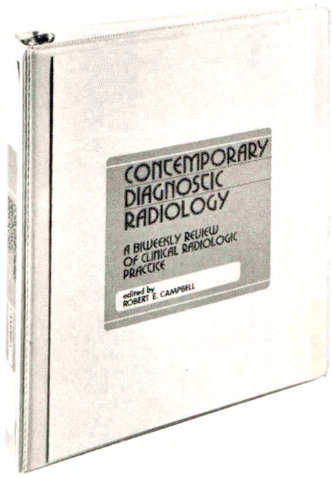
CONTEMPORARY DIAGNOSTIC RADIOLOGY

Editor: **Robert E. Campbell, M.D.**

A Biweekly Review of Clinical Radiologic Practice—26 issues a year!

One of your toughest jobs is keeping up with the many new developments that affect radiology. That's why you want **Contemporary Diagnostic Radiology**... an effective and convenient way to perfect your skills and maintain your professional status.

Contemporary Diagnostic Radiology is designed as a continuing education program that lets you work at your own pace. Every two weeks you'll receive an issue that covers a single topic or procedure in detail. Read the information and study the clearly reproduced radiographs—and then, if you choose, respond to a comprehensive examination in the strictest confidence. You set the pace.
Each biweekly lesson brings you pertinent review of the basics in bone radiology... gastrointestinal radiology... pediatric radiology... genitourinary radiology... MR imaging... and all of the topics you want to know more about.



Contemporary Diagnostic Radiology works *two ways*. You may choose to subscribe to the non-scoring version, receiving every issue as an important element of your professional reading. The scoring version, however, supplements your reading and computer-coded examinations with confidential result responses, making you eligible for Continuing Medical Education credits co-sponsored by the University of Pennsylvania School of Medicine.

"As an organization for continuing medical education, the University of Pennsylvania School of Medicine designates this continuing medical education activity as meeting the criteria for 1 credit hour per bi-weekly issue in Category I for Educational Materials for the Physician's Recognition Award of the American Medical Association provided it has been completed according to instructions."

You can begin this ongoing program **today**. **Contemporary Diagnostic Radiology** is a year-round program, so you can join at any time. To begin your lessons, just fill out the enclosed card and return it to us. Or call **FREE** 1-800-638-6423 (except from Alaska). In Maryland call **COLLECT** 528-4105. You'll find that **Contemporary Diagnostic Radiology** is the most efficient and inexpensive way to keep up with your dynamic field.

Williams & Wilkins

P.O. Box 23291
Baltimore, Maryland 21203

266 Fulham Road
London SW10 9EL England

clip & mail

CONTEMPORARY DIAGNOSTIC RADIOLOGY

☐ **Yes!** I want to keep pace in my field! Begin my 26-issue subscription:
☐ Send me the scoring version ($220)
☐ Send me the non-scoring version ($180)
☐ Send me the resident non-scoring version ($160)
(add $35 for optional air mail delivery outside the U.S.)
☐ new subscription
☐ renewal

name

address

city/state/zip

payment options
☐ payment enclosed ☐ bill me
☐ American Express ☐ MasterCard ☐ VISA

printed in USA

card # expiration date

signature/P.O. #

Maryland residents add 5% sales tax. Subscriptions outside the U.S. must be prepaid in U.S. dollars only. Rates subject to change without notice. Please allow 8 weeks for delivery of your first issue, up to 16 weeks for surface delivery outside the U.S. Optional airmail rates: add $35 per subscription.

Residents are eligible for the special in-training rate for up to three years. When requesting this rate, please include training status and institution.

Don't forget: you can order with a **FREE** phone call at 1-800-638-6423 (except from Alaska). In Maryland, call collect 528-4105.

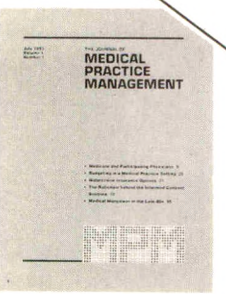
Williams & Wilkins

P.O. Box 23291
Baltimore, Maryland 21203

266 Fulham Road
London SW10 9EL England

CDRAD 95191 87

Control the future of your practice



NEW!

The Journal of MEDICAL PRACTICE MANAGEMENT

Editor: **Marcel Frenkel, MD, MBA**

A new journal gives you the management skills you need to pull ahead

Right now you need information on some important topics that weren't covered in medical school. Topics that are having a profound impact on private practice and hospital-based physicians across the country.

Like competition from HMOs. Industrialization of medicine. The sheer number of physicians competing for your patients. Increasing costs.

You know the issues. What you need to know is the best way to face them so your practice will flourish in years to come.

And that's where **The Journal of Medical Practice Management** comes in.

Keep up with the issues that are changing your way of practice forever

The Journal of Medical Practice Management is a new quarterly publication that covers *your* concerns...issues affecting the way you practice now — and the way you'll practice in the future.

Four times a year, an expert editorial board headed by Dr. Marcel Frenkel brings you concise, readable coverage of today's issues and tomorrow's trends.

You'll find departments covering • office procedures and management • malpractice • marketing • manpower • computers • taxation • legal and legislative affairs • and health policy.

You'll also find pertinent features like the **Washington Report,** telling you what's up in the nation's capital and how it affects you...a **Letter from Abroad,** offering perspectives on how physicians are handling health care issues in other countries...and profiles of profit and not-for-profit health care delivery systems.

A multidisciplinary editorial board

Members of the editorial board for **The Journal of Medical Practice Management** have been carefully chosen for their knowledge of the management aspects of practicing medicine. These experts, many with experience in more than one field, give you the perspectives you need from medicine, law, management, government, and education.

You can control the future of your practice

The issues you can't afford to ignore are in **The Journal of Medical Practice Management.** It's a lot of information for a little money. And that's good business for you.

Reserve your charter subscription today!

Just return the attached coupon, or **call our FREE number,** 800-638-6423, from anywhere in the US except Alaska. In Maryland, call 528-4105 collect. **Quarterly**

Williams & Wilkins

428 East Preston Street
Baltimore, Maryland 21202

266 Fulham Road
London SW10 9EL England

YES, I want to control the future of my practice!

Please enter my subscription to **The Journal of Medical Practice Management** (quarterly)

☐ Individuals and Institutions $40

All subscribers: add $10 outside the U.S.

☐ Check enclosed ☐ Bill me
☐ MasterCard ☐ American Express ☐ VISA

Card # Exp. date

Signature

Name

Address

City/State/Zip

Maryland residents add 5% sales tax. Subscriptions outside the US must be prepaid. All subscriptions must be paid in US dollars. Rates valid through April 30, 1988.

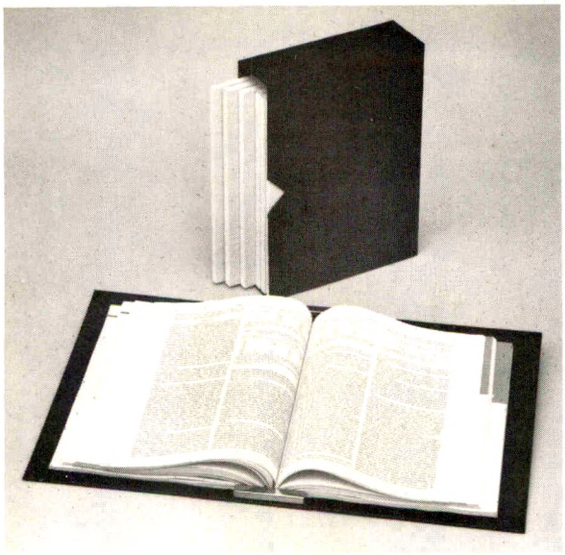
Please allow 8 weeks for delivery of your first issue, up to 16 weeks for surface delivery outside the US. Airmail rates available on request.

Williams & Wilkins

P.O. Box 23291
Baltimore, Maryland 21203

266 Fulham Road
London SW10 9EL England

MPMAD 95048 87



Protect your copies of

AJR: AMERICAN JOURNAL OF ROENTGENOLOGY

with Jesse Jones Binders or Files

Keep your journals clean, orderly, and readily accessible with Jesse Jones Binders or Files. Two Binders or two box style Files are all you need to accommodate a full year's worth of issues. Both Binders and Files are handsomely made with rich black leatherette covers and gold leaf embossed lettering.

Jesse Jones Binders open flat for easy reading and reference and are economically priced at only $9.95 each; 3 for $27.95, or 6 for $52.95 postpaid. The rugged, compact box Files are only $7.95 each; 3 for $21.95, or 6 for $39.95. Add $1.00/unit postage and handling. (Outside the U.S. add $2.50/unit.)

For charge orders call toll free 1-800-972-5858. ($15.00 minimum).

Free gold transfer slips included for indexing volume and year.

Please allow four to five weeks for delivery.

TO: Jesse Jones Industries
499 E. Erie Avenue, DEPT. AJR
Philadelphia, PA 19134

I enclose my check or money order for $_____
(PA residents add 6% sales tax)

Send me ____ ☐ Files ☐ Binders for my journals

Name

Address (will not ship to P.O. Box)

City/State/Zip

Satisfaction guaranteed.

INDEX TO ADVERTISERS

Ackrad Laboratories, Inc. A20

Adria Laboratories A15

Diasonics A21, A22, A23, A24, A25, A26, A27, A28

Eastman Kodak A6, A7

E-Z-EM Company . . . . . Cover 2

Fuji . . . . . Cover 3

General Electric A13, A29

Guthrie Clinic A20

Konica Medical Corporation A16, A17

Nuclear Associates A18

Ohio State University A20

Picker International A8, A9, A10

Precise Optics/PME, Inc. A19

E.R. Squibb & Sons, Inc. A30, A31, A32

S & S X-Ray A20

Tecnomed USA A2, A14

Winthrop Laboratories A11, A12, A35, A36

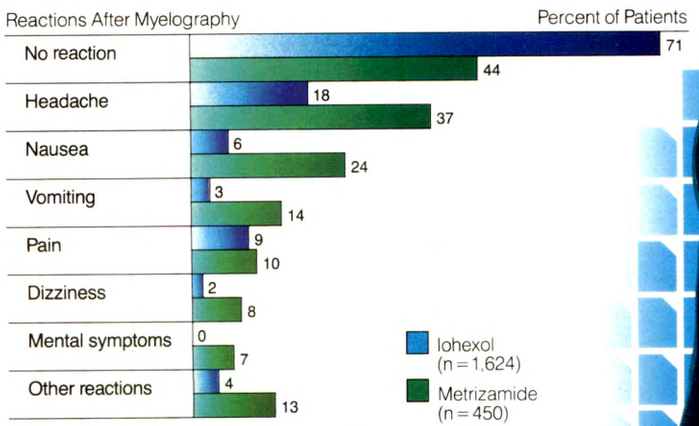
We try to present an accurate index. Occasionally this may not be possible because of a last-minute change or an omission.

In intrathecal imaging:

Because you can't be sure how every patient will react...

Improve the safety profile.

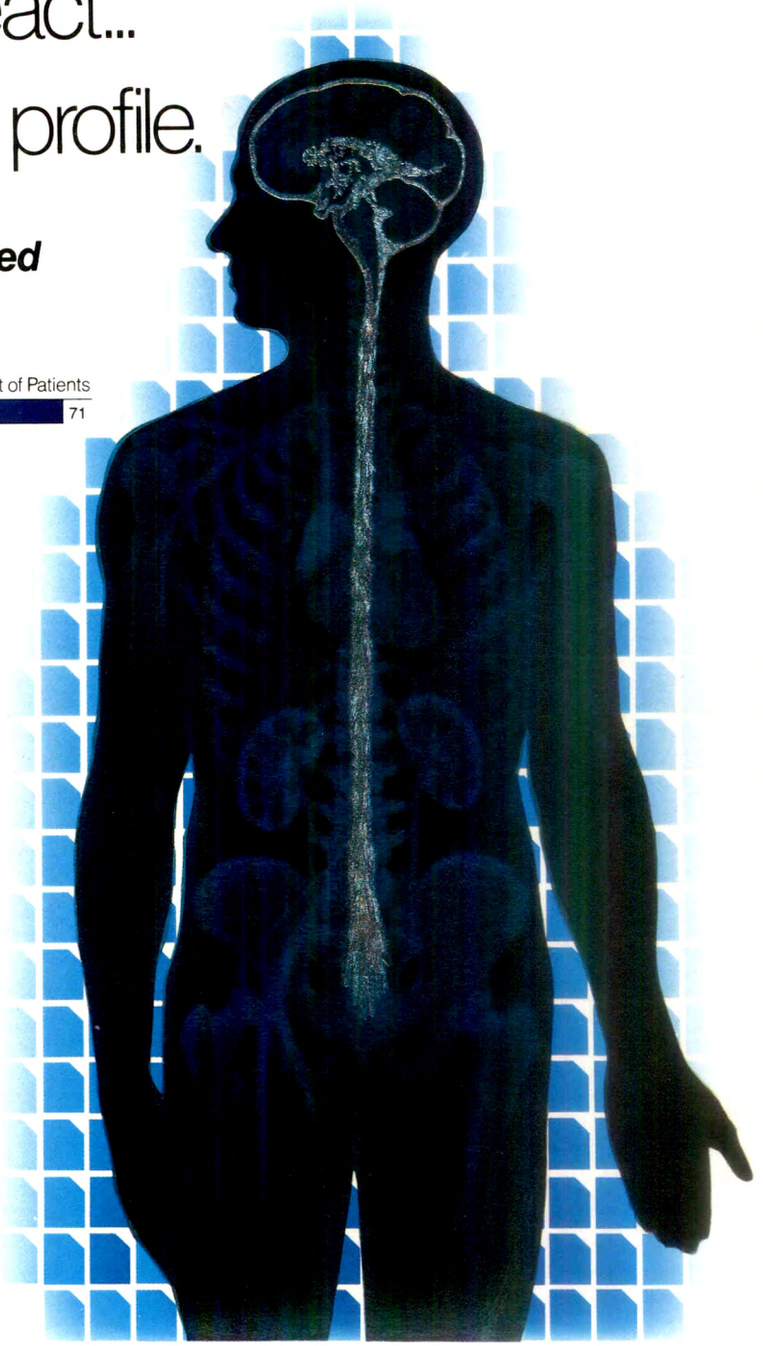
Better patient tolerance, measured subjectively and objectively.[1-5]



Adapted from Shaw el at.[2] Data on file, Winthrop Pharmaceuticals.[4] All adverse reactions reported are included and are irrespective of drug relationship. If a patient had more than one type of reaction, each is counted separately under the respective reaction type.

Lower incidence of EEG changes compared with iopamidol or metrizamide.[2,5]

Excellent diagnostic quality.



NONIONIC

OMNIPAQUE®

(IOHEXOL)

THE NEW STANDARD IN INTRATHECAL IMAGING.

See next page for important product information concerning contraindications, warnings, adverse reactions, patient selection, and precautionary recommendations.



OMNIPAQUE®
INJECTION (IOHEXOL)
INTRATHECAL

180

240

300

PLEASE CONSULT FULL PRODUCT INFORMATION BEFORE USING. A SUMMARY FOLLOWS:

DESCRIPTION: OMNIPAQUE is a nonionic, water-soluble radiographic contrast medium for intrathecal administration in concentrations of 180, 240, and 300 mgI/mL. Each milliliter of iohexol solution contains 1.21 mg tromethamine and 0.1 mg edetate calcium disodium with the pH adjusted between 6.8 and 7.7 with hydrochloric acid or sodium hydroxide. All solutions are sterilized by autoclaving, are nonpyrogenic, and contain no preservatives, so unused portions should be discarded.

CONTRAINDICATIONS–Intrathecal: OMNIPAQUE should not be administered to patients with a known hypersensitivity to iohexol. Myelography should not be performed in the presence of significant local or systemic infection where bacteremia is likely. Intrathecal administration of corticosteroids with OMNIPAQUE is contraindicated. Because of the possibility of overdosage, immediate repeat myelography in the event of technical failure is contraindicated.

WARNINGS–General: If grossly bloody CSF is encountered, the possible benefits of a myelographic procedure should be considered in terms of the risk to the patient.

Caution is advised in patients with a history of epilepsy, severe cardiovascular disease, chronic alcoholism, or multiple sclerosis.

Elderly patients may present a greater risk following myelography. The need for the procedure in these patients should be evaluated carefully. Special attention must be paid to dose and concentration of the medium used, hydration, and technique used.

Patients who are receiving anticonvulsants should be maintained on this therapy. Should a seizure occur, intravenous diazepam or phenobarbital sodium is recommended. In patients with a history of seizure activity who are not on anticonvulsant therapy, premedication with barbiturates should be considered.

Prophylactic anticonvulsant treatment with barbiturates should be considered in patients with evidence of inadvertent intracranial entry of a large or concentrated bolus of the contrast medium, since there may be an increased risk of seizure in such cases.

Drugs that lower the seizure threshold, especially phenothiazine derivatives, including those used for their antihistamine or antinauseant properties, are not recommended for use with OMNIPAQUE. Others include MAO inhibitors, tricyclic antidepressants, CNS stimulants, and psychoactive drugs described as analeptics, major tranquilizers, or antipsychotic drugs. While the contributory role of these medications has not been established, the use of such drugs should be based on physician evaluation of potential benefits and potential risks. Physicians have discontinued these agents at least 48 hours before and for at least 24 hours postprocedure. Care is required in patient management to prevent inadvertent intracranial entry of a large dose or concentrated bolus of the medium. Also, effort should be directed to avoid rapid dispersion of the medium causing inadvertent rise in intracranial levels (eg, by active patient movement). Direct intracisternal or ventricular administration for standard radiography (not CT) is not recommended.

In most reported cases of major motor seizures with nonionic myelographic media, one or more of the following factors were present. Therefore avoid:

- Deviations from recommended procedure or in myelographic management.
- Use in patients with a history of epilepsy.
- Overdosage.
- Intracranial entry of a bolus or premature diffusion of a high concentration of the medium.
- Medication with neuroleptic drugs or phenothiazine antinauseants.
- Failure to maintain elevation of the head during the procedure, on the stretcher, or in bed.
- Excessive and particularly active patient movement or straining.

PRECAUTIONS–General: Diagnostic procedures that involve the use of radiopaque diagnostic agents should be carried out under the direction of personnel with the prerequisite training and with a thorough knowledge of the particular procedure to be performed. Appropriate facilities should be available for coping with any complication of the procedure, as well as for emergency treatment of reactions to the contrast agent itself. After parenteral administration of a radiopaque agent, competent personnel and emergency facilities should be available, since delayed reactions have been reported (see ADVERSE REACTIONS).

Preparatory dehydration may be dangerous and may contribute to acute renal failure in patients with advanced vascular disease, diabetic patients, and in susceptible nondiabetic patients (often elderly with preexisting renal disease). Dehydration in these patients seems to be enhanced by the osmotic diuretic action of contrast agents. *Patients should be well hydrated prior to and following iohexol administration.*

The possibility of a reaction, including serious, life-threatening, fatal, anaphylactoid, or cardiovascular reactions, should always be considered (see ADVERSE REACTIONS). Therefore, it is of utmost importance that a course of action be carefully planned in advance for the immediate treatment of serious reactions, and that adequate and appropriate facilities and personnel be readily available in case of a severe reaction.

The possibility of an idiosyncratic reaction in susceptible patients should always be considered (see ADVERSE REACTIONS). The susceptible population includes patients with a history of a previous reaction to contrast media, patients with a known sensitivity to iodine per se, and patients with a known clinical hypersensitivity: bronchial asthma, hay fever, and food allergies.

A thorough medical history with emphasis on allergy and hypersensitivity prior to the injection of any contrast medium, may be more accurate than pretesting in predicting potential adverse reactions.

A positive history of allergy or hypersensitivity does not arbitrarily contraindicate the use of a contrast agent where a diagnostic procedure is thought essential, but caution should be exercised (see ADVERSE REACTIONS). Premedication with antihistamines or corticosteroids, to avoid or minimize possible allergic reactions in such patients, should be considered.

In patients with severe renal insufficiency or failure, compensatory biliary excretion of the drug is anticipated to occur, with a slow clearance into the bile. Patients with hepatorenal insufficiency should not be examined unless the possibility of benefit clearly outweighs the additional risk. Sterile technique must be used with any spinal puncture.

When OMNIPAQUE is to be injected using plastic disposable syringes, the contrast medium should be drawn into the syringe and used immediately. If nondisposable equipment is used, scrupulous care should be taken to prevent residual contamination with traces of cleansing agents. **Parenteral drug products should be inspected and discarded if particulate matter or discoloration is present.**

Repeat Procedures. If in the clinical judgment of the physician sequential or repeat examinations are required, a suitable interval of time between administrations should be observed to allow for normal clearance of the drug from the body.

Information for Patients: When receiving injectable radiopaque diagnostic agents, inform your physician: If you are pregnant; if you are diabetic; if you have multiple myeloma, pheochromocytoma, homozygous sickle cell disease, or known thyroid disorder; if you are allergic to any drugs or food or if you had any reactions to previous injections of dyes used for x-ray procedures; about any other medications you are currently taking, including nonprescription drugs, before you are administered this drug.

Drug Interactions (See WARNINGS–General): In nonelective procedures in patients on the drugs described, consider prophylactic use of anticonvulsants.

Carcinogenesis, Mutagenesis, Impairment of Fertility: No long-term animal studies have been performed to evaluate carcinogenic potential, mutagenesis, or whether OMNIPAQUE can affect fertility in men or women.

Pregnancy Category B: Reproduction studies have been performed in rats and rabbits with up to 100 times the recommended dose. No evidence of impaired fertility or harm to the fetus has been demonstrated due to OMNIPAQUE; there are, however, no studies in pregnant women. Because animal reproduction studies are not always predictive of human response, this drug should be used during pregnancy only if clearly indicated.

Nursing Mothers: It is not known to what extent iohexol is excreted in human milk. However, many injectable contrast agents are excreted unchanged in human milk. Although it has not been established that serious adverse reactions occur in nursing infants, caution should be exercised when intravascular contrast media are administered to nursing women. Bottle feedings may be substituted for breast feedings for 24 hours following administration of OMNIPAQUE.

Pediatric Use: Safety and effectiveness in children have not been established.

ADVERSE REACTIONS–Intrathecal: The most frequently reported adverse reactions with OMNIPAQUE 180, OMNIPAQUE 240, and OMNIPAQUE 300 are headache, mild to moderate pain including backache, neck ache and stiffness, nausea and vomiting. These reactions usually occur 1 to 10 hours after injection, and almost all occur within 24 hours. They are usually mild to moderate in degree, lasting for a few hours and usually disappearing within 24 hours. Rarely, headaches may be severe or persist for days. Headache is often accompanied by nausea and vomiting and tends to be more frequent and persistent in patients not optimally hydrated. Transient alterations in vital signs may occur and their significance must be assessed on an individual basis. Those reactions reported in clinical studies with OMNIPAQUE are listed below in decreasing order of occurrence, based on clinical studies of 1,624 patients.

Headaches: The most frequently occurring adverse reaction following myelography has been headache, with an incidence of approximately 18%. Headaches may be caused either by a direct effect of the contrast medium or by CSF leakage at the dural puncture site. However, in managing the patient, it is considered more important to minimize intracranial entry of contrast medium by postural management than to attempt to control possible CSF leakage (see PATIENT MANAGEMENT).

Pain: Mild to moderate pain including backache, neck ache and stiffness, and neuralgia occurred following injection, with an incidence of about 8%.

Nausea and Vomiting: Nausea was reported with an incidence of about 6%, and vomiting about 3% (see PATIENT MANAGEMENT). Maintaining normal hydration is very important. The use of phenothiazine antinauseants is not recommended (see WARNINGS–General). Reassurance to the patient that the nausea will clear usually is all that is required.

Dizziness: Transient dizziness was reported in about 2% of the patients.

Other Reactions: Other reactions occurring with an individual incidence of less than 0.1% included: feeling of heaviness, hypotension, hypertonia, sensation of heat, sweating, vertigo, loss of appetite, drowsiness, hypertension, photophobia, tinnitus, neuralgia, paresthesia, difficulty in micturition, and neurological changes. All were transient and mild with no clinical sequelae.

General Adverse Reactions to Contrast Media: Physicians should remain alert for the occurrence of adverse effects in addition to those discussed above, particularly the following reactions which have been reported in the literature for other nonionic, water-soluble myelographic media and rarely with iohexol. These have included, but are not limited to, aseptic and bacterial meningitis and CNS and other neurologic disturbances.

An aseptic meningitis syndrome has been reported rarely (less than 0.01%). It was usually preceded by pronounced headaches, nausea, and vomiting. Onset usually occurred about 12 to 18 hours postprocedure. Prominent features were meningismus and fever, sometimes with oculomotor signs and mental confusion. Lumbar puncture revealed a high white cell count and high protein content, often with a low glucose level and absence of organisms. The condition usually started to clear spontaneously about 10 hours after onset, with complete recovery over 2 to 3 days.

Allergy or Idiosyncrasy: Chills, fever, profuse diaphoresis, pruritus, urticaria, nasal congestion, dyspnea, and Guillain-Barré syndrome.

CNS Irritation: Mild and transitory perceptual aberrations, such as hallucinations, depersonalization, amnesia, hostility, amblyopia, diplopia, photophobia, psychosis, insomnia, anxiety, depression, hyperesthesia, visual or auditory or speech disturbances, confusion and disorientation. In addition, malaise, weakness, EEG changes, meningismus, hyperreflexia or areflexia, hypertonia or flaccidity, hemiplegia, paralysis, quadriplegia, restlessness, tremor, echoacousia, echolalia, asterixis, and dysphasia have occurred.

Profound mental disturbances have also rarely been reported; various forms and degrees of aphasia, mental confusion, or disorientation. Onset is usually at 8 to 10 hours and lasts for about 24 hours. Occasionally, they have been manifest as apprehension, agitation, or progressive withdrawal in several instances to the point of somnolence, stupor, and coma. In a few cases, these have been accompanied by transitory hearing loss or other auditory symptoms and visual disturbances (believed subjective or delusional), including unilateral or bilateral loss of vision, which may last for hours. In one case, persistent cortical loss of vision has been reported in association with convulsions. Ventricular block has been reported; amnesia of varying degrees may be present for the reaction event.

Rarely, persistent though transitory weakness in the leg or ocular muscles has been reported. Peripheral neuropathies have been rare and transitory. They include sensory and/or motor or nerve root disturbance, myelitis, persistent leg muscle pain or weakness, 6th nerve palsy, or cauda equina syndrome. Muscle cramps, fasciculation or myoclonia, spinal convulsion, or spasticity are unusual and have responded promptly to a small intravenous dose of diazepam.

In general, the reactions that are known to occur on parenteral administration of iodinated contrast agents are possible with any nonionic agent. Approximately 95% of adverse reactions accompanying the use of water-soluble contrast agents are mild to moderate in degree. However, severe, life-threatening, anaphylactoid, and fatal reactions, mostly of cardiovascular origin, have occurred. Adverse reactions to injectable contrast media fall into two categories: chemotoxic reactions and idiosyncratic reactions.

Chemotoxic reactions result from the physicochemical properties of the contrast medium, the amount of the dose and the speed of injection. All hemodynamic disturbances and injuries to organs or vessels perfused by the contrast medium are included in this category.

Idiosyncratic reactions occur more frequently in patients 20 to 40 years old and may or may not be dependent on the amount of dose injected, the speed of injection, and the radiographic procedure. They are subdivided into minor, intermediate, and severe. The minor reactions are self-limited and of short duration; the severe reactions are life-threatening, and treatment is urgent and mandatory.

The reported incidence of adverse reactions to the contrast medium in patients with a history of allergy is twice that of the general population. Patients with a history of previous reactions to a contrast medium are three times more susceptible than other patients. However, sensitivity to contrast media does not appear to increase with repeated examination.

Most adverse reactions to injectable contrast media appear within 1 to 3 minutes after the start of injection, but delayed reactions may occur.

OVERDOSAGE: Although clinical consequences of overdosage with OMNIPAQUE have not been reported, physicians should be aware that incorrect management of the patient can permit inadvertent early intracranial entry of normal doses of the medium, thereby increasing CNS reactions.

The intracisternal LD_{50} value of OMNIPAQUE (in grams of iodine per kilogram body weight) is greater than 2.0 in mice.

References: 1. Kieffer SA, Binet EF, Davis DO, et al: Lumbar myelography with iohexol and metrizamide: A comparative multicenter prospective study. *Radiology* 1984; 151:665-670. **2.** Shaw DD, Bach-Gansmo T, Dahlstrom K: Iohexol: summary of North American and European clinical trials in adult lumbar, thoracic, and cervical myelography with a new nonionic contrast medium. *Invest Radiol* 1985; 20(suppl 1):44-50. **3.** Latchaw RE, Hirsch WL Jr, Horton JA, et al: Iohexol vs metrizamide: Study of efficacy and morbidity in cervical myelography. *AJNR* 1985; 6:931-933. **4.** Data on file, Winthrop Pharmaceuticals. **5.** Lamb JT: Iohexol vs iopamidol for myelography. *Invest Radiol* 1985; 20(suppl 1):37-43.

© 1987 WINTHROP PHARMACEUTICALS 71171/3777

Winthrop PHARMACEUTICALS
Winthrop Pharmaceuticals
Division of Sterling Drug Inc.
New York, NY 10016



FUJI...Easier is Better!

FUJI FILM THERMAL IMAGING SYSTEM ■ World's only self-fixing, polyester base, thermal film ■ Sharper, clearer images ■ Superior archival quality ■ Fast! Records up to 4 images per minute ■ Hard copy in only 22 seconds ■ No trips to the darkroom ■ 100% room light loading (300 exposures per roll) **■ No film processor required ■ Tough film base eliminates wrinkling**

With the push of a button or foot switch you can make a hard copy from a standard video signal – in room light – in just 22 seconds and make duplicate or enhanced originals using the built-in image memory. FUJI Thermal Film produces images that are sharper, clearer and last longer when compared to conventional thermal paper. FUJI's MI (Micro-Isolating) technology protects the images from the effects of heat and chemicals. Contact your FUJI MEDICAL SYSTEMS representative for a demonstration.



The world's only self-fixing polyester base, thermal film.

FUJI QUALITY UNCOMMONLY CONSISTENT.

I&I *Imaging & Information*

FUJI MEDICAL SYSTEMS U.S.A., INC.
90 Viaduct Road, Stamford, CT 06907
(800) 431-1850 In CT – (203) 353-0300

CIRCLE 7 ON READER SERVICE CARD

Volume 149 **American Journal of Roentgenology** August 1987

SPECIAL REPORT

223 **High-temperature superconductors: will new materials take the chill off our magnets?** *Crooks LE, Kelley D*

BILIARY LITHOTRIPSY

227 **Perspective. Biliary lithotripsy: what will the issues be?** *Ferrucci JT*

233 **Perspective. The promise of extracorporeal shock-wave lithotripsy for the treatment of gallstones.** *Burhenne HJ*

CARDIOPULMONARY RADIOLOGY

237 **Measurement of myocardial infarct size at early and late time intervals using MR imaging: an experimental study in dogs.** *Caputo GR, Sechtem U, Tscholakoff D, Higgins CB*

245 **Instant images of the human heart using a new, whole-body MR imaging system.** *Rzedzian RR, Pykett IL*

251 **Vascular rings: MR imaging.** *Bisset GS III, Strife JL, Kirks DR, Bailey WW*

257 **Giant right atrium after mitral valve replacement: plain film findings in 15 patients.** *Rubin SA, Hightower CW, Flicker S*

261 **Case report. Compression of left main bronchus and left pulmonary artery by thoracic aortic aneurysm.** *Duke RA, Barrett MR II, Payne SD, Salazar JE, Winer-Muram HT, Tonkin IL*

265 **Nonspecific interstitial pneumonitis in patients with AIDS: radiologic features.** *Simmons JT, Suffredini AF, Lack EE, et al.*

269 **Thymic atrophy and regrowth in response to chemotherapy: CT evaluation.** *Choyke PL, Zeman RK, Gootenberg JE, Greenberg JN, Hoffer F, Frank JA*

273 **Case report. Congenital absence of the azygos vein: a cause for "aortic nipple" enlargement.** *Hatfield MK, Vyborny CJ, MacMahon H, Chessare JW*

275 **Evaluation of optical unsharp masking and contrast enhancement of low-scatter chest radiographs.** *Sorenson JA, Mitchell CR*

BREAST RADIOLOGY

283 **Two-view specimen radiography in surgical biopsy of nonpalpable breast masses.** *Rebner M, Pennes DR, Baker DE, Adler DD, Boyd P*

GASTROINTESTINAL RADIOLOGY

287 **Pictorial essay. Imaging of surgically relevant hepatic vascular and segmental anatomy. Part 1. Normal anatomy.** *Mukai JK, Stack CM, Turner DA, et al.*

293 **Pictorial essay. Imaging of surgically relevant hepatic vascular and segmental anatomy. Part 2. Extent and resectability of hepatic neoplasms.** *Mukai JK, Stack CM, Turner DA, et al.*

299 **Abdominal sonography after hepatic transplantation: results in 36 patients.** *Letourneau JG, Day DL, Ascher NL, et al.*

305 **Case report. Gallium-67 detection of occult gastric lymphoma in AIDS.** *Gianfelice D, Rosenthall L, Falutz J*

307 **Esophageal radiography and manometry: correlation in 172 patients with dysphagia.** *Ott DJ, Richter JE, Chen YM, Wu WC, Gelfand DW, Castell DO*

GENITOURINARY RADIOLOGY

313 **Case report. Urethroplasty with balloon catheter in prostatic hypertrophy.** *Castaneda F, Johnson S, Hulbert J, et al.*

315 **The accuracy of CT in the staging of carcinoma of the prostate.** *Platt JF, Bree RL, Schwab RE*

319 **Case report. Control of postoperative vaginal hemorrhage by embolization of the medial circumflex femoral artery.** *Odurny A, Colapinto RF*

321 **Case report. Duplex Doppler evaluation of puerperal ovarian vein thrombosis.** *Baran GW, Frisch KM*

MUSCULOSKELETAL RADIOLOGY

323 **Vertebral erosions in patients undergoing maintenance hemodialysis for chronic renal failure.** *Sundaram M, Seelig R, Pohl D*

329 **Stress fractures of the distal tibia and calcaneus subsequent to acute fractures of the tibia and fibula.** *Zlatkin MB, Bjorkengren A, Sartoris DJ, Resnick D*

333 **MR imaging of the shoulder: diagnosis of rotator cuff tears.** *Kneeland JB, Middleton WD, Carrera GF, et al.*

339 **Skeletal measurements using a flying spot digital imaging device.** *Wilson AJ, Ramsby GR*

345 **Technical note. A device for maintaining cervical spine stabilization and traction during CT scanning.** *Stimac GK, Burch D, Livingston RR, Anderson P, Dacey RG*

PALEORADIOLOGY

347 **Commentary. Arctic paleoradiology: portable radiographic examination of two frozen sailors from the Franklin Expedition (1845–1848).** *Notman DNH, Anderson L, Beattie OB, Amy R*

NEURORADIOLOGY

351 **MR signal abnormalities at 1.5 T in Alzheimer's dementia and normal aging.** *Fazekas F, Chawluk JB, Alavi A, Hurtig HI, Zimmerman RA*

357 **Reduced signal intensity on MR images of thalamus and putamen in multiple sclerosis: increased iron content?** *Drayer B, Burger P, Hurwitz B, Dawson D, Cain J*

365 **Study of movement disorders and brain iron by MR.** *Rutledge JN, Hilal SK, Silver AJ, Defendini R, Fahn S*

380 **Technical note. New needle for MR-guided aspiration cytology of the head and neck.** *Lufkin R, Teresi L, Hanafee W*

383 **MR of craniopharyngiomas: tumor delineation and characterization.** *Pusey E, Kortman KE, Flannigan BD, Tsuruda J, Bradley WG*

389 **Adverse reactions after iohexol lumbar myelography: influence of postprocedural positioning.** *Kuuliala IK, Göransson HJ*

PEDIATRIC AND FETAL RADIOLOGY

391 **Hepatic regenerating nodules in hereditary tyrosinemia.** *Day DL, Letourneau JG, Allan BT, et al.*

395 **Anorectal atresia: prenatal sonographic diagnosis.** *Harris RD, Nyberg DA, Mack LA, Weinberger E*

401 **Case report. Gallbladder contraction in biliary atresia.** *Weinberger E, Blumhagen JD, Odell JM*

403 **The coexistence of obstruction at the ureteropelvic and ureterovesical junctions.** *McGrath MA, Estroff J, Lebowitz RL*

407 **Multicystic dysplasia and crossed renal ectopia.** *Nussbaum AR, Hartman DS, Whitley N, McCauley RGK, Sanders RC*

COMPUTER PAGE

411 **Computerized reference management—filing the literature.** *Gurney JW, Wigton RS*

ARRS NEWS

415 **ARRS presidential address.** *Gagliardi RA*

418 **1987 ARRS awards for distinguished service to radiology.** *Gagliardi RA*

420 **ARRS secretary's report.** *Hartman GW*

422 **ARRS award-winning scientific exhibits, 1987**

424 **ARRS new members**

426 **ARRS membership invitation and application**

430 **ARRS 1988 meeting summary and calls for papers and exhibits**

OTHER CONTENT

264 **ARRS resident award papers**

312 **Editorial. AJR achieves goal to speed publication.** *Berk RN*

338 **Memorial, Alan Ward Shriver**

414 **Forthcoming articles**

435 **Resident education. Instruction in image processing for residents in diagnostic radiology.** *Huang HK, Bassett LW, Mankovich NJ, Cho P, Kangarloo H, Seeger L*

438 **Perspective. Women in academic radiology.** *Whitley NO*

440 **Letters**

442 **Review of current literature**

446 **News**

449 **Classified ads**

Book reviews 226, 232, 236, 244, 282, 298, 304, 328, 364

394 **Software review**

429 **American Roentgen Ray Society information**

A3 **Guidelines for Authors**

1988 ARRS Meeting: May 8–13, San Francisco, CA

AJR

Acc.
16.12.87

American
Journal of
Roentgenology

September 1987

Precise localization of non-palpable lesions ...from E-Z-EM

PercuGuide™

Regardless of your present method of marking non-palpable lesions, PercuGuide™ can improve upon it.

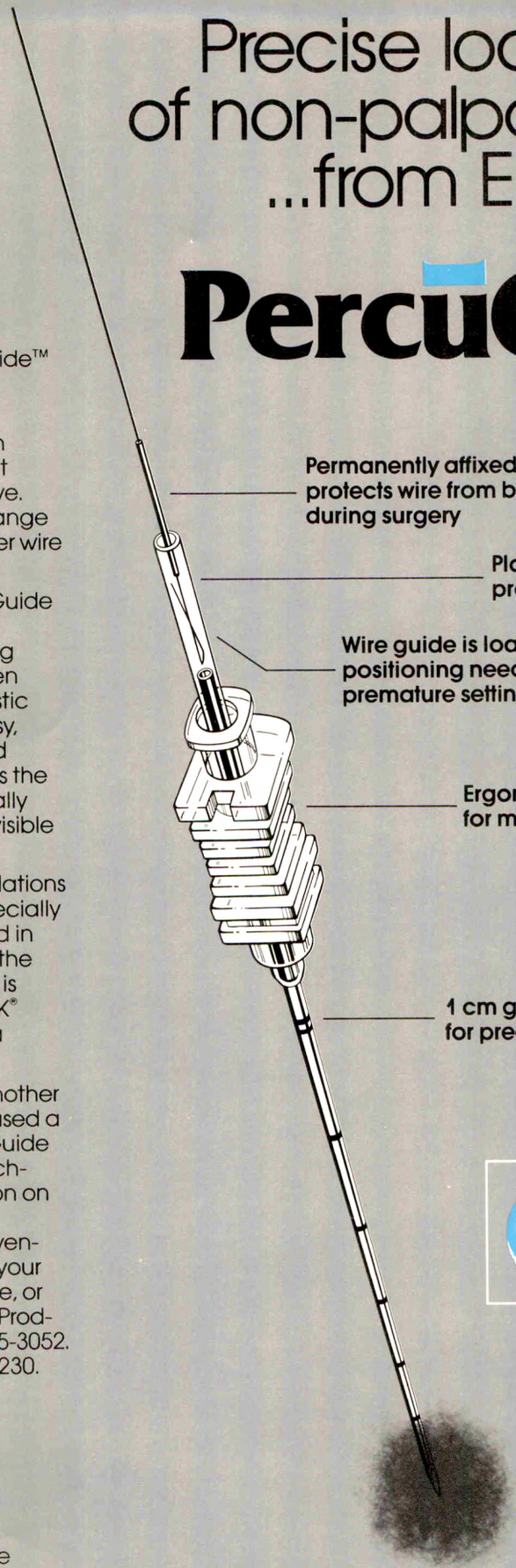
Unlike improvised markers, PercuGuide can't shift with patient movement. It won't disperse over time like a dye. And PercuGuide offers a range of refinements that no other wire guide system can match.

Afterloading of the PercuGuide wire guide eliminates any chance of the barb seating before the needle has been properly positioned. A plastic sheath makes loading easy, and a permanently affixed stiffening cannula protects the wire from being accidentally severed while it acts as a visible guide for the surgeon.

Clearly marked 1 cm gradations on the cannula, and a specially designed gripping hub aid in the precise placement of the needle. And each needle is supplied with an E-Z-MARK® radiopaque marker and a handy ruler.

If you're presently using another system, or if you've never used a wire guide before, PercuGuide can help improve your technique. For more information on PercuGuide, or on any of E-Z-EM's products for interventional medicine, contact your local E-Z-EM representative, or call E-Z-EM Interventional Products Marketing at 1-800-645-3052. In New York call 516-333-8230.

E-Z-EM
More than barium—
much more





E-Z-MARK® radiopaque marker provided with each PercuGuide needle

E-Z-EM®
E-Z-EM, Inc.,
7 Portland Avenue
Westbury, N.Y. 11590

© 1987 E-Z-EM, Inc.

CIRCLE 5 ON READER SERVICE CARD

Official Journal of the American Roentgen Ray Society

AJR

American Journal of Roentgenology
Diagnostic Imaging and Related Sciences

Editor-In-Chief Robert N. Berk, *San Diego, California*

Editor Emeritus Melvin M. Figley, *Seattle, Washington*

Associate Editor Saskia von Waldenburg Hilton, *San Diego, California*

Consulting Editor Juan M. Taveras, *Boston, Massachusetts*

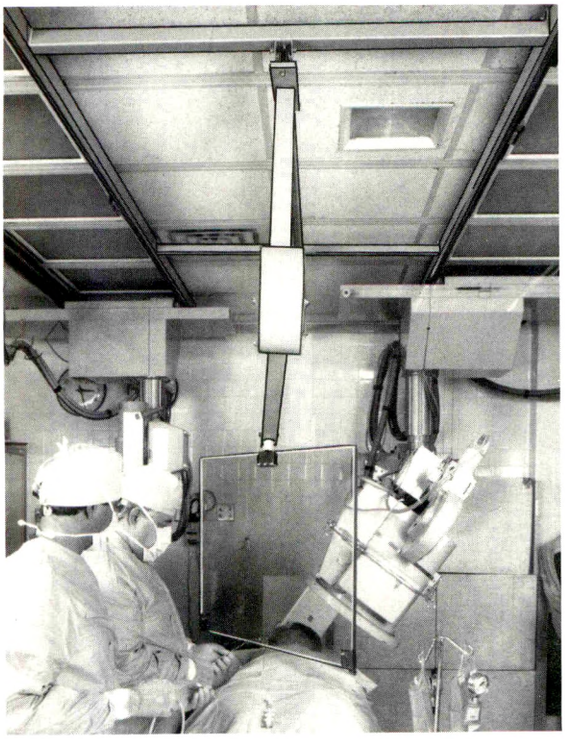
Assistant Editors

John R. Amberg
William L. Ashburn
Itamar Aviad
Lawrence W. Bassett
Charles C. Berry
Gregory P. Borkowski
William G. Bradley
Peter L. Cooperberg
Peter M. Doubilet
N. Reed Dunnick
David K. Edwards
Ronald G. Evens
David S. Feigin
William R. Hendee
Robert J. Herfkens
John R. Hesselink
Charles B. Higgins
Melvyn T. Korobkin
Thomas L. Lawson
Bruce L. McClennan
Albert A. Moss
Jeffrey H. Newhouse
Donald L. Resnick
Stewart R. Reuter
Stuart S. Sagel
David J. Sartoris
Edward A. Sickles
Barry A. Siegel
Eric vanSonnenberg
David D. Stark
Edward T. Stewart

Editorial Staff: Elizabeth A. Whalen, *publications supervisor*; Linda Wood, Barbara Rose, and Barbara L. Halliburton, *manuscript editors*; Nancy Rydbeck, *office manager*; Sandra Wood, *administrative assistant*; Geraldine Perillo, *administrative secretary*.

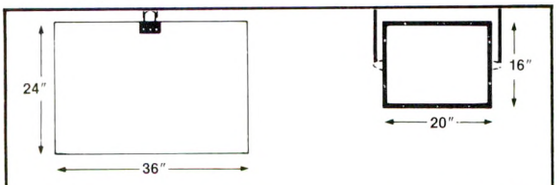
All business correspondence, including display (not classified) advertising, subscriptions, address changes, reprints, and permission requests should be addressed to Williams & Wilkins, 428 East Preston Street, Baltimore, MD 21202. Correspondence regarding editorial matters and classified advertising should be addressed to the editorial office, AJR, 2223 Avenida de la Playa, Suite 200, La Jolla, CA 92037-3218. For manuscript submission, see Guidelines for Authors, next page. Undelivered or damaged copies replaced within 60 days of publication; 90 days for foreign subscribers. Allow 90 days for address changes.
AJR AMERICAN JOURNAL OF ROENTGENOLOGY (ISSN 0361 803X) is published monthly by American Roentgen Ray Society, 428 E. Preston Street, Baltimore, MD 21202. Annual dues include $50 for journal subscription. Second class postage paid at Baltimore, MD and at additional mailing offices. Postmaster send address changes (Form 3579) to Williams & Wilkins, 428 East Preston St., Baltimore, MD 21202. Subscription rates $90 ($120 foreign); institutions $100 ($130 foreign); in training $25; single copy $16 ($19). Japanese yen price is available from our sole agent USACO Corporation, 13-12, Shimbashi 1-Chome, Minato-Ku, Tokyo 105, Japan, telephone 03-502-6471. Subscriptions in South Korea are available only through our sole agent in Korea: Korea-America Medical Books Co., Ltd. (KAMBOOK) 209 Yun kun-dong, Chongro-ku, Seoul, Korea (telephone: 745-3151; telex: K25211 KAMBC; FAX: 745-3153) All subscriptions to South Korea will be shipped by air freight after January 1, 1988. There is an air freight surcharge of $12.00 over the regular subscription rate for this journal in South Korea to partially compensate for air freight costs. Airmail rates furnished on request. Indexed by *Current Contents* and *Index Medicus*. Copyright © 1987 by American Roentgen Ray Society.
0361-803X/87 $2.00

THE UNMATCHED CHOICE BIGGER SHIELDING AREA... EASY TO USE



CLEAR-Pb® LEAD-PLASTIC OVERHEAD X-RAY BARRIER

For Cardiac Catheterization and Special Procedures Personnel



OURS: This is a CLEAR-Pb Lead-Plastic Overhead X-Ray Barrier. It measures 24″ × 36″.

THEIR BARRIER: Measures only 16″ × 20″.

Our CLEAR-Pb Overhead X-Ray Barrier is more than *twice* the size of *their* barrier. Shatter-resistant lead-plastic (0.5mm lead equivalency), provides *twice* as much protection from scatter radiation! Panoramic, crystal-clear visibility... protection for two people, if required. A counter-balanced ceiling suspension system with easy-glide overhead track saves space *and* allows for quick, exact barrier positioning.

For complete details, request Bulletin 373-C

NUCLEAR ASSOCIATES

VICTOREEN

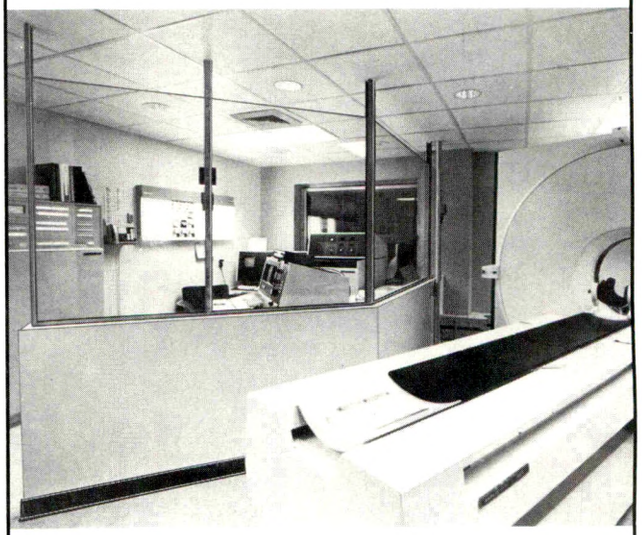
A Division of VICTOREEN, INC.
100 VOICE ROAD
CARLE PLACE, NY 11514-1593
(516) 741-6360
A Subsidiary of Sheller-Globe SG

® Victoreen, Inc.

For X-Ray Room Shielding...

HOSPITALS PREFER

CLEAR-Pb® Lead-Plastic Modular Barriers and Windows



- **Shatter-resistant transparent panels up to 6 x 8 ft. (larger sizes on request).**
- **Panoramic viewing areas, even in limited space.**
- **Quick, on-site modular installation.**
- **Attractive, space-saving, decorator look.**
- **Choice of lead equivalency — 0.5 to 1.5 mm.**

CLEAR-Pb is a lead-impregnated plastic sheet that combines superb light transmission with total radiation protection. When you specify a CLEAR-Pb Modular Barrier you get enormous design flexibility. Walls are only about 1½″ thick, and windows come in all sizes up to a panoramic 6 x 8 ft.

For more details, request Bulletin 3181-C

We'll also send you a FREE CLEAR-Pb Planning Guide illustrating dozens of user-designed applications, and a FREE sample of CLEAR-Pb lead-plastic. Write or phone our CLEAR-Pb Product Manager at (516) 741-7717.

NUCLEAR ASSOCIATES

VICTOREEN

A Division of VICTOREEN, INC.
100 VOICE ROAD
CARLE PLACE, NY 11514-1593
(516) 741-6360
A Subsidiary of Sheller-Globe SG

® Victoreen, Inc.

CIRCLE 16 ON READER SERVICE CARD

AJR Guidelines for Authors

Address new and revised manuscripts, correspondence, and classified ads to the Editor:

AJR Editorial Office
2223 Avenida de la Playa, Suite 200
La Jolla, CA 92037-3218 Telephone: (619) 459-2229

Inquiries regarding subscriptions, display advertising, reprints, or permission to republish *AJR* material should be addressed to the publisher:

The Williams & Wilkins Co.
428 E. Preston St.
Baltimore, MD 21202 Telephone: (301) 528-4133

The *AJR* publishes original contributions to the advancement of medical diagnosis and treatment. Submitted manuscripts should not contain previously published material and should not be under consideration for publication elsewhere. Papers dealing with neuroradiology should be addressed to: American Journal of Neuroradiology, Dept. of Radiology, Massachusetts General Hospital, Boston, MA 02114. At the discretion of the *AJR* Editor, *AJNR* articles that are of interest to the general reader may be republished in the *AJR*. Neuroradiologic papers sent to the *AJR* will be forwarded to the Editorial Office of the *AJNR*.

Manuscript decisions are based on peer review. Reviewers receive manuscripts without title pages to ensure an unbiased review. All accepted manuscripts are subject to editing. Statements made in the article, including changes made by the Editor or manuscript editor, are the responsibility of the author and not of the *AJR* or its publisher. Authors will be sent the edited manuscript, galley proof, and proofs of illustrations. If the corresponding author will be unavailable to review galleys, arrangements should be made for a coauthor or colleague to read and return the proof.

General Guidelines for Major Papers

Abstract. Clearly state (in 200 words or less) the purpose, methods, results, and conclusions of the study. Include actual data.

Introduction. Briefly describe the purpose of the investigation, including relevant background information.

Methods. Describe the research plan, the materials (or subjects), and the methods used, in that order. Explain in detail how disease was confirmed and how subjectivity in observations was controlled.

Results. Present results in a clear, logical sequence. If tables are used, do not duplicate tabular data in text, but do describe important trends and points.

Discussion. Describe the limitations of the research plan, materials (or subjects), and methods, considering both the purpose and the outcome of the study. When results differ from those of previous investigators, explain the discrepancy.

AUTHOR'S CHECKLIST

For priority handling, complete the following checklist, sign the copyright form on the reverse side of this page, and include both with the manuscript.

_____ Two copies of the manuscript (the original and a photocopy) and two complete sets of figures are submitted. One copy has been retained by the author.

_____ If appropriate, *AJR* Guidelines for case reports, technical notes, pictorial essays, or letters to the Editor have been followed. (See page A5.)

_____ The manuscript, including references, figure legends, and tables, is typed double-spaced on 8½ × 11 in. (21.6 × 27.9 cm) nonerasable paper. Right-hand margins are not justified.

_____ All manuscript pages are numbered consecutively beginning with the abstract. Authors' names do not appear on the manuscript pages.

_____ The manuscript is organized as follows: title page, blind title page (title only), abstract, introduction, methods, results, discussion, acknowledgments, references, tables, figure legends, and figures.

_____ Informed consent has been obtained from patients who participated in clinical investigations. If experiments were performed on animals, authors complied with NIH guidelines for use of laboratory animals.

_____ Use of unfamiliar acronyms and abbrevations is kept to a minimum. When abbreviations are used they are defined at first mention, followed by the abbreviation in parentheses.

_____ Metric measurements are used throughout, or the metric equivalent is given in parentheses.

_____ Names and locations (city and state only) of manufacturers are given for equipment and nongeneric drugs.

Title Page

_____ The following information is given: title of article; names and complete addresses (including zip code) of all authors; current addresses of authors who have moved since study; acknowledgment of grant or other assistance. The corresponding author is clearly identified, and a current address and phone number are given.

_____ Two copies of a blind title page are included giving only the title (without the authors' names) for use in the review process.

Abstract

_____ An abstract of approximately 200 words concisely states the purpose, methods, and results of the study in one paragraph. Actual data are included.

_____ No abbreviations or reference citations are used.

_____ Conclusions are stated in a second, summary paragraph.

References

_____ References (not to exceed 35) are typed double-spaced starting on a separate page and are **numbered consecutively in the order in which they appear in the text**.

_____ All references are cited in the text and are enclosed in brackets and typed on line with the text (not superscript).

_____ Unpublished data are not cited in the reference list, but are cited parenthetically in the text, for example, (Smith DJ, personal communication), (Smith DJ, unpublished data). This includes papers submitted, but not yet accepted, for publication.

_____ Inclusive page numbers (e.g., 333–335) are given for all references.

_____ Journal names are abbreviated according to *Index Medicus*.

_____ Style and punctuation of references follow the format illustrated in the following examples (all authors are listed when six or less; when seven or more authors, the first three are listed, followed by "et al."):

Journal article

1. Long RS, Roe EW, Wu EU, et al. Membrane oxygenation: radiographic appearance. *AJR* **1986**;146:1257–1260

Book

2. Smith LW, Cohen AR. *Pathology of tumors*, 6th ed. Baltimore: Williams & Wilkins, **1977**:100–109

Chapter in a book

3. Breon AJ. Serum monitors of bone metastasis. In: Clark SA, ed. *Bone metastases*. Baltimore: Williams & Wilkins, **1983**:165–180

Paper presented at a meeting

4. Lau FS, Kirk AN, Beck RA. MR imaging of the spine. Presented at the annual meeting of the American Roentgen Ray Society, Washington, DC, April 1986

Tables

_____ Each table is typed double-spaced on a separate page without vertical or horizontal rules; each has a short, descriptive title. Tables do not exceed two pages in length and contain at least four lines of data.

_____ Tables are numbered in the order in which they are cited in the text.

_____ Abbreviations are defined in an explanatory note below each table.

_____ Tables are self-explanatory and do not duplicate data given in the text or figures.

_____ All arithmetic (percentages, totals, differences) has been double checked for accuracy, and tabular data agree with data given in the text.

Figures and Legends

_____ Two complete sets of original figures are submitted unmounted in labeled envelopes.

_____ Figures are clean, unscratched, 5 × 7 in. (13 × 18 cm) glossy prints with white borders. A separate print is submitted for each figure *part*.

_____ All figure parts relating to one patient are in one figure.

_____ Each figure is labeled on the back with the figure number and an arrow indicating "top." Labeling is done on a gummed label, which is then affixed to the back of the print. (Never use ink on front or back of figures.)

_____ Author's names are *not* written on the backs of figures.

_____ Only removable (rub-on) arrows and letters are used on the figures. Symbols are uniform in size and style and are not broken or cracked.

_____ Images are uniform in size and magnification.

_____ Line drawings are done in black ink on a white background and are of professional quality. (Only glossy prints, not originals or photocopies, are acceptable.)

_____ Written permission has been obtained for use of all previously published illustrations (and copies of permission letters are included), and an appropriate credit line is given in the legends.

_____ Legends are typed double-spaced, and figure numbers correspond with the order in which the figures are cited in the text.

Transfer of Copyright Agreement and Exclusive Publication Statement

Complete copyright to the article entitled: _____

_____

is hereby transferred to the American Roentgen Ray Society (for United States government employees to the extent transferable), effective if and when the article is accepted for publication in the *American Journal of Roentgenology*. In the case of the authors who are officers or employees of the United States government, the American Roentgen Ray Society recognizes that works prepared by officers or employees of the United States government as part of their official government duties are in the public domain.

Authors reserve all proprietary rights other than copyright, such as patent rights and the right to use all or part of this article in future works of their own. The authors retain the right of replication, subject only to crediting the original source of publication and receiving written permission from the publisher.

Authors guarantee that this manuscript contains no matter that is libelous or otherwise unlawful, invades individual privacy, or infringes any proprietary rights.

Authors understand that they will receive no royalty or other compensation from the American Roentgen Ray Society or the publisher.

Finally, the authors certify that none of the material in this manuscript has been published previously or is currently under consideration for publication elsewhere.

_____	_____	_____
First author/date	Second author	Third author
_____	_____	_____
_____	_____	_____

This agreement must be signed by all authors in order for the manuscript to be published.

Case Reports

A case report is a brief description of a special case that provides a message that transcends the individual patient.

Format. There is no abstract. The introduction should be a short paragraph giving the general background and the specific interest of the case. No more than one case should be described in detail (similar ones can be mentioned briefly in the discussion). Emphasis should be on the radiologic aspects; clinical information must be limited to that necessary to provide a background for the radiology. The discussion should be succinct and should focus on the specific message and relevance of radiologic methods. A review of the literature is not appropriate.

Length. Maximum of five double-spaced, typewritten pages, including the references but not the title page or figure legends.

References. Maximum of eight.

Figures. Maximum of three or four, unless the text is shortened accordingly. Legends must not repeat the text.

Tables and Acknowledgments. Not appropriate in case reports.

Technical Notes

A technical note is a brief description of a specific technique or procedure, modification of a technique, or equipment of interest to radiologists.

Format. No abstract, headings, or subheadings are required. If headings are used, they should be a combination of "Case Report," "Materials and Methods," "Results," and "Discussion." A brief one-paragraph introduction should be included to give the general background. Discussion should be limited to the specific message, including the uses of the technique or equipment. Literature reviews and lengthy case reports are not appropriate.

Length. Maximum of five double-spaced, typewritten pages, including the references but not the title page or figure legends.

References. Maximum of eight.

Figures. Maximum of two, unless the text is shortened accordingly.

Tables and Acknowledgments. Not appropriate in technical notes.

Pictorial Essays

A pictorial essay is an article that conveys its message through illustrations and their legends. Unlike other *AJR* articles, which are based on original research, pictorial essays serve primarily as teaching tools, like exhibits at a scientific meeting. They are not encyclopedic book chapters. No abstract is necessary.

Length. Maximum of four double-spaced, typewritten pages, including the references but not the title page or figure legends.

References. Maximum of four.

Figures. Maximum of 30 figure *parts*. Number should be as few as necessary to convey the message of the paper.

Tables and Acknowledgments. Not appropriate in pictorial essays.

Letters to the Editor and Replies

Letters to the Editor and Replies should offer objective and constructive criticism of published articles. Letters may also discuss matters of general interest to radiologists.

Format. All letters should be typed double-spaced on nonletterhead paper, with no greeting or salutation. Signature and affiliation should appear at the end of the letter. Titles for letters should be short and pertinent. The title for a reply is simply "Reply."

Length. Maximum of two double-spaced, typewritten pages, including references.

References. Maximum of four.

Figures. Maximum of two.

Tables and Acknowledgments. Not appropriate in Letters to the Editor and Replies.

Opinions, Commentaries, and Perspectives

Opinions, commentaries, and perspectives are special articles dealing with controversial topics or issues of special concern to radiologists.

Format. Include a title page but no abstract. Headings may be used to break up the text.

Length. Maximum of five double-spaced, typewritten pages.

References. Maximum of five.

Tables and Figures. Maximum of four.

Computer Page Articles

Articles published on the computer page deal with practical computer applications to radiology.

Format. Include a title page but no abstract.

Length. Maximum of eight double-spaced, typewritten pages.

References. Maximum of five.

Figures and Tables. Maximum of five. Computer printouts are not acceptable. Figures must be submitted as 5 × 7 in. glossy prints.

All submissions to the *AJR* must be accompanied by a completed copy of the Author's Checklist and the signed Copyright Agreement.

YOUR PICTURE OF QUALITY FROM KODAK



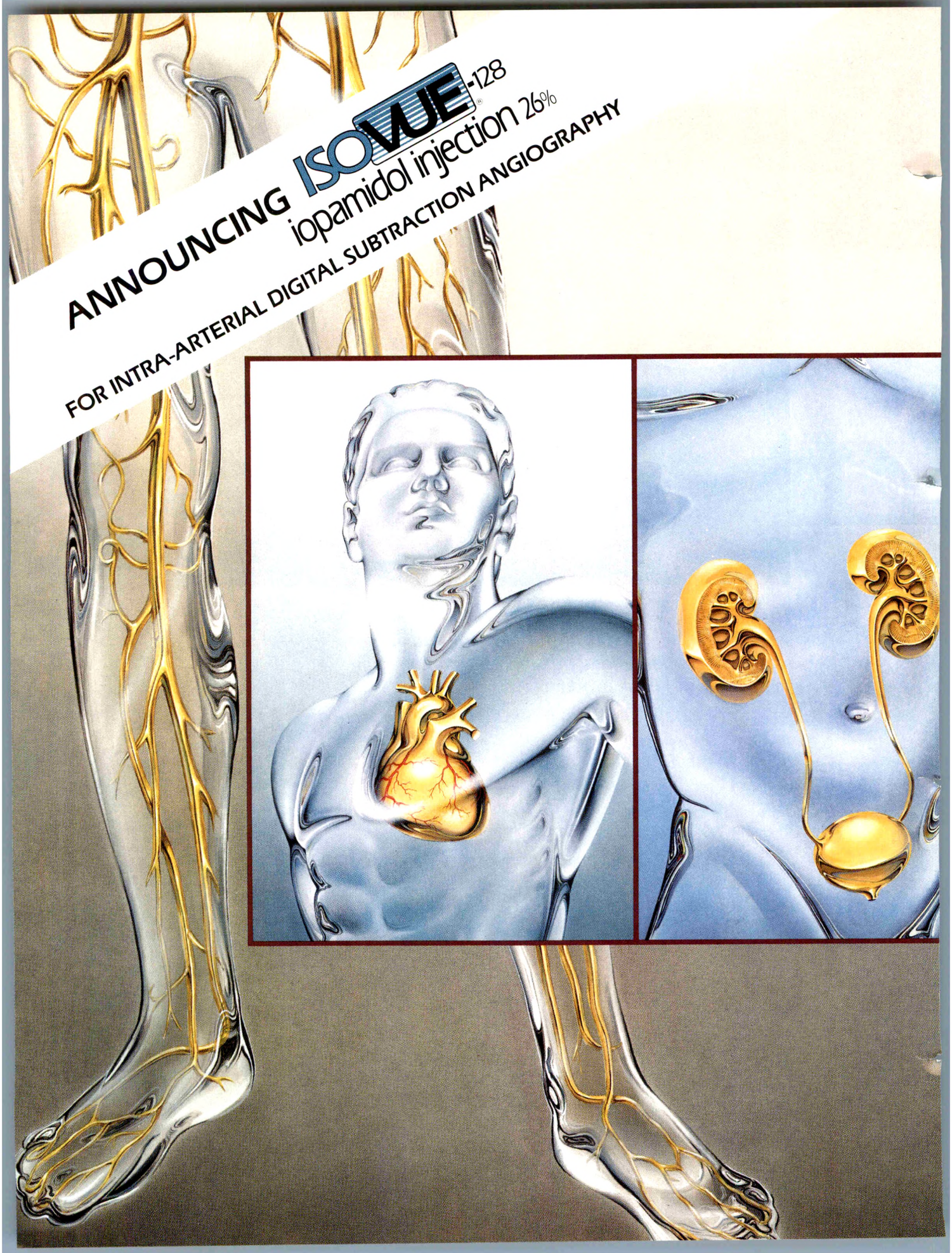
The engineers, representatives, researchers and service people of Kodak. Before, during and after the sale, their single-minded mission is to stand behind the quality of Kodak products.

You won't literally find them inside the yellow box, with the product. But, in spirit, they're very much there. They design in quality in the first place. They make sure you get all of it out that they put in. And, when there is a problem, they fix it right and fast. It's a dedication to quality instilled in every person in every part of Kodak.

Indeed, this dedication extends far beyond product, to phases of your operation as diverse as matters of finance, management and education. The program is called Kodak Resources for Healthcare Management. Your Kodak representative has the details.

The new vision of Kodak

© Eastman Kodak Company, 1987

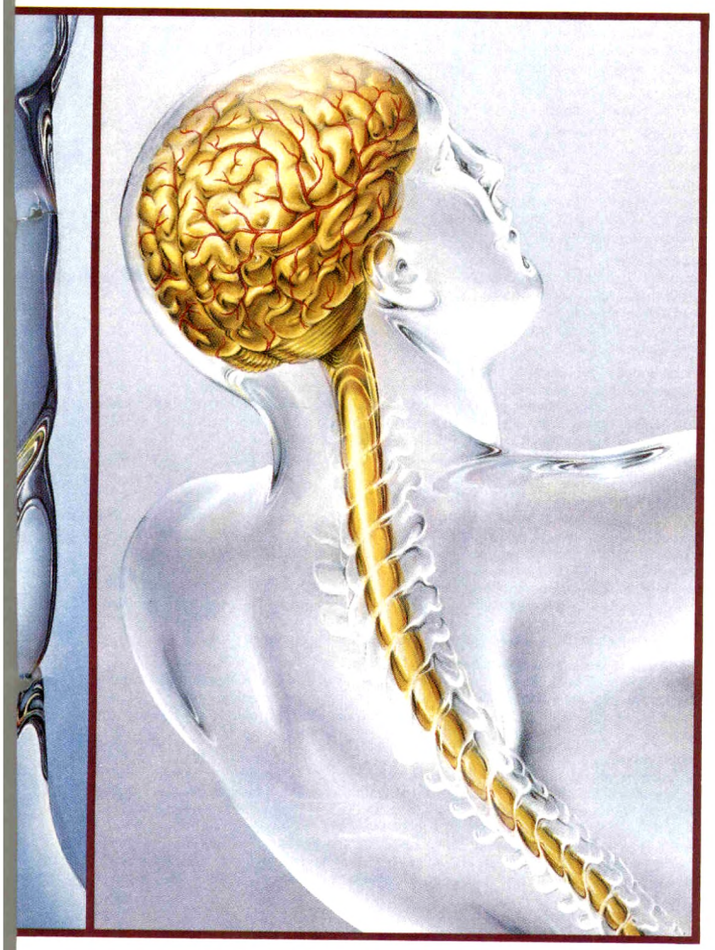

ANNOUNCING ISOVUE®-128
iopamidol injection 26%
FOR INTRA-ARTERIAL DIGITAL SUBTRACTION ANGIOGRAPHY

In radiologic contrast procedures

ISOVUE® iopamidol injection

ISOVUE®-M iopamidol injection

THE CLEAR CHOICE



A broad range of indications

Peripheral arteriography
Coronary arteriography and ventriculography
Excretory urography
Myelography (lumbar, thoracic, cervical, total columnar)
Cerebral arteriography
CT head and body imaging
CT cisternography and ventriculography
Selective visceral arteriography
Aortography
Intra-arterial digital subtraction angiography

The only nonionic contrast agent you need to stock

ISOVUE-M® 200
iopamidol injection 41%

ISOVUE-M® 300/ISOVUE®-300
iopamidol injection 61%

ISOVUE®-370
iopamidol injection 76%

ISOVUE®-128
iopamidol injection 26%

SQUIBB™ Diagnostics

Please see brief summary of prescribing information on following pages.

This product is under license from Bracco Industria Chimica, S.p.A. U.S. Patent #4,001,323

CIRCLE 14 ON READER SERVICE CARD

647-503

ISOVUE®-128 (Iopamidol Injection 26%)
ISOVUE®-300 (Iopamidol Injection 61%)
ISOVUE®-370 (Iopamidol Injection 76%)
ISOVUE-M® 200 (Iopamidol Injection 41%)
ISOVUE-M® 300 (Iopamidol Injection 61%)

INDICATIONS AND USAGE

ISOVUE (Iopamidol Injection) is indicated for intra-arterial digital subtraction angiography (DSA) of the cerebral and abdominal vasculature and for angiography throughout the cardiovascular system, including cerebral and peripheral arteriography, coronary arteriography and ventriculography, selective visceral arteriography and aortography, and intravenous excretory urography and intravenous contrast enhancement of computed tomographic (CECT) head and body imaging.

ISOVUE-M (Iopamidol Injection) is indicated for intrathecal administration in neuroradiology including myelography (lumbar, thoracic, cervical, total columnar), and for contrast enhancement of computed tomographic (CECT) cisternography and ventriculography.

CONTRAINDICATIONS

ISOVUE (Iopamidol Injection)

None.

ISOVUE-M (Iopamidol Injection)

Intrathecal administration of corticosteroids with iopamidol is contraindicated. Because of overdosage considerations, immediate repeat myelography in the event of technical failure is contraindicated (see interval recommendation under DOSAGE AND ADMINISTRATION). Myelography should not be performed in the presence of significant local or systemic infection where bacteremia is likely.

WARNINGS

ISOVUE-M (Iopamidol Injection)

The need for myelographic examination should be carefully evaluated. Iopamidol should be administered with caution in patients with increased intracranial pressure or suspicion of intracranial tumor, abscess or hematoma, those with a history of convulsive disorder, severe cardiovascular disease, chronic alcoholism, or multiple sclerosis, and elderly patients. Particular attention must be given to state of hydration, concentration of medium, dose, and technique used in these patients.

If frankly bloody cerebrospinal fluid is observed, the possible benefits of a myelographic examination should be considered in terms of risk to the patient.

Patients on anticonvulsant medication should be maintained on this therapy.

Direct intracisternal or ventricular administration for standard radiography (without computerized tomographic enhancement) is not recommended. Inadvertent intracranial entry of a large or concentrated bolus of the contrast medium, which increases the risk of neurotoxicity, can be prevented by careful patient management. Also, effort should be directed to avoid rapid dispersion of the medium causing inadvertent rise to intracranial levels (e.g., by active patient movement). If such intracranial entry of the medium occurs, prophylactic anticonvulsant treatment with diazepam or barbiturates orally for 24 to 48 hours should be considered.

Use of medications that may lower the seizure threshold (phenothiazine derivatives, including those used for their antihistaminic properties; tricyclic antidepressants; MAO inhibitors; CNS stimulants; analeptics; antipsychotic agents) should be carefully evaluated. While the contributory role of such medications has not been established, some physicians have discontinued these agents at least 48 hours before and for at least 24 hours following intrathecal use.

Focal and generalized motor seizures have been reported after intrathecal use of water-soluble contrast agents including iopamidol. In several of those cases reported with iopamidol, higher than recommended doses were employed. Therefore *avoid:*

- Deviations from recommended neuroradiologic procedure or patient management.
- Use in patients with a history of epilepsy unless medically justified.
- Overdosage.
- Intracranial entry of a bolus or premature diffusion of a high concentration of the medium.
- Failure to maintain elevation of the head during the procedure, on the stretcher, and in bed.
- Excessive and particularly active patient movement or straining.

ISOVUE (Iopamidol Injection)

Caution must be exercised in patients with severely impaired renal function, those with combined renal and hepatic disease, or anuria particularly when larger doses are administered.

Radiopaque diagnostic contrast agents are potentially hazardous in patients with multiple myeloma or other paraproteinemia, particularly in those with therapeutically resistant anuria. Myeloma occurs most commonly in persons over age 40. Although neither the contrast agent nor dehydration has been proved separately to be the cause of anuria in myelomatous patients, it has been speculated that the combination of both may be causative. The risk in myelomatous patients is not a contraindication; however, special precautions are required.

Contrast media may promote sickling in individuals who are homozygous for sickle cell disease when injected intravenously or intraarterially.

Administration of radiopaque materials to patients known or suspected of having pheochromocytoma should be performed with extreme caution. If, in the opinion of the physician, the possible benefits of such procedures outweigh the considered risks, the procedures may be performed; however, the amount of radiopaque medium injected should be kept to an absolute minimum. The blood pressure should be assessed throughout the procedure and measures for treatment of a hypertensive crisis should be available. These patients should be monitored very closely during contrast-enhanced procedures.

Reports of thyroid storm following the use of iodinated radiopaque diagnostic agents in patients with hyperthyroidism or with an autonomously functioning thyroid nodule suggest that this additional risk be evaluated in such patients before use of any contrast medium.

PRECAUTIONS

General

Diagnostic procedures which involve the use of any radiopaque agent should be carried out under the direction of personnel with the prerequisite training and with a thorough knowledge of the particular procedure to be performed. Appropriate facilities should be available for coping with any complication of the procedure, as well as for emergency treatment of severe reaction to the contrast agent itself. After parenteral administration of a radiopaque agent, competent personnel and emergency facilities should be available for at least 30 to 60 minutes since severe delayed reactions may occur.

Preparatory dehydration is dangerous and may contribute to acute renal failure in patients with advanced vascular disease, diabetic patients, and in susceptible nondiabetic patients (often elderly with preexisting renal disease). *Patients should be well hydrated prior to and following iopamidol administration.*

The possibility of a reaction, including serious, life-threatening, fatal, anaphylactoid or cardiovascular reactions, should always be considered (see ADVERSE REACTIONS). Patients at increased risk include those with a history of a previous reaction to a contrast medium, patients with a known sensitivity to iodine per se, and patients with a known clinical hypersensitivity (bronchial asthma, hay fever, and food allergies). The occurrence of severe idiosyncratic reactions has prompted the use of several pretesting methods. However, pretesting cannot be relied upon to predict severe reactions and may itself be hazardous for the patient. It is suggested that a thorough medical history with emphasis on allergy and hypersensitivity, prior to the injection of any contrast medium, may be more accurate than pretesting in predicting potential adverse reactions. A positive history of allergies or hypersensitivity does not arbitrarily contraindicate the use of a contrast agent where a diagnostic procedure is thought essential, but caution should be exercised. Premedication with antihistamines or corticosteroids to avoid or minimize possible allergic reactions in such patients should be considered (see CONTRAINDICATIONS). Reports indicate that such pretreatment does not prevent serious life-threatening reactions, but may reduce both their incidence and severity.

General anesthesia may be indicated in the performance of some procedures in selected patients; however, a higher incidence of adverse reactions has been reported with radiopaque media in anesthetized patients, which may be attributable to the inability of the patient to identify untoward symptoms, or to the hypotensive effect of anesthesia which can reduce cardiac output and increase the duration of exposure to the contrast agent.

Even though the osmolality of iopamidol is low compared to diatrizoate or iothalamate based ionic agents of comparable iodine concentration, the potential transitory increase in the circulatory osmotic load in patients with congestive heart failure requires caution during injection. These patients should be observed for several hours following the procedure to detect delayed hemodynamic disturbances.

In angiographic procedures, the possibility of dislodging plaques or damaging or perforating the vessel wall should be borne in mind during catheter manipulations and contrast medium injection. Test injections to ensure proper catheter placement are suggested. Following arteriographic procedures, gentle pressure hemostasis is required, followed by observation and immobilization of the limb for several hours to prevent hemorrhage from the site of arterial puncture.

The inhibitory effects of nonionic contrast media on mechanisms of hemostasis have been shown, in vitro, to be less than ionic contrast media at comparable concentrations. For this reason, standard angiographic procedures should always be followed: angiographic catheters should be flushed frequently, and prolonged contact of blood with contrast in syringes and catheters should be avoided.

Selective coronary arteriography should be performed only in selected patients and those in whom the expected benefits outweigh the procedural risk. The inherent risks of angiocardiography in patients with chronic pulmonary emphysema must be weighed against the necessity for performing this procedure. Angiography should be avoided whenever possible in patients with homocystinuria, because of the risk of inducing thrombosis and embolism.

If nondisposable equipment is used, scrupulous care should be taken to prevent residual contamination with traces of cleansing agents.

Information For Patients

Patients receiving injectable radiopaque diagnostic agents should be instructed to:

1. Inform your physician if you are pregnant.
2. Inform your physician if you are diabetic or if you have multiple myeloma, pheochromocytoma, homozygous sickle cell disease, or known thyroid disorder (see WARNINGS).
3. Inform your physician if you are allergic to any drugs, food, or if you had any reactions to previous injections of substances used for x-ray procedures (see PRECAUTIONS, General).
4. Inform your physician about any other medications you are currently taking, including nonprescription drugs, before you have this procedure.

Drug Interactions

Renal toxicity has been reported in a few patients with liver dysfunction who were given oral cholecystographic agents followed by intravascular contrast agents. Administration of intravascular agents should therefore be postponed in any patient with a known or suspected hepatic or biliary disorder who has recently received a cholecystographic contrast agent.

Other drugs should not be admixed with iopamidol.

Drug/Laboratory Test Interactions

The results of PBI and radioactive iodine uptake studies, which depend on iodine estimations, will not accurately reflect thyroid function for up to 16 days following administration of iodinated contrast media. However, thyroid function tests not depending on iodine estimations, e.g., T3 resin uptake and total or free thyroxine (T4) assays are not affected.

Any test which might be affected by contrast media should be performed prior to administration of the contrast medium.

Laboratory Test Findings

In vitro studies with animal blood showed that many radiopaque contrast agents, including iopamidol, produced a slight depression of plasma coagulation factors including prothrombin time, partial thromboplastin time, and fibrinogen, as well as a slight tendency to cause platelet and/or red blood cell aggregation (see PRECAUTIONS, General).

Transitory changes may occur in red cell and leucocyte counts, serum calcium, serum creatinine, serum glutamic oxalacetic transaminase (SGOT), and uric acid in urine; transient albuminuria may occur.

These findings have not been associated with clinical manifestations.

Carcinogenesis, Mutagenesis, Impairment Of Fertility

In animal reproduction studies performed on rats, intravenously administered iopamidol did not induce adverse effects on fertility or general reproductive performance.

In studies to determine mutagenic activity, iopamidol did not cause any increase in mutation rates.

Pregnancy Category B

No teratogenic effects attributable to iopamidol have been observed in teratology studies performed in animals. There are, however, no adequate and well controlled studies in pregnant women. It is not known whether iopamidol crosses the placental barrier or reaches fetal tissues. However, many injectable contrast agents cross the placental barrier in humans and appear to enter fetal tissues passively. Because animal teratology studies are not always predictive of human response, this drug should be used during pregnancy only if clearly needed.

Radiologic procedures involve a certain risk related to the exposure of the fetus to ionizing radiation.

Labor and Delivery

It is not known whether use of contrast agents during labor or delivery has immediate or delayed adverse effects on the fetus, prolongs the duration of labor or increases the likelihood that forceps delivery or other obstetrical intervention or resuscitation of the newborn will be necessary.

Nursing Mothers

It is not known whether iopamidol is excreted in human milk. However, many injectable contrast agents are excreted unchanged in human milk. Although it has not been established that serious adverse reactions occur in nursing infants, caution should be exercised when intravascular contrast media are administered to nursing women because of potential adverse reactions, and consideration should be given to temporarily discontinuing nursing.

Pediatric Use

Safety and effectiveness in children have not been established.

ADVERSE REACTIONS

ISOVUE (Iopamidol Injection)

Adverse reactions following the use of iopamidol are usually mild to moderate, self-limited, and transient.

In a clinical trial with 100 patients undergoing intra-arterial DSA, adverse reactions possibly attributed to ISOVUE-128 administration were nausea (2%), headache (1%) and vomiting (1%). One patient with preexisting renal impairment and severe bilateral renal vascular disease experienced renal failure, possibly secondary to a subsequent acute episode of congestive heart failure and/or drug administration (see Warnings).

In angiocardiography (597 patients), the adverse reactions with an estimated incidence of one percent or higher are: hot flashes 3.4%; angina pectoris 3.0%; flushing 1.8%; bradycardia 1.3%; hypotension 1.0%; hives 1.0%.

Intravascular injection of contrast media is frequently associated with the sensation of warmth and pain, especially in peripheral arteriography; pain and warmth are less frequent and less severe with ISOVUE (Iopamidol Injection) than with diatrizoate meglumine and diatrizoate sodium injection.

The following table of incidence of reactions is based on clinical studies with ISOVUE in about 1835 patients.

Adverse Reactions

System	Estimated Overall Incidence > 1%	≤ 1%
Cardiovascular	none	tachycardia hypotension hypertension myocardial ischemia circulatory collapse S-T segment depression bigeminy extrasystoles ventricular fibrillation angina pectoris bradycardia transient ischemic attack thrombophlebitis
Nervous	pain (1.7%) burning sensation (1.4%)	vasovagal reaction tingling in arms grimace faintness
Digestive	nausea (1.2%)	vomiting anorexia
Respiratory	none	throat constriction dyspnea pulmonary edema
Skin and Appendages	none	rash urticaria pruritus flushing
Body as a Whole	hot flashes (1.5%)	headache fever chills excessive sweating back spasm
Special Senses	warmth (1.1%)	taste alterations nasal congestion visual disturbances
Urogenital	none	urinary retention

Regardless of the contrast agent employed, the overall estimated incidence of serious adverse reactions is higher with *coronary arteriography* than with other procedures. Cardiac decompensation, serious arrhythmias, or myocardial ischemia or infarction may occur during *coronary arteriography and left ventriculography.* Following coronary and ventricular injections, certain electrocardiographic changes (increased QTc, increased R-R, T-wave amplitude) and certain hemodynamic changes (decreased systolic pressure) occurred less frequently with ISOVUE (Iopamidol Injection) than with diatrizoate meglumine and diatrizoate sodium injection; increased LVEDP occurred less frequently after ventricular iopamidol injections.

In *aortography,* the risks of procedures also include injury to the aorta and neighboring organs, pleural puncture, renal damage including infarction and acute tubular necrosis with oliguria and anuria, accidental selective filling of the right renal artery during the translumbar procedure in the presence of preexisting renal disease, retroperitoneal hemorrhage from the translumbar approach, and spinal cord injury and pathology associated with the syndrome of transverse myelitis.

Adverse effects reported in clinical literature for iopamidol include arrhythmia, arterial spasms, hematuria, periorbital edema, involuntary leg movement, malaise, and triggering of deglutition; some of these may occur as a consequence of the procedure. Other reactions may also occur with the use of any contrast agent as a consequence of the procedural hazard; these include hemorrhage or pseudoaneurysms at the puncture site, brachial plexus palsy following axillary artery injections, chest pain, myocardial infarction, and transient changes in hepatorenal chemistry tests. Arterial thrombosis, displacement of arterial plaques, venous thrombosis, dissection of the coronary vessels and transient sinus arrest are rare complications.

ISOVUE-M (Iopamidol Injection)

The most frequently reported adverse reactions following intrathecal administration of iopamidol are headache, nausea, vomiting and musculoskeletal pain. These reactions usually occur 1 to 10 hours after injection, almost all occurring within 24 hours. They are usually mild to moderate in degree lasting for a few hours and usually disappearing within 24 hours. Rarely, headaches may be severe or persist for days. Headache is often accompanied by nausea and vomiting, and tends to be more frequent and persistent in patients not optimally hydrated.

Backache, neck stiffness, numbness and paresthesias, leg or sciatic-type pain occurred less frequently, often in the form of a transient exacerbation of preexisting symptomatology. Transient alterations in vital signs may occur and their significance must be assessed on an individual basis.

The following table of incidence of reactions is based on clinical studies with ISOVUE-M (Iopamidol Injection) in about 615 patients.

Adverse Reactions

System	Estimated Overall Incidence > 1%	≤ 1%
Body as a Whole	headache (18.1%)	pyrexia muscle weakness hot flashes malaise fatigue weakness
Digestive	nausea (7.3%) vomiting (3.7%)	diarrhea heartburn
Musculoskeletal	back pain (2.3%) leg pain (1.4%) neck pain (1.1%)	leg cramps sciatica cervicobrachial irritation meningeal irritation radicular irritation, lumbosacral other musculoskeletal pain involuntary movement burning sensation
Cardiovascular	hypotension (1.1%)	tachycardia hypertension chest pain

Adverse Reactions (con't)

System	Estimated Overall Incidence > 1%	≤ 1%
Nervous	none	emotional stress dizziness paresthesia confusion hallucinations lightheadedness syncope numbness cold extremities
Urogenital	none	urinary retention
Respiratory	none	dyspnea
Skin and Appendages	none	rash
Miscellaneous	none	injection site pain

Other adverse effects reported in clinical literature for iopamidol include facial neuralgia, tinnitus, and sweating.

Major motor seizures have been reported in the clinical literature and since market introduction in the United States. Early onset of seizures (less than two hours) is indicative of early substantial intracranial entry. Transitory EEG changes occur and usually take the form of slow wave activity.

While not observed in controlled clinical studies with ISOVUE-M (Iopamidol Injection), or reported in clinical literature, the following adverse reactions may occur because they have been reported with other nonionic contrast agents: cardiovascular (arrhythmias); aseptic meningitis syndrome; allergy or idiosyncrasy (chills, pruritus, nasal congestion, Guillain-Barre syndrome); CNS irritation (psycho-organic syndrome: mild and transitory perceptual aberrations such as depersonalization, anxiety, depression, hyperesthesia, disturbances in speech, sight, or hearing, and disorientation; in addition, hyperreflexia or areflexia, hypertonia or flaccidity, restlessness, tremor, echoacousia, echolalia, asterixis or dysphasia have occurred). Profound mental disturbances have rarely been reported (various forms and degrees of aphasia, mental confusion or disorientation); the onset is usually at 8 to 10 hours and lasts for about 24 hours without aftereffects.

However, occasionally they have been manifest as apprehension, agitation, or progressive withdrawal to the point of stupor in several instances. In a few cases, these have been accompanied by transitory hearing loss or other auditory symptoms and visual disturbances (believed subjective or delusional). Persistent cortical loss of vision in association with convulsions, and ventricular block have been reported. Rarely, persistent though transitory weakness in the leg or ocular muscles has been reported. *Peripheral neuropathies* have been rare and transitory. They include sensory and/or motor or nerve root disturbances, myelitis, persistent leg muscle pain or weakness, or sixth nerve palsy, or cauda equina syndrome. Muscle cramps, fasciculation or myoclonia, spinal convulsion, or spasticity are unusual.

General Adverse Reactions To Contrast Media

Reactions known to occur with parenteral administration of iodinated ionic contrast agents (see the listing below) are possible with any nonionic agent. Approximately 95 percent of adverse reactions accompanying the use of other water-soluble intravascularly administered contrast agents are mild to moderate in degree. However, life-threatening reactions and fatalities, mostly of cardiovascular origin, have occurred.

Reported incidences of death from the administration of other iodinated contrast media range from 6.6 per 1 million (0.00066 percent) to 1 in 10,000 patients (0.01 percent). Most deaths occur during injection or 5 to 10 minutes later, the main feature being cardiac arrest with cardiovascular disease as the main aggravating factor. Isolated reports of hypotensive collapse and shock are found in the literature. The incidence of shock is estimated to be 1 out of 20,000 (0.005 percent) patients.

Adverse reactions to injectable contrast media fall into two categories: chemotoxic reactions and idiosyncratic reactions. Chemotoxic reactions result from the physico-chemical properties of the contrast medium, the dose, and the speed of injection. All hemodynamic disturbances and injuries to organs or vessels perfused by the contrast medium are included in this category. Experience with iopamidol suggests there is much less discomfort (e.g., pain and/or warmth) with peripheral arteriography. Fewer changes are noted in ventricular function after ventriculography and coronary arteriography.

Idiosyncratic reactions include all other reactions. They occur more frequently in patients 20 to 40 years old. Idiosyncratic reactions may or may not be dependent on the amount of drug injected, the speed of injection, the mode of injection, and the radiographic procedure. Idiosyncratic reactions are subdivided into minor, intermediate, and severe. The minor reactions are self-limited and of short duration; the severe reactions are life-threatening and treatment is urgent and mandatory.

The reported incidence of adverse reactions to contrast media in patients with a history of allergy is twice that for the general population. Patients with a history of previous reactions to a contrast medium are three times more susceptible than other patients. However, sensitivity to contrast media does not appear to increase with repeated examinations. Most adverse reactions to intravascular contrast agents appear within one to three minutes after the start of injection, but delayed reactions may occur (see PRECAUTIONS, General).

Because measurable plasma levels are attained following the intrathecal administration of iopamidol, adverse reactions reported with the use of intravascular contrast agents are theoretically possible. In addition to the adverse drug reactions reported for iopamidol, the following additional adverse reactions have been reported with the use of other intravascular contrast agents and are possible with the use of any water-soluble iodinated contrast agent:

Cardiovascular: vasodilation, cerebral hematomas, petechiae, hemodynamic disturbances, sinus bradycardia, transient electrocardiographic abnormalities, ventricular fibrillation.

Digestive: nausea, vomiting, severe unilateral or bilateral swelling of the parotid and submaxillary glands.

Nervous: paresthesia, dizziness, convulsions, paralysis, coma.

Respiratory: increased cough, asthma, laryngeal edema, pulmonary edema, bronchospasm, rhinitis, dyspnea.

Skin and Appendages: injection site pain usually due to extravasation and/or erythematous swelling, skin necrosis.

Urogenital: osmotic nephrosis of proximal tubular cells, renal failure, pain.

Special Senses: bilateral ocular irritation; lacrimation; conjunctival chemosis, infection, and conjunctivitis; itching.

The following reactions may also occur: neutropenia, thrombophlebitis, flushing, pallor, weakness, severe retching and choking, wheezing, cramps, tremors, and sneezing.

HOW SUPPLIED

ISOVUE-128: 10x50 mL vials; ISOVUE-300: 10x50 mL vials and 10 x 100 mL bottles; ISOVUE-370: 10x50 mL vials and 10 x 100 mL, 10 x 150 mL and 10x200 mL bottles; ISOVUE-M 200: 10x20 mL vials; ISOVUE-M 300: 10 x 15 mL vials.

STORAGE

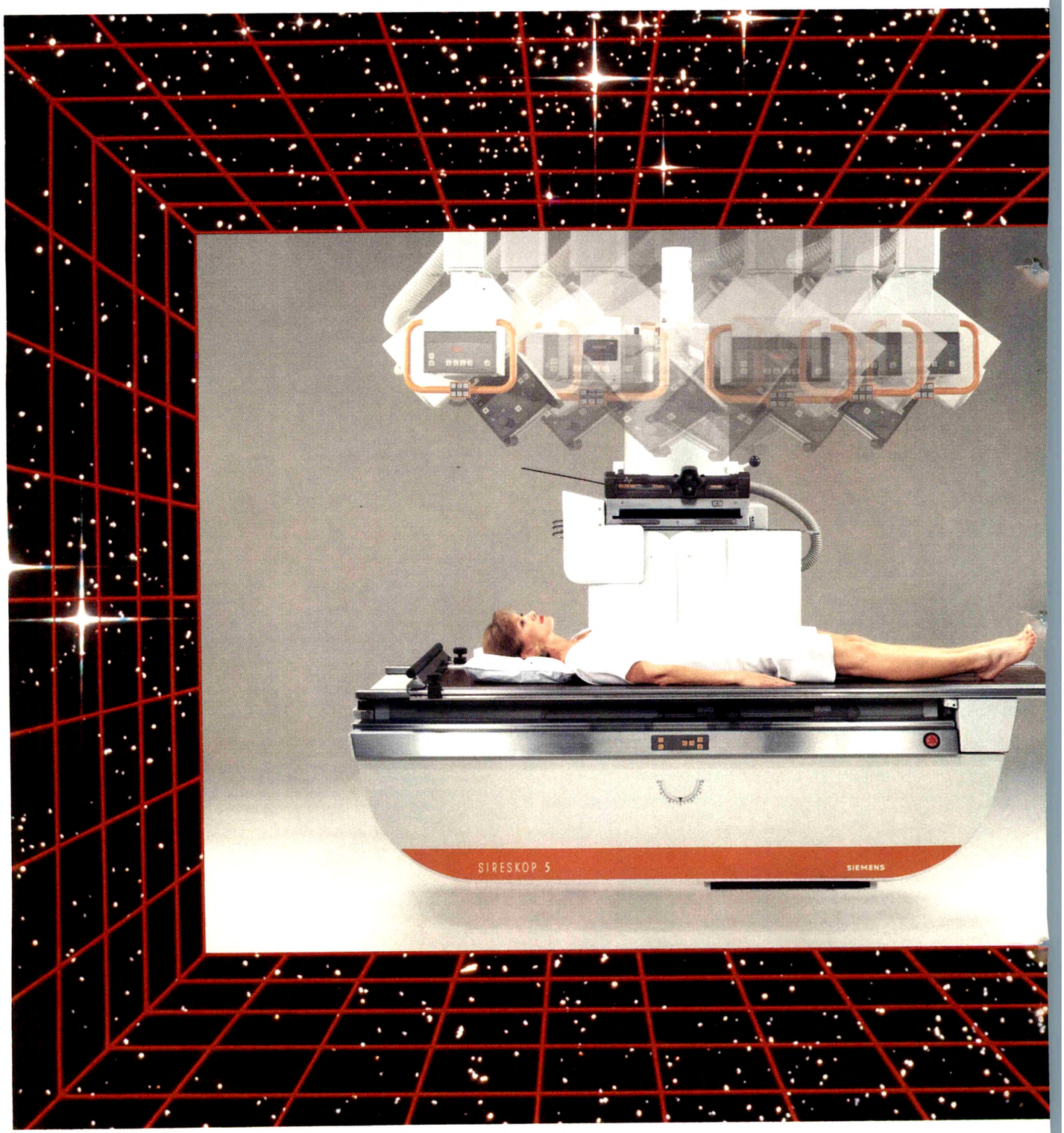
ISOVUE® and ISOVUE-M® (iopamidol injection) should be stored at room temperature not exceeding 86° F. Protect from light.

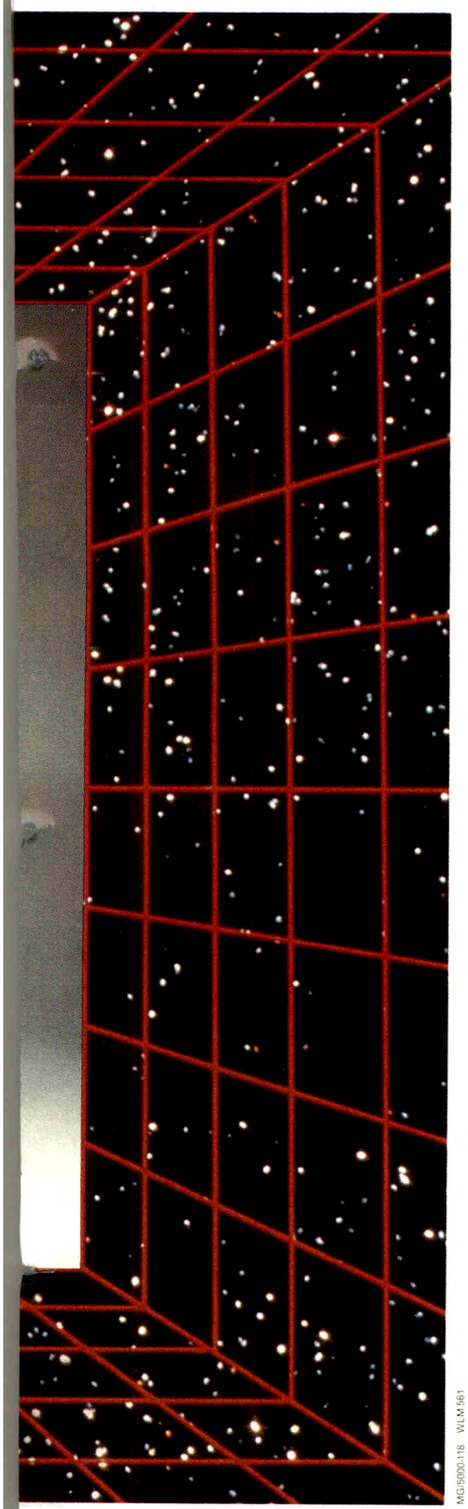
For full prescribing information consult package insert.

J3-702A/J3-652D/J3-653E.

© 1987 E.R. Squibb & Sons, Inc., Princeton, NJ 647-503 Issued: June 1987

SIEMENS





While exotic imaging technologies are making headlines, chances are the bulk of your routine imaging and the success of your bottom line depends on your R/F systems...

If you thought today's R/F systems couldn't be improved...Think again!

That's why we've introduced two improved "workhorse" systems that set new standards—the SIRESKOP® 5 for tableside control and the SIREGRAPH® D3 for remote operation.

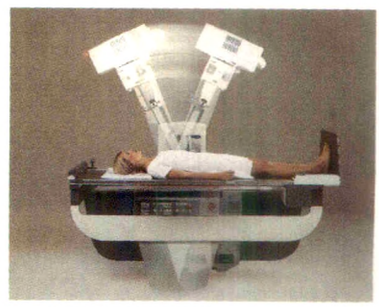
Greater versatility...
Both systems increase room utilization and productivity by performing not only routine R/F exams but also angiography, DSA, tomography, interventional radiography, and endoscopic radiography. *Digital radiography* is possible with the new DS 1000, a low dose, instantaneous imaging system with real-time image processing and storage capabilities.

Better images...
A shorter tabletop to film distance enhances geometrical sharpness. The SIRESKOP 5 outperforms the leading competitor by nearly *50% shorter distance.* Plus, a new collimation design refines image quality by reducing "scatter". And these systems offer the *fastest* fluoro to exposure time in the industry—**0.6** seconds!

Simpler to use...
Total microprocessor design makes operation simple and straightforward. Exclusive *electronic tomography* with the SIRESKOP 5 (see photo opposite) completely eliminates conventional mechanical coupling for operator efficiency. The POLYMATIC®, a *totally new* ADR system, automates the imaging process for demonstrably better results in all modalities.

...And cost effective technology
Modern software programming enables routine upgrades to be made without major expense. And through computerized system diagnosis, time spent on installation and service is significantly reduced.

Tableside or remote, these new R/F systems offer an **unconventionally** sound investment!



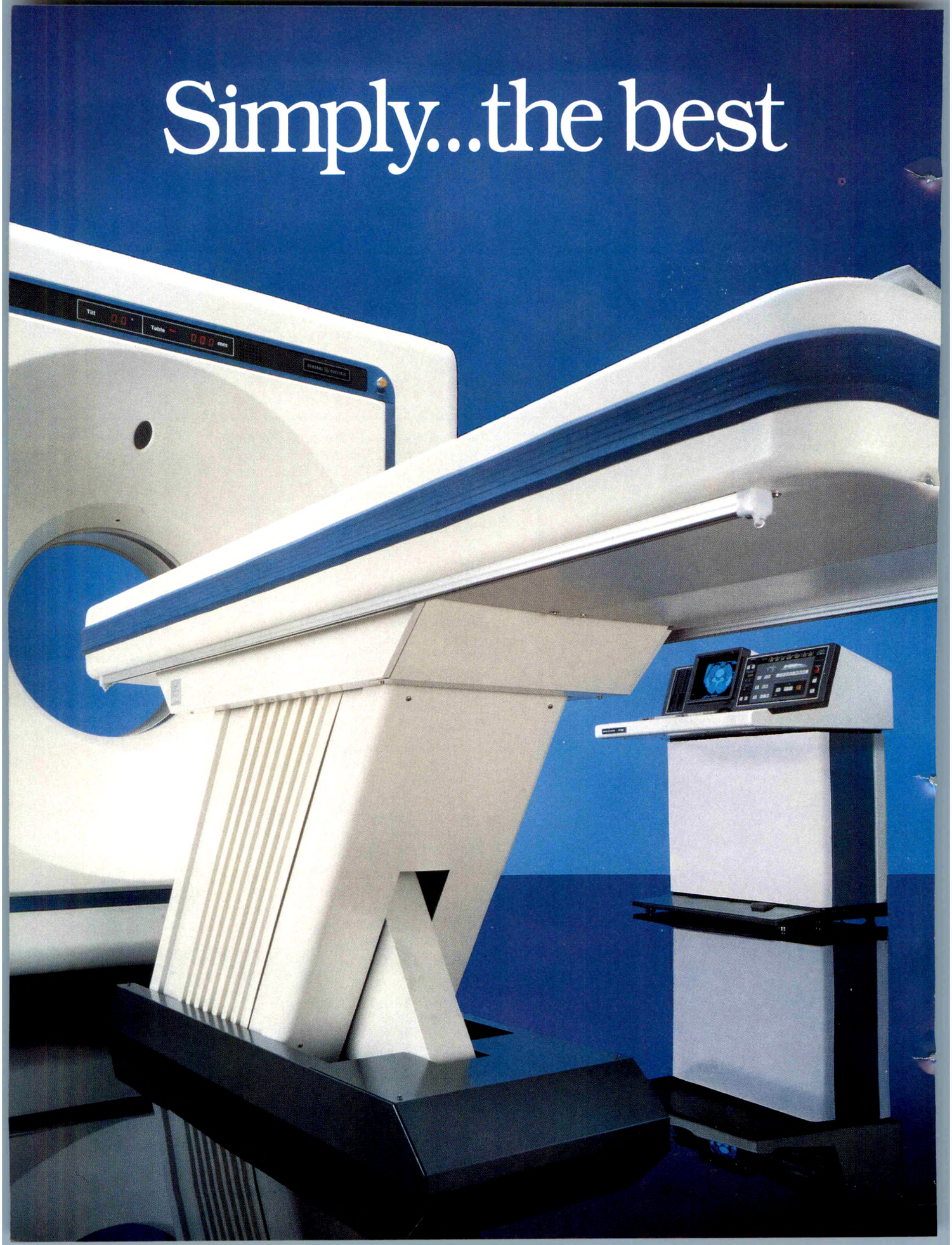
SIREGRAPH D3 Remote System

Siemens Medical Systems, Inc.
186 Wood Avenue South
Iselin, NJ 08830

CIRCLE 8 ON READER SERVICE CARD

Siemens...
technology with integrity.

MG-5000-118 WLM-561

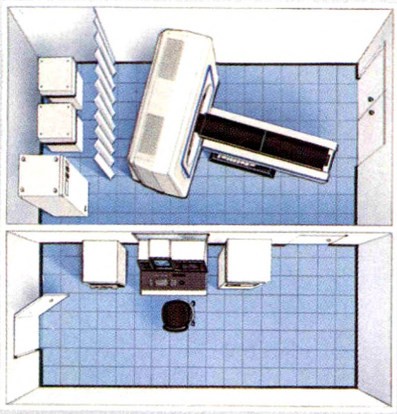

Simply...the best

CT 9000 from GE... an uncomplicated system that's the best in its class

When you're buying a CT system to handle routine procedures, the last thing you want is unnecessary complexity. Complexity can compromise the economy you're looking for in such a system . . . it can raise your overhead, increase downtime, and slow down throughput.

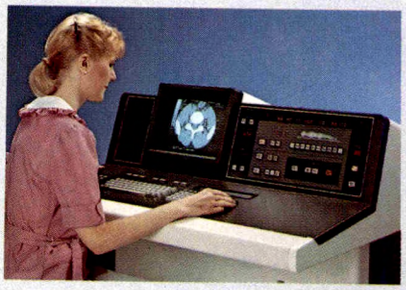
That's why the CT 9000 from General Electric has become the best-selling system in its class: it's remarkably uncomplicated.

Simple installation: The entire computer system is housed in the operator's console. That means you



don't need a separate computer room with special air conditioning requirements. And the CT 9000 fits into a room as small as 20 x 20 feet . . . in most cases, it can be installed without renovation.

Uncomplicated operation: The CT 9000 incorporates advanced micro-electronic technology to streamline operation and enhance



operator efficiency. Operation is so easy that training can be completed in as little as one day. Routine protocols can be initiated with the touch of a button. And the unique AutoVoice synthesizer automatically relays proper breathing instructions to the patient, letting the operator concentrate on the procedure at hand. Because the CT 9000 system is so easy to use, most procedures can be completed faster...enhancing patient throughput even further.

Uncommonly reliable: The CT 9000's modular electronics not only give you scan versatility, they also set a new standard in system reliability. You get consistently excellent performance, day after day, with minimum downtime and maximum throughput.

Financing made easy: GE offers a complete range of financing and lease plans that can be tailored to fit your budget and cash flow requirements. Our Super Saver lease plan, for example, offers a fixed lease rate as low as 4.8%* with no payments for the first 90 days of operation . . . that means your CT 9000 system will begin earning income for your facility immediately.

More information? Contact your General Electric sales representative, or call us and find out how the CT 9000 system can fit into your healthcare delivery plans.

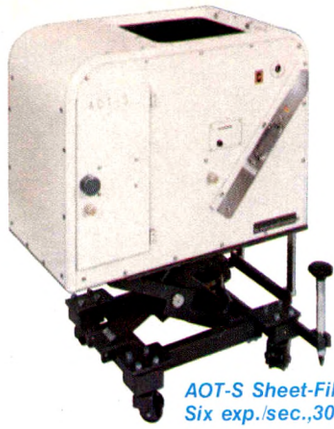
800-433-5566 Ext. 5303

*Rate in effect for a limited time only. Some restrictions apply. Contact your GE sales representative for details.



GENERAL ELECTRIC

ELEMA-SCHONANDER



AOT-S Sheet-Film Changer.
Six exp./sec.,30-film capacity.

FILMCHANGERS... where service is as dependable as the product itself.

PUCK UD®.
Position-Independent.

PUCK Sheet-Film Changers... four exp./sec., 20-film capacity. Single plane... biplane simultaneous or alternating mode.

PUCK U®.
Frontal and Lateral Projections.

Your filmchangers must function day in, day out. And should you have a problem, service must be prompt and effective.

In our headquarters Training Center, we train the x-ray companies' service engineers to maintain and repair Elema-Schonander filmchangers. And our own staff of product specialists, strategically located around the country, is available to assist if necessary.

A complete inventory of spare parts is maintained to immediately meet any need.

Service can be vitally important. We make sure it's good— and we make sure it's *available.*

For further information contact:
Elema-Schonander, Inc.
2360 North Palmer Drive
P.O. Box 94517
Schaumburg, IL 60173-3887
Telephone (312) 397-5900

elema-schonander

MG/5810-032

CIRCLE 4 ON READER SERVICE CARD

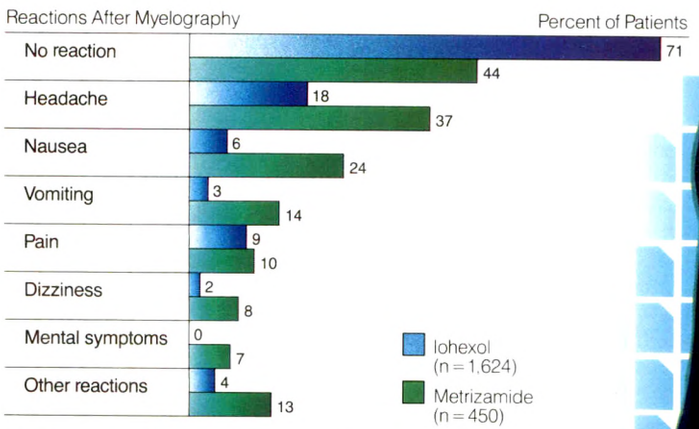
87212

In intrathecal imaging:

Because you can't be sure how every patient will react...

Improve the safety profile.

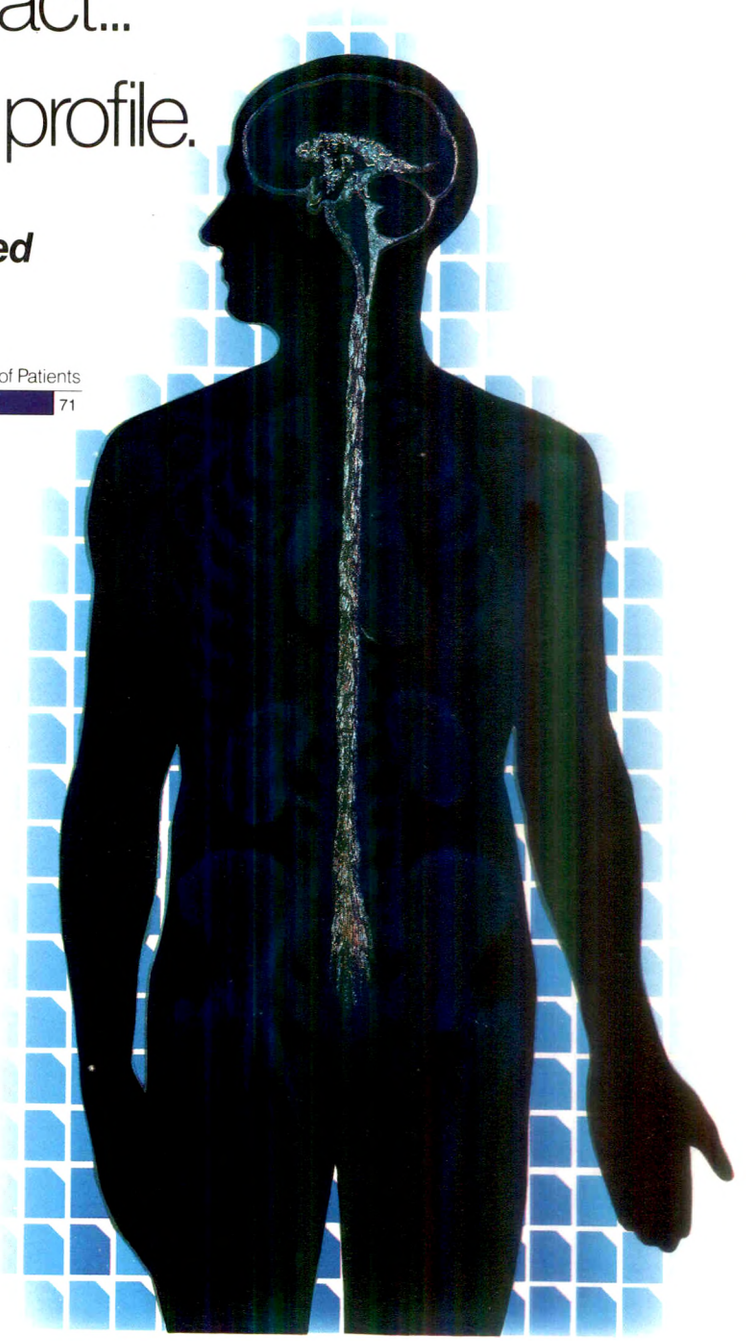
Better patient tolerance, measured subjectively and objectively.[1-5]



Adapted from Shaw el at.[2] Data on file, Winthrop Pharmaceuticals.[4] All adverse reactions reported are included and are irrespective of drug relationship. If a patient had more than one type of reaction, each is counted separately under the respective reaction type.

Lower incidence of EEG changes compared with iopamidol or metrizamide.[2,5]

Excellent diagnostic quality.



NONIONIC

OMNIPAQUE®

(IOHEXOL)

THE NEW STANDARD IN INTRATHECAL IMAGING.

See next page for important product information concerning contraindications, warnings, adverse reactions, patient selection, and precautionary recommendations.



OMNIPAQUE®
INJECTION (IOHEXOL)
INTRATHECAL

180

240

300

PLEASE CONSULT FULL PRODUCT INFORMATION BEFORE USING. A SUMMARY FOLLOWS:

DESCRIPTION: OMNIPAQUE is a nonionic, water-soluble radiographic contrast medium for intrathecal administration in concentrations of 180, 240, and 300 mgI/mL. Each milliliter of iohexol solution contains 1.21 mg tromethamine and 0.1 mg edetate calcium disodium with the pH adjusted between 6.8 and 7.7 with hydrochloric acid or sodium hydroxide. All solutions are sterilized by autoclaving, are nonpyrogenic, and contain no preservatives, so unused portions should be discarded.

CONTRAINDICATIONS–Intrathecal: OMNIPAQUE should not be administered to patients with a known hypersensitivity to iohexol. Myelography should not be performed in the presence of significant local or systemic infection where bacteremia is likely. Intrathecal administration of corticosteroids with OMNIPAQUE is contraindicated. Because of the possibility of overdosage, immediate repeat myelography in the event of technical failure is contraindicated.

WARNINGS–General: If grossly bloody CSF is encountered, the possible benefits of a myelographic procedure should be considered in terms of the risk to the patient.

Caution is advised in patients with a history of epilepsy, severe cardiovascular disease, chronic alcoholism, or multiple sclerosis.

Elderly patients may present a greater risk following myelography. The need for the procedure in these patients should be evaluated carefully. Special attention must be paid to dose and concentration of the medium used, hydration, and technique used.

Patients who are receiving anticonvulsants should be maintained on this therapy. Should a seizure occur, intravenous diazepam or phenobarbital sodium is recommended. In patients with a history of seizure activity who are not on anticonvulsant therapy, premedication with barbiturates should be considered.

Prophylactic anticonvulsant treatment with barbiturates should be considered in patients with evidence of inadvertent intracranial entry of a large or concentrated bolus of the contrast medium, since there may be an increased risk of seizure in such cases.

Drugs that lower the seizure threshold, especially phenothiazine derivatives, including those used for their antihistamine or antinauseant properties, are not recommended for use with OMNIPAQUE. Others include MAO inhibitors, tricyclic antidepressants, CNS stimulants, and psychoactive drugs described as analeptics, major tranquilizers, or antipsychotic drugs. While the contributory role of these medications has not been established, the use of such drugs should be based on physician evaluation of potential benefits and potential risks. Physicians have discontinued these agents at least 48 hours before and for at least 24 hours postprocedure. Care is required in patient management to prevent inadvertent intracranial entry of a large dose or concentrated bolus of the medium. Also, effort should be directed to avoid rapid dispersion of the medium causing inadvertent rise in intracranial levels (eg, by active patient movement). Direct intracisternal or ventricular administration for standard radiography (not CT) is not recommended.

In most reported cases of major motor seizures with nonionic myelographic media, one or more of the following factors were present. Therefore avoid:

- Deviations from recommended procedure or in myelographic management.
- Use in patients with a history of epilepsy.
- Overdosage.
- Intracranial entry of a bolus or premature diffusion of a high concentration of the medium.
- Medication with neuroleptic drugs or phenothiazine antinauseants.
- Failure to maintain elevation of the head during the procedure, on the stretcher, or in bed.
- Excessive and particularly active patient movement or straining.

PRECAUTIONS–General: Diagnostic procedures that involve the use of radiopaque diagnostic agents should be carried out under the direction of personnel with the prerequisite training and with a thorough knowledge of the particular procedure to be performed. Appropriate facilities should be available for coping with any complication of the procedure, as well as for emergency treatment of reactions to the contrast agent itself. After parenteral administration of a radiopaque agent, competent personnel and emergency facilities should be available, since delayed reactions have been reported (see ADVERSE REACTIONS).

Preparatory dehydration may be dangerous and may contribute to acute renal failure in patients with advanced vascular disease, diabetic patients, and in susceptible nondiabetic patients (often elderly with preexisting renal disease). Dehydration in these patients seems to be enhanced by the osmotic diuretic action of contrast agents. *Patients should be well hydrated prior to and following iohexol administration.*

The possibility of a reaction, including serious, life-threatening, fatal, anaphylactoid, or cardiovascular reactions, should always be considered (see ADVERSE REACTIONS). Therefore, it is of utmost importance that a course of action be carefully planned in advance for the immediate treatment of serious reactions, and that adequate and appropriate facilities and personnel be readily available in case of a severe reaction.

The possibility of an idiosyncratic reaction in susceptible patients should always be considered (see ADVERSE REACTIONS). The susceptible population includes patients with a history of a previous reaction to contrast media, patients with a known sensitivity to iodine per se, and patients with a known clinical hypersensitivity: bronchial asthma, hay fever, and food allergies.

A thorough medical history with emphasis on allergy and hypersensitivity, prior to the injection of any contrast medium, may be more accurate than pretesting in predicting potential adverse reactions.

A positive history of allergy or hypersensitivity does not arbitrarily contraindicate the use of a contrast agent where a diagnostic procedure is thought essential, but caution should be exercised (see ADVERSE REACTIONS). Premedication with antihistamines or corticosteroids, to avoid or minimize possible allergic reactions in such patients, should be considered.

In patients with severe renal insufficiency or failure, compensatory biliary excretion of the drug is anticipated to occur, with a slow clearance into the bile. Patients with hepatorenal insufficiency should not be examined unless the possibility of benefit clearly outweighs the additional risk. Sterile technique must be used with any spinal puncture.

When OMNIPAQUE is to be injected using plastic disposable syringes, the contrast medium should be drawn into the syringe and used immediately. If nondisposable equipment is used, scrupulous care should be taken to prevent residual contamination with traces of cleansing agents. **Parenteral drug products should be inspected and discarded if particulate matter or discoloration is present.**

Repeat Procedures. If in the clinical judgment of the physician sequential or repeat examinations are required, a suitable interval of time between administrations should be observed to allow for normal clearance of the drug from the body.

Information for Patients: When receiving injectable radiopaque diagnostic agents, inform your physician:

If you are pregnant; if you are diabetic; if you have multiple myeloma, pheochromocytoma, homozygous sickle cell disease, or known thyroid disorder; if you are allergic to any drugs or food or if you had any reactions to previous injections of dyes used for x-ray procedures; about any other medications you are currently taking, including nonprescription drugs, before you are administered this drug.

Drug Interactions (See WARNINGS–General): In nonelective procedures in patients on the drugs described, consider prophylactic use of anticonvulsants.

Carcinogenesis, Mutagenesis, Impairment of Fertility: No long-term animal studies have been performed to evaluate carcinogenic potential, mutagenesis, or whether OMNIPAQUE can affect fertility in men or women.

Pregnancy Category B: Reproduction studies have been performed in rats and rabbits with up to 100 times the recommended dose. No evidence of impaired fertility or harm to the fetus has been demonstrated due to OMNIPAQUE; there are, however, no studies in pregnant women. Because animal reproduction studies are not always predictive of human response, this drug should be used during pregnancy only if clearly indicated.

Nursing Mothers: It is not known to what extent iohexol is excreted in human milk. However, many injectable contrast agents are excreted unchanged in human milk. Although it has not been established that serious adverse reactions occur in nursing infants, caution should be exercised when intravascular contrast media are administered to nursing women. Bottle feedings may be substituted for breast feedings for 24 hours following administration of OMNIPAQUE.

Pediatric Use: Safety and effectiveness in children have not been established.

ADVERSE REACTIONS–Intrathecal: The most frequently reported adverse reactions with OMNIPAQUE 180, OMNIPAQUE 240, and OMNIPAQUE 300 are headache, mild to moderate pain including backache, neck ache and stiffness, nausea and vomiting. These reactions usually occur 1 to 10 hours after injection, and almost all occur within 24 hours. They are usually mild to moderate in degree, lasting for a few hours and usually disappearing within 24 hours. Rarely, headaches may be severe or persist for days. Headache is often accompanied by nausea and vomiting and tends to be more frequent and persistent in patients not optimally hydrated. Transient alterations in vital signs may occur and their significance must be assessed on an individual basis. Those reactions reported in clinical studies with OMNIPAQUE are listed below in decreasing order of occurrence, based on clinical studies of 1,624 patients.

Headaches: The most frequently occurring adverse reaction following myelography has been headache, with an incidence of approximately 18%. Headaches may be caused either by a direct effect of the contrast medium or by CSF leakage at the dural puncture site. However, in managing the patient, it is considered more important to minimize intracranial entry of contrast medium by postural management than to attempt to control possible CSF leakage (see PATIENT MANAGEMENT).

Pain: Mild to moderate pain including backache, neck ache and stiffness, and neuralgia occurred following injection, with an incidence of about 8%.

Nausea and Vomiting: Nausea was reported with an incidence of about 6%, and vomiting about 3% (see PATIENT MANAGEMENT). Maintaining normal hydration is very important. The use of phenothiazine antinauseants is not recommended (see WARNINGS–General). Reassurance to the patient that the nausea will clear usually is all that is required.

Dizziness: Transient dizziness was reported in about 2% of the patients.

Other Reactions: Other reactions occurring with an individual incidence of less than 0.1% included: feeling of heaviness, hypotension, hypertonia, sensation of heat, sweating, vertigo, loss of appetite, drowsiness, hypertension, photophobia, tinnitus, neuralgia, paresthesia, difficulty in micturition, and neurological changes. All were transient and mild with no clinical sequelae.

General Adverse Reactions to Contrast Media: Physicians should remain alert for the occurrence of adverse effects in addition to those discussed above, particularly the following reactions which have been reported in the literature for other nonionic, water-soluble myelographic media and rarely with iohexol. These have included, but are not limited to, aseptic and bacterial meningitis and CNS and other neurologic disturbances.

An aseptic meningitis syndrome has been reported rarely (less than 0.01%). It was usually preceded by pronounced headaches, nausea, and vomiting. Onset usually occurred about 12 to 18 hours postprocedure. Prominent features were meningismus and fever, sometimes with oculomotor signs and mental confusion. Lumbar puncture revealed a high white cell count and high protein content, often with a low glucose level and absence of organisms. The condition usually started to clear spontaneously about 10 hours after onset, with complete recovery over 2 to 3 days.

Allergy or Idiosyncrasy: Chills, fever, profuse diaphoresis, pruritus, urticaria, nasal congestion, dyspnea, and Guillain-Barré syndrome.

CNS Irritation: Mild and transitory perceptual aberrations, such as hallucinations, depersonalization, amnesia, hostility, amblyopia, diplopia, photophobia, psychosis, insomnia, anxiety, depression, hyperesthesia, visual or auditory or speech disturbances, confusion and disorientation. In addition, malaise, weakness, EEG changes, meningismus, hyperreflexia or areflexia, hypertonia or flaccidity, hemiplegia, paralysis, quadriplegia, restlessness, tremor, echoacousia, echolalia, asterixis, and dysphasia have occurred.

Profound mental disturbances have also rarely been reported; various forms and degrees of aphasia, mental confusion, or disorientation. Onset is usually at 8 to 10 hours and lasts for about 24 hours. Occasionally, they have been manifest as apprehension, agitation, or progressive withdrawal in several instances to the point of somnolence, stupor, and coma. In a few cases, these have been accompanied by transitory hearing loss or other auditory symptoms and visual disturbances (believed subjective or delusional), including unilateral or bilateral loss of vision, which may last for hours. In one case, persistent cortical loss of vision has been reported in association with convulsions. Ventricular block has been reported; amnesia of varying degrees may be present for the reaction event.

Rarely, persistent though transitory weakness in the leg or ocular muscles has been reported. Peripheral neuropathies have been rare and transitory. They include sensory and/or motor or nerve root disturbance, myelitis, persistent leg muscle pain or weakness, 6th nerve palsy, or cauda equina syndrome. Muscle cramps, fasciculation or myoclonia, spinal convulsion, or spasticity are unusual and have responded promptly to a small intravenous dose of diazepam.

In general, the reactions that are known to occur on parenteral administration of iodinated contrast agents are possible with any nonionic agent. Approximately 95% of adverse reactions accompanying the use of water-soluble contrast agents are mild to moderate in degree. However, severe, life-threatening, anaphylactoid, and fatal reactions, mostly of cardiovascular origin, have occurred. Adverse reactions to injectable contrast media fall into two categories: chemotoxic reactions and idiosyncratic reactions.

Chemotoxic reactions result from the physicochemical properties of the contrast medium, the amount of the dose and the speed of injection. All hemodynamic disturbances and injuries to organs or vessels perfused by the contrast medium are included in this category.

Idiosyncratic reactions occur more frequently in patients 20 to 40 years old and may or may not be dependent on the amount of dose injected, the speed of injection, and the radiographic procedure. They are subdivided into minor, intermediate, and severe. The minor reactions are self-limited and of short duration; the severe reactions are life-threatening, and treatment is urgent and mandatory.

The reported incidence of adverse reactions to the contrast medium in patients with a history of allergy is twice that of the general population. Patients with a history of previous reactions to a contrast medium are three times more susceptible than other patients. However, sensitivity to contrast media does not appear to increase with repeated examination.

Most adverse reactions to injectable contrast media appear within 1 to 3 minutes after the start of injection, but delayed reactions may occur.

OVERDOSAGE: Although clinical consequences of overdosage with OMNIPAQUE have not been reported, physicians should be aware that incorrect management of the patient can permit inadvertent early intracranial entry of normal doses of the medium, thereby increasing CNS reactions.

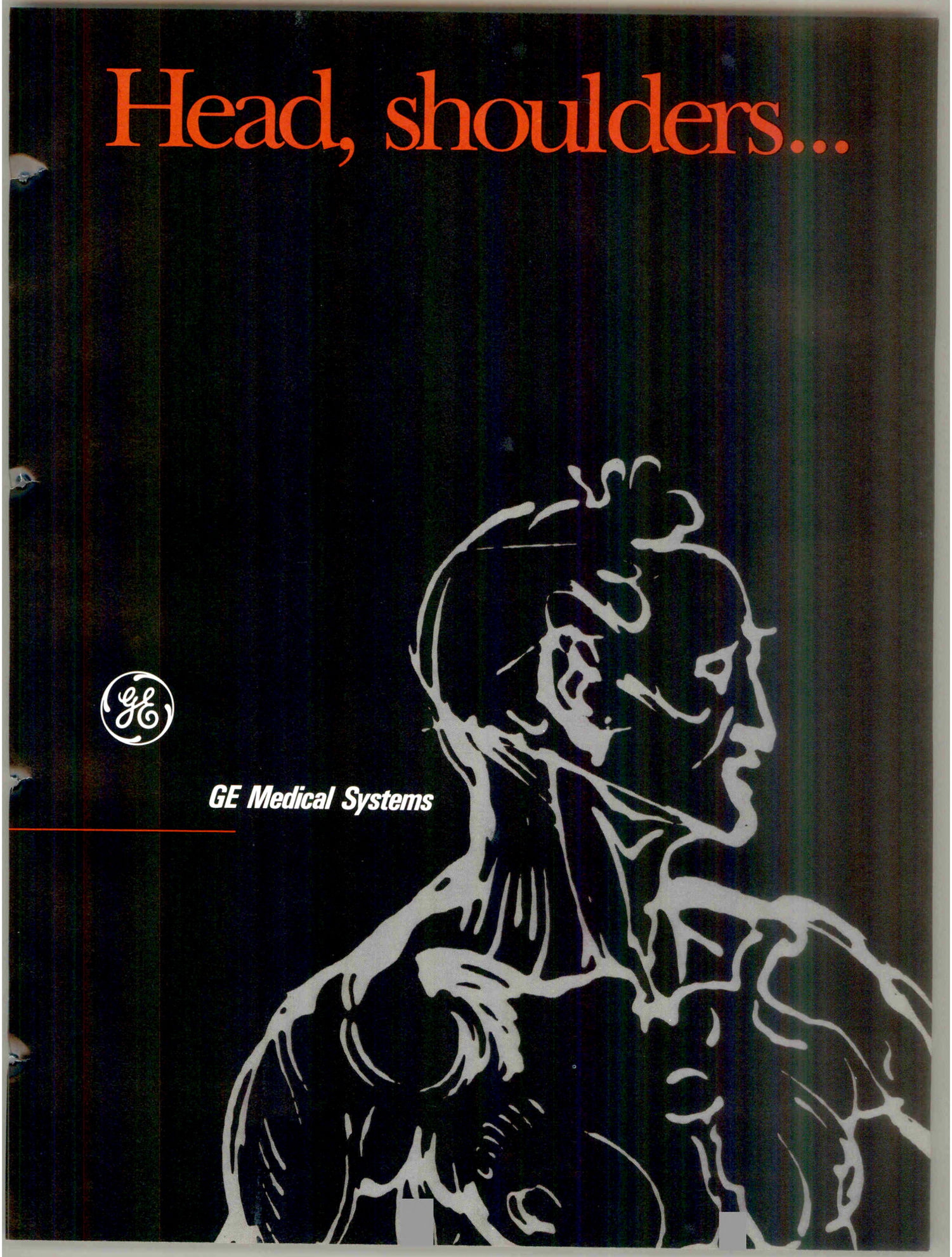
The intracisternal LD_{50} value of OMNIPAQUE (in grams of iodine per kilogram body weight) is greater than 2.0 in mice.

References: 1. Kieffer SA, Binet EF, Davis DO, et al: Lumbar myelography with iohexol and metrizamide: A comparative multicenter prospective study. *Radiology* 1984; 151:665-670. **2.** Shaw DD, Bach-Gansmo T, Dahlstrom K: Iohexol: summary of North American and European clinical trials in adult lumbar, thoracic, and cervical myelography with a new nonionic contrast medium. *Invest Radiol* 1985; 20(suppl 1):44-50. **3.** Latchaw RE, Hirsch WL Jr, Horton JA, et al: Iohexol vs metrizamide: Study of efficacy and morbidity in cervical myelography. *AJNR* 1985; 6:931-933. **4.** Data on file, Winthrop Pharmaceuticals. **5.** Lamb JT: Iohexol vs. iopamidol for myelography. *Invest Radiol* 1985; 20(suppl 1):37-43.

© 1987 WINTHROP PHARMACEUTICALS 71171/3777

Winthrop PHARMACEUTICALS
Winthrop Pharmaceuticals
Division of Sterling Drug Inc.
New York, NY 10016

Head, shoulders....



GE Medical Systems

spine & body

Signa... the reference point in MR

The true test of an MR system is day-to-day clinical performance. And from head to toe, the Signa® system delivers.

Excellent image quality. Comprehensive applications. High throughput. And continuing development of advanced software and hardware that keeps Signa sites the community leaders in MR.

Success in MR depends on having a system that can do it all. Signa can.

A head start

Right from the top, Signa imaging gives you a distinct advantage. Many Signa users report that, on the average, a complete high resolution head scan takes only 30 minutes.

Signa enables you to routinely combine single excitation imaging with small FOVs and thin slices to get superb resolution and contrast —quickly. Which is one reason why Signa sites typically build a strong neurological referral base—very quickly.

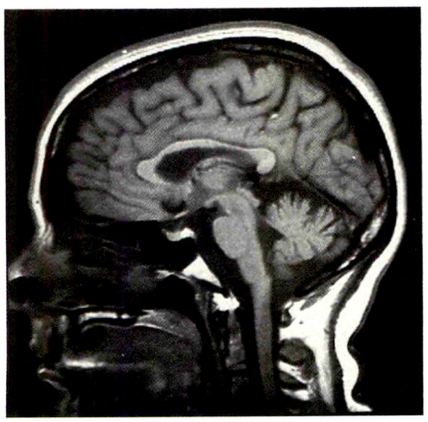
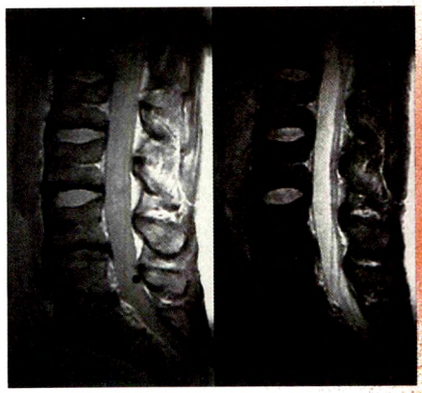


Image courtesy of University Diagnostic Institute, Tampa, FL.

The backbone of referral strength

Signa MR imaging provides superior visualization of spine anatomy. And with Signa's standard fast scanning, spine studies are completed with an efficiency that both patients and technologists appreciate.



Oblique imaging is another advantage. Signa's multi-slice, multi-angle acquisitions mean greater diagnostic sensitivity, particularly in the lumbar spine.

Important to both lumbar and cervical spine studies is the "myelographic effect"—easily achieved with Signa's standard fast



above the rest

scan and flow compensation techniques, and with the peripheral gating option.

Extraordinary extremities

Orthopedic studies are among the fastest growing applications at Signa sites. For good reason. Signa surface coils can provide submillimeter resolution images of the knee, TMJ or shoulder in less than

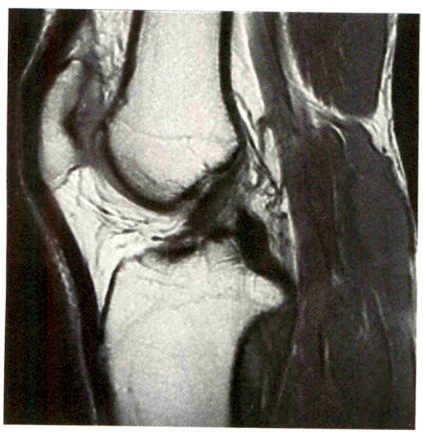


Image courtesy of Sunrise Diagnostic Center, Las Vegas, NV.

20 minutes. Minute changes in anatomy—rotator cuff and meniscal tears, TMJ derangements, and collateral ligament disease—can be clearly visualized due to Signa's high sensitivity and specificity, and its capability for small, off-center FOV imaging.

A growing body of work

Excellent body studies have become a clinical reality for Signa users, due to innovative new motion compensation software.

This software includes new

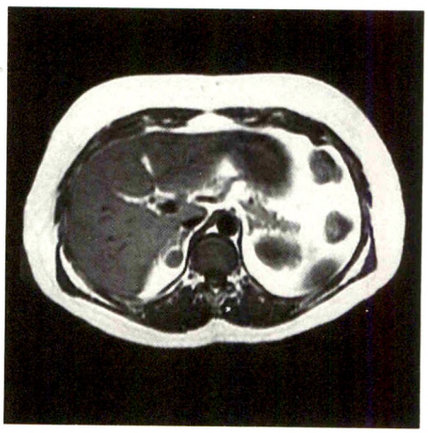


Image courtesy of Diagnostic Imaging, Chattanooga, TN.

blood flow compensation pulse sequences that virtually eliminate artifacts caused by pulsatile blood flow—without increasing acquisition time. And EXORCIST pulse sequences that keep respiratory motion artifacts to a minimum.

These advancements enhance Signa's already excellent contrast and spatial resolution for detailed studies of the liver, kidneys, vasculature and genitourinary tract.

A continuum of excellence

Our recent innovations in body imaging are just one example of other Signa applications to come, including MR angiography*, cine cardiac* and routine spectroscopy.* Also, the integrated exam—combining imaging and spectroscopy—which is now being performed at a number of Signa research sites.

*These Signa system features are currently classified as investigational and limited by federal law to investigational use. As such, they cannot be made commercially available until necessary government approvals are granted.

CIRCLE 3 ON READER SERVICE CARD

From head studies that helped establish the diagnostic power of MR to new applications that will determine its future, Signa continues to be the leader in MR.

For more information about the Signa system, please call GE Medical Systems.

(800) 624-5692.



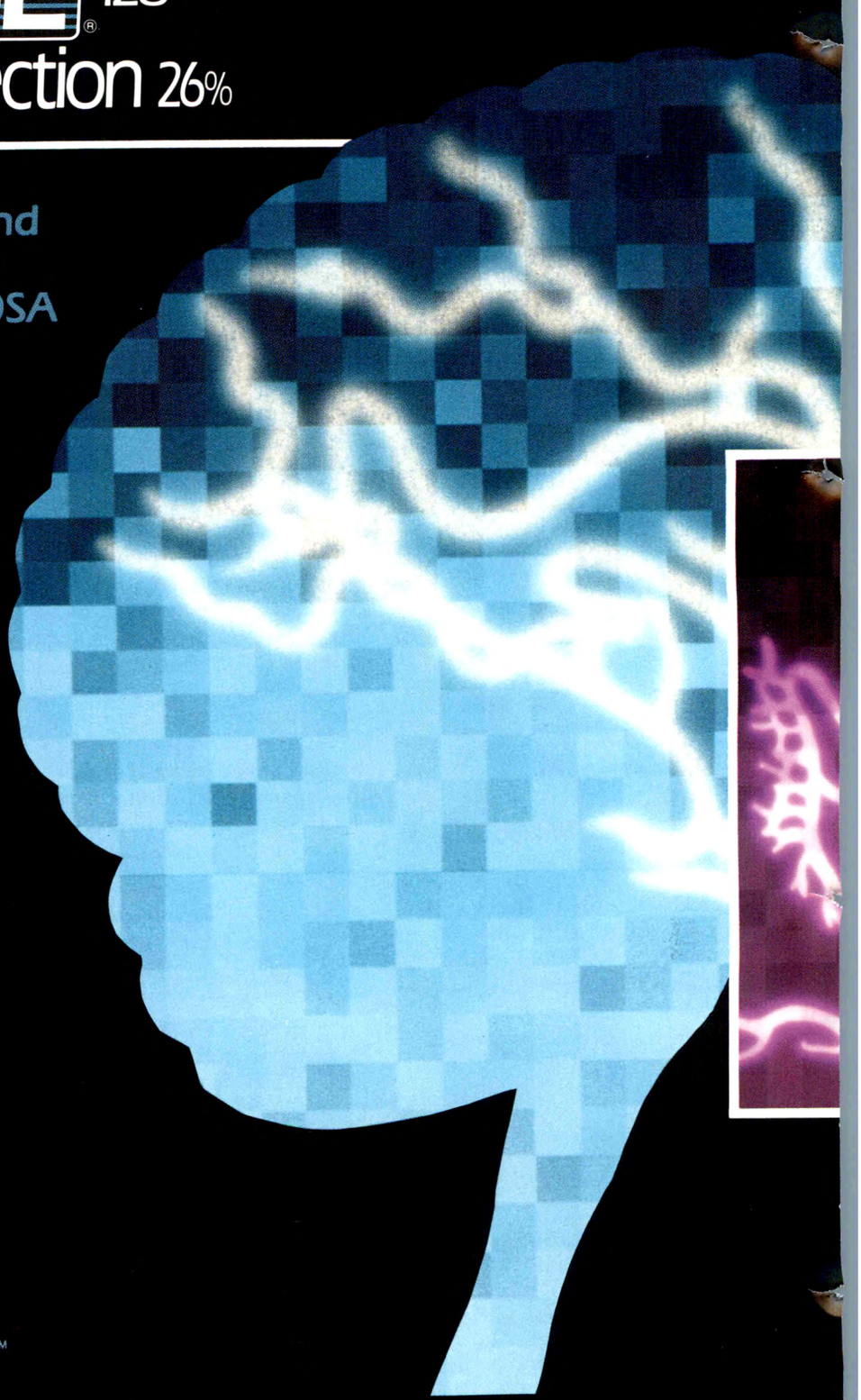
GE Medical Systems

ANNOUNCING

ISOVUE®-128

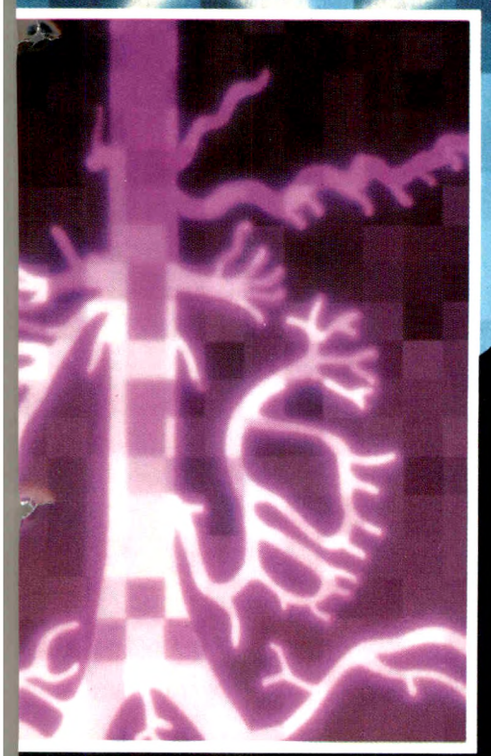
iopamidol injection 26%

For cerebral and abdominal intra-arterial DSA



From SQUIBB™ Diagnostics

THE ONLY NONIONIC, LOW-OSMOLALITY CONTRAST AGENT INDICATED FOR INTRA-ARTERIAL DSA



The ISOVUE Advantages:

Approximately isotonic to plasma.

The osmolality of ISOVUE-128 is 290 mOsm/kg H_2O, compared with 285 mOsm/kg H_2O for plasma. As with all injectable contrast agents, patients with CHF may experience a transient increase in circulatory osmotic load.

Low incidence of patient motion.

Well-tolerated ISOVUE-128 has been associated with a low incidence of patient motion, which may mean fewer retakes. In a clinical trial, 2% (9 of 520) sets of images were technically inadequate due to patient motion.*

High-quality images.

For both cerebral and abdominal studies, ISOVUE-128 has been shown to produce images of diagnostic quality in 98% (502 of 511) of cases.*

As with all injectable contrast agents, the possibility of severe adverse reactions should be borne in mind. (See brief summary on adjacent page for WARNINGS, PRECAUTIONS, and ADVERSE REACTIONS.)

*Data on file, Squibb Institute for Medical Research.

This product is under license from Bracco Industria Chimica, S.p.A.
U.S. Patent #4,001,323

ISOVUE®-128
iopamidol injection 26%

© 1987 E.R. Squibb & Sons, Inc., Princeton, NJ

647-505

Issued: August 1987

ISOVUE®-128
Iopamidol Injection 26%

INDICATIONS AND USAGE
ISOVUE-128 (iopamidol Injection 26%) is indicated for intra-arterial digital subtraction angiography (DSA) of the cerebral and abdominal vasculature.

CONTRAINDICATIONS
None.

WARNINGS
Caution must be exercised in patients with severely impaired renal function, those with combined renal and hepatic disease, or anuria, particularly when larger doses are administered.

Radiopaque diagnostic contrast agents are potentially hazardous in patients with multiple myeloma or other paraproteinemia, particularly in those with therapeutically resistant anuria. Myeloma occurs most commonly in persons over age 40. Although neither the contrast agent nor dehydration has been proved separately to be the cause of anuria in myelomatous patients, it has been speculated that the combination of both may be causative. The risk in myelomatous patients is not a contraindication; however, special precautions are required.

Contrast media may promote sickling in individuals who are homozygous for sickle cell disease when injected intravenously or intraarterially.

Administration of radiopaque materials to patients known or suspected of having pheochromocytoma should be performed with extreme caution. If, in the opinion of the physician, the possible benefits of such procedures outweigh the considered risks, the procedures may be performed; however, the amount of radiopaque medium injected should be kept to an absolute minimum. The blood pressure should be assessed throughout the procedure and measures for treatment of a hypertensive crisis should be available. These patients should be monitored very closely during contrast enhanced procedures.

Reports of thyroid storm following the use of iodinated radiopaque diagnostic agents in patients with hyperthyroidism or with an autonomously functioning thyroid nodule suggest that this additional risk be evaluated in such patients before use of any contrast medium.

PRECAUTIONS
General
Diagnostic procedures which involve the use of any radiopaque agent should be carried out under the direction of personnel with the prerequisite training and with a thorough knowledge of the particular procedure to be performed. Appropriate facilities should be available for coping with any complication of the procedure, as well as for emergency treatment of severe reaction to the contrast agent itself. After parenteral administration of a radiopaque agent, competent personnel and emergency facilities should be available for at least 30 to 60 minutes since severe delayed reactions may occur.

Preparatory dehydration is dangerous and may contribute to acute renal failure in patients with advanced vascular disease, diabetic patients, and in susceptible nondiabetic patients (often elderly with preexisting renal disease). *Patients should be well hydrated prior to and following iopamidol administration.*

The possibility of a reaction, including serious, life-threatening, fatal, anaphylactoid or cardiovascular reactions, should always be considered (see ADVERSE REACTIONS). Patients at increased risk include those with a history of a previous reaction to a contrast medium, patients with a known sensitivity to iodine per se, and patients with a known clinical hypersensitivity (bronchial asthma, hay fever, and food allergies). The occurrence of severe idiosyncratic reactions has prompted the use of several pretesting methods. However, pretesting cannot be relied upon to predict severe reactions and may itself be hazardous for the patient. It is suggested that a thorough medical history with emphasis on allergy and hypersensitivity, prior to the injection of any contrast medium, may be more accurate than pretesting in predicting potential adverse reactions. A positive history of allergies or hypersensitivity does not arbitrarily contraindicate the use of a contrast agent where a diagnostic procedure is thought essential, but caution should be exercised. Premedication with antihistamines or corticosteroids to avoid or minimize possible allergic reactions in such patients should be considered. Recent reports indicate that such pretreatment does not prevent serious life-threatening reactions, but may reduce both their incidence and severity.

General anesthesia may be indicated in the performance of some procedures in selected patients; however, a higher incidence of adverse reactions has been reported with radiopaque media in anesthetized patients, which may be attributable to the inability of the patient to identify untoward symptoms, or to the hypotensive effect of anesthesia which can reduce cardiac output and increase the duration of exposure to the contrast agent.

Although the osmolality of iopamidol 128 mgI/mL is comparable to that of plasma, the potential transitory increase in circulatory volume load in patients with congestive heart failure requires caution during injection. These patients should be observed for several hours following the procedure to detect delayed hemodynamic disturbances.

In angiographic procedures, the possibility of dislodging plaques or damaging or perforating the vessel wall should be borne in mind during catheter manipulations and contrast medium injection. Test injections to ensure proper catheter placement are suggested. Following arteriographic procedures, gentle pressure hemostasis is required, followed by observation and immobilization of the limb for several hours to prevent hemorrhage from the site of arterial puncture. Angiography should be avoided whenever possible in patients with homocystinuria, because of the risk of inducing thrombosis and embolism.

Drug Interactions
Renal toxicity has been reported in a few patients with liver dysfunction who were given oral cholecystographic agents followed by intravascular contrast agents. Administration of intravascular agents should therefore be postponed in any patient with a known or suspected hepatic or biliary disorder who has recently received a cholecystographic contrast agent.

Other drugs should not be admixed with iopamidol.

Drug/Laboratory Test Interactions
The results of PBI and radioactive iodine uptake studies, which depend on iodine estimations, will not accurately reflect thyroid function for up to 16 days following administration of iodinated contrast media. However, thyroid function tests not depending on iodine estimations, e.g., T3 resin uptake and total or free thyroxine (T4) assays are not affected.

Any test which might be affected by contrast media should be performed prior to administration of the contrast medium.

Laboratory Test Findings
In vitro studies with animal blood showed that many radiopaque contrast agents, including iopamidol, produced a slight depression of plasma coagulation factors including prothrombin time, partial thromboplastin time, and fibrinogen, as well as a slight tendency to cause platelet and/or red blood cell aggregation.

Transitory changes may occur in red cell and leucocyte counts, serum calcium, serum creatinine, serum glutamic oxalacetic transaminase (SGOT), and uric acid in urine; transient albuminuria may occur.

These findings have not been associated with clinical manifestations.

Carcinogenesis, Mutagenesis, Impairment of Fertility
In animal reproduction studies performed on rats, intravenously administered iopamidol did not induce adverse effects on fertility or general reproductive performance.

In studies to determine mutagenic activity, iopamidol did not cause any increase in mutation rates.

Pregnancy Category B
No teratogenic effects attributable to iopamidol have been observed in teratology studies performed in animals. There are, however, no adequate and well controlled studies in pregnant women. It is not known whether iopamidol crosses the placental barrier or reaches fetal tissues. However, many injectable contrast agents cross the placental barrier in humans and appear to enter fetal tissues passively. Because animal teratology studies are not always predictive of human response, this drug should be used during pregnancy only if clearly needed.

Radiologic procedures involve a certain risk related to the exposure of the fetus to ionizing radiation.

Labor and Delivery
It is not known whether use of contrast agents during labor or delivery has immediate or delayed adverse effects on the fetus, prolongs the duration of labor or increases the likelihood that forceps delivery or other obstetrical intervention or resuscitation of the newborn will be necessary.

Nursing Mothers
It is not known whether iopamidol is excreted in human milk. However, many injectable contrast agents are excreted unchanged in human milk. Although it has not been established that serious adverse reactions occur in nursing infants, caution should be exercised when intravascular contrast media are administered to nursing women because of potential adverse reactions, and consideration should be given to temporarily discontinuing nursing.

Pediatric Use
Safety and effectiveness in children have not been established.

ADVERSE REACTIONS
Adverse reactions following the use of iopamidol are usually mild to moderate, self-limited, and transient.

In a clinical trial with 100 patients, adverse reactions possibly attributed to ISOVUE-128 administration were nausea (2%), headache (1%) and vomiting (1%). One patient with preexisting renal impairment and severe bilateral renal vascular disease experienced renal failure, possibly secondary to a subsequent acute episode of congestive heart failure and/or drug administration (see Warnings).

The following table of incidence of reactions is based on clinical studies with ISOVUE in about 1835 patients. While the following reactions may or may not occur with ISOVUE-128 with the same frequency, the data are presented to provide a more complete profile of ISOVUE (Iopamidol Injection).

Adverse Reactions

System	Estimated Overall Incidence >1%	≤1%
Cardiovascular	none	tachycardia hypotension hypertension myocardial ischemia circulatory collapse S-T segment depression bigeminy extrasystoles ventricular fibrillation angina pectoris bradycardia transient ischemic attack thrombophlebitis
Nervous	pain (1.7%) burning sensation (1.4%)	vasovagal reaction tingling in arms grimace faintness
Digestive	nausea (1.2%)	vomiting anorexia
Respiratory	none	throat constriction dyspnea pulmonary edema
Skin and Appendages	none	rash urticaria pruritus flushing
Body as a Whole	hot flashes (1.5%)	headache fever chills excessive sweating back spasm
Special Senses	warmth (1.1%)	taste alterations nasal congestion visual disturbances
Urogenital	none	urinary retention

In *aortography,* the risks of procedures also include injury to the aorta and neighboring organs, pleural puncture, renal damage including infarction and acute tubular necrosis with oliguria and anuria, accidental selective filling of the right renal artery during the translumbar procedure in the presence of preexisting renal disease, retroperitoneal hemorrhage from the translumbar approach, and spinal cord injury and pathology associated with the syndrome of transverse myelitis.

Adverse effects reported in clinical literature for iopamidol include arrhythmia, arterial spasms, hematuria, periorbital edema, involuntary leg movement, malaise, and triggering of deglutition; some of these may occur as a consequence of the procedure. Other reactions may also occur with the use of any contrast agent as a consequence of the procedural hazard; these include hemorrhage or pseudoaneurysms at the puncture site, brachial plexus palsy following axillary artery injections, chest pain, myocardial infarction, and transient changes in hepatorenal chemistry tests. Arterial thrombosis, displacement of arterial plaques, venous thrombosis, dissection of the coronary vessels and transient sinus arrest are rare complications.

General Adverse Reactions To Contrast Media
Reactions known to occur with parenteral administration of iodinated ionic contrast agents (see the listing below) are possible with any nonionic agent. Approximately 95 percent of adverse reactions accompanying the use of other water-soluble intravascularly administered contrast agents are mild to moderate in degree. However, life-threatening reactions and fatalities, mostly of cardiovascular origin, have occurred. Reported incidences of death from the administration of other iodinated contrast media range from 6.6 per 1 million (0.00066 percent) to 1 in 10,000 patients (0.01 percent). Most deaths occur during injection or 5 to 10 minutes later, the main feature being cardiac arrest with cardiovascular disease as the main aggravating factor. Isolated reports of hypotensive collapse and shock are found in the literature. The incidence of shock is estimated to be 1 out of 20,000 (0.005 percent) patients.

Adverse reactions to injectable contrast media fall into two categories: chemotoxic reactions and idiosyncratic reactions. Chemotoxic reactions result from the physicochemical properties of the contrast medium, the dose, and the speed of injection. All hemodynamic disturbances and injuries to organs or vessels perfused by the contrast medium are included in this category. Experience with iopamidol suggests there is much less discomfort (e.g., pain and/or warmth) with peripheral arteriography. Fewer changes are noted in ventricular function after ventriculography and coronary arteriography.

Idiosyncratic reactions include all other reactions. They occur more frequently in patients 20 to 40 years old. Idiosyncratic reactions may or may not be dependent on the amount of drug injected, the speed of injection, the mode of injection, and the radiographic procedure. Idiosyncratic reactions are subdivided into minor, intermediate, and severe. The minor reactions are self-limited and of short duration; the severe reactions are life-threatening and treatment is urgent and mandatory.

The reported incidence of adverse reactions to contrast media in patients with a history of allergy is twice that for the general population. Patients with a history of previous reactions to a contrast medium are three times more susceptible than other patients. However, sensitivity to contrast media does not appear to increase with repeated examinations. Most adverse reactions to intravascular contrast agents appear within one to three minutes after the start of injection, but delayed reactions may occur (see PRECAUTIONS, General).

In addition to the adverse drug reactions reported for iopamidol, the following additional adverse reactions have been reported with the use of other intravascular contrast agents and are possible with the use of any water-soluble iodinated contrast agent:

Cardiovascular: vasodilation, cerebral hematomas, petechiae.
Nervous: paresthesia, dizziness, convulsions, paralysis, coma.
Respiratory: increased cough, asthma, laryngeal edema, pulmonary edema, bronchospasm, rhinitis.
Skin and Appendages: injection site pain usually due to extravasation and/or erythematous swelling, skin necrosis.
Urogenital: osmotic nephrosis of proximal tubular cells, renal failure, pain.
Special Senses: bilateral ocular irritation; lacrimation; conjunctival chemosis, infection, and conjunctivitis.

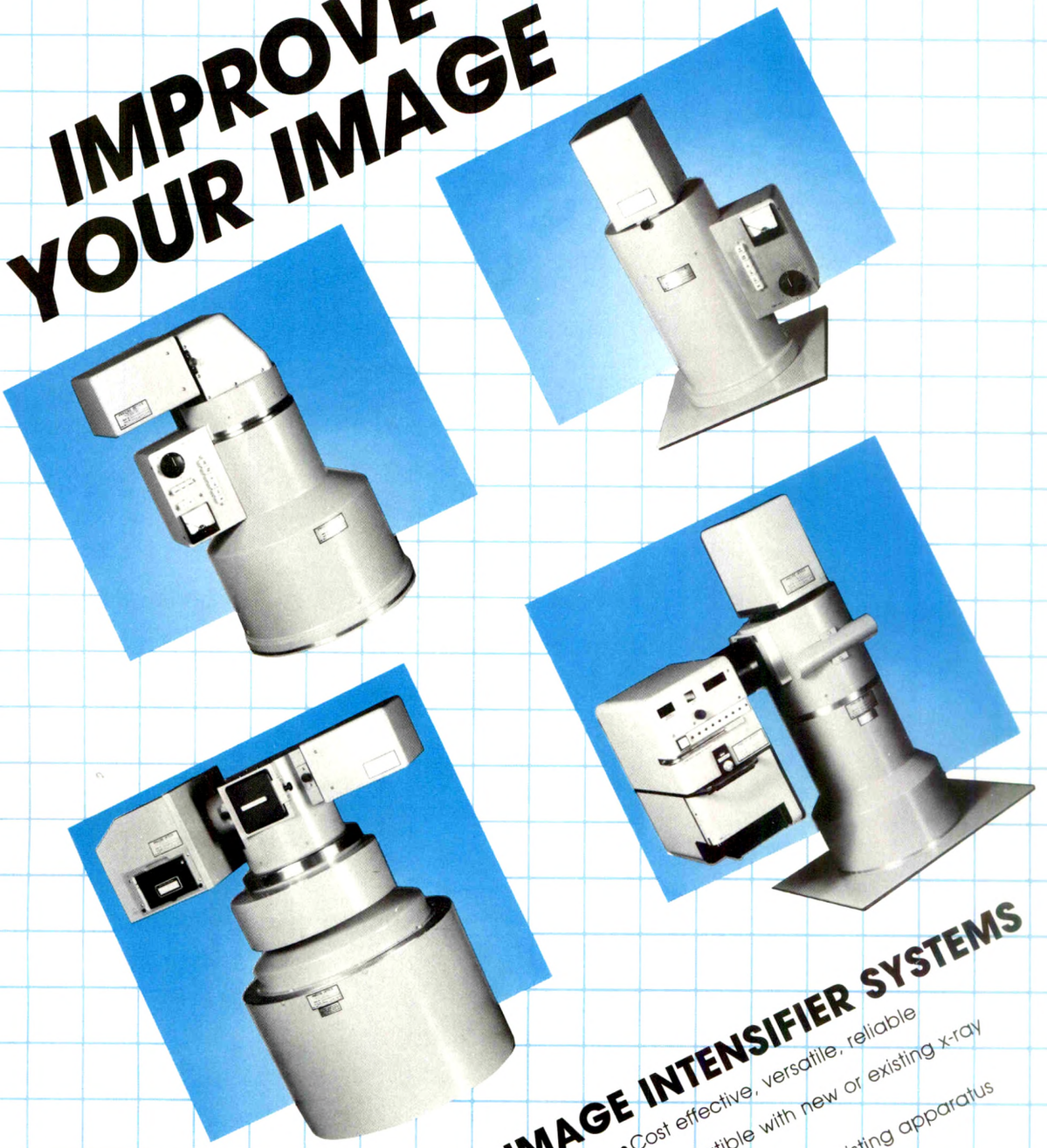
The following reactions may also occur: neutropenia, thrombophlebitis, flushing, pallor, weakness, severe retching and choking, wheezing, cramps, tremors, and sneezing.

OVERDOSAGE
Treatment of an overdose of an injectable radiopaque contrast medium is directed toward the support of all vital functions, and prompt institution of symptomatic therapy. Intravenous LD_{50} values (gI/kg) for iopamidol in animals: 21.8 (mice), 13.8 (rats), 9.6 (rabbits), 17.0 (dogs).

HOW SUPPLIED
ISOVUE-128 (Iopamidol Injection 26%)
Ten 50 mL single dose vials (NDC 0003-2153-10) J3-702 A

© 1987 E.R. Squibb & Sons, Inc., Princeton, NJ 647-505 Issued: August 1987

IMPROVE YOUR IMAGE



WITH PRECISE OPTICS IMAGE INTENSIFIER SYSTEMS

- The world's largest independent manufacturer of Image Intensifier Systems and components
- Over 30 years of experience in design and manufacture
- 6,9,12, and 16-Inch latest series image tubes for optimum performance
- 525/875/1023 line CCTV's, 6fps 100mm/105mm cameras
- Cost effective, versatile, reliable
- Compatible with new or existing x-ray equipment
- Extend the life of existing apparatus
- Worldwide dealer network

Precise Optics®
PHOTO MEDIC EQUIPMENT, INC.

239 South Fehr Way
Bay Shore, New York 11706
Tel.: 516 242-6600
TWX: 510-227-9837

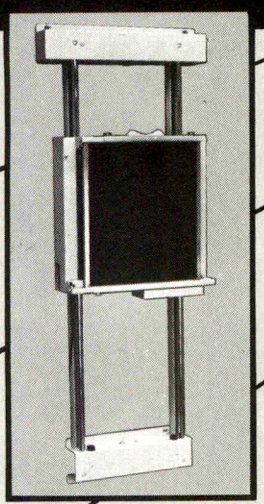
CIRCLE 6 ON READER SERVICE CARD

There are reasons
S.&S. X-RAY ACCESSORIES
are preferred...

PROVEN the best in X-Ray Departments throughout the world

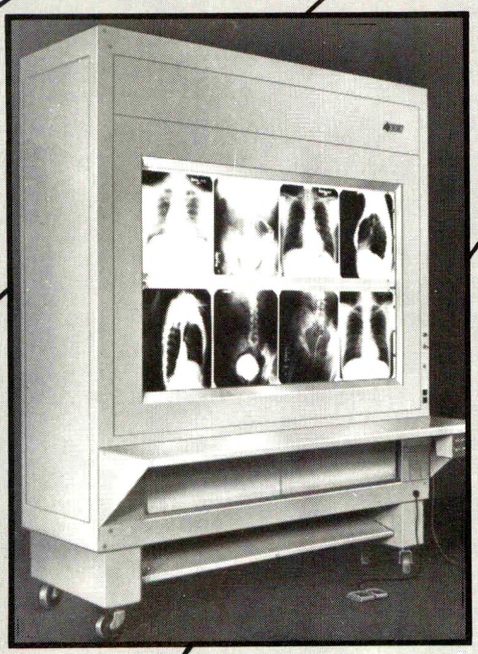
UNEQUALLED in design, construction and—quality

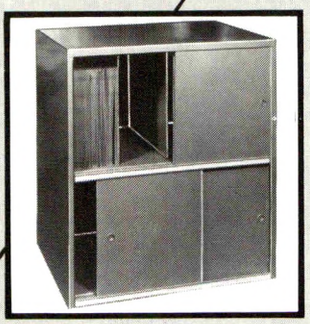
REPUTATION unmatched for RELIABILITY and PERFORMANCE





- Motorized Viewers
- Illuminators
- Transfer Cabinets
- File Cabinets
- Protective Panels
- Protective Aprons
- Wall Cassette Holders
- Dryers
- Safelights
- Dark Room Cabinets
- Storage Chests
- Loading Bins
- X-Ray Accessories





For more than 30 years, S. & S. has been meeting Radiologists' needs with a complete line of illuminators and accessories.

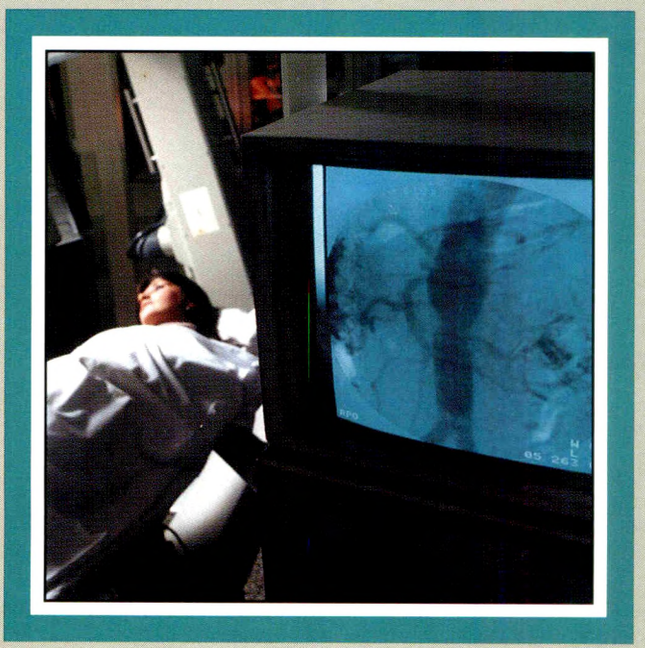
Contact S. & S. or your local x-ray dealer for additional information.

MANUFACTURED BY
S. & S. X-RAY PRODUCTS INC.

The Complete Line of X-Ray Accessories
Call Toll Free: 800-221-6634

Telephone: 718-649-8500
1101 LINWOOD STREET, BROOKLYN, NY 11208

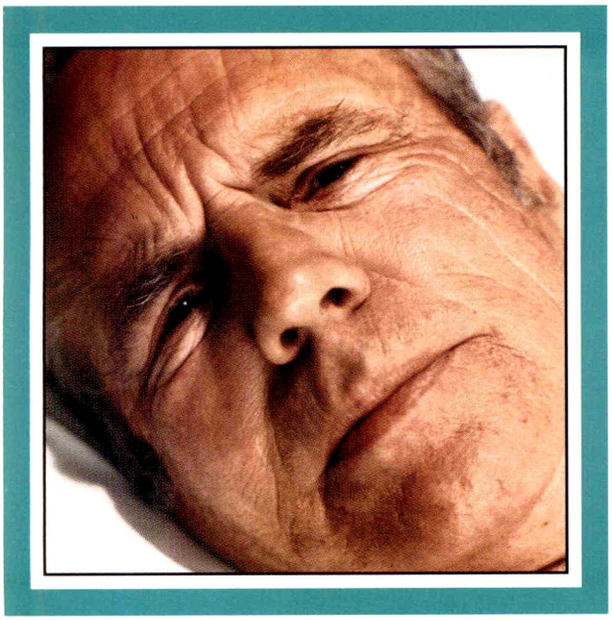
Because you really care...



...about patient comfort
...about diagnostic quality
...about clinical experience

HEXABRIX†

(Ioxaglate Meglumine 39.3% and
Ioxaglate Sodium 19.6% Injection)



Because you care

about patient comfort, tolerance, safety and well-being... you want a contrast agent known for:

- **Reduced pain**
- **Reduced heat**
- **Minimum patient movement**
- **Better patient compliance and cooperation**
- **Completing the procedure with fewer retakes**
- **Visualization comparable to conventional ionic media**
- **Improved nephrotoxic[1-3] and cardiovascular[4-7] profiles versus conventional ionic contrast media**



Because you care

about diagnostic quality...

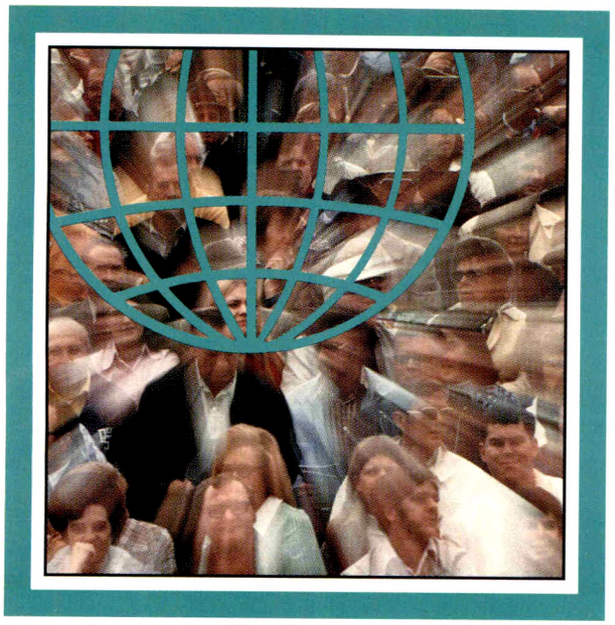
you want the low-osmolality contrast agent that has proved itself time and time again.

- **Hexabrix**—the low-osmolality ionic contrast medium—has been the agent of choice in over 5,000,000 procedures worldwide.
- **Hexabrix** has an osmolality lower than other currently available water-soluble contrast agents with comparable iodine concentrations—*including iopamidol and iohexol.*
- **Hexabrix** helps provide high-quality studies with enhanced patient comfort and fewer procedural problems.
- A recent multi-center U.S. study (893 patients) supports the efficacy and patient tolerance of Hexabrix:
  —95% of patients studied showed good-to-excellent visualization...*and*
  —96% of patients exhibited good-to-excellent toleration in angiographic procedures*

*Data on file at Mallinckrodt

HEXABRIX†

(Ioxaglate Meglumine 39.3% and Ioxaglate Sodium 19.6% Injection)



Because you care

about clinical experience...

you want a proven contrast agent that has passed the test of clinical scrutiny.

Study after study shows that Hexabrix delivers quality diagnostic images with reduced pain, reduced heat and greater patient comfort.[3-6,8-16]

Now...expanded clinical indications to meet procedural requirements for:

- **Peripheral Arteriography,** including percutaneous transluminal angioplasty
- **Selective Visceral Arteriography,** including percutaneous transluminal angioplasty
- **Cerebral Angiography**
- **Selective Coronary Arteriography** (with or without left ventriculography, including percutaneous transluminal coronary angioplasty)
- **Pediatric Angiocardiography**
- **Aortography**
- **Intra-arterial Digital Subtraction Angiography**
- **Intravenous Digital Subtraction Angiography**
- **Peripheral Venography**
- **Excretory Urography**
- **Contrast Enhancement of Computed Tomographic Head Imaging and Body Imaging**
- **Arthrography**
- **Hysterosalpingography**



Because you care

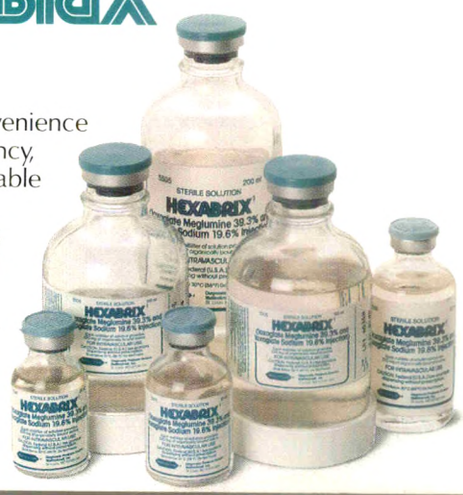
about your patients... and the professionals you work with...

you want the advantages of HEXABRIX†

- **Reduced pain...reduced heat.** ***Patients appreciate that.***
- **Better patient cooperation and compliance throughout the procedure.** ***Nurses and technologists appreciate that.***
- **Hexabrix helps you maintain a smooth-running schedule...cuts costly (and annoying) retakes... helps reinforce patient confidence.** ***Everyone appreciates that.***

HEXABRIX†

For greater convenience and cost-efficiency, Hexabrix is available in a wide range of package sizes to fit procedural needs and minimize waste.



Mallinckrodt®

HEXABRIX† (Ioxaglate Meglumine 39.3% and Ioxaglate Sodium 19.6% Injection)

HEXABRIX®

Each milliliter of HEXABRIX contains 393 mg of ioxaglate meglumine, 196 mg of ioxaglate sodium and 0.10 mg edetate calcium disodium as a stabilizer. The solution contains 3.48 mg (0.15 mEq) sodium in each milliliter and provides 32% (320 mg/mL) organically bound iodine.

CONTRAINDICATIONS

HEXABRIX is contraindicated for use in myelography. Refer to PRECAUTIONS concerning hypersensitivity. Hysterosalpingography should not be performed during the menstrual period; in pregnant patients; in patients with known infection in any portion of the genital tract; or in patients in whom cervical conization or curettage has been performed within 30 days. Arthrography should not be performed if infection is present in or near the joint.

WARNINGS

Serious or fatal reactions have been associated with the administration of iodine containing radiopaque media. It is of utmost importance to be completely prepared to treat any contrast medium reaction.

As with any contrast medium, serious neurologic sequelae, including permanent paralysis, can occur following cerebral arteriography, selective spinal arteriography and arteriography of vessels supplying the spinal cord. The injection of a contrast medium should never be made following the administration of vasopressors, since they strongly potentiate neurologic effects.

In patients with subarachnoid hemorrhage, a rare association between contrast administration and clinical deterioration, including convulsions and death, has been reported. Therefore, administration of intravascular iodinated contrast media in these patients should be undertaken with caution.

A definite risk exists in the use of intravascular contrast agents in patients who are known to have multiple myeloma. In such instances anuria has developed, resulting in progressive uremia, renal failure and eventually death. Although neither the contrast agent nor dehydration has separately proved to be the cause of anuria in myeloma, it has been speculated that the combination of both may be a causative factor. The risk in myelomatous patients is not a contraindication to the procedure; however, partial dehydration in the preparation of these patients for the examination is not recommended since this may predispose to precipitation of myeloma protein in the renal tubules. No form of therapy, including dialysis, has been successful in reversing the effect. Myeloma, which occurs most commonly in persons over 40, should be considered before instituting intravascular administration of contrast agents.

Administration of radiopaque materials to patients known or suspected to have pheochromocytoma should be performed with extreme caution. If, in the opinion of the physician, the possible benefits of such procedures outweigh the considered risks, the procedures may be performed; however, the amount of radiopaque medium injected should be kept to an absolute minimum. The blood pressure should be assessed throughout the procedure, and measures for treatment of a hypertensive crisis should be available.

Since intravascular administration of contrast media may promote sickling in individuals who are homozygous for sickle cell disease, fluid restriction is not advised.

In patients with advanced renal disease, iodinated contrast media should be used with caution and only when the need for the examination dictates, since excretion of the medium may be impaired. Patients with combined renal and hepatic disease, those with severe hypertension or congestive heart failure and recent renal transplant recipients present an additional risk.

Renal failure has been reported in patients with liver dysfunction who were given an oral cholecystographic agent followed by an intravascular iodinated radiopaque agent and also in patients with occult renal disease, notably diabetics and hypertensives. In these classes of patients there should be no fluid restriction and every attempt made to maintain normal hydration prior to contrast medium injection, since dehydration is the single most important factor influencing further renal impairment.

Caution should be exercised in performing contrast medium studies in patients with endotoxemia and/or those with elevated body temperatures.

Reports of thyroid storm occurring following the intravascular use of iodinated radiopaque agents in patients with hyperthyroidism or with an autonomously functioning thyroid nodule, suggest that this additional risk be evaluated before use of this drug. Iodine-containing contrast agents may alter the results of thyroid function tests which depend on iodine estimation, e.g., PBI, and may also affect results of radioactive iodine uptake studies. Such tests, if indicated, should be performed prior to the administration of this preparation.

PRECAUTIONS

Diagnostic procedures which involve the use of iodinated intravascular contrast agents should be carried out under the direction of personnel skilled and experienced in the particular procedure to be performed. All procedures utilizing contrast media carry a definite risk of producing adverse reactions. While most reactions are minor, life-threatening and fatal reactions may occur without warning, and this risk must be weighed against the benefit of the procedure. A fully equipped emergency cart, or equivalent supplies and equipment, and personnel competent in recognizing and treating adverse reactions of all types should always be available. If a serious reaction should occur, immediately discontinue administration. Since severe delayed reactions have been known to occur, emergency facilities and competent personnel should be available for at least 30 to 60 minutes after administration. (See ADVERSE REACTIONS.)

Preparatory dehydration is dangerous and may contribute to acute renal failure in infants, young children, the elderly, patients with pre-existing renal insufficiency, patients with multiple myeloma, patients with advanced vascular disease and diabetic patients.

Acute renal failure has been reported in diabetic patients with diabetic nephropathy and in susceptible non-diabetic patients (often elderly with pre-existing renal disease) following the administration of iodinated contrast agents. Therefore, careful consideration of the potential risks should be given before performing this radiographic procedure in these patients.

Severe reactions to contrast media often resemble allergic responses. This has prompted the use of several provocative pretesting methods, none of which can be relied on to predict severe reactions. No conclusive relationship between severe reactions and antigen-antibody reactions or other manifestations of allergy has been established. The possibility of an idiosyncratic reaction in patients who have previously received a contrast medium without ill effect should always be considered. Prior to the injection of any contrast medium, the patient should be questioned to obtain a medical history with emphasis on allergy and hypersensitivity. A positive history of bronchial asthma or allergy (including food), a family history of allergy, or a previous reaction or hypersensitivity to a contrast agent may imply a greater than usual risk. Such a history may be more accurate than pre-testing in predicting the potential for reaction, although not necessarily the severity or type of reaction in the individual case. A positive history of this type does not arbitrarily contraindicate the use of a contrast agent when a diagnostic procedure is thought essential, but does call for caution. (See ADVERSE REACTIONS.)

Prophylactic therapy including corticosteroids and antihistamines should be considered for patients who present with a strong allergic history, a previous reaction to a contrast medium, or a positive pre-test since in these patients the incidence of reaction is two to three times that of the general population. Adequate doses of corticosteroids should be started early enough prior to contrast medium injection to be effective and should continue through the time of injection and for 24 hours after injection. Antihistamines should be administered within 30 minutes of the contrast medium injection. Recent reports indicate that such pre-treatment does not prevent serious life-threatening reactions, but may reduce both their incidence and severity. A separate syringe should be used for these injections.

General anesthesia may be indicated in the performance of some procedures in selected patients; however, a higher incidence of adverse reactions has been reported in these patients, and may be attributable to the inability of the patient to identify untoward symptoms or to the hypotensive effect of anesthesia which can prolong the circulation time and increase the duration of contact of the contrast agent.

Angiography should be avoided whenever possible in patients with homocystinuria because of the risk of inducing thrombosis and embolism.

PRECAUTIONS FOR SPECIFIC PROCEDURES

Pediatric Angiocardiography: It is advisable to monitor for ECG and vital signs changes throughout the procedure.

When large individual doses are administered, sufficient time should be allowed for any observed changes to return to or near baseline prior to making the next injection.

Caution should be used when making right heart injections in patients with pulmonary hypertension or incipient heart failure, since this may lead to increased right side pressures with subsequent bradycardia and systemic hypotension. Patients with pulmonary disease present additional risks.

Caution is advised in cyanotic infants since apnea, bradycardia, other arrhythmias and a tendency to acidosis are more likely to occur.

Since infants are more likely to respond with convulsions than are adults, the amount of total dosage is of particular importance. Repeated injections are hazardous in infants weighing less than 7 kg, particularly when these infants have pre-existing compromised right heart function or obliterated pulmonary vascular beds.

Selective Coronary Arteriography with or without left ventriculography: During the administration of large doses of HEXABRIX, continuous monitoring of vital signs is desirable. Caution is advised in the administration of large volumes to patients with incipient heart failure because of the possibility of aggravating the pre-existing condition. Hypotension should be corrected promptly since it may result in serious arrhythmias.

Special care regarding dosage should be observed in patients with right ventricular failure, pulmonary hypertension, or stenotic pulmonary vascular beds because of hemodynamic changes which may occur after injection into the right heart outflow tract.

Peripheral Arteriography: Moderate decreases in blood pressure occur frequently with intra-arterial (brachial) injections. This change is usually transient and requires no treatment; however, the blood pressure should be monitored for approximately ten minutes following injection.

Extreme caution during injection of the contrast agent is necessary to avoid extravasation and fluoroscopy is recommended. This is especially important in patients with severe arterial disease.

Cerebral Angiography: Cerebral angiography should be performed with special caution in patients with advanced arteriosclerosis, severe hypertension, cardiac decompensation, senility, recent cerebral thrombosis or embolism, and migraine.

Intra-Arterial Digital Subtraction Angiography: The risks associated with IA-DSA are those usually attendant with catheter procedures. Following the procedure, gentle pressure hemostasis is required, followed by observation and immobilization of the limb for several hours to prevent hemorrhage from the site of arterial puncture.

Patient motion, including respiration and swallowing, can result in misregistration leading to image degradation and non-diagnostic studies.

Intravenous Digital Subtraction Angiography: The risks associated with IV-DSA include those usually attendant with catheter procedures and include intramural injections, vessel dissection and tissue extravasation. The potential risk is reduced when small test injections of contrast medium are made under fluoroscopic observation to insure that the catheter tip is properly positioned and, in the case of peripheral placement, that the vein is of adequate size.

Patient motion, including respiration and swallowing, can result in misregistration leading to image degradation and non-diagnostic studies.

Peripheral Venography: Special care is required when venography is performed in patients with suspected thrombosis, phlebitis, severe ischemic disease, local infection or a totally obstructed venous system.

Extreme caution during injection of contrast media is necessary to avoid extravasation and fluoroscopy is recommended. This is especially important in patients with severe arterial or venous disease.

Excretory Urography: Infants and small children should not have any fluid restrictions prior to excretory urography. (See WARNINGS and PRECAUTIONS concerning preparatory dehydration.)

Contrast Enhancement in Body Computed Tomography: Patient cooperation is essential since patient motion, including respiration, can markedly affect image quality. The use of an intravascular contrast medium can obscure tumors in patients undergoing CT evaluation of the liver, resulting in a false negative diagnosis. Dynamic CT scanning is the procedure of choice for malignant tumor enhancement.

Arthrography: Strict aseptic technique is required to prevent the introduction of infection. Fluoroscopic control should be used to insure proper introduction of the needle into the synovial space and prevent extracapsular injection. Aspiration of excessive synovial fluid will reduce the pain on injection and prevent the dilution of the contrast agent. It is important that undue pressure not be exerted during the injection.

Hysterosalpingography: Caution should be exercised in patients suspected of having cervical or tubal carcinoma to avoid possible spread of the lesion by the procedure. Delayed onset of pain and fever (1-2 days) may be indicative of pelvic infection.

Carcinogenesis, Mutagenesis, Impairment of Fertility: No long-term animal studies have been performed to evaluate carcinogenic potential. However, animal studies suggest that this drug is not mutagenic and does not affect fertility in males or females.

Pregnancy Category B: Reproduction studies have been performed in rats and rabbits at doses up to two times the maximum adult human dose and have revealed no evidence of impaired fertility or harm to the fetus due to HEXABRIX. There are, however, no adequate and well-controlled studies in pregnant women. Because animal reproduction studies are not always predictive of human response, this drug should be used during pregnancy only if clearly needed.

Nursing Mothers: Ioxaglate salts are excreted unchanged in human milk. Because of the potential for adverse effects in nursing infants, bottle feedings should be substituted for breast feedings for 24 hours following the administration of this drug.

Pediatric Use: Safety and effectiveness in children has been established in pediatric angiocardiography and intravenous excretory urography. Data have not been submitted to support the safety and effectiveness of HEXABRIX in any other indication.

(Precautions for specific procedures receive comment under that procedure.)

ADVERSE REACTIONS

Adverse reactions to injectable contrast media fall into two categories: chemotoxic reactions and idiosyncratic reactions.

Chemotoxic reactions result from the physiochemical properties of the contrast media, the dose and the speed of injection. All hemodynamic disturbances and injuries to organs or vessels perfused by the contrast medium are included in this category.

Idiosyncratic reactions include all other reactions. They occur more frequently in patients 20 to 40 years old. Idiosyncratic reactions may or may not be dependent on the dose injected, the speed of injection, the mode of injection and the radiographic procedure. Idiosyncratic reactions are subdivided into minor, intermediate and severe. The minor reactions are self-limited and of short duration; the severe reactions are life-threatening and treatment is urgent and mandatory.

NOTE: Not all of the following adverse reactions have been reported with HEXABRIX. Because HEXABRIX is an iodinated intravascular contrast agent, all of the side effects and toxicity associated with agents of this class are theoretically possible, and this should be borne in mind when HEXABRIX is administered.

Severe, life-threatening anaphylactoid reactions, mostly of cardiovascular origin, have occurred following the administration of HEXABRIX as well as other iodine-containing contrast agents. Most deaths occur during injection or 5 to 10 minutes later; the main feature being cardiac arrest with cardiovascular disease as the main aggravating factor. Isolated reports of hypotensive collapse and shock are found in the literature. Based upon clinical literature, reported deaths from the administration of conventional iodinated contrast agents range from 6.6 per 1 million (0.00066 percent) to 1 in 10,000 patients (0.01 percent).

Regardless of the contrast agent employed, the overall estimated incidence of serious adverse reactions is higher with coronary arteriography than with other procedures. Cardiac decompensation, serious arrhythmias, or myocardial ischemia or infarction may occur during coronary arteriography and left ventriculography.

The most frequent adverse reactions are nausea, vomiting, facial flush and a feeling of body warmth. These are usually of brief duration. In double-blind clinical trials, HEXABRIX produced less discomfort upon injection (pain and heat) when compared to various other contrast agents. Other reactions include the following:

Hypersensitivity reactions: Dermal manifestations of urticaria with or without pruritus, erythema and maculopapular rash. Dry mouth. Sweating. Conjunctival symptoms. Facial, peripheral and angioneurotic edema. Symptoms related to the respiratory system include sneezing, nasal stuffiness, coughing, choking, dyspnea, chest tightness and wheezing, which may be initial manifestations of more severe and infrequent reactions including asthmatic attack, laryngospasm and bronchospasm with or without edema, pulmonary edema, apnea and cyanosis. Rarely, these allergic-type reactions can progress into anaphylaxis with loss of consciousness, coma, severe cardiovascular disturbances, and death.

Cardiovascular reactions: Generalized vasodilation, flushing and venospasm. Occasionally thrombosis or, rarely, thrombophlebitis. Extremely rare cases of disseminated intravascular coagulation resulting in death have been reported. Severe cardiovascular responses include rare cases of hypotensive shock, coronary insufficiency, cardiac arrhythmia, fibrillation and arrest. These severe reactions are usually reversible with prompt and appropriate management; however, fatalities have occurred.

Technique reactions: Extravasation with burning pain, hematomas, ecchymosis and tissue necrosis, vascular constriction due to injection rate, thrombosis and thrombophlebitis.

Neurological reactions: Spasm, convulsions, aphasia, syncope, paresis, paralysis resulting from spinal cord injury and pathology associated with the syndrome of transverse myelitis, visual field losses which are usually transient buy may be permanent, coma and death.

Other reactions: Headache, trembling, shaking, chills without fever, hyperthermia and lightheadedness. Temporary renal shutdown or other nephropathy.

Pediatric angiocardiography has been complicated by intramural injection with marked adverse effects on cardiac function.

During selective coronary arteriography with or without left ventriculography, patients may have clinically insignificant ECG changes. The following adverse effects have occurred in conjunction with the administration of iodinated intravascular contrast agents for this procedure: hypotension, shock, anginal pain, myocardial infarction, cardiac arrhythmias (bradycardia, ventricular tachycardia, ventricular fibrillation) and cardiac arrest. Fatalities have been reported. Complications to the procedure include dissection of coronary arteries, dislodgement of atheromatous plaques, perforation, hemorrhage and thrombosis.

Following peripheral arteriography, hemorrhage and thrombosis have occurred at the puncture site of the percutaneous injection. Brachial plexus injury has been reported following axillary artery injection.

The major causes of cerebral arteriographic adverse reactions appear to be repeated injections of the contrast material, administration of doses higher than those recommended, the presence of occlusive atherosclerotic vascular disease and the method and technique of injection. Adverse reactions are normally mild and transient. A feeling of warmth in the face and neck is frequently experienced. Infrequently, a more severe burning discomfort is observed. Transient visual hallucinations have been reported. Serious neurological reactions that have been associated with cerebral angiography and not listed under Adverse Reactions include stroke, amnesia and respiratory difficulties. Visual field defects with anopsia and reversible neurological deficit lasting from 24 hours to 48 hours have been reported. Confusion, disorientation with hallucination, and absence of vision sometimes lasting for one week have also been reported. Cardiovascular reactions that may occur with some frequency are bradycardia and either an increase or decrease in systemic blood pressure. The blood pressure change is transient and usually requires no treatment. Arthrography may induce joint pain or discomfort which is usually mild and transient but occasionally may be severe and persist for 24 to 48 hours following the procedure. Effusion requiring aspiration may occur in patients with rheumatoid arthritis. Fever and pain, cramping and tenderness of the abdomen have been reported following hysterosalpingography.

OVERDOSAGE

Overdosages may occur. The adverse effects of overdosage are life-threatening and affect mainly the pulmonary and cardiovascular systems. The symptoms may include cyanosis, bradycardia, acidosis, pulmonary hemorrhage, convulsions, coma and cardiac arrest. Treatment of an overdose is directed toward the support of all vital functions and prompt institution of symptomatic therapy.

Ioxaglate salts are dialyzable.

The intravenous LD_{50} values of HEXABRIX (in grams of iodine/kilogram body weight) were 11.2 g/kg in mice, >8 g/kg in rats, >6.4 g/kg in rabbits and >10.2 g/kg in dogs.

DOSAGE AND ADMINISTRATION

Details on dosage are provided in the package insert. *CONSULT FULL PACKAGE INSERT BEFORE USE.*

REFERENCES

1. Nilsson PE, Aspelin P, et al: Tolerance and biochemical effects from intravenous injection of ioxaglate in healthy volunteers. *Acta Radiol* (Diagn) 25(6):523-528, 1984.

2. Dawson P: Contrast agent nephrotoxicity. An appraisal. *BR J Radiol* 58:121-124, 1985.

3. Nilsson PE, Holtas SL, Tejler LT: Subjective responses and albuminuria induced by ioxaglate during renal angiography in man. *Radiology* 144:509-512, 1982.

4. Svenson RH: Comparison of the hemodynamic effects of Hexabrix and Renografin 76 following left ventriculography and coronary arteriography. *Invest Radiol* 19(Supp 6):S333-S334, 1984.

5. Hirshfeld Jr JW, Laskey W, Martin JL, Groh WC, Untereker W, Wolf GL: Hemodynamic changes induced by cardiac angiography with ioxaglate: Comparison with diatrizoate. *J AM Coll Cardiol* 2(5):954-957, 1983.

6. Cumberland D: Low-Osmolality Contrast Media in Cardiac Radiology. *Invest Radiol* 19(Supp 6): S270-S274, 1984.

7. Weikl A, Hubmann M: A survey of contrast media used in coronary angiography. *Cardiovasc Intervent Radiol* 5:202-210, 1982.

8. Spataro RF: A comparison of Hexabrix and Renografin-60 in Intravenous Urography. *Invest Radiol* 19(Supp 6):S360, 1984.

9. Ramsey RG, Czervionke L, et al: A double-blind clinical study comparing the safety and efficacy of Hexabrix and Hypaque Meglumine 60% in contrast-enhanced computed cranial tomographic scanning. *Invest Radiol* 19(Supp 6):S317, 1984.

10. Anthony CL, Tonkin ILD, et al: A double-blind randomized clinical study of the safety, tolerability, and efficacy of Hexabrix in pediatric angiocardiography. *Invest Radiol* 19(Supp 6):S335-343, 1984.

11. Tonkin ILD: A double-blind randomized clinical study of the use of Hexabrix in pediatric angiocardiography. *Invest Radiol* 19(Supp 6):S344-349, 1984.

...because you really care

HEXABRIX†
(Ioxaglate Meglumine 39.3% and Ioxaglate Sodium 19.6% Injection)

Mallinckrodt®

Diagnostic Products Division
Mallinckrodt, Inc.
Post Office Box 5840
St. Louis, MO 63134

For orders, medical and/or professional assistance call
(800) 325-3688 TOLL FREE

© Mallinckrodt, Inc. 1987

†Licensed by Guerbet, S.A. Registered U.S. Patent and Trademark Office

THE INNOVATION CONTINUES

We're building a case for being #1 in Ultrasound.



EXAMINE THE EVIDENCE

Exhibit A: Symme

The best sector images in the industry.

Who really provides the best image quality and technology? We believe the evidence is there for everyone to see. Take a close look at Diasonics' superior images. Then you be the judge.

With our SPA 1000, you'll find the superior spatial and contrast resolution that leads to greater diagnostic confidence. And the ease of use that increases patient throughput.

Quite simply put, the SPA 1000 produces the best sector imaging available anywhere. Superior image quality is established by our wide aperture, symmetrical phased array technology, with all of its inherent advantages over standard phased linear and annular array technologies.

Symmetrical focusing produces the thinnest tomographic sector slice over the entire depth. Our wider apertures — up to 30 mm — allow you to see the subtle gray scale tissue differences that you miss with other technologies.

Our 10 MHz probe technology and digital RF signal processing set the industry standard for vascular and small parts imaging. The higher frequencies achievable with symmetrical phased array technology enable you to visualize subtle pathologies.

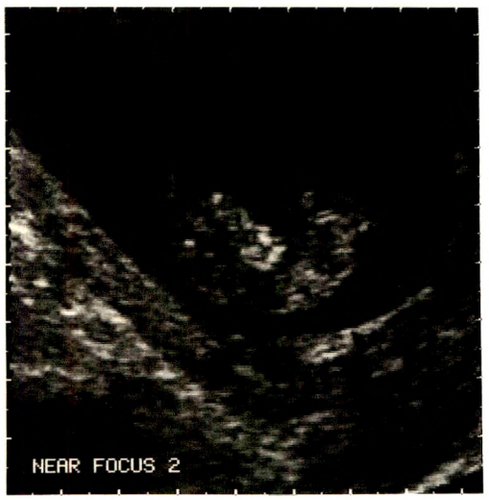


Symmetrical phased arrays provide superior sensitivity, which permits you to scan obese patients at higher frequencies. There's no need to revert to the lower resolution produced by lower transducer frequencies.

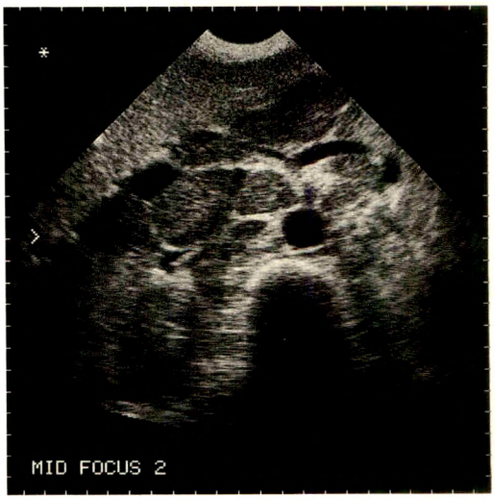
Along with such extensive imaging advantages, the SPA 1000 provides deep abdominal Doppler to analyze the hemodynamics of blood flow and expand your clinical capabilities.

That's only some of the evidence that proves the superiority of the Diasonics SPA 1000. But don't take our word for it. Examine the images and the technology, and judge for yourself.

trical Phased Array



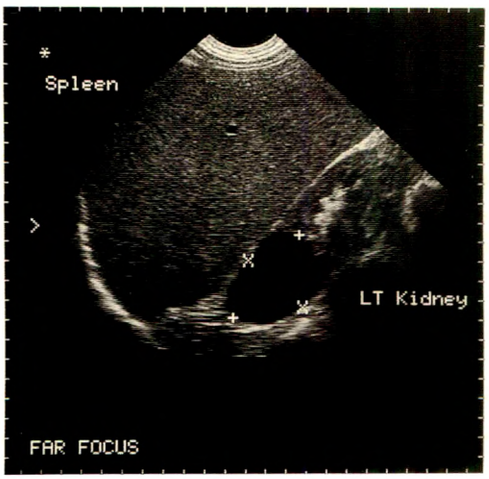
Excellent spatial resolution shows facial detail on a 9-week fetus.



Transverse view of the upper abdomen showing enlargement of the lymph nodes due to chronic lymphocytic leukemia.



Both renal arteries are visualized with excellent detail as they branch from the abdominal aorta.

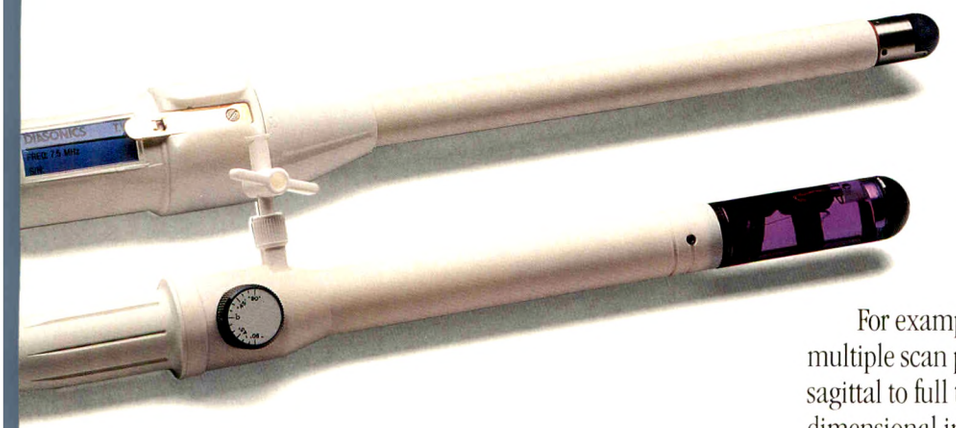


Intercostal sagittal scan demonstrating a large cyst on the upper pole of the left kidney and an enlarged spleen.

DIASONICS

A Habit of Innovation

Exhibit B: The



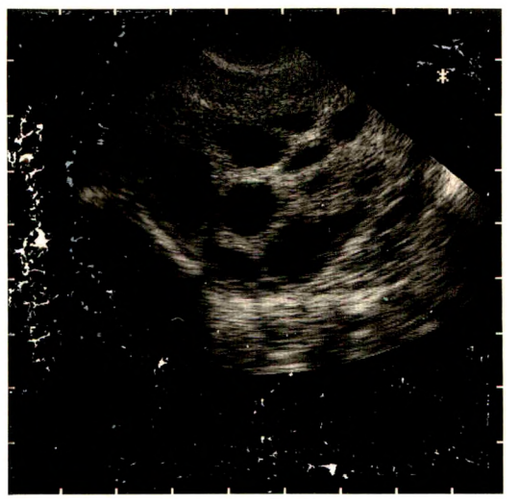
The right technology for the right clinical application.

Some ultrasound companies claim that a single probe can work for many different applications. But they don't tell you about the compromises they made to generalize their probe technology.

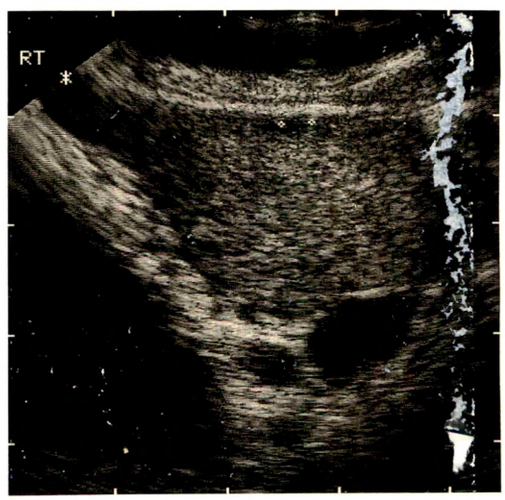
We're more specific about our probe technology. We've developed a wide variety of probes, each one optimized for a specific clinical application. That way, you never have to compromise on performance or your diagnosis.

For example, our unique transrectal probe gives you multiple scan planes for continuous imaging from full sagittal to full transverse. As a result, you achieve full, three-dimensional interrogation of the prostate, something you can't do with either linear or phased arrays.

Our transvaginal probe, which operates at 7.5 MHz, was specifically designed for early fetal viability studies, IVF and other obstetric and pelvic applications. This probe produces a wider sector image with higher resolution, so you



7.5 MHz transvaginal scan depicting multiple follicles in the right ovary.



7.5 MHz transrectal sagittal scan demonstrating a 2.7mm lesion in the peripheral zone of the prostate.

Specialty Probes

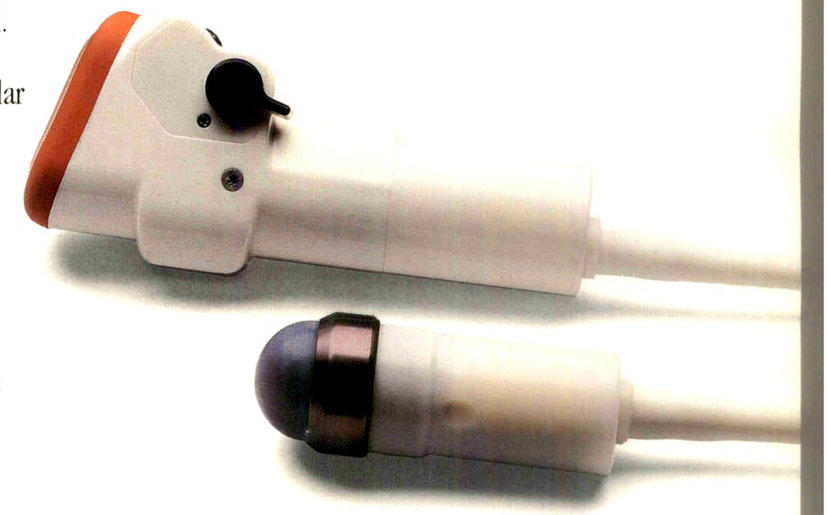
see the detail and structures that other probes fail to reveal.

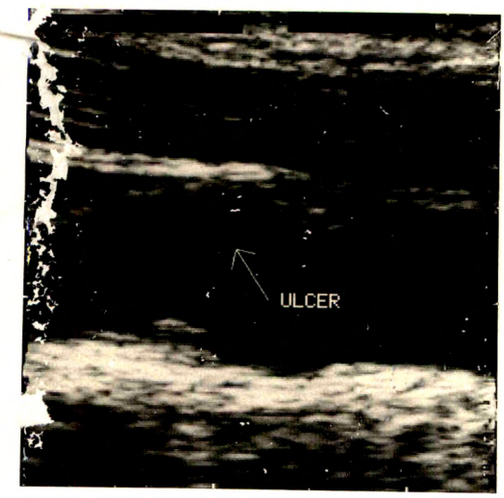
For simultaneous imaging and Doppler for vascular exams, you need the higher resolution of our 10 MHz vascular and small parts probe. To eliminate the compromises of single-transducer probes, our unique design incorporates two separate transducers: one clinically optimized for Doppler, the other for imaging.

The 10 MHz probe also provides the high resolution you need for confident diagnoses in thyroid, breast and testicular exams.

Our Micro-Sector probe provides high-quality images and sensitive pulsed Doppler for precise deep abdominal studies. The probe's small size facilitates ease of use and improves anatomical accessibility.

There's only one way to find out if an ultrasound company is using the right technology for the right application. Ask some probing questions. We have the answers.





True 10 MHz axial and lateral resolution provides the ability to detect a 4 mm ulceration in a soft plaque.

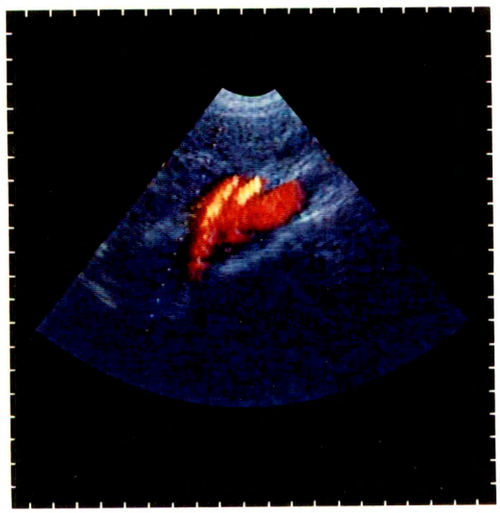


High-resolution 10 MHz sagittal image of an abnormal neonatal spine.

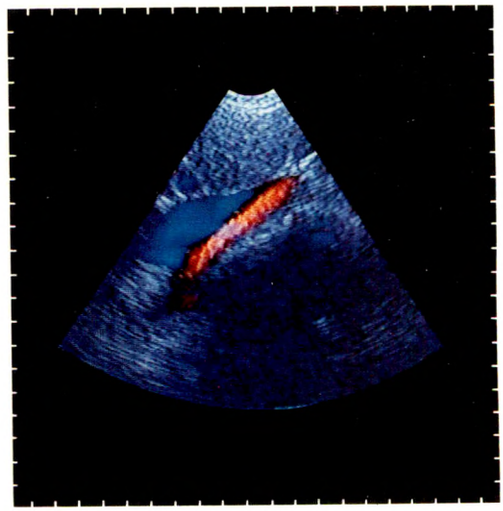
DIASONICS

A Habit of Innovation

Exhibit C: Color



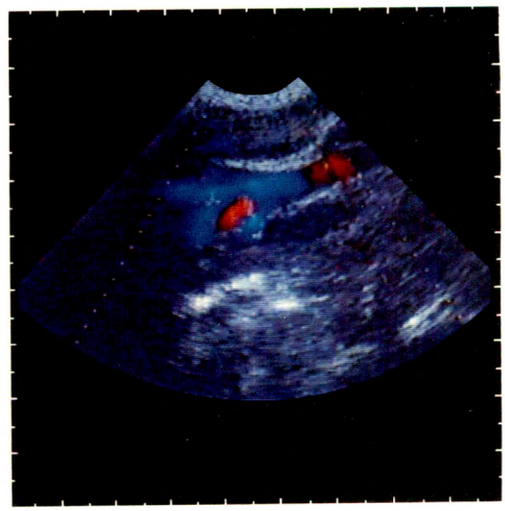
A sagittal image depicting the origin of the celiac trunk and SMA branching from the abdominal aorta.



Coronal scan through the liver demonstrating the IVC and right renal artery.



High-resolution abdominal array image showing blood flow within the IVC and portal venous system.



Carotid bifurcation showing the CCA, ECA, ICA and the superior thyroid artery posterior to the bifurcation.

Flow Mapping

Whole-body CFM without clinical compromise.

For abdominal Doppler and high-resolution peripheral vascular exams, Color Flow Mapping adds new dimensions to your diagnoses. CFM allows you to quickly see blood flow and complements your gray scale image to increase the speed and accuracy of your exams.

These advantages are being established in cardiology, where Diasonics is a CFM leader. Now we're bringing all of our CFM experience and expertise to abdominal and vascular ultrasound.

In keeping with our philosophy of the right technology for the right application, we're developing a series of clinically optimized CFM probes for a variety of specific applications.

Other companies may try to get by with one CFM probe for many different clinical applications. But we won't settle for clinical compromises.

Only a company with expertise in CFM technology and proven abilities in high-resolution imaging can provide the ultrasound medical community with the best Color Flow Mapping system. Diasonics has clearly demonstrated abilities in probe technology, image processing, Doppler and mainframe system architecture — the essential components of the best CFM system.

That's the kind of sound experience we bring to Doppler Color Flow Mapping. Soon you'll be able to see for yourself exactly what we mean.

DIASONICS

A Habit of Innovation

YOU BE THE JUDGE

A commitment that extends beyond product excellence.

Diasonics has designed a customer support program that's as advanced and complete as our products.

To begin with, we've built out obsolescence — bringing our product advances back to our installed base as upgrades. No one is left behind because we still offer upgrades on our very first products.

All Diasonics products are built for reliable performance and maximum uptime. For example, we feel so confident about the dependability of our SPA 1000 symmetrical phased array system that we offer the industry's first 36-month warranty.

We also support our products with direct national service, clinical educational support, and a research and development program devoted exclusively to medical imaging.

So before you judge which ultrasound company is best for your needs, examine all the evidence.

800-538-7021. In California, 800-662-6293.

DIASONICS

A Habit of Innovation

U.S.
Ultrasound
1656 McCarthy Boulevard
Milpitas, CA 95035
408-432-9000
800-662-6293 (in CA)
800-538-7021

Europe
Sonotron Holding AG
Steinhauserstrasse 74
P.O. Box 4737
CH-6304 Zug
Switzerland
(41) 42 41 64 64

Australia
Diasonics Pty Ltd
576 St. Kilda Road
Melbourne 3004
Australia
(03) 529-6111

1987 ARRS Executive Council Award

Intraarterial Fibrinolytic Therapy for Popliteal and Tibial Artery Obstruction: Comparison of Streptokinase and Urokinase

Paul D. Traughber[1]
Philip S. Cook[2]
Timothy J. Micklos[1]
Franklin J. Miller[1]

Experience with using intraarterial fibrinolysis in the treatment of occlusive disease of the popliteal artery and runoff vessels is limited. We describe the techniques and results in 25 patients with 30 fibrinolytic infusions of the popliteal and tibial arteries and compare them with the initial and long-term results of treatment using streptokinase and urokinase. The roles of catheter delivery systems and systemic heparin in the prevention of pericatheter thrombus were also studied. Urokinase was initially successful in 18 (90%) of 20 intraarterial infusions, whereas streptokinase was effective in 8 (80%) of 10 intraarterial infusions. Urokinase had the advantages of a shorter effective infusion time and fewer complications. Long-term follow-up was available in 20 of the successfully treated patients. Sixteen of these patients were doing well with an average follow-up of 27 months. The duration of the initial occlusion may be useful in identifying patients at risk for early reocclusion. No limbs were lost because of complications of therapy. The coaxial catheter system with a divided fibrinolytic dose provided protection against pericatheter thrombus, while systemic heparin was ineffective.

Our results suggest that urokinase is more effective than streptokinase for intraarterial infusion in the treatment of occlusion of the popliteal and tibial arteries; this procedure is an important alternative to surgery or an adjuvant to surgery in selected patients.

Surgical bypass at and below the knee is currently the standard therapy for thromboembolic occlusive disease, but it is associated with significant mortality and morbidity [1–3]. Fibrinolytic therapy combined with surgery or percutaneous angioplasty in the arteries above the knee has been efficacious in thromboembolic occlusive disease [4–9]. Our experience with fibrinolysis is limited to the popliteal and trifurcation arteries [10, 11]. We present a series of 25 patients ranging in age from 14 to 88 years who had 30 intraarterial infusions of fibrinolytic agents in the popliteal and trifurcation arteries. The results of treatment using streptokinase are compared with those using urokinase.

The purpose of this study was to determine the optimal fibrinolytic agent. Other areas investigated included (1) the relationship between the age of the thrombus and the initial and long-term success, and (2) prevention of pericatheter thrombus formation.

Materials and Methods

Twenty-five patients underwent 30 intraarterial fibrinolytic infusions at the Saint Joseph Hospital in Denver and at the University of Utah Medical Center in Salt Lake City. Seventeen of the patients had nonhealing ulcers or rest pain, six had disabling claudication, and two had postangioplasty complications. Patients were treated regardless of the apparent duration of the thromboembolic occlusion. There were 10 intraarterial infusions of streptokinase and 20 intraarterial infusions performed with urokinase.

The only absolute contraindications for therapy included active gastrointestinal bleeding, recent stroke, known intracranial aneurysm, or a devitalized limb. Any patient who was suspected of having emboli from the heart underwent echocardiography.

Received February 24, 1987; accepted after revision June 2, 1987.

Presented in part at the annual meeting of the American Roentgen Ray Society, Miami Beach, FL, April 1987; winner of an ARRS Executive Council award.

[1] Department of Radiology, University of Utah Medical Center, 50 N. Medical Dr., Salt Lake City, UT 84132. Address reprint requests to F. J. Miller.

[2] Department of Radiology, St. Joseph Hospital, 1835 Franklin St., Denver, CO 80218.

AJR 149:453–456, September 1987
0361–803X/87/1493–0453
© American Roentgen Ray Society

The patients were treated with different urokinase protocols at the two hospitals. At the University of Utah Medical Center, the urokinase was given as described by McNamara and Fischer [8]. This regimen uses higher initial doses of 240,000 units/hr tapered to 60,000 or 120,000 units/hr depending on the rate of fibrinolysis. At Saint Joseph Hospital the urokinase dose was a constant 100,000 units/hr in all but two patients. Streptokinase was begun at doses of 2500 to 5000 units/hr. Systemic heparin was administered during the infusion only in patients on the McNamara protocol [8].

Vascular access was obtained by means of the Seldinger technique in every patient. Early in the series procedures were performed with a single catheter with the tip at or into the occlusion. Later procedures using urokinase were often performed with a coaxial system either to treat pericatheter thrombus that had developed on the single catheter or to prevent its formation. This coaxial system was maintained by infusing 25% of the urokinase dose into the proximal catheter; the remaining 75% was administered via the distal catheter. The coaxial system most commonly used was either a 5-French catheter through a 7-French sheath or a 0.038-inch (0.097-cm) injectable guidewire placed through a 6-French sheath or a 6.5-French catheter.

When possible, a guidewire was advanced through the occlusion before fibrinolysis was begun to provide a channel and an increased surface area for fibrinolytic activity. During negotiation of the calf arteries, a steerable 0.015- to 0.018-in. (0.038- to 0.046-cm) platinum-tipped cardiac guidewire allowed reliable selective catheterization of these vessels. An injectable 0.038-in. (0.097-cm) guidewire was backloaded on the cardiac wire when it was necessary to use a larger balloon (i.e., 5–7 mm on a 7-French shaft) rather than the smaller cardiac balloons for angioplasty. Nitroglycerin administered sublingually and/or intravenously in 100 μg boluses was used liberally when angioplasty was performed.

Laboratory studies including prothrombin time, partial prothrombin time, thrombin time, platelet count, hematocrit, and fibrinogen level were recorded for baseline purposes; the partial prothrombin time was then followed when heparin was used and kept at 2.0–2.5 times the baseline level. The hematocrit, fibrinogen level, and thrombin time were monitored approximately every 12 hr. All of the patients were placed in the intensive care unit for the duration of the infusion.

Fifteen angioplasties of the popliteal and trifurcation arteries were performed. In three patients a more proximal angioplasty was also performed to improve inflow. Surgery was performed in ten patients associated with 11 fibrinolytic procedures. Surgery was performed following successful fibrinolytic therapy to correct an identified abnormality such as graft stenosis, popliteal artery entrapment, popliteal artery aneurysm, or failed percutaneous transluminal angioplasty.

The majority of patients at both hospitals were given systemic heparin after completion of therapy and removal of the catheter. Twenty patients received warfarin therapy at the time of discharge.

Successful treatment was defined as resolution of claudication, successful limb salvage, or treatment resulting in a simplified or less extensive surgical procedure.

The duration of therapy, number of complications, and the initial and long-term successes were compared for urokinase and streptokinase. In addition, the initial success and long-term follow-up were compared with the estimated age of the initial occlusion.

Results

Treatment was successful initially in 18 of 20 urokinase infusions and in eight of 10 streptokinase infusions. Long-term follow-up was available in 19 of the successfully treated patients (Table 1). There were three patients with late occlusions occurring an average of 4 months after the initial therapy. The remaining 16 patients were doing satisfactorily with an average follow-up of 27 months (Table 1).

The estimated age of initial thromboembolic occlusion and response to therapy were reviewed. No patients with an initial occlusion estimated to have been present for more than 1 month failed to respond to the initial therapy. After successful initial therapy for an occlusion estimated to have been present less than 1 month, only one patient (case 11) had recurrent thrombosis. Seven patients were treated for occlusions estimated to have been present for more than 1 month (range, 2–18 months). Three of the seven patients with occlusions estimated to have been present for more than 1 month have had recurring thrombosis during long-term follow-up. Only one of these three patients had recurring occlusions when being treated with warfarin (case 19).

The duration of streptokinase infusions averaged 84 hr. The patients treated with high-dose regional urokinase had infusions averaging 24 hr. The average duration of therapy in patients treated with the constant-dose infusion of 100,000 units of urokinase/hr was 31 hr, while the average duration of therapy in patients placed on the McNamara protocol [8] was 17 hr.

Three of the 17 patients treated for limb salvage required below-the-knee amputations when all therapeutic techniques failed. In no case did complications of fibrinolysis result in limb loss.

The coaxial system was used 17 times and a single catheter was used 19 times; in six treatments both were used. Pericatheter thrombus was encountered six times, with all episodes occurring during urokinase infusions. Five cases with pericatheter thrombus involved a single catheter. The single catheter was exchanged for a coaxial system in three of these cases, and in two the thrombus resolved. The coaxial system was used only with urokinase. One patient with pericatheter thrombus was a treatment failure because of a stenosis resulting from a hard rubberlike plaque at the site of a patch graft that was unresponsive to fibrinolysis and high-pressure balloon angioplasty.

Systemic heparinization was used in eight patients being treated with urokinase, and three developed pericatheter thrombus during the infusion. These three procedures were begun with a single catheter. In twelve infusions without systemic heparinization, three cases of pericatheter thrombus were encountered during urokinase infusions, one of which was encountered with a coaxial system.

Complications requiring transfusion or surgical intervention were defined as major complications. Major complications were seen in five of the 10 streptokinase procedures. Two of the 20 urokinase infusions resulted in a complication requiring surgery. Both patients required local repair at the puncture site because of persistent bleeding. The streptokinase cases with complications requiring therapy had local or deep hematomas that required transfusions. There were no cerebral vascular accidents, gastrointestinal bleeding episodes, or deaths in this series during fibrinolytic therapy.

Discussion

The results of this review of 30 intraarterial fibrinolytic infusion treatments in 25 patients with occlusion of the pop-

TABLE 1: Etiology of Occlusion, Related Therapy, and Long-Term Follow-up

Case No.	Final Diagnosis	Angioplasty	Surgery	Follow-up in Months
1	Peripheral vascular disease	−	−	Asymp × 40 months[a]
2	Peripheral vascular disease	−	+	Initial BKA
3	Diabetes mellitus	−	+	Initial BKA
4	Atrial fibrillation	−	−	Asymp × 41 months[a]
5	Popliteal artery entrapment	−	+	Asymp × 42 months[a]
6	Popliteal artery stenosis	−	−	Asymp × 54 months[a]
7	Ergotamine use	−	−	Asymp × 48 months[a]
8	Popliteal artery aneurysm	−	+	Asymp × 60 months[a]
9	Arrhythmia	−	−	No follow-up available[a]
10	Popliteal artery entrapment	−	+	Asymp × 66 months[a]
11	Bypass graft stenosis	+	−	Asymp × 2 months[a]
	Bypass graft stenosis	+	+	Asymp × 5 months[a]
	Bypass graft stenosis	+	−	Asymp × 6 months[a]
	Bypass graft occlusion	−	+	Required BKA
12	Anastomotic pseudoaneurysm	−	−	Asymp × 24 months[a]
13	Popliteal artery stenosis	+	−	Asymp × 7 months
14	Popliteal artery stenosis	+	−	Asymp × 7 months[a]
15	Bypass graft stenosis	+	−	Asymp × 6 months[a]
16	Peripheral vascular disease	+	−	Asymp × 20 months[a]
17	Popliteal artery stenosis	+	−	Asymp × 1 month, then reoccluded
18	Chondrosarcoma	−	+	Slight decreased pulses at 3 months, later occluded off warfarin[a]
19	Buerger's disease	+	−	Asymp × 7 months, then reoccluded[a]
20	Peripheral vascular disease	+	−	Asymp × 7 months
21	Peripheral vascular disease	+	−	Asymp × 10 months
22	Patch graft stenosis	+	+	Initial failure (see text)
23	Peripheral vascular disease	+	+	Asymp × 3 months
24	Peripheral vascular disease	+	−	Asymp × 3 months[a]
25	Popliteal stenosis/aneurysm	+	−	Asymp × 10 days[a]

Note.—Patients 1–10 were treated with streptokinase and patients 10–25 were treated with urokinase. The McNamara protocol was used in cases 17–24; other cases were treated with urokinase as described in the text. Patient 10 had two treatments and patient 11 had four separate treatments. Asymp = asymptomatic; BKA = below-the-knee amputation. Plus (+) sign indicates that procedure was done; minus (−) sign indicates that procedure was not done.

[a] Discharged on warfarin.

liteal and trifurcation arteries suggests that the procedure is a satisfactory option to surgery in selected patients and a successful adjuvant to surgery in others.

The numbers of patients having successful treatment initially with urokinase and streptokinase infusions were similar. These results agree with those of a study comparing the agents for intracoronary thrombolysis [12], but others report a higher success rate using urokinase in other arteries [4, 5]. Studies using urokinase-lysyl plasminogen show that this regimen has no significant advantage over urokinase alone [13–14].

Our results and those of others show a higher rate of complications with streptokinase [4, 6, 8–9, 15–16]. Distal emboli during infusion were not seen in our patients, in contrast to the experience of others [13, 17]. Urokinase is the fibrinolytic agent of choice because of its lower number of complications and its shorter duration of therapy.

Two regimens of urokinase were used in this study and both achieved comparable results. High-dose regional therapy, as outlined in this series and others [4, 8], results in a larger number of successful outcomes as compared with those in studies using lower urokinase doses (40,000 units/hr) [18–20]. The results of this study indicate that using higher initial doses (McNamara protocol) may decrease the therapy time and reduce the total dose required for effective therapy.

The coaxial system results in a lower frequency of pericatheter thrombus during urokinase infusion than do procedures requiring a single catheter. A coaxial system was also necessary to place a 3.0-French catheter, infusion guidewire, or the cardiac angioplasty system into trifurcation arteries to optimize infusion therapy and to perform angioplasty. We divided our fibrinolytic dose rather than administer heparin through the proximal component. Dividing the dose may obviate the use of heparin during the infusion. The results suggest that the use of systemic heparinization during urokinase infusion does not prevent pericatheter thrombus. However, we believe that systemic heparinization is indicated after fibrinolytic therapy is concluded.

Although we reviewed fibrinogen levels and thrombin time in our patients, we did not find this information to be useful on a case-by-case basis in adjusting our therapy, and the value of monitoring these coagulation parameters remains uncertain [16, 21].

The age of the occlusion as determined by the patient's

history was not useful in predicting initial failures, as it was in other studies [22–23]. This experience supports that of others suggesting that chronic occlusions of 4–12 months duration may be responsive to therapy [7, 24]. However, the length of time that the initial occlusion has been present may be a predictor of early reocclusion. Regardless of the fibrinolytic agent used, patients whose occlusions were less than 1 month old had fewer reocclusions. The observation that patients with older occlusions may be at higher risk for early reocclusion has been reported by others [11]. After successful fibrinolytic therapy, long-term systemic anticoagulation with warfarin was used in 19 patients (Table 1). Two of the three patients with reocclusion were among the six patients not on warfarin (Table 1). Comparison of initial and long-term results suggests that anticoagulation following the patient's discharge may prevent early reocclusion.

Indications for therapy are not currently well defined. We recommend that any patient presenting for limb salvage should be considered for fibrinolytic therapy, particularly if surgical revascularization is not an option. Patients with embolic disease should be considered for this treatment, but caution is advised. Whether the patients with a cardiac source for arterial emboli should undergo fibrinolytic therapy remains controversial, since systemic effects of therapy could put them at risk for further emboli as well as systemic complications including cerebral vascular accident. Any patient with thromboembolism following angioplasty should be considered for fibrinolytic therapy [25]. Our experience and that of others suggest that patients with occluded popliteal artery aneurysms, particularly those with occluded runoff arteries, should receive preoperative fibrinolytic therapy [10, 26].

The decision about whether to treat patients for claudication with fibrinolysis of popliteal and trifurcation arteries remains unclear. Patency rates are important considerations in treating patients with peripheral vascular occlusive disease. Surgical therapy has proved successful, with the greatest success seen in patients treated with in situ saphenous vein grafts [2]. The 5-year patency rate of autogenous femoral-popliteal bypass grafts approaches 75% [1], while other materials such as the human umbilical vein can show less satisfactory results as low as 30% [27]. However, successful fibrinolytic therapy may allow the patient to retain his saphenous vein for future coronary surgery. Follow-up of our successfully treated patients showed that 80% continue to have good results for an average of 27 months (Table 1). In the study by Taylor et al. [10] using streptokinase, follow-up in seven patients for an average of 13 months revealed that all patients had patent arteries. Other considerations for determining appropriate therapy include surgical morbidity and mortality that can range from 5% to 35% and from 0.5% to 2.0%, respectively [1, 3]. The morbidity and mortality rates increase with more distal procedures and in patients requiring another operation [1, 3, 9, 27], with the mortality rates ranging from 2.5% to 5.7% [1, 3, 9]. In conclusion, we disagree with those who would consider using fibrinolytic therapy only in those patients who refuse surgery or who are not considered to be good candidates for surgery [17, 24].

ACKNOWLEDGMENTS

The authors express their gratitude to the other physicians who participated in the care of these patients; Craig Carpenter, Steve Holt, Stephen Shealy, James Wolff, and Myron Wojtowycz. In addition, we appreciate the expert help of Rebecca Wesselman in preparing the manuscript.

REFERENCES

1. Brewster DC, LaSalle AJ, Robison JG, Strayhorn EC, Darling C. Femoropopliteal graft failures: clinical consequences and success of secondary reconstructions. *Arch Surg* **1983**;118:1043–1047
2. Bush HL, Corey CA, Nasbeth DC. Distal in situ saphenous vein grafts for limb salvage: increased operative blood flow and postoperative patency. *Am J Surg* **1983**;145:542–548
3. Rhodes RS, Krasniak CL, Jones PK. Factors affecting length of hospital stay for femoropopliteal bypass: implications of the DRG's. *N Engl J Med* **1986**;314:153–157
4. Eckstein MR, Geller SC, Brown K, et al. Intra-arterial thrombolysis: comparison of streptokinase and urokinase. Presented at the annual meeting of the Radiological Society of North America, Chicago, November **1985**
5. Harrington DP, Koltun W, Gardiner GA, et al. Thrombolytic therapy in peripheral vascular occlusive disease. Presented at the annual meeting of the Radiological Society of North America, Chicago, November **1985**
6. Hurley JJ, Burrell MJ, Auer AI, Woods JJ Jr, Binnington HB, Hershey FB. Surgical implications of fibrinolytic therapy. *Am J Surg* **1984**;148:830–835
7. Katzen BT, Edwards KC, Albert AS, van Breda A. Low-dose direct fibrinolysis in peripheral vascular disease. *J Vasc Surg* **1984**;1:718–722
8. McNamara TO, Fischer JR. Thrombolysis of peripheral arterial and graft occlusions: improved results using high-dose urokinase. *AJR* **1985**;144:769–775
9. Gardiner GA, Koltun W, Kandarpa K, et al. Thrombolysis of occluded femoropopliteal grafts. *AJR* **1986**;147:621–626
10. Taylor LM, Porter JM, Bauer GM, Hallin RW, Peck JL, Eidemiller LR. Intraarterial streptokinase infusion for acute popliteal and tibial artery occlusion. *Am J Surg* **1984**;147:583–588
11. Lammer J, Pilger E, Neumayer K, Schreyer H. Intraarterial fibrinolysis: long-term results. *Interven Radiol* **1986**;161:159–163
12. Tennant SN, Dixon J, Venable TC, et al. Intracoronary thrombolysis in patients with acute myocardial infarction: comparison of the efficacy of urokinase with streptokinase. *Circulation* **1984**;69:756–760
13. Fiessinger J-N, Vitoux J-F, Pernes J-M, Roncato M, Aiach M, Gaux J-C. Complications of intraarterial urokinase-lysyl-plasminogen infusion therapy in arterial ischemia of lower limbs. *AJR* **1986**;146:157–159
14. Pernes J-M, Vitoux J-F, Brenoit P, et al. Acute peripheral arterial and graft occlusion: treatment with selective infusion of urokinase and lysyl plasminogen. *Radiology* **1986**;158:481–485
15. Belkin M, Belkin B, Bucknam CA, Straub JJ, Lowe R. Intraarterial fibrinolytic therapy: efficacy of streptokinase vs urokinase. *Arch Surg* **1986**;121:769–773
16. Totty WG, Gilula LA, McClennan BL, Ahmed P, Sherman L. Low-dose intravascular fibrinolytic therapy. *Radiology* **1982**;143:59–69
17. Kakkasseril JS, Cranley JJ, Arbaugh JJ, Roedersheimer R, Welling RE. Efficacy of low-dose streptokinase in acute arterial occlusion and graft thrombosis. *Arch Surg* **1985**;120:427–429
18. Sicard GA, Schier JJ, Totty WG, et al. Thrombolytic therapy for acute arterial occlusion. *J Vasc Surg* **1985**;2:65–78
19. Fiessinger JN, Vayssairat M, Juillet Y, et al. Local urokinase in arterial thromboembolism. *Angiology* **1980**;31:715–720
20. Perler BA, White RI, Ernst CB, Williams GM. Low-dose thrombolytic therapy for infrainguinal graft occlusions: an idea whose time has passed? *J Vasc Surg* **1984**;2:799–805
21. Murray PD, Garnic JD, Bettmann MA. Pharmacology of angioplasty and intravascular thrombolysis. *AJR* **1982**;139:795–803
22. Dardik H, Sussman BC, Kahn M, et al. Lysis of arterial clot by intravenous or intra-arterial administration of streptokinase. *Surg Gynecol Obstet* **1984**;158:137–140
23. Rush DS, Gewertz BL, Lu CT, et al. Selective infusion of streptokinase for arterial thrombosis. *Surgery* **1983**;93:828–833
24. Hess H, Ingrisch H, Mietaschk A, Rath H. Local low-dose thrombolytic therapy of peripheral arterial occlusions. *New Engl J Med* **1982**;307:1627–1630
25. Wilson AR, Fuchs JCA. Percutaneous transluminal angioplasty. The radiologist's contribution to the treatment of vascular disease. *Surg Clin North Am* **1984**;64:121–150
26. Schwarz W, Berkowitz H, Taormina V, Gatti J. The preoperative use of intraarterial thrombolysis for a thrombosed popliteal artery aneurysm. *J Cardiov Surg* **1984**;25:465–468
27. Robison JG, Brewster DC, Abbott WM, Darling RC. Femoropopliteal and tibioperoneal artery reconstruction using human umbilical vein. *Arch Surg* **1983**;118:1039–1042

MR Imaging of the Musculoskeletal System:
Current and Future Status

David J. Sartoris[1]
Donald Resnick

Although MR imaging has become an important diagnostic method in all subspecialty areas of radiology, its impact ultimately may be greatest in the evaluation of musculoskeletal disorders [1–4]. Combining the sensitivity of scintigraphic techniques with the spatial resolution of CT, MR imaging has greatly enhanced the detection and determination of the extent of disease processes involving bone marrow. In addition, its superior contrast discrimination capabilities as compared with CT have provided new insight into a variety of conditions affecting musculoskeletal soft-tissue structures (Fig. 1). This review summarizes the proved and potential applications of MR to disorders of bone, joints, and associated soft tissues, emphasizing its advantages and limitations as contrasted with conventional imaging methods. The interested reader is referred elsewhere for detailed information on imaging strategies and insight relevant to scan interpretation [5, 6].

Bone-Marrow Disease

T1 relaxation times for normal bone marrow in the lumbar vertebral bodies decrease, whereas T2 relaxation times increase with age in both genders owing to replacement of hematopoietic marrow by fat. Gender-related differences in these phenomena may be due to the more rapid and significant loss of bone among women [7].

Chemical-shift imaging has been used to evaluate bone marrow in normal volunteers and patients with metabolic, inflammatory, traumatic, and neoplastic disorders [8]. Normally, hematopoietic marrow yields low signal intensity on phase-contrast images, whereas abnormal conditions typically result in relatively increased signal intensity owing to accumulated lipid or water. Because of its high fat content, yellow marrow normally yields high signal intensity on phase-contrast images, whereas abnormal conditions usually result in relatively diminished signal intensity caused by increased tissue water [8].

MR has been shown to be a sensitive method of detecting malignant foci within bone marrow toward which biopsy can be directed, although focal fat deposition constitutes a potential pitfall in interpretation [9, 10]. In patients with metastatic disease, areas of decreased signal intensity are observed on T1-weighted images. Patients with multiple myeloma manifest similar abnormalities [11]. Marrow involvement by Hodgkin's lymphoma is manifested as diffuse infiltration with superimposed focal areas of even lower signal intensity. MR in patients with chronic myelogenous leukemia prior to bone-marrow transplantation and acute leukemia in relapse demonstrates a markedly decreased marrow signal, consistent with replacement of fat by neoplastic tissue; chemical-shift imaging facilitates identification of leukemic marrow [12, 13]. Measurement of T1 relaxation times can assist in differentiating children with newly diagnosed leukemia as well as relapse from normals and those in remission [14]. Increased marrow signal intensity occurs in untreated aplastic anemia [13]. MR has also detected abnormalities in the bone marrow of

Received April 23, 1987; accepted after revision June 2, 1987.

[1] Both authors: Department of Radiology, University of California, San Diego, Medical Center and Veterans Administration Medical Center, San Diego, CA. Address reprint requests to D. J. Sartoris, UCSD Medical Center, Dept. of Radiology, 225 Dickinson St., San Diego, CA 92103.

AJR 149:457–467, September 1987
0361–803X/87/1493–0457
© American Roentgen Ray Society

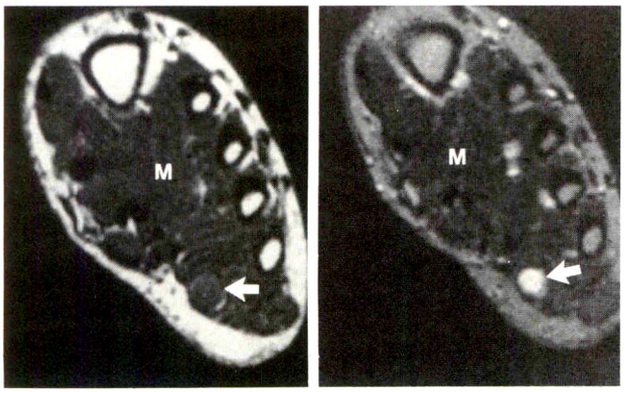


Fig. 1.—Neuroma of lateral plantar nerve.
***A*, T1-weighted image. No definite abnormalities are seen, as lesion (*arrow*) exhibits signal intensity identical to that of plantar musculature (M).**
***B*, T2-weighted image. Neuroma (*arrow*) is strikingly seen as well-encapsulated area manifesting signal intensity much greater than that of adjacent muscle (M). Through application of different pulse sequences, as in this case, full contrast-discrimination capabilities of MR (which exceed those of CT) are exhibited.**

children with metastatic neuroblastoma [15].

MR promises to be useful for determining therapeutic efficacy in hematologic disorders. Serial MR studies of cervical bone marrow have been performed in patients undergoing bone-marrow transplantation for chronic granulocytic leukemia and in patients with aplastic anemia given antilymphocytic globulin. Acute increases in signal intensity and T1 values of marrow during the treatment of leukemia reflect the effects of chemotherapy and radiation therapy, whereas decreases in these parameters during the chronic phases of both diseases are potentially beneficial in predicting a favorable outcome [13]. MR of spinal marrow after radiation treatment demonstrates well-defined areas of increased signal intensity on T1-weighted sequences. These zones are best demonstrated in the sagittal plane and are readily differentiated from involvement by tumor. Such alterations are presumably caused by replacement of marrow by fat, and they correspond closely with radiation therapy portals [16].

MR has been performed in children with acute, subacute, chronic, and recurrent osteomyelitis [17]. Reduction in the signal intensity of bone marrow corresponds well with abnormalities seen on radiographs, CT scans, and radionuclide scans. Contrast between normal and abnormal marrow is most pronounced on inversion-recovery sequences, suggesting increased water content in inflamed marrow. MR abnormalities may be present when CT and radionuclide studies are normal or equivocal [18].

Homogeneous, low-intensity areas have been found in the marrow of long bones, vertebrae, and hips in patients with Gaucher's disease, indicative of infiltration extent [19]. Similarly, the signal intensity of bone marrow is diffusely decreased in the axial and peripheral skeleton of patients with sickle cell anemia on spin-echo images with short and long repetition (TR) and echo (TE) times, indicating hematopoietic marrow hyperplasia as confirmed by isotope marrow scans [20].

The infantile form of osteopetrosis is characterized by a complete lack of signal from the marrow alternating with a signal intensity equivalent to that of the intervertebral disks, resulting in a "stepladder" appearance. In the benign form or after successful marrow transplantation in the infantile malignant form, intermediate or high signal intensity in the vertebrae is observed, suggesting the presence of marrow elements [21].

Ischemic Necrosis of Bone

MR imaging in patients with ischemic necrosis reveals areas of low intensity in the femoral heads [22], differing from the normal MR appearance that has been described in both children and adults [23]. The abnormal areas may manifest as homogeneous regions, inhomogeneous areas, bands of diminished signal, or rings of low signal with higher intensity centrally (Fig. 2). No correlation has been found among specific MR patterns, stage of disease, radiographic appearance, and scintigraphic findings. MR imaging is abnormal in all cases in which radiographs or bone scans or both are abnormal. MR is also occasionally abnormal in the setting of false-negative radiography or scintigraphy [24, 25]. In a controlled statistical study including CT and scintigraphy, MR was the most sensitive imaging technique for the early diagnosis of ischemic necrosis [26].

Patients with ischemic necrosis exhibit fatty marrow in the femoral capital epiphysis and greater trochanter at an earlier age than in most younger normal subjects. The early conver-

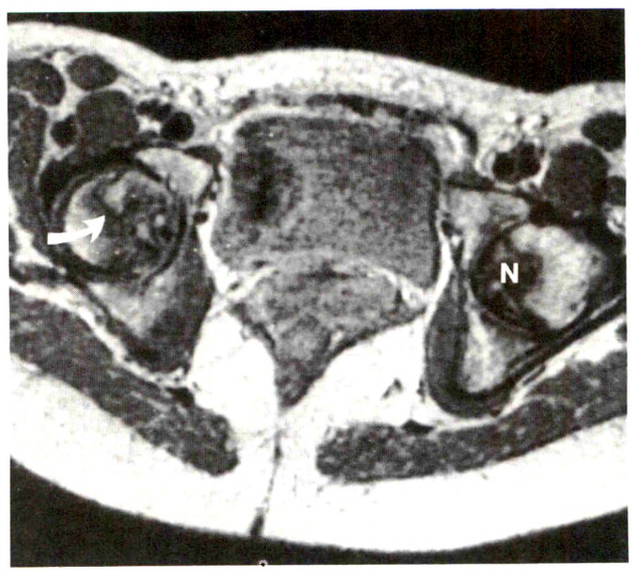


Fig. 2.—Steroid-induced ischemic necrosis affecting hip joints in patient with systemic lupus erythematosus. On T1-weighted axial image, inhomogeneous pattern is noted in weight-bearing aspects of both femoral heads. On right, curvilinear geographic pattern is evident (*arrow*), whereas left femoral head exhibits more widespread loss of normally intense marrow signal intensity in necrotic zone (N).

sion to fatty marrow in the disease as depicted by MR imaging may be caused by diminished vascularity and can facilitate identification of the population at increased risk [27].

The characteristic margin of peripheral sclerosis seen by CT in ischemic necrosis corresponds to a line of low intensity on MR. On T1-weighted images, subchondral fractures are not clearly delineated, whereas on T2-weighted images, they exhibit high intensity but are depicted less clearly than by CT, which remains preferable for staging. On T1-weighted images, most avascular zones with fracture appear less intense centrally than does fat, as opposed to those zones without fractures, which appear similar in intensity to fat [28].

Symptoms related to ischemic necrosis are least severe in lesions that are isointense with fat and most severe in lesions with low-intensity central regions on both T1- and T2-weighted images. A peripheral double-line sign on T2-weighted images may add specificity to the diagnosis of the disease by MR. A chronologic evolution of central signal features has been described, which may allow staging of the disease [29].

Small amounts of fluid are present both in normal hips and in those with ischemic necrosis, and MR is highly sensitive for its detection. In the disease, increased joint fluid may be present before radiographic abnormalities occur, but it is greater subsequent to collapse of the femoral head [30].

In children with Legg-Calvé-Perthes disease, areas of bone infarction within the secondary ossification center of the proximal femur produce little or no signal. In addition, the normal halo effect produced by the articular surface, subchondral region, and secondary ossification center is absent. MR is at least as sensitive as scintigraphy for early disease detection, and reliably determines the extent of altered signal intensity within the ischemic femoral epiphysis [31]. MR also may provide insight into the revascularization process in both children and adults with ischemic necrosis. Problems related to current application include limitations in spatial resolution, long image acquisition times that may require sedation in children, and the expense of the procedure [32].

T1-weighted MR is slightly less sensitive than scintigraphy in depicting carpal ischemic necrosis, but T2-weighted sequences render the former technique more specific. While bone scanning remains the preferred technique to screen patients with wrist pain and normal plain radiographs, MR can add significant diagnostic information in cases with positive scintigraphic findings [33].

Focal areas of decreased signal intensity have been observed on T1-weighted images of both painful and painless joints among patients with sickle cell anemia. In acutely painful joints, these zones convert to high signal intensity on long TR/TE images (presumably owing to the edema of acute marrow infarction), whereas in painless articulations, they remain of low signal intensity (compatible with old infarction or fibrosis). Thus, MR imaging allows dating of marrow infarcts in patients with sickle cell anemia and may be capable of monitoring or directing therapy [20]. In the setting of acute bone pain, higher marrow signal intensity related to fluid accumulation after an avascular episode may also be observed in patients with Gaucher's disease [19].

Osseous Neoplasms

MR is a sensitive method of detecting and staging primary bone tumors [34]. Intramedullary and extraosseous components of such lesions are better delineated by MR than by plain films and CT. MR provides definite advantages relative to CT, but exhibits poor specificity. Differentiation of tissue components, such as hematoma, fat, necrosis, and cystic areas, leads to a specific diagnosis only in rare cases. Radiography and CT are superior to MR in assessing the biologic activity and differential diagnosis of bone tumors and tumor-like lesions [35].

For demonstrating the extent of tumor in marrow and soft tissue, MR is superior or equal to CT in most instances [36]. CT is preferable for demonstrating calcific deposits, cortical involvement, and pathologic fractures. In patients with metal prostheses or surgical clips, MR is superior to CT in documenting recurrent tumor because of artifactual degradation of CT images. Direct sagittal and coronal MR images permit accurate assessment of tumor relationships to adjacent normal structures, including the physis, joints, and neurovascular bundle [37, 38]. Several different pulsing strategies may be required to distinguish tumors of the lower extremity from normal muscle and marrow [39].

MR features of aneurysmal bone cyst include multiple internal septations, fluid-fluid levels of varying intensity, and an intact rim of low-intensity signal completely surrounding the lesion [40]. MR imaging of giant cell tumor reveals low-intensity bone-marrow replacement with cortical thinning and destruction. The extent of tumor involvement is clearly delineated and corresponds well with radiographic and surgical findings [41].

In osteogenic and Ewing's sarcomas, MR is superior to CT in identifying tumor spread within bone marrow and adjacent soft tissues. MR identifies cortical disease but compared with CT it has inferior spatial resolution and defines calcium poorly. MR can be used to monitor tumor response to chemotherapy [15], and the relationship of tumor to adjacent vasculature can be determined without the use of contrast agents. Bone involvement is best assessed on T1-weighted sequences, whereas soft-tissue extension is best determined on T2-weighted sequences [42].

MR is superior to unenhanced CT and equal to contrast-enhanced CT in delineating characteristics of spinal tumors, including bone involvement, spinal canal invasion, paraspinal soft-tissue extension, and vascular compromise [43]. MR is at least equal to CT in demonstrating sacrococcygeal chordoma. MR provides superior contrast to surrounding soft tissues because of the prolonged T1 and T2 relaxation times of these tumors. Either MR or direct coronal CT images are needed for demonstration of tumor involving the sacral nerve roots.

High-resolution ^{31}P MR spectra have been obtained in patients with bone tumors of the extremities. The spectra of active tumors indicate high adenosine triphosphate and inorganic phosphate content, as well as low phosphocreatine concentration. Phosphodiester and phosphomonoester me-

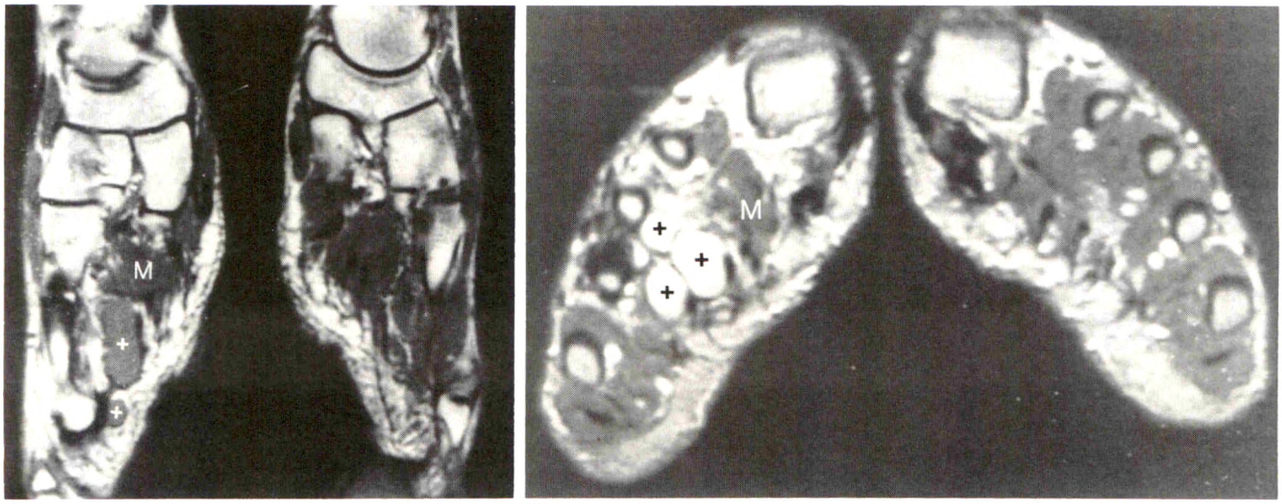


Fig. 3.—Recurrent multifocal schwannoma.
***A*, For surgical, planning purposes, localization of lesions (*plus signs*) on T1-weighted image in plantar plane proved extremely useful, despite isointensity with normal muscle (M).**
***B*, Contrast between abnormal masses (*plus signs*) and adjacent tissue is best on T2- weighted axial image, where signal intensity exceeds that of muscle (M) and intra- and extraosseous fat.**

tabolites have been found also, and spectral alterations have been documented after chemotherapy [44].

Soft-Tissue Neoplasms

MR is better than CT in demonstrating the size and extent of most musculoskeletal soft-tissue masses, as well as their relationships to vascular and nonvascular structures. Bone destruction is more difficult to appreciate by MR, and with the exception of fatty tumors, the method is not helpful in identifying tissue type. Subjective criteria are of limited value in distinguishing benign from malignant lesions, and T1 or T2 measurements are not helpful in this regard [45].

Lesions within muscles or intramuscular septa are best seen with T2-weighted sequences (Figs. 1 and 3), whereas those within subcutaneous fat are best outlined on T1-weighted sequences (Fig. 4). Both protocols are necessary to completely represent extent, although MR may fail to demonstrate soft-tissue calcification and gas [46].

The T1 and T2 relaxation times as well as spin density of benign lipomatous tumors are similar to those of normal subcutaneous fat. Differentiation between lipomas and liposarcomas is possible with both MR and CT. By using a short TR, liposarcomas exhibit lower signal intensity than do lipomas [47].

Surface-coil MR is an ideal technique for evaluating neurofibromatosis involving the spinal canal and paraspinal soft tissues. Neurofibromas exhibit slightly greater signal intensity than muscle on T1-weighted images and markedly increased signal intensity on T2-weighted images. Central areas of decreased signal intensity within the lesions may be shown on T2-weighted images, corresponding to fibrous areas surrounded by myxoid matrix. In patients with neurofibromatosis,

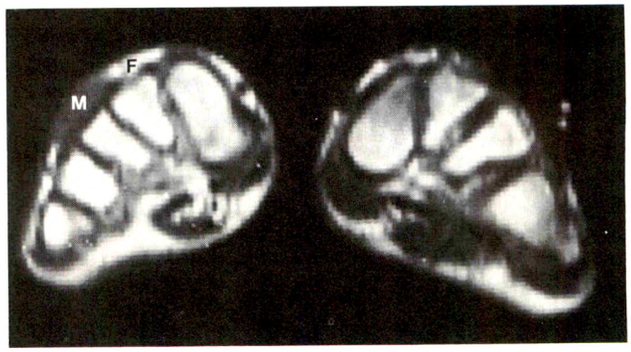


Fig. 4.—Aggressive juvenile fibromatosis. At level of metatarsal bases, lesion (M) is well delineated on T1-weighted sequence, where its relatively low signal intensity contrasts sharply with bright subcutaneous fat (F).

MR has demonstrated plexiform neurofibromas, lateral meningoceles, neurofibrosarcomas, and extradural spinal cord compression [48].

MR can be more accurate than CT in determining the extent of soft-tissue hemangiomas, owing to their marked hyperintensity compared with skeletal muscle on T2-weighted images. Small cavernous hemangiomas are homogeneous, well-defined round or oval lesions, while large hemangiomas consist of dilated, tortuous vascular channels. MR may be useful for distinguishing cavernous hemangiomas from other soft-tissue tumors, particularly sarcomas [49, 50].

Congenital arteriovenous malformations appear with MR as accumulations of dilated tortuous blood vessels infiltrating the involved muscles, whereas posttraumatic acquired lesions may exhibit large feeding vessels, pseudoaneurysm forma-

tion, or a soft-tissue mass [51]. MR provides details concerning the size and extent of these malformations including relationship to specific muscle groups, bones, and vascular structures. Although major feeding and draining vessels are readily identified, the exact arteries and veins supplying and draining the lesion cannot always be ascertained. MR and angiography are thus complementary techniques for the initial evaluation, follow-up examination, and treatment planning of arteriovenous malformations involving the extremities [51].

Trauma and Postoperative Evaluation

MR has been shown to be valuable for a variety of posttraumatic abnormalities affecting the musculoskeletal system [52]. Displaced fractures of the paranasal sinuses are well shown by MR, although nondisplaced and minimally displaced fractures are better evaluated with CT [53]. MR has also been used to document stress fractures (Fig. 5) [54].

In patients with orthopedic hardware, the conspicuity of artifacts is related to the composition, mass, orientation, and position of the metallic implant. In most instances, such artifacts do not significantly interfere with image interpretation (Fig. 6), as they do with CT [55].

Muscle and Tendon Disorders

Disorders of muscle including Duchenne's dystrophy, limb-girdle dystrophy, facioscapulohumeral dystrophy, spinal muscular atrophy, amyotrophic lateral sclerosis, hereditary sensorimotor neuropathy, cerebral palsy, poliomyelitis, and Kearn-Sayre mitochondrial disease have been studied by MR. General patterns of abnormality common among these diseases include decreased or increased muscle size and a spectrum of fatty replacement. A proton map of patients with muscle dysfunction can ensure that meaningful phosphorus-31 spectroscopic information is obtained from an appropriate tissue volume [56].

Increased signal intensity on T2-weighted images has been shown in skeletal muscle adjacent to neoplasms and nonneoplastic processes including infection, myositis, or hematoma. In patients who have not undergone previous surgery or radiation therapy and do not have an inflammatory mass, this phenomenon may be a useful indicator of malignancy [57].

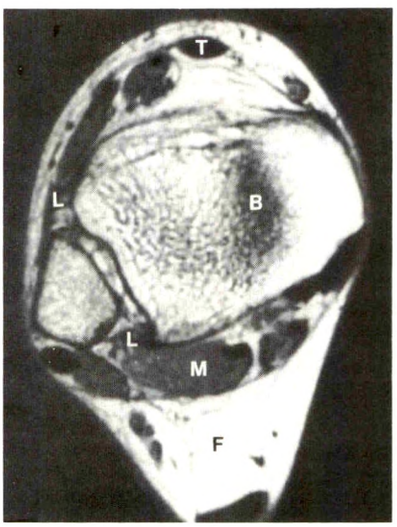
MR provides better discrimination between normal and abnormal psoas muscles than does CT, although calcifications and air bubbles within abscesses are seen less well [58]. Patients with neoplasms, inflammatory disease, retroperitoneal hemorrhage, iliopsoas bursitis, and hypertrophy have been studied. Axial images alone generally are adequate to determine the origin and margins of disease, although the sagittal plane is useful in defining vertebral extension. T1-weighted images provide the best contrast between the muscles and adjacent tissues, while T2-weighted images are more useful for depicting disease within the muscles themselves [59].

Through the use of surface coils and reduced field of view to enhance spatial resolution, MR imaging has become valuable for evaluating tendons [60]. Advantages over conventional methods include exquisite depiction of anatomic detail, superior contrast resolution, and the potential for multiplanar imaging. In the hands and feet, the technique has identified acute posttraumatic rupture, acute tenosynovitis, chronic tendonitis, and postsurgical complications [61].

Specific Anatomic Sites

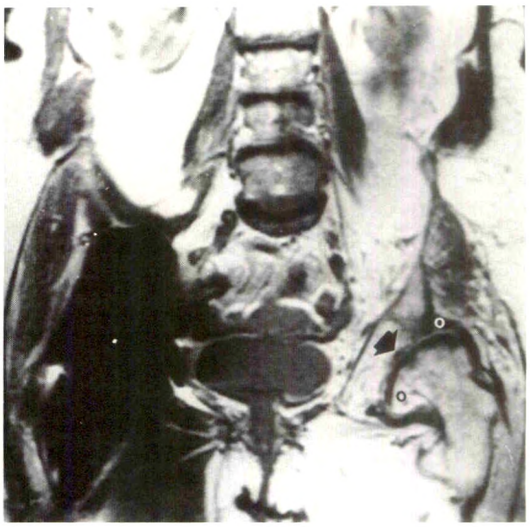
MR imaging has been useful in the evaluation of a broad spectrum of articular disorders (Fig. 6) and is likely to be of value for the early diagnosis of arthritis [62, 63].

The value of pulse sequences with long TRs to increase the signal intensity of intraarticular fluid has been documented



5

Fig. 5.—Normal soft-tissue anatomy with distal tibial stress fracture. As seen on high-resolution T1-weighted axial surface-coil image at level of distal tibiofibular joint, MR readily discriminates among skeletal muscle (M), tendons (T), capsular ligaments (L), and subcutaneous fat (F). Also, subtle abnormalities of bone marrow (B) (in this case a stress fracture) are seen as areas of diminished signal intensity.



6

Fig. 6.—Osteoarthritis of hip. On T2-weighted image, osteophytosis (o) and superior migration of deformed femoral head, secondary to joint space narrowing (*arrow*), are characteristic findings in affected left hip. Prominent zone of absent signal on right represents artifact induced by presence of total joint prosthesis.

(Figs. 7 and 8) [64]. Hip-joint effusions are readily shown by MR imaging and are easily differentiated from articular cartilage. Experimentally introduced intraarticular blood and saline have long T1 and T2 values, and one investigation has indicated that they cannot be confidently distinguished from one another [65].

Spine

Pathologic conditions of the spine studied by MR have included canal stenosis, herniated disk, metastatic tumor, neurofibroma, trauma, and rheumatoid arthritis [66, 67]. MR imaging provides diagnostic information comparable to CT or myelography in showing normal and pathologic intervertebral disks [68, 69], and may become the initial procedure of choice with further technical advances [70].

T2 values are significantly longer in the normal as compared with the degenerated nucleus pulposus. Absence of the intranuclear cleft in the presence of increased signal intensity suggests a disease process such as inflammation [69]. As contrasted with radiography, high-resolution CT, and myelography, MR imaging is more sensitive in identifying disk degeneration and infection. Herniation, spinal stenosis, and scarring can be identified as accurately with MR imaging as with CT or myelography [71]. MR imaging is least valuable in the evaluation of spondylosis and osseous encroachment upon the canal [72].

Normal or diminished signal intensity may be present within the nucleus pulposus of a herniated disk (Fig. 9). MR reveals retraction of the diskal protrusion and diminished nuclear signal intensity after chemonucleolysis. Postoperative fibrosis exhibits intermediate to high signal intensity on MR and is readily distinguished from adjacent thecal sac and disk material [73]. MR is also useful in screening patients for lumbosacral dysraphism [74]. CT and MR imaging can be considered complementary studies, and MR can be an alternative to myelography [75].

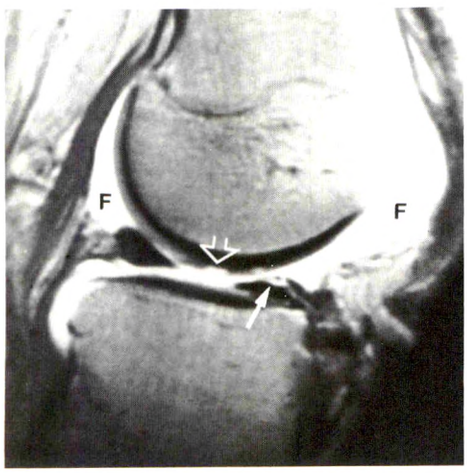
Surface-coil MR is a viable alternative to metrizamide myelography in the setting of cervical radiculopathy (Fig. 10), but CT may also be required. Oblique images may contribute information not available on sagittal or axial views [76, 77]. In general, MR is as sensitive as CT myelography for identification of disease level, but not as specific for type of disease. Patients with chronic atlantoaxial subluxation from either degenerative disease or congenital dysplasia of the dens have been shown to have benign fibrous masses in this region by MR, which is superior to myelography and CT in delineating the extent of such lesions [78].

The appearance of vertebral osteomyelitis by MR is characteristic (Fig. 11), and the technique exhibits accuracy and sensitivity comparable to radionuclide scanning in this setting [79]. In advanced tuberculous spondylitis, MR shows disk-space abnormalities and paravertebral extension of inflammation to best advantage in the coronal plane. Gadolinium-DTPA assists in delineating communications between vertebral and paravertebral components of inflammation. Further experience is needed to evaluate the potential of MR to distinguish tuberculous from nontuberculous spondylitis [80].

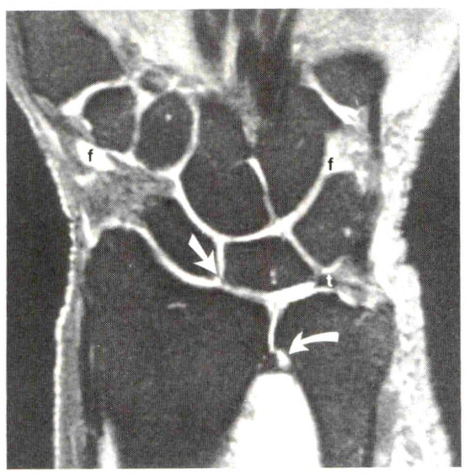
A protocol has been proposed for MR imaging of the lumbar spine that yields high-resolution sagittal and oblique images without a surface coil, by using heavily T1-weighted images with phase encoding. This technique affords a large field of view and a reduction of total imaging time [81]. A simple, inexpensive, and reliable method for providing cervical traction within the magnet room has also been described for imaging patients with acute cervical injury [82].

Temporomandibular Joint

Comparison of MR with arthrography, CT, and surgical findings has shown that surface coil MR provides accurate depiction of both normal and abnormal temporomandibular joints. High-resolution MR affords definition of soft-tissue structures (including the meniscus) that is superior to conven-



7



8

Fig. 7.—MR arthrography of knee. On T2-weighted image in sagittal plane, bright intraarticular fluid (F) outlines subtle defects in hyaline cartilage of femoral condyle (*open arrow*) as well as hairline anterior-horn meniscal tear (*solid arrow*).

Fig. 8.—MR arthrography of wrist. On T2-weighted image in coronal plane, intraarticular fluid (f) affords clear delineation of scapholunate ligaments (*straight arrow*). Opacification of distal radioulnar joint (*curved arrow*) is diagnostic of tear in triangular fibrocartilage (t).

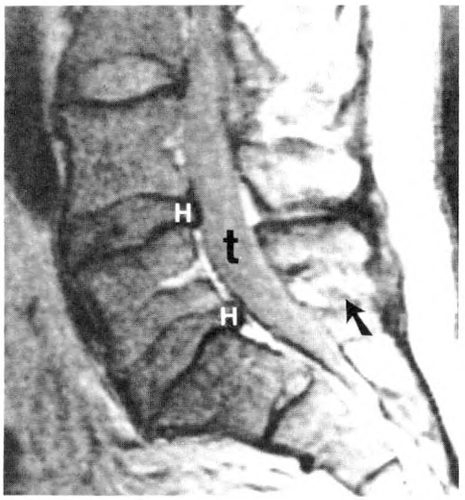


Fig. 9.—Lumbar intervertebral disk disease. On T1-weighted surface-coil image in sagittal plane, L4–L5 and L5–S1 disks exhibit lower nuclear signal intensity than normal L3–L4 disk. Prominent posterior convexities (H) with impingement on thecal sac (t) at both abnormal levels are compatible with diskal herniation. Incidental note is made of normal obliquely oriented interspinous ligaments (*arrow*) between L5 and S1 spinous processes.

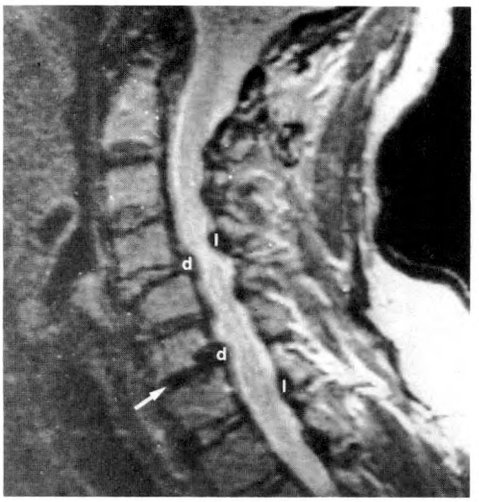


Fig. 10.—Degenerative disk disease in the cervical spine. On T2-weighted sagittal image, irregular impingement on thecal sac by posteriorly protruding disk material (d) and ligamentum flavum thickening (l) is evident. Diminished signal intensity in nucleus pulposus of C6–C7 disk (*arrow*) indicates dessication related to degenerative disease. Narrowing can be appreciated at lowest three intercervical disk levels.

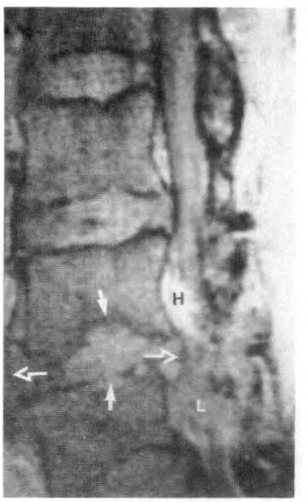


Fig. 11.—Intervertebral disk-space infection. On T2-weighted sagittal image of lumbar spine, narrowing and bulging (*open arrows*) of L4–L5 interspace is apparent, in association with irregular destruction of adjacent end plates (*solid arrows*). Posterior extension of process has resulted in epidural abscess, characterized by mixed areas of high (H) and low (L) signal intensity.

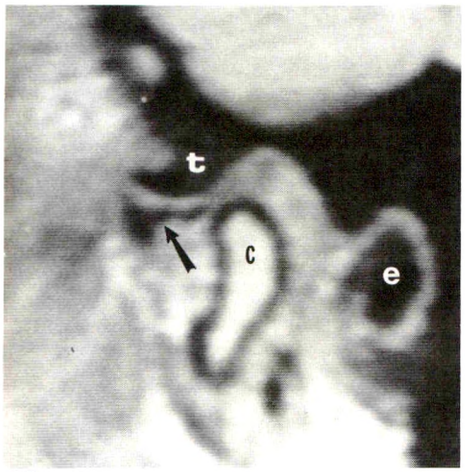
tional imaging methods, whereas osseous detail is comparable in quality to the other methods [83]. MR can provide information about meniscal position, morphology, and histology that is not available by either arthrography or CT alone. Anterior displacement of the joint meniscus is clearly visible on sagittal MR images in the open-mouth position (Fig. 12) [84]. The noninvasive and nonhazardous characteristics of MR render it a preferred technique for the evaluation of temporomandibular joint pain and dysfunction [85].

Knee

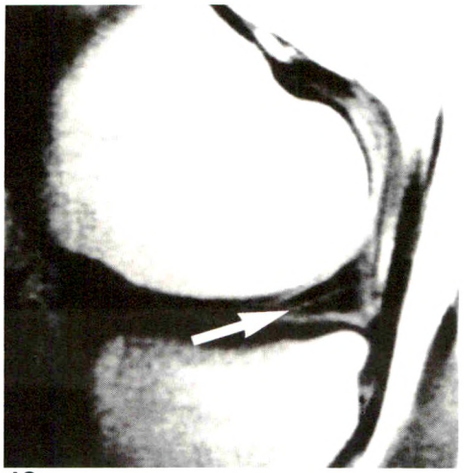
High-resolution, thin-section MR imaging has the potential to become a major imaging method for the evaluation of soft-tissue injuries to the knee [86, 87]. Nonorthogonal views of the anterior cruciate ligament are useful for showing both the femoral and tibial attachments in the same section. The posterior cruciate ligament is usually well seen on sagittal images. T2-weighted images are helpful for showing collateral ligament tears, and thin sections (1–5 mm) are necessary to define many cruciate ligament tears [88]. By MR criteria, the cruciate ligaments are considered torn if they appear disrupted or are not seen in their normal anatomic positions. The collateral ligaments are considered torn if abnormal high-intensity signal is noted in adjacent soft tissues on T2-weighted images or if disruption is apparent [89].

Both retrospective and blinded analyses have indicated that MR imaging is an effective technique for preoperative evaluation of suspected meniscal injuries (Fig. 13). The majority of false-positive MR studies involve the posterior horns of the menisci, the sites of most false-negative arthroscopic diagnoses [90]. In experiments performed on swine knees, vertical tears in the midportion of either meniscus are best seen on sagittal views, whereas lesions of the anterior and posterior horns are best visualized on coronal images [91]. T1-weighted images are adequate to detect most meniscal tears, although T2-weighted images are useful for providing an "arthrogram effect" in the presence of joint effusion (Fig. 7) [92]. Of menisci rated by MR as definitely or probably torn, approximately 80% have been found to be torn at subsequent arthroscopy; the predictive value of negative MR imaging is 100%. MR has been found to be 92% accurate in predicting clinical outcome among patients with suspected meniscal tears who do not undergo surgery [93]. Advantages of MR imaging over arthrography in the knee include noninvasiveness, absence of ionizing radiation, and excellent soft-tissue contrast resolution [91].

MR imaging is useful in determining the integrity of articular cartilage overlying subchondral osseous defects (osteochondritis dissecans, osteonecrosis) and in detecting gross cartilaginous lesions in arthritis (Fig. 7), but is less sensitive than arthroscopy in evaluating moderate changes in hyaline cartilage [92]. MR imaging can also differentiate complete disruption of the patellar tendon from partial tears, ligamentous inflammation, and localized effusion of the infrapatellar bursa [94]. The status of synthetic grafts of the anterior cruciate



12



13

Fig. 12.—Dislocation of temporomandibular-joint meniscus. On T1-weighted sagittal image, fibrocartilaginous disk (*arrow*) of low signal intensity is displaced anterior to mandibular condyle (c), limiting its range of forward excursion. t = temporal eminentia; e = external auditory canal.

Fig. 13.—Posterior-horn meniscal tear. On T1-weighted surface-coil image in sagittal plane, distinct bright horizontal line (*arrow*) traverses normally low-signal-intensity fibrocartilage of meniscus and surfaces at its apex.

ligament can be ascertained as well [93]. Posterior cruciate ligament avulsions, old osteochondral fractures, femoral condylar chondromalacia, and semimembranous tendon reinsertion can also be evaluated. MR imaging can depict additional knee abnormalities including degenerative joint disease, medullary infarcts, synovial and subchondral cysts, joint effusions (Fig. 7), intraarticular soft-tissue tumors, inflammatory disease (including rheumatoid arthritis, Fig. 14), leukemic infiltration of bone marrow, Osgood-Schlatter disease, and nonossifying fibroma. MR has depicted bone infarcts around the knee that were occult both scintigraphically and radiographically. MR can detect soft-tissue masses as in pigmented villonodular synovitis or osteochondral fragments that are potentially overlooked by arthroscopy [95].

In general, MR findings correlate well with results of double-contrast arthrography or surgery. Because of its ability to readily show small meniscal lesions and ligamentous injuries, surface-coil MR may eventually replace arthrography [96]. The technique is currently beneficial as a screening test as it can provide information that might otherwise require multiple, sometimes invasive diagnostic procedures.

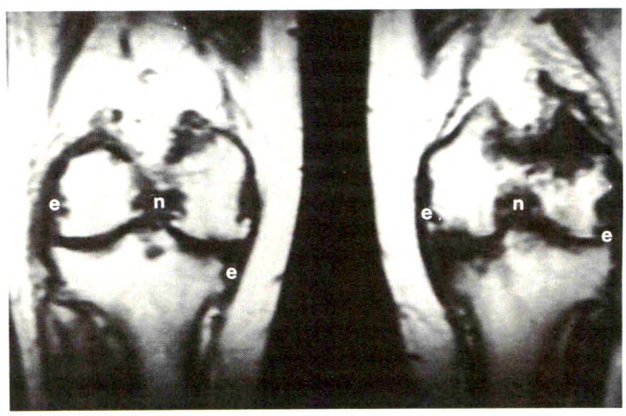


Fig. 14.—Rheumatoid arthritis. On T1-weighted coronal image of both knees, diffuse symmetric joint space loss is observed, in association with prominent marginal erosions (e) and widened intercondylar notches (n). Menisci have been destroyed by pannus and cannot be identified.

Shoulder

MR imaging has significant potential as a noninvasive tool for evaluation of the shoulder region. Anatomic structures including the rotator cuff, long head of the biceps tendon, articular capsule, muscles, and bones are well visualized, with coronal and sagittal views being most useful for showing the rotator cuff [97, 98]. MR imaging also has great potential in the evaluation of the supraclavicular fossa, the detailed normal anatomy of which has been outlined [99]. Difficulties in using MR to establish the diagnosis of rotator cuff tear in the shoulder relate to anatomic complexity, positioning problems, and the need for specially designed surface coils [64]. Relatively poor spatial resolution has been obtained on MR images of the shoulder because it must be positioned at the periphery of the magnetic field. Anatomically shaped surface coils afford demonstration of normal shoulder anatomy in different planes with high spatial resolution [98]. In the axial plane, anatomy analogous to that seen by CT is depicted. Patient-dependent variations in scapular position render the reproducibility of sagittal and coronal images difficult; this is not the case with oblique images, for which the plane is chosen from axial images and on which obliquely oriented structures including the rotator cuff are best evaluated in detail [100]. By using counter-rotating current loop-gap resonators as a coil designed specifically for the shoulder, the rotator cuff appears as a complex, heterogeneous band of tissue superficial to the humeral head. The individual tendons of the cuff exhibit low-signal intensity and can be distinguished from each other as well as from the intervening components of the cuff, which exhibit moderate intensity [101]. Additional technical improve-

ments may render MR valuable for the diagnosis of rotator cuff tears.

Wrist

MR imaging affords anatomic definition of the hand and wrist that is unmatched by other diagnostic methods and can delineate fine structures including nerves, ligaments, tendons, and blood vessels as well as osseous and cartilaginous morphology (Fig. 8) [102]. The technique reliably depicts the flexor retinaculum and carpal bones, thus defining the carpal tunnel. The median nerve is visualized as an ovoid structure of moderate signal intensity that is readily distinguished from the flexor tendons, which are separated from each other by their sheaths. Anatomic variations demonstrable by MR include anomalous positioning of the lumbrical muscle origins, persistent median arteries, and median-nerve interposition between the flexor pollicis longus and superficial flexor tendon of the index finger. In patients with carpal tunnel syndrome, segmental and diffuse swelling or distortion of the median nerve and thickening of the tendon sheaths may be observed [103].

MR can also detect and characterize marrow and articular alterations in the wrist earlier and more accurately than can conventional methods [104, 105]. Navicular nonunion or pseudarthrosis, rheumatoid arthritis, recent fractures, ganglions, arteriovenous malformations, other soft-tissue alterations, and bone tumors have been evaluated successfully.

Ankle

Surface-coil MR can provide excellent delineation of the ligaments and cartilaginous structures of the ankle (Fig. 5) [106, 107]. The potential of MR to show abnormalities at this articulation remains to be fully explored.

Clinical Impact and Future Applications

With regard to the ultimate future of MR imaging in the setting of musculoskeletal disease, it will complement rather than replace existing technologies. Conventional radiography and tomography remain preferable in situations demanding high spatial resolution of cortical and cancellous osseous architecture. Cross-sectional depiction of calcified and ossified tissue is better performed by CT. Since the practical application of MR is confined to localized anatomic regions, scintigraphic techniques will remain important for total body screening despite their inferior spatial resolution. Owing to the disappointingly poor tissue specificity of MR, percutaneous aspiration and biopsy of musculoskeletal lesions will continue to be indicated in certain situations. The overall impact of MR on contrast arthrography as a means of evaluating intraarticular pathology is yet to be established on the basis of additional clinical studies.

Areas of potentially promising clinical application for MR in the future include pelvimetry, quantitative bone-marrow densitometry for monitoring infiltrative disorders and possibly metabolic bone disease, three-dimensional image reconstruction, and intraarticular administration of contrast agents before examination of joints (Figs. 7 and 8) [108, 109]. Of major practical importance, the current high cost of MR is a significant disincentive for its use in situations in which the desired information can be obtained by other less expensive diagnostic imaging techniques. With optimization of pulse-sequence strategies for specific musculoskeletal disorders and the resulting increased patient throughout per unit time, improvement in this most undesirable attribute of MR theoretically should occur.

The potential utility of IV and intraarticular administration of gadolinium-DTPA and other paramagnetic contrast agents in the evaluation of bone and joint disease remains to be explored [109]. Similarly, the practical clinical role of phosphorus-31 and hydrogen spectroscopy as applied to muscle and other musculoskeletal soft tissues is yet to be established. Chemical-shift imaging of bone marrow, rapid scanning techniques [81, 110], improvements in surface-coil design, and oblique imaging planes promise to enhance the future efficacy of MR in the evaluation of the musculoskeletal system.

REFERENCES

1. Moon KL Jr, Genant HK, Helms CA, Chafetz NI, Crooks LE, Kaufman L. Musculoskeletal applications of nuclear magnetic resonance. *Radiology* **1983**;147:161–171
2. Berquist TH, Ehman RL, Richardson ML, eds. *Magnetic resonance imaging of the musculoskeletal system*. New York: Raven, **1987**
3. Pettersson H, Hamlin DJ, Mancuso A, et al. Magnetic resonance imaging of the musculoskeletal system. *Acta Radiol [Diagn]* (Stockh) **1985**;26:225–234
4. Burt CT, Koutcher J, Roberts JT, London RE, Chance B. Magnetic resonance imaging of the musculoskeletal system. *Radiol Clin North Am* **1986**;24:321–331
5. Richardson ML. Optimizing pulse sequences for magnetic resonance imaging of the musculoskeletal system. *Radiol Clin North Am* **1986**;24:137–144
6. Richardson ML, Helms CA. Artifacts, normal variants, and imaging pitfalls of magnetic resonance imaging of the musculoskeletal system. *Radiol Clin North Am* **1986**;24:145–177
7. Dooms GC, Fisher MR, Hricak H, Richardson M, Crooks LE, Genant HK. Bone marrow imaging: magnetic resonance studies related to age and sex. *Radiology* **1985**;155:429–432
8. Wismer GL, Rosen BR, Buxton R, Stark DD, Brady TJ. Chemical shift imaging of bone marrow: preliminary experience. *AJR* **1985**;145:1031–1037
9. Hajek PC, Baker LL, Goobar JE, et al. Focal fat deposition in axial bone marrow: MR characteristics. *Radiology* **1987**;162:245–249
10. Porter BA, Shields AF, Olson DO. Magnetic resonance imaging of bone marrow disorders. *Radiol Clin North Am* **1986**;24:269–289
11. Daffner RH, Lupetin AR, Dash N, et al. MRI in the detection of malignant infiltration of bone marrow. *AJR* **1986**;146:353–358
12. Olson DO, Shields AF, Scheurich CJ, Porter BA, Moss AA. Magnetic resonance imaging of the bone marrow in patients with leukemia, aplastic anemia, and lymphoma. *Invest Radiol* **1986**;21:540–546
13. McKinstry CS, Steiner RE, Young AT, Jones L, Swirsky D, Aber V. Bone marrow in leukemia and aplastic anemia: MR imaging before, during, and after treatment. *Radiology* **1987**;162:701–707
14. Moore SG, Gooding CA, Brasch RC, et al. Bone marrow in children with acute lymphocytic leukemia: MR relaxation times. *Radiology* **1986**; 160:237–240
15. Cohen MD, Klatte EC, Baehner R, et al. Magnetic resonance imaging of bone marrow disease in children. *Radiology* **1984**;151:715–718
16. Ramsey RG, Zacharias CE. MR imaging of the spine after radiation therapy: easily recognizable effects. *AJR* **1985**;144:1131–1135

17. Modic MT, Pflanze W, Fieglin DHI, Belhobek G. Magnetic resonance imaging of musculoskeletal infections. *Radiol Clin North Am* **1986**; 24:247–258
18. Fletcher BD, Scoles PV, Nelson AD. Osteomyelitis in children: detection by magnetic resonance. *Radiology* **1984**;150:57–60
19. Lanir A, Hadar H, Cohen I, et al. Gaucher disease: assessment with MR imaging. *Radiology* **1986**;161:239–244
20. Rao VM, Fishman M, Mitchell DG, et al. Painful sickle cell crisis: bone marrow patterns observed with MR imaging. *Radiology* **1986**;161: 211–215
21. Rao VM, Dalinka MK, Mitchell DG, et al. Osteopetrosis: MR characteristics at 1.5 T. *Radiology* **1986**;161:217–220
22. Gillespy T III, Genant HK, Helms CA. Magnetic resonance imaging of osteonecrosis. *Radiol Clin North Am* **1986**;24:193–208
23. Littrup PJ, Aisen AM, Braunstein EM, Martel W. Magnetic resonance imaging of femoral head development in roentgenographically normal patients. *Skeletal Radiol* **1985**;14:159–163
24. Totty WG, Murphy WA, Ganz WI, Kumar B, Daum WJ, Siegel BA. Magnetic resonance imaging of the normal and ischemic femoral head. *AJR* **1984**;143:1273–1280
25. Markisz JA, Knowles RJR, Altchek DW, Schneider R, Whalen JP, Cahill PT. Segmental patterns of avascular necrosis of the femoral heads: early detection with MR imaging. *Radiology* **1987**;162:717–720
26. Mitchell MD, Kundel HL, Steinberg ME, Kressel HY, Alavi A, Axel L. Avascular necrosis of the hip: comparison of MR, CT, and scintigraphy. *AJR* **1986**;147:67–71
27. Mitchell DG, Rao VM, Dalinka M, et al. Hematopoietic and fatty bone marrow distribution in the normal and ischemic hip: new observations with 1.5 T MR imaging. *Radiology* **1986**;161:199–202
28. Mitchell DG, Kressel HY, Arger PH, Dalinka M, Spritzer CE, Steinberg ME. Avascular necrosis of the femoral head: morphologic assessment by MR imaging with CT correlation. *Radiology* **1986**;161:739–742
29. Mitchell DG, Rao V, Dalinka MK, et al. Femoral head avascular necrosis: correlation of MR imaging, radiographic staging, radionuclide imaging, and clinical findings. *Radiology* **1987**;162:709–715
30. Mitchell DG, Rao V, Dalinka M, et al. MRI of joint fluid in the normal and ischemic hip. *AJR* **1986**;146:1215–1218
31. Bluemm RG, Falke THM, Ziedses des Plantes BG Jr, Steiner RM. Early Legg-Perthes disease (ischemic necrosis of the femoral head) demonstrated by magnetic resonance imaging. *Skeletal Radiol* **1985**;14:95–98
32. Coles PV, Yoon YS, Makley JT, Kalamchi A. Nuclear magnetic resonance imaging in Legg-Calve-Perthes disease. *J Bone Joint Surg [Am]* **1984**;66:1357–1363
33. Reinus WR, Conway WF, Totty WG, et al. Carpal avascular necrosis: MR imaging. *Radiology* **1986**;160:689–693
34. Richardson ML, Kilcoyne RF, Gillespy T III, Helms CA, Genant HK. Magnetic resonance imaging of musculoskeletal neoplasms. *Radiol Clin North Am* **1986**;24:259–267
35. Bohndorf K, Reiser M, Lochner B, de Lacroix WF, Steinbrich W. Magnetic resonance imaging of primary tumours and tumour-like lesions of bone. *Skeletal Radiol* **1986**;15:511–517
36. Aisen AM, Martel W, Braunstein EM, McMillin KI, Phillips WA, Kling TF. MRI and CT evaluation of primary bone and soft tissue tumors. *AJR* **1986**;146:749–756
37. Zimmer WD, Berquist TH, McLeod RA, et al. Bone tumors: magnetic resonance imaging versus computed tomography. *Radiology* **1985**; 155:709–718
38. Rosenthal DI, Scott JA, Mankin HJ, Wismer GL, Brady TJ. Sacrococcygeal chordoma: magnetic resonance imaging and computed tomography. *AJR* **1985**;145:143–147
39. Brady TJ, Rosen BR, Pykett IL, McGuire MH, Mankin HJ, Rosenthal DI. NMR imaging of leg tumors. *Radiology* **1983**;149:181–187
40. Beltran J, Simon D, Levy M, Herman L, Weis L, Mueller CF. Aneurysmal bone cysts: MR imaging at 1.5 T. *Radiology* **1986**;158:689–690
41. Brady TJ, Gebhardt MC, Pykett IL, et al. NMR imaging of forearms in healthy volunteers and patients with giant-cell tumor of bone. *Radiology* **1982**;144:549–552
42. Boyko OB, Cory DA, Cohen MD, Provisor A, Mirkin D, DeRosa GP. MR imaging of osteogenic and Ewing's sarcoma. *AJR* **1987**;148:317–322
43. Beltran J, Noto AM, Chakeres DW, Christoforidis AJ. Tumors of the osseous spine: staging with MR imaging versus CT. *Radiology* **1987**;162:565–569
44. Nidecker AC, Muller S, Aue WP, et al. Extremity bone tumors: evaluation by P-31 MR spectroscopy. *Radiology* **1985**;157:167–174
45. Petasnick JP, Turner DA, Charters JR, Gitelis S, Zacharias CE. Soft tissue masses of the locomotor system: comparison of MR imaging with CT. *Radiology* **1986**;160:125–133
46. Totty WG, Murphy WA, Lee JKT. Soft tissue tumors: MR imaging. *Radiology* **1986**;160:135–141
47. Dooms GC, Hricak H, Sollitto RA, Higgins CB. Lipomatous tumors and tumors with fatty component: MR imaging potential and comparison of MR and CT results. *Radiology* **1985**;157:479–483
48. Burk DL Jr, Brunberg JA, Kanal E, Latchaw RE, Wolf GL. Spinal and paraspinal neurofibromatosis: surface coil MR imaging at 1.5 T. *Radiology* **1987**;162:797–801
49. Levine E, Wetzel LH, Neff JR. MR imaging and CT of extrahepatic cavernous hemangiomas. *AJR* **1986**;147:1299–1304
50. Kaplan PA, Williams SM. Mucocutaneous and peripheral soft-tissue hemangiomas: MR imaging. *Radiology* **1987**;163:163–166
51. Cohen JM, Weinreb JC, Redman HC. Arteriovenous malformations of the extremities: MR imaging. *Radiology* **1986**;158:475–479
52. Ehman RL, Berquist TH. Magnetic resonance imaging of musculoskeletal trauma. *Radiol Clin North Am* **1986**;24:291–319
53. Zimmerman RA, Bilaniuk LT, Hackney DB, Goldberg HI, Grossman RI. Paranasal sinus hemorrhage: evaluation with MR imaging. *Radiology* **1987**;162:499–503
54. Stafford SA, Rosenthal DI, Gebhardt MC, Brady TJ, Scott JA. MRI in stress fracture. *AJR* **1986**;147:553–556
55. Laakman RW, Kaufman B, Han JS, et al. MR imaging in patients with metallic implants. *Radiology* **1985**;157:711–714
56. Murphy WA, Totty WG, Carroll JE. MRI of normal and pathologic skeletal muscle. *AJR* **1986**;146:565–574
57. Beltran J, Simon DC, Katz W, Weis LD. Increased MR signal intensity in skeletal muscle adjacent to malignant tumors: pathologic correlation and clinical relevance. *Radiology* **1987**;162:251–255
58. Lee JKT, Glazer HS. Psoas muscle disorders: MR imaging. *Radiology* **1986**;160:683–687
59. Weinreb JC, Cohen JM, Maravilla KR. Iliopsoas muscles: MR study of normal anatomy and disease. *Radiology* **1985**;156:435–440
60. Fullerton GD, Cameron IL, Ord VA. Orientation of tendons in the magnetic field and its effect on T2 relaxation times. *Radiology* **1985**;155:433–435
61. Beltran J, Noto AM, Herman LJ, Lubbers LM. Tendons: high-field-strength, surface coil MR imaging. *Radiology* **1987**;162:735–740
62. Terrier F, Hricak H, Revel D, et al. Magnetic resonance imaging and spectroscopy of the periarticular inflammatory soft tissue changes in experimental arthritis of the rat. *Invest Radiol* **1985**;20:813–823
63. Sims RE, Genant HK. Magnetic resonance imaging of joint disease. *Radiol Clin North Am* **1986**;24:179–188
64. Kneeland JB, Carrera GF, Middleton WD, et al. Rotator cuff tears: preliminary application of high-resolution MR imaging with counter rotating current loop-gap resonators. *Radiology* **1986**;160:695–699
65. Beltran J, Noto AM, Herman LJ, Mosure JC, Burk JM, Christoforidis AJ. Joint effusions: MR imaging. *Radiology* **1986**;158:133–137
66. Modic MT, Weinstein MA, Pavlicek W, Boumphrey F, Starnes D, Duchesneau PM. Magnetic resonance imaging of the cervical spine: technical and clinical considerations. *AJR* **1983**;141:1129–1136
67. Modic MT, Masaryk T, Paushter D. Magnetic resonance imaging of the spine. *Radiol Clin North Am* **1986**;24:229–245
68. Pech P, Haughton VM. Lumbar intervertebral disk: correlative MR and anatomic study. *Radiology* **1985**;156:699–701
69. Aguila LA, Piraino DW, Modic MT, Dudley AW, Duchesneau PM, Weinstein MA. The intranuclear cleft of the intervertebral disk: magnetic resonance imaging. *Radiology* **1985**;155:155–158
70. Edelman RR, Shoulimas GM, Stark DD, et al. High-resolution surface-coil imaging of lumbar disk disease. *AJR* **1985**;144:1123–1129
71. Modic MT, Pavlicek W, Weinstein MA, Boumphrey F, Ngo F, Hardy R, Duchesneau PM. Magnetic resonance imaging of intervertebral disk disease. *Radiology* **1984**;152:103–111
72. Han JS, Kaufman B, El Yousef SJ, et al. NMR imaging of the spine. *AJR* **1983**;141:1137–1145
73. Chafetz NI, Genant HK, Moon KL, Helms CA, Morris JM. Recognition of lumbar disk herniation with NMR. *AJR* **1983**;141:1153–1156
74. Barnes PD, Lester PD, Yamanashi WS, Prince JR. MRI in infants and children with spinal dysraphism. *AJR* **1986**;147:339–346

75. Modic MT, Masaryk T, Boumphrey F, Goormastic M, Bell G. Lumbar herniated disk disease and canal stenosis: prospective evaluation by surface coil MR, CT, and myelography. *AJR* **1986**;147:757–765
76. Modic MT, Masaryk TJ, Ross JS, Mulopulos GP, Bundschuh CV, Bohlman H. Cervical radiculopathy: value of oblique MR imaging. *Radiology* **1987**;163:227–231
77. Modic MT, Masaryk TJ, Mulopulos GP, Bundschuh C, Han JS, Bohlman H. Cervical radiculopathy: prospective evaluation with surface coil MR imaging, CT with metrizamide, and metrizamide myelography. *Radiology* **1986**;161:753–759
78. Sze G, Brant-Zawadzki MN, Wilson CR, Norman D, Newton TH. Pseudotumor of the craniovertebral junction associated with chronic subluxation: MR imaging studies. *Radiology* **1986**;161:391–394
79. Modic MT, Feiglin DH, Piraino DW, et al. Vertebral osteomyelitis: assessment using MR. *Radiology* **1985**;157:157–166
80. de Roos A, van Persijn van Meerten EL, Bloem JL, Bluemm RG. MRI of tuberculous spondylitis. *AJR* **1986**;147:79–82
81. Reicher MA, Gold RH, Halbach VV, Rauschning W, Wilson G, Lufkin RB. MR imaging of the lumbar spine: anatomic correlations and effects of technical variations. *AJR* **1986**;147:891–898
82. McArdle CB, Wright JW, Prevost WJ, Dornfest DJ, Amparo EG. MR imaging of the acutely injured patient with cervical traction. *Radiology* **1986**;159:273–274
83. Harms SE, Wilk RM, Wolford LM, Chiles DG, Milam SB. The temporomandibular joint magnetic resonance imaging using surface coils. *Radiology* **1985**;157:133–136
84. Roberts D, Schenck J, Joseph P, et al. Temporomandibular joint: magnetic resonance imaging. *Radiology* **1985**;155:829–830
85. Katzberg RW, Bessette RW, Tallents RH, et al. Normal and abnormal temporomandibular joint: MR imaging with surface coil. *Radiology* **1986**;158:183–189
86. Li DBK, Adams ME, McConkey JP. Magnetic resonance imaging of the ligaments and menisci of the knee. *Radiol Clin North Am* **1986**;24:209–227
87. Reicher MA, Rauschning W, Gold RH, Bassett LW, Lufkin RB, Glen W Jr. High-resolution magnetic resonance imaging of the knee joint: normal anatomy. *AJR* **1985**;145:895–902
88. Gallimore GW Jr, Harms SE. Knee injuries: high-resolution MR imaging. *Radiology* **1986**;160:457–461
89. Turner DA, Prodromos CC, Petasnick JP, Clark JW. Acute injury of the ligaments of the knee: magnetic resonance evaluation. *Radiology* **1985**;154:717–722
90. Reicher MA, Hartzman S, Duckwiler GR, Bassett LW, Anderson LJ, Gold RH. Meniscal injuries: detection using MR imaging. *Radiology* **1986**;159:753–757
91. Beltran J, Noto AM, Mosure JC, Bools JC, Zuelzer W, Christoforidis AJ. Meniscal tears: MR demonstration of experimentally produced injuries. *Radiology* **1986**;158:691–693
92. Burk DL Jr, Kanal E, Brunberg JA, Johnstone GF, Swensen HE, Wolf GL. 1.5 T surface-coil MRI of the knee. *AJR* **1986**;147:293–300
93. Reicher MA, Hartzman S, Bassett LW, Mandelbaum B, Duckwiler G, Gold RH. MR imaging of the knee. Part I. Traumatic disorders. *Radiology* **1987**;162:547–551
94. Reicher MA, Bassett LW, Gold RH. High-resolution magnetic resonance imaging of the knee joint: pathologic correlations. *AJR* **1985**;145:903–909
95. Hartzman S, Reicher MA, Bassett LW, Duckwiler G, Mandelbaum B, Gold RH. MR imaging of the knee. Part II. Chronic disorders. *Radiology* **1987**;162:553–557
96. Beltran J, Noto AM, Mosure JC, Weiss KL, Zuelzer W, Christoforidis AJ. The knee: surface coil MR imaging at 1.5 T. *Radiology* **1986**;159:747–751
97. Huber DJ, Sauter R, Mueller E, Requardt H, Weber H. MR imaging of the normal shoulder. *Radiology* **1986**;158:405–408
98. Seeger LL, Ruszkowski JT, Bassett LW, Kay SP, Kahmann RD, Ellman H. MR imaging of the normal shoulder: anatomic correlation. *AJR* **1987**;148:83–91
99. Kellman GM, Kneeland JB, Middleton WD, et al. MR imaging of the supraclavicular region: normal anatomy. *AJR* **1987**;148:77–82
100. Kieft GJ, Bloem JL, Obermann WR, Verbout AJ, Rozing PM, Doornbos J. Normal shoulder: MR imaging. *Radiology* **1986**;159:741–745
101. Middleton WD, Kneeland JB, Carrera GF, et al. High-resolution MR imaging of the normal rotator cuff. *AJR* **1987**;148:559–564
102. Weiss KL, Beltran J, Shamam OM, Stilla RF, Levey M. High field MR surface coil imaging of the hand and wrist. Part I. Normal anatomy. *Radiology* **1986**;160:143–146
103. Middleton WD, Kneeland JB, Kellman GM, et al. MR imaging of the carpal tunnel: normal anatomy and preliminary findings in the carpal tunnel syndrome. *AJR* **1987**;148:307–316
104. Koenig H, Lucas D, Meissner R. The wrist: a preliminary report on high-resolution MR imaging. *Radiology* **1986**;160:463–467
105. Weiss KL, Beltran J, Lubbers LM. High-field MR surface-coil imaging of the hand and wrist. Part II. Pathologic correlations and clinical relevance. *Radiology* **1986**;160:147–152
106. Beltran J, Noto AM, Mosure JC, Shamam OM, Weiss KL, Zuelzer WA. Ankle: surface coil MR imaging at 1.5 T. *Radiology* **1986**;161:203–209
107. Hajek PC, Baker LL, Bjorkengren A, Sartoris DJ, Neumann CH, Resnick D. High-resolution magnetic resonance imaging of the ankle: normal anatomy. *Skeletal Radiol* **1986**;15:536–540
108. Stark DD, McCarthy SM, Filly RA, Parer JT, Hricak H, Callen PW. Pelvimetry by magnetic resonance imaging. *AJR* **1985**;144:947–950
109. Hajek PC, Baker L, Sartoris DJ, Neumann CH, Resnick D. MR arthrography: anatomic-pathologic investigation. *Radiology* **1987**;163:141–147
110. Enzmann DR, Rubin JB, Wright A. Cervical spine MR imaging: generating high-signal CSF in sagittal and axial images. *Radiology* **1987**;163:233–238

Book Review

Radiology of the Pediatric Chest. Clinical and Pathological Correlations. By Alvin H. Felman. New York: McGraw-Hill, 484 pp., 1987. $80

An earlier version of this text was published by Charles C Thomas, Publisher, Springfield, IL, in 1983 under the title of *The Pediatric Chest: Radiological, Clinical, and Pathological Observations*. The organization, content, and illustrations are similar in this new version, but a 70-page section by Mervyn Cohen on chest imaging has been added at the end of the book. It consists of chapters on CT, MR imaging, and sonography.

The main portion of the book is composed of six sections: congenital abnormalities, neonatal disorders, mediastinum, roentgenographic patterns in pulmonary disease, infections and infestations, and selected parenchymal diseases. Most of the illustrations are radiographs, but pictures of histologic sections and gross anatomic specimens are scattered throughout the book—all in black and white. The new publisher has reproduced each illustration in a smaller size but with greatly improved contrast and clarity compared with the earlier version of the book. Useful correlations between radiologic and pathologic findings appear only infrequently.

Although most of the information presented appears accurate, the discussion is sometimes confusing because of peculiar phrasing, anecdotal or emotion-laden style, unusual use of words, and unusual words (e.g., pathosis). A few glaring errors are present, for example, the statement on page 101 that pneumopericardium is asymptomatic in 75% of affected neonates. The chapters on CT and MR imaging are written in outline form and give a general overview of these techniques. Most of the CT images are of good quality. The chapter on sonography is appropriately brief.

Despite its shortcomings, the book does present a large number of satisfactory radiographs of many important thoracic diseases as well as some extremely rare and obscure conditions. Because few texts devoted solely to this subject are available, some departments may want to acquire this volume.

Joel D. Blumhagen
Children's Hospital and Medical Center
Seattle, WA 98105

Reliability of Selective Pulmonary Arteriography in the Diagnosis of Pulmonary Embolism



Michael F. Quinn[1]
Caroline J. Lundell[1]
Thomas A. Klotz[2]
Ethel J. Finck[1]
Michael Pentecost[3]
William G. McGehee[2]
J. Daniel Garnic[3]

To test the reliability of conventional selective pulmonary arteriography in the diagnosis of pulmonary embolism, three angiographers reviewed the arteriograms of a series of 60 patients retrospectively, independently, and without benefit of additional data. Pulmonary arteriograms had been interpreted as positive for pulmonary embolism in 25 of these patients during their hospitalizations. Angiographers A, B, and C judged the arteriograms of 24, 29, and 25 patients, respectively, as positive for pulmonary embolism. Mean interobserver agreement was 86%. Interobserver agreement was not associated significantly with the quality of the arteriogram or with selective injection of a lobar vs a pulmonary artery, but was associated strongly with the magnitude of thromboembolism. All angiographers agreed that the arteriograms were positive in 18 cases of pulmonary embolism graded as massive, lobar, or segmental, but agreed in only two of 15 cases graded as subsegmental.

We conclude that conventional selective pulmonary arteriography is reliable in the detection of embolus in segmental or larger pulmonary arteries. Observer disagreement becomes considerable for embolus limited to subsegmental pulmonary arteries, indicating that emboli of this size are at the resolution limit of the technique.

Pulmonary arteriography is considered the most specific test for pulmonary thromboembolism and is usually the final and definitive step in the diagnostic workup of this disorder. Most such patients respond to anticoagulant therapy, and surgical or postmortem confirmation of the diagnosis is not obtained. Thus, pulmonary arteriograms are interpreted as positive or negative for thromboembolism, but there usually is no straightforward means of determining the accuracy of the arteriographic diagnosis. As a result, the standard indexes of diagnostic performance (i.e., accuracy, sensitivity, and specificity) cannot be measured for the arteriographic diagnosis of pulmonary embolism in clinical practice.

An alternative standard of merit for diagnostic performance is reliability [1]. Diagnostic reliability usually is measured as interobserver agreement and assessed by comparison of the independent interpretations of multiple observers. Classification of test interpretations as true or false according to some more definitive diagnostic standard is not required.

The shortcoming of reliability as a measure of diagnostic performance is that in theory observers may interpret a diagnostic test with low accuracy but high reliability. If the discussion is limited to a binary test (interpreted as positive vs negative), observers who always interpret the test incorrectly would have an accuracy of 0% but a reliability of 100%. Such observers no doubt quickly would realize that by reversing their diagnostic criteria, their accuracy also would become 100%. In real situations, the worst case would be unskilled observers interpreting the test by guessing; this can be modeled as a random process, such as the tossing of a fair coin. Accuracy and reliability both would approach 50% as a limit. If the test were a good one, skilled observers would have an accuracy much closer to 100%. It is easily verified that as accuracy approaches 100%, reliability also must approach 100%. This relationship makes reliability a useful measure of

Received February 23, 1987; accepted after revision April 14, 1987.

[1] Department of Radiology, Los Angeles County/University of Southern California Medical Center, 1200 N. State St., Los Angeles, CA 90033. Address reprint requests to M. F. Quinn.

[2] Department of Internal Medicine, Los Angeles County/University of Southern California Medical Center, Los Angeles, CA 90033.

[3] Department of Radiology, Glendale Memorial Hospital and Health Center, 1420 S. Central Ave., Glendale, CA 91204.

AJR 149:469–471, September 1987
0361–803X/87/1493–0469
© American Roentgen Ray Society

diagnostic performance when (1) the observers are skilled, (2) the test is a good one, and (3) the accuracy of the test cannot be measured because a more definitive diagnostic standard to serve as "truth" is unavailable.

If the reliability of experts who independently interpret a standard set of test cases without benefit of additional data is determined, an upper limit of reliability is derived that reflects the intrinsic value of the diagnostic test. We have used this approach to assess the reliability of conventional selective pulmonary arteriography in the diagnosis of pulmonary embolism. We measured interobserver agreement between three experienced angiographers, who reviewed a series of pulmonary arteriograms retrospectively, independently, and without benefit of additional data. We also have assessed whether reliability is associated with (1) the quality of the arteriogram, (2) selective injection of a lobar vs a pulmonary artery, and (3) the magnitude of thromboembolism.

Materials and Methods

Sixty patients who underwent arteriography for suspected pulmonary embolism during a 24-month period were studied. Fifty-four patients underwent ventilation-perfusion lung scans before arteriography with 3.5 mCi (129.5 MBq) ^{99m}Tc-macroaggregated albumin, constant-flow ^{81m}krypton, and a 37 photomultiplier tube Anger camera. In most cases, the lung scan was of intermediate probability or indeterminate for embolism. Choice of lung or lobe to be examined arteriographically was guided by scintigraphically shown perfusion defects. Pulmonary arteriograms had been interpreted as positive for pulmonary embolism in 25 patients and as negative in 35.

The pulmonary arteriograms were conventional sheet-film studies obtained on a General Electric single-plane angiographic unit by using an AOT-R rapid film changer (Elema-Schonander Corp., Schaumburg, IL). Meglumine diatrizoate contrast material with an iodine concentration of 37 g/dl was used. A percutaneous femoral or internal jugular venous puncture was performed, and an 8.3-French Grollman catheter (Cook Inc., Bloomington, IN) was advanced through the right side of the heart into the right or left pulmonary artery. Pressures in the right side of the heart and the main pulmonary artery were obtained. Contrast material was injected into the right or left pulmonary artery at a rate of 30–40 ml/sec for 2 sec. Films were obtained in the anteroposterior and posterior oblique projections at a rate of at least three per second for the first 3 sec after injection. In one-half of cases, lobar arteriograms also were obtained.

The pulmonary arteriograms reviewed in this study were cleaned of all notations made by the original interpreters, placed in the original filming sequence, and put into unmarked jackets. Pulmonary arteriograms were interpreted by three experienced angiographers who had not performed any of the procedures. Interpretations were performed independently and separately by each angiographer, without knowledge of any clinical, pathologic, or additional radiologic data. The criterion for a positive diagnosis of pulmonary embolism was demonstration of an intraarterial filling defect or an arterial occlusion. Each angiographer filled out a questionnaire for each case, indicating each pulmonary lobe shown as positive or negative for embolus and indicating any shortcomings in the quality of the arteriogram. All cases judged positive by at least one angiographer were reviewed and graded according to the magnitude of thromboembolism by one of the angiographers. For each case, the largest pulmonary arteries in which the luminal diameter was occluded by at least 50% were identified, and the case was graded accordingly as massive (occlusion of at least two lobar arteries), lobar, segmental, or subsegmental pulmonary embolism.

The 95% confidence interval for mean interobserver agreement was calculated as the Student's t-interval of the relative frequency of interobserver agreement for each patient. The hypotheses that there was no association between interobserver agreement and the quality of the arteriograms, lobar artery injection, and magnitude of thromboembolism were tested by using the Fisher exact probability test and chi-square test of association for 2 × 2 contingency tables.

Results

Interpretation of Pulmonary Arteriograms

Table 1 lists individual responses of angiographers A, B, and C. Angiographers A, B, and C judged 24, 29, and 25 cases, respectively, as positive. The angiographers disagreed whether the pulmonary arteriogram was positive for embolism in 13 of 60 cases. Angiographers A vs B disagreed in nine cases (15%). Angiographers A vs C also disagreed in nine cases. Angiographers B vs C disagreed in eight cases (13%). Mean interobserver agreement was 86% (95% confidence interval, 78–93%).

Magnitude of Thromboembolism vs Angiographer Agreement

At least one angiographer interpreted the pulmonary arteriograms as positive in 33 cases. Table 2 lists these cases according to magnitude of thromboembolism vs the number of angiographers who judged the arteriogram to be positive. All angiographers agreed that the arteriograms were positive in 18 cases of pulmonary embolism graded massive, lobar, or segmental. Angiographers disagreed in 13 of 15 cases graded subsegmental. The association between interobserver agreement and magnitude of thromboembolism was strong ($p < 10^{-6}$).

Quality of the Arteriogram

At least one angiographer criticized the quality of the arteriograms in 18 of 60 cases. The angiographers criticized 12

TABLE 1: Interpretations of Pulmonary Arteriograms

Angiographer			No. of Cases
A	B	C	
+	+	+	20
−	+	+	3
+	−	+	0
+	+	−	2
+	−	−	2
−	+	−	4
−	−	+	2
−	−	−	27
Total			60

Note.—Plus and minus signs denote positive and negative interpretations for embolism, respectively.

TABLE 2: Magnitude of Pulmonary Thromboembolism vs Angiographer Agreement

Magnitude	No. of Angiographers Judging Arteriogram Positive		
	3	2	1
	No. of Cases		
Massive	2	0	0
Lobar	4	0	0
Segmental	12	0	0
Subsegmental	2	5	8

of 47 cases in which they all agreed on the diagnosis and six of 13 cases in which they disagreed. No significant association was found between interobserver agreement and the quality of the arteriogram ($p > .1$). The most common criticisms were inadequate arterial opacification due to recoil of the catheter into the main pulmonary artery from a selective position, failure to repeat an injection in a second projection, failure to perform a specific selective lobar injection, and overpenetrated films.

Selectivity of Catheterization

Injections into a lobar or a descending branch artery were performed in 30 of 60 cases. In the remaining cases, most selective injections were of the right or left pulmonary artery. Injections into a lobar or a descending branch artery were performed in 22 of the 47 cases in which all angiographers agreed on the diagnosis and in eight of the 13 cases in which they disagreed. No significant association was found between interobserver agreement and the selectivity of arterial catheterization ($p > .3$).

Discussion

Pulmonary arteriography often is called the gold standard in the diagnosis of pulmonary thromboembolism. Bookstein [2] and Bookstein et al. [3] have shown that emboli as small as 1 mm in diameter can be shown arteriographically, both in humans and in dogs, by using selective injection of segmental pulmonary arteries. Other techniques useful for showing small pulmonary emboli include magnification arteriography, segmental balloon-occlusion arteriography, and balloon-occlusion cineangiography [4, 5]. Digital subtraction arteriography can be used to examine the larger pulmonary arteries [5]. Each of these modifications of pulmonary arteriography has proponents. Conventional selective pulmonary arteriography remains an accepted standard of practice and a yardstick against which the aforementioned techniques can be measured.

Arteriography is not a perfect detector of pulmonary embolism in clinical practice, however. Interobserver agreement between experts has been estimated to be 80–95% [6]. Greenspan measured interobserver disagreement between three angiographers in the analysis of 310 pulmonary arteriograms in the Urokinase Pulmonary Embolism Trial and reported that it exceeded 10% [7, 8]. Our finding of a mean interobserver agreement of 86% is consistent with these published values. No significant association was found between interobserver agreement and quality of the arteriogram or selective injection of a lobar vs a pulmonary artery. Interobserver agreement was associated strongly with the magnitude of thromboembolism. Disagreement between angiographers occurred only in cases in which embolus was limited to subsegmental arteries.

The extent of angiographer disagreement about embolism of subsegmental arteries observed in this study was a surprise to us but perhaps should not have been. Overall interobserver disagreement was no greater than that encountered by others. It is no surprise that angiographers should have a harder time detecting the smallest lesions rather than larger ones. Hence, we think that angiographers who repeat this study will have similar results.

This study is a retrospective analysis and therefore subject to hidden biases. For example, it is reasonable to expect that selective injection of a lobar artery would display emboli better than injection of a pulmonary artery and therefore would be associated with greater observer agreement. However, pulmonary arteriography often is terminated at first demonstration of an embolus. Because injection of a pulmonary artery usually is performed first, injections of a lobar artery tend to be omitted in those cases in which embolus is most obvious. The result is a bias toward association of injection of pulmonary rather than lobar arteries with greater observer agreement. Therefore, the data of this study justify no conclusion about the relative value of selective injection of lobar vs pulmonary arteries. Similarly, the lack of association between the quality of the arteriogram and observer agreement justifies no general conclusion about the importance of the quality of pulmonary arteriograms.

This study provides evidence that the reliability of conventional selective pulmonary arteriography is high for detection of emboli in segmental pulmonary arteries or larger arteries but declines significantly for embolism limited to subsegmental pulmonary arteries. We suggest the following explanation. Injection of a pulmonary or lobar artery opacifies the arteries of several overlapping segments. The result is a profusion of crossing and overlapping subsegmental arterial shadows, a background against which it is difficult to pick out small arterial filling defects. The difficulty is increased when subsegmental arteries are crowded together by atelectasis. As a result, subsegmental embolism is at the resolution limit of conventional selective pulmonary arteriography.

Opacification of individual segmental arterial beds may be required in some cases to make a reliable diagnosis of subsegmental pulmonary embolism. Our findings lend support to recommendations that selective segmental balloon-occlusion arteriography or cineangiography and magnification arteriography be used when a digital subtraction or conventional selective pulmonary arteriogram shows no embolism [3–5]. Observer agreement can be used as a measure of diagnostic performance in clinical studies that compare the various pulmonary arteriographic techniques used in the diagnosis of pulmonary embolism.

ACKNOWLEDGMENTS

We thank S. P. Azen and Charles Berry for statistical advice. We thank Roberta Bliss for manuscript preparation.

REFERENCES

1. Fleiss, JL. The measurement of interrater agreement. In: *Statistical methods for rates and proportions*, 2nd ed. New York: Wiley, **1981**:211–236
2. Bookstein JJ. Segmental arteriography in pulmonary embolism. *Radiology* **1969**;93:1007–1012
3. Bookstein JJ, Feigen DS, Kwan WS, Alazraki N. Diagnosis of pulmonary embolism. *Radiology* **1980**;136:15–23
4. Bynum LJ, Wilson JE, Christensen EE, Sorenson RT. Radiographic techniques for balloon occlusion pulmonary arteriography. *Radiology* **1979**;133:518–520
5. Ferris EJ, Holder JC, Lim WN. Angiography of pulmonary emboli: digital studies and balloon occlusion cineangiography. *AJR* **1984**;142:369–373
6. Sostman HD, Rapoport S, Gottschalk A, Greenspan RH. Imaging of pulmonary embolism. *Invest Radiol* **1986**;21:443–454
7. Greenspan RH. Angiography of pulmonary embolism. In: Abrams HL, ed. *Abrams Angiography*, 3rd ed. Boston: Little, Brown, **1983**:803–817
8. Urokinase pulmonary embolism trial. A national cooperative study. *Circulation* **1973**;47[Suppl 2]:1–108

Book Review

Pediatric Body CT. By Alan Daneman. New York: Springer-Verlag, 374 pp., 1987, $160

This unique text fulfills a need for which no adequate book previously was available. The book is written with a large radiology audience in mind. Details of CT technique and an adequate discussion of pediatric diseases are included so that a general radiologist will find this book a complete guide and reference. The book is fairly complete in its scope (absent are cine CT, quantitative bone CT, and some applications in orthopedics), and pediatric radiologists in large centers will find valuable reference information.

Throughout the text most images, which were obtained with a state-of-the-art CT scanner, are of excellent quality. Examples of common and many rare entities are well illustrated throughout each chapter. Many of the captions to the illustrations are, however, lengthy, in small print, and difficult to read. Labeling of the prints could have been done more clearly to facilitate understanding of the illustrations. The author has reviewed the literature well and summarized the experience of others by using appropriate references. Throughout the text he also conveys the vast experience obtained at the Hospital for Sick Children in Toronto. His personal experience in pediatric body CT is obviously extensive, and his comments add perspective to rare or unusual entities.

An introductory section of the book includes discussion about the choice of CT as an imaging technique and a summary about CT technique in children. The four other sections deal with the chest, abdomen, neck, and musculoskeletal system. Each section is subdivided into chapters that include anatomy and special technique as well as discussion of the pathology involving each organ. The organization of each section and chapter is fairly consistent.

Discussions of alternative approaches to imaging are mentioned throughout the book. One chapter, titled "Approach to Abdominal and Pelvic Mass, Inflammation, and Trauma," is dedicated almost entirely to choosing the proper imaging studies. Although germane to a general pediatric radiology text, at times these lengthy discussions distract from the theme of the book.

The only other available text extensively covering pediatric body CT, *Body Imaging in Pediatrics*, by Sty, Hernandez, and Starshak, although well written, suffers from outdated CT images. *Pediatric Body CT* provides quality illustrations essential to a state-of-the-art CT text and should become a part of the library of any radiology office or institution performing imaging studies in children.

James S. Donaldson
The Children's Memorial Hospital
Chicago, IL 60614

Intrathoracic Manifestations of Metastatic Testicular Seminoma: A Comparison of Chest Radiographic and CT Findings

Michael P. Williams[1]
Janet E. Husband
Christine W. Heron

The chest radiographs and CT scans of 200 patients with pure testicular seminoma were reviewed. The radiographs showed evidence of intrathoracic metastatic disease in 25 patients (12.5%). Of these, 17 had an abnormal mediastinal contour, seven had pulmonary metastases, five had pleural effusions, and two had discrete pleural masses. CT showed evidence of intrathoracic metastatic disease in 30 patients (15%). This included mediastinal nodal enlargement in 21, pulmonary metastases in 12, pleural effusions in six, and pleural masses in two. CT not only showed disease in five patients with normal chest radiographs, but also showed additional sites of disease in four other patients with abnormal chest radiographs.

The results suggest that mediastinal nodal enlargement is the most common intrathoracic manifestation of metastatic testicular seminoma. CT is more accurate than chest radiography in the detection of metastatic seminoma in the chest and defines the extent of metastatic disease more precisely.

Pure seminomas account for approximately one-third of testicular tumors [1, 2]. In over 90% of patients the disease at the time of presentation is limited to the primary site and infradiaphragmatic lymph nodes [3]. Metastatic spread beyond these areas occurs both at presentation and after apparently successful initial treatment. The most common sites for such metastases are the mediastinal and supraclavicular lymph nodes and the lungs [4, 5]. This paper reports the pattern of intrathoracic metastatic disease from seminoma of the testis and compares the findings on chest radiography and CT.

Subjects and Methods

The study group included 200 patients referred to the testicular tumor unit at the Royal Marsden Hospital between 1980 and 1986. All patients had a diagnosis of pure testicular seminoma and had both chest radiographs and CT scans available for review. The diagnosis of pure seminoma was based on histology of the original sections, an absence of staining for alpha-fetoprotein in those sections, and an absence of raised serum levels of alpha-fetoprotein. The serum level of beta human chorionic gonadotrophin was also measured in each patient. Patients with a histologic diagnosis of seminoma but who also had elevated serum alpha-fetoprotein were considered to have mixed seminoma and teratoma and were excluded from the study [6]. The age of the patients ranged from 22 to 74 years (mean, 38 years). Intrathoracic metastases were diagnosed in 30 patients, at the time of the original presentation in 11 and at relapse in 19. The diagnosis of intrathoracic relapse was based on unequivocally abnormal chest CT scans and chest radiographs that were associated with cervical lymphadenopathy in seven patients, abdominal masses in eight, and elevation of serum beta human chorionic gonadotrophin in 11. Biopsy proof of metastatic seminoma was obtained from mediastinal nodes, pleural masses, or pulmonary metastases in 12 patients. In the remainder, regression of the visualized abnormalities on chemotherapy was taken as confirmation of tumor involvement. The relapses occurred from 5 to 35 months after orchidectomy (mean, 19 months). All 19 patients who relapsed had been treated by infradiaphragmatic irradiation to the ipsilateral pelvic nodes and paraaortic regions. Two patients also received supradia-

Received March 11, 1987; accepted after revision June 1, 1987.

This work was supported by the Cancer Research Campaign, 2 Carlton House Terr., London SW1, U.K.

[1] All authors: Cancer Research Campaign Radiology Research Group, Royal Marsden Hospital, Downs Rd., Sutton, Surrey SM2 5PT, England.

AJR 149:473–475, September 1987
0361–803X/87/1493–0473
© American Roentgen Ray Society

phragmatic irradiation. In 10 patients relapse was recognized on routine radiographic follow-up, while nine patients had clinical signs or symptoms of relapse that prompted chest radiography and CT.

All patients had standard posteroanterior chest radiographs and chest CT scans performed at the time of the original diagnosis. Routine follow-up included standard posteroanterior chest radiographs at 2-month to 3-month intervals and chest CT scans at yearly intervals. If there was clinical suspicion of relapse, both standard radiography and chest CT scans were obtained at that time.

The chest CT scans were obtained using a Siemens Somatom 2 or DRH CT scanner. Contiguous 8-mm sections through the chest were obtained with suspended respiration. No IV contrast medium was used. The chest radiographs and the CT studies were reviewed independently by two radiologists.

Results

Of the 200 patients in the series 30 had evidence of intrathoracic metastases at CT. Twelve had isolated mediastinal lymphadenopathy, four had mediastinal nodal enlargement with a pleural effusion, three had mediastinal nodal enlargement and pulmonary metastases, and two had mediastinal nodal enlargement, pulmonary metastases, and pleural effusions. Seven patients had pulmonary metastatic disease alone, and two patients had isolated pleural masses.

Twenty-five of the 30 patients had an abnormal chest radiograph on review (although only 22 had been reported to be abnormal at the original viewing). An abnormal mediastinal contour was evident in 17 patients, pulmonary metastases in seven, a pleural effusion in five, and pleural masses in two.

All of the abnormalities seen on chest radiography were detected on CT. In addition to demonstrating intrathoracic metastases in five patients with a normal chest radiograph, CT also showed additional sites of involvement in four other patients. Unsuspected mediastinal disease was identified in one patient, and unsuspected pulmonary metastases were found in three. In the 21 patients with mediastinal disease, CT made it possible for us to determine the individual nodal stations involved. The numbers of patients showing nodes involved in each station, as classified by the American Thoracic Society Classification [7], is shown in Table 1.

In the 12 patients in whom pulmonary metastases were shown by CT, at least one of the metastases was greater than 1 cm in diameter. CT showed between one and three pulmonary nodules less than 1 cm in diameter in 12 additional patients who had had a normal chest radiograph. Serial CT studies suggested that these did not represent pulmonary metastases. In six patients the nodules were unchanged in the absence of systemic treatment on follow-up over a period of more than 1 year. In three patients the nodules resolved without treatment. In an additional three patients, the nodules remained unchanged despite satisfactory resolution of large intraabdominal masses following systemic chemotherapy.

TABLE 1: Lymph Node Groups Involved by Metastatic Testicular Seminoma as Shown by CT

Group	Mediastinal Nodal Stations[a]	No. of Patients
High right paratracheal	2 (R)	2
High left paratracheal	2 (L)	7
Low right paratracheal and tracheobronchial angle	4 (R)/10 (R)	7
Low left paratracheal and left peribronchial	4 (L)/10 (L)	1
Subcarinal	7	13
Posterior mediastinal	8	11
Right hilum	11 (R)	1
Left hilum	11 (L)	1

Note.—(R) = right; (L) = left.

[a] Based on the American Thoracic Society classification [7].

Discussion

This study demonstrates the distribution of intrathoracic metastatic disease from testicular seminoma and compares the use of chest radiography and CT scanning in the detection of such disease. The results showed that, unlike patients with testicular teratoma [8], those with seminoma have a higher prevalence of mediastinal metastases than pulmonary metastases. Mediastinal disease was seen in 70% of patients with intrathoracic metastases, whereas pulmonary metastases were present in only 40%. Furthermore, the mediastinum may be the only site of intrathoracic disease in seminoma and this is an infrequent finding in testicular teratoma. In a series of 432 patients with malignant testicular teratoma, only 9% showed intrathoracic metastases limited to the mediastinum [9]. As metastases occur most commonly in the subcarinal and posterior mediastinal nodes, it is particularly important that the chest radiographs in patients with testicular seminoma are adequately penetrated. Radiographs on which the azygoesophageal recess and lateral margin of the descending aorta cannot be identified are inadequate.

Anterior mediastinal involvement did not occur in this group of patients with metastatic seminoma, whereas the anterior mediastinum is the favored site of involvement in patients with primary mediastinal seminoma [10]. Posterior mediastinal involvement is not a feature of primary germ-cell tumors and indeed is not expected in view of their proposed thymic origin [11, 12]. This difference may help to separate the two groups, and thus avoid a search for a primary site in patients with an anterior mediastinal seminoma [13].

Pulmonary metastases were seen less frequently than was mediastinal involvement. Isolated pulmonary metastatic disease occurred in only seven patients. Thus, this is a rather unusual feature of pure seminoma. Patients with pulmonary metastases showed other features atypical of classic seminoma. In 58% of those with pulmonary metastases, the serum level of beta human chorionic gonadotrophin was greater than 100 IU/l, and in 25% coexistent abdominal masses had low-density cystic areas. The presence of an occult element of choriocarcinoma is suggested by these findings since cystic abdominal masses are more typical of teratoma [14], and although a modest rise in beta human chorionic gonadotrophin levels may be a feature of advanced pure seminoma [15], four of our patients had particularly high levels (greater than 1000 IU/l).

CT was considerably more sensitive in the detection of pulmonary metastases than was chest radiography, showing

disease in 12 patients whereas plain radiographs detected abnormalities in only seven. The greater sensitivity of CT over chest radiographs in detecting pulmonary nodules is well known [16]. The unexpected finding, however, was the prevalence of nonmetastatic pulmonary nodules (6%). A previous study also from the United Kingdom [17] showed only two nonmetastatic pulmonary nodules in a series of 100 chest CT scans in adult patients. Both nodules were calcified and visible on the plain chest radiographs. In the present series none of the nonmetastatic nodules were visible on plain films and none were of obvious calcific density, although the CT numbers of the nodules were not measured pixel by pixel. Our results suggest that with present-generation CT scanners, the CT demonstration of up to three pulmonary nodules less than 1 cm in diameter should not be considered diagnostic of pulmonary metastatic disease in adult oncology patients in the United Kingdom. In patients with a primary tumor such as seminoma, in which pulmonary metastases are rare and when they do occur tend to be greater than 1 cm in diameter, we would suggest that such patients be followed up by serial CT scanning to avoid overtreatment.

There was little difference between chest radiography and CT in their ability to detect pleural disease. Pleural plaques of tumor, seen in two patients, were equally well shown by both techniques, and five out of six pleural effusions seen on CT were also shown on chest radiography. All six patients with pleural effusions had associated mediastinal nodal enlargement, shown on chest radiography in five patients and on chest CT in six. The presence of an apparently isolated pleural effusion on plain radiographs in a patient with a history of seminoma is an indication for chest CT in order to search for occult mediastinal disease.

The analysis of this series of patients has revealed the characteristic sites of intrathoracic metastases from testicular seminoma and compared the abnormalities shown on chest radiography and chest CT. CT is superior to conventional chest radiography in the detection of intrathoracic metastatic disease and shows the extent of disease more clearly. Chest CT should be an integral part of the initial staging procedure for patients with seminoma and should also be employed whenever relapse is clinically suspected and in the follow-up of patients who are at high risk of developing mediastinal relapse even when they have a normal chest radiograph.

ACKNOWLEDGMENTS

We wish to thank the Testicular Tumour Unit for allowing us to study their patients. We also acknowledge the help of Julie Leggatt and Janice O'Donnell in the preparation of this manuscript.

REFERENCES

1. Pugh RCB. Testicular tumors—introduction. In: Pugh RCB, ed. *Pathology of the testis*. Oxford: Blackwell, **1976**:139–163
2. Anderson CK. Seminoma: aspects of pathology. In: Jones WG, Milford Ward A, Anderson CK, eds. *Advances in the biosciences: germ cell tumours II*. Oxford: Pergamon Press, **1985**:55, 193–201
3. Caldwell WL, Kademian MT, Frias Z, Davis TE. The management of testicular seminomas. *Cancer* **1980**;45:1768–1774
4. Read G. The treatment of supradiaphragmatic metastatic seminoma. *Clin Radiol* **1980**;31:349–353
5. Thomas GM, Rider WD, Dembo AJ, et al. Seminoma of the testis: results of treatment and patterns of failure after radiation therapy. *Int J Radiat Oncol Biol Phys* **1981**;8:165–174
6. Grigor KM. The role of histopathology in germ cell tumours: a review. In: Jones WG, Milford Ward A, Anderson CK, eds. *Advances in the biosciences: germ cell tumours II*. Oxford: Pergamon, **1985**;55:37–43
7. Tisi GM, Friedman PJ, Peters RM, et al. Clinical staging of primary lung cancer. American Thoracic Society node mapping scheme. *Am Rev Respir Dis* **1985**;127:659–669
8. Husband JE, Barrett A, Peckham MJ. Evaluation of computed tomography in the management of testicular teratoma. *Br J Urol* **1981**;53:179–183
9. Peckham MJ. Investigation and staging: general aspects and staging classification. In: Peckham M, ed. *The management of testicular tumours*. London: Edward Arnold, **1981**:89–101
10. Raghavan D, Barrett A. Mediastinal seminomas. *Cancer* **1980**;46:1187–1191
11. Kountz SL, Connolly JE, Cohn R. Seminoma-like (or seminomatous) tumors of the anterior mediastinum. *J Thorac Cardiovasc Surg* **1963**;45:289–301
12. Lattes R. Thymoma and other tumors of the thymus. *Cancer* **1962**;15:1223–1260
13. Bohle A, Studer UE, Sonntag RW, Scheidegger JR. Primary or secondary extragonadal germ cell tumours? *J Urol* **1985**;135:939–943
14. Husband JE, Peckham MJ, Macdonald JS. The role of abdominal computed tomography in the management of testicular tumours. *Comput Tomogr* **1980**;4:1–16
15. Peckham MJ, Horwich A, Hendry WF. Advanced seminoma: treatment with cis-platinum–based combination chemotherapy or carboplatin. *Br J Cancer* **1985**;52:7–13
16. Schaner EG, Chang AE, Doppman JL, Conkle DM, Flye MW, Rosenberg SA. Comparison of computed and conventional whole lung tomography in detecting pulmonary nodules: a prospective radiologic-pathologic study. *AJR* **1978**;131:51–54
17. Edwards SE, Kelsey Fry I. Prevalence of lung nodules on computed tomography of patients without known malignant disease. *Br J Radiol* **1982**;55:715–716

1988 AMERICAN ROENTGEN RAY SOCIETY MEETING

MAY 8–13, 1988
SAN FRANCISCO HILTON HOTEL
SAN FRANCISCO, CA

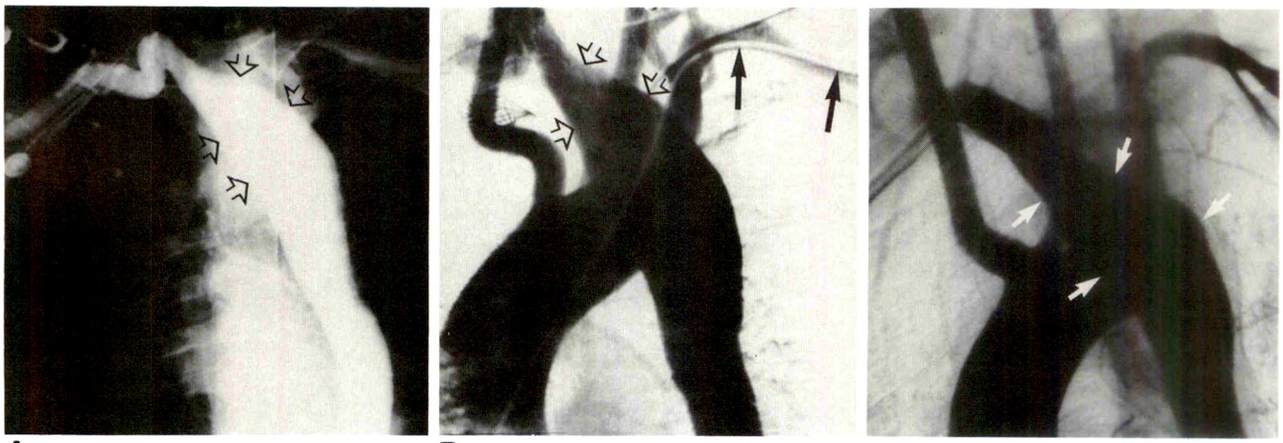
See page 656 and forthcoming issues for further information.

Case Report

Aberrant Right Subclavian Artery with a Large Diverticulum of Kommerell: A Potential for Misdiagnosis

T. Gregory Walker[1] and Stuart C. Geller

An aberrant right subclavian artery arising from the descending thoracic aorta, distal to the left subclavian artery, may be associated with an outpouching at its origin, the "diverticulum of Kommerell" [1–4]. This diverticulum is usually asymptomatic and is most often an incidental finding. It may mimic more serious disease such as thoracic aortic aneurysm, dissection, or aortic tear with mediastinal hematoma. This becomes especially important in certain clinical situations,



A B

Fig. 1.—68-year-old man who presented with chest pain and a widened mediastinum on chest radiograph.

***A*, Thoracic aortogram. Contrast injection was made with the catheter tip within a diverticulum of Kommerell (*arrows*). This was misinterpreted as representing catheter entry into the false channel of an aortic dissection.**

***B*, Arch aortogram performed via left axillary approach (*solid arrows*). This reveals a diverticulum of Kommerell (*open arrows*) and an aberrant right subclavian artery with an otherwise normal aorta. Linear defect in descending thoracic aorta is due to artifacts.**

Fig. 2.—Arch aortogram in a 23-year-old man suspected of having a traumatic aortic tear caused by a high-speed automobile accident. Plain chest radiograph revealed a widened and indistinct left superior mediastinum. Arteriogram reveals an aberrant right subclavian artery arising from a large diverticulum of Kommerell (*arrows*), but study is otherwise unremarkable.

Received February 26, 1987; accepted after revision April 20, 1987.

[1] Both authors: Department of Radiology, Massachusetts General Hospital and Harvard Medical School, Boston, MA 02114. Address reprint requests to T. G. Walker at Massachusetts General Hospital.

AJR **149:477–478, September 1987** 0361–803X/87/1493–0477 © American Roentgen Ray Society

such as in patients who present with chest pain or those who are evaluated following trauma or after sustaining deceleration injuries. We describe three patients with aberrant right subclavian artery and associated diverticulum of Kommerell, whose clinical presentation and initial radiographic studies suggested a more significant abnormality of the aorta.

Case Report

A 68-year-old man presented to an outside hospital with chest pain. On the basis of clinical presentation and an initial chest radiograph that revealed a widened mediastinum, aortic dissection was suspected. Arch aortography from a transfemoral approach was attempted, but difficulty was encountered in negotiating the transverse portion of the arch. The catheter preferentially entered the right subclavian artery. An injection of contrast material was made, but it failed to show the ascending aorta, either carotid artery, or the left subclavian artery (Fig. 1A). The arteriogram was misinterpreted as representing catheter entry into the false lumen of an aortic dissection that involved the proximal ascending aorta. The patient was referred to our institution for surgery. Before surgery a second attempt was made to visualize the ascending aorta. Repeat aortography via a left axillary approach revealed an aberrant right subclavian artery with a diverticulum of Kommerell (Fig. 1B). Because no aortic dissection was present, unnecessary surgery was avoided. The patient subsequently did well and was discharged.

We subsequently encountered two similar cases of aberrant right subclavian artery with a large diverticulum of Kommerell (Figs. 2 and 3). Again the clinical presentation and initial chest radiographs suggested severe aortic disease, resulting in referral for aortography. At catheterization, it was difficult to negotiate the aortic arch by using the transfemoral approach.

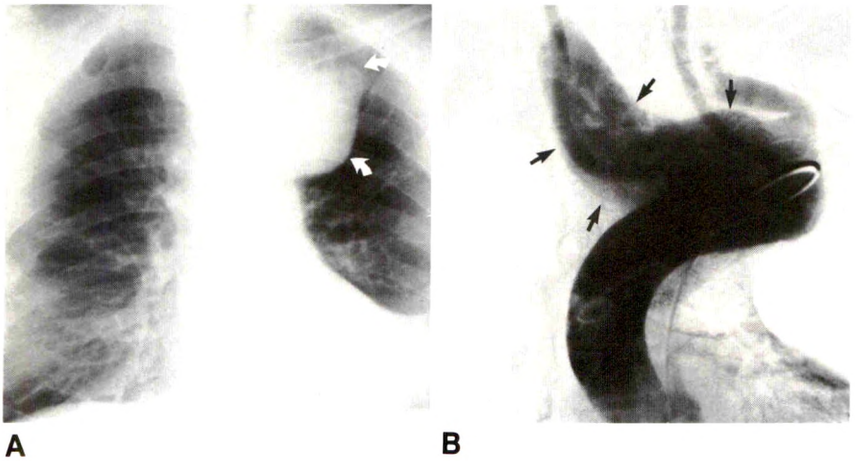
Discussion

An aberrant right subclavian artery is the most common vascular anomaly of the thoracic arch, occurring in approximately 0.5% of the normal population [2–5]. It originates as the fourth branch of the aortic arch just distal to the left subclavian artery, and courses behind the esophagus obliquely and superiorly to the right. In the majority of cases (up to 60%), the aberrant right subclavian artery originates from a diverticulum-like structure of the aorta [5]. This finding was first described in 1936 by Kommerell [1]; hence the eponym "diverticulum of Kommerell" [3, 4, 6]. This diverticulum is variable in size [2, 3]. Occasionally the diameter is large, approximating the diameter of the distal aortic arch [2]. In such cases, it may be misinterpreted. Confusion with other diseases such as a mediastinal mass, arch, or innominate aneurysm has been known to occur, and could lead to unnecessary surgery [2, 7, 8].

In the three cases we report, the clinical presentation and preliminary radiographic studies resulted in an erroneous initial clinical diagnosis. Although the angiographic study finally led to the correct diagnosis, all of these procedures involved a technically complicated catheterization because of the size of the diverticulum. In each case the catheter tip selectively entered the large diverticulum at the origin of the aberrant right subclavian artery, despite use of a pigtail catheter. Thus, when injections were made, the ascending aorta and the other great vessels were not visualized. Subsequent negotiation of the arch depended on recognition of the anomalous anatomy so that the catheter could be maneuvered past the diverticulum. Placement of the catheter tip within the ascending aorta from a transfemoral route can be quite difficult, and if the angiographer fails to recognize the anatomy, a misdiagnosis of aortic dissection may result. In one of our patients the aortogram was successfully completed and the correct diagnosis was obtained only after a left transaxillary route was chosen. In cases that prove difficult from a transfemoral route, this approach permits relatively simple passage of the catheter into the ascending aorta, bypassing the diverticulum and aberrant right subclavian artery. The resultant arteriogram should correctly delineate the anomalous anatomy and prevent angiographic misdiagnosis.

REFERENCES

1. Kommerell B. Verlagerung des Osophagus durch eine abnorm verlaufende Arteria subclavia dextra (Arteria lusoria). *ROFO* **1936**;54:590–595
2. Blake HA, Manion WC. Thoracic arterial arch anomalies. *Circulation* **1962**;26:251–265
3. Schmidt J. Die Arteria lusoria. *Arch Kreislaufforschg* **1953**;19:1–37
4. Felson B, Cohen S, Courter SR, McGuire J. Anomalous right subclavian artery. *Radiology* **1950**;54:340–348
5. Stewart JR, Kincaid OW, Edwards JE. *An atlas of vascular rings and related malformations of the aortic arch.* Springfield: Thomas, **1964**
6. Salomonowitz E, Edwards JE, Hunter DW, Castaneda-Zuniga WR, Lund G, Cragg AH, Amplatz K. The three types of aortic diverticula. *AJR* **1984**;142:673–679
7. Hunter JA, Dye WS, Hushang J, Najafi H, Julian OC. Arteriosclerotic aneurysm of anomalous right subclavian artery. *J Thorac Cardiovasc Surg* **1970**;59:754–758
8. McCallen AM, Schaff B. Aneurysms of an anomalous right subclavian artery. *Dis Chest* **1968**;54:63–66



A **B**

Fig. 3.—*A*, Chest radiograph in a 70-year-old man shows a large left superior mediastinal mass (*arrows*) suspected to be a thoracic aortic aneurysm.

***B*, Arch aortogram made with the catheter in the ascending aorta shows that mediastinal widening is due to a large diverticulum of Kommerell (*arrows*) and an aberrant right subclavian artery. Additionally, there is a tortuous but otherwise normal aorta. Left subclavian and both vertebral arteries are not yet opacified.**

Selective Intraarterial DSA of the Parathyroid Glands in Patients with Hyperparathyroidism after Parathyroidectomy

Pascal Lacombe[1]
Denis Foster[1]
Claude Dubost[2]
Elisabeth Schouman-Claeys[3]
Guy Frija[3]
Pierre Assens[2]
Victor Bismuth[1]

Eighteen patients with recurrent hyperparathyroidism after parathyroidectomy were prospectively examined with selective intraarterial digital subtraction angiography (DSA) of the brachiocephalic arteries. The results were compared with findings at reoperation. Seventeen of the 21 remaining abnormal parathyroid glands were correctly detected by selective DSA (sensitivity = 81%). In the neck and mediastinum, sensitivities were 73% (8/11) and 90% (9/10), respectively. All patients with histopathologic confirmation of primary hyperparathyroidism (17/18) became normocalcemic postoperatively.

We conclude that selective intraarterial DSA is indicated in patients with recurrent hypercalcemia after parathyroidectomy when the results of noninvasive imaging techniques are uncertain.

Up to 95% of patients with primary hyperparathyroidism can be cured by a single cervical parathyroidectomy with or without the help of localization techniques [1]. With recurrence, however, reoperation is less successful and has a higher morbidity. In these cases, it is important to locate the remaining parathyroid tissue. The most accurate angiographic method for this purpose is believed to be selective parathyroid arteriography [2].

Recently, several authors have reported the results of digital subtraction angiography (DSA) [3–5]. We report here our experience with intraarterial DSA performed by selective injection of contrast media into the brachiocephalic arteries in patients with persistent hypercalcemia after parathyroidectomy for primary hyperparathyroidism.

Materials and Methods

Since 1982, a prospective study has been conducted to assess the value of selective intraarterial DSA for parathyroid localization in patients requiring reoperation for persistent or recurrent primary hyperparathyroidism.

The study included 18 patients (12 women and 6 men) ranging in age from 18 to 66 years (mean age, 47 years; SD, 12.5). Patients were included in the series if they had hypercalcemia after an initial parathyroidectomy. Fifteen patients had persistent hypercalcemia and three had recurrent hypercalcemia. Eight patients had nephrolithiasis, three had multiple endocrine neoplasia, and five had severe bone resorption. Two patients were asymptomatic.

All patients underwent a second operation and the surgical localizations of normal and abnormal glands were compared with the results of preoperative selective intraarterial DSA.

A parathyroid gland was considered normal if its size at surgery and histology (if biopsied) were normal. When an abnormal gland was resected at reoperation, the remaining parathyroid glands were considered normal if the patient was cured after surgery (follow-up, 8 months to 4 years). A parathyroid gland was considered abnormal when an adenoma or a hyperplasia was detected by histopathologic studies, whatever the size and weight of the gland.

All studies were performed with a Polydiagnost C U-arm fluoroscope (Philips, Eindhoven, Holland) with 23-cm (9-in.) image intensifier, using a 1.2-mm focal spot. An Adac DPS 4100 digital system (Adac Laboratories, San Jose, CA) with a 512 × 512 matrix was used for image processing.

Received November 5, 1986; accepted after revision May 14, 1987.

[1] Service de Radiologie, Hôpital Ambroise Paré, 9 avenue Charles de Gaulle, F92100 Boulogne, France. Address reprint requests to P. Lacombe.

[2] Service de Chirurgie, Hôpital Saint-Louis, 40 rue Bichat, F75010 Paris, France.

[3] Service de Radiologie, Hôpital Raymond Poincaré, 104 boulevard Raymond Poincaré, F92380 Garches, France.

AJR 149:479–483, September 1987
0361–803X/87/1493–0479
© American Roentgen Ray Society

After local anesthesia an end-hole 5- or 6-French catheter was inserted by femoral approach into the origin of the left subclavian, left common carotid and innominate, or right subclavian arteries. Dilute contrast medium was used to decrease osmolality and viscosity and to reduce the symptoms related to injection into the subclavian arteries. For the same purpose, an arm cuff was inflated beyond systolic arterial pressure before each injection. These proximal injections used 32% sodium and meglumine ioxaglate diluted with 30% of distilled water (osmolality = 450 mOsm/kg) at a rate of 5 ml/second. A vol of 20 ml was injected into the innominate artery, 15 ml into subclavian arteries, and 10 ml into the left common carotid artery. An amount of 130 to 160 ml of 30% diluted contrast material was injected.

Filming was carried out at a rate of 2.5 images/sec (exposure factors: 65 KV, 800 mA, and 40 msec). Frontal and oblique views with neck rotation were centered on both neck and mediastinum. Flour bags were used as contrast equalizers for the neck, upper chest, and lung area. Mean duration of the procedure was 40 min.

On intraarterial DSA, the appearance of parathyroid adenoma or hyperplasia is similar to that seen on conventional angiography [2]. Enlarged glands are detected as abnormal round or ovoid regions of contrast staining adjacent to or separated from the thyroid. A lesion was considered present if there was an unequivocal localized contrast stain in the late arterial phase that persisted in the venous phase. In cases where the parathyroid was superimposed over the thyroid, oblique views were necessary. In case of concomitant thyroid disease, additional injections in oblique or transverse projections were necessary. The thyroid staining seen on intraarterial DSA was compared with the thyroid gland as shown on radionuclide scan.

Twenty-one abnormal parathyroid glands were found and excised at reoperation. These abnormal glands were found in 17 patients. There were 12 adenomas, 9 primary hyperplastic glands, and no carcinomas. All but one of the reoperated patients became normocalcemic postoperatively. The 40-year-old woman for whom reoperation was not successful had a slightly elevated parathormone level but a normal intraarterial DSA. Her persistent hypercalcemia was later related to bone metastases from an undiagnosed breast cancer (case 5). In three cases the excised gland was a supernumerary fifth gland, and in another case a sixth gland was recovered. Their surgical location is illustrated in Figure 1.

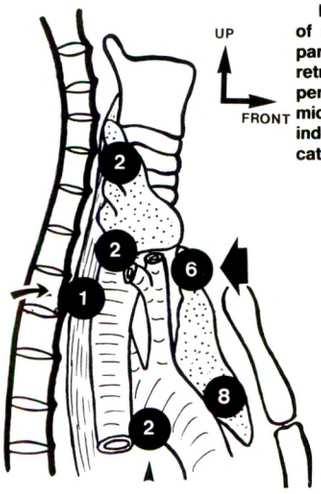


Fig. 1.—Schematic representation of the surgical sites of 21 remaining parathyroid glands. Curved arrow = retroesophageal location; arrow = upper pole of thymic lobe; arrowhead = middle mediastinum. Circled numbers indicate number of tumors in each location.

Results

Seventeen of the 21 abnormal glands were correctly located by preoperative selective DSA (sensitivity = 81%) (Tables 1 and 2).

TABLE 1: Angiographic Findings and Results of Reoperation

Case	Age	Gender	Selective Digital Arteriography		Histopathology
			Neck	Mediastinum	
1	45	F	True +, R	Negative	Hyperplasia
			False −, L		Hyperplasia
2	53	F	Negative	True +, R	Adenoma
3	56	F	Negative	True +, L	Adenoma
4	66	F	False −, L	True +, R and L	Hyperplasia (2 glands)
5	40	F	Negative	Negative	Normal
6	54	F	Negative	False +, R	
				True +, L	Hyperplasia
7	42	M	False −, L	False +, L	Adenoma
8	60	M	True +, L	Negative	Adenoma
9	60	F	Negative	False +, R	
				True +, L	Adenoma
10	64	F	Negative	True +, L	Adenoma
11	40	M	True +, R	Negative	Adenoma
12	45	F	Negative	True +, L	Adenoma
13	49	F	True +, L	Negative	Adenoma
14	48	F	True +, R	Negative	Hyperplasia
15	18	F	Negative	False −, L	Adenoma
16	33	M	True +, R	Negative	Adenoma
17	32	F	True +, L	True +, R	Hyperplasia (2 glands)
				True +, R	Hyperplasia
18	41	M	True +, R	Negative	Adenoma

Note.—R = right; L = left; + = positive; − = negative.

TABLE 2: Results of Intraarterial Digital Subtraction Angiography

	True Positive	False Positive	False Negative	Sensitivity (%)	PPV (%)
Intraarterial DSA (21 glands)	17	3	4	81	85
Neck	8	0	3	73	100
Mediastinum	9	3	1	90	75

Note.—PPV = positive predictive value; DSA = digital subtraction angiography.

In the neck, eight of the 11 remaining abnormal glands were detected angiographically (sensitivity = 73%) (Figs. 2 and 3). The mean weight of correctly detected glands was 1250 mg (SD = 1580); the smallest weighed 100 mg. Three glands were overlooked. Two were small, and one was the same size and weight as a normal gland (60 mg). The third, supplied by the left superior thyroid artery, was missed because the left common carotid artery was not injected.

There were no false-positive results in the cervical area. In the mediastinum, nine of the 10 remaining abnormal glands were correctly detected (sensitivity = 90%) (Fig. 4). The only false-negative result, still unexplained, involved a 1000-mg adenoma. The smallest diseased gland detected in the mediastinum weighed 80 mg and the largest weighed 12,000 mg (mean weight = 2935 mg; SD, 3621).

On the other hand, there were three false-positive results in the mediastinal area. In one case, abnormal staining in the anterior mediastinum was highly suggestive of an abnormal gland (Fig. 5). No abnormal mediastinal mass was detected by the surgeon. In this case the persistent hypercalcemia was caused by a cervical adenoma excised during a third surgical procedure. In the two other cases, two abnormal mediastinal glands were angiographically suspected in each case, but only one abnormal gland was subsequently found at surgery.

Discussion

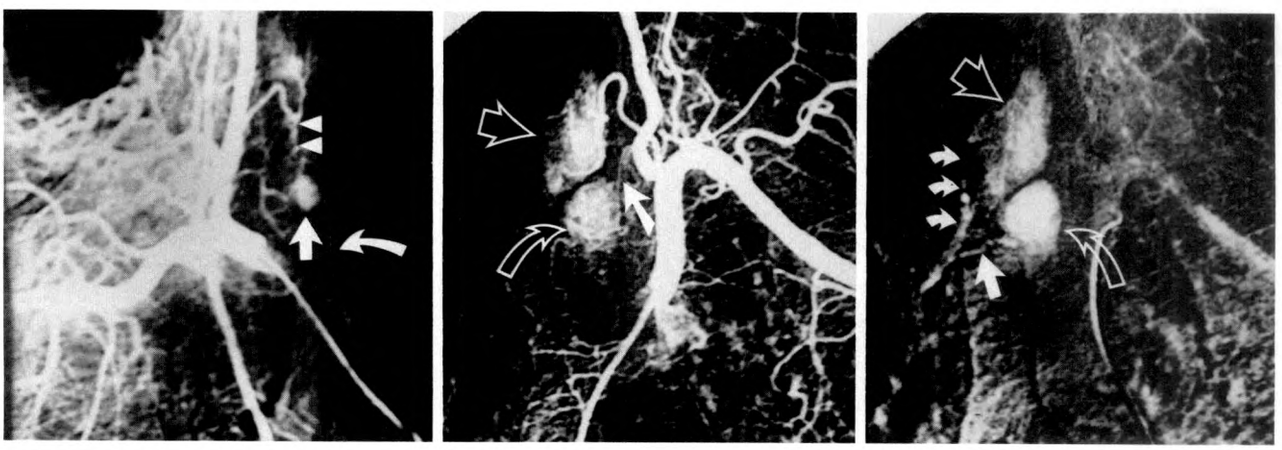
There are several causes of unsuccessful initial neck surgery for primary hyperparathyroidism [6–8]. These include failure to identify parathyroid glands in either a normal or abnormal location, inadequate resection of a parathyroid hyperplasia, and supernumerary glands.

Despite modern imaging procedures like sonography [9–12], CT [13–15], computer-assisted double-isotope scanning [16, 17], and MR imaging [18, 19], the localization of remaining abnormal parathyroid glands may still be possible in only 31% of cases [20].

Sensitivity of selective thyroid and thymic venous samples for parathormone assay is decreased when there are thyroid-thymic vein connections and distortion of the venous anatomy by previous surgery [6, 10, 21]. The detection rate is high when sampling is used in association with selective parathyroid arteriography [2].

Selective arteriography of both superior and inferior thyroid arteries, both internal mammary arteries, and occasionally lingual [22] or thyroidea ima [23] arteries is considered the most sensitive angiographic procedure [9, 14, 21]. Krudy et al. [4] located 11 of 16 cervical enlarged glands in previously operated patients (69%). In another series, 67% of glands in the mediastinum were correctly detected, with the smallest measuring 0.5 cm [2]. Nevertheless, selective parathyroid arteriography cannot be considered the ideal method of locating the parathyroid glands. The prolonged catheterization time often required increases the risks of stroke, radiation exposure, and renal complications in patients who already may have compromised renal function [2].

The good results for IV DSA reported by Levy et al. [3] have not been confirmed in larger series [4, 5]. In previously



A B

Fig. 2.—Right cervical location of parathyroid adenoma in a 45-year-old woman after resection of both hyperplastic superior parathyroid glands for primary hyperparathyroidism. Selective digital subtraction angiography (DSA) of right subclavian artery (frontal view). A tumor blush is visible under right inferior thyroid pole (*straight arrow*). Feeding artery is visible (*arrowheads*) as well as draining veins (*curved arrow*). At reoperation, a hyperplastic right lower parathyroid weighing 500 mg was retrieved; another 60-mg hyperplastic lower parathyroid gland, undetected by arterial DSA, was found on left side of neck.

Fig. 3.—Left cervical parathyroid adenoma.

***A*, Selective digital subtraction angiography (DSA) of left subclavian artery. Right posterior oblique projection (30°). Feeding arteries of adenoma arise from left inferior thyroid artery (*white arrow*). Thyroid (*open straight arrow*) and adenoma (*open curved arrow*) stains.**

***B*, DSA late phase. Localized stains of adenoma (*open curved arrow*) and thyroid (*open straight arrow*). Draining veins of both thyroid (*white curved arrows*) and adenoma (*white straight arrow*) are visible. At surgery, a 4000-mg adenoma was detected under inferior pole of left thyroid lobe.**

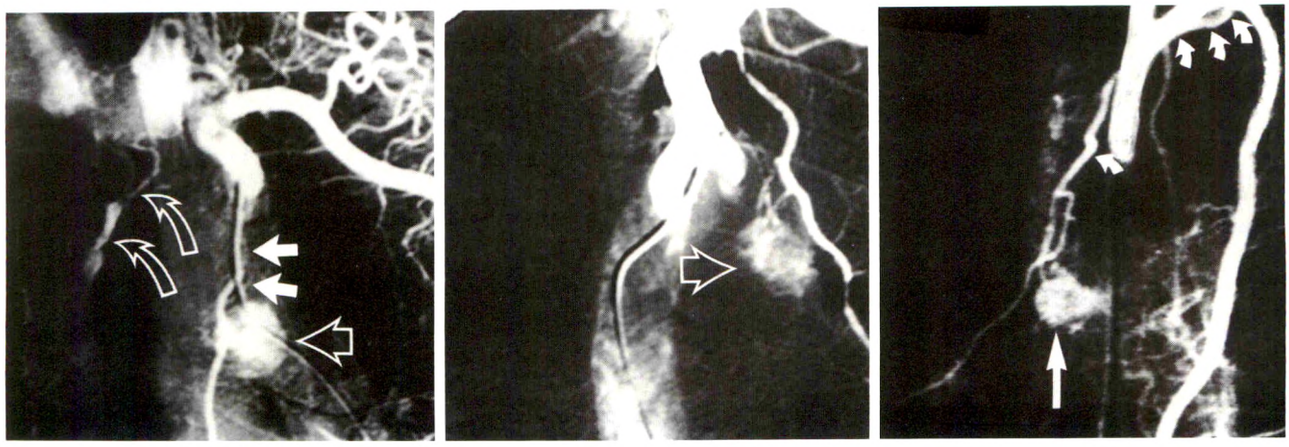


Fig. 4.—Mediastinal location of parathyroid adenoma.

***A*, Selective digital subtraction angiography (DSA) of left subclavian artery (frontal view). Left inferior thyroid artery supplies most of thyroid gland. Small arteries coming from internal mammary artery supply adenoma (*white arrows*). Contrast staining of mediastinal adenoma is seen (*open straight arrow*). Note inferior thyroid veins (*open curved arrows*).**

***B*, Left posterior oblique view. Adenoma lies behind left internal mammary artery (*arrow*). A 3500-mg adenoma of a fifth parathyroid gland was detected at reoperation; it abutted the left main pulmonary artery in a more posterior location than that suspected by intraarterial DSA. It was found at surgery that another feeding artery of the adenoma came directly from the aortic arch.**

Fig. 5.—False-positive examination. Patient with multiple endocrine neoplasia (MEN II A). A tumor blush in the mediastinum is disclosed by selective digital subtraction angiography of left subclavian artery (frontal view, *straight arrow*). Feeding artery originates from left internal mammary artery (*curved arrows*). Left common carotid artery has not been injected. At mediastinal exploration a total excision of thymus and anterior mediastinal fat was performed; a single normal parathyroid was found in right thymic lobe. Hypercalcemia persisted. Subsequently, a total thyroidectomy was performed; an 850-mg adenoma of the left upper parathyroid was recovered high in the neck.

operated patients, intraarterial DSA has been performed either by nonselective injection via the ascending aorta or by selective injections into brachiocephalic arteries [24]. In a report by Krudy et al. [4], seven (44%) of 16 cervical glands were found by aortic arch injection. In this series selective intraarterial DSA did not disclose more diseased glands than did aortic arch injections; sensitivity of both techniques was higher than that of IV DSA (31%).

A large series of previously operated patients examined by selective intraarterial DSA has been reported by Miller et al. [25]. Eighteen (49%) of 37 adenomas were located accurately by this technique, with only one false-positive finding. In the same series, sensitivity was slightly higher for selective parathyroid arteriography (60%) than for selective DSA. Invasive procedures (intraarterial DSA, selective arteriography, parathyroid venous sampling, and intraoperative sonography) permitted localization of adenomas in 95% of cases.

From out study of 18 patients, however, it appears that intraarterial DSA of brachiocephalic vessels can locate most of the remaining abnormal cervical or mediastinal glands, confirming the theoretical advantages of digital imaging over selective parathyroid arteriography. The sensitivity (neck = 73%, mediastinum = 90%) of this technique is higher than that of selective parathyroid arteriography. The specificity, negative predictive value, and overall accuracy of intraarterial DSA, as well as other imaging procedures of parathyroid glands, cannot be evaluated because normal glands cannot be visualized and therefore the number of true-negative results cannot be estimated.

Injection of all brachiocephalic arteries must be systematic, whatever the result of first injections. In our study false-negative results occurred because some injections were omitted. A false-negative result may also occur if a microadenoma lies inside a normal-size gland or when a gland is supplied by a vessel arising directly from the aortic arch. The latter can explain our single false-negative result in the mediastinum.

In the present study, false-positive results did not occur in the cervical area. However, motion artifacts and thyroid tumors can simulate parathyroid enlargement. Motion artifacts are common, but it is usually easy to detect them by reviewing image series in real time. Tumor staining of a thyroid adenoma or carcinoma can mimic a parathyroid tumor, especially in the frontal view. The lateral view of the neck is the best way of distinguishing an intrathyroid from an extrathyroid staining. But confusion can still occur. In fact, most thyroid tumors are detected by preoperative sonography and are resected at the first operation. False-positive results occurred only in the mediastinum (Fig. 5). In this area, tissues are thicker than in the cervical region, and images of tumor blush can be created by lung and heart motion.

How can the important differences between previous reports and our own experience be explained? Injections into brachiocephalic arteries were performed at the same rate and with the same dilution of contrast material (30%). But digital

systems were different and the matrix was only 256 × 512 pixels [4, 24]. Moreover, we have no information concerning exposure factors and the use of equalizing filters [25]. These technical differences may explain such different results.

In summary, localization procedures are strongly recommended in patients requiring reoperation for primary hyperparathyroidism. Among them, selective intraarterial DSA of brachiocephalic arteries appears to be accurate for both cervical and mediastinal parathyroid locations. This technique is easy to perform and well tolerated. Information provided by intraarterial DSA was judged sufficient by the surgeon for reoperation site selection. All reoperated patients with confirmed primary hyperparathyroidism were cured. Intraarterial DSA should be performed when results of noninvasive imaging methods do not concur on the location of remaining glands.

ACKNOWLEDGMENTS

We thank Marie Anne Bourdiol for the photography and Claudine Thepault for secretarial assistance.

REFERENCES

1. Dubost CI, Boucaut PH. Hyperparathyroidie primaire: étude rétrospective de 500 cas. *Presse Med* **1982**;11:443–446
2. Krudy AG, Doppman JL, Brennan MF, et al. The detection of mediastinal parathyroid glands by computed tomography, selective arteriography, and venous sampling. *Radiology* **1981**;140:739–744
3. Levy JM, Hessel SJ, Dippe SE, McFarland JO. Digital subtraction angiography for localization of parathyroid lesions. *Ann Intern Med* **1982**;97: 710–712
4. Krudy AG, Doppman JL, Miller DL, et al. Work in progress—abnormal parathyroid glands: comparison of nonselective arterial digital arteriography, selective parathyroid arteriography, and venous digital arteriography as methods of detection. *Radiology* **1983**;148:23–29
5. Obley DL, Winzelberg GG, Jarmolowski CR, Hydovitz JD, Danowski TS, Wholey MH. Parathyroid adenomas studied by digital subtraction angiography. *Radiology* **1984**;153:449–451
6. Wang CA. Parathyroid re-exploration. A clinical and pathological study of 112 cases. *Ann Surg* **1977**;186:140–145
7. Akerstrom G, Malmaeus J, Bergstrom R. Surgical anatomy of human parathyroid glands. *Surgery* **1984**;95:14–21
8. Thompson NW, Eckhauser FE, Harness JH. The anatomy of primary hyperparathyroidism. *Surgery* **1982**;92:814–821
9. Brennan MF, Norton JA. Reoperation for persistent and recurrent hyperparathyroidism. *Ann Surg* **1985**;205:40–44
10. Clark OH, Stark DD, Gooding GAW, et al. Localization procedures in patients requiring reoperation for hyperparathyroidism. *World J Surg* **1984**;8:509–521
11. Krudy AG, Shawker TH, Doppman JL, et al. Ultrasonic parathyroid localization in previously operated patients. *Clin Radiol* **1984**;35:113–118
12. Reading CC, Charbonneau JW, James EM, et al. Postoperative parathyroid high-frequency sonography: evaluation of persistent or recurrent hyperparathyroidism. *AJR* **1985**;144:399–402
13. Stark DD, Gooding GAW, Moss AA, Clark OH, Ovenfors C-O. Parathyroid imaging: comparison of high-resolution CT and high-resolution sonography. *AJR* **1983**;141:633–638
14. McGarity WC, Goldman AL. Reoperation for primary hyperparathyroidism. *Ann Surg* **1981**;194:134–139
15. Doppman JL, Shawker TH, Krudy AG, et al. Parathymic parathyroid: CT, US, and angiographic findings. *Radiology* **1985**;157:419–423
16. Winzelberg GG, Hydovitz JD, O'Hara KR, et al. Parathyroid adenomas evaluated by Tl-201/Tc-99m pertechnetate subtraction scintigraphy and high-resolution ultrasonography. *Radiology* **1985**;155:231–235
17. Percival RC, Blake GM, Urwin H. Assessment of thallium-pertechnetate subtraction scintigraphy in hyperparathyroidism. *Br J Radiol* **1985**;58: 131–135
18. Kier R, Herfkens RJ, Blinder RA, Leight GS, Utz JA, Silverman PM. MRI with surface coils for parathyroid tumors: preliminary investigation. *AJR* **1986**;147:497–500
19. Spritzer CE, Gefter WB, Hamilton R, Greenberg BM, Axel L, Kressel HY. Abnormal parathyroid glands: high-resolution MR imaging. *Radiology* **1987**;162:487–491
20. Miller DL, Doppman JL, Shawker TH, et al. Localization of parathyroid adenomas in patients who have undergone surgery. Part I. Non-invasive imaging method. *Radiology* **1987**;162:133–137
21. Brennan MF, Doppman JL, Krudy AG, Mark SJ, Spiegel AM, Aurbach GD. Assessment of technique for pre-operative parathyroid gland localization in patients undergoing reoperation for hyperparathyroidism. *Surgery* **1982**;91:6–11
22. Krudy AG, Doppman JL, Brennan MF, Saxe AW, Marx SJ, Parthemore JG. Arteriographic localization of parathyroid adenoma in the presence of lingual thyroid. *AJR* **1981**;136:1227–1230
23. Krudy AG, Doppman JL, Brennan MF. The significance of the thyroidea ima artery in arteriographic localization of parathyroid adenomas. *Radiology* **1980**;136:51–55
24. Krudy AG, Doppman JL, Miller DL, et al. Detection of mediastinal parathyroid glands by nonselective digital arteriography. *AJR* **1984**;142:693–695
25. Miller DL, Doppman JL, Krudy AG, et al. Localization of parathyroid adenomas in patients who have undergone surgery. Part II. Invasive procedures. *Radiology* **1987**;162:138–141

Book Review

The Radiologic Clinics of North America. Organ Transplantation. Guest editors: John F. Cardella and Kurt Amplatz. Philadelphia: Saunders, March 1987; 25(2). By subscription, 4 issues annually, $60

Organ transplantation has become a widely accepted medical therapy although it remains enormously expensive. Therefore, the search for noninvasive methods that can predict graft rejection and other complications of transplantation has intensified. Imaging techniques play an essential role in pre- and postoperative evaluation and in therapeutic intervention.

This issue of the *Radiologic Clinics of North America* was conceived with the purpose of providing a concise reference for the most effective diagnostic and interventional imaging techniques, with overviews of clinical considerations. Regrettably, the editors failed to include the topic of radionuclide evaluation, despite the fact that this technique has been used extensively to evaluate blood flow and function of transplanted organs.

This book is a collection of 13 papers by 32 contributors. It deals primarily with angiographic, sonographic, CT, and MR imaging evaluation of renal, hepatic, pancreatic, and cardiac transplantation. Surgeons who are authorities in the respective fields have written about the clinical and surgical considerations involved in using various imaging procedures and making decisions on clinical management.

The material on each topic is clearly written, readable, and concise. The illustrations are excellent. The authors quote the literature extensively, although they did not include references for all the data on quantitative evaluation (resistance or pulsatility indexes) by duplex sonography. The discussion on pre- and postoperative angiographic assessment of organ transplants is particularly comprehensive and excellent.

Despite unfortunate exclusion of a discussion of nuclear imaging, this book should appeal to diagnostic radiologists, transplant surgeons, and nephrologists to meet their need for an up-to-date guide to the latest radiologic information about organ transplantation. This book may also be of considerable interest to anyone (nuclear physicians, nurses) engaged in the evaluation of transplant patients. It is easy to handle and is recommended for inclusion in personal and departmental libraries.

E. Edmund Kim
University of Texas Medical School
Houston, TX 77030

Memorial Award of the SGR

Cholangiographic Findings in Hepatic Artery Occlusion After Liver Transplantation

Albert B. Zajko[1]
William L. Campbell[1]
Gregory A. Logsdon[1]
Klaus M. Bron[1]
Andreas Tzakis[2]
Carlos O. Esquivel[2]
Thomas E. Starzl[2]

Because the hepatic artery provides the only blood supply to the biliary tree of a liver allograft, posttransplantation arterial occlusion may result in a biliary complication. Cholangiograms were reviewed retrospectively in 31 transplant patients who had proved complete or partial occlusions of the hepatic artery (thrombosis in 29 and marked stenosis in two). Cholangiograms were abnormal in 26 (84%). The most common abnormality, seen in 16 patients, was nonanastomotic contrast leakage from the donor intra- or extrahepatic bile ducts. Strictures of the donor biliary tree occurred in 14 patients, four of whom also had a nonanastomotic bile leak. In 12 of the 14, the strictures were nonanastomotic. Other findings included poor filling of the intrahepatic bile ducts, generalized donor ductal dilatation and irregularity, and intraductal filling defects. Sixteen (89%) of 18 transplants with nonanastomotic contrast leakage had occlusions of the hepatic artery. Of 21 transplants with nonanastomotic strictures, 12 (57%) had occlusions of the hepatic artery. Only two (10%) of 20 transplants with biliary anastomotic strictures had arterial occlusion.

We conclude that liver transplant recipients who exhibit nonanastomotic contrast leakage or nonanastomotic strictures on cholangiography should be evaluated for occlusion of the hepatic artery as the probable cause.

Occlusion of the hepatic artery (thrombosis or stenosis) is an important cause of morbidity and mortality after liver transplantation. Thrombosis of the hepatic artery is the most common and most serious vascular complication after transplantation [1]. It is usually a devastating event that requires retransplantation for survival in most cases [2, 3]. Mortality is 73% without retransplantation and 27% if retransplantation is performed [2]. Stenosis of the hepatic artery anastomosis may require surgical revision or balloon angioplasty. Prompt recognition that occlusion of the hepatic artery is the cause of a poor postoperative course is important to patient survival.

Because the blood supply of the allograft biliary tree is entirely dependent on the hepatic artery, occlusion (thrombosis or stenosis) may result in a biliary complication. Often, the clinical signs of occlusion of the hepatic artery are nonspecific. If the patient has signs of a possible biliary complication, cholangiography may be performed before the diagnosis of occlusion of the hepatic artery is known. In this paper we review the cholangiographic findings in 31 liver transplant patients who had complete or partial occlusions of the hepatic artery. The cholangiographic abnormalities presented are those that should alert the radiologist and surgeon to occlusion of the hepatic artery as the cause of an abnormal postoperative course.

Materials and Methods

During the 6-year period ending January 1, 1987, 742 patients (278 children and 464 adults) received 968 orthotopic liver transplants. We studied all patients with proved partial or complete occlusions of the hepatic artery who also had postoperative cholangiography. Seventy-two (7.4%) of the transplants (in 46 children and 26 adults) had thromboses of the

Received March 19, 1987; accepted after revision May 8, 1987.

Presented at the annual meeting of the Society of Gastrointestinal Radiologists, Scottsdale, AZ, February 8–13, 1987. Recipient of the Memorial Award of the Society of Gastrointestinal Radiologists.

[1] Department of Radiology, University of Pittsburgh School of Medicine, Presbyterian-University Hospital, DeSoto at O'Hara Sts., Pittsburgh, PA 15213. Address reprint requests to A. B. Zajko.

[2] Department of Surgery, University of Pittsburgh School of Medicine, 1084 Scaife Hall, Pittsburgh, PA 15261.

***AJR* 149:485–489, September 1987**
0361–803X/87/1493–0485
© American Roentgen Ray Society

hepatic artery documented by angiography, surgery (retransplantation), or autopsy. Another eight transplants had angiographically proved stenoses of the hepatic artery anastomoses. Cholangiography was performed only in those patients with suspected biliary complications. Thirty-one patients (29 with thromboses and two with marked stenoses) underwent transhepatic or T-tube cholangiography after transplantation. Retrospective review of these cholangiograms forms the basis of this study.

These cholangiograms were compared with a group of 75 transhepatic cholangiograms performed during the study period of liver transplants that had no occlusions of the hepatic artery.

Results

Cholangiograms were abnormal in 26 (84%) of the 31 cases with occlusions of the hepatic artery. Major abnormalities were nonanastomotic contrast leakage and biliary strictures. Biliary strictures were classified as either anastomotic or nonanastomotic (Table 1). Nonspecific findings, such as narrowing and poor filling of peripheral intrahepatic ducts, were seen in three patients. Two patients had normal cholangiograms.

TABLE 1: Prevalence of Hepatic Artery Occlusion in Liver Transplants with Nonanastomotic Bile Leakage and Biliary Strictures

Cholangiographic Findings	Hepatic Artery Occlusion (%)
Nonanastomotic contrast leakage (N = 18)	16 (89)
Nonanastomotic strictures (N = 21)	12 (57)
Isolated anastomotic strictures (N = 20)	2 (10)

Note.— N = number of transplant patients.

Contrast Leakage

Nonanastomotic contrast leakage from the donor intra- or extrahepatic bile ducts was seen in 16 patients (nine children and seven adults) who had occlusions of the hepatic artery (sensitivity, 52%). The bile leaks were hilar or intrahepatic in 15 of the 16 cases. Eight of these were seen as focal collections of contrast material within the hilum and parahilar area (Fig. 1). Four patients had intrahepatic bilomas; three of these also had bilomas in the hilar area (Fig. 2). Diffuse leakage from the central intrahepatic bile ducts was observed in two patients (Fig. 3). In addition to bilomas, one patient also had irregularity, dilatation, and intraluminal filling defects in the entire donor biliary tree (Fig. 4). An extrahepatic nonanastomotic bile leak was seen in one patient (Fig. 5). Poor filling of the intrahepatic ducts (Figs. 2 and 3) and intraluminal filling defects (Figs. 1 and 4) accompanied bile leakage in six and four cases, respectively.

Nonanastomotic intrahepatic contrast leakage was observed in two cases in the group of patients with patent hepatic arteries (specificity, 97%).

The mean interval between the diagnosis of occlusion of the hepatic artery and the demonstration of contrast leakage was 36 days (range, 0–130). In four of the 16 cases, the cholangiographic diagnosis of nonanastomotic bile leak was the initial finding that prompted angiographic evaluation. In the remaining 12 cases, the diagnosis of occlusion of the hepatic artery was known before the cholangiograms were obtained.

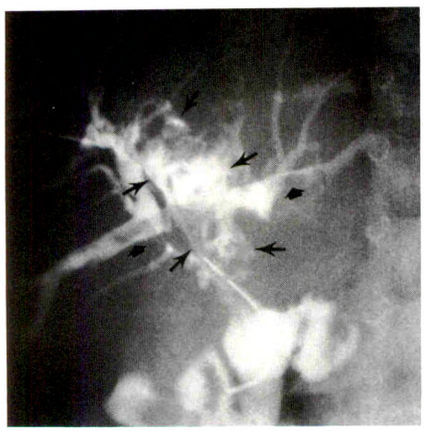


Fig. 1.—Hilar and parahilar biloma. Transhepatic cholangiogram shows contrast leakage into a central biloma cavity (*long arrows*) and filling defects within main right and left hepatic ducts (*short arrows*). Main left hepatic duct cannot be identified. Histologic examination of the hepatectomy specimen after retransplantation showed an infected central biloma cavity with necrosis of main left hepatic duct. Filling defects in right and left hepatic ducts probably represent necrotic debris and biliary sludge.

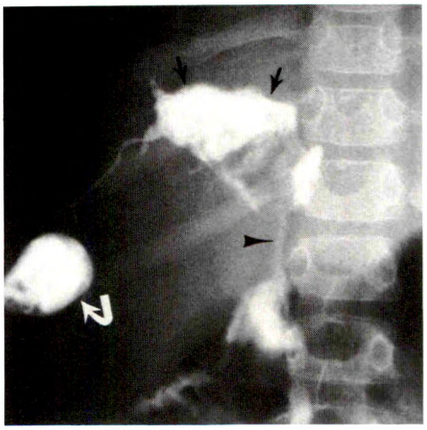


Fig. 2.—Intrahepatic and hilar bilomas. After percutaneous drainage of a peripheral intrahepatic biloma (*curved arrow*), a central hilar biloma (*straight arrows*) is seen to fill via a small right hepatic bile duct. Filling of intrahepatic biliary tree is poor, and main right and left hepatic ducts cannot be identified. Filling of common duct (*arrowhead*) and a Roux limb of jejunum is seen. Histologic examination of hepatectomy specimen after retransplantation showed necrosis of hilar structures with a bile abscess cavity.

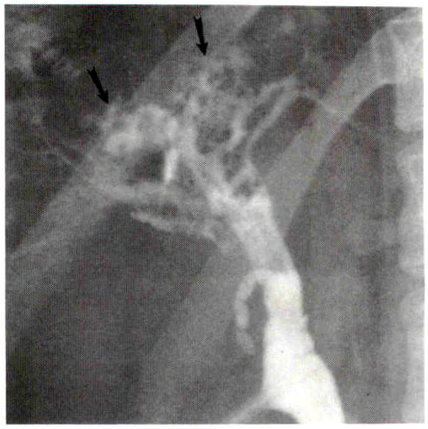


Fig. 3.—Diffuse bile leak. T-tube cholangiogram shows extensive contrast leakage (*arrows*) from central hepatic bile ducts. Ductal irregularity and poor filling of peripheral intrahepatic bile ducts are evident. Histologic examination of hepatectomy specimen after retransplantation showed bile duct necrosis with multiple hepatic infarcts and abscesses. (Reproduced with permission from Campbell and Zajko [4].)

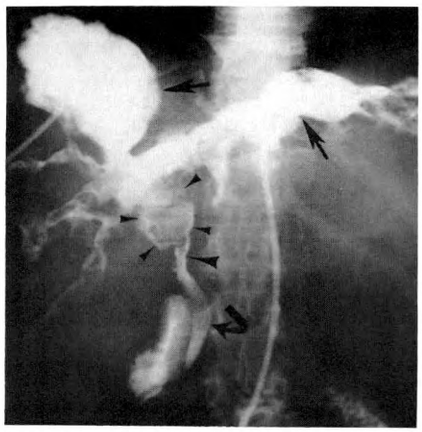


Fig. 4.—Necrosis of entire donor biliary tree. Sinogram 6 weeks after percutaneous drainage of fluid collections in right and left hepatic lobes (*straight arrows*) shows communication with biliary tree. Generalized ductal irregularity and dilatation with diffuse intraluminal filling defects are seen. Note hilar biloma cavity (*small arrowheads*) that replaces donor common duct. Recipient common bile duct (*curved arrow*) below biliary anastomosis (*large arrowhead*) is normal. Histologic examination of the hepatectomy specimen after retransplantation showed bile duct necrosis with purulent and necrotic material filling donor biliary tree.

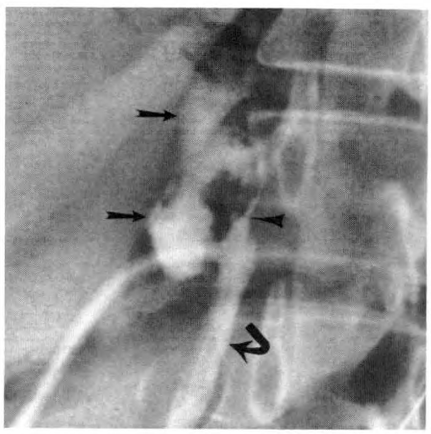


Fig. 5.—Nonanastomotic extrahepatic bile leak. T-tube cholangiogram shows contrast leakage (*straight arrows*) above choledochocholedochostomy (*arrowhead*) with no filling of donor biliary tree. Recipient common bile duct (*curved arrow*) is normal. Donor common duct was completely necrotic at laparotomy.

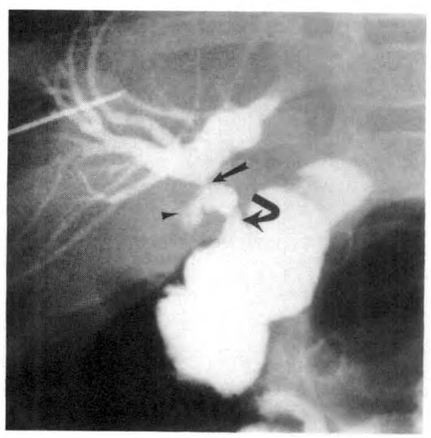


Fig. 6.—Nonanastomotic biliary stricture. Transhepatic cholangiogram shows partial biliary obstruction due to a severe stricture in common hepatic bile duct (*straight arrow*). Note that choledochojejunostomy anastomosis (*curved arrow*) is patent. Remnant (*arrowhead*) of donor cystic duct is also filled.

Biliary Strictures

Biliary strictures occurred in 14 patients (eight children and six adults) who had occlusions of the hepatic artery. Nonanastomotic strictures occurred in 12 of the 14 patients (sensitivity, 39%), three of whom also had bilomas. None of these strictures occurred at the previous site of a T-tube insertion. In two of the 12, choledochojejunostomy stricture was also present. In seven patients, the stricture developed in the common hepatic duct (Fig. 6); in four of these seven, the stricture extended into the bifurcation and involved both the main right and left hepatic ducts. Intrahepatic strictures of secondary and tertiary branches occurred in the other five patients. One of the five patients had a single stricture (Fig. 7A) that progressed to complete obstruction within 16 days (Fig. 7B). This patient also had an intrahepatic biloma. Multiple intrahepatic strictures developed in the other four patients (Fig. 8).

Isolated anastomotic strictures at a Roux-en-Y choledochojejunostomy were observed in two of the 14 patients, one of whom also had a biloma.

If two children in whom biliary stricture was discovered at 12 and 20 months after occlusions of the hepatic artery are excluded, the mean interval between the diagnosis of arterial occlusion and the cholangiographic demonstration of biliary stricture was 62 days (range, 1–154).

Five of the 14 patients presented with suspected biliary obstruction. The cholangiographic diagnosis of nonanastomotic biliary stricture prompted angiographic evaluation. In the remaining nine patients, the diagnosis of occlusion of the hepatic artery was known before the cholangiograms were obtained.

In the group of patients with patent hepatic arteries, nonanastomotic biliary strictures were observed in nine cases (specificity, 88%). Anastomotic strictures occurred in 18 cases.

Discussion

The arterial blood supply to the biliary tree is complex. The hepatic artery is the major blood supply to the hilar and portal tract structures [5, 6]. The intrahepatic biliary tree (above the common hepatic duct bifurcation) is supplied mainly by hepatic arterial branches [6–8]. The extrahepatic bile duct receives its blood supply from several sources, most commonly the retroduodenal branch of the gastroduodenal artery, the retroportal artery from the celiac axis or superior mesenteric artery, and the descending branches of the right hepatic artery [7].

At donor hepatectomy, the retroportal artery and the branches from the gastroduodenal artery are severed. This leaves the hepatic artery to provide the entire blood supply to the donor biliary system after transplantation. Arterial occlusion due to thrombosis or stenosis of the hepatic artery therefore may lead to ischemia and cause donor intra- or extrahepatic bile duct complications.

Biliary complications will not develop clinically in all transplant patients who have occlusion of the hepatic artery. In most transplant patients who have occlusion, the diagnosis

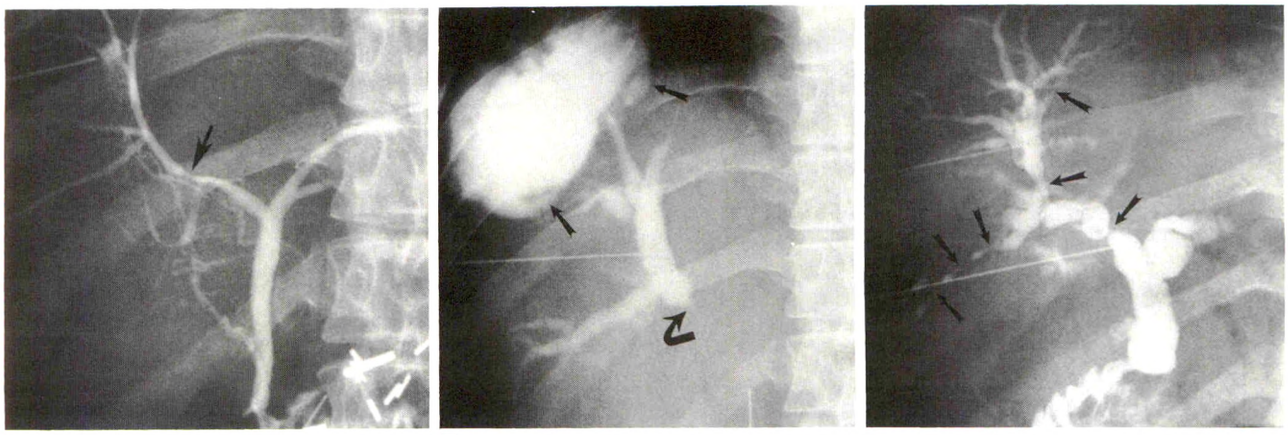


Fig. 7.—Intrahepatic biliary stricture.
A, Transhepatic cholangiogram shows stricture of right hepatic duct (*arrow*).
B, Transhepatic cholangiogram 16 days later shows complete obstruction of previously strictured right hepatic duct (*curved arrow*). Contrast leakage occurred from obstructed duct and filled a peripheral intrahepatic biloma cavity (*straight arrows*) that had been drained percutaneously earlier the same day.

Fig. 8.—Transhepatic cholangiogram shows multiple intrahepatic biliary strictures (*arrows*). Histologic examination of liver at autopsy showed arterial occlusion due to severe chronic rejection, with multiple bile duct infarcts and strictures.

is made early. Most of these patients undergo retransplantation for liver failure or hepatic necrosis before biliary complications develop.

The three main clinical presentations of posttransplantation thrombosis of the hepatic artery are fulminant hepatic necrosis, bile leak, and relapsing bacteremia [2]. Sonography often is performed in these settings to evaluate patency of the hepatic artery (by means of pulsed Doppler examinations) [9] and to evaluate for possible biliary abnormalities, especially if a bile leak or obstruction is suspected. Duplex Doppler sonography is an excellent screening test for detection of thrombosis of the hepatic artery [9]. However, we have observed a high false-negative rate with sonography for suspected biliary complications in transplant patients (Zajko AB, unpublished data). In the immunosuppressed liver transplant recipient, serious biliary complications are associated with a high mortality if not diagnosed and treated promptly. For this reason, cholangiography may be the first procedure performed in transplant patients who have suspected biliary complications.

In transplant patients, the indications for cholangiography are not absolute. The most common indication is suspected biliary obstruction. Other common indications include unexplained elevation of liver enzyme levels or fever and suspected biloma on noninvasive imaging [10, 11]. Bilomas usually appear as parahilar fluid collections on CT and sonography. Because of their high association with thrombosis of the hepatic artery, occasionally these findings have led directly to angiographic evaluation. A complete analysis of noninvasive imaging in posttransplantation thrombosis of the hepatic artery, including duplex sonography and CT, is currently underway and will be the subject of a separate report.

Bile leakage is the most common complication after transplantation in patients with biliary anastomosis via choledochocholedochostomy [12]. Most bile leaks occur at the T-tube choledochotomy and, if small, may close spontaneously [10]. Leaks occurring at the choledochocholedochostomy or choledochojejunostomy sites generally require revision of the anastomosis [12]. The demonstration of nonanastomotic contrast leakage on cholangiography strongly suggests that occlusion of the hepatic artery has occurred. Of 18 transplants with nonanastomotic contrast leakage seen on cholangiography, 16 (89%) had occlusion of the hepatic artery (Table 1). Retransplantation usually is required for survival. Two patients with patent hepatic arteries had intrahepatic contrast leakage into liver abscesses that communicated with the biliary tree [11].

Nonanastomotic leaks may occur from the extra- or intrahepatic donor biliary tree (Figs. 1–5). Tzakis et al. [2] reported their findings in seven transplant patients with extrahepatic bile leaks and thromboses of the hepatic artery; all had donor common duct necrosis at laparotomy (Fig. 5). If thrombosis of the hepatic artery results in necrosis of intrahepatic bile ducts, a hilar or intrahepatic biloma may develop (Figs. 1, 2, and 4). These bilomas frequently become secondarily infected. We have performed percutaneous drainage in most cases until such time as a suitable donor liver was available for retransplantation [11]. Bile duct necrosis [13] and cysts [14, 15] also have been reported to occur in nontransplant patients after occlusion of the hepatic artery by embolization.

Two patients had diffuse bile leakage from the central intrahepatic bile ducts (Fig. 3). This finding may represent the earliest cholangiographic change in bile duct ischemia and necrosis before formation of a frank biloma. In the first patient, the amount of leakage was small and was overlooked at first. A central biloma eventually formed, which was drained percutaneously. The patient required retransplantation after several months. In the second patient, the sole indication for the

cholangiogram (Fig. 3) was elevation of liver enzyme levels. On demonstration of the nonanastomotic bile leak, angiography was performed, which showed thrombosis of the hepatic artery. The patient underwent retransplantation 3 days later.

Biliary stricture is the most common cause of biliary obstruction after transplantation [11]. Biliary strictures can be classified as anastomotic or nonanastomotic. Most anastomotic strictures can be explained on the basis of scar formation with retraction and narrowing, although ischemia also may be a factor [7, 16]. Of 20 liver transplants with isolated anastomotic strictures, only two (10%) had occlusions of the hepatic artery (Table 1).

Most nonanastomotic strictures in the liver transplant biliary tree probably are due to ischemia. Of 21 transplants with nonanastomotic strictures, 12 (57%) had occlusions of the hepatic artery (Table 1). In patients without transplants, bile duct strictures have been shown to occur after peripheral hepatic artery embolization [17]. These strictures result from occlusion of the end arterial supply of the bile duct, the peribiliary vascular plexus. Strictures have not been reported to occur after more proximal occlusion of the hepatic artery. With proximal occlusions in patients without transplants, collateral arterial inflow develops rapidly and protects the liver [14]. However, in liver allografts, thrombosis of the hepatic artery effectively produces complete dearterialization of the liver because all potential extrahepatic collateral pathways have been severed.

Extrahepatic hepatopetal arterial collaterals have been shown in approximately 30% of children with liver transplants who have thromboses of the hepatic artery [1]. These collaterals probably are responsible for allograft survival in most of these children. Arterial collaterals also have been documented in several children in the current study. We have not observed these collaterals in adults who have transplants. In patients without transplants, hepatopetal collaterals develop rapidly after arterial occlusion and prevent ischemic injury. However, in liver allografts, these collaterals probably require a longer time to develop because they must arise de novo. Therefore, they may not be effective in preventing hepatic ischemic injury in all cases.

We speculate that posttransplantation nonanastomotic biliary leaks and strictures may represent a spectrum of ischemic injury from occlusion of the hepatic artery. Biliary strictures may develop after less severe ischemic disease, which allows the bile duct to heal with fibrosis and ductal stenosis. Bile leaks, on the other hand, result from duct necrosis, probably due to severe ischemia. Among other possible unknown factors, collateral circulation may have a role in preventing severe ischemic injury in some cases.

Ischemic injury also may occur during organ harvesting [18, 19] or result from chronic rejection. Severe chronic rejection can produce vascular compromise and ischemia by causing progressive narrowing and eventual occlusion of intrahepatic arteries [5]. Of the 21 transplants with nonanastomotic biliary strictures diagnosed by cholangiography, nine did not have occlusions of the hepatic artery. The cause of strictures in these patients is uncertain. Potential causes include harvesting injury, recurrent sclerosing cholangitis, ascending cholangitis, cytomegalovirus infection, and cholangiocarcinoma.

ACKNOWLEDGMENT

We thank Maggie Zdrodowski for manuscript preparation.

REFERENCES

1. Wozney P, Zajko AB, Bron KM, Point S, Starzl TE. Vascular complications after liver transplantation: a 5-year experience. *AJR* **1986**;147:657–663
2. Tzakis AG, Gordon RD, Shaw BW Jr, Iwatsuki S, Starzl TE. Clinical presentation of hepatic artery thrombosis after liver transplantation in the cyclosporine era. *Transplantation* **1985**;40:667–671
3. Shaw BW Jr, Gordon RD, Iwatsuki S, Starzl TE. Hepatic retransplantation. *Transplant Proc* **1985**;17:264–271
4. Campbell WL, Zajko AB. Radiology of liver transplantation. *In*: Taveras JM, Ferrucci JT, eds. *Radiology: diagnosis/imaging/intervention*. Philadelphia: Lippincott (in press)
5. Demetris AJ, Jaffe R, Starzl TE. A review of adult and pediatric posttransplant liver pathology. In: Rosen PP, Fechner RE, eds. *Pathology annual*, part II. Norwalk, CT: Appleton-Century-Crofts (in press)
6. Rappaport AM. Physioanatomic considerations. In: Schiff L, Schiff ER, eds. *Diseases of the liver*, 5th ed. Philadelphia: Lippincott, **1982**:1–57
7. Northover JMA, Terblanche J. A new look at the arterial supply of the bile duct in man and its surgical implications. *Br J Surg* **1979**;66:379–384
8. Cho KJ, Lunderquist A. The peribiliary vascular plexus: the microvascular architecture of the bile duct in the rabbit and in clinical cases. *Radiology* **1983**;147:357–364
9. Segel MC, Zajko AB, Bowen A, et al. Doppler ultrasound as a screen for hepatic artery thrombosis after liver transplantation. *Transplantation* **1986**;41:539–541
10. Zajko AB, Campbell WL, Bron KM, et al. Cholangiography and interventional biliary radiology in adult liver transplantation. *AJR* **1985**;144:127–133
11. Zajko AB, Bron KM, Campbell WL, Behal R, Van Thiel DH, Starzl TE. Percutaneous transhepatic cholangiography and biliary drainage after liver transplantation: a five-year experience. *Gastrointest Radiol* **1987**;12:137–143
12. Lerut J, Gordon RD, Iwatsuki S, et al. Biliary tract complications in human orthotopic liver transplantation. *Transplantation* **1987**;43:47–51
13. Makuuchi M, Sukigara M, Mori T, et al. Bile duct necrosis: complication of transcatheter hepatic arterial embolization. *Radiology* **1985**;156:331–334
14. Doppman JL, Dunnick NR, Girton M, Fauci AS, Popovsky MA. Bile duct cysts secondary to liver infarcts: report of a case and experimental production of small vessel hepatic artery occlusion. *Radiology* **1979**;130:1–5
15. Peterson IM, Neumann CH. Focal hepatic infarction with bile lake formation. *AJR* **1984**;142:1155–1156
16. Terblanche J, Allison HF, Northover JMA. An ischemic basis for biliary strictures. *Surgery* **1983**;94:52–57
17. Doppman JL, Girton ME. Bile duct scarring following ethanol embolization of the hepatic artery: an experimental study in monkeys. *Radiology* **1984**;152:621–626
18. McMaster P, Walton RM, White DGD, Medd RK, Syrakos TP. The influence of ischaemia on the biliary tract. *Br J Surg* **1980**;67:321–324
19. Esquivel CO, Jaffe R, Gordon RD, Iwatsuki S, Shaw BW Jr, Starzl TE. Liver rejection and its differentiation from other causes of graft dysfunction. *Semin Liver Dis* **1985**;5:369–374

Book Review

Computed Tomography of the Gastrointestinal Tract. Edited by Alec J. Megibow and Emil J. Balthazar. St. Louis: Mosby, 463 pp., 1986. $67.50

This excellent and valuable book by editors Megibow and Balthazar and nine contributing authors aims to evaluate the "role, significance, indications, and limitations of computed tomography of the gastrointestinal tract." The book deals specifically with CT examination of the normal and abnormal digestive tube from esophagus to anus. Conditions affecting the peritoneal cavity and mesentery are presented also. Primary CT evaluation of the solid abdominal viscera (liver and biliary tract, pancreas, spleen) is not included.

The heart of the book consists of five chapters on the esophagus, stomach, duodenum, small intestine, and colon. Each chapter develops logically, beginning with indications for CT evaluation and moving through examination techniques, normal anatomy, and pathologic conditions. A valuable first chapter is devoted to a detailed discussion of techniques for performing gastrointestinal CT, including conventional methods of oral, rectal, and IV contrast administration as well as air contrast techniques. A useful discussion of percutaneous drainage of abdominal abscesses and fluid collections is provided. The final chapter is an appendixlike atlas of radiologic-pathologic correlations.

The book is succinctly and clearly written. Although the text is multiauthored, the writing styles blend well. Overlap of subject matter is minimal. Numerous illustrations are provided; most are high-quality, recent-generation CT images. Figures are large, and only rarely are featured abnormalities difficult to appreciate. Correlative barium studies are provided when appropriate.

The authors are careful to remind the reader that in most gastrointestinal disease, CT is complementary to barium studies and endoscopy. They point out conditions in which CT is particularly useful. Where available, quantitative data, for example, on detection rates, accuracy, sensitivity, and specificity, are provided to give the reader perspective. Discussion and recommendations on currently unsettled topics, such as the value of CT in tumor staging, are measured and balanced.

This work is organized differently than another recent book on the same subject, *Computed Tomography of the Gastrointestinal Tract, Including the Peritoneal Cavity and Mesentery* by Meyers. The latter contains chapters based primarily on diseases or disease groups. It is a somewhat smaller book, both in number of pages and page size. These two books together make up a valuable resource on gastrointestinal tract CT. The Megibow and Balthazar book is particularly noteworthy for its breadth of conditions discussed, the quality of its illustrations, and its authoritative emphasis on optimal technique.

On the negative side, it is perhaps quibbling to note that it contains a smattering of typographical errors and misspellings. Some diseases are not discussed, but they are not serious omissions. The material on radiologic-pathologic correlation, although interesting and well done, probably does not warrant a separate chapter.

In conclusion, this book admirably meets the authors' stated aims. Radiologists who perform body CT will benefit from this book, whether they are specifically examining the gastrointestinal tract or are seeking information about an abnormality serendipitously discovered. The book also will be useful to radiology residents, to gastroenterologists, and to surgeons involved in the treatment of gastrointestinal tract disease.

William L. Campbell
University of Pittsburgh School of Medicine
Pittsburgh, PA 15213

Focal Fatty Change of the Liver Adjacent to the Falciform Ligament: CT and Sonographic Findings in Five Surgically Confirmed Cases

Jun Yoshikawa[1]
Osamu Matsui[1]
Tsutomu Takashima[1]
Hitoshi Sugiura[2]
Kanji Katayama[3]
Yoshio Nishida[3]
Masahiko Tsuji[4]

Five cases of surgically confirmed focal fatty infiltration of the liver were detected by CT and sonography. In all five cases, the abnormality was located at the anterolateral edge of the medial segment of the liver. It was seen as a small area of low attenuation adjacent to the falciform ligament on CT and as an echogenic area next to the ligamentum teres on sonography. Dynamic CT performed during infusion of contrast medium via the superior mesenteric artery (arterial portography) showed portal blood flow within the lesion and was useful for excluding the presence of a hepatic tumor.

Focal fatty infiltration of the liver adjacent to the falciform ligament constitutes a diagnostic pitfall on CT and sonography.

Irregular [1] or focal [2, 3] fatty infiltration of the liver is a well-recognized entity. On CT and sonography, it usually can be distinguished from space-occupying lesions in the liver by its nonspherical or geographic pattern, absence of mass effect, and penetration by branches of the hepatic and portal veins [4–6]. However, when it has the appearance of a small nodule, it can be confused with various focal hepatic diseases [7–9]. We describe five surgically confirmed cases of this abnormality that were detected adjacent to the falciform ligament by CT and sonography.

Materials and Methods

Between June 1985 and December 1986, we encountered five patients in whom focal fatty change of the liver adjacent to the falciform ligament was discovered incidentally on CT and sonographic examinations performed to detect cholelithiasis or liver metastasis. CT scans and sonograms were analyzed, and the patients' clinical records were reviewed. All of the patients were women (average age, 64 years; range, 47–57 years) and had cholelithiasis (three cases) or sigmoid colon cancer (one case) or both (one case). Their liver function tests were normal except for one patient whose alkaline phosphatase level was slightly elevated. One had diabetes. None had a history of alcoholism. CT studies were performed with a Somatom DR2 scanner with a section thickness of 8 mm (three cases) or with a GE CT/T9800 scanner with a section thickness of 10 mm (two cases). All CT scans were obtained with and without IV contrast material. Sonography was performed in all cases with a 3.5- or 5-MHz transducer of Aloka SSD-270 or Toshiba SAL 77A. Angiography was done in two cases. Dynamic CT was carried out during injection of contrast medium (65% meglumine amidotrizoate) in one case. The medium was injected via a catheter in the superior mesenteric artery at an estimated rate of 1 ml/sec, with a total dose of 10 ml [10]. In all patients, the lesion was resected during surgery performed for unrelated reasons, and the diagnosis of focal fatty infiltration of the liver was established histologically.

Results

CT scans showed a small area of low attenuation in the anterolateral part of the medial segment of the liver adjacent to the falciform ligament (Fig. 1). In all but one case, the lesions were shown on both plain and enhanced CT scans. In this case,

Received February 11, 1987; accepted after revision May 22, 1987.

[1] Department of Radiology, School of Medicine, Kanazawa University, Takaramachi 13-1, Kanazawa, 920 Japan. Address reprint requests to J. Yoshikawa.

[2] Department of Pathology, School of Medicine, Kanazawa University, Takaramachi 13-1, Kanazawa, 920 Japan.

[3] Department of Surgery, Kurobe Municipal Hospital, Mikkaichi 1108-1, Kurobe, 938 Japan.

[4] Department of Surgery, Toyama Prefectural Central Hospital, Nishinagae 2-2-78, Toyama, 930 Japan.

AJR 149:491–494, September 1987
0361–803X/87/1493–0491
© American Roentgen Ray Society

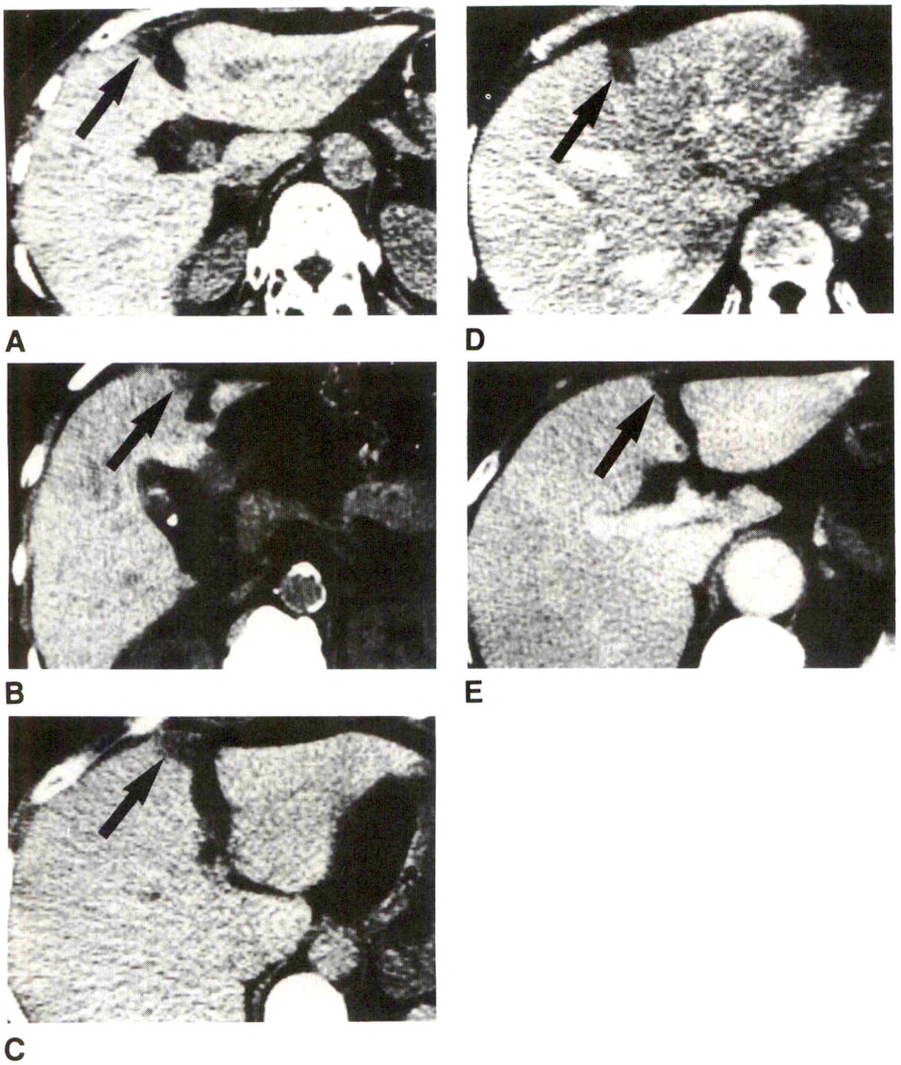


Fig. 1.—CT findings in five cases show a well-circumscribed area of low attenuation (*arrows*) in anterolateral part of medial segment of liver adjacent to falciform ligament.
A–C, Plain CT scans.
D and *E*, Enhanced CT scans.

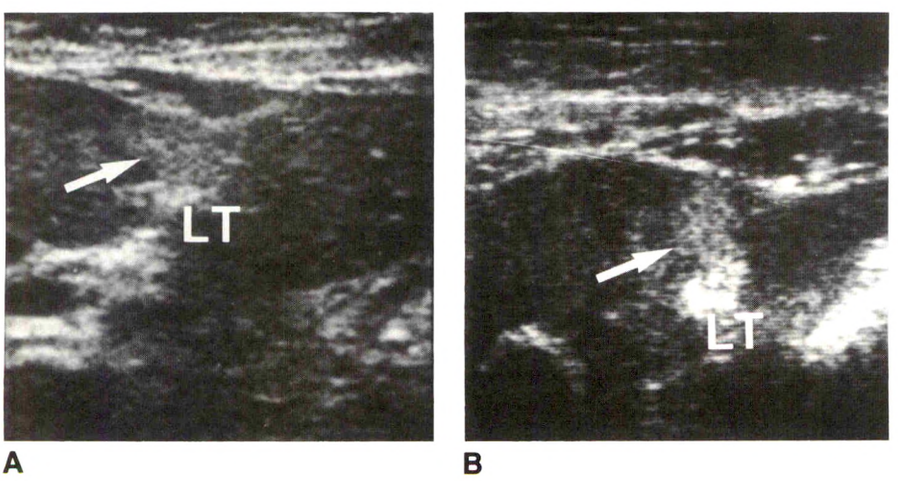


Fig. 2.—Transverse sonograms of two cases show an echogenic area (*arrows*) adjacent to highly echogenic ligamentum teres (LT). *A*, 62-year-old woman. *B*, 56-year-old woman.

the lesion was not shown on plain CT because of the patient's inadequate breath-holding. The mean attenuation value ranged from 0 to 25 H on plain CT, and only slight enhancement was observed when IV contrast medium was administered. In two cases, sonography showed an echogenic area next to the ligamentum teres (Fig. 2). Selective hepatic arteriography and arterial portography showed no abnormality. Dynamic CT performed during arterial portography in one case showed portal blood flow within the lesion (Fig. 3).

In all cases, the lesion was seen at surgery as a well-circumscribed yellow area in the anterior surface of the medial segment of the liver adjacent to the falciform ligament. In one patient, a similar yellow area was seen in the lateral segment of the liver adjacent to the falciform ligament. In two cases, the lesion bulged slightly from the surface of the liver and resembled a true hepatic tumor. In all cases, histologic examination showed focal fatty infiltration of the liver surrounded by normal or a slightly fatty liver parenchyma (Fig. 4).

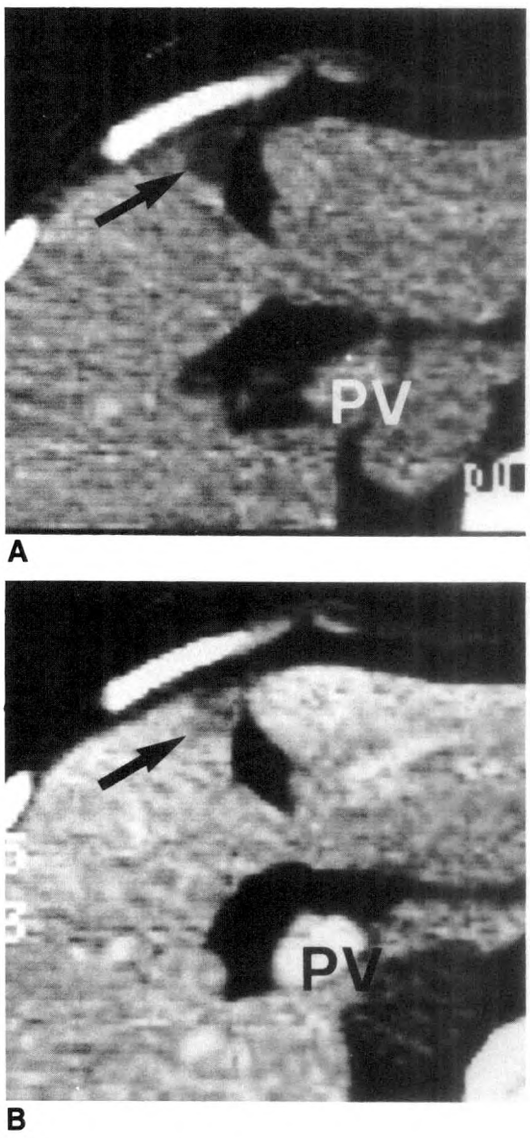


Fig. 3.—Dynamic CT performed during infusion of contrast medium into superior mesenteric artery. Lesion is enhanced, and contrast medium is seen in portal vein (PV), suggesting portal blood flow within lesion (*arrows*). *A*, Before infusion. *B*, Dynamic study.

Discussion

Fatty infiltration of the liver is a well-recognized entity both histologically and radiologically. Generally, it is diffuse, but occasionally it is irregular or focal [1–3]. It is associated most commonly with alcohol abuse, but it also is seen with morbid obesity, diabetes mellitus, pregnancy, steroid therapy, malnutrition, chemotherapy, and hyperalimentation. The cause of focal fatty infiltration is uncertain. Brawer et al. [11] postulated that focal tissue hypoxia might explain the focal nature of the fatty infiltration.

Typically, focal fatty infiltration of the liver is seen as a nonspherical, fan- or geographic-shaped lesion of decreased attenuation on CT and as a hyperechoic area on sonography without significant displacement of adjacent hepatic and portal veins. Sulfur colloid scintigraphy shows no corresponding photon-deficient area [1, 2], but selective uptake and retention of xenon on xenon ventilation scans have been reported [12].

Usually, focal fatty infiltration of the liver can be distinguished easily from space-occupying lesions. However, when it assumes the configuration of a nodule, as in the cases presented here, accurate diagnosis may be difficult. In these cases, differential diagnosis includes true hepatic tumors, such as hepatocellular carcinoma; metastasis; and cavernous hemangioma. When the diagnosis is uncertain, invasive procedures, such as percutaneous liver biopsy [8, 9] or peritoneoscopy [13], are needed. In one of our cases, dynamic CT during arterial portography revealed portal blood flow within the lesion, suggesting that it was not a true hepatic tumor, so fatty infiltration of the liver was considered. This method is less invasive than percutaneous liver biopsy and peritoneoscopy.

Brawer et al. [11] reported a case of focal fatty change that occurred adjacent to the falciform ligament at the watershed of the arterial blood supply, an area in which hepatic infarction has been observed. Kawashima et al. [13] also reported a case of focal fatty infiltration similar to ours in which the diagnosis was confirmed by peritoneoscopy. We consider that the regional tissue hypoxia leading to focal fatty change tends to occur around the falciform ligament in the liver, although the exact reason for this is unclear. Because a small area of low attenuation at the edge of the medial segment of the liver may be attributed to partial volume phenomenon, with fat in the hepatic hilum, it is possible that focal fatty infiltration has been overlooked in the past. We predict that these lesions will be noted with increased frequency through use of high-resolution, thin-slice CT scanners.

The findings in our patients suggest that if a focal area of low attenuation on CT or an echogenic area on sonography is identified adjacent to the falciform ligament, focal fatty infiltration of the liver is likely, and further diagnostic proce-

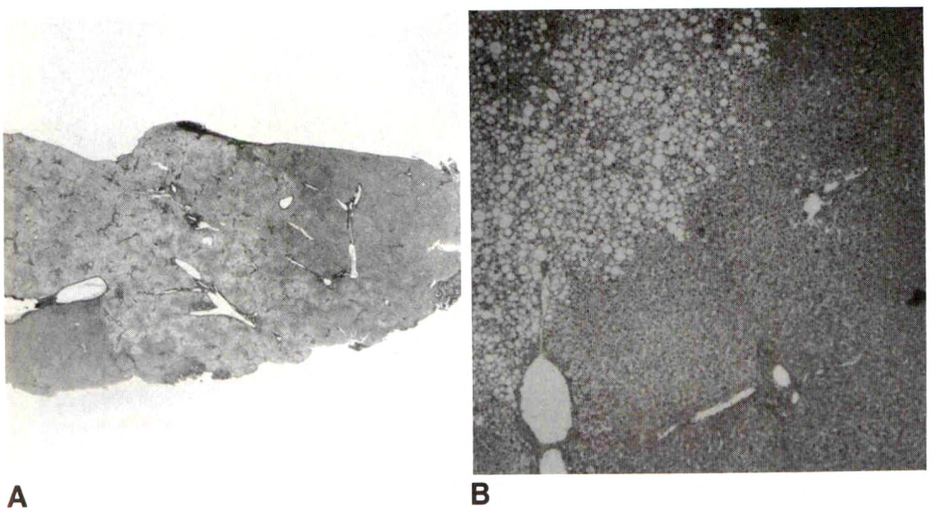


Fig. 4.—Resected specimen from a 62-year-old woman shows focal fatty liver surrounded by normal liver parenchyma.
***A*, Gross specimen.**
***B*, Photomicrograph.**

dures should be avoided. However, in a patient with a known extrahepatic malignancy or liver cirrhosis, a follow-up imaging examination in 2 or 3 months is recommended because the CT and sonographic appearances do not distinguish focal fatty infiltration from a true neoplasm.

REFERENCES

1. Scott WW, Sanders RC, Siegelman SS. Irregular fatty infiltration of the liver: diagnostic dilemmas. *AJR* **1980**;135:67–71
2. Halvorsen RA, Korobkin M, Ram PC, Thompson WH. CT appearance of focal fatty infiltration of the liver. *AJR* **1982**;139:277–281
3. Bashist B, Hecht HL, Harley WD. Computed tomographic demonstration of rapid changes in fatty infiltration of the liver. *Radiology* **1982**;142: 691–692
4. Sawada S, Kawa S, Murata T, Tanaka Y, Konishi T, Fukagae N. Localized fatty infiltration of the liver: CT demonstration of its disappearance on treatment. *Acta Radiol Diagn* **1983**;24:359–361
5. Clain JE, Stephens DH, Charboneau YW. Ultrasonography and computed tomography in focal fatty liver. *Gastroenterology* **1984**;87:948–952
6. Gale ME, Gerzof SG, Robbins AH. Portal architecture: a differential guide to fatty infiltration of the liver on computed tomography. *Gastrointest Radiol* **1983**;8:231–236
7. Baker ME, Silverman PM. Nodular focal fatty infiltration of the liver: CT appearance. *AJR* **1985**;145:79–80
8. Flournoy JG, Potter JL, Sullivan BM, Gerza CB, Ramzy I. CT appearance of multifocal hepatic steatosis. *J Comput Assist Tomogr* **1984**;8:1192–1194
9. Yates CK, Streight RA. Focal fatty infiltration of the liver simulating metastatic disease. *Radiology* **1986**;159:83–84
10. Matsui O, Kadoya M, Suzuki M, et al. Dynamic sequential computed tomography during arterial portography in the detection of hepatic neoplasms. *Radiology* **1983**;146:721–727
11. Brawer MK, Austin GE, Lewin KJ. Focal fatty change of the liver, a hitherto poorly recognized entity. *Gastroenterology* **1980**;78:247–252
12. Patel S, Sandler CM, Rauschkolb EN, McConnel BJ. ^{133}Xe uptake in focal hepatic fat accumulation: CT correlation. *AJR* **1982**;138:541–544
13. Kawashima A, Suehiro S, Murayama S, Russel WJ. Focal fatty infiltration of the liver mimicking a tumor: sonographic and CT features. *J Comput Assist Tomogr* **1986**;10:329–331

The Inferior Accessory Hepatic Fissure:
Sonographic Appearance

Jae Hoon Lim[1]
Young Tae Ko[1]
Man Chung Han[2]
Chu Wan Kim[2]
Byung Ihn Choi[2]
Jung Gi Im[2]

The inferior accessory hepatic fissure, a coronal or parasagittal fissure through the parenchyma of the posterior segment of the right hepatic lobe, was observed sonographically in 15 of 2000 patients. The fissure was seen as a thin, echogenic membrane stretching downward from the right branch of the portal vein to the inferior surface of the right hepatic lobe. On cadaveric sections, the fissure was an invagination of peritoneum directed laterally and slightly posteriorly from the medial inferior surface of the right hepatic lobe below the porta hepatis.

Although the sonographic and CT appearance of the major hepatic fissures have been well described in the literature [1, 2], there has been no discussion of an accessory fissure that occurs in the posterior segment of the right hepatic lobe. This fissural variation, however, has been present in several published illustrations of anatomic sections [3, 4]. Since our first sonographic observation of a short coronal fissure in the posterior segment of the right hepatic lobe, we observed the fissure on sonograms in 15 patients. In this article, we describe the sonographic appearance of the fissure and correlate it with anatomic findings in a cadaver.

Materials and Methods

We have observed an accessory fissure in the posterior segment of the right lobe of the liver in 15 of 2000 abdominal sonograms performed from October 1986 to January 1987. Sonograms were obtained with commercially available real-time scanners using a 3.5-MHz transducer. Longitudinal, oblique, and transverse scans of the liver were made with the patient in the supine position.

For the further study of the fissural anatomy, we reviewed anatomic sections from two cadavers. One cadaver was sectioned transversely and the other was sectioned sagittally. These cadavers were not prepared specifically for the hepatic fissures but for the general sectional anatomy.

Results

The inferior accessory hepatic fissure, demonstrated sonographically in 15 patients, was seen as a thin, echogenic membrane 0.5 mm thick. Lying in or between the coronal or parasagittal planes, the fissure passes inferiorly through the parenchyma of the posterior segment of the right hepatic lobe (Figs. 1 and 2). Its upper limit is the right branch of the portal vein and its posterior branch (Fig. 1B); its medial limit is the inferior surface of the right hepatic lobe (Fig. 2); its lateral limit is an imaginary vertical line through the middle of the posterior segment of the right hepatic lobe (Fig. 1A). Usually its medial end reached the gallbladder neck (Fig. 1A). Sometimes the caudal end of the fissure came into direct contact with the anterior margin of the right kidney (Fig. 1B).

Received March 9, 1987; accepted after revision May 14, 1987.

[1] Department of Diagnostic Radiology, Kyung Hee University Hospital, 1 Hoe Ki-Dong, Dong Dae Mun-Ku, Seoul 131, Korea. Address reprint requests to J. H. Lim.

[2] Department of Radiology, Seoul National University Hospital, 28 Yeon Gun-Dong, Chong Ro-Ku, Seoul 110, Korea.

AJR 149:495–497, September 1987
0361–803X/87/1493–0495
© American Roentgen Ray Society

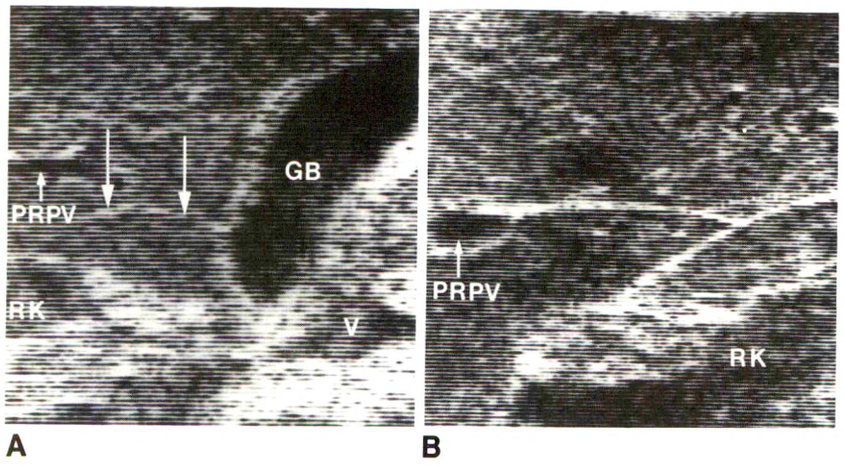


Fig. 1.—Sonogram showing inferior accessory hepatic fissure.
A, Transverse scan. Linear echoes (*arrows*) represent inferior accessory hepatic fissure. GB = gallbladder; PRPV = posterior branch of right branch of portal vein; RK = right kidney; V = inferior vena cava.
B, Parasagittal scan. Inferior accessory hepatic fissure extends downward from posterior branch of right branch of portal vein (PRPV) and comes in direct contact with anterior margin of right kidney (RK).

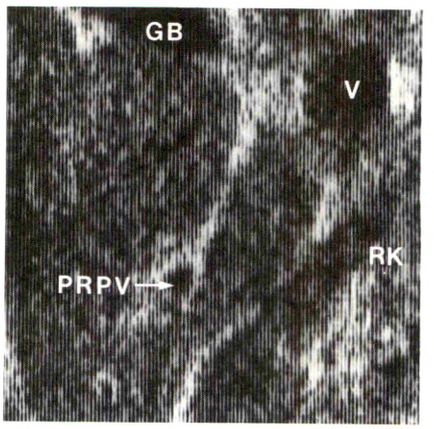


Fig. 2.—Scan made from the flank. Inferior accessory hepatic fissure extends laterally and posteriorly from gallbladder neck (GB) to posterior branch of right branch of portal vein (PRPV). Compare with Fig. 3B. RK = right kidney; V = inferior vena cava.

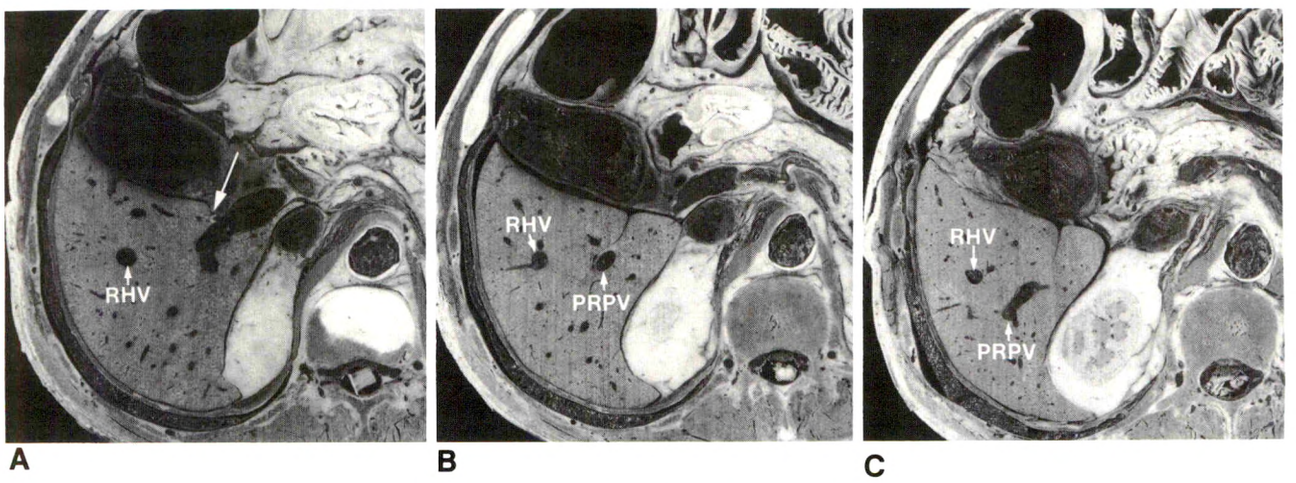


Fig. 3.—Photograph of axial cadaver sections through lower part of right lobe of liver. RHV = right hepatic vein.
A, Transverse section just below porta hepatis. Peritoneum invaginates (*arrow*) posteriorly from right side of porta hepatis, where right branch of portal vein enters the liver.
B, Transverse section 1 cm caudal to *A*. Peritoneal invagination directs posterolaterally and comes in direct contact with posterior branch of right branch of portal vein (PRPV).
C, Transverse section 1 cm caudal to *B*. Fissure extends farther down apart from posterior branch of right branch of portal vein (PRPV).

Review of the anatomic sections from one cadaver that was sectioned transversely disclosed a fissure in the posterior segment of the right hepatic lobe. The other cadaver did not have the fissure. The fissure was an invagination of peritoneum directed laterally and posteriorly from the medial inferior surface of the right hepatic lobe (Fig. 3). Invagination started from the right side of the porta hepatis at the level of the right branch of the portal vein and followed the proximal part of the posterior branch of the right branch of the portal vein (Fig. 3B). The depth of the invagination was 3 cm and the craniocaudal length was 5 cm.

Discussion

From the level of the porta hepatis near the neck of the gallbladder, an inferior accessory hepatic fissure passes downward through the posterior segment of the right hepatic lobe in or between the coronal or parasagittal plane (Figs. 1–

3). While the interlobar fissure is related to the right branch of the portal vein and more or less with its anterior branch, the inferior accessory fissure is related to the right branch of the portal vein and its posterior branch [4]. The fissure does not divide the right hepatic lobe into the anterior and posterior segments, but does divide the posterior segment of the right hepatic lobe into the anterolateral and posteromedial parts, although not exactly into two halves.

Furrowings in the surface of the liver caused by invaginations of the diaphragm and peritoneum have been referred to as accessory fissures [1], but these are not genuine fissures. Supernumerary hepatic fissures not associated with diaphragmatic invagination are rare [1]. The inferior accessory fissure is a true fissure caused by an infolding of peritoneum. To our knowledge, it has not been described in the literature. We identified the fissure in 15 (0.8%) of 2000 sonograms on patients referred for various abdominal problems. This rate might have been higher if we had specifically searched for the fissure in these cases. It is not certain how common the fissural variation is because the prevalence was not studied in a large series of cadavers or surgical patients.

The significance of the inferior accessory hepatic fissure is uncertain. Sonographic delineation of the fissure is important for proper localization of a tumor before surgery.

ACKNOWLEDGMENT

The authors wish to express their thanks to Nan Ok Yeo for her secretarial assistance.

REFERENCES

1. Auh YH, Rubenstein WA, Zirinsky K, et al. Accessory fissures of the liver: CT and sonographic appearance. *AJR* **1984**;143:565–572
2. Sexton CC, Zeman RK. Correlation of computed tomography, sonography, and gross anatomy of the liver. *AJR* **1983**;141:711–718
3. Whalen JP. Radiology of the abdomen: anatomic basis. Philadelphia: Lea & Febiger, **1976**:8
4. Weinstein JB, Heiken JP, Lee JKT, et al. High resolution CT of the porta hepatis and hepatoduodenal ligament. *RadioGraphics* **1986**;6:55–74

Book Review

Gastrointestinal Angiography, vol. 1, 3rd ed. By Stewart R. Reuter, Helen C. Redman, and Kyung J. Cho. Philadelphia: Saunders, 480 pp., 1986. $47.95

This is the third edition of this remarkable work. The first edition, published in 1972, was a major contribution to the angiographic literature. Each successive edition has been an improvement, and the third edition represents the "state of the art" in gastrointestinal angiography. The authors provide an overall view of the role of angiography and an approach to the angiographic workup in patients with gastrointestinal diseases. Therapeutic angiography is discussed also, although not as extensively.

The chapter on vascular anatomy is superb, thoroughly covering the normal vascular anatomy and the common variants. It is a must for the beginning angiographer. The chapter on vascular diseases encompasses atherosclerosis with all its ramifications, syndromes associated with vascular disease, and uncommon vascular lesions.

The chapter on tumors in the gastrointestinal tract is a classic. Angiographic characteristics of various gastrointestinal neoplasms are described extensively and illustrated beautifully. The role of angiography in the workup of these tumors is discussed in detail. Both the diagnostic and therapeutic aspects of gastrointestinal bleeding are covered.

The chapter on cirrhosis and portal hypertension is thorough, covering both the various angiographic techniques and the physiology necessary to interpret the hepatic studies. The other chapters cover trauma, inflammatory diseases, and radiologic equipment.

The major strength of the book continues to be its concise treatment of the subject and its easily readable style. The book is well organized. The diagrams are superb, and the excellent illustrations clearly depict the points made in the text.

This book will be a useful addition to the libraries of physicians with an interest in gastrointestinal disease. It is recommended for the novice as well as for those with experience in angiography of the gastrointestinal tract. This concise, yet comprehensive, book should be required reading for all radiology residents with an interest in angiography.

Charles John Tegtmeyer
University of Virginia Medical Center
Charlottesville, VA 22908

Sonographic Features of Amebic and Pyogenic Liver Abscesses: A Blinded Comparison

Philip W. Ralls[1]
Peter F. Barnes[2]
D. Randall Radin[1]
Patrick Colletti[1]
James Halls[1]

We blindly compared the sonographic findings in amebic (112 lesions) and pyogenic (30 lesions) liver abscesses. Two sonographic features were significantly more prevalent in amebic abscesses: (1) the lesions had a round or oval shape and (2) the lesions had an echogenicity that was lower than that of normal liver and were internally homogeneous on high-gain scans. Amebic abscesses were round or oval in 92 instances (82%), while 18 pyogenic abscesses (60%) ($p < .01$) had these shapes. Fifty-nine (58%) of 101 amebic abscesses displayed low echogenicity and homogeneous internal echoes with high-gain settings compared with nine (36%) of 25 pyogenic abscesses ($p < .04$). Despite these different sonographic patterns, image findings alone were inadequate in distinguishing pyogenic from amebic liver abscesses. However, when the sonographic findings were coupled with clinical and laboratory data, a correct diagnosis was possible in 83 (86%) of 96 patients with amebic abscess.

It appears that, although some sonographic features of amebic abscess differ from those of pyogenic abscess, these differences are not sufficient to allow a specific diagnosis on the basis of sonography alone. Sonography can expedite abscess detection and, when coupled with clinical and laboratory data, can aid in differentiating pyogenic from amebic liver abscesses.

Sonography has been successful in the diagnosis of amebic liver abscess [1–4]. We previously described five sonographic features that occur in amebic liver abscesses [2]: (1) absence of significant wall echoes, (2) round or oval shape, (3) lower echogenicity than normal liver with fine, homogeneous low-level internal echoes at high gains, (4) contiguity with the liver capsule, and (5) distal sonic enhancement (through-transmission) (Fig. 1). About one-third of patients with amebic abscess showed all five features—a pattern we considered suggestive, but not pathognomonic, of amebic liver abscess.

Because it is clinically important to distinguish amebic from pyogenic liver abscesses, we evaluated our ability to differentiate these entities by using the five sonographic features previously described.

Materials and Methods

A search of medical records at the Los Angeles County–University of Southern California Medical Center from May 1, 1983, to June 30, 1985, revealed 96 patients with amebic liver abscesses. The diagnosis in 88 patients was based on positive amebic serology coupled with response to specific amebicidal therapy (chloroquine and/or metronidazole). In eight patients, the diagnosis was made by negative bacteriologic studies and positive clinical response to specific amebicidal drugs.

A medical records' search between July 1, 1979, and December 31, 1985, (6 years) yielded 48 individuals with pyogenic abscesses. Diagnostic criteria included (1) positive blood or abscess cultures, negative or borderline amebic serology, and clinical response to appropriate antibiotics (41 patients); (2) autopsy findings (four patients); (3) positive image findings with negative blood and abscess cultures but response to antibiotics, not including amebicidal agents (two patients); and (4) negative blood cultures, no abscess culture, negative amebic

Received January 30, 1987; accepted after revision May 14, 1987.

[1] Department of Radiology, Los Angeles County/University of Southern California Medical Center, and University of Southern California School of Medicine, 1200 N. State St., Los Angeles, CA 90033. Address reprint requests to P. W. Ralls.

[2] Department of Internal Medicine, Los Angeles County/University of Southern California Medical Center, and University of Southern California School of Medicine, Los Angeles, CA 90033.

AJR 149:499–501, September 1987
0361–803X/87/1493–0499
© American Roentgen Ray Society

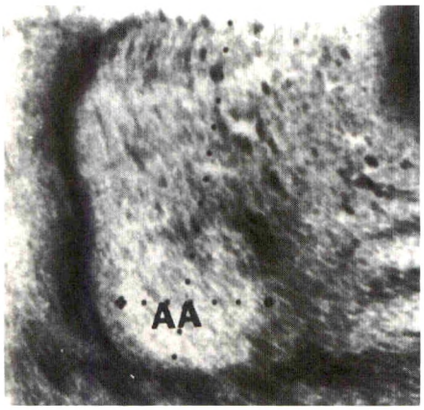


Fig. 1.—Longitudinal sonogram of liver. Amebic liver abscess (AA) has features previously considered suggestive but not pathognomonic of amebic abscess.



Fig. 2.—Longitudinal sonogram of liver. Poorly defined pyogenic liver abscess (PA) is of mixed echogenicity with strands of increased and areas of decreased echogenicity.

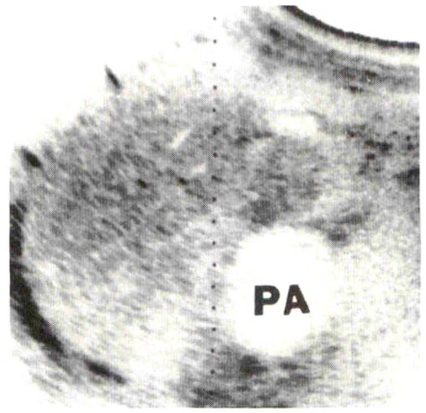


Fig. 3.—Longitudinal sonogram of liver. Pyogenic liver abscess (PA) displays all features "suggestive" of amebic abscess. Sonographic findings alone cannot differentiate amebic and pyogenic abscesses; this distinction depends on combination of clinical, laboratory, and sonographic information.

serology, and response to antibiotics that included metronidazole (one patient).

All available sonograms were reviewed by an experienced sonographer. The presence or absence of the five features listed above was noted. The radiologist was blinded to the diagnosis, the patient's name (since amebic abscesses occur with higher frequency among Hispanics), and the proportion of cases with each diagnosis within the total group. Sonograms were available from 85 patients with amebic abscesses and 22 patients with pyogenic abscesses. Since a number of patients had more than one abscess, 112 amebic and 30 pyogenic abscesses were analyzed.

Results

Review of the medical records revealed that 83 of 96 patients with amebic liver abscess were correctly diagnosed from a combination of clinical and laboratory data coupled with sonographic findings. In the other 13 patients, diagnostic aspiration was performed.

Sonograms of 112 amebic and 30 pyogenic liver abscesses were available for review. Ninety-two amebic abscesses (82%) were round or oval in shape compared with only 18 (60%) of the pyogenic abscesses. Hypoechoic appearance with fine, homogeneous low-level echoes throughout at high gain occurred in 59 (58%) of 101 amebic lesions for which high-gain sonograms were available. This pattern occurred in nine (36%) of 25 pyogenic abscesses. Distal sonic enhancement (through-transmission) was found in 84 (84%) of 100 amebic lesions and in 19 (70%) of 27 pyogenic abscesses. Ninety-three (86%) of 108 amebic abscesses were contiguous to the liver capsule compared with 26 (87%) of 30 pyogenic lesions. Lastly, no significant peripheral echoes were present in 68 (61%) amebic lesions vs 20 (67%) pyogenic lesions.

Analysis of these data (chi-square) yielded significant differences between amebic and pyogenic abscesses in two categories: (a) round or oval shape ($p < .01$) and (2) hypoechoic appearance throughout with fine, homogeneous low-level echoes at high gain ($p < .04$) (Fig. 2). Distal sonic enhancement (through-transmission) did not occur significantly more often in either type of abscess. The last two categories (contiguity with the liver capsule and lack of significant wall echoes) occurred with an essentially identical frequency in both types of lesions.

The suggestive pattern (Fig. 1), that is, presence of five of five criteria, occurred in 26 (31%) of 84 amebic abscesses. It also occurred in five pyogenic lesions (23% of 22 abscesses) (Fig. 3). This difference was not statistically significant. In some patients only four criteria could be assessed, usually because high-gain scans had not been obtained. Four of four criteria were present in 13 (50%) of 26 amebic and in two (25%) of eight pyogenic abscesses in this group.

Discussion

The most common serious error in detecting and managing hepatic amebic abscess is failure to consider the diagnosis, which can lead to potentially catastrophic results. Our previous retrospective analyses of amebic abscess patients were designed to elucidate the spectrum of sonographic findings, enabling sonographers to suggest the diagnosis when other clinicians failed to do so.

We blindly assessed the utility of these sonographic signs in differentiating amebic from pyogenic liver abscesses. These results indicate that our "suggestive pattern," that is, the presence of all five signs, is not adequate to definitively distinguish amebic from pyogenic liver abscesses. Two sonographic signs—(1) round or oval shape and (2) hypoechoic

appearance with fine, homogeneous echoes throughout at high gain—were more prevalent in hepatic amebic abscess to a statistically significant degree. In individual cases, even these signs were not sufficient to differentiate amebic from pyogenic abscesses.

It is no surprise that a definitive differential diagnosis cannot be based on sonographic findings alone. As a practical matter, diagnosis of hepatic amebic abscess is based on sonographic findings, clinical data, and laboratory data. Confirmation is usually obtained by appropriate response to amebicidal therapy. Percutaneous aspiration can be used (13 [13.5%] of 96 in our series) when clinical doubt remains after the analysis of the sonograms and clinical and laboratory data.

REFERENCES

1. Ralls PW, Colletti PM, Quinn MF, Halls J. Sonographic findings in hepatic amebic abscess. *Radiology* **1982**;145:123–126
2. Ralls PW, Meyers HI, Lapin SA, Rogers W, Boswell WD, Halls J. Gray-scale ultrasonography of hepatic amoebic abscess. *Radiology* **1979**; 132:125–129
3. Sukov RJ, Cohen LJ, Sample WF: Sonography of hepatic amebic abscesses. *AJR* **1980**;134:911–915
4. Landay MJ, Setiawan H, Hirsch G, Christensen EE, Conrad MR. Hepatic and thoracic amebiasis. *AJR* **1980**;135:449–454

Technical Note

Double-Contrast Examination of the Colon with Carbon Dioxide: The Use of Effervescent Powder

Rubem Pochaczevsky[1]

CO_2 has distinct advantages over room air for double-contrast examination of the colon [1–4]. Not only has CO_2 been proved safe, but also it has been shown to be absorbed much more rapidly from the gastrointestinal tract than is the nitrogen in room air (absorption occurs 30 to 100 times faster) [1, 2]. Thus, with CO_2, there is a marked decrease in bowel distension over a much shorter period of time, with resultant increased comfort after the barium enema examination [2]. This paper describes a simplified method of using CO_2 for double-contrast examination of the colon that eliminates the need to employ or store a CO_2 tank.

Materials and Methods

The proposed simplified effervescent techniques use a specially formulated effervescent powder containing citric acid and sodium bicarbonate to generate CO_2 as needed.

Method 1: Separate CO_2 Bag

In this method, CO_2 is generated by mixing a 25-g packet of effervescent powder with approximately 10–15 ml of water in a modified empty enema bag (the effervescent powder packet and bag cost approximately $1 and $2, respectively, and were supplied by E-Z-EM Inc., Westbury, NY). The tubing originating from the bag is situated centrally so that the small amount of water remaining from the effervescent reaction is always trapped at the bottom of the bag, regardless of how the bag is hung. Therefore, only CO_2 gas enters the tubing. Approximately 1.5 l of CO_2 are promptly produced on mixing, an amount that is both safe and sufficient for double-contrast examination of the colon (Fig. 1A). After mixing, the CO_2-distended bag is attached to the barium-containing enema kit by means of an adapter connected to an insufflator (Fig. 1B).

The insufflator (Fig. 1B) delivers an operator-controlled amount of CO_2 from the bag to the colon, whose distension is continuously monitored fluoroscopically. However, although the one-way valves incorporated within the insufflator and the air vent of the rectal catheter ordinarily serve to interrupt reflux into the bag, the system may not be foolproof in preventing transmission of infectious agents. This is particularly noteworthy in view of current concerns with immunocompromised patients in general, and with AIDS patients in particular, unless the insufflator and the bag are discarded after each patient. Therefore, an alternate step is favored by the author that serves to eliminate the use of the insufflator by connecting the tubing of the CO_2-containing bag directly to the rectal catheter air vent. Colonic insufflation is then accomplished by gentle manual pressure of the bag itself, whose set amount of CO_2 also prevents inadvertent colonic overdistension. The one-way valve in the rectal catheter air vent prevents reflux of gas from the colon. A relative disadvantage of this alternate technique is that, initially, control of the rate of gas insufflation may not be as precise as it is with an insufflator. However, adequate control of gas insufflation can be achieved with continued experience, and a feel for the degree of intracolonic distension or spastic contraction may be gained by the ease or difficulty of manual squeezing. Usually no sudden rush of gas insufflation is encountered, since no liquid barium (which has to be initially overcome) is present in the tubing. The author also recommends discarding the bag after each examination.

Received February 25, 1987; accepted after revision May 4, 1987.
[1] Department of Radiology, Long Island Jewish Medical Center, New Hyde Park, NY 10042. Address reprint requests to R. Pochaczevsky.

AJR **149:502–504, September 1987** 0361–803X/87/1493–0502 © American Roentgen Ray Society

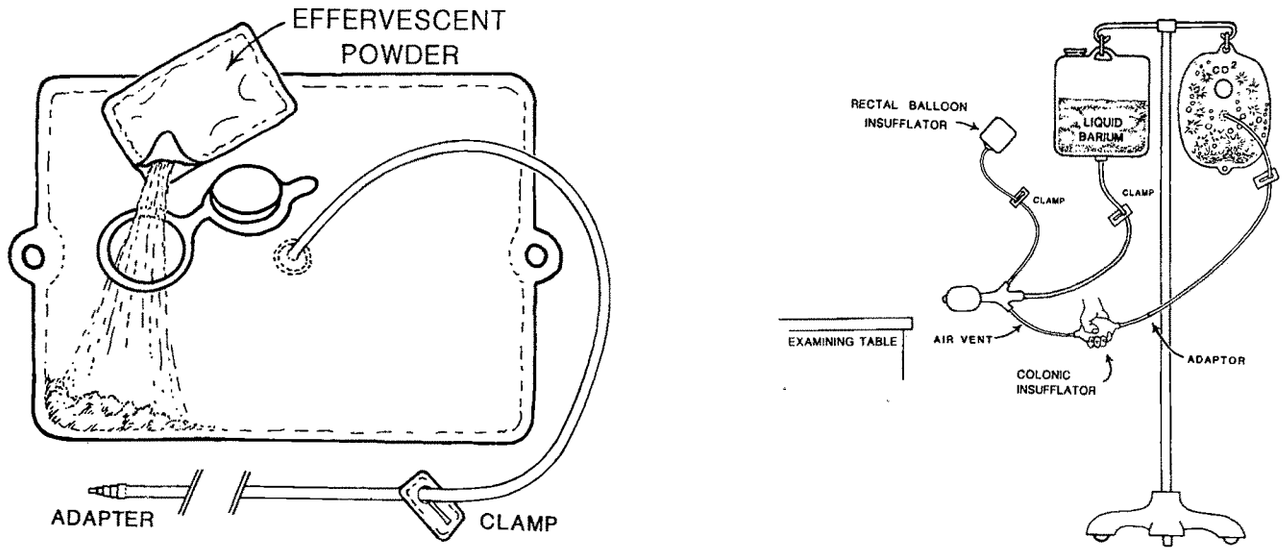


Fig. 1.—First method uses a separate CO_2 bag.

***A*, A packet of effervescent powder is poured into a corner of an empty modified enema bag whose tubing is clamped. Approximately 10–15 ml of water, directed away from the powder to avoid premature reaction, are then poured into bag. The bag, after being capped, is shaken to facilitate mixing of effervescent powder with water.**

***B*, The bag, distended with generated carbon dioxide, is then connected to colonic insufflator of barium enema kit with an adapter and hung on a stand next to barium enema bag. By squeezing the insufflator, which has a built-in one-way valve, a controlled amount of carbon dioxide is delivered into the colon.**

Method 2: CO_2 Generation in the Enema Bag

This second method consists of emptying the packet of effervescent powder directly into the enema bag containing the liquid barium suspension (Fig. 2). CO_2 will also be promptly generated. When the gas contrast stage of the examination is reached, CO_2 is insufflated into the colon by simply inverting the bag and gently squeezing it manually under fluoroscopic control. This technique was previously described using a tank reservoir as a source of CO_2 [1]. A tank is not needed with the current method. The advantage of this second method is that it does not require another bag or an insufflator. A relative disadvantage of this method, as in the alternative step in method 1, is that there may be a loss of precise control of the rate of gas insufflation. In addition, barium in the tubing may render the initial insufflation of gas more difficult to control. Another minor shortcoming of this method is the tendency of the colonic gas to reflux into the bag, since one-way valves are not present. However, reflux can be avoided by clamping the tubing before releasing manual pressure on the bag.

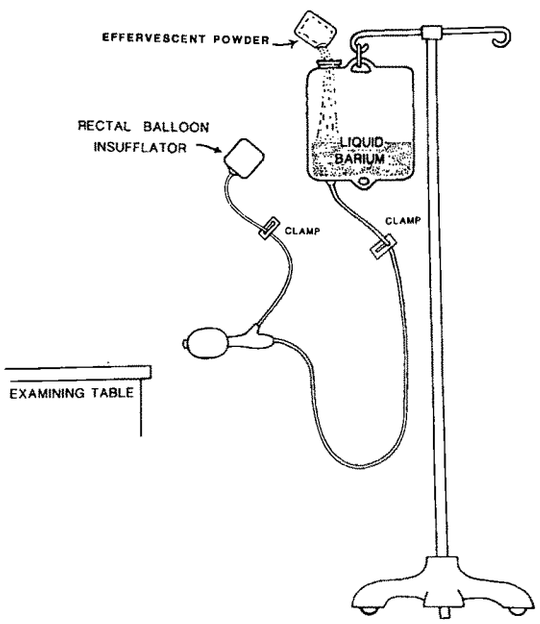


Fig. 2.—Second method. CO_2 generation in the enema bag. A packet of effervescent powder is emptied into the enema bag containing liquid barium suspension. After capping and shaking, 1.5 l of CO_2 are generated within 1 min. Barium is first instilled, and CO_2 is then insufflated into the colon under fluoroscopic control by inverting the bag and gently squeezing it manually.

Discussion

A closed-system CO_2 insufflation technique in conjunction with a prepackaged barium enema kit was described in 1963 [1]. A safe and inexpensive CO_2 delivery system was readvocated more than 20 years later [3]. More recently, a method of preinsufflation of CO_2 into a bag from a tank reservoir was described [4] with the CO_2-filled bag subsequently connected to the barium enema kit by means of a manual insufflator. All

the above methods, however, require the use, availability, and storage of a CO_2 tank, which may be cumbersome or undesirable. This may be particularly impractical in an office setting.

The simplified CO_2 double-contrast barium enema techniques described here have been successfully employed for several years. The quality of the resultant double-contrast enema is equivalent to and indistinguishable from that obtained using room air. Although CO_2 is absorbed faster than air, our experience in four institutions indicates that sufficient intracolonic gas remains for a long enough period of time to be adequately documented on postfluoroscopic overhead films. The effervescent powder does not, in our opinion, affect the mucosal coating properties of the barium suspension. Coblentz et al. [2] additionally noted that the quality of radiographs was equal in the CO_2 and air double-contrast groups. The technique is, furthermore, simultaneously practical and relatively inexpensive.

REFERENCES

1. Pochaczevsky R, Sherman RS. A new technique for the roentgenologic examination of the colon. *AJR* **1963**;89:787–796
2. Coblentz CL, Frost RA, Mollinaro V, Stevenson GW. Pain after barium enema: effect of CO_2 and air on double-contrast study. *Radiology* **1985**;157:35–36
3. Bernier P, Coblentz C. CO_2 delivery system for double-contrast examinations. *Radiology* **1986**;159:264
4. Bessette JR, Maglinte DDT. Double-contrast barium enema study: simple conversion to CO_2. *Radiology* **1987**;162:274–275

Case Report

Focal Acute Acalculous Cholecystitis

David Warshauer,[1] Glynis Scott,[2] and Alexander Gottschalk[1]

Acute acalculous cholecystitis, like calculous cholecystitis, generally shows diffuse inflammation throughout the gallbladder and cystic duct obstruction. Nonvisualization of the gallbladder on hepatobiliary scanning is typical [1, 2].

We report an unusual case of acute acalculous cholecystitis in which acute inflammation was focal but severe enough to result in perforation. Hepatobiliary scanning showed both a patent cystic duct (i.e., gallbladder filling) and free intraperitoneal spill of radionuclide.

Case Report

A previously healthy 39-year-old man came to the emergency room with crampy right upper quadrant pain. He was afebrile and had a normal WBC count. Plain radiography of the abdomen was unremarkable, and the patient was sent home after the pain abated with a diagnosis of either renal or biliary colic. He returned the next day with crampy pain now radiating to the right shoulder. Evaluation showed the patient to be febrile (37.8°C) with a positive Murphy's sign. No history of alcoholism, drug abuse, or recent fasting was obtained.

Sonography showed a distended gallbladder containing sludge with significant thickening of the gallbladder wall in the neck. No stones or pericholecystic fluid collections were observed.

Technetium-99m disofenin scan afforded prompt visualization of the gallbladder on the 5-min film. Excretion of radionuclide into the small bowel was noted on the 2-hr images. This delay was thought to be from spasm of the sphincter of Oddi caused by narcotics administered in the emergency room. Extrabiliary and extraintestinal activity was seen beginning on the 25-min film; extravasation continued on later films (Fig. 1).

The patient underwent cholecystectomy. The peritoneal cavity contained bile, and a pinpoint perforation was seen in the fundus of the gallbladder. No stones were identified within the peritoneal cavity, nor were any seen on an intraoperative cholangiogram. Cultures of gallbladder bile showed no growth. After surgery, the patient made a relatively uneventful recovery.

Pathologic examination of the gallbladder showed no stones. Microscopic examination showed a scattered mild chronic inflammatory cell infiltrate with thickening of the gallbladder wall and Rokitansky-Aschoff sinuses throughout. In the fundus of the gallbladder in an area of deep Rokitansky-Aschoff sinuses a 1-mm perforation with focal necrosis and microabscess formation was noted. The exact relationship of the abscess to the Rokitansky-Aschoff sinuses could not be determined because of accompanying necrosis. There was no evidence of vasculitis.

Discussion

Calculous cholecystitis typically shows diffuse inflammation of the gallbladder resulting from an obstructed cystic duct. Less commonly in acalculous cholecystitis, cystic duct obstruction is a secondary event, being caused by a generalized inflammatory process from bile stasis, ischemia, or infection [2, 3].

In our case, however, acute cholecystitis with perforation occurred without evidence of either generalized acute inflammation or cystic duct obstruction. Although a vasculitic, embolic, or hypotensive process could have been responsible for inducing focal necrosis, no evidence for these could be obtained. In view of the widespread and deep Rokitansky-Aschoff sinuses (some coming within microns of the gallblad-

Received February 4, 1987; accepted after revision May 5, 1987.
[1]Department of Diagnostic Radiology, Yale University School of Medicine, 333 Cedar St., New Haven, CT 06510. Address reprint requests to D. Warshauer.
[2]Department of Pathology, Yale University School of Medicine, New Haven, CT 06510.

AJR **149:505–506, September 1987** 0361–803X/87/1493–0505 © American Roentgen Ray Society

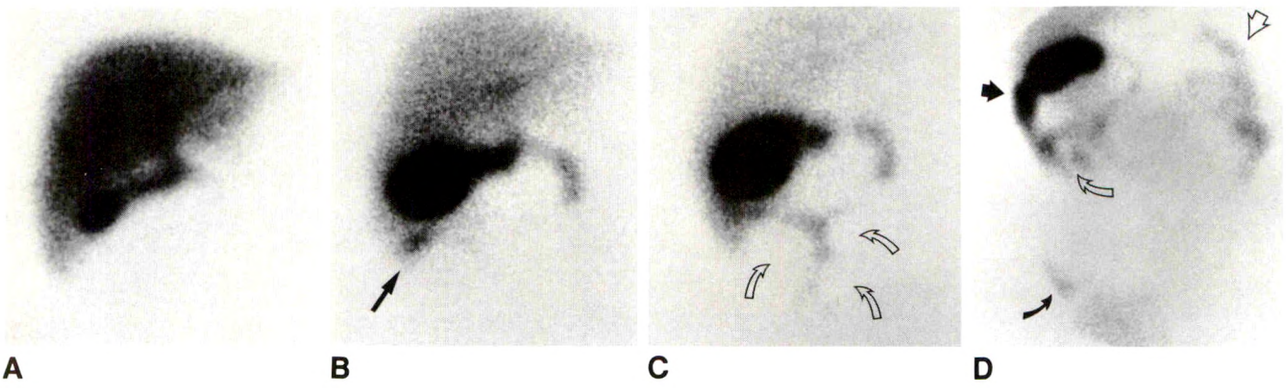


Fig. 1.—*A*, 5-min image from hepatobiliary scan.
***B*, 25-min image. Free intraperitoneal radionuclide is now seen (*arrow*).**
***C*, 45-min image. Bowel loops (*open arrows*) are outlined by radionuclide.**
***D*, 2-hr image. Free intraperitoneal radionuclide is collecting adjacent to gallbladder fundus (*black straight arrow*), outlining bowel loops (*open curved arrow*) and in right paracolic gutter (*black curved arrow*). Radionuclide within small bowel is seen in jejunal loops (*straight open arrow*).**

der surface), a mechanism first proposed by Glenn and Moore [4] seems more likely. They suggested that focal perforation of the gallbladder could be caused by abscess formation around an obstructed Rokitansky-Aschoff sinus in a fashion analogous to diverticular perforation in the large bowel. The limited focal nature of the resultant process would also explain our patient's relative paucity of clinical signs and symptoms.

The apparent rarity of the combination of findings in this patient—no stones, a patent cystic duct, and focal but severe acute inflammation—is fortunate given the inherent difficulty in making a diagnosis of acute cholecystitis without either stones or cystic duct obstruction. With current imaging techniques the demonstration of perforation may be the earliest diagnostic sign of serious disease in cases like this.

REFERENCES

1. Swayne LC. Acute acalculous cholecystitis: sensitivity in detection using technetium-99m iminodiacetic acid cholescintigraphy. *Radiology* **1986**; 160:33–38
2. Howard RJ. Acute acalculous cholecystitis. *Am J Surg* **1981**;141:194–198
3. Glenn F. Acute acalculous cholecystitis. *Ann Surg* **1979**;189:458–465
4. Glenn F, Moore SW. Gangrene and perforation of the wall of the gallbladder. A sequela of acute cholecystitis. *Arch Surg* **1942**;44:677–680

Pancreas Transplantation with Pancreatico-Duodeno-Cystostomy for Exocrine Drainage: Cystographic Findings

Edward J. Woolsey[1]
John R. Tauscher[1]
Donald C. Dafoe[2]

Pancreatic transplantation is becoming accepted therapy for a select subset of patients with type I insulin-dependent diabetes. At many centers, whole-organ transplants with pancreatico-duodeno-cystostomy for drainage of exocrine secretions is the preferred surgical procedure. We obtained 21 cystograms in nine patients who underwent this procedure who were suspected of having anastomotic leaks and possible abscess. Positive findings included extrinsic bladder compression (nine patients), filling of the transplanted duodenal segment (three patients), edematous bladder wall (four patients), intraperitoneal (two patients) and extraperitoneal (four patients) leaks, and fistulae (two patients). Intraperitoneal extravasation resulted in abscess formation and cutaneous fistulae, and these transplants were subsequently removed.

We conclude that cystography is a useful technique in evaluating the site and extent of anastomotic leaks and fistulae.

The number of patients with type I diabetes in the United States who will develop serious complications is about 5000 per year (25/million population) [1]. Evidence indicates that some of the secondary complications of diabetes may be halted, prevented, or even reversed by maintaining a euglycemic state in these patients [2]. Pancreatic transplantation is an exciting prospect for therapy to achieve this goal.

Pancreatico-duodeno-cystostomy is used with increasing frequency because it is technically simple to perform, a sterile field can be maintained as opposed to anastomosis with the intestine, and graft function can be easily monitored by following the concentration of pancreatic enzymes in the urine [3, 4]. At the University of Michigan, this is considered the procedure of choice for drainage of exocrine secretions.

Whole-organ cadaveric transplantation, rather than segmental pancreatic transplantation from living related donors, is performed. The donor pancreas and a portion of the duodenum are placed intraperitoneally, usually in the left iliac fossa. The portal vein of the graft is sutured to the recipient's left external iliac vein and the celiac axis of the graft is sutured to the recipient's left internal iliac artery. After revascularization, the duodenal segment of the transplant is anastomosed to the dome of the bladder (Fig. 1).

Previous reports have discussed the role of CT [5], sonography [6], and nuclear imaging [7] in evaluating peritransplant fluid collections and blood flow to the transplant. The purpose of this study is to describe the cystographic findings in pancreas transplantation and to assess the role of cystography in the diagnosis of complications of pancreas transplantation.

Subjects and Methods

From September 1985 to September 1986, 12 patients underwent whole-pancreas transplantation with pancreatico-duodeno-cystostomy. All 12 had synchronous renal transplanta-

Received December 10, 1986; accepted after revision May 6, 1987.

[1] Department of Radiology, Box 30, University of Michigan Medical Center, 1500 E. Medical Center Dr., Ann Arbor, MI 48109. Address reprint requests to E. J. Woolsey.

[2] Department of Surgery, University of Michigan Medical Center, Ann Arbor, MI 48109.

AJR 149:507–509, September 1987
0361–803X/87/1493–0507
© American Roentgen Ray Society

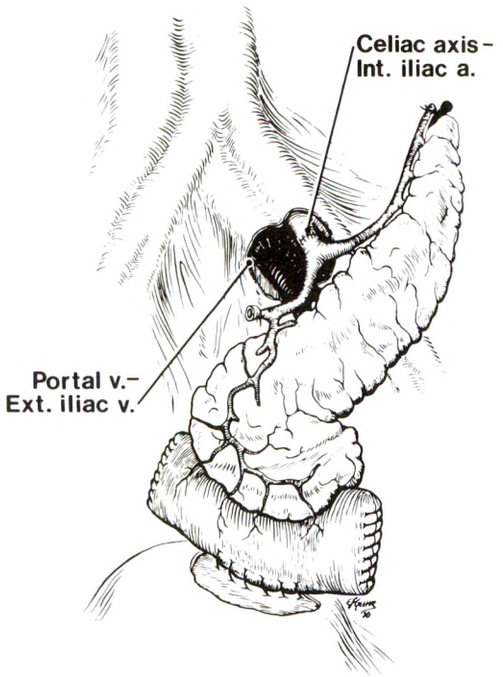


Fig. 1.—Whole cadaveric pancreatic transplant with long duodenal segment placed intraperitoneally and anastomosed to bladder dome. Peritoneum is disrupted at bladder dome. a. = artery; v. = vein; Int. = internal; Ext. = external.

tion in the right iliac fossa secondary to end-stage diabetic nephropathy. In the first nine patients, a small duodenal stump was used at the pancreas-bladder anastomoses. In the last three patients, about 8 cm of duodenum were used.

In nine of the 12 patients, cystography was performed in the postoperative period when an anastomotic leak and possible abscess were suspected clinically. Cystography was performed with about 200 ml of Hypaque 50% (Winthrop-Breon, New York, NY) instilled by gravity through a Foley catheter inserted per urethra. Care was taken to fill the duodenal segment for complete evaluation. Fluoroscopy was performed with frontal, oblique, and lateral spot radiographs.

Results

Nine patients had a total of 21 cystograms. A constant finding on all cystograms was an extrinsic defect on the bladder dome located anterolaterally on the left, caused by compression from the transplanted pancreas-duodenum (Fig. 2). On cystograms obtained within 10 days of surgery a markedly irregular bladder wall was a constant finding (Fig. 3A). In the four patients who had sequential cystograms, this irregularity resolved within 10–21 days of the initial cystogram.

In five patients no leak was shown, and these patients had uneventful postoperative recoveries. Cystograms in the other four patients showed extravasation of contrast material from the pancreatico-duodeno-cystostomy into either the extraperitoneal or intraperitoneal compartment or both (Figs. 3B and 4). In two of these four patients, extravasation was only

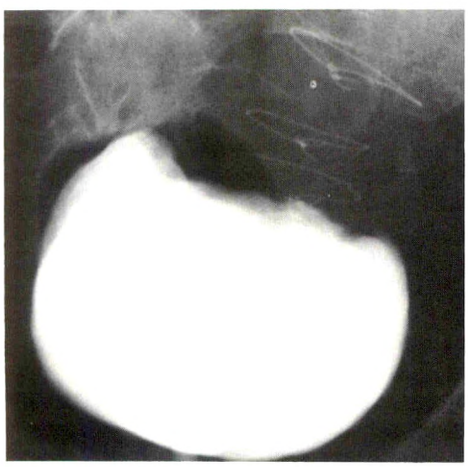
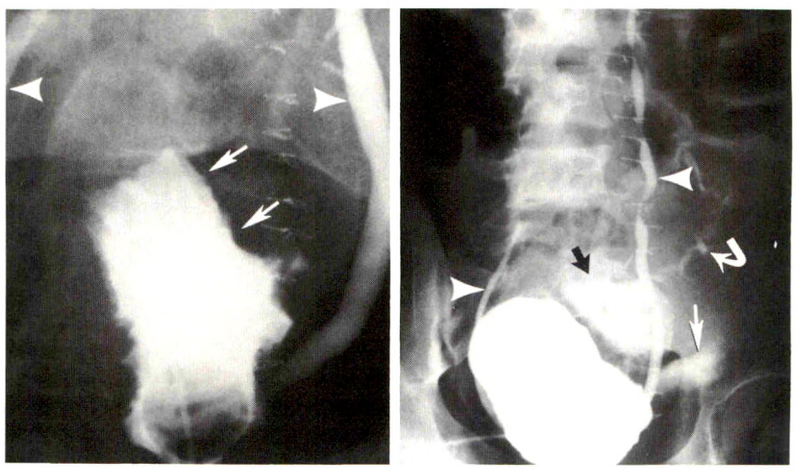


Fig. 2.—Cystogram (14 days after transplantation) shows left anterolateral extrinsic compression by transplant.



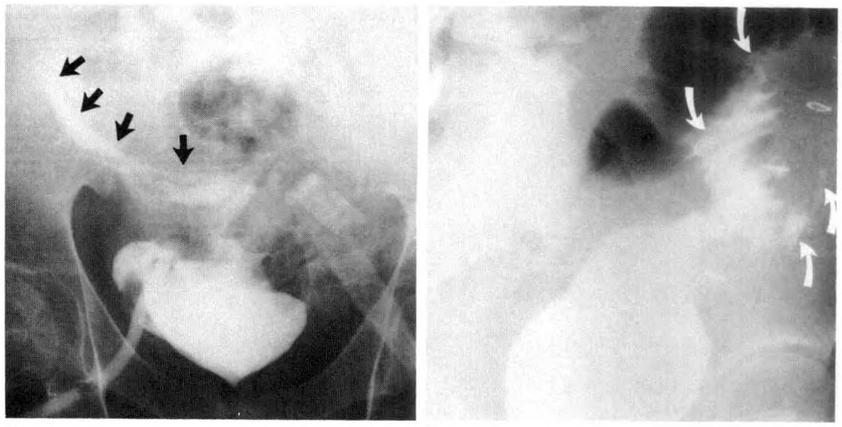
A B

Fig. 3.—*A*, Cystogram in febrile patient 6 days after transplantation. Markedly irregular and contracted bladder, extrinsic compression by transplant (*arrows*), and reflux into native ureters (*arrowheads*). Ureteral reflux is most likely incidental.

B, Reexamination 12 days later because of persistent fever and new cutaneous fistula. Cystogram shows smoother bladder wall, reflux into both native ureters (*arrowheads*), extrinsic compression by transplant, and new development of loculated intraperitoneal (*black arrow*) and extraperitoneal (*straight white arrow*) extravasation, as well as vesicocutaneous fistula (*curved arrow*).

Fig. 4.—Cystogram in febrile patient 7 days after transplantation shows free intraperitoneal extravasation (*arrows*). Note edematous bladder wall and extrinsic compression on dome by transplant. At surgery duodenocystostomy was necrotic.

Fig. 5.—Cystogram in left posterior oblique position shows filling of long duodenal segment (*arrows*) anastomosed to bladder. Note contrast material extending to radiopaque suture lines. This duodenal filling must not be mistaken for extravasation.



4 5

extraperitoneal, and these leaks eventually closed with conservative management. The other two patients had intraperitoneal as well as extraperitoneal extravasation complicated by vesicocutaneous fistulae and their transplants subsequently had to be removed.

Variable findings included (1) reflux up the native ureters in two patients (Fig. 3), (2) reflux up the ureter of the renal transplant in one patient, (3) irregular filling defects in the bladder due to blood clots in one patient, and (4) filling of the transplanted duodenal segment in three patients (Fig. 5). The pancreatic duct was not seen in any patient.

Discussion

The major role of cystography in patients with pancreas transplantation with pancreatico-duodeno-cystostomies is to determine the presence of an anastomotic leak, the size of the leak, and the location of extravasation. We found leaks in four of nine patients in whom a leak was clinically suspected. Extravasation may be in the intraperitoneal or extraperitoneal compartment or both. The location of the extravasation is important, as intraperitoneal leaks must be surgically repaired because of the potential for peritonitis, electrolyte disturbances, and azotemia from spillage of urine onto the peritoneal surface. Extraperitoneal leaks often can be managed conservatively, as shown in two of our patients. All of the leaks that occurred were in patients with a small stump of duodenum anastomosed to the bladder. More recently, about 8 cm of descending duodenum attached to the pancreatic head have been used for anastomoses with the bladder, and not one of these patients has developed a leak (Fig. 5).

Bladder-wall irregularity was a constant finding in the immediate postoperative period (Fig. 3A). In the four patients with more than one cystogram, this irregularity resolved within 10–21 days (Fig. 3B), suggesting that the finding was due to postsurgical edema.

Minimal to marked extrinsic bladder compression from the pancreatic transplant occurred in all patients (Figs. 2–4).

Reflux of contrast material into the duodenal segment can be confused with extravasation. Misdiagnosis usually can be avoided by careful fluoroscopy and complete filling of the segment, which is usually clearly demarcated by two radiopaque suture lines (Fig. 5).

While scintigraphy can provide indirect evidence of the functional status of the graft by evaluating blood flow, and sonography and CT are useful for finding peritransplant fluid collections, we believe cystography is the procedure of choice for identifying the site and magnitude of anastomotic leaks, as well as for delineating fistulous tracts.

ACKNOWLEDGMENTS

We thank Peter Hedlesky and Judi Wilson for assistance in manuscript preparation.

REFERENCES

1. Sutherland DER. Selected issues of importance in clinical pancreas transplantation. *Transplant Proc* **1984**;16(3):661–670
2. Corry RJ, Nghiem DD, Schulak JA, Beutel WD, Gonwa TA. Surgical treatment of diabetic nephropathy with simultaneous pancreatic duodenal and renal transplantation. *Surg Gynecol Obstet* **1986**;162:547–555
3. Sollinger HW, Cook K, Kamps D, Glass NR, Belzer FO. Clinical and experimental experience with pancreaticocystostomy for exocrine pancreatic drainage in pancreas transplantation. *Transplant Proc* **1984**;16(3):749–751
4. Sollinger HW, Kalayoglu M, Hoffmann RM, Deierhoi MH, Belzer FO. Experience with pancreaticocystostomy in 24 consecutive pancreas transplants. *Transplant Proc* **1985**;17:141–143
5. Maile CW, Crass JR, Frick MP, Feinberg SB, Goldberg ME, Sutherland DER. CT of pancreas transplantation. *Invest Radiol* **1985**;20:609–612
6. Crass JR, Sutherland DER, Feinberg SB. Sonography of the segmental human pancreatic transplant. *JCU* **1982**;10:149–152
7. Crass JR, Feinberg SB, Sutherland DER, Loken M, Gedgaudas EG. Radiology of the human segmental pancreatic transplant. *Gastrointest Radiol* **1982**;7:153–158

American Roentgen Ray Society
Resident Award Papers, 1988

The ARRS announces competition for the 1988 President's Award and two Executive Council's Awards for the best papers concerning the clinical application of the radiologic sciences.

Awards

The winner of the President's Award will receive a certificate and a $1000 prize. The winners of the two Executive Council Awards will each be given a certificate and a prize of $500. The winners will be announced on March 15, 1988. Winning papers will be presented at the ARRS annual meeting at the San Francisco Hilton Hotel, San Francisco, CA, May 7–12, 1988. Winning papers will be submitted for early publication in the *American Journal of Roentgenology*. All other papers will be returned to the authors.

Regulations

Eligibility is limited to residents or fellows in radiology who have not yet completed 4 years of approved training in a radiologic discipline. A letter from the resident's department chairman attesting to this status must accompany the manuscript. The resident must be the sole or senior author and be responsible for all or most of the project.

Submitted manuscripts must not exceed 5000 words and have no more than 10 illustrations. Four copies of the manuscript and illustrations are required.

Deadline for submissions is January 29, 1988. Send papers to:

B. G. Brogdon, M.D.
Chairman, Committee on Education & Research
American Roentgen Ray Society
Department of Radiology
University of South Alabama Medical Center
2451 Fillingim Street
Mobile, AL 36617

Case Report

Ascaris-Induced Pancreatitis

J. W. C. Leung,[1] S. D. Mok,[2] and C. Metreweli[3]

Pancreatitis associated with *Ascaris lumbricoides* infestation develops as a result of the passage of a worm into the pancreatic duct or bile duct through the sphincter of Oddi [1]. Usually the worm migrates up the biliary system. We report a case in which the worm had migrated into the pancreatic duct resulting in acute pancreatitis.

Case Report

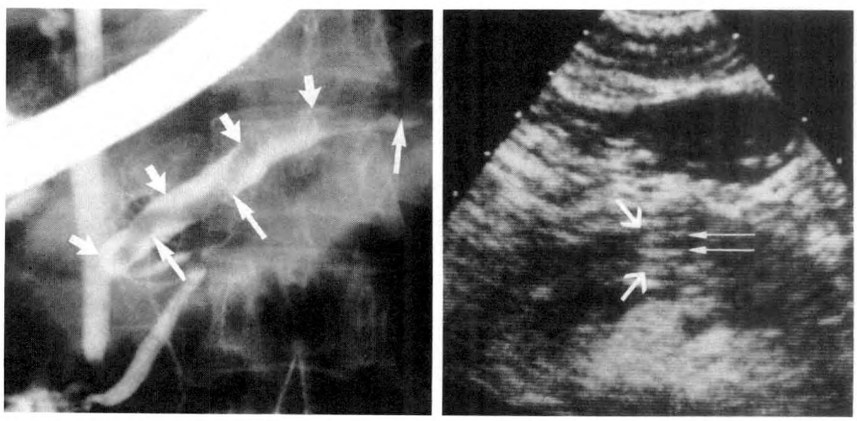
A 32-year-old woman was admitted because of abdominal pain, fever, and vomiting for 1 day. She had enjoyed good health, but did have a previous history of passing worms in the stool. Physical examination revealed tenderness and guarding in the epigastrium. There was no jaundice. Laboratory investigation revealed a raised serum amylase of 2700 iu/l (normal up to 200 iu/l), and leukocytosis of 14.6×10^9. She was managed conservatively and the pain subsided.

A sonogram of the abdomen showed a prominent pancreatic duct with swelling of the pancreas. An endoscopic retrograde cholangiopancreatography (ERCP) showed a tubular filling defect in the pancreatic duct, which was dilated (Fig. 1). A repeat sonogram showed the worm in the pancreatic duct (Fig. 2).

Endoscopic removal of the worm was attempted using a balloon catheter, but was unsuccessful.

Fig. 1.—ERCP shows an ascaris (*long arrows*) in the dilated pancreatic duct (*short arrows*) causing obstruction.

Fig. 2.—Transverse sonogram showing the ascaris (*long arrows*) in a dilated pancreatic duct (*short arrows*).



1 2

Received March 9, 1987; accepted after revision April 16, 1987.

[1] Department of Medicine, Prince of Wales Hospital, The Chinese University of Hong Kong, Shatin, N.T., Hong Kong. Address reprint requests to J. W. C. Leung.
[2] Department of Surgery, Prince of Wales Hospital, The Chinese University of Hong Kong, Shatin, N.T., Hong Kong.
[3] Department of Radiology, Prince of Wales Hospital, The Chinese University of Hong Kong, Shatin, N.T., Hong Kong.

AJR **149:511–512, September 1987** 0361–803X/87/1493–0511 © American Roentgen Ray Society

Because of persistent symptoms, a laparotomy was performed. A small incision was made in the pancreatic duct in the body of the pancreas and a 15-cm-long ascaris was removed.

Discussion

Ascaris lumbricoides is a recognized cause of acute pancreatitis [1]. The attacks occur usually as a result of the worm migrating up the biliary tree causing obstruction or spasm of the sphincter of Oddi. In our series of 84 patients admitted with acute pancreatitis, ascaris was identified as the etiologic factor in five patients (6%). The acute attack usually resolves with conservative treatment. The diagnosis is often made by the discovery of the adult worm in the biliary tree or in the second part of the duodenum at the time of ERCP or endoscopy [2, 3].

In rare situations, the presence of an ascaris within the pancreatic duct has been reported [4]. Sonography is useful in identifying the ascaris in the bile duct [5]. However, our experience suggests that the delineation of the worm in the pancreatic duct may be missed unless there is a high index of suspicion and careful transverse scans of the pancreas are made. A pancreatogram is undoubtedly more specific in making the diagnosis.

REFERENCES

1. Choi TK, Wong J. Severe acute pancreatitis caused by parasites in the common bile duct. *J Trop Med Hyg* **1984**;87:211–214
2. Chen YS, Den BX, Huang BI, Xu LZ. Endoscopic diagnosis and management of ascaris induced acute pancreatitis. *Endoscopy* **1986**;18:127–128
3. Leung JWC, Chung SCS, King WWK. Round worm pancreatitis: endoscopic worm removal without papillotomy. *Br J Surg* **1986**;73:925
4. Khuroo MS, Zargar SA. Biliary ascariasis: a common cause of biliary and pancreatic disease in an endemic area. *Gastroenterology* **1985**;88:418–423
5. Cerri GG, Leite GJ, Simoes JB, et al. Ultrasonographic evaluation of ascaris in the biliary tract. *Radiology* **1983**;146:753–754

Technical Note

Esophageal Deviation: Pushed or Pulled?

Marc S. Levine[1] and Alison M. Gilchrist[1,2]

Esophageal deviation to one side of the chest usually results from an extrinsic mediastinal mass on the opposite side that is compressing and displacing the esophagus from its normal midline position. Less frequently, esophageal deviation may be caused by pulmonary, pleural, or mediastinal scarring with retraction of the esophagus toward the diseased hemithorax. Unless an obvious mass is observed radiographically, however, it can be difficult to determine whether the esophagus has been "pushed" or "pulled" from its normal position in the mediastinum. In two well-known radiology textbooks, Sutton [1] and Eisenberg [2] indicate that traction on one wall of the esophagus due to fibrosis in the apex of the lung occasionally may produce an asymmetric "pseudodiverticular appearance." However, Eisenberg specifically states that retraction of the esophagus by apical pleuropulmonary fibrosis can simulate the radiographic appearance of an extrinsic mass arising from the opposite side [2]. We therefore wish to describe a simple radiologic sign that can be used on single- or double-contrast barium studies to determine whether the esophagus has been pushed or pulled from its normal midline position.

Description of Sign

Esophageal displacement by a mediastinal mass can be differentiated from esophageal retraction by pleuropulmonary scarring on single- or double-contrast esophagrams, using the radiologic sign illustrated in Figure 1. When the esophagus is displaced or pushed by an extrinsic mass in the mediastinum, the near wall of the esophagus (i.e., the wall abutting the mass) is usually displaced more than the far wall, so that the esophagus tends to be narrower at this level than it is above or below the deviated segment (Figs. 1A and 2). When the esophagus is retracted or pulled by pleuropulmonary scarring and volume loss, however, the near wall (i.e., the wall abutting the diseased hemithorax) is also deviated more

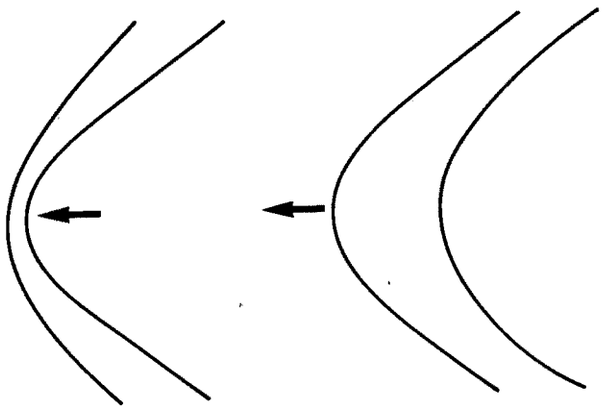


Fig. 1.—Diagram of "pushed" vs "pulled" esophagus.
***A*, When esophagus is displaced or pushed by extrinsic mediastinal mass, it tends to be narrower at this level (*arrow*) than above or below deviated segment.**
***B*, When esophagus is retracted or pulled by pleuropulmonary scarring and volume loss, however, it tends to be wider at this level (*arrow*) than above or below deviated segment.**

Received March 16, 1987; accepted after revision April 14, 1987.
[1] Department of Radiology, Hospital of the University of Pennsylvania, 3400 Spruce St., Philadelphia, PA 19104. Address reprint requests to M. S. Levine.
[2] Present address: Department of Radiology, Royal Victoria Hospital, Grosvenor Rd., Belfast, Northern Ireland.

AJR **149:513–514, September 1987** 0361–803X/87/1493–0513 © American Roentgen Ray Society

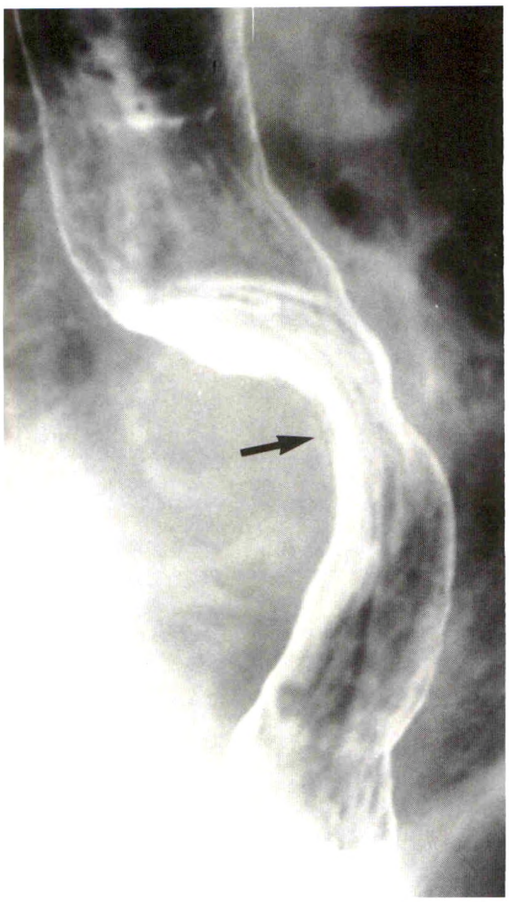
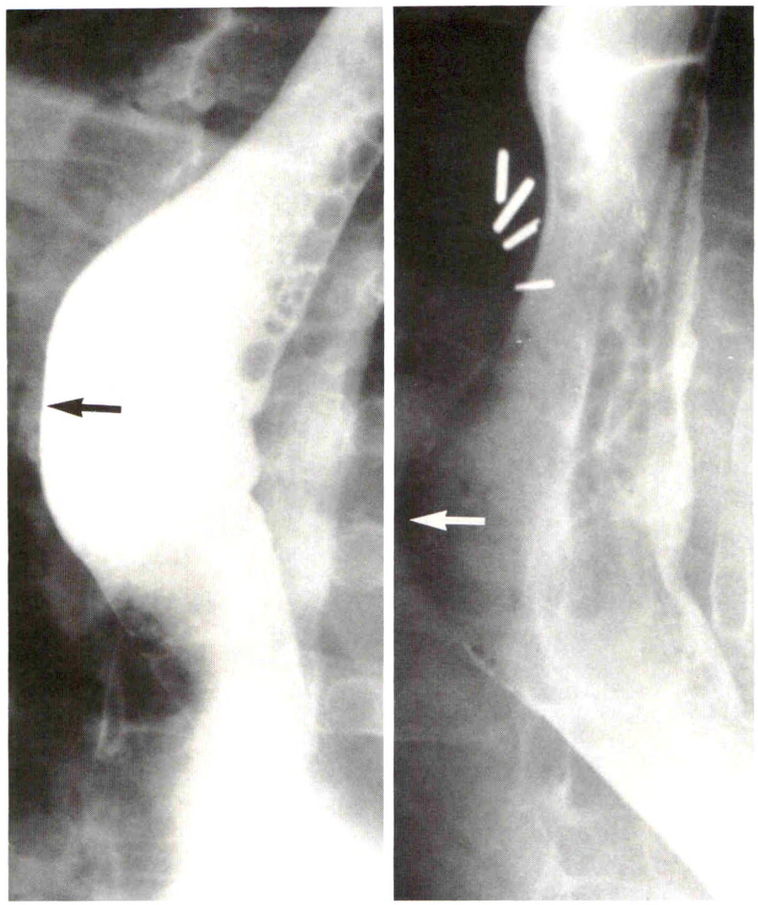


Fig. 2.—A 79-year-old woman with an ectatic descending thoracic aorta compressing and displacing distal esophagus to left (*arrow*) on double-contrast esophagram. Note how esophagus is narrowed at level of deviation.



A B

Fig. 3.—*A*, A 62-year-old man with right upper lobe tuberculosis causing deviation of upper thoracic esophagus to right (*arrow*) on single-contrast esophagram. Note how esophagus is widened at level of deviation. Chest radiographs showed extensive fibronodular changes of right upper lobe tuberculosis with associated fibrothorax and volume loss on that side.

B, A 54-year-old man known to have previously undergone pneumonectomy for carcinoma of lung has deviation of midthoracic esophagus to right (*arrow*) on single-contrast esophagram. However, localized esophageal widening at this level indicates retraction of esophagus toward side of surgery rather than displacement by mass on opposite side.

than the far wall, so that the esophagus tends to be wider at this level than it is above or below the deviated segment (Figs. 1B and 3). This localized widening or bulging of the esophagus has a characteristic appearance on single- or double-contrast esophagrams that permits differentiation from an extrinsic mass indenting and displacing the esophagus from the opposite side.

Discussion

The radiologic sign described above can be used on barium studies to determine whether the esophagus has been "pushed" or "pulled" from its normal midline position. Esophageal displacement by a mediastinal mass causes localized narrowing at the level of deviation (Fig. 2), whereas esophageal retraction by pleuropulmonary scarring causes characteristic widening at this level (Fig. 3). The latter finding indicates "pulling" of the esophagus toward the side of scarring rather than displacement by a mass on the opposite side. When esophageal retraction is suspected on barium studies, chest radiographs should confirm the presence of tuberculosis, radiation, postsurgical changes, or other signs of scarring and/or volume loss in the affected hemithorax.

A simple radiologic sign can therefore be used to determine whether the deviated esophagus has been pushed or pulled from its normal midline position. This differentiation is important, since esophageal retraction due to pleuropulmonary scarring can be noted and dismissed as an incidental finding, whereas esophageal displacement by a mediastinal mass may require further investigation to determine the nature and extent of the mass lesion.

REFERENCES

1. Sutton D, ed. *A textbook of radiology and imaging*, 3rd ed. New York: Churchill Livingstone, **1980**:679
2. Eisenberg RL. *Gastrointestinal radiology: a pattern approach*. Philadelphia: Lippincott, **1983**:42

Appendicitis as the Initial Manifestation of Crohn's Disease: Radiologic Features and Prognosis



Farooq P. Agha[1]
Gary G. Ghahremani[1]
Joseph S. Panella[1]
Michael W. Kaufman[2]

Twenty-five patients 15–47 years old presented with appendicitis as the initial manifestation of Crohn's disease. This entity accounted for 1.8% of all appendicitis patients undergoing surgery at our institution during a recent 9-year period. Preoperative radiologic studies in 18 (72%) of 25 cases showed abnormalities indicating the presence of appendicitis or periappendiceal abscess, but not the specific diagnosis of Crohn's disease as the underlying cause. Histopathologic evidence for an isolated, transmural, or granulomatous appendicitis was found in 20 patients; in two of these there was a local recurrence within 3 years after surgery, while 18 others have remained asymptomatic during follow-ups of up to 8 years. In the other five patients Crohn's disease caused appendicitis with concurrent inflammation of the cecum or terminal ileum; three of these cases were complicated by progressive granulomatous ileocolitis within 2 years.

The data presented herein indicate that (1) Crohn's disease can originate in and be confined to the appendix, yet manifest clinical symptoms leading to emergency laparotomy; (2) preoperative radiologic findings are similar to those of suppurative appendicitis, but visualization of a markedly thickened appendiceal wall with patent or irregularly narrowed lumen supports the diagnosis of Crohn's appendicitis; and (3) primary Crohn's disease of the appendix has a favorable long-term prognosis after simple appendectomy, despite a 10% incidence of recurrence as granulomatous ileocolitis.

Since the original description of regional enteritis by Crohn et al. [1] it has become apparent that the same histopathologic process may either originate in or secondarily involve any part of the alimentary tract. In approximately 20% of patients undergoing surgery for granulomatous ileocolitis, the resected specimen reveals evidence for appendiceal involvement as well [2]. However, primary Crohn's disease of the appendix is uncommon, and fewer than 100 cases have been reported in the literature [3–10].

This article describes our experience with 25 patients in whom the initial clinical presentation of Crohn's disease as appendicitis led to laparotomy. These cases were analyzed retrospectively to (1) determine the radiologic features that may indicate a correct preoperative diagnosis and (2) assess the potential risk of postappendectomy recurrence of Crohn's disease and its associated complications.

Materials and Methods

Histopathologic diagnosis of granulomatous or transmural nonsuppurative appendicitis caused by Crohn's disease was made in 25 patients who underwent appendectomy at the Evanston Hospital–McGaw Medical Center of Northwestern University (Evanston, IL) between January 1978 and December 1986.

The series consisted of 14 men and 11 women 15–47 years old (mean, 26). Twenty patients (80%) presented with clinical symptoms and physical findings suggestive of acute appendicitis or periappendiceal abscess. The remaining five patients had a history of recurrent right lower abdominal pain during the preceding 6 months to 3 years. Preoperative evaluation of these 25 patients included plain radiographs of the abdomen in 20, barium enemas in 13,

Received March 19, 1987; accepted after revision May 27, 1987.

Presented at the annual meeting and scientific session of the Society of Gastrointestinal Radiologists, Scottsdale, AZ, February 1987.

[1] Department of Diagnostic Radiology, Evanston Hospital–McGaw Medical Center of Northwestern University, 2650 Ridge Ave., Evanston, IL 60201. Address reprint requests to G. G. Ghahremani.

[2] Department of Pathology and Laboratory Medicine, Evanston Hospital–McGaw Medical Center of Northwestern University, Evanston, IL 60201.

AJR 149:515–518, September 1987
0361–803X/87/1493–0515
© American Roentgen Ray Society

upper gastrointestinal series with small-bowel follow-through in six, abdominal sonography in five, and CT in three.

All patients subsequently underwent laparotomy. Appendectomy with or without periappendiceal drainage was performed in 21 patients, while four others had segmental ileocecal resection. The specimens were examined by two experienced pathologists, and the diagnosis of appendiceal Crohn's disease was established on the basis of the same criteria as those for regional enteritis. The characteristic microscopic features included thickening of the appendiceal wall and constriction of its lumen, mucosal ulceration with crypt abscesses, fissure or fistula formation, transmural inflammation containing prominent lymphoid follicles, noncaseating epithelioid granulomas, submucosal and subserosal fibrosis, associated lymphangiectasia, and hypertrophy of muscularis mucosae and myenteric plexus of the appendix.

Results

Abnormalities indicative of appendicitis or periappendiceal abscess were recognized on preoperative radiologic studies in 18 (72%) of our 25 patients. The specific diagnosis of Crohn's appendicitis was not made in any instances, although regional enteritis was often mentioned among differential diagnostic possibilities.

Preoperative abdominal radiographs in 20 patients included both the supine and upright views. These showed a calcified appendicolith in two cases and a soft-tissue-mass density in the right lower quadrant in five. Small-bowel dilatation or air-fluid levels suggesting an obstruction were present in four cases. Of the 13 patients who underwent barium-enema examination, eight showed nonfilling of the appendix associated with extrinsic compression defect of the cecum and displacement of terminal ileum (Fig. 1). Three patients had a partially patent appendix with an irregular lumen (Fig. 2), while in the remaining two cases the opacified lumen seemed unremarkable except for a mild irregularity of its contour.

An upper gastrointestinal series with a small-bowel follow-through showed a nodular mucosa of the terminal ileum, probably caused by lymphoid hyperplasia, in three of six patients. However, three others had edematous folds or ulcerated mucosa of the distal ileum associated with deformity of the cecum and separation from adjacent segments (Fig. 3).

Sonograms of the lower abdomen were obtained in five patients, three of whom had a markedly thickened appendix measuring 2–3 cm in diameter (Fig. 3C). In one of these an appendicolith and periappendiceal abscess were also noted (Fig. 4A).

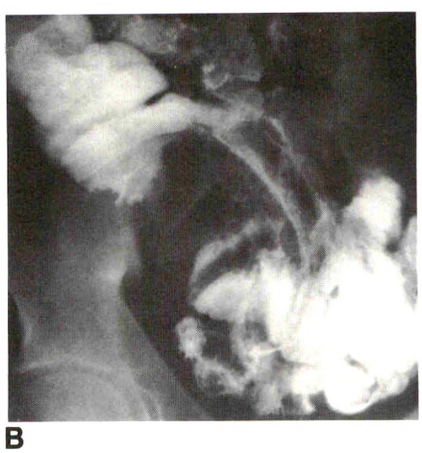
CT of the pelvis and abdomen in two of three patients examined by this technique revealed right lower quadrant abnormalities, primarily consisting of appendiceal wall thickening with periappendiceal inflammatory changes (Fig. 4B).

At laparotomy the appendix of all 25 patients was found to have a thickened wall with evidence of serositis on its external surface and the attached mesoappendix (Fig. 3D). Adhesions to the cecum and/or terminal ileum were frequently present, and five patients had periappendiceal phlegmon or abscess. The observed inflammatory changes were confined to the appendix in 20 patients, and they underwent appendectomy with or without drainage. Five other patients had Crohn's disease involving the appendix as well as the adjacent terminal ileum or cecum or both. A segmental ileocolic resection and ileoascending colostomy was performed in four of these cases, while the remaining patient had the appendix and the inflamed cecal tip removed.

The characteristic noncaseating epithelioid granulomas were found in only 15 of these cases, although their absence in the appendectomy specimen did not preclude the diagnosis of Crohn's disease when other typical histopathologic features were present. However, bacteriologic studies including Gram staining and/or cultures for enteric pathogens were performed to exclude infectious etiologies. In addition, each



A



B

Fig. 1.—Crohn's disease presenting as acute appendicitis and periappendiceal inflammatory mass in a 30-year-old man. Spot film of ileocecal region (*A*) and postevacuation film of barium enema examination (*B*) reveal nonfilling of appendix and extrinsic compression of ileocecal region. Note changing appearance of cecum and terminal ileum due to intermittent spasm and nonspecific inflammatory reaction to surgically proved granulomatous appendicitis.

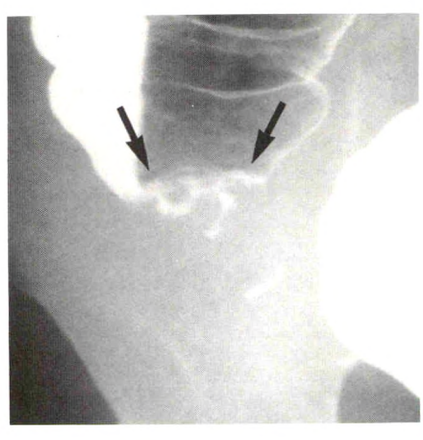


Fig. 2.—Crohn's disease of appendix and cecal tip in 28-year-old man with 2-month history of mild but persistent tenderness in right lower abdomen. Air-contrast view shows irregularly narrowed appendix associated with localized mucosal inflammation and deformity of cecum (*arrows*).

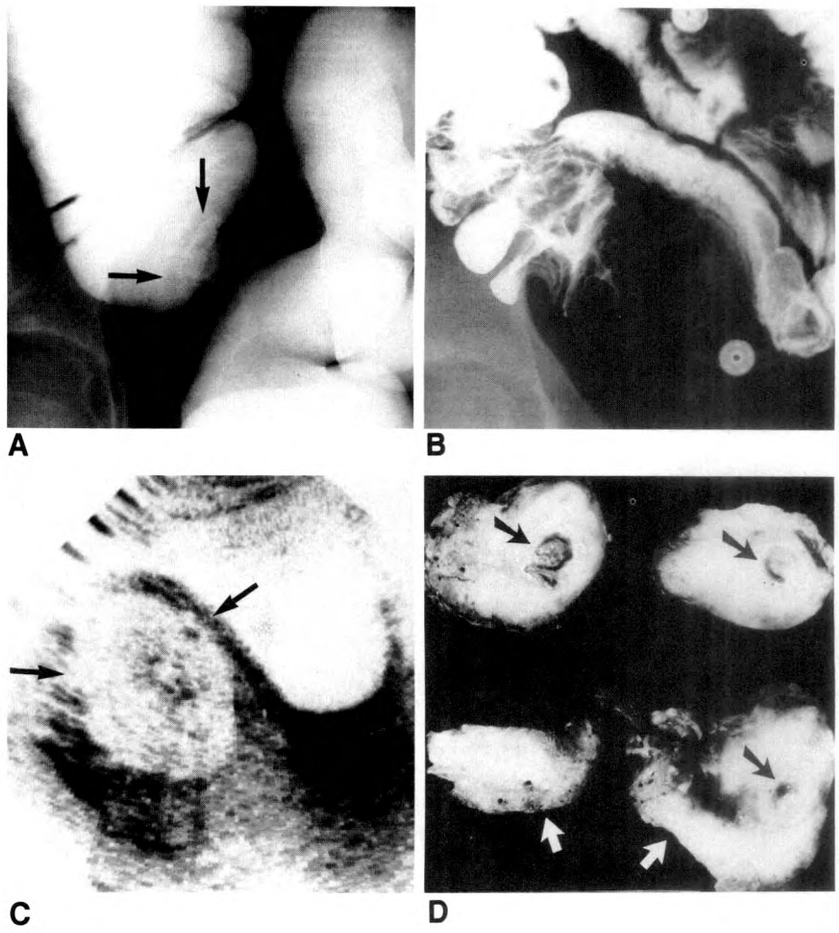


Fig. 3.—Acute appendicitis caused by Crohn's disease in a 15-year-old boy.

***A*, Barium enema shows slightly irregular and locally tender cecal tip (*arrows*), but nonfilling of appendix or terminal ileum.**

***B*, Small-bowel series 2 days later shows contracted cecum with thickened folds, finely nodular mucosa of terminal ileum, and suggestion of periappendiceal mass causing extrinsic compression on ileocecal segment.**

***C*, Sonogram of the right lower abdomen 2 days later reveals well-defined mass representing enlarged appendix (*arrows*) with some internal echoes from its eccentric lumen.**

***D*, Cross sections of resected appendix show its constricted lumen (*black arrows*), with marked thickening of the wall as well as attached mesoappendix (*white arrows*), from Crohn's disease. Note correlation with sonographic appearance.**

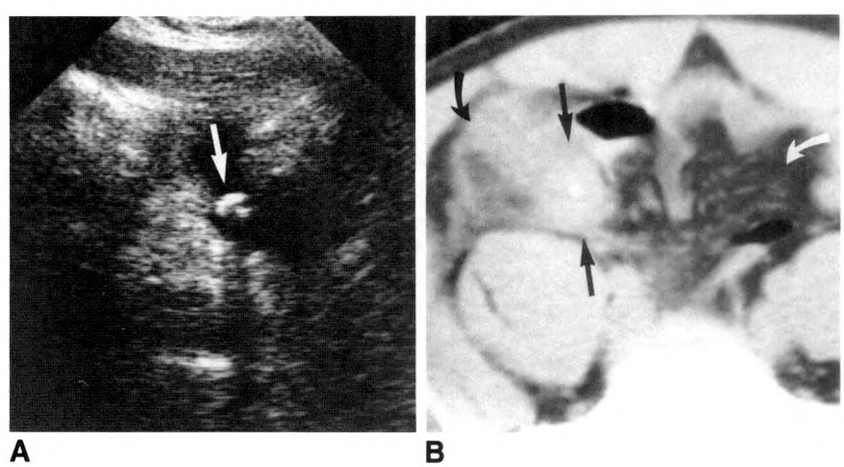


Fig. 4.—Crohn's appendicitis in 24-year-old man with fever, malaise, leukocytosis, and right lower abdominal pain.

***A*, Sonogram of right lower abdomen shows appendicolith (*arrow*) causing acoustic shadowing through periappendiceal inflammation.**

***B*, CT section shows radiopaque appendicolith in center of markedly thickened appendix (*black arrows*), as well as adjacent inflammatory process (*black curved arrow*) and mesenteric vascular engorgement (*white curved arrow*). Perforated appendix with periappendiceal abscess was found at surgery; histopathologic evaluation revealed a transmural granulomatous appendicitis with acute and chronic inflammation.**

case was carefully reviewed by two experienced pathologists to ascertain that the observed abnormalities were consistent with the diagnosis of Crohn's appendicitis.

Two (10%) of 20 patients with isolated Crohn's appendicitis subsequently developed granulomatous ileocolitis. It began as a postappendectomy enterocutaneous fistula in one case, while the other patient presented with recurrence nearly 2 years after surgery. Furthermore, three of five patients who had appendicitis with concurrent ileal or cecal involvement have manifested progressive Crohn's disease 2–4 years after their initial operation. The remaining 20 patients have been followed for up to 8 years at our institution or elsewhere; they have not shown any clinical or radiologic findings to suggest recurrent Crohn's disease.

Discussion

Approximately 100 cases of Crohn's disease first presenting as appendicitis have been described in the medical literature, most of them as anecdotal observations or incidental

findings [3–10]. Our experience represents the largest series reported from a single institution and indicates that this entity may be more common than generally realized. We encountered 25 cases among nearly 1400 consecutive appendectomies done over a 9-year period. This 1.8% incidence of Crohn's appendicitis might be due in part to a higher prevalence of inflammatory bowel disease in the population served by our hospital.

Although preoperative diagnosis of Crohn's appendicitis is difficult, it should be considered in adolescents and young adults who present with a history of intermittent right lower abdominal pain and moderate degrees of local tenderness, fever, and leukocytosis. Eighteen (72%) of our 25 cases had abnormal radiologic findings that indicated the presence of appendicitis but not its specific cause. On retrospective analysis, however, Crohn's disease as the underlying process might have been suspected if certain features were more clearly seen on preoperative studies. For example, barium-enema examination may show a patent but irregularly narrowed appendiceal lumen (Fig. 2) with coexistent inflammation and aphthous ulcers in the cecum terminal ileum or both (Figs. 1–3). Sonographic or CT demonstration of a markedly thickened appendix (Figs. 3C and 4) may also suggest the diagnosis of Crohn's disease, particularly when adjacent small-bowel loops or the colon show the CT features of this entity [11, 12].

Our radiologic findings of Crohn's appendicitis are based on a rather limited series, and only a few previous publications on this subject have commented on radiographic abnormalities. Two articles reported a total of five patients in whom the preoperative barium enema or small-bowel series showed extrinsic compression of the cecum or terminal ileum suggestive of a nonspecific appendiceal mass [4, 6]. However, Balthazar et al. [13] recently illustrated a case of Crohn's disease presenting as perforated appendicitis. CT of the abdomen in their patient showed a pericecal phlegmon associated with thickened walls of the cecum and terminal ileum.

There are two major concerns when isolated Crohn's appendicitis is diagnosed at the time of emergency laparotomy or during subsequent evaluation of the resected specimens: (1) Is there concurrent involvement elsewhere in the gastrointestinal tract? and (2) What is the potential risk of local recurrence or development of disease elsewhere in the gastrointestinal tract?

Both issues are of obvious critical importance for the best management of these patients. Yang et al. [8] and Timmcke [10] reviewed the literature on the subject and noted that concurrent Crohn's disease elsewhere in the gastrointestinal tract was present in approximately 25% of patients with Crohn's appendicitis. In our series five (20%) had concurrent involvement of the cecum or the terminal ileum at the time of laparotomy, and these inflammatory changes were evident on preoperative barium studies in four cases.

The recurrence rate after appendectomy for localized Crohn's disease has been reported as 14–50% [5, 8, 10]. However, only two (10%) of our 20 patients with isolated Crohn's appendicitis subsequently developed granulomatous ileocolitis. One of these patients had a fecal fistula from the appendectomy site, a complication previously seen in up to 20% of such cases [6–8]. Recurrent Crohn's disease was also detected in three of five patients whose appendicitis had been associated with concurrent inflammation of distal ileum or cecum or both. Nevertheless, two of these patients as well as 18 others with Crohn's disease confined to the appendix have remained asymptomatic anywhere from 2 to 8 years after surgery. Therefore, the uneventful postoperative course in 80% of the entire series would suggest a relatively favorable prognosis for appendiceal Crohn's disease. A somewhat similar conclusion was reached in a recent article by Ariel et al. [9]. They reviewed 25 patients undergoing surgery for primary Crohn's disease of the appendix and could confirm the diagnosis on reevaluation of pathologic slides in 22 of them. Their postoperative follow-up included periodic physical examination, barium studies of the small and large bowel, and proctosigmoidoscopy. Signs and symptoms of Crohn's disease at other sites in the gastrointestinal tract did not occur during the average follow-up period of 6.4 years after appendectomy. However, their review of other published reports indicated that Crohn's appendicitis had been followed by subsequent involvement of other intestinal segments in 7% of cases.

A number of other entities occasionally may manifest as granulomatous appendicitis, including tuberculosis, sarcoidosis, and *Yersinia pseudotuberculosis* [10, 14, 15]. In our series, therefore, the histopathologic evaluation of the resected specimens was complemented with bacteriologic studies using Gram stain to exclude an infectious cause. Furthermore, none of our patients had clinical or radiographic findings of pulmonary or systemic disease to suggest the remote possibility of appendiceal involvement by sarcoidosis or tuberculosis.

REFERENCES

1. Crohn BB, Ginzberg L, Oppenheimer GD. Regional ileitis, a pathological and clinical entity. *JAMA* **1932**;99:1323–1328
2. Lockhart-Mummery HE, Morson BC. Crohn's disease (regional enteritis) of the large intestine and its distinction from ulcerative colitis. *GUT* **1960**;1:87–105
3. Hall JH, Hellier MD. Crohn's disease of the appendix presenting as acute appendicitis. *Br J Surg* **1969**;56:390–392
4. Cohen WN, Denbesten L. Crohn's disease with predominant involvement of the appendix. *AJR* **1970**;110:361–363
5. Ewens SWR, Anderson J, Galloway JMD, Miller JDB, Kyle J. Crohn's disease initially confined to the appendix. *Gastroenterology* **1971**;60:853–857
6. Threatt B, Appelman H. Crohn's disease of the appendix presenting as acute appendicitis: report of 3 cases with a review of the literature. *Radiology* **1974**;110:313–317
7. Weiss Y, Durst AL. Crohn's disease of the appendix: presentation of a case with review of literature. *Am J Gastroenterol* **1975**;63:333–339
8. Yang SS, Gibson P, McCaughey RS, Arcari FA, Bernstein J. Primary Crohn's disease of the appendix: report of 14 cases and review of the literature. *Ann Surg* **1979**;189:334–339
9. Ariel I, Vinograd I, Hershlag A, et al. Crohn's disease isolated to the appendix: truths and fallacies. *Hum Pathol* **1986**;17:1116–1121
10. Timmcke AE. Granulomatous appendicitis. Is it Crohn's disease? Report of a case and review of the literature. *Am J Gastroenterol* **1986**;81:283–287
11. Goldberg HI, Gore RM, Margulis AR, Moss AL, Baker EL. Computed tomography in the evaluation of Crohn's disease. *AJR* **1983**;140:277–282
12. Yeh HS, Rabinowitz JG. Granulomatous enterocolitis: findings by ultrasonography and computed tomography. *Radiology* **1983**;149:253–260
13. Balthazar EJ, Megibow AJ, Hulnick D, Gordon RB, Naidich DP, Beranbaum ER. CT of appendicitis. *AJR* **1986**;147:705–710
14. Payan HM, Gilbert EF, Hafez R. Granulomatous appendicitis. *Dis Colon Rectum* **1981**;24:432–436
15. El-Maraghi NBH, Mair NS. The histopathology of enteric infection with *Yersinia pseudotuberculosis*. *Am J Clin Pathol* **1979**;71:631–639

Opinion

Primary Panendoscopy: A Radiologist's Response

David W. Gelfand,[1] David J. Ott, and Yu Men Chen

Most radiologists are aware that gastroenterologists advocate substitution of primary panendoscopy for the initial radiologic examination of the upper gastrointestinal tract. A recent publication in *Gastrointestinal Endoscopy* by Overholt et al. [1] contains a strategy, widely discussed among gastroenterologists, that is designed to encourage performance of primary panendoscopy rather than the upper gastrointestinal series. Curiously, two points in this strategy have merit.

First, Overholt et al. [1] advise that endoscopists reduce the cost of their studies to compete more aggressively with the lower costs of the radiologic examination. This is commendable considering the relatively low equipment costs and brief time required for the endoscopic examination. Most patients (and physicians) would welcome a reduction in endoscopic fees, which generally are regarded as excessive. However, it is our observation that the fees for endoscopy are not being reduced.

Second, it is suggested that diagnostic endoscopy be performed on brief referral, that the patient be returned to the care of the primary physician with a report of the endoscopic findings. Although this strategy is designed mainly to placate the referring physician's concern that the gastroenterologist might usurp the care of the patient, it does have the merit of avoiding the conflict of interest inherent in the present widespread self-referral of these highly remunerative procedures. Almost certainly, this self-referral encourages performance of more endoscopic procedures than would be the case otherwise. As an example, it is known that physicians who own their own equipment order radiologic examinations twice as often as physicians who refer their patients to other facilities [2]. The present self-referral of endoscopies likely results in a similar increase in the numbers of procedures performed.

In advocating primary panendoscopy instead of an initial radiologic examination, however, Overholt et al. [1] refer to radiologic results that are among the worst reported [3–5]. Similar reference to poor radiologic results gathered by endoscopists is almost universal in publications that advocate endoscopy instead of radiologic examinations. On the other hand, the radiologic literature suggests that radiologic detection of important pathologic entities in the upper gastrointestinal tract, such as gastric and esophageal carcinoma, esophageal strictures, and large peptic ulcers, is, in fact, comparable with endoscopic detection. The continuing usefulness of the upper gastrointestinal series is illustrated by the substantial numbers of studies obtained in Japan for detection and delineation of gastric cancer, despite the availability of endoscopy at a cost lower than that of the radiologic study.

Although gastroenterologists have created the impression that the error rate of endoscopy is negligible, it is probable that the accuracy of endoscopy is both lower and more variable than generally appreciated within the medical community. For example, in a recent report by Danish gastroenterologists [6] on the accuracy of the endoscopic diagnosis of gastric ulcer, the endoscopic error rate implied by interobserver disagreements was higher than the error rates generally found in radiologic publications. The gastroenterologists performing endoscopy agreed with the radiologic report more often than with each other.

If we assume that endoscopy has a modestly higher sensitivity for detecting small or superficial lesions, it is legitimate

Received April 27, 1987; accepted May 6, 1987.

[1] All authors: Department of Radiology, Bowman Gray School of Medicine, Wake Forest University, Winston-Salem, NC 27103. Address reprint requests to D. W. Gelfand.

AJR **149:519–520, September 1987** 0361–803X/87/1493–0519 © American Roentgen Ray Society

to ask if patients benefit when endoscopy is used as the initial procedure. Read et al. [7], in an analysis of diagnostic and therapeutic strategies for treating patients with dyspepsia or ulcerlike symptoms, projected the mortality rates presented in Table 1. These indicate that the small differences among strategies are considerably less than any published estimate of the mortality rate associated with endoscopy [7, 8]. Thus, endoscopy appears to present a far greater risk to a patient with ulcerlike symptoms than the risk from any curable disease likely to remain undiagnosed after an initial radiologic study, which causes virtually no deaths. Furthermore, the risk from endoscopy may be greater than the risk from any disease likely to be present after blind ulcer therapy unaccompanied by any diagnostic procedure.

On the other hand, the usefulness of an initial radiologic examination, with endoscopy performed only as necessary, was shown in a recent investigation of the clinical results of 199 upper gastrointestinal studies in hospitalized patients [9]. As verified by the 44 endoscopic procedures eventually performed, diagnostic failures of the radiologic examinations were limited almost entirely to minor entities. Furthermore, follow-up of the 199 patients for 1–2 years failed to reveal any mortality or morbidity due to a lesion missed by this sequence of studies. In these patients, the costs of diagnosis would have been increased twofold if endoscopy had been performed as the initial procedure. Furthermore, performing the radiologic examination as the initial study largely avoided the 1% to 2% risk of mortality engendered in the panendoscopy of 200 patients.

On the basis of these considerations, the wisdom of performing panendoscopy as the initial diagnostic procedure in perference to the radiologic examination must be challenged seriously. The performance of endoscopy as a substitute for the several million radiologic upper gastrointestinal series currently performed in the United States will result in several hundred deaths due to endoscopic complications each year. As suggested by the extremely small difference in mortality rates among the diagnostic strategies used in patients with ulcerlike symptoms, there is no prospect that primary endoscopy annually will save the several thousand lives required to justify such an "up-front" toll.

TABLE 1: Mortality Rates of Strategies for Patients with Ulcer Symptoms and for Panendoscopy

Strategy	Mortality Rate
Ulcer therapy only	0.016407
UGI, then ulcer therapy	0.016387
UGI, then endoscopy for gastric ulcers	0.016371
Panendoscopy (estimated rate)	0.000050–0.000650

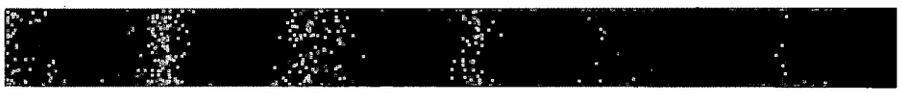
Note.—Rates for ulcer strategies from Read et al. [7]. Rates for panendoscopy from Read et al. [7] and Shamir and Schuman [8]. UGI = upper gastrointestinal series.

The concept of primary endoscopy will continue to be promoted by gastroenterologists, both among themselves and in the medical community as a whole. However, it presents the unfortunate prospect of simultaneously increasing both costs and the number of patient deaths.

REFERENCES

1. Overholt BF, Hargrove RL, Farris RF, Porter FR. Primary panendoscopy. *Gastrointest Endosc* **1987**;33:1–3
2. Childs AF, Hunter ED. Non-medical factors influencing use of diagnostic x-ray by physicians. *Med Care* **1972**;10:323–335
3. Tedesco FJ, Griffin JW, Crisp WL, Anthony HF. "Skinny" upper gastrointestinal endoscopy—the initial diagnostic tool: a prospective comparison of upper gastrointestinal endoscopy and radiology. *J Clin Gastroenterol* **1980**;2:27–30
4. Martin TR, Vennes JA, Ansel HJA. A comparison of upper gastrointestinal endoscopy and radiography. *J Clin Gastroenterol* **1980**;2:21–25
5. Dooley CP, Larson AW, Stace NH, et al. Double-contrast barium meal and upper gastrointestinal endoscopy: a comparative study. *Ann Intern Med* **1984**;101:538–545
6. Gjørup T, Agner E, Jensen LB, Jensen AM, Møllman KM. The endoscopic diagnosis of gastric ulcer. *Scand J Gastroenterol* **1985**;20:554–558
7. Read L, Pass TM, Komaroff AL. Diagnosis and treatment of dyspepsia: a cost-effectiveness analysis. *Med Decision Making* **1982**;2:415–438
8. Shamir M, Schuman BM. Complications of fiberoptic endoscopy. *Gastrointest Endosc* **1980**;26:86–91
9. Munitz HA, Gelfand DW, Ott DJ. Upper gastrointestinal series: patient management and a study of 199 cases. *Gastrointest Radiol* **1985**;10:277–281

The Distinction Between Acute Renal Transplant Rejection and Cyclosporine Nephrotoxicity: Value of Duplex Sonography



Ann R. Buckley[1]
Peter L. Cooperberg[1]
Charles E. Reeve[2]
Alexander B. Magil[3]

Although sonography is useful in the evaluation of renal transplants, there are no objective sonographic findings for reliably differentiating acute rejection from cyclosporine nephrotoxicity. This study was undertaken to determine the role of pulsed Doppler flow analysis (duplex sonography) in making this distinction. Duplex Doppler sonography was performed in 106 patients with normally functioning transplanted kidneys and in 34 patients with renal transplant dysfunction who underwent percutaneous biopsy. Renal vascular impedance was estimated in the segmental, interlobar, and arcuate arteries by calculating the ratio of end-diastolic minimum velocity to systolic peak velocity (diastolic/systolic ratio). In the healthy control subjects, the diastolic/systolic velocity ratios varied in the different arterial segments, ranging from a mean of 0.23 in the segmental arteries to a mean of 0.32 in the arcuate arteries. Seventeen patients experienced acute rejection: eight of the nine with acute vascular rejection had abnormal Doppler ratios; eight patients with acute cellular rejection had normal ratios. Nine patients with cyclosporine nephrotoxicity all had normal duplex scans. Seven patients with chronic rejection had normal ratios. One patient with hemolytic-uremic syndrome had an abnormal flow pattern.

These findings indicate that duplex sonography may be useful in differentiating acute vascular rejection from cyclosporine nephrotoxicity in the transplanted kidney.

Sonography has been used extensively in the evaluation of renal transplants [1–13]. Sonographic imaging can definitively show hydronephrosis, peritransplant fluid collections, and enlargement of the kidney due to edema. There are sonographic signs that have been used to try to differentiate rejection, cyclosporine nephrotoxicity, and acute tubular necrosis [1–9]. These are based on altered echogenicity of the cortex, medulla, and renal sinus. However, these findings are subjective and have not proved to be reliable, definitive, or specific [10].

With the improvement in quality and ease of use of pulsed Doppler sonography combined with real-time scanning (duplex sonography), it is now possible to detect and analyze blood flow velocity patterns. Since the renal transplant is superficial and relatively immobile, it is particularly amenable to duplex sonographic evaluation, especially using higher frequency transducers. It has been suggested that peripheral vascular resistance increases in certain types of renal transplant dysfunction [14–19]. Peripheral vascular resistance can be estimated by a ratio of diastolic and systolic flow velocities [20–22]. We undertook to evaluate diastolic/systolic (D/S) ratios in normal and dysfunctional renal allografts and to see if cyclosporine nephrotoxicity could be differentiated from rejection by using this technique.

Materials and Methods

The study group consisted of 119 examinations in 106 patients with normally functioning renal transplants who were referred for routine postoperative and yearly follow-up sonography, as well as 65 examinations in 34 patients with renal transplant dysfunction who had undergone percutaneous biopsies. All transplants were from cadaveric donors.

For the control population, lack of abnormality of renal function was confirmed by biochem-

Received August 29, 1986; accepted after revision May 19, 1987.

[1] Department of Radiology, University of British Columbia and Vancouver General Hospital, 855 W. 12th Ave., Vancouver, B.C., Canada V5Z 1M9. Address reprint requests to P. L. Cooperberg.

[2] Department of Medicine, University of British Columbia and Vancouver General Hospital, Vancouver, B.C., Canada V5Z 1M9.

[3] Department of Pathology, University of British Columbia and Vancouver General Hospital, Vancouver, B.C., Canada V5Z 1M9.

AJR 149:521–525, September 1987
0361–803X/87/1493–0521
© American Roentgen Ray Society

ical, radioisotope, sonographic, and urographic studies. The age range was 21 to 64 years (mean, 36.4 years), and the male/female ratio was 2:1. The time since transplantation ranged from 3 days to 22 years (mean, 4.4 years). Of the 106 patients, 21 patients had 34 studies within 3 months after transplantation; usually at 2 weeks, 1 month, and 3 months. The studies done at 2 weeks were done before they were discharged. The remaining 85 patients were assessed at the time of their yearly routine evaluation.

The 34 patients with renal transplant dysfunction were scanned 65 times from 4 days to 5 years after transplantation. Renal transplant dysfunction was defined as a persistent elevation of serum creatinine ≥1.5 mg/dl. Percutaneous biopsies were performed on all 34 patients with a 16-gauge Tru-Cut biopsy needle under sonographic guidance. The duplex studies were done at the same time as the biopsies. The cores were divided for histologic, electron microscopic, and direct immunofluorescent examination [23]. The results of the duplex scans were compared with the clinical diagnosis mainly on the basis of the pathologic interpretation. Seven patients eventually required allograft nephrectomy. These were performed 3 to 9 days (average, 5 days) after the last duplex scan.

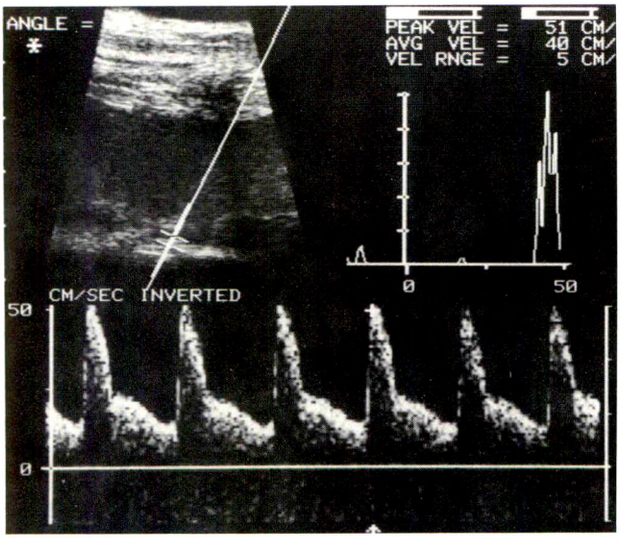


Fig. 1.—Duplex scan showing sample volumes superimposed over B-scan image in region of a segmental renal artery and typical normal velocity flow pattern. Calculated D/S ratio was 0.26. Histogram in upper right corner shows velocity distribution in systole.

All studies were performed with a Diasonics DRF 400 duplex scanner (Diasonics, Milpitas, CA). Initial imaging of the allograft was performed using a 5.0-MHz real-time mechanical sector scanner. Then, a duplex transducer using a 7.5- or 10-MHz imaging transducer and a 3.0- or 4.5-MHz, range-gated, pulsed Doppler transducer was used to evaluate Doppler signals from the regions of the segmental, interlobar, and arcuate arteries. These vessels were not actually visualized on the real-time image. However, the Doppler cursor was placed in the appropriate anatomic site and adjusted until a clear flow pattern was obtained (Fig. 1). The arterial signals obtained from the renal sinus were assumed to be from the segmental branches and from the deep portion of the cortex between the pyramids (the interlobar branches); those signals from the region of the corticomedullary junction were assumed to be from arcuate arteries. We measured the peak velocity in systole and the minimum velocity in diastole using one to three samples from each region. The built-in software was used to calculate the ratio of end-diastolic minimum velocity to systolic peak velocity (D/S ratio). Since the direction of blood flow could not be determined, absolute values for blood flow velocity could not be obtained. However, as we only compared diastolic and systolic velocities within each blood vessel, the angle between the Doppler sound beam and the direction of blood flow in the vessel was not important. When more than one sample was obtained from one region, the D/S ratios were averaged.

Results

Table 1 shows the results of diastolic/systolic velocity ratios in the different arterial segments. These are divided into an early group (≤3 months after transplantation) and a late group (>3 months after transplantation). The D/S ratios in the early renal transplants are more widely scattered than in the later group (Figs. 2–4). However, there is no statistically significant difference between the mean values in the two groups. The D/S ratios in both the early and the late studies increase from central to peripheral, with a mean of 0.23 in the segmental arteries to a mean of 0.32 in the arcuate arteries. However, there is considerable overlap and no significant statistical difference ($p < .1$). An example of a normal segmental arterial pattern and D/S ratio is shown in Figure 1.

The Doppler results and pathology findings in the 34 patients with renal transplant dysfunction are presented in Table 2. In addition, Figures 2–4 show scattergram comparisons of the D/S ratios in the different arterial segments in the two control groups and in the abnormal subjects. The normal and

TABLE 1: D/S Ratios in Control Groups

	Segmental Artery	Interlobar Artery	Arcuate Artery
≤3 months after transplantation (21 patients, 34 studies):			
Mean	0.23 ± 0.09[a]	0.25 ± 0.08[a]	0.28 ± 0.08[a]
Range	0.1 – 0.39	0.11 – 0.45	0.13 – 0.43
>3 months after transplantation (85 patients, 85 studies):			
Mean	0.26 ± 0.06[a]	0.29 ± 0.06[a]	0.32 ± 0.07[a]
Range	0.14 – 0.41	0.18 – 0.45	0.13 – 0.52

Note.—D/S ratio = ratio of end-diastolic minimum blood flow velocity to systolic peak blood flow velocity.
[a] Two standard deviations.

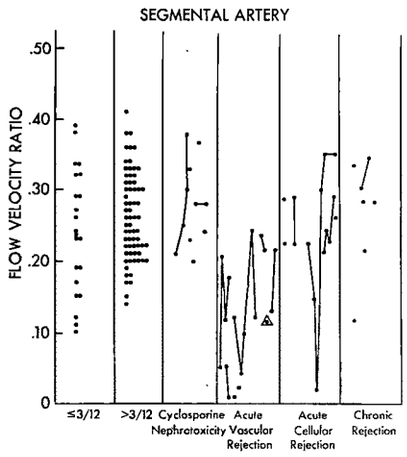


Fig. 2.—Scattergram of D/S ratios in segmental arteries of two control groups and in abnormal subjects. A continuous line implies serial studies in a single patient. Point enclosed in triangle shows patient with hemolytic-uremic syndrome. 3/12 = 3 months.

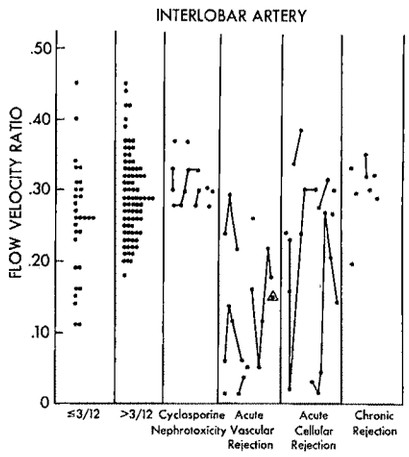


Fig. 3.—Scattergram of D/S ratios in interlobar arteries of two control groups and in abnormal subjects. A continuous line implies serial studies in a single patient. Point enclosed in triangle shows patient with hemolytic-uremic syndrome. 3/12 = 3 months.

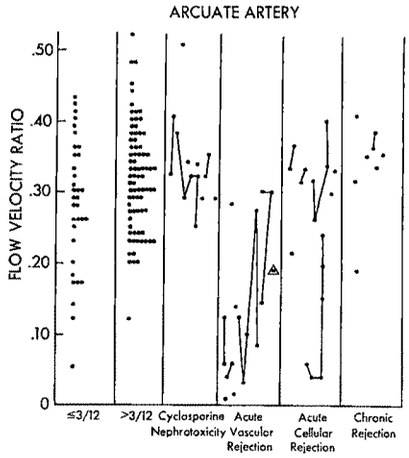


Fig. 4.—Scattergram of D/S ratios in arcuate arteries of two control groups and in abnormal subjects. A continuous line implies serial studies in a single patient. Point enclosed in triangle shows patient with hemolytic-uremic syndrome. 3/12 = 3 months.

TABLE 2: Summary of D/S Ratios and Pathologic Results in Patients with Renal Transplant Dysfunction

Results of Pathology	D/S Ratio
Acute cellular rejection	6 normal
	2 transiently abnormal
Acute vascular rejection	1 low normal
	8 abnormal[a]
Chronic rejection	6 normal
	1 low normal
Cyclosporine nephrotoxicity	9 normal
Hemolytic-uremic syndrome	1 abnormal

Note.—D/S ratio = ratio of end-diastolic minimum blood flow velocity to systolic peak blood flow velocity.

[a] Six patients had diastolic flow reversal.

abnormal Doppler flow velocity patterns usually are obviously different on inspection alone, especially if there is diastolic flow reversal. The measured and calculated D/S ratios best differentiated normal from abnormal at a level of 0.2 in the more peripheral arteries.

Nine patients with allograft dysfunction and biopsy-proved cyclosporine nephrotoxicity had duplex scans that showed normal anatomy, normal flow patterns, and normal D/S ratios. Eight patients improved when therapy was changed to azothioprine. The ninth patient continued to have elevated creatinine levels, and a second biopsy was consistent with azothioprine hypersensitivity. A repeat duplex scan at the time of the second biopsy was again normal. This patient is now well on cyclophosphamide maintenance therapy.

Nine of the seventeen patients had acute vascular rejection (Fig. 5), and eight showed cellular rejection, but without a vascular component. Of the nine with vascular rejection, the initial biopsy in three showed only cellular rejection. However, a subsequent biopsy in one and a nephrectomy in two showed evidence of arteriolar involvement to indicate vascular rejection. Two of the patients with acute cellular rejection were diagnosed on repeat biopsy, but the initial sample only showed acute tubular necrosis. All eight patients with cellular rejection showed normal flow patterns with normal or low normal D/S ratios. In eight of the nine cases with vascular rejection, there was no diastolic flow and diastolic reversal in six patients (Fig. 6). The ninth patient had a D/S ratio of 0.22.

One patient with hemolytic-uremic syndrome, occurring 3 years after transplantation, had a low D/S ratio (0.19). The biopsy showed a thrombotic microangiopathy. Seven patients with chronic rejection had normal D/S ratios, although one was in the lower range (0.21).

Discussion

After renal transplantation, patients are routinely treated with immunosuppressive drugs to minimize the risk of allograft rejection. Cyclosporine is widely used for this purpose. However, cyclosporine has well-recognized nephrotoxic effects [24]. There are no distinguishing clinical features to differentiate cyclosporine nephrotoxicity from acute transplant rejection. Such a distinction is clinically critical, as the treatment of rejection requires an increase in the cyclosporine dose whereas cyclosporine nephrotoxicity requires its reduction or elimination. At present, the distinction is based on the results of renal biopsy. On occasion, even the histology can be nonspecific, with evidence of both toxicity and rejection appearing on a single biopsy. Our results suggest that patients with renal transplant dysfunction and normal D/S velocity ratios are more likely to have either cyclosporine nephrotoxicity or cellular rejection (with a good prognosis) rather than vascular rejection (with a poor prognosis). However,

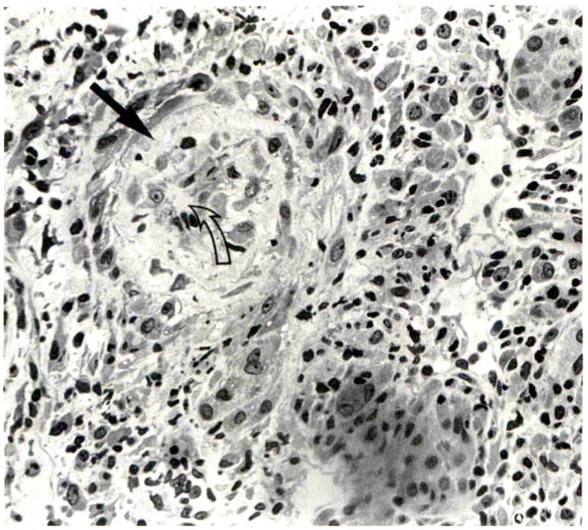


Fig. 5.—Histologic section showing an interlobular artery (*black arrow*) with swollen endothelial cells, intimal thickening, and a stenotic lumen (*open arrow*). Interstitium contains a mononuclear cell infiltrate characteristic of an acute cell-mediated allograft rejection. (H and E ×200)

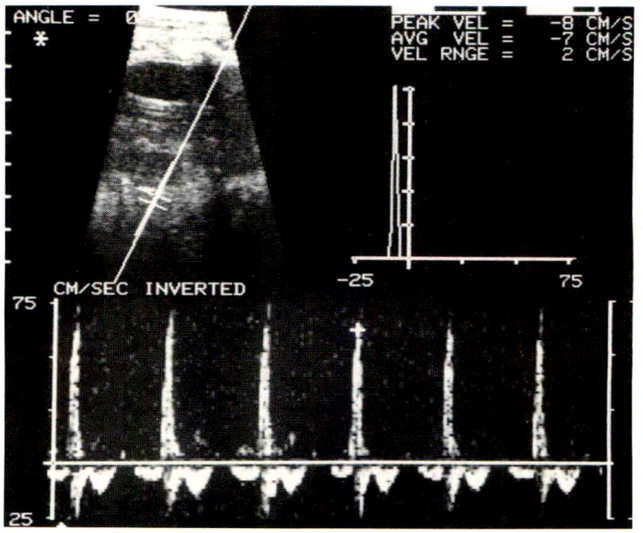


Fig. 6.—Duplex scan in a transplant with acute severe vascular rejection showing diastolic flow reversal.

duplex sonography cannot discriminate between cyclosporine nephrotoxicity, acute cellular rejection, and other causes of renal transplant dysfunction that do not affect vascular resistance.

In the early postoperative period, cyclosporine nephrotoxicity is primarily an abnormality of the tubules with no significant vascular changes [24]. We therefore would not expect to see any alterations in the D/S velocity ratios or waveform patterns during early cyclosporine nephrotoxicity. Later, arteriolar involvement may develop. These vascular changes tend to have a patchy distribution throughout the kidney, and probably do not significantly alter the overall peripheral resistance.

In this study, patients with persistently low D/S ratios, decreased diastolic flow, or diastolic flow reversal all had acute severe vascular rejection, with a very poor prognosis. To date, five of these nine patients have required allograft nephrectomy. In three patients with acute vascular rejection, the Doppler studies more accurately reflected the global status of the transplanted kidneys than did biopsies performed at the same time. In these three cases, the initial percutaneous biopsy in each was interpreted as only cellular rejection. However, a subsequent biopsy or nephrectomy showed clear evidence of arteriolar and small arterial abnormalities, indicative of vascular rejection; this finding correlated better with the duplex results. We presume that the erroneous interpretation of the initial biopsy result was due to a sampling error, the biopsy being taken from an area of milder involvement.

Two patients with early acute tubular necrosis and subsequent acute cellular rejection showed diastolic flow reversal, but in a focal distribution. The significance of these focal changes is still unclear. It is interesting, however, to note that both of these patients required a nephrectomy within 4 months of transplantation. Perhaps it would be useful in these cases to guide a percutaneous biopsy to an area of focal flow abnormality instead of performing a biopsy indiscriminately. The other six patients with acute cellular rejection had normal duplex scans. In each case, the rejection was mild to moderate, and the patients responded favorably to medical therapy. These normal duplex scans presumably reflect the lack of significant vascular compromise in mild-to-moderate cellular rejection.

Seven patients with chronic rejection also had normal duplex scans. The abnormality in chronic rejection involves progressive narrowing of the lumen in not only the small arteries and arterioles but also in the more central segmental arteries and even in the main renal arteries [25]. If it were possible to measure the actual peak systolic velocity, one could perhaps assess the more uniform narrowing in chronic rejection. This is, however, impossible to measure accurately, especially since the angle of the beam relative to the direction of flow cannot be ascertained.

The one patient with hemolytic-uremic syndrome had vascular occlusive changes similar to those of acute vascular rejection, and showed similar Doppler flow patterns and D/S velocity ratios.

It is the clinical practice in our hospital not to perform a renal transplant biopsy unless the renal dysfunction persists for more than 10 days. Some of the cases in the early control group showed low D/S ratios. It is possible that these patients had acute tubular necrosis or mild rejection with a transient increase in peripheral resistance; however, their condition improved and thus there was no need for a biopsy. It took longer for their creatinine levels to fall, but otherwise these patients were considered normal.

In the original reports on the relationship of flow to peripheral resistance, the Pourcelot Index (or, more recently, the pulsatility index) was calculated [20–22]. The Pourcelot Index {[S-D]/S} is equivalent to 1 – D/S. This should be proportional to peripheral resistance. We simplified this to D/S, which should be inversely related to the peripheral resistance. For the pulsatility index, the difference of end-diastolic flow from systolic peak flow is divided by the mean flow velocity. Perhaps the pulsatility index will be a more reliable estimate of peripheral resistance. However, the estimate of average flow velocity is much more complex, and more work is needed to find out if the results justify the added complexity compared with the simpler D/S ratio.

In renal transplant dysfunction, duplex sonography does appear to reflect the underlying pathologic vascular changes. However, Doppler cannot discriminate between the different causes of vascular involvement. After the early posttransplant period, a duplex study showing abnormal velocity flow patterns and persistently low D/S velocity ratios is strongly suggestive of severe acute vascular rejection with a poor prognosis. A normal Doppler study in a patient with renal dysfunction is suggestive of cyclosporine nephrotoxicity or mild cellular rejection (with a good prognosis). Although duplex sonography cannot yet substitute for biopsy, our preliminary experience suggests that this can be a useful adjunct in the evaluation of patients with renal transplant dysfunction.

REFERENCES

1. Hricak H, Toledo-Pereyra LH, Eyler WR, Madrazo BL, Sy GS. Evaluation of acute post transplant renal failure by ultrasound. *Radiology* **1979**;133:443–447
2. Hricak H, Cruz C, Eyler WR, Madrazo BL, Romanski RN, Sandler MA. Acute post-transplantation renal failure: differential diagnosis by ultrasound. *Radiology* **1981**;139:441–449
3. Maklad NF, Wright CH, Rosenthal SJ. Gray scale ultrasonic appearance of renal transplant rejection. *Radiology* **1979**;131:711–717
4. Barrientos A, Leiva O, Diaz-Gonzalez R, et al. The value of ultrasonic scanning in the differentiation of acute post transplant renal failure. *J Urol* **1981**;126:308–312
5. Delmonico FL, McKusick KA, Cosimi ABN, Russell PS. Differentiation between renal allograft rejection and acute tubular necrosis by renal scan. *AJR* **1977**;128:615–628
6. Rosenfield AT, Zeman RK, Cicchetti DV, Siegel NJ. Experimental acute tubular necrosis: US appearance. *Radiology* **1985**;157:771–774
7. Hricak H, Cruz C, Romanski RN, et al. Renal parenchymal disease: sonographic-histologic correlation. *Radiology* **1982**;144:141–147
8. Rosenfield AT, Siegel NJ. Renal parenchymal disease: histopathologic-sonographic correlation. *AJR* **1981**;137:793–798
9. Nomura G, Kinoshita E, Yamagata Y, Koga N. Usefulness of renal ultrasonography for assessment of severity and course of acute tubular necrosis. *JCU* **1984**;12:135–139
10. Linkowski GD, Warvariv V, Filly RA, Vincenti F. Sonography in the diagnosis of acute renal allograft rejection and cyclosporine nephrotoxicity. *AJR* **1987**;148:291–295
11. Singh A, Cohen WN. Renal allograft rejection: sonography and scintigraphy. *AJR* **1980**;135:73–77
12. Dubovsky EV, Logic JR, Diethelm AG, Balch CM, Tauxe WN. Comprehensive evaluation of renal function in the transplanted kidney. *J Nucl Med* **1975**;16:1115–1120
13. Reinitz ER, Goldman MH, Sais J, et al. Evaluation of transplant renal artery blood flow by Doppler sound-spectrum analysis. *Arch Surg* **1983**;118:415–419
14. Arima M, Ishibashi M, Usami M, et al. Analysis of the arterial blood flow pattern of normal and allografted kidneys by directional ultrasonic Doppler technique. *J Urol* **1979**;122:587–591
15. Avasthi PS, Voyles WF, Greene ER. Noninvasive diagnosis of renal artery stenosis by echo-Doppler velocimetry. *Kidney Int* **1984**;25:824–829
16. Siegel NJ, Gunstream SK, Handler RI, Kashgarian M. Renal function and cortical blood flow during the recovery phase of acute renal failure. *Kidney Int* **1977**;12:199–204
17. Taylor KJW, Burns PN, Woodcock JP, Wells PNT. Blood flow in deep abdominal and pelvic vessels: ultrasonic pulsed-Doppler analysis. *Radiology* **1985**;154:487–493
18. Arima M, Takahara S, Ihara H, et al. Predictability of renal allograft prognosis during rejection crisis by ultrasonic Doppler flow technique. *Urology* **1982**;19:389–394
19. Rigsby CM, Taylor KJW, Weltin G, et al. Renal allografts in acute rejection: evaluation using duplex sonography. *Radiology* **1986**;158:375–378
20. Johnston KW, Taraschuk I. Validation of the role of pulsatility index in quantitation of the severity of peripheral arterial occlusive disease. *Am J Surg* **1976**;131:295–297
21. Berland LL, Lawson TL, Adams MB, Melrose BL, Foley WD. Evaluation of renal transplants with pulsed Doppler duplex sonography. *J Ultrasound Med* **1982**;1:215–222
22. Norris CS, Barnes RW. Renal artery flow velocity analysis: a sensitive measure of experimental and clinical renovascular resistance. *J Surg Res* **1984**;36:230–236
23. Jones E, Magil A. Nonsystemic mesangiopathic glomerulonephritis with "full house" immunofluorescence. Pathological and clinical observations in 5 patients. *Am J Clin Pathol* **1982**;78:29–34
24. Mihatsch MJ, Thiel G, Spichtin HP, et al. Morphological findings in kidney transplants after treatment with cyclosporine. *Transplant Proc* **1983**;15[Suppl 1]:2821–2835
25. Morris PJ. *Kidney transplantation. Principles and practice.* New York: Grune & Stratton, **1984**:364–370

1988 AMERICAN ROENTGEN RAY SOCIETY MEETING

MAY 8–13, 1988
SAN FRANCISCO HILTON HOTEL
SAN FRANCISCO, CA

See page 656 and forthcoming issues for further information.

The Evaluation of Gross Hematuria in Anticoagulated Patients: Efficacy of IV Urography and Cystoscopy

John T. Cuttino, Jr.[1]
Richard L. Clark[1]
Samuel H. Feaster[1,2]
Dianne L. Zwicke[1,3]

To determine the efficacy of investigating gross hematuria in anticoagulated patients, records were reviewed of 24 patients who had gross hematuria while being treated with warfarin for various thromboembolic disorders. All had IV urography, and half had cystoscopy. Sources of bleeding were found in seven (29%) of 24 patients by IV urography and in five (42%) of 12 patients by cystoscopy. Abnormalities considered responsible for bleeding included renal stones (four), transitional cell carcinoma (one), calcified renal mass (one), lymphoma (one), bladder tumors (two), hemorrhagic cystitis (two), and a bleeding prostate tumor (one). Additionally, an enlarged prostate was the only abnormal finding in five patients. If an enlarged prostate is considered a source of bleeding, the workup that included both IV urography and cystoscopy identified a cause of bleeding in 17 (71%) of 24 patients.

The results suggest that IV urography and cystography are warranted in patients who take anticoagulants and who have gross hematuria.

Use of anticoagulants is associated with hemorrhage in approximately 10% of patients [1]. The most common site of bleeding is the urinary tract; hematuria is noted in approximately 40% of patients [1]. The prevalence of gross hematuria in anticoagulated patients varies from 4% [2] to 21% [3].

To determine the efficacy of investigating gross hematuria in anticoagulated patients, we analyzed the results of IV urography and cystography in a series of 24 patients who had gross hematuria while they were taking anticoagulants.

Materials and Methods

The results of IV urography and cystoscopy performed between January 1982 and July 1986 at North Carolina Memorial Hospital to determine the sources of gross hematuria in 24 patients who were taking warfarin were analyzed retrospectively. Patients whose clotting parameters were within the prothrombin time therapeutic range (1.5–2 × control) constituted the study population. All 24 patients had gross hematuria and had IV urography as the initial investigative procedure. The studies were performed by using standard doses (1 ml/kg) of 60% contrast media and routine radiography, which included nephrotomography. Half of the patients had routine cystoscopy performed by urologists. In seven patients, the source of bleeding was detected by urography, so cystoscopy was considered unnecessary. Five patients who had normal urograms did not have cystoscopy. In these patients, hematuria resolved before cystoscopy was performed, and it was decided to follow these patients clinically. The results of cystoscopy, biopsies, treatment, and clinical outcome as reported in the medical records were reviewed, and the urograms were analyzed.

The age range of the patients was 32 to 80 years (mean, 61). The group had 16 men and eight women. The disorders being treated with warfarin included pulmonary embolisms (eight), deep venous thromboses (four), conditions secondary to cardiac valve replacement (six), transient ischemic cerebral attacks (two), myocardial infarction (one), postoperative aorta–peripheral artery bypass grafts (two), and mesenteric embolus (one).

Received March 13, 1987; accepted after revision May 5, 1987.

Presented in part at the annual meeting of the Society of Uroradiology, St. Thomas, VI, March 1985.

[1]Department of Radiology, University of North Carolina, School of Medicine, Chapel Hill, NC 27514. Address reprint requests to J. T. Cuttino, Jr.

[2]Present address: Department of Radiology, University of Florida, School of Medicine, Gainesville, FL 32610.

[3]Present address: Department of Medicine, Mount Sinai Medical Center, Milwaukee, WI 53201.

AJR 149:527–528, September 1987
0361–803X/87/1493–0527
© American Roentgen Ray Society

Results

Abnormalities on IV urography were found in 14 (58%) of 24 patients. These included six with enlarged prostates; four with caliceal stones; and one each with transitional cell carcinoma of the renal pelvis, calcified renal mass (biopsy results indeterminate), ureteral obstruction secondary to retroperitoneal lymphoma, and chronic pyelonephritis. In seven, the lesions discovered were considered likely sources for hematuria (stones, carcinoma, mass, ureteral obstruction). These were corroborated by findings at surgery or by resolution of the hematuria after treatment of the abnormality.

Cystoscopy detected seven abnormalities (58% of the 12 patients studied by cystoscopy). These included bladder tumors (two), hemorrhagic cystitis (two), prostatic hypertrophy (two), and bleeding prostate tumor (one). A bleeding site was visualized in five (all but the two with prostatic hypertrophy). The patients with bladder tumors and hemorrhagic cystitis had normal urograms. Their lesions were too small to be detected, even retrospectively.

Both IV urography and cystoscopy detected the same abnormality (enlarged prostate) in two patients. However, in no case did both diagnostic studies detect an abnormality that was considered to be a source of bleeding. In two patients, IV urography and cystoscopy detected different abnormalities; one of these patients had chronic pyelonephritis (detected by urography) and hemorrhagic cystitis (cystoscopy), and the other had transitional cell carcinoma of the renal pelvis (urography) and an enlarged prostate (cystoscopy).

Likely or definite sources of bleeding were found by IV urography in seven patients and by cystoscopy in five (a total of 12 of 24 or 50%). Additionally, an enlarged prostate was the only abnormal finding in five patients. Because hematuria is a well-known symptom of prostatic hypertrophy [3], it could be argued that a total of 17 (71%) of 24 patients had findings positive for hematuria. In all of the seven patients who had negative findings, follow-up revealed no recurrence of hematuria.

Discussion

Hemorrhage is the most frequent and important complication of anticoagulant therapy. The prevalence varies but reported percentages range from as low as 4% by Roos and van Joost [4] to as high as 16% by Peyman [5] and 24% by Mosley et al. [2]. Hemorrhagic complications occur more often in ambulatory patients than in hospitalized patients [5], probably because of increased physical activity and poorer control of clotting parameters. In hospitalized patients, the prevalence is approximately 10% [1]. Sites of bleeding include the gastrointestinal tract, brain, retroperitoneum, peritoneal cavity, and, most commonly, the urinary tract (up to 40%) [1].

Hematuria in nonanticoagulated patients is almost always a hallmark of clinically significant disease of the urinary system and usually requires investigation. In a study of 270 patients with unexplained hematuria, Barkin et al. [6] found a causative lesion on IV urography and cystoscopy in more than 90%. Their series included 17 patients who experienced gross hematuria while receiving anticoagulants. In this group, the source of bleeding was found in only three (18%). Antolak and Mellinger [7] reported that they found a cause of hematuria in 81% of their patients who had gross hematuria while being treated with anticoagulants. If the low frequency of positive results reported by Barkin et al. is correct, follow-up of these patients rather than performance of diagnostic studies seems justified. However, like Antolak and Mellinger [7], we had a higher number of positive studies (71%), findings that appear to justify the use of IV urography and cystography in these cases.

The causes of the hematuria in our patients were similar to those reported by Antolak and Mellinger [7] and to the causes of hematuria reported in nonanticoagulated patients of similar age [8]. The lesions detected included stone disease, tumors, and inflammatory conditions. These patients have all done well after treatment. None of the patients with prostatic hypertrophy was treated, and in all the hematuria cleared. None of these patients had significant symptoms referable to prostatic enlargement.

Gross hematuria was found to be the result of serious, treatable conditions in 12 (50%) of our patients. In five additional patients, prostatic hypertrophy was considered a possible source of the gross hematuria. Whether the detection rate is 50% (12 of 24) or 71% (17 of 24), the percentage of positive findings suggests that IV urography and cystoscopy should be performed in the evaluation of anticoagulated patients with gross hematuria.

REFERENCES

1. Zweitler AJ, Coon WW, Willis PW III. Bleeding during oral anticoagulant therapy. *Am Heart J* **1966**;71:118–123
2. Mosley DH, Schatz IJ, Breneman GM, Keyes JW. Long-term anticoagulant therapy: complications and control in a review of 978 cases. *JAMA* **1963**;186:914–916
3. Walsh PC. Benign prostatic hyperplasia. In: Walsh PC, Gittes RF, Perlmutter AD, Stamey TA, eds. *Campbell's urology*, 5th ed. Philadelphia: Saunders, **1986**:1259
4. Roos J, van Joost HE. The cause of bleeding during anticoagulant treatment. *Acta Med Scand* **1965**;178:129–131
5. Peyman MA. The significance of haemorrhage during the treatment of patients with the Coumarin anticoagulants. *Acta Med Scand* **1958**;162[Suppl 339]:1–62
6. Barkin M, Lopatin W, Herschorn S, Comisarow R. Unexplained hematuria. *Can J Surg* **1983**;26:501–503
7. Antolak SJ Jr, Mellinger GT. Urologic evaluation of hematuria occurring during anticoagulant therapy. *J Urol* **1969**;101:111–113
8. Coe FL. Proteinuria, hematuria, azotemia, and oliguria. In: Petersdorf RG, Adams RD, Braunwald E, Isselbacher KJ, Martin B, Wilson JD, eds. *Harrison's principles of internal medicine*, 10th ed. New York: McGraw-Hill, **1983**:213

Case Report

Spermatic Granuloma Complicating Abdominoperineal Resection of the Rectum: Diagnosis by CT, MR Imaging, and Percutaneous Biopsy

Samuel H. Feaster,[1] Richard E. Kinard,[2] Judith M. Yancey,[1] and Robert L. Marsh[3]

Urinary complications after abdominoperineal resection of the rectum are not uncommon [1]. However, to our knowledge, spermatic granuloma complicating this procedure has not been reported previously. We present the CT, MR imaging, and percutaneous biopsy findings in such a case in which the spermatic granuloma simulated recurrent carcinoma.

Case Report

A 60-year-old man underwent abdominoperineal resection of the rectum for moderately well-differentiated adenocarcinoma. The pericolic lymph nodes were free of tumor, but numerous metastatic nodules were noted in the liver at the time of surgery. The patient did not receive radiation therapy. Four months after surgery, a CT scan showed a presacral mass near the surgical site in the pelvis (Fig. 1). On MR imaging, the mass had a high signal intensity on the T2-weighted image (Fig. 2), suggesting that the lesion was recurrent tumor or inflammation rather than postoperative fibrosis. A CT-guided percutaneous biopsy was performed with an 18-gauge needle by using a transgluteal approach. Pathologic examination of the specimen was diagnostic for a spermatic granuloma; it showed innumerable sperm, many of which had been engulfed by reactive histiocytes.

Discussion

Diagnosis of recurrent tumor in the pelvis after abdominoperineal resection is a well-known clinical problem [2–6]. The value of CT in detection of recurrence has been established, and the early detection it provides increases the chance for prolonged survival and better local therapy [3]. A baseline CT is recommended in the immediate postoperative period and at selected intervals (usually 6 months) to assess subsequent changes [3]. However, it is often difficult to distinguish recurrent tumor from postoperative and/or radiation fibrosis, and percutaneous biopsy often is required [2–4].

MR imaging shows promise for use in distinguishing recurrent tumor from radiation fibrosis [7]. However, relatively high signal intensity on T2-weighted images is not specific for tumor recurrence and may be seen in acute radiation change, infection, and hemorrhage [7]. MR imaging may be helpful, however, because if a mass has relatively low signal intensity on T2-weighted images, it is more likely to be due to fibrosis than to recurrent tumor. As radiologists gain more experience with this finding, it may obviate biopsy in selected cases.

This case represents the first known report of a spermatic granuloma complicating abdominoperineal resection of the rectum. Spermatic granulomas evolve from leakage of sperm into the soft tissues, resulting in an intense inflammatory and histiocytic reaction [8]. They are not an uncommon complication of vasectomy, but they are otherwise rare. In this case, the leakage of sperm probably resulted from the injury to the seminal vesicles or vas deferens at the time of surgery. The intense inflammatory response probably accounts for the high signal intensity of the mass on the T2-weighted images.

Received February 9, 1987; accepted after revision March 31, 1987.
[1] Department of Radiology, University of Florida College of Medicine, Gainesville, FL 32605.
[2] Department of Radiology, North Florida Regional Medical Center, Gainesville, FL 32605. Address reprint requests to R. E. Kinard.
[3] Department of Medicine, University of Florida College of Medicine, Gainesville, FL 32605.

AJR 149:529–530, September 1987 0361–803X/87/1493–0529 © American Roentgen Ray Society

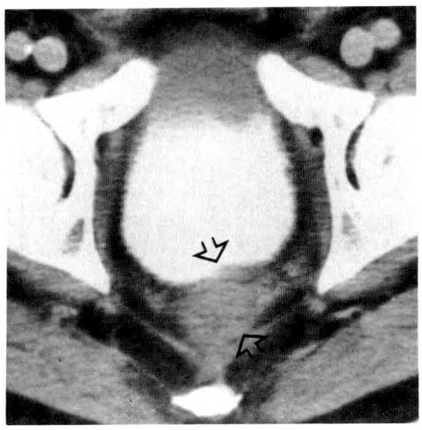


Fig. 1.—Axial CT image 6 months after resection of rectum shows a presacral mass (*arrows*).

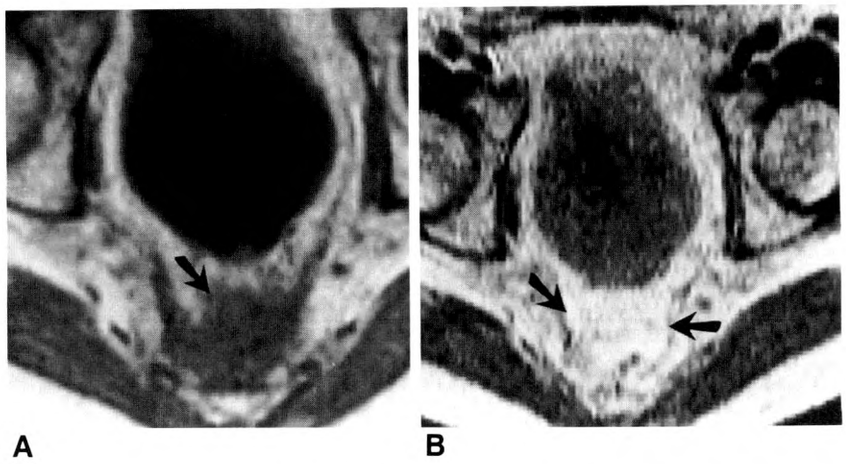


Fig. 2.—*A*, Axial T1-weighted image (TR 500 msec, TE 30 msec) shows a mass with a low signal intensity (*arrow*).

B, Axial T2-weighted image (TR 2000 msec, TE 60 msec) shows mass has a high signal intensity (*arrows*). Long T2 suggests lesion is due to recurrent tumor or inflammation rather than postoperative fibrosis. Biopsy showed lesion was a spermatic granuloma.

This report describes the effective combined use of CT, MR imaging, and percutaneous biopsy in the detection and evaluation of a postoperative mass after abdominoperineal resection for carcinoma of the rectum. Although rare, spermatic granuloma should be included in the differential diagnosis of a mass in this setting.

REFERENCES

1. Watters GR, Bokey EL, Chapuis PH, Maher PW, Pheils MT. Urologic complications following abdominoperineal excision of the rectum for carcinoma. *Aust NZ J Surg* **1983**;53:445–447
2. Butch RJ, Wittenburg J, Mueller PR, Simione JF, Meyer JE, Ferrucci JT. Presacral masses after abdominoperineal resection for colorectal carcinoma: the need for needle biopsy. *AJR* **1985**;144:309–312
3. Freeny PC, Marks WM, Ryan JA, Bolen JW. Colorectal carcinoma evaluation with CT: preoperative staging and detection of postoperative recurrence. *Radiology* **1986**;158:347–353
4. Zelas P, Haaga JR, Lavery IC, Fazio VW. The diagnosis by percutaneous biopsy with computed tomography of a recurrence of carcinoma of the rectum in the pelvis. *Surg Gynecol Obstet* **1980**;151:525–527
5. Lee JKT, Stanley RJ, Sagel SS, Levitt RG, McClennan BL. CT appearance of the pelvis after A-P resection for rectal carcinoma. *Radiology* **1981**;141:737–741
6. Reznek RH, White FE, Young JWR, Kelsey Fry I, Nichols RJ. The appearances on computed tomography after abdominoperineal resection for carcinoma of the rectum: a comparison between the normal appearances and those of recurrence. *Br J Radiol* **1983**;56:237–240
7. Glazer HS, Lee JKT, Levitt RG, et al. Radiation fibrosis: differentiation from recurrent tumor by MR imaging. *Radiology* **1985**;156:721–726
8. Glassy FJ, Mostofi FK. Spermatic granulomas of the epididymis. *Am J Clin Pathol* **1956**;26:1303–1313

MR Imaging of Marrow Changes Adjacent to End Plates in Degenerative Lumbar Disk Disease

Albert de Roos[1,2]
Herbert Kressel[1]
Charles Spritzer[1]
Murray Dalinka[1]

MR studies of the lumbar spine in 41 patients were analyzed at 203 disk interspaces to assess the appearance and frequency of bone marrow signal changes in the vertebral bodies adjacent to normal and degenerated disks. Degenerative changes were found at 58 interspaces; an abnormal bone marrow signal was identified in 29 (50%) of these. On spin-echo pulse sequences with short and long repetition times (TRs) and echo times (TEs), an area of relative increased signal intensity was seen in the vertebral body adjacent to the disk in 24 cases (17 were bandlike on both sides of the disk, four were focal on one side of the disk, and three were bandlike and focal on one or both sides of the disk). In one patient decreased signal was noted on both short and long TR/TE imaging. In the other four patients decreased signal was noted on short TR/TE pulse sequences and increased signal was evident on long TR/TE. These marrow changes were not present adjacent to normal disks. The relatively high signal intensity on both short and long TR/TE pulse sequences suggests that the increased signal resulted from the conversion of normal hemopoietic bone marrow to fatty marrow.

We conclude that bandlike or focal areas of high signal intensity in the bone marrow adjacent to degenerated intervertebral disks occur commonly on MR images of the spine and must not be confused with signal changes from tumors or infections involving the disk space and adjacent vertebral end plates.

MR imaging is an exquisite method for detecting bone-marrow abnormalities [1]. Normal vertebral bone marrow consists of hemopoietic marrow that demonstrates an intermediate signal intensity on MR pulse sequences with both short and long repetition times (TRs) and echo times (TEs) [2]. Bone-marrow changes adjacent to the vertebral end plates have been noted on MR in a variety of pathologic conditions [3]. We have observed focal alterations in bone-marrow signal intensity adjacent to the end plates in patients with degenerated disks. The purpose of this study was to assess the appearance and frequency of this finding in 41 MR examinations of the spine and to determine the pathophysiologic basis for these marrow changes.

Materials and Methods

MR studies were performed with a General Electric 1.5-T superconductive system, with a flat surface coil (15 × 24 cm) for spine imaging. Short TR, short TE spin-echo pulse sequences were obtained in the sagittal plane (TR = 800 msec, TE = 25 msec). The matrix size was 128 × 256 with a field of view of 20 cm. The slice thickness was 5 mm. The data were acquired with two excitations. In some patients, high-resolution images were obtained with a 3-mm slice thickness, four excitations, and a 256 × 256 matrix. In addition, axial images were obtained with short TR/TE (TR = 600–800 msec, TE = 25 msec) pulse sequences, and sagittal images were obtained with long TR/TE (TR = 2000–2500 msec, TE = 80 msec) pulse sequences. All patients were studied at least with short and long TR/TE pulse sequences in the sagittal plane and short TR/TE pulse sequences in the axial plane.

MR studies of the lumbar spine were reviewed in 31 consecutive patients with degenerative disease examined over a 15-month period. Disk degeneration was considered present when

Received September 8, 1986; accepted after revision April 7, 1987.

[1] Department of Radiology, The David W. Devon Medical Imaging Center, Hospital of the University of Pennsylvania, 3400 Spruce St., Philadelphia, PA 19104. Address reprint requests to H. Y. Kressel.

[2] Present address: Department of Diagnostic Radiology, University Hospital, Leiden, The Netherlands.

AJR **149:531–534, September 1987**
0361–803X/87/1493–0531
© American Roentgen Ray Society

there was loss of height and decreased signal intensity of the intervertebral disk on long TR/TE pulse sequences. The MR studies of a group of 10 patients with normal lumbar spines were also reviewed for comparison. A total of 203 disk levels were analyzed in 41 patients (22 women and 19 men 16–83 years old; mean, 52 years). Degenerated disks were noted in 58 of 203 disk interspaces.

The MR findings were correlated with clinical findings and plain radiographs (20 patients), CT examinations (four patients), and bone scintigraphy (four patients).

Results

Altered signal intensity in the bone marrow adjacent to the end plates was observed in 29 (50%) of 58 degenerated disks. This was not encountered at any normal disk levels. In 24 of the 29 abnormal disk levels there was increased signal intensity on short and long TR/TE pulse sequences. These marrow alterations were bandlike, focal, or mixed bandlike and focal on both sides of the disk (Fig. 1). The focal areas were typically posterior and adjacent to the disk. In one patient, decreased signal intensity was observed adjacent to the disk on both short and long TR/TE pulse sequences (Fig. 2). In four patients, decreased marrow signal intensity on short TR/TE pulse sequences and relatively high signal intensity on long TR/TE pulse sequences was demonstrated (Fig. 3). Patients with degenerative disk disease and altered marrow signal tended to be somewhat older than patients with degenerated disk and normal marrow signal (mean ages, 58 and 47, respectively). Spotty areas of increased signal intensity were seen in 65% of otherwise normal spines; however, extensive marrow alteration in the absence of degeneration was noted in only one patient.

Review of plain radiographs in 20 patients revealed degenerative disk disease in all cases. In one patient with decreased signal intensity along the disk on both short and long TR/TE pulse sequences sclerosis of the end-plates was observed (Fig. 2); in the other patients with altered marrow signal intensity on MR imaging no focal marrow abnormalities were observed on plain radiographs.

Bone scintigraphy in four patients did not show increased radionuclide uptake corresponding to the marrow changes; in two cases with a compressed vertebral body there was focal increased signal on MR with short TR/TE pulse sequences and an increased uptake on bone scintigraphy, probably related to compression.

CT studies in four patients did not show focal abnormalities in the vertebra, which demonstrated marrow alterations on MR. However, in two patients with bandlike increased signal intensity on both short and long TR/TE pulse sequences, CT showed extensive osteopenia at the corresponding levels. In one patient who had decreased marrow signal on short TR/TE pulse sequences and increased signal intensity on long TR/TE pulse sequences, CT showed a vacuum disk phenomenon at the level of disk degeneration seen on MR.

Discussion

The normal lumbar vertebral body has intermediate signal intensity on both short and long TR/TE pulse sequences due to the signal contribution of fat and hemopoietic marrow [2, 3]. The normal intervertebral disk demonstrates relatively homogeneous low signal intensity on short TR/TE pulse sequences. On long TR/TE sequences, the normal nucleus pulposus has a high signal intensity and a central cleft [4, 5].

We found alterations in marrow signal intensity adjacent to the intervertebral disks in 50% of cases with degenerative disks. MR imaging with short TR/TE pulse sequences showed the finding to best advantage. Three basic patterns of marrow changes were observed: (1) increased signal on short TR/TE

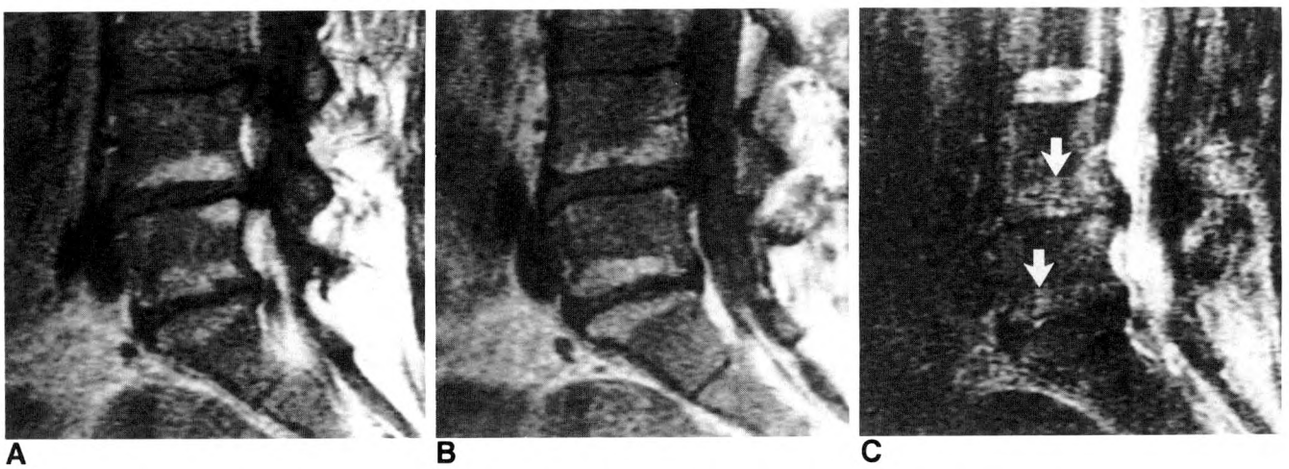


Fig. 1.—Regions of focal and bandlike increase in marrow signal adjacent to degenerated disks on short and long TR/TE pulse sequences suggesting fatty marrow conversion.

***A* and *B*, Consecutive parasagittal MR images (TR = 600 msec, TE = 25 msec) show bandlike increased bone marrow signal intensity on both sides of L5–S1 disk level and bandlike and focal area of increased signal intensity on either side at L4–L5 level. Note loss of intervertebral disk height at L4–L5 and L5–S1.**

***C*, Sagittal MR scan with long TR/TE pulse sequence (TR = 3000 msec, TE = 100 msec) shows degenerated disks at L4–L5 and L5–S1. Areas of relatively higher marrow signal intensity adjacent to degenerated disks are compatible with local increase in fatty marrow (*arrows*).**

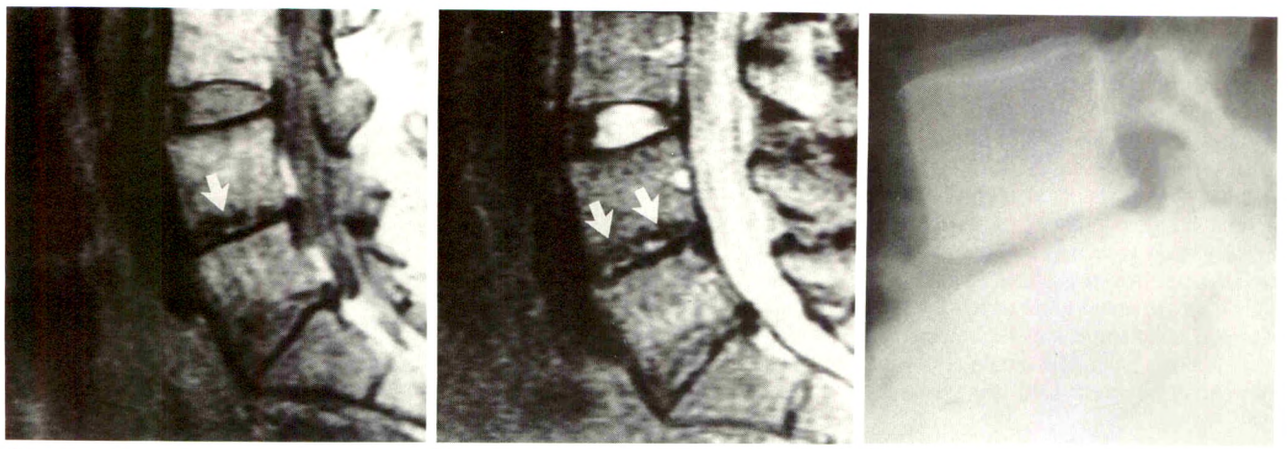


Fig. 2.—Bandlike signal decrease in marrow signal adjacent to degenerative disk on both long and short TR/TE pulse sequences in patient with end-plate sclerosis on plain-film radiography.

***A*, Sagittal MR image (TR = 800 msec, TE = 60 msec) shows decreased height of L4–L5 disk with bandlike decreased signal intensity adjacent to degenerated disk (*arrow*).**

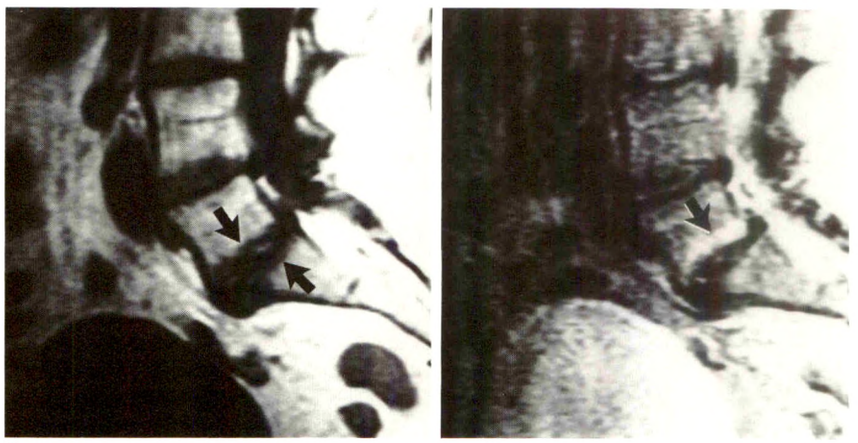
***B*, Sagittal MR image (TR = 2000 msec, TE = 60 msec) shows degenerated disk at L4–L5 and L5–S1 levels. Note decreased signal intensity adjacent to lower end plate of L4 (*arrows*).**

***C*, Lateral plain radiograph shows decreased disk height at L4–L5 level with adjacent end-plate sclerosis.**

Fig. 3.—Mixed pattern of altered signal adjacent to degenerated disk.

***A*, Sagittal MR image (TR = 600 msec, TE = 20 msec) shows bandlike decreased marrow signal intensity on both sides of L5–S1 disk (*arrows*).**

***B*, Sagittal MR scan (TR = 2000 msec, TE = 80 msec) shows increased marrow signal intensity adjacent to lower end-plate of L5 (*arrow*). Note disk degeneration at L3–L4, L4–L5, and L5–S1.**



and long TR/TE scans, (2) decreased signal on short TR/TE and long TR/TE scans, and (3) decreased signal on short TR/TE with increased signal on long TR/TE scans.

The increased signal intensity on both pulse sequences suggests the finding is caused by a local increase in marrow fat. Hajek et al. [6] recently noted a high frequency of spotty bone marrow alterations compatible with focal fatty infiltration in otherwise normal spines. However, in our cases the marrow abnormalities were more extensive and often had a bandlike appearance.

A pivotal role of end plates in the pathogenesis of degenerative disk disease has been suggested, because diffusion of nutrients into the disk mainly takes place across the end plates [7, 8]. Focal histologic changes in the cartilaginous end plates appear to precede histologic changes in the nucleus pulposus and anulus fibrosus [9]. In addition, during aging a vascular network along the end plates atrophies, and local marrow ischemia can cause a conversion of normal hemopoietic to fatty marrow [10–12]. Furthermore, bony trabeculae adjacent to the end plate become thickened, resulting in sclerosis as part of the degenerative process.

We believe that the focal fatty marrow conversion adjacent to degenerated disks, which we suspect accounts for the increased signal, reflects the local stress and ischemia involved in degenerative disk disease, which subsequently may result in end-plate compression and sclerosis. Conceivably, end-plate sclerosis could occur independently in a subgroup of patients with degenerative disk disease.

Local depositions of marrow fat may be the cause of focal areas of increased signal intensity on both short and long

TR/TE pulse sequences. Bandlike decreased signal intensity on both short and long TR/TE pulse sequences may relate to sclerosis or fibrosis adjacent to the disk. Decreased bandlike signal intensity along the disk on short TR/TE pulse sequences and relatively high signal intensity on long TR/TE pulse sequences were also noted. This pattern can be differentiated from the findings seen in infection by the absence of increased signal intensity of the disk on long TR/TE pulse sequences [13]. We hypothesize that in patients with this pattern of marrow alterations an increase in the water fraction of the marrow space is present. Conceivably this change may reflect local inflammation and/or ischemia. This hypothesis is strengthened by similar changes in marrow signal intensity that can occur in patients with ischemic necrosis of the hip [14].

ACKNOWLEDGMENTS

We thank Marcy Kreamer for manuscript preparation and Alexandra Kilger for help in data collection.

REFERENCES

1. Daffner RH, Lupetin AR, Dash N, Deeb ZL, Sefczek RJ, Schapiro RL. MRI in the detection of malignant infiltration of bone marrow. *AJR* **1986**;146:353–358
2. Wismer GL, Rosen BR, Buxton R, Stark DD, Brady TJ. Chemical shift imaging of bone marrow: preliminary experience. *AJR* **1985**;145:1031–1037
3. Modic MT, Masaryk TJ, Weinstein MA. Magnetic resonance imaging of the spine. In: Kressel HY, ed. *Magnetic resonance annual*. New York: Raven, **1986**:37–54
4. Modic MT, Pavlicek W, Weinstein MA, et al. Magnetic resonance imaging of intervertebral disk disease. Clinical and pulse sequence considerations. *Radiology* **1984**;152:103–111
5. Murphy WA, Totty WG. Musculoskeletal magnetic resonance imaging. In: Kressel HY, ed. *Magnetic resonance annual*. New York: Raven, **1986**: 1–35
6. Hajek PC, Baker LL, Goobar JE, et al. Focal fat deposition in axial bone marrow: MR characteristics. *Radiology* **1987**;162:245–249
7. Urban J, Holm S, Maroudas A, Nachemson A. An in vivo study of the penetration of the sulphate ion into the canine intervertebral disc and of its incorporation into the matrix. *J Bone Joint Surg [Br]* **1976**;58:255
8. Bernick S, Caillet R. Vertebral end-plate changes with aging of human vertebrae. *Spine* **1982**;7:97–102
9. Pritzker KPH. Aging and degeneration in the lumbar intervertebral disc. *Orthop Clin North Am* **1977**;8:65–77
10. Resnick D. Degenerative disease of the vertebral column. *Radiology* **1985**;156:3–14
11. Trueta J, Harrison MHM. The normal vascular anatomy of the femoral head in adult man. *J Bone Joint Surg [Br]* **1953**;35:442–461
12. Mitchell DG, Rao VM, Dalinka M, et al. Hematopoietic and fatty bone marrow distribution in the normal and ischemic hip: new observations with 1.5 Tesla MR imaging. *Radiology* **1986**;161:199–202
13. Resnick D, Niwayama G. Degenerative disease of the spine. In: Resnick D, Niwayama G, eds. *Diagnosis of bone and joint disorders*. Philadelphia: Saunders, **1981**:1368–1415
14. Mitchell DG, Rao VM, Dalinka M, et al. MRI of the normal and ischemic hips at 1.5 Tesla: observations utilizing T2 contrast. Presented at the annual meeting of the American Roentgen Ray Society, Washington, DC, April **1986**

The Effect of Restricting the Indications for Lumbosacral Spine Radiography in Patients with Acute Back Symptoms

Stephen R. Baker[1]
Andrew Rabin[1]
George Lantos[1]
E. John Gallagher[2]

A prospective study was performed to evaluate the effect of using a special requisition form on the utilization of lumbosacral spine radiography for patients presenting in the emergency room with acute lower back complaints. Over a 1-year period, emergency room house officers were encouraged to complete a special form that listed only three acceptable indications for lumbosacral spine radiographs: history of trauma, evidence of focal neurologic abnormality, and "other." Neurologic abnormalities included hypesthesia, hyperesthesia or anesthesia of lumbar or sacral dermatomes, weakness or hyporeflexia of the lower extremities, and bladder or bowel incontinence. If the indication "other" was chosen, radiographs were done only if the form contained both a one- to two-sentence history and the signed approval of a supervising attending physician. The number and results of lumbosacral spine examinations were compared with those from the previous year, which served as a control. In the control year 1443 examinations were performed, and in the experimental year only 759 were done (a decrease of 47%). The percentage of patients with vertebral fractures increased from 5.1% to 5.8% in the experimental year if only the detection of new fractures was considered positive, and from 9.1% to 13.4% if the detection of fractures of all ages was regarded as significant.

The use of the special requisition form appears to be a simple and effective means of reducing unnecessary lumbosacral radiography in the emergency room setting.

The costs [1], radiation dose [2, 3], and questionable effectiveness of lumbosacral spine radiography challenges the appropriateness of its continued widespread use [4–7]. There is a need to develop and implement guidelines that will limit the use of lumbosacral spine radiography to only those cases in which it can help establish an unequivocal diagnosis or influence patient management. The purpose of this paper is to report our experience with a special written form designed to restrict the indications for lumbosacral spine radiography in patients with acute lower back complaints.

Materials and Methods

The study was performed at the Bronx Municipal Hospital Center, a designated trauma center and a major teaching facility of the Albert Einstein College of Medicine. Each patient was seen in the emergency room by surgery, internal medicine, or emergency medicine house officers who obtained the medical history, performed the initial physical examination, and initiated requests for radiologic examinations. Forty percent of the house officers were full-time emergency room physicians. The other residents spent no more than 1 month on emergency room duty each year. The house staff was supervised by attending physicians who specialized in emergency medicine and by consultants in neurology and neurosurgery who were on call.

Beginning February 1, 1982, a special requisition form was instituted for lumbosacral radiography that listed only three indications: (1) trauma, (2) focal neurologic findings, and (3) "other." Neurologic abnormalities included hypesthesia, hyperesthesia or anesthesia of lumbar or sacral dermatomes, weakness or hyporeflexia of the lower extremities, and bladder or bowel incontinence. If the category "other" was chosen, a one- to two-sentence summary of

Received March 9, 1987; accepted after revision May 21, 1987.

[1] Department of Radiology, Albert Einstein College of Medicine, 1300 Morris Park Ave., Bronx, NY 10461. Address reprint requests to S. R. Baker.

[2] Department of Medicine, Albert Einstein College of Medicine, 1300 Morris Park Ave., Bronx, NY 10461.

AJR 149:535–538, September 1987
0361–803X/87/1493–0535
© American Roentgen Ray Society

clinical findings was required along with the signed approval by either an attending physician in Emergency Medicine or a consultant in Neurology or Neurosurgery. House officers were strongly encouraged to use the new form, although submitted requests for lumbosacral spine radiography on the preexisting general radiography requisition form were not rejected. This form, too, had space for clinical information but did not require attending countersignature. Examinations requested with the preexisting form were included in the compilation of data.

All emergency lumbosacral spine examinations over a 1-year experimental interval were tabulated and compared with those performed during the preceding year, when no attempt was made to restrict requests for lumbosacral spine films and only the general requisition form was used.

A negative study for acute changes included normal examinations, degenerative changes of the spine with or without disk-space narrowing, spondylolysis without spondylolisthesis, and minor congenital abnormalities such as spina bifida occulta, transitional lumbosacral vertebra, and unfused transverse process. Mild scoliosis and diffuse osteopenia without fracture were also placed in the negative category.

All radiographic reports from both the control and experimental years were further divided according to clinical indications. In the control year, placement into one of the three categories—trauma, neurologic change, or "other"—was determined on the basis of the requisition form. For both years, all urgent lumbar myelography and lower spine CT examinations performed on patients referred directly from the emergency room were also tabulated to determine if plain film findings influenced the decision to seek these more definitive examinations.

The form has been in continuous use since February 1, 1982. Aggregate annual examinations were compiled in the experimental year and in the three successive years ending January 31, 1986. For each year, a randomly selected sample of 100 examinations was selected to determine compliance with use of the special lumbosacral spine requisition form.

Results

The number of examinations decreased from 1443 in the control year to 759 in the experimental year, a decline of 47% (Fig. 1). The reduction in use of lumbosacral spine radiography was immediately apparent in the first month, with the February 1982 total being 42% less than that of February 1981. Along with a reduction in the number of annual examinations, there was less variation in the number of examinations performed from month to month.

The radiologic reports on 832 patients in the control year and 445 patients in the experimental year were available for analysis. Twenty-two reports from the control year and 12 from the experimental year were excluded because no clinical information was supplied, leaving 810 and 433, respectively, for further investigation. In the experimental year, 79% of lumbosacral spine studies were requested with the limited indication form. For the other 21%, the house staff used the preexisting general requisition form. All patients were assigned to one of four groups on the basis of age and gender. The percentage distribution of these four groups was remarkably similar during the 2 years of the study. In each year the number of examinations was divided equally between men and women. Men less than 50 years of age were examined most often, 35% in the control year and 36% in the experimental year. Men 50 years old or older were the least frequently studied, 15% in both years. Women less than 50 years of age made up 27% of patients in the control year and 25% in the experimental year. Women 50 years old or older made up 23% in the control year and 24% in the subsequent year.

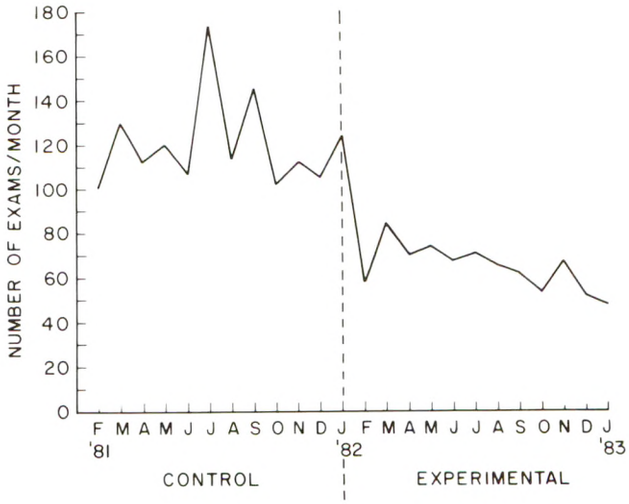


Fig. 1.—Monthly total of lumbosacral radiography in the control and experimental years.

Indications for examinations were determined from historic information provided on the general requisition form or tabulated directly from the special form. During both years, approximately half the examinations were done for the evaluation of trauma. In the control year, acute neurologic change was the reason for lumbosacral spine examination in 10%, while all "other" indications prompted 42% of requests. In the experimental year, neurologic change and the indication "other" each accounted for 24% of requests. The most frequent explanation for examination in the "other" category in both years was persistent back pain.

Each vertebral fracture was assessed according to two standards. A strict interpretation attributed as positive only those fractures that the radiologist deemed to be unequivocally new. Factors that suggested a new fracture included point tenderness at the fractured vertebra, absence of spurring or sclerosis across the fracture line, and lack of evidence of fracture on previous films. A liberal interpretation included every vertebral fracture, even if it was thought to be of questionable or indeterminate age.

With the strict standard, the overall percentage of fractures increased slightly from 5.1% to 5.8% in the control year, and in none of the four categories of patients was the positive rate greater than 16%. Under the liberal standard, the percentage of positive studies rose from 9.1% to 13.4% in the experimental period (Table 1). In both years, abnormal plain films were most frequent in women over 50 years of age, a finding that most likely reflects the high prevalence of osteoporosis and vertebral collapse in this population. This is substantiated by the disproportionate increase in positive

TABLE 1: Percentage Distributions and Number of Patients with Positive Lumbosacral Studies by Age, Gender, and Clinical Indication

	Percentage Males <50		Percentage Females <50		Percentage Males ≥50		Percentage Females ≥50		All Patients	
Control Year	A	B	A	B	A	B	A	B	A	B
Trauma	6.5 (10/155)	7.7 (12/155)	6.4 (7/110)	6.4 (7/110)	1.9 (1/54)	9.3 (5/54)	6.8 (5/74)	25.7 *(19/74)	5.8 (23/396)	10.9 (43/396)
Neurologic Change	4.3 (1/23)	4.3 (1/23)	4.2 (1/24)	4.2 (1/24)	0 (0/14)	0 (0/14)	15.8 (3/19)	21.1 (4/19)	6.3 (5/80)	7.5 (6/80)
"Other"	3.9 (4/103)	6.8 (7/103)	2.4 (2/84)	2.4 (2/84)	9.4 (5/53)	18.9 *(10/53)	2.1 (2/94)	6.4 (6/94)	3.9 (13/334)	7.5 (25/334)
Experimental year										
Trauma	5.8 (6/103)	9.7 (10/103)	5.4 (3/56)	5.4 (3/56)	4.8 (1/21)	9.5 (2/21)	11.1 (5/45)	37.8 *(17/45)	6.7 (15/225)	14.2 (32/225)
Neurologic Change	3.7 (1/27)	11.1 (3/27)	0 (0/25)	0 (0/25)	4.3 (1/23)	4.3 (1/23)	6.7 (2/30)	23.3 (7/30)	3.8 (4/105)	10.5 (11/105)
"Other"	0 (0/25)	4.0 (1/25)	6.9 (2/29)	6.9 (2/29)	5.3 (1/19)	26.3 (5/19)	10.0 (3/30)	23.3 (7/30)	5.8 (6/103)	14.6 (15/103)

Note.—A = Strict interpretation; B = liberal interpretation. Asterisks (*) indicate a significant difference from the total ($p < .05$).

studies in women over 50 years old who present with trauma. This increase is based on the liberal interpretation of acute fracture and on the lack of a statistically significant increase using the strict interpretation. The moderate overall rise in the percentage of positive studies in the experimental year is probably related to a selection bias engendered by the limited indication form, which served to deny examination to healthier postmenopausal women with minor back complaints. This tended to exclude those patients who were more apt not to have an acute fracture.

In both years, lumbar myelography and CT were available at all times for emergency room patients. The results of lumbosacral spine radiography had little influence on the decision to seek an additional imaging examination. There were 13 patients referred for myelography and CT studies in the control year, and only three of these had an abnormal lumbosacral spine examination. In the experimental year, seven of 15 patients who underwent CT or lumbar myelography also had a positive preliminary lumbosacral spine examination. In two-thirds of these cases, neurologic changes were the reason for the decision to proceed with CT or myelography.

Figure 2 reveals that the total number of lumbosacral spine requests has remained relatively unchanged since the imposition of the limited indication form. The yearly number of examinations continues to be well below the annual figures for each of the 2 years prior to the introduction of the special requisition form. What has changed in the past 4 years is the increasing acceptance of the new form. In the experimental year, 21% of requests used the preexisting general requisition form. Since then, the noncompliance rate has decreased every year and, in 1985, was only 4%.

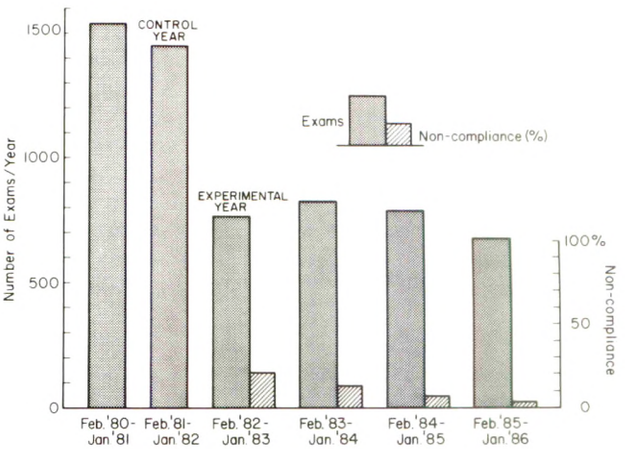


Fig. 2.—Annual emergency lumbosacral radiography from February 1980 to January 1986 and percentage compliance with limited indications form.

Discussion

Plain film examination of the lumbar spine is often obtained for the evaluation of low back pain. Recent investigations have clearly demonstrated that for many pain syndromes, plain radiographs of the lower back are frequently negative or reveal information unrelated to the patient's complaints [8–11]. Several studies have shown that minor developmental abnormalities, such as transitional vertebra or spina bifida occulta, are equally common in patients with and without backache [12–14]. Spondylosis and disk degeneration may cause pain the severity of which bears little relationship to the extent of changes demonstrated on plain films [15, 16]. Nerve root impingement can produce low back pain, but its severity is not necessarily proportional to plain film findings and its exact delineation requires further evaluation, usually by CT [17].

Limiting the use of spine radiographs almost exclusively to patients with trauma or acute neurologic change was an attempt to restrict the examination only to those who might derive benefit from it. The inclusion of the category "other" was a recognition of exceptional circumstances for which lumbosacral radiography could have special value. In most cases, patients in this group had a long history of pain that

did not resolve with time or therapy. Nonetheless, in both the control and experimental years, the yield in the "other" category was less than 5% in patients under the age of 50 years.

Postmenopausal women had the highest positive rate in both years. It is especially difficult in this group of patients to distinguish between the symptomatic woman with acute fracture and the patient with a painful back and an incidental fracture of uncertain age. Comparison with previous examinations, which could resolve the problem in many cases, was often not possible at the time of initial interpretation in the emergency room.

Plain radiographs of the spine have long been advocated as an essential examination in view of malpractice concerns [18, 19]. Certainly, the demonstration of an acute fracture has medicolegal implications that favor continued use in the evaluation of trauma to the spine. Yet patients at low risk for fracture should not be required to undergo this examination simply for fear of a lawsuit. In the 4 years since the special form has been in use, the Risk Management Committee of the Bronx Municipal Hospital Center has not been informed of any legal action contemplated against it because an emergency lumbosacral spine examination was not performed.

In both the control and the experimental years, the results of conventional lumbosacral spine radiographs bore little relation to the determination to seek further evaluation of the spinal canal by CT or myelography. Such a decision was usually reached on clinical grounds alone. Moreover, digital scout radiographs of the lower back can be obtained in the frontal and lateral projections during CT examinations, and scout radiographs are frequently obtained before myelography.

The introduction of a limited indication form was readily accepted by house officers assigned to the emergency room. Other investigators have suggested that forced modifications of practice routines will not persist because with the relaxing of surveillance to ensure that desired changes are carried out comes a reversion to former habits [20]. The 21% noncompliance rate in the experimental year was due to a lack of familiarity with the new requisition form. There was no attempt to alert house officers about the special form before they came on the emergency room rotation; further education about its presence and purpose took place on the job.

There are several reasons for the continuing approval of the limited indication form by the emergency room house staff. In our institution, there is a consensus shared by residents and attending physicians alike that lumbosacral spine radiography should be governed by strict guidelines. The provision of a new form that also included similar limited indications for skull radiography was a tangible reminder of the desire to reduce unnecessary studies [21]. The form is simple to fill out and does not create a paperwork burden. House officers were receptive to the requirement for attending involvement in the "other" category, which allowed them to defer decision-making to a higher authority in difficult cases. At present, after 4 years experience, the special requisition form is now well accepted by all physicians who provide care in the emergency room.

REFERENCES

1. Eisenberg RL, Akin JR, Hedgcock MW. Single, well centered lateral view of lumbosacral spine: is coned view necessary? *AJR* **1979**;133:711–713
2. *The National Ambulatory Medical Care Survey: office visits involving X-rays, United States, 1977*. Publication 79-1250. Washington, DC: Department of Health, Education and Welfare, **1979**
3. Webster EW, Merrill OE. Radiation hazards II: measurements of gonadal dose in radiographic examinations. *N Engl J Med* **1957**;257:811–819
4. Hall FM. Overutilization of radiological examinations. *Radiology* **1976**;120:443–448
5. Gehweiler JA, Daffner RH. Low back pain: the controversy of radiologic evaluation. *AJR* **1983**;140:109–112
6. Nachemson AL: The lumbar spine—an orthopedic challenge. *Spine* **1976**;1:59–71
7. Kelen GD, Noji EK, Doris PE. Guidelines for use of lumbar spine radiography. *Ann Emerg Med* **1986**;15:245–251
8. Scavone JG, Latshaw RF, Rohrer GV. Use of lumbar spine films: statistical evaluation at a university teaching hospital. *JAMA* **1981**;246:1105–1108
9. Rockney PH, Tompkins RD, Wood RW, et al. The usefulness of x-ray examination in the evaluation of patients with back pain. *J Fam Pract* **1978**;7:455–465
10. Witt I, Vestergaard A, Rosenklint A. A comparative analysis of x-ray findings of the lumbar spine in patients with and without lumbar pain. *Spine* **1984**;9:298–300
11. White AWM. Low back pain in men receiving Workman's Compensation. *Can Med Assoc J* **1966**;95:50–56
12. Fullenlove TM, Williams AJ. Comparative roentgen findings in symptomatic and asymptomatic backs. *Radiology* **1957**;68:572–574
13. Torgerson WR, Dotter WE. Comparative roentgenographic study of the asymptomatic and symptomatic lumbar spine. *J Bone Joint Surg [Am]* **1976**;58A:850–853
14. Splithoff CA. Lumbosacral junction: roentgenographic comparison of patients with and without backaches. *JAMA* **1953**;152:1610–1613
15. Hirsch C. Studies on the pathology of low back pain. *J Bone Joint Surgery [Br]* **1959**;41B:237–243
16. Waddel G. An approach to backache. *Br J Hosp Med* **1982**; 28(3):187–219
17. Chafetz N, Genant HK. Computed tomography of the lumbar spine. *Orthop Clin North Am* **1983**;14:147–169
18. Lusted LB. *A study of the efficacy of diagnostic radiologic procedures: final report of diagnostic efficacy*. Chicago: American College of Radiology, **1977**
19. Eisenberg RL, Hedgcock MW, Gooding GAW. Compensation examination of the cervical and lumbar spines. Critical disagreement in radiographic interpretation. *AJR* **1980**;134:519–522
20. Cummins RO. Clinicians' reasons for overuse of skull radiographs. *AJR* **1980**;135:549–552
21. Baker SR, Gaylord GM, Lantos G, Tabbaddor K, Gallagher EJ. Emergency skull radiography: the effect of restrictive criteria on skull radiography and CT use. *Radiology* **1985**;156:409–413

Percutaneous Biopsy of the Cervical Spine Using CT Guidance

Susan V. Kattapuram[1]
Daniel I. Rosenthal

CT was used during the percutaneous needle biopsies of seven cervical spine lesions. Four were primary bone tumors, and there was one case each of metastasis, fibrous dysplasia, and infection. Two of the lesions were located in the lateral masses of C1 and one was in the pedicle of C2. The other four were in the lower cervical spine (C4–C6). Accurate diagnosis was obtained on the first attempt in six (86%) of seven cases. No complications were encountered.

This experience suggests that needle biopsy performed with CT guidance is both safe and effective.

Adequate treatment of musculoskeletal lesions often depends on knowledge of the histologic diagnosis. Therefore, biopsy may be necessary before therapy of a skeletal lesion can begin. When a percutaneous approach can be substituted for an open biopsy, a specific diagnosis can be obtained with substantially reduced patient morbidity and cost. Percutaneous biopsy of the spine using radiographic or fluoroscopic guidance is a well-established procedure, especially for lumbar lesions [1–4]. Percutaneous biopsy of the cervical spine has been avoided, often because of concern for complications.

CT has been used to assist in the biopsies of a variety of anatomic sites and greatly enhances the safety and adequacy of this procedure [5–8]. With CT guidance and appropriate precautions, biopsy of the cervical spine can be performed with relative ease. Biopsies were done on lesions of the cervical spine in seven individuals and the diagnostic yield was satisfactory, with no complications.

Materials and Methods

Four men and three women underwent percutaneous biopsy of cervical spine lesions using CT guidance. All of them presented with neck pain of varying duration. The lesion was solitary in all seven. Ages ranged from 19 to 72 years (mean, 45). Purely lytic, mixed lytic, and sclerotic lesions were all included.

Preoperative evaluation included cervical spine radiographs and a radionuclide bone scan. Hematocrit, prothrombin time, partial thromboplastin time, and a platelet count were performed. A careful history of any bleeding tendency or ingestion of nonsteroidal anti-inflammatory drugs was obtained.

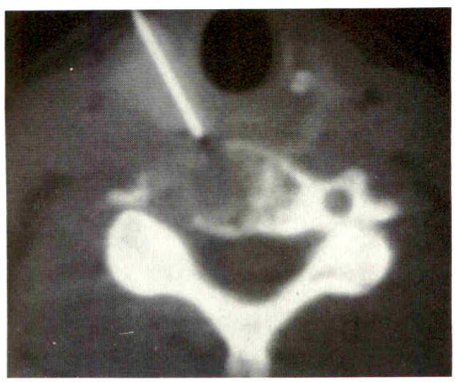
The type of biopsy needle used was based in part on the size of the lesion and the necessity of having densely mineralized bone in the sample. When it was not necessary to transgress cortical bone, a Tru-Cut needle (Travenol Laboratories, Inc., Deerfield, IL) was used to obtain a large, soft-tissue core. For biopsies through an intact vertebral cortex, a trephine needle such as the Turkel needle (Turkel Instruments Inc., Southfield, MI) was used. For small lesions or for lesions in particularly difficult anatomic sites, a 20-gauge cutting needle was preferred.

In the cervical spine, an anterior approach was used for the vertebral bodies. The patient was supine, and the needle was advanced between the pharynx and the carotid artery (Fig. 1). In some cases it was helpful to manually retract the great vessels laterally. For the

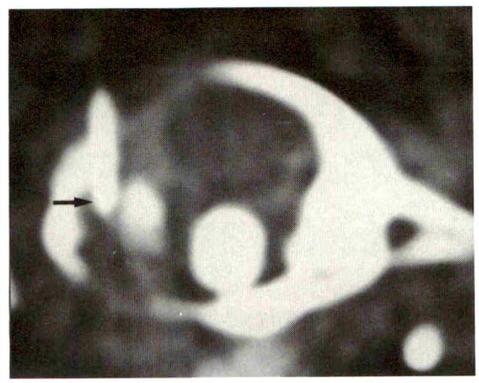
Received January 20, 1987; accepted after revision April 14, 1987.

[1] Both authors: Department of Radiology, Massachusetts General Hospital and Harvard Medical School, Boston, MA 02114. Address reprint requests to S. V. Kattapuram.

AJR 149:539–541, September 1987
0361–803X/87/1493–0539
© American Roentgen Ray Society



1



2

Fig. 1.—Case 2: Metastasis. Axial scan through C5 body shows anterolateral approach of biopsy needle medial to vascular triangle.

Fig. 2.—Case 3: Giant-cell tumor. Posterior parasagittal approach. Needle (*arrow*) is positioned caudal to C1 lamina and and medial to foramen transversarium.

posterior approach the patient was prone. The thecal sac and vertebral artery were carefully avoided, especially at the C1–C2 level. Because the vertebral artery courses along the upper (cranial) surface of the C1 lamina, it was possible to safely perform the biopsy of the lateral masses of C1 by angling the needle caudal to the lamina (Fig. 2). Local anesthetic was used for all biopsies. We used a tandem needle technique in which a 20-gauge spinal needle was introduced by increments using CT guidance. Anesthetic (1% lidocaine) was administered as the needle was advanced. If radicular symptoms were produced, the needle was slightly redirected. When the tip of the needle encountered the lesion, it was left in place. The biopsy needle was then placed adjacent to it along the same path. For large-gauge needles such as the Tru-Cut or Turkel, a small skin incision was made with a blade to allow easy passage of the large-caliber needle along the path marked by the spinal needle. Position of the large needle was confirmed by CT scans when the tip of the needle encountered bone, and again when the biopsy needle was within the lesion.

In each case, two core biopsies and an aspiration sample were attempted. Each of the procedures lasted from 40 min to 1 hr.

Results

A summary of the cases, techniques used, and the diagnoses are given in Table 1. The correct diagnosis was made in six (86%) of the seven cases. One biopsy of fibrous dysplasia was done because the presence of pain and the highly lytic, expanded appearance of the lesion raised the question of a neoplasm. The biopsy showed no tumor cells, although the tissue recovered was insufficient for diagnosis of fibrous dysplasia.

The patients experienced only mild discomfort, which was adequately controlled by local anesthetic. No complications were encountered.

Discussion

Biopsy of the cervical spine poses special problems because of the proximity of many vital organs. Although we encountered no problems in this small series, the potential for bleeding and damage to nerves and spinal structures certainly exists. This procedure should be undertaken only if adequate surgical and neurosurgical support is available, because compromise of the airway or hemorrhage into the spinal canal could require rapid intervention.

Because of the relatively high level of difficulty and risk involved in this procedure, a more complete prebiopsy evaluation than for conventional bone biopsies is necessary. This should include cervical spine radiographs. Performing a radionuclide bone scan is advisable to ascertain if the lesion is solitary or if other lesions more accessible to biopsy are present. Hematocrit, prothrombin time, partial thromboplastin time, and a platelet count should be performed. Because aspirin and many similar substances can increase bleeding time up to 2 weeks after their use is discontinued [9], a history of ingestion of nonsteroidal anti-inflammatory drugs should be obtained.

Complication rates reported for vertebral body biopsies have varied widely. Although significant complications have been reported [10], fluoroscopic needle biopsy is considered safe [11, 12]. This is especially true if a fine needle is used [12, 13]. However, the histologic diagnosis of primary bone neoplasms can be difficult. In our experience, which includes hundreds of needle biopsies of bone in various locations, cytologic aspirates are satisfactory for metastatic disease and for most infections, but large-core biopsies are preferable for primary tumors [7–10]. With CT, both the safety and efficacy of this procedure have been greatly enhanced. The relationship of the skeletal lesion to adjacent structures can be established, allowing a safe route to be selected. Therefore, we attempt to maximize the diagnostic yield by use of large-bore needles and to minimize the hazards by use of CT guidance.

Pain is mild to moderate with this technique. It is preferable to use only local anesthetic whenever possible. Destructive lesions appear to impair sensation so that relatively little pain is produced if there has been adequate soft-tissue anesthetic. A patient who is alert and cooperative can warn the examiner if the needle approaches a spinal sensory nerve. Occasionally, it may be necessary to supplement the xylocaine anesthetic with IV morphine.

We correctly diagnosed single cases of myeloma, chordoma, chondrosarcoma, giant-cell tumor, metastatic cancer, and infection (Table 1). One example of fibrous dysplasia

TABLE 1: Summary of Cases

Case No.	Age (yr.)	Spine Level	Patient Position	Needle Used	Type of Biopsy	Biopsy Diagnosis
1	39	C4	Supine	20-gauge Westcott	Core and aspirate	Chordoma
2	39	C5	Supine	14-gauge Tru-Cut, 11–13 gauge Turkell	Core and aspirate	Metastasis
3	26	C1	Prone	20-gauge spinal needle	Aspirate	Giant-cell tumor
4	67	C6	Supine	20-gauge Westcott	Core and aspirate	Myeloma
5	72	C5–C6–C7	Supine	14-gauge Tru-Cut	Core and aspirate	Infection
6	19	C1	Prone	20-gauge Westcott	Core	Fibrous dysplasia
7	54	C2	Prone	14-gauge Tru-Cut	Core	Chondrosarcoma

yielded tissue that was insufficient for diagnosis. Perhaps the fibrous texture of the lesion precluded adequate aspiration [14] or we simply failed to trap sufficient tissue in the biopsy needle. Even retrospective review of the histology with knowledge of the diagnosis did not reveal diagnostic tissue, suggesting that the problem was not due to the pathologist's lack of confidence with a small sample.

One shortcoming of this procedure is the limitation of the amount of tissue that can be obtained. Because of the hazards of bleeding in the anatomic confines of the neck, the close proximity to major nerves and vessels, and the frequent necessity of transgressing the thyroid using the anterior approach, we have been reluctant to make more than two passes at the lesion with a large-caliber needle.

REFERENCES

1. Frankel CJ. Aspiration biopsy of the spine. *J Bone Joint Surg [Am]* **1954**;36A:69–74
2. Armstrong P, Chalmers AH, Green G, Irving FD. Needle aspiration/biopsy of the spine in suspected disc space infection. *Br J Radiol* **1978**;51:333–337
3. Debnam JW, Staple TW. Needle biopsy of bone. *Radiol Clin North Am* **1975**;13:157–164
4. Hewes RC, Vigorita VJ, Freiberger RH. Percutaneous bone biopsy: the importance of aspirated osseous blood. *Radiology* **1983**;148:69–72
5. Hardy DC, Murphy WA, Gilula LA. Computed tomography in planning percutaneous bone biopsy. *Radiology* **1980**;134:447–450
6. deSantos LA, Zornoza J. Bone and soft tissue. In: Zornoza J (ed). *Percutaneous needle biopsy*. Baltimore, MD: Williams & Wilkins, **1981**:141–178
7. Bernardino ME. Percutaneous biopsy. *AJR* **1984**;142:41–45
8. Zornoza J. *Percutaneous needle biopsy*. Baltimore, MD: Williams & Wilkins, **1981**
9. Lind SE. Prolonged bleeding time. *Am J Med* **1984**;77:305–312
10. Fyfe IS, Henry APJ, Mulholland RC. Closed vertebral biopsy. *J Bone Joint Surg [Br]* **1983**;65B:140–143
11. Murphy WA, Destouet JM, Gilula LA. Percutaneous skeletal biopsy 1981: a procedure for radiologists—results, review, and recommendations. *Radiology* **1981**;139:545–549
12. Adler O, Rosenberger A. Fine needle aspiration biopsy of osteolytic metastatic lesions. *AJR* **1979**;133:15–18
13. Valls J, Ottolenghi CE, Schajowicz F. Aspiration biopsy in diagnosis of lesions of vertebral bodies. *JAMA* **1948**;136:376–382
14. Ayala AG, Zornoza J. Primary bone tumors: percutaneous needle biopsy. Radiologic-pathologic study of 222 biopsies. *Radiology* **1983**;149:675–679

Book Review

Basic Bone Radiology, 2nd ed. By Harry J. Griffiths. Norwalk, CT: Appleton & Lange, 221 pp., 1987. $29.95

The author, a well-known authority on musculoskeletal imaging, has done a magnificent job improving on the important first edition of this primer. The book constitutes a practical introduction to bone radiology for medical students; residents in radiology and orthopedic surgery; and allied health professionals, including nurses, physical therapists, occupational therapists, and chiropractors. The text and illustrations have been revised and updated to reflect the impact of newer imaging techniques, including CT and MR imaging. The content of the book is more complete owing to the addition of some less common entities and a glossary of eponymous terms used in skeletal radiology. The second edition features a total of 263 impressive illustrations.

Bone formation and related background information are discussed in the first section, and the six subsequent chapters cover the major disorders in the categories of congenital, traumatic, infectious, metabolic, arthritic, and neoplastic disease. An additional section discusses a series of miscellaneous diseases and situations of interest. The final chapter features a discussion of specialized radiographic procedures relevant to the skeleton, including arthrography, CT, sonography, MR imaging, scintigraphy, and percutaneous biopsy.

Specific advantages of the book include its concise and informative text, carefully selected high-quality illustrations, and numerous supplementary tables and diagrams. The index and glossary are extremely useful for accessing specific information, and the handy size and paperback format are conducive to the book's intended function as a practical manual. Disadvantages of the book include the limited depth of its text and its rather short reference lists, both of which are unavoidable owing to the nature of the audience to whom it is directed.

As a consequence of its length, the book is far less comprehensive but infinitely more readable than G. B. Greenfield's well-known introductory textbook on musculoskeletal imaging, *The Radiology of Bone Diseases*.

This publication would be of greatest practical utility in an academic setting, as an instructional aid for medical student clerkships, the first year of residency in radiology or orthopedics, and related health care training programs. The book also would be useful to radiology residents as a review for board examinations, as well as to any practicing radiologist who feels the need for a brief refresher course on the subject. This practical guide is well worth its low cost and would be a valuable addition to the library of any radiology department. Unquestionably, the book more than accomplishes its stated purpose of helping the reader to learn and remember some of the important facts about basic bone radiology.

David J. Sartoris
University of California, San Diego, Medical Center
San Diego, CA 92103

Pictorial Essay

MR Imaging of the Normal Elbow: Anatomic Correlation

William D. Middleton,[1,2] Stephanus Macrander,[1] J. Bruce Kneeland,[1] W. Froncisz,[1,3] Andre Jesmanowicz,[1] and James S. Hyde[1]

We investigated the MR appearance of the normal elbow. Comparison of the MR images of normal volunteers with anatomic sections obtained from cadaveric elbows documented MR's ability to visualize essentially all of the important articular and periarticular anatomy. This paper describes a detailed MR anatomic correlation of the anatomy of the elbow.

Materials and Methods

All imaging was performed on a GE Signa MR system operating at 1.5 T. An adjustable axial pair of counterrotating current loop-gap resonators (Medical Advances, Wauwatosa, WI) was used as a local RF receiver and the body coil as a transmitter. A 3-mm slice thickness was used in either a contiguous mode or with a 1.5-mm gap. A 256 × 256 matrix was used with 12- and 16-cm fields-of-view. Two excitations were obtained in all cases. The images presented in this paper all were obtained with a T1-weighted pulse sequence (TR = 500 msec, TE = 25 msec).

Six asymptomatic normal volunteers were imaged in axial, sagittal, and coronal planes. The volunteers were positioned in either the supine or prone position with the arm extended overhead. Off-center field-of-view data acquisition was used for obtaining the axial and coronal images. Imaging was performed with the arm in both pronation and supination.

The anatomic sections were obtained from three cadaveric elbows in axial, sagittal, and coronal planes using a cryomicrotome (LKB 2250, Gaithersburg, MD). Blocks of tissue were frozen and placed in the cryomicrotome stage. As each millimeter of tissue was removed, a photograph of its surface was taken. These photographs were carefully compared with the MR images to confirm the identity of the various structures seen on MR.

Results

Relatively T1-weighted images were best for defining the anatomy of the elbow. Corresponding pairs of axial, sagittal, and coronal MR images and cryomicrotomes are shown in Figures 1–3.

The elbow is actually composed of three joints [1]. The trochlear-ulnar articulation and the capitular-radial head articulation are best imaged in the sagittal (Fig. 2) and coronal (Fig. 3) planes. The articular cartilage of these joints is seen as a layer of moderate intensity separating the black cortical bone. The superior radial ulnar joint is best seen on axial images (Figs. 1C and 1D). The small depression in the lateral surface of the coronoid process of the ulna into which the radial head rests is called the radial notch. The annular ligament attaches to the anterior and posterior aspect of the radial notch and surrounds the radial head, thus securing it in its socket (Fig. 4). Because the articular cartilage of the radial head appears gray and extends distally around the outer circumference of the radial head in the region where it articulates with the ulna, it allows for segmental separation of the black annular ligament and the black cortical bone of the radial head along the anterior aspect of the radial head (Figs. 1C and 1D).

Received March 4, 1987; accepted after revision April 28, 1987.
This work was supported in part by NIH grants RR01008, CA41464-01, and AM33667.
[1] Department of Radiology, Medical College of Wisconsin, Milwaukee, WI 53226.
[2] Present address: Mallinckrodt Institute of Radiology, 510 S. Kingshighway Blvd., St. Louis, MO 63110. Address reprint requests to W. D. Middleton.
[3] On leave from the Department of Radiology, Jagiellarian University, Krakow 31-120, Poland.

 0361–803X/87/1493–0543 © American Roentgen Ray Society

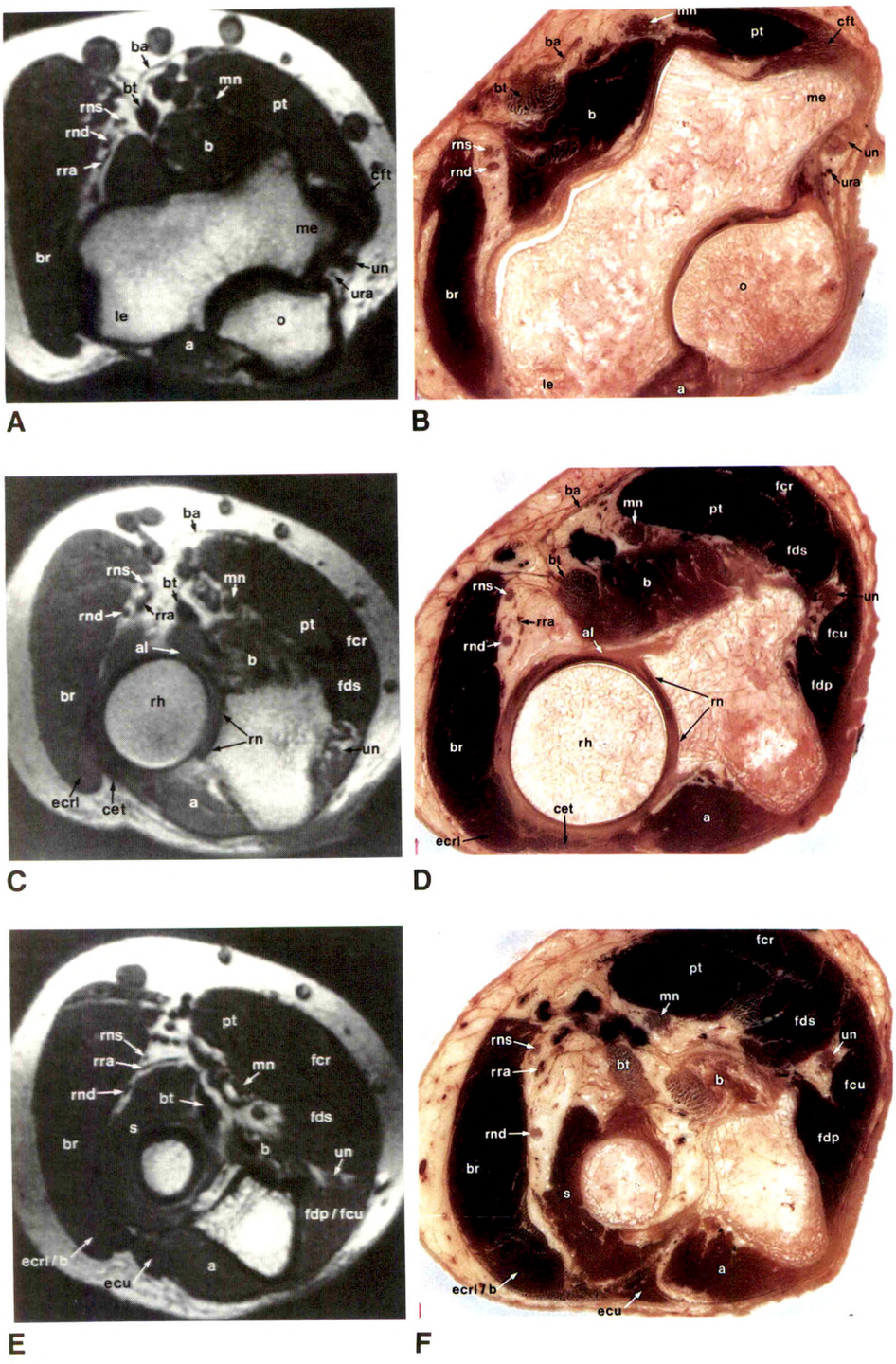


Fig. 1.—Axial MR images and cryomicrotome sections through the superior (*A* and *B*), middle (*C* and *D*), and inferior (*E* and *F*) elbow. Imaging parameters were TR = 500 msec, TE = 25 msec, field of view = 12 cm, slice thickness = 3 mm, excitations = 2. Muscular and neurovascular structures are well seen in axial plane.

The lateral (radial) collateral ligament originates from the lateral epicondyle and attaches to the annular ligament [1] (Fig. 4A). The lateral collateral ligament is thin but can be identified on high-quality MR images (Fig. 3).

The medial collateral ligament arises from the medial epicondyle and spreads out in a fanlike fashion to attach to the trochlear notch of the ulna [1]. Its anterior aspect is cordlike (Fig. 4B) and is seen on MR (Fig. 3).

A large number of muscles originate and insert at the elbow (Fig. 5). Knowledge of these origins and insertions is crucial

Key to Abbreviations Used in Figures

a	anconeus
afp	anterior fat pad
al	annular ligament
apl	abductor pollicis longus
b	brachialis
ba	biceps aponeurosis
br	brachioradialis
bt	biceps tendon
c	capitellum
cet	common extensor tendon
cft	common flexor tendon
cp	coronoid process
ecrl	extensor carpi radialis longus
ecrl/b	extensor carpi radialis longus and brevis
ecu	extensor carpi ulnaris
fcr	flexor carpi radialis
fcu	flexor carpi ulnaris
fdp	flexor digitorum profundus
fds	flexor digitorum superficialis
fpl	flexor pollicis longus
lcl	lateral collateral ligament
le	lateral epicondyle
mcl	medial collateral ligament
me	medial epicondyle
mn	median nerve
o	olecranon
pfp	posterior fat pad
pt	pronator teres
rh	radial head
rn	radial notch
rnd	radial nerve (deep branch)
rns	radial nerve (superficial branch)
rra	radial recurrent artery
rs	radial styloid
s	supinator
t	triceps
tr	trochlea
tt	triceps tendon
u	ulna
un	ulnar nerve
ura	ulnar recurrent artery

in understanding the muscular anatomy of the elbow [2, 3]. The muscles of the elbow can be conveniently divided into posterior, anterior, medial, and lateral groups. The posterior group includes the triceps and anconeus muscles. In the region of the elbow, the three heads of the triceps fuse into a single musculotendinous unit. The thick central tendon inserts into the posterior-superior surface of the olecranon and is well seen on axial and sagittal (Fig. 2C) MR images.

The anconeus is a small, fan-shaped muscle originating from the posterior surface of the medial epicondyle and crossing the elbow joint to insert along the posterior lateral aspect of the olecranon. It is thought to represent a detached portion of the triceps [3]. Axial (Fig. 1) and sagittal (Fig. 2A) MR images show the anconeus best.

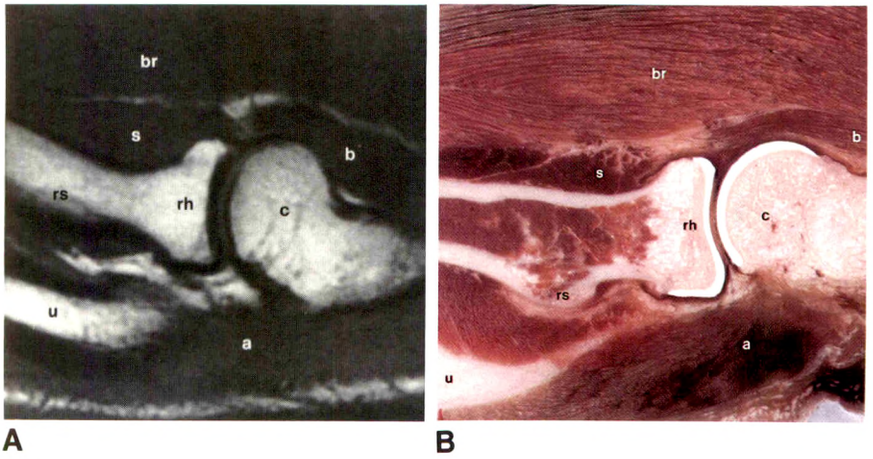
The anterior muscle group consists of the biceps brachii and brachialis muscles. The brachialis muscle originates from the anterior-inferior humerus, crosses the elbow joint, and inserts into a tuberosity of the ulna just distal to the coronoid process [2]. Unlike the biceps, the muscle belly of the brachialis extends all the way to its insertion, with its central tendon imbedded within the substance of the muscle. The brachialis is best imaged in the axial (Fig. 1) and sagittal (Figs. 2C and 2D) planes.

The two heads of the biceps brachii muscle converge distally and, in the region of the elbow, become mostly tendinous [2]. The tendon runs along the superficial surface of the brachialis and inserts onto the radial tuberosity (Fig. 4). When the arm is pronated (as in Figs. 1–3), the biceps tendon wraps around the medial aspect of the radius and becomes positioned between the radius and ulna. Axial (Fig. 1) and sagittal (Fig. 2C) images show the biceps tendon best. Associated with the biceps tendon is a prominent fascial band called the bicipital aponeurosis [1]. It runs obliquely from the distal biceps tendon to the superficial surface of the pronator teres and is best seen on axial images (Figs. 1A and 1C).

The lateral muscle group includes the supinator, the extensors of the digits and wrist, and the brachioradialis. The deepest of these muscles is the supinator [2]. The supinator arises from the posterolateral aspect of the ulna and runs obliquely, inferiorly, and laterally to wrap around the lateral aspect of the radius (Fig. 5). With the arm pronated, the supinator completely surrounds the proximal radius. It is well seen in all planes.

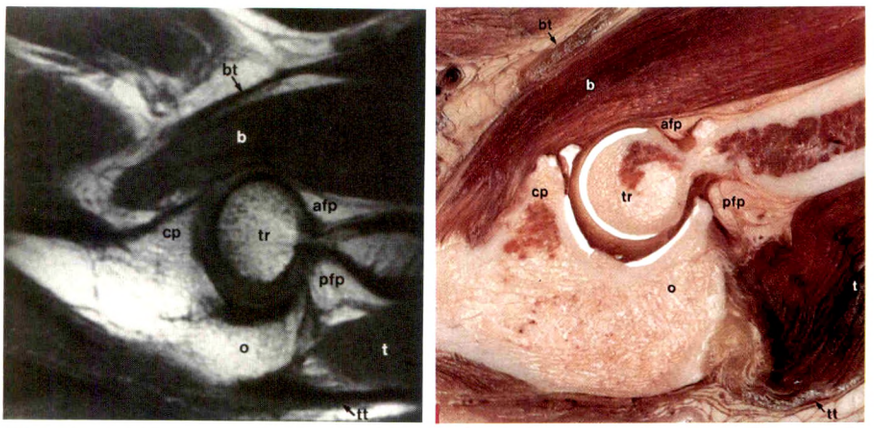
The other muscles of the lateral group are more difficult to differentiate from each other. The brachioradialis is the most anterior muscle in this group. It arises from the lateral aspect of the distal third of the humerus (Fig. 5). Posterior to the brachioradialis is the extensor carpi radialis longus, which originates from the lateral humerus just inferior to the brachioradialis (Fig. 5). Posterior to the extensor carpi radialis longus are the extensor carpi radialis brevis, the extensor digitorum, the extensor digiti minimi, and the extensor carpi ulnaris. These four muscles arise from a common tendon of origin on the most inferior aspect of the lateral epicondyle (Fig. 5) and are difficult to separate from each other in the region of the elbow [1]. The axial plane is best suited for identifying these muscles (Fig. 1).

The medial muscle group includes the pronator teres, the flexors of the hand and wrist, and the palmaris longus. The pronator teres is located most anteriorly. It arises from the distal humerus just proximal to the medial epicondyle and partially from the common tendon of origin of the other flexor muscles [1]. It also has a deep portion that arises from the proximal ulna (Fig. 5A). The other muscles all arise from the common flexor tendon and are arranged from anterior to posterior as the flexor carpi radialis, the palmaris longus, the flexor carpi ulnarus, and the flexor digitorum superficialis [2]. Because of their common origin, these muscles are also difficult to separate proximally in the region of the elbow; however, if the intervening fascia is prominent, they may be identifiable even in the region of the elbow (Fig. 1).

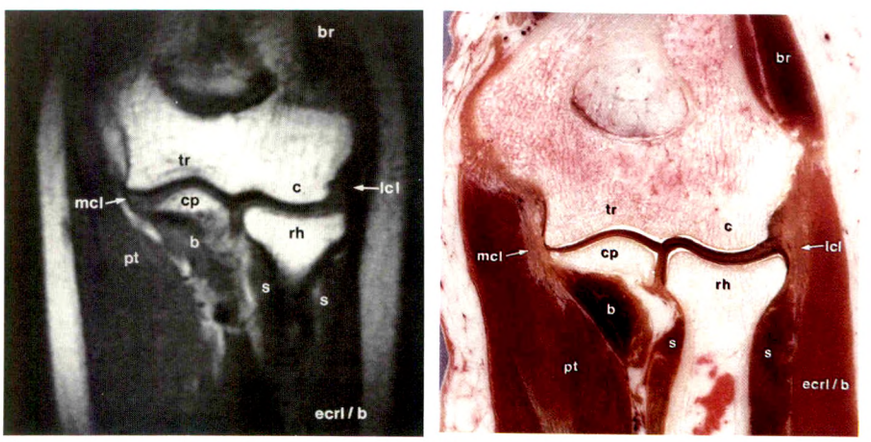


A B

Fig. 2.—Sagittal MR images and cryomicrotome sections through lateral (*A* and *B*) and medial (*C* and *D*) elbow. Imaging parameters same as for Fig. 1. Capitular-radial head and trochlear-ulnar articulations are well seen in sagittal plane.



C D



A B

Fig. 3.—Coronal MR image (*A*) and cryomicrotome section (*B*) through mid-elbow. Imaging parameters same as for Figures 1 and 2. Articular cartilage and collateral ligaments are identified well in coronal plane.

The only major artery in the elbow is the brachial artery. It runs just superficial to the brachialis muscle and medial to the biceps muscle and tendon. It divides into the radial and ulnar arteries at a variable level, but usually about 1 to 2 cm distal to the elbow. The radial artery then runs distally between the brachioradialis and pronator teres, while the ulnar artery runs deep to the pronator teres [1]. Both the radial and ulnar arteries have recurrent branches that travel superiorly adja-

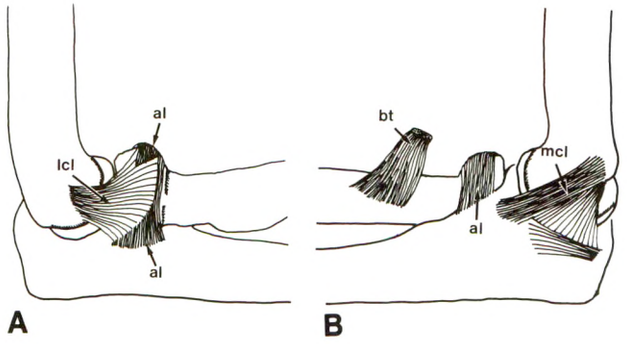


Fig. 4.—Ligaments of the elbow. Radial aspect (*A*) and ulnar aspect (*B*) of elbow.

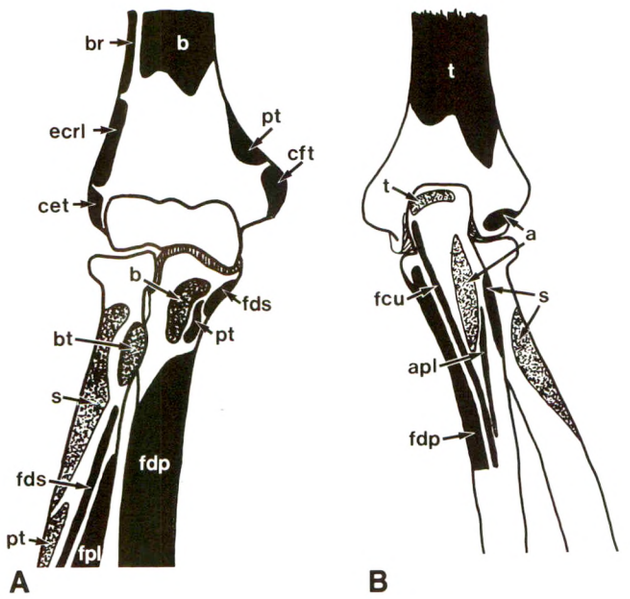


Fig. 5.—Origins (black) and insertions (stippled) of muscles and tendons of the elbow. Anterior aspect (*A*) and posterior aspect (*B*) of the elbow.

cent to the radial and ulnar nerves (Fig. 1). Because the brachial, radial, and ulnar arteries each have corresponding veins, it may be difficult to differentiate the deep arteries and veins.

Three major nerves are present in the region of the elbow. The median nerve runs along the superficial surface of the brachialis muscle medial to the brachial artery. Distally, the nerve runs between the superficial and deep heads of the pronator teres [1]. Visualization of the median nerve depends on the amount of adjacent fat and is usually easiest on proximal axial sections (Figs. 1A and 1C). Distally, the nerve becomes surrounded by muscles (brachioradialis and pronator teres) and since they both have similar signal intensities, the nerve is frequently difficult to identify.

The radial nerve runs between the brachialis and brachioradialis [1]. Like the median nerve, visualization depends on the amount of fat separating it from the adjacent muscles. Division of the radial nerve into deep and superficial branches occurs at the elbow. The more superficial position of the nerves with respect to the recurrent radial artery is helpful in differentiating these structures (Fig. 1).

The last nerve present at the elbow is the ulnar nerve. It is best seen on axial images just posterior to the medial epicondyle (Figs. 1A and 1C). Distally, it is difficult to identify as it runs in a triangular region formed between the flexor digitorum superficialis, the flexor digitorum profundus, and the flexor carpi ulnaris.

Discussion

The elbow is a complex joint. It contains three separate articulations oriented in multiple planes and has multiple muscles and tendons originating and inserting on it. This intricate bony and soft-tissue anatomy is difficult to portray in its entirety with conventional imaging techniques. This study shows that MR is well suited for defining the anatomy of the elbow. Differences in relaxation times and proton density of the various structures allow for high contrast resolution, and use of local coils improves spatial resolution and the signal-to-noise ratio such that images of exquisite quality can be obtained. Add to this the multiplanar imaging capability of MR, and most of the important articular and periarticular structures can be well visualized with this technique. Given the remarkable anatomic detail that is achievable with MR, it becomes essential that radiologists acquire a firm knowledge of the normal appearance and cross-sectional spatial relationships of the various structures of the elbow. Only then will interpretation allow for improved identification, localization, and quantitation of elbow abnormalities.

ACKNOWLEDGMENTS

We thank Shirley Laszewski and Carla Claussen for manuscript preparation, Bruce Nowicki for preparation of the cryomicrotomes, and Lisa Klotz, Marie Bye, Julie Strandt, Beth Beck, and Steve Censky for assistance in scanning the normal volunteers.

REFERENCES

1. Goss MG. *Gray's anatomy*, 29th ed. Philadelphia: Lea & Febiger **1973**:326–331, 458–472, 614–624, 700–703, 971–978
2. Grant JCB. *Grant's atlas of anatomy*, 6th ed. New York: Williams & Wilkins, **1972**:45–79
3. Basmajian JV. *Primary anatomy*, 7th ed. Baltimore: Williams & Wilkins, **1976**:152–165

Book Review

The Radiology of Acute Cervical Spine Trauma, 2nd ed. By John H. Harris, Jr., and Beth Edeiken-Monroe. Baltimore: Williams & Wilkins, 295 pp., 1987. $45

In cutting and polishing jewels, too many facets or asymmetry can ruin an intrinsically lovely stone. This has not happened in this second edition of what was considered a gem in the first edition. The organization of the book is a pleasure in itself. Although it would be tempting to classify injuries as per topography, the authors instead have classified according to mechanism of injury. This classification is particularly appealing because it is well known that complexes of abnormalities occur in a relatively stereotypical fashion after certain types of injury. As before, the emphasis is on plain films. This underscores the central role of such images in the evaluation of all acute spinal injuries. The next level of emphasis is appropriately placed on CT and film-screen laminography, with only superficial coverage of sonography and MR imaging. This is absolutely appropriate in the evaluation of acute injuries.

Although at first glance the book appears to be highly specialized and apparently of interest only to radiologists intimately associated with the imaging evaluation of trauma, even a brief reading proves this is to be untrue. The compositional style is friendly but precise. Any physician involved in the evaluation of trauma will be able to follow the book and learn a significant amount about imaging evaluation from it. Some who consider themselves experts in the field will be surprised that the book also provides a depth of information and an excellent reference source that will satisfy even their needs. One of the strongest tests of a radiology reference book is its appeal to busy clinicians. In my review of this work I planned to seek the opinions of my neurosurgical and orthopedic surgical colleagues. That opinion was sought and received without my saying a single word. Prominently displayed on the shelf in the neurosurgeon's office and in the hand of the orthopedic surgeon was the Harris and Edeiken-Monroe book.

We are all only too aware that the most beautiful gem is also usually the most expensive. This is the only place where that analogy fails. This hardcover book with well-registered half-tone, black-and-white illustrations costs $45.

Stephen S. Gebarski
The University of Michigan Medical School
Ann Arbor, MI 48109

Sonography in the Detection of Meniscal Injuries of the Knee: Evaluation in Cadavers

Bayne Selby[1]
Michael L. Richardson[1]
Brent D. Nelson[2]
Daniel O. Graney[3]
Laurence A. Mack[1]

We evaluated the ability of high-resolution, real-time sonography to identify and characterize artificially produced lesions in the menisci in human cadaveric knee specimens. In total, 20 lesions created in 10 specimens from five knees were prepared and examined sonographically. Four different types of lesions were created: eight vertical concentric tears, four horizontal tears, four vertical radial tears, and four complex lesions including displaced or amputated meniscal edges. All 20 (100%) of the lesions were visualized sonographically. The vertical concentric tears were the easiest to locate and identify, and appeared as highly echogenic lines in the menisci. Tears of this type as small as 2 mm could be visualized. The vertical radial tears were the most difficult to visualize, and no lesions of this type smaller than 5 mm could be seen.

Our study shows that under optimal experimental conditions, sonography is capable of reliably demonstrating even small meniscal tears. On this basis, we believe that further clinical studies of the efficacy of meniscal sonography are both reasonable and necessary.

One of the most common injuries to the knee is disruption of the meniscus, a painful and disabling condition that may be difficult to diagnose. Currently the definitive diagnosis of meniscal tears involves the use of an invasive procedure such as arthrography, arthroscopy, or both. With recent refinements in instrumentation and technique, arthroscopy has largely replaced arthrography in many centers. Even more recently, CT and MR have been shown to be diagnostically useful noninvasive adjuncts [1–9]. Although sonography of the menisci has received little attention [10, 11], it is noninvasive, rapidly performed, widely available, readily accepted by patients, uses no ionizing radiation, and is relatively inexpensive compared with CT and MR, making it a potentially attractive screening examination for knee injuries. In a recent study [11], we were able to visualize not only normal anatomic structures, but also several meniscal lesions. However, the sensitivity, specificity, and accuracy of this technique in vivo remain unknown. Before embarking on a double-blinded clinical trial of sonography in the evaluation of knee injuries, we studied the ability of sonography to reveal meniscal tears under optimal conditions in vitro.

Materials and Methods

Five cadaveric knees were obtained from the Department of Biological Structure at the University of Washington. All knees were specimens that included the intact joint capsule and approximately 15 cm of normal lower extremity both above and below the joint. Four of the specimens were fixed; the remaining knee was fresh frozen.

The knees were examined under fluoroscopy to exclude any specimen with surgical or congenital anomalies. At the time of fluoroscopy, 18-gauge needles were placed on both the ventral and dorsal surfaces of the specimen to identify a sagittal plane that would bisect the intercondylar fossa and the intercondylar eminence of the tibial plateau. Each specimen was initially bisected with a bandsaw in this sagittal plane. Subsequently, two equally spaced

Received February 24, 1987; accepted after revision June 5, 1987.

Presented in part at the annual meeting of the American Roentgen Ray Society, Miami Beach, FL, April 1987; winner of the President's Award for best paper by a radiology resident.

[1] Department of Radiology SB-05, University of Washington, 1956 NE Pacific St., Seattle, WA 98195. Address reprint requests to M. L. Richardson.

[2] School of Medicine SC-64, University of Washington, 1956 Pacific St., Seattle, WA 98195.

[3] Department of Biological Structure SM-20, University of Washington, 1956 NE Pacific St., Seattle, WA 98195.

AJR 149:549–553, September 1987
0361–803X/87/1493–0549
© American Roentgen Ray Society

coronal cuts were made with the saw. This resulted in the production of six pieces of tissue 1–2 cm thick, containing sections of the anterior, middle, or posterior horns of each meniscus (Fig. 1). These tissue slabs were radiographed before sonography.

Ten meniscal specimens were selected from the five cadaveric knees obtained on the basis of their relative state of preservation. Some specimens were not usable after cutting and thawing, and these were discarded. Five medial and five lateral menisci were used for scanning. Of the lateral meniscal specimens, three were from the central portion of the meniscus and two were from the posterior portion. Of the medial meniscal specimens, three were from the central portion, one was from the anterior portion, and one was from the posterior portion.

Sonographic imaging was done with a 5.0-MHz, phased linear array transducer (Acuson, Mountain View, CA). The specimens were placed in a plastic holder made of lucite to maintain them in an appropriate position for imaging. The specimen and holder were then placed in a water bath, and air bubbles were removed from the specimen. The transducer was then held at the surface of the water bath, parallel to the specimen and over the area of the meniscus. The knee specimens were slightly distracted to help separate the meniscus from surrounding structures and to reproduce the effects of displacement of the lower leg as done in arthrography [12]. Before the creation of simulated meniscal lesions, each specimen was photographed and a baseline scan was performed.

A total of 20 different artificial tears were then created with a scalpel. These tears were initially made on a cutting board. However, this technique was subsequently refined by creating the cuts under water in an attempt to minimize the possibility of small air bubbles being trapped within the lesion. The initial cuts were approximately 2 mm deep into the meniscus and 2 mm wide. The dimensions of these cuts were gradually increased in a stepwise fashion and then rescanned to determine the sensitivity of sonography to the size of the tear. None of the scans were interpreted blindly at any time. The sonographer was cognizant of the presence, orientation, location, and size of the tear in each case. These cuts were made in four different orientations to simulate various types of meniscal lesions (Fig. 2): (1) vertical concentric tears (eight cuts), (2) horizontal tears (four cuts), (3) vertical radial tears (four cuts), and (4) complex tears (four cuts), including amputated meniscal tips.

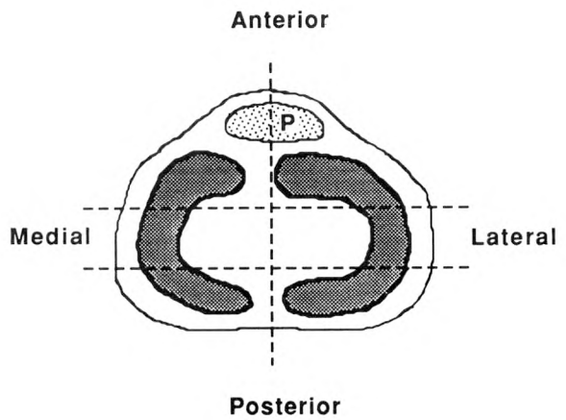


Fig. 1.—Diagram of knee specimen. Dashed lines indicate planes used for sawing the knee specimens. P = patella.

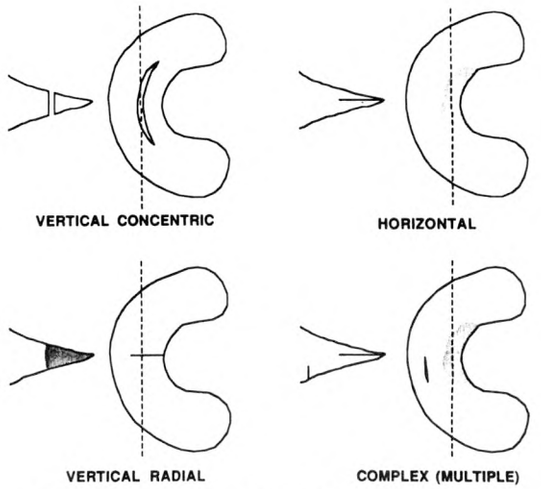


Fig. 2.—Types of artificial tears produced in meniscal specimens. Each tear is depicted not only as it might appear at arthrography (tangentially), but also as seen from above (en face).

After each cut was made, the specimen was again photographed to document the lesion. In some cases in which the artificially produced tear was too small to be readily visible, the edges of the tear were slightly displaced for easier photographic documentation. When this was done, the edges were then allowed to reapproximate before the sonographic examination.

Results

On the initial baseline scans, the meniscal specimens appeared as homogeneously echogenic triangular structures, with the apex of the triangle pointed toward the middle of the joint. In the lateral meniscal specimens containing a portion of the posterior horn with the popliteus tendon defect, the defect was visualized sonographically as an area of hypoechogenicity in all cases. No unexpected tears were found in the specimens during the initial visual inspection or during baseline sonography.

All 20 (100%) of the artificially produced tears were eventually identified at the time of sonography, although in certain orientations, the tears could not be visualized if they were less than a certain size. The vertical concentric tears were the easiest pattern to locate and identify, and were consistently visualized as a hyperechoic line perpendicular to the sonographic beam (Fig. 3). Both partial-thickness tears as small as 2 mm and full-thickness tears through the meniscus could be identified in all specimens. The horizontal lesions also resulted in the formation of a highly echogenic but more discrete focus in the body of the relatively homogeneous meniscus (Fig. 4). In some cases it appeared as a small, nondiscrete, but identifiable area. The smallest detectable horizontal cut was approximately 3–4 mm deep. The vertical radial tears were the most difficult to visualize of the simple tears. These lesions were visible in all scans but could not be well characterized (Fig. 5). The smallest detectable tear of this type was approximately 5 mm wide and through the full thickness of the meniscal specimen.

These three simple patterns of tear were combined in various patterns to produce four complex tears. One tear pattern included amputation of the tip of the meniscus, reproducing the findings one would encounter in a displaced bucket-handle tear. The other complex tears were a combination of randomly produced lesions in a variety of orientations. These more complex tears were easily seen. When viewed with real-time sonography, we were able to identify the specific types of tears that were part of the complex tear (i.e., vertical concentric and horizontal). The amputated menisci were recognized by the appearance of a blunted tip.

Discussion

An understanding of the anatomy of the knee and meniscus is necessary if sonography is to be used to identify meniscal lesions. The menisci are located between the femoral condyles and the tibial plateaus, and are essentially triangular in their cross-sectional shape. Their function is not only to provide stability to the knee, but also to aid in load transmission from the femur to the tibia [13]. The medial and lateral menisci are not mirror images of each other. The medial meniscus is "C"-shaped, while the lateral meniscus is nearly circular. The medial meniscus also is different in that its posterior cornu or horn is wider than its anterior one. The medial meniscus is firmly attached to the joint capsule throughout, whereas the lateral meniscus has no connection with the capsule.

The anatomy of the lateral meniscus is complicated by the fact that the popliteus tendon courses through its substance from the lateral femoral condyle in a downward and posterior fashion. Knowledge of the normal appearance of this popliteus defect is important not only with arthrography, but also with sonography of the menisci, so that this normal structure will not be mistaken for a peripheral tear [11, 12]. We had no problems distinguishing this defect from a tear, since the defect was sonographically visible as an area of hypoechogenicity, while the tears we saw were all hyperechoic.

Sonographic imaging of the menisci of the knee has previously been used in a limited number of subjects [10, 11]. In

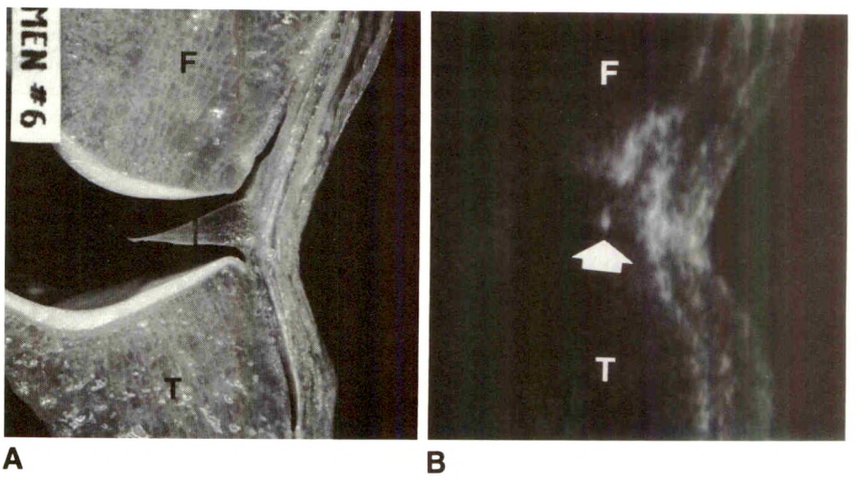


Fig. 3.—Vertical concentric tear of a medial meniscal specimen, with medial femoral condyle (F) above and medial tibial plateau (T) below. Sonogram is positioned vertically to match specimen photograph, with femur superior to tibia.
***A*, Specimen photograph with a tear.**
***B*, Sonogram of same meniscal specimen showing a high-intensity line (*arrow*) at site of tear.**

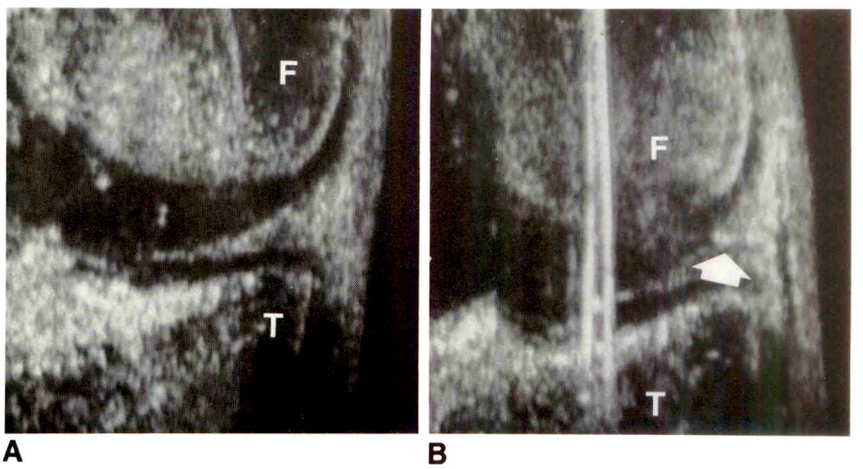


Fig. 4.—Sonography of a medial meniscal specimen. Sonograms are positioned vertically, with femur (F) superior to tibia (T).
***A*, Normal meniscal specimen.**
***B*, Meniscus after creation of a 4-mm horizontal tear on femoral surface of the meniscus. A small, focal area of echogenicity is noted (*arrow*) corresponding to tear. A large vertically oriented streak artifact, incidentally noted, was caused by the lucite specimen holder.**

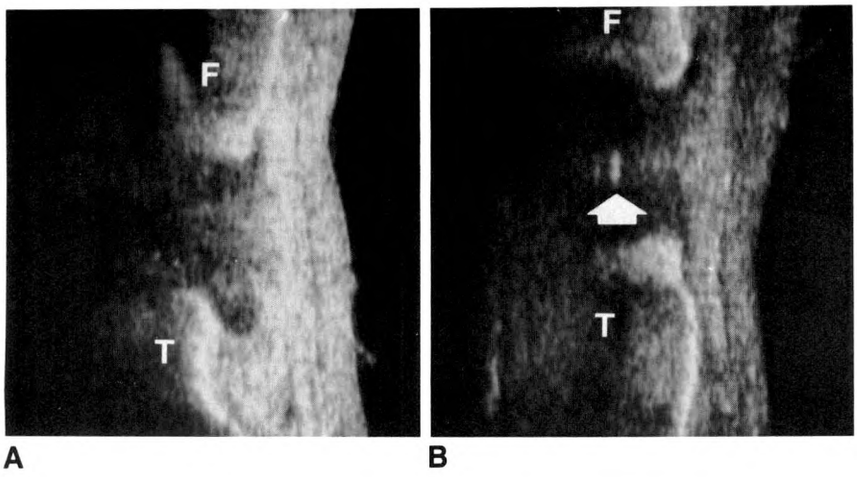


Fig. 5.—Sonography of a medial meniscal specimen. Sonograms are positioned vertically, with the femur (F) superior to the tibia (T).
***A*, Normal meniscus.**
***B*, Meniscus after creation of a 5-mm vertical radial tear on femoral surface. A focal area of echogenicity (*arrow*) corresponds to the tear.**

our previous study of meniscal sonography [11], we performed sonography on 10 normal volunteers and on 10 patients with symptomatic knees. The symptomatic patients all underwent arthroscopy. The sonographic findings were unremarkable in all of the normal patients. Five symptomatic patients had normal menisci both arthroscopically and sonographically. The other five symptomatic patients included three with tears of the posterior horn (two lateral, one medial) and two patients with a history of meniscectomies. All three of the tears and one of the meniscectomies were visualized by sonography.

The current study further verifies the ability of sonography to show not only anatomically normal menisci, but also meniscal tears. More importantly, however, the current study defines the size, shape, and orientation of tears that one could expect to visualize in vivo under optimum imaging conditions.

The results were as one would predict from a knowledge of sonographic physics and tear geometry. As expected, the vertical concentric tears were the ones most easily visualized. The perpendicular orientation of the tear to the sonographic beam consistently yielded intense specular reflections of the beam, allowing lesions as small as 2 mm to be identified. Horizontal tears were also well seen, although the smallest visible lesion was slightly larger, ranging from approximately 3 to 4 mm. As expected, the vertical radial tears were the most difficult to image, because of the parallel orientation of the tear to the beam, and no lesions smaller than 5 mm were identified. With practice, we were able to identify specific types of tears that were part of a complex tear (i.e., vertical concentric and horizontal).

Several potential scanning problems were investigated during the study. The first concerned the possibility that small air bubbles might have become trapped in the meniscus at the time the tear was created, thereby creating the areas of observed echogenicity. To test this possibility, several cuts were made under water. However, these cuts appeared just as echogenic as the cuts made in air.

A second potential problem related to the fact that the images obtained in this study, although adequate, were inferior to those we have seen in living subjects. This finding is consistent with previously reported findings that in vitro sonography of isolated specimens produces images of lesser quality than scans performed in vivo [14]. This was also the experience of one of the authors during previous work on sonography of the rotator cuff. Since four of our five cadaveric knees were fixed specimens, it was thought that poor propagation of the sound waves could be the result of decreased water content of the tissue. In addition, the specimens had been exposed to air for at least 1 day before being examined. To evaluate this possibility, the specimens were subsequently submerged in tap water for approximately 6–10 hr before they were scanned. This resulted in an improvement in the images, although they still did not attain the quality of in vivo images. The one fresh-frozen knee used in our study did provide better images than the fixed knees, but these were also inferior to those seen in vivo. Thus, while decreased tissue water may play some role in degrading in vitro images, we suspect that changes in tissue elasticity may be more important.

As with all in vitro experiments, certain aspects of the study depart from what would normally be possible in a clinical setting. In an earlier study [11], we were able to visualize much of the sonographic interface between the menisci and the adjacent hyaline articular cartilage in normal volunteers in the absence of a knee effusion. However, we also found that stress views and the presence of knee-joint effusions improved visualization of this interface in some of the symptomatic patients. The degree of distraction obtainable during distraction of a bandsawed specimen is greater than that which can be seen in an intact knee. We did not attempt to precisely measure the amount of distraction achieved. We tried by visual reckoning to distract the specimens to a degree similar to that obtainable in vivo, but we may have exceeded that amount in some cases. Likewise, the amount of fluid surrounding the meniscal specimens was variable, but sometimes it may have exceeded what would be expected even in an acutely injured joint. However, distraction and fluid were

primarily useful in visualizing the edges of the menisci separate from the hyaline articular cartilage of the femur and tibia, and did not noticeably affect visualization of the meniscal tears.

A further concern is whether sonography can consistently visualize all portions of the menisci. In our initial clinical study [11] we were able to visualize the posterior horn in 90% of the menisci scanned, but we could not consistently visualize the outlines of the middle or anterior horn of either meniscus. However, in the current study, we had no difficulty consistently visualizing the meniscal specimens containing anterior or middle horns. This improvement may have been due to the water bath in which the specimens were scanned. We hope to design a suitable water bath or its equivalent for scanning knees in vivo to test this hypothesis. In any event, the posterior horns of the menisci are by far the most frequently injured [15], and are also the site least amenable to conventional arthroscopic diagnosis. For this reason, we believe that sonography would be worthwhile even if it were useful only for the evaluation of the posterior meniscal horns.

Another potential problem is the evaluation of amputations of the meniscal tip. Both in this study and in our previous clinical study [11], we frequently were unable to visualize the tip of the medial and lateral menisci. Therefore, we think it likely that such lesions could frequently be missed by sonography.

No intact knees were scanned in this study, although the possibility was considered. In the initial stages of this study, we attempted to create meniscal lesions in an intact knee specimen via an arthroscope, but an experienced arthroscopist was unable to cut or tear the menisci using any of the endoscopic instruments available. We therefore abandoned this approach in favor of bandsawed slabs of tissue, so that we could not only create the meniscal lesions, but also control their orientation, location, and size with precision.

As with other body regions, sonography of the knee is an operator-dependent study. A certain degree of familiarity with both normal anatomy and the appearance of lesions is thus necessary to obtain optimal results. The dynamic nature of real-time sonography makes it much easier to visualize lesions than it would appear from the static images shown here.

On the basis of our previous experience with several different transducers [11], we believe that a high-resolution linear transducer is required for optimal visualization of the menisci. We found it much more difficult to visualize the menisci with a sector scanner, most likely because of transducer geometry and inferior near-field resolution.

MR imaging is becoming increasingly important in the evaluation of knee injuries and is not only noninvasive, but provides accurate diagnostic information about the menisci and ligaments of the knee. However, MR imaging remains far more expensive than sonography and is much less widely available. Even with the advent of recent fast-scanning techniques, an MR examination of the knee requires considerably more time than does a sonographic examination, and the waiting time for an MR study in our hospital is several times longer than that for a sonographic examination. Sonography is also widely available and portable. If sonography of the menisci can be shown to have an acceptable level of sensitivity and accuracy, it could become an attractive screening examination for knee injuries.

In summary, diagnosis of meniscal lesions of the knee can be difficult. Sonography is noninvasive, rapidly performed, widely available, readily accepted by patients, uses no ionizing radiation, and is relatively inexpensive compared with other conventional imaging studies of the menisci, making it a potentially attractive screening examination for knee injuries. However, the sensitivity, specificity, and accuracy of this technique in vivo remain unknown. Our study shows that under optimal experimental conditions, sonography is capable of reliably showing even small meniscal tears. On this basis, we conclude that further clinical studies of the efficacy of meniscal sonography are both reasonable and necessary.

REFERENCES

1. Passariello R, Trecco F, de Paulis F, Masciocchi C, Bonanni G, Zobel BB. Meniscal lesions of the knee joint: CT diagnosis. *Radiology* **1985**;157:29–34
2. Beltran J, Noto AM, Mosure JC, Bools JC, Zuelzer WA, Christoforidis AJ. Meniscal tears: MR demonstration of experimentally produced injuries. *Radiology* **1986**;158:691–693
3. Beltran J, Noto AM, Mosure JC, Weiss KL, Zuelzer WA, Christoforidis AJ. The knee: surface-coil MR imaging at 1.5 T. *Radiology* **1986**;159:747–751
4. Reicher MA, Hartzman S, Duckwiler GR, Basset LW, Anderson LJ, Gold RH. Meniscal injuries: detection using MR imaging. *Radiology* **1986**;159:753–757
5. Gallimore GW Jr, Harms SE. Knee injuries: high-resolution MR imaging. *Radiology* **1986**;160:457–461
6. Burk DL Jr, Kanal E, Brunberg JA, Johnstone GF, Swensen HE, Wolf GL. 1.5-T surface-coil MRI of the knee. *AJR* **1986**;147:293–300
7. Ghelman B. Meniscal tears of the knee: evaluation by high-resolution CT combined with arthrography. *Radiology* **1985**;157:23–27.
8. Reicher MA, Hartzman S, Bassett LW, Mandelbaum B, Duckwiler G, Gold RH. MR imaging of the knee. Part I. Traumatic disorders. *Radiology* **1987**;162:547–551
9. Hartzman S, Reicher MA, Bassett LW, Duckwiler GR, Mandelbaum B, Gold RH. MR imaging of the knee. Part II. Chronic disorders. *Radiology* **1987**;162:553–557
10. Dragonat P, Claussen C. Sonographische meniskusdarstellungen. *Fortschr Röntgenstr* **1980**;133:185–187
11. Selby B, Richardson ML, Montana MA, Teitz CC, Larson RV, Mack LA. High resolution sonography of the menisci of the knee. *Invest Radiol* **1986**;21:332–335
12. Kaye JJ, Himmelfarb E. Knee arthrography. *Orthop Clin North Am* **1979**;10:51–59
13. Henning CE, Lynch MA. Current concepts of meniscal function and pathology. *Clin Sports Med* **1985**;4:259–265
14. Graf R. The ultrasonic image of the acetabular rim in infants. *Arch Orthop Trauma Surg* **1981**;99:35–41
15. Wolfe RD. *Knee arthrography: a practical approach*. Philadelphia: Saunders, **1984**

1988 AMERICAN ROENTGEN RAY SOCIETY MEETING

MAY 8–13, 1988
SAN FRANCISCO HILTON HOTEL
SAN FRANCISCO, CA

See page 656 and forthcoming issues for further information.

Technical Note

A CT Table Attachment for Parasagittal Scanning of the Axilla

Douglas J. Roger[1] and William R. Richli[2]

Many soft-tissue and bony structures of the axilla are easily shown with conventional CT scanning techniques. However, some structures in this area are not well imaged because they are scanned tangentially rather than axially, and when the arm is adducted during conventional CT scanning, the axilla is collapsed. We constructed a device for positioning the patient in the scanner that circumvents these problems.

Materials and Methods

The device has three parts: an adapter, a table, and a tripod (Fig. 1A). The adapter is made of half-inch Lucite. It is 16 in. (40 cm) wide and 60 in. (150 cm) long, with four semielliptical supports that conform to the surface of the CT table. These supports elevate the surface of the adapter, converting the cradle of the CT table into a flat platform. There is a 2½-in. (6-cm) circular hole in the adapter that receives the cylindrical head of the second part of the apparatus, the table. The adapter is secured to the end of the CT table by two guide screws.

The table, on which the patient lies, is composed of a Lucite infrastructure and a Lexan top. Because Lucite and Lexan will not bond, nylon screws must be used to fasten the two together. The top surface of the table is scaphoid. The bottom surface is flat and contains a cylindrical head which is approximately 2½ in. (6 cm) in diameter. The cylindrical head protrudes 2 in. (5 cm) from the bottom surface and fits into the hole of the adapter. One end of the table is thus fastened to the CT table by way of the adapter. The other end is supported by a movable tripod, so that the table attachment as a whole moves with and indexes with the CT table. The angle the table attachment makes with the CT table can vary according to the examination being done, but it remains fixed by the weight of the patient when the table attachment is in use.

The patient is placed in a supine position on the table attachment. The attachment is positioned so that it forms an angle of approximately 45° with the CT table, and the patient's arm is abducted and placed in the gantry (Fig. 1B). To view the muscular, ligamentous, and bony structures of the axilla, contiguous 5-mm-thick slices are obtained from the level of the proximal humerus to the midscapular region. For images of the brachial plexus, 1.5-mm slices are made at the level of the cords.

We used a GE 9800 CT scanner, although this device is adaptable to virtually any type of CT scanner.

Discussion

We constructed a device that makes it possible to position patients for parasagittal scans of the axilla. The table is constructed out of Lucite, Lexan, and nylon screws. These materials are radiolucent and do not interfere with the radiographic image. The table attachment positions the patient so that the areas to be scanned are in the middle of the scanning field. This assures the validity of the X-ray attenuation coefficients, and allows for an optimal field of view. The patient is positioned so that scans are made transversely with respect to the long axis of the neurovascular bundle. This allows axial visualization of structures that are usually seen tangentially, as, for example, the axillary artery and vein (Fig. 2A). This principle was used by Beltran et al. [1] in performing direct sagittal CT of the shoulder.

Received March 23, 1987; accepted after revision April 30, 1987.
This work was supported in part by the John S. Dunn Research Foundation.
[1] 11548 Chapman St., Loma Linda, CA 92354.
[2] Department of Diagnostic Radiology, University of Texas, M.D. Anderson Hospital and Tumor Institute, 6723 Bertner Ave., Houston, TX 77030. Address reprint requests to W. R. Richli.

AJR **149:555–556, September 1987** 0361–803X/87/1493–0555 © American Roentgen Ray Society

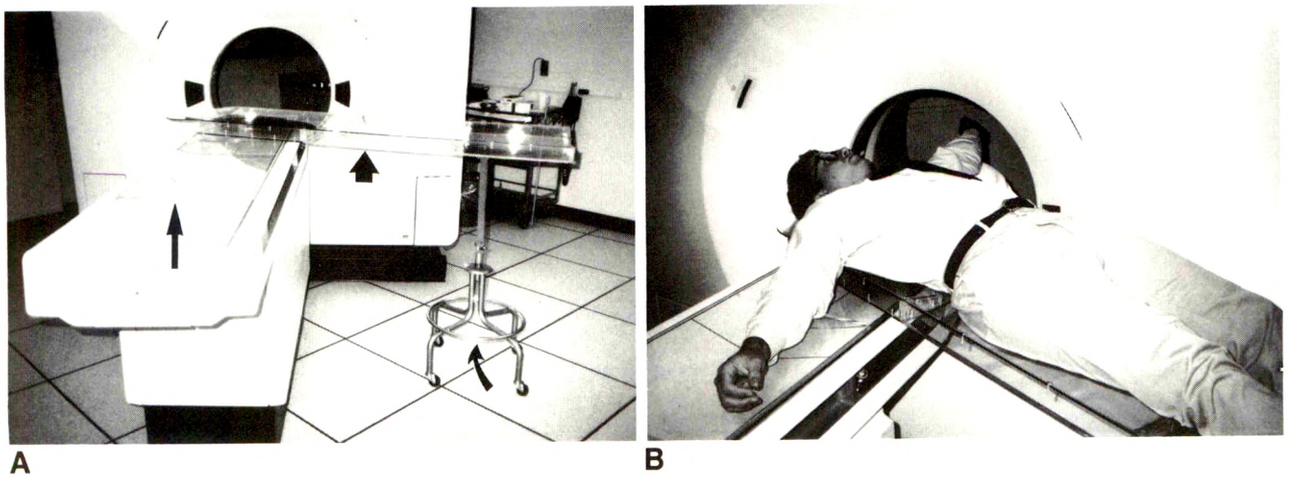


Fig. 1.—*A*, Photograph of the apparatus showing the three parts: adapter (*long arrow*), table (*thick arrow*), and tripod (*curved arrow*). *B*, Photograph showing use of the apparatus. Patient's arm is abducted. Axilla is positioned in the center of the CT gantry.

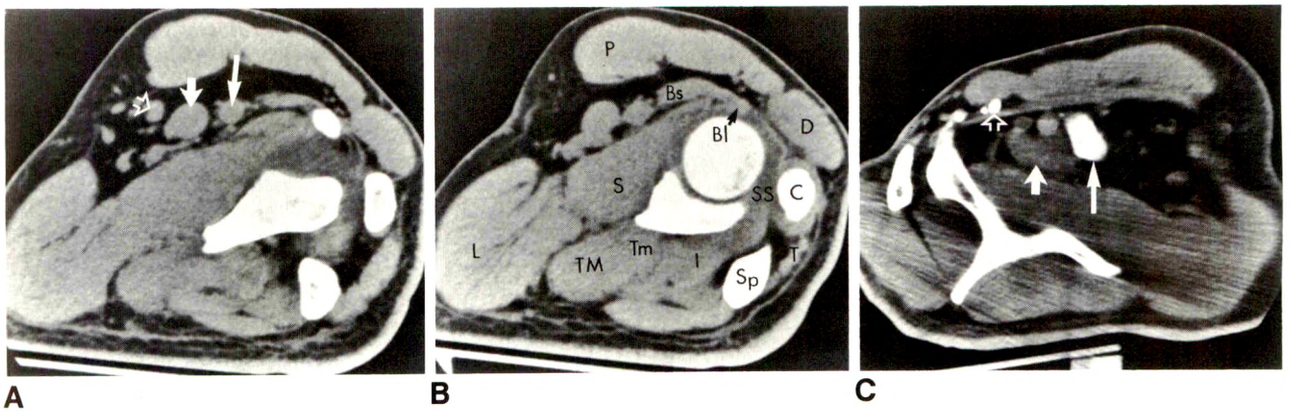


Fig. 2.—CT scans of shoulder made using apparatus. With arm abducted, axillary contents are easily identified.
A, Small axillary node (*open arrow*), axillary vein (*short arrow*), and axillary artery surrounded by cords of the brachial plexus (*long arrow*).
B, Shoulder girdle and constituents of rotator cuff are clearly seen. Pectoralis major (P), deltoid (D), trapezius (T), infraspinatus (I), supraspinatus (SS), teres major (TM), teres minor (Tm), latissimus dorsi (L), subscapularis (S), short head of biceps (Bs), long head of biceps (Bl), clavicle (C), spine of scapula (Sp).
C, A mass (neurofibrosarcoma) in posterior cord of brachial plexus is evident (*short arrow*). Axillary (*long arrow*) and cephalic veins (*open arrow*) are opacified with contrast material.

The arm is abducted during scanning so that images of an expanded axilla are obtained. This allows for excellent visualization of the shoulder girdle and constituents of the rotator cuff (Fig. 2B). The anatomic relationships between neural and vascular components of the neurovascular bundle are clearly shown (Fig. 2C). Because the attachment is supported by a movable tripod, indexing with the CT table is possible. This allows for easy repositioning of the patient should biopsy of a lymph node be desired.

REFERENCE

1. Beltran J, Gray LA, Bools JC, Zuelzer W, Weis LD, Unverferth LJ. Rotator cuff lesions of the shoulder: evaluation by direct sagittal CT arthrography. *Radiology* **1986**;160:161–165

MR Imaging of Solitary Osteochondromas: Report of Eight Cases

Joong K. Lee[1]
Lawrence Yao[1]
Carl R. Wirth[2]

MR imaging was performed in eight patients with osteochondromas, and the results were compared with the histologic findings in six of these cases. MR imaging effectively showed the essential anatomic features of lesions and was particularly useful in assessing the presence and thickness of the cartilage cap. The cartilage cap was clearly seen as a region of high signal intensity on T2-weighted images. A superficial zone of low signal intensity was seen covering the cartilage cap, corresponding to an intact perichondrium, in all of the five cases in which histologic examination confirmed the presence of an intact perichondrium.

The results of MR in these cases suggest that MR is useful in the preoperative planning of cases in which excision of an osteochondroma is necessary. Optimal surgical resection of the lesion requires complete excision of an intact perichondrium to prevent possible recurrence of the tumor.

Osteochondromas, also known as osteocartilaginous exostoses, are the most common benign tumors of bone. Osteochondromas possess a cartilage cap that typically ossifies with maturation of the skeleton, marking the end of exostotic growth. On occasion, remnants of a quiescent cartilage cap may persist far into adult life [1].

Osteochondromas, although generally asymptomatic, occasionally come to clinical attention for various reasons. Symptoms may result from exostotic impingement on adjacent neural, vascular, or periarticular structures. Pain may result from the fracture of an osteochondroma. The presence of a visible mass may create a cosmetic problem. The exostotic cartilage cap may rarely undergo malignant degeneration, giving rise to chondrosarcomas of the so-called peripheral type [2]. The incidence of malignant degeneration is thought to be about 1% for solitary osteochondromas and from 5% to 25% in cases of hereditary multiple exostoses [3].

We describe the MR findings in eight patients with symptomatic, solitary osteochondromas. In six cases in which surgery was performed, gross and histologic examination of the osteochondroma was performed for correlation with the MR findings.

Subjects and Methods

Solitary osteochondromas were studied in eight patients 4–25 years old. The locations of the osteochondromas included the femur (five), the humerus (one), the tibia (one), and the pelvis (one).

MR imaging was performed on a GE Signa unit operating at 1.5 T. Spin-echo sequences were performed by using a repetition time (TR) of 600–800 msec and an echo time (TE) of 20–30 msec for T1-weighted images; a TR of 1200–2000 msec and TE of 20–80 msec was used for T2-weighted images. Contiguous slices 5 or 10 mm in thickness were obtained in the axial, coronal, and/or sagittal planes and were reconstructed by using a 128 × 256 matrix size.

Received March 26, 1987; accepted after revision May 26, 1987.

[1]Department of Diagnostic Radiology, Albany Medical College/Albany Medical Center Hospital, New Scotland Ave., Albany, NY 12208. Address reprint requests to J. K. Lee.

[2]Department of Orthopedic Surgery, Albany Medical College/Albany Medical Center Hospital, Albany, NY 12208.

AJR 149:557–560, September 1987
0361–803X/87/1493–0557
© American Roentgen Ray Society

Six of the eight patients underwent surgical excision of their osteochondromas, and subsequent histologic examination was performed.

Results

In all cases, MR scans identified continuity of the exostotic cortex and medullary cavity with the cortex and medullary cavity of the bone from which the lesion arose (Fig. 1). In these cases histologic sections showed the full thickness of the cartilage cap and an intact perichondrium. Dense exostotic mineralization noted on plain radiographs was well seen by MR as areas of signal absence intervening between the higher signal areas of the cartilage cap and medullary bone (Fig. 2).

MR imaging identified cartilage caps in all five cases with histologically proved cartilage caps ranging in thickness from 0.3 to 3.0 cm. The cartilage cap, not typically detected on plain radiographs, was well seen on T2-weighted MR images as a region of high signal (Figs. 1–3). Cartilage-cap thickness as estimated by MR imaging was within 2 mm of the thickness found on gross examination in four of the five cases. Fragmentation of the specimen in the fifth case precluded determination of cap thickness (Fig. 3). An osteochondroma in one of the six cases in which histologic examination was performed showed no cartilage cap by MR and histologic examination. Quantitative comparison of cartilage-cap thickness as determined by MR vs gross examination was not considered meaningful, given the intrinsic variability in orientation of the sectioning plane of examination and the complex contours involved.

In all of the five cases in which histologic examination confirmed the presence of an intact perichondrium, continuity of the perichondrium was clearly shown by MR imaging. In all cases, the perichondrium was seen as a low-signal zone overlying the higher signal region of the cartilage cap on T1- and T2-weighted images and was best seen in the presence of large, nonossified cartilage caps on T2-weighted images (Figs. 1 and 2).

Discussion

Our experience suggests that MR imaging effectively shows the essential anatomic features of benign osteochondromas. MR clearly demonstrates continuity of the exostotic cortex and medullary cavity with that of the parent bone, a hallmark of osteochondromas that distinguishes them from

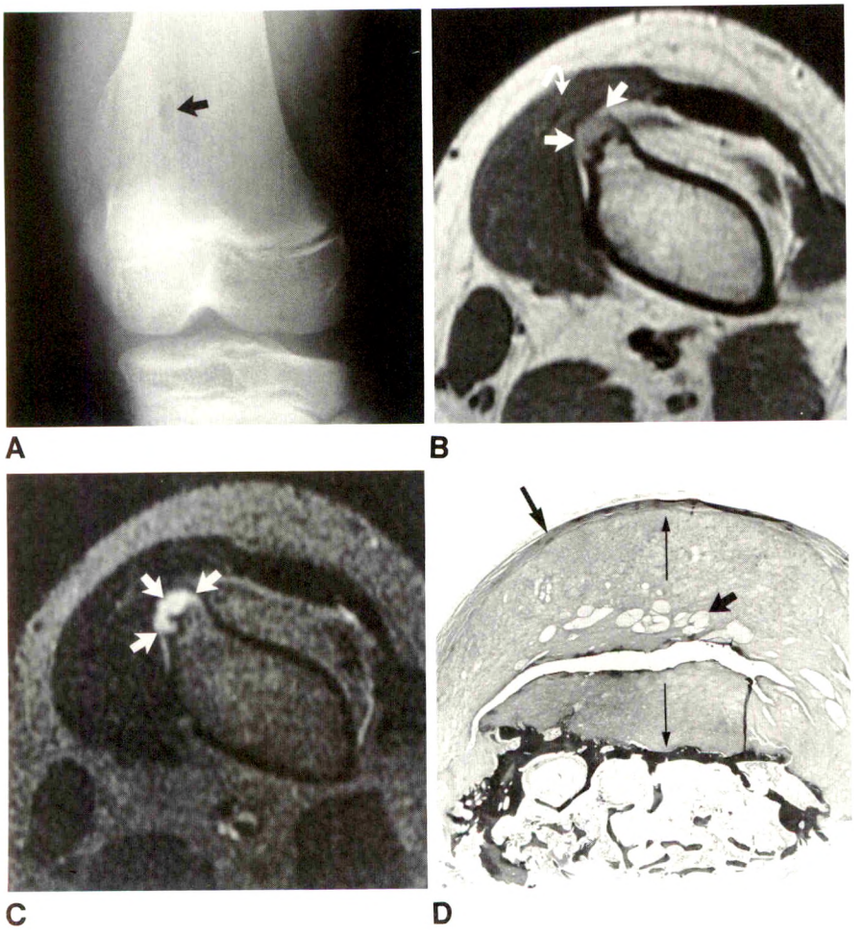


Fig. 1.—12-year-old boy with pain after local trauma.

***A*, Radiograph of distal left femur shows sessile osteocartilaginous excrescence. There is continuity of exostotic cortex and medullary bone with cortex and medulla of femoral metaphysis. Small, well-defined, ovoid radiolucency in metaphysis is posteriorly located fibrous cortical defect (*arrow*).**

***B*, Transaxial MR image (TR = 1500 msec, TE = 20 msec). Lesion is seen displacing vastus medialis muscle (*curved arrow*) Low-signal zone at periphery of lesion represents perichondrium (*straight arrows*).**

***C*, T2-weighted transaxial MR image (TR = 1500 msec, TE = 80 msec). Exostotic cartilage cap is seen as area of intense signal (*arrows*).**

***D*, Histologic section of excised exostosis shows full thickness of smooth, nonossified cartilage cap (*long thin arrows*) with areas of cystic degeneration within it (*short thick arrow*) and overlying layer of perichondrium (*long thick arrow*).**

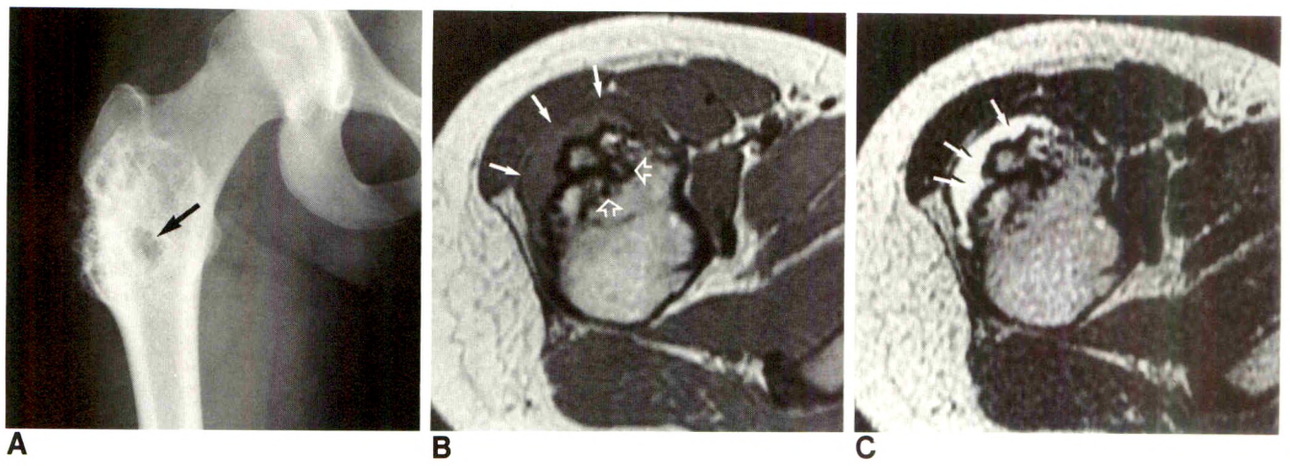


Fig. 2.—19-year-old woman.

***A*, Radiograph of right proximal femur shows anteriorly protruding osteochondroma containing irregular areas of mineralization and poorly defined external margin. Radiolucency is seen in subtrochanteric region of proximal femur (*arrow*), suggesting malignant degeneration. Subsequent histologic examination showed this to represent an area of nonossified cartilage.**

***B*, Transaxial MR image (TR = 1200 msec, TE = 20 msec). Intact perichondrium is seen as low-signal zone (*arrows*). Irregular areas of signal absence in base of lesion are consistent with extensive matrix mineralization (*open arrows*).**

***C*, More T2-weighted transaxial MR image (TR = 1200 msec, TE = 75 msec). Exostotic cartilage cap is seen as area of high signal (*arrows*).**

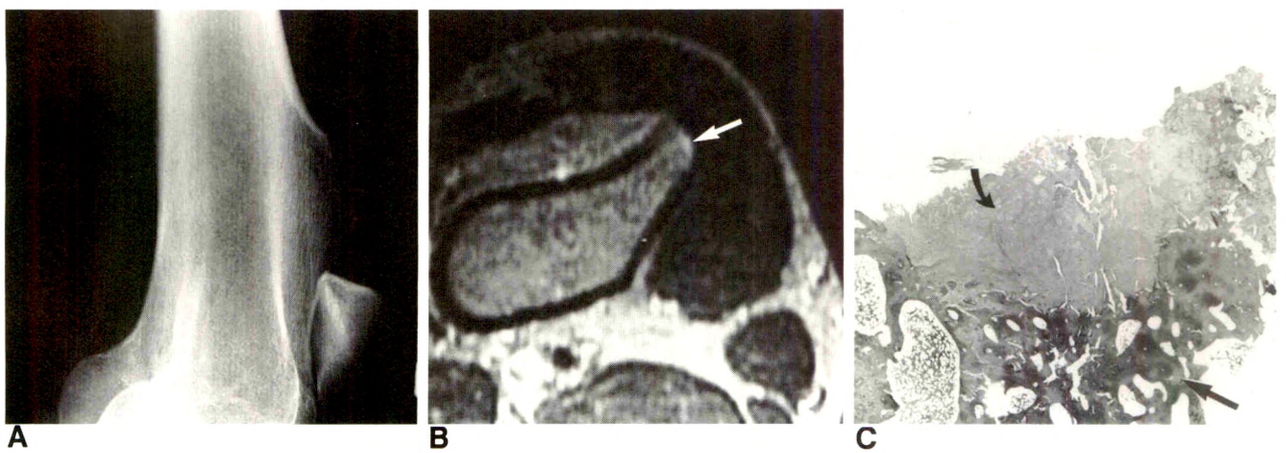


Fig. 3.—25-year-old man with palpable suprapatellar mass.

***A*, Lateral radiograph of distal left femur shows anterior, sessile osteochondroma and no evidence of persistent cartilage cap.**

***B*, T2-weighted transaxial MR image (TR = 2000 msec, TE = 80 msec) shows thin, 3-mm cartilage cap (*arrow*). Continuity of exostotic medullary cavity with that of parent bone is clearly seen.**

***C*, Histologic section of excised osteochondroma shows partially ossified cartilage cap (*curved arrow*) overlying irregular trabecular bone (*straight arrow*). Perichondrium is not preserved because of fragmentation of excised specimen.**

other juxtacortical lesions such as ossifying hematomas or juxtacortical chondromas. MR provides information regarding the degree of exostotic mineralization, showing areas of exostotic cortex as areas of signal absence intervening between the cartilage cap and the exostotic and parent medullary bone. An outer perichondrium is clearly seen on T2-weighted images as a smooth, low-signal region opposing the high-signal areas of the cartilage cap. Accurate demonstration of the cartilage cap, in addition to confirming the potential for further exostotic growth, facilitates assessment of the regularity of the external contour of the cap, one relative sign of benignity [4, 5].

CT has been shown to be effective in demonstrating exostotic cartilage caps that are greater than 2.5 cm in thickness [6]. The degree of thickening of the cartilage cap that is suggestive of malignant change has been disputed. Some authors state that peripheral chondrosarcomas are generally associated with cartilage caps thicker than 3 cm [7]. Others report cartilage-cap thicknesses of 0.1–3.0 cm in benign osteochondromas and thicknesses of 2 cm or greater in

chondrosarcomas [8]. In any discussion of cartilage cap thickness, however, the age of the patient should be considered, as the expected thickness of the cartilage cap would be greater in younger patients before the cessation of bone growth has occurred [7]. Our experience suggests that MR clearly demonstrates cartilage caps as thin as 3 mm, or those in the "benign" range. Correlation between actual and MR-determined cartilage-cap thicknesses would also appear to depend on the degree of cartilage calcification, with a better correlation expected in noncalcified cartilage caps, those found more commonly in younger patients.

Osteochondromas may recur after apparent surgical excision [9]. When surgical removal of an osteochondroma is warranted, optimal surgical resection requires excision of the lesion with an intact perichondrium, as recurrence of tumor growth may arise from perichondrium left behind [10]. By defining the local soft-tissue anatomy and delineating the extent of the cartilage cap and its overlying perichondrium, MR imaging facilitates precise preoperative planning.

REFERENCES

1. Dahlin DC. *Bone tumors*, 3d ed. Springfield, IL: Thomas, **1978**:17–27, 90–217
2. Lichtenstein L, Jaffe HL. Chondrosarcoma of bone. *Am J Pathol* **1943**;19:553–589
3. Garrison RC, Unni KK, McLeod RA, Pritchard DJ, Dahlin DC. Chondrosarcoma arising in osteochondroma. *Cancer* **1982**;49:1890–1897
4. Norman A, Sissons JA. Radiographic hallmarks of peripheral chondrosarcoma. *Radiology* **1984**;151:589–596
5. Kenney PJ, Gilula LA, Murphy WA. The use of computed tomography to distinguish osteochondroma and chondrosarcoma. *Radiology* **1981**; 139:129–137
6. Hudson TM, Springfield DS, Spanier SS, Enneking WF, Hamlin DJ. Benign exostoses and exostotic chondrosarcomas: evaluation of cartilage thickness by CT. *Radiology* **1984**;152:595–599
7. Spjut KJ, Dorfman HD, Fechner FE, Ackerman LV. *Tumors of bone and cartilage*. Washington, DC: Armed Forces Institute of Pathology, **1970**: 84–110
8. O'Neal LW, Ackerman LV. Chondrosarcoma of bone. *Cancer* **1952**;5: 551–577
9. Schmidt W. Exostoses, osteochondroma, and osteochondromatosis: clinical findings and therapy. *Zentralbl Chir* **1969**;94:1515–1524
10. Lichtenstein L. *Bone tumors*, 5th ed. St. Louis: Mosby, **1977**:26

Perspective

Arthrography: Past, Present, and Future

Ferris M. Hall[1]

Technological advances in arthroscopy and the imaging techniques of sonography, CT, and surface-coil MR have had a substantial impact on conventional arthrographic procedures in the past decade. An individual's perception of the usefulness of arthrography is influenced by personal interests and those of orthopedic colleagues, referral patterns, access to newer imaging techniques, and recently published data. A survey was done to assess the current and future status of arthrography in relationship to its past use.

A questionnaire was sent to 146 radiologists who were interested in arthrography. Replies were received from 67% (98/146). The respondents, almost two-thirds of whom were members of the International Skeletal Society, were from 13 countries; 77% (75/98) practiced in the United States or Canada. Seventy-eight percent (76/98) considered their practice to be primarily academic, 16% (16/98) were hospital-based nonacademic radiologists, and 6% (6/98) had primarily an office practice. The 98 respondents, representing 92 departments, performed or supervised a total of more than 33,000 arthrograms each year (i.e., for each respondent, 337 per year or six to seven per week).

The number of arthrograms performed during the past 5–10 years decreased approximately 20% overall; 30% of departments experienced a decrease, and 15% experienced an increase. The decline in examinations was greater in academic centers, perhaps reflecting the fact that arthrography was a relatively new technique 10 years ago and was used by fewer private practitioners.

Knee examinations accounted for 55% of all arthrograms currently performed. The number of knee studies done during the past 5–10 years decreased 50% overall; 85% of respondents experienced a decrease, 10% had no change, and only 5% showed an increase. All respondents mentioned arthroscopy as the major factor resulting in this decline. Those practicing in prepaid systems, such as a health maintenance organization or the British Health Service, generally experienced less reduction, and this was attributed to different economic considerations in orthopedic practice. Some arthrographers thought that their only orthopedic referrals were patients with relative contraindications to arthroscopy, such as those who were debilitated, elderly, or overweight; or those who had medicolegal problems or refused arthroscopy.

A majority of respondents thought that knee arthrography would continue to decline. A minority thought that continued emphasis on cost containment and the growth of health maintenance organizations would result in a modest increase. A general concern was that arthrography, particularly of the knee, would suffer because of a lack of adequate experience among recent trainees and current radiology residents.

Few respondents thought that CT or CT-arthrography would play a significant role in assessment of knee problems in the foreseeable future. On the other hand, noninvasive MR imaging was thought by many to be an excellent technique for assessing the menisci and probably the cruciate ligaments. Those respondents with personal experience in MR imaging of the knee had a throughput of two to three patients per hour and an accuracy that was thought to be almost equivalent to that for arthrography. Some thought that MR imaging, despite its present cost, eventually would replace both arthroscopy and arthrography as the technique of choice for assessment of suspected internal knee injuries.

Shoulder arthrograms accounted for 20% of the total ar-

Received March 24, 1987; accepted after revision April 20, 1987.

[1] Department of Radiology, Beth Israel Hospital and Harvard Medical School, Boston, MA 02215. Address reprint requests to F. M. Hall, Dept. of Radiology, Beth Israel Hospital, 330 Brookline Ave., Boston, MA 02215.

AJR **149:561–563, September 1987** 0361–803X/87/1493–0561 © American Roentgen Ray Society

thrograms performed. Thirty percent of respondents had experienced a recent increase in these examinations; 10% showed a decrease. The overall increase was thought to be related to a better orthopedic understanding of the syndrome of tendonitis/impingement/adhesive capsulitis, with earlier and more aggressive treatment and more satisfactory surgical results. A few respondents attributed their increases to therapeutic arthrographic distension of adhesive capsulitis. Most thought that a modest increase in demand for arthrography of the shoulder would continue.

A few respondents thought that sonography largely could replace arthrography in assessment of the rotator cuff. However, most were sceptical about a major role for sonography of the shoulder, although, admittedly, these individuals usually had less experience with this technique. The additional information available with CT-arthrography, particularly as regards the glenoid labrum, was acknowledged, but this information was thought to be useful only if the clinical problem was one of instability. Few respondents had experience with arthroscopy or MR imaging of the shoulder. These techniques were thought to be potentially exciting, but none of the respondents anticipated that they would have much impact on the role of arthrography in the near future.

Arthrograms of the temporomandibular joint accounted for almost 10% of all examinations in this survey. Use of this study has increased dramatically in recent years; few such arthrograms were performed 10 years ago. Use of temporomandibular arthrograms was extremely variable; they accounted for more than one-half of the arthrograms performed in some large series, but 60% of respondents rarely or never performed them. Both CT and MR imaging have affected temporomandibular arthrography adversely, although many of those in the field thought that the dynamic information available from fluoroscopy ensured a continued important role for this examination. Those respondents who ventured an opinion thought that the overall underutilization of temporomandibular arthrography outweighed any impact of CT and MR imaging and that in absolute terms the use of this examination would continue to increase. This was the only joint for which mention was made of nonradiologists performing the arthrograms, with resultant turf battles.

Wrists accounted for 5–10% of arthrograms, with recent increases experienced by most respondents. Range of usage was wide. The examination was most popular in academic institutions, presumably because they have more hand specialists. There were differences of opinion in this survey as to whether wrist arthrography will continue to grow in popularity. This may reflect a controversy in orthopedics as to the long-term success of carpal fusion in the treatment of wrist instability.

Hips accounted for slightly more than 5% of all arthrograms. This examination, like temporomandibular and wrist arthrography, had a wide range of popularity. This reflects orthopedic practice because, with the exception of pediatrics, the great majority of hip arthrograms are done to assess symptomatic arthroplasties. The number of hip arthrograms performed has changed little recently, and no immediate increase was predicted. This may reflect an improvement in surgery because hip arthroplasty has become the most common major surgical procedure performed in the United States. Newer imaging techniques are unlikely to affect the major indications for hip arthrography: assessment of infection before contemplated surgery and, to a lesser extent, the diagnosis of prosthetic loosening.

Taken together, elbows and ankles accounted for <5% of arthrograms. These examinations usually were obtained to assess the presence of loose joint bodies or defects in the articular cartilage. Presently ankle arthrography is rarely performed for the assessment of acute ligamental injury. The few comments received suggest that, whatever the indications, these examinations rarely contribute useful information. A few respondents thought that they were performed more for the benefit of the referring physician than the patient. Given this pessimistic view, it is not surprising that the respondents were cautiously optimistic about some role for CT, CT-arthrography, or MR imaging of these joints in lieu of conventional arthrography. Spinal facet-joint arthrography usually was performed as part of a somewhat controversial therapeutic procedure, and only a few of the respondents had personal experience with this examination.

Arthrography is changing. However, in overall numbers it has diminished only modestly over the past 5–10 years. Its popularity is based on a vast clinical experience, an extremely low prevalence of complications, and low cost in comparison with arthroscopy and MR imaging.

Sonographic Measurements of the Normal Bladder Wall in Children

Sigrid Jequier[1]
Odette Rousseau

The thickness of the bladder wall was measured sonographically in 410 children (1 day to 19 years old) and in 10 adults. None had complaints related to the urinary tract. The bladder wall thickness varied mostly with the state of bladder filling and only minimally with age and gender. The normal bladder wall had a mean thickness of 2.76 mm when the bladder is almost empty and 1.55 mm when it is distended.

There is a linear relationship between bladder fullness and bladder wall thickness; the upper limits are 3 and 5 mm for a full or empty bladder respectively.

The normal bladder wall is difficult to assess radiographically. A smooth bladder contour on positive contrast studies and absence of elevation of its base during voiding tend to indicate a normal bladder. A thickened bladder wall can often be seen on IV urogram as a rim of soft tissue between the contrast material in the bladder and the perivesical fat. CT also allows demonstration of a thickened bladder wall [1]. However the normal bladder wall thickness is not well seen on radiographs, and we were unable to find any radiographic data on normal bladder wall thickness in children and its possible relation to age, sex, and state of bladder filling. On sonography with appropriate gain setting, the bladder wall can be seen clearly in most cases. The more echogenic mucosa can often be distinguished from the more echolucent detrusor muscle. Having noted a "thick" bladder wall in some children on chemotherapy or with urinary tract infection, neurogenic bladder, posterior urethral valves, or hematuria, we recognized a need for normal values of bladder wall thickness in order to delineate clearly abnormal vs normal measurements.

Materials and Methods

The study included 410 children (age range, 1 day to 19 years) and 10 adults (age range, 19 to 42 years). There were 33 neonates (19 males [M] and 14 females [F]); 57 children 1 month to 1 year old (28 M, 29 F); 134 patients 1 to 6 years old (69 M, 65 F); 135 6 to 12 years old (69 M, 66 F); and 61 patients over 12 years of age (33 M, 28 F). A total of 218 males and 202 females. All came for a sonographic examination for reasons unrelated to the urinary tract (e.g., abdominal pain, questionable mass, questionable congenital anomaly, remote tumor, family screening) or for follow-up of a remote urinary tract problem (e.g., check on renal growth 1 year after a urinary tract infection, remote reimplantation). Patients with urinary tract symptoms were excluded. All sonographic examinations were done with a real time ATL machine (Bothel, WA), with 7.5- or 5-MHz probes for children under 5 years of age. A Diasonics machine (Sunnyvale, CA) with a 5-MHz probe was used for older children and adults. The bladder wall thickness was measured on transverse and sagittal cuts, usually in an area of the bladder floor posterolateral to the trigone. Care was taken not to include the vagina, rectum, or peritoneal reflection of the bladder dome into the measurements. The volume of the bladder was measured, assuming the bladder to be a sphere and calculating the radius (r) by adding sagittal, transverse, and anteroposterior diameter divided by 8 and using the formula: $V = \frac{4}{3} \pi r^3$. The calculated volume was compared with the normal bladder

Received November 3, 1986; accepted after revision May 4, 1987.

Presented at the meeting of The Society for Pediatric Radiology, Washington, DC, April 1986.

[1] Both authors: Department of Radiology, The Montreal Children's Hospital, 2300 Tupper St., Montreal, Quebec H3H 1P3, Canada. Address reprint requests to S. Jequier.

AJR **149:563–566, September 1987**
0361–803X/87/1493–0563
© American Roentgen Ray Society

capacity of the patient's age group as indicated by Koff [2]. The bladder was considered empty when it contained less than 10% of its normal capacity, ±full with 10–25% of its capacity, full with 26–90%, and full++ when it was filled close to its capacity (Fig. 1).

All recorded data on bladder wall thickness were analyzed statistically as to their relation to the patient's age, gender, and filling state of the bladder. A factorial analysis of variance [3] was done and a graphic curve of the findings was obtained (Figs. 2–4).

Results

The mean bladder wall thickness of all patients combined was 2.13 mm with a standard deviation of 0.59 mm. Calculating the mean bladder wall thickness of children of different age groups, we found a minimal increase of the thickness occurring with age. The mean bladder wall thickness was 2.21 mm (SD, 0.54 mm) in 33 neonates; 1.96 mm (SD, 0.6 mm) in 57 children, ages 1 month to 1 year; 2.09 mm (SD, 0.61 mm) in 134 children, ages 1 to 6 years; 2.23 mm (SD, 0.56 mm) in 135 children, ages 6 to 12 years; and 2.20 mm (SD, 0.62 mm) in 61 patients who were older than 12 years. This difference is barely significant ($p < .04$) (Fig. 2).

Grouping the patients according to gender, we found that boys tended to have a minimally thicker bladder wall (mean, 2.19 mm) than girls (mean, 2.08 mm). This difference was not statistically significant ($p < .07$) (Fig. 3).

Measuring and comparing the bladder wall thickness of empty, ±full, full, and distended (full++) bladders, we found a highly significant relation between the degree of bladder distension and wall thickness ($p < .0001$). Indeed the mean bladder wall thickness of an empty bladder was 2.76 mm (SD, 0.58 mm; maximum, 4.5 mm; minimum, 2 mm) and decreased to a mean of 1.55 mm (SD, 0.56 mm; maximum, 3 mm; minimum, 1 mm) in a distended bladder. Nomogram with estimated percentiles is shown in Fig. 4.

Assessing group interaction, we found no significant relationship between age and gender ($p < .16$), age and state of filling ($p < .83$), or gender and state of filling ($p < .45$).

The mean values of bladder wall thickness with normal variants according to age and state of bladder filling are indicated in Table 1.

Discussion

Only a few reports in the literature discuss the sonographic appearance of the normal bladder wall [4, 5]. A thickness of 5 mm was mentioned for normal adult bladder walls, but it appeared that the perivesical fat was included in these measurements.

When structures as thin as the bladder wall are being measured, several factors have to be considered. The axial or lateral resolution of the transducer becomes increasingly important. As the axial resolution is better than the lateral resolution, measurements of the wall should be made at the bladder floor using the correct transducer. We found the 7.5- or 5-MHz sufficient for all cases. Using a 3.5-MHz probe for transrectal sonography, Perkash and Friedland [6] could not evaluate the bladder wall. It is best to measure within the focal zone of the transducer, which may be difficult in a distended bladder. The bladder wall may not be seen at all without careful gain setting, and the measurements are operator dependent.

The site of measurement is important. At the dome of the bladder the peritoneal reflection will add 1 mm to the apparent wall thickness. The wall of the vagina or rectum can be included mistakenly within the measurement when one is measuring at the bladder floor. The posterior inferior wall of the bladder on sagittal views and the bladder floor lateral to the trigone on transverse views are optimal sites for measurements.

It is difficult to see the anterior bladder wall because of the

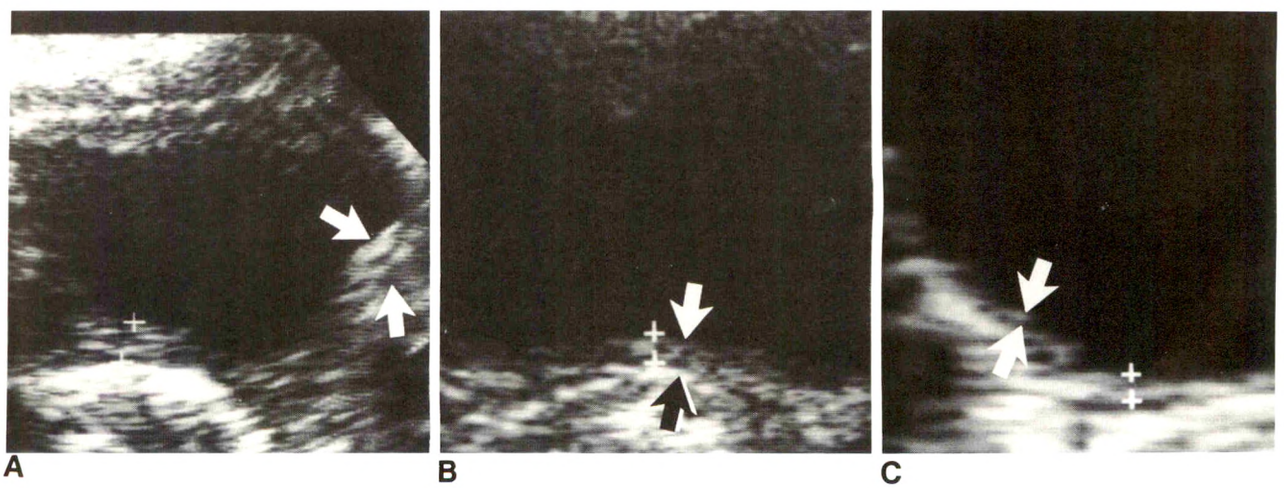


Fig. 1.—Transverse bladder sonograms: *arrows* outline bladder wall.
***A*, "Empty" bladder in a 1-month-old boy with hydroceles. Wall is 3 mm thick.**
***B*, Bladder ±full in a 7-year-old boy with remote renal contusion. Wall is 2.9 mm thick.**
***C*, Bladder full. Close-up view in a 9-year-old boy with lactose intolerance. Wall is 1.4 mm thick.**

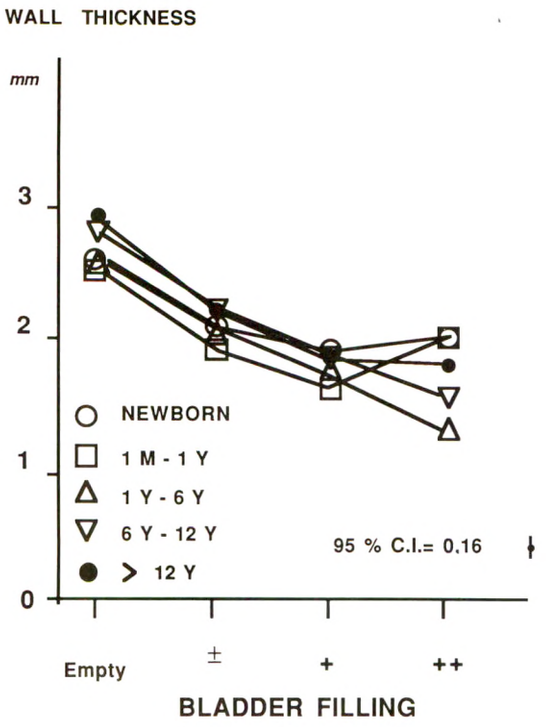


Fig. 2.—Nomogram of bladder wall thickness according to age. See Table 1 for definitions of bladder fullness. c. i. = confidence interval.

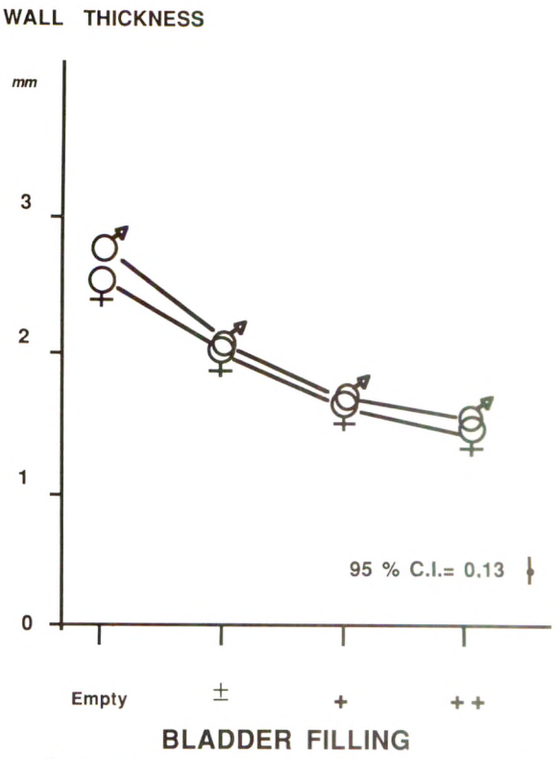


Fig. 3.—Nomogram of bladder wall thickness according to gender. See Table 1 for definitions of bladder fullness. c. i. = confidence interval.

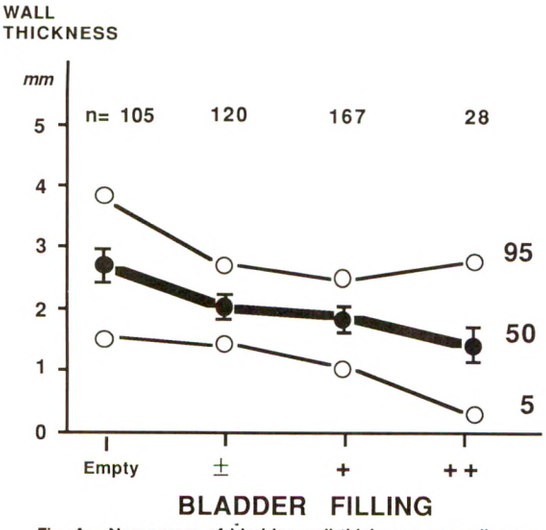


Fig. 4.—Nomogram of bladder wall thickness according to state of filling. n = number of patients in each group. 5, 50, 95 = estimated percentiles. See Table 1 for definitions of bladder fullness.

ring-down artifact of the anterior abdominal wall; therefore, one cannot obtain a true anteroposterior diameter and must estimate bladder volume. Another source of inaccuracy of this study is the electronic calipers of the ATL machine indicating full millimeters only. A bladder wall measured to be 2 mm thick could therefore range from 1.6 to 2.4 mm.

In addition, the variable shape of the bladder with different degrees of filling leads to errors in the calculation of the bladder volume. The normal bladder gets indented by the surrounding organs (bowel, uterus). It adapts to the bladder floor. When the bladder is empty, the transverse diameter is usually larger than the anteroposterior or sagittal diameter. With progressive filling, it becomes more spherical. Any proposed method of volume measurement is therefore inaccurate as none applies for both full and empty bladders. The method of Hakenberg et al. [7], for instance, has an error factor of ± 25% and is recommended for small volumes only. Orgaz et al. [8] advocate an empirical formula for sonographic bladder volume calculations: vol. = 12.56 × radius × height. They also stress the impossibility of an accurate measurement of an organ that changes its shape with filling. Their maximum error of a calculated volume compared with a known volume by retrograde filling was 31.8%.

We compared our data on bladder volume with those of Hakenberg et al. [7], who calculated the volume as the product of sagittal maximum diameter H × transverse diameter W × [(anteroposterior diameter on transverse cut + anteroposterior diameter on sagittal cut) ÷2] × 0.6. In general, our method of volume measurement tends to underestimate slightly the amount of fluid in the bladder.

Recognizing the limitations of this study, we conclude that the bladder wall thickness in children is independent of age and gender but varies significantly with the state of bladder filling. Regardless of the patient's age and gender, the wall of a normal empty bladder should measure less than 5 mm and that of a well distended bladder should measure less than 3 mm.

TABLE 1: Mean Bladder Wall Thickness in mm (±SD) According to Age and State of Bladder Filling

Age	Empty	±Full	Full	Full++
<1 mo.	2.62 ± 0.51 (8)	2.10 ± 0.31 (10)	1.92 ± 0.51 (12)	1.67 ± 0.57 (3)
1 mo.–1 yr.	2.61 ± 0.62 (14)	1.93 ± 0.27 (14)	1.65 ± 0.47 (27)	2 (2)
1–6 yr.	2.76 ± 0.73 (29)	2.06 ± 0.35 (39)	1.87 ± 0.37 (57)	1.44 ± 0.52 (9)
6–12 yr.	2.82 ± 0.46 (36)	2.17 ± 0.32 (43)	1.97 ± 0.42 (49)	1.43 ± 0.53 (7)
>12 yr.	2.83 ± 0.51 (18)	2.18 ± 0.32 (14)	1.89 ± 0.39 (22)	1.64 ± 0.74 (7)

Note.—Numbers in parentheses indicate numbers of patients in each group. mo. = month; yr. = year. Empty = bladder contained <10% of its normal capacity; ±full = bladder contained 10–25% of capacity; full = bladder contained 26–90% of capacity; full++ = bladder contained >90% of capacity.

ACKNOWLEDGMENTS

We thank Thierry Petitjean-Roget for statistical analysis, Isabell Webb for secretarial assistance, Denis Giguère for the graphics, and Michel Leblanc for the illustrations.

REFERENCES

1. Korobkin M, Callen PW, Fish AE. CT of the pelvic region. Advances in uroradiology. *Radiol Clin North Am* **1979**;XII(2):313–319
2. Koff SA. Estimating bladder capacity in children. *Urology* **1983**;21:248
3. BMDP Statistical Package 1985. Program BMDP4F. Los Angeles: University of California Press, **1985**
4. Singer D, Itzchak Y, Fischelovitch Y. Ultrasonographic assessment of bladder tumors. II. Clinical staging. *J Urol* **1981**;126:34–36
5. Abu-Yousef MM, Narayana AS, Brown RC, Franken EA Jr. Urinary bladder tumors studied by cystosonography. *Radiology* **1984**;153:227–231
6. Perkash I, Friedland GW. Transrectal sonographic urodynamics. In: Hricak H, ed. *Clinics in diagnostic ultrasound*, vol. 18. *Genito-urinary ultrasound*. New York: Churchill Livingstone, **1986**:181–193
7. Hakenberg OW, Ryall RL, Langlois L, Marshall VR. The estimation of bladder volume by sonocystography. *J Urol* **1983**;130:249–251
8. Orgaz RE, Gomez AZ, Ramirez CT, Torres JLM. Applications of bladder ultrasonography. I. Bladder content and residue. *J Urol* **1981**;125:174–176

Case Report

Cor Triatriatum: Diagnosis by MR Imaging

George S. Bisset III,[1,2] Donald R. Kirks,[1,2] Janet L. Strife,[1,2] and David C. Schwartz[3]

Cor triatriatum is a rare congenital cardiac anomaly that classically results in left ventricular inflow obstruction. A fibromuscular membrane divides the left atrium into an accessory chamber, which receives pulmonary venous return, and an anteroinferior chamber, which communicates with the left atrial appendage and the left ventricle. A single orifice, or small fenestrations, provide the only source of communication between the two chambers.

We present a case in which MR imaging provided a specific diagnosis of cor triatriatum, despite nondiagnostic echocardiography and angiography.

Case Report

A 15-year-old boy had been followed for many years with a history of "asthma" associated with moderate exertional dyspnea. During the 2 years prior to admission, the patient had experienced intermittent episodes of hemoptysis. On physical examination, there was right ventricular enlargement, a loud single second heart sound, and no cardiac murmur. These findings were believed to be consistent with cor pulmonale secondary to chronic lung disease.

Chest radiography showed prominent central pulmonary arteries. Two-dimensional echocardiography did not reveal the cause of the pulmonary hypertension. Cineangiography was performed in the anteroposterior plane with contrast injection in the main pulmonary artery. The transit time was delayed, but the pulmonary veins appeared anatomically normal. No membrane was identified prospectively. The patient developed increasing tachypnea following the angiogram; a chest radiograph showed pulmonary edema (Fig. 1).

MR imaging of the heart was performed using a General Electric 1.5-T Signa System. ECG-gated, 5-mm-thick axial and sagittal images were obtained using a spin-echo, multislice technique with an echo time (TE) of 20 msec and a repetition time (TR) of 667 msec (determined by R-R interval). An accessory chamber was identified posterior to the normal left atrium (Fig. 2). Intermediate signal intensity within this chamber indicated slow (obstructed) flow. The pulmonary

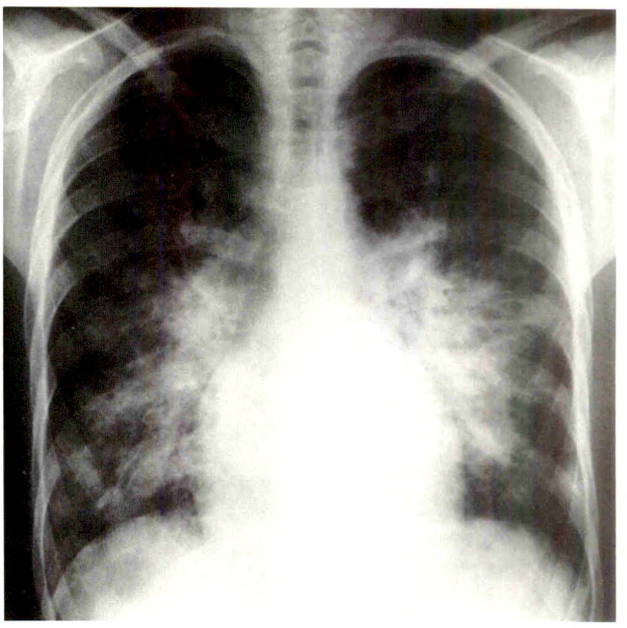


Fig. 1.—Posteroanterior chest radiograph shows perihilar distribution of pulmonary edema. Cardiac size appears normal.

Received March 31, 1987; accepted after revision May 4, 1987.

[1] Department of Radiology, Children's Hospital Medical Center, Elland and Bethesda Aves., Cincinnati, OH 45229–2899. Address reprint requests to G. S. Bisset III.

[2] Departments of Radiology and Pediatrics, University of Cincinnati College of Medicine, Cincinnati, OH 45267.

[3] Department of Pediatric Cardiology, Children's Hospital Medical Center, Elland and Bethesda Aves., Cincinnati, OH 45229-2899.

AJR **149:567–568, September 1987** 0361–803X/87/1493–0567 © American Roentgen Ray Society

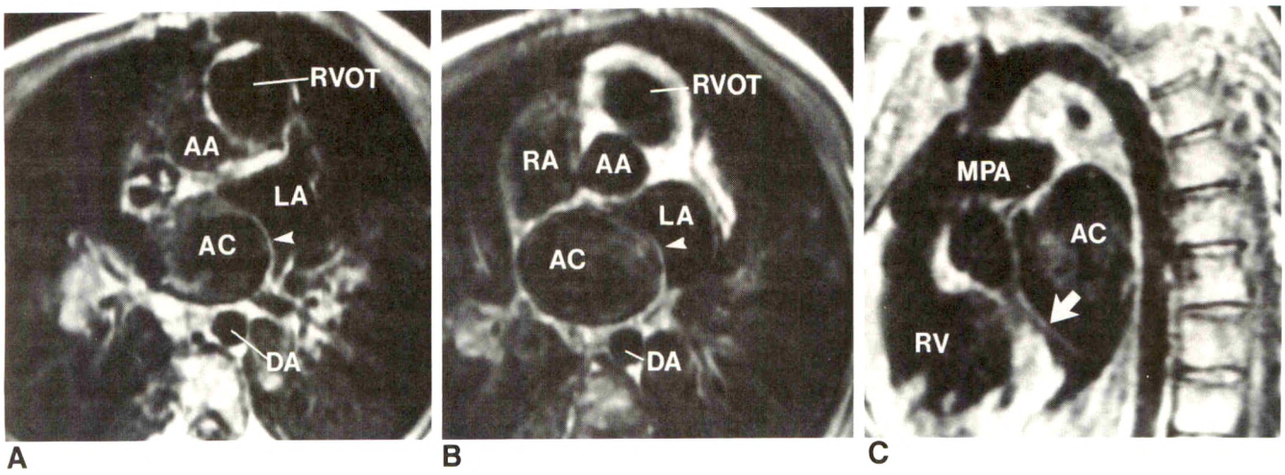


Fig. 2.—*A* and *B*, Contiguous axial 5-mm-thick MR scans (SE 667/20) through mid left atrium.
***C*, 5-mm-thick sagittal scan through left atrium. *Arrow* = fibromuscular diaphragm.**
AC = accessory chamber; LA = anterior chamber (normal left atrium); *arrowhead* = fibromuscular diaphragm; AA = ascending aorta; DA = descending aorta; RA = right atrium; RV = right ventricle; RVOT = right ventricular outflow tract; MPA = main pulmonary artery.

veins were dilated and emptied into the posterior chamber. Increased signal intensity in the lung parenchyma was most consistent with pulmonary edema. No atrial septal defect was identified.

At surgery, cor triatriatum was confirmed, and after an uneventful surgical resection of the fibromuscular diaphragm, the patient was discharged in good condition. He is currently asymptomatic.

Discussion

Cor triatriatum is a rare form of congenital left ventricular inflow obstruction that may be difficult to diagnose using currently available imaging techniques.

M-mode echocardiography may not detect the intraatrial membrane because of the superior anatomic location of this structure and the lack of spatial orientation inherent in the technique [1, 2]. Two-dimensional echocardiography is usually accurate in establishing the diagnosis [3]; however, occasional errors are made (as in this case) because of confusion with other cardiac structures or ultrasonic artifacts [2, 3]. Also, because of limited acoustic windows, the membrane may not be imaged in an optimal plane. Transesophageal echocardiography lends further sensitivity to the technique, but may be impractical in certain clinical situations (e.g., with small children).

Although the venous return phase of pulmonary angiography (with angled views) is usually diagnostic of this condition, this technique may still have limitations in detecting the left atrial membrane [1, 4–6]. Additionally, angiography may be harmful in patients with pulmonary hypertension. Pulmonary edema, acute right heart failure, and death may occur with injections of large volumes of contrast material in patients with pulmonary hypertension.

MR imaging is effective in imaging congenital heart disease [7]. In this case, MR imaging provided excellent preoperative delineation of the intraatrial membrane and obstructed flow in the accessory chamber of cor triatriatum. Other causes of obstructive pulmonary venous hypertension, including supravalvar left atrial stenosing ring, mitral stenosis/atresia, and left atrial myxoma, were excluded. This imaging technique may be helpful in the evaluation of children with unexplained pulmonary hypertension.

REFERENCES

1. Jacobstein MD, Hirschfeld SS. Concealed left atrial membrane: pitfalls in the diagnosis of cor triatriatum and supravalve mitral ring. *Am J Cardiol* **1982**;49:780–786
2. Schluter M, Langenstein BA, Thier W, et al. Transesophageal two-dimensional echocardiography in the diagnosis of cor triatriatum in the adult. *J Am Coll Cardiol* **1983**;2:1011–1015
3. Snider AR, Roge CL, Schiller NB, Silverman NH. Congenital left ventricular inflow obstruction evaluated by two-dimensional echocardiography. *Circulation* **1980**;61:848–855
4. Marin-Garcia J, Tandon R, Lucas RV, Edwards JE. Cor triatriatum: study of 20 cases. *Am J Cardiol* **1975**;35:59–66
5. Lang D, Wagenvoort CA, Kupferschmid C, Kleihauer E. Cor triatriatum masked by primary pulmonary hypertension. *Pediatr Cardiol* **1985**;6:161–164
6. Jegier W, Gibbons JE, Wiglesworth FW. Cor triatriatum: clinical, hemodynamic and pathological studies: surgical correction in early life. *Pediatrics* **1963**;31:255–267
7. Jacobstein MD, Fletcher BD, Nelson AD, Goldstein S, Alfidi RJ. ECG-gated nuclear magnetic resonance imaging: appearance of the congenitally malformed heart. *Am Heart J* **1984**;107:1014–1020

Case Report

Atrial Ventricular Diverticulum: Sonographic Diagnosis

Michael G. Karnaze,[1] Gary D. Shackelford, and Charles L. Abramson

Diverticulum of the lateral ventricle is an uncommon occurrence in patients with hydrocephalus [1–5]. Confusing this entity with similar-appearing abnormalities such as arachnoid cysts, cystic neoplasms, or the trapped fourth ventricle must be avoided to ensure proper mangement [6–8]. Although the pathologic and CT features have been described [1], the sonographic appearance is not widely known. Given the role that cranial sonography has assumed in evaluating the neonatal brain, it is essential that sonographers recognize this unusual entity. We report two cases of lateral ventricular diverticulum diagnosed with sonography, one with CT correlation.

Case Reports

Case 1

A 2½-month-old girl was evaluated for an enlarged head. The infant had weighed 3340 g at birth following a full-term pregnancy complicated by persistent vaginal bleeding, and the mother had noted the child's head to be large during early infancy. Physical findings at presentation included an enlarged head, bulging of the anterior fontanelle, split sutures, mild right esotropia, and downward gaze. CT showed marked dilatation of the lateral and third ventricles, a nondilated fourth ventricle, and a large cystic structure in the region of the quadrigeminal cistern (Fig. 1A). A lateral ventricular diverticulum was suspected, although an arachnoid cyst was also considered as a possible diagnosis. Cranial sonography revealed a communication between the "cyst" and the trigone of the left lateral ventricle, confirming the abnormality to be a ventricular diverticulum (Figs. 1B and 1C). A shunt catheter was placed in the right frontal horn. Postoperative sonograms showed no immediate resolution of the hydrocephalus or diverticulum. CT 6 weeks after shunting showed a mild decrease in the hydrocephalus and no change in the size of the diverticulum.

Case 2

A newborn premature infant girl with an estimated gestational age of 27 weeks and a birth weight of 830 g was noted on the second day of life to have multiple petechiae, bleeding from puncture sites, and prolonged prothrombin and partial thromboplastin times. Physical examination was otherwise normal except for mild right esotropia. Sonography showed a large hemorrhage in the region of the head of the right caudate nucleus, which progressed to involve the right lateral ventricle and periventricular white matter. Dilatation of the lateral ventricles developed and a follow-up sonogram on the 14th day of life demonstrated a diverticulum of the left lateral ventricle and dilatation of the lateral ventricles (Fig. 2). The patient later developed a large porencephalic cyst communicating with the right lateral ventricle, and a ventriculoperitoneal shunt was inserted at age 3 months. Postoperative sonography showed a decrease in the ventricular dilatation and disappearance of the ventricular diverticulum.

Discussion

Ventricular diverticulum is a recognized complication of hydrocephalus and has been reported to occur at a variety of locations. A diverticulum can arise from the third ventricle at its posterior recess, floor, or anteriorly at the lamina terminalis, and also from the lateral ventricle at its trigone [1–4]. Lateral ventricular diverticulum can also occur at the site of needle puncture of a dilated lateral ventricle [5]. Spontaneous rupture of the diverticulum or of a dilated ventricle into the subarachnoid space, termed ventriculocisternostomy, is known to occur, sometimes with resolution of hydrocephalus [2–4]. Ventricular diverticula may reach a size of 7 cm and may be unilateral or bilateral [1]. Their true prevalence is unknown.

The anatomic basis of lateral ventricular diverticulum has been well described by Naidich et al. [1]. The superomedial wall of the atrium of the lateral ventricle is formed by the splenium of the corpus callosum, which is thinned, elevated, and displaced posteriorly as the atrium expands in hydrocephalus. The crus of the fornix—which, along with the alveoli of the hippocampus, forms the inferomedial atrial wall—is thinned and displaced inferiorly. The alveoli are stretched between the elevated splenium and depressed crus. This region of the alveoli and the crus of the fornix becomes progressively thinned and lies medial to the free edge of the tentorium and superior to the incisura. Focal dehiscence of this thin alveolar-crural sheet creates an ostium in the inferomedial atrial wall through which pia and CSF can protrude. Separated from the subarachoid space by this thin pial covering, the resulting diverticulum may extend downward through the incisura. This may result in displacement of the fourth ventricle inferiorly, the quadrigeminal plate and pineal anteroinferiorly, and the straight sinus and tentorium posterosuperiorly.

This article appears in the July/August 1987 issue of *AJNR* and the September 1987 issue of *AJR*.

Received September 15, 1986; accepted after revision January 8, 1987.

[1]All authors: Mallinckrodt Institute of Radiology, 510 South Kingshighway Blvd., St. Louis, MO 63110. Address reprint requests to G. D. Shackelford.

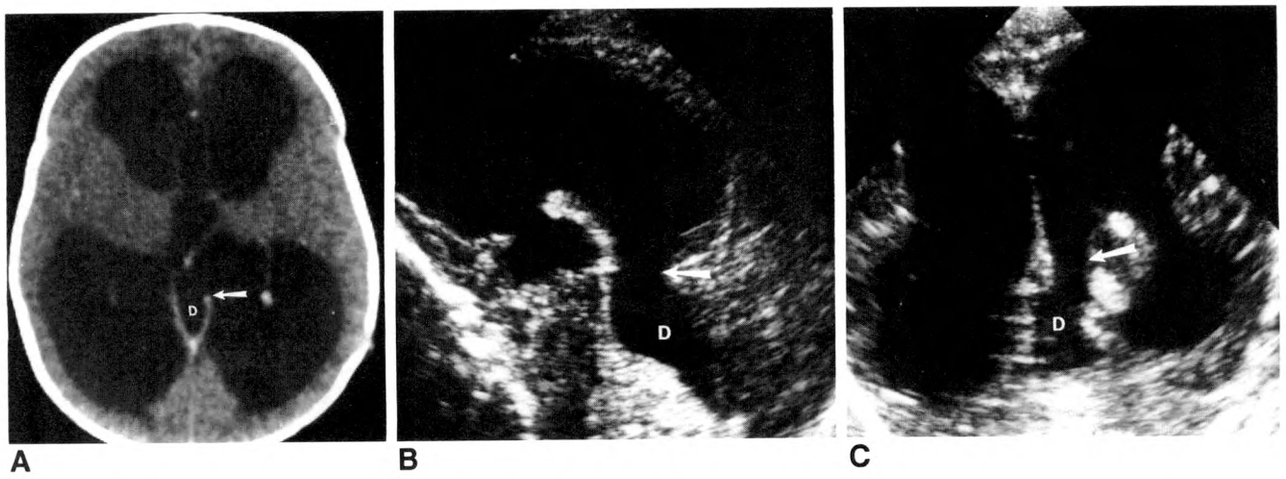


Fig. 1.—Case 1.
A, Axial contrast-enhanced CT with 4-mm collimation shows dilatation of lateral and third ventricles. Anterior edge of left tentorial band is shortened, typical of lateral ventricular diverticulum (*arrow*). D = diverticulum.
B, Sagittal sonogram through dilated left lateral ventricle shows this diverticulum (D) and its point of communication with lateral ventricle (*arrow*). Diverticulum extends posteroinferiorly from trigone and is seen superior to cerebellum.
C, Coronal image clearly shows communication of diverticulum (D) with left lateral ventricle (*arrow*).

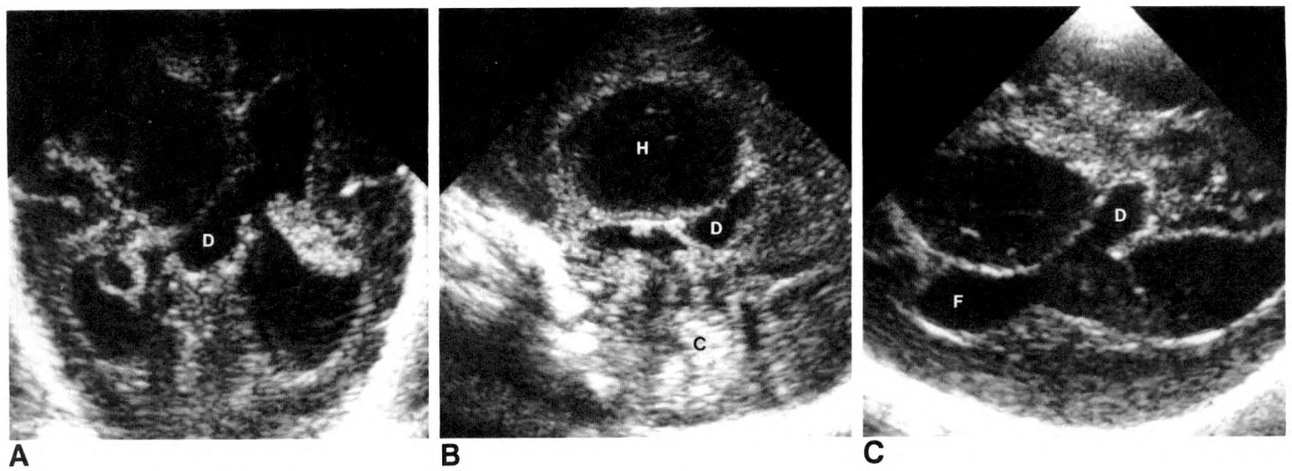


Fig. 2.—Case 2.
A, Coronal sonogram through trigone shows diverticulum (D) extending from left lateral ventricle.
B, Midsagittal scan shows that diverticulum (D) lies superior to cerebellum (C) and tentorium. H = hemorrhage.
C, Axial scan clearly defines communication between diverticulum (D) and left lateral ventricle. F = frontal horn of lateral ventricle.

In our two cases, sonography revealed hydrocephalus and an asymmetrical cystic structure extending from the inferomedial aspect of the trigone. The point of communication of the diverticulum with the trigone was clearly evident in both our cases, but has not always been identified with CT [1]. This communication could be seen on sonography with careful sagittal and coronal scanning but was more clearly demonstrated in the axial plane in the one case in which axial scanning was performed (Fig. 2C). Coronal scans displayed the relationship of the diverticulum to the tentorium in both cases, although the location of the diverticulum superior to the tentorium in the second case was better shown on sagittal images (Figs. 2A and 2B).

Lateral ventricular diverticula, which are secondary to hydrocephalus and can be treated by shunting, must be differentiated from entities that can cause hydrocephalus, such as arachnoid cysts and cystic neoplasms [6]. The dilated posterior recess of the third ventricle, trapped fourth ventricle, or trapped posterior recess of the third ventricle may also be mistaken for a lateral ventricular diverticulum [7, 8]. A dilated posterior third ventricular recess communicates with the third ventricle. The trapped fourth ventricle and the less common

trapped posterior third ventricle typically occur following shunting of hydrocephalus [7, 8]. Cystic tumors may show an associated soft-tissue mass. Arachnoid cysts may be more symmetric than diverticula and do not have a communication with the lateral ventricle [6]. It is the absence of this communication with the lateral ventricle and the presence of intact ventricular walls that differentiate all of these abnormalities from a lateral ventricular diverticulum.

In summary, diverticulum of the lateral ventricle is an uncommon complication of hydrocephalus, but one that must be recognized by the sonographer. A diverticulum should not be confused with other abnormalities, some of which can cause hydrocephalus and thus have different therapeutic implications. We have described two cases in which sonography was diagnostic by depicting the actual communication between the diverticulum and the lateral ventricle.

REFERENCES

1. Naidich TA, McLone DG, Hahn YS, Hanaway J. Atrial diverticula in severe hydrocephalus. *AJNR* **1982**;3:257–266
2. Tandon PK, Harkmark W. Spontaneous ventriculocisternostomy with relief of obstructive hydrocephalus. *Neurology* **1959**;9:699–703
3. Miller CF, White RJ, Roski RA. Spontaneous ventriculo-cisternostomy. *Surg Neurol* **1981**;54:98–100
4. Liss L, Mervis L. Spontaneous ventriculostomy through lamina terminalis with arrest of hydrocephalus. *J Neurosurg* **1965**;23:211–213
5. Grainger RG, Lorber J. Development of ventricular diverticula following ventricular puncture in hydrocephalic infants. *Acta Radiol* **1963**;1:569–576
6. Lee BCP. Intracranial cysts. *Radiology* **1979**;130:667–674
7. Scotti G, Musgrave MA, Fitz CR, Harwood-Nash DC. The isolated fourth ventricle in children. *AJR* **1980**;135:1233–1238
8. Babcock DS, Han BK. *Cranial ultrasonography of infants*. Baltimore: Williams & Wilkins, **1981**:154

ASNR: The Silver Anniversary

Neuroradiology: The Next 25 Years

Juan M. Taveras[1]

The President of the American Society of Neuroradiology (ASNR), Derek Harwood-Nash, asked me as founder of the Society to write an essay on the occasion of its 25th anniversary. I am extremely happy and highly honored to respond to this request but wonder if I can do justice to such an important occasion.

The founding of the ASNR in 1962 was an important step in the development of neuroradiology in the United States and in a broader sense in the development of subspecialization within radiology in this country. Before 1962, Ernest Wood, the director of radiology at the Neurological Institute of New York, was *the only full-time* neuroradiologist in the United States, and after his departure in 1962 (to become Chairman of the Department of Radiology at the University of North Carolina in Chapel Hill) I was appointed director of the Department and again became virtually the only practicing full-time neuroradiologist in the country. This continued for several years and, slowly, partly because of the stimulus engendered by the IV Symposium Neuroradiologicum, which took place in London in 1955, more radiologists in this country became interested in the subspecialty and some of them sought training outside the United States. In the late 1950s, Torgny Greitz, from Sweden, was invited to come to the Mallinckrodt Institute of Radiology at Washington University in St. Louis to spend a couple of years practicing and teaching neuroradiology. At that time, neuroradiology in Europe, particularly in Sweden, was far more developed than in the United States, and training opportunities were available there as well as in England. One reason why neuroradiology was not developed at that time in the United States was that the concept of subspecialization within radiology was really nonexistent and generally opposed by most chairmen of radiology departments [1].

It was obvious that neuroradiology could not grow as a subspecialty until the chairmen of radiology departments around the country accepted the need for such development. The same applied to other subspecialties within radiology.

One important factor that slowed the development of neuroradiology was the need to perform invasive procedures such as angiography, pneumoencephalography, and myelography. Because radiologists were not accustomed to performing invasive procedures, these were carried out by the neurosurgeons and sometimes by the neurology residents in training who wanted to acquire the skills to perform such procedures. The idea that radiologists were capable of developing these skills had yet to be established and put into practice.

A significant development in the early 1960s was the introduction of training programs in clinical neurology financed by the National Institutes of Health through the then National Institute of Neurological Diseases and Blindness (NINDB). At that time there was no opportunity for an individual who had completed full training in diagnostic radiology to obtain postresidency fellowship training because no financing was available from hospitals. Following the model established in clinical neurology, the NINDB provided an opportunity to establish training programs in neuroradiology by offering special training fellowships to individuals who had completed full training in diagnostic radiology. I was fortunate to have been able to establish the first training program in the United States at the Neurological Institute, Columbia Presbyterian Medical Center, in New York; the second was established almost simultane-

This article appears in the May/June 1987 issue of *AJNR* and the September 1987 issue of *AJR*.

[1] Department of Radiology, Massachusetts General Hospital, 32 Fruit St., Boston, MA 02114. Address reprint requests to J. M. Taveras.

***AJR* 149:572–574, September 1987** 0361–803X/87/1493–0572 © American Roentgen Ray Society

ously by Manny M. Schechter at the Albert Einstein Medical Center, also in New York. Shortly thereafter, other training programs were organized. This allowed us to accept qualified individuals for training in neuroradiology for a period of 1, 2, or 3 years. Interestingly, this started slowly but grew rapidly so that by 1963 I already had seven fellows in the program, all of them agreeing to undergo the 2 years of training that I felt was the minimum needed to become a true subspecialist.

I believe the ASNR was the first formally organized subspecialty society within diagnostic radiology in the United States. It became a successful organization early after its founding and has continued to grow steadily throughout its 25 years.

Some of its success can be attributed to the requirements for membership. From the beginning, becoming a member of the ASNR was an achievement in itself, since membership required having had 2 years of training in the subspecialty under a recognized neuroradiologist. These standards have been maintained to the present and have been tightened rather than relaxed. The strict membership requirements have, in my mind, created a homogeneity and fostered a sense of belonging to an achiever group, which has contributed to the success and prestige that the society enjoys. Despite such stringent requirements, the number of members has been increasing, reaching 1,000 in 1986.

It is possible that the ASNR is looked upon as an elite society, and some might oppose it because of that. Certain expressions, such as "splitting or dismemberment of the specialty of radiology" or "disenfranchising of the general radiologist," are often heard. These refer mainly to the development of neuroradiology, but also to other subspecialties within diagnostic radiology. I wonder if these expressions would be used if anyone who is board-certified in radiology could become a member of the ASNR simply by applying. The creation and maintenance of standards of competence is apt to create opposition from groups that do not qualify and to be applauded by those that do. The medical profession is constantly required to elevate its standards if it is to provide the best care possible. I wonder how much opposition followed the creation of the American Board of Radiology in 1935. Some physicians obviously were disenfranchised; and with the establishment of specialty boards in other areas of medicine the accusation of "splitting" or "dismemberment" was undoubtedly voiced.

But how are we to achieve progress and apply it for the common good: by denying that progress has taken place and needs to be incorporated into medical care, or by recognizing those who have agreed through considerable sacrifice to comply with defined requirements? Are we to deny that there has been a great expansion of special knowledge in the field of neuroradiology and that society would demand that these achievements be fully applied in the practice of medicine? And can we be satisfied with the *partial* application of this expanded knowledge on a permanent basis solely to satisfy the desire of the general radiologist? Society would never forgive the medical profession for such behavior; neither is it consistent with what has occurred in surgery, medicine, pediatrics, and pathology. Is not radiology, like those other fields, a specialty of medicine dealing with every organ system in the body?

The Journal

In 1978 the society decided to start a new journal, to be called the *American Journal of Neuroradiology* (*AJNR*). After considerable discussion a decision was made to associate with the *American Journal of Roentgenology* (*AJR*) and the American Roentgen Ray Society. Preparations to publish the first volume began in June 1979, and the first bimonthly issue came out in timely fashion on January 1, 1980. By all standards the *AJNR* can be considered a very successful journal. And it has been a great honor and privilege to be its first editor—even though at times it has not been easy.

Since January 1986, the journal has been wholly owned by the ASNR, but dual publication of some articles in the *AJR* will continue, which I feel is advantageous.

I believe the *AJNR* will continue to prosper as long as high standards are maintained in all aspects of its publication.

The Future

The success of the ASNR has gone beyond my dreams; how can I express my deep satisfaction at having been able to witness this in my lifetime? I am optimistic about the future of neuroradiology and believe that increased recognition and acceptance will undoubtedly take place as time goes on. In spite of my remarks in the preceding paragraphs, I believe some kind of official recognition of special competence or added qualifications will take place in years to come. However, it is my earnest hope that when a decision is made to grant recognition through examination that a *2-year training period*, the same as that required for membership in the ASNR, be instituted as a minimum for admission to the examination. It is the firm opinion of most members of the ASNR that 2 years are necessary to reach the level of competence required in this special field.

Only one thing has worried me in the past and continues to worry me: the relative scarcity of true research by members of the ASNR. This was aptly expressed in an editorial by Murray Goldstein, Director of the National Institute of Neurological and Communicative Disorders and Stroke, entitled "Where Are You? You Are Needed!" [2]. Neuroradiologists, with few exceptions, share with the rest of radiologists a lack of training in basic research. On many occasions in the past I have spoken to the Society about the need to develop research in neuroradiology. Fortunately, technological developments have favored us because the new instrumentation has been applied first to the brain and the spinal cord, allowing neuroradiologists to become "pioneers" in the clinical application of these new imaging techniques: CT, MR, radionuclide scanning, and even sonography, initially. However, we need to go beyond this to develop programs of basic research, to delve into the biology of disease, to study physiology and pathophysiology using our unique imaging methods to elucidate phenomena, and to generate new information.

How can we accomplish this important goal of developing research? The answer is not simple, but I would like to say something about how it can be started. First, we need the determination to promote research carried out by neuroradiologists. Second, we must commit financial support as needed in the beginning, from our clinical funds, to the measure of our ability, to equip laboratories and to support personnel. We must build an infrastructure made up of Ph.D.s and well-trained technologists, and, most important, we must *enthusiastically support research training* for young neuroradiologists. How can we generate the financial support to maintain these young investigators? Perhaps a special fund can be created for this purpose. The Society of Neurological Surgeons has developed a national program for support of research training in neurosurgery. A special fund has been created from financial contributions made mostly by individual members of the society. Once the fund reaches a certain level, the interest derived from it is used *only* to support deserving individuals while they obtain research training in an appropriate environment. More recently the RSNA has established a program to support young investigators; this is progressing well and will undoubtedly grow in the future.

Establishing a research program in a specialty like neuroradiology is not easy. What are suitable areas for true research in neuroradiology? In the last 16 years many developments have assisted the subspecialty by creating a feeling among our peers in other specialties that investigation in pure neuroradiology is alive and well. These developments were in interventional neuroradiology, for which credit goes mostly to radiologists, and in the technological developments in CT and MR mentioned above. This provided a great opportunity to study the clinical utility of these new techniques, which is continuing. But as a group, neuroradiologists can claim little originality in the creation of this new knowledge. CT offers virtually no investigative opportunities at present, but MR does; there is much to be done in this area. Nevertheless, can a retrospective analysis of 10, 50, or 100 cases of a certain disease process with or without CT comparison, with or without contrast media, be considered true research? To be sure, in radiodiagnosis, as well as in earlier medicine and surgery, description and careful analysis of findings have been important and have filled most of the radiologic literature. Perforce, this must be retrospective in the majority of cases. But how long can this go on? In CT this is virtually over; in MR there is still some time to go both for MR alone and for comparison with other techniques, mostly CT.

In MR, however, there is much true research to be carried out in spectroscopy, first on the basic side and then, after laying a solid foundation in this area, on the clinical applications, both with protons and with other nuclei. In addition, there is the broad area of development and application of contrast media for MR imaging.

MR (chemical-shift imaging, spectroscopy, and contrast media development) is an exceedingly important field for us in research. Let us not abandon it to others!

Research in all aspects of cerebral vascular disease is another appropriate area for neuroradiologists. Any research project or program designed to achieve the earliest possible diagnosis of a disease process is appropriate research for a neuroradiologist. This may require a collaborative effort with other specialists and an acquisition of considerable knowledge about the biology of the disease under study.

Prospective (as opposed to retrospective) clinical investigation is a vast area for which the neuroradiologist is well suited, and I hope to see more of this in our journals in the future.

One of the most important research areas in radiology involves the study of contrast media. This applies to contrast media for vascular visualization, myelography, and cisternography, and also to contrast media for MR, which may in the future require a variety of compounds for different organs or disease processes, to contrast media for nuclear medicine, a vast area of basic and clinical research, and possibly to contrast media for other uses.

Basic research is tedious and often disappointing, and clinical application of knowledge acquired through basic research may take a long time. Impatience in research usually goes unrewarded because the investigator is apt to give up too soon. Often the most painstaking research goes nowhere, at times it cannot even be published, particularly if it turns out that it was poorly controlled and poorly planned. But that is precisely the nature of research; that is one of the reasons why *good research training is needed.*

Radiologists have been extremely preoccupied with maintaining clinical skills. They feel that if they leave clinical radiology for one or more years to do research they'll forget everything and lose their trained eye. This is simply not so. Do internists forget clinical medicine, do surgeons lose their skills simply because they spend time in the laboratory? If the surgeon was skillful to start with he'll simply become better through his experience with research. Moreover, after research training, the internist or the surgeon has a solid foundation that allows him to continue to carry out or direct investigations. Sustained basic research requires the creation of an environment and the addition of interested Ph.D.s to the laboratory. Initially, they must be supported from clinical funds, but later enough research support can be attracted to provide most or all of their salaries.

I hope that the next 25 years will see an active increase in the quantity and quality of research by members of our Society, and that research will become progressively more sophisticated and basic with the passage of time. I would like to see special research sessions at the annual meeting. I also hope that the Society is able to establish a special fund to support research training in a manner similar to that done by the Society of Neurological Surgeons and by the RSNA. The Society is most grateful to the Berlex Corporation for its support in creating the ASNR Basic Science Fellowship. This may be a good beginning!

REFERENCES

1. Taveras JM. Aubrey O. Hampton lecture. Subspecialization in radiology: response to a need. *AJR* **1987**;148:465–469
2. Goldstein M. Where are you? You are needed! *AJNR* **1986**;7:1106

Lymphomas of the Head and Neck: CT Findings at Initial Presentation

Ya-Yen Lee[1]
Pamela Van Tassel
Craig Nauert
Luceil B. North
Bao-Shan Jing

CT findings were reviewed in 68 patients with untreated head and neck lymphoma. More than half of the patients with either Hodgkin's disease or non-Hodgkin's lymphoma were detected in the earlier stages (stage I or II). Four types of abnormalities were identified with CT: nodal involvement alone (type 1), extranodal involvement alone (type 2), a combination of extranodal and nodal disease (type 3), and multifocal extranodal disease with or without nodal involvement (type 4). In the 18 patients with Hodgkin's disease, a subgroup of mixed cellularity was most common; type 1 was the prevailing CT presentation, and no type 2 or 4 lesions were observed. In the 50 patients with non-Hodgkin's lymphoma, diffuse large-cell lymphoma was the most common histologic subtype, and the most common CT presentation was type 2, followed by type 3. Lymphomatous nodes may be extensive and confluent, but often they are smaller than 2 cm and rarely are necrotized. The most frequent extranodal sites of head and neck lymphomas are Waldeyer's ring, paranasal sinuses, and nasal cavity. Extranodal lymphoma cannot be differentiated reliably from the more commonly occurring carcinoma, although it is less often associated with invasion and destruction of adjacent bony structures. Multiple sites of extranodal involvement, with or without neck lymphadenopathy, may suggest a diagnosis of non-Hodgkin's lymphoma.

Hodgkin's disease and non-Hodgkin's lymphoma often involve the head and neck region, and many clinical articles have been published on head and neck lymphomas [1–14]. However, to our knowledge there are no thorough radiologic evaluations of head and neck lymphomas, particularly ones that emphasize CT findings. In this paper, we report our analysis of the CT findings of untreated head and neck lymphomas in 68 patients to establish CT patterns and to correlate them with histopathologic and staging classifications.

Materials and Methods

Between October 1981 and July 1986, 68 untreated patients with a diagnosis of lymphoma involving the head and neck region were referred to the Department of Diagnostic Radiology at the University of Texas M. D. Anderson Hospital and Tumor Institute at Houston for CT evaluation of tumor extent in the head and neck. The CT studies were performed with a GE 8800, GE 9800, Siemens Somatom 2, or Siemens DR-3 scanner after an IV bolus injection of contrast medium (either 300 ml of 30% iodine or 150 ml of 60% iodine). Consecutive 4- or 5-mm-thick axial images were obtained routinely from the sphenoid sinus to the angle of the mandible, and sections 8 or 10 mm thick from there to the sternal notch. For those patients with lesions suspected in the orbit or paranasal sinuses, both direct coronal and axial 4- or 5-mm-thick images were obtained.

Nodal and extranodal lesions were confirmed by pathologic studies. The histopathologic classification of these 68 patients was made according to the Rye classification [15] for Hodgkin's disease and the working formulation classification [16] for non-Hodgkin's lymphoma. The Ann Arbor staging classification [17] was used for both Hodgkin's and non-Hodgkin's lymphomas after a complete staging workup, which included chest radiography, chest CT in selected cases, lymphangiography and/or CT of the abdomen, and bone-marrow

This article appears in the July/August 1987 issue of *AJNR* and the September 1987 issue of *AJR*.

Received October 20, 1986; accepted after revision January 21, 1987.

[1] All authors: Division of Diagnostic Imaging, Department of Diagnostic Radiology, M. D. Anderson Hospital and Tumor Institute, University of Texas System Cancer Center, 1515 Holcombe Blvd., Houston, TX 77030. Address reprint requests to Y-Y Lee.

***AJR* 149:575–581, September 1987**
0361–803X/87/1493–0575
© American Roentgen Ray Society

TABLE 1: Classification of Head and Neck Lymphomas

Type of Lymphoma: Category	No. by Stage									
	IA	IEA	IIA	IIEA	IIIA	IIIEA	IIIB	IVA	IVB	Total
Hodgkin's disease:										
Nodular sclerosis	0	0	2	1	1	0	2	0	0	6
Mixed cellularity	1	0	2	2	0	0	0	3	1	9
Lymphocytic predominance	2	0	1	0	0	0	0	0	0	3
Subtotal	3	0	5	3	1	0	2	3	1	18
Non-Hodgkin's lymphoma:										
Diffuse, small lymphocytic	0	1	0	2	0	0	0	0	0	3
Follicular, small cleaved	1	1	0	0	1	0	0	2	0	5
Follicular, mixed	0	0	1	0	0	0	0	0	0	1
Follicular and diffuse, large	0	0	0	0	0	1	0	1	0	2
Diffuse, mixed	0	2	0	0	0	0	0	1	2	5
Diffuse, large	2	11	1	10	0	0	0	3	0	27
Diffuse, small noncleaved	0	4	0	0	0	0	0	0	0	4
Lymphoblastic	0	0	0	0	0	1	0	0	0	1
Unclassified	0	2	0	0	0	0	0	0	0	2
Subtotal	3	21	2	12	1	2	0	7	2	50
Total	6	21	7	15	2	2	2	10	3	68

biopsy. Eighteen patients had Hodgkin's disease and 50 had non-Hodgkin's lymphoma (Table 1).

Results

CT Patterns

Four CT patterns of head and neck lymphomas were identified (Table 2).

In Hodgkin's disease, six were type 1A, nine were 1B, and three were 3A. In non-Hodgkin's lymphoma, five were type 1A, two were 1B, five were 2A, 20 were 2B, eight were 3A, seven were 3B, two were 4A, and one was 4B (Table 3).

Histopathologic correlation.—In Hodgkin's disease, the mixed-cellularity subgroup was observed most often (nine of 18 patients), followed by the nodular sclerosis subtype. Nodal involvement occurred in all 18 cases. Among these, three patients presented with additional extranodal lesions in Waldeyer's ring (type 3A): one in the nasopharynx, one in the tonsil, and one at multiple sites). No cases were observed of isolated extranodal presentation (type 2).

Twenty-seven (54%) of 50 non-Hodgkin's patients had diffuse large-cell lymphomas. The predominant feature was extranodal presentation, 25 (50%) without (type 2) and 15 (30%) with (type 3) nodal involvement. Isolated nodal involvement (type 1) was observed in only seven (14%) of 50 cases. The most common single CT pattern was type 2B, occurring in 20 patients (40%). The most common sites of extranodal involvement were Waldeyer's ring, the paranasal sinuses, and the nasal cavity (Table 4). Waldeyer's ring involvement in non-Hodgkin's lymphoma was found at more than one site in eight of 13 patients and was associated with nodal disease in eight of 13. Conversely, 12 of 13 patients whose disease involved the paranasal sinuses and nasal cavity were free of nodal involvement.

TABLE 2: CT Patterns of Head and Neck Lymphomas

Type, Description
1, Nodal lymphomas:
1A, Unilateral
1B, Bilateral
2, Extranodal lymphomas:
2A, Extranodal lesion(s) confined within Waldeyer's ring
2B, Extranodal lesion outside Waldeyer's ring (extralymphatic)
3, Nodal and extranodal lymphomas (combined types 1 and 2):
3A, Waldeyer's ring lesion(s), with nodal involvement
3B, Extralymphatic lesion, with nodal involvement
4, Multifocal extranodal lymphomas:
4A, Without nodal involvement
4B, With nodal involvement

Staging correlation.—In Hodgkin's disease, more than half (11 of 18) the patients had earlier staging (stage I or II) at presentation. The same observation was made in non-Hodgkin's lymphoma (38 of 50). Most of the patients in both groups were free of constitutional symptoms (for example, fever, sweats, pruritis, and unexplained weight loss of more than 4.5 kg).

Anatomic Considerations

Nodal involvement.—In 13 (72%) of 18 patients the involved lymph nodes in Hodgkin's disease measured less than 2 cm in greatest diameter on CT (Fig. 1). All cases had involvement of the deep lymphatic chains, particularly the internal jugular chains, either unilaterally (10 of 18) or bilaterally (eight of 18). Additional superficial nodes were involved in only one case. One case showed evidence of extracapsular spread and nodal necrosis.

TABLE 3: Distribution of Head and Neck Lymphomas by CT Pattern

Type of Lymphoma: Category	No. by CT Pattern								
	1A	1B	2A	2B	3A	3B	4A	4B	Total
Hodgkin's disease:									
Nodular sclerosis	2	3	0	0	1	0	0	0	6
Mixed cellularity	2	5	0	0	2	0	0	0	9
Lymphocytic predominance	2	1	0	0	0	0	0	0	3
Subtotal	6	9	0	0	3	0	0	0	18
Non-Hodgkin's lymphoma:									
Diffuse, small lymphocytic	0	0	0	1	2	0	0	0	3
Follicular, small cleaved cell	2	0	2	1	0	0	0	0	5
Follicular, mixed cell	1	0	0	0	0	0	0	0	1
Follicular and diffuse, large cell	0	0	0	2	0	0	0	0	2
Diffuse, mixed cell	0	1	0	2	2	0	0	0	5
Diffuse, large cell	2	1	3	8	3	7	2	1	27
Diffuse, small noncleaved	0	0	0	4	0	0	0	0	4
Lymphoblastic	0	0	0	0	1	0	0	0	1
Unclassified	0	0	0	2	0	0	0	0	2
Subtotal	5	2	5	20	8	7	2	1	50
Total	11	11	5	20	11	7	2	1	68

Note.—CT patterns are defined in Table 2.

TABLE 4: Extranodal Sites of Head and Neck Lymphomas

Type of Lymphoma: Site	No.
Hodgkin's disease:	
Waldeyer's ring:	
Nasopharynx	1
Tonsil	1
Multiple sites	1
Subtotal	3
Total	3
Non-Hodgkin's lymphoma:	
Waldeyer's ring:	
Nasopharynx	3
Tonsil	2
Multiple sites	8
Subtotal	13
Paranasal sinuses and nasal cavity	13
Cheek:	
Skin	4
Buccal mucosa	3
Subtotal	7
Thyroid gland	4
Nose	1
Orbit	1
Parotid gland	1
Multifocal:	
Nasopharynx plus submandibular gland	1
Nasopharynx plus paranasal sinus	1
Waldeyer's ring plus cheek	1
Subtotal	3
Total	43

In non-Hodgkin's lymphoma, most (15) of the 23 involved nodes also measured less than 2 cm. However, in seven (30%) of 23 cases the largest node was more than 5 cm; of these, six had extracapsular and three had nodal necrosis (Fig. 2). Of interest, in three cases very large nodes were present (greater than 10 cm in the largest), but none showed evidence of central necrosis (Fig. 3). As in Hodgkin's disease the deep lymphatic chain was always involved in cases in which non-Hodgkin's lymphoma appeared in the neck lymph nodes unilaterally (13 of 23) or bilaterally (10 of 23). However, the superficial lymphatic chains were involved in nine (39%) of 23 patients because associated disease was common at extralymphatic sites such as the cheek or thyroid gland.

Extranodal involvement (Table 4).—Waldeyer's ring was the site at which extranodal disease occurred most often in head and neck lymphomas (Fig. 4). In our series there were three in Hodgkin's disease and 16 in non-Hodgkin's lymphoma, and the disease often infiltrated more than one site within the ring. However, in several cases isolated lesions were found in the nasopharynx or tonsil. None of the Waldeyer's-ring lesions had associated destruction of the base of the skull.

All the extranodal lymphomas outside the Waldeyer's ring (extralymphatic) were in non-Hodgkin's lymphoma, predominantly the diffuse large-cell subgroup (Table 3). The paranasal sinuses and nasal cavity were the sites at which extralymphatic disease was found most often (Fig. 5). Minimal adjacent bone destruction was seen in nine of 13 cases. Tumor calcification occurred in only one case, appearing in the ethmoid sinus with extensive bone destruction and intracranial extension (Fig. 6).

All four cases of thyroid lymphoma in our series had a preceding history of goiter with a histologic background of chronic lymphocytic thyroiditis detected microscopically. All of these lymphomas were aggressively infiltrating the adjacent aerodigestive tract and had extensive nodal involvement (Fig. 7). The cheek lesions, either originating in skin or buccal submucosa, extended into the maxillary sinus or nasal cavity,

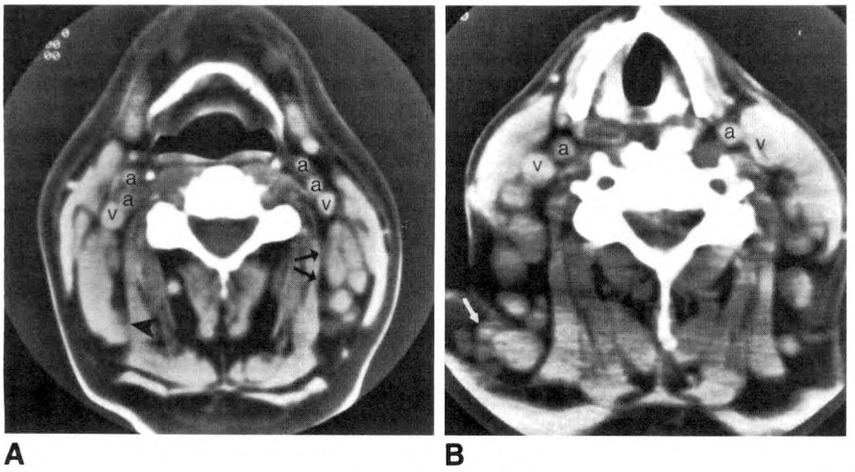


Fig. 1.—*A* and *B*, Bilateral nodal disease in 20-year-old man with nodular sclerosing Hodgkin's disease involving deep lymphatic chains. Large, right, nonnecrotic spinal accessory node (*arrowhead*) is confluent with jugular nodes. Clusters of left jugular nodes (*black arrows*) and right transverse cervical nodes (*white arrow*) all measured less than 1 cm in diameter. a = common internal and external carotid arteries; v = internal jugular veins.

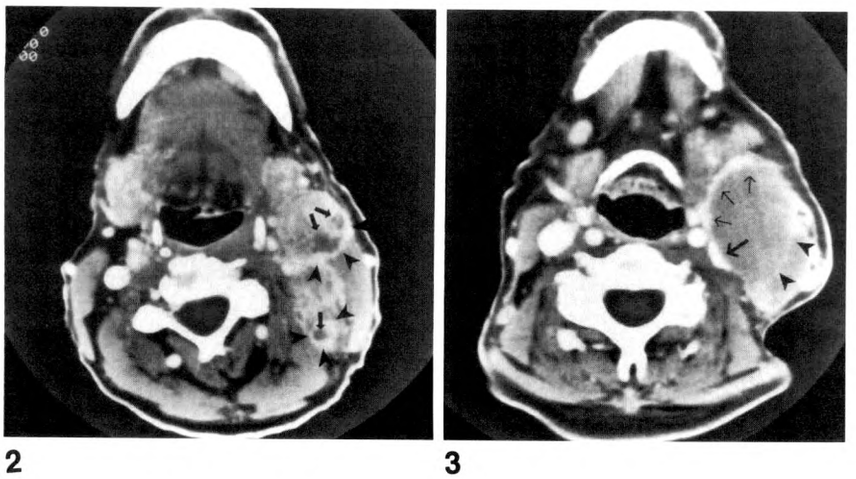


Fig. 2.—Confluent nodal involvement along with left deep jugular and spinal accessory chains in 62-year-old woman with diffuse large-cell lymphoma. Nodal necrosis is manifested as central hypodensity within lymph nodes (*arrows*); in addition, extracapsular spread is shown as thick pericapsular enhancement obliterating normal fasciae (*arrowheads*).

Fig. 3.—Left nodal involvement along deep jugular chain in 63-year-old woman with follicular small-cleaved-cell lymphoma. Internal jugular vein (*large arrow*) and facial vein (*small arrows*) are displaced by large confluent node that shows extracapsular spread into overlying sternomastoid muscle (*arrowheads*). However, no nodal necrosis is evident.

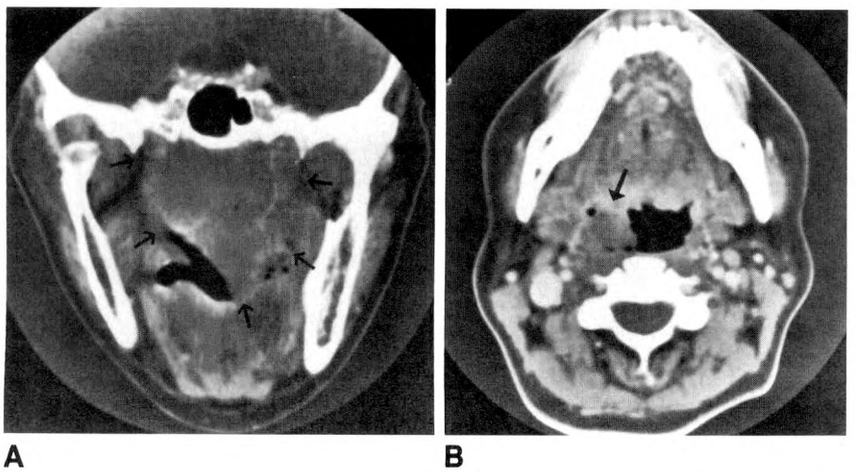


Fig. 4.—*A*, Multiple-site involvement of Waldeyer's ring (*arrows*) of diffuse large-cell lymphoma without nodal disease in 68-year-old woman. There is no destruction of base of skull or extension into sphenoid sinus despite extensive disease in nasopharynx.

B, Isolated, diffuse large-cell lymphoma in right tonsillar fossa (*arrow*) projects into oropharynx in 48-year-old woman.

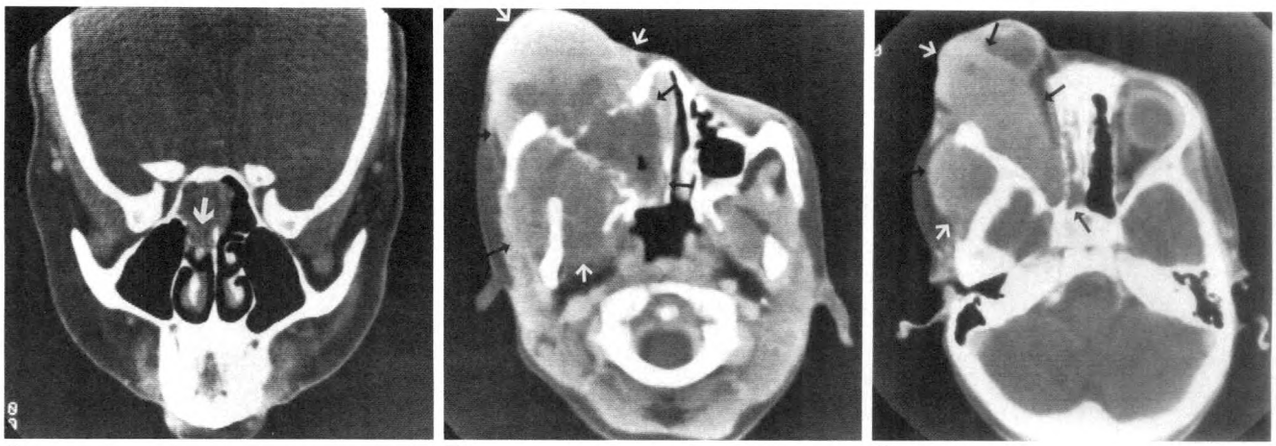


Fig. 5—*A*, Diffuse large-cell lymphoma involving sphenoid sinus in 43-year-old woman. Minimal bone destruction (*arrow*) but no intracranial extension. *B* and *C*, Extensive infiltrative lymphoma (*arrows*) of diffuse, small, noncleaved subtype (non-Burkitt's) in 4-year-old boy originates from right maxillary sinus and has extensive bone destruction. There is direct extension into right orbit, temporal fossa, infratemporal fossa, and right nasal cavity.

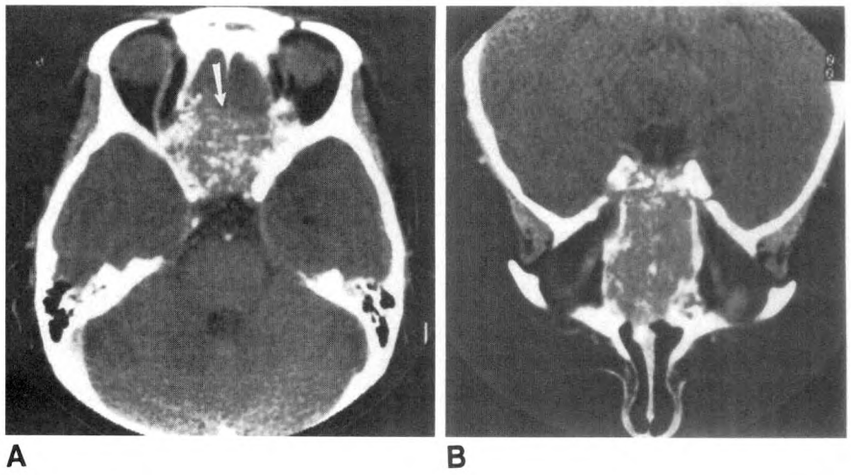


Fig. 6.—Axial (*A*) and coronal (*B*) views. Diffuse involvement of nasal cavity and ethnoid sinuses with bone destruction and intracranial extension (*arrow*) in 49-year-old woman with diffuse large-cell lymphoma. Note scattered tumoral calcifications.

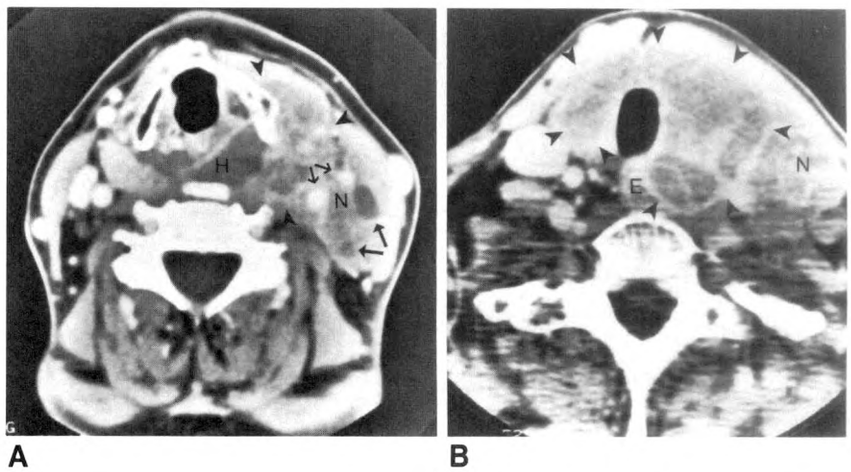


Fig. 7.—*A* and *B*, Diffuse thyroid lymphoma (*arrowheads*) of diffuse large-cell subtype with extensive regional extension and nodal disease (N) in 60-year-old woman. Note extension into hypopharynx (H) and esophagus (E). Nodal necrosis (*large arrows*) is seen in confluent nodal involvement. Common carotid artery and internal jugular vein (*small arrows*) are encased by tumor infiltration.

with bone destruction in three of seven patients. Three patients had multifocal extranodal disease, all from diffuse, large-cell lymphomas (Fig. 8).

Discussion

The malignant lymphomas are a heterogeneous group of solid lymphoreticular neoplasms. Hodgkin's disease is a subgroup of lymphomas that originate from cells of the monocyte-histiocyte series, and it accounts for 25% of all malignant lymphomas [18]. The other lymphomas are grouped together as non-Hodgkin's lymphomas.

One of the most common initial presentations of Hodgkin's disease is painless lymph-node enlargement in the head and neck region. Hodgkin's disease spreads in a predictable fashion from one lymph-node group to the next contiguous group by lymphatic channels [19]. Extranodal presentation of Hodgkin's disease is rare, even with nodal involvement. Conversely, non-Hodgkin's lymphoma frequently involves extranodal structures in the head and neck region, which is the second most common site of extranodal lymphoma after the gastroenterologic tract [7, 11–13]. More than half of the patients with extranodal head and neck lymphomas present with disease localized to the site of origin, and less often associated with nodal involvement [1]. The extranodal sites most frequently involved are Waldeyer's ring, the paranasal sinuses, and the nasal cavity. The histologic subtypes are usually intermediate or high-grade, particularly diffuse, large-cell lymphomas [1, 3, 10, 14].

When neck nodes are involved in either Hodgkin's or non-Hodgkin's lymphoma, the disease spreads into multiple nodes. Whether the nodal involvement is unilateral or bilateral, the deep lymphatic chains are almost always involved, particularly the internal jugular chain. The middle and lower jugular nodes are often diseased when lymphomas present in the nodal pattern (type 1). Isolated lymphomatous involvement of the superior internal jugular chain or superficial nodes is unusual; this is in contrast to the carcinomatous nodal involvement of unknown primary site. The size of the involved lymph node can be quite variable, with larger ones more than 10 cm in diameter and smaller ones less than 5 mm. Frequently, multiple nodes of varying sizes are involved. Sometimes they are elliptical in shape, although a rounded appearance is most common. It is of interest to note that nodal necrosis was found in only one (5%) of our 18 patients with Hodgkin's disease and three (13%) with non-Hodgkin's lymphoma, even when the disease was extensive. Since necrosis is prevalent in carcinomatous nodes, its absence may warrant a prebiopsy diagnosis.

The extranodal lesions in Waldeyer's ring can be isolated by their appearance, which resembles squamous carcinoma; however, more often there are multiple sites of involvement within the ring. Rarely does nasopharyngeal lymphoma present with skull-base destruction, even with extensive involvement. This is in contrast to the frequent bone destruction seen with squamous carcinoma. The extralymphatic lesions in the paranasal sinus and oral cavity can be small or extensive and often are associated with sinus obstruction. This observation is nonspecific, and these lesions are indistinguishable from other slow-growing neoplasms. Tumor calcification, previously unreported, was observed in one of our cases, and its cause is undetermined.

Thyroid lymphoma tends to diffusely infiltrate the adjacent soft tissue, including the aerodigestive tract, and is often accompanied by extensive nodal involvement. As mentioned [20, 21], all four cases in our series had associated chronic lymphocytic thyroiditis histologically, suggesting a strong relationship between the two. Lymphoma originating from the cheek, either in the skin or buccal submucosa, tends to extend regionally into the nasal cavity, maxillary sinus, and orbit, and is often associated with bone destruction. Again, this finding mimics that of other slow-growing neoplasms.

In summary, the extranodal presentation of head and neck lymphoma is nonspecific and indistinguishable from the more commonly occurring carcinoma. However, multiple sites of involvement within or outside Waldeyer's ring, without or with nodal disease, should alert radiologists to the possible diagnosis of a lymphoreticular neoplasm.

Treatment of both Hodgkin's and non-Hodgkin's lymphoma

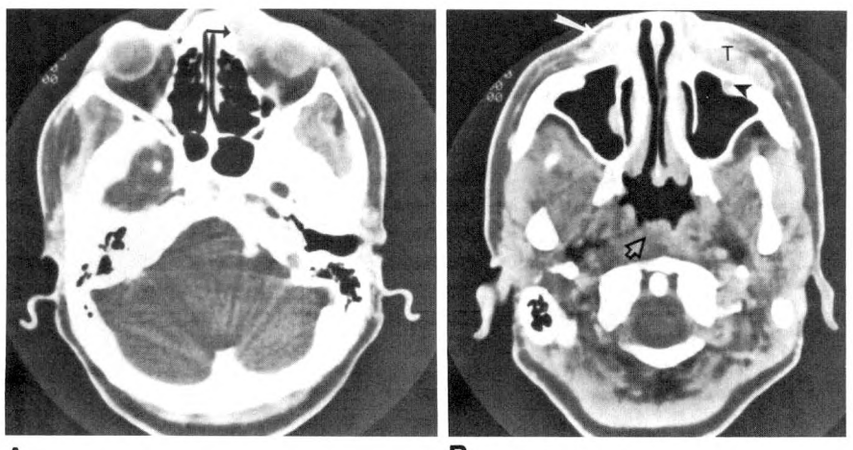


Fig. 8.—*A* and *B*, Multicentric involvement of diffuse large-cell lymphoma in 36-year-old woman. Note extensive regional infiltration of left cheek lesion (T) into left medial orbital canthus (*solid black arrow*), left infraorbital canal (*arrowhead*), and right cheek (*white arrow*). Second lesion is identified in nasopharynx (*open arrow*).

is based on the histologic classification and anatomic staging of disease, the latter of which has been influenced by modern diagnostic imaging. The diagnosis and management of head and neck lymphoma, in particular non-Hodgkin's, often varies with the site of extranodal disease. The precise definition of the anatomic extent of disease is critical to effective treatment when radiotherapy is used alone. Therefore, the decision to obtain a CT scan should be made according to the histologic classification and clinical involvement of disease [22]. It is the practice in our institute not to obtain a CT scan of the head and neck routinely unless the findings will dictate the treatment planning of the lymphoma. Generally, nodal lymphoma does not require a CT evaluation. A CT scan of the head and neck is needed for identifying a possible extranodal primary site when there are isolated superficial nodes positive for lymphoma. Waldeyer's-ring lymphoma may require a CT scan for evaluation of exact tumor extent for radiotherapeutic portal definition. A CT evaluation is definitely desired in extranodal extralymphatic lymphomas for diagnosis and staging purposes as well as for determining radiation portals.

REFERENCES

1. Fienstein JT, Thawley SE. Lymphoma of the head and neck. *Laryngoscope* **1978**;88:582–593
2. Mill WB, Lee FA, Franssila KO. Radiation therapy treatment of stage I and II extranodal non-Hodgkin's lymphoma of the head and neck. *Cancer* **1980**;45:653–661
3. Reddy S, Pellettiere E, Saxena V, Hendrickson FR. Extranodal non-Hodgkin's lymphoma. *Cancer* **1980**;46:1925–1931
4. Plantenga KF, Hart G, Van Heerde P, Tierie AH. Non-Hodgkin's malignant lymphomas of upper digestive and respiratory tracts. *Int J Radiat Oncol Biol Phys* **1981**;7:1419–1427
5. Evans C. A review of non-Hodgkin's lymphomata of the head and neck. *Clin Oncol* **1981**;7:23–31
6. Horiuchi J, Okurama T, Matsubara S, Shibura H, Suzuki S, Kamiyama R. Extranodal non-Hodgkin's lymphoma in the head and neck: irradiation and clinical course. *Acta Radiol [Oncol]* **1982**;21:393–399
7. Kong JS, Fuller LM, Butler JJ, et al. Stages I and II non-Hodgkin's lymphomas of Waldeyer's ring and the neck. *Am J Clin Oncol* **1984**;7:629–639
8. Aozasa K, Nara H, Ikeda H, et al. The influence of histologic type on survival in early extranodal non-Hodgkin's lymphoma in head and neck. *Oncology* **1984**;41:164–169
9. Larson DL, Robbins KT, Butler JJ. Lymphoma of the head and neck: a diagnostic dilemma. *Am J Surg* **1984**;148:433–437
10. Robbins KT, Fuller LM, Vlasak M, et al. Primary lymphomas of the nasal cavity and paranasal sinuses. *Cancer* **1985**;56:814–819
11. Jacobs C, Hoppe R. Non-Hodgkin's lymphomas of head and neck extranodal sites. *Int J Radiat Oncol Biol Phys* **1985**;11:357–364
12. Albada J, Hordijk GJ, van Unnik JAM, Dekker AW. Non-Hodgkin's lymphoma of Waldeyer's ring. *Cancer* **1985**;56:2911–2913
13. Shidnia H, Hornback NB, Lingeman R, Barlow P. Extranodal lymphoma of the head and neck area. *Am J Clin Oncol* **1985**;8:235–243
14. Jacobs C, Weiss L, Hoppe RT. The management of extranodal head and neck lymphomas. *Arch Otolaryngol Head Neck Surg* **1986**;112:654–658
15. Lukes RJ, Butler JJ, Hicks EB. Natural history of Hodgkin's disease as related to its pathologic pictures. *Cancer* **1966**;19:317–344
16. National Cancer Institute sponsored study of classification of non-Hodgkin's lymphomas. Summary and description of a working formulation for clinical usage. *Cancer* **1982**;49:2112–2135
17. Carbone PP, Kaplan HS, Musshoff K, Smithers EW, Tubiana M. Report of the committee on Hodgkin's disease staging. *Cancer Res* **1971**;31:1860–1861
18. Canellos GP. Malignant lymphomas. In: Rubenstein E, Federman DD, eds. *Scientific medicine.* New York: Scientific American, **1986**:1–15
19. Castellino RA. Hodgkin's disease: practical concepts for the diagnostic radiologist. *Radiology* **1986**;159:305–310
20. Aozasa K, Inoue A, Yoshimura J, et al. Intermediate lymphocytic lymphoma of the thyroid. *Cancer* **1986**;57:1762–1767
21. Aozasa K, Inoue A, Tajima K, Mirauchi A, Matsuzuka T, Kuma K. Malignant lymphomas of the thyroid gland. *Cancer* **1986**;58:100–104
22. Bragg DG, Colby TV, Ward JH. New concepts in the non-Hodgkin's lymphomas: radiologic implications. *Radiology* **1986**;159:289–304

American Roentgen Ray Society:
Officers, Committees, and Meeting Information

Officers

President: Raymond A. Gagliardi
President-elect: Lee F. Rogers
1st Vice-president: Gerald D. Dodd
2nd Vice-president: Rosalind H. Troupin
Secretary: Glen W. Hartman
Treasurer: Ronald G. Evens

Executive Council: E. Gedgaudas, J. F. Wiot, L. F. Rogers, R. A. Gagliardi, R. G. Evens, R. N. Berk, F. L. Angell, J. E. Madewell, M. P. Capp, G. W. Hartman, B. G. Brogdon, R. H. Troupin, G. R. Leopold, G. D. Dodd, A. K. Poznanski, A. E. James, Jr., J. T. Ferrucci, Jr., T. C. Beneventano, E. J. Ferris, J. A. Kirkpatrick, Jr., chairman

Committees 1987–1988

Editorial Policy: S. S. Sagel, W. J. Casarella, J. T. Ferrucci, Jr., N. C. Whitley, S. Hilton, J. M. Taveras, R. N. Berk, M. P. Capp, chairman

Education and Research: C. E. Putman, A. R. Margulis, B. J. Hillman, R. A. McLeod, J. T. Ferrucci, Jr., ex officio, B. G. Brogdon, chairman

Finance and Budget: B. P. Wood, L. R. James, J. A. Kirkpatrick, Jr., A. E. James, Jr., F. L. Angell, chairman

Nominating: W. J. Casarella, H. C. Carlson, A. E. James, Jr., chairman

Publications: W. J. Casarella, S. S. Sagel, N. C. Whitley, C. A. Rohrmann, Jr., M. P. Capp, chairman

Membership: E. J. Ferris, G. R. Leopold, A. K. Poznanski, A. E. James, Jr., chairman

Representatives to Other Organizations

American Board of Radiology: E. C. Klatte, L. F. Rogers, T. C. Beneventano

American College of Radiology: L. F. Rogers, G. A. Kling, R. A. Gagliardi, J. M. Dennis, E. J. Ferris, J. E. Madewell

American Medical Association House of Delegates: S. F. Ochsner, K. L. Krabbenhoft, alternate

American National Standards Institute: M. Haskin

National Council on Radiation Protection and Measurements: E. L. Saenger, H. L. Friedell

Meeting Arrangements

Annual Meetings: May 8–13, 1988, Hilton, San Francisco; May 7–13, 1989, Hilton, New Orleans; May 13–18, 1990, Sheraton Washington, Washington, DC

Annual Meeting Committee: H. C. Carlson, G. P. Janetos, G. D. Dodd, T. C. Beneventano, chairman

Instruction Courses: R. A. McLeod, associate chairman, J. T. Ferrucci, Jr., chairman

Scientific Program: R. A. Gagliardi, G. W. Hartman, J. A. Kirkpatrick, Jr., A. E. James, Jr., M. P. Capp, J. E. Madewell, B. G. Brogdon, J. T. Ferrucci, Jr., G. A. Kling, S. A. Feig, G. P. Janetos, L. F. Rogers, chairman

Scientific Exhibits: K. H. Vydareny, A. V. Proto, S. M. Goldman, J. E. Madewell, chairman

ARRS Membership

Applications: An application form is printed in this issue of the Journal. For consideration at the 1988 ARRS meeting, send completed forms before February 1, 1988, to Paul Fullagar, administrative director, American Roentgen Ray Society, 1891 Preston White Dr., Reston, VA 22091. Active members are graduates of an approved medical school or hold an advanced degree in an allied science. They must practice radiology or work in an associated science in the United States or Canada and be certified by the American Board of Radiology or the Royal College of Physicians of Canada or otherwise adequately document training and credentials. Corresponding members are foreign radiologists or scientists who are active in radiology or an allied science. Members-in-training are residents or fellows in radiology or postgraduate students in an allied science. Additional application forms can be obtained from the ARRS offices in Reston, VA.

Business Information

Business Office: Paul Fullagar, administrative director, American Roentgen Ray Society, 1891 Preston White Dr., Reston, VA 22091; (703) 648-8900

An Early CT Sign of Ischemic Infarction: Increased Density in a Cerebral Artery

Barry D. Pressman[1]
E. James Tourje[1]
Joseph R. Thompson[2]

The diagnosis of ischemic cerebral infarction by CT usually is not possible for 12–24 hr after the event. A sign that allows earlier diagnosis is increased density of a cerebral vessel secondary to a thrombus or embolus. We report 19 cases of increased density in a middle cerebral artery or one of its major branches visible on the initial CT scan of patients subsequently clinically proven to have suffered a cerebrovascular accident. In three cases angiography confirmed the presence of embolus or thrombus as seen on the CT scans. In several cases subsequent CT scans showed the density to dissipate, thereby confirming its nature as thrombus or embolus. Recognition of this finding will allow earlier diagnosis of ischemic infarction, which may be important in instituting an appropriate therapeutic regimen.

The early diagnosis of ischemic infarction by CT depends on the recognition of often subtle changes of reduced attenuation and slight mass effect [1, 2]. A sign of cerebral infarction that may be present shortly after the ictus is increased density in a major cerebral artery. Gacs et al. [3] reported this finding in a retrospective study, and they considered it most likely secondary to intraluminal clot.

We have found this sign to be useful in the early recognition of nonhemorrhagic cerebral infarction. It has been seen in a number of patients in the first 24 hr after the ictus, and frequently it is the only CT finding or is an important corroborative finding in association with other subtle changes of infarction.

Subjects and Methods

CT examinations were performed on high-resolution scanners. The posterior fossa and basal cisterns were evaluated with contiguous 5-mm thick sections at Cedars-Sinai Medical Center and with 1.5-mm sections at 3-mm intervals at Loma Linda University Hospital, these being the routine examinations at these institutions. At both hospitals the remainder of the brain was studied with 10-mm sections at 10-mm intervals. All examinations were performed without contrast and, in addition, three patients also had contrast examinations.

Nineteen patients had increased density in the middle cerebral artery or one of its major branches, and their clinical information was reviewed and correlated with the radiographic findings. Fourteen of these cases were from Cedars-Sinai Medical Center and were collected from a total of 747 CT brain examinations in patients suspected of having acute cerebral infarction. This results in an incidence of 1.9% in this series. Seven patients underwent a second CT within 10 days of their initial scan. Cerebral angiograms were obtained in three patients within 48 hr of the ictus.

Results

In all 19 patients with CT scan findings of increased density in the middle cerebral artery, the clinical evaluation indicated signs and symptoms consistent with acute cerebral infarction of the ipsilateral hemisphere. These patients included 10 men and nine women, ranging in age from 36 to 90 years (mean age, 62 years).

This article appears in the July/August 1987 issue of *AJNR* and the September 1987 issue of *AJR*.

Received June 25, 1986; accepted after revision January 13, 1987.

Presented at the annual meeting of the American Society of Neuroradiology, New Orleans, February 1985.

[1] Department of Radiology, Cedars-Sinai Medical Center, 8700 Beverly Blvd., Los Angeles, CA 90048. Address reprint requests to B. D. Pressman.

[2] Department of Radiology, Loma Linda University Medical Center, 11234 Anderson Drive, Loma Linda, CA 92350.

***AJR* 149:583–586, September 1987**
0361–803X/87/1493–0583
© American Roentgen Ray Society

On the basis of suggestive clinical histories—including previous carotid endarterectomy, transient ischemic attacks, cardiac arrhythmias temporally related to the cerebral infarction, bilateral simultaneous infarction, and mitral valve prolapse—10 patients were thought to have had embolic episodes [4].

Fifteen patients showed increased density in the middle cerebral artery on the initial scan (performed within 24 hr after the ictus). An additional two patients also showed increased density in the middle cerebral artery on the initial scan, but the exact time of the ictus could not be determined. One patient had a negative scan on the day of the ictus but increased density of the middle cerebral artery was seen on a scan on day 5. Another patient was scanned only once, 4 days after the infarction, and increased density was seen in the middle cerebral artery. In one patient who was studied by CT both with and without contrast, there was decreased density on the postcontrast scan in the area of increased density seen on the precontrast scan.

Of the 17 patients with density visible in the vessel on the initial scan, nine had no other CT evidence of cerebral infarction, six had only slight edema or minimal mass effect, and only two had obvious edema. Therefore, in 15 patients, the density in the vessel was either the only abnormality on CT or was helpful in identifying other subtle abnormalities. In five patients, the density diminished on the follow-up scan, which was performed within 1–2 weeks.

Three patients underwent cerebral angiography. In each, an occluded vessel was seen at the site of the increased density shown on the CT scan. In two patients, a 36-year-old woman 3 weeks postpartum and a 42-year-old woman with mild mitral valve prolapse, the angiograms strongly suggested embolus as the cause of the occlusion. In the third patient, occlusion was nonspecific.

Case Reports

Case 1

A 42-year-old woman on oral contraceptives developed a sudden right facial droop with eyes deviating to the left. Her condition progressed to stupor. The initial CT scan performed approximately 6 hr after the ictus showed a small density in the left sylvian fissure but was otherwise normal (Figs. 1A and 1B). An angiogram 24 hr later showed an occluded branch of the middle cerebral artery at the same

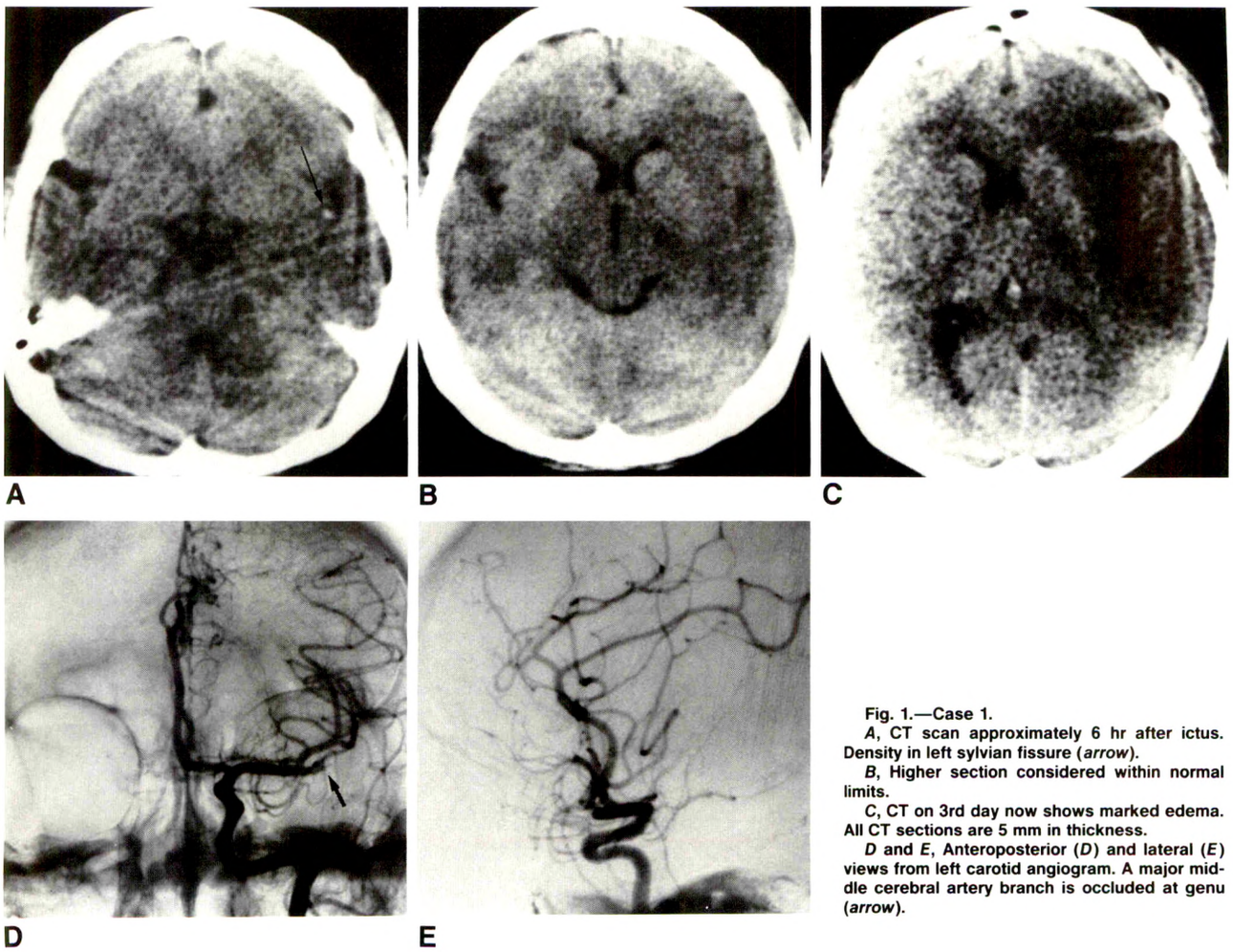


Fig. 1.—Case 1.
***A*, CT scan approximately 6 hr after ictus. Density in left sylvian fissure (*arrow*).**
***B*, Higher section considered within normal limits.**
***C*, CT on 3rd day now shows marked edema. All CT sections are 5 mm in thickness.**
***D* and *E*, Anteroposterior (*D*) and lateral (*E*) views from left carotid angiogram. A major middle cerebral artery branch is occluded at genu (*arrow*).**

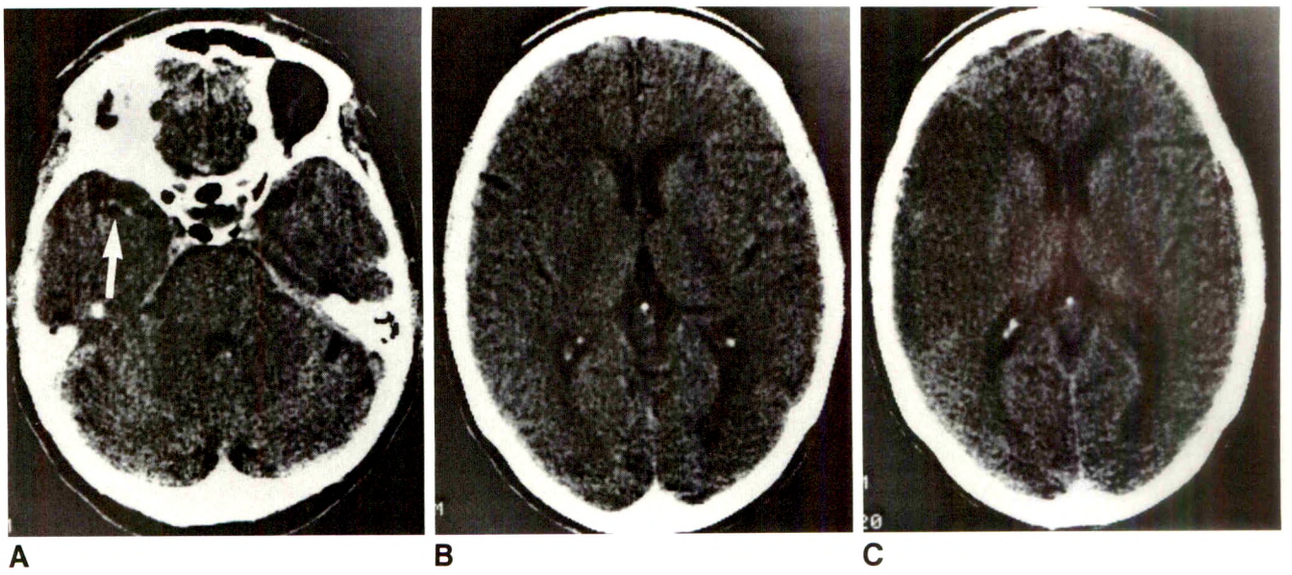


Fig. 2.—Case 2.
***A*, CT scan approximately 5 hr after onset of left hemiparesis. Density is present along course of horizontal right middle cerebral artery (*arrow*).**
***B*, Higher section at same time as *A* shows questionable edema in right hemisphere.**
***C*, CT scan on 10th day, at same level as *B*, now shows definite edema on right. *A* is 1.5 mm in thickness and *B* and *C* are 10 mm in thickness.**

location as the increased density seen on the CT scan. There was some retrograde filling of the middle cerebral artery branches. The shape of the occlusion suggested an embolus. A follow-up CT scan on the third day showed edema in the left temporal lobe and an even more obvious area of increased density within the middle cerebral artery (Fig. 1C). The patient gradually improved but was left with a profound aphasia.

Case 2

A 73-year-old woman had undergone a right radical mastectomy 14 years previously. Two days before the onset of left hemiparesis a lump on her right chest wall was removed. Approximately 5 hr after the development of left hemiparesis a CT scan showed increased density in the distribution of the right middle cerebral artery with questionable associated edema (Figs. 2A and 2B). A CT scan on the 10th day showed reduction of the density within the vessel distribution with development of definite edema (Fig. 2C).

Case 3

A 72-year-old woman developed acute right hemiparesis and aphasia. A CT scan within the first 24 hr showed increased density along the course of the horizontal left middle cerebral artery without edema (Figs. 3A and 3B). At approximately 36 hr a CT scan showed the development of basal ganglia edema. A CT scan performed on the 10th day showed that the density in the left middle cerebral artery had almost totally resolved (Fig. 3C).

Discussion

The increased density seen on the CT scans of these 19 patients may reasonably be presumed to represent thrombus or embolus in the middle cerebral artery for the following reasons: (1) in all cases the location of the increased density was along the course of the middle cerebral artery or one of its major branches; (2) in five patients the density that was seen on the initial scan had diminished or disappeared on the follow-up scan performed within 10 days; (3) in one patient the density developed on the fifth day but was not present on the first day; (4) in the three patients who underwent angiography, all had occlusion of the middle cerebral artery in a location corresponding to the CT finding; (5) in all cases there was clinical evidence of acute cerebral infarction in the distribution of the middle cerebral artery. Furthermore, the densities clearly followed the contours of the vessels and their appearance could not be explained either by parenchymal or subarachnoid hemorrhage.

Calcification of the vessel wall was excluded in five patients by the disappearance of the density on the follow-up scan within 10 days and, in another patient, by its development on the second scan when it was not present on the initial scan 5 days previously. One other possible consideration would be subintimal hemorrhage, which cannot be excluded in the patients who did not undergo angiography.

The clinical diagnosis in each of these patients was consistent with the radiologic diagnosis of acute infarction in the distribution of the vessel with the increased density. Ten patients were thought to have had embolic episodes on the basis of clinical circumstances, including previous carotid endarterectomy, transient ischemic attacks, cardiac arrhythmias temporally related to the cerebral infarction, bilateral simultaneous infarction, and mitral valve prolapse [4]. However, at this time, we cannot suggest that there is any specificity of the CT findings with regard to embolus vs thrombus.

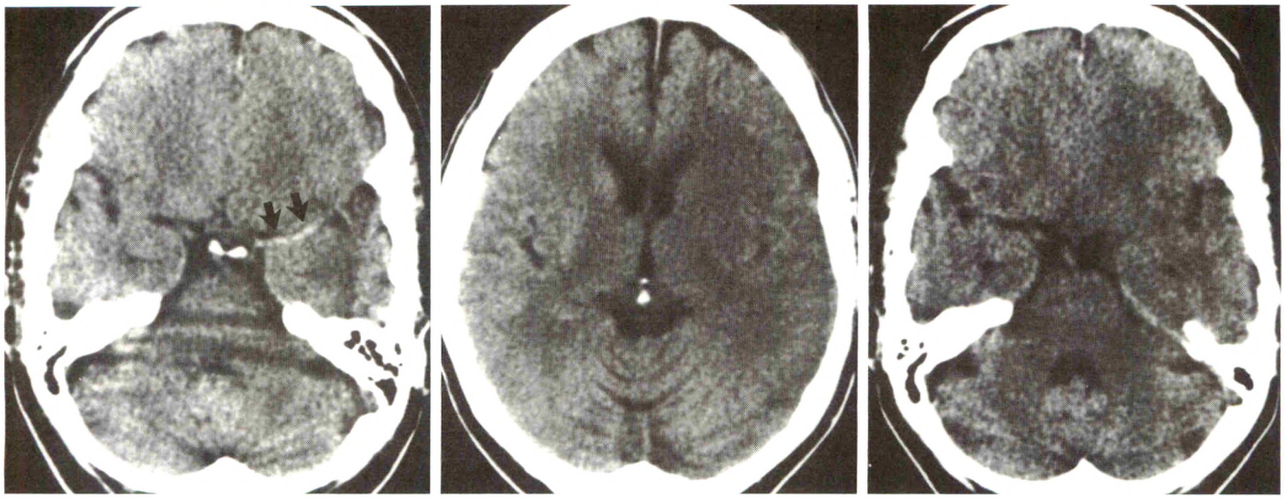


Fig. 3.—Case 3.
A, **CT scan within 24 hr of onset of right hemiparesis. Increased density along course of left middle cerebral artery (*arrows*).**
B, **Section at higher level considered within normal limits.**
C, **On 10th day, density in left middle cerebral artery has resolved. All CT sections are 5 mm in thickness.**

Recognition of increased density along the distribution of a major intracranial vessel may be extremely valuable in the early CT diagnosis of infarction. In 15 patients the density in the vessel was either the only abnormality or was helpful in properly identifying other subtle abnormalities. It may be especially useful in the first 24 hr, when there are frequently no other CT changes to suggest infarction.

It is quite likely that the CT technique used in our institutions increased the frequency with which increased density within the basal vessels was seen. Patients were evaluated with 1.5-mm or 5-mm-thick sections through the posterior fossa and basal vessels, these being the routine examinations at each of these institutions. Ten-millimeter (10-mm) sections would probably decrease the likelihood of recognizing this finding. Obtaining thinner sections through basal vessels in patients studied for the possibility of acute cerebral infarction, therefore, merits consideration.

Early positive diagnosis of acute cerebral infarction may become more significant as new therapeutic regimens are developed. Recognition of increased density in the middle cerebral artery, one of its major branches, or in other major cerebral arteries (Gacs et al. [3] reported a case involving the posterior cerebral artery in their series), will allow the neuroradiologist to make an earlier and/or more definitive diagnosis of cerebral infarction.

REFERENCES

1. Inoue Y, Takemoto K, Miyamoto T, et al. Sequential computed tomography scans in acute cerebral infarction. *Radiology* **1980**;135:655–662
2. Wall SD, Brant-Zawadzki M, Jeffrey RB, Barnes B. High frequency CT findings within 24 hours after cerebral infarction. *AJNR* **1981**;2:553–557, *AJR* **1982**;138:307–311
3. Gacs G, Fox AJ, Barnett HJM, Viñuela F. CT visualization of intracranial arterial thromboembolism. *Stroke* **1983**;14:756–762
4. Charness ME. Controversies in the medical management of stroke—medical staff conference, UCSF. *West J Med* **1985**;142:74–78

Carotid Cavernous Fistulae:
Indications for Urgent Treatment

Van V. Halbach[1]
Grant B. Hieshima[1]
Randall T. Higashida[1]
Murray Reicher[2]

Angiographic and clinical data from 155 patients with carotid cavernous fistulae were retrospectively reviewed to determine angiographic features associated with increased risk of morbidity and mortality. These features included presence of a pseudoaneurysm, large varix of the cavernous sinus, venous drainage to cortical veins, and thrombosis of venous outflow pathways distant from the fistula. Clinical signs and symptoms that characterized a hazardous carotid cavernous fistula included increased intracranial pressure, rapidly progressive proptosis, diminished visual acuity, hemorrhage, and transient ischemic attacks. Cortical venous drainage from the carotid cavernous fistula is secondary to occlusion or absence of the normal venous outflow pathways and is associated with signs and symptoms of increased intracranial pressure and an increased risk of intraparenchymal hemorrhage. Angiographic demonstration of a cavernous sinus varix, with extension of the sinus into the subarachnoid space, is associated with an increased risk of fatal subarachnoid hemorrhage. Identification of these high-risk features provides a basis for making decisions about treatment.

Carotid cavernous fistulae (CCFs) are spontaneous or acquired connections between the carotid artery and the cavernous sinus, and can be classified as direct or indirect. Direct connections between the internal carotid artery and cavernous sinus may occur as a consequence of trauma, ruptured intracavernous carotid aneurysms, collagen deficiency syndromes, arterial dissection, fibromuscular dysplasia, and direct surgical trauma [1–10]. Indirect fistulae are usually supplied from dural branches of the external carotid artery but can be supplied from dural branches of the internal carotid artery. Although the cause is often unknown, factors associated with the development of indirect fistulae include pregnancy, sinusitis, trauma, surgical procedures, and cavernous sinus thrombosis. Symptoms caused by CCFs are related to their size, duration, location, adequacy and route of venous drainage, and presence of arterial and venous collaterals [11].

Surgical and angiographic techniques that have been described for the closure of CCFs include carotid occlusion; trapping procedures; direct surgical exposure and closure; and embolization with muscle, glue, thrombus, wires, and, more recently, detachable balloons [12–19].

Unfortunately, the natural history of CCFs is incompletely understood. Spontaneous closure, which is more common in indirect than direct CCFs, as well as closure following diagnostic angiography, has been documented by Seeger et al. [20]. Carotid compression therapy has been successful in closure of 17% of direct and 30% of indirect CCFs [21]. While aggressive forms of therapy may be successful in closure of CCFs, no technique is without risk. Ideally, the decision to institute a potentially hazardous treatment should be based on full understanding of the disease's natural history.

To identify those patients whose poor natural history mandated the need for emergent or aggressive therapy, we evaluated the angiographic and clinical data from 155 patients with CCFs. The delineation of high-risk features enables rational choices to be made regarding the timing and method of treatment.

This article appears in the July/August 1987 issue of *AJNR* and the September 1987 issue of *AJR*.

Received August 20, 1986; accepted after revision December 31, 1986.

[1] Department of Diagnostic and Interventional Neuroradiology, UCSF Medical Center, San Francisco, CA 94143. Address reprint requests to V. V. Halbach.

[2] Department of Radiology, UCLA Medical Center, Los Angeles, CA 90024.

***AJR* 149:587–593, September 1987**
0361–803X/87/1493–0587
© American Roentgen Ray Society

Materials and Methods

The radiographic findings and clinical records of 150 patients treated for CCF over the past 10 years were reviewed retrospectively. There were 122 direct fistulae and 28 indirect fistulae. Radiographic and clinical findings from five additional patients who died before treatment could be instituted were also reviewed. Before treatment, specific attention was given to the signs, symptoms, and angiographic features associated with a poor clinical outcome, and these were recorded.

Results

Several angiographic and clinical signs and symptoms were found to be associated with a poor clinical outcome, all of which occurred prior to treatment. These are summarized in Table 1.

Hemorrhage

Hemorrhage occurred in 13 (8.4%) of 155 patients with direct CCFs, and was associated with a poor outcome. In eight patients, hemorrhage occurred at least 3 weeks after the event, usually trauma, that was responsible for the development of the fistula. The remaining five patients, all with pseudoaneurysms, hemorrhaged within a week of onset of the fistula. Four patients experienced massive subarachnoid hemorrhage, which was rapidly fatal in all cases. None were associated with a sentinal bleed, as is common with aneurysms. Three of the patients with subarachnoid hemorrhage had a large varix of the cavernous sinus that extended beyond the normal sinus wall confines. Although three of the patients who suffered fatal subarachnoid hemorrhage demonstrated a large varix of the cavernous sinus, 18 other patients who did not bleed also demonstrated this finding. We define a cavernous sinus varix as a dilated cavernous sinus with extension into the subarachnoid space.

Figure 1 shows a varix of the cavernous sinus involved in a CCF. There is occlusion of the inferior petrosal drainage and narrowing of the junction of the cavernous sinus with the superior ophthalmic vein. Angiographic differentiation between a cavernous sinus varix and a pseudoaneurysm may be difficult or impossible. In a pseudoaneurysm, the walls of both the carotid artery and cavernous sinus have been torn and only thrombus or brain parenchyma remain. Figure 2 shows a pseudoaneurysm in the fourth patient who suffered a massive subarachnoid hemorrhage and died before treatment could be instituted. The onset of the pseudoaneurysm is usually coincidental with the trauma, as opposed to the delayed onset of a varix, which develops after the occlusion of venous outflow pathways.

Four patients suffered intracerebral hemorrhage; one had a fatal pontine bleed, another had a temporal lobe hemorrhage, one had temporal and frontal lobe hemorrhages, and the last had multifocal hemorrhages. Each of these patients exhibited cortical venous drainage from the fistula, which correlated with the site of the hemorrhage. All four patients had occlusion of the normal outflow pathways of the cavernous sinus and diversion of flow into cortical veins. Figure 3 shows cortical venous drainage from a direct CCF in a patient who subsequently developed a frontal and temporal hematoma. Although all four patients who suffered from an intracerebral hemorrhage demonstrated cortical venous drainage secondary to occlusion of outflow pathways, this finding was also observed in seven other patients who did not bleed. All these patients had fluctuating neurologic signs presumed to be from the cortical venous hypertension. After closure of the CCF with detachable balloons there was prompt resolution of symptoms in all patients. The four patients who hemorrhaged suffered no further hemorrhages after their fistulae were closed with detachable balloons.

Five patients (3.2%) had external hemorrhage with one case of otorrhagia and four cases of massive epistaxis. Of the four cases of epistaxis, two were fatal. All four of the cases had a pseudoaneurysm or venous pouch that entered the sphenoid sinus via a communication through a basal skull fracture. Figure 4 is a lateral common carotid angiogram showing a traumatic CCF and a pseudoaneurysm posteriorly with communication into the sphenoid sinus through a clival fracture. The patient suffered a massive fatal epistaxis before treatment could be instituted. The patient with otorrhagia (Fig. 5) had minor external bleeding from dilated draining veins involving the ear canal. The two surviving patients with epistaxis and one patient with otorrhagia were treated with detachable balloon embolization and had no further episodes of hemorrhage.

Twelve patients (7.7%) have subconjunctival hemorrhages from rupture of dilated arterialized veins. None of these patients had a poor outcome. After closing the CCFs in these patients, no further episodes of hemorrhage occurred.

TABLE 1: Complications in Direct and Indirect Carotid Cavernous Fistulae

Complication	Direct (n = 127)	Indirect (n = 28)	Total (n = 155)
Hemorrhage			
Intracerebral	4 (3.1%)	0	4 (2.6%)
Epistaxis	4 (3.1%)	0	4 (2.6%)
Otorrhagia	1 (0.8%)	0	1 (0.6%)
Subarachnoid	4 (3.1%)	0	4 (2.6%)
Total	13 (10.2%)	0	13 (8.4%)
Increased intracranial pressure	11 (8.7%)	1 (3.6%)	12 (7.7%)
Decreased visual acuity	41 (32.3%)	7 (25.0%)	48 (31.0%)
Blindness	4 (3.1%)	3 (10.7%)	7 (4.5%)
Rapidly progressive proptosis	2 (1.6%)	0	2 (1.3%)
Cerebral ischemia	1 (0.8%)	0	1 (0.6%)
Fatalities	5 (3.9%)	0	5 (3.2%)

Increased Intracranial Pressure and Cortical Venous Hypertension

Twelve patients (7.7%) presented with signs and symptoms of increased intracranial pressure, including nausea, vomiting, papilledema, and waxing and waning neurologic signs. Eleven

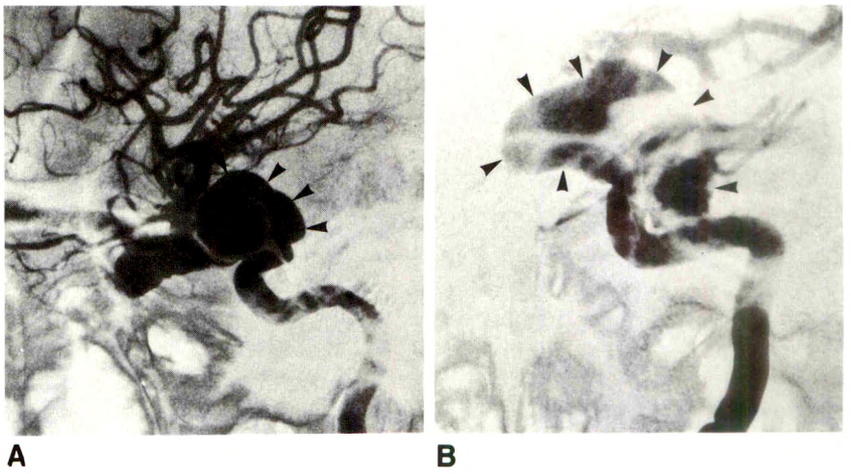


Fig. 1.—*A*, Internal carotid artery injection, lateral view, showing a varix (*arrowheads*) of cavernous sinus involved in direct carotid cavernous fistula.

B, Anteroposterior view of same patient. Note extension of varix (*arrowheads*) outside normal cavernous sinus confines.

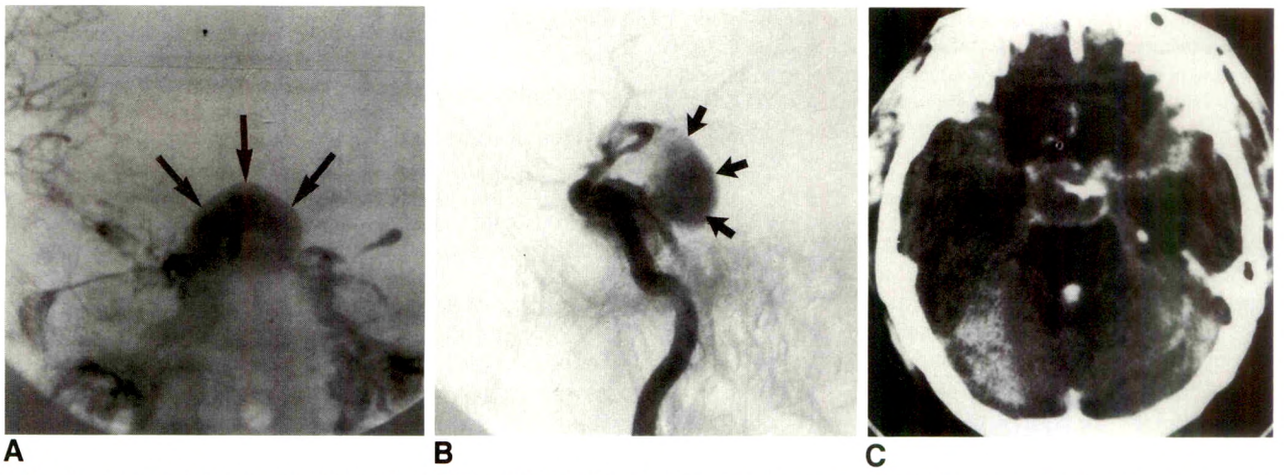


Fig. 2.—Anteroposterior (*A*) and lateral (*B*) internal carotid injection showing pseudoaneurysm (*arrows*) involving carotid cavernous fistula. *C*, Unenhanced CT scan at level of pseudoaneurysm shows massive subarachnoid hemorrhage.

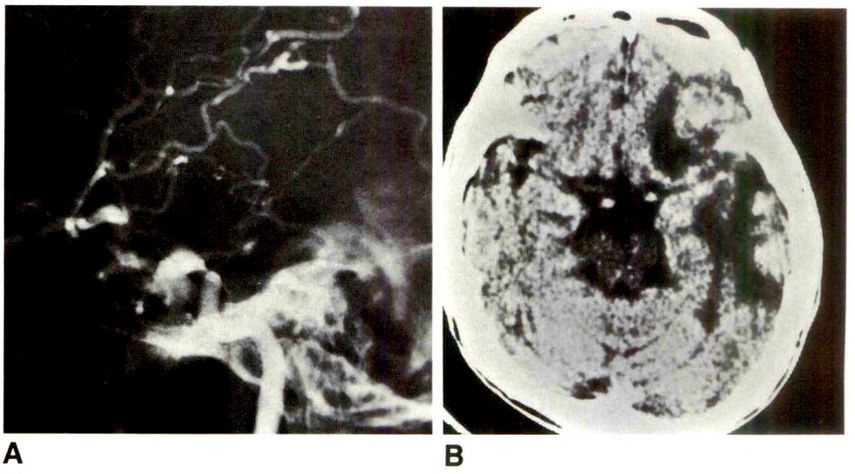


Fig. 3.—*A*, Lateral internal carotid injection showing cortical venous drainage from a direct carotid cavernous fistula.

B, Noncontrast CT scan with frontal and temporal hematomas.



4



5

Fig. 4.—Common carotid injection, lateral view. Note *arrowhead* at site of clival fracture creating a communication of precavernous carotid artery with sphenoid sinus. *Arrow* indicates drainage to superior ophthalmic vein.

Fig. 5.—Left internal carotid artery injection, lateral view, showing venous drainage from cavernous sinus to superior (*arrows*) and inferior petrosal sinus. Superior petrosal drainage resulted in engorgement of ear veins, causing otorrhagia.

patients demonstrated cortical venous drainage resulting from occlusion or hypoplasia of the normal cavernous sinus drainage pathways. After closure of the fistulae in these patients there was complete resolution of their symptoms of increased intracranial pressure. Figure 6 shows cortical venous drainage from an indirect CCF that resulted in severe headaches, retroorbital pain, papilledema, and fluctuating level of consciousness.

Elevation of intracranial pressure also occurred in one patient who demonstrated drainage to the sigmoid and transverse sinuses. This patient suffered a traumatic direct CCF and presented with increased intracranial pressure (40 mm Hg) and coma. Angiography demonstrated venous drainage through the inferior petrosal sinuses to the sigmoid sinuses. Figure 7 is a subarachnoid pressure tracing made during balloon occlusions of the fistula. During occlusion of the fistula there was an immediate drop in intracranial pressure and concomitant improvement in the patient's clinical status. However, during detachment, the balloon shifted, and the fistula reopened. This was associated with a prompt increase in intracranial pressure and clinical deterioration. After reclosure of the CCF with a second balloon, the intracranial pressure again fell to normal (7 mm Hg) with immediate improvement in the patient's clinical status.

Decreasing Visual Function

Twenty-five percent (7/28) of indirect CCFs and 32.3% (41/127) of direct CCFs were associated with diminishing visual acuity. Seven (4.5%) of the 155 patients had total visual loss in the involved eye, with bilateral blindness occurring in three patients (1.9%). Minor decreases in visual acuity were reversible with closure of the fistula. Visual decline can progress rapidly, and if it is severe (to the point of light perception only) it is often irreversible, even with prompt closure of the fistula. This event occurred in five of six patients. However, one exception was a patient who progressed to total blindness and was treated 48 hr later with balloon embolization and closure of the fistula. He gradually recovered vision over the next 4 days to a 20/40 acuity.

Progressive Proptosis

Proptosis occurred in 75% (21/28) of indirect CCFs and in 77% (98/127) of direct CCFs. Rapidly progressive proptosis associated with severe pain and visual deterioration occurred in two patients, and in each case angiography revealed thrombosis of the superior ophthalmic vein distal to the site of the fistula. One patient developed a direct CCF after a motor vehicle accident with few symptoms for a period of 2 years. After a bout of retching and vomiting, he developed severe retroorbital pain, visual loss, and progressive proptosis. Follow-up angiography demonstrated interval thrombosis of the distal superior ophthalmic vein and diversion of venous drainage to cerebral veins (Fig. 8). After the fistula was closed, the patient's symptoms and proptosis abated.

Cerebral Ischemia

Delayed cerebral ischemia occurred in one patient who had a direct CCF treated by internal carotid ligation 30 years before developing repeated transient ischemic attacks. Repeat angiography revealed the fistula supplied by massively enlarged anterior and posterior communicating arteries as well as retrograde flow through an enlarged ophthalmic artery (Fig. 9). Tortuosity of the communicating arteries precluded endovascular treatment; therefore, a surgical clipping of the supraclinoid carotid artery to complete a surgical trapping procedure was attempted. Immediately after applying the clip there was massive cerebral edema and the patient died.

Discussion

Retrospective review of the radiographic and clinical findings of 155 patients with CCF revealed several features associated with a poor clinical outcome.

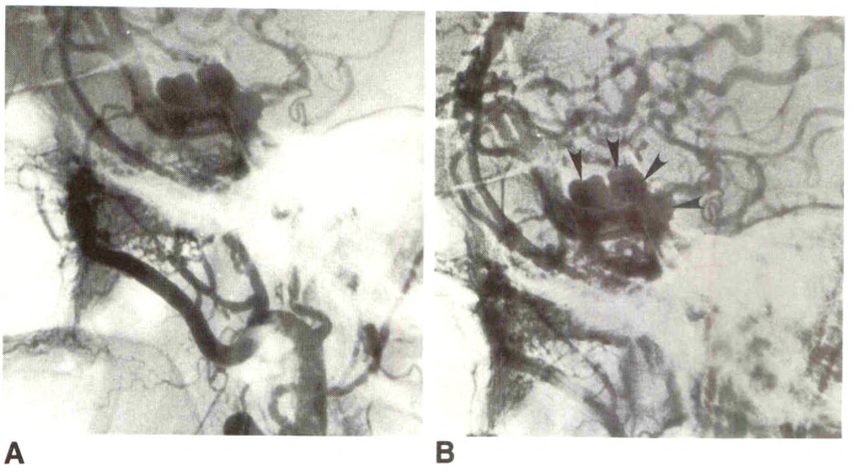


Fig. 6.—Common carotid injection, lateral view, early (*A*) and later (*B*) arterial phase. *Arrowheads (B)* outline cavernous sinus involved in indirect carotid cavernous fistula with venous drainage to cortical veins.

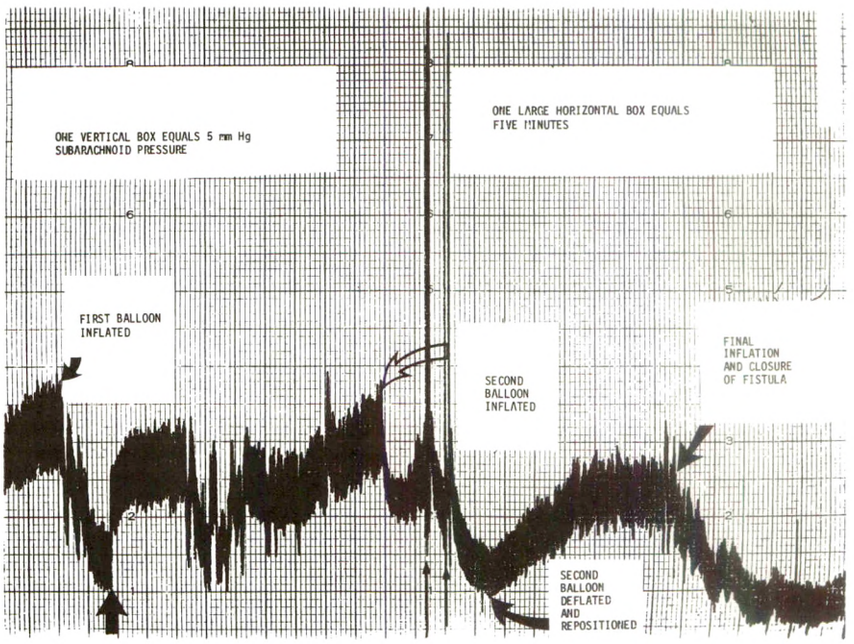


Fig. 7.—Subarachnoid pressure tracing during embolization of direct carotid cavernous fistula. *Small curved arrow* (top left) indicates the time first balloon was inflated with fistula closure. *Straight arrow* (bottom left) is the point at which first balloon shifted during detachment with partial reopening of fistula. *Curved open arrow* (top middle) indicates the time of inflation of second balloon with closure of fistula. *Large curved arrow* (bottom middle) indicates the time when balloon was deflated and repositioned in cavernous sinus. *Slanted arrow* (top right) indicates final balloon inflation with complete closure of fistula. *Thin straight arrows* (bottom middle) indicate artifacts from patient coughing.

Hemorrhage is a devastating complication of a carotid cavernous fistula. The first reported case, in 1908, was by deSchweinitz and Holloway [22]. In 1930, Sattler [23] reviewed 322 cases of CCF reporting the incidence of 1.5% fatal epistaxis and 0.9% intracerebral hematomas. In our series, 13 (8.4%) of 155 patients had hemorrhage, with four (2.6%) having fatal subarachnoid hemorrhage. Although three patients with subarachnoid hemorrhage had a varix of the cavernous sinus, this angiographic sign was not specific, being found in 18 other patients who did not bleed. However, considering the outcome of subarachnoid hemorrhage in our series (100% fatal), we feel that any patient with angiographic findings of a cavernous sinus varix should have emergent treatment to eliminate the risk of subarachnoid hemorrhage. Patients with angiographic evidence of a pseudoaneurysm have a grave prognosis and should also receive immediate treatment.

All 11 patients with cortical venous drainage were symptomatic with signs and symptoms suggestive of increased intracranial pressure. All had hypoplasia or occlusion of normal cavernous sinus outflow pathways with diversion of venous outflow into the cortical veins. Following closure of the fistula these symptoms abated. Kosnik et al. [24] in discussing symptoms of dural arterial venous malformations stated: "Flow problems in these patients are created more by the increased venous pressure and consequent passive conges-

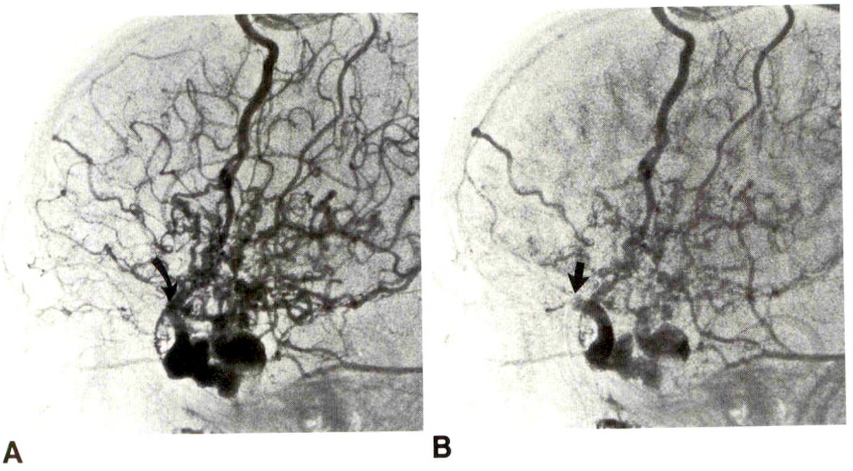


Fig. 8.—*A*, Mid-arterial internal carotid injection, lateral view, showing thrombosis of mid portion of superior ophthalmic vein (*arrow*) with diversion of venous drainage from fistula to cortical veins.

B, Late venous phase, same projection. There is stasis in superior ophthalmic vein (*arrow*).

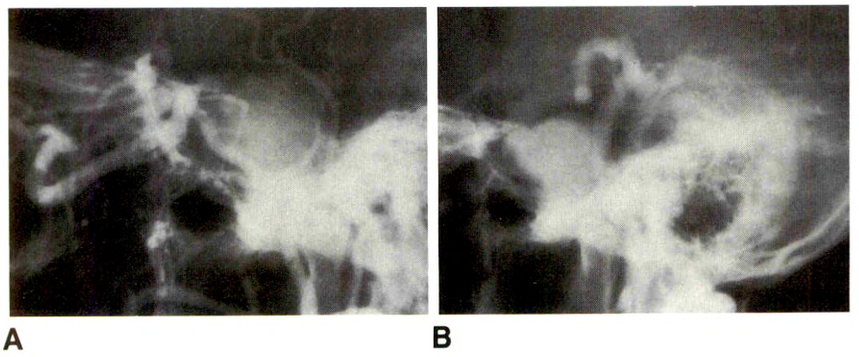


Fig. 9.—*A*, Common carotid injection, lateral view, shows retrograde flow in ophthalmic artery filling a carotid cavernous fistula.

B, Vertebral artery injection, lateral view, shows enlarged posterior communicating artery supplying fistula.

tion of the brain than by arterial steal." Lasjaunias et al. [11] stated in a review of neurologic manifestations of dural arterial venous malformations that "these symptoms appear to be related to chronic passive congestion due to retrograde increased venous pressure towards the venous drainage routes of the normal brain." Of the 11 patients with cortical venous drainage, all with signs and symptoms of increased intracranial pressure, four suffered intracerebral hemorrhage. Turner et al. [25] reported three intracerebral hematomas associated with CCF, each of which demonstrated cortical venous drainage in the region of the hemorrhage. Therefore, patients who demonstrate cortical venous drainage are at risk for intracerebral hemorrhage and should receive emergent therapy.

Increased intracranial pressure can also be present in patients with fistula drainage to the sigmoid sinuses. Proposed mechanisms of elevated intracranial pressure in dural fistulae involving the sigmoid and transverse sinuses include an increase in cerebral blood volume and dural sinus pressure with concomitant dimunition of cerebral fluid absorption resulting in an increase in intracranial pressure [26–28].

Decreased visual acuity is an ominous finding, and, if untreated, may result in blindness. Many factors contribute to the ischemic changes in the orbit associated with CCF. These include venous hypertension and diminished arterial pressure resulting from reversal of flow in the supraclinoid carotid artery and steal away from the ophthalmic artery into the fistula [29]. In our series, visual decline was observed in 31% (48/155) of patients, with blindness occurring in 4.5% (7/155). Because severe visual loss is often irreversible, and mild degrees of visual loss are completely reversible, we feel that all patients with CCFs should have frequent ophthalmologic examinations as well as daily self-evaluation of visual function. Any visual decline is an indication that urgent treatment is needed.

Rapidly progressive proptosis may signify spontaneous thrombosis of venous outflow pathways to the orbit. Because of the severe symptoms associated with this occurrence, such a finding is an indication for immediate treatment.

Fortunately, cerebral ischemia occurred in only one patient with CCF, but this patient died after surgical closure of the fistula. This symptom may signify the cerebral vasculature's impaired autoregulation secondary to chronic long-standing steal and may indicate the need for staged closure to prevent normal perfusion pressure breakthrough and cerebral edema during treatment.

In conclusion, patients presenting with major external hemorrhage such as epistaxis have a high mortality rate and require emergent treatment. Patients with cortical venous

drainage have symptoms of increased intracranial pressure and are at risk to develop intraparenchymal hemorrhage. These patients should also be given urgent treatment. The angiographic demonstration of a cavernous sinus varix is associated with an increased risk of development of fatal subarachnoid hemorrhage and should be treated immediately. Visual loss associated with CCFs is common, and if treated promptly can be entirely reversible. Severe visual loss, however, is often irreversible; therefore, treatment is warranted for any rapid or severe visual decline. With the recognition of these signs, symptoms, and angiographic features that indicate an increased morbidity and mortality from CCFs, immediate definitive treatment can be instituted to improve the outcome.

REFERENCES

1. Delens E. De la communication de la carotide interne et du sinus caverneux (anevrysme arterioveineux). These de Paris, A Parent, **1870**
2. Dandy WE. Carotid cavernous aneurysms (pulsating exophthalmos). *Zentralbl Neurochir* **1937**;2:77–113, 2:165–204
3. Hamby WB. *Carotid cavernous fistula.* Springfield: Charles C Thomas, **1966**
4. Davie JC, Richardson R. Distal internal carotid thromboembolectomy using a Fogarty catheter in total occlusion. *J Neurosurg* **1967**;22:171–177
5. Takahashi M, Killeffer F, Wilson G. Iatrogenic carotid cavernous fistula. *J Neurosurg* **1969**;30:498–500
6. Motarjene A, Keifer JW. Carotid cavernous sinus fistula as a complication of carotid endarterectomy: a case report. *Radiology* **1973**;108:83–84
7. Sorig IC, Bromberg BE. Carotid cavernous sinus fistula occurring after a rhinoplasty. *Plast Reconstr Surg* **1975**;55:92–96
8. Eggers F, Lukin R, Chambers AA, Tomsick TA, Sawaya R. Iatrogenic carotid cavernous fistula following Fogarty catheter thromboembolectomy. *J Neurosurg* **1979**;51:543–545
9. Lister JR, Sypert GW. Traumatic false aneurysm and carotid cavernous fistula: a complication of sphenoidotomy. *Neurosurgery* **1979**;5:473–475
10. Pedersen RA, Troost BT, Schramm VL. Carotid cavernous sinus fistula after external ethmoid-sphenoid surgery. *Arch Otolaryngol* **1981**;107:307–309
11. Lasjaunias P, Ming C, Brugge KT, Atul T. Neurological manifestations of intracranial dural arteriovenous malformations. *J Neurosurg* **1986**;64:724–730
12. Parkinson D. Carotid cavernous fistula: direct repair with preservation of the carotid artery. *J Neurosurg* **1973**;38:99–106
13. Sedzimir CB, Occleshaw JV. Treatment of carotid cavernous fistula by muscle embolization and Jaeger's maneuver. *J Neurosurg* **1967**;22:309–314
14. Ohta T, Nishimura S, Kikuchi II, Toyama M. Closure of carotid cavernous fistula with polyurethane foam embolus. *J Neurosurg* **1973**;38:107–114
15. Bank WO, Kerber CW, Drayer BP, et al. Carotid cavernous fistula: endarterial cyanoacrylate occlusion with preservation of carotid flow. *J Neuroradiol* **1978**;5:279–285
16. Hosobuchi Y. Electrothrombosis of carotid cavernous fistula. *J Neurosurg* **1975**;42:76–85
17. Serbinenko FA. Balloon occlusion of a cavernous portion of the carotid artery as a method of treating carotid cavitary anastomoses. *Zh Vopr Neirokhir* **1971**;6:3–8
18. Prolo DJ, Hanbery JW. Intraluminal occlusion of a carotid cavernous sinus fistula with a balloon catheter. *J Neurosurg* **1971**;35:237–242
19. Picard L, Lepoire J, Montaut J, Hepner H, Roland J, Guyonnard JC. Endarterial occlusion of carotid cavernous sinus fistulae using a balloon-tipped catheter. *Neuroradiology* **1974**;8:5–10
20. Seeger JF, Gabrielsen TO, Gianotta S, Lotz P. Carotid cavernous sinus fistulae and venous thrombosis. *AJNR* **1982**;1:141–148
21. Higashida RT, Hieshima GB, Halbach VV, Goto KG. Compression of cervical carotid artery and jugular vein for treatment of carotid cavernous fistula. *Acta Radiol* (in press)
22. deSchweinitz GE, Holloway TB. *Pulsating exophthalmos: its etiology, symptomatology, pathogenesis and treatment.* Philadelphia: Saunders, **1908**
23. Sattler CH. *Pulsierender exophthalmus. Handbuch der Gesamten Augenheilkunde.* Berlin: Springer, **1920**, 1–268
24. Kosnik EJ, Hunt WE, Miller CA. Dural arteriovenous malformations. *J Neurosurg* **1974**;40:322–329
25. Turner DM, VanGilder JC, Mojtahedi S, Dierson EW. Spontaneous intracerebral hematoma in carotid cavernous fistula. *J Neurosurg* **1983**;59:680–686
26. Vinuela F, Fox AJ, Pelz DM, Drake CG. Unusual clinical manifestations of dural arteriovenous malformations. *J Neurosurg* **1986**;64:554–558
27. Kuhner A, Krastel A, Stoll W. Arterial venous malformations of the transverse sinus. *J Neurosurg* **1976**;45:12–19
28. Tomsick TA, Tew JM Jr, Lukin RR, et al. Intracranial arteriovenous malformations with increased intracranial pressure: response to embolization. In: Smith RR, Haerer AF, Russel WF, eds. *Vascular malformations and fistulae of the brain.* New York: Raven Press, **1982**:119–127
29. Sanders MD, Hoyt WF. Hypoxic ocular sequelae of carotid cavernous fistulae. *Br J Ophthalmol* **1969**;53:82–97

1988 AMERICAN ROENTGEN RAY SOCIETY MEETING

MAY 8–13, 1988
SAN FRANCISCO HILTON HOTEL
SAN FRANCISCO, CA

See page 656 and forthcoming issues for further information.

Pitfalls in the CT Diagnosis of Atlantoaxial Rotary Subluxation

Henryk M. Kowalski[1]
Wendy A. Cohen[1]
Paul Cooper[2]
Jeffrey H. Wisoff[2]

CT was used to examine six patients with clinically evident atlantoaxial rotary fixation, two patients with torticollis, and six normal subjects who had turned their heads to the side as far as voluntarily possible. The CT appearances of the atlantoaxial complex were identical in all three groups. To differentiate these groups, we propose a functional scan through C1–C2 in which patients are scanned initially as they present, with their heads fixed in lateral rotation. Subsequent scans are obtained with their heads turned to the maximum contralateral rotation. CT scans in patients with atlantoaxial rotary fixation demonstrate no motion at C1–C2 during this maneuver, while those in patients with transient torticollis show a reduction or reversal of the rotation of C1 on C2.

Atlantoaxial rotary fixation is a clinical syndrome consisting of rotation with lateral tilt of the head, painful limitation of motion, and inability to turn the head voluntarily to the contralateral side. The condition often follows insignificant cervical trauma or upper respiratory infection [1, 2]. It is distinguished from torticollis by its failure to resolve within a few weeks. Radiographic evaluation of the patient with this condition is difficult because of the patient's rotated head position. Before the advent of CT, radiologic diagnosis traditionally required careful functional examination with cineradiography [2, 3].

Axial CT scans through C1–C2 in patients with the clinically diagnosed atlantoaxial rotary fixation demonstrate the rotated position of C1 on C2 [4–6]. However, when we evaluated the CT scan of a patient with transient torticollis, the atlantoaxial complex appeared as it would in atlantoaxial rotary fixation. We performed this study to attempt to distinguish between these two conditions.

Subjects and Methods

Eight patients with symptoms referable to the occipitoatlantoaxial joint complex were studied by cervical CT. Six of these patients were diagnosed as having atlantoaxial rotary fixation and represent all the cases of this type seen between 1984 and 1986. The other two patients, diagnosed as having torticollis, were the only patients with this condition admitted to the neurosurgery service during this period. Atlantoaxial rotary fixation was diagnosed clinically when the signs and symptoms of torticollis did not resolve within 3–4 weeks. Six normal volunteers had no symptoms referable to the cervical spine.

Scans were obtained from the base of the skull to the top of the vertebral body of C3 by using 3- or 5-mm contiguous sections at a gantry angulation of 0°. The hard palate was included in the examination whenever possible as a reference point for determining the orientation of the skull. A functional examination was performed in both patients with torticollis and in one patient with rotary fixation by scanning the patient's cervical spine with the head in the rotated position in which it was fixed and in the maximum voluntary contralateral rotation. The other patients were studied at rest. The normal volunteers were scanned with their heads turned as far as possible to the side. Bone- and soft-tissue windows were obtained in all examinations. The degree of rotary displacement was quantitated by comparing the anteroposterior axes of the head (line congruent with the nasal septum), atlas (line

This article appears in the July/August 1987 issue of *AJNR* and the September 1987 issue of *AJR*.

Received November 7, 1986; accepted after revision February 10, 1987.

[1] Department of Radiology, New York University Medical Center, 550 First Ave., New York, NY 10016. Address reprint requests to H. M. Kowalski.

[2] Department of Neurosurgery, New York University Medical Center, New York, NY 10016.

***AJR* 149:595–600, September 1987**
0361–803X/87/1493–0595
© American Roentgen Ray Society

connecting the anterior tubercle to the spinous process), and axis (line connecting the base of odontoid to the spinous process). Occipitoatlantal rotary subluxation was defined as malalignment of the axes of the head and atlas.

Results

All eight patients had histories of mild to moderate neck trauma with neck pain, stiffness, and rotational deformity (Table 1). They all held their heads in varying degrees of lateral rotation and lateral tilt ("cock-robin" position) with painful limitation of motion and an inability to rotate their heads to the oppostie side. Cranial nerve deficits were present in two patients, both of whom also had occipitoatlantic rotary subluxation, defined as malalignment of the axes of the head and atlas [5]. Duration of symptoms before presentation varied from hours in patients with torticollis to 4 years in one patient with C1–C2 rotary fixation. The initial treatment consisted of skeletal traction and muscle relaxants in all symptomatic patients. Arthrodesis was recommended in three patients.

Plain films, available in three patients, demonstrated asymmetry of the distance between the odontoid and the lateral masses of C1 on the open-mouth view. The lateral view did not aid in diagnosis. Functional examinations were not performed with plain-film techniques.

Axial CT easily established the diagnosis of occipitoatlantic rotary subluxation in two patients (Fig. 1) and demonstrated rotational displacement of the atlantoaxial complex in all patients. The spatial relationship of the vertebral bodies was appreciated better in those patients who were studied with 5-mm rather than 3-mm sections. This difference was most pronounced in patients with a significant lateral tilt of the cervical spine.

Without functional imaging, scans through C1–C2 in the patients with clinically fixed C1–C2 rotary fixation (Figs. 1–3) were radiographically indistinguishable from either the patients with reversible torticollis (Fig. 4) or a group of normal subjects who were scanned with their heads turned as far as possible to the side (Fig. 5). No one finding on the static examination appeared to be helpful in the CT diagnosis of fixation. An eccentric location of the odontoid with respect to the anterior arch of C1 was seen in one patient with torticollis and in one with rotary fixation. The extent of rotational displacement did not correlate with fixation, as was evidenced by two of the patients who had minimal rotation by CT examination. In one, whose inability to rotate his head resolved, the minimal rotation demonstrated on CT appeared no different from that of the other patient, whose CT rotation remained unchanged despite halo traction.

We performed functional examinations by scanning the occipitoatlantoaxial complex in the rotated position in which the patient presented and in maximum voluntary contralateral rotation. In a patient with rotary fixation there was no change in the relationship of the atlas and axis during this maneuver (Fig. 3). In the two patients with torticollis the functional scan resulted in reduction and actual reversal of the subluxation (Fig. 4). In the normal volunteers, scanning with the head turned yielded a range of motion of 29–44° (average, 34°) at the atlantoaxial joint (Table 2).

TABLE 1: Clinical Summary in Rotary Subluxation

Cause: Case No.	Age	Gender	Neurologic Findings	CT Appearance	Pre-CT Duration	Treatment	Follow-up
Motor vehicle accident:							
1	16	F	Pain	C1–C2 rotation	4 mo	Halo traction; fusion C1–C2	Diminished pain
2	30	F	Pain	C1–C2 rotation	4 yr	Cast immobilization	No change
3	22	F	Pain	C1–C2 rotation	3–4 days	Traction for 2 weeks	Diminished pain; CT unchanged
4	34	M	Transient left hand weakness	Fracture of C2; lateral mass; C1–C2 rotation	6 mo	Halo traction	Limitation of motion
Head turning:							
5	17	F	Cranial nerves X and XII	Occiput–C1 dislocation; C1–C2 rotation	5 mo	Traction C1–C2; fusion occiput–C2	Improved nerve function
Fall:							
6	7	M	Pain	C1–C2 rotation	2 mo	Halo traction	Diminished pain
7	9	M	Pain	C1–C2 rotation; able to turn head	3–4 days	Muscle relaxants	Resolved
8	12	F	Pain	C1–C2 rotation	Hours	Collar	Resolved

Note.—All patients had limited rotational head movement when initially evaluated. mo = months; yr = years.

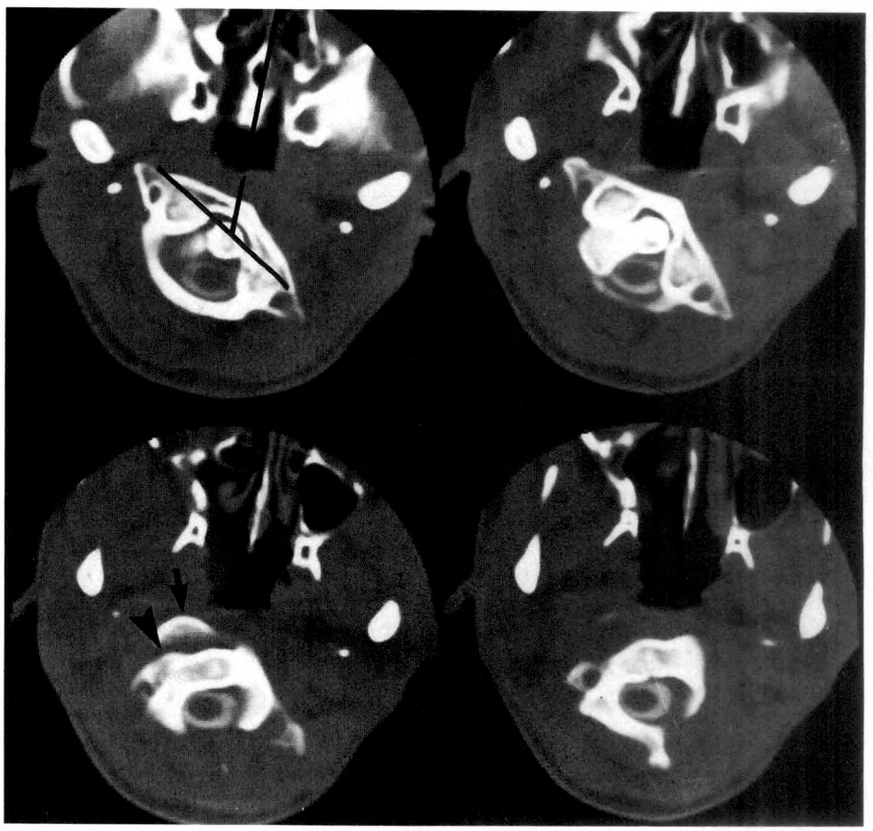


Fig. 1.—Case 5: 17-year-old girl with no history of trauma. Her head was fixed in rotation to the left and she had difficulty swallowing. Sequential CT scans from metrizamide myelogram show occipitoatlantal dislocation and atlantoaxial rotary fixation. Septal axis forms acute angle with transverse axis of atlas. Right lateral mass of C1 (*arrow*) is displaced anterior to superior articular surface of C2 (*arrowhead*). Odontoid remains in normal relationship to anterior arch of atlas, suggesting that transverse ligament remains intact.

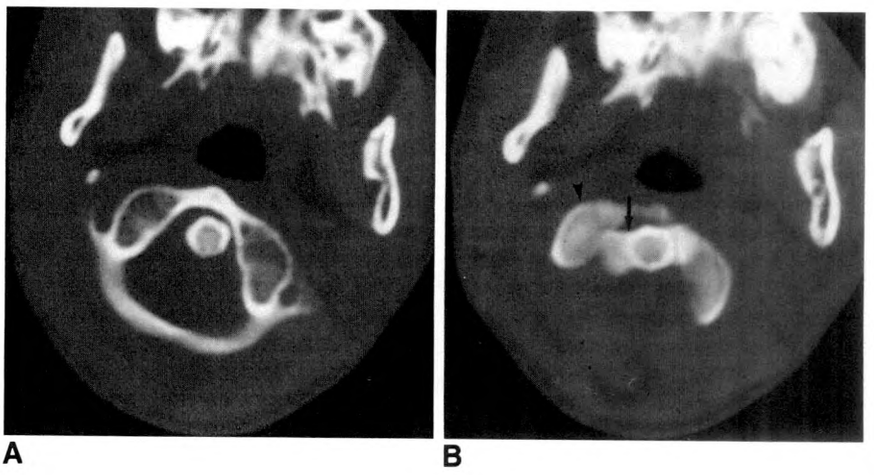


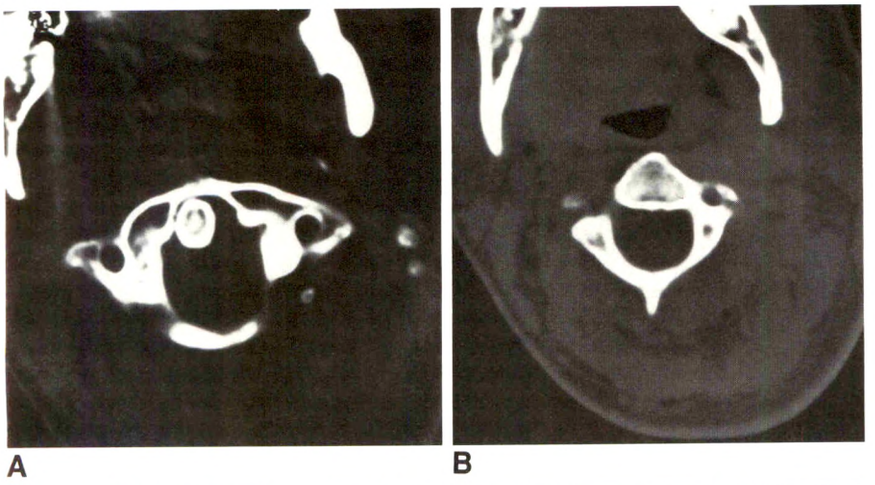
Fig. 2.—Case 6: 7-year-old boy whose head was fixed in rotation to the left.

***A*, Septal axis remains perpendicular to transverse axis of C1. Odontoid lies eccentrically between lateral masses of C2.**

***B*, Right lateral mass of C1 (*arrowhead*) lies anterior to anterior articular surface of C2 (*arrow*). Transverse axis of C1 is no longer perpendicular to axis of C2.**

Discussion

Atlantoaxial rotary fixation was described extensively in the pre-CT literature [1–3, 7, 8]. It occurs after minor neck trauma or an upper respiratory tract infection. The atlas, which normally rotates 45° in either direction on a relatively immobile axis [9, 10], is fixed in a position that could be attained during normal rotation. At initial presentation, the patient with atlantoaxial rotary fixation may be indistinguishable from someone with torticollis. In both conditions there may be neck pain, an inability to turn the head, and fixation of the head in a "cock-robin" position [1–3]. Clinical recognition of atlantoaxial rotary fixation depends on failure of the symptoms to resolve after a short period of time. Although the cause of rotary fixation



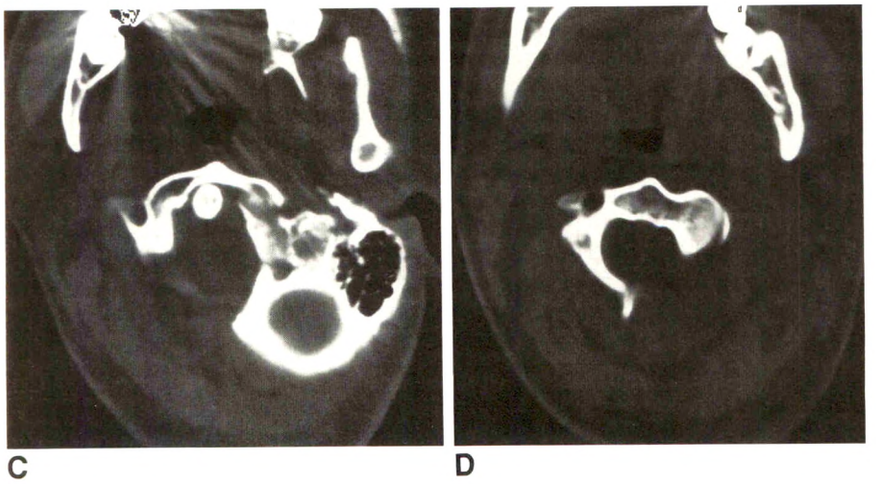


Fig. 3.—Case 2: 30-year-old woman 4 years after automobile accident.

***A* and *B*, Patient lies normally. She presented with her head fixed in rotation to the right. Odontoid lies eccentrically between lateral masses of atlas. Transverse axis of C1 is no longer perpendicular to axis of C2, indicating rotation at atlantoaxial joint.**

***C* and *D*, After trying to turn her head as far as possible to the left. No change in relationship between transverse axis of C1 and axis of C2, confirming rotary fixation.**

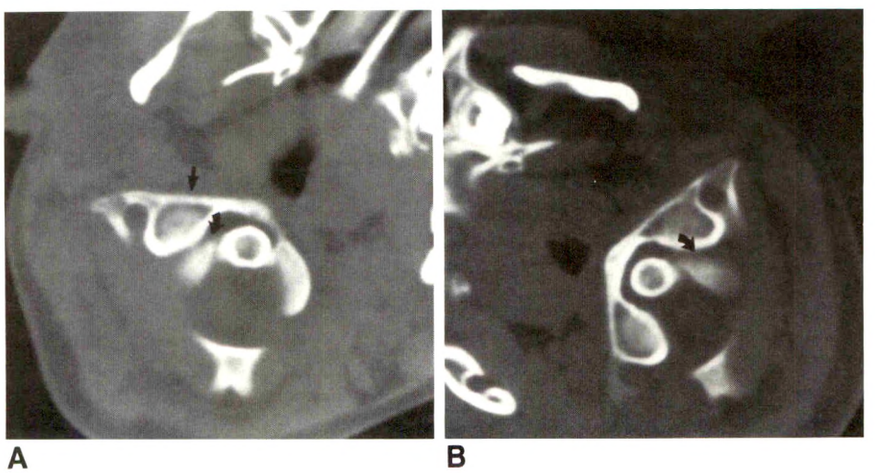


Fig. 4.—Case 8: 12-year-old girl with transient torticollis who presented with her head turned to the left.

***A*, With head in comfortable "neutral" position. Right lateral mass of C1 (*straight arrow*) lies anterior to articular surface of C2 (*curved arrow*).**

***B*, After trying to turn her head to the right. Left lateral mass of C1 now lies anterior to articular surface of C2 (*curved arrow*).**

remains uncertain, postulated mechanisms include entrapment of inflamed synovium combined with muscle spasm or a tear and invagination of capsular ligaments between the articular facets of C1 and C2 [1, 3, 4].

Plain films in all patients whose heads are rotated, whether voluntarily or pathologically, as in atlantoaxial rotary fixation or torticollis, show a rotated appearance of C1 on C2, with asymmetry of the distance between the odontoid and the

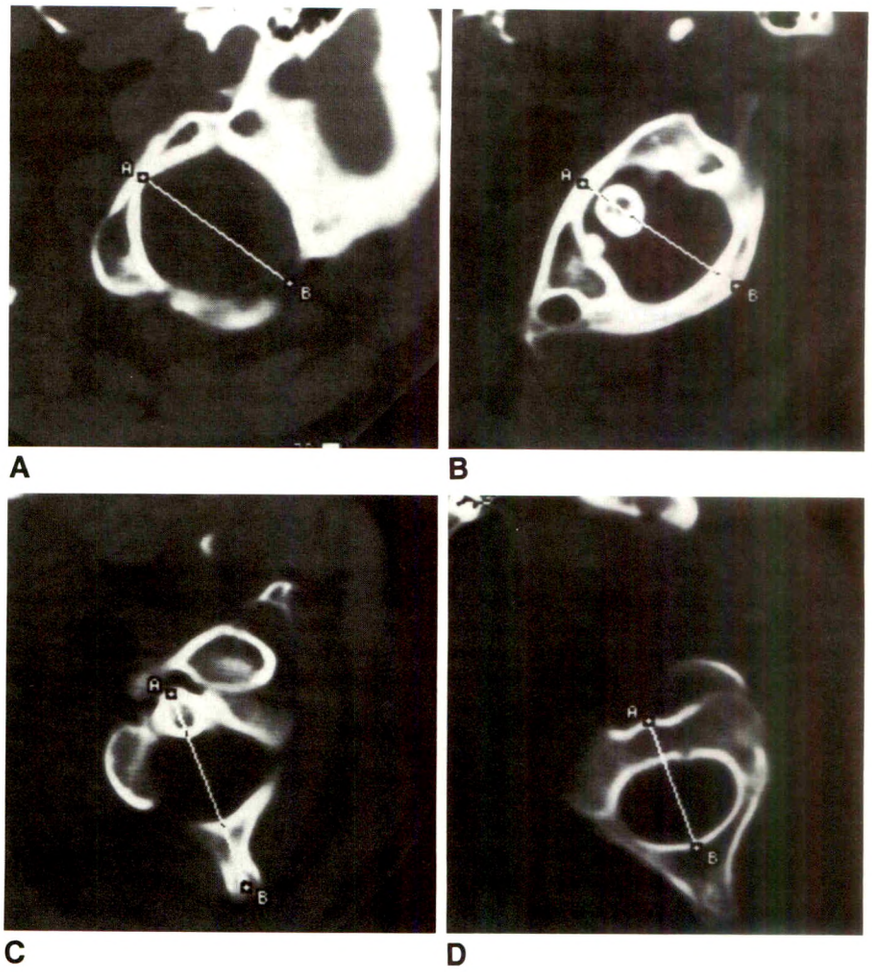


Fig. 5.—Normal volunteer asked to turn his head as far as possible to the right.

***A*, Through foramen magnum. Anteroposterior axis of head is parallel to nasal septum.**

***B*, Through atlas. Anteroposterior axis line of C1 remains parallel to anteroposterior axis of head.**

***C* and *D*, Through C2. Anteroposterior axis of C2 is no longer parallel to anteroposterior axis of C1. Lateral mass of C1 is rotated anteriorly on articular surface of C2.**

TABLE 2: Maximum Rotation at the Atlantoaxial Joint in Normal Volunteers

Age	Gender	Rotation (degrees)
2	M	34
32	M	32
37	M	41
72	M	24
66	F	36
67	F	39

Note.—The average rotation was 34°.

lateral masses of C1 [2, 3]. Cineradiography of the atlantoaxial joint during turning of the head from side to side has been proposed as a method of diagnosis because actual fixation at the atlantoaxial joint could be demonstrated [9, 11]. Reports of the CT appearance of patients with the clinical syndrome of atlantoaxial rotary fixation have consisted of case studies [4, 5] or of discussions of the efficacy of CT in delineating the rotation of C1 on C2 [6]. The problem of distinguishing relatively normal head turning (torticollis) from pathologic fixation has not been addressed.

We began using functional CT studies after encountering a patient with transient torticollis whose initial static CT scan demonstrated C1–C2 rotation indistinguishable from that of previous patients with clinically proven rotary fixation. On functional examination the rotary deformity reversed, prompting further investigation of both the limitations of static scans and the utility of functional examinations. In our experience, the static CT examination is quite adequate for demonstrating the pathology in patients with either occipitoatlantal subluxation or atlantoaxial subluxation with associated anterior displacement of the atlas on the axis. However, the static examination cannot differentiate between patients with *isolated* C1–C2 rotary fixation, patients with reversible torticollis, and normal volunteers who are scanned with their heads held in rotation. By using a functional examination we were able to demonstrate reduction and reversal of the subluxation in the patients with torticollis, thereby excluding the diagnosis of rotary fixation. Conversely, this maneuver did not produce any change in the relationship of the atlas and axis in the patients with clinical rotary fixation who were thus studied, radiographically proving fixation. A similar method of proving fixation radiographically in a patient whose head was fixed in rotation for 9 months was described by Rinaldi et al. [4];

however, they did not comment on the use of functional CT to exclude a transient rotational deformity. Functional scanning has also been used in children with congenital abnormalities of C1–C2 to evaluate stability before surgical immobilization [12]. The advantage of CT over cineradiography is the ease of performance and interpretation.

Additional investigation of the functional examination in the diagnosis of atlantoaxial rotary fixation is still necessary. Our sample size was small and we did not investigate the option of a single set of CT scans with the patient's head turned to the side opposite the deformity. The latter procedure would offer the advantage of decreased radiation and scanning time; however, it is possible that a patient might be unable to turn his head fully past midline because of muscular discomfort rather than actual fixation. We postulate that the demonstration of cervical rotation without movement at C1–C2 is necessary to establish the diagnosis of rotary fixation.

REFERENCES

1. Fielding JW, Hawkins RJ. Atlanto axial rotatory fixation. *J Bone Joint Surg [Am]* **1977**;59:37–44
2. Fielding JW, Hawkins RJ, Hensinger RN, Francis WR. Atlantoaxial rotary deformities. *Orthop Clin North Am* **1978**;9:955–967
3. Wortzman G, Dewar FP. Rotary fixation of the atlantoaxial joint: rotational atlantoaxial subluxation. *Radiology* **1968**;90:479–487
4. Rinaldi I, Mullins WJ Jr, Delaney WF, Fitzer PM, Tornberg DN. Computerized tomographic demonstration of rotational atlanto-axial fixation. *J Neurosurg* **1979**;50:115–119
5. Fielding JW, Stillwell WT, Chynn KY, Syropoulos EC. Use of computed tomography for the diagnosis of atlanto-axial rotatory fixation. *J Bone Joint Surg [Am]* **1978**;60:1102–1104
6. Baumgarten M, Mouradian W, Boger D, Watkins R. Computed axial tomography in C1–C2 trauma. *Spine* **1985**;10:187–192
7. Jacobson G, Adler DC. Examination of the atlantoaxial joint following injury. *AJR* **1956**;76:1081–1094
8. Akbarnia BA, Vafaie M. Atlantoaxial rotary fixation. *Spine* **1983**;8:907–909
9. White AA, Panjabi MM. The clinical biomechanics of the occipitoatlantoaxial complex. *Orthop Clin North Am* **1978**;9:867–878
10. Dvorak J, Panjabi M, Wichman C. CT functional diagnostic instability of the upper cervical spine. Presented at the annual meeting of the Cervical Spine Research Society, Cambridge, MA, December **1985**
11. Fielding JW. Cineradiography of the normal cervical spine. *J Bone Joint Surg [Am]* **1957**;39:1280–1288
12. Roach JW, Duncan D, Wegner DR, Maravilla A, Maravilla K. Atlanto-axial instability and spinal cord compression in children—diagnosis by computerized tomography. *J Bone Joint Surg [Am]* **1984**;66:708–714

Role of CT in Excluding Major Arterial Injury After Blunt Thoracic Trauma

Stuart E. Mirvis[1]
Irene Kostrubiak[1]
Nancy O. Whitley[1]
Laurence D. Goldstein[1]
Aurelio Rodriguez[2]

The role of CT in the diagnosis of major vascular rupture following blunt decelerating chest trauma is controversial. Its value in excluding major arterial injury has not yet been determined. During a 12-month period we obtained dynamic enhanced thoracic CT studies in 20 patients with blunt decelerating thoracic trauma who had abnormal or equivocal mediastinal contours on chest radiographs. In all cases diagnosis was confirmed by either digital subtraction (18 patients) or conventional thoracic angiography (two patients). CT scans showed evidence of direct aortic injury in three patients and evidence of mediastinal hematoma in five others. Four of these eight patients had major arterial injury verified angiographically and at surgery. In two patients the CT scan was considered equivocal; both patients had normal thoracic angiograms. CT excluded direct vascular injury or mediastinal hematoma in 10 patients. All 10 had normal thoracic angiograms.

This preliminary study suggests that, in patients sustaining blunt decelerating thoracic trauma, thoracic CT may be more valuable than chest radiography in excluding major vascular injury and, in some cases, may reduce the need for thoracic angiography.

Currently, chest radiography serves as the principal screening method for detecting mediastinal hemorrhage and great vessel injury following blunt decelerating chest trauma [1–7]. Chest radiographs obtained in this critical setting are frequently of poor quality owing to power limitations of single-phase, line-operated mobile radiographic systems, short focal film distance, poor inspiratory effort, and motion due to limited cooperation from patients [8, 9]. Further, in patients with multisystem injury, only the supine anteroposterior view can be obtained. Because of these limitations, in a major trauma center as many as seven to eight patients may undergo thoracic angiography for each patient who actually sustains a major arterial injury [4–6].

The role of CT in the diagnosis of traumatic thoracic vascular injury is controversial [10–14]. Heiberg et al. [10] documented the potential of CT to identify mediastinal hemorrhage, as well as to provide direct evidence of thoracic aortic injury following blunt thoracic trauma in a small series of patients. Others have cast considerable doubt regarding the potential efficacy of CT in diagnosing aortic and great vessel injury and have discouraged its use for this purpose [11–13].

In light of this controversy we have performed a prospective study in which both dynamic enhanced CT and thoracic angiography, using digital or conventional methods, were done in 20 patients with blunt decelerating thoracic trauma in whom admission chest radiographs indicated possible mediastinal hemorrhage. Our results suggest that contrast-enhanced CT may substantially reduce the need for thoracic angiography in these patients.

Methods and Materials

The study group consisted of 17 males and three females ranging in age from 11 to 75 years (mean, 36 years). Sixteen were victims of motor vehicle accidents, three suffered falls

Received March 23, 1987; accepted after revision May 21, 1987.

[1] Department of Diagnostic Radiology, University of Maryland Medical System, 22 S. Greene St., Baltimore, MD 21201. Address reprint requests to S. E. Mirvis.

[2] Maryland Emergency Medical Services System, University of Maryland Medical System, 22 S. Greene St., Baltimore, MD 21201.

AJR **149:601–605, September 1987**
0361–803X/87/1493–0601
© American Roentgen Ray Society

from a substantial height, and one was a pedestrian struck by a van. Admission chest radiographs, CT scans, and thoracic angiograms were available in all cases. The study protocol was approved by the Research Committee of the Maryland Institute for Emergency Medical Services Systems and was in effect for 12 months. In cases in which informed consent for thoracic CT could not be obtained expeditiously, the clinical physician acted as the patient's advocate in deciding on inclusion in the study. The following protocol was established: (1) All patients were victims of blunt decelerating thoracic trauma with possible mediastinal hemorrhage as evidenced principally by an ill-defined mediastinal contour, particularly obscuration of the aortic arch and descending aorta on admission chest radiographs [1–7]. (2) All patients required CT to assess existing cerebral or abdominopelvic injury.

Thoracic CT studies were performed using a GE 9800 (Milwaukee, WI) scanner. An anteroposterior scout view was done to ensure adequate removal or repositioning of cutaneous monitor lines and tubes away from the scan planes. Nasogastric tubes were present in 13 patients, and were left in place to mark the position of the esophagus. These did not produce significant artifacts in any case. Dynamic CT scanning was performed in 1-cm contiguous sections beginning at the level of the top of the manubrium to the level of the carina. Immediately before scanning, a bolus injection of 30–40 ml of Angiovist 282 (76% diatrizoate meglumine/sodium) were injected rapidly into a central venous catheter or large antecubital line. After a second 30–40 ml bolus of IV contrast material, dynamic scanning was continued to the diaphragm. All CT studies obtained were considered to be of adequate diagnostic quality. Two patients had contrast-enhanced thoracic CT studies performed at other institutions before being transferred to our facility.

Because of the increased dose of contrast material required to perform both enhanced CT and thoracic angiography, all patients were required to have a serum creatinine of <1.5 mg/dl and a serum urea nitrogen of <40 mg/dl in order to be included in the study. The total time required to perform the dynamic thoracic CT scan was 5–15 min (average, 11 min), depending on the clinical needs of the patient.

While CT images were undergoing reconstruction, the patients were transferred to the angiographic suite. In 18 cases an intraarterial DSA was performed, as previously described [15]. Two patients had conventional biplane cut-film aortograms.

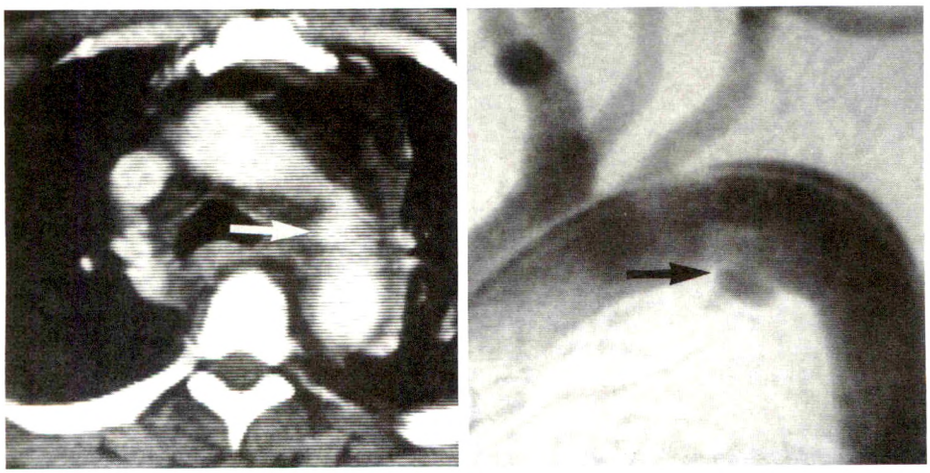
CT studies were reviewed by two staff radiologists who had expertise in CT but who had no knowledge of the results of angiography. Assessment of CT scans was by consensus and included the following classifications: (1) direct aortic injury based on identification of a focal bulge or irregularity in the vessel contour and/or an intraluminal lucency suggesting an intimal flap; (2) focal periaortic hematoma with or without tracheal or esophageal displacement; (3) diffuse mediastinal hematoma; and (4) focal mediastinal hematoma not adjacent to the aorta. The CT interpretations were then compared with the angiographic results.

Results

In three patients CT suggested evidence of direct aortic injury. Two of these patients had aortic pseudoaneurysms confirmed by thoracic angiography and at surgery, and one had a normal thoracic angiogram (Figs. 1 and 2). Four patients had a focal periaortic hematoma or diffuse mediastinal hemorrhage by CT. One of these had a rupture of the proximal left subclavian artery, and one had a 99% transsection of the aorta at the level of the ligamentum arteriosum (Fig. 3) by angiography and at surgery. The other two had normal thoracic angiograms. One patient had a focal small anterior mediastinal hematoma and normal thoracic angiography. Two other patients had equivocal CT findings, including one adolescent with an anterior mediastinal soft-tissue mass that could not be differentiated from the thymus gland and one patient with right upper-lobe atelectasis partially obscuring the periaortic region. These patients had normal thoracic arteriograms. Finally, all 10 patients believed to be normal on the basis of CT scans of the mediastinum were normal by angiography as well. All patients with normal arteriograms were managed without surgery and all have been discharged with normal follow-up chest radiographs.

Discussion

During the past 20 years many plain radiographic signs of mediastinal hemorrhage and possible aortic and proximal



A B

Fig. 1.—CT scan shows rupture of thoracic aorta.

***A*, CT section after bolus contrast enhancement shows peculiar bulge in aortic contour and lucent line crossing aorta compatible with an intimal flap (*arrow*).**

***B*, DSA aortogram confirms small pseudoaneurysm projecting from undersurface of aortic arch (*arrow*) corresponding to abnormality detected on CT scan. Aortic rupture at this site subsequently confirmed at surgical repair.**

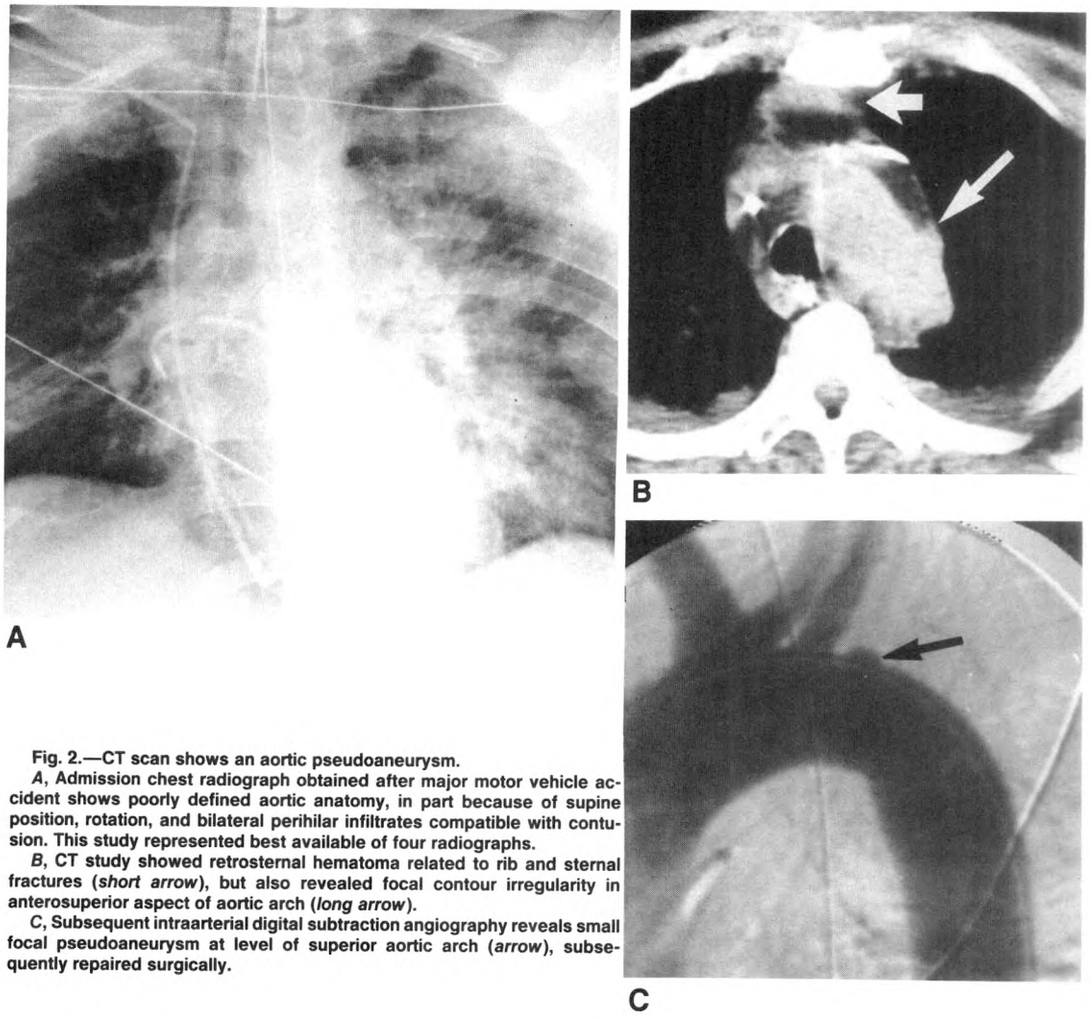


Fig. 2.—CT scan shows an aortic pseudoaneurysm.

***A*, Admission chest radiograph obtained after major motor vehicle accident shows poorly defined aortic anatomy, in part because of supine position, rotation, and bilateral perihilar infiltrates compatible with contusion. This study represented best available of four radiographs.**

***B*, CT study showed retrosternal hematoma related to rib and sternal fractures (*short arrow*), but also revealed focal contour irregularity in anterosuperior aspect of aortic arch (*long arrow*).**

***C*, Subsequent intraarterial digital subtraction angiography reveals small focal pseudoaneurysm at level of superior aortic arch (*arrow*), subsequently repaired surgically.**

great vessel injury have been suggested [1–7]. Unfortunately, no single plain radiographic sign is completely sensitive or specific, and even frequently observed signs lack high positive predictive value [6, 16]. On the other hand, only the simultaneous absence of several signs in combination has been shown to have a reasonably high negative predictive value [4, 6]. Previous studies at our institution indicate that 80% of patients sustaining blunt decelerating thoracic trauma who do not have major thoracic arterial injury show signs of mediastinal hemorrhage on supine chest radiographs, while 52% of these patients show signs of mediastinal hemorrhage on erect chest radiographs [6]. The low specificity of many signs of mediastinal hemorrhage requires as many as seven or eight thoracic arteriograms in order to exclude major vascular injury for each patient diagnosed with such an injury [6, 8, 9]. The role of CT in evaluating acute thoracic trauma has not been well established, and, specifically, the use of CT in evaluating great vessel injury has been controversial [10–14]. In a series of 10 patients, Heiberg et al. [10] showed the ability of contrast-enhanced CT to detect aortic wall injury in four patients and to exclude it in six others, as evidenced by angiographic correlation. In their series, the extent of mediastinal hematoma did not correlate with the presence of aortic injury. On the other hand, Egan et al. [11] reported CT findings in five patients with thoracic trauma and mediastinal widening on chest radiographs. All five had mediastinal hematomas, one of which was periaortic, but none had aortic injury by angiography. This article is widely quoted as support for the poor performance of CT of diagnosing acute aortic injury [12, 17, 18]. Goodman and Teplick [17] described five patients who had no history of upper thoracic trauma, but who had widened mediastina on chest radiography. Four of these patients showed no evidence of mediastinal hematoma or aortic injury, and all had benign clinical courses. A single patient with a normal CT scan also had a negative thoracic aortogram.

In our literature review, we found three cases of false-negative CT scans for thoracic aortic injury. Kubota et al. [19] described a single patient with an equivocal CT scan, but two intimal tears of the lower descending thoracic aorta on angiography. The tears were considered non–life threatening and were not treated. White et al. [20] described two patients

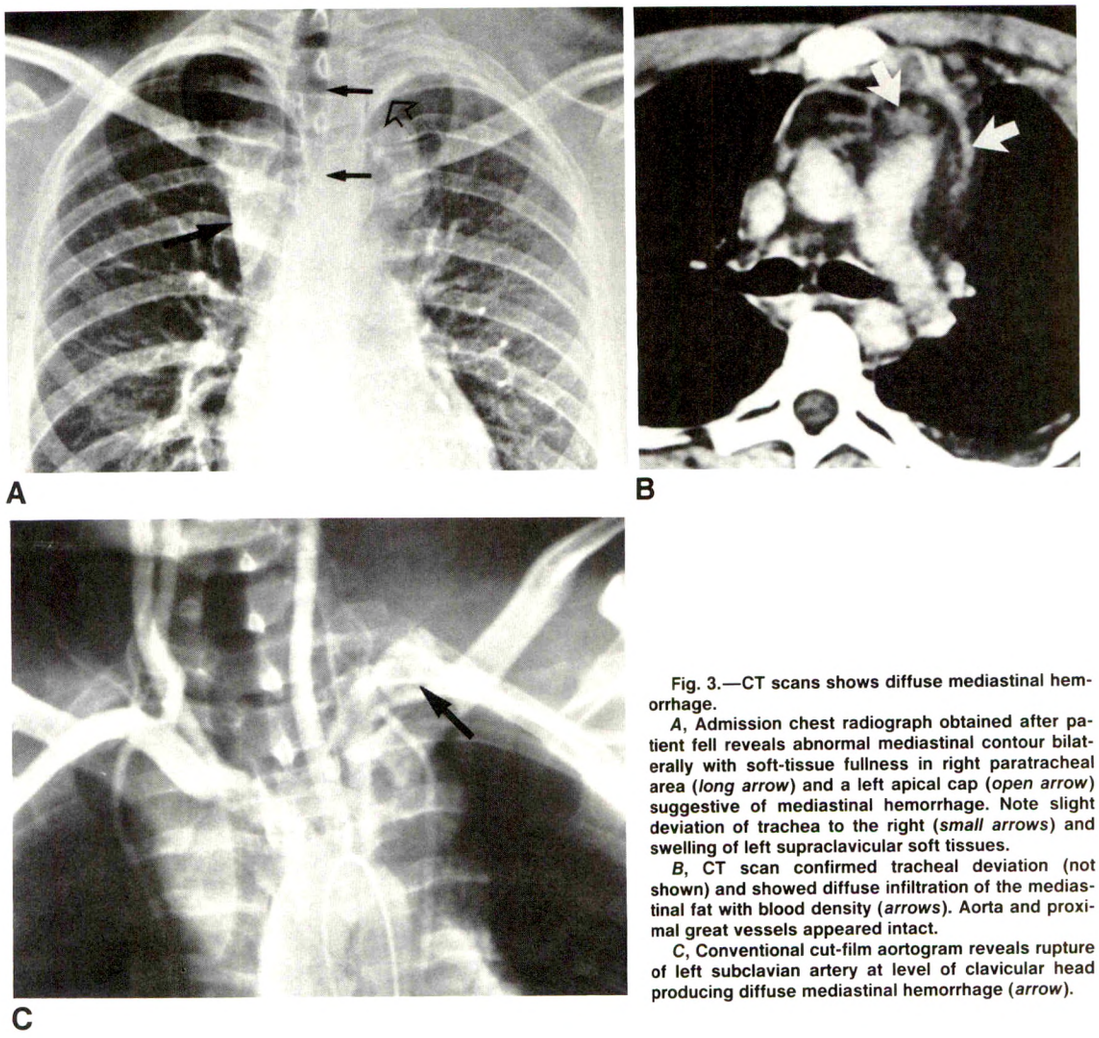


Fig. 3.—CT scans shows diffuse mediastinal hemorrhage.

***A*, Admission chest radiograph obtained after patient fell reveals abnormal mediastinal contour bilaterally with soft-tissue fullness in right paratracheal area (*long arrow*) and a left apical cap (*open arrow*) suggestive of mediastinal hemorrhage. Note slight deviation of trachea to the right (*small arrows*) and swelling of left supraclavicular soft tissues.**

***B*, CT scan confirmed tracheal deviation (not shown) and showed diffuse infiltration of the mediastinal fat with blood density (*arrows*). Aorta and proximal great vessels appeared intact.**

***C*, Conventional cut-film aortogram reveals rupture of left subclavian artery at level of clavicular head producing diffuse mediastinal hemorrhage (*arrow*).**

who had partial aortic transsections but no evidence of direct aortic injury. One patient did have evidence of mediastinal hematoma, but the other was not discussed specifically. Both authors recommended against the use of CT scanning in screening for possible aortic injury.

In their recent text on CT of trauma, Toombs and Sandler [14] acknowledge the role of CT in identifying mediastinal hematoma, despite a normal chest radiograph, and suggested a possible future role for CT in screening for aortic injury. However, in two other recent texts, the authors advise against the use of CT in the evaluation of potential aortic or great vessel injury [12, 13]. Problems with lack of cooperation from patients and potential volume averaging of small intimal injuries or psuedoaneurysms are cited as factors against the use of CT [12, 13, 21].

In view of the controversy surrounding this subject and because of the excessive number of negative thoracic aortograms being performed in the setting of blunt thoracic trauma, we have attempted to assess the role of CT in evaluating patients with possible major thoracic vascular injury following blunt decelerating chest trauma. We evaluated the performance of CT of the thorax and compared the blinded readings against angiography and surgical results in all cases. In four patients with aortic or proximal great vessel injury, we were able to either directly visualize the aortic injury or detect diffuse or focal periaortic hematomas on CT. We would most certainly recommend confirmatory angiography in such patients. Three other patients were believed to have similar findings on CT, but had normal aortograms. Three additional patients had either equivocal CT results (two) or a focal mediastinal hematoma not adjacent to the aorta. We would also recommend angiography in these patients. Most importantly, 10 patients with abnormal or equivocal mediastinal contours on admission chest radiographs were found to have normal mediastina by CT, and all had normal thoracic angiograms.

Traditionally, the presence of plain radiographic signs of mediastinal hemorrhage has been used to indicate possible

major vascular injury following blunt chest trauma. This hemorrhage is in all probability not directly related to the presence of major vascular injury as discussed by Ayella et al. [22], but it is probably a marker of significant mediastinal trauma, with bleeding from veins and perhaps small arteries. It is this association that we depend on largely to diagnose those patients with major arterial injury. While the detection of a focal or diffuse mediastinal hematoma by CT does not necessarily indicate vascular injury, we do not yet believe that the sensitivity of CT to major arterial injury in the mediastinum has been clearly established. Therefore, given the high rate of mortality associated with this injury, we believe that the CT demonstration of diffuse or focal mediastinal hematoma constitutes sufficient evidence of mediastinal injury to recommend thoracic angiography.

On the basis of this initial experience with CT in the evaluation of mediastinal trauma, we recommend and have adopted the following diagnostic algorithm. Any patient with unequivocal radiographic evidence of mediastinal hematoma should have an angiogram promptly. With equivocal mediastinal contours thoracic CT should be performed, particularly if the patient is already scheduled to have CT to evaluate other injuries. CT evidence of direct aortic injury or mediastinal hematoma is also an indication for angiography. Following this algorithm would have eliminated the need for thoracic angiography in 50% of our patients.

REFERENCES

1. Stark, P. Traumatic rupture of the thoracic aorta: a review. *CRC Crit Rev Diagn Imaging* **1984**;21:239–255
2. Sturm JT, Olsen FR, Cicero JJ. Chest roentgenographic findings in 26 patients with traumatic rupture of the thoracic aorta. *Ann Emerg Med* **1983**;12(10):598–600
3. Gundry SR, Burney RE, Mackenzie JR, et al. Assessment of mediastinal widening associated with traumatic rupture of the aorta. *J Trauma* **1983**;23:293–299
4. Marnocha KE, Maglinte DDT. Plain-film criteria for excluding aortic rupture in blunt chest trauma. *AJR* **1985**;144:19–21
5. Gundry SR, Williams S, Burney RE, MacKenzie JR, Cho KJ. Indications for aortography. Radiography after blunt chest trauma: a reassessment of radiographic findings associated with traumatic rupture of the aorta. *Invest Radiol* **1983**;18:230–237
6. Mirvis SE, Bidwell JK, Buddemeyer EU, et al. Value of chest radiography in excluding traumatic aortic rupture. *Radiology* **1987**;163:487–493
7. Woodring JH, Loh FK, Kryscio RJ. Mediastinal hemorrhage: an evaluation of radiographic manifestations. *Radiology* **1984**;151:15–21
8. Sherrier RH, McAdams HP. Digital processing of portable films can reduce need for repeat studies. *Diagn Imag* **1986**;8:117–118
9. Ovenfors C, Hedgecock MW. Intensive care unit radiology: problems of interpretation. *Radiol Clin North Am* **1978**;16:407–439
10. Heiberg E, Wolverson MK, Sundaram M, Shields JB. CT in aortic trauma. *AJR* **1983**;140:1119–1124
11. Egan TJ, Neiman HL, Herman RJ, Malave SR, Sanders JH. Computed tomography in the diagnosis of aortic aneurysm dissection or traumatic injury. *Radiology* **1980**;136:141–146
12. Goodman PC. CT of chest trauma. In: Federle MP, Brant-Zawadzki M, eds. *Computed tomography in the evaluation of chest trauma*, 2nd ed. Baltimore: Williams & Wilkins, **1986**:168–190
13. Chakravarty M. Utilization of angiography in trauma. *Radiol Clin North Am* **1986**;24(3):383–396
14. Toombs BD. Acute chest trauma. In: Toombs BD, Sandler CM, eds. *Computed tomography in trauma*. Philadelphia: Saunders, **1987**:11–26
15. Mirvis SE, Pais SO, Gens DR. Thoracic aortic rupture: advantages of intraarterial digital subtraction angiography. *AJR* **1986**;146:987–991
16. Mirvis SE, Bidwell JK, Buddemeyer EU, Diaconis JN, Pais SO, Whitley JE. Radiologic diagnosis of thoracic aortic rupture: four years experience at a major trauma center. *Invest Radiol* **1987**;22:187–196
17. Goodman LR, Teplick SK. Computed tomography in acute cardiopulmonary disease. *Radiol Clin North Am* **1983**;21:741–758
18. Godwin JD, Korobkin M. Acute disease of the aorta: diagnosis by computed tomography and ultrasonography. *Radiol Clin North Am* **1983**;21:551–574
19. Kubota RT, Tripp MD, Tisnado J, Cho S. Evaluation of traumatic rupture of descending aorta by aortography and computed tomography: case report with follow-up CT. *J Comput Tomogr* **1985**;9:237–240
20. White RD, Lipton MJ, Higgins CB, et al. Noninvasive evaluation of suspected thoracic aortic disease by contrast-enhanced computed tomography. *Am J Cardiol* **1986**;57:282–290
21. Godwin JD. The pericardium, heart, and great vessels. In: Godwin, JD, ed. *Computed tomography of the chest*. Philadelphia: Lippincott, **1984**: 293–372
22. Ayella RJ, Hankins JR, Turney SZ, Cowley RA. Ruptured thoracic aorta due to blunt trauma. *J Trauma* **1977**;7:199–205

Book Review

Diagnostic Angiography. By Saadoon Kadir. Philadelphia: Saunders, 736 pp., 1986. $85

The emergence of interventional radiology and new sophisticated surgical procedures for the treatment of disease have rejuvenated interest in diagnostic angiography. The need for precise information, however, has necessitated changes. A simple midstream angiogram is no longer adequate. Superselective studies and hemodynamic measurements are now needed to provide adequate information.

This book contains 23 chapters spanning the field of diagnostic angiography, excluding cerebral and cardiac angiography. The chapters are organized on the basis of regional anatomy. The book deals with the indications and interpretations of vascular studies. Each chapter contains a complete description of the angiographic findings and discusses the angiographic pitfalls resulting from interpretative errors or angiographic "look alikes." Care of patients and the technical aspects of angiography are covered also. The first section of the book contains seven chapters devoted to the equipment necessary to perform angiography. The entire spectrum is covered, from radiologic equipment to catheters and guidewires. Special emphasis is placed on angiographic technique. The second section of the book contains six chapters devoted to regional angiography of the aorta and the extremities. The third section of the book contains four chapters covering visceral angiography of the gastrointestinal tract, kidneys, and spine. Angiography of the endocrine system is dealt with in Section 4. The venous system and pulmonary angiography are covered in Section 5. Other sections cover the lymphatic and biliary systems and the complications of angiography.

The book is illustrated profusely, with more than 1345 angiograms, drawings, and tables. If the book has any shortcoming, it is that the physiology associated with the angiographic interpretation is not covered in great depth. This book was written for radiologists with an interest in angiography. Radiology residents also will find the book of value.

Charles John Tegtmeyer
University of Virginia Medical Center
Charlottesville, VA 22908

Penetrating Injuries of the Thoracic Aorta and Brachiocephalic Arteries:

Angiographic Findings in 18 Cases

Richard G. Fisher[1]
Yoram Ben-Menachem[2]

Eighteen patients with surgically proved penetrating injuries to the thoracic aorta or brachiocephalic arteries were evaluated preoperatively with angiography. Fifteen injuries resulted from direct penetration of a vessel and three were concussion or blast injuries. Arteriography correctly showed vessel damage in 16 (89%), although one was identified only in retrospect. There were two false-negative examinations. False aneurysms were present in nine. Other findings included occlusion, wall irregularity, and an arterial-arterial fistula.

Our results show that angiography is an accurate means of detecting penetrating injuries to the thoracic aorta or brachiocephalic arteries.

Preoperative angiography is not used commonly in the assessment of suspected penetrating injuries to the thoracic aorta or its branches. Frequently the catastrophic nature of such injuries demands immediate surgery [1–3]. However, in selected patients, angiography can be useful in the patient's management by establishing the diagnosis and locating the site of injury preoperatively. Life-threatening injuries may be clinically silent for a period of time, and aggressive use of angiography is essential for their prompt diagnosis [4–6].

We report our experience with 18 cases of proved intrathoracic penetrating vascular injury at two major trauma centers in Houston (Ben Taub General and Hermann hospitals).

Materials and Methods

In the two hospitals, 1000–1200 patients with penetrating thoracic injury are seen annually. Over a 10-year period, about 110 have had angiography before surgery. Eighteen of these 110 proved to have injuries to the aorta or brachiocephalic arteries.

Angiography was performed via a femoral-artery approach in all, and there were no complications from the examination. Indications for performing the procedure were the possibility of an injury in the region of the aorta or brachiocephalic vessels (proximity injury), evidence of mediastinal hematoma on chest radiograph, or the presence of a pulse deficit (diminished or absent pulse).

Results

Angiography showed vascular injury in 16 of the 18 patients with surgically proved vessel damage (Table 1). In one, a subtle injury was identified only in retrospect (Fig. 1). The angiograms were obtained promptly after the injury in 16 patients. In one other patient angiography was done immediately after surgical repair of a laceration of the ascending aorta (Fig. 2). The remaining case was studied 6 years after injury.

The aorta was damaged in six patients and the brachiocephalic arteries in 12. Four of those 12 cases had multiple intrathoracic arterial injuries. Twelve injuries

Received January 26, 1987; accepted after revision April 20, 1987.

[1] Department of Radiology, Baylor College of Medicine, 1 Baylor Plaza, Houston, TX 77030. Address reprint requests to R. G. Fisher.

[2] Department of Radiology, University of Texas Health Science Center, Houston, TX 77030. Present address: Department of Radiology, Baylor College of Medicine, Houston, TX 77030.

AJR 149:607–611, September 1987
0361–803X/87/1493–0607
© American Roentgen Ray Society

TABLE 1: Angiography of Penetrating Injuries of the Thoracic Aorta and Brachiocephalic Arteries

Case No.	Age (yr.)	Gender	Clinical Indications	Vessel Injured	Angiographic Diagnosis	Surgical Diagnosis
1	35	M	Proximity[a]	Aortic arch	Normal[b]	5-cm puncture wound in arch
2	40	M	Bullet embolus	Descending aorta[c]	Wall irregularity[d]	Puncture
3	23	M	Proximity[a]	Aortic arch	Normal[e]	Through-and-through puncture
4	33	M	Mediastinal hematoma[f]	Aortic arch	False aneurysm	4-mm puncture wound, arch
5	37	M	Hemothorax	Descending aorta	Two areas of extravasation	Through-and-through perforation
6	20	M	Proximity[a]	Ascending aorta	Wall irregularity[d]	Blast injury to intima
				Left internal mammary artery	Occlusion	Transection
7	35	M	Mediastinal hematoma[f]	Innominate artery[g]	False aneurysm	Puncture posterior wall
8	25	M	Proximity[a,e]	Innominate artery	False aneurysm	Puncture
9	24	M	Right apical mass	Right subclavian artery	False aneurysm[h]	False aneurysm
10	28	M	Absent pulse, left axillary artery and proximity[a]	Left common carotid and subclavian arteries	Arterial-arterial fistula and occlusion, left subclavian artery	Through-and-through perforation; bullet lodged in left subclavian artery
11	31	M	Mediastinal hematoma[f]	Innominate artery	False aneurysm	Puncture
12	40	M	Mediastinal hematoma[f] and shock	Right common carotid artery	False aneurysm and extravasation	Puncture
13	35	M	Mediastinal hematoma[f]	R common carotid artery	Occluded	Transection
				R subclavian artery	Wall irregularity	Puncture
				R vertebral artery	Occluded	Transection
14	46	M	Proximity[a]	Innominate artery	False aneurysm and extravasation	Puncture
15	29	M	Proximity[a]	Innominate artery	Wall irregularity[d]	Blast injury to intima
16	25	F	Proximity[a]	Innominate artery	False aneurysm and extravasation	Puncture
				R common carotid artery	False aneurysm	Puncture
				R subclavian artery	False aneurysm	Puncture
17	21	M	Proximity[a]	Innominate artery	False aneurysm	Through-and-through puncture
				L common carotid artery	False aneurysm and clot	One puncture and incomplete transection
				R vertebral artery	Occlusion	Transection
18	30	M	Proximity[a]	R common carotid artery	Normal	Avulsion of adventitia and media

Note.—All injuries were from handguns except in cases 1, 3, 4, and 8 (stab wounds) and 5, 16, and 17 (shotgun injuries). R = right; L = left.

[a] Suspected injury in the vicinity of the aorta or brachiocephalic arteries.

[b] False aneurysm recognized in retrospect.

[c] Bullet embolized to popliteal artery.

[d] Injury to intima.

[e] Died from surgical complications.

[f] Detected on chest radiograph.

[g] Diagnosed immediately after ascending aortic repair and bullet embolectomy, right femoral artery.

[h] Diagnosed 6 years after injury.

were inflicted by handgun, three by shotgun, and three were stab wounds. Two resulted in bullet embolization to the lower extremities (Table 1). In 15, vessel damage was the result of direct puncture, and three were caused by concussion or blast injuries (cavitary blast effect from a high-velocity missile). Proximity of the injury to major vessels was the primary indication for angiography in eight (44%) of the 18 patients. The remainder had more specific signs such as mediastinal hematoma or pulse deficit.

In 16, vessel injuries were readily recognized on the basis of one or more of five angiographic signs of injury described by Snyder et al. [4]. These include obstruction, extravasation, early venous filling, wall irregularity or filling defect, and false aneurysm.

Nine of 18 patients had false aneurysms (Fig. 2). Frank extravasation was present in four (Fig. 3). In the four patients with multiple vascular injuries, mixed findings were the rule: fistula and occlusion, intimal defect and occlusion, false aneurysms with and without extravasation, and false aneurysms plus occlusion (Table 1). One had an arterial-arterial fistula (Fig. 4). Subtle injuries were present in seven. Two of these had identical mechanisms of injury (stabbed through the thoracic inlet) and similar angiographic abnormalities (Figs. 1 and 5). One patient with a concussion or blast injury sustained a subtle innominate lesion (Fig. 6), while another had a small but fairly obvious ascending aortic injury (Fig. 7). The two false-negative arteriograms were in patients who proved to have puncture wounds (Table 1).

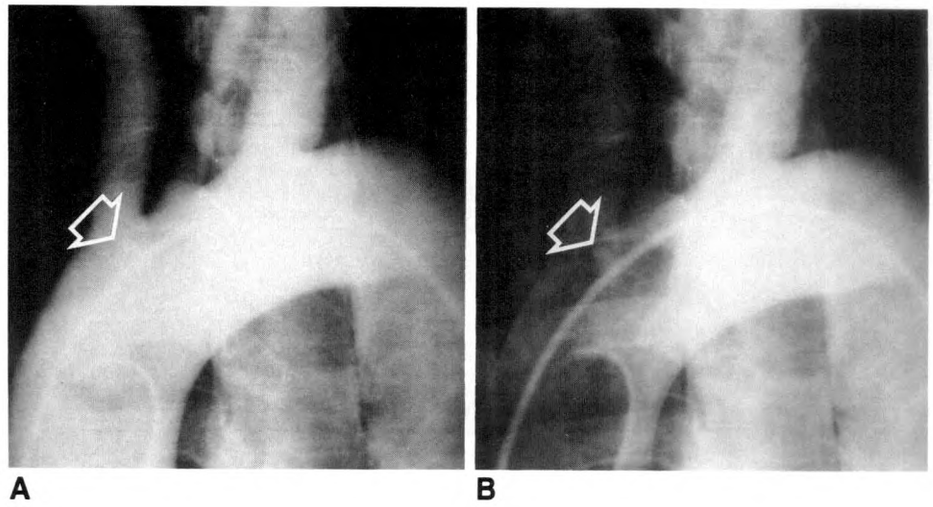


Fig. 1.—Case 1: 35-year-old man stabbed through thoracic inlet. Early-phase (*A*) and late-phase (*B*) arch aortogram shows subtle false aneurysm near orifice of innominate artery (*arrows*) that was recognized only in retrospect. Puncture of arch in this location was found at surgery.

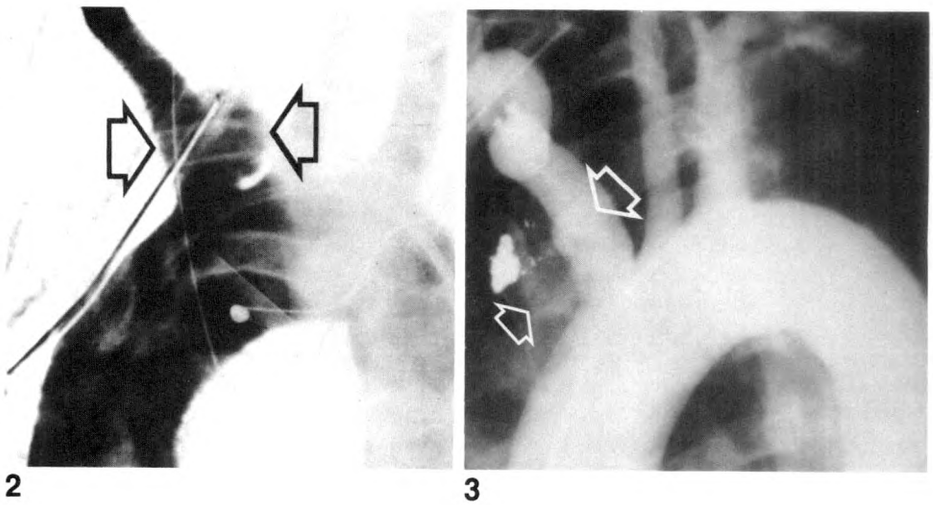


Fig. 2.—Case 7: 35-year-old man with multiple gunshot wounds. Surgery revealed entry hole in ascending aorta from a bullet that embolized to the right superficial femoral artery. Acute swelling of patient's neck developed while he was in the recovery room. Chest radiograph showed marked mediastinal widening; emergency aortogram reveals large false aneurysm arising from injury to proximal innominate artery (*arrows*).

Fig. 3.—Case 14: 46-year-old man with gunshot wound to the chest. Arch aortogram shows false aneurysm arising from innominate artery (*large arrow*) with adjacent frank extravasation (*small arrow*).

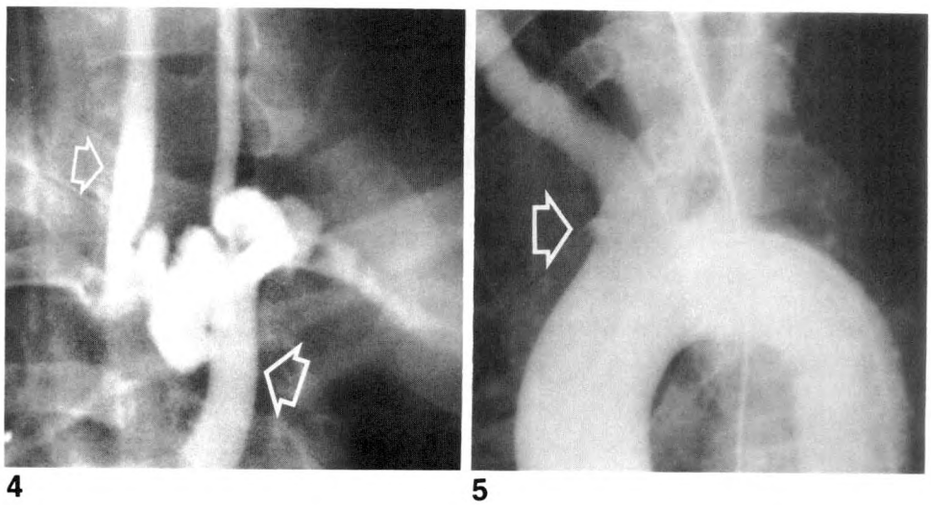
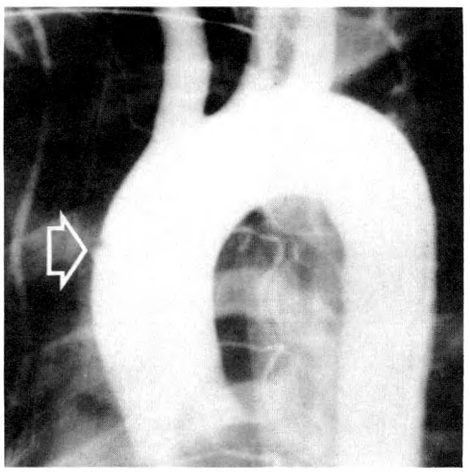


Fig. 4.—Case 10: 28-year-old man with gunshot wound to the chest. Selective left subclavian arteriogram shows large, multilobular false aneurysm and arterial-arterial fistula between left subclavian artery (*large arrow*) and left common carotid artery (*small arrow*).

Fig. 5.—Case 4: 33-year-old man with stab wound through thoracic inlet. Arch aortogram shows false aneurysm (*arrow*) arising from aortic arch near origin of innominate artery. Surgery revealed a 4-mm puncture wound in aortic arch.



6



7

Fig. 6.—Case 15: 29-year-old man with gunshot wound to the chest. Arch aortogram reveals irregular area in wall of innominate artery (*arrow*). At surgery this proved to be a concussion or blast injury.

Fig. 7.—Case 6: 20-year-old man with gunshot wound to the thorax. Chest radiograph indicated the bullet traversed the mediastinum. Arch aortogram shows subtle defect (*arrow*) in wall of ascending aorta. Left internal mammary artery (not shown) was occluded. Surgery revealed external surface of aorta to be intact. Palpable ridge in ascending aorta indicative of concussion or blast injury to media and/or intima was oversewn. Internal mammary artery proved to be transected and was ligated.

Discussion

There are relatively few reported examples of the angiographic diagnosis of penetrating intrathoracic vascular injuries. Two were described by Rich and Spencer [7] in 1978 and five more were subsequently recorded [8–12]. Other authors mentioned the use of preoperative angiography but did not provide good documentation of numbers of cases [13, 14]. Eighteen of the approximately 110 patients we evaluated proved to have aortic or brachiocephalic injuries.

Fifteen of 18 patients described here were accurately diagnosed preoperatively by angiography. One other patient deteriorated rapidly 2 days after a "negative" aortogram. Emergency surgery revealed a large puncture wound in the aortic arch between the innominate and left carotid arteries. A faint collection of contrast material from a false aneurysm was recognized in retrospect (Fig. 1). Nine injuries were clinically silent and nine had clinical and/or chest radiographic signs suspicious for vascular injury (Table 1).

Suspected proximity injury (injury in the vicinity of major vessels) on the basis of clinical evaluation and/or chest radiography was the sole indicator for angiography in the majority of our 110 cases, including seven of 16 positive studies (Table 1). This is sufficient reason for angiographic exploration in the stable patient, because some injuries can be clinically silent. O'Gorman et al. [6] convincingly demonstrated the significance of this concept in the evaluation of peripheral vascular injuries. In their series of 515 arteriograms, 352 (68%) were done with suspected injury close to a major vessel as the only indication; 59 (17%) of 352 were positive.

Most penetration vascular injuries are caused by direct perforation by a missile or knife. However, high-velocity missiles can produce a temporary cavity due to blast effect that greatly exceeds the diameter of the bullet-entry wound. This effect can stretch a vessel with considerable force. The thicker adventitial layer subsequently recoils, but the media and intima may be transected at that moment [15]. We prefer to describe these as concussion or blast injuries and reserve the term *proximity injury* for describing any penetrating injury (e.g., gunshot wound, stab wound) close to a major vessel. Arteriography can show concussion injuries, although they are indistinguishable from contact injuries (Figs. 6 and 7).

Snyder et al. [4] noted a sizable number (14) of false-positive arteriograms and one false-negative study in a series of 117 patients with penetrating injuries of the extremities. O'Gorman et al. [6] reported one false-negative and four false-positive arteriograms in 515 studies for penetrating extremity injuries. Allen et al. [16] and Hewitt et al. [17] each reported one false-negative thoracic aortogram in patients with a gunshot and stab wound, respectively.

Two of our 18 aortograms were false-negative results. There were no false-positive results. A subtle false aneurysm was overlooked (Fig. 1). A remarkably similar injury several years later was accurately diagnosed before surgery (Fig. 5). The diagnosis in a patient with a normal arteriogram (case 18) might have been established if multiple projections had been used. Surgery in this case revealed damage to the adventitia and media of the common carotid artery. The other patient with a false-negative angiogram (case 3) did not show a defect despite a through-and-through gunshot wound of the descending aorta.

Our experience shows the accuracy of arteriography in selected patients with penetrating thoracic injuries. Life-threatening injuries can be detected, many of which are clinically silent. In our series there were few false-negative or false-positive results.

REFERENCES

1. Parmley LF, Mattingly TW, Manion WC. Penetrating wounds of the heart and aorta. *Circulation* **1953**;17:953–973
2. Rich NM, Spencer FC. Injuries of the thoracic aorta. In: *Vascular trauma*. Philadelphia: Saunders, **1978**:425–440
3. Reul GJ Jr, Rubio PA, Beall AC Jr. The surgical management of acute injury to the thoracic aorta. *J Thorac Cardiovasc Surg* **1974**;67:272–291
4. Snyder WH III, Thal ER, Bridges RA, Gerlock JA, Perry MO, Williams JF. The validity of normal arteriography in penetrating trauma. *Arch Surg*

1978;113:424–428
5. Smith PL, Lim WN, Ferris EJ, Casali RE. Emergency arteriography in extremity trauma: assessment of indications. *AJR* **1981**;137:803–807
6. O'Gorman RB, Feliciano DV, Bitondo CG, Mattox KL, Burch JM, Jordan GL. Emergency center arteriography in the evaluation of suspected peripheral vascular injuries. *Arch Surg* **1984**;119:568–573
7. Rich NM, Spencer FC. Injuries of the intrathoracic branches of the aortic arch. In: *Vascular trauma*. Philadelphia: Saunders, **1978**:287–306
8. Shin M, Soto B, Baxley WA. Azygos dilatation due to traumatic aortoazygos fistula. *AJR* **1979**;133:758–759
9. Martinez E, Miller J, Godoy M, Lourenco J, Herrmann V, Buffolo E. Arteriovenous fistula of the thoracic aorta: report of a case presenting with superior vena cava obstruction. *Thorax* **1981**;36:315–318
10. Snow N, Johnson P. Traumatic fistula between the descending thoracic aorta and the left main pulmonary artery. *J Trauma* **1985**;25:263–265
11. Syracuse DC, Seaver PR Jr, Amato JJ. Aortic gunshot injury and paraplegia: preoperative definition with arteriography and computerized axial tomography. *J Trauma* **1985**;25:271–273
12. Cooley RN, Schreiber MH. Trauma to the heart and great vessels. In: *Radiology of heart and great vessels*, 3rd ed. Baltimore: Williams & Wilkins, **1978**:562–569
13. Sclafani SJA, Cooper R, Shaftan GW, Goldstein AS, Glanz S, Gordon DH. Arterial trauma: diagnostic and therapeutic angiography. *Radiology* **1986**;161:165–172
14. Robbs JV, Baker LW, Human RR, Vawda IS, Duncan H, Rajaruthnam P. Cervicomediastinal arterial injuries. *Arch Surg* **1981**;116:663–667
15. Rapaport A, Feliciano DV, Mattox KL. An epidemiologic profile of urban trauma in America—Houston style. *Tex Med* **1982**;78:44–50
16. Allen TW, Reul GJ Jr, Morton JR, Beall AC Jr. Surgical management of aortic trauma. *J Trauma* **1972**;12:862–868
17. Hewitt RL, Smith AD, Becker ML, Lindsey ES, Dowling JB, Drapanas T. Penetrating vascular injuries of the thoracic outlet. *Surg* **1974**;76:715–722

FORTHCOMING ARTICLES

PROGRESS IN RADIOLOGY

Intravascular contrast media: adverse reactions. *Cohan RH, Dunnick NR*

CARDIOPULMONARY RADIOLOGY

Noninfectious complications of long-term central venous catheters: radiologic evaluation and management. *Cassidy FP Jr, Zajko AB, Bron KM, Reilly JJ Jr, Peitzman AB, Steed DL*

Thrombosis of upper extremity thoracic inlet veins: diagnosis with duplex Doppler sonography. *Falk RL, Smith DF*

Accuracy of CT in evaluating mediastinal lymph nodes in lung cancer: influence of the lobar site of the primary neoplasm. *Platt JF, Glazer GM, Gross BH, Quint LE, Francis IR, Orringer MB*

CT of interpectoral lymph nodes. *Holbert BL, Holbert JM, Libshitz HI*

Ventricular septal defect: visualization of shunt flow and determination of shunt size by cine MR Imaging. *Sechtem U, Pflugfelder P, Cassidy MC, Holt W, Wolfe C, Higgins CB*

Pictorial essay. The anatomy of the pericardial space: a study in cadavers and patients. *Choe YH, Jung-Gi I, Park JH, Han MC, Kim C-W*

Case report. Strut fracture of a Bjork-Shiley mitral valve prosthesis. *Hayne LA, Schmidt R, Marglin SI*

BREAST RADIOLOGY

The halo sign and malignant breast lesions. *Swann CA, Kopans DB, Koerner FC, McCarthy KA, White G, Hall D*

GASTROINTESTINAL RADIOLOGY

Hemodynamic Changes in Portal Circulation After Portosystemic Shunts: Use of duplex sonography in 43 patients. *Lafortune M, Patriquin H, Pomier G, et al.*

Mesoatrial shunt for the treatment of Budd-Chiari syndrome: radiologic evaluation in eight patients. *Chezmar JL, Bernardino ME*

Intrahepatic portosystemic venous shunt: occurrence in patients with and without liver cirrhosis. *Mori H, Hayashi K, Fukuda T, et al.*

Intraperitoneal hemorrhage due to spontaneous rupture of hepatocellular carcinoma: treatment by hepatic artery embolization. *Hsieh J-S, Huang C-J, Huang Y-S, Sheen P-C, Huang T-J*

Case report. Hepatocellular carcinoma: MR appearance mimicking focal nodular hyperplasia. *Wilbur AC, Gyi B*

MR imaging of ferrite-enhanced detection splenic lesions: in rats. *Weissleder R, Hahn PF, Stark DD, et al.*

Splenic trauma: false-negative CT diagnosis in cases of delayed rupture. *Pappas D, Mirvis SE, Crepps JT*

Case report. Dorsal pancreas presenting as a mass in the chest. *Coral A, Jones SN, Lees WR*

Case report. Esophageal mucocele after surgical isolation of the esophagus. *Glickstein MF, Gefter WB, Low D, Stephenson LW*

Sonographic diagnosis of neutropenic typhlitis. *Teefey SA, Montana MA, Goldfogel GA, Shuman WP*

Case report. Strangulation of the colon caused by an intestinal decompression tube: radiographic findings. *Yoshino MT, Boyle RR Jr*

GENITOURINARY AND OBSTETRIC RADIOLOGY

Subchorionic hemorrhage: sonographic diagnosis and clinical significance. *Abu-Yousef MM, Bleicher JJ*

Case report. Diagnosis of ureteral stump transitional cell carcinoma by CT and MR imaging. *Jaffe J, Friedman AC, Seidmon EJ, Radecki PD, Lev-Toaff AS, Caroline DF*

MUSCULOSKELETAL RADIOLOGY

Radiographic evaluation of joints resurfaced with osteochondral shell allografts. *Kusnick C, Hayward I, Sartoris DJ, et al.*

CT arthrographic patterns in recurrent glenohumeral instability. *Singson RD, Feldman F, Bigliani L*

High-resolution CT of the wrist: initial experience with scaphoid disorders and surgical fusions. *Bush C, Gillespy T III, Dell PC*

Technical note. Identification of torn intercarpal ligaments by using fluoroscopy after the injection of contrast material. *Gilula LA, Hardy DC, Totty WG, Reinus WR*

Hemangiomas of skeletal muscle: MR findings in five patients. *Yuh WTC, Kathol MH, Sein MA, Ehara S, Chiu L*

Case report. An unusual form of tibial sarcoidosis. *Beasley EW III, Peterman SB, Hertzler GL*

INTERVENTIONAL RADIOLOGY

Sonography of thigh abscess: detection, diagnosis, and drainage. *van-Sonnenberg E, Wittich GR, Casola G, Cabrera OA, Gosink BB, Resnick DL*

Treatment of frostbite with IV streptokinase: an experimental study in rabbits. *Salimi Z, Wolverson MK, Herbold DR, Vas W, Salimi A*

Technical note. Modified use of the tip-deflecting wire in manipulation of foreign bodies. *Nemcek AA Jr, Vogelzang RL*

NEURORADIOLOGY

Commentary. Imaging recommendations for head trauma: a new comprehensive strategy. *Thornbury JR, Masters SJ, Campbell JA*

Non-Hodgkin's lymphoma of the head and neck: CT evaluation of nodal and extranodal sites. *Harnsberger HR, Bragg DG, Osborn AG, et al.*

"Papilledema": neuroradiologic evaluation of optic disk protrusion with dynamic orbital CT. *Jinkins JR*

The diagnostic accuracy of preoperative CT scanning in the evaluation of pituitary ACTH-secreting adenomas. *Marcovitz S, Wee R, Chan J, Hardy J*

MR evaluation of Hydrocephalus. *El Gammal T, Allen MB Jr, Brooks BS, Mark EK*

MAGNETIC RESONANCE IMAGING

Perspective. MR sequence parameter optimization: an algorithmic approach. *Bradley WG Jr, Tsuruda JS*

Hybrid color MR imaging display. *Weiss KL, Stiving SO, Herderick EE, Cornhill JF, Chakeres DW*

Review article. The biophysical basis of tissue contrast in extracranial MR imaging. *Mitchell DG, Burk DL Jr, Vinitski S, Rifkin MD*

Magnetite albumin suspension: a superparamagnetic oral MR imaging contrast agent. *Widder DJ, Edelman RR, Grief WL, Monda L, Widder KJ*

Technical note. MR imaging of ventilator-dependent patients: preliminary experience. *Mirvis SE, Borg U, Belzberg H*

DIGITAL RADIOLOGY

A digital radiology imaging system: description and clinical evaluation. *Templeton AW, Dwyer SJ IV, Cox GG, et al.*

Evaluation of dry silver hard copies in digital radiography. *Trefler M, Yrizarry J*

Angiography in Patients with Arterial Trauma: Correlation Between Angiographic Abnormalities, Operative Findings, and Clinical Outcome

Steven C. Rose[1]
Ernest E. Moore[2]

The arteriograms and clinical course of 280 consecutive patients with suspected arterial trauma were reviewed to correlate the angiographic abnormalities with operative findings and to assess the impact of these findings on surgical management and prognosis. Major angiographic abnormalities were found in 77 patients. Arterial occlusion (46 patients) was caused by intimal flap injury or arterial transection with subsequent thrombosis and frequently presented with an acutely ischemic extremity (27 patients, three of whom required subsequent amputations). Intraluminal defects typical for intimal flaps (20 patients) were the most difficult pathologic entity to diagnose, accounting for two false-positive angiograms and the sole false-negative examination. Focal luminal widening (five patients) corresponded with a partial-thickness injury of the arterial wall. Major angiographic extravasation of contrast material (19 patients) was caused by arterial laceration or transection and usually presented with clinical signs of acute hemorrhage; massive pelvic hemorrhage was the cause of death in three patients. Acute arteriovenous fistulas (four patients) were from arterial laceration with venous communication. Arterial narrowing with a smooth margin (50 patients) was a finding associated with a benign clinical course, except when combined with slowed arterial flow—a characteristic finding of compartment syndrome (six of 13 patients). An irregular beaded pattern of arterial narrowing (23 patients) was associated with severe injuries, subsequent poor fracture healing, and wound infection.

A detailed angiographic map is of considerable value in planning surgical management. The absence of major angiographic abnormalities usually eliminates the need for surgical exploration; the location of injury and routes of distal blood flow affect the feasibility of conservative therapy; the length of occlusion influences the necessity of saphenous vein harvesting; the location of arterial extravasation determines the advisability of surgical ligation or transcatheter embolization; and the need for fasciotomy may be suggested first by the angiographic features of compartment syndrome.

Surgical repair of vascular injuries has improved substantially since World War II, and the incidence of acute trauma resulting in vascular injuries continues to rise [1, 2]. These developments have increased the need for angiography to screen patients with suspected arterial injury [3, 4]. The goals of diagnostic angiography are to document the presence or absence of vascular injury and secondarily to locate and characterize the injury and collateral circulation. Although a range of specific angiographic abnormalities have been described, questions have arisen as to how these arteriographic findings relate to the actual vascular injury observed during surgery and whether surgical management or patient prognosis is affected by the type of angiographic abnormality found. The purpose of this review was to characterize the angiographic abnormalities, correlate them with operative findings, and evaluate their significance with respect to operative or angiographic intervention as well as clinical outcome.

Materials and Methods

During the 7 years ending December 31, 1985, 300 consecutive angiograms were obtained in 297 acutely injured patients suspected to have acute extremity or torso arterial injuries;

Received March 20, 1987; accepted after revision May 19, 1987.

[1] Department of Radiology, Denver General Hospital, Denver, CO 80204. Present address: Department of Radiology, Duke University Medical Center, Box 3808, Durham, NC 27710. Address reprint requests to S. C. Rose.

[2] Department of Surgery, Denver General Hospital, Denver, CO 80204.

AJR 149:613–619, September 1987
0361–803X/87/1493–0613
© American Roentgen Ray Society

these did not include cases of blunt decelerating chest trauma in which aortic transection was suspected. Two hundred seventy-nine charts and 246 angiographic studies were available and were reviewed for injury mechanism, physical findings, angiographic features, operative reports, and clinical follow-up. Adequate information was available in 280 of the 297 cases to correlate the angiographic abnormalities with the operative findings (when performed) and clinical course.

Arch aortography was performed with 6- or 7-French pigtail catheters, abdominal aortic injections with 6-French pigtail or multiple-side-hole straight catheters, and selective extremity or visceral injections with 6-French end-hole selective catheters. Renografin 76% (Squibb, Princeton, NJ) was the contrast agent used in all but the carotid or renal artery injections, in which Renografin 60% was used. Neither arterially injected tolazoline nor reactive hyperemia was used. The mode of contrast injection was aortic (retrograde) in 40%, antegrade selective arterial in 55%, retrograde selective arterial in 3%, and unrecorded in 1%. Conventional serial filming was used in all studies.

The cause of injury was a gunshot wound in 163 (55%), laceration in 51 (17%), and blunt injury in 82 (27%). Four cases (1%) did not fit well into the above categories and included two arterial-puncture-site complications of cardiac catheterization, one leg degloving injury (extensive flaplike soft-tissue avulsion involving an extremity), and one near amputation of a shoulder.

Mean age was 31.8 years old (range, 3–90); 248 (89%) patients were men. Mean hospitalization time was 13.4 days (range, 1–187 days); mean follow-up period was 8.3 months (range, 1 day to 6 years 10 months); and mean number of follow-up visits and readmissions was 4.5 (range, 0–46).

Major vessels were defined as those that provide blood flow to the head, distal extremities, viscera, or pelvis. These included the brachiocephalic vessels; the axillary, brachial, iliac, femoral, and popliteal arteries; the trifurcation vessels of both upper and lower extremities; the main and segmental renal arteries; and large pelvic arterial branches. The deep femoral artery was included with minor vessels. Major arterial injury was categorized as a major vessel affected by a major angiographic abnormality. All other combinations were classed as minor arterial injuries.

Major angiographic abnormalities were defined as occlusion of the lumen, the presence of a constant filling defect within the opacified lumen, focal widening of the arterial lumen with prompt washout of contrast material (pseudoaneurysm formation), arteriovenous fistulization, and extravasation of contrast material [5, 6]. Arterial extravasation was distinguished by contrast material flowing from the arterial lumen to an extravascular space via a narrow neck. Minor angiographic abnormalities were defined as narrowing of the arterial lumen, deviation of the arterial course, and slowed arterial flow. Luminal narrowing was assessed for severity (mild, less than 25%; moderate, 25–75%; or marked, greater than 75%), length (short, less than 5 cm; medium, 5–10 cm; or long, greater than 10 cm), and wall characteristics (smooth or irregular). Slow flow was arbitrarily defined as the presence of contrast material in the arterial phase for more than 20 sec after termination of injection.

Results

Major abnormalities

Seventy-seven (28%) of our 280 patients had a major arterial injury on angiography. Operative exploration of the arteries was performed in 74 patients, including 60 of 77 patients angiographically noted to have major arterial injury and 14 of 203 patients with either minor or no angiographic abnormalities.

Arterial occlusion.—Occlusion of the arterial lumen was the most common major angiographic abnormality, occurring in 59 (21%) patients. In 13 (5%) of these patients occlusion was limited to minor vessels, and no clinical sequelae were noted. The other 46 (16%) patients had a total of 58 major vessel occlusions; 44 cases involved extremity arteries and two cases involved segmental renal arteries (Table 1). Simultaneous injury of multiple arteries occurred primarily in parallel vessels (eight patients) rather than in vessels in series (one case). The length of occlusion in 56 affected major extremity arteries was short (<5 cm) in six (11%), medium (5–10 cm) in three (5%), and long (>10 cm) in 47 (84%). Distal reconstitution was angiographically present in 19 (34%) of 56 major extremity artery occlusions. The likelihood of reconstitution varied greatly depending on the anatomic site. Distal reconstitution was present in 12 (86%) of 14 cases of extremity artery occlusions that occurred proximal to the elbow or thigh adductor hiatus, but in only seven (17%) of 42 cases of arterial occlusion distal to these landmarks.

Operative correlation was available in 36 of 44 patients with occlusion of major extremity arteries. Vessel transection with thrombosis was present in 23 cases and an intimal flap with thrombosis in 11. The angiographic appearance was

TABLE 1: Summary of Vascular and Nonvascular Complications for Individual Major Angiographic Abnormalities

Angiographic Abnormality	No. of Patients ($n = 77$)	No. of Injured Arteries	Mean Follow-Up (months)	No. of Patients (%)			
				Vascular Deaths	Amputation	Delayed Union of Fractures	Wound Infection
Occlusion	46	58	10	0	3[a] (7)	11/29 (38)	12 (26)
Intimal flap	20	23	11	0	0	6/15 (40)	4 (20)
Pseudoaneurysm	5	6	7	0	0	1/3 (33)	0
Extravasation	19	19	13	2[b] (11)	1[a] (5)	0/10	0
Arteriovenous fistula	4	4	16	0	0	0/2	0

[a] A patient who underwent a delayed amputation had occlusion of the anterior tibial and peroneal arteries with extravasation of contrast material from the posterior tibial artery.

[b] Does not include one additional patient who died from complications arising from a massive pelvic hemorrhage treated with external pelvic fixation before angiography.

identical in both groups. Angiographically, the popliteal artery tapered to full occlusion in one patient with compartment syndrome of the calf; after fasciotomy, the popliteal artery was normal by external inspection and intraoperative angiography. Arterial occlusion was caused by entrapment within a pelvic fracture in another case; after operative release, the external iliac artery appeared normal and distal pulses returned. Wound debridement without arterial exploration was used in eight patients.

Intraluminal defects.—Constant intraluminal defects of the major arteries were present in 30 patients. Twenty-three (77%) of these defects in 20 patients were interpreted as probable intimal flap injuries (Table 1). The angiographic films were available for analysis of the morphologic appearance in 19 cases. Inconstant filling defects were believed to represent flow artifacts caused by unopacified blood, and were not associated with clinical sequelae. In five patients the defects were contiguous to an occlusion, longitudinally oriented with respect to the vessel, and interpreted as the trailing edge of thrombus (Fig. 1). Surgical correlation was available in three patients. All contained intraarterial thrombus with underlying vessel transection (two cases) or an intimal flap (one).

Angiograms were interpreted as probable intimal flaps in 14 patients: the filling defects were attached to the vessel wall on at least one projection and were not adjacent to an occlusion. Surgical proof was obtained in seven cases, and it confirmed isolated intimal injury. The intraluminal filling defects appeared as either a thin transverse strip (Fig. 2) or a globule (Fig. 3). In no case did a proven intimal flap appear angiographically as a thin longitudinal strip—a helpful differential point with respect to flow artifacts.

Focal lumen widening (pseudoaneurysm).—Focal widening of the major arterial lumen suggestive of pseudoaneurysm formation was noted in five patients. Operative exploration in one patient confirmed the presence of an intimal flap injury with extension into the tunica media and pseudoaneurysm formation.

Extravasation of contrast material.—Extravasation from a major artery was evident in 19 patients with 19 lesions that involved the extremity arteries (nine patients), segmental renal arteries (five patients), and pelvic branch arteries (five patients). Operative correlation was available in 12 cases. Arterial laceration was found in nine patients and arterial transection in three.

Arteriovenous fistulas.—Four acute arteriovenous fistulas were identified. Three had no distal arterial flow, presumably because of arteriovenous shunting. Operative correlation was available in two cases in which arterial laceration with venous communication was confirmed.

Minor Abnormalities

Arterial narrowing.—Angiographic narrowing of major arteries occurred in 109 vessels in 76 patients. Multiple artery involvement was common in the calf (52) and forearm (nine). Angiographic studies were available for review in 73 of the 76 patients with arterial narrowing (Table 2). Arterial narrowing appeared either as a smooth, gradually tapered segment (50 patients) or as multiple areas of irregular constriction (23 patients) (Fig. 4). The irregular type of arterial narrowing was distinguished from stationary-wave artifacts by the presence of a narrowed lumen and the absence of regular periodicity. Generally, narrowed arterial segments were not explored; therefore, operative correlation was unavailable. In one case of severe posterior tibial artery narrowing, an intimal flap injury was discovered at exploration.

Slow arterial flow.—Slowed blood flow within major arteries was present in 13 patients. Five cases (38%) occurred in patients with compartment syndrome. Upstream flow limiting arterial lesions not associated with compartment syndrome

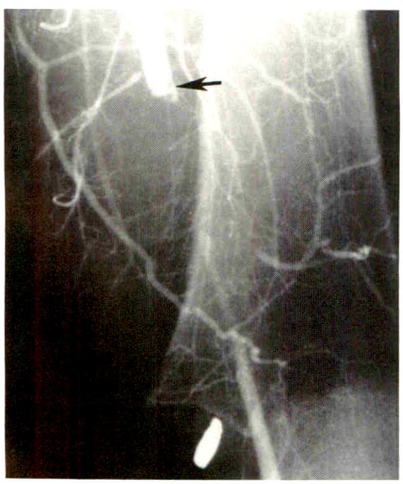


Fig. 1.—Intraluminal filling defect created by operatively proved thrombus (*arrow*) extending axially from occluded distal superficial femoral artery. Bullet fragment is present distally.

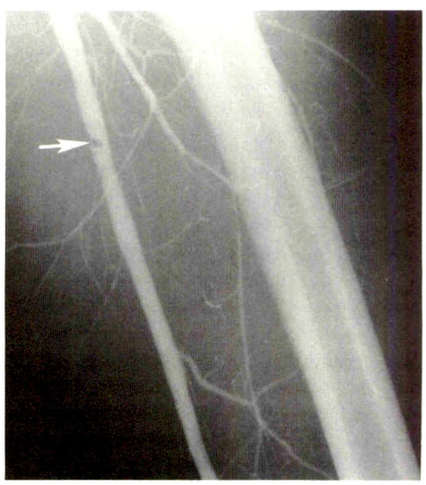


Fig. 2.—Intraluminal filling defect created by operatively documented intimal flap (*arrow*) of superficial femoral artery, transverse type, in patient with gunshot wound.

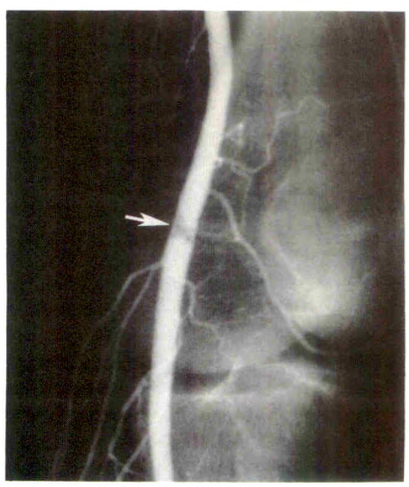


Fig. 3.—Lateral view of globular intraluminal filling defect created by operatively documented intimal flap (*arrow*) involving popliteal artery.

TABLE 2: Association of Nonvascular Sequelae with Morphologic Appearance and Severity of Arterial Narrowing

Arterial Characteristic	No. of Patients (%)			
	Total	With Wound Infections	With Associated Fractures	With Delayed Union or Nonunion
Appearance of vessel wall:				
Smooth	50	3 (6)	25 (50)	2/25 (8)
Irregular	23	5 (22)	22 (96)	11/22 (50)
Severity of narrowing:				
Mild	42	3 (7)	23 (55)	3/23 (13)
Moderate	12	2 (17)	7 (58)	3/7 (43)
Severe	19	3 (16)	17 (89)	7/17 (41)

Note.—Narrowing is mild if it is less than 25% of lumen diameter, moderate if 25–75% of lumen diameter, and severe if more than 75% of lumen diameter.

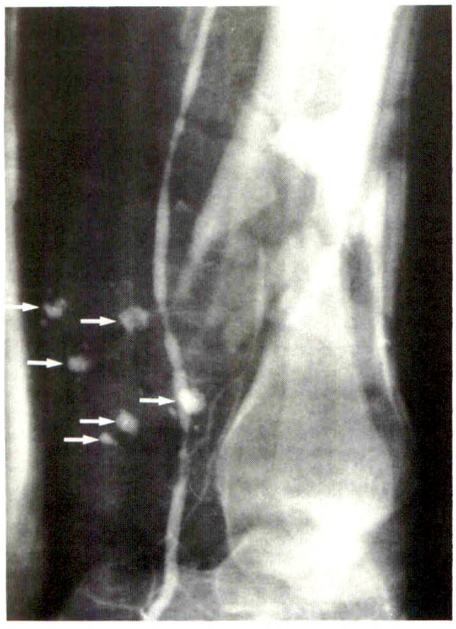


Fig. 4.—Lateral view of distal leg shows the irregular-type narrowing of anterior and posterior tibial arteries adjacent to comminuted distal tibial and fibular fractures. Peroneal artery is occluded at more proximal fracture site, with distal reconstitution. Gravel is present posteriorly (*arrows*). Subsequent course was complicated by fracture nonunion.



Fig. 5.—Lateral view of leg in patient with documented compartment syndrome. All arteries are smoothly narrowed and arterial flow is slow (film obtained 25 sec after injection of contrast material).

was found in six (46%) patients: one occlusion, three intimal flaps, and two areas of moderate-to-severe narrowing. In two (15%), the distal pulses were normal, as were the angiographic examinations.

Arterial deviation.—The course of a major artery was deviated in 45 patients. In no case was arterial deviation responsible for pulse abnormality, subsequent vascular compromise, or surgical intervention.

Compartment syndrome. Compartment syndrome was diagnosed clinically in 13 patients and confirmed by elevated compartment pressures and bulging pale musculature at the time of fasciotomy. Eleven occurred in the calf, one in the forearm, and one in the upper arm. Major arterial injury was found angiographically in nine patients (69%). Nonreconstituted occlusion of the popliteal artery (two patients) or trifurcation arteries (five patients) was the arterial injury found in seven cases of calf compartment syndrome. Brachial artery occlusion occurred in the one case of upper-arm compartment syndrome. Extravasation from the ulnar artery was present in the case of forearm compartment syndrome. Six (46%) of the 13 patients with compartment syndrome displayed long segments of arterial narrowing and five of six had slowed arterial flow of multiple calf trifurcation vessels (Fig. 5). The one normal angiogram preceded the onset of compartment syndrome by 4 hr.

Surgical Management

Occlusion.—Location of extremity arterial occlusion and the presence or absence of distal ischemia determined which patients underwent primary vascular repair. Surgical management in 17 patients was limited to wound debridement (11

patients) or arterial ligation (six patients); calf injury was usually involved, with at least one patent trifurcation artery and no clinical signs of ischemia (14 patients). Alternatively, most patients with extremity artery occlusion proximal to the knee or elbow (17 patients) underwent primary vascular repair. In addition, vascular repair was performed in nine patients with occlusion of multiple calf trifurcation arteries and ischemia.

The type of primary vascular repair reflected the length of angiographic arterial occlusion. Five patients with short segmental arterial occlusion underwent vascular repair; resection of the injured segment with end-to-end anastomosis was performed in each case. Only six of 21 patients who had medium- or long-segment angiographic occlusion were repaired with resection and end-to-end anastomosis; 15 required saphenous vein interposition grafting.

Intimal flap.—Twenty patients had angiographic intraluminal filling defects interpreted as probable intimal flap injury. Six cases were managed by observation; two other cases were explored and found to have normal popliteal arteries by external inspection. In retrospect, one of these was most likely an angiographic flow artifact (false-positive angiogram) and the other an operatively missed intimal injury with the normal appearance of the arterial adventitia (false-negative surgery). Twelve cases were managed with primary vascular repair. Resection with end-to-end anastomosis was the most commonly employed technique of vascular repair (nine patients), with occasional use of primary arterial wall repair (one patient), vein patch angioplasty (one patient), and resection with saphenous vein interposition grafting (one patient).

Focal lumen widening (pseudoaneurysm).—Primary vascular repair was performed in only one of three patients with pseudoaneurysm formation of a major extremity artery; resection with end-to-end anastomosis was performed. Two cases of pseudoaneurysm formation of extremity arteries as well as one case with segmental renal artery involvement were followed expectantly. An additional patient with injury to three segmental renal arteries underwent successful transcatheter embolization.

Extravasation.—Surgical intervention included arterial ligation (three patients, all with calf trifurcation-artery injuries), primary suture repair of the arterial laceration (two patients), resection with end-to-end anastomosis (five patients), resection with saphenous vein bypass graft (one patient with avulsion of a long arterial segment), and external pelvic fixation (two patients). Transcatheter embolization successfully achieved hemostasis in four cases of arterial extravasation: three segmental renal artery injuries and one pelvic injury. Embolotherapy in a fourth renal injury failed because of the massive flow rate through a large arterial laceration. Two cases (one patient with segmental renal artery injury and one patient with calf trifurcation-artery injury) were observed.

Arteriovenous fistulas.—The two patients with arteriovenous fistulas of large extremity arteries underwent primary vascular repair. Two additional cases were managed expectantly (one patient with segmental renal artery injury and one patient with tibioperoneal trunk injury).

Minor or no abnormalities.—In 203 cases, arteries were angiographically normal or exhibited only minor abnormalities; 182 (90%) of these patients were spared operative exploration and sustained no vascular sequelae. The other 21 cases that were explored surgically had clinical findings that strongly suggested arterial injury and/or required repair of adjacent venous or neural structures; arterial normalcy was confirmed and local wound care rendered.

Prognosis

Occlusion.—Thirty-two (11%) of the 280 patients presented with physical signs of an acutely ischemic extremity manifested by absent or diminished distal pulses in conjunction with extremity coolness, cyanosis, pallor, or poor capillary refill. Twenty-seven (84%) had major arterial injury; all of these had arterial occlusion as part of the injury complex. Limb amputation occurred in three of the 280 reviewed patients; in all cases, arterial occlusion was the dominant angiographic finding. Nonvascular sequelae are summarized in Table 1.

Intimal flaps.—Intimal flaps identified angiographically were not repaired in seven cases. No early vascular sequelae occurred. One patient with bilateral popliteal pseudoaneurysms and intimal-flap injuries developed new-onset claudication and loss of the pedal pulses bilaterally 2.5 years after the initial injury. This patient did not return for a repeat angiographic study and was lost to follow-up. Another patient with an intimal-flap injury on the initial angiogram had repeat angiography 1 month later; the second study demonstrated an angiographic pseudoaneurysm that was subsequently repaired. The remaining patients who underwent vascular repairs have not had vascular complications during a mean follow-up of 11 months. Nonvascular complications are presented in Table 1.

Focal lumen widening (pseudoaneurysm).—In one case, an initial angiographic intraluminal filling defect (intimal flap) progressed to focal lumen widening (confirmed pseudoaneurysm) 4 weeks later. Another patient with bilateral intimal flaps and pseudoaneurysm of the popliteal artery developed late claudication. Both cases were discussed under intimal flaps. A third patient with an angiographic pseudoaneurysm was studied again 1 month later; the angiographic appearance remained unchanged. He remained asymptomatic for 4 months, at which point he was lost to clinical follow-up. Hematuria in both patients with involvement of segmental renal arteries resolved. Nonvascular sequelae are given in Table 1.

Extravasation of contrast material.—Most of the 19 patients with major angiographic extravasation presented with clinical signs of substantial blood loss, including hypotension in nine (47%), acute anemia in eight (42%), expanding or large hematoma in five (26%), pulsatile external bleeding in three (16%), gross hematuria in five (26%), and widened mediastinum in one (5%). The mean transfusion requirement in these patients was nine units of blood. Three deaths related to vascular injury occurred in the 280 reviewed patients; all were multiple trauma patients with massive pelvic hemorrhage. In two cases, angiography showed extravasation from pelvic branch arteries; the third case confirmed hemostasis after placement of external pelvic fixators. Fracture nonunion and

wound infections did not occur in these 19 patients. Fifteen patients had extravasation from minor branch arteries. None of these patients had clinical sequelae, though arterial ligation was used frequently during subsequent wound debridement.

Arteriovenous fistulas.—All four patients had uneventful recoveries and no nonvascular complications occurred.

Arterial narrowing.—Surgical intervention and vascular clinical sequelae were related only to concomitant major arterial injury (25 cases). However, late nonvascular complications were common in the patients with morphologically irregular or severe arterial narrowing (Table 2); both of these features were commonly observed in patients with more severe injuries.

Discussion

Angiography is an excellent method of assessing the presence or absence of major arterial trauma in injured patients [3, 4, 6, 7]. The angiographic image should reflect the gross pathologic state, and therefore provide insight to the severity of the arterial injury, existence of concomitant compartment syndrome, urgency and manner of corrective action, and likelihood of complicated healing.

In our series, angiographic arterial occlusion was caused by arterial transection with secondary vasoocclusion or intimal injury with secondary thrombosis; the angiographic appearance was identical [6, 8]. Arterial occlusion of the proximal extremities was likely to be reconstituted, whereas distal occlusion was not. In most cases, patients without signs of extremity ischemia and at least one patent major artery distal to the elbow or knee were safely treated conservatively. Those patients with evidence of ischemia, multiple vessel injury distal to the knee or elbow, or major arterial occlusion proximal to these landmarks were managed with primary vascular repair. Short-segment involvement angiographically was an indication that arterial repair could be accomplished with an end-to-end anastomosis. Long segments of arterial occlusion may be rendered patent with the use of a Fogarty-balloon thrombectomy catheter, allowing limited resection and end-to-end anastomosis in selected cases. However, in our series the angiographic finding of long-segment arterial occlusion was commonly suggestive that saphenous vein harvest for interposition grafting may be necessary. As expected, major extremity arterial occlusion was frequently associated with abnormal distal pulses and signs of ischemia. The limb-threatening nature of arterial occlusion was confirmed by the fact that all three patients who required amputation had arterial occlusion angiographically. Nonvascular complications of healing—specifically, poor osseous union of associated fractures, osteomyelitis, or soft-tissue infections—were relatively common.

Intraluminal filling defects may represent thrombus, intimal injury, or lamellar flow artifacts. In our series, filling defects that protruded axially into the lumen from an occluded segment were found to represent the trailing edge of thrombus. If the defect was relatively constant over time and appeared as a thin transverse band or as an oblique globule, the diagnosis of an intimal flap was secure [9]. Lamellar flow defects were evanescent longitudinal strips that extended from curved arterial surfaces. A missed intimal flap contributed the one false-negative angiogram, and intraluminal filling defects accounted for one and possibly two false-positive angiograms. From a diagnostic standpoint, intimal flaps remain the most challenging type of major arterial injury. The limited nature of intimal-flap injuries permitted resection with end-to-end anastomosis in most cases. The natural history of angiographically identified nonocclusive intimal flaps has not been addressed in the literature. Our limited experience with seven patients suggests that arteries having isolated intimal-flap injuries at the time of angiography are unlikely to thrombose in the near future, though there is increased risk of late occlusion or progression to chronic pseudoaneurysm formation. The incidence of nonvascular sequelae are also increased in the presence of angiographic intimal flaps.

Focal widening of the arterial lumen with rapid washout of contrast material was an infrequent angiographic finding that correlated with a partial-thickness injury of the arterial wall (acute pseudoaneurysm) [5, 10]. Vascular repair involved limited resection. The number of patients with angiographic acute pseudoaneurysm formation was too small to draw conclusions regarding the natural history of this abnormality.

Extravascular contrast material that communicated with the arterial lumen via a narrow neck, occupied a cavity with smooth or feathered margins, and had delayed washout correlated well with the operative finding of a full-thickness arterial wall injury (arterial laceration or transection) [5, 6]. Arterial occlusion via surgical ligation (extremity injuries), transcatheter embolization (renal or pelvic injuries), or orthopedic compression (pelvic injuries) was used to arrest hemorrhage in noncrucial arteries [6, 11–15]. Arteries requiring continued patency were repaired with suture of the laceration or resection and end-to-end anastomosis [2]. The serious hemodynamic consequences of major arterial extravasation were apparent by the many clinical signs of acute hemorrhage manifested in our patient group. This point was underscored by the occurrence of three vascular deaths in patients with massive pelvic fractures.

Arteriovenous fistulas were infrequent angiographic findings in our series and correlated with arterial laceration and venous communication [10]. Early venous shunting caused by loss of small-vessel vasomotor tone in ischemic or contused regions may simulate an arteriovenous fistula [16]. Identification of a discrete point of brisk artery to vein communication allows differentiation.

Arterial narrowing was present in two relatively distinct forms. In one, the outer margin was smoothly tapered. Most likely this narrowing was secondary to arterial spasm or extrinsic compression. The association of long-segment, smooth-type arterial narrowing and concomitant slow arterial flow was noted in several cases of documented compartment syndrome. Usually the diagnosis of compartment syndrome is made on the basis of ischemic symptoms and neurologic abnormalities and confirmed by measurement of intracompartmental pressures [17]. In comatose patients or those with multiple injuries, the clinical findings of compartment syndrome may be easily overlooked; recognition of the constellation of angiographic findings in this abnormality may be instrumental in detecting compartment syndrome at a reversible stage.

The second morphologic type of arterial narrowing was

characterized by irregular margins of the lumen, often with a beaded appearance. The zone of transition to the more normal artery was frequently abrupt. Patients in this group almost invariably had an associated fracture that frequently was complicated by delayed union; skeletal or wound infections were also common complications of healing. Only one of these irregularly narrowed injuries was explored surgically, and it proved to be an intimal injury. Clinical follow-up of the others showed that vascular integrity (intact distal pulses) had been maintained. Although further evaluation is needed to ascertain the significance of this angiographic sign, this irregular type of arterial narrowing may be a useful marker for injuries caused by severe shock-wave or shearing-type forces, with regional tissues devitalized either directly or indirectly by microvascular insult. Laasonen [18] reported a high rate of limb amputation when severe angiographic arterial narrowing was present. The irregular morphology may be secondary to separation of the intima and media or to localized intense arterial spasm.

Slowed arterial flow in most cases was attributable either to angiographically definable arterial inflow lesions or to compartment syndrome. Slowed arterial flow in those patients with otherwise normal angiograms may be secondary to altered arteriolar or capillary basal motor tone, such as that seen in soft-tissue contusions [19]. Deviation in the arterial course is unassociated with vascular complications. When the major type of angiographic features occurred in minor arteries, no vascular complications occurred and no surgical intervention was undertaken, except that extravasating branch arteries were ligated if the wound was explored or debrided.

ACKNOWLEDGMENTS

We thank Michael F. Mestek and Delmar H. Knudsen for access to the angiographic data and Simon D. Braun for assistance in manuscript preparation.

REFERENCES

1. DeBakey ME, Simeone FA. Battle injuries of the arteries in World War II, an analysis of 2,471 cases. *Ann Surg* **1946**;123:534–579
2. Reynolds RR, McDowell HA, Diethelm AG. The surgical treatment of arterial injuries in the civilian population. *Ann Surg* **1979**;189:700–708
3. Snyder WH III, Thal ER, Bridges RA, Gerlock AJ, Perry MO, Fry W. The validity of normal arteriography in penetrating trauma. *Arch Surg* **1978**;113:424–428
4. Geuder JW, Hobson RW II, Padberg FT Jr, Lynch TG, Lee BC, Jamil Z. The role of contrast arteriography in suspected arterial injuries of the extremities. *Am Surg* **1985**;51:89–93
5. Gerlock AJ Jr, Mathis J, Goncharenko V, Maravilla A. Angiography of intimal and intramural arterial injuries. *Radiology* **1978**;129:357–361
6. Sclafani SJA, Cooper R, Shaftan GW, Goldstein AS, Glanz S, Gordon DH. Arterial trauma: diagnostic and therapeutic angiography. *Radiology* **1986**;161:165–172
7. Rose SC, Moore EE. Emergent trauma angiography: accuracy, safety, and pitfalls. *AJR* **1987**;148:1243–1246
8. Sturm JT, Kenton CB, Rothenberger DA, Perry JF. Arterial injuries of the extremities following blunt trauma. *J Trauma* **1980**;20:933–936
9. Hare RR, Gaspar MR. The intimal flap. *Arch Surg* **1971**;102:552–555
10. Rich NM, Hobson RW II, Collins GJ Jr. Traumatic arteriovenous fistulas and false aneurysms: a review of 558 lesions. *Surgery* **1975**;78:817–828
11. Lang EK. Transcatheter embolization of pelvic vessels for control of intractable hemorrhage. *Radiology* **1981**;140:331–339
12. Sclafani SJA, Becker JA. Traumatic presacral hemorrhage: angiographic diagnosis and therapy. *AJR* **1982**;138:123–126
13. Sclafani SJA, Shaftan GW. Transcatheter treatment of injuries to the profunda femoris artery. *AJR* **1982**;138:463–466
14. Clark RA, Gallant TE, Alexander ES. Angiographic management of traumatic arteriovenous fistulas: clinical results. *Radiology* **1983**;147:9–13
15. Moreno C, Moore EE, Rosenberger A, Cleveland HC. Hemorrhage associated with major pelvic fracture: a multispecialty challenge. *J Trauma* **1986**;26:987–994
16. Kohler R, Viljanen V. Angiographically demonstrated arteriovenous shunting in circulatory obstructions in the lower extremities. *Acta Radiol [Diagn]* (Stockh) **1964**;2:473–486
17. Matsen FA III, Krugmire RB Jr. Compartment syndromes. *Surg Gynecol Obstet* **1978**;147:943–949
18. Laasonen EM. Emergency angiography in extremity trauma, prognostic aspects. *Acta Radiol [Diagn]* (Stockh) **1978**;19:42–48
19. Sandegard J, Zachrisson BE. Angiography and hemodynamic measurements in extensive soft tissue trauma to the extremity. *Acta Radiol [Diagn]* (Stockh) **1975**;16:279–296

Invitation to Membership in the American Roentgen Ray Society

During the American Roentgen Ray Society's (ARRS) 1985 meeting in Boston, society members approved several fundamental changes in the membership application process and created a new category of membership: members-in-training. Also, active members are no longer required to document contributions to radiology by way of teaching or scientific publications.

Active Membership

Candidates for active membership must be graduates of an approved medical school or hold an advanced degree in one of the physical, chemical, or biological sciences. Each must be board certified and active in the practice of radiology or one of its branches in the United States or Canada. Applicants must be endorsed by two members of the ARRS, not necessarily residents of the same community.

Members-in-Training

The new members-in-training membership category is reserved for physicians in a radiology residency or a postresidency program approved by the Radiology Residency Review Committee of the American Council of Graduate Education and for postgraduate students in allied sciences. The status is limited to 5 years, starting with the entrance date into the radiology residency. In the fifth year, members-in-training are eligible for transfer to active membership.

Corresponding Members

Corresponding members shall be physicians and/or scientists residing in foreign countries who are active in the science of radiology or allied sciences and who are in good ethical standing in the respective countries. They shall pay dues, but shall not have the privilege of voting nor of holding elective office. They may be members of special committees.

Dues and Initiation Fees

A new schedule of fees and dues has been established. Initiation fee for active members is $50. There is no initiation fee for members-in-training. Annual dues for active and corresponding members are $125, payable on July 1 of each year. The dues payment includes a 1-year subscription to the *American Journal of Roentgenology* (*AJR*) and waiver of the annual meeting registration fee. Dues for members-in-training are $25 and include a year's subscription to the *AJR* and waiver of meeting fees. *AJR* subscription rates for domestic nonmembers will be $90 for 1987. The resident subscription rate will remain $25 for residents who do not elect to become members-in-training. Nonmember residents will have a $25 meeting registration fee.

A membership application form is in this issue of the journal. Applications for active membership should be received by February 1 for action during the annual meeting in May. Members-in-training will be eligible for membership upon receipt and processing of the completed application form.

Initiation fees and dues should not accompany the application but are payable after election upon notice by the treasurer.

The American Roentgen Ray Society continues to be a vital force in providing an educational forum for the radiologic community. As it embarks on a program of a broader base of membership, we cordially welcome all those who are eligible. Thus, I urge you to complete the application and forward it to Paul Fullagar, Administrative Director, ARRS, 1891 Preston White Dr., Reston, VA 22091

Glen W. Hartman
Secretary

American Roentgen Ray Society Membership Application

Date _____ Category (check one) ☐ Active ☐ Corresponding ☐ In-Training

Name (in full) _____ Age _____

Address & zip code _____ Date of Birth _____

_____ Birthplace _____

Education | Institution | Years | Degree/Type

Undergraduate: _____

_____

Graduate (medical school, graduate school, etc.):

_____

_____

Postgraduate (internship, residency, fellowship, etc.):

_____

_____

_____

Licensed to practice _____ (type) in _____ (state, province, etc.)

Active and corresponding membership applicants, complete this section. In-training applicants, turn to reverse side.

Practice limited to radiology or one of its branches for _____ years, since (date) _____

Present appointments: Academic _____

_____

Hospitals _____

_____

Membership in scientific societies _____

_____

Offices or committee memberships in scientific societies _____

_____

Government service (military, civilian) _____

Credentials

I hereby certify that I was issued a certificate of qualification in _____

by the _____ (an American Medical Specialty Board or the Royal College of Canada)

continued overleaf

Other credentials _____

Signature _____

We, active members in good standing of the American Roentgen Ray Society and personally acquainted with the applicant, do recommend him/her for Active Membership in the society. **Two references are required.**

Name (print/type) _____ _____

Address _____ _____

_____ _____

Signature _____ _____

In-training applicants must complete this section

Credentials

I certify that I am serving as a resident/fellow in _____

at _____ (institution) Date program begins (began) is _____

_____. It ends _____. I understand the in-training membership is limited to 5 years and in my 5th year I may transfer to active membership.

Signed _____

Program director or department chairman (name and address) _____

_____

Training director's certification.

I certify the applicant is a trainee at the institution named and qualifies for enrollment as a member-in-training of the American Roentgen Ray Society. Name (print) _____ Signature _____

Address _____

General Information

Candidates for Active Membership

1. An active member must be a graduate of an approved medical school or hold an advanced degree in one of the physical, chemical, or biological sciences and be certified by the American Board of Radiology, the Royal College of Physicians of Canada, or document training and credentials that are adequate to qualify for membership. Active members shall actively practice radiology or one of its branches in the United States or Canada. Such members are eligible to participate in all activities of the society, including membership on committees, and have full voting privileges.
2. Application must be on an official form, signed by the applicant and at least two active members of the American Roentgen Ray Society, in good standing, who endorse the applicant.
3. Initiation fee is $50.
4. Annual dues are $125, payable on July 1 of each year. Of this amount, $50 is for a 1-year subscription to the *American Journal of Roentgenology*, beginning with the July issue for the year following election to membership.
5. Application must be received by February 1 for action during the 1988 meeting.

Candidates for In-Training Membership

1. In-training members must be serving in a radiology residency or a postresidency fellowship program approved by the Radiology Residency Review Committee of the American Council of Graduate Medical Education or be a postgraduate student in an allied science. Training status must be verified by the program director. In-training members have special consideration in fees and subscription rates to the society journal. Such members cannot hold society offices or vote.
2. Application must be on an official form and signed by the applicant and by the applicant's training or residency program director.
3. In-training status is limited to 5 years starting with the entrance date into the radiology residency. In the fifth year, each in-training member will receive an application for transfer to active membership from the society secretary. Those who do not apply for transfer to active membership shall be dropped from membership at the end of the fifth year.
4. There is no initiation fee. Annual dues are $25. Membership includes a subscription to the *American Journal of Roentgenology* and admission to the annual meeting without registration fees.
5. Membership applications will be acted on when received.

All Applicants

1. Do not remit initiation fee or dues until requested by the treasurer.
2. Send completed forms to: Paul Fullagar
   Administrative Director
   American Roentgen Ray Society
   1891 Preston White Dr.
   Reston, VA 22091

Technical Note

Use of Light Localizer in Fluoroscopically Guided Percutaneous Procedures

David B. Hayt[1]

The use of the radiographic-fluoroscopic–tube light localizer in conjunction with fluoroscopically guided percutaneous procedures can reduce the amount of fluoroscopy time necessary. When the needle hub shadow is projected directly over the point of entrance of the needle into the skin, the fluoroscopic central ray, the needle, and the structure to be punctured (previously centered fluoroscopically) are all coaxial, and the needle can be advanced with the light localizer substituting for much of the fluoroscopy. This technique is applicable for all equipment in which the fluoroscopic X-ray tube, equipped with a light localizer, is used.

In our institution this method has been used for various types of fluoroscopically guided procedures in three remotely controlled fluoroscopic-radiographic rooms equipped with rotating cradles (Siemens Siregraph A 90, Siregraph 2, Iselin, NJ).

Technique

After review of the patient's previous imaging procedures, the best possible path for the fluoroscopically guided percutaneous procedure is selected. Where appropriate, this includes angulation of the fluoroscopic tube and/ or rotation of the patient cradle [1, 2]. The structure or lesion to be punctured is then centered in the fluoroscopic field to avoid parallax [3], and a lead marker is placed on the skin. The marker is carefully aligned with the structure to be punctured, either by moving the marker or by realigning the fluoroscopic beam by angulating the tube and/or rotating the patient until the marker is properly superimposed on the targeted structure. At this point, the central ray of the fluoroscopic beam, the lead marker, and the structure to be punctured are all in perfect alignment (Fig. 1A). An appropriate needle is then introduced at the site of the marker with the light localizer on, making certain that the shadow of the hub of the needle is projected directly over the point of entrance of the needle into the skin. Since the properly adjusted light localizer emits light following a path identical to that of the fluoroscopic beam, it may substitute for fluoroscopy. The shadow of the needle may therefore substitute for the fluoroscopic image of the needle, which should be coaxial to the previously aligned fluoroscopic beam, the point of entrance in the skin, and the structure to be punctured.

If the shadow of the hub of the needle is not superimposed on the point of entrance of the needle when the operator releases the needle (Figs. 1B and 1C), it indicates that the needle is off course and must be repositioned in a direction opposite the shadow of the hub until the hub shadow is again superimposed on the point of entrance of the needle (Fig. 1D). The shadow serves as a substitute for fluoroscopy (Fig. 1E) for all but the final guidance of the needle, which usually requires some fluoroscopy.

Alternatively, if the needle shadow projection appears to be only slightly misaligned, it is possible to reangulate the fluoroscopic tube and/or rotate the cradle until the light localizer again projects the hub of the needle over the point of entrance into the skin. At this point, the examiner can fluoroscope the patient to determine whether the needle direction is on target. If so, redirection and manipulation are avoided, and the needle is advanced to the appropriate depth.

Discussion

The light localizer method has been used in approximately 50 patients and has reduced fluoroscopy time in percutaneous lung biopsies, shoulder arthrography, wrist and ankle

Received January 5, 1987; accepted after revision March 17, 1987.

[1] Department of Radiology, Our Lady of Mercy Medical Center, 600 E. 233rd St., Bronx, NY 10466. Address reprint requests to D. B. Hayt, Dept. of Radiology, The New York Hospital–Cornell Medical Center, 525 E. 68th St., ST-8A33, New York, NY 10021.

AJR 149:623–624, September 1987 0361–803X/87/1493–0623 © American Roentgen Ray Society

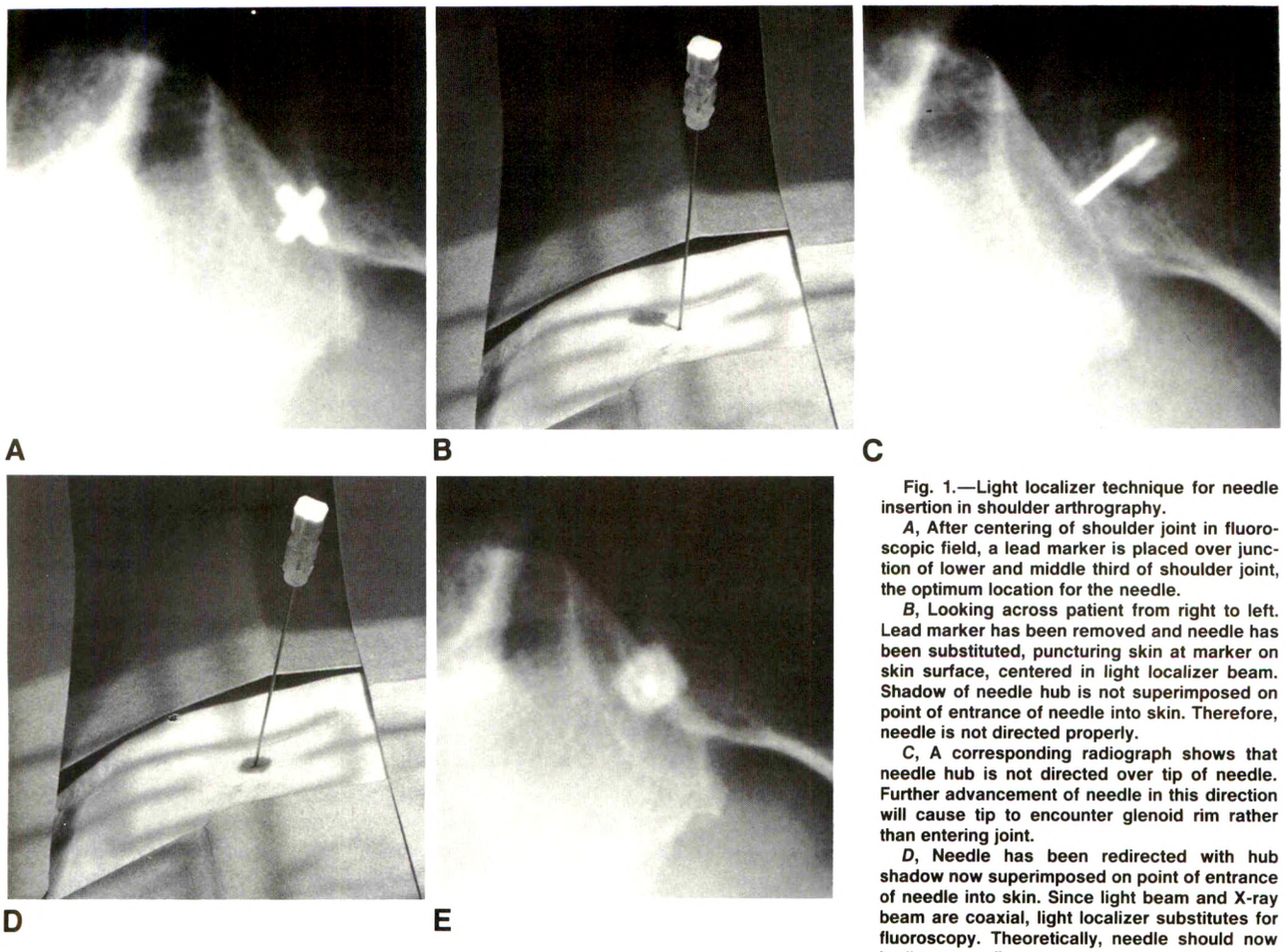


Fig. 1.—Light localizer technique for needle insertion in shoulder arthrography.

***A*, After centering of shoulder joint in fluoroscopic field, a lead marker is placed over junction of lower and middle third of shoulder joint, the optimum location for the needle.**

***B*, Looking across patient from right to left. Lead marker has been removed and needle has been substituted, puncturing skin at marker on skin surface, centered in light localizer beam. Shadow of needle hub is not superimposed on point of entrance of needle into skin. Therefore, needle is not directed properly.**

***C*, A corresponding radiograph shows that needle hub is not directed over tip of needle. Further advancement of needle in this direction will cause tip to encounter glenoid rim rather than entering joint.**

***D*, Needle has been redirected with hub shadow now superimposed on point of entrance of needle into skin. Since light beam and X-ray beam are coaxial, light localizer substitutes for fluoroscopy. Theoretically, needle should now be "on target."**

***E*, Radiograph shows that light localizer beam, fluoroscopic-radiographic beam, needle, and joint space are now all aligned. Needle may now be advanced directly into joint space.**

arthrography, and myelography. With remotely controlled fluoroscopy, the small amount of fluoroscopy required could be performed by the radiologist-operator from the control booth, obviating the wearing of lead aprons. In biliary drainage procedures and in percutaneous nephrostomies, the method was less satisfactory because of greater complexity of these procedures.

The light localizer has previously been used in CT-guided biopsy procedures [4]. To our knowledge, the shadow cast by the hub of the needle over the point of entrance of the needle has not been used to correct the guidance of the needle as a substitute for fluoroscopy in fluoroscopically guided procedures.

A number of caveats apply to the use of the light localizer as a substitute for fluoroscopy: (1) The point of entrance on the skin and the structure to be punctured must be perfectly centered in the fluoroscopic field and bisected by the cross hairs of the light localizer. (2) The light localizer itself must be in perfect adjustment with regard to the X-ray tube target. When perfectly adjusted, the cross hairs of the light localizer may also be used directly to mark the puncture site without a lead marker if desired. (3) Narrow-diameter needles tend to bend [5, 6] and are more deflected by tissue in a direction away from the bevel [7]. This is especially true when the tissue is firm. For this reason, it is better to select a thicker needle, such as a 20-gauge as opposed to 22-gauge, whenever practical. (4) When the structure to be punctured is deep, more fluoroscopic guidance is necessary.

REFERENCES

1. Gobien RP, Skucas J, Paris BS. CT-assisted fluoroscopically guided aspiration biopsy of central hilar and mediastinal masses. *Radiology* **1981**;141:443–447
2. Smith DF, Doust BD. Angulated fluoroscopy for needle biopsy localization. *AJR* **1982**;138:765–767
3. House AJS. Biopsy techniques in the investigation of diseases of the lung, mediastinum, and chest wall. *Radiol Clin North Am* **1979**;17:393–412.
4. Fredrick PR, Brown TH, Miller MH, Bahr AL, Taylor KH. A light-guidance system to be used for CT-guided biopsy. *Radiology* **1985**;154:535–536
5. Hawkins IF, Caridi JG. Curved stylus for redirection of the fine-needle guide. *Radiology* **1984**;151:530
6. Lalli AF, McCormack LJ, Zelch M, Reich NE, Belovich D. Aspiration biopsies of chest lesions. *Radiology* **1978**;127:35–40
7. Mirfakhraee M, Gerlock AJ, Giyanani VL, Sadree A. Thin spinal or biopsy needle guidance. *Radiology* **1985**;154:240–242

Technical Note

Percutaneous Atheroma Removal Using a Wire Basket

Ducksoo Kim,[1] David H. Turkel,[1] Dan E. Orron,[1] and Michael L. Steer[2]

Several methods for direct removal of atheroma exist, including open endarterectomy, semiclosed endarterectomy, and laser ablation. When successful, percutaneous transluminal angioplasty (PTA) provides a less invasive method of improving distal blood flow and reducing the hemodynamic significance of the stenotic region. However, in patients with severely fibrotic atheroma, PTA may be less effective [1]. We have recently percutaneously removed two atherosclerotic plaques using a Dormia-type wire basket catheter. This percutaneous atherectomy with a wire basket was attempted after an unsuccessful treatment of a long segmental occlusion with PTA and thrombolysis due to a noncompressible atheroma. Although we stress that significant risks are involved with this technique, additional laboratory work and animal studies may be warranted.

Case Report

A 51-year-old white male smoker with 34-year history of juvenile-onset insulin-dependent diabetes presented with a chief complaint of 3 months of increasing claudication involving the left leg and a nonhealing ulcer of the left foot. Examination of the extremities revealed bilaterally nonpalpable dorsalis pedis and posterior tibial pulses.

The left femoral arteriogram showed a moderate degree of stenosis in the midportion of the superficial femoral artery (SFA) and a 14-cm-long occlusion of the distal SFA with distal reconstitution at the popliteal artery via collaterals (Fig. 1A). In addition, occlusions were present in the mid anterior tibial, proximal posterior tibial, and proximal peroneal arteries (not illustrated). There was also a small filling defect in the popliteal artery immediately distal to the long occlusion. After left antegrade femoral puncture, 180,000 units of urokinase were infused into the occluded artery over a 2-hr period. A digital angiogram after 2 hr of infusion showed no significant change in the proximal stenosis, but some contrast material flow was observed through the previously occluded distal segment. PTA was then performed to dilate the focal stenosis of the mid SFA using a 7-French catheter with a 6-mm balloon. The region of the popliteal occlusion was dilated using a 6-French catheter with a 4-mm balloon. A post-PTA angiogram showed moderate improvement in lumen caliber but also some intimal dissection at the site of the stenosis in the mid SFA. Flow through the popliteal lesion had further increased but with evidence of persistent thrombus in the proximal segment of this area. Infusion of urokinase was therefore continued at 2000 u/min over the next 16 hr. At this time a posterior tibial pulse had become detectable by Doppler sonography. A repeat angiogram showed some moderate improvement. Urokinase was infused locally into the thrombosed area through an Sos-type open-ended guidewire (1.0 mm, Bard, Billerica, MA) as well as in the proximal sheath at a total rate of 3000 u/min over the next 24 hr.

The next day, follow-up angiograms showed continued improvement, but with two areas of significant arterial compromise remaining. The lesion in the midportion of the SFA was considered most likely to represent an avulsed plaque because of its origin after the angioplasty and its unchanged appearance thereafter; the distal lesion was believed to contain thrombus as it successively diminished in size.

The atheroma at the mid SFA was noted fluoroscopically on test injections to be undulating in the bloodstream and only loosely adherent to the wall. Impending embolization was considered a strong possibility. In consultation with our collaborating vascular surgeon, we concluded that this angiographic finding justified an attempt to remove the unstable plaque by means of catheter intervention. We also believed that such a procedure, even if unsuccessful or complicated by plaque dislocation, would not have changed our contemplated alternative surgical approach, which was to consist of a femoral-posterior tibial artery bypass procedure because of the mul-

Received December 1, 1986; accepted after revision March 31, 1987.
[1]Department of Radiology, Beth Israel Hospital, 330 Brookline Ave., Boston, MA 02115. Address reprint requests to D. Kim.
[2]Department of Surgery, Beth Israel Hospital, 330 Brookline Ave., Boston, MA 02115.

AJR 149:625–628, September 1987 0361–803X/87/1493–0625 © American Roentgen Ray Society

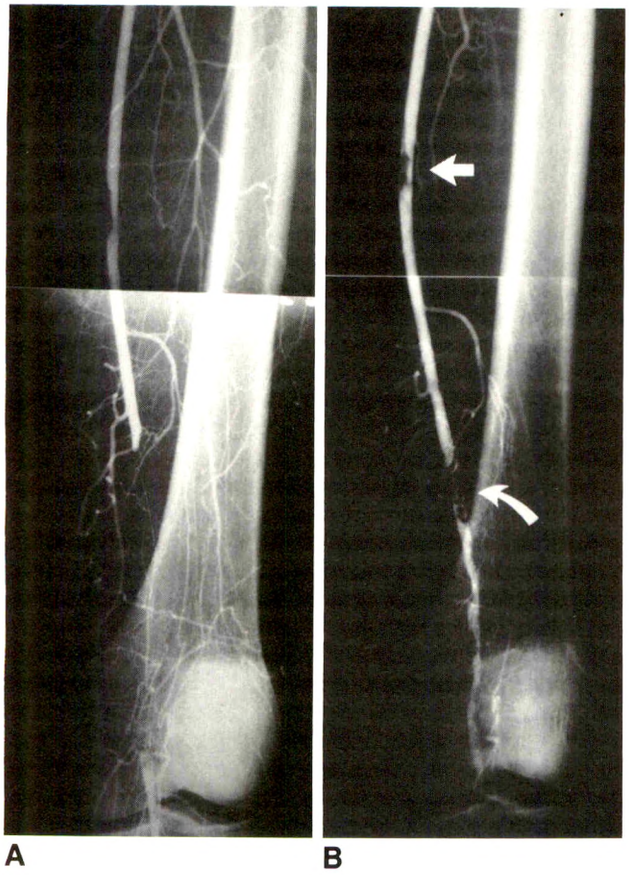


Fig. 1.—*A*, Initial angiogram shows long occlusion of distal superficial femoral and popliteal artery, in addition to stenosis of mid superficial femoral artery.

***B*, After urokinase infusion and angioplasty, there remains a stenosis, with intimal dissection, at mid superficial femoral artery (*straight arrow*) and additional stenoses more distally (*curved arrow*).**

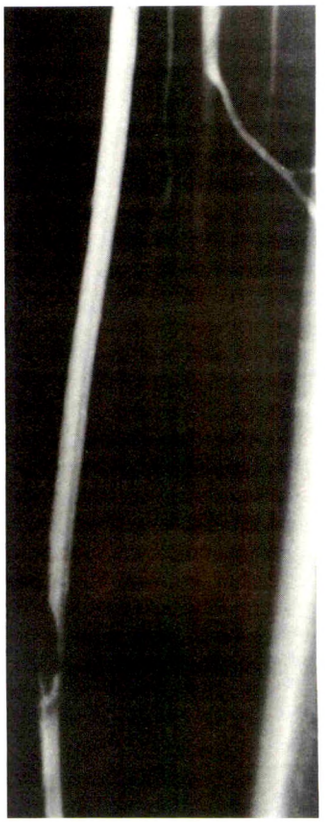


Fig. 2.—Mid superficial femoral artery plaque is seen before basket removal.

tiple distal occlusions observed in the initial angiogram.

Subsequently, a 5-French Schwartz-Pfister (V. Mueller del Caribe, Puerto Rico) wire basket was introduced through the 7-French sheath and advanced to the site of the large atheroma located in the midportion of the SFA. Using superimposition of fluoroscopy on the angiogram provided through the road mapping algorithm (Fluoro Plus, AMS, Millburn, NJ), We easily captured the large fragment in the wire basket by a gentle twisting of the basket. After a gentle tug, the large atheroma was mobilized along with a large portion of its base (Fig. 2). The fragment (Fig. 3) was pulled to the level of the sheath, and as it was unable to pass through the sheath, which was too small, the sheath, basket, and fragment were pulled out of the patient together, with loss of arterial access.

The femoral artery was recatheterized. Urokinase was again infused through a distally placed open-ended guidewire for lysis of distal thrombi. The follow-up angiogram shows normal caliber with no definite wall abnormality at the site of the previous distal femoral artery defect.

Angiography after an additional 18 hr of urokinase infusion showed some new areas of thrombosis involving the popliteal artery, beginning at the proximal segment of the stenotic distal superficial femoral lesion. After dissolution of this new thrombus by local urokinase infusion, the second loosely adherent atheroma was seen, which was thought to be inducing new thrombus formation. This intraarterial defect was similarly removed with a wire basket, but arterial access

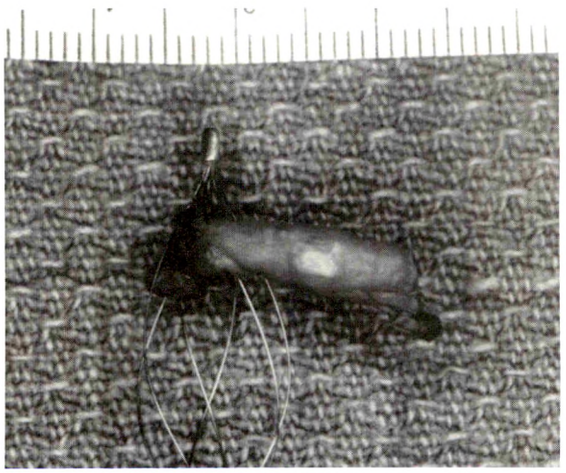


Fig. 3.—Gross appearance of plaque in wire basket after removal. Millimeter scale is shown at top of figure.

was maintained by placement of a long (0.41 mm), platinum-tipped wire (Bard, Billerica, MA) parallel to the sheath, through the same arterial puncture. The angiogram after basket removal showed normal

caliber of the popliteal artery with minimal irregularity of the vessel wall (Fig. 4).

After additional urokinase infusion the angiogram was repeated (Fig. 4) and showed satisfactory restoration of lumen of the previously occluded artery, with no evidence of intimal flaps or free intraluminal thrombus. Improved distal runoff was seen. The patient reported subjective improvement with increased warmth in the left foot and a new absence of left leg pain. The ankle-brachial index (ABI) before the procedures measured 0.41. After the procedures, the left leg ABI had increased to 0.70, with considerable improvement in the Doppler flow waveform. The patient was clinically well for 4 months after the procedure and then had symptomatic reocclusion, confirmed angiographically at another institution.

Both lesions removed by wire basket underwent pathologic microscopic analysis. The larger proximal plaque measuring 25 × 5 × 5 mm was a firm atherosclerotic plaque with foamy fat-laden cells along one surface and marked fibrosis elsewhere. Gomori trichrome stain failed to reveal smooth muscle, indicating that the media of the artery was not included in the specimen. Elastin stain did not show a definite internal elastic membrane, indicating absence of true intima in the large specimen. The smaller distal fragment was also interpreted as fibrotic plaque, without additional vascular elements.

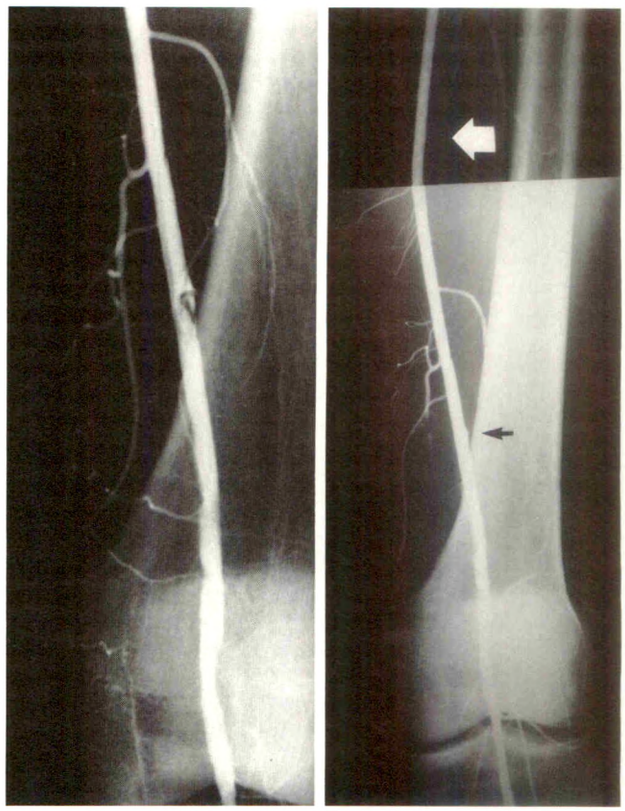


Fig. 4.—*A*, Distal superficial femoral artery plaque is seen before removal by wire basket.
***B*, Final angiogram with markedly improved appearance. *Large arrow* is at site of previous proximal superficial femoral artery lesion; *small arrow* is at site of previous distal superficial femoral artery lesion.**

Discussion

Since the technique of PTA was first described by Dotter and Judkins [2] in 1964, it has become a widely practiced treatment for atherosclerotic occlusive disease. In 1980 Castaneda-Zuniga et al. [3] suggested the currently prevailing concept that the mechanism of angioplasty involves predominantly cracking of the intima and separating it from the media while the muscular layer is stretched. Once freed from the encasement of the plaque and exposed to a normal pulsatile blood flow, the improved luminal caliber is maintained [4, 5].

The post-PTA angiogram in our case indicated that the proximal lesion was likely to be a firm fibrotic atheroma, since it was unchanged in length (2.5 cm) and configuration after multiple balloon dilatations, an occurrence thought to be indicative of severe atherosclerosis [1]. This, in combination with the undulating appearance of the lesion on fluoroscopy strongly suggested a loosely attached plaque partially liberated by the preceding angioplasty. Although clinically significant embolization of atheroma fragments is uncommon, its occurrence has been described [6]. Of equal concern, and a motivating factor in the removal of the atheroma, was the narrowing of the vessel lumen by the plaque.

The distal atheroma, which was subsequently removed, was located at the proximal end of the recurrent thrombosis of the popliteal artery, which suggested to us a causal role. Our main reason for removing this second lesion was its potential catalytic action for thrombus formation and subsequent obstruction.

The Schwartz-Pfister basket, originally designed for removal of urinary stones, has been used in the vascular system for retrieval of foreign bodies [7]. It was chosen in our case because we thought its mechanism of action would be less traumatic than forceps (Fig. 5). We believe that the success of our intervention was facilitated by fluoroscopic road-mapping equipment available to us.

Histopathologic examination of the arterial specimens retrieved by us revealed that they most closely resembled those removed by endarterectomy and thus confirmed our tentative diagnosis of a dehisced plaque as seen in the sequential angiograms.

We believe that our approach in this case was justified to correct an unusual complication of balloon angioplasty, especially since the presence of widely disseminated arterial occlusions would not have adversely affected the surgical alternative of femoral-posterior tibial bypass. Other potential complications of endarterectomy, such as arterial rupture, must be considered. Therefore, considering the uncertain risks of this procedure, its use cannot be recommended widely on the basis of this limited experience and will require further investigation in a laboratory setting. The initial success demonstrated its feasibility for use in cases in which PTA would fail because of hard plaque and in cases in which PTA is complicated by severe dissection.

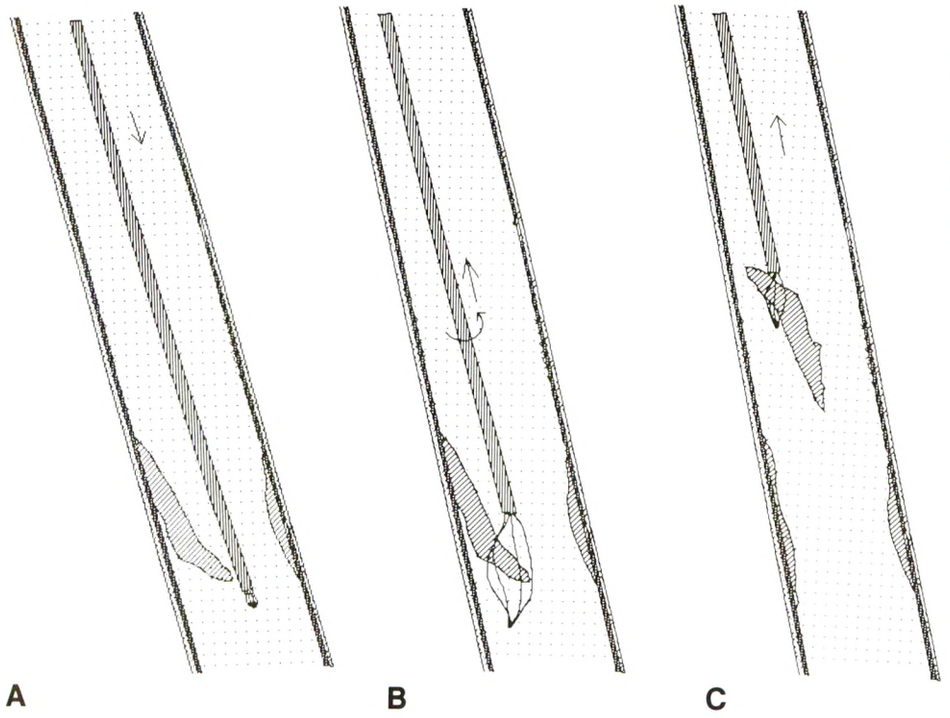


Fig. 5.—*A*, For percutaneous endarterectomy, wire basket is advanced past the free edge of the atheroma in a closed conformation to minimize arterial abrasion.

***B*, Wire basket is opened around neck of atheroma with a twisting motion, and then closed, capturing the atheroma.**

***C*, Atheromatous plaque is gently pulled free from artery wall and removed.**

REFERENCES

1. Probst P, Cerny P, Owens A, Mahler F. Patency after femoral angioplasty: correlation of angiographic appearance with clinical findings. *AJR* **1983**;140:1227–1232
2. Dotter CT, Judkins M. Transluminal treatment of arteriosclerotic obstructions: description of a new technique and a preliminary report of its application. *Circulation* **1964**;30:654–657
3. Castaneda-Zuniga WR, Formanek A, Tadavarthy M, et al. The mechanism of balloon angioplasty. *Radiology* **1980**;135:565–571
4. Kinney TB, Chin AK, Rurik AW, et al. Transluminal angioplasty: a mechanical-pathological correlation of its physical mechanisms. *Radiology* **1984**;153:85–89
5. Block PC, Fallon JT, Elmer D. Experimental angioplasty: lessons from the laboratory. *AJR* **1980**;135:907–912
6. Aueron F, Gruentzig A. Distal embolization of coronary artery bypass graft atheroma during percutaneous transluminal coronary angioplasty. *Am J Cardiol* **1984**;53:953–954
7. Clouse ME, Costello P, O'Leary DH. Removal of intravascular foreign bodies using modified Grollman catheter and Dormia basket. *J Can Assoc Radiol* **1984**;35:305–307

Technical Note

Improved Guidewire Immobilization Technique for Interventional Procedures

Morris L. Gavant[1]

Guidewire immobilization with continued access to a catheter's lumen for further flushing and contrast medium injection or to a stent's lumen for fluid drainage is commonly desired during and after diagnostic and interventional procedures [1–3]. When guidewire fixation is required during vascular procedures, an airtight seal is necessary to prevent air embolization. I have developed a new flow control device, that is, a stopcock, with an optional conventional side-arm adapter as an improved method of guidewire immobilization.

Materials and Methods

When catheter immobilization is desired during or after a procedure, a transparent FloSwitch HP high-pressure stopcock (Medi-tech, Watertown, MA) is attached to an opaque plastic side-arm fitting (Cook, Bloomington, IN). The male luer-lock of the stopcock is attached to the nonangled female luer-lock. A less expensive conventional stopcock is attached to the side-arm's female luer-lock as an injection port or drainage site (Fig. 1).

The FloSwitch HP stopcock is a transparent plastic flow control mechanism using a switch that can be easily opened and closed with the thumb and index finger. The blue switch is marked with "on" for open and "off" for closed positions. As the switch is closed, a ball bearing is forced to compress a short, flexible tube within the stopcock. As the sides of the tube coapt, a seal is established preventing backbleeding or leakage (Fig. 2). With a guidewire through the stopcock, the plastic tube's sides obviously do not completely coapt, but they do tighten sufficiently around the wire to provide a high-friction, airtight seal.

During intravascular procedures, the device is attached to the catheter hub. To assure an airtight seal the open FloSwitch stopcock is filled with clear flush by injecting saline from a syringe attached to the side-arm port. As the flush spills out of the FloSwitch stopcock, it is closed. Gentle aspiration can then be performed through the side-arm port until blood return or backflow is evident. The clear FloSwitch stopcock is kept under direct vision to prevent air aspiration into the side-arm adapter. Once backflow is established, contrast medium or flush may be injected. The smaller the guidewire through the catheter the easier the aspiration of blood or injection of contrast medium/flush.

In nonvascular procedures, a drainage bag can be attached to the side arm while the guidewire is left fixed in place to provide access at a later time. This allows the stented organ or space to drain satisfactorily if the draining fluid is not highly viscous.

I have used this device successfully in the past 20 patients undergoing percutaneous transluminal angioplasty and in the past 10 patients requiring guidewire fixation after percutaneous nephrostomy for renal stone removal.

Discussion

In the past the best way to immobilize a guidewire was by using a Tuohy-Borst side-arm adapter (Cook, Bloomington, IN) [1]. However, distortion of the adapter's rubber gasket around the small-diameter wire can lead to an unsatisfactory airtight seal. This prevents injection of flush or contrast medium for fear of air embolization. The screwlike, rotating adapter can be clumsy to use when a guidewire needs to be left in place after a procedure. This can lead to guidewire kinking during procedures. Accidental guidewire dislodgment

Received February 27, 1987; accepted after revision April 14, 1987.

[1] Department of Radiology, University of Tennessee, Memphis, and Memphis Veterans Administration Medical Center, 865 Jefferson Ave., Memphis, TN 38163. Address reprint requests to M. L. Gavant at the VA Medical Center.

AJR 149:629–630, September 1987 0361–803X/87/1493–0629 © American Roentgen Ray Society

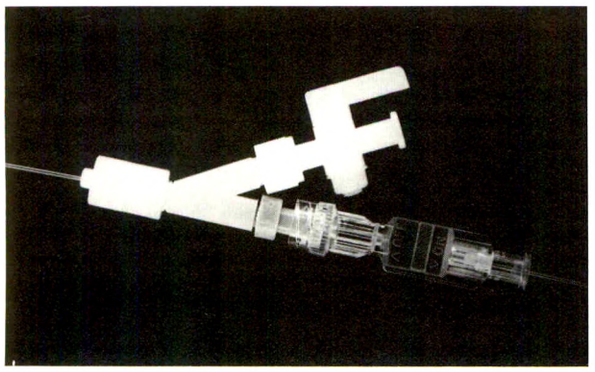


Fig. 1.—High-flow switch connected to side-arm fitting for use during interventional procedures.

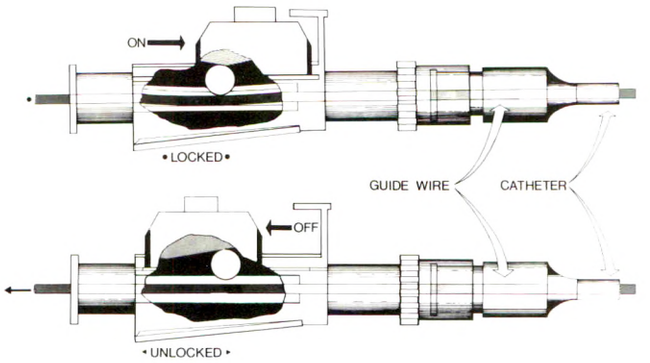


Fig. 2.—Diagram of ball bearing/tube system within high-pressure switch. In locked position the sides of the tube coapt, preventing backflow. In unlocked position ball bearing recedes and allows injection, drainage, and retrograde flow to occur.

after the examination may occur if surgical staff, residents, or nursing personnel caring for the patient are not familiar with the device.

Evaluation of the results immediately after percutaneous transluminal angioplasty commonly requires that a guidewire be left across the site in case the relatively stiff angioplasty catheter has to be repositioned for redilatation [2]. The balloon-tipped catheter is withdrawn proximal to the angioplasty site, or a catheter with a side hole proximal to the balloon is left in place across the stenosis. Contrast injection through the side arm with the stopcock switch closed around the guidewire allows conventional or digital angiographic evaluation. The clear stopcock material also allows visual inspection for possible trapped air bubbles.

Percutaneous nephrostomy placement before removal of urinary tract calculi is commonly performed as a two-stage procedure in separate rooms or on different days. A guidewire is left in place to provide the endourologist access to the pelvocalyceal system [3]. Usually a sufficient length of the guidewire can be placed down the ureter into or near the bladder so that accidental dislodgment is unlikely. No guidewire immobilization is generally necessary. The extracorporeal portion of the wire is left within the closed urinary drainage system: nephrostomy catheter, connecting drainage tubing, and collection bag. This allows urine to drain around the wire in the nephrostomy stent and into the drainage bag.

However, when negotiation of the ureter is unsuccessful a smaller length of guidewire is left within the collecting system. This wire is prone to accidental removal or dislodgment while the patient is hospitalized waiting for the procedure or during the dilatation of the nephroscope tract. The FloSwitch HP stopcock attached to the properly stabilized nephrostomy stent can be used in this situation to fix the guidewire in place. If there is no urinary tract obstruction, the switch is simply closed around the wire and the external portion is coiled in bandaging against the patient's side. Alternatively, the exposed guidewire is covered with a straight end-hole catheter or stiffener and is then coiled and bandaged. Where external drainage is desired, the side-arm adapter is attached. The guidewire is fixed in place through the FloSwitch HP stopcock, and the drainage bag is connected to the angled side arm.

REFERENCES

1. Gerlock AJ, Mirfakhraee M. *Essentials of diagnostic and interventional angiographic techniques*. Philadelphia: Saunders, **1985**;81:200–202
2. Kadir S. Percutaneous transluminal angioplasty of the iliac and common femoral arteries and their accessory vessels. In: Jang GD, ed. *Angioplasty*. New York: McGraw-Hill, **1986**:44–48
3. Smith AD, Castaneda-Zuniga WR. Dilatation of the nephrostomy tract. In: Smith AD, Castaneda-Zuniga WR, Bronson JG, eds. *Endourology: principles and practice*. New York: Thieme, **1986**:89–90

An Improved Method for Estimating the Entrance Exposure in Diagnostic Radiographic Examinations

Robert G. Zamenhof[1]
Siamak Shahabi[2]
Hugh T. Morgan[1,3]

There is currently a widespread consensus on the importance of monitoring patient radiation exposures during radiographic examinations. Diagnostic facilities under federal jurisdiction already legislate maximum patient exposure limits for various diagnostic radiologic examinations, while an increasing number of state legislatures have instituted such regulations. Compliance requires that institutions be capable of assessing each patient's entrance exposures. A method is proposed that would facilitate the acquisition of such patient exposure information in a relatively straightforward and accurate manner, requiring a minimum number of measurements and access to a suitable programmable calculator. A standardized set of exposure measurements obtained on an accurately calibrated three-phase radiographic unit has been fitted by an analytic function. The average accuracy of the fit between the limits of 40–140 kVp and 2.5- to 6.0-mm aluminum filtration was 0.3%. The concept of linear scaling was employed to allow the analytic function to accurately reproduce the exposure outputs of different radiographic units. Validation experiments on patients indicated that an overall accuracy of 10% can be expected when using well-calibrated radiographic equipment.

The method described permits institutions to verify their compliance with federal and/or state regulations and to confirm that their radiation exposures are consistent with national averages.

During the past decade the large decrease in patient radiation exposures has resulted mainly from the advent of rare-earth intensifying screens. The increasing prevalence of three-phase X-ray generators and the employment of greater amounts of X-ray beam filtration than the minimum necessary for federal compliance have also helped to lower patient exposures. The recent introduction of K-edge X-ray filters, such as erbium, promises further significant reductions in patient exposures, while the advent of digital radiography will allow exposures to be further lowered to an irreducible quantum-limited minimum consistent with acceptable image quality.

Paralleling these technological advances have been increasing efforts by federal and state agencies to ensure that patient exposures are kept to an acceptable level based on prevailing standards. At the federal level the Environmental Protection Agency has enacted regulations governing maximum patient entrance exposures in federal health-care facilities [1]. The Food and Drug Administration's Center for Devices and Radiological Health (CDRH) has recommended that institutions be aware of the radiation exposures they deliver and that they take corrective action if these exposures fall outside the generally expected ranges [2]. At the state level, Vermont and Illinois legislatures, for example, have specified actual maximum permitted entrance exposures for a number of common radiographic projections for patients of average size [3, 4].

In view of this increasing consciousness about radiation exposure, we developed a straightforward method by which technologists, radiologists, or medical physicists can comply with the radiation protection philosophy embodied by the CDRH. The proposed method allows one to obtain with sufficient accuracy (we estimate

Received January 28, 1987; accepted after revision June 2, 1987.

S. Shahabi was supported by National Research Service Award 5T32CA09045 from the National Cancer Institute, Department of Health, Education, and Welfare. Picker International provided access to the radiographic and measurement equipment used and supported the travel of R. G. Zamenhof.

[1] Department of Radiation Oncology, Box 246, New England Medical Center, 750 Washington St., Boston, MA 02111. Address reprint requests to R. G. Zamenhof.

[2] Present address: Department of Radiation Oncology, University of Wisconsin, Madison, WI 53792.

[3] Picker International, Cleveland, OH 44143.

AJR 149:631–637, September 1987
0361–803X/87/1493–0631
© American Roentgen Ray Society

approximately 10%) free-air entrance exposure (FAEE) estimates without the need for deploying dosimeters on patients or relying on average values derived from measurements on phantoms. Knowledge of FAEEs is also necessary for the purpose of estimating organ doses, such as the dose received by the embryo or fetus of a pregnant patient exposed to diagnostic radiographs.

Materials and Methods

The work described here consisted of four parts: (1) measurement of internally consistent FAEE data for various three-phase kilovoltages and thicknesses of aluminum filtration, (2) derivation by the least-squares method of an analytic function to fit the above data accurately, (3) validation of the hypothesis that exposure data measured on one radiographic unit (that is, our "standard" exposure data) can be employed as a basis for estimating exposures produced by other radiographic units, and (4) a field test of the proposed method on patients undergoing diagnostic radiographic examinations to evaluate the accuracy of the derived analytic function for estimating actual FAEEs.

Measurement of Standard FAEE Data

Standard FAEE data were measured on a three-phase, 12-pulse X-ray generator (VTX-1050, Picker, Cleveland, OH) driving an X-ray tube (Picker PX-1432CQ Dynamax) having a nominal 1.4- by 1.4-mm focal spot and 13.5° target angle. An X-ray exposure monitor (Model 1015C, with 0.6-cc ion chamber, MDH Industries, Monrovia, CA) was used to measure exposure. This instrument was cross-calibrated with an identical instrument owned by the Massachusetts Department of Public Health, which possessed a National Bureau of Standards' traceable calibration. Every exposure made was monitored by a voltage divider (Machlett Dynalyzer Machlett Lab., Stamford, CT) having digital readout of kilovoltage, milliamperage, and exposure time. All exposure times were fixed at 2 sec to (1) minimize the milliamperage and thereby reduce any undesirable effects of power loading during exposure and (2) ensure that the kilovoltage rise and decay times would be insignificantly short relative to the total exposure time. Two replicate exposures were made for each combination of kilovoltage and aluminum filtration. After every 24 exposures a reference exposure was made by using standard technique factors to verify the consistency of the output of the X-ray tube. In total, approximately 175 exposures were made in this way over a period of approximately 10 hr. Narrow-beam geometry was used at all times by masking the X-ray tube port and ion chamber with a lead sheet that was 0.25 in. (0.625 mm) thick. The X-ray tube's inherent aluminum first half-value layer (HVL) was measured by the method of Trout et al. [5] both before and after the standard exposure data were measured, and at both 60 and 100 kVp. All four of these HVL measurements were found to yield the same equivalent aluminum thickness to within 0.2 mm and therefore were averaged. The average HVL so obtained was converted to equivalent aluminum thickness by using conversion data for three-phase waveforms (Randall B, Keithley Instruments, Inc., Cleveland, personal communication). The inherent equivalent aluminum filtration of the X-ray tube was thus estimated as 1.63 mm. This value was subsequently added to the aluminum filter thicknesses introduced into the X-ray beam.

Fitting an Analytic Function to the Standard Exposure Data

A number of different polynomial type functions were used to fit the measured exposure data as a function of kilovoltage and aluminum filtration. Finally, a bivariate cross-term third-order polynomial function was chosen. The form of the function is given below, with FAEE as the dependent variable and V (kVp) and F (aluminum filtration thickness in mm) as the two independent variables cross-linked by first- and second-order terms: $FAEE = A1 + A2\,(V) + A3\,(F) + A4\,(V^2) + A5\,(F^2) + A6\,(V^3) + A7\,(F^3) + A8\,(V \times F) + A9\,(V^2 \times F) + A10\,(V \times F^2)$. A1–A10 are the constants to be determined by the least-squares fitting procedure. The FAEE is calculated in units of R/100 mAs at a distance of 100 cm from the focal spot.

The fitting procedure was designed to enable freely chosen weighting factors to be applied to each unit of data entry. This permitted the accuracy of the fit to be maximized within certain boundaries at the expense of reduced accuracy outside of those boundaries. For example, at less than 40 kVp and less than 2.5 mm of aluminum filtration, the fitting errors were allowed to increase slightly so that the fit could be forced to greater accuracy within the domain of kilovoltage and filtration more frequently used in diagnostic radiology.

The choice of a third-order polynomial was influenced by the fact that a second-order polynomial produced a significantly less accurate fit, while a fourth-order polynomial did not significantly improve the accuracy of the fit. Contrary to expectations, the introduction of a logarithmic transformation of the kilovoltage and/or filtration values prior to least-squares fitting did not significantly improve the accuracy of the fit. However, the inclusion of the first- and second-order cross terms in the fitting function made a large difference in its interpolative accuracy. This was discovered by performing the fitting both including and excluding the cross terms, and omitting the alternate lines and columns of input data. The two derived fitting functions were then used to estimate the values of the missing input data. The function that contained the cross terms was more accurate by these criteria.

Experimental Validation of the Proposed Method

To determine in a preliminary fashion whether analytically generated FAEE data can accurately predict (after linear scaling) the exposure output of other X-ray units, measurements were performed on a relatively new radiographic installation in our hospital and the resulting exposures compared with analytically generated exposures. The X-ray unit was a Philips C-850 three-phase, 12-pulse generator driving a Philips D401206 X-ray tube. The scaling factor to be used was measured at a set value of 80 kVp. This particular radiographic unit was relatively well calibrated in terms of kilovoltage accuracy, exposure vs milliamperage linearity, and exposure timer accuracy.

Preliminary Field Test of the Proposed Method

For a preliminary field test of the proposed method, we used the Philips radiographic room in which the validation measurements described earlier were performed. This room is located in the emergency admissions area of our hospital. The routine annual quality-assurance measurements performed on this equipment indicated that the kilovoltage was accurate to within ±4 kVp from 50 to 125 kVp (measured by using a Photon Physics Digital kVp Meter, Model KV1, Detroit, MI). Similarly, the exposure vs milliamperage linearity was better than ±5% (maximum variation) from 5 to 100 mAs. The unit was calibrated for absolute exposure output at 77.3 kVp (true) and 20 mAs. The HVL, measured at a true 77.3 kVp, was found to be 2.60 mm of aluminum. The technologists working in this radiographic room were asked to record for each patient and body part examined the set kilovoltage, milliamperage, and focus-to-skin distance used (by using the tape measure built into the collimator). First, FAEEs were generated for this room for an arbitrary focus-to-skin distance of 100 cm. Second, referring to the notes made by the technologists, inverse-square corrections were calculated for each exposure, and the final analytically generated FAEEs were obtained. Third, the technique factors and focus-to-skin distances used for each examination were reproduced, and the actual FAEEs were measured.

Results

Table 1 shows the measured FAEE exposure data averaged as previously described and normalized to 100 mAs and 100-cm distance from the focal spot (the midline of the ionization chamber was assumed to be the point of measurement). Note that the filtration values are the added aluminum plus the measured 1.63-mm inherent aluminum equivalent, and that the kilovoltages are not the values set on the generator console but the actual kilovoltages as measured by the voltage divider.

In Table 2, our currently measured exposure data are compared with the experimental exposure data from a report of the National Council on Radiation Protection (NCRP) [6] and Birch et al. [7]. It is evident that there is a systematic discrepancy between our data and those from the NCRP-report, with the latter showing a more rapid increase in exposure with increase in kilovoltage. The NCRP data were measured on single-phase equipment, and they were interpolated and normalized from different sources. It is difficult to understand, however, why the relative variation of exposure with kilovoltage should be that different for single- and three-phase equipment; indeed our own measurements have indicated that there is no detectable difference within the estimated errors of measurement. On the other hand, the agreement between our data and the three-phase data of Birch et al. is more favorable in terms of exposure variation with kilovoltage and filtration; the small absolute offset is of no concern to us since we propose to scale our exposure data linearly to agree at some fixed reference point with the output of each individual radiographic unit.

The coefficients, A1–A10, of the polynomial fitting function shown earlier are: A1 = −1.50470; A2 = 8.15696×10^{-2}; A3

TABLE 2: Comparison of Our Measurements with Measured Single-Phase Exposure Data from NCRP [6] and Three-Phase Exposure Data from Birch et al. [7]

kVp	NCRP [6]/Our Data		Birch et al. [7]/Our Data	
	2.5 mm Al	4.0 mm Al	2.0 mm Al	4.0 mm Al
50	0.94	—	0.94	—
60	0.94	—	0.88	—
80	0.90	0.85	0.88	0.91
100	1.08	0.96	0.95	0.96
120	—	1.07	—	0.96
125	1.16	—	—	—
140	—	1.06	—	—

Note.—Our data were divided by the factor 1.7 [8] when comparing them with data from the National Council on Radiation Protection (NCRP) [6]. Dash indicates data not available.

TABLE 1: Normalized Exposures in R/100 mAs at 100 cm from the Focal Spot for a Three-Phase, 12-Pulse Waveform

Aluminum Filtration (mm)	Normalized Exposure (R/100) by kVp											
1.63	kVp	32.5	42.0	51.0	63.0	71.0	81.5	92.0	101.0	110.5	122.0	132.5	141.5
	R/100	0.1969	0.4284	0.6839	0.9858	1.2181	1.5226	1.8606	2.1084	2.3690	2.7355	3.0452	3.3022
2.63	kVp	33.0	42.0	51.5	62.5	71.0	82.0	92.5	102.5	111.5	121.0	132.0	140.5
	R/100	0.0782	0.2072	0.3690	0.5832	0.7484	0.9652	1.2026	1.4323	1.6723	1.9174	2.1935	2.4542
3.63	kVp	32.5	42.0	51.0	62.3	72.0	82.0	93.0	102.5	111.0	122.5	132.0	141.5
	R/100	0.0387	0.1244	0.2395	0.4026	0.5548	0.7226	0.9161	1.1071	1.2981	1.5613	1.7626	2.000
4.63	kVp	33.0	42.0	52.0	62.3	70.5	82.5	93.5	102.0	111.0	122.5	132.0	141.0
	R/100	0.0222	0.0826	0.1729	0.3045	0.4103	0.5703	0.7561	0.9136	1.0839	1.3058	1.4994	1.7213
5.63	kVp	33.0	42.0	51.5	62.3	71.5	82.5	93.0	102.0	111.5	123.0	131.0	140.5
	R/100	0.0140	0.0573	0.1265	0.2341	0.3226	0.4568	0.6142	0.7484	0.9084	1.1097	1.2774	1.4606
6.63	kVp	33.0	42.5	52.0	63.0	70.5	82.0	94.0	102.0	111.5	122.5	131.5	141.5
	R/100	0.0098	0.0434	0.1001	0.1866	0.2606	0.3819	0.5239	0.6426	0.7923	0.9781	1.1303	1.3136
7.63	kVp	33.0	42.0	52.0	63.0	71.0	82.5	94.0	101.5	111.5	122.5	131.5	141.5
	R/100	0.0067	0.0310	0.0770	0.1502	0.2111	0.3148	0.4413	0.5419	0.6813	0.8439	0.9806	1.1510

Note.—Estimated relative accuracy is better than ±5% over range of energies measured.

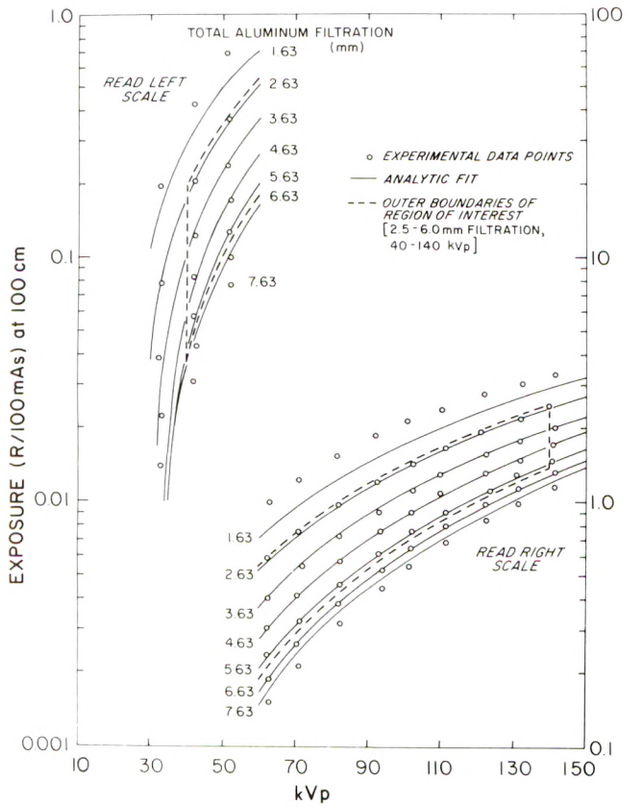


Fig. 1.—Comparison of measured and analytically fitted exposure data. Measured exposures are shown by *circles* and fitted polynomial function is shown by *solid lines*. *Broken line* encloses region for which fitted polynomial is accurate to within an average discrepancy of 0.3% and maximum discrepancy of 3% (at 90 kVp, 2.5 mm of aluminum). Read *right* scale for lower family of curves and *left* scale for upper family of curves.

$= 9.32482 \times 10^{-3}$; A4 $= 3.55244 \times 10^{-4}$; A5 $= 6.47732 \times 10^{-2}$; A6 $= -4.48768 \times 10^{-7}$; A7 $= -4.85248 \times 10^{-3}$; A8 $= -2.23978 \times 10^{-2}$; A9 $= 7.04024 \times 10^{-6}$; and A10 $= 1.25783 \times 10^{-3}$.

Figure 1 shows the measured exposure data points and the corresponding curves as given by the polynomial fitting function. By manipulating the weighting factors during the fitting process, as described earlier, the accuracy of the fitting function within the dotted boundaries was forced to be high at the expense of lower accuracy outside these boundaries. In the kilovoltage range of 40–140 kVp and filtration range of 2.5–6.0 mm of aluminum (the region within the dotted boundary), the worst discrepancy between measured and fitted data was 3% (90 kVp, 2.5-mm aluminum filtration), while the average discrepancy was 0.3%.

Figure 2 shows curves generated by the polynomial fitting function, within the constraints of kilovoltage and aluminum filtration specified above. These curves enable exposure values to be read off without the need to interpolate more than one of the two independent variables.

An additional piece of information that can be obtained from the polynomial exposure function is the functional dependence of exposure vs kilovoltage and aluminum filtration when mathematically modeled as a simple power law. It is a commonly stated rule-of-thumb that exposure varies with kilovoltage approximately according to the power law: exposure = constant × (kilovoltage)^n, where n frequently is assigned the value 2 [9, 10].

The above power law was fitted to the polynomial FAEE function, with n as a variable dependent on kilovoltage and filtration, in order to examine the validity of the n = 2 rule. Figure 3 shows the most appropriate value of n to use in the power law above as a function of kilovoltage and aluminum filtration. It is gratifying to observe that the accepted rule-of-

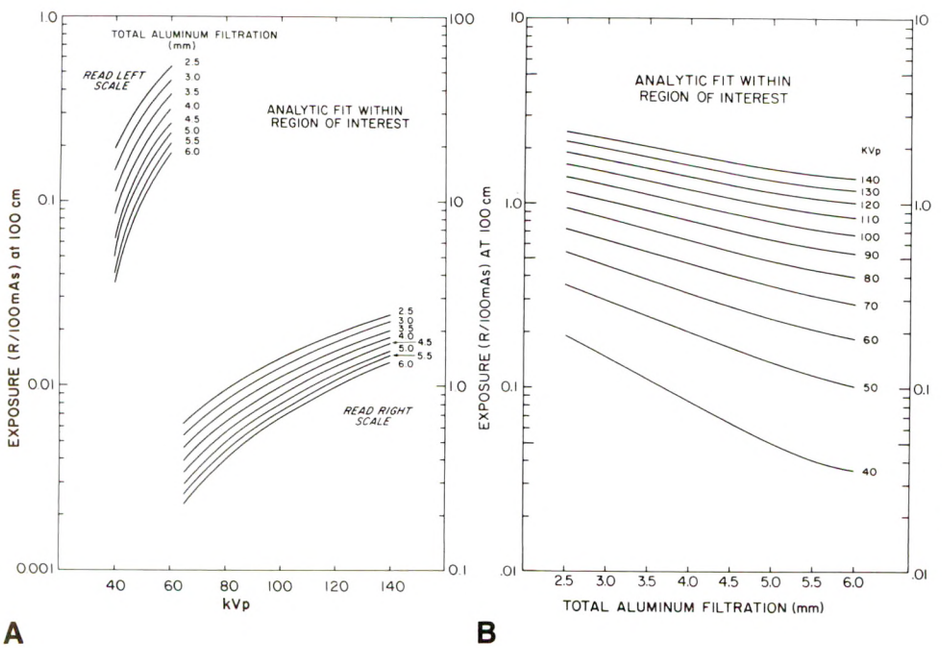


Fig. 2.—Analytically calculated exposure data with more realistic values of aluminum filtration and limited to region over which analytic representation is valid (40–140 kVp, 2.5–6.0 mm of aluminum).

***A*, Read *right* scale for lower family of curves; use *left* scale for upper family of curves.**

***B*, Axes have been interchanged.**

thumb, which assumes that n = 2, is actually quite accurate at the intermediate values of kilovoltage and moderate values of aluminum filtration used in diagnostic radiology. At low kilovoltages and for large amounts of aluminum filtration n increases to more than 4, while at high kilovoltages and for small amounts of aluminum filtration n decreases to 1.7.

Table 3 shows the discrepancies between the analytically generated exposures and the actual measured exposures in the Philips radiographic room where the validation measurements were performed. The discrepancies are extremely small in all cases. The linear scaling factor that was applied to the analytic function was equal to 0.810. This means that if no scaling had been performed the analytically generated exposures would have been approximately 19% too high. This difference in absolute exposure output between different three-phase radiographic units, supposedly operated under identical kilovoltage and milliamperage factors, is difficult to explain, but it does underscore the value of performing linear scaling for each individual radiographic unit.

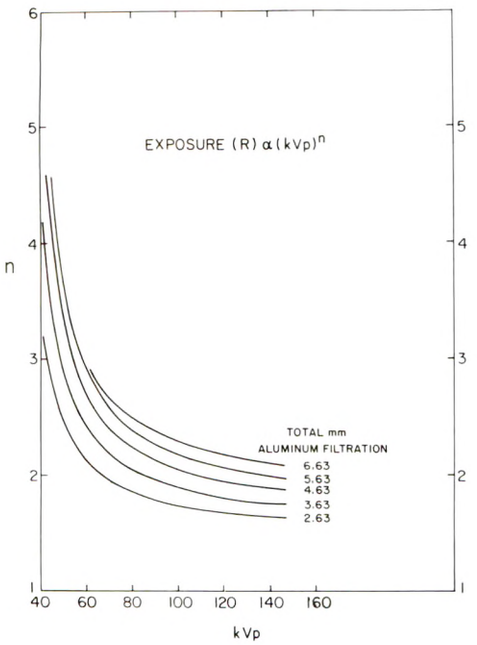


Fig. 3.—Assuming that exposure vs kilovoltage can be modeled as a power-law relationship with n as exponent of kVp, curves show actual values of n that are most accurate for various kVps and amounts of aluminum filtration.

TABLE 3: Accuracy of the Proposed Method in Predicting Exposures of a Philips Radiographic Unit at Tufts–New England Medical Center

kVp		Exposure (mR)		% Difference
Set	Measured[a]	Calculated	Measured	
60	57.70	341	344	+0.9
80	77.25	642	633	−1.4
100	95.03	934	954	+2.1
120	116.1	1335	1338	+0.2
140	135.4	1737	1766	+1.6

[a] Measured with Photon Physics Digital kVp meter model KV1.

Table 4 shows the results of the comparison between analytically calculated FAEEs and FAEEs measured under field-test conditions and shows that under idealized circumstances the accuracy of the proposed method can be very high. It should be noted, however, that the calibration exposure was entered with the true kilovoltage and also that the "calculated" FAEEs listed in Table 4 were obtained by reading true kilovoltages into the FAEE tables. In practice, both the calibration exposure and the technique factors for the actual patient examinations would be entered by using set rather than true kilovoltages. Consequently, the comparison shown in Table 4 was reevaluated by using set rather than true kilovoltages. The differences under these more realistic conditions were found not to exceed 5%. If the X-ray generator is putting out a kilovoltage that is inaccurate by the same absolute amount (in kilovoltage) over the entire range of kilovoltages used, the use of set rather than true kilovoltages in the proposed method will incur little additional error. Only if the error in kilovoltage varies over the kilovoltage range, as was the case in the equipment considered here, will larger additional errors in FAEE estimation occur. Nevertheless, we believe that for radiographic equipment in a relatively good state of calibration the overall errors in our proposed method should not exceed 10%.

Discussion

For the proposed method to be accepted readily and used routinely the exposure information must be presented in a straightforward and user-friendly manner. In our hospital, we have adopted the following approach.

A simple computer program (written in FORTRAN and available from the authors on request) prints individualized (scaled) exposure tables for each X-ray tube and generator combination in our hospital. Suppose, for example, that we have a radiographic room with one table Bucky. For the table Bucky, a focus-to-film distance of 102 cm is always used. For this particular table the distance from table top to film is 5 cm. The focus-to-skin distance will therefore range from approximately 95 cm (for an anteroposterior film of the hand) to approximately 65 cm (for an anteroposterior abdominal film of an obese patient). A single calibration exposure is performed at 80 kVp (set) and at a known focus-to-ion chamber distance and milliamperage (in practice three replicate exposures are made and the results averaged). The 80-kVp setting is arbitrarily chosen to be approximately in the middle of the range of kilovoltages that would be used in this particular radiographic room. The focus-to-ion chamber distance is measured by using the measuring tape built into the collimator. The equivalent aluminum filtration (HVL measurement and conversion curves obtained from Bryan R, Keithley Instruments, Cleveland), kilovoltage, milliamperage, focus-to-ion chamber distance, and calibration exposure are entered into the computer program, together with the focus-to-skin distance for which the printed FAEE table is to apply. Seven

TABLE 4: Field Test of Proposed Method in a Clinical Setting with Philips Radiographic Unit at Tufts–New England Medical Center

Examination	FSD (cm)	kVp (set/true)	mAs	Skin Exposure in Air (mR)		
				Calculated	Measured	% Difference
Chest:						
PA	152	115/110.8	4	21.3	21.4	−0.5
Lateral	145	120/116.1	17	108.2	109.0	−0.7
Skull:						
Lateral	80	70/67.5	40	301	301	+0
Abdomen:						
AP	76	70/67.5	60	502	503	−0.20
Lumbar spine:						
AP	82	70/67.5	28	201	205	−2.0
Lateral	70	80/77.3	80	1035	1033	+0.19
Hand:						
AP	92	65/62.6	7	33.2	34.1	−2.7
Lateral	88	65/62.6	10	79.7	80.3	−0.7

Note.—Exposures were measured with an MDH model 1015C X-ray monitor with 0.6-cc ion chamber. Equipment: radiographic unit—three-phase, 12-pulse table Bucky; X-ray tube—Philips D401206; generator—Philips Maximus C850; focal spot—0.6 mm; filtration—2.60 mm Al @ 77.25 kVp; screen-film combination—DuPont Quanta V with Cronex 8L film. FSD = focus-to-skin distance; PA = posteroanterior; AP = anteroposterior.

scaled FAEE tables are generated, with focus-to-skin distances ranging from 65 to 95 cm in 5-cm increments. Each of these tables consists of a matrix of FAEEs with different milliamperage values (1–200 mAs) defining the columns and different kilovoltage values (40–140 kVp) defining the rows. These seven FAEE tables are collated and placed in the radiographic room near the control console. When a technologist, radiologist, or physicist needs to determine the FAEE for a specific radiologic examination, he/she measures the actual focus-to-skin distance while the patient is on the table and observes the kilovoltage and milliamperage settings used for the exposure. He/she then selects the FAEE table having the closest focus-to-skin distance to the actual measured value and, with linear interpolation in kilovoltage and milliamperage, obtains the FAEE. The errors in FAEE introduced by using FAEE tables calculated at 5-cm incremental distances are a maximum of 5–8%, depending on the thickness of the body part being radiographed. If desired, this inverse-square error can be eliminated retrospectively by making an additional inverse-square correction to the FAEE.

The earliest systematically organized FAEE data pertaining to diagnostic radiographic applications can be found in the NCRP report [6]. These data are based on interpolations and averages of older measured data [11, 12] for full-wave, rectified, single-phase radiographic equipment. The data are tabulated over a range of 70–150 kVp and 1–4 mm of total equivalent aluminum filtration. McCullough and Cameron [8] published exposure data that theoretically were calculated by using Kramers' mathematical model for bremsstrahlung X-ray production. Kilovoltages of 40–150 kVp and aluminum filtration values of 1–4.5 mm were considered. More recent data from Birch et al. [7] are based on a theoretical model of X-ray production in tungsten targets and agree with limited measurements (by the same authors) to within a few percentage points. However, at the higher aluminum-filtration values used today, particularly in digital subtraction angiography and digital projection radiography, the range of kilovoltage values covered by the data of Birch et al. is not adequate. For example, for 3-mm aluminum filtration the kilovoltage range is 80–140 kVp, while for 4 mm the range is 100–140. Also, as in the case of the NCRP data [6], 4 mm of aluminum is the highest filtration considered. Wilson and Palmer [13] reported a method, similar in concept to the proposed method, where the theoretical X-ray production data of Storm [14] was fitted by a polynomial function and used to estimate patient exposures based on kilovoltage, HVL of the X-ray beam, milliamperage product (mAs), and focus-to-skin distance. Despite the fact that no attempt was made to correct the predictive polynomial for the individual characteristics of each radiographic unit, the average accuracy of this method, when compared with thermoluminescent dosimetric measurements on patients, was estimated to be approximately ±20%.

The actual radiation output of a specific radiographic unit as a function of kilovoltage and aluminum filtration is dependent on factors other than simply the physics of X-ray production in the tungsten target. Such factors include pitting effects in the target material [13], the precise shape of the kilovoltage waveform applied [8], and the accuracy of the calibration of the specific X-ray unit in terms of kilovoltage, milliamperage, and exposure time. For this reason we suggested in earlier work that the physics of X-ray production should be used only as a parametric description of the variation in X-ray output with kilovoltage and filtration, while the absolute value of the output should be "pegged" by an absolute measurement performed for each specific X-ray unit [15]. Shrimpton [16] and McGuire and Dickson [17] have also proposed this concept.

We are currently investigating the possibility of mounting on the X-ray tube collimator an ultrasonic photographic range finder, available from Polaroid Corp. (Cambridge, MA), to automatically measure the focus-to-skin distance for each radiographic examination. An analog-to-digital converter and

a microprocessor programmed with the polynomial function that we have described would provide a straightforward method for FAEEs to be recorded automatically.

REFERENCES

1. *Radiation protection guidance for diagnostic X-rays. Federal Register, 43 FR 4377, Washington, DC,* **1978**
2. Burkhart RL. *Recommendations for evaluation of radiation exposure in diagnostic radiology examinations*. HHS publication no. (FDA)85–8247, Washington, DC, **1985**
3. State of Vermont Division of Occupational and Radiological Health. *Regulation for radiation protection*. **1977**: Authority 13 VSA, section 102, and 18 VSA, chapt 32, section 5-305, Burlington, VT
4. Department of Nuclear Safety. *Radiation regulations*, part F, section 6. Chicago: State of Illinois Office of Radiation Safety, **1981**
5. Trout ED, Kelley JP, Lucas AC. Determination of half value layer. *AJR* **1960**;84: 729–740
6. National Council on Radiation Protection and Units. *Medical X-ray and gamma-ray protection for energies up to 10 MeV*. NCRP report no. 33, Washington, DC, **1968**
7. Birch R, Marshall M, Ardran GM. *Catalogue of X-ray spectra for diagnostic X-rays*. London: Hospital Physicists' Association, **1979**
8. McCullough EC, Cameron JR. Exposure rates from diagnostic X-ray units. *Br J Radiol* **1970**;43:448–451
9. Curry TS, Dowdey JE, Murry RC. *Christensen's introduction to the physics of diagnostic radiology*, 3rd ed. Philadelphia: Lea & Febiger, **1984**
10. Johns HE, Cunningham JR. *The physics of radiology*, 4th ed. Springfield, IL: Thomas, **1983**
11. Trout ED, Kelley JP. Leakage radiation through lead glass fluoroscopic screen assemblies. *Radiology* **1964**;82:977–981
12. Hale J. The homogeneity factor for pulsating potential X-ray beams in the diagnostic energy region. *Radiology* **1966**;86:147–151
13. Wilson CR, Palmer DW. Prediction of patient doses in diagnostic radiology. *Proc SPIE* **1980**;233:122–128
14. Storm ES. Calculated bremsstrahlung spectra from thick tungsten targets. *Phys Rev* **1972**;A5:2328–2337
15. Shahabi S, Zamenhof RG, Kalend A, Sternick ES, Morgan HT. Screening radiation exposures in diagnostic radiology by using machine-specific exposure lookup tables (abstr). *Med. Phys* **1984**;11:407
16. Shrimpton PC. Calculation of patient skin dose from diagnostic X-ray procedures. *Br J Radiol* **1985**;58:483–485
17. McGuire EL, Dickson PA. Exposure and organ dose estimates in diagnostic radiology. *Med Phys* **1986**;13:913–916

Opinion

Wall Street Entrepreneurs and Imaging Centers: An Insidious Threat to Radiology

Leonard Berlin[1]

The advertisement is eye-catching: it features a color photograph of a radiologist sitting at a console that displays multiple images of an MR examination. Alongside him is a bank of view boxes on which hang various images of a CT scan. The radiologist has a contented smile on his face and is looking directly at the reader. Below the photograph, in large black type, are the words, "I have an M.D., not a M.B.A. I want to practice medicine, not manage an MRI clinic." The sponsor of this ad is a Texas-based company that describes itself as a specialist "in creating successful inpatient and outpatient MRI clinics throughout the United States." It adds, "We handle all business aspects of each center's operation—and our physicians concentrate on the practice of medicine."

Another attention-getting ad, sponsored by a California-based developer of MRI clinics, shows three apparently happy radiologists studying MR images on a view box. Testimonials from the radiologists are placed alongside the photograph. One reads, "Physicians must have access to high-technology medical imaging equipment, preferably without the complications associated with running the business."

The two advertisements have appeared often in radiologic journals and magazines during the past 18 months. They underscore a relatively new phenomenon in radiology: the emergence of a separate, nonmedical organization to purchase and operate radiologic equipment, most commonly MR imagers or CT scanners, which cost from 1 to 2 million dollars. These companies provide many additional services, including researching the optimal location for establishment of a facility to house the equipment, building the facility, installing and maintaining the equipment, hiring professional and nonprofessional personnel, managing the business affairs of the installation, and marketing the facility. Additionally, these companies usually provide the funds, or raise the funds from investors, to finance the entire project.

A unique nomenclature has evolved as a result of this phenomenon. What used to be called an "X-ray office" is now an "imaging center." Banks that used to give loans have been replaced by "venture capitalists." New terms have entered the radiological vocabulary: "Wall Street entrepreneurs," "joint ventures," "cash-flow turnaround," "neutral party interface," and "freestanding clinics."

A lot of money seems to be flowing into a number of privately or publicly owned companies that have already opened or are planning to open imaging centers. A New York brokerage house is said to have raised 25 million dollars in just 18 days for this purpose [1]. Many hundreds of these centers are expected to be operating throughout the United States during the next several years [1, 2].

Economic and ethical considerations of joint ventures and imaging centers have been exhaustively debated in numerous recent articles in both the scientific and popular literature, and thus are not the subject of this communication. The subject of this discussion is of far greater importance to every radiologist: the role, indeed the entire future, of the radiologist in this new era of imaging centers. Is it realistic for the radiologist in the ad who says that he wants to practice medicine instead of managing an MRI clinic to be as contented as he appears? Is it realistic for the radiologist in the other ad who says that he prefers to practice without the complications of running the business to be as happy as he seems?

Received April 24, 1987; accepted May 8, 1987.
[1] Department of Radiology, Rush North Shore Medical Center, 9600 Gross Point Rd., Skokie, IL 60076. Address reprint requests to L. Berlin.

 0361–803X/87/1493–0638 © American Roentgen Ray Society

Most American physicians, including those radiologists who have opted to practice outside a hospital setting, have historically practiced as heads of small businesses. They established offices; hired nursing, technical, and secretarial personnel; handled the payroll and patient billings; and ordered and paid for supplies, either by themselves or possibly with the help of a business manager. Those radiologists who decided to go into private practice purchased the equipment themselves, often supported by loans from their friendly banker. While the types of the practices among American doctors were quite diverse, they all had one characteristic in common: independence. The doctor himself was in control of his practice; he was his own boss. Radiologists, of course, were not entirely independent, in that they had to rely on the goodwill of their nonradiologist colleagues for the referral of patients. Nonetheless, these radiologists, along with other physicians in private practice, answered only to themselves with regard to working schedules and day-to-day business and professional decisions.

Most radiologists chose a different track and confined their practices to hospitals. In comparison with their counterparts in private offices, the independence of these radiologists was limited, for the hospital generally owned the equipment, and hired and fired the technical and secretarial personnel. But the hospital-based radiologist remained relatively autonomous: he generally had considerable input into the management of the radiology department. While he may not have had true self-determination, still he did have the security of possessing medical staff privileges in his hospital, he usually had either membership on, or at least influence with, the hospital executive committee, he most likely set his own professional fees, and he generally had a solid relationship with a stable hospital management. The radiologist's ultimate position in the hospital was usually dependent on the quality of service he gave, rather than on how much profit was generated in the radiology department.

But over the past decade the economic climate has changed drastically. Not only did the price of conventional X-ray equipment skyrocket, but more importantly, equipment that had never even been envisioned in the 1950s and 1960s began to appear on the scene. CT scanners, when introduced in the early 1970s, carried a price tag of over a half-million dollars, rising in the next decade to the million-dollar range. MR imagers appeared in the marketplace in the early 1980s, with prices ranging from 1.5 to 2 million dollars. Hospitals, which until recent years were more than happy to spend big dollars on capital equipment because their costs were reimbursed by Medicare and private insurance, now found themselves pinched for funds: hospital utilization was down and third-party reimbursement was sharply curtailed. Government now found it cheaper to promote care outside, rather than inside, the hospital. Outpatient care, rather than inpatient care, became the buzzword. Thus the stage was set for the moving of the expensive CT and MR equipment away from the hospital, in both the financial as well as the geographic senses. Simultaneously a vacuum—and a business opportunity—were created.

It is easy to understand why the business community moved in to fill the vacuum. The million-dollar equipment was there to be bought and the hospitals wanted no part of it. Radiologists for the most part did not want to undertake the risks of such expensive purchases. The "venture capitalists" thus appeared on the scene, gearing themselves up to provide facilities with the equipment and personnel in place ("turnkey operations") and then to hire a radiologist to provide the necessary professional service. Superficially it seemed like a good deal for the radiologist: no risk, no money down, no responsibility, no headache. He could devote all his time to rendering professional opinions of CT and MR images, and would not have to concern himself with any other aspects of the operation. Seemingly he could not lose a thing; it was a perfect situation.

The founder of the business organization that published one of the ads mentioned earlier epitomized the displacement of the radiologist from a supervisory to a subservient capacity by commenting in a recent magazine article [1] that radiologists who become involved in imaging centers find "it's hard to be a physician and run an MRI business on the side." Perhaps we should ask ourselves whether it really is that hard. Perhaps we should ask ourselves whether the intrusion of outside management companies and Wall Street entrepreneurs into the radiology profession is really as harmless as some may think. And perhaps we should consider the answers to the following other pertinent questions: Hasn't the radiologist who relinquishes ownership and management of a radiologic facility lost something important? Hasn't he lost his independence, his ability to be the head of his own business, the privilege of making decisions? Hasn't the Wall Street entrepreneur rather insidiously usurped much of what the radiologist has been trained to do and what he ought to do? Ought not the radiologist know specifications and applications of radiologic equipment—including MR—better than a layperson? Ought not the radiologist be able to provide competent and efficient technician coverage in a more knowledgeable fashion than a layperson? Ought not the radiologist be able to educate his referring physicians about the indications and limitations of imaging procedures more effectively than a layperson? Should not the radiologist, rather than a nonradiologist with an M.B.A. degree, have the authority to fix the price of a radiologic procedure and his professional fee? Should not the radiologist make a reasonable and fair return on his investment and his professional ability, rather than forfeiting a large portion of it to an entrepreneur who may be more profit-oriented than concerned with good patient care? Could not the radiologist finance the cost of purchasing the MR or CT equipment, either by himself or with partners who are either radiologists or nonradiologist physicians? Could not the radiologist himself stay in charge of the project? Isn't it the radiologist who can best handle the scheduling of patients, to whose medical needs he can more easily respond with sensitivity, the hiring and firing of technicians and secretaries, whose idiosyncrasies he understands so well, and the billing of patients, whose hardships and financial problems he can readily deal with in a humanitarian fashion? Isn't it the radiologist who, in the long run, can best convince fellow doctors to refer patients to him on the basis of quality of

service rather than by slick marketing brochures? And isn't it the radiologist who has a better chance of assuring high quality in the entire operation because his basic outlook is predicated on good medical care rather than profit margins? Isn't it the radiologist who, in short, best knows the radiology business?

If the answers to these questions are affirmative, then the conclusions we can draw are ominous for the future of radiology. By permitting management companies to do what the radiologist himself should do, the radiologist is abdicating something that he may never to able to regain: self-determination. He is giving up the long-term right to be independent for the immediate gratification of being able to function without worry or responsibility. Let there be no illusions: the nonradiologist manager will set the policies of the facility and determine the income and working conditions of the radiologist. Aside from ensuring his own income, that manager's sole duty is to generate profits for the owner-investors of the operation. And as increasing competition begins to cut into profit margins, it is not unlikely that he may have to accomplish this by continually lowering the radiologist's remuneration and by eventually compromising good patient care [3, 4].

One wonders whether the smiling, apparently blissful radiologists who appear in ads praising the benefits of entrepreneurial management companies shouldn't better be soberly contemplating whether they can ever reclaim their lost status. And perhaps they should be asking themselves whether radiologists who want only to "practice medicine" rather than conduct the business of radiology, with its inherent risks and rewards, may find themselves one day permanently relegated to the employee category of itinerant "film reader." And perhaps they should be wondering whether they themselves are helping to create an environment wherein Wall Street entrepreneurs control so many imaging centers such that future graduates of radiology residencies will find themselves ordinary laborers instead of proud members of a distinguished profession.

REFERENCES

1. Davis JE. High-tech medicine heads for the malls. *Business Week*. **1986**; July 14:70
2. Crane M, Paxton HT. Joint ventures: which deals are the big winners. *Med Econ* **1987**;64 (March 30):41–45
3. Thomas MC. Joint ventures: who knows what evil lurks. *Med Econ* **1987**;64 (March 30):47–51
4. Economic glut, practice pressures are hurting outlook for radiology. *Radiol Today* **1987**;4 (March):1, 12–13

Opinion

Risk Management for the Radiologist

Justin P. Smith[1]

Malpractice claims against radiologists can only increase as established practice is evaluated against new standards [1]. Faced with the inevitability of greater risks of malpractice claims, what can radiologists do to protect themselves?

Risk management offers a direct approach to reduce claims. Rather than forcing society to march at "tortpoint," risk management helps physicians practice and document good care. The goal of risk management is prevention. Watching for problems, documenting efforts to practice properly, and learning from mistakes are its fundamentals. Risk management is common sense [2–4].

Strategy for risk management must approach medical malpractice as a legal issue. The court is not a medical disciplinary board, and only in the most exceptional case will the court dictate a standard of care [5]. Rather, the court hears a complaint and seeks to resolve that complaint by applying legal tests. If the plaintiff's argument and evidence meet those tests, the jury will find that malpractice has occurred. How can radiologists prevent unavoidable imperfection or disagreements on standards from becoming grounds for malpractice? They must understand how these legal tests will be applied to their actions.

Strategy for risk management also must approach medical malpractice as an issue of human relations. Few doubt that smoking causes lung cancer, yet most smokers do not develop lung cancer. Certain factors heighten the risk, but the answer to "why me?" lies with the individual rather than with the group. Few doubt that bad outcomes lead to malpractice suits, yet most bad outcomes do not generate suits. Certain factors heighten the risk, such as a bad outcome from a minor operation on a child. The answer to "Why was a suit filed?" often lies with the patient rather than with the type of injury. Radiologists must understand that the radiographic "miss" itself is only a small factor in motivating a patient to pursue a malpractice claim. The major determinant of whether a mistake will become a claim is patient dissatisfaction. Dissatisfaction grows from little things: a rude receptionist, an inconsiderate technician, inadequate pain relief, lack of concern for the patient's modesty, a brusque physician, or a long, unexplained wait in the reception room. Gradually, dissatisfaction becomes anger, and, should an injury occur, this anger may transform injury into suit [6].

Does risk management work? No controlled studies, only anecdotes, support its effectiveness. However, as a strategy to counter legal tactics and trends, as a way to ensure the best care for patients, and as a way to renew the satisfaction of medical practice, risk management costs little and offers much. It is a positive approach to increasingly negative societal developments and requires only common sense and humane concern.

This is the first of three short articles on selected aspects of risk management. Two others, "Building a Winning Team: Risk Management for Employees" and "Suit Pending: Action Required," will appear in future issues of *AJR*.

Good Documentation Is the Best Insurance

Adverse outcomes must be documented thoroughly [7]. The common notion that documentation of an adverse out-

Received January 6, 1987; accepted after revision May 5, 1987.
[1]Department of Radiology, SB-05, University of Washington, Seattle, WA 98195. Address reprint requests to J. P. Smith.

 0361–803X/87/1493–0641 © American Roentgen Ray Society

come makes it more likely that a suit will be filed is wrong. On the contrary, it is the lack of documentation that cripples a defense and disenchants a jury [8]. When the medical record shows what happened, what the physician did, and what arrangements were made for follow-up, the record is the physician's ally. When the medical record is incomplete, and when the physician's reasoning is not shown, the quality of care becomes a matter of conjecture. An incomplete record leaves actions open to question. A problem may have been recognized immediately and proper steps taken to manage it, but good care begins to appear substandard if a late complication does develop, and the record shows only "Patient experienced hives. No sequelae." Ambiguity is the marble from which the plaintiff's attorney will sculpt a malpractice case [9]. It is better to describe carefully the circumstances surrounding a bad outcome and to admit an honest mistake than to leave a few vague statements in the hope that "the whole thing will blow over." A few minutes spent describing an adverse outcome may preclude months of litigation. Furthermore, when an adverse outcome has occurred, the liability insurer must be notified promptly. Although different insurers may have slight differences in their expectations of when a physician must report a potential claim, three circumstances usually obligate the physician to notify the carrier: when a medical outcome occurs that the physician believes could lead to a claim, when the physician or the physician's staff receives a request or subpoena from an attorney for medical records that may be related to a malpractice claim, or when the physician or the physician's staff is served with a "summons and complaint." To ignore these requirements is to risk denial of coverage by the insurer [10]. Remember, surprise is the plaintiff's ally.

The medical record must never be altered surreptitiously. The court will view such alteration as tampering. No matter how honest the intent, evidence of tampering destroys the defendant physician's credibility and makes a medically defensible case legally indefensible [11, 12]. If the record must be edited, a single line should be drawn through the erroneous text, leaving the original text legible. The new text should be added in the margin and signed with the date and the author's initials. An amended report may be preferable. No law requires a pedestrian to look both ways before crossing a street, and no law requires a radiologist to assure that the referring physician is aware of an amended report. In both circumstances common law yields to common sense. If delayed awareness of the amended report could harm the patient, the referring physician should be notified by telephone [13]. The wise radiologist will include a statement in the record that this notification was made.

Reports must be phrased for public as well as professional scrutiny. Reports should not contain words that could be considered an admission of negligence: oversight, iatrogenic, mistake, and inadvertent. Why use "inadvertent"—meaning "careless" to the court—when "unintentional" avoids the implication of negligence [14, 15]? Furthermore, the referring physician's work should not be impugned. How will 12 laypersons interpret "the distal fracture fragment is poorly aligned"? As shorthand for anatomic description, such comments may save seconds during dictation but may lead to months of litigation for both the referring physician and the radiologist [16]. Likewise, does the report respect the clinician's autonomy, or does it force action—perhaps against the clinician's judgment—to avoid the implication of negligence? Although the cold nodule in the thyroid may be cancer, does the report's conclusion of "fine-needle aspiration biopsy strongly recommended" obligate the clinician? If the clinician does not have a reliable cytopathologist, is an alternative available? When the results are unexpected or may require immediate action, telephone contact with the clinician is desirable and should be documented. These calls can be noted either in the report or in a logbook. The law does not require such contact, but the radiologist may be found negligent if the failure to communicate contributes to a patient's injuries. The written report is necessary but may not be sufficient in such circumstances [17].

Reports should show that the author is sincere and careful. Sincere, caring radiologists are seen to make forgivable mistakes; insincere, hasty radiologists are seen to commit malpractice. Imagine the jury listening to the defendant radiologist reading the report. Are they wondering how anyone could sue such a conscientious doctor, or are they interpreting his inappropriate humor (e.g., "positive Throckmorton's sign") as disrespect for the patient? Radiologists would find little difference between "normal chest" and "The trachea is midline. The heart is not enlarged, and the pulmonary vasculature is normal. No pulmonary nodules, effusions, or infiltrates are identified. The osseous structures are intact. Impression: Normal chest." Suppose these reports fail to mention an indistinct, rounded carcinoma in the peripheral right lung; the opportunity for a curative resection is lost. Will a malpractice suit be filed? Under the contingency-fee system, the likelihood of a malpractice suit being filed depends, in part, on the likelihood of economic recovery for the plaintiff's attorney. When the attorney seeks to show that the radiologist was negligent, which report will make it easier to convince the jury of hasty, substandard care? The radiologist who dictated "normal chest" may have studied the radiograph with far more care than did the more descriptive radiologist, yet it will be easier to convince a jury of the first radiologist's "haste" on the basis of the succinct report.

The report should speak for itself. Technical limitations should be described: was the patient on a ventilator, was the patient in pain and unable to cooperate fully, did the fluoroscope malfunction, did the patient ask that the examination be limited, did distended bowel obscure the appendix? Was a useful clinical history provided? Were comparison studies available? Such limitations are far more convincing when they are part of the report rather than offered as "after-the-fact" excuses [18]. Without such a description, the failure to achieve technical excellence may raise doubts about the defendant radiologist's competence, especially when the plaintiff's attorney reads to the jury: "Making sure that the films are of adequate quality is the radiologist's responsibility, and no excuses are acceptable if they are of poor quality" [19].

Finally, informed consent must be acquired realistically and

documented. Is the consent form specific to the procedure, easy to read, and comprehensive [20]? Legal boilerplate does not inform the patient; it does render the defendant's sincerity suspect. Twelve lay persons may not look favorably on a consent form whose apparent intent is to protect the physician first and the patient second. Are the forms readable? A simple test is to imagine patients reading the forms aloud in court. How will they fare with any abbreviations? Will they stumble over "percutaneous transluminal femoral angioplasty"? Can they explain in their own words what they have read? True, the form was signed, but did the patient understand it—was the consent informed? Did the patient and the patient's family have the opportunity to ask questions? The report should contain a brief statement documenting the patient's comprehension, even though the patient has signed a separate consent form: "After I explained the procedure, Mr. Jones and his wife said they understood and that they had no questions. He then signed the consent form" [5].

Good documentation requires only common sense. Prefer the specific to the vague, be diligent in the correction of those inevitable mistakes, and place the patient's interests first. Patients, courts, and conscience can ask no more.

REFERENCES

1. Berlin L. Malpractice and radiologists, update 1986: an 11.5-year perspective. *AJR* **1986**;147:1291–1298
2. Holzer JF, Current concepts in risk management. *Int Anesthesiol Clin* **1984**;22:91–116
3. Pollack BR. Risk management in the dental office. *Dent Clin North Am* **1985**;29:557–580
4. Jones DB. Risk management: one way to fight malpractice suits. *Tex Med* **1985**;81:64–66
5. King JH. *The law of medical malpractice*, 2nd ed. St. Paul, MN: West, **1986**:49–52, 163
6. Sommers PA. Malpractice risk and patient relations. *Leg Aspects Med Pract* **1985**;13:1–4, 8
7. Applebaum M. Malpractice and radiologists, update 1986 (letter). *AJR* **1986**;148:830–831
8. Williams CW. Guide to hospital incident reports. *HCM Review* **1985**;10:19–25
9. Freilich H, Finkelstein SF. You must identify non-medical issues that can lead to liability. *Hosp Top* **1985**;63:36–37, 39
10. Crinean CL. Patient-physician privilege clarified. *Washington Physicians Q* **1987**;1(2):1, 4
11. Gage SM. Alteration, falsification, and fabrication of records in medical malpractice actions. *Med Trial Tech Q* **1981**;27:476–488
12. Hirsh HL. Tampering with medical records. *Med Trial Tech Q* **1978**;25:450–455
13. Gregory DR. Patient must be informed of misdiagnosis. *Leg Aspects Med Pract* **1985**;13:4–6
14. Mayhew JF. Use of *inadvertent* for *unintentional* is negligent (letter). *JAMA* **1985**;254:357
15. Black HC, ed. *Black's law dictionary*, 4th ed. rev. St. Paul, MN: West, **1968**:903
16. Renner RR, Mauler GG, Ambrose JL. The radiologist, the orthopedist, the lawyer, and the fracture. *Semin Roentgenol* **1978**;13:7–18
17. Schreiber MH, Winslade WJ. Rights, roles, and relationships in radiology. *Radiology* **1987**;163:269–270
18. Radiologist may be liable for negligently failing to inform treating physicians of limited scope of x-rays. *Health Law Digest* **1985**;13:26–27
19. Jones B, Braver JM. *Essentials of gastrointestinal radiology*. Philadelphia: Saunders, **1982**:45
20. Reuter SR. An overview of informed consent for radiologists. *AJR* **1987**;148:219–227

Letters

Prudent Diplomacy: Shared Radiology, not Radiation

Since the start of the nuclear age, conflict between nations has been held in check by the threat of global annihilation. However, the continuing proliferation of atomic weapons and the growing possibility of accidental deployment suggest that this delicate balance of peace cannot go on forever. The key to lasting world peace, in my opinion, lies in mutual understanding at all levels of society. Unfortunately, suspicion and mistrust within governments and public misconceptions fueled by the mass media have rendered this goal a virtual impossibility. As the scientist frequently is blamed for bringing the burden of potential nuclear holocaust to bear upon humanity, the radiology community should aspire to contribute positively toward international communication.

To date, the sharing of knowledge in the field of diagnostic medical imaging between Eastern and Western bloc countries has been far less than optimal, even within international societies. I was initially impressed by this deficiency during attendance at annual meetings of the International Skeletal Society, the membership of which includes not a single physician from a Communist nation. Similarly, the major diagnostic imaging meetings and journals in the United States are characterized by a noticeable absence of such radiologists, despite impressive foreign representation by other free countries. Conversely, although a small minority of the radiology community in the United States may have had the opportunity to visit the Soviet Union or the People's Republic of China, most American radiologists (including me) lack insight into the practice of our specialty in these nations.

The radiologist is, nevertheless, in an ideal position to bridge the ideological barriers that currently exist between democratic and socialist countries. As we interact chiefly with images during the course of our daily work, the problem of language barriers is minimized. In serving the needs of our clinical colleagues, we as radiologists are also skilled in interpersonal communication and instruction.

Therefore, more active endeavors should be aimed at interaction with radiologists from socialist nations at all levels of activity within our subspecialty. Although a broad spectrum of possibilities exists to achieve this purpose, the following appear potentially most fruitful: (1) Scientific papers and guest lecturers should be invited from Eastern countries for inclusion in the programs of refresher courses and major American radiology meetings, including the Radiological Society of North America and the American Roentgen Ray Society. (2) Radiologist exchange programs should be established between the United States and Eastern countries at a variety of levels, including postgraduate academic staff, fellowship, and residency. (3) Major American diagnostic imaging journals should encourage submission and publication, with appropriate translation, of manuscripts authored by radiologists from socialist nations. (4) The number of postgraduate refresher courses for American radiologists that include visits to Eastern bloc countries should be increased. (5) Technological information from both sides should be shared, via scientific meetings, newsletters, and manufacturer demonstrations organized specifically for this purpose.

In conclusion, by adopting strategies such as these, the radiology community in America can take an important first step toward mutual understanding between members of our specialty on both sides of the Iron Curtain.

David J. Sartoris
University of California, San Diego, Medical Center
San Diego, CA 92103-1990

Diverticulitis: Evaluation by CT and Contrast Enema

The recent publication by Johnson et al. [1] compared contrast enema and CT in the diagnosis of diverticulitis and reported CT to be "diagnostic" in 41% of patients, "consistent" in 38%, and "falsely negative" in 21%. Contrast enema was reportedly "correct" in 77%, "falsely negative" in 15%, and "indeterminate" in 7%. They claimed that in only one of their patients was management altered by CT interpretation. We are surprised by their relatively poor results with CT because in our experience CT has proved to be superior to contrast enema in the diagnosis of diverticulitis, more accurate in showing the extent of the inflammation, and extremely useful in guiding patient management (2, 3]. The following comments may help explain our different results.

First, 41% of their patients did not have surgical or pathologic proof of diverticulitis, and readers can be skeptical about the true pathologic diagnosis in at least some of these patients. In fact, we have found that a good-quality normal CT examination is useful in *excluding* the diagnosis of diverticulitis in those patients whose clinical presentation is nonspecific.

Second, diagnostic accuracy in CT depends on good technique, and Johnson et al. did not use optimal CT technique in several regards. In 30% of their CT examinations, scans 10 mm thick were obtained at 20-mm intervals. In essence, in these patients half of the area of interest was not included in the scans obtained. More closely spaced and thinner sections would undoubtedly increase CT accuracy. Johnson et al. performed CT after colon distension with dilute

barium, a "positive contrast," in 43% of their cases and postulated that use of rectal contrast in more CT examinations would have resulted in a higher accuracy. We concur that lumen distension with contrast improves CT accuracy and encourage its use when it is not clinically contraindicated. However, we think that the method of choice for contrasting the colon lumen for CT examination is instillation of air to act as a "negative" contrast agent [4, 5]. Compared with positive opacification, negative opacification results in better delineation of the bowel lumen and wall. Also, although Johnson et al. administered glucagon for contrast enemas, it was not used for any of their CT studies, thereby introducing another bias against the CT examination.

Third, Johnson et al. biased their statistics by applying loose criteria for the "correct" diagnosis of diverticulitis by contrast enema and rigid criteria for the "correct" diagnosis by CT. The CT findings of mural thickening and pericolic inflammation are, at the least, equivalent findings to thickening and tethering of the mucosal folds shown by contrast enema and should be judged as equally diagnostic or correct. In fact, by either technique the respective findings are not pathognomonic of diverticulitis but rather, in the appropriate clinical setting, consistent with and highly suggestive of this diagnosis. If Johnson et al. had used the same radiologic criteria in interpreting their CT data as they did their contrast enema data, most, if not all, of the consistent CTs would be added to the diagnostic CTs to yield sensitivities and accuracies at least as high as those of contrast enema.

Fourth, Johnson et al. reported that CT showed fluid- or gas-containing pericolic abscess in 41% of their cases. In how many of these same patients did contrast enema show such a pericolic abscess? The obvious conclusion is that unlike CT, contrast enema is not useful in distinguishing uncomplicated diverticulitis from diverticulitis accompanied by abscess or other complication. In our initial series [2], as well as in our continued experience, CT has proved to be not only more sensitive than contrast enema in the diagnosis of diverticulitis but also, most importantly, more accurate in reflecting the extent of the pericolic inflammation. The indirect evidence of pericolic inflammation perceived on contrast enema may be seen on CT to represent a spectrum of abnormality ranging from mild edema to phlegmon to frank abscess. Although we agree that the ultimate decision to treat the patient surgically or medically remains based on clinical judgment, we disagree with the assumption that radiologic investigation is or should be used "primarily" for diagnostic purposes and not for treatment planning. On the contrary, at our institution radiologic investigation is requested only partly to confirm the clinical diagnosis of diverticulitis but primarily to stage the extent of the inflammatory process. In the setting of diverticulitis, the questions that must be answered are as follows: Is there abscess or only pericolic inflammation? Where precisely is the inflammation? Is the urinary or genital tract involved? Is there distant abscess? If surgery is contemplated, is a single-stage procedure feasible? Is the patient a candidate for percutaneous abscess drainage?

In summary, we believe that the report by Johnson et al. is compromised by the inclusion of unproved cases, bias against CT because of discrepant rigidity in accepting the radiologic diagnoses based on CT findings vs diagnoses based on contrast enema findings, and, too often, suboptimal CT technique. We do not disagree that contrast enema has a proved value in the diagnosis of diverticulitis, outlining fistulas, and aiding differential diagnosis by directly depicting mucosal detail. However, it must be emphasized that diverticulitis is an extraluminal disease imaged only indirectly by luminal studies, either radiologic or endoscopic. The mural and pericolic tissues are where we must direct our attention, and here CT is clearly advantageous. At out institution, our initial conclusions have been strengthened by continued experience. In patients in whom the clinical diagnosis is in doubt and in patients with a strong presumptive clinical diagnosis of diverticulitis, CT has supplanted contrast enema as the primary radiologic technique.

Donald H. Hulnick
Alec J. Megibow
Emil J. Balthazar
New York University Hospital and Bellevue Hospital Medical Center
New York University Medical Center
New York, NY 10016

REFERENCES

1. Johnson CD, Baker ME, Rice RP, Silverman P, Thompson WM. Diagnosis of acute colonic diverticulitis: comparison of barium enema and CT. *AJR* **1987**;148:541–546
2. Hulnick DH, Megibow AJ, Balthazar EJ, Naidich DP, Bosniak MA. Computed tomography in the evaluation of diverticulitis. *Radiology* **1984**; 152:491–495
3. Balthazar EJ, Megibow AJ, Gordon RB, Hulnick DH. Cecal diverticulitis: evaluation with CT. *Radiology* **1987**;162:79–81
4. Megibow AJ, Zerhouni EA, Hulnick DH, et al. Gas contrast CT of the gastrointestinal tract. Presented as an exhibit at the annual meeting of the American Roentgen Ray Society, Boston, April **1985**
5. Zerhouni EA, Megibow AJ, Hulnick DH, et al. Gas contrast CT of the gastrointestinal tract. Presented as an exhibit at the annual meeting of The Radiological Society of North America, Washington, DC, November **1985**

Reply

We appreciate the interest and comments by Drs. Hulnick, Megibow, and Balthazar. Our interest in the CT evaluation of diverticulitis was indeed sparked by their published experience and recommendations [1]. Our purpose was to evaluate the sensitivity of contrast enemas and CT in diverticulitis and to determine if the additional information provided by CT changed clinical management. We also investigated whether contrast enemas were contraindicated in diverticulitis in the acute setting. We shall respond to the comments concerning our article first and then summarize our conclusions.

Because diverticulitis encompasses a spectrum of severity and often is treated conservatively, we included nonsurgical patients to avoid bias toward the more severe form of the disease. In fact, we think that the conclusions reached by Hulnick et al. may be based on such a bias. Hulnick et al. [1] have indicated that surgery was performed in 78% of their patients. This suggests their series included an unusually large percentage of patients with frank abscess. In Zollinger's series [2], only 21% of patients required surgery. Therefore, for a balanced perspective, both clinical and surgical patients must be included in a series of diverticulitis. It should be noted that the CT findings in our series were consistent with or diagnostic in more than half of the patients whose diverticulitis was diagnosed clinically.

In their letter, Hulnick et al. state that a "good-quality normal CT examination is useful in excluding the diagnosis of diverticulitis in those patients whose clinical presentation is nonspecific." They further state, "In our initial series, as well as in our continued experience, CT has proved to be not only more sensitive than contrast enema in the diagnosis of diverticulitis . . ." No prospective evidence supports either of these statements [3]. Furthermore, we think that many of our negative findings on CT when 2-cm intervals were used to search for abscesses occurred because the diverticulitis was minimal.

We agree that proper CT technique is essential in evaluation for diverticulitis. Our population was gleaned from the diagnostic registry and not from patients prospectively evaluated for this disease. CT examinations in which we used 2-cm intervals were "abscess searches." We routinely perform these at 2-cm intervals, with recuts at 1-cm intervals only if abnormalities are detected. Although it is possible that minimal disease was missed, management would not have been changed. These patients were included because accept-

able CT technique was used for an abscess survey with adequate evaluation of the pelvis (the sigmoid and pelvic fat was normal in these patients). This group also raises questions concerning the sensitivity of CT when diverticulitis may not be suspected.

We are pleased that the authors agree that "lumen distension with contrast improves CT accuracy . . ." In their article, one of the advantages of CT over contrast enema is that it is "less invasive to the inflamed bowel, since distension with contrast material is not necessary."

We know of no prospective evidence that documents the superiority of negative (air) rectal contrast over positive contrast material. Furthermore, the administration of glucagon for enema studies and not for CT could not have introduced a bias against CT. The use of air and glucagon could have facilitated the detection of wall thickening on CT, but this is a nonspecific finding.

Our criteria for "diagnosis" via contrast enema and CT reflect the fact that once a diseased segment of the sigmoid colon is identified, the differentiation between diverticulitis and carcinoma is essential. Critical to this diagnosis is the identification of an intact mucosa in the affected segment. Thickening of the bowel wall on CT can be seen in uncomplicated diverticulosis, ischemic colitis, Crohn's disease, carcinoma, and diverticulitis [4, 5]. In fact, in half of our patients evaluated by CT, only thickening of the bowel wall or masslike thickening was detected (without mesenteric change). Without an abscess, these were considered consistent with, but not diagnostic of, diverticulitis. In many, carcinoma had not been excluded. We think the mucosal changes and tethering seen on contrast enema are much more specific than bowel-wall thickening and/or mesenteric change detected on CT.

We agree that CT is superior in showing extracolonic disease. We have shown in our patient population that the detection of extracolonic disease does not significantly alter patient management. Most of the fluid collections in our series were small and amenable to conservative therapy with antibiotics and bowel rest.

Before a physician considers what test is best for a patient, at least two things must be considered: (1) Which test is most sensitive and specific? (2) What management changes will occur if the results are positive or negative? To date, no prospective study has evaluated the sensitivity and specificity of both contrast enema and CT in the detection of diverticulitis. Furthermore, it is unclear that the ability of CT to detect extracolonic abnormalities necessarily changes management. We think that our results and conclusions differ from those reported by Hulnick et al. because their population appears to have had more severe disease [1, 6].

At Duke, where conservative management is the rule, contrast enema remains the primary imaging study for the initial diagnosis and treatment of diverticulitis. Contrast enema is not contraindicated in the acute setting and, in most cases, it is the only test necessary for successful diagnosis and therapy. In our institution, initial CT has not been shown to alter therapy in most patients with diverticulitis. CT is reserved for patients with suspected distant abscesses, those considered for percutaneous drainage, and those with disease not responsive to medical therapy. We think that our population reflects a broader spectrum of disease, and therefore our findings are more applicable to the general population.

Mark E. Baker
Reed P. Rice
Duke University Medical Center
Durham, NC 27710
C. Daniel Johnson
Mayo Clinic
Rochester, MN 55905
Paul M. Silverman
Georgetown University Hospital
Washington, DC 20007
William M. Thompson
University of Minnesota Hospital and Clinics
Minneapolis, MN 55455

REFERENCES

1. Hulnick DH, Megibow AJ, Balthazar EJ, Naidich DP, Bosniack MA. Computed tomography in evaluation of diverticulitis. *Radiology* **1984**;152:491–495
2. Zollinger RW. The prognosis in diverticulitis of the colon. *Arch Surg* **1968**;97:418–421
3. Hall FM. Computed tomography in the evaluation of diverticulitis (letter). *Radiology* **1985**;154:835
4. Feldberg MAM, Hendricks MJ, van Waes PFGM. Role of CT in diagnosis and management of complications of diverticular disease. *Gastrointest Radiol* **1985**;10:370–377
5. Morris J, Stellato TA, Haaga JR, Lieberman J. The utility of computed tomography in colonic diverticulitis. *Ann Surg* **1986**;204:128–132
6. Hulnick DH, Megibow AJ, Balthazar EJ, Naidich DP, Bosniack MA. Computed tomography in the evaluation of diverticulitis (response to letter). *Radiology* **1985**;154:836

Medication-induced Esophagitis: Diagnosis by Double-Contrast Esophagography

In the April issue of *AJR*, Bova et al. [1] present convincing data that in addition to endoscopy, double-contrast esophagography is an excellent technique for the diagnosis of medication-induced esophagitis. However, one area prompts questions as to the validity of their study. Their sample population consisted of nine patients who had both double- and single-contrast studies. The nine double-contrast studies showed the typical clustered, ovoid ulcerations, and the single-contrast studies showed only a few ulcers. Two of the nine patients underwent endoscopy, which confirmed the findings of their previous double-contrast studies. The authors implied that esophagography is a sensitive and specific study as it does identify correctly those who have the disease. Validity would have been better measured if the authors had performed endoscopy on all nine patients, thereby excluding the possibility of error due to technique or observer bias. I am still interested to know if medication-induced esophagitis would have been diagnosed by means of endoscopy in the remaining seven patients.

Janá M. Williams
Meharry Medical College
Nashville, TN 37208

REFERENCE

1. Bova JG, Dutton NE, Goldstein HM, Hoberman LJ. Medication-induced esophagitis: diagnosis by double-contrast esophagography. *AJR* **1987**;148:731–732

Reply

We appreciate Ms. Williams's interest in our manuscript concerning the diagnosis of medication-induced esophagitis by double-contrast esophagography. Her suggestion is true that endoscopy in all of our patients would optimize the scientific correlation. However, a major significance of this manuscript is that the sensitivity of double-contrast esophagography obviates endoscopy in most instances. In our opinion, it is appropriate in the clinical evaluation of this type of patient that endoscopy not be performed. The referring clinicians in these cases thought that the clinical presentation, radiographic findings, and subsequent resolution of symptoms were sufficient.

James G. Bova
The University of Texas Health Science Center at San Antonio
San Antonio, TX 78284

An Academic Career: The Rest of the Story

As an academic radiologist about to enter private practice, I found the *Opinions* of Drs. Schreiber [1] and Sartoris [2] of timely interest. I have known and enjoyed the four-dimensional rewards of academic radiology that they mention—teaching, patient care, research, and administration—for 6 years. I have thoroughly learned my subspecialty, applied its most recent innovations, and introduced them to the private sector, but not without first educating the general radiologist and referring clinician about the advantages and pitfalls of these innovations. To improve patient care within the community while serving as a consultant/teacher is satisfying and similar to what Dr. Schreiber noted for the private practitioner.

Because of my academic interest, I will continue to promote excellence in patient care, and I will continue to teach—clinicians now more often than medical students or residents. But of necessity, research and its end product, publication, will be limited. Some might argue that it already is limited; however, I have done my "homework" this past winter, producing several articles and a book chapter, but not without significantly curtailing my teaching and patient care responsibilities. Even though I would like to be judged for what I do best—teaching and patient care—I know that research and its publication are, in reality, the only measurable parameters for promotion in academia.

Therefore, residents and fellows in training who are considering the option of *the* "exciting and rewarding road to travel within the profession" should understand the method of judgment. You may be promoted and tenured for being an excellent three-dimensional academician—teacher, administrator, and patient-care provider—but probably not. You must do research and publish to attain the security afforded by promotion and tenure. Also, an aspiring academic radiologist must become a member of, be active in, and be comfortable with the peer-review organization of academic radiology, the Association of University Radiologists (AUR). I recommend that you attend their annual meeting, present your research, and see if you can realize a "good fit."

The hypocycloidal logo of the AUR implies equal emphasis on teaching, patient care, and research. Examination of the AUR scientific program, memorial awards, and committee makeup, however, reveals heavy weighting toward research. For example, the Scientific Program Committee has grown from six to 14 members between 1982 and 1987, except for 1986 when the committee had 18 members. In 1983, the five-member Ad-Hoc Committee on Teaching in Radiology was formed. Today, it continues as an ad-hoc committee with a membership of seven. Since 1984, it has successfully presented a half-day teaching symposium at the annual AUR meeting. Of 182 papers presented at the 1987 meeting, 12 (6.6%) were teaching papers, and 170 (93.4%) were scientific/research papers.

Although I do not disagree with the substance of Dr. Sartoris's opinion, I think that any guide to an academic career choice should include information on the method of acceptance and advancement both by the peer group (the AUR) and by the institutional group (the university promotion and tenure committee). With few exceptions, you will be judged by your research and publications. If this best represents your goals and interests, go for the academic career. If you like to teach, administrate, and care for patients, you probably can find these satisfactions in private practice and, at the same time, enjoy greater economic security.

Lawrence M. McNiesh
Community Radiology Associates
Olney, MD 20832

REFERENCES

1. Schreiber MH. Opinion. Academic and private practice: competition, concession, and conciliation. *AJR* **1987**;148:1027–1028
2. Sartoris DJ. Opinion. Beyond radiology training: a guide to career choice. *AJR* **1987**;148:1029

Reply

The points raised by Dr. McNiesh in his response to my *Opinion* concerning careers in academic vs private practice radiology are certainly well taken. Although it is true that academic promotion does depend heavily on the quality of research and publications in general, it is my feeling that certain institutions place much more emphasis upon this aspect of academia than others do. Although I myself truly enjoy the challenge and excitement of research, it is less important to me than teaching and patient-care activities, which provide a more immediate sense of fulfillment. When I recognized this priority order within myself as a fourth-year resident, I voiced concerns similar to those of Dr. McNiesh to one of my most highly regarded instructors at Stanford (who, I might add, is a tenured professor at this highly regarded university and does not have an extensive background in basic research). His encouraging response to me was, "You *can* be yourself in academics; people will respect you for being good at what you do best, and if that doesn't conform with the promotion policies of the school where you find yourself, take your talent elsewhere and look upon it as their loss, not yours." As my career has progressed, I have come to know quite a number of "well-balanced" academicians who have been promoted at an expected pace, and I therefore believe that there are, in fact, institutions that recognize teaching and patient-care abilities as well as research achievements. With regard to Dr. McNiesh's criticisms concerning the Association of University Radiologists, I am unable to comment as I am a relatively new member who lacks extensive involvement with its policies and procedures. However, I do recognize the fact that their Gold Medal this year was awarded to another of my mentors, Dr. Henry Jones, an exceptional radiologist and human being who for years has devoted his time and effort to high-quality patient care and excellence in instruction. I think that Dr. McNiesh errs in implying that the AUR is not interested in teaching and the clinical practice of radiology. Although much of its meeting program may, in fact, be composed of scientific/research papers, most of this work has been performed by radiology trainees, under the tutelage of academicians. In conclusion, the three facets of academic radiology are not mutually exclusive; rather, they coexist in nearly every activity, thus enhancing the excitement and challenge of this career choice. One need only approach this overall environment with energy, enthusiasm, and a positive attitude. Quality in all three areas will result, without the need for conscious direction of effort toward an area that is thought to be of greatest importance to a promotions committee or peer group.

David J. Sartoris
University of California, San Diego, Medical Center
San Diego, CA 92103-1990

Heterotopic Excretion of IV Contrast Material by the Appendix

In the past, vicarious excretion of renographic compounds, especially by the liver, was not uncommon. Biliary excretion has been reported in as many as 20% of patients after an average dose of Urokon (sodium acetrizoate) [1]. With ionic contrast agents, opacification of the gallbladder or bowel is most unusual in the absence of impaired renal function [2].

The following report illustrates a case of ectopic excretion of Renografin-60 (meglumine diatrizoate) by a normal appendix in the absence of renal failure. In the workup of a young woman with cervical cancer, laboratory studies and an IV pyelogram were performed. All the laboratory studies had normal results. The IV pyelo-

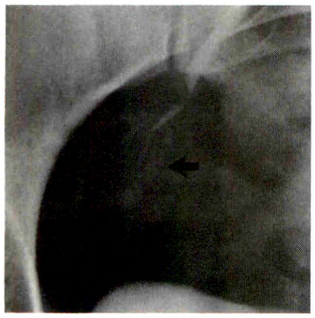


Fig. 1.—Radiograph made 15 min after injection of contrast material for an IV pyelogram shows opacification of appendix (*arrow*). Appendix was not visible on preliminary radiograph.

gram with 60 ml of Renografin-60 showed good delineation of the urinary tract. On films made 10 and 15 min after injection of the contrast agent, a coiled tubular-appearing opacity not present on preliminary films was seen in the right lower quadrant (Fig. 1). The proximal part of the opacity had the typical configuration of a contrast-enhanced intestinal wall with a lumen containing gas. Except for its fainter density, its appearance was identical to that of a barium-filled appendix.

A radical hysterectomy and an incidental appendectomy were performed. Examination of the uterus revealed a stage IB squamous carcinoma of the cervix. The gross and histologic examination of the appendix was normal.

There are three possible explanations for opacification of the appendix in this patient who has an apparently normal urinary tract. First, excretion of the contrast medium by the mucosa of the small bowel might be followed by its concentration in the large bowel and drainage into the appendix. Second, abnormal communication might exist between the bowel and the urinary tract, and, third, the contrast medium might have been excreted directly into the lumen of the appendix via the appendiceal mucosa.

We reject the first explanation because (1) the initial pyelogram showed no opacification of any portion of the gastrointestinal tract other than the appendix, and (2) the contrast agent appeared in the appendix 10 min after it was given intravenously.

The second possible explanation also is unlikely because (1) the patient had no history of any previous illness or injury; (2) no contrast material was seen outside the urinary tract; (3) at the time of surgery, no abnormality of the urinary or gastrointestinal systems was encountered; and (4) on pathologic examination of the surgical specimens, the appendix was normal.

Therefore, it seems likely that opacification of the appendix was the result of heterotopic excretion of contrast material by the mucosa of the appendix, with subsequent accumulation of the contrast material in the lumen.

Roy J. Siragusa
University of Florida College of Medicine
Gainesville, FL 32610
John Faunce Roach
Albany Medical Center Hospital
Albany, NY 12208

REFERENCES

1. Porporis AA, Eliott GV, Fisher GL, et al. Mechanism of Urokon excretion. *AJR* **1954**;72:995–1003
2. Jackson DA. Heterotrophic excretion of diatrizoate. *Lancet* **1968**;1:1286–1288

Review of Current Literature

Initials and addresses of corresponding authors are provided in parentheses for each article so that the reader can obtain reprints directly. Abstracts are printed verbatim from each journal.

CLINICAL LITERATURE

The New England Journal of Medicine

Compensatory enlargement of human atherosclerotic coronary arteries. Glagov S, Weisenberg E, Zarins CK, Stankunavicius R, Kolettis GJ (SG, Dept. of Pathology, University of Chicago, 5841 S. Maryland Ave., Chicago, IL 60637). *N Engl J Med* 316(22):1371–1375, 1987

Whether human coronary arteries undergo compensatory enlargement in the presence of coronary disease has not been clarified. We studied histologic sections of the left main coronary artery in 136 hearts obtained at autopsy to determine whether atherosclerotic human coronary arteries enlarge in relation to plaque (lesion) area and to assess whether such enlargement preserves the cross-sectional area of the lumen. The area circumscribed by the internal elastic lamina (internal elastic lamina area) was taken as a measure of the area of the arterial lumen if no plaque had been present. The internal elastic lamina area correlated directly with the area of the lesion ($r = 0.44$, $P < 0.001$), suggesting that coronary arteries enlarge as lesion area increases. Regression analysis yielded the following equation: Internal elastic lamina area = 9.26 + 0.88 (lesion area) + 0.026 (age) + 0.005 (heart weight). The correlation coefficient for the lesion area was significant ($P < 0.001$), whereas the correlation coefficients for age and heart weight were not. The lumen area did not decrease in relation to the percentage of stenosis (lesion area/internal elastic lamina area × 100) for values between zero and 40 percent but did diminish markedly and in close relation to the percentage of stenosis for values above 40 percent ($r = -0.73$, $P < 0.001$).

We conclude that human coronary arteries enlarge in relation to plaque area and that functionally important lumen stenosis may be delayed until the lesion occupies 40 percent of the internal elastic lamina area. The preservation of a nearly normal lumen cross-sectional area despite the presence of a large plaque should be taken into account in evaluating atherosclerotic disease with use of coronary angiography.

Cancer

Prophylactic cranial irradiation in adenocarcinoma of the lung: a possible role. Jacobs RH, Awan A, Bitran JD, et al. (RHJ, 5841 S. Maryland Ave., Box 420, Chicago, IL 60637). *Cancer* 59:2016–2019, 1987

Seventy-eight patients with modified Stage II or Stage IIIMO adenocarcinoma of the lung were evaluated retrospectively with regard to the impact of prophylactic cranial irradiation (PCI) (30 Gy in 15 fractions) in preventing central nervous system (CNS) metastases. Twenty patients received PCI and 58 did not. There were no significant differences between these groups with respect to age, sex, stage, or median survival (17.4 months with PCI *versus* 16.9 months without PCI; $P = 0.6$). One (5%) of 20 patients receiving PCI developed CNS metastases, compared with 14 (24%) of 58 patients not receiving PCI ($P = 0.06$). The time from diagnosis to development of CNS metastases and survival after CNS involvement was 51 weeks and 14 weeks, respectively, for the patient who received PCI; and a median time of 50 weeks and 26 weeks, respectively, for the patients not receiving PCI. In nine (64%) of the 14 non-PCI patients the CNS was the first and only site of relapse. A Cox regression analysis demonstrated that nodal involvement was significantly associated with an increased risk of CNS metastases. These data suggest that PCI may decrease the incidence of CNS metastases, and that it may be beneficial in the management of patients with N1 or N2 disease.

Reprinted with permission by the American Cancer Society.

Chest

Thoracocentesis: clinical value, complications, technical problems, and patient experience. Collins TR, Sahn SA (SAS, Pulmonary/Critical Care Medicine, Medical University of South Carolina, Charleston, SC 29425). *Chest* 91(6):817–822, June 1987

A prospective study of 129 consecutive thoracocenteses in 86 patients at a university medical center evaluated the clinical value, complications, and patient experience with thoracocentesis. Pleural fluid analysis in conjunction with the clinical presentation placed 78 pleural fluids into diagnostic categories: definitive 14 (18 percent), presumptive 44 (56 percent), and nondiagnostic 20 (26 percent). Fourteen of 78 (18 percent) of the nondiagnostic fluids were useful, while only six (8 percent) were not useful clinically; therefore, 92 percent of thoracocenteses provided clinically useful information. Using sequential data analysis, initial diagnostic categorizations of eight of 78 patients were upgraded from presumptive or nondiagnostic to definitive based on data available 24 hours following thoracocentesis. Thus, 70 patients were categorized based on the pleural fluid data obtained within the first 24 hours of thoracocentesis. Thirty-four objective complications occurred in 26 of 129 (20 percent) thoracocenteses. The most common complications were pneumothorax, 15 of 129 (12 percent), and cough, 12 of 129 (9 percent). Sixty-five subjective complications occurred in 56 of 123 (46 percent) thoracocenteses. Anxiety, 26 of 123 (21 percent), and site pain, 24 of 123 (20 percent), were the most common subjective complications noted. Thirty technical problems occurred in 129 (23 percent) thoracocenteses with blood contamination, 14 of 129 (11 percent), and dry tap, nine of 129 (7 percent), being the most common. We conclude

that diagnostic thoracocentesis is a clinically valuable procedure if used in conjunction with the patient presentation with an understanding of its limitations for providing a specific etiologic diagnosis. When performed by physicians in training, the number of complications are substantial and the operator often underestimates the degree of patient discomfort. Awareness of the clinical value and complications of thoracocentesis should lead to improved use and safety of this procedure.

Editor's note: *Chest* has published a supplement with its June 1987 issue. The supplement contains papers from the International Workshop on the Etiology of Asthma.

Circulation

Angiographic and histologic consequences of laser thermal angioplasty: comparison with balloon angioplasty. Sanborn TA, Haudenschild CC, Garber GR, Ryan TJ, Faxon DP (TAS, Dept. of Cardiology, University Hospital, 75 Newton St., Boston, MA 02118). *Circulation* 75(6):1281–1286, 1987

The angiographic and histologic consequences of laser thermal angioplasty were examined and compared with those of conventional balloon angioplasty in an atherosclerotic rabbit iliac artery preparation immediately and 4 weeks after the procedure. Nineteen vessels in 13 rabbits underwent either laser thermal or balloon angioplasty in random order. Laser thermal angioplasty was performed in a total of nine vessels with either a 1.5 or 2.0 mm laser-heated metallic-capped fiber by delivery of 6 or 8 W, respectively, of argon laser energy for 5 sec duration during continuous advancement through the stenosis. Balloon angioplasty was performed in a total of 10 stenotic lesions with a 2.5 mm balloon catheter. The immediate enlargement of the angiographic luminal diameters was similar for both procedures: from 1.0 ± 0.2 to 1.9 ± 0.2 mm for laser thermal angioplasty vs 1.0 ± 0.1 to 2.0 ± 0.2 mm for balloon angioplasty. However, 4 weeks later the vessels treated with laser thermal angioplasty had less restenosis, defined as a 20% or greater reduction in luminal diameter (two of nine vessels [22%] vs 10 of 10 vessels [100%]; $p < .001$), and a significantly larger mean luminal diameter (1.6 ± 0.5 vs 1.0 ± 0.4 mm) than those treated with conventional balloon angioplasty ($p < .02$). Histologic examination 4 weeks after the procedure revealed less fibrocellular proliferation after laser thermal angioplasty, whereas those vessels treated with balloon angioplasty demonstrated evidence of prior fracture and dissection of the vessel wall with more of a fibrocellular proliferative response. Morphometric analysis of these histologic cross-sections confirmed a significantly larger lumen after laser thermal angioplasty compared with balloon angioplasty (1.24 ± 0.62 vs 0.64 ± 0.45 mm^2; $p < .05$). In summary, in rabbit iliac artery stenoses, laser thermal angioplasty was associated with less restenosis and produced a significantly larger mean luminal diameter and mean luminal area than conventional balloon angioplasty. Differences in the pathophysiologic mechanisms of angioplasty with these two techniques may be responsible for this observation and may have clinical relevance.

Gastroenterology

Percutaneous endoscopic gastrostomy: indications, success, complications, and mortality in 314 consecutive patients. Larson DE, Burton DD, Schroeder KW, DiMagno EP (DEL, Division of Gastroenterology, Dept. of Internal Medicine, Mayo Clinic, Rochester, MN 55905). *Gastroenterology* 93:48–52, 1987

The aim of this study was to determine the indications, success rate, procedure-related mortality, and major and minor complication rates in 314 consecutive patients in whom we attempted a percutaneous endoscopic gastrostomy. The most common indications for placement of the gastrostomy tube were neurologic ($n = 235$, 75%) and oropharyngeal disorders ($n = 42$, 13%). We noted that the gastrostomy tube was successfully placed in 299 (95%) of the 314 patients. Ninety-three percent ($n = 291$) of the patients had the procedure performed in the hospital and 7% ($n = 23$) were outpatients when the procedure was performed. In those patients with stable underlying conditions, the procedure can safely be performed in the outpatient setting. A low rate of procedure-related mortality (1%), major complication (3%), and minor complication (13%) was noted. Our experience suggests that the percutaneous endoscopic gastrostomy is safe and has a low mortality rate even in patients who are medically debilitated secondary to their underlying disease.

Reprinted with permission by the American Gastroenterological Association.

Digestive Diseases and Sciences

Radiologic appearance of gallstones and its relationship with biliary symptoms and awareness of having gallstones: observations during epidemiological studies. Rome Group for the Epidemiology and Prevention of Cholelithiasis (GREPCO) (Attili AF, Largo Forano 3, 00199, Rome, Italy). *Dig Dis Sci* 32(4):349–353, April 1987

In the course of two cross-sectional epidemiological surveys carried out by the Rome Group for Epidemiology and Prevention of Cholelithiasis (GREPCO), cholecystography was performed in 82 of 126 subjects identified by means of ultrasonography as having gallstones. In four subjects gallstones were not detected by cholecystography. The x-ray characteristics of the gallbladder and gallstones of the remaining 78 subjects were related to age, sex, presence of biliary symptoms in the five years prior to the study, and awareness of having gallstones. Twenty-three of the 78 gallstone subjects (29.5%) showed a nonvisualized gallbladder. Among the 55 subjects with visualized gallbladder, 16 (29.1%) and 28 (50.9%) showed radiopaque and solitary stones, respectively. The mean diameter of the largest stone was $19.7 \text{ mm} \pm 11.2$ (SD). Age was related inversely to the number of stones. X-ray characteristics of gallstones did not differ between men and women. Presence of biliary symptoms in the five years prior to the study or awareness of having gallstones were not related to any radiologic feature, either in univariate or multivariate statistical analysis which included age, sex, weight, and height as possible confounding variables. Nineteen (24.3%) of the 78 subjects showed gallstones which would have been suitable for medical therapy with bile acids (ie, radiolucent, with a diameter of less than 20 mm, and in a visualized gallbladder).

The Journal of Bone and Joint Surgery

Complications and mortality associated with bilateral or unilateral total knee arthroplasty. Morrey BF, Adams RA, Ilstrup DM, Bryan RS (BFM, Dept. of Orthopaedics, Mayo Clinic and Mayo Foundation, Rochester, MN 55905). *J Bone Joint Surg [Am]* 69A:484–488, 1987

The incidence of complications, the need for secondary surgical procedures, and the mortality rate associated with bilateral replacement of the knee performed simultaneously, performed during the same hospitalization, or performed during separate hospitalizations were compared with those after unilateral replacement of the knee. The incidence of complications after 290 simultaneous bilateral procedures was 9.3 percent, which compares favorably both with the incidence of 7.0 percent after 228 bilateral procedures that were done during the same hospitalization and incidence of the 12.0 percent after 234 bilateral procedures that were performed during separate hospitalizations. The incidence for each of these groups compares favorably with the incidence of complications of 11.0 percent after 501 unilateral procedures. The incidence of reoperation was 2.4, 4.8, 8.5, and 5.6 percent, respectively, in the four groups, and the incidence of mortality was 5.5, 0.9, 3.8, and 7.0 percent. None of these differences were statistically significant.

These data indicate that the incidence of morbidity and mortality that is associated with simultaneous bilateral total knee arthroplasty is no greater than when the procedure is performed during the same hospitalization or separate hospitalizations.

The Journal of Urology

Clinical significance of hematuria in patients on anticoagulant therapy. Schuster GA, Lewis GA (GAS, Ste. 303, 330 N. Madison St., Joliet, IL 60435). *J Urol* 137:923, May 1987

We evaluated 29 consecutive patients in whom gross or microscopic hematuria developed while they were on heparin or warfarin anticoagulant therapy. Patients who had bleeding as a result of anticoagulant overdosage and/or from an additional organ system(s) other than the urinary tract were excluded from this review.

Significant pathological findings consisting of carcinoma, calculi, renal infarction, infection, benign prostatic hyperplasia and/or adult polycystic renal disease were identified in 17 patients. Insignificant or incidental pathological findings classified as posterior urethritis, simple renal cyst or renal scarring were noted in 6 patients. No pathological condition was found in the remaining 6 patients. We concluded that a thorough and appropriate evaluation of the urinary tract should be conducted in patients on anticoagulant therapy who have gross or microscopic hematuria, since a pathological lesion of variable clinical significance often is discovered.

British Journal of Urology

Surgical treatment of renal cancer with vena cava extension. Neves RJ, Zincke H (RJN, Depts. of Surgery and Urology, Mayo Clinic and Mayo Foundation, Rochester, MN 55905) *Br J Urol* 59:390–395, May 1987

Fifty-four patients with renal cancer and vena cava tumour thrombus underwent radical nephrectomy and removal of the thrombus; the operative mortality rate was 9.3% (5 patients). The extent of the vena cava thrombus did not affect survival.

Of 36 patients with no known pre-operative metastases and complete (29 patients) and incomplete (7 patients) removal of the vena cava tumour thrombus, the 5-year survival rate was 68 and 17%, respectively ($P = 0.01$). Thirteen patients (45%) who underwent complete removal of the vena cava tumour thrombus are alive and free of disease, with a mean follow-up of 51.2 months (range 4–144); three died without disease 110, 31 and 23 months after operation.

The 2-year and 5-year survival rates of 18 patients with known pre-operative metastases was 37.5 and 12.5% respectively; 14 died between 1 and 27 months post-operatively (mean 11.6) of metastatic disease. Two of these 18 patients experienced long-term remission: one died of unrelated causes 151 months after operation; the other was lost to follow-up 219 months after operation, with no evidence of disease. Of 14 patients with positive regional nodes, the mean survival in those with metastases compared with those without metastases was 7.5 versus 15 months, respectively; only one patient survived at 14 months.

Operative intervention in patients without metastatic disease (systemic or regional) and complete removal of the vena cava thrombus achieved a 5-year survival rate of 68%. Variables which significantly decreased survival and may be considered contraindications for operation were systemic metastasis, regional lymph node involvement and incomplete removal of the vena cava thrombus.

Pediatrics

Prolonged mechanical ventilation and intracranial hemorrhage: impact on developmental progress through 18 months in infants weighing 1,200 grams or less at birth. Bozynski MEA, Nelson MN, Matalon TAS, et al. (MAB, University of Michigan Medical Center, Department of Pediatrics, Section of Newborn Services, L3023 Women's Hospital, Box 0254, Ann Arbor, MI 48109-0254). *Pediatrics* 79(5):670–676, May 1987

In this prospective, longitudinal study, the relative impact of intracranial hemorrhage and prolonged mechanical ventilation on developmental progress during the first 18 months of life of infants weighing 1,200 g or less at birth was examined. A total of 159 surviving infants were divided into two groups: infants with and those without intracranial hemorrhage. These groups were then subdivided into groups of infants receiving prolonged mechanical ventilation (>21 days) and those mechanically ventilated for 21 days or less, thus creating four subgroups. Group 1 (intracranial hemorrhage and prolonged mechanical ventilation) and group 3 (intracranial hemorrhage and no prolonged mechanical ventilation) showed no statistically significant differences for severity of intracranial hemorrhage, persistence of ventriculomegaly, or presence of periventricular leukomalacia. A repeated-measures analysis of variance demonstrated a main effect for prolonged mechanical ventilation on outcome as measured by the Bayley Mental Development Index and Bayley Psychomotor Development Index at 4, 8, 12, and 18 months of age (corrected for prematurity). Forward stepwise regression revealed prolonged mechanical ventilation to be the best predictor of Bayley indexes at all ages except 4 months of age, for which the Psychomotor Development Index was best predicted by length of hospitalization. No main effect for intracranial hemorrhage was demonstrated, but the motor performance of infants with intracranial hemorrhage declined significantly with age. By contrast prolonged mechanical ventilation was associated with uniformly poor performance at every age and serves as a powerful marker for poor developmental progress during the first 18 months of life in infants weighing 1,200 g or less at birth.

Reproduced with permission by *PEDIATRICS* © 1987.

The Journal of Pediatrics

Hemostasis and thromboembolism in children with nephrotic syndrome: differences from adults. Mehls O, Andrassy K, Koderisch J, Herzog U, Ritz E (OM, Division of Pediatric Nephrology, University Children's Hospital Heidelberg, Im Neuenheimer Feld 150, D-6900 Heidelberg, West Germany). *J Pediatr* (110(6):862–867, June 1987

Eleven of 204 children with nephrotic syndrome had thrombotic complications: arterial thrombosis in five, venous thrombosis in four, and pulmonary embolism in two. Fifty-one episodes of thromboembolism were recognized in 116 adult patients with nephrotic syndrome. Despite the lower incidence, thromboembolic complications tended to be more severe in children. In vitro indices of hemostasis and clinical evidence of thromboembolic complications were compared in children and adults. Antithrombin III concentrations and activities were abnormal in seven of 10 children, but in only two of 32 adults. In both groups, α_2-macroglobulin was elevated, but more markedly so in children. No evidence for circulating granulocyte-derived proteases (elastase/antielastase complexes) was noted in either group. Protein C was significantly elevated in children with nephrotic syndrome, but was normal in adults. Children also differed from adults with nephrotic syndrome in laboratory evidence of subthreshold disseminated intravascular coagulation (i.e., elevated soluble fibrinogen monomeric complexes and fibrin degradation products) and indicators of in vivo platelet activation (elevated β-thromboglobulin). The more severe coagulation abnormalities in children may be linked to the more pronounced hypoalbuminemia.

RADIOLOGY SUBSPECIALTY JOURNALS

Pediatric Radiology

Children with AIDS—is pathologic diagnosis possible based on chest radiographs? Zimmerman BL, Haller JO, Price AP, Thelmo WL, Fikrig S (BLZ, Dept. of Radiology, Kings County Hospital, Downstate Medical Center, Brooklyn NY). *Pediatr Radiol* 17:303–307, 1987

In a review of the clinical, radiographic and pathologic data of 36 patients with AIDS we found 29 with pulmonary infections (Cyto-

megalic virus, Pneumocystis carinii, etc.) and 7 who had varying types of lymphocytic infiltration and interstitial changes on chest radiographs but did not have opportunistic infection. Pathologic diagnosis included lymphocytic interstitial pneumonitis, bronchus associated lymphoid tissue, chronic interstitial pneumonitis, desquamative interstitial pneumonitis and immunoblastic sarcoma. The chest X-rays were not predictive in making a specific diagnosis.

Gastrointestinal Radiology

Granular small bowel mucosa: a reflection of villous abnormality. Jones B, Hamilton SR, Rubesin SE, Bayless TM, Ravich WJ, Hendrix TR (BJ, Dept. of Radiology, The Johns Hopkins Hospital, 600 N. Wolfe St., Baltimore, MD 21205). *Gastrointest Radiol* 12:219–225, 1987

Diffuse mucosal granularity was reported recently in small bowel Crohn's disease. The radiographic appearance corresponded on histopathologic examination to villous hypertrophy, fusion, or epithelial bridge formation. We have observed similar granularity in Crohn's disease but also in several other conditions, including radiation enteritis, pancreatic glucagonoma, protein-losing enteropathy, and small bowel ischemia. Histopathologic examination demonstrated various alterations in villous morphology, such as edema, hyperplasia, clubbing, or fusion. In Crohn's disease, this appearance was sometimes an indication of early inflammatory disease but was also seen following extensive small bowel resection, possibly due to villous enlargement resulting from intestinal adaptation. These findings suggest that granular mucosa in the small bowel is a nonspecific finding reflecting an alteration in villous structure.

The Journal of Nuclear Medicine

Volume expansion diuretic renal scan in urinary tract obstruction. Howman-Giles R, Uren R, Roy LP, Filmer RB (RH-G, Dept. of Nuclear Medicine, The Children's Hospital, P.O. Box 34, Camperdown, N.S.W. 2050, Australia). *J Nucl Med* 28:824–828, 1987

The diuretic renal scan is used to differentiate the obstructed dilated urinary system from the nonobstructed dilated system. The technique, however, has a false-positive and indeterminate rate of 10%–15%. This usually is due to variables such as the degree of dilatation of the pelvicalyceal system or ureter, the degree of bladder distention, the diuretic dose, and the state of hydration. We developed the volume expansion diuretic renal scan (VEDRS) to overcome these variables and to improve the accuracy of the technique. Twelve patients who had obstructive patterns on the diuretic renal scan were evaluated. Ten patients were shown to be dilated but not obstructed. Two patients were confirmed as obstructed. This technique improves the accuracy of the diuretic renal scan.

Journal of Ultrasound in Medicine

Sonographic evaluation of the kidney following extracorporeal shock wave lithotripsy. Kaude JV, Williams JL, Wright PG, Bush D, Derau C, Newman RC (JVK, Box J-374, JHMHC, University of Florida College of Medicine, Gainesville, FL 32610). *J Ultrasound Med* 6:299–306, 1987

We investigated the value of real-time sonography for determination of pelvicaliceal dilatation 24–48 h after extracorporeal shock wave lithotripsy (ESWL) in 369 patients (419 treated kidneys). A varying degree of hydronephrosis was present in 121/419 (29%) kidneys. Fragmented stones post-ESWL were demonstrable in 346/419 kidneys (82%), but were missed by ultrasound in three kidneys (<1%). In four kidneys (1%), stone fragments which were shown to be present by ultrasound were not detectable on radiographs. In 25/419 kidneys (6%), evidence of renal trauma caused by ESWL was demonstrated by ultrasound. The most important incidental finding was a small renal cell carcinoma of the contralateral (untreated) kidney. KEY WORDS: renal ultrasound; extracorporeal shock wave lithotripsy; kidney stones; hydronephrosis.

Reprinted with permission by the American Institute of Ultrasound in Medicine.

Magnetic Resonance Imaging

Proton relaxation enhancement by manganese(III)TPPS$_4$ in a model tumor system. Fiel RJ, Button TM, Gilani S, et al. (RJF, Dept. of Biophysics, Roswell Park Memorial Institute, 666 Elm St., Buffalo, NY 14263). *Mag Reson Imag* 5:149–156, 1987

Manganese(III)tetraphenylporphine sulfonate [Mn(III)TPPS$_4$] has been investigated as a tumor specific paramagnetic contrast agent for magnetic resonance imaging (MRI) of L1210 solid tumors in mice. Mn(III)TPPS$_4$ was found to clear rapidly from the blood and concentrate in the kidneys, tumor and liver. Although relatively high ratios of tumor to normal tissues could be obtained (e.g., >90 for tumor/muscle), the kidneys were found to have the highest concentration of the metalloporphyrin at all doses and time periods tested. A significant decrease in the longitudinal relaxation time was measured for excised tissues (kidney, tumor, liver, muscle) from mice that were treated with Mn(III)TPPS$_4$. A linear correlation was observed between the longitudinal relaxation rate determined for L1210 tumor and the corresponding concentration of Mn(III)TPPS$_4$ found at various injected doses and time intervals between the injection and analysis. A small animal radiofrequency receiver coil designed for use with a 0.15-T clinical imager was employed to evaluate the ability of Mn(III)TPPS$_4$ to selectively increase the signal intensity of the implanted L1210 tumor. The images show a conspicuous enhancement in the contrast between the tumor and adjacent tissue upon treatment with this agent. The results indicate that Mn(III)TPPS$_4$ is a useful prototype paramagnetic metalloporphyrin MRI contrast agent with a significant affinity for the L1210 tumor.

News

Radiation, Physics, and Biology

The NYU Medical Center will sponsor Radiation, Physics, and Biology, Aug. 31–Sept. 4, at the NYU Medical Center in New York City. This course, especially designed for residents in diagnostic radiology and nuclear medicine, is an intensive review and preparation for the written board examination in Radiology and Nuclear Medicine. It is also of value for those preparing for the oral examination. Students are advised to read one or more of the basic texts in diagnostic radiologic physics and radiation biology beforehand. Category 1 credit: 32 hr. Fee: physicians, $550; residents, $413. Information: NYU Medical Center, Post-Graduate Medical School, 550 First Ave., New York, NY 10016; (212) 340-5295 (24-hr service).

Computed Tomography and Magnetic Resonance Imaging of the Brain, Head, Neck, and Spine

The Dept. of Diagnostic Radiology, Rush-Presbyterian-St. Luke's Medical Center, will hold its 14th annual course on Computed Tomography and Magnetic Resonance Imaging of the Brain, Head, Neck, and Spine, Sept. 14 and 15, at the Westin Hotel in Chicago. The course material will cover the interpretation of CT and MR images of the brain, head, neck, and spine and the performance of these examinations. Guest faculty: R. N. Bryan, D. O. Davis, M. H. Gado, D. C. Harwood-Nash, S. K. Hilal, T. P. Naidich, P. F. J. New, Enrique Palacios, D. L. Reede, E. J. Russell, P. M. Som, J. M. Taveras, and R. D. Zimmerman. Category 1 credit: 16 hr. Information: M. S. Huckman, M.D., Director of Neuroradiology, Rush-Presbyterian-St. Luke's Medical Center, 1753 Congress Pkwy., Chicago, IL 60612; (312) 942-5781.

Correlative Imaging in the Endocrine System

Ann Arbor Veterans Administration Medical Center and The University of Michigan Medical School are sponsoring Correlative Imaging in the Endocrine System: Current Status and Clinical Applications, Sept. 28, at Ann Arbor. The conference will present up-to-date information on the imaging evaluation of the endocrine system and changes that occur with endocrine disease. The complex issues of the imaging approach and relative roles of various techniques will be placed in perspective. Category 1 credit: 6 ACCME hr of the PRA. Fee: physician, $100; allied health care professional, $70. Information: Debbie DeSmyther, The Office of Continuing Medical Education, The University of Michigan Medical School, Towsley Center, Box 0201, Ann Arbor, MI 48109-0201; (313) 763-1400.

Quantitative Thallium Myocardial Tomography

The Dept. of Radiology, Division of Nuclear Medicine, Emory University School of Medicine, is sponsoring Quantitative Thallium Myocardial Tomography, Sept. 28 and 29, Oct. 19 and 20, and Dec. 14 and 15, at Emory University, Atlanta, GA. This program is designed for cardiologists, radiologists, and nuclear medicine physicians. It is intended to familiarize participants with basic principles as well as the clinical usefulness of quantitative thallium tomography. Category 1 credit: 13.5 hr. Fee: $500. Information: Continuing Medical Education, Emory University School of Medicine, 1440 Clifton Rd., N. E., 110 WHSCAB, Atlanta, GA 30322; (404) 727-5695.

Jack R. Dreyfuss Fellowship

The Massachusetts General Hospital, Harvard Medical School, Boston, MA, has announced the creation of the Jack R. Dreyfuss Fellowship for research in gastrointestinal radiology. The fellowship, which is for 1 year, will begin July 1, 1988. The program will include participation in ongoing research in gastrointestinal radiology, including MR, CT, ultrasound, interventional radiology, and biliary lithotripsy. Applicants must be board eligible and should anticipate a career in academic radiology. The deadline for receipt of applications in Oct. 1, 1987. Information: J. T. Ferrucci, M.D., Abdominal Imaging Section, Dept. of Radiology, Massachusetts General Hospital, Boston, MA 02114; (617) 726-8387.

Laser Angioplasty and Interventional Radiology

The Dept. of Radiology and Radiological Science, The Johns Hopkins University School of Medicine, is sponsoring Laser Angioplasty and Interventional Radiology, Oct. 12–14, at The Johns Hopkins Medical Institutions, Baltimore, MD. This course is designed to give on-line demonstrations of techniques in biliary stenting, embolotherapy, and transluminal angioplasty. The argon "hot tip" laser will be demonstrated during the course. The audience will be able to interact with the faculty in the auditorium and in the angiographic suite. Course director: R. I. White, Jr. Category 1 credit: 25 hr. Fee: physicians, $400; residents, nurses, technicians, $200. Information: Carlita M. Kearney, Program Coordinator, Office of Continuing Education, Turner 22, 720 Rutland Ave., Baltimore, MD 21205; (301) 955-3168.

Fall Symposium on Diagnostic Imaging

The faculty of the Dept. of Radiology, Duke University Medical Center, will present its 14th annual Fall Symposium of Diagnostic Imaging, Oct. 12–16, at the Southampton Princess, Bermuda. This 5-day postgraduate course is designed to update participants in a number of the newer imaging techniques in diagnostic radiology and to review the role of conventional imaging in relation to these techniques. The course is limited to 150 participants. Program director: N. R. Dunnick. Category 1 credit: 22 hr. Fee (U. S. dollars): before Aug. 10, $450; after Aug. 10, $495. Information: C. E. Ravin, M.D.,

Dept. of Radiology, Duke University Medical Center, P. O. Box 3808, Durham, NC 27710; (919) 681-5268.

2nd Hellenic Radiological Symposium of Modern Imaging Modalities

The Hellenic Radiological Society is sponsoring the 2nd Hellenic Radiological Symposium of Modern Imaging Modalities, Oct. 15–18, in Athens, Greece. The course will feature the impact of new imaging techniques in diagnostic and therapeutic radiology. Topics will be presented by local faculty and guest speakers. The first day of the symposium, the University of Athens, School of Medicine, Dept. of Radiology, Areteion Hospital, Athens, Greece, will sponsor a satellite Conference on the Radiology of Thalassemias. Fee (U. S. dollars): physicans, $150; residents, $100. Information: Secretariat, Public Relations Center, Ltd., 56 Ippokratous St., 106-80 Athens, Greece.

International Congress of Oral Cancer and Jaw Tumors

The World Health Organization and The International Union Against Cancer are cosponsoring the 1st International Congress on Oral Cancer and Jaw Tumors, Nov. 9–14, in Singapore. The congress is being organized by the Division of Oral and Maxillofacial Surgery, The Johns Hopkins Medical Institutions, in conjunction with the Dept. of Oral and Maxillofacial Surgery of the National University of Singapore. The purpose of the congress is to bring together distinguished and well-known international leaders on the subject to establish the current status of this disease and the state of the art in management. The intent is to provide a stimulus for future avenues of creative endeavors for improvements in diagnosis, treatment, reconstruction, and rehabilitation. Congress coordinator: Dr. R. W. Van Bowen, The Johns Hopkins Medical Institutions; (301) 955-2083 or 955-6664. Information: Dr. N. Ravindranthan, Organizing Secretary, First International Congress on Oral Cancer and Jaw Tumors, Dept. of Oral Surgery, Faculty of Dentistry, National University of Singapore, Kent Ridge, Singapore 0511.

Interventional Neuroradiology

The Dept. of Radiology and Radiological Science, The Johns Hopkins University School of Medicine, will sponsor Interventional Neuroradiology: Current Practices and Technique, Dec. 7–9, at The Johns Hopkins Medical Institutions, Baltimore, MD. The course will feature both a didactic component and practicum given by leading authorities in the fields of interventional neuroradiology, neurosurgery, neurology, plastic surgery, otolaryngology, and ophthalmology. The focus will be the crucial collaborative relationship between neuroradiologic and surgical expertise in the management of patients with complex medical problems. Course director: Gerard Debrun. Category 1 credit: 22.5 hr. Fee: physicians, $500; technicians, $400. Information: Carlita M. Kearney, Program Coordinator, Office of Continuing Education, Turner 22, 720 Rutland Ave., Baltimore, MD 21205; (301) 955-3168.

3-D Imaging in Medicine

The Dept. of Radiology, Hospital of the University of Pennsylvania, is sponsoring a conference, 3-D Imaging in Medicine, Dec. 10–12, at the Penn Tower Hotel in Philadelphia. The course is organized to meet the educational needs of radiologists, surgeons, orthopedists, radiation therapists, and others who are interested in the rapidly expanding medical applications of three-dimensional imaging. The goals are to acquaint the participants with the basic principles of three-dimensional imaging, the broad scope of its clinical applications, the wide variety of available software and hardware, and the prospects for future developments and advances. Category 1 credit: 15 hr (pending). Fee: $125. Information: Janice Ford, CME Coordinator, Dept. of Radiology, Hospital of the University of Pennsylvania, 3400 Spruce St., Philadelphia, PA 19104; (215) 662-6904 or 662-6982.

Breast Imaging 1988

Massachusetts General Hospital, Harvard Medical School, will offer the postgraduate course Breast Imaging 1988 at Frenchman's Reef Beach Resort, St. Thomas, U. S. Virgin Islands, Feb. 1–5, 1988. This practical, comprehensive course on breast cancer detection and diagnosis emphasizes interaction with the faculty and includes various approaches to mammographic screening. Guest faculty: M. L. Moskowitz and E. A. Sickles. Program director: D. B. Kopans. Category 1 credit: 20 hr. Fee: physicians, $500; residents and fellows, $400. Information: Harvard Continuing Education, Boston, MA 02114; (617) 732-1525.

International Congress on Interventional Radiology in Cardio-Vascular Diseases

The International Congress on Interventional Radiology in Cardio-Vascular Diseases will be held Feb. 3–5, 1988, in Toulouse, France. The congress will consider the present and future of different techniques of interventional radiology, including transluminal angioplasty, thrombolysis, embolization therapy, valvuloplasty, laser angioplasty, vascular endoprosthesis, percutaneous vena cava filter, atherectomy, sympatholysis, and angioscopy. The congress is being organized by the Depts. of Angiology, Cardiology, and Radiology (Chu Rangueil, Toulouse, France). Information: Prof. F. Joffre, Service de Radiologie, Chu Rangueil, Chemin du Vallon, 31054 Toulouse Cedex; telephone: 61554478 or 61531133, ext. 3081 or 3047.

12th Annual Big Sky Radiology Conference

The Dept. of Radiology, Sacred Heart Medical Center, Spokane, WA, and the Dept. of Medical Education, Columbus Hospital, Great Falls, MT, will sponsor the 12th annual Big Sky Radiology Conference, Feb. 7–12, 1988, at the Huntley Lodge, Great Falls, MT. General topics to be covered include neuroradiology, bone and chest radiology, and interventional radiology. Category 1 credit: 20 hr (pending). Fee: General, $350; residents, $150 (with letter from program director). Information: Audrey Goyette, Educational Services Dept., Columbus Hospital, 500 15th Avenue South, Great Falls, MT 59405; (406) 727-3333, ext. 5592.

Palm Beach Magnetic Resonance Imaging Update

Boston University Medical Center, Boston, MA, and JFK Memorial Hospital, Lake Worth, FL, will sponsor an MR imaging update, Feb. 14–17, 1988, at the Hyatt Palm Beaches in West Palm Beach, FL. Course directors: A. M. Green and Neil Steinmetz. Category 1 credit: 18 hr. Fee: physicians, $385; residents and technologists, $285. Information: Dept. of CME, Boston University School of Medicine, 80 E. Concord St., Boston, MA 02118; (617) 638-4605.

Pediatric Radiology 1988

Pediatric Radiology 1988 will be held at the Children's Hospital of Philadelphia, March 17–19, 1988. Sponsored by the Dept. of Radiology, the course will be an in-depth presentation of state-of-the-art imaging in infants and children. Lectures, workshops, and refresher courses will cover a wide gamut of pediatric diseases and the appropriate applications for sonography, MR imaging, CT, scintigra-

phy, and Doppler sonography. Program director: H. K. Rosenberg. Category 1 credit: 17 hr. Fee: physicians, $300; residents and technologists, $220. Information: H. K. Rosenberg, M.D., Dept. of Radiology, The Children's Hospital of Philadelphia, 34th St. and Civic Center Blvd., Philadelphia, PA 19104; (215) 596-9308.

International Symposium on the Planning of Radiological Departments

The 5th meeting of the International Symposium on the Planning of Radiological Departments will be held April 20–23, 1988, in Florence, Italy. A call for papers is being sent out. Information: Dr. Antonio Chiesa, Clas Editoriale, Via Pace, 8-25122 Brescia, Italy.

Nebraska Radiological Society Elects Officers

The Nebraska Radiological Society has announced the election of the following officers for the 1987–1988 term: president, T. R. Rusthoven; vice-president, James Call; secretary-treasurer, O. D. Osterholm; councilors, Charles Dobry and J. E. McGill; alternate councilors, Thomas Gapp and Farooq Jaffer.

Meeting and Course Review

For reader convenience, a summary of upcoming meetings and courses is provided. Detailed listings are given in the *AJR* issue noted in parentheses.

Fellowships in Imaging and Interventional Radiology for Physicians, 1987–1988, times arranged, San Diego, CA (Aug)
Visiting Fellowships in MR Imaging, times arranged, San Diego, CA (Aug)
International Continuing Medical Education Series, Sept. 5–12, Banff, Canada (Oct)
Sarcoidosis and Granulomatous Disorders, Sept. 6–11, Milan, Italy (June 1986)
Wendell G. Scott Lecture, Sept. 9, St. Louis, MO (Aug)
Magnetic Resonance Imaging: A Technologist's New World, Sept. 10–12, Orlando, FL (June)
Advances in Sectional Imaging, Sept. 10–12, San Diego, CA (July)
Doppler Echocardiography Seminar, Sept. 10–12, Tarpon Springs, FL (Aug)
Physics of Diagnostic Radiology, Nuclear Medicine and Radiation Biology, Sept. 10–13, Davis, CA (June)
Magnetic Resonance Imaging for Technologists, Sept. 11–12 and Dec. 4–5, Houston, TX (June)
Radiology in Yorkshire, Sept. 13–20, Yorkshire, England (March)
Physics of Radiology, Nuclear Medicine, and Radiobiology, Sept. 14–16, New York, NY (June)
Organ Imaging Review—Toronto 1987, Sept. 14–18, Toronto, Ontario (July)
Registry Review Courses for Sonographers, Sept. 14–19, Arlington, VA (May)
Refresher Course of the International Skeletal Society: Musculoskeletal Disorders, Sept. 16–19, Cannes, France (July)
Diagnostic Ultrasound Course, Sept. 17–19, Ann Arbor, MI (April)
Diagnostic Ultrasound in Obstetrics and Gynecology, Sept. 18–20, Baltimore, MD (July)
Ultrasound Update, Sept. 19–20, Sacramento, CA (July)
Nuclear Cardiology Symposium, Sept. 21–22, Milwaukee, WI (July)
Asian-Oceanian Congress of Radiology, Sept. 21–25, Seoul, Korea (Aug)
International Workshop on Bone and Soft Tissue Densitometry, Sept. 22–25, Buxton, Derbyshire, UK (March)
Breast Imaging Conference, Sept. 27–29, Palm Springs, CA (Aug)
Computed Tomography/MRI Update: 1987, Sept. 28–Oct. 2 (July)
MRI and Neuroimaging, Oct. 1–3, Bordeaux, France (July))
Congress on Ultrasonic Examination of the Breast, Oct. 4–5, New Orleans, LA (July)
Angiography and Interventional Radiology: 1987, Oct. 5–8, Cambridge, MA (July)
Mammography Courses, Oct. 5–8, Nov. 2–5, Boston, MA (Jan)
American Institute of Ultrasound in Medicine Convention, Oct. 6–9, New Orleans, LA (Aug)
The American Board of Radiology Examinations. Written examinations: Oct. 8–9, 1987; Oct. 6–7, 1988; Oct. 5–6, 1989. **Oral examinations:** May 23–27, 1988; June 5–9, 1989, all oral examinations at Louisville, KY (Dec 1986)
Practical Radiology, Oct. 12–14, Charlottesville, VA (July)
Society for Medical Decision Making Meeting, Oct. 12–14, Philadelphia, PA (Aug)
Neuroradiology and Head and Neck Radiology Course, Oct. 12–16, Boston, MA (April)
Chest Disease: 1987, Oct. 13–16, Boston, MA (July)
Current Trends in Diagnostic Radiology, Intervention, and Cross-Sectional Imaging—1987, Oct. 19–22, Boston, MA (April)
Twelfth Annual San Diego Postgraduate Course, Oct. 19–23, Coronado, CA, San Diego (July)
International Symposium on Diagnostic Imaging, Oct. 19–23, Barcelona, Spain (July)
American Society for Therapeutic Radiology and Oncology Meeting, Oct. 19–23, Boston, MA (July)
Advanced Applied Ultrasound in Obstetrics, Nov. 5–7, Naples, FL (Aug)
Recent Advances in the Systemic Therapy of Genitourinary Malignancies, Nov. 11–14, Houston, TX (July)
Temporomandibular Joint Conference, Nov. 12–14, Philadelphia, PA (July)
Progress in Impotence: Workshops/Seminars, Nov. 12–14, San Diego, CA (Aug)
The Johns Hopkins Medical Institutions Courses in Abdominal and Obstetric Ultrasound: Basic Practicum, Nov. 16–20; **Advanced Practicum in Ultrasound,** Dec. 7–11, Baltimore, MD (Feb)
Computed Tomography Head to Toe, Dec. 14–19, New York (Aug)
Congress of the Indian Radiological and Imaging Association, Jan. 14–16, 1988, Coimbatore, India (June)
The Society of Gastrointestinal Radiologists Meeting and Postgraduate Course, Jan. 16–20, 1988, Nassau, Bahamas (July)
The Society of Thoracic Radiology—Annual Postgraduate Course, March 27–31, 1988, Washington, DC (July)

AJR carries announcements of courses, symposia, and meetings of interest to its readers if received a minimum of 5 months before the event. There is no charge; receipt of items by the *AJR* Editorial Office is not acknowledged. Submit items for publication typed double spaced. Provide title, date, location, brief description, sponsor, course directors, fees, category I credit, and address and telephone number for additional information. Faculty from the host institution will not be listed. Guest faculty names will appear **only** if initials are provided. Mail news items to *AJR* Editorial Office, 2223 Avenida de la Playa, Suite 200, La Jolla, CA 92037-3218.

American Roentgen Ray Society 88th Annual Meeting May 8–13, 1988, San Francisco, CA San Francisco Hilton Hotel

Registration and Hotel Reservations

Forms for advance registration and hotel reservations will be in the February and March 1988 issues of the *AJR*.

Scientific Program

Abstracts of papers to be considered for the program must reach the president-elect, Lee F. Rogers, by October 1, 1987. Forms on which to submit abstracts are in this issue of the *AJR*. Please photocopy if additional copies are needed. The ARRS Program Committee will select papers in October and notify the authors by November 1. The *AJR* has first rights to all papers accepted for presentation at the ARRS meeting. Send abstract to:

Lee F. Rogers, M.D.
Dept. of Radiology
Olson Pavillion, Rm. 3426
Northwestern University Medical School
710 N. Fairbanks
Telephone (312) 908-5103 Chicago, IL 60611

Refresher Course Program

A summary of the refresher courses will appear in the *AJR* in February along with advance registration forms. Early registration is an advantage in assuring preferred courses in this popular program. J. T. Ferrucci, Jr., is program director.

Scientific Exhibits

Proposals for scientific exhibits must reach the Chairman of Exhibits by October 1. Forms, which may be photocopied, are in this issue of the *AJR*. Send completed form to:

John E. Madewell, M.D.
Dept. of Radiology
Baylor College of Medicine
One Baylor Plaza
Telephone (713) 799-6362 Houston, TX 77030

Local Program

A program of sightseeing, shopping, and entertainment will be developed by George Janetos, the Local Arrangements Chairman. Information and advance registration forms will be in the February issue of the *AJR*.

Residents' Award Papers

The society offers several cash awards for the best scientific papers prepared by residents in radiology. The President's Award has a $1000 prize. There are two Executive Council awards of $500 each. All are presented at the annual meeting. Papers should be submitted by January 31, 1988, for consideration in this competition. Send entries to:

B. G. Brogdon, M.D.
Dept. of Radiology
University of South Alabama Medical Center
2451 Fillingim St.
Mobile, AL 36617

Associated Society Meetings

Society for Pediatric Radiology

The Society for Pediatric Radiology will hold its 31st annual meeting April 27–May 1, 1988, at the Hotel Del Coronado, Coronado, CA (San Diego, CA). The SPR 1989 annual meeting will be April 5–9, 1989, at The Four Seasons Hotel, San Antonio, TX. For details, contact Donald R. Kirks, M.D., Secretary, Society for Pediatric Radiology, c/o Dept. of Radiology, Childrens Hospital Medical Center, Elland and Bethesda Aves., Cincinnati, OH 45229-2899, (513) 559-8058.

Deadlines

Abstracts of papers: October 1, 1987
Scientific exhibit proposals: October 1, 1987
Residents' Award papers: January 31, 1988

Call for Papers

American Roentgen Ray Society 1988 Annual Meeting: May 8–13, 1988, San Francisco, CA

FOR COMMITTEE USE

Received _____ No. _____
Subject _____ Score _____
Rejected _____ Accepted _____
Assigned: Day _____ Session _____
Time _____ No. _____

Title of Paper:

Names of Authors (Last, First, Middle):
(Use asterisk to indicate who will present paper.)

Degree (one only) | Member ARRS? Yes | No

_____

_____

_____

Professional Address of Corresponding Author: _____

_____

City State Zip Code Telephone

Type Abstract in This Space Single Spaced:
(Instructions are on reverse.)

Has this been presented elsewhere? _____yes _____no. If yes, please describe on reverse.

Projection Requirements: _____ 35 mm (2 × 2), single or double (circle which); _____ 16 mm silent movie. (Note: video tapes must be converted to 16-mm films.)

(This Form May Be Photocopied)

Instructions for Scientific Abstracts

Proposals are judged by topic and content. New information is preferred, but careful reviews of subjects important to the practice of radiology are also acceptable. The content is treated as confidential information. If the material has been presented elsewhere, notice to that effect is required.

The abstract should contain the four essentials of a scientific communication. It should describe the purposes of the study, the material and methods used, the principal observations, and their significance to radiologic practice. Brevity is desired but not at the expense of information. Factual data are essential. The abstract should be a succinct summary of work done rather than a promissory note. Acceptance for publication is encouraged by well-organized, factual abstracts. The abstract will remain confidential until the program is distributed at the meeting.

PLEASE USE TYPEWRITER. Supplemental information may be attached. Photocopies of the abstract will be distributed to the Program Committee for evaluation. Keep a copy for yourself.

Manuscripts presented on the scientific program become the property of the Society and will be considered for publication in the *American Journal of Roentgenology*. If publication is not offered by the Journal, publication rights return to the author.

Deadline for submission of abstract is October 1, 1987

Telephone (312) 908-5103

Mail abstract to: Lee F. Rogers, M.D.
Dept. of Radiology
Olson Pavillion, Room 3426
Northwestern University Medical School
710 N. Fairbanks
Chicago, IL 60611

Call for Scientific Exhibits

American Roentgen Ray Society 1988 Annual Meeting: May 8–13, 1988, San Francisco, CA

FOR COMMITTEE USE ONLY

Date Received _____ Application No. _____
Subject _____ Score _____
Rejected _____ Accepted _____
Assigned _____ Space No. _____

Principal Exhibitor's Professional Mailing Address:

Name: _____ Institution: _____

Department: _____ Street Address: _____ City: _____

State: _____ Zip Code: _____ Telephone: office ( ) _____ home ( ) _____

Are you a member of ARRS? (Please circle one.) yes or no

Names of Exhibitors:
(List principal exhibitor first and telephone number of each person.)

Last	First	Middle	Telephone	Degree (one only)	Member ARRS? Yes	No

Title of Exhibit:

Type Abstract in This Space Single Spaced:
(Instructions are on reverse.)

Instructions for Abstract

A brief resume of the exhibit is requested. State purpose, principal information, and conclusions. Promissory statements are not acceptable. Type single-spaced in the space provided on the reverse side. Brevity is desirable but not at the expense of factual information. The abstract **will appear in the program book as submitted.** Exhibitors will receive detailed instructions for exhibit preparation. Please use typewriter and complete the application form on both sides. Type must be fully legible. List space requirements.

What Sort of Exhibit Is Proposed? (Check one and complete all appropriate places.)

_____**Free Standing.** This is a self-contained display created in total by the exhibitor and may be a fold-open unit, a unit shipped in cases and assembled on site, or a table top unit. Linear feet required: _____

_____**Poster Board (Backboard Panels).** Backboard panels are 4 × 6 or 4 × 8 feet. Number of panels required: _____ 4 × 6 or _____ 4 × 8. If two panels are needed, there will be a ¼-in frame separating the panels, thus requiring a separation in the presentation.

_____**Viewbox.** Mounted materials (radiographs and other transparencies) for display on the society's illuminators. Each illuminator is 39.5 × 59.5 inches. Number of illuminators required: _____ . Slides should be nonglass mounted.

_____**Audiovisual.**

Please Indicate Most Appropriate Category for Your Exhibit.

Diagnostic Radiology:
_____Bone _____ Cardiovascular System _____ Chest _____ Pediatric Radiology
_____Gastrointestinal Tract _____ Genitourinary Tract _____ Neuroradiology

Other:
_____Medical Physics _____ Nuclear Medicine _____ Radiation Oncology _____ Radiobiology
_____Ultrasound

Has the exhibit been shown in whole or part at any previous meeting? _____ (Previous display does not preclude acceptance.)

Where? _____When? _____

Nature of meeting or name of society _____

_____
Signature of Principal Exhibitor

Applications must be received no later than October 1, 1987.
Mail original (*and five copies) to:* John E. Madewell, M.D.
Department of Radiology
Baylor College of Medicine
One Baylor Plaza
Houston, TX 77030

Telephone (713) 799-6362

Classified Advertisements

Positions Available

THE UNIVERSITY OF ARIZONA, DEPT. OF RADIOLOGY is recruiting a Section Head of Thoracic Radiology and abdominal imaging radiologist for the University Medical Center and a General Radiologist for the VA Medical Center. Candidates should be trained in appropriate imaging modalities and invasive techniques, and interested in teaching and research. Income and academic rank are negotiable. The University of Arizona is an affirmative action/equal opportunity employer. Contact Bruce J. Hillman, M.D., Vice-Chairman, Dept. of Radiology, University of Arizona Health Sciences Center, Tucson, AZ 85724; (602) 626-7368. 9–2a

UNEXPECTED OPENING: SECTION CHIEF, CT AND ULTRASONOGRAPHY—We are seeking a board-certified radiologist with fellowship training in CT and ultrasonography to direct a thriving section in a busy University Hospital. The individual should have a proven background in teaching and research, as well as patient care. The section includes state-of-the-art CT scanners and ultrasound equipment. Currently, there are 4 full-time faculty and 2 fellows in the section. Stony Brook is located on the highly desirable North Shore of Long Island, with convenient access to New York City. The medical center provides the benefits of academic practice in a suburban setting. Please send CV to Morton A. Meyers, M.D., Professor and Chairman, Dept. of Radiology, Health Sciences Center, Level 4, Room 147, State University of New York at Stony Brook, Stony Brook, NY 11794-8460. SUNY Stony Brook is an affirmative action/equal opportunity educator and employer. 9a

VASCULAR INTERVENTIONAL RADIOLOGIST, UNIVERSITY OF VIRGINIA MEDICAL CENTER—Dept. of Radiology. Tenure-track position at rank of Assistant Professor to Professor. Salary and academic rank will be commensurate with experience and qualification. Minimum requirements include M.D. with board certification in radiology and competence in angiography, interventional radiology, and special procedures. Starting date: Negotiable. Please provide CV and names and addresses of 3 references. Contact Charles J. Tegtmeyer, M.D., Professor and Chief, Division of Angiography, Interventional Radiology, and Special Procedures, Box 170, Charlottesville, VA 22908; (804) 924-9401. Equal opportunity/affirmative action employer. 9 & 11a

ULTRASOUND/CT/MRI—Seeking board-certified radiologist specializing in sectional body imaging to pursue academic practice at the University of Alabama at Birmingham. Expanding 1400-bed medical complex performs over 10,000 imaging examinations per yr with state-of-the-art equipment, including 2 Acuson units, 2 GE 9800 CT scanners, and high- and low-field MRI units. Special interest in abdominal Doppler ultrasound. Position includes clinical, teaching, and research responsibilities. Send CV to Lincoln L. Berland, M.D., Dept. of Radiology, University of Alabama at Birmingham, 619 S. 19th St., Birmingham, AL 35233. 9a

DIAGNOSTIC RADIOLOGIST—An 8-man diagnostic radiology group situated in southwestern Oregon, near 3 wilderness areas plus numerous lakes and streams, seeks a board-certified diagnostic radiologist. The community has excellent schools as well as a local state college. The practice consists of 2 offices, 2 hospitals, and includes CT, ultrasound, vascular ultrasound, angiography, and some interventional procedures, plus routine films. MRI will be installed August 1987. This is the regional medical referral area for southern Oregon and northern California. Please send inquiries to Stephen J. Cook, M.D., 692 Murphy Rd., Medford, OR 97504. 9a

DIRECTOR OF MUSCULOSKELETAL RADIOLOGY—The University of Michigan Medical School is seeking to recruit a board-certified radiologist to serve as Director of Musculoskeletal Radiology in the Dept. of Radiology. In-depth experience in musculoskeletal radiology in an academic dept. is essential. This individual will direct the clinical service, medical student and house officer education, and research programs of the skeletal division. The dept. provides excellent facilities and academic opportunities. Rank and salary commensurate with experience. Contact William Martel, M.D., Chairman, Dept. of Radiology, University Hospital B1G503/0030, 1500 E. Medical Center Dr., Ann Arbor, MI 48109-0030. A nondiscriminatory, affirmative action employer. 9a

ULTRASOUND/CT/MRI—THE DEPT. OF RADIOLOGY, GEORGETOWN UNIVERSITY HOSPITAL is seeking a board-certified, academic radiologist with experience in body imaging. Appointment will be at the Assistant or Associate Professor level. Equipment includes Acuson and ATL ultrasound units, GE 9800 CT scanners, Siemens 1.5T MR, and a Varian 4.7T spectral imager for animal research. Over 10,000 body imaging studies are performed annually including a wide range of invasive procedures, Doppler ultrasound, endovaginal and transrectal sonography, and neurosonography. Submit CV in confidence to Robert K. Zeman, M.D., Professor and Clinical Director of Diagnostic Radiology, Georgetown University Hospital, 3800 Reservoir Rd., N.W., Washington, DC 20007. An equal opportunity/affirmative action employer. 9–10a

HOSPITAL-BASED GROUP IN PACIFIC NORTHWEST with private practice limited to ultrasound and nuclear medicine seeks associate with extensive training in these subspecialties. BC/BE in nuclear medicine/radiology preferred. Send CV to Michael Daly, M.D., Nuclear Medicine/Ultrasound Section, 2801 N. Gantenbein Ave., Portland, OR 97227. 9–10ap

SEEKING ACADEMIC ASSOCIATE IN NEURORADIOLOGY at Assistant or Associate Professor level. Clinical experience at University Hospital, VA Hospital, Children's Hospital. Research opportunity, equal opportunity employer, latest generation MRI, CT, and angiography. Salary negotiable. Contact Edgardo Angtuaco, M.D., University of Arkansas for Medical Sciences, Slot 581, 4301 W. Markham, Little Rock, AR 72205. 9–11a

RADIOLOGIST, HAWAII—Unique opportunity to live and work in the beautiful sunny state of Hawaii. The Honolulu Medical Group, a well-established, growing, 50-physician, multispecialty clinic is seeking a board-certified/board-eligible radiologist. Attractive salary/benefits package and an excellent working environment. Interested applicants should send their CV to Medical Director, The Honolulu Medical Group, 550 S. Beretania St., Honolulu, HI 96813. An equal opportunity employer. 9ap

RADIOLOGIST—A board-certified/board-eligible radiologist with experience is needed to join the staff of the Alaska Native Medical Center, a 170-bed referral facility for a state-wide system of Indian Health Service hospitals and clinics. Practice stimulating and challenging radiology in a relaxed and casual atmosphere. State-of-the-art in-house CT, sonography, and mammography. Send CV to W. M. Cox, M.D., P.O. Box 10-7741, Anchorage, AK 99510-7741. EOE. 9–2a

PEDIATRIC RADIOLOGIST—Large metropolitan hospital with busy pediatric practice needs pediatric radiologist. Practice should be more than 50% pediatric. Very busy in ICU. Board certification mandatory. Practice includes CT/MRI. Write or call Randy Greene, M.D., 2801 N. Gantenbein, Portland, OR 97227; (503) 280-4032. 9–11a

GENERAL DIAGNOSTIC RADIOLOGIST to join 9-man private group practicing in active 450-bed teaching hospital in desirable southwestern Connecticut community. Radiology dept. equipped with GE 8800 and GE 9800 CT scanners, state-of-the art Special Procedure Suite, and a very active ultrasound lab. MRI to be added soon. Candidate must be board certified and have at least 1 yr of postresidency training. Skills in general angiography essential. Experience in CT and ultrasound required. MRI experience and immediate availability desirable. Please direct inquiries and CV to William B. Goldstein, M.D., Chairman, Dept. of Radiology, Danbury Hospital, 24 Hospital Ave., Danbury, CT 06810. 9–10a

INTERVENTIONAL RADIOLOGIST—The University of Mississippi Medical Center is seeking an interventional radiologist to assume a leadership role in the Division of Special Procedures. Modern equipment in 600-bed hospital. Salary competitive and working conditions excellent. Send CV to R. Brent Harrison, M.D., University of Mississippi Medical Center, Dept. of Radiology, 2500 N. State St., Jackson, MS 39216-4505. E/O/E/M/F/H/V. 9ap

RADIOLOGISTS NEEDED—The VA Medical Center in Syracuse is creating an inhouse Dept. of Radiology, and is recruiting for Chief of Radiology Services and for 3 staff radiologists; the positions will be available July 1, 1988. This Medical Center is closely associated with the SUNY Health Science Center at Syracuse, and candidates should have interests in teaching and research, and be able to qualify for faculty appointments at the appropriate level. Candidates for the position of Chief should have leadership ability and administrative credentials. Excellent federal benefits include 30 days paid vacation, 15 days of sick leave, and 10 paid holidays. Applications including a CV should be directed to H. R. Hellstrom, M.D., Chairman, Radiology Search Committee, VA Medical Center, 800 Irving Ave., Syracuse, NY 13210. Equal opportunity employer, 9–10a

PARTNER DESIRED—Board-certified/eligible radiologist desired to share position in a small, stimulating community hospital in a desirable vacation area of northeastern Wisconsin. Must enjoy general radiology, mammography, nuclear medicine, ultrasound, and CT. Please send CV to Box X21, *AJR* (see address this section). 9–10a

CHAIRPERSON, DEPT. OF RADIOLOGY—The individual is responsible for the growth of the dept., for the development of programmatic goals and objectives consistent with those of Children's Hospital National Medical Center and for providing patient care, education, and leadership in research and child advocacy. The position requires experience in administrative leadership and the management and supervision of professional, technical, and administrative staff. The individual must have demonstrated academic leadership as proven by national recognition and productivity. The position encompasses administrative, medical, professional, and academic responsibilities commensurate with that of a dept. chairperson. The individual must have a broad background in imaging techniques currently available and new modalities under development. The position carries joint academic appointment in the Dept. of Radiology and the Dept. of Child Health and Development of the George Washington University School of Medicine and the Health Sciences. No applications will be accepted after Dec. 15, 1987. Reply with CV and at least 3 references to William J. Rodriguez, M.D., Ph.D., Chairman, Search Committee for Radiology Dept., Chairman, Children's Hospital National Medical Center, 111 Michigan Ave., NW, Washington, DC 20010. EOE. 9a

CHAIRPERSON, DEPT. OF RADIOLOGY—297-bed, growing community hospital in suburban Pittsburgh. Candidate should be board certified in radiology with demonstrated broad clinical expertise, as well as significant administrative experience. Please send letter outlining above as well as full CV to David Berk, M.D., 9104 Babcock Blvd., Pittsburgh, PA 15237. 9–10a

NEURORADIOLOGIST to join 9 board-certified radiologists in metropolitan southwestern city. Group consists of an interventional radiologist, 2 neuroradiologists, and 2 radiation therapists. Need due to increased volume. Sophisticated medical community. Excellent modern facilities and equipment. Compensation determined by certification and experience. Reply Box X14, *AJR* (see address this section). 9a

DIAGNOSTIC RADIOLOGIST to work with a group covering both hospital and private practice. CT, ultrasound, and angiography. 1 hr from Boston. Please reply to Box X16, *AJR* (see address this section). 9–11ap

PROGRESSIVE, SOUTHERN CALIFORNIA, PRIVATE-RADIOLOGY GROUP seeking cardiac radiologist for major cardiology/cardiac surgery practice with substantial adult and pediatric material. Please send inquiries and CV to Box X18, *AJR* (see address this section). 9–10a

RADIOLOGIST—Cross-sectional imaging specialist required for 18-man, private radiology group based primarily at 750-bed Abbott Northwestern Hospital in Minneapolis, MN. Candidate must have a strong background in body CT, ultrasound, and MRI. Hospital dept. runs 2 GE 9800 scanners and will have a second Siemens Magnetom (1.5T) by spring 1988. Young, aggressive, expanding group offers competitive salary and benefits package. Contact T. J. Koelz, M.D., Consulting Radiologists Ltd., 453 Medical Arts Bldg., Minneapolis, MN 55402; (612) 863-4261. 9ap

NEURORADIOLOGIST—Opening for experienced neuroradiologist with fellowship training to join partnership of 4 radiologists in outpatient office and 200-bed general hospital. MR experience essential. Currently considering MRI addition to be operational in 12 mo. Practice is in Coeur d' Alene, ID. Beautiful recreational, fishing, and hunting facilities. Excellent opportunity for university-trained radiologist seeking full, private-practice partnership situation. Send letters of inquiry with CV to Richard Hehn, M.D., Radiology Associates of North Idaho, 1104 Ironwood Dr., Coeur d' Alene, ID 83814. 9ap

BC/BE RADIOLOGIST to join 2 other radiologists in hospital-based practice in southeastern US. Town has a population of 15,000 with a broad economic base and a large referral area. Near the Gulf of Mexico and Atlantic Ocean. CT, MRI, ultrasound, angiography, mammography, and general diagnostic work. Prefer individual with fellowship or additional training in MRI. Send CV to Box X25, *AJR* (see address this section). 9–11a

BC/BE RADIOLOGIST—Immediate opportunity available to join 6-member group. All modalities present. Group services 2 hospitals and has 2 offices in south Florida, East Coast. Interventional fellowship would be beneficial. David Harr, M.D., 1845 Tarpon Ln., G-101, Vero Beach, FL 32960. 8–9ap

ISRAEL, DIAGNOSTIC RADIOLOGY. Opportunities for 3–4 week or longer working vacations in a number of Israeli medical centers, on a volunteer basis. Positions varied, arrangements flexible. For information contact: Jonathan H. Fish, M.D., 1844 San Miguel Dr., #302, Walnut Creek, CA 94596; (415) 947-0560. 8xa

DIAGNOSTIC RADIOLOGIST—7-man group seeking BC/BE radiologist to join busy practice in 530-bed community hospital. State-of-the-art in all modalities. Position available 10/87. Nuclear medicine training a plus. Contact Arthur E. Bishop

SOUTH ORANGE COUNTY DIAGNOSTIC RADIOLOGIST—Excellent position available, ASAP, in multispecialty hospital and office practice located in Orange County (Southern California). Position is for interventional radiologist with training in cardiovascular radiology. Excellent salary and benefits. Hospital is in a beautiful, growing area. Reply with CV to Box W54, *AJR* (see address this section). 8–9ap

ULTRASOUND/CT/MRI—Seeking board-certified radiologist specializing in sectional body imaging to pursue academic practice at the University of Alabama at Birmingham. Expanding 1400-bed medical complex performs over 10,000 imaging examinations per yr with state-of-the-art equipment, including 2 Acuson units, 2 G.E. 9800 CT scanners, and high- and low-field MRI units. Special interest in abdominal Doppler ultrasound. Position includes clinical, teaching, and research responsibilities. Send CV to Lincoln L. Berland, M.D., Dept. of Radiology, University of Alabama at Birmingham, 619 S. 19th St., Birmingham, AL 35233. 8–11a

RADIOLOGIST, BOARD-CERTIFIED/ELIGIBLE—4 Mayo Clinic-trained radiologists have a position available in a hospital-based practice that includes angiography and other invasive procedures, diagnostic radiology, CT, ultrasound, nuclear medicine, and MRI. 4-yr university training required. Liberal vacation and seminar time. Low buy-in and early full partnership. Locum tenens assistance desired until a permanent associate is obtained. Send CV and 3 references with initial letter of inquiry to Box 2818, Waterloo, IA 50704. 8–10a

BC/DIAGNOSTIC RADIOLOGIST WITH NEURORADIOLOGY OR MR FELLOWSHIP TRAINING to join progressive 5-man group in central Maine. 1.0-T MR unit to go on-line 1/88. 280-bed hospital. 52,000 exams/yr. 5000 CT. Brand new dept. to be completed by 1990 with state-of-the-art equipment. Position available 1/88–7/88. Excellent salary and benefits to partnership in 2 yr. Unique opportunity to join a progressive private group doing university-level practice in a regional referral center. Send CV to X-Ray P.A., 583 Main St., Lewiston, ME 04240; (207) 795-2400. 8–9a

DIRECTOR, SECTION OF INTERVENTIONAL RADIOLOGY—The Dept. of Radiology at Harper Hospital is seeking a board-certified radiologist with competence in all aspects of interventional radiology. Harper Hospital is the major institution in the Detroit Medical Center and is affiliated with Wayne State University. Please send CV or inquiries to George A. Kling, M.D., Chairman, Dept. of Radiology, Harper Hospital, 3990 John R, Detroit, MI 48201; (313) 745-8405. 7–9a

CT/ULTRASOUND—The University of Texas Health Science Center, San Antonio is seeking a board-certified radiologist with experience in CT/ultrasound to join our faculty. Contact Robert L. Siegle, M.D., Chief, Diagnostic Radiology, Dept. of Radiology, University of Texas Health Science Center at San Antonio, 7703 Floyd Curl Dr., San Antonio, TX 78284. Equal Opportunity/Affirmative Action Employer. 7–9a

DIAGNOSTIC RADIOLOGIST with special interest in CT and ultrasound to join growing hospital-based practice. 125-bed hospital with adjoining office building located near downtown Seattle. Send CV to K. Wade Brunette, M.D., 16775 16th Ave. NW, Seattle, WA 98177; (206) 583-2675. 7–9a

BOARD-CERTIFIED RADIOLOGIST, university trained, wanted for a salaried position in a free-standing imaging center and part-time hospital practice. The center facilities include an Acuson 128, GE 9800, Low-Rad dedicated mammography, dedicated digital angiography, and routine fluoroscopic and radiographic imaging. Regular hours with minimal on-call responsibilities. Beautiful town in Indiana-Illinois-Kentucky tri-state. Part-

DIAGNOSTIC RADIOLOGIST. Need aggressive associate to perform all aspects of diagnostic radiology in well-equipped hospital with large outpatient component in South Texas. MR training a plus but not essential. Excellent salary and early partnership available. For confidential consideration please submit CV to Box H70, *AJR* (see address this section). 11xa

ASSOCIATE DIAGNOSTIC RADIOLOGIST needed for new community hospital in scenic Michigan upper-peninsula town. Practice includes ultrasound (Doppler), nuclear medicine, CT, mammography, and some special procedures. Generous salary and liberal benefits leading to early partnership. Send CV to Mario Nunez, M.D., 750 Lake Shore Dr., Escanaba, MI 49829; (906) 786-7350. 7–9ap

BOARD-CERTIFIED RADIOLOGIST to join 12-member dept. and 625-bed hospital and associated private office. All modalities of radiology performed. Have a 1.5-T GE MRI operation and 2 CT scanners, one of which is a GE 9800 quick scan. Large ultrasound and nuclear medicine section. New angiographic suite being completed. Active residency program. Please send resume to H. E. Yeagley, M.D., Dept. of Radiology, Reading Hospital and Medicine Center, Reading, PA 19603. 7–10a

NEURORADIOLOGIST—Applications are being sought for a neuroradiologist for a 560-bed teaching hospital/private office. New 1.5-T MRI unit soon to be operational. Candidate should be board certified preferably with 2 yr of neuroradiology fellowship. Training in MR, CT, angiography, and myelography necessary. Send current CV to R. William McConnell, M.D., Chairman, Dept. of Radiology, Number 9, Doctor's Park, Greenville, NC 27834. 7–12a

EXCELLENT OPPORTUNITY—Seeking board-certified radiologist with additional training in interventional radiology or board certification in nuclear medicine to join 12-man private-practice group covering 2 hospitals in suburban St. Louis. Applicant should have experience in CT, nuclear medicine, ultrasound, and mammography. Very competitive salary with excellent benefits. Send CV to A. C. Hooper, M.D., Ernst Radiology Clinic, Inc., Ste. 110, 14377 Woodlake Dr., Chesterfield, MO 63017; (314) 878-4680. 7–9ap

BOARD-CERTIFIED RADIOLOGIST wanted for community of 10,000 (45,000 service area) in the lush Yakima Valley of central Washington. Superior diagnostic radiologic skills required with experience in ultrasound, angiography, and CT. Generous practice assistance package. Excellent school system and outdoor recreation. Contact PROSEARCH, 305 NE 102nd Ave., Portland, OR 97220; (503) 256-2070. 7–9ap

Positions Desired

HUSBAND AND WIFE, UNIVERSITY-TRAINED, BOARD-ELIGIBLE RADIOLOGISTS seeking permanent positions on east coast to begin after 8/88. His training in neuroradiology, including MRI. Her training in pediatric radiology. Both due to complete fellowships in Philadelphia in 6/88. Reply to 55 Bryn Mawr Ave., Lansdowne, PA 19050; (215) 284-6591. 9bp

DIAGNOSTIC RADIOLOGIST—ABR-certified and eligible for special competency certification in nuclear medicine seeks hospital-contract/private-practice opportunity in a community within 50 mi of a major city. Has fellowship training in neuroradiology, CT, ultrasound, angiography, interventional radiology, special competency training in nuclear medicine (including SPECT), and limited experience in MRI. Available before Jan. 1988.

BOARD-CERTIFIED AIR FORCE RADIOLOGIST desires general outpatient (private/HMO/multispecialty) position beginning August 1988. Has 12-yr experience that includes chairmanships of three major USAF Medical Center dept. Reply A. Daley, M.D., 6306 Wilmington Dr., Burke, VA 22015; office (301) 981-4222. 7–10b

Fellowships and Residencies

FELLOWSHIPS IN (1) ULTRASOUND/CT/MRI, (2) CARDIOVASCULAR?INTERVENTIONAL, (3) NEURORADIOLOGY/ENT, (4) CARDIOPULMONARY—The Dept. of Radiology at Thomas Jefferson University Hospital offers these 4 subspecialty fellowships each yr. We have a very large and extensively equipped ultrasound division that offers training in all phases of ultrasound including cardiac, vascular, and obstetric. The dept. also has 3 modern CT scanners and a GE 1.5-T MRI unit. The Cardiovascular/Interventional Division is currently being renovated and will house state-of-the-art angiography equipment with DSA. This division performs a full range of both vascular and nonvascular interventional procedures. Neuroradiology is housed in a brand new Neurosciences Imaging Center containing all imaging modalities in a single comprehensive facility. For information and applications to these 4 programs, contact Barry B. Goldberg, M.D. (Ultrasound/CT/MRI); Geoffrey Gardiner, Jr., M.D. (Cardiovascular/Interventional); Carlos Gonzalez, M.D. (Neuroradiology); or Robert Steiner, M.D. (Cardiopulmonary) at the Dept. of Radiology, Thomas Jefferson University Hospital, Philadelphia, PA 19107. 9c

BOSTON UNIVERSITY MEDICAL CENTER offers imaging fellowships beginning July 1, 1988. If you would like to be considered for the following fellowships, please submit a current CV, 2 letters of recommendation (1 from your program director), and rank order of fellowships desired. (1) CT/MRI, address inquiries to Peter D. Franklin, M.D., Chief Body CT/MRI, 75 E. Newton St., Boston, MA 02118. (2) Ultrasound/MRI, address inquiries to Ewa Kuligowska, M.D., Chief Ultrasound, 75 E. Newton St., Boston, MA 02118. (3) Nuclear/MRI, address inquiries to Victor Lee, M.D., Chief Nuclear Medicine, 818 Harrison Ave., Boston, MA 02118. 9–10c

FELLOWSHIP IN NUCLEAR MEDICINE—The State University of New York at Stony Brook and Brookhaven National Laboratory are sponsoring a 2-yr fellowship in nuclear radiology that combines clinical experience in a university tertiary-care facility with research experience in a national laboratory. Prerequisites are 3 yr training in diagnostic radiology or 2 yr in a nuclear medicine program. Experience with SPECT, PET and general nuclear medicine should be an excellent preparation for an academic career. Contact Harold L. Atkins, M.D., Dept. of Radiology, Health Sciences Center, State University of New York, Stony Brook, NY 11794-8460. 9c

INTERVENTIONAL RADIOLOGY FELLOWSHIP—The Mallinckrodt Institute of Radiology announces a new 1-yr fellowship position starting July 1, 1988, in Vascular and Interventional Radiology. Mallinckrodt Institute of Radiology provides radiology services to Barnes Hospital and Children's Hospital totaling approximately 1300 beds. The fellow will be involved in all ranges of vascular and nonvascular interventional radiology including angiography, venography, lymphangiography, percutaneous transhepatic cholangiography, biliary drainage and biliary stone management, percutaneous nephrostomy and percutaneous renal stone management, abscess drainages, gastrostomy placements, angioplasty, embolization, thrombolysis, percutaneous vena cava filter placement, and percutaneous endoscopy. Send inquiries to Daniel Picus, M.D., Chief, Vascular and Interventional Radiology, Mal-

ANGIOGRAPHY/NEURORADIOLOGY FELLOWSHIP, BOSTON—Unexpected new position available immediately. Fellows participate in cerebral, peripheral, and abdominal angiography; interventional procedures and myelography; CT and MRI. Send inquiries to Laura Feldman, M.D., Head, Angiography Section, VAMC, 150 S. Huntington Ave., Boston, MA 02130; (617) 739-3435. 7–9c

PEDIATRIC NEURORADIOLOGY FELLOWSHIP—Childrens Hospital of Los Angeles has an opening for a pediatric neuroradiology fellow starting July 1, 1988, for 1 yr. Childrens Hospital of Los Angeles is the largest children's hospital on the West Coast. The neuroradiology facilities include a new Siemens angiographic suite and a GE 9800 scanner; a GE magnetic resonance imager has been ordered. Applications should be sent to John L. Gwinn, M.D., Radiology, Childrens Hospital of Los Angeles, 4650 Sunset Blvd., Los Angeles, CA 90027. Childrens Hospital of Los Angeles is an equal opportunity employer. 8–9c

IMAGING FELLOWSHIP IN DIAGNOSTIC IMAGING with emphasis on diseases of children and women. Diasonics MRI, Imatron CT, and Acuson Ultrasound. Opportunity for clinical or basic research. Must be eligible for oral board exam. Reply Jerald Kuhn, M.D., Director, Radiology Dept., Children's Hospital, 219 Bryant St., Buffalo, NY 14222; (716) 878-7525. 7–10c

IMAGING FELLOWSHIP, BOSTON—Unexpected new position available immediately. Fellows participate in CT, ultrasound, nuclear medicine, MRI, and related procedures. Send inquiries to Stephen Gerzof, M.D., Chief, Ultrasound and Body CT, VAMC, 150 S. Huntington Ave., Boston, MA 02130; (617) 739-3435. 7–9c

Tutorials/Courses

AUSTRALIA-NEW ZEALAND—IMAGING DOWN UNDER, MARCH 12–27, 1988. International faculty. Auckland, New Zealand, March 13–14; Sydney, Australia, March 18–20; and Melbourne, Australia, March 25–26. Information: Medical Seminars, 21915 Roscoe Blvd., Ste. 222, Canoga Park, CA 91304; (818) 719-7380. 9/2d

MAUI, HAWAII—12TH ANNUAL BODY IMAGING CONFERENCE—October 10–18, 1987. Diagnostic Imaging, Category I Accreditation, University Faculty. Registration and information: Body Imaging Conference, 21915 Roscoe Blvd., Ste. 222, Canoga Park, CA 91304; (818) 719-7380. 7–9d

MRI TUTORIAL PROGRAM—Diagnostic Radiological Imaging Medical Group offers 1-wk training programs in clinical MRI for physicians with limited or no experience in MRI. The program is individualized to the applicant, and the physician may subscribe to 1 or more weeks. Only 2 physicians per week are accepted. The 1.5-T MRI scanner is used in an outpatient imaging facility and 12–16 examinations per day are performed. Individual tutorials in MRI physics, equipment evaluation, clinical indications for MRI examination, performance of MRI studies, discussion of case material, and review of an extensive teaching file are offered. The faculty are A. B. Dublin and M. H. Reid. The fee is $600 and 40 hr Category I credit are available/week. For further information contact Michael H. Reid, Ph.D., M.D., Diagnostic Radiological Imaging, 79 Scripps Dr., Ste. 100, Sacramento, CA 95825. (916) 921-1300. 6–9d

Other

RADIOLOGY OFFICE FOR LEASE, SALE, OR JOINT VENTURE in rapidly growing area. Hospital and 3 medical-building complex, 30-plus physicians. Reply Box X12, *AJR* (see address this section). 9e

NEED ON-SITE MRI TRAINING?—Fellowship trained radiologist with MRI consultant experience offers on-site MRI training and over-reading for your group, tailored to your needs. M. Barnett, M.D., 2413 Bayview, Manhattan Beach, CA 90266; (213) 545-5886. 9e

PRIVATE PRACTICE OPPORTUNITY. 1348-ft furnished and equipped radiology office in best north Dallas location. Sell or lease. Will help finance. Opportunity for radiologist considering practice change, or semiretirement, in "carriage trade" Woodhill Medical Park. Call (214) 960-9727 after 7 p.m. 9ep

WANTED, RADIOLOGY PRACTICE—Desire private-office practice or outpatient clinic. Prefer sunbelt/mountain location. Reply Box W58, *AJR* (see address this section). 8–9d

AJR Classified Advertisements Information

Box Responses and Address for Ad Placement

Write Box _____, AJR, Suite 200, 2223 Avenida de la Playa, La Jolla, CA 92037; (619) 459-2229.

How to Place an Ad

AJR accepts classified advertising for Positions Available, Positions Desired, Fellowships and Residencies, and Tutorials/Courses. Ads are accepted by mail or telephone. Institutions should supply purchase orders.

Rates: $6.00/line with a $30 minimum charge. Box service is $10 additional for each month the ad appears. There are discounts for multiple insertions: 10% for 2–3 insertions; 20% for 4 or more. To estimate lines, count all words and divide by 5.5.

Billing: Ads may be prepaid or invoices will be sent after the ad appears.

Deadlines. 6 weeks prior to issue date. For specific deadlines telephone the AJR editorial office.

Estimating Ad Charges

Line charge: divide total words by 5.5 and multiply by $6.00 . . . . $ _____

Multiple insertions? If so, multiply by number . . . . . × _____

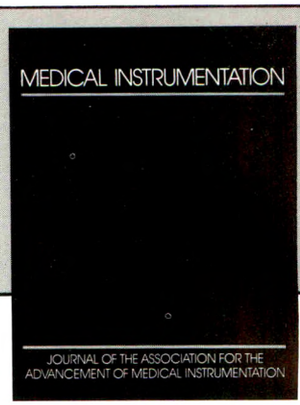
Subtotal . . . . . $

Box response requested? If so, multiply number of months by $10.00 . . . . . + _____

Subtotal . . . . . $

Discount applies to two or more insertions. Subtract 10% if ad

Get the complete story on the new medical technologies and instrumentation of today...and tomorrow



MEDICAL INSTRUMENTATION

The official journal of the Association for the Advancement of Medical Instrumentation

Editor-in-Chief: Charles A. Rawlings, Ph.D., C.C.E.

If you are involved in the design, manufacturing, clinical application, specification, regulation, or administrative facets of medical device technology, make MEDICAL INSTRUMENTATION the first journal you reach for when you want the latest developments, innovations, and advances in this fast-paced field.

Each bimonthly issue alerts you to trends and forecasts in the development, design, regulation, and clinical applications of medical instruments, devices, and systems. Original papers and timely articles help you keep pace with changes in the field that can have great effect on your work...new government standards and codes...new clinical uses...new approaches to enhancing quality, reliability, safety...key technologic breakthroughs ...and more.

Several special issues yearly are carefully planned around a single topic of current interest. Recent and upcoming special issues include —

- Environmental Therapeutic Devices for Infants
- Lasers in Medicine
- Neurologic Instrumentation and Techniques
- Alternative Communication Devices
- Respiratory Equipment

MEDICAL INSTRUMENTATION's coverage spans the disciplines, giving you a well-rounded perspective on trends in many areas — instrumentation for cardiovascular monitoring...clinical engineering...certification...instrumentation in anesthesiology.

Keep pace with technology and subscribe to **MEDICAL INSTRUMENTATION** today! Just clip out the coupon below or call **FREE** 1-800-638-6423 from anywhere in the U.S. (except Alaska), or call **COLLECT** in Maryland at 528-4105.

Williams & Wilkins

GET UP TO 3 YEARS AT THESE LOW RATES!

MEDICAL INSTRUMENTATION

The official journal of the Association for the Advancement of Medical Instrumentation

Keeping pace with the technologies of today... and tomorrow

☐ 3 years ☐ 2 years ☐ 1 year
☐ Individual $60/year
☐ Institution $75/year
☐ In-training $30/year
(Please add $10/year outside U.S.)

☐ Check enclosed ☐ Bill me
☐ VISA ☐ MasterCard ☐ American Express

card # expiration date

signature/PO#

name

address

city/state/zip

Maryland residents please add 5% sales tax. Subscriptions outside the U.S. must be prepaid, in U.S. dollars only. Please allow up to 8 weeks for delivery of first issue. Surface deliveries outside the U.S. may take up to 16 weeks. Airmail rates available on request.

Mail to:
Williams & Wilkins
P.O. Box 23291
Baltimore, MD 21203

266 Fulham Road
London SW10 9EL England

DIAGNOSTIC RADIOLOGIST

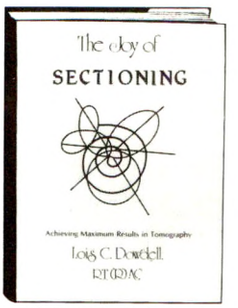
Guthrie Clinic recruits a diagnostic radiologist to join 9 other radiologists with general and subspecialty interests. This tertiary level, multispecialty group staffs 160 physicians representing all disciplines in medicine and surgery.

The Guthrie Clinic affords physicians a dynamic and progressive practice opportunity, excellent salaries and benefits as well as a rural, Northeast Pennsylvania setting.

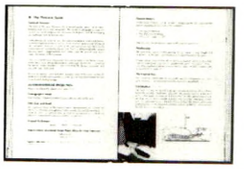
Candidates should submit their CV and three references to:

Donald R. Weaver, M.D.
Medical Director
Guthrie Clinic Ltd.
Sayre, PA 18840
(717) 888-5858

This excellent book will become your most valuable tomography reference.



240 pages • Durable hard cover
270 photos and illustrations



- Concise, easy-to-read, consistent style of presentation and format
- Emphasis on patient care and positioning
- Adaptable to any tomography unit and any tomographic mode
- Typical techniques with details on processing and section levels
- Typical focal plane dose measurements for each patient position
- Examples of normal, abnormal tomograms
- 40 different patient positions and tomographic procedures described in step-by-step approach
- Satisfaction guaranteed!

Examine your copy free for 10 days!

Easy to read! Easy to use!
You've never seen a tomography book that's as handy, easy to read, and so ready to use! "The Joy of Sectioning — Achieving Maximum Results in Tomography" is certain to become your most valuable tomography reference.

You'll appreciate the logical chapter segments . . . the frequent and consistent section headings . . . the large type. There are all kinds of photographs (270 in all), showing positions, procedures, and — most important — excellent examples of radiographs.

The Author
Lois Dowdell knows tomography. She achieved her Advanced Certification in radiography in 1977, with credits in anatomy and physiology in radiography, image recording radiography, radiographic procedures, positioning and pathology, radiobiology, radiation protection and patient care, and hospital department management.

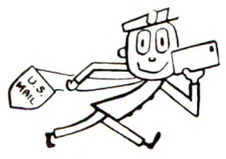
Examine your new book free for 10 days. No obligation whatever!
You can examine your own copy of "The Joy of Sectioning — Achieving Maximum Results in Tomography" now, with absolutely no obligation. You'll receive your copy by return mail. Then, you look it over for 10 days. Only if you agree it is everything you expected will you pay the accompanying invoice for $29.95, plus $3.00 for shipping, handling and cartoning. If not, then simply return the book in the original mailing carton within 10 days, and the invoice will be cancelled, with no obligation whatever.

Better still, save yourself $3.00.
Send your check or money order for $29.95 now, and you'll be able to put $3.00 in your pocket, because we'll absorb the shipping, handling and cartoning costs. (That's a saving of 10%). Be sure to send your order in right away.

How to order your book:
Send $3 shipping, cartoning and handling. Send check or money order for US$29.95 OR: Advise Hospital / Lab / Clinic name for invoicing purposes ($29.95 plus $3.00)
Unconditional guarantee: you must be satisfied or your money back! *Prices subject to change.*

Railfare Enterprises Limited, Box A-248, Hanover, New Hampshire, USA 03755

Help us to serve you better.....



USE YOUR ZIP CODE

Remember, your zip code provides faster, more direct delivery of your journals. Use it on all correspondence, too.

Director, Department of Radiology

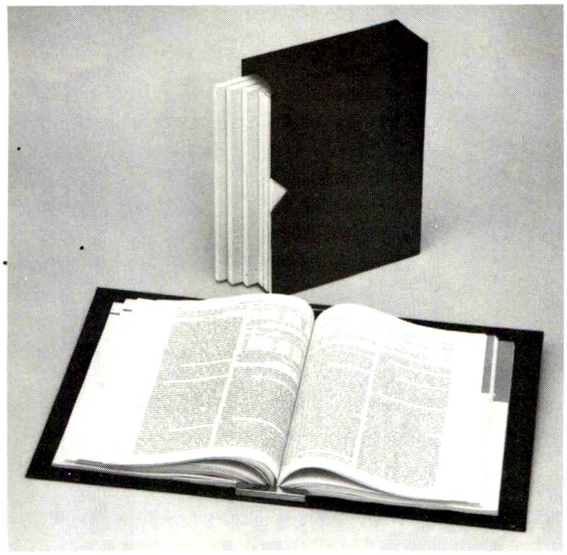
Lenox Hill Hospital

Our 698 bed, JCAH-accredited teaching institution in Manhattan, is seeking a highly qualified physician to become Director of Radiology. Candidate must have or be eligible for New York State license. Specialty Board certification in radiology is required. Applicant must be eligible to obtain a faculty appointment at affiliated medical college. Extensive experience in administration, teaching and research required. Compensation is competitive. The Department currently has an active staff of 114 and among these are 10 attending radiologists. The service in 1986 performed 106,109 procedures. This included CT scans, diagnostic radiology, ultrasound, nuclear medicine and radiation therapy. The Department has a fully accredited 4-year residency training program, with 3 residents at each level.

Interested candidates should direct inquiries, curriculum vitae and references to:

Hugh. R. K. Barber, M.D.
Chairman, Selection Committee
Lenox Hill Hospital
100 East 77 Street
New York, New York 10021

Lenox Hill Hospital is a university affiliate of New York Medical College and is an Equal Opportunity Employer.



Protect your copies of

AJR: AMERICAN JOURNAL OF ROENTGENOLOGY

with Jesse Jones Binders or Files

Keep your journals clean, orderly, and readily accessible with Jesse Jones Binders or Files. Two Binders or two box style Files are all you need to accommodate a full year's worth of issues. Both Binders and Files are handsomely made with rich black leatherette covers and gold leaf embossed lettering.

Jesse Jones Binders open flat for easy reading and reference and are economically priced at only $9.95 each; 3 for $27.95, or 6 for $52.95 postpaid. The rugged, compact box Files are only $7.95 each; 3 for $21.95, or 6 for $39.95. Add $1.00/unit postage and handling. (Outside the U.S. add $2.50/unit.)

For charge orders call toll free 1-800-972-5858. ($15.00 minimum).

Free gold transfer slips included for indexing volume and year.

Please allow four to five weeks for delivery.

TO: Jesse Jones Industries
499 E. Erie Avenue, DEPT. AJR
Philadelphia, PA 19134

I enclose my check or money order for $_____
(PA residents add 6% sales tax)

Send me ____ ☐ Files ☐ Binders for my journals

Name

Address (will not ship to P.O. Box)

City/State/Zip

Satisfaction guaranteed.

INDEX TO ADVERTISERS

Diasonics A31, A32, A33, A34 A35, A36, A37, A38

Eastman Kodak A6, A7

Elema Schonander, Inc. A16

E-Z-EM Company . . . . . Cover 2

FUJI . . . . . Cover 3

General Electric A14, A15, A19, A20, A21

Guthrie Clinic A31

Lenox Hill Hospital A31

Mallinckrodt, Inc. A27, A28, A29, A30

Nuclear Associates A2

Precise Optics/PME, Inc. A25

Railfare Enterprises A31

Siemens Medical Systems, Inc. A12, A13

E. R. Squibb & Sons, Inc. A8, A9, A10, A11, A22, A23, A24

S & S X-Ray A26

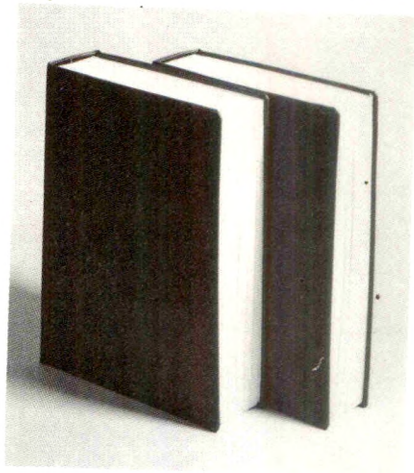
Winthrop Laboratories A17, A18, A41, A42

We try to present an accurate index. Occasionally this may not be possible because of a last-minute change or an omission.

AJR: AMERICAN JOURNAL OF ROENTGENOLOGY

Bound Volume Offer

A trouble-free way to keep your reference library up to date



As an **AJR: American Journal of Roentgenology** subscriber, you know how much useful information is packed into each issue. But you also probably know how frustrating and time-consuming it can be to try and locate one particular article from a back issue.

Find that back issue quickly and easily

Now you can get a year's worth of articles in bound volume form — a special offer available only to subscribers. So the information you need will be at your fingertips, handsomely preserved and ready for years of future reference.

You get the timely coverage only a journal can provide — penetrating discussions of the topics that interest you most, by the brightest names in your field — with all the durability and convenience of a hard-cover edition. With bound volumes, you'll never again spend frustrating hours sifting through dog-eared back issues, only to discover that the article you need has been torn out. You'll have a year's worth of vital information all arranged and indexed in one sturdy source. And each carefully crafted volume will make a handsome addition to your permanent library.

Send in your paid order by October 31, 1987 and SAVE

Act now and receive the **1987 Bound Volumes** for only $73.00 for all prepaid orders, $2.00 off the regular price of $75.00. (Please add $10.00 to all orders outside the US.) Bound volumes are available for the current year only, and are in addition to the regular subscription price.

We'll help you keep your reference library up to date

Once a year, we'll send you a reminder so you can order the latest bound volumes. When you send in your paid order, a set will be reserved for you, to be sent as soon as available on 30-day approval. If you do not want the bound volumes for any reason, simply return them to us within 30 days for a courteous refund. It's that easy.

Williams & Wilkins
P.O. Box 23291 Baltimore, Maryland 21203
266 Fulham Road London SW10 9EL England

EASY ORDERING

Please send me the **AJR: American Journal of Roentgenology 1987 Bound Volumes** at $75.00 ($85.00 outside the US). I understand that I can save $2.00 by sending in my prepaid order (check or charge) by October 31, 1987. I also understand that this offer is in addition to my regular subscription, that it is available only to subscribers, and that I will have the option of ordering bound volumes for subsequent years as long as I remain a subscriber. I will receive my 1987 bound volumes in early 1988.

☐ Check enclosed ☐ Bill me
☐ VISA ☐ MasterCard ☐ American Express

Card # _____ Exp. date _____

Signature/P.O. # _____

Please pay in US dollars. MD residents, please add 5% sales tax. Orders outside the US and Canada must be prepaid. Rates subject to change without notice. **All orders must be received by December 31, 1987.**

Name _____

Address _____

City/State/Zip _____

Date of order _____

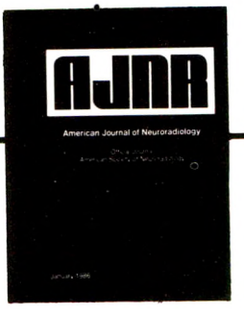
ORDER FREE BY PHONE. Call **1-800-638-6423** from anywhere in the US except AK. MD residents, call **528-4105** collect.

Williams & Wilkins
P.O. Box 23291 Baltimore, Maryland 21203
266 Fulham Road London SW10 9EL England

Printed in US

AJRBNDV 1000 87

Increase your expertise in evaluating CNS lesions



AJNR
American Journal of Neuroradiology

Editor: **Juan M. Taveras, MD,** Harvard Medical School; MGH

Outstanding clinical papers on every aspect of CNS imaging, including spinal diagnosis...informed coverage of head and neck radiology...clear, readable CTs, angiographs, MR imaging and ultrasound studies. These are the features you demand of a quality professional journal. You'll find them in every issue of **AJNR: American Journal of Neuroradiology.**

As you are called upon to perform and interpret more and more sophisticated diagnostic tests — from myelography to CT to newborn ultrasound studies — you need a comprehensive, reliable journal that can keep you abreast of all the latest developments. Each bimonthly issue of **AJNR** brings you timely, clinically pertinent information, as well as important clinical research presented with an eye toward immediate practical application.

Here are just a few of the many excellent articles from the November/December 1986 issue:

The MR Appearance of Syringomyelia: New Observations. *Sherman, et al.*

Cranial MR in Spinal Cord MS: Diagnosing Patients with Isolated Spinal Cord Symptoms. *Edwards, et al.*

Time-Dependent Changes in Image Contrast in Brain Tumors After Gadolinium-DTPA. *Schörner, et al.*

Physiology of the CSF Flow-Void Sign: Modification by Cardiac Gating. *Citrin, et al.*

Percutaneous Laser Catheter Recanalization of Carotid Arteries in Seven Cadavers and One Patient. *Choy, et al.*

Focal Necrosis of the White Matter (Periventricular Leukomalacia): Sonographic, Pathologic, and Electroencephalographic Features. *Bejar, et al.*

If you can benefit from articles like these, then you should be a regular reader of **AJNR.** Use the attached coupon to subscribe today.

Bimonthly
Personal $100/yr **Institutions** $120/yr
In-training $65/yr *(add $20.00 outside the US)*

ORDER FREE BY PHONE. Just call 1-800-638-6423 from anywhere in the US except AK. Maryland residents, call 528-4105 *collect.*

Williams & Wilkins
P.O. Box 23291 Baltimore, Maryland 21203
266 Fulham Road London SW10 9EL England

Subscribe to AJNR for 3 years and SAVE

Avoid future rate increases and ensure uninterrupted service by placing a multi-year subscription at current rates.

☐ New subscription ☐ Renewal
☐ 3 yrs ☐ 2 yrs ☐ 1 yr
☐ **Personal** $100 ☐ **Institutions** $120 ☐ **In-training** $65
(add $20.00 outside the US)

☐ Also send me the **1987 Bound Volume** at $45.00 ($50.00 outside the US). $2.00 discount for orders placed before October 1, 1986, and for prepaid orders. I understand that the bound volume is *in addition to* my regular subscription and is available only to subscribers. (To be shipped in early 1988. Sorry, bound volumes for years prior to 1987 are not available.) *All bound volume orders must be received by December 31, 1987.*

☐ Check enclosed ☐ Bill me
☐ VISA ☐ MasterCard ☐ American Express

card # exp.

signature/P.O. #

printed in USA

Name

Address

City/State/Zip

MD residents, please add 5% sales tax. Subscription orders from outside the US must be prepaid in US dollars only.

Residents, Fellows, Interns, and Students: when applying for the in-training rate, available for 3 years, please specify name of institution and training status. Rates valid through October 31, 1987.

Please allow 8 weeks for order processing and delivery of your first issue. Surface mail delivery to countries outside the US may take up to 16 weeks. Airmail rates available upon request.

Williams & Wilkins
P.O. Box 23291
Baltimore, Maryland 21203

266 Fulham Road
London SW10 9EL
England

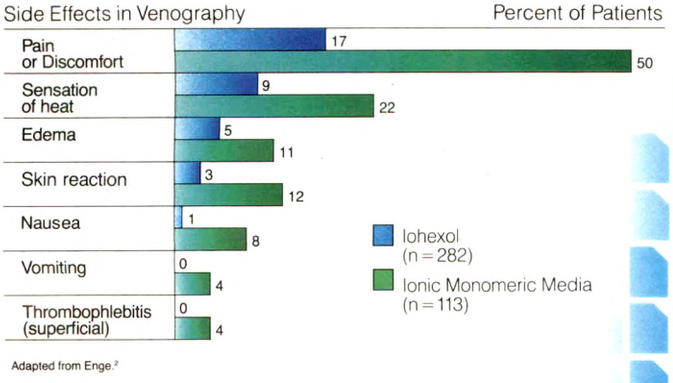
AJNRAD 94625 87

In peripheral arteriography/venography:

Because you can't be sure how every patient will react...

Improve the safety profile.

Significant improvement in patient comfort.
Lower incidence of adverse reactions than with conventional ionic media.[1-4]

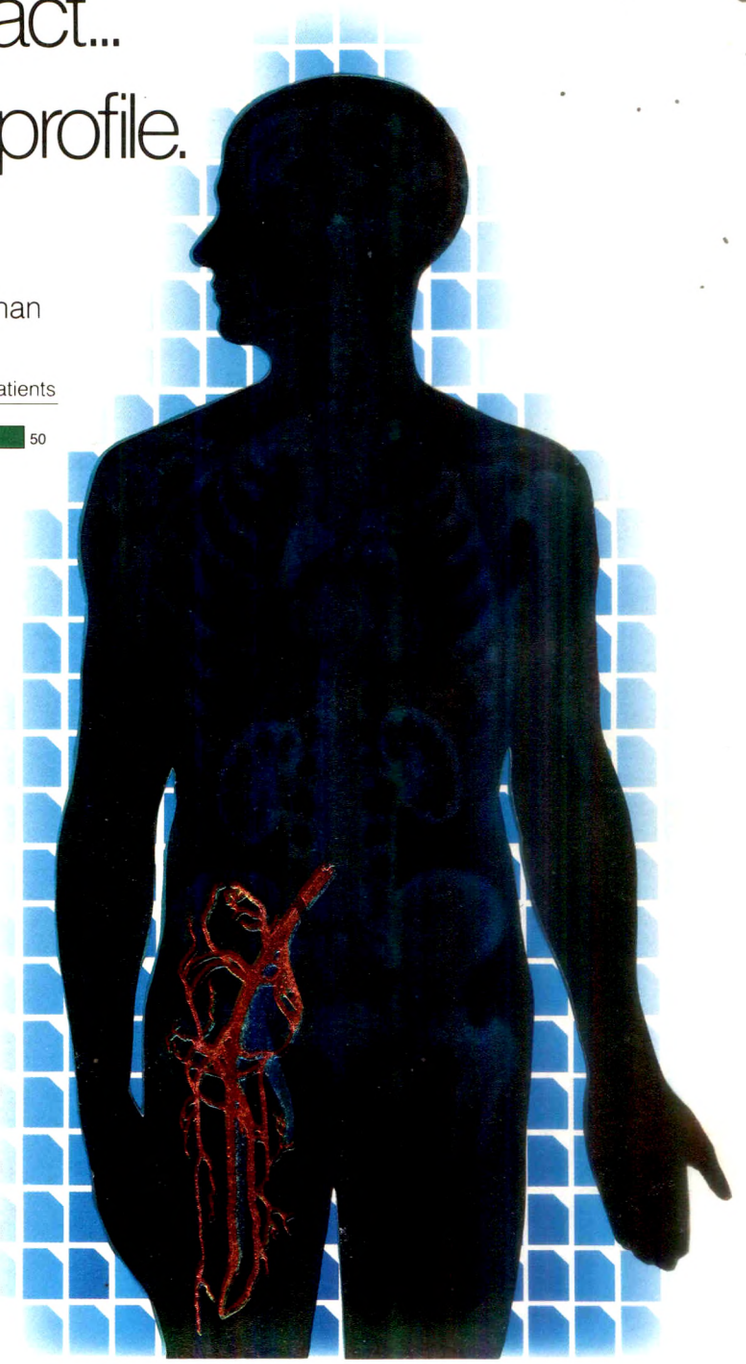


Adapted from Enge.[2]

Excellent vascular tolerance.
Lower incidence of thrombophlebitis.[2]

Excellent cardiovascular profile.
Reduced effect on blood pressure and heart rate.[4,5]

Pulsation should be present in the artery to be injected.



NONIONIC

OMNIPAQUE®

(IOHEXOL)

THE NEW STANDARD IN

See next page for important product information concerning contraindications, warnings, adverse reactions, patient selection, and precautionary recommendations.



OMNIPAQUE®
INJECTION (IOHEXOL)
INTRAVASCULAR

240

300

350

PLEASE CONSULT FULL PRODUCT INFORMATION BEFORE USING.
A SUMMARY FOLLOWS:

DESCRIPTION: OMNIPAQUE is a nonionic, water-soluble radiographic contrast medium for intravascular administration and is provided in iodine concentrations of 240, 300, and 350 mgI/mL. Each milliliter of iohexol solution contains 1.21 mg tromethamine and 0.1 mg edetate calcium disodium with the pH adjusted between 6.8 and 7.7 with hydrochloric acid or sodium hydroxide, but it contains no preservatives.

CONTRAINDICATIONS: OMNIPAQUE should not be administered to patients with a known hypersensitivity to iohexol.

WARNINGS: OMNIPAQUE should be used with extreme care in patients with: severely impaired renal and/or hepatic function; severe thyrotoxicosis, hyperthyroidism, or an autonomously functioning thyroid nodule, diabetes with a serum creatinine level above 3 mg/dL. Not recommended for use in patients with anuria.

Patients with known or suspected pheochromocytoma should receive a minimum of contrast medium if benefit of the exam is judged to outweigh risk; blood pressure should be monitored throughout the procedure, and measures for the treatment of hypertensive crisis should be readily available.

Contrast agents are potentially hazardous in patients with multiple myeloma or other paraproteinemia, particularly those with therapeutically resistant anuria. The combination of contrast agent and dehydration may precipitate myeloma protein in the renal tubules. No form of therapy, including dialysis, has been successful in reversing the effect. Myeloma, which occurs most commonly in persons over age 40, should be considered before instituting intravascular administration of contrast agents.

PRECAUTIONS: Diagnostic procedures that involve the use of radiopaque diagnostic agents should be carried out under the direction of personnel with the prerequisite training and with a thorough knowledge of the particular procedure to be performed. Appropriate facilities should be available for coping with any complication of the procedure, as well as for emergency treatment of severe reactions to the contrast agent itself. Competent personnel and emergency facilities should be available for at least 30 to 60 minutes postprocedure. The possibility of serious, life-threatening, fatal, anaphylactoid, or cardiovascular reactions should always be considered (see ADVERSE REACTIONS). It is of utmost importance that a course of action be carefully planned in advance for immediate treatment of serious reactions. Preparatory dehydration is dangerous and may contribute to acute renal failure in patients with advanced vascular disease, diabetic patients, and in susceptible nondiabetic patients (often elderly with preexisting renal disease). *Patients should be well hydrated prior to and following iohexol administration.* Careful consideration to the potential risk of acute renal failure should be given before performing excretory urography in diabetic patients with diabetic nephropathy and in susceptible nondiabetic patients (often elderly with preexisting renal disease). Immediately following surgery, excretory urography should be used with caution in renal transplant recipients. The possibility of an idiosyncratic reaction in susceptible patients should always be considered (see ADVERSE REACTIONS). The susceptible population includes patients with a history of a previous reaction to contrast media, patients with a known sensitivity to iodine per se, and patients with a known clinical hypersensitivity: bronchial asthma, hay fever, and food allergies. A thorough medical history with emphasis on allergy and hypersensitivity, prior to the injection of any contrast media, may be more accurate than pretesting in predicting potential adverse reactions.

A positive history of allergies or hypersensitivity does not arbitrarily contraindicate the use of a contrast agent where a diagnostic procedure is thought essential, but caution should be exercised (see ADVERSE REACTIONS). Premedication with antihistamines or corticosteroids to avoid or minimize possible allergic reactions in such patients should be considered. Recent reports indicate that such pretreatment does not prevent serious, life-threatening reactions but may reduce both their incidence and severity.

Even though the osmolality of OMNIPAQUE is low compared to diatrizoate- or iothalamate-based ionic agents of comparable iodine concentration, the potential transitory increase in circulatory osmotic load in patients with congestive heart failure requires caution during injection. These patients should be observed for several hours following the procedure to detect delayed hemodynamic disturbances.

Angiography should be avoided whenever possible in patients with homocystinuria, because of the risk of inducing thrombosis and embolism.

In angiographic procedures, the possibility of dislodging plaques or damaging or perforating the vessel wall should be borne in mind during the catheter manipulations and contrast medium injection. Test injections to ensure proper catheter placement are recommended.

Selective coronary arteriography should be performed only in those patients in whom the expected benefits outweigh the potential risk. The inherent risks of angiocardiography in patients with chronic pulmonary emphysema must be weighed against the necessity for performing this procedure.

When OMNIPAQUE is to be injected using plastic disposable syringes, the contrast medium should be drawn into the syringe and used immediately.

The inhibitory effects of nonionic contrast media on mechanisms of hemostasis have been shown, in vitro, to be less than those of ionic contrast media at comparable concentrations. For this reason, standard angiographic procedures should always be followed: angiographic catheters should be flushed frequently, and prolonged contact of blood with contrast media in syringes and catheters should be avoided.

If nondisposable equipment is used, scrupulous care should be taken to prevent residual contamination with traces of cleansing agents.

Drug/Laboratory Test Interaction: If iodine-containing isotopes are to be administered for the diagnosis of thyroid disease, the iodine-binding capacity of thyroid tissue may be reduced for up to 2 weeks after contrast medium administration. Thyroid function tests which do not depend on

Carcinogenesis, Mutagenesis, Impairment of Fertility: No long-term animal studies have been performed to evaluate carcinogenic potential, mutagenesis, or whether OMNIPAQUE can affect fertility in men or women.

Pregnancy Category B: Reproduction studies have been performed in rats and rabbits with up to 100 times the recommended human dose. No evidence of impaired fertility or harm to the fetus has been demonstrated due to OMNIPAQUE. There are, however, no studies in pregnant women. Because animal reproduction studies are not always predictive of human response, this drug should be used during pregnancy only if clearly needed.

Nursing Mothers: It is not known to what extent iohexol is excreted in human milk. However, many injectable contrast agents are excreted unchanged in human milk. Although it has not been established that serious adverse reactions occur in nursing infants, caution should be exercised when intravascular contrast media are administered to nursing women. Bottle feedings may be substituted for breast feedings for 24 hours following administration of OMNIPAQUE.

Pediatric Use: Safety and effectiveness in children have not been established.

ADVERSE REACTIONS: Usually mild to moderate in severity. However, serious, life-threatening, and fatal reactions, mostly of cardiovascular origin, have been associated with the administration of iodine-containing contrast media including OMNIPAQUE. The injection of contrast media is frequently associated with the sensation of warmth and pain, especially in peripheral angiography; pain and warmth are less frequent and less severe with OMNIPAQUE than with many contrast media.

Cardiovascular System: Arrhythmias including PVCs and PACs (3%), angina/chest pain (2%), and hypotension (1%). Others including cardiac failure, asystole, bradycardia, tachycardia, and vasovagal reaction were reported with an individual incidence of less than 0.8%. In controlled clinical trials involving 900 patients, one fatality occurred. A cause-and-effect relationship between this death and iohexol has not been established.

Nervous System: Pain (6%), photomas (3%), headache (2%), and metallic taste (0.8%). Others including anxiety, blurred vision, dizziness, fever, motor and speech dysfunction, convulsion, lightheadedness, paresthesia, somnolence, vertigo, stiff neck, hemiparesis, and nystagmus were reported, with an individual incidence of less than 0.3%.

Respiratory System: Dyspnea and laryngitis, with an individual incidence of 0.1%.

Gastrointestinal System: Nausea (2%) and vomiting (0.5%). Others including diarrhea, dyspepsia, and dry mouth were reported, with an individual incidence of 0.1%.

Skin and Appendages: Urticaria (0.3%) and purpura (0.1%).

General Adverse Reactions to Contrast Media: The following reactions have been reported after administration of other intravascular iodinated contrast media. *Reactions due to technique:* hematomas and ecchymoses. *Hemodynamic reactions:* vein cramp and thrombophlebitis following intravenous injection. *Cardiovascular reactions:* rare cases of cardiac arrhythmias, reflex tachycardia, chest pain, cyanosis, hypertension, hypotension, peripheral vasodilatation, shock, and cardiac arrest. *Renal reactions:* occasionally, transient proteinuria; rarely, oliguria or anuria. *Allergic reactions:* asthmatic attacks, nasal and conjunctival symptoms, dermal reactions such as urticaria with or without pruritus, as well as pleomorphic rashes, sneezing, and lacrimation; rarely, anaphylactic reactions. Rare fatalities have occurred due to these or unknown causes. *Signs and symptoms related to the respiratory system:* pulmonary or laryngeal edema, bronchospasm, dyspnea; or *to the nervous system:* restlessness, tremors, convulsions. *Other reactions:* flushing, pain, warmth, metallic taste, nausea, vomiting, anxiety, headache, confusion, pallor, weakness, sweating, localized areas of edema (especially facial cramps), neutropenia, and dizziness. Rarely, immediate or delayed rigors can occur, sometimes accompanied by hyperpyrexia. Infrequently, "iodism" (salivary gland swelling) from organic iodinated compounds appears 2 days after exposure and subsides by the sixth day.

In general, the reactions that are known to occur upon parenteral administration of iodinated contrast agents are possible with any nonionic agent. Approximately 95% of adverse reactions accompanying the use of water-soluble intravascularly administered contrast agents are mild to moderate in degree. However, severe, life-threatening anaphylactoid reactions, mostly of cardiovascular origin, have occurred.

Reported incidences of death range from 6.6 per 1 million (0.00066%) to 1 in 10,000 (0.01%). Most deaths occur during injection or 5 to 10 minutes later, the main feature being cardiac arrest, with cardiovascular disease as the main aggravating factor. Isolated reports of hypotensive collapse and shock are found in the literature. The incidence of shock is estimated to be 1 out of 10,000 (0.005%) patients.

Adverse reactions to injectable contrast media fall into two categories: chemotoxic reactions and idiosyncratic reactions.

Chemotoxic reactions result from the physicochemical properties of the contrast media, the amount of dose injected, and the speed of injection. All hemodynamic disturbances and injuries to organs or vessels perfused by the contrast medium are included in this category.

Idiosyncratic reactions include all other reactions. They occur more frequently in patients 20 to 40 years old. Idiosyncratic reactions may or may not be dependent on the amount of dose injected, the speed of injection and the radiographic procedure. Idiosyncratic reactions are subdivided into minor, intermediate, and severe. The minor reactions are self-limited and of short duration; the severe reactions are life-threatening and treatment is urgent and mandatory.

The reported incidence of adverse reactions to contrast media in patients with a history of allergy is twice that in the general population. Patients with a history of previous reactions to a contrast medium are three times more susceptible than other patients. However, sensitivity to contrast media does not appear to increase with repeated examinations.

Most adverse reactions to injectable contrast media appear within 1 to 3 minutes after the start of injection, but delayed reactions may occur.

Regardless of the contrast agent employed, the overall estimated incidence of serious adverse reactions is higher with angiocardiography than with other procedures. Cardiac decompensation, serious arrhythmias, angina pectoris, or myocardial ischemia or infarction may occur during angiocardiography and left ventriculography. Electrocardiographic and hemodynamic abnormalities occur less frequently with OMNIPAQUE than with diatrizoate meglumine and diatrizoate sodium injection.

References: 1. Gordon IJ, Skoblar RS, Chicatelli PD, et al: A comparison of iohexol and Conray-60 in peripheral arteriography. *AJR* 1984; 142:563-565. **2.** Enge I: Phlebography: Survey and present state. *Acta Radiol* 1983; suppl 366, pp 50-53. **3.** Wolf GL: Adult peripheral angiography: Results from four North American randomized clinical trials of ionic media versus iohexol. *Acta Radiol* 1983; suppl 366, pp 166-170. **4.** Egsgaard H, Hørup A, Praestholm J: Iohexol and diatrizoate in aortofemoral angiography: a controlled clinical trial. *Acta Radiol* 1983; suppl 366, p 173. **5.** Higgins CB, Mancini GBJ, Bloomquist JN, et al: Cardioangiography in man using iohexol and meglumine-Na diatrizoate: A comparison of hemodynamic and electrocardiographic effects. *Acta Radiol* 1983; suppl 366, pp 111-114.

Winthrop PHARMACEUTICALS

Winthrop Pharmaceuticals
Division of Sterling Drug Inc.

CONSISTENCY...

U.S. Currency – recognized world wide as a standard of consistency.



From the beginning of Fuji's effort to manufacture the highest quality medical x-ray films in the world, one thing was apparent. Quality that can't be reproduced with *every sheet* is no quality at all. That's why Fuji designed and constructed what remains today the most modern and sophisticated medical x-ray film factory in the world. So with the same assurance you would have that these 100-dollar bills are identical, one to another, it is with this mind set that Fuji manufactures medical x-ray film. The result: From sheet-to-sheet, box-to-box, no manufacturer produces a *more consistent medical x-ray* film than FUJI. NO ONE!

The point is – If you're not getting this kind of consistency from your current film, you are wasting *hundreds of dollars.*

Let Fuji show your radiology department the difference between consistent and *UNCOMMONLY CONSISTENT.* Call your local Fuji Representative, or 800-431-1850.



**FUJI QUALITY...
UNCOMMONLY
CONSISTENT.**

I&I *Imaging & Information*

FUJI MEDICAL SYSTEMS, U.S.A., INC.
90 Viaduct Road, P.O. Box 4960, Stamford, CT 06907

CIRCLE 7 ON READER SERVICE CARD

Volume 149 American Journal of Roentgenology September 1987

1987 ARRS EXECUTIVE COUNCIL AWARD

453 **Intraarterial fibrinolytic therapy for popliteal and tibial artery obstruction: comparison of streptokinase and urokinase.** *Traughber PD, Cook PS, Micklos TJ, Miller FJ*

PROGRESS IN RADIOLOGY

457 **MR imaging of the musculoskeletal system: current and future status.** *Sartoris DJ, Resnick D*

CARDIOPULMONARY RADIOLOGY

469 **Reliability of selective pulmonary arteriography in the diagnosis of pulmonary embolism.** *Quinn MF, Lundell CJ, Klotz TA, et al.*

473 **Intrathoracic manifestations of metastatic testicular seminoma: a comparison of chest radiographic and CT findings.** *Williams MP, Husband JE, Heron CW*

477 **Case report. Aberrant right subclavian artery with a large diverticulum of Kommerell: a potential for misdiagnosis.** *Walker TG, Geller SC*

ENDOCRINE RADIOLOGY

479 **Selective intraarterial DSA of the parathyroid glands in patients with hyperparathyroidism after parathyroidectomy.** *Lacombe P, Foster D, Dubost C, et al.*

GASTROINTESTINAL RADIOLOGY

485 **Memorial award of the SGR. Cholangiographic findings in hepatic artery occlusion after liver transplantation.** *Zajko AB, Campbell WL, Logsdon GA, et al.*

491 **Focal fatty change of the liver adjacent to the falciform ligament: CT and sonographic findings in five surgically confirmed cases.** *Yoshikawa J, Matsui O, Takashima T, et al.*

495 **The inferior accessory hepatic fissure: sonographic appearance.** *Lim JH, Ko YT, Han MC, Kim CW, Choi BI, Im JG*

499 **Sonographic features of amebic and pyogenic liver abscesses: a blinded comparison.** *Ralls PW, Barnes PF, Radin DR, Colletti P, Halls J*

502 **Technical note. Double-contrast examination of the colon with carbon dioxide: the use of effervescent powder.** *Pochaczevsky R*

505 **Case report. Focal acute acalculous cholecystitis.** *Warshauer D, Scott G, Gottschalk A*

507 **Pancreas transplantation with pancreatico-duodenocystostomy for exocrine drainage: cystographic findings.** *Woolsey EJ, Tauscher JR, Dafoe DC*

511 **Case report. Ascaris-induced pancreatitis.** *Leung JWC, Mok SD, Metreweli C*

513 **Technical note. Esophageal deviation: pushed or pulled?** *Levine MS, Gilchrist AM*

515 **Appendicitis as the initial manifestation of Crohn's disease: radiologic features and prognosis.** *Agha FP, Ghahremani GG, Panella JS, Kaufman MW*

519 **Opinion. Primary panendoscopy: a radiologist's response.** *Gelfand DW, Ott DJ, Chen YM*

GENITOURINARY RADIOLOGY

521 **The distinction between acute renal transplant rejection and cyclosporine nephrotoxicity: value of duplex sonography.** *Buckley AR, Cooperberg PL, Reeve CE, Magil AB*

527 **The evaluation of gross hematuria in anticoagulated patients: efficacy of IV urography and cystoscopy.** *Cuttino JT Jr, Clark RL, Feaster SH, Zwicke DL*

529 **Case report. Spermatic granuloma complicating abdominoperineal resection of the rectum: diagnosis by CT, MR imaging, and percutaneous biopsy.** *Feaster SH, Kinard RE, Yancey JM, Marsh RL*

MUSCULOSKELETAL RADIOLOGY

531 **MR imaging of marrow changes adjacent to end plates in degenerative lumbar disk disease.** *de Roos A, Kressel H, Spritzer C, Dalinka M*

535 **The effect of restricting the indications for lumbosacral spine radiography in patients with acute back symptoms.** *Baker SR, Rabin A, Lantos G, Gallagher EJ*

539 **Percutaneous biopsy of the cervical spine using CT guidance.** *Kattapuram SV, Rosenthal DI*

543 **Pictorial essay. MR imaging of the normal elbow: anatomic correlation.** *Middleton WD, Macrander S, Kneeland JB, Froncisz W, Jesmanowicz A, Hyde JS*

549 **Sonography in the detection of meniscal injuries of the knee: evaluation in cadavers.** *Selby B, Richardson ML, Nelson BD, Graney DO, Mack LA*

555 **Technical note. A CT table attachment for parasagittal scanning of the axilla.** *Roger DJ, Richli WR*

557 **MR imaging of solitary osteochondromas: report of eight cases.** *Lee JK, Yao L, Wirth CR*

561 **Perspective. Arthrography: past, present, and future.** *Hall FM*

PEDIATRIC RADIOLOGY

563 **Sonographic measurements of the normal bladder wall in children.** *Jequier S, Rousseau O*

567 **Case report. Cor triatriatum: diagnosis by MR imaging.** *Bisset GS III, Kirks DR, Strife JL, Schwartz DC*

569 **Case report. Atrial ventricular diverticulum: sonographic diagnosis.** *Karnaze MG, Shackelford GD, Abramson CL*

NEURORADIOLOGY

572 **ASNR: the Silver Anniversary. Neuroradiology: the next 25 years.** *Taveras JM*

575 **Lymphomas of the head and neck: CT findings at initial presentation.** *Lee Y-Y, Van Tassel P, Nauert C, North LB, Jing B-S*

583 **An early CT sign of ischemic infarction: increased density in a cerebral artery.** *Pressman BD, Tourje EJ, Thompson JR*

587 **Carotid cavernous fistulae: indications for urgent treatment.** *Halbach VV, Hieshima GB, Higashida RT, Reicher M*

595 **Pitfalls in the CT diagnosis of atlantoaxial rotary subluxation.** *Kowalski HM, Cohen WA, Cooper P, Wisoff JH*

VASCULAR RADIOLOGY

601 **Role of CT in excluding major arterial injury after blunt thoracic trauma.** *Mirvis SE, Kostrubiak I, Whitley NO, Goldstein LD, Rodriguez A*

607 **Penetrating injuries of the thoracic aorta and brachiocephalic arteries: angiographic findings in 18 cases.** *Fisher RG, Ben-Menachem Y*

613 **Angiography in patients with arterial trauma: correlation between angiographic abnormalities, operative findings, and clinical outcome.** *Rose SC, Moore EE*

INTERVENTIONAL RADIOLOGY

623 **Technical note. Use of light localizer in fluoroscopically guided percutaneous procedures.** *Hayt DB*

625 **Technical note. Percutaneous atheroma removal using a wire basket.** *Kim D, Turkel DH, Orron DE, Steer ML*

629 **Technical note. Improved guidewire immobilization technique for interventional procedures.** *Gavant ML*

RADIOLOGIC PHYSICS

631 **An improved method for estimating the entrance exposure in diagnostic radiographic examinations.** *Zamenhof RG, Shahabi S, Morgan HT*

OPINIONS

638 **Wall Street entrepreneurs and imaging centers: an insidious threat to radiology.** *Berlin L*

641 **Risk management for the radiologist.** *Smith JP*

OTHER CONTENT

510 **1988 Residents' award paper announcement**

582 **American Roentgen Ray Society information**

612 **Forthcoming articles**

620 **ARRS membership invitation and application**

644 **Letters**

649 **Review of current literature**

653 **News**

656 **1988 ARRS meeting summary, calls for papers and exhibits**

661 **Classified ads**

Book reviews 468, 472, 484, 490, 498, 542, 548, 606

A3 **Guidelines for authors**